NUCLEAR SCIENCE ABSTRACTS

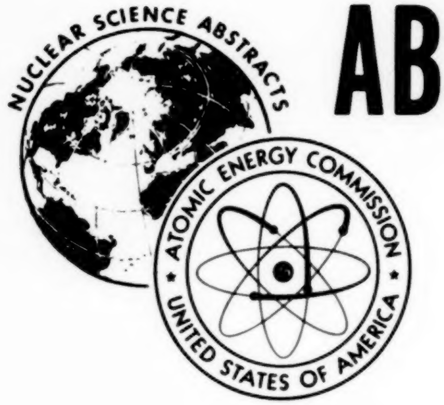

Volume 25 Number 7

Abstracts 12921-15469

April 15, 1971

UNITED STATES ATOMIC ENERGY COMMISSION
Division of Technical Information

REPORT COLLECTIONS IN THE UNITED STATES

The libraries listed below purchase and maintain microfiche collections of USAEC and foreign reports that are abstracted in *NSA*. Their collections also include *NSA* and its indexes, AEC's Technical Progress Reviews, AEC-sponsored translations, conference proceedings published by AEC, and various bibliographic tools. Most of these libraries have microfiche reader-printers or other photocopy facilities with which to reproduce enlarged copies from microfiche. Charges for reproduction services vary.

ALABAMA
Auburn, Auburn University
Tuskegee Institute, Tuskegee Institute
ALASKA
College, University of Alaska
ARIZONA
Tucson, University of Arizona
ARKANSAS
Fayetteville, University of Arkansas
CALIFORNIA
Davis, University of California
Los Angeles, University of California
COLORADO
Boulder, University of Colorado
DISTRICT OF COLUMBIA
Washington, Library of Congress (by deposit)
FLORIDA
Gainesville, University of Florida
GEORGIA
Atlanta, Georgia Institute of Technology
HAWAII
Honolulu, University of Hawaii
IDAHO
Pocatello, Idaho State University
ILLINOIS
Evanston, Northwestern University
Urbana, University of Illinois
INDIANA
Lafayette, Purdue University
IOWA
Ames, Iowa State University
KANSAS
Manhattan, Kansas State University
KENTUCKY
Lexington, University of Kentucky
Louisville, University of Louisville
LOUISIANA
Baton Rouge, Louisiana State University
New Orleans, Tulane University
MARYLAND
Baltimore, Johns Hopkins University
College Park, University of Maryland
MASSACHUSETTS
Cambridge, Massachusetts Institute of Technology
MICHIGAN
Ann Arbor, University of Michigan
MISSISSIPPI
State College, Mississippi State University
MISSOURI
Kansas City, Linda Hall Library
NEVADA
Las Vegas, University of Nevada
NEW JERSEY
Princeton, Princeton University
NEW MEXICO
Albuquerque, University of New Mexico
NEW YORK
Albany, New York State Library
Buffalo, State University of New York at Buffalo
Ithaca, Cornell University
New York, Columbia University
Rochester, University of Rochester
Syracuse, Syracuse University
Troy, Rensselaer Polytechnic Institute
NORTH CAROLINA
Raleigh, North Carolina State University
OHIO
Cincinnati, University of Cincinnati
Columbus, Ohio State University
Toledo, University of Toledo
OKLAHOMA
Norman, University of Oklahoma
PENNSYLVANIA
Philadelphia, University of Pennsylvania
Pittsburgh, Carnegie Library
University Park, Pennsylvania State University
PUERTO RICO
San Juan, University of Puerto Rico
SOUTH CAROLINA
Columbia, University of South Carolina
TENNESSEE
Knoxville, University of Tennessee
Nashville, Joint University Libraries
Oak Ridge, Oak Ridge Associated Universities
TEXAS
Austin, University of Texas
College Station, Texas A & M University
Houston, Rice University
UTAH
Salt Lake City, University of Utah
VIRGINIA
Blacksburg, Virginia Polytechnic Institute
Charlottesville, University of Virginia
WASHINGTON
Pullman, Washington State University
Seattle, University of Washington
WEST VIRGINIA
Morgantown, West Virginia University
WISCONSIN
Madison, University of Wisconsin
WYOMING
Laramie, University of Wyoming

The following governmental and international organizations offer for sale USAEC reports abstracted in *Nuclear Science Abstracts:*

National Technical Information Service, U. S. Department of Commerce
Springfield, Virginia 22151
International Atomic Energy Agency, Vienna, Austria
National Lending Library, Boston Spa, England

Volume 25, Number 7, April 15, 1971

NUCLEAR SCIENCE ABSTRACTS

A semimonthly publication of the USAEC Division of Technical Information, Edward J. Brunenkant, Director,
Published by the USAEC Division of Technical Information Extension, Robert L. Shannon, Extension Manager.

Nuclear Science Abstracts provides the only comprehensive abstracting and indexing coverage of international nuclear science literature. *Nuclear Science Abstracts* covers scientific and technical reports of the U. S. Atomic Energy Commission and its contractors, other U. S. Government agencies, other governments, universities, and industrial and research organizations. In addition, books, conference proceedings, individual conference papers, patents, and journal literature on a worldwide basis are abstracted and indexed. Each issue of *Nuclear Science Abstracts* includes four indexes: subject, personal author, corporate author, and report number.

The following organizations scan and abstract the nuclear science literature in their respective countries:

Atomic Energy of Canada Limited
Australian Atomic Energy Commission
Danish Atomic Energy Commission
Finnish Atomic Energy Commission
French Atomic Energy Commission
Japan Atomic Energy Bureau–Atomic Energy Research Institute
Institutt for Atomenergi (Norway)
Aktiebolaget Atomenergi (Sweden)
United Kingdom Atomic Energy Authority

Numerous organizations, societies, and publishers throughout the world provide *Nuclear Science Abstracts* with advance page-proof copy of their publications, e.g., in the United States the American Institute of Physics provides page-proof copy of its publications.

A list of the journals scanned regularly and the abbreviations used appears in Issue 1 (January 15) of each volume of *Nuclear Science Abstracts* and is supplemented in Issues 7, 13, and 19. Issue 1 of each volume also describes the scope and arrangement of the subject matter covered in *Nuclear Science Abstracts.* The subject matter covered is also described in TID-4552, *Subject Scope of Nuclear Science Abstracts,* available free from the USAEC Division of Technical Information Extension, P.O. Box 62, Oak Ridge, Tennessee 37830. An outline of the subject categories appears in the Contents of each issue.

AVAILABILITY OF PUBLICATIONS ABSTRACTED

Public availability of all U. S. Atomic Energy Commission reports is indicated in the report number indexes. The availability of other reports, when known, is also indicated. The availability of some unnumbered reports is given in the abstract.

Dissertations abstracted in *Dissertation Abstracts* and included in *Nuclear Science Abstracts* are available from University Microfilms, Inc., 315 N. First Street, Ann Arbor, Michigan 48103.

Information on the availability of the published literature and unpublished conference papers abstracted in *Nuclear Science Abstracts* can be obtained from the USAEC Division of Technical Information Extension, P.O. Box 62, Oak Ridge, Tennessee 37830.

HOW TO OBTAIN NUCLEAR SCIENCE ABSTRACTS

Nuclear Science Abstracts is available to the public on a subscription basis from the Superintendent of Documents, U. S. Government Printing Office, Washington, D. C. 20402.

For the 24 regular issues, the yearly rate is $42.00 for domestic subscribers and $52.50 for foreign subscribers. A single issue costs $1.75, domestic rates, or $2.19, foreign rates. Domestic rates apply to the United States, Canada, Mexico, and Central and South American countries except Argentina, Brazil, Guyana, French Guiana, Surinam, and British Honduras.

For a yearly subscription to the cumulative indexes, the rates are $38.00 for domestic subscribers and $47.50 for foreign subscribers.

The following cumulative indexes are available:

From Johnson Reprint Corporation, 111 Fifth Avenue, New York, N. Y. 10003:
  Vols. 1–4, Subjects and Authors (1948–1950), $30.00.

From Superintendent of Documents, U. S. Government Printing Office, Washington, D. C. 20402:

Vols. 5–10, Subjects and Authors (1951–1956), $5.25.

Vols. 11–15, Subjects (1957–1961), $19.00.
Vols. 11–15, Personal Authors (1957–1961), $14.25.
Vols. 11–15, Corporate Authors (1957–1961), $2.50.

Vols. 16–20, Subjects (1962–1966), $36.00.
Vols. 16–20, Personal Authors (1962–1966), $22.50.
Vols. 16–20, Corporate Authors (1962–1966), $3.75.

Vol. 21, Subjects and Authors (1967), $16.00.
Vol. 22, Subjects and Authors (1968), $26.00.
Vol. 23, Subjects and Authors (1969), $25.75.
Vol. 24, Subjects and Authors (1970), $22.50.

Cumulative Report Number Index, Vols. 1-15 Revised, $4.00.
Cumulative Report Number Index, Vols. 16-20 Revised, $5.50.
Cumulative Report Number Index, Vols. 21-24, $4.25.

Nuclear Science Abstracts is available on an exchange basis to universities, research institutions, industrial firms, and publishers of scientific information. Government agencies may obtain *NSA* free of charge. Inquiries should be directed to the USAEC Division of Technical Information Extension, P. O. Box 62, Oak Ridge, Tennessee 37830.

INDEXES TO NSA

Comprehensive indexes appear in each issue and are cumulated quarterly and annually. Multivolume cumulations have been issued as indicated above.

All documents abstracted are indexed by subjects and personal authors. Report literature is indexed also by corporate author and report number. Each of these indexes in every issue is preceded by an introduction explaining in detail the organization of the index and the principles by which it is compiled. The reader is referred to these explanations for information not found in the brief summary below.

Personal Authors

Each author's name is indexed in the form appearing on the document abstracted:

ISHIHARA, T., Accumulation of fallout ^{137}Cs in newborn infants, 23:50538
ISHIHARA, Toyokuki, Shielding effect of paraffin, water, soil, concrete, Fe, and Pb for nigh-energy neutrons, 23:51748

Subjects

The subject index consisting of specific materials, objects, and processes is arranged alphabetically. Modifying phrases specific to these subjects in turn are arranged alphabetically under the subjects.

MELPHALAN
  effects on proliferation of cultured antigen-stimulated spleen cells from mice, dose-response curve for, 23:50820
MEMBRANE FILTERS
  design for removal of cell-free Streptococcus faecalus from bacteria cultures in fermentation tank, 23:49996 (UCRL-18667, pp 322-9)
MENDELEVIUM
  separation from einsteinium and fermium by electrolysis, 23:49772 (UCRL-18667, pp 277-312)
  separation from sodium acetate solutions by solvent extraction using sodium amalgam, 23:49772 (UCRL-18667, pp 277-312)
  stability of divalent state of, 23:49772 (UCRL-18667, pp 277-312)

Corporate Authors

Technical report literature is indexed from the name of the organization or institution responsible for the issuance of the report.

51093 (LA-4164) FABRICATION OF BORON CARBIDE RINGS AND DISKS. Sheinberg, H.; Herrera, T.; Kostacopoulos, J. **(Los Alamos Scientific Lab., N. Mex.)**. Apr. 25, 1969. Contract W-7405-eng-36. 11p. Dep. CFSTI.

is indexed as:

LOS ALAMOS SCIENTIFIC LAB., N. MEX.
  Fabrication of boron carbide rings and disks, 23:51093 (LA-4164)

Report Numbers

Technical report literature is also indexed by report numbers. This index includes information on where individual reports may be obtained. While not reports, patents and conference papers are indexed here as a matter of convenience.

JPRS-	(Non-AEC)	
46949	23-51587	CFSTI
48330	23-52305	CFSTI
48331	23-52451	CFSTI
48481	23-50889	CFSTI
48743	23-51034	CFSTI
49025	23-51706	CFSTI (U. S. Sales Only)
JUL-	(German)	
571-RG	23-52269	Dep
578-PP	23-51624	Dep. CFSTI (U. S. Sales Only)
581-FN	23-51079	Dep. CFSTI (U. S. Sales Only)
584-RG	23-52313	Dep
586-FN	23-51035	Dep. CFSTI (U. S. Sales Only)
K-		
1777	23-50987	Dep. CFSTI
1778	23-50988	Dep. CFSTI
KFK-	(German)	
743	23-52461	Dep
743	23-52447	For translation see EURFNR-613
781/I	23-52462	Dep
824	23-52397	Dep. CFSTI (U. S. Sales Only)

XUM

TABLE OF CONTENTS

Volume 25, Number 7, April 15, 1971

Category *Page*

- **CHEMISTRY** 1255
  - Analytical Chemistry 1255
    - *Chemical and Spectral Procedures* 1255
    - *Isotope Dilution Procedures* 1258
    - *Radiometric and Radiochemical Procedures* 1258
    - *Activation Procedures* 1258
  - Inorganic, Organic, and Physical Chemistry 1261
    - *Chemical Properties* 1261
    - *Isotope Effects and Exchange* 1261
    - *Physical Chemistry* 1265
  - Radiation and Nuclear Chemistry 1267
    - *Radiation Effects* 1267
    - *Radiation Processes* 1267
    - *Radiolysis* 1269
    - *Radioisotope Production* 1271
    - *Recoil Production and Reactions* 1271
  - Radiochemistry 1272
  - Separation Processes 1272
- **EARTH SCIENCES** 1276
  - Geology and Hydrology 1276
  - Meteorology 1277
  - Mineralogy and Exploration 1278
  - Oceanography 1279
  - Seismology 1279
- **ENGINEERING** 1280
  - Nuclear Explosions 1280
  - Facilities and Equipment 1280
  - Heat Transfer and Fluid Flow 1282
  - Isotope Technology 1283
  - Materials Testing 1285
  - Protective Structures 1285
  - Radioactive Material Handling 1286
- **INSTRUMENTATION** 1289
  - Radiation Detection Instruments 1289
    - *General Detectors and Monitors* 1289
    - *Nuclear Spectroscopic Instrumentation* 1291
    - *High Energy Physics Instrumentation* 1291
  - Radiation Dosimeters 1297
  - Radiometric Instruments 1297
  - Miscellaneous Instruments and Components 1298
  - Radiation Effects on Instruments and Instrument Components 1299
- **LIFE SCIENCES** 1300
  - Biochemistry, Physiology, and Molecular Biology 1300
    - *Basic Processes* 1300
    - *Metabolism, Physiology, and Toxicology* 1301
    - *Radiation Effects* 1303
    - *Immunology* 1306
  - Ecology 1306
  - Genetics and Cytogenetics 1308
  - Health Physics and Safety 1310
    - *Radioactive Contamination and Decontamination* 1310
    - *Dosimetry and Monitoring* 1311
    - *Radiation Protection* 1313
    - *Safety Procedures* 1314

Category *Page*

LIFE SCIENCES (Cont'd.)

    - *Civil Defense* 1314
    - *Legal Aspects* 1314
  - Medicine 1314
    - *Protective Substances* 1314
    - *Radiation Sickness and Injuries* 1315
    - *Radiodiagnosis* 1316
    - *Radiotherapy* 1319
  - Radiation Effects on Animals 1321
    - *Invertebrates* 1322
    - *Vertebrates* 1322
    - *Man* 1325
  - Radiation Effects on Plants 1326
  - Radiation Effects on Microorganisms 1327
  - Radiosterilization and Radiopreservation 1329
- **METALS, CERAMICS, AND OTHER MATERIALS** 1330
  - Metals and Alloys 1330
    - *Corrosion and Erosion* 1330
    - *Preparation and Fabrication* 1331
    - *Properties Evaluations* 1332
    - *Structure and Phase Studies* 1338
    - *Radiation Effects* 1340
  - Ceramics and Cermets 1342
    - *Corrosion and Erosion* 1342
    - *Preparation and Fabrication* 1342
    - *Properties Evaluations* 1343
    - *Structure and Phase Studies* 1344
    - *Radiation Effects* 1346
  - Plastics and Other Materials 1347
- **PHYSICS (GENERAL)** 1348
  - Astrophysics and Cosmology 1348
    - *Cosmic Ray Exposure Ages* 1348
    - *Stars* 1348
    - *Quasi-Stellar, Radio, and X-Ray Sources* 1351
    - *Solar Phenomena* 1354
    - *Galaxies* 1359
    - *Cosmology* 1361
    - *Planetary Phenomena* 1363
  - Atomic and Molecular Physics 1364
    - *Atomic, Electron, Ion, and Molecular Beams and Their Reactions* 1364
    - *Atomic and Molecular Properties* 1366
    - *Positronium, Muonium, and Mesic Atoms and Molecules* 1367
    - *Collision Phenomena* 1368
    - *Atomic Theory* 1374
  - Cosmic Radiation 1375
  - Direct Energy Conversion 1377
  - Fluid Physics 1378
  - Geophysics (Upper Atmosphere) 1380
  - Low-Temperature Physics and Cryogenic Equipment 1383
    - *Superfluidity* 1383
    - *Superconductivity* 1385
    - *Equipment and Devices* 1392
  - Plasma and Thermonuclear Physics 1394
    - *Confinement and Heating* 1394
    - *Diagnostics* 1395

TABLE OF CONTENTS (continued)

Category *Page*

PHYSICS (GENERAL) (Cont'd.)
- *Kinetics (General)* . . . 1398
- *Kinetics (Experimental)* . . . 1399
- *Kinetics (Theoretical)* . . . 1400
- *Production* . . . 1404
- *Stability* . . . 1404
- *Thermonuclear Processes* . . . 1406
- *Wave Phenomena* . . . 1407

Shielding . . . 1410
Solid-State Physics . . . 1412
- *Radiation Effects* . . . 1412
- *Physical Properties* . . . 1415
- *Moessbauer Effects and NMR* . . . 1420
- *Theory* . . . 1421

Theoretical Physics . . . 1422

PHYSICS (HIGH-ENERGY) . . . 1424
Particle Interactions and Properties (Experimental) . . . 1424
- *Electromagnetic* . . . 1424
- *Weak* . . . 1426
- *Strong (Baryon-Induced)* . . . 1427
- *Strong (Meson-Induced)* . . . 1429

Particle Interactions and Properties (Theoretical) . . . 1432
- *General* . . . 1432
- *Electromagnetic* . . . 1433
- *Weak* . . . 1436
- *Strong (General)* . . . 1438
- *Strong (Baryon No. = 0)* . . . 1440
- *Strong (Baryon No. = 1)* . . . 1442
- *Strong (Baryon No. ≥ 2)* . . . 1444

Particle Invariance Principles and Symmetries . . . 1446
- *General* . . . 1446
- *Applications (Electromagnetic and Weak)* . . . 1447
- *Applications (Strong)* . . . 1448

Field Theories . . . 1448
- *General* . . . 1448
- *Quantum Field Theory* . . . 1448
- *Gravitation and General Relativity* . . . 1452

Scattering Theory . . . 1452
Particle Accelerators . . . 1454

Category *Page*

PHYSICS (NUCLEAR) . . . 1458
Neutron Interactions with Matter . . . 1458
Nuclear Properties and Reactions, A ≤ 5 . . . 1460
Nuclear Properties and Reactions, 6 ≤ A ≤ 19 . . . 1461
Nuclear Properties and Reactions, 20 ≤ A ≤ 89 . . . 1464
Nuclear Properties and Reactions, A ≥ 90 . . . 1472
Nuclear Theory . . . 1490

REACTOR TECHNOLOGY . . . 1498
Commercial Power Reactors . . . 1498
- *Operation and Economics* . . . 1498
- *Safety and Siting* . . . 1499

Power Reactor Development . . . 1503
- *Kinetics and Dynamics* . . . 1504
- *Control Systems* . . . 1505
- *Cooling Systems* . . . 1505
- *Fuels* . . . 1506
- *Auxiliary and Emergency Systems* . . . 1507
- *Operation and Economics* . . . 1507
- *Safety and Siting* . . . 1508
- *Power Conversion Systems* . . . 1508

Research and Test Reactors . . . 1508
Rocket and Space Reactors . . . 1510
Reactor Theory . . . 1511
- *Kinetics* . . . 1511
- *Experimental Applications* . . . 1512

Reactor Components, Fuels, and Accessories . . . 1512

GENERAL . . . 1514

CORPORATE AUTHOR INDEX . . . INDEX-1

PERSONAL AUTHOR INDEX . . . INDEX-11

SUBJECT INDEX . . . INDEX-64

REPORT NUMBER INDEX . . . INDEX-162

JOURNAL LIST . . . APPENDIX-1

STAFF OF NUCLEAR SCIENCE ABSTRACTS

John W. Norris
Managing Editor

Donald D. Davis
Assistant Managing Editor

David E. Bost
Production Manager

Sidney F. Lanier
Subject Heading Specialist

J. Paul Meredith
Descriptive Cataloging Specialist

Frederick E. Marsh, Jr.
Computer Index Coordinator

Clara L. Fox
Corporate Author Specialist

Helen W. White
Report Number Specialist

Section Editors

Everett J. Hoffman
Chemistry

Robert C. Kelly
Engineering; Earth Sciences; Metals, Ceramics, and Other Materials

Lee M. Thompson
General Physics

Charles E. Stuber
High Energy Physics; Instrumentation

Helen G. Donald
Life Sciences

Lawrence T. Whitehead
Nuclear Physics

James M. Jacobs
Reactor Technology

Evaluators

Thomas S. Chapman
Rose V. Jermain
John H. Mitchell
Mary H. Newman
Polly C. Summers

Abstractors

F. S. Armstrong*
Ellis R. Bedford
Mary M. Brown
Jane G. Buchanan
D. Lamar Cason
Gloria M. Caton
David C. Cunningham
James R. Dulaney
Helga B. Gerstner
Mary C. Grissom
Phyllis C. Hansen
Carolyn D. Houston
Elaine E. Huber
Rose V. Jermain
W. Hugh Kinser, Jr.
Lisbeth C. Lieberman
Betty L. McDowell
Patricia B. McEwen
Fay M. Martin
William D. Matheny
Dora H. Moneyhun
Jean F. Peckham
Henry D. Raleigh
Mona H. Raridon
Julia S. Redford
Jessie W. Rushing
Robert W. Rutkowski
Francis L. Sachs
Lila B. Smith
Anne G. Ward
Helen L. Ward
Milton O. Whitson
Juanita Wilson

---

*Atomic Energy of Canada, Ltd.

Charles R. Bruce
Publishing Coordinator

Communication concerning the editorial policy and content of *Nuclear Science Abstracts* should be addressed to the Managing Editor, *Nuclear Science Abstracts*, USAEC Division of Technical Information Extension, P. O. Box 62, Oak Ridge, Tennessee 37830.

Use of funds for printing this publication approved by the Director of the Bureau of the Budget, June 26, 1969.

Volume 25, Number 7 April 15, 1971

NUCLEAR SCIENCE ABSTRACTS

CHEMISTRY

Analytical Chemistry

Refer also to abstracts 13195, 13625, 13626, and 13651.

12921 SEPARATION OF RHENIUM FROM MOLYBDENUM, VANADIUM, TUNGSTEN, AND OTHER ELEMENTS BY TRIBENZYLAMINE–CHLOROFORM EXTRACTION FROM PHOSPHORIC ACID. Yatirajam, V.; Kakkar, L. R. (Kurukshetra Univ., Haryana, India). Anal. Chim. Acta; 52: 555-9(Dec 1970).

Some tertiary amines were investigated for separation of rhenium from other elements in various media. The highest extraction was found from sulfuric and phosphoric acids. Tribenzylamine was cheaper than the other tertiary amines with equally high extraction and thus was examined further. The wide applicability of the method was shown by the satisfactory analyses of a variety of samples. (M.C.G.)

Chemical and Spectral Procedures

Refer also to abstracts 13098, 13116, 13309, 13310, 13312, and 13319.

12922 (WHAN-SA-44) DETERMINATION OF RARE EARTHS IN PLUTONIUM–URANIUM MIXED OXIDES. Ko, Roy (WADCO Corp., Richland, Wash.). 31 Aug 1970. Contract AT(45-1)-1830. 4p. (CONF-701017–3). Dep. NTIS.

From 14th Annual Conference on Analytical Chemistry in Nuclear Technology, Gatlinburg, Tenn.

A method to determine all the rare earths in Pu–U mixed oxide fuels by amine extraction-emission spectrography was developed. Rare earth solutions were equilibrated with tri-n-octylamine (TNOA), an internal standard of yttrium then added, and the rare earth–Y intensity ratios compared against those obtained without the extraction step. An average recovery of 96% was obtained. The relative standard deviation varied from ±2 to ±13% with an average of ±7.4%. Based on the recovery and precision measurements, the error in the analysis was estimated to be less than 25% at the 95% confidence level. (P.C.H.)

12923 (WHAN-SA-47) USE OF AMINE EXTRACTION AND EMISSION SPECTROGRAPHY IN THE ANALYSIS OF PLUTONIUM. Ko, Roy (WADCO Corp., Richland, Wash.). 5 Oct 1970. Contract AT(45-1)-1830. 11p. (CONF-701025–2). Dep. NTIS.

From Conference on Chemistry and Spectroscopy, San Francisco, Calif.

Methods for the determination of impurities in Pu by the combination of amine extraction using tri-n-octylamine (TNOA) and emission spectrography are described. The impurities determined include: Ta, Ti, W, Zr, and rare earths. Studies were also made on the effects of HF on amine extraction of Pu in the presence of Ta. (P.C.H.)

12924 (WHAN-SA-62) WATER AND GAS DETERMINATIONS IN MIXED OXIDES. Plucinski, C. E. (WADCO Corp., Richland, Wash.). 26 Oct 1970. Contract AT(45-1)-1830. 5p. (CONF-701017–4). Dep. NTIS.

From 14th Annual Conference on Analytical Chemistry in Nuclear Technology, Gatlinburg, Tenn.

Problems involved in the determination of H_2O and gas in mixed oxide fuels are discussed. A moisture analyzer that operates on a conductometric readout was used for the determination of H_2O. A residual gas analyzer, which has the capability of gas identification as well as quantity measurements, was used for the determination of gas content. The gas was identified as primarily H_2 (>90%) by mass spectrographic analysis. From the analytical viewpoint it was discovered that the presence of H_2 was affecting the water measurement. (P.C.H.)

12925 (WHAN-SA-77) WATER AND SORBED-GAS CONTENT OF HYPOSTOICHIOMETRIC MIXED OXIDE FUEL PELLETS. Carlson, M. C. J. (Battelle-Northwest, Richland, Wash. Pacific Northwest Lab. WADCO Corp., Richland, Wash.). 28 Sep 1970. Contract AT(45-1)-2170. 9p. (CONF-701017–2). Dep. NTIS.

From 14th Annual Conference on Analytical Chemistry in Nuclear Technology, Gatlinburg, Tenn.

Studies were made on the water content and gas sorption behavior of mixed oxide fuel pellets, which were produced by mechanical blending of UO_2 and PuO_2 powders to provide the fuel composition 75% UO_2–25% PuO_2. Densified pellets were produced by pressing and sintering at temperatures between 1600 and 1700°C in Ar–8% H_2. From the results it was concluded that the sorbed gas contents of as-sintered fuel pellets are highly dependent on the density of the pellets. Sorbed gas contents increased significantly with decreasing density. Sorbed gas contents for as-sintered low-density fuel pellets were significantly greater than the present specification limit (0.09 cc/g). The sorbed gas was principally hydrogen. Vacuum outgassing at 850°C for four hours was adequate to reduce the sorbed gas contents for 90% TD pellets to less than 0.05 cc/g. Pellet gas contents increased during storage of outgassed pellets in a nitrogen glove box atmosphere. (P.C.H.)

12926 ANALYTICAL STUDY OF DIBROMOPYROGALLOL-SULFONEPHTHALEIN (DBPSP). COMPLEXATION WITH URANIUM AND ALUMIUM. Bokra, Yobou; Luca, Constantin (Poitiers Univ., France). Bull. Soc. Chim. Fr.; 10: 3761-7 (Oct 1970). (In French).

Bromopyrogallol red belongs to the group of triphenylmethane colorants used as pH indicators. An investigation was made on the absorption spectra, in the visible range and on the acid-base dissociation products of bromopyrogallol red. The visible absorption spectra and the equilibria of formation of its complexes with UO_2^{2+} and Al^{3+} ions were also studied. Analytical applications to the spectrophotometric determination of uranium and aluminum were made. (auth) (France)

12927 RESEARCH OF CORRECTION COEFFICIENTS FOR ELEMENTARY QUANTITATIVE ANALYSIS BY SPARK MASS SPECTROMETRY. APPLICATION TO URANIUM AND PLUTONIUM DIES. Billon, J. P. (CEA, Montrouge, France). Method. Phys. Anal.; 6: 231-6(Sep 1970). (In French).

In spark mass spectrometry, a quantitative relation has been established by Ménétrier between the composition of the ion beam and that of the sample. Experimental correction factors were determined for U and Pu. They are in good agreement with the calculated correction factors. (France)

12928 ASSAY OF BORON ISOTOPES AT THE BAND HEADS OF THE BO MOLECULE. Strohner, G. (Institut fuer Stabile Isotope, Leipzig). Isotopenpraxis; 6: 323-4(Sep 1970). (In German).

An emission spectroscopic method for the determination of the boron isotope ratio $^{10}B/^{11}B$ in boron trifluoride–ether complex $[BF_3(C_2H_5)_2O]$ was studied. The complex was chemically transformed into BF_3 gas and this was excited by a high-frequency oscillator discharge. The emitted light was analyzed by a spectrograph or a monochromator and recorded by a photoplate or a recorder. A distinct emission spectrum of the α-system of the BO-bands was obtained. The determination of boron isotope ratio may be possible by utilizing the isotopic displacement of the 2-0 band at 384.7 nm and of the 2-0 band at 382.99 nm. (auth)

12929 STUDY OF THE OPTIMAL CONDITIONS FOR POTENTIOMETRIC TITRATION OF FLUORIDE WITH LANTHANUM AND THORIUM IN UNBUFFERED MEDIA. **Eriksson, T.; Johansson, G.** (Univ. of Umea, Sweden). Anal. Chim. Acta; 52: 465-73(Dec 1970).

Some of the difficulties encountered in the titration of fluoride with fluoride-selective electrodes and lanthanum and thorium titrants were studied in unbuffered media. The solubility product of lanthanum fluoride decreases with time as the precipitate ages and this accounts for a drift of the potential towards decreasing fluoride activity after the end-point. The solubility product of lanthanum fluoride was determined to be $10^{-17.66}$ at 25.0°C in 1$\underline{M}$ potassium nitrate or 1$\underline{M}$ sodium chloride and the β_1 value of $La^{3+} + F^- \rightarrow LaF^{2+}$ was found to be $10^{5.15}$ under the same conditions. In accurate titrations of fluoride, lanthanum is recommended for fluoride solutions stronger than 1 m$\underline{M}$, with computer evaluation. Thorium is recommended as a titrant in the range 0.2 to 1 m$\underline{M}$ fluoride. (auth)

12930 SPECTROPHOTOMETRIC DETERMINATION OF MOLYBDENUM WITH GALLEIN AND CETYLTRIMETHYLAMMONIUM BROMIDE. **Leong, C. L.** (Geological Survey Federal Headquarters, Ipoh, Malaysia). Analyst; 95: 1018-22(Dec 1970).

A ternary complex system between molybdenum, gallein, and cetyltrimethylammonium bromide is proposed for the determination of microgram amounts of molybdenum. The complex has an absorbance maximum at 618 nm. The sensitivity of the reaction is 0.0026 μg cm^{-2} of molybdenum for log $I_0/I = 0.001$. The development of this method for the determination of molybdenum included a study of the effect of pH, temperature, reagent concentration, rate of complex formation, and conformity to Beer's law. (auth) (UK)

12931 METHOD FOR DETECTING ONE OF HEAVY WATER AND ORDINARY WATER IN THE PRESENCE OF THE OTHER OF HEAVY WATER AND ORDINARY WATER. **Brown, Donald P.; Garlick, George F.; Porter, Newell S.** (to United States Atomic Energy Commission). U. S. Patent 3,538,434. 3 Nov 1970. Filed 9 Jun 1967.

A method for determining water-d_2 and ordinary water in the presence of each other includes generating a microwave signal at a predetermined frequency value selected such that water-d_2 and ordinary water exhibit different polarization-attenuation characteristics for the microwave signal, passing a portion of the signal through the sample, attenuating the other portion of the signal, and then comparing the signal detected passing through the sample with the attenuated signal portion. (B.L.M.)

12932 ATOMIC ABSORPTION SPECTROPHOTOMETRY UNIT FOR THE ANALYSIS OF RADIOACTIVE SOLUTIONS. **Benhamou, Andre; Ganivet, Michel** (to Commissariat a l'Energie Atomique). French Patent 1,586,938. 26 Jan 1970. Filed 1 Oct 1968. (In French).

An atomic absorption spectrophotometry unit for the analysis of radioactive solutions of plutonium nitrate is described. It includes a burner equipped with combustion gas inlets, a device to spray the solution into the burner flame, a light source, and a spectrometer to measure the light absorbed by the atoms produced in the flame by the element to be analyzed. The burner is housed inside a closed airtight vessel, fitted with optical passages for the beam traveling from the source through the flame towards the spectrometer. This vessel includes a system to cool and evacuate the burned gases, a radioactive waste recovery device placed in the path of these gases, and safety units, which supervise the flame and check the gas flow-rate and temperature. (France)

12933 EXTRACTION–PHOTOMETRIC DETERMINATION OF MOLYBDENUM AS A COMPLEX TRIHYDROXYFLUORONATE. **Nazarenko, V. A.; Shustova, M. B.; Shelikhina, E. I.** (Inst. of General and Inorganic Chemistry, Odessa). Zh. Anal. Khim.; 25: 2139-41(Nov 1969). (In Russian).

An extraction–photometric method for determining micro amounts of molybdenum is described. The method is based on the extraction of a molybdenum-salicylfluorone-antipyrine-bromide complex with chloroform after its separation by extraction as diethyl dithio carbamate and displacing back extraction by means of copper(II). The method has been used for determining molybdenum as impurity in caustic alkalies and metallic titanium. (auth)

12934 EXTRACTION–PHOTOMETRIC DETERMINATION OF IRON WITH TIRON. **Busev, A. I.; Rudzit, G. P.; Tsurika, I. A.** (Moscow State Univ. Latvian State Univ., Riga). Zh. Anal. Khim.; 25: 2151-4(Nov 1970). (In Russian).

Of three compounds that are formed by Fe(III) with tiron, only the 1 : 3 compound is readily extracted by organic solvents in the presence of diphenylguanidinium cations. The maximum extraction is observed at pH 5 to 6. An extraction variant of the photometric determination of iron with tiron has been developed. Mo(VI), V(IV), V(V), and small amounts of Ti(IV) are separated by extraction at pH 2, after that the Fe(III) compound is extracted at pH 5 to 6 U(VI) and Cu(II) ions are masked with sodium fluoride and thiourea, respectively. Only higher amounts of Ti(IV) interfere with Fe(III) determination. (auth)

12935 COMPLEX FORMATION AND EXTRACTION OF BROMO-TELLURATE WITH VICTOR BLUE 4R. **Kish, P. P.; Kremeneva, S. G.** (Uzhgorod State Univ., USSR). Zh. Anal. Khim.; 25: 2200-3(Nov 1970). (In Russian).

The interaction of tellurium(IV) with Victoria Blue 4R (VB4R) in the presence of Br-ions produces a complex that can be extracted by a mixture of benzene or carbon tetrachloride with nitrobenzene and has an absorption maximum at 602 nm. The ratio of $TeBr_6^{2-}$ to VB4R in the extracted complex is 1 : 2. Its molar extinction coefficient is 80,000. Optimum conditions for the formation and extraction of the complex compound have been found. A method has been developed for the extraction–photometric determination of tellurium in solutions of its salts and in semiconductor alloys. (auth)

12936 SPECTROPHOTOMETRIC DETERMINATION OF FLUORINE IN ORGANIC COMPOUNDS WITH THORIUM CHLORANILATE AFTER HYDROPYROLYTIC DECOMPOSITION OF LEAD FLUORIDE. **Papay, K. M.; Mazor, L.; Takacs, J.** (Technical Univ., Budapest). Acta Chim. Acad. Sci. Hung.; 66: 13-88 (1970).

Developing an earlier method, a procedure is given for the determination of fluorine in organic compounds. The fluorine bound by a layer of red lead is hydropyrolyzed and distilled as hydrogen fluoride, then determined spectrophotometrically in the distillate with thorium chloranilate as reagent. The opinion of American authors that the color intensity of chloranilic acid is increased by Methyl Cellosolve is disputed. It is shown that this increase in color intensity is due to iron(III) impurities in Methyl Cellosolve forming a violet complex with chloranilic acid. Fluorine contents of a few organic compounds are reported. (auth)

12937 CARMINIC ACID AS A REAGENT FOR THE PHOTOMETRIC DETERMINATION OF THE RARE EARTH ELEMENTS. **Poluektov, N. S.; Lauer, R. S.; Sandu, M. A.** (Inst. of General and Inorganic Chemistry, Odessa). Zh. Anal. Khim.; 25: 2118-24(Nov 1970). (In Russian).

The reaction of the rare earth ions with carminic acid has been studied spectrophotometrically. It has been found that $MeOH^{2+}$ ions participate in the reaction, and complexes at a ratio of Me : R = 1 : 2 are formed. The formation constants of the complex compounds of La, Gd, Lu, and Y have been found. A photometric method has been developed for determining Yb and Lu in a mixture with Y which is gased on masking with sodium fluoride. (auth)

12938 SIMULTANEOUS DETERMINATION OF URANIUM(IV) AND URANIUM(VI) BY THE MOVING BOUNDARY METHOD. **Luginin, V. A.; Frolova, L. V.; Tserkovnitskaya, I. A.** (Leningrad State Univ.). Zh. Anal. Khim.; 25: 2142-5(Nov 1970). (In Russian).

A method has been developed for the quantitative determination of uranium(IV) and uranium(VI) in solutions by the method of moving boundary using the AIP-I analyzer of ionic mobilities. The results obtained have been treated by the mathematical statistics method. The possibility of using the method of moving boundary for determining the above valence forms of uranium with reasonable accuracy is discussed. (auth)

12939 METHODS FOR THE ANALYSIS OF NATURAL MATERIALS CONTAINING RUTHENIUM AND OSMIUM. **Alimarin, I. P.; Khvostova, V. P.; Shlenskaya, V. I.** (Moscow State Univ.). Zh. Anal. Khim.; 25: 2167-76(Nov 1970). (In Russian).

The literature data and studies on the methods for decomposition of the samples containing small amounts of osmium and ruthenium are systematized. Some practical recommendations are given on the choice of oxidants that are used to convert osmium and ruthenium into OsO_4 and RuO_4, and on the choice of substances for their absorption. (auth)

XUM

12940 ON INCREASING THE SENSITIVITY OF THE SPECTROGRAPHIC DETERMINATION OF SELENIUM AND TELLURIUM IN SULFUR. Romanova, L. V. (Scientific-Research Inst. of Mining-Chemical Raw Materials, Lyubertsy, USSR). Zh. Anal. Khim.; 25: 2197-9(Nov 1970). (In Russian).

A method has been worked out for the direct spectrographic determination of not less than 2 × 10^{-3}% of selenium and 1 × 10^{-4}% of tellurium in sulfur. The region of the spectrum in the wave length range of 2030 to 2200 A is used, which has been achieved by means of the optimum scheme of the illuminating system. (auth)

12941 MASS-SPECTROMETRIC METHOD FOR DETERMINING MICROIMPURITIES IN INERT GASES OF HIGH PURITY. Talakin, O. G.; Golovin, Yu. I.; Dykhno, N. M.; Avdon'kin, V. V.; Bludova, L. N. (All-Union Scientific-Research Inst. of Cryogen Machine Building, Moscow). Zh. Anal. Khim.; 25: 2204-7(Nov 1970). (In Russian).

A mass spectrometric method has been worked out for determining H in neon and helium with a sensitivity of 1 × 10^{-4}% (vol) and an error of not more than 12%. The method is based on the preliminary accumulation of H by adsorption on the activated charcoal. A mass spectrometric method has been developed for determining N, O, Ar, and H in xenon, and H in krypton and argon which is based on accumulating microimpurities in the gas phase by condensation of the main component. The sensitivity is 2 × 10^{-4}% (vol) at a gas sample of 200 to 300 ml. The error is 15%. One determination takes 30 min. A mass spectrometric method has also been developed for determining CO_2 and individual hydrocarbons in argon, krypton, helium, neon, and hydrogen which is based on accumulating microimpurities by freezing-out at the temperature of liquid nitrogen or oxygen. The sensitivity is 3 × 10^{-5}% (vol) at a gas sample of 800 ml. The error is 12%. One determination takes 30 min. (auth)

12942 COMPOSITION AND STABILITY CONSTANTS OF CERIUM–CHROMOTROPE 2R CHELATE AND THE SPECTROPHOTOMETRIC DETERMINATION OF CERIUM. Shah, Vasant L.; Sangal, Satendra P. (Nagpur Univ., India). Microchem. J.; 15: 548-56(Dec 1970).

The composition and stability of the pinkish violet chelate of cerium–CTR (Chromotrope 2R) (λ_{max} 550 m_μ) were established by the method of continuous variation and the mole ratio method. The stoichiometric ratio was found to be 1:1 (metal:ligand) at pH 6.0. The conditional stability constant of the chelate was determined by the method of Mukherji and Dey and the mole ratio method at pH 6.0 and at 28°C. The value of log K by the method of Mukherji and by mole ratio method are 3.81 and 4.8, respectively. Suitable conditions for the determination of the metal in micro amounts were worked out. The range for adherence to Beer's law is 0.56 to 10.16 ppM. The molar absorption coefficient is 6650. Sensitivity is 1.41 γ/cm^2. The pH range suitable for determination of metal ion is 5.6 to 6.4. Effect of the various forms of ions on the chelate was also studied. (auth)

12943 PRECIPITATION OF TELLURIUM WITH BISMUTHIOL II. Wang, Jui-chang; Cheng, K. L. (Univ. of Missouri, Kansas City). Microchem. J.; 15: 607-21(Dec 1970).

A gravimetric method using Bismuthiol II (potassium salt of 5-mercapto-3-phenyl-1,3,4-thiadiazole-2-thione) as a reagent for determining tellurium was developed with a very favorable gravimetric factor of 0.1240. Tellurium(IV) is quantitatively precipitated in the presence of tartaric acid and (ethylenedinitrilo) tetraacetic acid (EDTA) by Bismuthiol II at pH 3.0 to 3.5. The yellow precipitate decomposes on heating, but it can be vacuum-dried at room temperature at $Te(C_8H_5N_2S_2)_4$. The structure of the precipitate is discussed based on its infrared spectrum. The solubility of the precipitate in various solvents and other factors affecting the precipitation have been studied. A selective precipitation can be made in the presence of tartaric acid and EDTA. Many interfering ions such as Ni(II), Al(III), Cr(III), Fe(III), Bi(III), Pu(II), and As(III) can be masked by EDTA, but Hg(II), Cu(II), Se(IV), and Ag(I) still interfere. The samples containing 10 to 50 mg of tellurium were analyzed. An accuracy of ±0.5% or better was obtained. The proposed method for tellurium will be valuable for the stoichiometric analysis of telluride compounds where accuracy is of prime concern. (auth)

12944 TRACE METAL ANALYSIS BY COMBINED THIN-LAYER CHROMATOGRAPHY INCORPORATING FLUORESCENT SUPPORT AND RING OVEN COLORIMETRY. Johri, K. N.; Mehra, Harish C. (Univ. of Delhi). Microchem. J.; 15: 642-52(Dec 1970).

Clean and rapid analytical separation of microgram quantities of Pb(II), Bi(III), U(VI), and Th(IV); and Cu(II), Ni(II), Co(II), and Cd(II) from their mixed solutions was made possible by ascending thin-layer chromatography. For the evaluation of different metal ions, the resulting delineated spots were scooped out with the help of a Mottier gadget and the collected material was transferred to the paper set on the ring oven. Separate rings were obtained for the individual metal ions and the computation of results was made possible by ring colorimetry, using PTC (potassium thiocarbonate) and other chromogenic reagents. (auth)

12945 GENERAL ALLOY ANALYSIS WITH A GAS SHEATHED TUBULAR ELECTRODE ARC. Muntz, James H. (Air Force Materials Lab., Wright-Patterson AFB, Ohio). Appl. Spectrosc.; 25: 47-53(Jan-Feb 1971).

The gas-sheathed tubular electrode arc was investigated and applied to general alloy analysis. One set of six solution standards containing 18 different elements was used. Matrix effects were mostly controlled by using a 1-mg/ml sample or standard in a solution containing 6 mg/ml of sodium as the chloride. Fourteen different standard alloys (NBS and Alcoa) were tested, representing seven different base metals. The over-all accuracy was about ±8% deviation from the certified value. This would permit identification of alloy type, but for greater accuracy standards more closely approximating the sample should be used. Precision for the technique is normally ±3% to 4% relative standard deviation with photographic detection. (auth)

12946 EMISSION SPECTROMETRIC DETERMINATION OF TRACE ELEMENTS IN BIOLOGICAL FLUIDS. Niedermeier, William; Griggs, James H.; Johnson, Richard S. (Univ. of Alabama, Birmingham). Appl. Spectrosc.; 25: 53-6(Jan-Feb 1971).

An emission spectrometric method of analysis is described, in which trace quantities of copper, iron, aluminum, barium, manganese, nickel, cesium, tin, strontium, chromium, zinc, lead, molybdenum, and cadmium were determined in blood serum. The sample preparation, starting with 2.0 ml of blood serum, is discussed in detail. The source of excitation was a 10-A dc arc. Quantitation was achieved with a direct reading emission spectrometer. The metal concentration, in micrograms per 100 ml of blood serum, was calculated from the experimental data by means of a computer. (auth)

12947 SPECTROPHOTOMETRIC DETERMINATION OF TANTALUM WITH METHYLENE BLUE. Onishi, Hiroshi; Nagai, Hitoshi (Japan Atomic Energy Research Inst., Tokai). Jap. Anal.; 20: 86-90(Jan 1971). (In Japanese).

A spectrophotometric method is described for the determination of 4–20 μg of tantalum. Seven ml of 8 N sulfuric acid and 2.5 ml of 5% hydrofluoric acid solution are added to the sample solution. The solution is diluted to 25 ml with water and allowed to stand for 30–60 min. One ml of 0.001 M Methylene Blue is added and the solution is shaken with 10.0 ml of 1,2-dichloroethane. The organic phase is filtered through dry paper and diluted with an equal volume of 1,2-dichloroethane. The absorbance of the solution is measured at 660 nm against 1,2-dichloroethane. The apparent molar absorptivity is 1.0 × 10^5 at 660 nm and the sensitivity is 0.0018 μg Ta/cm^2 for an absorbance of 0.001. Microgram amounts of boron and perchlorate and 0.1 mg of niobium interfere. However, microgram amounts of tantalum can be separated from 10 mg of niobium by extraction of the former with methyl isobutyl ketone from a solution that is 1 N in hydrofluoric acid and 2 N in hydrochloric acid. The tantalum is back-extracted with hydrogen peroxide. (auth)

12948 X-RAY EXCITED OPTICAL LUMINESCENCE ANALYSIS OF TRACE RARE EARTHS IN HIGH PURITY YTTRIUM AND GADOLINIUM OXIDES. Sato, Matsuji; Matsui, Hiroshi; Matsubara, Tadao (Shin-Etsu Chemical Industry Co., Ltd., Takefu, Japan). Jap. Anal.; 20: 70-8(Jan 1971). (In Japanese).

Analysis by x-ray excited optical luminescence was applied to the determination of trace amounts of rare earths as impurities in yttrium and gadolinium oxides. In order to establish fundamental conditions, studies were made on the method for purification of base materials, the effects of temperature and time of ignition of test specimens, and mutual interferences of different rare earths and (or) non-rare earth metals. An internal standard was employed for the compensation of the self-quenching of emission spectra. Yttrium and gadolinium oxides used for the base materials were purified by ion exchange. They were further purified twice by homogeneous precipitation to remove non-rare earth impurities. The ignition of the oxalates into oxides was done at 1200°C for 4 hours. The self-quenching effect in emission spectra of rare earth impurities increased with the amounts of other co-existing rare earths, especially of terbium and (or) praseodymium. The effect was much larger in gadolinium oxide than in yttrium oxide. The use of praseodymium and dysprosium as the internal standard elements respectively for the analyses of yttrium and gadolinium oxides eliminated the influences of those impurities. The coefficients of variation in the results of analysis were 6.6–8.6% for 2 ppM of terbium, europium, and dysprosium in yttrium oxide and 5.2–8.2% for 2 ppM of terbium, europium, and praseodymium in gadolinium oxide. (auth)

Isotope Dilution Procedures

Refer also to abstract 13081.

12949 MICROANALYSIS OF COBALT BY ELECTROPHORETIC FOCUSSING WITH RADIOACTIVE TRACER. Popper, E. (Inst. of Medicine and Pharmacy, Cluj); Szabo, A.; Szentgyoergyi, P. Rev. Roum. Chim.; 15: 1447-51(Sep 1970).

An isotopic dilution method, combined with electrophoretic focusing on paper, for cobalt microanalyses is presented. These analyses may be carried out with small volume of samples using ^{60}Co as tracer. The solution to be analyzed is labeled with radioactive cobalt; the cobalt is substoichiometrically complexed with EDTA solution; and then the complexed anions and noncomplexed cations are separated by electrophoretic focussing. The concentration of cobalt is calculated knowing the radioactivities of both anions and cations and the concentration of the EDTA solution. The sensitivity of the method is 0.5×10^{-4} gram atom Co per liter. (auth)

Radiometric and Radiochemical Procedures

Refer also to abstracts 13214, 13221, 13230, and 13231.

12950 (BRH/NERHL-70-2) LIQUID WASTE EFFLUENTS FROM A NUCLEAR FUEL REPROCESSING PLANT. Magno, P.; Reavey, T.; Apidianakis, J. (Bureau of Radiological Health, Winchester, Mass. Northeastern Radiological Health Lab.). Nov 1970. 59p. NTIS.

The liquid waste effluents from Nuclear Fuel Services were studied in detail during the six-month period May through October 1969. The concentrations and amounts of individual radionuclides discharged from the plant were measured and the amounts of sedimentation of individual radionuclides in the lagoon system were estimated. Tritium, ruthenium-106, strontium-90, cesium-137, and cesium-134 were the principal radionuclides discharged to the environment during this period. No relationship could be established between the amount and burnup of fuel processed and the amount of activity discharged from the plant to the lagoon system during this study. For the Yankee fuel campaign of May to August 1969, the waste management practice and not the amount of fuel processed was the controlling factor in the amount of activity discharged from the plant to the lagoon system. During June and November 1969 simultaneous sampling was carried out at the point of discharge of the waste and several locations on the Buttermilk and Cattaraugus Creeks. Tritium, ruthenium-106, and strontium-90 were the radionuclides present in the highest concentrations in these streams during these periods. Stream dilution and absorption factors were calculated for individual radionuclides at various locations along the stream system. A comparison of the concentrations of the radionuclides in Cattaraugus Creek with 10CFR20 discharge concentration limits showed that strontium-90 was about 20 percent of the concentration limit during both sampling periods. All other radionuclides were less than 10 percent of the concentration limits during these periods. (auth)

12951 (USGS-474-83) RADIOCHEMICAL ANALYSES OF WATER FROM SELECTED STREAMS, WELLS, SPRINGS, AND PRECIPITATION COLLECTED PRIOR TO REENTRY DRILLING. PROJECT RULISON. Rulison-6. Voegeli, Paul T. Sr.; Claassen, Hans C. (Geological Survey, Denver, Colo.). 1971. Contract AT(29-2)-474. 16p. (PNE-R-42). Dep. NTIS.

Water samples obtained from selected streams, wells, springs, and from precipitation were analyzed for tritium, gross α, and gross β activity. A description of the procedures used in collection, analysis, and reporting of data is included to permit evaluation of the quality of the data presented and to permit a direct comparison between data obtained by the Geological Survey and by other agencies. (P.C.H.)

12952 DESIGN AND EVALUATION OF A MICRORADIOMETRIC DETECTOR FOR COLUMN LIQUID CHROMATOGRAPHY. Van Urk-Schoen, A. M.; Huber, J. F. K. (Univ., Amsterdam). Anal. Chim. Acta; 52: 519-27(Dec 1970).

The theory of radiometric detection is discussed. An expression for sensitivity is derived; peak-broadening owing to mixing phenomena in the feed line and the detector cell is described. The significance of the noise is discussed. The detector was tested with respect to peak-broadening effects, sensitivity, linearity, precision, and detection limit. The results demonstrate its excellent performance. It proves to be very suitable for high-speed column liquid chromatography. (auth)

12953 METHODS FOR THE DETERMINATION OF THE RADIOACTIVITY OF SAMPLES, DOUBLE-LABELED WITH TRITIUM, OR ^{14}C. Glick, H. (Univ., Munich). Isotopenpraxis; 6: 310-16(Sep 1970). (In German).

A method has been developed for the possible determination of the radioactivity of tritium- or ^{14}C-labeled material on chromatographic or pherographic paper, making use of a liquid scintillation spectrometer. This method provides counting of double-labeled samples with a T-to-^{14}C ratio of $\frac{1}{2}$ as a maximum, the statistical 2 σ-error being no more than ±15%. At the same time, optimum measuring conditions have been provided for the determination of the radioactivity of tritium hamamelose hydrazone, and of fission fragments, which originated as a result of decomposition. Furthermore, the necessary calibration graphs were plotted. (auth)

12954 THE IDENTIFICATION AND MEASUREMENT OF IMPURITIES IN NEUTRON-IRRADIATED GRAPHITES BY HIGH RESOLUTION γ-RAY SPECTROMETRY. Reed D.; Hilton, D. A. (Central Electricity Generating Board, Berkeley, Eng.). Radiochem. Radioanal. Lett.; 5: 293-301(31 Dec 1970).

A high resolution γ-ray spectrometer was used to identify nuclides in neutron-irradiated graphite. The technique used is nondestructive and the impurity elements Co, Mo, Sm, Eu, La, Sc, Re, Cu, As, W, Na, Mn, and Cr were determined in several graphites. The data obtained are of value in assessing the relative quality of graphites with respect to their neutron absorption characteristics. (auth)

12955 RADIO-RELEASE DETERMINATION OF pH USING RADIOACTIVE KRYPTONATE OF THALLIUM. Toelgyessy, J.; Varga, S.; Jesenak, V.; Lukac, P.; Dillinger, P. (Technical Univ., Bratislava). Radiochem. Radioanal. Lett.; 5: 331-4 (31 Dec 1970).

The radioactive kryptonate of thallium was used for the determination of pH. Hydrogen ions react with the surface layer of radioactive kryptonate of thallium, and release radioactive krypton in amounts proportional to the pH value of the solution. (auth)

12956 GAMMA-RAY SPECTROMETRIC ANALYSIS APPLIED TO ESTIMATION OF RADIONUCLIDES IN REACTOR COOLANT WATER. Marathe, S. G.; Pai, S. A.; Rao, C. L.; (and others) (Bhabha Atomic Research Centre, Trombay, India). Radiochim. Acta; 14: 141-3(Nov 1970).

The estimation of radionuclides present in the CIRUS primary coolant water by gamma spectrometry is described. The major activities present were found to be ^{24}Na, ^{56}Mn, ^{64}Cu, ^{95}Zr, ^{95}Nb, and ^{239}Np. The gamma spectrometric values calculated manually and by means of a computer are compared with radiochemical values. (auth)

Activation Procedures

12957 (LYCEN-7076) DETERMINATION OF THE INTERNAL AND SUPERFICIAL OXYGEN CONTENT OF MOLYBDENUM OBTAINED USING 54 MeV α PARTICLES AND LOW ENERGY DEUTERONS. Mazagol, Lyliane; Tousset, Jean (Lyon Univ. (France). Institut de Physique Nucleaire); Boissier, Michele (Commissariat a l'Energie Atomique, Grenoble (France). Centre d'Etudes Nucleaires). 28 Oct 1970. 14p. (In French). Dep. NTIS (U. S. Sales Only).

The internal oxygen content of molybdenum samples was determined by activation with 55-MeV alpha particles. This method yielded a mean value for the oxygen content of a volume of target with a variable depth between 20 and 360 μ. The oxygen distribution profile in the immediate vicinity of the surface was studied using nuclear reactions. The oxygen content beneath the oxide layer up to a depth of about 4 μ was determined from the shape, at low energy, of the proton peak in the ^{16}O(d,p$_1$) reaction. Rapid coincidence measurements yielded the α spectra in the (d,α) reaction. (France)

12958 (TKK-F-A-136) DETERMINATION OF THE ISOTOPIC RATIO ^{238}U/^{235}U BY NEUTRON ACTIVATION. Aalto, H. (Technical Univ. of Helsinki, Otaniemi (Finland). Dept. of Technical Physics). 15 Dec 1970. 31p. Dep. NTIS.

A method is described for the nondestructive and accurate determination of the isotopic ratio ^{238}U/^{235}U by neutron activation. The high-resolution Ge(Li) x-ray detector used permits easy identification of the 210-keV gamma of ^{239}Np formed from ^{238}U and the 140-keV gamma peak of fission product ^{99}Mo formed from ^{235}U during activation. The ratio of the peak intensities is proportional to the ^{238}U/^{235}U ratio in the sample. The statistical deviation of one determination is 1% in the upper and 3% in the lower limit of the range $18 < {}^{238}\text{U}/{}^{235}\text{U} < 138$. (auth) (Finland)

12959 ADSORPTION OF VANADIUM ON ALUMINUM AND ZIRCONIUM OXIDES AND ITS APPLICATION TO ANALYTICAL

XUM

SEPARATIONS. Kosta, L.; Ravnik, V.; Levstek, M. (Jozef Stefan Nuclear Inst., Ljubljana, Yugoslavia. Univ. of Ljubljana, Yugoslavia). Radiochim. Acta; 14: 143-6(Nov 1970).

Vanadium can be separated by adsorption on oxides from dilute solutions with essentially quantitative yields. Experimental adsorption coefficients are from 10^3 to more than 10^4 in the range between pH 3 to 9 for chromatographic quality aluminum oxide as well as for zirconium oxide. A method for determining traces of vanadium by activation analysis in aluminum matrices was devised based on this property. The sensitivity of the spectrophotometric procedure for vanadium was also increased by introducing an absorption stage followed by elution with phosphotungstic acid reagent. (auth)

12960 PULSED-NEUTRON ACTIVATION ANALYSIS SYSTEM FOR SHORT-LIVED RADIOISOTOPES. Naughton, William F.; Jester, William A. (Pennsylvania State Univ., University Park). Nucl. Appl. Technol.; 9: 851-5(Dec 1970).

A pulsed neutron activation analysis system capable of handling and analyzing short-lived radioisotopes with half-lives as short as one to two seconds was developed. Since a single reactor pulse will induce more activity for short-lived neutron reaction products than continuous irradiation to saturation at a normal reactor power level, experimental procedures were formulated to analyze quantitatively a few important fast neutron reactions with short-lived products and to establish limits of detection for these reactions using this system. To augment the fast neutron reactions, a cadmium-lined in-core terminus was utilized to reduce (n,γ) interference reactions. The reactions analyzed were $^{16}O(n,p)^{16}N$, $^{19}F(n,\alpha)^{16}N$, $^{19}F(n,\gamma)^{20}F$, $^{23}Na(n,p)^{23}Ne$, $^{23}Na(n,\alpha)^{20}F$, $^{34}S(n,p)^{34}P$, and $^{31}P(n,\alpha)^{28}Al$. The detection limits which were attained for these reactions utilizing this system were: 54.8 μg for ^{16}O, 0.23 and 0.19 μg for ^{19}F; 1.8 and 8.0 μg for ^{23}Na; 150 μg for ^{34}S; and 2.6 μg for ^{31}P. Most of these limits are an order of magnitude or more lower than those reported by users of the Cockroft-Walton neutron generators usually employed for these analyses. (auth)

12961 PROTON MICROPROBE ANALYSIS OF THE SURFACE OF STRANDED WIRE IN THE LUNAR MODULE. Padawer, Gerald M. (Grumman Aerospace Corp., Bethpage, N. Y.). Nucl. Appl. Technol.; 9: 856-60(Dec 1970).

Proton microprobe analysis utilizing the strong, narrow 0.874-MeV resonance in the $^{19}F(p,\alpha\gamma)^{16}O$ reaction was employed to identify fluorine as a contaminant and to measure its concentration profile in the surface of silver-coated copper wiring on the Lunar Module (LM). (auth)

12962 LABORATORY AND ENVIRONMENTAL MINERAL ANALYSIS USING A ^{252}Cf NEUTRON SOURCE. Perkins, R. W.; Rancitelli, L. A.; Cooper, J. A.; Brown, R. E. (Battelle Memorial Inst., Richland, Wash.). Nucl. Appl. Technol.; 9: 861-74(Dec 1970). (BNWL-SA-3173).

Rapid nondestructive mineral analysis can be performed with use of a ^{252}Cf neutron source and a lithium-drifted germanium [Ge(Li)] diode gamma-ray detector. Also, in situ analysis of terrestrial and marine mineral deposits appears practical. Laboratory studies show that a one- or two-minute exposure of mineral samples to the thermalized neutron flux from a 1-mg ^{252}Cf source followed by a one- or two-minute count with an 80-cc Ge(Li) diode will allow the measurement of most elements at concentrations of 10- to 100-fold below the levels of economic interest. The technology developed for laboratory mineral analysis is described and its applicability to in situ terrestrial and seabed mineral exploration is discussed. (auth)

12963 USE OF DIETHYL DITHIOCARBAMATES FOR ACTIVATION ANALYSIS WITH SUBSTOICHIOMETRIC SILVER SEPARATION. Kukula, F. (Inst. of Nuclear Research, Rez, Czech.). Isotopenpraxis; 6: 303-6(Sep 1970). (In Russian).

For direct substoichiometric silver separation in activation analysis, silver was extracted as diethyl dithiocarbamate. Combination of fast transfer of the irradiated sample out of the reactor by means of a pneumatic transfer device with substoichiometric silver separation rendered possible use of the radioisotope ^{108}Ag, having a half-life of 2.4 minutes, for the analysis, at the same time providing high separation selectivity. Determination of silver was made on lead oxide and zinc sulfide samples. The accuracy of silver determination through the isotope ^{108}Ag ranged 10^{-7} g (provided optimum experimentation and measuring conditions; measurement was carried out with germanium (lithium) radiation detectors having an active volume of 20 cm). NaI(Tl) measurement with a detector having a volume of 10 × 10 cm provided an accuracy that was higher by two orders. (auth)

12964 POSSIBILITIES OF THE APPLICATION OF ACTIVATION ANALYSIS IN MEDICINE. Draskovic, R. (Boris Kidric Inst. of Nuclear Sciences, Vinca, Yugoslavia). Isotopenpraxis; 6: 300-3(Sep 1970). (In French).

A review is given on the uses of activation analysis in the fields of medicine, biology, and biochemistry, as well as in the fields of production and control of radioisotopes destined for medical use. It was concluded that activation analysis is used more in medicine. It has become indispensable in the analysis of microcomponents of organs of living things (in vitro or in vivo). The use of Ge(Li) detectors eliminates chemical operations. The method is presently indispensable for the determination of the radioactivity of radioisotopes destined for medical use. (57 references). (P.C.H.)

12965 ACTIVATION ANALYSIS OF AIRBORNE SELENIUM AS A POSSIBLE INDICATOR OF ATMOSPHEF SULFUR POLLUTANTS. Pillay, K. K. Sivasankara; Thomas, Charles C. Jr.; Sondel, James A. (Western New York Nuclear Research Center, Inc., Buffalo). Environ. Sci. Technol.; 5: No. 1, 74-7(Jan 1971).

Neutron activation analysis was used to measure the Se content of air pollutants. These results were compared with the total S content of air pollutants determined by gravimetric analysis. The Se/S ratios of airborne pollutants from Buffalo, N. Y., monitored during 1968 to 1969, range from 0.5 to 1.6×10^{-3}. The results were contrasted with Se/S ratios in fossil fuels reported previously. The Se contents of both particulate and gaseous pollutants have been separately determined and reported. If the Se/S ratio of air pollutants in a region is known, neutron activation analysis of Se may be used for an estimate (an order of magnitude or less) of the sulfur content of air pollutants. (auth)

12966 NEUTRON-ACTIVATION ANALYSIS USING MONOENERGETIC GAMMA-RAY SPECTRA. Robinson, Edgar Larry. Blacksburg, Va.; Virginia Polytechnic Institute (1970). 72p. University Microfilms Order No. 70-19,189.

Thesis.

Computer programs for performing both qualitative and quantitative neutron activation analysis using monoenergetic γ spectra were developed. Qualitative analysis is based on the spectrum stripping technique. Quantitative analysis is based primarily on the absolute calibration of the counting system; however, the comparator technique can be used with the present program. The methods used are described and a test case is presented to illustrate the use and capability of the programs. (Diss. Abstr. Int., B)

12967 APPLICATION OF GAMMA-GAMMA COINCIDENCE COUNTING TECHNIQUES TO THE NONDESTRUCTIVE ACTIVATION ANALYSIS OF METEORITIC MATERIALS. McKown, David Melvin. Lexington, Ky.; Univ. of Kentucky (1969). 165p. University Microfilms Order No. 70-16,979.

Thesis.

A fast coincidence gated γ spectrometer was set up to measure coincidence activities in complex samples such as irradiated meteorites. The signal outputs from two 3" × 3" NaI(Tl) detector-photomultiplier tube assemblies are each fed through a double delay amplifier and "jitter-free" single channel pulse height analyzer to a fast coincidence unit. The output of the fast coincidence unit is fed to the slow coincidence gate of a multichannel analyzer. The multichannel analyzer input pulses are taken, through a variable delay line, from one of the detector outputs. With this counting system, an energy spectrum of coincidence events is accumulated only if the coincidence pulses from both detectors fall within the pulse-height regions selected by the single channel analyzers. Placing the discrimination electronics before the fast coincidence module provides the energy selection necessary to reduce the high Compton coincidence activity in the lower energy regions of the meteorite spectra. Coincidence resolution times of approximately 26 nanoseconds (FWHM of a ^{60}Co delay curve) may be obtained with this system. Experiments were carried out to determine the stability of the total detector-coincidence system with respect to short term variations, long term drift, and count rate variations as a function of source intensity. For single detector pulse rates less than about 5×10^5 pulses/min, this counting system provides reliable quantitative analysis of coincidence activities in complex samples, and no coincidence loss corrections are required. Techniques were developed for the nondestructive determination of Ir in meteorites using neutron activation followed by gamma-gamma coincidence spectrometry. This nondestructive technique avoids the potential sources of error associated with radiochemical separations for Ir. An alternating current dissolution method for the preparation of accurate Ir standards was also developed. Evidence is presented that the earlier Ir determinations via radiochemical separations may be subject to significant analytical error. Iridium abundances for the various chondrite groups as determined by this work are (in units of ppb by weight, Ir): C1-490, C2-608, C3-645, Enstatite-618, H-group-781, L-group-453, LL-group-371. Coincidence spectrometry was also used to determine the concentrations of Ni, Na, Co, and Sc in some samples used for the Ir analyses.

XUM

These data are evaluated and compared to data obtained using other nondestructive counting techniques. (Diss. Abstr. Int., B)

12968 DETERMINATION OF ANTIMONY IN NATURAL MATERIALS BY NEUTRON ACTIVATION. Tanner, James Thomas. Lexington, Ky.; Univ. of Kentucky (1966).
Thesis.

After a thermal neutron irradiation in sealed quartz vials for 14 days at a flux of 1×10^{13} n cm^{-2} sec^{-1}, the samples were dissolved by successive treatment with various acids. Antimony carrier solution was added at the beginning of the dissolution to permit determination of the chemical yield. The separation of Sb involved several precipitations of Sb as the sulfide and a final reduction of Sb to the metal with $CrCl_2$. The Sb activity was determined by measuring the area under both the 0.60 MeV and the 1.69-MeV γ photopeaks of the 60-day ^{124}Sb. Abundances were calculated based on the activities of flux monitors irradiated simultaneously with the sample vials. The flux monitors consisted of sealed quartz vials containing "Spec-pure" SiO_2 onto which had been evaporated an aliquot of a standard solution of Sb. The flux monitors were processed by the identical procedure used for the samples. Antimony was determined in 23 chondrites, 8 achondrites, 3 siderites, 5 separated meteoritic phases, 12 tektites, 6 natural glasses, 11 standard rocks, 11 selected terrestrial rocks, and 8 deep-sea sediments. The data confirm the expectation that antimony has appreciable siderophilic and chalcophilic properties in meteoritic matter. The Sb abundances on a weight basis among the ordinary chondrites (average of 0.089 ppM) were found to be very uniform with the maximum variation from the mean for 13 analyses being only approximately a factor of two and the mean deviation less than 20%. Similarly, major variations were not found among the various types of enstatite chondrites (average of 0.18 ppM) or carbonaceous chondrites (average of 0.14 ppM), although both of these groups exhibited an average of Sb abundance approximately a factor of two larger than that found for the ordinary chondrites. The cosmic atomic abundance of Sb was calculated and compared with various reference models. The cosmic atomic abundance for Sb relative to Si = 10^6 was found to be 0.11 based on the ordinary chondrites, 0.40 based on the Type I carbonaceous chondrites, and 0.20 based on the Type III carbonaceous chondrites. The cosmic atomic abundance values of Sb were calculated using the Si content of the specific meteorite samples analyzed. The use of the model based on the ordinary chondrites gave the closest agreement to predictions based on theories of nucleosynthesis. The standard and terrestrial rocks were divided into groups ranging from the most acid to the most basic and the average Sb abundances for each group determined. These Sb abundances compare favorably with recent determinations in the literature. A crustal abundance computed from a 1 : 1 ratio of basalt and granite yielded an abundance of 0.2 ppM in agreement with the crustal abundance previously reported in the literature. In addition deep-sea sediments from a mid-Pacific core and an Argentine Basin core were analyzed for Sb. Values ranged from 0.36 ppM to 7.03 ppM. The data suggest an increase of Sb concentration with depth for the mid-Pacific core but only a random distribution for the Argentine Basin core. Tektites, natural glasses (Libyan Desert and Darwin glass), and impact glass were also analyzed for Sb. Antimony was found to be enriched in going from west to east in the Australian tektites. However, on the basis of these few Sb data in tektites no simple pattern for the volatilization processes in the tektites from a meteorite impact could be determined. (Diss. Abstr.)

12969 MULTI-ELEMENT NEUTRON ACTIVATION ANALYSIS: DEVELOPMENT AND APPLICATION TO A TRACE ELEMENT STUDY OF THE BRUDERHEIM CHONDRITE. Allen, Ralph Orville Jr. Madison, Wis.; Univ. of Wisconsin (1970). 243p. University Microfilms Order No. 70-13,900.
Thesis.

Procedures for the determination by neutron activation of 38 elements in small (~$\frac{1}{4}$ gm) geological samples were developed. In order to take maximum advantage of the improved resolution of lithium-drifted germanium detectors for γ spectrometry, the 38 elements were chemically separated into 12 groups (4 of which are single elements) for radioassay. The separation procedure was designed to obtain elements of proven geochemical interest. The order of the separations was chosen according to the half-lives of the elements. The procedure was tested by analyzing a U.S.G.S. standard rock (BCR-1) and a cosmochemically interesting object, the Bruderheim chondritic meteorite. Six separate chips of the Bruderheim chondrite, varying in size from 0.36 to 0.76 gm, were analyzed to determine the inhomogeneities in trace element distribution and the sampling errors arising from use of small samples. Samples of the major mineral phases, olivine, pyroxene, troilite, and metal, and important minor phases, feldspar and whitlockite, were also analyzed. Using a modal analysis for Bruderheim and the trace element concentrations, a satisfactory mass balance was obtained for most of the elements. The minor mineral whitlockite was found to be the most important carrier of a number of lithophilic elements, including the lanthanides (except Eu), Sc and Ba. The feldspar contains most of the Eu, Ba, Ga, and K. The pyroxene contains higher concentrations of all of the trace elements than does the olivine, except for Ni. The variations in concentrations from chip to chip for the strongly siderophilic elements to be due to differences among the samples in the amounts of metal phase. Some of the variations observed for chalcophile elements may be due to variations of the amount of troilite or, possibly, to variations of minor accessory sulfide minerals. Among the strongly lithophilic elements, only the lanthanides, Sc, and Zn show definite variations in concentration of more than 10% from chip to chip. (Diss. Abstr. Int., B)

12970 NONDESTRUCTIVE DETERMINATION OF SILICON AND OXYGEN IN METEORITES BY FAST NEUTRON-ACTIVATION ANALYSIS. Vogt, James Robert. Lexington, Ky.; Univ. of Kentucky (1966).
Thesis.

A highly automated system for rapid and precise fast neutron activation analysis, and its application to the nondestructive determination of Si and O in a wide variety of stony meteorites was developed. An automated pneumatic tube sample transfer system was constructed, which permits samples to be sent 200 feet (from a 250-kV Cockcroft–Walton accelerator to a counting room) in less than four sec. Two solenoid operated pneumatic sample spinner assemblies were built to permit rotation of the samples during irradiation and counting. Rotation of the sample container in the neutron beam and in front of the detector minimizes errors due to flux attenuation in the sample, self-absorption, inhomogeneity of the sample, and non-reproducible geometry. A solenoid operated beam-stop assembly was developed, which permits turning the neutron beam on and off in a time interval on the order of millisec. An irradiation control system permits automatic control of all irradiation and counting processes, and a computer program was developed for automatic processing of the data. Techniques were developed for the nondestructive determination of Si and O in stony meteorites, and a total of 884 individual analyses were made. The samples were irradiated with 14-MeV neutrons and counted using a 3" × 3" NaI(Tl) crystal and a 400 channel analyzer. An IBM 1410 computer was used to normalize the data for variations in neutron flux, irradiation time, delay time, and dead time. Usually one standard sample is run for every 10 to 20 analyses. Silicon abundance data for 107 chondrites and 11 achondrites, and oxygen abundance data for 34 chondrites and 5 achondrites are tabulated. Other studies on target cooling, sample packaging, photomultiplier tube voltage divider network design, radiofrequency ion-source operation, nanosec coincidence counting, and lithium-drifted germanium detectors were also conducted. (Diss. Abstr.)

12971 DETERMINATION OF B, C, AND O IN SILICON BY ACTIVATION ANALYSIS USING CHARGED PARTICLES AND γ PHOTONS. Engelmann, Ch.; Gosset, J.; Rigaud, J. M. (CEN, Saclay, France). Radiochem. Radioanal. Lett.; 5: 319-29(31 Dec 1970). (In French).

Results of the determination of B, C, and O in monocrystalline and polycrystalline silicon are given. It was found that the electric resistivity measured by the 4-point method does not vary proportionately with the boron content when the latter is less than 10^{-2} μg/g. It was also established that in these samples the nitrogen and fluorine concentrations are lower than 5×10^{-3} μg/g. (auth)

12972 QUANTITATIVE DETERMINATION OF IMPURITIES IN BORON CARBIDE BY NEUTRON ACTIVATION ANALYSIS. Gueckel, W.; Born, H.-J.; Staerk, H. (Technische Univ., Garching, Ger.). Radiochem. Radioanal. Lett.; 5: 357-64(31 Dec 1970). (In German).

Impurities in boron carbide were determined by neutron activation analysis. Three methods are described which either avoid the inhomogeneous activation of the samples caused by thermal neutrons and resonance neutrons or take into account the self-shielding effects using a correction factor. (auth)

12973 THERMAL NEUTRON ACTIVATION ANALYSIS OF COUNTERFEIT AND GENUINE JAPANESE POSTAGE STAMPS. Landolt, R. R.; Tyler, V. E. (Purdue Univ., Lafayette, Ind.). Radiochem. Radioanal. Lett.; 5: 365-8(31 Dec 1970).

Thermal neutron activation analysis was used to measure differences in trace constituents of a genuine and a counterfeit Japanese postage stamp. ^{198}Au was detected in the genuine but not in the forgery in addition to ^{24}Na and ^{56}Mn which were detected in both stamps. The method appears to be potentially useful for detecting postage stamp forgeries. (auth)

XUM

12974 DETERMINATION OF STRONTIUM IN SEA WATER BY PHOTON ACTIVATION ANALYSIS. Gordon, C. M.; Larson, R. E. (Naval Research Lab., Washington, D. C.). Radiochem. Radioanal. Lett.; 5: 369-73(31 Dec 1970).

Photon activation analysis of seawater was used to measure strontium concentrations. The radioactive strontium was produced by $^{86}Sr(\gamma,n)^{87m}Sr$ and $^{87}Sr(\gamma,\gamma')^{87m}Sr$ reactions in a 30-MeV bremsstrahlung flux of γ rays from the NRL Linac. The results are in substantial agreement with those obtained by other methods. (auth)

12975 DETERMINATION OF SCANDIUM, CHROMIUM, IRON, COBALT, ZINC, AND ANTIMONY IN DEPOSITS AND AIRBORNE PARTICULATE BY NEUTRON ACTIVATION ANALYSIS. Bando, Shoji; Imahashi, Tsuyoshi (Japan Atomic Energy Research Inst., Ibaraki). Jap. Anal.; 20: 49-56(Jan 1971). (In Japanese).

A neutron activation method has been developed for the determination of trace amounts of scandium, chromium, iron, cobalt, zinc, and antimony as the long-lived nuclide in the deposits and airborne particulates. Collected samples in sealed quartz tubes were irradiated for 200 hours in a JRR-2 reactor (thermal neutron flux: 4×10^{13} n/cm^2 · sec) and were analyzed either by the nondestructive method which used Ge(Li) detector or the chemical separation method which used anion exchange separation followed by extraction with TTA–benzene and DDTC–carbon tetrachloride. The two results were in good agreement. Consequently, the nondestructive method with a Ge(Li) detector was recommended as an efficient means for analyzing many samples of deposits and airborne particulates at a time with high sensitivity. (auth)

12976 OPTIMUM CONDITIONS FOR CARRYING OUT A NEUTRON ACTIVATION ANALYSIS IN THE CONTINUOUS DETERMINATION OF FLUORITE IN A PULP FLOW. Prokopchik, V. I. At. Energ. (USSR); 29: 50-1(Jul 1970). (In Russian).

Fluorite can be determined by counting the gamma radiation of ^{16}N (half-life = 7.5 sec; gamma energies of 6.13 and 7.11 MeV), which is formed as a result of the $^{19}F(n,\alpha)^{16}N$ reaction with the use of fast neutrons. Under optimum conditions a part of the slurry is withdrawn from the main flow, and is irradiated in a chamber with neutrons from a Po–Be or Pu–Be source. The induced activity is counted on a NaI(Tl) crystal 40 × 40 mm in size. The count rate is about one pulse per second per 1% CaF_2 in the pulp with a neutron source giving 10^7 neutrons per sec. The relative error of analyzing a pulp containing 1 to 2% CaF_2 does not exceed ±20%. This method is sensitive enough to be used for the continuous control of fluorite content in flotation pulp. (TTT)

Inorganic, Organic, and Physical Chemistry

Refer also to abstracts 13625, 13626, and 13669.

Chemical Properties

Refer also to abstract 15368.

12977 KINETIC STUDY OF THE OXIDATION OF TRIVALENT URANIUM SULFURIC ACID SOLUTIONS. Avrain, Ch.; Duflo-Plissonnier, M. (Univ., Paris). Rev. Chim. Miner.; 7: 701-12 (1970). (In French).

The oxidation of $6.10^{-3}\underline{M}$ $U^{(III)}$ in sulfuric acid solutions, prepared by electrolytic reduction and carefully degassed, was studied with an absorption spectrophotometer. The reaction rate is low: $k \leq 1.7.10^{-6}$ s^{-1}; the $U^{(III)}$ concentration varies only by 5% during 8 hr; thus, the oxygen desorption from the walls may alter the kinetics. The rate is independent of sulfuric acid concentration between 0.05 and 1$\underline{M}$, but increases under strong acidity (3 or 5$\underline{M}$ H_2SO_4). The addition of Fe^{2+} ions or N_2O doubles the oxidation rate. It may be explained by intermediary H-atom formation. $U^{(IV)}$ is not reduced by the H atoms. Zn^{2+} ions in a high concentration and Cd^{2+} ions are instantaneously reduced by $U^{(III)}$. (France)

12978 PROTACTINIUM(V) FLUORIDES. Brown, D.; Easey, J. F. (Atomic Energy Research Establishment, Harwell, Eng.). J. Chem. Soc., A; No. 19, 3378-81(1970).

The protactinium pentafluoride hydrates $PaF_5 \cdot 2H_2O$ and $PaF_5 \cdot H_2O$ were obtained from reactions between vacuum-dried protactinium(V) hydrous oxide and gaseous hydrogen fluoride at 40 and 60°C, respectively. Diprotactinium(V) oxide octafluoride, Pa_2OF_8, was obtained from this reaction at 140°C and was the ultimate product when solutions of protactinium(V) in aqueous hydrofluoric acid were evaporated to dryness in vacuo. Pa_2OF_8 decomposed when heated in the atmosphere at 220 to 290°C to yield protactinium(V) dioxide monofluoride, PaO_2F, which was converted into triprotactinium(V) heptaoxide monofluoride, Pa_3O_7F, at 560 to 580°C. At intermediate temperatures a series of structurally related solid solutions were obtained whilst above 650°C Pa_2O_5 was formed. PaO_2F appeared to be identical to the phase originally believed to be β-Pa_2O_5; Pa_3O_7F was isostructural with high-temperature U_3O_8. These reactions, and others involving hydrofluorination or fluorination of various protactinium(V) oxide halides, are discussed together with some chemical properties, i.r. spectral results, and x-ray powder diffraction results. (auth) (UK)

12979 EIGHT-COORDINATE COMPLEXES OF NIOBIUM, TANTALUM, AND URANIUM TETRAHALIDES. Deutscher, R. L.; Kepert, D. L. (Univ. of Western Australia, Nedlands). Inorg. Chem.; 9: 2305-10(Oct 1970).

In order to assign the d–d spectral transitions in dodecahedral complexes, further eight-coordinate complexes of niobium tetrahalides of the type $NbX_4(diars)_2$ (where X is Cl, Br, or I) with diarsine-like ligands (where diars is o-phenylenebis(dimethylarsine)) were prepared from the tetrahalides in acetonitrile solution. The d–d bands were assigned by studying variations in their energies for different halides and for different ligands. The complexes $NbX_4(C_2H_5diars)_2$ (where X is Cl or Br and C_2H_5 diars is o-phenylenebis(diethylarsine)) dissolve unchanged in toluene but partially dissociate in acetonitrile and completely dissociate in pyridine. Under the same conditions tantalum tetrachloride forms only monoadducts of the type $TaCl_4(diars)$, although $TaCl_4(diars)_2$ can be obtained in an impure form from a sealed-tube reaction. The uranium complex $UCl_4(diars)_2$ was also prepared and characterized. (auth)

12980 PRECIPITATION OF SOME ACTINIDE ELEMENT COMPLEX IONS BY USING HEXAMMINE COBALT(III) CATION. I. THE PRECIPITATION OF THORIUM AND PLUTONIUM(IV) CARBONATE COMPLEX IONS WITH HEXAMMINE COBALT(III) CHLORIDE. Ueno, Kaoru; Hoshi, Michio (Japan Atomic Energy Research Inst., Tokai). J. Inorg. Nucl. Chem.; 32: 3817-22(Dec 1970).

The precipitation behavior of thorium, neptunium(V), plutonium(IV), and americium(III) in ammonium carbonate solution with hexaamminecobalt(III) chloride was studied. Orange and green-yellow precipitates were produced in the case of thorium and plutonium(IV), respectively, while no precipitate of americium(III) was observed under the same conditions. On the other hand, neptunium(V) was precipitated as a white compound in ammonium carbonate solution before hexaamminecobalt(III) chloride was added. The composition of the thorium and plutonium(IV) compounds were dihexaaminecobalt(III) thorium pentacarbonate aquo trihydrate, $[Co(NH_3)_6]_2[Th(CO_3)_5 \cdot H_2O] \cdot 3H_2O$, and dihexaamminecobalt(III) plutonium(IV) pentacarbonate aquo tetrahydrate, $[Co(NH_3)_6]_2[Pu(CO_3)_5 \cdot H_2O] \cdot 4H_2O$. Chemical and crystallographic properties of the two compounds and crystallographic property of the uranium(VI) compound were also studied. (auth)

12981 PHOTOSENSITIZATION OF VINYL POLYMERIZATION BY URANYL IONS. Venkatarao, K.; Santappa, M. (Univ. of Madras). J. Polym. Sci., Part A-1; 8: 3429-33(Dec 1970).

Monomer acrylamide was used as quencher of uranyl ion fluorescence, and Stern–Volmer plots were constructed at three monochromatic wavelengths of exciting radiation. The results indicated that the reaction between excited uranyl ion and monomer is one of energy transfer. The rate parameters $k_p/k_t^{1/2}$ and k'_d/k_i were calculated from the polymerization kinetics at high monomer concentrations. A general mechanism for the photopolymerization of vinyl monomers sensitized by uranyl ions is proposed and discussed. (auth)

Isotope Effects and Exchange

Refer also to abstracts 13044, 14016, 14041, and 14439.

12982 DEUTERIUM EXCHANGE OF C-METHYL PROTONS IN LUMAZINE DERIVATIVES. McAndless, J. M.; Stewart, Ross (Univ. of British Columbia, Vancouver). Can. J. Chem.; 48: 263-70(15 Jan 1970).

Proton magnetic resonance spectroscopy was used to examine the deuterium exchange of the methyl protons in two lumazine derivatives. The exchange occurs at the C-7 methyl group in 6,7,8-trimethyllumazine and at the C-6 methyl group in 1,7-dihydro-6,7,8-trimethyllumazine. The former reaction is subject to both general acid- and general base-catalysis but the latter only to general acid-catalysis. Plausible mechanisms for the reactions of both compounds are advanced, involving in the second case acid-catalyzed addition of water across the C_6–N_5 double bond. (auth) (Canada)

XUM

12983 MECHANISM OF INITIATION IN THE THERMAL POLYMERIZATION OF STYRENE. KINETIC DEUTERIUM ISOTOPE EFFECTS IN THE INITIATION STEP OF THE THERMAL POLYMERIZATION OF SOME DEUTERATED STYRENES. **Kopecky, Karl R.; Evani, Syamalarao (Univ. of Alberta, Edmonton). Can. J. Chem.; 47: 4049-58(1 Nov 1969).**

A convenient synthesis of 2,6-dideuteriostyrene starts with N,N-dimethyl-(1-phenylethyl)-amine, which is deuterated in the 2 and 6 positions by a series of exchanges using n-butyllithium followed by deuterium oxide. The deuterium isotope effects at 70°C on the rates of the thermal polymerization, R_{pH}/R_{pD}, of 2,6-dideuterio-, α-deuterio-, and β,β-dideuteriostyrene are 1.29, 1.00, and 0.78, respectively. The deuterium isotope effects at 70°C on the 2,2′-azobis-(2-methylpropionitrile) initiated rates of polymerization, R'_{pH}/R'_{pD}, are 0.96, 0.86, and 0.81, respectively. From these values the deuterium isotope effects on the rates of initiation of the thermal polymerization, k_{iH}/k_{iD}, are calculated to be 1.80, 1.31, and 0.92, respectively. At 147°C the presence of 1.5% potassium t-butoxide decreases the rate of the thermal polymerization of neat styrene by a factor of 17, and results in the formation of 1-phenyltetralin as the greatly predominant dimer. The results support the suggestion that the thermal polymerization of styrene is initiated by hydrogen transfer from 1-phenyl-1,2,3,9-tetrahydronaphthalene, formed by a concerted dimerization of two molecules of styrene, to a third molecule of styrene. (auth) (Canada)

12984 HEAT CAPACITY OF ACTIVATION FOR THE HYDROLYSIS OF METHANESULFONYL CHLORIDE AND BENZENESULFONYL CHLORIDE IN LIGHT AND HEAVY WATER. **Robertson, R. E.; Rossall, B.; Sugamori, S. E.; Treindl, L. (National Research Council of Canada, Ottawa). Can. J. Chem.; 47: 4199-4206(15 Nov 1969).**

Rates of solvolysis of methanesulfonyl chloride and benzenesulfonyl chloride were determined in H_2O and D_2O. The free energy, enthalpy; entropy, and heat capacity of activation were calculated. The exceptional accuracy of the data permitted an estimation of $d\Delta C^{\ddagger}_p/dT$ from a four parameter temperature dependence of the kinetic rates. From these data it was concluded that both sulfonyl chlorides hydrolyse by the same mechanism (S_N2). The change in R from CH_3 to C_6H_5 in RSO_2Cl did not alter $\Delta C^{\ddagger}_p$ but $\Delta S^{\ddagger}$ (20°) was changed from −8.32 to −13.25 cal deg^{-1} mole^{-1}, respectively. The significance of this difference is attributed to the probability of bond formation rather than to differences in solvent reorganization. (auth) (Canada)

12985 CONCENTRATION DEPENDENCE OF VAPOR PRESSURE ISOTOPE EFFECT OF METHYLAMINE AND N-DEUTERIOMETHYLAMINE IN HEXANE. **Wolff, H. (Univ., Heidelberg). J. Phys. Chem.; 75: 160-1(7 Jan 1971).**

The concentration dependence of the vapor pressure isotope effect of dimethylamine and N-deuteriodimethylamine in hexane was previously described by the two-state function $p/p' = (p/p')^{1-x}_{\text{bonded}}(p/p')^{x}_{\text{free}}$, (1), where p/p′ is the ratio of partial pressures of the heavy (p) and of the light (p′) isotopic compound at the fraction x of molecules with free amino groups. $(p/p')_{\text{free}}$ and $(p/p)_{\text{bonded}}$ are the ratios at the limit of dilution and at the hypothetical state of complete association which can be calculated from the intramolecular vibrations of gaseous compounds and from the inter- and intramolecular vibrations of monomers or associated compounds in the liquid state. In order to check eq 1 in more detail the ratios of methylamine and N-deuteriomethylamine in solution with hexane were investigated. A straight line was obtained when ln p/p′ was plotted vs the fraction x of molecules with free groups. Results indicate that the dependence of the vapor pressure isotope effect of methylamine and N-deuteriomethylamine in hexane on concentration is shown in eq 1. The model of association used in the calculation is thus supported. (J.G.B.)

12986 DYNAMICS OF SOME EXCHANGE REACTIONS. **Wong, Wing-hing. Ontario, Can.; Univ. of Toronto (1969).**

Thesis.

The dynamics of several three-center exchange reactions were studied by numerically integrating Hamilton's equations of motion in three dimensions. The location of the saddle point on a potential surface had a very profound effect on the detailed dynamics of the reaction. With the saddle point in the "entrance valley," the initial translational energy was most effective for barrier-crossing, and a large fraction of the available energy was channelled into product vibration. However, if the saddle point was in the "exit valley," vibrational energy of the reactant was indispensable, and the reaction product had lower vibrational excitation. In a "hot-atom" reaction it was found that the computation could reproduce the experimental data on the relative yields of "abstraction" and "displacement" products if the interaction potential provided sufficient interaction time between the very fast attacking atom and the target molecule. The detailed dynamics of collisions leading to abstraction, displacement or fragmentation were analyzed in terms of specimen trajectories and in terms of the pattern of forces controlling them. It was found that both abstraction and displacement involved "direct interaction," in the sense that once the old bond started to dissolve it extended continuously. Even at the very high energy of 12 eV, the dynamics were only approaching the limit of spectator-stripping, owing to the effect of product repulsion in broadening the angular and energy distributions. The reaction dynamics of the isotopic systems Cl + HI and Cl + DI were studied by Monte Carlo sampling techniques. The difference in product vibrational distributions of these two systems, observed experimentally, was satisfactorily reproduced by a highly-repulsive potential-energy surface. Classical mechanics predicts a shift in k(v) toward higher v in Cl + DI than in Cl + HI, in close accord with experiment. From examination of specimen trajectories, and of the pattern of forces governing them, secondary collisions were shown to play an important part in the reaction dynamics. The computations lend further support to the contention that classical mechanics can provide an approximate but adequate description of reactive collisions. (Diss. Abstr. Int., B)

12987 KINETICS OF THE HOMOGENEOUS, BIOMOLECULAR ISOTOPE EXCHANGE REACTIONS $D_2 + CH_4 \rightarrow HD + CH_3D$, $D_2 + H_2S \rightarrow HD + HDS$ AND $HD + HD \rightarrow H_2 + D_2$ AS STUDIED IN SINGLE-PULSE SHOCK TUBES. **Lewis, David Kenneth. Ithaca, N. Y.; Cornell Univ. (1970). 216p. University Microfilms Order No. 70-17,090.**

Thesis.

A group of related atom-switching reactions between simple hydrogen and deuterium containing species was studied under homogeneous conditions in single-pulse shock tubes. The reactions $D_2 + CH_4 \rightarrow HD + CH_3D$ and $D_2 + H_2S \rightarrow HD + HDS$ were investigated, thereby completing the series $[D_2 + H_2, SH_2, NH_3,$ and $CH_4]$. Also, additional data were collected on the exchange reaction $H_2 + D_2 \rightarrow {}_2HD$, and a complete study was made of the reverse of this reaction, $2HD \rightarrow H_2 + D_2$. The $D_2 + CH_4$ reaction was studied over the temperature range 1440 to 1755°K. D_2/CH_4 ratios were varied from ⅓ to 10, and sample densities ranged from 1.5×10^{-2} to 4.7×10^{-2} moles/l. The empirical power rate expression was found to be approximately first order with respect to D_2 and one-half order with respect to CH_4 and to the Ar diluent (94 to 97% of the total sample). When the data were reduced on this basis, an activation energy of 50 ± 3 kcal/mole was obtained. The $D_2 + H_2S$ reaction was studied in two different shock tubes over the temperature range 1250 to 1590°K and density range 6×10^{-3} to 4×10^{-2} moles/l. D_2/H_2S ratios were varied from ¼ to 4. The agreement between the two sets of data was good, and both sets could be fitted by a second order expression in which the rate is first order in D_2 and about one-half order in H_2S and the Ar diluent. The deduced activation energy is 53 + 3 kcal/mole. The HD HD exchange was studied over the temperature range 1120 to 1659°K, at densities ranging from 1×10^{-2} to 7×10^{-2} moles/l. Samples consisted of 1 to 4.5% HD in Ar. The power rate expression, again second order overall, was approximately 1.4 order with respect to HD and 0.6 order in Ar. The activation energy was found to be 36 + 2 kcal/mole. The data from these three reactions support a mechanism similar to that proposed for other exchange reactions in this series. In this model, the probability for exchange during a collision of two reactant molecules is greatly enhanced when one of them is excited to or above a critical vibrational level. The overall exchange rate is limited by the rate of repopulating that level via collisions with other reactant molecules and with the Ar diluent. Energy transfer probabilities for collisions of the various species present, calculated from these kinetic data assuming this mechanism, are internally compatible and in agreement with independent measurements of vibrational relaxation times. A comparison of the data from these experiments with recent theoretical work on 4-center transition states has shown that these homogeneous atom-switching reactions probably do not occur via formation of transition states that are either square planar, rectangular, rhombic or tetrahedral. However, less symmetrical transition state configurations of lower relative energy, such as isosceles trapezoid or "kite" shapes, are suggested. (Diss. Abstr. Int., B)

12988 DIPOLE MOMENT AND HYPERFINE PARAMETERS OF $H^{35}Cl$ AND $D^{35}Cl$. **Kaiser, Edward William Jr. Cambridge, Mass.; Harvard Univ. (1970). 141p. University Microfilms Order No. 70-18,341.**

Thesis.

The molecular-beam electric resonance spectra of $H^{35}Cl$ and $D^{35}Cl$ were analyzed. The molecular constants obtained in the observed states are as follows. All constants are given in units of kilohertz with the exception of the dipole moment, which is in debye. The notation is standard with eqQ_X and C_X representing the quadrupole coupling constant and spin-rotation interaction of

XUM

nucleus X. Numbers in parenthesis are the 95% confidence limits in the final significant figures presented for the indicated vibrational and rotational state. $H^{35}Cl$: (v = 0, J = 1) $eqQ_{Cl} = -67618.93$ (47), $C_H = -41.80(25)$, $C_{Cl} = +53.851(42)$, $\mu_v = 1.10847$; (v = 1, J = 1) $eqQ_{Cl} = -69272.89(93)$, $C_H = -41.09(24)$, $C_{Cl} = +58.597(45)$, $\mu_v = 1.13888(26)$; (v = 2, J = 1) $eqQ_{Cl} = -70908.1(2.4)$, $C_H = -39.94(94)$, $C_{CL} = +63.68(17)$, $\mu_v = 1.16835(60)$; (v = 0, J = 2) $eqQ_{Cl} = -67638.53$ (15). $D^{35}Cl$: (v = 0, J = 1) $eqQ_D = +187.36(30)$, $eqQ_{Cl} = -67393.38(9)$, $C_D = -3.295(46)$, $C_{Cl} = +27.426(7)$, $\mu_v = 1.10312(8)$; (v = 1, J = 1) $eqQ_D = +184.8(3.8)$, $eqQ_{Cl} = -68583.1(1.0)$, $C_D = -3.25(7)$, $C_{Cl} = +29.121(62)$, $\mu_v = 1.12515(35)$. (v = 0, J = 2) $eqQ_{Cl} = -67403.32(29)$; (v = 0, J = 3) $eqQ_{Cl} = -67418.01(10)$. The above dipole moments, μ_v, are defined as the dipole moments in the J = 0 state of the vibrational state v. The error limits quoted in these dipole moments are the precisions of the measurement of the dipole moment of the given state relative to the moment of the $H^{35}Cl$ (v = 0) level. The absolute accuracy of these dipole moment determinations is 0.05%. The above relative dipole moments were used in conjunction with available absolute infrared intensity measurements of vibrational bands to obtain the dipole moment functions of the molecules. The derivatives of the dipole moment operator with respect to the internuclear distance R evaluated at R_e for $H^{35}Cl$ are: $\mu_e = 1.0929(5)$; $(d\mu/dR)_e = +0.925(20)$ D/Å; $(d^2\mu/dR^2)_e = +0.16(11)$ D/Å^2; $(d^3\mu\ dR^3)_e = -3.83(90)$ D/Å^3; $(d^4\mu/dR^4)_e = -9.3(4.5)$ D/Å^4. In addition, an isotope effect on the dipole moment due to a vibrationally induced violation of the Born-Oppenheimer approximation was observed by comparing the HCl and DCl dipole moments. The electronic polarizability anisotropy was also determined in magnitude and sign: $\alpha_{||} - \alpha_{\perp} = +0.29(10)$ Å^3. Two distance derivatives of the field gradient, q_{Cl}, were obtained in this study: $(dq_{Cl}/dR)_e = +13.52(55) \times 10^{15}$ (esu/cm^3)/Å; $(d^2q_{Cl}/dR^2)_e = -23.9(3.3) \times 10^{15}$ (esu/cm^3)/Å^2. The rotational magnetic moment of $H^{35}Cl$ (v = 0, J = 1) was measured, yielding the molecular g value: $g_J = +0.47(03)$. This parameter, when combined with other available data, permitted a very precise determination of the relative values of R_e in $H^{35}Cl$ and $D^{35}Cl$: $Re(H^{35}Cl) - R_e(D^{35}Cl) = +4.8(5) \times 10^{-15}$Å. There is a significant difference in the equilibrium distances due to a mass dependent adiabatic breakdown of the Born–Oppenheimer approximation. (Diss. Abstr. Int., B.)

12989 ISOTOPIC NON-ISOMORPHISM OF $Rb(H_{1-x}D_x)_3(SeO_3)_2$ CRYSTALS. Shuvalov, L. A.; Ivanov, N. R.; Kirpichnikova, L. F.; Gordeyeva, N. V. (Moscow Inst. of Crystallography). Phys. Lett.; 33A: 490-1(28 Dec 1970).

On H → D substitution the ferroelectric properties of $Rb(H_{1-x}D_x)_3(SeO_3)_2$ decrease up to complete disappearance but the phase transition remains approximately at the same temperature. (auth)

12990 VOLUME VISCOSITY AND STRUCTURE OF D_2O USING ULTRASONICS. Kor, S. K.; Deorani, S. C. (Univ. of Allahabad, India). Phys. Lett.; 33A: 489-90(28 Dec 1970).

Hall's theory of structural relaxation was applied to calculating two adiabatic volume viscosities, η_v and η'_v; the mole fraction in the open packed state, x_2; and the relaxational thermal expansion, β_r, of D_2O in the temperature range 5 to 50°C. The values K_T, $\infty = 17 \times 10^{-12}$ cm^2/dyn and $\Delta V/V = 0.47$ were taken for computation. The results agree fairly well at low temperatures with those available for H_2O and D_2O. The value of thermodynamic parameters give support to Hall's two state model up to 10°C. (auth)

12991 OXYGEN AND HYDROGEN ISOTOPE EXCHANGE IN ALCOHOLS. Pisarev, Yu. N.; Zel'venskii, Ya. D.; Shal'gin, V. A. (Inst. of Chemistry Technology, Moscow). Isotopenpraxis; 6: 365-8(Oct 1970). (In Russian).

The catalytic hydrogen and oxygen exchange of CH_3OH, C_2H_5OH, and C_3H_7OH were studied in the temperature range 200 to 300°C. Using the most active coal catalyst, AGN, the activation energy for the oxygen exchange with $H_2{}^{18}O$ was 10, 8, and 6 kcal/mole and for the C–H hydrogen-exchange with D_2O 21, 18, and 15 kcal/mole. It is possible to prepare ^{18}O-, T, and D-substituted alcohols by this procedure. (auth)

12992 SOME STUDIES ON ISOTOPE EXCHANGE REACTIONS IN DIFFERENT BF_3-COMPLEX SYSTEMS. Voloshchuk, A. M.; Katal'nikov, S. G.; Dmitrevskii, L. L. (Inst. for Chemistry Technology, Moscow). Isotopenpraxis; 6: 359-65(Oct 1970). (In Russian).

The isotope equilibrium in the system BF_3-BF_3–complex was studied. The following compounds were used as complexing agents: β-chlorophenetole, p-chlorophenetole, p-fluorophenetole, p-bromophenetole, and p-nitrophenetole. A method for calculation of α by using Hammet–Taft relation is described. Calculation of π-electron density and bending order was made by the Molkao method and the "Hückel-A" program. (auth)

12993 SHOCK TUBE EXPERIMENTS ON THE PYROLYSIS OF DEUTERIUM-SUBSTITUTED ETHYLENES. Skinner, Gordon B.; Sweet, Ronald C.; Davis, Steven K. (Wright State Univ., Dayton, Ohio). J. Phys. Chem.; 75: 1-12(7 Jan 1971).

Dilute mixtures of C_2H_4, $C_2H_4 + C_2D_4$, trans-1,2-$C_2H_2D_2$, and $C_2H_2 + D_2$ in argon were pyrolyzed in a single-pulse shock tube. Empirically, in ethylene pyrolysis the order with respect to argon was 0 ± 0.2, and that with respect to ethylene 1.2 ± 0.2. Pyrolysis data are summarized in terms of first-order (in ethylene) rate constants as follows: $8.9 \times 10^8 e^{-46,400/RT}$ sec^{-1} for 0.1% C_2H_4, $1.05 \times 10^9 e^{-48,800/RT}$ sec^{-1} for 0.05% C_2H_4 + 0.05% C_2D_4 and 0.1% $C_2H_2D_2$, and $1.8 \times 10^9 e^{-48,800/RT}$ sec^{-1} for 0.25% C_2H_4 + 0.25% C_2D_4 and 0.5% $C_2H_2D_2$, at 3 atm total reaction pressure, and 1100 to 1500°K. The isotopic distribution of ethylene after reaction indicated that isotope exchange is nearly first order in ethylene, the rate constant for the step producing C_2H_3D and C_2HD_3 from C_2H_4 and C_2D_4 being $3.4 \times 10^7 e^{-32,000/RT}$ sec^{-1}. Rates of subsequent steps are governed by the statistics of the reactions. Isotope distributions of acetylene and hydrogen (the chief decomposition products of ethylene) and of ethylene produced by hydrogenation of acetylene indicate that both ethylene decomposition and acetylene hydrogenation occur by free-radical rather than molecular mechanisms. Isotope exchange reactions were considerably faster than either ethylene decomposition or acetylene hydrogenation. (auth)

12994 INFRARED SPECTRUM OF HDO IN WATER AND IN NaCl SOLUTION. Wyss, H. R.; Falk, M. (National Research Council of Canada, Halifax, Nova Scotia). Can. J. Chem.; 48: 607-14(15 Feb 1970).

The molar absorptivity of dilute HDO in water and in aqueous NaCl solutions was determined at temperatures between 10 and 85°C in the spectral region from 4000 to 2000 cm^{-1}. The infrared band profiles for the OH and OD stretching fundamentals are single-peaked and devoid of shoulders, in contrast to the high-frequency shoulders recently observed in the Raman spectrum. It is shown that such shoulders do not contradict a single-peaked distribution of OH oscillators with respect to intermolecular geometry. Absence of resolvable sub-bands in the spectrum of HDO in concentrated salt solutions indicates a wide distribution of ion–H_2O interactions, akin to the distribution of H_2O-H_2O interactions in water. (auth) (Canada)

12995 SYSTEM FOR DETERMINATION OF PRECISE ISOTOPIC VAPOR PRESSURE DIFFERENCES FROM -20 TO 110°C INCLUDING TEMPERATURE CONTROL TO 0.001 OVER THAT RANGE. Pupezin, J. (Boris Kidrich Inst. of Nuclear Sciences, Belgrade); Jancso, G.; Taylor, J. W.; Van Hook, W. A. Isotopenpraxis; 6: 319-22(Sep 1970).

The system designed for the precise measurement of small isotopic vapor pressure differences over the range –20 to 110°C consists of a cell designed to hold two isotopically different samples at identical temperatures, a thermostat to maintain the cell at constant temperature, pressure transducers to measure the isotopic pressure differences and the total pressure, heated connecting lines, an auxiliary vacuum system, and a thermometer. An example of data obtained with the apparatus is given for the vapor pressure isotope effect of H_2O (liq) vs D_2O (ice) over an 0.8°C interval. Very low dispersion about the correlation line nicely demonstrated the efficiency of the system as a whole. (P.C.H.)

12996 SOME DATA TO THE REACTION BETWEEN METHYL IODIDE AND ALKALINE IODIDE. Pataki, L.; Beronius, P.; Kocsis, E. (Eoetvoes Lorand Univ., Budapest). Radiochem. Radioanal. Lett.; 5: 313-17(31 Dec 1970).

The reaction order of the components in the isotopic exchange reaction between methyl iodide and potassium iodide in ethanol at 35°C was determined. By the measurements $\alpha = \beta = 1$, the reaction is a first order one, both for organic and for inorganic components. (auth)

12997 ISOTOPE EFFECT IN THE RAMAN SPECTRA OF A DKDP CRYSTAL. Popova, E. A.; Savatinova, I. T.; Velichko, I. A. (Ioffe Inst. of Physics and Tech., Leningrad). Sov. Phys.-Solid State (Engl. Transl.); 12: 1543-6(Jan 1971).

Translated from Fiz. Tverd. Tela; 12: 1941-4(Jul 1970).

The Raman scattering of the ferroelectric KD_2PO_4 (DKDP) was studied in natural and polarized light. Comparison with the spectrum of ordinary KDP showed that the broad, intense wing of the Rayleigh line, characteristic of the Raman spectrum of KDP, is far weaker in the case of DKDP. A considerable (10–15 cm^{-1}) isotope shift of OPO deformation vibrations is noted. Especially pronounced changes in the spectrum are noted in the region of valence vibrations of the PO bond. The isotope shift in the symmetric vibration of the PO ions, observed on replacement of hydrogen by deuterium and amounting to 30 cm^{-1}, and the appearance of a very intense band at 960 cm^{-1} in the Raman spectrum of DKDP can hardly be explained from the viewpoint of the ordinary kinematic effect of isotopic substitution. Investiga-

XUM

tions of the Raman spectrum of DKDP in polarized light enabled the determination of the symmetry of normal vibrations in the crystal. (auth)

12998 EFFECTS OF DEUTERATION ON THE SPECIFIC HEAT OF $NH_4H_2PO_4$ (ADP) CRYSTALS. Amin, M.; Strukov, B. A. (Moscow State Univ.). Sov. Phys.-Solid State (Engl. Transl.); 12: 1616-18(Jan 1971).

Translated from Fiz. Tverd. Tela; 12: 2035-8(Jul 1970).

Results are reported for $NH_4H_2PO_4$ (ADP) and $ND_4D_2PO_4$ (DADP) over the antiferroelectric transition. A difference from KH_2PO_4 (KDP) is that the entropy of transition is reduced by deuteration. This quantity is 1.10 ± 0.01 and 0.73 ± 0.02 cal/mole/deg for ADP and DADP, respectively. (auth)

12999 KINETICS OF ANTIMONY(III AND V) EXTRACTION. Iofa, B. Z.; Nesmeyanov, An. N.; Kireev, G. I.; Abramov, A. A. Vestn. Mosk. Univ., Ser. II. Khim.; 11: 537-41(Sep-Oct 1970). (In Russian).

The effects of concentration of antimony and hydrogen chloride on extraction rate and isotopic exchange rate in aqueous phase has been studied. The mass transfer coefficients for extraction and isotopic exchange were calculated. The hydrolysis and rehydrolysis rate constants for antimony(V) in aqueous phase were estimated. (auth)

13000 BASE-CATALYZED HYDROGEN–DEUTERIUM EXCHANGE OF N-SUBSTITUTED PYRIDINIUM IONS. INDUCTIVE EFFECTS AND INTERNAL RETURN. Zoltewicz, John A.; Helmick, Larry S. (Univ. of Florida, Gainesville). J. Amer. Chem. Soc.; 92: 7547-52(30 Dec 1970).

Rates of hydrogen–deuterium exchange of N-substituted pyridinium ions in D_2O at 75.0°C were obtained by the use of an nmr method. Deprotonation is catalyzed by deuteroxide ion. Catalysis by buffer bases is negligible. Relative rates of exchange for substituents O^-, $CH_2C_6H_5$, CH_3, C_6H_5, ND_2, and OCH_3 are 1.0, 1.1×10^2, 1.4×10^2, 5.3×10^2, 2.7×10^3, and 1.3×10^6, respectively. Rates show a good correlation with the Taft σ_I inductive parameter; ρ_I is 15. The substituent rate factor for positively charged nitrogen is estimated to be about 10^{14-16}. The absence of substantial buffer base catalysis for these reactions giving pyridinium ylide intermediates is consistent with internal return during exchange. Generalizations concerning the structure of carbon acids, general base catalysis, and internal return are given. (auth)

13001 CATALYTIC ACTIVITY AND REACTIVITY OF AROMATIC NITRILE AND ALKALI METAL ION RADICAL SALT. I. HOMOGENEOUS AND HETEROGENEOUS CATALYSIS OF BENZONITRILE-CESIUM ION RADICAL SALT. Tsuda, Motoyuki; Inokuchi, Hiroo (Tokyo Univ.). Bull. Chem. Soc. Jap.; 43: 3410-14(Nov 1970).

Homogeneous and heterogeneous mechanisms of parahydrogen conversion and hydrogen–deuterium exchange reactions were investigated in the presence of a benzonitrile–cesium ion radical salt. Studies of their activation energies and rate constants showed that the heterogeneous reaction on the solid-ion radical salt occurs mainly through the chemisorption mechanism and the exchange mechanism, but the homogeneous reaction over the salt solution in benzonitrile takes place only through the physical mechanism. According to these results, it was concluded that the catalytic activity and reactivity of the ion radical salt must be due to the nature of its solid phase, not to that of its aromatic anion or free-ion radical pair. (auth)

13002 CATALYTIC ACTIVITY AND REACTIVITY OF AROMATIC NITRILE AND ALKALI METAL ION RADICAL SALT. II. HYDROGEN EXCHANGE ON BENZONITRILE ION SALT AS A FUNCTION OF ALKALI METALS. Tsuda, Motoyuki (Tokyo Univ. Waseda Univ., Tokyo). Bull. Chem. Soc. Jap.; 43: 3415-19(Nov 1970).

The para-ortho hydrogen conversion (rate constant k_e^H and the deuterium exchange reaction (rate constant k_e^D) over the benzonitrile–alkali metal ion radical salt were investigated as functions of the donor component–alkali metal. The sort of alkali metals in the ion radical salts greatly affected the catalytic activity and the reactivity. The activation energies obtained from the temperature dependence of k_e^H and k_e^D, E^H and E^D, and the value of α (depending on the ratio of k_e^H to k_e^D, decreased as Na → K → Rb, but those values showed an irregular trend for the Cs complex. The results suggest that the catalytic activity cannot be understood only in terms of the nature of the components; must also be considered the structural nature of the solid phase of the ion radical salt. (auth)

13003 $\pi-\pi^*$ ELECTRONIC ABSORPTION SPECTRA OF p-DIBROMOBENZENES-D_4 AND -H_4. Shukla, J. V.; Upadhya, K. N.; Thakur, S. N. (Banaras Hindu Univ., India). Appl. Spectrosc.; 25: 85-9(Jan-Feb 1971).

The uv absorption spectra of p-dibromobenzenes-H_4 and -D_4 were recorded on a Hilger E_1 large quartz spectrography in the regions 35370 to 39540 cm^{-1} and 35340 to 39470 cm^{-1}, respectively. The assignments of vibronic bands were made using the results from the two isotopic molecules. Some of the previous assignments were revised in the light of the data from the present investigations. (auth)

13004 OPTICAL HETERODYNE MEASUREMENT OF XENON ISOTOPE SHIFTS. Dhsgrt, J. Hoestf (National Bureau of Standards, Boulder, Colo. Univ. of Colorado, Boulder, Colo.). Phys. Rev., A; 3: 752-7(Feb 1971).

Isotope-shift measurements with a precision of two parts in 10^9 of the optical transition frequency were made for the 2.02-μ line of the three even isotopes of xenon: ^{132}Xe, ^{134}Xe, and ^{136}Xe. This shift is extremely small due to the large xenon mass, the proximity of the xenon isotopes to the neutron magic number N = 82, and the weak interaction of the nucleus with the 5d and 6p electron states. The measurements were 500 ± 300 kHz ($0.17 \pm 0.01 \times 10^{-3}$ cm^{-1}) for $^{132}Xe-^{134}Xe$ and $1500 \pm 0.01 \times 10^{-3}$ cm^{-1}) for $^{134}Xe-^{136}Xe$, where the lighter isotope had the larger transition frequency in each case. These two shifts are sufficiently different to suggest that nuclear field effects contribute to the results. (auth)

13005 CARBON ISOTOPES AND THE ORIGIN OF PETROLEUM. Vinogradov, A. P.; Galimov, E. M. (Inst. of Geochemistry and Analytical Chemistry, Moscow. Inst. of the Petrochemical and Gas Industry, Moscow). Geochem. Int. (Engl. Transl.); 7: 217-35(Nov 1970).

Translated from Geokhimiya; No. 3, 275-96(Mar-Apr 1970).

Transformation of petroleum and the origin of its components are discussed on the basis of new data on the carbon isotopic composition of petroleum and associated gases from a single petroliferous province (Perm' Province). There are persistent regularities in the distribution of carbon isotopes in petroleum. The gaseous hydrocarbons are enriched in ^{12}C. Methane is the richest in the lighter carbon isotope, with the average $\delta^{13}C$ = 4.86% ethane is isotopically heavier than methane (average $\delta^{13}C$ = 3.83%), but lighter than propane and butane. The carbon isotopic composition of the last two gases approaches that of petroleum, and is sometimes enriched in ^{13}C as compared with it. The aromatic hydrocarbons (average $\delta^{13}C$ = –2.45%) are systematically different in carbon isotopic composition from the paraffin–naphthene hydrocarbons (average $\delta^{13}C$ = –2.94%). Fractions boiling at temperatures of 60° to 187° (average $\delta^{13}C$ = –2.92%) have similar carbon isotopic compositions except for the 60° to 95°C fraction (average $\delta^{13}C$ = –2.81%), which is systematically enriched in ^{13}C among the samples investigated. Paraffins (average $\delta^{13}C$ = –2.71%) and asphaltenes (average $\delta^{13}C$ = –2.70%) have practically identical isotopic compositions both in individual samples and on the average, and are poorer in ^{12}C than the crude petroleum (average $\delta^{13}C$ = –2.89%). Solid paraffins (average $\delta^{13}C$ = –3.02%) are enriched in ^{13}C as compared with crude petroleum and liquid paraffins. Comparison of theoretical effect of temperature on the thermodynamics of the isotope effects in the $CH_4-C_2H_6-C_3H_8$ series with the separation factor for carbon isotopes leads to the conclusion that the temperature at which petroleum forms cannot be high. Analysis of the carbon isotopic composition in the components of petroleum and organic matter shows that only a part of organic matter can be regarded as the source of petroleum. It is assumed that the biochemical components of organic matter from which petroleum was derived were fatty acids and lignin-like substances, the former serving as the source of the paraffin–naphthene fractions of petroleum, and the latter, for the most part, of the aromatic hydrocarbons. (auth)

13006 ULTRAVIOLET ABSORPTION SPECTRA OF ACETONE AND ACETONE-d_6. Rao, C. N. R.; Chaturvedi, G. C.; Randhawa, H. S. (Indian Inst. of Tech., Kanpur). Chem. Phys. Lett.; 7: 563-4(15 Dec 1970).

Ultraviolet absorption spectra of acetone and acetone-d_6 were photographed under fairly high resolution and vibrational analyses carried out. The results indicate that the C(CO)C skeleton of the excited state of acetone is nonplanar; CNDO/2 calculations also substantiate this observation. (auth)

13007 COMPENSATION EFFECT IN A PROTOPHILIC DEUTERIUM-EXCHANGE REACTION ASSOCIATED WITH A CHANGE IN SOLVATION OF THE CATALYST CATION. Marchenko, V. A.; Yakushin, F. S.; Shatenshtein, A. I. (Inst. of Physical Chemistry, Moscow). Dokl. Akad. Nauk SSSR; 194: 1123-6(11 Oct 1970). (In Russian).

The reaction between 9-d-fluorene and tertiary butanol during catalysis by lithium tert-butoxide was followed in the presence of electron-donor additives. In all experiments the concentration of lithium tert-butoxide was fixed at 0.13 moles/l, while the concentration of additive (tetramethyl urea (TMU), dimethylsulfoxide

(DMSO), methyl-di-(methoxymethyl)-phosphine oxide (MDP), and 1,2-dimethoxyethane (DME)) was varied within the limits of 1.3 to 5.0 mole % with respect to the tert-butanol. The ratio between the number of moles of additive and catalyst was varied from 1 : 1 to 4 : 1. The rate constants (k, sec^{-1}) were measured at 3 to 4 temperatures in the interval of 25 to 50°C. The value of k_0 at 25°C in the absence of additive was found to be 3.3×10^{-5} sec^{-1}. The relative reaction rates k/k_0 at a concentration of additive = 3.4 mole % were 2.4 for DME, 4.9 for TMU, 13.6 for DMSO, and 200×10^{-5} sec^{-1} for MDP. Values of the activation energy, heat of reaction and entropy are tabulated for these reactions at 1.3, 2.0, 3.4, and 5.0 mole % of additive in each reaction. With increasing solvating ability and concentration of additive, the heat of reaction decreases and the negative value of the entropy increases. A decrease in enthalpy is accompanied by a fall in entropy as given by the following equation: $\Delta S = -69.7 + 2.80 \times 10^{-3}\ \Delta H$. (TTT)

Physical Chemistry

Refer also to abstracts 13027, 13032, 13653, 13712, 13753, 13761, 14437, 14466, 14482, 15372, and 15374.

13008 COMPLEX FORMATION BETWEEN TECHNETIUM AND CHELATE-FORMING LIGANDS. II. **Gorski, B.; Koch, H. (Institut fuer Angewandte Radioaktivitaet, Leipzig). J. Inorg. Nucl. Chem.; 32: 3831-6(Dec 1970). (In German).**

Complex formation of tetravalent technetium with chelate-forming ligands such as nitrilotriacetic acid, ethylenediaminetetraacetic acid, and cyclohexanediaminetetraacetic acid in aqueous solution was studied by means of ion exchange and electrophoresis. The composition of the complexes formed and their stability constants were determined. (auth) (UK)

13009 QUINQUEVALENT PROTACTINIUM AND QUADRIVALENT ACTINIDE TROPOLONATES. **Brown, D.; Rickard, C. E. F. (Atomic Energy Research Establishment, Harwell, Eng.). J. Chem. Soc., A; No. 19, 3373-83(1970).**

Protactinium pentachloride, pentabromide, and oxide tribromide react with an excess of tropolone in nonaqueous solvents to yield tetrakis(tropolonato)protactinium(V) halides of the type $Pa(trop)_4 \times$ (trop = $C_7H_5O_2^-$; X = Cl or Br). Attempts to prepare $Pa(trop)_5$ were unsuccessful. Reactions in ethanol involving lithium tropolonate and the tetrakis(tropolonato)metal(V) halides, or $Pa(trop)_4$ and tropolone, resulted in the precipitation of $Pa(trop)_4^-$ OEt, which on the addition of hydrochloric acid–acetone mixtures was converted into $Pa(trop)_4Cl$. This formed a 1 : 1 adduct $Pa(trop)_4Cl$, DMSO with dimethyl sulphoxide but did not react with dimethylformamide. The quadrivalent tropolonates $Pa(trop)_4$, $Np(trop)_4$, and $Pu(trop)_4$ were prepared by reactions in either aqueous or nonaqueous solvents. $Pa(trop)_4$, but neither $Np(trop)_4$, nor $Pu(trop)_4$ reacted with lithium tropolonate to form a pentakis-complex. Oxidation of $Pa(trop)_4$ in perchloric acid solution yielded $Pa(trop)_4ClO_4$. Some chemical properties, ir spectra, and crystallographic results are reported for these compounds and for some quadrivalent thorium tropolonates. (auth) (UK)

13010 THE CRYSTAL STRUCTURE AND ANISOTROPIC THERMAL EXPANSION OF β-URANYL DIHYDROXIDE, $UO_2(OH)_2$. **Bannister, M. J.; Taylor, J. C. (Australian Atomic Energy Commission Research Establishment, Lucas Heights). Acta Crystallogr., Sect. B; 26: 1775-81(1970).**

Single-crystal and powder x-ray diffraction techniques were used to determine improved positional, thermal vibration, and lattice parameters for the orthorhombic β-$UO_2(OH)_2$. Values obtained for lattice parameters at 21°C are: a = 5.6438 ± 0.0001, b = 6.2867 ± 0.0001, c = 9.9372 ± 0.0002 Å. Thermal expansion of this material was studied by elevated temperature x-ray diffraction and hot-stage optical microscopy. Thermal expansion up to 260°C was strongly anisotropic, with large contractions in a, large expansions in b, and a smaller cyclic change in c. Expansion at higher temperatures was almost isotropic. Using the structural and vibrational data, the anisotropic thermal expansion is interpreted in terms of a thermally induced rotation of the oxygen octahedra surrounding all uranium atoms. (auth) (Denmark)

13011 REFINEMENT OF THE CRYSTAL STRUCTURE OF $AmCl_3$. **Burns, John H.; Peterson, J. R. (Oak Ridge National Lab., Tenn.). Acta Crystallogr., Sect. B; 26: 1885-7(1970).**

A refinement of the parameters of $AmCl_3$, which is of the UCl_3 structure type, was carried out using single-crystal x-ray diffraction data. An ionic radius of 0.984 ± 0.003 Å for Am^{3+} was derived. (auth) (Denmark)

13012 CONTINUOUS URANIUM PRECIPITATION PROCESS AND APPARATUS. **Delpech, Andre (to Commissariat a l'Energie Atomique). French Patent 1,588,805. 16 Mar 1970. Filed 10 May 1968. (In French).**

A process of continuous precipitation of uranium in the form of uranyl formate is described. Uranyl nitrate in concentrated aqueous solution is fed into the top of a vertical column, together with formic acid at the rate of at least 0.35 ml per gram of uranium. The lower part of the column is heated to a temperature above 100°C to vaporize the water and release nitrous vapors, and uranyl formate is collected in powder form at the bottom. The system includes a vertical column, the lower part taken up by a bed of glass or teflon beads resting on a grid with holes smaller than these beads, a propeller keeping the beads in motion, systems to supply uranyl nitrate solution and formic acid to the top of the column and to mix them, a means to collect the formate as dry powder after passage through the grid and, an adjustable heat supply to the beads. (auth) (France)

13013 PHYSICO-CHEMICAL BEHAVIOR OF RUTHENIUM IN SEAWATER. **Gueguenlat, P. (CEA, Cherbourg, France). Bull. Inform. Sci. Tech. (Paris); No. 151, 27-32(Sep 1970). (In French).**

A physicochemical study is made of nitrosyl ruthenium derivatives discharged into the sea by spent fuel processing plants. Soluble, insoluble, or intermediate forms are distinguished by ion exchange separation, the percentages varying as a function of time and with certain characteristics of the oceanic medium. Because of their higher contaminating power, the particle forms were rigorously studied. (auth) (France)

13014 SPECTROPHOTOMETRIC INVESTIGATIONS OF THE SYSTEM $Th(NO_3)_4$–VIOLURIC ACID. **Popea, Florica; Banciu, A.-C. (Institut fuer Physikalische Chemie, Bucarest). Rev. Roum. Chim.; 15: 1319-29(Sep 1970). (In German).**

Complex formation is aqueous solutions of $Th(NO_3)_4$ and violuric acid (5-isonitrosobarbituric acid) was investigated spectrophotometrically. The use of several methods, which are suitable for investigation of the formation of several complexes, did not give clear results, but allowed several simultaneously formed complexes to be suspected. The molar ratio method was used to detect complexes with metal: ligand ratios of 1 : 1, 1 : 2, 1 : 3, and 1 : 4. Stability constants for all these complexes were calculated to be on the order of 10^2, 10^5, 10^7, and 10^{10}. (tr-auth)

13015 COMPRESSIBILITY STUDIES IN MIXED AQUEOUS ELECTROLYTES. **Kulkarni, A. G. (Poona Univ., India). Indian J. Chem.; 7: 333-5(Apr 1969).**

Ultrasonic velocities were measured for mixed electrolytes in aqueous medium by secondary interference method at 2.1 Mc/s and 25°C. The systems studied are $Pb(NO_3)_2-KNO_3$, $Pb(NO_3)_2-NH_4NO_3$, $KNO_3-NH_4NO_3$, $LiNO_3-KNO_3$, $UO_2(NO_3)_2-NH_4NO_3$, $Mg(NO_3)_2-NH_4NO_3$, $MgCl_2-NH_4Cl$, $BaCl_2-NH_4Cl$, $NaCl-KCl$, $MgSO_4-(NH_4)_2SO_4$. Measurements of twenty-three compositions with constant total molarity (1M) were carried out for every system. The velocity and the observed adiabatic compressibility data were plotted as a function of the composition of one of the salts in the mixture. The plots are presented only for the systems $Pb(NO_3)_2-KNO_3$, $UO_2(NO_3)_2-NH_4NO_3$, $BaCl_2-NH_4Cl$ and $MgSO_4-(NH_4)_2SO_4$. The breaks in the compressibility versus concentration plots at stoichiometry are ascribed to the changes in the hydration number of cations and the changes in the structure of the water molecule. (auth)

13016 NEW COORDINATION COMPOUNDS OF URANIUM(V). **Pribble, Mary Jo. Baton Rouge, La.; Louisiana State Univ. (1970). 178p. University Microfilms Order No. 70-18,554. Thesis.**

Uranium(V) compounds containing U–P, U–As, and U–Bi bonds were prepared. It has been found in this study that the reaction $UCl_5 \cdot TCAC + xL \rightarrow UCl_5 \cdot xL + TCAC^a$, where TCAC = trichloroacrylyl chloride, can be carried out in benzene solution with a variety of ligands to produce compounds, $UCl_5 \cdot xL$. Compounds of this type are $UCl_5 \cdot Ph_3P$; $UCl_5 \cdot$ diphos, where diphos = ethylenebisdiphenylphosphine; $UCl_5 \cdot 2C_9H_7NO$, where C_9H_7NO = 8-hydroxyquinoline; and $UCl_5 \cdot 4C_9H_7NO$. A different type of reaction occurs with tropolone, $C_7H_5O_2^- = T^-$, as the ligand in reaction with a solution of $UCl_5 \cdot TCAC$. In this case TCAC and one chlorine are replaced and the resulting compound is $UCl_4T \cdot 4HT$. Reactions of other ligands with $UCl_5 \cdot TCAC$ have produced the following ionic compounds: $[UCl_4dipy]Cl$, where dipy = 2, 2^1-dipyridyl; $[U_2Cl_9(Ph_3As)]Cl$; and $[U_2Cl_9(Ph_3Bi)]Cl$. Impure products were obtained with Ph_3Sb, Ph_2SO and other phosphines and arsines. The new compounds, with one exception, are extremely unstable to moisture and oxygen and preparation of the compounds and subsequent studies were done under an argon atmosphere and in anhydrous, oxygen-free solvents. $UCl_4T \cdot 4HT$ is unique among U(V) compounds in that it is stable in dry air for several days. The compounds were characterized by elemental analyses, conductance measurements, magnetic susceptibility measurements, and mass spectra. The U(V) oxidation state was confirmed in

XUM

the compounds by electron spin resonance, magnetic susceptibility measurements, and the electronic spectra. The g_{av} ESR values for all the compounds except $UCl_4T \cdot 4HT$ and $UCl_5 \cdot 4C_9H_7NO$ are very close to the value for the free electron. The ESR spectra of all the compounds except $UCl_5 \cdot 4C_9H_7NO$ and $UCl_4T \cdot 4HT$ show a very narrow signal width. These data suggest that the 5f electron of the U is strongly delocalized into the low energy molecular orbitals of the atomatic ring systems in the ligands. Infrared absorption studies of the CsI region have made possible the assignment of U–N, U–P and U–Cl frequencies. The U–N stretching frequency in $[UCl_4dipy]Cl$ has been assigned as 492 cm^{-1} and in $UCl_5 \cdot 4C_9H_7NO$ as 507 cm^{-1}. The U–P frequency has been assigned as 265 cm^{-1} and 273 cm^{-1} in $UCl_5 \cdot Ph_3P$ and $UCl_5 \cdot$ diphos, respectively. In agreement with previous assignments the U–Cl frequencies are assigned at 325 cm^{-1} and 318 cm^{-1} in $UCl_5 \cdot Ph_3P$, at 330 cm^{-1} and 318 cm^{-1} in $UCl_5 \cdot$ diphos, at 305 cm^{-1} in $[U_2Cl_9(Ph_3As)]Cl$ and at 327 cm^{-1}, 315 cm^{-1} and 310 cm^{-1} in $[UCl_4dipy]Cl$. The electronic spectra of these new U(V) compounds are quite complex. The four groups of bands corresponding to the four predicted transitions for an octahedral $5f^1$ system were assigned for all the new compounds. (Diss. Abstr.)

13017 LUMINESCENCE OF URANIUM GLASSES. Eubanks, Alfred Guion. College Park, Md.; Univ. of Maryland (1969). 101p. University Microfilms Order No. 70-15,500.
Thesis.

A series of uranium glasses was developed which have cathodoluminescent and photoluminescent efficiencies superior to those of any glasses reported previously. The most efficient glass is of composition 29.40 wt% B_2O_3, 58.80 wt% SiO_2, 9.80 wt% Na_2O, and 2.00 wt% UO_2. It has an intrinsic cathodoluminescent efficiency of (1.1 ± 0.1)% and a photoluminescent radiant efficiency of (12 ± 1)%. The absolute radiant emittance spectra of the glasses were determined during excitation with 100- to 350-keV electrons and with 253.7 nm light. The spectra are the same for both excitation processes. The glasses luminesce over the wavelength range 470 to 630 nm. Three maxima are apparent in the spectra. These occur at 518, 534, and 563 nm. The measured absolute cathodoluminescent spectral radiant emittances, calculated electron depth-dose distributions, and the Kubelka–Munk theory of light scattering and absorption in a powder were used to calculate the intrinsic cathodoluminescent efficiencies of the glasses. In the course of making the efficiency determinations, measurements of the optical scattering, absorption and reflection properties of the glass powders were made as a function of wavelength. To test the basic assumptions underlying the cathodoluminescent efficiency calculations, a study was made of the effect of particle size on efficiency. If it is assumed that the scattering coefficient varies inversely with and the absorption coefficient is independent of particle size, the calculated effect of particle size agrees with measured results. The photoluminescence measurements were made with 253.7 nm ultraviolet light incident on powdered glass targets. The light source was calibrated by means of radiant emittance measurements on a National Bureau of Standards standard phosphor of known radiant efficiency and absorptance. The calibrated monochromator-photomultiplier system was used to detect the emitted light. The photoluminescent radiant emittances, the irradiance of the exciting source, and the measured absorptances of the glass powders for the exciting radiation were used to calculate the photoluminescent radiant efficiencies. (Diss. Abstr. Int., B)

13018 SOME MAGNETIC, SPECTROSCOPIC, AND CRYSTALLOGRAPHIC PROPERTIES OF BERKELIUM, CALIFORNIUM, AND EINSTEINIUM. Fujita, Dennis Ken. Berkeley, Calif.; Univ. of California (1969). 182p. University Microfilms Order No. 70-17,563.
Thesis.

During the course of these studies, ~100 μg ^{249}Bk, ~40 μg ^{249}Cf, and ~15 μg ^{253}Es were made available. Procedures for the purification, assay, and evaluation of sample purity are discussed in detail. The experimental techniques used to study the magnetic susceptibilities of Bk metal, Bk^{3+}, and Cf^{3+} are described. The susceptibilities of Bk^{3+} and Cf^{3+} follow the Curie–Weiss relationship with μ_{eff} (Bk^{3+}) = 9.40 ± 0.06 B.M. and μ_{eff} (Cf^{3+}) = 9.14 ± 0.06 B.M. Among 3 samples of Bk metal both ferromagnetism and antiferromagnetism were detected at low temperature; at higher temperatures the susceptibilities follow the Curie–Weiss law. Effective magnetic moments derived from the high temperature data suggest that greater than 3 electrons per atom occupy bonding orbitals. The effective moment of the more pure Bk metal sample (8.83 B.M.) corresponds to a metallic valence of ~3.4. A recently developed, light-pipe microabsorption cell used to obtain the solution absorption spectra of Bk^{3+} and Es^{3+} in dilute HCl solutions is described. The confirmatory experiments verified most of the previously-detected Bk^{3+} and Es^{3+} absorption peaks. Seven additional Bk^{3+} and 12 new Es^{3+} absorption bands are reported. The most intense Es^{3+} peaks are observed at 4225 Å and 4950 Å. Techniques to prepare several ^{249}Bk, ^{249}Cf, and ^{253}Es compounds on the microgram scale are discussed. Standard x-ray diffraction powder methods are applied in the determinations of the crystal structures and lattice parameters of the Bk and Cf compounds. The extremely high specific radioactivity of ^{253}Es required the development of special techniques for the preparation and x-ray analysis of Es compounds. Face-centered cubic Bk metal (a = 4.987 ± 0.001 Å) is prepared by Li vapor reduction of BkF_3. Attempts to prepare Cf metal by similar reductions of CfF_3 with Li and K were unsuccessful due to the high vapor pressure of elemental Cf. CfF_3 samples exhibiting the orthorhombic YF_3-type structure (a = 6.651 ± 0.007 Å, b = 7.040 ± 0.002 Å, and c = 4.393 ± 0.004 Å) are prepared. The monoclinic lattice constants of $CfBr_3 \cdot 6H_2O$ are a = 9.992 ± 0.053 Å, b = 6.716 ± 0.025 Å, c = 8.146 ± 0.006 Å, and β = 93.50 ± 0.14 Å. $CfBr_3$ crystallizes in a structure that remains uncharacterized; however, similar structures have been observed in $BkBr_3$ and $GdBr_3$. CfOBr and CfOI exhibit the tetragonal PbFCl-type structure. Lattice constants of CfOBr are a = 3.900 ± 0.003 Å and c = 8.110 ± 0.007 Å. CfOI lattice parameters are a = 3.97 ± 0.02 Å and c = 9.13 ± 0.08 Å. Thermal expansion coefficients for CfOCl are reported: $\alpha_a = (1.14 \pm 0.01) \times 10^{-5}{}^{\circ}C^{-1}$ and $\alpha_c = (1.85 \pm 0.03) \times 10^{-5}{}^{\circ}C^{-1}$. Successful preparation of $CfCl_2$ by hydrogen reduction of $CfCl_3$ contradicts tracer experiments, which have been interpreted as evidence for a moderately stable +2 oxidation state of Cf. The first compounds of ^{253}Es are reported. $EsCl_3$ exhibits the hexagonal UCl_3-type structure between 400 to 450°C; the lattice parameters corrected to 20°C are a = 7.40 ± 0.02 Å and c = 4.07 ± 0.02 Å. EsOCl crystallizes in the tetragonal PbFCl-type structure at 400–450°C. The lattice constants at 20°C are a = 3.948 ± 0.004 Å and c = 6.702 ± 0.019 Å. (Diss. Abstr. Int., B)

13019 STRUCTURES AND PROPERTIES OF La_2O_3–BaO–B_2O_3 GLASSES. Malmendier, Joseph William. New Brunswick, N. J.; Rutgers–The State Univ. (1970). 308p. University Microfilms Order No. 70-16,939.
Thesis.

Melts were made of three compositions near the apices of the approximately triangular glass-forming region in the La_2O_3–BaO–B_2O_3 system. These were chemically analyzed and experimental melts were prepared from mixtures of these three protogenic melts. Differential thermal and thermogravimetric analyses were used to determine optimum melting conditions. A special technique was developed to achieve homogeneous glasses. Similar thermal histories were established for all glasses by one thermal treatment. Density, refractive index, thermal expansion, dielectric constant, and power factor were determined for each composition. The manner in which these properties varied with composition was related to the structure of the glasses in the system. X-ray diffraction measurements were made of devitrified and vitreous compositions. The coordination structure of lanthanum in La_2O_3–B_2O_3 glasses was determined. Electron microscopy was employed to determine the presence and extent of sub-solidus phase separation. It appears that the ternary compositions are mixtures of $La_2O_3 \cdot xB_2O_3$ and $BaO \cdot yB_2O_3$ networks. Lanthanum is found in A-type cation coordination. Barium is in the B-type except at higher concentrations, where it may be found in both forms. Lanthanum has a greater contracting effect on the glass volume than barium does. Calculations were made for B_2O_3, and the BaO–B_2O_3, La_2O_3–B_2O_3, and Na_2O–B_2O_3 systems to estimate structural units and groups. The calculations were based on concepts found in the literature. A model for B_2O_3 was constructed. (Diss. Abstr. Int., B)

13020 POLAROGRAPHIC STUDIES OF LANTHANIDES AND CIS- AND TRANSURANIUM ELEMENTS. David, F. (Institut de Physique Nucleaire, Orsay, France). Radiochem. Radioanal. Lett.; 5: 279-85(31 Dec 1970). (In French).

Radiopolarography was applied to the study of the reduction of Eu(III), Gd(III), Yb(III), Ac(III), Am(III), Cm(III), and Cf(III) in perchlorate medium (pH 1 to 6). The polarograms present two waves. The first corresponds to the reaction $M^{2+} \rightarrow M^0$ and the second seems to be attributable to the reaction $M^{3+} \rightarrow M^0$. The following standard potentials were calculated from the observed half-wave potential: –2.62 V (Ac^{3+}/Ac^0), –2.31 V (Cm^{3+}/Cm^0), and –2.32 V/N.H.E. (Cf^{3+}/Cf^0). The potentials of the first wave $[M^{2+} \rightarrow M(Hg)]$ are consistent with the potentials of M^{3+}/M^{2+} couples that were derived from amalgamation experiments for Gd, Ac, Am, Cm, and Cf. (auth)

13021 BEHAVIOR OF URANIUM OXIDE PARTICLES IN REDUCING FLAMES. Tischer, Robert L.; Schiller, Karl

XUM

(Wright-Patterson Air Force Base, Ohio). Combust. Flame; 15: 199-202(Oct 1970).

An analysis was made of the experimental data of Bulewicz, et al., (1969) on the emittance of uranium oxide particles in nitrogen-diluted rich hydrogen-oxygen flames. They interpreted the radiation as gray body in character, calculated particle temperatures as significantly greater than the adiabatic flame temperature, and concluded that radical recombination at the surface was responsible. Present results demonstrate that the emission need not necessarily be taken as gray body, particle temperatures are not uniquely determinable without knowledge of the spectral emissivity, and heating of the particles may be attributed more plausibly to gas–solid reaction than to radical recombination. (auth) (UK)

13022 THERMODYNAMIC PARAMETERS OF THORIUM FLUORIDE COMPLEXES FROM MEASUREMENTS WITH THE FLUORIDE-SELECTIVE ELECTRODE AT 5, 25, AND 45°C. Baumann, Elizabeth W. (E. I. du Pont de Nemours and Co., Aiken, S. C.). Contract AT(07-2)-1. J. Inorg. Nucl. Chem.; 32: 3823-30(Dec 1970).

Stability quotients for the thorium fluoride and hydrogen fluoride systems in 0.01M NH_4NO_3 at 5, 25, and 45°C were determined from measurements of free fluoride ion concentration by the lanthanum fluoride membrane electrode. Thermodynamic stability constants, standard enthalpies, and standard entropies were derived from the experimental data for formation of ThF^{3+}, ThF_2^{2+}, ThF_3^+, ThF_4, and HF. (auth) (UK)

13023 IONIZATION (HETEROLYSIS) OF COVALENT COMPOUNDS AS A COORDINATION-CHEMICAL PHENOMENON. Gutmann, Viktor (Technische Hochschule, Vienna). Angew. Chem. Int. Ed. Engl.; 9: 843-60(Nov 1970).

The ionization of a covalent compound into a cation and an anion is a coordination-chemical phenomenon. The ions are formed with coordination either by nucleophilic attack of an electron pair donor or by electrophilic attack of an electron pair acceptor. The dielectrically controlled component of the ionization affects only the degree to which it occurs. It is shown that the ionization generally increases with increasing donor strength of the donor or with increasing acceptor strength of the acceptor. For a given M, the ease of ionization of the M–X bond increases in the order X = fluoride < chloride < bromide < iodide. These general aspects are discussed with the aid of examples, including thorium and uranium halides. (auth)

13024 MASS SPECTROMETRIC INVESTIGATION OF THE THERMAL DESORPTION OF ATMOSPHERIC GASES FROM PLUTONIUM DIOXIDE. I. RADIOLYTICALLY PRODUCED NITRIC OXIDE. Stakebake, Jerry L.; Loser, Robert W.; Chambers, Carey A. (Dow Chemical Co., Golden, Colo.). Appl. Spectrosc.; 25: 70-6(Jan-Feb 1971).

A technique was developed for measuring the thermal desorption of one or more gases using the time-of-flight mass spectrometer. With this method the adsorbed population, gas–solid bond energy, and preexponential kinetic factor can be determined for each adsorbed gas. The thermal desorption of nitric oxide from plutonium dioxide was measured over the temperature range 100° to 900°C and typical spectra are presented. The activation energy of desorption was found to be 19.4 kcal/mole. The probable mechanism for adsorption is also discussed. (auth)

Radiation and Nuclear Chemistry

Refer also to abstract 14837.

Radiation Effects

Refer also to abstracts 12954 and 14411.

13025 PARAMAGNETIC SPECIES PRODUCED BY ULTRAVIOLET IRRADIATION OF LITHIUM, POTASSIUM, SODIUM, MAGNESIUM, AND CADMIUM IN 3-METHYLPENTANE AT 77°K. Froben, F. W.; Willard, J. E. (Univ. of Wisconsin, Madison). Contract AT(11-1)-1715. J. Phys. Chem.; 75: 35-40(7 Jan 1971).

An ESR singlet with characteristics expected for the signal of trapped electrons was observed when Li, K, Na, Mg, or Cd in a 3-methylpentane matrix deposited from the vapor at 77°K was irradiated at wavelengths in the region of 250 nm. This is flanked by lines from another species which grow to the photostationary state and decay from it with a half-life of less than 0.2 sec, in parallel with the singlet. The flanking lines may be due to a cationic species with which the electron recombines. A photosensitized decomposition of the matrix to produce relatively stable free radicals also occurs in the case of sodium. For all the metals the photoionization threshold is lower than the gas phase ionization potential and (with the possible exception of Mg) higher than the photoelectric work function. The short trapping lifetime of the electron and the narrowness of the ESR singlet indicate that the available electron trapping sites in the matrix deposited from the vapor are weaker than those in a matrix formed by cooling liquid 3-methylpentane to 77°K. (auth)

13026 COMMENT ON THE PAPER "AQUOLUMINESCENCE: AN ALTERNATIVE MODE OF RELEASE OF ENERGY STORED IN γ-IRRADIATED CRYSTALS". Adloff, J. P. (Centre de Recherches Nucleaires, Strasbourg). Radiochem. Radioanal. Lett.; 5: 303-4(31 Dec 1970).

A rebuttal is given to a paper published previously and abstracted in NSA as 25: 2227. Evidence is offered through the citing of various references that the claim of priority concerning the phenomenon of luminescence accompanying the solution of irradiated crystals is not accurate. (J.G.B.)

13027 ELECTRICAL CONDUCTIVITY OF 2-PENTENE IRRADIATED AT 77°K DURING WARMING TO 125°K. Stachowicz, W.; Owczarczyk, A. (Inst. of Nuclear Research, Warsaw). Radiochem. Radioanal. Lett.; 5: 305-12(31 Dec 1970).

The electric conductivity technique was adapted to the study of the transient charged species appearing in the range of 77 to 125°K in glassy (2-pentene) following its γ-irradiation. Three peaks corresponding to different species were observed. (auth)

13028 UNSTABLE INTERMEDIATES. PART LXXX. AN ELECTRON SPIN RESONANCE INVESTIGATION OF THE $[Ag–Cd]^{2+}$ AND Cd^{3+} DIATOMIC CATIONS. Eachus, R. S.; Symons, M. C. R. (Univ. of Leicester, Eng.). J. Chem. Soc., A; No. 18, 3080-4(1970).

Exposure of frozen aqueous acids and alcohols containing Cd^{2+} salts to γ rays at low temperatures results in the formation of a species which has the properties expected for Cd^+. When the matrices are annealed, this reacts with excess Cd^{2+} to form the diatomic Cd_2^{3+}. In environments containing excess of Ag^+ ions the analogous species $[Ag–Cd]^{2+}$ is formed when the matrix is warmed. (auth) (UK)

Radiation Processes

13029 (AAEC/LIB/Bib–259) RADIATION-INDUCED POLYMERIZATION. PART I. WOOD-PLASTIC COMPOSITES. A Bibliography. Newland, E. A. (comp.) (Australian Atomic Energy Commission Research Establishment, Lucas Heights). Oct 1970. 22p. Dep. NTIS (U. S. Sales Only).

One hundred fifty-two references are listed, covering the period 1960 to May 1970. The references are arranged chronologically by year and alphabetically by author within each year. Abstracting services that provide abstracts of each article are also given. (Australia)

13030 (AAEC/LIB/Bib–260) RADIATION-INDUCED POLYMERIZATION. PART II. CONCRETE-POLYMERS: AN IMPROVED TYPE OF CONCRETE OBTAINED BY USING RADIATION TO COMBINE CONVENTIONAL CONCRETE AND PLASTIC. A Bibliography. Newland, E. A. (comp.) (Australian Atomic Energy Commission Research Establishment, Lucas Heights). Nov 1970. 6p. Dep. NTIS (U. S. Sales Only).

Thirty-one references are listed, covering the period 1964 to July 1970. Arrangement is alphabetical by author within each year. Abstract references for each article are also given, where applicable. (Australia)

13031 (AAEC/LIB/Bib–261) RADIATION-INDUCED POLYMERIZATION. PART III. FORMATION OF POLYMER COATINGS ON SUBSTRATES. A Bibliography. Newland, E. A. (comp.) (Australian Atomic Energy Commission Research Establishment, Lucas Heights). Nov 1970. 24p. Dep. NTIS (U. S. Sales Only).

One hundred twenty references are listed covering the period 1956 to July 1970. The references are arranged alphabetically by author within each year. Reference is made to an abstract for each article, where applicable. (Australia)

13032 CONCERNING KINETICS OF ISOPROPYL ALCOHOL RADICALS BY ELECTRON SPIN RESONANCE-FLOW TECHNIQUES. Burchill, C. E. (Univ. of Manitoba, Winnipeg). J. Phys. Chem.; 75: 167-70(7 Jan 1971).

A critical examination of previously reported studies on rates of reaction of the radicals $(CH_3)_2\dot{C}OH$ and $CH_3CHOH\dot{C}H_2$ with H_2O_2 in the system aqueous Ti(III)–H_2O_2–2-propanol is presented. In order to determine the effect of Ti(IV) on the free-radical chain reaction of H_2O_2 and 2-propanol, a series of deaerated aqueous solutions 0.5$\underline{M}$ in 2-propanol and 0.05$\underline{M}$ in H_2O_2 was γ-irradiated to initate reaction. The addition of 0.005$\underline{M}$ Ti(IV) introduced only a slight inhibition of the chain reaction. An alternative mechanism for the reaction is suggested. (J.G.B.)

13033 ELECTRON SPIN RESONANCE STUDIES OF RADIATION DAMAGE. PART IV. THE EFFECT OF PHOTOBLEACHING ON THE TRAPPED RADICALS IN GAMMA-IRRADIATED 2-METHYLTETRAHYDROFURAN GLASSES AT 77°K. **Sargent, F. P. (Atomic Energy of Canada Ltd., Pinawa, Manitoba). Can. J. Chem.; 48: 3453-9(1 Nov 1970). (AECL-3699).**

The concentration of trapped radicals was found to decrease during the course of photobleaching of trapped electrons in gamma irradiated 2-methyltetrahydrofuran glasses at 77°K. (auth) (Canada)

13034 ESR STUDY ON MOLECULAR MOTION OF PEROXY RADICALS OF POLYTETRAFLUOROETHYLENE. **Moriuchi, S.; Nakamura, M.; Shimada, S.; Kashiwabara, H.; Sohma, J. (Japan Victor Co., Yokohama). Polymer; 11: 630-9(Dec 1970).**

Temperature variations of the line shapes of ESR spectra from the γ radioinduced radicals of polytetrafluoroethylene(PTFE) were investigated in detail and the results were quantitatively analyzed based on Kneubühl's theory (1960) on the line shape. Two kinds of rapid molecular motions were found of which the correlation times were about 10^{-9} s, for the peroxy radicals of PTFE; the rotational motion related to the peroxy chain radical, and the three dimensional motion associated with the peroxy end radical. The activation energies of these molecular motions were estimated as 0.52 and 0.26 kcal/mole for the rotational motion and the three dimensional motion, respectively. Origins of such rapid motions are discussed in connection with the other molecular motions of polymers, which were found by other experimental methods. (auth) (UK)

13035 PROCESS FOR THE PREPARATION OF PERFLUORINATED CARBOXYLIC ACIDS. **Ferse, Armin; Koch, Wolfgang (to Institut fuer Silikonund Fluorkarbon-Chemie). British Patent 1,214,498. 2 Dec 1970. Filed 1 Dec 1967.**

An irradiation process is described for the preparation of perfluorinated carboxylic acids. The process enables the working up of polytetrafluoroethylene waste in a favorable way to produce valuable perfluorinated acids. The PTFE (or its thermal decomposition products or related fluorinated polymers such as the homopolymers of other perfluorinated alkenes such as hexafluoropropene or octafluorobutene, as well as the copolymers of two or more perfluorinated alkenes, and their thermal decomposition products) is broken down into chain fragments by the use of high energy radiation and then oxidized to the desired perfluorinated mono- and dicarboxylic acids. In this way, in general, chain fragments containing 5 to 20 C atoms are obtained when carrying out the process at 10 to 250°C, using radiation doses of 8×10^8 to 5×10^{10}R. The oxidizing agent may be aqueous $KMnO_4$. A mixture of high and low molecular weight perfluorinated mono- and dicarboxylic acids is obtained, which can be separated into its components by distillation or can be used directly or worked up in a desired manner. The preferable irradiation temperature is 20° to 80°C and the irradiation dose 5×10^9 to 1×10^{10}R. (UK)

13036 RADIATION TREATMENT OF MINE WASTE WATERS. **Steinberg, Meyer; Pruzansky, Jacob (to United States Atomic Energy Commission). U. S. Patent 3,537,966. 3 Nov 1970. Filed 3 Nov 1967.**

A process for treating acidic mine waste waters containing ferrous compounds dissolved in the waters comprises exposing the waters having a pH below 6.0 to ionizing radiation having an intensity of at least 1000 Rad/hr while aerating the solution to substantially convert all the ferrous compounds to ferric compounds and then contacting the solution containing the ferric compounds with a solution of calcium carbonate to precipitate ferric oxide. (B.L.M.)

13037 IONS AND EXCITATIONS IN ORGANIC RADIATION CHEMISTRY: I. THE GAMMA RADIATION INDUCED REACTIONS OF 1,3-CYCLOHEXADIENE. II. THE RADIATION INDUCED ISOMERIZATION OF 1,2-DIPHENYLPROPENE IN CYCLOHEXANE. Penner, Thomas Lorne. Pasadena, Calif.; California Inst. of Technology (1970). 178p. University Microfilms Order No. 70-14,847.

Thesis.

Irradiation of 1,3-cyclohexadiene with γ rays leads to dimerization, either in benzene solution or in the neat liquid. Relative amounts of the products vary widely with reaction conditions but the composition of the mixtures can be expressed as consisting of variable amounts of two groups. One set of products corresponds to those formed in thermal dimerization and the other has the distribution found in photodimerization induced by triplet sensitizers. Formation of the "thermal" dimers is inhibited by 2-propanol, a cation scavenger, and promoted by electron scavengers, so a cationic mechanism is postulated. The other, "photo" dimers, are presumably formed from triplet diene. Ring cleavage to give 1,3,5-hexatriene is also observed and attributed to an excited singlet state of 1,3-cyclohexadiene. Since ring opening is not affected by electron scavengers whereas "photo" dimers are quenched, it is inferred that excited singlets are formed in primary excitation processes and that triplets are largely produced by charge neutralization. In benzene solution charge and excitation transfer from the solvent are involved in the production of diene products. A chain dimerization also seems to be present in benzene solution. The cis and trans isomers of 1,2-diphenylpropene are isomerized in cyclohexane by irradiation of solutions with γ radiation. At low solute concentrations both isomers appear to react through the triplet state of the 1,2-diphenylpropene, which is formed by charge neutralization. At higher alkene concentrations and especially at low radiation doses a cationic chain reaction contributes to cis → trans isomerization. The value for isomerization of the trans isomer at high solute concentration gives a G for solute triplet of 4.4. (Diss. Abstr.)

13038 CHEMICAL INTERACTIONS OF ACCELERATED CARBON-14 IONS AND ATOMS WITH BENZENE. **Lin, Tz-Hong. Berkeley, Calif.; Univ. of California (1969). 222p. University Microfilms Order No. 70-17,606.**

Thesis.

Solid benzene at –196° was irradiated with monoenergetic beams of $^{14}C^+$ ions and atoms with kinetic energy ranging from 5 eV to 15 keV. About 28% of the ions striking the target benzene were identified as ^{14}C-labeled benzene, toluene, cycloheptatriene, phenylacetylene, styrene, biphenyl, diphenylmethane, phenylcycloheptatriene, benzaldehyde, tropone, phenol, and $n\text{-}C_3\text{–}C_7$ unsaturated alkylbenzenes. The nature of the reactions involved was investigated by total degradations of toluene; partial degradations of toluene (from 5 to 5000 eV irradiations) and benzaldehyde (from 15- to 5000-eV irradiations); and partial degradations of phenylacetylene, biphenyl, diphenylmethane, and phenylcycloheptatriene from a 5000-eV irradiation. The mechanisms for the product formations were interpreted in terms of the intermediate carbenes and radicals resulting from the C–H and C=C bond insertions of hot $C(^3P)$, $C(^1D)$, and $C(^1S)$. These intermediates were evidenced by the presence of benzaldehyde, tropone, and phenol, which could result from the interactions of such intermediates with oxygen from an unknown source. The dependence of the radiochemical yields of the products upon the energy of the irradiating $^{14}C^+$ ions was consistent with these hypotheses. It was concluded that in an accelerated C-benzene system, the hot and thermal $C(^1S)$ species react similarly. However, the reactions of hot (C^3P) and $C(^1D)$ are different from that of the thermal counterparts. (Diss. Abstr.)

13039 THE PERMEATION OF GASES THROUGH MODIFIED POLYMER FILMS. II. GAS PERMEABILITY AND SEPARATION CHARACTERISTICS OF GAMMA RAY-IRRADIATED POLYETHYLENE. **Kanitz, Peter J. F.; Huang, Robert Y. M. (Univ. of Waterloo, Ontario). J. Appl. Polym. Sci.; 14: 2739-51(Nov 1970).**

A study has been made of the diffusion, solubility, and separation of nitrogen and methane gases in a series of air- and vacuum-irradiated polyethylene films in the temperature range of 15 to 50°C. Samples were air irradiated to 90 Mrads and vacuum irradiated to 80 Mrads. The major structural differences between the modified films were the presence of oxygenated species in the air-irradiated samples. The oxidation of these samples reduced the amount of crosslinking normally found in vacuum-irradiated samples. Diffusion and permeability coefficients for both gases decreased with irradiation dose. The solubility coefficients for the air-irradiated samples increased with increasing irradiation dose while little change was observed for vacuum-irradiated film. The gas mixture permeabilities could be predicted from the pure component permeabilities, and the methane–nitrogen separation factor decreased with increasing irradiation dose. (auth)

13040 EFFECT OF TEMPERATURE ON THE COMPOSITION OF PRODUCTS IN RADIATIVE INDUCED OXIDATION OF ISOOCTANE. **Pichuzhkin, V. I.; Saraeva, V. V. Vestn. Mosk. Univ., Ser. II. Khim.; 11: 612-14(Sep-Oct 1970). (In Russian).**

The main products from the radioinduced oxidation of isooctane were found to be alcohols and hydroperoxides containing 8 and 4 carbon atoms. The yields of these products increased with temperature as a result of chain reactions. (auth)

13041 ENHANCING THE PERMEATION CHARACTERISTICS OF POLYETHYLENE BY MEMBRANE IRRADIATION IN THE

XUM

FULLY SWOLLEN STATE. Siegel, Richard D. (Northern Research and Engineering Corp., Cambridge, Mass.); Coughlin, Robert W. J. Appl. Polym. Sci.; 14: 2431-9(Oct 1970).

Fully swollen, low-density polyethylene films were irradiated, vacuum dried, reswollen, and subsequently permeability tested using tritiated toluene and benzene as penetrants. The treatment improved the permeability of polyethylene up to 88%, with the enhancement strongly dependent on the choice of the irradiation solvent. These results suggest a potentially practical process for improving the performance of semipermeable membranes. (auth)

13042 MECHANICAL PROPERTIES OF RADIATION-INDUCED GRAFT COPOLYMERS OF STYRENE TO POLYETHYLENE. Machi, Sueo; Silverman, Joseph (Univ. of Maryland, College Park). J. Polym. Sci., Part A-1; 8: 3529-32(Dec 1970).

Measurements were made of the tensile properties of polyethylene–styrene grafts prepared by γ-irradiating polyethylene films in liquid styrene. The films contained true graft and occluded styrene homopolymer. It was found that yield strength, tensile strength, and initial modulus of elasticity increase while elongation decreases with increasing polystyrene content. The tensile strength and elongation were reduced when the grafted film was soaked in benzene more than 15 hr. The film prepared by a post-irradiation graft gave higher tensile strength and elongation than those of grafts formed by simultaneous irradiation of the film and the monomer. These results indicate that radioinduced grafting makes the system of polyethylene and polystyrene compatible and potentially useful, provided the samples are not subjected to drastic solvent extraction procedures for the removal of homopolymer. (auth)

Radiolysis

Refer also to abstracts 13024, 13075, 13093, and 13305.

13043 STUDY OF THE OXYGEN ISOTOPE EFFECT IN RADIOLYSIS OF CRYSTALLINE KNO_3. Ladov, Edwin Neil. College Park, Md.; Univ. of Maryland (1969). 113p. University Microfilms Order No. 70-15,375.

Thesis.

A kinetic isotope effect in the radiolysis of crystalline $KN^{18}O_3$ was observed. It has a maximum of 19 ± 3% at an absorbed dose of 0.5×10^{21} eV/g. The isotope effect is explained by the simultaneous occurrence of two reaction paths, which produce an additive isotope effect. One of these paths involves an exciton-induced reaction of randomly diffusing oxygen molecules at preferred lattice sites. The amount of decomposition occurring via this reaction path is a function of the concentration of these "preferred" sites which in the case of most inorganic solids is on the order of 10^{17} to 10^{19} per cm^3. The other reaction path is that associated with direct decomposition of excited or ionized nitrate ions. The economics of utilizing this isotope effect for the production of the heavy isotopes of oxygen was examined. Results indicate that the kinetic isotope effect may be profitably used for the manufacture of isotopically substituted oxyanions by utilizing the radioinduced back reaction between oxygen and a lower oxidation state of the oxyanion. The preparation of enriched NO feed stock for use in the distillation process for concentrating the heavy isotopes of nitrogen and oxygen was shown to be profitable provided the cost of radiation may be neglected or is minimal. It has also been shown that Raman spectroscopy is a valuable analytical tool for determining the heavy oxygen concentration in isotopically substituted oxyanions. (Diss. Abstr. Int., B)

13044 CONTRIBUTION OF H ATOMS TO G/sub H2/ IN THE RADIATION CHEMISTRY OF AQUEOUS SOLUTIONS. Peled, E.; Mirski, U.; Czapski, G. (Hebrew Univ., Jerusalem). J. Phys. Chem.; 75: 31-5(7 Jan 1971).

G_{H_2} was determined in neutral and in 1$\underline{M}$ NaOH air-saturated solutions as a function of $[N_3^-]$. It was found that N_3^- reduces G_{H_2} from 0.43 at 10^{-3} $\underline{M}$ N_3^- to 0.157 at 5$\underline{M}$ N_3^- in neutral solutions and from 0.37 at 0.5$\underline{M}$ N_3^- to 0.21 at 4$\underline{M}$ N_3^- in alkaline solutions. Through pulse radiolysis studies it was found that the value of the rate constant $k_{e_{aq}+N_3^-}$ was $\leq 1.5 \times 10^6$ $\underline{M}^{-1}$ sec^{-1} and that N_3^- had no effect on Ge_{aq}. In competition experiments between N_3^- and isopropyl alcohol, $k_{H+N_3^-} = 2.7 \times 10^9$ $\underline{M}^{-1}$ sec^{-1} was obtained. From the decrease of G_{H_2} by efficient electron scavengers it was concluded that the reaction $H + e_{aq} \rightarrow H_2 + OH^-$ in spurs makes a major contribution to G_{H_2}. This conclusion together with other experimental results makes necessary the assumption that in addition to a distribution in the number of radicals in various spurs there is a distribution of concentrations of radicals in each kind of spur. The condensed spurs (spurs with higher initial concentration of radicals) make an important contribution to G_{H_2}. (auth)

13045 RADIOLYSIS OF CARBON TETRACHLORIDE. RADICAL YIELDS AND THE FORMATION OF TETRACHLOROETHYLENE AS AN INITIAL PRODUCT. Bibler, Ned E. (E. I. du Pont de Nemours and Co., Aiken, S. C.). Contract AT(07-2)-1. J. Phys. Chem.; 75: 24-30(7 Jan 1971).

The radiolysis of liquid, air-free carbon tetrachloride containing a variety of solutes at 25° was investigated in detail. With Br_2 and HI as radical scavengers, the measured initial 100-eV yield of CCl_3 radicals was equal to 7.0 ± 0.2. The organic products resulting from spur reactions in these solutions were C_2Cl_4 and C_2Cl_6 (G = 0.08 and 0.47 molecule/100 eV, respectively). The total yield of scavengeable chlorine was 8.3 atoms/100 eV. With these two scavengers, evidence for the existence of intermediates other than Cl and CCl_3 was obtained. When I_2 was the scavenger, ICl was the most abundant product. The other major product, CCl_3I, was very susceptible to radical attack, and eventually all the initial iodine atoms appeared as ICl. In solutions containing ICl as a scavenger, G(–ICl), $G(I_2)$, and $G(CCl_3I)$ were all equal to zero. With each of the above scavengers, tetrachloroethylene was an initial product; in the absence of scavengers, tetrachloroethylene presumably is removed by reaction with Cl or Cl_2. To explain C_2Cl_4 formation in the presence of ICl, and ICl_2 intermediate is proposed. Other scavengers suitable for Cl atoms included NH_3, C_2H_4, CH_2Cl, CH_2Cl_2, and $CHCl_3$; CCl_2Br was not an efficient scavenger as suggested by the absence of C_2Cl_4 as a product. In solutions containing NH_3, a precipitate containing Cl^- ions was formed by the radiolysis. Also, in the presence of the chloromethanes, CH_2Cl_2 and $CHCl_3$, the radical yield in carbon tetrachloride was lowered considerably, apparently by an energy- or charge-transfer mechanism. (auth)

13046 INFLUENCE OF TEMPERATURE ON THE γ RADIOLYSIS OF ISOPROPYL ALCOHOL VAPOR. EFFECT OF MOLECULAR STRUCTURE ON THE NONCHAIN AND CHAIN DECOMPOSITIONS OF ALCOHOL VAPORS. van der Linde, H. J.; Freeman, G. R. (Univ of Alberta, Edmonton). J. Phys. Chem.; 75: 20-4 (7 Jan 1971).

Isopropyl alcohol vapor at a density of 0.78 g/l was irradiated to a dose of 3.2×10^{19} eV/g at temperatures from 125 to 400°. The yields of all the measured products except pinacol were independent of temperature between 125 and 205°. The G values were H_2, 7.2; CH_4, 4.8; CO, 0.52; C_2H_4, 0.21; C_2H_6, 0.16; CH_3CHO, 2.9; C_2H_5OH, 0.66; C_3H_6, 2.5; $(CH_3)_2CO$, 4.0; diisopropyl ether, 0.36; and pinacol, 1.0 to 1.5. The results are compared with those from the radiolyses of methanol and ethanol vapors. As the alcohol molecule size increases the amounts of C–O and C–C bond cleavage increase at the expense of C–H and O–H cleavage. The total ionization yield and the net amount of alcohol decomposition do not vary greatly from one alcohol to the next: G(ionization) = 4.1 ± 0.2 and G(–alcohol) = 14 ± 1 for each of the alcohols in the nonchain decomposition region of temperatures. At temperatures above about 250° chain reactions became important in isopropyl alcohol vapor. There were four modes of radiation induced chain decomposition. The stoichiometric representation of the modes, with their G values at 380° and activation energies (kcal/mol) were $C_2H_7OH \rightarrow H_2 + (CH_3)_2CO$, 600 (32 ± 4); $C_3H_7OH \rightarrow CH_4 + CH_3CHO$, 43 (18 ± 2); $C_3H_7OH \rightarrow H_2O + C_3H_6$, ~1200 (40 ± 10); $2C_3H_7OH \rightarrow H_2O + (C_3H_7)_2O$, 300 (41 ± 2). The activation energies were similar to those of the corresponding modes in the radioinduced pyrolysis of ethanol under similar conditions. However, the rates of all the modes except demethanation were an order of magnitude greater in isopropyl alcohol than in ethanol. Demethanation occurred at similar rates in the two alcohols. (auth)

13047 VIBRONIC TRANSITIONS IN RADICALS IN IRRADIATED NAPHTHALENE SINGLE CRYSTALS. Chong, Taisu; Itoh, Noriaki (Nagoya Univ., Japan). Mol. Cryst.; 11: 315-18 (Oct 1970).

The vibronic structures for the α-hydronaphthyl radicals and other unidentified radicals, from electron radiolysis of naphthalene monocrystals, are presented. It is suggested that one is associated with β-hydronaphthyl radicals and the other is the radical with a hydrogen added to binaphthyl. (UK)

13048 RADIOLYSIS OF LIQUID HYDROCARBONS CONTAINING DEUTERIUM SULFIDE. Stone, J. A.; Holland, P. T. (Queen's Univ., Kingston, Ont.). Can. J. Chem.; 48: 3282-90 (1 Nov 1970).

The radiolysis of hydrocarbons containing dissolved D_2S led to HD, D_2, and H_2 formation, the total hydrogen yields being greater than those in the absence of D_2S. A limiting yield of HD was attained at low D_2S concentrations (~5 mole %) in all solvents studied. This limiting yield was equal to G(H·) in ethane at 195°K but not in $c\text{-}C_6H_{12}$ at 298°K when G(HD) was much greater than accepted values of G(H·). D_2S behaved as both an electron and a positive ion scavenger, most of the D_2 and probably some of the HD being formed in these processes. The use of D_2S to determine H atom and ion yields in irradiated alkanes is not recommended. (auth) (Canada)

13049 EFFECTS OF ^{60}Co γ RADIATION ON XENON TRIOXIDE IN AQUEOUS SOLUTIONS. Heitz, Ch.; Simon, F. (Centre de Recherches Nucleaires, Strasbourg). Radiochem. Radioanal. Lett.; 5: 341-7(31 Dec 1970). (In French).

Aerated and deaerated aqueous solutions of xenon trioxide were irradiated with ^{60}Co γ rays. The radiolysis of the solute leads to the production of xenon and oxygen. The initial G values for the radiolytic decomposition of XeO_3 vary from 6 to 12 in the concentration range 10^{-4} to 10^{-1} M. (auth)

13050 TRANSIENT SPECTRUM AND KINETICS OF SHORT-LIVED INTERMEDIATES IN METHYLCYCLOHEXANE RADIOLYSIS. Reitberger, T. (Royal Inst. of Tech., Stockholm). Radiochem. Radioanal. Lett.; 5: 349-55(31 Dec 1970).

A pulse radiolysis study of short-lived intermediates in methylcyclohexane was carried out at room temperature. A transient spectrum ($\lambda_{max} \cong 245$ nm), assigned to the methylcyclohexyl radical, was determined. The transient disappeared in a second-order reaction that might be diffusion-controlled. (auth)

13051 ESR STUDY OF IRRADIATED SINGLE CRYSTAL OF p-TOLUIDINIUM CHLORIDE. Krishnamurthy, M. V.; Venkataraman, Balu (Tata Inst. of Fundamental Research, Bombay). Proc. Indian Acad. Sci., Sect. A; 72: 155-72(Oct 1970).

Electron spin resonance has been observed in γ-irradiated single crystals of p-toluidinium chloride. The spectra obtained for different orientations of the crystal are analyzed on the basis of the formation of cyclohexadienyl type of radicals. Partially deuterated p-toluidinium-ND_3 chloride sample was studied to confirm these results. A qualitative study of irradiated o-toluidinium bromide and the related deuterium labeled compounds has supported the formation of such radicals. (auth)

13052 ELECTRON SPIN RESONANCE STUDIES OF IRRADIATED SINGLE CRYSTALS OF L-TYROSINE HYDROCHLORIDE AND L-PHENYLALANINE HYDROCHLORIDE. Fasanella, Edwin Lane. Durham, N. C.; Duke Univ. (1969). 118p. University Microfilms Order No. 70-18,081.

Thesis.

Single crystals of the aromatic amino acids L-tyrosine HCl and L-phenylalanine-HCl were irradiated at room temperature in a ^{60}Co γ source. The free radicals that formed were studied at room temperature with electron spin resonance (ESR). Analysis of the ESR spectra from the irradiated single crystal of L-tyrosine-HCl indicated a long-lived radical formed by loss of a hydrogen atom from the hydroxyl group attached to the ring. The principal values and directions of the g-factor indicated that the electron spin density was distributed in the ring. The principal g-values are $g_x = 2.0023 \pm 0.0005$, $g_y = 2.0067 \pm 0.0005$, and $g_z = 2.0045$, with g_x perpendicular to the plane of the ring and g_y along the CO bond to the ring. Anisotropic hyperfine couplings of the unpaired electron to two hydrogens were observed. In addition, isotropic coupling to another hydrogen by hyperconjugation was measured. Although L-phenylalanine is similar in structure to tyrosine, the radiation damage to phenylalanine as revealed by ESR is more serious and probably irreversible. The principal effect of irradiation on the single crystal of L-phenylalanine-HCl was breakage of a C–C bond releasing the benzyl radical. The electron spin density in the benzyl radical is also distributed in the ring. Hyperfine structure due to proton couplings of the two methylene hydrogens and of three hydrogens on the ring of the benzyl radical was observed and analyzed to give the electron spin density on the various carbons. The g-factor of the benzyl radical was found to be nearly isotropic with a value near 2.003. In both of these aromatic amino acids, radicals formed by hydrogen addition to the aromatic rings were shown to occur when powdered samples are subjected to gaseous hydrogen atoms; however, no hydrogen addition radicals were observed in this study of γ-irradiated single crystals. (Diss. Abstr. Int., B)

13053 PULSE RADIOLYSIS OF GASES: N_2–NO AND He–N_2 SYSTEMS. Rushbrook, Peter Roys. Troy, N. Y.; Rensselaer Polytechnic Institute (1970). 210p. University Microfilms Order No. 70-19,950.

Thesis.

In pulse radiolysis studies of gas mixtures of N_2–NO and He–N_2, the source of radiation was a pulsed 1-MeV Van de Graaff electron accelerator with a power output of 0.5 joules per pulse, and a pulse width of 0.5×10^{-6} seconds. The reaction cell was pressurized to 20 atm with the appropriate gas mixtures. The primary band systems that appeared in the gross spectra of many of the mixtures were the NO(γ), N_2 2nd positive, and N_2^+ 1st negative systems. Other bands and lines also appeared, which were due to minute impurities in the mixtures. The specific band systems studied in both gas mixtures, with the available instrumentation, were the NO(γ) and the NH 3360 Å systems. Many NO(γ) bands appeared in the gross spectra, but only the v′ = 0 progression was intense enough for a study of formation lifetimes. All the observed decays followed first order kinetics; the half-lives varied inversely with the NO concentration in the N_2–NO mixtures and inversely with the N concentration in the He–N_2 mixtures. The reaction was determined to be an energy transfer between the Vegard–Kaplan state of N and the ground state of NO. The reaction is: $N_2(A\ ^3\Sigma_u^+) + NO(X\ ^2\pi)\ \ N_2(X\ ^1\Sigma) + NO(A\ ^2\Sigma^+)$. The average rate constant was found to be $2.00 \pm 0.19 \times 10^{-12}$ cm^3/particle-sec in mixtures, which contained between 140 ppM and 1160 ppM NO. At greater than 1160 ppM, the decay half-lives were shorter than the 0.5×10^{-6} sec pulse width; thus no measurements could be made. This rate constant is in fair agreement with a published value of 3×10^{-11} cm^3/particle-sec. The lifetime of the NH* formation was also measured in the same mixture as the NO* formation. The similar lifetime and concentration dependency led to the conclusion that the formation of the NH* is also by an energy transfer process between N in the Vegard–Kaplan state and NH in the ground state. The reaction is: $N_2(A\ ^3\Sigma_u^+) + NH(X\ ^3\Sigma^-)$, $N_2(X\ ^1\Sigma) + NH(A\ ^3\pi)$. The average rate constant for this reaction was not calculated since the NH concentration could not be measured. The rate constant is believed to be larger than that found for the formation of the NO* by about a factor of ten, due to the greater reactivity of the NH radical compared with the NO molecule. A sequential irradiation of mixture of N and 0.64% NO indicated a $-G_{NO} = 3.00$, in good agreement with published values. It also revealed that, over relatively short periods of time, no NO_2 is observed in the gas phase, but rather, migrates to the walls of the reaction vessel and can form a condensation product, $2HNO_3 \cdot N_2O_5$. Nitrous oxide and O are ultimately produced as final products upon the decomposition of the condensation product. The NO decomposes to an equilibrium concentration of a few hundred ppM, and upon long term irradiation, the O and NO also tend to approach an equilibrium concentration. The formation lifetimes of the other observed emissions were too short to be measured. (Diss. Abstr. Int., B)

13054 EFFECTS OF ULTRAVIOLET LIGHT AND X RAYS ON AQUEOUS SOLUTIONS OF POLY-L-GLUTAMIC ACID. Ishikawa, M. (International Christian Univ., Tokyo). Biophysik; 7: 1-7(1970).

Poly-L-glutamic acid (PLGA) in aqueous solution in helical or random coil form was irradiated in air by x rays or ultraviolet light. It was observed that both x rays and ultraviolet light caused degradation of PLGA in either form. The changes in molecular weight of PLGA in alkaline solutions caused by x irradiation were larger than those in acidic solutions. This fact indicates that the coil form suffers more degradation than the helix form. X-rays caused little change in the conformation of PLGA, while ultraviolet light effectively broke the helix form. The decrease in helix content brought about by ultraviolet exposure could not be explained just by degradation. (auth)

13055 EFFECT OF KIND AND ENERGY OF IRRADIATION ON RADIOLYSIS OF POLYPROPYLENE. Staren'kii, A. G.; Lavrentovich, Ya. I.; Kabakchi, A. M. (Inst. of Physical Chemistry, Kiev). Vysokomol. Soedin.; Ser. A; 12: 2476-80(Nov 1970). (In Russian).

Isotactic polypropylene has been irradiated with γ rays and with α particles with energy of 28 MeV. The effects of structure of the track of the charged particles on the chemical processes were studied. At low doses polypropylene was degraded with a yield of 0.86 bonds per 100 eV, at higher doses it was crosslinked. With γ irradiation the gel-fraction was revealed at 25 Mrad, with α particles at 50 Mrad. The rate of accumulation of vinylidene bonds was higher with α irradiation, but the rate of diene and triene sequence formation was higher with γ irradiation. The mechanism of the primary reactions in the radiolysis is discussed. (auth)

13056 CHEMICAL EFFECTS OF ENERGETIC RADIATION ON FROZEN SOLUTIONS AND SOLID ORGANIC MATERIALS. Schulte-Frohlinde, Dietrich (Max-Planck Instituts fuer Kohlenforschung, Muelheim, Ger.). Ber. Bunsenges. Phys. Chem.; 74: 1196-1202(Nov 1970). (In German).

The effect of γ irradiation on product formation as a function of temperature and matrix structure is described and some possibilities for the minimization of radiation damage are discussed. (auth)

13057 STUDIES OF ZEOLITE CATION INFLUENCE ON γ RADIOLYSIS OF ADSORBED AMMONIA BY THE EPR METHOD. Sorokin, Yu. A.; Tupikov, V. I.; Malkova, A. I.; Pshezhetskii, S. Ya.

XUM

(Inst. of Physics and Chemistry, Moscow). Teor. Eksp. Khim.; 6: 693-8(Sep-Oct 1970). (In Russian).

The EPR method was used to study the γ radiolysis of ammonia adsorbed on synthetic zeolites containing H^+, Li^+, Na^+, K^+, and Cs^+ at 77°K. The results showed that the concentration and type of zeolite cations influence the radiative yield and steady concentration of radicals in the wide range of surface saturation. The effect was assumed to be related to the various defects during NH_3 radiolysis near the cation. (R.V.J.)

13058 DECAY OF FREE RADICALS IN IRRADIATED PMMA AT HIGH PRESSURES STUDIED BY ESR. Szocs, F. (Deutsches Kunststoff-Institut, Darmstadt, Ger.). J. Appl. Polym. Sci.; 14: 2629-33(Oct 1970).

The decay of free radicals in irradiated PMMA (poly methyl methacrylate) subjected to high pressures was studied by the method of ESR. The rate constants and activation energies were determined for the decay of free radicals at the pressures of 5000 and 10,000 atm over the temperature range of 100 to 170°C. The rate of decay was reduced essentially by the effect of high pressure. The mechanism of the decay of free radicals in solid polymers is being discussed. The influence of the motion of macromolecule segments on the course of radical reactions in solid phase is considered. (auth)

Radioisotope Production

Refer also to abstract 15001.

13059 THE SYNTHETIC ACTINIDES: FROM DISCOVERY TO MANUFACTURE. Seaborg, Glenn T. (Atomic Energy Commission, Washington, D. C.). Nucl. Appl. Technol.; 9: 830-50(Dec 1970).

The first synthetic actinide element, neptunium, was discovered in 1940. The last element of the actinide series, lawrencium, was created for the first time in 1961. These and the nine other intervening elements have added a new dimension to science, technology, industry, medicine, and politics in an extraordinarily short period of time. Each synthetic actinide element from atomic number 93 to atomic number 98 (with the exception of berkelium, atomic number 97) can now be manufactured in essentially any desired quantity, a truly remarkable achievement. (auth)

13060 SZILARD–CHALMERS EFFECT FOR PRODUCTION OF ^{203}Hg IN HIGH SPECIFIC ACTIVITY. Angelberger, P.; Grass, F. (Univ., Vienna. Oesterreichische Hochschule, Vienna). Radiochim. Acta; 14: 130-5(Nov 1970). (In German).

A systematic investigation of Szilard–Chalmers reactions in inorganic and organic mercury compounds was undertaken with the aim of preparation of the internal conversion radioisotopes ^{197}Hg and ^{203}Hg in high specific activity. Several separation procedures were used for recoil Hg^0 and Hg(II). After a 30-minute irradiation og Hg-Dibenzyl, $Hg(CH_2\Phi)_2$, with thermal neutrons ($1.75 \cdot 10^{12}$ n · cm^{-2} s^{-1}) at dry ice temperature and extraction of a benzene solution with 0.1 m NaCN, ^{197}Hg or ^{203}Hg (no isotope effect) could be recovered in 30% yield with an enrichment factor of 130. With Hg-Diphenyl, $Hg\Phi_2$, under the same conditions the yield was 10%, enrichment 160. By one hour irradiation of the highly toxic Hg-Diethyl, $HgEt_2$, and adsorption on precipitated MnO_2 from acetone solution, enrichment factors up to 170 with yields approximately 15% were obtained. In these experiments it could be shown that the unusually high enrichment of 2.5×10^5 reported by Nefedov et al., for the same procedure is due to an error in their method. (auth)

13061 PREPARATION OF ^{85}Sr AND /sup 87m/Sr FOR BONE SCINTIGRAPHY. Sorantin, H.; Umek, H.; Czembirek, H. (Reaktorzentrums, Seibersdorf, Austria. Medizinische Univ., Vienna). Atompraxis; 16: 383-6(Nov-Dec 1970). (In German).

Preparation methods of ^{85}Sr and ^{87m}Sr from natural or enriched Sr by direct activation and the clinical application for bone scintigraphies are discussed. The use of ^{87m}Sr for faster availability of results, better quality of scintigrams, and lower costs is recommended. Only the distribution range is limited by the short half-life of 2.8 hours. (auth)

13062 CARRIER-FREE SEPARATION OF ^{131}Cs FROM IRRADIATED BARIUM SALTS WITH THE HELP OF COUNTER CURRENT ELECTROLYSIS. Bilal, B. A. (Hahn-Meitner-Institut fuer Kernforschung, Berlin). Radiochim. Acta; 14: 151-4(Nov 1970). (In German).

With the aid of countercurrent electromigration carrier-free ^{131}Cs was continuously separated from its parent nuclide ^{131}Ba. The method described is generally suitable for carrier-free nuclide separation in other nuclide generators. (auth)

13063 PRODUCTION OF ^{52}Fe FOR MEDICAL USE. Greene, M. W.; Lebowitz, E.; Richards, P.; Hillman, M. (Brookhaven National Lab., Upton, N. Y.). Int. J. Appl. Radiat. Isotop.; 21: 719-23(Dec 1970).

A method is described for producing practical quantities of ^{52}Fe by the ^{52}Cr(^{3}He, 3n)^{52}Fe reaction. The excitation function was measured for this reaction and a simple chemical separation method was developed. (auth) (UK)

Recoil Production and Reactions

13064 (INR–1211) LCAO–SCF CALCULATIONS OF THE ELECTRON ENERGIES FOR THE TRANSITION STATES: BROMINE + AROMATIC MOLECULE. Palczewski, A. (Institute of Nuclear Research, Warsaw (Poland)). 1970. 11p. Dep. NTIS (U. S. Sales Only).

Calculations of the electron energies for the transition states were performed. These energies were calculated for the nucleophilic, radical, and electrophilic substitutions of bromine by reactions of recoil ^{82}Br in ortho, meta, and para positions of nitrobenzene, toluene, and bromobenzene. (auth)

13065 NUCLEAR TRANSFORMATIONS OF ^{35}S GENERATED IN NEUTRON-IRRADIATED ALKALI METAL CHLORIDES AND OXYCHLORIDES. Abdel-Rassoul, A. A.; Abdel-Aziz, A.; Aly, H. F. (Atomic Energy Establishment, Cairo). Radiochim. Acta; 14: 113-6(Nov 1970).

The distribution of different oxidation states of ^{35}S generated in neutron-irradiated NaCl, KCl, RbCl, $KClO_3$, and $KClO_4$ was determined. The forms evidenced include: S^{2-}, S^0, S^{2+}, S^{4+}, S^{6+} and other unidentified S ions as well. Mutual separation is readily achieved by ion-exchange chromatography. A general trend for the distribution of different sulfur species is the increase in S^{6+} and respective decrease in other forms as the chlorine content decreases in the various targets experimented. The data obtained are interpreted on the basis of the S^{2-} precursor primarily formed and the induced cavities in the host lattice. The effect of thermal annealing by aging at ambient temperature was also investigated. (auth)

13066 HOT-ATOM RECOIL REACTIONS OF ^{18}F IN PERFLUOROCYCLOBUTANE AND PERFLUOROCYCLOBUTENE IN THE LIQUID PHASE. Hinkson, Thomas Clifford. Fayetteville, Ark.; Univ. of Arkansas (1970). 180p. University Microfilms Order No. 70-17,158.

Thesis.

Hot atom recoil reactions of ^{18}F atoms generated by the ^{19}F (n,2n)^{18}F nuclear reaction were studied in the liquid phase with perfluorocyclobutane and perfluorocyclobutene. The method of analysis was by radiogaschromatography. The influence of the free radical scavengers isobutene and iodine was examined. In the perfluorocyclobutane system over twenty-five labeled products were observed including as major identified products CF_4, C_2F_4, C_2F_6, n-C_3F_6, C_3F_8, n-C_4F_{10}, cyclo-C_4F_8, cis-2-C_4F_8, perfluoroethylcyclobutane, -butylcyclobutane, and -1,4-diclobutylbutane. The mechanism of ^{18}F atom labeling consistent with the observed product distribution and scavenger effects includes: (1) a substitution reaction to produce labeled excited perfluorocyclobutane, which subsequently is either stabilized to labeled parent molecules or decomposes to labeled and unlabeled perfluoroethane; (2) an insertion reaction followed by ring opening to produce labeled perfluoronormalbutane radicals; (3) decomposition of excited nonlabeled perfluorocyclobutane molecules produced by inelastic collisions with the recoiling ^{18}F atoms; and (4) recombination of the reactive fragments within a liquid cage. In the perfluorocyclobutene system the major identified products included C_2F_4, n-C_3F_6, cyclo-C_4F_8, 1,3-C_4F_6, and tentatively identified C_7, C_8, C_{10}, and C_{12} compounds. The labeling mechanism is similar to that of perfluorocyclobutane, differing in that (1) the initial substitution product having excess energy, labeled cyclo-C_4F_6, isomerizes to perfluorobutadiene rather than decomposing and (2) the ^{18}F atoms are self-scavenged by the unsaturated parent molecules to form labeled perfluorocyclobutyl radicals which recombine with the reactive decomposition fragments, rather than recombining as free atoms. (Diss. Abstr. Int., B)

13067 IODINE HALIDES AS RADICAL SCAVENGERS. Hawke, John; Wolfgang, Richard (Univ. of Colorado, Boulder). Radiochim. Acta; 14: 116-19(Nov 1970).

The iodine halides ICl and IBr were used as radical scavengers in the system T + CH_4 and T + H_2-D_2 where T was produced by recoil in the reaction ^{3}He(n,p)T. The results agree well with data obtained previously using Br_2 and I_2 both in moderated and unmoderated systems and have the advantage of considerably greater vapor pressures than I_2, allowing their use in the hydrogen system without heating. A further advantage for analysis by chromatography lies in the greater volatility of the scavenged products that appear as chlorides or bromides rather than iodides. (auth)

XUM

13068 CHEMICAL CONSEQUENCES OF THE NUCLEAR REACTIONS ^{58}Fe(n,γ)^{59}Fe AND ^{57}Co(EC)^{57}Fe IN SOLUBLE PRUSSIAN BLUE. Fenger, J. (Cambridge Univ., Eng.); Maddock, A. G.; Siekierska, K. E. J. Chem. Soc., A; No. 19, 3255-61(1970).

KFe[Fe(CN)$_6$], H$_2$O was prepared with ^{58}Fe in either the cation or the complex, and both samples were neutron-irradiated and analyzed for free and complexed ^{59}Fe. Parallel experiments were performed on K$_4$[Fe(CN)$_6$], 3H$_2$O. In Prussian Blue the retention in the hexacyano-complex is ca. 5% and can be increased only slightly by annealing, whereas it is ca. 20% in the simple hexacyanide and increases to 30% on annealing. It is suggested that the low retention in Prussian Blue is due to competition between recoil ^{59}Fe and inactive Fe^{3+} for re-formation of the complex. Moessbauer experiments were performed on KFe[Fe(CN)$_6$], H$_2$O doped with ^{57}Co as cation or in the complex. The spectra showed that ^{57}Fe formed by the ^{57}Co(EC)^{57}Fe process in the cationic ^{57}Co does not enter the complex. ^{57}Fe formed from [^{57}Co(CN)$_6$] however appears principally in a different complex species, probably losing a CN$^-$ ligand to form a pentacyanide. (auth) (UK)

13069 DIRECT LABELLING REACTIONS OF RECOILING ^{35}S AND ^{32}P ATOMS. Turcanu, C. N. (Inst. for Atomic Physics, Bucharest). Radiochem. Radioanal. Lett.; 5: 287-91(31 Dec 1970).

Direct labeling reactions of carrier-free ^{35}S and ^{32}P formed in anhydrous AlCl$_3$ and FeCl$_3$ by (n, p) and (n, α) nuclear reactions, respectively, with S$_2$Cl$_2$, SCl$_2$, SOCl$_2$, SO$_2$Cl$_2$, PSCl$_3$, POCl$_3$, and PCl$_3$, were studied. The radiosulphur and the radiophosphorus atoms present in AlCl$_3$ and FeCl$_3$ targets show some differences in these reactions. The study presents a new labeling method for some chlorine–sulfur compounds. (auth)

13070 CHEMICAL BEHAVIOR OF HOT ATOMS OF ^{14}C AND ^{13}N IN SEVERAL SOLID INORGANIC COMPOUNDS. I. METALLIC NITRIDES. Kuhry, J. G. (Centre de Recherches Nucleaires, Strasbourg). Radiochim. Acta; 14: 122-6(Nov 1970). (In French).

^{14}C produced by ^{14}N(n,p) is found in metallic nitrides as carbide ^{14}CMe, cyanide ^{14}CN-, cyanamide ^{14}CN$_2$=, and isocyanide O^{14}CN-. The last two species result from secondary processes activated by the radiation flux involving ^{14}CN-. The carbide and the cyanide are created in replacement collisions of ^{14}C with nitrogen and metal atoms, but these forms become stabilized only after long irradiation times. The chemical forms of ^{13}N formed in the ^{14}N(n,2n) process in the nitrides are ^{13}NMe(nitride) and ^{13}NN(molecular nitrogen). The behaviour of ^{13}N suggests a low recoil energy of the hot atom. (auth)

13071 CHEMICAL FORMS OF ^{37}S RESULTING FROM NEUTRON IRRADIATION OF LiCl IN SOLUTION IN METHANOL. Meyer, J. P. (Centre de Recherches Nucleaires, Strasbourg). Radiochim. Acta; 14: 154-6(Nov 1970). (In French).

The chemical forms of ^{37}S produced by the ^{37}Cl(n,p) reaction in methanolic solutions of lithium chloride were determined. 60% of the activity was found as monoatomic neutral sulfur, the residual activity being distributed among sulfate (16%), sulfite (10%), and sulfide (14%). In the presence of water, the sulfur atoms are oxidized to sulfate. The formation of S$^+$ ions leading to sulfate and of another species giving sulfate in aqueous solution and sulfite with a reducing agent are considered. (auth)

13072 CHEMICAL BEHAVIOR OF HOT ATOMS OF ^{14}C AND ^{13}N IN SEVERAL SOLID INORGANIC COMPOUNDS. II. ALKALI CYANIDES. Kuhry, J. G. (Centre de Recherches Nucleaires, Strasbourg). Radiochim. Acta; 14: 127-30(Nov 1970). (In French).

The chemical forms of ^{13}N in sodium and potassium cyanides are cyanide C^{13}N–, cyanamide ^{13}NCN=, and molecular nitrogen ^{13}NN. These compounds result from reactions of ^{13}N with the fragments of CN ligands and from an addition process on CN–. The pile irradiation of the cyanides yields the following ^{14}C compounds: CN–, CC, elementary C, and CN$_2$=. The formation of these species is explained by similar processes and by secondary thermal activated reactions with radiolytic decomposition products of the targets. (auth)

Radiochemistry

Refer also to abstracts 13068 and 13374.

13073 COULOMB FRAGMENTATION FOLLOWING THE DECAY OF ^{131}I. Langhoff, H. (Franklin Inst., Swarthmore, Pa.). Phys. Rev., A; 3: 1-5(Jan 1971).

The fragmentation of several diatomic iodine compounds as a consequence of β^- decay was investigated. Information about the velocity spectra of the ^{131}Xe fragments was obtained by analyzing the profiles of their γ lines using the nuclear resonance fluorescence technique. Experimental cross sections for resonance fluorescence obtained with gaseous ^{131}I sources were in satisfactory agreement with predictions using a simple model for the fragmentation process. (auth)

13074 NUCLEAR GAMMA-RESONANCE STUDY OF PRODUCTS OF β-DECAY OF ^{121m}Sn. Lebedev, R. A.; Babeshkin, A. M.; Nesmeyanov, An. N.; Popov, E. A. Vestn. Mosk. Univ., Ser. II. Khim.; 11: 627-8(Sep–Oct 1970). (In Russian).

The products of β decay of ^{121m}Sn in solid inorganic tin compounds have been studied by nuclear gamma-resonance. Conclusions concerning the state of electron shells of daughter antimony atoms were drawn from the isomeric shifts. (auth)

13075 ON THE MECHANISM OF FORMATION OF ANOMALOUS CHARGE STATES OF IRON AFTER ^{57}Co ELECTRON CAPTURE IN Co COMPLEXES. Friedt, J. M.; Baggio-Saitovitch, E.; Danon, J. (Centro Brasileiro de Pesquisas Fisicas, Rio de Janeiro). Chem. Phys. Lett.; 7: 603-5(15 Dec 1970).

The Moessbauer absorption spectra of ferric acetylacetonate irradiated with electrons, are similar to the emission spectra after electron capture in ^{57}Co-labeled Co(AcAc)$_3$. This result indicates that an autoradiolysis mechanism is responsible in molecular compounds for the stabilization of the anomalous iron charge states. (auth)

Separation Processes

Refer also to abstracts 12923, 12933–12935, 12947, 12999, 13039, 13043, 13625, and 13626.

13076 (AECL–2503) REVIEW OF HEAVY WATER PRODUCTION PROCESSES. Rae, H. K. (Atomic Energy of Canada Ltd., Chalk River (Ontario)). Aug 1969. 21p. (CONF-651019–1; CRL–91). Dep. NTIS (U. S. Sales Only). AECL $1.00.

From 15th Canadian Chemical Engineering Conference, Quebec City, Canada.

The rapid growth of Canadian heavy-water-power-reactor capacity has renewed interest in D$_2$O production. The economic source for large quantities of D$_2$O today is considered to be water. Processes include hydrogen distillation (where pure hydrogen streams are available for stripping) and several chemical exchange reactions. Chemical exchange of deuterium and hydrogen between two compounds leads to the preferential accumulation of the deuterium in one. Choosing a gas and a liquid, efficient countercurrent multistage operation is possible giving large enrichment factors in a single tower. To obtain reflux the deuterium transfer must be reversed outside the tower using chemical conversion or another exchange tower operating at a higher temperature. Chemical exchange between water and hydrogen sulfide has been used at the USAEC Savannah River plant for 16 years and is the process chosen for the three large heavy water plants being built in Canada. Ammonia–hydrogen exchange and amine–hydrogen exchange are other processes. (auth)

13077 (ANL–7755) CHEMICAL ENGINEERING DIVISION FUEL CYCLE TECHNOLOGY QUARTERLY REPORT, JULY–SEPTEMBER 1970. Webster, D. S.; Jonke, A. A.; Bernstein, G. J.; Levitz, N. M.; Pierce, R. D.; Steindler, M. J.; Vogel, R. C. (Argonne National Lab., Ill.). Oct 1970. Contract W-31-109-eng-38. 55p. Dep. NTIS.

Work has been done during the period July through September 1970 on fuel cycle technology projects in the following areas: (1) development of a head-end process for LMFBR fuels, consisting of removal of stainless steel cladding in a zinc bath and subsequent reduction of the fuel oxide to metal, (2) laboratory-scale and pilot-scale work to develop a fluid-bed process for the conversion of uranium nitrate and plutonium nitrate solutions to an oxide form suitable for the fabrication of fuel shapes for LMFBR fuel, (3) development of x-ray fluorescence spectrometry as an in-line analytical method for determining the Pu/U ratio of oxide fuels during fabrication, and (4) development of a centrifugal contractor of small diameter and large length-to-diameter ratio for the plutonium isolation steps in the solvent extraction of LMFBR fuels. (auth)

13078 (DOCKET-50201–60) WEST VALLEY REPROCESSING PLANT. License No. CSF-1. Technical Specifications Change No. 13. (Division of Materials [and] Licensing (AEC), Washington, D. C.). 26 Jan 1971. 11p. Dep. NTIS.

Revision to Section 5.1 of the Technical Specifications (Effluent and Environmental Monitoring) is presented. It was concluded that the change does not present significant safety hazards considerations. (M.C.G.)

13079 (DOCKET-50201–61) WEST VALLEY REPROCESSING PLANT. Quarterly Report, October 1–December 31, 1970.

XUM

(Nuclear Fuel Services, Inc., West Valley, N. Y.). 21 Jan 1971. 8p. Dep. NTIS.

Environmental monitoring, low level liquid effluents, stack effluents, and periodic testing are reported. (M.C.G.)

13080 (DOCKET-50201-62) WEST VALLEY REPROCESSING PLANT. Environmental Sample Data. (Division of Materials [and] Licensing (AEC), Washington, D. C.). 31 Aug 1970. 122p. Dep. NTIS.

Data on radiation monitoring for the first three quarters of 1969 are presented. Data for grass α, β, and γ in plants, soils, Buttermilk Creek, Cattaraugus Creek, drinking water, and hold-up and burial lagoons are given. Tritium data are given for drinking water and tritium and ^{90}Sr data are included for the creeks and lagoons. (M.C.G.)

13081 (NP-18577) INVESTIGATION OF REPROCESSING INPUT MEASUREMENT USING TRACER TECHNIQUE. Bokelung, H. (European Company for the Chemical Processing of Irradiated Fuels, Mol (Belgium)). Oct 1970. 31p. (ETR-266). Dep. NTIS (U. S. Sales Only).

The quantities of uranium and/or plutonium fed into a reprocessing plant are currently found by multiplying the dissolver solution batch size (volume or weight) by the concentrations of these elements as found by analyses of samples taken from the batch. An independent verification of the volume measurement using tracer techniques is proposed. The basic concept is that of isotope dilution mass spectrometry applied to the dissolver solution into which, at the outset, a known amount of ^{7}Li is mixed as tracer. Samples of the solution are spiked with ^{6}Li, ^{233}U, and ^{242}Pu for mass spectrometry. The measured ratio ^{6}Li/^{7}Li verifies the batch size (volume or weight), whereas the concentration ratios U/Li and Pu/Li give the quantities of these fissile materials, (kg), in the batch. The solution of the ^{6}Li spike is calibrated against a dilution of the ^{7}Li solution used to trace the dissolver solution; the batch size can thus be found merely as a ratio of two ^{6}Li/^{7}Li ratios, thereby circumventing the complicated absolute standardization of the ^{7}Li additive. The assets of the Li concept are discussed in terms of process compatibility, analytical sensitivity, precision, and price. The chemical separation of Li from the dissolver solution prior to its determination by mass spectrometry is described. Results on simulated input solutions show the capability of the system under laboratory conditions to be about 0.3% relative standard deviation. (auth)

13082 (RLO-2225-T-11-1) DYNAMICS OF SOLVENT EXTRACTION SYSTEMS. III. Progress Report No. 3, October 1, 1969–September 30, 1970. Babb, Albert L.; Garlid, Kermit L. (Washington Univ., Seattle. Dept. of Nuclear Engineering). Oct 1970. Contract AT(45-1)-2225. 83p. Dep. NTIS.

Controlled cycling operation of a pulsed, sieve-plate extraction column was studied. The significance of design variables and operating variables on extraction efficiency and column throughout was established. Random variations in organic phase holdup were measured and analyzed. A computer model was developed for describing typical dynamic operation of extraction systems. (M.C.G.)

13083 (WHAN-FR-33) APPLICATION OF AQUEOUS TECHNOLOGY TO LMFBR SEPARATIONS PROCESSES. PROGRAM PLAN FOR TASK T-2: FUEL DISSOLUTION CHARACTERISTICS. Lerch, R. E. (WADCO Corp., Richland, Wash.). Dec 1970. Contract AT(45-1)-2170. 38p. Dep. NTIS.

A development program for investigating the effects of fuel fabrication variables and irradiation history on the dissolution characteristics of LMFBR fuels in nitric acid is outlined. Studies will include measurements on the dissolubility and dissolution rate of various unirradiated and irradiated mixed plutonium–uranium oxides in nitric acid. An effort will be made to establish how dissolubility and dissolution properties vary with composition, fabrication, and conditions of breeder reactor exposure. Methods for predicting dissolubility and dissolution behavior of unirradiated and irradiated mixed oxide fuels from fabrication and irradiation parameters will be developed. Initial experiments were made to determine feasibility of the studies and to establish fractionation variables to be considered. (J.G.B.)

13084 ION EXCHANGE PROPERTIES OF CRYSTALLINE ZIRCONIUM PHOSPHATE. Harvie, Sylvia J.; Nancollas, George H. (State Univ. of New York, Buffalo). J. Inorg. Nucl. Chem.; 32: 3923-37(Dec 1970).

Equilibrium and kinetic studies were made at 25°C of the exchange of lithium, sodium, potassium, calcium, and strontium ions on crystalline zirconium phosphate. The results are consistent with the existence of several distinct crystalline phases of the metal forms. As was found for the semicrystalline material, the properties of crystalline zirconium phosphate are to some extent dependent on the method of preparation of the particular form. (auth) (UK)

13085 CONTRIBUTION TO THE ELEMENTARY INTEGRATION OF NONLINEAR TRANSPORT EQUATIONS IN ISOTOPE SEPARATION. PART I. Zieger, K. (Institut fuer Stabile Isotope, Leipzig). Isotopenpraxis; 6: 316-18(Sep 1970). (In German).

A large class of isotope separation procedures can be described uniformly by Cohen's transport equations. In the simplest case a system of two first order partial differential equations of the hyperbolic type exist. This nonlinear system is reduced by a suitable substituion to a linear differential equation of second order. Then problem formulations are confined, for which not only the differential equation but also the boundary and initial conditions are linear after the reduction. (auth)

13086 INVESTIGATION OF SPONTANEOUS SILVER PRECIPITATION ON POWDERY PLATINUM IN NITRIC SOLUTIONS. Toth, G.; Fuessy, E. (Inst. for Isotope, Budapest). Isotopenpraxis; 6: 307-9(Sep 1970). (In German).

It was found that silver ions precipitate on hydrogenated platinum powder, while with nitric acid concentration between 5 and 0.001 N the maximum precipitated quantity does not come up to the value equaling the monomolecular layer. Though the values obtained through measuring with regard to the dependence of the precipitation upon concentration formally seem to cover the Langmuir equation, the values determined by means of this equation showed some dependence on pH values, and did not correspond with the BET surface. Spontaneous silver precipitation on platinum powder can be used for the separation of radioactive silver isotopes. (auth)

13087 ASSAINISSEMENT ET DECHETS RADIOACTIFS. (Antipollution and Radioactive Wastes). Rodier, Jean; Vernhes, Claude. Paris: Dunod (1970). 127p.

The dangers connected with radioactive wastes and their administrative consequences are examined. Radioactive wastes and their different treatments are classified and their conditioning and final disposal discussed. The cost of administrating radioactive wastes is estimated. (France)

13088 CHEMICAL SEPARATION OF RUTHERFORDIUM. Silva, R.; Harris, J.; Nurmia, M.; Eskola, K.; Ghiorso, A. (Lawrence Radiation Lab., Berkeley, Calif.). Inorg. Nucl. Chem. Lett.; 6: 871-7(Dec 1970).

Element 104 is expected to fall into group IVB, i.e., to be eka-hafnium. It is predicted to have a valence and ionic radius similar to Zr and Hf and to exhibit similar chemical properties. Previous studies with actinide elements showed that cation exchange columns using chelating agents as eluants could provide rapid chemical separations on one atom at a time and yield sources suitable for alpha energy analysis. These methods were developed further in order to test the above predictions. The behavior of the activity assigned to element 104 with mass 261 was found to be entirely different from trivalent and divalent actinide elements but similar to Hf and Zr as predicted. (UK)

13089 POTENTIAL CHLORIDE ELECTROLYTES FOR RECOVERING THE METALS Ti, Zr, AND Hf BY FUSED SALT ELECTROLYSIS. Flengas, S. N.; Pint, P. (Univ. of Toronto). Can. Met. Quart.; 8: 151-66(Apr-Jun 1969).

The properties of potential electrolytes for recovery of Ti, Zr, and Hf by a fused salt electrolytic process employing solutions of $TiCl_4$, $ZrCl_4$, and $HfCl_4$ in alkali and alkaline earth chloride melts are discussed in terms of thermal stability. Pressure–temperature relationships for these systems are analyzed, and methods for calculating activities of complex ionic species in solution are presented. (auth) (Canada)

13090 PROCEDURE FOR RECOVERY OF FISSILE MATERIALS IN CHEMICAL DECLADDING SOLUTIONS. Faugeras, Pierre; Kikindai, Tivadar (to Commissariat a l'Energie Atomique). French Patent 1,586,431. 12 Jan 1970. Filed 20 Aug 1968. (In French).

A decladding solution, obtained from the dilute nitric acid attack of metal cladding, is subjected to a selective crystallization of the salts present in order to eliminate the crystals of cladding metal nitrate, the soluble nitrates of fissile materials being left in solution. The solution collected, after elimination of the crystals, is sent to the unit where the rods of fissile material are dissolved after decladding. (auth) (France)

13091 ION-EXCHANGE SELECTIVITY OF THE SYNTHETIC ZEOLITE LINDE A IN ANHYDROUS AND MIXED MEDIA. Barrett, R. B.; Marinsky, J. A. (State Univ. of New York, Buffalo). Contract AT(30-1)-2269. J. Phys. Chem.; 75: 85-9(7 Jan 1971).

The selectivity coefficients for the ion exchange of cesium with sodium A zeolite and cesium and sodium with potassium A zeolite were determined in nonaqueous and mixed media. The exchanging ions were at radioactive tracer level concentrations so that the fraction of the macroion of the zeolite was essentially unity in both the zeolite and external liquid phase. The dramatic increase in ion selectivity at very high alcoholic content of the liquid phase could only be qualitatively examined and was attributed to the significant solvation of the zeolite by the alcohol in the alcohol-rich media. Quantitative interpretation of the data obtained in the mixed media prior to this sharp increase in selectivity was attempted by assuming that the zeolite phase may be treated as a highly concentrated electrolyte solution having only one diffusible ion and as a crosslinked network which exerts a pressure on the internal solution phase. The special properties of the zeolite, rigidity, resistance to electrolyte incursion, and high selectivity for water, were believed to permit recourse to this model in mixed media over an alcohol–water weight per cent composition ranging from 0 to 70%. Correlation of experimental and calculated selectivity points was sufficiently good to support the validity of this approach. (auth)

13092 COMPLEX FORMATION IN THE SOLVENT EXTRACTION SYSTEM: NEODYMIUM NITRATE–WATER–DI-(2-ETHYLHEXYL) PHOSPHORIC ACID. Lloyd, Robert C. **University, Miss.; Univ. of Mississippi (1970). 201p. University Microfilms Order No. 70-16,400.**

Thesis.

The system, neodymium nitrate–water–di-(2-ethylhexyl) phosphoric acid (HDEHP), was studied to obtain information about the stoichiometries, which describe the extraction of rare earths from aqueous solutions by the organic solvent. The structures of the organometallic complexes formed due to rare earth extraction were also determined. Equilibrium studies were made using water-equilibrated HDEHP as the solvent for extracting neodymium from aqueous solutions of neodymium nitrate. Concentrations of neodymium in the aqueous phase ranged from 1.17 to 2.2 molal. In this study molality was defined as moles of neodymium per thousand grams of material other than neodymium. Concentrations lower than 1.17 molal were not examined because of gel formation in the organic phase attributed to hydrolysis of the neodymium ions. Three material balance methods were used to test possible extraction stoichiometries by evaluating the amount of water transferred from the organic to the aqueous phases. Nitrate analyses on the equilibrated organic phases, hydrogen ion balances on the equilibrated aqueous phases, and infrared studies (qualitative and quantitative) on the equilibrated organic phases gave independent data for correlation with the material balance data. The infrared data were coupled with Raman polarization studies to describe the structures of the extracted neodymium and lanthanum complexes. The combined results of the above studies suggest that several extraction stoichiometries may be active at various parts of the concentration range for the neodymium system. These extraction stoichiometries are (1) $ND^{3+} + 3[(HDEHP)_2 \cdot H_2O] \rightleftharpoons Nd[H(DEHP)_2]_3 + 3H_2O + 3H^+$, (2) $Nd(OH)_2^{1+} + (HDEHP)_2 \cdot H_2O \rightleftharpoons Nd(OH)_2H(DEHP)_2 + H_2O + H^+$, (3) $NdNO_3^{2+} + 2[(HDEHP)_2 \cdot H_2O] \rightleftharpoons NdNO_3[H(DEHP)_2]_2 + 2H_2O + 2H^+$, and (4) $Nd(NO_3)_2^{1+} + (HDEHP)_2 \cdot H_2O \rightleftharpoons Nd(NO_3)_2H(DEHP)_2 + H_2O + H^+$ where DEHP represents the acid monomer less a hydrogen ion. Reactions 1 to 3 are possible extraction stoichiometries at the lowest concentration studied (1.17 aqueous neodymium molality). However, reactions 2 and 3 are probably the dominant ones. In the mid concentration range reactions 2 and 3 are the controlling extraction stoichiometries. Near saturation reaction 4 probably dominates but the infrared spectra indicate that reaction 2 may be influential over the entire concentration range. The infrared data support the extraction stoichiometries proposed by Cheng for the lanthanum system. The data also suggest that the hydrolysis reaction of Equation 2 may be active. The infrared spectra indicate that the rare earth-oxygen bonds of the solvent are probably covalent. The nitrate-metal bonds in the neodymium and lanthanum complexes are also indicated to be covalent by the infrared spectra. Raman polarization studies suggest that the bonding is bidentate or bridging instead of monodentate. The position of the nitrate bands suggests that the nitrate is bonded to the metal in a bidentate fashion instead of bridging. (Diss. Abstr. Int., B)

13093 RADIOLYTIC DEGRADATION OF THE TOLUENE–NITRIC ACID SYSTEM: STUDIES ON THE ROLE OF SOME PRIMARY DEGRADATION PRODUCTS IN THE EXTRACTION OF ^{95}Zr. Dworschak, Heinz; Gasparini, Giulio M. (CNEN, Rome). Radiochim. Acta; 14: 136-41(Nov 1970).

The radiolytic degradation of toluene, the simplest alkyl aromatic hydrocarbon, by means of gamma rays was studied in the presence of nitric acid. Some primary degradation products containing nitrogen were investigated with respect to their role as possible intermediates in the formation of Zr-complexing species responsible for the retention of ^{95}Zr by the organic phases in the liquid-liquid extraction reprocessing of irradiated fuels. A comparison of the extractive behavior of the organic solutions after degradation by gamma rays and of the stability of the ^{95}Zr complexes, as well as an analysis of these complexes by radio-thin layer chromatography, showed that the main Zr-extracting products obtained by degradation of three model compounds were not identical with those of the direct toluene degradation. Some considerations and hypotheses were made on the degradation mechanism. (auth)

13094 **IMPROVEMENTS IN OR RELATING TO THE REMOVAL AND DISPOSAL OF RADIOACTIVE IMPURITIES FROM CONTAMINATED LIQUIDS. (to Union Tank Car Co.). British Patent 1,215,397. 9 Dec 1970. Priority date 29 May 1967, United States.**

A method is described for cleaning a filter having finely divided radioactive particles and/or filtered radioactive solids deposited on it. A gas is passed in reverse flow through the filter while it is submerged in a cleaning liquid. The cleaning fluid is then removed from the filter, and a backwash liquid is passed through the filter in reverse flow. The cleaning and backwash liquids are then routed away from the filter. The solids and particles are allowed to settle, and the settled particles are centrifuged to remove the liquid. The solid waste is then discarded. (B.L.M.)

13095 ELECTROCHEMICAL STUDIES OF YTTRIUM AND YTTRIUM–ZINC ALLOYS IN FUSED LiCl–KCl EUTECTIC. **Hoshino, Yoshio; Plambeck, James A. (Univ. of Alberta, Edmonton). Can. J. Chem.; 48: 685-7(15 Feb 1970).**

The electromotive force of cells of the type $Y(s)/YCl_3 + LiCl-KCl$ (eutectic)/Y – Zn alloy (saturated liquid) was measured over the temperature range 450 to 570°C. Thermodynamic values for the limiting solid YZn_{12} existing in this region are: ΔG_f^0, –48.7 kcal/mole at 450°C; ΔH_f^0, –74.9 kcal/mole; ΔS_f^0, –36 cal/deg mole. The standard molar potential of the Y(III)–Y(0) couple was determined to be –2.831 V against Pt(II)–Pt(0). This work is of interest in the possible electrochemical separation of fission product impurities. (auth) (Canada)

13096 EXTRACTION OF U(VI) AND SELECTED M(III) CATIONS BY BIS N-OCTYL PHOSPHORIC ACID IN TWO DIFFERENT HYDROCARBON DILUENTS. **Mason, G. W.; Schofer, N. L.; Peppard, D. F. (Argonne National Lab., Ill.). J. Inorg. Nucl. Chem.; 32: 3899-3909(Dec 1970).**

The extraction of Ce^{3+}, Pm^{3+}, Eu^{3+}, Tm^{3+}, Y^{3+}, Am^{3+}, Cm^{3+}, and UO_2^{2+} from an aqueous chloride phase into a solution of $(n\text{-}C_8H_{17}O)_2PO(OH)$, HDOP, in benzene or in n-heptane was studied as a function of concentration of extractant in the organic phase and of hydrogen ion in the aqueous phase and the stoichiometries of extraction obtained. Corresponding to the stoichiometries, values of K, F, and $[H^+]$ obtained from the hydrogen ion dependency plots were inserted in the equation: $K = K_sF^a/[H^+]^b$ to obtain values of K_s. (K is the observed distribution ratio, F the concentration of HDOP in the organic phase and $[H^+]$ the concentration of hydrogen ion in the aqueous phase following equilibration, and a and b the respective extractant and hydrogen ion dependencies. The equation is applied specifically to a system embodying 1.0 F (NaCl + HCl) at 22 ± 2°C). The K_s (n-heptane) value is higher than the K_s (benzene) value for each of the cations studied. However, although the ratio of the two K_s values is large for each of the seven M(III) cations, ranging from 50 to 200, it is only 10 for U(VI). From these observations, it is apparent that the term carrier diluent is preferable to the term inert diluent. Comparisons with systems employing $[C_4H_9CH(C_2H_5)CH_2O]_2PO(OH)$ and $(n\text{-}C_8H_{17})_2PO(OH)]$ as extractants are made in terms of acidity of the extractant, structure of extractant, that is C–P or C–O–P bonds, steric effects within the extractant molecule, and effect of diluent (aromatic or saturated hydrocarbon). (auth) (UK)

13097 EXTRACTION OF YTTRIUM IN THE SYSTEM $Y(NO_3)_3$–HNO_3–H_2O–DI(2-ETHYLHEXYL) PHOSPHORIC ACID. **Harada, Takeo; Bautista, Renato G.; Smutz, Morton (Ames Lab., Iowa). Met. Trans.; 2: 195-7(Jan 1971).**

The extraction equilibrium in the system $Y(NO_3)_3$–HNO_3–H_2O–D2EHPA in Amsco as the solvent was studied as a function of the D2EHPA concentration, acidity, and aqueous yttrium concentration, and the results were compared to the chloride system. The ratio of the distribution ratios for nitrate and chloride system was found to vary from 0.5 to 7.0. (auth)

13098 **EXTRACTION OF ALKALINE EARTH METALS AS IONIC ASSOCIATES WITH THENOYLTRIFLUOROACETONE AND RHODAMINE S. Poluektov, N. S.; Bel'tyukova, S. V. (Inst. of General and Inorganic Chemistry, Odessa). Zh. Anal. Khim.; 25: 2106-9(Nov 1970). (In Russian).**

XUM

Conditions have been studied for the formation and extraction of Ca, Mg, and Sr ionic associates with thenoyltrifluoroacetone and Rhodamine S. The ratio of Me : HTTA : Rhod in the complexes is 1 : 1 : 1. An extraction–photometric method for determining magnesium with a sensitivity of 0,003 μg/ml has been developed. (auth)

13099 SEPARATION OF RADIOIODIDE, RADIOIODATE, AND RADIOPERIODATE BY THIN-LAYER CHROMATOGRAPHY. Palagyi, S.; Zaduban, M. (Pavla Jozeta Safarika Univ., Kosice, Czech.). Chem. Zvesti; 23: 876-80(Nov-Dec 1969).

A rapid method for the separation of radioiodide, radioiodate, and radioperiodate on a thin layer of silica gel and starch is described. Using the system methanol–25% ammonium hydroxide–water–10% acetic acid (9 : 1 : 1 : 0.5) good separation has been achieved within 45 to 50 minutes. The method is suitable for the separation of carrier-free radioiodine or radioiodine with a carrier of the concentration up to 10^{-3} M. (auth)

13100 RECOVERY OF REACTOR-PRODUCED ^{231}Pa. Karraker, D. G. (E. I. du Pont de Nemours and Co., Aiken, S. C.). Contract AT(07-2)-1. Radiochim. Acta; 14: 158(Nov 1970).

A manganese dioxide precipitation for purification of ^{233}U from 27.4-day ^{233}Pa is reported. ^{231}Pa was also carried on the MnO_2 and the precipitated MnO_2 was processed to recover the ^{231}Pa after a 2-year storage period to allow the ^{233}Pa to decay. The ^{231}Pa was purified by anion exchange. (M.C.G.)

13101 PROCESS FOR RECOVERING PLUTONIUM AND URANIUM FROM REACTOR FUEL ELEMENTS IRRADIATED AT VARIOUS DEGREES. Larsson, Alf; Hultgren, Ake (to Aktiebolaget Atomenergi). French Patent 1,560,128. 3 Feb 1969. Priority date 21 Apr 1967, Sweden. (In French).

The procedure for the recovery of Pu and U from reactor fuel elements that have been irradiated, for example in a fast reactor, consists of dissolving the elements separately according to the amount of irradiation received to form an aqueous HNO_3 solution. The Pu is then converted to an insoluble form and the Pu and U are separated by separately using different solvents. The solvent used for Pu is tridodecylamine or tridodecylmethylamine, and for U the solvent is either TBP, dibutylcarbinol, diamylbutyl phosphate, or dibutyl phenylphosphonate. (P.C.H.)

EARTH SCIENCES

Geology and Hydrology

Refer also to abstracts 13005, 13078–13080, 13120, 13186, and 15336.

13102 (NCG-TR-27) SEEPAGE CHARACTERISTICS OF EXPLOSIVELY PRODUCED CRATERS IN SOIL AND ROCK. Sherman, W. C.; Banks, D. C. (Army Engineer Waterways Experiment Station, Vicksburg, Miss.). Aug 1970. 75p. Dep. NTIS.

For Army Engineer Nuclear Cratering Group, Livermore, Calif.

A review is presented of the permeability characteristics of soil and rock formations in both disturbed and undisturbed conditions which are likely to occur in the zones surrounding craters. Methods for determining permeability are discussed, and typical values of permeability in a variety of materials are tabulated. Factors which affect the seepage characteristics of craters are discussed, and a few examples are presented to illustrate the influence of seepage on stability calculations. The data indicate that laminar-flow conditions will prevail in soil and rock formations, dependent upon the size of the pore opening and hydraulic gradient. For a given pore opening, a critical gradient exists above which the flow is found to be turbulent; the technique of constructing flow nets for turbulent flow is illustrated. The correct assessment of seepage conditions in the zones surrounding a crater will depend to a large extent upon the correct evaluation of boundary conditions, such as geological discontinuities and sources of seepage. (auth)

13103 (NP–18639) TRITIUM CONTENT MEASUREMENTS ON A VARIETY OF WATER SAMPLES. SECOND LISTING. Technical Memorandum 3/1970. Hughes, M. W. (Commonwealth Scientific and Industrial Research Organization, Adelaide (Australia). Div. of Soils). 2 Oct 1970. 7p. Dep. NTIS (U. S. Sales Only).

Analysis of water samples for tritium at 7 sites in Australia between September 1969 and January 1970 is given. (Australia)

13104 (UCRL–50855) K-DIVISION EXPERIMENTAL WORK. PART I. GEOPHYSICS RESEARCH FOR UNDERGROUND EXPLOSION TECHNOLOGY. Hearst, Joseph R.; Carlson, Richard C.; Rambo, John T. (California Univ., Livermore. Lawrence Radiation Lab.). 17 Apr 1970. 172p. Dep. NTIS.

A detailed discussion of all the research carried out by the Geophysics Research Group during the past four years is presented. Descriptions are given of tests of a dry hole acoustic log, a shear-wave downhole survey, and comparisons between commercial logging systems and other logging methods. Computer programs for reducing logging data to physical properties are also discussed, as are programs for correlation and storage of logs. A proposed new method for measuring shear strength in place is also discussed. (auth)

13105 (USGS–474-84) HYDRAULIC TESTING OF HOLE UAe-7h, AMCHITKA ISLAND, ALASKA. Ballance, Wilbur C. (Geological Survey, Denver, Colo.). 1970. Contract AT-(29-2)-474. 35p. Dep. NTIS.

Five zones of hole UAe-7h were hydraulically tested by isolating them with straddle packers. Water bypass around the packers occurred during two of the tests. Because of unstable borehole-wall conditions, favorable locations for setting packers were scarce. The hole was drilled into an intrusive contact zone consisting of highly fractured, hydrothermally altered andesites, metamorphosed breccias, hornfels, and intrusive diorites. The hole was very difficult to drill because the fractured rock constantly caved from the hole wall and considerable time was required to clean the caved material from the hole. The constant caving resulted in an enlarged borehole often beyond the capacity of the packers to expand. The relative specific capacity (computed from injection test data) of the tested intervals ranges from 0.65 to 1.94 cubic meters per day per meter of drawdown. Due to the unfavorable hole conditions for conducting the tests and the high permeability of the fractured rocks, some of the data are only approximate. (auth)

13106 MEASUREMENT OF THE RADIOACTIVITY OF NATURAL WATERS. Biro, Tomas; Grisanti, Alvaro; Tori, Paolo. Ann. Ist. Super. Sanita; 6: 95-105(1970).

The exposure of man to external and internal radiation is determined by environmental radioactivity that may contribute significantly to the overall radiation exposure. The radiochemical techniques suitable for the analysis of water for controlling the radioactivity present in the natural waters from the Fontana Nuova well in Buggiano (Spoleto), are described. A careful radiochemical study of this water and of the normal tap-water used in Rome was then undertaken. (auth)

13107 NATURAL ENVIRONMENTAL RADIOACTIVITY IN SOUTH FLORIDA SANDS AND SOILS, FEBRUARY–JUNE 1968. Keefer, Douglas H.; Dauer, Maxwell (Dept. of Health, Education, and Welfare, Washington, D. C.). Radiol. Health Data Rep.; 11: 441-8(Sep 1970).

An investigation of the naturally occurring gamma-emitting radionuclides present in selected sands and soils of south Florida was conducted. Although the primary interest was in the natural environmental radioactivity from ^{238}U, ^{226}Ra, ^{232}Ta, and ^{40}K the concentrations of five fission products were also determined to minimize the error in computing the concentrations of the four naturally occurring radionuclides. The determination of these nine radionuclides in 45 environmental samples was performed by the linear least-squares method of analysis utilizing a computer. (auth)

13108 TRITIUM IN STREAMS IN THE UNITED STATES, 1961–1968. Wyerman, T. A. (Geological Survey, Washington, D. C.); Farnsworth, R. K.; Stewart, G. L. Radiol. Health Data Rep.; 11: 421-39(Sep 1970).

As part of its program of water resources investigations, the U. S. Geological Survey has been analyzing the tritium content of stream water since the early 1960's. The results of this sampling program for 20 streams in the conterminous United States and Alaska are tabulated along with relevant stream discharge data. The data show the effect on stream tritium concentration caused principally by thermonuclear detonations, and also seasonal, latitudinal, and continental effects. (auth)

13109 FAST-NEUTRON THERMALIZATION TIME IN SILICATE ORES OF VARYING MOISTURE CONTENT. Kolesov, B. M.; Ganichev, G. I.; Ovchinnikov, A. K.; Khaikovich, I. M.; Timofeeva, T. V. At. Energ. (USSR); 29: 51-3(Jul 1970). (In Russian).

In pulse neutron borehole surveying it is of interest to know the time characteristics of the neutrons because of moderation and thermalization. A model of a borehole was set up in the form of a cube 3 mm on edge penetrated by an aluminum tube having a wall thickness of 5 mm and an internal diameter of 100 mm. Measurements were made on sand having a moisture content of 4 and 19 wt. %. The neutrons were counted on a ZnS + B – 10 scintillation counter. The distribution of counts was studied over an interval of 10 to 1000 microseconds after the neutron pulse. An analysis of the data showed that the neutron thermalization times in the relatively dry and wet sands were equal to about 100 and 80 microseconds respectively, while the average lifetimes of the thermal neutrons were 650 and 410 microseconds respectively (calculated theoretical values for a Maxwellian neutron distribution are 730 and 350 microseconds). (TTT)

13110 SOIL WATER CONTENT FROM GAMMA RAY ATTENUATION: A COMPARISON OF IONIZATION CHAMBER AND SCINTILLATION DETECTORS. Topp, G. C. (Canada Dept. of Agriculture, Ottawa). Can. J. Soil Sci.; 50: 439-47(Oct 1970).

Scintillation detection systems are commonly used to measure gamma ray attenuation by soil in the determination of its water content. The performance of a specially designed ionization chamber detector and electrometer was evaluated relative to that of a commercially available scintillation system. Quantitative assessments were made of the absorption coefficients of water, equipment response times, stabilities, accuracies, and costs for the two systems. The ionization chamber showed a constant absorption coefficient and gave greater combined accuracy and response time as well as better stability with respect to both time and temperature. Although it was not entirely commercially available, the ion chamber system employed simpler electronic components and was both easier to operate and less expensive to purchase and maintain than was the scintillation system. (auth)

13111 DISCUSSION OF PAPER BY WALTER E. REED, TRANSPORT OF WATER AWAY FROM A BURIED HEAT SOURCE WITH SPECIAL REFERENCE TO HYDROLOGIC PHENOMENA OBSERVED AT AARDVARK NUCLEAR DETONATION. Davis, Stanley N. (Univ. of Missouri, Columbia). J. Geophys. Res.; 76: 630-4(10 Jan 1971).

A possible explanation of the abnormally high water level in a

XUM

well near the Aardvark detonation, a Nevada Test Site underground nuclear test in tuff, is presented. It suggests that, contrary to the theses of other investigators, mechanical compaction of the saturated and porous zones near the explosion was the most important factor causing the well water level to rise. (L.C.L.)

13112 FISSION TRACK DATING AND URANIUM CONTENTS OF OBSIDIAN. I. Suzuki, Masao (Tokyo Univ.). Dai-4-Ki Kenkyu; 8: 123-30(Dec 1969). (In Japanese).

Obsidian is a volcanic glass which was widely used as an important material for making stone implements and found in archaeological sites all over Japan. As original sources of obsidian are limited to about twenty localities in number, it might be of use to trace the trading area in prehistoric Japan, if the original sources could be determined with regard to obsidian materials found from these archaeological sites. The fundamental experiments were carried out for determining original sources of archaeological obsidian materials by means of the age of rock formation and its uranium concentration of the materials. The results of these experiments together with some results of assays obtained so far on obsidian from several original sources are presented. Obsidian samples from four outcrops in Wada-pass in Central Honshu gave almost the same ages of formation (0.85×10^6 yr) in good accordance with the potassium–argon dates of the same samples. Uranium contents of these samples were also almost the same (6.8 ppM by weight). On the other hand, obsidian samples from Mt. Kirigamine near Wada-pass were clearly different from those of Wada-pass in fission track dates (1.30×10^6 yr) as well as uranium contents (3.2 ppM by weight). (auth) (Japan)

13113 INVESTIGATION OF THE SCATTERED GAMMA SPECTRA IN NUCLEAR GEOPHYSICS APPLICATIONS. Czubek, Jan Andrzej. Zesz. Nauk. Akad. Gorn.-Hutn. Krakow., Rozpr.; No. 208, 97-107(1969). (In Polish).

Research on scattered gamma spectra in rock media, performed at the Nuclear Geophysics Laboratory of the Institute of Nuclear Techniques in Cracow, are presented. This work was done for natural gamma ray logging, natural selective gamma ray logging, bulk density measurements by the gamma–gamma method, and for selective gamma–gamma logging. In each case the final information about the method of interest was obtained by the treatment of the scattered gamma ray spectra in the rock media considered. (auth)

13114 EVOLUTION OF THE CHEMICAL COMPOSITION OF THE ROCKS IN THE SHIELDS AND SEDIMENT COVER OF THE RUSSIAN AND NORTH AMERICAN PLATFORMS. Ronov, A. B.; Migdisov, A. A. (Inst. of Geochemistry and Analytical Chemistry, Moscow). Geochem. Int. (Engl. Transl.); 7: 294-325(Nov 1970).

Translated from Geokhimiya; No. 3, 403-38(Mar-Apr 1970).

Over 8000 analyses are used to compare the mean compositions over geological time. It is found that the mean composition of the granite layer is almost the same and the sediment layer is surprisingly similar between the different continents. Major stages are traced in the evolution of the chemical composition of the sediments from the Archean onwards, and it is found that common trends are involved, which are closely related to organic evolution and compositional change in the outer layers of the Earth. (71 references) (auth)

13115 PHYSICOCHEMICAL MODEL FOR ELEMENT SEPARATION DURING MANTLE DIFFERENTIATION. Vinogradov, A. P.; Yaroshevskii, A. A.; Il'in, N. P. (Inst. of Geochemistry and Analytical Chemistry, Moscow). Geochem. Int. (Engl. Transl.); 7: 283-93(Nov 1970).

Translated from Geokhimiya; No. 3, 389-402(Mar-Apr 1970).

On the basis of published data and new results of element separation during zone melting of chondrite silicate phase, a model of phase equilibria in silicate systems at high pressures is presented. The model is based on incongruent melting of metasilicates, with accumulation of silica and most of the lithophilic elements in the liquid, the latter forming compounds with the silica or dissolving in the liquid to lower the liquidus temperature. The dynamics of element separation during zone melting of the mantle and the physicochemical concepts on which the model is based are discussed. (auth)

13116 CONCENTRATION OF URANIUM BY LIVING AND DEAD PEAT-FORMING PLANTS. Lopatkina, A. P.; Komarov, V. S.; Sergeev, A. N.; Andreev, A. G. Geochem. Int. (Engl. Transl.); 7: 277-82(Nov 1970).

Translated from Geokhimiya; No. 3, 372-7(Mar-Apr 1970).

Exposed parts of plants, hydromorphic soils, and water from a marshy floodplain of a small stream flowing on mesozoic granites were analyzed for uranium. Water, peat, various mosses, and dead plants from several bogs were also analyzed. It was found that in the humid zone the exposed parts of trees and grasses absorb one tenth to one thousandth of the uranium absorbed by the hydromorphic soil in which they grow, regardless of the concentration of uranium in ground waters. It is concluded that these plants cannot be the source of the high concentrations of uranium in peat. The roots of higher plants, plant debris, and the humus of hydromorphic soils absorb much more uranium if they are in direct contact with water. The lower plants, mosses, etc. absorb considerable amounts of uranium, the amount absorbed depending on the concentration of the element in the ground waters and probably, on the area of contact between plant tissues and water. (J.G.B.)

Meteorology

Refer also to abstracts 12965, 13078–13080, 13103, 13136, 13138, 13144, 13145, 13322, 13323, and 13430.

13117 (AD–711532) EXPERIMENTAL COMPARISON OF FALLOUT FIELD SIMULATION TECHNIQUES. Maloney, Joseph C.; Meredith, John L. (Ballistic Research Labs., Aberdeen Proving Ground, Md.). Jul 1970. 130p. (BRL–1485). NTIS.

Activities are reported in a program to compare directly the results obtained from using the techniques and isotopes employed in experimental fallout field simulation and thus, to determine ground effects factors and dose-distance relationships that would affect decontamination operations. In the experiment the cumulative fractions of the infinite field exposure as a function of distance is the same for the circulating point source and spread source systems. Therefore each system can be used to experimental advantage, the results compared directly and applied to operational requirements in fallout fields. The air lift point source system with cobalt or cesium sources is an adequate technique for simulating fallout fields only for heights of detection above 25 feet. Ground roughness affects the exposure fields from circulating point and distributed particulate sources. For the Camp McCoy test area these factors are 0.90 for cobalt circulating point sources, 0.85 for cesium circulating point sources, and 0.57 for lanthanum tagged particles at 3 ft elevation. (auth) (USGRDR)

13118 (COO–414-17) DETAILED CHARACTERIZATION OF SOIL AND VEGETATION ON SELECTED SITES. Technical Progress Report, March 1, 1970–November 26, 1970. Haghiri, F. (Ohio Agricultural Research and Development Center, Wooster). 27 Nov 1970. Contract AT(11-1)-414. 45p. Dep. NTIS.

Data on the effects of soil and crop management practices on the fate of strontium-90 in soil, plant and run off and leachate water are presented. The percent of the initial application of strontium-90 removed by run off (water + sediment) decreased while its loss by leachate water increased with time over an eight year period. During this period, the net rates of percent strontium-90 removed by run off from continuous corn and gravel mulch plots diminished at a slower rate as compared with other treatments. The net rate of percent strontium-90 removed by leachate water from gravel mulch plots was considerably greater than other treatments. The total fractions (%) of applied strontium-90 removed by runoff, leachate and plant uptake over an eight year period were 18.37, 17.02, 16.40, 13.38, and 11.20 for gravel mulch rotation (low lime), continuous corn, rotation (high lime) and permanent grass, respectively. The effect of burning of vegetation containing strontium-90 on the availability of this isotope to plants from soils with different chemical properties was studied. The uptake of ^{90}Sr (^{90}Y) by oats was significantly higher from soils spiked with ashed plant materials containing ^{90}Sr (^{90}Y) than from soils spiked with non-ashed plant tissue containing ^{90}Sr (^{90}Y). The uptake of this isotope by the test plants was markedly affected by soil pH. A field study on the vertical transfer of ^{90}Sr in high clay content soils suggested that some fractions of the fallout strontium-90 on the soil surface can be washed into the cracks, which are formed under drought conditions, by intensive sheet erosion. Isotopic dilution of the ^{90}Sr labeled non-displaceable Sr in a peat soil with more unlabeled Sr in an amount approximately equivalent to the non-displaceable Sr was completed. The dilution was completed rapidly (1 hour) with approximately equal amounts of Sr from the two sources being present in the final solution. The rapid dulution would support a hypothesis of selective bonding sites for Sr being responsible for the non-displaceable fraction of adsorbed Sr. Ashing of corn and black alder plant material at 200, 300, and 400°C has been completed. The weights of the residues were greatest for alder at 200°C and greatest for corn at 400°C indicating that the alder had more materials stable at 200°C while corn had more materials stable at 400°C. The dark colored organic material from the ash at 400°C was classified as neutral compounds by solubility test. An IR spectra indicated hydroxyls are a major functional group. The ^{90}Sr labeled plant material will be produced by the same method used to produce the plants containing unlabeled Sr. The material from the anode compartment in the Bradfield cell analysis of run-off water was found to contain a water insoluble, HCl soluble material with which the $^{90}Sr^{++}$ tended to be associated. An IR spectra of this material indicates the presence of NH_2 groups and some carbonyl groups. The use of KCl, KSCN, K_2SO_4, or KH_2PO_4 to K^+ saturate peat samples before equilibration with Sr had no major effect of the anion on the adsorption or retention of Sr by the peat when equilibrated with NH_4OA_c and $Cu(OA_c)_2$ as in previous adsorption studies. (auth)

13119 (JAERI-Memo-4175) ENVIRONMENTAL MONITORING AT JAERI, TOKAI IN 1969. (Japan Atomic Energy Research Inst., Tokyo). Oct 1970. 34p. Dep. NTIS (U. S. Sales Only).

The environmental monitoring program at JAERI, Tokai consists of monitoring of the gamma exposure in the environment, measurement of the radioactivity in the environmental materials, and meteorological and oceanographic observations. Fallout nuclides produced by nuclear detonation tests were also investigated. The results of the monitoring performed in 1969 are summarized except for the meteorologic and oceanographic observations. No abnormal radioactivity was found in the environment in association with the discharge of radioactive materials from the facilities of the Institute in 1969. It should be noted that the average concentrations in air of relatively short-lived radionuclides were two to three times as high as those in the preceding year, although the total amount of radioactivity in fallout remained on the same level. This fact suggests that new injections of nuclides into the atmosphere were brought about by the recent nuclear tests. (auth) (Japan)

13120 (NP-18638) TRITIUM CONTENT MEASUREMENTS ON A VARIETY OF WATER SAMPLES. Technical Memorandum 31/1969. Hughes, M. W. (Commonwealth Scientific and Industrial Research Organization, Adelaide (Australia). Div. of Soils). 17 Sep 1969. 10p. Dep. NTIS (U. S. Sales Only).

Tabulations of tritium content of rainfall for various centers in Australia (New South Wales, Western Australia, South Australia) are given for 1968 with some results for the 1967 and 1969. Some figures for surface and sub-surface water samples around the same period are also given. (Australia)

13121 (TID-25314) ATMOSPHERIC TRANSPORT PROCESSES. PART II. CHEMICAL TRACERS. Atmospheric Science Paper No. 133. Reiter, Elmar R. (Colorado State Univ., Fort Collins. Dept. of Atmospheric Science). Jan 1971. 382p. Dep. NTIS.

Work done by various investigators dealing with the distribution of chemical tracers in the atmosphere is reviewed in detail in order to provide information on global transport processes in the atmosphere. The chemical tracers discussed include CO_2, O, O_3, water vapor, and others. (L.C.L.)

13122 DATA. SECTION III. AIR AND DEPOSITION. Radiol. Health Data Rep.; 11: 467-72(Sep 1970).

Surveillance data on radioactivity in airborne particulates and precipitation were collected by the U. S. Public Health Service, the Canadian Department of National Health and Welfare, the Mexican Commission of Nuclear Energy, and the Pan American Health Organization. Tables are presented to show monthly average gross beta radioactivity in surface air particulates and deposition by precipitation during May, 1970, in the United States, Canada, and South America. (H.L.W.)

13123 DIFFUSIONAL DEPOSITION FROM A FLUID FLOWING RADIALLY BETWEEN CONCENTRIC, PARALLEL, CIRCULAR PLATES. Mercer, T. T. (Univ. of Rochester, N. Y.); Mercer, Robert L. J. Aerosol Sci.; 1: 279-85(Nov 1970).

A theoretical study was made of the diffusional losses of particles from a fluid flowing radially inward between concentric, parallel, circular plates of radius, R_0. The relative number of particles remaining in the fluid at a distance, r, from the axis of the plates is $(N/N_0) = 0.9104\ e^{-2.8278\gamma} + 0.0531\ e^{-32.147\gamma} + 0.0153\ e^{-93.475\gamma} + 0.0068\ e^{-186.805\gamma} + \ldots$ where $\gamma = 4\pi D(R_0^2 - r^2)/3\ Qh$, D is the diffusion coefficient of the particles, Q is the volumetric flow rate, and 2h is the separation between the plates. The practical application of the system is discussed. The same equation applies to parallel flow through a duct of rectangular cross-section if $\gamma = 4DBl/3Qh$, where B and I are respectively the duct width and length. It is more accurate than equations now in use to describe this process. (auth)

13124 TRANSFER OF ^{85}Kr FROM AIR TO GRASS. Voilleque, Paul G.; Adams, Donald R.; Echo, John B. (Atomic Energy Commission, Idaho Falls, Idaho). Health Phys.; 19: 835(Dec 1970).

An experiment was performed to determine the transfer velocity, V_d, for ^{85}Kr from air to grass (V_d = ^{85}Kr transferred per unit horizontal area of grass/time-integrated air concentration) in a laboratory exposure chamber with 69% humidity and no wind simulation. V_d for ^{85}Kr was found to be 2.3×10^{-11} cm/sec and was compared with V_d for ^{131}I which was found to be 7.2 ± 0.9 cm/sec measured under the same conditions. Reasons for the relatively high value of V_d for ^{131}I were considered. As these were equally applicable to the ^{85}Kr measurement, it was believed that a value of 10^{-10} cm/sec for V_d (^{85}Kr) could be used as a conservative upper limit. (UK)

Mineralogy and Exploration

13125 (RME-160) PRELIMINARY RECONNAISSANCE FOR URANIUM IN NEW MEXICO, 1950 TO 1958. (Grand Junction Office (AEC), Colo.). Nov 1970. 223p. Dep. GPO $1.75.

Preliminary information related to uranium deposits in 26 counties in New Mexico is presented. For each area examined data are given on the location of the deposit, property owner, date examined, mining history, measured radioactivity, and the geology, mineralogy, and topography of the deposit. (L.C.L.)

13126 ENERGY PRODUCERS. MARY KATHLEEN URANIUM LIMITED. Willett, K. (Queensland Dept. of Mines, Brisbane). Queensland Govt. Mining J.; 71: 207-10(May 1970).

An account of the economic history of Mary Kathleen Uranium Ltd., is given, covering the period from its formation in August 1954 to the annual meeting of April 1970. Uranium ore reserves announced in November 1969 were: indicated ore above R. L. 550 and within the boundaries of the extended open cut design—7,037,000 short tons of ore at an average grade of 2.48 lbs U_3O_8/short ton; possible ore delineated by diamond drilling above R. L. 200 and outside the boundaries of the extended opencut design—2,052,000 short tons of ore at an average grade of 1.91 lbs U_3O_8/short ton; and stockpiled ore—480,000 short tons at an average grade of 1.22 lbs U_3O_8/short ton. These grades allow for dilution in mining. The project was placed on a care and maintenance basis in December 1963 and its re-implementation is dependent on the writing of suitable sales contracts. These grades are expected to be available for sales from 1974 onwards and some spot sales are anticipated before then. (Australia)

13127 ROLES OF THE GEOLOGICAL SURVEY OF CANADA IN FORMER URANIUM PROGRAMS. Lang, A. H. (Dept. of Energy, Mines, and Resources, Ottawa). CIM (Can. Mining Met.) Bull.; 62: 1210-8(Nov 1969).

A review of events that led to the discovery and development of past and present sources of uranium in Canada is presented in the belief that knowledge of approaches that were successful and unsuccessful could benefit present and future searches for additional ores. The history of Canadian discoveries is traced from the time when uranium deposits were scientific curiosities, through the periods when they were in demand; first for their contained radium, then for military uses of uranium and later when demands for peaceful purposes caused a boom in prospecting the production. Most mines evolved from a series of events commonly occurring over long periods and forming complex "chains" or "patterns" in mineral exploration. The most critical events involved prospectors and companies, but supporting incidents generally contributed to the successes. The Geological Survey of Canada was responsible for a wide variety of such "assists." An indication of the value of the work of the Geological Survey is suggested by comparing the total cost of the Survey's work with the estimated value of the ore in the most productive uranium district—Elliot Lake—where the Survey assisted in several ways. Appropriations for the Survey from 1842 to 1968, for all parts of Canada and for any purpose, totaled $96 million. The gross value of production and reserves at Elliot Lake is estimated by the writer to be at least $5.5 billion. On that basis, the total cost of the Survey is about 1.8 percent of the value of this one district—and many other districts producing uranium or other commodities have benefited from Survey data. (auth) (Canada)

13128 PHASE TRANSFORMATIONS OF BRANNERITE DURING HEATING. Krivokoneva, G. K. Dokl. Akad. Nauk SSSR; 194: 1168-71(11 Oct 1970). (In Russian).

Chemical analyses of the brannerite samples gave a content of about 33% TiO_2, 35% UO_2, 14.5% UO_3 and small amounts of SiO_2, Al_2O_3, Fe_2O_3, MgO and CaO. In the natural state the samples showed no structure, but became crystalline on heating. On heating in air, crystallization starts at about 600°C with formation of the brannerite structure. X ray analysis results showed that at temperatures above 700°C the following phases crystallize out

XUM

along with brannerite: a small amount of U_3O_8 at 800°C; U_3O_8 and an unknown phase X at 900°C; phase X at 1000°C, and U_3O_8 at 1100 and 1200°C. These phase transformations are due to oxidation and reduction of uranium in the mineral. Oxidation of uranium takes place up to 900°C, while reduction of uranium sets in above 900°C. Results of the Debyegram analyses phase X showed that the crystal structure of this phase is a derivative of the $U_3O_8-UTa_2O_8$ show that the crystals have rhombic symmetry, and are characterized by the following cell parameters: a = 6.380, b = 7.415, and c = 11.77. Apparently phase X is the compound $U^{6+}Ti_2O_7$. The occurrence of the phase transformations is not affected by the ratio of UO_2 to UO_3 in the initial sample. (TTT)

Oceanography

Refer also to abstract 13103.

Seismology

13129 (AD–713521) FAR-FIELD CHARACTERISTICS OF GROUND SHOCK INDUCED BY EXPLOSIONS. Drake, J. L.; Sakurai, A. (Army Engineer Waterways Experiment Station, Vicksburg, Miss.). 1970. 9p. NTIS.

General formulas for the ground motions from an explosion source were derived and their results compared with high explosive and nuclear weapons test data. The comparisons show reasonably good agreement may be obtained by using a simple elastic description for the earth as long as the explosion is properly modeled. (auth (USGRDR)

13130 (UCRL–13329(Pt.2)) RESPONSE OF EARTH DAMS TO SEISMIC DISTURBANCES. PART II. DIGITAL COMPUTER CODES. Keightley, W. O. (Montana State Univ., Bozeman. Engineering Research Labs.). Aug 1970. 101p. Dep. NTIS.

Digital computer codes, in FORTRAN, used to derive ground acceleration from seismometer records, to assemble stiffness and mass matrices of plane strain and three dimensional finite element assemblages representing earth dams, to find the natural frequencies and mode shapes of the assemblages, and to compute and plot the acceleration response of the assemblages to foundation accelerations are presented. The codes were used to compute the response of Fort Peck Dam to base motions caused by a distant underground explosion. Only a plane strain representation was used because computer storage was inadequate to permit a three-dimensional representation. Two different finite element assemblages yielded almost the same response. Using rigid base excitation and 10% critical damping, the codes predicted maximum accelerations of several points on the dam with good accuracy, but they underestimated by 50% the greatest response, which was vertical acceleration approximately midway between the crest and the toe. A vertical acceleration, almost as large, closer to the toe, was satisfactorily predicted. Except for vertical acceleration near the toe, the envelopes of computed response did not agree well with the observations. The effects of using different assumptions for base motion and degree of critical damping in the computations are discussed. More tests of the codes and measured data on real structures must be made before their range of usefulness can be established. (L.C.L.)

ENGINEERING

Nuclear Explosions

Refer also to abstracts 12951, 13102, 13111, 13129, 13130, 13322, 13323, 13328, 13430, and 13445.

13131 (AAEC/LIB/BIB-255) PHYSICS OF THE DYNAMIC GROWTH OF MUSHROOM CLOUDS, ASSOCIATED WITH NUCLEAR EXPLOSIONS. A Bibliography. Newland, E. A. (comp.) (Australian Atomic Energy Commission Research Establishment, Lucas Heights). Sep 1970. 8p. Dep. NTIS (U. S. Sales Only).

Forty five references are listed, covering the period 1950 to 1969. Arrangement is chronologically by year and alphabetically by author within each year. Where applicable, reference is made to an abstract for each item. (Australia)

13132 (AD-711021) ASSESSMENT OF NUCLEAR WEAPON REQUIREMENTS FOR ASSURED DESTRUCTION. Final Report. Miller, Carl F. (URS Research Co., San Mateo, Calif.). Feb 1970. Contract DAHC20-69-C-0142. 144p. (URS-757-6). NTIS.

The results of rudimentary nuclear-war-damage-assessment calculations are presented as part of an investigation of the size and composition of nuclear forces that would be required for the "assured destruction" of the entire population of the United States. The latter result would be a reduced version of the simplistic view of the consequences of an exchange of nuclear explosions between the Soviet Union and the United States in which the total destruction of mankind is anticipated. The calculational results indicate that the total megatonnage required for a given level of population coverage by a given minimum overpressure would be much less if (many) low yield weapons were used instead of (few) high yield weapons. The calculational results also show that, if the population were sheltered in concrete buildings with a protection factor of 130 or more, the extent or coverage of the lethal radiological hazard from surface burst 100-kt weapons would be reduced to the assured lethal coverage of air burst 100-kt weapons. A direct connection exists between the civil defense capability to provide the necessary fallout protection and the capability of the U.S. arsenal to provide deterrence since both are apparently related to the size of the nuclear force that the Soviet Union may deploy over a period of time. This conclusion must be true as long as the nation's political leaders, newsmen, scientists, and even military leaders discuss the consequences of nuclear war in terms of the destruction of mankind. Rejection of this illusion is necessary before questions of societal recovery from a nuclear war can be given proper consideration. (auth) (USGRDR)

13133 (AD-711861) CRATERING IN GREENLAND ICECAP SNOW. Final Report. Conway, John A.; Meyer, John W. (Army Engineer Waterways Experiment Station, Vicksburg, Miss.). Jul 1970. 37p. NTIS.

Predicting cratering effects from explosions in various media and with various charge geometries is a primary purpose of nuclear weapons research. Crater formation resulting from high-explosive surface bursts in a snow medium are examined. The test program for which crater data were obtained consisted of nine 256-pound TNT charges, one 500-pound C-4 charge, one 1,860-pound C-4 charge, and two 4,180-pound C-4 charges. All were surface bursts fired on the Greenland icecap. Results show that craters produced in snow are larger than those produced in other media, presumably due to greater vaporization and compaction of material. These craters have a characteristic wide, shallow appearance; it is believed that pseudoelastic rebound is the mechanism that diminishes crater depth. Analysis of the crater data shows that scaling exponents for craters in snow are lower than cube-root or other scaling exponents generally used for craters in soil or rock media. (auth) (USGRDR)

13134 (AD-713418) EVALUATION OF SYSTEMS OF FIRE DEVELOPMENT. Final Report. Weisbecker, Leo W.; Lee, Hong (Stanford Research Inst., Menlo Park, Calif.). Aug 1970. Contract DAHC20-67-C-0116. 88p. NTIS.

Three fire spread models recently developed for the Office of Civil Defense are compared for utility, accuracy, and efficiency when applied to civil defense fire information requirements. The fire spread modeling was essentially limited to the radiation fire spread mechanism. All three models provided procedures for calculating fire spread under a limited range of conditions, but all suffered to some degree from inadequate modeling of urban configurations and the fire parameters associated with urban structures that significantly affect fire spread mechanisms. (auth) (USGRDR)

13135 (AD-713574) CONCEPT OF ROW CRATER ENHANCEMENT. Redpath, Bruce B. (Army Engineer Nuclear Cratering Group, Livermore, Calif.). 1970. 15p. NTIS.

Linear craters formed by the simultaneous detonation of a row of buried explosives will probably have a wider application than single charges in the explosive excavation of engineering structures such as canals, channels and harbors. Most cratering experience to date has been with single charges, and an analytical procedure for the design of a row of charges to excavate a crater with a specified configuration has been lacking. There are no digital computer codes having direct application to a row of charges as there are for single charges. A simple relationship is derived which can be used to design row charges with some assurance of achieving the desired result and with considerable flexibility in the choice of explosive yield of the individual charges. (auth) (USGRDR)

13136 (ARLV-351-15) WEATHER FOR INDUSTRIAL NUCLEAR EXPLOSIONS. Allen, Philip W. (Environmental Science Services Administration, Las Vegas, Nev. Air Resources Lab.). [1970]. 23p. (CONF-710103-1). Dep. NTIS.

From 51st Annual Meeting of the American Meteorological Society, San Francisco, Calif.

Nuclear explosives are a major energy source and, as man's use of natural resources progresses toward lower-grade minerals and ores, and he engages in larger construction efforts, these large detonations will become a more necessary and more frequent mining and engineering tool. The risk of an accidental release of radioactivity to the atmosphere is very low. Some minor releases may be planned, but the potential impact of any such release is very great, so that extensive safety precautions will be taken, providing for the protection of people in the path of any such radioactive cloud. An essential part of this capability is the knowledge of such paths well ahead of the detonations, and this involves predictions of winds, trajectories, turbulence, precipitation, and related transport phenomena. The philosophy of weather controls on the scheduling of detonations is explored, the preparations and procedures involved in such a weather service are outlined, and the meteorological problems encountered in two recent detonations for the stimulation of natural gas wells near Farmington, New Mexico, and Rulison, Colorado, are described. (auth)

13137 (NP-18659) LEGAL FRAMEWORK FOR INDUSTRIAL PLOWSHARE APPLICATIONS. (Atomic Industrial Forum, Inc., New York). May 1969. 16p. Atomic Industrial Forum, Inc. $6.00.

The background, current status, and critical analysis of proposed legislation (H.R. 18448 and S.3783) which would authorize the AEC to provide nuclear explosion services to U. S. industry and foreign users, at reasonable compensation to the government, are presented. From the analytical study it was concluded that the proposed legislation constitutes a flexible and workable charter for progress in the industrial applications of Plowshare technology and that matters of concern which are not covered in the proposed legislation can best be dealt with administratively until more experience is gained. (L.C.L.)

13138 PARTICLE SIZE DISTRIBUTION IN CLOUDS FROM NUCLEAR AIRBURSTS. Nathans, M. W.; Thews, R.; Holland, W. D.; Benson, P. A. (Electronics Corp., Richmond, Calif.). J. Geophys. Res.; 75: 7559-72(20 Dec 1970).

The theory of self-preserving size distributions of Friedlander and Wang has been applied to particle formation after nuclear air bursts. The parameters at the start of coagulation are those derived from nucleation theory as applied by Stewart and by Edvarson. Brownian motion with and without slip correction has been considered. The results are compared with the log normal distribution having a logarithmic standard deviation of 2.0 such that both distributions have the same value of the geometric mean diameter. At constant mass $\langle a \rangle$ varies slowly with yield, namely, it varies as $W^{-0.23}$. Contours of constant $\langle a \rangle$ as a function of mass and yield have been calculated. The results are compared with size distributions measured on cap and stem samples from eight air bursts of the 1962 Dominic series. (auth)

Facilities and Equipment

Refer also to abstracts 13123, 13181, 13628, 13630, and 13653.

XUM

13139 (AERE-R-4852) EXPERIMENTAL STUDY OF SPOUTING BEDS OF SPHERES. Charlton, B. G.; Morris, J. B.; Williams, G. H. (Atomic Energy Research Establishment, Harwell (England)). Jun 1965. 35p. Dep. NTIS (U. S. Sales Only).

The spouted bed behavior of systems of spheres was studied in a 3-in. diameter vessel fitted with a conical base section. The particle size varied from 0.050 to 0.64 cm and density varied from 1.3 to 11.0 g/cm^3. Air, helium and carbon dioxide at room temperature and pressure were used, the gas being admitted, through a single orifice in the size range 0.13 to 0.95 cm in diameter. It was found that four main types of pressure-drop/gas-flowrate curve could be obtained, starting from the normal fluidized condition and going through two types of spouted bed condition to a slugging bed. Progression through this series could be achieved by increasing the sphere size, the gas density, the particle density, and the bed volume, or by reducing the size of the gas inlet orifice. The minimum spouting velocity for gases having a viscosity of about 10^{-4} poise could be approximately correlated by an equation of the form: $U_{msp} = K \times V^a \times \rho^b \times \rho_s^c \times d_s^e \times d_i^f$ where a, b, c, e and f are constants. However, a, b, and f appeared to be functions of the system variables. (auth) (UK)

13140 (BMBW-FBK-70-26) INFLUENCE OF DIMENSIONS OF GAS FLUIDIZED BEDS ON GAS MIXING. Lentzsch, B. (Technische Hochschule, Hanover (West Germany). Institut fuer Technische Chemie). Nov 1970. 80p. (In German). Dep. NTIS (U. S. Sales Only).

The influence of the length and diameter of fluidized bed reactors on gas mixing was investigated at various velocities of the fluidizing gas. Coefficients of axial, radial, and back mixing of the gas were derived by means of a dispersion model. The diameters of the reactors were 19.2, 35.2, and 50.0 cm. The ratio of length to diameter was varied between 25 to 50 and 80 to 20. Quartz sand with an average particle diameter of 162 μm was used as solid material; it was fluidized by air. The intensity of axial mixing increased with the square root of the bed height and approached with increasing bed diameter as well as velocity a limiting value. The intensity of radial and back mixing amounted to 5 to 10% of axial mixing. (auth)

13141 MEASUREMENT OF FILM THICKNESS BY ELECTRON BACKSCATTERING. Levenes, Guy (Societe Industrielle de Combustible Nucleaire, Veurey, France). Energ. Nucl. (Paris); 12: 417-25(Sep-Oct 1970). (In French).

Electron backscattering is used for thickness measurements in conjunction with plated films on foils or heavier gage sheets. Electron backscattering increases with the thickness of the plated film until a saturation condition is reached; it is proportional to the atomic number of the diffusing material. Using suitably designed gages, films of thicknesses varying between 0.01 and 100 μm deposited on the outer or inner surfaces of hollow structures of irregular shape, can be measured. (auth) (France)

13142 FACILITY FOR IN-PILE CREEP EXPERIMENTS ON CLADDING TUBES UNDER THERMAL AND STRESS CYCLING. Schmidt, L.; Will, H. (Kernforschungszentrum, Karlsruhe, Ger.). Nucl. Eng. Design; 14: 109-16(Oct 1970).

The irradiation facility described is for the BR2 Reactor at Mol for use in testing breeder fuel cladding tubes in in-pile creep behavior under thermal and stress cycling. These stresses occur during startup, shutdown, and load changes of the reactor. The facility was designed initially for tests of cladding tube specimens for the sodium-cooled fast breeder. However, by different arrangement of the specimens it is possible also to simulate the operating conditions of the gas and steam cooled breeders, respectively. The different requirements and the details of design, construction and operation of the irradiation facility are outlined. The test specimens can be loaded with gas pressures up to 500 kg/cm^2 at electrically controlled temperatures of up to 900°C. The development of the facility has been based on all the experiences gathered from a similar test device which has been run for some years. The axial temperature distribution in the test specimens was greatly improved. The facility is presently under construction. The in-pile tests are scheduled to be started in the fall of 1971. (auth)

13143 TEST FACILITY FOR SODIUM-HEATED STEAM GENERATORS (CGVS). Milliat, J. P. (Electricite de France, Chatou); Lecocq, P.; Beaufrere, J.; Chanudet, L.; Chauvin, M. Energ. Nucl. (Paris); 12: 397-405(Sep-Oct 1970). (In French).

The CGVS test facility for sodium-heated steam generators for future fast breeder reactor power stations is described. It comprises two main circuits: a sodium circuit supplying heat to the steam generator under test, and a water and steam circuit designed to extract and dissipate the heat. With its 50 MW thermal power output the CGVS facility can be used both to reproduce the full range of operating conditions in a nuclear power plant and to endurance-test the steam generators over prolonged periods of time. (auth) (France)

13144 SOME COMMENTS ON THE PRODUCTION AND MEASUREMENT OF SPHERES OF POLYSTYRENE LATEX. Billard, F.; Madelaine, G.; Delhaye, J. (CEA-CEN, Fontenay-aux-Roses, France). J. Aerosol Sci.; 1: 357-67(Nov 1970). (In French).

The main results obtained when dispersing spheres of polystyrene latex are given. The ratio of particles to latex suspension, under different conditions of generation, was evaluated by means of a condensation nucleus counter and a Royco spectrometer. The retention of spheres of latex by diffusion batteries and systems of channels is affected by the electric charge on the particles. Neutralization of the charge and making the particles radioactive results in the formation of a number of parasitic particles. (auth)

13145 NEW METHOD FOR THE GENERATION OF AEROSOLS OF INSOLUBLE PARTICLES. Kanapilly, G. M.; Raabe, O. G.; Newton, G. J. (Lovelace Foundation for Medical Education and Research, Albuquerque, N. Mex.). J. Aerosol Sci.; 1: 313-23 (Nov 1970).

A method for the controlled generation of spherical aerosol particles of insoluble metal oxides has been developed. The method consists of nebulizing a solution (or suspension) of the chosen metal in chelated or other form, drying the droplets, passing the aerosol through a high temperature heating column to produce the spherical oxide particles, and cooling the aerosol with the addition of diluting air. This procedure provides a continuous source of insoluble aerosols suitable for animal inhalation exposures or other experimental uses. The size distribution of an aerosol produced by this method depends upon the distribution of the nebulized droplets. This technique has been used with a Fulwyler Droplet Generator to produce monodisperse aerosols. The physical and chemical nature of aerosols of zirconium and lanthanum compounds generated by this method were studied. Physical characteristics were ascertained by electron-microscopic observations, particle density measurements, and aerodynamic sampling; and chemical properties by tracer and instrumental techniques. (auth)

13146 CURIUM PROCESS EQUIPMENT (8 Nov 1969) (Engineering Materials). (Savannah River Operations Office (AEC), Aiken, S. C.). (CAPE-2047).
36 drawings.

Equipment used in processing solutions containing Cm, Am, Cf, and fission products to produce CmO$_2$ is described. The equipment includes sixteen-stage mixer-settlers, solvent washers, precipitators, filters and a calciner. The arrangement of the caves used in the process is also described. The mixer-settler is a sealed-down Jumbo type which is described in CAPE-676. A four-bladed paddle is used instead of the volute-vaned Jumbo impeller. Each stage consists of the following sections: interface, weir, aqueous inlet, solvent inlet, mixing and settling. The mixer-settlers are used in the solvent extraction cycles in which nitric acid solutions of Cm, Am, and fission products are converted to a chloride solution. Solvent washers permit reuse of the solvent used in the solvent extraction steps. The spent solvent and wash solution are fed to an axial mixing compartment with a residence time of 2 to 3 min. The mixed dispersion flows over the circular weir at the top of the settling section. The volume ratio of the separated organic and aqueous phases is controlled by adjusting the height of the aqueous weir. Residence time of the organic phase is ~20 min. After separation from Cf and fission products, Cm and Am are separated from each other by precipitation and filtration. Precipitators consist of a stainless-steel vessel with a 333 rpm agitator driven by an air motor, cooling jacket, gas purge, liquid level bubbler, off-gas exhaust, thermocouple, and sparge. Filters have a removal Pt-lined filter and a Pt frit in a stainless steel housing. The calciner used in preparing the CmO$_2$ and AmO$_2$ has a 130 W heater around the central cavity which holds the Pt-filter boat. Insulation consists of two layers of ½ in. Fiberfrax. An air-cooled jacket between the insulation and the heaters shortens cooling time. A thermocouple monitors and controls the temperature and process material during calcination. Feed and product evaporators are 75-liter cylindrical Ta tanks fitted with condensers for removal of the distillate. Waste evaporators are similar but larger (150 and 300 liters). Electric immersion heaters heat the evaporators. For CmO$_2$ shipping cask see CAPE-2046. (For details see TID-4100 Suppl. 62) (see also NSA 24: 31341.) (F.S.)

13147 EVALUATE YOUR COST OF COOLING STEAM TURBINES. Hauser, L. G. Elec. Light Power (Boston); 49: No. 1, 32-4(Jan 1971).

Guidelines for evaluating and comparing the cost of power plant

XUM

cooling systems are presented. Cooling requirements for fossil-fueled and nuclear power plants are compared. A method for calculating the approximate water loss for both types of plants is illustrated. Tabulated data on the capital costs for various methods of cooling water supply, on increases in power generation cost due to costs of cooling water supply, and on the total economic impact of cooling water supply on plant location are presented using a 1000 MW(e) nuclear plant as an example. It is concluded that, in the siting of power plants, all the variables affecting cooling costs must be carefully considered and that evaluating the alternative can result in considerable savings to a utility. (L.C.L.)

13148 RADIOACTIVE TRACERS TEST NUCLEAR STEAM TURBINES EASIER, BETTER. Cotton, K. C.; Holloway, J. H.; Gilbert, R. S.; Herzog, W. G.; Morris, F. S. Elec. Light Power (Boston); 49: No. 1, 36-8(Jan 1971).

Feasibility tests were conducted on a radioactive tracer technique for determining the enthalpy of wet steam in nuclear turbines. Careful consideration of all the requirements related to the tracer resulted in the selection of ^{24}Na. The instrumentation, equipment, injection method, and sampling and counting procedures are described. It was concluded that the ^{24}Na injection method results in the smallest error possible in effectiveness of moisture removal, and that use of this tracer technique can improve the accuracy and reduce the cost of enthalpy tests on steam turbines operating in nuclear power plants. (L.C.L.)

Heat Transfer and Fluid Flow

Refer also to abstracts 13123, 13139, 13148, 13167, 13168, 13176, 13630, 15213, 15363, 15370, and 15382.

13149 (EUR-4561) HEAT TRANSFER COEFFICIENT AS A FUNCTION OF STEAM QUALITY FOR HIGH-PRESSURE ONCE THROUGH FLOW BOILING, WITH DETERMINATION OF THE TRANSITION POINTS BETWEEN THE REGIONS OF PARTICULAR HEAT TRANSFER. Nobel, L. (European Atomic Energy Community, Ispra (Italy). Joint Nuclear Research Center). Nov 1970. 70p. Dep. NTIS (U. S. Sales Only). EUR FF 11,-.

In once-through steam generators, the water enters the generator at a temperature far below the saturation temperature and leaves it as superheated steam; heat transfer taking place according to different mechanisms, each of which is active over a limited length of the tubes. As far as the present state of knowledge permits, the heat transfer coefficient for a particular heat transfer region is determined analytically as a function of the mathematical steam quality X, for different heat and mass fluxes and pressures between 170 and 210 bar. Also, for X values indicating the transition between the different regions of heat transfer, equations have been set up as functions of the same parameters. The theoretical background of these equations differs in some cases from the actual theories. One of the most unconventional approaches to the problem is the assumption that the pipe length over which film boiling takes place can be determined by using an analogy with a water-jet-gas-pump aggregate. This method indeed seems to give a useful correlation equation. (auth)

13150 (GEAP-10253) TWO-PHASE FLOW AND HEAT TRANSFER IN MULTIROD GEOMETRIES. Nineteenth Quarterly Progress Report, April 1-June 30, 1970. (General Electric Co., San Jose, Calif. Atomic Power Equipment Dept.). Jul 1970. Contract AT(04-3)-189. 40p. Dep. NTIS.

Multirod critical heat flux (CHF) data were obtained, using an array of nine uniformly heated rods held in their correct positions in a square channel by means of five grid-type spacers typical of modern water-cooled and moderated power reactors. Five combinations of axial position of heated length in relation to end of channel, and axial position of spacers with respect to end of heated length, were tested at various mass velocities and pressures. The effect on CHF of moving the end of the heated length from a position 2 inches before the end of the channel (test channel No. 4) to a position 3½ feet before the end of the channel (test channel No. 2) was to reduce the CHF at low qualities. The effect on CHF of moving the last spacer from a position just past the end of the heated length (test channel No. 2) to a position just before the end of the heated length (test channel No. 1) was generally to raise the CHF, particularly at low qualities and high flows. The effect on the magnitude of CHF of adding a diversion plate 6 inches past the end of the heated length (test channel No. 2A) was insignificant, but the location of CHF moved from the corner rods to the center rod. The effect on CHF (relative to test channel No. 2) of removing the last spacer (test channel No. 3) was to raise the CHF at low qualities and lower the CHF at high qualities. The presence of the spacer just past the end of the heated length helped CHF at high qualities. At pressures greater than 1000 psia, the CHF decreases as the pressure is increased. This inverse pressure effect is stronger at higher flows. Sixteen-rod results were compared with nine-rod results (test channel No. 4) where, for both the sixteeen-rod and the nine-rod channels, the rods were uniform, the ends of the heated lengths were even with the ends of the chamber, and the axial positions of the spacers were the same. The sixteen-rod points agree well with the nine-rod data at $G = 0.5 \times 10^6$ lb/h-ft^2, but lie above the nine-rod data at $G = 1.0 \times 10^6$ lb/h-ft^2. (auth)

13151 (NP-18642) REFRIGERANT FORCED-CONVECTION CONDENSATION INSIDE HORIZONTAL TUBES. Report No. DSR 72591-71. Bae, Soonhoon; Maulbetsch, John S.; Rohsenow, Warren M. (Massachusetts Inst. of Tech., Cambridge. Engineering Projects Lab.). 1 Dec 1970. 55p.

High vapor velocity condensation inside a tube was studied theoretically. The heat transfer coefficients were calculated by the momentum and heat transfer analogy. The Von Karman universal velocity distribution was applied to the condensate flow. Pressure drop was calculated by the Lockhart-Martinelli method and the Zivi void fraction equation. Experimental data were obtained for the mass velocities from 150,000 to 555,000 lbm/ft^2 hr for R-12 and R-22 condensing in a 0.493" ID 18 ft long test section. The measured heat transfer coefficients agreed with the prediction within 10% except a few points in the very low quality region. (auth)

13152 (SU-326-P-13-5) STUDY OF RADIATION-INDUCED NUCLEATION OF BUBBLES IN SUPERHEATED WATER. Progress Report. Whitehouse, H. T.; Christensen, R. N.; Pilati, D. A.; Connolly, T. J. (Stanford Univ., Calif. Dept. of Mechanical Engineering). 18 Dec 1970. 38p. Dep. NTIS.

Efforts to measure bubble nucleation caused by alpha particles or, more specifically, caused by the products of the ^{10}B(n,α)^{7}Li reaction are described. Whereas the previous fission-fragment measurements required operation of the bubble chamber at pressures up to 500 psi and temperatures to 440°F, the alpha-particle measurements require pressures to 1100 psi and temperatures up to 550°F. These more severe conditions required substantial changes in the system design and some of the system components. Initial experiments to observe bubble nucleation by alpha particles were unsuccessful due to large numbers of background bubbles. The experimental procedure was extended during the period to include high-speed (1000 frames per second) photography of the bubble chamber. The resulting motion pictures led to a more complete understanding of the occurrences during bubble nucleation and growth than had been possible by the previous technique of one still photograph per run. Calculations for bubble nucleation by alpha particles in the light of new "stopping power" or "linear energy transfer" data were carried out and thermodynamic properties of water were studied. It became apparent that deviations in predictions of superheat threshold for bubble formation caused by uncertainties in water surface-tension data exceeded the probable experimental error in the measurements. Better surface-tension data are needed if discrepancies between predictions and measurements are to be adequately explained. (auth)

13153 (ZJE-66) EXPERIMENTAL INVESTIGATION OF FILM HEAT-TRANSFER COEFFICIENT IN THE FUEL ELEMENT SPACERS AREA. Vlcek, J.; Weber, P. (SKODA Concern, Pilsen (Czechoslovakia). Nuclear Power Plant Div.). 1970. 24p. Dep. NTIS (U. S. Sales Only).

Results of heat transfer experiment in annulus with different spacers are reported. Aspects of the problem are reviewed along with descriptions of basic equations, and descriptions of experimental devices; some results are presented. The conclusion is made as to the experimental data utilization and extension for both power design of reactor fuel elements and hot spot factor analyses. (auth)

13154 BEHAVIOR OF LIQUID SODIUM IN A SINUSOIDAL PRESSURE FIELD. Nystrom, R. E.; Hammitt, F. G. (Univ. of Michigan, Ann Arbor). J. Basic Eng.; 92: 671-80(Dec 1970).

Utilizing an ultrasonic vibratory cavitation facility, the onset of cavitation was observed in liquid sodium for different liquid sodium temperatures and at various sinusoidal pressure field frequencies. It was observed that the pressure oscillation required to initiate cavitation decreases linearly as the temperature of the sodium is increased from 500 to 1500°F. For frequencies below 20 kHz the cavitation threshold pressure amplitude is essentially independent of frequency. For frequencies above 20 kHz the cavi-

XUM

tation threshold begins to increase sharply. Using the onset of cavitation data and the saturation temperature-pressure data for liquid sodium, the superheat required to produce nucleate boiling in liquid sodium was calculated. As the saturation temperature of liquid sodium is increased the calculated superheat decreases. For frequencies below 20 kHz the calculated sodium superheat requirements, which are independent of frequency, are in good agreement with steady-state sodium superheat data reported in the literature. (auth)

13155 TWO-DIMENSIONAL CONDUCTION HEAT TRANSFER IN LIQUID-METAL BONDED FAST REACTOR FUEL ELEMENT WITH PELLET AND CANNING ECCENTRICITY. **Wolf, L.; Johannsen, K. (Technische Univ., Berlin). Nucl. Sci. Eng.; 43: 237-9(Feb 1971).**

The design of container-type fast-reactor fuel elements of high thermal performance is strongly affected by the heat transfer between pellet and canning. To demonstrate the effect of possible pellet and canning eccentricities on fuel rod temperatures separately from other circumferential effects, heat-source density as well as heat-transfer coefficient between canning surface and coolant have been taken as constant for calculating typical results. The numerical calculations have been performed by the computer program ECFUEL II for fuel rod temperatures T above the coolant average temperature; characteristic data for LMFBR fuel rods have been used. It was found that the temperature variation increases with increasing pellet eccentricity and nominal gap width. Liquid-metal bonding reduces the temperature variation due to pellet eccentricity. The application of liquid-metal bonding in order to reduce canning temperature variations is more stringent for carbide elements. Because of pellet eccentricity the gap width should be as small as possible regardless of the gap filling used. (J.R.D.)

13156 HEAT TRANSFER AND BOILING DURING FORCED CONVECTION OF SODIUM IN AN INDUCTION-HEATED TUBE. **Schleisiek, Karl (Kernforschungszentrum, Karlsruhe, Ger.). Nucl. Eng. Design; 14: 60-8(Oct 1970).**

A series of forced convection boiling and heat transfer experiments has been performed in the sodium boiling loop (NSK). The test section was an h-f induction-heated Ni-tube of 9 mm inner diameter and 168 mm heated length. The results of the preliminary liquid-phase heat transfer measurements at heat fluxes up to 720 W/cm^2 can be correlated by the equation $Nu = 5.3 + 0.018 \cdot Pe^{0.85}$. The boiling experiments have been performed under the following conditions: heat flux: 170 to 600 W/cm^2, pressure: 0.3 to 1 atm abs, mass flow: 0.06 to 0.12 kg/sec, and inlet subcooling: 85 to 170°C. The incipient boiling wall superheat was between 40 and 125°C. It increased with increasing heat flux and decreased with increasing sodium velocity. In the whole range of parameters the phenomenon observed was violently pulsating boiling with partial discharge and subsequent refilling of the test section and strong oscillations of wall temperature. The course of the boiling process was mainly determined by the liquid phase pressure drop before the test section and the heat flux. At low pressure drops dryout of the test section occurred at heat fluxes of about 250 W/cm^2. At high pressure drop generated by throttling, no dryout could be observed at heat fluxes up to 400 W/cm^2. (auth)

13157 GENERAL RELATION FOR CALCULATING HEAT TRANSFER DURING DEVELOPED BOILING OF ALKALI METALS. **Subbotin, V. I.; Sorokin, D. N.; Kudryavtsev, A. P. At. Energ. (USSR); 29: 29: 45-6(Jul 1970). (In Russian).**

The heat transfer coefficient of liquid metals can be described as a power function of the thermal flux, the pressure, and a constant coefficient depending on the physical properties of the liquid heat transfer medium. The thermal flux is usually taken to the 0.7 or two-thirds power. If the reduced pressure (pressure with respect to the critical pressure) is plotted as a function of K which involves the heat transfer coefficient divided by the thermal flux raised to the two-thirds power and other physical constants, the data for liquid sodium and cesium fall on straight line sections. Equations are given for the heat transfer coefficients below a reduced pressure of 10^{-3} and above a reduced pressure of 10^{-5}. These equations can be used to calculate heat transfer coefficients for potassium, cesium and other alkali metals in the range of reduced pressures from 4×10^{-5} to 2×10^{-2}. (TTT)

13158 DYSYS: A DIGITAL COMPUTER PROGRAM FOR SIMULATION OF GENERAL DYNAMIC PROBLEMS. **Schlechtendahl, E. G. (Kernforschungszentrum, Karlsruhe, Ger.). Nucl. Eng. Design; 14: 104-8(Oct 1970).**

The principles of operation of the digital Dynamic System Simulator DYSYS for analysis of continuous and discontinuous changes of state of a system with up to 500 state variables are described. A brief summary of the conventions for usage are given. The program is applicable to a broad range of problems, including those which require changes in the structure of the equations during the course of a dynamic system simulation. (auth)

13159 THEORETICAL SOLUTIONS FOR LOW-PECLET-NUMBER THERMAL-ENTRY-REGION HEAT TRANSFER IN LAMINAR FLOW THROUGH CONCENTRIC ANNULI. **Hsu, Chia-jung (Brookhaven National Lab., Upton, N. Y.). Int. J. Heat Mass Transfer; 13: 1907-24(Dec 1970).**

Exact temperature solutions and theoretical Nusselt curves, valid for Péclét numbers ranging from 1 to ∞, were obtained for thermal-entry-region heat transfer for laminar flow through concentric annuli, subject to a step jump in wall heat flux at $z = 0$. To allow for the effect of axial conduction, which is significant at low Péclét numbers, the inlet fluid temperature was taken to be uniform at $z = -\infty$, and the first twenty eigenconstants were computed for the adiabatic region ($-\infty < z \leq 0$) and the heated region ($0 \leq z < \infty$), separately. By constructing two sets of orthonormal functions from the non-orthogonal eigenfunctions, the series expansion coefficients were then determined such that both the temperatures and longitudinal temperature gradients for the two regions match at $z = 0$. The temperature solutions corresponding to the limiting case of $N_{Pe} = \infty$ show excellent agreement with results of other work, where the entry-region problem was analysed by neglecting axial conduction. (auth) (UK)

13160 TURBULENT HEAT EXCHANGE AND MASS TRANSFER. **Millionshchikov, M. D. At. Energ. (USSR); 29: 411-16 (Dec 1970). (In Russian).**

The theory of heat and mass transfer in turbulent liquid flow based on the principle of the cumulative effect of molecular and turbulent transfer factors and using concepts of laminar sublayers is described. (R.V.J.)

Isotope Technology

Refer also to abstracts 13148, 13180, 13310, and 13529.

13161 (BNWL-SA-3169) NEUTRON RADIOGRAPHY WITH ^{252}Cf: A PORTABLE CAMERA. **Cason, J. L. (Battelle-Northwest, Richland, Wash. Pacific Northwest Lab.). [1970]. 10p. Dep. NTIS.**

Battelle-Northwest is conducting a research program to determine the usefulness of ^{252}Cf as a source for portable thermal neutron radiography. Emphasis has been on developing a device using ^{252}Cf that could be used for laboratory, hot cell or field radiography. The use of ^{252}Cf for neutron radiography in a portable device has been evaluated both analytically and experimentally. A 268 μgm ^{252}Cf source was used for experimental testing. This source has a neutron yield of 6.4×10^8 neutrons/sec. A first generation portable device which completely contains the ^{252}Cf has been designed and built and is presently being evaluated. Preliminary work included flux measurements and neutron radiographs. (auth)

13162 (JINR-P13-5369) OPTIMIZATION OF ION SOURCE AND ION OPTICAL PARAMETERS OF THE ISOTOPE SEPARATOR IN THE YASNAPP-1-FACILITY. **Piotrowski, A.; Raiko, V. I.; Tyrroff, H. (Joint Inst. for Nuclear Research, Dubna (USSR). Lab. of Nuclear Problems). 1970. 16p. (In Russian). Dep. NTIS (U. S. Sales Only).**

The operating conditions that give the highest possible efficiency and resolving power for an isotope separator of the ISOLDE type are given. A magnetron ion source with end extraction along the magnetic field lines of a cylindrical ion beam and a 4-electrode system for the ion beam formation have been used. By measuring the dependence of the opening angle θ for the ion beam and the resolution power of the mass-lines at the collector for the accelerating voltage $U_\alpha = 25$ kV and $U_\alpha = 40$ kV—on the ion current for various values of the extraction voltage U_e, the distance between the electrodes d and the diameter of the exit hole, it was confirmed that: the highest possible resolving power is to be obtained only for a certain value of the opening angle $\theta = \theta_{opt}$; the absolute value of the resolving power for fixed acceleration voltage U_α depends on the ion current I and increases with increasing U_α or decreasing δ. The behavior of the resolving power on the ion current is explained by the pulsation of the ion current density in the plasma discharge and by the amplification process of these pulsations in the ion beam via the strong dependence θ (I). The absolute value of the resolving power also depends on the ion beam perveance in the vacuum chambers of the machine. The results are used to find the dependence of the opening angle θ on the scale parameters. P contains the most essential ion source and beam forming parameters U_e, d, I, M, θ(P) can be used to find the optimum conditions

XUM

for any kind of ions. The efficiency of the ion source (η) is the highest possible one for the minimum working pressure in the ion source. The absolute value of η decreases with decreasing δ. By opposing the efficiency and resolving power curves for several values U_e and δ as functions of the ion current, the necessary compromise between efficiency and resolution can be obtained. (auth)

13163 (MLM-1652) METALLOGRAPHIC ANALYSIS OF THE SNAP-19B (IRHS) CAPSULE. Kelly, M. D.; Selle, J. E. (Mound Lab., Miamisburg, Ohio). 15 Jul 1969. Contract AT(33-1)-Gen-53. 28p. Dep. NTIS.

Two SNAP-19B heat source capsules, exposed for 130 days in seawater, were given a detailed metallographic examination. The graphite heat shield of one of these capsules was found to be cracked. Seawater penetrated to the Haynes alloy No. 25 inner liner interface, producing a corrosion product and pitting of the cracked capsule. Also a thick deposit containing calcium, silicon, magnesium, sodium, and chlorine was formed on the surface of the tantalum canister of this heat source. Examination of the uncracked capsule revealed seawater penetration to the tantalum canister. At the fuel-Haynes alloy No. 25 interface chromium and manganese depletion was found along with a buildup of silicon and iron. (auth)

13164 (MLM-1670) METALLOGRAPHIC ANALYSIS OF THE SNAP-15C HEAT SOURCE CAPSULE. Kelly, M. D.; Roesch, D. L.; Selle, J. E. (Mound Lab., Miamisburg, Ohio). 30 Sep 1969. Contract AT(33-1)-Gen-53. 23p. Dep. NTIS.

Alpha contamination was detected on the outside surface of a SNAP-15C heat source after 3 yr of operation at 427°C. Metallographic examination of the heat source revealed that all the welds in both the Hastelloy C and Ta-10 wt % W containers were physically sound. There was no apparent penetration of plutonium into the Ta-10 wt % W inner container. A combination of pressure at the operating temperature and diffusion of plutonium through the fibrous structure of the cold-worked Ta-10 wt % W may have caused a crack. Once the plutonium penetrated the Ta-10 wt % W inner container it reacted with the constituents of the Hastelloy C and Lithobraze. (auth)

13165 (MLM-1753) STABLE GASEOUS ISOTOPE SEPARATION AND PURIFICATION: APRIL-JUNE 1970. (Mound Lab., Miamisburg, Ohio). 12 Nov 1970. Contract AT(33-1)-Gen-53. 51p. Dep. NTIS.

Research progress is summarized on carbon isotope separation by Co distillation, thermal diffusion, chemical exchange, Freon 11 distillation, liquid thermal diffusion, and conversion separations. Activities in work directed to separation of stable isotopes of Ne, Ar, Kr, and Xe are also summarized. Other work on thermal diffusion and low temperature methods are also reported. (J.R.D.)

13166 (MMM-4187-1) SNAP-23A PROGRAM: THERMOELECTRIC CONVERTER DEVELOPMENT PROGRAM. Final Report. (Minnesota Mining and Mfg. Co., St. Paul. Electrical Products Group). 30 Dec 1970. Contract AT(30-1)-4187. 360p. Dep. NTIS.

Research and development on Phases II and III of the SNAP-23 converter development program are summarized. Development and testing of an experimental mockup converter and a prototype mockup converter is reported. Technical developments include: establishment of thermopile operating temperature, increased converter efficiency, demonstrated reliability, establishment of performance data for evaluation of production legs used in converters, and achievement of long-time operation of converters. (J.R.D.)

13167 (N-70-41092) PRELIMINARY THERMAL ANALYSIS OF AN AERODYNAMICALLY SHAPED HEAT SOURCE FOR USE WITH THE ISOTOPE BRAYTON SPACE POWER SYSTEM. Burns, Raymond K. (National Aeronautics and Space Administration, Cleveland, Ohio. Lewis Research Center). Sep 1970. 38p. (NASA-TM-X-52891). NTIS.

A two-dimensional thermal analysis was used to demonstrate the thermal advantage of using an isotope heat source aerodynamically shaped for predictable orientation during individual heat source atmospheric reentry. One side of the heat source, designed to lead during reentry, is insulated for thermal protection. The opposite side (uninsulated) is used as a heat transfer path during power system operation. This approach is intended to eliminate the conflict between reentry and steady-state operation thermal requirements which exist for the present Pioneer-type design being considered for use with the Brayton power system. (auth) (STAR)

13168 (N-70-41276) CONCEPTUAL DESIGN STUDY OF A NUCLEAR BRAYTON TURBOALTERNATOR-COMPRESSOR, PHASES 1-3. Final Report. Brooks, R. D. (ed.) (General Electric Co., Cincinnati, Ohio. Nuclear Systems Programs). [1970]. Contract NAS3-13449. 543p. (NASA-CR-113925; GESP-493). NTIS.

The Brayton turboalternator-compressor (TAC) study was conducted with a number of component designs and lubrication systems as candidates for selection. It was concluded that the radial in-flow turbine, centrifugal compressor, and 1200 Hz Rice-Lundell alternator, mounted on gas lubricated bearings met the requirements. Modifications were found to be necessary for the low temperature application and the modified requirements necessitated additional geometric changes and the 400 Hz Lundell alternator was selected. The principal features of the TAC include a titanium alloy compressor wheel with back-swept blades to obtain maximum efficiency. The alternator rotor is of bimetallic construction with 4340 and Inconel 718 to be bonded by HIP welding. Cooling is provided for the pole face losses by circulation of the working fluid through the gap and stack to a heat exchanger cooled by oil along the periphery of the stator. The reference voltage is 240 (L-N) with reconnectability to 480 volts. The insulation systems considered included high temperature ceramic materials previously developed by NASA and inorganic insulation for lower temperature application. (auth) (STAR)

13169 (NUMEC-3731-24) RADIOISOTOPE POWERED CARDIAC PACEMAKER PROGRAM. Final Term Report, Phase I, January 31, 1969-January 31, 1970. (Nuclear Materials and Equipment Corp., Apollo, Pa. Energy Conversion Div.). 24 Jun 1970. Contract AT(30-1)-3731. 149p. Dep. NTIS.

Progress in the Radioisotope Powered Cardiac Pacemaker Program from Feb. 1, 1969, to Feb. 1, 1970, is described. During this period, the electrically heated mock-up system continued to operate in a vacuum system and accumulated 24,588 hours of operation without the degradation of any component. Eight additional high-fueled experimental model RPCP's were constructed and put on test, as were six prototype model RPCP's. Seven of these units, including three experimental and four prototype units, were implanted in dogs. Development work on various components and sub-systems pertaining to both experimental prototype models is described, including work done on electrical feedthroughs, thermal analysis, shock, drop and vibration testing, safety and dose rate testing, and materials testing and purchasing procedures. Comparisons are presented to demonstrate the close agreement between predicted performance and measured performance of the prototype units. (auth)

13170 (SNC-2708-1) DEVELOPMENT OF THE SIREN CAPSULE, PHASE I. Anderson, R. W.; Deschamps, N. H.; Rexford, H. E.; Talbot, M. (Sanders Nuclear Corp., Nashua, N. H.). 3 Oct 1969. Contract AT(29-2)-2708. 372p. Dep. NTIS.

The feasibility of the SIREN isotopic fuel capsule was evaluated by means analyses and tests of design aspects critical to its successful performance. The feasibility of the SIREN concept was evaluated for fabricability and fueling of the capsule, ability to perform long-term missions, ability to withstand reentry conditions, and ability to confine the fuel after impact. Results of test data evaluations and analyses indicate the SIREN concept could develop into a successful isotopic fuel system using PuO_2 fuel as either microspheres or solid forms. The status of the technologies required for fabrication of the SIREN capsule is discussed and the areas requiring further development are identified. (auth)

13171 (SNC-2708-2) DEVELOPMENT OF THE SIREN CAPSULE, PHASE IA. Final Report, September 1969-January 1970. Anderson, Robert W.; Rexford, H. Eugene (Sanders Nuclear Corp., Nashua, N. H.). Contract AT(29-2)-2708. 54p. Dep. NTIS.

A study was performed of various parameters that affect the impact resistance of the SIREN capsule—a non-metallic encapsulation system for radioisotopic heat sources. A series of 22 SIREN test capsules were fabricated and impact tested. Relative impact resistance of the respective capsules was based on the condition of the simulated fuel core, the condition of the graphite structural shell, and the degree of post impact containment. Evaluation of the test data showed that solid cores of the ThO_2-Mo fuel simulant can be impacted intact when protected by the SIREN capsule. It was also found that higher strength graphite yarn can improve the impact resistance of the structural shell and that post impact containment of the fuel core could be provided by three independent methods. (auth)

13172 ^{15}N PROGRAM OF THE INSTITUTE OF STABLE ISOTOPES. Kretzschmann, G. (Institut fuer Stabile Isotope, Leipzig). Isotopenpraxis; 6: 354-8(Oct 1970). (In German).

Production, determination, and uses of ^{15}N are discussed along with production of ^{15}N-labeled compounds. (M.C.G.)

XUM

13173 OVERHEATING PROTECTION DEVICE FOR THERMIONIC ELEMENTS HEATED BY NUCLEAR ENERGY. Gross, Franz; Krapf, Rudolf (to Brown, Boveri and Cie AG). U. S. Patent 3,546,496. 8 Dec 1970. Priority date 9 Dec 1966, Germany.

An overheating protection device for thermionic converters which are heated by nuclear energy is described. A container filled with a highly heat-conducting fluid, e.g., a gas having great thermal conductivity, such as helium, is connected with a discharge or electrode interspace through a sealing means of determined melting point and having thermal contact with the emitter. When the temperature of the thermionic element rises above the melting point of a fusible joint, such as solder, this causes the fluid, e.g., helium contained within the container to flow into the electrode interspace and to cause the excess heat of the emitter to flow into the collector. (Offic. Gaz.)

13174 EKONOMICHESKAYA EFFEKTIVNOST' PRIMENENIYA RADIOAKTIVNYKH IZOTOPOV V PROMYSHLENNOSTI. (Economic Effectiveness of Using Radioactive Isotopes in Industry). Pasechnik, L. A. Kiev; Naukova Dumka (1969). 168p.

Information concerning results of experiments on methods for using radioisotopes in industry are presented. The efficiency of radioisotope use and results of progressive investigations are evaluated along with production of reserves for use in automation, and control and checking functions. The most promising directions and the possibilities for use of radioisotopes are considered along with questions associated with methods and economic parameters. (tr-auth)

13175 MAJOR CHANGES RECOMMENDED BEFORE DEUTERIUM'S PLANT OPERATIONAL. Chem. Can.; 21: 33-4 (Nov 1969).

Major modifications and repairs are required before the heavy water plant of Deuterium of Canada Ltd. (DCL) at Glace Bay, N. S. can be successfully started and operated. These are necessitated by inadequacies of the plant that have been compounded by equipment failure and damage during startup. It is estimated that $30 million will be required to place the plant in an operable condition, and that from 20 to 24 months' time will be required for the redesign and reconstruction after a decision to proceed is made. The estimate covers modifications and repair of the first three stages of the 5-stage plant only. (auth) (Canada)

13176 RADIOISOTOPE MEASUREMENTS OF THE FLOW PARAMETERS OF THE POSTFLOTATION SLURRY. Korbel, Kazimierz (Inst. of Nuclear Physics, Krakow); Hubert, Jerzy; Krzuk, Jerzy; (and others). Nukleonika; 15: 365-70(1970).

Radiometric measurements of flow parameters of the postflotation slurry transported hydraulically by a horizontal pipe line are described. In particular the flow velocity and the density distribution of the slurry were measured. Good agreement between the results obtained by conventional and radiometric methods was obtained. No significant vertical gradient of density distribution for a wide range of flow velocities was ascertained. (auth)

13177 HOW NEUTRONS TAKE ON PROCESS CONTROL. Downs, W. E. (Atomic Energy of Canada Ltd., Ottawa). Can. Contr. Instrum.; 8: 42-4(Dec 1969).

The use of neutrons in process control is relatively new, but there are three functions that can be performed in an industrial control environment, such as continuous elemental analysis, gauging, and continuous production of tracers for flow studies. (auth) (Canada)

13178 USE OF ^{238}Pu RADIATION SOURCES IN CARDIAC PACEMAKERS. Berger, R.; Boucher, R.; Jampsin, B.; Hot, M. (CEA, Fontenay-aux-Roses, France). Inform. Bull. Isotop. Generators; No. 10, 3-21(Nov 1970). (In French).

The design of a ^{238}Pu sealed source was studied in terms of size and mass considerations, and safety tests in connection with radiation protection, thermomechanical stress resistance (percussion, collapse, shock and thermal tests) and chemical corrosion resistance. (auth) (France)

13179 DESIGNING MULTICOMPONENT ISOTOPE SEPARATION CASCADES. Kolokol'tsov, N. A.; Minenko, V. P.; Nikolaev, B. I.; Sulaberidze, G. A.; Tret'yak, S. A. At. Energ. (USSR); 29: 425-9(Dec 1970). (In Russian).

The multicomponent separation cascades with an unbroken profile for separating isotopes (or groups of isotopes) with intermediate atomic weight were theoretically investigated. A method of calculating real square cascades and simulating the unbroken form cascades, is proposed. It is shown that any sector of the multicomponent unbroken form cascade may be replaced by a square section. Examples of calculations are also presented. (auth)

Materials Testing

Refer also to abstracts 13141–13143, 13177, 13627, 13656, 13658, 13662, 13668, and 14861.

13180 (JAERI-Memo-4163) NONDESTRUCTIVE TESTING OF AIRCRAFT STRUCTURES BY RADIOISOTOPES. (Japan Atomic Energy Research Inst., Tokyo). Oct 1970. 153p. (In Japanese). Dep. NTIS (U. S. Sales Only).

Joint research carried out between the Radioisotope Center, JAERI and the Engineering Department, Japan Air Lines from March 1970 to June 1969 is reported. The preparation and radiological characteristics of ^{170}Tm and ^{192}Ir gamma sources, and the nondestructive testing of structural parts for aircraft using gamma sources, are discussed. (auth)

13181 (WAPD-TM-976) FRACTURE MECHANICS EVALUATION OF STRESS INTENSITY FACTORS FOR VARIOUS CRACK GEOMETRIES AND LOADING CONDITIONS. Bhatt, S. J. (Bettis Atomic Power Lab., Pittsburgh, Pa.). Dec 1970. Contract AT(11-1)-Gen-14. 79p. Dep. NTIS.

More recent references on fracture mechanics solutions, limited to plane strain are summarized. Emphasis was placed upon solutions for various flaw geometries and arbitrary stress fields. The crack geometries analyzed and treated are straight-line cracks in plane bodies and circular flaws, parabolic flaws, and elliptical flaws in three-dimensional bodies. A variety of loadings are treated, including uniform stress, concentrated body forces, bending moments, and those arising from specified crack surface temperature or uniform heat fluxes. A method for approximating the stress intensity due to a flat circular or an elliptical flaw subjected to a non-uniform normal stress is also presented. (auth)

13182 INFLUENCE OF DIMENSIONAL INACCURACIES ON THE STRESS CALCULATION OF PIPING SYSTEMS. Krieg, Rolf (Kernforschungszentrum, Karlsruhe, Ger.). Nucl. Eng. Design; 14: 168-74(Oct 1970).

In general, calculations on the propagation of errors in the stress analysis of statically indeterminate framed structures (e.g. piping systems) lead to the problem; there are given ranges of variation of certain physical parameters (dimensions, loads, material characteristics) from which the coefficients and constants of a system of linear equations are calculated. The stress in the system are a function of the solution vector of this system of linear equations. For the critical stresses the range of variations are required which are caused by the variations of the physical parameters. The difference which exists between this problem and the problem encountered when the coefficients and constants—independently—are subject to some variation, for instance, as a result of inaccuracies in the calculation is considered. Furthermore, a method is indicated which facilitates the approximate calculation of the maximum variation of a critical stress even in cases where a relatively great number of parameters is subject to variations independent of each other. (auth)

13183 METHOD OF THERMAL SHOCK ANALYSIS. Lang, W. (Kernforschungszentrum, Karlsruhe, Ger.). Nucl. Eng. Design; 14: 151-67(Oct 1970).

A method of solving problems related to transient thermal stresses is described. The method is based on the experimental determination of frequency response functions and weighting functions for thermal stresses. With the use of Duhamel's integral, it is employed to determine the time curves of the temperatures and thermal stresses generated in a structural component as a result of fast variations of the coolant temperature during reactor operation. Moreover, it provides the means to evaluate the effects of cyclic thermal loads encountered in reactor operation which may cause fatigue of the structure in long-term operation. A representative structural component of reactor technology (hollow cylinder of 100 mm inside diameter with an abrupt change of wall thickness from 20 mm to 2 mm), which is particularly sensitive to thermal stresses, was equipped with thermocouples and strain gages and investigated in a helium circuit, in order to test the proposed method. The validity of the method was demonstrated in a comparison of the results of a real thermal shock on the helium circuit with the results calculated in advance with the help of weighting functions which also had been determined experimentally. (auth)

Protective Structures

Refer also to abstracts 13117 and 13132.

13184 CIVIL DEFENSE IMPLICATIONS OF A PRESSURIZED WATER REACTOR IN A THERMONUCLEAR TARGET AREA.

Chester, C. V.; Chester, R. O. (Oak Ridge National Lab., Tenn.). Nucl. Appl. Technol.; 9: 786-95(Dec 1970).

The Turkey Point Pressurized Water Reaction was analyzed as a Civil Defense problem in a nuclear attack. It is postulated that the reactor presents no additional hazard in a target area unless a large fraction of the fission product inventory in the core can be promptly released due to weapon effects. High explosives tests on scale models of the pressure vessel and pertinent shielding were employed to determine the required delivery accuracy of nuclear weapons to rupture the pressure vessel and release the core fission product inventory. It was concluded that the presence of a power reactor in a target area will not add significantly to the number of casualties produced by a nuclear weapon unless the reactor receives essentially a direct hit. Further, preferentially targeting a PWR would be prohibitively expensive because with existing missile accuracies a large number of weapons would have to be targeted on the reactor in order to ensure getting a direct hit. (auth)

Radioactive Material Handling

Refer also to abstracts 13087 and 13230.

13185 (AERE-R-6338) EVACUABLE GLOVE-BOX FOR THE HANDLING OF LIQUID SODIUM, AND APPARATUS FOR THE ANALYSIS OF CARBON IN SODIUM AND OTHER METALS. Ainsley, R.; Holroyd, P. M.; Long, G.; Stratton, L. P. (Atomic Energy Research Establishment, Harwell (England)). Dec 1970. 25p. Dep. NTIS (U. S. Sales Only).

A stainless steel dry box constructed for the safe and contamination-free handling of liquid sodium is described and operating experience summarized. Operations are carried out with the box either filled with high purity argon or evacuated. The box is designed to permit easy modification and is suitable for the handling of other highly reactive materials. Also described is the apparatus used for the analysis by combustion of total carbon (as natural carbon and/or labelled with ^{14}C) in sodium and other metals (iron, nickel, zirconium), and the method and equipment used to determine the nature and quantity of carbonaceous species present in sodium. (auth) (UK)

13186 (BNWL-1503) ANALYSIS OF HYDROLOGICAL FACTORS INFLUENCING THE OPERATION OF THE 100-N EMERGENCY WASTE DISPOSAL CRIB. Cearlock, D. B.; Mudd, R. D. (Battelle-Northwest, Richland, Wash. Pacific Northwest Lab.). Nov 1970. Contract AT(45-1)-1830. 34p. Dep. NTIS.

A mathematical model was used to simulate ground water flow conditions near the 100-N Emergency Waste Disposal (EWD) Crib beside the Columbia River and to determine the effects of hydrological factors on the safe operation of the EWD Crib. This evaluation showed a significant advantage in operating the EWD Crib in conjunction with the 1301-N Crib. Operation with both cribs showed a 99.8 and 94% reduction in maximum total iodine and tritium, respectively, entering the Columbia River over that obtained through use of the 1301-N Crib. The EWD Crib with 1301-N Crib deactivated showed a 55% and 6% reduction in total I and H_3, respectively, entering the Columbia River over that obtained through use of the 1301-N Crib. This analysis was based on continuous discharges, and no attempt was made to determine the discharge rate to the 1301-N Crib that would provide the maximum reduction of wastes entering the river from discharges to the EWD Crib. (L.C.L.)

13187 (BNWL-1512) CRITICALITY SAFETY ANALYSIS: MODEL 60 SHIPPING PACKAGE FOR FFTF DRIVER FUEL PINS. Brown, C. L. (Battelle-Northwest, Richland, Wash. Pacific Northwest Lab.). Nov 1970. Contract AT(45-1)-1830. 16p. Dep. NTIS.

The Model 60 is a Fissile Class II shipping container designed for transporting FTR driver fuel pins. The design consists of an 18 × 18 × 112.5-inch metal birdcage with a centrally mounted 6-inch ID × 102.5-inch long containment vessel. The criticality safety evaluation shows that each container may be loaded with up to 120 FTR-type fuel pins enriched to 31 wt % $PuO_2-U(Nat)O_2$ (6.75 kg Pu); and that a single Fissile Class II shipment may consist of up to 12 containers (1440 fuel pins). The Transport Index is 4.0. (auth)

13188 (BNWL-B-34) SURVEY OF ALPHA WASTE GENERATION AND DISPOSAL AS SOLIDS IN THE U. S. NUCLEAR FUEL INDUSTRY. Van Tuyl, H. H.; Winegardner, W. K.; Hilliard, R. K.; Cooley, C. R. (Battelle-Northwest, Richland, Wash. Pacific Northwest Lab.). Dec 1970. Contract AT(45-1)-1830. 43p. Dep. NTIS.

Nine commercial fuel element fabrication and four spent fuel reprocessing companies were surveyed to learn their current practices regarding generation and disposal of solid alpha-contaminated wastes. The information was obtained by visiting processors throughout the United States in June 1970. Special emphasis was placed on wastes contaminated with plutonium. Current practices are reported for each of the two industries, and extrapolations are made to the year 1990. (auth)

13189 (CEA-CONF-1712) STUDY OF A MARINE SITE WITH A VIEW TO RADIOACTIVE EFFLUENT DISCHARGE. Ancellin, J.; Avargues, M.; Bovard, P. (Commissariat a l'Energie Atomique, Fontenay-aux-Roses (France). Centre d'Etudes Nucleaires). [1970]. 18p. (In French). (CONF-701203-1). Dep. NTIS (U. S. Sales Only).

From Conference on Marine Pollution and its Effects on Living Resources and Fishing, Rome, Italy.

The three fields of activity of the La Hague Laboratory are reviewed: experimental contamination of marine species (algae, molluscs, crustaceans and fish) carried out in aquaria in order to obtain over-all concentration factor values; observations in situ; physicochemical study of ^{106}Ru. (auth) (France)

13190 (JAERI-Memo-4153) BIBLIOGRAPHY ON WASTES OF PLUTONIUM. Kato, Kiyoshi (ed.) (Japan Atomic Energy Research Inst., Tokyo). Sep 1970. 19p. (In Japanese). Dep. NTIS (U. S. Sales Only).

A bibliography compiled from Nuclear Science Abstracts for 1945 to 1969 on plutonium-containing radioactive wastes is presented. The references are classified into three groups: treatment (removal, recovery, separation, etc.); disposal; and methods for determining plutonium content. (auth) (Japan)

13191 (JPRS-51948) TREATMENT AND DISPOSAL OF RADIOACTIVE WASTES. Translation of Selected Papers from Symposium on Treatment of Medium- and Low-level Radioactive Wastes held in Aix-en-Provence, France, 7-11 September 1970. 100p NTIS.

Seven papers selected from the Symposium on Treatment of Medium- and Low-Level Radioactive Wastes, held in Aix-en-Provence, France on Sept. 7 to 11, 1970 are presented. Information on the disposal and processing of both liquid and solid wastes is included. (L.C.L.)

13192 (NACAR-10012) FILTER SYSTEM DESIGN, INSTALLATION AND TESTING FOR RADIOACTIVE CONTAMINANT REMOVAL. Kovach, J. Louis (North American Carbon, Inc., Columbus, Ohio. Research and Development Dept.). [1970]. 16p. (CONF-701115-1).

From American Association of Contamination Control, North Central Conference, Chicago, Ill.

An analysis of capabilities and limitations of filter systems is presented. The results of this analysis are presented. It was concluded that filter systems capable of maintaining 99.95+% removal efficiencies can be attained only if careful consideration is given to all factors related to the contaminants to be filtered. The additional hazard of radioactivity extends to both operating personnel and residents of the surrounding area if mistakes are not corrected before startup. This factor, above all, sets high efficiency filter systems for radioactive contaminants in a separate class from conventional clean rooms and other non-radioactive contaminant filtration systems. Past experience indicates some lack of appreciation and understanding in the design, installation, and operation of high efficiency air filtration systems. High reliability of individual filter components is no substitute for a reliable, tested filter system. (auth)

13193 (SZS-16/70) PRINCIPLES FOR CONTROL OF NUCLEAR MATERIAL IN THE GDR. Burkhardt, W.; Gegusch, M.; Schimmel, W. (Staatliche Zentrale fuer Strahlenschutz, Berlin (East Germany)). Sep 1970. 24p. (In German). Dep. NTIS (U. S. Sales Only).

The Radiation Protection Center presents a concept for the control of nuclear material in the GDR with regard to the Non-Proliferation Treaty. The principles laid down include the handling of nuclear materials, responsibilities, safeguards procedures, records, institutional regulations for the handling of nuclear material and records, reports, performance of controls, and distribution of expenses for records and inspection. (auth)

13194 (SZS-19/70) ILLUSTRATION OF THE SPECIFICATIONS FOR THE TRANSPORT OF RADIOACTIVE MATERIALS OF HIGH ACTIVITY AND FISSIONABLE MATERIALS. PRINCIPLES OF CRITICALITY SAFETY IN THE TRANSPORT OF FISSIONABLE MATERIALS. Richter, D.; Birkigt, W.; Albrecht, L. (Staatliche Zentrale fuer Strahlenschutz, Berlin (East Germany)). Sep 1970. 34p. (In German). Dep. NTIS (U. S. Sales Only).

Regulations for the transport of highly radioactive and fissile materials in East Germany are described. For those materials, the requirements relating to packaging, transport, and approval are given. The regulations are based on the 1967 Regulations of the IAEA. Insignificant differences from the IAEA Regulations are discussed. (auth)

13195 (WHAN-SA-91) MOCK-UP OF REMOTELY OPERATED HIGH-PURITY INERT-ATMOSPHERE SODIUM ANALYSIS FACILITY. **Lust, L. F.; Scott, F. A.; Jarosch, J. F. (Battelle-Northwest, Richland, Wash. Pacific Northwest Lab. WADCO Corp., Richland, Wash.). [1970]. Contract AT(45-1)-1830. 21p. (BNWL-SA-3437; CONF-701102-14). Dep. NTIS.**

From Meeting of the American Nuclear Society, Washington, D. C.

Operation of the Fast Flux Test Facility (FFTF) requires chemical characterization of the radioactive sodium coolant. One means to obtain this characterization is by sampling and laboratory analysis. Since no remotely operated facilities have been developed which have an atmosphere of sufficient purity to permit the analysis of metallic sodium, new technology is required. To aid in the development of this technology, a special mock-up facility was constructed. A hermetically sealed cell was constructed of stainless steel plate. It was furnished with sealed master-slave manipulators, an evacuable air lock, a viewing window and a recirculating gas purification system. Following an argon purge, an atmosphere containing less than 1 ppM oxygen and 0.5 ppM water was attained. The quality of the atmosphere was continuously monitored for two months, during cell operation, and the ability to maintain this purity level was demonstrated. Results of determinations of oxygen in sodium, performed in the remote facility, are comparable to those obtained in conventional sodium analysis facilities. Sufficient information has been obtained to predict with a high degree of certainty that highly radioactive sodium can be analyzed by conventional procedures if the proper facilities are available. These facilities can be constructed using commercially available components and proven construction techniques. (auth)

13196 PROTECTIVE SHELL FOR THE TRANSPORT OF LEAD CASKS. **Lacheteau, Herve (to Commissariat a l'Energie Atomique). French Patent 1,586,726. 19 Jan 1970. Filed 2 Oct 1968. (In French).**

The protective shell for a lead transport cask consists of a cylindrical outer container, its parallel sheet metal lateral wall and base enclosing a space filled with a heat-insulating material, a removable cover fitting into the opening of the container, and a system to block this cover. (auth) (France)

13197 THE FEASIBILITY OF INCORPORATING RADIOACTIVE WASTES IN ASPHALT OR POLYETHYLENE. **Fitzgerald, C. L.; Godbee, H. W.; Blanco, R. E.; Davis, W. Jr. (Oak Ridge National Lab., Tenn.). Nucl. Appl. Technol.; 9: 821-9(Dec 1970).**

Residues from aqueous and organic intermediate-level radioactive waste can be incorporated in asphalt or polyethylene to reduce the mobility of radionuclides after burial or storage of the solidified waste product. Asphalt or polyethylene products containing up to 60 wt % of nonoxidizing inorganic solids have a chemical resistance similar to that of pure asphalt or polyethylene. Leach rates projected over 200 years indicate that about 5% of a soluble element (sodium or cesium) or 0.6% of an insoluble nuclide (^{106}Ru) would be leached from a 55-gal drum of product submerged in water. Polyethylene accommodated up to 40 wt % of organic liquids, such as tributyl phosphate (TBP), while asphalt products containing 25 wt % TBP were not entirely satisfactory. Polyethylene products were also superior to asphalt products in flammability and radiation stability tests. Incorporation in asphalt is not recommended for waste solids containing significant amounts of oxidants. (auth)

13198 AN EMPIRICAL FORMULA WHICH PREDICTS THE CRITICAL PARAMETERS OF A PLANAR ARRAY OF URANIUM-SOLUTION-FILLED CYLINDERS. **Clark, Harold E.; Tuck, Grover (Dow Chemical Co., Golden, Colo.). Nucl. Appl. Technol.; 9: 814-20(Dec 1970).**

An empirical formula was developed for determining the individual diameter of essentially unreflected cylinders in a critical planar array. The formula is $D_a = \{[k_1 + k_2 (\sqrt{N}/S)/H - k_3] + k_4 e^{-0.44N/S}\}[(k_5/C - k_6) + k_7](G/k_8)$. The independent variables are N, the number of cylinders in the array; S, the edge-to-edge spacing between adjacent cylinders; H, the solution height in the array; C, the concentration of the solution [U ~ 93 wt-% ^{235}U]; G, the geometry factor determined by the shape of the array; and k_i (i = 1, 2, ..., 8), the constants determined by the type of solution; either uranyl nitrate or uranyl fluoride. These independent variables, the formula ranges, and approximations are discussed. The critical cylinder diameter, calculated by this formula, is within ±8% of the experimentally measured diameter for 112 experimental data points. Therefore, the formula can be used as a guide-line for nuclear criticality safety. (auth)

13199 COUPLING. **Bergeret, Marcel; Borrel, Louis; Simeone, Marius (to Commissariat a l'Energie Atomique). British Patent 1,216,426. 23 Dec 1970. Priority date 24 May 1967, France.**

A coupling designed to be assembled or dismantled by means of a remote-handled bolting device is described. The coupling is intended for use in assembling components of hot cells for fuel reprocessing under dry conditions. (J.R.D.)

13200 REMOTE MANIPULATION TOOL. **Bergeret, Marcel; Borrel, Louis; Simeone, Marius (to Commissariat a l'Energie Atomique). British Patent 1,216,425. 23 Dec 1970. Priority date 24 May 1967, France.**

A remote-manipulation tool is described which is designed so that two diametrically opposite fastening nuts and bolts can be positioned then tightened or slackened without direct operation by the user. The tool is comprised of slideways engaged around a guide. Bolts and nuts for insertion in the flanges are carried in a magazine. Provision is made for insertion and rotation of the bolts in the flanges by remote control. (J.R.D.)

13201 CONCEPTION OF INTEGRITY OF TYPE A AND B PACKAGING FOR SHIPMENT OF RADIOACTIVE MATERIALS. **Richter, D.; Birkigt, W. (Staatliche Zentrale fuer Strahlenschutz, Berlin). Isotopenpraxis; 6: 369-77(Oct 1970). (In German).**

On the basis of an analysis of the requirements for the integrity of packages for the shipment of radioactive materials currently in use, the relationships are outlined which make it possible to derive the necessary radiological integrity (activity leakage rates) or engineering integrity (gas leakage rates) from radiation protection parameters. Some representative examples are calculated for Type A and B packages for radioactive materials of medium activity. Proposals are made for more precise regulations on integrity. (auth)

13202 CURIUM SHIPPING CASK (29 May 1968) **(Engineering Materials). (Savannah River Operations Office (AEC), Aiken, S. C.). (CAPE-2046).**

12 drawings.

A water-filled stainless steel shipping cask used to ship CmO_2 is described. The cask withstands normal and accident conditions of transport without the release of any CmO_2. Sixteen vents with low-melting alloy plugs are provided. The vents are situated so that one or more vents will be in the vapor space above the cooling water for all cask orientations. The alloy plugs will not melt below the water line. Modifications needed for mounting the cask on a flatbed trailer are described. Four platinum-lined capsules, each enclosed in a case, hold the CmO_2. Each cask may hold up to 144 g of Cm. See also CAPE-2047 for equipment used in producing the CmO_2. (For details see TID-4100 Suppl. 62) (see also NSA 24: 31640.) (F.S.)

13203 REMOVABLE HEAD FOR PNEUMATIC TRANSFER DEVICE AND TRANSPORT SYSTEM INCLUDING APPLICATION. **Baudoin, J.-C.; Drieu, F.; Marlin, H.; Oger, R.; Pennincq, A. (to Commissariat a l'Energie Atomique). French Patent 1,587,616. 16 Feb 1970. Filed 20 Jun 1968. (In French).**

The invention concerns a removable head for a pneumatic transfer device and a system intended for the transfer of objects from one point to another in a hot cell. The head, designed to be mounted at the end of a duct, includes a case which can be connected hermetically to and disconnected from the duct by a bolting mechanism, a block mounted to slide on the case between an upper and a lower position where it can support the object to be transferred, a remote-control system to move the block from its upper position, and means of adjusting the pressure at the bottom of the casing. (auth) (France)

13204 IMPROVEMENTS IN AND RELATING TO A TRANSPORT FLASK ESPECIALLY FOR RADIOACTIVE MATERIAL. **Marsault, Jacques (to Commissariat a l'Energie Atomique). British Patent 1,220,041. 20 Jan 1971. Priority date 26 Jan 1968, France.**

A lead-shielded container is described for use in transporting materials which are to be isolated from the external atmosphere. The flask is supported by a pivotable base which incorporates a means of moving the flask from the horizontal conveying position into a vertical position for charging and discharging. Two half shutters are provided at the lowest position on the flask which can be opened, closed, locked, and unlocked by remote contol. (J.R.D.)

13205 TRANSPORT FLASK FOR NUCLEAR FUEL ELEMENTS. Capet, Henri (to Commissariat a l'Energie Atomique). British Patent 1,220,027. 20 Jan 1971. Priority date 30 Aug 1968, France.

A transport container for fuel elements is described which provides shielding and stable internal recesses for housing the elements to be transported. The recesses are brought in line with a plugged port for loading and unloading the fuel by rotating the body of the container. The rotating means are outside of the shielding, affording maximum radiation protection. (J.R.D.)

13206 IMPROVEMENTS TO MASTER-SLAVE MANIPULATORS. Townsend, Eric (to Commissariat a l'Energie Atomique). British Patent 1,219,876. 20 Jan 1971. Priority date 23 Apr 1968, France.

A manipulator is described which comprises a slave assembly adapted to reproduce the movements of a master assembly. Each of these assemblies comprises a number of articulated members or elements. A potentiometer is associated with each element the cursor of which is sensed by movement and sets up imbalance in Wheatstone bridge circuits between master members and slave members which control electric drive motors for the slave members. (J.R.D.)

13207 ITALIAN REGULATIONS ON RADIOACTIVE WASTE DISPOSAL IN CONNECTION WITH THE USE OF RADIOISOTOPES. Com. Naz. Energ. Nucl., Notiz.; 16: No. 11, 103-6(Nov 1970). (In Italian).

An analysis of the Italian regulations on radioisotopes is presented with emphasis on the standards for radioactive waste disposal. Regulations on possession, sale, trading, and use were discussed previously. (auth)

13208 FLUID SUPPORTED CAPSULE HOLDER FOR HOMOGENEOUSLY IRRADIATING SAMPLES. Ricci, Enzo; Handley, Thomas H.; Willey, Melvin G. (to United States Atomic Energy Commission). U. S. Patent 3,549,492. 22 Dec 1970. Filed 12 May 1969.

A spherical multisample holder is employed so as to permit transfer from a remote loading position to an irradiating position. This holder may then be held by a column of fluid, such as air, for a sufficient irradiation time during which its orientation changes randomly due to its unique structure to thus effect a homogeneous irradiation of all samples. The spherical holder may then be returned to a remote unloading position. (Office. Gaz.)

INSTRUMENTATION

Radiation Detection Instruments

General Detectors and Monitors

Refer also to abstracts 13318, 13329, 13487, 13514, 13520, 14228, and 14403.

13209 (COO–1671-28) UNIFIED TRACK THEORY. Katz, Robert (Nebraska Univ., Lincoln. Behlen Lab. of Physics). [1970]. Contract AT(11-1)-1671). 29p. (CONF-700705–1). Dep. NTIS.

From 7th International Conference on Corpuscular Photography and Visual Solid Detectors, Barcelona, Spain.

A theory for particle track formation in emulsion and other physical and biological media is discussed. It is attempted to couple the dose-response function of a medium to gamma rays with the spatial distribution of dose from secondary electrons to yield the spatial distribution of response about the path of a charged particle. Measured and calculated data are presented for particle track formation in emulsion etchable track formation in dielectrics, the response of scintillation counters to heavy ions, and the inactivation of dry enzymes and viruses and cells by heavy ions. (W.H.K.)

13210 (JINR–P3-5421) THRESHOLD DETECTORS USED FOR THE NEUTRON SPECTRUM MEASUREMENT. Koshaeva, K. K.; Kraitor, S. N.; Pikel'ner, L. B. (Joint Inst. for Nuclear Research, Dubna (USSR). Lab. of Neutron Physics). 1970. 25p. (In Russian). Dep. NTIS (U. S. Sales Only).

Spectrometer characteristics of the threshold detector set, consisting of ^{235}U, ^{235}U + Cd, ^{235}U + 1 g/cm^2 ^{10}B, ^{237}Np, ^{238}U, ^{32}S are considered, and the optimal values of the effective cross-sections and the threshold energies for neutron spectra are calculated. The accuracy of the measurements, performed by this set for a number of characteristic spectra, is estimated. Special attention is paid to the measurements below the ^{237}Np fission threshold. New interpretation of data is proposed that allows the measurement accuracy to be enhanced in this energy region. The construction of the neutron spectrum of the pulsed fast reactor IBR (JINR) are described. (auth)

13211 (JINR–P13-5402) SPECTROMETER CHANNEL OF EXPERIMENTAL IONIZATION CHAMBERS WITH THE ARGON AND XENON CONDENSATES. Ryabtsov, V. D.; Silaev, E. A. (Joint Inst. for Nuclear Research, Dubna (USSR). Lab. of High Energy). 1970. 12p. (In Russian). Dep. NTIS (U. S. Sales Only).

A spectrometric channel is described, used in the investigations of ionization chambers with xenon condensates. The demands to the spectrometric equipment are formulated taking into account the specific peculiarities of these media. A schematic diagram of the chamber preamplifier is presented. The basic technical characteristics of the channel are given. (auth)

13212 (NP–18653) DESIGN, CONSTRUCTION, AND CHARACTERISTICS OF SOME Ge(Li) DETECTORS AND SPECTROMETERS. Suominen, Pekka (Jyvaskyla Univ. (Finland). Dept. of Physics). Aug 1970. 115p. Dep. NTIS (U. S. Sales Only). Thesis.

Experience obtained in preparing different kinds of Ge(Li) detectors is presented. The preparation method used involves an unusual sodium hypochlorite etching procedure. A method for externally cooling the field effect transistor of a standard preamplifier is presented and some test results are described. A "semitoroidal" detector configuration intended for making large Ge(Li) detectors with approximately homogeneous electric fields is described in detail. Test measurements have been carried out with a relatively small semitoroidal detector. Some data obtained with an anti-Compton spectrometer, which results in a peak-to-tail ratio of 200 for ^{137}Cs spectrum, are presented. Cryogenic and electronic problems concerning the performance of the anti-Compton spectrometer are discussed in detail. Some two-crystal pair spectrometers have been tested and possibilities for further development are discussed. Efficiency and line shape problems involved in a summing Compton spectrometer have been examined both theoretically and experimentally. On the basis of optimizing work a summing Compton spectrometer has been constructed. A very simple "analog on-line-computer" has been employed in connection with the spectrometer which renders it possible that gamma quanta with energies down to 100 keV might be recorded. The spectrometer resulted in spectra with higher peak-to-tail ratios than the ratios obtained with anti-Compton spectrometers. Further development of the summing Compton spectrometer employing, for instance, a Si(Li)–Ge(Li) detector pair, is discussed. (42 references). (auth) (Finland)

13213 (UCRL–71508) EVALUATION OF TRAPPING AND TAILING EFFECTS IN Ge(Li) DETECTORS. Armantrout, G. A. (California Univ., Livermore. Lawrence Radiation Lab.). 22 Jan 1969. 11p. Dep. NTIS.

Day's model of trapping effects in detectors has been simplified and applied to the case of Ge(Li) detectors. With this model it is possible to easily determine τ_t for any given detector. τ_t, the mean time before trapping of a carrier, is related to the trap density and trap capture cross section and is a useful parameter for characterizing the trapping properties of Ge. A number of ingots have been evaluated. In general, horizontally grown ingots closely follow the expected behavior of the model, and values of τ_t = 10 to 30 μsec have been found. However, vertically grown ingots, which have larger values of τ_t (>50 μsec), appear to be subject to thermal defects which ultimately result in nonlinear collection fields. The nonlinear fields cause large deviations from the response predicted by the simple model and are the cause of much of the tailing seen in vertically pulled material. (auth)

13214 AROMATIC NITRILES: A NEW FAMILY OF SCINTILLATION SOLUTES. Velazquez, C.; Castrillon, J. (Univ. of Puerto Rico). Radiochem. Radioanal. Lett.; 5: 243-5(15 Dec 1970).

Several aromatic nitriles were examined as scintillator solutes in comparison with the standard compounds, terphenyl (PPP) and 2,5-diphenyloxazole (PPO). Although none of the compounds studied, 9,10-anthracenedicarbonitrile, 4,4'-biphenyldicarbonitrile, terphenyl-4-carbonitrile, and terphenyl-4,4'-dicarbonitrile, surpassed the standard solutes, PPP or PPO, they showed considerable promise for this chemical family in the search for better scintillators and could be used for tritium counting. (P.C.H.)

13215 NEUTRON DETECTOR WITH A FLAT ENERGY RESPONSE FOR USE IN TIME-OF-FLIGHT EXPERIMENTS. Coates, M. S.; Hunt, G. J.; Rae, E. R. (Atomic Energy Research Establishment, Harwell, Eng.). pp 211-19 of Nuclear Data for Reactors. Vol. I. Vienna; International Atomic Energy Agency (1970).

From 2nd International Conference on Nuclear Data for Reactors, Helsinki, Finland. See STI/PUB-259(Vol.1); CONF-700605–(Vol.1).

Monte-Carlo calculations have been carried out to assess the feasibility of making a neutron detector suitable for time-of-flight work whose efficiency can be accurately predicted (~±2%) ideally over the energy region 100 eV to several MeV. Accurate flux measurements are needed in this region to determine partial neutron cross-sections for use in fast-reactor design. The detector was taken to be a spherical homogeneous mixture of ^{10}B and vaseline with a radial re-entrant hole to allow a parallel neutron beam to fall near the sphere center. Neutrons are moderated and captured in the ^{10}B to produce 478-keV γ-rays in the reaction ^{10}B(n,α)^{7}Li*, γ^{7}Li which are detected at the surface of the sphere in NaI scintillation counters. On the basis of the calculations a 12 cm radius counter has been built containing ~1 kg ^{10}B with a re-entrant hole 8 cm deep and 2.5 cm diameter. The counter is predicted to have an efficiency which is flat within 4% between 100 eV and 700 keV. The time response is such that an incident fast neutron has a probability of 0.99 of being captured within 0.67 μs. Measurements are being carried out on a 300 m flight path of the Harwell 45 MeV electron linac to test the theoretical predictions. If these are successful the flat response detector will be used as a standard for calibrating the counters actually used for flux determination in fast neutron partial cross-section measurements. The measured characteristics of the detector are presented and compared with the theoretical predictions. (auth)

13216 DEVELOPMENT OF METHODS FOR THE ABSOLUTE MEASUREMENTS OF FAST NEUTRON FLUXES IN THE RANGE OF 10 keV TO 1 MeV. Leroy, J. L.; Huet, J. L.; Szabo, I.; Fort, E. (Centre d'Etudes Nucleaires, Cadarache, France). pp 243-52 of Nuclear Data for Reactors. Vol. I. Vienna; International Atomic Energy Agency (1970). (In French).

From 2nd International Conference on Nuclear Data for Reactors, Helsinki, Finland. See STI/PUB-259(Vol.1); CONF-700605–(Vol.1).

The absolute measurement of a neutron flux is a necessary stage in the determination of all the reaction cross-sections. In the energy range of 10 keV to 1 MeV precise flux measurements are difficult. To provide a sound basis for cross-section measurements, a systematic comparison was made between the following monokinetic flux measurement techniques: the associated-particle method with neutrons produced by the $T(p,n)^3He$ reaction, using both the coincidence variant and the absolute counting variant for ^3He-particles; the manganese sulphate bath method in combination with a collimator for neutron selection; and the method based on the use of recoil proton proportional counter. Since this comparative study was carried out over a fairly extended period, these different methods have been applied successively for the calibration of the same measurement instrument, the stability of which with time was carefully verified. This instrument consists of a BF_3-counter assembly in a paraffin block; it is fitted with a collimator for selecting the neutrons for measurement and a shield to eliminate the background due to scattered neutrons. The efficiency of this apparatus is virtually independent of energy. Calculations were made by the Monte-Carlo method. Overall the theoretical and measurement results are in good agreement. The authors consider this instrument capable at the present time of measuring neutron fluxes to an accuracy of ±2% within the energy range 10 keV to 1 MeV. (auth)

13217 IMPROVEMENT OF RESPONSIVE LAYER DEPTH AND ENERGY RESOLUTION BY COOLING OF CZECHOSLOVAK SURFACE-BARRIER SILICON DETECTORS DURING THE DETECTION OF HEAVY CHARGED PARTICLES. Habanec, Josef; Fukatko, Tomas; Spalek, Vaclav (Inst. of Nuclear Research, Rez, Czech.). Jad. Energ.; 17: 30-1(Jan 1971). (In Czech).

Cooling of surface barrier radiation Si-detectors substantially improved the response layer depth and energy resolution of these detectors. Performance data are given. (auth)

13218 CONSTRUCTION OF AN INSTRUMENT FOR MORE ACCURATE, REPEATED BLOOD VOLUME DETERMINATIONS USING HSA-^{131}I. Bojsen, J.; Funch-Rosenberg, H.; Mueller, Th. (Finsen Inst., Copenhagen). Int. J. Appl. Radiat. Isotop.; 21: 691-5(Dec 1970).

The construction of an instrument for up to five repeated blood volume determinations on one patient by means of Human Serum Albumin(HSA)-^{131}I is presented. The system is characterized by great accuracy as well as the possibility to separate the technical uncertainties from the biological uncertainties in each determination. (auth) (UK)

13219 NUCLEAR TRACK METHODS IN SOLIDS AND ITS DEVELOPMENT. PART I. FUNDAMENTALS, AND THE TRACKS IN MINERAL AND IN GLASS. Sakanoue, Masanobu (Kanazawa Univ., Japan). Kagaku No Ryoiki; 24: 124-37(Feb 1970). (In Japanese).

The fundamentals of the method for observing charged particle tracks formed in various dielectric solids by etching with a chemical reagent are explained. They involve the formation mechanism of tracks and sensitivity (1), the etching process (2), the influence of external conditions (3), and the observation method (4). The tracks in various minerals and their application are described and include the following subjects: 1. the distribution and concentration measurement of fissile nuclides such as uranium; 2. neutron flux distribution and dose measurement; 3. nuclear-chemical investigation such as the measurement of cross section for nuclear fission reaction; 4. age determination; and 5. α recoil tracks and other tracks. The tracks in glassy substances and their application are described with mention of uranium concentration and age determination and neutron dose measurement. (TACHIYA, M) (Japan)

13220 TRIPLET-TRIPLET INTERACTIONS IN ORGANIC SCINTILLATORS. Birks, J. B. (Argonne National Lab., Ill.). Chem. Phys. Lett.; 7: 293-5(15 Oct 1970).

Data on the prompt and delayed scintillation emission of an organic liquid solution are analyzed to obtain the triplet-triplet interaction parameters. (auth)

13221 CALIBRATION FIGURES FOR THE TYPE 1383A IONIZATION CHAMBER. Woods, M. J. (National Physical Lab., Teddington, Eng.). Int. J. Appl. Radiat. Isotop.; 21: 752-3(Dec 1970).

A comprehensive list of calibration figures for the NPL γ-chamber used with and without liner are tabulated. The values apply to 1g of solution in an NPL type 2 ml ampoule. Responses for the following radioactive nuclides are given: ^{22}Na, ^{24}Na, ^{42}K, ^{46}Sc, ^{51}Cr, ^{54}Mn, ^{56}Mn, ^{57}Co, ^{59}Fe, ^{60}Co, ^{75}Se, ^{82}Br, ^{85}Sr, ^{87m}Sr, ^{95}Nb, ^{99m}Tc, ^{113m}In, ^{131}I, ^{132}I, ^{137}Cs, ^{139}Ce, ^{141}Ce, ^{198}Au, and ^{203}Hg. Errors in the measurements are discussed. (UK)

13222 REVIEW OF COMMERCIAL STATIC SYSTEMS OF CAMERAS USED IN NUCLEAR MEDICINE. Husak, Vaclav (University Hospital, Olomouc, Czech.). Jad. Energ.; 17: 15-26(Jan 1971). (In Czech).

A review of literature data on scintillation cameras produced by Nuclear Chicago, Picker Nuclear, Nuclear Enterprises, Baird Atomic and Brevatome is presented. The principles of the design of individual instruments (Anger's camera, Ter-Pogossioan' and spark camera, Bender and Blau's autofluoroscope) and characteristics used for their evaluation (resolution, sensitivity, homogeneity linearity, resolution time) are briefly described. Some improvements of commercial cameras that have been described in the literature, the application possibilities in radiodiagnostics and comparison results with rectilinear seamers are reported. (69 references) (auth)

13223 ^{133}Xe PULMONARY-FUNCTION ANALYZER. Blum, A. S. (Broward General Medical Center, Fort Lauderdale, Fla.). Isotop. Radiat. Technol.; 8: 226-36(1970-71).

A mobile system is described for the automatic, separate measurement of the function of each lung. External measurement of the gamma radiation of ^{133}Xe eliminates the need to seal catheters within the bronchial tree. Lung-volume data are computed and displayed digitally in liters. A volumetric maneuver that calibrates the entire system, including the patient, makes this computation possible. The radioactive gas, supplied in a tank of compressed air, is metered and dispensed by an electrically operated valve. Radioactivity in exhaled air is removed by a trap; this minimizes the problem of handling radioactivity and avoids environmental contamination. (auth)

13224 PUNCHED TAPE OUTPUT OF VAKUTRONIK MEASURING EQUIPMENT WITH OUTPUT PRINTER. Franke, J.; Winkler, K. (Zentralinstitut fuer Physikalische Chemie, Berlin). Isotopenpraxis; 6: 288(Aug 1970). (In German).

A schematic diagram for the printer adjustment for a Vakutronik liquid scintillation output printer is presented. (W.H.K.)

13225 FREQUENCY OF SPURIOUS ALARMS IN RADIATION MONITORING BY THE ANALOG AND BY THE DIGITAL METHODS. Andresen, E. G. (Staatliche Ingenieurakademie Grauss, Berlin). Kerntechnik; 12: 399-405(Sep 1970). (In German and English).

Spurious alarms occurring in the digital monitoring method are investigated on the basis of the same criteria as for the analog method. The two methods are compared critically. It is found that the digital method is distinctly superior. (auth)

13226 MEASUREMENT OF FAST REACTOR TYPE NEUTRON SPECTRA BY FOIL ACTIVATION TECHNIQUES. Chiocchio, O.; Dierckx, R.; Maracci, G. (EURATOM-CCR, Ispra, Italy). Nucl. Instrum. Methods; 91: 45-56(1971).

Four unfolding methods are described in order to evaluate from integral activation data, the differential neutron spectrum of the fast reactor type. A simulated experiment is executed. In five prechosen, 16-group spectra, activation data are calculated for a series of foil detectors. Each of the unfolding methods is tested, using these activation data as input. The resulting differential spectra are compared between each other. The unfolding methods are experimentally verified. The spectra measured are the transmission of thermal reactor spectra through a ^{10}B capsule. In the experiments standard spectra for intercalibration of detectors are used in order to eliminate the errors of absolute counting and first order errors in activation cross sections. (auth)

13227 ROCKET INSTRUMENT FOR MEASURING ENERGY SPECTRUM AND DIRECTIONAL DISTRIBUTION OF MEDIUM ENERGY PROTONS IN THE AURORAL ZONE. Raethjen, H.; Ulmann, R. (Institut fuer Reine und Angewandte Kernphysik, Kiel. AEG-Telefunken-Forschungsinstitut, Ulm, Ger.). Atompraxis; 16: 395-402(Nov-Dec 1970). (In German).

To measure protons in the energy range $0.15 \leq E \leq 8$ MeV, an instrument for operation on sounding rockets has been developed. The sensor consists of one semiconductor detector as thick as the 8 MeV proton range in silicon. An electronic system is connected, which allows both the energy determination by precision pulseheight analysis in connection with an analog output, and the high speed counting of all incident particles in three integral energy channels. In order to get a sufficient energy resolution by using a linear multichannel analyser, the analog part is nonlinear in amplification. An aperture with 15 degrees half angle assures the directional sensitivity to the sensor. A sweep magnet removes incident electrons with energies <1 MeV and prevents them from entering the detector. High energy protons and electrons are ruled out from analysis by an anticoincidence detector. By two further counting channels the frequency of anticoincidences and the background counting rate are recorded. (auth)

13228 PLASMA DELAY AND PLASMA TIME JITTER IN SUBNANOSECOND TIMING WITH A SURFACE BARRIER DETECTOR. Moszynski, M.; Bengtson, B. (Univ. of Aarhus, Denmark). Nucl. Instrum. Methods; 91: 73-7(1971).

XUM

The influence of plasma on subnanosecond timing with a surface barrier detector for α-particles was studied. An initial delay was found to be inversely proportional to the electric field and it was about 1 ns for 10^4 V/cm. A time resolution study showed a significant time jitter also inversely proportional to the electric field. This effect is interpreted as being associated with the plasma discharge and it is called plasma time jitter. A time resolution of 180 ps fwhm was obtained for 5.7 MeV α-particles detected by the 50 pF surface barrier detector in coincidence with about 200 keV electrons detected by a plastic scintillation counter. The time resolution of the surface barrier detector alone was estimated to be 130 ps fwhm. (auth)

Nuclear Spectroscopic Instrumentation

Refer also to abstracts 12967 and 14841.

13229 (CEA-CONF-1647) AUTOMATION OF A SERIES OF RADIOACTIVE MEASUREMENTS ON BIOLOGICAL SPECIMENS. Farges, L. (Commissariat a l'Energie Atomique, Fontenay-aux-Roses (France). Centre d'Etudes Nucleaires). [1970]. 22p. (In French). (SM-142/46; CONF-701023-1). Dep. NTIS (U. S. Sales Only).

From Symposium on the Use of Nuclear Techniques in the Measurement and Control of Environmental Pollution, Salzburg, Austria.

Three generations in the development of the automation of laboratories can be distinguished: cable assemblies, simple programmed assemblies, and developed programmed assemblies. The characteristics of each of these are summarized. Automatic α, β, and γ measurements, which are all of the cable assembly type, are described. The direct connection of a spectrograph with a computer for the measurement of biological specimens is discussed, and the spectral analysis possible with this combination is described. (J.S.R.)

13230 (WCAP-7562-1) PLANT INSTRUMENTATION PROGRAM. Quarterly Progress Report for the Period Ending June 30, 1970. Limpert, J. C. (Westinghouse Electric Corp., Pittsburgh, Pa. Nuclear Energy Systems [Div.]). Aug 1970. Contract AT(30-1)-64. 58p. Dep. NTIS.

GAMMA SPECTROMETERS—development of lithium-drifted germanium, for scanning analysis of plutonium-bearing fuel rods and process waste
—development of sodium iodide, for scanning analysis of plutonium-bearing fuel rods and process waste
RADIOACTIVE WASTE—analysis for plutonium, development of spectrometer systems for gamma and neutron scanning
REACTOR FUEL ELEMENTS—analysis for plutonium, development of spectrometer systems for gamma and neutron scanning (W.H.U.)

13231 APPLIED γ RAY SPECTROMETRY. Second Edition Revised and Enlarged. Adams, F.; Dams, R. International Series of Monographs in Analytical Chemistry. Volume 41. Oxford, Pergamon Press (nd.). 771p. Pounds 12.

The subject is dealt with under the following headings; intrinsic variables (types of emission and decay schemes of unstable nuclei, interaction processes of radiation with matter, γ ray detectors); scintillation detectors (principles of scintillation, the detection of scintillations, sodium iodide-thallium activated crystals); semiconductor gamma detectors (general considerations, the lithium ion drift process and the germanium–lithium system, fabrication of lithium drifted detectors, germanium–lithium drifted detector characteristics, other semiconductor gamma detectors, silicon–lithium drifted detectors); proportional counters as spectrometers for low energy applications (proportional gas counter, semiconductor detectors with internal amplification); instrumentation (amplification equipment, analyzing equipment, special spectrometer arrangements, design of the detector shielding and analysis of the sources of the detector background), energy and time resolution (scintillation spectrometer statistics, energy resolution of germanium (lithium) detectors, energy resolution of the proportional gas counter); calibration of the detectors (computed efficiency of sodium iodide detectors, experimental efficiency calibration of sodium iodide detectors, calibration of germanium detectors); gamma spectrometric determination of identity, purity and quantity of radionuclides (source preparation, determination of identity and energy calibration, purity control and effects complicating gamma-ray spectra, determination of the peak area, limits of qualitative detection and quantitative determination, data reduction); specific applications (tracer applications, activation analysis, fission product studies, whole-body counters, scanners, and scintillation cameras, nondispersive x ray spectrometry). Appendices give: x ray critical absorption and emission energies in keV, a compilation of gamma-ray spectra (sodium iodide detector), a compilation of gamma-ray spectra (germanium detectors), intrinsic efficiencies of right cylindrical sodium iodide crystals, internal conversion coefficients, photon energy, atomic number, and half-life sequences of the nuclides, a compilation of precise gamma-ray energies of isotopes produced by neutron bombardment. (UK)

13232 FAST NEUTRON SPECTROMETER WITH FAST COINCIDENCE TECHNIQUE IN PROPORTIONAL COUNTERS. Mizuho, M.; Yamanaka, T. (Japan Atomic Energy Research Inst., Tokyo). Nucl. Instrum. Methods; 91: 57-60(1971).

The preliminary results on a gas-recoil proportional fast neutron spectrometer, in which a new method of electronic collimation is employed, are reported. The principle and typical performance of the electronic collimation for alpha particles are first reviewed, and in the following part, the performance of the spectrometer is described for monoenergetic neutrons of 0.6 to 1.5 MeV. The dispensation with a conventional collimator in a neutron spectrometer, by introducing an electronic collimation, was expected to reduce the background due to the collimator material, but a background continuum was still observed in the present method. However, this continuum was removed by combining the present method with a rise time discrimination method which has been described previously. (auth)

High Energy Physics Instrumentation

Refer also to abstracts 14838 and 14839.

13233 (CEA-N-1397) SIMPLIFIED METHOD OF OBTAINING INFORMATION FROM BUBBLE CHAMBER PHOTOGRAPHS AND THE USE OF AUTOMATIC SELECTION TECHNIQUES. Bouchez, Jacques; Cadiet, Francoise; Fabie, Adrienne; Laurens, Georges (Commissariat a l'Energie Atomique, Saclay (France). Centre d'Etudes Nucleaires). Dec 1970. 28p. (In French). Dep. NTIS (U. S. Sales Only).

A simplified method of obtaining information from bubble chamber photographs is presented. This method allows geometric and kinematic reconstruction followed by automatic selection. It was used to study the $\pi^- p \rightarrow \pi^- \pi^+ N$ reaction. This simplified method has been used with the HPD automatic measurement apparatus. (auth) (France)

13234 (CERN-70-21(Vol.1)) INTERNATIONAL CONFERENCE ON DATA HANDLING SYSTEMS IN HIGH-ENERGY PHYSICS, CAVENDISH LABORATORY, CAMBRIDGE, MARCH 23-25, 1970. Proceedings, Vol. I. Lord, D. H.; Powell, B. W. (eds.) (European Organization for Nuclear Research, Geneva (Switzerland)). 24 Jul 1970. 518p. (CONF-700323-(Vol.1)).

Separate abstracts were prepared for 28 of the 29 papers presented. The remaining paper was previously included in NSA and appears as 24: 44313. (W.H.K.)

For abstracts of individual papers see: 13235–13262.

13235 (CERN-70-21(Vol.1), pp 5-18) CALIBRATION, PRECISION, AND FILTERING QUESTIONS FOR THE CERN SPIRAL READER. Boeck, R. K.; Dobrzynski, L.; Eichmann, E.; Krischer, W.; Martin, F.; Pichon, G.; Rossa, E. (European Organization for Nuclear Research, Geneva (Switzerland)).

From International conference on data handling systems in high-energy physics, Cavendish Laboratory, Cambridge, March 23-25, 1970.

Preliminary precision and efficiency results of test and production measurements on individual chamber tracks and on artificial patterns performed on CERN's Spiral Reader (LSD) are summarized. The precision studies show that random errors can, with sufficient care in the calibration procedure, be brought well below the level of conventional hand-measuring apparatus. The maximum remaining systematic errors do not reach the magnitude of the x–y least count (2 μ). About 25,000 measurements of two- and four-prong events are available for judging filtering and reconstruction capabilities. Reject rates and the reasons for rejection are such that remeasurement of all rejected events may not be necessary. (auth)

13236 (CERN-70-21(Vol.1), pp 19-36) DESCRIPTION AND PERFORMANCE OF THE CERN SPIRAL READER (L.S.D.) Brandon, G.; Budde, R.; Geissler, K.; Gouache, J. C.; Nappey, P.; Ponssen, H.; Regad, G.; Rossa, E.; Trembley, J. (European Organization for Nuclear Research, Geneva (Switzerland)).

From International conference on data handling systems in high-energy physics, Cavendish Laboratory, Cambridge, March 23-25, 1970.

The main differences between the CERN and Berkeley spiral

XUM

readers are briefly described. The digitizing system and the procedure for the automatic measurement of fiducial marks are discussed. Also, the current status of the CERN spiral reader is outlined. (W.H.K.)

13237 (CERN-70-21(Vol.1), pp 39-46) ON-LINE MEASURING SYSTEM USING VISUAL DISPLAYS FOR OPERATOR GUIDANCE. Edwards, M.; Lambert, P. G.; Petmezas, G.; Smith, I. L.; Zacharov, B. (Daresbury Nuclear Physics Lab. (England)).

From International conference on data handling systems in high-energy physics, Cavendish Laboratory, Cambridge, March 23–25, 1970.

A film plane digitizer connected on-line to a computer is described. A number of data links are connected to an IBM 1800 computer which acts as a satellite buffer-multiplexer computer to a central IBM 360/65 computer. (W.H.K.)

13238 (CERN-70-21(Vol.1), pp 47-58) VAST: A VIDEO ASSISTED SCAN TABLE. Shaylor, H. R. (Birmingham Univ. (England). Dept. of Physics).

From International conference on data handling systems in high-energy physics, Cavendish Laboratory, Cambridge, March 23–25, 1970.

VAST, a three-view scanning table using electronic displays, is described. A precision C. R. T. will be used as a flying spot raster scanning system with a resolution of $10\mu-20\mu$. The video output will be displayed on a television display tube with 500 lines resolution. A variable magnification facility will be used so that any selected area of the picture can be enlarged to fill the whole of a separate display tube enabling the resolution to be increased to see fine detail. The magnification and area selection controls will be designed to be easy to use and co-ordinate. A graticule will be used to point to any specific area on the film and enable the co-ordinates of a track within the area to be transmitted to a computer. There will also be facilities for co-ordinates from the computer to be displayed on the screen. The computer could be programmed for collecting road guidance co-ordinates, and for giving assistance such as projecting tracks back to the point of origin and presenting alternate views of a given track in order to help track identification. Eventually, perhaps a fully automatic scanning system could be developed. (auth)

13239 (CERN-70-21(Vol.1), pp 61-88) OXFORD PEPR SYSTEM. Berge, J. P.; Harris, J. F.; Loken, J. G. (Oxford Univ. (England). Nuclear Physics Lab.).

From International conference on data handling systems in high-energy physics, Cavendish Laboratory, Cambridge, March 23–25, 1970.

The performance of the Oxford PEPR system in measuring some 13,000 π^-p 2 prong events is reported. The exposures were at 690 and 740 MeV/c in the Saclay 80 cm chamber. Working with zone guidance of 4 mm × 4 mm on a single view the system measured events at an average of 150 events/hour including on-line operator helping. The pass rate through Match and Geometry was 87%. Working with the vertex predigitized to 1 mm on a single view, and anti-selecting at the scan table events with a confused beam, the current system measures at 400 events/hour without operator assistance. In this mode the pass rate through Match/Geometry was 91%. (auth)

13240 (CERN-70-21(Vol.1), pp 89-104) PEPR FOR BEBC? Willder, S. S.; Brooks, C. B. (Oxford Univ. (England). Dept. of Nuclear Physics).

From International conference on data handling systems in high-energy physics, Cavendish Laboratory, Cambridge, March 23–25, 1970.

The performance of the Oxford PEPR I and PEPR II systems for scanning BEBC film is studied. Track detectability, film signal-to-noise ratio, the signal processor, and performance data are discussed. (W.H.K.)

13241 (CERN-70-21(Vol.1), pp 105-11) HEIDELBERG AUTOMATIC EVENT RECOGNITION (HAER). Klein, F.; Reiss, G.; Schmidt, R.; Schneider, H. (Heidelberg Univ. (West Germany). Institut fuer Hochenergiephysik); Brokate, K.; Erbe, R.; Keppel, E.; Kropp, D. (IBM Scientific Center, Heidelberg (West Germany)).

From International conference on data handling systems in high-energy physics, Cavendish Laboratory, Cambridge, March 23–25, 1970.

The PEPR system at Heidelberg for automatic film analysis is briefly described. The Astrodata PEPR device with an f/2 lens and one-view film transport delivered by LEITZ is connected on-line to a PDP 10 computer. (W.H.K.)

13242 (CERN-70-21(Vol.1), pp 113-24) ARNULF: A PDP-10 PROGRAM FOR RAPID ACQUISITION OF COMPLETE FILM INFORMATION BY A PEPR-DEVICE. Klein, F.; Reiss, G.; Schmidt, R.; Schneider, H. (Heidelberg Univ. (West Germany). Institut fuer Hochenergiephysik).

From International conference on data handling systems in high-energy physics, Cavendish Laboratory, Cambridge, March 23–25, 1970.

The essential operations of ARNULF are described. The bubble chamber picture is divided into scan cells of typical size 2 × 4 mm^2 (2 mm LE = length, 4 mm sweep amplitude). These cells can be partly overlapping. All cells are treated completely independently of each other. Each cell is swept by the PEPR-line element at equally spaced angles over an angle-interval of about 100°. From the hits detected in this scanning process LE's are "recognized." These LE's are precision measured in a slow sweep of small amplitude (PE-mode) at only one angle: the one averaged in the element recognition. Several PE-sweeps are performed to reduce statistical uncertainty. At the same time the critical threshold (blackening) of the track element is determined. In order to get ionization information the track element is probed with a light spot, giving a bubble bit pattern and/or bubble count. There are about 300 to 1000 scan cells per picture and one also obtains about 300 to 1000 LE's per view. All the LE's are written onto magnetic tape. The output from one roll of film (1000 frames, one view only) fits onto one reel of magnetic tape. The output from ARNULF is analyzed by the event-recognition program BERTA. (auth)

13243 (CERN-70-21(Vol.1), pp 125-39) BERTA: A FORTRAN PROGRAM FOR AUTOMATIC RECOGNITION AND RECONSTRUCTION OF BUBBLE CHAMBER EVENTS. PART I. TWO DIMENSIONS. Klein, F.; Reiss, G.; Schmidt, R.; Schneider, H. (Heidelberg Univ. (West Germany). Institut fuer Hochenergiephysik); Brokate, K.; Erbe, R.; Keppel, E.; Kropp, D. (IBM Scientific Center, Heidelberg (West Germany)).

From International conference on data handling systems in high-energy physics, Cavendish Laboratory, Cambridge, March 23–25, 1970.

The program BERTA was designed to extract all physically interesting information contained in a whole bubble chamber frame (not just one event) and to present it in such a form that (after some selection) it is ready to go into the kinematics program GRIND. A triad of output tapes from the line element acquisition program ARNULF serves as input for BERTA. In the first part of the program each view is handled separately: The LE's are combined into track pieces using circle extrapolation and circle fits in case of conflict. Fiducial marks are identified and removed from the set of LE's. The track pieces ordered according to decreasing lengths are connected to complete tracks. Tracks with recognized kinks are divided. Beam tracks are identified and counted. The bubble density of each track is determined. The number of LE's per track is reduced to a standard number. Finally a search for vertex-candidates takes place. Each track end can give rise to one or more vertex candidates. (auth)

13244 (CERN-70-21(Vol.1), pp 141-75) BERTA: A FORTRAN PROGRAM FOR AUTOMATIC RECOGNITION AND RECONSTRUCTION OF BUBBLE CHAMBER EVENTS. PART II. THREE DIMENSIONS. Klein, F.; Reiss, G.; Schmidt, R.; Schneider, H. (Heidelberg Univ. (West Germany). Institut fuer Hochenergiephysik); Brokate, K.; Erbe, R.; Keppel, E.; Kropp, D. (IBM Scientific Center, Heidelberg (West Germany)).

From International conference on data handling systems in high-energy physics, Cavendish Laboratory, Cambridge, March 23–25, 1970.

The three dimensional operations start with matching the vertex candidates to obtain space vertices. Two vertices superimposed in one view are admitted. All tracks are checked if they cross through an established vertex and if so, they are broken in two. Further search for "far away" tracks belonging to the vertex is done in each view. Vertices verified from only two views are recomputed in the third view and there possible tracks belonging to this vertex are looked for. Then track matching begins. First the tracks that led to a vertex are handled. A hierarchy of tests is applied to all possible track pair and triple combinations. Tracks accidentally crossing a vertex in one or two views will be discovered and removed from the vertex. Tracks not forming a vertex are matched now. All matched tracks go into a geometry program which is part of the system. It uses the method of the Hamburg geometry program WELAGA. All vertices are carefully fitted in space and tracks in fact missing the vertex are detected and detached from the vertex. The result is a tape carrying the reduced, interesting, geometrically identified information from the bubble chamber film. By a simple scanning routine the physicist may call certain classes of events from this tape and send them into GRIND. (auth)

13245 (CERN-70-21(Vol.1), pp 177-86) CARL: A FORTRAN PROGRAM FOR PEPR CALIBRATION USING CHEBYSHEV POLY-

XUM

NOMIALS. Klein, F.; Stroebele, H. (Heidelberg Univ. (West Germany). Institut fuer Hochenergiephysik).
From International conference on data handling systems in high-energy physics, Cavendish Laboratory, Cambridge, March 23–25, 1970.

A new PEPR calibration program, CARL, is described, putting emphasis on the numerical techniques to fully exploit the precision of PEPR. (W.H.K.)

13246 (CERN-70-21(Vol.1), pp 187-96) THE PRESENT STATUS OF THE HEIDELBERG-PEPR-HARDWARE AND PRODUCTION SYSTEM. Klein, F.; Stroebele, H. (Heidelberg Univ. (West Germany). Institut fuer Hochenergiephysik).
From International conference on data handling systems in high-energy physics, Cavendish Laboratory, Cambridge, March 23–25, 1970.

The installation and performance of the PEPR system at Heidelberg are briefly described. (W.H.K.)

13247 (CERN-70-21(Vol.1), pp 199-211) ELKE: A GRID GUIDANCE PROGRAM FOR THE RAPID MEASUREMENT OF BUBBLE CHAMBER FILM ON A PEPR FILM SCANNER CONNECTED TO A PDP-10 COMPUTER. Grimm, H.-J. (Heidelberg Univ. (West Germany). Institut fuer Hochenergiephysik).
From International conference on data handling systems in high-energy physics, Cavendish Laboratory, Cambridge, March 23–25, 1970.

The grid guidance program, ELKE, in PDP-10 assembler language and FORTRAN IV for measuring bubble chamber photographs on the PEPR device is described. Data preparation and output of measurements, event finding, hardware/software interface, programming techniques, program control, and timing are discussed. (W.H.K.)

13248 (CERN-70-21(Vol.1), pp 233-42) STATUS OF MIT'S PEPR'S. Watts, T. L. (Massachusetts Inst. of Tech., Cambridge. Lab. for Nuclear Science).
From International conference on data handling systems in high-energy physics, Cavendish Laboratory, Cambridge, March 23–25, 1970.

Developments on the PEPR system at MIT including film processing and a three-view scanning program are outlined. (W.H.K.)

13249 (CERN-70-21(Vol.1), pp 243-60) THE UCLA SMP SYSTEM. Slater, W. E. (California Univ., Los Angeles).
From International conference on data handling systems in high-energy physics, Cavendish Laboratory, Cambridge, March 23–25, 1970.

A brief review of the development of the Scanning and Measuring Projector (SMP) is given, and current development of the SMP at UCLA is reviewed. The computer and program configuration are described, and the routines in which people and computer interact most heavily are discussed including Scan, Measure, Plot and Azimuth Test, and Zoning. Plans for future development of a POLLY system are outlined. (W.H.K.)

13250 (CERN-70-21(Vol.1), pp 273-83) THE PRINCETON AUTOMATIC TRACK READER: A THREE-VIEW CRT SCANNING SYSTEM. Sekely, M. E.; Bopp, C.; Currie, J.; Gruters, M.; Knapp, B.; Maguire, W.; Sanders, H.; Wright, K. (Princeton Univ., N. J. Dept. of Physics).
From International conference on data handling systems in high-energy physics, Cavendish Laboratory, Cambridge, March 23–25, 1970.

The Princeton Automatic Track Reader (PATR) for automatic measurement of bubble and spark chamber film is described. Interfaces, digital subsystems, analog subsystems, CRT and deflection coils, the optical system, the view changer, film clamping gates, film transport, film drives, and the scan table are briefly discussed. PATR is now routinely scanning and measuring spark chamber pictures at the rate of 1500 frames/hour. (W.H.K.)

13251 (CERN-70-21(Vol.1), pp 285-92) SWEEPNIK II, AN IMPROVED TRACK MEASURING MACHINE. Frisch, O. R.; Davies, D. J. M.; Street, G. S. B. (Cambridge Univ. (England). Cavendish Lab.).
From International conference on data handling systems in high-energy physics, Cavendish Laboratory, Cambridge, March 23–25, 1970.

The development of Sweepnik II at the Cavendish Laboratory for semi-automatic measurement of bubble and spark chamber film is briefly described. (W.H.K.)

13252 (CERN-70-21(Vol.1), pp 293-308) THE PERFORMANCE OF SWEEPNIK I. Baker, R. D.; Davies, D. J. M.; Street, G. S. B. (Cambridge Univ. (England). Cavendish Lab.).
From International conference on data handling systems in high-energy physics, Cavendish Laboratory, Cambridge, March 23–25, 1970.

Results of some measurements of conventional bubble chamber events with Sweepnik I are discussed, and recent developments in the system are outlined. (W.H.K.)

13253 (CERN-70-21(Vol.1), pp 311-21) PROGRESS IN AUTOMATIC SCANNING AT COLUMBIA. Baltay, C.; Alvarez, F.; Burd, D.; (and others) (Columbia Univ., New York).
From International conference on data handling systems in high-energy physics, Cavendish Laboratory, Cambridge, March 23–25, 1970.

The automatic system for automatic scanning of bubble and spark chamber film at Columbia University which consists of an HPD with an IBM 360/91 computer is discussed. Studies of Σ leptonic decays and $\omega^0 \to 2\pi$ decays are described. (W.H.K.)

13254 (CERN-70-21(Vol.1), pp 325-55) AUTOMATIC SCANNING AND MEASUREMENT OF BUBBLE CHAMBER FILM ON POLLY II. Allison, W. W. M.; Beck, F.; Charlton, G.; Hodges, D.; Loken, J. G.; Musgrave, B.; Phillips, H. B.; Royston, R.; Sunde, R. A. (Argonne National Lab., Ill.).
From International conference on data handling systems in high-energy physics, Cavendish Laboratory, Cambridge, March 23–25, 1970.

An exposure of 600,000 hydrogen bubble chamber pictures of 2.3 GeV/c $\bar{p}p$ interactions in the 30-inch Argonne–MURA chamber is being scanned and measured for 2, 4, 6, and 8 prong interactions by POLLY II, a computer-controlled CRT device. The performance of the automatic scanning and measuring is assessed on the basis of the first 160,000 events processed. The control program searches for beam tracks and finds interactions without prescanning. It digitizes the tracks, measures bubble density and outputs master point information ready for direct input to the geometrical reconstruction program. The operator is an integral part of the system and is available to give assistance when required. Film is processed at 70 to 100 events per hour. (auth)

13255 (CERN-70-21(Vol.1), pp 357-70) PROGRESS ON POLLY AT GLASGOW. Benetta, R.; Browning, G. K. S.; Conway, A. P.; Findlay, T.; McCormick, J. W. P.; O'Donnell, H. A.; O'Neill, R.; Robinson, C. J. (Glasgow Univ. (Scotland). Dept. of Natural Philosophy).
From International conference on data handling systems in high-energy physics, Cavendish Laboratory, Cambridge, March 23–25, 1970.

The version of Polly being built at Glasgow is in principle the same as Polly II at Argonne. However, several changes have been made both to the hardware and the software, and the current progress of the system is described. (auth)

13256 (CERN-70-21(Vol.1), pp 371-81) THE USE OF COCCINELLE, A CRT DIGITIZER TO SCAN AND MEASURE BIG BUBBLE CHAMBER PICTURES. Equer, B.; Fontaine, G.; Reboul, G. (College de France, Paris. Laboratoire de Physique Nucleaire).
From International conference on data handling systems in high-energy physics, Cavendish Laboratory, Cambridge, March 23–25, 1970.

The CRT scanner Coccinelle for automatic pattern recognition and event measurement on bubble chamber photographs is described, and its application to Mirabella and other big bubble chamber pictures is briefly discussed. (W.H.K.)

13257 (CERN-70-21(Vol.1), pp 383-97) AUTOMATIC GAIN CONTROL IN SIGNAL PROCESSING FOR BUBBLE CHAMBER PICTURES. Fontaine, G.; Reboul, G. (College de France, Paris. Laboratoire de Physique Nucleaire).
From International conference on data handling systems in high-energy physics, Cavendish Laboratory, Cambridge, March 23–25, 1970.

Background variations are expected to be more and more important on pictures from the new bubble chambers which will lead to difficulty in data extraction. Therefore, a theoretical justification of automatic gain control and a review and comparison of different methods are presented. The analog division method, variable gain photomultiplier method, and the variable gain amplifier method are discussed. (W.H.K.)

13258 (CERN-70-21(Vol.1), pp 401-25) "PANGLOSS," A CRT DEVICE FOR BUBBLE CHAMBER PICTURES. Antoine, Pierre; Cech, Jan; Guignard, Claude; Guiollot, Michel; Gutmann, Micheline; Ouannes, Claude; Passeneau, Jacques; Prinzie, Michel; Robert, Marie-Josee (Paris Univ., Orsay (France). Institut de Physique Nucleaire).
From International conference on data handling systems in high-energy physics, Cavendish Laboratory, Cambridge, March 23–25, 1970.

XUM

A CRT device for bubble chamber picture analysis called PANGLOSS is described for the new generation of big bubble chambers. The detection unit, controller, track analyzer processor, and software are discussed. (W.H.K.)

13259 (CERN-70-21(Vol.1), pp 427-65) LUCY, A CRT FILM MEASURING DEVICE: A BRIEF DESCRIPTION OF THE PROTOTYPE AND RESULTS OF DETAILED HARDWARE PERFORMANCE MEASUREMENTS. Anders, H.; Jacobs, D.; Krischer, W.; (and others) (European Organization for Nuclear Research, Geneva (Switzerland)).

From International conference on data handling systems in high-energy physics, Cavendish Laboratory, Cambridge, March 23-25, 1970.

LUCY, a PDP-9 computer-controlled CRT measuring device for track chamber film, is described. Test measurements on a prototype single-view system are discussed. (W.H.K.)

13260 (CERN-70-21(Vol.1), pp 467-96) GEOMETRICAL RECONSTRUCTION FOR THE NEW BUBBLE CHAMBERS. Aderholz, M.; Bettels, J.; Bruyant, F.; (and others) (European Organization for Nuclear Research, Geneva (Switzerland)).

From International conference on data handling systems in high-energy physics, Cavendish Laboratory, Cambridge, March 23-25, 1970.

The Large Bubble Chamber Geometry (LBCG) program which is being written at CERN primarily for Gargamelle, Mirabelle, and the European 3.7-meter bubble chamber is discussed. Features of the new chambers affecting the reconstruction and the LBCG program in ASA FORTRAN are described. (W.H.K.)

13261 (CERN-70-21(Vol.1), pp 497-503) GLOBAL METHOD OF FIDUCIAL RECOGNITION WITH FISH-EYE LENSES. Thompson, M. A. (Wisconsin Univ., Madison. Dept. of Physics).

From International conference on data handling systems in high-energy physics, Cavendish Laboratory, Cambridge, March 23-25, 1970.

A global method for fiducial crosses where the fiducial arms are at the same angle is described which locates the unknown frame positions by recognizing fiducials in the midst of extreme noise due to scratches, delta rays, poor illumination, and crossing tracks. Development of the system is discussed, and advantages and disadvantages are outlined. (W.H.K.)

13262 (CERN-70-21(Vol.1), pp 505) THE STATUS OF SATR. Thompson, M. A. (Wisconsin Univ., Madison. Dept. of Physics).

From International conference on data handling systems in high-energy physics, Cavendish Laboratory, Cambridge, March 23-25, 1970.

The present status of the SATR system for bubble and spark chamber film analysis at the University of Wisconsin is outlined, and plans for the future are briefed. (W.H.K.)

13263 (CERN-70-21(Vol.2)) INTERNATIONAL CONFERENCE ON DATA HANDLING SYSTEMS IN HIGH-ENERGY PHYSICS, CAVENDISH LABORATORY, CAMBRIDGE, MARCH 23-25, 1970. Proceedings, Vol. II. Lord, D. H.; Powell, B. W. (eds.) (European Organization for Nuclear Research, Geneva (Switzerland)). 24 Jul 1970. 491p. (CONF-700323-(Vol.2)).

Separate abstracts were prepared for 33 of the 34 papers included. One paper was previously included in NSA and the abstract appears as 24: 39349. (W.H.K.)

For abstracts of individual papers see: 13264–13294, 14838, and 14839.

13264 (CERN-70-21(Vol.2), pp 539-48) WIRE SPARK CHAMBER DESIGN AND PERFORMANCE USING FET, CAPACITOR READOUT. Nunamaker, T. A.; Neumann, M. (Chicago Univ., Ill. Enrico Fermi Inst.).

From International conference on data handling systems in high-energy physics, Cavendish Laboratory, Cambridge, March 23-25, 1970.

The spark chambers have three electrodes: the center electrode is a thin aluminum pulse electrode and the outside electrodes are X and Y readout grid wires. The design, operation, and performance of the capacitor memory FET readout circuit are described. (W.H.K.)

13265 (CERN-70-21(Vol.2), pp 551-9) FOCUS REMOTE ACCESS SYSTEM. Palandri, E. M. (European Organization for Nuclear Research, Geneva (Switzerland)).

From International conference on data handling systems in high-energy physics, Cavendish Laboratory, Cambridge, March 23-25, 1970.

The FOCUS system, a small-scale multi-access data-acquisition and file-handling system, is described. It has been designed and implemented at CERN on a CDC 3100 computer which is connected to CERN's central computers, a CDC 6600 and CDC 6500. The system was developed to provide fast turn-around for sample calculations on data produced by wire and spark chamber experiments. (W.H.K.)

13266 (CERN-70-21(Vol.2), pp 581-606) COST-EFFECTIVENESS OF DIFFERENT SPARK CHAMBER READ-OUT AND DIGITISING SYSTEMS. Osmon, P. E.; Strong, J. A. (Westfield Coll., London (England)).

From International conference on data handling systems in high-energy physics, Cavendish Laboratory, Cambridge, March 23-25, 1970.

The characteristics and costs of five kinds of spark chamber readout systems are reviewed. The film flying spot digitizer, television (vidicon), sonic, magnetic core, and magnetostrictive systems are compared. Digitizing and temporary storage, computers, cost comparison, and readouts for spark chambers in magnetic fields are discussed. (W.H.K.)

13267 (CERN-70-21(Vol.2), pp 607-15) THE HPD-IBM 360/44 SYSTEM REALIZED AT C.N.A.F. FOR BUBBLE CHAMBER DATA ANALYSIS. I. THE SYSTEM CONFIGURATION AND ITS PERFORMANCE IN ROAD GUIDANCE. Cecchet, G.; Dameri, M.; Luvisetto, M. L.; Masetti, M.; Misuri, G.; Romagnoli, U.; Sala, A.; Venturi, D.; Zanotti, U. (Istituto Nazionale di Fisica Nucleare, Bologna (Italy)).

From International conference on data handling systems in high-energy physics, Cavendish Laboratory, Cambridge, March 23-25, 1970.

The system is briefly described, and block diagrams of the hardware system configuration and the GATE processing system for FSD data are given. The over-all geometry rejection rate of the HPD road guidance system determined on 3041 four-prong events was ≈14%. The exact percentage of the different causes of these rejects and uncertainties has not been determined. (W.H.K.)

13268 (CERN-70-21(Vol.2), pp 617-24) THE HPD-IBM 360/44 SYSTEM REALIZED AT C.N.A.F. FOR BUBBLE CHAMBER DATA ANALYSIS. II. SOFTWARE AND HARDWARE DEVELOPMENTS OF THE HPD 360/44 SYSTEM AT C.N.A.F. FOR BUBBLE CHAMBER DATA ANALYSIS. Castelvetri, A.; Fonti, L.; Ghiselli, A.; Luvisetto, M. L.; Masetti, M.; Misuri, G.; Romagnoli, U.; Sini, G. P.; Venturi, D.; Zanotti, U. (Istituto Nazionale di Fisica Nucleare, Bologna (Italy)).

From International conference on data handling systems in high-energy physics, Cavendish Laboratory, Cambridge, March 23-25, 1970.

A flow chart for the IBM 360/44 and the IBM 7094 is presented and briefly discussed. Also, the CRT display and light pen are mentioned. (W.H.K.)

13269 (CERN-70-21(Vol.2), pp 625-30) THE HPD-IBM 360/44 SYSTEM REALIZED AT C.N.A.F. FOR BUBBLE CHAMBER DATA ANALYSIS. III. THE NEW OFF-LINE GLOBAL FILTER PROGRAM. Castelvetri, A.; Masetti, M. (Istituto Nazionale di Fisica Nucleare, Bologna (Italy)).

From International conference on data handling systems in high-energy physics, Cavendish Laboratory, Cambridge, March 23-25, 1970.

The FILTER program for off-line bubble chamber event reconstruction for the IBM 360/44 is briefly described. (W.H.K.)

13270 (CERN-70-21(Vol.2), pp 633-49) ADAM+EVA, A UNIVERSAL SCANNING AND MEASURING MACHINE FOR FILM FROM THE LARGE BUBBLE CHAMBERS. Altaber, J.; Chanel, G.; Dodd, P.; Eastwood, D.; Fucci, A.; Mazzari, C.; Stuerzinger, P.; Verkerk, C.; Wiskott, D.; Vaghin, A. I. (European Organization for Nuclear Research, Geneva (Switzerland)).

From International conference on data handling systems in high-energy physics, Cavendish Laboratory, Cambridge, March 23-25, 1970.

ADAM + EVA is a universal scanning and measuring machine for one-pass treatment of the film from the large European bubble chambers. It is a highly-automated manually-operated film-plane digitizer. The projector, the PDP8/L control computer, the interface for the PDP8/L and the CDC 3200 computers, and the hardware facilities for aid in scanning are described. (W.H.K.)

13271 (CERN-70-21(Vol.2), pp 651-64) SCANNING AND MEASURING OF HEAVY LIQUID FILM ON-LINE. Burmeister, H.; Cundy, D. C.; Sletten, H. I.; Venus, W. (European Organization for Nuclear Research, Geneva (Switzerland)).

From International conference on data handling systems in high-energy physics, Cavendish Laboratory, Cambridge, March 23-25, 1970.

XUM

To deal with the difficulties in scanning and measuring Gargamelle film, a highly interactive on-line system is being developed in the CERN heavy liquid bubble chamber group. It allows computer-guided scanning and measuring with complete geometrical reconstruction and also minimizes the manual book-keeping effort. It is based on a working system of seven measurement tables on-line to a CDC 3100 with full geometry. The present system is briefly reviewed and the philosophy and main features of the one planned are given. (auth)

13272 (CERN–70-21(Vol.2), pp 665-73) DATA PROCESSING FOR BUBBLE CHAMBERS FROM THE POINT OF VIEW OF A SMALL LABORATORY. Graebsch, W.; Hein, P.; Kirst, H.; (and others) (Deutsche Akademie der Wissenschaften zu Berlin (East Germany). Institut fuer Hochenergiephysik).

From International conference on data handling systems in high-energy physics, Cavendish Laboratory, Cambridge, March 23–25, 1970.

The development of a bubble chamber film measuring system in East Germany is discussed. The scanning table and ZMP measuring projector are described. A small TPA computer (12 bit, 12 K, 10 nsec) is used. (W.H.K.)

13273 (CERN–70-21(Vol.2), pp 679-85) RESULTS ON THE USE OF A SIMPLE GEOMETRY PROGRAM FOR FILTERING HPD DATA. de La Vaissiere, Ch.; Leguey, A. (Paris Univ., Orsay (France). Institut de Physique Nucleaire); Ton That, B. (College de France, Paris).

From International conference on data handling systems in high-energy physics, Cavendish Laboratory, Cambridge, March 23–25, 1970.

The HPD is connected to a small CDC 160 A computer which performs the real time operations including a rough gating and the writing of digital images on magnetic tapes. These tapes enter as input for off-line filtering on a CDC 6600. A simple track filtering program by geometrical reconstruction is briefly described. (W.H.K.)

13274 (CERN–70-21(Vol.2), pp 689-707) THE BRUSH SYSTEM FOR AUTOMATIC PROCESSING OF BUBBLE CHAMBER PICTURES. Status Report, March 1970. Billing, H.; Ruediger, A.; Schilling, R.; Schnupp, L.; Kaufhold, R.; Gandini, F. (Max-Planck-Institut fuer Physik und Astrophysik, Munich (West Germany)).

From International conference on data handling systems in high-energy physics, Cavendish Laboratory, Cambridge, March 23–25, 1970.

The BRUSH system is intended for automatic track detection, track following, and 3D track reconstruction of bubble chamber pictures. Track detection and track following are done in the special purpose BRUSH computer, on line with the HPD. A special geometry program for the IBM 360/91 is being written to reconstruct the tracks from the track elements found by the BRUSH computer. The special hardware used for detection of track elements from the individual digitizings (Track Detection Unit) has been completed and has been attached to a general purpose computer to speed up the simulations of the BRUSH computer. The use of an active program memory and the addition of a magnetic drum will result in more program flexibility in the BRUSH computer. Modifications of the BRUSH program result in improved track following and allow detection and flagging of beam tracks to speed up the subsequent geometry program. The general concept of the geometry program is discussed. A significant feature is the direct 3D approach. First results of this geometry program are quoted. (auth)

13275 (CERN–70-21(Vol.2), pp 709-20) THE HPD–CDC 3200 SYSTEM AT AMSTERDAM. de Boer, R. J.; van Dam, P. H. A.; Harting, D.; Hertzberger, L. O.; Holthuizen, D. J.; van Leeuwen, W. M.; Snoek, C. (Amsterdam Univ. (Netherlands). Zeeman-Laboratorium).

From International conference on data handling systems in high-energy physics, Cavendish Laboratory, Cambridge, March 23–25, 1970.

The hardware configuration and digitizing method are briefly discussed, and the main features of the Minimum Guidance program are described. Preliminary results of the ionization measurements and future developments such as BEBC and Zero Guidance are discussed also. (W.H.K.)

13276 (CERN–70-21(Vol.2), pp 721-7) EXPERIENCES WITH COUPLED COMPUTERS TO CONTROL AN HPD. Mueck, H. J.; Nagel, H.-H.; Selonke, F. (Bonn Univ. (West Germany). Institut fuer Physikalische); Blobel, V.; Hellwig, B.; Moenkemeyer, D.; Raubold, E. (Deutsches Elektronen-Synchrotron, Hamburg (West Germany). Hamburg Univ. (West Germany). II. Institut fuer Experimentalphysik).

From International conference on data handling systems in high-energy physics, Cavendish Laboratory, Cambridge, March 23–25, 1970.

A different approach by the Bonn–Hamburg collaboration for computer control of an HPD is described. The HPD is controlled by a small PDP 9 computer which is directly connected to the large IBM/360–75 central computer at DESY via a 1.2 Mbyte/sec data channel and a separate Direct Control Feature (DCF). The DCF enables both computers to interrupt each other in order to transmit an 8-bit Byte of control information. (W.H.K.)

13277 (CERN–70-21(Vol.2), pp 729-34) USE OF IBM DATA MANAGEMENT TO CONTROL BUBBLE CHAMBER DATA FLOW. Raubold, E. (Deutsches Elektronen-Synchrotron, Hamburg (West Germany)).

From International conference on data handling systems in high-energy physics, Cavendish Laboratory, Cambridge, March 23–25, 1970.

The available cataloging facilities of the IBM 360 Operating System are briefly described; and the uses of the facility are outlined including managing a tape library and data set retrieval, automatic generation of new data set names, and automatic transfer of data between jobs. (W.H.K.)

13278 (CERN–70-21(Vol.2), pp 737-52) THE STATUS OF THE HPD MINIMUM GUIDANCE PROGRAMS AT CERN. Altaber, J.; Ferran, P.; Gerard, M.; Head, A.; Krischer, W.; Messerli, R.; Sambles, A.; Williams, D. (European Organization for Nuclear Research, Geneva (Switzerland)).

From International conference on data handling systems in high-energy physics, Cavendish Laboratory, Cambridge, March 23–25, 1970.

The HPD Minimum Guidance chain of programs for bubble chamber particle track analysis is described, and recent developments in the program chain are discussed. (W.H.K.)

13279 (CERN–70-21(Vol.2), pp 753-60) DEVELOPMENT OF TRACK CHAMBER PICTURE PROCESSING SYSTEMS AT THE JOINT INSTITUTE FOR NUCLEAR RESEARCH. Govorun, N. N.; Inkin, V. D.; Karzhavin, Yu. A.; Mescheryakov, M. G.; Moroz, V. I.; Pose, R.; Shigaev, V. N.; Shkundenkov, V. N. (Joint Inst. for Nuclear Research, Dubna (USSR)).

From International conference on data handling systems in high-energy physics, Cavendish Laboratory, Cambridge, March 23–25, 1970.

A brief survey of the status of the track chamber processing system is given. Semi-automatic measuring devices (PUOS) on-line to the BESM-4 and MINSK-22 computers, HPD on-line to the CDC-1604A computer, CRT automatic scanner on-line to the BESM-4 computer, and bubble and spark chamber picture processing programs are described. (W.H.K.)

13280 (CERN–70-21(Vol.2), pp 761-804) PERFORMANCE OF THE DAPR SYSTEM. White, H. S.; Hall, D. (California Univ., Berkeley. Lawrence Radiation Lab.).

From International conference on data handling systems in high-energy physics, Cavendish Laboratory, Cambridge, March 23–25, 1970.

Results of a comparison experiment to determine the performance of the Digital Automatic Pattern Recognition (DAPR) system for bubble chamber particle track analysis are presented and discussed. The DAPR hardware consists of a Hough–Powell FSD and an IBM 7094-II computer. (W.H.K.)

13281 (CERN–70-21(Vol.2), pp 813-24) BUBBLE CHAMBER FILM MEASUREMENT ON HPDs AT CERN. Blair, W. M. R.; Powell, B. W. (European Organization for Nuclear Research, Geneva (Switzerland)).

From International conference on data handling systems in high-energy physics, Cavendish Laboratory, Cambridge, March 23–25, 1970.

The present status and plans for future development of the HPD systems at CERN for bubble chamber film measurement are reviewed. Bubble chamber experiments completed or in progress on CERN HPD's are listed in a table. (W.H.K.)

13282 (CERN–70-21(Vol.2), pp 825-30) SYSTEM FOR ON-LINE CONTROL OF BUBBLE CHAMBER MEASUREMENTS. Blomqvist, G.; Holmgren, S. O.; Hulth, P. O.; Svedin, U. (Stockholm Univ. (Sweden). Inst. of Physics).

From International conference on data handling systems in high-energy physics, Cavendish Laboratory, Cambridge, March 23–25, 1970.

A hardware system that connects a measuring device for bubble chamber pictures, "Enetra," on-line to a CDC 8090 computer has been constructed by the Stockholm group. The software is under development. The measurements will be performed using a measurement list. Auxiliary data such as event type and ionization will be entered through a set of thumbwheel-switches, and demands will be given by the operator through push-buttons each with a specific function. The operator will be guided in the measurements by a label display and a set of message lamps. No typewriter is necessary in the system. The data from the measurements will be stored on magnetic tape. The on-line system will be used as a complement to a future Spiral Reader System. (auth)

13283 (CERN-70-21(Vol.2), pp 831-50) PATTERN RECOGNITION METHODS FOR OMEGA AND SFM SPARK CHAMBER EXPERIMENTS. Bourgeois, F.; Grote, H.; Lassalle, J-C. (European Organization for Nuclear Research, Geneva (Switzerland)).

From International conference on data handling systems in high-energy physics, Cavendish Laboratory, Cambridge, March 23–25, 1970.

The basic ideas of the pattern recognition programs being developed at CERN for the different types of particle detectors that are likely to be used in the Omega and the Split Field Magnet projects are presented. Optical spark chambers operated inside the Omega magnet, multiwire proportional chambers operated in the Split Field Magnet system, and filmless methods for the Omega project are discussed. (W.H.K.)

13284 (CERN-70-21(Vol.2), pp 851-7) THE DIGITIZED MICROSCOPE (OR DM): A MEASURING DEVICE FOR THE EVALUATION OF PHOTO EMULSIONS IN HIGH-ENERGY PHYSICS AT MPI IN MUNICH, GERMANY. Brettel, H.; Carathanassis, C.; Kollmeder, L. (Max-Planck-Institut fuer Physik und Astrophysik, Munich (West Germany)).

From International conference on data handling systems in high-energy physics, Cavendish Laboratory, Cambridge, March 23–25, 1970.

A computer-based microscope system for the automatic scanning and measuring of bubble and spark chamber film is described. The system consists of a microscope and its associated electronics, parts of the HPD electronics and data connections, a PDP-8, and an IBM 360/91. (W.H.K.)

13285 (CERN-70-21(Vol.2), pp 859-78) ARIANE II: AN AUTOMATIC DEVICE FOR THE ANALYSIS OF SPARK CHAMBER PHOTOGRAPHS. Dillet, A.; Goldwasser, M.; Michau, J. C.; Mullie, J.; Pichard, B.; Riols, G. (Commissariat a l'Energie Atomique, Saclay (France). Centre d'Etudes Nucleaires).

From International conference on data handling systems in high-energy physics, Cavendish Laboratory, Cambridge, March 23–25, 1970.

ARIANE II, a flying-spot CRT controlled by a small on-line computer (CDC 8090) for automatic analysis of spark chamber photographs, is described. The hardware, main features, analysis of a frame, centering the spot on a line, and measuring are discussed. (W.H.K.)

13286 (CERN-70-21(Vol.2), pp 879-905) AN EVALUATION OF REVERSE DEVELOPED FILM MEASURED ON HPD 2. Eastwood, D. (European Organization for Nuclear Research, Geneva (Switzerland)).

From International conference on data handling systems in high-energy physics, Cavendish Laboratory, Cambridge, March 23–25, 1970.

The advantages and disadvantages of reverse developed (dark field) film from bubble and spark chambers for analysis in flying-spot digitizers are discussed. A roll of 700 frames of film exposed in the CERN 2-meter hydrogen bubble chamber was reverse developed and a similar quantity of film was normally developed and measurements were made on the film with the CERN HPD 2 system. It was found that reverse developed film offers two definite advantages for automatic measuring machines: the signal-to-noise ratio was improved for track detection and the average number of digitizings per frame was considerably reduced. (W.H.K.)

13287 (CERN-70-21(Vol.2), pp 907-9) THE PRESENT DATA ANALYSIS SYSTEM OF THE BUBBLE CHAMBER GROUP AT THE MPI MUNICH. Freund, P.; Seyerlein, J. (Max-Planck-Institut fuer Physik und Astrophysik, Munich (West Germany)).

From International conference on data handling systems in high-energy physics, Cavendish Laboratory, Cambridge, March 23–25, 1970.

A brief description is given of the bubble chamber track analysis system, which consists of one SOM ENETRA and two Vanguard film-plane digitizers, six home-made scanning and image-plane measuring tables equipped with modified DMAC-pencil followers, and one HPD flying spot digitizer. One PDP 8 is used to collect the data from the film-plane and image-plane digitizers. (W.H.K.)

13288 (CERN-70-21(Vol.2), pp 911-20) THE IBM 1130 COMPUTER ON-LINE SYSTEM AT TORINO. Gamba, D.; Werbrouck, A. (Istituto Nazionale di Fisica Nucleare, Turin (Italy)).

From International conference on data handling systems in high-energy physics, Cavendish Laboratory, Cambridge, March 23–25, 1970.

The hardware configuration, actual measurement procedure, dialogue, and background analysis procedure for the IBM 1130 on-line system for bubble chamber track analysis at Torino are described. (W.H.K.)

13289 (CERN-70-21(Vol.2), pp 921-30) OPERATIONAL EXPERIENCE WITH THE BROOKHAVEN ON-LINE DATA FACILITY. Lindenbaum, S. J.; Ozaki, S. (Brookhaven National Lab., Upton, N. Y.).

From International conference on data handling systems in high-energy physics, Cavendish Laboratory, Cambridge, March 23–25, 1970.

The hardware, local data handling equipment, and satellite computers for the Brookhaven On-Line Data Facility for on-line experiments utilizing electronic digitized detectors such as counters, counter and spark chamber hodoscopes, etc., are described. Typical configurations of users utilizing the PDP-6 facility and the combined PDP-6 and PDP-10 facility are shown. (W.H.K.)

13290 (CERN-70-21(Vol.2), pp 931-40) OPERATOR INTERVENTION IN THE IMPERIAL COLLEGE HPD SYSTEM. Penney, B. K. (Imperial Coll. of Science and Technology, London (England). Dept. of Physics).

From International conference on data handling systems in high-energy physics, Cavendish Laboratory, Cambridge, March 23–25, 1970.

A light pen and CRT system is described which allows operator remeasurement of tracks that have been inadequately filtered after HPD digitization. A flow chart of the light pen measurement procedure is given and some test results are discussed. (W.H.K.)

13291 (CERN-70-21(Vol.2), pp 941-8) PRELIMINARY TESTS WITH PICTURES FROM MIRABELLE. Seite, G.; Sellier, J. C. (Commissariat a l'Energie Atomique, Saclay (France). Centre d'Etudes Nucleaires).

From International conference on data handling systems in high-energy physics, Cavendish Laboratory, Cambridge, March 23–25, 1970.

An automatic gain control for an HPD system for bubble chamber track analysis of dark background film from Mirabelle is described. (W.H.K.)

13292 (CERN-70-21(Vol.2), pp 949-52) BIRMINGHAM TRACK ANALYSIS SYSTEM. Simmons, J. (Birmingham Univ. (England). Dept. of Physics).

From International conference on data handling systems in high-energy physics, Cavendish Laboratory, Cambridge, March 23–25, 1970.

The system is based on a conventional HPD attached online, via a 2701, 16 bit parallel data adapter, to a semi-dedicated IBM 360/44 computer with a memory of 256 K bytes, 2 high speed channels and a multiplexer channel. The 2701 is attached to one of the high speed channels and the 2 system disks (IBM 2311 with 7M bytes capacity each) and four 1600 b.p.i. tape drives to the other. The low speed multiplexer services the usual low speed devices, card reader, printer and console typewriter, together with a single disk drive, a channel to channel link to an IBM 1800 computer and an IBM 2250 display unit. (W.H.K.)

13293 (CERN-70-21(Vol.2), pp 953-62) THE WEIZMANN INSTITUTE SPIRAL READER SYSTEM. Ronat, E. E.; Brafman, H.; Eisenberg, Y.; Reuter, B.; Shapira, A.; Yaari, R.; Yekutieli, G. (Weizmann Inst. of Science, Rehovoth (Israel). Dept. of Nuclear Physics).

From International conference on data handling systems in high-energy physics, Cavendish Laboratory, Cambridge, March 23–25, 1970.

The mechanical-optical hardware, the PDP-9 computer, the control electronics, on-line software, and checkout and performance results of the Weizmann Institute spiral reader system for particle track analysis are discussed. (W.H.K.)

13294 (CERN-70-21(Vol.2), pp 963-77) GLOSSARY OF ON-LINE MEASURING DEVICES. Beck, F. (Argonne National Lab., Ill.).

From International conference on data handling systems in high-energy physics, Cavendish Laboratory, Cambridge, March 23–25, 1970.

A table of manual, semi-automatic, and automatic particle track measuring machines attached to computers that was compiled from data from questionnaires circulated at the Cambridge conference is presented. The systems are listed by installation, machine description or name, computers, person to contact, year started, and current status. (W.H.K.)

XUM

13295 (JINR–P13-5404) EXPERIMENTAL IONIZATION CHAMBER FILLED WITH LIQUID AND SOLID ARGON. Golovanov, L. B.; Ryabtsov, V. D.; Silaev, E. A.; Tsvinev, A. P. (Joint Inst. for Nuclear Research, Dubna (USSR). Lab. of High Energy). 1970. 12p. (In Russian). Dep. NTIS (U. S. Sales Only).

A plane-parallel ionization chamber filled with liquid and solid argon is described. The results of investigations of ionization processes in argon are presented. 100% of the ionizations are collected in solid argon tested in relativistic π^--meson beam. (auth)

13296 (JINR–P13-5472) PROPORTIONAL CHAMBER FOR COMPENSATION OF COUNTER GEOMETRY IN THE TIME-OF-FLIGHT MEASUREMENTS. Zanevskii, Yu. V.; Peshekhonov, V. D.; Ronzhin, A. I.; Turala, M.; Tsisek, Z. (Joint Inst. for Nuclear Research, Dubna (USSR)). 1970. 11p. (In Russian). Dep. NTIS (U. S. Sales Only).

The compensation for counter geometry in time-of-flight spectrometers using a proportional chamber is described. The proposed method reduces completely the effect of the counter geometry on the time resolution of the π^- spectrometer. (auth)

13297 (JINR–P13-5473) SYSTEM OF PROPORTIONAL WIRE CHAMBERS ON-LINE WITH A COMPUTER. Zanevskii, Yu. V.; Nigmanov, T. S.; Peshekhonov, V. D.; Pugachevich, V. P.; Turala, M. (Joint Inst. for Nuclear Research, Dubna (USSR). Lab. of High Energy). 1970. 11p. (In Russian). Dep. NTIS (U. S. Sales Only).

A system of two proportional wire chambers on-line with a computer or analyzer is described. Results obtained by operating the system in the 4.03 GeV/c π^- beam are presented. (auth)

13298 (NAL–48-2624) SAFETY REPORT: 15-FOOT BUBBLE CHAMBER. (National Accelerator Lab., Batavia, Ill.). Nov 1970. 147p. Dep. NTIS.

The purpose of this document is to show that the NAL 15-foot hydrogen bubble chamber is safe for operation. The hazards associated with the facility have been considered and provisions incorporated into the design to insure a minimum risk to equipment and operators. The material necessary for the final design of the buildings and facilities was studied, and descriptions of all the equipment which plays an important role in the layout and arrangement of the area are given. A detailed stress analysis report on the 22-foot diameter vacuum tank, a failure mode analysis of a large rupture of the bubble chamber with spillage of liquid into the vacuum vessel, and a cryogenic systems safety report are presented. (W.H.K.)

13299 RELATIVISTIC INCREASE OF IONIZATION AND IONIZATION EFFECTS IN NUCLEAR PHOTOEMULSIONS. III. THE EXPERIMENTAL CONFIRMATION OF THE NEW MODEL. Skirda, N. V. Zh. Nauch. Prikl. Fotogr. Kinematogr.; 15: 173-9(May-Jun 1970). (In Russian).

Confirmation was given to the previously developed model for the process of relativistic increase of grain density, based on the determining role of the average sensitivity of the emulsion crystals. Experimental agreement with predictions was established. (tr-auth)

13300 SHOWER COUNTERS OF GAMMA QUANTA AND ELECTRONS. Strugalski, Z. S. (Joint Inst. for Nuclear Research, Dubna, USSR). Acta Phys. Pol.; B1: 453-65(Oct-Dec 1970).

A discussion of the methods of energy measurement of gamma-quanta and electrons is given based on results of a systematic investigation of the electron–photon propagation process in matter. Typical gamma and electron shower counters are described. (auth)

13301 HIGH RESOLUTION WIRE SPARK CHAMBER. Willis, W. J.; Hungerbuehler, V.; Tanenbaum, W.; Winters, I. J. (Yale Univ., New Haven). Contract AT(30-1)-2726. Nucl. Instrum. Methods; 91: 33-6(1971).

A magnetostrictive wire spark chamber has been constructed with a wire spacing of eight wires per mm and a 1.2 mm gap. Operated at a pressure of 15 atm of a neon–helium mixture, it has been found to give a track position accuracy of better than 75 μm. (auth)

13302 HIGH RESOLUTION OPTICAL SPARK CHAMBER. Willis, W. J. (Yale Univ., New Haven); Majka, R.; Bergmann, W. Contract AT(30-1)-2726. Nucl. Instrum. Methods; 91: 29-31(1971).

An optical spark chamber was constructed with 3 mm gaps, capable of operation at high pressures. With twenty atmospheres of a neon–helium mixture, a resolution of about 70 μm was achieved, a considerable improvement over conventional chambers. (auth)

13303 LASER BEAMS AS FIDUCIAL LINES IN BUBBLE CHAMBERS. Leutz, H. (CERN, Geneva); Wenninger, H.; Klamann, H.; Muuss, H.; Schmelzer, Ch. Nucl. Instrum. Methods; 91: 5-11(1971).

It is proposed to base the fiduciary system of large volume bubble chambers on laser beams originating from theodolite-fixed positions and thus traversing the liquid at well defined space coordinates. From a series of experiments some important conditions for this proposal have been established: Rayleigh-scattering on molecular concentration fluctuations in the chamber liquid is responsible for the visibility of laser beams which can be photographed under angles up to 90° within reasonable exposures. Small-angle random deflections of the laser beam were observed which are due to thermal turbulence in the chamber liquid and yield a rms net deflection angle of ±0.075 $\text{mrad/m}^{1/2}$. This error in angular position is about one order of magnitude smaller than that caused by multiple Coulomb scattering on the track of a 10 GeV particle. (auth)

Radiation Dosimeters

13304 (RT/PROT–(70)23) THE DOSIMETRIC USE OF BERYLLIUM OXYDE AS A THERMOLUMINESCENT MATERIAL: A PRELIMINARY STUDY. Scarpa, G. (Comitato Nazionale per l'Energia Nucleare, Rome (Italy)). 23 Jul 1970. 32p. (CONF-700505–15). Dep. NTIS (U. S. Sales Only).

From 2nd Congress of the International Radiation Protection Association, Brighton, England.

Results of a preliminary study on the dosimetric characteristics of three different grades of commercial beryllium oxide are reported. The samples were made available by a British firm in the form of sintered disks. Among useful features of this promising thermoluminescent material, a very low sensitivity to thermal neutrons (0.2 gamma rads per 10^{10} neutrons/cm^2), a fairly high sensitivity to gamma rays, and a good energy response are emphasized. These parameters allow beryllium oxide to be used in mixed fields of thermal neutrons and gamma rays, such as in nuclear reactors facilities. Sensitivity to fast neutrons was found to be between 6 and 9% of that to ^{60}Co gamma rays. Other parameters tested were glow-curve, fading, linearity with dose, and light decay. (auth)

13305 SOME PRACTICAL RESULTS OF FERROUS-SULFATE (FRICKE) DOSIMETRY. Koch, W. (Zentralinstitut fuer Festkoerperphysik und Werkstofforschung, Dresden). Isotopenpraxis; 6: 337-44(Oct 1970). (In German).

The Fricke dosimeter is one of the chemical dosimeters, which meets nearly perfectly some main requirements of practical dosimetry. By application of a 10^{-4} to 10^{-2} $\underline{m}$ solution of $FeSO_4$ in 0.4 to 2.0 $\underline{m}$ H_2SO_4, saturated with air, the Fricke dosimeter can be used as a standard for comparing the results of different laboratories for doses up to 5×10^4 rad. The $FeSO_4$ dosimeter is applicable as a secondary standard to the calibration of other chemical dosimeters. (108 references) (auth)

13306 DOSIMETRY OF IONIZING RADIATION THROUGH SOLID-DYE SYSTEMS. Prokert, K.; Stolz, W. (Technische Univ., Dresden). Isotopenpraxis; 6: 325-30(Sep 1970). (In German).

A solid dye dosimeter, used for absorbed-dose measurement ranging from $5 \cdot 10^3$ to $5 \cdot 10^7$ rad is described. Polystyrene is used as base material, in which leuco compounds of triphenyl methane dyes (crystal violet leuco cyanide or leuco malachite green) and 1,4-diiodiobenzene are incorporated. Only exposure to ionizing radiation produces dye formation proportional to the absorbed dose, which renders possible safe determination of the absorbed dose through spectrophotometric measurement. The dosimeter is especially suitable for use on radioprocesses (radiosterilization, food irradiation, radiation chemistry etc.) taking place in intensive radiation fields, of gamma-ray irradiation plants or electron accelerators. The description covers manufacture, properties, and some typical uses of the dosimeter. The reaction mechanism is discussed. (auth)

Radiometric Instruments

Refer also to abstracts 13110 and 13141.

13307 NUCLEAR SYSTEM INDICATES BLAST FURNACE LEVELS. Can. Contr. Instrum.; 8: 32(Dec 1969).

A brief account is given for more accurate control with a nuclear instrumentation system which converts transmitted radiation into an electrical current to operate indicating lights and recording instruments. Seven radioisotope sources of ^{60}Co and seven corresponding Geiger–Mueller detector tubes make up the system. Three sources are mounted in a vertical row on one side of the furnace about one foot apart. The other four are mounted at right angles to the first three and in a vertical row about one foot apart. As the stock passes through the radiation beam, it is attenuated and the appropriate indicating lights are activated and a recording made on a circular chart. The strength of the ^{60}Co sources can be low enough for safe practical use since the radiation does not have to penetrate the blast furnace wall because of a system of ports. (Canada)

13308 CONTROLLING THE VOLUMETRIC WEIGHT OF LIGHT CONCRETES IN ENCLOSING MEMBERS BY SCATTERED GAMMA RADIATION. Breitman, Z. M. Beton Zhelezobeton; 15: No. 7, 34-6(1969). (In Russian).

The design and performance of developed gamma radiometric devices for measurements of the weight of light concretes in construction are described. The optimum parameters and conditions are evaluated. The results show that the highest efficiency and statistically accurate data were obtained with 55 to 60 mm transducers, ^{137}Cs gamma radiation sources with activity of 0.08 to 0.1 mg. equiv. radium and a scintillation detector with a NaI(Tl) crystal. The relative order of error of the device did not exceed 2.1%. (R.V.J.)

13309 AUTOMOBILE EXHAUST ANALYSIS FOR LEAD USING A NUCLEAR TECHNIQUE. Sciaraffa, P. L. (Millipore Corp., Bedford, Mass.); Ziegler, C. A. Isotop. Radiat. Technol.; 8: 163-4(1970-71).

The feasibility of measuring the level of lead in the atmosphere by air sampling with a Millipore filter and then using a radioisotope-excited x-ray fluorescence analyzer to determine the lead collected is studied. Instrument design and operation, sample collection, x-ray fluorescence analysis, and calibration procedures are discussed. (W.H.K.)

13310 PORTABLE RADIOISOTOPE X-RAY ANALYZERS: TECHNIQUES AND APPLICATIONS. Rhodes, J. R. (Columbia Scientific Research Inst., Austin, Tex.). Isotop. Radiat. Technol.; 8: 153-61(1970-71).

The characteristics and uses of various commercially-available portable x-ray fluorescence analyzers are reviewed. (29 references) (W.H.K.)

13311 ON-LINE SILVER ANALYZER FOR NON-DESTRUCTIVE DETERMINATION OF SILVER SURFACE DENSITY ON CURRENT FILM STRIP. Johannes, E. (VEB RFT Messelektronik, Dresden). Isotopenpraxis; 6: 264-8(Aug 1970). (In German).

A description is given of the construction, operating mode, and sensibility of a device for continuous silver determination of films on production, operating according to the backscattering principle (^{241}Am source). (auth)

13312 SILVER ANALYZER FOR DISCONTINUOUS DETERMINATION OF THE SILVER CONCENTRATION IN EMULSION SAMPLES. Hildebrandt, J. (VEB RFT Messelektronik, Dresden). Isotopenpraxis; 6: 260-3(Aug 1970). (In German).

A description is given of the construction, operating mode, and sensibility of a device for the determination of silver concentration in photographic emulsion. The operating mode of the device is based on x-ray transmission principle (^{241}Am-source). (auth)

13313 HALF-MINUTE COUNTS FOR NEUTRON PROBES. Rogerson, T. L. (Dept. of Agriculture, Harrison, Ark.). Soil Sci.; 110: 359-60(Nov 1970).

Results of a test are presented and discussed which show that by using a 100 mC americium–beryllium neutron source in the drillhole neutron-radiometric moisture gage, counting intervals of one-half minutes are adequate to give accurate measurements. Standard deviations for measured moisture content are presented for one-minute count intervals and one-half-minute count intervals. (W.H.K.)

13314 CORRECTIONS TO OBSERVED BETA-RAY ATMOSPHERIC DENSITOMETER VALUES AS CAUSED BY COSMIC RAYS. Ballard, Harold N. (White Sands Missile Range, N. Mex.); Izquierdo, Miguel; Smith, Jack; Whitacre, John. J. Appl. Meteorol.; 9: 933-9(Dec 1970).

Theoretical and experimental studies have led to the development and fabrication of a rocketborne beta-ray densitometer for the direct determination of atmospheric density in the 30–65 km atmospheric interval. Comparison of atmospheric density profiles determined by the Betasonde densitometer with temperature-derived atmospheric density profiles showed excellent agreement to 35 km. Above 35 km, however, the two profiles gradually diverged until at 50 km the Betasonde-determined density was 35 to 40% greater than the temperature-derived density. This paper discusses the results of the cosmic ray count determination in the 0–50 km region with a cosmic ray detector, identical in configuration and sensitivity to the Betasonde, which served as a part of the instrument package on a high-altitude balloon flight from White Sands Missile Range, to 50 km on 22 September 1969. These results indicate that the differences in the comparison atmospheric density values can be attributed to cosmic rays which are detected by the Betasonde. (auth)

13315 PORTABLE NUCLEAR GAGE FOR MEASURING CEMENT CONTENT OF PLASTIC CONCRETE. Berry, P. F. (Nuclear-Chicago Corp., Austin, Tex.). Isotop. Radiat. Technol.; 8: 146-51(1970-71).

The radiometric gage can be operated in the transmission mode or the backscatter mode. NaI(Tl) scintillation detectors were used and a variety of x-ray and low-energy gamma-ray sources were used including americium-241, cadmium-109, and cobalt-57. The design, calibration, operation, and performance of the gage are discussed. (W.H.K.)

13316 MINIMIZING ERRORS IN GAMMA-RAY BACKSCATTER DENSITY GAGES: EXISTING GAGES AND NEW DESIGN CONCEPTS. McDougall, F. H.; Dunn, W. L. (North Carolina State Univ., Raleigh). Isotop. Radiat. Technol.; 8: 165(1970-71).

Research in design optimization of gamma backscatter densimeters for soil density measurements is described. (W.H.K.)

Miscellaneous Instruments and Components

Refer also to abstracts 13628, 13748, 13875, 14067, 14837, and 15411.

13317 (NP-18655) FUNDAMENTAL PRINCIPLES ON DIMENSIONING OF A COUNTER–TIMER SYSTEM. Tradowsky, K. (Kernforschungszentrum, Karlsruhe (West Germany). Labor fuer Elektronik und Messtechnik). Oct 1970. 10p. (In German). Dep. NTIS (U. S. Sales Only).

The counting of statistical events is described to establish requirements for specifications for a scaler-timer system. The calculation shows the requirements for such a system depending on dead time and pulse repetition rate at a given accuracy. (auth)

13318 (ORNL-4620) INSTRUMENTATION AND CONTROLS DIVISION ANNUAL PROGRESS REPORT FOR PERIOD ENDING SEPTEMBER 1, 1970. Sadowski, G. S. (comp.) (Oak Ridge National Lab., Tenn.). Nov 1970. Contract W-7405-eng-26. 169p. Dep. NTIS.

CONTROL SYSTEMS—development at ORNL
DATA ACQUISITION SYSTEMS—development at ORNL
DATA PROCESSING SYSTEMS—development at ORNL
ELECTRONIC EQUIPMENT—development at ORNL
FAST FLUX TEST FACILITY—instrumentation for, development of,
IN-PILE LOOPS—instrumentation for, development at ORNL of,
INSTRUMENTS—development at ORNL
LINEAR ACCELERATORS—control systems and instruments for ORELA, development of,
ORNL HIGH-FLUX ISOTOPE REACTOR—instrumentation for, development of,
PROCESS EQUIPMENT—development at ORNL
PULSE ANALYZERS —development at ORNL
RADIATION DETECTORS—development at ORNL
REACTOR CONTROL SYSTEMS—development at ORNL
REACTOR SAFETY—research at ORNL
REACTOR SIMULATORS—development at ORNL
REACTORS—instrumentation for, development at ORNL of,
THERMOCOUPLES—development at ORNL
VAN DE GRAAFF ACCELERATORS—control systems and instruments for ORNL, development of (W.H.K.)

13319 (ORNL-4643) ANALYTICAL MASS SPECTROMETRY AT OAK RIDGE NATIONAL LABORATORY. Cameron, A. E.; Christie, W. H.; McKown, H. S.; Rainey, W. T. Jr.; Smith, D. H. (Oak Ridge National Lab., Tenn.). Jan 1971. Contract W-7405-eng-26. 67p. Dep. NTIS.

The mass spectrometry group of the Analytical Chemistry Division has designed and built several mass spectrometers. These spectrometers, as well as the electronic equipment and computer programs associated with their use, are described. These instruments include those of two and three stages used primarily for the isotopic analysis of heavy metals and those of high and low resolution used for the analysis of organic compounds. Techniques and equipment used for accumulation of data are discussed. (auth)

13320 (RI-70/13) AMPLITUDE DISCRIMINATOR ON A LARGE DYNAMIC SCALE WITH PRECISE TIME DEFINITION. Delachoux, Jean-Claude (Paris Univ., Orsay (France). Laboratoire de l'Accelerateur Lineaire). Oct 1970. 58p. (In French). Dep. NTIS (U. S. Sales Only).

The discussion of the pulse discriminator covers discrimination modes and dynamic scale, data fluctuations in time and the passage to zero principle, standardization of emitted data, and the definition and precision of dead time. The passage-to-zero discriminator, the discriminator circuits, measurements and performance, and time measurement by scintillator signals simulated by diode light emitters are also discussed. (J.F.P.)

13321 (RISO-M-1270) SEMI-ANNUAL REPORT [ON ELECTRONICS], OCTOBER 1, 1969–MARCH 31, 1970. (Danish Atomic Energy Commission, Risoe. Research Establishment). Jul 1970. 14p. Dep. NTIS (U. S. Sales Only).

Topics include the DR 2 computer system; software for the hybrid computer system; evaluation of uranium reserves in Southern Greenland; field gamma-spectroscopy; determination of rare-earth elements in rock surfaces by x-ray spectrometry; fission track autoradiography; data handling system for the isotope laboratory; measurement of two-phase flow by means of laser techniques; and instrumentation for the cold neutron source in the DR 3. Also, a list of publications and lectures is included. (W.H.K.)

13322 (UCRL-50892(Vol.4)(Pt.1)) WEAPONS EFFECTS DISPLAY SYSTEM (WEDS MOD II): MAINTENANCE MANUAL. PART 1. FALLOUT DISPLAY SYSTEM. Cooper, J. H.; Peschel, D. J. (California Univ., Livermore. Lawrence Radiation Lab.). Nov 1970. 79p. Dep. NTIS.

The fallout display portion of the Weapons Effects Display System (WEDS MOD II) is described. The fallout display system computes radioactive fallout based on console-entered weapons parameters and meteorological data. Resultant patterns are displayed as an overlay on a projected map. (auth)

13323 (UCRL-50892(Vol.4)(Pt.2)) WEAPONS EFFECTS DISPLAY SYSTEM (WEDS MOD II): MAINTENANCE MANUAL. PART 2. PROMPT EFFECTS SYSTEM. Goodman, R. A.; Peschel, D. J. (California Univ., Livermore. Lawrence Radiation Lab.). Sep 1970. 185p. Dep. NTIS.

A detailed description of the prompt effects portion of the Weapons Effects Display System (WEDS MOD II) is presented together with procedures for checking out the data interface and for isolating faulty components. Detailed maintenance and troubleshooting information is presented in appendices. (auth)

13324 (UUIP-715) APPROXIMATION AND ACCURACY IN THE DESIGN OF A DOUBLE-FOCUSING FLAT SPECTROMETER. Besev, C.; Castman, B.; Groth, T. (Uppsala Univ. (Sweden). Inst. of Physics). Aug 1970. 20p. Dep. NTIS (U. S. Sales Only).

The problem of calculating accurate magnetic fields from a configuration of air-cored coils was systematically investigated by using current-sheets, current-loops and extended coils as approximations of the real coils of an existing well-established iron-free double-focusing spectrometer. The relative accuracy of the various approximations was judged on the basis of iso-aberration contours as calculated in the corresponding magnetic fields. The influence of constructional errors on the quality of the spectrometer was investigated by adding random errors to the physical parameters of the coils. The corresponding effect on the transmission-resolution characteristics was illustrated. The disturbing effect of magnetic fields from outside was investigated. The choice of a proper model for the field calculation is suggested in view of the effect of plausible constructional errors. (auth) (Sweden)

13325 REALIZING OF Z FOCUSING IN CYLINDRICAL ELECTROSTATIC ANALYZERS. Jacobs, D.; Suares, Kh. B.; Timushev, G. F.; Fuentes, Kh. (Havana State Univ.). Vestn. Mosk. Univ., Ser. III. Fiz. Astron.; 11: 466-7(Jul-Aug 1970). (In Russian).

It is shown that, in an electric field with axial symmetry, it is possible to develop radial and z focusing similar to the magnetic double-focusing analyzer. In order to produce such focusing it was necessary to create a nonhomogeneous electric field, symmetrical with the median plane of the analyzer, which decreased in absolute magnitude with increased radius. Moreover, in the median plane it should be $\sim 1/mn$, where $n > 1$. A complete double focusing was found for $n = 2$ and the angle of charged particle flight equal to π. It was also observed that at $n > 2$ the Z focusing can be achieved at smaller angles. Calculations indicate that, for measuring β-particles polarization, in order to increase the luminosity it is more efficient to use strong Z focusing without the radial focusing. In such cases the radial direction of the analyzer would perform only as a velocity selector. (R.V.J.)

13326 THERMOCOUPLE FOR ACCURATE HIGH-TEMPERATURE MEASUREMENTS IN A VACUUM AND IN THE PRESENCE OF REACTOR RADIATION. Fraktovnikova, A. F.; Gushehin, G. I.; Druzhinina, I. P.; Vladimirskaya, T. M. Meas. Tech. (USSR) (Engl. Transl.); No. 6, 865-7(Jun 1970).

Translated from Izmer. Tekh.; No. 6, 40-1(Jun 1970).

The development and testing of molybdenum–platinum/molybdenum–platinum thermocouples for in-core high-temperature measurements are described. The negative electrode was composed of a platinum alloy with 1% molybdenum and the positive electrode was composed of a platinum alloy with 5% molybdenum. Fabrication, annealing, calibration, and results of stability tests are discussed. (W.H.K.)

Radiation Effects on Instruments and Instrument Components

13327 (LCIE-364) INFLUENCE OF VARIOUS FACTORS IN DETERMINING THE VARIATION IN THE ELECTRICAL CHARACTERISTICS OF CAPACITORS EXPOSED TO GAMMA RADIATION OR ELECTRONS. (Laboratoire Central des Industries Electriques, Fontenay-aux-Roses (France)). Sep 1970. 34p. (In French). Dep. NTIS (U. S. Sales Only).

The changes in the electrical characteristics of several types of capacitors after exposure to high energy radiation were investigated. In order to obtain a better understanding of these effects, the influences of different parameters of the radiation, the environment, and the component geometries were studied. (France)

13328 (ORNL-TM-2830) EFFECTS OF NUCLEAR EMP ON AM RADIO BROADCAST STATIONS IN THE EMERGENCY BROADCAST SYSTEM. Nelson, D. B. (Oak Ridge National Lab., Tenn.). Jan 1971. Contract W-7405-eng-26. 77p. Dep. NTIS.

The effects of EMP on AM broadcast stations of the Emergency Broadcast System are studied. Interviews with station personnel and other efforts to identify typical station construction and practice, as well as analytical treatments of the transients induced by EMP on station antennas and power lines were studied. Most likely sources of damage are determined and the possibility and time requirements of effecting repairs are estimated. Station experience with lightning and a comparison of direct lightning strokes to the antenna with the EMP caused surges are included. Recommendations are given for measures which may reduce EMP damage or the extent of its effects. In most cases these are limited to procedures or low cost improvements. Conservative overdesign to achieve very high reliability is not currently recommended for stations participating in the EBS. (auth)

13329 RADIATION DAMAGE OF SEMICONDUCTOR SURFACE BARRIER DETECTORS IN MEASURING NEUTRON FLUX DENSITY DISTRIBUTIONS IN REACTORS. Graul, J.; Ruge, I. (Technische Hochschule, Munich). Kerntechnik; 12: 393-8 (Sep 1970). (In German and English).

The radiation in nuclear reactors (thermal neutrons, fast neutrons, hard gamma radiation and the conversion alpha particles of the detector itself) change the electric parameters of semiconductor barrier layers, namely the carrier lifetime, the carrier mobility and the pn-characteristics, and thus the counting properties of semiconductor detectors. Estimates of displacement cross-sections, defect generation rates, alterations of impurity concentrations owing to nuclear reactions, and the radiation resistance of silicon carbide are presented. (auth)

13330 TESTING OF ORGANOSILICATE PRESS-MATERIAL VNPM-1 IN THE REACTOR IVV-2 CORE. Kharitonov, N. P.; Krotikov, V. A.; Lysikov, B. V. At. Energ. (USSR); 29: 184-6 (Sep 1970). (In Russian).

Insulators fabricated by the method of direct hot-pressing from press-material VNPM-1 were tested before and after their irradiation in the reactor IVV-2 core. The integral dose was about $2 \cdot 10^{21}$ neutron/cm^2 under neutron flux of $5 \cdot 10^{13}$ neutron/cm^2 sec, γ-radiation of 10^8 roentg/h, and heating of components of up to 140 to 159°C. The insulation resistance R_{ins} before the tests was within the limits of 1 to $2 \cdot 10^{11}$ ohm (at 200 to 300°C) and $1 \cdot 10^8$ to $1 \cdot 10^{11}$ ohm (at 400 to 600°C). After removal of the details from the core R_{ins} was found to be $3 \cdot 10^8$ to $2 \cdot 10^{10}$ ohm, and the mechanical strength corresponded to the primary level. The press-material VNPM-1 can be recommended for fabrication of electric insulators which are used in nuclear reactors. (auth)

LIFE SCIENCES

Biochemistry, Physiology, and Molecular Biology

Refer also to abstract 13116.

Basic Processes

Refer also to abstracts 13223 and 13604.

13331 (LA-4551) PRODUCTION OF CANDIDA UTILIS WITH 93 AT. PERCENT ^{13}C ACETIC ACID AS THE SOLE CARBON SOURCE. Kollman, V. H.; Adams, W. H.; Buchholz, J. R.; Christenson, C. W.; Langham, J.; Price, R.; Fowler, Eric B. (Los Alamos Scientific Lab., N. Mex.). Sep 1970. Contract W-7405-eng-36. 9p. Dep. NTIS.

The yeast Candida utilis has been adapted to grow on acetate as a sole source of carbon. Adaptation has been followed by mass production of the organism on doubly labeled ^{13}C acetate. Concentration of ^{13}C in the acetate was 92.7% and reached 87.4% in the organism. An inhibition of growth (cell numbers) was observed when the culture was initially transferred to ^{13}C acetate. The inhibition was statistically significant at about 20 hr when ^{12}C and ^{13}C growth curves were compared. This inhibition and other observations are interpreted as an isotope effect of ^{13}C. (auth)

13332 TECHNETIUM-LABELED RED BLOOD CELLS. Eckelman, W.; Richards, P.; Hauser, W.; Atkins, H. (Brookhaven National Lab., Upton, N. Y.). J. Nucl. Med.; 12: 22-4(Jan 1971).

A method is described for the preparation of ^{99m}Tc-labeled red blood cells in dogs and rabbits. The method seemingly overcomes some of the problems previously encountered in labeling attempts. Following preparation, the stability of the labeled red blood cells was determined in vitro and in vivo. (E.R.B.)

13333 CHOLINESTERASE ACTIVITY OF THE SPINAL CORD OF ANIMALS AFTER X-RAY IRRADIATION. Snisar, I. A.; Reva, A. D. (Dnepropetrovsk State Univ., USSR). Byull. Eksp. Biol. Med.; 69: No. 6, 47-9(Jun 1970). (In Russian).

The total cholinesterase activity of different structures of the spinal cord is dissimilar: it is highest in the grey matter of the anterior and posterior horns. Phasic changes in the enzymatic activity are seen 1, 24, and 48 hours after whole-body x irradiation with a single dose of 1200 R to cats. (auth)

13334 INVESTIGATION OF VITAMIN B_{12}–^{58}Co RADIOMETRIC METHOD OF THE WHOLE BODY AFTER RESECTION OF THE STOMACH. Kaplan, M. A.; Gabuniya, R. I.; Berdov, B. A. (Inst. of Medical Radiology, Obninsk, USSR). Med. Radiol.; 15: No. 11, 34-9(Nov 1970). (In Russian).

A study of vitamin B_{12}-^{58}Co metabolism in patients after different operations on the stomach by means of whole-body radiometry demonstrates assessment of the functional state of the gastrointestinal tract. Methods for prevention of development of vitamin B_{12} hypovitaminosis are outlined. The degree of vitamin B_{12} assimilation depends on the markedness of the dumping syndrome and decreases in its severe form. Percentages of assimilated vitamin B_{12} are presented for various types of stomach surgery. (P.B.M.)

13335 MODIFICATIONS IN PHOSPHORATED ^{32}P ERYTHROCYTIC METABOLISM IN THE 2nd AND 3rd PHASE OF G.A.S. Szantay, I. (Univ., Cluj); Szirmai, E. Nucl. Hematol. (Publ. Nucl. Energy); 11: 154-6(Sep-Oct 1970).

A study was made of the correlation between the 2nd and 3rd phase of General Adaptation Syndrome (GAS) and between the Phosphorated Erythrocytic Metabolism (PEM) by the determination in vivo of the coefficient ^{32}P Plasma/^{32}P Blood and of the incorporation of $^{32}PO_4$ in the erythrocytes of rats submitted to simple stress and severe combined stress. It has been established that whereas the 2nd phase of "GAS" is characterised by the diminution of the coefficient ^{32}P Plasma/^{32}P Blood and equally by the increase in the incorporation of $^{32}PO_4$ ions in the erythrocytes, the 3rd phase of "GAS" presents this increased coefficient, a fact which denotes a diminution of the concentration of erythrocytic ^{32}P. In determining the same parameters of "PEM" in insulin shock we have demonstrated that the results obtained are obviously equal to the data recorded in the 3rd phase of "GAS." These results allow one to accept the hypothesis that in the case of combined stress one of the determining causes of the disturbance of "PEM" is the biochemical lesion of the "lack of glucose substrate" type. (auth) (UK)

13336 UPTAKE CURVE IN TRACER KINETICS. Gunn, Robert B.; Patlak, Clifford S. (National Inst. of Mental Health, Bethesda, Md.). Math. Biosci.; 6: 19-24 (1970).

The uptake function for a stationary, open, compartmental system was shown to be equal to the steady-state value less the washout function for the same system: $g_{in}(t) = G - g_{out}(t)$. This relation between an uptake experiment and a washout experiment and the established convexity of the washout curve directly proved that uptake curves must be concave. The usual semilogarithmic plot of the tracer function was shown to be equivalent to graphing the normalized washout function, whose logarithmic convexity was shown previously for a large class of systems including passive systems. Underestimation of G in such a system may cause this curve to be log concave. It was shown, however, that the complete uptake curve and thus the correct G in all systems can be constructed from an incomplete uptake curve and the elution curve starting from the end point of the uptake experiment. (auth)

13337 LOCALIZATION OF DNA SYNTHESIS AND MIGRATION OF CELLS IN LAYERS OF HAIR FOLLICLES IN LAMBS. Vsevolodov, E. B.; Babkina, E. M. (Inst. of Experimental Biology, Alma Ata, USSR). Izv. Akad. Nauk Kaz. SSR, Ser. Biol.; No. 5, 67-72(1969). (In Russian).

An autoradiographic method was used for localization of DNA synthesis and following the cell migration from cambial follicular zones. The root-sheath-dermal relationship and control of the hair growth was observed in three lambs one to three days old following injection with thymidine-^{3}H. (R.V.J.)

13338 SIGNIFICANCE OF THE TOTAL-BODY HEMATOCRIT IN MEASUREMENTS OF BLOOD COMPARTMENTS. Kirsch, Karl A.; Johnson, Raleigh F.; Gorten, Ralph J. (Duke Univ., Durham, N. C. Veterans Administration Hospital, Durham, N. C.). J. Nucl. Med.; 12: 17-21(Jan 1971).

Red cell mass and plasma volume were measured simultaneously with dual-tracer dilution techniques in 29 patients referred because of suspected abnormalities in red cell mass. A second value for each patient's red cell mass was calculated using the measured plasma volume and the venous hematocrit times a correction factor. This often-used timesaving calculation was found, on comparisons with measured values, to be subject to unpredictable and often serious error. This was evident particularly in patients with elevated values of red cell mass. These discrepancies are caused by an unpredictable difference between the correction factor applied to the venous hematocrit and an individual's total body hematocrit-to-venous hematocrit ratio. This is partly explained by the observation that the relation between red cell mass and venous hematocrit is more likely to be exponential rather than linear. For clinical or investigational purposes, red cell mass should be measured rather than indirectly calculated. Total blood volume should be determined by summation of independently measured plasma volume and red cell mass. If saving time is essential and red cell mass is to be calculated using the venous hematocrit, the magnitude of the error can be reduced in patients with hematocrits under 40% by using the correction factor 0.86 (instead of 0.91). In patients suspected of having polycythemia, no compromise should be made, and red cell mass should be measured with the red cell tagging technique. Similarly, total blood volume in these patients can only be adequately determined by dual tracer techniques for independent measurements of the plasma and red cell compartments. (auth)

13339 WHOLE BODY ^{40}K LOSS AS A PREDICTOR OF HEAT TOLERANCE IN CATTLE. Kamal, T. H.; Johnson, H. D. (Univ. of Missouri, Columbia). J. Dairy Sci.; 53: 1734-8(Dec 1970).

Eleven nonlactating Holstein cows were exposed for 3 days at 18.3°C and 50% relative humidity followed by 3 days at 32.2°C and 50% relative humidity in the climatic laboratory. Feed and water were provided ad libitum. Liquid scintillation whole body counting of ^{40}K was performed at the end of each climatic exposure. Heat caused an increase in rectal temperature ($P < 0.01$) and decreases in whole body ^{40}K ($P < 0.01$), nitrogen retention ($P < 0.01$), and body weight ($P < 0.05$). Predicted heat tolerance was measured by subtracting the percentage decrease in body potassium, due to heat exposure, from 100. The coefficient ranged from 75 to 102 among the cows studied. It was possible to arrange

XUM

the animals arbitrarily into 6 classes of predicted heat tolerance in the ascending order of: 70 to 75, 76 to 80, 81 to 85, 86 to 90, 91 to 95, and 96 to 100. The ^{40}K of the rumen contents decreased insignificantly with heat exposure and such a decrease was too low compared to the whole body ^{40}K loss; thus, it did not interfere with accuracy of the test. There was no significant correlation ($P > 0.05$) between the final rise in rectal temperature and the percentage decrease in ^{40}K or in body weight caused by heat exposure. The percentage decreases in body weight and in ^{40}K due to heat also were not correlated ($P > 0.05$). (auth)

Metabolism, Physiology, and Toxicology

Refer also to abstracts 13118, 13395, 13396, 13485, 13486, 13501, 13503, 13506, and 13593.

13340 (NP–18382) ^{137}Cs FROM GLOBAL FALLOUT IN FOODSTUFFS AND THE HUMAN ORGANISM. Prokof'ev, O. N.; Nevstrueva, M. A.; Perova, A. A.; Shvydko, N. S.; Shapiro, E. L.; Dzyubenko, I. I.; Krisyuk, E. M. (Gosudarstvennyi Komitet po Ispol'zovaniyu Atomnoi Energii SSSR, Moscow). 1969. 21p. (In Russian). Dep. CFSTI (U. S. Sales Only).

The rate of decrease of the level of contamination with ^{137}Cs of the principal food stuffs and the human organism in recent years was significantly reduced as a consequence of the role of the soil source in the uptake of ^{137}Cs in biological chain. Together with the fact that the rate of decontamination of different foodstuffs varied, therefore the contribution of different components of foods in the uptake of ^{137}Cs by the population of the RSFSR from 1965 to 1968 significantly changed: grain products was reduced from 50 to 35%, of meat from 15 to 30%, and potatoes from 8 to 14%. The zoning in levels of contamination of milk and meat with ^{137}Cs was observed: the ^{137}Cs contamination in zone I (principally stall content of cattle) is two times lower than in zone 2 (principally pasturage content of cattle). The surface and soil contamination coefficients for ^{137}Cs were evaluated in wheat grains, milk, potatoes, food, and the human organism. The size of the genetically significant dose from the incorporation of ^{137}Cs from 1962 to 1968 was only 6 mrem. The period for the half-elimination of ^{137}Cs from man, on the basis of the results of mass measurements, is in the interval from 60 to 120 days. (tr-auth)

13341 EFFECT OF DEOXIDIZED GLUTATHIONE (TATHION) ON EXCRETION OF ^{203}Hg–MHP IN KIDNEY. Oshiumi, Yoshihiko (Hiroshima Atomic Bomb Hospital); Matsuura, Keiichi; Komaki, Senichiro. Nippon Igaku Hoshasen Gakkai Zasshi; 29: 1038-46(Nov 1969).

The effect of reduced glutathione was studied as one means to minimize the renal dose of ^{203}Hg-MHP. Experiments on mice revealed that reduced glutathione (Tathion) was as effective as 1,propanol,2,3-dimercapto (BAL) with doses of 2 mg/g injected intraperitoneally. Clinical applications of 2 mg/g Tathion appeared to be impossible due to the large amount required. Therefore, 7,000 mg Tathion with 200 mg BAL was applied to determine the renal excretory rate of ^{203}Hg-MHP. The renal excretory rate was slightly greater in the treated group than in the control group. Tathion was also investigated in cases of normal renal function, and the weekly mean urinary excretory rate was observed to be 10% in the controls and 24.5% in the treated group. Urinary excretory rates were affected by renal function. It was concluded that reduced gluthathione possessed a beneficial effect on the excretion of ^{203}Hg-MHP from the kidney to reduce the renal dose. However, in the clinical cases, dosage and method of administration was not determined. It was assumed that reduced glutathione could be useful for the reduction of renal dose by using ^{197}Hg-MHP instead of ^{203}Hg, and a highly sensitive scanner. (auth) (Japan)

13342 STUDIES ON RECOVERY OF COLPODA FROM POTENTIALLY LETHAL X AND ULTRAVIOLET RADIATION INDUCED DAMAGE. Griggs, Henry Gaston. Lexington, Ky.; Univ. of Kentucky (1969). 166p. University Microfilms Order No. 70-12,354.

Thesis.

Investigations were undertaken to determine the extent and nature of systems that repair potentially lethal x- and uv-radioinduced damage in a strain of surface water Colpoda and a strain of cave Colpoda. X-ray resistances shown by the two strains were comparable to those observed for other ciliates. Both strains showed an extremely high resistance to ultraviolet radiation. Photoreactivation increased survival at higher doses but decreased survival in a range of lower doses in the surface strain. Cave strain organisms did not show photoreactivation. Ultraviolet radioinduced division delay studies revealed that the first division delay increased with dose after lower doses in both strains. Division delay decreased with dose within a range of higher doses in the cave strain. Postirradiation caffeine treatments indicated that concentrations of this purine that did not slow growth rates of unirradiated organisms resolved the dark repair mechanism of Colpoda into a caffeine sensitive system that functioned primarily after lower doses and a system, less sensitive to caffeine, that functioned primarily after higher doses. Experiments designed to determine the effect of temperature on repair system activity indicated that the dark repair system of both strains functioned more efficiently at temperatures a few degrees below optimal growth temperatures. Studies in which synchronized organisms were irradiated in different periods of the interdivision growth cycle, indicated that the x-ray resistances of the two strains varied little throughout the cycle. Administration of low doses of uv radiation to the organisms immediately after exposure to x irradiation, indicated that significant uv reactivation of x-ray damage could be accomplished in both strains. Many of the results of these studies were interpreted as indicating that there are at least two dark repair systems in Colpoda that contribute significantly to the high degree of uv radiation resistance observed in these organisms. One system functions primarily after lower doses and the other system, functioning primarily after higher doses, is activated by some component of accumulated radiation induced damage in DNA. (Diss. Abstr.)

13343 UPTAKE STUDIES IN CANINE ABDOMINAL ORGANS FOLLOWING ^{75}Se-SELENOMETHIONINE ADMINISTRATION BY A VARIETY OF INTRAVASCULAR INJECTION TECHNIQUES. Kupic, Edward A.; Kasenter, Albert G.; Janney, Clinton D. (Univ. of Vermont, Burlington). J. Nucl. Med.; 12: 35-9(Jan 1971).

Measurements were obtained of the uptake of ^{75}Se-selenomethionine in the canine pancreas, liver, spleen, and kidney following a variety of injection techniques. In many instances secretin and/or pancreozymin were used before the radiopharmaceutical. Pancreatic uptake of selenium was extremely variable, and although in some instances the use of hormone stimulants and selective arterial injection increased pancreatic uptake, the effect was not consistent. The route of administration does not seem to be of major importance for clinical scanning. (auth)

13344 AVIDIN EFFECT ON INTENSITY OF ^{14}C INCORPORATION FROM NaH^{14}CO$_3$ AND GLYCINE-1-^{14}C INTO PROTEINS AND LIPIDS OF RAT LIVER HOMOGENATES. Gulyi, M. F.; Mel'nichuk, D. O. (Inst. of Biochemistry, Kiev). Ukr. Biokhim. Zh.; 42: 322-4(1970). (In Ukrainian).

The avidin effect was studied on intensity of ^{14}C incorporation from NaHC^{14}O$_3$ and glycine-1-^{14}C into proteins and lipids of rat liver homogenates. It was shown that avidin, inhibiting the fixation of CO$_2$, approximately to the same degree inhibits the incorporation of ^{14}C from glycine-1-^{14}C into proteins and lipids. (auth)

13345 DETERMINATION OF ^{14}C IN TISSUES PROTEIN BY THE LOW-EFFECTIVE COUNTERS. Zhurbin, G. I. (Inst. of Biochemistry, Kiev). Ukr. Biokhim. Zh.; 42: 381-5(1970). (In Ukrainian).

A simple and convenient method is described to prepare samples for measuring radioactivity of ^{14}C labeled tissue proteins. A sample of denatured, washed and dried protein is solved in the known amount of concentrated formic acid and is applied to the flat metallic targets without deepening. Protein weight in the sample must not exceed 1 mg. When using microamount of protein it is not necessary to make a correction for selfabsorption, as the radioactivity of the preparation in this case is directly proportional to the amount of protein. The standard error of the average in the parallel samples does not exceed ±3%. (auth)

13346 CHANGE IN COMPOSITION OF RAT BLOOD AS AFFECTED BY ^{237}Np. Kreslov, V. S.; Mushkacheva, G. S. (Inst. of Biophysics, Moscow). Ukr. Biokhim. Zh.; 42: 489-93 (1970). (In Russian).

In rats, investigated during two to four wks after intravenous administration of ^{237}Np-nitrate in a dose of 1 μCu (1.5 mg), changes in some biochemical indexes of blood serum were observed: increase in the content of total protein at the expense of the globulin fractions in the content of residual nitrogen and sugar in the alkali and acidic phosphatase activity. These shifts, conditioned mainly by the chemical not the radiation effect of the element, showed disturbance of the functional state of the liver and kidneys when the organism was affected with neptunium in toxic amounts. The greatest changes in the blood composition of rats were observed three days after priming in the period of maximal death of the animals. This may be of both diagnostic and prognostic importance. (auth)

13347 ^{131}I RECONCENTRATION FACTOR. George, K. D. (Union Carbide Corp., New York). Health Phys.; 19: 699(Nov 1970).

To assess the correctness of the reconcentration factor, the relative magnitudes of the ^{131}I dose to a child's thyroid from a given air concentration are estimated via two routes. These are the direct inhalation route using data given by Bryant (NSA 23: 38519) and the milk route using both the data given by Burnett (NSA 24: 12086) for the relationship between air and milk concentrations and the data given by Bryant for milk intake and child's thyroid dose. The results suggest a value of 88 for the reconcentration factor. However, because of the variability in some of the parameters involved in the milk route a value for the reconcentration factor of about 200, is felt to be a more realistic estimate. (UK)

13348 EFFECT OF SUBLETHAL AND LETHAL DOSES OF IRRADIATION ON EXTRACELLULAR AND INTRACELLULAR DISTRIBUTION OF WATER IN SOME TISSUES OF RATS. Shamrai, E. F.; Sokolova, V. I. (Kiev Medical Inst.). Ukr. Biokhim. Zh.; 42: 494-8(1970). (In Ukrainian).

A decrease in water content of the brain, liver, kidneys, and skeletal muscles of rats was observed following radiation. The dehydrating effect of lethal (900 R) doses of radiation was more pronounced than with sublethal (600 R) doses. Dehydration was accompanied by an increase in the volume of plasma and extracellular fluids and a decrease of intracellular fluids. Shifts of water distribution in tissues were greater with lethal doses of radiation than with sublethal doses. Water distribution disturbances in the organ occurred before changes in total content of water were observed. (E.E.H.)

13349 PROTEOLYSIS OF PARTIALLY DENATURED ALBUMIN IN ISOLATED PERFUSED INTESTINE OF NORMAL AND IRRADIATED RATS. Gerber, G. B.; Remy-Defraigne, J.; Kocmierska-Grodzka, D. (CEN-SCK, Mol, Belgium). Strahlentherapie; 139: 744-9(Jun 1970). (In German).

The uptake and degradation of ^{131}I labeled denatured albumin were investigated in isolated perfused intestine from fed, starved, and starved irradiated rats (24 h after 800 R). Protein degradation is smaller in perfused intestine than in perfused liver and in contrast to liver decreases during starvation. Irradiation did not produce any significant changes. A modified method for perfusing isolated rat intestine is described. (auth)

13350 ^{6}Li INCORPORATION INTO TISSUES, ORGANS, AND TRANSPLANTABLE TUMORS. Letov, V. N.; Ivanov, V. N.; Ryabukhin, Yu. S.; Uspenskii, V. A.; Gorvat, F. Yu. (Inst. of Medical Radiology, Obninsk, USSR). Med. Radiol.; 15: No. 11, 50-5(Nov 1970). (In Russian).

The distribution of ^{6}Li in tissues and organs of rats was investigated with subcutaneously transplantable fibrosarcoma in intraperitoneal and intravenous routes of introduction of the preparation. In intraperitoneal injection the concentration of nuclide was the highest in 2 hrs, in intravenous, in ½ hr in the kidneys, liver, blood serum, and skin. In intravenous injection in the tumor the maximal concentration of ^{6}Li was noted in one hour, in intraperitoneal, in 3 hrs. In intraperitoneal injection the maximal concentration in the lungs is seen in 3 hrs, in the muscles in 6 hrs. In intravenous injection in the muscles between 0.5 to 8 the concentration steadily rises. In the period between 2 to 8 hrs the concentration is virtually independent of routes of injection. The nature of curves of temporal ^{6}Li distribution in the skin is similar in both routes of introduction. The most marked capacity to include ^{6}Li is endowed by the above mentioned tumor, the least by Walker carcinosarcoma 256; sarcoma-256 occupies an intermediate position. The features specific to each of the two routes of ^{6}Li injection are discussed from the viewpoint of experimental neutron capturing therapy. (auth)

13351 EFFECTS OF CONTINUOUS EXPOSURE TO RADIOACTIVE PHOSPHORUS (^{32}P) IN IONIC FORM. RESEARCH ON THE DAMAGE INDUCED IN CONTINUOUS KB CELL CULTURES. Ferrero, B.; Cirillo, R.; Piccotti, F.; Calderini, P. (Univ., Turin). Cancro; 20: 694-723(1967). (In Italian).

Cell colonies of about 100 cells each were obtained from a line of KB cells in continuous culture. Groups of these colonies were subjected to the action of scalar activities (466; 233; 116.5; 58.25 microcuries/ml) of ^{32}P dissolved in the culture medium. (auth)

13352 COMPARISON OF ^{46}Sc AND ^{144}Ce AS NONABSORBED REFERENCE MATERIALS IN STUDIES WITH CATTLE. Miller, J. K.; Byrne, W. F. (Univ. of Tennessee, Oak Ridge). Contract AT(40-1)-GEN-242. J. Nutr.; 100: 1287-91(Nov 1970).

The suitability of ^{46}Sc as a nonabsorbed reference material for cattle was investigated by simultaneous within-animal comparison with ^{144}Ce which has previously been used for this purpose. Excretions and tissue distributions of ^{46}Sc and ^{144}Ce were compared in six calves and twelve mature cattle. Tracer levels of both nuclides were given to two calves intravenously, to two as single oral doses, and to two as daily oral doses. Older animals were given either ^{46}Sc or ^{144}Ce as daily oral doses. Blood ^{46}Sc and ^{144}Ce, expressed as percentages of concentrations found 5 minutes after intravenous administration, decreased respectively from 88 and 30% at 15 minutes to 33 and 0.9% at 10 hours. Urinary ^{46}Sc and ^{144}Ce averaged 0.1 and 0.2% of intravenous doses. Neither radioisotope was detected in blood or urine after oral dosage, and recovery in feces was almost complete. Similar gastrointestinal distributions of the two nuclides were found at slaughter, and adsorption to undigested residues averaged 92% of the ^{46}Sc and 95% for ^{144}Ce. Tissues accounting for totals of 40 and 36% of intravenous ^{46}Sc and ^{144}Ce doses contained barely detectable traces of oral doses. These results indicate ^{46}Sc is as suitable as ^{144}Ce for use as a nonabsorbed reference material for cattle. Scandium-46 could substitute in mixtures with certain other radioisotopes where ^{144}Ce would be unsuitable because of its counting characteristics. (auth)

13353 PINOCYTOSIS AND MEMBRANE DILATION IN URANYL-TREATED PLANT ROOTS. Wheeler, Harry (Univ. of Kentucky, Lexington); Hanchey, Penelope. Science; 171: 68-71(8 Jan 1971).

Electron-dense crystals formed in plant roots exposed to uranyl acetate were used to identify binding sites and to follow the pinocytotic uptake of uranyl in the oat rootcap. Before uranyl enters the protoplast, the plasmalemma is greatly dilated. After uranyl is sequestered in vacuoles, the tonoplast is similarly dilated. (auth)

13354 RADIATION EFFECTS ON ^{75}Se INCORPORATION IN TUMORS FOLLOWING ADMINISTRATION OF $Na_2{}^{75}SeO_3$. Wenzel, M.; Woellgens, P. (Univ., Zurich). Klin. Wochensch.; 48: 1367-8(15 Nov 1970). (In German).

After in vitro irradiation, rat diaphragm and rat livers showed only a slight decrease in ^{75}Se incorporation when incubated with $Na_2{}^{75}SeO_3$. By contrast, the ^{75}Se incorporation increased in tumor cells after irradiation. After selective irradiation with 1500 R of tumor bearing hamsters, the affinity of different tissues for ^{75}Se remains almost unchanged in comparison with non-irradiated animals. But the ratio of the ^{75}Se activity in muscle and tumor per gram of tissue decreased significantly if the tumor was selectively irradiated with 500 R daily over 5 days and if $Na_2{}^{75}SeO_3$ was injected thereafter. As a result, scintigrams with $Na_2{}^{75}SeO_3$ may show quite different aspects before and after tumor radiotherapy. (auth)

13355 DEMONSTRATION OF A CIRCULATING FACTOR REGULATING BLOOD PLATELET PRODUCTION USING ^{35}S-SULFATE IN RATS AND MICE. Cooper, George W.; Cooper, Barbara; Chang, Chung-yueh (City Coll., New York). Proc. Soc. Exp. Biol. Med.; 134: 1123-7(Sep 1970).

Platelet counts and ^{35}S-sulfate incorporation were studied in rats and mice following injection of saline or homologous plasma from normal or platelet-depleted animals. Donor rats were treated with antiplatelet serum 5 to 8 hr before sacrifice, and donor mice were injected with neuraminidase 40 hr before exsanguination. To prevent the injection of platelet antibody, the simulated and control plasmas were either boiled at acid pH for 10 to 15 min, or precipitated with goat antirabbit gamma globulin antiserum (GAGGA). The sulfate incorporation into platelets of animals given plasma from depleted donors was significantly increased over control values to levels as high as 116%. These data demonstrated the existence of thrombopoietin control over platelet production. The radiosulfate incorporation method appeared to be more sensitive than assays making use of platelet counts alone. (auth)

13356 ^{14}C-1-PALMITATE INCORPORATION BY RAT LUNG: EFFECT OF NITROGEN DIOXIDE. Thomas, Thomas Jr.; Rhoades, Rodney A. (Pennsylvania State Univ., University Park). Proc. Soc. Exp. Biol. Med.; 134: 1181-3(Sep 1970).

The effect of breathing nitrogen dioxide (NO_2) on the in vivo incorporation and turnover of ^{14}C-1-palmitate in rat lung lecithin was studied. Continuous exposure to 5 ppm or NO_2 for 14 days markedly decreased lecithin turnover. The suggestion is made that changes in lecithin turnover may lead to alterations in the surface-active material on the alveolar surface which in turn may account for some of the damage observed in NO_2-exposed lungs. (auth)

13357 PRODUCTION OF HEPARIN RELATED MUCOPOLYSACCHARIDES BY MAMMALIAN CELLS IN CULTURE. Dietrich, Carl P.; Montes de Oca, H. (Univ. of Saskatchewan, Saskatoon). Proc. Soc. Exp. Biol. Med.; 134: 955-62(Sep 1970).

Radioactive mucopolysaccharides were isolated from HeLa, L, mouse embryo, and rat embryo cells grown in culture medium in the presence of radioactive inorganic sulfate, for 72 hr. The isolated mucopolysaccharides were submitted to mild acid hydrolysis as well as to the action of several mucopolysaccharidases and the degradation products were characterized by their migration in several chromatographic systems and on electrophoresis. It was demonstrated that part of these mucopolysaccharides are chondroitin sulfate A/C and part N-sulfated-heparin-like compounds susceptible to hydrolysis by heparinases releasing glucosamine 2, 6-disulfate as the major amino sugar residue. (auth)

13358 SPECIFICITY OF TRITIATED THYMIDINE AS A PRECURSOR OF DNA UNDER CONDITIONS OF PROLONGED ADMINISTRATION. Grieder, A.; Odartchenko, N.; Cottier, H.; Cronkite, E. P.; Schindler, R. (Swiss Inst. for Experimental Cancer Research, Lausanne, Switzerland. Univ. of Bern. Brookhaven National Lab., Upton, N. Y.). Proc. Soc. Exp. Biol. Med.; 134: 1026-9(Sep 1970).

After 90 injections of thymidine-methyl-^{3}H into adult mice at intervals of 8 hr, the radioactivities of several biochemical fractions (acid-soluble material, lipids, RNA, DNA, and protein) were determined in homogenates of various organs. A high specificity of incorporation of labeled thymidine into DNA was observed in tissues characterized by a high rate of cell proliferation, while this specificity was of a lower degree in tissues exhibiting a low rate of cell proliferation. With few exceptions, the amounts of radioactivity (per gram wet weight) in the fractions other than DNA were similar for all organs tested. Approximately 70% of label contained in the acid-soluble fraction were in tritiated water, whereas no free thymidine-^{3}H could be detected 1 hr after the last injection of this precursor. (auth)

13359 ^{47}Ca STUDIES IN ADULT COELIAC DISEASE AND OTHER GASTROINTESTINAL CONDITIONS WITH PARTICULAR REFERENCE TO OSTEOMALACIA. Harris, O. D.; Philip, Helen M.; Cooke, W. T.; Pover, W. F. R. (General Hospital, Birmingham, Eng. Univ. of Birmingham, Eng.). Scand. J. Gastroenterol.; 5: 169-75(1970).

Following oral administration of ^{47}Ca in the early plasma levels and, using a whole-body counter, the 6-day retention of the isotope, was studied in 31 patients, 17 with adult coeliac disease and 14 with other gastrointestinal disorders. Osteomalacia was present in 19. Though there was significant correlation between 120-minute plasma levels and 6-day retention of ^{47}Ca, the percentage retention at any given plasma level might range between 40 and 70, which precluded the use of the method as a measure of calcium absorption. No correlation between the percentage retention and the presence or absence of osteomalacia was found. (auth) (Norway)

13360 EFFECTS OF TOBACCO MOSAIC VIRUS INFECTION ON PHOTOSYNTHETIC CO_2 FIXATION AND $^{14}CO_2$ INCORPORATION INTO PROTEIN IN TOBACCO LEAVES. Doke, N.; Hirai, T. (Nagoya Univ, Japan). Virology; 42: 68-77(Sep 1970).

Photosynthetic $^{14}CO_2$ fixation was slightly increased in tobacco leaves infected for one day with tobacco mosaic virus (TMV). Although significant differences in the fixation activity between inoculated and noninoculated leaves were not detected 2, 3, and 4 days after inoculation by chemical determination, a local activation was found by radioautography of inoculated leaves exposed to $^{14}CO_2$. The amount of $^{14}CO_2$ incorporated into protein was less in inoculated leaves than in noninoculated leaves when $^{14}CO_2$-fed leaves were chased for 5 hours, but was much greater when chased for 24 hours. Rates of incorporation of $^{14}CO_2$ into the acid-insoluble fraction of chloroplasts and fraction 1 protein were decreased by infection. However, incorporations into TMV and soluble antigen were stimulated in inoculated leaves by chasing for a long time. More amino acids—aspartic acid, glutamic acid, alanine, glycine, and serine—synthesized through photosynthesis were incorporated into protein (especially viral protein) in inoculated leaves than in noninoculated leaves. Utilization of $^{14}CO_2$ fixed through photosynthesis for TMV synthesis is discussed. (auth)

13361 FISSION OF NATURAL URANIUM IN NEOPLASTIC AND NORMAL TISSUE. Kukiel, E.; Majewski, C.; Wszolek, B. (Strus Municipal Hospital, Poznan, Poland). Pol. Med. J.; 7: 717-22(1968).

Previous studies revealed the presence of natural Th and U in a kidney removed surgically because of clear-cell carcinoma. The highest concentrations of Th and U were in the tissue adjacent to the neoplasm. This was associated with intense α radiation in the area. It was expected that other nuclear processes induced by the presence of Th and U would be more intense. Clear-cell carcinoma tissue, tissue adjacent to the tumor, and normal tissue from the opposite pole of the kidney exhibiting no abnormalities were examined for spontaneous fission of ^{238}U present in natural U. The method involved autoradiography with Polish nuclear plates, type M_3 with emulsion 100 μ thick. In the tissue assumed to be normal, one case of fission of U was recorded, two in paraneoplastic tissue, and nine in the tumor tissue on the basis of 0.03 g of tissue exposed for 6 weeks. From the results of the calculations, it was suggested that fission of U in tumor tissue depended on neutron-induced fission of ^{235}U rather than spontaneous fission of ^{238}U. (BBB) (TSS)

Radiation Effects

Refer also to abstracts 13411, 13527, 13570, 13572, and 13598.

13362 (CEA-R-4039) INFLUENCE OF RADIATION AND AMOUNT OF PALMITATE-1-^{14}C ON THE DISTRIBUTION OF THIS FATTY ACID IN THE DIFFERENT LIPID CLASSES OF THE EHRLICH ASCITES. Polverelli, Michel; Teoule, Robert (Commissariat a l'Energie Atomique, Grenoble (France). Centre d'Etudes Nucleaires). Oct 1970. 23p. (In French). Dep. NTIS (U. S. Sales Only).

The distribution of palmitate-1 ^{14}C in lipids of Ehrlich ascites depends on the total quantity of fatty acid incorporated (high uptake occurs in the phospholipids when small amounts of palmitate are incorporated). The biosynthesis of triglycerides increases with the palmitate/albumin ratio. With high fatty acid concentrations palmitate uptake occurs preferentially in the triglycerides and decreases in phospholipids. There is no modification in the incorporation and the distribution of palmitate-1 ^{14}C after its irradiation with ^{60}Co gamma rays (between 4,500 and 18,000 rads). (France)

13363 SEPARATION ON PHOSPHATE CELLULOSE OF THE PRODUCTS OF DEGRADATION OF DEOXYRIBONUCLEOPROTEIN FORMED AFTER IRRADIATION AND ENZYMATIC ACTIN IN VITRO. Ermolaeva, N. V.; Vodolazskaya, N. A. (Inst. of Biophysics, Moscow). Biokhimiya; 35: 641-7(Jul-Aug 1970). (In Russian).

Chromatography on phosphate cellulose was used to fractionate salt extract obtained from lymphoid tissue of appendix and thymus of the rabbit (in health and 3 to 6 hrs after γ-irradiation in a dose of 800 R). Three fractions were isolated such as: non-sorbed, slightly sorbed and rapidly sorbed on phosphate cellulose. On the basis of distribution between fractions of DNA and protein from salt extract; a suggestion is made that about 30% of DNA occurs in free state or is bound to small amount of protein, 55% constitutes a complex with histones which is slightly sorbed on phosphate cellulose, and about 15% of DNA is rapidly sorbed on the column together with the bulk of histones. Marked similarity in fractional distribution of the products of DNP degradation obtained after irradiation of rabbits and after enzymic action in vitro allows a conclusion that decomposition of DNP after irradiation occurs by means of nuclear nucleases. The data obtained indicate the low probability of involvement of cell proteases or dissociation of nucleoprotein complex in this process. (auth)

13364 STRUCTURE AND FUNCTION OF E. COLI FORMYLMETHIONYL tRNA. I. EFFECT OF MODIFICATION OF PYRIMIDINE RESIDUES ON AMINOACYL SYNTHETASE RECOGNITION. Schulman, LaDonne H. (Albert Einstein Coll. of Medicine, Bronx, N. Y.). Proc. Nat. Acad. Sci. U. S.; 66: 507-14(Jun 1970).

Escherichia coli formylmethionyl tRNA (tRNA^{fMet}) has been irradiated with ultraviolet light in the presence of Mg^{2+} to the extent of 50% inactivation of amino acid acceptance. Separation of active and inactive molecules after irradiation has shown that ultraviolet light modification of the uridine in the anticodon, the uridine in the small loop, the 4-thiouridine, and the pyrimidines in the double-stranded stem adjacent to the dihydrouridine loop has no effect on aminoacylation or transformylation. The ultraviolet light-induced inactivation of methionine acceptance by tRNA^{fMet} is due almost entirely to modification of the cytidine residues in the 3′-terminal CCA-OH sequence. (auth)

13365 ASPARAGINE SYNTHETASE FROM γ-IRRADIATED POTATOES. Nair, P. Madhusudanan (Bhabha Atomic Research Center, Bombay). Arch. Biochem. Biophys., 133: 208-15(Sept. 1969).

Gamma irradiation of potatoes at sprout-inhibiting dose was found to enhance the asparagine synthetase activity. This activation was dose-dependent and maximum activation was obtained between 5 and 25 krads; 10 krad being the optimum dose. Asparagine synthetase was purified to about 50-fold. L-Asparagine was identified as the product of the reaction. The reaction was specific for L-aspartic acid and devoid of transferase activity. Hydroxylamine at very high concentration could replace NH_4^+ for substrate. The reaction showed a definite requirement for NH_4^+, ATP, and Mg^{2+}. The mechanism of enzyme activity resembled that reported for other higher plants, where L-asparagine, ADP, and Pi are the products of the reaction. No AMP was detected as the product of the enzyme reaction. There was strict stoichiometry between asparagine and ADP formed and Pi liberated during the reaction. Mn^{2+} ions could replace Mg^{2+} for activity. But the pH optima shifted from 7.2 to 6.0 when Mg^{2+} ions were supplemented in the reaction. (auth)

13366 SECRETORY ACTIVITIES OF PROSTATES AND SEMINAL VESICLES AFTER LOCALIZED X-IRRADIATION OF RAT TESTES. Gupta, G. S.; Bawa, S. R. (Panjab Univ., Chandigarh, India). J. Reprod. Fert.; 21: 329-31(1970).

White, albino male, adult rats were anesthetized by chloroform and x-irradiated at a single surface dose of 2400 R. Tissues were analyzed for contents of nucleic acid, citric acid, fructose, and acid phosphatase; loss of nucleic acid was used as the criterion of testicular cell injury. The unit of enzyme activity was defined as the amount of inorganic phosphate in μg liberated by 1 g of tissue in 1 hr at 37°C and pH 5.6. Losses of DNA from wet and dry tissues were 25 and 30% respectively; RNA losses were, however, less pronounced (22 to 23%). Fructose levels in dorsolateral prostates of irradiated animals were 27% less than values for controls, and citric acid levels in the seminal vesicles were reduced 20% by irradiation. Acid phosphatase activities were 60% that of controls. It is suggested that the lowered production of fructose and acid phosphatase by the prostates and of citric acid by the seminal vesicles in irradiated animals resulted from a decrease in production of testosterone and other androgens by interstitial cells of the testes. (P.B.M.)

13367 RADIATION STIMULATED INCORPORATION OF ^3H-THYMIDINE INTO DIPLOTENE OOCYTES OF THE GUINEA-PIG. Crone, M. (Finsen Inst., Copenhagen). Nature (London); 228: 460(31 Oct 1970).

Evidence is presented that x irradiation of a 1 day female guinea pig with 5,000 R was followed by a small but autoradiographically detectable incorporation of injected ^3H-thymidine into the DNA of diplotene oocytes. By comparing the number of autoradiograph grains over the oocyte nuclei with the number of grains over the follicle cells that were in normal S-phase at the time of ^3H-thymidine injection the radiation stimulated incorporation of the thymidine was estimated as less than 10% of the amount incorporated during normal replication of DNA, and this result was of the same order of magnitude as observed in the radiation stimulated incorporation of DNA precursor in human blood lymphocytes in vitro. Whether some of the ^3H-thymidine incorporated into guinea-pig oocytes after irradiation is a result of repair replication is not clear. Guinea-pig oocytes appear to be much more resistant to irradiation than oocytes of mice and rats, and the question arises whether the unscheduled DNA synthesis observed after irradiation can be correlated with the higher radiation resistance. In some mice experiments the incorporation of ^3H-thymidine into oocytes was investigated after 200 R x irradiation, that kills almost all oocytes within 24 hrs; there was no autoradiographically detectable incorporation, in accordance with the suggestion of a correlation between the extent of unscheduled DNA synthesis and repair synthesis, and survival of the oocytes after irradiation. (UK)

13368 INVESTIGATIONS ABOUT COMBINATION INJURIES. Messerschmidt, Otfried; Seydewitz, Vera; Koslowski, Leo (Univ., Freiburg i. B. Univ., Tuebingen, Ger.). Strahlentherapie; 139: 724-34(Jun 1970). (In German).

With the fluorometric method of Shore, the histamine content was measured in skin, lung, small intestine, and blood of male albino rats. The animals received whole-body irradiation of 690 or 810 R, either alone or combined with a skin wound before or after an irradiation of 690 R. A remarkable decrease of histamine was observed a few hours after irradiation, demonstrating the profound effect of the irradiation on histamine metabolism. Its causes are discussed. (auth)

13369 OSCILLOPOLAROGRAPHIC DETERMINATION OF CYSTEIC ACID LEVEL IN THE FINGERNAILS FOLLOWED CHRONIC IRRADIATION IN HUMANS. Grozdanovic, J.; Ulbert, K. (Health Inst. of Uranium Industry, Pribram-Zdabor, Czech. Inst. of Macromolecular Chemistry, Prague). Strahlentherapie; 139: 735-7(Jun 1970).

Chromatographic and oscillopolarographic analysis of hydrolysates of fingernails removed from miners of uranium, mineral ores and kaolin, and from military personnel, revealed a significant decrease in the cysteic acid content in the fingernails of uranium miners. The phenomenon is explained as being due to radon. The results support our previous conclusions based on electron-spin resonance analysis. (auth)

13370 INFLUENCE OF TOTAL X-RAY IRRADIATION ON THE SYNTHESIS OF BILE ACIDS IN ALBINO FEMALE RATS (CHROMATOGRAPHIC INVESTIGATION). Skakun, N. P.; Drogovoz, S. M. (Medical Inst., Ternopol, SSR). Byull. Eksp. Biol. Med.; 70: No. 9, 40-1(Sep 1970). (In Russian).

In experiments carried out on 38 albino female rats it is established that inhibition of synthesis of bile acids in the liver occurs in acute radiation sickness. In particular, the formation of primary bile acids from cholesterol and conversion of deoxycholic acid into cholic ones becomes impaired. Besides, the conversion of free bile acids into conjugated (taurocholic and glycolic acids) is impeded. At late stages of radiation this fact becomes very manifest. At this time the concentration of cholic acid in the bile rises, taurocholic acid decreases, whereas glucocholic acid completely disappears from the bile. (auth)

13371 COMPARATIVE STUDY OF DNAse ACTIVITY UNDER THE TREATMENT OF CELLS ESCHERICHIA COLI K12 (λ) WITH VARIOUS INDUCING AGENTS. Guberniev, M. A.; Drozhennikov, V. A. (Inst. of Experimental Biology, Moscow). Zh. Obshch. Biol.; 31: 600-8(Sep-Oct 1970). (In Russian).

The activity of endonuclease I, exonucleases II, and III, and inducible exonuclease in the extracts of the lysogenic strain E. coli K 12 (λ) was determined by means of microexpress-method. The effects of gamma radiation, ultraviolet, and high energy protons were compared. The content of DNA and total protein in cell extracts was determined. The levels of the activity of DNAses under study underwent no changes under the doses of inducing agents which caused the maximum induction of vegetative phage. It apparently followed that these DNAses played no immediate part in the induction of vegetative phage. DNAses of host cell were sensitive and specific with respect to different inducing agents: mitomycin C in the bactericide concentrations, unlike other agents, increased the activity of free endonuclease I and exerted no effect upon the activity of exonuclease III. Unlike DNAses of host cell, the inducible λ-exonuclease was being active as the development proceeded, correlating with the degree of induction irrespective of the nature of inducing agent. (auth)

13372 INHIBITION OF HEPATIC MICROSOMAL MIXED FUNCTION OXIDASES BY D_2O. Holtzman, Jordan L.; Carr, Matthew L. (National Cancer Inst., Baltimore. Emory Univ., Atlanta). Life Sci., Part I; 9: 1033-8(15 Sep 1970).

Aniline hydroxylase, 3,4 benzpyrene hydroxylase, and ethylmorphine N-demethylase were inhibited 22 to 30% by 99% D_2O. Endogenous NADPH oxidase was not inhibited nor was the unstimulated NADPH-cytochrome P-450 reductase. On the other hand both the NADPH oxidase and NADPH-cytochrome P-450 reductase stimulation seen on the addition of ethylmorphine were inhibited 31 and 26% respectively. NADPH-cytochrome c reductase activity was inhibited only 13%. These results indicate the participation of water in mixed function oxidases either through hydration of the proteins or heme, or through a cryptic protonolysis. (auth)

13373 METABOLISM OF THE ISOLATED PERFUSED RAT LIVER FOLLOWING IRRADIATION IN VITRO. THIRD REPORT: INCORPORATION OF TRITIUM-LABELED LEUCINE INTO PROTEINS OF THE LIVER OR PERFUSED PLASMA. Staehler, Fritz (Univ., Hamburg). Strahlentherapie; 140: 330-40(Sep 1970). (In German).

Irradiation provokes an increased plasma protein synthesis in the isolated and perfused rat liver. The liver is irradiated 20 minutes after the beginning of the perfusion with 1000 or 5000 R 200 keV x-rays. The absolute content of protein and the incorporation of tritium-labeled leucine are both increased. The content of free (acid-soluble) leucine in the cytoplasm of the liver also is increased. From the more rapid uptake of acid-soluble tritium-compounds in the perfusion plasma, with an almost constant free leucine content, it can be concluded than an increased exchange between the intra- and extracellular space takes place. (auth)

13374 RADIOCHEMICAL PROCESSES IN 6-RING COMPOUNDS. Wolter, Helmut. Strahlentherapie; 140: 341-6(Sep 1970). (In German).

Radiochemical reactions generated large interest in biology and medicine. Hypericin is active in normal metabolism, but is dangerous when irradiated. The behavior of acridinic substances, of rhodopsins and the photochemical synthesis of ascaridine from chlorophyl is described. Studies of carbon, radiochemistry, and radiosensibilization with noble gases are described. As an example of radical formation by photolysis, hexaphenylethane is cited. Chemical causes of biologic radiolesions, or mutagenic effects, were described for uracil. Research done with pyrimidine bases, and concerning the influence of the ribonucleic acids is useful for radiotherapy. The photochemistry of the Dewar-benzols has theoretical and practical implications. Photochemistry is of interdisciplinary interest for general chemistry. (auth)

13375 CHOLINESTERASE ACTIVITY OF SPINAL CORD FOLLOWING RADIATION. Snisar, I. A.; Reva, O. D. (Dnepropetrovsk State Univ., USSR). Ukr. Biokhim. Zh.; 42: 469-71(1970). (In Ukrainian).

Total cholinesterase activity was determined by the electrometric method in functionally and morphologically different areas of the lumbar enlargement of cats totally x-irradiated with a dose of 1200 R 1, 24, 48 hrs, 5–6 and 9 to 10 days after irradiation. Phase changes were found in total cholinesterase activity. Considerable inhibition of enzyme activity was observed an hr and 5 to 6 days after irradiation in motor and sensitive zones of the spinal cord. An hr after local irradiation of the lumbarsacral region, changes analogous to those evoked by whole-body radiation were found. Intramuscular injection of cysteine before irradiation has a protective effect and the found changes were not observed. (auth)

13376 INVESTIGATION OF SPLEEN AND LIVER POLYSOMES OF NON-IMMUNIZED AND IMMUNIZED RATS WITH ACUTE RADIATION DAMAGE. Vasilchenko, V. M.; Todorov, I. M.; Dyachenko, A. H.; Vasil'eva, E. S. (Physical-Technical Inst. of Low Temperatures, Kharkov. Sector of Molecular Biology and Genetics, Kiev). Ukr. Biokhim. Zh.; 42: 499-507(1970). (In Ukrainian).

In experiments in vivo and in vitro the state of polysomal apparatus of the spleen and liver was investigated in albino rats subjected to separate as well as to combined effect of ionizing radiation in lethal doses and to immunization. It was established that 24 hrs after irradiation of the non-immunized animals the protein-synthetic activity of the liver polysomes rises with a simultaneous destruction of the spleen polysomes and corresponding drop in their synthetical activity. With immunization, a considerable activation of the protein synthesis was observed in the liver and especially in the spleen. Irradiation 24 hrs after immunization did not result in a noticeable drop of the functional activity of the polysomal apparatus in the spleen as compared with these indices of immunized non-irradiated animals whereas, in the liver, under these conditions, the protein synthesis on polysomes was considerably decreased (also in comparison with the immunized non-irradiated rats). An assumption was advanced on a temporary, compensatory participation of the liver in immunogenesis with acute radiation damage of an organism. Possible reasons were also considered of the radioprotective effect of preliminary immunization on a polysomal apparatus of the irradiated animal spleens. (auth)

13377 LACK OF PHOTOREACTIVATION IN HUMAN CELLS GROWN IN VITRO. Trosko, J. E.; Isoum, M. (Michigan State Univ., Ann Arbor). Int. J. Radiat. Biol.; 18: 271-5(1970).

Direct photoreactivation was looked for in human amnion (AV_3) and HeLa cells by examining pyrimidine dimers and DNA synthesis after uv irradiation. Ultraviolet light was predominantly 2537 Å and the incident dose-rate 20 ergs/mm^2/sec. Photoreactivation of AV_3 cells was carried out by illumination from above for up to 120 min using three blacklight bulbs predominantly 3650 Å and one GE 15.W daylight fluorescent bulb placed to deliver 4800 ergs/mm^2/min through 1 cm plate glass. HeLa cells were treated with four blacklight bulbs, the incident dose-rate being 5100 ergs/mm^2/min. DNA synthesis and pyrimidine dimer assay were carried out using ^{3}H-thymidine. The uv radiation suppressed DNA synthesis in both types of cells. Photoreactivation did not ameliorate inhibition, but appeared of itself to impair DNA synthesis in unirradiated cells. (UK)

13378 RESULTS OF HISTOCHEMICAL STUDIES OF GLYCOGEN AND LIVER CELLS ULTRASTRUCTURE OF IRRADIATED RATS. Khamidov, D. Kh.; Mirakhmedov, A. K.; Neganova, N. L. (Inst. of Biochemistry, Tashkent). Uzb. Biol. Zh.; No. 3, 27-8(1970). (In Russian).

Data of histochemical studies of glycogen and liver cells ultrastructure of rats irradiated by gamma rays (^{60}Co) in doses of 400 and 1200 rad were presented. It was found that glycogen decrease is connected with destructive changes in intercellular organoids. (auth)

13379 MAIN RESULTS OF INVESTIGATIONS CONCERNING RADIATION ENZYMOLOGY. Savitskii, I. V. (Odessa Medical Inst.). Ukr. Biokhim. Zh.; 42: 294-301(1970). (In Ukrainian).

Experimental studies, performed on organs of rats and rabbits, are presented that show considerable reversibility of a number of enzymatic disturbances rising with the effect of radiation and radiomimetics as only under this condition the injection of nicotinamide and ATP may favor the normalization of NAD and NADP content and activity of some dehydrogenases in the subcellular structures. There are interesting possibilities in the field of reparation enzymotherapeutics and new preconditions of further researches of the enzymic mechanisms with the effect of penetrative radiation and radiomimetics on an organism. (auth)

13380 FACTORS INFLUENCING EXOGENOUS NUCLEOSIDE UTILIZATION IN DNA SYNTHESIS BY IRRADIATED HUMAN CELLS. Little, J. B. (Harvard Univ., Boston). Exp. Cell Res.; 62: 368-74(Oct 1970).

The relative rate of incorporation of exogenous nucleoside precursors into DNA of four strains of cultured human cells immediately after irradiation was affected by the growth phase of the culture, the concentration of the specific nucleoside in the growth medium, the precursor used, the position of the radioactive label on the precursor, and the concentration of other pyrimidine nucleosides in the medium. Although the radiation-induced depression in the rate of thymidine uptake by these human cells may reflect a decrease in net DNA synthesis, caution should be used in equating rates of incorporation of any single labelled precursor under specific experimental conditions with actual synthetic rates. (auth)

13381 COMBINED ACTION OF ETHYLENEIMINE AND X RAYS ON ASPERGILLUS ORYZAE. Pashev, I.; Kibarska, T. Compt. Rend. Acad. Bulg. Sci.; 23: 839-42(1970).

The combined action of ethylenimine and x radiation on the amylolytic enzymes, in particular α-amylase were studied in Aspergillus oryzae. The results indicated that the amylolytic activity was decreased with the combined treatment. (P.B.M.)

13382 GREATER VULNERABILITY OF THE INFECTING VIRAL STRAND OF REPLICATIVE-FORM DEOXYRIBONUCLEIC ACID OF BACTERIOPHAGE phiX174. Datta, B.; Poddar, R. K. (Saha Inst. of Nuclear Physics, Calcutta). J. Virol.; 6: 583-8(Nov 1970).

Four types of ϕX-infected cells of Escherichia coli CR, a thymine-requiring strain of E. coli C, were prepared in which the parental replicative-form deoxyribonucleic acid (RF DNA) was labeled with same specific amounts of bromouracil in both strands, only the infecting viral strand, only the complementary strand, and neither strand. The sensitivity of each type of infected cell toward irradiation by ultraviolet light, visible light, and x rays was measured. The results indicate that a certain amount of radiation damage in the infecting viral strand of the parental RF was more inhibitory to the production of progeny phage than when the damage was in the complementary strand. Similar conclusions were also drawn from suicide experiments of the phage-infected complexes containing ^{32}P of the same specific activity on either strand of the parental RF DNA. The results suggest that the beta decay occurring in the infecting viral strand was more effective in inactivating the plaque-forming ability of the complex. (auth)

13383 PROCEEDINGS OF THE SECOND ANNUAL SYMPOSIUM ON AUTOMATED, HIGH-RESOLUTION ANALYSES IN THE CLINICAL LABORATORY, OAK RIDGE, TENNESSEE, MARCH 12–13, 1970. Clin. Chem.; 16: 623-725(Aug 1970). (CONF-700334).

Separate abstracts were prepared for two papers presented at the conference. An additional 14 papers were presented on various concepts and applications of automated, high-resolution analyses. (H.L.W.)

For abstracts of individual papers see: 13384 and 13506.

13384 SERUM ORGANIC ACIDS IN SHEEP EXPOSED TO NEUTRON–GAMMA IRRADIATION, AIR BLAST, OR BOTH. Henderson, Thomas R.; Jones, Robert K. (Lovelace Foundation for Medical Education and Research, Albuquerque, N. Mex.). Clin. Chem.; 16: 697-701(Aug 1970).

From 2nd Annual Symposium on Automated, High-Resolution Analyses in the Clinical Laboratory, Oak Ridge, Tenn. See CONF-700334.

Organic acids were measured in serum from sheep that had been exposed to neutron-gamma irradiation, air blast, or both to determine which concentrations change after experimental injury. Samples were directly analyzed by partition chromatography and indicator titration. The semiautomated instrument efficiently separates mixtures of monocarboxylic acids. Monocarboxylic acids in serum seem to be sensitive indicators of biological injury. Survey experiments showed that lactate and propionate accumulate in sheep serum after severe air-blast injury, but only propionate after irradiation. Propionate-loading studies suggested that the utilization of injected propionate is impaired, to various degrees, in fasting, irradiation, and air blast. However, presumptive impairment of propionate utilization occurred earlier in sheep exposed to irradiation and blast than in only irradiated animals, and earlier in irradiated animals than in fasting controls. Air blast exposure resulted in effects of only borderline significance. (auth)

13385 CHANGES IN DNP HISTONES AFTER IRRADIATION AND CONTACT WITH HEPARIN. Kolibalova, Anna (Inst. of Biophysics, Brno). Folia Biol. (Prague); 16: 356-62(1970).

Histones extracted from rat liver, spleen, and thymus and from the same tissues six and 20 hrs after irradiation with an exposure of 600 R were chromatographed on carboxymethyl cellulose. Three fractions were isolated: f1 (very lys-rich), f2 (slightly lys-rich), and f3 (arg-rich). Irradiation was followed by a distinct decrease in the histone content of fractions f1 and f2 in all the organs except the thymus, in which it did not fall in the f1 fraction. The histone content of the f3 fraction fell in the liver and thymus, but rose in the spleen. The action of heparin on DNP obtained from the same organs six hrs after irradiation resulted in a decrease in the histone content of the f1 chromatographic fraction in the liver, spleen, and thymus (compared with material not treated with heparin); no significant changes occurred in the other two fractions (f2 and f3). (auth)

13386 THREE CISTRONS IN BACTERIOPHAGE Qβ. Horiuchi, Kensuke; Matsuhashi, Sachiko (Tokyo Univ.). Virology; 42: 49-60(Sep 1970).

Amber mutants of bacteriophage Qβ were isolated and classified into three groups by complementation tests. Physiological studies showed that the three cistrons of Qβ could be related to the three known genes of the f2 group of RNA phages. Gene I mutants do not produce either phage RNA polymerase or phage specific RNA in Su$^-$ hosts. Gene II mutants in Su$^-$ hosts produce defective phage particles which are lighter in density than viable phage particles. Gene III mutants do not grow on either Su-2 or Su-3 suppressor strains; they hyperproduce double-stranded RNA and viral RNA polymerase on these hosts. On Su$^-$ hosts they appeared to have a polar effect on the synthesis of phage RNA polymerase. None of the Qβ mutants lysed nonpermissive hosts. (auth)

Immunology

13387 PLAQUE-FORMING CELLS OF TWO DIFFERENT ORIGINS IN SINGLE HEMOLYTIC FOCI. Vann, D. C.; Campbell, P. A. (Scripps Clinic and Research Foundation, La Jolla, Calif. Univ. of California, San Diego, La Jolla). J. Immunol.; 105: 1584-6(Dec 1970).

Small numbers of spleen cells and heterologous red blood cells as antigens were injected into lethally γ-irradiated mice, regions of hemolytic antibody forming cell activity, hemolytic foci, was detected in the spleens of these recipients mice. The results of the experiment indicate that the formation of hemolytic foci may depend on the interaction between at least two cell types, one an antigen reactive cell required for initiation of antibody production and the other a precursor cell which is the direct progenitor of antibody forming cells. (P.B.M.)

13388 TUMOR-INDUCED SKIN HETEROGENIZATION. III. IMMUNOLOGIC AND IMMUNOGENETIC MECHANISMS. Liozner, Alexander L.; Svet-Moldavskii, George J.; Mkheidze, Demuri M. (Inst. of Experimental and Clinical Oncology, Moscow). J. Nat. Cancer Inst.; 45: 485-94(Sep 1970).

Skin heterogenizing virus (SHV) obtained from K-237 sarcoma of C57BL/6J mice was strain specific. SHV produced syngeneic skin rejection in C57BL/6J mice inoculated with any type of virus-containing materials, i.e., tumors, skin grafts, or cell-free tumor homogenates. However, SHV produced no such effect on BALB/c, CBA, C3HA, C3H, C3Hf, and T6T6 mice. Hybrid mice (C57BL/6J X BALB/C)F_1 also resisted the heterogenizing action of SHV, despite the fact that K-237 sarcoma always grew progressively in these hosts. Sensitivity to SHV action seemed to be controlled by a recessive gene (or genes). The C57BL/6J strain was probably homozygous in respect to the hypothetical gene. A part of F_2 hybrid mice appeared sensitive to the heterogenizing action of SHV. Furthermore, some sensitive F_2 mice acquired the ability to infect C57BL/6J mice with SHV as a result of skin grafting. Thus sensitive F_2 mice were, in this respect, similar to sensitive mice of the parental strain C57BL/6J. Various immunosuppressive treatments not only delayed rejection of heterogenized skin but often abolished it. Far from being accelerated, the rejection of secondary grafts of C57BL/6J heterogenized skin was delayed 2 to 4 days. However, the second-set rejection of C57BL/6J heterogenized skin occurred after it was transplanted to (C57BL/6J) X BALB/c)F_1 mice sensitized with similar grafts 3 weeks before. K-237 sarcoma cells failed to produce the new transplantation antigen present in skin cells. Skin cells, on the contrary, always produced this antigen, but did not provide mature virus reproduction. Possible explanations for these contradictory results are briefly discussed. (auth)

13389 QUANTITATIVE DETECTION OF CYTOTOXIC ANTIBODIES AGAINST TUMOR-SPECIFIC ANTIGENS OF MURINE SARCOMAS INDUCED BY 3-METHYLCHOLANTHRENE. Bloom, Eda T. (Univ. of California, Los Angeles). J. Nat. Cancer Inst.; 45: 443-53(Sep 1970).

The antibody response to the tumor-specific antigen(s) (TSA) of a murine sarcoma induced by 3-methylcholanthrene was studied in isogeneic mice. Of recent origin, the tumor was indigenous to the C57BL/10 strain. A new microtechnique was used to detect and assay cytotoxic antibody against TSA. Only microliter quantities of serum were necessary for multiple titrations. The following evidence supports the conclusion that the cytotoxic effect in vitro resulted from a true tumor-specific antibody response: The reproducibility of the method was demonstrated at a high level of significance; the cytotoxic effect depended on the addition of exogenous complement; the detectable antibody titers were specific for the sensitizing sarcoma; antiserum activity resided in the IgG and IgM immunoglobulin fractions; and the cytotoxic effect, induced by antigenic stimulation, was boosted with further challenge. The routine titration of tumor-specific antibody promises to facilitate greatly definitive studies of tumor immunity and tumor enhancement. (auth)

13390 DISSOCIATION OF SPLENOMEGALY FROM GRAFT-VERSUS-HOST DISEASE BY HOST X-IRRADIATION. Hilgard, Henry R. (Naval Medical Research Inst., Bethesda, Md.). Transplantation; 10: 396-402(Nov 1970).

Twenty-four hours after receiving 300 or 500 R of x-irradiation, F_1 hybrid mice were injected with parental strain lymphoid cells in order to cause a graft-versus-host reaction. Spleen index values obtained from these mice 8 days after thymus cell injection were increased (300 R) or decreased (500 R) in comparison to the values obtained from unirradiated hosts. Hosts x-irradiated with 500 R and injected with parental strain spleen or thymus cells showed decreased spleen index values, in comparison to controls receiving irradiation only, or irradiation and hybrid cells. X-irradiation with 500 R therefore abolishes the usual host proliferative response of splenomegaly. In spite of the absence of splenomegaly, the 500 R x-irradiated hosts developed graft-versus-host disease earlier than the 300 R x-irradiated hosts in which splenomegaly was present. It is concluded that host proliferative responses such as splenomegaly play no essential role in the pathogenesis of graft-versus-host disease. (auth)

13391 INCREASE IN ANTIBODY TITER AGAINST THE EBV-ASSOCIATED MEMBRANE ANTIGEN COMPLEX IN BURKITT'S LYMPHOMA AND NASOPHARYNGEAL CARCINOMA AFTER LOCAL IRRADIATION. Einhorn, Nina; Klein, George; Clifford, Peter (Karolinska Hospital, Stockholm. Kenyatta National Hospital, Nairobi, Kenya). Cancer; 26: 1013-21(Nov 1970).

Sera of two African patients with Burkitt's lymphoma and three with nasopharyngeal carcinoma were examined for antibodies against the EBV-associated membrane antigen complex by titrating their blocking activity against an FITC-conjugated reference immunoglobulin (F-Mutua), derived from a case of Burkitt's lymphoma in long-term remission. The sera were tested before, at the termination, and 6–9 weeks after applying local radiotherapy to the tumor. Burkitt lymphoma-derived, EBV-carrying lymphoblastoid cell lines were used as target cells. Three patients with other tumors receiving radiotherapy served as controls (a case of Hodgkin's disease, laryngeal carcinoma and lymphosarcoma, respectively). Six to 9 weeks after irradiation of the tumor, there was a significant increase in the titer of membrane-reactive antibodies, in both cases of Burkitt's lymphoma, and in all 3 cases of nasopharyngeal carcinoma, but not in the control tumors. (auth)

Ecology

Refer also to abstracts 13124, 13393, 13431–13434, and 13436.

13392 (EUR-3945(Pt.2)) COMPARISON OF THE RADIOACTIVE CONTAMINATION OF THE TOTAL DIET OF ADOLESCENTS IN THE COMMUNITY. II. INSTITUTIONAL DIET PROGRAMME RESULTS AND COMMENTS. Smeets, J.; Van Der Stricht, E. (European Communities, Luxembourg. Commission). Nov 1970. 70p. Dep. NTIS (U. S. Sales Only).

Results of a comparative institutional diet study performed in the Member States of the European Community in the period October 1965 to 31 December 1967 are presented. Ten institutes geographically widespread, participated. The purpose was to find out to what extent differences in food habits within the Community influenced the intake of radionuclides. During the period concerned, samples were taken every month for a whole week and measured for the concentrations of ^{90}Sr, ^{137}Cs, stable Sr, Ca, K, ^{226}Ra, and U. A significant difference in contamination between institutes was noted, particularly if milk and grain formed an important proportion of the food consumed. The mean values of pCi^{90}Sr/gCa for various institutes appear to differ by less than a factor two; the intake seemed to deviate very little from the mean value for the whole population. (auth)

XUM

13393 (NYO-2577-12) STUDY OF NATURAL RADIOACTIVITY IN BRAZIL. (Pontificia Universidade Catolica do Rio de Janeiro (Brazil). Instituto de Fisica). Nov 1970. 30p. Dep. NTIS.

Procedures used to estimate the radiation dose to permanent residents of Guarapari, Brazil, a region of high natural background radioactivity, are described. Lithium fluoride dosimeters worn by about 500 residents showed an average dose of 630 mR/yr. Measurements were also made of the radioactivity in breath samples. Food and water samples analyzed showed little radioactivity. A program to monitor radioactivity in the air and for the whole-body counting of residents to determine their radionuclide body burdens is described. (C.H.)

13394 (RLO-2099-1) STUDIES OF THE NATURAL ALPHA-EMITTING RADIOISOTOPES IN MARINE ORGANISMS. Annual Progress Report, 1969-1970. Beasley, Thomas M. (Washington Univ., Seattle. Lab. of Radiation Ecology). 19 Dec 1969. Contract AT(45-1)-2099. 7p. Dep. NTIS.

An alpha spectrometer system utilizing four separate diode inputs was assembled and calibrated. Three total alpha counters were assembled and are in the testing stage. Ten species of marine vertebrates and 14 species of invertebrates were collected, identified, processed for wet/dry weights, and analyzed for ^{210}Pb, ^{210}Po, and stable lead. The specimens represented pelagic and benthic open ocean organisms and inshore organisms. Fish protein concentrates were obtained from six species of fish and analyzed for contents of ^{210}Pb, ^{210}Po, and the artificial radionuclides, ^{40}K, ^{54}Mn, ^{60}Co, ^{137}Cs, ^{90}Sr, and ^{55}Fe. (H.L.W.)

13395 (SWRHL-90-r) PLANT RADIOIODINE RELATIONSHIPS: A REVIEW. McFarlane, James C.; Mason, Benjamin J. (Public Health Service, Las Vegas, Nev. Southwestern Radiological Health Lab.). Jul 1970. 53p. Dep. CFSTI.

The term deposition velocity has been widely used to describe iodine contamination of plants. The physics of iodine transfer from air to plants is a complex problem involving both chemistry and physics of the fallout, various forces that cause movement of the particles in the atmosphere, and the behavior and extent of the boundary layer that surrounds each leaf surface. In 1966, Fisher developed a model that can be used to predict the deposition velocity to within a factor of three. Increases in wind speed or particle size cause a corresponding increase in deposition velocity. It has been recognized that different plant species collect contamination at different rates. These differences were not clearly defined, but before a complete understanding of deposition velocity can be attained, differences in deposition on various species must be understood in relation to their physiology and leaf morphology. Some of the factors that should be evaluated are differences in deposition under light and dark conditions, differences caused by variations in leaf morphology, and differences caused by change in humidity. Absorption of iodine through the roots was shown to be dependent on the iodine concentration, pH, and plant species. Although it was not documented, it appears that iodine absorption is by an active uptake mechanism. At levels above 1 μg/ml in a culture solution, iodine was toxic to plants. After being absorbed by a plant tissue, iodine is only very slowly translocated. Contamination of plants through the roots by fallout iodine was shown to be of little importance in the total contamination of plants. Foliar absorption, on the other hand, provided a route whereby iodine could be fixed against most decontamination measures. Foliar absorption of iodine by plants is largely dependent on the chemical and physical form of the contaminant. Very small particles and gases can enter the plant through the stomata while dissolved iodine enters through the cuticle mainly in the areas of ectodesmata. The effective half-life of iodine on plant tissues includes both radioactive decay and other loss processes. Effective decay rates have been reported from 3.5 to 6.3 days. There are three methods of loss that need to be considered in evaluating half life data: apparent loss caused by dilution resulting from plant growth; loss from the exterior surface, suggested methods of loss are particle removal, volatilization, and cuticle flaking; and loss from inside plants, there is very little translocation of iodine but iodine can possibly escape via transpiration or other gaseous exchanges. The significance of these three routes was not evaluated but must be understood in order to accurately predict effective half-lives. Experiments show that the effective decay rate of iodine from plants occurs in two phases. At first the loss rate is rapid, presumably caused by the loss of surface contamination. Later the loss rate is less with dilution by growth and loss of absorbed iodine becoming the principal processes. Various authors working with radioiodine have reported their results on the basis of wet weight, dry weight, leaf area, and the total ground area covered by plants. Evidence that areas of ground cover and wet weight are poor bases for data expression is presented. Dry weight, although not perfect, is a much sounder basis for expressing contamination data than either of the others. Predictions of contamination cannot accurately be made until the differences between species are understood and these will never be understood unless there is a standard method for data expression. (auth)

13396 (UCRL-72511) FATE OF SCHOONER FALLOUT RADIONUCLIDES INGESTED BY THE DAIRY COW. Potter, G. D.; Vattuone, G. M.; McIntyre, D. R. (California Univ., Livermore. Lawrence Radiation Lab.). 20 Oct 1970. 18p. (CONF-701102-6). Dep. NTIS.

From Meeting of the American Nuclear Society, Washington, D. C.

Fallout from the Plowshare Schooner Project was administered orally to a lactating dairy cow and to a six-month pregnant cow. Data are presented on excretion rate in milk, urine, and feces of the lactating cow of ^{54}Mn, ^{58}Co, ^{74}As, ^{88}Y, ^{89}Zr, ^{103}Ru, ^{131}I, ^{132}Te, ^{140}Ba, ^{140}La, ^{181}W, ^{187}W, ^{188}W, ^{188}Re, and ^{196}Au. The distribution of ^{74}As, ^{131}I, ^{140}Ba, ^{181}W, ^{185}W, ^{188}W, and ^{188}Re in maternal and fetal tissues was determined for the pregnant cow. (C.H.)

13397 ANALYSIS OF ^{131}I DATA IN BOVINE THYROIDS, OCTOBER 1964 THROUGH FEBRUARY 1969. Russell, John L.; Pliner, Gerald A. (Bureau of Radiological Health, Rockville, Md.). Radiol. Health Data Rep.; 11: 573-9(Nov 1970).

A detailed analysis of the ^{131}I bovine thyroid data from October 1964 through February 1969, as reported in RHD&R, shows that most positive results can be related to various nuclear tests with known atmospheric intrusions. The widespread nature of various samples having positive concentrations of short-lived fission products and the rapid increase of levels in these samples indicate the source to be a major atmospheric intrusion. Estimates determining thyroid dose in man from ^{131}I concentrations in bovine thyroids appear to be feasible under selected conditions but are of little use in evaluating nationwide network data. The lower limit of detectability is 1 pCi ^{131}I/g bovine thyroid, and most samples at this level have a 2-standard deviation error greater than the measured quantity. (auth)

13398 DATA. SECTION IV. OTHER DATA. Radiol. Health Data Rep.; 11: 649-57(Nov 1970).

Summaries of environmental radioactivity data for Lawrence Radiation Laboratory, California and Shippingport Atomic Power Station, Pennsylvania, during 1969 are presented. (C.H.)

13399 DATA. SECTION III. AIR AND DEPOSITION. Radiol. Health Data Rep.; 11: 641-8(Nov 1970).

Data are presented on the gross β activity in samples of atmosphere and precipitation collected at various locations throughout North, Central, and South America during July 1970. (C.H.)

13400 DATA. SECTION II. WATER. Radiol. Health Data Rep.; 11: 637-9(Nov 1970).

Samples of surface waters collected at eight stations located on major U.S.A. river systems during January to July 1970 were analyzed for tritium content. The data are tabulated. (C.H.)

13401 DATA. SECTION I. MILK AND FOOD. Radiol. Health Data Rep.; 11: 617-36(Nov 1970).

Data are reported on the content of ^{137}Cs, ^{131}I, and ^{90}Sr in milk samples collected at locations throughout North, Central, and South America during July 1970. The data are compared with data from the previous 12-month period. Samples of hospital diets collected at 20 selected geographical areas in California between 1965 and 1970 were analyzed for ^{89}Sr, ^{90}Sr, ^{226}Ra, and stable Ca, K, and Sr. Typical diets of school children sampled throughout the U.S.A. during December 1969 were analyzed for ^{137}Cs, ^{89}Sr, ^{90}Sr, and stable Ca and K. (C.H.)

13402 RADIOCONTAMINATION OF SOILS AND CROPS. Bovard, P. (CEA, Fontenay-aux-Roses, France). Prot. Civ. Secur. Ind.; No. 187, 10-13(May 1970). (In French).

The different origins of radioactivity are listed: natural radioactivity, fall-out (^{90}Sr and ^{137}Cs) and radioactive industrial wastes. The cycles of radioelement transfer in the environment are described. The influence of water pollution (rainfall, irrigation) on contamination is discussed, together with the radionuclide distribution variation as a function of type of soil and organic matter. Next follows a study of the contamination of different crops either through the soil or directly, by radioactive aerosol deposition or by irrigation with contaminated water. Direct contamination is the main cause of contamination of the aerial parts of plants. The influence of technology on the contamination of food products is mentioned. The short-term risk is bound up with the presence of short-lived fission products (^{131}I) and the long-term risk with that of ^{90}Sr and ^{137}Cs. (France)

13403 EXPERIMENTAL STUDY OF THE ACCUMULATION OF RADIONUCLIDES ^{90}Sr AND ^{144}Ce FROM SEA WATER BY

ALGINIC ACID. Lazorenko, G. E.; Polikarpov, G. G. (Inst. of Biology of the Southern Seas, Sevastopol). Dopov. Akad. Nauk Ukr. RSR, Ser. B; No. 5, 445-8(May 1970). (In Ukrainian).

Alginic acid-polysaccharide obtained by extraction of brown algae is capable of accumulating ^{90}Sr and ^{144}Ce quickly from sea water to high concentration factors values (about 100 and 500 units, respectively). On the other hand, alginic acid does not accumulate ^{137}Cs, ^{65}Zn and ^{204}Tl. Correlation between concentration factors of ^{90}Sr and ^{144}Ce accumulation by alginic acid and their concentration factors in brown algae and high stability of alginic acid to external influences make it possible to assume that alginic acid or its compounds might take part in extraction of strontium and cerium by these algae from sea water. (auth)

Genetics and Cytogenetics

Refer also to abstracts 13374, 13452, 13614, and 13621.

13404 DOSE-RESPONSE CURVE FOR THE YIELD OF TRANSLOCATIONS IN MOUSE SPERMATOGONIA AFTER REPEATED SMALL RADIATION DOSES. Lyon, Mary F.; Phillips, Rita J. S.; Glenister, P. (MRC Radiobiology Unit, Harwell, Eng.). Mutat. Res.; 10: 497-501(Nov 1970).

Male mice were given small doses of about 10.4 Rad γ rays at high dose rate (17 to 18 Rad/min) on 5 days/wk for 12 wk. The yield of translocations in spermatocytes irradiated as spermatogonia was less than after the same total dose (620 Rad) given in a single exposure. A dose-response curve for the yields of translocations after 3, 6, 9, or 12 wk of such daily repeated irradiation was linear but with intercept on the ordinate significantly different from the control. The interpretation was that reduced effect of repeated small doses was due to change in susceptibility of the spermatogonial cell population after repeated irradiation. (auth)

13405 NUCLEAR DNA COMPLEMENT IN YOUNG PROEMBRYOS OF BARLEY. Mericle, L. W.; Mericle, R. P. (Michigan State Univ., East Lansing). Mutat. Res.; 10: 515-18(Nov 1970). (COO-1400-29).

The DNA content of early proembryo stages of Hordeum distichum was studied. It was found that 1 and 2-celled proembryos exhibit high lethality rates following acute irradiation, however before abortion they undergo a few cell divisions without mitotic delay or prolongation of the mitotic cycle. In unirradiated proembryos, nuclear volume decreases about 8.5 fold between 1- and 1000-celled stages. Microspectrophotometry was employed to determine the DNA content of the proembryos. (P.B.M.)

13406 SPECIFICITY OF UV MUTAGENESIS IN E. COLI. Cheung, M. K.; Bockrath, R. C. (Indiana Univ., Indianapolis). Mutat. Res.; 10: 521-3(Nov 1970).

The specificity of uv mutagenesis was studied using Escherichia coli. Nutrient supplement was found to enhance the number of suppressor containing revertants. Arginine revertants developed on nutrient broth supplemented medium were compared to revertants developed on arginine supplemented medium. A greater number of revertants were found on the former medium and a large majority of these revertants were the result of class 2 amber suppressors. Control, unirradiated cultures were assayed to determine the number and distribution of spontaneous revertants. The values were taken into account when determining the net arginine revertants produced by uv and their distributions. The preferential production of class amber suppressors by uv suggests that GC to AT transitions result from uv irradiation. (P.B.M.)

13407 ULTRAVIOLET-SENSITIVE MUTANTS OF STREPTOMYCES COELICOLOR. II. GENETICS. Harold, Richard J.; Hopwood, David A. (Univ. of Glasgow. John Innes Inst., Norwich, Eng.). Mutat. Res.; 10: 439-48(Nov 1970).

Genetic analysis of 23 uv sensitive (uvs) mutants of Streptomyces coelicolor led to the recognition of 6 loci, uvsA-F. Three of the loci, uvsA,C,D, are closely linked in a cluster, 2 others, uvsB,E are located diametrically to the A,C,D cluster, and uvsF is distant from the other loci. (auth)

13408 MAPPING OF THE UVR GENE OF SALMONELLA TYPHIMURIUM. Andreeva, I. V.; Kiryushkina, A. A.; Pokrovskii, V. N.; Skavronskaya, A. G. (Inst. for Epidemiology and Microbiology, Moscow). Mutat. Res.; 10: 506-8(Nov 1970).

A gene (hcr) was located on the Salmonella typhimurium genetic map. This gene permits the repair of uv damage to phage that infect the cell (host cell reactivation). Mapping was carried out by conjugation. Chromosomal position was established on the basis of the frequency of recombinations in the crosses with suitable Hfr strains. (P.B.M.)

13409 INDUCTION BY X-RAYS OF ISOCHROMOSOMES IN THE GERM CELLS OF DROSOPHILA MELANOGASTER MALES. EVIDENCE FOR NUCLEAR SELECTION IN EMBRYOGENESIS. Leigh, B.; Sobels, F. H. (Univ. of Leiden. Cohen Inst. for Radiopathology and Radiation Protection, Leiden). Mutat. Res.; 10: 475-87(Nov 1970).

Drosophila melanogaster males, heterozygous for markers on either the second or third chromosomes, were irradiated and mated to females in which the corresponding homologous pair were present as isochromosomes. Gametes at different stages of development at irradiation were sampled by serially mating the males in 5 2-day broods. All normal zygotes were inviable; most of the viable progeny carried newly induced isochromosomes or were triploid. The new isochromosomes were either heterozygous or homozygous for the paternal markers. The former, heteroiso's, were only induced in diploid cells and the latter, homoiso's, were induced in all of the germ cell stages which were tested. The rates of induction could not be measured directly but were estimated from the results of some calibration tests. Spermatocytes and spermatogonia appear to be about 30 times more sensitive than spermatozoa and mature spermatids for the induction of homoiso's. The unexpected finding is that homoiso's, which presumably result from a chromatid type exchange, can be recovered from irradiated spermatozoa and late spermatids. The survival of such induced homoiso's is explained by taking into account the process of gametic fusion of Drosophila. Only one of the first two fusion nuclei will be genetically balanced and competent to produce an adult. Triploids resulted from the production of diploid female gametes. The data provide a strong indication that this is not a random process. (auth)

13410 TERTIARY STRUCTURE OF CHROMOSOMES. Wolff, Sheldon (Univ. of California, San Francisco). Mutat. Res.; 10: 405-14(Nov 1970).

Chromosomes consist of both nucleic acids and protein, the actual organization of these components in chromosomes as they are seen in mitosis is still unsure. Radiation studies in which chromosome aberrations are induced at various stages of the cell cycle have indicated that chromosomes react as though they were single-stranded structures (i.e., give rise to chromosome aberrations) during most of G_1 and then behave double-stranded (i.e., give rise to chromatid aberrations) during S and G_2. Studies of human lymphocytes have indicated that this transition from singleness to doubleness occurs in the absence of both DNA and protein synthesis. This was interpreted to mean that chromosomes are multistranded structures that simply loosen at the time of transition. Attempts were made to modify this tertiary structure of chromosomes to gain some insight into the nature of the binding involved in the lateral organization of chromosomes. If freshly drawn human lymphocytes are treated for 15 to 30 min with glycerol, which can change the dielectric constants within the cell, or with urea, which can disrupt hydrogen bonds, then radiation can induce chromatid breaks in cells that ordinarily respond to give only chromosome aberrations. It seems as though hydrogen bonds and ionic bonds are involved in maintaining the tertiary structure of chromosomes and that this structure can be modified in living cells. (auth)

13411 T4 ENDONUCLEASE INVOLVED IN REPAIR OF DNA. Yasuda, Seiichi; Sekiguchi, Mutsuo (Kyushu Univ., Fukuoka). Proc. Nat. Acad. Sci. U. S. A.; 67: 1839-45(15 Dec 1970).

An enzyme activity, named T4 endonuclease V, was purified from T4-infected Escherichia coli. The enzyme induces single-stranded breaks in uv-irradiated DNA but does not act on native or heat denatured DNA. The enzyme activity is dependent on the dose of uv irradiation, and the number of the breaks formed is approximately equal to the number of pyrimidine dimers present in the DNA. Denatured DNA, which was exposed to uv light, is also attacked by the enzyme although the extent of the reaction is greater with irradiated native DNA. The enzyme shows optimal activity at pH 7.5 and does not require added divalent ions. When the enzyme treated, irradiated DNA is subjected to stepwise degradation by spleen phosphodiesterase, dimers are released more rapidly than thymine into the acid soluble fraction, suggesting that the enzyme induces a break at the 5′-side of a pyrimidine dimer. The enzyme, whose formation is controlled by the v^+ gene of T4, appears to be responsible for the first step of excision repair. (auth)

13412 MUTATION AND RECOMBINATION OF BACTERIOPHAGE LAMBDA: EFFECT OF ULTRAVIOLET RADIATION. Miura, Akiko; Tomizawa, Jun-ichi (National Inst. of Health, Tokyo. Osaka Univ.). Proc. Nat. Acad. Sci. U. S. A.; 67: 1722-6(15 Dec 1970).

Defects in Escherichia coli recB or recC or phage red or int gene did not impair uv-radioinduced clear mutations of λ phage. Clear mutants of cI and cII genes were not enriched among RecA-promoted uv-radioinduced recombinants between the N and O

XUM

genes which closely encompass the c genes. No correlation was observed between uv-radioinduced mutation and genetic recombination. (auth)

13413 RADIATION DOSE FRACTIONATION, MITOTIC INDEX, AND MULTIPLE FIXATION STUDIES ON CHROMOSOME ABERRATIONS IN VICIA FABA. Miller, Morton W.; Colaiace, Joyce D. (Univ. of Rochester, N. Y.). Mutat. Res.; 10: 449-62(Nov 1970). (UR-49-1204).

Soaked seeds of Vicia faba were x-irradiated with 800 R, 400 R, or two 400 R exposures separated by 1 to 8 hr and harvested during the first mitotic peak. The yield of rings and dicentrics initially fell with increased time between the 1st and 2nd hr split doses, rose significantly at the 3rd hr split dose, fell again at the 4th and 5th hr split doses, then rose to a yield which approximated that produced by a single unsplit dose, and then fell again at the 7th and 8th hr split doses. The split dose yield was compared to that produced by half (400 R) and single (800 R) exposures at that hourly interval. Dose squared kinetics were not obtained, and some split dose yields fell to or considerably below the base line (2 × 400 R) yield. Further investigation showed that the yields of a single (800 R), half (400 R), and split doses (400 + 400 R) varied fixation time and time of irradiation during G_1, indicating a heterogeneity of the cells to radiosensitivity and time. It was concluded that the root tip of Vicia faba cannot be regarded as a simple homogeneous system and that the results and interpretations of split dose two-hit chromosome aberration yields based on a single fixation time are unreliable. (auth)

13414 ULTRAVIOLET-SENSITIVE MUTANTS OF STREPTOMYCES COELICOLOR. I. PHENOTYPIC CHARACTERISATION. Harold, Richard J.; Hopwood, David A. (Univ. of Glasgow. John Innes Inst., Norwich, Eng.). Mutat. Res.; 10: 427-38(Nov 1970).

Twenty three uv sensitive (uvs) mutants of Streptomyces coelicolor were isolated by a replica plating technique after mutagenesis by uv or nitrosoguanidine. Phenotypic classification of the uvs mutations were defined in 6 loci, uvsA to F. Mutations in uvsA to E result in an increased uv sensitivity of strains carrying them; mutations in uvsF, on the other hand, confer no increased sensitivity alone but enhance the sensitivity of strains carrying uvsA, C, or D mutations. None of the uv sensitive mutants is x ray sensitive. Mutations in none of the uvs genes had a major effect on recombination frequencies between pairs of strains, both carrying the same mutation. Wild type strains of S. coelicolor were found to be heterogeneous in respect to photoreactivability. (auth)

13415 X-RAY INDUCED CHLOROPHYLL MUTATION IN SESAMUM ORIENTALE L. Nayar, G. G. (Bhabha Atomic Research Centre, Bombay). Sci. Cult. (Calcutta); 35: 631-2(Nov 1969).

A chlorophyll mutant obtained from Sesamum orientale var. T10 is described. Seeds were x-irradiated (75 to 125 kR) and mutants were selected in the X_3 generation. Out of 31 plants selected, one showed chlorophyll deficiency that persisted throughout development. The mutant was retarded in growth and had reduced fertility. It bred true and exhibited monofactorial segregation when backcrossed. (M.M.B.)

13416 VARIABILITY OF BAC. MESENTERICUS INDUCED BY UV RAYS, FAST NEUTRONS, AND ETHYLENE IMINE. Luginina, T. N. (Inst. of Microbiology and Virology, Alma-Ata, USSR). Mikrobiol. Zh.; 29: 507-10(1967). (In Russian).

A study was made of some regularities of induced variability of the strain PB-8 Bacillus mesentericus. Ultraviolet rays, fast neutrons, and ethylene imine were used as mutagens. An aqueous suspension of a 7-day culture of B. mesentericus having about 10^7 spores per ml was treated with the mutagens. The effect of each mutagen on variability was studied by the gelatinase formation index in five doses. The results analyzed by statistics showed the peak and drop of the curve under the effect of different survival level, i.e., different mutagen effects. For fast neutrons, the maximum of plus-vaspores, for ultraviolet rays this dose is equal to 6000 ergs/mm^2, and the survival accounts for no more than 0.0003%. The maximum accumulation of variants with an increased gelatinase activity in the experiments with ethylenimine was observed when treating the spores with the preparation at a dilution of 1:1000. In this case, the survival amounted to 0.065%. In all the cases, the frequency of plus-variants in the experiments with the mutagens definitely differed from the one under natural seeding conditions, i.e., it depended entirely on the mutagen effect. (JPRS)

13417 CHROMOSOMAL DOSIMETRY OF SWINE LYMPHOCYTES IRRADIATED IN VITRO BY ^{60}Co. Haag, J.; Nizza, P. (Commissariat a l'Energie Atomique, Jouy-en-Josas, France). Ann. Genet. (Paris); 13: No. 2, 87-9(1970). (In French).

The effects on chromosomes of exposure in vitro to ^{60}Co were studied using blood from swine. The incidence of dicentric and ring formation appeared proportional to the square of the exposure dose. (France)

13418 PRODUCTIVITY OF SOME MUTANTS OF THE PEA (PISUM SATIVUM L.) AND THEIR HYBRIDS. A CONTRIBUTION TO THE HETEROSIS PROBLEM IN SELF-FERTILIZING SPECIES. Gottschalk, W. (Univ., Bonn). Euphytica; 19: 91-7(Feb 1970).

The favorable yielding capacity of a group of x-radioinduced Pisum sativum mutants makes them attractive for pea breeding. The fasciated mutant 489C produced as much as 32–92% more seed than the corresponding values of the initial line. Hybrids of all mutants with the fasciated 489C showed a marked heterosis effect for increased vigour and stem length resulting in a conspicuously high seed production. (P.B.M.)

13419 VARIATION AND COVARIATION OF SEED WEIGHT AND ITS COMPONENTS IN WHEAT FOLLOWING IRRADIATION, EMS, AND HYBRIDIZATION. Khadr, F. H. (Univ. of Alexandria, Egypt). Theor. Appl. Genet.; 40: 280-5(9 Nov 1970).

Seeds from two hexaploid wheat varieties, Giza 150 and Sonora 64, and the F_2 seeds of their hybrid were given two mutagenic treatments, γ irradiation and ethyl methanesulfonate (EMS), to study the type of variation and covariation in seed weight, width, and length induced by irradiation, EMS, and hybridization. Measurements of seed weight and its components were taken on 30 replicated lines derived from each treated and non-treated material. Both irradiation and EMS produced significant variability in seed weight and its components in the pure genetic background. The hybrid genetic background somewhat depressed the expression of irradiation-induced variability. The variations resulting from EMS and hybridization were to a great extent independent and cumulative. (P.B.M.)

13420 MUTAGENICITY OF RADIATIONS AND CHEMICAL MUTAGENS IN SORGHUM. Ramulu, K. Sree (Agricultural Coll. and Research Inst., Coimbatore, India). Theor. Appl. Genet.; 40: 257-60(9 Nov 1970).

A comparative study on the relative mutagenicity of x and γ rays and chemical mutagens EMS, MMS, deS, and NEU in inducing chlorophyll, viable and total mutations was made on three cultivated varieties of Eu-Sorghum. A critical comparison of the chlorophyll, viable and total mutations shows that the mutation rate increased with an increase in dose up to a certain dose level, beyond that the saturation effect was observed. EMS was found to be the most potent mutagen in inducing chlorophyll, viable and total mutations. The treatments with NEU (viable mutations) and dES (viable and total mutations) also proved to be effective. In a large number of cases the relationship between chlorophyll and total mutations was more close than that of viable to total mutation rates. (auth)

13421 BASE-CHANGE MUTAGENESIS AND PROPHAGE INDUCTION IN STRAINS OF ESCHERICHIA COLI WITH DIFFERENT DNA REPAIR CAPACITIES. Kondo, Sohei; Ichikawa, Haruko; Iwo, Kazuhiro; Kato, Takesi (Osaka Univ.). Genetics; 66: 187-217(Oct 1970).

Base-pair reversion (from argF_{am} to prototrophy) and prophage induction (ϕ80) by various mutagens were compared in Escherichia coli strains that differ in DNA repair capacity. These include wild type, exc (unable to excise pyrimidine dimers), res (polymeraseless), and recA (recombinationless). Mutability and prophage induction patterns were strikingly similar. Reversion patterns lead to the conclusion that base change mutations require not only premutational DNA damage (an excisable one after uv and 4-nitroquinoline-1-oxide, an unexcisable one after x rays and methyl methanesulfonate, and repair errors after mitomycin C) but also recombinational events; premutational damage only provokes recombination which in turn induces mutation probably through recombinational errors. Mutations also can be induced, by passing recombination mechanisms, by ethyl methanesulfonate. N-methyl-N'-nitro-N-nitrosoguanidine induces mutations by a combination of these two mechanisms. Since spontaneous mutation and spontaneous prophage induction are lower in the recA strain but higher in the res strain than in wild type, both phenomena seem to require, at least partly, the action of recombination machinery; DNA polymerase, which is defective in the res strain, and may participate in repair of spontaneous recombination errors. (auth)

13422 GENETIC ANALYSIS OF THE HISTIDINE OPERON IN ESCHERICHIA COLI K12. Goldschmidt, Eugene P. (Univ. of Houston, Tex.); Cater, Margot S.; Matney, Thomas S.; Butler, Mary Ann; Greene, Anne. Genetics; 66: 219-29(Oct 1970).

Histidineless mutations in Escherichia coli involving eleven cistrons and corresponding to eight of the nine gene functions in Salmonella typhimurium were identified. The mutations were in-

XUM

duced by either uv or x irradiation. The gene sequence is similar if not identical in the two operons: G, D, C, B, H, A, F, I, (E). Dissimilarities were found in that no recombination was observed in interspecific hybrids and an extended deletion of the entire operon was the most prevalent type of mutation in E. coli. (P.B.M.)

13423 GENETIC AND MORPHOLOGICAL PROPERTIES OF UNDIFFERENTIATED AND INVASIVE VARIANTS OF ASPERGILLUS NIDULANS. Dorn, Gordon L. (Wadley Insts. of Molecular Medicine, Dallas). Genetics; 66: 267-79(Oct 1970).

A total of nine morphological mutants, called fluffy, were uv-irradiated and isolated in Aspergillus nidulans. These mutants displayed varying degrees of delayed differentiation and were capable of invading into established non fluffy cultures. Four flu loci and two extracistronic suppressor loci were tentatively identified. On the basis of morphological properties, drug response, and genetic differences, it was possible to place each fluffy variant into a distinct category. (P.B.M.)

13424 NEW CRISP GENES AND CRISP-MODIFIERS IN NEUROSPORA CRASSA. Garnjobst, Laura; Tatum, E. L. (Rockefeller Univ., New York). Genetics; 66: 281-90(Oct 1970).

Sixteen crisp strains or dwarf strain of Neurospora crassa were examined. From linkage tests and results of interstrain crosses and complementation tests, it was concluded that the crisp (cr) phenotype is determined by mutation at any one of three loci in the right arm of linkage group I. The order appears to be cr-1, cr-3, cr-2, with cr-1 closest to the centromere. Genetic modifications of the crisp phenotype found included apparent reversions of cr-1 and mutant genes which modify crisp morphology (m-1, m-2, and m-3) or completely suppress it (m-4 and m-5) in the double mutants. The phenotype of the modified crisp (cr-1; m-1) was not readily expressed in heterocaryons with cr-1 (cr-1 + cr-1; m-1) formed by spontaneous mutation or produced experimentally. (P.B.M.)

13425 RELATION OF MITOTIC RECOMBINATION TO DNA REPLICATION IN YEAST PEDIGREES. Wildenberg, Judith (Brooklyn Coll.). Genetics; 66: 291-304(Oct 1970).

Histidine prototrophic cells were selected from x ray treated synchronous Saccharomyces cerevisiae cultures. The isolation of the first few division products of each diploid cell ensured the recovery of all genetic strands present at the time of recombination. The genotypes of the mother cell, first bud, and any other phenotypically unique segregant were resolved by tetrad analysis and allele identification tests. The data indicate that both reciprocal and nonreciprocal products of recombination originated at the two strand stage in a large fraction of the analyzed pedigrees. Events that are probably similar to phage heterozygosis and postmeiotic segregation were observed as well. (P.B.M.)

13426 GENE CONVERSION IN HIGHER ORGANISMS: HALF-TETRAD ANALYSIS OF RECOMBINATION WITHIN THE ROSY CISTRON OF DROSOPHILA MELANOGASTER. Chovnick, Arthur; Ballantyne, Graeme H.; Baillie, David L.; Holm, David G. (Univ. of Connecticut, Storrs). Genetics; 66: 315-29(Oct 1970).

A study of gene conversion and recombination between separable mutants of the rosy cistron in x-irradiated Drosophila melanogaster was carried out in half-tetrads utilizing compound third chromosomes. The progeny of mass matings were grown on a purine enriched selective medium which permits survival only of offspring with significant xanthine dehydrogenase activity. Analysis of exceptional ry$^+$ survivors permits their classification as either classical recombinants or convertants. Both classes share features which implicate a single process as their mode of origin. A three point intracistronic half-tetrad analysis was carried out utilizing a mutant heterozygous half-tetrad of the type a + c/ + b +, and possessing flanking markers. A high frequency of ry$^+$ half-tetrads were recovered, and all of these, upon analysis were convertants of the middle allele. The data are entirely consistent with the extensive studies of gene conversion and allele recombination in fungal systems, and are interpretable in terms of nonreciprocal events involving breakage and repair synthesis of DNA as the mechanism of recombination. Moreover, a consideration of recent research on allele recombination in Drosophila suggests that the relative frequency of nonreciprocal to reciprocal events is directly related to the length of the genetic interval between the markers under study. (P.B.M.)

13427 GENETIC BASIS OF VIRULENCE IN DERMATOPHYTES. Hejtmanek, M.; Lenhart, K. (Palacky Univ., Olomouc, Czech.). Folia Biol. (Prague); 16: 363-6(1970).

The virulence of the dermatophyte, Nannizzia incurvata Stockdale, is controlled at the gene level. Crosses between a virulent strain, Microsporum gypseum (st. perf. Nannizzia incurvata), and two avirulent uv-induced mutants revealed that the virulence has a polyfactorial basis. (auth)

13428 GENETIC AND MOLECULAR CHARACTERISTICS OF X-RAY-SENSITIVE MUTANTS OF ESCHERICHIA COLI DEFECTIVE IN REPAIR SYNTHESIS. Kato, Takesi; Kondo, Sohei (Osaka Univ.). J. Bacteriol.; 104: 871-81(Nov 1970).

Alleles responsible for x ray-sensitive characteristics of three mutants of Escherichia coli B, that were also sensitive to uv irradiation, were mapped near metE locus, and named res-1, res-2, and res-3. All the res$^-$ mutants showed no host cell reactivability (Hcr$^-$) for transducing DNA of P1 phage irradiated by uv but they were Hcr$^+$ for infective DNA of P1 phage. They showed no detectable activity of DNA polymerase. Characteristics of allele res-1 were studied in detail. The mutant res-1 uvr$^+$ showed an extensive degradation of DNA after uv irradiation. Double mutants carrying res-1 uvrA$^-$, res-1 uvrB$^-$, and res-1 uvrC$^-$ showed no marked increase in uv sensitivity beyond that of the uvr$^-$ single mutants and only negligible uv-induced DNA degradation. The uvr$^-$ mutations showed no such suppressive effect on DNA degradation induced by x rays in these double mutants. It was concluded that res$^-$ mutants were defective in the second step (repair synthesis) of the excision repair process and that DNA polymerase is partly responsible for the assumed resynthesis step. (auth)

Health Physics and Safety

Refer also to abstracts 13169 and 13471.

13429 PLOWSHARE: NEW CHALLENGE FOR THE HEALTH PHYSICIST. Cohen, J. J. (Univ. of California, Livermore). Health Phys.; 19: 633-9(Nov 1970).

Radiation safety problems encountered by Plowshare researchers are discussed. To help health physicists understand these problems the history of the Plowshare program is outlined and the peaceful uses for nuclear explosives under development are explained. The question of how to weigh the benefits of using nuclear explosions for these purposes against the risk involved is raised, and a possible solution is offered. (auth) (UK)

Radioactive Contamination and Decontamination

Refer also to abstracts 13079, 13080, 13122, 13124, 13189, 13394, 13395, and 13397–13403.

13430 (UCRL-72830) PLOWSHARE AND THE ENVIRONMENT. Holzer, Alfred (California Univ., Livermore. Lawrence Radiation Lab.). Nov 1970. 23p. (CONF-701102-5). Dep. NTIS.

From Meeting of the American Nuclear Society, Washington, D. C.

Deeply-buried underground nuclear explosions used in the recovery of minerals and natural gas can have a positive impact on the environment. To put this on a quantitative base, one can compute emissions from a hypothetical 1000 MW(e) plant using coal, oil, or nuclearly-stimulated gas and examine the relative effects downwind from the plant. The trade-offs between SO$_2$ emissions from coal and oil, and tritium and krypton from the nuclearly-stimulated gas can then be evaluated under identical conditions. Using natural gas, the plant energy requirement of 90 billion ft^3 per year can be met by a field development consisting of 15 wells the first year and decreasing to 2 wells per year after five years. Four 100-kt explosives are assumed needed to stimulate each well. Tritium and krypton-85 concentrations are computed to decrease from first-year values of 10 pCi/cm^3 and 52 pCi/cm^3, respectively, to 1.4 and 7.2 pCi/cm^3 after five years, as new formation gas replaces the original chimney gas and the number of new wells decreases. For the reasonable meteorological conditions which are assumed to remain constant, the maximum effluent concentration occurs 4.3 km from the plant. There the ground-level values of SO$_2$ for coal, oil, and natural gas use are 0.18, 0.044, and 0.00002 parts per million, respectively. Converting the radionuclide concentration at the same location to dose shows that whole-body tritium doses decrease from 0.14 mrem/year for the first year to 0.018 mrem/year after six years, and that the whole-body krypton-85 dose decreases from 0.009 to 0.001 over the same time span. These doses can be compared with those from neutral and manmade radioactive sources. The annual dose from a power plant using nuclearly-stimulated natural gas is comparable to that from TV sets and luminous dial watches. (auth)

13431 DATA. SECTION IV. OTHER DATA. Radiol. Health Data Rep.; 11: 473-82(Sep 1970).

Data are tabulated on ^{90}Sr content of human bone in various geographical regions of the United States during October through December, 1969. A summary is presented of environmental levels of radioactivity during 1969 at Atomic Energy Commission installations. Tables are presented to show gross α, β, and γ radio-

XUM

activity in Bettis Laboratory liquid effluent; ^{89}Sr and ^{90}Sr in stream silt at Bettis; β radioactivity in air and precipitation at Los Alamos; β radioactivity and uranium concentrations in outdoor air samples at Paducah; concentration of β particle emitters and uranium in water at Paducah; and external γ radiation levels at Paducah. (H.L.W.)

13432 DATA. SECTION II. WATER. Radiol. Health Data Rep.: 11: 463-5(Sep 1970).

Water sampling and analysis programs of the Public Health Service and other state and local agencies are discussed. Levels of radioactivity in surface waters of Kansas were monitored by the Kansas State Department of Health. Tables are presented to show gross alpha and gross beta radioactivity in the total solids in Kansas surface waters during 1969. (H.L.W.)

13433 DATA. SECTION I. MILK AND FOOD. Radiol. Health Data Rep.: 11: 449-61(Sep 1970).

Data on radioactive contamination of milk are reported by the Pasteurized Milk Network sponsored by the Bureau of Radiological Health and the Bureau of Foods, Pesticides and Product Safety, Food and Drug Administration of the U. S. Public Health Service. A study on accuracy of data from various milk networks was conducted on milk samples containing known concentrations of ^{89}Sr, ^{90}Sr, ^{131}I, ^{137}Cs, and ^{140}Ba. The various milk surveillance networks that report regularly were surveyed for information on analytical methodologies, sampling and analysis frequencies, and estimated analytical errors associated with the data. A summary of the guidance provided by the Federal Radiation Council for specific environmental conditions is presented. Tables are presented to show guidelines and related information on environmental levels of ^{137}Cs, ^{131}I, ^{89}Sr, and ^{90}Sr as set forth by the FRC for conditions under which Radiation Protection guides are applicable during normal peacetime operations and an acute contaminating event. Federal and state agencies engaged in evaluating the significance of radioactivity in foods and diets are as follows: California Diet study, Connecticut Diet study, PHS study of Radionuclides in Institutional Diet Samples, and HASL study of ^{90}Sr in Tri-City Diets. (H.L.W.)

13434 FALLOUT ^{90}Sr IN BEER. Shirashi, Yoshiyuki; Ichikawa, Ryushi (National Inst. of Radiological Sciences, Chiba, Japan). Health Phys.; 19: 443-4(Sep 1970).

The fallout ^{90}Sr content in Japanese beer was determined in order to compare its annual change with that of ^{137}Cs which depended on the deposition rate of atmospheric ^{137}Cs due primarily to nuclear weapon tests. The concentration of ^{90}Sr and ^{137}Cs in beer and the monthly deposition of ^{90}Sr in the Tokyo area from 1959 to 1969 was shown graphically. The results indicated that the accumulation of ^{90}Sr in the soil was more easily absorbed by plant roots than ^{137}Cs. A table giving the ^{90}Sr and Ca content in raw materials, spent residues, and 1 liter of beer in 1967 is presented and discussed. The balance of ^{90}Sr and Ca between the raw and spent materials both comprising malt, side materials, and hops, was in good agreement with the values measured in beer. 60% to 70% of both ^{90}Sr and Ca was transferred from raw materials to beer during the manufacturing process. (UK)

13435 ASSESSMENT OF IRRADIATION HAZARDS PRODUCED BY NON-EQUILIBRIUM EMANATIONS. Bad'in, V. I.; Sayapina, R. Ya.; Alferov, M. V.; Novikov, V. I. Gig. Sanit.; No. 7, 51-4(Jul 1970). (In Russian).

It was found that the maximum permissible concentration of the non-equilibrium emanation is equal to the ratio of the balanced maximum permissible concentration of radioactive gas and that of the extent of balance of its secondary dissociation product (RaB, ThB, AcB). In the field this phenomenon proved to be true in the changes noted in the balance of dissociation products emanations depending on the extent of airing of premises. The method suggested simplifies the process of monitoring in the assessment of irradiation hazards due to non-equilibrium emanations and shortens the time of their fulfilment. (auth)

13436 RADIATION HAZARDS. Gibbs, W. J.; Moroney, J. R.; Stevens, D. J.; Titterton, E. W. (Australian Atomic Weapons Tests Safety Committee, Ascot Vale, Victoria). Nature (London); 228: 297-8(17 Oct 1970).

It is pointed out that the results of the present measurements on fallout from nuclear weapons tests in French Polynesia were assessed by the Australian National Radiation Advisory Committee and found to have no significance as a health hazard to the Australian community. Measurements on shorter-lived fission products in fallout over Australia and New Guinea, following the French nuclear weapons tests of 1966 to 68, indicate that the highest γ-radiation dose to the whole body from all these tests was 3.3 mR and the highest dose to thyroid in young children due to ^{131}I in milk consumed in any year in this period was 226 mR. Weathering, shielding and other effects would reduce whole body doses by a factor of 3 to 5, while decay of ^{131}I before consumption of milk would result in substantially lower thyroid doses. Furthermore, the stratospheric burden of ^{90}Sr in the southern hemisphere decreased from 1,200 kCi in 1963 to 50 kCi in mid-1968, and annual deposit of ^{90}Sr in Australia fell from 2.1 mCi/km^2 in 1964 to 0.4 in 1968. High yield nuclear weapons tests in Polynesia in August–September 1968 added 130 kCi to a total stratospheric burden of 180 kCi ^{90}Sr and an annual deposit of ^{90}Sr of 0.6 mCi/km^2 in 1969. Some data are also given on migratory fish. (UK)

13437 ENVIRONMENTAL CONTAMINATION ASSOCIATED WITH THE DEVELOPMENT OF NUCLEAR POWER. Takahashi, Kanji (Kyoto Univ.). Doboku Gakkaishi; 55: No. 2, 41-2(Feb 1970). (In Japanese).

According to the long-range atomic-power development program in Japan, the nuclear power generation will be about 6,000,000,000 kWe in 1975 and 30,000,000,000 kWe in 1985. Then, under this situation, the main sources of environmental contamination are fuel processing plants and atomic power stations. The environmental contamination associated nuclear-power development is described as follows: Environmental-contamination criteria for radioactive materials—MPC$_{s}$ are specified for over 200 nuclides. The control on the release of radionuclides alone is not sufficient; the environmental-contamination medium is closely associated with the intake by human beings. Atomic power stations as a source of environmental contaminations—Thermal power stations and nuclear power stations, in this connection, are compared. Contamination due to tritium; the particular nature of contamination by tritium is explained. (OGAWA, H) (Japan)

13438 INVITED COMMENTS ON A DERIVATION OF THE "FACTOR OF 700" FOR ^{131}I. Hull, A. P. (Brookhaven National Lab., Upton, N. Y.). Health Phys.; 19: 698-9(Nov 1970).

The factor for ^{131}I is used in reactor hazards calculations and applied by the AEC Division of Licensing and Regulation to the annual release limits for halogens from power reactors. The note is intended to clarify the basis and applications of this factor. It is pointed out that Burnett's calculations (NSA 24: 12086) although they lead to the AEC's value of 700, include a somewhat arbitrary choice of highly variable parameters, few of which have been established for reactor effluent ^{131}I. It is considered that the factor of 700 thus obtained is conservative by about a factor of 2. (UK)

13439 RADIOACTIVITY IN THE DIET IN HIGH BACKGROUND AREAS OF BRAZIL. Penna-Franca, E.; Fiszman, M.; Lobao, N.; (and others) (Univ. Federal do Rio de Janeiro, Brazil). Health Phys.; 19: 657-62(Nov 1970).

Two types of high background regions were studied in Brazil—the monazite sand region along the Atlantic Coast and the zone of volcanic intrusives in the inland state of Minas Gerais. In both regions there are groups of people living on variable fields of radiation ranging from 0.03 to 1.0 mR/hr. To evaluate the extent of the radioactive intake and internal contamination of representative populations, an extensive survey was carried out. In villages in the monazite sand region, the local production of food was found to be insignificant and the radioactive contents were practically within normal ranges. In the volcanic intrusive zone, two villages were selected for having extensive agriculture production cultivated, to a large extent, in soils containing thorium and uranium minerals. The radioactivity in local produce is appreciable, mostly due to ^{228}Ra and daughters, that in some types of foodstuff reach two orders of magnitude above average normal values. A dietary injury is reported. (UK)

Dosimetry and Monitoring

Refer also to abstracts 13513, 13533, 13534, 13536, 13538, 13568, 13581, and 14403.

13440 DATA. SECTION II. WATER. Radiol. Health Data Rep.; 11: 399-401(Aug 1970).

The gross β radioactivity in domestic water supplies, most of which are of surface origin, in California during July to December 1968 is presented. The monthly data for specific sampling sites are presented in tabular form. A map locating the sampling sites is also included. (E.R.B.)

13441 DATA. SECTION III. AIR AND DEPOSITION. Radiol. Health Data Rep.; 11: 403-11(Aug 1970).

The results of surface air and precipitation surveillance activities are presented by the Radiation Alert Network (RAN), the Canadian Air and Precipitation Monitoring Program (CAPMP), the Mexican Air Monitoring Program (MAMP), and the Pan American Air Sampling Program (PAASP). The RAN data include the gross β radioactivity in surface air and precipitation at 73 selected sites during April 1970 and a monthly and yearly

XUM

profile of β radioactivity in air during 1964 to April 1970 at eight selected sites. The CAPMP data include the gross β radioactivity in surface air and precipitation at 24 selected sites during April 1970. The MAMP data include the gross β radioactivity of airborne particulates at 16 selected sites during December 1969. The PAASP data include the gross β radioactivity in surface air at 12 selected sites during April 1970. The RAN data also include the ^{238}Pu and ^{239}Pu activities in airborne particulates at 11 selected sites during January to March 1969. All data are presented in tabular form. (E.R.B.)

13442 DATA. SECTION I. MILK AND FOOD. Radiol. Health Data Rep.; 11: 383-93(Aug 1970).

The average concentrations of ^{90}Sr, ^{131}I, and ^{137}Cs in milk samples collected during April 1970 are presented and comparisons are made with the 12-month averages from May 1969 through April 1970. The samples were obtained at sampling stations throughout the Western Hemisphere by the Canadian Milk Network, Pasteurized Milk Network, and Pan American Milk Sampling Program. The concentrations and intake of stable calcium and potassium and ^{89}Sr, ^{90}Sr, and ^{137}Cs in institutional diets of children (9 to 12 yrs) and adults in the U. S. during October to December 1969 are given as are the 1969 annual average concentrations of stable calcium and potassium and ^{90}Sr, ^{137}Cs, and ^{226}Ra for the same sampling stations. All data are presented in tabular form. (E.R.B.)

13443 STANDBY MILK SURVEILLANCE NETWORK. Sharpe, Thomas J.; Stein, John L. (Bureau of Radiological Health, Las Vegas, Nev.). Radiol. Health Data Rep.; 11: 379-82(Aug 1970).

The operation of the Standby Milk Surveillance Network of the Southwestern Radiological Health Laboratory is described. Portions of the network were activated on several occasions. Fresh fission products were defined in a number of samples collected from processing plants in the network, although in all cases the concentrations of the radionuclides present were well below the recommendations of the Federal Radiation Council. (auth)

13444 DISPOSAL OF RADIOACTIVE WASTES FROM U. S. NAVAL NUCLEAR-POWERED SHIPS AND THEIR SUPPORT FACILITIES, 1969. Mangeno, J. J.; Miles, M. E. Radiol. Health Data Rep.; 11: 373-7(Aug 1970).

Data on disposal of radioactive wastes from U. S. Naval nuclear-powered ships and their support facilities and results of environmental monitoring performed to confirm adequacy of waste disposal limits and procedures are summarized. The waste disposal data presented show that the total long-lived radioactivity in liquid waste discharges associated with operation and maintenance of Naval nuclear-powered ships totaled 0.05 Ci in 1969 for all harbors. This is comparable to the average of 0.2 Ci discharged per year during the preceding 3 years for all harbors and is less than the average of 4 Ci reported discharged per year during the preceding 5 years. Results of environmental surveys of harbor water and bottom sediment for gross radioactivity and for ^{60}Co have shown that no increase in radioactivity above normal background levels was detected in harbor water, discharges of liquid wastes for U. S. Naval nuclear-powered ships have not caused a measurable increase in the general background radioactivity of the environment, and low-level ^{60}Co radioactivity is detectable in localized areas of harbor bottom sediment around a few piers at operating bases and shipyards where maintenance and overhaul of Naval nuclear-powered ships have been conducted over a period of several years. This report confirms that procedures used by the Navy to control discharges of radioactivity from U. S. Naval nuclear-powered ships and their support facilities are effective in protecting the health and safety of the general public. (auth)

13445 DATA. SECTION IV. OTHER DATA. Radiol. Health Data Rep.; 11: 412-18(Aug 1970).

Environmental levels of radioactivity during July to December 1969 are reported for the following AEC installations: Atomics International—Canoga, California; Feed Materials Production Center—Fernald, Ohio; and Neutron Devices Department—St. Petersburg, Florida. Seismic signals originating in the Semipalatinsk nuclear test area, presumably from Soviet underground nuclear explosions in the 20 to 200 kiloton TNT equivalent range, were recorded by the United States Atomic Commission on July 20 and 23, 1970. (E.R.B.)

13446 INVESTIGATIONS ABOUT ENERGY DEPENDENCE OF DOSIMETERS IN A 42-MeV BETATRON. Fehrentz, Dieter; Franz, Klaus-Dieter (Univ., Heidelberg). Strahlentherapie; 140: 71-7(Jul 1970). (In German).

Several dosimeters and dose measuring procedures were examined in a 42-MeV-betatron as to the dependence of their indications on the irradiation energy. Some of the usual ionization dosimeters and one flat chamber with lateral air walls were employed. Furthermore, films, LiF-thermoluminescence dosimeters and iron sulfate dosimeters were used. (auth)

13447 PENDULUM RADIATION WITH TRANSVERSAL SHIFT OF THE AXIS DURING ^{60}Co-TELETHERAPY. PART III. TRANSVERSAL SHIFT OF THE PENDULUM AXIS DURING RAPID TRANSLATION MOTION. Kuttig, Helmut; Froeling, Monika; Schneider, Heidemarie (Univ., Heidelberg). Strahlentherapie; 140: 53-62(Jul 1970). (In German).

Dose distribution of cobalt-60-teletherapy in pendulum translation with a transverse shifting of the axis into the direction of the angle-bisecting line, as well as in the corresponding vertical plane is discussed. A translation vertical to the angle-bisecting line effects two dose maxima of butterfly shape of low isodoses. A translation into the direction of the angle-bisecting line causes a stronger dose maximum emigration into the direction of the surface, as well as a stronger extension of the isodoses in the translation plane. (auth)

13448 ISODOSE MEASUREMENT OF THE BLADDER DOSE IN RADIUM THERAPY. Nieminen, U.; Forss, M.; Unnerus, C. E. (University Central Hospital, Helsinki). Strahlentherapie; 140: 280-2(Sep 1970).

Parallel determinations were made of the amounts of radiation received by the urinary bladder in Ra therapy in 109 cases, using a Siemens gammameter and isodose curves plotted on the roentgenograms. A small amount of contrast medium was injected into the bladder via a catheter. The bladder wall was clearly visualized in a lateral exposure of the pelvis, and the radiation dose to the bladder was read from the isodoses plotted. The doses calculated from isodose curves were consistently higher than those measured by the gammameter. Although the dose calculated from isodose curves is an approximate quantity that includes errors, these errors were not significant as those measured by gammameter. An advantage of the method is the shortening of the application time and the smaller amounts of radiation received by the nursing staff. (auth)

13449 COMPUTER METHOD FOR CALCULATING MULTI-FIELD AND ROTATIONAL DOSE DISTRIBUTIONS IN ^{60}Co TELETHERAPY. Jayaraman, S. (International Atomic Energy Agency, Vienna). Strahlentherapie; 140: 283-5(Sep 1970).

A method for calculating the multi-field and rotational dose distributions in Co-60 teletherapy is presented. The method is based on an empirical formula for tissue-air ratio for rectangular fields and estimates primary dose and scatter dose at each point separately. Homogenetics and the effect of contour shapes are also mentioned. (auth)

13450 RADIATION PROTECTION AGAINST NEUTRONS IN A BETATRON BEAM. Eipper, Hermann Hans; Manegold, Karlheinz (Strahlenklinik im Staedtische Krankenhaus, Cologne). Strahlentherapie; 140: 286-90(Sep 1970). (In German).

Distribution measurements of thermal, of medium fast, and of fast neutrons as well as of the neutron dose were carried out in the Radiation Clinic Köln-Merheim at the Siemens-42-MeV Betatron. Two different devices were used, a BF_3-counting tube with double moderator, and the AEG Neutron monitor ELM 714 LMS. Measuring results showed that in the examined irradiated space (with a sluice room, length = 5.5 m) it is not necessary to place a paraffin inlay into the door of the irradiation space in order to screen off the neutrons. (auth)

13451 INTERRELATIONSHIP BETWEEN CELL SURVIVAL, RADIATION PORTALS, AND DOSE GRADIENTS. Matschke, Siegfried (Zentralinstitut fuer Biologie und Medizin, Berlin). Strahlentherapie; 140: 291-5(Sep 1970). (In German).

The effect of an error in adjustment of dose distribution can be considerable in fractionated radiation used in tumor therapy. A general relation between error in adjustment, dose gradient, and total error is stated. This relation is correlated to different grades of cell survival curves, so as to have the possibility to state the error of the cell survival number depending on the adjustment error of different dose distributions. (auth)

13452 X RAYS FROM DOMESTIC COLOUR TELEVISION RECEIVERS IN BRITAIN. O'Riordan, M. C.; Casbolt, P. N. (Radiological Protection Service, Sutton, Eng.). Nature (London); 228: 420-1(31 Oct 1970).

It is stated that with British domestic colour television receivers the genetic dose from x rays is negligible, and the x-ray emission from individual sets is normally well within the internationally accepted limit. (UK)

13453 DETERMINATION OF THE RADIATION LOADING IN ROENTGENODIAGNOSTIC INVESTIGATION WITH THE AID OF

XUM

THERMOLUMINESCENT DOSIMETRY. Gubatova, D. Ya.; Nemiro, E. A. (Inst. of Medicine, Riga). Med. Radiol.; 15: No. 11, 61-5(Nov 1970). (In Russian).

Thermoluminescent dosimetry was used in determining the radiation loading in roentgenodiagnostic procedures. The exposure doses of x ray radiation were measured in patients with different diseases of the lungs and mediastinum (40 cases), 40 patients with alimentary diseases and 42 apparently healthy persons (prophylactic examination). The exposure doses in alimentary diseases were higher than in examination of thoracic organs. The exposure doses in the irradiation field are quite irregular differing up to 60 R. The convenience and simplicity of thermofluorescent dosimetry on the basis of lithium chloride, a relatively small energy dependence, a large range of measured doses, and tissue-equivalent monitor were stressed. (auth)

13454 RESULTS OF MEASUREMENTS OF RADIOACTIVITY IN THE SEWAGE IN MILAN FOR DETERMINING POSSIBLE CONTAMINATION BY RADIOISOTOPES. Colangelo, S. (Politecnico, Milan); Cortellessa, G. C.; Terrani, S. Ig. Sanita Pubblica; 26: 165-78(May-Jun 1970). (In Italian).

During the winter of 1968 to 69 a program of measurements on the waste solutions in sewer trunks of the hospital and the main sewer trunk lines sited downstream of the discharges was carried out in order to collect data on the possible radioactive contamination of a city-wide sewer system. The city of Milan was selected because of its elaborate dynamic sewer system and the fact that the city of Milan produces a large amount of waste waters, due to its high industrial level. Measurements were made of the content of γ-emitting nuclides, especially ^{131}I, ^{203}Hg, and ^{198}Au using a multichannel spectrometer. The radioactivity of the waste waters at the outlet of the production sites was found sometimes to be higher than 10^{-5} microCi/ml; however the dilution factor in the dynamic sewer of Milan generally lowered, within a few meters, the concentrations by a factor 10^2 to 10^3. At the outlet of the main sewer trunk lines, activities were found to be no higher than 10^{-10} microCi/ml. (auth)

13455 RECTANGULAR MOULDS: A FOOTNOTE TO PATTERSON-PARKER. Porter, E. H. (New York Univ. Medical Center). Brit. J. Radiol.; 43: 445-7(Jul 1970).

A study was made of dose-distributions, produced by square and rectangular radium and ^{60}Co slug distributions in moulds. Calculations were based on a computer program of Schlessinger and Porter and the results confirmed the Paterson-Parker dose estimation system. The classical distribution rules gave small areas in which ±10%, but never ±12%, of the mean calculated dose agreed with the tabular dose to 2 to 3½%. Modifications to the distribution rules gave a uniformity of ±5%, to which the Paterson-Parker tables could be applied with the same accuracy as moulds following the classical rules. Extended rules were concerned with dose-rate, corners, two or more inner lines, short lines, gaps, alternating sources, and long thin moulds. (UK)

13456 SOME UNEXPECTED DOSIMETRIC PROBLEMS IN AN APPARATUS FOR MAMMALIAN RADIOBIOLOGY. Moore, J.; Pritchard, J. A. V.; Sutherland, W. H.; Harper, M. W. (Velindre Hospital, Cardiff, South Wales). Int. J. Radiat. Biol.; 18: 287-9(1970).

HeLa S_3 (OXF) cells were irradiated with ^{60}Co γ rays. The cells were attached to 5.0 cm diameter glass or polystyrene Petri dishes contained in a Perspex box, (20 × 20 × 12 cm), divided into two compartments by a central partition of lead of such thickness that the four dishes on the top shelf should have received half the dose delivered to those on the shelf in the lower compartment, with the beam being directed vertically up through the box. The results suggested that the "backward-going" radiation from the shelf contributed to the dose received on the lower shelf by more than the 10% expected due to back-scattering from ^{60}Co radiation of approx. 1.2 MeV energy. The difference in the dose measured by different volumes of ferrous sulphate and with 2mm thick aluminum sheet added to the load, suggested that the "backward-going" radiation was of low energy and absorbed by the surface layers of ferrous sulphate. Simulation experiments were carried out using samples of lithium fluoride placed immediately above, and within 1 cm below a 2.5 mm lead sheet. The dose to the lower sample was 100% higher than to the higher one. If a 2.5 cm sheet of Perspex was substituted for lead, the doses above and below agreed with the predictions of the inverse square law. The dose to the lithium fluoride over the Perspex and lead was almost entirely due to the primary beam, whereas 50% of the dose below was due to the "backward-going" radiation. Experiments using carbon, Perspex, aluminum, copper, tin, tungsten and lead showed that the "backward-going" radiation varied directly with the atomic number of the material used. The half-value thickness of the "backward-going" radiation was about 0.65 mm aluminum, corresponding to photon energy of 20 keV or electron energy of 200 keV. (UK)

13457 RADIATION PROTECTION AGAINST X-RAY DIFFRACTION APPARATUS. Nishi, Tatsuo; Yamada, Norikazu; Minami, Kentaro; Hasegawa, Keisuke; Mito, Norio (Japan Atomic Energy Research Inst., Oarai). Hoken Butsuri; 5: No. 2, 69-74(Jun 1970). (In Japanese).

For the purpose of radiation protection against x ray diffraction apparatus, the following studies were made: measurements of the exposure rates of the primary and scattered x rays produced from the apparatus, determinations of the sensitivity of many types of surveymeters for the low energy x rays from the apparatus, and experiments on the shielding effect of many kinds of materials such as vinyl sheet, and rubber. Exposure rates of about 600 R/min were observed for the primary x rays at the sample holder of the apparatus during the normal operation. For the 8 keV x rays emitted from the apparatus, the readings of an ionization chamber type surveymeter (ICS-101C) that was designed for x-rays were in good agreement with those of the Victoreen r-meter, whereas the readings of the ionization chamber type surveymeter made for γ rays indicated about one half of those of the Victoreen r-meter. The shielding effects of several materials such as polyethylene, rubber, and cotton cloth were measured. Among them, vinyl sheet had the greatest shielding effect. Survey technique and assessment of absorbed dose were described in appendix. (auth) (Japan)

13458 INTERFERENCE OF MEDICALLY ADMINISTERED ^{57}Co WITH TRANSURANIC ELEMENT IN VIVO LUNG MEASUREMENTS. Andersen, B. V.; Jech, J. J. (Battelle Memorial Inst., Columbus, Ohio). Health Phys.; 19: 693-5(Nov 1970).

The presence of internally deposited ^{57}Co may interfere with lung counter evaluations and may not be readily identifiable by its normally expected photopeak. (auth) (UK)

Radiation Protection

Refer also to abstracts 13457 and 13461.

13459 PRIORITY SYSTEM FOR THE INSPECTION OF X-RAY FACILITIES. Dillard, Bobby L.; Hardin, Charles M. (Kentucky State Dept. of Health, Frankfort). Radiol. Health Data Rep.; 11: 367-72(Aug 1970).

A method of establishing a priority system for performing radiation safety inspections of specific x-ray facilities by a state radiation control program is described. Data obtained from past inspections of radiographic fluoroscopic and dental x-ray facilities are evaluated, and a priority number is assigned to these facilities. Those facilities with the highest priority number will be surveyed first on the next round of inspections. (auth)

13460 ADDITIONAL RADIATION BURDEN TO THE PATIENT CAUSED BY SHIELDING DURING DEEP X-RAY THERAPY. Vogel, Karl-Heinz; Breitling, Gerhard (Univ., Tuebingen, Ger.). Roentgenpraxis; 23: 207-12(Sep 1970). (In German).

Based on literature survey and on phantom measurements, the problem of patient shielding during deep x-ray therapy is analyzed. It can be shown that the surface dose is significantly increased by shielding material around the entrance field, along the lateral aspects of the body, and especially at the exit area where strong backscatter occurs. Therefore such shielding is useless and should be avoided. Under conditions of modern depth therapy, lead shielding of the patient should be abandoned. (tr-auth)

13461 OPTIMUM PLANNING FOR RADIATION FACILITIES. BASIC CONCEPT OF RADIATION PROTECTION. Fujii, Shoichi (Shibaura Inst. of Tech., Tokyo). Genshiryoku Kogyo; 16: No. 5, 6-10(May 1970). (In Japanese).

In order to protect personnel and the surrounding population from radiation hazards, it is necessary to follow the proper procedures for handling radioactive materials and to have completely protected radiation facilities. In designing radioactive installations, optimum planning involves the type of work performed, the degree of danger involved, the type of radiation generator, the radiation energy, and the types and amounts of radionuclides involved. The fundamental considerations in designing radioactive installations are the location including the site, buildings and rooms; maximum permissible doses; shielding against radiations; control of discharged air, water; control of surface contaminations, and prevention of accidents. (YOSHIMURA, S) (Japan)

13462 DOSE REDUCTION FACTORS OF A LEAD-LINED GIRDLE. Smith, Roy H.; Willhoit, Donald G. (Univ. of North Carolina, Chapel Hill). Health Phys.; 19: 830-2(Dec 1970).

Two models of foundation garments for female radiation workers are described which incorporate flexible panels of lead impregnated vinyl material. The material does not crack even after repeated flexing and has a shielding equivalence of 0.2 mm of lead. Radiation measurements for 1.0 mm Al HVL to 3.3 mm Cu HVL x rays were made with dosimeters placed within a pelvic phantom enclosed in one of the lead girdles. Data obtained indicated that the use of the girdle may reduce gonadal dose from x ray exposure by a factor of between 1.6 and 19 depending on radiation quality and direction of the x rays. (UK)

Safety Procedures

Refer also to abstracts 13078, 13519, and 13586.

13463 PRELIMINARY SURVEY OF X-RAY PRODUCING DEVICES IN KANSAS SCHOOLS, 1968. **Spencer, Leo W. Jr. (Kansas State Dept. of Health, Topeka). Radiol. Health Data Rep.; 11: 613-15(Nov 1970).**

A survey was made of the use and safety of x-ray sources used in schools in Kansas during 1968. The results indicate that the amount of exposure received by students in school work was small, although three x-ray tubes and four Crookes tubes were found that gave a maximum exposure calculated to be 750 mR to the hands of 10 high school students over a school year. (C.H.)

13464 RESULTS OF 33,911 X-RAY PROTECTION SURVEYS OF FACILITIES WITH MEDICAL OR DENTAL DIAGNOSTIC X-RAY EQUIPMENT, FISCAL YEARS 1961–1968. **Fess, Lawrence R.; McDowell, Richard B.; Jameson, Wayne R.; Alcox, Ray W. (Public Health Service, Rockville, Md.). Radiol. Health Data Rep.; 11: 581-604(Nov 1970).**

The results of radiation surveys of 33,911 medical and dental x-ray facilities are presented and analyzed. It was found that a high percentage of x-ray machines in medical facilities have improper collimation and inadequate filtration. In addition, a large proportion of the facilities do not possess adequate accessory patient or operator shielding. The use of an open-end aiming device high-speed film and the need to improve darkroom procedures were the primary recommendations made for dental facilities. (auth)

13465 MEDICAL SUPERVISION OF RADIATION WORKERS. Hill, S. M. B. (United Kingdom Atomic Energy Authority, Harwell, Eng.). Brit. J. Radiol.; 43: 751(Oct 1970).

It is believed that at a simple medical examination, it is not possible to detect physical conditions which render an individual more sensitive to ionizing radiation exposure, precluding him working under normal control conditions at less than maximum permissible exposure. The requirements of the Codes of Practice and the Ionizing Regulations should be reviewed. (UK)

13466 ^{192}Ir CONTACT IRRADIATION WITH CLINICAL SEQUELAE (RADIATION ACCIDENT). **Chone, B.; Schneider, G. J.; Fehrentz, D. (Univ., Heidelberg. Univ., Freiburg i. B.) Strahlentherapie; 140: 113-22(Jul 1970). (In German).**

The origin, mechanism, course, and direction of an irradiation accident caused by an iridium-192-radiation vehicle are discussed. A group of six construction workers was involved in the accident. Only with one of the persons, visible contact lesions were present together with sequelae, as this worker had inadvertently kept the vehicle in his pocket for some hours. According to the circumstances, a high partial-body dose in the regions of the left body side, pelvis and thigh, had to be presumed. The estimated physical dose at the contact surfaces was about 4,000 to 8,000 R. The peak stress in the region of the radiation ulcer, however, was higher to an essential degree (about 10,000 to 20,000 R). A whole-body stress of 100 to 200 R could be derived from these circumstances. Nominal values corresponded to the consecutive local irritative defects at the surface of the skin, as well as to the distant effects in the gonadal region. Consequences of the permanent secondary lesions can, at present, not yet be defined, especially as far as gonadal function is concerned. The contact lesions of the skin healed. The radiation ulcer in the middle of the thigh had to be corrected by an operation. (auth)

13467 RADIATIONAL SAFETY IN THE USE OF RADIOISOTOPIC METHODS IN ENGINEERING INDUSTRY. Lyarskii, P. P.; Moiseitsev, P. I.; Volkovitskaya, V. V.; Korenkov, I. P. Gig. Sanit.; No. 9, 48-51(Sep 1970). (In Russian).

Features of the radioisotopic investigation methods and their hygienic assessment are discussed. The finding was that when radiation safety regulations were fulfilled the extent of external radiation of the personnel did not exceed 400 to 700 mber a year. (auth)

13468 STATISTICAL CONSIDERATIONS REGARDING MEDICAL JUDGMENTS OF UNSUITABILITY FOR WORK INVOLVING RISKS OF RADIOACTIVE EXPOSURE. **Pulcinelli, Mario (Univ., Pisa, Italy). Securitas; 55: 187-204(1970). (In Italian).**

After having recalled the legislative bases that concern the individual protection of workers in nuclear establishments, a statistical analysis of 3069 judgments of unsuitability or conditional suitability given by the health authorities at the military nuclear establishment of San Piero at Grado was made. In view of the particular structure of this establishment and the special modalities that govern the hiring of personnel, these judgments are made by categories of suitability. The more important reasons for exclusion are emphasized, and then the individual judgments both as regards their overall incidence and in relation to the age of the workers concerned are examined. The data obtained in this manner acquire particular importance because they relate to a sample population (i.e. military personnel) that was already selected and checked from a health point of view. (auth)

Civil Defense

Refer also to abstract 13134.

Legal Aspects

Refer also to abstract 13437.

13469 (ORNL-NSIC-75(Rev.1)) PERSONNEL INVOLVED IN THE DEVELOPMENT OF NUCLEAR STANDARDS IN THE UNITED STATES. **(Oak Ridge National Lab., Tenn.). Dec 1970. 626p. Dep. NTIS.**

The personnel involved in the development of nuclear standards in the United States are listed. The listings, prepared by machine sorting, are alphabetical by: personal name (white pages); company affiliation (blue pages); and standards, organizations, and committee titles (green pages). A KWIC (Keyword in Context) index of topics (yellow pages) giving the name of the committee or group working on a given topic is included. A list of the members of the Nuclear Technical Advisory Board is also given. (E.R.B.)

13470 CHEMICAL AND HYGIENIC STUDIES ON NATURAL RADIOACTIVE SPA. 3. NATURAL RADIOACTIVE NUCLIDES IN HOT SPRING WATER AT MASUTOMI SPA AREA. **Kametani, Katsuaki; Tanaka, Akira; Kido, Yasumasa; Hasegawa, Akira; Ikebuchi, Hideharu (National Inst. of Hygienic Sciences, Tokyo). Eisei Kagaku; 16: No. 1, 15-18(Feb 1970). (In Japanese).**

Natural radioactive nuclides in the spring water at Masutomi spa area were investigated to determine its safety for drinking. Samples of spring water were collected from 12 places in the Masutomi spa area in 1963, and from six places in 1964 and 1965. The mean value of concentration of ^{226}Ra was 21.7 pCi/l and that of ^{222}Rn was 1.3×10^{-2} μCi/l at six sampling places where the water was used for drinking. The maximum concentration of natural U was 2.3 μg/l. Compared to $^1/_{30}$ of the maximum permissible concentration in water for personnel that was recommended by ICRP and NBS in the USA, the concentration of ^{226}Ra and ^{222}Rn was higher, than that of natural U. It was recommended that the mean daily intake of spring water be less than 300 ml based on the ^{226}Ra content and 150 ml based on the ^{222}Rn content. (Japan) (TSS)

13471 SAFE CONTROL OF ENVIRONMENTAL RADIOACTIVITY AROUND ATOMIC ENERGY PLANTS. **Saiki, Masamichi (National Inst. of Radiological Sciences, Chiba, Japan). Genshiryoku Kogyo; 16: No. 6, 28-32(Jun 1970). (In Japanese).**

Radiation exposure of human beings is through the contact or proximity to radioactive materials. The protection of personnel in nuclear installations is due largely to the development and improvement of the installation itself and pretection devices. On the other hand, the radiation exposure of the general population, as against that of nuclear personnel, is via the surrounding environment. Radioactivity measures for the general population in the area around a nuclear installation are described: safety control of radioactive wastes, measures following major accidents, investigation of background radiations, including natural radioactivity and fallout ecology concerning radiation protection, and environmental radiation monitoring, both normal and emergency. (KOIZUMI, I) (Japan)

Medicine

Refer also to abstracts 12964 and 14837.

Protective Substances

Refer also to abstracts 13567 and 13604.

13472 PROTECTION BY PHYTOHEMAGGLUTININ OF HUMAN BLOOD LYMPHOCYTES IRRADIATED IN VITRO. **Cir-**

XUM

kovic, Dimitrije (Boris Kidric Inst. of Nuclear Sciences, Belgrade). Strahlentherapie; 140: 318-24(Sep 1970).

The effects of phytohemagglutinin (PHA) on human peripheral blood lymphocytes irradiated in vitro with 500–5000 R were studied. The direct cytolytic action of irradiation on the PHA-treated and the control cultures of lymphocytes was followed by counting the cells after four days incubation. The cell counts showed exponential decrease with the increase in radiation dose. In PHA-treated cultures there was a considerably higher number of cells as compared to the controls. It appeared that the protective effect of PHA in regard to the number of cells in cultures depends on the concentration of this agent in the culture medium. Data concerning the examination of DNA synthesis in PHA-treated lymphocyte cultures demonstrated the reduction in cell number with the increase of radiation dose. The extent of blast transformation was unaffected by radiation which demonstrated that surviving lymphocytes undergo morphological changes as normal lymphocytes and that PHA protects both unstimulated and transformed cells. It appears that the protective effect of PHA on irradiated lymphocytes may result from intensive metabolic changes in initial phase of PHA action. (auth)

13473 GROWTH INHIBITION THROUGH GAMMA RADIATION ON TRANSPLANTED SARCOMAS IN MICE. **Hilscher, Werner; Ritzl, Friedrich; Stockhausen, Wolfgang; Witt, Inge (Univ., Duesseldorf. Kernforschungsanlage, Juelich, Ger.). Strahlentherapie; 140: 325-9(Sep 1970). (In German).**

Methyl-cholanthrene induced sarcomas in mice showed a clear radiosensitivity for gamma-rays. Healing can be obtained without damage to neighboring tissues. With the optimal dose of 1090 R, neither epilation was observed nor any lesion of the irradiated limb. The optimal dose was 1090 R. Healing was obtained in 30% of the cases. The same cure rate could be obtained by neutron capture irradiation. Any relevant difference in RBE was not noted. The animals, irradiated in the reactor or by a cesium source were followed for their fertility. No difference was noted either in size or frequency of litters. No external malformation was observed. (auth)

13474 EXPERIMENTAL TESTS ABOUT TIME FACTOR EFFECTS. **Kaufmann, Horst (Ruhr-Univ., Bochum, Ger.). Strahlentherapie; 140: 296-301(Sep 1970). (In German).**

It is discussed that the protective effect of anabolic hormones (methylprednisolone, Urbason) is due to an enhancement of the restorative processes after irradiation as was observed in studies with mice. This means and confirms that, for the interpretation of time factor effects in fractionated irradiation schemes, one must take into account that lesion and recovery occur at the same time. (auth)

13475 EFFECTS OF AN EXTRACT OF CALVES-BLOOD ON RADIOINDUCED MUCOSA LESIONS IN THE AREA OF LARYNX AND PHARYNX. **Hoefer-Janker, Hans; Scheef, Wolfgang; Dockter, Juergen (Strahlenklinik Janker, Bonn). Strahlentherapie; 139: 701-6(Jun 1970). (In German).**

To 40 patients with mucosal reaction and its painful syndrome caused by radiotherapy, a protein free extract of cattle-blood, Actihaemyl, was administered. In the group treated with Actihaemyl, 17/20 favorably responded with decrease of pain, in the placebo group only 6 patients. The negative results, when studied by the test of Mantel-Haenszel, showed a statistically significant difference with p smaller than 0.001. This activity and demonstrable effect of Actihaemyl on the mucosal radiotherapy reactions were due to an increase in tolerance to the irradiation. An analgesic or antiphlogistic effect was not evident. It seemed probable that Actihaemyl has a protective effect only for the mucosa, and had a sensitizing effect on the tumor cells. In many clinical observations, the protective effect could already be shown during the irradiation for cervical and bladder carcinomas. The possibility to increase the tumor dose improved the prognosis in many patients. (auth)

13476 EFFECTS OF TANDERIL ON RADIOSENSITIVITY. **Muehleisen, Hermann; Voertler, Hans-Hellmut (Staedtsche Marienkrankenhaus, Amberg, Ger.). Strahlentherapie; 139: 707-12(Jun 1970). (In German).**

Comparative examinations in carcinoma irradiations over a longer period proved significant differences in cutaneous radioreactions with patients to whom tanderil was given prophylactically and during irradiation, and with patients of the placebo group. Radioreaction is weaker owing to the inhibition of the inflammative reaction during tanderil therapy, i.e., stronger tumor doses can be given at equal radioreaction. There are no objections as to the application of tanderil before and during a carcinoma irradiation. (auth)

13477 EFFECT OF DIMETHYL SULPHOXIDE ON THE RADIATION RESPONSE OF THE ROUGH-SKINNED NEWT (TARICHA GRANULOSE). **Lappenbush, William L. (Bureau of Radiological Health, Rockville, Md.); Willis, David L.** Int. J. Radiat. Biol.; 18: 217-23(1970).

Newts were collected, acclimatized, and maintained unfed at 10°C both before and after irradiation. Exposures ranging up to 30 kR were given with 300 kVp x rays and ^{60}Co γ rays. Half the newts were pre-treated with the maximum sublethal dose of dimethyl sulphoxide DMSO (i.p.), the remainder were untreated. The mean survival-time—exposure curves for both groups of animals were typically sigmoid. However, the mean survival times of the DMSO-treated newts were significantly longer for all exposures between 200 R and 15 kR. Absolute protection was afforded by DMSO up to 500 to 600 R, while the lethal threshold dose for untreated irradiated newts was 100 to 200 R. The degree of radioprotection afforded by DMSO varied according to the time of administration, concentration of DMSO, and radiation exposure. DMSO prevented skin ulceration and caused splenomegaly and hepatomegaly after 650 R, which in turn was associated with a degree of plethora and haemoconcentration, or possibly real polycythaemia. (auth) (UK)

13478 STUDY OF WEIGHT CHANGES IN THE SPLEEN AS A FUNCTION OF IRRADIATION DOSE IN PROTECTED OR UNPROTECTED IRRADIATED MICE. **Frossard, Henri; Fatome, Marc; Perles, Rene; Gerard, Abadie; Holleville, Patrick (Centre de Recherches du Service de Sante des Armees, Clamart, France). Compt. Rend., Ser. D; 271: 442-5(27 Jul 1970). (In French).**

Five days after irradiation, the spleen of the mouse decreases in weight. The spleen weight-irradiation dose relation is linear in log-probit coordinates. This effect provides a radioprotection test applicable at sublethal doses. The test was used with AET and with a cocktail made up of serotonin, AET, glutathion, and DNA. (France)

13479 SKIN ALLOGRAFT SURVIVAL IN MICE AFTER RADIOPROTECTION WITH SODIUM S-(2-AMINOETHYL) PHOSPHOROTHIOATE AND SUPRALETHAL TOTAL BODY X-IRRADIATION. **Saltzstein, Edward C.; Rimm, Alfred A.; Bortin, Mortimer M. (Marquette School of Medicine, Inc., Milwaukee. Mount Sinai Hospital, Milwaukee). Transplantation; 10: 451-3 (Nov 1970).**

Mice were injected intraperitoneally with sodium s-(2-aminoethyl) phosphorothioate (WR638) and x-irradiated in doses of 400 to 1100 R. Paired skin isografts and allografts were performed the same day. Observations were made on survival, isograft survival, and allograft survival. The sharp decline in 30-day survival above 950 R suggested that the dose-reducing effects of WR638 did not lower the effective radiation dose below an apparent threshold level. The fact that 10% of the animals survived 30 days after receiving 1100 R indicated some radioprotective effect of WR638. It was concluded that the hypothesis that supralethal irradiation plus radioprotection with WR638 will prolong allograft survival was not supported by these experiments. (H.L.W.)

13480 NEW METHOD OF TREATING RADIATION-INDUCED BRACHIAL PLEXUS PARESIS, AFTER OPERATIONS FOR CARCINOMA OF THE BREAST. **von Albert, H.-H.; Mackert, B. (Univ., Munich). Deut. Med. Wochenschr.; 95: 2119-22(16 Oct 1970). (In German).**

In seven patients operated on for carcinoma of the breast with postradiation brachial plexus lesions and brachial plexus paresis in another patient with axillary lymphosarcoma, administration of actihemyl, a protein-free blood extract, in high doses and for periods of up to 24 months, achieved rapid clinical improvement and electromyographically demonstrable remission of neurological defects. Trophic disorders, atrophies and pareses regressed and function and sensory perception improved. The results will have to be checked in a larger series of patients before this method of treatment is accepted. Two additional observations on the rapid regression of chronic indurating lymphatic edema after radiotherapy of a malignoma of the pelvis, pain and leg swellings, suggest that the described treatment may be of value in this condition, too. (auth)

Radiation Sickness and Injuries

13481 EFFECT OF IRRADIATION ON LYMPH FLOW AND FILTRATION FUNCTION OF LYMPH NODES. **Sinha, B. K.; Goldenberg, G. J. (Univ. of Manitoba, Winnipeg. Manitoba Cancer Treatment and Research Foundation, Winnipeg). Cancer; 26: 1239-45(Dec 1970).**

The effect of irradiation on lymph flow and filtration function of lymph nodes was investigated in rats using colloidal ^{198}Au. The popliteal node region of Wistar male rats was irradiated with a single dose of 500 to 3000 rads x radiation and quantitative measurements of lymph flow and lymph node filtration function were

XUM

made two weeks following irradiation. Lymph flow, as measured by disappearance of colloidal gold from the injection site, decreased only in rats treated with 3000 rads. A marked decrease in the concentration of isotope in irradiated nodes and increased bypass to the lumbar nodes and thoracic duct lymph was found at all dose levels; these findings suggest that radiation therapy decreases filtration capacity of lymph nodes for colloidal gold. (auth)

Radiodiagnosis

Refer also to abstracts 13218, 13222, 13332, 13338, 13339, 13341, 13343, 13459, 13464, and 13580.

13482 (CONF-661071) FIRST CONGRESS OF THE LATIN AMERICAN ASSOCIATION OF SOCIETIES OF BIOLOGY AND NUCLEAR MEDICINE, LIMA, PERU, 2–8 OCTOBER 1966. (Sociedad Peruana de Biologia y Medicina Nuclear, Lima). 303p. (In Spanish).

Sixty-two of the 114 papers presented at the Lima Congress are compiled. They deal with the use of radioisotopes in endocrinology, hematology, nephrology, and other aspects of biology and nuclear medicine not readily classified. (J.S.R.)

13483 DIAGNOSIS OF MALIGNANT LESIONS OF THE LIVER BY RADIOCOLLOID AND ^{131}I FIBRINOGEN. Riccioni, N. (Univ., Pisa, Italy). J. Nucl. Biol. Med.; 13: 160–6(Oct–Dec 1969).

The external counting isotope method developed to differentiate malignant from non malignant lesions of the liver was reported. The method is based on the study of the time course of radioactivity, after injection of ^{131}I-fibrinogen (RIF), on the cold areas detected by liver radiocolloid scan. The RIF study was carried out in 92 patients: 57 with malignant lesions and 35 with non malignant lesions of the liver. In 45 patients the diagnosis could be established anatomically; in the remaining 47 cases there were no histologic studies, but sufficient follow up data were available for a reliable clinical diagnosis. The RIF study gave a positive result in 48 out of 57 malignant lesions (84%) and a negative result in 32 out of 35 non malignant lesions (91%). All together the RIF study gave a correct result in 80 out of 92 patients examined. (auth)

13484 CHANGES IN LUNG SCAN PATTERN RELATED TO FREE FLUID AND CARDIAC POSITION. Partlow, W. F.; McCormack, K. R. (St. Mary's Hospital, San Francisco. Mt. Zion Hospital, San Francisco). J. Nucl. Med.; 12: 2–4(Jan 1971).

The lateral decubitus scan of the dependent lung by an inferior probe on a dual-headed rectilinear scanner can demonstrate displacement of radioactivity by free fluid and an enlarged heart. Free fluid appears as deficient activity along the fissure lines and in the most dependent parts of the pleural spaces. The cardiac impression on the left lower lobe is markedly accentuated by the enlarged heart in a dependent position. These deficits in activity can be distinguished from perfusion defects since they disappear when the same lateral projection is attained in the nondependent lateral position. (auth)

13485 ^{125}I FOR MEASURING THE RADIOIODINE UPTAKE OF THE THYROID. Rollo, F. David (Upstate Medical Center, Syracuse, N. Y.). J. Nucl. Med.; 12: 8–13(Jan 1971).

The results of a study of 80 patients indicate that ^{125}I can be used reliably and accurately to measure the radioiodine uptake of the thyroid gland with the 2D method of measurement. The 2D method requires one additional patient measurement requiring only a few minutes, besides the measurements of the standard ORINS technique. For the procedure, ^{125}I as the uptake agent has the following advantages. The 2D method corrects for variations in the depth of the gland and can therefore be used at a decreased thyroid-to-detector distance. The resulting increase in counting efficiency can be used to decrease the administered dose or improve counting statistics. The correction for gland depth variation of absorption and scattering should remove apparent inaccuracies included in conventional uptake measurements such as those made with the ORINS phantom. Iodine-125 has a high relative photon merit ratio compared with ^{131}I and when used provides a significant reduction of radiation dose in thyroid function studies. The high counting efficiency and low absorbed dose associated with ^{125}I make this radioisotope particularly attractive for pediatric studies. The 57-day half-life of ^{125}I has definite advantages in terms of shipping, storage, and infrequent need for preparing a stock solution. In addition, the long half-life would permit long-term evaluation of the biological retention of iodine within the thyroid. Iodine-125 has been accepted as a routine thyroid scanning agent in many institutions because of the improved resolution this radioisotope offers over other agents. Consequently, the introduction of the 2D technique for uptake measurements would allow a single radioisotope to be used for total thyroid evaluation. The low absorbed dose associated with ^{125}I would permit the routine administration of 100 μCi of this radioisotope for routine clinical thyroid studies. This dose would permit total thyroid evaluation of all patients (uptake and scan). Consequently, patients originally scheduled for uptakes only, but whose uptake study suggests a scan should be made, can have a scan performed without a second administration of radioactive material. The low-energy (20 to 35 keV) associated with ^{125}I would permit followup studies with ^{131}I at any time without fear of counting cross contamination. The energy characteristics of ^{125}I are such that several simplifications of counting instrumentation are possible. (auth)

13486 RETENTION OF ^{113m}In–^{59}Fe–FERRIC HYDROXIDE IN THE MOUSE. Barker, S. L.; Gusmano, E. A.; Smith, T. D.; Murty, D. R. K.; Bruno, G. A. (Squibb Inst. for Medical Research, New Brunswick, N. J.). J. Nucl. Med.; 12: 5–7(Jan 1971).

The pulmonary retention of ^{59}Fe in mice following injection of ^{113m}In-^{59}Fe-Fe(OH)$_3$ particles was determined. Based on the retention data reported here and on the lack of consensus regarding the toxicity of Fe(OH)$_3$ particles, it was concluded that more extensive investigation is required for a definitive evaluation of the safety of these labeled particles for lung scanning. (E.R.B.)

13487 USE OF LITHIUM-DRIFTED GERMANIUM DETECTORS FOR CLINICAL RADIONUCLIDE SCANNING. Hoffer, Paul B.; Beck, Robert N.; Lembares, Nicholas; Charleston, Donald B.; Gottschalk, Alexander (Univ. of Chicago. Argonne Cancer Research Hospital, Chicago). J. Nucl. Med.; 12: 25–7(Jan 1971).

The advantages and disadvantages of using lithium-drifted germanium detectors for imaging in clinical radioisotope scanning are considered. Among the disadvantages are: the fact that large germanium crystals are not available, therefore, the detector systems have low sensitivity; and the requirement that these detectors be operated at liquid nitrogen temperatures. The potential advantages offered by the detectors include: the excellent energy resolution of the detector systems; applications in fluorescent scanning; use with radioisotopes emitting multiple γ radiations; and efficiency in dual-radioisotope scanning. Initial clinical results on a limited number of patients are reported as encouraging. (E.R.B.)

13488 EARLY VISUALIZATION OF ^{99m}Tc-PERTECHNETATE IN METASTATIC THYROID CANCER IN A PATIENT WITH GRAVES' DISEASE. Carr, H. A.; Temple, T. E.; Staab, E. V. (Vanderbilt Univ., Nashville). J. Nucl. Med.; 12: 40–2 (Jan 1971).

Small areas of papillary thyroid carcinoma will concentrate pertechnetate. Until further information becomes available, when imaging for metastatic thyroid carcinoma with pertechnetate, both early and late studies should be obtained. The dynamic serial studies of the Anger camera were superior to the static rectilinear scans in both delineation and resolution of this metastatic thyroid lesion with pertechnetate. (auth)

13489 UNUSUAL SCAN IN CEREBRAL INFARCTION. Rothfeld, B. (Veterans Administration Hospital, Perry Point, Md.). J. Nucl. Med.; 12: 47–8(Jan 1971).

A case involving an abnormal ^{99m}Tc brain scan, obtained just 4 months following a completely negative scan, is reported. The scan, performed after the patient suddenly became unconscious, was considered unusual because the entire visualized right cerebrum manifested increased activity. Possible explanations for the extent of this cerebral infarction included: simultaneous obstruction of both basilar and internal carotid arteries; or the basilar artery was compromised before the acute episode and the collateral circulation from the internal carotid, and its branches prevented clinical signs from developing until they were subsequently occluded. A small area of normal activity in the occipital region was explained by the fact that the area of infarction was so large the radioisotope could not diffuse all the way through. The scan was still positive 187 days after the acute episode. (E.R.B.)

13490 URETERAL KINKING AND HYDRONEPHROSIS IN A TRANSPLANTED KIDNEY MIMICKING THE REJECTION PHENOMENON. Weiss, Edward R.; Winston, Martin A.; Krishnamurthy, G. T.; (and others) (Wadsworth General Hospital, Los Angeles. Univ. of Southern California, Los Angeles. Univ. of California, Los Angeles). J. Nucl. Med.; 12: 43–6(Jan 1971).

A patient who had received a renal homotransplant suddenly appeared to manifest the rejection phenomenon, with fever and a rising serum creatinine. Increased doses of azothioprine and prednisone were administered. Dynamic radioisotope studies with the scintillation camera revealed a tortuous, kinked ureter compressed between the bladder and the transplant causing obstruction to urinary flow and severe hydronephrosis. (auth)

XUM

13491 COPPER TEST MAY DIAGNOSE CYSTIC FIBROSIS. J. Amer. Med. Ass.; 212: 2039(22 Jun 1970).

Nail clippings are obtained from infants and the resulting sample is irradiated with thermal neutrons. Using activation analysis the copper content is determined from the amount of anninilation radiation of a resulting isotope, ^{64}Cu. Analysis of nail clippings has shown a higher copper content in the nails of cystic fibrosis patients than in those of normal subjects. Hence, a measurement of the copper content in nail clippings from newborn infants may provide a useful screening technique for cystic fibrosis. (H.L.W.)

13492 ANGIOGRAMS HELP IN JAUNDICE DIAGNOSIS. J. Amer. Med. Ass.; 211: 191(12 Jan 1970).

The accuracy of a technique combining angiography and percutaneous transhepatic cholangiography (PTC) for diagnosing drug-induced jaundice was tested. The angiogram and PTC give complementary information. Angiography demonstrates the vascular anatomy and will also help define a carcinoma. PTC demonstrates the biliary ducts and will show the level and extent of biliary obstruction. If the angiogram and PTC indicate an obstruction, a percutaneous liver biopsy will confirm the diagnosis. If the jaundice is due to phenothiazine, the biopsy will show typical changes of bile stasis. (E.R.B.)

13493 FUNCTIONAL AUTONOMY IN MULTINODULAR GOITER. Miller, J. Martin; Block, Melvin A. (Henry Ford Hospital, Detroit). J. Amer. Med. Ass.; 214: 535-9(19 Oct 1970).

Forty-six of 70 patients with large multinodular goiters had significant radioactive iodine uptake after liothyromine sodium (T_3) administration. The scintiscan patterns during suppression were comparable to those of 49 patients with similar goiters and non-Graves' hyperthyroidism. The distribution of radioactive iodine uptake varied from localization in one of the many nodules to a patchy but diffuse picture which microscopically involved several types of follicular architecture. It is hypothesized that the gradual increment of the autonomous tissue causes transition from a euthyroid to a hyperthyroid state based on gland autonomy rather than on a humoral stimulator. Autonomous function must be suspected in all large multinodular goiters and evaluated before levothyroxine sodium treatment. If such function is present, a replacement dose of thyroid hormone will actually be an additive one, and hyperthyroidism may be produced. (auth)

13494 ANGIOGRAPHIC DIAGNOSIS OF HYDATID DISEASE OF THE LIVER. Steckenmesser, R.; Bayindir, S.; Heger, N. (Univ., Giessen, Ger.). Deut. Med. Wochenschr.; 95: 2288-91 (6 Nov 1970). (In German).

Three cases of hydatid disease of the liver are reported, one cystic and the others alveolar in character. The definitive diagnosis and exact localization were achieved by a combination of selective arteriography, injection of radioisotopes, and biochemical, and immunological tests. The angiographic pictures made it possible to distinguish between cystic and alveolar hydatid. (auth)

13495 RADIOISOTOPES IN THE DIAGNOSIS OF GASTRIC TUMORS. Fridrich, R. (Universitaets-Instituts fuer Roentgendiagnostik und Strahlentherapie, Basel); Stalder, G. A.; Locher, J.; Heinis, P. Deut. Med. Wochenschr.; 95: 2261-5(6 Nov 1970). (In German).

Recently refined radioisotope methods for the diagnosis of gastric tumors, suitable for routine use, are discussed. Benign and malignant gastric tumors can be distinguished by measuring ^{32}P incorporation rate or by scintigraphy with ^{99m}Tc. Serial or camera scintigraphy makes it possible to measure the time that the test meal is retained in the stomach and the rate with which the stomach empties. (auth)

13496 THINNER CONTRAST MATERIAL IMPROVES IMAGE QUALITY. J. Amer. Med. Ass.; 211: 189(12 Jan 1970).

With the recent availability of a contrast medium containing 15% iodine by weight, a comparative study was conducted to determine whether the 15% variety produced better myelographs than did the standard contrast medium containing 30% iodine by weight. It was found that a preparation containing 22% iodine by weight (equal parts of 15% and 30% mixed) worked better than either of the other preparations. (E.R.B.)

13497 NEUTRON-ACTIVATION AUTORADIOGRAPHY OF THE THYROID GLAND IN EXPERIMENTAL RADIATION SICKNESS. Tkachev, A. V. (Inst. of Medical Radiology, Moscow). Med. Radiol.; 15: No. 11, 46-9(Nov 1970). (In Russian).

With the aid of the technique of neutron autoradiography, endogenous iodine was found in different concentrations in the thyroid gland in August and Wistar rats. In acute radiation sickness caused by gamma-irradiation doses of 900 R protein-bound iodine contents were reduced in the thyroid gland. On the 3rd day of acute radiation sickness in August rats the reaction of the thyroid gland to exogenous thyrostimulating hormone decreased. (P.B.M.)

13498 INFRARED THERMOGRAPHY WITH A COLOR SCANNER USED IN NUCLEAR MEDICINE. Poser, H.; Lange, D.; Moersdorf, D. (Univ., Heidelberg). Strahlentherapie; 140: 123-7(Jul 1970). (In German).

Color thermography is proving to be a reasonable supplement to X-ray diagnostic and nuclear medical research. More than 100 patients were examined. The connection of an infrared detector to a nuclear-medical color scanner is described. The advantage of semi-quantitative (colored) differentiation possibilities of differences in cutaneous temperatures is strengthened by a mechanical compensation of the line joggle. (auth)

13499 SEQUENTIAL SCINTIGRAMS OF THE KIDNEY WITH ^{131}I-O-IODO-HIPPURIC ACID AND ^{113m}In-EDTA. Haubold, Ulrich; Jost, Heidemarie; zum Winkel, Karl (Freie Univ., Berlin). Strahlentherapie; 140: 89-96(Jul 1970). (In German).

Sequential scintigrams of the kidneys were performed in 27 patients, comparing ^{131}I-o-iodohippuric acid and ^{113m}In-EDTA. 18 patients with chronic pyelonephritis and one patient with chronic glomerulonephritis were examined, besides 8 normal cases. The results are discussed. (auth)

13500 SIMULTANEOUS DOUBLE-ISOTOPE SCINTIGRAPHY WITH AN ANGER CAMERA FOR REPRESENTATION OF PERFUSED AND AIR-CONTAINING LUNG TISSUE. Schenck, Peter; Lange, Dieter; Schnabel, Klaus (Univ., Heidelberg). Strahlentherapie; 140: 97-104(Jul 1970). (In German).

A simple scintigraphic recording, arranged simultaneously, of perfused and inflated lung tissue by means of an Anger scintillation camera is demonstrated. Advantages and disadvantages compared to simultaneous ventilation tests with radioisotopes are considered. According to tests, blood circulation must be regarded as the most delicate scintigraphic indication of a reduced lung function. With regard to fibrotic and malignant processes of the lungs, scintigraphy of inflated lung tissue can be considered as sufficiently competent. (auth)

13501 Sn–^{113m}In TRACERS FOR USE IN LUNG, LIVER, AND SPLEEN SCINTIGRAPHIES. Morcellet, J. L.; Le Mignant, A.; Francois, Y. (Hopital d'Instruction des Armees, Toulon, France). J. Biol. Med. Nucl.; 5: No. 20, 13-22(May-Jun 1970). (In French).

The masses of In involved in scintigraphic explorations are extremely small and those of Sn, employed as carried, lie well below the toxic doses. The toxicity of Sn–^{113m}In combinations was tested. One of the advantages of ^{113m}In is its low radiotoxicity due to its half-life (1.7 hours) and to the emission of a single gamma (390 keV); scintigraphies are carried out with activities of 1 to 2 mCi of ^{113m}In and the dose delivered is about a rad. The other acknowledged advantage is practical: the ^{113m}In-generator is available twice a day and can be used for 6 months (half-life of ^{113}Sn: 18 days). The distribution of Sn–^{113m}In combinations in the liver, spleen, kidneys and lungs of rats is presented, together with scintigraphies carried out on animals and on man. (France) (auth)

13502 USE OF A ^{113m}In-GELATINE PREPARATION AT pH4 FOR PLACENTAL SCINTIGRAPHY. Planiol, T.; Garnier, G. (Centre Hospitalier Regional Bretonneau, Tours, France). J. Biol. Med. Nucl.; 5: No. 20, 7-12(May-Jun 1970). (In French).

A preparation of ^{113m}In stabilized on gelatine at pH4 remains for several hours in the blood stream and is particularly suitable for exploration of the placenta. The very slight irradiation, lower than that delivered by x rays, presents almost no danger for the foetus. Other physical methods of placental localization, ultrasonics and thermography, give results difficult to interpret and even erroneous. Isotopic localization using ^{113m}In stabilized on gelatine at pH4 seems to be the method providing the largest number of data in a single examination. (France)

13503 CONSIDERATIONS OF THE VALUE OF TOTAL BODY SCANNING FOR STUDIES ON REGIONAL DISTRIBUTION USING RADIOACTIVE TRACERS. Abbati, A.; Rossi, A.; Turba, E. (Maggiore Ospedali, Bologna). Boll. Soc. Ital. Biol. Sper.; 45: 290-2(15 Mar 1969). (In Italian).

The scintigrams obtained in six cases of total body scanning are given. It is shown that this procedure can yield a valuable orientation point for more detailed studies on the localization of commonly used diagnostic and therapeutic radioisotopes, on the dose received by various organs, and on the existence of singularities in the radioisotope distribution in individual cases. (J.S.R.)

13504 SCANNING HELPS TO IDENTIFY LESIONS. J. Amer. Med. Ass.; 215: 32(4 Jan 1971).

A radioisotope procedure is described that is useful for the differential diagnosis of benign and malignant neoplasms of the kidneys. Iron-ascorbic acid complex labeled with metastable ^{99}Tc is injected intravenously and a series of γ camera pictures followed one hour later by a rectilinear scan or γ camera image shows typical distribution of the tracer in benign and malignant lesions. (C.H.)

13505 INTERVAL BRAIN SCANNING WITH SODIUM PERTECHNETATE ^{99m}Tc FOR TUMOR DETECTABILITY. Gates, Gary F. (Memorial Hospital, Long Beach, Calif.). Dore, Earl K.; Taplin, George V. J. Amer. Med. Ass.; 215: 85-8(4 Jan 1971).

Brain scans were performed on patients during the first hour following injection of sodium pertechnetate ^{99m}Tc and selected patients were rescanned one to 24 hours later. Eighty brain tumors were found among nearly 1,500 patients scanned during a two-year period. Diagnoses were established for 74 through histological examination, and for six through clinical, scan, and neuroradiological findings. Forty were scanned twice, and in 15 the early scans were normal or equivocal. Fourteen of these 15 had abnormal findings upon rescanning. Twenty-six nondiagnostic to moderately abnormal early scans increased in their degree of abnormality upon rescanning. The detectability of brain tumors improved from 80% with routine early scanning, to 93% with rescanning. The optimal time for repeated scanning is three to four hours following tracer injection. (auth)

13506 DIAGNOSTIC APPLICATION OF METABOLIC STUDIES WITH ISOTOPES. Hutterer, Ferenc; Sarkozi, Laszlo; Roboz, John; Bacchin, Paolo (Mount Sinai Hospital, New York). Clin. Chem.; 16: 633-6(Aug 1970).

From 2nd Annual Symposium on Automated, High-Resolution Analyses in the Clinical Laboratory, Oak Ridge, Tenn. See CONF-700334.

The mechanism of the maintenance of normoglycemia in chloroform intoxication in rats was studied with isotopes. Metabolic pathways were altered before the concentration of blood glucose changed significantly. Measurement of the incorporation of precursors rather than the determination of the concentration of the metabolic end products (e.g., glucose) may provide more diagnostic information and may more sensitively detect early diseases or disease stages. (auth)

13507 PROBLEMS CONCERNING RADIOLOGICAL EXAMINATION OF THE PARANASAL SINUSES. Martin, Margrit (Univ., Tuebingen, Ger.). Roentgenpraxis; 23: 213-19(Sep 1970). (In German).

In order to yield optimal diagnostic information, x-ray films of each paranasal sinus must avoid superimposure of other skull bone structures; the x-ray beam must be directed toward the largest spacial extension of the sinus, and the patient must be in a sitting position for clear presentation of fluid levels. Five standard projections are required for a systematic examination of all paranasal sinuses. Thus far, optimal positioning of the patient resides in manual dexterity as well as in anatomical knowledge. (H.B.G.)

13508 INTERNATIONAL CONFERENCE ON PROCTOLOGY. SECTION OF PROCTOLOGY WITH THE AMERICAN PROCTOLOGIC SOCIETY AND THE SECTION OF COLONIC AND RECTAL SURGERY OF THE ROYAL AUSTRALASIAN COLLEGE OF SURGEONS, London, 23-6 JUNE 1969. Proc. Roy. Soc. Med.; 63: Suppl., 1-160(1970). (CONF-690645-(Suppl.).

Seventy-eight papers were presented. Separate abstracts were prepared for two of these. Topics included basic science, treatment of carcinoma of the colon, diverticular disease, inflammatory diseases, and irradiation injury to the bowel and rectum. (F.M.M.)

For abstracts of individual papers see: 13588 and 13589.

13509 ROENTGENOLOGIC-PHOTOMETRIC METHOD FOR BONE MINERAL DETERMINATIONS. Ekman, B.; Ljungquist, K. G.; Stein, U. (County Hospital, Vanersborg, Sweden). Acta Radiol., Diagn.; 10: 305-25(1970).

A new technically simple method of determining the mineral content of the radius and ulna is reported. This demands only standard equipment for roentgen films and for photometric scanning. Normal ranges for males and females of different ages were recorded in a population study of 426 subjects and agree with those in the literature on the incidence of senile osteoporosis. (auth) (Sweden)

13510 HOT HEPATIC HEMANGIOMA: A UNIQUE RADIOCOLLOID-CONCENTRATING LIVER SCAN LESION. Volpe, Joseph A.; Johnston, Gerald S. (Letterman General Hospital, San Francisco). J. Surg. Oncol.; 2: 373-7(1970).

The unique case is reported of a liver hemangioma that appeared on scintiscan as an area of increased concentration of radiogold—a hot lesion. The scintiscan appearance described was explained by the presence of increased amounts of reticuloendothelial tissue in the tumor over that in the surrounding normal tissue. The usual scan picture of liver hemangioma is that of a cold lesion. (auth)

13511 SCINTISCANNING IN THE DIAGNOSIS OF RUPTURE OF THE SPLEEN. O'Mara, Robert E.; Hall, Robert C.; Dombroski, Daniel L. (State Univ. of New York, Syracuse). Surg. Gynecol. Obstet.; 131: 1077-84(Dec 1970).

In five patients, the diagnosis of splenic rupture was made by scintiscanning with technetium sulfur colloid. Splenic scanning is a simple, safe, and rapid procedure that can be performed in any hospital capable of thyroid scanning. Scanning, even with present limitations, is preferable to angiography because specific anatomic information, both of the liver and spleen, is provided simply. One patient had a negative result from abdominal paracentesis but a positive scan; a ruptured spleen was removed. Scanning should lower the mortality from delayed splenic bleeding by providing conclusive evidence of injury to the spleen in suspicious cases. Patients with sufficient trauma to rupture the spleen, especially those with fractured ribs, or patients with suggestive pain in the left upper quadrant after trivial trauma are candidates for splenic scanning if the diagnosis cannot be confirmed by other means. (auth)

13512 VALUE OF SCINTISCANS IN THE DIAGNOSIS OF SPLENIC ABSCESS. Zook, Elvin G.; Bolivar, Juan C.; Epstein, Leonard I. (Indiana Univ., Indianapolis. West Tenth Street Veterans Administration Hospital, Indianapolis). Surg. Gynecol. Obstet.; 131: 1125-9(Dec 1970).

In the past two yrs, three patients with splenic abscess were encountered. In two, the diagnosis was made prior to operation, and they did well after splenectomy. In the third patient, rupture occurred with generalized peritonitis and death, despite surgical treatment. Recent methods of diagnosis, including pneumoperitoneum and spleen scintiscans, were used. Roentgenograms of the upper gastrointestinal tract, barium enema, intravenous pyelogram, and roentgenograms of the chest and abdomen also were valuable in reaching a diagnosis. Early diagnosis is imperative. Delay may result in spontaneous rupture of the abscess attendant with a high mortality rate or prolonged period of morbidity. (auth)

13513 DETECTION OF BONE METASTASES BY AN ISOTOPIC METHOD. Thibault, M.; Langelier, R.; Beaudoin, L. (Hotel-Dieu, Quebec). Laval Med.; 37: 1051-5(Dec 1966). (In French).

The use of ^{85}Sr to detect bone metastases was reviewed and discussed. Strontium-85 did not emit any corpuscular radiation, therefore irradiation of the patient was lessened. Although ^{85}Sr scintigraphy indicated areas of hyperactive calcification better than x-ray studies, it could not differentiate the etiology of the hyperactivity precisely. A fracture, a lytic metastasis, a Ewing tumor, an osteosarcoma, and Paget's disease gave similar photoscans. Disadvantages of the use of ^{85}Sr included its long retention in bony tissue and its long half-life of 65 days. It was estimated that with an average injection of 150 mCi the whole-body irradiation dose was about 1R and the bone dose was about 7R. These values may be acceptable for older patients. If the patient has a cancerous lesion, the long term radiation effects would be relatively small. (BBB) (TSS)

13514 SIMPLIFIED MOBILE EQUIPMENT FOR ^{133}Xe-RADIOSPIROMETRY. Arborelius, M. Jr.; Kendrup, I.; Lilja, B. (Univ. of Lund, Sweden). Scand. J. Clin. Lab. Invest.; 26: 125-8(Sep 1970).

Radiospirometry with ^{133}Xe is a useful method for the study of regional lung function. A modified equipment was described that is light and mobile and can be used on subjects in any body position, thereby making possible studies during and after operations as well as under varying physiological conditions. The apparatus uses four probes that are placed either in front of or behind the subject. The information obtained thus comes mainly from the parts of the lungs closest to the detectors. This has both advantages and disadvantages. Some applications in the clinic and in research are discussed. (auth) (Norway)

13515 INDIRECT PARASTERNAL LYMPHOSCINTIGRAPHY IN MAMMARY CARCINOMAS. ANALYSIS OF 62 PATIENTS. Seifert, J.; Betzner, J. (Ruhr Univ., Bochum, Ger.). Fortschr. Geb. Roentgenstr. Nuklearmed.; 113: 457-62(Oct 1970). (In German).

Parasternal lymphatic scanning with radioactive colloidal gold was carried out in 62 patients with carcinoma of the breast and in more than two thirds involvement of the parasternal lymph nodes was demonstrated. Early spread depended more on histology than on the position of the primary tumor, but also on tumor size. It was concluded that this examination should be added for the purpose of staging of mammary carcinomas and for evaluation of appropriate treatment. (F. St.)

XUM

13516 BLOODPOOL SCINTIGRAPHY WITH SHORTLIVED RADIONUCLIDES. **Langhammer, H.; Buell, U.; Hoer, G.; Frey, K. W.; Pabst, H. W. (Univ., Munich. Technische Hochschule, Munich). Fortschr. Geb. Roentgenstr. Nuklearmed.; 113: 462-71(Oct 1970). (In German).**

The development of blood pool scanning into a routine diagnostic method depended on the introduction of short-lived ^{113m}Indium. Our experience with ^{113m}In in cardiac and placental scanning in 95 patients is described. The clinical indications are discussed and the results of placentography are compared with those using ^{99m}Tc-marked erythrocytes. The advantages of ^{113m}In compared with ^{99m}Tc are indicated; they result from its radio-chemical, biological, and physical properties. Clinical applications are described. (F. St.)

13517 PLACENTOGRAPHY: INDICATIONS AND COMPARATIVE INVESTIGATIONS ABOUT PROCEDURES IN NUCLEAR MEDICINE. **Huenermann, B.; Klink, R.; Akhtar, M.; Winkler, C. (Univ., Bonn). Fortschr. Geb. Roentgenstr. Nuklearmed.; 113: 472-9(Oct 1970). (In German).**

Indications for placental localization and available methods are enumerated. In order to determine the usefulness of radioactive methods, and their optimal use, three different substances were investigated with two scanning methods. It was found that ^{99m}Tc-Fe^{3+}, ^{99m}Tc-marked erythrocytes and ^{113m}In serum proteins showed little difference and all resulted in good localization. A scintillation camera was found to be definitely superior to scanning with a mobile detector. Results of placental localization were particularly satisfactory with the use of a computer for digital evaluation of the results. Among 90 patients a placenta previa was demonstrated on three occasions and a double placenta, with twins, in one patient. Placentas were demonstrated in all their usual positions. The results were checked by ultra-sound and clinical examination. No errors were made and present experience suggested 100% accuracy in placental localization, if appropriate methods and suitable scanning are used. (F. St.)

13518 EXPERIMENTAL ANIMAL STUDIES CONCERNING SCINTIGRAPHIC DETECTION OF ACUTE THROMBOSIS. **Fernholz, H.-J.; Mueller, G. (Technische Hochschule, Aachen). Fortschr. Geb. Roentgenstr. Nuklearmed.; 113: 487-93(Oct 1970). (In German).**

Experimentally produced thrombi were demonstrated by scanning, using ^{131}I fibrinogen which does not lose its biological activity during marking. In a growing thrombus there is a high concentration without loss of the radioactive indicator. It is therefore possible to obtain a positive scan of a fresh thrombus. First results in animal experiments are demonstrated. The findings on scanning always correspond with the length of the thrombus. Fibrinogen as the tracer and ^{131}I as the radioactive substance provide the most satisfactory results, compared with other substances, in the early diagnosis of thrombosis by scanning, and as a means of further observation. (F. St.)

13519 RADIOPHARMACEUTICALS IN NUCLEAR MEDICINE. Petersen, D. A. (Australian Atomic Energy Commission Research Establishment, Lucas Heights); Boyd, R. E.; Lane, E. A.; Morris, J. At. Energy Aust.; 13: 2-8 (Jul 1970).

A review is given on the use of radionuclides in medical diagnosis and treatment. Aspects covered include choice of radionuclide, diagnostic techniques, production, transport, safety, and cost. (Australia)

13520 DORSAL AND/OR VENTRAL DETECTORS IN STUDIES OF REGIONAL LUNG FUNCTION BY ^{133}Xe RADIOSPIROMETRY. Aulin, I.; Lilja, B.; Lindell, S.-E.; Mioerner, G. (Malmoe General Hospital, Sweden). Scand. J. Clin. Lab. Invest.; 26: 129-36(Sep 1970).

In 92 patients with various lung diseases, the results obtained using ventral and dorsal detectors were compared with those obtained with only ventral or dorsal detectors. There was a good agreement as regards the estimate of the right lung's part of total pulmonary perfusion, ventilation, and volume. With ventral detectors only, there was an over-estimation of the right lung's part of perfusion, ventilation, and volume, especially when comparing the basal parts of the lungs. The advantage of separating the information from dorsal and ventral detectors was discussed. (auth) (Norway)

Radiotherapy

Refer also to abstracts 13391, 13447–13449, 13451, 13455, 13503, 13578, 13582, 13584, 13585, 13587–13589, 13591, 13592, 13594, and 13596.

13521 RADIOTHERAPY OF MALIGNANT BONE TUMORS. **Kuttig, Helmut; Fornusek, Arthur Henry; Radermacher, Ernst (Univ., Heidelberg). Strahlentherapie; 140: 1-7(Jul 1970). (In German).**

Radiotherapy is faced with a difficult task, in the treatment of bone tumors, because of the low radiosensitivity and early formation of metastases. This treatment can only be carried out, because of the high focal doses needed, by megavolt therapy, especially with cobalt-60-gamma rays. One hundred and forty-four primary bone tumors in patients of the University Radiation Clinic Heidelberg are reported as well as the respective results of therapy of osteosarcomata, chondrosarcomata, and Ewing sarcomata. (auth)

13522 RESULTS OF RADIOTHERAPY FOR BRONCHIAL CARCINOMA OBTAINED AT THE GIESSEN UNIVERSITY CLINIC FROM 1962 TO 1967: ORTHO- AND MEGAVOLTTHERAPY, TREATMENT WITH FRACTIONATED RADIATION AND CYTOSTATIC AGENTS. **Ringleb, Dietrich; Heidenreich, Roger (Univ., Giessen, Ger.). Strahlentherapie; 139: 635-51(Jun 1970). (In German).**

Between 1962 and 1967, primary radiotherapy was done, at the Röntgen Clinic of Giessen, for 406 cases of bronchogenic carcinomas of these, 50 cases were treated after an exploratory thoracotomy. Histologic verification was not obtained in 133 patients. The results are as follows: average survival 5.6 months, survival after one year 22%, and after two years 6.7%. The results for megavoltage radiotherapy are superior to orthovoltage, whatever stage or histologic form is considered. Results with a split-course irradiation are better than with a continuous series, but this may be due to selection of patients. For indifferentiated carcinomas, combination of radiotherapy with chemotherapy yielded statistically significantly better results: with chemotherapy: average survival 7.1 months, survival after one year 23%, and after 2 years 3.3%; radiotherapy alone resulted in average survival of four months, survival after one year 10.3%, and after two years 1.8%. An associated chemotherapy for differentiated carcinomas did not improve the palliative effect. Improvement of objective symptoms was noticed in more than two thirds of the patients; subjective improvement in even more. The use of megavoltage instead of orthovoltage increased survival for about 10% in many institutes. (auth)

13523 EARLY RESULTS OF TELECOBALT THERAPY OF BRONCHIAL CARCINOMAS. **Willner, Birge; Schmidt-Hermes, Heinz-Josef (Univ., Homburg, Ger.). Strahlentherapie; 139: 652-5(Jun 1970). (In German).**

Results of telecobalt irradiation of bronchial carcinomas with 34.4% surviving patients after one year of therapy are reported. Treatment results lie within the varying width that remained constant over a period of 10 years, showing a rate of survivors, after one year, of 18.2 to 39.0%. Therapy with high-energy electrons will probably bring about an improvement in the results. (auth)

13524 STRUMA MALIGNA: 3, 5, AND 8-YEAR RESULTS IN 259 CASES. **Heinze, H. G.; Pabst, H. W. (Univ., Munich). Strahlentherapie; 139: 656-64(Jun 1970). (In German).**

Two hundred and fifty-nine cases of thyroid carcinomas treated by various methods (surgery, external radiotherapy, radio-iodine, or thyroid hormones) are reported. The five-year survival is 18%. 66% of the deaths occur within the first year of the beginning of therapy. The male patient has a worse prognosis than the female. Patients below 40 years of age have a survival of 50% at 5 years, patients over 40 years only of 0.9 years. The 50% survival time for the different histological types is 2.75 years for differentiated adenocarcinomas, 2.25 years for the struma of Langhans, and 0.75 years for the anaplastic carcinomas and sarcomas. The extent of the tumors, presence of metastases, and iodine uptake in metastases profoundly affect the results of treatment. (auth)

13525 HIGH VOLTAGE THERAPY IN BLADDER CARCINOMAS. **Graefe, K. H.; Frohmueller, H. (Univ., Wuerzburg, Ger.). Strahlentherapie; 139: 665-70(Jun 1970). (In German).**

Fifty-nine patients with advanced bladder carcinoma were treated with telecobalt after various surgical treatments. For a tumor dose of about 4000 R, the one or multiple field technique was used, while even in 11 cases a supplementary dose of 3500 R was given later. In three patients an extensive subcutaneous necrosis was observed, and in 2 patients a small bladder. In the observation period of 6 years, 28.8 patients survived with a mean survival time of 21.1 months. The necessity of an accurate classification of the tumors, prior to treatment, is stressed. Concerning the urologic handling which should precede radiotherapy, it is shown, after analysis of the post-radiation complications, that transurethral resection was preferable to suprapubic operations. (auth)

13526 GEOMETRICAL ARRANGEMENT OF RADIOGOLD PREPARATIONS IN TUMOR IMPLANTS. **Keller, H. L.; Hettner, G. (Institut fuer Roentgenologie und Physikalische Therapie, Munich). Strahlentherapie; 139: 675-83(Jun 1970). (In German).**

The use of gold-198-seeds in tumor filling irradiation has essential advantages compared to interstitial radium irradiation. When preparations of 10 mCi each are used, positioning of the seeds in triangle form is recommended. Distances of 13 to 17 mm are necessary between the preparations in simple geometrical arrangements, so as not to underpass the minimum doses of 6000 to 10,000 R. If there are a greater number of seeds in one plane or in several planes of the space, the distances may be enlarged to a small extent. Furthermore, it is possible to adjust differences between the present activity and the nominal activity of 10 mCi by varying the seed distances. The dose distributions of one preparation and of eight different combined preparations are demonstrated, by diagrams, in profile and as isodoses. (auth)

13527 PROBLEMS CONCERNING CHEMOTHERAPY OF CERVICAL CARCINOMAS BASED ON EXPERIENCES AT THE GYNECOLOGICAL CLINIC: UNIVERSITY OF GOETTINGEN. **Paeschke, Karl-Dietrich (Univ., Goettingen, Ger.). Strahlentherapie; 139: 698-700(Jun 1970). (In German).**

Based on experimental research, the clinical use of a simultaneously combined cancer therapy by x-rays and Proresid ® was introduced which justifies some hope in clinical treatment in dealing with cancer, as long as we do not dispose of antitumoral chemotherapeutics which bring about the effect of tumor destruction. With research into lactate Dehydrogenase to be found in serum it was attempted to evaluate the course and success of x-ray-therapy with and without cytostatics. (auth)

13528 METHOTREXATE FAILS TO IMPROVE IRRADIATION RESULTS. **J. Amer. Med. Ass.; 211: 191(12 Jan 1970).**

In a randomized study of 75 patients with advanced head and neck cancer, doctors were unable to demonstrate any beneficial effect from sequential low dose intravenous methotrexate and irradiation. Patients in a high dose methotrexate group had a significantly higher rate of complications resulting from irradiation. (E.R.B.)

13529 IMPLANTABLE RADIATION ASSEMBLY FOR CIRCULATING SYSTEMS. Anderson, Donald R.; Ballinger, Edwin R. (to Secretary of the Air Force). U. S. Patent 3,434,467. 25 Mar 1969. Filed 15 Aug 1966.

An implantable radiation assembly for radiating body fluids which has an α or β emitter enclosed in a shielding material such as a stainless steel container is described. The body fluids are passed through the container either by the body duct such as a vein being positioned within the container or by connecting the body ducts to a plastic tubing that passes through the container. (Offic. Gaz.)

13530 RESULTS OF CONFORMATION RADIOTHERAPY IN CERVIX CARCINOMAS. **Morita, Kozo; Takahashi, Shinji (Nagoya Univ., Japan). Strahlentherapie; 140: 8-12(Jul 1970). (In German).**

The results of radiotherapy in 588 patients with cancer of the uterine cervix were reported. The influence of the conformation radiotherapy, a new type of the moving-field therapy, to the 5 year cure rate was discussed. By the conformation radiotherapy the beam focus can always coincide with the lesion. The 5 year cure rate obtained by stationary irradiation technique versus that by conformation technique revealed no statistical difference. No severe complications of skin and bladder were seen in the group irradiated by conformation radiotherapy. (auth)

13531 RESULTS AND COMPLICATIONS IN MEGAVOLT THERAPY OF CERVIX CARCINOMAS. **Frischbier, H.-J.; Lohbeck, H. U. (Univ., Hamburg). Strahlentherapie; 140: 13-19(Jul 1970). (In German).**

About 1500 female patients with a collum carcinoma of the stages I to IV were examined, and the results of therapy recorded after conventional x-radiation therapy and megavolt therapy, combined with surgery of radium therapy. The patients mentioned were treated, from 1951 until 1963, at the University Frauenklinik Hamburg-Eppendorf. The five-year healing results in the stages II and III were improved for about 10% by the addition of a 15 MV x-irradiation or a cobalt-60-gamma irradiation to the percutaneous therapy. This difference was of statistical significance. (auth)

13532 MEGAVOLT THERAPY OF MALIGNANT NEOPLASMS OF THE STOMACH. **Wieland, Cuno; Hymmen, Ursula (Univ., Heidelberg). Strahlentherapie; 140: 20-6(Jul 1970). (In German).**

Case histories of 29 patients suffering from malignant stomach neoplasms and treated with ^{60}Co-γ megavolt irradiation were reported. 113 results could be interpreted; average age was 62 years. 106 carcinomas were adenocarcinomas with various kinds of differentiation. Furthermore, 5 reticulosarcomas, one round-cell sarcoma, and one lymphogranulomatosis were treated. Survivals were as follows in the carcinoma cases: 3 years $^{9}/_{82}$ (11%); 5 years $^{5}/_{72}$ (7%); 10 years $^{1}/_{25}$ (4%). The indication for irradiation therapy was demonstrated. Grid irradiation therapy represents a procedure that is safer to an especially high degree. (auth)

13533 POSTOPERATIVE RADIOTHERAPY OF MAMMARY CARCINOMA WITHOUT IRRADIATION OF THE THORAX WALL. **Kuttig, Helmut; Harbst, Hans; Lachmann, Ute; Misri, Hassan; Zunter, Franjo (Univ., Heidelberg). Strahlentherapie; 140: 27-31(Jul 1970). (In German).**

A method of high-dose postoperative ^{60}Co-γ irradiation of mammary carcinomas within the region of the lymphatic excretory passages that are not accessible by surgery is described. Routine irradiation of the thorax wall was not performed. The early results of treatment in, so far, 192 patients justified recommendation of this method for further examination in order to achieve further improvements in therapy. (auth)

13534 TELECOBALT IRRADIATION OF AORTIC LYMPH NODES. **Frischbier, Hans-Joachim; Karl, Brigitte (Univ., Hamburg). Strahlentherapie; 140: 32-6(Jul 1970). (In German).**

Biaxial telecobalt pendulum therapy, comprising four sectors of 90 degrees each is described for aortal lymph node metastases. This irradiation method permits the optimal adjustment of dose distribution to the position of the aortal lymph nodes. Adjustment technique and dosage are described. (auth)

13535 IRRADIATION PLANNING FOR MEGAVOLT THERAPY OF LYMPH NODES. **Alth, G.; Kaercher, K. H. (Univ., Vienna). Strahlentherapie; 140: 37-44(Jul 1970). (In German).**

It is demonstrated that exact planning of irradiation measures by using the corresponding localization devices is necessary before carrying out radiotherapy by means of megavolt apparatuses. The use of different kinds of irradiation is emphasized. A new method is introduced for ultrahard x rays that permits a homogenous, irradiation of lymph node chains. (auth)

13536 STUDIES OF MOST EFFICIENT ENERGIES FOR IRRADIATION OF BONE PROCESSES. **Fornusek, Arthur Henry; Kuttig, Helmut (Univ., Heidelberg). Strahlentherapie; 140: 45-9(Jul 1970). (In German).**

Dose distribution and energy doses in the irradiation of bone tissues were examined by phantom measuring methods by means of 200 kV x rays, cesium-137-, and cobalt-60-gamma radiation, as well as by hyperenergetic electrons. It was concluded that cobalt-60-gamma radiation is the method of choice for therapy of malignant bone processes. (auth)

13537 NEW RADIOTHERAPEUTIC ASPECTS IN THE TREATMENT OF TUMORS IN LONG BONES. **Kaercher, K. H.; Alth, G. (Univ., Vienna). Strahlentherapie; 140: 50-2(Jul 1970). (In German).**

It is demonstrated that a homogenous irradiation of long bones is guaranteed by ionometric measuring methods and new irradiation procedures. Herein, the use of ultrahard X-rays in the range of 43.5 MeV is regarded as the method of choice. The use of fast electrons in an energy range of 10 to 30 MeV is unsatisfactory because of the strong absorption in more deep seated bones. (auth)

13538 IRRADIATION OF LARGE SURFACES WITH HIGH-ENERGY BEAMS. **Kaercher, K. H.; Alth, G. (Univ., Vienna). Strahlentherapie; 140: 63-6(Jul 1970). (In German).**

The possibility of irradiation of large surfaces by fast electrons of different energy, irradiation consisting of vertical field rays or longitudinal pendulation, is discussed. Extended malignant processes of the skin, metastatic or primary, are especially appropriate for this irradiation procedure. In the same way, lung metastases and pleural and peritoneal carcinomas can be treated by higher electron energies. Dosage for malignant processes is 100 to 200 rd daily. In order to influence systemic diseases, that are very radiosensitive, whole-body irradiations of minimum doses of 10 to 30 R can be applied. (auth)

13539 COMPARISON OF HIGH-ENERGY RADIATION APPLIED THROUGH PLASTER CASTS. **Franz, Klaus-Dieter; Hymmen, Ursula; Kuttig, Helmut; Misri, Hassan; Wieland, Cuno (Univ., Heidelberg). Strahlentherapie; 140: 67-70(Jul 1970). (In German).**

XUM

Comparisons of different ray qualities with regard to radiation through plaster casts are made (ultrahard X-rays, fast electrons, ^{60}Co γ, and ^{137}Cs γ). The curves of the depth doses and the influence on the buildup effect are demonstrated. Especially ultrahard X rays and ^{60}Co γ radiation are suitable for irradiations through plaster casts. (auth)

13540 PUNCH CARD CONTROL OF TELECOBALT THERAPY. **Weishaar, Julius; Reuss, Albrecht; Rummel, Wulf** (Univ., Erlangen, Ger.). Strahlentherapie; 140: 78-83(Jul 1970). (In German).

Telecobalt therapy for carcinoma of the cervix at the Gynecological Clinic of the University of Erlangen since 1960 is reviewed. Some developments are described as to cones that allow compression without losing the skin sparing effect; also discussed is the use of supplementary diaphragms. The use of perforated cards conducting the teletherapy machine is described. (auth)

13541 ISOLATED LYMPHOGRANULOMAS OF THE STOMACH. **Wendenburg, H.-H.; Kelleter, H.** (Univ., Heidelberg). Strahlentherapie; 140: 84-8(Jul 1970). (In German).

One of the rare cases of Morbus Hodgkin is reported, in which only a manifestation at the stomach could be proved. Clinical evidences are not characteristic; a radiodiagnostic differentiation in comparison to a stomach carcinoma or a stomach sarcoma is possible only in few cases. Stomach resection and consecutive radiotherapy are considered as the therapy of choice; prospects for recovery are favorable. (auth)

13542 RADIOTHERAPY OF ESOPHAGAL FISTULAS CAUSED BY LYMPHOGRANULOMATOSIS. **Hoffmann, Klaus** (Univ., Tuebingen, Ger.). Strahlentherapie; 140: 268-72(Sep 1970). (In German).

A lymphogranulomatous fistula of the lower esophagus appeared in a 34 years old female patient suffering, since 11 years, from lymphogranulomatosis. This fistula closed after telecobalt irradiation and made possible, for more than three years, an undisturbed esophageal passage. Ten cases were reported and analyzed. Radiotherapy was the only promising method of treatment. (auth)

13543 UNUSUAL DELAY OF METASTASES RECURRENCE FOLLOWING RADIOTHERAPY OF A MEDIASTINAL TUMOR. **Ratkoczy, Nandor** (Univ., Budapest). Strahlentherapie; 140: 273-4(Sep 1970). (In German).

A mediastinal tumor of a young man was irradiated, in January 1933, by the focus destructive dose that was introduced at that time. Biopsy of the cervical knot showed a lymphogranuloma. A negative result was stated by the radiographs made by the author in 1936, 1938, 1952 and by those made in Tel Aviv 1968. The patient died in March 1970 from the consequences of a lung tumor, that was discovered in Tel Aviv in 1969. He was without any relapse for 36 years. (auth)

13544 RESULTS OF THE TREATMENT OF TESTICULAR TUMORS IN THE RADIOTHERAPEUTICAL INSTITUTE OF ROTTERDAM. **van der Werf-Messing, B.** (Radio Therapeutisch Instituut, Rotterdam). Ned. Tijdschr. Geneesk.; 114: 1281-4 (1 Aug 1970).

Reference is made to an analysis of the case records of 279 patients with testicular tumours which shows that supervoltage irradiation of the regional lymph-node station of the testicle, the lumbar lymph-node territory, results in more efficacious elimination of the local metastases than orthovoltage irradiation. Consequently supervoltage irradiation reduces further spread from the lumbar region to intrathoracic and other localizations and increases survival rates both for seminoma patients and for patients with malignant teratomata. The prognosis for the patients with a trophoblastic teratoma, on the other hand, is still unfavourable. (Netherlands)

13545 COMBINED THERAPY FOR CANCER OF THE LARYNGOPHARYNX. **Goldman, Joseph L.; Gunsberg, Melvin J.; Friedman, William H.; Ryan, John R.; Bloom, Bruce S.** (Mount Sinai Medical Center, New York). Arch. Otolaryngol.; 92: 221-5(Sep 1970).

Fifty-three patients with laryngeal cancer were treated with combined preoperative γ irradiation (daily fractions of 250 rads to total dose of 5,500 rads) followed by radical surgery. Thirty-five were alive and well. Six are dead of disease and only three of these patients developed local recurrences. Three had distant metastases. A histopathological study consisting of en bloc serial sectioning of laryngeal and neck specimens has demonstrated several advantages to the use of combined therapy. Among these are the recognition and total surgical extirpation of isolated post-radiation nests of laryngeal cancer cells throughout the original tumor site. In addition, incubation of laryngeal cancer in vitro with tritiated thymidine has demonstrated cell viability after 5,500 rads of preoperative radiation. (auth)

13546 CLINICAL EXPERIENCES DURING A TEN-YEAR PERIOD IN AN ONCOLOGICAL INSTITUTE IN ANTINEOPLASTIC TREATMENT WITH TELECOBALT THERAPY. **Carnevali, G.; Banfi, A.; Ricci, S. Basso; Milani, F.** (Univ., Milan). Radiaz. Alta Energ.; 9: 47-73(Apr 1970). (In Italian).

The results obtained during a ten-year period in the treatment by telecobaltherapy of oro-pharyngeal and thorax-abdominal neoplastic diseases, by the Institute of Radiology of the University and Radiological Department of the National Cancer Institute of Milan are discussed. (auth)

13547 METHOD FOR MAPPING THE SPATIAL DISTRIBUTION OF STOPPING π^- MESONS IN TISSUE. **Sperinde, J.; Perez-Mendez, V.; Miller, A. J.; Rindi, A.; Raju, M. R.** (Univ. of California, Berkeley). Phys. Med. Biol.; 15: 643-7(Oct 1970).

A method is discussed for locating the stopping position of π^- mesons in tissue. The γ-rays emitted following the capture process are collimated and converted to electrons. They are detected with a plastic scintillator and their position is determined with a magnetostrictive wire spark chamber. The sensitivity and resolution of the system are measured. (auth) (UK)

13548 LINAC DYNAMIC BOOSTER PROJECT AND ITS APPLICATION TO MEDICINE AND BIOLOGY. **Kikuchi, Akira** (Tohoku Univ., Sendai). Rinsho Hoshasen; 15: 140-6(Feb 1970). (In Japanese).

At present, the highest thermal neutron flux obtainable by a Japanese reactor is about 10^{14} n/cm^2 sec., and higher flux such as 10^{15} or 10^{16} n/cm^2 sec. is desired for researching the property of matter, activation analysis, producing transuranium elements, or thermal neutron capture therapy. For obtaining this higher thermal neutron flux, a pulsed reactor surpasses a steady reactor. Tōhoku University adopted a pulsed reactor with an electron-Linac (dynamic booster) as the most suitable installation, and three steps of construction, namely, setting up of electron-Linac, installation of booster, and then assembling a Linac-pulsed reactor, was planned. In medicine and biology, a reactor is used for producing radioisotope, activation analysis, irradiation experiments, and thermal neutron capture therapy. In radioisotope production, this dynamic booster does not show any proper advantage, but in activation analysis, this makes it possible to try the on-beam measurement of nuclides having very short half lives. In irradiation experiments, this makes pulsed irradiation possible, but is not suitable for fast neutron irradiation because of γ-ray contamination is the same as with a steady reactor. In thermal neutron capture therapy, this pulsed reactor has the following advantage. Epithermal neutrons can be picked up discriminatively by eliminating γ rays and fast neutrons with a chopper, utilizing their different velocities and the distance from the center of the reactor to the exit aperture, and these neutrons produce more evenly distributed (n,α) reactions in tissues than do thermal neutrons. (auth) (Japan)

Radiation Effects on Animals

Refer also to abstracts 13351, 13377, 13378, 13389, 13472, and 13615.

13549 INFLUENCE OF EXOGENIC SEROTONIN ON THE AGGREGATION OF BLOOD PLATELETS AND SOME BLOOD COAGULATION INDICES IN EXPERIMENTAL ACUTE RADIATION SICKNESS. **Dorofeev, V. M.; Khnychev, S. S.** (Inst. of Medical Radiology, Obninsk, USSR). Byull. Eksp. Biol. Med.; 69: No. 6, 21-3(Jun 1970). (In Russian).

Wistar rats on the seventh day after irradiation (^{60}Co gamma-rays, 600 r, 6 r/sec) were injected with serotonin creatinine sulfate in a dose of 0.1 mg/kg into the femoral vein. Two to three minutes after serotonin injection the aggregation of blood platelets and some indices of the blood coagulation was determined. Serotonin exerted no essential influence on the indices studied in irradiated rats. It was concluded that disturbances of aggregation of blood platelets and the blood coagulation process in acute radiation sickness are not associated with reduced serotonin concentration in the blood. (auth)

13550 CIRCADIAN VARIATIONS IN THE EFFECT OF X-IRRADIATION ON THE HAEMATOPOIETIC STEM CELLS OF MICE. **Vacek, A.; Rotkovska, D.** (Inst. of Biophysics, Brno). Strahlentherapie; 140: 302-6(Sep 1970).

Mice, adapted to cyclic change of light and darkness (12 hours light, 12 hours darkness), were irradiated at different times within

24 hours. It was observed that, after x-ray exposure during the day (11 – 17 hours), the number of endogenous colonies in the spleen was higher than that after irradiation by night (20 hours). The transplantation of bone-marrow cells indicated a higher colony-forming ability for cells from adapted mice killed in the middle of the day than from those killed at night. Survival of irradiated adapted mice was higher when irradiation was performed at 14 hours than at 2 hours. It is suggested that a higher number of survived hematopoietic stem cells in mice, irradiated during daytime, can be the cause of the differences in the mortality of mice irradiated at light or dark phases of the light regime of adaptation. (auth)

13551 PROBLEM OF RELATIVE BIOLOGICAL EFFICACY OF TRITIUM OXIDE. Moskalev, Yu. I.; Zhuravlev, V. F.; Istomina, A. G.; (and others) (Inst. of Biophysics, Moscow). Gig. Sanit.; No. 9, 43-8(Sep 1970). (In Russian).

The investigation was carried out on 726 rats that were subjected to the action of tritium oxide and γ-irradiation with ^{137}Cs in equivalent doses. The relative biological effectiveness (RBE) of tritium in comparison with γ-irradiation with ^{137}Cs judging by the reaction of leucocytes and lymphocytes amounted to 1.84 – 0.16 and 1.87 – 0.59 respectively. Judging by the reaction of neutrophiles, the RBE of tritium oxide equaled to 2.09 on the 7th day. The RBE of tritium according to changes in the weight of the thymus gland on the 1st, 3rd, 7th, and 14th day was from 1.61 to 2.09 and changes in the weight of the spleen on the 3rd and 7th day equaled 1.74 and 1.89 respectively. (auth)

13552 ENHANCEMENT OF VIRAL TRANSFORMATION BY ULTRAVIOLET LIGHT. Lytle, C. D.; Hellman, K. B.; Telles, N. C. (Bureau of Radiological Health, Rockville, Md.). Int. J. Radiat. Biol.; 18: 297-300(1970).

Ultraviolet irradiation of mouse cells enhanced their transformation by the DNA tumour virus SV_{40}. The survival curves of infected and uninfected cells showed that the colony forming ability of both fell within the range 60 to 75 erg/mm^2 for D_0 and 6 to 13 for the extrapolation number. In the infected cells, the number of transformed colonies decreased with irradiation although more slowly than the colony forming ability, and the uninfected irradiated controls had no identifiable transformed colonies. The relation between the fraction of survivors transformed and the uv dose was plotted and the uv dose necessary to enhance the transformation by a factor of e (analogous to D_0 for inactivation) was about 310 erg/mm^2. (UK)

13553 RADIATION-ENHANCED ONCOGENESIS BY SV40. Coggin, J. H.; Harwood, S. E.; Anderson, N. G. (Univ. of Tennessee, Knoxville. Oak Ridge National Lab., Tenn.). Contract AT(40-1)3646. Proc. Soc. Exp. Biol. Med.; 134: 1109-11(Sep 1970).

Exposure of hamster and mouse embryo cells to x-irradiation prior to infection with Simian virus 40 (SV40) significantly increased the frequency of transformation in vitro. Neonatal hamsters were tested for increased sensitivity to SV40 tumorigenicity after exposure to localized, low-level x-ray at the site of virus inoculation in vivo. Results showed that irradiation of a target area prior to infection markedly decreased the time to tumor appearance and increased the frequency of tumor occurrence. No tumors occurred in irradiated animals that did not receive virus. Although low doses of localized x-ray may have resulted in modest immunologic suppression, this was not a primary factor in tumor enhancement. Tumors appearing in SV40-infected animals uniformly possessed viral neoantigens. (auth)

13554 TEMPERATURE DEPENDENCE OF THYMIDINE UPTAKE AND STABILITY OF THYMIDINE INCORPORATED DURING UNSCHEDULED DNA SYNTHESIS IN IRRADIATED AND UNIRRADIATED HeLa CELLS. Evans, R. G.; Djordjevic, B.; Perez, A. G. (Sloan-Kettering Inst. for Cancer Research, New York). Int. J. Radiat. Biol.; 18: 277-80(1970).

There appeared to be a marked difference in the temperature dependence of uv stimulated unscheduled DNA synthesis (UDS) and spontaneous UDS taking place in HeLa cells from 39 to 42°C. The spontaneous UDS decreased by a factor of 7 and the net uv UDS increased by a factor of 3. UDS was measured by the uptake of tritium-labelled thymidine that appeared to be stable through subsequent phases of the cell cycle. Ultraviolet radiation was carried out at 4 ergs/mm^2/sec at 2537 Å. (UK)

Invertebrates

Refer also to abstracts 13409 and 13623.

13555 INVESTIGATIONS ON RADIOSENSITIVE AND RADIORESISTANT POPULATIONS OF DROSOPHILA MELANOGASTER. I. DECREASED RADIOSENSITIVITY IN STAGE-7 OOCYTES OF THE IRRADIATED POPULATION ROE I. Noethel, H. (Freie Univ., Berlin). Mutat. Res.; 10: 463-74(Nov 1970).

An approach was made to study the genotype dependent mechanisms which modify the response of higher organisms to ionizing radiations. A Drosophila melanogaster population with an irradiation history (RO I) and an unirradiated control population (+60) were tested, both being derived from the Berlin wild stock. RO I was given an exposure of 2100 R of x rays in each generation; it was maintained by using treated stages 6 to 14 oocytes, sperm, and late spermatids. Comparisons between +60 and RO I were made after 220 generations of irradiation. Although x irradiation causes a reduction of fertility, equal numbers of viable offspring are produced by the 2 populations when identical culture conditions, except the irradiation, are used. At least 2 mechanisms contribute to this adaptation of RO I to x rays: an increased oviposition rate, and a decreased radiosensitivity for the induction of reduced egg-to-adult survival. Data are presented on the sensitivity of stage 7 oocytes. The dose response relationships for the x ray induction of dominant lethals and X chromosome loss are probit linear in both populations. They demonstrate that the radiosensitivity of RO I is only half that of +60. In addition, sex-linked recessive lethals are induced at lower frequencies in RO I than in +60. The sensitivity differences between +60 and RO I are statistically significant. They are not due to a shift in stages sampled from the 2 populations. Their possible relation to differences in chromosome breakage events was discussed with special emphasis on the fact that nondisjunction does not contribute to the differences in induced X chromosome loss, and that a 2-hit component, apparent for the induction of sex-linked recessive lethals in +60, disappeared in RO I. (auth)

13556 STUDY OF THE DEVELOPMENT OF PARAMECIUM AURELIA IN AN UNDERGROUND LABORATORY: INFLUENCE OF NATURAL IONIZING RADIATION. Planel, H.; Tixador, R.; Vedrenne, G.; Richoilley, G. (Univ., Toulouse). Compt. Rend. Soc. Biol.; 164: 654-8(1970). (In French).

The C.N.R.S. underground laboratory of Moulis (Ariege) behaves as a natural radiation shielding system and the changes observed in the development of Paramecium aurelia cultures are bound up with an attenuation of the natural irradiation. A comparative study of biological responses and spectrographs shows that delays in growth or lengthenings of the cell cycle are all the greater as the irradiation level around the cultures is lower. The facts confirm the biological action of natural irradiation and suggest the role with a decrease in this irradiation could play in the origins of certain features of cave-dwelling fauna. (France)

13557 REDUCTION OF SEXUAL AGGRESSIVENESS OF MALE CODLING MOTHS TREATED WITH TEPA OR GAMMA IRRADIATION. Hathaway, D. O.; Butt, B. A.; Lydin, L. V. (U. S. Dept. of Agriculture, Yakima, Wash.). J. Econ. Entomol.; 63: 1881-3(15 Dec 1970).

Sexual aggressiveness of male Laspeyresia pomonella was measured by comparing the longevity of female codling moths confined at various ratios with untreated males or with males treated with tepa or γ irradiation. Females held without males lived 9.3 days, females caged at a ratio of 7 untreated males per female lived 4.2 days, and females confined at the same ratio with males treated with 40 kR of γ irradiation or with 15 or 30 μg of tepa, lived 5.1, 6.1, and 7.6 days, respectively. Also, when untreated males were caged with females at ratios of 1 : 1 and 7 : 1, the females contained 2.1 and 3.9 spermatophores, respectively; those caged at the same ratios with males treated with 15 μg of tepa contained 1.7 and 4.3 spermatophores, respectively. (auth)

13558 EFFECTS OF ^{60}Co GAMMA RADIATION ON THE EGG AND LARVAL STAGES OF THE RICE WEEVIL, SITOPHILUS ORYZAE (L.). Towheed, Syed Manzoor; Kabir, Syed M. Humayun (East Pakistan Agricultural Univ., Mymensingh). Nucleus (Karachi); 7: 59-64(Jan-Apr 1970).

Eggs and larvae of the rice weevil, Sitophilus oryzae (L.) were exposed to various levels of γ radiation from a ^{60}Co source. Maize grain, with approximately 14% moisture content, was used as the medium. The dose rate of the source was 24,000 R/hr at the time of radiation. The larvae were found to be more tolerant than the eggs. The eggs and larvae, respectively, failed to emerge as adults at 1000 and 5000 R. (auth)

Vertebrates

Refer also to abstracts 13333, 13346, 13348, 13349, 13366, 13367, 13370, 13373, 13375, 13376, 13383–13385, 13387, 13390, 13404, 13426, 13474, 13477–13479, and 13502.

13559 MELATONIN SYNTHESIS IN RAT PINEAL GLANDS INHIBITED BY X-IRRADIATION. Barfuss, D. W.; Tait, G.

XUM

Robert: Ellis, LeGrande C. (Utah State Univ., Logan). Proc. Soc. Exp. Biol. Med., 132: 35-6(Oct. 1969).

Melatonin synthesis was measured in individual male rat pineal glands in vitro. When compared with control animals 24 hr after treatment, rats irradiated with 450 R of x rays demonstrated a striking decrease in the activity of the melatonin-synthesizing enzyme hydroxyindole-O-methyl transferase in the pineal glands. (auth)

13560 EFFECT OF OVARIAN STEROIDS AND X-RAY IRRADIATION ON PREIMPLANTATION BLASTOCYSTS OF THE RAT. Wu, Jung-tsung. Madison, Wis.; Univ. of Wisconsin (1969). 194p. University Microfilms Order No. 69-22,513. Thesis.

When delayed blastocysts were cultured in vitro in medium containing estradiol-17β, washed, and transferred into the uterus of the progesterone-treated ovariectomized rat, no implantation sites were observed. It was concluded that estrogen-treated blastocysts cannot implant in the progesterone-stimulated uterus. Ultrastructural changes in the delayed blastocysts were studied at different times following the injection of an implantation dose of estrogen. The changes in inner cell mass cells were: an increase in the number of cytoplasmic processes which sometimes penetrate deeply into neighboring inner cell mass cells; an increase in the number of polysomes; the presence of slightly electron-dense material in expanded rough-surfaced endoplasmic reticula. In trophoblastic cells the glycogen granules and vesiculation of dense bodies appear first at 16 hrs., followed by multivesicular bodies. It was postulated that the dense bodies were transformed into membranous bodies directly, or indirectly through the formation of multigranular bodies. Multigranular bodies may also fuse with multivesicular bodies prior to membrane formation. The ovariectomized pregnant rats were administered 300R of whole-body x-irradiation on day 5 of pregnancy, and blastocysts were recovered 24 and 96 hrs. later (days 6 and 9, respectively) and processed for ultrastructural studies. Cytoplasmic blebs were seen only in the irradiated blastocysts and persisted up to day 9. More autophagic vacuoles and crystal-like aggregates were present in the irradiated than the sham-irradiated day 6 blastocysts, although the difference was not statistically significant. These two structures were seen only rarely in both groups of day nine blastocysts. Thus, the structures related to the digestion of damaged components in cells were considerably reduced by 72 hrs after irradiation. Means for the disposal of autophagic vacuoles into the blastocoele were discussed. (Diss. Abstr.)

13561 ACTION OF IONIZING RADIATIONS ON SOME BIOCHEMICAL AND BIOELECTRICAL ACTIVITIES OF THE CENTRAL NERVOUS SYSTEM. La Grutta, G.; Abbadessa, S.; Avellone, S.; Natale, E.; Di Gregorio, I.; Montalbano, M. E.; Ortolani, E. A.; Zagami, M. T. (Univ., Palermo, Italy). Arch. Fisiol., 65: 271-312(Dec. 1967). (In Italian).

The effects of ionizing radiations on some biochemical and bioelectrical activities of the central nervous system were studied in rabbits. The results are as follows: Cholinesterase activity (true and pseudo) appears variously increased in the cerebral cortex, basal ganglia and cerebellum, while there is no important modification in the blood; γ-amino butyric acid (GABA) concentration is also increased in the same structures showing a typical temporal evolution; glutamic decarboxylase (GDC) activity increases parallely with GABA concentration; lactate dehydrogenase (LDH) activity is not altered; spontaneous bioelectric activity (E.Co.G.) results are variously impaired: irritative spikes (1 hr after irradiation) and slow-waves (8 to 12 hr after irradiation) are seen; convulsive threshold of Metrazol and Novocaine i.v. is largely increased; convulsive threshold of strychnine, picrotoxin and folic acid applied on cortico-cerebral acoustic area is also increased; central nervous system reactivity to some drugs (penicillin, folic acid and thiamine) is modified. Possible interpretations of these experimental data are discussed. (auth)

13562 INTERACTION OF X-RADIATION AND MALNUTRITION. A STUDY OF KINETICS OF CELLULAR PROLIFERATION IN THE JEJUNUM OF PROTEIN-DEFICIENT RATS. Verma, Kusum; Deo, M. G.; Sharma, Urmil; Ramalingaswami, V. (All-India Inst. of Medical Sciences, New Delhi). Amer. J. Pathol.; 61: 341-55(Dec 1970).

Some aspects of the cell generative cycle in protein deficiency were investigated. The mitotic phase of the cell generative cycle of the jejunal crypt cells and the pattern of recovery in these cells after 200 R whole-body x radiation were studied in a group of young growing rats rendered protein deficient. Two groups of control animals were studied similarly. One group was fed isocaloric amounts of a high protein diet and the other was a weight control group fed a stock diet. After x radiation, the rate of disappearance of mitoses was slowed in the protein deficient animals. This was explained on the basis that the mitotic phase in protein deficiency was prolonged. The rate of recovery, as judged by the rate of resumption of mitosis and cumulative mitoses using colchicine after 200 R whole-body x radiation was markedly decreased in the protein deficient animals as compared to those fed the high protein and stock diets. The ^{3}H-thymidine labeling index in the crypt cells 4 hrs after 200 R whole-body x radiation was similar in both the high protein and the protein deficient animals. Evidence of cytoplasmic and nuclear damage and of associated inflammatory reaction in the jejunal mucosa was much less in the protein deficient animals than in the controls. There is thus a paradox of less tissue damage associated with a more prolonged recovery after x radiation in the protein deficient animals. (auth)

13563 DYNAMIC OF RESTORATION OF THE BONE MARROW IN ITS LOCAL IRRADIATION IN MICE AND RATS. Strelin, G. S.; Tavrovskaya, T. V. (Central Roentgenoradiological Inst., Leningrad). Byull. Eksp. Biol. Med.; 70: No. 9, 85-8(Sep 1970). (In Russian).

Albino mongrel mice and rats were investigated. Local irradiation of the shin was carried out on RUM-3 apparatus in doses of 1500, 2000 and 3000 r. Follow-up observations were conducted for a period of six months after irradiation. Changes occurring in the locally irradiated bone marrow were evaluated by the total number of nucleus-containing bone marrow elements in the shin. The data derived testify that there are significant species differences in the rats and degree of restoration of locally irradiated bone marrow in mice and rats. In mice the level of bone marrow elements normalizes about the 15th day postradiation, whereas in rats the process of repopulation occurs much slower and does not normalize. Secondary reduction of the number of myeloid cells in the irradiated shin in rats and mice seen at the end of the observation period is associated with developing sclerotic manifestations. (auth)

13564 MALIGNANT TUMOURS OF THE RAT ADRENAL GLAND INDUCED BY FISSION NEUTRON IRRADIATION. Vogel, H. H. Jr.; Zaldivar, R. (Univ. of Tennessee, Knoxville). Int. J. Radiat. Biol.; 18: 267-70(1970).

The incidence of malignant tumors in the adrenal glands of male Buffalo rats treated with fission neutron irradiation (single exposure 300 to 364 rads whole-body irradiation, including 15% γ ray sublethal contamination) was compared with incidence in control rats untreated or treated with gum acacia. The difference between the number of adrenal cancers in control and neutron-irradiated rats (1.1% and 13.1%) was significant ($P < 0.01$). The neoplasms were diagnosed as cortical carcinomas and in one case a pleomorphic sarcoma. The neoplasms were late radiation effects, age at death ranging from 414 to 1311 days. (UK)

13565 EFFECT OF OPTICAL QUANTUM GENERATOR RADIATION ON ELECTRICAL PARAMETERS OF FRESH TISSUE. Volkov, Yu. N.; Sidorik, E. P.; Danko, M. I. (Kiev State Univ. Inst. of Experimental and Clinical Oncology, Kiev). Fiziol. Zh., Akad. Nauk Ukr. RSR; 16: 480-3(Jul-Aug 1970). (In Ukrainian).

Changes were investigated in electric parameters of skin at different times after radiation, the histomorphological investigations being carried out simultaneously. The greatest changes in the electric parameters of skin were observed a day after radiation. Histomorphologically deep injuries in the radiation zone were observed, testifying to the coagulative necrosis. An existence is shown of connection between the changes in electric parameters of skin and degree of radiation effects. (auth)

13566 EFFECT OF SUBLETHAL AND LETHAL RADIATION DOSES ON EXTRACELLULAR AND INTRACELLULAR DISTRIBUTION OF SODIUM AND POTASSIUM IN THE BRAIN, LIVER, KIDNEYS, AND MUSCULAR TISSUE OF RATS. Shamrai, E. F.; Sokolova, V. I. (Medical Inst., Kiev). Fiziol. Zh., Akad. Nauk Ukr. RSR; 16: 513-18(Jul-Aug 1970). (In Ukrainian).

With a sublethal radiation dose (600 R) the total content of sodium in brain and muscular tissues decreased somewhat; with a lethal radiation dose (900 R) the total content of sodium sharply increased on the 9th, 11th, and 13th days after radiation. With 600 R the total extra- and intracellular content of potassium in the investigated tissues did not change. With an increase of the dose up to 900 R essential shifts took place in extracellular and intracellular content of potassium. Essential changes were observed in the distribution of sodium ions between the cell and environment. (auth)

13567 EFFECT OF X RAYS ON CYTOLOGICAL CHANGES OF BONE MARROW CELLS AS A FUNCTION OF THE IMMUNOBIOLOGICAL STATE OF THE RETICULO-ENDOTHELIAL SYSTEM. Stepanyan, E. D.; Petrosyan, R. A.; Grigorenko, L. P.;

Zakharyan, E. G. (Inst. of Zoology, Erevan). Biol. Zh. Arm.; 23: 59-65(Jan 1970). (In Russian).

White rats 100 to 150 g in weight were given x ray doses of 300 and 500 R alone and in combination with administrations of adrenalin (0.1 mg/100 g), pilocarpine (1 mg/100 g), or bacterial antigen. At intervals of three hrs, one day, four days, and eight days after irradiations, tests were made to determine the mitotic activity and chromosome aberrations in bone marrow cells and the ability of the reticulo-endothelial system to remove Congo red dye from the blood. Sharp suppression of mitotic activity was noted with the use of radiation alone, especially at 500 R. It was possible to correlate phagocytic activity of the reticuloendothelial system with mitotic activity of the bone marrow cells. Adrenalin and pilocarpine stimulated phagocytosis after a brief suppression at three hours after treatment. The combined treatment of radiation and adrenalin or pilocarpine led to a cancelling out of opposite effects with only a slight gain in mitotic activity and phagocytosis. Vaccination of the animals with a bacterial antigen had a significant radioprotective effect in that the number of chromosomal aberrations was much lower than observed with the use of radiation alone. The survival of animals irradiated with an x ray dose of 750 R was 86% at 10 minutes after vaccination, while it was only 47% when the irradiation was carried out 4 days after vaccination with the bacterial agent. Thus preliminary vaccination significantly increases the radioresistance of the animal. (TTT)

13568 BIOLOGICHESKOE DEISTVIE BYSTRYKH NEITRONOV. VYPUSK 1. (Biological Effects of Fast Neutrons. Number 1). Gorodetskii, A. A. (ed.). Kiev; Izdatel'stvo Naukova Dumka (1969). 123p.

Twenty-three Russian-language papers discuss the results of experimental studies on the biological effects of fast neutrons on experimental animals, plants, and microorganisms. Several method used for fast neutron dosimetry in various animal tissues and organs are described. (C.H.)

13569 EFFECT OF RADIOPHOSPHORUS ON THE DEVELOPMENT OF GONADS IN MICE. **Srivastava, Pratap N.; Chadha, Sudha R. (Univ. of Rajasthan, Jaipur, India). Strahlentherapie; 139: 738-43(Jun 1970).**

Thirty day old C-57 strain mice were intramuscularly injected with ^{32}P at a dose rate of 1.3 μCi/g body weight. On day 60, the animals were autopsied and the effect of ^{32}P on ovaries and testes was studied. The ovaries showed complete damage. Injections of estradiol and FSH did not bring about any change in the ovary indicating that no normal oocyte or follicle was present on day 60. The seminiferous tubules of the testes did not show uniform degree of damage. Some of the tubules were damaged completely, others only partially, while still others showed no damage at all. (auth)

13570 ELECTROMAGNETIC FIELDS AND LIFE. Presman, A. S. New York; Plenum Press (1970). 350p. $25.00. Translation of Elektromagnitnye Polya i Zhivaya Priroda by F. L. Sinclair.

Separate abstracts were prepared for the three sections of the book. A list of approximately 700 references and a subject index is included. (H.L.W.)

For abstracts of individual sections see: 13571, 13572, and 13581.

13571 EXPERIMENTAL INVESTIGATIONS OF THE BIOLOGICAL ACTION OF ELECTROMAGNETIC FIELDS. pp 87-195 of Electromagnetic Fields and Life. /Presman, A. S. New York; Plenum Press (1970).

Chapters on the following topics are presented: irreversible and permanent effects of electromagnetic fields in entire organisms; effect of electromagnetic fields on neurohumoral regulation in entire organisms; effects on reproduction and development of organisms; effects at the cellular and molecular levels; and mechanisms of the experimentally observed biological effects of electromagnetic fields. (H.L.W.)

13572 ROLE OF ELECTROMAGNETIC FIELDS IN THE REGULATION OF THE VITAL ACTIVITY OF ORGANISMS. pp 197-280 of Electromagnetic Fields and Life. /Presman, A. S. New York; Plenum Press (1970).

A chapter on environmental electromagnetic fields and the vital activity of organisms is concerned with the following topics: relationship between biological phenomena and solar activity and the role of electromagnetic fields in these effects; the biological clock and natural electromagnetic fields; orientation of living organisms in relation to the earth's magnetic and electric fields; effect of natural low and high-frequency electromagnetic fields on chemical and biological systems; and mechanisms of the effect of natural electromagnetic fields on the vital activity of organisms. A chapter is presented on electromagnetic fields within the organism and their role in the regulation of vital processes. A chapter on the role of electromagnetic fields in informational interconnections between organisms is concerned with sensations and unconditioned reflexes due to electromagnetic fields, electromagnetic fields created close to cells and organs, bioinformation transfer and electromagnetic fields, and parapsychological investigations. A chapter on practical applications is concerned with therapy, diagnosis, hygienic factors, agricultural practice, space biology, and biological activity of electromagnetic fields in relation to bionics. (H.L.W.)

13573 ELECTRORETINOGRAM OF A FROG EXPOSED TO ULTRAVIOLET LIGHT OF ABOUT 366 nm. **Berger, Helmut; Seidel, Karl-Heinz (Friedrich-Schiller Univ., Jena, Ger.). Acta Biol. Med. Ger.; 25: 243-50(1970). (In German).**

The effectiveness of stimulation with ultraviolet light of about 366 nm is tested electroretinographically. The eye of the frog responds only to high intensities of irradiation. Since the stimulating light induces self-fluorescence of the lens and retina, it is supposed that the irritation is elicited indirectly. The uv-insensibility of the frog demonstrated earlier with other methods is thus corroborated. The indirect action of radiation is essentially increased by injection of fluorescein sodium solutions. The fluorescent light emitted by the organic dye includes 3 wavelengths (527, 570 and 640 nm). The former two are well absorbed by the pigments of vision. As the fluorescein molecules cannot pass the retinal blood-tissue barrier, the fluorescence light is emitted from out of the vessels. The effect of fluorescein is dependent on concentration. (auth)

13574 X RADIATION EFFECTS ON ANIMALS PRE-TREATED WITH UV RADIATION. **Isaenko, V. I. (Kiev Inst. of Physiology). Fiziol. Zh., Akad. Nauk Ukr. RSR; 16: 681-4(Sep-Oct 1970). (In Ukrainian).**

Preliminary exposure of dogs to uv irradiation reduced the changes induced by 200 and 400 R whole-body x-irradiation in the albumin concentrations in the serum and blood fractions. The preliminary uv irradiation also reduced changes in the erythrocytes of dogs irradiated with 400 R. Mineral composition of blood (calcium, potassium, and sodium) reflected less change in the x-irradiated dogs pre-treated with uv as compared to animals not treated with uv. (R.V.J.)

13575 INTRACEREBRAL TEMPERATURE CHANGES AFTER X IRRADIATION IN THE RABBIT. **Leith, J. T.; Levy, C. K. (Univ. of California, Berkeley). Int. J. Radiat. Biol.; 18: 291-5(1970).**

Intracranial temperature was measured after doses of x radiation of 9000 to 12000 R to the heads of New Zealand rabbits (3 to 5 kg weight). There was an initial temperature response, apparently unrelated to body-temperature, in all animals, of 0.03°C per min, reaching a maximum value of 0.7 to 1.1°C above pre-irradiation levels 30 to 40 min after irradiation, and returning to pre-irradiation levels within 1 to 2 hr. In animals with thermistors located in the superior colliculus region of the optic system, a second temperature rise was recorded, which could have been dose dependent, occurring 2.5 to 3.5 hr after irradiation, correlating with epileptiform seizures and a general rise in body temperature. The rate of increase of the second temperature rise was 0.005°C per min, reaching a maximum of 0.2 to 0.7°C above pre-irradiation levels. (UK)

13576 ABSORPTION, DISTRIBUTION, AND ELIMINATION OF ^{14}C-DIMECARBINE IN HEALTHY AND IRRADIATED ANIMALS. **Byrikhin, V. I.; Shadurskii, K. S.; Trofimov, F. A. Farmakol. Toksikol.; 33: 44-7(1970). (In Russian).**

Tests conducted on rabbits demonstrated the appearance of ^{14}C-dimecarbine in the blood 45 to 60 min after its introduction into the stomach. With single and multiple introduction of ^{14}C-dimecarbine to healthy and irradiated animals, its distribution in the organism and tissues is nonuniform. The preparation is eliminated chiefly through the kidneys and gastrointestinal tract. Carbon-14-labeled dimecarbine is passed with the urine either unchanged or in the form of two metabolites. (auth)

13577 EFFECT OF IONIZING RADIATION ON THE FREQUENCY AND ULTRASTRUCTURE OF MAST CELLS IN MOUSE SPLEEN. **Viklicky, V.; Trebichavsky, I. (Inst. of Experimental Biology and Genetics, Prague. Inst. of Microbiology, Prague). Folia Biol. (Prague); 16: 347-52(1970).**

A whole-body sublethal γ irradiation (^{60}Co) of mice was followed by changes in both the frequency and ultrastructure of mast cells in the spleen. Following the exposure, the number of cytoplasmic granules increased while their electron-density decreases. Simultaneously with lysis of the original granules, signs of formation of new granules tend to appear. However, some phenomena, that ap-

XUM

peared to be due to active substances being released from mast cell granules (the decreased density and formation of light areas around the granules), tended to persist for the whole time of observation. It was concluded that the observed changes in the frequency and fine structure of mast cells represent a component of the regeneration processes in the irradiated tissue rather than its direct reaction to irradiation. (auth)

Man

Refer also to abstracts 13410, 13452, 13460, 13465, 13466, 13470, 13476, 13480, 13508, 13513, 13522–13525, 13530, and 13532.

13578 LIVER SCANS AFTER PRIMARY TREATMENT OF TUMORS IN CHILDREN. Samuels, Larry D. (Ohio State Univ., Columbus); Grosfeld, Jay L.; Kartha, Mukund. Surg. Gynecol. Obstet.; 131: 958-64(Nov 1970).

The livers of children are quite sensitive to doses of 2,000 to 3,000 rads of megavoltage radiation to adjacent organs, when fractionated over two to three weeks, especially but not exclusively when administered concomitantly with dactinomycin. Both hepatic parenchymal and reticuloendothelial cells appear to be equally sensitive with respect to decreased uptake of radionuclide and subsequent atrophy. A characteristic pattern of regeneration leading to right-to-left reversal of the usual liver lobe dominance following radiation therapy to the right renal fossa is described. A closer investigation of the sequence of changes in the livers of children, during and after such therapy, appears in order and is underway. At least in children, the liver is not as radioresistant an organ as previously widely believed. (auth)

13579 THYROID GLAND GROWTH AND THYROID HYPERFUNCTION IN ANTERIOR-PITUITARY INSUFFICIENCY. **Pickardt, C. Renate; Scriba, P. C. (Univ., Munich). Deut. Med. Wochenschr.; 95: 2166-9(23 Oct 1970). (In German).**

Three cases of anterior-pituitary insufficiency with thyroid abnormalities are reported. In one, a malignant goiter developed five years after an adenoma of the anterior pituitary had been surgically removed. In the second case, hyperthyroidism developed after ^{90}Y implantation for the treatment of acromegaly had caused anterior-pituitary insufficiency. In the third case, toxic adenoma developed after operative removal of a chromophobe anterior-pituitary adenoma. In the differential diagnosis of such cases of TSH-independent thyroid gland enlargement, with or without thyroid hyperfunction, possible causes to be considered include malignant thyroid tumor, thyroiditis, acromegaly, hyperthyroidism, and autonomous thyroid adenoma. (auth)

13580 RADIATION BURDEN TO THE PATIENT DURING A GASTROINTESTINAL PASSAGE. **Schulte-Brinkmann, Wolfgang; Lindner, Helmut (Univ., Duesseldorf). Strahlentherapie; 140: 307-17(Sep 1970). (In German).**

The gonadal dose received during the radiological examinations of the stomach and of the intestine is measured in phantoms and in patients (100 cases). The following mean values are derived. Skin dose 52 R; incident dose 4359 R · cm^2; integral dose 39.1 rd kg; male gonadal dose 8.37 mR. The dose and the somatic and genetic dose can thus be considered as very low. The influence of the radiation quality, the examination technique, and the qualification of the examiner are discussed. The possible ways of further reduction of this dose are outlined. (auth)

13581 PHYSICAL PRINCIPLES AND EXPERIMENTAL METHODS OF INVESTIGATION OF THE BIOLOGICAL ACTION OF ELECTROMAGNETIC FIELDS. **pp 15-86 of Electromagnetic Fields and Life. /Presman, A. S. New York; Plenum Press (1970).**

Physical characteristics of electromagnetic fields are discussed with regard to the dielectric constant, specific electrical conductivity, magnetic permeability, permeance, and interactions with physical media. The earth's electric and magnetic fields, atmospherics, and radio emission of the sun and galaxies are described as natural sources of electromagnetic fields in the habitats of organisms. Artificial sources of electromagnetic fields in the habitats of organisms are generators and the radio background created by the transmission of numerous radio and television stations. A discussion of electric properties of tissues of living organisms includes properties of tissues in constant fields, dispersion of electric parameters of tissues in alternating fields, and values of electric parameters of animal and human tissues in various frequency ranges. Physical principles of the interaction of electromagnetic fields with biological objects are discussed. Problems of dosimetry of electromagnetic fields in biological and medical investigations are as follows: physical quantities; relation between the intensity of the electromagnetic field measured in the medium surrounding the living object and the biologically effective intensity acting directly on the object; and techniques and instruments used to measure the intensity of electromagnetic fields. (H.L.W.)

13582 LATE SEQUELAE AFTER EXPOSURE TO ^{90}Sr SKIN IRRADIATORS OBSERVED EIGHT AND MORE YEARS LATER. **Bekerus, Milos (Medical Faculty, Belgrade). Strahlentherapie; 140: 105-7(Jul 1970). (In German).**

Late alterations in the skin are reported that manifested 8 to 10 years after application of ^{90}Sr-irradiation. The following items are observed: achromia, slight atrophy, teleangiectases, and pigmentations. (auth)

13583 STUDIES OF THE INFLUENCE OF WAVELENGTH ON BIOLOGICAL EFFECTS. TIME AND DOSE DIFFERENTIALS AT RADIATION ACTION SITES IN THE SKIN. **Jolles, Benjamin; Harrison, Raymond (General Hospital, Northampton, Eng.). Strahlentherapie; 139: 716-23(Jun 1970).**

It is shown that certain skin vascular changes following exposure to X-rays (50–250 kV) are absent when a ^{60}Co beam is used. The finding cannot be accounted for by the build-up effect below the skin surface and by the RBE alone. The importance of the varying strengths of tissue filtration and of the biologically active function sites in skin structures and the dose differentials in these in both time and space are brought forward as an explanation of phenomena which up to the present are not considered in the concept of the RBE of radiations of different wavelengths. The role of enzymes and their inhibitors and of vasoactive compounds effective at different levels of the epidermis and dermis, stimulating or cancelling each other, is discussed. (auth)

13584 RADIATION INJURIES FOLLOWING ELECTRON THERAPY FOR MAMMARY CARCINOMAS. **Frischbier, H.-J.; Lohbeck, H. U. (Univ., Hamburg). Strahlentherapie; 139: 684-94(Jun 1970). (In German).**

Between 1958 and 1964, 173 patients with breast carcinomas were treated with electron beams. In 121 patients, radiotherapy was followed by Halsted surgery. For preoperative and postoperative cases, the dose was 4500 to 6000 R, delivered by a 15 MeV betatron. The survival results are 38.4% at 5 years. Effects of radiotherapy on the skin are early or late. Chronic ulcers were observed in less than 5%. Edema of the arm was noted in 42.8%, whereas severe edemas were rare. Radionecrosis of the first and/or second ribs and of the clavicula were observed in 10.4%. Lung fibrosis was observed in 13.3%. The most serious complications encountered are lesions of the brachial plexus. We noted this in 33% of the patients. For all patients followed during more than six years, 72.2% presented these symptoms. 34 cases presented paraesthesias and paresis, and in 23 only sensory deficits were noted. The cause of the lesions is not a direct radiation effect on the nerves, but more certainly a progressive sclerotic inclusion in the subcutaneous fibrosis in the supraclavicular field. (auth)

13585 MALIGNANT THYROID ADENOMAS FOLLOWING X RADIATION DURING CHILDHOOD. **Gilly, L.; Meese, D. (Knappschaftskrankenhaus, Recklinghausen, Ger.). Strahlentherapie; 139: 695-7(Jun 1970). (In German).**

A case of an 18 year old male with thyroid cancer is reported 15 years after roentgen therapy for bilateral cervical lymph node adenomas. The genesis of a thyroid carcinoma after roentgen therapy of the neck and the upper infantile thorax is discussed. (auth)

13586 INFLUENCE OF INSULIN ON THE SYMPATHO-ADRENAL SYSTEM OF PERSONS WORKING WITH RADIATION SOURCES. **Kogan, I. A. (Research Inst. of Medical Radiology, Kharkov). Med. Radiol.; 15: No. 11, 39-46(Nov 1970). (In Russian).**

The functional possibilities of the sympatho-adrenal system were studied by means of loading tests with small doses of insulin in persons working with different radiation sources. A total of 172 persons were examined, 77 of whom were not previously subjected to irradiation and served as controls. Prior to the administration of insulin (0.15 U/kg of body weight intramuscularly), catecholamine levels were determined in diurnal urine and in four portions, collected during the following day and night. After the injection of insulin, collection of the urine was continued fractionally for 1 to 2 days. Adrenal stimulation, insufficiency of mediator chain of the sympatho-adrenal system, hypoadrenaline, and a perversed type of shifts in catecholamine excretion were dose dependent. (P.B.M.)

13587 X-RAY THERAPY AND THYROID TUMORS. Epstein, Ervin. J. Amer. Med. Ass.; 215: 486(18 Jan 1971).

Two of four children in a family were given x-ray therapy for acne during childhood. The two younger children, not having acne, were not irradiated. Of the two younger (unexposed) children, the boy developed thyroid cancer at the age of 22. The unexposed female sibling, at the age of 22, underwent surgical exploration, revealing a benign thyroid tumor. The two older (irradiated) children remained free of thyroid neoplasms. There was no family history of thyroid tumors. (E.R.B.)

13588 STUDY OF 200 PATIENTS WITH PRURITUS ANI. Bowyer, A.; McColl, I. (Guy's Hospital, London. St. Mark's Hospital, London. St. Bartholomew's Hospital, London). Proc. Roy. Soc. Med.; 63: Suppl., 96-8(1970).

From International Conference on Proctology, London, England. See CONF-690645-(Suppl.).

An investigation was made on 200 patients complaining of itching in the perianal region. The conditions found included erythrasma, thrush, intertrigo, contact dermatitis and hemorrhoids. X-ray damage was observed in four patients. These all had long-standing Pruritus ani and had received x-ray therapy in the past. X-ray therapy may relieve symptoms for a while, but does not eradicate any original cause of the itching and may result in permanent damage to the perianal skin. A combined dermatological and surgical approach to the problem of Pruritus ani is recommended. (F.M.M.)

13589 IRRADIATION INJURY TO THE BOWEL AND RECTUM. Blank, W. A. (St. Vincent Hospital and Medical Center, Toledo). Proc. Roy. Soc. Med.; 63: Suppl., 98-100(1970).

From International Conference on Proctology, London, England. See CONF-690645-(Suppl.).

Irradiation damage to the rectum and sigmoid colon is a complication that develops in a significant number of instances despite recent improvements in methods and techniques in the treatment of uterine and cervical carcinoma with radium and cobalt. In a large percentage of cases the irradiation damage appears in 2 to 6 weeks, and many of these will heal spontaneously or respond satisfactorily to steroid retention enemas. A colostomy should be used to relieve obstruction or to supplement repair or anastomosis. Pain, hemorrhage and fistula formation are not relieved by colostomy. Tissues affected by irradiation heal poorly; hence the necessity for supplementing resections and repair work with a diversionary colostomy. (auth)

13590 POSSIBILITY OF WHOLE-BODY ACTIVATION AUTORADIOGRAPHY. Matsuoka, Osamu; Kashima, Masatoshi; Joshima, Hisamasa; Noda, Yutaka (National Inst. of Radiological Sciences, Tokyo). Radioisotopes (Tokyo); 19: 511-17(Nov 1970).

A new autoradiographic technique of whole body activation autoradiography was developed to utilize whole body autoradiographic techniques in studies of non-radioactive materials. This technique is expected to be useful in several areas of biological research. However, several difficult problems associated with interference from induced radioactivities in natural occurring elements in the specimen remain to be solved. Target elements such as Au, Mn, Hg, As, Pr and Eu were given to mice and rats. Freeze-dried whole body sections were irradiated by neutrons in the reactor where neutron flux is 4.0×10^{12} n/sec/cm^2 in pneumatic tube. The activated specimens were placed in contact with x-ray film after adequate cooling. Results showed that the whole body activation autoradiography would be applicable in practical purpose under the limited condition of well selected materials and well designed irradiation and cooling. Several factors which influence minimum detectable amounts were discussed. (auth)

13591 EXPERIENCES WITH ^{32}P IN ADVANCED CARCINOMA OF THE PROSTATE. Corwin, Stephen H.; Malament, Maxwell; Small, Maurice; Strauss, Herbert D. (Veterans Administration Hospital, East Orange, N. J. New Jersey Coll. of Medicine and Dentistry, East Orange). J. Urol.; 104: 745-8(Nov 1970).

Twenty patients with stage 4 carcinoma of the prostate and severe debilitating pain requiring narcotics received 24 courses of ^{32}P therapy. Following a multi-disciplined protocol, 75 percent of the cases received almost complete relief of pain. Although radioactive phosphorus provides an excellent therapeutic modality for treating hormonally refractive patients, bone marrow depression may occur especially when multiple courses of therapy are given. Increased bone pain can result from the androgenic preparation and may be a contributory factor in the onset of paraplegia. Occasionally, a beneficial subjective improvement is encountered by the use of androgens alone. (auth)

13592 TREATMENT OF DELAYED INTRACTABLE HEMORRHAGIC CYSTITIS FOLLOWING RADIATION OR CHEMOTHERAPY. Lapides, Jack (Univ. of Michigan, Ann Arbor). J. Urol.; 104: 707-8(Nov 1970).

Delayed, intractable, gross hematuria following cobalt irradiation to the bladder or prolonged cytoxan therapy for malignancies in general is often due to bleeding from telangiectasia. Abrupt cessation of the hemorrhage can be accomplished readily by searing the telangiectatic capillaries in the bladder with electrocautery using a ball-tip electrode and an electric current of intensity just barely sufficient to accomplish coagulation. (auth)

13593 MALIGNANCY FROM RADIUM. Loutit, J. F. (Medical Research Council Radiobiology Unit, Harwell, Eng.). Brit. J. Cancer; 24: 195-207(Jun 1970).

Human experience of the toxicity of radium acts as a guide for the setting of occupationally permissible levels for radioactive nucleides, especially bone-seekers. Reviewing the published statements and photomicrographs in early reports, one can make a case that malignancy was induced in bone-marrow (leukaemia, malignant myelosclerosis) as well as in bone (osteosarcoma) by radium, especially with large doses. Three case reports of radium intoxication in Britons are noted as compatible with this suggestion, after revised interpretation in two of them. (auth) (UK)

13594 NEW EXPERIMENTAL FINDINGS CONCERNING THE DEFINITION OF TOXIC THYROID ADENOMAS. Ramdohr, B.; Freyschmidt, P.; Karguth, K. (Freie Univ., Berlin). Fortschr. Geb. Roentgenstr. Nuklearmed.; 113: 479-87(Oct 1970). (In German).

In the majority of toxic thyroid adenomas, thyroid function is clinically and biochemically normal. Following therapeutic radioiodine, curves of marked thyroid hormone concentration indicate a rate of hormone synthesis equal to that in patients with normal thyroids. Only a small proportion of toxic adenomas is associated with hyperthyroxinemia, and among these an increased rate of synthesis can be demonstrated. Only these toxic adenomas can be classified as hyperthyroid. By thin layer chromotography, an increased tri-iodothyronin content was found in all toxic adenomas; this always exceeded that found in hyperthyroidism. An increased tri-iodothyronin is due to increased thyroid iodine turnover, resulting in a decreased thyroid iodine pool. The current concept of so-called decompensated-toxic or compensated-toxic adenoma resulting from more or less marked reduction of TSH secretion, due to thyroid hormone, can no longer be maintained. The effect of the adenoma-to-thyroid mass ratio on radio-iodine storage in the thyroid is discussed. (auth)

13595 HYGIENIC INVESTIGATION OF THE EFFECT PRODUCED BY SMALL CONCENTRATIONS OF URANIUM ON THE HUMAN BODY. Novikov, Yu. V.; Pushkina, N. N.; Tambovtseva, A. M. (Scientific Research Inst. of Hygiene, Moscow). Gig. Sanit.; No. 6, 39-44(Jun 1968). (In Russian).

Effects of small concentrations of uranium in drinking water on the following indices were studied: blood content of aminonitrogen, catalase, aldolase, prothrombin, and sulfhydryl groups; 17-ketosteroids of urine; vitamins C, B_1, B_2, and PP; and pyrotartaric acid. No significant differences could be detected in these indices among persons living in regions where the uranium content of water was at levels of 0.04 to 0.05 and 0.002 to 0.004 mg/1. Examination of the protein fraction of the blood serum by means of paper electrophoresis revealed certain differences in the value of the albumin–globulin coefficient. Data from animal experiments did not confirm observations on protein fractions of man. (auth)

13596 RADIO-IODINE THERAPY TO OUT-PATIENTS: THE CONTAMINATION HAZARD. Sear, R. (London Hospital). Brit. J. Radiol.; 43: 751(Oct 1970).

In the case of patients treated for thyroid carcinomas with radioiodine, as much as 75% of the administered activity can be excreted in the first 24 hours after administration. In view of the fact that the activity may be as much as several hundred millicures and urine contain as much as 1Ci per millilitre, it is suggested that protective controls of outpatients should not be abandoned. (UK)

Radiation Effects on Plants

Refer also to abstracts 13365, 13405, 13413, 13415, 13418–13420, 13423–13425, 13427, and 13568.

13597 (NP-18606) THE EFFECT OF GAMMA IRRADIATION ON PHOSPHOROUS METABOLISM AND NUCLEIC ACID SYNTHESIS IN WHEAT SEEDLINGS. Auda, H.; Mirjan, J. (Atomic Energy Commission, Baghdad (Iraq). Nuclear Research Inst.). Sep 1970. 16p. (B-1). Dep. NTIS (U. S. Sales Only).

Biochemical processes and active uptake of phosphate in wheat seedlings are found to be affected by irradiation. The influence of 5, 10, 20, 30, and 50 krad of γ irradiation on seedlings from irradiated seeds and seedlings of nonirradiated seeds was studied. A fractionation following absorption of phosphate-^{32}P at 26°C and

XUM

constant light showed that the relative incorporation into the acid soluble fraction, alcohol fraction, RNA, and DNA increased as the time incubation was increased. Also the rate of irradiation showed a large effect on absorption of phosphate-^{32}P, where it was increased specially for 5, 10, and 20 krad and decreased as the dose rate increased. Irradiated seedlings showed less response to irradiation after 24 hrs. There were slight changes in the content of inorganic phosphate except for 5 krad treatment which gave higher radioactivity for all fractions. (auth)

13598 EFFECT OF IONIZING RADIATION ON THE CONTENTS OF ORTHO-OXYPHENOL IN POPLAR SHOOTS. Kreitsberg, Z. N.; Sergeeva, V. N.; Grabovskii, Ya. K. (Inst. of Wood Chemistry, Riga). Khim. Drev.; No. 2, 13-15(1968). (In Russian).

Studies of poplar shoots raised from scions of Populus trychocarpa irradiated by γ rays with doses up to 5000 R and fast neutrons of up to 1000 R showed an increase in ortho-oxyphenol to over twice the amount observed in the control shoots. Data obtained confirmed Kuzin's theory on the increase of orthophenols in irradiated growing tissue. (R.V.J.)

13599 TAUTSAIMNIECIBA DERIGIE AUGI. V. (Plants in National Agriculture. V). Ripa, A. (ed.). Riga; Izdevnieciba Zinatne (1970). 236p.

Twenty chapters are included that discuss the selection of plants for use in agriculture and as folk medications. The biology and physiology of plants, including legumes, tobacco, apples, and tomatoes are discussed as well as effects of various minerals on amino acid synthesis and the translocation of nutrient elements. The influence of γ rays on the harvest and stimulation of growth of hot-house cucumbers was estimated. Effects of pre-sawing γ irradiation of seeds on sexual differentiation of plants were also considered. (R.V.J.)

13600 OPTICAL PROPERTIES OF LEAVES OF PLANTS OBTAINED FROM IRRADIATED SEEDS. Dzhavrshyan, Dzh. M. (Erevan State Univ.). Biol. Zh. Arm.; 23: 80-5(Jan 1970). (In Russian).

Air-dried bean seeds were given x ray doses of 0.1, 0.5, 2, 4, 6, 8, and 10 kR at a dose rate of 50 R/min. The seeds were raised under hothouse conditions. The absorption, reflection, and transmission spectra of the leaves were measured on a spectrophotometer. The greatest spectra changes took place at a 10 kR dose which produced small thick leaves whose surface was about 10% smaller than in the control leaves. The surface mass in the control leaves was 0.0175 g/cm^2, while it was 0.0229 g/cm^2 in leaves obtained from seed given a dose of 10 kR. The increase in optical density and smoothing out or leveling of the spectral maxima were brought about because of the increase in surface mass of the leaves, the occurrence of a rough surface, and the formation of white spots on the leaves by irradiation. These factors led to scattering and reflection of light by the leaf. The pigment content of the leaves was found by paper chromatography to be the following in mg per 1 g of dry leaves whose seed had a 10 kR dose: chlorophyll a 1.1500; chlorophyll b 0.5650; carotene 0.0464; violaxantin 0.0597; and lutein 0.0259, while the control leaves showed 1.5000, 0.7460, 0.0485, 0.0865, and 0.0277 respectively for these pigments. (TTT)

13601 INFLUENCE OF TEMPERATURE SHOCKS AFTER THE IRRADIATION OF POLLEN FROM NICOTIANA TABACUM ON THE FORMATION OF SEEDS AND PLANTS. Dryanovska, O. A. (Dept. of Cytogenetics, Sofia). Compt. Rend. Acad. Bulg. Sci.; 23: 995-8(1970).

Investigations were carried out to study the effects of a temperature shock of low-high temperature immediately following γ irradiation of Nicotiana tabacum on the formation of seeds and plants. Immediately following irradiation the pollen was placed at 0°C for 4 hr, after which pollination was carried out under conditions of hothouse cultivation 20 to 25°C. The results indicated that low temperature following irradiation intensified the repair processes in the pollen and tended to reduce the damaging effects of the radiation. (P.B.M.)

13602 EFFECTS OF ^{60}Co γ RAYS ON THE EARLY RIPENING AND HARVEST OF COTTON AT VARIOUS LIGHT CONDITIONS. Sadykov, S. S.; Avtonomov, V. A. (Inst. of Experimental Plant Biology, Tashkent). Uzb. Biol. Zh.; 14: No. 4, 58-9(1970). (In Russian).

Effects of day-light duration on the early ripening and harvest of 1306-DV and C-460 cotton seeds irradiated with γ rays with the 1000, 2000, and 6000 R doses were studied. It was found that irradiation with 6000 R and short day-light (10 hr) resulted in ripening of the 1306-DV plants 16 days earlier and 2 days earlier in C-460. Irradiation with 6000 R in a prolonged day light (24 hr) strongly injured both types of plants and produced many sterile plants. Doses of 1000 and 2000 R during 10 hr day light did not produce any effects on the examined cotton plants. (R.V.J.)

13603 EFFECT OF REPEATED GAMMA IRRADIATION ON THE RADIOSENSITIVITY AND MUTABILITY OF TWO-ROWED SPRING BARLEY. Yankulov, Merko (Inst. of Genetics and Plant Breeding, Sofia). Genet. Selek.; 2: 305-12(1969). (In Bulgarian).

The present study was designed to investigate the radiosensitivity of the two-rowed spring barley varieties Fraja and Imperial to repeated ^{60}Co gamma-radiation in doses of 5, 10, 15, and 20 kR with a rate of 78 and 240 R/min. It was found that the inhibitory effect of repeated radiation on height and survival of plants is weaker by two-fold than that of a single treatment. The emergence period was prolonged and plant sterility augmented as a result of repeated radiations. Plants of both varieties show a higher radiosensitivity at greater radiation doses. (auth)

13604 STUDIES IN RADIOSENSITIVITY AND DNA METABOLISM INHIBITION. SITES OF THE INHIBITION ARE TMP SYNTHESIS OR dCMP SYNTHESIS. Munechika, Hirotsugu (Showa Univ., Tokyo). Showa Igakkai Zasshi; 29: 504-17(Sep 1969). (In Japanese).

Experimental studies on the relation of radiosensitivity to the growing phase, to inhibition of DNA metabolism, and to labeled TdR uptake in respect to DNA synthesis were performed on yeast cells. The sites of the inhibition were TMP synthesis or dCMP synthesis. The following results were obtained: In the incorporation of labeled TdR into the cell, the time of its high rate was in agreement with the time of radiosensitivity. It was suggested that the initial induction of enzymes involved in TMP synthesis was the key to the radiosensitivity. The incorporation of labeled TdR into the cells was increased by irradiation. These results might show that there were some questions in labeled TdR incorporation being used as an adequate indicator of DNA synthesis. However, the incorporation was much less in yeast cells than in Escherichia coli or in mammalian cells. Enhancement of irradiation with 5-FU was remarkable but not with BUdR in yeast cells. The administration of TMP, dUMP, AdR, GdR, and hydroxyurea in high concentration caused cell growth inhibition and this inhibition was slightly prevented by addition of dCMP to the medium. Hydroxyurea inhibition was slightly prevented by addition of dCMP, AdR, and GdR. From the results, it was suggested that the substances were inhibitors in the deoxyribosidation step from CDP to dCDP. The inhibitions did not change the radiosensitivity, excepting hydroxyurea, that enhanced it when used for pretreatment. (auth) (Japan)

13605 GAMMA-RAY-INDUCED SPORE GERMINATION OF DICTYOSTELIUM DISCOIDEUM. Khoury, A. T.; Deering, R. A.; Levin, G.; Altman, G. (Pennsylvania State Univ., University Park). J. Bacteriol.; 104: 1022-3(Nov 1970).

Cobalt-60 γ rays induced germination of the spores of the cellular slime mold, Dictyostelium discoideum, in the absence of heat shock, amino acids, or bacteria food source. About 65% amoeba emergence occurred 13 hr after a dose of 180 krad. (auth)

Radiation Effects on Microorganisms

Refer also to abstracts 13342, 13386, 13406–13408, 13411, 13412, 13414, 13416, 13421, 13422, 13428, 13568, 13617, 13620, and 13623.

13606 UV-SENSITIVITY OF THE WILD-TYPE AND DIFFERENT UVS MUTANTS OF SCHIZOSACCHAROMYCES POMBE. INFLUENCE OF GROWTH STAGES AND DNA CONTENT OF THE CELLS. Fabre, F. (Faculte des Sciences, Orsay, France). Mutat. Res.; 10: 415-26(Nov 1970).

Cells of a wild type strain of the yeast Schizosaccharomyces pombe are more uv resistant during the logarithmic phase than during the stationary phase of growth. With caffeine in the post-irradiation medium, this difference in sensitivity is maintained. For most uv sensitive strains studied, the inverse result was obtained: cells are more sensitive at low doses if irradiated during the logarithmic phase. Liquid holding of cells irradiated during the stationary phase increases the lethality for the wild type strain, and the survival for some uv sensitive mutants. During the logarithmic phase, liquid holding of cells induces lethality even of unirradiated cells. The more uv resistant the cells, the more rapid is this induction of lethality. An interpretation of these results is that there are at least two repair mechanisms. One that would be responsible for the high resistance of the wild type strain. A second one, not sensitive to caffeine, would act in most uv sensitive strains studied. Study of the uv sensitivity of cells whose genetic material is duplicated (2c cells) or not duplicated (1c cells) shows that for the wild type strain and several uv sensitive mutants the 1c cells are more uv sensitive. The shoulder of the survival curves is smaller and the final slope more accentuated. However, cells 2c and 1c of one uv sensitive mutant have the same uv sensitivity. This indicates that the higher resistance of the 2c cells is due to a repair mechanism which acts only if the genetic material is duplicated. (auth)

13607 ROLE OF PYRIDINE NUCLEOTIDES IN THE CONTROL OF RESPIRATION IN ULTRAVIOLET-IRRADIATED ESCHERICHIA COLI B/r CELLS. Swenson, P. A.; Schenley, R. L. (Oak Ridge National Lab., Tenn.). J. Bacteriol.; 104: 1230-5(Dec 1970).

Escherichia coli B/r cells grown on glycerol containing medium and irradiated with uv to about 1% survival respire for about 1 hr and then cease completely for several hours. The results of studies on cell-free respiration and analyses of pyridine nucleotide levels at various times after uv irradiation show that the cessation of respiration is associated with two changes—loss of glycerol kinase activity and complete disappearance of pyridine nucleotides. Under other cultural conditions in which respiratory inhibition is less complete and more transitory, the losses of pyridine nucleotides are smaller, and the rises that follow are correlated with increases in respiratory activity. (auth)

13608 REQUIREMENT OF CELLULAR SYNTHESIS FOR KILHAM RAT VIRUS REPLICATION. Tennant, Raymond W.; Hand, Russell E. Jr. (Oak Ridge National Lab., Tenn.). Virology; 42: 1054-63(Dec 1970).

X irradiation of rat embryo cells before infection with Kilham rat virus (KRV) impaired the capacity of the cells to synthesize the virus. Dose response assays indicated that the cell population was composed of a radiosensitive fraction with an approximate mean lethal dose (D_0) of 82 R and a radioresistant fraction with a D_0 of about 1990 R. Irradiation with uv light likewise abolished cellular capacity for virus synthesis; and, as with the x rays, the dose response assay could be resolved into a two component curve. A dose of approximately 8 ergs/mm^2 was the D_0 for the radiosensitive fraction of cells and 129 ergs/mm^2 the D_0 for the resistant fraction. Finally, treatment of cells with 5-fluorouracil prior to infection also impaired capacity for replication of KRV, but neither x radiation, uv light, nor 5-fluorouracil decreased the capacity of rat embryo cells to support pseudorabies virus replication. Therefore, KRV requires cell function(s) not required by other DNA viruses which replicate in the nucleus, and evidence suggests that the function(s) involves DNA synthesis. (auth)

13609 INACTIVATION OF MURINE SARCOMA AND LEUKEMIA VIRUSES BY ULTRA-VIOLET IRRADIATION. Kelloff, Gary (National Cancer Inst., Bethesda, Md.); Aaronson, Stuart A.; Gilden, Raymond V. Virology; 42: 1133-5(Dec 1970).

Murine sarcoma virus contains both transforming sarcoma virions (MSV) and nontransforming leukemia virions (MuLV). This study was undertaken to distinguish the transforming function of MSV from the replicating function of MuLV by comparing their rates of inactivation by uv. The results showed that the inactivation of both functions followed single-hit kinetics and exhibited very similar inactivation rates. (P.B.M.)

13610 EFFECTS OF REDUCTONE ON IRRADIATED E. COLI. Gomes, R. Alcantara; Mayr, L. M.; de Souza, C. M.; Caldas, L. R. (Univ. Federal, Rio de Janeiro). Int. J. Radiat. Biol.; 18: 439-49(1970). (In French).

The keto-aldehyde reductone ($HOCH_2COCHO$) blocks macromolecular (DNA, RNA, and protein) syntheses and respiration in Escherichia coli. The blockage is reversible and apparently due to the inhibition of oxydative phosphorylation. $10^{-2}-10^{-3}$M reductone has a negligible lethal effect on unirradiated cells. However, if bacteria are submitted to uv rays (2537 Å) and then treated with reductone, a significant lethal effect is observed. The lethal effect decreases as a function of the time elapsed between irradiation and treatment of cells with reductone. Experiments made with starved bacteria show that the lethal effect of the keto-aldehyde is not related to the blockage of oxydative phosphorylation. However, the experiments which show the decreasing lethal effect of reductone as a function of the time elapsed between uv irradiation and treatment of cells with the keto-aldehyde, and the similarity of the effects of reductone and caffeine on bacteria previously submitted to uv rays, suggest that the lethal effect of the keto-aldehyde is due to an inhibition of repair mechanisms. (auth) (UK)

13611 RADIATION SURVIVAL OF BACTERIAL SPORES IN NEUTRAL AND ACID ICE. Grecz, Nicholas; Upadhyay, J. (Illinois Inst. of Tech., Chicago). Can. J. Microbiol.; 16: 1045-9 (Nov 1970).

Spores of Clostridium botulinum 33A were γ-irradiated at pH 2, 3, 4, 5, 6, and 7 to 0.6, 0.7, and 0.9 Mrad. Temperatures were controlled at −196°C to 0°C in distinct intervals. The survival data presented a complex wave-like pattern that appeared to be influenced by pH, temperature, and radiation dose. Three typical survival patterns could be recognized. Pattern A (at −190°C) showed peaks of high survival at pH 4 and 7 and low survival at pH 2 and 6. Pattern B (at −50, −40, and −30°C) showed peaks of high survival at pH 3 and 6 and low survival at pH 2, 4 to 5, and 7.0. Pattern C (at 0°C) was similar to pattern A but had generally higher peaks and deeper troughs. Between the temperatures showing typical A, B, and C patterns, the survival profiles indicated various degrees of transition from A to B or from B to C. The effect of pH appears to be related to its influence on yield of radicals in water such as, for example, ·OH which may result in highly lethal conditions within the region of low spore survival, and extinction of ·OH by reaction with H· at the peaks of spore survival. (auth) (Canada)

13612 COMPARISON OF THE LETHAL EFFECTS OF ^{32}P AND ^{33}P DECAY IN E. COLI AND IN BACTERIOPHAGES. Krisch, Robert E. (Argonne National Lab., Ill.). Int. J. Radiat. Biol.; 18: 259-66(1970).

The lethal effects of ^{32}P and ^{33}P were compared for T1 and T4 bacteriophages and for radio-sensitive and -resistant strains of Escherichia coli. A ^{33}P decay in either bacteriophage, stored at −196°C, is only about half as likely to be lethal as is a ^{32}P decay, implying that about half of all ^{32}P lethalities under these conditions are due to nuclear recoil. At a storage temperature of +4°C the lethal efficiency per decay due to nuclear recoil is about the same as at −196°C, although overall lethal efficiency per decay is considerably higher at +4°C for both isotopes. In the four strains of E. coli tested, B_{s-1}, K−12 AB2463, K−12 AB1157 and 15THU, all stored at −196°C during decay, there is no evidence for a greater lethal efficiency per decay for ^{32}P than from ^{33}P, implying that nuclear recoil is unimportant in ^{32}P killing of E. coli. A model is proposed that explains the greater sensitivity of bacteriophage to lethality from nuclear recoil by the interruption of transfer of phage DNA into the host cell. (auth) (UK)

13613 INFLUENCE OF CHLORAMPHENICOL ON IRRADIATED BACTERIA. Mukherjee, P.; Bhattacharjee, S. B. (Saha Inst. of Nuclear Physics, Calcutta). Z. Naturforsch.; 25b: 1071-2(Sep 1970).

A study was made of the response of x-irradiated and uv-irradiated Escherichia coli to treatment with chloramphenicol. The results showed that the bacteria that were normally insensitive to the action of chloramphenicol with respect to their colony-forming ability became sensitive following exposure to x rays. Chloramphenicol used in the culture media of uv-irradiated cells did not influence the survival rate of the bacteria. X-irradiated cells incubated in a buffer showed a gradual decrease in population due to peroxide formation. This indicated that the death of x-irradiated bacteria due to the presence of chloramphenicol and the death of uv-irradiated cells in its presence or absence were not a manifestation of peroxide action. The reasons for increased chloramphenicol mortality among x-irradiated cultures while uv-irradiated bacteria showed no sensitivity were not clear. (E.E.H.)

13614 ISOLATION AND CHARACTERIZATION OF THYMINELESS MUTANTS FROM ULTRAVIOLET-SENSITIVE BACILLUS SUBTILIS STRAINS. Felkner, Ira C. (Univ. of Texas, Dallas). J. Bacteriol.; 104: 1030-2(Nov 1970).

Thymineless mutants of Bacillus subtilis 168 ind, hcr-9 were isolated by using trimethoprim. These and other Thy$^-$ strains differed drastically from Thy$^+$ ones in their patterns of [^{3}H]thymidine uptake and growth in trimethoprim-containing medium. Transformation was negligible between most mutants derived from the uv-sensitive strain 168 ind, hcr-9 but significant between 168 ind, thy, and these mutants. The latter and these new mutants all grow in the presence of trimethoprim plus thymidine or thymine and fail to grow if thymine or thymidine is omitted. (auth)

13615 ANALYSIS OF SV40-INDUCED TRANSFORMATION OF HAMSTER KIDNEY TISSUE IN VITRO. VII. INDUCTION OF SV40 VIRUS FROM TRANSFORMED HAMSTER CELL CLONES BY VARIOUS AGENTS. Rothschild, Henry; Black, Paul H. (Massachusetts General Hospital, Boston). Virology; 42: 251-6 (Sep 1970).

Chemical agents and physical treatments were utilized to: increase the yield of infectious virus from inducible clones; determine whether the noninducible clones could be induced directly by these agents; and gain insight into mechanisms of induction of infectious virus from virogenic mammalian cell lines. Cell monolayers were exposed to uv radiation for 30 to 600 sec or were x-irradiated with 250 to 5000 rad. The cells were then washed and acriflavine, BUdR, caffeine, or mitomycin C was added. A table is

XUM

presented to show results of induction of infectious SV40 from T8-APl by these agents. Results of other investigators are discussed with regard to induction of cell lines by agents used in combination, induction of other cell lines, effect of visible light on the induction process, effect of prolonged exposure to BUdR, and chromosome changes. (H.L.W.)

13616 RELATIONSHIP BETWEEN THE SYNTHESIS OF DNA AND THE SYNTHESIS OF PHAGE LYSOZYME IN ESCHERICHIA COLI INFECTED BY BACTERIOPHAGE T4. Mark, Kaikeung (Univ. of Oregon, Eugene). Virology; 42: 20-7(Sep 1970).

In *Escherichia coli* cells infected by uv-irradiated bacteriophage T4, lysozyme synthesis may occur in the absence of DNA synthesis. The rate of lysozyme synthesis that is observed to occur in the absence of DNA synthesis is a function of the multiplicity of infection. In experiments where the level or the time of initiation of DNA synthesis was affected, the rate of lysozyme synthesis again showed a dependence on the number of phage DNA present in the infected cells. (auth)

Radiosterilization and Radiopreservation

13617 (COO-1183-32) GROWTH CHARACTERISTICS OF TYPE E CLOSTRIDIUM BOTULINUM IN THE TEMPERATURE RANGE 34 TO 50°F. Final Report, January 15, 1969–January 14, 1970. (Continental Can Co., Inc., Chicago, Ill. Metal Div. Research and Development). 24 Feb 1970. Contract AT(11-1)-1183. 59p. Dep. CFSTI.

In a second inoculated pack study on fresh cod, the following combinations of inoculation dose, incubation temperature, and radiation dose yielded the following results. When inoculated with spores of *Clostridium botulinum* at 10^6 spores/g and incubated at 46°F after exposure, samples given radiation doses of 0, 100, and 200 Krads showed Type E toxin development at 3/4 X (6 days), 1/2 X (7 days), and X (15 days). The value of X in days is the maximum product storage life of the sample as determined by a consumer panel. When inoculated with 10^4 spores/g, the same radiation doses and incubation temperature resulted in values of 1½ X (12 days), 3/4 X (10 days), and X (15 days). Samples inoculated with 10^4 spores and incubated at 50°F following irradiation, showed Type E toxin development at 3/4 X (6 days), 1/2 X (7 days), and 3/4 X (11 days) following doses of 0, 100, and 200 Krads. At 10^2 spores/g these same radiation doses gave values of 1¼ X (10 days), 1/2 X (7 days), and 3/4 X (11 days) at 50°F. Cultural studies were conducted on marine isolates of *Cl. botulinum* type C. The following factors were investigated: growth and sporulation on Egg Meat Medium; effects of preheat treatment on viable spore count; sugar fermentation ability; effects of $NaHCO_3$ on spore recovery with Beef Infusion agar; Type C toxin production on different media; effects of trypsin on toxin activation; low temperature growth ability; sodium chloride sensitivity of strains; pH sensitivity of strains; and heat resistance of spores. (E.R.B.)

13618 CHEMICAL AND PHYSICAL CHANGES IN IRRADIATED AND FROZEN BOMBAY DUCK. Kumta, U. S.; Gore, M. S. (Bhabha Atomic Research Centre, Bombay). J. Food Sci.; 35: 456-60(Jul-Aug 1970).

Bombay duck (*Harpodon nehereus*), a tropical fish, is readily susceptible to drip losses leading to textural alterations. These changes occur during storage at 0 or −20°C for 3 days and also by irradiation and storage at 0 or 10°C for 3 days. In situ denaturation of fibrillar proteins of Bombay duck occurs as evidenced by a decrease in salt-soluble proteins. Loss in extractability occurring at 0 or −20°C parallels increased drip loss, but appears to be arrested by pre-dip treatment in 10% sodium tripolyphosphate solution for 15 min. The radiation-induced drip loss also correlates with loss in the extractability at a radiation dose of 3 Mrad, but at 0.5 Mrad the drip loss occurs without appreciable decrease in the extractability. Pre-dip treatment in 10% sodium tripolyphosphate solution reduces the drip loss caused by 3 Mrad, but this is not reflected in the recovery of extractable proteins. Loss in the extractability could be attributed to the aggregation phenomenon of fibrillar proteins induced by irradiation. The radiation-induced off-odors appear to originate from the sarcoplasmic proteins. (auth)

13619 RADIATION PASTEURIZATION OF FRESH AND BLANCHED TROPICAL SHRIMPS. Kumta, U. S.; Mavinkurve, S. S.; Gore, M. S.; (and others) (Bhabha Atomic Research Centre, Bombay). J. Food Sci.; 35: 360-3(Jul-Aug 1970).

The storage life of fresh, peeled and deveined tropical shrimps at 10 to 12°C is extended to 10 to 14 and 18 to 21 days with 0.15 and 0.25 Mrad, respectively, as against spoilage of unirradiated samples within 4 days. Blanching treatment (steaming of 4 min) with or without brine (3.0% NaCl) extends the storage life up to 30 days at 10 to 12°C, the former retaining the shell-fish flavor. However, the blanched products develop musty odor and slimy texture during storage; subjected to irradiation (0.15 Mrad) these are devoid of undesirable attributes and are acceptable for 60 and 130 days, respectively, at 10 to 12°C and 2 to 4°C. Bacterial counts exceeding 10^8/g and high levels of TMAN and TVBN concur with spoilage of unirradiated shrimps. In contrast, low levels of TMAN and TVBN, despite high TBC, corroborate with high acceptability of radiation-processed shrimps. In blanched as well as blanched and irradiated shrimps TBC, TMAN and TVBN are low. Samples subjected to blanching only have low acceptability as against the improvement in quality by irradiation. These alterations in storage property have been discussed in the light of shifts in microflora. (auth)

13620 RECOVERY OF SALMONELLAE FROM IRRADIATED AND UNIRRADIATED FOODS. Licciardello, J. J.; Nickerson, J. T. R.; Goldblith, S. A. (Massachusetts Inst. of Tech., Cambridge). Contract AT(30-1)-3325. J. Food Sci.; 35: 620-4(Sep-Oct 1970).

Maximum recovery of salmonellae from artificially contaminated irradiated and unirradiated foods was usually obtained on tryptic soy yeast extract agar, a nonselective medium. Recovery on various selective media depended, in general, upon the serotype and the substrate. Irradiated cells were definitely inhibited on Salmonella–Shigella agar or desoxycholate citrate agar, but only slightly, if at all, on brilliant green, bismuth sulfite or MacConkey agars. The highest count of irradiated cells of *Salmonella newport* by the MPN method was obtained with tetrathionate broth, yet this medium was inhibitory to *Salmonella oranienburg* and *Salmonella heidelberg*. In this latter situation, pre-enrichment in nutrient broth prior to inoculation into tetrathionate broth was beneficial. (auth)

13621 CYTOLOGICAL EFFECTS OF JUICE OR PUREE FROM IRRADIATED STRAWBERRIES. Ross, Sarah T.; Bradley, Muriel V.; Oka, Janet A. (Univ. of California, Davis). Contract AT(11-1)-34. J. Food Sci.; 35: 549-50(Sep-Oct 1970). (UCD-34-P-73-29).

Vicia faba roots were treated 4 hr with undiluted juice or puree from strawberries irradiated with 200 or 400 Krad of gamma radiation from ^{60}Co and from control berries. 200 Krad would be the highest feasible dose for strawberries as a fungicidal treatment to extend shelf life without causing unfavorable changes in fruit quality. The differences between percentages of abnormal anaphases after treatments with juice or puree from irradiated and control berries were not significant at the 1% level ("t" test) in all the 7 experiments with 200 Krad as the radiation dose, and in 6 of 7 experiments when the dose was 400 Krad. In 1 experiment with a 400-Krad dose, the difference between percentages of abnormal anaphases was barely significant at the 5% level of confidence. (auth)

13622 ON THE COMMERCIALIZATION OF IRRADIATED FOOD. Ulmann, R. M. (Stichting Proefbedrijf voor Voedselbestraling, Wageningen, Netherlands). Ind. Obst- Gemueseverwert.; 55: 269-70(1970). (In German).

Pilot studies were made on the commerical applications of mushroom and potato radiopreservation. During three successive years 80, 16, and 80 tons of potatoes were irradiated in semitechnical tests. The dose was reduced from 13 to 8 krad in order to avoid damage and to reduce costs. A general license for the sale of irradiated potatoes was expected before the 1970 harvest. A general license for mushroom preservation was available in late 1969. Negotiations with a wholesale firm are underway and sale to consumers will begin in 1970. Irradiation of packaged goods for increased shelf-life was quite successful and progress with other foods (spices, pot-herb, fruit) was reported. (E.E.H.)

13623 FOOD PRESERVATION WITH IONIZING RADIATION. ACTION OF ENZYMES. Venosa, Francesco. Ind. Aliment. (Pinerolo, Italy); 5: No. 25, 52-8(30 Oct 1966). (In Italian).

The present state of knowledge in the area of food preservation by ionizing radiations was summarized. The types of radiation used and the effects of radiation on microorganisms and insects in the preservation of meats, fruits, and grains were considered. The economic aspects of this process are also indicated. (J.S.R.)

13624 HYGIENIC ASSESSMENT OF CHICKEN MEAT IRRADIATED WITH PASTEURIZING DOSES OF γ-RAYS. Shillinger, Yu. I.; Kachkova, V. G. (Inst. of Nutrition, Moscow). Gig. Sanit.; No. 6, 44-8(Jun 1968). (In Russian).

Rats were fed chicken meat treated with 600 Krad doses of γ irradiation. The chicken meat made up 60% of the protein and 50% of the fat of the diet. No harmful effects were observed following daily feeding for a period of six months. (auth)

METALS, CERAMICS, AND OTHER MATERIALS

Metals and Alloys

13625 PLUTONIUM-DOKUMENTATION. Referate-Zeitschrift mit Anhang Transplutonium-Elemente. September 1970. Band 4, Heft 9. 195 Referate (Register-Nr.3021-3378) 72 Referate (Register-Nr.407T-478T). (Plutonium-Documentation. Abstract Journal With Appendix on Transplutonium Elements. September 1970. Vol. 4, No. 9. 195 Abstracts (Register No. 3021-3378) 72 Abstracts (Register No. 407T-478T)). Karlsruhe, Ger.; Gesellschaft fuer Kernforschung m.b.H (1970). 115p. (In German and English).

13626 PLUTONIUM-DOKUMENTATION. Referate-Zeitschrift mit Anhang Transplutonium-Elemente. November 1970. Band 4, Heft 11. 220 Referate (Register-Nr.3842-4285) 55 Referate (Register-Nr.534T-588T). (Plutonium-Documentation. Abstract Journal With Appendix on Transplutonium Elements. November 1970. Vol. 4, No. 11. 220 Abstracts (Register No. 3842-4285) 55 Abstracts (Register No. 534T-588T)). Karlsruhe, Ger.; Gesellschaft fuer Kernforschung m.b.H (1970). 126p. (In German and English).

13627 INTEGRATED PROGRAM LIBRARY FOR MATERIAL PROPERTY DATA. Pee, A.; Schumann, U. (Gesellschaft fuer Kernforschung mbH, Karlsruhe, Ger.). Nucl. Eng. Design; 14: 99-103(Oct 1970).

A program system for material property data (MAPLIB) is introduced which is available for incorporating large quantities of material data in a form suitable for computer programs. MAPLIB consists of a multitude of Fortran Function subprograms — one for each material property — which are in accordance with some conventions relative to form, nomenclature and units. The data can be retrieved by problem programs in a flexible mode. As far as possible errors in retrieval requests are supervised. For the integration of new data functions in MAPLIB a utility is available. (auth)

13628 PRINCIPLES OF ELECTRON MICROSCOPY AT HIGH VOLTAGES AND A COMPARISON 100 TO 200 kV. Warlimont, Hans (Max-Planck-Institut fuer Metallforschung, Stuttgart). Prakt. Metallog.; 7: 654-78(Dec 1970). (In German and English).

The use of higher accelerating voltages in electron microscopy was studied with reference to the different influences of elastic and inelastic scattering on contrast, resolving power and image intensity. The results are presented of a comparison of images produced at 100 and 200 kV accelerating voltage. Radiation damage to specimens in the electron microscope is also discussed. It is noted that these effects are currently being investigated. (J.R.D.)

Corrosion and Erosion

Refer also to abstract 15357.

13629 (EIR-184) CORROSION OF ZIRCONIUM ALLOYS IN SUPERHEATED STEAM: RESULTS OF THE PROLONGED EXPERIMENTS. Gruetter, A. (Eidgenoessisches Institut fuer Reaktorforschung, Wuerenlingen (Switzerland)). Jul 1970. 63p. (In German). Dep. NTIS (U. S. Sales Only).

The corrosion behavior of seven alloys (Ozhennite, Zr–1.5 Nb, Zr–Cu–Fe, Zr–Cr, Zr–Cr–Si, Zircaloy-2, and Zr–2.5 Nb) was investigated in steam at 50 atm and 350 and 450°C over a prolonged period. The behavior both at 350 and 450°C varies sharply among the alloys. With the exception of Zr–1.5 Nb, an exponent of about 3 at 350°C and about 2.5 at 450°C was established for all the alloys in the pretransition range. The alloys vary greatly with respect to the transition point data. The time up to the transition point, for example, varies at both temperatures from several days (Zr–Cr) to over 750 days (Zr–Cu–Fe). The phenomenon of transition is connected with a "cloud formation" observed under the microscope and it is very probably conditional on hollow formation in or under the oxide layer. The appearance of the transition cannot be correlated with the formation of microscopically observable fissures perpendicular to the surface. In Zr–Cr and Zr–Cr–Si, transition is strongly localized in which large surface pieces with penetration oxide surface areas with thick post-transition oxide occur next to each other for prolonged periods. The curve is not strictly linear in the post-transition region. Zircaloy-2 shows also at both temperatures in the post-transition region a cyclic behavior. During grinding hollows were observed in all post-transition oxides. These are very often arranged in layers parallel to the surface. In Zr–2.5 Nb marked local attacks were observed. Fissure formation perpendicular to the surface occurs relatively late in the post-transition region. Zr–Cu–Fe at 450°C is an exception. An effect of this fissure formation on the weight increase-time curve could not be established. The results show clearly that it is possible on the basis of the behavior in the post-transition region to predict the appearance of the transition or the behavior in the post-transition region. The transition time is shown to be unusable since Ozhennite, Zr–1.5 Nb, Zircaloy-2, and Zr–2.5 Nb are independent of the layer thickness reached at 450°C and not mentioning deviation at 350°C show a curve which is very similar to that of a blank at 350°C. The transition time of samples of Zr–Cr–Si shows abnormally high corrosion rates at 350°C. In Zr–Cu–Fe the post-transition region was not attained and Zr–Cr corrodes too fast to permit transition studies. With respect to the hydrogen uptake, there is in general in the post-transition region a linear relation with the oxygen uptake. Very large variations were found in which Zr–2.5 Nb absorbs 20% of the theoretical hydrogen, but Zr–Cr–Si absorbs 100%. The hydrogen absorption in the pre-transition region at 450°C is negligibly small in comparison with that in the post-transition region. At 350°C the rates with respect to hydrogen absorption are too uncertain to permit conclusions. (tr-auth)

13630 (EUR-4298) CORROSION IN HIGH-TEMPERATURE LITHIUM HEAT PIPES WITH NIOBIUM–ZIRCONIUM AND TANTALUM AS WALL MATERIAL. Busse, C. A. (European Atomic Energy Community, Ispra (Italy). Joint Nuclear Research Center). 1969. 32p. Dep. NTIS (U. S. Sales Only).

In Nb–1 Zr or Ta heat pipes with Li as working fluid, operated at temperatures of 1500 or 1600°C, corrosion can cause a wall perforation in the heating zone within a few hours. Analysis of such heat pipes, together with fluiddynamic and thermodynamic considerations, leads to the conclusion that the corrosion is caused by the initial oxygen content of the wall material. The corrosion mechanism consists in the transition of oxygen from the wall material of the cooling zone to the liquid Li, the transport of the oxygen to the heating zone, the local increase of the oxygen concentration in the liquid Li by the evaporation process and finally the wall attack by this oxygen-rich Li. The corrosion can be strongly reduced or completely inhibited by deoxidation of the wall material, by the addition of Ca to the Li, or of Y to the Ta. (auth)

13631 ANODIC DISSOLUTION OF Mo IN CHLORIDE–MOLYBDATE MELTS. Shunailov, A. F.; Baraboshkin, A. N.; Martynov, V. A. Tr. Inst. Elektrokhim., Akad. Nauk SSSR, Ural. Filial; No. 13, 40-8(1969). (In Russian).

The anodic dissolution of metallic Mo in $CaCl_2$–$CaMoO_4$ melts at 800 to 1000°C was studied. Results revealed that dependent on anode current density three processes evolve. At low current densities the dissolution proceeds with the formation of molybdate ions. With increase of CaO content the saturated current of the process increases and the potential is shifted to negative. At higher current densities an anodic film forms which is about the composition of Mo_2O_3 and then gaseous molybdenum chlorides are formed. Timed potentiometric measurements were used to determine the rates of oxygen-ion and molybdate-ion diffusion in the melt. At 900°C they are equal to 3.4×10^{-5}, and 1.8×10^{-6} cm^2/sec^{-1}, respectively. (tr-auth)

13632 PERSPECTIVES ON CORROSION OF MATERIALS. Fontana, Mars G. Met. Trans.; 1: 3251-66(Dec 1970).

Perspectives on corrosion look back 10 years or so and into the seventies. General ignorance by many engineering disciples and others and resultant costly failures are emphasized. The scope of the corrosion problem is described. Discussed are forms of corrosion and methods for combatting; secondary reactions; effects of materials structure; advances in techniques for measuring corrosion; important developments; and needs for the 1970's. Need for involvement by metallurgists is emphasized. (auth)

13633 INTERCRYSTALLINE CORROSION OF THE N70M28-TYPE ALLOYS. Pavlov, S. S.; Svistunova, T. V. (Inst. for Chemical Machine Construction, Moscow. Central Scientific Research Inst. for Ferrous Metallurgy, Moscow). Metalloved. Term. Obrab. Metal.; No. 10, 20-2(1970). (In Russian).

The influence of tungsten, titanium, and zirconium on the tendency of the Ni–Mo N70M28-type alloys toward intercrystalline corrosion was investigated by developing a temperature-time-corrosion diagram for the tempered and annealed specimens. The study was based on metallographic examination after im-

XUM

mersing the specimens into boiling, 21% HCl solution for 240 hours. The alloy was found to exhibit intercrystalline corrosion at elevated temperatures; this was attributed to the presence of a continuous network of carbides at the grain boundaries. It was found that introduction of 3.5 to 5.3% of tungsten eliminated this tendency; on the other hand, additions of 1.1 to 2.6% of titanium and 0.012 to 0.23% of zirconium accelerated the corrosion. The intercrystalline corrosion at both high and low temperatures was attributed to the formation of an intermetallic Ni_4Mo phase, resulting in stresses. The strong carbide formers, such as tungsten, titanium, and zirconium did not affect this tendency at low temperatures. (TTT)

13634 MOLYBDENUM TREATMENT FOR INCREASING THE STABILITY OF STEEL NO. Kh18N9T IN LIQUID LITHIUM. **Dubinin, G. N.; Karpman, M. G.; Benediktova, G. P.; Granovskii, E. B. (Moscow Inst. of Aviation). Metalloved. Term. Obrab. Metal.; No. 10, 54-6(1970). (In Russian).**

Treatment with molybdenum was used to increase the resistance of austenitic chromium–nickel steels against liquid lithium. The treatment was carried out by the contact method with molybdenum powder applied at the vacuum of 10^{-3} to 10^{-4} mm of Hg. The treated Kh18N9T-type steel was tested in lithium and in air at 900°C. The results indicated that the molybdenum-treated specimens had a higher resistance against lithium than the untreated ones. This may be attributed to the slowing down of the diffusion of chromium, nickel, and titanium toward the surface and their dissolution in the lithium. The diffusion layer also serves as a barrier which delays the migration of dislocations toward the outside and thus inhibits the formation of microcracks. (TTT)

13635 CHANGES IN THE SURFACE OF URANIUM AND ITS HYDRIDES DURING SUCCESSIVE HYDROGENATIONS AND DEHYDROGENATIONS AT VARIOUS TEMPERATURES. **Caralp-Amilhat, Francoise; Destriau, Michel (Bordeaux Univ., Talence, France). Compt. Rend., Ser. C; 271: 1265-8(23 Nov 1970). (In French).**

A great difference exists between the volumic masses of U and its hydride; in consequence, when it is subjected to successive hydrogenation and dehydrogenation cycles, the metal becomes increasingly powdery. Its specific surface increases up to a limiting value for which powder production by hydrogenation is compensated by the agglomeration during the dehydrogenation. (auth) (France)

13636 CORROSION WEEK. **41st Manifestation of the European Federation of Corrosion, 7–12 October, 1968 in Budapest. Farkas, T. (ed.). Budapest; Akademiai Kiado (1970). 1084p. (In several languages). (CONF-681084).**

Approximately 126 lectures concerning recent research results on corrosion and surface protection, are presented. Information is included on theory of corrosion, use of inhibitors, metallic coatings, surface protection by paints and plastics, electroplating, corrosion testing, and procedures for temporary corrosion protection (J.R.D.)

13637 SELECTIVE GROWTH OF PITS ON A STAINLESS STEEL IN A CHLORINATED OXIDIZING MEDIUM. Monnier, Anne; Coriou, Henri; Pinard-Legry, Gerard; Plante, Georges (CEA, Fontenay-aux Roses, France). Compt. Rend., Ser. C; 271: 981–4(19 Oct 1970). (In French).

In a chlorinated oxidizing solution, stainless steel corrodes by pitting; for the most part these corrosion sites, which can be numerous, become passive again with time; only a few pits develop and then offer a protection to the whole metal. (auth) (France)

Preparation and Fabrication

Refer also to abstracts 13169 and 13743.

13638 (ORNL–4313-3) FABRICATION PROCEDURES AND ACCEPTANCE DATA FOR ASTM A-533 WELDS AND A 10-IN. THICK ASTM A-543 PLATE OF THE HEAVY SECTION STEEL TECHNOLOGY PROGRAM, DOCUMENTARY REPORT 3. **Childress, C. E. (Oak Ridge National Lab., Tenn.). Jan 1971. Contract W-7405-eng-26. 86p. Dep. NTIS.**

Several heavy-gage ASTM A-533 grade B steel plates have been purchased for evaluation by the Heavy Section Steel Technology (HSST) program. The fabrication histories of these plates were presented in ORNL-4313 and ORNL-4313-2. To provide weldments for investigation, practically all of the edge material from the first HSST plate was used to fabricate submerged-arc and shielded-metal-arc weldments. The weldments were made by fabricators who produce nuclear reactor pressure vessels and related components to the requirements of Sect. III of the ASME Code for Nuclear Vessels. Each of the weldments was made in accordance with Code requirements, and the welding parameters and available test data are presented. An effort was made to procure an electroslag weldment made to the requirements of Sect. III. However, no vendors were currently using this process in the fabrication of nuclear pressure vessels. A portion of an electroslag weldment was donated to the HSST program by the General Electric Corporation. Data relative to this weldment are presented in addition to the data for submerged-arc and shielded-metal-arc weldments. To provide additional base material for investigation, a 10-in.-thick ASTM A-543 steel plate was purchased. This report provides the fabrication and processing history of that A-543 plate. (auth)

13639 (ORNL–4590, pp 1-19) PROGRAM ADMINISTRATION AND PROCUREMENT. **(Oak Ridge National Lab., Tenn.).**

From Heavy-Section Steel Technology Program.

The Heavy-Section Steel Technology (HSST) Program was initiated to study the structural behavior of thick-section plates and pressure vessels fabricated from such plates for use in light-water power reactor systems. The broad spectrum of investigations of the HSST program covers metallurgy, chemistry, material properties, inspection, analytical and experimental stress and strain analyses, environmental effects, fracture mechanics, and the general area of fracture behavior. During this reporting period six subcontract or subcontract extensions were negotiated. Bids were solicited for fabricating the first six intermediate test vessels. After review the award was made to Taylor Forge Division of Gulf and Western Products Company. Fabrication was started immediately. A major effort was the revising and updating of the HSST program plan. The revised program was completed. (J.R.D.)

13640 (TRG-Report–2040) THE MATRIX PRECIPITATION OF NbC IN 20/25/Nb STAINLESS STEEL. Rowcliffe, A. F.; Winton, J. (United Kingdom Atomic Energy Authority, Springfields (England). Reactor Group). 1 Jun 1970. 12p. Dep. NTIS (U. S. Sales Only). UK 3s. 0d.

A series of heat treatments carried out on a 20/25/Nb stainless steel are described, the aim of which was to define the conditions necessary to attain a fine homogeneous dispersion of NbC. Solution heat-treatment temperatures above 1200°C are essential to attain sufficient solute supersaturation, and the most consistent results are subsequently obtained by quenching direct to an aging temperature of about 700°C. If the material is cooled to room temperature before aging, the cooling rate for successful precipitation is very critical. The correct heat treatment conditions would not be easily attained in commercial practice. (auth)

13641 (UCRL-Trans–10503) PROCESS FOR THE REMOVAL OF GASES HELD IN INTERSTITIAL SITES FROM TITANIUM, ZIRCONIUM, HAFNIUM, OR THORIUM. Rieck, G. D.; Bruning, H. A. C. M. Translated by R. Dewar for Univ. of California Lawrence Radiation Lab., Livermore, from German Patent 1,188,301. 6p. Dep. NTIS.

An abstract of this paper, prepared from the original language, appeared as NSA 19: 36564. (auth)

13642 NIOBIUM PRECIPITATION ON LIQUID ZINC CATHODE. **Ivanovskii, L. E.; Kozlov, F. N.; Plekhanov, A. F. Tr. Inst. Elektrokhim., Akad. Nauk SSSR, Ural. Filial; No. 13, 63-7 (1969). (In Russian).**

Results of investigation are reported of the precipitation on liquid Zn cathode in electrolysis of alkali metal chloride melts incorporating a soluble anode and effecting reduction of $NbCl_3$ and K_2NbF_7 by Zn. It was found that Zn is useful as liquid cathode or as reducing agent for preparing powders of Nb and Nb alloys. (tr-auth)

13643 PREPARATION AND SOME MECHANICAL PROPERTIES OF HIGH-PURITY VANADIUM. **Beale, H. A.; Arsenault, R. J. (Univ. of Maryland, College Park). Met. Trans.; 1: 3355-60(Dec 1970).**

Electron beam melting of vanadium at total dynamic pressures of less than 10^{-9} was shown to reduce the oxygen content. Internal friction analyses and chemical analyses showed good agreement. The purification was attributed to the metallic vapor envelope around the molten zone which may have the effect of reducing the partial pressure of oxygen below 10^{-13} adjacent to the molten metal and also to the vaporization of VO molecules from the surface of the molten zone. Three stages of work hardening were shown to exist in vanadium. However, a small interstitial concentration was required to observe stage II. Optical microscope examination revealed that secondary slip lines appeared as stage II proceeded. The maximum rate of work hardening of 14 kg per sq mm was in good agreement with the rate of work hardening observed in other bcc metals. (auth)

XUM

13644 INFLUENCE OF TEMPERATURE IN THE CONTACT AREA ON THE STATIC WELDING CHARACTERISTICS OF ELECTRICAL CONTACTS. Sato, Mitsunori; Hijikata, Masayuki; Morimoto, Ichiro (National Research Inst. for Metals, Tokyo). J. Jap. Inst. Metals; 34: 1067-74(Nov 1970). (In Japanese).

The mutual relationship between the static welding behavior and physical characteristics of contact materials was obtained with an X–Y recorder and an oscilloscope for various metals and alloys. Light welding or sticking occurred at the softening temperature of the material in the contact area, and heavy welding occurred at its melting temperature. The temperature of the contact area which has influence on the welding behavior was correlated to the current density in the contact area. The I/d is given by $(I/d) = \{[4L(T^2 - T_r^2)]^{1/2}/\rho_r[1 + \frac{2}{3}\alpha(T - T_r)]\}$ where I is the contact current, d is the diameter of the circular contact area, T is the maximum temperature in the contact area, T_r is room temperature, ρ_r is the electrical resistivity at room temperature, α is the temperature coefficient of electrical resistivity, and L is the Wiedemann–Franz constant and is equal to 2.45×10^{-8} $(V/deg)^2$. The higher the melting temperature or the larger the temperature coefficient of electrical resistivity of the contact material, it is more difficult for the contact area to attain its melting state. It is considered that the stationary melting state cannot exist in the static contact area. (auth)

13645 CLADDING TUBES FOR ATOMIC REACTORS ARE PRODUCED AT RAUFOSS. Maskin; 3: No. 9, 30(12 Nov 1970). (In Norwegian).

A/S Raufoss Ammunisjonsfabrikker have in cooperation with the Institutt for Atomenergi built a factory for the production of Zircaloy cladding tubes for nuclear fuel. The production processes and machinery are briefly described. The plant has a projected capacity of 100 tons of cladding tube per year. (Norway)

13646 STABILITY OF A PLANAR SOLID/LIQUID INTERFACE FOR ALLOYS OF INDIUM IN TIN. Davis, K. G.; Fryzuk, P. (Dept. of Energy, Mines, and Resources, Ottawa). J. Cryst. Growth; 8: 57-60(Jan 1971).

Alloys of indium in tin were solidified unidirectionally, under controlled conditions, and examined for solute substructure by autoradiography. The observed growth conditions, under which solute substructures form, are compared with those predicted by theoretical treatments of the stability of a planar advancing solid/liquid interface. At low G/R, the observations were not in accord with predictions based on the Mullins–Sekerka perturbation analysis. (auth)

13647 EXPLOSIVE WELDING PLUGS INTO HEAT EXCHANGER TUBES. Johnson, Wayne R. (Babcock and Wilcox Co., Alliance, Ohio). Weld. J. (N. Y.); 50: 22-32(Jan 1971).

The design, development, and evaluation of explosive plug welding techniques for making repairs in heat exchanger tubes from a remote location are discussed. Major areas of development included: plug and charge design, environmental conditions for explosive welding, and ignition system and tooling. The plug and tubing materials consisted of the nickel base alloy, ASME SB-166 and 163, respectively. The tubing dimensions were 0.625 in. OD × 0.035 in. wall. The basic plug design consisted of a hollow cylindrical plug with one end closed, with the basic charge design consisting of nitroguanidine (explosive) and a length of mild detonating fuse (MDF). Several modifications of the basic plug and charge design were evaluated. Tests conducted to evaluate weld quality consisted of: photomicrographs of wave formations, hydrostatic and helium leak testing, microhardness traverses, microprobe analysis of weld interface, chemical analysis of explosive by-products, shear tests, effect of thermal cycling on weld quality, and effect of oxide and water films between the plug and the tube. The ignition system and tooling used to demonstrate the technique of explosively plugging tubes from a remote location are shown and discussed. (auth)

13648 BONDING GRAPHITE TO METALS WITH TRANSITION PIECES. Hammond, J. P.; Slaughter, G. M. (Oak Ridge National Lab., Tenn.). Weld. J. (N. Y.); 50: 33-40(Jan 1971).

Joining graphite to structural metals by conventional brazing techniques invariably produces thermal cracking as a result of wide differences in coefficients of thermal expansion. Isotropic graphites have coefficients of 4.5 to 8×10^{-6} °C^{-1} compared with 12.5 to 18.5×10^{-6} °C^{-1} for nickel- and iron-base alloys. A graded transition piece to join nuclear graphite to Hastelloy N for a nuclear application involving fused fluoride salts as fuels was developed. Special alloys were developed for the transition pieces in which heavy metals (tungsten or molybdenum) were dispersed in nickel-rich matrices. Coefficients of expansion of the alloys can be varied by changing the heavy metal-matrix ratio. Segments of these alloys are fabricated by sintering and machining; then they are copper-brazed to form a composite varying gradually in expansion coefficient over its length. Of several ternary and quaternary systems explored for the transition piece, tungsten with Ni-30 Fe (wt-%) as the matrix had the most suitable properties. Joining the segments to isotropic graphite was very difficult since most commercial brazing filler metals did not adequately wet graphite. Consequently, a unique technique was developed in which a Cr_3C_2 coating was formed on the graphite; this coating was readily wetted by ductile, corrosion-resistant copper. Excellent graphite-to-graphite and graphite-to-metal bonds were achieved with good reproducibility. Tubular transition joints withstood rapid cycling 24 times between 700°C and room temperature (8 min cool-down time) without cracking. All of the segment and braze materials were metallurgically compatible with one another and chemically compatible with the molten fluoride. (auth)

Properties Evaluations

Refer also to abstracts 13095, 13154, 13164, 13170, 13988, 14172, 14208, 14209, 14438, 14440, 14452, 14455, 14458, and 15379.

13649 (AD–713191) TOTAL MATERIAL VARIABLES INFLUENCING A DUCTILE–BRITTLE TRANSITION TEMPERATURE FOR MOLYBDENUM. Pink, E.; Armstrong, R. W. (Maryland Univ., College Park. Engineering Materials Group). Sep 1970. Contract N00014-67-A-0239-0011. 22p. (TR–1). NTIS.

The ductile-brittle transition temperature for a coarse grained re-crystallized molybdenum material was found to be lower than for the original fine grained metal from which it was produced. The coarse grain size resulted from a critical straining and subsequent annealing treatment at a low recrystallization temperature. It is concluded from an analysis of various strength parameters which are either measured or estimated for this material that an improved grain boundary strength and a considerable influence of the dislocation substructure are responsible for the less brittle behavior of the coarse grained molybdenum. (auth) (USGRDR)

13650 (AI-Trans–289) AEROSOLS PRODUCED BY EVAPORATION OF URANIUM WIRE. Morel, Colette ([Commissariat a l'Energie Atomique, Fontenay-aux-Roses (France). Centre d'Etudes Nucleaires]). Translated for Atomics International, Canoga Park, Calif., from report CEA-R–3473. 44p. Dep. NTIS.

This paper was abstracted from the original language and appeared in NSA as 23: 982.

13651 (ANL/ST–4) SODIUM TECHNOLOGY QUARTERLY REPORT, JULY–SEPTEMBER 1970. Kesser, G. M. (comp. and ed.) (Argonne National Lab., Ill.). Dec 1970. Contract W-31-109-eng-38. 67p. Dep. NTIS.

A national meter program was implemented to characterize instrumentation for on-line monitoring of oxygen, carbon, and hydrogen impurities in sodium and for detecting leaks in steam generators, and to establish commercial availability of the on-line meters, which will be built to RDT standards. In the analytical standards program, the management effort continued, with the goal of formulating standard analytical and sampling methods to be uniformly applied throughout the national sodium technology program; development work proceeded on methods for determining oxygen, carbon, nitrogen, and trace metals in sodium. Work continued on the definition of radioactivity problems associated with the repair and maintenance of LMFBRs, the development of methods for detecting and characterizing fuel failures, and the evaluation of problems created by sodium aerosol in cover gas. Studies of the chemistry of sodium included investigation of the nature of nitrogen-bearing species in sodium, elucidation of phase relations in the sodium-rich region of the Na–O–H ternary system, and measurement of the solubility of xenon in sodium. Work on the purification of sodium continued with development of methods for characterization of cold-trapped sodium. Studies of materials-coolant compatibility included investigations of the transport of carbon in sodium-steel systems and of the adequacy of vanadium alloys as cladding for LMFBR fuels. (auth)

13652 (GAMD–8219(Rev.)) INSTANTANEOUS AND TIME-DEPENDENT COLLAPSE OF EXTERNALLY PRESSURIZED CIRCULAR TUBES WITH INITIAL OUT-OF-ROUNDNESS. Buttemer, D. R. (Gulf General Atomic, Inc., San Diego, Calif.). 6 Nov 1970. Contract AT(04-3)-167. 32p. Dep. NTIS.

The collapse characteristics of externally pressurized circular tubes with an initial out-of-roundness were investigated analytically. A computer program was developed to calculate the pres-

XUM

sure required to instantaneously collapse a tube with an initial out-of-roundness as well as to determine the time to cause collapse at operational conditions due to progressive creep deformation. Both primary and secondary creep were considered and the computer program had both Hastelloy-X and Type 316 stainless steel creep data built into it as functions of temperature and stress level. An option is also available that allows other materials to be investigated if their creep properties are known. Results of a case representative of a GCFR fuel-rod application are included herein. (auth)

13653 (LA–4521) ADIABATIC CALORIMETRIC ENTHALPY MEASUREMENTS FOR α, β, AND γ URANIUM AND THE HEATS OF THE TRANSFORMATIONS $\alpha \rightarrow \beta$ AND $\beta \rightarrow \gamma$. Clifton, David G. (Los Alamos Scientific Lab., N. Mex.). Sep 1970. Contract W-7405-eng-36. 13p. Dep. NTIS.

Enthalpy of the α, β, and γ phases of high-purity depleted ^{238}U was measured, and values for the heats of the $\alpha \rightarrow \beta$ and $\beta \rightarrow \gamma$ transformations were obtained. These measurements were made during development of an adiabatic calorimeter designed to measure heat effects on condensed-phase samples in the temperature range from about 500 to 1000°C. The calorimeter is described. (auth)

13654 (MLM–1734) SOLUBILITY OF TRITIUM IN ANNEALED AND COLD-WORKED COPPER. Braun, J. D.; Chaney, K. F.; Downs, G. L.; Powell, G. W. (Mound Lab., Miamisburg, Ohio). 8 Jan 1971. Contract AT-33-1-GEN-53. 6p. Dep. NTIS.

The solubility and diffusivity of tritium in both cold-worked and annealed copper is being investigated as a continuation of work on metals with face-centered cubic structures. Samples were exposed to a tritiated gas mixture over a range of 100 to 300°C. Preliminary results indicated the tritium solubility at 300°C is much greater than that reported in the previous literature. Possible errors in experimental techniques which might explain the results obtained are being investigated. (auth)

13655 (NP–18625) TEXTURE AND ANISOTROPY OF ZIRCONIUM RELATED TO PLASTIC DEFORMATION. Kaellstroem, Krister (Sandvik Steel Works, Sandviken (Sweden)). 1970. 40p. (In Swedish). Dep. NTIS (U. S. Sales Only).

Thesis. Submitted to Kungliga Tekniska Hogskolan, Stockholm, Sweden.

An investigation of the influence of the manufacturing procedure on texture and resulting anisotropic qualities of zirconium in general and zircaloy tubes in special is reported. A formalism and method were developed for estimation and description of texture, mechanical anisotropy and anisotropic precipitation of zirconium hydride. Experimental investigations are presented that partly prove or modify properties predicted earlier. Dependency between deformation, texture, and anisotropy were evaluated regarding deformation viz. strain conditions; texture and mechanical anisotropy; texture changes during recrystallization; changes of hydride orientation during recrystallization and deformation; mechanical tests of tubes with three different textures; Knoop hardness flow boundary surface and real flow boundary surface; and texture softening. (Sweden)

13656 (ORNL–4590) HEAVY-SECTION STEEL TECHNOLOGY PROGRAM. Semiannual Progress Report for Period Ending February 28, 1970. (Oak Ridge National Lab., Tenn.). Oct 1970. Contract W-7405-eng-26. 256p. Dep. NTIS.

Results of research and development are summarized in five sections. A separate abstract was prepared for each section. (J.R.D.)

For abstracts of individual sections see: 13639, 13657–13659, and 13724.

13657 (ORNL–4590, pp 20-99) INVESTIGATION OF UNIRRADIATED MATERIALS. (Oak Ridge National Lab., Tenn.).

From Heavy-Section Steel Technology Program.

The material investigations are divided, in general, into studies of unirradiated materials and studies of irradiation effects. The studies of unirradiated material include inspection, characterization, variability determinations, transition-temperature investigations, fracture mechanics studies, and fatigue-crack-propagation tests. The current work in these areas is discussed. (J.R.D.)

13658 (ORNL–4590, pp 135-232) PRESSURE VESSEL INVESTIGATIONS. (Oak Ridge National Lab., Tenn.).

From Heavy-Section Steel Technology Program.

Three pressure vessel investigations are currently under way involving complex stress state studies, simulated service tests, and specific safety research studies. The complex stress state studies include development of processes for manufacturing epoxy models of the intermediate test vessels and the simulated service test vessels, fabrication of epoxy models and steel models of the intermediate test vessels, crack preparation studies on the epoxy models, fatigue-crack growth studies in epoxy, and straingage analyses of the nozzle-cylindrical shell region of an epoxy model of the intermediate test vessel. Design and procurement of the intermediate test vessels and continued testing of the 6-in.-thick large tensile specimens comprise the principal current activities under the simulated service test program. Further investigations of the hypothetical thermal shock problem are included in the specific safety research studies. A study of the relationship between impact test data and fracture toughness (K_{Ic} and K_c) data has also been undertaken. (auth)

13659 (ORNL–4590, pp 233-48) DISCUSSIONS. (Oak Ridge National Lab., Tenn.).

From Heavy-Section Steel Technology Program.

Discussions of research results are presented on correlations of test data from transition temperature and fracture mechanics tests. (J.R.D.)

13660 (ORNL-TM-3211) TENSILE AND IMPACT PROPERTIES OF THICK-SECTION PLATE AND WELDMENTS. Canonico, D. A.; Berggren, R. G. (Oak Ridge National Lab., Tenn.). Jan 1971. Contract W-7405-eng-26. 30p. (CONF-700935–2). Dep. NTIS.

From Symposium on the Technology of Pressure-Retaining Steel Components, Vail Village, Colo.

Most nuclear pressure vessels have been fabricated from ASTM A533, grade B, class 1 steel plate. This steel is quenched and tempered in order to obtain its optimum properties in section sizes from 6 to 12 in. in thickness. The quench-and-temper heat treatment results in a variation in mechanical properties through the thickness of the plate. The room-temperature ultimate tensile strength varies from nearly 97,000 psi at the plate surface to about 89,500 psi at the midsection ($\frac{1}{2}$ T). The greatest effect of the quench is observed in the nil ductility transition temperature. The 30 ft-lb Charpy V-notch temperature varies from –150°F at the surface to +10°F at the $\frac{1}{8}$ T location. Anisotropy due to the rolling is reflected in the upper shelf values of the longitudinal, transverse, and through-the-thickness properties of the plate. These values are 115, 100, and 80 ft-lb, respectively, for the three directions. Three welding processes are employed in the fabrication of the pressure vessels. These are the submerged arc process, the shielded metal-arc process, and the electroslag process. The subarc and shielded metal-arc processes employ multipass welding techniques and the weldments resulting from these processes are only stress relieved after welding. The electroslag weld consists of a coarse-grained (ingot-like) structure which is unacceptable in the as-welded condition. The electroslag weldment is quenched and tempered after welding. The ultimate tensile strength of the welds is uniform through their thicknesses. Their ultimate tensile strengths are all similar, about 80,000 to 85,000 psi. The impact properties of the electroslag and multipass weldments are not similar. The electroslag weld metal has an upper shelf Charpy V-notch energy of about 80 ft-lb, whereas the multipass welds (subarc and shielded metal-arc) have shelf values of from 120 to 150 ft-lb. Further, the 30 ft-lb C_V temperature of the subarc and shielded metal-arc welds are near –50 to –70°F. The temperature for the electroslag weld metal for the same energy value is –20°F. (auth)

13661 (UCRL–72627) DISPERSION HARDENING OF A Mo–1 AT. PERCENT Hf ALLOY BY INTERNAL HARDENING. Himmel, L.; Mitchell, J. B. (California Univ., Livermore. Lawrence Radiation Lab.). 19 Aug 1970. 7p. (CONF-700819–9). Dep. NTIS.

From 2nd International Conference on the Strength of Metals and Alloys, Pacific Grove, Calif.

The microstructure and high-temperature tensile properties of an internally nitrided Mo–1 at. % Hf alloy were studied. The strength levels, though not optimum, were far superior to those of the best commercial high-strength TZM and TZC Mo-base alloys. (G.M.C.)

13662 NEW METHOD FOR CALCULATING THE DESIGN STRENGTH OF FUEL CANS FOR LIQUID METAL COOLED FAST REACTORS. Schmidt, G. (Kernforschungszentrum, Karlsruhe, Ger.). Nucl. Eng. Design; 14: 117-35(Oct 1970).

The method described provides a possibility for calculating the maximum design pressure and corresponding fission gas plenum length for cladding tubes of liquid metal-cooled fast reactors with oxide fuel. The material properties—especially the creep behavior—as well as temperature and power distributions are specified. Creep relaxation of a composite mechanical-thermal stress state is solved on the basis of Norton's formula. Using integral relations for the strain rates the initial equations are transformed into a system of integrodifferential equations. These, after sub-

XUM

stitution of the integrals by easily calculated constant mean values for only few and relatively long periods of time, change into ordinary differential equations for which an approximate analytic solution can be quoted. This solution is further simplified and finally leads to the definition of a limiting stress analogous to the yield strength of the material. Thus the problem is reduced to the well-known case of an elastic-plastic tube under internal pressure and intermittent heat flux; its solution can be generalized to yield a criterion for the limitation of the tube loading caused by intolerable cyclic growth, the so-called thermal ratchetting. The method is applied to several examples with the aid of two small digital computer programs, and the results lead to conclusions for the appropriate design of fuel pin claddings. (auth)

13663 THERMAL CONDUCTIVITY AND TOTAL EMITTANCE OF TUNGSTEN FROM 1800 TO 2800°K. **Jun, C. K.; Ebrahim, S.; Hoch, M. (Univ. of Cincinnati). High Temp.-High Pressures; 2: 43-54(1970).**

Measurements are reported on six tungsten samples prepared by different manufacturers using either arc-casting or powder metallurgy techniques. The values obtained for the thermal conductivity (2000 < T < 2800°K) were 1.00 ± 0.03 and 0.92 ± 0.03 W cm^{-1} deg^{-1}, respectively, and for the total emittance (2500°K) 0.28 and 0.26, respectively, for the arc-cast and powder metallurgy samples. (auth) (UK)

13664 MEASUREMENT OF THE SPECIFIC HEAT AND THE HEAT OF FUSION OF TUNGSTEN AT HIGH TEMPERATURES BY THE WIRE EXPLOSION TECHNIQUE. **Dikhter, I. Ya.; Lebedev, S. V. (Inst. for High Temperatures, Moscow). High Temp.-High Pressures; 2: 55-8(1970).**

The measurements were carried out by passing current with a density of 4.25×10^6 A cm^{-2} through 80 μm tungsten wire and recording the voltage drop and the current (i.e. the energy input rate), and the luminescence (from which the temperature of the wire was calculated). The specific heat was determined by graphical differentiation of the temperature dependence of the energy input rate, and in the 2600 to 3500°K range found to agree within 10% with the results of other investigators. The specific heat of liquid tungsten was measured up to 4500°K. The heat of fusion is given as 80 ± 4 cal g^{-1}. (auth) (UK)

13665 ENTHALPY AND SPECIFIC HEAT OF THE 80 PERCENT W-20 PERCENT Mo ALLOY AT HIGH TEMPERATURE. **Chekhovskoi, V. Ya.; Tarasov, V. D.; Zhukova, I. A. (Inst. of High Temperatures, Moscow). High Temp.-High Pressures; 2: 59-61(1970).**

The enthalpy of the 80% W-20% Mo alloy in the range 1400 to 3000°K was measured by drop calorimetry and the results are compared with those calculated from the values for W and Mo. The additivity law holds up to 2700°K but near the melting point the measured enthalpy of the alloy is higher than the calculated enthalpy, probably due to the vacancy contribution. Equations fitting the results are derived for the temperature dependence of the enthalpy and the specific heat of the alloy. (auth) (UK)

13666 TOTAL HEMISPHERICAL EMISSIVITY OF TUNGSTEN, MOLYBDENUM, AND RHENIUM SINGLE CRYSTALS AT HIGH TEMPERATURES. **Peletskii, V. E.; Druzhinin, V. P. (Inst. of High Temperatures, Moscow). High Temp.-High Pressures; 2: No. 1, 69-74(1970).**

The total hemispherical emissivity was determined for monocrystalline tungsten at 1200 to 3200°K, monocrystalline molybdenum at 1200 to 2600°K, and mono- and polycrystalline rhenium at 1200 to 2800°K, using electron-beam heating of small cylindrical specimens. Comparison with the data for polycrystalline materials reported by other workers shows that grain-boundary contribution to the total emissivity of these metals is negligible. The results for molybdenum and rhenium conform to Davisson's equation; those for tungsten depart from it by up to 27%. (auth) (UK)

13667 RESEARCH ON THERMOPHYSICAL PROPERTIES OF SOLIDS AT HIGH TEMPERATURES AT THE INSTITUTE FOR HIGH TEMPERATURES OF THE USSR ACADEMY OF SCIENCES. **Sheindlin, A. E.; Chekhovskoi, V. Ya.; Shipl'rain, E. E. (Inst. of High Temperatures, Moscow). High Temp.-High Pressures; 2: 1-15(1970).**

The research reviewed was mainly directed at obtaining new experimental data on properties of substances at high temperatures with stress on maximum possible accuracy and extension of the results to very high temperatures. The substances investigated were chosen primarily to meet the requirements of modern technology in various fields. The requirements of theory were also taken into consideration and certain classes of substances were studied and rules sought governing the variation of the properties among the substances within the given class. Composite research was carried out on the different thermophysical properties of a given substance and attempts made to correlate these properties. The basic lines of the research work and the results are outlined and attention drawn to special features of the techniques employed. Composite research on the thermophysical properties of solids included investigations of enthalpy, specific heat, thermal conductivity, coefficient of thermal expansion, electrical resistivity, integral emissivity, spectral emissivity in the visible and near-infrared regions, temperatures and heats of phase transitions. The solids investigated were: zirconium, tantalum, niobium, alumina, magnesia, hafnium, titanium, pyrolytic zirconium, graphites, and silicon carbides; tantalum, zirconium, tungsten, niobium and molybdenum metals and their alloys; corundum, zirconium dioxide, and titanium diboride. (UK)

13668 EXPERIMENTAL INVESTIGATIONS OF SELF-WELDING OF STRUCTURAL MATERIALS UNDER SODIUM. **Bendorf, K. (Kernforschungszentrum, Karlsruhe, Ger.). Nucl. Eng. Design; 14: 83-98(Oct 1970).**

Within the framework of the German Fast Breeder Program static load tests in sodium were carried out on structural materials with the purpose of investigating the self-welding tendency of these materials. Besides austenitic materials also a stabilized ferritic steel and a nickel base alloy as well as several hard facing and hard metal alloys were used in the tests. The test temperatures were 580 and 700°C, the compressive load ranged up to 5 kg/mm^2 and the tests lasted for 168 hr. The oxygen content of the cold-trapped sodium was nearly 20 ppM. The results show a more or less pronounced tendency of all the materials to weld together. While the austenitic and ferritic steels showed a marked tendency to weld together at 700°C the behavior of the hard facing and the hard metal alloys is not uniform. The nickel base alloy, which up to now has been investigated in one experiment only, does not weld together—with one exception. Micrographs made of some different-material couples seem to indicate that the welding was caused by recrystallization after previous strong deformation of the contact region. (auth)

13669 ADSORPTION OF WATER VAPOR ON POLYCRYSTALLINE TUNGSTEN. **Waclawski, B. J.; Hughey, L. R. (National Bureau of Standards, Washington, D. C.). Surface Sci.; 19: 464-8(Feb 1970).**

Features of room temperature water vapor reactions with tungsten during initial stages of adsorption are discussed. Emphasis is placed on the dynamics of H evolution during the adsorption process and changes of work function during this process. It is noted that there is initially an induction period during which no H is evolved. This is followed by spontaneous evolution, the total amount of which is fixed. The H evolution is accompanied by a positive charge contribution to the surface dipole layer. (J.R.D.)

13670 SOLID-SOLUTION STRENGTHENING AT 77°K IN CADMIUM SINGLE CRYSTALS CONTAINING ZINC. **Lukac, P. (Charles Univ., Prague); Brown, A. F. Phys. Status Solidi (a); 3: K169-72(16 Nov 1970).**

The variation of the critical resolved shear stress τ_0 and activation volume V of Cd with alloying of Zn up to 0.53 at. % was investigated at 77°K. A plot of τ_0 vs $c^{1/2}$ (c = concentration of Zn) shows a straight line; the plateau stress (athermal component) reported by Prochazka also shows a straight line with a lower slope. The activation volume V decreases with $c^{-1/2}$; this is in agreement with a flexible dislocation model. (D.L.C.)

13671 NUCLEATION OF CRACKS BY A SPARK DISCHARGE IN MOLYBDENUM SINGLE CRYSTALS. **Vesely, D. (Univ. of Liverpool). Phys. Status Solidi (a); 3: 669-77(16 Nov 1970).**

The nucleation of cracks by a spark discharge was studied using optical and transmission electron microscopy. It was found that in molybdenum single crystals, dislocations are produced by the spark discharge and low-angle boundaries are found on {100} and {110} planes. It is proposed that the high density of ⟨100⟩ dislocations in these walls may be responsible for the initial crack nucleation. The crack tip in thin foils as well as in bulk specimen was always found to be blunted by plastic deformation. In a few cases in the bulk specimens renucleation of crack at the crack tip was observed and seemed to be related to twinning. (auth)

13672 EFFECT OF MICROSTRUCTURE ON THE STRENGTH, TOUGHNESS, AND STRESS-CORROSION CRACKING SUSCEPTIBILITY OF A METASTABLE BETA TITANIUM ALLOY(Ti-11.5Mo-6Zr-4.5Sn). **Feeney, J. A. (Boeing Co., Renton, Wash.); Blackburn, M. J. Met. Trans.; 1: 3309-23(Dec 1970).**

The influence of microstructure on the mechanical properties of the alloy Ti-11.5Mo-6Zr-4.5Sn is described. The phase trans-

XUM

formations were similar to those that occurred in binary Ti-Mo alloys containing 10 to 12% Mo. Thus, the β phase can be retained by quenching from above 1400°F. The β phase deformed in a complex manner, including mechanical twinning, and was characterized by low strength, high ductility, and high toughness. The ω phase, which also formed on quenching, was stable at temperatures up to 800°F. Yield strengths of up to 220 ksi were measured in $(\beta + \omega)$ structures, the strength level being dependent on the size and volume fraction of the ω phase. In contrast, fracture toughness reached a minimum value of ~20 ksi $\sqrt{\text{in.}}$ when the ω particle size $\geq$100Å $(\beta + \alpha)$ structures showed good combinations of yield strength and fracture toughness. Unfortunately, the best combinations were susceptible to stress-corrosion cracking in aqueous solutions containing halide ions. (auth)

13673 NITROGEN DIFFUSION AND SOLUBILITY IN TUNGSTEN. Wagner, R. L. (Oak Ridge National Lab., Tenn.). Met. Trans.; 1: 3365-70(Dec 1970).

The diffusion and solubility of nitrogen in tungsten were determined using an ultrahigh vacuum- and mass-spectrometric technique capable of measuring concentrations of 10^{-2} ppM and degassing rates of 10^{-3} ppM N per hr. The technique is based on measuring the degassing rate of nitrogen as a function of time from a resistivity heated tungsten wire previously engassed with nitrogen between 1 and 25 torr. The diffusion and solubility constants between 1000 and 1800°C may be summarized by $D = (2.37 \pm 0.43) \times 10^{-3} \exp[(-35{,}800 \pm 3900)/RT]$ cm^2/sec, and $S = (0.21 \pm 0.06) \exp[(-17{,}600 \pm 5900)/RT]$ torr · liter cm^{-3} torr$^{-1/2}$. The concentration of nitrogen tungsten at 760 torr according to these results are 0.4 and 9.2 ppM at 1000 and 2000°C, respectively. The expression for the permeation constants calculated from D and S is $K = 5 \times 10^{-4} \exp(-53{,}400/RT)$ torr · liter cm^{-1} torr$^{-1/2}$. (auth)

13674 RECOVERY CREEP OF NIOBIUM-STABILISED AUSTENITIC STAINLESS STEELS. Williams, K. R.; McLauchlin, I. R. (Berkeley Nuclear Labs., Eng.). J. Mater. Sci.; 5: 1063-72(Dec 1970).

The creep properties of niobium-stabilized stainless steels of carbon contents in the range 0.01 to 0.05% carbon can be accounted for by the general recovery theory of creep. The high stress dependencies of recovery and creep rate can be adequately explained through an internal friction stress or impedance term, retarding recovery. Measurement of this friction term by dislocation density and stress relaxation techniques provides the correct stress dependencies when applied to the modified recovery theory. (auth) (UK)

13675 SURFACE AND INTERIOR MEASUREMENTS OF GRAIN BOUNDARY SLIDING DURING CREEP. Bell, R. L. (Univ. of Southampton, Eng.); Graeme-Barber, C. J. Mater. Sci.; 5: 933-44(Nov 1970).

Measurements of grain boundary sliding were made on polycrystalline specimens of Magnox AL80, a magnesium-0.78 wt % aluminum alloy, at successive strains during creep at 200°C under a stress of 2800 psi. Three independent methods were used to determine the strain due to sliding (ϵ_{gb}) at the surface and two to determine ϵ_{gb} in the interior of the specimens. The one direct method of measuring ϵ_{gb} in the interior used oxide markers introduced by extruding a composite billet. The values of ϵ_{gb} obtained from the offsets in these interior markers were found to agree with those given by the three sets of measurements made on the surface, but not with those from the indirect method for the interior which relies on the measurement of grain strain via grain shape changes. (auth) (UK)

13676 DIFFUSION OF CESIUM IN MONO- AND POLYCRYSTALLINE MOLYBDENUM. Korolev, A. A.; Pavlinov, L. V. Fiz. Metal. Metalloved.; 29: 1326-8(Jun 1970). (In Russian).

Additives with low solubility in crystals are expected to be concentrated preferentially near structural defects, such as grain boundaries or dislocations. This problem was studied by examining the diffusion of low-solubility cesium in various types of molybdenum, such as high-purity single-crystals and polycrystalline, hot-wrought rods. Deformed, deformed and annealed at 1200°C, and deformed and annealed at 1600°C polycrystalline specimens were used for the experiments. The diffusion was determined by autoradiography, using the ^{134}Cs isotope. Measurement of the diffusion coefficient and energy of activation of diffusion indicated that the diffusion mechanism of cesium and other low-solubility impurities differed from the usual vacancy-type mechanism. (TTT)

13677 ANELASTIC PIEZORESISTANCE DUE TO STRESS-INDUCED ORDERING OF DEFECTS. Venkataraman, Krishnamurthi. Pittsburgh; Univ. of Pittsburgh (1970). 120p. University Microfilms Order No. 70-22,753. Thesis.

The anelastic piezoresistance due to stress-induced ordering of O-interstitials in tantalum and of N-interstitials in α-iron was studied. By means of a phase detection technique, the 0° and 90° components of the anelastic piezoresistance were measured in polycrystalline wires of tantalum containing 0.3 at. % of O and α-iron containing 0.3 at. % of nitrogen. The 90° component of piezoresistance gives rise to a relaxation peak having the characteristics of a Debye peak. In tantalum, the anelastic stress coefficient of piezoresistance β_a was found to be equal to $(0.30 \pm .03) \times 10^{-9}$ cm^2/g as measured from the 0° component and the variation in β due to 90° component was found to be $(\sim 0.18 \pm .02) \times 10^{-9}$ cm^2/g. Experiments on α-iron show definite variation of β over the familiar Snoek peak range both in the 0° and 90° component data. β_a for this case was measured to be $(0.13 \pm .01) \times 10^{-9}$ cm^2/g. The anelastic longitudinal piezoresistance coefficient π_a assumes a value equal to $(0.23 \pm .03) \times 10^{-9}$ cm^2/g for Ta and for α-iron it was found to be too small ($\pi_a \leq .02 \times 10^{-9}$ cm^2/g) to be measured by the present apparatus. The theoretical study of electron scattering due to the strain field surrounding a defect region was considered. Expressions are obtained for the residual resistance due to spherically symmetric and asymmetric types of strain field. In the case of asymmetric defects, the theoretical anisotropy of defect scattering, defined by the ratio $(\rho_\perp - \rho_{||}/\rho_R)$, was found to be 0.9 by means of an approximate calculation where $\rho_\perp$ and $\rho_{||}$ are the resistivities of the asymmetric defect described in terms of a double-force model when the axis of the defect is aligned perpendicular and parallel to the $\bar{E}$ field respectively. The experimentally attainable anisotropy, determined by the ratio $(\rho_P - \rho_R/\rho_R)$, is about 5×10^{-4} where ρ_P is the resistivity due to a collection of double forces under the influence of a stress and ρ_R is the resistivity for a random arrangement of double-forces in the absence of a stress. The present theoretical study indicates that the strain scattering is a substantial part of the residual resistance and that the anisotropy of the strain scattering results in a substantial contribution to the anelastic piezoresistance. (Diss. Abstr. Int., B)

13678 EFFECT OF RADIATION INDUCED GAS ON THE STRESS RUPTURE PROPERTIES OF AN ALUMINIUM–LITHIUM ALLOY. Smith, I. O.; Russell, B. (Univ. of Queensland, St. Lucia, Australia). J. Nucl. Mater.; 38: 1-16(Jan 1971).

The changes in stress-rupture properties of an aluminum–lithium alloy induced by the presence of inert gas bubbles after neutron irradiation were investigated in the temperature range of 175 to 300°C. A bubble distribution with a mean diameter of 47 Å at an average spacing of 1400 Å produced a decrease in the minimum creep rate of two orders of magnitude below that for the bubble-free material under the same test conditions. For very fine bubble distributions and distributions which contained a narrow size range of large bubbles, a breakaway to a very high stress-sensitivity at low stresses occurred. This was absent in alloys which contained stronger bubble obstacle arrays which included a wide range of bubble sizes. All inert gas concentrations reduced creep ductility of aluminum–lithium alloy but the severity of embrittlement increased markedly with gas concentration and testing temperature. The existence of a critical bubble size for breakaway growth of grain boundary voids is implied by the experimental evidence. For a given bubble distribution a critical stress exists below which grain boundary degeneration does not occur. As the gas concentration is increased, the fracture mechanism tends increasingly towards inter-granular failure. (auth)

13679 CONTINUOUS COOLING TRANSFORMATION BEHAVIOUR OF ZIRCONIUM–NIOBIUM–OXYGEN ALLOYS. Hunt, C. E. L.; Niessen, P. (Univ. of Waterloo, Ont.). J. Nucl. Mater.; 38: 17-25(Jan 1971).

The continuous cooling transformation behavior of zirconium alloys containing up to 5 at. % niobium and 3 at. % oxygen was examined using thermal analysis and metallographic techniques. Two types of reactions were found; nucleation and growth reactions which showed the familiar C-curve kinetics, and the athermal martensite reaction. The nucleation and growth reactions were identified as the formation of α-zirconium at the β-grain boundaries and the transformation $\beta_{Zr} \rightarrow \alpha_{Zr} + \beta_{Nb}$ throughout the grains. Increasing niobium content lowered the temperature and increased the time required to obtain the thermal arrests. Increasing oxygen raised the temperature of both reactions and caused grain boundary nucleation to occur sooner and nucleation within the grains to occur later. The martensite start temperature was not affected by oxygen but decreased linearly with niobium content. Clustering of solute atoms within the β-phase has been suggested by other workers. The results show that this must be an equilibrium condition. Clusters will not disperse with increased solution time as previously proposed. (auth)

13680 EFFECT OF ZIRCONIUM ADDITION ON THE OXIDATION RESISTANCE AND MECHANICAL PROPERTIES OF Fe–Al–

XUM

Cr ALLOYS. Ikeda, Seiichi; Ohashi, Shigeo; Ito, Goro (National Research Inst. for Metals, Tokyo). J. Jap. Inst. Metals; 34: 1140-4(Nov 1970). (In Japanese).

The oxidation resistance of Fe–Al–Cr alloys containing 1 to 3% zirconium in carbon dioxide at temperatures of 600 to 900°C under a pressure of 10 kg/cm^2 and mechanical properties of their alloys were studied. The oxidation resistance of Fe–Al–Cr alloys decreased with increase in zirconium content. Oxidation occurred especially for the alloys containing 3% zirconium at the testing temperatures of 600 and 700°C. Violent oxidation phenomenon was attributed to the precipitation of Zr and Cr carbide and internal oxidation of aluminum in the alloys due to carburization from carbon dioxide. The ductility of the alloy was improved by the addition of zirconium. The ductility and tensile strength of the tested alloys were highest when they were water quenched from 800°C. The high temperature creep strength of the alloys was improved with increasing zirconium content. (auth)

13681 EQUATION OF STATE OF SOLIDS. Rodionov, K. P. (Inst. of Metal Physics, Moscow). Fiz. Metal. Metalloved.; 29: 1169-76(Jun 1970). (In Russian).

The widely used equation of state derived by P. W. Bridgman contains baric coupling coefficients; the physical interpretation of these parameters is presented. The previously used graphic method for their determination was replaced by a more precise analytical technique. The values calculated from volume change data determined as a function of pressure were tabulated for 35 elements in the pressure range up to 100,000 kg/cm^2. The equation of state was also used for deriving a simplified formula to express the dependence of the true compressibility, thermal expansion, heat capacity, baric and thermal coefficients on the pressure. In some cases this coefficient was also calculated for atmospheric pressure. Previous data on the heat capacity of lead and copper at 30,000 kg/cm^2 were used to indicate the relative changes of C_P and C_V as a function of pressure. (TTT)

13682 SOME PROPERTIES OF TUNGSTEN–RHENIUM ALLOYS. Yoda, Renpei (National Research Inst. for Metals, Tokyo); Itagaki, Takehiko; Hamada, Takeo. J. Jap. Inst. Metals; 34: 1092-7(Nov 1970). (In Japanese).

Tungsten–rhenium alloys in general attract much attention because of their favorable ductility characteristics. In the present study some properties of 0.5 mm ϕ wires of doped tungsten containing 0 to 26% Re prepared by powder metallurgy process were investigated. Both the hardness and the tensile strength of wrought or annealed specimens increased with increasing rhenium content. The elongation of the wrought specimens of both doped tungsten and tungsten–rhenium alloys was smaller than 4%. However, with increasing annealing temperature, the elongation of doped tungsten further decreased and that of tungsten–rhenium alloys increased markedly. The elongation of annealed tungsten–rhenium alloys became higher with decreasing rhenium content, and the annealing temperature shifted to the higher temperature side. The recrystallization temperature of doped tungsten increased markedly with 3% Re addition, but it decreased with the addition of more than 3% rhenium. The high temperature tensile strength at 1100 to 1600°C was the highest for 10 to 20% Re alloys, but that at 2000°C did not show any large difference between doped tungsten and tungsten–rhenium alloys. The bending transition temperature decreased markedly with the addition up to 10% Re, but the temperature became almost constant above its rhenium content. The emf of a tungsten/tungsten-26 rhenium thermocouple was higher than that of a platinum/platinum-10 rhodium thermocouple, and increased linearly with increasing temperature from about 300 to 2200°C. At temperatures above 2200°C, however, the emf of the tungsten/tungsten-26 rhenium thermocouple decreased gradually with heating time. Hence, it is desirable that the couple be used in the temperature range below 2200°C. (auth)

13683 CYCLIC DEFORMATION BEHAVIOR OF SOME ENGINEERING MATERIALS. Burbach, J. (Fried-Krupp, Essen). Tech. Mitt. Krupp, Forschungsber.; 28: 55-101(Sep 1970). (In German).

Newly developed apparatus is described for the exact determination of the cyclic stress-strain behavior. The Bauschinger effect was treated theoretically for microscopic deformation without strain hardening and without removal of strain hardening. The second order elastic constants were measured. The influence of non-linear elastic effects upon the measured value was eliminated. Geometric relationships existed between $\sigma(t)$ and $\epsilon(t)$ at stabilized hysteresis and given $\sigma(t)$ or $\epsilon(t)$. The velocity, time and temperature-dependent effects were normal. The elastic and plastic energy were balanced during cyclic deformation. Pronounced yield strength and propagation of Lüders lines were found. Phenomena relating to work-hardening and removal of work-hardening were found. The following were also studied: climbing and migration of hysteresis loops; inverse velocity dependence of the creep stress in aluminum–copper alloys; quasi-work-hardening during cyclic deformation; and cyclic stress-strain curves and fatigue. Criticism of the conventional theories pertaining to the accumulation of damage was given. (auth)

13684 IMPACT STRENGTH AND FRACTURE STRUCTURE OF BERYLLIUM. Kornienko, L. A.; Papirov, I. I. (Physical-Tech. Inst., Kiev). Metalloved. Term. Obrab. Metal.; No. 10, 74-5(1970). (In Russian).

In view of the contradictory data in the literature, the temperature dependence of the impact strength of beryllium was determined, studying also the structure of fractures of the deformed metal. The 99.9% pure specimens were tested at temperatures ranging from 20 to 900°C, after polishing them and subjecting them to recrystallization annealing at 850°C. The impact strength of the specimens was found to range from ~0.05 kgm/cm^2 at 20°C to 0.2 kgm/cm^2 at 450°C, then decreasing to 0.04 kgm/cm^2 at 900°C. Electron-microscopic examination of the fractures revealed that the high-temperature reduction of the impact strength was due to changes in the mode of failure. Static tensile-strength tests indicated that the plasticity of beryllium increased continuously with increasing temperature from 20 to 900°C; however, at a rapid application of the force, failure along the grain boundaries preceded the deformation of the matrix. Recrystallization along the grain boundaries was responsible for the marked decrease of the impact strength of beryllium at high temperature. (TTT)

13685 THERMAL CONDUCTIVITY OF THE 29NK-TYPE ALLOY AT TEMPERATURES BETWEEN 80 AND 293^{0}K. Rad'kov, A. I.; Kalmykov, A. N.; Tret'yakova, S. M. (Central Scientific Research Inst. for Ferrous Metallurgy, Moscow). Metalloved. Term. Obrab. Metal.; No. 10, 38-41(1970). (In Russian).

Iron-nickel base alloys are widely used for low-temperature applications. In view of its importance on the martensitic transition at low temperatures, the thermal conductivity was measured by the absolute, stationary method on alloys with a composition close to that of 29 NK; the specimens used contained 29.2 to 28.0 wt % nickel and 16.5 to 18.2 wt % cobalt with the rest being iron. It was found that at temperatures from 293°K to liquid nitrogen temperature, the thermal conductivity of the alloys, which as a result of the heat treatment, had a homogeneous austenitic structure, ranged from 0.18 to 0.205 W/sec degree and was found to be dependent on the cobalt content: an increase of 1 wt % of the cobalt concentration increased the thermal conductivity by 6 to 10%. (TTT)

13686 MASS SPECTROMETRIC INVESTIGATION OF SURFACE IONIZATION. VI. DESORPTION OF Th$^+$, Np$^+$, AND Pu$^+$ FROM TUNGSTEN SURFACES. Smith, David H. (Oak Ridge National Lab., Tenn.); Cameron, A. E.; Dean, John A. J. Chem. Phys.; 54: 170-4(1 Jan 1971).

The mean residence times of Th$^+$, Np$^+$, and Pu$^+$ on polycrystalline tungsten surfaces were determined as functions of temperature using the modulated beam technique. The desorption parameters, determined from the relationship $1/\tau = \omega_0 \exp(-E_i/kT)$, are in the following order: Ion, ω_0(sec^{-1}), E_i(eV); Th$^+$, (1.7 ± 1.5) × 10^{14}, 7.83 ± 0.25; Np$^+$, (6.8 ± 3.8) × 10^{13}, 6.32 ± 0.12, and Pu$^+$, (1.6 ± 0.9) × 10^{12}, 4.99 ± 0.15. (auth)

13687 MIXED ADSORPTION OF ETHYLENE AND NITROGEN ON TUNGSTEN. Rye, Robert R. (Cornell Univ., Ithaca, N. Y.). Surface Sci.; 20: 245-57(Apr 1970).

Flash filament spectroscopy was applied to mixed adsorption of nitrogen and ethylene on polycrystalline tungsten. The order of dosing was found to be critically important in determining whether nitrogen is adsorbed. With ethylene preadsorbed at either 95°K or 300°K no nitrogen is adsorbed; but, if nitrogen is preadsorbed, both nitrogen and ethylene adsorb with the resultant spectrum being approximately a composite of separate nitrogen and ethylene spectra. The surface chemistry of ethylene as reflected by adsorption, stability and hydrogenation activity was identical to that on a clean tungsten surface. The drastic shift in nitrogen adsorption with changing dosing sequence indicated that nitrogen was adsorbed on independent sites under the chemisorbed ethylene layer with nitrogen bonded in the surface and ethylene bonded to the surface. Preadsorbed nitrogen was perturbed by subsequent ethylene adsorption. The onset of β-nitrogen desorption was shifted ~300°K lower in temperature, and at the same time the amount of β-nitrogen in spectra resulting from adsorption at 95°K was greatly enhanced over the amount resulting from nitrogen adsorption without ethylene at the same temperature. The total amount of nitrogen, however, was equal to the maximum amount obtained for a saturated dose at 300°K. It is suggested that the small amount of β-nitrogen resulting from a dose of nitrogen alone results from rapid pumping of desorbed nitrogen by the cold walls, and that an

XUM

ethylene dose subsequent to nitrogen dosing neutralizes this pumping action. (auth)

13688 PECULIARITIES OF URANIUM DEFORMATION FOR TENSION AT CONSTANT VELOCITY. Voloshchuk, A. I.; Zelenskii, V. F.; Konotop, Yu. F.; Miroshnichenko, Yu. T. At. Energ. (USSR); 29: 416-22(Dec 1970). (In Russian).

Tests of reactor-pure uranium and its alloy with 0.5% beryllium oxide were carried out. Uranium and its alloy were deformed to destruction at constant velocity. The structure of fractured specimens was studied. On the bais of tension curves, strength characteristics, and the structure, the existence of three high-temperature mechanisms for uranium deformation by creep was supported. Conditions of cavity formation in uranium and its alloy at different temperatures were under investigation. An analogy between uranium deformation conditions and peculiarities of cavitation swelling under irradiation was established. (auth)

13689 QUENCHING OF VACANCY DEFECTS INTO MOLYBDENUM. Evans, J. H. (Atomic Energy Research Establishment, Harwell, Eng.). Phil. Mag.; 22: 1261-4(Dec 1970).

The results of high-speed quenching investigations on zone-refined molybdenum are presented to support the inference of Burke, Köthe and Werth that vacancies cannot be efficiently quenched into molybdenum. Evidence is given to show that the quenching results of Meakin, Lawley and Koo, which are interpreted in terms of retained vacancies, can be fully explained by contamination effects. The implications of the molybdenum results on recent helium quenching work on tungsten are discussed. (auth) (UK)

13690 INTERSTITIAL SOLUTION HARDENING IN TANTALUM SINGLE CRYSTALS. Smialek, R. L.; Mitchell, T. E. (Case Western Reserve Univ., Cleveland). Phil. Mag.; 22: 1105-27 (Dec 1970).

The strong temperature dependence of the flow stress of body-centered cubic metals at temperatures below ~0.1 T_m has generally been attributed to the inherent lattice friction of the bcc structure (the Peierls stress). To test this hypothesis, very high purity (with regard to interstitials) tantalum single crystals were prepared. The purification treatment greatly reduced the temperature dependence of the flow stress as well as the athermal component of the yield stress of Ta which was given six zone-refining passes only. Small, controlled additions of interstitial oxygen, nitrogen and carbon (10 to 1000 at. ppM) were introduced into the pure Ta. Yield and flow stresses were found to increase rapidly with interstitial content over the temperature (4.2 to 550°K) and composition ranges investigated. Solution hardening could be divided into two regions: from 0 to ~300 at ppM the yield stress increases as the square root of concentration and is strongly temperature dependent; the rate of solution hardening is greatest for nitrogen, followed by carbon and then oxygen. In the region from ~300 to 1000 at ppM, the yield stress increases linearly with concentration and the rate of solution hardening is independent of temperature and the type of interstitial. Although interstitial impurity elements can make a major contribution to the temperature dependence of the flow stress, it appears that the residual temperature dependence after purification is due to the Peierls stress. (auth) (UK)

13691 CONTACT ANGLES OF GOLD AND SILVER ON A CLEAN TUNGSTEN SUBSTRATE. Sugita, Toshio; Ebisawa, Shigeo; Kawasaki, Koji (Electrotechnical Lab., Tokyo). Surface Sci.; 20: 417-20(Apr 1970).

Contract angles were measured for gold and silver on a clean tungsten substrate under an ultrahigh vacuum by the sessile drop method. Substrate temperatures were 960 to 1200°C. (G.M.C.)

13692 UNIDIRECTIONAL SOLIDIFICATION OF EUTECTIC ALLOYS. Beghi, Giorgio; Piatti, Giovanni (EURATOM, Ispra, Italy). Euro-Spectra; 9: 117-23(Dec 1970).

Production and properties of composites prepared by unidirectional solidification of eutectics is described. Composites prepared by this method contain fibers which are formed in place and in this way are grown in the matrix involving only one operation. The conditions under which the two phases are produced are close to equilibrium thus creating structures which are stable at high temperatures. (J.R.D.)

13693 WORK FUNCTION MEASUREMENTS ON MACROSCOPIC TUNGSTEN SPECIMENS. Van Someren, L. (Thermo Electron Corp., Waltham, Mass.). Contract AT(30-1)-3874. Surface Sci.; 20: 221-34(Apr 1970).

Accurate work function values are tabulated for carefully characterized macroscopic tungsten surfaces. It was found that the surface preparation can alter the work function values obtained by as much as 0.6 eV. Values greater than 5.1 eV were obtained on three types of substrate, up to 3 cm^2 in area. The values found for electropolished (111) and (100) single crystal surfaces lay between 4.5 and 4.6 eV. Large curved surfaces with $\varphi > 5$ eV could be obtained by vapor deposition from the chloride. Reference is made to detailed measurements of the performance of one surface as an emitter in a cesiated converter. (auth)

13694 COMPRESSIBILITY OF THE RARE EARTH-TRANSITION METAL INTERMETALLIC COMPOUNDS. Maury, Roland (CNRS, Grenoble, France). Compt. Rend., Ser. B; 271: 950-3(2 Nov 1970). (In French).

A strain gage was used to determine the compressibilities of intermetallic compounds A_nB_m between a rare earth A and a transition metal B. (France)

13695 VARESTRAINT TEST FOR REFRACTORY METALS. Lessmann, G. G.; Gold, R. E. (Westinghouse Electric Corp., Pittsburgh). Weld. J. (N. Y.); 50: 1s-8(Jan 1971).

The principles of the Varestraint test were applied to the evaluation of refractory metal alloys. This required development of a special test apparatus employing a modest specimen size for improved economy and compatible with the high purity inert atmosphere required for welding these alloys. Minimum specimen size is desirable because of high cost of these alloys and also to permit timely testing of limited production developmental alloys. The Varestraint apparatus satisfies these requirements, providing a timely and economic test for hot crack sensitivity. This test can be used both for alloy development and production surveillance. The test apparatus was designed for use in vacuum purged dry boxes and is completely compatible with high purity inert atmosphere. Augmented strain can be varied continuously from $\frac{1}{4}$ through 4%. In addition to varying the augmented strain—the primary Varestraint variable—the effect on hot cracking of varying other weld parameters such as unit weld length heat input have also been studied. Test reproducibility, in terms of bending or strain rate, was demonstrated using high speed photography. Alloys evaluated in demonstrating this apparatus included the alloys FS-85, B-66, and SCb-291, and the tantalum alloys Ta-10W, T-111, T-222, and ASTAR-811C. All of these are commercially available except ASTAR-811C (Ta-8W-1Re-0.7Hf-0.025C) which is an advanced alloy scaled up to production for the first time in this program. Primary emphasis was directed toward the tantalum-base alloys T-111 and ASTAR-811C due to their current importance for space power system applications requiring a combination of excellent weldability, ductility, and high temperature strength. B-66 is a particularly useful alloy for demonstrating the flexibility and range of this apparatus in defining hot crack sensitivity as a function of Varestraint test parameters. The propensity this alloy exhibits for hot cracking has been explained in terms of a theoretically derived correlation based on the relationship of Mo-V-Zr contents. In contrast to B-66 the other alloys are relatively insensitive to compositional variations or weld parameter selections. Excellent correlation was achieved using this test. (auth)

13696 WELD CRACKING AND MECHANICAL PROPERTIES OF 17 PERCENT CHROMIUM STEEL WELDMENT. Nishio, Y.; Ohmae, T.; Yoshida, Y.; Miura, Y. (Mitsubishi Heavy Industries, Ltd., Japan). Weld. J. (N. Y.); 50: 9s-18(Jan 1971).

A study was carried out on the cause for the weld cracking and embrittlement of the heat-affected zone of 17% chromium steel. It was found that by means of promoting the ferritizing and refining of the weld metal structure by adding of Nb, Ti, and Al to 17% chromium weldment, crack sensitivity is reduced, enabling the production of sound weld metal without preheating. Compared with structural low alloy steels, the 17% chromium weldment is apt to cause delayed cracking with a long incubation period. The embrittlement of the heat-affected zone is due to the formation of retained austenite and martensite structure; however, ductility can be recovered by decomposing these structures using postweld heat treatments. At postweld heat temperatures of 150 to 250°C, a phenomenon is evident in which the retained austenite is transformed to martensite, resulting in a decrease of ductility at the heat-affected zone. (auth)

13697 MEASUREMENT OF RESIDUAL STRESSES. Cepolina, A. G.; Canonico, D. A. (Oak Ridge National Lab., Tenn.). Weld. J. (N. Y.); 50: 31s-8(Jan 1971).

A modification of the Sachs "boring-out" method for determining residual stresses has been developed. This technique permits the determination of the distribution of the stresses and their levels over extremely short increments of distances. This technique was used for measuring the residual stresses present in gas tungsten-arc welds made in Hastelloy N, an alloy that is currently being employed in the Molten Salt Reactor Experiment. The specimen was $\frac{1}{2}$ in. thick plate, 12 in. in diameter. Circular welds 6 in. in diameter were simultaneously deposited on both flat faces. The equations applicable for the calculation of residual stresses in this specimen geometry are as follows: $(\sigma_R)_R =$

$(E\epsilon_T/2)[(R_0^2/R_2 - 1)]$, $\sigma_T = \sigma_R + (Rd\sigma_R/d_R)$, where σ_R = radial stress and σ_T = tangential stress. It was found that the maximum value of tangential residual stress was about 50,000 psi and was not particularly affected by either the shielding gas or heat input. Stress relieving at 1600°F for 4.5 hr proved to be the optimum heat treatment and reduced the tangential residual stress to about 5000 psi. Lowering of the maximum residual stress to about 10,000 psi was achieved at 1400°F after 6 hr; however, lower temperatures even for times as long as 100 hr only reduced the maximum residual stress by about 25%. (auth)

Structure and Phase Studies

Refer also to abstracts 14456, 14457, 14459, and 14461.

13698 DEFORMATION OF INDIUM. Harrod, Donald Lee. Pittsburgh; Univ. of Pittsburgh (1969). 110p. University Microfilms Order No. 70-16,367.

Thesis.

Slip, twinning, and deformation (kink) bands were observed as operative modes of deformation in indium single crystals strained in tension in the temperature range 0.01 to 0.95 T_m (T_m = 428°K). The crystallography of these modes of deformation was determined by surface trace analyses using optical microscopy in conjunction with Laue x-ray diffraction patterns. Indium had a tetragonal crystal structure and could be indexed as either face-centered-tetragonal or body-centered-tetragonal. The two descriptions differed merely by a 45° rotation about the C-axis. In the following, the planes and directions given refer to the face-centered-tetragonal structure. The slip planes were identified as {111}, (112), (212), (113), and {101}. Slip on {111} planes was observed at all temperatures except at 0.95 T_m, where the slip planes could not be identified, and were the only slip planes observed at 0.01 T_m. The other slip planes became operative with increasing temperature. The slip directions were identified as ⟨101⟩ and ⟨110⟩, though this was based on limited experimental observations. Twinning was observed as a prominent mode of deformation only at 0.01 T_m. The twinning system was identified as {101} ⟨101⟩. Deformation (kink) bands were observed on several crystals. They were observed in connection with primary slip on $(11\bar{1})$ at 0.01 T_m, $(21\bar{2})$ at 0.44 T_m, and $(1\bar{1}3)$ at 0.7 T_m. For the latter two slip planes, the plane of the kink band was identified as (101) and (110), respectively. The kink bands were more prominent at the higher temperature. The critical resolved shear stress decreased from 80 to 90 psi at 0.01 T_m to 10 to 20 psi at 0.95 T_m, though this was not based on a fixed slip system. At 0.01 T_m, the resolved shear stress for twinning was about the same as that for slip. Three-stage hardening curves were not observed, but several crystals exhibited features resembling a yield-point type elongation. (Diss. Abstr. Int., B)

13699 UNUSUAL DISSOCIATION OF DISLOCATIONS IN Ni_3Ta. Hayashi, Y.; Delavignette, P.; Amelinckx, S. (SCK-CEN, Mol, Belgium). Phys. Status Solidi; 42: 637-44(1 Dec 1970).

Dislocations in ordered Ni_3Ta are examined by transmission electron microscopy. [100] super-dislocations dissociate visibly into two dislocations both of which presumably consist of closely spaced partial dislocations. [001] super-dislocations dissociate into two dislocations, one of which is a partial dislocation and the other consists presumably of three very closely spaced partial dislocations. These dissociations seem to occur when the antiphase boundary energy is much larger than the stacking fault energy. The dissociation of the [100] super-dislocations allows an estimation of the order fault energy which is found to be of the order of 130 erg/cm^2. (auth)

13700 STRUCTURE AND WORK FUNCTION OF FILMS OF GADOLINIUM ON MOLYBDENUM. Bondarenko, B. V.; Makhov, V. I. (Moscow Physical-Technical Inst.). Sov. Phys.-Solid State (Engl. Transl.); 12: 1525-6(Jan 1971).

Translated from Fiz. Tverd. Tela; 12: 1915-17(Jul 1970).

The structure of gadolinium films on the (110) face of a single crystal of molybdenum, and the work function $\varphi(t)$ as a function of the time of deposition are investigated using the diffraction of slow electrons. In the region of the minimum value of $\varphi(t)$, where φ_{min} = 3.2 eV, the system has a surface structure of the form $Mo_{(110)} - C(1 \times 2)$ Gd. The work function on the $\varphi(t)$ plateau is characterized by the completion of a new layer of gadolinium with hexagonal packing. The changes in the structure and the work function of thick layers of gadolinium in the 300–1600°K temperature range are traced. (auth)

13701 ADSORPTION OF BARIUM ON A (110) FACE OF A MOLYBDENUM SINGLE CRYSTAL. Bondarenko, B. V.; Makhov, V. I. (Moscow Inst. of Tech. Physics). Sov. Phys.-Solid State (Engl. Transl.); 12: 1522-4(Jan 1971).

Translated from Fiz. Tverd. Tela; 12: 1912-14(Jul 1970).

Slow-electron diffraction has been applied to the structure of these films, with simultaneous measurement of the work function. If the barium is deposited with the source and target inadequately outgassed, the film is amorphous and the work function $\varphi(t)$ falls monotonically, whereas cleaner conditions produce an ordered structure and a dip φ_{min} = 2.3 eV on the $\varphi(t)$ curve even for deposition on a substrate at 300°K. This φ_{min} corresponds to surface structure $C(2 \times 2)Ba - Mo_{(110)}$. The plateau in $\varphi(t)$ at 2.7 eV represents completion of a second (denser) monolayer close to (0001). The structure and thermal stability of the films have been examined at 300–1300°K. (auth)

13702 STRUCTURE AND WORK FUNCTION OF LANTHANUM FILMS ON A (110) MOLYBDENUM SINGLE CRYSTAL SURFACE. Bondarenko, B. V.; Makhov, V. I. (Moscow Physical-Technical Inst.). Sov. Phys.-Solid State (Engl. Transl.); 12: 1646-8(Jan 1971).

Translated from Fiz. Tverd. Tela; 12: 2073-5(Jul 1970).

The structure of lanthanum films on a (110) molybdenum single crystal surface was studied using low-energy electron diffraction. The structural changes of the system and its work function dependence $\varphi(t)$ on deposition time were noted. $AC(2 \times 1)-La \cdot Mo_{(110)}$ structure was seen to form at φ_{min} = 2.8 eV. The emergence of a plateau on the $\varphi(t)$ curve is characteristic of the addition of a second hexagonal close-packed monolayer with its (0001) plane parallel to the substrate and work function equal to 3.0 eV. The thermal stability of the lanthanum film was studied in the 300–1500°K temperature range. (auth)

13703 ACTIVATION ENERGY OF ISOTHERMAL MARTENSITIC $\beta-\alpha'$ TRANSFORMATION. Mihajlovic, A. (Boris Kidric Inst. for Nuclear Sciences, Belgrade). J. Mater. Sci.; 5: 955-9 (Nov 1970).

The kinetics of isothermal $\beta-\alpha'$ martensitic transformation in the U−0.45 wt% Mo alloy were investigated. The specimens were quenched from the β region (690° C) and held isothermally at temperatures from 120 to −196° C (liquid nitrogen). By quantitative metallographic methods the percentage of the newly formed α'-phase was determined and the half-thickness c and radius r of plates calculated. The activation energy for nucleation period was estimated. It was found that ΔG depends linearly on temperature. The nucleation rate N was determined to be a parabolic function of temperature. A part of the T-T diagram below the M_s temperature was determined. (auth) (UK)

13704 SURFACE STATE OF BERYLLIUM AND FARADAIC YIELD OF ITS ANODIC DISSOLUTION. Epelboin, I.; Froment, M.; Garreau, M. (Univ., Paris). Corros.-Trait., Prot., Finition; 18: 433-40(Nov 1970). (In French).

Examination was made with a scanning electron microscope of the surface of beryllium samples after an anodic dissolution in electrolytes containing ClO_4^- ions: ternary ethanol-water-$LiClO_4$ mixtures and carbonate of propylene-water-$LiClO_4$. The change of the yield of the faradic dissolution is associated with the surface state under varying conditions. An attempt is made to explain this change in terms of the anodic layer structure. (auth) (France)

13705 EFFECTIVE SIZE OF AMERICIUM DISSOLVED IN LANTHANUM. Hill, H. H.; Ellinger, F. H. (Los Alamos Scientific Lab., N. Mex.). J. Less-Common Metals; 23: 92-4(1971).

The lattice parameters for lanthanum and lanthanum–americium alloys deviated only slightly from the Vegard line thus indicating that the effective size of Am in La (at least at dilute concentrations) is very close to that of elemental Am. (G.M.C.)

13706 METASTABLE PHASE $(Al_{0.5}Nb_{0.5})Ni_3$. Giessen, B. C.; Ray, R. (Northeastern Univ., Boston). J. Less-Common Metals; 23: 95-7(1971).

Small specimens of an $Al_{0.125}Nb_{0.125}Ni_{0.75}$ alloy were splat quenched in an inert gas atmosphere in an attempt to produce a $TiNi_3$-type phase in nonequilibrium. Three phases were identified namely: γ was a metastable extension of pseudobinary $(Al_{1-x}Nb_x)Ni_3$ solid solution with $x_{equil.} \leq 0.35$; ϵ was a new metastable phase isostructural with $(Al_{0.5}Ta_{0.5})Ni_3$; and β was a metastable phase, possibly an extension of the binary phase AlNi into the ternary system. A metastable phase $NbNi_2$ analogous to $TaNi_2$ could not be prepared. (G.M.C.)

13707 STRUCTURAL AND MAGNETIC CHARACTERISTICS OF THE PSEUDOBINARY SYSTEM $PrMn_2$–$ErMn_2$. Oesterreicher, H. (Oregon Graduate Center, Portland). J. Less-Common Metals; 23: 7-19(1971).

Alloys were prepared by induction melting and subsequent annealing at 950°K. Replacement of Er by Pr in $ErMn_2$ resulted in increasing lattice parameters in the hexagonal $MgZn_2$-type

XUM

structure. From $Pr_{0.283}Er_{0.05}Mn_{0.667}$ to $Pr_{0.163}Er_{0.17}Mn_{0.667}$ the alloys crystallized with a cubic face-centered structure with lattice parameters from 12.308 to 12.601 Å, isotypical with Th_6Mn_{23} (G-phase). This was also the structure of $(TmPr)Mn_2$. $PrMn_2$ crystallized as α-Mn type (x-phase), body-centered cubic, with a = 8.902 Å at 950°K, and as G-phase with a = 12.690 Å at 1000°K. In the liquid He range, Pr and Er magnetic moments aligned antiferromagnetically in the $MgZn_2$-type structure. High saturation moments at 4.2°K in the face-centered cubic phase suggested complex behavior. These alloys showed two Curie temperatures around 60 and 420°K and remained ferromagnetic above room temperature. Neutron diffraction at 4.2 and 300°K did not reveal antiferromagnetic ordering within crystallographic sites. Some kind of magnetic order may be retained beyond 1000°K. The compounds did not follow the Curie–Weiss law to 1000°K. $PrMn_2$ (x-phase) had a Weiss constant of –80°K and may order antiferromagnetically below 4.2°K on Pr sites. (auth)

13708 PHASE TRANSFORMATIONS IN NEAR EQUIATOMIC Ta–Ru ALLOYS. **Schmerling, M. A.; Das, B. K.; Lieberman, D. S.** (Univ. of Illinois, Urbana). Met. Trans.; 1: 3273-8 (Dec 1970).

Phase transitions in near equiatomic alloys of Ta-Ru were investigated with x-ray powder patterns at room temperature and resistance, metallography, and susceptibility measurements as a function of temperature. The results suggested a two-step cubic-to-tetragonal-to-orthorhombic martensitic transformation with decreasing temperature in alloys with compositions in the immediate vicinity of 50–50 at. % while those slightly farther away in composition exhibited a single transition from cubic-to-tetragonal on cooling to room temperature. (auth)

13709 EUTECTOID REGION OF THE Zr–Ga SYSTEM. **Easton, D. S.** (Oak Ridge National Lab., Tenn); **Betterton, J. O. Jr.** Met. Trans.; 1: 3295-9(Dec 1970).

The zirconium-rich portion of the Zr-Ga phase diagram was determined by the optical examination of microstructures of isothermally annealed and quenched alloys. A deviation from binary equilibrium was observed even though careful selection of materials and techniques held impurities to a minimum and produced alloys with a purity of at least 99.9%. The slopes of the α-β boundaries were depressed and the range of solubility of the solid solution phases was restricted when compared to the phase diagrams of other Group IIIB elements, apparently as a result of the large difference in atomic size between zirconium and gallium. The a_0 and c_0 lattice constants of cph zirconium were contracted and the axial ratio was expanded by the addition of gallium. The change in c/a at 1 at. % was very close to the change observed in Zr-In alloys, in agreement with general dependence of these properties in zirconium alloys upon electron to atom ratio. A eutectoid reaction occurred at 860°C with β solid solution (1.8 at. % Ga), decomposing into α solid solution (0.8 at. % Ga) and Zr_3Ga. Cast microstructures suggested a eutectic reaction in which liquid (21.0 at. % Ga) decomposed into β (8.0 at. % Ga) and Zr_5Ga_3. It is proposed that intermediate phases are formed at 25.0 at. % Ga (Zr_3Ga), 37.5 at. % Ga (Zr_5Ga_3), and 50.0 at. % Ga (ZrGa) although the exact composition was not determined. (auth)

13710 DEFORMATION IN WROUGHT Mg–9Wt. PERCENT Y. **Eckelmeyer, Kenneth H.; Hertzberg, Richard W.** (Lehigh Univ., Bethlehem, Pa.). Met. Trans.; 1: 3411-14(Dec 1970).

Considerable tensile-compressive yield strength anisotropy is normally associated with textured wrought magnesium alloys. The ease of $\{10\bar{1}2\}$ twinning is responsible for the lower compressive yield strengths of these materials. In Mg-9 wt % Y, however, approximately equal tensile and compressive yield strengths of about 50 ksi were previously reported. This investigation was performed to study the deformation of wrought Mg-9 wt % Y with the purpose of understanding its unusual isotropic behavior. It was found that almost no $\{10\bar{1}2\}$ twinning occurred in this alloy, thus accounting for the absence of anisotropy. Initial plastic deformation both in tension and compression occurred almost entirely by slip, primarily on the basal plane. Subsequent deformation occurred by a combination of slip and $\{11\bar{2}1\}$ twinning with short $\{10\bar{1}2\}$ twins appearing only occasionally. (auth)

13711 REGULAR NETWORK OF ANTI-PHASE BOUNDARIES IN THE X-PHASE OF THE SYSTEM Fe–Cr-Mo-Ti. **Meulemans, M.; Delvignette, P.; Garcia-Gonzales, F.; Amelinckx, S.** (CEN–SCK, Mol, Belgium). Mater. Res. Bull.; 5: 1025-30(Dec 1970).

Very striking, regular networks of anti-phase boundaries were observed in the X-phase of composition $Fe_{36}Cr_{12}Mo_5Ti_5$. (auth)

13712 PHASE DIAGRAM FOR Zr–Co SYSTEM. **Bataleva, S. K.; Kuprina, V. V.; Burnasheva, V. V.;** (and others). Vestn. Mosk. Univ., Ser. II. Khim.; 11: 557-61(Sep–Oct 1970). (In Russian).

The phase diagram for the Zr–Co system is given. Data on the various phases in the system as a function of temperature are tabulated. (P.C.H.)

13713 RECOVERY OF LOW-TEMPERATURE ELECTRON-IRRADIATED COBALT CRYSTALS. **Maury, F.** (CNRS, Orsay, France); **Roux, G.; Vajda, P.;** (and others). Cryst. Lattice Defects; 1: 361-2(Dec 1970).

The recovery of monocrystalline hcp cobalt specimens irradiated with 0.7 and 1.7 MeV electrons at ~7°K was studied. Both energy and orientation dependences were observed. In substages I_A–I_B, recovery of close pairs created in the focussing $\langle 11\bar{2}0\rangle$ direction was particularly important, while in substages I_D–I_E, migration of interstitials produced in the (0001) crystal was predominant. (auth)

13714 ETCHING DISLOCATIONS IN ZIRCONIUM. **Dickson, J. I.; Dedo, A.; Craig, G. B.** (Univ. of Toronto). J. Nucl. Mater.; 38: 116-17(Jan 1971).

An etching technique which reveals fresh glide dislocations on all crystallographic faces of alpha-zirconium was developed. The etchant consisted of 250 ml of water, 35 ml of nitric acid, 21 ml of hydrochloric acid, and 1 ml of hydrofluoric acid. The etching time was 5 to 20 sec. The etchant revealed pure edge, pure screw and mixed dislocations but not dislocations lying on a plane which makes a small angle with the surface. (auth)

13715 ELECTRON MICROSCOPY STUDY OF THE PRECIPITATION PROCESSES IN Cu–2 WT. PERCENT Be ALLOY. **Shimizu, Ken'ichi** (Osaka Univ.); **Mikami, Yasuharu; Mitani, Hiroyasu; Otsuka, Kazuhiro.** J. Jap. Inst. Metals; 34: 1108-15 (Nov 1970). (In Japanese).

In order to make clear the precipitation processes in Cu–Be alloy, the structural changes upon aging of the 2 wt % Be alloy were examined in detail through an electron microscope with the use of the selected-area electron diffraction technique. The change of electron diffraction patterns with increasing aging time or temperature was as follows. In the earliest stage the long streaks appeared in the ⟨001⟩ directions due to the formation of Guinier–Preston (G. P.) zones. Upon prolonged aging the streaks became shorter and intensity maxima appeared at about ⅔ of $\{002\}_\alpha$ reciprocal lattice vectors. This stage was distinct from the G. P. zones and may be designated as the γ'' phase. The structure of γ'' was considered to be body-centered tetragonal, Cu atom being at the corner and Be atom at the body-center, and was different from that proposed by Geisler. Aging at higher temperatures caused another superlattice reflection (CuAu(I) type, γ') to appear and ⅔ reflections mentioned above to split. This splitting corresponded to the formation of the γ phase. From these observations, it was concluded that the aging sequence in this alloy was $\alpha \rightarrow$ G. P. zone $\rightarrow \gamma' \rightarrow \gamma' \rightarrow \gamma$. The structure of the final precipitate γ was identified to be the same as that of the equilibrium phase with the lattice constant 2.71Å. The new orientation relationship between the γ and α was proposed, such that $\{103\}_\gamma // \{1\bar{1}3\}_\alpha$, $\langle 010\rangle_\gamma // \langle 110\rangle_\alpha$. Among several orientation relationships reported so far, only this one was consistent with experimental results. In spite of the identity in structure, the final precipitates γ were associated with strain contrast around themselves, in contrast to the equilibrium phase. This fact suggests that the transformation γ' to γ might be martensitic in the nucleation stage. The mechanism of transformation γ' to γ is discussed along this line and from the viewpoint of coherency. (auth)

13716 METASTABLE CONSTITUTION AND THE SUPERCONDUCTING TRANSITION BEHAVIOR OF Zr–Ta ALLOYS. **Narasimhan, S. L.; Taggart, R.; Polonis, D. H.** (Univ. of Washington, Seattle). Contract AT(45-1)-2225-T13. J. Nucl. Mater.; 38: 83-7(Jan 1971). (RLO-2225-T13-3).

The metastable constitution and superconducting transition temperature were studied for a series of Zr–Ta alloys over the composition range from 0 to 20 at. % Ta. The transition temperatures of the as-quenched martensitic and retained beta alloys increased as the tantalum content was increased. The precipitation of the metastable omega phase on aging the as-quenched alloys led to a net decrease in the transition temperature and a broadening of the superconducting transition. These studies also reveal that Zr–Ta alloys are potentially important for superconducting applications. (auth)

13717 METASTABLE PHASE TRANSFORMATIONS IN BCC TRANSITION METAL ALLOYS. **Perkins, Arthur Jeffery.** Cleveland; Case Western Reserve Univ. (1969). 359p. University Microfilms Order No. 70-25,988.

Thesis.

Transmission electron microscopy and diffraction have been used to study the isothermal and athermal omega transformations in Zr–Nb alloys, and the pre-martensitic transition in near-equiatomic Ti–Ni alloys. The morphology and microstructural distribution of the aged omega phase have been determined. The particles are cuboidal, with $\{100\}_\beta$ faces, and aligned in $\langle 100\rangle_\beta$ directions in a three dimensional modulated array. These things are interpreted in terms of precipitate-matrix lattice mismatch and elastic strain energy considerations. The critical factors are a high mismatch and the lower stiffness of an anisotropic beta matrix having soft $\langle 100\rangle$ directions. The kinetics of development of a modulated beta : omega microstructure have been examined through quantitative electron micrographic measurements, and are revealed to be representative of a selective nucleation and coarsening process, with the average particle size increasing according to a $(\text{time})^{1/3}$ growth law during the period when this process operates. The aged omega phase initially nucleates heterogenously from the retained beta phase, and sequentially adds cuboidal particle members to small aligned groups; the particles are added without regard to the particular crystallographic orientation variant, of which there are four possible. The close-spaced particles within these groups resist gross coarsening. Once precipitation is complete, in terms of the development of a completely modulated microstructure, further coarsening is resisted. Coherency of the particles is maintained up to the largest particle sizes developed, ≈1000 Å. At long aging times, the equilibrium alpha phase precipitates from the metastable beta–omega microstructure. This phase utilizes the strained beta–omega interfaces as nucleating sites and later extends into needle-like plates. In the Zr-12% Nb alloy, which has a high ω_s temperature, the pre-aging precipitation of a finely dispersed athermal omega phase is found to have an important role in the subsequent rapid isothermal development of a modulated microstructure. Without the assistance of such a prior structure, there is a much lower degree of isothermal nucleation. This type of role for athermal omega is not found to be general for all of the alloys which develop a modulated structure. Athermal omega in Zr–Nb forms as stacks of parallel thin discs with $\{112\}_\beta$ habit planes and stack axes near the appropriate $\langle 112\rangle$ direction. This morphology and distribution is a reflection of the diffusionless shuffle mechanism of the lattice transformation and is not affected by elastic strain considerations such as for the diffusion-controlled aged phase. The "diffuseness" of the athermal phase increases with solute content and is found by electron diffraction to be accompanied by a characteristic distribution of scattered intensity in reciprocal space. This distribution has the same form in several systems examined (Zr–Nb, Hf–Nb, Ti–V), consisting of structured $\{111\}_\beta$ reciprocal walls of diffuse intensity and streak intersections consistent with high angle $\langle 112\rangle$ streaks from relpoints in neighboring zones. This distribution is believed to be due to thermal diffuse scattering from a particular transverse lattice vibration mode, namely $\langle 112\rangle$ $\langle 111\rangle$, which operates in the beta phase as the initial manifestation of lattice instability, and which precedes the actual change of basis to the new (omega) structure when the temperature is reduced further. An analogous sequence to the athermal omega transition is found to precede the low-temperature martensitic transformation in near-equiatomic Ti–Ni alloys. In this case, the diffuse intensity distribution is also $\{111\}$ walls, with intersections consistent with $\langle 312\rangle$ and $\langle 210\rangle$ streaks, reflecting possible $\langle 312\rangle$ $\langle 111\rangle$ and $\langle 210\rangle$ $\langle 111\rangle$ transverse vibration modes. The structure of the pre-martensitic phase which develops on further cooling has not yet been determined rigorously; it is not the hexagonal omega structure. Both of these transitions are felt to arise from the same general tendency of the beta-type structure to become distorted to a more closely packed or lower symmetry structure at low temperatures. (Diss. Abstr. Int., B)

13718 TWINS OF TETRAHEDRAL FORM IN BERYLLIUM. Avotin, S. S.; Papirov, I. I.; Tikhinskii, G. F. (Inst. of Technical Physics, Kiev). Sov. Phys.-Cryst. (Engl. Transl.); 15: 671-4 (Jan-Feb 1971).

Translated from Kristallografiya; 15: 783-7(Jul-Aug 1970).

On deforming high-purity beryllium single crystals, twins of tetrahedral form are observed. The conditions underlying the formation of these twins are discussed and their precise shape is determined. The twins are in fact bounded by planes of the $\{10\bar{1}2\}$ and $\{12\bar{3}0\}$ or $\{13\bar{4}0\}$ type. The formation of tetrahedral twins is accompanied by the development of cracks leading to the rupture of the beryllium on subjecting to complex forms of deformation. (auth)

13719 CORRELATION OF AUGER EMISSION SPECTROSCOPY, LEED AND WORK FUNCTION MEASUREMENTS FOR THE EPITAXIAL GROWTH OF THORIUM ON A W(100) SUBSTRATE. Pollard, J. H. (Franklin Inst., Swarthmore, Pa.). Surface Sci.; 20: 269-84(Apr 1970).

Auger emission spectra of the Th–W (100) system were measured and a coverage calibration of thorium Auger peaks, observed at 64 and 78 V, was made by correlating with existing work function data. Carbon and sulphur peaks, observed impurities, were calibrated relative to W Auger peaks of the clean surface. With the substrate at room temperature and pressures $<5 \times 10^{-10}$ torr during evaporation, the measurements show CO to be a major impurity in the thorium overlayers. The co-adsorption of CO and Th was precluded by heating the W substrate to 1400°C during evaporation. Under these conditions the LEED patterns showed that thorium formed initially a $c2 \times 2$ structure followed by a 1×1 ionic pseudomorphic monolayer. Further thorium adsorbed at random filling $c2 \times 2$ sites on this overlayer and thereafter nucleated forming islands of bulk thorium with random orientation relative to the substrate. Photomicrographs taken of the surface with 25 monolayers equivalent coverage of thorium support these conclusions. (auth)

13720 β-TO-α MASSIVE TRANSFORMATIONS IN SILVER–ZINC, SILVER–CADMIUM, AND COPPER–ZINC ALLOYS. Ayers, Jack Duane. Pittsburgh; Carnegie-Mellon Univ. (1970). 198p. University Microfilms Order No. 70-20,892.

Thesis.

The β to α massive transformations in Ag–Zn, Ag–Cd, and Cu–Zn alloys were studied under adiabatic conditions by pulse-heating retained β phase samples from room temperature to higher temperatures and measuring the resistivity changes during the subsequent reactions. The upper temperature limit of massive growth was determined in the alloys studied, and it was found that massive growth in these alloys was limited at high temperatures by the occurrence of the competitive transformation of the β phase to Widmanstätten α. It was also found that in all three alloy systems there was a competitive interaction between the massive transformations and bainitic transformations at low temperatures, and it is thought that massive growth at low temperatures is limited by this competitive interaction. The temperature-composition limits of massive growth did not correspond to the $\alpha/\alpha + \beta$ phase boundary in any of the alloys studied, and it is therefore concluded that the limits of massive growth are determined by the competitive interactions between massive and alternative transformation modes, and not by thermodynamic considerations. (Diss. Abstr. Int., B)

13721 DEPENDENCE OF RADIATION DAMAGE ON DEVIATION FROM THE BRAGG ANGLE. Shoaib, K. A.; Segall, R. L. (Univ. of Warwick, Eng.). Phil. Mag.; 22: 1269-72(Dec 1970).

A sensitive method of detecting radition damage in metals, by electron microscope observation of the shrinking of small, faulted, vacancy loops produced by prior quenching, was used to study displacement damage in electron-irradiated aluminum. It was shown that the difference in damage rate between specimens oriented for anomalous transmission and absorption is sufficiently small to be accounted for on the basis of present theories. (auth) (UK)

Radiation Effects

Refer also to abstracts 13782, 14427, and 14430.

13722 (JUL-658-FN) MEASUREMENT OF STORED ENERGY IN ELECTRON-IRRADIATED PLATINUM BELOW 40°K. Feese, Klaus (Kernforschungsanlage, Juelich (West Germany). Institut fuer Festkoerper- und Neutronenphysik). Apr 1970. 47p. (In German). Dep. NTIS (U. S. Sales Only).

Caloric measurements on electron-irradiated Pt were reported. After irradiation with 3-MeV electrons at temperatures below 10°K the stored energy released in the annealing of the radioinduced Frenkel pairs was measured between 15 and 40°K. A study of the possible annealing methods and caloric measurement methods with respect to the set requirements led to the selection of a twin calorimeter in which the effective heat capacity of an irradiated sample in time-linear heating was compared quantitatively with that of an unirradiated sample. The surroundings of the samples were maintained at 4.2°K. A basic analysis of the heat transfer in the calorimeter together with suitable blank measurements led to an extensive consideration of construction-caused asymmetries. The reproducibility and the absolute measurement certainty were proved by blank measurements and measurements with electrically simulated stored energy. For values in the order of magnitude of the integral stored energy to be expected in irradiation, a total measurement uncertainty of ±8% was obtained. The recovery curves measured after irradiation of the 20 μm thick Pt foils showed systematic deviations from that observed by other authors in resistance recovery. These deviations corresponded to a supplementary energy release increasing steadily with temperature. It could be shown that this type of energy release occurred when the samples were irradiated with subthreshold electrons (1.4 MeV), which are not in a position to produce Frenkel pairs. This effect can be explained principally by ionization effects in the gas layer adsorbed on the sample surface. After correction of the recovery curves with respect to this background, the value $\Delta E/m\phi = 1.0 \times 10^{-19} [W_{sec}/g\ cm^{-2}]$ ±24% was given for the integral stored energy in the range of the recovery stages I_c to I_E. The uncertainty given can be traced principally to the uncertainty of the energy release caused by subthreshold irradiation. From the value of this ratio, the effective cross section of defect production can be calculated for 3-MeV electrons on Pt. By use of a theoretical estimated value for the formation energy of a Frenkel pair in Pt of E_F = 6 eV, the value of the effective cross section of defect production is given as $\sigma_D = (50 \pm 25)$b. An uncertainty in the theoretical estimation of E_F of about ±30% is contained in the error given in addition to the measurement uncertainty. From the effective cross section measured in the present study one obtains from the experimentally well verified damage rate for 3-MeV electrons the resistance contribution of the unit concentration in Frenkel pairs as $\rho_F = (20 \pm 10) \times 10^{-4}$ Ωcm. (tr-auth)

13723 (JUL–664-FN) LATTICE PARAMETER MEASUREMENTS ON ALUMINUM AFTER ELECTRON IRRADIATION AT LOW TEMPERATURES. Wagner, Hans (Kernforschungsanlage, Juelich (West Germany). Institut fuer Festkoerper- und Neutronenphysik). Jun 1970. 58p. (In German). Dep. NTIS (U. S. Sales Only).

The lattice parameter with a resolution of $\Delta a/a = 6.5 \times 10^{-6}$ and the electrical resistance were measured simultaneously in high purity Al after irradiation with 3 MeV electrons. Liquid helium flowed around the samples during the irradiation and during the measurement. The experiment consisted of four irradiations at two different irradiation doses—3×10^{19} and 12×10^{19} el/cm^2. After irradiation with the maximum dose a great change of the lattice parameter of $\Delta a/a = 9 \times 10^{-4}$ occurred; the corresponding increase of the residual resistance was $\Delta\zeta = 600$ nΩcm. It was shown that up to saturation the ratio of lattice parameter change and resistance change remained constant. The value was $\Delta(\Delta a/a)/\Delta\zeta = \eta = (1.61 \pm 0.10) \times 10^3$ (Ωcm)$^{-1}$. From the constancy of the ratio η it follows that the specific resistance ζ_F is independent of the defect concentration. The possibility that both properties show the same non-linear dependence on the defect structure can be concluded with good probability. At the conclusion of all four irradiations the samples were isochronously recovered. The recovery of the lattice parameter corresponds well with the resistance recovery. The ratio is constant for all recovery stages and equals the value in the irradiation. It was concluded that the specific resistance of the defects does not depend on the configuration. Interstitial atom agglomerates contribute to the resistance just as do the corresponding interstitial atoms when they are present individually in the lattice. The saturation behavior of Al was also studied. At higher concentration a linear decrease of the damage rate was measured. The extrapolated saturation value for the resistance was $\zeta_\infty = 995 \pm 10$ nΩcm. In both measurement methods a non-linear decrease of the damage rate curve from small up to average defect concentrations was observed. From the analogous behavior of both material properties it follows that the increased damage rate at small concentrations lies in the mechanism of the defect production. (tr-auth)

13724 (ORNL–4590, pp 100-34) INVESTIGATIONS OF IRRADIATED MATERIALS. (Oak Ridge National Lab., Tenn.).

From Heavy-Section Steel Technology Program.

Results of investigations of radiation effects on pressure vessel steels are reported. Heavy-section specimens of Type A533B were neutron irradiated and subjected to postirradiation Charpy-V notch testing. (J.R.D.)

13725 ACCELERATION OF CLIMB-CONTROLLED CREEP BY NEUTRON IRRADIATION. Lewthwaite, G. W. (United Kingdom Atomic Energy Authority, Caithness, Scotland). J. Nucl. Mater.; 38: 118-20(Jan 1971).

From theoretical considerations it was concluded that if a material creeps by a process whereby dislocations overcome obstacles to slip by climb then, in principle, the creep rate may be accelerated by a flux of damaging neutrons. (auth)

13726 EFFECTS OF NEUTRON IRRADIATION ON U_2Ti. Baran, Z.; Bazin, J.; Bloch, J.; Accary, A. (CEN, Saclay, France). J. Nucl. Mater.; 38: 67-76(Jan 1971). (In French).

The completely ordered, hexagonal U_2Ti phase was submitted to a sequence of neutron irradiations at a temperature of about 100°C. After each irradiation the x-ray diffraction pattern was determined using an x-ray diffractometer specially designed for radioactive materials examination. It was found, that the diffraction pattern progressively changed from the one characteristic of the ordered phase to the one corresponding to the cubic disordered phase. Comparing the intensities of the superlattice lines to those of the fundamental lines of the phase, the degree of order was measured as a 0 value for a fluence of 10^{18} n/cm^2. This experimental result is interpreted assuming, that every elementary fission causes the complete disordering in a small volume of the ordered matrix. The value of this volume is calculated and equals 3.2×10^{-17} cm^3. This volume consists roughly of 1.7×10^6 atoms. (auth)

13727 DAMAGE IN ALUMINUM BY 200 kV ELECTRONS. Wolfenden, A. (Oak Ridge National Lab., Tenn.). J. Nucl. Mater.; 38: 114-15(Jan 1971).

Electron displacement damage was observed in high-purity aluminum at voltages as low as 200 keV. The damage became visible after about 20 min exposure to the 200 keV electron beam and was in the form of loops that could be tilted in and out of contrast. (G.M.C.)

13728 ELECTRON-MICROSCOPIC EXAMINATION OF NICKEL IRRADIATED WITH α PARTICLES. Ibragimov, Sh. Sh.; Reutov, V. F. Fiz. Metal. Metalloved.; 29: 1268-73(Jun 1970). (In Russian).

Radioinduced defects in metals were studied by exposing 99.99% pure nickel foil to 42 to 44 MeV α particles in the cyclotron at a mean integral flux of 3.8×10^{17} α particles/cm^2. Electron-microscopic examination of the specimens revealed that the irradiation produced 100 to 1000 Å dislocation loops with a mean density of about 10^5 loops/cm^2. Heating of the specimens by the electron beam generated dislocations probably as a result of the motion and action of the dislocation loops. Helium-field pores were also noted primarily along the dislocation lines. Pores located at the grain boundaries and at the intersection of several dislocations were found to be much larger than those in other positions. This was attributed to the accelerated diffusion of helium atoms through the so-called dislocation cannals. The rate of motion of the pores in the case of temperature gradient was found to be indirectly proportional with their radii. Cyclic heating caused the pores to become octahedral in shape. The helium pores tended to fix the dislocations to a given position and to prevent their motion. (TTT)

13729 ANOMALOUS BEHAVIOR OF CARBON ATOMS AT LOW TEMPERATURES IN MARTENSITE IRRADIATED BY ELECTRONS. Kritskaya, V. K.; Narkhov, A. V. (Inst. of Metal Science and Physics of Metals, Moscow). Fiz. Metal. Metalloved.; 29: 1293-4(Jun 1970). (In Russian).

It was earlier found that at room temperature, carbon atoms in the irradiated martensitic carbon steels tended to increase the tetragonal character (c/a ratio) of the lattice; this was attributed to disorder reactions during the exposure, followed by ordering at room temperature. Roentgenographic study of martensitic specimens irradiated with a ~ 2 MeV electron beam at a dose of ~ 10^{19} electrons/cm^2 while the temperature of the specimens was kept between 40 and 68°C, indicated a sharp decrease of the tetragonal character. This unexpected effect was discovered after the specimens were chilled to temperatures between −40 and −50°C. This low-temperature change of the lattice parameter was not caused by changes in the carbon concentration but by its redistribution caused by the sudden transition of carbon from the octahedral holes along the tetragonal c axis in the radiation-induced point defects in the martensite. These transitions did not require long-range diffusion of carbon but occurred at the elementary cell boundaries. (TTT)

13730 RADIATION AGING OF CHROMIUM. Kritskaya, V. K.; Kuznetsova, A. P.; Sharov, B. V. (Inst. of Metal Science and Physics of Metals, Moscow. Inst. of Theoretical and Experimental Physics, Moscow). Fiz. Metal. Metalloved.; 29: 1296-9(Jun 1970). (In Russian).

A previous study of the properties of neutron-irradiated metals and alloys revealed that chromium undergoes radiation aging. The phenomenon was found to depend on the dislocations and impurities present in the metal before the irradiation. This problem was further examined on electrolytic chromium specimens of varying structure. Some of the specimens were recrystallized in an inert atmosphere; others were subjected to various mechanical and heat treatments. The resulting recrystallized, polygonized, and 30%-deformed specimens possessed widely different dislocation densities. They were exposed within a month to an integral dose of ~10^{19} n/cm^2 at ~80°C and an energy of $E_n > 1$ MeV. It was found that the joint effect of deformation-irradiation or irradiation-deformation decreased or completely eliminated the effect of aging in chromium. Study of microhardness changes as a function of annealing temperature of the deformed, unirradiated and polygonized, irradiated specimens indicated that radiation aging occurred at lower temperatures than deformation aging. (TTT)

13731 VACANCY TETRAHEDRA IN COPPER DUE TO ELECTRON IRRADIATION IN THE HIGH-VOLTAGE MICROSCOPE. Ipohorski, M.; Spring, M. S. (Cambridge Univ., Eng.). Phil. Mag.; 22: 1279-83(Dec 1970).

Under suitable conditions of irradiation in the high-voltage microscope, stacking-fault tetrahedra were found to form in copper specimens. These defects are thought to be of vacancy-type, in contrast to the more usually observed displacement damage, which is of interstitial type. (auth) (UK)

13732 DISLOCATION LOOP GROWTH IN AN ELECTRON IRRADIATED THIN FOIL. Norris, D. I. R. (Berkeley Nuclear Labs., Eng.). Phil. Mag.; 22: 1273-8(Dec 1970).

Large faulted dislocation loops were grown in thin foils of nickel at 450°C by electron irradiation in the beam of a high-voltage electron microscope. Loop size was directly proportional to time, implying that surfaces are the dominant sinks for interstitials. A model of loop growth under these conditions was developed and predicts a growth rate in agreement with that observed. (auth) (UK)

13733 DIRECTIONAL DEPENDENCE OF ATOMIC DISPLACEMENTS IN COBALT CRYSTALS. Maury, F. (CNRS, Orsay, France); Vajda, P.; Lucasson, A.; (and others). Phil. Mag.; 22: 1265-7(Dec 1970).

Monocrystalline cobalt specimens were irradiated below ~7°K in various crystallographic directions by electrons. Results in the energy range 0.45 to 0.90 MeV are presented. The damage rate was highest for the electrons incident perpendicularly to the (0001) plane and lowest for the $(11\bar{2}0)$ plane. The threshold energies for displacement are deduced to 22.0 ± 2 eV in the $\langle 0001 \rangle$ direction and 25.0 ± 2 eV in the $\langle 11\bar{2}0 \rangle$ direction. For the $(10\bar{1}0)$, $(30\bar{3}4)$ and $(30\bar{3}8)$ specimens, the damage rates and the threshold energies are intermediate between those of the (0001) and $(11\bar{2}0)$ specimens. (auth) (UK)

Ceramics and Cermets

Refer also to abstracts 13625–13628.

13734 STRUCTURE ET PROPRIETES DES SURFACES DES SOLIDES. (Structure and Properties of the Surfaces of Solids). International Conference, Paris, France, 7–11 July 1969. Paris; Centre National de la Recherche Scientifique (1970). 232p. (In several languages). (CONF-690728).

Thirty-one papers were presented at the conference. A separate abstract was prepared for one paper. The remaining papers were not in scope for NSA. (France)

For an abstract of one paper see: 13735.

Corrosion and Erosion

Refer also to abstract 13636.

13735 STUDY OF GRAPHITE OXIDATION BY LOW ENERGY ELECTRON DIFFRACTION. David, G.; Escard, J.; Goldsztaub, S. (Univ., Strasbourg). pp 179-82 of Structure et Proprietes des Surfaces des Solides. Paris; Centre National de la Recherche Scientifique (1970). (In French).

From Conference on Structure and Properties of the Surfaces of Solids, Paris, France. See CONF-690728.

The oxidation of graphite under high vacuum was studied. By careful cleavage, (0001) surfaces without large ledges were obtained and diffraction patterns with ternary symmetry were observed. In the case of stacked hexagonal layers, changes in parity of the surface layer were detected. On heating a crystal in oxygen at 10^{-5} torr, it was found that graphite oxidation occurs above 570°C. This oxidation is followed by a change in symmetry and orientation of the diffraction pattern. After several successive oxidations, the electron diffraction pattern with ternary symmetry becomes hexagonal and then reverts back to ternary symmetry with an orientation different from the original. (auth) (France)

Preparation and Fabrication

Refer also to abstracts 12924 and 12925.

13736 (EUR-4551) NUCLEAR FUEL WITH BURNABLE POISON. PART 2. PREPARATION AND OUT-OF-PILE EVALUATION OF Gd_2O_3 POISONED UO_2 PELLETS. Topical Report, January 1, 1969–May 31, 1970. Abate-Daga, G.; Amato, I.; Grappiolo, G. (FIAT, Turin (Italy). Sezione Energia Nucleare. ANSALDO S.p.A., Genoa (Italy)). Nov 1970. 40p. Dep. NTIS (U. S. Sales Only). EUR FF 6.65.

Gd_2O_3 microspheres about 500 microns in diameter were molybdenum-coated by metal vapor deposition in a fluidized bed. The coating thickness was maintained in the range 25 to 30 microns. The optimum density of gadolinia microspheres, in order to maintain coating integrity at high temperature, was in the range 85 to 90% of theoretical density (TD). UO_2 pellets poisoned with 1200 ppM of Gd_2O_3 were obtained at about 95% TD. Tests performed at high temperature both under gradient and isothermal conditions showed an acceptable behavior of molybdenum-coated gadolinia microspheres in UO_2 pellets. (auth)

13737 (KFK-1292) THE PRECIPITATION OF VANADIUM ON UO_2 SPHERES FROM THE GAS PHASE. Schneider, Helga; Schoenwald, Dieter (Kernforschungszentrum, Karlsruhe (West Germany). Institut fuer Material und Festkoerperforschung). Oct 1970. 19p. (In German). Dep. NTIS (U. S. Sales Only).

A method is described to provide for fluidized bed coating of spherical UO_2 with metallic vanadium having a chlorine content <0.01%. By reduction of VCl_4 above 950°C in the presence of hydrogen, up to 45 vol.% of vanadium was vapor deposited on batches of 30 to 50 g of UO_2 spheres. The coatings had bright surfaces, were of good quality, and were dense and uniform. The coated particles were used for fabrication of UO_2/V cermets of ideal structure and could be packed satisfactorily by isostatic hot compaction. (auth)

13738 PROCESS FOR PRODUCING URANIUM MONOCARBIDE. (to Snam Progetti SpA). British Patent 1,216,633. 23 Dec 1970. Priority date 24 Jan 1968, Italy.

A process for carburizing metallic U or U contained in low-melting alloys to obtain UC, UC_2 or U_2C_3 is described. The U or U-containing alloy is reacted with gaseous CH_4-H_2 mixtures. The reaction is effected at 700 to 1050°C. (J.R.D.)

13739 CARBON-INDUCED LATTICES OF BORON. I. Tetragonal $(B_{12})_4B_2C$ AND $(B_{12})_4B_2C_2$. Ploog, K.; Amberger, E. (Univ., Munich). J. Less-Common Metals; 23: 33-42(1971). (In German).

During the pyrolysis of BBr_3 and H_2 on tantalum wires at 900 to 1300°C under very clean conditions, elementary boron was formed with the II-tetragonal or α-rhombohedral structure in a reproducible manner. These lattices of pure boron disappeared when very small quantities of CH_4 or $CHBr_3$ were added to the BBr_3-H_2 mixture (maximal CH_4: BBr_3 = 0.03 : 1 mole %). By increasing the small carbon supply, the following lattices were induced: first the β-rhombohedral boron (which probably contained carbon) was obtained and then the new boron-rich borides $(B_{12})_4B_2C$ and $(B_{12})_4B_2C_2$ were formed. In these two borides with the lattice constants a = 8.77 and c = 5.07 Å the unstable lattice $(B_{12})_4B_2$ of the so-called I-tetragonal boron was stabilized by occupying one or two more tetrahedral holes in the icosahedron framework by single carbon atoms. When the carbon supply was further increased the two known rhombohedral phases $B_{13}C_2$ and B_4C were obtained. (auth)

13740 FORMATION OF LATTICES OF PURE BORON. Amberger, E.; Ploog, K. (Univ., Munich). J. Less-Common Metals; 23: 21-31(1971).

On the pyrolysis of a mixture of BBr_3 and H_2, on tantalum wires at 900 to 1300°C and in the absence of any foreign atoms, the following boron lattices were obtained: the glassy amorphous boron, α-rhombohedral boron, and II-tetragonal boron. Temporarily, these were certainly the only genuine modifications of boron formed. The I-tetragonal lattice was never formed. The so-called I-tetragonal boron, therefore, did not represent a modification of pure boron but a boron-rich boride, induced by doping with foreign atoms. The same probably applies to the β-rhombohedral boron, but with less certainty. Previous analysis of two-dimensional x-ray diffraction data by applying the convolution molecule method shows that nearly regular icosahedral groups are present in II-tetragonal boron. (auth)

13741 NUCLEAR FUEL ELEMENT MANUFACTURING PROCESS AND FUEL ELEMENTS OBTAINED BY APPLICATION OF THE PROCESS. Moreau, Claude (to Commissariat a l'Energie Atomique). French Patent 1,588,611. 9 Mar 1970. Filed 23 Sep 1968. (In French).

A method is described for the manufacture of nuclear fuel elements made up of a nucleus of refractory fuel (U or Pu oxides, carbides or nitrides) dispersed in a carbon matrix, and a carbon envelope surrounding the nucleus. These fuel elements are designed for use in reactors cooled by a high temperature gas. The process involves: the coating of refractory nuclear fuel particles with a layer of graphite by projection of a mixture containing graphite and an organic diluant; preparation of an envelope by shaping and drying of a paste made up of graphite powder and a binder; filling of the envelope with the coated particles; plugging of the envelope by a plug made of the same paste; baking and pyrocarbon impregnation of the envelope in a single operation by heating to a temperature between 850 and 1100°C, preferably between 900 and 1000°C, in an atmosphere of gaseous hydrocarbons. The nuclear fuel particle size before coating corresponds to passage through the 1000 μ sieve and if possible the 400 μ sieve. (auth) (France)

13742 METALLOGRAPHIC PREPARATION OF URANIUM–SILICON ALLOYS. Moore, Donald A.; Walker, Durham E. Y.

XUM

(United Kingdom Atomic Energy Authority, Salwick, Eng.). Prakt. Metallog.; 7: 698-706(Dec 1970). (In English and German).

Methods of polishing and etching uranium-silicon alloys (1.8 to 4 wt % Si) are described and the results obtained with the most satisfactory techniques are discussed. Normal etches distinguished between α−U, U_3Si_2 and U_3Si, but it was only with a line etch that the microstructure of the latter alloy was revealed. (auth)

13743 SINTERING OF METALS, CARBIDES, AND OXIDES BY HOT-PRESSING. Samsonov, G. V.; Petrikina, R. Ya. (Inst. for Development of Materials, Kiev). Phys. Sintering; 2: No. 3, 1-20 (Sep 1970).

Results of investigations concerning the densification processes in various materials by sintering and hot-pressing at various temperatures and under various pressures are presented. The metals titanium, zirconium, niobium, chromium, molybdenum, tungsten, and rhenium were studied. Carbides of the transition metals within the limits of their homogeneity such as TiC_x, ZrC_x, HfC_x, NbC_x, and TaC_x, and transition metal oxides such as TiO_2, ZrO_2, HfO_2, NbO_2, and Cr_2O_3 were investigated. (auth)

13744 EFFECT OF GAS TRAPPED WITHIN PORES DURING SINTERING AND DENSITY REGRESSION OF CERAMIC BODIES. Amato, Ignazio (FIAT, Turin). Mater. Sci. Eng.; 7: 49-53 (1 Jan 1971).

The effects of non-diffusible gases trapped within the pores of ceramic bodies were examined. It is shown that non-diffusible gases trapped during the second stage of the sintering process do not hinder the material in reaching a high sintered density such as 95 to 98% of the theoretical value; in this situation, the dense ceramic bodies contain stationary bubbles in equilibrium. During grain growth, the grain-boundary movements sweep the stationary bubbles and they coalesce to form new equilibrium bubbles with volume larger than the sum of the volume of the primary stationary bubbles. According to the grain boundary energy field, the coalescence of the bubbles occurs preferentially at grain boundaries. A confirmation of the above summarized behavior is given in a set of experiments on urania. (auth)

13745 METHOD OF COATING FUEL ELEMENT CLADDING. Alecu, Marian (to Commissariat a l'Energie Atomique). French Patent 1,586,737. 19 Jan 1970. Filed 7 Oct 1968. (In French).

The process involves applying a suspension of graphite in a nitro-cellulose solution to the surface of the fuel cladding and heating the coated cladding to a temperature high enough to eliminate the nitro-cellulose solvent. The method can be used for Mg-clad U or U alloy fuel elements and Zr-clad UO_2-based fuel elements. (auth) (France)

13746 NUCLEAR FUEL MATERIAL BASED ON URANIUM MONOCARBIDE. Guinet, Philippe; Vaugoyeau, Henri (to Commissariat a l'Energie Atomique). French Patent 1,588,604. 9 Mar 1970. Filed 20 Sep 1968. (In French).

The fuel material is made up of grains of stoichiometric uranium monocarbide, UC, bound by a matrix containing Be_2C combined with small quantities of UBe_{13}, the atomic proportion of beryllium being between 1 and 12% and preferably about 8%. The uranium content of the material lies between 44 and 46.5% with the optimum around 44.5%. The substance is prepared by fusion of a mixture of uranium carbide and UBe_{13} in an inert atmosphere, or by heating of a mixture of uranium oxide, carbon and pieces of beryllium dioxide in a carburetting atmosphere to complete reduction and carburization, then fusion of the carburetted mixture. (auth) (France)

13747 NUCLEAR FUEL MATERIAL BASED ON URANIUM CARBIDE. Guinet, Philippe; Vaugoyeau, Henri (to Comissariat a l'Energie Atomique). French Patent 1,588,605. 9 Mar 1970. Filed 20 Sep 1968. (In French).

The manufacture of a nuclear fuel material based on uranium carbide for a high-temperature fluid-cooled reactor is described. The fuel is made up of fine grains of uranium monocarbide, UC, containing inclusions of UC_2 and surrounded by Be_2C, the atomic proportion of beryllium being between 1 and 12% and preferably about 8%. The atomic uranium content of the material lies between 42 and 44%, ideally about 43%. It is prepared by fusion of a mixture of uranium carbide and UBe_{13} in an inert atmosphere or by heating of a mixture of uranium oxide, carbon and pieces of beryllium dioxide in a carburetting atmosphere to complete reduction and carburization, then fusion of the carburetted mixture. (auth) (France)

13748 VAPOR DEPOSITION AND CHARACTERIZATION OF METAL OXIDE THIN FILMS FOR ELECTRONIC APPLICATIONS. Wang, C. C.; Zaininger, K. H.; Duffy, M. T. (RCA Labs., Princeton, N. J.). RCA Rev.; 31: 728-41(Dec 1970).

The rapid progress of solid-state electronics technology has stimulated the development of chemical vapor-deposition techniques for thin-film materials with functional properties for device applications. Research results are reviewed on the vapor deposition and characterization of transition-metal oxides (TiO_2, Ta_2O_5, and Nb_2O_5) dielectric films and lead oxide (PbO) photoconductive films. Potential device applications are presented. (auth)

Properties Evaluations

Refer also to abstracts 13667, 14435, 14469, 14470, 14476, and 15354.

13749 (EUR-4568) THERMAL CONDUCTIVITY OF URANIUM DIOXIDE. Review Report. Marchandise, H. (European Communities, Luxembourg. Commission). Nov 1970. 158p. (In French). Dep. NTIS (U. S. Sales Only). EUR FF 23,35.

The main available data are collected on the thermal conductivity of UO_2 in pile and out of pile, on the conductivity integral, and on their variations under the influence of such parameters as stoichiometry, porosity. Both sintered and vibro-compacted fuels are considered. The conductivity integral (from 500 to 2,800°C) of pellet UO_2 fuels (95% td) seemed to be about 68 ± 5 W/cm. Vibro-compacted fuels, 85% td had only half of this value under fast heating conditions. After redistribution of UO_2 at high temperatures, the conductivity integral of compacted fuels could approach 59 W/cm. (auth)

13750 (GAMD-9335) THERMODYNAMIC DATA FOR CARBONACEOUS SYSTEMS. Winchell, P. (Gulf General Atomic, Inc., San Diego, Calif.). 20 Nov 1970. Contracts AT(04-3)-167; AT(04-3)-633. 46p. Dep. NTIS.

An updated compilation and evaluation of thermodynamic data for carbonaceous materials which are used in high-temperature reactor technology is presented. For some systems experimental data are not available; in these cases estimates are given. (J.R.D.)

13751 CALCULATION OF THE ELASTIC MODULI OF BINARY COMPOSITES. Wang, Franklin F. Y. (State Univ. of New York, Stony Brook). Mater. Sci. Eng.; 17: 109-16(Feb 1971).

A modification was introduced to Hashin and Shtrikman's variational approach to calculate the elastic moduli of binary composites. The distribution effect of dispersed phases was taken into account. As a first approximation, a normal distribution was assumed. The calculations of moduli of nine systems were compared with the results of experiments for concentrations up to 50%. The introduction of a distribution effect showed distinct improvement. (auth)

13752 RECENT RESULTS OF CEMENTED CARBIDE RESEARCH AND PROBLEMS ENCOUNTERED. Ruediger, O.; Ostermann, G.; Kolaska, H. (Fried-Krupp, Essen). Tech. Mitt. Krupp, Forschungsber.; 28: 33-54(Sep 1970). (In German).

The following were discussed: inspection and testing methods for the materials used in making cemented carbides; qualitative and quantitative methods for analyzing the grain structure; method for determining the mechanical properties; grinding and sintering; properties of carbides, binding agent, and finished products; and applications. (auth)

13753 EQUATIONS OF STATE OF THE FUEL MATERIALS UC AND PuC. Hoffmann, H.; Thurnay, K. (Kernforschungszentrum, Karlsruhe, Ger.). J. Nucl. Mater.; 38: 105-13(Jan 1971). (In German).

Thermal and caloric equations of state were developed for the fuels UC and PuC. The temperature range of the equations was from 0 to nearly 16,000°K and a constant reduced volume of 0.8 was used. Below the melting point T_F the caloric equations were calculated using the specific heats of the carbides; the thermal equation equalled the carbide vapor pressure in this region. The melting points of the carbides were interpreted as dissociation points; with this approximation the energy and the pressure of the carbide are the sum of the energies in respect to the pressures of the components in the region $T > T_F$. The contributions of the metals are estimated using the principle of corresponding states and the tables of Hougen et al., for the carbon extrapolated specific heat and vapor pressure functions were applied. A short review of the different methods to calculate the equations of state and the critical properties of the carbides is added. (auth)

13754 NUCLEAR MAGNETIC RESONANCE STUDIES OF IRRADIATED BERYLLIUM OXIDE. II. Walter, J. A.; Troup, G. J. (Monash Univ., Clayton, Australia). J. Nucl. Mater.; 38: 51-66(Jan 1971).

XUM

Following an earlier paper which presented observations of defect-induced quadrupole broadening of the nuclear magnetic resonance of ^{9}Be in BeO at a variety of neutron-irradiation doses, an attempt is made to obtain some independent information on the types of defects responsible. Considerations of the effect of defect charge and lattice strain indicated that the defects annealing below 600°C in material irradiated at < 100°C were predominantly charged point defects (interstitial Be^{2+} and O^{2-} ions and the corresponding vacancies). The angular dependence of quadrupole broadening provided further evidence for the presence of planar defect clusters, and the results are compatible with a recent model for the anisotropic lattice expansion of BeO. (auth)

13755 ELECTRICAL AND TENSILE PROPERTIES OF Cu–ThO_2, Au–ThO_2, Pt–ThO_2, Au–Al_2O_3, AND Pt–Al_2O_3 ALLOYS. Fuschillo, N.; Gimpl, M. L. (Rutgers—The State Univ., New Brunswick, N. J.). J. Mater. Sci.; 5: 1078-86(Dec 1970).

Dispersion-strengthened alloys of Pt, Au and Cu containing ThO_2 and Al_2O_3 were prepared by precipitating the elements from a solution containing a suspension of the oxide phase. The precipitate deposited on the oxide particles of 0.05 μm average diameter and produced dispersions of good homogeneity on compaction. Alloys containing less than 2 vol % oxide phase had sufficient ductility to permit fabrication of wire. Tensile strength and elongation, hardness, and electrical resistivity were measured as a function of temperature up to 1000°C. The dispersion-strengthening caused a relatively small increase in the resistivity of the alloys compared to the resistivity of the metals. The alloys are useful where high electrical or thermal conductivity combined with superior tensile strength, hardness and oxidation resistance at elevated temperatures are desirable. (auth) (UK)

13756 NATURE OF THE ACTIVATION VOLUME-STRESS DEPENDENCE IN THE HIGH TEMPERATURE PLASTICITY OF UO_2. Roberts, J. T. A. (Argonne National Lab., Ill.). J. Nucl. Mater.; 38: 35-41(Jan 1971).

The stress relaxation technique was used to measure activation volumes in sintered polycrystalline UO_2 as a function of stress (200 to 2000 kg/cm^2), temperature (1324 to 1800°C), and strain rate (0.092 to 0.92/hr). The activation volume, V, was more sensitive to stress than to temperature, and varied with the inverse of the applied stress, above 1400°C. The activation work, W, defined as the product $V\sigma^*$, where σ^* is the effective stress, was 18 ± 1.8 kcal/mole. It was approximately independent of stress, temperature, and strain rate. It was shown that steady-state creep under high stresses had a similar activation volume-stress dependence. The average value of the activation work was 17 ± 1 kcal/mole. The stress dependence of the activation volume could not be accounted for by either of the contemporary models for high-temperature deformation. (auth)

13757 STRUCTURE AND MECHANICAL PROPERTIES OF ISOTROPIC PYROLYTIC CARBONS DEPOSITED BELOW 1600°C. Kaae, J. L. (Gulf General Atomic Inc., San Diego, Calif.). J. Nucl. Mater.; 38: 42-50(Jan 1971).

The relations between the deposition conditions, structure, and mechanical properties of isotropic pyrolytic carbons deposited at temperatures less than 1600°C were investigated. The carbons were deposited in a fluidized bed at a number of different temperatures and fractions of propane in the fluidizing gas. Structures were characterized by density, crystallite size, and Bacon anisotropy factor, and the fracture stress and Young's modulus were measured in three-point bending. These carbons were about twice as strong and twice as tough as isotropic carbons deposited at higher temperatures. At constant crystallite size, the fracture stress, Young's modulus, and strain energy to fracture all increased with increasing density. The fracture stress, elastic modulus, and strain energy to fracture also increased with decreasing crystallite size at constant density. (auth)

13758 DETERMINATION OF THE DISTRIBUTION OF FISSION PRODUCTS IN FUEL PARTICLE COATINGS BY THE SPUTTERING TECHNIQUE. Betz, G.; Dobrozemsky, R.; Viehboeck, F. P.; Wotke, H. (Reactor Center, Seibersdorf, Austria). J. Nucl. Mater.; 38: 77-82(Jan 1971).

For the retention of fission products, high temperature fuel particles normally are coated with pyrolytic carbon and silicon carbide layers. The knowledge of the distribution of the fission products in these coatings for a given history of irradiation is very important for the prediction of the lifetime of fuel particles and for the improvement of the retainment factor. Due to their chemical resistivity and porous structure, the peeling off of the coating layers by chemical or mechanical methods is very difficult and only rough steps of peeling off were achieved up to now. A new method is investigated: peeling off by sputtering, using an Ar^+ ion beam of 40 keV energy. The sputtered material was condensed on collecting foils and the fission products were determined by Ge(Li)-γ-spectrometry. The method and the experimental setup are described and first results on the fission product distribution in PyC and PyC–SiC–PyC-coatings are given. (auth)

13759 CREEP MECHANISMS IN STOICHIOMETRIC URANIUM DIOXIDE. Langdon, T. G. (Univ. of British Columbia, Vancouver). J. Nucl. Mater.; 38: 88-92(Jan 1971).

High temperature creep data for stoichiometric polycrystalline uranium dioxide suggested that a dislocation mechanism was probably rate-controlling at high stresses, but at low stress levels deformation occurred by the stress-directed diffusion of vacancies either through the lattice or along the grain boundaries. The creep rates calculated from theoretical models at the low stresses were in reasonable agreement with those observed experimentally, but the diffusion coefficients are not known with sufficient accuracy to determine the diffusional path. By considering the temperature dependence of the creep rate, it appears that diffusion via the grain boundaries may contribute more than ≈0.3 of the total creep rate for a material having a grain size of 10 μm tested at 1430°C. (auth)

13760 X-RAY DETERMINATION OF THE EXPANSION COEFFICIENTS OF LANTHANUM AND YTTRIUM BORIDES. Zhuravlev, N. N.; Belousova, I. A.; Manelis, R. M.; Belousova, N. A. (Moscow State Univ.). Sov. Phys.-Cryst. (Engl. Transl.); 15: 723-4(Jan-Feb 1971).

Translated from Kristallografiya; 15: 836-8(Jul-Aug 1970).

The thermal expansion of YB_2, YB_4, YB_6, YB_{12}, LaB_4, LaB_6, and LaB_6 + B (= LaB_{12}) were measured: hexagonal YB_2: $\alpha_\perp = 9.4 \pm 1.0 \times 10^{-6}$ and $\alpha_{||} = 8.5 \pm 0.9 \times 10^{-6}$; tetragonal YB_4: $\alpha_\perp = 7.6 \pm 0.5 \times 10^{-6}$ and $\alpha_{||} = 6.4 \pm 0.6 \times 10^{-6}$; cubic YB_6: $\alpha_\perp = 6.02 \pm 0.6 \times 10^{-6}$; cubic YB_{12}: $\alpha_\perp = 6.6 \pm 0.6 \times 10^{-6}$; tetragonal LaB_4: $\alpha_\perp = 7.17 \pm 1.16 \times 10^{-6}$ and $\alpha_{||} = 8.36 \pm 1.03 \times 10^{-6}$; cubic LaB_6: $\alpha_\perp = 7.4 \pm 0.5 \times 10^{-6}$; and cubic LaB_6 + B: $\alpha_\perp = 6.6 \pm 0.6 \times 10^{-6}$ deg^{-1}. (D.L.C.)

13761 MASS-SPECTROMETRIC DETERMINATION OF THE DISSOCIATION ENERGY OF ScC_2 AND ScC_4. Kohl, Fred J.; Stearns, Carl A. (Lewis Research Center, Cleveland). J. Chem. Phys.; 54: 1414-16(1 Feb 1971).

The method described in J. Chem. Phys. 52: 6310 (1970) was used to study the vapor phase above the Sc–C system at 2165 to 2328°K. ScC_2^+ and ScC_4^+ were identified as ions whose precursors originated in the Knudsen cell. Reaction enthalpies were measured for the reactions $Sc(g) + 2C(s) \rightarrow ScC_2(g)$ and $Sc(g) + 4C(s) \rightarrow ScC_4(g)$. Fundamental vibrational frequencies were calculated for ScC_2 and ScC_4. Dissociation (atomization) energies were calculated to be: 565 ± 21 (1155 ± 21) kJ/mole for ScC_2 and 1217 ± 22 (2397 ± 21) kJ/mole for ScC_4. (D.L.C.)

Structure and Phase Studies

Refer also to abstracts 14442 and 14454.

13762 (AD–713153) PHASE EQUILIBRIA INVESTIGATION OF BINARY, TERNARY, AND HIGHER-ORDER SYSTEMS. I. THE PHASE DIAGRAMS OF THE SYSTEMS Ti–Nb–C, Ti–Ta–C, AND Ti–Mo–C. Rudy, E. (Aerojet-General Corp., Sacramento, Calif. Materials Research Lab.). Aug 1970. Contract F33615-67-C-1513. 148p. (AFML-TR–69-117(Pt.1)). NTIS.

The ternary alloy systems Ti–Nb–C, Ti–Ta–C, and Ti–Mo–C were investigated by means of x-ray, melting point, DTA, and metallographic techniques; phase diagrams for all three systems from 1500°C through the melting range were established. The solid state phase relationships in all three systems are similar. The cubic monocarbides are completely miscible, whereas the subcarbides, Nb(Ta,Mo)C2 show limited solubility and are terminated by three-phase equilibria Me + Me2C + MeCl-x in the ternary. The sublattice order-disorder transition in the subcarbides are lowered by titanium substitutions. The monocarbide solutions in all three systems show a regular melting behavior. The phase relationships of the three systems are discussed and the differences in particular equilibria related to the thermodynamic properties of the phases in the boundary systems. (auth) (USGRDR)

13763 (AD–713154) EXPERIMENTAL PHASE EQUILIBRIA OF SELECTED BINARY, TERNARY, AND HIGHER-ORDER SYSTEMS. V. THE PHASE DIAGRAM W–B–C. Rudy, E. (Aerojet-General Corp., Sacramento, Calif. Materials Research Lab.). Aug 1970. Contract F33615-67-C-1513. 62p. (AFML-TR–69-117(Pt.5)). NTIS.

The ternary alloy system W–B–C was investigated by means of x-ray, melting point, DTA, and metallographic techniques using hot-pressed and heat-treated, as well as melted specimens, and a phase diagram at 1500°C through the melting range established. No ternary phases are formed in the system and the mutual solu-

XUM

bilities between carbide and boride phases are small. The solid state sections (<2000°C) are characterized by two-phase equilibria existing between the phase pairs W2B + W2C, W2B + WC, WC + WB, WB + C, W2B5 + C, W2B5 + B4C, and WB approximately 4 + B4C. The two-phase equilibrium W2B + WC is replaced by an equilibrium W2C + WB above 2150C. Fifteen ternary isothermal reactions were found. Five are associated with pseudobinary eutectic equilibria, six with ternary eutectics, and the remaining four with class II ternary four-phase reaction isotherms. (auth) (USGRDR)

13764 (KFK-1260) BEHAVIOR OF FISSION PRODUCT Mo, Tc, Ru, Rh, AND Pd IN A CARBIDE FUEL ELEMENT AND STRUCTURE OF THE SYSTEM Mo-Ru-C. Holleck, H. (Kernforschungszentrum, Karlsruhe (West Germany). Institut fuer Material und Festkoerperforschung). Sep 1970. 31p. (In German). Dep. NTIS (U. S. Sales Only).

From the fission product elements Mo, Tc, Ru, Rh, and Pd the metals Mo and Ru have been taken as typical and most frequent examples to investigate the behavior of alloys of the above elements with carbon. Temperature-sections of the phase diagram Mo−Ru−C are given for 2000, 1500, and 1100°C. There exists a fcc high temperature phase $(Mo_yRu_{1-y})C_{1-x}$ (with y ~ 0.5, x ~ 0.5 at 1500°C). The homogeneous region of this phase becomes larger in the direction of $\alpha-MoC_{1-x}$ with increasing temperature. The existence of certain types of binary or ternary phases in systems with the components Mo, Tc, Ru, Rh, Pd, and C is discussed. The stability of phases occurring in the Mo−Ru−C system has been estimated, i.e., calculated assuming ideal solution. The occurring phases are too unstable to prevent a reaction of the fission products Mo and Ru with UC. (auth)

13765 (RD/B/N-1770) CHARACTERISATION OF THE SURFACE ROUGHNESS OF GRAPHITE. Gordelier, S. C. (Central Electricity Generating Board, Berkeley (England). Berkeley Nuclear Labs.). Aug 1970. 35p. Dep. NTIS (U. S. Sales Only).

The surface roughness of graphite will be important in Mark III gas-cooled reactors in that it affects both thermal contact resistance and fluid friction. It is shown that graphite roughness differs from that of most other surfaces in having two components. Methods of roughness measurement are considered and an optical technique is used to produce results for a particular graphite. The method of formation and geometry of the roughness is discussed. (auth)

13766 (SRO-552-6) QUANTITATIVE DETERMINATION OF THE STRUCTURE: PROPERTY RELATIONSHIPS IN NUCLEAR FUEL ELEMENT MATERIALS. Quarterly Progress Report, September 15–December 15, 1970. Rhines, F. N.; DeHoff, R. T.; Whitney, E. D. (Florida Univ., Gainesville. Engineering and Industrial Experiment Station). Dec 1970. Contract AT(39-1)-552. 22p. Dep. NTIS.

Continued experimental progress has been achieved in the areas of quantitative microstructural analysis, gas permeability studies, short time mechanical properties, and thermal conductivity measurements on both sintered nickel and sintered uranium dioxide powders. In broad terms, the path of microstructural change followed by both powders, and the dependence of properties upon geometric state, may be predicted on the basis of the results of earlier work on copper sinterings. (auth)

13767 B−C SYSTEM IN THE KINETIC FORMATION REGION: PYROLYTIC FORMATION OF CARBON-RICH B−C PHASES. Amberger, E.; Druminski, M.; Ploog, K. (Univ., Munich). J. Less-Common Metals; 23: 43-52(1971). (In German).

In the kinetically controlled temperature range of formation (900 to 1200°C) the primitive rhombohedral lattice of $B_{13}C_2$ (space group $R\bar{3}m$) dominated. All phases of higher C content were derived from this lattice. In detail, the following regions could be defined, in order of increasing C content: thermodynamically stable $B_{13}C_2$ (14.4 % C, d = 2.48 g/ml) and thermodynamically less stable $B_{13}C_2$ with interstitial C atoms and a small phase width: $(B_{13}C_2)C$ $(B_{13}C_2C_{0.95-1}$, 20.1 to 20.4 % C, d = 2.52 g/ml). The $B_{13}C_2$ lattice could not take up more carbon; there was no formation of B_4C (21.7 % C, d = 2.512) but of graphite. In this case $(B_{13}C_2)C$ and graphite formed a very close association of high density, hardness, and phase width, which was similar to a compound $(B_{13}C_2)C \cdot xC_{\text{graphite}}$ (31.4 to 35.4 % C, $B_{2.04 \text{ to } 2.42}C$, d = 2.44 to 2.47 g/ml). At 36 % C there appeared a sharp boundary to the soft, loose conglomerate of $(B_{13}C_2)C$ and pyrographite (d = 1.36 to 1.87 g/ml). Starting from the broad boundary region at 84 to 90 % C the densities of hard pyrolysis products, again formed, increased from d = 2.16 g/ml up to 2.21 g/ml (the density of pyrographite). As in the B−C phase diagram, under similar thermodynamical conditions (>2200°C) there were no (kinetically favored metastable) B−C phases between 35 and 100 % carbon. Also in the kinetic range of formation of B−C phases, the B_{12} icosahedron predominated over the layer structure of graphite, the boron atoms did not form other coordination polyhedrons. (auth)

13768 HABIT PLANE OF VANADIUM HYDRIDE IN VANADIUM. Westlake, D. G. (Argonne National Lab., Ill.). J. Less-Common Metals; 23: 89-91(1971).

Experimental results indicated that the habit plane of vanadium hydride in vanadium was at, or near, {227}, in direct contradiction of prediction of {001} habit planes. The (227) was in the $[1\bar{1}0]$ zone, lying 22° from the (001). (G.M.C.)

13769 HIGH-TEMPERATURE RADIOGRAPHIC STUDIES OF OXIDES. II. ZIRCONIUM DIOXIDE REACTIONS WITH YTTRIUM OXIDE. Zubankov, V. N.; Strekalovskii, V. N.; Pal'guev, S. F. Tr. Inst. Elektrokhim., Akad. Nauk SSSR, Ural. Filial; No. 13, 112-19(1969). (In Russian).

Results of the investigation showed that at about 2000°C fluorite phases form. Below 1500°C coexisting fluorite and tetragonal phases were observed in ZrO_2 and in free U_2O_3. The experimental data were used as the basis of a model of fluorite-cubic solid solutions in these oxides. (tr-auth)

13770 PHASE EQUILIBRIA IN THE HIGH MAGNESIA CORNER OF THE SYSTEM $MgO-ThO_2-B_2O_3$ AT 1200°C. Whitaker, A.; Darby, I. A. (Brunel Univ., London). J. Mater. Sci.; 5: 1087-90(Dec 1970).

Phase equilibria in the high magnesia corner of the system $MgO-ThO_2-B_2O_3$ were investigated at 1200°C using x-ray powder diffraction techniques. The two magnesium borates reported previously at this temperature were confirmed, but no magnesium thorate and no ternary phases were found. Solid solution effects were investigated; for the binary phases by comparison of patterns, for magnesium oxide and thorium oxide by comparison of lattice parameters. No solid solutions were detected. Phase equilibria in the system $MgO-ThO_2$ were investigated at 1500°C, again no binary compound was found and no solid solution detected. A suggestion is made to reconcile the latter observation with previous work. (auth) (UK)

13771 STRUCTURE OF OXIDE FILMS FORMED ON NIOBIUM IN HIGH-TEMPERATURE WATER AND WATER VAPOR. Osaka, Toshiaki; Nakayama, Tadayuki (Waseda Univ., Tokyo). J. Jap. Inst. Metals; 34: 1163-8(Nov 1970).

Niobium samples were heated in an 18-8 stainless steel autoclave filled with deionized water and water vapor. After heating, the oxide films were identified by means of reflection and transmission electron diffraction, and then component elements in the thin films were detected by using an electron probe micro-analyzer. The film formed on Nb in deaerated high-temperature water by oxidation at 300°C for 1 hr was composed of the rutile-type crystal alone. In addition, the presence of Fe and Nb was detected by means of the x-ray micro-analysis of the film, indicating that the film was composed of $(Fe,Nb)O_2$. However, the oxide film produced by oxidation for 24 hr gave a diffraction pattern corresponding to the pseudohexagonal δ-phase. The oxide films on Nb in deaerated high-temperature water vapor and in the pyrex glass tube together with deionized water at 300°C for 1 hr also consisted of a normal rutile-type oxide, and were thought to be NbO_2. The unit cell dimensions for the above oxide were a_0 = 4.75Å, c_0 = 3.09Å, c_0/a_0 = 0.65. Further, after heating in deaerated water vapor for 24 hr, the electron diffractogram of the film indicated the presence of δ-phase. The film formed on Nb in aerated high-temperature water by oxidation at 300°C for 1 hr or 24 hr was a hexagonal-type oxide; a_0 = 5.84Å, c_0 = 4.69Å, c_0/a_0 = 0.80. Characteristic spectra $CrK\alpha_1^2$ and $NbL\alpha_1^2$ were detected from the film, and Cr^{6+} ions were detected from water after oxidation. Therefore the Cr ions may contribute to the formation of the hexagonal-type oxide. After heating in aerated high-temperature water vapor at 300°C for 1 hr or 24 hr, the δ-phase was found on the Nb surface. (auth)

13772 STUDIES OF THE SYSTEM URANIUM MONONITRIDE–MOLYBDENUM AND URANIUM MONONITRIDE–TUNGSTEN AT HIGH TEMPERATURES. Politis, C.; Thuemmler, F.; Wedemeyer, H. (Kernforschungsanlage, Karlsruhe, Ger.). J. Nucl. Mater.; 38: 93-104(Jan 1971). (In German).

Mixtures of uranium mononitride and molybdenum were studied between the temperatures of 2100 and 2700°C. By means of several melt specimens the liquidus line and the eutectic line were determined. Under a pressure of 650 torr nitrogen for the eutectic, a composition of 58 wt % molybdenum and 42 wt % uranium nitride was obtained at a eutectic temperature of 2400 ± 20°C. Particularly in uranium-rich specimens the components of the uranium-rich phase (U_2Mo containing nitrogen) were observed. Additional experiments at higher and lower nitrogen pressures showed displacements of the eutectic composition and temperature. A few special experiments in the analogous system uranium mononitride-tungsten were carried out and the resulting composition for the eutectic, with 96 wt % uranium nitride, was found to lie near the pure uranium nitride. One can suppose that the eutectic melting point is at about 2700°C. (auth)

13773 DISORDERED CRYSTALLOGRAPHIC SHEAR IN WO_{3-x} CRYSTALS. Allpress, J. G. (Univ. of Melbourne); Gado, P. Cryst. Lattice Defects; 1: 331-42(Dec 1970).

Crystals of $WO_{\sim 2.90}$ were prepared under non-equilibrium conditions and examined by x-ray and electron optical techniques. Their structures were related to that of β-tungsten oxide ($W_{20}O_{58}$), but there was considerable disorder in the spacing and direction of crystallographic shear planes. The results indicated that individual fragments may exhibit variations in composition at the unit cell level, and provide a basis for a limited discussion of the processes involved in the formation of shear defects and their subsequent diffusion. (auth)

13774 STRUCTURAL STUDIES BY ELECTRON MICROSCOPY: POLYMORPHISM OF $ZrO_2.12Nb_2O_5$. Allpress, J. G. (Univ. of Melbourne); Roth, R. S. J. Solid State Chem.; 2: 366-76(Nov 1970).

Three polymorphs of $ZrO_2 \cdot 12Nb_2O_5$ were identified by the combined use of x-ray diffraction and electron optical techniques. The α form, which was the initial product of the reaction of ZrO_2 with Nb_2O_5 in the molar ratio 1 : 12, was isostructural with $TiNb_{24}O_{62}$. The monoclinic β form, produced by long annealing, had a more complex structure, and may contain intergrowths of a third, γ, polymorph. Lattice images of the β form, together with the diffraction data, are used to derive possible structures for these materials. (auth)

13775 EFFECT OF OXIDE ADDITIONS ON THE POLYMORPHISM OF TANTALUM PENTOXIDE. IV. THE SYSTEM Ta_2O_5–Ta_2WO_8. Roth, R. S.; Waring, J. L.; Parker, H. S. (National Bureau of Standards, Washington, D. C.). J. Solid State Chem.; 2: 445-61(Nov 1970).

The low-temperature form of pure Ta_2O_5 was found to exist in two slightly different modifications. The lowest temperature form had a b axis multiplicity of 14 whereas the highest temperature form (about 1350°C) had a multiplicity of 11. At intermediate temperatures an infinite number of at least partially ordered sequences of these two modifications existed in equilibrium. The addition of WO_3 to Ta_2O_5 caused the stabilization of an infinite number of phases similar in structure to the low temperature form of Ta_2O_5. From just less than 10 mole % WO_3 to the last compound in the series at 26⅔ mole % WO_3 these phases were in equilibrium with liquid, and the high temperature structure type of pure Ta_2O_5 was eliminated from the phase diagram. One compound, $15Ta_2O_5 \cdot 2WO_3$ with a multiplicity of 8, was found to melt congruently at about 1815°C and the last phase, $11Ta_2O_5 \cdot 4WO_3$ with a multiplicity of 13, melted incongruently at about 1605°C. (auth)

13776 CHEMICAL AND STRUCTURAL INVESTIGATION OF THE AB_2O_8 COMPOUNDS OF Mo-V-O, U-V-O, AND U-Mo-O SYSTEMS. Mahe-Pailleret, Paulette (Univ., Paris). Rev. Chim. Miner.; 7: 807-48(1970). (In French).

Single crystals of the AB_2O_8 type compounds: MoV_2O_8, $MoV_2O_{7.8}$, UV_2O_8, and UMo_2O_8 encountered in the different systems were prepared. Their structures were determined by classical methods: Patterson functions, generalized projections, and electron density sections. MoV_2O_8 is in the MnO_{3n-1} series through the association of the distorted MoO_6 and VO_6 octahedra. $MoV_2O_{7.8}$ exhibits the same arrangement, a stacking fault explains its deviation from stoichiometry. UV_2O_8 consists of an array of pyramids with pentagonal bases for the uranium and triangular bipyramids for the vanadium. UMo_2O_8 consists of distorted oxygen octahedra, surrounding the molybdenum, connected to pyramids with hexagonal bases in the center of which the uranium is located. (auth) (France

13777 PHASE DIAGRAM OF THE URANIUM–OXYGEN SYSTEM. Kovba, L. M. (Moscow State Univ.). Dokl. Akad. Nauk SSSR; 194: 98-100(1 Sep 1970). (In Russian).

Previously published data and new results were combined to plot a more complete phase diagram of the uranium–oxygen system. The quantitative phase analysis of quenched specimens was used to determine that the upper boundary of homogeneity of the $U_4O_{9\pm y}$ phase at 1000°C was $UO_{2.260}$ and at 700°C it was $UO_{2.257}$. The phase diagram for the $UO_{2.15}$ to $UO_{2.30}$ range at 800 to 1150°C showed agreement between the data obtained by various methods. The oxygen content in $\beta-U_3O_7$ was lower than in γ and $\delta-U_3O_7$; the two latter phases had practically identical compositions. The $\alpha-U_3O_7$ consisted of a mixture of $\beta-U_3O_7$ and UO_2. The experimentally determined decomposition temperatures of the β and γ U_3O_7 after extended heating did not agree with the equilibrium data because no inverse reactions took place at those temperatures. Different conditions prevailed when high pressures were used, as the formation of β, γ, and $\delta-U_3O_7$ from U_4O_9 and U_8O_{21} was accompanied by a volume reduction of about 8.5%. The $\alpha-U_3O_8 \rightleftharpoons \alpha'-U_3O_8$ reaction was probably a second order transformation; the $U_8O_{21\pm x} \rightarrow \alpha'-U_3O_{8-x}$ was a first-order one. (TTT)

13778 PHASE RELATIONS AND THE ELECTRICAL CONDUCTIVITY IN THE SYSTEM ZrO_2–Sc_2O_3. Spiridonov, F. M. (Moscow State Univ.); Popova, L. N.; Popil'skii, R. Ya. J. Solid State Chem.; 2: 430-8(Nov 1970).

Phase relations in the $ZrO_2-Sc_2O_3$ system were investigated by the methods of high-temperature x-ray analysis, dilatometry, differential thermal analysis, and electrical conductivity measurements in the composition range 3 to 40 mole % Sc_2O_3 and the temperature range 20 to 2000°C. The phase diagram was constructed in its subsolidus regions. Existence regions were refined for three known compounds, $Sc_2Zr_7O_{17}$, $Sc_2Zr_5O_{13}$, and $Sc_4Zr_3O_{12}$, and the region corresponding to high temperature, cubic, fluorite-type solid solutions was established. The character of the thermal dependence of the electrical conductivity for the compositions studied agreed with the phase transformations. The maximum value of the electrical conductivity at 1200°C was observed for the composition 7.5 to 9 mole % Sc_2O_3. With increasing temperature, in the field of the high-temperature solid solutions, there occurred a broadening of this maximum and a lateral displacement to higher content of scandium oxide. (auth)

Radiation Effects

Refer also to abstracts 13028, 14430, and 15366.

13779 (DP-MS-70-44) SELF-RADIATION DAMAGE IN ^{244}Cm OXIDE AND ALUMINATE. Mosley, W. C. (Du Pont de Nemours (E. I.) and Co., Aiken, S. C. Savannah River Lab.). 15 Oct 1970. 21p. (CONF-701116-1). Dep. NTIS.

From Basic Science and Nuclear Division Meering of the American Ceramic Society, Gatlinburg, Tenn.

Self-radiation from α-decay of ^{244}Cm causes lattice swelling, phase transformations, and metamict state formation in several curium compounds. In curium oxides, the percentage swelling at saturation decreases with decreasing symmetry; swelling in bcc C-type Cm_2O_3 is about half that in fluorite CmO_2 (about 0.3%); monoclinic Cm_2O_3 does not swell. CmO_2 swells with time according to $(\Delta a/a_0) = 0.003[1 - e^{-1.7 \times 10^{4}\lambda t}]$, essentially the same relation as for PuO_2 and AmO_2. The rate of structure loss of curium oxides decreases with increasing temperature of prior heatings. In curium aluminate, the metamict state is produced before swelling reaches saturation. Radiation-induced transformation at room temperature produces metastable phases which normally exist at higher temperatures, e.g., bcc C-type Cm_2O_3 transforms to hexagonal A-type Cm_2O_3, and rhombohedral $CmAlO_3$ becomes cubic. (auth)

13780 (GEAP-12147) FISSION GAS RE-SOLUTION RATES. Quarterly Report No. 1, July 1–September 30, 1970. Marlowe, M. O. (General Electric Co., Pleasanton, Calif. Nucleonics Lab.). Sep 1970. Contract AT(04-3)-189. 10p. Dep. NTIS.

A description is given of the basis and experimental approach to the measurement of the re-solution rate of fission gases in oxide nuclear fuels. Twenty-eight UO_2 disks were irradiated up to 3.8×10^{20} fissions/cm^3. The specimens were characterized by optical, scanning electron, and transmission electron microscopy in the unirradiated condition. A technique for preparing specimens for transmission electron microscopy was proven out-of-cell, but some experimental difficulties were encountered in cell. A furnace for high-temperature anneals in-cell (1300 to 1600°C) was obtained, and suitable auxiliary equipment for atmosphere control is being fabricated. Work is in progress on the theoretical significance and temperature regime over which the re-solution process may be important in the interpretation of fuel behavior. (auth)

13781 (JUL-677-RG) INVESTIGATIONS OF THE DIFFUSION OF ^{6}Li FROM IRRADIATED BERYLLIUM OXIDE. Roehrig, Heinz Dieter (Kernforschungsanlage, Juelich (West Germany). Institut fuer Reaktorentwicklung). Jul 1970. 123p. (In German). Dep. NTIS (U. S. Sales Only).

Thesis. Submitted to Technische Hochschule, Aachen, Ger.

Investigations on ^{6}Li diffusion from irradiated BeO are reported. The measurement methods and apparatus developed were described. The measurement results obtained are given and interpreted. The release isotherms determined indicate a pattern deviating sharply from the normal diffusion behavior. This behavior was explained as a post-sintering process of the relatively slightly sintered samples. A semiempirical formula with which the measured curves could be quantitatively described was derived. The time constants of the texture changes obtained

XUM

from the release curves are in qualitative agreement with the measured changes in density and the open porosity. From the temperature dependence of these time constants result activation energies in similar heights as the Q values for sinters of BeO known from the literature. The diffusion itself was described by a reduced diffusion coefficient, for which a straight line was given in the Arrhenius diagram. From its slope an activation energy of 71 kcal/mole was determined. The lower value determined by Stieglitz and Zumwalt could be traced to the higher radiation damage of the beryllium oxide used. Since the reduced coefficient given relates to the extrapolated final state of the texture where grain boundaries and isolated pores are still present, but plays no role for the diffusion mechanism it should be possible to calculate the absolute diffusion coefficient from the reduced diffusion coefficient and the macroscropic sample dimensions. Since the model developed is in the position of explaining the extremely abnormal appearing release curves measured as diffusion process, it can be applied to the clarification of the very complex fission product diffusion proceeding from ceramic fuels. (tr-auth)

13782 (JUL-685-PA) DIFFERENT MODELS FOR CALCULATION OF NUCLIDE TRANSPORT IN CLAD SPHERICAL FUEL PARTICLES FOR HIGH-TEMPERATURE REACTORS. Baurmann, Karl-Wilhelm (Kernforschungsanlage, Juelich (West Germany)). Aug 1970. 73p. (In German). Dep. NTIS (U. S. Sales Only).

Various models for nuclide transport in multiple clad spherical fuel particles (coated particles) were developed. With the knowledge of the concentration profile and nuclide amounts within and outside the fuel particles obtained in post-irradiation studies, transport and evaporation coefficients can be calculated with the help of the solution represented; the latter are determinate for a poisoning of the cooling gas of a high-temperature reactor. The coefficients which describe the transient starting behavior of the transport were developed to solutions. These solutions correspond to that of a semi-infinite expanding transport range and were represented in the form of Gauss error integrals which guarantee a sufficient convergence of the solutions. The solutions for the long-term behavior have the form of infinite series in whose calculation transcendent determinant equations of the eigenvalues must be considered. In the treatment of the boundary conditions a time-constant concentration transition (partition coefficient) on the surface of two transport media flowing by each other and an evaporation coefficient on the particle surface were considered. For an evaporation constant approaching infinity the solutions given describe the transport of the gaseous fission products, whereas a finite value of the evaporation constant gives the transport behavior of solid fission products. The stationary solution terms permit the calculation of the nuclide release rate from spherical fuel elements when a constant production rate corresponding to the equilibrium state occurs in them. The differential equations describing the transport problem were treated with the help of the Laplace transformation in the subregion. It is recommended to solve numerically the differential equations when the number of transport ranges exceeds two. (tr-auth)

13783 (UCRL-20369) DEFECTS AND PHASE TRANSFORMATIONS IN COBALT FERRITES. De Jonghe, Lutgard C. (California Univ., Berkeley. Lawrence Radiation Lab.). Nov 1970. Contract W-7405-eng-48. 138p. Dep. NTIS. Thesis.

Defects and phase transformations in ferrimagnetic cobalt ferrites, with a Co/Fe ratio between 0.54 and 0.76, have been studied by means of high voltage transmission electron microscopy. The origin and characterization of ion radiation damage, ferrimagnetic domains, dislocations, and phase transformations in air and in the electron microscope are discussed. Ferrimagnetic domains have been observed in single phase specimens, when the foils were symmetrically oriented with respect to the field of the objective lens. The domain wall images have been found to be in agreement with the contrast that is expected from 90° Bloch walls. The configuration and motion of these 90° walls is shown to depend on the foil geometry, and on the presence of mechanical stresses. Phase transformations in the reducing atmosphere of the microscope have been examined in detail. It is shown that (Co,Fe)O precipitates in cobalt ferrite, after heating in air at 1230°C. The precipitates initially are shaped as square prisms and are fully coherent up to a size of at least 1200Å. Between 1200 and 1500Å they lose coherency, and also become more or less spherical in shape. The nature of the semi-coherent interface is discussed in detail. The presence of undissociated interface dislocations is shown. Micropores were found to migrate along with the semicoherent interfaces. Their origin is discussed. A possible mechanism by which the precipitates lose coherency is described. (auth)

13784 ACTIVATION ENERGY OF THE FIRST STAGE OF ANNEALING OF IRRADIATED $^{238}PuO_2$. Kapshukov, I. I.; Sudakov, L. V.; Yakovlev, G. N. Sov. Phys.-Solid State (Engl. Transl.); 12: 1718(Jan 1971).

Translated from Fiz. Tverd. Tela; 12: 2157(Jul 1970).

An x-ray diffraction investigation was conducted of the changes in the lattice parameter of $^{238}PuO_2$ during isothermal annealing at 300 and 400°C. The activation energy was determined to be 0.15 ± 0.05 eV. (D.L.C.)

13785 MECHANISMS OF SWELLING AND GAS RELEASE IN URANIUM DIOXIDE. Hilbert, R. F.; Storhok, V. W.; Chubb, W.; Keller, D. L. (Battelle Memorial Inst., Columbus). Contract W-7405-eng-92. J. Nucl. Mater.; 38: 26-34(Jan 1971).

Data on the external dimensional changes and gas release behavior of uranium dioxide irradiated in tungsten—rhenium claddings at surface temperatures from 1325 to 1900°C are presented. External dimensional changes and gas release fractions increased with increasing temperatures; but the density of the uranium dioxide showed little change. Microstructures of the uranium dioxide showed long, columnar grains associated with lenticular voids at temperatures over 1600°C. A theory to explain these observations postulates that the uranium dioxide swells by the formation of small, relatively immobile fission gas bubbles. This swelling results in small, permanent external dimensional changes. However, periodically portions of the uranium dioxide are swept by lenticular voids. This vapor-phase zone-refining process reconstitutes the uranium dioxide down the temperature gradient maintaining its density essentially constant. The large external dimensional changes occurring when this sequence is repeated many times represent the summation of a large number of repetitive steps involving small density decreases in the uranium dioxide followed by redensification by the zone-refining process. The zone-refining process is instrumental in collecting fission gas and in forming channels for gas release. The process is a major, although probably not the sole mechanism of gas release from uranium dioxide at temperatures over 1600°C. (auth)

Plastics and Other Materials

Refer also to abstract 13725.

13786 A STUDY OF THERMALLY GENERATED ELECTRICAL CURRENTS IN GAMMA-IRRADIATED LUCITE. Murphy, Paul Henry. Lawrence, Kan.; Univ. of Kansas (1970). 139p. University Microfilms Order No. 70-25,380.

Thesis.

This study was concerned with the generation of electrical currents in a solid dielectric, Lucite, upon heating it after exposure to x- or gamma radiation. These currents are generated without the application of an external electric field. Insight into the nature of the potential gradient responsible for charge carrier movement was obtained by observing the currents generated under various heating and irradiation arrangements. Heating was carried out both with and without a net temperature gradient in a direction normal to the electrode surfaces. Samples were irradiated both isotropically and directionally with ^{60}Co gamma rays and directionally with 250 kVp x rays. Different sample thicknesses and temperature gradients were employed along with externally applied electric fields to obtain some information on the magnitude of the potential gradients. Samples were irradiated directionally with thin filters (160 mg/cm^2) on the entrance and/or exit sides. This irradiation configuration resulted in trapped space charges in the samples. The effects of these trapped space charges on the magnitude and the polarity of the thermally induced currents were studied. For samples heated in the presence of a net temperature gradient, it was concluded that the potential gradient responsible for charge movement is thermovoltaic in nature. The direction of the currents is such that the colder electrode is always positive. This indicates that the sign of the mobile charge carrier during heating an irradiated sample is positive. For samples heated in the absence of a net temperature gradient, the direction of the potential gradient is determined by the direction of the gamma rays through the sample. Upon heating, the exit side of the sample always becomes positive. The magnitude of this potential gradient appears to increase as the proton energy increases. Results obtained using thin lead filters during directional irradiation of samples suggested that production of trapped internal space charges, associated with regions of under or overdose, can also serve as sources of electric fields in the sample for the movement of thermally released trapped charge carriers. Using filters of different atomic numbers, the variation of the magnitude of the underdose, for ^{60}Co radiation, at the filter/Lucite interface, was measured. These results agreed with those of others who obtained them by ionization measurements. A limited investigation of the consequences of applying an external electric field during heating of an irradiated sample in a net temperature gradient yielded results suggesting that Ohm's Law was followed for the doses and field strengths employed (up to 120 kilorads and 800 volts/cm.). (Diss. Abstr. Int., B)

XUM

PHYSICS (GENERAL)

Astrophysics and Cosmology

Refer also to abstract 14876.

Cosmic Ray Exposure Ages

Refer also to abstracts 12967–12970.

13787 COMPOSITION OF STONY METEORITES. IX. ABUNDANCE TRENDS OF THE REFRACTORY ELEMENTS IN CHONDRITES, BASALTIC ACHONDRITES, AND APOLLO 11 FINES. **Ahrens, L. H. (Univ. of Cape Town). Earth Planet. Sci. Lett.; 10: 1-6(Dec 1970).**

The paper is in three parts: (i) a critical examination of the Ca/Al ratio in chondrites: the weight ratio (Av. = 1.08) is remarkably uniform, as indicated in previous work, and is much greater than that in plagioclase (maximum = 0.74); no Ca–Al mineral known to the writer has the chondrite ratio; (ii) a general examination of the enrichment trends of the refractory elements (Ca and Al excepted) in the sequence: chondrites, eucrites Stannern and/or Nuevo Laredo, Sea of Tranquillity fines; and (iii) the arrangement, on a tentative basis, of various chondrites and basaltic achondrites in a sequence according to their refractory element content. (auth)

Stars

Refer also to abstracts 13851 and 14650.

13788 (AD–711364) STELLAR STANDARDS AT 10 MICRONS. Air Force Surveys in Geophysics. Price, Stephan D. (Air Force Cambridge Research Labs., L. G. Hanscom Field, Mass.). 13 Jul 1970. 19p. (AFCRL–70-0402; AFCRL-AFSIG–221). NTIS.

There is a need for reliable 10-μ standards with which to reference the background measurements. A literature search was conducted to compile a list of nonplanetary celestial sources that have fluxes $> 5 \times 10^{-17}$ W/μcm^2 at 10μ. "Standard" stars are chosen from the list and recommended flux values are assigned to them. (auth) (USGRDR)

13789 (N–70-38166) GENERAL SURVEY OF CLASSICAL CEPHEID VARIABLE STARS. Wilson, Robert M. (National Aeronautics and Space Administration, Huntsville, Ala. George C. Marshall Space Flight Center). 16 Sep 1969. 89p. (NASA-TM-X-53920; MSFC-IN-SSL-T-68-16). NTIS.

Cepheid variable stars (description, characteristics, and spectra) are discussed. The interstellar medium, infrared radiation (history, detection, and atmospheric effects), and the H–R diagram are also considered. The topics of immediate concern are Cepheids (Types 1 and 2) the light curve, the velocity curve, pulsation theory (without mathematical proof), and distance modulation. (auth) (STAR)

13790 PHOTOMETRIC RECOGNITION OF RAPID ROTATORS AND SUPERGIANTS AMONG B STARS. Furenlid, Ingemar (Stockholm Observatory). Astrophys. Lett.; 7: 147-9(Dec 1970).

A photometric scheme for distinguishing normal main-sequence B stars from rapid rotators and supergiants is proposed. Numerical experiments with several different filter combinations indicate that stars with projected rotational velocities greater then 250 km/sec can best be distinguished with a Balmer-line index that uses filters which are 10 and 30 Å wide at half transmission. Since this index is also temperature sensitive, it must be used in conjunction with another temperature index, such as the magnitude of the Balmer jump. This combination of indices also permits recognition of very rapid rotators seen pole-on. Conveniently, this scheme can also be used to distinguish B supergiants. (auth)

13791 RADIAL VARIATION IN THE RATIO OF BLUE TO RED SUPERGIANTS IN THE GALAXY. Hartwick, F. D. A. (Univ. of Victoria, B. C.). Astrophys. Lett.; 7: 151-2(Dec 1970).

It is shown that there is a systematic variation in the ratio of blue to red supergiants with respect to radial distance from the center of the Galaxy. The amplitude of the variation and its sense are similar to those found in M33 by Walker. (auth)

13792 OUTER LAYERS OF MODEL MOVING ATMOSPHERES. **Fischel, D.; Nethery, C. M.; Sparks, W. M. (Goddard Space Flight Center, Greenbelt, Md.). Astrophys. J.; 163: 649-51(1 Feb 1971).**

In evaluating the divergence of the flux through the optically thin outer layers of model moving atmospheres, the large difference between the areas of the inner and outer surfaces causes an unreal temperature decrease. This numerical difficulty can be removed by including physically exact weighting functions in the energy-balance equation. (auth)

13793 PULSATIONAL STABILITY OF PURE-HELIUM STARS OF LOW MASS. **Hansen, C. J.; Spangenberg, W. (Univ. of Colorado, Boulder). Astrophys. J.; 163: 653–4 (1 Feb 1971).**

A set of models near the minimum mass of the zero-age helium main sequence were analyzed for pulsational instability and it was found that models with masses less than ~0.35 $M_\odot$ are unstable with periods of about 1 minute. The connection with unstable hot subdwarfs is considered briefly. (auth)

13794 COMPARISON OF THEORETICAL AND OBSERVATIONAL RESULTS FOR PLEIONE'S SHELL EPISODE, 1938–1954. **Marlborough, J. M. (Univ. of Western Ontario, London). Astrophys. J.; 163: 525-31(1 Feb 1971).**

The time variations of the line profiles for the Balmer lines Hα, H15, H25, and H35 are presented for the model envelope determined by Limber which best agrees with the observations of Pleione's shell phase between 1938 and 1954. The theoretically predicted variations of the lines in the upper Balmer series agree quite well with Limber's results. The observed approximate equality of R and V during most of the shell phase and R > V during the later stages is reproduced by the model. The theoretical Hα profile at the time of maximum rate of ejection of matter by the star appears to be similar to a tracing of the observed Hα profile in 1945. A problem concerning the time scale of the ejection rate is evident in that the emission at Hα does not begin early enough and disappears too quickly as compared with the observations. A suggestion to remove this problem is briefly discussed. (auth)

13795 EVIDENCE FOR HYDROGEN-TO-CARBON RATIOS IN ACCORDANCE WITH THE CNO BI-CYCLE IN SEVERAL CARBON STARS. **Thompson, Rodger I.; Schnopper, Herbert W.; Rose, William K. (Massachusetts Inst. of Tech., Cambridge). Astrophys. J.; 163: 533-42(1 Feb 1971).**

Equivalent widths of a C_2 and several CO infrared absorption bands were measured in four carbon stars (W Ori, X Cnc, U Hya, and 19 Psc). Line-of-sight abundances of C_2 and CO were computed from the observed equivalent widths. Model-atmosphere calculations were then used to predict theoretical C_2 and CO abundances for various H : C : N : O abundance ratios. Two cases were considered: (1) a high carbon-to-hydrogen ratio which is indicative of either high initial carbon abundance or mixing of products of the triple-α process and (2) a low carbon-to-hydrogen ratio which is indicative of a hydrogen-to-carbon ratio derived from the CNO bi-cycle. A comparison of the observed C_2 and CO abundances with the best available theoretical models indicated agreement with the predicted CNO bi-cycle hydrogen-to-carbon ratio. (auth)

13796 DEUTERIUM BURNING AS THE ORIGIN OF THE OUTBURSTS OF THE STAR HL TAURUS 76. **Vila, Samuel C. (Univ. of Pennsylvania, Philadelphia). Astrophys. J.; 163: 543-6(1 Feb 1971).**

It is shown that central deuterium burning can be the cause of the energy release in the periodic outbursts of the variable star HL Tau 76 on an assumed deuterium abundance in that star of the order of that of the Earth. (auth)

13797 ORDINARY STARS, WHITE DWARFS, AND NEUTRON STARS. **Green, Louis C. (Strawbridge Observatory, Haverford, Pa.). Sky Telesc.; 41: 18-20(Jan 1971).**

Stellar evolution from ordinary main-sequence stars to white dwarfs to neutron stars and supernovae is briefly discussed. Hydrostatic equilibrium, energy transport in a star, states of matter, and neutron-star properties are considered. (W.D.M.)

13798 METHOD FOR THE SIMULTANEOUS DETERMINATION OF HELIUM AND METAL ABUNDANCES IN OLD OPEN CLUSTERS. **Demarque, Pierre; Heasley, James N. Jr. (Yale Univ. Observatory, New Haven). Astrophys. J.; 163: 547-53(1 Feb 1971).**

A method for the simultaneous determination of the helium content Y, and metal content Z, for stars in old open clusters is described. The method is independent of the distance modulus

XUM

of the cluster and of color corrections. It is found that the maximum luminosity during the phase of evolution in which hydrogen is burned in a thick shell is proportional to Y for fixed Z. By using this effect and the analysis of the dependence of the gap width upon Y for fixed Z determined by Aizenman, Demarque, and Miller it is possible in principle to determine Y and Z for an old open cluster. In order to calibrate this new effect a series of theoretical evolutionary tracks was computed for stars evolving from the main sequence to the base of the giant branch for different chemical compositions. Problems of observational comparison are considered. (auth)

13799 LOW-MASS WHITE DWARFS AND THE COOLING SEQUENCES IN THE HYADES CLUSTER. **Chin, Chao-wen; Stothers, Richard (Goddard Inst. for Space Studies, New York). Astrophys. J.; 163: 555-65(1 Feb 1971).**

Detailed evolutionary sequences were constructed for models of white dwarfs with very low mass (0.1, 0.2, and 0.3 $M_{\odot}$) and with a variety of chemical compositions. Convection near the surface was taken fully into account in the models with hydrogen envelopes. Down to a luminosity of at least $\log (L/L_{\odot}) = -3.3$, the basic properties of the models were not affected significantly by the presence of convection in the hydrogen-rich layers. All the models with envelopes assumed to be in radiative equilibrium were insensitive to the choice of chemical composition of the envelope, at least as long as the mass of the envelope encompassed 1%, or less, of the total mass. The color-magnitude diagram of the white dwarfs in the Hyades was reinterpreted. Two major mass sequences were isolated: a "blue" sequence at ~1 $M_{\odot}$ and a probable "red" sequence at ~0.1 $M_{\odot}$, with a scatter of intermediate-mass stars. The observed luminosity functions seem to be in good agreement with the theoretical ones. If the red sequence is real, then the bifurcation of the white-dwarf masses occurs at a parent mass of 2.4 ± 0.4 $M_{\odot}$. A speculative picture is presented of the origin of the white-dwarf sequences. (auth)

13800 ROTATIONAL DECELERATION OF MAGNETIZED STARS. **Kulsrud, Russell M. (Princeton Univ., N. J.). Astrophys. J.; 163: 567-76(1 Feb 1971).**

The possibility was investigated that magnetic stars are rotationally decelerated solely by the radiation of hydromagnetic waves with no mass loss. It is shown that two classes of stars should be considered: those with periods smaller than a few thousand days and those with longer periods. For the shorter-period class, such a strong influence on the surrounding medium is exerted by the radiation that it must be calculated in the perturbed medium. For the slow rotators, this effect can be ignored. It is shown that a few stars with very large fields or initially small rotation may be decelerated to very long periods by this mechanism. The rest are relatively unaffected. (auth)

13801 MEMBERSHIP IN THE OPEN CLUSTER NGC 7062. **Jones, B. F. (Univ. of California, Santa Cruz); van Altena, W. F. Astron. Astrophys.; 9: 86-94(Nov 1970).**

Proper motions with an average accuracy of 0.0007/yr were determined for 334 stars in the region of the open cluster NGC 7062. Membership probabilities were determined for all stars within 12 arc minutes of the cluster center. The color–magnitude diagram for probable members showed the cluster to be very similar to the Hyades or Praesepe, and thus older than previous indications. (auth)

13802 PERTURBATION TREATMENT OF CLOSE BINARIES IN THE N-BODY PROBLEM. **Aarseth, S. J. (Inst. of Theoretical Astronomy, Cambridge, Eng.). Astron. Astrophys.; 9: 64-9 (Nov 1970).**

The variation of parameters method developed by Pines (1961) was used to study close binaries in the N-body problem. Direct treatment of the two components was replaced by an integration of the perturbed relative motion as well as the corresponding center of mass. The use of osculating two-body elements permitted a significant reduction in the number of integration steps while at the same time increasing the accuracy. Unperturbed relative motion may be assumed for small perturbations whereas strong interactions must still be calculated by the direct integration method. Dynamically invariant criteria were used when selecting suitable binaries for special treatment and an arbitrary number of close pairs may be studied simultaneously. A comparison was made with the direct method for a simple three-body problem. Extensive results were obtained for several systems with 250 particles which will be discussed in a subsequent paper. (auth)

13803 $^{14}N/^{12}C$, $^{12}C/^{13}C$, AND $^{14}N/^{15}N$ IN THE CARBON STAR UU AUR. **Querci, M.; Querci, F. (Observatoire de Paris, Meudon, France). Astron. Astrophys.; 9: 1-14(Nov 1970).**

Absolute molecular curves of growth for the carbon star UU Aurigae were constructed from the $C^{12}N^{14}$ red system and the $C^{12}C^{12}$ Phillips system in the region λλ 7626 to 8718 Å, using a spectrum of 6.4 Å/mm dispersion. It was found that $C^{12}N^{14}/C^{12}C^{12} \approx 116$; this value leads to $N^{14}C^{12} \approx 37$ for an excitation temperature of 2500°K and $\log P_g \approx 0$, following the theoretical molecular equilibrium calculations of Morris and Wyller. The molecular ratio CN/C_2 should also be an indicator of the C/O ratio, equal to 3.4. It followed that the mass of UU Aur was about 6 $M_{\odot}$. C^{12}/C^{13} was found to be about 12 to 20. The first value was determined from the $C^{12}N^{14}$ and $C^{13}N^{14}$ curves of growth, and was of low weight because of the uncertainty in the latter. The value of 20 was obtained from the intensity ratios of weak lines in the $C^{12}C^{12}$ and $C^{12}C^{13}$ Phillips system. The variation of these abundance ratios was relatively insensitive to temperature within a range of 600°K. The excess of N^{14} and the lack of appreciable C^{13} in this star cannot be explained by the CNO process alone. The HCN molecule and tentatively the CH_2 molecule were identified from wavelength measurements. An attempt was also made to identify the $C^{12}N^{15}$ molecule as an indicator of the N^{14}/N^{15} ratio. (auth)

13804 DETECTION OF RADIO EMISSION FROM ANTARES. **Wade, C. M.; Hjellming, R. M. (National Radio Astronomy Observatory, Green Bank, W. Va.). Astrophys. J.; 163: L105-6(1 Feb 1971).**

Radio emission from the M1 Ib supergiant Antares (α Scorpii) was detected at 11.1-cm wavelength, at a flux density of (0.005 ± 0.001) flux units. (auth)

13805 OBSERVATION OF PERIODIC SHELL ACTIVITY BY HR 2142. **Peters, Geraldine J. (Univ. of California, Los Angeles). Astrophys. J.; 163: L107-9(1 Feb 1971).**

Spectroscopic observations of the Be star HR 2142 during 1969–1970 confirmed that a short-term, conspicuous shell phase reappears regularly every 80 days. A sequence of profiles observed in 1970 September is presented to demonstrate the effect. (auth)

13806 LIMB-DARKENING TABLES FOR F0–K0 MAIN-SEQUENCE STARS. **Margrave, Thomas E. Jr. (Univ. of Montana, Missoula). Astrophys. Space Sci.; 9: 199-205(Nov 1970).**

Limb-darkening tables for blanketed model atmospheres fitted to main-sequence stars in the F0–K0 spectral range are presented. The tables cover the wavelength range λλ 3,646 to 24,000. (auth)

13807 MASS OF THE CRAB NEBULA. **Trimble, Virginia; Woltjer, Lodewyk (Inst. of Theoretical Astronomy, Cambridge, Eng.). Astrophys. J.; 163: L97-8(1 Feb 1971).**

The absence of differences in the acceleration of bright and faint filaments in the Crab Nebula makes it improbable that the presence of neutral matter can significantly increase the previously estimated values of the mass of the filamentary shell. (auth)

13808 HIGH-FREQUENCY STELLAR OSCILLATIONS. VI. R548, A PERIODICALLY VARIABLE WHITE DWARF. **Lasker, Barry M.; Hesser, James E. (Observatorio Interamericano de Cerro Tololo, La Serena, Chile). Astrophys. J.; 163: L89-93 (1 Feb 1971).**

The white dwarf R548 is a periodic variable with a dominant period of 212.864 ± 0.031 sec and a secondary period of 273.0 ± 0.6 sec. The amplitude of the former is 0.01 mag, while that of the latter fluctuates between 0.001 and 0.01 mag on a time scale of ≲24 hours. Light curves are given for both variations. This star and the other confirmed periodically variable white dwarfs, HL Tau 76 and G44-32, lie near the lower junction of the DA boundary and the blackbody line in the [(U – B), (B – V)] diagram, but other stars in this region of the two-color plane appear quiescent. The variations of these white dwarfs cannot be readily interpreted as pulsations, and the need for other physical models is discussed. (auth)

13809 QUANTITATIVE CLASSIFICATION OF STARS BY STROEMGREN PHOTOMETRY. **Stepien, Kazimierz (Univ. of Warsaw). Postepy Astron.; 18: 345-54(Dec 1970). (In Polish).**

The definition of Strömgren photometry, its calibration, and basic principles are considered. An application of the photometry to classification of stars according to their age, chemical composition, and other physical parameters is discussed. (auth)

13810 FORMATION OF SOLAR RARE-EARTH LINES INSIDE AND OUTSIDE H AND K. **Canfield, R. C. (Sonnenborgh**

Observatory, Utrecht). Astron. Astrophys.; 10: 64-72(1 Jan 1971).

The solar spectra of many lanthanide rare-earths consist entirely of weak lines, and the atomic structure of the ions of interest in the visible solar spectrum encourages interlocking effects. Calculations were made that mimic the essential features of these ions in the solar atmosphere. It is shown that the mechanism of interlocking via photo-excitations and de-excitations can quantitatively explain the characteristic behavior of solar lines of rare-earth ions, both in normal continuum regions in the visible spectrum and in the wings of the H and K lines. (auth)

13811 RADIAL VELOCITY OBSERVATIONS OF SX PHOENICIS. Stock, J.; Tapia, S. (Univ. of Chile, Santiago de Chile). Astron. Astrophys.; 10: 134-46(1 Jan 1971).

A radial velocity curve for SX Phoenicis was derived from nearly five hundred spectra. An analysis of this curve, together with photometric data, showed that the observations cannot be reconciled with the model of a single pulsating star. This conclusion was confirmed by the behavior of the absorption line profiles. In addition, the intensities and profiles of the absorption lines varied rapidly, often within minutes. This characteristic was different from line to line. SX Phoenicis is possibly a binary, or even a multiple system. (auth)

13812 LINE-INTENSITY VARIATIONS IN THE SPECTRUM OF SX PHOENICIS. Stock, J.; Tapia, S. (Univ. of Chile, Santiago de Chile). Astron. Astrophys.; 10: 147-54(1 Jan 1971).

Line intensities for 31 absorption lines during 74 separate time intervals, covering four subcycles of the variation of SX Phoenicis, are given. (auth)

13813 OBSERVATION OF EARLY-TYPE STARS FROM OGO-VI. Metzger, P. H.; Clark, M. A. (Aerospace Corp., El Segundo, Calif.). Astron. Astrophys.; 10: 155-8(1 Jan 1971).

Stellar fluxes of the order of 10^{-8} erg s^{-1} cm^{-2} $Å^{-1}$ for 10-eV photons were observed for several bright ultraviolet-emitting stars. These observations were made from the OGO-VI scanning Lyα experiment whose resonance absorption filter suppressed the strong HLyα airglow, enabling weak external enhancements to be observed. Five separate orbits of data revealed point-source enhancements. Observations with an SrF_2 background light filter establish that less than 10% of the observed signals could be at spurious wavelengths. (auth)

13814 STARK BROADENING AND RADIO RECOMBINATION LINES IN NGC 7027. Hoang-Binh, D. (Observatoire, Meudon, France). Astron. Astrophys.; 10: 159-60(1 Jan 1971).

The observed upper limit for the ratio T_L/T_C of central H109α line to continuum brightness temperatures in NGC 7027 (Terzian and Balick, 1969) is shown to be consistent with an electron density $N_e \gtrsim 10^5$ cm^{-3}. The lower limit of $\sim 10^5$ cm^{-3} for N_e is smaller by a factor ~10 than that found by Goldberg (1970), who did not consider Stark broadening. Further, an emission measure considerably larger than the value derived by high-frequency flux measurements is not found necessary to account for the upper limit for T_L/T_C. (auth)

13815 STARS WITH CENTRAL HELIUM BURNING AND OCCURRENCE OF LOOPS IN THE H–R DIAGRAM. Lauterborn, D.; Refsdal, S.; Weigert, A. (Hamburger Sternwarte, Hamburg. Univ. of Nebraska, Lincoln). Astron. Astrophys.; 10: 97-117 (1 Jan 1971).

The occurrence of loops during central He burning is discussed by considering separately the effects of changes in the following basic parameters of a model: mass and radius of the He core and the X profile above the core. It is shown that only the effect from the X profile can produce a loop. The variation of the loops with the total mass as well as the influence of an assumed mass loss is discussed. (auth)

13816 DEVIATIONS FROM LOCAL THERMODYNAMIC EQUILIBRIUM IN WEAK COMPLEX SPECTRA. Canfield, Richard C. (Sonnenborgh Observatory, Utrecht). Astron. Astrophys.; 10: 54-63(1 Jan 1971).

The equations of statistical equilibrium are solved for an atom or ion whose energy level structure is complex and whose spectral lines are all weak. Semi-empirical expressions are used to calculate atomic cross sections for idealized multilevel atoms. A linear Planck function $B(\tau)$ is assumed, i.e., there is no chromospheric temperature rise in the atmospheric model. Solutions of the statistical-equilibrium equations are obtained for a variety of model atoms and atmospheres. When interlocking via permitted radiative excitations and de-excitations can take place, the source function is photo-excitation controlled. As a result, LTE does not normally obtain. Calculations made for atoms of up to 24 levels plus continuum demonstrate the extent of representative deviations from LTE. (auth)

13817 OPTICAL SPECTRUM OF THE OH AND INFRARED EMITTER VX SAGITTARII. Wallerstein, George (Univ. of Washington, Seattle). Astrophys. Lett.; 7: 199-200(Jan 1971).

The general appearance of the spectrum and the velocity structure of the OH and optical features of VX Sgr are very similar to those of VY CMa. VX Sgr does not show a visible nebula nor does it show a low-excitation emission spectrum. The main-velocity data for both VX Sgr and VY CMa can be understood by a model with a central object surrounded by a shell expanding at about 40 km/sec. (auth)

13818 UNUSUAL OH EMISSION FROM A MIRA VARIABLE. Robinson, B. J.; Caswell, J. L.; Goss, W. M. (CSIRO, Sydney). Astrophys. Lett.; 7: 163-5(Jan 1971).

Previously known OH-infrared objects have been characterized by strong OH emission at 1612 MHz. It is reported here that the Mira-type variable R Hor does not emit at 1612 MHz, but does emit on the main OH lines at 1665 and 1667 MHz. (auth)

13819 CLUSTERING OF NUCLEONS IN LOW-DENSITY NEUTRON-STAR MATTER. Buchler, Jean-Robert; Barkat, Zalman (California Inst. of Tech., Pasadena). Astrophys. Lett.; 7: 167-70(Jan 1971).

A new approach to the study of the composition and the properties of neutron star matter at subnuclear densities is proposed. The approach is based on an improved Thomas–Fermi model for nuclei and on realistic nuclear matter calculations. Preliminary results are given. In particular, the proton number of the clusters is found to be relatively small ($Z \sim 26$ to 33). The need for such an approach is emphasized by a demonstration of the vulnerability of previous methods. (auth)

13820 REGION OF FORMATION OF THE NARROW EMISSION LINES OF NOVA DELPHINI. Friedjung, M.; Malakpur, I. (Institut d'Astrophysique, Paris). Astrophys. Lett.; 7: 171-4(Jan 1971).

A study of the centers of the emission lines of Nova Delphini shows that they are formed in a region of radius near 3×10^{13} cm. It is concluded that they were formed in the atmosphere of the other component of the binary system. (auth)

13821 STRUCTURE AND EVOLUTION OF STARS WITH VARIOUS CHEMICAL COMPOSITIONS. Masevich, A. G.; Frantsman, Yu. L. Vestn. Akad. Nauk SSSR; No. 12, 23-9(Dec 1970). (In Russian).

The age of various stars in different groupings was determined by comparisons in the Hertzsprung–Russell diagram with the data of star evolution. Data obtained indicated that various postulations on the initial chemical composition of stars could increase the calculated age–magnitude relation by two. (R.V.J.)

13822 THERMAL INSTABILITY AND THE CONVECTIVE STABILITY OF STELLAR CHROMOSPHERES. Defouw, Richard John. Pasadena, Calif.; California Inst. of Tech. (1970). 107p. University Microfilms Order No. 70-18,033.

Thesis.

It is generally believed that stellar chromospheres are stable against convection since the Schwarzschild criterion indicates stability when temperature increases with height. It is shown, however, that the Schwarzschild criterion does not apply to chromospheres because it ignores the possibility of thermal instability. In the absence of a magnetic field, thermally unstable regions of a chromosphere will be overstable if the temperature inversion is sufficiently steep. This overstability may explain the origin of a certain class of oscillations in the solar chromosphere. Thermally unstable regions containing magnetic fields are monotonically unstable for all values of the temperature gradient. It is suggested that this monotonic instability of magnetic regions is responsible for spicule formation in the solar chromosphere. Elementary considerations of thermal balance predict that the temperature gradient should diverge at levels of marginal stability. The chromospheric region of spicule formation should, therefore, be bounded below by an abrupt temperature jump. The above results are derived by analyzing the stability of a simple model chromosphere in which all neutral hydrogen atoms are assumed to be in the ground state. Although the model chromosphere emits only free–bound radiation, its thermal instability is caused by the same ionization effects that lead to instability in plasmas emitting line radiation. Thermally unstable regions of a stellar chromosphere, although not represented in detail by the model, should behave in a similar fashion. (Diss. Abstr. Int., B)

13823 PULSATIONAL CHARACTERISTICS OF A LOW-MASS CEPHEID MODEL INCLUDING CONVECTION EFFECTS. Jones,

XUM

Eric Manning. Madison, Wis.; Univ. of Wisconsin (1970). 47p. University Microfilms Order No. 70-13,918.

Thesis.

The model parameters are: mass 0.93 $M_\odot$, $M_{bol} = -1.7$, and log $T_e = 3.75$. Convection is treated by a time-dependent, mixing-length type theory where the eddy velocity is assumed to exponentially approach the equilibrium value computed in Bohm–Vitense's formulation. The dynamical evolution of the model is computed by a code based on the method of Cox, Brownlee, and Eilers. The model is found to be marginally unstable to pulsation driven by the hydrogen ionization zone. A long-period (≈6 days) oscillation moves the model back and forth across the high-temperature boundary of the instability region ($\delta R/R \approx 0.03$). Consequently, the amplitude of the motion of the material above the hydrogen ionization zone is irregular and the period varies in the range $(1.1 \pm 0.1) \times 10^5$ sec. The model is unstable with convection present although the rise of convective flux at maximum compression probably decreases the effectiveness of the driving mechanisms. The ratio of mixing length to pressure-scale height is taken to be 1.5. When convection is not included, the absence of turbulent pressure causes a decrease in the total radius and the model becomes stable. (Diss. Abstr. Int., B)

13824 SCANNER ABUNDANCE STUDY OF LATE G AND K DWARFS. Taylor, Benjamin Joseph. Berkeley, Calif.; Univ. of California (1969). 187p. University Microfilms Order No. 70-17,668.

Thesis.

A technique developed by Spinrad and Taylor for obtaining metal abundances of late-type stars, and used by them in an earlier investigation of evolved stars, was applied to field dwarfs in the solar vicinity and the Hyades. The following major conclusions were reached: (1) Super-metal-rich dwarfs (i.e., dwarfs with higher metal content than the Hyades) are to be found in the solar neighborhood; this conclusion is in accord with previous investigations. The fractions of stars that are super-metal-rich in each metal range from 3% for Fe to 9% for Na —about 4% of the stars studied have mean metallicities greater than that of the Hyades. (2) The tight correlation between N, Na, and Fe abundances found by Spinrad and Taylor for evolved stars exists for dwarfs as well. Mg and Ca are also correlated with Fe, but with some intrinsic scatter. α-rich stars of solar metallicity exist, but moderately iron-poor, α-poor stars apparently do not. (3) Dwarfs for which $e > 0.35$ and/or $|W| > 40$ km/sec and which have solar or higher metallicities exist, contrary to the results of Eggen, Lynden-Bell, and Sandage. Little certain correlation between kinematic properties and overall metal abundance is found in the sample studied. α-rich stars generally (but not always) have high velocities; no other generalizations about them appear possible. (4) The abundance heterogeneity observed by Breger in the Hyades moving group probably exists in the 61 Cyg group as well. (5) Helium abundances ranging from fractions of 0 to 0.5 by weight may well be found among some stars in the solar neighborhood. (Diss. Abstr. Int., B)

13825 SPECTROSCOPIC INVESTIGATION OF FOUR O-TYPE SUBDWARFS. Peterson, Arsine Victoria. Pasadena, Calif.; California Inst. of Tech. (1970). 156p. University Microfilms Order No. 70-18,044.

Thesis.

The spectra of four O-type subdwarfs, of the class with strong nitrogen lines and very weak carbon and oxygen lines, were studied in some detail. Model atmospheres were constructed for the stars HZ 44, +25°4655, and HD 127493, and the computed profiles of selected hydrogen and helium lines were compared with the observed profiles. The effective temperatures of the model atmospheres were $T_e \geq 40{,}000$ °K and the surface gravities $g \geq 5 \times 10^5$ (cgs). A mass of approximately 0.5 $M_\odot$ and an absolute visual magnitude of about +4 for the stars HZ 44 and HD 127493 was found to be consistent with the available data. The star +25°4655 is probably less luminous. High helium abundances were inferred for these stars —from $Y \approx 0.4$ for HZ 44 to $Y \approx 0.9$ for +25°4655. Chemical abundances were derived for heavier elements in a fine analysis. The nitrogen-to-carbon, and nitrogen-to-oxygen ratios derived for these stars were two orders of magnitude greater than is observed in the Sun and in other main-sequence stars. The high helium abundance and the observed CNO ratios were consistent with abundances predicted for material that has undergone hydrogen-burning in the CNO cycle. (Diss. Abstr. Int., B)

13826 INFRARED OBSERVATIONS OF H II REGIONS. Hilgeman, Theodore William. Pasadena, Calif.; California Inst. of Tech. (1970). 198p. University Microfilms Order No. 70-18,037.

Thesis.

Spectral data are presented, giving intensities of the Brackett B_γ line at six positions in M42 and of the Brackett ten through fourteen ($B_{10}-B_{14}$) lines plus the He $4d^3D-3p^3P^0$ line at three positions in M42. Observations of the Brackett B_γ line are also given for the planetary nebulae NGC 7027 and IC 418. Brackett gamma is shown to exhibit an anomalous satellite line in NGC 7027. Broadband data are presented, giving intensities at effective wavelengths of 1.25, 1.65, 2.2, 3.5, and 4.8 μ for three positions in M42. Comparisons with visual and radio data as well as 12-μ and 20-μ data are used to derive reddening, electron temperatures, and electron densities for M42 and the two planetaries, as well as a helium abundance for M42. A representative electron temperature of 8400 ± 1000°K, an electron density of $1 \pm 0.1 \times 10^3$ cm^{-3}, and a He/H number density ratio of $0.10^{+0.10}_{-0.05}$ are derived for the central region of M42. The electron temperature is found to increase slightly with distance from the Trapezium. M42 is shown to emit in excess of the predicted recombination radiation throughout the entire infrared spectrum. The variations in the excess with wavelength and with position are analyzed to determine which of several physical processes may be operating. The longer-wavelength infrared excess is shown to be dominated by dust emission, while the shorter wavelength infrared excess is caused by dust scattering. The dust is shown to be larger than the average interstellar particle. A new feature of the Orion red star ORS-1 is found in that it appears to have a reflection nebula around it. (Diss. Abstr. Int., B)

13827 DISTANCES AND DISTRIBUTION OF PLANETARY NEBULAE. Cahn, J. H.; Kaler, J. B. (Univ. of Illinois, Urbana). Astrophys. J., Suppl. Ser.; 22: No 189, 319-68(Jan 1971).

Distances, or upper limits to the distances, of more than 600 planetary nebulae were determined by the photometric method, based upon an assumption of mean nebular parameters. For this program the extinction coefficients of about 100 nebulae were computed and these were used to find a dust model of the Galaxy for use in self-consistent calculations of extinctions and distances. The dust model was then used to estimate the distances of several optically thick planetaries for which the extinctions have been measured. The local density of those optically thin nebulae with $0.08 < R < 0.4$ pc was found to be about 50 kpc^{-3}. The total number of optically thin planetaries in the Galaxy is about 3×10^5 if the distance to the galactic center is 8 kpc and 4×10^5 if it is 10 kpc. The estimated birthrate of planetary nebulae is in agreement with the birthrate of white dwarfs. (auth)

13828 AXISYMMETRIC BLACK HOLE HAS ONLY TWO DEGREES OF FREEDOM. Carter, B. (Cambridge Univ., Eng.). Phys. Rev. Lett.; 26: 331-3(8 Feb 1971).

The theorem described establishes the claim that, in a certain canonical sense, the Kerr metrics represent "the" (rather than merely "some possible") exterior fields of black holes with the corresponding mass and angular-momentum values. (auth)

13829 ATOMS IN SUPERSTRONG MAGNETIC FIELDS. Newton, Roger G. (Indiana Univ., Bloomington). Phys. Rev., D; 3: 626-7(15 Jan 1971).

It is pointed out that because of possible large radiative corrections, the mass and magnetic moment of an electron in the presence of magnetic fields above 10^{13} G, which may be present in pulsars, are unknown. Calculations of ionization energies of atoms in such fields may therefore be meaningless unless the quantum-electrodynamic corrections are included. (auth)

13830 POSSIBILITY OF OBSERVING NEUTRINOS FROM COLLAPSING STARS AND NEUTRINO OSCILLATIONS. Domogatskii, G. V.; Zatsepin, G. T. Bull. Acad. Sci. USSR, Phys. Ser. (Engl. Transl.); 33: 1639-42(Nov 1969).

Translated from Izv. Akad. Nauk SSSR, Ser. Fiz.; 33: 1796-9 (Nov 1969).

It is shown that a scintillation detector weighing a few hundred tons and located deep underground could be expected to detect the neutrino flux from a collapsing star in the Milky Way. (W.D.M.)

Quasi-Stellar, Radio, and X-Ray Sources

13831 (AD-711300) GALACTIC HYDROGEN ABSORPTION AT 21 cm WAVELENGTH IN THE DIRECTION OF VIRGO A. Report No. 1970-8. Colvin, R. S.; Hughes, M. P.; Thompson, A. R.; Verschuur, G. L. (Owens Valley Radio Observatory, Pasadena, Calif.). 1970. Contract N00014-67-A-0094-0008. 18p. NTIS.

The 21-cm optical depth in the direction of Virgo A is 0.017 ± 0.003 near the velocity of the peak of the galactic background emission, and the corresponding gas temperature lies within the range 180 to 460°K. In the negative-velocity wing of the emission profile the optical depth is less than 0.002, which indicates a minimum gas temperature of 600°K. (USGRDR)

XUM

13832 (AD-711397) MODEL OF PULSARS. Sturrock, P. A. (Stanford Univ., Calif. Inst. for Plasma Research). May 1970. Contract F44620-69-C-0008. 82p. (SU-IPR-365). NTIS.

The model comprises a rotating neutron star (R ~ 1,000,000 cm) with a strong magnetic field (B ~ 10^{12} gauss). Magnetic field lines that reach the light cylinder are open field lines that connect to the surface of the star at the "polar caps." Each polar cap contains two zones, an "electron polar zone" (EPZ) and a "proton polar zone" (PPZ) from which electrons and protons, respectively, stream from the star. Acceleration of each stream is effected, close to the surface of the star. The optical, x-ray, and gamma-ray flux expected from a model of the Crab pulsar can be reconciled with observation if the rotation axis, dipole axis, and line of sight are so related that radiation is received from the PPZ's but none from the EPZ's. (USGRDR)

13833 (AD-711611) SYNTHESIS OF THE POLARIZATION PROPERTIES OF 3C10 AND 3C58 AT 1420 AND 2880 MHz. Report No. 1970-6. Weiler, K. W.; Seielstad, G. A. (Owens Valley Radio Observatory, Pasadena, Calif.). 1970. Contract N00014-67-A-0094-0008. 57p. NTIS.

An Earth-rotation aperture-synthesis technique was combined with the methods of interference polarimetry to study the total intensity and linear polarization properties of the two radio sources 3C 10 and 3C 58 with a resolution of approximately one minute of arc at both 1420 and 2880 MHz. These data were then used to calculate the distributions of spectral index, rotation measure, intrinsic position angle, and polarization for the sources. (auth) (USGRDR)

13834 EXTENDED RADIO SOURCE IN THE DIRECTION OF THE PULSAR CP 1919. Caswell, J. L.; Goss, W. M. (CSIRO, Sydney). Astrophys. Lett.; 7: 141-5(Dec 1970).

An extended radio source in the direction of the pulsar CP 1919 was detected. The observations at 178 and 2700 MHz suggest that the source is nonthermal, and its brightness distribution suggests that it is not extragalactic. It is proposed that the extended source may be a supernova remnant associated with CP 1919. Some of the consequences which follow if the association is real are explored, including the possibility that at least some pulsars initially have quite long (≈1 sec) periods. (auth)

13835 INTERPRETATION OF RADIO SPECTRA OF EXTRAGALACTIC SOURCES. Hirth, W. (Institut fuer Radioastronomie, Bonn). Astrophys. Lett.; 7: 153-6(Dec 1970).

It is proposed to interpret the curvature of type C-radio spectra by the assumption of relativistic Maxwellian distributions. The power law spectra of type S appear to be the result of a spatial variation of temperature in the sources. (auth)

13836 PULSAR NUMBER-PERIOD DISTRIBUTIONS AND THE OBLIQUE ROTATOR: A FINITE AND EVOLVING POPULATION. Henriksen, R. N. (Queen's Univ., Kingston, Ont.). Astrophys. Lett.; 7: 89-94(Dec 1970).

The number–period distribution predicted for a homogeneous pulsar population by the oblique rotator model (aligning and braking due to electromagnetic and gravitational-radiation torques) is given for various geometries. Three principal qualitative features may be isolated: (i) the "luminosity-limited" distribution at the long periods; (ii) the "aging-rate" distribution at short periods for a finite pulsar population; and (iii) the "pile-up" at the period P_∞ at which the rotator is aligned, in a spiral-arm population. It is argued that these features may be recognized in the presently available pulsar sample. (auth)

13837 KINEMATIC DISTANCE ESTIMATES FOR FOURTEEN GALACTIC SUPERNOVA REMNANTS USING MOLECULAR ABSORPTION LINES. Wilson, T. L. (Max-Planck-Institut fuer Radioastronomie, Bonn). Astrophys. Lett.; 7: 95-9(Dec 1970).

Minimum distances to a number of supernova remnants are estimated by use of OH and H_2CO absorption line velocities, together with the Schmidt-model velocity-distance relation. Comparisons with the theoretical distance estimates of Milne are made. (auth)

13838 ATTENUATION OF RADIO WAVES BY THE ATMOSPHERE AT THE FREQUENCY 1415 MHz. Encrenaz, P. J. (Observatoire de Paris, Meudon, France); Penzias, A. A.; Wilson, R. W. Astron. Astrophys.; 9: 51-2(Nov 1970).

New observations of the atmospheric attenuation at the frequency of 1415 MHz were carried out using the horn antenna of the Bell Telephone Laboratories in Holmdel. The atmospheric emission and the extinction of Cas A as a function of zenith angle lead to the same value of the zenithal absorption: 0.035 ± 0.002 dB. (auth)

13839 SYNTHESIS OF THE POLARIZATION PROPERTIES OF 3C 10 AND 3C 58 AT 1420 AND 2880 MHz. Weiler, K. W.; Seielstad, G. A. (California Inst. of Tech., Pasadena). Astrophys. J.; 163: 455-78(1 Feb 1971).

An Earth-rotation aperture-synthesis technique was combined with the methods of interference polarimetry to study the total intensity and linear-polarization properties of the two radio sources 3C 10 and 3C 58 with a resolution of approximately 1 minute of arc at both 1420 and 2880 MHz. These data were then used to calculate the distributions of spectral index, rotation measure, intrinsic position angle, and depolarization for the sources. The source 3C 10 (Tycho's supernova, SN 1572) is thought to be the remnant of a Type I supernova 5000 pc distant and ~120 pc above the galactic plane. The total radiation has an annular structure with a sharp outer edge and with little emission from the central regions. The polarized flux density has a similar, though less complete, ringlike shape. Although the integrated emission shows little polarization, many areas are polarized in excess of 5% at 21.1 cm and 10% at 10.4 cm. The rotation measure ranges from –6 to +60 rad m^{-2} with no obvious positional organization. The distribution of intrinsic position angles implies the existence of a radial component to the magnetic field. The depolarization distribution is seemingly random. A search for relations among the various source parameters failed to reveal any strong correlations. The source 3C 58, on the basis of the present work, is thought to be the remnant of a supernova ~5000 pc distant and ~270 pc above the galactic plane. In the total radiation it has a simple shape, brightest in the center and falling off slowly to zero at the edges, with an east–west elongation. The distribution of polarized emission is quite complex with some possibly unresolved regions. Although the source has little integrated polarization, when resolved, many regions exhibit polarizations exceeding 10% at 21.1 cm and 15% at 10.4 cm. The spectral index appears to be relatively flat in the central and south–central regions of the source and steeper toward the edges. The rotation measure changes smoothly from –67 rad m^{-2} in the eastern region to –125 rad m^{-2} in the western region. The distribution of intrinsic position angles implies an organized component of the magnetic field parallel to the major east–west axis over the full extent of the source. The depolarization distribution is seemingly random. Again, no strong correlations could be found between the various source parameters. (auth)

13840 OBSERVATIONS OF RADIO RECOMBINATION LINES WITH $\Delta n = 1$ TO 5. Davies, R. D. (National Radio Astronomy Observatory, Green Bank, W. Va.). Astrophys. J.; 163: 479-93(1 Feb 1971).

Observations near a wavelength of 6 cm are described for the 110α, 138β, 158γ, 173δ, and 186ε recombination lines from W3, Orion A, NGC 2024, M16, M17, W43, and W51. Line integrals for each of the sources are tabulated. Since the observations of the different lines are made with nearly the same beamwidths, the data for different lines for a given source can be strictly intercompared. It is shown that the observed lines cannot be understood in terms of local thermodynamic equilibrium (LTE) but require the full non-LTE treatment. The data are discussed from the point of view of turbulence, the helium-to-hydrogen ratio, line shapes, Stark broadening, and anomalous recombination-line emission. (auth)

13841 ULTRAVIOLET ABSORPTION-LINE SPECTRA PRODUCED BY H I REGIONS. Silk, Joseph (Princeton Univ. Observatory, N. J.); Brown, Robert L. Astrophys. J.; 163: 495-502 (1 Feb 1971).

The ionization equilibria of the more abundant ions in H I regions are calculated for the case of x-ray heating and ionization. Significant differences emerge in the abundances of the higher states of ionization in H I regions heated either by energetic particles or by photons. The corresponding absorption-line strengths of the ultraviolet resonance lines are evaluated. Resolution of ~0.1 Å in the ultraviolet would be adequate to distinguish between the two heating models. (auth)

13842 THEORY OF RADIATION MECHANISMS OF PULSARS. I. Chiu, H. Y.; Canuto, V. (Goddard Space Flight Center, New York). Astrophys. J.; 163: 577-94(1 Feb 1971).

A possible mechanism for pulsar radiation is proposed. A maserlike action is shown to take place on account of a nonthermal distribution of the electrons due to the presence of an electric field. The radiation process takes place via Coulomb bremsstrahlung of the electrons in the presence of a strong quantizing magnet field. The model predicts that the amplification of radiation in the radio range gives brightness temperatures ranging from 10^{21} to over 10^{31}°K, depending on the individual pulsar. This is the range of the observed brightness temperature of pulsars. (auth)

XUM

13843 RADIO SPECTRA OF QUASI-STELLAR OBJECTS. Hirasawa, Toshiaki; Tabara, Hiroto (Rikkyo Univ., Tokyo). Astrophys. Lett.; 7: 121-3(Dec 1970).

The radio spectra of quasars with a peak in the frequency range from 1 to 5 GHz can be explained by the superposition of the radio spectra of remnant clouds produced by the successive explosions. Both gradual and steep slopes on the low-frequency side of the peak in the radio spectra can be explained by taking suitable physical parameters. (auth)

13844 NATURE OF PULSARS. Ostriker, Jeremiah P. Sci. Amer.; 224: No. 1, 48-60(Jan 1971).

A review is presented on pulsars which includes the initial observations, theorizing by elimination, confirmation of the neutron star hypothesis, properties of neutron stars, pulse emission mechanisms, and the Crab Nebula. (W.D.M.)

13845 STUDIES OF GALACTIC INTERSTELLAR FORMALDEHYDE. Barrett, Alan H. (Massachusetts Inst. of Tech., Cambridge). Comments At. Mol. Phys.; 11: 98-102(Aug-Sep 1970).

New insight into the physical processes of the interstellar gas has been gained from the discovery of formaldehyde, CH_2O, by absorption of 4830-MHz radiation from galactic sources. The detection and first observational results showed that CH_2O was throughout the galactic plane, had an excitation temperature less than 3°K in some clouds, and a typical line-of-sight in the galactic plane was thought to contain 10^{13} to 10^{14} molecules/cm^2. The $1_{10} \rightarrow 1_{11}$ rotational transition at 4830 MHz shows that CH_2O has a rich microwave spectrum and some of its other lines have been detected. The observations were conducted with the U. S. Naval Research Laboratory 85-foot antenna. The CH_2O lines are valuable probes of the interstellar medium and galactic structure because the angular resolution obtainable is a factor of three greater than with the H or OH lines for a given antenna. (J.C.W.)

13846 STARQUAKES: HAVE THEY BEEN OBSERVED? Green, Louis C. (Haverford Coll., Pa.). Sky Telesc.; 41: 76-9(Feb 1971).

Topics discussed in some detail include gravitational radiation, pulsar models, runaway stars, and pulsar crusts and starquakes. (W.D.M.)

13847 SECULAR BEHAVIOR OF X-RAY AND RADIO EMISSION FROM SUPERNOVA REMNANTS. Tucker, Wallace H. (American Science and Engineering, Cambridge, Mass.). Astrophys. Space Sci.; 9: 315-31(Nov 1970).

General models for the secular behavior of the radio and x-ray emission from supernova remnants were examined and compared with the observations. Hot plasma and synchrotron models for the x-ray emission were considered. Among other things, it was concluded that (1) the total kinetic energy released in most supernova outbursts is probably less than about 10^{51} ergs; (2) continuous injection probably occurs for at least 10 yr in every case and about 1000 yr in most supernova remnants, in which case the supernova remnants 3C 392, W28, Pup A, and IC 443 should produce 1 to 10-keV x-ray fluxes $\approx 10^{-10}$ ergs/cm^2 sec; and (3) the x-ray sources in the Crab Nebula, Cas A and Tycho, can be explained in terms of a model wherein continuous injection occurs for 300 yr for the Crab Nebula, much less than 250 yr for Cas A, and much longer than 400 yr for Tycho. Finally, it is shown that if Tycho and Cas A contain an x-ray star, such as NP 0532, it is quite possible that the x-ray emission from those sources is predominantly due to the x-ray star. (auth)

13848 PULSAR NP 0532: DISAPPEARANCE OF THE PRECURSOR PULSE AT 606 MHz. Rankin, J. M. (Univ. of Iowa, Iowa City); Heiles, Carl; Comella, J. M. Astrophys. J.; 163: L95-6(1 Feb 1971).

For the first time a series of observations of the Crab Nebula pulsar was carried out at 606 MHz. No precursor-pulse component was observed. (auth)

13849 ENERGY SPECTRUM OF A NOVA-LIKE X-RAY SOURCE. Kitamura, T. (Osaka City Univ.); Nakagawa, M.; Takagishi, K.; (and others). Nature (London); 229: 31-3(1 Jan 1971).

Reference is made to a new x-ray source, designated GX 333 + 25, which appeared near or in the Centaurus constellation during July 6–9, 1969. This source reached a maximum intensity approximately twice that of Sco X-1 within a few days, the intensity then remaining nearly constant for about two months, but then diminishing until the source became unobservable at the end of September. Measurements of this source in the energy range 2 to 20 keV were reported in Nature, 224: 784 (1969) using proportional counters on the sounding rocket Kappa-9M, launched on Aug. 7, 1969 from the Kagoshima Space Center. The present communication gives the results of further analysis of the data from Kappa-9M, together with data obtained from the rocket S-210, launched on Aug. 8. The spectrum obtained suggested a thermal origin for the source, with a strong gas absorption of the flux in the energy range <3 keV, indicating the existence of a dense circumstellar gas. Details are given of the apparatus and technique employed; also of the data analysis technique. No definite optical identification of the source was made. Whether the existence of a dense circumstellar cloud has any genetic relation to the sudden appearance of the source is open to question; if the cloud also contained dust the fact that the source was not optically observed may be reasonably understood. The sudden appearance of two sources in the past few years makes it reasonable to expect the appearance of more sources, and investigation of these new sources may be important to a deeper understanding of x-ray sources. (UK)

13850 MAGNETIC FIELD STRUCTURE AROUND THE CRAB PULSAR. Forman, W.; Visvanathan, N. (Howard Coll. Observatory, Cambridge, Mass.). Nature (London); 229: 39-40(1 Jan 1971).

Linear polarization observations of the Crab Nebula at optical wavelengths are described, indicating that the magnetic field is uniform in direction over a region of ~0.5 pc around the pulsar. The observations were made with an automatic sky-compensated polarimeter–photometer, with photomultiplier and filter, in conjunction with the 84-inch Kitt Peak telescope. The results of polarization observations with different size apertures centered on the Crab pulsar are tabulated. The observations were made in Nov. 1969 and Feb. 1970. On the assumption that the nebular radiation is of synchrotron origin the uniform field was at an angle of 68°, and assuming that the observed wisps are plasma waves generated by relativistic particles from the pulsar, the angle through which the magnetic field is rotated by the passage of a suprathermal hydromagnetic wave is calculated. Although the general field around the pulsar is at an angle of 68°, the field in the wisps may lie along their axes, and the calculated rotation of about 28° away from the direction of the general field may be caused by the propagation of suprathermal waves through the nebula. (UK)

13851 GUM NEBULA: FOSSIL STROEMGREN SPHERE OF THE VELA X SUPERNOVA. Brandt, John C. (Goddard Space Flight Center, Greenbelt, Md.); Stecher, Theodore P.; Crawford, David L.; Maran, Stephen P. Astrophys. J.; 163: L99-104(1 Feb 1971).

A physical model for the Gum Nebula was derived from dispersion measures of pulsars, the nebular Hα emission measure, rocket observations of the Lα absorption in the spectra of γ^2 Vel and ζ Pup, and photometry of stars near γ^2 Vel. The objects γ^2 Vel and ζ Pup are not capable of ionizing the nebula. It is suggested that the nebula was produced by radiation from the supernova outburst that gave rise to the Vela X remnant and pulsar PSR 0833−45. (auth)

13852 STUDY OF SCO X-1. Mook II, Delo Emerson. Ann Arbor, Mich.; Univ. of Michigan (1970). 151p. University Microfilms Order No. 70-21,736.

Thesis.

Photometric monitoring of Sco X-1 simultaneously in the V and B bands of the UBV system was used to establish a mean color–magnitude relation for the object. As an example of how this relation can be used in evaluating models for the Sco X-1 system, the self-absorption bremsstrahlung model is discussed in some detail. It was concluded that there are not yet sufficient simultaneous x-ray and optical observations of the object to permit construction of definitive models. Spectra, polarization, and UBV measurements of field stars around Sco X-1 were used to estimate both the distance to the object and the amount of interstellar reddening suffered by its radiation; the distance was found to be between 200 and 300 parsecs and the reddening was between 0.20 and 0.24 magnitudes excess in B−V. These values depend critically upon observations of one field star; a more accurate estimate of both quantities will be possible with an extension of the present work to a larger sample of field stars. (Diss. Abstr. Int., B)

13853 PULSE BROADENING DUE TO ANGULAR SCATTERING IN THE INTERSTELLAR MEDIUM. Lang, Kenneth R. (Cornell-Sydney Univ. Astronomy Center, Arecibo, Puerto Rico). Astrophys. Lett.; 7: 175-8(Jan 1971).

Average pulse profiles of several pulsars exhibit an exponential broadening whose 1/e decay time scales as the fourth power of frequency. This pulse broadening is consistent with that expected from interstellar scattering, and agrees with a thin-screen scattering model in which the screen lies halfway between the Earth and the pulsar. The broadening measurements are also shown to agree with previous measurements of decorrelation frequency. (auth)

13854 RADIO STRUCTURE OF THE REMNANT OF KEPLER'S SUPERNOVA. Hazard, C.; Sutton, J. (Inst. of Theoretical Astronomy, Cambridge, Eng.). Astrophys. Lett.; 7: 179-83(Jan 1971).

The brightness distribution across Kepler's supernova can be interpreted as arising either in two halves of a broken expanding shell of diameter 3 arc min with little radiation between the two halves, or in two separate sources each with a shell-type structure. A comparison is made with the remnants associated with other Type I supernovae. (auth)

13855 POLARIZATION OF THE 150-MHz RADIATION FROM FOUR PULSARS. Schwarz, U. J.; Morris, D. (CSIRO, Sydney). Astrophys. Lett.; 7: 185-9(Jan 1971).

The variation of polarization across the average pulse from PSR 0628, CP 0834, CP 0950, and CP 1133 is presented. For PSR 0628, CP 0950, and CP 1133 the degree of linear polarization is larger at 150 MHz than at higher frequencies and gives no evidence of depolarization at low frequencies. The interstellar Faraday rotation estimated from measurements at adjacent radio frequencies is similar to that determined from neighboring extragalactic radio sources. The maximum value found for the galactic magnetic field is +2.3 μ gauss. No significant circularly polarized component was detected in the average pulse. (auth)

13856 GAMMA RADIATION FROM THE CELESTIAL X-RAY SOURCE SCO X-1. Apparao, Krishna M. V. (Tata Inst. of Fundamental Research, Bombay). Proc. Indian Acad. Sci., Sect. A; 72: 103-7(Sep 1970).

Gamma radiation from the x-ray source Sco X-1 due to Compton-synchrotron process was calculated. Comparison with the upper limits set by an experimental survey for sources of gamma rays with energy greater than 100 MeV was made and constraints on the size of the source and its magnetic field are discussed. The flux predicted in the energy range 10^{11} to 10^{12} eV is above the observable lower limit of present-day detectors. An observation of this flux will serve as a test of the synchrotron origin of the x-radiation. (auth)

13857 1- TO 10-keV X-RAY SKY NEAR THE GALACTIC CENTER. Bradt, H.; Burnett, B.; Mayer, W.; Rappaport, S.; Schnopper, H. (Massachusetts Inst. of Tech., Cambridge). Nature (London); 229: 96-9(8 Jan 1971).

Some experiments carried out with sounding rockets during 1967−9 are described, the object being to resolve source confusion in the region of the galactic centre and to measure source positions with good precision. Spectral and angular size measurements were also made during the flights. As a result, it was possible to obtain a picture of the overall appearance of the sky in this region, and to eliminate various hypotheses concerning possible types of optical and radio counterparts. Information was also obtained concerning source distances. Data are tabulated concerning the sources GX 340 + 6, 340 + 0, 342 − 8, 349 + 2, 358 − 8, 3 + 1, 5 − 1, 9 + 9, 9 + 1, 13 + 1, and 17 + 2, including galactic coordinates, angular size, and observed intensity. (UK)

Solar Phenomena

Refer also to abstracts 14070, 14076, 14107, and 14245.

13858 (AD-710629) MODELS FOR MAGNETOFLUID DYNAMICS OF THE SUN. Final Report, June 15, 1967–June 15, 1970. Gilman, Peter A. (Colorado Univ., Boulder). Contract F19628-67-C-0304. 18p. (AFCRL-70-260). NTIS.

The report summarizes a number of theoretical models developed for: (a) baroclinic and Rossby waves in magnetic fields, and Rossby-wave dynamos; (b) interaction of thermal convection with rotation and shear flow; (c) magnetic buoyancy instabilities. These models elucidate mechanisms for the maintenance of solar differential rotation and large-scale magnetic fields. (auth) (USGRDR)

13859 (AD-711398) POLARIZATION MEASUREMENTS OF SOLAR TYPE-III RADIO BURSTS AT 25.3 MHz. Chin, Y. C.; Fung, P. C. W.; Lusignan, B. B. (Stanford Univ., Calif. Inst. for Plasma Research). Nov 1969. Contract F44620-69-C-0008. 42p. (SU-IPR-338). NTIS.

Reported are the results of 1966, 1968, and 1969 polarization measurements of Solar Type 3 radio noise bursts made by recording the output of two orthogonally polarized receiving channels and subsequent digital processing of selected data. The processed data yield total intensity, degree of polarization, ellipticity, and polarization ellipse orientation at 1 second intervals. The measurements were made in a 100 Hz bandwidth to minimize the influence of the propagating medium on the measurements. The mean degree of polarization was found to be about 65% in contrast to previous studies which indicated that Type 3 events were more weakly polarized. By assuming that Type 3 bursts are flare related the polarization characteristics of Type 3 bursts were studied as a function of the solar longitude of the related flares. The relation between Type 3 event polarization characteristics and flare importance was also investigated. The significance of polarization measurements in studies of solar radio events is pointed out and relevant suggestions for further theoretical research are given. (auth) (USGRDR)

13860 (AD-711784) OBSERVATION OF 3.3-mm BURSTS AND THEIR CORRELATION WITH SOFT X-RAY BURSTS. Report for March 1968–December 1969. Shimabukuro, Fred I. (Aerospace Corp., El Segundo, Calif.). 3 Sep 1970. Contract F04701-70-C-0059. 27p. (TR-59(6230)-30)-5; SAMSO-TR-70-331). NTIS.

Observations of 3.3-mm bursts show that, in most cases, these bursts have slower rise times and are longer lived than the impulsive centimeter bursts. There is a good temporal correlation between the 3.3-mm and soft x-ray bursts, indicating that these bursts have their origin in the same thermal source mechanism, although these emissions may not arise from the same electrons. (auth) (USGRDR)

13861 (N-70-37452) SOLAR FLOW PARAMETERS. Schocken, Klaus (National Aeronautics and Space Administration, Huntsville, Ala. George C. Marshall Space Flight Center). 16 Sep 1969. 30p. (NASA-TM-X-53916; MSFC-IN-SSL-T-68-4). NTIS.

The solar plasma is assumed to be a fully ionized mixture of two species. Nine important nondimensional parameters are obtained from the fundamental equations of plasma flow. Some thermodynamic properties of the solar plasma, based on a computed solar model, are presented in tables. (auth) (STAR)

13862 (N-70-38381) HEAT TRANSFER IN THE CONVECTIVE ENVELOPE OF THE SUN. Schocken, Klaus (National Aeronautics and Space Administration, Huntsville, Ala. George C. Marshall Space Flight Center). 16 Sep 1969. 18p. (NASA-TM-X-53928; MSFC-R-SSL-INT-67-8). NTIS.

The heat flux in the convective layer of the Sun is derived by two different methods. The first method is conventional and starts with the condition of thermodynamic equilibrium. If in radiative equilibrium due to adiabatic expansion a rising mass of gas becomes warmer than its surroundings, its motion will continue. Under this condition convection currents are stable and can be produced only if the amount of the adiabatic temperature gradient is smaller than the radiative gradient. The convective heat flux is computed from the energy balance during convection. The second method is based on the photon transport equation. The convective flux is derived from the equation of radiative transfer, applying to nonequilibrium photon transport processes, by substituting convective for radiative parameters. The two formulas for the same quantity yield a relation between the temperature gradients occurring in the equations. (auth) (STAR)

13863 (N-70-39828) SOLAR X-RAY ASTRONOMY SUMMARY AND BIBLIOGRAPHY. Wilson, Robert M.; Reynolds, John M.; Fields, Stanley A. (National Aeronautics and Space Administration, Huntsville, Ala. George C. Marshall Space Flight Center). Jan 1970. 143p. (NASA-TM-X-53991). NTIS.

A review of solar x-ray astronomy is given with tables summarizing some of the results of the survey. A list of observed solar spectral lines and a tabulation of all x-ray flight experiments from the literature surveyed are provided. The bibliography is annotated and cross-referenced. (auth) (STAR)

13864 ISOTOPIC ABUNDANCE OF ^{26}Mg AND LIMITS ON ^{26}Al IN THE EARLY SOLAR SYSTEM. Schramm, David N.; Tera, F.; Wasserburg, G. J. (California Inst. of Tech., Pasadena). Earth Planet. Sci. Lett.; 10: 44-59(Dec 1970).

The isotopic composition of Mg was investigated in meteoritic, lunar and terrestrial feldspar samples, and standard reagents using a mass spectrometer with on-line data processing. Isotopically enriched standards were run, demonstrating a resolution of better than five parts in 10^4 for the ^{26}Mg/^{24}Mg ratio. No ^{26}Mg/^{24}Mg anomalies were found in any samples analyzed to within experimental errors. (These analyses included some samples run by Clarke, de Laeter, Schwarcz and Shane and found by them to have ^{26}Mg/^{24}Mg anomalies of 4 to 6 parts in 10^3 relative to terrestrial values.) There is at the present time no positive evidence indicating the existence of ^{26}Al in the early solar system. From these results, limits were placed on the amount of ^{26}Al($\tau_{1/2} = 7.4 \times 10^5$ yr) and the resulting heating effects in the solar system at the time of crystallization of the meteorites. It

XUM

is clear that when the meteorites solidified, ^{26}Al was not an important heat source; however, this would not rule out the possibility that a few million years prior to solidification ^{26}Al was a major heat source. (auth)

13865 ABUNDANCE OF LITHIUM IN SUNSPOTS. Traub, W.; Roesler, F. L. (Univ. of Wisconsin, Madison. Kitt Peak National Observatory, Tucson, Ariz.). Astrophys. J.; 163: 629–44(1 Feb 1971).

The absorption line of lithium at 6708 Å that is found in sunspots was observed with a high-resolution interferometric spectrometer, and a theory of line formation applicable to medium-strength lines was used to interpret the line. If the measured equivalent width of 133 ± 3 mÅ is used, and if a sunspot model suggested by Zwaan is adopted, then the lithium abundance was found to be $\log [n(Li)/n(H)] = -11.32$, in general agreement with estimates obtained from observations of the disk spectrum. There may be an uncertainty of up to a factor of 2 in the calculated abundance, depending upon the model chosen for reduction of the data. The isotope ratio was $n(^6Li)/n(^7Li) = 0.04 \pm 0.02$. The line-shape parameters, including Zeeman shifts, of twenty-one other lines found in the spot spectrum near 6708 Å are also given. (auth)

13866 SPECTRUM OF PLASMA-DENSITY IRREGULARITIES IN THE SOLAR WIND. Hewish, A. Astrophys. J.; 163: 645-7 (1 Feb 1971).

It is shown that the observed wavelength dependence of interplanetary scintillation is not consistent with a spectrum of density fluctuations similar to that observed for the magnetic field. A satisfactory explanation of both spacecraft and scintillation data requires a separate regime for small-scale irregularities of plasma density. (auth)

13867 SOLAR MICROWAVE BURSTS AS INDICATORS OF THE INTENSITY OF SOLAR PROTON EMISSIONS. Croom, D. L. (Air Force Cambridge Research Labs., Bedford, Mass.). Astrophys. Lett.; 7: 133-5(Dec 1970).

The total energy in fixed-frequency solar microwave bursts that exceed certain threshold values, when normalized in terms of the peak intensity of the burst, is a much better guide to the intensity of associated solar proton fluxes than either the peak burst intensity itself or the total, un-normalized, energy produced in the burst. (auth)

13868 EVIDENCE FOR MHD PULSATIONS IN THE SOLAR CORONA. Rosenberg, H. (Astronomical Inst., Utrecht). Astron. Astrophys.; 9: 159-62(Nov 1970).

Observed broad-band intensity fluctuations associated with Type IV solar radio emission at meter wavelength may be explained by mhd pulsations in flux tubes in the corona. (auth)

13869 INFLUENCE OF AN INTERPLANETARY DISTURBANCE ON SOLAR FLARE PROTON PROPAGATION. Barouch, E.; Raguideau, J. (CEN, Saclay, France). Astron. Astrophys.; 9: 146-50(Nov 1970).

The scattering of cosmic rays by interplanetary shock waves is examined. Solar proton time–intensity profiles calculated according to these considerations are presented. The solar cosmic-ray anisotropy is discussed. (auth)

13870 SOLAR LITHIUM ABUNDANCE. Engvold, O.; Moe, Kjeldseth O.; Maltby, P. (Univ. of Oslo). Astron. Astrophys.; 9: 79-85(Nov 1970).

The abundance of lithium was determined from selected sunspot spectra. The best sunspot spectra obtained during 10 months of observation were analyzed. Taking into account the scattered light of the instrument and the atmosphere as well as the effect of the instrumental profile a larger depth of the Li λ 6707.8 line was found than derived by earlier observers. The Li resonance doublets were found to be blended with lines of TiO in the sunspot spectrum. The resulting line profile of the magnetic active resonance doublets was calculated together with the molecular lines using the theory of Kjeldseth Moe (1968) for magnetic active lines. Comparison of observed and calculated line profiles gave $\log N(Li) = 0.80 \pm 0.25$ on the scale of $\log N(H) = 12.00$. The Li^6/Li^7 isotope ratio was found to be less than 0.20. (auth)

13871 THEORY OF TYPE II AND TYPE III SOLAR RADIO BURSTS. I. THE IMPOSSIBILITY OF NONTHERMAL EMISSION DUE TO COMBINATION SCATTERING OFF THERMAL FLUCTUATIONS. Melrose, D. B. (Australian National Univ., Canberra). Aust. J. Phys.; 23: 871-84(Dec 1970).

"Combination scattering" as proposed by Ginzburg and Zheleznlakov involves the coalescence of electron plasma waves from a nonthermal distribution with electron plasma waves from the distribution of thermal charge fluctuations. Reabsorption is neglected. Here it is shown that reabsorption is a major effect which limits the emitted radiation to that of a black body at twice the local electron temperature. Existing models for type-II and -III bursts are discussed critically and found to be inadequate. An alternative model is indicated. (auth) (Australia)

13872 THEORY OF TYPE II AND TYPE III SOLAR RADIO BURSTS. II. ALTERNATIVE MODEL. Melrose, D. B. (Australian National Univ., Canberra). Aust. J. Phys.; 23: 885-903(Dec 1970).

It is argued that observational data on type-III bursts point to the exciting agent for a burst being a bunch of fast electrons that experience no strong two-stream instability. Ways in which the two-stream instability might be suppressed are discussed. A model for type-III bursts based on a bunch of electrons passing through the corona and generating electron plasma waves incoherently is explored. It is found that the emission at the fundamental frequency results from the coherent scattering of electron plasma waves into electromagnetic waves. Coherent scattering of electron plasma waves into electron plasma waves is found to be the major effect allowing emission at the second harmonic to arise from the coalescence of electron plasma waves into electromagnetic waves. Reasonable agreement with observation is found for 10^{33} to 10^{34} electrons per bunch. (auth) (Australia)

13873 COMPARISON OF SIMULTANEOUS MEASUREMENTS OF THE POLAR MAGNETIC FIELDS MADE AT CRIMEA AND MOUNT WILSON. Kotov, V. A. (Crimean Astrophysical Observatory, USSR); Stenflo, J. O. Solar Phys.; 15: 265-72(Dec 1970).

Measurements of the polar magnetic fields of the Sun made in August 1968 with the Crimean and Mt. Wilson magnetographs are compared. The agreement between the results obtained at the two observatories is rather satisfactory. The correlation coefficient between the Crimean and Mt. Wilson values of the observed average field strength at different latitudes is 0.7 for the north and 0.5 for the south polar region. The earlier conclusion based on the Mt. Wilson material that a polarity reversal of the field occurred at latitudes +70° and −55° in the north and south hemispheres (Stenflo, 1970) is confirmed by the Crimean data. (auth)

13874 DESCRIPTION OF AN OBSERVATIONAL METHOD FOR DETERMINING ABSOLUTE INTENSITIES IN THE SOLAR SPECTRUM BETWEEN λ 2962 A AND λ 4087 A. Houtgast, J. (Astronomical Inst., Utrecht). Solar Phys.; 15: 273-87(Dec 1970).

The results of measurements of absolute intensities in the spectrum of the center of the Sun's disk in the wavelength region 2977 to 4087 Å have already been published (Houtgast 1965, 1968) and use has been made of them on different occasions. The intensities at 206 spectral points have been given, chosen as much as possible between the Fraunhofer lines, but well divided over the region. Each strip of the Utrecht (Minnaert et al., 1940) and Göttingen (Brückner, 1960) Atlases contains at least two points. Later (Houtgast and Namba, 1968) four more points were added below λ 2977 Å. In order to judge the reliability of the published intensities one requires a description of the observational method. This description included the apparatus, the correction for atmospheric extinction, and the number of observations from which the final mean values of the absolute intensities are deduced. Finally, a discussion of the most important sources of error is given. (auth)

13875 GRAZING INCIDENCE SPECTRA OF THE SUN. Freeman, F. F.; Jones, B. B. (Culham Lab., Abingdon, Eng.). Solar Phys.; 15: 288-308(Dec 1970).

Intensity-calibrated grazing-incidence spectrographs were flown on three Skylark sounding rockets to record the solar soft x-ray and xuv spectra over a wide wavelength range. This paper describes the instrumentation and calibration procedures, and presents wavelength and intensity data, for each of the flights. (auth)

13876 HIGH-RESOLUTION PHOTOGRAPHY OF THE SOLAR CHROMOSPHERE. VIII. COMPUTER CONTROL OF A TUNABLE $\frac{1}{8}$ A FILTER. Bray, R. J.; Winter, J. G. (CSIRO, Sydney). Solar Phys.; 15: 309-16(Dec 1970).

Computer control of a tunable $\frac{1}{8}$-Å filter is described. The filter is installed in the 30-cm chromospheric telescope of the CSIRO Solar Observatory, Culgoora. (auth)

13877 MASS MOTION IN THE SOLAR CHROMOSPHERE. Jones, R. A.; Rense, W. A. (Univ. of Colorado, Boulder). Solar Phys.; 15: 317-21(Dec 1970).

A high-resolution profile of the solar O I 1304.9-Å line was measured from rocket spectrograms. The profile was nearly flat-topped, showing only a slight solar reversal after instrument effects and absorption due to atomic oxygen in the Earth's atmosphere were allowed for. A theoretical analysis of this line, under the assumption of non-LTE conditions and a homogeneous, spherically symmetric chromosphere, predicted a rather deep solar reversal. The theoretical profile may be made consistent with the observed profile if mass motion is present in the chromospheric region where the line is formed. A Gaussian distribution of up and down velocities with a root mean square velocity of about 7 km/sec gave best agreement between the predicted and observed profile. This result was consistent with the conclusion made from a study of high-resolution profiles of solar lines in the visible spectrum that mass vertical velocities increase with height above the photosphere. (auth)

13878 COMPARISON OF COMPUTED AND OBSERVED LINE PROFILES AND FLASH INTENSITIES IN THE PHOTOSPHERE–CHROMOSPHERE TRANSITION REGION. van Dessel, E. L. J. (Astronomical Inst., Utrecht). Solar Phys.; 15: 322-37(Dec 1970).

This paper mainly deals with the development of a method for the interpretation of eclipse observations in the extreme limb–lower chromosphere transition region. Line profiles emitted by a column of 1 cm^2 cross section along the line of sight were computed and, by integration, profiles and total (flash) intensities from a slice of 1-cm width beyond the Moon's edge, at various heights with respect to the solar limb were determined. The solar models used are mentioned and method and approximations are described. Calculations were made for some Fe I lines with various equivalent widths; the results are discussed. It appears that the method enables one to distinguish between the various models. Particularly, line intensities just inside the limb are very important. The computed results were compared with some observations made by Houtgast. The main conclusion was that a BCA-type temperature distribution alone does not agree with observations. An excitation temperature of Holweger's type was assumed. (auth)

13879 CONTINUUM WINDOWS IN SPECTRA OF UMBRAE (4000 TO 8000 A). Woehl, H. (Univ., Goettingen, Ger.). Solar Phys.; 15: 338-41(Dec 1970).

A list of continuum windows in umbral spectra is given and briefly discussed. (auth)

13880 ROTATIONAL TEMPERATURES OF UMBRAE. Woehl, H. (Univ., Goettingen, Ger.). Solar Phys.; 15: 342-4 (Dec 1970).

The equivalent widths of molecular lines have been used to determine the temperatures of umbrae by several authors. At a first glance this method of temperature determination is believed to have the very important advantage of being rather insensitive to photospheric false light scattered into umbrae. An attempt is made here to show that, for several reasons, the temperature values derived by this method are rather unreliable. (W.D.M.)

13881 UPPER LIMIT OF THE SWAN BAND INTENSITY IN A SUNSPOT SPECTRUM. Schadee, Aert (Astronomical Inst., Utrecht). Solar Phys.; 15: 345-8(Dec 1970).

There is no evidence for the $C_2(0,1)$ band in an investigated sunspot spectrum. Upper limits are given for the band intensity. (auth)

13882 VERTICAL STRUCTURE OF PLAGES. Stoyanova, M. N. (Pulkovo Observatory, USSR). Solar Phys.; 15: 349-55 (Dec 1970).

A new spectroscopic method of deriving the three-dimensional information ("escalation") worked out at the Pulkovo Observatory was applied to observations of solar faculae. The size of the investigated area was 70″ × 18″. Two series of spectra were obtained simultaneously in four spectral regions (Hα, $D_{1,2}$ (NaI), Hβ, and H, K (CaII)) with a quadruple-camera spectrograph attached to the second horizontal solar telescope at Pulkovo on August 13, 1968. It was found from the analysis of the maps of brightness distribution in the cores of the lines and continuum that the facular emission lies in ropes which incline to the solar surface. (auth)

13883 CONNECTION BETWEEN N–S AND E–W SOLAR ASYMMETRIES. Cantu, A. M. (Osservatorio Astrofisico, Arcetri, Italy); Godoli, G.; Poletto, G. Solar Phys.; 15: 356-8 (Dec 1970).

In a previous paper (Godoli and Poletto, 1969) it was pointed out that an influence on the solar activity of the motion of the Sun towards the solar apex would result in: (1) a variation with heliographic latitude of the N–S asymmetry; and (2) a variation during the year of the E–W asymmetry. An attempt is made to deduce the expected variations. (W.D.M.)

13884 MAGNETIC FIELDS IN QUIESCENT PROMINENCES. Tandberg-Hanssen, Einer (National Center for Atmospheric Research, Boulder, Colo.). Solar Phys.; 15: 359-71(Dec 1970).

A discussion is presented on the longitudinal component of the magnetic field, $B_{||}$, based on data from about 135 quiescent prominences observed at Climax during the period 1968–1969. The measurements were obtained with the magnetograph which records the Zeeman effect on hydrogen, helium, and metal lines. Use of the following lines, Hα; HeI, D_3, HeI, 4471 Å; NaI, D_1 and D_2, leads to the same value for the observed magnetic field component in these prominences. For more than half of the prominences their mean field, $\overline{B}_{||}$, satisfied the inequalities $3\ G \le \overline{B}_{||} \le 8\ G$, and the overall mean value for all the prominences was 7.3 G. As a rule, the magnetic field enters the prominence on one side and exits on the other, but in traversing the prominence material, the field tends to run along the long axis of the prominence. (auth)

13885 VARIATION IN O VII X-RAY LINE-EMISSION FROM THE SOLAR CORONA. Rugge, H. R.; Walker, A. B. C. Jr. (Aerospace Corp., El Segundo, Calif.). Solar Phys.; 15: 372-9 (Dec 1970).

The variation in intensity of the solar x-ray resonance ($1s^2\ ^1S_0$–$1s2p\ ^1P_1$), intercombination ($1s^2\ ^1S_0$–$1s2p\ ^3P_1$), and forbidden ($1s^2\ ^1S_0$–$1s2s\ ^3S_1$) lines of helium-like O VII with 2800-MHz solar radio flux is presented for three solar rotations. A high correlation ($r \approx 0.80$) exists between the intensities of all three x-ray lines and the 2800-MHz solar flux. The ratio of the forbidden to the intercombination line intensities is found to be essentially independent of long-term solar activity. This ratio is used to determine upper limits on the coronal electron density and to make inferences concerning the change in density with solar activity. (auth)

13886 HIGH QUANTUM NUMBER EMISSION AND ABSORPTION LINES OF Fe VIII, Fe XV, O III, O VII OF THE SUN. Greve, A. Solar Phys.; 15: 380-2(Dec 1970).

The results of an investigation are briefly reported in which the effects of dielectronic recombination on lines of high n (n = principal quantum number) and for transitions $n \rightarrow n-1$ of Fe VIII, Fe XV, O III, and O VII were calculated. (W.D.M.)

13887 PROGRAM OF MONOCHROMATIC PHOTOGRAPHY OF CORONAL EMISSIONS FOR THE PERIOD 1973–1976. Leroy, Jean-Louis; Roesch, Jean (Observatoire du Pic-du-Midi, Bagneres de Bigorre, France). Solar Phys.; 15: 383-6(Dec 1970). (In French).

A cooperative international program is suggested for monochromatic coronal photography by means of interference filters. (auth)

13888 MAUNO LOA CORONAGRAPH OBSERVATIONS AROUND THE MARCH 7, 1970 ECLIPSE. Hansen, Richard T.; Hansen, Shirley F.; Garcia, Charles J. (National Center for Atmospheric Research, Kamuela, Hawaii). Solar Phys.; 15: 387-93(Dec 1970).

The locations of seven principal coronal features observed in projection at the March 7, 1970 eclipse were established from synoptic coronagraphic measurements. (auth)

13889 COOLING OF FLARE-PRODUCED PLASMAS IN THE SOLAR CORONA. Culhane, J. L. (University Coll., London. Lockheed Palo Alto Research Labs., Calif.); Vesecky, J. F.; Phillips, K. J. H. Solar Phys.; 15: 394-413(Dec 1970).

Solar-flare x rays, at energies less than 10 keV, are emitted by hot plasmas located in the corona. Three plasma cooling models are examined in detail. The cooling of the electrons by Coulomb collisions with ions at a lower temperature would require the observed material to occupy very large volumes. Cooling could take place by conduction or by radiation, and observations are proposed that would allow the dominant cooling mechanism to be established. (auth)

13890 71-GHz (4.2 mm) SOLAR RADIO BURSTS IN THE PERIOD JULY 1967 TO DECEMBER 1969. Croom, D. L. (SRC Radio and Space Research Station, Ditton Park, Eng.). Solar Phys.; 15: 414-23(Dec 1970).

The results of $2\frac{1}{2}$ years (July 1967–December 1969) monitoring of solar radio bursts at 71 GHz ($\lambda = 4.2$ mm) at the Radio and Space Research Station, Slough, are presented. During this period only seven events were positively identified as 71-GHz bursts. One of these events (July 6, 1968) is among the largest solar bursts ever recorded anywhere in the microwave millimetre-wave band ($47{,}000 \times 10^{-22} Wm^{-2}Hz^{-1}$), and the associated magnetic field may possibly have exceeded 7200 G. Another event (March 27, 1969) demonstrated that bursts at 71 GHz can be both intense ($4700 \times 10^{-22} Wm^{-2}Hz^{-1}$) and complex. On other occasions, the absence of any detectable event at 71 GHz helps to define the high-frequency spectrum of the burst, this being an important factor in determining the initial energy distribution of the electrons ejected by the associated flare. On one such occasion (March 21, 1969) the de-

XUM

rived energy distribution index γ is ≥ 8, in contrast with the more usual values of 2 to 4. (auth)

13891 OBSERVATION OF 3.3-mm BURSTS AND THEIR CORRELATION WITH SOFT X-RAY BURSTS. Shimabukuro, F. I. (Aerospace Corp., El Segundo, Calif.). Solar Phys.; 15: 424-32(Dec 1970).

Observations of 3.3-mm bursts show that, in most cases, these bursts have slower rise times and are longer lived than the impulsive centimeter bursts. There is a good temporal correlation between the 3.3-mm and soft x-ray bursts, indicating that these bursts have their origin in the same thermal source mechanism, although these emissions may not arise from the same electrons. (auth)

13892 TYPE-III SOLAR RADIO BURST STORMS OBSERVED AT LOW FREQUENCIES. II. AVERAGE EXCITER SPEED. Fainberg, Joseph; Stone, R. G. (Goddard Space Flight Center, Greenbelt, Md.). Solar Phys.; 15: 433-45(Dec 1970).

Storms of Type-III solar radio bursts observed from 5.4 to 0.2 MHz consist of a quasi-continuous production of Type-III events observable for half a solar rotation but persisting, in some cases, for well over a complete rotation (Fainberg and Stone, 1970). The observed burst drift rates are a function of the heliographic longitude of the associated active region. This apparent drift rate dependence is a consequence of the radio emission propagation time from source to observer. Based on this dependence, a least squares analysis of 2500 drift rates between frequencies in the 2.8 to 0.7 MHz range yields an average exciter speed of 0.38 c for the height range from approximately 11 to 30 $R_{\odot}$. In conjunction with the available determinations of exciter speeds of 0.33 c close to the Sun, i.e., less than 3 $R_{\odot}$, and with in situ measurements of 40-keV solar electrons by space probes, the present results suggest that the exciters are electron packets that propagate with little deceleration over distances of at least 1 AU. (auth)

13893 PRELIMINARY OBSERVATIONS OF CORONAL MAGNETIC FIELDS BEFORE AND AFTER SOLAR PROTON EVENTS. Valdez, Jesusa; Altschuler, Martin D. (National Center for Atmospheric Research, Boulder, Colo.). Solar Phys.; 15: 446-52(Dec 1970).

Maps of the coronal magnetic field before and after several proton flares were examined. There are indications that large-scale changes occur in both the photospheric and coronal magnetic field as a consequence of large proton flares. (auth)

13894 EMISSION AND PROPAGATION OF ~40-keV SOLAR-FLARE ELECTRONS. II. ELECTRON EMISSION STRUCTURE OF LARGE ACTIVE REGIONS. Lin, R. P. (Univ. of California, Berkeley). Solar Phys.; 15: 453-78(Dec 1970).

Electrons of ~40 keV energy observed at 1 AU were used as tracers to map the emission structure of a large active region, McMath plage 8905, which crossed the visible disk in July—August, 1967. The acceleration of 10 to 100-keV electrons was found to be a property of active regions with a certain stage of development, and was signaled by the emission of $\gtrsim$20-keV x rays. The emission of electrons into the interplanetary medium may be separate from the acceleration of the electrons. Type-III radio emission at long wavelengths appears to indicate the escape of the electrons into the interplanetary medium. The subsequent electron propagation in the interplanetary medium is essentially scatter-free, and the profile of the electron appears to be determined predominantly by transport/storage processes in the solar corona. The emission structure for active-region McMath plage 8905 consisted of (1) an open cone of ~70° extent in solar longitude where electrons have direct access to interplanetary field lines; (2) a cone of propagation of 100° width in solar longitude, surrounding and including the open cone in which impulsive electron events were observed; and (3) an overall ~200° extent of solar longitude over which low, nonimpulsive fluxes from the active region were observed. A model is presented to account for the observed structure. This type of emission structure may be present in other electron-active regions. (auth)

13895 ALPHA-PARTICLE OBSERVATIONS IN THE SOLAR WIND. Formisano, V. (CNR, Rome. Univ., Rome); Palmiotto, F.; Moreno, G. Solar Phys.; 15: 479-98(Dec 1970).

The plasma experiment on board the ESRO satellite HEOS-1 detects solar-wind positive ions in the energy range from 200 to 16,000 eV/Z. α-particles were observed for 10% of the time, from December 1968 to March 1969, when in the interplanetary medium α-particle and proton bulk velocities were on average, equal. The average relative abundance of α particles was 5.5%. Although in general the two species, hydrogen and helium, have a similar behavior, very often α particles have an independent time history. Strong discontinuities may be observed in one species, without occurring in the other, or having different characteristics. At certain times, α particles seem to behave as an independent fluid. Well defined fluxes of α particles were observed within the magnetosheath: in several cases, α particles, present in the unperturbed solar wind, were found with unchanged energy spectrum through a certain layer behind the proton shock front inside the magnetosheath. This suggests that thermalization of α particles does not occur at the same place as that of protons. (auth)

13896 SOURCE SURFACE THEORY COROLLARY: THE MEAN SOLAR FIELD-INTERPLANETARY FIELD CORRELATION. Schatten, K. H. (Goddard Space Flight Center, Greenbelt, Md.). Solar Phys.; 15: 499-503(Dec 1970).

The correlation of the mean solar magnetic field and the interplanetary magnetic field reported by Wilcox et al. (1969) and Severny et al. (1970) has been interpreted by comparing the relationship of the measurement of the mean solar field with the physics involved in the formation of the interplanetary field. The high correlation observed is thus interpreted as a fortuitous correspondence between two integrals. The high correlation thus provides further support for the source surface model involved in these calculations. A new method is suggested for observing the "mean solar field" that might improve the correlations slightly. (auth)

13897 X-RAY CONTROL OF THE IONOSPHERIC ABSORPTION OF HF RADIO WAVES. Triska, P.; Lastovicka, J. (Geophysical Inst., Prague). Solar Phys.; 15: 504-6(Dec 1970).

For the sake of comparison, the solar x-ray data from the SOLRAD 9 satellite and the absorption data from Panská Ves Observatory were used as measured by the A3 method (Tříska 1962) at a frequency of 2775 kHz. The analysis was made for the period April—Oct. 1969, using only the data measured at 1200 UT. (W.D.M.)

13898 INFLUENCE OF THE LINE ABSORPTION ON POLARIZATION OF THE CONTINUUM SPECTRUM. Dumont, S.; Pecker, Pecker, J.-C. (College de France, Paris). Astron. Astrophys.; 10: 118-27(1 Jan 1971). (In French).

The polarization in Fraunhofer lines is computed from a detailed statistical analysis of five spectral bands of the solar spectrum. The assumptions, that are necessary to treat several thousands of lines, are necessarily rather crude: rectangular profiles; lines divided into four categories: weak—pure absorption; averaged strong—pure absorption; weak—pure scattering; averaged strong—pure scattering. The results show that the line resonance polarization is of the right order of magnitude to explain the observations; but that a proper treatment of collisional depolarization and new measurements are highly necessary to reach definitive conclusions. (auth)

13899 DAMPING AND SOLAR ABUNDANCE OF SODIUM FROM Na I FRAUNHOFER LINES. Holweger, H. (Univ., Kiel). Astron. Astrophys.; 10: 128-33(1 Jan 1971).

Empirical damping constants of six strong solar Na I lines ($\lambda\lambda$ 4497 to 23348 Å) were determined by comparing, similar to Weidemann (1955), the corresponding abundances with those computed from weak, damping-independent sodium lines, the f-values being known with sufficient accuracy. Agreement between strong and weak lines may be obtained by increasing their van der Waals interaction constants, C_6, uniformly by $\Delta \log C_6 = +0.8 \pm 0.2$ over the theoretical value predicted by Unsöld's (1938, 1955) approximation. Within these limits this correction is independent of the term properties. Repulsive interatomic forces, whose astrophysical importance for collisional broadening by hydrogen atoms was suspected by Roueff and Van Regemorter (1969) and Roueff (1970), are therefore either insignificant or their effect on solar sodium lines can quantitatively be represented by uniformly increased van der Waals attraction. Stark broadening and radiative damping are found to be of minor importance for the line abundances. If C_6 is modified accordingly, the scatter of abundances, including the D lines, becomes remarkably low, due to the accuracy of f-values and equivalent widths. A mean solar sodium abundance $\log \epsilon_{Na} = 6.30 \pm 0.07$ (referring to $\log \epsilon_H = 12.00$) is deduced. Deviations from LTE or from true absorption are shown to have a negligible effect on abundances. Some remarks on the solar abundance of magnesium and silicon are given. (auth)

13900 CuH LINES IN THE SUNSPOT SPECTRUM AND THE SOLAR ISOTOPE RATIO OF COPPER. Hauge, Oe. (Univ., Oslo). Astron. Astrophys.; 10: 73-5(1 Jan 1971).

CuH lines from the R and P branches of the $^1\Sigma - X^1\Sigma(0,0)$ band are shown to exist in sunspot spectra obtained at Kitt Peak. A determination of the copper isotope ratio from the very weak CuH lines is rather uncertain. More reliable results on the solar copper isotope ratio are obtained from Cu I lines. From two lines of relatively high isotope shifts an isotope ratio $^{63}Cu/^{65}Cu = 2 \pm 1$ is obtained. (auth)

13901 NEW DESCRIPTION OF THE SOLAR FIVE-MINUTE OSCILLATION. Leibacher, J. (Harvard Coll. Observatory, Cambridge, Mass.); Stein, R. F. Astrophys. Lett.; 7: 191-2(Jan 1971).

A model is proposed for producing oscillations in the solar photosphere; it is suggested that the upper portion of the convection zone acts as a resonant cavity and drives the photosphere as a whole, at frequencies for which waves are nonpropagating. The existence of such a cavity depends on a reflecting upper boundary that results from decreasing temperature and on the postulated existence of a reflecting lower boundary which, for waves of 300-sec period, lies 1000 to 2000 km below the top of the convection zone. (auth)

13902 CORONAL ELECTRON TEMPERATURES ASSOCIATED WITH SOLAR FLARES. Horan, Donald Martin. Washington, D. C.; Catholic Univ. of America (1970). 133p. University Microfilms Order No. 70-22,133.

Thesis.

X-ray emission from seventeen x-ray flares was analyzed to obtain electron temperatures and emission measures associated with the source region in the solar corona. The source region was assumed to be isothermal with a Maxwellian electron velocity distribution. The primary determination of electron temperature and emission measure is derived from the ratio of energy fluxes in the 0.5 to 3 and 1 to 8 Å bands measured by ionization chambers. Electron temperatures obtained from ratios of x-ray emission for segments of the continuum spectrum measured by a Bragg crystal spectrometer were used to provide a check on the primary temperature determinations in several instances. Flares that were characterized by a rapid initial x-ray flux increase were found to also have a rapid initial rise in electron temperature and emission measure. Flares that were characterized by a gradual initial x-ray energy flux increase were found to have a less-rapid initial rise in electron temperature and emission measure. In all flares studied the peak temperature chronologically preceded the peak x-ray flux, and the peak x-ray flux preceded the peak emission measure. The bases for the analysis and the time histories of the seventeen individual events studied are presented. (Diss. Abstr. Int., B)

13903 ANISOTROPY OF DIFFUSE SOLAR RADIATION. Morris, Charles Wayne. Lubbock, Tex.; Texas Tech. Univ. (1969). 100p. University Microfilms Order No. 70-20,693.

Thesis.

An experimental study of the intensity distribution of the diffuse component of solar radiation was performed over a one year period. The results clearly indicate that the isotropic assumption is not a valid description of the scattered radiation for most atmospheric weather conditions. The probable causes of the intensity distributions are discussed and a new calculation technique is presented which, for clear skies, takes into account the actual diffuse radiation intensity variation. The mathematical model, when compared to diffuse radiation measurements, showed a significant improvement over past calculation methods. Cloudy sky data produced several general conclusions about the diffuse radiation intensity distribution on cloud surfaces, but only the average diffuse radiation can be predicted accurately. (Diss. Abstr. Int., B)

13904 ISOTOPIC ABUNDANCE OF MAGNESIUM IN THE SUN. Kumar, Cidambi Krishna. Ann Arbor, Mich.; Univ. of Michigan (1970). 75p. University Microfilms Order No. 70-21,706.

Thesis.

The isotopic abundance of magnesium in the Sun was determined by an analysis of the profiles of the lines of the $A^2\pi - X^2\Sigma^+$ ($\Delta v = 0$ sequence) bands of MgH in the 5100 to 5160 Å region of the sunspot spectrum. The profiles were calculated using a model atmosphere for the spot characterized by $\theta_{spot} - \theta_{ph} = 0.3$. Effects of blends due to Swan band lines of C_2 and due to atomic lines were taken into account. Also included was the influence of photospheric and penumbral light scattered into the sunspot spectrum. Neglect of this effect results in an overestimation of the relative abundance of the heavier isotopes of Mg. The following values of the dissociation energy of MgH and the chemical abundance of Mg were used: $D_0(MgH) = 2.49$ eV, and $\log(Mg/H) = -4.7$. The synthesized spectra were compared with intensity tracings of 7 mm/Å spectra of sunspots obtained at the McMath–Hulbert Observatory. It was found that the isotopic ratio $^{24}Mg : ^{25}Mg : ^{26}Mg$ in the Sun is 64 : 18 : 18 as against the terrestrial value of 79 : 10 : 11. In addition, line profiles were computed using Zwaan's $\Delta\theta = 0.48$ model for the spot. Reasonable line profiles could be obtained only by reducing $D_0(MgH)$ to 2.08 eV and log (Mg/H) to −5.15. Computations carried out, using a model with temperature gradient lower than that of the above models, result in lower abundances of the heavier isotopes of magnesium. However, the general agreement with observations is not as satisfactory as in the case of the $\Delta\theta = 0.3$ model. Hence, it is suggested that the enrichment of ^{25}Mg and ^{26}Mg in the Sun is probably real. (Diss. Abstr. Int., B)

13905 INTERACTION OF THE SOLAR WIND WITH OPTICALLY THIN ATMOSPHERES. Mitchell, Archer Sylvester Jr. Pittsburgh; Carnegie-Mellon Univ. (1970). 123p. University Microfilms Order No. 70-21,596.

Thesis.

The reactive hydromagnetic equations are derived for flow situations in which the bulk velocity of the plasma is perpendicular to the magnetic field, and accounting for the generation of ions in the flow. Due to the requirements of the continuum assumption of the flow, the generation terms, appearing in the equations, must be averaged over the cyclotron period, resulting in an anisotropic momentum generation term. The one-dimensional solution to these equations is discussed, and is considered to render "zeroth" order modifications in the flow, thus, allowing "first"-order perturbation solutions for the flow velocity and magnetic field. The result of this analysis is then applied to exemplary models of the lunar and cometary atmospheres. Resulting from this analysis are several dimensionless parameters which are found to characterize the interaction effects. The flow is found to diverge in planes perpendicular to the magnetic field and to converge in the ecliptic plane. The wake angle of the Moon is estimated to be on the order of 1° for flow in the polar plane containing the Sun–Moon vector, and to be negligible for flow in the ecliptic plane. The relative abundances of the solar-wind constituents impinging on the lunar surface are evaluated and the extent to which the lunar atmosphere will modify the makeup of the surface flux is estimated. The character of the flow in the optically thin region of comets is described and discussed. (Diss. Abstr. Int., B)

13906 GEGENSCHEIN. Roosen, Robert George. Austin, Tex.; Univ. of Texas (1970). 177p. University Microfilms Order No. 70-18,283.

Thesis.

The optical properties of the interplanetary medium in the direction of the gegenschein were investigated in detail both theoretically and observationally. The characteristics considered theoretically were: 1) the apparent phase function of the particles producing the gegenschein; 2) the distribution of these particles with respect to distance from the Earth and the Sun; and 3) the effect of the Earth's shadow on the illumination of these particles. All previous explanations for the gegenschein found in the literature were considered; the only one found tenable is that the gegenschein is caused by light reflected from particles of dust in heliocentric orbits. Models for the zodiacal light that assume that the spatial distribution of particles follows an inverse power law R^{-P} (where R is heliocentric distance and $P \geq 0$) cannot satisfactorily explain the gegenschein. There must be an increase in the spatial density of reflecting material outside the Earth's orbit. The asteroid belt is suggested as the source of the material. Both the asteroid belt and comets have long been considered as possible sources of the zodiacal material. The relative merits of these models are discussed in the light of the present observations and recent results reported in the literature. At least outside the Earth's orbit, the asteroidal model is found to be preferable. Precise photometric measurements in the antisolar direction have also yielded observational evidence of possible inhomogeneities in the zodiacal cloud. These inhomogeneities may be due to debris from comet Encke. (Diss. Abstr. Int., B)

13907 ENERGY SOURCE FOR THE SOLAR CORONA. Hashemi-Tafreshi, Jafar. Stillwater, Okla.; Univ. of Oklahoma (1970). 71p. University Microfilms Order No. 70-23,009.

Thesis.

It is proposed that heat is transported to the corona through the agency of neutrons originating in the photospheric layer of the Sun. A steady-state model for the corona is developed. A flux of neutrons is assumed to reach the base of the corona. The neutrons decay in the corona and release electrons and protons that collide with the coronal gas and distribute their energy. Neutrons are assumed to be produced in the solar photosphere by returning protons that have been unable to escape the solar magnetic field. (Diss. Abstr. Int., B)

13908 HEATING OF THE CHROMOSPHERIC NETWORK BY HYDROMAGNETIC WAVES. Milkey, Robert William. Bloomington, Ind.; Indiana Univ. (1970). 82p. University Microfilms Order No. 70-19,096.

Thesis.

The nonhomogeneous nature of the chromosphere, even in quiet regions of the disk, is quite apparent on a Ca II, H or K line spectroheliogram. This calcium emission network is correlated with

XUM

regions of intensified magnetic field, which in turn are correlated with the boundaries of the photospheric supergranules. The chromospheric magnetic field will retain some of the characteristics of the network structure in the photospheric field and it has been suggested that these magnetic fields are responsible for enhanced heating of the regions from which the calcium emission arises. In this work the propagation and dissipation of hydromagnetic waves are considered for the purpose of demonstrating the effect of concentrated magnetic fields on the height distribution of energy deposition in the solar atmosphere; the goal is to illustrate a mechanism for the origin of the calcium network. The study was carried out for a range of temperature and magnetic field models using a geometrical optics technique for studying the transport of energy by fast-mode magneto–acoustic shocks. The technique is subject to the limitations that the wavelengths are short compared to the scale for variation of the quantities governing the propagation and that the shock strength remains less than unity so that the Brinkley–Kirkwood shock damping theory may be applied. The application of this technique indicates that, in the absence of a magnetic field, the heating per gram of the chromosphere by dissipation of acoustic shocks is approximately constant with height. The introduction of a concentrated magnetic field, like that in the boundary of a supergranule, causes the heating per gram to increase with height in the region where the field is concentrated. This increase in heating is offered as an explanation of the network structure of the chromosphere. (Diss. Abstr. Int., B)

13909 LEPTON CHARGE AND NEUTRINO ASTROPHYSICS. Pontecorvo, B. M. Bull. Acad. Sci. USSR, Phys. Ser. (Engl. Transl.); 33: 1631-4(Nov 1969).

Translated from Izv. Akad. Nauk SSSR, Ser. Fiz.; 33: 1787-91 (Nov 1969).

It is emphasized that the results of experiments on solar neutrinos not only involve astrophysical and nuclear physical uncertainties, but also depend essentially on the still-unknown properties of neutrinos as elementary particles. The question of the conservation of lepton charge is considered. (W.D.M.)

13910 UPPER CUTOFF IN THE SPECTRUM OF SOLAR PARTICLES. Heristchi, Dj.; Trottet, G. (Laboratoire de Physique Cosmique, Verrieres le Buisson, France). Phys. Rev. Lett.; 26: 197-200(25 Jan 1971).

Arguments are advanced in favor of the existence of an upper cutoff in the spectrum of solar protons. In the case of the event of January 28, 1967, on the basis of the recordings made by the worldwide network of neutron monitors, this cutoff is found to be 4.3 ± 0.5 GeV. (auth)

Galaxies

Refer also to abstract 14058.

13911 (AD-711299) NEUTRAL HYDROGEN ABSORPTION IN THE Irr II GALAXY M82. Report No. 1970-7. Guelin, M.; Weliachew, L. (Owens Valley Radio Observatory, Pasadena, Calif.). 1970. Contract N00014-67-A-0094-0008. 20p. NTIS.

Absorption by neutral hydrogen was detected in the galaxy M82. Measurements were carried out with the transit radio telescope at Nancay. Emission and absorption do not occur at the same velocities. The velocity and width of the absorption profile are in agreement with emission lines detected previously at optical wavelengths along the major axis and close to the center of the galaxy. The neutral absorbing gas is related to the noncircular motions near the center of the galaxy rather than to the rotation as derived from optical absorption lines. The neutral hydrogen temperature cannot be estimated because emission was not detected at the central absorption velocity. (auth) (USGRDR)

13912 SMALL-SCALE IRREGULARITIES IN THE INTERSTELLAR GAS. Scheuer, P. A. G. (Cavendish Lab., Cambridge, Eng.); Tsytovich, V. N. Astrophys. Lett.; 7: 125-7(Dec 1970).

Calculations by Pikelner and Tsytovich (1969) and Lifshitz and Tsytovich (1970) show that nonlinear processes in plasmas tend to convert all turbulence generated on small scales into one particular spectrum. When this theory is applied to the interstellar medium, the predicted turbulence is comparable with that required to account for pulsar scintillations; difficulties concerning the damping of the waves are discussed. (auth)

13913 GALAXIES AND THE UNIVERSE. Oort, J. H. (Univ., Lieden). Science; 170: 1363-70(25 Dec 1970).

This brief review illustrates that the properties of the Universe are revealed by the rotation of galaxies and their distribution in space. Topics covered include black-body radiation, intergalactic gas, average density in the Universe, large-scale features, rotation and origin of galaxies, evolution effects, and nuclei of galaxies and their instability. (W.D.M.)

13914 GALACTIC CENTER REGION OBSERVED AT 80 MHz. Dulk, G. A. (CSIRO, Sydney). Astrophys. Lett.; 7: 137-40(Dec 1970).

Observations of the Sagittarius A region with the 80 MHz radioheliograph (3.8 arc min beam diameter) reveal no small-diameter source with flux density greater than 5 flux units. (auth)

13915 OPTICAL OBSERVATIONS OF THE GALAXY ASSOCIATED WITH 3C 386. van den Bergh, Sidney (Univ. of Toronto, Richmond Hill, Ont.). Astrophys. Lett.; 7: 107-9(Dec 1970).

The galaxy associated with 3C 386 appears to be a compact dwarf elliptical with $M_V \simeq -12.5$. Spectroscopic observations show a low internal velocity dispersion and hint at a low metal abundance. (auth)

13916 STEPHAN'S QUINTET OR QUARTET? Tammann, G. A. (Carnegie Institution of Washington, D. C. California Inst. of Tech., Pasadena). Astrophys. Lett.; 7: 111-13(Dec 1970).

Arguments are given that NGC 7320 is not a physical member of Stephan's quintet but is rather a companion galaxy to the foreground galaxy NGC 7331. (auth)

13917 NUMERICAL STUDY OF THE STOCHASTICITY OF DYNAMICAL SYSTEMS WITH TWO DEGREES OF FREEDOM. Froeschle, C. (Observatoire de Nice). Astron. Astrophys.; 9: 15-23(Nov 1970).

Numerical results were compared with the second-order Birkhoff's method and there was good agreement in a zone surrounding a stable invariant point. In the ergodic zone the numerical results seem to follow the general behavior of the C-systems. (auth)

13918 PHYSICAL PARAMETERS OF THE EMISSIVE GAS IN THE NUCLEUS OF NGC 3031. Alloin, D. (Institut d'Astrophysique, Paris). Astron. Astrophys.; 9: 45-50(Nov 1970). (In French).

The physical parameters deduced from the intensities of the emission lines in the nucleus of NGC 3031 are considered. It is shown that the lines from a given element in different stages of ionization come from different regions in the nucleus. It is found that the abundances of O, N, and Ne are not solar; the ratio N(N)/N(O) being six to ten times higher than the solar value. This abnormal ratio can be explained by either a nitrogen overabundance due to ejection of matter from evolved stars or by an underabundance of oxygen due to the formation of H_2O molecules. The latter explanation would require the presence of dust in the nucleus. (auth)

13919 INTERPRETATION OF THE SURFACE BRIGHTNESS OF DARK NEBULAE. Mattila, K. (Univ. of Helsinki). Astron. Astrophys.; 9: 53-63(Nov 1970).

The surface brightness measurements of the author (Mattila, 1970) in two dark nebulae, the Coalsack and a dark nebula in Libra, are interpreted in terms of the albedo and the form of the scattering function of the interstellar particles. In a theoretical study on radiative transfer in spherical models for interstellar dust clouds, the Monte Carlo method is used to find the intensity of the scattered light for a parallel beam of incident light. The illumination of dark nebulae by the Milky Way is then discussed, and theoretical values of the scattered light are calculated for the various particle models. Then, a comparison with the observations gives the albedo a and the asymmetry factor g of the interstellar particles in an unambiguous way, when it is assumed that the Coalsack and the Libra Cloud consist of the same kind of particles. Their values are found to be: $a = 0.65$, $g = 0.85$, with an uncertainty of about ±0.1 for both. A reinterpretation of Witt's observations of the diffuse galactic light in Cygnus and Taurus–Auriga is presented, and it gives support to these values. (auth)

13920 OPTICAL SPIRAL TRACERS AND GALACTIC STRUCTURE. Isserstedt, J. (Ruhr Univ., Bochum, Ger.). Astron. Astrophys.; 9: 70-8(Nov 1970). (In German).

New observational material from H II regions, young open clusters (Becker and Fenkart, 1969), Population I Wolf–Rayet stars (Smith, 1968), and stellar rings (Isserstedt, 1968a) is used to discuss the local galactic structure up to 5 kpc distance from the Sun. Structure elements found previously from the distribution of the stellar rings are in very good agreement with the other spiral tracers. The galactic structure is shown, defined by the above spiral tracers, schematized in a way that the spiral filaments cover just half of the total area. The concentra-

XUM

tion to the spiral features then can be described by the fraction of objects which lie in these arms: H II-regions 100%, clusters O–b 2.5 99%, stellar rings 96%, WR-stars 94%, Bpe, dBOe stars 83%, X-ray sources 80%, δCep ($P > 9^d$) 60%. Be-stars and x-ray sources also are strongly concentrated in these spiral filaments whereas δ Cephei stars appear to be only slightly concentrated. The galactic structure as represented by the space distribution of 1070 stellar rings does not show an overall two-armed spiral. The galaxy consists of many filaments of varying length and thickness. The distance to the galactic center is 10.8 kpc, using a minor ring diameter of 7.1 pc. (auth)

13921 PHOTOMETRY OF BRIGHT STARS IN THE SMALL MAGELLANIC CLOUD. **Dachs, J. (Ruhr Univ., Bochum, Ger.). Astron. Astrophys.; 9: 95-109(Nov 1970).**

Photoelectric photometry in the UBV system down to a limiting visual magnitude of about 14.5m is presented for 118 stars in three fields of the Small Magellanic Cloud. Two of the fields are located in the Bar, the third one in the Wing of the SMC. Because of the small interstellar absorption in the SMC, it is possible to distinguish early-type bright giant and supergiant stars which are probable SMC members, from a large fraction of the main sequence (foreground) stars by plotting the (U–B) vs. (B–V) two-color diagram. About one star out of three selected at random in the three fields in the visual magnitude range 10m to 14.5m probably is a physical member of the SMC, 50% turn out to be probable foreground stars, while for the remaining objects no certain decision upon SMC membership is possible by means of UBV photometry. Among the 49 stars found to be certain or probable SMC members according to the results of the present photometry, 35 were previously known or suspected members, including 16 H_α emission-line stars selected for the photometry from the catalogue of Henize (1956). Probable spectral types and luminosity classes have been derived from the two-color diagram for all SMC and foreground stars, assuming the distance modulus of the SMC to be 19.2m. Color excesses could be obtained for 39 SMC members and 32 foreground stars, by comparing the observed colors to intrinsic colors of similar unreddened galactic stars. No difference is found between the mean reddening of the SMC members in the Bar and in the Wing of the SMC. The mean color excess $E_{(B-V)}$ is 0.12m ± 0.04m for SMC emission-line stars, as compared to 0.06m ± 0.05m for nonemission SMC bright giant and supergiant stars, and 0.07m ± 0.05m (r.m.s. error) for foreground stars. This leads to the conclusion that the mean dust content of the H I component in the SMC is much smaller than in the Galaxy. (auth)

13922 DIFFUSION OF ENERGETIC PARTICLES FROM RADIO GALAXIES. **De Young, D. S. (National Radio Astronomy Observatory, Green Bank, W. Va.). Astron. Astrophys.; 9: 125-9 (Nov 1970).**

A mechanism is described that allows the escape of relativistic particles from radio galaxies in times of 10^6 to 10^7 years. This process, which depends upon fluctuations in the magnetic-field orientation, is consistent with observations and can account for the lack of steep high-frequency spectra pointed out by van der Laan and Perola. Implications of the resulting particle flux with regard to the diffuse x-ray background are discussed. (auth)

13923 SPECTROGRAPHIC OBSERVATIONS OF TWENTY-EIGHT MARKARIAN GALAXIES. **Ulrich, Marie-Helene J. (Institut d'Astrophysique, Paris. Univ. of Texas, Austin). Astrophys. J.; 163: 441-7(1 Feb 1971).**

Spectrographic observations of twenty-eight galaxies of Markarian's second and third lists were made at 207 Å mm^{-1} in the spectral range 3400 to 6800 Å. The galaxies of this sample presented a wide variety of spectral characteristics and absolute luminosities: nine of them were fainter than $M = -18$, and six were brighter than $M = -21$. The three brightest ones were the Seyfert-type galaxies Nos. 79, 141, and 205 of absolute magnitudes –21.9, –22.0, and –23.2, respectively. Positive identification of Markarian galaxies with common types of galaxies, like spirals or irregular-I, cannot be made without direct photographs. (auth)

13924 LIGHT VARIATIONS OF THE SEYFERT GALAXY NGC 4151. III. LONG-TERM PHOTOGRAPHIC B-VARIATIONS AND INFRARED K-DATA. **Pacholczyk, A. G. (Univ. of Arizona, Tucson). Astrophys. J.; 163: 449-54(1 Feb 1971).**

Examination of Harvard patrol plates taken during the years 1932–1952, and of Steward Observatory plates taken between the years 1956 and 1968, indicates irregular changes of the photographic magnitude of the Seyfert galaxy NGC 4151 within the range 10.7 to 12.7 mag, with one recorded outburst of 9.9 mag and one low of 13.2 mag. The presence of a cycle of about 5 years in the light variations of this object is a possibility not incompatible with the photographic data. Measurements in the infrared at 2.2 μ performed since 1967 do not exclude the possibility of variations in brightness of the order of 1 mag, but more sensitive observations are needed to establish the variations definitely. (auth)

13925 THREE-COLOR PHOTOMETRY OF A FIELD AT THE BORDER OF THE SCUTUM CLOUD. **Schubarth, A. (Univ., Basel). Astron. Astrophys.; 9: 130-41(Nov 1970). (In German).**

In a field S4 of 0.097 square degree 1648 stars up to the limiting magnitude G = 17.5 mag were measured photometrically in three colors of the RGU-System. Fifteen plates taken with the 48 inch Palomar–Schmidt telescope were used. The two color diagrams for given intervals of apparent magnitude were used for the determination of the interstellar reddening in that direction. Up to distances of 1.6 kpc the reddening is constant $E(G - R) = 0.19$ mag. It is caused by an interstellar cloud in a distance smaller than 200 pc. In distances larger than 1.6 kpc an increase of the reddening is observed. The luminosities of the main sequence stars were taken from the calibrated two color diagrams. The late-type giants were identified according to three criteria: shift and gap in the two color diagrams and according to the calculated space density. The distances were determined using $M\ (G) = 1.0$ as a mean value of the absolute magnitude for late-type giants. The space densities were determined for main sequence stars of the interval $3.0 \leq M\ (G) \leq 6.0$ and for late-type giants. The main sequence stars show a density maximum between 0.6 and 1.2 kpc, which exists also in the other Scutum fields S1–S3 and which clearly defines the Scutum Cloud itself. The density function for late-type giants can be calculated only for distances larger than 2 kpc because of the scarcity of nearer stars. It shows a maximum between 2 and 4 kpc and a uniform increase of density for larger distances in spite of the increase of the distance from the galactic plane. Since in this direction the minimum distance from the galactic center is 4 kpc, some mixing with late type giants of Population II may occur. The luminosity function was determined only for main-sequence stars of the interval $3.0 \leq M\ (G) \leq 6.0$ and compared with the functions found in the other three Scutum fields and with van Rhijn's function. All the luminosity functions of the Scutum fields lie above van Rhijns function and are steeper than this function. (auth)

13926 PLACES OF ORIGIN OF STARS IN THE GALAXY. **Hube, D. P. (Univ. of Alberta, Edmonton). Astron. Astrophys.; 9: 142-5(Nov 1970).**

Meridional galactic orbits were computed for a sample of nearby, late B-type stars. Using ages obtained by the $(U-B)_0$, β method, places of origin were derived. No support was found for a recent suggestion that stars tend to be formed in extreme portions of their orbits as a result of the action of nongravitational forces on the interstellar gases. (auth)

13927 NEUTRAL HYDROGEN ABSORPTION IN THE IRR II GALAXY M82. **Guelin, M.; Weliachew, L. (Observatoire de Paris, Meudon, France). Astron. Astrophys.; 9: 155-8(Nov 1970).**

Absorption by neutral hydrogen was detected in the galaxy M82. Measurements were carried out with the transit radio telescope at Nançay. Emission and absorption do not occur at the same velocities. The velocity and width of the absorption profile are in agreement with emission lines detected previously at optical wavelengths along the major axis and close to the center of the galaxy. The neutral absorbing gas is related to the noncircular motions near the center of the galaxy rather than to the rotation as derived from optical absorption lines. The neutral hydrogen temperature cannot be estimated because emission was not detected at the central absorption velocity. (auth)

13928 STREAMING MOTIONS IN THE CARINA–CENTAURUS REGION. **Humphreys, Roberta M. (Univ. of Arizona, Tucson). Astrophys. J.; 163: L111-13(1 Feb 1971).**

An analysis of new velocity data for a large number of supergiants confirms results presented earlier that streaming motions of 8 km sec^{-1} occur between the sides of the spiral feature in the Carina–Centaurus region. (auth)

13929 CLASSIFICATION OF GALAXIES. **Flin, Piotr (Univ. of Jagellonian, Krakow). Postepy Astron.; 18: 355-62 (Dec 1970). (In Polish).**

A short review on the classification of galaxies is presented. (auth)

13930 GALACTIC STRUCTURE DERIVED FROM NEUTRAL HYDROGEN OBSERVATIONS USING KINEMATIC MODELS BASED ON THE DENSITY-WAVE THEORY. **Burton, W. B. (Leiden Observatory). Astron. Astrophys.; 10: 76-96(1 Jan 1971).**

XUM

Observations of neutral hydrogen near the galactic plane in the first quadrant of longitude reported earlier by the author are interpreted here in terms of two sorts of kinematic models of the galactic velocity field. The existence of large-scale streaming motions such as the streaming associated with the Sagittarius and other major spiral arms makes interpretation in terms of circular galactic rotation unsatisfactory. Failures of kinematic models based on circular rotation are pointed out. It is shown that application of a velocity field of the type predicted by the density-wave theory as formulated by Lin et al. (1969) leads to a more satisfactory interpretation. Model I based on this theory and on the observations of large-scale patterns in the observed velocity–longitude diagram, systematic irregularities in the run of terminal velocities with longitude, and steps in the variation of integrated brightness along the galactic equator, has streaming amplitudes between 3 and 8 km s^{-1}. The arm–interarm hydrogen density contrast in this model is typically 3 to 1 and the tilt of the spiral pattern is about 7°. On the whole the fit to the observations is quite satisfactory. It is emphasized that the velocity field of the Galaxy and the hydrogen density distribution must be studied simultaneously. It is shown that the profiles are more sensitive to small variations in the streaming motions than to small variations in the hydrogen density. In the galactic plane, density variations cannot therefore be determined directly from observation. They can only be derived from a theory relating the velocity and density fields. As an illustration it is shown how a model V based on the model I streaming motions superimposed on a completely uniform distribution of hydrogen represents the observations as well as model I itself. However, on general grounds a model like I is to be preferred, because the streamings will always be accompanied by systematic density variations. Characteristics of the geometry inherent in the observed velocity–longitude diagram which can lead to the appearance of pseudo concentrations of hydrogen are illustrated by a model (VI) based on circular rotation and uniform hydrogen distribution. These model-independent geometrical effects and the effects of systematic streaming are such that it is not possible to determine the true velocity dispersion from observations in the plane. A map of nondetailed galactic structure in the region of the Sagittarius spiral arm is produced using density-wave theory kinematics. The method used to derive the map places emphasis on the agreement of the observed profiles with model profiles calculated from the velocity and density distributions in the map. (auth)

13931 STRUCTURE OF THE WING OF THE SMALL MAGELLANIC CLOUD. Westerlund, B. E. (European Southern Observatory, Santiago de Chile). Glaspey, J. Astron. Astrophys.; 10: 1-7(1 Jan 1971).

Direct plates taken in visual and ultraviolet light of the Wing of the Small Magellanic Cloud were blinked for blue stars. Over 2000 objects were identified to a limiting magnitude of about V = 18.5. They define a fairly irregular band through the 16 square degrees covered in the investigation. Several concentrations of faint blue stars were found but also fairly large areas in the band with a pronounced lack of blue stars. The borders of the band were well defined. Photographic photometry in U, B, V was carried out of all stars inside two areas of 0.1 square degrees each to a limiting magnitude of V = 17. In this way the completeness of the survey was checked to this magnitude and the definition of the blue stars confirmed by color measurements. The galactic stars included in this photometry were of both halo and disc population, as was to be expected. (auth)

13932 GALACTIC PARAMETERS AS A CONSEQUENCE OF COSMOLOGICAL TURBULENCE. Ozernoi, L. M.; Chibisov, G. V. (Lebedev Inst. of Physics, Moscow). Astrophys. Lett.; 7: 201-4(Jan 1971).

A simple model of the evolution of primeval cosmological turbulence explains well enough, without arbitrary assumptions, the main parameters of galaxies. (auth)

13933 INFRARED SPECTRA OF INTERSTELLAR GRAINS. Martin, P. G. (Cambridge Univ., Eng.). Astrophys. Lett.; 7: 193-8(Jan 1971).

Infrared observations of spectral features caused by interstellar grains provide an important means of chemical identification. Using the infrared complex refractive index, which can be determined in the laboratory, it is possible to calculate the spectrum for grains of all sizes. Contrary to assumptions made recently in the literature, even for submicron-sized grains the linear absorption coefficient γ is not necessarily a good approximation to the shape of the absorption spectrum, and the absorbance as measured by Lyon (1963) does not give a suitable estimate of γ because of saturation effects. Polarized features characteristic of aligned elongated grains are pointed out, and brief mention is made of the emission spectrum. (auth)

13934 STUDIES OF INTERSTELLAR EXTINCTION AT INFRARED WAVELENGTHS. Knacke, Roger Fritz. Berkeley, Calif.; Univ. of California (1969). 114p. University Microfilms Order No. 70-17,596.

Thesis.

A study of interstellar extinction between 1 and 12 μ was made. Calculations are presented for extinction cross sections for grains composed of water ice, quartz, silica, and graphite and silica surrounded by an ice mantle. Laboratory spectra of the position, strength, and shape of the strong ice band at 3.07 μ confirm that the calculations are valid for ice at interstellar temperatures. Infrared spectra of the reddened stars VI Cyg No. 12 (1 to 5.5 μ), CIT 11 (1 to 3.5 μ), HD 183143 (1 to 3.5 μ), and 119 Tau (2.9 to 12 μ) were obtained to test the theoretical predictions. No absorption band at 3.07 μ stronger than 10, 10, 50, and 20%, respectively, of the expected absorption of ice grains can be fitted to the spectra of these stars. It is concluded that the interstellar grains contain very little ice. The extinction spectrum of VI Cyg No. 12 does not contain any strong absorption bands at the wavelengths studied. Broad absorption features at 5 and 8 μ in the spectrum of 119 Tau are attributed to the fundamental vibration–rotation bands of CO and SiO in the stellar atmosphere. Additional features at 9.7 and 10.6 μ may be produced by a silicate mineral in the interstellar grains. (auth) (Diss. Abstr. Int., B)

13935 STELLAR-POPULATION SAMPLES AT THE GALACTIC POLES. II. UBVRI PHOTOMETRY OF M STARS NEAR THE SOUTH POLE. Eggen, O. J. (Australian National Univ., Canberra). Astrophys. J., Suppl. Ser.; 22: No. 188, 289-318 (Dec 1970).

About 950 UBV and 850 RI observations were obtained for 109 red stars near the South Galactic Pole. All except nine of the HD stars of types Ma, Mb, and Mc within 30° of the South Galactic Pole and all except eleven of the Ma stars within 20° were included. Of the Ma stars, 14% were found to be variable, with 11% showing erratic (EC) variations and 3 percent being quasi-periodic (P). A total of thirty-eight, or 72%, of the Mb stars are variable; four of these are named variables. The variables of class Mb are equally divided between nineteen EC and nineteen P types. All Mc and Md stars are variable. The 105 HD stars of type M observed yielded a total of sixty variables, of which forty-three are new. Four additional known variables, U, X, SY, and TT Scl, which are near the South Galactic Pole but not in the HD, were also observed. Proper motions were collected, or derived, for most of the stars, and the luminosities obtained from the $(M_I, R - I)$-relation yielded relatively accurate space-motion components (U, V), with which population discrimination can be made. Also the position in the $(U - B, R - I)$-plane is discussed and used as a population indicator. The young disk stars reach a ceiling at about 400 pc from the plane, the old disk stars at about 900 pc, and the halo objects are distributed up to 1200 pc. The old disk variables have a space density of about four per 10^7 pc^3; the halo variables, one per 10^7 pc^3. Observations of early-type stars, on the UBV system, indicated a uniform reddening of $E(B - V) = +0.025$ mag at the South Galactic Pole. (auth)

Cosmology

Refer also to abstracts 14080 and 14788.

13936 (AD–711829) THEORETICAL STUDY OF NONTHERMAL PHENOMENA OF ASTROPHYSICS. Final Report, May 1966–June 30, 1970. Sturrock, P. A. (Stanford Univ., Calif. Inst. for Plasma Research). Aug 1970. Contract N00014-67-A-0112-0006. 31p. (SU-IPR-382). NTIS.

The research program was concerned with nonthermal phenomena exhibited by extragalactic objects. Particular attention was given to quasars and to active galaxies such as Seyfert galaxies and radio galaxies. It has become clear, in recent years, that there is a close similarity between quasars and the nuclei of active galaxies. For this reason, special attention was given to galactic nuclei. Study of quasars is closely linked with study of the intergalactic medium and of cosmology. (auth) (USGRDR)

13937 INTRODUCING THE BLACK HOLE. Ruffini, Remo; Wheeler, John A. (Princeton Univ., N. J.). Phys. Today; 24: No. 1, 30-6; 39; 41(Jan 1971).

The physics of black holes is discussed in terms of equilibrium configurations, neutron stars or black holes, continuing collapse, process of formation, dust clouds, light cones, the Kruskal diagram, departures from symmetry, angular momentum, gravitational radiation, and search for black holes. (W.D.M.)

13938 LINEAR MAGNETOHYDRODYNAMIC THEORY OF THE DEVELOPMENT OF INHOMOGENEITIES IN AXIALLY SYMMETRIC MODELS OF THE UNIVERSE WITH A COSMOLOGIC MAGNETIC FIELD. Sibgatullin, N. (Moscow State Univ.). Dokl. Akad. Nauk SSSR; 193: 1267-70(21 Aug 1970). (In Russian).

The potential solutions of Einstein's equation of a gravitating ideal gas in a three-parameter group of motion were reexamined in order to derive a model of the homogeneous Universe within the framework of the general theory of relativity. Properties of the various solutions of the Einstein–Maxwell equation were studied for the case of the close, plane, and open models. One of the solutions was considered as the basic cosmologic background, superposing on it the arbitrarily small perturbation of the distributions and speed of matter, and the gravitational and electromagnetic fields assuming that the matter possesses ideal electric conductivity. The considerations indicated that the singular collapse into the "needle" and "pancake" shape is always unstable. The results correct previously published conclusions of Doroshkevich. (TTT)

13939 PHOTO-IONIZATION OF INTERGALACTIC MATTER. Bergeron, J. (Institut d'Astrophysique, Paris); Salpeter, E. E. Astrophys. Lett.; 7: 115-19(Dec 1970).

For cosmological models which require a large present matter density, most of this matter could be in the form of highly ionized intergalactic gas. The possibility was investigated of photoionization of the intergalactic gas by uv radiation from quasars, for a closed Friedman model (F), where $\sigma_0 = q_0 = 1$, and for a Lemaître model (L), where $\sigma_0 = 0.05$, $\Lambda = 1.02\Lambda_c$. The discrepancy between the present observational estimate for the total uv emissivity F(0), due to quasars, and the required one for both models (F) and (L), is quite large. For Friedman models, this discrepancy could be easily removed by considering open models with $\sigma_0 = q_0 \lesssim 0.1$; for Lemaitre models, this discrepancy could be removed easily only if F(0) is underestimated by an appreciable factor, or if most of the matter is not in the form of intergalactic gas. (auth)

13940 ELEMENTARY OBSERVATIONS ON GRAVITATIONAL COLLAPSE. Treder, H.-J. (Institut fuer Relativistische und Extragalaktische Forschung, Babelsberg, Ger.). Monatsber. Deut. Akad. Wiss. Berlin; 11: 856-72(1969). (In German).

Gravitational collapse is reconsidered from elementary physical principles. From the generality of these principles, it is inferred that gravitational collapse is, as indicated by Oppenheimer, Einstein, and Wheeler, an unavoidable phenomenon in the framework of the gravitational theories of Newton and Einstein. The equilibrium theory of gravitational collapse and the question of the possible equilibrium states of gravitating matter are considered. The dynamics of gravitational collapse is treated. (M.C.G.)

13941 THEORY OF INVERSE COMPTON SCATTERING IN A COLD PLASMA. Goldstein, Melvyn L.; Lenchek, Allen M. (Univ. of Maryland, College Park). Astrophys. J.; 163: 515-23(1 Feb 1971).

A theory was derived for inverse Compton scattering in a cold collisionless plasma. In the absence of a magnetic field, the general shape of the scattered-photon spectrum is qualitatively similar to the vacuum spectrum. The average rate of electron-energy loss is three-quarters of the vacuum value if the frequency of the incident photons is close to the plasma frequency. In order for the plasma to have a large effect on the scattered-photon spectrum, the incident radiation must propagate below the plasma frequency, which is possible if a magnetic field is present. As an example, gyrosynchrotron photons propagating in the ordinary mode below the plasma frequency were used as the source of incident photons. When these photons are scattered, the spectrum is greatly suppressed compared with the vacuum results. The total scattering cross-section is also sharply decreased in a magnetoactive plasma. (auth)

13942 THEORETICAL FRAMEWORKS FOR TESTING RELATIVISTIC GRAVITY. I. FOUNDATIONS. Thorne, Kip S.; Will, Clifford M. (California Inst. of Tech., Pasadena). Astrophys. J.; 163: 595-610(1 Feb 1971).

This is the first in a series of theoretical papers which will discuss the experimental foundations of general relativity. This paper reviews, modifies, and compares two very different theoretical frameworks, within which one devises and analyzes tests of gravity. The Dicke framework assumes almost nothing about the nature of gravity; and it uses a variety of experiments to delineate the gross features of the gravitational interaction. Two of its tentative conclusions (the presence of a metric, and the "gravitational response equation," $\nabla \cdot T = 0$, for stressed matter) become the postulates of the Parametrized Post-Newtonian framework. The PPN framework encompasses most, if not all, of the theories of gravity that are currently compatible with experiment. Future papers in this series will develop the PPN framework in detail, and will use it to analyze a variety of relativistic gravitational effects that should be detectable in the solar system during the coming decade. (auth)

13943 THEORETICAL FRAMEWORKS FOR TESTING RELATIVISTIC GRAVITY. II. PARAMETRIZED POST-NEWTONIAN HYDRODYNAMICS, AND THE NORDTVEDT EFFECT. Will, Clifford M. (California Inst. of Tech., Pasadena). Astrophys. J.; 163: 611-28(1 Feb 1971).

Chandrasekhar's post-Newtonian equations of hydrodynamics were generalized to encompass any metric theory of gravity by the use of arbitrary metric parameters. The resultant Parametrized Post-Newtonian (PPN) hydrodynamical equations were then used to calculate the Newtonian acceleration of the center of mass of a massive body of perfect fluid toward a very distant point mass. This acceleration can be written in terms of a gravitational-mass tensor and the gradient of the Newtonian potential: $ma^\alpha = m^{\alpha\beta} U_{,\beta}$. The gravitational-mass tensor $m^{\alpha\beta}$ is equal to the isotropic inertial mass ($m\delta^{\alpha\beta}$), plus a small correction ("Nordtvedt effect"), which depends on the gravitational internal energy of the body and on the metric parameters that characterize the particular theory being used. In general relativity, the gravitational mass is precisely equal to the inertial mass (correction terms vanish), in accordance with the equivalence principle. In Brans–Dicke theory the two masses differ by a small isotropic correction which varies from body to body, in violation of the equivalence principle. A simple explanation of these two results is discussed. This work generalizes and substantially agrees with previous calculations by Nordtvedt. (auth)

13944 DOES A PRIMEVAL MAGNETIC FIELD EXIST? Reinhardt, Michael (Univ., Bonn); Thiel, Manfred A. F. Astrophys. Lett.; 7: 101-6(Dec 1970).

Systematic differences in the distribution of rotation measures in galactic coordinates were found for 88 distant ($z > 0.25$) and nearby ($z < 0.25$) radio sources with known rotation measures and redshifts. This indicates an intergalactic contribution to the Faraday rotation observed in distant radio sources and corroborates earlier conclusions drawn by Sofue et al. (1969), from data on 40 radio sources, in favor of an intergalactic magnetic field running in the direction $l^{II} \approx 280°$, $b^{II} \approx +30°$ to $l^{II} \approx 100°$, $b^{II} \approx -30°$. (auth)

13945 IS THE 8°K BACKGROUND RADIATION UNIVERSAL? Anand, K. C.; Apparao, Krishna M. V. (Tata Inst. of Fundamental Research, Bombay). Proc. Indian Acad. Sci., Sect. A; 72: 62-6 (Aug 1970).

The high-energy gamma-ray flux (energy greater than 10^{12} eV) resulting from high-energy protons interacting with photons of the recently observed sub-millimeter microwave radiation in metagalactic space is calculated. Comparison of the flux of these gamma rays with experimental observations indicates that the observed sub-millimeter radiation may not be universal. (auth)

13946 PARADOX IN THE INTERACTION OF THE GRAVITATIONAL AND ELECTROMAGNETIC FIELDS? Reinhardt, M. (Univ., Bonn). Nature (London); 229: 36-7(1 Jan 1971).

Reference is made to Woodward and Yourgrau (Nature, 226: 619(1970)) who suggested that the influence of gravitation on the propagation of electromagnetic waves depends on the frequency of the radiation. These authors argued from the finding that light deflection by the Sun's gravitational field, as found from optical studies at solar eclipses, appeared somewhat larger than predicted by the Einstein theory of gravitation. The results of Muhleman (Phys. Rev. Lett., 24: 1377(1970)) and Seielstad (loc. cit. 24: 1373(1970)), who measured light deflection by the Sun at 2.388 and 9.602 GHz, were however in close agreement with the predictions of general relativity, and were very much smaller than given by the predictions of Woodward and Yourgrau. Reasons for this are discussed, and it is concluded that the possibility of a frequency dependence of the interaction of gravitational and electromagnetic fields, at least of the strength assumed by Woodward and Yourgrau, is precluded. A reply from Woodward and Yourgrau is included, which points out some interesting features of the results reported by Reinhardt, and states that it is possible to formulate a plausible theory of electromagnetic–gravitational field interaction that easily explains all of the empirical data, including anomalies in the observations that indicate frequency dependence. (UK)

13947 COSMOLOGICAL THEORY BASED ON LYRA'S GEOMETRY. Halford, W. D. (Univ. of Toronto). Aust. J. Phys.; 23: 863-9(Dec 1970).

Using a Robertson–Walker metric in a modified Riemannian

XUM

manifold, a cosmological theory is obtained which gives rise to nonstatic perfect-fluid world models. The cosmological equations are formally identical to those of the normal relativistic theory with cosmological constant Λ. The advantage gained by the present theory is that the cosmological constant arises naturally from the geometry. Inspection of the field equations shows that Hoyle's C-field theory can be placed naturally within the framework of Lyra's geometry. (auth) (Australia)

13948 INVESTIGATION OF THE GRAVITATIONAL INTERACTION OF ELECTROMAGNETIC RADIATION AND MATTER AS A CAUSE OF THE COSMOLOGICAL RED SHIFT. Hegarty, John Christopher. Boston; Boston Univ. (1970). 127p. University Microfilms Order No. 70-22,367.

Thesis.

Although the cosmological red shift is regarded almost universally as a Doppler effect resulting from the expansion of the Universe, numerous attempts have been made to explain it as a consequence of the gravitational interaction of the electromagnetic radiation and the matter of the Universe. Previous work by Zwicky, Tolman, Westervelt, Havas, and Goldberg is discussed at length. (TSS) (Diss. Abstr. Int., B)

13949 COSMIC-BACKGROUND MEASUREMENTS IN THE FAR INFRARED. Shivanandan, Kandiah. Washington, D. C.; Catholic Univ. of America (1970). 177p. University Microfilms Order No. 70-21,921.

Thesis.

Measurements of the cosmic background temperature in the decimeter and centimeter wavelengths (λ = 0.3 cm to 7 cm) indicate that the radiation is that of a 2.7°K blackbody whose peak is at a wavelength of $\lambda \sim 0.2$ cm. In order to establish the true blackbody character of the spectrum, it is essential to determine its curvature, which lies in the far-infrared. Ground-based observations at wavelengths shorter than 0.3 cm are not possible because of strong atmospheric H_2O and CO_2 atmospheric bands. A complete liquid-helium-cooled telescope was designed at the Naval Research Lab. and Cornell Univ. to carry out rocket observations above the atmosphere. The far-infrared detector used was n-type InSb suitably fabricated for flight. Calibrations were carried out using conventional infrared techniques at room temperature and in the flight telescopes assimilating cold environment. Of the materials tested for blackbody, black velvet seems to have a good emissivity in the far-infrared. The Cornell experiment was successfully flown, and the results indicated a background temperature corresponding to an 8°K blackbody in the wavelength region of 0.4 mm to 1.3 mm. The flux measured was two orders of magnitude higher than the expected 2.7°K blackbody spectrum. Some theoretical implications of this excess infrared flux is discussed in relation to gamma- and x-ray background observations. (Diss. Abstr. Int., B)

13950 ARGUMENTS CONCERNING RELATIVITY AND COSMOLOGY. Klein, Oskar (Univ., Stockholm). Science; 171: 339-45(29 Jan 1971).

The true foundation of Einstein's theory of general relativity, the so-called principle of equivalence, according to which there is no essential difference between "genuine" gravitation and inertial forces, well known from accelerated vehicles is reviewed. By means of a comparison with Gaussian geometry of curved surfaces—the background of Riemannian geometry, the tool used by Einstein for the mathematical formulation of his theory—it is made clear that this principle is incompatible with the idea proposed by Mach and accepted by Einstein as an incitement to his attempt to describe the main situation in the Universe as an analogy in three dimensions to the closed surface of a sphere. In the later attempts toward a mathematical description of the Universe where Einstein's cosmology was adapted to the discovery by Hubble that its observed part is expanding, the so-called cosmological postulate has been used as a kind of axiomatic background which, when analyzed, makes it probable that this expansion is shared by a very big, but still bounded system. This implies that our expanding metagalaxy is probably just one of a type of stellar objects in different phases of evolution, some expanding and some contracting. Some attempts toward the description of this evolution are sketched with the hope that further investigation, theoretical and observational, may lead to an interesting advance in this part of astrophysics. (auth)

13951 STUDY OF GAMMA RADIATION WITH THE SATELLITE KOSMOS-135 AND THE POSSIBLE EXISTENCE OF ANTIMATTER METEORS. Konstantinov, B. P.; Aptekar, R. L.; Bredov, M. M.; (and others). Bull. Acad. Sci. USSR, Phys. Ser. (Engl. Transl.); 33: 1660-5(Nov 1969).

Translated from Izv. Akad. Nauk SSSR, Ser. Fiz.; 33: 1820-6 (Nov 1969).

A way to test the antimatter meteor hypothesis is to look for the annihilation radiation that should arise in the upper atmosphere under the action of antimeteors. The intensity of electron–positron annihilation radiation during passage through the Geminid, Ursid, and Quadrantid meteor streams was investigated with Kosmos-135 as part of its program of recording the spectra and intensities of γ radiation in circumstellar space. (W.D.M.)

13952 ARE PROTARS SPINARS? Stecker, F. W. (Goddard Space Flight Center, Greenbelt, Md.). Nature (London); 229: 105(8 Jan 1971).

It has been suggested (Morrison, Astrophys. J. Lett. 157: L73(1969)) that quasi-stellar radio sources and pulsars are basically similar in every respect except scale, and that both are centrally condensed magnetised spinning masses with a luminous lifetime governed by the rotational work done on charged particles by the moving magnetic fields. Morrison proposes that the term "spinar" be applied to QSOs, pulsars, and other highly condensed core objects that may exist in the nuclei of Seyfert galaxies and extragalactic radio sources. A possible connection between this hypothesis and those of Harrison (Mon. Not. Roy. Astron. Soc., 148: 119(1970)) and Gunn and Ostricker (Phys. Rev. Lett., 22: 728(1969)) is discussed. Harrison suggested that, even during its earliest stages, the Universe was structured with protogalactic configurations that were relatively dense and possessed spins, and that these "spinning cores" may have accounted for the origin of present galactic magnetic fields. Gunn and Ostricker showed that such "spinars" may be capable of accelerating cosmic-ray protons to energies of $\sim 10^{21}$eV. Gamma rays produced by interactions of these cosmic rays would be observable out to redshifts of ~100, and in fact, may have already been observed. If protars are the "spinars" of an early Universe epoch, a qualitative outline of a cosmology consistent with and suggestive of primordial inhomogeneities is arrived at. (UK)

13953 HOT-UNIVERSE MODEL AND THE DIRAC MONOPOLE. Domogatskii, G. V.; Zheleznykh, I. M. Bull. Acad. Sci. USSR, Phys. Ser. (Engl. Transl.); 33: 1635-8(Nov 1969).

Translated from Izv. Akad. Nauk SSSR, Ser. Fiz.; 33: 1792-5 (Nov 1969).

An attempt is made to obtain limitations on the properties of the hypothetical magnetic charge, the Dirac monopole, through astrophysical considerations. (W.D.M.)

Planetary Phenomena

13954 CORRELATION BETWEEN ROCK TYPE AND IRRADIATION HISTORY OF APOLLO 11 IGNEOUS ROCKS. Eberhardt, P.; Geiss, J.; Graf, H.; (and others) (Univ., Bern). Earth Planet. Sci. Lett.; 10: 67-72(Dec 1970).

High-K and low-K Apollo 11 lunar rocks show different distributions of exposure ages T_e. The low-K rocks group around 100×10^6 y ($65 \times 10^6 \leq T_e \leq 130 \times 10^6$ y; except one rock out of 9) whereas the high-K rocks have either ages between 30 and 55×10^6 y or between 240 and 450×10^6 y. From the $(^{78}Kr/^{83}Kr)_{sp}$ versus $(^{131}Xe/^{126}Xe)_{sp}$ correlation diagram it is concluded that the low-K rocks were systematically exposed to a harder irradiation than the high-K rocks. The observed grouping of exposure ages is essentially in agreement with only three impacts originally ejecting the Apollo 11 rocks analyzed so far. Three models explaining the systematically higher shielding of the high-K rocks are discussed. Model A suggests that high-K rocks were initially one (or several) large boulder(s), reduced to present size by space erosion and break-up on the lunar surface. Low-K rocks were directly ejected as small rocks. Model B requires a stratigraphy of the lunar bedrock. High-K material must be closer to the surface than low-K material and has received a substantial preirradiation prior to the ejection. Model C requires that the high-K rocks came from small local craters, whereas the low-K rocks were ejected from a larger, more distant crater. Independent of any model, the exposure age group found for the low-K rocks corresponds to the time of formation of the crater or craters which produced these rocks. (auth)

13955 RARE EARTH ABUNDANCES IN SOIL AND ROCKS FROM THE OCEAN OF STORMS. Gast, P. W.; Hubbard, N. J. (Columbia Univ., Palisades, N. Y.). Earth Planet. Sci. Lett.; 10: 94-100(Dec 1970).

The rare-earth abundance patterns in Apollo 12 basalts have much lower concentrations and smaller Eu anomalies than Apollo 12 soil and all analyzed Apollo 11 samples. The rare-earth abundance patterns of Apollo 12 basalts are similar to and overlap those of achondritic meteorites. A partial melting model can explain the rare-earth data for lunar samples. (auth)

13956 LATITUDINAL AND LONGITUDINAL VARIATION OF A PLANETARY ATMOSPHERE AND THE OCCULTATION EX-

PERIMENT. Pirraglia, J.; Gross, S. H. (Polytechnic Inst., Brooklyn). Planet. Space Sci.; 18: 1769-84(Dec 1970).

The distribution of neutral and ionized particles about a planet depends, at any time, on angular coordinates (latitude and longitude) as well as altitude. Measurements of the Venusian and Martian atmospheres and ionospheres were made by means of the "occultation" experiment on-board the Mariner spacecrafts, and the same or similar experiment is planned for future missions to the planets. The conventional method of reducing the residual doppler data assumes spherical symmetry, in which the refractivity of the medium depends only on radius from the center of the planet, or altitude. It is shown that the neglect of angular dependence may introduce serious errors, even for media in which this dependence is slight compared to that in the radial direction, when the plane of motion of the spacecraft about the planet is inclined with respect to the direction of the Earth. The magnitude of the errors may be greatest for a planet such as Mercury and least for Jupiter, if planetary size and atmospheric temperature are the principal factors considered, Mars and Venus being intermediate. These results are most significant for an orbiter in which the orbital plane is inclined to obtain planetary coverage in a matter of months of measurements. Results of calculations for a particular model show that scale-height measurements, and, thereby, atmospheric temperature, may be in error by a factor greater than 2 for inclined orbital configurations. (auth) (UK)

13957 JUPITER'S MAGNETOSPHERIC ROTATION PERIOD. Carr, Thomas D. (Univ. of Florida, Gainesville). Astrophys. Lett.; 7: 157-62(Jan 1971).

Five independent decametric determinations of the mean value of Jupiter's rotation period averaged over approximately one orbital period yield a value of 09 hr 55 min 29.76 ± 0.04 sec. An analysis of all the available decametric data meeting certain criteria confirms the existence of a cyclic effect which is probably due to the variation in the Jovicentric declination of the Earth. The most probable value of the Jovian magnetospheric rotation period, based on both decametric and decimetric observations, is 09 hr 55 min 29.75 ± 0.04 sec. (auth)

13958 EXTRALUNAR DUST IN APOLLO CORES. Barber, D. J.; Hutcheon, I.; Price, P. B. (Univ. of California, Berkeley). Contract AT(04-3)-34. Science; 171: 372-4(29 Jan 1971).

Densities of nuclear tracks exceed 10^{11}/cm^2 in several percent of the micrometer-size silicate grains from all depths in the 12- and 60-cm lunar cores. Either these grains were irradiated in space as extralunar dust or the ratio of iron to hydrogen in low-energy (about 10^6 eV/nucleon) solar particles is orders of magnitude higher than in the photosphere. (auth)

Atomic and Molecular Physics

Atomic, Electron, Ion, and Molecular Beams and Their Reactions

Refer also to abstract 14353.

13959 (UCRL-19719) ENERGY SPECTRA OF BACKSCATTERED ELECTRONS AND POSITRONS BY MONTE CARLO CALCULATIONS. Tillmann, Klaus-Dieter (California Univ., Berkeley. Lawrence Radiation Lab.). 5 Mar 1970. Contract W-7405-eng-48. 36p. Dep. NTIS.

The energy spectra and angular distribution of backscattered electrons and positrons from thick targets of Li, Be, Al, Fe, Cu, and Sn for 1.0-MeV particles and from Be and Sn targets for 0.5- and 2.0-MeV particles normally incident on the targets are presented. These spectra were calculated by a random-sampling Monte Carlo program on a CDC 6600 digital computer. Backscattering coefficients are found to fit a dependence for $Z > 13$. The shapes of the energy spectra depend strongly on the atomic number Z and are found to be in good agreement with experimental data. The angular distribution fits a $\cos(\pi - \alpha) \cdot e^{-(\pi-\alpha)^2/2}$ dependence. The energy spectra, angular distributions, and backscattering coefficients depend on the angle β between the initial beam and the target surface. For decreasing angles β, the most probable energy shifts toward the initial energy. (auth)

13960 EFFECT OF CRYSTALLINITY AND INTEGRATED FLUX ON THE RANGE OF CESIUM IONS INJECTED AT 20 keV INTO ALUMINUM. Siekhaus, Wigbert Josef. Berkeley, Calif.; Univ. of California (1969). 129p. University Microfilms Order No. 70-17,656.

Thesis.

The concentration profile of ions injected into a metal target was investigated both theoretically and experimentally as a function of the integrated flux of the bombarding ions. A theoretical solution for the time-dependent concentration is given, and it is proven that the number of bombarding ions contained in a target at saturation is increased if the ions diffuse throughout the target. Polycrystalline and monocrystalline aluminum was bombarded with radioactive cesium for increasing values of integrated flux. The total number of cesium atoms contained in the target after bombardment and the number of cesium atoms contained in the target after removal of successive layers were measured by counting the beta radiation emitted by cesium. The layers were removed by anodization and chemical stripping. These experiments give the integrated flux of bombarding ions necessary for saturation of monocrystalline and polycrystalline aluminum bombarded with 20-keV cesium ions and the number of cesium atoms contained in the target at saturation. The results are consistent with a theory that assumes diffusion in the range of the bombarding particles. They show that the mean depth of the concentration decreases with increasing integrated flux. In a monocrystalline lattice the concentration extends even at saturation deeper into the target than in polycrystalline aluminum. The highest concentration in aluminum is achieved for bombardment along the 110 direction. These measurements suggest that diffusion in the range of penetration is an important factor in determining the shape of the concentration. The diffusion constant near the surface is found to be approximately three times higher in monocrystalline aluminum than in polycrystalline aluminum. Two polycrystalline and one monocrystalline targets were bombarded to saturation with ^{133}Cs and then bombarded with 6×10^{12} ions/cm^2 of radioactive ^{134}Cs. Comparison of the radioactivity of these samples to the activity of samples bombarded with the same number of radioactive ^{134}Cs ions gives the ratio of the accommodation coefficient for saturated aluminum to the accommodation coefficient for pure aluminum as .92. The range of Cs ions in a saturated aluminum target (polycrystalline or monocrystalline bombarded along the 100 direction) is reduced by at least a factor 4 compared to the range in unsaturated aluminum. (Diss. Abstr. Int., B)

13961 THEORY OF BACKSCATTERING OF FAST ELECTRONS FROM A CONDENSED MEDIUM. I. NONRELATIVISTIC CASE. Kalashnikov, N. P.; Mashinin, V. A. (Moscow Engineering-Physics Inst.). Zh. Eksp. Teor. Fiz.; 59: 2025-34(Dec 1970). (In Russian).

A quantum mechanical approach to the problem of backscattering of fast charged particles from condensed media is developed. The backscattering differential cross section can be expressed as a series, the nth term of which describes n large-angle elastic scattering acts; between collisions resulting in large-angle scattering, the particle suffers multiple small-angle inelastic and elastic scattering. It is shown that for not too large values of Z the first term of the series yields a reasonable approximation for the backscattering differential coefficient, which agrees with the experimental results. (auth)

13962 THICK-TARGET YIELDS OF CHARACTERISTIC X RAYS BY p, d, ^{3}He$^+$, AND ^{4}He$^+$ BOMBARDMENTS. Shima, Kunihiro; Sakisaka, Masakatsu; Kokado, Masayuki; Yamamoto, Takehisa; Makino, Isao (Kyoto Univ.). Jap. J. Appl. Phys.; 9: 1297-1305(Nov 1970).

Characteristic x-ray yields by p, d, ^{3}He$^+$, and ^{4}He$^+$ bombardments were measured for various thick metallic elements in the incident energy range from 90 to 360 keV. The combination of incident particles, target materials, and produced characteristic x-rays is given as: (a) Al-K, Ti-K, Ni-K, Cu-K, Ni-L, Cu-L, Zr-L, Mo-L, Ag-L, Cd-L, Sn-L, Ta-M, W-M, Pt-M, and Pb-M for proton bombardment, (b) Al-K, Ti-K, Cu-K, Ni-L, Cu-L, Zr-L, Mo-L, Ag-L, Cd-L, Sn-L, Ta-M, W-M, Pt-M, and Pb-M for deuteron bombardment, (c) Al-K, Ni-L, Cu-L, Mo-L, Ag-L, and W-M for ^{3}He$^+$ bombardment, (d) Al-K, Ni-L, Cu-L, Mo-L, Ag-L, W-M, Pt-M, and Pb-M for ^{4}He$^+$ bombardment. The thick-target yields against particle energy were found to increase more steeply as target atomic number becomes larger. The behaviors of yield ratios of $I\mu(d)/I\mu(p)$ and $I\mu(^4He^+)/I\mu(^3He^+)$ have been qualitatively explained by the effect of average charge of the incident particles. (auth)

13963 AN INVESTIGATION OF ION-INDUCED ELECTRON EMISSION FROM METALLIC OXIDES. Stein, John D. Troy, N. Y.; Rensselaer Polytechnic Inst. (1970). 123p. University Microfilms Order No. 70-19,956.

Thesis.

Secondary electron yields produced by ion impact on aluminum oxide, titanium oxide, and beryllium oxide were measured. Results are reported for alkali metal and alkaline earth ions (Ba, Sr, Li, Cs) having energies ranging from 10 to 40 keV. The mean electron yield varied between 2 and 9, as a function of ion energy

XUM

and ion–target combination. A new mass spectrometer was developed in order that the mass and energy of the primary ion beam could be determined completely. This instrument consists of a large homogeneous electromagnet containing multiple ion trajectories. Small (10^{-15} to 10^{-16} ampere), well-collimated ion beams were focused onto a target. These target samples were biased to negative potentials ranging from 10 to 30 kV. Electrons produced by ion impact of the sample surface were then accelerated through these potentials and focused onto a reverse-bias surface-barrier detector. Output pulses from the detector and charge-sensitive amplifier were then routed to a multichannel analyzer. For a given accelerating potential, the magnitude of the output pulses corresponded to the number of electrons striking the detector simultaneously. The pulse-height spectrum, therefore, gave not only a direct measurement of the electron yield, but also indicated the statistical distribution of the number of secondary electrons produced by single ion impacts. This new method for secondary electron measurement yields results that are less subject to error than classical measurements because the detector is insensitive to negative ions. In addition, this method allows the measurement of electron yields of semiconducting and insulating materials, where low primary ion currents are desirable to prevent charge buildup or contamination. It has also been demonstrated that this new method for measuring secondary electron distributions can measure the dead layer or "window thickness" of a reversed-bias p–n junction. The dead-layer thickness is observed by determining the change in the number of electron–hole pairs produced by electrons of varying kinetic energies. (TSS) (Diss. Abstr. Int., B)

13964 CHARGE DISTRIBUTION PRODUCED BY 4- TO 24-MeV ELECTRONS IN ELEMENTAL MATERIALS. Tabata, Tatsuo (Radiation Center of Osaka Prefecture); Ito, Rinsuke; Okabe, Shigeru; Fujita, Yoshiaki. Phys. Rev., B; 3: 572-9(1 Feb 1971).

Charge-deposition distributions of monoenergetic electrons normally incident on thick absorbers of Be, Al, Cu, Ag, and Au were measured with a thin collector moved through the absorber thickness. The measurements were made at incident energies of 4.09, 7.79, 11.5, and 14.9 MeV, and also at 23.5 MeV for absorbers other than Be. Values of the most probable charge-deposition depth x_m and the charge-deposition straggling w were determined from the distributions observed. The ratio of x_m to the theoretical mean range L of the incident electrons decreases with decreasing incident energy E_0 and with increasing atomic number Z of the absorber, reflecting the effect of multiple-scattering detours of the primary electrons. The ratio w/L shows an increase with increasing E_0 in the region of $E_0 \gtrsim 11$ MeV for Al and in the entire energy region of the present experiment for Cu, Ag, and Au; this trend is considered mainly due to bremsstrahlung energy-loss straggling. The contribution to the measured distributions of electrons mediated by bremsstrahlung was found to be less than about 1×10^{-3} cm^2/g absorbed electron. Some of the distributions are compared with the Monte Carlo results of Berger and Seltzer. Agreement between the experimental and calculated results is rather good except in the case of the Be absorber. (auth)

13965 SCATTERING CROSS SECTIONS FOR MULTISPECIES QUANTUM FLUIDS. Allen, Kenneth R. (Univ. of Florida, Gainesville). Phys. Rev., A; 3: 638-42(Feb 1971).

The various possible ground-state structure factors are defined for a multispecies quantum fluid. These structure factors are then used to construct the Born approximation to the scattering cross sections for the multispecies fluid. The cross sections are used in conjunction with the results of an earlier paper to discuss the scattering of (i) charged particle, (ii) neutrons, and (iii) x rays from a two-species system composed of electrons and nuclei at high densities. (auth)

13966 ANGULAR DISTRIBUTION OF THE SPUTTERED MATERIAL IN ION BOMBARDMENT OF SINGLE CRYSTALS. Dubinskii, V. E.; Lebedev, S. Ya. Sov. Phys.-Solid State (Engl. Transl.); 12: 1516-21(Jan 1971).

Translated from Fiz. Tverd. Tela; 12: 1906-11(Jul 1970).

^{40}Ar ions of 70-keV energy were used to bombard $\{110\}$ and $\{100\}$ planes of single crystals of gold and gold–25 at. % copper. The angle of incidence ranged from 0 to 70°. Cylindrical collectors show spots corresponding to escape of atoms along the $\langle 110\rangle$, $\langle 100\rangle$, $\langle 211\rangle$, $\langle 310\rangle$, $\langle 111\rangle$, $\langle 312\rangle$, $\langle 411\rangle$, $\langle 210\rangle$, $\langle 332\rangle$, and $\langle 521\rangle$ directions as well as bands representing traces of the $\{111\}$ and $\{100\}$ planes. The signs of the $\langle 431\rangle$, $\langle 510\rangle$, $\langle 221\rangle$, and $\langle 611\rangle$ directions are not explicit. The emergence in high-index directions and bands is relatively weakened when the angle of incidence approaches the transmission directions. There is a relation between the traces of the directions and the distances between the atoms in the corresponding rows. (auth)

13967 INELASTIC SCATTERING OF SLOW ELECTRONS IN GERMANIUM AND SILICON. Borisov, V. L.; Kazeev, Yu. I. (Leningrad Polytechnic Inst.). Sov. Phys.-Solid State (Engl. Transl.); 12: 1746-7(Jan 1971).

Translated from Fiz. Tverd. Tela; 12: 2186-7(Jul 1970).

Secondary electron-emission coefficients σ were measured for (111) Sb-doped Ge and P-doped Si single crystals excited by 400-eV electrons. Monoatomic Ba coatings were used to increase the electron yield. It was found that σ dropped with temperature (20 to 400°C) and with the density of free carriers (10^{13} to 10^{18} cm^{-3}). It is concluded that the mechanism for the σ decrease is the pair interactions of the electron–electron and electron–hole type. (D.L.C.)

13968 SPECTRA OF THE ENERGY LOST BY SLOW ELECTRONS IN CRYSTALS OF AROMATIC HYDROCARBONS. Bubnov, L. Ya.; Frankevich, E. L. (Inst. of Chemical Physics, Chernogolovka, USSR). Sov. Phys.-Solid State (Engl. Transl.); 12: 1726-7(Jan 1971).

Translated from Fiz. Tverd. Tela; 12: 2164-6(Jul 1970).

Characteristic energy loss spectra of 115-eV electrons were measured for polycrystalline pyrene and tetracene and single-crystal anthracene. The strongest lines of anthracene and tetracene correspond to the $^1A_{1g}$–$^1B_{2u}$ transition, while the other lines are attributed to the $^1A_{1g}$–$^1B_{1u}$ transitions. The energy losses are in good agreement with the excitation energies of the vapors of the compounds. Possible reasons for the discrepancy between the losses and the optical absorption spectra are discussed. (D.L.C.)

13969 ANGULAR DISTRIBUTION OF SECONDARY ELECTRONS EMITTED BY A NIOBIUM SINGLE CRYSTAL DUE TO BOMBARDMENT WITH IONS. Begrambekov, L. B.; Kurnaev, V. A.; Sotnikov, V. M.; Tel'kovskii, V. G. (Moscow Engineering Physics Inst.). Sov. Phys.-Solid State (Engl. Transl.); 12: 1738-9 (Jan 1971).

Translated from Fiz. Tverd. Tela; 12: 2178-9(Jul 1970).

Measurements were made on secondary electrons emitted from the (111) plane of a Nb single crystal bombarded with 25-keV Ar ions at ~450°C. The shape of the angular distribution obeys the cosine law but has many small maxima and minima. A shift of the maxima toward larger emission angles relative to the crystal axes is observed. (D.L.C.)

13970 ANISOTROPIC SPATIAL DISTRIBUTION OF IONS SCATTERED BY A SINGLE CRYSTAL. Aissa, M.; Mashkova, E. S.; Molchanov, V. A.; Skripka, Yu. G. (Moscow State Univ.). Sov. Phys.-Solid State (Engl. Transl.); 12: 1643-5(Jan 1971).

Translated from Fiz. Tverd. Tela; 12: 2070-2(Jul 1970).

In an experimental study of the anisotropy in the spatial distribution of 30-keV argon ions scattered by various faces of a Cu single crystal, the anisotropy was found to depend significantly on both the packing density of the atomic rows and on the separation between neighboring rows. (auth)

13971 STUDY OF THE SPUTTERING YIELD AND THE COEFFICIENT OF SECONDARY EMISSION FOR POLYCRYSTALLINE METALLIC TARGETS BOMBARDED WITH Hg^+ IONS IN THE ENERGY RANGE 5 TO 30 keV. Ismail, H. (Paris Univ., Orsay, France). Rev. Phys. Appl.; 5: 759-64(Oct 1970). (In French).

Using a monoenergetic Hg^+ ion beam, a study of the variation in the sputtering yield S and the electron secondary emission coefficient γ as a function of the ion energy E was made for various polycrystalline materials, which could be used in ion sources (or ionic motors). Large variations in S were observed in each period of the periodic table. Smaller values of S were obtained with carbon, titanium, molybdenum, and tantalum (2 to 3 atoms per ion at E = 20 keV). Molybdenum and tantalum gave weak electron secondary emission. The evaporation heat E_1 appeared to be an important parameter, and the sputtering yield varied approximately as a decreasing exponential function of E_1 for a given value of the ion energy. (auth) (France)

13972 DISSOCIATION OF A FAST H_2^+ MOLECULAR ION BEAM COLLIDING WITH THIN CARBON TARGETS. Poizat, J.-C.; Remillieux, J. (Univ., Lyon). Phys. Lett.; 34A: 53-4 (25 Jan 1971).

The cross section for the nondissociation of 2-MeV H_2^+ ions going through thin carbon targets was measured for thicknesses increasing from 3 to 50 μg/cm^2. (auth)

13973 OPTICAL AND INFRARED EMISSION SPECTRA OF ELECTRON-BOMBARDED LIQUID HELIUM. Dennis, Wiley Sam. Houston, Tex.; Rice Univ. (1970). 128p. University Microfilms Order No. 70-23,498.

Thesis.

Liquid helium was bombarded with a beam of 160-keV electrons, and the resulting optical and infrared emission spectra were recorded and analyzed. Great care was taken to ascertain that the recorded spectra resulted from liquid helium rather than beam-vaporized helium. Identification of spectral features was facilitated by comparison of the liquid emission features with those of electron-bombarded dense helium gas. The emission spectrum of liquid helium was found to consist primarily of certain transitions of the He_2^* system: $d^3\Sigma_u^+ \rightarrow b^3\Pi_g(0-0)$, $D^1\Sigma_u^+ \rightarrow B^1\Pi_g(0-0)$, $d^3\Sigma_u^+ \rightarrow c^3\Sigma_g^+(0-0)$, $c^3\Sigma_g^+ \rightarrow a^3\Sigma_u^+(0-0)$ and vibrational structure, and $C^1\Sigma_g^+ \rightarrow A^1\Sigma_u^+(0-0)$ and vibrational structure. The presence of vibrational transitions originating on other than the ground vibrational states (indicating lack of vibrational equilibration) is understood in terms of the structure of the He_2^* states. The lack of vibrational structure in some cases is explained in terms of small Frank–Condon factors. It was found that molecular spectral features of the liquid were slightly shifted (~10 cm^{-1}) toward the violet. It was observed that the singlet spectral features were stronger relative to the corresponding triplet features in the liquid than in the dense gas. This was thought to result from an increased probability of parental recombination of beam-produced ions and electrons in the denser medium, i.e., liquid. In addition to the molecular transitions discussed above, the $3^1S \rightarrow 2^1P$, $3^3S \rightarrow 2^3P$, and $2^3P \rightarrow 2^3S$ atomic lines were tentatively identified. Absence of other atomic features was explained in terms of the reaction $He^* + He \rightarrow He_2^+ + e^-$, which very effectively converts all atomic states lying above 23 eV into He_2^+. Given the correctness of the $2^3P \rightarrow 2^3S$ identification, both the atomic and the diatomic metastable states (2^3S and $a^3\Sigma_u^+$) are present in the liquid. If both states have comparable lifetimes in the liquid, then absolute spectral intensity measurements indicate that the neutral excitation can likely be identified as the diatomic metastable $a^3\Sigma_u^+$ state of He_2^*. (TSS) (Diss. Abstr. Int., B)

Atomic and Molecular Properties

Refer also to abstracts 14277, 14280, 14302, 14316, 14409, 14929, and 14981.

13974 FREE–FREE ABSORPTION COEFFICIENT OF THE NEGATIVE HYDROGEN ION. Stilley, Jerry Lee. Baton Rouge, La.; Louisiana State Univ. (1970). 101p. University Microfilms Order No. 70-18,562.

Thesis.

The dipole adiabatic exchange wave functions of polarized orbital theory were employed to obtain the S → P and P → D contributions to the free–free absorption coefficient of H^- in the dipole length and dipole velocity formulations. The length and velocity results have been found to be in good agreement, 3% or less at the longer wavelengths where free–free absorption dominates bound–free absorption. These results were found to be in good agreement with other recent calculations and with solar observations. The effects of atomic distortion were found to be small at longer wavelengths (1% for length formulation and 6% for velocity formulation) making inclusion thereof relatively unimportant for astrophysical applications. Asymptotic matrix elements convergent over all space reproduce the full results to within 10%. (Diss. Abstr. Int., B)

13975 THEORETICAL STUDY OF THE $^3\Pi_g$ AND $^1\Pi_g$ STATES OF He_2. Watson, Mary Beatrice Nelson. Austin, Tex.; Univ. of Texas (1970). 87p. University Microfilms Order No. 70-18,308.

Thesis.

Ab initio quantum mechanical calculations are made on the He_2 states $^3\Pi_g$ and $^1\Pi_g$. The calculations of these electronic potential surfaces are made first using small wave functions of nine and six terms, respectively, and then larger wave functions of 57 and 39 terms, respectively, are used. The potential curves obtained using the large wave functions are then adjusted using a semi-empirical technique. Vibrational levels and the five lowest rotational levels of each vibrational level are then fitted to both the ab initio potential curves obtained using the large wave functions and also the adjusted curves. These results are then compared with experimental values. (Diss. Abstr. Int., B)

13976 SCREENING NUMBERS AND THE SCALED HYDROGEN-LIKE WAVE FUNCTIONS FOR SOME SYSTEMS WITH LARGE ATOMIC NUMBERS. Saxena, K. M. S. (Simon Fraser Univ., Burnaby, B. C.). Can. J. Phys.; 48: 2824-30(1 Dec 1970).

Values of the screening numbers σ_{nl} for obtaining the analytic scaled hydrogen-like wave functions are calculated for a large number of atoms and ions from Z = 87 to Z = 103. (auth) (Canada)

13977 BREAKDOWN OF THE 2^1P AND 2^3P LEVELS OF He IN A GLOW DISCHARGE. Vasilenko, L. S.; Lisitsyn, V. N.; Notkin, G. E.; Chebotaev, V. P. Opt. Spectrosc. (USSR) (Engl. Transl.); 28: 584-8(Jun 1970).

Translated from Opt. Spektrosk.; 28: 1085-92(Jun 1970).

The processes of breakdown of the 2^1P and 2^3P levels under electronic and atomic collisions in a helium discharge were studied. The method of selective optical excitation was used as the basis of the investigation. It has been shown that the 2^1P and 2^3P helium levels under consideration have a cross section $<10^{-16}$ cm^2 for breakdown by atom–atom collisions. Study of the magnitude and sign of the modulation of the population of a number of levels caused by selective optical excitation of the 2^1P level permits formation of an opinion about the general excitation pattern of the levels of helium. (auth)

13978 CLASSICAL-PATH CALCULATION OF THE IMPACT-BROADENING OPERATOR FOR THE STARK BROADENING OF H_α. Bacon, M. E. (Aerospace Research Labs., Wright-Patterson AFB, Ohio). Phys. Rev., A; 3: 825-8(Feb 1971).

The impact-broadening operator Φ for the hydrogen line H_α is calculated by solving numerically for the S matrices using the straight-line classical-path approximation. All contributing multipoles in the perturber (free-electron)–atom interaction [V(t)] are included; time ordering of the operators in the S matrices is retained. The matrix elements are compared with previous approximations based on the same model; the effects on the H_α line profile are considered. (auth)

13979 MASS-SPECTROMETRIC INVESTIGATION OF SURFACE IONIZATION. VII. THE FIRST IONIZATION POTENTIAL OF CURIUM. Smith, David H. (Oak Ridge National Lab., Tenn.). J. Chem. Phys.; 54: 1424-5(1 Feb 1971).

The surface ionization comparison technique was used to determine the first ionization potential of Cm. The technique involves measuring the ratio of the intensity of the ion beam of the element in question to that of a standard after desorption from a hot surface. The curium sample consisted largely of ^{248}Cm, the standard was ^{238}U, and the surface was polycrystalline W. The value obtained for the first ionization potential of Cm was 6.18 ± 0.09 eV. (A.G.W.)

13980 ATOMIC L-SHELL COSTER–KRONIG, AUGER, AND RADIATIVE RATES AND FLUORESCENCE YIELDS FOR Na THROUGH Th. McGuire, Eugene J. (Sandia Labs., Albuquerque, N. Mex.). Phys. Rev., A; 3: 587-94(Feb 1971).

Calculated Auger, Coster–Kronig, and radiative transition rates are used to compute atomic L-shell Coster–Kronig and fluorescence yields. The results are compared with the other calculations, experimental yield determinations, and radiative half-width measurements. (auth)

13981 QUANTUM MECHANICS OF A DOUBLE PERTURBATION: APPLICATION TO THE ZEEMAN EFFECT OF METASTABLE HYDROGEN MOLECULES. Lichten, William (New Haven Public Schools). Phys. Rev., A; 3: 594-603(Feb 1971).

A general theorem is derived, which applies to any quantum-mechanical system subject to two perturbations H and G. It is shown that the eigenvalues of the system can be found by first solving exactly the secular equation in H. Then the first-order perturbation of the energy by G can be written explicitly without solving for the eigenfunctions. This leads to a simple method for finding the exact Landé g factors for the Zeeman effect of any quantum-mechanical system. These results are applied to the Zeeman effect of the hydrogen molecule in the metastable $c^3\pi_u$ state. Jette and Cahill's theory of the Zeeman effect is extended to cover all magnetic fields. Excellent agreement is found between experimental g factors and theory. At higher magnetic fields, "anti-crossings" are found between pairs of states for which $\Delta J = \pm1, \pm2$, $\Delta F = 0, \pm1, \pm2$, and $\Delta M_F = 0$. The repulsion between these levels is very small, of the order of a few Mcps. This causes the noncrossing rule of von Neumann and Wigner to be violated experimentally. The Landau–Zener theory of level crossings is applied. It is shown that the observed loss of quantization in the molecular-beam experiments is consistent with theory. (auth)

13982 ENERGY DEPENDENCE OF AUTO-IONIZATION IN BETA DECAY. der Mateosian, E. (Brookhaven National Lab., Upton, N. Y.). Phys. Rev., A; 3: 573-7(Feb 1971).

Auto-ionization accompanying β decay was studied in an equilibrium mixture of $^{90}Sr-^{90}Y$ by a comparison of the intensities of K x rays accompanying these decays. Since both nuclides undergo β decay of the unique first-forbidden type, the main difference between the two decays is a factor of ~4 in endpoint energy. The ratio of the amount of x rays accompanying the ^{90}Y decay to the amount accompanying ^{90}Sr decay was found to be

1.3. This is interpreted to mean that the direct collision process plays an unimportant role in auto-ionization in these two isotopes and that it is most likely that the probability of auto-ionization in β decay is independent of the energy of the β particle in decays with endpoint energies high compared with the K-shell ionization energy. (auth)

13983 QUADRUPOLE CRYSTALLINE ELECTRIC FIELD SHIELDING AND ANTISHIELDING FACTORS AT SOME RARE-EARTH AND HEAVY IONS. **Gupta, R. P.; Rao, B. K.; Sen, S. K. (Univ. of Manitoba, Winnipeg, Can.). Phys. Rev., A; 3: 545-53(Feb 1971).**

The results of calculations of Sternheimer crystalline electric-field shielding and antishielding factors for Pr^{3+}, Tm^{3+}, W^+, and Au^+ ions at all the core electronic sites, the unfilled valence electron site, and the nuclear site of each ion are reported. The calculations take into account the effect of polarization of all the closed shells within the ions, including the exchange interaction terms. Mann's relativistically corrected Hartree–Fock (HF) wave functions were used in the computations. The calculations thus extend and improve upon the previous calculations by Sternheimer and others who did the computations for rare-earth ions at the location of the 4f electron and at the nuclear site only. The present values of shielding and antishielding factors λs at the location of the 4f electron and at the nuclear site for Pr^{3+} and Tm^{3+} ions agree well with previous calculations and measurements. The possibility of experimentally determining the quadrupole splittings of the atomic-core level by the recently developed technique of electron spectroscopy for chemical analysis (ESCA), which underlines the great significance of these calculations, is discussed. (auth)

13984 LONG-RANGE INTERMOLECULAR FORCES USING GAUSSIAN BASIS FUNCTIONS: A MODEL CALCULATION. **Singh, T. R.; Meath, William J. (Univ. of Western Ontario, London). J. Chem. Phys.; 54: 1137-41(1 Feb 1971).**

The charge-induced dipole induction energy and the dipole–dipole dispersion energy for the ground state $H-H^+$ and $H-H$ interactions are used as model energies for investigating the feasibility of using Gaussian basis functions to calculate long-range intermolecular forces. The use of various types of Gaussian basis sets to represent the first-order wave function, $\Psi^{(1)}$, in the calculation of the interaction energies and the errors introduced into the calculations by using Gaussian representations of the exact zeroth-order wave functions for the isolated atoms are considered. Satisfactory long-range forces, at least for the simple interactions considered here, can be obtained by using small Gaussian basis sets to represent the interaction, that is $\Psi^{(1)}$, and/or the zeroth-order wave function. (auth)

13985 ON THE USEFULNESS OF APPROXIMATE EXCHANGE INTEGRALS IN CALCULATIONS OF THE LONG-RANGE FORCES. **Piela, L. (Univ. of Warsaw). Chem. Phys. Lett.; 6: 591-2 (15 Dec 1970).**

The usefulness of Mulliken and Mataga–Nishimoto approximations in perturbational calculations is investigated. The calculations are carried out for the hydrogen molecule in its ground and first excited states by a method similar to the Jansen–Byers Brown method. (auth)

13986 PRECISION MEASUREMENT OF THE HYPERFINE STRUCTURE OF ^{175}Lu WITH THE ATOMIC BEAM MAGNETIC RESONANCE METHOD. **Figger, H.; Wolber, G.; Penselin, S. (Univ., Bonn). Phys. Lett.; 34A: 21-2(25 Jan 1971).**

The hyperfine-structure separations of both doublet states of the ground configuration $6s^2$ 5d of ^{175}Lu were remeasured with high precision with the atomic-beam magnetic-resonance method. Despite the greater accuracy a quadrupole hfs anomaly between ^{175}Lu and ^{176m}Lu was not found. (auth)

Positronium, Muonium, and Mesic Atoms and Molecules

Refer also to abstracts 14290 and 14441.

13987 POSITRON DIFFUSION AND ANNIHILATION IN HELIUM GAS. **Leung, Cho Yuk. Ontario, Can.; Univ. of Toronto (1969). National Library of Canada, Ottawa.**
Thesis.

Positron annihilation and diffusion in helium gas was studied by the method of delayed coincidence timing of annihilation using a ^{22}Na source of positrons. A special system of instrumentation was designed and built for this purpose. To achieve high purity of helium for this experiment, a special "molecular sieve filter" capable of removing unwanted gas molecules from the helium supply was designed. A special chamber capable of standing up to 600 psi at 77°K with built-in accelerating rings for electrostatically accelerating positrons was constructed. A high-speed low-jitter fast-current-mode trigger was designed and built for delayed coincidence time measurement to give a system resolution with large NaI (Te) counters of ~4 nsec fwhm. Coincidence timing experiments were performed both at room temperature and at 77°K with helium gas density ranging from 20 to 70 amagats. The nonexponential shoulder in the free positron component of the annihilation time spectrum was confirmed for helium and was found to have a breadth of more than 1300 nsec amagat, corresponding to a Ramsauer–Townsend type minimum in the diffusion cross section Q of about 0.04 πa_0^2. Contrary to the findings of Marder et al. (1956), positronium enhancement was not observed up to an applied accelerating field of 33 volts/cm amagat. It was found that around 17.7 eV, $Q > 0.115\ \pi a_0^2$. The effective number of electrons per atom, taking part in annihilation, was found to be $Z_{eff} = 3.680 \pm 0.025$ at thermal energy, dropping to about 3.3 near 1 eV. These results are in agreement with the findings of Lee and Jones (1969) and are also compatible with Drachman's (1968) theoretical predictions. The Ps annihilation rates are not compatible with a linear quenching curve as is usually assumed, though they are unlike Celitan's findings for argon. A parabolic fit seems to be called for. No logical support for such a fit was eminent. There is, however, a subtle suggestion that a third component such as the 2S state of Ps representing longer-lived annihilation may be present in the annihilation spectrum. (Diss. Abstr. Int., B)

13988 POSITRON ANNIHILATION RATES IN LANTHANUM HYDRIDES. **Green, Richard; Bos, William G.; Huang, W. F. (Univ. of Louisville, Ky.). Phys. Rev., B; 3: 64-8(1 Jan 1971).**

Positron annihilation rates λ_1 and λ_2 are reported for a series of lanthanum hydride samples of compositions from $LaH_{2.0}$ to $LaH_{2.9}$. From $LaH_{2.0}$ to $LaH_{2.7}$, λ_1 was approximately constant at 3.36 nsec^{-1}. At higher compositions, λ_1 increased with increasing hydrogen content. A slower rate component λ_2 was observed for annihilation in lanthanum hydrides, but the associated intensity was very low. New data are also reported for lithium hydride as follows: $\lambda_1 = 3.12$ nsec^{-1}, $\lambda_2 = 0.68$ nsec^{-1}, and $I_2 = 6.30\%$. (auth)

13989 SLOW MUON DEPOLARIZATION IN A SINGLE CRYSTAL OF GYPSUM ($CaSO_4.2H_2O$). **Schenck, Alexander (Univ. of Washington, Seattle); Crowe, Kenneth M. Phys. Rev. Lett.; 26: 57-61(11 Jan 1971).**

Polarized muons were stopped in a single crystal of $CaSO_4 \cdot 2H_2O$ placed in a magnetic field. Muon precession displayed a beat behavior and a slow —μsec— decrease of the muon spin polarization; these effects were found to be strongly dependent on crystal orientation in the field. Consistent explanation of the results was achieved by assuming that the muon occupied a normal proton site and by considering the local field effects due to the dipole–dipole interaction of muon–proton pairs. (auth)

13990 ORDER $(m_e/m_\mu)\alpha^2 \ln\alpha^{-1}$ CORRECTIONS TO THE MUONIUM HYPERFINE STRUCTURE. **Fulton, Thomas (Johns Hopkins Univ., Baltimore); Owen, David A.; Repko, Wayne W. Phys. Rev. Lett.; 26: 61-3(11 Jan 1971).**

A calculation of the $(m_e/m_\mu)\alpha^2 \ln\alpha^{-1}$ corrections to the hyperfine splitting (ν_m) of the muonium ground state is reported. The result, $\Delta\nu_m = 24(m_e/m_\mu)^2[1 + (m_e/m_\mu)]^{-5}c\alpha^4 R_\infty \ln\alpha^{-1} = 0.0252$ MHz (5.6 ppM), shifts the theoretical value for ν_m to within one standard deviation of the most recent experimental determination of the muonium hyperfine interval by the Chicago–Illinois group. (auth)

13991 METASTABILITY OF THE 2s STATE OF MUONIC HYDROGEN. **Kodosky, G.; Leon, M. (Rensselaer Polytechnic Inst., Troy, N. Y.). Nuovo Cim.; 1B: 41-7(11 Jan 1971).**

It was found that the otherwise metastable 2s level of muonic hydrogen will rapidly be depopulated by collisions with neighboring hydrogen atoms at reasonable hydrogen densities, $\sigma \simeq 4a_0^2$. This is because of the Stark transitions $2s \rightleftharpoons 2p$ that take place when the mesic atom passes through a hydrogen atom. The conclusion fails for slow (kinetic energy $\lesssim$ 0.3 eV) μp atoms, but these are expected to be rare. (auth)

13992 PHOTON–PHOTON SCATTERING CONTRIBUTION TO THE DECAY RATE OF ORTHOPOSITRONIUM. **Pascual, P.; de Rafael, E. (CERN, Geneva). Lett. Nuovo Cim.; 4: 1144-6(12 Dec 1970).**

The contribution of photon–photon scattering to the 3-gamma-ray annihilation rate of orthopositronium was calculated by two different methods. Each method gave a negative correction; this result increases the existing discrepancy between theoretical and experimental values. (A.G.W.)

13993 POSITRON ANNIHILATION IN METHANE GAS. Smith, P. M.; Paul, D. A. L. (Univ. of Toronto). Can. J. Phys.; 48: 2984-90(15 Dec 1970).

The annihilation of positrons in methane gas at room temperature was measured at pressures below 2 atm. The annihilation rate for the free positron component is proportional to the gas density and corresponds to an effective number of electrons per molecule taking part in annihilation, $Z_{eff} = 139.6 \pm 1.0$ (standard error). The quenching of orthopositronium corresponds to $^1Z_{eff} = 0.57 \pm 0.07$. Resonance annihilation is discussed in a general way. (auth) (Canada)

13994 PION FINITE SIZE AND MESIC ATOMS. Daniel, H. (Technische Hochschule, Munich). Z. Naturforsch.; 25a: 1510-11(Oct 1970).

Contrary to the point-like muon the pion has a spatial extension. The effect of this finite size on levels of π-mesic atoms is estimated to be small but not necessarily negligible. (auth)

Collision Phenomena

13995 (AD–711664) TABLES OF SCATTERING AMPLITUDES AND SPIN POLARIZATIONS OF 25, 50, 75, 150, 175, 200, 300, 400, 600, 800 eV ELECTRONS SCATTERED ELASTICALLY FROM H, He, C, Ne, Ar, Kr, Rb, Xe, Cs, Au, Hg, Pb, AND Bi. I. Fink, Manfred; Yates, Albert C. (Texas Univ., Austin. Electronics Research Center). 15 May 1970. 156p. (TR–88; AFOSR–70-1652-TR). NTIS.

In order to investigate the influence of the spin in elastic low-energy electron scattering from gaseous atoms, the Dirac equation was solved numerically. The complex scattering amplitudes, which describe the scattering process, are given. From the tables it is possible to determine the elastic differential cross section, the spin polarization of elastically scattered electrons, the asymmetry of scattered electrons when the incoming electrons are already polarized, and the change of the polarization vector in a scattering experiment. The employed scattering potentials are relativistic Hartree potentials. The exchange of the electrons was not included since it contributes very little, with the exception of the smallest angles. In this angular range the uncertainty in the wave functions for very large impact parameter is so significant that the addition of the approximation exchange would have distorted the values even further. Thus the scattering factors for theta < 10° have to be used with special care. (auth) (USGRDR)

13996 ABSOLUTE DOUBLY DIFFERENTIAL IONIZATION CROSS SECTIONS FOR Ne^+–Ne AND Ar^+–Ar COLLISIONS. Cacak, Robert Kent. Lincoln, Nebr.; Univ. of Nebraska (1970). 204p. University Microfilms Order No. 70-17,709.

Thesis.

Absolute differential ionization cross sections for the collisions of neon ions with a neon gas target and argon ions with an argon gas target were measured. The cross sections were doubly differential in angle and energy of the ejected electrons. The energy range of the ions was 50 to 300 keV. An ion beam from a Cockcroft–Walton accelerator passed into the chamber containing the target gas. Electrons produced by the ion–atom collisions passed through a nearly field-free region into an electrostatic energy analyzer. After being energy-analyzed, the electrons were individually counted by an electron-multiplier detector. The angle that the detector–analyzer assembly made with the ion beam was variable, and the assembly's position determined the angle at which the electrons were observed. From a knowledge of the geometry of the scattering chamber and target-defining slits, the number of electrons ejected, the number of ions passing through the gas, the pressure of the target gas, and the efficiency of the detection system, an absolute cross section was determined. The experimental results are compared with the predictions of the Fano–Lichten electron-promotion model, and the consequences of the model agree with the experimental results. Calculations based on the results of the Russek statistical evaporation model are also compared with experiment. A simple model for Auger excitation is compared to the cross section for Auger electron emission, and the results tend to support the Fano–Lichten model. (Diss. Abstr. Int., B)

13997 CROSS SECTIONS FOR EXCITATION OF N_2^+ FIRST NEGATIVE AND MEINEL BANDS BY ELECTRON IMPACT. Mirza, Ishaq Muhammad. College, Alaska; Univ. of Alaska (1969). 100p. University Microfilms Order No. 70-20,679.

Thesis.

The absolute emission cross sections for the (0,0), (0,1), and (0,2) N_2^+ first negative bands and (4,1), (2,0), and (3,1) N_2^+ Meinel bands produced by 0.07- to 4.0-keV electrons were measured. A photon counting technique was used. The maximum emission cross sections for the (0,0), (0,1) and (0,2) N_2^+ first negative bands are 16.86×10^{-18}, 6.06×10^{-18}, and 1.16×10^{-18} cm², respectively, and for the (4,1), (2,0), and (3,1) N_2^+ Meinel bands are 6.76×10^{-19}, 6.02×10^{-18}, and 2.35×10^{-18} cm² respectively, at 90 to 110 eV. The average ratio of the cross sections for the (0,0), (0,1), and (0,2) N_2^+ first negative bands is 1 : 0.34 : 0.065 and for the (2,0), (3,1), and (4,1) N_2^+ Meinel bands is 1 : 0.4 : 0.12. The results of the present investigation are compared with the available experimental and theoretical results. The average ratio of the total ionization cross section of N_2 to the emission cross section of λ3914Å is 15. The apparent absolute excitation cross sections of the three vibrational levels (v′ = 2, 3 and 4) of the N_2^+ A $^2\Pi_u$ state are calculated using Franck–Condon factors. The experimentally determined relative vibrational populations are compared with the theoretical values obtained from the Franck–Condon factors of excitation. The apparent excitation cross section of the A $^2\Pi_u(N_2^+)$ state is twice the apparent excitation cross section of the B $^2\Sigma_2^+$ (N_2^+) state. The excitation functions of both the N_2^+ first negative and the Meinel bands are similar in nature. The excitation of the v′ = 0 vibrational level of B $^2\Sigma_2^+$ (N_2^+) state is of the order of 0.1 of the total ionization cross section of N_2 by electron impact. This corresponds to an energy flux of 60 ergs cm^{-2} sec^{-1} for the incident electrons in a type of IBC III aurora. The emission cross sections of both the N_2^+ first negative and N_2^+ Meinel bands display an E^{-1} ln E dependence as described by the Bethe–Born approximation above 300 eV. (TSS) (Diss. Abstr. Int., B)

13998 MEASUREMENT OF THE EFFECTIVE CROSS SECTIONS AND EXCITATION FUNCTIONS FOR BANDS OF THE FIRST NEGATIVE SYSTEM OF THE MOLECULAR ION N_2^+ ON EXCITATION OF NITROGEN BY FAST ELECTRONS. Koppe, V. T.; Koval, A. G.; Fizgeer, B. M.; Fogel, Ya. M.; Ivanov, S. I. (Kharkov State Univ.). Zh. Eksp. Teor. Fiz.; 59: 1878-83(Dec 1970). (In Russian).

The effective cross sections for the (0,0), (0,1), (0,2), (0,3), (1,2), (1,3), and (1,4) bands of the first negative system of the N_2^+ ion and the multiplet lines λ = 5001 to 5005 Å in the N II spectrum are measured at energies between 0.5 and 20 keV. Nitrogen was excited by electrons with energies between 0.5 and 20 keV. In the region of overlapping energies the experimental effective cross sections are in good agreement with the data of others. The course of the excitation function of the bands and lines investigated at energies between 0.8 and 20 keV can be satisfactorily described by a formula. (auth)

13999 FORMATION OF SLOW ATOMIC NEGATIVE OXYGEN IONS IN COLLISIONS BETWEEN FAST PROTONS OR HYDROGEN ATOMS AND O_2 MOLECULES. Gusev, V. A.; Oksyuk, A. A.; Fogel, Ya. M.; Pilipenko, D. V. (Physical-Technical Inst., Kharkov). Zh. Eksp. Teor. Fiz.; 59: 1909-16(Dec 1970). (In Russian).

A method is developed for investigation of processes involving the formation of negative ions in collisions between fast ions or atoms and gas molecules. The effective cross sections for O^- ion production in collisions between 3- to 50-keV hydrogen ions or atoms and oxygen molecules are measured in relative units. (auth)

14000 EFFECTIVE CROSS SECTIONS FOR ELECTRON EXCITATION OF TRANSITIONS BETWEEN EXCITED STATES IN Ba^+ AND Sr^+ IONS. Beigman, I. L.; Vainshtein, L. A.; Dronov, A. P.; Kudryavtsev, E. M. (Lebedev Inst. of Physics, Moscow). Zh. Eksp. Teor. Fiz.; 59: 1991-8(Dec 1970). (In Russian).

The effective cross sections for inelastic scattering of electrons by excited Ba^+ and Sr^+ ions are found from data on the electron width of the corresponding spectral lines. The investigations are performed with a shock tube, and the electron concentrations required for the calculations are determined by two independent methods. The experimental values of the cross sections are in good agreement with results of calculations based on the Born–Coulomb approximation with normalization. (auth)

14001 CHARGE EXCHANGE OF CARBON AND NITROGEN IONS IN NITROGEN GAS. Tonuma, Tadao; Miyazawa, Yoshitoshi; Karasawa, Takashi; Kohno, Isao (Inst. of Physical and Chemical Research, Saitama, Japan). Jap. J. Appl. Phys.; 9: 1306-11 (Nov 1970).

Electron-loss and-capture cross sections of carbon and nitrogen ions were measured at 3.5 to 7 MeV/nucleon, i.e. velocities of 2.6 to 3.7×10^9 cm/sec in nitrogen gas. Cross sections obtained were σ_{45}, σ_{56}, and σ_{65} for carbon ions and $\sum_{k=5}^{7} \sigma_{4k}$ for nitrogen ions when they passed through the charge-exchange (collision) chamber. Cross sections of single electron loss σ_{45} and σ_{56} are nearly proportional to v_0/v and those of single electron capture σ_{65} are proportional to $(v_0/v)^6$ where v_0 is the atomic unit of velocity and v is ion velocity. The beam attenuation of N^{4+} ions, accelerated in the IPCR 160-cm cyclotron, caused by charge exchange at collisions with residual gases is compared with the attenuation calculated from measured $\sum_{k=5}^{7} \sigma_{4k}$ in nitrogen gas. (auth)

14002 ELECTRON IMPACT EXCITATION AND IONIZATION STUDIES OF THE RARE GASES. Grissom, John Thomas. Knoxville, Tenn.; Univ. of Tennessee (1970). 177p. University Microfilms Order No. 70-20,308.

Thesis.

The trapped-electron technique has been used in conjunction with the retarding potential difference technique to measure the electron-impact excitation spectra of He, Ne, and Ar from the energy threshold of the first excited state up to approximately 80 eV with an energy resolution of 0.1 to 0.3 eV. Below the ionization threshold the excitation spectra exhibit structure corresponding to the usual singlet–singlet and singlet–triplet transitions. In the slow-electron continuum region above the ionization potential the spectra were found to have structure in the energy regions corresponding to p-subshell double-electron excitation and s-subshell single-electron excitation. In addition, at least some and possibly many of the spectral features in these energy regions may be due to interference resonances resulting from the formation of negative-ion compound states in the electron scattering interaction. Previously reported negative-ion resonances are observed in He, and conclusive evidence of new negative-ion states is presented for Ne. Unambiguous interpretation of the observed structure in the analogous energy region of the Ar spectrum is complicated by the presence of many autoionizing levels. The general behavior of the slow-electron continuum appears to warrant additional consideration. The cross section for producing slow electrons in direct ionization was measured for several incident electron energies above the first ionization potential for He, Ne, and Ar. New structure in the ionization cross section of He at 57.21 and 58.31 eV corresponding to the previously observed negative-ion states He^- $(2s^22p)$ ^2P and $(2s2p^2)$ ^2D, respectively, was observed. The ionization cross sections of He, Ne, Ar, Kr, and Xe were measured from threshold to 150 eV. The results are compared to previous measurements. (Diss. Abstr. Int., B)

14003 SMALL-ANGLE SCATTERING OF 10-keV ELECTRONS IN He, Ne, AND Ar. van der Wiel, M. J. (FOM-Instituut voor Atoom-en Molecuulfysica, Amsterdam). Physica; 49: 411-24(26 Oct 1970).

An experiment is reported in which fast electrons scattered by He, Ne, and Ar are detected in coincidence with the ions formed. From the measurements of the scattering intensity at small angles, optical oscillator strengths were calculated. For singly charged ions these oscillator strengths agree with those obtained from photoionization and -absorption cross sections up to the threshold for double ionization. Above this threshold deviations are found for Ne and Ar, which are ascribed to the contribution of multiple ionization in the photon experiments. (auth)

14004 CROSS SECTIONS FOR Ar L-SHELL AND Ne K-SHELL X-RAY EMISSION IN HEAVY ION–ATOM COLLISIONS. Saris, F. W.; Onderdelinden, D. (FOM-Instituut voor Atoom- en Molecuulfysica, Amsterdam). Physica; 49: 441-60(26 Oct 1970).

Cross-section measurements for soft-x-ray emission produced by Ar^+, Ne^+, and H^+ on Ar and Ne^+ on Ne are reported. The x radiation, which is detected by a proportional counter, corresponds to vacancies in the Ar L shell and Ne K shell. The cross section appears several orders of magnitude smaller for proton impact than for heavy-ion bombardment; this shows the difference in excitation mechanisms. Mean fluorescence yields are deduced from the experimental emission cross sections and the Auger excitation cross sections of the inner shells involved. It is observed that the fluorescence yield is influenced by the mechanism for primary vacancy creation. Finally, from the energy dependence of the cross section near threshold, critical internuclear distances for inner-shell excitation are determined. (auth)

14005 TOTAL CROSS SECTION MEASUREMENTS OF K ON RARE GASES IN THE VELOCITY RANGE OF 300 TO 15000 m/s. Politiek, J.; Schipper, J. J. M.; Los, J. (FOM-Instituut voor Atoom- en Molecuulfysica, Amsterdam). Physica; 49: 165-91 (19 Oct 1970).

Cross sections of potassium on noble gases were measured for two angular resolutions in the velocity interval of 300 to 15000 m/sec. The thermal oven (300 to 1500 m/sec) and the sputter source (1200 to 15000 m/sec) were used as atom sources. The measurements in the high-velocity range were analyzed with a Lennard–Jones (LJ) (n, 6) potential model. It was found that an n = 7 gives the best fit to the measurements. The Van der Waals constant C_6, being $7\epsilon\gamma_m^6$ for a LJ (7, 6) potential model, is far too large compared with the theoretical value. This means that the attractive part of the LJ (7, 6) potential is too strong for large intermolecular distances. However, when determining the C_6 value from the thermal measurements, a good agreement was found between experiment and theory. For the system K–Ar the measurements were also analyzed with an exp(α, 6) potential model. It was found that an $\alpha = 10.25$ describes the measurements better than a LJ (7, 6) potential model does. The ϵ and γ_m values agree very well with those determined by Düren et al. from thermal measurements. The exp(10.25, 6) potential model was used when correcting the two series of incomplete cross sections. After the correction was applied, the deviation between the two series was about 1%. (auth)

14006 ELECTRON CAPTURE BY POSITRONS FROM MOLECULAR HYDROGEN. Sural, D. P.; Mukherjee, S. C. (Indian Association for the Cultivation of Science, Calcutta). Physica; 49: 249-60(19 Oct 1970).

The cross sections for electron capture by positrons from molecular hydrogen forming positronium are calculated in the Born approximation for different incident energies. The exact numerical results are compared with those obtained using a simple peaking approximation. (auth)

14007 ANOMALIES IN THE Z DEPENDENCE OF MEAN CHARGES OF HEAVY IONS IN HELIUM AND AIR. Petrov, L. A.; Karnaukhov, V. A.; Bogdanov, D. D. (Joint Inst. for Nuclear Research, Dubna, USSR). Zh. Eksp. Teor. Fiz.; 59: 1926-31(Dec 1970). (In Russian).

The mean charges of heavy ions moving through air or helium with a velocity ~10^9 cm/sec are measured between krypton and tungsten by means of a gas-filled mass separator. It is shown that the mean charge is approximately proportional to the velocity (for krypton). Deviations from proportionality can be accounted for by the expression $\bar{e} = av + b$; b having different signs for helium and air. For ions lying between Kr and Cs the dependence of the mean charge on Z obeys the formula $\bar{e} \sim Z^n$ where $n = 0.57 \pm 0.07$ for helium and $n = 0.6 \pm 0.1$ for air. The situation changes for the rare earth elements, growth of $\bar{e}$ ceasing with increase of Z. For terbium the mean charge is 15% lower than expected on the basis of the extrapolation. This anomaly is ascribed to shell effects. Evidently, filling up of the inner 4f shell results in a decrease of the cross section for electron loss. The relation between the directly measured charge and the effective charge defining energy losses is discussed. (auth)

14008 ELECTRON-EXCITATION CROSS SECTIONS FOR X-RAY SERIES OF CHLORINE, ARGON, AND XENON. Dolgov-Savelev, G. G.; Panchenko, V. E. Opt. Spectrosc. (USSR) (Engl. Transl.); 28: 575-8(Jun 1970).

Translated from Opt. Spektrosk.; 28: 1065-71(Jun 1970).

The dependence of the electron-excitation cross sections for the K series of chlorine and argon and for the L series of xenon on electron energy in the range from 3 to 16 keV was investigated using total intensities of these series. (auth)

14009 TWO AUTODETACHING STATES OF O^-. Edwards, A. K.; Risley, J. S.; Geballe, R. (Univ. of Washington, Seattle). Phys. Rev., A; 3: 583-6(Feb 1971).

Two autodetaching states of O^- were found by observing the electron energy spectrum of O^- ions excited in collisions with a He target at keV beam energies. The energies of the states were measured as 10.112 and 12.115 ± 0.010 eV. The H^- ^1S, ^3P, and ^1D autodetaching states below the n = 2 hydrogen level are excited in O^- on H_2 collisions, and the Ar^- autodetaching states below the first excited argon level are formed in O^- on Ar collisions. No structure in the electron energy spectrum was seen for collisions of O^- on O_2 or Ne. (auth)

14010 FADDEEV EQUATIONS FOR ATOMIC PROBLEMS. IV. CONVERGENCE OF THE SEPARABLE-EXPANSION METHOD FOR LOW-ENERGY POSITRON–HYDROGEN PROBLEMS. Kramer, Paul J.; Chen, Joseph C. Y. (Univ. of California, San Diego, La Jolla). Phys. Rev., A; 3: 568-73(Feb 1971).

The separable-expansion method for solving the Faddeev equations is applied to the positron–hydrogen system at energies below the positronium-formation threshold. The results for the scattering length and phase shift are compared with those obtained by other methods. The three-body bound state and resonance obtained using only the first few terms in the separable expansion are shown to disappear when more terms are included in the expansion. The problem of convergence of the separable-expansion method in the Strumian-function representation is discussed. (auth)

XUM

14011 CHARGE-TRANSFER EXCITATION PRODUCED IN COLLISIONS OF He^+ AND N_2^+ WITH ALKALI ATOMS. Salop, A.; Lorents, D. C.; Peterson, J. R. (Stanford Research Inst., Menlo Park, Calif.). J. Chem. Phys.; 54: 1187-95(1 Feb 1971).

Optical excitation produced in collisions of He^+ and N_2^+ with alkali atoms was investigated using a crossed-beam apparatus. Studies of the spectral radiation were made in the near uv and visible wavelength region for ion kinetic energies 50 to 1600 eV. For He^+ on K and Rb, the spectra observed were identified primarily with excited alkali ions resulting from electron capture into the ground state of He. The relative weakness of near-resonant excitations and the generally small magnitude of the emission cross sections are explained by the fact that the active electron moves from a closed shell of K or Rb to the 1s shell of He; orbital overlap requires a close encounter in which the atoms are strongly perturbed. For N_2^+ on K, the predominant spectra are the bands of the second positive system in N_2 resulting from electron capture into the excited C $^3\Pi_u$ states of N_2. Emission cross sections were large (10^{-17} to 10^{-16} cm^2) having energy dependence characteristic of near-resonant charge-transfer reactions and the population distribution of the various vibrational states corresponded to the Franck–Condon factors for transitions between N_2^+(X) and N_2(C). These features arise because the outermost electron of the alkali moves to an excited orbital of N_2 so that orbital overlap favors a transfer at large distances, a process in which the collision partners are only slightly perturbed. (auth)

14012 ENERGY TRANSFER BETWEEN N_2 AND ELECTRONICALLY EXCITED INERT GAS ATOMS AND IONS. Kassal, T. T.; Fishburne, E. S. (Grumman Aerospace Corp., Bethpage, N. Y.). J. Chem. Phys.; 54: 1363-8(1 Feb 1971).

Collisions of the second kind between N_2 and metastable inert gas atoms and ions were studied in order to investigate the energy exchange mechanism. Excited inert gas atoms are created by means of an electron beam. The state of the nitrogen molecule immediately after the energy exchange is determined by examining the spectra produced by the excited nitrogen molecule. A nonthermal rotational excitation appears to accompany most of the electronic energy transfer processes. In the case of the reaction between Kr^+ and N_2, the rotational excitation is limited to the N_2^+ (B $^2\Sigma_u^+$) v = 1 level. With the collision between a metastable argon atom and N_2, the rotational excitation is limited to the v = 0 level of the N_2 (C $^3\Pi_u$) state. The Franck–Condon factors for the change in vibrational levels during an electronic transition are not obeyed during either of these processes. (auth)

14013 ELECTRON-IMPACT EXCITATION FUNCTIONS FOR THE α $^1\Pi_g$ AND D $^3\Sigma_u^+$ STATES OF N_2. Freund, Robert S. (Bell Telephone Labs. Inc., Murray Hill, N. J.). J. Chem. Phys.; 54: 1407-9(1 Feb 1971).

The emission spectrum of N_2 excited by ~16-eV electrons and observed with 2.5-nm optical resolution is reported. Optical excitation functions for the C $^3\Pi_u$, a $^1\Pi_g$, and D $^3\Sigma_u^+$ states of N_2 are also shown. Possible sources of error and interpretation of results are discussed briefly. (A.G.W.)

14014 INELASTIC ELECTRON SCATTERING FROM NITROUS OXIDE BETWEEN 5.0 AND 20.0 eV ENERGY LOSS. Weiss, M. J.; Mielczarek, S. R.; Kuyatt, C. E. (National Bureau of Standards, Washington, D. C.). J. Chem. Phys.; 54: 1412-14(1 Feb 1971).

The electron scattering spectrum for N_2O between 5 and 20 eV was obtained with 115-eV electrons. The onsets for three dissociative continua are indicated. Oscillator strengths for the scattering spectrum were determined and compared with results of uv studies. Agreement is good. (A.G.W.)

14015 ELECTRON-IMPACT EXCITATION OF RARE GAS ATOMS IN THE DISTORTED-WAVE APPROXIMATION. Shelton, W. N.; Leherissey, E. S. (Florida State Univ., Tallahassee). J. Chem. Phys.; 54: 1130-6(1 Feb 1971).

The distorted-wave formalism is applied to the inelastic scattering of electrons on rare gas atoms. Both the direct and exchange contributions are included. The multiparticle aspects of the problem are handled by means of the fractional parentage expansion. In particular, the case of a transition from the LS coupled ground state to a Jl coupled excited state is worked out. (auth)

14016 NONSTATISTICAL BEHAVIOR FOR HYDROGEN ATOM RECOMBINATION CALCULATED BY THE ORBITING RESONANCE THEORY. Roberts, R. E. (Indiana Univ., Bloomington). J. Chem. Phys.; 54: 1422-3(1 Feb 1971).

Since ortho–para conversion is forbidden in recombination of H atoms in the presence of a third body, the overall rate constant k_r can be partitioned as $k_r = k_r^{ortho} + k_r^{para}$. The orbiting resonance theory was used to calculate ortho–para ratios for the recombination of H atoms in the presence of H_2 or He. The results indicate that the partitioning is predominantly determined by the distribution of the complex quasi-bound states and is not critically dependent upon the third body. A possible experiment that could be used to check the validity of the resonance theory is suggested. (A.G.W.)

14017 NONITERATIVE SOLUTIONS OF INTEGRAL EQUATIONS FOR SCATTERING. V. AUXILIARY $T^{(kj)}$ MATRIX FORMALISM. Hayes, Edward F. (Rice Univ., Houston, Tex.); Kouri, Donald J. J. Chem. Phys.; 54: 878-90(1 Feb 1971).

The homogeneous integral solution method is used to develop a scheme for direct computation of the T matrix. The method involves calculation of auxiliary matrices $T^{(kj)}$ in terms of which the true T matrix is obtained. The auxiliary $T^{(kj)}$ matrices can be obtained by solving either integral or first-order linear nonhomogeneous differential equations. The relationship of calculations based on these equations to those based on the wave function integral equations is discussed. Numerical studies of the general behavior of the homogeneous integral solution procedure are presented. These studies deal with rotationally inelastic collisions of an atom and a rigid rotator interacting via a Morse-type potential. An investigation of some higher-order numerical schemes for solving the integral and differential equations for the auxiliary matrices and the integral equations for the wave function is reported. The results indicate that the use of higher-order procedures such as the Runge–Kutta method or Simpson's quadrature scheme permit one to use step sizes 5 to 10 times larger than those required with the trapezoidal quadrature scheme (or equivalently, the uncorrected Euler method for the differential equation) to achieve a given accuracy. The role of the potential function is studied by a comparison of the $|T|^2$ matrix elements for Lennard–Jones (12–6) and Morse potentials having the same well depth, curvature, and equilibrium position. In addition, hybrid potentials constructed by splicing together Morse and Lennard–Jones potentials are studied. The results indicate that, at the energy considered, the long-range portion of the potential has a dominant effect on the elastic and inelastic scattering. (auth)

14018 INFLUENCE OF THE SHORT-RANGE ATOMIC FORCES ON THE MOLECULAR TERM SPLITTING IN THE (A,A) SYSTEM. APPLICATION TO O^-–O RESONANT CHARGE TRANSFER. Davidovic, D. M.; Janev, R. K. (Boris Kidric Inst. of Nuclear Science, Belgrade). Phys. Rev., A; 3: 604-6 (Feb 1971).

A general asymptotic expression for the energy separation $\Delta(R)$ of the symmetrical and antisymmetrical states in the (A^-, A) system is derived. A great influence of the atomic short-range forces on $\Delta(R)$ has been found. At large values of the atomic effective range γ_0, the present expression for $\Delta(R)$ leads to the previous result of the authors, and for small γ_0, a Smirnov-like behavior of the molecular term splitting is obtained. As an application of the result obtained for $\Delta(R)$, the resonant charge transfer in O–O collisions is calculated, and a comparison with the experimental data is made. (auth)

14019 LOW-ENERGY SCATTERING BY LONG-RANGE POTENTIALS. Hinckelmann, Otto; Spruch, Larry (New York Univ., N. Y.). Phys. Rev., A; 3: 642-8(Feb 1971).

The phase shift for low-energy scattering by a potential consisting of a long-range and a short-range part, to first order in the long-range potential, is derived using the two-potential formula of scattering theory. For the r^{-4} and for the r^{-6} potentials and for their superposition, $\tan\eta_0$ is calculated up to and including the k^5 lnk terms, where η_0 is the zero-angular-momentum (L = 0) phase shift. For the r^{-4} potential and L > 0, $\tan\eta_L$ is calculated up to and including the k^{2L+3} lnk term. Finally, the long-range correction to the matrix element for photodissociation of negative ions is calculated. (auth)

14020 TRIPLE SCATTERING FOR LOW-ENERGY ELECTRONS: DEPOLARIZATION DUE TO SPIN FLIP. Fink, M.; Schmiedekamp, C.; Spalinger, D. (Univ. of Texas, Austin. Electronics Research Center, Austin, Tex.). Phys. Rev., A; 3: 650-6(Feb 1971).

Numerical solutions of the Dirac equation applied to low-energy electron scattering are presented. The calculated complex scattering amplitudes are used to discuss single, double, and triple scattering. Although knowledge of all three experiments leads theoretically to the explicit scattering amplitudes, the calculations show that the amplitudes can be determined with a reasonable uncertainty only from high-precision experimental data. This is a consequence of the fact that |g| is normally very small

XUM

compared to |f|. However, for very selective combinations of the experimental parameters, a very strong influence of the spin on the scattering process is predicted. Use of this result in studies of electron exchange scattering and in investigations of spin-flip processes is discussed. The important quantities for triple scattering from tungsten were calculated for different scattering potentials in an energy range 50 eV to 200 keV. The dependency of the observables on the incident-electron energy and scattering potential is shown. (auth)

14021 NONADIABATIC ATOM–ATOM COLLISIONS: TWO-STATE IMPACT-PARAMETER CALCULATION OF THE H(1s) + H(1s) = H(1s) + H(2s) CROSS SECTION INCLUDING ELECTRON EXCHANGE. **Ritchie, Burke (Goddard Space Flight Center, Greenbelt, Md.). Phys. Rev., A; 3: 656-65(Feb 1971).**

The cross section for the 1s–2s excitation of hydrogen atoms by incident hydrogen atoms is calculated for laboratory energies 1 to 56.25 keV. The calculation is made in the coupled-state impact-parameter approximation, including electron exchange. All exchange potentials are calculated as a function of internuclear distance and velocity. The cross section is much larger at low energies than that predicted by an unsymmetrized state expansion, and at higher energies it shows a very smooth undulatory behavior as a function of velocity. The calculation establishes the importance of electron exchange for incident energies at least as high as 100 keV. (auth)

14022 TOTAL CROSS SECTIONS FOR INELASTIC SCATTERING OF CHARGED PARTICLES BY ATOMS AND MOLECULES. V. EVALUATION TO THE NEXT ORDER BEYOND THE BETHE ASYMPTOTE. **Kim, Yong-ki; Inokuti, Mitio (Argonne National Lab., Ill.). Phys. Rev., A; 3: 665-78(Feb 1971).**

The Bethe procedure to obtain an asymptotic expression for the total cross section for inelastic scattering is extended to include three constants instead of the usual two. Within the first Born approximation, the third constant is essentially related to the total number of electrons in the target. By subtracting the sum of the cross sections for discrete excitations from the total cross section, the ionization cross section can also be given in an asymptotic form with three constants. The Mott formula is used to estimate the correction for electron exchange in the ionization cross section. The resulting cross sections compare favorably with experiments on the ionization of H, He^+, H^-, He, and Li^+ by fast charged particles. (auth)

14023 COLLISION CROSS SECTIONS FOR THE EXCITATION OF THE SCHUMANN–RUNGE DISSOCIATION CONTINUUM IN MOLECULAR OXYGEN BY 20 TO 110-keV PROTONS. **Park, John T.; Schowengerdt, F. D.; Schoonover, D. R. (Univ. of Missouri, Rolla). Phys. Rev., A; 3: 679-84(Feb 1971).**

Absolute cross sections for the excitation of the Schumann–Runge dissociation continuum of molecular oxygen were obtained from inelastic energy-loss spectra induced by 20- to 110-keV protons incident on gaseous targets of molecular oxygen. Apparent differential energy-loss cross sections, ionization cross sections, and total inelastic cross sections are also obtained from the energy-loss spectra. The proton energy-loss spectra have an energy resolution of about 2 eV. The energy location of the first peak in the energy-loss spectra of O_2 is in general agreement with the findings of photoabsorption and electron energy-loss-spectra measurements. The cross section for the Schumann–Runge dissociation continuum for 20- to 110-keV protons varies between 5 and 7×10^{-17} cm^2 and has a broad maximum at about 60 keV. Existing theoretical treatments show poor agreement with these reported cross sections for the excitation of the dissociation continuum with respect to both absolute magnitude and curve shape. (auth)

14024 VARIATIONAL PRINCIPLE FOR SCATTERING WITH BOUNDS ON THE PHASE SHIFT. **Miller, Kenneth J. (Rensselaer Polytechnic Inst., Troy, N. Y.). Phys. Rev., A; 3: 607-12(Feb 1971).**

A variational principle possessing a minimum, i.e., $I = \int (LG - X)^2 dr \geq 0$, is examined for the case of an electron scattered off the static field of hydrogen with and without exchange effects. $L = H - E$, where H may be either an effective one-electron Hamiltonian or the total Hamiltonian operator, and X contains the exchange interactions. The positive definite character of I eliminates the occurrence of false resonances, which appear in the Kohn and Huithén procedures. Bounds on the phase shift based on Kato's identity and related to $\int |LG - X|\, dr$ are derived, which are useful in estimating the error in the phase shifts not only for the Kohn and Hulthén variational principles, but also in the one proposed. Through Schwartz's inequality, these bounds are also related to $\sqrt{I}$. (auth)

14025 MEASUREMENT OF THE TOTAL CROSS SECTION FOR SINGLE-ELECTRON TRANSFER IN COLLISIONS OF He^+ WITH He IN THE ENERGY RANGE 2 TO 22 keV. **Shelton, W. N.; Stoycheff, P. A. (Florida State Univ., Tallahassee). Phys. Rev., A; 3: 613-19(Feb 1971).**

The total cross section for electron transfer between a ground-state singly ionized helium atom and a ground-state helium atom was measured in the energy range 2 to 22 keV. The method used was that of collection of the slow ions produced by the charge transfer process. The collection was made via parallel plates with an electric field imposed perpendicular to the ion beam. The results are estimated to be accurate to 5%. The data are compared with the theories of Rapp and Francis; Sural, Mukherjee, and Sil; and Moiseiwitsch. (auth)

14026 THEORY OF THE QUENCHING OF METASTABLE HYDROGEN ATOMS BY HELIUM. **Byron, F. W. Jr. (Univ. of Massachusetts, Amherst); Gersten, Joel I. Phys. Rev., A; 3: 620-34(Feb 1971).**

The quenching of metastable hydrogen atoms by helium is analyzed in the energy range below roughly 250 eV. Two methods are discussed. In one, a perturbation-theory approach is used; in the other, a pseudopotential is employed, which attempts to relate the quenching matrix elements of low-energy-electron elastic scattering data. At thermal energies, both methods predict very large quenching cross sections. The pseudopotential approach gives a result of about $80\pi a_0^2$; the perturbation analysis yields $40\pi a_0^2$. As one goes to higher energies, the cross sections decrease, with the pseudopotential result falling off much less rapidly than the perturbation-theory result. Reasonable agreement between experiment and the pseudopotential method is found at about 300 eV, which is the lowest energy experimentally available at present. (auth)

14027 ELASTIC SCATTERING OF BERYLLIUM DOUBLY CHARGED IONS IN HELIUM. **Giffen, W. C.; Berry, H. W. (Syracuse Univ., N. Y.). Phys. Rev., A; 3: 635-8(Feb 1971).**

The scattering of Be^{++} ions of energy 100 to 800 eV by He was measured by observing the energy-loss spectrum of the ions on traversing various path lengths of the scattering gas. The scattering data were analyzed to determine an interaction energy for Be^{++} and He for the internuclear separations from 0.15 to 1.0 Å. While not strictly logarithmic, the results can be approximately fitted by an expression for the interaction which is $V(r) = 6.0 \times 10^2 \times e^{-5.70r}$ eV, with r in Å. A Thomas–Fermi–Dirac calculation of the interaction energy fits the experimental result well for $r > 0.3$ Å. (auth)

14028 NONRESONANT VIBRATIONAL EXCITATION OF CO_2 BY ELECTRON COLLISION. **Itikawa, Yukikazu (Tokyo Univ.). Phys. Rev., A; 3: 831-2(Feb 1971).**

Experimental cross sections for the electron-impact vibrational excitation of CO_2 are compared with the theoretical calculation in the Born approximation. It is found that the optically forbidden mode (100) can be excited through the polarization interaction, whereas the dipole interaction is responsible for the excitation of both the infrared-active modes (010) and (001). (auth)

14029 LARGE ANGLE SCATTERING IN SLOW H^+–H(1s) COLLISIONS. **Bates, D. R.; Sprevak, D. (Queen's Univ., Belfast). J. Phys., B (London); 3: 1483-91(Nov 1970).**

Collisions between H^+ ions and H(1s) atoms are studied theoretically, allowance being made for the fact that the relative motion of the nuclei is not rectilinear. A simple physical argument is given for supposing that if the encounter is sufficiently close and fast and if the axis of quantization is taken to be parallel to the final direction of the velocity of relative motion vector then the probability of excitation to the $2p_{\pm 1}$ state around either nucleus is $\frac{1}{2} \sin^2\theta$ where θ is the scattering angle in the center of mass system. This prediction is verified by computations in which the electronic motion is treated by the perturbed stationary state method (in a 4-state approximation) and the motion of the nuclei is treated semiclassically with a forced common turning point. Other aspects of H^+–H(1s) collisions are covered by the computations. The results are in accord with the results of the full quantal investigation recently carried out by Knudson and Thorson (1970). Special attention is given to the case of 6° scattering. Satisfactory agreement with the measurements of Lockwood and Everhart (1962) is achieved. (auth) (UK)

14030 PRODUCTION OF N_2^+ IN COLLISIONS BETWEEN N^+ AND N_2. **Murad, E. (Air Force Cambridge Research Labs., Bedford, Mass.); Maier II, W. B. Chem. Phys. Lett.; 7: 624-6 (15 Dec 1970).**

The cross section for $N^+ + N_2 \rightarrow N_2^+ + N$ was measured for kinetic energies between 1 and 67 eV in the center-of-mass system. Kinetic energy analysis of the products and isotopic substitution show that both electron- and atom-transfer reactions occur. (auth)

14031 CLASSICAL THEORY OF RESONANT CHARGE EXCHANGE. Smirnov, B. M. Zh. Eksp. Teor. Fiz.; 59: 1225-9 (Oct 1970). (In Russian).

The cross section for resonant charge exchange between an ion and excited atom is calculated for the case when charge exchange is determined by a nonbarrier transition of an electron from the field of one ion to the field of another. The region of applicability of the classical theory is estimated. (auth)

14032 MUTUAL NEUTRALIZATION AT THERMAL ENERGIES. Bates, D. R. Comments At. Mol. Phys.; 2: 107-13(Oct-Nov 1970).

Calculations on mutual neutralization, $X^- + Y^+ \rightarrow X + Y + \Delta E$, carried out using the Landau--Zener formula for the probability of a transition on passing through a pseudocrossing are discussed. Comparison of results of such calculations with measured values shows that the measured values are rather larger than can readily be reconciled with the maxima allowed by the Landau-Zener formula even taking into account the possible increase (at most a doubling) due to the occurrence of several pseudocrossings or of dissociation. An empirical formula consistent with six of seven cited measured values is suggested. 15 references. (A.G.W.)

14033 GYROSCOPIC INTERPRETATION OF TWO-STATE HYPERGEOMETRIC MODELS OF NON ADIABATIC COUPLING. Nikitin, E. E. Comments At. Mol. Phys.; 2: 118-23(Oct-Nov 1970).

Extension of the so-called linear approximation to a general two-state Hamiltonian to some models beyond the limits of the linear one is considered. A gyroscopic model that permits interpretation of the time evolution of the density matrix for the system considered in terms of the precession of a classical magnetic moment around a time-dependent effective magnetic field is used to simplify the presentation. Specific models considered include the original Landau-Zener model, an extended Landau-Zener model, the Rosen-Zener model, the Nikitin and Ellison-Borowitz model, and the Demkov-Kunicke model. 17 references. (A.G.W.)

14034 ELASTIC AND INELASTIC DIFFERENTIAL SCATTERING OF LOW-ENERGY ELECTRONS BY POTASSIUM. Slevin, James A. New York; City Univ. (1970). 133p. University Microfilms Order No. 70-24,492.

Thesis.

A new method for studying excitation processes in low-energy electron-atom collisions is introduced, and inelastic differential cross sections for the 4S-4P transition in potassium are presented at electron impact energies of 3.0, 4.4 and 5.2 eV. The method utilizes in a crossed electron-atom beam configuration certain of the kinematic properties of the recoiling atom beam to distinguish between elastic events and excitation to various atomic levels. With observations made on the scattered atoms, absolute values for the cross sections are easily obtainable since these determinations depend only on the ratio of scattered to unscattered atom current; a precise knowledge of the detector efficiency is thus unnecessary. Differential cross sections for elastic scattering are also presented at 1.0, 3.0, 4.4, and 5.2 eV. The experimental data are compared to close-coupling calculations by Karule and Peterkop. The agreement is good in all cases, especially in the order of magnitude of the cross sections. (Diss. Abstr. Int., B)

14035 OBSERVATION AND ANALYSIS OF ELASTIC RESONANCE SCATTERING OF ELECTRONS BY RARE GASES. Hoeper, Phillips Stephen. Boston; Boston Univ. (1970). 107p. University Microfilms Order No. 70-22,394.

Thesis.

An investigation of the resonances in the elastic scattering of electrons from rare gases was made. The two resonances investigated in argon lie approximately 0.5 eV below the inelastic threshold. Because of the small width of the resonances, an electron beam of very good energy resolution is required, and to obtain such a beam, a Purcell-type electron monochromator was constructed. The elastic scattering was observed at three angles, 54, 90, and 126°, by means of Faraday cups connected to a vibrating-reed electrometer. Scattered currents were of the order of 5 to 10×10^{-12} A. The scattered current, as a function of energy at each angle, was recorded on an x-y recorder, and numerical values of scattered current and electron energy were derived from these graphs. The data were fitted by computing a cross section from seven parameters: the two resonance energies, three potential scattering phase shifts, the natural width of the two resonances (assumed the same for both), and the detector resolution. These parameters were varied until the fit to the data, in the least-squares sense, was optimized. In order to obtain initial values for the iterative analysis method, the previous (nonresonant) data of Ramsauer and Kollath were analyzed by a least-squares procedure to extract the potential scattering phase shifts. A numerical method of solving Laplace's equation in spherical polar coordinates for geometries with axial symmetry is described. The method used successive overrelaxation and was employed in the design of the electron gun. Analysis of the present data yields values of the first three potential scattering phase shifts for elastic scattering of electrons from the resonances in argon of 275, 135, and 60°. The natural width of the resonances is found to be approximately 0.6 MeV, and the resolution of the apparatus used was approximately 65 MeV fwhm. (Diss. Abstr. Int., B)

14036 IONIZATION OF CESIUM ATOMS IN COLLISIONS WITH ATOMIC OXYGEN. Woodward III, Benjamin Weston. Boulder, Colo.; Univ. of Colorado (1970). 176p. University Microfilms Order No. 70-23,767.

Thesis.

A new technique was used to measure the absolute cross section for the electron transfer reaction, $O + Cs \rightarrow O^- + Cs^+$, for both the ^3P and ^1D states of the oxygen atom. The O atoms are obtained by photodetachment from a .2- to 1.8-keV negative-oxygen-ion beam using high-power pulsed lasers. By a suitable choice of laser wavelength, O atoms are produced either entirely in the ground ^3P state or with a known fraction in the metastable ^1D state. The fraction of negative ions undergoing photodetachment is great enough that the absolute neutral flux can be determined by measuring the loss in the negative-ion beam with a gated detector. The cesium beam is a collimated thermal beam produced in an effusive source. The reaction products, both charged particles, are electrostatically separated from the neutral atoms and accelerated to approximately 5 keV for detection by open electron multipliers. Individual events are counted in both channels, and delayed coincidence is employed to provide a high signal-to-noise ratio. The cross section for electron transfer with $O(^3P)$ atoms is of the order of 10×10^{-16} cm^2 across the energy range studied; the total cross section for ionization of cesium is less than 30% larger. The electron transfer cross section using $O(^1D)$ atoms is definitely different only at 1 keV, where the cross section is much smaller than that for $O(^3P)$ atoms. In addition the total absolute cross section for ionization of Cs in collisions with O^- ions is found to be of the order of 4×10^{-16} cm^2 across the same energy range. (Diss. Abstr. Int., B)

14037 ELASTIC AND INELASTIC SCATTERING BETWEEN 2^3S METASTABLE AND GROUND-STATE HELIUM ATOMS AND BETWEEN HELIUM IONS AND 2^3 ^1S METASTABLES. Evans, Stephen Anderson. Houston, Tex.; Rice Univ. (1970). 157p. University Microfilms Order No. 70-23,506.

Thesis.

A two-state close-coupling approximation is used to calculate both elastic and inelastic cross sections for collisions between 2^3S metastable and ground-state helium atoms. Comparisons between elastic close-coupling and adiabatic (no coupling) partial-wave cross sections for scattering in the $^3\Sigma_g^+(1s2s^3S)$ and $^3\Sigma_g^+(1s2p_0{}^3P)$ molecular states at E = 10, 20, 50, 100, and 200 eV demonstrate that the adiabatic approximation is a reasonable assumption within this range of energy. Structure observed at 50 and 100 eV in the elastic close-coupling Q^{l}_{11} is shown to result from small nonadiabatic effects. Comparisons between close-coupling and Landau-Zener inelastic cross sections are made for $^3\Sigma^+(1s2s^3S \rightarrow 1s2p_0{}^3P)$ transitions. A three-state close-coupling approximation is used to calculate both elastic and inelastic cross sections for helium-ion-metastable (atom) collisions. A comparison of elastic close-coupling and adiabatic (no coupling) partial-wave cross sections is made for scattering in the $^2\Sigma_g^+(1s^2\ ^1S)$, $^2\Sigma_g^+(1s2s^3S)$, and $^2\Sigma_g^+(1s3s^1S)$ molecular states of He_2^+. The results indicate that the collision system cannot be described adiabatically at E = 75 eV. Also, the effect of the coupling matrix elements is studied by relating the behavior of the elastic partial-wave cross sections to variations in these elements. (Diss. Abstr. Int., B)

14038 VACANCY CASCADE SPECTROSCOPY: A CONVENIENT METHOD OF STUDYING HIGHLY IONIZED ATOMS AND MOLECULES. Erman, P.; Berry, H. G. (Research Inst. for Physics, Stockholm). Phys. Lett.; 34A: 1-2(25 Jan 1971).

Vacancy cascades were created in gas jets of He, N_2, O_2, CO_2, Cl_2, Ar, and Xe by bombardment with a monoenergetic beam of 2 to 10-keV electrons. The resulting spectra, observed at 500 to 2500 Å, are comparable to beam-foil spectra but have several orders of magnitude higher intensity, with a broad distribution

XUM

of ionization stages. This technique can be used to measure atomic and molecular lifetimes; other applications are discussed as well. (auth)

14039 SPIN POLARIZATION AND DIFFERENTIAL CROSS SECTIONS IN INELASTIC ELECTRON–ATOM COLLISIONS. Eitel, W.; Kessler, J. (Univ., Karlsruhe, Ger.). Z. Phys.; 241: 355-68(1971). (In German).

Measurements of electron spin polarization resulting from inelastic electron scattering by mercury (excitation of the 6^1P_1 state, 6.7-eV energy loss) are reported. Differential cross sections and angular dependences of the polarization were measured for incident energies of 25, 30, 50, and 180 eV. (auth)

14040 EXCITATION FUNCTIONS OF THE SPECTRAL LINES OF Kr II. Rozgachev, K. I.; Yaroslavtseva, A. T. Opt. Spectrosc. (USSR) (Engl. Transl.); 28: 578-9(Jun 1970).

Translated from Opt. Spektrosk.; 28: 1072-5(Jun 1970).

Results of measurements of electronic excitation functions of the spectral lines of Kr II under electron-gun conditions are given. (auth)

14041 DYNAMICS OF ION–MOLECULE REACTIONS. George, Thomas Frederick. New Haven; Yale Univ. (1970). 270p. University Microfilms Order No. 70-25,267.

Thesis.

The kinetic model for atom–diatom reactions is extended to ion–molecule reactions. The ion is represented as a hard sphere and the molecule as two hard spheres infinitesimally separated. The molecule is assumed to initially have no vibrational or rotational energy. The reactants approach each other through an induced polarization potential up to the point of collision. Energy and momentum transfers among the three particles are calculated from hard-sphere interactions; reaction probabilities are assigned on the basis of the results of the kinematic analysis. Reaction cross sections are calculated for the $Ar^+ + H_2$ and $Ar^+ + D_2$ systems in the relative energy range 1 to 10 eV. Good agreement with experiment is obtained. The model predicts a small isotope effect favoring the reaction of Ar^+ with D_2 over H_2 when compared at the same relative energy. The criteria for the outcome of a collision event have been extended to include the potential well and centrifugal barrier of products. These added criteria are significant only at the lowest energy for total reaction cross sections, which are lowered below experiment. Under the new criteria, calculations are extended to predict angular and velocity distributions and differential cross sections. The model tends to predict more of the total energy available to go into the internal motion of the products than does experiment. However, there is generally good agreement with nonreactive scattering and with reactive scattering up through 4.55 eV. It has been shown within the model that the angular distributions of products are dependent on the final potential between them as well as on the kinematic analysis. Isotope effects from the $Ar^+ + HD$ system have been calculated, where consideration is taken of the torque arising from the difference between the centers of mass and charge on the molecule. The torque causes the molecule to have a small rotational energy (less than .1 eV) upon impact with the ion. It is found that the torque for this system is significant only at energies below 1 eV, where the formation of ArD^+ is significantly decreased. Over the entire energy range (from .7 to 7 eV) the model shows an isotope effect favoring ArH^+ more than in experiment. The main conclusion is that the difference in masses, upon which the kinematic model relies heavily for the prediction of isotope effects, is not sufficient in a prediction for the system $Ar^+ + HD$. (Diss. Abstr. Int., B)

14042 ELECTRON CAPTURE AND LOSS IN COLLISIONS OF HEAVY IONS WITH ATOMIC OXYGEN BELOW 2 MeV: A NOVEL EXPERIMENTAL APPROACH TO STUDY ELECTRON IMPACT EXCITATION OF THE 2P STATE OF HELIUM ION. Lo, Hsi Hu. Pittsburgh; Univ. of Pittsburgh (1969). 157p. University Microfilms Order No. 70-11,818.

Thesis.

Electron-capture and -loss cross sections for various gaseous (N^+, O^+, Ar^+, Kr^+, Xe^+) and metallic (Al^+, K^+, Fe^+, Ba^+, and Ba^{++}) ions in collisions with atomic oxygen were measured in the energy range 30 keV to 2 MeV. Beam-in-static-gas techniques were employed. Ions formed by an electron-impact ion source were mass-selected by a rf quadrupole mass filter and were accelerated by a Van de Graaff accelerator into a fast, well collimated ion beam. This ion beam was then steered through an atomic-oxygen target chamber developed to provide a collision region containing thermally dissociated oxygen atoms in the ground state. The charge states of the emerging fast ion beam were measured and this information along with knowledge of the atomic oxygen target thickness within the target chamber was used to deduce the electron capture and loss cross sections of the particular fast heavy ion on neutral atomic oxygen. Comparisons with theoretical calculations and other experimental data were made whenever possible. In another experiment, the electron-impact excitation of He^+ to the 2P state was studied with the goal of developing a new experimental approach in which the relative kinetic energy between the collision partners is given to the ion rather than to the electron in attempting to avoid the electron-beam-generated noise. The He^+ ions accelerated by the Van de Graaff accelerator were passed through a space-charge-limited electron cloud inside tungsten chamber. Photons emerging from a slit running along the length of the tungsten chamber were filtered by C and Al thin-film filters and were detected either by an electron multiplier or by a Geiger–Mueller counter. Several possible sources of noise in this experiment were considered. Some findings were drawn from the data obtained. (Diss. Abstr. Int., B)

14043 FORMATION AND DESTRUCTION OF EXCITED HYDROGEN ATOMS AT HIGH IMPACT VELOCITIES. Edwards, Joseph Lee. Atlanta; Georgia Inst. of Tech. (1970). 128p. University Microfilms Order No. 70-24,372.

Thesis.

The charge-transfer processes whereby fast neutral atoms of hydrogen are formed in the 3s, 3p, and 3d excited states as a result of the impact of protons on targets of helium and of nitrogen were studied. The procedure involved quantitative measurement of the Balmer alpha radiation emitted in spontaneous decay of the excited atoms. The fact that the 3s, 3p, and 3d states have substantially different lifetimes permitted the use of a time-of-flight technique to identify separately their contributions to the emission. It was necessary to assess the influence of processes whereby the excited atoms were collisionally destroyed before undergoing spontaneous radiative decay. Detailed measurements of the collisional formation and destruction processes are presented for targets of He and N_2 for impact energies from 75 to 400 keV. An assessment is also made of the effect on the measurements of other secondary processes: cascade contributions from more highly excited states and the formation of ground state neutral atoms of hydrogen in the beam with the subsequent excitation or ionization of these atoms. Comparisons are made with theoretical predictions and with other experimental measurements. (TSS) (Diss. Abstr. Int., B)

14044 SCATTERING OF He^+ IONS BY NOBLE GASES AT HIGH ENERGIES. Taylor, George Ormsbee. Atlanta; Georgia Inst. of Tech. (1970). 178p. University Microfilms Order No. 70-11,193.

Thesis.

The scattering of He^+ projectiles by impact on the noble gases, He, Ne, and Ar, was investigated in the energy range 120 to 830 keV under single-collision conditions. Specifically, the experiment measured, as a function of angle in the range one to eight degrees, the total differential scattering cross section as well as the differential scattering cross sections for scattering without change of charge, for scattering with charge transfer, and for scattering with electron stripping. Also, the fraction of particles in a particular charge state was measured as a function of energy at fixed scattering angle. The sum of the differential cross sections for scattering He^0, He^+, and He^{2+} through an angle θ was equal to the measured total differential cross section. The absolute error associated with the total differential cross section is ±23%, the random error is estimated to be ±10%. This total differential cross section was found to equal the theoretical differential scattering cross section based on a classical calculation using a screened Coulomb-type potential. Thus, the scattering of the particles in these close encounters is determined by the mutual nuclear repulsion and may be adequately described by classical mechanics. The four differential scattering curves were parallel over the angular range investigated, indicating that P_n, the fraction of particles in a particular charge state n, was independent of the scattering angle. This result is consistent with theory and with experiments performed at slightly lower energies. There was excellent agreement for the energy dependence of P_n in all three target gases with data at lower energies. The random error in P_n is estimated to be ±10%. (TSS) (Diss. Abstr. Int., B)

14045 ABSOLUTE AND RELATIVE MEASUREMENT OF THE DISSOCIATIVE EXCITATION CROSS SECTION FOR PRODUCTION OF METASTABLE 2s ATOMS BY ELECTRON IMPACT UPON MOLECULAR DEUTERIUM. Cox, Donald Martin. Boulder, Colo.; Univ. of Colorado (1970). 169p. University Microfilms Order No. 70-23,700.

Thesis.

The energy dependence and the absolute value of the cross section for the production, through dissociative excitation by electron impact, of the metastable $(2\ ^2S_{1/2})$ state of atomic deuterium were measured. The metastable atoms were quenched by an rf field at the Lamb-shift frequency (1059 MHz), applied directly at the excitation region. The slow modulation of the rf field then resulted in an incremental change in the emitted Lyman-alpha radiation, which is quite specifically attributed to the 2s atoms decaying to the ground state by an induced transition to the $2\,^2P_{1/2}$ state. This Lyman-alpha radiation emitted from the quenching region was then detected by a solar-blind photomultiplier located perpendicular to the electron beam. The energy dependence of the cross section was studied over the electron energy range from 10 eV to 500 eV. The threshold for metastable production was found to be 14.8 ± 0.3 eV. The threshold for Lyman-alpha production by the dissociative excitation to the 2p atomic state was found to be 14.8 ± 0.6 eV. These values are in good agreement with the expected value corresponding to the sum (14.7 eV) of the dissociation energy (4.5 eV) and the excitation energy (10.2 eV) to the n = 2 state of atomic deuterium. The 2s dissociative excitation cross section was found to rise steeply within a few volts of threshold, rounding off at about 20 eV to a slow rise to a broad maximum at about 60 eV, before falling off again at higher energies. A concentrated effort was made in the energy range below 45 eV where structure might be anticipated, but no significant features were observed. In the energy range below 15 eV, an indication of 2p Lyman-alpha radiation from the dissociative attachment process was observed, but no indication of the 2s Lyman-alpha radiation could be observed. The absolute cross section was measured at two electron energies 23.8 eV and 39.0 eV. The signal was found to be linear with electron current and gas pressure over all values of pressure and current examined. The absolute value of the cross section for the production of 2s metastable atoms through the dissociative excitation of deuterium by electron impact was found to be 3.33×10^{-18} cm^2 at 39 eV. (Diss. Abstr. Int., B)

Atomic Theory

Refer also to abstract 13816.

14046 MANY-BODY THEORY FOR PROPERTIES OF INTERACTING ATOMS. Dutta, Chizuko Matsubara. Riverside, Calif.; Univ. of California (1969). 137p. University Microfilms Order No. 70-19,232.

Thesis.

The Brueckner–Goldstone many-body perturbation procedure was applied to study various properties of interacting atoms, utilizing the response functions of individual atoms to time-dependent external fields. The frequency-dependent polarizabilities of hydrogen, helium, and neon were calculated. The results were compared with earlier work and experiments. Also, various excitation energies and ionization energies were obtained from the singularities of $\alpha(\omega)$ functions. They are uniformly in good agreement with experiments, the error being less than 0.75% for the case of helium and less than 7% for neon. The necessity of taking account of the pressure effects in comparing theoretical $\alpha(\omega)$ with experimental data is discussed in detail. These $\alpha(\omega)$ functions were extended to the imaginary frequency region and used for calculation of the Van der Waals constants of two- and three-body interactions. The present results were compared with some earlier works and semi-empirical results. A formulation for calculating fractional frequency shifts of the hyperfine interaction of a paramagnetic atom in a rare gas atmosphere was carried out by a similar approach, using appropriate response functions besides $\alpha(\omega)$. Application was made to H–He and H–Ne systems. The fractional frequency shifts of a hydrogen atom due to the long-range interaction obtained by the present method were compared with other one-electron variational and semi-empirical calculations. In the present method, one can analyze neatly the contributions from one-electron and from consistency and correlation effects. The present one-electron results compared well with earlier one-electron calculations, and the final results with consistency and correlations were in very good agreement with the semi-empirical results. (Diss. Abstr. Int., B)

14047 ELEMENTARY ATOMIC STRUCTURE. Woodgate, G. K. London; McGraw-Hill (1970). 225p. 70s.

The subject is considered under the following headings: introduction (empirical aspects, orders of magnitude); the hydrogen atom gross structure (the Schroedinger equation, stationary states, expectation values, solution of Schroedinger's equation for a Coulomb field, the quantum numbers l and m_l; the hydrogen energy spectrum); radiative transitions (Einstein's A and B coefficients, transition probabilities, the electric dipole approximation, selection rules for l and m_l, higher-order radiation); the hydrogen-atom fine structure (electron spin, the interaction terms, the vector model, the Lamb shift, summary of the hydrogen spectrum); two-electron systems (electrostatic interaction and exchange degeneracy, the ground state of helium, the excited states of helium, electron spin functions and the Pauli exclusion principle, the periodic system); the central field approximation (the central field, Thomas–Fermi potential, the gross structure of the alkali metals); angular problems in many-electron atoms (the LS coupling approximation, allowed terms in LS coupling, fine structure in LS coupling, relative intensities in LS coupling the j–j coupling approximation and other types of coupling); interaction with static external fields (Zeeman effect in LS coupling, quadratic Stark effect, linear Stark effect, relative intensities in the Zeeman effect); hyperfine structure and isotope shift (magnetic dipole interaction, determination of nuclear spin from magnetic hyperfine structure, determination of μ_I from magnetic hyperfine structure, magnetic hyperfine structure in two-electron spectra, electric quadrupole interaction, Zeeman effect of hyperfine structure isotope shift). Appendices cover some theorems of quantum mechanics, results of time-dependent perturbation theory, notes on angular momentum, ground states of the elements, and units. (UK)

14048 LAMB LEVEL SHIFT OF INNER ELECTRONS IN HEAVY ATOMS. Labzovskii, L. N. (Lenningrad State Univ.). Zh. Eksp. Teor. Fiz.; 59: 2165-74(Dec 1970). (In Russian).

The self-energy of an inner electron in a heavy atom is calculated by expanding the electron propagator into a series in powers of the nuclear potential. Terms that contain the first and second powers of the potential are calculated. The residue is calculated by means of a variational principle. Calculation of the self-energy of an electron in the $1s_{1/2}$ state in an atom with Z = 137 is performed by taking into account the finite size of the nucleus R. Senior terms of the order of $\alpha \ln^2 R$ are calculated. (auth)

14049 THEORY OF PERTURBATIONS OF THE AUTOIONIZATION LEVELS OF TWO-ELECTRON ATOMS. Matulis, A. Yu.; Safronova, U. I. Opt. Spectrosc. (USSR) (Engl. Transl.); 28: 580-4(Jun 1970).

Translated from Opt. Spektrosk.; 28: 1076-84(Jun 1970).

By using the Green function of a two-electron system, the energy and width of autoionization levels is discussed within the framework of second-order perturbation theory. It is shown that in higher orders there exist diagrams whose contributions diverge at a small level width. A partial summation of these diagrams is made. Several autoionization levels of the He atom are discussed as an illustration of the method. (auth)

14050 EFFECT OF DOPPLER BROADENING ON THE LINE SHAPE OF SPONTANEOUS RADIATION. Lazarev, A. V. Opt. Spectrosc. (USSR) (Engl. Transl.); 28: 572-4(Jun 1970).

Translated from Opt. Spektrosk.; 28: 1060-4(Jun 1970).

The expression for the relaxation function that determines the Doppler line broadening is obtained in the quadratic approximation with respect to the velocity of the source of emission for the transition frequency being observed. It is shown that the corrections are essential for the emission of both long and short wavelengths. (auth)

14051 FINE STRUCTURE OF TERMS FOR A SEQUENCE OF STATES OF LIGHT ATOMS. Safronova, U. I.; Kharitonova, V. N. Opt. Spectrosc. (USSR) (Engl. Transl.); 28: 562-7(Jun 1970).

Translated from Opt. Spektrosk.; 28: 1039-49(Jun 1970).

The Breit operator was considered for the purpose of calculating the fine structure of terms. Perturbation theory was employed. The results are shown in the form of a series in Z^{-1}. The calculation was carried out for terms of the configuration $1s^2 2s^{n_1} 2p^{n_2}$. (auth)

14052 RELATIVISTIC CORRECTIONS TO TERMS FOR A NUMBER OF STATES OF LIGHT ATOMS. Safronova, U. I. Opt. Spectrosc. (USSR) (Engl. Transl.); 28: 568-72(Jun 1970).

Translated from Opt. Spektrosk.; 28: 1050-9(Jun 1970).

For calculating relativistic corrections, all terms of Breit's operator which describe the shift of terms were investigated. The results are presented in the form $E^{rel} = (\alpha^2/4) \times (E^{(0)} Z^4 + \Delta E^{(1)} Z^3)$. Values of $E^{(0)}$ and $E^{(1)}$ were calculated for the terms of the $1s^2 2s^{n_1} 2p^{n_2}$ $(2 \geq n_1 \geq 0,\ 6 \geq n_2 \geq 0)$ configurations. (auth)

14053 STABILITY CONDITIONS FOR THE SOLUTIONS OF THE HARTREE–FOCK EQUATIONS FOR ATOMIC AND MOLECULAR SYSTEMS. V. THE NONANALYTIC BEHAVIOR OF THE BROKEN-SYMMETRY SOLUTIONS AT THE BRANCHING POINT. Cizek, J.; Paldus, J. (Univ. of Waterloo, Ont.). Phys. Rev., A; 3: 525-7(Feb 1971).

It is shown that both the energy and the wave function of the stable Hartree–Fock solution are nonanalytic functions of the

XUM

coupling constant at the branching point, dividing the symmetry-adapted and the broken-symmetry solutions. The π-electronic model of benzene is used to illustrate this fact for the case of the Hartree–Fock singlet instability. It is indicated that the same type of nonanalytical behavior is found in other types of instabilities, i.e., nonsinglet (triplet) instabilities for closed shells and doublet instabilities for simple open shells. This nonanalyticity persists even after the projection on the totally symmetric subspace is carried out, and can only be avoided by projecting before the variational principle is applied. (auth)

14054 TIME-DEPENDENT PERTURBATION CALCULATIONS BASED ON THE HYDRODYNAMIC ANALOGY TO QUANTUM MECHANICS. **Weiner, J. H.; Askar, A.** (Brown Univ., Providence). **J. Chem. Phys.; 54: 1108-13(1 Feb 1971).**

A new formulation is presented for the problem of the time-dependent perturbation of bound states. It is based on the hydrodynamic analog to quantum mechanics and leads to the physical picture of a continuum of particles that oscillate in the vicinity of their equilibrium positions under the influence of the perturbing field. The corresponding mathematical formulation involves a single partial differential equation, which is second-order in time and fourth-order in the spatial coordinates. The procedure is applied to the time-dependent polarizability of the hydrogen atom in its ground state. It was possible to obtain an exact series solution, which yields results in full agreement with those previously obtained by other methods. (auth)

14055 CORRELATED PSEUDO-POTENTIAL APPROACH FOR MOLECULES. **David, D. J.** (Laboratoire de Chimie, Paris). **Chem. Phys. Lett.; 7: 577-80(15 Dec 1970).**

A somewhat semiempirical pseudopotential procedure of dealing with the electron-correlation problem is presented. It consists of the introduction of a correlation factor in coulombic bielectronic integrals. Influence of kinetic energy upon the correlation factor is taken into account, providing satisfactory variation along Z for the isoelectronic series of helium. The formalism is directly applicable for molecules, and preliminary results for H_2 and F_2 are given. (auth)

14056 NONCOMPACT GROUP FOR RADIAL EIGENFUNCTIONS. **Judd, B. R. Comments At. Mol. Phys.; 2: 132-5(Oct-Nov 1970).**

A method proposed by Armstrong in a paper presented at the Centre National de la Recherche Scientifique Colloquium Theorie de la Structure Atomique, Paris–Gif sur Yvette, July 1970 (to be published in J. Phys. (Paris)), for theoretical treatment of the radial properties of an atom is discussed. The method makes use of the noncompact group 0(2,1) and makes it possible to cast properties regarded as purely radial in character in the language of angular-momentum theory. The limitations and possible extensions of the method are considered briefly. (A.G.W.)

14057 LINE SHIFTS AND ELASTIC SCATTERING BY SLOW ELECTRONS. **Bederson, Benjamin. Comments At. Mol. Phys.; 2: 114-17(Oct-Nov 1970).**

The Fermi theory (1934) for the pressure shift of highly excited states of the alkali metals in the presence of foreign gases is based partly upon the assumption that the highly excited valence electron is quasi-free, so that it interacts with the foreign-gas atoms as though it were a free electron possessing an energy equal to its average orbital kinetic energy, i.e., the interaction is effectively that of elastic scattering between a free electron and a ground-state perturbing atom. This effect is described qualitatively, and attempts of various investigators to use the effect for study of very-low-energy elastic collisions are reviewed. 8 references. (A.G.W.)

Cosmic Radiation

Refer also to abstracts 13949, 14127, 14509, and 14845.

14058 ACCELERATION AND HEATING OF INTERSTELLAR GAS BY COSMIC RAYS. **Wentzel, Donat G.** (Univ. of Maryland, College Park). **Astrophys. J.; 163: 503-14(1 Feb 1971).**

When cosmic rays try to stream along the magnetic field of the Galaxy, they are scattered and must diffuse down a cosmic-ray density gradient. The associated pressure gradient acts on the interstellar gas, with the hydromagnetic waves that cause the scattering acting as a clutch which couples gas and cosmic rays. When the cosmic rays have diffused down a density scale height, they have lost a major fraction of their momentum and energy. Therefore, they may be a major source of the observed interstellar kinetic and thermal energies. This energy transfer is a collective, plasma-physical process that does not ionize the gas.

For applications, one must distinguish the cosmic rays that are "engaged by the clutch" from those that are not. The former have energies up to a few GeV and carry much of the energy and pressure of the cosmic rays. The engaged cosmic rays may raise neutral hydrogen several hundred parsecs above spiral arms, as observed. They may aid in star formation. Their confinement to spiral arms helps to explain the pressure balance in inter-arm regions, and perhaps in the galactic halo. (auth)

14059 DECAY OF ^{7}Be IN COSMIC RAYS. Yiou, F.; Raisbeck, G. M. (Centre de Spectrometrie Nucleaire et de Spectrometrie de Masse, Orsay, France). Astrophys. Lett.; 7: 129-32(Dec 1970).

Calculations were made on the probability that ^{7}Be will capture an electron and subsequently decay in cosmic rays. It was concluded that significant decay will occur only for ^{7}Be nuclei of less than 25 MeV/nucleon. (auth)

14060 MULTIPLE MUON EVENTS OBSERVED UNDERGROUND. **Krishnaswamy, M. R.** (Tata Inst. of Fundamental Research, Bombay); **Menon, M. G. K.; Narasimham, V. S.;** (and others). **Proc. Indian Acad. Sci., Sect. A; 72: 55-61(Aug 1970).**

Observations are reported on events involving multiple penetrating particles recorded in a scintillator-neon flash tube telescope, at a depth of 1500 hg/cm^2 in the Kolar Gold Mines. From these, it is shown that: (1) the cross-section for nuclear interaction of muons of average energy ~200 GeV is $\sim 6 \times 10^{-30}$ cm^2/nucleon; (2) the decoherence curve for events involving two parallel muons is uniform over the range of distances from 0 to 2 meters; and (3) the angular distribution of double-parallel muons closely resembles that of single muons, implying that these two types of events are probably produced in the atmosphere in a similar manner. (auth)

14061 LYMAN-α PRODUCTION BY SUPRATHERMAL PROTONS. Silk, Joseph (Princeton Univ. Observatory, N. J.); Steigman, Gary. Astrophys. Space Sci.; 9: 304-14(Nov 1970).

At sufficiently low energies, cosmic-ray protons capture electrons from interstellar H I and become neutral. In the subsequent cascade to the ground state, a Doppler-shifted Ly-α photon may be emitted. The neutral cosmic ray will be excited collisionally by further encounters with the ambient interstellar gas, emitting additional Doppler-shifted Ly-α photons. The form of the cosmic-ray spectrum is given down to 10 keV, assuming that there is no cosmic-ray injection below 1 MeV. The neutral fraction is evaluated as a function of energy, and the diffuse ultraviolet flux is calculated. Comparison is made with observations in the range 1225 to 1340 Å. It is concluded that far more stringent limits on the flux of subcosmic rays may be obtained by consideration of the heating and ionization of H I regions. (auth)

14062 CONSIDERATION OF THE OBSERVED ISOTROPIC γ-RAY BACKGROUND. Cavallo, Giacomo (Univ. of California, San Diego, La Jolla). Phys. Rev., D; 3: 299-305(15 Jan 1971).

The experimental data on the isotropic component of the diffuse γ-ray background at energies $E_\gamma > 100$ MeV are shown to be inconsistent with the explanation of the isotropic x-ray background as due to the inverse Compton effect of secondary electrons (i.e., due to the decay of mesons produced in nuclear collisions) on the 3°K (or 8°K) blackbody radiation. The possibility of the coexistence of a dense intergalactic medium ($n_0 \gtrsim 10^{-7}$ cm^{-3}) and a universal cosmic-ray flux is also examined, in the context of an evolutionary and of a steady-state cosmology, and restrictions are found. The inner-bremsstrahlung explanation of the diffuse x-ray background is found to be not inconsistent with the π^0-decay explanation of the diffuse γ-ray background, and a set of useful parameters can therefore be suggested. (auth)

14063 BACKGROUND TO THE OBSERVATION OF DIRECT MUON PRODUCTION BY NEUTRAL COSMIC RAYS NEAR SEA LEVEL. **Shelby, Robert Nelson. Washington, D. C.; Catholic Univ. of America (1970). 78p. University Microfilms Order No. 70-22,086.**

Thesis.

For a number of years several experiments have been performed at the Catholic University of America in a search for direct muon production by neutral cosmic rays. These studies have been directed toward achieving a thorough understanding of the background to the observation of direct muon production. One of these experiments has used a large internally triggered spark chamber to study muon production. In this discussion the data from 2412 hours of operation of the spark chamber are analyzed to determine the production rate, range distribution, zenith-angle distribution, and charge ratio of the neutral-produced particles observed. The background contribution of stopping cosmic-ray muons and neutron production of pions is discussed, and the results of a calculation of spark chamber response to neutron production of pions are given.

It is determined that, with the exception of production rate, the characteristics of the events observed are consistent with neutron production of pions. The two published values for neutron flux at sea level are used to demonstrate that, while up to one half of the events could be interpreted as direct production of muons, it is possible to explain all events by neutron production of pions. (Diss. Abstr. Int., B)

14064 SOLAR-CYCLE MODULATION OF FAST NEUTRONS IN THE ATMOSPHERE. Merker, Milton. New York; New York Univ. (1970). 139p. University Microfilms Order No. 70-19,020.
Thesis.

The effect of the solar-cycle modulation on the production of neutrons in the atmosphere was studied. During the period of increasing solar activity from 1965 to 1969, a series of measurements of the fast-neutron flux in the atmosphere was made. The long-term variation of the neutron flux from 2 to 10 MeV was seen to be similar to the modulation of the integral flux of galactic cosmic-ray protons of rigidity greater than 1.3 GV. The shape of the neutron energy spectrum did not change during this period. For a differential energy spectrum power law fit, the average spectral index was 1.17 ± 0.1 at the transition maximum and 1.08 ± 0.1 near the top of the atmosphere. From 1965 to 1968 when the Deep River neutron monitor counting rate decreased about 10%, the high latitude transition maximum fast-neutron flux decreased 37%. A Monte Carlo calculation of neutron production and transport in the atmosphere was made to compare with the results of the experiment and to determine the low-energy neutron distribution, the neutron leakage flux, and the radiocarbon production rate. (Diss. Abstr. Int., B)

14065 SEARCH FOR FRACTIONALLY CHARGED PARTICLES IN COSMIC RAYS AND A THEORETICAL INTERPRETATION OF THE RESULTS. Orth, Charles Douglas. Pasadena, Calif.; California Inst. of Tech. (1970). 285p. University Microfilms Order No. 70-18,042.
Thesis.

An array of two spark chambers and six trays of plastic scintillation counters was used to search for unaccompanied fractionally charged particles in cosmic rays near sea level. No acceptable events were found with energy losses by ionization between 0.04 and 0.7 that of unit-charged minimum-ionizing particles. New 90%-confidence upper limits were thereby established for the fluxes of fractionally charged particles in cosmic rays, namely, $(1.04 \pm 0.07) \times 10^{-10}$ and $(2.03 \pm 0.16) \times 10^{-10}$ $\text{cm}^{-2}\ \text{sr}^{-1}\ \text{sec}^{-1}$ for minimum-ionizing particles with charges $^1\!/_3$ and $^2\!/_3$, respectively. In order to be certain that the spark chambers could have functioned for the low levels of ionization expected from particles with small fractional charges, tests were conducted to estimate the efficiency of the chambers as they had been used in this experiment. These tests showed that the spark-chamber system with the track-selection criteria used might have been over 99% efficient for the entire range of energy losses considered. Lower limits were then obtained for the mass of a quark by considering the above flux limits and a particular model for the production of quarks in cosmic rays. In this model, which is one involving the multi-peripheral Regge hypothesis, the production cross section and a corresponding mass limit are critically dependent on the Regge trajectory assigned to a quark. If quarks are "elementary" with a flat trajectory, the mass of a quark can be expected to be at least 6 ± 2 BeV/c^2. If quarks have a trajectory with unit slope, just as the existing hadrons do, the mass of a quark might be as small as 1.3 ± 0.2 BeV/c^2. For a trajectory with unit slope and a mass larger than a couple of BeV/c^2, the production cross section may be so low that quarks might never be observed in nature. (Diss. Abstr. Int., B)

14066 COSMIC-RAY METEOROLOGICAL EFFECTS. Dorman, L. I.; Kaminer, S. N. Bull. Acad. Sci. USSR, Phys. Ser. (Engl. Transl.); 33: 1759-62(Nov 1969).
Translated from Izv. Akad. Nauk SSSR, Ser. Fiz.; 33: 1926-9 (Nov 1969).

Interest in the meteorological effects in cosmic-ray data has increased greatly in the last few years, following the development of a network of supermonitors and supertelescopes. Results are presented of a number of investigations carried out in the last few years that were aimed at improving the theory and experimental study of cosmic-ray variations of atmospheric origin. (W D.M.)

14067 SYSTEM FOR PROCESSING MESON-TELESCOPE DATA. Kokh, I.; Shomodi, A.; Vagner, I.; Valash, D.; Varga, A. Bull. Acad. Sci. USSR, Phys. Ser. (Engl. Transl.); 33: 1763-5 (Nov 1969).
Translated from Izv. Akad. Nauk SSSR, Ser. Fiz.; 33: 1930-2 (Nov 1969).

The data-processing system described is used to analyze the results of measurements with underground semicubical meson telescopes. The system has four inputs and outputs. The system is so constructed as to have the minimum possible number of intrinsic errors and at the same time to have the maximum possible capability of detecting telescope errors. The basis of the data-processing system is an ICT−1905 computer. (W.D.M.)

14068 BACKWARD AND FORWARD FLOWS OF 100 TO 1500-MeV ELECTRONS AT VARIOUS HEIGHTS IN THE ATMOSPHERE. Bezus, V. A.; Gal'per, A. M.; Grigorov, N. L.; (and others). Bull. Acad. Sci. USSR, Phys. Ser. (Engl. Transl.); 33: 1666-70 (Nov 1969).
Translated from Izv. Akad. Nauk SSSR, Ser. Fiz.; 33: 1827-31 (Nov 1969).

Results of balloon measurements during 1967−1968 on 100- to 1500-MeV electron streams are given. The equipment is described. The intensities of electron streams and the indexes of the differential energy spectrum at different heights were determined. It is mentioned that at atmospheric depths of $p < 100$ g/cm^2 additional streams of electrons are sometimes observed, the appearance of which correlates with change of the index of geomagnetic activity. (W.D.M.)

14069 COSMIC-RAY VARIATIONS. Dorman, L. I. Bull. Acad. Sci. USSR, Phys. Ser. (Engl. Transl.); 33: 1671-95(Nov 1969).
Translated from Izv. Akad. Nauk SSSR, Ser. Fiz.; 33: 1832-57 (Nov 1969).

A survey is given of investigations of cosmic-ray variations. Special attention is given to the topics meteoritic method of investigation, microvariations, the relation between transport range for scattering and the structure of the interplanetary magnetic field, and 11-year and sidereal variations. (W.D.M.)

14070 COSMIC-RAY VARIATIONS AND THE INTERPLANETARY MEDIUM. Krymskii, G. F. Bull. Acad. Sci. USSR, Phys. Ser. (Engl. Transl.); 33: 1695-1707(Nov 1969).
Translated from Izv. Akad. Nauk SSSR, Ser. Fiz.; 33: 1858-69 (Nov 1969).

The modulation of galactic cosmic rays by the interplanetary medium is considered. Topics discussed include extent of the solar wind, phase−amplitude characteristics of the variations, nonspherical modulation of cosmic rays, structure of the magnetic field, anisotropy of cosmic rays and magnetic-field structure during forbush decreases, streaming structure of the solar wind, second spherical harmonic and orientation of the interplanetary magnetic field, and microstructure of the interplanetary magnetic field. (W.D.M.)

14071 NEW INFORMATION ON THE TIME AND SPACE VARIATIONS OF COSMIC RAYS IN THE SOLAR SYSTEM (FROM METEORITE DATA). Lavrukhina, A. K. Bull. Acad. Sci. USSR, Phys. Ser. (Engl. Transl.); 33: 1708-14(Nov 1969).
Translated from Izv. Akad. Nauk SSSR, Ser. Fiz.; 33: 1870-6 (Nov 1969).

New information obtained by investigation of meteorites and modeling of cosmic-ray-induced nuclear processes was examined. Conclusions obtained include: (1) modulating region for cosmic rays is at 4 to 5 AU; (2) the intensity of primary cosmic radiation in the asteroidal belt is 1.6 ± 0.1 times the average intensity at the top of the atmosphere during the last solar cycle; (3) the intensity 300 to 900 my ago was three times lower than it is now. (W.D.M.)

14072 STUDIES OF COSMIC PLASMA WITH THE YAKUTSK COSMOPHYSICAL AND AERONOMIC COMPLEX. Shafer, Yu. G. Bull. Acad. Sci. USSR, Phys. Ser. (Engl. Transl.); 33: 1715-26 (Nov 1969).
Translated from Izv. Akad. Nauk SSSR, Ser. Fiz.; 33: 1877-89 (Nov 1969).

The objects of the Yakutsk studies are the circumstellar, interplanetary, and interstellar plasmas, which are highly ionized, are associated with magnetic fields, and are in the collisionless regime. The possibility of investigating the physical conditions in quasi-stationary and disturbed cosmic plasma of different scales and the possibility of studying the interaction of plasma media under cosmic conditions are considered. (W.D.M.)

14073 FORBUSH DECREASES: THEORY AND EXPERIMENT. Dorman, L. I. Bull. Acad. Sci. USSR, Phys. Ser. (Engl. Transl.); 33: 1726-31(Nov 1969).
Translated from Izv. Akad. Nauk SSSR, Ser. Fiz.; 33: 1890-4 (Nov 1969).

It is stated that the leaky-piston model gives a basically correct description of the physics of a forbush decrease but requires

XUM

progressive elaboration if the many new experimental results are to be accounted for. In particular, a model has been proposed in which it is assumed that behind the piston there is no particle exchange in the radial direction, but only diffusion in the transverse direction, due to which the cosmic-ray intensity recovers exponentially after a forbush decrease. However, since the magnetic field behind the piston is mainly radial, the assumption of free particle exchange in the radial direction may be closer to reality. This case is examined, and an attempt is made to take into account possible changes in the properties of the magnetic piston as it recedes from the Sun as well as the decrease in its velocity. (W.D.M.)

14074 EFFECT OF SMALL MAGNETIC STORMS ON THE DIURNAL VARIATION OF THE COSMIC-RAY NEUTRON COMPONENT. Akhababyan, N.; Grueva, T. (Inst. of Physics, Sofia). Bull. Acad. Sci. USSR, Phys. Ser. (Engl. Transl.); 33: 1731-3 (Nov 1969).

Translated from Izv. Akad. Nauk SSSR, Ser. Fiz.; 33: 1895-7 (Nov 1969).

An investigation is reported on the effect of small magnetic storms on the diurnal variation of the neutron component, using data continuously recorded at Mt. Musala (23° 35′ E, 42° 11′ N, 2925 m altitude) with a standard neutron monitor of the Simpson type. (W.D.M.)

14075 COSMIC-RAY ANISOTROPY IN THE PERIODS FOLLOWING PROTON OUTBURSTS. Dorman, L. I.; Inozemtseva, O. I. Bull. Acad. Sci. USSR, Phys. Ser. (Engl. Transl.); 33: 1734-42(Nov 1969).

Translated from Izv. Akad. Nauk SSSR, Ser. Fiz.; 33: 1898-1907(Nov 1969).

The hypothesis of the origin of the diurnal variation of cosmic rays based on the anisotropic diffusion model is now widely accepted. The mean amplitude of the diurnal variation in the vicinity of the Earth's orbit is estimated as ~0.4% of the average intensity, assuming that the mean cosmic-ray density gradients are close to zero. The diffusion model describing the cosmic-ray anisotropy following proton flares was examined for the case when the amplitude of the diurnal variation increases sharply and the cosmic-ray density gradients may differ appreciably from zero. (W.D.M.)

14076 REACTION OF COSMIC RAYS ON THE SOLAR WIND. Dorman, I. V.; Dorman, L. I. Bull. Acad. Sci. USSR, Phys. Ser. (Engl. Transl.); 33: 1742-51(Nov 1969).

Translated from Izv. Akad. Nauk SSSR, Ser. Fiz.; 33: 1908-17 (Nov 1969).

Topics discussed include radial deceleration of the solar wind by cosmic rays, lag between changes in solar activity and cosmic-ray intensity, and focusing effect of cosmic rays on the solar wind. (W.D.M.)

14077 COSMIC RAYS AND PLASMA TURBULENCE. Tsytovich, V. N. Bull. Acad. Sci. USSR, Phys. Ser. (Engl. Transl.); 33: 1642-57(Nov 1969).

Translated from Izv. Akad. Nauk SSSR, Ser. Fiz.; 33: 1800-16 (Nov 1969).

Successful approaches in the study of the physics of turbulent plasmas are discussed and the relation between cosmic rays and plasma turbulence is analyzed. The questions of the generation of cosmic rays by plasma turbulence and the problem of the spectra of cosmic electrons and ions were examined. (W.D.M.)

14078 SEARCH FOR MAGNETIC MONOPOLES IN COSMIC RAYS. Ashton, F.; Burchuladze, A. A.; King, J.; Smith, N. I.; Mamidzhanyan, E. A. Bull. Acad. Sci. USSR, Phys. Ser. (Engl. Transl.); 33: 1658-60(Nov 1969).

Translated from Izv. Akad. Nauk SSSR, Ser. Fiz.; 33: 1817-19 (Nov 1969).

An upper bound to the flux of relativistic magnetic monopoles in cosmic rays at sea level is 1.3×10^{-10} cm^{-2} sec^{-1} sr^{-1}. This is sufficient to exclude the possibility that monopoles with energies of 10^{18} eV are present in primary cosmic rays provided the elementary electric charge is e, but if the elementary charge is e/3 (i.e., if quarks exist) such monopoles might be present. (W.D.M.)

14079 SOME REMARKS ON THE THEORY OF THE ORIGIN OF COSMIC RAYS. Ginzburg, V. L.; Syrovatskii, S. I. (Lebedev Inst. of Physics, Moscow). Bull. Acad. Sci. USSR, Phys. Ser. (Engl. Transl.); 33: 1615-20(Nov 1969).

Translated from Izv. Akad. Nauk SSSR, Ser. Fiz.; 33: 1770-5 (Nov 1969).

The present state of knowledge of the origin of cosmic rays is briefly summarized. The external problem is discussed in terms of the role of metagalactic cosmic rays, the origin and region of confinement of the majority of the cosmic rays observed near the Earth, possible sources of cosmic rays, the relationship between the various components, the role of cosmic rays in the dynamics of the interstellar medium, and the nature of their motion in the Galaxy. The clarification of these points is an essential preliminary to the solution of the internal problem—the theory of the physical processes leading to the acceleration of cosmic rays and the formation of their energy spectrum and chemical composition in the source. (W.D.M.)

14080 COSMIC RAYS IN AN EXPANDING UNIVERSE. Prilutskii, O. F.; Rozental, I. L. Bull. Acad. Sci. USSR, Phys. Ser. (Engl. Transl.); 33: 1621-30(Nov 1969).

Translated from Izv. Akad. Nauk SSSR, Ser. Fiz.; 33: 1776-86 (Nov 1969).

Ways of using certain aspects of cosmic-ray physics to estimate cosmological parameters are discussed. Specifically, two parameters are considered: the evaluation of the cosmic-ray sources and the time of their formation. Certain processes accompanying the passage of high-energy cosmic rays through the metagalaxy, which have not previously been investigated, are analyzed. (W.D.M.)

Direct Energy Conversion

Refer also to abstracts 14097 and 14098.

14081 (AD-711351) INVESTIGATION OF A LARGE SCALE NONEQUILIBRIUM MAGNETOHYDRODYNAMIC GENERATOR. Annual Report, August 1, 1969–July 31, 1970. Zauderer, B. (General Electric Co., Philadelphia, Pa. Space Div.). Contract Nonr-3867(00). 15p. NTIS.

A large portion of the effort of the present contract year was devoted to "technology problems," namely, the development of a satisfactory cesium seeding technique, the development of the thermionically emitting electrodes compatible with the shock-tube MHD generator, the design of a large MHD magnet, the design of a new MHD channel, and the development of additional diagnostic techniques. A considerable number of MHD experiments with cesium-seeded, noble gases were performed. An analytical study of power optimization in linear MHD generators was undertaken. A study of the effect of molecular gases on the generator performance was undertaken. (auth) (USGRDR)

14082 (N-70-39764) TESTING OF A CASCADED THERMOELECTRIC MODULE. Final Report. Miller, N. C. (Atomics International, Canoga Park, Calif.). 14 Jul 1970. Contract NAS3-13452. 14p. (NASA-CR-72700; AL-70-56). NTIS.

The life testing of a cascaded thermoelectric converter, which had been fabricated and tested to 3450 hours, was extended to about 3930 hours. At that time the coolant pump of the heat rejection system failed, resulting in severe damage to the module. The test was subsequently terminated. During the first 450 hours of testing, the power output of the module remained essentially constant. (auth) (STAR)

14083 (N-70-39884) OPERATION OF A THERMIONIC CONVERTER WITH A (112) TO (114) ORIENTED TUNGSTEN EMITTER AND A NIOBIUM COLLECTOR WITH OXYGEN PRESENT. Wilson, V. C.; Podkulski, S. P. (General Electric Co., Schenectady, N. Y.). Sep 1970. Contract NAS3-8511. 78p. (NASA-CR-1661; GESP-9006). NTIS.

A parallel plane, variable-spaced, thermionic converter with a fluoride-vapor-deposited emitter, a niobium collector and a niobium guard ring was built and tested. Current–voltage characteristics were obtained from a range of emitter temperatures from 1670 to 2153K, collector temperatures from 773 to 1073K, cesium reservoir temperatures from 513 to 641K, and spacings from 2 to 20 mils. The results are compared to those of a converter using a polycrystalline tungsten emitter and a niobium collector. (auth) (STAR)

14084 (SC-RR-70-804) STUDY OF THE EFFECT OF THE EVAPORATIVE EROSION ON THERMOELECTRIC ELEMENTS ON THE PERFORMANCE OF THERMOELECTRIC GENERATORS. Kinney, Ragon D. (Sandia Labs., Albuquerque, N. Mex.). Nov 1970. 19p. Dep. NTIS.

A model is presented and an analysis made of the material losses from thermoelectric elements in some thermoelectric generators, and the effect of such loss on generator performance is determined. (auth)

14085 CAESIUM PLASMA DIODES SEEDED WITH MERCURY OR CADMIUM AND THE PENNING EFFECT. Kaufman, A. J.; Schrenk, G. L. (Univ. of Pennsylvania, Philadelphia). J. Phys., D (London); 3: 1855-67(Dec 1970).

In recent years considerable research has been devoted to techniques for improving the performance of caesium plasma diodes. One such proposal is that increasing the ionization rate might enhance the performance; in fact, Badareu and co-workers have recently reported that they experimentally observed such an effect when seeding a caesium plasma diode with mercury or cadmium. This enhancement is believed to be due to the Penning effect. A theoretical investigation was made of the effects of seeding a caesium plasma diode with mercury or cadmium. A model for both a pure caesium and a caesium seeded diode in the presence of the Penning effect was developed; results from this model compare favorably with available experimental data. It was found that the electron temperature for a pure caesium diode operating in the ignited mode lies in the 2300 to 2800 K range. This model, covering both the ignited and unignited modes, shows clearly where significant enhancements due to seeding can be expected; unfortunately, as will be shown, the region where significant enhancements are obtained are not near the maximum power point. (auth) (UK)

14086 LONGITUDINAL END EFFECTS OF INDUCTIVE THREE-PHASE MHD CONVERTERS WITH OPEN MAGNETIC CIRCUIT AND THEIR SIMULATION ON SEGMENT STATOR ASYNCHRONOUS MACHINES. Schulz, Tilo. Wiss. Ber. AEG-Telefunken; 43: 139-52(1970). (In German).

In the study of the longitudinal end effects of MHD converters with loose coupling between stator and rotor, the problem, complex in more general terms, whereby the secondary section (rotor and working medium) exercises reactive effects on the primary section (inductor) is described. Converters with nonbanked and banked windings are dealt with. The magnet fields, powers, and efficiencies are calculated, details about the phase symmetry also being considered. Great value was attached to the examination of the magnetic field in the active section, above all to the conditions in the air gap (or working channel). Numerical evaluations of the calculation results were performed for converters with high magnetic Reynolds members (tight coupling). The stators examined had nonbanked windings and an even number of poles without unwound ends, as well as banked windings and an odd number of poles without projecting ends. The segment stator asynchronous (SSAS) machines, which have been discussed for some time, are suitable test models on which the longitudinal end effects may be simulated in simple manner. They are induction machines incorporating segment stator and normal squirrel-cage rotor, in which the opening of the magnetic circuit entails special features resembling those of inductive linear MHD converters. In order to render possible a direct comparison between calculation and measurement, the calculations of the first section had to be extended, however, because the rotor stray field of SSAS machines must be considered in contrast to MHD converters. The experiments on SSAS machines cover the field, power, efficiency, and balance, stators having banked and nonbanked windings being used. In general, the measurement and calculation results agree satisfactorily. The results are also compared with various published theories, and methods for preventing the negative influence of the end effects are indicated. (auth)

14087 ELECTRICAL EFFECTS IN THE ELECTRODE BOUNDARY LAYER IN AN FARADAY-TYPE MHD GENERATOR. Celinski, Zdzislaw (Inst. of Nuclear Research, Swierk, Poland). Nukleonika; 15: 499-514(1970).

Some interesting physical phenomena occur in the gas in the Faraday-type MHD generator when the gas parameters vary in the direction of the induced electric field. They are concentrated first of all in the electrode boundary layers, where the gradients of the gas velocity and gas temperature are the largest. The distributions of the electrical quantities in the electrode boundary layers are calculated, and some physical effects occurring there are discussed. (auth)

14088 ANALYTICAL AND EXPERIMENTAL STUDIES OF THERMIONICALLY EMITTING ELECTRODES IN CONTACT WITH DENSE, SEEDED PLASMAS. Koester, John Kent. Pasadena, Calif.; California Inst. of Tech. (1970). 178p. University Microfilms Order No. 70-24,302.

Thesis.

The electrode current–voltage characteristics and the limiting-cathode current density for thermionically emitting electrodes in contact with high-pressure, seeded, nonequilibrium MHD plasmas were determined analytically and experimentally. The theoretical model is based on the coupling of the adsorption phenomena of alkali-metal seed particles onto electrode surfaces with that behavior due to the plasma in the electric boundary layer adjacent to the electrode surface. The desorption rates of electrons and seed atoms and ions (which are given by quoted functions of the surface temperature, the surface degree of coverage, and the electric field at the surface) are related to the appropriate boundary conditions for the governing continuum-type plasma equations in the electric boundary layer. An algorithm is given for the simultaneous solutions of both the surface state and the electric boundary layer. Machine-computed results are presented for a potassium-seeded argon plasma (at 2000°K and one atmosphere pressure) in axially symmetric stagnation flow over a tungsten electrode and display the effects of varying the parameters of surface temperature and seed fraction. These results indicate an order-of-magnitude increase in the thermionic limiting current density due to coupling effects. Experimentally, the electrode phenomena were studied in a nonequilibrium discharge produced in the same plasma–electrode system as used for the machine computations. The electrode behavior was determined from voltage probes, photomultiplier measurements, and photographs. As the thermionic limit was approached, a transition to an arc mode of cathode operation occurred at some breakdown voltage drop. The experimental current–voltage characteristics for the cathode agreed with the machine results, and the predicted enhancement of the thermionic limiting current density was observed. (Diss. Abstr. Int., B)

Fluid Physics

14089 MHD RAYLEIGH PROBLEM WITH UNSTEADY WALL MOTION. Shih, Pei-chong. Baton Rouge, La.; Louisiana State Univ. (1970). 94p. University Microfilms Order No. 70-18,556.

Thesis.

The flow of an electrically conducting, viscous, incompressible fluid, due to the decelerating impulsive motion as well as accelerating motion of an infinite flat wall, is first discussed. A transverse, uniform, fixed-in-space magnetic field is supposed to be present. The induced magnetic field is retained in the governing equations given by Ludford (1959), and nondimensional variables introduced by Steketee (1964) are applied. Laplace transform techniques are used. The wall velocity is assumed to be (I(t) U. exp(–wt)) in the case of decelerating impulsive wall motion and (I(t) U.{1 – exp(–wt)}) in the case of accelerating wall motion. I(t) is the unit step function at t = O, w and U. are constants and t is the time. The classical Rayleigh problem and MHD Rayleigh problem are two special cases of the problem of decelerating wall motion. The solution for the accelerating wall motion follows immediately from that for the decelerating impulsive wall motion by superposition. The solution, in general, is very complicated and can not be expressed in terms of known functions. However, the solutions in certain cases have been found for $((\eta^{1/2} + \nu^{1/2})^2 w/a^2 \le 1)$ even though the corresponding solution does not exist in ordinary fluid mechanics. a is the Alfvén velocity, η and ν are the magnetic diffusivity and kinematic viscosity of the fluid respectively. For the decelerating impulsive wall motion, it is observed that, in the case of equal diffusion coefficients, the shear stress at the interface and the disturbances in both the velocity and magnetic field increase with an increase in the wall conductivity or the applied magnetic field, and with a decrease in w. The speed of the diffusing Alfvén wave is modified to $(a^2 - 4\eta w)^{1/2}$, leaving the solution dominated by the effect of the viscous boundary layer diffusing from the wall. The induced magnetic field is, in general, not neglible. For the accelerating wall motion, it is found that, in the case of equal diffusion coefficients, the shear stress at the interface and the disturbances in both the velocity and magnetic field increase as time advances with the increase in the wall conductivity or the value of w and with the decrease in the applied magnetic field. The induced magnetic field is not negligible except for small time. The concept of the characteristic signal lines, together with the exact solution previously obtained, is then applied and a general transient solution for a nondissipative fluid is obtained for the arbitrary motion of a perfectly conducting or nonconducting wall. (Diss. Abstr. Int., B)

14090 EFFECTS OF VARIABLE PROPERTIES ON MHD FLOW IN FINITE DUCTS. Thomson, W. J.; Bopp, G. R. (Univ. of Idaho, Moscow). J. Appl. Mech.; 37: 954-8(Dec 1970).

Numerical solutions are obtained of the coupled partial differential equations that describe variable-property MHD flow in finite rectangular ducts. The fluid properties are allowed to vary to the extent that electrical conductivity and viscosity are assumed to be temperature-dependent. It is shown that it is not possible to account for fluid-property variations in terms of "weighted" fluid parameters such as average Hartmann numbers. Analysis leads to the conclusion that it is the nature of the current distributions in the duct that is important in predicting the behavior of nonisothermal MHD duct flow. It is possible that this conclusion may aid in the evaluation and correlation of experimental data. It is also shown that consideration of variable fluid properties results in friction factors and flow rates that differ from constant-property solutions by as much as a factor of two and by 50%, even for small variations. (auth)

XUM

14091 MAGNETOHYDRODYNAMIC GENERALIZED COUETTE FLOW (WITH UNIFORM SUCTION; TIME-DEPENDENT PRESSURE GRADIENT; AND ARBITRARY INITIAL VELOCITY). Wadhwa, Y. D. (Birla Inst. of Tech. and Science, Pilani, India). J. Appl. Mech.; 37: 1189-90(Dec 1970).

A general method of solving linear time-dependent fluid flow problems is demonstrated which splits the given problem into the simultaneous solution of a number of boundary and initial-value problems. The special cases of no suction, no magnetic field, and no suction and no magnetic field are included. (M.H.R.)

14092 MAGNETOGASDYNAMIC BOUNDARY LAYER. Perez De Tejada, Hector Antonio. Boulder, Colo.; Univ. of Colorado (1970). 164p. University Microfilms Order No. 70-23,743.

Thesis.

The boundary-layer problem is formulated for a perfectly conducting plasma flow past a flat plate, with a magnetic field imposed along the flow direction. The equations describing the system are analyzed, using Howarth's transformation and a modified version of Meksyn's technique. An expression is derived for the slope of the boundary layer near the wall as a function of the Mach number of the freestream flow, the β parameter of the plasma, and for various forms of the viscosity function $\mu(T)$. The results obtained are found to agree with the numerical integration of the problem. A critical case for which the density of the flow is preserved constant all across the boundary layer is recognized and identified. (Diss. Abstr. Int., B)

14093 SOME INTRINSIC MOTIONS IMPORTANT IN MAGNETOHYDRODYNAMICS. I. Gheorghiev, Gheorghe; Ignat, Margareta. Atti Accad. Naz. Lincei, Rend., Cl. Sci. Fis., Mat. Natur.; 48: 57-63(Jan 1970). (In Italian).

Certain notable intrinsic magnetohydrodynamic motions of a perfect incompressible fluid are studied, choosing as intrinsic reference the trihedron formed, at a given point, by the directions of the velocity and the magnetic field and by the direction perpendicular to them. In this system, making use of suitable Pfaffian forms, the fundamental equations of magnetohydrodynamics are expressed, deducing various important geometrical properties of the motion and considering slow motions in particular. (auth)

14094 SOME INTRINSIC MOTIONS IMPORTANT IN MAGNETOHYDRODYNAMICS. II. Gheorghiev, Gheorghe; Ignat, Margareta. Atti Accad. Naz. Lincei, Rend., Cl. Sci. Fis., Mat. Natur.; 48: 215-19(Feb 1970). (In Italian).

Using the results of Note I, a study is made of the helicoidal motions in which the vorticity vector is parallel to the velocity vector and the conduction current vector is parallel to the magnetic field. That is to say, the field concerned is one of free force, important for astrophysical applications. Finally, the so-called quasi-rigid motions are studied, where the deformation tensor of the velocities cancels out. (auth)

14095 TEMPERATURE FIELD IN MAGNETOHYDRODYNAMIC OSCILLATORY FLOW. Messiha, S. A. S. (Univ. of Ife, Nigeria). Atti Accad. Sci. Torino. I. Cl. Sci. Fis., Mat. Natur.; 104: 483-96(Jul-Oct 1970).

The energy equation for an incompressible electrically conducting fluid in the presence of an external magnetic field along an infinite unmagnetized, but conducting, plane porous wall is considered. It is assumed that the viscous and magnetic Reynolds numbers are equal. The suction velocity normal to the wall, as well as the external velocity parallel to the wall, varies periodically with time about a nonzero constant mean. The temperature field in the boundary layer is obtained in terms of a suction parameter A, two magnetic parameters K and S, Eckert number E, and the Prandtl number P. Two cases are considered, namely (i) the case of thermally insulated wall for which the wall temperature is obtained and (ii) the case of constant wall temperature for which the temperature gradient at the wall is obtained. (auth)

14096 MAGNETOHYDRODYNAMICS OF A DROP, MAGNETOHYDRODYNAMICS IN A CONE, AND SINKS IN UNIFORM MAGNETIC FIELDS. Narain, Jai Prakash. Boulder, Colo.; Univ. of Colorado (1970). 98p. University Microfilms Order No. 70-23,737.

Thesis.

The nature of deformation and drag on a spherical, viscous, conducting and incompressible fluid drop under axisymmetric current distribution is considered. The drop fluid and the ambient fluid phases are nonreacting, nondiffusive and free of charge separation and space charges. The well-known matched asymptotic expansion method is used in analysis. The converging flow of conducting, viscous, incompressible fluid inside an infinite cone under radial converging (or diverging) current field is investigated. These situations are encountered in electric arcs and in the solar atmosphere. The flow is divided into two parts: (1) flow at large distances from apex, and (2) flow near the apex of the cone. The motion due to a line sink situated in a uniform magnetic field is considered. The fluid is assumed to be inviscid, incompressible and conducting in nature. The exact solution obtained showed that motion is confined in a narrow region parallel to magnetic field. (TSS) (Diss. Abstr. Int., B)

14097 REGENERATIVE AMPLIFICATION AND DAMPING OF IONIZATION WAVES IN MHD CHANNELS AND THEIR INFLUENCE ON THE EFFECTIVE ELECTRIC CONDUCTIVITY, THE EFFECTIVE HALL PARAMETER, AND THE AVERAGE ELECTRON TEMPERATURE. **Valentini, H.-B. (Zentralinstitut fuer Elektronenphysik, Berlin). Beitr. Plasmaphys.; 10: 23-36(1970). (In German).**

The phase velocity, amplification rate, and critical Hall parameter are theoretically determined for ionization waves in a weakly ionized plasma streaming across a strong external magnetic field and bearing a current flowing perpendicular to both the magnetic field and the stream velocity. The investigations hold for seeded rare gases at any degree of seed ionization. The critical Hall parameter β_c depends on the degree of ionization, the ionization energy, and the temperatures of the electron gas T_θ and neutral gas T_g. β_c is always greater than one, if $0 < T_\theta - T_g \ll T_\theta$ holds. The three-dimensional treatment indicates the existence of waves with a nonvanishing wave vector component in the direction of the magnetic fields. The influence of ionization waves on mean current density, mean Hall field intensity, and mean electron temperature is determined up to second-order terms in the relative fluctuations of the electron temperature. The amplification of ionization waves reduces the effective electric conductivity, the effective Hall parameter, and the mean electron temperature compared to the undisturbed state. Similar results are also obtained for steady-state homogeneous isotropic turbulence and a special case of axially symmetric turbulence. Furthermore, a component of the electric field in direction or in opposite direction to the magnetic field vector may be generated by nonisotropic and nonhomogeneous turbulence. (auth)

14098 REGENERATIVE AMPLIFICATION AND DAMPING OF MAGNETO-ACOUSTIC WAVES IN MHD CHANNELS AND THEIR INFLUENCE ON AVERAGE CURRENT DENSITY AND AVERAGE HALL FIELD STRENGTH. **Valentini, H.-B. (Zentralinstitut fuer Elektronenphysik, Berlin). Beitr. Plasmaphys.; 10: 207-22(1970). (In German).**

Magneto-acoustic waves generated by fluctuations in the Hall parameter, the electric conductivity, and the stream velocity are theoretically investigated in a weakly ionized plasma streaming across a strong external magnetic field and bearing a current flowing perpendicularly to both magnetic field and stream velocity. The investigations hold for seeded-rare gas plasmas at any degree of seed ionization, but are restricted to waves propagating in parallel or antiparallel direction to the current density vector and in parallel or antiparallel direction to the stream velocity vector and to wavelengths which are small in comparison to the interaction length which occurs as a characteristic wavelength. The influence of these waves on the mean current density and the mean Hall field intensity is calculated for the case of small amplitudes and low degree of seed ionization up to second-order terms. Omitting Ohmic heating, the dispersion equation can be solved exactly. A phase shift exists between the fluctuations in gas density and gas velocity. The phase velocity and the amplification rate depend on the wavelength. Typical results are represented in a diagram. For both types of waves, the phase velocity rises slightly with increasing wavelength, while the amplification rate decreases. Waves propagating in opposite direction to the current density vector are amplified if the electron velocity exceeds a critical value. They reduce the mean current density and the mean Hall field intensity. Waves propagating in opposite direction to the steam velocity vector are also amplified, except for very high degrees of seed ionization. The threshold current density is greater than that for the waves of the first type by approximately the Hall parameter as factor. At an extremely high degree of seed ionization, the phase velocity is directed opposite to the direction occurring at weakly ionized seed. Waves of the second type decrease the mean current density but increase the mean Hall field intensity. (auth)

14099 FORMATION OF A BOUNDARY LAYER DISSIPATING MAGNETIC ENERGY NEAR A NEUTRAL PLANE. **Antonini, Gerard; Quemada, Daniel (Univ., Paris). Compt. Rend., Ser. A; 271: 1193-6(9 Dec 1970). (In French).**

The variations with respect to time of a magnetic field near its neutral plane resulting from the flow of a fluid of finite electrical conductivity were studied. The existence of Joule dissipation of the magnetic energy at the boundary layer was demonstrated. (auth) (France)

14100 DECREASE IN INTENSITY OF Hg LINES NEAR THE SOURCE IN WEAKLY IONIZED MERCURY GAS FLOW. **Nishikawa, Masahiro; Fujiie, Yoichi; Suita, Tokuo (Osaka Univ.). J. Phys. Soc. Jap.; 30: 258-66(Feb 1971).**

In a flowing mercury afterglow with dc discharge source, rapid decrease in intensity of Hg lines near the source are investigated. Both the axial intensity distribution along the flow downstream and the radial one are interpreted in connection with diffusion of electrons to the wall and electron attachment. The effective diffusion coefficient is found to be $D_{\delta,\gamma} = 2.7 \times 10^3/p(cm^2/sec)$, which is close to the ambipolar diffusion coefficient under the experimental conditions i.e., $n_e = 5 \times 10^8/cm^3$ and $T_e = 2$ eV. As for the resonance line ($6^3P_1-6^1S_0$), slow decrease in intensity as compared with decrease in intensity of lines emitted from the higher levels is taken to be due to the radiative capture and, in consequence, the absorption coefficient of this line is obtained as 1.2×10^{-13} n_0/cm and the quenching cross section of the state 6^3P_1 due to the collisions with mercury atoms as $\langle\sigma\rangle_{10} = 0.048$ Å^2. (auth)

Geophysics (Upper Atmosphere)

Refer also to abstracts 13328 and 13897.

14101 (AD-712045) SOLAR ELECTRON ACCESS TO CLOSED FIELD LINES. **Vampola, Alfred L. (Aerospace Corp., El Segundo, Calif.). 15 Aug 1970. Contract F04701-70-C-0059. 27p. (TR-59(6260-20)-8; SAMSO-TR-70-352). NTIS.**

Solar electron fluxes, by virtue of their spectra, pitch-angle distributions, and temporal and spatial behavior, are used as test particles in investigating the quasi-trapping region of the geomagnetosphere. A number of features of these fluxes are demonstrated using data from magnetic electron spectrometers on the polar-elliptical oribiting satellite OV1-19 (1969-25C) during the period April 12 to April 17, 1969. The results indicate that although the particles are readily injected onto closed field lines, inward radial diffusion is slow compared with longitudinal drift and electrons do not become stably trapped in significant quantities unless the diffusion mechanism is an energy-dependent one in which low energy particles are preferentially diffused inward. Sharp persistent gradients between the quasi-trapped zone and the polar plateau (a region of uniform isotropic fluxes) are regarded as indicating there is an abrupt transition between a region of the geomagnetic field which consists entirely of closed field lines (i.e., permit conjugate point mirroring), and a second region in which the field lines either connect directly to the interplanetary field or extend into a tail which is very turbulent on the scale of the gyro-radius of .1 to 2 MeV electrons. (auth) (USGRDR)

14102 (N-70-19848) ATOMIC PHYSICS AND THE POLAR CAP. **Green, A. E. S.; Strickland, D. J. (Florida Univ., Gainesville. Dept. of Physics and Astronomy). [1969]. 87p. (NASA-CR-108236). CFSTI.**

Fundamental mechanisms in polar-cap phenomena are discussed from the standpoint of atomic physics. Emphasis is placed on processes stimulated either by photons, electrons, or protons. A characterization of the special morphological features of polar-cap phenomena, distinct from auroral-zone or other atmospheric phenomena, is included. A state-of-the art review is given on atomic physics and planetary aeronomy. (STAR)

14103 AURORAL-PARTICLE PRECIPITATION AND TRAPPING CAUSED BY ELECTROSTATIC DOUBLE LAYERS IN THE IONOSPHERE. **Albert, R. D. (Physics International Co., San Leandro, Calif.); Lindstrom, P. J. Science; 170: 1398-1401 (25 Dec 1970).**

Interpretation of high-resolution angular distribution measurements of the primary auroral electron flux detected by a rocket probe launched into a visible aurora from Fort Churchill in the fall of 1966 leads to the following conclusions: the auroral electron flux is nearly monoenergetic and has a quasi-trapped as well as a precipitating component; the quasi-trapped flux appears to be limited to a region defined by magnetic-mirror points and multiple electrostatic double layers in the ionosphere; the electrostatic field of the double-layer distribution enhances the aurora by lowering the magnetic-mirror points and supplying energy to the primary auroral electrons. (auth)

14104 CHANGES OF LOWER IONOSPHERE ELECTRON DENSITIES WITH SOLAR ZENITH ANGLE. **Mechtly, E. A. (Univ. of Illinois, Urbana); Smith, L. G. Radio Sci.; 5: 1407-12(Dec 1970).**

A series of four Nike–Apache rockets were launched from Wallops Island, Virginia, on July 24, 1968 for the study of changes of lower-ionosphere electron densities with solar-zenith angle on the same day. An improved method of data analysis is outlined. Profiles of electron density for each of the four rockets are presented and compared with two profiles from years of quiet Sun, 1964 and 1965. Evidence is found for an initial increase of free electrons followed by a decrease and then an increase in electron number density as the solar-zenith angle changes from 94 to 18°. This pattern suggests a sequence of processes; i.e., electron detachment, recombination, and photo-ionization. (auth)

14105 UNIFIED DESCRIPTION OF THE TIDAL EFFECTS IN f_0F_2. **Rush, C. M. (Air Force Cambridge Research Labs., Bedford, Mass.); St. John, D. E.; Venkateswaran, S. V. Radio Sci.; 5: 1413-28(Dec 1970).**

The ionospheric spectrum of the critical frequency of the F_2 region, f_0F_2, is studied in detail at 35 locations during solar maximum and at 21 stations during solar minimum. The spectra contain prominent lines superposed on background continua. The most prominent lines correspond to solar periods of 24, 12, and 8 hours. Lines at half a lunar day (period of 12.48 solar hours) and at two lunisolar periods were also detected in all the spectra investigated. The lunisolar lines have statistically significant amplitudes only at the low-latitude stations. The analysis indicates the influence in the F region of plasma transport processes such as E × B drift, ambipolar diffusion, and ion-drag effects of the neutral air wind generated by the thermospheric diurnal density variations. An assessment of the roles of some of these processes is attempted in terms of the results obtained from the analysis. (auth)

14106 NATURE OF AURORAL MAGNETO-IONOSPHERIC PERTURBATIONS. **Van'yan, L. L.; Osipov, N. K.; Pivovarov, V. G. Dokl. Akad. Nauk SSSR; 194: 77-9(Sep-Oct 1970). (In Russian).**

Ionization of the auroral ionosphere is increased strongly by streams of energetic particles, which play an important role in creating magneto–ionospheric perturbations. Interaction of the particles with the atmosphere at altitudes below 1000 km may result in charge separation in an originally quasi-neutral stream. This means that uncompensated electrical charges are brought in at the 100- to 120-km level by the auroral particles, creating a meridional electric field. Thus, the auroral perturbations involve ionization of the ionosphere, generation of electric currents by the space charge as the conductivity of the ionosphere is increased, and excitation of the magnetic fields by the auroral currents. The structure of the electric field of the space charge transported into the ionosphere by the electron currents and the associated proton flux is represented graphically. It is pointed out that, in the auroral region where the lines of force are almost vertical, the magnetic fields of magnetospheric and Pedersen currents mutually compensate each other and the final effect involves the Hall current. The magnetic field directly above the auroral region is estimated at $H \approx 100\ \gamma$. (TTT)

14107 OXYGEN AURORAL LINES: NEW THEORY AND EXPERIMENT ON FORBIDDEN TRANSITION PROBABILITIES. **Sinanoglu, Oktay (Yale Univ., New Haven). Comments At. Mol. Phys.; 11: 79-83(Aug-Sep 1970).**

Experimental and theoretical results have previously been discussed on the allowed-transition probabilities of atoms like C, N, O, F, Ne and their ions. New methods now give few-percent accuracy on this property. Forbidden transitions of [O I], [O II], [O III], [N I], and [N II] occur in aurorae, night airglow, gaseous and planetary nebulae, and solar corona. They are mainly quadrupole (E2) or magnetic dipole (M1) transitions. A detailed study of the [O I] lines and the new calculation method are given. The few experiments on [O I] depend on the elimination of the O ($^1S_0$) number density by essentially looking at two transitions that start from the same level. An absolute A(5577) measurement was made recently. In the same oxygen–helium discharge, the O ($^1S_0$) allowed λ1218-A, vacuum-uv absorption gives indirectly the number density that is combined with the λ5577 intensity measurement. (J.C.W.)

14108 INVERSE COMPTON EFFECT IN THE ELECTRONS OF THE VAN ALLEN RADIATION BELT. **Albano, Jorge Raul (Univ., Nacional de La Plata). Astrophys. Space Sci.; 9: 332-7(Nov 1970).**

A first estimate of the energy that reaches the Earth's surface and is produced by the inverse Compton effect between the electrons in the Van Allen belt and the solar flux was made. Since in the belt there are electrons with energies between 0.5 and 7 MeV, it was possible to use the Klein–Nishina formula in an approximate form and estimate the energy that is Compton-scattered by all the electrons in the Van Allen belt by using Vette, Lucero, and

XUM

Bright's model. The result was compared (a) with the measurements of the continuum in the regions of soft x rays, and (b) with the energy that is produced by the trapped electrons through the synchrotron mechanism. (auth)

14109 LATITUDE-WIDE ENHANCEMENT OF 6300-A EMISSION IN NIGHTGLOW. **Pal, S. R.** **(Meteorological Service of Canada, Toronto). Planet. Space Sci.; 18: 1829-31(Dec 1970).**

In observations at Mt. Abu, India, the 6300-Å nightglow emission was found to show post-twilight decay to around midnight and post-midnight enhancement from about midnight until dawn. Studies with a scanning photometer at other latitudes along the same meridian (72° 43′ E) indicated a latitude-wide development of emission enhancement. These enhancements are discussed, and the results are compared with studies made at other stations. Corrections were made for atmospheric scattering and extinction. Results are presented for very clear and geomagnetically quiet nights during April and May, 1967. The enhancements may have been due to both ambipolar diffusion of ionisation and ionospheric vertical drifts. (UK)

14110 COUPLING BETWEEN SOLAR WIND AND IONOSPHERE. **Burkard, O. M.** **(Univ., Graz). Planet. Space Sci.; 18: 1832-4(Dec 1970).**

Some relationships are established between the velocity of the solar wind and the electron density of the F2 layer. Pioneer VI solar-wind data for the period Dec. 16, 1965 to May 10, 1966 are used for the calculations, and critical frequencies f_0F2, measured at the ionospheric station at Lindau, are used to characterise the F2 ionisation. A significant correlation was found only for daytime data. With increasing solar-wind velocity typical storm phenomena appeared. The influence of the interplanetary magnetic field is discussed. A significant correlation was found between solar wind and height of the F2 layer. The fact that no night-time relationship was found means that the increase in electron density cannot be attributed to penetration of solar-wind particles into the ionosphere on the night side through the magnetospheric tail. The question remains, however, whether such penetration occurs on the day side or the density increase is attributable to change of shape or volume of the ionosphere. Further investigations are required to examine how far the derived relationships are modified by solar wind particle density. (UK)

14111 NATURE OF THE DAILY VARIATION OF GEOMAGNETIC FIELD. **Kane, R. P.** **(Physical Research Lab., Akmedabad, India). Planet. Space Sci.; 18: 1834-6(Dec 1970).**

The daily variation of geomagnetic field is usually attributed to dynamo current systems in the spherical ionospheric shell. Sarabhai and Nair (1969), however, proposed an alternative explanation, in that the daily variation is due to a weakening of the ambient field on the night side. It is shown, however, that the quiet-day daily variation is caused mainly by daytime increases, in mid and low latitudes, and not by night-time depletions as proposed by Sarabhai and Nair. It does not follow, however, that the source of these variations is necessarily the ionospheric current systems; there may be magnetospheric contributions. The effects need further quantitative studies. (UK)

14112 COMMENTS ON THE PAPER OF V. C. LIU AND R. I. HUNG "DOUBLE SCATTERING OF THE PLASMA STREAMS IN A BI-THERMAL IONOSPHERE." **Al'pert, Y. L.; Bud'ko, N. I.; Vas'kov, V. V.** (Dept. of Solar-Terrestrial Research, Moscow). Planet. Space Sci.; 18: 1843-5(Dec 1970).

Liu and Hung (Planet. Space Sci., 16: 845(1968)) studied the far wake of a body moving in a rarefied plasma with a velocity V, $v_i \ll V \ll v_e$, v_i and v_e being the thermal velocities of ions and electrons, but it is noted that the results obtained by these authors do not agree with those of other authors and lead to a wrong conclusion concerning the structure of a body wake. An analysis of this discrepancy is given. The case when the external magnetic field is absent is first considered, and the influence of an external magnetic field then considered. It is also stated that Liu and Hung obtained some wrong expressions for the case of double scattering, that is, plasma disturbance by a tandem of bodies. (UK)

14113 GEOMAGNETIC TAIL STRUCTURE NEAR THE NULL SHEET. **Mihalov, J. D.** **(Ames Research Center, Moffett Field, Calif.). Planet. Space Sci.; 18: 1845-7(Dec 1970).**

A study of geomagnetic tail structure normal to the solar-magnetospheric X–Y coordinate plane is described, using hourly average field-magnetometer data from Explorers 33 and 35. The data suggest that the near-Earth field depression is not necessarily pronounced, and support the view of a broad and shallow field-magnitude depression, rather than a sharp profile. A decrease and/or dissipation of plasma sheet particle-energy density at lunar distances in the geomagnetic tail may be indicated. The data are also consistent with the finding by Hones (1969) that the quiet-time tail field-magnitude gradient down the tail within the plasma sheet is less steep than in the remainder of the tail. Any central field-magnitude depression is identified with the plasma sheet. No significant dependence of tail-field latitude angle on geocentric radial distance, geomagnetic-activity index or coordinate Y was found for either the north or south lobe of the tail. Evidence was also obtained that tail-field latitude angles are increased at coordinate $Z \sim 0$ only at moderate geocentric distances where a field-magnitude depression is noticeable. (UK)

14114 LOW-LATITUDE SUBPROTONOSPHERIC AND ION CYCLOTRON WHISTLERS GENERATED BY THE SAME LIGHTNING DISCHARGE. **Egeland, A.; Leer, E.** **(Norwegian Inst. of Cosmic Physics, Oslo). Planet. Space Sci.; 18: 1848-50(Dec 1970).**

Whistler phenomena, generated by lightning discharges and observed in the OVI-10 electric field experiment, are discussed. Ac electric-field measurements were analysed with an electric sonograph and a spectrum analyser. The data were obtained in Dec. 1966 at about geomagnetic midnight and 10 to 30° geomagnetic latitude. Electron whistlers above 600 Hz followed the Eckersley equation, with a dispersion close to 5 $sec^{½}$, but below 300 Hz the dispersion was about 20% larger. Proton whistlers were always observed, and there were indications of He^+ whistlers. Proton and He gyrofrequencies were calculated, together with fractional concentrations of H^+ and He^+. The disappearance of whistler energy below 585 Hz meant that the proton concentration down to <450 km was high enough to cause polarisation reversal. An interesting point was the occurrence of additional traces on the spectrogram; these are discussed. The generation of subprotonospheric whistlers is also discussed. (UK)

14115 MIDDLE-LATITUDE AURORAE AT THE CURRENT SOLAR MAXIMUM. **Truttse, Y. L.; Shefov, N. N.** **(Inst. of Physics of the Atmosphere, Moscow).** Planet. Space Sci.; 18: 1850-4(Dec 1970).

In recent years information has been obtained concerning the behaviour of upper-atmosphere emissions in the middle-latitude zone during intense geomagnetic disturbances. It was thought desirable to check the results during the present solar maximum cycle. The geomagnetic storm of March 24, 1969, which followed a solar burst on March 23, was considered to be of great interest, and data are given on the upper atmosphere emissions as obtained at the Zvenigorod Observatory; the total intensities of 6300 and 6364-Å emissions were measured. It was found that the earlier-established regularity in the behavior of the 6300-Å emission remained valid. Observations concerning the Doppler temperature were also confirmed. The Doppler temperature was not more than 700°K at night during quiet geomagnetic conditions indicating that, during strong geomagnetic storms, there is an increase in temperature of the neutral and ionic components of the atmosphere. The overall global energy released during the storm of March 24, on the night side, within the limits ±60° geomagnetic latitude, is estimated as 3×10^{22} ergs. The behavior of OH emission during and after the storm was also investigated. (UK)

14116 CONSIDERATIONS THAT THE SOURCE OF AURORAL ENERGETIC PARTICLES IS NOT A PARALLEL ELECTROSTATIC FIELD. **O'Brien, Brian J.** **(Univ. of Sydney). Planet. Space Sci.; 18: 1821-7(Dec 1970).**

It is shown that electrostatic fields parallel (E_{11}) to the geomagnetic field cannot be the major mechanism that accelerates charged particles to auroral energies. Principal arguments are that electron and proton precipitation occur simultaneously, and also that precipitated electrons with energies less than 100 eV are found to accompany the electrons with energies of 1 to 10 keV that excite auroral luminosity. It is further shown that essentially all the ambient plasma in an entire tube of flux is required to sustain this intense low-energy precipitation, and this places a severe constraint on any replenishment process. It is found that generally the upper limit of E_{11} throughout the auroral regions of the ionosphere and magnetosphere is of order 10 μV/m and it may be appreciably less. Relevant measurements are reviewed briefly. It is concluded that while there may occasionally be significant E_{11} fields, they play only a minor role, if any, in auroral phenomena. (auth) (UK)

14117 ON THE RESONANT MODES OF A CAVITY AND THE DYNAMICAL PROPERTIES OF MICROPULSATIONS. **McClay, J. F.** **(Air Force Cambridge Research Labs., Bedford, Mass.). Planet. Space Sci.; 18: 1673-90(Dec 1970).**

Certain classes of micropulsations are customarily explained in terms of guided (toroidal) and isotropic (poloidal) hydromagnetic waves in the magnetosphere. The physical properties of these waves are not well understood and their utility in explaining observed polarization patterns is questionable. In an effort to understand and explain the physics underlying these modes, a study is made of a cylindrical cavity (the hydromagnetic wedge), filled with a plasma having a large but finite conductivity and magnetized by an azimuthal magnetic field. Coupling between the toroidal and poloidal modes is effected by the inclusion of the Hall current in the generalized Ohm's law. Physically meaningful solutions to the wave equation are obtained and the toroidal eigenfunctions are demonstrated to be non-degenerate and well-behaved throughout the configuration, and exhibit for each mode a unique spatial resonance whose location, given by a line of force, is specified by the corresponding eigenvalue. The non-degenerate, discrete, and spatially independent eigenvalues for the modes are shown to obey a selection rule that limits the spectrum. For a given mode, the states of polarization of the transverse field are determined and it is shown (as has been observed) that, depending on the line of force singled out, the magnetic polarization may be linear, elliptical, or circular, right- or left-handed, and whatever the state, it is immutable along the line of force. More complicated polarization patterns are derived and explained by superposing different modes vectorially. Classical concepts such as guided and isotropic modes and vibrating field lines are reinterpreted and evaluated in terms of the model. To examine the dependence of modal amplitude on source, the amplitude is expressed in terms of a sinusoidal-driving pressure for a simple steady-state case. Symmetries of the model and the magnetosphere are specified and the detailed numerical results are "scaled" for plasmaspheric application. The resonant spectrum, encompassing Pc 2–4, is described and the variation of period spectrum with magnetic latitude and activity is presented. The agreement between the semi-quantitative analysis and the observational results is sufficiently close to indicate that the basic physics of the model encompasses the fundamental dynamics of Pc activity. (auth) (UK)

14118 CONJUGATE AND CLOSELY-SPACED OBSERVATIONS OF AURORAL RADIO ABSORPTION. IV. THE MOVEMENT OF SIMPLE FEATURES. **Hargreaves, J. K. (Univ. of Lancaster, Eng.). Planet. Space Sci.; 18: 1691-1705(Dec 1970).**

Although the time structure of auroral-radio absorption, measured with riometers at high-latitude stations, is generally complex, some features are seen that have a relatively simple structure. Multiple riometer data from the magnetically conjugate stations Great Whale River and Byrd demonstrate that many of these features show movements over a 250-km baseline. Both the velocities and the directions of movement are consistent with the substorm movements that have been detected in other auroral work, for example by visual observations or by auroral radar. The velocities range between 80 m/sec and 3.3 km/sec, the directions being predominantly westward in the evening sector and eastward in the morning. The observed behaviour is essentially the same in both hemispheres, though event-by-event comparisons show some differences of velocity. The data are applied to determine the instantaneous corresponding points in the two hemispheres; it is found that the corresponding point wanders by 130 km about its mean position. Some implications of the results are discussed. (auth) (UK)

14119 SMALL-SCALE AURORAL ARC DISTORTIONS. **Hallinan, Thomas J.; Davis, T. Neil (Univ. of Alaska, College). Planet. Space Sci.; 18: 1735-44(Dec 1970).**

Small-scale spatially-periodic distortions of auroral forms were studied utilizing low-light level television observations made at various locations in the northern and southern hemispheres. The most commonly observed features were folds and vortex-like curl formations. The curls, identified here with the Kelvin–Helmholtz instability due to fluid shear, invariably had a counterclockwise rotational shape and motion when viewed in a direction anti-parallel to the Earth's magnetic field. The typical measured wavelength (~5 km) and measured growth rate (4.2 $\sec^{-1}$) were used to evaluate the Kelvin–Helmholtz dispersion relation for the apparent shear $\omega_s = \partial v_x/\partial y$ (28 $\sec^{-1}$). The apparent horizontal velocities of both folds (0 to 5 km/sec) and curls (0 to 22 km/sec) were invariably observed to be counterclockwise with respect to the multiple arc centre when viewed antiparallel to B. Consistent agreement between rotational shape and rotational motion suggests that the apparent growth rate and the apparent horizontal velocities closely approximate the actual values. If the shear results from E × B drifts in a space charge field, the calculated value for ω_s implies an unneutralized electron density ~0.1 cm^{-3} and a ΔE across the arc element ~500 mV/m. The velocity measurements indicate that the ΔE values for individual elements can combine to produce transient electric fields at the edges of multiple arcs as high as 1000 mV/m. (auth) (UK)

14120 MAGNETOSPHERIC REFLECTION OF WHISTLERS. **Lyons, L. R.; Thorne, R. M. (Univ. of California, Los Angeles). Planet. Space Sci.; 18: 1753-67(Dec 1970).**

An analytical description of the propagation of magnetospherically reflecting, nonducted whistler-mode waves is given, and an attempt is made to evaluate which features of the magnetospheric plasma govern the wave-reflection process. A new approximate wave-dispersion relationship is derived, valid for wave-propagation vectors nearly normal to the ambient-field direction and for frequencies below the lower-hybrid frequency. This is then used to evaluate the instantaneous radius of curvature of nonducted whistler-ray paths. It is found that the major contribution to the ray curvature results from the gradient in the magnetic-field strength along the direction of the field. Analytical expressions for the whistler-ray paths suggest that waves near the lower-hybrid frequency bounce back and forth across the geomagnetic equatorial plane, more or less along a given field line. At lower frequencies the waves are more confined to the equatorial plane, and their penetration on each bounce across field lines is larger. (auth) (UK)

14121 IONOSPHERIC RESPONSE TO AN ISOTROPIC SPECTRUM OF INTERNAL GRAVITY WAVES. **Hooke, William H. (ESSA Research Labs., Boulder, Colo.). Planet. Space Sci.; 18: 1793-7(Dec 1970).**

The computer-produced tonal-value plots in which darkness or intensity are used to display the ionospheric response to an isotropic spectrum of internal gravity waves are presented. Each plot shows at a glance those portions of the wave spectrum, i.e., those wave periods and azimuths of propagation, producing the ionospheric irregularities of greatest magnitude. Arrays of the plots illustrate the variations of this response with time of day, season, latitude, geomagnetic dip, and height. (auth) (UK)

14122 NONLINEAR PARTICLE TRAJECTORIES IN A WHISTLER-MODE WAVE PACKET. **Ashour-Abdalla, M. (Imperial Coll. of Science and Tech., London). Planet. Space Sci.; 18: 1799-1812(Dec 1970).**

Particle trajectories for the case of a whistler-wave packet propagating in the direction of the ambient magnetic fields are computed. The computed trajectories enable the study of the distortion of a loss cone by such a wave. Currents are obtained and comparison with linear theory show that nonlinear effects reduce the current. It is found that the time behaviour of the fields is such as to make the packet grow at the front and decay at the rear. (auth) (UK)

14123 ELECTROSTATIC FIELD THEORY UNDER IONOSPHERIC CONDITIONS. **Gershman, B. N.; Samsonov, A. V. (Gorky State Univ., USSR . Izv. Vyssh. Ucheb. Zaved., Radiofiz.; 13: 1312-20(1970). (In Russian).**

Equations are derived for the potential of the electrostatic field in the presence of sources under ionospheric conditions. These fields may be due to neutral-gas motion. The study is made taking into account the factors responsible for ambipolar plasma diffusion. The effectiveness of excitation, and especially the penetration degree, is shown to be essentially associated with horizontal scales of the fields. (auth)

14124 ADDITIONAL CALCULATIONS OF THE RATE OF PRODUCTION OF ELECTRONS IN THE LOWER IONOSPHERE BY SOLAR COSMIC RAYS. **Dorman, L. I.; Krupitskaya, T. M. Bull. Acad. Sci. USSR, Phys. Ser. (Engl. Transl.); 33: 1766-72 (Nov 1969).**

Translated from Izv. Akad. Nauk SSSR, Ser. Fiz.; 33: 1933-9 (Nov 1969).

Calculations of the rates of electron production by solar corpuscular streams with different charge and energy spectra are given. From flares in Nov. 1960, the average energy required to form a single ion pair was found. The results of numerical calculations are given in the form of diagrams and tables. (W.D.M.)

14125 OBSERVATION OF LOW-ENERGY PROTON FLUX PARALLEL TO THE GEOMAGNETIC FIELD LINES IN THE AURORAL IONOSPHERE. **Reme, Henri; Bosqued, Jean-Michel (Univ., Toulouse, France). Compt. Rend., Ser. B; 271: 1145-8(9 Dec 1970). (In French).**

The low-energy proton flux (0.5 to 5 keV) measured during the flight of the Dragon rocket in a diffuse aurora was parallel to the geomagnetic field lines for 115 seconds and associated with intense electron precipitation (5 to 30 keV). The experimental results obtained during this part of the flight imply a potential difference of about 1 kilovolt along the field lines. (auth) (France)

14126 EFFECT OF THE PROPERTIES OF SOLAR CORPUSCULAR STREAMS ON THE RATE OF PRODUCTION OF

XUM

ELECTRONS IN THE LOWER IONOSPHERE. Velinov, P. Bull. Acad. Sci. USSR, Phys. Ser. (Engl. Transl.); 33: 1751-3 (Nov 1969).

Translated from Izv. Akad. Nauk SSSR, Ser. Fiz.; 33: 1918-20 (Nov 1969).

Earlier results on polar cap absorption are generalized to take into account the well-known change in the angular distribution of the particles of an intruding solar corpuscular stream as they penetrate into the atmosphere. (W.D.M.)

14127 27-DAY VARIATIONS IN THE LOWER IONOSPHERE ASSOCIATED WITH COSMIC-RAY AND GEOMAGNETIC VARIATIONS. Nestorov, G.; Velinov, P.; Letfus, V. (Inst. of Geophysics, Sofia. Astronomical Observatory, Prague). Bull. Acad. Sci. USSR, Phys. Ser. (Engl. Transl.); 33: 1754-8(Nov 1969).

Translated from Izv. Akad. Nauk SSSR, Ser. Fiz.; 33: 1921-5 (Nov 1969).

The galactic cosmic rays produce a layer with an electron density of $\sim 10^{-2}$ cm^{-3} at a height of 50 to 80 km in the lower ionosphere. The detection of 27-day variations in this layer is reported, and a method is presented for studying this variation theoretically. (W.D.M.)

Low-Temperature Physics and Cryogenic Equipment

Superfluidity

Refer also to abstracts 14492 and 14500.

14128 (COO-1574-17) DEPENDENCE OF THE HELIUM II FILM TRANSFER RATE ON PRESSURE HEAD, FILM HEIGHT, AND SUBSTRATE. Duthler, Carl James (Michigan State Univ., East Lansing). 1970. 81p. Dep. NTIS.

Thesis.

Helium film transfer rates, σ, were measured as a function of level difference, z, and height, h, to the beaker rim, for filling clean glass and neon-coated beakers. Measured transfer rates as a function of level difference or pressure head are described by: $\sigma(z) = 1/[A - B \ln z(\text{cm})]$. For T = 1.65K and h = 7 cm, the values A = $(1.80 \pm 0.09) \times 10^4$ sec/cm^2 and B = $(8.9 \pm 1.9) \times 10^2$ sec/cm^2 are found. For T = 1.28K and h = 7 cm, the values A = $(1.35 \pm 0.02) \times 10^4$ sec/cm^2 and B = $(8.4 \pm 1.4) \times 10^2$ sec/cm^2 are found. The dependence of the transfer rate on height is: $\sigma(h) = 10(\rho_s/\rho)h^{-(0.26\pm0.05)} \times 10^5$ cm^3/sec-cm. These observations give the dependence $P_s \propto \exp[f(h,T)/v_s]$, of the frictional pressure, P_s, which opposes the flow, on superfluid velocity, v_s. The dependence $v_c \propto d^{-1/4}$, of the critical velocity, v_c, on film thickness, d, is also determined from these results. A 16% decrease is observed in σ going from a clean glass substrate to a neon-coated substrate in the same apparatus. This result is in reasonable agreement with the calculated helium film thickness for a neon substrate of $2.3\,h^{-1/3} \times 10^{-6}$ cm. (auth)

14129 (COO-1574-19) COUPLING BETWEEN PRESSURE AND TEMPERATURE WAVES IN LIQUID HELIUM. Fritz, Garold F. (Michigan State Univ., East Lansing). 1970. 90p. Dep. NTIS.

Thesis.

When the thermal expansion coefficient α is retained in the linearized hydrodynamic equations of the two-fluid model of superfluid liquid helium, pressure and temperature waves are not independent. Thus, a periodically varying temperature source produces not only temperature waves in liquid helium, but also two pressure waves, p_1' and p_2', which propagate at the velocity of first and second sound, respectively. Similarly, a vibrating diaphragm produces not only pressure waves but also two temperature waves, T_1' and T_2', which also propagate at the velocity of first and second sound, respectively. Lifshitz has shown that the amplitudes of these cross modes should be proportional to α. This coupling is investigated here by observing and studying the two pressure waves p_1' and p_2' produced by a heater and the temperature wave T_2' produced by a capacitor microphone. The temperature dependence of the amplitude of these waves is studied, using both pulse- and standing-wave techniques in the temperature range from 1.2°K to the λ point. Good agreement with theory results only for the p_1' mode. (auth)

14130 ACOUSTIC FLOW IN A SUPERFLUID LIQUID. Boguslavskii, Yu. Ya.; Ioffe, A. I.; Statnikov, Yu. G. (Inst. of Physics of High Pressures, Moscow). Zh. Eksp. Teor. Fiz.; 59: 1999-2002(Dec 1970). (In Russian).

Acoustic currents arising during propagation of first and second sound in a superfluid liquid are considered, with an accuracy to the second approximation. (auth)

14131 KINETIC PHENOMENA IN THE PROPAGATION OF SECOND SOUND IN He II WITH A LARGE THERMAL FLUX. Arkhipov, R. G. (Inst. of Physics of High Pressures, Moscow). Zh. Eksp. Teor. Fiz.; 59: 2055-8(Dec 1970). (In Russian).

The equation set for propagation of second sound in He II with an arbitrary difference between the normal and superfluid velocities is investigated. For internal motion, velocities of the order of second-sound-velocity shock-wave formation become possible. The temperature dependence of the critical velocities is found. (auth)

14132 CRITICAL HEAT FLUX IN LIQUID HELIUM II CLOSE TO THE λ TRANSITION. Winer, Bette Marcia. College Park, Md.; Univ. of Maryland (1969). 88p. University Microfilms Order No. 70-14,951.

Thesis.

For the specific case of liquid helium II near its λ transition, Ferrell et al. suggested that the dominant consideration is fluctuations in the second sound modes of the system which become very large at the transition. Using this idea and the criterion of Landau, Mikeska developed a theory for the coupling of the superfluid to these critical fluctuations and the resulting breakdown of superfluidity. One characteristic of the superfluid state is the inability of He II to support a temperature gradient. The absence of this gradient results in boiling of the liquid unaccompanied by the usual presence of bubbles below its free surface. This experiment uses both the appearance of bubbles and the onset of a finite temperature gradient as indications that superfluidity has broken down. Specifically, the breakdown of superfluidity due to the excitation of second sound modes as predicted by Mikeska's theory is measured. (TSS) (Diss. Abstr. Int., B)

14133 NUCLEATION OF CAVITATION BY ALPHA-PARTICLE IRRADIATION OF LIQUID HELIUM. Shadley, John Russell. Houston, Tex.; Univ. of Houston (1970). 147p. University Microfilms Order No. 70-18,024.

Thesis.

A review is given of cavitation in normal liquids and liquid helium, vortex and radiation-induced cavitation, and the creation of vortex rings in helium II by ions. The presence of an α source in the vicinity of the sound field is shown to markedly reduce the cavitation threshold in helium II while having no discernible effect in helium I. Furthermore, neither the presence of a beta source, nor electric fields affects the nucleation. Several similarities can be observed, however, to the behavior of the threshold in the presence of a rotating shaft. It is concluded that the threshold lowering is not due to the formation of microbubbles at hot spots as in the Seitz theory, or ions, but rather to the formation of vortices by the α particles. A clear demonstration of the existence of two distinct regions of audible cavitation, hissing and popping, is provided by graphic records of the cavitation noise, along with evidence for the existence of a hysteresis effect in the incipient and desinent step thresholds associated with the popping noise. The hysteresis effect is found to be strongly temperature dependent and exists at temperatures just below the lambda point only. It is proposed that audible cavitation in helium II involves the growth, by a rectified heat transfer process, of vaporous cavities, a few angstroms in radius, arising spontaneously along the cores of normal fluid-filled vortices. Calculations show that the growth of a bubble in helium I by rectified heat transfer is possible. The reasons for the differences between the hissing and popping noises and the cause of the hysteresis effect in audible cavitation are discussed in light of the above-mentioned nucleation process. (Diss. Abstr. Int., B)

14134 AMPLITUDE EFFECTS FOR THE OSCILLATING DISK IN LIQUID He II. Roger, Robert Patrick. Baton Rouge, La.; Louisiana State Univ. (1970). 53p. University Microfilms Order No. 70-18,555.

Thesis.

The amplitude variation of the logarithmic decrement D of a disk (radius ≈2.5 cm) performing torsional oscillations in liquid He II was found to depend on the history of the helium bath. Two types of damping curves are observed: (1) The first (called "steep") occurs when the height, h, of the bath above the disk is greater than some critical height, h′, ($15.8 \leq h' \leq 16.8$ cm) and the time interval Δt between reaching the lambda temperature T_λ and the initial deflection of the disk is short ($\Delta t < 30$ min); (2) The second (called "flat") occurs when either $h < h'$, or if $h > h'$ then Δt must be long ($\Delta t > 60$ min). There is a critical velocity v_c associated with each type of curve. For the steep curves v_{c1} increases with temperature (from 1.33 to 2.15°K) and varies with period as $\tau^{-1/4}$ for periods between 3.9 sec and 19.6 sec. For the flat curves v_{c2} is independent of temperature (from 1.4 to 2.156°K), is larger than v_{c1}, and has a period dependence given by $v_{c2}\tau^{-1/2}$ = 1.4 (cgs units) for periods between 3.9 sec and 45.0 sec. The difference between steep and flat curves is attributed to the presence of a long-lived motion of the superfluid (possibly an ordered array of quantized vortex lines) in the subcritical flow for the steep case and the absence of this motion for the flat case. The low amplitude logarithmic decrement D_0 is found to be the same for the steep and flat curves. The relative change in D_0 from the calculated value $((D_0 - D_{calc})/D_0)$ is found to increase as h/λ decreases (λ is the penetration depth). The excess damping slightly above v_c cannot be explained by the effect of mutual friction. The relative change in moment of inertia $(I_a - I_{a0})/I_{a0}$ at high amplitudes (up to 2.5 rad) indicates that for the steep curves about 30% of the superfluid is entrained for a 4 sec period and 5% for a 12 sec period. No entrainment is indicated for the flat curves. (Diss. Abstr. Int., B)

14135 SUPERFLUIDITY IN ^{3}He: INHIBITION BY POLARIZATION. **Bookbinder, James H. (Univ. of California, San Diego, La Jolla). Phys. Rev., A; 3: 372-82(Jan 1971).**

The previous treatments of the question of superfluidity in ^{3}He, which have not shown conclusively whether this phase should or should not occur are summarized. The most promising calculation was by Pitaevskii, whose determination of the screened quasi-particle transition amplitude $\tilde{\mathcal{F}}_j$ was carried out in the limiting case of large angular momentum j. In estimating T_c this was extrapolated to j = 2 by Gor'kov and Pitaevskii (GP). The work of GP was found to contain an inadequate approximation (the D-wave Born approximation) plus also an algebraic error. When these corrections are made, their formula for T_c then yields the unattainably low value $T_c \sim 10^{-100}$ deg. $\tilde{\mathcal{F}}_j(0 \le j \le 10)$ was projected precisely in second-order perturbation theory. The off-energy-shell K matrix, the particular form of which was chosen so that K would satisfy two exact identities (Ward identities), was used as the bare vertex function. It was found that GP's extrapolation underestimates the effective D-wave interaction. In fact, the polarization (particle–hole) diagram is an attractive correction for K_j, for j = 2 and j ≥ 6, in contrast to Pitaevskii's result that the second-order diagram for $\tilde{\mathcal{F}}_j$ is repulsive. The three approximations involved in Pitaevskii's large-j calculation are studied carefully. Theoretical arguments are given, and numerical evidence is furnished, which indicate that as j increases, Pitaevskii's limit is being approached asymptotically, but so slowly that his analytical result does not hold for angular momenta of interest (i.e., for j < 20). The possibility of D-state superfluidity is discussed. The transition temperature is such a sensitive function of the calculated theoretical parameters that it is difficult to furnish a precise estimate for T_c. (auth)

14136 He II–He I TRANSITION IN THE PRESENCE OF A HEAT CURRENT. **Bhagat, S. M.; Lasken, R. A. (Univ. of Maryland, College Park). Phys. Rev., A; 3: 340-5(Jan 1971).**

The He II–He I transition was investigated by measuring the temperature at which the conductivity of He II exhibits a sharp drop. It was found that this temperature is a function of the heat current Q. A qualitative explanation in terms of the Ginzburg–Pitaevskii phenomenological theory is suggested. (auth)

14137 HYDROKINETIC THEORY OF LIQUID HELIUM II. Goodman, Seymour Evan. Pasadena, Calif.; California Inst. of Tech. (1970). 74p. University Microfilms Order No. 70-24,298.

Thesis.

The kinetic theory of excitations in flowing liquid He II is developed to a higher order than that carried out previously, by Landau and Khalatnikov, in order to demonstrate the existence of nonequilibrium terms of a new nature in the hydrodynamic equations. It is then shown that these terms can lead to spontaneous destabilization in counter currents when the relative velocity of the normal and super fluids exceeds a critical value that depends on the temperature, but not on geometry. There are no adjustable parameters in the theory. The critical velocities are estimated to be in the 14–20 m/sec range for T ≤ 2.0°K, but tend to zero as $T \to T_\lambda$. The possibility that these critical velocities may be related to the experimentally observed "intrinsic" critical velocities is discussed. A semi-classical investigation of roton-quantized vortex line interactions is presented. An essentially classical model is used for the collision and the behavior of the roton in the vortex field is investigated in detail. From this model it is possible to derive the HVBK mutual friction terms that appear in the phenomenological equations of motion for rotating liquid He II. Estimates of the Hall and Vinen B and B′ coefficients are in good agreement with experiments. The claim is made that the theory does not contain any arbitrary adjustable parameters. (Diss. Abstr. Int., B)

14138 HIGH-ENERGY NEUTRON SCATTERING AND THE MIHARA–PUFF THEORY OF THE STRUCTURE FACTOR FOR LIQUID ^{4}He. **Sposito, Garrison (Sonoma State Coll., Rohnert Park, Calif.). Phys. Rev., A; 3: 820-3(Feb 1971).**

The ostensible correctness of the Mihara–Puff theory of the structure factor for liquid ^{4}He and well-known sum-rule expressions are combined to suggest two limiting forms for the dynamic structure factor. One of them is exact in the limit $k \to \infty$ and has the form proposed by Hohenberg and Platzman. It is shown that it should provide information about Bose condensation if inelastic neutron scattering can be done for $k > 40$ Å^{-1}. The other is a simple phenomenological form which applies to the range 3 Å$^{-1} < k <$ 8 Å^{-1} and is shown to describe successfully the scattering experiments of Cowley and Woods. (auth)

14139 HYDRODYNAMIC EQUATIONS FOR THE CONDENSATE AND THE DEPLETION OF HELIUM II. **Haug, H.; Weiss, K. (Philips Research Labs., Eindhoven, Netherlands). Phys. Rev., A; 3: 717-24(Feb 1971).**

The equations of motion for the reduced density matrices of an interacting Bose system are treated, using the concept of off-diagonal long-range order. The equations are decoupled on the one-particle level. With this approximation, the hydrodynamic equations for the densities and the velocities of the condensate and the depletion are derived. The interaction between the two fluid components depends on density variations and on the relative velocity. The latter interaction terms appear as kinetic pressure terms and a Magnus force term. Via the equation for the total momentum, a connection between the velocities of the condensate and the depletion, and the velocities in Landau's two-fluid model is derived. The excitation spectrum of the system is investigated in the phonon region. A comparison of the resulting velocities for the first and second sound with the experimentally determined ones shows that the functional dependence of the condensate density on temperature is similar to that of the superfluid component. (auth)

14140 FLUCTUATIONS, LONG-RANGE ORDER, AND SUPERFLUIDITY. **Sonin, E. B. (Inst. of Semiconductors, Leningrad). Zh. Eksp. Teor. Fiz.; 59: 1416-28(Oct 1970). (In Russian).**

Long-range order over very large distances in three-dimensional systems and, in particular, Bose condensation to a level with a momentum p = 0 do not exist for arbitrary relations between the linear dimensions of the system. This, however, does not lead to a dependence of thermodynamic functions on these relations. It is shown that superfluid persistent currents can exist in rings without ODLRO at T = 0 and T > 0. It is pointed out, in particular, that such currents may exist in the one-dimensional Lieb and Liniger model, which can be solved exactly. (auth)

14141 HEAT CAPACITY NEAR THE SUPERFLUID TRANSITION IN ^{4}He AT SATURATED VAPOR PRESSURE. **Ahlers, Guenter (Bell Telephone Labs., Murray Hill, N. J.). Phys. Rev., A; 3: 696-716(Feb 1971).**

Apparatus and experimental procedures suitable for a number of high-precision measurements of properties of liquid helium near the superfluid transition temperature T_λ are described. Experimental determinations near T_λ of the heat capacity at saturated vapor pressure are presented. On the basis of these measurements, the asymptotic temperature dependence of the heat capacity at constant pressure C_p is examined and compared with current theories of critical phenomena. Although there is some latitude in the interpretation of the results in terms of the asymptotic behavior of C_p, no interpretation fully in agreement with the original formulations of the scaling laws for critical phenomena, and with a divergent C_p, is consistent with the measurements. It is expected that an extensive discussion of the thermodynamics of the λ line at higher pressure, based on measurements of the heat capacity at constant volume C_v, will be presented in a later publication. (auth)

14142 BEYOND THE HARTREE-LIQUID MODEL OF SUPERFLUID BOSONS. **Cummings, F. W. (London Univ.); Herold, J. S.; Sarfatt, J. Physica; 50: 15-26(23 Nov 1970).**

A model of interacting superfluid bosons is proposed that is intended to extend the usual Hartree-liquid model in the case of the stationary state. The result is a coupled set of three differential equations relating the order parameter, a purely rotational velocity field, and a depletion scalar field. The latter two fields play a role similar to that of the vector and scalar potentials coupled to a complex matter field, and the formulation thus closely

XUM

resembles the Landau–Ginzberg equation of superconductivity coupled to the electromagnetic field. (auth)

14143 STATISTICAL MECHANICS OF PERSISTENT CURRENTS IN QUANTUM FLUIDS. Garrison, John C. (Univ. of California, Livermore); Wong, Jack; Morrison, Harry L. Phys. Rev., A; 3: 685–90(Feb 1971).

The Landau condition, $\vec{\nabla} \times \vec{v}_s = 0$, for He II and the analogous Meissner effect in superconductors are shown to follow from the existence of persistent currents by the use of a new definition of the quasiequilibrium state. The novel aspect of this definition is the requirement that the effective Hamiltonian defining the density matrix is invariant under infinitesimal quasi-Galilei transformations. In applications to He II and superconductors, the existence of a condensate implies that the density matrix does not have the full symmetry of the effective Hamiltonian. By slightly relaxing the quasiequilibrium conditions the usual Landau equations for $\vec{v}_s$ (for the case that $\vec{v}_n = 0$) are obtained. (auth)

14144 MOTION OF IONS AT FINITE VELOCITIES IN HELIUM II. Strayer, Donald M. (Univ. of Oregon, Eugene); Donnelly, Russell J.; Roberts, Paul H. Phys. Rev. Lett.; 26: 165–9(25 Jan 1971).

The drag force on an ion moving through liquid helium II at finite velocities is discussed in terms of localized roton states near the ion. These ideas are compared with experiments on positive and negative ions below 1°K. (auth)

14145 SUPERFLUIDITY IN QUANTUM CRYSTALS. Guyer, R. A. (Univ. of Massachusetts, Amherst). Phys. Rev. Lett.; 26: 174–7(25 Jan 1971).

The speculations of Chester, Andreev and Lifshitz, and Leggett concerning the possibility of Bose–Einstein condensation and/or superfluidity in quantum crystals are examined. The existing body of experimental data on these systems places extremely strong constraints on the experimental realization of these speculations. (auth)

14146 MEASUREMENT OF SUPERFLUID CRITICAL VELOCITIES IN WIDE CHANNELS UTILIZING PHASE COUPLING. Corke, Henry Edwin. Houston, Tex.; Univ. of Houston (1970). 106p. University Microfilms Order No. 70-16,011.

Thesis.

The superfluid component of He II flows without viscosity or dissipation below a critical velocity. Previously measured critical velocity values for flow in wide channels ($>10^{-3}$ cm) fall into two conflicting ranges. Values in the higher range vary with the characteristic channel size (d) as $d^{-1/4}$ and show no temperature dependence, while the lower reported values vary approximately as d^{-1} with reported temperature dependence. It has been suggested that these lower values are the result of detecting normal fluid turbulence. The higher reported values have no firm theoretical explanation. However, the lower-valued critical velocities are justifiable by the Feynman vortex model. Quantum-mechanical phase coherence in He II has been previously observed, which demonstrates that a coupling between elements of the superfluid places restrictions on the flow profile. Here, this phase coupling is utilized to control the superfluid flow in parallel channels to indicate the first signs of flow impedance. A sensitive pressure-measuring device is located in a flow channel to monitor the velocity and detect the superfluid critical velocity. Critical velocity data for isothermal as well as heat current flow are obtained. The results substantiate the concept of phase coupling and indicate that a superfluid critical velocity exists as a result of vortex generation and is not dependent upon normal fluid flow in the temperature range 1.71 to 2.15°K. In this temperature range little or no temperature dependence is found. At velocities well above critical, flow transitions are observed which indicate the onset of superfluid turbulence. These turbulent critical velocities have values in the range corresponding to previous data with the $d^{-1/4}$ dependence. (Diss. Abstr. Int., B)

Superconductivity

Refer also to abstracts 13716 and 14215.

14147 (AD–711826) TUNNELING INTO SUPERCONDUCTING RHENIUM SINGLE CRYSTALS. Ochiai, Shin I.; MacVicar, Margaret L. A.; Rose, Robert M. (Massachusetts Inst. of Tech., Cambridge. Dept. of Metallurgy and Materials Science). 24 Sep 1970. Contract N00014-67-A-0204-0041. 13p. (TR–2). NTIS.

Tunneling into rhenium single crystals from amorphous carbon barriers was used to measure the dependence of the energy gap on temperature, orientation, and magnetic field. Both gap and gap anisotropy were different for the cases of data from single-particle and double-particle events, respectively, indicating the importance of selection rules. Field and temperature dependences were those of a classified Type-I BCS-type superconductor. Comparison with Fermi surface and phonon spectrum anisotropies indicate that, for Re, phonon effects dominate, in contrast to the case of Nb. (auth) (USGRDR)

14148 SUPERCONDUCTIVITY OF THE F.C.C. TRANSITION METALS, AND OF THEIR ALLOYS, AND F.C.C. CARBIDES. Lawson, A. C. (Univ. of California, San Diego, La Jolla). J. Less-Common Metals; 23: 103-6(1971).

The discovery of new ternary superconductors connected two regions of the previously known variation of T_c with electron concentration among the fcc transition metals, alloys, and binary and ternary carbides. Superconducting properties varied in a simple way among the fcc transition metal superconductors. Unfortunately, it appears that any hope for a dramatic increase in T_c obtained by raising e/a (electrons per atom) in fcc carbides or nitrides must now be abandoned. (auth)

14149 OPTICAL PROPERTIES AND ELECTRON CHARACTERISTICS OF NIOBIUM–TIN ALLOYS. Golovashkin, A. I.; Donner, E. D.; Levchenko, I. S.; Motulevich, G. P. (Lebedev Inst. of Physics, Moscow). Zh. Eksp. Teor. Fiz.; 59: 1967-74(Dec 1970). (In Russian).

An optical method for studying the electron characteristics of Nb–Sn alloys was employed. The complex refractive index in the 1- to 10-μ spectral range, superconducting characteristics, and the density and static conductivity and its temperature dependence were measured on a given sample. Most of the alloys investigated contained from 6 to 55% of tin by weight. The following quantities were also determined: conductivity-electron concentration, electron velocity on Fermi surface, total area of Fermi surface, effective electron collision frequency, frequency of collisions between electrons and phonons or defects, electron mean free path, and depth of skin layer. The correlation between the conductivity-electron concentration and transition temperature to the superconducting state is considered. (auth)

14150 PROCESS FOR THE MANUFACTURE OF SUPERCONDUCTING MATERIALS. (to Radio Corp. of America). French Patent 1,572,805. 19 May 1969. Filed 4 Jul 1968. (In French).

A procedure for depositing a crystalline coating of niobium and of tin on a substrate is described. The substrate, which is an insulating material, semiconducting or metallic, is warmed in a reducing gaseous atmosphere containing hydrogen and vaporous chlorides of niobium and tin at 900 to 1200°C. Upon reduction, the metallic fractions are deposited as crystalline Nb_3Sn on the substrate. The method is characterized by addition to the atmosphere of a gas that induces imperfections in the crystal lattice of the deposit. This gas may be carbon monoxide, carbon dioxide, nitrogen, or a gaseous hydrocarbon having a molecular weight greater than 16, and should be of quantity sufficient to produce a large number of defects per unit volume. (J.G.B.)

14151 SUPERCONDUCTIVITY IN NEARLY ONE-DIMENSIONAL WIRES. Possin, George Edward. Stanford, Calif.; Stanford Univ. (1970). 85p. University Microfilms Order No. 70-18,458.

Thesis.

The effect of intrinsic fluctuations on the superconducting transition was studied. For this purpose tin wires with diameters between 450 and 1000Å and lengths of the order of 14 microns were prepared. The resistance ratios indicate low-temperature mean free paths limited by the wire diameter. The wires are prepared by electroplating from acid solution into small holes etched in mica. The holes are produced by etching out the damage tracks produced by high-energy fission fragments. A search was made for the effect of thermodynamic fluctuations on the superconducting transition. The experimental results can be divided into three parts: The transition widths vary but the smallest transition widths for each diameter can be described by the formula $\Delta T_w = 0.9d^{-1/2}$K, where d is in 1000Å units. This is what would be expected from free-energy estimates with an activation parameter ~3.6 or a $\gamma = 10$ in a theory due to Langer and Ambegaokar. Agreement was found with the prediction of Langer and Ambegaokar for the temperature dependence of the critical current near the transition temperature although no fit for their γ parameter was made because of experimental problems. A microscopic theory due to Aslamazov and Larkin predicts that the dc resistance of a superconductor with diameter $<\xi(T)$ should satisfy: $R/R_N = 1 - (\Delta T_0/\Delta T)^{3/2}$ when $(R_N - R)/R_N \ll 1$ and $T/T_c < 3/2$. Good agreement with the predicted temperature dependence and the theoretical magnitude of ΔT_0 is found if their calculation for a "dirty" wire is taken. A field-dependent complex rf impedance in thin aluminum films and the inertial inductance due to the superconducting electrons were also measured. The field-dependent impedance was identified with a model of vortices undergoing heavily damped harmonic motion in their pinning wells. (TSS) (Diss. Abstr. Int., B)

14152 MASS ENHANCEMENT AND SUPERCONDUCTING TRANSITION TEMPERATURE CALCULATIONS FOR METALS AND SEMICONDUCTORS. **Allen, Philip Brown. Berkeley, Calif.; Univ. of California (1969). 137p. University Microfilms** Order No. 70-17,493.

Thesis.

The theory of the electron–phonon interaction and the renormalization of electronic properties in degenerate systems is developed and applied to three problems. The first problem is the superconducting transition temperature of the degenerate semiconductors SnTe and GeTe. Intravalley electron–electron interactions, especially the coupling via polar phonon modes, is considered in detail and shown to be inadequate to explain superconductivity in these compounds. A simple model is proposed to include the effects of intervalley electron–phonon interactions, and this serves very well to explain the observed dependence of the superconducting transition temperature on carrier density. The second problem is the mass enhancement and superconducting transition temperature of the nontransition metals. A simple calculation is presented of the electron–phonon coupling parameter λ, using pseudopotential matrix elements of the electron–phonon interaction within a single orthogonalized plane wave approximation. Theoretical values of the superconducting transition temperature are calculated using the McMillan equation. Particularly good agreement with experiment is found for the hexagonal divalent metals beryllium, zinc, and cadmium. It is predicted that lithium and magnesium should be superconducting at low temperatures. Certain systematic patterns of superconductivity in the periodic table are discussed. The third problem is the temperature dependence of the electron–phonon mass enhancement. Calculations of the temperature shift of the mass enhancement are presented for sixteen nontransition metals, using a slight modification of the single orthogonalized plane wave method. The results are in good agreement with recent experiments on zinc. (Diss. Abstr. Int., B)

14153 THERMAL CONDUCTIVITY AND THERMAL EFFECTS IN SUPERCONDUCTING NIOBIUM. **Wasim, Syed Mohammad. Baton Rouge, La.; Louisiana State Univ. (1970). 111p. University Microfilms** Order No. 70-18,570.

Thesis.

Thermal conductivity measurements on a niobium plate of intermediate purity ($l \simeq \xi_0$) were performed in the normal, superconducting, and mixed states. The lattice and electronic components of the conductivity in the superconducting state are separated. The critical temperature and the energy gap are found to be $T_c = 9 \pm 0.1$°K and $2\epsilon\ (o) = 3.96KT_c$, respectively. The temperature dependence of the minimum in the thermal conductivity in the mixed state suggests a decrease in both the phonon and the electron conductivities just above H_{c1}. The comparative importance of each depends on a combination of temperature range and purity of the sample. The slope $\partial K_m/\partial H$ and upper critical field parameter $\kappa_1(t)$ are found to change with temperature much faster than predicted by relevant theories. The temperature dependence of the magnetocaloric effect, its distribution over the mixed state and the magnetization were measured in a niobium single crystal. From these results magnetocaloric cooling, enthalpy, and free energy are calculated and discussed. The irreversible hysteretic heating in the mixed state and its field temperature dependence have been discussed in terms of the pinning forces in the light of Morton's theory. The reduced upper critical field h^* and the reduced Ginsburg–Landau parameter $\kappa_1(t)/\kappa_1(1)$ as obtained from magnetocaloric measurements are again found to increase faster with decreasing temperature than predicted by the theory. The "flux flow" resistivity and the corresponding heat dissipation in both parallel and perpendicular fields were measured and, from the results, H_{c3}/H_{c2} was determined, and proportionality between flow resistance and rate of heat dissipation is found. (Diss. Abstr. Int., B)

14154 INVESTIGATION OF THE ELECTROMAGNETIC INTERACTION OF SUPERCONDUCTORS NEAR T_c USING TRANSVERSE HYPERSOUND. Page, Edward A. College Park, Md.; Univ. of Maryland (1969). 81p. University Microfilms Order No. 70-15,508.

Thesis.

The attenuation of transverse hypersonic waves was measured in a superconductor, single-crystal tin, near the superconducting transition temperature T_c. This is a particularly useful technique in the study of superconductivity since transverse ultrasonic waves have the unique ability to establish a transverse electromagnetic field of a single wave number q within the bulk of a superconductor. The response of a superconductor to this transverse electromagnetic field can be expressed directly in terms of the superconducting conductivities corresponding to given q values, and special information about superconductivity can be obtained. The results obtained confirmed heretofore unobserved properties of this attenuation mechanism which were theoretically predicted by Cullen and Ferrell. Measurements of the temperature and frequency dependence, at 395, 1016, and 1335 MHz, were in remarkable agreement with the theoretical predictions. These are the first ultrasonic measurements to exhibit the frequency dependence of the transverse electromagnetic interaction for propagating waves. The measured total transverse electromagnetic attenuations at 1016 and 1335 MHz were compared with the theoretical frequency dependence. The results were in good agreement and provided the first convincing demonstration of normal-state electron screening breakdown in ultrasonics. Analysis of the transition curves using the theoretical expressions of Cullen and Ferrell yielded values of the superconducting penetration depths corresponding to the three frequencies used in the experiment. These measurements provide a direct determination of q-dependent electromagnetic penetration depths. The results clearly indicate an enhancement of the penetration depth with increasing q values. This q dependence is in reasonable agreement with the nonlocal theoretical predictions. (Diss. Abstr. Int., B)

14155 APPLICATIONS OF SUPERCONDUCTIVITY. **Goodkind, John M. (Univ. of California, San Diego, La Jolla). Amer. J. Phys.; 39: 9-23(Jan 1971).**

A general review of current practical applications of the properties of superconductors is presented. The devices are classified into groups according to the property of superconductors which is of primary importance to the device. A brief introduction to each of these properties is given and extensive references to the literature are supplied so as to make it possible for a novice in the field to grasp the technical implications of superconductivity. (auth)

14156 PROBLEM OF HIGH-TEMPERATURE SUPERCONDUCTIVITY. II. **Ginzburg, V. L. Usp. Fiz. Nauk; 101: 185-215(Jun 1970). (In Russian).**

The photon and exciton mechanisms of superconductivity are reviewed in order to evaluate the possibility of the existence of high-temperature superconductors. It is concluded that a critical temperature T_c less than 40°K is the upper limit for a phonon mechanism of superconductivity (with the exception of metallic hydrogen which may have a critical temperature of 30 to 300°K). At present the highest critical temperature is 21°K. The production of materials with a critical temperature of 25 to 30°K would be of great practical importance, for it would be possible to use liquid hydrogen as a cooling agent on a wide scale. However, the exciton mechanism of superconductivity predicts much higher critical temperatures, even on the order of 10,000°K. Long-polymeric organic compounds with a conjugated double-bond system as the metallic conductor and side chains playing the role of polarizers are believed to be prospective candidates for high-temperature superconductors. Layer–lattice type of compounds is another class of compounds that are considered. The critical temperature of tantalum disulfide was increased from 0.7°K to 3.5°K on introducing pyridine into the TaS_2 molecule. It is possible that interactions between conduction electrons and organic molecules may be taking place in this layered compound by an exciton mechanism. (66 references) (TTT)

14157 WHAT FUTURE FOR SUPERCONDUCTIVITY? Froehlich. H. (Univ. of Liverpool). Nature (London); 228: 1145-6 (19 Dec 1970).

Progress in the theory of superconductors, particularly in regard to macrowave functions, is discussed in relation to opportunities for future development. (auth) (UK)

14158 SUPERCONDUCTING PROXIMITY EFFECT IN LAYERED SYSTEMS WITH A MAGNETIC FIELD APPLIED PERPENDICULAR TO THE INTERFACES. **Tilley, D. R.; Ward, R. (Univ. of Essex, Colchester, Eng.). Solid State Commun.; 8: 1983-5 (1 Dec 1970).**

The proximity effect in the dirty limit for a slab of material 1 of thickness d embedded in material 2 is calculated. The critical field varies from that of 1 for large d to that of 2 for small d. Critical field measurements on rolled Nb foils are also presented. (auth) (UK)

14159 SUPERCONDUCTING–NORMAL PHASE BOUNDARY OF SUPERCONDUCTORS CONTAINING NEARLY NONMAGNETIC IMPURITIES. **Huber, J. G.; Maple, M. B. (Univ. of California, San Diego, La Jolla). Solid State Commun.; 8: 1987-70(1 Dec 1970).**

XUM

For superconductors containing impurities with d or f electrons in resonant states, which are nonmagnetic or nearly so at low temperatures, the depression of the transition temperature is anomalously large initially and curves positively away from linearity with increasing impurity concentration. This is in contrast to the negative curvature deviation from linearity predicted by the Abrikosov–Gor'kov theory for magnetic impurities with well-defined noninteracting local moments. (auth) (UK)

14160 ULTRASONIC ATTENUATION OF TRANSVERSE WAVES IN DIRTY SUPERCONDUCTORS. Bearzatto, C.; Joffrin, J.; Levelut, A. (Faculte des Sciences Paris). Phys. Lett.; 33A: 473-4(28 Dec 1970).

The attenuation of transverse acoustic waves in mercury–indium alloy is measured. In the high-frequency limit it varies linearly with $(H_{c_2}-H)$, in agreement with theory. (auth)

14161 INDUCED SUPERCONDUCTIVITY IN GERMANIUM FILMS. Lipson, S. G.; Stupel, M. M. (Technion–Israel Inst. of Tech., Haifa). Phys. Lett.; 33A: 493-4(28 Dec 1970).

The voltage–current characteristics of films of Ge, sandwiched between Sn and Sn, and sandwiched between Sn and Al, were measured at helium temperatures. (auth)

14162 FLUCTUATION EFFECTS IN ONE- AND TWO-DIMENSIONAL SUPERCONDUCTORS. Masker, Warren E. Rochester, N. Y.; Univ. of Rochester (1970). 157p. University Microfilms Order No. 70-17,897.

Thesis.

The temperature region near the critical temperature of a superconductor was explored in an attempt to investigate the breakdown of mean field theory due to thermodynamic fluctuations. In one segment of the study, attention was focused on the broadening of resistive transition of two-dimensional superconducting films caused by fluctuations. The samples used in these experiments were granular aluminum films prepared by evaporating aluminum in the presence of oxygen. The conductivity as a function of temperature was examined over five orders of magnitude and the results compared with existing theories. It was found that above the transition temperature T_c, the data were in accord with the predictions of Aslamazov and Larkin, i.e., the excess conductivity increased with decreasing temperature as $(T-T_c)^{-1}$. Below T_c the resistivity showed an exponential falloff with a decay rate proportional to $R^n_\square$, the sample's normal resistance per square. A study of precursive superconductance (the excess conductivity due to Cooper pair formation above T_c) was also undertaken using aluminum films with a range of mean free paths spanning four orders of magnitude. It was found that in all cases, the resistivity as a function of temperature followed the "Curie–Weiss" law predicted by Aslamazov and Larkin. However, the prediction that τ_0/R^n be constant regardless of mean free path (where τ_0 is the Curie–Weiss parameter proportional to the width of the critical region) was not confirmed. The temperature dependence of the critical current I_c was studied in one-dimensional superconductors (thin film Sn microstrips and Sn whiskers). A small shift of the transition temperature ΔT_c away from its mean field value was detectable and the temperature dependence of the critical current showed a gradual departure from the mean field theory prediction that $I_c \propto [(T_c-T)/T_c]^{½}$. A qualitative comparison with the theory of Langer and Ambegaokar is presented. (TSS) (Diss. Abstr. Int., B)

14163 ANGULAR DEPENDENCE OF CRITICAL MAGNETIC FIELDS IN SUPERCONDUCTING FILMS. Kraetzig, E.; Keller, J. (Philips Forschungslaboratorium, Hamburg. Max von Laue/Paul Langevin Institut, Garching, Ger.). Phys. Status Solidi; 42: 725-32(1 Dec 1970).

The angular dependence of the critical magnetic field H_c in superconducting films is studied by measuring the attenuation of ultrasonic surface waves. In the case of thin films (phase transitions of second order), good agreement with an interpolation formula derived by Tinkham is found. Thick films (film thickness large compared to coherence length and penetration depth) are studied too showing first-order phase transitions or surface superconductivity in a magnetic field parallel to the film. In the case of surface superconductivity, the measurements are compared with a new interpolation formula for H_c, which can be derived from the Ginzburg–Landau equation. (auth)

14164 INTERMEDIATE STATE OF TYPE-II SUPERCONDUCTORS. Kraegeloh, U. (Max-Planck-Institut fuer Metallforschung, Stuttgart. Univ., Stuttgart). Phys. Status Solidi; 42: 559-76(1 Dec 1970). (In German).

For disks of lead–thallium alloys with Ginzburg–Landau parameters $\varkappa$ slightly exceeding $2^{-½}$, there were observed, by means of the decoration technique of Träuble and Essmann, intermediate-state patterns at T = 1.2°K, consisting of Meissner domains and Shubnikov domains with a constant lattice parameter. The coexistence of these domains indicates a positive boundary energy between them. This boundary energy and the boundary energy between Meissner and normal domains for type I superconductors were determined as a function of $\varkappa$ in the range $0.43 \leqq \varkappa \leqq 0.82$, using the models for domain structures of Landau, Lifshits, and Sharvin; S does not vanish for $\varkappa = 2^{-½}$. Shubnikov domains appearing as isolated domains surrounded by field-free material in the Meissner state are explained as a result of a hitherto unknown attractive interaction between flux lines, which, together with the better-known repulsive interaction, leads to a flux-line lattice with definite lattice parameter. The binding energy E_B between flux lines is estimated from the boundary energy S. (auth)

14165 CURRENT-INDUCED INTERMEDIATE STATE IN TYPE-I SUPERCONDUCTORS. Baird, D. C. (Royal Military Coll., Kingston, Ont.); Mukherjee, B. K. Phys. Rev., B; 3: 1043-5 (1 Feb 1971).

An improvement is made on the previous model of the intermediate state in type-I current-carrying superconductors. In addition to predicting a resistance transition in reasonable agreement with experimental observations, the model gives good agreement with experimental values for the radius of the intermediate-state core as obtained by Rinderer. (auth)

14166 THERMAL CONDUCTIVITY IN PURE TWO-BAND SUPERCONDUCTORS IN HIGH MAGNETIC FIELDS. Tang, I-ming (Reed Coll., Portland, Oreg.). Phys. Rev., B; 3: 1045-8(1 Feb 1971).

The theory proposed by Maki, for the electronic thermal conductivity in the gapless region of a pure type-II superconductor, is extended to include the presence of a second superconducting band so that it can be used to describe the mixed-state thermal conductivity in clean transition-metal superconductors near H_{c2}. The general features of Maki's one-band expression remain in the two-band expression. (auth)

14167 FLUCTUATIONS OF THE ORDER PARAMETER IN SMALL SUPERCONDUCTING SAMPLES. Hurault, J. P. (Laboratoire d'Etude et de Recherches Generales, Limeil Brevannes, France); Maki, K.; Beal-Monod, M. T. Phys. Rev., B; 3: 762-8 (1 Feb 1971).

A study is made of the effect of the time-dependent fluctuations of the order parameter in superconducting samples in which the dimensions are smaller than the coherence length. It is found that within the mean field theory, the static properties (specific heat, spin susceptibility), as well as the transport properties, nuclear-spin relaxation time, and the tunneling density of states, diverge as T approaches T_c. Therefore, the fluctuation corrections are much more important in those "zero-dimensional" superconductors than in the one-, two-, and three-dimensional ones. In particular, the width of the critical region is very large and increases when the size of the samples decreases. These effects should be observable if the problems of sample preparation can be solved. (auth)

14168 THEORY OF JOSEPHSON RADIATION. I. GENERAL THEORY. Lee, Patrick A.; Scully, Marlan O. (Univ. of Arizona, Tucson. Massachusetts Inst. of Tech., Cambridge). Phys. Rev., B; 3: 769-81(1 Feb 1971).

The problem of a Josephson junction interacting with a quantized electromagnetic field contained in a microwave cavity is considered. Inasmuch as the cavity has a quality factor Q, and an external current J flows in and out of the junction, this is a problem in nonequilibrium statistical mechanics. A technique is used that eliminates adiabatically the radiation field directly from the total-density-matrix equation of motion. The resulting equation for the reduced density matrix is found to have a simple physical interpretation. The spectrum of the voltage fluctuations and the linewidth of the emitted radiation are then calculated for the case when the resonance cavity is at absolute zero. (auth)

14169 ELECTRONIC STRUCTURE OF THE INTERMEDIATE STATE IN TYPE-I SUPERCONDUCTORS. Kuemmel, Reiner (Univ., Frankfurt am Main. Univ. Valle, Cali, Colombia). Phys. Rev., B; 3: 784-93(1 Feb 1971).

The quasi-particle wave functions and the energy–eigenvalue equations of the intermediate state in extreme type-I superconductors are calculated for the full range of the excitation spectrum. A WKBJ method of solving the Bogolyubov equations at any temperature below T_c is used. The periodicity of the pair potential leads to Bloch-type wave functions and a band structure of the energy spectrum for fixed momenta parallel to the phase boundaries. The magnetic field has an effect on the quasi-particle energies only by its influence on the structural and thermodynamic properties of the system. The width of the normal regions, and an effective variation length summing up the space dependence of the pair potential, are the variational parameters of the theory. From the general eigenvalue equations, explicit energy spectra are obtained for simplified models of the pair potential. (auth)

14170 MEASUREMENT OF DEPENDENCE ON FREQUENCY OF RESIDUAL RESISTANCE OF SUPERCONDUCTING LAYERS OF LEAD. **Szecsi, L. (Univ., Karlsruhe, Ger. Kernforschungszentrums, Karlsruhe, Ger.). Z. Phys.; 241: 36-44(1971). (In German).**

The surface resistance of lead was measured in a coaxial cavity at frequencies between 375 and 5000 MHz and temperatures between 4.2 and 1.5°K. The residual resistance was determined from these data. (auth)

14171 SURFACE NUCLEATION CRITICAL FIELD H_{c3}(T) OF TYPE II SUPERCONDUCTORS. Sarma, Pranab K. (Univ., Cologne). Z. Phys.; 241: 22-35(1971).

Near the critical temperature T_c, the thermodynamic potential of a semi-infinite superconductor in an external magnetic field parallel to the surface can be expanded asymptotically in a power series in $(1 - T/T_c)^{1/2}$. In this limit the order parameter decomposes into two parts, the gauge-invariant gradient of one of which is proportional to $(1 - T/T_c)^{1/2}$. This part satisfies asymptotically the Ginzburg–Landau (GL), the generalized GL equations and so on. The other part is of nonlocal nature, is asymptotically nonvanishing near the surface only, and influences the boundary conditions for the former part. In general these boundary conditions can be determined to any finite order of $(1 - T/T_c)^{1/2}$ by solving a finite set of inhomogeneous integral equations, all with the same kernel. It turns out that $H_{c3}(T)$ can be computed up to the order of $(1 - T/T_c)^{1/2}$ for specular and $(1 - T/T_c)^2$ for nonspecular reflection without solving the integral equations explicitly. The temperature dependence of $H_{c3}(T)/T_c(dH_{c2}/dT)_{T=T_c}$ is given up to the orders mentioned above. (auth)

14172 MAGNETISATION STUDIES OF SOME CRYOGENIC ALLOYS. **Larbalestier, D. C. London; Imperial Coll. of Science and Tech. (1970). 240p.**

Thesis.

The flux-pinning properties of superconducting alloys of indium with thallium, lead, and cadmium in the vicinity of the martensitic phase transformation were investigated. It was found that flux pinning reaches a peak in the partially transformed alloys of In–Tl and In–Pb, but that precipitation of the Cd-rich phase complicated the situation in In–Cd. These superconducting measurements also allowed the position of the low-temperature phase boundaries to be determined in the hitherto-uninvestigated In–Pb and In–Cd alloys. The magnetic properties of a wide variety of commerical austenitic iron–chromium–nickel stainless steels were also studied. All the standard AISI 300 grade steels were found to have significant magnetisations on cooling to 4.2°K. In the 18Cr/10Ni grades, a ferromagnetic martensitic transformation may occur in an antiferromagnetic or paramagnetic austenite matrix. The occurrence of the transformation was related both to the chemical composition variation within standard grades and to the room-temperature deformation properties. At higher alloy contents, such as AISI 309 (23Cr/14Ni), the austenite phase remained stable on cooling to 4.2°K and was antiferromagnetic, as in the 18/10 steels. On further increasing the alloy content to AISI 310 (25Cr/20Ni) and Incoloy 800 (20Cr/32Ni), however, the austenite became reversibly ferromagnetic. This change is believed to be due to the existence of two electronic states in γ–Fe, whose relative stability is a function of alloying content. An analysis of previous deformation work shows that all steels found to be antiferromagnetic in the present study became martensitic after tensile destruction at 4.2°K, while those that were ferromagnetic were structurally stable. This behaviour is also believed to be related to the two electronic states of γ–Fe and suggests the importance of the magnetic energy in determining the equilibrium structure of these steels. (auth) (UK)

14173 EFFECT OF SPECIMEN THICKNESS ON THE SUPERCONDUCTING CRITICAL TEMPERATURE OF INDIUM. **Gregory, W. D.; Superata, M. A.; Carroll, P. J. (Georgetown Univ., Washington, D. C.). Phys. Rev., B; 3: 85-7(1 Jan 1971).**

The superconducting critical temperature (T_c) is found to decrease inversely proportional to the boundary-limited mean free path (mfp) for thin single-crystal and polycrystal In plates. Since the boundary-limited mfp is not linearly related to specimen thickness for the sample thicknesses used (5 to 250 μm), these results are a stronger confirmation of the Markowitz–Kadanoff calculations than previously reported in the literature. The In results contrast with similar experiments using Ga single crystals reported by Gregory in which no mfp effect was observed. Possible reasons for this difference are discussed. The possible use of measurements such as these to determine the anisotropic-pairing interaction is discussed. (auth)

14174 INSTABILITIES OF HIGH-TEMPERATURE SUPERCONDUCTORS. **Matthias, B. T.; Corenzwit, E.; Cooper, A. S.; Longinotti, L. D. (Bell Telephone Labs., Inc., Murray Hill, N. J.). Proc. Nat. Acad. Sci. U. S. A.; 68: 56-7(Jan 1971).**

The transition temperatures of both the cubic and tetragonal phases of several high-temperature β-W superconductors were observed. The instability of the cubic lattice appears to be characteristic of high-temperature superconductors. (auth)

14175 PHONON EFFECTS IN THE FAR-INFRARED REFLECTIVITY OF SUPERCONDUCTING LEAD. **Gavini, A.; Timusk, T. (McMaster Univ., Hamilton, Ont.). Phys. Rev., B; 3: 1049-50(1 Feb 1971).**

Measurements of reflectivity of evaporated films of lead at 1.2°K show phonon structure above the energy gap. The frequencies of the peaks in the spectrum agree with phonon frequencies in lead observed by tunneling and neutron spectroscopy. (auth)

14176 MAGNETIC FLUX FLOW AND FLUCTUATION EFFECTS IN THIN-FILM SUPERCONDUCTORS. **Escher, John S.; Ginsberg, D. M. (Univ. of Illinois, Urbana). Phys. Rev., B; 3: 735-41(1 Feb 1971).**

Resistance measurements were used to investigate magnetic flux pinning, flux motion, and fluctuation effects in thin films of superconducting indium, thallium, and aluminum condensed onto cold substrates and maintained below 20°K throughout the measurements. The depinning threshold of vortex motion was studied as a function of transport-current density, applied perpendicular magnetic field, and temperature. The absence of the peak effect in films is explained in terms of Pearl's theory of long-range electromagnetic interactions between vortices in films. The critical-state data do not satisfy the empirical equation of Kim et al. which relates the current density to the critical depinning field in bulk samples. Vortex guiding was observed, and Hall-effect measurements are also reported. Measurements on superimposed films of indium and thallium suggest that the surfaces of these films play an important role in flux pinning. Measurements of the resistive transition in most of our samples showed a peak in resistance near the transition temperature, similar to resistance peaks noticed by some other investigators. This peak disappeared as a perpendicular magnetic field was applied. An explanation of the peak is suggested; it involves small-angle electron scattering from regions in which superconducting fluctuations are occurring. (auth)

14177 SUPERCONDUCTIVITY IN Mo–Re AND Nb–Ir σ PHASES. Koch, C. C.; Scarbrough, J. O. (Oak Ridge National Lab., Tenn.). Phys. Rev., B; 3: 742-8(1 Feb 1971).

Superconducting transition temperatures and low-temperature specific-heat capacities were measured for well-characterized Nb–Ir and Mo–Re σ-phase alloys. The transition temperatures T_c, and the electronic specific-heat-capacity coefficients γ were found to vary only slowly with composition in these alloys. By considering data from the literature on other σ-phase alloys as well as the present data, it was concluded that no clear correlation could be made between T_c and γ [and therefore the electronic density of states at the Fermi level $N_{bs}(0)$]. Good correlation was obtained, however, between McMillan's electron–phonon coupling constant λ and T_c. This suggests that the phonon spectrum may be more important than the electronic density of states at the Fermi level in controlling T_c for σ phases. The high value of T_c (9.8°K) reported in the literature for the Nb–40 at. % Ir σ phase is believed to be due to small quantities of a second superconducting phase. (auth)

14178 SUPERCONDUCTING TRANSITION TEMPERATURES AND LATTICE PARAMETERS OF SIMPLE-CUBIC METASTABLE Te–Au SOLUTIONS CONTAINING Fe AND Mn. **Newkirk, L. R.; Tsuei, C. C. (California Inst. of Tech., Pasadena). Phys. Rev., B; 3: 755-61(1 Feb 1971).**

The superconducting transition temperatures and lattice spacings of simple-cubic Te–Au–Fe and Te–Au–Mn alloys, prepared by rapid quenching from the liquid state, were measured and correlated with anomalies in the Te–Au system and the band structure proposed to explain those anomalies. The unusual behavior of these properties in the ternary alloys containing Fe and Mn is interpreted in terms of a Fermi-surface–Brillouin-zone interaction based on information obtained from studying binary Te–Au alloys. The results of this study lend additional support to the electronic band structure proposed for simple-cubic Te–Au alloys and, in addition, show a very distinct band-structure effect on the superconducting transition temperatures of the Te–Au–Fe alloys. (auth)

14179 SPECIFIC HEAT OF SUPERCONDUCTING TRANSITION METALS CONTAINING NONMAGNETIC IMPURITIES AT LOW TEMPERATURES. Burkel, Richard H.; Chow, W. S. (Univ. of Cincinnati). Phys. Rev., B; 3: 779-84(1 Feb 1971).

Green's-function theory is used for the calculation of the specific heat of superconducting transition metals containing nonmagnetic impurities at low temperatures, $T \gtrsim 0$. It is found that, in this temperature region, the s-band specific heat is lowered by the presence of the nonmagnetic impurities. The logarithm of the s-band specific heat obeys the following relation: $\ln C_s = \ln C_s^{(0)} - \Gamma/k_BT$ for $T \gtrsim 0$, where $C_s^{(0)}$ is the s-band specific heat for a pure two-band superconductor, and Γ is proportional to the density of impurities, the density of states at the d-band Fermi surface, and the strength of the interband impurity scattering. This relation agrees very well with the low-temperature experimental data of Shen, Senozan, and Phillips. (auth)

14180 PROPERTIES OF LEAD-INDIUM ALLOYS. II. SPECIFIC HEAT. Culbert, Harvey V. (Argonne National Lab., Ill.); Farrell, D. E.; Chandrasekhar, B. S. Phys. Rev., B; 3: 794-801(1 Feb 1971).

Specific-heat measurements were made on a series of lead-indium alloys containing from 0 to 60 at. % indium. For each sample the data yield precise (within 1%) values for both the normal-state electronic specific-heat coefficient γ and the Debye temperature θ_D. In addition, though with less precision, both the bulk thermodynamic critical field $H_c(0)$ and the first generalized Ginzburg-Landau parameter κ_1 were obtained. These results, together with those previously obtained for the magnetic properties of the same system, provide a set of comprehensive data for bulk thermal and magnetic properties of Pb-In alloys. The data are examined in order to establish to what extent strong-coupling and electronic structure effects may need to be incorporated into existing theoretical treatments. A combination of both effects is found to provide a quantitative explanation of the electronic specific-heat changes observed on alloying. (auth)

14181 ETTINGSHAUSEN EFFECT IN THE INTERMEDIATE STATE OF THIN SUPERCONDUCTING Pb FILMS. Rowe, V. A.; Huebener, R. P. (Argonne National Lab., Ill.). Phys. Rev., B; 2: 4489-94(1 Dec 1970).

Earlier measurements of the Nernst effect in thin films of Pb, Sn, and In have shown that below a critical film thickness d_c, the entropy per unit length and per unit flux transported by the vortices decreases strongly with decreasing film thickness. To check this behavior, the Ettingshausen effect in the intermediate state of superconducting Pb films at 4.2°K was measured as a function of the magnetic field. The films investigated were 0.75 and 3.16 μm thick. The Ettingshausen data clearly confirm the earlier results obtained from the Nernst effect. It is suggested that the decrease of the transport entropy with decreasing film thickness, found below d_c, is due to the increasing vortex interaction present in very thin type-I films. (auth)

14182 UNUSUAL STRAIN DEPENDENCE OF T_c AND RELATED EFFECTS FOR HIGH-TEMPERATURE (A-15-STRUCTURE) SUPERCONDUCTORS: SOUND VELOCITY AT THE SUPERCONDUCTING PHASE TRANSITION. Testardi, L. R. (Bell Telephone Labs., Murray Hill, N. J.). Phys. Rev., B; 3: 95-106(1 Jan 1971).

The sound velocities (elastic moduli) of V_3Ge and V_3Si are found to have very large discontinuities in their temperature derivatives at the superconducting transition. A thermodynamic treatment of these data (with the specific-heat behavior) for a second-order phase transition is shown to yield a general dependence of T_c on strain. It is found that all strains greater than roughly 10^{-3} will lower T_c for cubic V_3Si and raise T_c for V_3Ge. The results show that these strain dependences are very large, mainly quadratic, and directly responsible for some of the anomalous behavior of the superconductors. They predict, quantitatively for V_3Si: (a) the reduction in T_c which results from the structural transformation, (b) the arrest of the structural phase transformation at T_c, (c) the strain dependence of the specific-heat discontinuity at T_c, (d) the strain dependence of the structural-transformation temperature, and (e) the anisotropic stress dependence on T_c. The predicted dependence of T_c upon the lattice parameter is a major factor in accounting for the different T_c's among the A-15-structure compounds. The microscopic source of this large strain dependence is discussed in terms of the Labbe-Friedel (density-of-states peak) model. It is a surprising result that this model does not predict the large strain dependence of T_c for V_3Si. Finally, the "approximate" nature of the sound velocity data at a phase transition is discussed and the general thermodynamic form for the corrections to the nonideal case is given. (auth)

14183 UNUSUAL STRAIN DEPENDENCE OF T_c AND RELATED EFFECTS FOR HIGH-TEMPERATURE (A-15-STRUCTURE) SUPERCONDUCTORS: ELASTIC, THERMAL, AND ALLOY BEHAVIOR. Testardi, L. R.; Kunzler, J. E.; Levinstein, H. J.; Maita, J. P.; Wernick, J. H. (Bell Telephone Labs., Murray Hill, N. J.). Phys. Rev., B; 3: 107-12(1 Jan 1971).

The specific heats of V_3Ge and V_3Si, and the elastic behavior of V_3Ge are given. These data are used to calculate the strain dependence of T_c in the preceding paper and to confirm some of the predictions of that calculation. From measurements of specific heat and electrical resistance, it is found that T_c for tetragonal V_3Si is up to 0.4°K below that for the cubic state. This result, as well as the strain dependence of the specific-heat discontinuity at T_c, are in reasonable agreement with the calculated results obtained in the previous paper. Finally, the dependence of T_c on lattice parameter for V_3Si, V_3Ge, and V_3Ga, predicted in the previous paper, is compared with the results for V_3X alloys. The remarkable agreement obtained in this comparison indicates that the chemical changes on alloying are relatively unimportant in establishing the large changes in T_c. (auth)

14184 JOSEPHSON COUPLING ENERGY IN THE PRESENCE OF THERMAL FLUCTUATIONS. Zil'berman, L. A.; Ivanchenko, Yu. M. (Physical-Technical Inst., Donetsk, USSR). Sov. Phys.-Solid State (Engl. Transl.); 12: 1530-5(Jan 1971).

Translated from Fiz. Tverd. Tela; 12: 1922-30(Jul 1970).

The effect of internal and external thermal fluctuations on the coupling energy of an extended Josephson tunnel junction was studied. The nonlinear term in the equation for the phase difference between the order parameters of the two superconductors is not assumed to be small. The stochastic differential equation in partial derivatives with boundary conditions is compared to the multidimensional Fokker-Planck equation. It is shown that the thermal fluctuations always decrease the coupling energy and change its dependence on the external magnetic field. (auth)

14185 UNCERTAINTY OF PSEUDOMULTIPLICITY IN THE THEORY OF SUPERCONDUCTIVITY. Vonsovskii, S. V.; Svirskii, M. S. (Inst. of the Physics of Metals, Sverdlovsk, USSR. Chelyabinsk State Teacher's Coll., USSR). Zh. Eksp. Teor. Fiz.; 59: 1192-9(Oct 1970). (In Russian).

Population uncertainty and the consequent incertainty of pseudospin projections in a system described by the Bardeen-Cooper-Schrieffer (BCS) hamiltonian are considered. It is demonstrated that uncertainty of the population and energy gap related to it is independent of the anomalous means. An analysis method is developed that takes into account uncertainty of the total spin when the total number of electrons of the system is constant. An exact solution is given for the case of a single Cooper pair and two phase-space elements. The solution yields an energy that is independent of the sign of the interelectron interaction parameter and lies below the ground-state energy calculated by the BCS method. It is shown that the L. Cooper problem admits separation of the system ground state from continuum by an energy gap not only in the case of attraction but also in the case of sufficiently strong interelectron repulsion. A modification of the trial wave function, which permits one to include interelectron repulsion in the BCS method, is considered. The role of small and large pseudospins is elucidated for interelectron attraction or repulsion. (auth)

14186 ROLE OF COLLECTIVE OSCILLATIONS IN THE ELECTRONIC MECHANISM FOR SUPERCONDUCTIVITY. Geilikman, B. T. Sov. Phys.-Solid State (Engl. Transl.); 12: 1497-9 (Jan 1971).

Translated from Fiz. Tverd. Tela; 12: 1881-4(Jul 1970).

The dynamical effects connected with the emission and absorption by electrons of virtual acoustic plasmons are considered in the electronic mechanism for superconductivity with a high critical temperature in metals with overlapping bands. For the case of a metal with one wide and one narrow band, the dispersion relations for the various branches of collective oscillations that correspond to poles of the two-particle Green's function are found. The equation for the energy gap is solved, including the contribution from the vertex part related to the acoustic plasma collective oscillations. This effect increases the attraction between electrons due to the static interaction. Combinations of metals and organic compounds are discussed briefly. It is shown that the pairing of electrons in this case is analogous to the pairing in the electronic superconductivity mechanism for compounds of metals and nonmetals. (auth)

14187 ALTERNATING FIELD LOSSES IN SUPERCONDUCTING STRIP CONDUCTORS. Linford, R. M. F.; Rhodes, R. G. (Univ. of Warwick, Coventry, Eng.). J. Appl. Phys.; 42: 10-15 (Jan 1971).

From Applied Superconductivity Conference, Boulder, Colo. See CONF-700618.

A wattmeter technique is described that advances the measurement of alternating field losses in superconducting materials. In particular, it allows realistic experiments on strip conductors, the geometric form most promising for application to electrical power engineering. Uniform current distribution is acheived, contact problems are eliminated, and sample preparation is minimal. It is shown how the alterating field measurements can be interpreted to yield values for several properties of the material studied. Critical fields, the surface shielding currents, and the bulk currents can all be determined. When these quantities are inserted into expressions derived from a modified critical state model, a good match to the experimental results is obtained. Comparison of the measured alternating field dissipation with the area enclosed by magnetization curves, derived in slowly varying fields, confirms the validity of the technique and the applicability of critical state models to results obtained at audio frequencies. (auth)

14188 LOW-FREQUENCY ELECTROMAGNETIC LOSSES AT 4.2°K OF NEUTRON-IRRADIATED Nb. Sekula, S. T. (Oak Ridge National Lab., Tenn.). J. Appl. Phys.; 42: 16-21(Jan 1971).
From Applied Superconductivity Conference, Boulder, Colo. See CONF-700618.

Low-frequency (350 Hz) permeability measurements at 4.2°K using phase-sensitive techniques were carried out on a Nb sample irradiated in the Oak Ridge Research Reactor at 40°C to several fast neutron doses up to 6×10^{19} neutrons/cm^2 (E > 1 MeV). In the mixed-state region a signal proportional to the electromagnetic loss in the sample is observed which decreases with increasing fast neutron dose. Quantitative estimates of the power dissipation in irradiated Nb are given, which are then related to the magnetic field dependence of the critical current density $J_c(H)$. (auth)

14189 ALTERNATING-CURRENT LOSS MEASUREMENTS IN THIN-FILM TYPE II SUPERCONDUCTORS. Deis, D. W.; Gavaler, J. R.; Jones, C. K.; Patterson, A. (Westinghouse Research Labs., Pittsburgh). J. Appl. Phys.; 42: 21-6(Jan 1971).
From Applied Superconductivity Conference, Boulder, Colo. See CONF-700618.

An electrical technique is described for measuring the audio-frequency power dissipation in superconducting thin films as a function of the ac current density, frequency, and applied dc magnetic field. This system has been used to study the ac losses in thin films of Nb and NbN, and also the ac and dc critical current densities in these materials. The results can be explained by assuming that both hysteresis and eddy current losses contribute. (auth)

14190 ANALOG COMPUTER SIMULATION OF WEAKLY CONNECTED SUPERCONDUCTING RINGS. Simmonds, M. B.; Parker, W. H. (Univ. of California, Irvine). J. Appl. Phys.; 42: 38-45(Jan 1971).
From Applied Superconductivity Conference, Boulder, Colo. See CONF-700618.

A system comprising a weakly connected superconducting ring inductively coupled to a resonant L–C circuit was studied using an analog computer. The weak link was characterized either by a current–phase relation of the form $I = I_c \sin\phi$ or by "supercurrent breakdown," and the results were compared. The effects of a normal resistance shunting the junction were investigated, as well as the effects of thermal current noise in the ring. Some criteria for achieving optimum coupling to the superconducting ring are discussed. (auth)

14191 HIGH-FIELD SUPERCONDUCTIVITY OF ALLOYS IN POROUS GLASS. Watson, J. H. P. (Corning Glass Works, N. Y.). J. Appl. Phys.; 42: 46-50(Jan 1971).
From Applied Superconductivity Conference, Boulder, Colo. See CONF-700618.

Superconductors were prepared by impregnating porous glass with low-melting-point alloys such as those in the Pb–Bi–Sb system. The critical fields of many alloys in porous glass with a pore diameter of 32 Å are in excess of 100 kOe at 4.2°K. Samples were prepared having critical current densities near 10^5 A/cm^2 in low (<10 kOe) magnetic fields. (auth)

14192 PROPERTIES OF VERY THIN ALUMINUM FILMS. Meservey, R.; Tedrow, P. M. (Massachusetts Inst. of Tech., Cambridge). J. Appl. Phys.; 42: 51-3(Jan 1971).
From Applied Superconductivity Conference, Boulder, Colo. See CONF-700618.

Thin films of aluminum have been produced in the thickness range of 1000 to 30 Å in small-area samples with photoetched edges. The superconducting transition temperature T_c, the critical magnetic field H_c, and the room-temperature conductivity have been measured as a function of thickness d. The results indicate that films as thin as 30 Å act essentially as uniform layers in which the crystal size is approximately equal to the film thickness. The transition temperature was found to vary linearly with d^{-1}. $H_c(T)$ was measured from T_c to 0.4°K. For thickness from 1000 to 200 Å, $H_c \sim d^{-1/2}$, as expected from the Ginzburg–Landau theory. For d < 200 Å, H_c is paramagnetically limited to about 49 kOe = $19.6T_c$, slightly above the Clogston limit. (auth)

14193 VERY HIGH CRITICAL CURRENT AND FIELD CHARACTERISTICS OF NIOBIUM NITRIDE THIN FILMS. Gavalier, J. R.; Janocko, M. A.; Patterson, A.; Jones, C. K. (Westinghouse Research Labs., Pittsburgh). J. Appl. Phys.; 42: 54-7(Jan 1971).
From Applied Superconductivity Conference, Boulder, Colo. See CONF-700618.

Previous results indicated that NbN thin films possess critical current and field characteristics significantly superior to that of bulk NbN having a similar T_c. Further measurements made on NbN films, with thicknesses between 50 Å and 8 μ, now show that, at 4.2°K, certain of these films exhibit the highest current densities of any presently known superconductor in all fields from zero up to the limit of our measurement capability (210 kOe). In addition, anomalously high current and field values have been measured in very thin (<300 Å) films. These thinner films show no depressions in J_c (measured at 4.2°K) or in $H_{c2}(0)$ values despite decreases in T_c from almost 16°K (in the thicker films) down to 11°K. (auth)

14194 ANALYSIS OF CRITICAL POWER LOSS IN A SUPERCONDUCTOR. Rabinowitz, Mario (Stanford Univ., Calif.). J. Appl. Phys.; 42: 88-96(Jan 1971).
From Applied Superconductivity Conference, Boulder, Colo. See CONF-700618.

A critical power dissipation resulting from an oscillating magnetic field, $H_p \cos\omega t$, can produce a magnetic breakdown field $H_p' < H_c$, the critical field of the superconductor. The analysis shows, for example, why the breakdown field of a superconducting microwave cavity can be well below H_c in some cases, and indicates what the functional dependence of the cavity Q may be for values of H_p near H_p'. The effective resistivity of a single isolated oscillating fluxoid, as well as that of a stationary normal region, is also derived for both type I and type II superconductors. (auth)

14195 MAGNETIZATION AND SUSCEPTIBILITY MEASUREMENTS OF POLYCRYSTALLINE NIOBIUM. Brechna, H.; Allen, M. A.; Cobb, J. K. (Stanford Univ., Calif.). J. Appl. Phys.; 42: 103-5(Jan 1971).
From Applied Superconductivity Conference, Boulder, Colo. See CONF-700618.

Magnetization and susceptibility data are presented for niobium rod samples in the temperature range of 1.2 to 8.9°K. The niobium samples tested had a range of tantalum content from 700 to 4000 ppm. The samples were annealed and degassed in high vacuum at temperatures between 2100° and 2300°C. Values of κ_1, κ_2, H_{c1}, H_{c2}, and H_c are presented as a function of tantalum impurity, and these values are compared with theoretical predictions. (auth)

14196 MECHANISMS DETERMINING THE CRITICAL CURRENT IN HARD SUPERCONDUCTORS. Webb, W. W. (Cornell Univ., Ithaca, N. Y.). J. Appl. Phys.; 42: 107-15(Jan 1971).
From Applied Superconductivity Conference, Boulder, Colo. See CONF-700618.

It is well established that critical current densities in hard superconductors depend on pinning of the fluxoid lattice by microstructural inhomogeneities against electromagnetic forces. However, the connection between the measured critical current densities which are continuum quantities and the interactions between the pinning objects and the fluxoid lattice which are virtual point interactions has presented a rather complex problem that is the focus of this review. An experimental approach to diagnosis of the mechanisms and a rather general phenomenological theory are described and illustrated by a summary of some studies of hard superconductors containing high lattice-dislocation densities that provide a high density of rather weak pinning objects. Conclusions of general applicability are summarized. (auth)

14197 FLUX FLOW AND A NEW CRITICAL-CURRENT FORMULA. Urban, Eugene W. (Marshall Space Flight Center, Huntsville, Ala.). J. Appl. Phys.; 42: 115-27(Jan 1971).
From Applied Superconductivity Conference, Boulder, Colo. See CONF-700618.

An experimental study was conducted to measure the flow of magnetic flux through the wall of a specimen of Nb–25% Zr, and

XUM

thereby to infer the magnetic induction and currents in the material. It was found that if at some magnetic field the specimen were heated to above T_c and recooled, and the applied field then subsequently changed at a constant rate, the rate of flux flow into or out of the sample would increase linearly with time. If measured at a series of magnetic fields, the rates of these increases, or the flow rate slopes were found to be a smoothly increasing function of average applied field. Calculations based on eight published critical-current density models did not satisfactorily explain these observations. It was found, however, that the empirical current-density model $J_c = \alpha_c[(\mu_0 H_{c2} - B)/(B_0 + B)]$ did, in fact, give excellent agreement with the measured flow-rate behavior. The experimental and analytical results are described, and the new critical-current density model is compared with earlier ones. (auth)

14198 NOISE THERMOMETRY WITH THE JOSEPHSON EFFECT. Kamper, R. A.; Zimmerman, J. E. (National Bureau of Standards, Boulder, Colo.). J. Appl. Phys.; 42: 132-6(Jan 1971).

From Applied Superconductivity Conference, Boulder, Colo. See CONF-700618.

Thermal noise causes a random-frequency modulation of the self-oscillation of a Josephson junction, and the temperature of the noise source can be determined by analysis of the generated signal. It is shown that a thermometer based on this principle would be theoretically capable of measuring temperatures in the microkelvin range, and a prototype thermometer that has recorded noise temperatures down to 0.075 K is described. (auth)

14199 OBSERVATION OF SINGLE FLUXON DRIFT THROUGH A SUPERCONDUCTOR. Burnette, K. T.; Newhouse, V. L. (Purdue Univ., Lafayette, Ind.). J. Appl. Phys.; 42: 138-46(Jan 1971).

From Applied Superconductivity Conference, Boulder, Colo. See CONF-700618.

What is believed to be the first direct observation of the drift of single fluxons through a superconductor is reported. This was achieved by using an ultrasensitive cryotron amplifier to sense the changes in persistent current that occur in a superconducting film loop when a fluxon is drifting into or out of the loop. The loop is deposited on an insulated superconducting ground plane; this decreases the inductance sufficiently so that the current changes induced by single fluxons entering or leaving the loop can be sensed. It was found possible to nucleate single fluxons by current pulsing narrow films that are superimposed over but insulated from the loop. The fluxons are found to be nucleated at the intersections of the edges of the film loop with the superimposed films, and then swept into or out of the loop by the Lorentz force exerted by the loop current. The fluxon velocity component normal to this current was measured for tin and found to be less than a factor of two different from the values predicted by certain of the present theories of fluxon motion. (auth)

14200 HIGH-FREQUENCY LIMIT OF THE JOSEPHSON EFFECT. McDonald, D. G.; Evenson, K. M.; Wells, J. S.; Cupp, J. D. (National Bureau of Standards, Boulder, Colo.). J. Appl. Phys.; 42: 179-81(Jan 1971).

From Applied Superconductivity Conference, Boulder, Colo. See CONF-700618.

Coherent detection of applied radiation via a Josephson current step was achieved with an applied frequency approximately a factor of 3 higher than heretofore reported. The detected signal is at 2.5 THz (118 μ). The inadequacy of existing theory to predict the frequency dependence of the Josephson effect is discussed. (auth)

14201 CHARACTERISTICS OF NbN DAYEM BRIDGES. Janocko, M. A.; Gavaler, J. R.; Jones, C. K.; Blaugher, R. D. (Westinghouse Research Labs., Pittsburgh). J. Appl. Phys.; 42: 182-5(Jan 1971).

From Applied Superconductivity Conference, Boulder, Colo. See CONF-700618.

Dayem-bridge weak links were fabricated by sputter etching niobium nitride thin films having Tc's of ~15 K. These junctions exhibit a negative resistance region extending to 45 mV at 3.2 K, in which are seen self-induced subharmonic current steps and structure near the energy-gap voltage. Temperature dependence of these features and effects of applied microwave radiation are discussed, and possible explanations of the negative resistance region and of the self-induced step structure are given. (auth)

14202 SUPERCONDUCTIVITY AND SPIN FLUCTUATIONS IN THE Ir–Ni, Ir–Co, AND Ir–Fe ALLOY SYSTEMS. Riblet, G. (Univ. of Pennsylvania, Philadelphia). Phys. Rev., B; 3: 91-5 (1 Jan 1971).

The superconducting transition temperatures of Ir–Ni, Ir–Co, and Ir–Fe alloys were measured in the temperature interval 0.10 to 0.040°K. It is shown that the rates of change of $\ln T_c$ with impurity concentration for these systems provide quantitative evidence that localized spin fluctuations are responsible for the suppression of superconductivity when these rates are compared with the rates of increase of the specific-heat coefficient γ and the susceptibility χ. (auth)

14203 COMPOUNDS AND ALLOYS FOR SUPERCONDUCTING APPLICATIONS. Enstrom, R. E.; Hanak, J. J.; Cullen, G. W. (RCA Labs., Princeton, N. J.). RCA Rev.; 31: 702-14(Dec 1970).

Several variations of a chemical vapor deposition process for Nb_3Sn, based on the hydrogen reduction of niobium and tin chlorides, are reviewed. These methods are used for preparing Nb_3Sn in forms including single crystals and polycrystalline films on ceramic or metal substrates, particularly long lengths of ribbon. Growth techniques are described that make this material available (1) as a highly perfect nearly dislocation-free material suitable for basic studies of properties needed for theoretical work and (2) as a heavily doped material with maximum concentration of defects necessary for flux pinning and high current-carrying capability in high-field-solenoid applications. This technology has culminated not only in the construction of the highest-field superconducting magnets to date, but also in a successful commercial product. (auth)

14204 DC CURRENTS AND AC INDUCTIVE COUPLING IN JOSEPHSON JUNCTIONS, AND S-WAVE INSTABILITIES IN SUPERCONDUCTING MATERIALS. Owen, Charles Scott. Philadelphia; Univ. of Pennsylvania (1970). 164p. University Microfilms Order No. 70-25,714.

Thesis.

First, "vortices" in dc tunneling supercurrents are considered in long Josephson junctions where magnetic self-fields due to the currents themselves influence the shape of the vortices. The details lead to predictions for maximum total tunneling current as a function of junction length and applied magnetic field. Second, the coupling of a Josephson junction and a superconducting stripline is calculated. The coupling is an inductive one via magnetic field penetration through the superconducting films which the two structures have in common in a S–I–S–I–S configuration. An equivalent circuit model of the problem is presented. A criterion for matching is developed, and the power flow to be expected via the inductive coupling is estimated. The calculation of the s-wave instability in the normal metal particle–particle scattering matrix of a superconductor is presented. One such instability occurs at the transition temperature T_c in all metals which become superconducting. This transition is associated with a particular form of the space–time superconducting pair correlations and it is possible, in principle, to ask what additional particle–particle instabilities can be found in a system which is supercooled so that it remains in its normal phase at temperatures below T_c. This work indicates that there is only one s-wave instability (that associated with the superconducting transition) and gives a straightforward means of calculating T_c. (Diss. Abstr. Int., B)

14205 LOCAL REINFORCEMENT OF THE HF MAGNETIC FIELD NEAR THE ASPERITIES OF A SUPERCONDUCTING METALLIC SURFACE. Bergeret, Henri; Septier, Albert (Paris Univ., Orsay, France). Compt. Rend., Ser. B; 271: 1048-50 (23 Nov 1970). (In French).

The local maximum coefficient of reinforcement β_h in a mean magnetic field H_0 ($H_{local} = \beta_h H_0$) was calculated at the surface for two simple types of microrelief. For points of ellipsoidal cross section $1.5 \leq \beta_h \leq 2$ and for a ride of semicylindrical elliptical form, β_h may be much greater than 2. The asperities revert back to normal when H_0 is very much less than the critical field H_c. (auth)

14206 PROBLEM OF ZERO-BIAS ANOMALIES IN THE TUNNELING SPECTROSCOPY OF SUPERCONDUCTORS. Kaufmann, Frank P.; Holzer, Peter (Univ., Frankfurt am Main). Z. Phys.; 241: 308-12(1971).

Taking into account nonmagnetic energy-loss processes in the barrier as a model for zero-bias anomalies, an expression is derived for the derivative of the tunneling current with respect to the applied voltage as a function of the superconducting density of states in a superconductor/normal metal junction. It is assumed that boson-like excitations are created in the barrier region. The investigations show that the results of elastic-tunneling calculations have to be corrected by a term proportional to an integral over the superconducting density of states. (auth)

14207 VORTEX MOTION IN THE PRESENCE OF THERMODYNAMIC FLUCTUATIONS. Horn, P. M.; Masker, W. E.; Parks,

XUM

R. D. (Univ. of Rochester, N. Y.). Phys. Rev. Lett.; 26: 177-80(25 Jan 1971).

An exponential temperature dependence of the quantity $d\rho_f/dH$, where ρ_f is the flux-flow resistivity, was observed in thin-film superconductors in the reduced temperature interval $0.7 \lesssim T/T_c \lesssim 1.0$. The results can be explained qualitatively if it is assumed that the dominant contribution to the flux-flow viscosity is power dissipation resulting from the presence of thermodynamic fluctuations. (auth)

14208 EFFECTS OF V, Mo, OR Ta ADDITIONS ON SUPERCONDUCTING PROPERTIES OF Nb-40 Zr-10 Ti ALLOY. Kitada, Masahiro; Doi, Toshio (Hitachi Ltd., Kokubunji, Japan). J. Jap. Inst. Metals; 34: 1082-6(Nov 1970). (In Japanese).

The applied magnetic field vs critical current density, the superconducting transition temperatures, and the microstructures of Nb–Zr–Ti alloys were investigated. V, Mo, and Ta added as the fourth elements had bcc structures and were all superconducting. It is presumed that each metal dissolved in the Nb–40 Zr–10 Ti base alloy was of the substitutional type. From microstructural observation, the solubilities of V, Ta, and Mo were about 5, 5, and 2% in the base alloy, respectively. When the V, Mo, or Ta contents were larger than the above values, precipitation occurred and cold working of the alloys became more difficult than the base alloy. The critical current densities of Nb–Zr–Ti–(V or Mo) alloys were smaller than that of the base alloy, and the critical current densities of Nb–Zr–Ti–Ta alloys were nearly equal to that of the base alloy. Superconducting transition temperatures of the three alloys containing 5% V, 5% Ta, and 5% Mo were 6.7, 8.4, and 6.3°K, respectively, which were lower than that (9.3°K) of the base alloy. (auth)

14209 APPLIED MAGNETIC FIELD VS CRITICAL CURRENT DENSITY CHARACTERISTICS OF SUPERCONDUCTING Nb-60 Ti-5 Zr ALLOY SHEETS. Kitada, Masahiro; Doi, Toshio (Hitachi Ltd., Kokubunji, Japan). J. Jap. Inst. Metals; 34: 1075-81(Nov 1970). (In Japanese).

Applied magnetic field (H) vs critical current density (J_c) characteristics of rolled Nb–60 Ti–5 Zr sheets aged at 300 to 500°C were measured at 4.2°K in order to examine the anisotropic effect. The most suitable heat treatment to increase the magnitude of J_c of the sheets was aging at 300 or 350°C for at least about 500 or 100 hr, respectively. For the sheets aged at 350°C for 125 hr, the critical current densities $J_c(//)$ and $J_c(\perp)$, which corresponded to the rolled planes parallel and perpendicular to the direction of an applied magnetic field, were 1.1×10^5 and 5.8×10^4 A/cm² at 70 kOe and 3.7×10^4 and 1.8×10^4 A/cm² at 90 kOe, respectively. In case of aging at 400 to 500°C, the anisotropic effect of $H-J_c$ characteristics (the ratio of $J_c(//)$ to $J_c(\perp)$) increased with increasing aging temperature. The peak effect was observed in the $H-J_c(\perp)$ characteristics of the sheets and depended upon the aging temperature and time, while it was not shown in the $H-J_c(//)$ characteristics. (auth)

14210 ELECTRON-TUNNELING INVESTIGATING OF SUPERCONDUCTING AMORPHOUS STATE OF BISMUTH. Chen, Juei-Teng. Waterloo, Ont.; Univ. of Waterloo (1969). Thesis.

Electron tunneling measurements were made on $Al/Al_xO_y/Bi$ tunneling junctions in which the amorphous Bi film was condensed on a substrate kept at liquid helium temperature. The energy gap parameter, Δ_0, for amorphous Bi derived from the tunneling measurements was $\Delta_0 = 1.210 \pm 0.01$ MeV. Using the $T_c = 6.11 \pm 0.03$°K derived from the resistance vs temperature measurements on the amorphous Bi film and the value of Δ_0, it was found that the ratio $2\Delta_0/k_BT_c$ was 4.59 ± 0.05 for amorphous bismuth. The phonon spectrum for amorphous Bi was derived by using McMillan's inversion program on the tunneling data. The results are in the form of a plot of $\alpha^2(\omega)F(\omega)$, where $\alpha^2(\omega)$ is the energy dependent electron–phonon coupling parameter and $F(\omega)$ is the phonon density of states. The results indicate an extreme "softening of the phonon spectrum" from what is found for crystalline superconductors. The following parameters characterize the phonon spectrum: the total area under the $\alpha^2(\omega)F(\omega)$, $\alpha_1^2 = 3.50$ MeV; the electron–phonon coupling constant, $\lambda = 2.46$; the average phonon energy, $\langle\omega\rangle = 2.86$ MeV; the average phonon energy squared, $\langle\omega^2\rangle = 16.3\ (\text{MeV})^2$; the Coulomb pseudopotential, $\mu^* = 0.105$. The estimated errors are ± 10% on α_1^2, λ, and μ^* and ±20% on $\langle\omega\rangle$ and $\langle\omega^2\rangle$. The results support the theory of Garland et al., on the transition temperature of disordered and amorphous superconductors. Qualitatively, their theory predicts the decrease in $\langle\omega\rangle$, increase in λ, and broadening in the peaks of $F(\omega)$ that is observed in amorphous Bi in comparison with what is found in a crystalline superconductor. Quantitatively, the theory of Garland et al., predicts $T_c = 5.1$°K, when the values of the parameters for amorphous Bi are used, which is in reasonable agreement with the experimental $T_c = 6.11$°K. It was possible to test in the limit of extremely strong coupling the McMillan equation which predicts the maximum possible transition temperature for a given class of superconductor as a function of λ. The results suggest that the McMillan equation is incorrect in the limit of extremely strong coupling, and the maximum transition temperature is much less than that given by the McMillan expression. (Diss. Abstr. Int., B)

Equipment and Devices

Refer also to abstracts 14474, 14846, and 14860.

14211 (KFK-1217) MEASUREMENTS ON PULSED SUPERCONDUCTING MAGNETS. Juengst, K. P.; Krafft, G.; Ries, G. (Kernforschungszentrum, Karlsruhe (West Germany). Institut fuer Experimentelle Kernphysik). May 1970. 13p. (CONF-700503-8). Dep. NTIS (U. S. Sales Only).

From 3rd International Conference on Magnet Technology, Hamburg, Germany.

Several experiments with superconducting multifilament NbTi wires were performed to measure ac losses, degradation effects and reachable $\dot{H}$, in order to find a suitable conductor for an ac dipole. Solenoids were built with NbTi multicore wires having the following parameters: composite diameter 0.04 to 0.1 cm, Cu and Cu/CuNi (3-component) matrix, twist rate between 0.5 and 2 turns/cm, filament diameter 13 to 48 μm. The solenoids typically had an inner diameter of 2.5 cm, an outer diameter of 8.5 cm and a length of 5.5 cm, yielding a central field between 40 and 72 kG. The solenoids were not potted and reached 85 to 90% of short-sample critical current. For the chosen cooling conditions, a maximum $\dot{H}$ was reached of 95 kG/sec with a field amplitude of 52 kG. The measured ac losses agree with theoretically predicted ones. Significant additional self field losses could not be confirmed quantitatively. (auth)

14212 (UUIP-677) ³He-CRYOSTAT FOR SPECIFIC HEAT MEASUREMENTS. Lindqvist, Torsten; Spahr, Kurt; Marklund, Kari; Hoel, Lars; Larsson, Mats (Uppsala Univ. (Sweden). Inst. of Physics). Jan 1970. 26p. Dep. NTIS (U. S. Sales Only).

A conventional ³He cryostat for measurements of specific heat in the temperature range 0.5 to 4.2°K is described in detail. Data recording and data treatment is discussed. Calibration of Ge thermometers and measurements of the empty calorimeter are reported. Results from measurements on a copper standard sample are presented. (auth)(Sweden)

14213 EXPERIMENTS WITH ³He–⁴He DILUTION REFRIGERATION AND THEIR APPLICATION TO NUCLEAR MAGNETIC SUSCEPTIBILITY MEASUREMENTS IN SOLID ³He. Pipes, Paul Bruce Jr. Stanford, Calif.; Stanford Univ. (1970). 144p. University Microfilms Order No. 70-18,456. Thesis.

A theoretical analysis of the ³He–⁴He dilution refrigeration process is developed, based upon a "liquid–vapor" model for a phase-separated ³He–⁴He mixture at low temperatures. The dilution process is shown to be similar to the vaporization of a liquid. Experiments are described in which a temperature of .025°K is maintained continuously and the experiments are compared with the theory. This refrigerator was used in the measurements described. Measurements of the nuclear magnetic susceptibility of pure (1×10^{-5} ⁴He) solid ³He from .4°K to .04°K are described. The susceptibility is shown to obey a Curie–Weiss law $\chi = C/(T - \Theta)$ with $\Theta = -1.5 \times 10^{-3}$°K for a molar volume, v, of 23.3 cm³/mole, $\Theta = -4.0 \times 10^{-3}$°K for v = 23.6 cm³/mole and $\Theta = -5.4 \times 10^{-3}$°K for v = 24.2 cm³/mole. The negative values for Θ mean that solid ³He nuclei will order antiferromagnetically at very low temperatures. The experimental data are compared with current theories and other experiments.

14214 SIMPLE ³He–⁴He DILUTION REFRIGERATOR. Neganov, B. S. (Joint Inst. for Nuclear Research, Dubna, USSR); Safrata, R. S.; Sebek, J.; Svec, K. Czech. J. Phys.; B20: 1316-18(1970).

A very simple ³He–⁴He dilution refrigerator is described. The temperature 60 mK was achieved at a circulation of 3×10^{-5} mole ³He per second. The cooldown time is one hour. (auth)

14215 SUPERCONDUCTIVITY. 1970 Applied Superconductivity Conference, Boulder, Colorado, 15-17 June 1970. J. Appl. Phys.; 42: 1-189(Jan 1971). (CONF-700618).

Thirty-two papers, 14 "abstracts only," and 11 "titles only" are grouped in the following categories: levitation and monopoles, alternating-current losses in materials and coils, quantum interference devices, materials, magnets, high-frequency resonators and lines, flux motion and critical currents, instruments, power, and detectors. A separate abstract is included for each full-length paper. (M.H.R.)

For abstracts of individual papers see: 14187–14201, 14216–14230, 14356, and 14860.

14216 UNIVERSITY OF VIRGINIA SUPERCONDUCTING WIND-TUNNEL BALANCE. Zapata, R. N. (Univ. of Virginia, Charlottesville); Parker, H. M.; Moss, F. E.; Hamlet, I. L.; Kilgore, R. S. J. Appl. Phys.; 42: 3-5(Jan 1971).
From Applied Superconductivity Conference, Boulder, Colo. See CONF-700618.

The design of an electromagnetic balance using superconducting coils is reported. Both dc and ac coils are used to support aerodynamic models in a supersonic (Mach 3) wind tunnel and to simultaneously measure the forces acting on them along 3 orthogonal axes. Major design characteristics include: adoption of symmetrical coil arrangement to provide maximum space for the wind tunnel; 3 gradient–coil pairs capable of being driven between 0 and 350 A at a frequency of 30 Hz by specially designed power supplies; a vertical wind tunnel with a 6-in. test section located in the axial room-temperature access of a 250-liter liquid-helium Dewar. Results on ac losses for prototype gradient coils wound of three different superconducting materials are reported. (auth)

14217 VERSATILE SUPERCONDUCTING FEMTOVOLT AMPLIFIER AND MULTIMETER. Lukens, J. E.; Warburton, R. J.; Webb, W. W. (Cornell Univ., Ithaca, N. Y.). J. Appl. Phys.; 42: 27-30(Jan 1971).
From Applied Superconductivity Conference, Boulder, Colo. See CONF-700618.

The adaption and use of superconducting quantum interference magnetometers for the measurement of voltage, resistance, and inductance are described. The instrument which is discussed achieves the Nyquist noise limit, about 10^{-22} W of noise power in a 1-Hz bandwidth, over a wide range of conditions. This permits resistance measurements down to this power level and a voltage sensitivity of a few femtovolts for low-impedance sources. Using a 10-μA measuring current, inductance changes of 0.1 pH were measured. The noise limitations of the device and the design criteria for optimum performance are discussed in detail. Circuit and construction designs are presented that allow the device to be used, with minimal changes, for measurements over a wide range of parameters. (auth)

14218 RECENT DEVELOPMENTS IN SUPERCONDUCTING DEVICES. Zimmerman, J. E. (National Bureau of Standards, Boulder, Colo.). J. Appl. Phys.; 42: 30-7(Jan 1971).
From Applied Superconductivity Conference, Boulder, Colo. See CONF-700618.

A simple model of the electrical characteristics of thin-film-bridge, point-contact, and tunnel junction Josephson devices is given, along with some comments on their relative performance at very low and at very high frequencies. A particular example is the dc IV characteristic of a point contact at the center of a parallel-disk microwave cavity. Some recent developments in devices and the application of a point-contact loop (SQUID) device to magnetocardiography is described. (auth)

14219 COMPARISON OF NbTi AND Nb_3Sn MATERIAL TESTS WITH THE ACTUAL PERFORMANCE OF COILS. Coffey, D. L.; Gauster, W. F.; Lubell, M. S. (Oak Ridge National Lab., Tenn.). J. Appl. Phys.; 42: 59-65(Jan 1971).
From Applied Superconductivity Conference, Boulder, Colo. See CONF-700618.

A 100-kG, 8.26-cm-bore, 40-kJ Nb_3Sn magnet and a 75-kG, 10.2-cm-bore, 95-kJ twisted filament NbTi magnet were constructed and tested. A number of other magnets of smaller size using both the Nb_3Sn and twisted filament NbTi conductors are also described. Material evaluation tests leading to these magnet designs are reported. They include short sample tests with controlled surface-cooling conditions and cusp coil tests in which an external field is applied perpendicular to the cusp coil axis. Finally, two successful stabilization techniques for Nb_3Sn ribbon are presented with coil performance data before and after the stabilization has been employed. (auth)

14220 STATE OF THE ART OF SUPERCONDUCTING MAGNETS. Stekly, Z. J. J. (Magnetic Corp. of America, Cambridge, Mass.). J. Appl. Phys.; 42: 65-72(Jan 1971).
From Applied Superconductivity Conference, Boulder, Colo. See CONF-700618.

The superconducting magnet is a key component in various applications including high-energy physics, fusion research, magnetohydrodynamics, and electrical rotating machinery. The general characteristics of state of the art of superconducting magnets as far as design and performance are concerned are presented. The properties of superconductors are briefly discussed, and the basis for design of stable conductors is set forth. Examples of conductors and magnet systems are given and discussed. The current state of affairs is summarized in three plots showing size versus field achieved, current density in coils as a function of magnetic field, and specific weight versus stored magnetic energy. (auth)

14221 CONSTANT VOLTAGE CONTROLLER AND TRANSITION MONITOR FOR SUPERCONDUCTING MAGNETS. Lester, Donald H. (Los Alamos Scientific Lab., N. Mex.). J. Appl. Phys.; 42: 80-1(Jan 1971).
From Applied Superconductivity Conference, Boulder, Colo. See CONF-700618.

Superconducting magnets with long charge times require a power supply that will hold a constant voltage across a magnet during the charge, hold, and discharge periods. Conventional supplies regulate poorly during hold and lose control completely during discharge of the magnet. A simple circuit has been designed to connect between a magnet and the remote sense input of a conventional power supply which permits control and regulation at all times. During the testing of multisection superconducting magnets, it is desirable to know the order and approximate time interval in which each section undergoes a transition to the normal conducting state. A circuit has been designed which detects and displays this information. (auth)

14222 SURFACE RESIDUAL RESISTANCE OF HIGH-Q-SUPERCONDUCTING RESONATORS. Halbritter, J. (Univ., Karlsruhe, Ger. Kernforschungszentrum, Karlsruhe, Ger.). J. Appl. Phys.; 42: 82-7(Jan 1971).
From Applied Superconductivity Conference, Boulder, Colo. See CONF-700618.

The temperature-independent residual surface resistance R_{res} of high-Q-superconducting resonators is up till now not well understood. Experiments in lead-plated copper cavities and massive niobium cavities ($\nu \approx$ GHz) have shown $R_{res} \propto \omega^{1.8 \pm 0.2}$, which excludes normal conducting regions as a cause for the rf losses. An explanation is presented that can describe the observed dependencies on frequency and on surface treatment: the losses are caused by the generation of phonons in fissured surfaces by locally excited rf fields. These losses are temperature-independent, give $R_{res} \propto \omega^2$, and can also explain the observed mode dependence in lead-plated copper cavities. (auth)

14223 EFFECT OF TIN ADDITIVE ON INDIUM THIN-FILM SUPERCONDUCTING TRANSMISSION LINES. Mason, P. V. (California Inst. of Tech., Pasadena). J. Appl. Phys.; 42: 97-102(Jan 1971).
From Applied Superconductivity Conference, Boulder, Colo. See CONF-700618.

The effect of adding up to 23% tin to the indium film of a thin-film/tantalum-oxide/bulk-tantalum transmission line is reported. Addition of tin reduces the velocity and increases the delay for fixed length by 1.4% for each percent of tin. Agreement with the predictions of Pippard's nonlocal theory when mean-free path is reduced is excellent. Pulse attenuation and shape degradation are not increased by addition of tin. Attenuation as low as 10 dB per microsecond of delay was observed at 1.25 K. The added tin reduces by 50% the sensitivity of velocity to temperature near T_c, and improves the reproducibility of velocity from line to line. Critical temperature is increased to 6 K for 23% tin, in good agreement with previous measurements. (auth)

14224 NOISE ANALYSIS FOR AMPLIFIERS WITH SUPERCONDUCTING INPUT. Radhakrishnan, V.; Newhouse, V. L. (Purdue Univ., Lafayette, Ind.). J. Appl. Phys.; 42: 129-32(Jan 1971).
From Applied Superconductivity Conference, Boulder, Colo. See CONF-700618.

A method is developed to adapt the conventional definition of the noise temperature to amplifiers with superconducting inputs. In particular, this method is applied to a crossed-film cryotron amplifier with a superconducting input to calculate its noise temperature. It is then compared with that of other amplifiers and masers. In addition to the noise temperature, a new criterion is evolved here: to estimate the figure of merit of amplifiers and detectors. This involves a new parameter called herein the action factor, which is the product of the smallest energy measurable by a device, with its smallest possible response time. The action factor and the noise temperature are worked out for the cryotron and a few other amplifiers and detectors for comparison. The advantage of the cryotron amplifier is brought out. (auth)

14225 HIGH-CURRENT ac LOSSES IN LARGE SUPERCONDUCTING NIOBIUM TUBES. Meyerhoff, R. W.; Beall, W. T. Jr. (Union Carbide Corp., Tarrytown, N. Y.). J. Appl. Phys.; 42: 147-53(Jan 1971).

From Applied Superconductivity Conference, Boulder, Colo. See CONF-700618.

Loss measurements were made at 60 Hz on 6-m lengths of 1- and 3-cm-diam superconducting niobium tubes used as the inner conductor of a coaxial line. These tubes carried transport currents up to 1700 and 5300 A, respectively. The losses were found to fit the relation $P = fAE_{c1}(H/H_{c1})^n$, where f is the frequency, A is the surface area, E_{c1} is the energy loss per unit surface area per cycle at H_{c1}, the lower critical magnetic field, and H is the peak magnetic field at the surface of the superconductor. The exponent n equals 3 for $H \leq H_{c1}$ and $n \geq 4$ for $H \geq H_{c1}$. The ac losses showed a 25% linear increase with temperature from 4.2 to 5 K. For the case of an eccentric coaxial line, where the current and magnetic field vary about the circumference of the superconductor, the ac losses were found to agree with those predicted from calculated values of the current and magnetic field distributions. In particular, when the peak surface field is less than H_{c1} and R is the ratio of the maximum to minimum surface magnetic fields about the circumference of the superconductor, the losses were a factor $(3R^2 + 2R + 3)/4R$ greater than those found at an equivalent current for a concentric configuration. (auth)

14226 DESIGN FEATURES OF ac SUPERCONDUCTING CABLES. Long, H. M.; Notaro, J. (Union Carbide Corp.; Tonawanda, N. Y.). J. Appl. Phys.; 42: 155-62(Jan 1971).

From Applied Superconductivity Conference, Boulder, Colo. See CONF-700618.

Alternating current superconducting cables that can be readily integrated into utility systems require both a superconductor with low characteristic ac losses and a high-performance cryogenic system to minimize the cost of heat pumping the thermal losses to the atmosphere. Moreover, the resulting cable systems must operate with the long-term reliability expected of utility systems. Recent publications have treated the measurement of the superconducting material properties and the conceptual electrical and cryogenic design for a superconducting cable. Here, a cable configuration is discussed, and its electrical and cryogenic design features are examined, with principal emphasis placed upon the relationship of these features with present technological capabilities. Fabrication and installation feasibility and the expected levels of performance and reliability can be inferred from the practical operating cryogenic systems, which are used as a guide for the selection and design of the cryogenic enclosure for the cable. (auth)

14227 COMPARISON OF SUPERCONDUCTING AND SEMICONDUCTING BOLOMETERS. Bertin, C. L. (IBM Components Div., East Fishkill, N. Y.); Rose, K. J. Appl. Phys.; 42: 163-6 (Jan 1971).

From Applied Superconductivity Conference, Boulder, Colo. See CONF-700618.

Superconducting tin bolometers are now reasonably well understood, and the results of calculations of performance are given over a large range of sheet resistances (0.01 to 1000 Ω/□ at 4.2°K). Comparison of superconducting bolometers with semiconducting ones shows that tin and germanium are equivalent in performance. The superconducting devices have the additional advantage of simplicity of sample preparation and lower impedance levels permitting higher operating speeds if desired. (auth)

14228 NUCLEAR RADIATION DETECTION USING A SUPERCONDUCTING RESONANT CAVITY. Alworth, C. W.; Haden, C. R. (Texas A and M Univ., College Station). J. Appl. Phys.; 42: 166-9(Jan 1971).

From Applied Superconductivity Conference, Boulder, Colo. See CONF-700618.

Nuclear radiation is detected using a superconducting resonant circuit operated at 380 MHz. The technique uses a doped semiconductor crystal placed on the stub of a reentrant cavity. The cavity is lead-plated and cooled to 4.2°K, such that it becomes superconducting. The cavity then becomes the frequency-controlling element for a voltage-variable oscillator. Nuclear radiation impinging on the crystal causes a change in the relative dielectric constant, which in turn causes the resonant frequency of the cavity to change. The crystal exhibits a peculiar trap property at 70°K or below, which allows any electron-hole pairs generated in the crystal to be indefinitely trapped. The output frequency of the resonant circuit is then proportional to the total dose received by the crystal. Frequency shifts of the order of 4.051 kHz/min are observed in CdS, for a ^{14}C source of 1 μ Ci. (auth)

14229 MATERIAL-PROPERTIES ANALYZERS USING SUPERCONDUCTING RESONATORS. Hinds, James J.; Hartwig, William H. (Univ. of Texas, Austin). J. Appl. Phys.; 42: 170-9 (Jan 1971).

From Applied Superconductivity Conference, Boulder, Colo. See CONF-700618.

A low-temperature material-properties analyzer, using a superconducting microwave resonant cavity, is discussed. Placing semiconductor or dielectric material samples in the cavity perturbs the resonant frequency, absorbed microwave power, and cavity Q. Additional perturbations occur when the sample complex dielectric constant is altered by a thermal, nuclear radiation, or optical stimulus. In samples such as Si, GaAs, CdS, and CdTe, these perturbations have been used to determine such material properties as relaxation time, lifetime, Fermi level, trap ionization energy, trap density, capture cross section, free-carrier density, and trap population. A contactless experimental technique similar to the thermally stimulated conductivity experiment is proposed. The contactless ac measurement system is shown to be sensitive, accurate, useful with randomly shaped or powdered samples, and applicable to many types of insulators and semiconductors. (auth)

14230 SUPERCONDUCTING MICROSTRIP HIGH-Q MICROWAVE RESONATORS. DiNardo, A. J.; Smith, J. G.; Arams, F. R. (Airborne Instruments Lab., Melville, N. Y.). J. Appl. Phys.; 42: 186-9(Jan 1971).

From Applied Superconductivity Conference, Boulder, Colo. See CONF-700618.

Superconducting miniature microstrip resonators, operating at X band, were constructed using vacuum-deposited lead on low-loss sintered alumina substrate. Unloaded Q's as high as 200,000 and 500,000 were measured at 14.3 GHz at 4.2 and 1.8 K, respectively. (auth)

Plasma and Thermonuclear Physics

14231 (NP-18663) WILLS PLASMA PHYSICS DEPARTMENT TWENTIETH SIX-MONTHLY PROGRESS REPORT, JULY 1-DECEMBER 31, 1970. (Sydney Univ. (Australia). School of Physics). 11p. (PR-20). Dep. NTIS (U. S. Sales Only).

Research in the department is briefly reviewed. It covers the following aspects of plasma physics: (1) plasma sources; (2) hydromagnetic ionizing fronts; (3) hydromagnetic waves; (4) laser diagnostics; (5) plasma decay in SUPPER I; (6) electron cyclotron harmonic resonances in the 500-MHz to 2-GHz range of the SUPPER V discharge; (7) a performance study of the pulsed HCN laser at 337 μm and its dependence on the electrical discharge and other parameters. Recent research reports are listed. (Australia)

14232 ELECTRODE ABLATION IN A SPARK DISCHARGE AND IN AN ELECTROMAGNETIC SHOCK TUBE. Sharah, Abul. Ottawa; Carleton Univ. (1969). National Library of Canada, Ottawa.

Thesis.

The results of a study on the entry of electrode material into a spark discharge and into the plasma in an electromagnetic shock tube are presented. The theory of electrode ablation in a spark discharge is considered by treating the electrode as a semi-infinite solid having one face suddenly exposed to a constant heat flux. Expressions are derived for the ablation time, ablated mass, and depth of ablation of the cathode. An order-of-magnitude calculation is made to estimate these quantities for various cathode materials. An experimental investigation of electrode processes in a spark discharge was carried out in a specially designed apparatus that produced a discharge having an immobile spark channel. A number of electrode materials having a wide range of thermal and physical properties were investigated. Time-resolved spectrophotometric measurements yielded experimental values of ablation time for the cathode materials that were in fair agreement with theoretical predictions. The electrode ablation in a parallel-plate electromagnetic shock tube was also studied. The electrode ablation mechanism is believed to be the same as in a spark discharge. Expressions for the ablated mass of electrode material were derived by describing the motion of the plasma in the shock tube by a modified snow-plow model. Experimentally observed plasma velocities enabled the author to estimate the ablated masses. Various electrode materials were tested to determine their ablative performance in the shock tube. (TSS) (Diss. Abstr. Int., B)

Confinement and Heating

Refer also to abstract 14344.

14233 (JAERI-Memo-4186) JOULE HEATING IN JFT-2. Takeda, Tatsuoki; Itoh, Satoshi (Japan Atomic Energy Research Inst., Tokyo). Oct 1970. 20p. Dep. NTIS (U. S. Sales Only).

The time dependence of the plasma parameters in JFT-2 was investigated numerically. The calculations were carried out by solving the simultaneous differential equations composed of circuit equations and plasma energy-balance equations. Necessary one-turn resistance of a liner and the dependence of ion temperature and thermal conduction time on plasma parameters were obtained. (auth) (Japan)

14234 MAGNETIC AND DRIFT SURFACES USING A NEW STELLARATOR EXPANSION. Dobrott, D.; Frieman, E. A. (Princeton Univ., N. J.). Phys. Fluids; 14: 349-60(Feb 1971).

A new stellarator expansion was devised, wherein the depths of the helical and toroidal field modulations are comparable and the total rotational transform is finite. To accomplish this, one defines $\lambda = \rho/R \ll 1$ (R is the major radius, ρ is the minor radius) and choose p, the number of helical periods, to be of order $\lambda^{-1/2}$. Detailed calculations of vacuum magnetic field properties were carried out, including the magnetic surfaces, V'', shear, etc. For the particle surface calculations, the ratio of ion gyroradius to major radius of the torus, $\epsilon = R_L/R$, is chosen to be of order $\lambda^{1/2}$. Using the same methods as for the vacuum field calculations, analytic solutions are obtained for particle drift surfaces in stellarators with finite departures from axial symmetry. These surfaces, derived from perturbation techniques, are obtained for four particle classes that are, for the first time, precisely categorized according to trapping state. Transitions between classes are interpreted. Numerical calculation of integrals is carried out for comparison with approximate results. (auth)

14235 RESISTIVE PLASMA ROTATION AND SHOCK FORMATION IN TOROIDAL GEOMETRY. Hazeltine, R. D.; Lee, E. P.; Rosenbluth, M. N. (Inst. for Advanced Study, Princeton, N. J.). Phys. Fluids; 14: 361-70(Feb 1971).

The rotation of a toroidally confined plasma about its magnetic axis due to resistive diffusion is studied by means of a single fluid model in which the only dissipation occurs through a small scalar resistivity. The time evolution of the rotation is examined by considering the resistivity as inducing first-order time variation on a dissipationless steady state. The known instability of flows with small rotational velocity to rapidly speed up toward a critical speed is confirmed; more importantly, it is found that a shock which develops at the critical speed stabilizes the flow, so that the ultimate state of the system is characterized by steady rotation with a very weak shock front directed radially inward from the magnetic axis. The outward flux of plasma in this state is found to be essentially the Pfirsch–Schlüter flux enhanced by a factor of the square root of the aspect ratio. (auth)

14236 NUMERICAL MODEL FOR TOROIDAL PLASMA CONTAINMENT WITH FLOW. Winsor, Niels K.; Johnson, John L.; Dawson, John M. (Princeton Univ., N. J.). J. Comput. Phys.; 6: 430-48(Dec 1970).

A numerical model was developed to study the confinement of low-pressure plasmas in simple axially symmetric configurations. The equations contain the effects of resistivity, plasma inertia, and pressure gradients along the field. The model is applied to a simple magnetic geometry that includes the effects of curvature, rotational transform, and shear. An explicit difference scheme is derived for the numerical solution with this prescribed geometry. Results of calculations with the model are compared to a similarity solution for resistive diffusion in a cylinder, and to calculations of quasi-stationary diffusion in a torus. Finally, the onset of plasma rotation is demonstrated and its development to a steady-state rotation is observed. (auth)

14237 SELF-SIMILAR THERMAL WAVE IN A TWO-TEMPERATURE PLASMA HEATED BY A LASER PULSE. Anisimov, S. I. (Inst. of Theoretical Physics, Moscow). JETP Lett. (USSR) (Engl. Transl.); 12: 287-9(20 Oct 1970).

Translated from Zh. Eksp. Teor. Fiz., Pis'ma Red.; 12: 414-16(20 Oct 1970).

It is shown that the problem of heating and motion of a two-temperature plasma with allowance for the electron-ion relaxation and the electron thermal conductivity admits a self-similar solution in the case when the energy flux absorbed by the plasma increases linearly in time. The solution makes it possible to determine the qualitative features of the plasma heating process at different values of the pulse duration and of the absorbed energy. (M.O.W.)

14238 DIFFUSION-ELECTRIC PHENOMENA IN A PLASMA CONFINED IN TOKAMAK. Galeev, A. A. (Inst. of Nuclear Physics, Novosibirsk, USSR). Zh. Eksp. Teor. Fiz.; 59: 1378-89(Oct 1970). (In Russian).

The particle and heat fluxes due to the presence of a conductivity current and the electric field that produces it in the Tokamak are calculated. Additional fluxes are directed inside the plasma and, hence, diffusion resembles the well-known phenomenon of pinching of a current-carrying plasma column. The inward motion plasma velocity differs from the classical diffusion velocity by β_I^{-1} times ($\beta_I = 4\pi p/B_I^2$ where p is the plasma pressure and B_I the field strength of the proper current). An additional current resistance arises simultaneously. In a Coulomb plasma the resistance does not differ significantly from that calculated by Spitzer. In a rarefied plasma the longitudinal electric field induces a drift of "trapped" particles along the magnetic field and yields a comparable contribution to self-compression of the column. (auth)

14239 DEPENDENCE OF TRANSPORT COEFFICIENTS ON PLASMA PARAMETERS IN THE TOKAMAK INSTALLATION. Bobrovskii, G. A.; Kuznetsov, E. I.; Razumova, K. A. Zh. Eksp. Teor. Fiz.; 59: 1101-14(Oct 1970). (In Russian).

Results are presented of a separate study of transport coefficients in a plasma in the installation TM-3. The experimental diffusion and thermal conductivity coefficients are compared with those calculated by the theoretical formulas proposed by A. A. Galeev and R. Z. Sagdeev. For a sufficiently high plasma concentration, the experimental values of the energy losses are of the order of the classical values. Considerable divergence from the classical theory is observed in the case of a collisionless plasma, and an anomalously low plasma electric conductivity occurs. Under conditions of a relatively high electron temperature ($T_e > 500$ eV) and low concentration ($n_e < 6 \times 10^{12}$ cm^{-3}) protons are observed whose temperature in some cases cannot be explained by Coulomb transfer of energy from electrons to ions. The dependence of anomalous resistance on plasma parameters is investigated at hydrogen pressures $p_0 \approx 10^{-4}$ to 10^{-3} mm Hg, I = 7 to 35 kA, and H_z = 7 to 27 kOe. (auth)

14240 ION HEATING CAUSED BY ION-ACOUSTIC WAVES IN AN ION-STREAMING PLASMA. Honzawa, T.; Kawai, Y. (Nagoya Univ., Japan). Phys. Lett.; 33A: 481-2(28 Dec 1970).

It was found experimentally that ion heating occurs because of ion–acoustic waves arising from the drift of electrons in an ion-streaming plasma. (auth)

Diagnostics

Refer also to abstract 14359.

14241 (AD-710718) LASER-LIGHT SCATTERING AS A PLASMA DIAGNOSTIC TECHNIQUE. Pease, Alfred Anthony (Naval Postgraduate School, Monterey, Calif.). Jun 1969. 99p. NTIS.

Thesis.

The effort here was concerned with initiating a long-term experimental study to develop the method of laser-light scattering as a plasma diagnostic technique. This was done with a ruby laser and a grating spectrometer coupled with sensitive detectors, at the steady-state plasma facility at the Naval Postgraduate School. Although attempts to detect the extremely low levels of scattered light failed, excellent progress was made in determining existing apparatus limitations and in recognizing which system parameter may be adjusted in order to detect the scattered light; this will enable the future experimenter to progress with a minimum of overlap. (auth) (USGRDR)

14242 (AD-711095) EXPERIMENTAL STUDY OF THE CYLINDRICAL LANGMUIR-PROBE RESPONSE IN THE TRANSITION REGIME. Kirchhoff, R. H.; Peterson, E. W.; Talbot, L. (California Univ., Berkeley. Div. of Aeronautical Sciences). Dec 1969. 59p. (AS-69-13). NTIS.

Experiments were performed in a highly expanded low-density flowing argon plasma using both single and double probes. Results are obtained in the near free-molecule regime over a wide range of ratios of Debye length to probe radius, probe length to probe radius, and probe radius to relevant mean free path. The effect of collisions on the ion-saturation current, the retarding field electron current, the floating potential, and the inferred electron temperature was investigated experimentally. An existing approximate analysis describing the collisional single-probe ion-saturation current and the retarding-field electron current was extended to describe the collisional double-probe characteristic and magnitude of the single-probe floating potential. (auth) (USGRDR)

14243 (AD-711127) DIAGNOSTIC STUDIES IN AN INDUCTION-HEATED SUPERSONIC ARGON PLASMA. Fraser, Robert B. (California Univ., Berkeley. Coll. of Engineering). Jun 1970. 87p. (AS-70-5). NTIS.

Diagnostic studies were carried out in an induction-heated low-density supersonic plasma jet. The number of neutral densities was obtained from the calibrated intensity of the 4609A line of argon excited by a 25-kV electron beam. The contribution to the 4609A line due to the plasma self-emission was found to be negligible. The velocities and heavy-particle temperatures were determined by measuring the Doppler shift and Doppler-broadening of the 4609A line with a Fabry–Perot interferometer in two linearly independent directions, following a technique developed by Muntz. The density, impact pressure, and velocity along the free jet centerline all followed the isentropic source flow model up to the Mach disc. The temperature, however, showed an unexpected rise above the isentropic prediction. Ion number densities and electron temperatures were measured with a double Langmuir probe. The fraction of ionization was frozen at about 0.1% along the free-jet axis. Calculations are made of the fraction of the energy of recombination absorbed by the electrons and the fraction lost by radiation. (auth) (USGRDR)

14244 (AD-711669) ELECTRON TEMPERATURE AND NUMBER DENSITY MEASUREMENTS IN A NONEQUILIBRIUM PLASMA BOUNDARY LAYER. Brown, Robert T. (Stanford Univ., Calif. Inst. for Plasma Research). Jan 1970. Contract F44620-68-C-0051. 257p. (SU-IPR-350; AFOSR-70-2371-TR). NTIS.

Measurements of the electron temperature and electron number density in a nonequilibrium plasma boundary layer are presented, along with related analyses. The plasma consisted of atmospheric-pressure NaK-seeded argon at 2400°K flowing over a cooled flat surface that was electrically floating and nonemitting. The analyses proceed from consideration of the coupled-electron continuity and electron energy equations with boundary conditions appropriate to NaK-seeded argon. The entire electron continuity equation is retained, including the ionization–recombination source term. Various source terms are included in the electron energy equation to account for elastic collisions, inelastic collisions with seed atoms, and inelastic collisions with gas additives such as molecular nitrogen. The equations are transformed into boundary-layer coordinates using a "local similarity" transformation and are solved numerically for a range of plasma conditions. It is shown that the major nonequilibrium effects can be interpreted in terms of three characteristic lengths: δ, the thermal layer thickness; l_E, the characteristic length for electron energy exchange; and l_I, the characteristic length for ionization and recombination. (auth)

14245 INVESTIGATION OF AN IMPROVED IRON ARC. Richter, J.; Wulff, P. (Univ., Kiel). Astron. Astrophys.; 9: 37-44(Nov 1970).

Construction and properties of an improved low-current iron arc are described. Spectroscopic analysis of the arc plasma shows that the arc is a suitable light source for the measurement of wavelengths and oscillator strengths of weak iron lines. Fe I lines with a solar equivalent width of 1 mÅ can be observed and oscillator strengths can be measured down to equivalent widths of about 3 mÅ. Measured oscillator strengths of 38 weak Fe I lines are presented and compared with solar values. From the plasma analysis it follows that the arc column is not in LTE. In spite of this fact, the populations of the excited levels of the neutral iron obey a Boltzmann distribution. The excitation temperature in the axis of the arc is 6800°K. (auth)

14246 TIME-RESOLVED MEASUREMENTS OF THE ELECTRON ENERGY DISTRIBUTION IN UNSTABLE PLASMA. I. MEASUREMENT TECHNIQUE. Sicha, M.; Vessely, V.; Rezacova, V.; (and others) (Charles Univ., Prague). Czech. J. Phys.; 21: 62-70(1971).

The sampling technique for the direct measurement of the second derivative of the Langmuir-probe characteristic is described. It enables the study of the variation of the distribution function in the time-unstable plasma. The tests of the method and the discussion of its results are given. (auth)

14247 TIME-RESOLVED MEASUREMENTS OF THE ENERGY DISTRIBUTION IN UNSTABLE PLASMA. II. MEASUREMENT IN THE IONIZATION WAVES. Sicha, M.; Rezacova, V.; Tichy, M.; (and others) (Charles Univ., Prague). Czech. J. Phys.; 21: 71-6(1971).

A sampling technique was used for measurement of the electron distribution function. Two groups of electrons and changes of the distribution function along the ionization waves of small amplitude were found. (auth)

14248 EDUCATIONAL AID FOR HIGH-FREQUENCY PLASMA DIAGNOSTICS. **Baibulatov, F. Kh. (Novosibirsk State Univ., USSR). Usp. Fiz. Nauk; 101: 331-3(Jun 1970). (In Russian).**

High-frequency methods based on the interaction of short radio waves with a plasma are used in experimental plasma studies. In order to demonstrate this method based on the passage of waves along a plasma waveguide, a simple radio interferometer was developed, with which it is possible to make qualitative observations on the interaction of radio waves with the plasma and to carry out quantitative measurements of the electron density. The unit consists of a quartz discharge tube, with an external diameter of 27 mm and an internal diameter of 22 mm, connected with epoxy resin with two aluminum waveguide tubes. The ends of the discharge tube are covered with quartz windows fastened at the proper Brewster angle to avoid reflection of the radio waves from the windows. With each discharge of a condenser through the middle part of the metal discharge tube, a plasma forms that drifts to the ends of the tube fitted with adapters to convert the rectangular waveguide to a circular one. Both kinds of radio waves are mixed and sent to a detector. The discharge tube is evacuated through one of the electrodes. The interferograms clearly show the wave damping as a function of the magnitude of the constant electric field in the plasma. An increase in electron density is seen to occur in the presence of a large difference in potentials between the discharge-tube electrodes, i.e., in the presence of a strong longitudinal electrical field in the plasma. The presence of a constant electric field results in charged-particle drift and more collisions of the charged particles between themselves and neutral particles. Therefore, during this period, the adsorption of waves by the plasma is large, as shown by the interferogram. The electron concentration can be determined at the point where maximum adsorption of the signal is obtained. (TTT)

14249 ION CURRENT TO A PLANE PROBE IN A FLOWING PLASMA. **Freeston, I. L.; Kelk, J. E. (Univ. of Sheffield, Eng.). Electron. Lett.; 6: 810-11(10 Dec 1970).**

An expression is developed for the ion current to a plane probe in a flowing plasma for the probe surface parallel to the ion flow, neglecting ion thermal motion. The application of the result to the measurement of plasma density of a plasma torch is considered. (auth) (UK)

14250 MEASUREMENT OF ION DENSITY IN A PLASMA TORCH USING A PLANE PROBE. **Freeston, I. L.; Kelk, J. E. (Univ. of Sheffield, Eng.). Electron. Lett.; 6: 812-13(Oct 1970).**

The plasma density of the flame of a plasma torch was determined from the current to a plane probe using two theories. One includes only the ion flow motion; the other includes only the ion thermal motion. Comparison with spectroscopic results suggests that both motions should be included. (auth) (UK)

14251 VARIATION OF THE ADMITTANCE OF A PLASMA CAPACITOR WITH THE AMPLITUDE OF THE MEASURING POTENTIAL. **Freeston, I. L. (Sheffield Univ., Eng.). Electron. Lett.; 6: 672-3(Oct 1970).**

The measured admittance is unaffected up to a measuring rf potential of r.m.s. value five times the equivalent electron temperature, except in a frequency range in which the admittance is affected by a potential exceeding half the electron temperature. This range is also that of the resonance probe, but it is concluded that any connection between the two effects is indirect. (auth) (UK)

14252 VELOCITY DISTRIBUTIONS IN A GASEOUS PLASMA. I. DERIVATION OF FLOW TYPES WITHIN A HELIUM PLASMA. **Meubus, P.; Parent, J. R. (Univ. Laval, Quebec). Can. J. Chem. Eng.; 47: 542-7(Dec 1969).**

Velocity distributions in a plasma jet are generally determined by means of direct methods which are liable to alter the medium, especially at very high temperatures. A gas flow model is proposed, which is worked out from the luminous profile of a helium plasma jet, such as viewed through a dense orange glass filter. The knowledge of the luminous profile equation, temperature distribution, gas flow rate and energy balance completely determines the velocity distribution in the plasma. Boundary conditions lead, in certain cases, to the concept of an axial turbulent core. The helium plasma was operated at 27 kW, with a gas flow rate of 7.2 g/min. The jet was issuing into an atmosphere kept at 300-mm Hg in order to favor conditions leading to laminar flow. (auth) (Canada)

14253 VELOCITY DISTRIBUTIONS IN A GASEOUS PLASMA. II. APPLICATION OF A FLOW MODEL TO A HELIUM PLASMA. **Meubus, P.; Parent, J. R. (Univ. Laval, Quebec). Can. J. Chem. Eng.; 47: 548-52(Dec 1969).**

A mathematical model for gas velocity distributions and definition of flow types is applied to a helium plasma operated at 27 kW and a gas flow rate of 7.2 g/min under pressures of 760- and 300-mm Hg. The calculated velocity data are used to predict

XUM

values of thermal conductivity and viscosity for helium in the plasma. A good approximation to theoretical values is obtained, lending validity to the model of velocity distributions. (auth) (Canada)

14254 TEMPERATURE DISTRIBUTIONS IN A HELIUM PLASMA. **Meubus, P.; Parent, J. R. (Univ. Laval, Quebec). Can. J. Chem. Eng.; 47: 536-42(Dec 1969).**

Temperature distributions are determined in a helium plasma, the power used being 27 kW and the gas flow rate 7.2 g/min. Pressure conditions for the plasma under study are respectively 760- and 300-mm Hg. The spectroscopic method used for obtaining temperatures is that of Larenz or the method of maximum emission, applied to the 3,889-Å neutral helium line. A maximum temperature, on the plasma axis, of approximately 24,000°K is obtained. (auth) (Canada)

14255 PLASMA DIAGNOSTICS WITH LASER BEAMS. **Bito, Janos. Musz. Tud.; 43: 107-29(1970). (In Hungarian).**

A critical survey was made of the two characteristic groups of diagnostic methods with laser beams, that is to say, of the dispersion and interferometric measurements. 45 references. (M.O.W.)

14256 DISCREPANCY BETWEEN ELECTRON-DRIFT VELOCITIES OBTAINED FROM THE ION AND ELECTRON FEATURES OF LIGHT SCATTERING IN A z-PINCH PLASMA. **Kronast, B.; Pietrzyk, Z. A. (National Research Council of Canada, Ottawa). Phys. Rev. Lett.; 26: 67-9(11 Jan 1971).**

Light scattering by ion–acoustic waves was investigated in a z-pinch plasma. The asymmetry of the observed spectra varies with the angle between scattering wave number and longitudinal electron-drift velocity in a way that is in qualitative accord with light-scattering theory. However, the magnitudes of electron-drift velocities evaluated from these spectra are greatly at variance with values derived from the Doppler shift of the electron feature of light scattering. (auth)

14257 DECAY PROCESSES IN A HIGH DENSITY ARGON AFTERGLOW. **Donovan, B. V.; Sexton, M. C. (University Coll., Cork, Ireland). Proc. Roy. Irish Acad., Sect. A: 70: No. 6, 35-45(1970).**

Microwave and spectroscopic methods were used to analyse afterglow processes in argon within the electron density range 10^{13} to 10^{10} cm^{-3}. Both electron density and neutral gas temperature decay were monitored, using a 35-GHz microwave interferometer with the electron temperature decay inferred from the time-resolved spectral intensities of specific argon I lines, observed with a monochromator/photomultiplier arrangement. The collisional radiative type of electron–ion recombination was identified as the principal afterglow mechanism of electron removal, showing the expected decline with increase of electron density over the three orders of magnitude covered. Although precise agreement with theory was not possible since comprehensive calculations were available for a 250°K gas temperature only, the actual trend confirmed the existence of the measured elevated gas temperatures. (auth) (UK)

14258 ELECTRON TEMPERATURE AND NUMBER DENSITY MEASUREMENTS IN A NONEQUILIBRIUM PLASMA BOUNDARY LAYER. Brown, Robert Thomas. Stanford, Calif.; Stanford Univ. (1970). 255p. University Microfilms Order No. 70-22,156.

Thesis.

Measurements of the electron temperature and electron number density in a nonequilibrium plasma boundary layer are presented along with related analyses. The plasma consisted of atmospheric pressure NaK-seeded argon at 2400°K flowing over a cooled flat surface that was electrically floating and nonemitting. The analyses proceed from consideration of the coupled electron continuity and electron energy equations with boundary conditions appropriate to NaK-seeded argon. The entire electron continuity equation is retained, including the ionization-recombination source term. Various source terms are included in the electron energy equation to account for elastic collisions, inelastic collisions with the seed atoms, and inelastic collisions with gas additives such as molecular nitrogen. The equations are transformed into boundary layer coordinates using a "local similarity" transformation and are solved numerically for a range of plasma conditions. It is shown that the major nonequilibrium effects can be interpreted in terms of three characteristic lengths: δ, the thermal layer thickness; l_E, the characteristic length for electron energy exchange; and l_I, the characteristic length for ionization and recombination. Plasma conductivity profiles (which were determined primarily by the electron number density) were measured experimentally in the boundary layer described above using a small, traversing, electrical conductivity probe. Electron temperature profiles were measured using a spectroscopic technique. The experimental results, obtained for various values of the lengths l_E and l_I, were found to be in good agreement with the theoretical predictions. It is shown that for small values of the parameter δ/l_I, the electron number density profile is nearly frozen and is governed by convection and ambipolar diffusion effects. When δ/l_I is large, ionization–recombination effects dominate and the electron number density profile is similar to the electron temperature profile. For a NaK-seeded argon with no additives, it is shown that there is considerable nonequilibrium between the electron temperature and the gas temperature. When the parameter δ/l_E is increased, the electron temperature tends to equilibrate with the gas temperature. (Diss. Abstr. Int., B)

14259 RESONANCE CONES IN THE FIELD PATTERN OF A SHORT RADIO-FREQUENCY PROBE IN A WARM ANISOTROPIC PLASMA. Fisher, Raymond Kurt. Pasadena, Calif.; California Inst. of Tech. (1970). 79p. University Microfilms Order No. 70-24,296.

Thesis.

The angular field pattern of a small radio-frequency probe in a plasma in a magnetic field was investigated experimentally. The field was observed to become very large along a resonance cone whose axis is parallel to the static magnetic field and whose opening angle is observed to vary with incident probe frequency, electron cyclotron frequency, and electron plasma frequency in agreement with simple cold plasma dielectric theory. The use of the resonance cone angle as a diagnostic tool to measure the plasma density is discussed. It is noted that similar cones might be expected near the ion cyclotron frequency. The relationship of these cones to the limiting phase- and group-velocity cones, which appear in the theory of plane wave propagation, is discussed. The necessity for examining the allowed directions of the group velocity rather than the allowed directions of the phase velocity and customary phase velocity plots when determining whether propagation between two remote points in a plasma is possible, is emphasized. The addition of electron thermal velocities to the theory is examined in the limit of a large static magnetic field. The resonance cone angle is shifted to a slightly smaller angle than that predicted by cold plasma theory, and a fine structure appears inside the cones and is shown to result from an interference between a fast electromagnetic wave and a slow plasma wave. The interference structure is observed experimentally, and measurements of the angular interference spacing are shown to agree with the warm plasma theory. (Diss. Abstr. Int., B)

14260 METHOD FOR DETERMINATION OF THE VISCOSITY OF A PLASMA AT ATMOSPHERIC PRESSURE. **Rother, Wolfgang (Technische Hochschule, Ilmenau, Ger.). Beitr. Plasmaphys.; 10: 497-506(1970). (In German).**

A simple method to measure the viscosity of a plasma at atmospheric pressure is described. If spheres move through a cylindrical plasma perpendicular to the axis, they undergo a deflection from which the resistance coefficient can be calculated. Measuring, too, the dynamic pressure and the temperature, and knowing the resistance coefficient as a function of the REYNOLDS number, the viscosity can be computed. As an example, the measurement of the viscosity of a nitrogen plasma is reported. (auth)

14261 DIAGNOSTICS OF XENON PLASMAS WITH HIGHER PRECISION. **Guenther, K. (Zentralinstitut fuer Elektronenphysik, Berlin). Beitr. Plasmaphys.; 10: 469-85(1970). (In German).**

Several experimental methods for temperature measurements are discussed with respect to their qualities as diagnostic tools for xenon plasmas in the pulsed mode. In this work the continuum radiation intensity, corrected for infinite optical thickness, is used for the determination of plasma temperature. An uncertainty $\delta T = 1.5\%$ follows from a detailed error calculation. Results are given for $p = 6 \ldots 20$ at and $i = 1 \ldots 3.5$ kA/cm^2. It is proposed to use xenon pulse discharge as a calibration standard for black-body radiation at $T \approx 11{,}000$°K in a special pressure range, where the plasma temperature is nearly independent on pressure. (auth)

14262 DESENSITIVITY OF A MICROWAVE CAVITY TO MEASUREMENTS OF HOT-ELECTRON DENSITY. Brisset, C.; Geller, R.; Jacquot, B.; Jacquot, C.; Shohet, J. L. (CEN, Grenoble, France). Phys. Lett.; 34A: 71-2(25 Jan 1971).

Electron density measurements were made with a cylindrical microwave cavity operated in the TM 010 mode. The experimental results are consistent if it is assumed that the frequency shift is only produced by cold plasma. (auth)

14263 MEASUREMENT OF LOCAL ENTHALPY IN AN HF PLASMA WITH A CALORIMETRIC GAS-SAMPLING PROBE.

Cheylan, J.; Dauvergne, J. P.; Le Goff, P. (CNRS, Villers-les-Nancy, France). Chim. Ind., Genie Chim.; 103: 2679-86(Dec 1970). (In French).

Radial and axial enthalpy profiles in an hf plasma were measured with a calorimetric probe, whose hydrodynamic performance was adapted to the present problem. A model for the penetration of induced energy allowed the radial profiles of temperature to be established in the induction zone. (auth) (France)

Kinetics (General)

14264 (AD-711828) BASIC PLASMA PROCESSES. Final Report, July 1, 1969–September 30, 1970. Phelps, A. V.; Chen, C. L. (Westinghouse Research Labs., Pittsburgh, Pa.). Contract N00014-70-C-0128. 58p. NTIS.

A theory was developed describing the magnitude and wavelength dependence of the resonance radiation emitted as the result of thermal excitation. The predictions of the theory are compared with the results of measurements at a temperature of 788°K as obtained in a cell capable of operating up to 1050°K. The absorption coefficients and total absorption for the cesium resonance lines at 8944, 8521, 4593 and 4555 A for cesium in argon at pressures near atmospheric were measured over a wide range of cesium densities and found to scale as the product of the cesium and argon densities. These results are consistent with broadening as the result of binary collisions between cesium and argon atoms. The theory of resonance fluorescence for optically thick systems is found to give good agreement with experiments in which mercury was illuminated with a resonance line source. The dominant loss mechanism at moderate and high densities is diffusion to the window. Significant discrepancies remain between the theory and the measurements in cesium using a white light source. (auth) (USGRDR)

14265 PLASMA EXPANSION IN VACUUM AND THE FLOW OF A COLLISIONLESS PLASMA STREAM AROUND A PLATE. Alikhanov, S. G.; Belan, V. G.; Kichigin, G. N.; Chebotaev, P. Z. (Inst. of Nuclear Physics, Novosibirsk, USSR). Zh. Eksp. Teor. Fiz.; 59: 1961-6(Dec 1970). (In Russian).

The problem of flow of an ultrasonic plasma stream around a plate is reduced to the problem of expansion of a plasma into a vacuum and is solved numerically for the one-dimensional case by taking into account the Poisson equation. The solution of the problem of expansion of a nonisothermal collisionless plasma into a vacuum is compared with the self-similar solution. The structure of the perturbed zone in the track of a plate located in the stream of a nonisothermal plasma moving with a velocity M = 2 in the absence of a magnetic field is investigated. The density and potential distributions behind the plate are obtained. The results of the experiments and calculations are in good agreement. (auth)

14266 DISCHARGE MAINTAINED BY A DIRECT CURRENT AND HIGH FREQUENCY WAVES. **Allis, William P.; Leprince, Philippe; Matthieussent, Gilles (Paris Univ., Orsay, France). Compt. Rend., Ser. B; 271: 1054-7(23 Nov 1970). (In French).**

The deformation of the resonance curves of a plasma column subjected to electromagnetic radiation of frequency near to that of the plasma is due to density increases in the plasma resulting from the high-frequency power absorbed. The plasma is thus maintained in a state of resonance by the discharge current and the high-frequency waves. (auth) (France)

14267 LIMITING THE RADIAL EXPANSION OF ARC CURRENT BY AN AXIAL MAGNETIC FIELD. I. PROBLEMS, ARC MODEL, AND TYPICAL RESULTS. **Klueber, O. (Institut fuer Plasmaphysik, Garching, Ger.). Z. Naturforsch.; 25a: 1583-1600(Nov 1970). (In German).**

In an arc without external magnetic field the current-carrying region is identical with the conducting plasma column. This is not generally true if the arc is in an axial magnetic field and if the electrode radius is much smaller than the plasma radius. Radial current components then produce a rotational motion of the plasma and an azimuthal Hall current, and hence electromotive forces, which try to suppress the current perpendicular to the magnetic field. In a plasma with finite viscosity the rotation is determined by the Navier–Stokes equation, which is solved here for a homogeneous plasma simultaneously with generalized Ohm's law. The results show that the plasma rotation is always an essential, and often the dominant, mechanism for guiding the arc current parallel to the magnetic field lines. (auth)

14268 MEASUREMENT OF THE RADIAL DISTRIBUTION OF ELECTRIC CURRENT DENSITY AND TEMPERATURE IN HYDROGEN ARCS WITH AXIAL MAGNETIC FIELDS. **Schwenn, R. (Institut fuer Plasmaphysik, Garching, Ger.). Z. Naturforsch.; 25a: 1601-9(Nov 1970). (In German).**

The radial distribution of the axial electric current density in a stationary hydrogen arc with axial magnetic field was measured. This was done by shooting small induction-coil probes across the arc. The experiments confirmed that the arc current is almost completely restricted to the magnetic flux tube defined by the cathode radius, as discussed in a previous paper. In the case of a hollow anode a distinctly tube-like current density distribution was found. With the aid of the axial electric field measurements, temperature profiles in good agreement with other experimental methods were derived. In addition, the ohmic heat input into the arc could be determined. This is much larger than the energy that can be lost radially as a result of thermal conduction according to the measured temperature profile and the thermal conductivity known from the theory. The cause may be the Rayleigh–Taylor instabilities that were observed or radial mass flows directed outwards. Allowing for even relatively slow flows ($u_r < 10^4$ cm/sec) in the calculations, one obtains good agreement with the measured distributions. (auth)

14269 DISPLACEMENT OF WALL-STABILIZED ELECTRIC ARCS BY CURVATURE. **Nathrath, Norbert (Technische Univ., Munich). Z. Naturforsch.; 25a: 1609-17(Nov 1970). (In German).**

If an electric arc is forced to burn in a curved line by a toroidal container, its position is displaced in direction to the center of curvature due to the inhomogeneous ohmic heating and of the cooling by conduction. The self magnetic-field pushes the arc outwards. Corresponding measurements in argon at atmospheric pressure with currents from 0.5 to 20 A yield the eccentric positions depending on current and curvature. The measured functions compare favorably with theory, but only if the deviation from LTE in the calculation of electric conductivity is taken into account. (auth)

14270 AN INVESTIGATION OF THE COAXIAL PLASMA ACCELERATOR AND THE PRODUCTION OF SHOCK WAVES BY THE DENSE PLASMA FOCUS. Wolf, Randolph John. Boulder, Colo.; Univ of Colorado (1970). 109p. University Microfilms Order No. 70-23,765.

Thesis.

The general problem of shock wave production by a coaxial electromagnetic accelerator is examined. The linear accelerator employing a snow-plow model is first considered. Numerical solutions obtained demonstrate the importance of the inductance derivative in limiting the obtainable velocity and currents. Solutions are then obtained for various accelerators in the literature. It is shown that many of their measurements are consistent with one-dimensional snow-plow calculations. The snow-plow calculations are then extended to two-dimensions and compared in detail to current sheet, luminous front and pressure probe measurements made on a coaxial accelerator which is operating in a mode so as to form the dense plasma focus. Good agreement is obtained between computed and measured axial and radial current sheet speeds and shapes in regions where the current sheet is thin (i.e., away from electrodes). Detailed measurements of the magnetic fields within and external to the coaxial accelerator were made. The existence of regions of reversed current (i.e., eddy currents) was observed. The hot high density focused region obtained when the current sheet collapses off of the finite length center electrode was investigated with the use of an x-ray monitor system which measured the flux transmitted through various absorbed materials. (Diss. Abstr. Int., B)

14271 DYNAMIC VOLTAGE–CURRENT CHARACTERISTICS OF A MEGAWATT MPD-ARC THRUSTER. **Michels, Charles J.** (Lewis Research Center, Cleveland). AIAA (Amer. Inst. Aeronaut. Astronaut.) J.; 9: 173-6(Jan 1971).

The dynamic voltage–current characteristic of a hot-cathode, megawatt (MW), pulsed MPD-arc thruster is given for various axial magnetic fields (1.0 to 2.0 t). The arc is powered by a crowbarred capacitor bank, and the transient data are obtained for the 100-μsec period after crowbar time. Each shot shows a positive sloped characteristic. A series of these dynamic characteristics, spanning 2 to 14 kA, along with estimated static characteristics are given for argon and for nitrogen propellant. As the magnetic field increases, the dynamic curves tend to be more identifiable as part of a connected, positive sloped line. (auth)

14272 FORCE-FREE CONFIGURATION OF A HIGH-INTENSITY ELECTRON BEAM. **Yoshikawa, S. Princeton Univ., N. J.). Contract AT(30-1)-1238. Phys. Rev. Lett.; 26: 295-7 (8 Feb 1971).**

The equilibrium configuration of a neutralized electron beam is calculated, including the self-field (parallel to the beam) generated by the beam itself. The resultant equilibrium configuration allows an arbitrary current to be carried by the beam, the motion of electrons being unimpeded by the self-magnetic field. Electrons in this configuration travel almost parallel to the magnetic field; thus, the synchrotron radiation can be minimized. It is suggested that this type of configuration opens up the possibility of low-loss electron coils and, in particular, is useful for fusion reactors. (auth)

14273 PRODUCTION OF CONTINUOUS HIGH-POWER PLASMA FLOW. **Bonet, Claude; Lamos, Jean; Foex, Marc (CNRS, Montlouis, France). Entropie; No. 34-35, 36-51(Jul-Oct 1970). (In French).**

A device for producing high-power plasma flow is described (100 kW in the laboratory). A three-phase alternating current supply was used; under variable plasma conditions (flow rate, gas pressure, and nature of the gas) the efficiency was high (90% or more). The operating potential was measured between an electrode and a neutral point, for a constant current of 200 A (limit of supply) when the device was operating, with nitrogen as the plasma gas, at atmospheric pressure. The potential may be expressed in terms of the total plasma flow rate Q g/s and the interelectrode distance d : $V = 0.5\ Qd - 4.85\ Q + 3.6\ d + 66$ where $10\ \text{cm} \leq d \leq 21.5\ \text{cm}$. The axial gradients of the potential, the mean enthalpy, the mean temperature, and the heating efficiency were determined. Oscillograms of the voltage and the current were plotted. (auth) (France)

14274 PLASMA ACCELERATION AND SHOCK FORMATION BY ELECTROMAGNETIC FORCE FIELDS. Steinolfson, Richard Steingrimur. Boulder, Colo.; Univ. of Colorado (1970). 201p. University Microfilms Order No. 70-23,756.

Thesis.

When an electromagnetic force field is created in a channel containing a stationary fluid, the fluid is accelerated in the direction of the force, and an expansion wave travels in the opposite direction. Depending on the conditions under which the force field is created, the force field may either remain stationary or move in the direction of the force. This situation is analyzed theoretically using a single-fluid model, and both the initial value problem and the asymptotic state are investigated. A force field created by externally applied electric and magnetic fields and one created by a self-induced magnetic field are each considered. Both an infinite and a finite initial electrical conductivity of the fluid are also considered. The method of characteristics is used to solve the initial-value problem when the electrical conductivity is finite, and the Lax method is used when the electrical conductivity is infinite. Under most conditions a shock is formed ahead of the accelerated fluid. Another shock or expansion may be formed such that it remains between the first shock and the force field, and a shock may be formed such that it remains inside the force field. The time and position at which a shock first forms, the type of interaction between the fluid and the force field that exists in the asymptotic state, and the shock velocity and the velocity just upstream of the force field in the asymptotic state are determined as functions of the parameters. An initial difference in the fluid pressure across the force field is treated as a parameter when the magnetic field is self-induced. It is shown that, under most conditions of interest for a stationary force field, a shock is located inside the force field in addition to the shock ahead of the accelerated fluid. Substantial increases in the velocity of the accelerated fluid and the shock velocity can be obtained by maintaining an initial difference in fluid pressure across the force field. When the electrical conductivity is finite and when the force field is traveling at a supersonic velocity, the shock (or shocks) forms inside the force field. The time at which a shock first forms is relatively independent of the force field velocity, but the shock forms further back in the force field if the force field velocity is increased. When the electrical conductivity is infinite, the shock reaches its maximum strength sooner at larger values of the force; however, the position at which the maximum strength is attained is only slightly dependent on the magnitude of the force. (Diss. Abstr. Int., B)

14275 DIPOLE RADIATION IN COMPRESSIBLE PLASMA. Lin, Sing-hsiung. Berkeley, Calif.; Univ. of California (1969). 118p. University Microfilms Order No. 70-17,605.

Thesis.

A finite cylindrical antenna with (or without) a dielectric sheath in an isotropic compressible plasma was studied. The boundary-value problem is formulated in a set of four coupled integral equations through the application of the equivalent source principle and is solved numerically by the method of collocation. The effects of the plasma compressibility, the plasma collision frequency and the sheath on the antenna current, the input impedance and the maximum driving voltage (imposed by the linearization assumption) are investigated rigorously. The radiation of electro-acoustic waves may raise the input resistance of an electrically extremely short antenna by a factor of 10^8. The resonance frequency of the rf probe is found to be below the plasma frequency; and the half power width of the resonance is approximately equal to the plasma collision frequency. The formulation and the method used in this thesis can easily be modified to investigate a dielectric-sheathed antenna in free space. The effects of rain and snow on the performance of outdoor antennas can then be estimated by this approach. (Diss. Abstr. Int., B)

14276 FLAT-PLATE BOUNDARY-LAYER STUDIES IN A PARTIALLY IONIZED GAS. Tseng, Raymond Chi-jen. Berkeley, Calif.; Univ. of California (1969). 128p. University Microfilms Order No. 70-17,674.

Thesis.

A combined experimental and numerical investigation was conducted on the flat-plate boundary layer flow of a partially ionized gas. A free-molecule cylindrical Langmuir probe was used to measure charged-particle density, electron temperature, and plasma potential distributions in the boundary layer. The ambipolar diffusion flux to the plate surface was determined by an array of flush-mounted surface electrodes. A probe size-study was carried out, and an empirical formula was obtained to make correction for the sheath-fringing field effect on ion current collection to small flush probes. Numerical integrations were made of the charged species conservation and electron energy equations in the quasineutral region of the boundary layer for a thin plasma sheath. Mechanisms leading to the cooling of the electron gas were investigated. Numerical profiles of charged-particle density, electron temperature and plasma potential compared favorably with experimental results. Ambipolar diffusion fluxes predicted theoretically agreed very well with the measured flush-probe ion saturation current. The validity of employing such a flush-mounted surface in determination of the free-stream charged-particle density was then established. (Diss. Abstr. Int., B)

Kinetics (Experimental)

Refer also to abstracts 14100, 14334, and 14378.

14277 (AD-712024) OPTICAL SPECTROSCOPIC INVESTIGATION OF HELIUM AND NITROGEN PLASMAS. Manalis, Melvyn Samuel (California Univ., Santa Barbara). Jun 1970. Contract N00014-69-A-0200-8004. 161p. (TR-31). NTIS.

Thesis.

Energetic species and their respective energy-exchange processes in a cool, high-density helium plasma are reviewed. Light from a flowing helium afterglow was observed from 2500 to 10,500 Å using an Ebert double-pass scanning monochromator coupled to standard dc detecting equipment. Experimental data in the form of relative populations of atomic helium states provided motivation for a theory that may explain the manner in which ionization is maintained in the afterglow region of the helium plasma. A bimodal electron distribution was found to exist in this plasma. Molecular nitrogen was used as a probe to detect various energetic species present in the helium afterglow. In addition to the usual systems observed when N_2 is injected into the helium afterglow, light from many levels of atomic nitrogen and three new vibrational population distributions of the first positive system of molecular nitrogen were observed. Two independent mechanisms for exciting the atomic nitrogen were isolated. (auth) (USGRDR)

14278 (NP-18643) EXPERIMENTAL EVIDENCE OF ELEMENT AND ISOTOPE SEPARATION IN A ROTATING PLASMA. Bonnevier, B. (Kungliga Tekniska Hogskolan, Stockholm (Sweden)). 11 Jun 1970. 28p. Dep. NTIS (U. S. Sales Only).

An experimental investigation of separation effects in a rotating plasma and a method for collecting a separated plasma are described. The basic diagnostic technique used was mass spectrometry. Discharges in hydrogen–argon mixtures, hydrogen–deuterium mixtures, and neon were studied. (Sweden)

14279 ELECTRON HEATING AND INCOHERENT HARD RADIATION PRODUCED IN THE INTERACTION BETWEEN ULTRA-SHORT INTENSE LASER PULSES AND MATTER. **Bunkin, F. V.; Kazakov, A. E. (Lebedev Inst. of Physics, Moscow). Zh. Eksp. Teor. Fiz.; 59: 2233-43(Dec 1970). (In Russian).**

The major mechanisms of heating of the electron component of a plasma during interaction with picosecond laser pulses is considered for a broad range of pulse intensities. It is shown that, in certain intensity ranges, hard bremsstrahlung radiation from the plasma is not determined by electron temperature but by the energy corresponding to electron oscillations in the field of the laser radiation. (auth)

XUM

14280 CONTINUOUS ABSORPTION OF PARTIALLY IONIZED XENON IN THE VISIBLE REGION OF THE SPECTRUM. Gembarzhevskii, G. V.; Generalov, N. A.; Kozlov, G. I.; Roitenburg, D. I. Opt. Spectrosc. (USSR) (Engl. Transl.); 28: 593-5(Jun 1970).

Translated from Opt. Spektrosk.; 28: 1101-5(Jun 1970).

The distribution of the absorption coefficient in a xenon plasma behind the front of a reflected shock wave was measured by absorption spectroscopy over the 4000 to 7500 Å wavelength interval at a temperature of 10,600 K. The experimental results obtained agree with the theoretical values if the lowering of the photoionization threshold is taken into account. It is shown that the lowering of the photoionization threshold is in accordance with the Inglis–Teller theory. (auth)

14281 ACCELERATION PATTERNS IN QUASI-STEADY MPD ARCS. Jahn, Robert G.; Clark, Kenn E.; Oberth, Ronald C.; Turchi, Peter J. (Princeton Univ., N. J.). AIAA (Amer. Inst. Aeronaut. Astronaut.) J.; 9: 167-72(Jan 1971).

Argon exhaust velocities of the order of 25,000 m/sec are observed in a quasi-steady, self-field MPD accelerator operated at 17,500 A. The variation of measured exhaust velocity with input mass flow indicates a preferred or "matched" mass flow, at which the observed velocity substantially exceeds both the Alfvén critical speed and that computed from the electromagnetic thrust relation. Although the measured velocity corresponds roughly to the total electrode voltage, an electrostatic ion-acceleration mechanism is not supported by detailed maps of the potential contours within the arc chamber. Specifically, it is found that the bulk of the arc voltage gradient, exclusive of the electrode falls, occurs within two diameters of the cathode, and is normal to it. The remainder of the arc chamber, and all of the down-stream plasma is nearly equipotential, at a value close to anode sheath potential. Anode full voltage varies inversely with local current density, implying substantially lower anode losses at higher power arc operation. Bow shocks from small obstacles placed in the exhaust stream indicate supersonic, but not hypersonic flow. (auth)

14282 DIAMAGNETIC MOMENT OF A STRONG SHOCK WAVE FROM A HIGH-TEMPERATURE LIGHT EXPLOSION IN GASES. Askar'yan, G. A.; Savchenko, M. M.; Stepanov, V. K. (Lebedev Inst. of Physics, Moscow). Zh. Eksp. Teor. Fiz.; 59: 1133-45(Oct 1970). (In Russian).

Extensive experimental material pertaining to an investigation of diamagnetic perturbations of a strong shock wave from a light spark in various gases at different pressures is presented. A theoretical description of the phenomenon is given on the basis of the theory of strong shock waves. It is shown that a long life of the diamagnetic moment indicated a high temperature of the process in the light spark. Experiments on reflection and focusing of a shock wave and on its cumulative action on the fireball of the light spark are carried out with the aim of repeated utilization of a dense hot plasma. Some new possible effects of interaction between a strong magnetic field and the shock wave plasma are described. Practical applications of the results obtained are mentioned. (auth)

Kinetics (Theoretical)

Refer also to abstract 13941.

14283 (AD-710950) HIGH-ORDER PERTURBATION THEORY FOR A ONE-ELECTRON ION IMMERSED IN A PLASMA. Iafrate, Gerald J. (Army Electronics Command, Fort Monmouth, N. J.). Jul 1970. 84p. (ECOM-3305). NTIS.

High-order Rayleigh–Schroedinger perturbation theory is developed and applied to model problems in plasma spectroscopy; namely the separate problems of an electron bound in a screened Coulomb potential and a one-electron ion under the influence of long-range protons. (auth) (USGRDR)

14284 (AD-711086) MAGNETIC STRUCTURE OF OBLIQUE AND NORMAL IONIZING SHOCK WAVES. Report No. 50. Leonard, B. P. (Columbia Univ., New York. Plasma Lab.). Jul 1970. Contract AF49(638)-1634. 68p. (AFOSR-70-2284-TR). NTIS.

Oblique and normal ionizing shock waves are considered as a subclass of the skew shocks. It is shown explicitly that, for these cases, when the electrical conductivity is a scalar, the magnetic field and velocity vectors lie in a single plane throughout the shock structure. Details of the shock structure are given in the large-Ohmic-diffusion limit for a range of values of the upstream magnetic pressure ratio as the transverse electric field is varied parametrically. (auth) (USGRDR)

14285 (BMBW-FBK-70-29) COMPOSITION AND ELECTRICAL CONDUCTIVITY OF COMBUSTION PLASMAS. Raeder, J. (Institut fuer Plasmaphysik, G.m.b.H., Garching (West Germany)). Dec 1970. 53p. (In German). Dep. NTIS (U. S. Sales Only).

Equations are compiled that describe the composition of a mixture of chemically reacting gases in thermodynamic equilibrium. The method for the solution of this system of partially nonlinear equations is given. The ensuing sections deal with different approximations and methods for the calculation of the conductivity tensor components in a magnetized plasma. Finally, calculations are made for the composition and electrical conductivity of a plasma generated through combustion of CH_2, Al, and K with O_2. (auth)

14286 (N-70-40979) THEORY OF POLARIZATION TRANSFER IN INHOMOGENEOUS MAGNETIZED PLASMAS. Chin, Y. C.; Fung, P. C. W. (Stanford Univ., Calif. Inst. for Plasma Research). Aug 1970. Contract F44620-69-C-0008. 21p. (NASA-CR-113823; SU-IPR-378). NTIS.

The theory of polarization transfer in an inhomogeneous magnetized plasma medium is extended to include the effects of the mode-coupling phenomenon. The resultant system of polarization transfer equations is analyzed for several special cases of interest. (auth) (STAR)

14287 FLUCTUATIONS IN A MAGNETOHYDRODYNAMIC SHOCK WAVE. Akhiezer, A. I.; Polovin, R. V.; Rozhkov, V. V. (Physical-Technical Inst., Kharkov). Zh. Eksp. Teor. Fiz.; 59: 2180-6(Dec 1970). (In Russian).

The effect of fluctuations on a shock wave moving in a plasma perpendicular to an external magnetic field is investigated. The amplitude distribution function for the magnetic field behind a shock wave is determined. It is shown that fluctuations may lead to destruction of the shock wave. The lifetime of the shock wave is found. It is very small for Mach numbers close to unity. (auth)

14288 RADIATIVE INSTABILITY OF A NONEQUILIBRIUM PLASMA IN MAGNETIC TRAPS. Nekrasov, A. K.; Timofeev, A. V. Zh. Eksp. Teor. Fiz.; 59: 2175-9(Dec 1970). (In Russian).

A plasma in a magnetic field with a nonequilibrium momentum distribution of charged particles is considered. The distribution is δ-like with respect to all or to the transverse components of the momentum (in the latter case $p_{\perp 0} \gg p_{\|0}$). Negative energy oscillations with circular polarization moving along the magnetic field should be possible in such a plasma. In systems bounded along the magnetic field, such as in magnetic traps, negative energy oscillations build up as a result of energy flow to the vacuum. Thus, a magnetic trap may serve as a source of electromagnetic radiation. The unstable oscillation buildup mechanism may be predominant in sufficiently short systems with not-very-high plasma densities. (auth)

14289 COMPUTER SIMULATION OF A SPHERICALLY SYMMETRIC PLASMA. Barnes, Christopher Warren. Stanford, Calif.; Stanford Univ. (1970). 148p. University Microfilms Order No. 70-22,149.

Thesis.

One-dimensional plasma problems with planar and spherical symmetry are studied by means of numerical-simulation techniques. The finite-length planar diode problem with a beam traveling through a neutralizing background of oppositely charged particles is treated, and the effect of finite background mass and temperature on beam stability in this model is determined. These results are then used to explain the behavior of a proposed fusion confinement device. This machine consists of a number of high-energy ion guns arranged symmetrically on a spherical surface such that ion beams are directed radially inward. The objective is to confine a high-density energetic ion plasma within this spherical region by means of particle trapping in self-generated potential wells. Numerical-simulation techniques were used to determine the behavior of this device under various beam injection conditions. This behavior was then interpreted in terms of the above mentioned planar and spherical diode results. It was found that hot ions do not become trapped to a significant degree in the center of the sphere, indicating that, to the extent that this one-dimensional model provides an accurate characterization of this device, the device in the form initially conceived does not hold much promise as a fusion plasma machine. However, there is a wide range of variables in the design of such a device, and it is also possible that there may be important trapping mechanisms that depend on two-dimensional effects. Therefore, only this limited statement of the significance of the results presented is possible. (Diss. Abstr. Int., B)

14290 ANNIHILATION AND OTHER INTERACTIONS OF POSITRONS IN A PLASMA. Wolfer, Wilhelm G. Gainesville, Fla.; Univ. of Florida (1969). 142p. University Microfilms Order No. 70-20,625.

XUM

Thesis.

A consistent derivation of the nonrelativistic Hamiltonian for a many-body electron—positron system is given as well as a general formula for the annihilation probability in such a system. The derivations begin with the proper relativistic expressions and are based on a power expansion of the electron—positron field operators in terms of (k/K), where ħk is the nonrelativistic momentum of the particles and K the inverse of the electron Compton wavelength. The theory is carried out up to the second power in (k/K) for the Hamiltonian as well as the annihilation probability. An upper momentum cut-off $k_{max} = K$ is introduced to avoid divergences and ensure the convergence of the expansion. The annihilation rate and the angular correlation function are then evaluated for a plasma as a function of the electron temperature, assuming thermal equilibrium for electrons as well as positrons. Finally, a short survey of processes other than annihilation with free electrons is given. (Diss. Abstr. Int., B)

14291 CORRECTIONS TO THE QUASI-STATIONARY VALUE OF THE DIELECTRIC PERMEABILITY TENSOR OF A SMOOTHLY INHOMOGENEOUS ELECTRON PLASMA. Kravtsov, Yu. A.; Kugushev, A. I.; Chernykh, A. V. (Radiotechnical Inst., Moscow). Zh. Eksp. Teor. Fiz.; 59: 2160-4(Dec 1970). (In Russian).

The correction to the quasi-stationary value of the dielectric permeability tensor $\epsilon_{\alpha\beta}^0$ in a smoothly inhomogeneous electron plasma is calculated by geometrical optics methods. The hydrodynamic approximation is used for describing the electron motion. It is shown that besides the anti-Hermitian correction to $\epsilon_{\alpha\beta}^0$, which ensures conservation of energy flux in the ray tube, there is also a Hermitian correction that does not affect the magnitude of the field in the zero approximation of geometrical optics. (auth)

14292 COLLECTIVE SLOWING DOWN OF AN INTENSE RELATIVISTIC ELECTRON BEAM IN A DENSE PLASMA TARGET. Rudakov, L. I. Zh. Eksp. Teor. Fiz.; 59: 2091-2104 (Dec 1970). (In Russian).

Instability of a relativistic electron beam in a plasma is studied on the basis of the Vlasov kinetic equation. It is demonstrated that slowing down of an initially monoenergetic beam in accordance with the one-dimensional model is valid only for moderate-strength beams for which $(n'/n)^{1/3}\gamma \ll 1$. Here $\gamma = (1 - v^2/c^2)^{-1/2}$ and n′ and n are the beam and plasma densities respectively. Slowing down of more intense beams or beams with an initial angular velocity dispersion θ exceeding $(n'/n)^{1/3}\gamma^{-1/3}$ may occur only as the result of the induced Cherenkov effect ("kinetic" instability). However, even for kinetic instability, the quasi one-dimensional character of beam retardation remains. As a consequence, the characteristic instability increment is a function of the initial θ. The role of nonlinear scattering of Langmuir oscillations by plasma particles, which leads to saturation of the unstable oscillation amplitude, and also the effect of inhomogeneity of the plasma target are analyzed. A formula for the mean free path of a relativistic electron beam in a dense plasma target is presented. It is shown that beam instability may increase the effective scattering frequency of the plasma electrons. This may result in an increase of the rate of heating of the target due to ohmic dissipation of the inverse current and the beam slowing down involved. (auth)

14293 DARWIN MODEL AS A TOOL FOR ELECTROMAGNETIC PLASMA SIMULATION. Kaufman, Allan N.; Rostler, Peter S. (Univ. of California, Berkeley). Phys. Fluids; 14: 446-8(Feb 1971).

The Darwin model of electromagnetic interaction is presented as a self-consistent theory and is shown to be an excellent approximation to the Maxwell theory for slow electromagnetic waves. (auth)

14294 DEPENDENCE OF PLASMA DENSITY DISTRIBUTION ON LOCAL DECAY TIME. Uramoto, Johshin (Nagoya Univ., Japan). Phys. Fluids; 14: 440-2(Feb 1971).

A local increase in e-folding length in a density distribution across B is not related to an increase in diffusion coefficient, if a decay time of plasma along B increases locally with reflection of the plasma on two end sheaths. (auth)

14295 MOTT-SMITH SOLUTION OF THE FOKKER-PLANCK EQUATION. Koura, Katsuhisa (National Aerospace Lab., Tokyo). Phys. Fluids; 14: 435-6(Feb 1971).

The nonlinear Fokker—Planck equation describing the relaxation of the fully ionized gas is solved by the Mott—Smith method. The relaxation time obtained using the lower-moment equations is found to agree with the Spitzer self-collision time. (auth)

14296 NONLINEAR BEAM-PLASMA INTERACTIONS AND STOCHASTIC ACCELERATION. Dum, Christian T.; Sudan, R. N. (Cornell Univ., Ithaca, N. Y.). Phys. Fluids; 14: 414-23 (Feb 1971).

The development of an electron beam—plasma instability beyond the stage described by quasi-linear theory is investigated by means of kinetic equations for waves and particles that include the effects of spontaneous emission and scattering of waves. Characteristic times for the formation of a high-energy tail are computed, which at late times may extend significantly beyond the original beam velocity. Qualitative agreement is obtained with experiments. (auth)

14297 QUANTUM TRANSPORT CROSS SECTIONS FOR IONIZED GASES. Hahn, Hong-sup (Brown Univ., Providence); Mason, E. A.; Smith, Francis J. Phys. Fluids; 14: 278-87(Feb 1971).

Transport cross sections and collision integrals are calculated over a wide range of energies and temperatures for the attractive and repulsive screened Coulomb potentials. Results accurate to 1% over the whole range from classical to quantum-mechanical behavior are given in the form of numerical tables. Results of lower accuracy are given as analytical expressions. (auth)

14298 COLLISION FREE IONIZING SHOCK. Pert, G. J. (Univ. of Alberta, Edmonton). Phys. Fluids; 14: 332-8(Feb 1971).

The structure of an ionizing wave propagating into a low density un-ionized gas is considered. It is shown that due to phase mixing of the velocities of ions formed at different points in the wave, the oscillatory nature of the wave is damped and the front may form a shock transition. Only the existence of these waves is demonstrated; their stability is not considered. (auth)

14299 SHEATH GROWTH IN A LOW PRESSURE PLASMA. Andrews, J. G.; Varey, R. H. (Central Electricity Generating Board, Marchwood, Eng.). Phys. Fluids; 14: 339-43(Feb 1971).

The limits of very slow and very fast sheath growth in a low-pressure plasma can be described by Child's law and the ion matrix model, respectively. It is shown that if the sheath edge grows with constant speed, the range between these two extremes can be treated analytically by transforming the equations to the sheath edge frame of reference. This provides a continuous transition between the two extremes which reduces to Child's law for very slow growth and to the ion matrix model for very fast growth. The theoretical expression for sheath thickness calculated from the continuous transition model is found to be in good agreement with experimental results. (auth)

14300 COLLISIONLESS SHEATH NEAR AN ELECTRODE IN THE PRESENCE OF A MAGNETIC FIELD. Hassan, H. A.; Seals, R. K. Jr. (North Carolina State Univ., Raleigh). Phys. Fluids; 14: 344-8(Feb 1971).

Magnetic field effects on the structure of a collisionless sheath near a planar electrode are considered. The model assumes the distribution functions normal to the electrode to be Maxwellian. The case where the electric and magnetic fields are mutually perpendicular is discussed in detail. It is shown that, in this case, the sheath is always stable and one need not invoke a sheath criterion. The resulting nonlinear differential equations for the electric and magnetic potentials are solved by an exact numerical scheme for an argon plasma near an anode. The results predict the effect of magnetic fields on anode losses in arc jets rather well. (auth)

14301 LOW-CURRENT HELIUM DISCHARGE AT LOW PRESSURES. Masek, K.; Ruzicka, T. (Inst. of Physics, Prague). Czech. J. Phys.; 21: 43-61(1971).

On the basis of a good knowledge of the energy distribution function of electrons corresponding to the conditions of low-current discharge, the electrons as well as the excited helium atoms are balanced. A model of a helium atom possessing four excitation levels (2^3S, 2^1S, 2^3P, 2^1P) is assumed. The calculated volt—ampere characteristic is compared with an experiment and the relative densities of excited atoms are given. For these quantities approximate formulas are derived. The laws of similarity, ionization mechanism, and energy balance of the electron gas are discussed. (auth)

14302 ATOMIC PROCESSES IN A LOW-DENSITY HYDROGEN-HELIUM PLASMA. Gould, R. J.; Thakur, R. K. (Univ. of California, San Diego, La Jolla). Ann. Phys. (N. Y.); 61: 351-86(Dec 1970).

For a partially ionized hydrogen—helium plasma at 10^4 to 10^6°K the processes bremsstrahlung, radiative and dielectronic recombination, excitation of discrete levels, and collisional ionization due to electron collisions with various species are discussed. The steady-state ionization conditions are computed assuming a balance between collisional ionization and radiative and dielectronic recombination. This is done for the cases where the plasma is optically thin and optically thick to photons resulting from radiative captures to the ground states of the recombined species. The cooling rates for the plasma are computed for all of the above processes. A very brief discussion is given of the effects of deviations from a Maxwellian electron velocity distribution. Possible applications of the results in astrophysics are mentioned, the principal application being to the primordial gas after decoupling of the matter from the radiation. (auth)

14303 DC NOISE IN PLASMA DUE TO ELECTRON–ION COLLISIONS. Nandedkar, D. P.; Bhagavat, G. K. (Indian Inst. of Tech., Bombay). Int. J. Electron.; 29: 513-23(Dec 1970).

The dc noise in plasma at electron–ion collisions is quantum-mechanically analysed. Maximum frequency of noise generated is determined by number density of ions in the plasma. An expression for noise power per unit bandwidth of noise frequencies in the rf spectrum of electromagnetic radiations is obtained. (auth) (UK)

14304 POSSIBILITY OF PHASE TRANSITIONS IN AN IMPERFECT MULTIPLY IONIZED PLASMA. Valuev, A. A.; Medvedev, I. G.; Norman, G. E. (Inst. of High Temperature, Moscow). Zh. Eksp. Teor. Fiz.; 59: 2228-32(Dec 1970). (In Russian).

The equation of state and equation for ionization equilibrium of an equilibrium plasma are considered for various ionization multiplicities under conditions when the charge interaction energy is comparable with or exceeds the thermal energy of the charges. Two models of an imperfect plasma are used; assumedly, these models yield the upper and lower contributions of quantum effects, which ensure thermodynamic stability of a very imperfect plasma. It is shown that with growth of ionization multiplicity the division of a strongly imperfect plasma into two phases becomes more probable. Cases are considered when a phase transition for a definite ionization multiplicity possesses upper and lower critical temperatures and when overlapping of phase-transition regions occurs for successive ionization multiplicities. Application of the results to various elements of the periodic system is discussed. (auth)

14305 PHYSICS OF HOT PLASMAS. Rye, B. J.; Taylor, J. C. (eds.). Edinburgh; Oliver and Boyd (1970). 455p. £ 8.

Lectures presented at the Scottish Universities Summer School in Physics 1968 are reproduced. Topics include: introduction to kinetic theory of plasma, advanced kinetic theory, plasma waves and oscillations, plasma instabilities, computational problems in plasma physics and controlled thermonuclear research, turbulence, collisionless shocks, collisionless shock waves, laser-produced plasmas, the production and containment of high-density plasmas, light scattering experiments, and plasma diagnostics based on refractivity. (UK)

14306 SPECTROSCOPIC STUDY OF ION–NEUTRAL COUPLING IN PLASMA ACCELERATION. Malliaris, A. C.; Libby, D. R. (Avco Corp., Wilmington, Mass.). AIAA (Amer. Inst. Aeronaut. Astronaut.) J.; 9: 160-7(Jan 1971).

The acceleration of a partially ionized gas by electromagnetic means might be quite inefficient if the coupling between the ions and the neutrals, for momentum transfer, is weak. The absence or presence of a sufficiently strong coupling is generally revealed by velocity disparities determined spectroscopically, for several species, both ionic and neutral. Velocities are determined by Doppler-shift measurements of selected spectral lines. Results regarding two different situations are presented from experiments where two basically similar axisymmetric configurations operate under significantly different conditions. In the first case, a large disparity in ion–neutral velocities is observed, whereas in the second case, the said disparity disappears and the common ion–neutral velocities are in good agreement with the center-of-mass velocity, as determined independently from measurements of motionally induced potentials in the flow. A satisfactory interpretation of the results is obtained when the calculated mean free path for momentum exchange is compared with a typical dimension of the electromagnetic acceleration region. (auth)

14307 FINITE-DIFFERENCE METHODS FOR THE FOKKER–PLANCK EQUATION. Whitney, James C. (Columbia Univ., New York). J. Comput. Phys.; 6: 483-509(Dec 1970).

Two methods are developed for numerical solution of the time-dependent Fokker–Planck equation. First, a finite difference scheme is constructed that has the property of simultaneously conserving total system mass, energy, and momentum throughout the interior of velocity space, thereby reducing nonconservation errors to boundary contributions only. Second, the Fokker–Planck collision operator is expanded in Legendre polynomials and reduced to an equivalent system of one-dimensional problems. The expansion is carried out to all orders and is mathematically exact; no terms are neglected or linearized. The resulting system of one-dimensional equations is given explicitly. Both these formulations are given for the case of two-dimensional azimuthally symmetric distribution functions. As a test of the methods, the thermal equipartition of an isotropic deuterium–electron plasma is computed numerically. Over a range of initial conditions from $T_e/T_D = 0.01$ to $T_e/T_D = 100$ the electron and ion temperatures obtained from the Fokker–Planck equation agree to within 6% with those obtained from the Maxwellian model given by Spitzer. (auth)

14308 ABOUT THE INFLUENCE OF THE ENERGY DEPENDENCE OF THE ELECTRON COLLISION FREQUENCY ON THE ELECTRICAL CONDUCTIVITY OF WEAKLY IONIZED PLASMAS. Becker, R.; Kummer, J.; Nicol, K.; Schmidt, W. (Johann-Wolfgang-Goethe-Univ., Frankfurt am Main). Z. Phys.; 241: 380-94 (1971). (In German).

With regard to experimental applications in plasma diagnostics, numerical approximations are given for the Gurevich-type correction functions, which in the kinetic theory of weakly ionized plasmas describe the deviations from the Lorentzian electrical conductivity. The approximations are based either upon the dependence of the collision frequency on the power of the electron velocity, or on a first-order Taylor expansion around the most probable electron velocity of a Maxwellian distribution. For all assumptions regarding the velocity dependence of the collision frequency the influence of temperature (and pressure) on the effective collision frequency is indicated. (auth)

14309 ASYMPTOTIC SOLUTION IN THE PROBLEM OF ANOMALOUS PLASMA RESISTANCE. Vekshtein, G. E.; Ryutov, D. D.; Sagdeev, R. Z. (Inst. of Nuclear Physics, Novosibirsk, USSR). JETP Lett. (USSR) (Engl. Transl.); 12: 291-4(20 Oct 1970).

Translated from Zh. Eksp. Teor. Fiz., Pis'ma Red.; 12: 419-22(20 Oct 1970).

The distribution functions of the charged particles and the spectrum of the oscillations in the asymptotic regime are determined. It is also shown that there is no anomalous resistance in the asymptotic regime. (M.O.W.)

14310 AMPLITUDE MODULATION AND NONADIABATICITY IN STARK BROADENING OF HYDROGEN LINES IN A PLASMA. Sholin, G. V.; Lisitsa, V. S.; Kogan, V. I. Zh. Eksp. Teor. Fiz.; 59: 1390-1403(Oct 1970). (In Russian).

Deviations from the quasi-static Holtsmark shape of hydrogen spectral lines due to thermal motion of charged particles of the plasma are calculated. Effects are analyzed for the first time that are related to rotation of the electric microfield vector and that lead to nonadiabaticity and amplitude modulation of the light wave emitted by an atom. It is shown that amplitude modulation and nonadiabaticity of rotation play a decisive role in the deviations from the Holtsmark line shape. Thus, for example, for the "binary" wing of the L_α line the correction for thermal motion, which takes into account all indicated effects, is by almost two orders of magnitude greater than the correction considered hitherto and due only to phase modulation. The theory is extended to the plural case in which the simultaneous action of all perturbing particles on the emitting atom is taken into account; the complete line shape is thus obtained by taking into account deviations from quasi-staticity. The results are applied to an analysis and correction of the criteria of the quasi-static and adiabatic approximations underlying the theory of Stark line broadening. A number of related effects are discussed, e.g., the role of ions in broadening of the central Stark component, amplitude modulation for an arbitrary broadening mechanism, etc. (auth)

14311 CONTRIBUTION TO THE NONLINEAR THEORY OF EXCITATION OF A MONOCHROMATIC PLASMA WAVE BY AN ELECTRON BEAM. Onishchenko, I. N.; Linetskii, A. R.; Matsiborko, N. G.; Shapiro, V. D.; Shevchenko, V. I. (Physical-Technical Inst., Kiev). JETP Lett. (USSR) (Engl. Transl.); 12: 281-5(20 Oct 1970).

Translated from Zh. Eksp. Teor. Fiz., Pis'ma Red.; 12: 407-11(20 Oct 1970).

The nonlinear theory of excitation of a monochromatic plasma wave by means of a beam is considered for two limiting cases: when the electron beam is smeared, $\Delta v/v_0 \gg (n_1/n_0)^{1/3}$, and monoenergetic, $\Delta v/v_0 \ll (n_1/n_0)^{1/3}$ (Δv is the velocity spread in the beam, v_0 the mean velocity, and n_1 and n_0 the beam and plasma densities, with $n_1 \ll n_0$). (M.O.W.)

14312 DIELECTRIC PERMITTIVITY OF PLASMA IN A STRONG MAGNETIC FIELD. Nazaryan, A. Kh. (Erevan State

XUM

Univ.). Izv. Vyssh. Ucheb. Zaved., Radiofiz.; 13: 1325-8(1970). (In Russian).

Corrections for the complex dielectric tensor of plasma in a uniform magnetic field are derived, taking into account the Coulomb interactions. (auth)

14313 PROPAGATION OF A CHARGED PARTICLE THROUGH WEAK NONLINEAR PLASMA. Giorgadze, N. P.; Kaladze, T. D.; Lominadze, D. G. (Inst. of Physics, Tbilisi, USSR). Izv. Vyssh. Ucheb. Zaved., Radiofiz.; 13: 1329-34(1970). (In Russian).

The geometry of the nonlinear longitudinal field caused by the interaction of a particle with a weakly nonlinear isotropic plasma is considered. With the proper choice of parameters, the amplitude of the nonlinear wave field is shown to be an order smaller than the amplitude of the linear wave field. The differences in the spectral characteristics of these fields make it possible to observe the considered nonlinear effects. (auth)

14314 RADIATION INTENSITY FROM THE FRONT OF COLLISIONLESS SHOCK WAVES. Stepanov, A. V. (Gorky State Univ., USSR). Izv. Vyssh. Ucheb. Zaved., Radiofiz.; 13: 1342-9 (1970). (In Russian).

Spontaneous processes of Rayleigh and Raman scattering of plasma waves and electromagnetic waves in a collisionless shock front are considered. The scattering coefficients are determined. It is shown that, if the relative velocity of electrons and ions in the shock wave front exceeds the thermal velocity of electrons, the Rayleigh scattering coefficient is $(2a^4q^4)^{-1}$ times less than $(a^2q^2 \ll 1)$ as compared with that in the usual plasma. (auth)

14315 SIMULTANEOUS DETERMINATION OF ELECTRON CONCENTRATION AND ELECTRON COLLISION FREQUENCY IN A LOCALLY SLOWLY VARYING MAGNETOPLASMA. Muschler, W. (Max-Planck-Institut fuer Aeronomie, Lindau, Ger.). Z. Naturforsch.; 25a: 1578-83(Nov 1970). (In German).

Electron concentration and electron collision frequency are parameters of the Appleton–Hartree formula, which describes the complex refractive index of the medium penetrated by the wave. The refractive index can be expressed by the complex ratio of the electric and magnetic wave components if the WKB solutions of coupled wave equations are used. These are valid for a (locally) slowly varying medium. The complex wave polarization is another characteristic of the magnetoplasma. It is also defined by simple field-strength relations and presents itself for application in the experiment. When both refractive index and wave polarization are determined by amplitude and phase measurements, electron concentration and electron-collision frequency can easily be deduced from the complete Appleton–Hartree formula. (auth)

14316 SELF-CONSISTENT ANALYSIS OF THE EFFECT OF RADIATION ESCAPE ON THE ATOMIC STATE DENSITIES AND ELECTRON DISTRIBUTION FUNCTION. Cohn, A. (Air Force Cambridge Research Labs., Bedford, Mass.); Hollinger, H. B. Phys. Lett.; 33A: 495-6(28 Dec 1970).

The influence of resonance radiation escape on the atomic state densities in H is analyzed, with the electron distribution function calculated self-consistently. The degree of ionization can fall severely below the values calculated, assuming the Maxwellian distribution. (auth)

14317 COLLISIONLESS HEAT WAVE. (THE WAVE OF REPLACEMENT). Ivanov, A. A.; Istomin, I. N.; Kozorovitskii, L. L.; Rusanov, V. D. (Inst. of Atomic Energy, Moscow). Phys. Lett.; 33A: 509-10(28 Dec 1970).

Propagation of heat along a magnetic field is considered. The velocity of a nonlinear wave is found to be in accordance with the experiment. Collective effects are taken into account. (auth)

14318 SIMILARITY RULES IN PLASMA PHYSICS. Lacina, J. (Inst. of Plasma Physics, Prague). Czech. J. Phys.; 21: 97-9(1971).

Plasma is examined from the microscopic point of view. Similarity rules are derived for a plasma whose motion is describable by the Boltzmann equation with a collision term and by the Maxwell equations for self-consistent fields. Only the case of binary collisions is considered. (M.O.W.)

14319 EQUATION OF STATE AND IONIZATION EQUILIBRIUM OF HYDROGEN PLASMAS. Ebeling, W.; Kelbg, G.; Saendig, R. (Univ., Rostock, Ger. Moscow State Univ.). Beitr. Plasmaphys.; 10: 507-25(1970). (In German).

A recently developed quantum-statistical theory of low-density plasmas is extended and applied to hydrogen plasmas in thermal equilibrium. The theory is shown to be a generalization of the formulas by Abé, DeWitt, Vedenov and Larkin. Numerical and graphical representations of various characteristic plasma parameters, the equation of state, the degree of ionization, and the lowering of the ionization energy are given. The formation of hydrogen molecules is semi-quantitatively taken into account. (auth)

14320 THEORY OF A DOUBLE SHEATH BETWEEN TWO PLASMAS. Andrews, J. G. (Central Electricity Generating Board, London. Oxford Univ.); Allen, J. E. Proc. Roy. Soc. (London), Ser A; 320: 459-72(5 Jan 1971).

A model of a double sheath between two plasmas is presented in which reflected particles and the initial velocities of accelerated particles are considered. The model shows that, in addition to the voltage drop across the double sheath, the ions from the plasma acquire kinetic energy (comparable with the electron thermal energy) in a presheath region. The ratio of the ion and electron current densities can depart significantly from Langmuir's $(m/M)^{½}$. (auth) (UK)

14321 CALCULATION OF CURRENT DENSITY AND FIELD IN A QUASI-NEUTRAL ELECTRON-BEAM PLASMA. Wunderer, Bernd (Univ., Munich). Beitr. Plasmaphys.; 10: 271-84(1970). (In German).

The current density in a cylindrical beam-generated plasma with diffusion and attachment losses is calculated by introducing the magnetic field as a vector potential. The boundary values for the elliptic partial differential equation resulting from this procedure are submitted to certain restrictions for the case of a quasi-neutral plasma. The boundary-value problem is solved numerically. As an example, current densities and electrical fields of the negative glow of constricted anomalous H_2 discharges are computed. The results show that, even for higher degrees of constriction, the radial currents are ambipolar. Some aspects of comparison to experiments are discussed. (auth)

14322 QUANTUM STATISTICAL SECOND VIRIAL COEFFICIENT FOR REAL GASES AND PLASMAS. Ebeling, W.; Kraeft, W. D.; Kremp, D. (Univ., Rostock, Ger.). Beitr. Plasmaphys.; 10: 237-63(1970).

Using the resolvent representation of the binary Boltzmann operator, the second virial coefficient is expressed by a contour integral over the Jost function of the two-particle scattering problem. This new formula is useful for many general investigations and also for practical calculations if the Jost functions for the scattering problem are known. As special examples, real gases with hard-core potentials and fully ionized plasmas with Coulomb interactions are treated. For the plasma case, the second virial coefficient is derived without approximations with respect to the interaction parameter. The contribution of the bound states to the free energy is discussed and compared with the effect of ionic association on the classical free energy and the conductivity. (auth)

14323 EXPERIMENTAL TEST OF QUASI-LINEAR THEORY. Roberson, C.; Gentle, K. W.; Nielsen, P. (Univ. of Texas, Austin). Phys. Rev. Lett.; 26: 226-9(1 Feb 1971).

The shape and amplitude of the electron-plasma wave spectrum resulting from a "gentle bump" on the tail of the electron velocity distribution of a plasma is measured and found to be in good agreement with quasi-linear theory. (auth)

14324 NEAR-STEADY OBLIQUE SHOCK WAVES IN A COLLISIONLESS PLASMA. Olson, Lynn Mary. Madison, Wis.; Univ. of Wisconsin (1970). 82p. University Microfilms Order No. 70-20,864.

Thesis.

Waves of small amplitude ϵ that travel into an equilibrium plasma and whose head approaches steadiness are studied. The plasma is cold and the equilibrium magnetic field is inclined at an arbitrary angle θ to the propagation direction. The relevant double limit $\epsilon \xrightarrow{\text{lim}} 0\ t \xrightarrow{\text{lim}} \infty$ is treated in terms of equivalent sets of single limits. Near-steady waves that can lead from one equilibrium to another are shown to be possible only at propagation speeds corresponding to Alfvén Mach number 1 or $\cos\theta$. In the first case, either the magnetic pressure at the head of the wave decreases monotonically from its initial value and the wave spreads linearly with time, or else the head of the wave consists of a near-periodic train of conoidal waves, the first crest of which approaches a solitary wave solution. For $1\text{-}M^2\cot^2\theta > 0$, where $M = (m_+/m_-)^{½} - (m_-/m_+)^{½}$, the magnetic pressure in the near-periodic wave train always exceeds its initial equilibrium value. But for $1 - M^2\cot^2\theta < 0$, it always falls short of that equilibrium value. A transition with precursor waves is shown to be impossible for a cold collisionless plasma. At an Alfvén Mach number of $\cos\theta$, the only near-steady solution consists of a main wavefront followed by an oscillatory tail; however, on the length scale considered, the electric field becomes unbounded at the tail. (Diss. Abstr. Int., B)

14325 TEST-PARTICLE RADIATION IN MAGNETOPLASMA. Trulsen, Jan Karsten. San Diego, Calif.; Univ. of California (1970). 154p. University Microfilms Order No. 70-23,848. Thesis.

This work has two main objectives. The theory of the radiation from a charged particle moving in a spiral path through a cold magnetoplasma is reviewed and unified. Several errors in the literature are pointed out. Secondly, the effect of including thermal motions on the power loss suffered by the test particle is studied. The general results for the fields set up and the polarization and the statistical energy loss suffered by the particle in a hot magnetoplasma described by the linearized Vlasov equation are derived. The first loss is due to the polarization fields set up by the particle in the plasma. The second loss is caused by the fluctuating electric fields existing in hot plasma. (TSS) (Diss. Abstr. Int., B)

14326 EXISTENCE CONDITIONS OF HYDROMAGNETIC SHOCKS ALONG THE MAGNETIC FIELD IN THE VLASOV PLASMA. Kato, Y. (Nagoya Univ., Japan); Tajiri, M.; Taniuti, T. Phys. Lett.; 34A: 37-8(25 Jan 1971).

The existence condition of the steady shock-like waves along an applied magnetic field in a collisionless plasma is calculated by means of the Vlasov equation. Two types of waves are expected to appear for certain plasma configurations. (auth)

14327 PERTURBATION THEORY FOR TOROIDAL PLASMA. Burt, P. B. (Oak Ridge National Lab., Tenn. Clemson Univ., S. C.). Phys. Lett.; 34A: 47-8(25 Jan 1971).

The self magnetic field of an axially symmetric toroidal plasma is shown to contain positive powers of the aspect ratio and a logarithmic function of this quantity. The limit of large aspect ratio is finite. (auth)

14328 CONTRIBUTIONS TO THE KINETIC THEORY OF WEAKLY IONIZED PLASMAS IN AN EXTERNAL CONSTANT ELECTRIC FIELD. Stenflo, Lennart. Uppsala, Sweden; Univ. of Uppsala (1968). 10p. Thesis.

A homogeneous plasma, which is assumed to be so weakly ionized that inter-carrier collisions can be neglected, is assumed to be situated in an applied constant electric field. The effect of the external field in different situations of interest for gas-discharge physics as well as for semiconductor physics is considered. Thus, dispersion relations are derived and discussed for cases where the true collision integral can be replaced by different collision models, conductivities are calculated, runaway phenomena are studied, and the influence of non-parabolicity of the energy band is treated. (Diss. Abstr. Int., B)

14329 FINITE-LARMOR-RADIUS HYDROMAGNETIC FLOW PAST AN OBSTACLE. Morioka, Shigeki; Tanaka, Koichi (Osaka Univ.). J. Phys. Soc. Jap.; 30: 549-56(Feb 1971).

Effects of dispersion due to the finite Larmor radius on the steady flow of a collisionless plasma past a thin symmetrical semi-infinite wedge are considered on the basis of the modified Chew–Goldberger–Low theory. The flow field near the tip is given by the numerical integration of the Fourier transform. The asymptotic behavior of the flow field at a far distance from the wedge is estimated by using the method of stationary phase or Laplace's method. It is shown that the flow field is subject to a remarkable variety of the dispersion effect, according to the main flow conditions. (auth)

14330 GUIDING CENTER OF A CHARGED PARTICLE IN SUPERPOSED HELIOTRON AND BICONICAL CUSP FIELDS. Bhat, P. K.; Murthy, S. Narasimha (Indian Inst. of Science, Bangalore). J. Phys. Soc. Jap.; 30: 522-7(Feb 1971).

The allowed region for the guiding center of a charged particle gyrating in superposed Heliotron and biconical cusp fields was investigated by combining the motion of the guiding center and the rotation of the particle around it. This is done by finding the stationary values of the guiding center coordinates expressed as functions of the particle coordinates. It is found that the guiding center almost sticks to the leading line of force. Further, from the numerical integration of the nonlinear set of equations governing the motion of a single charged particle, it is found that the particle remains in the allowed region. A comparison shows that the two approaches are in qualitative agreement with each other. (auth)

Production

Refer also to abstract 14359.

14331 INVESTIGATION OF A HIGH-PRESSURE LASER SPARK IGNITED BY AN EXTRANEOUS PLASMA SOURCE. Mul'chenko, B. F.; Raizer, Yu. P.; Epshtein, V. A. (Inst. of Mechanical Problems, Moscow). Zh. Eksp. Teor. Fiz.; 59: 1975-82(Dec 1970). (In Russian).

A laser spark in argon at pressures up to 80 atm is ignited by an extraneous plasma source, the intensity of the supporting radiation being below the breakdown threshold. The threshold power of the radiation from a ruby laser required for maintaining the plasma is determined for pressures ranging from 16 to 80 atm and is found to lie between 70 and 10 kW. The plasma temperature (18,000 to 33,000°) and other parameters are measured. The results are in agreement with the theoretical calculations. (auth)

14332 PONDEROMOTIVE FORCE ON LASER-PRODUCED PLASMAS. Lindl, John D.; Kaw, Predhiman K. (Princeton Univ., N. J.). Phys. Fluids; 14: 371-7(Feb 1971).

The deconfining ponderomotive force exerted by an intense electromagnetic wave on a linearly inhomogeneous plasma layer is analytically investigated. Since the ponderomotive force maximizes near the region where the dielectric constant $\epsilon' \to 0$, an exact solution of the wave equation is required for a correct estimate of the maximum force. For the case of oblique incidence with the electric vector in the plane of incidence, the solution of the exact wave equation leads to an interesting resonance effect which predicts a force higher than that obtained by earlier workers using a WKB procedure. Physically, this enhanced ponderomotive force arises because of the large nonuniform longitudinal fields that are generated in the region $\epsilon' \approx 0$ for this geometry. (auth)

14333 EXPLANATION OF PLASMA DENSITIES HIGH ABOVE CRITICAL DENSITY IN A CYLINDER EXCITED BY AN rf HELIX. Aubert, A. E.; Messiaen, A. M.; Vandenplas, P. E. (Royal Military School, Brussels). Appl. Phys. Lett.; 18: 63-5(15 Jan 1971).

It is shown that the density characteristics of plasmas created by an rf helix are completely determined by the low-power resonance features of the bounded system, which is constituted by the plasma column and the surrounding helix of finite axial length. Whether a magnetic field is present or not, plasma densities high above critical density are obtained, in agreement with the general philosophy previously developed. Experiments already performed without magnetic field support the theoretical predictions. (auth)

14334 INTERACTION OF A LASER-CREATED PLASMA WITH A STRONG MAGNETIC INDUCTION. Schirmann, D.; Grelot, P.; Rabeau, M.; Tonon, G. (Center d'Etudes de Limeil, Villeneuve-Saint-Georges, France). Phys. Lett.; 33A: 514-15 (28 Dec 1970).

The effect of a few-hundred-kilogauss magnetic induction on the expansion of a laser plasma is observed during the laser pulse by means of optical interferometry. (auth)

14335 ARGON PLASMA GENERATOR WITH ELECTRON DENSITY WITHIN THE RANGE 5×10^{14} TO 5×10^{17} cm^{-3}. Leleu, C.; Chapelle, J.; Cabannes, F.; Bourasseau, D. (CNRS, Orleans, France). High Temp.-High Pressures; 2: 215-26(1970). (In French).

An argon plasma jet generator was studied over a wide range of pressures (10^{-2} to 10 atm) and electron densities (5×10^{14} to 5×10^{17} cm^{-3}). The thermal-balance method, which is very easy to use, gives plasma temperatures with as good an accuracy as the spectroscopic method. The measurements show that local thermodynamic equilibrium exists even at the lower end of the pressure range, where the electron density is much below Griem's critical density of 10^{16} cm^{-3}. (auth) (UK)

Stability

14336 (NP-18662) STUDY OF AN IONIC INSTABILITY IN THE PLASMA OF A LOW PRESSURE POSITIVE COLUMN SUBJECTED TO A MICROWAVE RESONATING ELECTRIC FIELD. Pointu, Anne-Marie (Paris Univ., Orsay (France). Laboratoire de Physique des Plasmas). Nov 1970. 134p. (In French). (LP-118). Dep. NTIS (U. S. Sales Only).

The origin of low-frequency oscillations excited in a plasma column by a microwave signal of several hundred mW is interpreted by an approximate theoretical model; this theory is experimentally valid. It is shown that the oscillations are due to a feedback mechanism resulting from a linear coupling between the incident microwave signal and an ion plasma perturbation that is excited on the discharge tube wall and propagated through the plasma sheath. (auth) (France)

XUM

14337 PERIODIC PULLING OF THE DRIFT INSTABILITY IN A THERMAL PLASMA. Abrams, Richard Henry Jr. College Park, Md.; Univ. of Maryland (1970). 128p. University Microfilms Order No. 70-21,316.

Thesis.

The experiment was performed on the University of Maryland Q machine, operated in the single-ended mode. Modes of the drift instability were perturbed by applying a signal from an external oscillator to the cold endplate. The behavior of the sideband spectrum of the perturbed mode is found to agree with the predictions of the theory. The signal associated with the pulled spectrum is found to be amplitude- and frequency-modulated. Low-amplitude oscillations in a Q machine are frequently observed at discrete, harmonically related frequencies. At higher oscillation amplitudes the spectrum becomes a continuous noise spectrum, characteristic of turbulence. The periodic pulling mechanism, which produces a multiplicity of sidebands for each perturbed mode, provides a possible explanation for this transition. The mechanism is characteristic of any distributed-parameter system that can be described by the van der Pol equation, and indicates that the random-phase approximation should be used with care in problems of weak plasma turbulence. (TSS) (Diss. Abstr. Int., B)

14338 SECOND-ORDER SHIFTS IN FREQUENCY AND AMPLITUDE IN THE NONLINEAR THEORY OF E X B INSTABILITY. Kim, John Jungyu. Rochester, N. Y.; Univ. of Rochester (1970). 89p. University Microfilms Order No. 70-17,886.

Thesis.

Using a single-mode analysis, a consistent method to calculate the shifts in amplitude and frequency to order Δ^2 in the E X B instability is presented, taking into account all nonlinear effects. Galerkin's method is applied to obtain approximate results. (Diss. Abstr.)

14339 PLASMA STABILITY IN BOUNDED SYSTEMS WITH APPLICATION TO A TWO-STREAM INSTABILITY IN SPHERICAL GEOMETRY. Porter, G. D. (Univ. of California, Livermore); Klevans, E. H. Phys. Fluids; 14: 428-34(Feb 1971).

A simple procedure for numerically obtaining the solution of a linear, differential boundary-value problem is presented. For an nth-order equation, the technique requires the solution of n initial-value problems. The solution of the boundary-value problem is then a linear combination of these solutions. The technique has very attractive features that should make it a convenient method for studying a variety of stability problems in bounded systems. As an example of these applications, the initial stability of the inertial containment device proposed by Hirsch is examined. It is found that the particular model studied is marginally stable. The results are compared with computer-simulation studies of the device. (auth)

14340 TWO-STREAM INSTABILITY IN TWO MAXWELLIAN, RESONANCE, AND TWO POLE MODELS FOR ARBITRARY STREAM TEMPERATURES AND DENSITIES. Skorupski, A.; Zakowicz, W.; Infeld, E. (Inst. of Nuclear Research, Warsaw). Phys. Fluids; 14: 438-40(Feb 1971).

The problem of stability of two hot streams of charged particles with Maxwellian distributions is solved, in principle, for arbitrary parameters. Stability limits are also found for two models often used for the velocity distributions, and comparisons are made. (auth)

14341 STABILIZATION OF UNIVERSAL INSTABILITY. Mishin, E. V. (Inst. of Nuclear Physics, Novosibirsk, USSR). Zh. Eksp. Teor. Fiz.; 59: 2252-5(Dec 1970). (In Russian).

Normal universal instability modes of a plasma in a large-shear magnetic field ($\Theta > a_i/R_p$) are considered. A condition for stabilization of the modes is derived that differs from that found recently by Berk and Pearlstein. (auth)

14342 ELECTROMAGNETIC INSTABILITY IN COUNTERSTREAMING PLASMAS. Lee, Kai Fong; Armstrong, James C. (Catholic Univ. of America, Washington, D. C.). Phys. Rev. Lett.; 26: 77-80(11 Jan 1971).

It is shown that, in a system of two counterstreaming plasmas, the growth rates of the ordinary-mode electromagnetic instability can be several times the plasma frequency even for nonrelativistic velocities. The electromagnetic instability therefore grows faster than the coexisting electrostatic instabilities of the two-stream type, contrary to the common belief that electromagnetic instabilities are only of interest if electrostatic ones are absent. (auth)

14343 LOW-FREQUENCY INSTABILITY OF AN ELECTRON-CYCLOTRON WAVE IN A PLASMA. Patrushev, B. I.; Ivanov, A. A.; Gozak, V. P.; Frank-Kamenetskii, D. A. Zh. Eksp. Teor. Fiz.; 59: 1080-2(Oct 1970). (In Russian).

Excitation of waves with a frequency ~100 MHz is observed in cyclotron heating of plasma electrons. The waves rapidly decay after the initial cyclotron wave is turned off. The peak in the excited-wave spectrum is close to the lower-hybrid frequency; they may thus be identified as anisotropic ion sound. The mechanism of their excitation may be explained as a result of distortion of the averaged electron distribution function by high-frequency currents. (auth)

14344 CURRENT-INTERCHANGE INSTABILITY IN TURBULENT HEATING OF A PLASMA BY A CURRENT. Kalinin, Yu. G.; Lin, D. N.; Rudakov, L. I.; Ryutov, V. D.; Skoryupin, V. A. Zh. Eksp. Teor. Fiz.; 59: 1056-66(Oct 1970). (In Russian).

Results are presented of a theoretical and experimental study of large-scale current–interchange instability under conditions of turbulent heating of a plasma by a current. The nonlinear equation describing variation of the longitudinal electric field in the plasma is solved, and it is shown that current-interchange instability results in a strong increase of the thermal conductivity along the magnetic field. This explains the limited growth of energy content of the plasma observed experimentally and the large losses at the ends of the installation. Measurements of electric field distribution in the plasma and the rate of perturbation growth are in satisfactory agreement with the theory proposed here. (auth)

14345 EXPERIMENTAL OBSERVATION OF DRIFT INSTABILITIES IN A COLLISIONLESS PLASMA. Brossier, P.; Deschamps, P.; Gravier, R.; Pellat, R.; Renaud, C. (EURATOM-CEN, Fontenay-aux-Roses, France). Phys. Rev. Lett.; 26: 124-7(18 Jan 1971).

Pressure-gradient-driven drift waves were identified in a collisionless ($n_0 = 10^{10}$ cm^{-3}, $T_e = 10$ eV), 5.4-m-long, hydrogen plasma. Measurements show large but finite parallel wavelengths and short transverse wavelengths as predicted by the theory. For these wavelengths, computations give the maximum linear theoretical growth rate. (auth)

14346 STABILITY OF A CYLINDRICAL PLASMA IN THE PRESENCE OF A MONOTONIC FIELD. II. Murthy, S. Narasimha (Indian Inst. of Science, Bangalore). Proc. Indian Acad. Sci., Sect. A; 72: 134-43(Sep 1970).

The stability of an incompressible inviscid, perfectly conducting, cylindrical plasma against azimuthal disturbances, in the presence of a monotonic decreasing magnetic field having a constant pitch, is discussed by using the energy principle. The results obtained by this principle are compared for the m = 1 mode (which is a dangerous mode in which there is a lateral shift of the entire column) with that obtained by normal-mode analysis. It is found that the m = 1 mode is always unstable. Further, an axial line current, external axial field, and the surface tension tend to stabilize m ≠ 1 modes. (auth)

14347 SMALL-AMPLITUDE NONLINEAR THEORY OF POSITIVE COLUMN SPIRAL INSTABILITY. Shiau, Jeng-nan. Rochester, N. Y.; Univ. of Rochester (1970). 108p. University Microfilms Order No. 70-17,909.

Thesis.

An analysis of the nonlinear behavior of the spiral instability of the positive column in a longitudinal magnetic field is presented. The finite amplitude and frequency shift of the single mode that results from raising the magnetic field slightly above the critical value are determined. The slope at the kink of the E–H curve also is obtained. The method is based on a general theory of nonlinear behavior in weakly ionized plasma. The nonlinear results depend on the ion species present in the discharge and agree favorably with experiments. (Disser. Abstr. Int., B)

14348 ION CYCLOTRON INSTABILITIES IN FINITE PLASMAS. Haste, Glenn Roy. Knoxville, Tenn.; Univ. of Tennessee (1969). 126p. University Microfilms Order No. 70-17,821.

Thesis.

The microinstabilities of two different plasma models are considered. The first model, the Burt–Harris model, is an infinitely long annular plasma cylinder. The second model is a short mirror-confined plasma. The Burt–Harris model is analyzed for the case of long axial wavelengths. Using this limit, the radial variation of the perturbed potential is determined, and unstable frequencies are found that are displaced slightly above and below the ion cyclotron harmonics. The stabilizing effect of finite ion and electron temperatures is determined, and the type of instability is determined. It is shown that the instability whose frequency lies below the ion cyclotron harmonics is an absolute instability, and that the instability whose frequency lies above the harmonics is convective. These calculations are compared with experimental

XUM

results from DCX-2. A short mirror plasma is analyzed with the assumption that the form of the perturbed potential is that of a plane wave. Marginally stable conditions are found for which the growth provided by the ions is just balanced by the electron damping. The principal frequencies of the instabilities are found to be displaced from the ion cyclotron harmonics by multiples of the bounce frequency, with the frequencies below the harmonics being more unstable than those above. In addition, instabilities are found whose frequencies lie slightly above the ion cyclotron harmonics, which are the modified negative mass instabilities. Finite temperature effects are found to be stabilizing for these instabilities. These calculations are applied to results from DCX-1.5. (Diss. Abstr. Int., B)

14349 INSTABILITIES IN A HOT ELECTRON PLASMA. Schwartz, Marvin Jack. Berkeley, Calif.; Univ. of California (1969). 139p. University Microfilms Order No. 70-17,650.

Thesis.

Instabilities of two distinct types were studied in a hot electron plasma created by adiabatic compression in a pulsed magnetic mirror field. Early in the compression history of the plasma, bursts of radiation occur, with frequencies below the electron cyclotron frequency and its harmonics, with no apparent loss of plasma. The anisotropy in velocity space of the plasma was determined by comparing the measured axial plasma distribution with theoretical profiles. A bi-Maxwellian distribution can be made to fit the experimental distribution by appropriate choice of the anisotropy parameter. The observed values of plasma density (cold plus hot), temperature, and anisotropy are used to find the unstable modes of the complete electromagnetic dispersion relation for all angles of propagation. The fastest-growing mode early in the compression cycle is an electrostatic mode occurring below the second harmonic; here ω_p/Ω (cold) $\approx$ 1.5, ω_p/Ω (hot) $\approx$ .35. Later in time, ω_p/Ω (cold) $\approx$ .5, ω_p/Ω (hot) $\approx$ .25, and the fastest growing mode is electromagnetic, occurring below the fundamental. These predictions are in agreement with the observed spectrum and polarization measurements. The second instability occurs near peak compression, and is often triggered by the crowbarring of the magnetic field at its peak value. The instability results in radial movement of most of the hot plasma across the magnetic field lines, resulting in increased x-ray emission when the plasma meets the wall of the chamber. Radial probes have verified the radial transport. The occurrence of the instability is dependent upon the base pressure and proximity of the metal source to the plasma. The experimental observations are in agreement with the theory of the interchange mode stabilized by the presence of a cold component. (Diss. Abstr. Int., B)

Thermonuclear Processes

14350 (AD-711003) CONSTRUCTION OF A THETA PINCH FOR THE GENERATION OF SHOCK WAVES IN A NITROGEN PLASMA. Budzik, Dennis Michael (Naval Postgraduate School, Monterey, Calif.). Jun 1970. 35p. NTIS.

Thesis.

A theta-pinch device was constructed for the production of shock waves in a nitrogen plasma. The device consisted of six 7-μF capacitors in parallel, and a one-turn coil through which the capacitors were discharged. The rise time of the current in the coil is 1 μsec, and the stored energy in the capacitors is 13 kJ at 25 kV. The large perturbation of the plasma is expected to produce large-amplitude Alfven waves, which would propagate up the plasma column. (auth) (USGRDR)

14351 (AD-711822) ANOTHER APPROACH TO THE INJECTION OF RELATIVISTIC ELECTRONS INTO AN ASTRON-LIKE DEVICE. Friedman, Moshe (Cornell Univ., Ithaca, N. Y. Lab. of Plasma Studies). Jun 1970. Contract N00014-67-A-0077-0002. 16p. (LPS-47). NTIS.

An approach to the injection phase of Astron-like devices was investigated. A rotating cloud of relativistic electrons was injected into three different magnetic field configurations. Preliminary results are presented. (auth) (USGRDR)

14352 (IPPJ-T-3) DIFFUSION OF MULTIPOLE MAGNETIC FIELDS THROUGH A CONDUCTIVE WALL OF A PLASMA CONTAINER. Kawasaki, Sunao (Nagoya Univ. (Japan). Inst. of Plasma Physics). Nov 1970. 19p. Dep. NTIS (U. S. Sales Only).

Diffusion of multipole magnetic fields (especially quadrupole) into a plasma container through its conductive cylindrical wall of finite thickness is studied with regard to the design of the system of the stabilizing field in BSG experiment. The lower limit of the diffusion time is estimated by solving the Maxwell equation with the special initial and boundary conditions, and evaluating the rate of evolution of the time-dependent solutions. It is found that the rate does not depend on the harmonic number of Fourier component of the initial field distribution. The theory is consistent with the experimental results. (auth) (Japan)

14353 EXPERIMENTAL STUDY OF INTENSE LOW-ENERGY ION BEAMS FOR FUSION RESEARCH. Morgan, Ora Billy Jr. Madison, Wis.; Univ. of Wisconsin (1970). 146p. University Microfilms Order No. 70-19,163.

Thesis.

This research results in the design of a system capable of producing intense H^+ beams in the energy range of 0.1 to 1.0 keV. The primary emphasis is on those problems that are peculiar to these low-energy ion beams. Space-charge extraction and neutralization are the most important of these problems. Successful solutions to both of these problems are discussed and evaluated. Total H^+ beams of 100 to 250 mA are extracted from a 2-cm-diameter plasma source produced by a modified duoplasmatron ion source. The brightness of these charged-particle beams is adequate for a 20 to 50 mA (equivalent) 1-keV H^0 injector for some plasma physics experiments. The understanding and ideas resulting from this research should be applicable in scaling these injectors to even greater ion currents at these low energies. (TSS) (Diss. Abstr. Int., B)

14354 APPLICATION OF SIMILARITY RULES TO CONTROLLED FUSION. Lacina, J. (Inst. of Plasma Physics, Prague). Czech. J. Phys.; 21: 100-3(1971).

Similarity relations are described for controlled fusion research. There are the following: similarity of magnetic traps, similarity of experiments carried out in similar traps, and similar time developments. (M.O.W.)

14355 NEUTRON YIELD OF A FOCUS DISCHARGE IN VARIOUS EXPERIMENTS. Bernard, A.; Coudeville, A.; Watteau, J. P. (Centre d'Etudes de Limeil, Villeneuve-Saint-Georges, France). Phys. Lett.; 33A: 477-8(28 Dec 1970).

The neutron yield of a focus discharge is increased by using higher capacitor bank energy, as long as no breakdown occurs behind the collapsing plasma sheet. (auth)

14356 OPERATION OF A LEVITATED SUPERCONDUCTING RING IN A PLASMA PHYSICS EXPERIMENTAL DEVICE. File, J.; Martin, G. D.; Mills, R. G.; Wakefield, K. E. (Princeton Univ., N. J.). J. Appl. Phys.; 42: 6-9(Jan 1971).

From Applied Superconductivity Conference, Boulder, Colo. See CONF-700618.

An isolated, isochoric Dewar and superconducting ring, operable up to 130,000 ampere turns, was installed in the Princeton Spherator, and plasma physics experiments were performed with the ring levitated and stabilized by means of a system similar to that discussed previously. The evolution of this device has progressed through three stages. Initially, the poloidal field coil was a conventional copper conductor ring within a vacuum jacket supported within the reaction chamber from top and bottom by four thin bars. In its second stage of development, the conventional coil was replaced by a superconducting coil and Dewar, supported by thin wire-like hangars. The present mode eliminates the need for mechanical supports of any sort. (auth)

14357 NUCLEAR CROSS SECTION REQUIREMENTS FOR FUSION REACTORS. Crocker, V. S. (United Kingdom Atomic Energy Authority, Abingdon, Eng.); Blow, S.; Watson, C. J. H. pp 67-91 of Nuclear Data for Reactors. Vol. I. Vienna; International Atomic Energy Agency (1970).

From 2nd International Conference on Nuclear Data for Reactors, Helsinki, Finland. See STI/PUB-259(Vol.1); CONF-700605-(Vol.1).

Nuclear cross-section requirements for the plasma and the surrounding blanket are considered. Both toroidal and open-ended (e.g. mirror) confinement systems are considered. From the permissible plasma pressure it appears that the former are limited to temperatures up to 100 keV (energy equivalent), while for open-ended machines the temperature limit appears to be as high as 1 MeV. Taking into account the various forms of energy loss from the plasma; and economic considerations related to magnetic-field winding costs, a relationship is derived for selecting possible thermonuclear reactions. In general, it excludes reactions with $Z > 10$, and all reaction with cross sections less than a millibarn at energies less than 10 MeV. The number of "interesting" reactions remaining is surprisingly large, and a table of data on reactions for Z up to 3 is given. A literature search has revealed the cross-section data to be poor for many of these reactions. Since the neutronic design of fusion reactors is still at a very early stage, a model blanket design is used to illustrate the importance of nuclear cross sections in various blanket problems. The blanket is designed around a fusion sys-

XUM

tem using the D–T reaction which emits 14.1-MeV neutrons. The accuracy of the nuclear cross sections and their effect on the neutron spectra, tritium breeding, heat generation, radiation damage and radioactivity, are commented on. (auth)

14358 EXPERIMENTAL STUDY OF A TRAVELING-WAVE MAGNETIC-FIELD PLASMA ACCELERATOR. Wilcox, Lowell Enrick. Rochester, N. Y.; Univ. of Rochester (1970). 179p. University Microfilms Order No. 70-17,915.
Thesis.

An experimental study is made of accelerating a plasma with a traveling-wave magnetic field. The accelerating channel is a diverging annulus between two nonconducting coaxial cones, the inner cone converging in the flow direction and the outer one diverging in the flow direction. Helical windings are placed outside the outer cone and inside the inner cone; silicon iron core material, laminated in an axial direction, is placed inside the inner windings and outside the outer windings. The windings are connected to a two-phase power supply so that an essentially radial magnetic field between the two cones moves in an axial direction. Argon introduced between the two cones is ionized by the traveling field and is then accelerated in an axial direction by the field. (TSS) (Diss. Abstr. Int., B)

14359 PRODUCTION AND DIAGNOSTIC MEASUREMENTS OF A PULSED HIGH-DENSITY KILOVOLT PLASMA EMPLOYING A NONCYLINDRICAL Z PINCH. Hilland, Carl Boyd. Columbus, Ohio; Ohio State Univ. (1970). 147p. University Microfilms Order No. 70-19,319.
Thesis.

Plasma focus experiments were conducted using a discharge chamber of the Filippov geometry. In the operation of the device, capacitively stored energy is used to cause the formation and eventual radial implosion of a noncylindrical current sheet between two concentric electrodes, thereby assembling a high-temperature deuterium plasma. The initial collapse and subsequent oscillations of the plasma can be understood in terms of a current-sheet-driven shock wave model which is consistent with the theory of the linear pinch. According to the interpretation assigned to data taken in these experiments, initial plasma heating is performed by the incident shock wave, followed by preferential heating of deuterium ions behind the axis-reflected shock wave. This reflected shock wave is retarded by electrodynamic forces acting radially inward and a second contraction phase occurs in which heating of both electrons and ions proceeds adiabatically with Maxwellian energy distributions being easily obtained during the applicable confinement times, although equilibrium between ions and electrons was not attained on these time scales. During the final compression, contraction of the plasma to a radius of approximately 1 mm with an implosion velocity on the order of 20 cm/μsec was observed by streak photography. Ion temperatures of 2.4 keV, electron temperatures of 1 keV, and particle densities in excess of 10^{19} cm^{-3} were attained at the time of the pinch. Neutron yields of 3×10^9 resulted from thermonuclear reactions among deuterium ions and a copious supply of x rays was observed to be emitted from the anode and anode vapors. These x rays resulted initially from anode bombardment by high-energy electrons with copper line radiation accounting for the softer portion of the spectrum occurring late in time. (Diss. Abstr. Int., B)

Wave Phenomena

Refer also to abstracts 14293, 14311, and 14343.

14360 (AD–711649) SURFACE AND BULK WAVES ON AXIALLY MAGNETIZED PLASMA COLUMNS. Research Report, September 1967–August 1968. Bevc, Vladislav (Aerospace Corp., El Segundo, Calif.). 1 Sep 1970. Contract F04701-70-C-0059. 50p. (TR–59(9220-2)-1; SAMSO-TR–70-309). NTIS.

The dispersion relation and field solutions of slow electromagnetic waves propagating along a cold, collisionless, cylindrical plasma in an axial magnetic field of finite magnitude are studied numerically. Field distribution and gradual metamorphosis of surface waves into bulk waves along the dispersion characteristics are investigated. It is shown that both surface waves and bulk waves belong to the same set of plasma modes. Criteria concerning conditions under which surface waves occur are extended to include transitional situations. Power-flow density along the plasma may, in certain cases, be in opposite directions inside and outside of the plasma both for forward surface waves as well as for backward cyclotron waves implying transfer of energy between propagation media. (auth) (USGRDR)

14361 INTERACTION OF AN OBLIQUELY INCIDENT p-POLARIZED PLANE ELECTROMAGNETIC WAVE WITH A HOT PLASMA HALF-SPACE. Bolduc, P. E. (Sandia Labs., Albuquerque, N. Mex.); Klevans, E. H. Phys. Fluids; 14: 378-86(Feb 1971).

Reflection and penetration of a p-polarized electromagnetic wave obliquely incident on a plasma half-space is investigated. The perturbed plasma is treated by use of the linearized relativistic Vlasov equation. Electrons are assumed to be specularly reflected from the boundary. The Laplace transform technique, recently employed by Ozizmir, is used to obtain the field solutions in the plasma. These field solutions consist of a transverse and a longitudinal part. Power reflection and transmission coefficients are also obtained. (auth)

14362 RESONANT INTERACTIONS BETWEEN PARTICLES AND NORMAL MODES IN A CYLINDRICAL PLASMA. Kaufman, Allan N. (Univ. of California, Berkeley). Phys. Fluids; 14: 387-97(Feb 1971).

A plasma configuration with cylindrical symmetry containing axial and azimuthal magnetic fields and a radial electric field, with arbitrary radial variations, is studied. The particle motion is parameterized by three exact action invariants: radial action, canonical angular momentum, and canonical axial momentum; in the limit of small gyroradius they are equivalent to magnetic moment, radial guiding-center position, and parallel velocity. The perturbed Vlasov–Maxwell equations lead to a set of normal modes, which can interact resonantly with the particles. The quantum rate equations for this interaction, together with the laws for conservation of energy, angular momentum, and axial momentum, lead (in the classical limit) to a Fokker–Planck equation in action space for the particles and to an equation of evolution for mode energy. These coupled kinetic equations satisfy an H theorem, which implies monotonic approach to a canonical distribution: a rigid-rotor distribution for particles and a generalized Rayleigh–Jeans distribution for the modes. This asymptotic state may, however, be unconfined. The quantum transition probability is deduced from a classical calculation of emissivity. Explicit expressions are obtained for the mode growth rate and for the particle diffusion tensor. Finally, the Vlasov conductivity kernel is deduced from the growth rates, by the use of the Kramers–Kronig relations. (auth)

14363 EXPERIMENTAL CHECK OF THE APPLICABILITY OF SINGLE BORN SCATTERING THEORY UP TO CRITICAL ELECTRON DENSITY FLUCTUATIONS. Richard, C.; Ghosh, A. K.; Johnston, T. W.; Shkarofsky, I. P. (RCA Ltd., Montreal). Phys. Fluids; 14: 398-409(Feb 1971).

The results of a theory–experiment comparison of the absolute electromagnetic wave backscatter for a neutral-gas-dominated turbulent argon-arc plasma jet are reported. The study is carried out at 16 GHz for various aspect angles and covers a range of rms electron density fluctuations extending beyond critical. The backscatter power is measured using a homodyne detection system. The calculation, based on the unmodified Born scattering model, consists of a volume weighting of the turbulent plasma properties, $\langle \delta n_e^2 \rangle$ and S(k), by the antenna illumination. The determination of S(k), the three-dimensional spectral density function, makes use of the measured space–time correlation function and frequency spectrum of electron density fluctuations, Taylor hypothesis, and a three-dimensional MacDonald function analysis. The Born theory is found to describe the backscatter within about 3 dB right up to critical. This result is thought to be due in part to attenuation of the coherent antenna field by large density fluctuations being roughly compensated for, both by decreasing wave number and by higher-order multiple scattering effects. (auth)

14364 APPLICATION OF A SIMPLE MODEL FOR CALCULATING SCATTER. Graf, K. A.; Guthart, H. (Stanford Research Inst. Menlo Park, Calif.). Phys. Fluids; 14: 410-13 (Feb 1971).

A simple model for calculating scatter from a turbulent medium is applied to a computer experiment with good results. The proposed calculation is a modification of a first-order Born calculation that accounts for attenuation due to absorption and scatter by energy conservation. Such a nonrigorous approach requires experiments to specify the scatter attenuation in a phenomenological way. The exact computer calculations by Hochstim and Martens constitute such an experiment. (auth)

14365 DISPERSION AND STABILITY OF COLLISIONAL DRIFT WAVES IN TWO-ION-SPECIES PLASMAS. Verheest, Frank (Rijksuniversiteit, Ghent). Phys. Fluids; 14: 424-7 (Feb 1971).

The Coppi–Perkins theory of collisional drift waves in low-β plasmas is extended to plasmas containing ions of two different types. Recent experiments call for such an extension. Before discussing the general results, the specialization to the usual plasma shows the destabilizing effect of a high ionic charge and of an electron temperature exceeding the ion temperature. As an application of the obtained criterion of marginal stability, the average ion mass is computed and compared to the intuitive linear formula, based only upon concentrations. Under the conditions present, almost no difference is detected, but for future experiments with higher temperatures and higher mass ratios, the correct formula is shown to give less-stable results than the intuitive one at the same relative concentration. This is also true for lower densities and shorter wavelengths. The discrepancies can become quite important. (auth)

14366 THREE WAVE MODE COUPLING THEORY OF NONRESONANTLY UNSTABLE WAVES. Ott, Edward (Cornell Univ., Ithaca, N. Y.). Phys. Fluids; 14: 442-4(Feb 1971).

The usual nonlinear three-wave-mode coupling theory is extended to include nonresonantly unstable waves near the marginal stability limit. Both coherent and incoherent (turbulent) coupling are investigated. (auth)

14367 NONLINEAR INSTABILITY OF MODULATED WAVES IN A MAGNETOPLASMA. Tang, Ting-wei; Sivasubramanian, A. (Univ. of Massachusetts, Amherst). Phys. Fluids; 14: 444-6 (Feb 1971).

The nonlinear instability of small but finite-amplitude modulated waves is investigated for R-, L-, O- and X-wave propagations in an electron magnetoplasma. Relativistic effects are included in the treatment. (auth)

14368 RESONANCE PHENOMENA IN AN ALKALI PLASMA LOCATED IN A VARIABLE ELECTRIC FIELD. Demirkhanov, R. A.; Khorasanov, G. L.; Sidorova, I. K. Zh. Eksp. Teor. Fiz.; 59: 1873-7(Dec 1970). (In Russian).

The behavior of a highly ionized thermal-cesium plasma on passage of a longitudinal high-frequency current through it is investigated. The high-frequency power is efficiently absorbed by the plasma in the frequency range $\Omega_0 \sim \omega_{pe}k_z/k$. The plasma heating observed is interpreted as a manifestation of parametric resonance in the magnetized plasma. (auth)

14369 SELF-SIMILAR WAVES IN COLD PLASMA WITH A MAGNETIC FIELD. Gintsburg, M. A. (Inst. of Terrestrial Magnetism, Ionosphere, and Radio-Wave Propagation, Moscow). Dokl. Akad. Nauk SSSR; 193: 1276-9(21 Aug 1970). (In Russian).

Nonstationary waves in a plasma with a magnetic field were examined. At a t = 0, a cylindrical pinch or a thin plasma layer that decreased with the distance from the axis, and with the electric and magnetic fields, or a spherical plasma cloud were considered, solving the motion of the plasma at t > 0. The Maxwellian and the two-liquid hydrodynamic equations were reduced to ordinary differential equations. Computer-based solution of these equations indicated that there are two boundary cases for the self-similar solution. A series of equations was obtained, describing the spreading of the system. The thermal motion was taken into account by means of a self-similar kinetic equation. Use of the Maxwell equation in its integral form allows to determine that in case of cylindrical symmetry there are charges at the axis. In the two-dimensional flow of cold plasma, the charges are magnetic; in the nonstationary flow of a plasma with hot electrons, they are electric. These prevent the outflow of electrons. (TTT)

14370 EXCITATION OF LANGMUIR OSCILLATIONS IN A PLASMA BY THE FIELD OF A TRANSVERSE WAVE. Andreev, N. E. (Lebedev Inst. of Physics, Moscow). Zh. Eksp. Teor. Fiz.; 59: 2105-9(Dec 1970). (In Russian).

Conditions for excitation of proper electron potential and nonpotential plasma oscillations by the field of an external monochromatic pumping wave whose frequency exceeds the doubled plasma frequency are investigated. It is shown that for not-very-small electron temperatures, instability with respect to buildup of such oscillations is of decisive importance since the instability development time is much smaller than the perturbation rise time in induced Mandelstam–Brillouin scattering or aperiodic instability. (auth)

14371 INFLUENCE OF THE TRANSFORMATION OF WAVES ON THE THRESHOLD CURRENTS OF THE BEAM INSTABILITY. Kopecky, V. (Inst. of Plasma Physics, Prague). Czech. J. Phys.; 21: 34-42(1971).

In a hot anisotropic plasma with an inhomogeneity across the magnetic field, eigenmodes are a superposition of long waves of cold plasma and the short-wave Bernstein modes. As a consequence of the fact that the Bernstein modes with non-zero wave numbers are damped more intensively than the waves of cold plasma, the threshold currents of the beam instability increase correspondingly compared with the case of homogeneous plasma. For frequencies between the first and second harmonics of the electron cyclotron frequency, the threshold current is from v_0/v_T to $(v_0/v_T)^3$ times greater, where v_0 is the beam velocity and v_T is the thermal velocity of plasma electrons. (auth)

14372 SPACE-CHARGE WAVES OF BOUNDED PLASMAS. Poularikas, A. D. (Univ. of Rhode Island, Kingston). Electron. Lett.; 6: 673-4(Oct 1970).

The approximate phase characteristics of the space-charge waves in bounded plasmas are developed, assuming the charge density to be statistically distributed. The influence of the correlation function of the charge distribution on the phase characteristics is also found. (auth) (UK)

14373 ANOMALOUS ABSORPTION OF ELECTROMAGNETIC WAVES BY A PLASMA. Pustovalov, V. V.; Silin, V. P. (Lebedev Inst. of Physics, Moscow). Zh. Eksp. Teor. Fiz.; 59: 2215-27(Dec 1970). (In Russian).

The spectral energy density of ion–sound oscillations in a nonisothermal plasma located in the field of an electromagnetic wave is found. The high-frequency conductivity of a weakly turbulent plasma with developed ion–sound noise is calculated for an electromagnetic wave frequency close to the plasma frequency. It is shown that the electromagnetic wave absorption coefficient associated with such conductivity is large compared with ordinary absorption determined by collisions between electrons and ions. (auth)

14374 TRAPPING OF ELECTROMAGNETIC WAVES BY NONLINEAR RESONANT INTERACTIONS WITH ION SOUND WAVES. Yeh, K. C.; Liu, C. H. (Univ. of Illinois, Urbana). Planet. Space Sci.; 18: 1813-20(Dec 1970).

Resonant wave–wave interaction among one ion-sound wave and two electromagnetic waves in an isotropic plasma is studied. The emphasis is on the possibility of trapping the electromagnetic wave. Equations for the three-wave system are derived. One particularly interesting case is that for which the frequency of ion-sound wave is much less than the frequency of electromagnetic waves. For this case it is shown that energy exchange takes place only between the two high frequency waves. The ion-sound wave does not participate in the energy exchange process but acts as a kind of catalyst for the interaction. Simple solutions are obtained. It is found that the electromagnetic energy is trapped within a certain spatial region. The trapping width is found to depend, among other parameters, on the magnitude of ion-sound wave perturbation. Possible application of the theory to topside ionospheric observations of field-aligned propagation is discussed. (auth) (UK)

14375 CHARACTERISTIC CURVE OF THE COLLECTIVE SCATTERING OF ELECTROMAGNETIC RADIATION IN A PLASMA. Petrov, G. D.; Yurchuk, E. F. Opt. Spectrosc. (USSR) (Engl. Transl.); 28: 647-8(Jun 1970).
Translated from Opt. Spektrosk.; 28: 1204-7(Jun 1970).

A brief mathematical analysis is given for electromagnetic scattering on plasma with varying electron densities. Several typical curves for the scattering are described. (M.O.W.)

14376 THEORY OF PARAMETRIC RESONANCE OF PLASMA IN A STRONG HF ELECTRIC FIELD. Andreev, N. E.; Kirii, A. Yu.; Silin, V. P. (Lebedev Inst. of Physics, Moscow). Izv. Vyssh. Ucheb. Zaved., Radiofiz.; 13: 1321-4(1970). (In Russian).

The values of the external field frequency and the intensity at which the instability increment takes the largest possible value are found, when taking into account the thermal-particle motion in the theory of parametric resonance for a plasma in a strong hf field. (auth)

14377 POSSIBILITY OF PARAMETRIC RESONANCE IN AN ELECTRON PLASMA. Tsintsadze, N. L. (Inst. of Physics, Tbilisi, USSR). Zh. Eksp. Teor. Fiz.; 59: 1251-3(Oct 1970). (In Russian).

An electron plasma located in a strong high-frequency electric field is investigated. It is demonstrated that oscillations of the electron mass in an external high-frequency field lead to parametric buildup of potential as well as nonpotential high-frequency oscillations. (auth)

14378 EXCITATION OF ION OSCILLATIONS BY BEAM–PLASMA INTERACTION. Vermeer, Abraham. Delft, Netherlands; Technological Univ. of Delft (1968).
Thesis.

An investigation into ion vibrations that propagate themselves in a beam–plasma system is described. After considering several ion oscillations, such as ion sound waves and waves in the neighborhood of the ion cyclotron and ion plasma frequencies, the research then concentrates on the observed ion oscillations, the frequency of which is just above the ion plasma frequency ω_{pi}. (TSS) (Diss. Abstr. Int., B)

14379 PROPAGATION OF A PLANE WAVE IN A PLASMA SUBJECTED TO A MAGNETIC FIELD. Agostinelli, Cataldo. Atti Accad. Naz. Lincei, Rend., Cl. Sci. Fis., Mat. Natur.; 48: 334-42(Mar 1970). (In Italian).

Plane-wave propagation is considered in an indefinite plasma, which initially is in a homogenous condition and at rest, subjected to a uniform magnetic field. The effect of collisions between ions and electrons is neglected, and the reaction of the electrons is equivalent to a pressure that depends on the variation of the electron density. (auth)

14380 ACOUSTIC OSCILLATIONS IN PARTIALLY IONIZED ARGON COLUMNS. O'Keiff, Gustav Mason. Houston, Tex.; Rice Univ. (1970). 131p. University Microfilms Order No. 70-23,561.

Thesis.

Standing acoustic waves were produced in an inductively heated argon plasma column. The frequency and the wavelength of the standing acoustic waves were measured and used to compute the velocity of sound of the plasma. The temperature of the plasma column was calculated using the measured velocity of sound. Power necessary to produce plasma at different pressures was measured. A simultaneous numerical solution of the energy equation and the magnetic field equations was obtained as a theoretical check for the experimentally measured parameters. For the plasmas studied the measured power input was approximately 50% greater than that predicted theoretically for the same center line temperature. The trend of increasing temperature of the plasma for a constant power input and increasing pressure obtained experimentally agrees very closely with the predicted trend for the same conditions. (Diss. Abstr. Int., B)

14381 PULSE STIMULATED EMISSION AND ECHOES AT UPPER HYBRID RESONANCE. Henderson, David Michael. New Haven; Yale Univ. (1970). 192p. University Microfilms Order No. 70-25,094.

Thesis.

An experimental study of the interaction at upper hybrid resonance of high-frequency radiation with a low-temperature, inhomogeneous plasma column is presented. This interaction is investigated through three types of measurements: scattering, single-pulse stimulated emission, and two-pulse stimulated-emission echoes. The linear processes of scattering and pulse-stimulated emission are studied. Results of these measurements are compared with the zero-temperature, electrostatic theory of resonant absorption by inhomogeneous plasma. The scattering measurements at upper hybrid resonance compare favorably with the theoretical scattering by a plasma cylinder computed by Baldwin and Ignat. The pulse-stimulated emission measurements leading to maximum upper hybrid radiation confirm the fundamental phase-mixing feature of the theory. Also presented is a related pulse excitation experiment with a nonmagnetized plasma column. The nonlinear process of two pulse-stimulated emission echo formation is investigated. Based on an approximate collision model of a Ramsauer gas, a theory is developed for upper hybrid resonance echoes in a low-density plasma, arising from velocity-dependent electron–neutral collisions. The experimental measurements are compared both with this theory and with the theory of Blum and Gould for echoes from nonlinear upper hybrid oscillations. Under these experimental conditions, the velocity-dependent collision process dominates. (Diss. Abstr. Int., B)

14382 UPPER HYBRID RESONANCE SCATTERING BY MAGNETOPLASMA COLUMNS. Greenwald, Raymond Albert. Hanover, N. H.; Dartmouth Coll. (1970). 80p. University Microfilms Order No. 70-25,530.

Thesis.

The upper hybrid resonance scattering spectrum of small-diameter plasma columns is examined. The general theory of scattering by uniform dielectric columns is extended to treat a nonuniform, anisotropic magnetoplasma. The wave equation is solved inside the plasma column, and the internal wave fields are matched to the external wave fields at the plasma/vacuum boundary. The external field is composed of an incident plane wave and an outgoing scattered wave. Scattering spectra are calculated in the vicinity of upper hybrid resonance for various density profiles. In general, one assumes $\omega_B^2 \gg \omega_p^2 \gg \nu^2$ where ω_B, ω_p, and ν are the cyclotron, plasma, and collision frequencies, respectively. The theory is also extended to study the effect of the glass tube containing the plasma on the scattered spectrum. Experimental observations were made of scattering spectra. The scattering experiments were performed on a thermally ionized potassium plasma column, 50 cm long and contained in a 31 mm I.D. Pyrex tube. The plasma and Pyrex tube shunt a section of L-band waveguide. Under typical operating conditions, the incident wave frequency is 1.5 GHz with 45 mW of microwave power incident on the plasma column. The entire system is in a Helmholtz coil field uniform to 0.03% over the section of plasma inside the waveguide. Finally, several Langmuir probes are immersed in the plasma to provide density profile information. Aside from providing spectral and density data, the experiment was used to test some of the conclusions of the theoretical model. Using the theoretical model, electromagnetic and quasi-static solutions to the scattering problem are compared. (TSS) (Diss. Abstr. Int., B)

14383 LOW-FREQUENCY ELECTROSTATIC WAVES IN A WEAKLY IONIZED PLASMA UNDER A WEAK MAGNETIC FIELD. Sato, Noriyoshi; Sugai, Hideo (Tohoku Univ., Sendai). J. Phys. Soc. Jap.; 30: 537-48(Feb 1971).

Propagating waves excited by a small coil surrounding a plasma column produced by a dc discharge at a pressure of a few μHg under a weak axial magnetic field were investigated. Measurements were made mainly of the (0, 2) mode excited on the cathode side of the exciting coil in the frequency range of 17 to 60 kc. The waves are observed to have a forward-wave dispersion for lower frequencies, but a backward-wave dispersion for higher frequencies in this range. Their phase velocities are directed toward the exciter. These waves are theoretically predicted to propagate in a weakly ionized, current-carrying, uniform plasma under a weak magnetic field. The experimental data are in reasonable agreement with the theoretical results. The (0, 1) and (1, 1) modes excited on the cathode and anode sides are also studied experimentally in some detail. (auth)

14384 GROWTH RATES OF THE ELECTROSTATIC WAVES IN AN ANISOTROPIC MEDIUM WITH OR WITHOUT A COLD PLASMA. Jacquinot, J.; Leloup, C. (EURATOM–CEN, Fontenay-aux-Roses, France). J. Phys. (Paris); 31: 881-91(Oct 1970). (In French).

The growth rates of electrostatic waves are calculated in an infinite homogeneous plasma containing a hot anisotropic electron population represented by a maxwellian distribution function with two temperatures and a cold plasma. The analysis is restricted to frequencies below the electron cyclotron frequency. A simplified analytical treatment and an exact numerical calculation are used to study the effect of various parameters: propagation angle, pressure anisotropy, and hot and cold plasma densities. (auth) (France)

14385 THERMAL CONDUCTIVITY AND LOW-FREQUENCY WAVES IN COLLISIONAL PLASMAS. Tsai, Shih-tung. Princeton, N. J.; Princeton Univ. (1970). 60p. University Microfilms Order No. 70-19,806.

Thesis.

Temperature perturbations and heat flow terms are retained in the two fluid equations used to derive a localized dispersion relation for low-frequency electrostatic waves in a nonuniform collision dominated slab plasma immersed in a magnetic field. The Nyquist analysis shows two unstable waves: the collisional drift instability and a new overstability of the entropy wave. The collisional drift wave is most easily excited for parallel wavenumbers given by $k_{||} = 0.15\,\alpha^2(m_e/m_i)^{1/2}$ where $\alpha \equiv |\nabla \ln n|$ (all quantities in cgs units). The stability condition at this $k_{||}$ is $B/k_\perp < 104(m_i n/\kappa T_e|\alpha|)^{1/2}$ gauss-cm. These are in markedly improved agreement with the experimental data, compared with the rigorous isothermal theory. Heat transport reduces the maximum growth rate, especially at high density. A small equilibrium temperature gradient tends to stabilize the drift waves in the large magnetic field region. The entropy-wave instability propagates along the ion drift direction and is found in the parameter range $0.4 \leqq \bar{d} \leqq 2$ with $\bar{d} \equiv 0.15[k_\perp^2\,\kappa T_i/\Omega_i^2 m_i]^2\,\nu_{ii}\nu_{ei}m_e/k_{||}\,\kappa T_e$. The maximum growth rate of entropy wave is given roughly by $k_{||}(\kappa T_i/m_i)^{1/2}\,(k_\perp^2\,\kappa T_e/m_i\Omega_i^2)(m_i/m_e)^{1/2}$, and occurs around $\bar{d} \simeq 0.8$. The ion thermal conductivity and temperature gradient are not significant for both instabilities. The normal mode structure along the magnetic field imposed by the end plates in Q machines is investigated. Particular emphasis is placed on how a dc electron current along the magnetic field can change this structure. The dispersion relation and the sheath boundary conditions resulting from both the particle and the heat flows are obtained. The case of electron flow velocity comparable to the ion-acoustic wave velocity is studied in detail. The dispersion relation indicates that the wave frequency and the growth rate change only very little for devices with end plates. The normal mode consists of two oppositely directed running drift waves, and two small-amplitude oppositely directed running entropy waves. The drift waves grow spatially in the direction of electron flow and the backward directed wave has a larger amplitude. Both drift waves have an axial phase variation, which depends on the electron current. (Diss. Abstr. Int., B)

14386 THE INTERACTION OF AN OBLIQUELY INCIDENT P-POLARIZED PLANE ELECTROMAGNETIC WAVE WITH A HOT PLASMA HALF-SPACE AND PLASMA SLAB. Bolduc, Paul Eugene. University Park, Pa.; Pennsylvania State Univ. (1969). 149p. University Microfilms Order No. 70-19,389.
Thesis.

A relativistic kinetic theory description of the interaction of a plane p-polarized electromagnetic wave obliquely incident on a hot plasma half-space and plasma slab is developed. The Laplace transform technique, together with the radiation condition and the condition of specular reflection of the electrons at the interface, is used to obtain unique linearized solutions for the fields and the particle distribution in a plasma half space. The above procedure is modified to treat the case of the plasma slab. A proof of self-consistency is presented in the treatment of both the slab and the half-space problems. The elementary nonequilibrium thermodynamics of the interaction is discussed in the case of the plasma half-space. Power reflection and transmission coefficients are obtained for both problems. The above theory is then applied to several problems in the limit of large $\beta = (m_0c^2/KT)$. The critical angle of incidence is obtained and the depths of penetration are computed for the half-space. The equivalent Fourier series representation is presented for the slab case with no limitations placed on β. A cursory study of the geometrical resonances in the large β limit is also presented. (Diss. Abstr. Int., B)

14387 CYCLOTRON ECHOES IN Cs VAPOR. Shaner, John Wesley. Berkeley, Calif.; Univ. of California (1969). 102p. University Microfilms Order No. 70-17,652.
Thesis.

Cyclotron echoes were studied in a weakly ionized cesium plasma in a magnetic field. The behavior of the multiple echoes following two resonant microwave pulses (two-pulse echoes) and those following three resonant microwave pulses (three-pulse echoes) are shown for various pulse spacings and neutral Cs densities. These results are compared with various theoretical models. On the basis of this comparison, the velocity dependence of the electron–neutral collision frequency is chosen as the mechanism for two-pulse echo generation. Several mechanisms are invoked to explain the three-pulse echoes, including scattering without diffusion, and diffusion across flux lines. A detailed comparison is made between the results from these models and the experimental results. (Diss. Abstr. Int., B)

14388 INTERACTION OF QUASI-TRANSVERSE AND QUASI-LONGITUDINAL WAVES IN AN INHOMOGENEOUS VLASOV PLASMA. Hedrick, Clyde Lewis. Los Angeles; Univ. of California (1970). 186p. University Microfilms Order No. 70-19,853.
Thesis.

The interaction of quasi-longitudinal and quasi-transverse modes in an inhomogeneous Vlasov plasma for frequencies between the electron cyclotron frequency and the maximum value of the upper-hybrid frequency is considered. Using a formalism which parallels that used for a homogeneous plasma, the Vlasov equation and Maxwell's equations are solved for propagation perpendicular to the dc magnetic field and obtain a set of coupled differential equations for the components of the electric field. These equations are truncated so that they are correct to order $k^2\rho_c^2$ and $k\kappa\rho_c$ where k indicates $-i(d/dx)$ operating on the electric field, $\kappa = (1/n_0)(dn_0/dx)$, n_0 is the density and ρ_c is the gyroradius. Fourth-order wave equations for the longitudinal component of the electric field E_x, as well as for the transverse component E_y, are solved for a linear density profile and connection formulas are derived. Comparison of the solutions for E_x and those for E_y provides considerable insight into the coupling that occurs near points where the frequency equals the local upper-hybrid frequency. Outside these coupling regions it is shown that the fourth-order wave equation decouples into two second-order systems: one for the quasi-longitudinal waves and one for the quasi-transverse waves. Using an idealized density profile for a bounded plasma, analytic expressions are obtained for the transmission and reflection coefficients. These expressions depend strongly on the number of "wavelengths" of the quasi-longitudinal modes between the points where the upper hybrid condition is satisfied, as well as the number of "wavelengths" of the quasi-transverse modes between these same points. In contrast to previous treatments, all approximations are made in a consistent and systematic fashion and the results apply to a much wider frequency range. (Diss. Abstr. Int., B)

14389 STEEPENING OF ION–ACOUSTIC WAVES AND FORMATION OF COLLISIONLESS ELECTROSTATIC SHOCKS. Taylor, Robert John. Los Angeles; Univ. of California (1970). 94p. University Microfilms Order No. 70-19,904.
Thesis.

Large-amplitude ($e\phi/\kappa T < 0.3$) ion–acoustic waves were studied experimentally in a nonmagnetized plasma with electron-to-ion temperature ratios in the range from 5 to 15 ($5 < T_e/T_i < 15$). The waves were excited in a target plasma by low-velocity ions injected from a driver plasma through a negatively biased fine mesh grid interface which blocks the flow of the electrons in both directions. Electrons in the target plasma neutralize the incoming ions. Due to the electron pressure, the neutralization is not quite complete and the ion flow gives rise to an ion–acoustic wave which, for small amplitudes, propagates approximately at the ion sound velocity, $(\kappa T_e/M_i)^{1/2}$. When a sinusoidal or a ramp excitation is used, classical overtaking (steepening) can be observed as given by the usual Riemann invariants. A comparison between experimental and theoretical wave profiles is made. Steepening is observed to continue until arrested by short-scale dispersive effects, resulting in a collisionless electrostatic shock, a few Debye lengths in thickness. In the transition region oscillations develop, forming a wave train. The damping length of the wave train depends on the temperature ratio but is always much less than can be accounted for by collisional dissipation. The shock Mach number and the wave number of the oscillations depend on the shock amplitude in accordance with predictions based on the results of Moiseev and Sagdeev, (1) who assumed cold ions and isothermal electrons, and constructed a simple model for a collisionless electrostatic shock. It is shown that their results qualitatively hold even when the ion temperature is finite. Depending on its amplitude, the shock also interacts with ions in the tail of the ion distribution and accelerates those ions that are going slightly slower than the wave, giving rise to a two-humped distribution ahead of the shock. Measurements of the resulting ion stream density agree with values computed based on a Maxwellian ion distribution using temperatures that are measured by an electrostatic ion energy analyzer. In plasmas with higher ion temperatures, the two-humped distribution is observed to be unstable mostly for frequencies about the ion plasma frequency. The electrons are found to obey the Boltzmann law for all wave potentials. This is related to the nature of the plasma source used. (Diss. Abstr. Int., B)

14390 ION–ION HYBRID RESONANCE. Babu, Ram. Austin, Tex.; Univ. of Texas (1970). 205p. University Microfilms Order No. 70-18,198.
Thesis.

The ion–ion hybrid resonance is investigated by choosing different theoretical models of plasma. The investigation is carried out for a partially ionized plasma with a view of analyzing the low-density laboratory plasma. It is known that the ion–ion hybrid resonance has been thought important for heating of ions because of the relatively predominant motion of the positive ions at this resonance. This is in contrast with the other well-known lower hybrid resonance where both ions and electrons move together. The cold collisionless plasma is reinvestigated for both perpendicular and slightly off the perpendicular directions. The effects of different ion concentrations of two ions of different charge to mass ratio is studied. Various density plasmas are studied next. The effect of the off-perpendicular propagation is to shift the hybrid resonances to the ion-cyclotron values of smaller magnitude as compared to the hybrid frequency itself. The accessibility condition is also investigated. Effects of pressure and the pressure with collisions are included from the kinetic equation point of view. For low pressures, as expected, the pressure effects do not alter the cold collisionless plasma model. The effects of collisions in the presence of pressure are included in an approximate way. The power transfer calculations are carried out to see the collisionless heating effects. The cyclotron damping is not important at the ion–ion hybrid resonance since each ion sees a frequency far from its cyclotron frequency. For a bounded plasma with azimuthal perturbations in the presence of temperature, the boundary conditions select a set of eigenvalues for the propagation vector and various resonances result. This result was investigated for a two-ion plasma. The resonances occur on either side of the lighter ion cyclotron field value. Similar results were reported earlier from the experimental investigation, and an interpretation based on these calculations is suggested. (TSS) (Diss. Abstr. Int., B)

Shielding

Refer also to abstracts 13209, 13964, 14486, 14865, and 14986.

14391 (AD–710963) NEUTRON STREAMING THROUGH TWO-LEGGED CONCRETE DUCTS WITH BAFFLES. Final Report. Donat, Klaus (Army Engineer Waterways Experiment Station, Vicksburg, Miss.). Jun 1970. 31p. NTIS.

The effectiveness of baffles in concrete ducts in the attenuation of nuclear radiation was determined. Five baffle configurations were tested in a two-legged concrete duct. The neutron source used was the Fast Burst Reactor at the Nuclear Effects Branch of the White Sands Missile Range. Neutron spectra at the entrance to and within the duct were measured with foil threshold detectors. (auth) (USGRDR)

14392 (AD–711005) ENERGY LOSS OF HIGH-ENERGY ELECTRONS IN TIN, LEAD, AND GADOLINIUM. Mosbrooker, Michael Lee; Sandquist, David Lee (Naval Postgraduate School, Monterey, Calif.). Jun 1970. 82p. NTIS.
Thesis.

The LINAC at the Naval Postgraduate School, Monterey, was used to accelerate electrons to energies ranging from 52 to 92 MeV in order to study the energy distributions of high-energy electrons before and after passing through layers of tin, gadolinium, and lead. The thickness of these materials ranged from 0.8 to 5.9 g/cm^2. The most probable energy losses agreed with the theory of Blunck and Westphal for all materials used, while distribution half-widths agreed only for absorbers of thickness less than 3.0 g/cm^2. The thickness at which theory and experiment began to exhibit a noticeable discrepancy was found to be dependent on the atomic number of the material. Where comparison was possible, results of this experiment generally agreed with the findings of similar works concluded previously. (auth) (USGRDR)

14393 (ANL–7689) ON THE MULTIPLE SCATTERING OF GAMMA RADIATION. Brockwell, P. J.; Greenspan, H. (Argonne National Lab., Ill.). Jun 1970. Contract W-31-109-eng-38. 31p. Dep. NTIS.

A method has been devised to calculate the joint and marginal distribution of the emergent wavelength λ and angle of emergence θ, given a quantum of gamma radiation incident on the left face of the slab $\{x: 0 \le x \le a\}$ with wavelength λ_0 and angle of incidence θ_0. The method has been applied in this instance to scattering cross sections $\sigma_\lambda(\theta)$ as given by the Klein–Nishina formula, but can be used with any other specified scattering law. Results obtained compare well with Monte Carlo calculations for marginal distributions, but the developed procedure yields more information regarding joint distributions for the same effort. (auth)

14394 (CEA-N–1382) MEASUREMENT OF THE NEUTRON ALBEDO OF ORDINARY CONCRETE. Brisbois, Jacques; Costa, Laurent; Lott, Michel (Commissariat a l'Energie Atomique, Fontenay-aux-Roses (France). Centre d'Etudes Nucleaires). Dec 1970. 27p. (In French). Dep. NTIS (U. S. Sales Only).

Measurements were made on the albedo of concrete and concrete covered with an iron shell, as a function of different neutron energy groups. The measurements were made inside a hollow concrete sphere; a neutron beam from the TRITON pile supplies the input flux. The experimental results and their interpretation using a monoenergetic calculation formalism, and for isotropic collision scattering, are given. (France)

14395 (CTC-INF–1017) RADIATION SHIELDING INFORMATION CENTER PROGRAM SETUP INSTRUCTIONS MANUAL. Jones, J. G.; Green, R. O. (Union Carbide Corp., Oak Ridge, Tenn. Computing Technology Center). 15 Dec 1970. Contract W-7405-eng-26. 108p. Dep. NTIS.

The following information is included: document update and SDI program, SDI edit program, document edit program, customer update program, customer search program, authority file creation program, and MT/ST conversion program. (M.H.R.)

14396 (N–70–37470) REVIEW AND UPDATING OF INFORMATION ON TRANSMISSION AND REFLECTION OF ELECTRONS BY ALUMINUM SHIELDS. (National Bureau of Standards, Washington, D. C.). 4 Aug 1970. 53p. (NASA-CR–112838). NTIS.

The available information regarding the transmission and reflection of high-energy electrons by aluminum shields is reviewed. The incident electron energies considered lie between 0.5 and 10.0 MeV, covering the region of interest for shielding against electrons in natural and artificial radiation belts. Emphasis is placed on summary parameters such as number and energy transmission coefficients, reflection coefficients, and practical ranges. Extensive new data calculated with the Monte Carlo computer program ETRAN 16 are tabulated. Numerous comparisons are also made with all pertinent experiments in order to review the experimental situation and to verify the validity of the method of calculation. (auth) (STAR)

14397 MONTE CARLO CALCULATION OF ELECTRON SLOWING-DOWN SPECTRA AT HIGH ENERGIES. Sugiyama, Haruo (Electrotechnical Lab., Tokyo). Denki Shikensho Iho; 34: 572-6(1970).

Slowing-down spectra for water, aluminum, and copper were calculated for initial electron energy E_0 = 20 and 30 mc^2. The results are in fairly good agreement with the ones by Spencer and Fano's theory. But the lower portion of the spectrum is larger than that by Spencer and Fano. (auth)

14398 MONTE CARLO STUDY OF HIGH ENERGY ELECTRON SPECTRA IN WATER AND ALUMINUM. Sugiyama, Haruo. Denki Shikensho Iho; 34: 577-81(1970). (In Japanese).

Energy spectra of the slowed-down electrons in water and aluminum were calculated for initial energies between 10 to 28 MeV. The results are summarized as follows: (1) at the lower portion of the spectrum, the effects of delta rays become important; (2) energy spectra in a material depend largely on the spectral shape of incident electrons; and (3) a large discrepancy was found between these results and the analytical calculation reported by Kessaris. (auth)

14399 MULTIPLE SCATTERING CALCULATIONS OF GAMMA PHOTON TRANSPORT. Cangiano, Sergio. College Park, Md.; Univ. of Maryland (1969). 179p. University Microfilms Order No. 70-11,615.
Thesis.

A method to solve the problem of three-dimensional photon transport is developed. The method solves the Boltzmann equation by expanding the flux in a Neumann series such that the nth term represents the flux of photons that have undergone n collisions. A computer program, SCAT, was written in order to calculate angular and energy spectra at different points in heterogeneous spherical media. The results were compared with moments-method calculations by Goldstein and Wilkins. Buildup factors and number flux versus energy for various source energies and materials were calculated. Reasonable agreement was obtained. (Diss. Abstr. Int., B)

14400 INVESTIGATION OF ENERGY DISSIPATION OF ELECTRONS IN Al AND Cu TARGETS BY MONTE CARLO METHOD. Shimizu, Ryuichi; Honji, Masahiro; Murata, Kenji (Osaka Univ.). Jap. J. Appl. Phys.; 9: 1291-6(Nov 1970).

Different formulas for the mean ionization potential J in Bethe's expression for stopping power were examined for use in calculating the energy-loss distribution of electrons and the depth distribution of x-ray production by the Monte Carlo method. The contributions of the mean ionization potential to final phenomena, such as energy dissipation, backscattering ratio, and x-ray production, were simulated by Monte Carlo calculation. The results are compared with the experiments on the normalized energy-loss distribution in silicon oxide reported recently by Hoff and Everhart and with experiments on the depth distribution of characteristic x rays. (auth)

14401 STOPPING POWER OF HAVAR FOR 2.5 TO 7.0 MeV DEUTERONS. Porter, L. E.; McIntyre, L. C.; Haeberli, W. (Univ. of Wisconsin, Madison). Nucl. Instrum. Methods; 89: 237-40(1970).

Energy losses of 2.5- to 7.0-MeV deuterons in thin Havar foils were measured. The results are fitted by means of the Bichsel energy-loss computer code with fixed-shell correction parameters common to the major-constituent elements and a variable mean excitation energy. The best fit value of the mean excitation energy is 15% lower than the value calculated from an assumed additivity of stopping effects. (auth)

14402 EFFECTIVE ATOMIC NUMBERS OF ALLOYS FOR PAIR-PRODUCTION PROCESS. Visweswar Rao, V.; Parthasaradhi, K. (Andhra Univ., Waltair, India). Indian J. Pure Appl. Phys.; 6: 643-4(1968).

Effective atomic numbers for pair-production processes in the gamma energy region 2.6 to 17.6 MeV are calculated for several alloys, viz., solder (67% Pb, 33% Sn), bell metal (25% Cu, 75% Sn), platinum–rhodium alloy I (60% Pt, 40% Rh) and II (80% Pt, 20% Rh). These values are found to be constant and are in satisfactory agreement with the theoretical values computed from the expressions of G. J. Hine (Phys. Rev., 85: 725(1952)) within the range of errors. (auth)

14403 ATTENUATION OF BETA-PARTICLE FLUXES IN ABSORBERS WHEN MEASURING ACTIVITIES WITH 2π-GEOMETRY. Chugunov, V. V. Instrum. Exp. Tech. (USSR) (Engl. Transl.); No. 1, 72-4(Jan-Feb 1970).
Translated from Prib. Tekh. Eksp.; No. 1, 67-70(Jan-Feb 1970).

The attenuation of β-particle fluxes in absorbers in direct contact with a thin source in 2π-geometry is studied. The results of the experiments are approximated by an expression of the form $K = m \exp(-0.69d/\Delta'_{1/2})$. The relation between the factor m and the half-value thickness $\Delta_{1/2}$ and the mean energy of the β spectrum is established. The estimates of the errors in the correction for the attenuation are given. (auth)

14404 GENERAL METHOD OF IMPORTANCE SAMPLING THE ANGLE OF SCATTERING IN MONTE CARLO CALCULATIONS. Burgart, Calvin E. (Oak Ridge National Lab., Tenn.); Stevens, P. N. Nucl. Sci. Eng.; 42: 306-23(Dec 1970).

The application of the Monte Carlo method to the solution of deep-penetration radiation transport problems requires the use of "importance sampling." A systematic approach to obtaining an importance function is to calculate the solution of the inhomogeneous adjoint transport equation (using the Monte Carlo estimator of the answer of interest as the source term) and to use this adjoint flux (or value function) as the importance function. The adjoint flux is calculated for simplified geometries using one-dimensional discrete-ordinates methods. In three-dimensional deep-penetration Monte Carlo calculations the alteration of both the transport and the collision kernel is desirable. The exponential transform is quite useful for altering the transport kernel. However, selection from the altered collision kernel is much more difficult. The approach taken here is to introduce an angular grid with 30 discrete directions fixed in the laboratory coordinate system, along which particles are required to travel. After determining appropriate scattering probabilities and values of the importance function for each of the discrete directions, the selection of the outgoing direction and, hence, energy from the resulting discrete distribution is easily performed. The effects of the discrete angular grid and the capability of angular-biased Monte Carlo were investigated for neutron transport by comparison with standard Monte Carlo and discrete-ordinates calculations, experiment, and exact analytic solutions for several configurations. In all cases the discrete grid alone (no angular biasing) was observed to have no significant effect on the results. Monte Carlo calculations were performed utilizing the exponential transform, nonleakage, source energy biasing, Russian roulette, and splitting plus the angular biasing. The results of these calculations illustrate the general usefulness of this discrete-grid approach to angular biasing in several ways. First, meaningful results were obtained with angular biasing at much greater distances from the source than were practically possible with the earlier biasing techniques. The answers, variances, and computer times were all on the same order or better than those obtained with the earlier biasing techniques. Finally, this method utilizing the discrete grid to incorporate angular biasing requires very little human interaction once the adjoint configuration is selected. (auth)

14405 EFFECTIVE ATOMIC NUMBERS FOR COHERENT SCATTERING PROCESS OF GAMMA RAYS IN ALLOYS. Murty, M. Sriramachandra; Rao, A. Lakshmana; Rama Rao, J.; Parthasaradhi, K. (Andhra Univ., Waltair, India). Nucl. Sci. Eng; 42: 423-4(Dec 1970).

Differential coherent scattering cross sections were measured in elements Sn, Ta, Pt, and Pb previously at energies 662, 1120, and 1330 keV. Using these data, effective atomic numbers for the differential coherent scattering process in three alloys, solder (Pb 67%, Sn 33%), plumber's solder (Pb 50%, Sn 50%), and solder soft (Pb 40%, Sn 60%) are estimated at three energies 662, 1120, and 1330 keV and discussed. (M.H.R.)

14406 RADIATION TRANSPORT IN ONE-DIMENSIONAL FINITE SYSTEMS. PART I. DEVELOPMENT IN THE ANISOTROPIC SOURCE–FLUX ITERATION TECHNIQUE. Gopinath, D. V.; Santhanam, K. (Bhabha Atomic Research Centre, Bombay). Nucl. Sci. Eng.; 43: 186-96(Feb 1971).

A semianalytical technique for the solution of neutron and gamma-ray transport in one-dimensional finite systems is developed. The method is applicable to multivelocity, multiregion systems with arbitrary degree of anisotropy. The transport equation is written in the form of coupled integral equations separating the spatial and energy–angular transmissions. Legendre polynomial approximation in the direction cosine and discrete-ordinate representation in energy and spatial domain are used for radiation source and flux. The space and energy–angle transmission kernels are evaluated analytically and the integral equations are then solved by a fast-converging iterative technique. For a plane parallel beam of radiation incident on a slab, the virgin and the first collision flux are not amenable to polynomial expansion because of the singularities. For such a case, up to second collision, the source is computed analytically and then recourse is taken to polynomial approximation. The computer code ASFIT written on the basis of the above formulation is briefly described. Convergence studies with the polynomial approximation, energy and spatial mesh width are described. (auth)

14407 RADIATION TRANSPORT IN ONE-DIMENSIONAL FINITE SYSTEMS. PART II. GAMMA-RAY TRANSPORT STUDIES WITH ASFIT. Gopinath, D. V.; Santhanam, K. (Bhabha Atomic Research Centre, Bombay). Nucl. Sci. Eng.; 43: 197-211 (Feb 1971).

Results of extensive calculations on gamma-ray transport in finite heterogeneous systems using the technique developed in Part I of this paper are presented. Systems studied are water, concrete, aluminum, iron, and lead, and data are presented on evolution of spectra with collisions, reflected and transmitted spectra, spectra at different depths, and buildup factors for different source energies and different thickness of each medium. Similar data are also presented for two-region systems of water–iron, iron–lead, and water–lead. Results observed include: (a) a step structure and a second peak in the low-energy part of the backscattered spectra from light media, (b) progressive buildup of a peak in the low-energy region of transmitted flux, and (c) significant dip in the buildup factors near the outer boundary of the systems. The results are discussed on the basis of the physical processes involved. Results are compared with published data. (auth)

14408 MILNE PROBLEM FOR POLARIZED RADIATION SCATTERED ACCORDING TO RAYLEIGH'S LAW. Kuzmina, M. G. (Inst. of Applied Mathematics, Moscow). Dokl. Akad. Nauk SSSR; 193: 308-12(11 Jul 1970). (In Russian).

The transport of polarized radiation in a semi-infinite plane atmosphere $z > 0$ was examined. It was assumed that the atmosphere was scattering according to Rayleigh's law and there was no incident external radiation at the $z = 0$ boundary. The problem may have a homogeneous azimuthal solution, corresponding to the field of a linearly polarized radiation, as the plane vectors of the internal normal to the $z = 0$ surface and the direction of propagation of the radiation in each point. This radiation field may be described by a 2-dimensional vector. An expression was derived on the basis of the transport equation, determining the numerical value of the needed coefficients by means of Laplace transforms. The problem was originally studied by S. Chandrasekhar, who derived an approximate solution by using the discrete-ordinate method. (TTT)

14409 PHOTON CROSS SECTIONS FROM 1 keV TO 100 MeV FOR ELEMENTS Z = 1 TO Z = 100. Storm, Ellery; Israel, Harvey I. (Los Alamos Scientific Lab., N. Mex.). Nucl. Data, Sect. A; 7: 565-81(Jun 1970).

Tables of photon cross sections of elements ($Z = 1$ to $Z = 100$) are given for photon energies in the range of 1 keV to 100 MeV. Supplementary tables of atomic energy levels and of x-ray line energies, average energies, and relative intensities are also presented. 112 references. (auth)

14410 INCOHERENT SCATTERING OF GAMMA RAYS BY K-SHELL ELECTRONS OF PLATINUM. Reddy, D. V. Krishna; Narasimhacharyulu, E.; Murthy, D. S. R. (Osmania Univ., Hyderabad, India). Proc. Indian Acad. Sci., Sect. A; 72: 185-95 (Oct 1970).

The differential cross section $d\sigma_K$ for the incoherently scattered gamma rays of energy 662 keV, coming from a 6.0-Ci cesium-137 source, by K-shell electrons of platinum was studied by experiment. The scattered gamma rays were selected in coincidence with the accompanying K x rays from the scatterer, using NaI (Tl) scintillation detectors and a fast–slow coincidence method. The differential cross section $d\sigma_K$ was compared with the Klein–Nishina cross section $d\sigma_F$ for free and stationary electrons at a scattering angle of 30° for different thicknesses of platinum scatterers. The ratio is found to be fairly constant (0.52) at thicknesses less than 20 mg/cm^2. The differential-cross-section ratio $d\sigma_K/d\sigma_F$ for the thinnest target is compared with different experimental and theoretical values. The agreement is satisfactory. The cross-section ratio is found to be less than unity because of small momentum transfer to the K-shell electrons at small angles of scattering. The energy spectrum of the gamma rays scattered by K-shell electrons, displayed on a twenty-channel analyzer, is also presented. (auth)

Solid-State Physics

Refer also to abstracts 13213 and 14630.

Radiation Effects

Refer also to abstracts 13733 and 14188.

14411 (AD–712321) EFFECTS OF HIGH-ENERGY ELECTRON IRRADIATION ON SINGLE CRYSTALS OF AMMONIUM AND SODIUM BIFLUORIDE. Van de Kieft, Lawrence J. (Ballistic Research Labs., Aberdeen Proving Ground, Md.). Aug 1970. 36p. (BRL–1490). NTIS.

Radiation effects in single crystals of ammonium bifluoride and sodium bifluoride were studied by electron spin resonance and optical methods following 1-MeV electron irradiations at 77°K.

The irradiations changed the samples from clear to deep blue-green and both crystal types showed paramagnetic resonances which were determined to result from F_2^- ions in anion sites. This defect resulted from the displacement of hydrogen atoms from their normal positions in the linear bifluoride FHF^- ions. Only in NH_4HF_2 were the displaced hydrogen atoms detected. Best-fit spin-Hamiltonian parameters for the F_2^- and H defects are given. Optical absorption measurements on the irradiated bifluorides are discussed. The ESR annealing characteristics for the F_2^- ions in both crystals appear to follow second-order kinetics. In two of the three inequivalent sites for F_2^- ions in NH_4HF_2, the orientation of the F_2^- molecular axis differs by eight degrees from the reported crystallographic axis of the corresponding bifluoride anion. This is interpreted to result from weaker hydrogen bonding between nitrogen and fluorine for the F_2^- ion than for the bifluoride ion in ammonium bifluoride, because of an increased N−H−F distance for the shorter F_2^- ions. (auth) (USGRDR)

14412 (N-70-39456) STUDY OF DOPANTS FOR RADIATION-RESISTANT SILICON. Final Report. Bass, R. F.; Curtis, O. L. Jr.; Srour, J. R. (Northrop Corporate Labs., Hawthorne, Calif.). Aug 1970. Contracts NAS7-100; JPL-952523. 59p. (NASA-CR-113550; NCL-70-51-R). NTIS.

For Jet Propulsion Lab., Pasadena, Calif.

Results are described of investigations of the effects of gamma irradiation on the electrical properties (primarily carrier lifetime) of both Al- and Li-doped silicon. The results of initial studies of the radiation sensitivity of Li-doped material were rendered uncertain due to an inhomogeneous distribution of Li throughout the bulk of the silicon samples employed. Subsequently, a procedure was developed involving a diffusion and distribution cycle employing considerably longer times and higher temperatures than previously used. Use of this technique resulted in the preparation of a considerably more homogeneous Li-doped sample. Studies of Al-doped material demonstrate that Czochralski-grown Al-doped Si that undergoes an appreciable resistivity change upon heat treatment apparently is significantly less sensitive to gamma irradiation than comparable B-doped crucible-grown material. (auth) (STAR)

14413 (NP-18645) DAMAGE IN GOLD BOMBARDED WITH MEDIUM MASS IONS. Hoegberg, G.; Norden, H. (Chalmers Tekniska Hogskola, Goteborg (Sweden)). 1969. 12p. (LF-24). Dep. NTIS.

Thin foils of gold were bombarded with ions of argon (4 to 50 keV), krypton (4 to 42 keV), and xenon (12 to 30 keV) at ambient temperature. The irradiated foils were studied in an electron microscope. The damage concentration was evaluated by counting the number of visible defects. The defects per incident ion values after bombardments with argon, krypton, and xenon ions all showed a similar energy dependence. Above the minimum energy required to produce defects of visible size, the number of defects per incident ion increased slowly with energy. (Sweden)

14414 FAST-NEUTRON SPUTTERING FROM POLYCRYSTALLINE AND MONOCRYSTALLINE GOLD. Fairand, Barry Philip. Columbus, Ohio; Ohio State Univ. (1969). 99p. University Microfilms Order No. 70-14,012.

Thesis.

The atomic sputtering by fast neutrons incident upon a polycrystalline gold target and ⟨100⟩ and ⟨111⟩ monocrystalline gold targets was determined. An upper limit for the atomic sputtering by thermal neutrons was also determined. The polycrystalline and ⟨100⟩ monocrystalline gold targets were irradiated in a separate vacuum facility from the ⟨111⟩ monocrystalline target. A cadmium and B_4C cover shielded the polycrystal and ⟨100⟩ monocrystal from thermal neutrons. Atoms ejected from the surface of a gold target were collected on quartz plates. A radioactive tracer technique was used to determine the number of sputtered atoms. A fraction of these atoms was activated by thermal neutrons and the total number of sputtered atoms were determined by measuring the activity of radioactive gold atoms collected on the quartz plates. In the ⟨111⟩ monocrystalline experiment, the radioactive gold atoms were generated "in-pile" by thermal neutron irradiation of the gold target and quartz plates simultaneously with sputtering by fast neutron irradiation of the target. In the other sputtering experiment, the atoms sputtered onto the quartz plates were activated by thermal neutrons in a separate irradiation facility. This irradiation was conducted adjacent to the reactor core face. The sputtering ratio (atoms of gold sputtered per fast neutron crossing the surface of the target) for the 0.0005-in.-thick polycrystalline gold target was $(1.5 \pm 0.4) \times 10^{-4}$. This value is in good agreement with an earlier measurement of $(1.0 \pm 0.3) \times 10^{-4}$. The fast-neutron sputtering ratios for the ⟨100⟩ and ⟨111⟩ monocrystalline gold targets, both greater than 1000 angstroms thick, were respectively $(0.9 \pm 0.2) \times 10^{-4}$ and $(0.8 \pm 0.4) \times 10^{-4}$. The good agreement between the two values for the polycrystalline sputtering ratios and the fact that in the earlier measurement the sputtered atoms were activated "in-pile" by thermal neutrons simultaneously with sputtering by fast neutron irradiation, confirms an earlier conclusion that fast neutrons are primarily responsible for the number of sputtered atoms. Because of the radioactive technique used to determine the number of sputtered atoms, an upper limit for sputtering by recoil atoms generated in the thermal neutron (n,γ) reaction with ^{197}Au is conservatively estimated to be 10^{-8}. The fast-neutron sputtering ratios observed for the monocrystalline gold targets and the polycrystalline gold target are in reasonable agreement with sputtering ratios predicted by a sputtering model where atom ejection is due to long-range focusing collisions along the ⟨110⟩ close packed crystal direction. A random sputtering mechanism which neglects the ordered nature of the crystal lattice and treats sputtering on a single knock-on atom basis underestimates the observed values by more than an order of magnitude. Based on the comparison between theory and experiment, a focusing mechanism appears to contribute significantly to the number of sputtered atoms while the random mechanism is of secondary importance. This conclusion is not inconsistent with reported results for 14-MeV neutron sputtering in gold. Qualitative arguments indicate that a sputtering mechanism based on clusters of atoms being ejected from the surface may contribute to the number of sputtered atoms. (Diss. Abstr. Int., B)

14415 F-CENTRE SATURATION PHENOMENA IN KCl DURING LOW-ENERGY ELECTRON IRRADIATION. Soul, P. B. (Univ. of Warwick, Coventry, Eng.). Phys. Status Solidi; 42: 801-12(1 Dec 1970).

The absorption levels in the F and M bands in KCl were monitored during controlled high-intensity irradiation with 5-keV electrons at room temperature, and novel saturation effects were observed. The F-center concentration rises to a maximum of between 4 and 7×10^{19} cm^{-3} (depending on the dose rate) and then decays slowly to an equilibrium level. The M-band absorption rises steadily except for a "plateau" coinciding with the F-center maximum. After irradiation, F-to-M-center conversion takes place, but this is reversed on re-irradiation. These effects can be explained using a model in which F centers produced less than about 25 Å apart aggregate spontaneously; in addition, M centers appear to be split up into F centers by the radiation itself. The relatively large amount of energy (45 keV) apparently expended in forming each vacancy suggests that there is also a high rate of recombination with interstitial defects during irradiation. (auth)

14416 VOIDS IN NICKEL AFTER ELECTRON IRRADIATION. Urban, K. (Max-Planck-Institut fuer Metallforschung, Stuttgart). Phys. Status Solidi (a); 3: K167-8(16 Nov 1970).

Electron irradiation and observation of (001)-oriented Ni samples were carried out in a 650-kV electron microscope. Irradiation of freshly thinned samples resulted in vacancy- and interstitial-type defect clusters but no voids. However, if thinned samples were allowed to oxidize in air to an oxide layer 1000-Å thick, subsequent irradiation at 5.5 A/cm^2 produced square-like features, which were identified as voids. After 2-hr irradiation, the density of these defects is 1.6×10^9 cm^{-2} and the diameter is 250 Å in a 3000-Å-thick foil. It is suggested that O_2 from the thick oxide layer penetrated into the sample and nucleated the resulting voids. (D.L.C.)

14417 CHANNELING PATTERNS BASED ON PENETRATION OF LOW-ENERGY IONS. Jech, C. (Inst. of Physical Chemistry, Prague). Phys. Status Solidi (a); 3: 579-83(16 Nov 1970).

A method for recording channeling patterns based on channeled penetration of low-energy radioactive inert-gas ions was improved by introducing a bombardment technique with a divergent ion beam of tracer ions. Channeling patterns were obtained with {111}, {110}, and {100} surfaces of silicon using 10-keV ^{85}Kr and ^{133}Xe ions as tracers. A good resolution of individual channeling directions and planes exhibiting enhanced penetration of low-energy ions was achieved. Alternative procedures for revealing channeling patterns are discussed. (auth)

14418 CHANNELING OF POSITRONS. Andersen, J. U. (Bell Telephone Labs., Murray Hill, N. J.); Augustyniak, W. M.; Uggerhoej, E. Phys. Rev., B; 3: 705-11(1 Feb 1971).

Axial and planar channeling in thin single-crystalline gold foils was investigated by wide-angle scattering of monoenergetic positrons. The beam was obtained by accelerating the positrons emitted from a ^{58}Co source in a 1-MeV Van de Graaff. The results are in good agreement with corresponding measurements for protons. For the planar case, classical calculations are compared to calculations based on the dynamical theory of diffraction. The results are very similar except for the "wiggles" due to wave interference, which appear in the quantum-mechanical calculation. These, however, are difficult to resolve experimentally. (auth)

14419 ENTRAPMENT OF HELIUM IONS AT (100) AND (110) TUNGSTEN SURFACES. **Kornelsen, E. V. (National Research Council of Canada, Ottawa). Can. J. Phys.; 48: 2812-23(1 Dec 1970).**

Two (100) and two (110) tungsten surfaces were bombarded with helium ions of selected energies between 5 and 2000 eV. The helium thermal desorption spectra obtained when the targets were subsequently heated at 40°K/sec were used to deduce the fraction of the incident particles trapped in the crystal and their binding energies. For ion energies $\leq$400 eV, the fractions trapped were small ($\sim 1 \times 10^{-3}$ on the (100) surfaces and $\sim 1 \times 10^{-2}$ on the (110) surfaces), and almost all the trapping occurred in surface-related sites with binding energies $\leq$2.1 eV. For ion energies >500 eV, trapping occurred predominantly in sites characteristic of the bulk material, the sites being created by the incoming ions as soon as their energy was sufficient to produce atomic displacements in the lattice (480 eV). At doses $<1 \times 10^{13}$ ions/cm^2, four characteristic binding energies were observed: 2.65, 3.05, 3.35, and 4.15 eV. At higher doses, additional binding states were observed with energies up to 5.4 eV. The results suggest that helium diffuses rapidly in tungsten at room temperature and that it is trapped within the crystals only if it encounters lattice defects. Estimates of the ion penetration depth lead to the tentative conclusion that in the annealed crystals (ion energies <400 eV) the fractional trap concentration is $<1 \times 10^{-9}$ and the helium incident at a few hundred eV energy becomes trapped at depths up to at least 1 μ. (auth) (Canada)

14420 RADIATION-ACCELERATED DIFFUSION OF GOLD IN SILICON. **Klimkova, O. A.; Niyazova, O. R. (Inst. of Nuclear Physics, Tashkent). Sov. Phys.-Solid State (Engl. Transl.); 12: 1760-1(Jan 1971).**

Translated from Fiz. Tverd. Tela; 12: 2199-2200(Jul 1970).

Single-crystal plates of n-type Si doped with P were coated with Au and irradiated with 50- or 100-kV x rays at 300°K. The Au distribution profile was determined by neutron-activation analysis of layers removed by etching. No penetration below 1 to 2 μ from the surface occurred in the unirradiated control samples; doses of 1 to 5×10^8 R resulted in diffusion depths of 150 to 200 μ. Gold diffusion into surface-barrier diodes changed the electrical properties of the diodes and resulted in the formation of p- and n-type regions. The diffusion coefficient under x irradiation at 300°C is $\sim 10^{-12}$ cm^2/sec, the same as the coefficient for nonirradiated material at 600°C. (D.L.C.)

14421 INFLUENCE OF WEAK DEFORMATION OF SINGLE-CRYSTAL COPPER FILMS ON THE CHANNELING OF PROTONS. **Markus, A. M.; Geguzin, Ya. E.; Fainshtein, A. L. (Physical-Technical Inst. of Low Temperatures, Kharkov). Sov. Phys.-Solid State (Engl. Transl.); 12: 1704-5(Jan 1971).**

Translated from Fiz. Tverd. Tela; 12: 2143-4(Jul 1970).

Single-crystal Cu films of (100) orientation and 6 to 8×10^{-7} m thickness were bombarded by ~170-keV protons. The films were oriented 45° to the beam for the strongest channeling effect, and were deformed during bombardment by means of a stretching device. The effects of a deformation less than $\epsilon = 10^{-3}$ were studied for beams traveling along the [110] or [101] direction. The deformation produced an increase in the proton current which reached saturation at 1.2 to 1.3 times the current in an undeformed film at $\epsilon \sim 0.05\%$. This increase was reversible except for $\epsilon > 10^{-3}$. (D.L.C.)

14422 RADIATION DAMAGE IN COPPER BOMBARDED WITH COPPER IONS. **Wilson, M. M. Oxford; Oxford Univ. (1970). 174p.**

Thesis.

The work is discussed under the following headings: study of copper ion damage in copper; two-beam theory of electron diffraction; experimental techniques used in specimen preparation, electron microscopy, and operation of a heavy-ion accelerator; the form of the defect clusters produced by copper-ion irradiation; the size, density and distribution of clusters produced by copper ions incident both in an off-axis direction and in a channelling direction; the mechanism of radiation damage production; and the fate of interstitials generated in a collision cascade. The following conclusions are presented: (1) The radiation damage produced in copper by Cu$^+$ ions of energies 30 and 90 keV consists of vacancy-type Frank sessile loops on $\{111\}$ planes; many of the loops show dissociation along parts of their circumference. (2) A clustering and diffusion calculation indicates that a substantial proportion of the interstitials formed in a 30-keV Cu$^+$ ion cascade will combine to form small clusters. (3) A 30-keV Cu$^+$ ion produces of the order of one cluster larger than 20Å in diameter, and on average, 2.5 to 3 such clusters are produced by each 90-keV ion. (4) The cluster size distributions for the two ion energies are similar, and have an exponential form for clusters larger than 30Å in diameter. (5) Channelling reduces the quantity of damage produced, the reduction being greater for clusters of large diameter. (6) The damaged layer produced by $\langle 110 \rangle$ irradiations with 30-keV Cu$^+$ ions extends deeper than that produced by off-axis irradiations. The mean depth of the clusters for an off-axis bombardment direction is 30Å. (UK)

14423 EFFECT OF ELECTRON IRRADIATION ON LITHIUM-DOPED SILICON. **Carter, J. R. Jr. (TRW Systems Group, Redondo Beach, Calif.). J. Phys. Chem. Solids; 31: 2405-16 (Nov 1970).**

Lithium-doped silicon was irradiated at room temperature with 1-MeV electrons. The initial carrier removal rate was 2.2 cm^{-1} in float-zone silicon. As larger quantities of carriers were removed, the carrier concentration varied exponentially with electron fluence. The changes in Hall coefficient after irradiation indicate that lithium is consumed in the production of defects. Changes in Hall mobility in float-zone silicon indicate production of a neutral defect that consumes one conduction electron for each lithium atom reacting. In quartz-crucible silicon, a different neutral defect results after intermediate Si A-center formation. Similar measurements in phosphorus-doped float-zone silicon indicate the formation of negatively charged defects which appear to be silicon "E" centers. (auth) (UK)

14424 RELEASE OF STORED ENERGY IN ANNEALING OF RADIATIONAL DEFECTS IN NaCl. **Zavadovskaya, E. K.; Golovchanskii, E. M.; Borisovskii, V. V. (Tomsk Polytechnic Inst., USSR). Izv. Vyssh. Ucheb. Zaved., Fiz.; No. 8, 12-16 (1970). (In Russian).**

Release of stored energy during annealing of radiation defects in NaCl crystals irradiated with 4.5-MeV protons with a dose of 90×10^{14} protons/sec was studied. The obtained spectrum of energy separation indicates a four-stage character of radiation defect annealing. The first stage was in the range from room temperature to 90°, the second from 90 to 130°, the third from 130 to 200, and the fourth from 200 to 250°C. Data on the release of stored energy resulting from destruction and annihilation of M and V centers were obtained. (R.V.J.)

14425 THERMOLUMINESCENCE OF NaCl DOPED BY STOICHIOMETRIC EXCESS. **Serpi, A.; Serpi Macciotta, P. (Univ., Cagliari, Italy). Lett. Nuovo Cim.; 4: 1136-8(12 Dec 1970).**

Additive coloring by a Na excess produces an excess concentration of F centers, which should influence the thermoluminescence following x-ray excitation. Experiments on pure and Na-coped NaCl crystals were performed at 77°K. The glow curve was made asymmetric by the doping, and the kinetic order α (exponent of the integrated area ΔS in the glow curve) was lowered from 1.3 to 1.0. The activation energy was likewise lowered by the doping. An explanation of the results is offered. (D.L.C.)

14426 SPACE-CHARGE-LIMITED CURRENT IN FAST-NEUTRON-IRRADIATED SILICON. **Vu, Quat Thuong. Pasadena, Calif.; California Inst. of Tech. (1970). 109p. University Microfilms Order No. 70-24,315.**

Thesis.

Dc and transient measurements of space-charge-limited currents through alloyed and symmetrical $n^+\nu n^+$ structures made of nominally 75 kΩcm ν-type silicon were studied, before and after the introduction of defects by 14-MeV neutron radiation. In the transient measurements, the current response to a large turn-on voltage step was analyzed. Right after the voltage step is applied, the current transient reaches a value which is called "initial-current" value. At longer times, the transient current decays from the initial current value if traps are present. Before the irradiation, the initial-current density–voltage characteristics J(V) agree quantitatively with the theory of trap-free space-charge-limited current in solids. For the electron mobility, a temperature dependence is obtained which indicates that scattering due to impurities is weak, as expected for the high-purity silicon used. The drift velocity-field relationships for electrons at room temperature and 77°K, derived from the initial current density–voltage characteristics, are shown to fit the relationships obtained with other methods by other workers. The transient current response for $t > 0$ remains practically constant at the initial value, thus indicating negligible trapping. Measurement of the initial (trap-free) current density–voltage characteristics after the irradiation indicates that the drift velocity-field relationship

XUM

of electrons in silicon is affected by the radiation only at low temperature in the low-field range. The effect is not sufficiently pronounced to be readily analyzed and no formal description of it is offered. In the transient response after irradiation for $t > 0$, the current decays from its initial value, thus revealing the presence of traps. To study these traps, in addition to transient measurements, the dc current characteristics were measured and shown to follow the theory of trap-dominated space-charge-limited current in solids. This theory was applied to a model consisting of two discrete levels in the forbidden band gap. Calculations and experiments agreed and the capture cross sections of the trapping levels were obtained. These results demonstrate the sensitivity of space-charge-limited current flow as a tool to detect traps and changes in the drift velocity-field relationship of carriers caused by radiation. They also establish that devices based on the mode of space-charge-limited current flow will be affected considerably by any type of radiation capable of introducing traps. (Diss. Abstr. Int., B)

14427 EFFECT OF PONT DEFECTS IN COPPER ON THE ANOMALOUS TRANSMISSION OF X RAYS. **Edelheit, Lewis Selig.** Urbana, Ill.; Univ. of Illinois (1970). 82p. University Microfilms Order No. 70-20,955.

Thesis.

Anomalous x-ray transmission (Borrmann) measurements were made at 4.2°K on nearly perfect copper single crystals before and after irradiation at 20°K with 3-MeV electrons (total integrated flux 0.87×10^{18} electrons/cm^2). The intensity in the diffracted direction was measured for the (111), (222), (333), and (220) reflecting planes. The measured intensity changes were 1.15 ± 0.4%, 4.52 ± 0.6%, 8.90 ± 0.8%, and 4.06 ± 0.8% respectively. A comparison of the observed intensity changes with theoretical predictions, assuming that the damage consists of isolated interstitials and vacancies, and using previously calculated displacements associated with these defects, indicates that the interstitial is not in the split (100) configuration. Possible configurations are the body-centered interstitial or the split (111) interstitial. Measurements after annealing at 80 and 300°K were made. The measurements indicated that defect clusters were formed when the irradiated crystal was heated to 80°K, and some clusters remained after annealing at room temperature. (Diss. Abstr. Int., B)

14428 PROPERTIES OF DEFECT CLUSTERS IN NEUTRON-IRRADIATED SILICON. **Sprague, James Alan.** Houston, Tex.; Rice Univ. (1970). 82p. University Microfilms Order No. 70-23,579.

Thesis.

Dislocation-free single crystals of three types of silicon were irradiated with fast-neutron fluences of 1.25×10^{19} nvt and 5×10^{19} nvt. The neutron-irradiated samples were studied by transmission-electron microscopy, infrared-absorption spectroscopy, Hall effect, and resistivity measurement. Diffraction-contrast analysis was used to determine that the defects visible in the electron microscope had nonspherical strain fields. The projections of the principal displacement directions for these defects on a (111) plane were 30° either side of the ⟨220⟩ directions. This symmetry was consistent with the displacements surrounding vacancy and interstitial Frank dislocation loops on {111} planes. The annealing of the visible defects was found to be at least a 2-stage process, the first stage(s) falling between 100 and 400°C, and the final stage centered around 625°C. The mean size of the defect images remained constant during annealing in high-resistivity phosphorus-doped Lopex silicon, but increased with annealing in low-resistivity phosphorus- and antimony-doped Lopex samples. The 3.3-μ infrared absorption band was observed in as-irradiated specimens of all types of silicon investigated. This absorption annealed out around 250°C. The Hall coefficient and resistivity of irradiated and annealed samples of both phosphorus- and antimony-doped silicon were measured. The electron trapping and mobility increase annealed in the same temperature range as the defect clusters observed in the electron microscope. This was interpreted as evidence that the defect clusters act as both electron traps and electron scattering centers. (Diss. Abstr. Int., B)

14429 TEMPERATURE DEPENDENCE OF RADIATION COLLOID PRODUCTION IN KCl CRYSTAL. **Kristapson, Ya. Zh.; Shvarz, K. K.** (Inst. of Physics, Riga). Latv. PSR Zinat. Akad. Vestis, Fiz. Teh. Zinat. Ser.; No. 4, 44-9(1970). (In Russian).

The optical absorption of KCl was measured. The samples were irradiated in a nuclear reactor to doses of 500 Mrad at different temperatures. The radiation colloid production was observed at 80 to 180°C, and the production of colloids in additively colored KCl was observed at 250 to 400°C. The optimal temperature of potassium colloid production depends on the radiation intensity, increasing with intensity. The impurity (silver, thallium) colloid production had no pronounced temperature dependence. (auth)

14430 ELECTRIFICATION OF SUBSTANCES BY GAMMA RADIATION. **Lenchenko, V. M.** At. Energ. (USSR); 29: 53-5 (Jul 1970). (In Russian).

It is known that alpha and beta emitters may become charged to potentials comparable to the energy of the emitted particle. High-voltage electrification of substances may also take place as a result of emission of charged recoil particles (for example, the emission of Compton electrons or photoelectrons during gamma irradiation). This high-voltage buildup may be a reason for the radiation instability of semiconducting and insulating substances. In heterogeneous systems individual particles can acquire a high charge, and such properties as particle flotation may change because of the charge acquisition. Equations are presented to calculate the electrification of a substance due to emission of Compton electrons and photoelectrons under irradiation. As an example it is known that the charge rate for a sphere 1 cm in radius in a ^{60}Co gamma field of 1000 rads is 10^{13} particles per sec. If charge leakage from the surface of the sphere is ignored, this charge rate would be sufficient to charge the substance up to hundreds of volts in one second. Thus an insulator may be rapidly charged to breakdown voltages. It is important to set up special experiments to study this problem. (TTT)

14431 MEASUREMENTS OF PROTON RADIATION DAMAGE AND CARRIER DIFFUSIVITIES IN SILICON THROUGH OBSERVATIONS OF THE DRIFT OF ELECTRON-BEAM-INDUCED CARRIERS. **Sigmon, Thomas William.** Stanford, Calif.; Stanford Univ. (1970). 93p. University Microfilms Order No. 70-18,476.

Thesis.

Measurements of (1) the variation of electron and hole diffusivity and drift velocity in the "warm electron" range of electric field (1 to 50 kV/cm) and (2) the introduction rate and annealing characteristics of damage resulting from implanting 2.8-MeV protons in the silicon lattice are presented in this work. Both measurements involved the observation and analysis of the transient currents produced as a thin layer of "warm" carriers pass through the depletion region of a $p^+-\nu-n^+$ diode structure. The diffusivity measurements show both the electron and hole diffusion coefficient decreasing slightly below field values (35 cm^2/sec for electrons and 12 cm^2/sec for holes) in the field range of 6 to 50 kV/cm for ⟨111⟩-oriented silicon at 300°K. Calculation of the equivalent electron temperature (T_{eq}) for electrons from the experimental data results in values for T_{eq} that are in reasonable agreement with those obtained by hot electron emissions from cesiated silicon surfaces. Electron and hole drift velocity measurements are presented; they extend the range of drift velocity measurements to higher electric fields. The measurements show that neither carrier velocity has reached saturation at electric fields of 50 kV/cm. Values of 9.27×10^6 cm/sec for electron drift velocity and 7.18×10^6 cm/sec for hole drift velocity are found at the electric field of 50 kV/cm. Measurements of the damage created by the 2.8-MeV protons as a function of proton fluence show a linear dependence for fluences from 8.2×10^{11} to 4×10^{13} protons/cm^2. The resulting lattice defects are found to be positively charged in the presence of a high electric field. The defect introduction rate is found to be 9.1×10^{-3} net (+) defects/2.8-MeV proton. Carrier trapping effects of the damage in low to medium electric fields (6 to 50 kV/cm) are negligible to within the sensitivity of the experiment. Annealing experiments indicate that the damage could be completely annealed (within experimental sensitivity) at a temperature of 450°C (20 minute anneal time). This annealing property identifies the damage introduced by the protons as isolated clusters of damaged silicon. (TSS)(Diss. Abstr. Int., B)

14432 DIELECTRIC PROPERTIES OF A γ-IRRADIATED KDP CRYSTAL. **Burdanina, N. A.; Kamysheva, L. N.; Zhukov, O. K.** (Voronezh State Univ., USSR). Sov. Phys.-Cryst. (Engl. Transl.); 15: 721-2(Jan-Feb 1971).

Translated from Kristallografiya; 15: 834-6(July-Aug 1970).

The effects of small γ doses up to 982 R on the dielectric constant and losses of KH_2PO_4 crystals were studied. The temperature dependence of the constant shows an increase at and below the Curie point. The initial maximum in the losses decreases and a second maximum at −165°C appears whose magnitude decreases somewhat with dose. The changes are stable with time. It is suggested that irradiation reduces the mobility of the domain walls. (D.L.C.)

Physical Properties

Refer also to abstracts 13018, 13663, 13667, 13693, 13707, 13713, 13755, 13778, 14172, 14213, and 15020.

14433 (ANL-7659) INVERSION OF DE HAAS-VAN ALPHEN DATA. I. CLOSED SURFACES WITH INVERSION SYMMETRY.

Aurbach, R. L.; Ketterson, J. B.; Mueller, F. M.; Windmiller, L. R. (Argonne National Lab., Ill.). Jul 1970. Contract W-31-109-eng-38. 311p. Dep. NTIS.

This report presents a collection of a series of mathematical techniques and detailed computer programs which allow the inversion of de Haas–van Alphen data on closed Fermi surfaces that possess inversion symmetry and have a single-valued radius vector measured from that center. De Haas–van Alphen data include extremal cross-sectional areas and cyclotron effective masses, whereas the techniques discussed allow the determination from such data of the Fermi radius and Fermi velocity. The programs have been applied to the platinum group near-noble metals and the arsenic group semimetals. Programs are presented, however, which are applicable to all ten of the point groups containing the inversion element. Also included are programs for the generation of Kubic harmonics as linear combinations of spherical harmonics. The coefficients for this expansion are tabulated to order $l = 60$. The programs employing Kubic harmonics have been used extensively and are therefore reasonably well "debugged." The programs built around the C_{2h} and D_{4h} point groups have been employed somewhat less, while the remaining point groups have not been tested at all. (auth)

14434 (CEA-CONF–1701) MAGNETIC PROPERTIES AND STRUCTURES OF THE CrB COMPOUNDS Tb–$Ge_{0.2}Si_{0.8}$, HoSi, ErSi, AND TmSi. Nguyen Van Nhung (Commissariat a l'Energie Atomique, Grenoble (France). Centre d'Etudes Nucleaires); Barlat, A.; Laforest, J. (Centre National de la Recherche Scientifique, Grenoble (France)). 1970. 13p. (In French). (CONF-700940–2). Dep. NTIS (U. S. Sales Only).

From International Conference on Magnetism, Grenoble, France.

The compounds $TbGe_{0.2}Si_{0.8}$, HoSi, ErSi, and TmSi of the CrB type are antiferromagnetic below 56, 25, 10, and 10°K, respectively. At 4.2°K, HoSi, ErSi, and TmSi are metamagnetic. The configurations of Tb, Ho, and Er moments are colinear; they all have the wave vector $\vec{K} = (1/2, 0, 1/2)$ and belong to the four-dimensional representation associated with this vector. These structures are stabilized by pseudodipolar exchange forces. TmSi has a colinear magnetic structure with a wave vector $\vec{K} = (0, 0, 1/2)$; it belongs to one of the four representations of the space group Cmcm associated with this $\vec{K}$ vector. (auth) (France)

14435 (IJS–587) THERMAL TREATMENT OF Cr–SiO CERMET THIN FILMS. Gasperic, J.; Navinsek, B. (Institut Jozef Stefan, Ljubljana (Yugoslavia)). Sep 1970. 8p. (CONF-701032–1). Dep. NTIS (U. S. Sales Only).

From Conference on Thin Films, Cannes, France.

Cr–SiO films were prepared in a Balzers evaporation unit using a BSF 101 flash evaporator. Cermet films were evaporated on pyrex, alumina, and fused quartz substrates at temperatures of 20 to 300°C. All substrates had pre-evaporated gold contacts. Films with and without SiO_2 protection layer were stabilized and aged in vacuum at 200 to 550°C and in the atmosphere at 100 to 200°C. The following properties of evaporated cermet films were investigated: thickness and mass, chemical composition, resistivities, and temperature coefficients of resistance (TCR) using the Tolansky and microgravimetric method, the quartz microbalance method, x-ray fluorescence and microprobe analysis, electrical measurements, and a monopole mass analyser (to study the influence of residual gases). (auth)

14436 (JAERI–1197) PROCEEDINGS OF THE THIRD CONFERENCE ON INELASTIC NEUTRON SCATTERING, TOKAI, 1969. (Japan Atomic Energy Research Inst., Tokai. Tokai Research Establishment). Mar 1970. 117p. (In Japanese and English). (CONF-691219). Dep. NTIS (U. S. Sales Only).

Two main subjects of the conference were collective excitations in disordered and magnetic systems and lattice dynamics of high-polymer substances. This report is a collection of the papers presented at the conference and the records of the discussions. (auth)

14437 (WHAN-SA–75) POLARIZATION EFFECTS IN OXIDE INSULATORS. Gordon, R. L.; Schemmel, R. R. (WADCO Corp., Richland, Wash.). [1970]. Contract AT(45-1)-2170. 19p. (CONF-701102–9). Dep. NTIS.

From Meeting of the American Nuclear Society, Washington, D. C.

An analysis is made of the factors affecting the reliability of the four-probe technique for resistivity measurements at high temperatures. The effects of polarization on measurements are considered, and results are reported of experiments on commercial-grade Al_2O_3 at 1165 and 1683°F. For currents more than 1 μA, the slope of V vs I becomes negative. The nonlinear distribution of potential over the sample and its possible effects are considered. (D.L.C.)

14438 STAGE I RECOVERY OF DEFORMED METALS. II. Swanson, M. L. (Atomic Energy of Canada, Ltd., Chalk River, Ont.). Phys. Status Solidi (a); 3: 551-67(16 Nov 1970).

Electric resistivity data on the stage I recovery of deformed fcc, hcp, and bcc metals are summarized, and the effects of impurities are discussed. Results from other experiments (thermal conductivity, superconductivity, stress-strain, etc.) are also considered. The identity of the defects produced by deformation and their annealing are discussed. It is concluded that the stage I recovery is due to rearrangement of point defects and dislocations, short-range migration of point defects, and long-range migration of point defects. (30 references) (D.L.C.)

14439 ISOTOPE DEPENDENCE OF THE SELF-TRAPPING ENERGY OF A LIGHT INTERSTITIAL IN A METAL, AND ITS EFFECT ON ACTIVATION ENERGIES IN DIFFUSION. Matthew, J. A. D. (Univ. of York, Heslington, Eng.). Phys. Status Solidi; 42: 841-7(1 Dec 1970).

The isotope dependence of the strain energy or "self-trapping energy" of a light interstitial in a metal is considered for a model in which the interstitial interacts with the lattice through a two-body potential. Estimates indicate that the difference in the volume of solution of hydrogen and deuterium in various metals will be at maximum only a few percent. These results suggest that the "self-trapping energy" barrier in the quantum mechanical diffusion theory of Flynn and Stoneham will not lead to large isotope effects in the activation energy. (auth)

14440 DIFFUSION COEFFICIENTS OF HYDROGEN AND DEUTERIUM IN VANADIUM, NIOBIUM, AND TANTALUM BY GORSKY-EFFECT MEASUREMENTS. Schaumann, G.; Voelkl, J.; Alefeld, G. (Kernforschungsanlage, Juelich, Ger.). Phys. Status Solidi; 42: 401-13(1 Nov 1970).

Gorsky-effect measurements on vanadium, niobium, and tantalum samples loaded with different concentrations (0.2 to 4.3 at. %) of hydrogen or deuterium are reported. From the relaxation strength the trace of the dipole-moment tensor of hydrogen and deuterium was determined and found to be consistent with the lattice parameter changes. From the relaxation time of the Gorsky effect, the diffusion coefficients of hydrogen and deuterium in vanadium, niobium, and tantalum were determined in the temperature range from 600 to about 270°K (in the case of hydrogen in niobium down to 120°K). The diffusion coefficients are very large and show only a weak exponential temperature dependence, which moreover decreases for hydrogen in niobium below 300°K. In contrast to classical rate theory, the activation energies are isotope-dependent, whereas the pre-exponential factors are isotope-independent within the experimental errors. (auth)

14441 POSITRON ANNIHILATION IN A ZIRCONIUM SINGLE CRYSTAL. Coussot, G. (Institut National des Sciences et Techniques Nucleaires, Saclay, France). Phys. Rev., B; 3: 1048-9 (1 Feb 1971).

The angular distribution of the γ quanta emitted in the two-photon annihilation of positrons in zirconium was measured along the (0001) direction of a single crystal. The results are compared with calculations by Gupta and Loucks in the augmented-plane-wave approximation. The data confirm that the curve at small angles falls significantly below the parabola expected for a free-electron gas and that there is a conspicuous contribution at large angles from the high-momentum components of the electron wave function. A small hump predicted near the zone boundary was not resolved. (auth)

14442 X-RAY DIFFRACTION STUDIES OF THE METAL INSULATOR TRANSITIONS IN Ti_4O_7, V_4O_7, AND VO_2. Marezio, M.; Dernier, P. D.; McWhan, D. B.; Remeika, J. P. (Bell Telephone Labs., Inc., Murray Hill, N. J.). Mater. Res. Bull.; 5: 1015-24 (Dec 1970).

The lattice parameters of Ti_4O_7 and V_4O_7 are reported from 77 to 298°K. The volume changes at the metal–insulator transitions were: $(V_M - V_I)/V_I = -0.004 \pm 0.001$ (Ti_4O_7), -0.0011 ± 0.0006 (V_4O_7), and $+0.001 \pm 0.003$ (VO_2). The volume change at the lower M – I transition in Ti_4O_7 was <0.001, and the extra reflections observed below this transition suggested a doubling of the unit cell. The pressure dependence of the M – I transition temperature in V_4O_7 was -0.2 ± 0.1°K/kbar. (auth)

14443 BULK-PLASMON DISPERSION SPECTRUM OF Be USING AN X-RAY SCATTERING TECHNIQUE. Miliotis, Demitrios M. (Univ. of Athens). Phys. Rev., B; 3: 701-5(1 Feb 1971).

Spectroscopic analysis of scattered x rays from Be irradiated by copper-target Kβ radiation establishes the existence of a first-order bulk-plasmon line. Dispersion of the plasmon energy as a

XUM

function of the scattering angle for momentum transfer $\hbar\vec{k}$ smaller than the critical $\hbar\vec{k}_c$ was observed, as predicted by Bohm and Pines, and Nozières and Pines. The plasmon energy for scattering angle zero was found to be 19.4 ± 0.4 eV. No appreciable dispersion was observed for $\hbar\vec{k} > \hbar\vec{k}_c$. Adopting the Drude–Zener model for the electron gas, the experimental half-width of the unfolded lines gives an estimated plasmon lifetime of the order of 1.4×10^{-16} sec, for scattering angle $\phi = 0$. (auth)

14444 SPIN-WAVE DISPERSION RELATION IN DYSPROSIUM METAL. Nicklow, R. M.; Wakabayashi, N.; Wilkinson, M. K.; Reed, R. E. (Oak Ridge National Lab., Tenn.). Phys. Rev. Lett.; 26: 140-3(18 Jan 1971).

The spin-wave dispersion relation for the c direction of dysprosium metal in the ferromagnetic phase at 78°K and in the helical magnetic phase at 98°K was measured by triple-axis neutron spectrometry. The energy gap measured in the ferromagnetic phase at $\vec{q} = 0$ is in poor agreement with that calculated from the macroscopic magnetostriction and crystal-field anisotropy constants. The Fourier-transformed exchange interaction $J(\vec{q}) - J(0)$ in the ferromagnetic phase posseses a peak near the wave vector that gives the periodicity of the helical structure just above the Curie temperature. (auth)

14445 LOCAL MAGNETIC FIELDS IN THE VANADIUM–MANGANESE ALLOY SYSTEM. von Meerwall, E. (Univ. of Illinois, Urbana); Schreiber, D. S. Phys. Rev., B; 3: 1-21 (1 Jan 1971).

A study of the nuclear magnetic resonance (NMR) lines shapes, Knight shifts, and linewidths of both ^{51}V and ^{55}Mn was made between 1.4 and 300°K in the vanadium–manganese alloy system, and is complemented by measurements of the magnetic susceptibility. The concentration dependence of the magnetic susceptibility shows a gradual decrease and is temperature-independent to 30% Mn in V, followed by a temperature-dependent increase. Both V and Mn Knight shifts decrease rapidly above 40% Mn, but without most of the temperature dependence displayed by the susceptibility. Both shifts and susceptibility are analyzed in terms of the details of the 3d-band structure in this and related alloy systems: a relatively flat 4s band is superimposed on two 3d subbands whose position is such that the Fermi level falls between their peaks in alloys at 45% Mn in V. In a more-detailed consideration of the susceptibility, and both Knight shifts, it is necessary to depart from the rigid-band model by taking into account solute–solvent local electron density differences. The much smaller temperature dependence of the observed NMR parameters, when compared to that of the susceptibility above 45% Mn, is speculatively explained by the magnetization of Mn atoms determined by local Mn concentration, in reasonable agreement with the results. A Curie–Weiss component of the susceptibility above 40% Mn may have its origin in an itinerant magnetism based on the Anderson–Wolff band model as elaborated on by Schrieffer and co-workers. Strong field-dependent increases in the susceptibility below 85°K are observed in alloys above 35% Mn, but the modest observed changes in the NMR parameters through this transition suggest that these magnetic phenomena originate in a small fraction of the sample volume. The effects of the nuclear quadrupole interaction, and of Knight-shift inhomogeneity, on the ^{51}V NMR are discussed in detail. The NMR in three σ-phase samples was observable for both nuclear species down to 1.4°K, and the susceptibility is only moderately temperature dependent; no evidence of magnetic ordering was found. (auth)

14446 BEHAVIOR OF THE INITIAL PARAPROCESS SUSCEPTIBILITY OF GADOLINIUM AND Ni_3Mn SINGLE CRYSTALS NEAR THE CURIE TEMPERATURE. Zotov, T. D.; Pronina, A. P. (Inst. of Metal Physics, Sverdlovsk, USSR). Sov. Phys.-Solid State (Engl. Transl.); 12: 1744-5(Jan 1971).

Translated from Fiz. Tverd. Tela; 12: 2184-6(Jul 1970).

The temperature dependence of the reciprocal of the initial paraprocess susceptibility near the Curie point θ_f is: $1/\chi_0 = A(T - \theta_f)^{\gamma}$. An experimental study was made of the anistropy of χ_0 in a Gd single crystal and of χ_0 in a partly ordered Ni_3Mn single crystal. Magnetization isotherms were measured at 280 to 368°K in fields up to 17,000 Oe. From graphs of $1/\chi_0$ vs $T - \theta_f$, the slopes yield $\gamma = 1.30 \pm 0.02$ for $H \| c$ and 1.09 ± 0.02 for $H \perp c$ in Gd, and $\gamma = 1.29 \pm 0.02$ for Ni_3Mn. (D.L.C.)

14447 EFFECT OF PRESSURE ON THE MAGNETIC SUSCEPTIBILITY OF VANADIUM–CHROMIUM AND CHROMIUM–MANGANESE ALLOYS. Panfilov, A. S.; Svechkarev, I. V. (Physical-Technical Inst. of Low Temperatures, Kharkov). Zh. Eksp. Teor. Fiz.; 59: 1156-9(Oct 1970). (In Russian).

The effect of hydrostatic pressure up to 4000 kg/cm² at room temperature on the magnetic susceptibility of chromium–vanadium and chromium–manganese alloys is investigated. The experimental results can be satisfactorily explained within the framework of a simple model of electron spectrum alterations induced by hydrostatic pressure in which d-zone deformation and a relative shift of the s and d zones are assumed. Values of the parameters that can be used to describe both mechanisms are obtained. (auth)

14448 SCATTERING OF CONDUCTIVITY ELECTRONS BY SPIN WAVES IN TERBIUM AND DYSPROSIUM SINGLE CRYSTALS. Volkenshtein, N. V.; Dyakina, V. P. (Inst. of the Physics of Metals, Sverdlovsk, USSR). Zh. Eksp. Teor. Fiz.; 59: 1160-4 (Oct 1970). (In Russian).

The temperature dependences of the electric resistance of terbium and dysprosium single crystals are measured along the [0001] c-axis and $[1\bar{2}10]$ a-axis at temperatures between 4.2 and 370°K. That part of the resistance due to electron scattering by spin waves is separated. It is shown that the magnetic part of the resistance is anisotropic throughout the whole temperature region. In the magnetic-ordered state $\rho_m^c(T) > \rho_m^a(T)$, and in the paramagnetic region $\rho_m^c < \rho_m^a$. Anisotropy of scattering by magnetic disordering ρ_m^a/ρ_m^c is 1.2 for dysprosium and 1.1 for terbium. Between 15 and 40°K, $\rho_m(T)$ varies almost quadratically with the temperature. (auth)

14449 SPACE-CHARGE-LIMITED ELECTRON CURRENTS IN SODIUM CHLORIDE. Lampson, Miles Landrum. Bethlehem, Pa.; Lehigh Univ. (1970). 82p. University Microfilms Order No. 70-26,153.

Thesis.

Measurements of the current–voltage characteristics in thin Harshaw crystals of sodium chloride in the temperature range 100 to 150°C are interpreted in terms of mixed electronic and ionic conduction. The theory of Rose is applied to the space-charge-limited electron current in order to determine the mobility, trap depth, and trap concentration in several samples. The average conduction band mobility in this temperature range is found to be 1 cm² volt-second, in agreement with predictions based on the low-temperature behavior of the mobility. This result indicates that steady-state values of the current were obtained. In some crystals, discrete trapping levels are found at about 1.07 eV below the conduction band with a density of about 10^{13} cm^{-3}. No evidence is found for the existence of a large concentration of anion vacancies which has been postulated to explain the rapid initial growth of the F-center concentration in these crystals on x-irradiation. (Diss. Abstr. Int., B)

14450 HEAT CAPACITY OF GADOLINIUM–LUTETIUM ALLOYS AT SUPERLOW TEMPERATURES. Kogan, A. V.; Nikulin, E. I.; Patrikeev, Yu. B. (Ioffe Inst. of Physics and Tech., Leningrad). Sov. Phys.-Solid State (Engl. Transl.); 12: 1565-8 (Jan 1971).

Translated from Fiz. Tverd. Tela; 12: 1969-72(Jul 1970).

The heat capacity of magnetic Gd–Lu alloys was measured at temperatures in the range 0.06 to 0.16°K, achieved by the adiabatic demagnetization of cerium–magnesium nitrate crystals, which also were used to measure the temperature. Samples having Lu contents of 10, 25, 40, 55, 70, 85, and 90% were used. The heat capacity of the alloy can be described by $C = AT + B/T^2$, where the first term corresponds to the electronic heat capacity, and the (predominant) second term corresponds to the nuclear heat capacity. The electronic heat capacity was evaluated, and the effective magnetic field at the lutetium nuclei was found: 280, 260, 240, 150, 120, 110, and 80 kOe, respectively. The possible transition to antiferromagnetism with increasing Lu content is discussed. (auth)

14451 DIRECT CONTRIBUTIONS OF THE CONDUCTION ELECTRONS TO THE CRYSTALLINE ELECTRIC FIELD AND NUCLEAR QUADRUPOLE INTERACTION IN RARE EARTH METALS. Das, K. C.; Ray, D. K. (Laboratoire de Spectrometrie Physique, Grenoble, France). Solid State Commun.; 8: 2025-8(1 Dec 1970).

The wave functions for the conduction electrons in dysprosium metal were constructed, following the APW formalism, to see how much they differed from the plane wave description in pure earth metals. These functions are used to calculate the direct contributions of the conduction electrons to the crystalline electric field and the nuclear quadrupole interaction in Dy metal. (auth) (UK)

14452 EFFECT OF ALLOYING ADDITIONS OF PLUTONIUM AND NEPTUNIUM ON THE LATTICE PARAMETERS OF α-URANIUM BETWEEN 4 AND 300°K. Marples, J. A. C. (Atomic Energy Research Establishment, Harwell, Eng.). J. Phys. Chem. Solids; 31: 2421-30(Nov 1970).

The effect of plutonium and neptunium in solution on the thermal expansion anomaly in α-uranium at 43°K was studied by x rays. Both solutes reduce the size of the anomaly and the temperature at which it occurs. The results support the theory that the cause of the anomaly is interband transfer of electrons. (auth) (UK)

14453 MAGNETIC SUSCEPTIBILITY OF THE INTERMETALLIC COMPOUNDS OF THE Sn–Sm SYSTEM. Percheron, Annick; Lethuillier, Philippe (CNRS, Meudon-Bellevue, France. CNRS, Grenoble, France). Compt. Rend., Ser. B; 271: 1129-32(9 Dec 1970). (In French).

The magnetic behavior of the Sn–Sm compounds $SmSn_3$, Sm_2Sn_3, and Sm_5Sn_3 in the crystalline state was determined between 2 and 900°K. The variation in the susceptibilities with respect to temperature of these compounds does not follow the Curie–Weiss law. The Néel temperatures of $SmSn_3$ and Sm_2Sn_3 are 9 and 11°K, respectively. There is an anomaly in the susceptibility of Sm_5Sn_3 between 120 and 160°K. The three compounds exhibit minima in their susceptibilities in the 400°K region. (France)

14454 X-RAY STUDY OF THE STRUCTURES OF UN, UP, US, AND USe AT CRYOGENIC TEMPERATURES. Marples, J. A. C. (Atomic Energy Research Establishment, Harwell, Eng.). J. Phys. Chem. Solids; 31: 2431-39(Nov 1970).

The structures and lattice parameters of the compounds UN, UP, US, and USe were determined between 4 and 300°K. UN has a negative expansion coefficient below the Néel temperature (52°K) and UP, while showing no change at its Néel temperature (122°K), exhibits a small expansion anomaly at 22°K. US and USe both become rhombohedral below their Curie temperatures (178 and 160°K). The lattice distortion may be correlated with published magnetisation results. (auth) (UK)

14455 INFLUENCE OF THERMIONIC EMISSION ON MEASUREMENTS OF ELECTRICAL PROPERTIES OF REFRACTORY MATERIALS AT HIGH TEMPERATURES. Loup, J.-P.; Jonkiere, Nicole; Anthony, Anne-Marie (CNRS, Orleans, France). High Temp.-High Pressures; 2: 75-88(1970).

Significant differences in published high-temperature ($T > 1700°K$) electrical resistivity data question the validity of some of the measurements. An analysis is presented of the leakage resistances occurring in furnaces used for such measurements. The widespread hypothesis of thermal ionization of the furnace atmosphere is found to be unreasonable. It is shown that leakage currents are due to thermionic emission, both from the walls of the furnace and from the sample material itself, the leakage resistances acting in parallel with the real resistance of the material tested. The effects of temperature, voltage, and sample shape are discussed in detail. To eliminate errors resulting from leakage currents, it is recommended actually to determine the latter for the purpose of correcting the resistivity result. Alternatively, measurements should be taken at high voltages (200 V) or with a setup employing a suitably constructed guard ring. (auth) (UK)

14456 STRUCTURE OF FILM PREPARED BY LOW-ENERGY SPUTTERING OF MOLYBDENUM. Nagata, Saburo; Shoji, Fumiya (Kobe Univ., Japan). Jap. J. Appl. Phys.; 10: 11-17(Jan 1971).

Dependence of the structure and electrical resistivity of sputtered molybdenum films on residual gas pressure, ion energy, ion current density, and substrate temperature is investigated in detail. Fcc structure is obtained when the residual gas pressure is high and the deposition rate is low. The film structure is bcc on substrates at 500°C, while the film of fcc structure does not transform to bcc when it is heated up to 700°C in vacuum. The lattice constant of fcc structure coincides with that of γ-Mo_2N obtained by reactive sputtering. From these results, it is concluded that the film of fcc structure is γ-Mo_2N. (auth)

14457 NATURE OF SOLID SOLUTIONS IN THE NIOBIUM–OXYGEN SYSTEM. Dekanenko, V. M.; Vavilova, V. V.; Lyashchenko, A. B. (Inst. of Metallurgy, Moscow). Fiz. Metal. Metalloved.; 29: 1319-21(Jun 1970). (In Russian).

In the interaction between niobium and oxygen, the latter acts as an electron donor, which indicates that solid solutions of this system may have a strong bond. The solubility of oxygen in niobium amounts to 6 at.% at 1780°C and decreases with decreasing temperature. The nature of the interatomic bond was studied on alloys containing 0.2 to 6 at.% oxygen by determining their modulus of elasticity and calculating the shift of atoms from the equilibrium position. It was found that introduction of niobium resulted in a marked increase of the modulus of elasticity and the decrease of the mean-square shift of the atoms, thus indicating that the interatomic bond in the solid solution lattice became stronger as oxygen up to 6 at.% was introduced into the niobium. This is indeed attributed to the donor nature of oxygen and to the ordered distribution of the oxygen atoms in the niobium lattice, even when the concentration is quite low. (TTT)

14458 THERMAL MAGNETIC EFFECT AND THE THERMOELECTROMOTIVE FORCE OF GADOLINIUM AT 90 TO 250°K. Kondorskii, E. I.; Galkina, O. S.; Markov, P. A.; Karneev, A. N. (Moscow State Univ.). Fiz. Metal. Metalloved.; 29: 1300-2 (Jun 1970). (In Russian).

The change of thermoelectromotive force of gadolinium in a longitudinal magnetic field of 38.5 kOe was studied in the temperature range from 90 to 250°K. A potentiometer and a photoelectro-optical amplifier were used for the measurements. In view of the absence of a generally applicable theory of the longitudinal thermomagnetic effect in ferromagnetic rare-earth metals, the experimentally observed complex correlations between ΔQ_s, which characterized the thermomagnetic saturation effect, and the temperature could not be clearly explained; however, the temperature dependence of the light magnetization axis of gadolinium was definitely established. There was also a correlation between ΔQ_s and the effective anisotropy field. As the Curie point was approached, the thermoelectromotive force decreased, indicating a large contribution of the nonlocalized magnetic electrons to the magnetic moment. This also indicated that, in addition to the localized 4f electrons in the magnetic moment of gadolinium, nonlocalized 5d electrons were also involved in the magnetic moment. (TTT)

14459 TEMPERATURE DEPENDENCE OF DISLOCATION ATTENUATION IN γ-IRRADIATED LEAD. Lenz, D.; Luecke, K. (Technische Hochschule, Aachen). Cryst. Lattice Defects; 1: 297-308(Dec 1970).

The ultrasonic attenuation of γ-irradiated single crystals of lead was measured between 77 and 300°K. Warmup experiments after low-temperature irradiation as well as isothermal irradiation experiments yielded two dislocation-pinning stages centered at about 130 and 200°K, respectively, and two dislocation-depinning stages at about 180 and 270°K, respectively. In addition, measurements of the recovery of attenuation following thermal deformation and temperature-cycling experiments were made. The results are discussed in terms of point-defect diffusivity and pinning-point behavior. Evidence was obtained that both pinning stages were due to vacancies (with an activation energy of about 0.25 eV for the 130°K stage). The depinning stages were attributed to the formation of cluster-like pinning points (in the 180°K stage) and to the thermal instability of pinning points (in the 270°K stage). (auth)

14460 SELF-POLARIZATION CONTRIBUTION TO MAGNETIC ORDERING IN SYSTEMS WITH SINGLET GROUND STATE. Mahanti, S. D.; Varma, C. M. (Bell Telephone Labs., Murray Hill, N. J.). Phys. Rev., B; 3: 189-92(1 Jan 1971).

Self-polarization effects on the f-electron magnetization is found to contribute significantly to the susceptibility and critical value of the exchange for ordering of the rare-earth–group-V intermetallic compounds where the ground state of the rare-earth ion is a crystal-field singlet. For PrBi, a typical example of such a system, the contribution from the self-polarization effect is found to be of the same order as the Ruderman–Kittel–Kasuya–Yosida contribution. (auth)

14461 MAGNETIC PROPERTIES OF $Y_{1-x}Sm_xCo_5$ COMPOUNDS. Shibata, Tsugio; Katayama, Toshikazu; Mizuhara, Takeshi (Electrotechnical Lab., Tokyo). Jap. J. Appl. Phys.; 10: 163-5(Jan 1971).

Lattice parameters, magnetic anisotropies Ku_1 and Ku_2, and coercive force were measured for seven compounds in the series $Y_{1-x}Sm_xCo_5$. The results, plotted as functions of the Sm content, show peaks at $x = 0.5$ to 0.6. (D.L.C.)

14462 PLASMA RESONANCE IN TiO, VO, AND NbO. Rao, C. N. R. (Indian Inst. of Tech., Kanpur); Wahnsiedler, W. E.; Honig, J. M. J. Solid State Chem.; 2: 315-17(Nov 1970).

Reflectance spectra of TiO, VO, and NbO were recorded. All these oxides showed reflectance minima due to plasma edges. The energy corresponding to the reflectance minumum in TiO varied with stoichiometry (in the homogeneity range) and this phenomenon was related to the transport properties of these oxides. (auth)

14463 ELECTRONIC STRUCTURE OF SOME HEXABORIDES OF THE CaB_6 TYPE. Etourneau, Jean; Mercurio, Jean-Pierre; Naslain, Roger; Hagenmuller, Paul (Faculte des Sciences, Bordeaux). J. Solid State Chem.; 332-42(Nov 1970). (In French).

High-purity cubic MB_6 (M = Th, La, Yb, Ca, Sr) were prepared either from the elements or by borothermic reduction of oxides. Magnetic susceptibility, thermoelectric power, and specific heat were measured to study the electronic structure of the compounds. All the specimens were sintered at high temperature except LaB_6

XUM

samples which were zone refined. Hexaborides of elements having an oxidation state higher than two (M = Th, La) exhibited a metallic behavior. In YbB_6 ytterbium was divalent. Hexaborides of elements having an oxidation state equal to two (M = Yb, Ca, Sr) were semiconductors. The electronic behavior of the compounds that were studied agreed with the H. C. Longuet-Higgins and M. de V. Roberts' model. (auth)

14464 EFFECT OF HIGH-TEMPERATURE HEATING ON MAGNETIC PROPERTIES OF (Ce-MM)-Cu-Co TERNARY ALLOYS. Kawaguchi, Toranosuke (Meiji Univ., Tokyo); Yamamoto, Hiroshi; Takata, Shinzo. J. Jap. Inst. Metals; 34: 1097-1102 (Nov 1970). (In Japanese).

Studies on magnetic properties of intermetallic compounds of 3d transition elements and rare-earth metals (R) have been carried out by many workers. Especially, RCo_5 of these compounds was investigated as a new fine-particle permanent magnet, in view of its large magnetocrystalline anisotropy. Recently, cast magnets of the RCo_5-RCu_5 system have become a subject of ever increasing attention. The present experiment was carried out to investigate the effect of composition and heat treatment on magnetic properties of cast (Ce-MM)-Cu-Co ternary alloys. The specimens were made by melting the above ternary alloys in the induction furnace filled with argon gas and casting into the metal or shell mold. These cast samples were heat treated in the temperature range from 200 to 1220°C. In the ternary alloys of $(Ce-MM)Cu_xCO_{4-x}$, $(Ce-MM)Cu_xCo_{4.5-x}$, and $(Ce-MM)Cu_xCo_{5-x}$, the best magnetic properties were obtained in the composition range from x = 0.6 to 1.0. The magnetic properties of these alloys were improved remarkably by heat treatment at a higher temperature such as 1180°C. The magnetic properties of a typical sample were as follows: $4\pi I_{10000} = 5650(G)$, $4\pi I_r = 5450(G)$, ${}_IH_C = 2450(Oe)$, ${}_BH_C = 1950(Oe)$, $(B \cdot H)_{max} = 3.7$ (MG·Oe). (auth)

14465 ACOUSTIC AND MAGNETIC MEASUREMENTS OF TITANIUM AND ZIRCONIUM ALLOYS. Doherty, James Edward. Cleveland; Case Western Reserve Univ. (1969). 118p. University Microfilms Order No. 70-25,951.

Thesis.

The magnetic susceptibility and the internal friction spectra of some titanium and zirconium alloys were measured from 4 to 300°K. The magnetic measurements show that the transformation from the beta to the omega phase is reversible and continuous with temperature. The internal friction spectra show a peak in the vicinity of 180°K (at 120 kHz). This peak was found to be associated with the β phase and not with the $\beta-\omega$ interface as has been previously suggested by Nelson et al., (1965). These data are discussed in terms of the special electronic properties of the titanium-group elements. An analysis of the omega structure suggests that titanium-group elements can exist in two different electronic configurations. The existence of these two electronic species in the bcc beta phase results in stabilized or bound vacancies, which account for the anomalous diffusion behavior in the titanium-group elements. These vacancies and their stabilizing complex constitute defects in the bcc lattice, and these defects are responsible for the internal friction peak observed in the vicinity of 180°K in bcc titanium-group-element alloys. (Diss. Abstr. Int., B)

14466 OPTICAL SPECTROSCOPY OF Np^{4+} IN CUBIC AND OCTAHEDRAL CRYSTALLINE ELECTRIC FIELDS. Menzel, Erhard Roland. Pullman, Wash.; Washington State Univ. (1970). 110p. University Microfilms Order No. 70-24,991.

Thesis.

The optical absorption spectrum of Np^{4+} in single-crystal ThO_2 has been investigated at 4°K, 77°K, and room temperature between 0.3 and 3 μ. Intermediate-coupling wave functions and eigenvalues of the ground-state $5f^3$ electronic configuration were generated by computer using the lowest six J-manifolds of the spectrum, since they are reasonably well isolated. The free-ion parameters $E^1 = 3185$, $E^2 = 18.50$, $E^3 = 323.2$, and $\zeta = 2009$ in cm^{-1} provide the best agreement between theory and experiment. Inclusion of configuration interaction effects produced no significant improvement. A first-order crystal field analysis of the lowest six J-manifolds on the assumption of cubic symmetry yielded reasonably good agreement between calculation and experiment for the values $B_4 = -410$ and $B_6 = 50.4$ in cm^{-1} of the crystal field parameters. A dynamic distortion lifts inversion symmetry so that electronic electric dipole transitions are observed. Resulting line widths can be described to good approximation by the fictitious Hamiltonian $H = B_2\alpha O_2^0$ for $B_2 = 150\ cm^{-1}$. The optical absorption spectra of single-crystal Cs_2NpCl_6 and $(TEA)_2NpCl_6$, both of near-octahedral symmetry, were investigated between 0.4 and 3 μ at room temperature and between 0.4 and 1 μ at 77°K. Analysis of the spectra was carried out in the same manner as that of Np^{4+} in ThO_2. The parameters $E^1 = 2955$, $E^2 = 17.4$, $E^3 = 313.8$, $\zeta = 1985$, $B_4 = 520$, and $B_6 = 150$ in cm^{-1} provide reasonably good agreement between theory and experiment for both crystals. Electronic electric dipole transitions are also observed for Cs_2NpCl_6 and $(TEA)_2NpCl_6$, but are due to a static distortion from octahedral symmetry. The validity of the first-order crystal field analysis for Np^{4+} was confirmed by carrying out a first-order calculation for the isolated levels of $Pa^{4+}(5f^1)$ in Cs_2ZrCl_6 and $U^{4+}(5f^2)$ in Cs_2UCl_6, where levels are not nearly as well isolated as those of Np^{4+}. (Diss. Abstr. Int., B)

14467 A STUDY OF THE LATTICE DYNAMICS OF ZIRCONIUM USING THE TECHNIQUE OF THERMAL NEUTRON SCATTERING. Bezdek, Hugo Frank. Boulder, Colo.; Univ. of Colorado (1970). 92p. University Microfilms Order No. 70-23,685.

Thesis.

With the use of the triple-axis spectrometer at the Materials Testing Reactor in Idaho, coherent inelastic neutron scattering techniques were employed to measure the phonon dispersion curves for zirconium at room temperature. Data were taken in the two high-symmetry direction, [0001] and $[01\bar{1}0]$. Analysis of the data was accomplished on the basis of a six-neighbor modified-axially-symmetric model, which features noncentral but harmonic forces. Results from the model calculation permitted a calculation of the frequency distribution of normal modes. In addition, these results allowed the calculation of the elastic constants, which made possible a comparison with the elastic constants measured by ultrasonic methods, thereby providing a check on the model calculation. Elastic constants were also determined using just the slopes of particular branches of the dispersion curves. A comparison of these values with the ultrasonic data seems to indicate that zero sound propagation was observed in zirconium. Unfortunately, only qualitative comparisons can be made. Theoretical calculations, being rather intractable, are not available. (Diss. Abstr. Int., B)

14468 HELICON MEASUREMENTS IN METALS. Giovanielli, Damon Vincent. Hanover, N. H.; Dartmouth Coll. (1970). 177p. University Microfilms Order No. 70-25,524.

Thesis.

A study was made of standing-wave resonances of helicons in flat-plate metal samples. The parameters of the resonances are functions of the elements of the resistivity tensor of the metal. Resonances were studied in polycrystalline indium samples. Both very large and "finite" sample plates were used. The results were compared to accepted theory. The resonance parameters were inverted to obtain the elements of the anisotropic resistivity tensor of single-crystal silver. Results are shown for the variations of the tensor elements with field direction relative to the crystal axes. The tensor elements were also measured as functions of field strength for field directions parallel to (100), (110), (111) and (211). (Diss. Abstr. Int., B)

14469 ELECTRICAL TRANSPORT IN RARE-EARTH OXIDES. Rao, G. V. Subba; Ramdas, S.; Mehrotra, P. N.; Rao, C. N. R. (Indian Inst. of Tech., Kanpur). J. Solid State Chem.; 2: 377-84(Nov 1970).

Sesquioxides and nonstoichiometric oxides of rare-earths (Ln) exhibited electrical conductivities in the range 10^{-9} to $10^{-1}\ \Omega^{-1}\ cm^{-1}$. The sesquioxides exhibited mixed conduction with some contribution from ionic conductivity and major contribution from electronic conductivity. Seebeck-coefficient data as well as the oxygen partial pressure dependence of conductivity indicated that LnO_x compounds were mixed-valence semiconductors where oxides with $1.50 \le x \le 1.75$ were p-type semiconductors and oxides with $1.75 < x \le 2.00$ were n-type semiconductors. The conductivity of LnO_x (Ln = Pr or Tb) went through a maximum at $x \approx 1.75$; Seebeck coefficients were sensibly constant with temperature and approached zero values at $x \approx 1.75$. Employing the conductivities and Seebeck coefficients, transport parameters were calculated. The mechanism of conduction in these oxides can be understood in terms of the hopping model and the small-polaron theory. Fully ionized cation vacancies seem to be the predominant defects contributing to the defect structure in rare-earth sesquioxides. (auth)

14470 SEMICONDUCTOR $\rightleftharpoons$ METAL PHASE TRANSITIONS. Hyland, G. J. (Univ. of Warwick, Coventry, Eng.). J. Solid State Chem.; 2: 318-31(Nov 1970).

Existing experimental data pertaining to the semiconductor $\rightleftharpoons$ metal phase transitions found in some of the lower oxides of Ti and V are collated and summarized, and the theoretical implications of the insulating ground states of these and other solid compounds of transition elements (e.g., NiO) are discussed. In particular, the effect of dynamical Coulomb correlations on the validity of the Bloch-Wilson band theory is examined with special reference to the establishment of the Mott-insulating state. Various models exhibiting thermally induced semiconductor $\rightleftharpoons$ metal phase transitions are qualitatively described and their relevance to V_2O_3, VO_2, and Ti_2O_3 investigated. (auth)

14471 INELASTIC SCATTERING OF NEUTRONS FROM ANTIFERROMAGNETS. Schulhof, M. P. (Brookhaven National Lab., Upton, N. Y. State Univ. of New York, Stony Brook). Int. J. Magnet.; 1: 45-52(Oct 1970).

The dynamic aspects of the critical scattering of neutrons are discussed with regard to antiferromagnets. Results are presented for the time dependence of the spin fluctuations as a function of temperature and neutron wave vector in the isotropic system $RbMnF_3$ and the anisotropic material MnF_2. When analyzed in the manner suggested by dynamical scaling, these data are found to be well described by the theory. The scaling functions applying above and below the phase transition are determined explicitly, and a comparison is made between the two systems. (auth)

14472 A STUDY OF LOW ENERGY ELECTRON DIFFRACTION (LEED) INTENSITIES FROM CLEAVED SURFACES OF ZINC AND BERYLLIUM. Baker, John Michael. Ithaca, N. Y.; Cornell Univ. (1970). 227p. University Microfilms Order No. 70-17,459.

Thesis.

The intensities of low-energy electrons diffracted from cleaved (0001) surfaces of zinc and beryllium crystals were studied as a function of the direction and energy of the incident beam, in order to determine the basic mechanism of low-energy electron diffraction. A review of the theory of LEED is presented. The crystals were cooled to liquid nitrogen temperature and cleaved in a vacuum of 10^{-10} torr or less. The intensity of the 00 beam was measured from the phosphor screen of the display apparatus with a spot photometer. The incident beam current was measured simultaneously with the diffracted intensity and the logarithm of their quotient was formed electronically and recorded. This technique automatically corrects for any variations in the incident beam current. The intensity curves are found to be generally quite complex. They are quite sensitive to the direction of incidence, showing that dynamical interactions among the excited beams are important, i.e., strong multiple scattering is taking place. The cause of a strong minimum in a Bragg peak of zinc is identified as a strong coupling to another beam. An effect which may be a surface wave resonance is discussed. On contamination with CO or O_2, neither metal forms a superstructure as evidenced by the lack of extra diffracted beams. Furthermore, the I–V curves change insignificantly with contamination; possible implications of this observation are discussed. Preliminary work function measurements were made to detect contamination. The intensity of Bragg peaks of zinc were studied as a function of temperature and the results interpreted in terms of increased vibrational amplitudes for surface atoms. Also peak widths were measured as a function of temperature and energy. The experimental results are compared with the intensity calculations of Strozier using a wave matching formalism and a simplified model of the crystal. Although the comparison is not too favorable there are cases of agreement which lead one to believe that this highly simplified approach is basically correct and that further refinements in the theory will substantially improve the agreement. (TSS) (Diss. Abstr. Int., B)

14473 THERMAL RESISTIVITY OF CADMIUM, MAGNESIUM, AND ALLOYS AT LOW TEMPERATURES. Bogaard, Ronald Henry. Lafayette, Ind.; Purdue Univ. (1970). 58p. University Microfilms Order No. 70-18,600.

Thesis.

The intrinsic thermal resistivity (W_i) of pure Cd and CdZn single crystals with residual resistance ratios in the range 5×10^4 to 500 (Zn content up to 0.6 at. %) were measured for both hexagonal and basal orientations in the temperature range $3°K < T < 100°K$. The Cd data were represented by $W_i \propto T^n$. In the case of pure Cd, $n = 2$ for $T < 3.5°K$, whereas for the most impure alloy, $n = 2$ for $T < 13°K$. For temperatures above the $n = 2$ region, n was found to be as large as 4.5 in the interval $4°K < T < 7°K$ in the case of the purest crystal. The known, rapid change of the specific heat Debye θ does not explain the large n. This would imply a diminished interaction between the electrons and transverse phonons. A comparison between the electrical and thermal resistivities indicates that the electrical and thermal scattering processes are more similar than generally has been assumed. It is suggested that because of the particular shape of the Fermi surface, Umklapp processes may be important in the temperature range where n is large. In addition, several samples of Mg comprising pure polycrystals and single crystals with resistance ratios ranging from 1700 to 210 as well as two alloys (MgZn and MgPb), each having 0.1 at. % impurity were studied. The results of Mg indicate that $W_i \propto T^2$ is generally correct for $T < 50°K$. The purity is not sufficient to observe an effect similar to that for Cd. Small anomalies observed for $T \lesssim 5°K$ were similar to effects reported earlier as being related to magnetic impurities or a lattice thermal conduction. (Diss. Abstr. Int., B)

14474 DILUTION REFRIGERATION AND A CALORIMETRIC MEASUREMENT OF THE QUADRUPOLE COUPLING CONSTANT IN RHENIUM METAL. Rockwood, Stephen Dell. Pasadena, Calif.; California Inst. of Tech. (1970). 169p. University Microfilms Order No. 70-18,046.

Thesis.

A dilution refrigerator capable of producing steady-state temperatures less than 0.075°K was constructed. The performance of the refrigerator is compared with the operating characteristics of three other dilution refrigerators in the literature. The refrigerator was used to measure the nuclear contribution to the low-temperature specific heat of pure, single-crystalline rhenium metal. Measurements were made in magnetic fields from 0 to 12.5 kOe for the temperature range 0.13 to 0.52°K. The expected nuclear contribution is not found when the sample is in the superconducting state. This is believed to be due to the long spin–lattice relaxation times in superconductors. In the normal state, for the temperature range studied, the nuclear contribution is given by A/T^2 where $A = 0.061 \pm 0.002$ mJ-K/mole. The value of A is found to increase to $A = 0.077 \pm 0.004$ mJ-K/mole when the sample is located in a magnetic field of 12.5 kOe. From the measured value of A, the splitting of the energy levels of the nuclear spin system due to the interaction of the internal crystalline electric field gradients with the nuclear quadrupole moments is calculated. A comparison is made between the predicted and measured magnetic dependence of the specific heat. Finally, predictions are made of future nuclear magnetic resonance experiments that may be performed to check the results obtained by calorimetry here and further, to investigate existing theories concerning the sources of electric field gradients in metals. (Diss. Abstr. Int., B)

14475 ETTINGSHAUSEN EFFECT IN RARE-EARTH METALS. Zecchina, L. (Istituto di Fisica, Parma, Italy). Phys. Status Solidi; 42: K153-6(1 Dec 1970).

The fact that the Lorenz number $k/\sigma T$ of the rare-earth metals is larger than predicted by the Wiedemann–Franz law, led Gallo (J. appl. Phys., 36: 3410(1965)) to postulate a bipolar mechanism of heat transport. This predicts that other transport properties, including the Ettingshausen effect, should be anomalous. Ettingshausen coefficients P were measured for Gd, Dy, Tb, and Y polycrystals at room temperature and found to be (in units of 10^{-6} cm $°KA^{-1}G^{-1}$): 11.6, 29.3, 30.4, and 75, respectively, in agreement with Gallo (the P of a good metal is $\sim 10^{-10}$ cm $°KA^{-1}G^{-1}$). The anomalous behavior is ascribed to the multiband structure of the rare-earth metals and to two types of carriers. P measured in Gd single crystals was 70×10^{-6} cm $°KA^{-1}G^{-1}$. (D.L.C.)

14476 ELECTRICAL CONDUCTIVITY IN CUBIC Y_2O_3–ZrO_2 SOLID SOLUTIONS. Krishnan, C. S.; Chakravorty, D. (Indian Inst. of Tech., Kanpur). Mater. Res. Bull.; 6: 91-6(Feb 1971).

Guarded measurements of the electrical conductivity of Y_2O_3–ZrO_2 solid solutions were made on polycrystalline samples in the range 700 to 1250°C under ambient oxygen pressure. The ionic contribution to the total conductivity as determined by the blocking-electrode polarization technique was found to be negligible. The data tend to support an anion interstitial defect model determined on the basis of density measurements. (auth)

Moessbauer Effects and NMR

Refer also to abstract 13754.

14477 INFLUENCE OF COMBINED STATIC AND TIME-DEPENDENT QUADRUPOLE INTERACTIONS ON ANGULAR CORRELATION IN NUCLEI WITH INTEGRAL SPIN. Andrade, P. da R.; Rogers, J. D. (Univ. Federal do Rio Grande do Sul, Porto Alegre, Brazil). Phys. Rev., B; 3: 1052-3(1 Feb 1971).

The application of the Bloch–Wangsness–Redfield theory of nuclear relaxation to the study of perturbed angular correlations in even-A nuclei subject to simultaneous static and time-dependent quadrupole interactions is treated. The differences in the perturbation factors as compared to the odd-A case are shown. (auth)

14478 ELECTRON SPIN RESONANCE OF AXIALLY SYMMETRIC Er^{3+} IONS IN A SINGLE THORIA CRYSTAL. Michoulier, Jean; Wasiela, Andre (Grenoble Univ., Saint-Martin-D'Heres, France). Compt. Rend., Ser. B; 271: 1002-5(9 Nov 1970). (In French).

The ESR of Er^{3+} ions, occupying axial symmetric sites in relation to the four [111] directions of a single thoria crystal, was observed. The experiment was performed at 20°K with a frequency of 35,400 MHz. The influence of an axial deformation on the fundamental level of the Er^{3+} ion in a cubic site was calcu-

XUM

lated. Information was thus obtained on the separation between the Γ_7 and Γ_8 levels. (auth) (France)

14479 QUADRUPOLE RELAXATION OF ^{11}B AND ^{10}B NUCLEI. Akitt, J. W. (Univ. of Newcastle-upon-Tyne, Eng.). J. Magn. Resonance; 3: 411-14(Nov 1970).

The often-accepted view that quadrupole relaxation of ^{10}B is faster than that of ^{11}B is shown to be in error since the effect of the larger ^{10}B quadrupole moment is more than compensated by its larger nuclear spin. The significance of this for the appearance of the spectra of spin-½ nuclei coupled to boron is discussed. (auth) (UK)

14480 ELECTRIC QUADRUPOLE INTERACTIONS IN SINGLE CRYSTALS OF Te METAL, Hf METAL AND $CaWO_4$ BY MOESSBAUER EFFECT. Boolchand, Punit. Cleveland; Case Western Reserve Univ. (1969). 155p. University Microfilms Order No. 70-25,938.

Thesis.

The Moessbauer effect in ^{178}Hf was studied with oriented single-crystal absorbers of hafnium metal at 4°K. Along the [0001] axis only the $|\Delta m| = 1$ component of the quadrupole spectrum is observed, and along the $[10\bar{1}0]$ axis only the $|\Delta m| = 1$ and $|\Delta m| = 2$ components are observed. Combining these observations with those made using a polycrystalline hafnium-metal absorber, the magnitude of the electric field gradient was found to be $V_{zz} = (0.95 \pm 0.04) \times 10^{18}$ volts/cm^2, and the asymmetry parameter $\eta < 0.1$. The Debye temperature of hafnium carbide was estimated to be (350 ± 10)°K, and the Debye temperature of hafnium metal was found to be (227 ± 10)°K and (192 ± 13)°K, for gamma rays propagating parallel to and perpendicular to the c-axis, respectively. The Moessbauer effect in Te single-crystal absorbers was studied along different crystal axes. Area ratios of the quadrupole doublet were used as an experimental parameter to extract the electric field gradient and mean square displacement tensors. Experimental data taken at 4°K fits well to collinear principal axes for the electric field gradient and mean square displacement tensors. Within the limits of experimental uncertainties, the Debye–Waller factor is found to be isotropic. $\Delta Eq = 7.74 \pm 0.10$ mms/sec, $\eta = 0.64 \pm 0.04$, and $\langle x^2\rangle = \langle y^2\rangle = \langle z^2\rangle = (1.6 \mp 0.05)\lambda^2$. The electric quadrupole interactions in ^{183}W (99.1 keV) $\frac{5}{2}^-$ state and in ^{182}W (100.1 keV) 2^+ state were studied in single crystals of $CaWO_4$ using the Moessbauer effect. For ^{182}W, along the c-axis only the $|\Delta m| = 1$ quadrupole component is observed, and along the a-axis only the $|\Delta m| = 1$ and $|\Delta m| = 2$ quadrupole components are observed. Combining these measurements with polycrystalline $CaWO_4$, the magnitude of the axially symmetry ($\eta \simeq 0$) quadrupole interactions at 4°K are found to be $e^2qQ(2^+)^- = (3.24 \pm 0.1)$ mms/sec and $e^2qQ(5/2)^- = -(7.53 \pm 0.3)$ mms/sec. This gives the quadrupole moment ratio $Q(5/2^-)/Q(2^+) = 0.91 \pm 0.04$. From the ^{183}W Moessbauer measurements with a thin tungsten-metal foil absorber, the lifetime of the $5/2^-$ state is found to be 0.99 ± 0.04 nsec. (Diss. Abstr. Int., B)

14481 ^{27}Al NUCLEAR MAGNETIC RESONANCE AND THE POSSIBILITY OF MAGNETIC ORDERING IN DELTA-PLUTONIUM. Fradin, F. Y.; Brodsky, M. B. (Argonne National Lab., Ill.). Int. J. Magnet.; 1: 89-91(Oct 1970).

The ^{27}Al nuclear magnetic resonance was used to look for a postulated magnetic transition in fcc delta-plutonium. No evidence for a magnetic transition or local moment formation was found. The ^{239}Pu resonance was sought between $0.31 \leq \nu/H \leq 0.89$ without success. (auth)

14482 ANALYSIS OF EPR SPECTRA OF OXIDIZING CATALYSTS. Trifiro, Ferruccio (Istituto G. Donegani, Novara, Italy); Nucciotti, Alessandro; Mognaschi, Ezio Roberto; Lanzi, Giuseppe. Atti Accad. Naz. Lincei, Rend., Cl. Sci. Fis., Mat. Natur.; 48: 358-63(Mar 1970). (In Italian).

EPR investigations were conducted of the paramagnetic centers formed during reduction at high temperature in vacuum of MoO_3, WO_3, Ta_2O_5, and Nb_2O_5. For all oxides, a signal was observed at g = 0.002, both at –170°C and at room temperature. This signal was destroyed reversibly by the presence of molecular oxygen; furthermore, it was not possible to observe any peroxidic species. The data are discussed in view of the hypothesis that the paramagnetic center is an F center or species O^-. Moreover, the EPR spectra of the studied oxides with metal–oxygen double bond are discussed in relation to those of oxides without such a metal–oxygen bond. (auth)

14483 HYPERFINE MAGNETIC FIELDS IN USb FROM MOESSBAUER SPECTROSCOPY. Shenoy, G. K.; Kalvius, G. M.; Ruby, S. L.; (and others) (Argonne National Lab., Ill.). Int. J. Magnet.; 1: 23-8(Oct 1970).

The hyperfine interaction in antiferromagnetic USb was investigated using the Moessbauer technique in both ^{121}Sb and ^{238}U. A saturation hyperfine magnetic field of 170 ± 5 kOe was detected at the Sb nucleus. The presence of a unique field value at all the nonmagnetic anions is consistent with the type-I antiferromagnetic structure, determined by neutron diffraction. The anion field per unit moment in USb is about four times the value found in the analogous compound UP. This ratio of the anion fields is shown to be about equal to the ratio of the atomic hyperfine fields of Sb and P. The hyperfine field at the U nucleus is 4500 ± 200 kOe. This value scales linearly with the ordered moment at the uranium when compared to UO_2 and the free U^{4+} ion. (auth)

14484 NONLOCAL PSEUDOPOTENTIAL CALCULATION OF CONTRIBUTIONS TO THE KNIGHT SHIFT IN BERYLLIUM METAL. Gerstner, Joseph. University Park, Pa.; Pennsylvania State Univ. (1969). 77p. University Microfilms Order No. 70-19,413.

Thesis.

Measurements of the Knight shift in beryllium were recently reported by Barnaal, Barnes, McCart, Mohn and Torgeson, and by Anderson, Ruhilig and Hewitt, who find, respectively, the $(\Delta H/H)$ value to be $-0.0027 \pm 0.0006\%$, and $-0.0025 \pm 0.0006\%$. All previous theoretical calculations have failed to explain this anomalously small shift or its sign, with the exception of a recent work by Jena, Mahanti, and Das; they have obtained the correct sign of the shift but only order of magnitude agreement with experiment. In this work, the principal contributions to this effect, viz., the hyperfine contact (p) and the diamagnetic (d) contributions were calculated. In order to compute the complete Knight shift, the results of the calculations were combined with core polarization (cp) effects. Wave functions and the effective mass on the Fermi surface were obtained by a nonlocal pseudopotential calculation using the OPW potential of Loucks and Cutler. Energies and wave functions were determined for 712 points in the 1/24th Brillouin zone, from which 190 points were obtained by interpolation on the Fermi surface chosen 0.95 ryd above the Γ-point energy. First and second derivatives of the energy function were also obtained at these points by interpolation. From these 190 points on the 1/24th portion of the Fermi surface, averages of the Knight shift due to hyperfine contact (p) interaction and to diamagnetic (d) susceptibility were obtained: $(\Delta H/H)_p = +0.00130\%$, and $(\Delta H/H)_d = -0.00374\%$. Using the work of Jena, Mahanti, and Das, one obtains a core polarization contribution of $(\Delta H/H)_{cp} = -0.00026\%$. The total calculated the Knight shift is found to be –0.0027%; there is now good agreement between the measured and theoretically calculated Knight shift in beryllium. The effect, for the first time, has been shown to be primarily the result of orbital contributions (diamagnetism), with the hyperfine interaction contributing less than originally predicted. (Diss. Abstr. Int., B)

14485 AMBIGUITY PROBLEM IN THE EVALUATION OF MOESSBAUER SPECTRA FOR ^{57}Fe. Dabrowski, L.; Piekoszewski, J.; Suwalski, J. (Inst. of Nuclear Research, Swierk, Poland). Nucl. Instrum. Methods; 91: 93-5(1 Jan 1971).

The relations between the nuclear energy levels of ^{57}Fe and hf parameters of Moessbauer-effect spectra are discussed. It is shown that, in a general case, there is more than one value of each of the EFG parameters that gives the same spectrum for a powder sample. The possible ambiguities in the determination of hf parameters from Moessbauer spectra are illustrated. (auth)

Theory

Refer also to abstract 14493.

14486 MULTIPLE PLASMON EFFECTS IN THE ENERGY-LOSS SPECTRA OF ELECTRONS IN THIN FILMS. Sunjic, M.; Lucas, A. A. (International Centre for Theoretical Physics, Trieste, Italy). Phys. Rev., B; 3: 719-29(1 Feb 1971).

The interaction of a fast electron (energy $\gtrsim$ 1 keV) with collective modes in a thin metallic or doped semiconductor film is studied, taking explicitly into account bulk and surface effects. Reducing the problem to an exactly soluble quantum-mechanical model, results to all orders of the interaction are obtained, and the multiple-plasmon contribution to the electron energy losses is investigated. The theory is applied to transmission as well as to reflection and a complete description of the loss spectra is obtained. It is shown that the zero-energy plasmon mode does not cause singularities in the low-energy excitation spectrum. The strength of the many-body processes is given by the "fine-structure constant" $e^2/\hbar v_\perp$, where $v_\perp$ is the electron velocity normal to the surface, and in some cases multiple-plasmon emission becomes important, especially so in the specular reflection at grazing-angle incidence. For a thicker slab ($a \sim 500$ to 1000 Å), this results in a series of sharp peaks in the loss spectrum that have maximum strengths corresponding to several excited plasmons. For a thin slab (a ~ few 100 Å), the dominant contribution to the loss spectrum is a broad structure with a high-energy ($\omega > \omega_p$) tail, characteristic for the recombinational effect of many emitted low-energy plasmons. (auth)

14487 INDIRECT EXCHANGE COUPLING OF MAGNETIC MOMENTS IN RARE-EARTH METALS. **Robinson, Lawrence Baylor** (Univ. of California, Los Angeles); **Ferguson, Lloyd N. Jr.; Milstein, Frederick.** Phys. Rev., B; 3: 1025-33(1 Feb 1971).

The Ruderman–Kittel–Kasuya–Yosida (RKKY) exchange mechanism is examined for its relevance to ferromagnetism in the rare-earth metals. More specifically, the experimental sensitivity of the exchange energy (or Curie temperature) to the interatomic spacing (applied pressure) of the rare earths is examined in terms of the RKKY interaction. The form in which the interaction is usually examined, i.e., with the coupling parameter J(r) given by a Dirac δ function, is unable to provide the observed sensitivity of Curie temperature to interatomic spacing. When this coupling parameter, or exchange interaction, is calculated with free-ion wave functions for the 4f electrons, instead of the δ-function approximation, agreement between theory and experiment is still not obtained. A modification of the coupling parameter is proposed which effectively takes into account some contribution of the crystal in determining the wave functions to be associated with the isolated magnetic moments. The procedure is phenomenological. Both the correct shape of the Curie-temperature–pressure curve and the sensitivity of the Curie temperature to pressure are obtained. Also the correct interlayer turn angle of the various elements is obtained. Undetermined multiplicative parameters appear in the final result that can be adjusted at some point in order to make the agreement quantitative. The conclusion is that the present modification of the RKKY interaction appears to account correctly for the origin of ferromagnetism in the rare-earth metals. (auth)

14488 ASSOCIATED-WAVE SCATTERING OF LIGHT AND SLOW NEUTRONS IN SEMICONDUCTOR ANTIFERROMAGNETS. **Bar'yakhtar, V. G.; Bass, F. G.; Makhmudow, Z. Z.** (Physical-Technical Inst., Kharkov). Sov. Phys.-Solid State (Engl. Transl.); 12: 1596-9(Jan 1971).

Translated from Fiz. Tverd. Tela; 12: 2009-14(Jul 1970).

The scattering of electromagnetic waves near resonance between longitudinal plasma waves and spin waves, and the scattering of slow neutrons near this resonance as well as near the resonance between helicoidal and spin waves are considered. Effective scattering cross sections are calculated. It is shown that the intensity of scattering of light by magnetic moment fluctuations increases sharply near resonance. A similar behavior is observed in the scattering of slow neutrons by electrical fluctuations. (auth)

14489 TEMPERATURE-DEPENDENT PROPERTIES OF ISOTOPIC DEFECTS IN A CUBIC LATTICE. **Eisenriegler, E.** (Kernforschungsanlage, Juelich, Ger.). Cryst. Lattice Defects; 1: 281-95(Dec 1970).

The x-ray scattering cross section of a crystal containing a small concentration of isotopic defects was calculated for temperatures T below the Debye temperature. In the case of heavy defects, low temperature expansions for the mean square displacement (MSD) of a single defect and for the specific heat are given for a temperature interval which includes the resonance frequency. For T = 0, an explicit expression for the MSD of a single defect as a function of the mass ratio is given. (auth)

Theoretical Physics

Refer also to abstract 13981.

14490 (AD-711681) DIFFICULTY AND POSSIBILITY OF KINETIC THEORY OF QUANTUM-MECHANICAL SYSTEMS. PART III. INCONSISTENT SCALE EFFECTS IN THE THEORY OF SCATTERING. PART IV. INCONSISTENCIES IN REPRESENTATION OF PHOTON–ELECTRON INTERACTION. **Koga, Toyoki** (Polytechnic Inst. of Brooklyn, N. Y. Dept. of Aerospace Engineering and Applied Mechanics). Jul 1970. Contracts Nonr-839(38); DAHC04-69-0077. 37p. (PIBAL-70-35). NTIS.

It is shown that results of the theory of scattering among unfixed particles vary inconsistently depending on the choice of volume scale employed for the second quantization. This situation demonstrates that the conventional quantization method is not feasible for treating interactions among unfixed particles. The paradox is an inevitable consequence of the theory of absolute indeterminism underlying the conventional method of quantization. Only by interpreting a wave function as an ensemble representation may one reach reasonable results. It is noted that the same paradox arises in common in classical mechanics, if one treats interactions among particles according to Gibbs concept of particle. Inconsistent scale effects and questionable momentum relations are shown to be involved in conventional representatives of the photon–electron interaction. The inconsistencies are similar to those that tend to occur in the classical kinetic theory. (auth) (USGRDR)

14491 ALGEBRAIC SOLUTION OF A SHORT-RANGE POTENTIAL PROBLEM. **Cordero, P.; Hojman, S.** (Univ. Catolica de Chile, Santiago). Lett. Nuovo Cim.; 4: 1123-4(12 Dec 1970).

The bound S-state energy spectrum of the Schroedinger equation with the Morse short-range central potential is solved using the SU(2,1) spectrum-generating algebra. (L.B.S.)

14492 DECAY OF ORDER IN ISOTROPIC SYSTEMS OF RESTRICTED DIMENSIONALITY. I. BOSE SUPERFLUIDS. **Jasnow, David; Fisher, Michael E.** (Cornell Univ., Ithaca, N. Y.). Phys. Rev., B; 3: 895-907(1 Feb 1971).

The off-diagonal ordering of one- and two-dimensional Bose-particle systems of finite thickness and cross section is considered, in the presence and absence of a symmetry-breaking field. It is shown rigorously, by applying Bogolyubov's inequality to a subdomain of the system, that no spontaneous ordering can occur; several definitions of long-range order are discussed. Explicit bounds on the order–order correlation function, integrated over a subdomain, are obtained which indicate how the short-range order decays with distance. Conditions under which information on the pointwise behavior of the correlation function can be inferred are also discussed. The inequalities are assessed numerically for real situations. (auth)

14493 DECAY OF ORDER IN ISOTROPIC SYSTEMS OF RESTRICTED DIMENSIONALITY. II. SPIN SYSTEMS. **Fisher, Michael E.; Jasnow, David** (Cornell Univ., Ithaca, N. Y.). Phys. Rev., B; 3: 907-24(1 Feb 1971).

The ordering of one- and two-dimensional spin systems of finite thickness and cross section is considered in the presence and absence of a symmetry-breaking magnetic field. The exchange interactions are allowed to vary randomly or regularly throughout the lattice. It is shown rigorously, by applying Bogolyubov's inequality to a subdomain of the system that, provided the (suitably averaged) exchange interactions do not fall off too slowly, no spontaneous ordering can occur. Explicit bounds on the spin–spin correlation function, summed over the sites in a subdomain, are obtained which indicate how the short-range order decays with distance. Detailed numerical plots for the order as a function of the subdomain size are presented for various realistic values of the temperature. Conditions under which these curves yield bounds on the spatial decay of the spin–spin correlation function are also discussed. (auth)

14494 NOTE ON THE PARTITION FUNCTION FOR SYSTEMS OF INDEPENDENT PARTICLES. **Ford, D. I.** (LeTourneau Coll., Longview, Tex.). Amer. J. Phys.; 39: 215-20(Feb 1971).

The N-particle Bose–Einstein and Fermi–Dirac canonical partition functions are expressed explicitly in terms of the single-particle partition function. The nature of the approximations made in using corrected Maxwell–Boltzmann statistics is thereby made more obvious. A recurrence relation is developed to facilitate calculations using the exact partition function. (auth)

14495 TIME EVOLUTION OF SIMPLE QUANTUM-MECHANICAL SYSTEMS. II. TWO-STATE SYSTEM IN INTENSE FIELDS. **Salzman, W. R.** (Univ. of Arizona, Tucson). Phys. Rev. Lett.; 26: 220-1(1 Feb 1971).

The Schrödinger equation for a two-state quantum-mechanical system with sinusoidal perturbation is numerically integrated with respect to time. From these results a general formula for the induced transition probability (as a function of time, perturbation frequency, and perturbation strength) is extracted. (auth)

14496 SOLUTION OF THE TIME-DEPENDENT SCHROEDINGER EQUATION BY THE LAPLACE TRANSFORM METHOD. **Lin, S. H.; Eyring, H.** (Arizona State Univ., Tempe. Univ. of Utah, Salt Lake City). Proc. Nat. Acad. Sci. U. S. A.; 68: 76-81 (Jan 1971).

The time-dependent Schroedinger equation for two quite general types of perturbation is solved by introducing the Laplace transforms to eliminate the time variable. The resulting time-independent differential equation can then be solved by the perturbation method, the variation method, the variation–perturbation method, and other methods. (auth)

14497 THE NUMERICAL SOLUTION OF COUPLED DIFFERENTIAL EQUATIONS ARISING FROM THE SCHROEDINGER

XUM

EQUATION. Allison, A. C. (Smithsonian Astrophysical Observatory, Cambridge, Mass.). J. Comput. Phys.; 6: 378-91 (Dec 1970).

Several step-by-step methods for the numerical solution of coupled differential equations are given and compared under realistic circumstances. A variant of the Numerov method is found to be the most efficient. A novel method that consists of approximating the solutions by sets of Airy functions is investigated. (auth)

14498 QUANTUM PROCESSES IN A CONSTANT ELECTRIC FIELD. Nikishov, A. I. (Lebedev Inst. of Physics, Moscow). Zh. Eksp. Teor. Fiz.; 59: 1262-72(Oct 1970). (In Russian).

The differential probability for emission of a photon by an electron moving in a constant electric field is derived. The differential probabilities of the remaining processes represented by the "three-tail" under consideration are also obtained. (auth)

14499 PROPAGATION OF ELECTROMAGNETIC WAVES IN RIEMANN SPACE. Volkov, A. M.; Izmest'ev, A. A.; Skrotskii, G. V. (Moscow Physical-Technical Inst.). Zh. Eksp. Teor. Fiz.; 59: 1254-61(Oct 1970). (In Russian).

The principal equations describing propagation of electromagnetic waves in Riemann space with an arbitrary metric as propagation in a certain anisotropic "medium" are derived and investigated. The nature of the anisotropy depends on the metric tensor. An analysis of the equations derived shows that double refraction of electromagnetic waves in an arbitrary gravitational field should always exist. A necessary and sufficient condition for absence of double refraction in any anisotropic medium is proportionality between the dielectric and magnetic permeability tensors. A general expression is found that permits one to determine the variation of parameters characterizing polarization of an electromagnetic wave moving in space with a given metric. (auth)

14500 FLUID-SOLID PHASE TRANSITION OF A HARD-SPHERE BOSE SYSTEM. Hansen, Jean-Pierre; Levesque, Dominique; Schiff, Daniel (Laboratoires de Physique Theorique et Hautes Energies, Orsay, France). Phys. Rev., A; 3: 766-80 (Feb 1971).

The ground-state energy of a system of hard-sphere bosons of diameter σ is calculated by a variational method using a Jastrow wave-function for the fluid phase and a "localized" Jastrow times a Gaussian wave function for the solid phase. The transition densities are $\rho_{\text{fluid}} = 0.23 \pm 0.02$ particles/σ^3 and $\rho_{\text{solid}} = 0.25 \pm 0.02$ particles/σ^3. (auth)

14501 GROUND-STATE ENERGY OF A MIXTURE OF FERMIONS AND BOSONS IN ONE DIMENSION WITH A REPULSIVE δ-FUNCTION INTERACTION. Lai, C. K.; Yang, C. N. (State Univ. of New York, Stony Brook). Phys. Rev., A; 3: 393-9(Jan 1971).

The ground-state energy of a mixture of spin-$\frac{1}{2}$ fermions and bosons in one dimension, interacting with a repulsive δ-function potential, is analyzed. The wave function is given by repeated use of a generalized Bethe hypothesis. The "momenta" in the hypothesis are determined by coupled Fredholm integral equations. Numerical solutions are given. No phase separation is found. (auth)

14502 CONCERNING A THOUGHT EXPERIMENT VIOLATING HEISENBERG'S UNCERTAINTY PRINCIPLE. Billette, J. J.; Campillo, C.; Lee, C.; McConnell, R. D.; Pariseau, G.; Fischer, G. (Univ. of Montreal). Can. J. Phys.; 47: 2415-6(Nov 1969).

It is shown that "Robinson's thought experiment" does not violate Heisenberg's uncertainty principle, contrary to the claim of its designer. (auth) (Canada)

14503 SIMPLE PROOF OF THE SEMI-CIRCLE' LAW FOR GAUSSIAN RANDOM MATRICES. Gervois, A. (CEN de Saclay, Gif-sur-Yvette, France). Nucl. Phys.; B25: 551-6(1971).

A functional property of the Gaussian function is used to derive an implicit equation for the asymptotic level density of random matrices belonging to the Gaussian real or unitary ensembles. A generalization to some other Gaussian Hermitian random matrices is described. (auth)

14504 DENSITY OPERATOR FOR UNPOLARIZED RADIATION. Prakash, H.; Chandra, N. (Univ. of Allahabad, India). Phys. Lett.; 34A: 28-9(25 Jan 1971).

In a recent note (Phys. Lett., 31A: 331(1970)) the authors calculated cross sections for second harmonic generation in scattering of radiation of a general nature by free electrons and pointed out that the currently used procedure for studying nonlinear interactions of unpolarized radiation is not correct. The purpose of this note is to report the form of the density operator for unpolarized radiation obtained by a simple method and to point out that the "unpolarized radiation," nonlinear interactions of which have been studied by several authors, is not actually unpolarized. An unpolarized beam of radiation is defined as one that is (i) symmetric about the direction of propagation, and (ii) remains so even on introducing arbitrary phase changes in its two orthogonally polarized components. (auth)

14505 SUPEROPERATOR TRANSFORMATION THEORY IN QUANTUM MECHANICS. Mandel, P. (Univ. Libre, Brussels). Physica; 50: 77-87(23 Nov 1970).

In the generalized transformation theory proposed by Prigogine et al. (Proc. Nat. Acad. Sci., 65: 789(1970)) a transformation operator $\overline{\gamma}$, introduced in the subspace spanned by one of the orthogonal operators Π, removes the off-diagonal elements of the subspace. The author (Physica, 48: 397(1970)) proposed a differential equation for that operator. The purpose of this note is to prove that the transformation operator is equivalent to a unitary transformation in quantum mechanics when the spectrum of the Hamiltonian is discrete and nondegenerate. Much of the note is devoted to showing how to write a unitary transformation in terms of superoperators. (L.M.T.)

14506 COVARIANT CLASSICAL MOTION OF ELECTRON IN A LASER BEAM. Meyer, James W. (Purdue Univ., Lafayette, Ind.). Phys. Rev., D; 3: 621-2(15 Jan 1971).

The classical motion of an electron interacting with a plane-wave electromagnetic pulse is calculated in a fully covariant manner, starting from the relativistic equation of motion neglecting radiation reaction. (auth)

14507 RELATIVISTIC MOTION IN A CONSTANT FIELD AND THE SCHOTT ENERGY. Herrera, J. C. (Brookhaven National Lab., Upton, N. Y.). Nuovo Cim.; 70B: 12-20(11 Nov 1970).

The Lorentz–Dirac equation of motion for a particle moving in a uniform magnetic field is solved in a form consistent with the idea of Bhabha that the physical solutions be continuous functions of the interaction constant when the value of the constant approaches zero. Using this solution, it is shown explicitly how the Schott energy plays an essential role in the energy balance characterizing the motion. Similar considerations for the Schott energy are shown to apply in the case of motion in a uniform electric field. An approximate expression for the Schott energy associated with a particle moving in an arbitrary constant field is derived. (auth)

14508 CAUSALITY AND LORENTZ INVARIANCE IN RELATIVISTIC QUANTUM MECHANICS. Ishikawa, Yoshiko. San Diego, Calif.; Univ. of California (1970). 78p. University Microfilms Order No. 70-17,790.

Thesis.

In the Fock space of the physical states of a single spinless particle, an attempt is made to construct an interaction Hamiltonian. The following conditions on the Hamiltonian are imposed: (1) it is Hermitian; (2) it does not affect the vacuum and single particle states; and (3) the S-matrix given by Dyson's formula is Lorentz invariant. Any interaction Hamiltonian in field theory does not satisfy the second condition, since the Fock space of the theory consists of bare states instead of physical states. As it is the case in field theory, the Lorentz invariance of the S-matrix is possibly attained through an interaction Hamiltonian which can be expressed by the space integral of a causal and Lorentz invariant interaction Hamiltonian density. It is found, however, that an interaction Hamiltonian density in the physical Fock space, made of a sum of terms, each of which has finite number of creation and annihilation operators, ($a^{+}_{k_1} \ldots a^{+}_{k_s} a^{+}_{s+1} \ldots a^{+}_{k_n}$ with n finite) can probably not satisfy both Lorentz invariance and causality simultaneously. The question whether a meaningful Hamiltonian density, made of infinite series including terms with infinite number of creation and annihilation operators, can fulfill both the conditions, is open. Since the way described is not a unique one to attain the invariance of S-matrix, other possibilities are considered. A fairly simple way is found to construct an interaction Hamiltonian without a causal and invariant density, which gives a Lorentz invariant S-matrix. It is even possible to obtain an interaction Hamiltonian that leads to exactly the same S-matrix as that given by field theory. The detail is investigated using the S-matrix given by the φ^4 model of scalar field theory. It is concluded that the properties of S-matrix (Lorentz invariance, analyticity, etc.) do not necessarily require causality and Lorentz invariance of an interaction Hamiltonian density. (Diss. Abstr. Int., B)

XUM

PHYSICS (HIGH ENERGY)

Particle Interactions and Properties (Experimental)

Refer also to abstracts 14583, 14837, and 14925.

Electromagnetic

Refer also to abstract 13300.

14509 (INP-718) COMPARISON OF THE K/π RATIO IN MULTIPLE PRODUCTION AT ENERGIES 60 GeV AND ~ 1000 GeV. Babecki, J.; Furmanska, B. (Institute of Nuclear Physics, Krakow (Poland)). 1970. 8p. Dep. NTIS (U. S. Sales Only).

In 200 jets with $N_h \leq 5$ originated by 60-GeV pions from the Serpukhov accelerator and in 203 comsic-ray jets with energies ~1000 GeV found in nuclear emulsion the identification of relativistic secondary particles emitted at the angles ≥20° and of grey tracks was performed. It was found that in the region of large normalized longitudinal momenta $(-p_\parallel^* > 0.2)$ the K/π-ratio is equal 1.50 ± 0.62 for high energy cosmic-ray jets and only 0.24 ± 0.10 for accelerator jets. (auth)

14510 PHOTON REST MASS. Franken, P. A.; Ampulski, G. W. (Univ. of Michigan, Ann Arbor). Phys. Rev. Lett.; 26: 115-17(11 Jan 1971).

Experiments were performed with very low-frequency parallel resonance circuits which, subject to some questions of theoretical validity, set a new upper limit for the photon rest mass of 10^{-49} g. This value is more than an order of magnitude smaller than the previous limit established by satellite measurements of the earth's magnetic field. (auth)

14511 PHOTOPRODUCTION OF HIGH-MASS DI-PION PAIRS AT 15 BeV. Bulos, F. (Stanford Univ., Calif.); Busza, W.; Giese, R.; (and others). Phys. Rev. Lett.; 26: 149-51(18 Jan 1971).

The cross section was measured for the photoproduction of dipions in the mass range 0.9 to 2.2 GeV/c^2. The experiment was performed with a 16-GeV bremsstrahlung beam on a Be target. Upper limits on the cross section for photoproduction of high-mass vector mesons are determined. (auth)

14512 PHOTOPRODUCTION OF ω MESONS FROM HYDROGEN AND DEUTERIUM. Behrend, H.-J. (Univ. of Rochester, N. Y.); Lee, C. K.; Lobkowicz, F.; (and others). Phys. Rev. Lett.; 26: 151-4(18 Jan 1971).

The ω-meson photoproduction cross sections, summed over elastic $(\gamma N \rightarrow \omega N)$ and inelastic $(\gamma N \rightarrow \omega N^*)$ channels, were measured from hydrogen and deuterium targets. The results agree with a calculation which includes only elastic and $N^*(1236)$ channels, suggesting that photoproduction of higher resonances is small. No evidence is found for I = 1 natural-parity (e.g., A_2) exchange. (auth)

14513 MEASUREMENT OF THE Σ^+ MAGNETIC MOMENT. Alley, P. W.; Benbrook, J. R.; Cook, V.; (and others) (Univ. of Washington, Seattle). Phys. Rev., D; 3: 75-80(1 Jan 1971).

The magnetic moment of the Σ^+ hyperon was measured to be 2.7 ± 1.0 nuclear magnetons. (auth)

14514 SEARCH FOR AN ELECTRON MASS SHIFT IN ^{133}Cs IN AN INTENSE ELECTROMAGNETIC FIELD. Mowat, J. Richard (Univ. of California, Berkeley); Johnson, Charles E.; Shugart, Howard A.; Ehlers, Vernon J. Phys. Rev., D; 3: 43-51(1 Jan 1971).

The possibility that the mass of a bound electron changes when placed in an intense electromagnetic field is studied here both theoretically and experimentally. The atomic-beam magnetic-resonance technique was used to examine hyperfine-structure frequency shifts in ^{133}Cs that occur when the atom is subjected to an intense, nonresonant radio-frequency magnetic field perpendicular to the static "C" field. A 2921-MHz TM_{010} cavity produced the perturbing field and was situated between Ramsey separated oscillatory loops, which induced the resonant transitions of interest. Shifts were observed for six $\Delta m_F = \pm 1$ transitions at field-independent points. No evidence was found for an electron mass shift. Good agreement is found between all observed shifts and those expected from a multilevel Bloch–Siegert effect. (auth)

14515 VALIDITY OF THE LEPTONIC SELECTION RULES FOR THE (μeγ) VERTEX AT HIGH FOUR-MOMENTUM TRANSFERS. Alles-Borelli, V.; Bernardini, M.; Bollini, D.; (and others) (CERN, Geneva. Istituto Nazionale di Fisica Nucleare, Bologna. Univ., Bologna. CNEN, Frascati, Italy). Lett. Nuovo Cim.; 4: 1151-5(12 Dec 1970).

A colliding-beam experiment was performed in search for the possible existence of the process $e^+ + e^- \rightarrow \mu^\mp + e^\pm$, which, in the one-photon approximation, can take place if at the μ–e–γ vertex the currently known leptonic selection rules are violated. An analysis was made of data at energies from 0.8 GeV to 1 GeV, in the angular range of 45 to 135°. No good candidate was found for a muon–electron pair event. (L.B.S.)

14516 RECOIL PROTON POLARIZATION FROM NEUTRAL PION PHOTOPRODUCTION ON HYDROGEN IN THE ENERGY RANGE FROM 1200 TO 1800 MeV. Tanaka, Nobuyuki. Medford, Mass.; Tufts Univ. (1969). 260p. University Microfilms Order No. 70-18,013.

Thesis.

The polarization of the recoil proton in neutral pion photoproduction on hydrogen was measured for incident photon energies from 1200 to 1800 MeV and a mean pion production angle of 65° in the center-of-mass. The experiment was performed at the 6-GeV alternating gradient electron synchrotron at the Cambridge Electron Accelerator during the autumn of 1967. A large carbon-plate spark chamber was utilized for the measurement of scattering asymmetry and range. A total of approximately 160,000 events in the incident photon energy range of 900 to 1800 MeV were recorded on film. The polarization values were calculated by a maximum-likelihood method using existing analyzing power data for proton-carbon scattering. Analysis was done on a portion of such events for incident photon energies above 1200 MeV The results indicate that the polarization changes sign from negative to positive values around 1300 MeV photon energy. Plotting the polarization vs four momentum transfer squared, one sees a structure between –0.5 and –0.6 $(GeV)^2$. The agreement with the Caltech group is good within two standard deviations. The steep variation of polarization as a function of the center-of-mass angle, seen earlier at the California Institute of Technology, was confirmed in the present experiment. The polarization seems to cross the axis at around $|t| = 0.5$ from negative to positive. This is the region of ω-dip where ω-trajectory goes through zero. (Diss. Abstr. Int., B)

14517 LIMITS ON THE ELECTROMAGNETIC PRODUCTION OF HEAVY LEPTONS. Alles-Borelli, V.; Bernardini, M.; Bollini, D.; (and others) (CERN, Geneva. Istituto Nazionale di Fisica Nucleare, Bologna. Univ., Bologna. CNEN, Frascati, Italy). Lett. Nuovo Cim.; 4: 1156-9(12 Dec 1970).

The possible production of a heavy lepton with electron and muon decay modes was studied in a colliding-beam $e^+ + e^-$ experiment at 0.8 to 1 GeV. No evidence was found for the existence of a heavy lepton with mass less than 780 MeV. (L.B.S.)

14518 BROKEN CHANNELS IN π^+-PHOTOPRODUCTION ON ^{3}He. Guardiola, R.; Sanchez-Gomez, J. L. (International Centre for Theoretical Physics, Trieste, Italy). Nuovo Cim.; 1A: 243-54(21 Jan 1971).

The reactions $\gamma + {}^3He \rightarrow \pi^+ + n + d$ and $\gamma + {}^3He \rightarrow \pi^+ + n + n + p$ are studied in the impulse approximation. The angular distributions of the π's as well as the total cross sections for both reactions are calculated. Final-state interaction effects are investigated for the first reaction. (auth)

14519 γ PARTIAL CROSS SECTIONS UP TO 12 GeV AND THE ISOVECTOR–ISOSCALAR INTERFERENCE. Alexander, G.; Bar-Nir, I.; Dagan, S.; (and others) (Tel Aviv Univ., Ramat, Israel). (Phys. Rev. Lett.; 26: 340-3(8 Feb 1971).

γn reactions are studied in a 40-in. bubble chamber filled with deuterium. Cross sections for channels with no neutral particles in the final state are presented up to a photon energy of 12 GeV. For channels with one neutral particle the cross sections are presented at 7.5 GeV only. Comparison of γn reactions with their charge-symmetric γp reactions indicates a considerable isovector-isoscalar interference contribution. (auth)

14520 EXPERIMENT ON 2 γ-QUANTUM ANNIHILATION ON THE VEEP-2. Balakin, V. E.; Budker, G. I.; Pakhtusova, E. V.; (and others) (Inst. of Nuclear Physics, Novosibirsk, USSR). Phys. Lett.; 34B, 99-100(18 Jan 1971).

The results of 2 γ-quantum annihilation of e^+e^- pairs at the total energy of 2E = 1 GeV and large angles of the outgoing quanta are given. Simultaneously the same apparatus detects the elastic scattered electrons. Comparison of the measured ratio of γ-quanta to electrons with the calculated ratio, allows the validity limit of quantum electrodynamics Λ > 1.3 GeV to be obtained. (auth)

XUM

14521 REACTIONS $\gamma n \rightarrow p\pi^+\pi^-\pi^-$, $p\pi^+\pi^-\pi^-\pi^0$ AND $n\pi^+\pi^+\pi^-\pi^-$ AT 4.3 GeV. Eisenberg, Y.; Haber, B.; Kogan, E.; (and others) (Weizmann Inst. of Science, Rehovot, Israel). Nucl. Phys.; B25: 499-509(1971).

A study of γd interactions leading to multi-pion final states is presented. No quasi-two-body reactions are observed. The multi-body reactions $\gamma n \rightarrow V^0\pi^-p$ ($V^0 = \rho^0,\omega^0$) are seen and the conjectured production mechanism is discussed. Evidence for other resonance production is also shown. (auth)

14522 PHOTOPRODUCTION OF ETA MESONS IN THE FORWARD DIRECTION. Ito, Albert Shunji. Ithaca, N. Y.; Cornell Univ. (1970). 142p. University Microfilms Order No. 70-23,118.

Thesis.

The η photoproduction cross section was measured from hydrogen in the forward direction with incident photon energies ranging from 1.465 to 1.815 GeV. A bremsstrahlung beam from the Cornell 2.2-GeV synchrotron struck a liquid hydrogen target and the photoproduced eta mesons were detected via the two photon decay mode. Each photon was detected by one of a pair of identical detection arms, each consisting of a scintillation anticounter, a lead-plate optical spark chamber, a 5 × 3 scintillation counter hodoscope and a total-absorption, lead-glass Cherenkov counter. The range of incident photons was limited by means of a bremsstrahlung subtraction. The measured cross section agrees with the t-channel exchange theory of Gorczyca et al., and gives a value for $S^2d\sigma/dt$, which agrees within experimental errors with the higher energy data. Comparison of results with the prediction of the generalized interference model of Bajpai et al., indicates that their inclusion of the $D_{13}(2030)$ resonance into their theory is incorrect and that the addition of a ρ^0 exchange, which was an alternative they mentioned, is probably needed. Also a crude measurement was made of the cross section for the reaction with a pi meson plus an eta in the final state. The measurement disagrees with the model of Celeghini et al. (Diss. Abstr. Int., B)

14523 THE RATIO OF NEGATIVE TO POSTIVE PIONS IN FORWARD PION PHOTOPRODUCTION. Ramanauskas, Algimantas. Ithaca, N. Y.; Cornell Univ. (1970). 137p. University Microfilms Order No. 70-12,643.

Thesis.

The ratio $[\sigma(\gamma d \rightarrow \pi^-pp)/\sigma(\gamma d \rightarrow \pi^+nn)]|_{\theta=0^\circ}$ was measured as a function of incident photon energy between 600 and 1700 MeV. A triple focusing magnet spectrometer was used to detect the forward going pion. Electron contamination was eliminated by placing about one radiation length of material at the first focus as well as using a gas Čerenkov anti-counter in conjunction with an optical shower spark chamber. This measurement of the π^-/π^+ ratio and the well-known measurements of the $\gamma p \rightarrow \pi^+n$ cross section in the forward direction have been used to determine A_S and A_V, the isoscalar and isovector pion photoproduction amplitudes in the exact forward direction, as a function of energy. It was assumed that the forward production amplitudes are predominantly real and that Re $A_V \gg$ Re A_S. A substantial isoscalar contribution which varied rapidly with energy was found in the region between 600 and 1300 MeV. This is also the region where the $I = \frac{1}{2}$ baryon resonances $D_{13}(1520)$, $P_{11}(1470)$, $S_{11}(1550)$, $F_{15}(1690)$, and $D_{15}(1650)$ are located, and their excitation is believed to cause the main contribution to A_S. Also the values of A_V are compared with predictions obtained from fixed-t dispersion relations and have found fairly good agreement for energies below 900 MeV. In the energy range between 900 and 1700 MeV the values of A_V were lower than the predicted background amplitude and this is a result of contributions coming from the $I = \frac{3}{2}$ baryon resonances which are located in this energy region, such as $F_{37}(1950)$, $F_{35}(1910)$, etc. No evidence was found for the production of Roper's resonance $P_{11}(1470)$ and therefore one was not able to draw conclusions about its SU(3) classification. The $[\sigma(\gamma d \rightarrow \pi^+nn)/\sigma(\gamma d \rightarrow \pi^+n)|_{\theta=0^\circ}$ ratio was also measured and found to be equal to ~0.67, in agreement with theoretical predictions. It was pointed out however that these theoretical discussions may not be reliable since they used the closure approximation which is open to serious question in the exact forward direction. Finally, measurements of the π^-/π^+ ratio which had been corrected for final state Coulomb effects according to the method of Baldin was used to find the forward cross section for π^- photoproduction from a free neutron target. (Diss. Abstr. Int., B)

14524 HIGH ENERGY PHOTOPRODUCTION OF NEUTRAL MESONS. Kreinick, David Louis. Pasadena, Calif.; California Inst. of Tech. (1970). 167p. University Microfilms Order No. 70-12,439.

Thesis.

Cross sections for the photoproduction of neutral pi, eta, rho and phi mesons on hydrogen were measured at the Stanford Linear Accelerator Center using a missing-mass spectrometer technique. The data cover photon energies between 5.0 and 17.8 GeV and four momentum transfer squared t between −.12 and −1.38 $(\mathrm{GeV}/c)^2$. Pion differential cross sections at lower energies show a peak at low momentum transfers, a distinctive dip and secondary maximum for t in the region −.4 to $-.9(\mathrm{GeV}/c)^2$, and a smooth decrease at higher momentum transfers. As photon energy increases, the dip becomes less pronounced, in contradiction to the expectations of simple Regge theories based on the exchange of omega and B trajectories only. Eta photoproduction was measured only below 10 GeV. The cross section has about the same magnitude as the pion production cross section, but decreases exponentially with t, showing no dip. Rho mesons appear to be diffractively produced. The differential cross section varies approximately as $\exp(8.5t + 2t^2)$. It falls slowly with energy, decreasing about 35 percent from 6 GeV to 17.8 GeV. A simple quark model relation appears to describe the data well. Phi meson cross sections are also consistent with diffraction production. The differential cross section varies approximately as exp(4t). The cross section tends to decrease slightly with photon energy. Production of particles with masses between 1100 and 2000 MeV was sought. A broad resonance with mass 1240 ± 20 MeV was observed. It is tentatively identified with the B meson. No particle of mass between 1300 and 2000 MeV and width less than 200 MeV was produced with a cross section larger than about 10 percent of the rho's. (Diss. Abstr. Int., B)

14525 THE DIRECT PRODUCTION OF ELECTRON PAIRS IN NUCLEAR EMULSION BY 13.75 GeV ELECTRONS. Cary, Arthur Simmons. Riverside, Calif.; Univ. of California (1969). 84p. University Microfilms Order No. 70-11,983.

Thesis.

The observation of events in nuclear emulsion appearing to be tridents caused by the direct production of a primary electron has resulted in an uncertainty as to whether the trident cross section may not be considerably higher than that predicted by quantum electrodynamics. However, previous workers have been hampered in their efforts to resolve this difficulty because of poor statistics, uncertainty of the energy of primary electron and unsatisfactory approximation methods for correcting pseudo-tridents produced by bremsstrahlung radiation. The nuclear emulsions in this experiment were exposed to the Stanford Linear Accelerator electron beam at an energy of 13.75 GeV. Forty-five meters of electron track were scanned, and 1085 trident-like events were observed. Two techniques were applied in determining the number of real tridents and the mean free path for trident production. A correction technique, depending on the numerical integration of the Bethe−Heitler equations for bremsstrahlung radiation and pair production, was carried out. The number of bremsstrahlung pairs that one would expect to find in a radiation length was determined by this correction method. The other method depends on the fact that the creation of bremsstrahlung pairs varies quadratically with the distance; while, the yield for tridents varies linearly with the distance. A direct measure of the trident mean free path can be obtained by plotting the differential probability of the total distribution of apparent tridents in distance and by extrapolating the best fitting straight line to zero distance. The correction for pseudo-tridents using a numerical integration technique leads to values of the mean free path for direct pairs which are smaller than that predicted by theory. The method of extrapolating the differential distribution leads to values of the mean free path that are in excellent agreement with theory. (Diss. Abstr. Int., B)

14526 PHOTOPRODUCTION OF PION PAIRS WITH HIGH INVARIANT MASS. Alvensleben, H.; Becker, U. J.; Bertram, William K.; (and others) (Deutches Elektronen-Synchrotron, Hamburg. Massachusetts Inst. of Tech., Cambridge). Phys. Rev. Lett.; 26: 273-6(1 Feb 1971).

The yield of $\pi^+\pi^-$ pairs from the reaction $\gamma + C \rightarrow C + \pi^+ + \pi^-$ in the invariant-mass region $0.6 < m < 1.8\ \mathrm{GeV}/c^2$ was measured. The result, based on 10^5 events, shows that the data, at high energy and very small momentum transfer, exhibit an enhancement in the region $1.3 < m < 1.8\ \mathrm{GeV}/c^2$. (auth)

14527 DETERMINATION OF THE PHOTOPRODUCTION PHASE OF ρ^0 MESONS. Alvensleben, H.; Becker, U.; Chen, M.; (and others) (Deutsches Elektronen-Synchrotron, Hamburg. Massachusetts Inst. of Tech., Cambridge). Nucl. Phys.; B25: 342-50(1971).

Large-angle electron-positron pairs from the reaction $\gamma + \mathrm{Be} \rightarrow \mathrm{Be} + e^+ + e^-$ in the e^+e^- invariant-mass region of $610 < m < 850\ \mathrm{MeV}/c^2$ were measured. The phase of the photoproduction amplitude of the ρ-meson at 4.1 to 6.1 GeV was found to deviate from pure imaginary by 11.8° ± 4.4° which corresponds to a ratio of the real to imaginary ρ-nucleon amplitude of $\beta = -0.2 \pm 0.1$. (auth)

14528 OBSERVATION OF COHERENT INTERFERENCE PATTERN BETWEEN ρ, ω DECAYS. Alvensleben, H.; Becker,

XUM

U.; Bertram, William K.; (and others) (Deutsches Elektronen-Synchrotron, Hamburg. Massachusetts Inst. of Tech., Cambridge). Nucl. Phys.; B25: 333-41(1971).

A high-statistics experiment measuring the structure of e^+e^- mass spectrum from photoproduction of ρ- and ω-mesons is reported. At 5.1 GeV, based on 4000 events, analysis of the spectra yields a ratio of vector-meson-photon coupling constants $\gamma_\omega^2\sigma_{\rho N}/\gamma_\rho^2\sigma_{\omega N} = 9.4$ and a ρ, ω production phase difference $\varphi_{\omega\rho} = 41° \pm 20°$. (auth)

14529 WIDE-ANGLE BREMSSTRAHLUNG: ANGULAR DEPENDENCE. Lichtenstein, Carl Arthur. Ithaca, N. Y.; Cornell Univ. (1970). 148p. University Microfilms Order No. 70-12,632.

Thesis.

The cross section for wide angle bremsstrahlung was measured by electron-photon coincidences, using the circulating beam of the Cornell 10-GeV electron synchrotron. Earlier work with the electron spectrometer and photon detector placed symmetrically about the incident beam was extended by placing the detectors in two asymmetric arrangements, thus varying the ratio of timelike to spacelike masses contributing. Data were taken around the point of transverse momentum balance (minimum momentum transfer to the nucleus) at several energies in each arrangement. In the large photon angle arrangement, a background of electroproduced pions prevented an accurate measurement. For the large electron angle case, the data confirm the predictions of quantum electrodynamics. The best quadratic and quartic fits to the ratio of experimental rate to predicted rate are $R = (1.00 \pm 0.039) + (0.060 \pm 0.075)m_T^2$ and $R = (1.00 \pm 0.039) + (0.060 \pm 0.070)m_T^4$. These can be interpreted in terms of a cutoff distance Λ^{-1}; 95% confidence upper limits of this parameter for these fits are $\Lambda_2^{-1} = 6.5 \cdot 10^{-15}$ cm and $\Lambda_4^{-1} = 11 \cdot 10^{-15}$ cm. The data are also interpreted in terms of upper limits for the coupling constant for heavy electron production. The calculation of contributions from inelastic nuclear states is described in more detail. (Diss. Abstr. Int., B)

Weak

Refer also to abstract 14762.

14530 MEASUREMENT OF THE BRANCHING RATIO $K_L^0 \to 2\pi^0/K_L^0 \to 3\pi^0$. Oliver, William Parker. Berkeley, Calif.; Univ. of California (1969). 62p. University Microfilms Order No. 70-17,632.

Thesis.

The rate of the decay $K_L^0 \to 2\pi^0$ was measured relative to that of $K_L^0 \to 3\pi^0$ using a monoenergetic K_L^0 beam and a nearly 4π solid-angle detection system of lead-plate spark chambers and shower counters. The analysis of the fraction (40%) of the data at the Lawrence Radiation Laboratory gives for the branching ratio 0.0100 ± 0.0018 (statistical) ±0.0009 (systematic). This result leads to a value for the branching ratio $[\Gamma(K_L \to 2\pi^0)/\Gamma(K_L \to \pi^+\pi^-)]$ of 1.37 ± .25 (statistical) ± .14 (systematic). The significant difference between this ratio and the $[\Gamma(K_L \to 2\pi^0)/\Gamma(K_L \to \pi^+\pi^-)]$ implies that CP violation must occur at least in part in the $K^0 \to 2\pi$ decay process itself. (Diss. Abstr. Int., B)

14531 PRECISE MEASUREMENT OF THE K^+ LIFETIME. Ott, R. J.; Pritchard, T. W. (Queen Mary Coll., London). Phys. Rev., D; 3: 52-6(1 Jan 1971).

A measurement of the K^+ mean lifetime was made to resolve the discrepancy of 4.5 standard deviations between the two previous best measurements. An accurate timing system was used, enabling a precision of nearly 1 part in 1000 to be obtained. The result was a mean lifetime of 12.380 ± 0.016 nsec. The time spectrum over six mean lifetimes showed no deviations from a pure exponential at a 0.1% level. (auth)

14532 COMMENTS ON SOME RECENT MUON EXPERIMENTS. Hickey, F. R. (Clarkson Coll. of Tech., Potsdam, N. Y.); McNulty, P. J.; Shivpuri, R. K.; Wixon, N. J. Phys. Rev., D; 3: 254-5(1 Jan 1971).

Several studies have appeared in the literature based on emulsion exposures to either 10.1-GeV/c μ^+ or 15.8-GeV/c μ^- at the Brookhaven AGS in 1966. The effect of discrepancies in the values of the primary momenta of both beams on their results is discussed. (auth)

14533 EXPERIMENTAL TEST OF THE $\Delta S = \Delta Q$ RULE IN LEPTONIC DECAYS OF NEUTRAL K MESONS. Webber, Bryan R.; Solmitz, Frank T.; Crawford, Frank S. Jr.; Alston-Garnjost, Margaret (Univ. of California, Berkeley). Phys. Rev., D; 3: 64-74(1 Jan 1971).

The final results are reported of a study of the time distribution of decays of neutral K mesons produced in the reaction $K^- + p \to \bar{K}^0 + n$. Independent results based on 81 electronic and 38 muonic decays are presented. Combining these with 133 ambiguous events, for the $\Delta S = -\Delta Q$ parameter x the value $\mathrm{Re}(x) = 0.25^{+0.07}_{-0.09}$, $\mathrm{Im}(x) = 0.00 \pm 0.08$ is found. This value lies about 2.5 standard deviations away from the point x = 0, and to this extent the experiment suggests a violation of the $\Delta S = \Delta Q$ rule. In the course of an investigation of background processes, the rate of the radiative decay $K_S \to \pi^+\pi^-\gamma$ is identified and measured. (auth)

14534 MEASUREMENT OF THE $K_{\mu 3}^+$ DECAY PARAMETERS. Haidt, D. (Technische Hochschule, Aachen); Stein, J.; Natali, S.; (and others). Phys. Rev., D; 3: 10-37(1 Jan 1971).

A sample of K^+ mesons stopped in the CERN 1.1-m^3 heavy-liquid bubble chamber was used to study the Dalitz-plot density and the μ^+ polarization in $K_{\mu 3}^+$ decay and to measure the $K_{\mu 3}^+$ and K_{e3}^+ branching ratios. All three analyses are described in detail, and they are used, separately and combined, to study the form of the strangeness-changing, semileptonic weak interaction. This is found to be consistent with a coupling of vector currents and to be invariant under time reversal. The vector form factors are studied with a wide range of assumptions as to their possible four-momentum (q^2) dependence, and the results of all three measurements are in agreement. If λ_+ is fixed at 0.029 (the average value from K_{e3}^+ experiments) and if ξ is assumed to be independent of q^2, then the result is $\xi = -0.65 \pm 0.13$. Assuming that $f_+(q^2)$ and $\xi(q^2)$ are both linear functions of q^2, a three-parameter fit gives $\lambda_+ = 0.060 \pm 0.019$, $\xi(0) = -1.0 \pm 0.5$, and $\xi(5.1m_\pi^2) = -0.97 \pm 0.20$. (auth)

14535 EXPERIMENTAL RESULTS ON STOPPING MUONS AT 60 AND 300 m.w.e. Bergamasco, Laura; Castagnoli, Carlo; Tabasso, M. Cristina; Picchi, Pio. Atti Accad. Naz. Lincei, Rend., Cl. Sci. Fis., Mat. Natur.; 48: 423-6(Apr 1970).

In the experiment performed liquid scintillators were used rather than emulsions for well-known efficiency problems, and a detector of large volume and spherical symmetry was used to reduce the geometrical effects. Curves are shown describing the experimental results on the traversing muon intensity, the stopping muon rate, and the ratio of the traversing muons to the stopping muons rate. (J.F.P.)

14536 EXPERIMENTAL STUDY OF THE DECAY SPECTRUM OF $K_L^0 \to \pi^+\pi^-\pi^0$. Smith, Richard Cecil. College Park, Md.; Univ. of Maryland (1970). 193p. University Microfilms Order No. 70-23,320.

Thesis.

An experimental study of the decay $K_L^0 \to \pi^+\pi^-\pi^0$ based on a final sample of 4580 events is described. The experiment was performed in a 30° neutral beam at the Brookhaven AGS by use of a counter-triggered wide-gap chamber in a 10.4 kilogauss magnetic field. The data are compared to results generated by Monte-Carlo techniques to determine a best-fit value of the slope parameter, σ_0, of the linear-spectrum approximation $|M|^2 \sim 1 + 2\sigma_0 (m_K/m_{\pi^0}) (2T_{\pi^0} - T_{\pi^0 \max})$ with the result $\sigma_0 = -0.300 \pm 0.018$. The error includes both a statistical contribution and other effects which are described. Systematic effects are also considered. Both the matrix element, M, as well as $|M|^2$ are found to be consistent with having no quadratic dependence on T_{π^0}. When compared to results from K^+ decay, the results of this experiment appear to be in disagreement with the theoretical predictions of the $\Delta I = 1/2$ rule. However, the value of σ_0 is shown to be in rather good agreement with theoretically predicted values based on current algebra using PCAC and including $\Delta I = 3/2$ transitions. In addition, as a search for possible CP violation, the $\pi^+\pi^-$ asymmetry, a, on the Dalitz plot is calculated. No indication of CP violation is found as the value obtained is: a = 0.000 ± 0.018. (Diss. Abstr. Int., B)

14537 BUBBLE CHAMBER SEARCH FOR $K_S^0 \to \pi^+\pi^-\pi^0$. Haggerty, Herman Frederick. Madison, Wis.; Univ. of Wisconsin (1970). 132p. University Microfilms Order No. 70-19,147.

Thesis.

The CP violating three pion decay mode of the short lived neutral kaon ($K_S^0 \to \pi^+\pi^-\pi^0$) was searched for in the Argonne-Michigan 40″ heavy liquid bubble chamber. No statistically significant evidence for the process was found. (Diss. Abstr. Int., B)

14538 TEST OF THE $\Delta S = \Delta Q$ RULE IN NEUTRAL K-e3 DECAY. Littenberg, Laurence Stephen. San Diego, La Jolla, Calif.; Univ. of California (1969). 181p. University Microfilms Order No. 70-13,225.

Thesis.

Neutral K-e3 decay was studied in the K^0-$\bar{K}^0$ interference region. K^0's were produced by the charge exchange of 1 GeV/c separated K^+ beam. The three charge exchange targets were separated by spark chambers to allow determination of the charge exchange point. The K's decayed in a thin foil spark chamber situated in a magnetic field. Electrons were identified by their showers in a 12-gap spark chamber with 1/8-inch lead plates between the gaps. One and three tenths million pictures were scanned to obtain ~40,000 leptonic candidates. These were measured and the ~4000 events which were kinematically most likely to be K-e3 decays were rescanned by physicists. After a final kinematic selection 686 events remained. The visual and kinematical filtering procedure reduced the competing decay modes (primarily $K_S \rightarrow \pi^+\pi^-$) from >400:1 to <0.10:1 in the most sensitive region ($\tau < 3\ \tau_S$). The lifetime distributions of the selected $e^+\pi^-\nu$ and $e^-\pi^+\nu$ events were fit to the theoretical distributions: $N^{\pm}(\tau) = k\ \{|1 + x|^2 e^{-\Gamma_S\tau} + |1 - x|^2 e^{-\Gamma_L\tau} + 4\ \mathrm{Im}(x) \sin(\delta\ \tau)\ e^{-\frac{1}{2}(\Gamma_S+\Gamma_L)\tau} \pm 2(1 - |x|^2) \cos(\delta\ \tau)\ e^{-\frac{1}{2}(\Gamma_S+\Gamma_L)\tau}\}$ (where $\Gamma_{S,L}$ is the $K_{S,L}$ decay rate, and δ is the K_S-K_L mass difference) using a Monte Carlo-calculated detection efficiency curve. The parameter x is the ratio of the $\Delta S = -\Delta Q$ amplitude to the $\Delta S = \Delta Q$ amplitude. CP conservation requires x to be real. There are found Re x = $.09^{+.14}_{-.16}$, Im x = $-.11^{+.10}_{-.11}$. If CP is assumed to be conserved (Im x ≡ 0) it is found that x = 0 ± .12. This assumption might be appropriate in view of the fact that, of all particle reactions studied in the last four years, still the only example of CP violation is the $K_L \rightarrow 2\pi$ decay, and it seems, more and more, that $\eta_{00} = \eta_{+-}$, that is the CP violation is confined to the fact that the compositions K_S,K_L are not CP eigenstates rather than to CP violation in the decay interaction. If one assumes x = 0 and fits for $\delta = .48^{+.066}_{-.060}$ are obtained in units of $\hbar/\tau_S$. If the best fit value is assumed for x, $\delta = .485^{+.058}_{-.053}$ is obtained. (Diss. Abstr. Int., B)

14539 ASYMMETRY PARAMETERS IN $\Sigma^- \rightarrow ne\ \bar{\nu}$ AND $\Sigma^+ \rightarrow p\gamma$. Gershwin, Lawrence Kenneth. Berkeley, Calif.; Univ. of California (1969). 123p. University Microfilms Order No. 70-13,053.

Thesis.

An experiment was performed in the Lawrence Radiation Laboratory 25-inch hydrogen bubble chamber. There were 1.3×10^6 pictures taken of the interactions of a K^- beam ranging in momentum from 270 to 470 MeV/c, with most of the pictures taken in the vicinity of 390 MeV/c, where the $Y_0^*(1520)$ resonance is formed. The interference of the resonant amplitude with that of the predominantly S-wave background produces polarized Σ's in the reactions $K^-p \rightarrow \Sigma^-\pi^+$ and $K^-p \rightarrow \Sigma^+\pi^-$. From a sample of 85,000 $\Sigma^- \rightarrow n\pi^-$ decays and 57,000 $\Sigma^+ \rightarrow p\pi^0$ decays we have found 53 examples of $\Sigma^- \rightarrow ne\ \bar{\nu}$, 8 of $\Sigma^- \rightarrow n\mu\ \bar{\nu}$, and 61 of $\Sigma^+ \rightarrow p\gamma$. The leptonic Σ^- decays were analyzed to measure the correlation between the Σ^- polarization and the direction of the charged lepton, as described by the lepton distribution $(1 + \alpha\ P_\Sigma \cos\theta)$. The asymmetry parameter α for the electron events was found to be $\alpha = -0.26 \pm 0.37$. The asymmetry parameter is related to g_A/g_V, the ratio of the axial-vector to vector weak coupling constants. It was found that $g_A/g_V = 0.16 \pm {}^{0.19}_{0.18}$ for the electron events. The sign convention is such that $g_A/g_V = -1.2$ for $n \rightarrow pe\ \bar{\nu}$. Assuming μ-e universality, $g_A/g_V = 0.19 \pm {}^{0.20}_{0.17}$ was found for the combined electron and muon events. A comparison with Cabibbo's theory of semi-leptonic decays showed reasonable agreement with the prediction of the theory when a fit was carried out to presently published data for baryon leptonic decays. For the 61 $\Sigma^+ \rightarrow p\gamma$ events, the asymmetry parameter expressing the correlation of the Σ^+ polarization with the direction of the proton was measured, obtaining $\alpha = -1.03^{+0.52}_{-0.42}$. The branching ratio $(\Sigma^+ \rightarrow p\gamma)/(\Sigma^+ \rightarrow p\pi^0) = (2.76 \pm 0.51) \times 10^{-3}$ was measured, using 31 of the $\Sigma^+ \rightarrow p\gamma$ events. Both the branching ratio and asymmetry parameter were found to be in agreement with some theoretical calculations, although the asymmetry parameter is two standard deviations from the value α = 0 predicted by SU(3) invariance. (Diss. Abstr. Int., B)

Strong (Baryon-Induced)

14540 (IFVE-SEF-70-16) OBSERVATION OF anti ^{3}He. Antipov, Yu. M.; Vishnevskii, N. K.; Gorin, Yu. P.; (and others) (Gosudarstvennyi Komitet po Ispol'zovaniyu Atomnoi Energii SSSR, Serpukhov. Institut Fiziki Vysokikh Energii). 1970. 31p. (In Russian). Dep. NTIS (U. S. Sales Only).

$^3\widetilde{He}$ nuclei were observed in the negative beam, produced by 70-GeV protons on an AL traget. Five $^3\widetilde{He}$ have been identified among $2{,}4\text{-}10^{11}$ particles that passed through the apparatus. Scintillation and Čerenkov counters were used to measure electrical charge and velocity of particles. The mass of $^3\widetilde{He}$ is obtained to be $M_{^3\widetilde{He}} = (1.00 \pm 0.03)\ 3m_p$, the charge is $z = (0.99 \pm 0.05)2e$. The ratio of differential production cross sections of $^3\widetilde{He}$ (P = 20 GeV/c) and π^- (P = 10 GeV/c) equals $2(10^{-11})$. This corresponds to antihelium-3 production cross section $d^2\sigma_{^3\widetilde{He}}/d\Omega dP = 2.0(10)^{-35}$ cm²/ster (GeV/c) per AL nuclei and $2.2(10)^{-36}$ cm²/ster (GeV/c) per nucleon. (auth)

14541 (JINR-P1-5399) SEARCH FOR A NEW TYPE OF RADIOACTIVITY IN ALUMINUM AND TUNGSTEN TARGETS IRRADIATED BY 70-GeV PROTONS. Dem'yanov, A. V.; Kulikov, A. V.; Kuptsov, A. V.; Mkrtchyan, G. G.; Nemenov, L. L.; Pontekorvo, B. M.; Smirnov, G. I.; Fedunov, A. G.; Khazins, D. M.; Chirkin, Yu. M. (Joint Inst. for Nuclear Research, Dubna (USSR). Lab. of Nuclear Problems). 1970. 11p. (In Russian). Dep. NTIS (U. S. Sales Only).

A method was previously proposed suitable for searching for hypothetical quasi-stable elementary particles which might be produced in high-energy collisions. The method is based on the idea that such particles may be trapped in nuclear matter and thereby originate a new type of radioactivity characterized by a comparatively high energy of its disintegration products (tens of MeV or more). The first results are given of a search for a radioactivity with the emission of high-energy gamma quanta from targets irradiated for a long time by 70-GeV protons at Serpukhov. Lifetimes in the range from one day to several years were considered. The experimental set-up consists of three scintillation counters, an optical spark chamber, a water Cherenkov counter and a total absorption glass Cherenkov spectrometer. The pulses from all the detectors were fed to a five-beam oscilloscope for the time-amplitude analysis. No events with gamma emission were observed. The upper limits of the nuclear cross section for production by 70-GeV protons of the radioactive quasi-nucleus emitting the high-energy photons are 10^{-38} to 10^{-37} cm² for Al and 10^{-36} to 10^{-35} cm² for W. (auth)

14542 CROSS SECTIONS FOR $p + p \rightarrow d + \rho^+$ FROM 4.0 TO 12.3 GeV/c AND A SEARCH FOR THE δ^+. Anderson, H. L. (Univ. of Chicago); Dixit, M.; Evans, H. J.; (and others). Phys. Rev. Lett.; 26: 108-12(11 Jan 1971).

Forward differential cross sections for isospin-1 bosons produced in $p + p \rightarrow d + x^+$ were measured using a deuteron missing-mass spectrometer at a small angle between 4.0- and 12.3-GeV/c incident momentum. Differential cross sections for π^+ and ρ^+ were extracted from the spectra using phase-space backgrounds. They range from 10.4 to 0.4 μb/sr for π^+ and from 1.4 to 0.3 μb/sr for ρ^+. A bump near 6 GeV/c appears in both $d\pi$ and $d\rho$ channels. No clear evidence is seen for higher-mass bosons. The possible δ^+ cross sections average less than 0.01 μb/sr. (auth)

14543 PROTON-PROTON DIFFERENTIAL [illegible]ROSS SECTIONS FROM 600 TO 1800 MeV/c. Ryan, B. A. (Le[illegible]niv., Bethlehem, Pa.); Kanofsky, A.; Devlin, T. J.; Mischke, [illegible] E.; Shepard, P. F. Contract AT(30-1)-4159. Phys. Rev., D; 3: 1-9(1 Jan 1971).

Proton-proton elastic differential cross sections were measured for incident laboratory momenta of 600 to 1800 MeV/c and cm angles of 5° to 90°. The data span, in a single experiment, the intermediate energy region from isotropic differential cross sections at lower energies to the development of a clear diffraction peak at higher energies. Parameters for phenomenological formulations derived from the experimental results are presented. (auth)

14544 BY WAY OF ANTIPLASMA TOWARDS ANTIMATTER. Boudker, Guersch (Inst. of Nuclear Physics, Novosibirsk, USSR). Energ. Nucl. (Paris); 12: 426-9(Sep-Oct 1970). (In French).

Research into particle accelerators with crossed beams, or intersecting storage rings, was undertaken in the Soviet Union. The first installations accelerated electrons. Currently protons and antiprotons are being studied. An accelerator with crossed beams of protons and antiprotons of 25 GeV, is under construction at Novosibirsk. The possible existence of quarks can be investigated. Soviet research workers hope to achieve the synthesis of antimatter. (France)

14545 MEASUREMENTS OF PROTON-PROTON BREMSSTRAHLUNG AT 20 MeV. Storm, Derek Walton. Seattle; Univ. of Washington (1970). 125p. University Microfilms Order No. 70-19,663.

Thesis.

The cross section, $d\sigma/d\Omega_1 d\Omega_2$ was measured for proton-proton bremsstrahlung, with 20-MeV incident proton energy, detecting the protons in coincidence at 25 deg. on either side of the beam and at 30 deg. on either side of the beam. Also the photon angular distributions, $d\sigma/d\Omega_1 d\Omega_2 d\theta_\gamma$, and the photon energy spectra, $d\sigma/d\Omega_1 d\Omega_2 dE_\gamma$ were determined. The experimental techniques are standard, except that a method of reducing the pileup effects due to a high counting rate of elastically scattered particles was developed. This technique enabled one to maintain fairly good (75 keV) resolution in the proton counters in spite of a 3×10^4 count/sec counting rate. After correcting for the finite azimuthal angular acceptance of the counters, $d\sigma/d\Omega_1 d\Omega_2 = .68 \pm .07$ μb/sr² was found for equal proton angles of 25 deg. and $d\sigma/d\Omega_1 d\Omega_2 = .69 \pm .07$ μb/sr² for equal proton angles of 30 deg. These results appear to be consistent with theoretical predictions based on potential model calculations. (Diss. Abstr. Int., B)

14546 A MEASUREMENT OF THE LIFETIMES OF THE $\Sigma^\pm$-HYPERONS. Barker, A. M. (Zeemanlaboratorium, Amsterdam); Hoogland, W.; Kluyver, J. C.; (and others). Lett. Nuovo Cim.; 1: 37-40(2 Jan 1971).

The reactions $K^- + d \to p + \Sigma^-(\Sigma^+) + \pi^+(\pi^-) + \pi^-$ produced in a bubble chamber from 3-GeV/c negative kaon interactions are studied to determine the lifetimes of the Σ^- and Σ^+ hyperons decaying into a charged pion and a neutron. Cross sections are determined for the considered reactions, and the Σ^- and Σ^+ hyperon lifetimes are respectively (1.42 ± 0.05) $(10)^{-10}$ and (0.83 ± 0.04)$(10)^{-10}$ seconds. (J.F.P.)

14547 NEW CLASS OF GRAVITATIONAL WAVE DETECTORS. Douglass, D. H. (Univ. of Rochester, N. Y.); Tyson, J. A. Nature (London); 229: 34-6(1 Jan 1971).

Reference is made to Weber (Phys. Rev. Lett. 17: 1228 (1966) and 18: 498 (1967)) who derived the equations of motion and the response of mass quadrupole detectors to tensor gravitational waves, and also constructed a detector comprising a cylindrical rod tuned to its fundamental longitudinal acoustic resonance. Such devices, known as class-1 detectors, show a definite relation between resonant frequency and dimensions, and become very large and expensive for low frequencies. They become difficult to build for frequencies <1,000 Hz. There are other mechanically resonant devices, for example tuning forks, rings and "hollow" squares, and known as class-2 detectors, that show a different relation between resonant frequency and dimensions; the useful frequency range of these can be extended down to ~30 Hz, with a sensitivity at the lower frequencies comparable with class-1 detectors. The application of these detectors is mathematically analyzed, and the case of the "hollow" square specifically considered, particularly with regard to the quadrupole vibrational mode. Class-2 detectors can also distinguish between scalar and tensor radiation, and can afford a "pure quadrupole" channel and a "pure scalar" channel. Furthermore, the "hollow" square antenna is sensitive to only one state of tensor polarization, hence by rotation polarization studies of sources can be made. (UK)

14548 ANNIHILATION $\bar{p}n \to \pi^+\pi^-\pi^-$ BETWEEN 1.0 AND 1.6 GeV/c AND ITS COMPARISON WITH THE VENEZIANO MODEL. Bettini, A. (Univ., Padua. Istituto Nazionale di Fisica Nucleare, Padua); Cresti, M.; Mazzucato, M.; (and others). Nuovo Cim.; 1A: 333-44(21 Jan 1971).

The reaction $\bar{p}n \to \pi^-\pi^+\pi^-$ between 2.08 and 2.29 GeV c.m. energy was analyzed. The population of the 3π Dalitz plot (a total of 2328 events at all energies) is strongly nonuniform and shows a structure that can be qualitatively interpreted with simple Veneziano-type formulas. The moments of the angular distributions of the three-pion plane are also examined. (auth)

14549 $n + p \to d + \pi^0$: A TEST OF CHARGE INDEPENDENCE FROM THRESHOLD THROUGH RESONANCE PEAK. Hammerman, Ira Saul. Princeton, N. J.; Princeton Univ. (1969). 167p. University Microfilms Order No. 70-14,212.

Thesis.

The differential and total cross sections for $n + p \to d + \pi^0$ were measured for neutron energies from the threshold through the region of the first resonance peak. Total cross section data are presented in 10 MeV bins from 280 to 720 MeV. The overall normalization is not known, but the relative normalization as a function of energy is known well. Differential cross section data are presented in 10 bins of 40 MeV from 280 to 680 MeV. A test is made of the predictions of charge independence: $\sigma_{pp \to d\pi^+}(\theta^*,E) = 2\sigma_{np \to d\pi^0}(\theta^*,E)$. No evidence for a violation is seen. The experiment was performed at the Princeton-Pennsylvania Accelerator (PPA) in conjunction with a study of $n + p \to d + \gamma$ testing time reversal invariance. Neutrons of measured time of flight interacted in a liquid hydrogen target. Decay photons from the π^0 were detected in a lead and aluminum plate spark chamber array. The deuteron track was measured in thin plate spark chambers and its momentum was analyzed by bending in a magnet. About two million pictures were taken. The results presented are based on 90,000 events. (Diss. Abstr. Int., B)

14550 STRANGE PARTICLE PRODUCTION IN anti Pd ANNIHILATIONS IN FLIGHT. Sehgal, Narender Kumar. Madison, Wis.; Univ. of Wisconsin (1970). 210p. University Microfilms Order No. 70-8331.

Thesis.

Results are presented from a study of Pd annihilations at four incident antiproton ($\bar{P}$) momenta between 1.25 and 1.67 GeV/c. A total of 159,000 pictures taken in the deuterium-filled 30 inch MURA chamber at Argonne was used. Only events with at least one V(visible charged decay of K_1°, Λ or $\bar{\Lambda}$) were considered for this study. Cross sections for the following processes were measured. (a) $\bar{p}n \to K^-K_1^\circ(\pi^\circ)$, $\pi^-K_1^\circ(K^\circ)$, $\pi^-K_1^\circ K_1^\circ$, $\pi^-K_1^\circ K_1^\circ(\pi^\circ)$, $K^\pm\pi^\mp\pi^-K_1^\circ$, $K^\pm\pi^\mp\pi^-K_1^\circ$, $K^\pm\pi^\mp\pi^-K_1^\circ(\pi^\circ)$, and $\pi^+\pi^-\pi^-K_1^\circ(K^\circ)$, (b) $\bar{p}p \to K^\pm\pi^\mp K_1^\circ$, $\pi^+\pi^-K_1^\circ(K^\circ)$, $\pi^+\pi^-K_1^\circ K_1^\circ$, $K^\pm\pi^\mp K_1^\circ(\pi^\circ)$ $\pi^+\pi^-K_1^\circ K_1^\circ(\pi^\circ)$ and $K^\pm\pi^\mp\pi^+\pi^-K_1^\circ$, and (c) $\bar{p}d \to \Lambda^\circ$ + (MM) where (MM) refers to missing mass. Reactions (a) and (b) comprised the bulk of our events. The impulse approximation was used wherever the number of available kinematic constraints necessitated it. The spectator momenta, for the most part, agreed well with the appropriately normalized and modified Hulthen distributions. In both (a) and (b) K*(890) was found to be abundantly produced. Besides K*(890), there is clear evidence for the production of some well known and established resonant states like ρ(765), ω(783), A_2(1310), E(1420), etc. A search for new or relatively poorly established resonances like B(1210), A_1(1080), π(1640), η(1830), etc., and K*'s in the region between 1080 and 1600 MeV, did not produce any evidence, for or against, their existence. One of the significant results of this study is the fairly consistent domination of the isospin zero (I = 0) amplitude over the isospin one (I = 1) amplitude in (a) and (b). This effect is especially pronounced in the case of $\bar{P}n$ and $\bar{P}p$ final states involving two pions and two kaons. The cross section for Λ-production in (c) seems to vary little in the available range of $\bar{P}d$ center-of-mass energy. A study of data for the process (c) is interpreted to rule out certain mechanisms for Λ-production in $\bar{P}d$ annihilations. This fact makes the explanation of Λ-production phenomenon even more elusive. A speculation is made about other mechanisms but lack of sufficient evidence prevents one from calling it an explanation of this phenomenon. Also cross sections were measured for some rare two-body final states like $\bar{P}p \to K_1^\circ$ (K°), $\bar{P}p \to K_1^\circ K_1^\circ$, $\bar{P}p \to \Lambda(\bar{\Sigma}/\bar{\Lambda})$, or $\bar{\Lambda}(\Sigma/\Lambda)$ and $\bar{P}n \to K^-K_1^\circ$. (Diss. Abstr. Int., B)

14551 INVESTIGATION OF THE REACTION $np \to pp\pi^-$ FOR THE INCIDENT NEUTRON MOMENTA FROM 2 UP TO 10 GeV/c. Gasparyan, A. P.; Nikitin, A. V.; Troyan, Yu. A. (Joint Inst. for Nuclear Research, Dubna, USSR). Yadern. Fiz.; 12: 987-93(Nov 1970). (In Russian).

The manifestly peripheral nature of the $np \to pp\pi^-$ reaction is established. Abundant resonance production in the neutron vertex is observed. The N*(1470) isobar dominates at the neutron momenta $p_n > 4$ GeV/c, the fact indicating an essential contribution from the zero-isospin exchange. Total cross section of the reaction and the production cross sections for the isobar states Δ(1236), N*(1470), N*(1688) are measured as functions of the incident neutron momentum. (auth)

14552 EVIDENCE FOR A NARROW N*(1470). Ma, Z. Ming (Michigan State Univ., East Lansing); Colton, Eugene. Phys. Rev. Lett.; 26: 333-7(8 Feb 1971).

A narrow I = ½ enhancement at a mass of 1.462 ± 0.006 GeV/c² with a width of 0.049 ± 0.012 GeV/c² was observed in $p\pi^0$ and $n\pi^+$ modes produced in pp collisions at 6.6 GeV/c. The effect, having a 6-standard-deviation significance, is narrower in width than has been observed before in missing-mass-spectrometer experiments. (auth)

14553 ANTIPROTON-NEUTRON ANNIHILATION AT REST INTO FINAL STATES OF 5 AND 6 PIONS. Hagerty, Patrick Edwin. Syracuse, N. Y.; Syracuse Univ. (1969). 73p. University Microfilms Order No. 70-12,779.

Thesis.

The subject is antiproton annihilations at rest with neutrons into final states with five charged pions. The antiprotons were produced by the 30-Gev proton Alternating Gradient Synchrotron (AGS) at Brookhaven National Laboratory (BNL). The antiprotons were then separated from undesired particles and brought to rest in the BNL-Columbia 30-inch hydrogen bubble chamber. The chamber was filled with deuterium, and the neutrons upon which the antiprotons annihilated were bound in the deuterium nuclei. Analysis of events in which the proton of the deuterium nucleus was invisible (5 prong events) and visible (6 prong events) yielded events of the types $\bar{p}n \to 3\pi^-2\pi^+$ and $\bar{p}n \to 3\pi^-2\pi^+\pi^0$. The branching ratios of these final states with respect to all $\bar{p}n$ annihilations are (4.2 ± 0.23) × 10^{-2} and (6.93 ± 0.36) × 10^{-2} respectively. The dynamics of the $3\pi^-2\pi^+$ final state differ markedly from the theoretical predictions of any of the models which were examined. There appears to be copious ρ^0 production (and possibly even double rho production), but the $\pi^+\pi^-$ invariant mass distribution shows no clear rho signal. The "A_1" effect may also be occurring, but it cannot be clearly separated out. No satisfactory theoretical description of this channel was achieved. The $3\pi^-2\pi^+\pi^0$ final state proceeds through the reactions $\bar{p}n \to \omega^0 2\pi^-\pi^+$ and $\bar{p}n \to 3\pi^-2\pi^+\pi^0$, with intermediate ω formation (88.4 ± 9.3)% of the time. The B meson is not observed in this channel. Since the analysis assumes S-capture of antiprotons and the fact that the nonannihilating nucleon behaves as a spectator, both of these assumptions were tested and limits for their validity are discussed. It is found that 80% of the annihilations satisfy the spectator hypothesis, while the entire deuteron participates in the remaining 20%. (Diss. Abstr. Int., B)

XUM

14554 FOUR-PRONGED ANTIPROTON-DEUTERIUM INTERACTIONS AT 7.0 GeV/c. Goodman, Gerald Joseph. Baltimore; Johns Hopkins Univ. (1969). 197p. University Microfilms Order No. 70-11,786.

Thesis.

Antiproton-deuterium interactions are studied for an incident beam momentum of 7.0 GeV/c. The five following four-pronged final states are investigated in some detail and the accompanying cross sections for visible spectator events are found: $\bar{p}d \to \pi^- \bar{p} \pi^+$ (p) n, 889 ± 29 μb (1), $\bar{p}d \to \pi^- \bar{p} \pi^+$ d, 204 ± 10 μb (2), $\bar{p}d \to \pi^- \bar{p}$ p(p), 329 ± 14 μb (3), $\bar{p}d \to \pi^- \bar{p}$ p(p) π^0, 519 ± 19 μb (4), and $\bar{p}d \to \pi^- \pi^-$ p(p) $\bar{n}$, 334 ± 14 μb (5). Reaction (1) exhibits two outstanding characteristics. The first is the existence of two distinct enhancements in the $\bar{\Delta}^{--} \pi^+$ effective mass distribution at 1470 and 1750 MeV. These enhancements are determined to be of isotopic spin ½ which makes them consistent with resonances reported in recent phase shift analysis work. The other very noticeable facet found in the investigation of reaction (1) is a broad peak around 2250 MeV in the $p_s\ n\ \pi^+$ mass spectrum which appears to be associated with the fact that the spectator protons do not have an isotropic angular distribution as expected but are peaked forward. The study of reaction (2), an example of coherent scattering shows copious $\bar{\Delta}^{--}$(1238) production. Also present is a substantial amount of the so-called d^*, an enhancement around 2170 MeV in the d^+ effective mass distribution. A final state interaction model is used to demonstrate that the d^* can be accounted for by assuming that the pion interacts with one of the nucleons to form a Δ which then decays in a manner that enables the deuteron to maintain its identity. The most interesting aspect of the investigation of reaction (3) comes in the $\pi^- \bar{p}$ mass spectrum. Clearly distinguishable are the Δ(1238) and Δ(1920) resonances. An attempt to explain the distribution by means of the one pion exchange model modified by the Ferrari–Selleri form factor, which was successful in an analogous pp interaction, results in the theoretical differential cross sections being consistently high. It is argued that the model may have to be altered to allow for a significant amount of B exchange. Reaction (4) shows much Δ(1238) production in various charge states. The quasi three-body subsample of events containing a $\bar{\Delta}^{--}$ is analyzed in terms of double Regge pole exchange. Once allowance is made for the presence of a Δ^+ signal, the model's predictions are in extremely good agreement with the experimental results. The study of reaction (5) is complicated somewhat by the presence of a pair of identical particles in the final state. Nevertheless, the production of Δ^0 and $\bar{\Delta}^{--}$ is noted. The $\bar{n}\pi^-\pi^-$ effective mass distribution gives no clear indication of the reported resonance at 1640 MeV. (Diss. Abstr. Int., B)

14555 $\bar{p}d$ TOPOLOGICAL CROSS SECTIONS IN THE MOMENTUM RANGE 50 TO 920 MeV/c. Burrows, R. D.; Caro, D. E.; Gold, E.; (and others) (Univ. of Melbourne, Parkville, Australia). Aust. J. Phys; 23: 819-21(Dec 1970).

The total and topological cross sections are presented for events seen in the interaction of 50 to 920 MeV/c antiprotons with deuterium in the BNL 30-in. bubble chamber. (auth) (Australia)

14556 MEASUREMENT OF PROTON–PROTON BREMSSTRAHLUNG CROSS SECTIONS AT 42 MeV. Jovanovich, J. V.; Greeniaus, L. G.; McKeown, J.; (and others) (Univ. of Manitoba, Winnipeg). Phys. Rev. Lett.; 26: 277-9(1 Feb 1971).

The results of a proton-proton bremsstrahlung experiment are reported. The cross sections were measured over wide angular ranges using a wire-chamber spectrometer. Where possible, comparisons are made with the theoretical predictions of the Hamada–Johnston potential. (auth)

Strong (Meson-Induced)

Refer also to abstract 14714.

14557 (FSU-HEP–70-3-1) PARTIAL WAVE ANALYSIS OF THE REACTION $K^-n \to \Sigma^-\pi^+\pi^-$ FROM 1.62 TO 1.74 GeV. Harrison, William Craig (Florida State Univ., Tallahassee. High Energy Physics Lab.). Mar 1970. 76p.

Thesis.

An explicit formalism was given for a relativistic partial wave analysis of the reaction $1 + 2 \to a + b + g$ with arbitrary spins incorporating an isobar or sequential decay model by the parametrization of the reduced matrix elements. This formalism was applied to a study of the reaction $K^-n \to \Sigma^-\pi^+\pi^-$ in the center-of-mass energy region from 1620 to 1740 MeV. The model is capable of reproducing all experimental distributions well and permits a straightforward interpretation of the reaction studied in this region, which is consistent with all available information on the $\bar{K}N$ system from two-body reactions. The analysis is consistent with the observation that the Σ(1660) $J^P = 3/2^-$ state formed from $\bar{K}N$ couples only weakly to Λ(1405) and supports a previous conclusion that there may exist two distinct Σ(1660)'s of $J^P = 3/2^-$. (auth)

14558 (INP-708) PION PRODUCTION MECHANISM IN HIGH MULTIPLICITY π^+p INTERACTIONS AT 8 GeV/c. Coghen, T.; Czyzewski, O.; Eskreys, A.; (and others) (Institute of Nuclear Physics, Krakow (Poland)). 1970. 23p. (CONF-700806-55). Dep. NTIS (U. S. Sales Only).

From 15th International Conference on High Energy Physics, Kiev, USSR.

The mechanism of pion production in eight-prong π^+p reactions is discussed in terms of two models: the "fireball" model and multiperipheral CLA model. Both models give adequate description of the general features of the experimental data, however, they fail in the prediction of fine details of the process. (auth)

14559 (INP-731) DECAY DISTRIBUTIONS IN THE REACTION $\pi^+p \to K^+Y^{*+}$(1385) AND THE POLARIZATION OF THE Λ HYPERON FROM Y^{*+}(1385) DECAY AT 8 GeV/c PRIMARY MOMENTUM. Kisielewska, D. (Institute of Nuclear Physics, Krakow (Poland)). 1970. 9p. Dep. NTIS (U. S. Sales Only).

The study of the decay distributions of the Y^{*+}(1385) resonance produced in the reaction $\pi^+p \to K^* \Lambda \pi^+$ at 8 GeV/c and of the Λ hyperon polarization from Y^{*+}(1385) decay is presented. Statistical tensors both of even and odd rank were calculated and a complete comparison with quark model predictions was done. On the level of the statistics for reaction $\pi^+p \to K^+ Y^{*+}$(1385) available at the moment agreement is observed between the experimental values of the statistical tensors and their quark model predicted values. (auth)

14560 (JINR-E1-5349) STUDY OF THE EFFECTIVE MASS SPECTRA OF THE $\gamma\gamma$, $\pi^0\gamma$, $\pi^0\gamma\gamma$, $\pi^0\pi^0$, $\pi^0\eta^0$, $\pi^0\pi^0\gamma$, $\pi^0\pi^0\pi^0$ SYSTEMS IN THE MASS VALUE REGION M $(\gamma.......\gamma) \leq 1.3$ GeV. Strugal'skii, Z. S.; Chuvilo, I. V.; Gemesy, T.; Ivanovskaya, I. A.; Jablonski, Z.; Kanarek, T.; Krasnovsky, S.; Okhrimenko, L. S.; Pinter, G.; Slowinski, B. (Joint Inst. for Nuclear Research, Dubna (USSR). Lab. of High Energy). 1970. 45p. Dep. NTIS (U. S. Sales Only).

The production and decays of neutral bosons decaying into π^0 and gamma quanta were searched in a xenon bubble chamber exposure to a 2.34 GeV/c π^+ beam. Interactions of the type $\pi^+ + n \to X + p$, where n is a quasi-free neutron in the xenon nucleus and X is any particle decaying into π^0's and gamma quanta, were studied. Among the produced neutral bosons studied are the f^0, η^0, and ω^0. (J.F.P.)

14561 (JINR-P1-5460) MEASUREMENT OF THE TOTAL CROSS SECTIONS OF THE π^--p INTERACTION IN THE ENERGY RANGE FROM 4.0 TO 6.0 GeV WITH THE SYSTEMATIC ERROR NOT MORE THAN 30 mμb. Giordenesku, N.; Zubarev, V. N.; Ivanov, V. I.; Moroz, N. S.; Radomanov, V. B.; Stavinskii, V. S. (Joint Inst. for Nuclear Reserach, Dubna (USSR). Lab. of High Energy). 1970. 14p. (In Russian). Dep. NTIS (U.S. Sales Only).

Using the Čerenkov hodoscope the total cross sections of the π^--p interactions in the energy region from 4.0 to 6.0 GeV were measured with the systematic error no more than 30 μb. (auth)

14562 (TID-25640) OBSERVATION OF A 2400-MeV 5π MASS ENHANCEMENT IN 6-PRONG π^-p EVENTS AT 12 GeV/c. Johnson, A. D.; Peters, M. W.; Stenger, V. J.; Yee, A. (Hawaii Univ., Honolulu). [1970]. Contract AT(04-3)-511. 9p. Dep. NTIS.

All six-prong events from the exposure of a heavy-liquid bubble chamber to a 12-GeV/c π^- beam were measured. The production of Δ^{++}(1236) and ρ^0(765) was observed. Also observed was a $\rho\rho\pi$ (2420) enhancement having a width of 80 MeV. The branching ratio of this enhancement was calculated. (J.F.P.)

14563 QUASI-TWO-BODY PRODUCTION IN π^+p INTERACTIONS INTO FOUR PRONGS AT 1.95 GeV/c. Chapman, J. W.; Fortney, L. R.; Fowler, E. C. (Duke Univ., Durham, N. C.). Phys. Rev., D; 3: 38-42(1 Jan 1971).

The quasi-two-body reactions $\pi^+p \to \Delta^{2+}\rho^0$ and $\pi^+p \to \Delta^{2+}\omega^0$ were extracted from the four- and five-body final states in π^+p interactions at 1.95 GeV/c momentum. The total and differential cross sections for these two reactions were determined and density-matrix elements of the resonances were determined as a function of t′ (the square of the four-momentum transferred minus the minimum value.) (auth)

14564 PROTON MOMENTUM SPECTRUM IN πN INELASTIC INTERACTIONS AT 17.2 GeV/c. Bozoki, G. (Central Research Inst. for Physics, Budapest); Fenyves, E.; Gombosi, E.; Vanicsek, L. Acta Phys. Acad. Sci. Hung.; 28: 401-17(1970).

The momentum spectrum of protons produced in πN interactions at 17.2 GeV/c was investigated in nuclear emulsion. The results support the earlier observations concerning the existence of the double maximum in the proton momentum spectrum as well as the difference in its shapes for πp and πn interactions. An attempt was made to explain the two-maximum structure of the spectrum on the basis of the multi Regge model taking into account the effect of the superposition of "pure" inelastic reaction channels. (auth)

14565 AZIMUTHAL SYMMETRY IN 17.2-GeV/c π^- JETS. Rao, Y. V.; Kamal, A. A. (Osmania Univ., Hyderabad, India). Acta Phys. Acad. Sci. Hung.; 28: 307-13(1970).

Azimuth angles of shower particles produced in 17.2 GeV/c π^- interactions were analyzed by two methods, method of consecutive angles and method of "minimum fallout." The results do not indicate any deviation from isotropy. (auth)

14566 ANALYSIS OF NEGATIVE-PION PHOTOPRODUCTION NEAR THE P_{33} RESONANCE: TEST OF THE $\Delta I \leq 1$ RULE AND TIME-REVERSAL INVARIANCE. Berardo, P. A. (Univ. of California, Los Angeles); Haddock, R. P.; Helland, J.; (and others). Phys. Rev. Lett.; 26: 205-8(25 Jan 1971).

Angular distributions for the reaction $\pi^- p \rightarrow \gamma n$ are analyzed. Existing sets of multipoles do not agree with the data. An acceptable fit is obtained with the Sanda–Shaw model of an electromagnetic current with an isotensor component of $-0.1 > x > -0.4$. The model of Christ and Lee is used to estimate the magnitude of a possible T-invariance violation implied by the difference between the data at $\widetilde{E} = 1245$ MeV and the inverse reaction deduced from γd work. A strong violation in the isovector or isotensor amplitude is excluded, but a maximum violation in the isoscalar amplitude is possible. (auth)

14567 MEASUREMENT OF INVERSE PION PHOTOPRODUCTION NEAR THE $P_{33}{}^0(1236)$ RESONANCE. Berardo, P. A. (Univ. of California, Los Angeles); Haddock, R. P.; Nefkens, B. M. K.; (and others). Phys. Rev. Lett.; 26: 201-4(25 Jan 1971).

The differential cross sections for $\pi^- + p \rightarrow \gamma + n$ at $40° < \widetilde{\theta}_\gamma < 150°$ at c.m. total energies 1245 and 1337 MeV are presented. The results do not agree with predictions based on the $\Delta I \leq 1$ rule for the electromagnetic current and fixed-t dispersion relations. The data can be fitted with the Sanda–Shaw model, in which the electromagnetic current contains an isotensor component. The angular distribution at 1337 MeV agrees with the inverse reaction as deduced from γd work; however, there is some disagreement at 1245 MeV. (auth)

14568 STUDY OF $K^- + \rightarrow \Sigma^0 + \pi^0$ NEAR 1670 MeV. Smith, William Malcolm. Durham, N. C.; Duke Univ. (1970). 90p. University Microfilms Order No. 70-23,413.

Thesis.

The reaction $K^- + p \rightarrow \Sigma^0 + \pi^0$ was studied in a search for the reported T = 0 S-wave resonance with a mass of approximately 1675 MeV. The angular distribution of the Λ and the distribution of $M^2(x)$ from the reaction $K^- + p \rightarrow \Lambda + x$ were studied. A maximum likelihood fit to the data was carried out to obtain the coefficients of the Legendre expansions of the differential cross sections of the reactions $K^- + p \rightarrow \Lambda + \pi^0$ and $K^- + p \rightarrow \Sigma^0 + \pi^0$. The Legendre expansion is $(d\sigma/d\Omega) = \lambda^2 \Sigma_m A_m P_m (\cos\theta)$ where λ is the center of mass wavelength of the incident particle divided by 2π, the A_m are energy dependent coefficients, and the $P_m (\cos\theta)$ are the Legendre polynomials. There is a set of A_i for each final state. The A_i obtained in this experiment agreed with those presented in the literature. An attempt was made to fit a set of partial-wave amplitudes to the A_i that were determined for the $\Sigma^0\pi^0$ final state. However, the energy spread that was available for this experiment was so small as to make a true partial wave analysis very difficult. Within the limits of the data, it was found that an acceptable fit to the data was possible when the S-wave amplitude was composed of a combination of complex, nonresonant and Breit–Wigner resonant terms. The parameters of the S-wave resonance term (the width, partial width, and mass) were compatible with those obtained in other experiments. (Diss. Abstr. Int., B)

14569 STUDY OF THE INTERACTION $K^-d \rightarrow K^-\pi^-\pi^+d$ AT 7.3 GeV/c. Godden, Gerald Dean. Boulder, Colo.; Univ. of Colorado (1970). 152p. University Microfilms Order No. 70-23,711.

Thesis.

A study of the interaction $K^-d \rightarrow K^-\pi^-\pi^-d$ was made from 100,000 photographic exposures of the Brookhaven National Laboratory 80-inch deuterium-filled bubble chamber exposed to a negative kaon beam of 7.3 GeV/c momentum. Partial cross sections are measured and resonance production is studied. High peripherality and strong $K^*(890)$ production is noted. The cross section for the above interaction for events with a visible deuteron is $232 \pm 43\ \mu b$. (Diss. Abstr. Int., B)

14570 SINGLE-PION PRODUCTION IN π^-p INTERACTIONS AT 2.3 GeV/c. Hagopian, Sharon Lee Ford. Philadelphia; Univ. of Pennsylvania (1970). 180p. University Microfilms Order No. 70-25,655.

Thesis.

The analysis is presented of 25,000 two-prong events from 350,000 pictures taken in the 15-inch Princeton-Pennsylvania hydrogen bubble chamber with an incident π-beam momentum of 2.3 GeV/c. These events were measured on a flying spot digitizer (Hough–Powell Device) and processed through the Penn automatic track following and minimum guidance pattern recognition programs, which had an effective efficiency of 84%. A detailed study of the reaction $\pi^-p \rightarrow \pi\pi N$ was made, with special emphasis on the ρ resonance region, in order to obtain a clearer understanding of the various resonances and production mechanisms involved. Both the production and decay angular distributions of the ρ events with small 4-momentum transfer between the nucleons are well described by the one pion exchange model modified by absorptive effects, but some new features are clearly visible. The production angular distribution of the ρ^- has a secondary peak which is associated with an exchange particle, probably the ω^0. The ρ^- polarization, even at low values of momentum transfer to the nucleon, shows a behavior different from that of the ρ^0; this difference is possibly due to ω^0 exchange. The ρ^0 production angular distribution has a small central peak, whose source is unclear, and a backward peak, which is presumably associated with baryon exchange. The decay angular distribution for these backward ρ^0 events was found to be anisotropic. The $\Delta(1236)$ isobar was observed but its effect was found to be small for low-momentum transfer events. (Diss. Abstr. Int., B)

14571 MULTIPION PRODUCTION IN $\pi^-\rho$ INTERACTIONS AT 2.3 GeV/c. O'Donnell, Robert Michael. Philadelphia; Univ. of Pennsylvania (1970). 215p. University Microfilms Order No. 70-25, 709.

Thesis.

A study was made of the four-pronged final states from $\pi^-\rho$ interactions at an incident momentum of 2.3 GeV/c in the 15″ rapid cycling hydrogen bubble chamber at the Princeton-Pennsylvania Accelerator. The events were digitized by the Hough–Powell Device at the University of Pennsylvania and processed using the Automatic Track Following system. The cross sections for the different multipion channels were determined. The $\pi^-\pi^-\rho\pi^+$ final state is dominated by the production of the $N^{*++}(1238)$ isobar. Some $\rho^0(765)$ production is observed. The $\pi^-\pi^-(T = 2)$ scattering cross section as a function of $\pi^-\pi^-$ mass was extracted from the $N^{*++}\pi^-\pi^-$ events using the form factor models of Salzman–Salzman and Durr–Pilkuhn. The $\pi^-\pi^-\rho\pi^+\pi^0$ final state shows strong $\omega^0(785)$ and $N^{*++}(1238)$ production. The $\omega^0\pi^-$ decay of the $B^-(1220)$ meson is observed. The $N^{*-}(1238)$ is the only resonance seen in the $\pi^-\pi^-\pi^+\pi^+n$ final state. Upper limits to the following branching ratios were determined. $(\rho^0 \rightarrow \pi^+\pi^+\pi^-\pi^-/\rho^0 \rightarrow \pi^+\pi^-) < 0.002 \pm 0.001$ and $(\rho^- \rightarrow \pi^-\pi^+\pi^-\pi^0/\rho^- \rightarrow \pi^-\pi^0) < 0.008 \pm 0.002$. (Diss. Abstr. Int., B)

14572 $\pi^+\pi^0\pi^-$ PRODUCTION IN K^-p INTERACTIONS AT 5.5 GeV/c. Chandler, Gerald David. Urbana, Ill.; Univ. of Illinois (1970). 127p. University Microfilms Order No. 70-20,936.

Thesis.

The separated K^- beam and the 30-inch MURA hydrogen bubble chamber at the Argonne National Laboratory were used to obtain more than 400,000 stereoscopic photographs in which K^--proton interactions centered at a beam momentum of 5.46 GeV/c were recorded. From these photographs 2042 examples of the reaction $K^-p \rightarrow K^-p\pi^+\pi^0\pi^-$ were identified and studied. The following are the primary results of this study: The total cross section for the reaction is 0.6 ± 0.2 mb. The K^- in the final state tends to travel in the same direction as the beam K^- and the proton in the final state tends to travel (when considered in the overall center-of-mass) in the same direction as the target proton. Copious production of well known resonances occurs. In particular approximately 17% of the events have present an ω^0, 20% a K^{*0}, 10% a K^{*-}, 13% a Δ^{++}, and 13% a Δ^+. Other known resonances, including ρ, Δ^0, and γ^*'s, are produced less copiously. As the result of the presence of these resonances there are numerous quasi-two, three, and four-body states. The quasi-three-body states $K\omega p$, $K^{*-}\pi^-\Delta^{++}$, and $K^{*0}\pi^-\Delta^+$ were studied and found to be describable by a double peripheral model. An investigation of the $M_{\pi\pi\pi}$ spectrum led to the conclusion that the $A_1(1070)$ is not produced in the data studied. (Diss. Abstr. Int., B)

14573 SEARCH FOR RESONANT STATES $p-{}^5_\Lambda He$ AND $\alpha-{}^5_\Lambda He$. van de Graaf, M. Skorko; Skrzypczak, E.; Tymieniecka, T. (Univ., Warsaw). Acta Phys. Pol.; B1: 401-7(Oct-Dec 1970).

A sample of 164 K^- interactions with emulsion nuclei with ${}^5_\Lambda He$ hypernuclei among secondaries was studied. The invariant mass distributions for ${}^5_\Lambda He-p$ and ${}^5_\Lambda He-\alpha$ systems in these stars were

XUM

obtained and analysed. No maxima corresponding to particle-unstable ${}^{6}_{\Lambda}$Li or ${}^{9}_{\Lambda}$Be* systems (decaying into ${}^{5}_{\Lambda}$He and a proton or into ${}^{5}_{\Lambda}$He and an α-particle, respectively) were observed; this indicates a low, if not zero, value of cross section for production of such systems. (auth)

14574 TWO- AND THREE-BODY FINAL STATES IN K^+p INTERACTIONS AT 7.3 GeV/c. Mellema, Dwight Joel. Los Angeles; Univ. of California (1970). 269p. University Microfilms Order No. 70-24,365.

Thesis.

The production of two- and three-body final states in K^+p interactions is studied at an incident beam momentum of 7.3 GeV/c. The data were obtained in two exposures of the Brookhaven National Laboratory 80" hydrogen bubble chamber to an r.f.-separated K^+p beam in April, 1966, and in April, 1968. The two-prong and two-prong vee topologies were analyzed for the following reactions: $K^+p \to K^+p$ (1), $K^+p \to pK^+\pi^0$ (2), $K^+p \to p\pi^+K^0$ (3), $K^+p \to K^+\pi^+n$ (4), $K^+p \to \bar{\Lambda}pp$ (5), and $K^+p \to \Lambda K^+K^+$ (6). A cross section of 3.86 ± 0.38 mb is obtained for K^+p elastic scattering (1) at 7.3 GeV/c. The reaction is characterized by a forward diffraction peak which fits the distribution $(d\sigma/dt) = (d\sigma/dt)_0\, e^{\alpha t + \beta t^2}$ with $(d\sigma/dt)_0 = (20.6 \pm 2.6)$ mb/(GeV/c)^2, $\alpha = (5.46 \pm 0.29)$ (GeV/c)$^{-2}$ and $\beta = (0.38 \pm 0.25)$ (GeV/c)$^{-4}$. The ratio $|\mathrm{Re}\, f(O)/\mathrm{Im}\, f(O)|$ for the forward scattering amplitude is 0.60 ± 0.14. Kaon-nucleon forward elastic scattering is discussed in terms of a Regge pole model with an exchange degenerate combination of the ω and f trajectories in addition to the Pomeron pole. One elastic scatter was found in the backward direction, leading to a cross section of (0.5 ± 0.5) μb for K^+p backward elastic scattering at 7.3 GeV/c. The energy dependence of K^+p backward elastic scattering is well accounted for by a Reggeized hyperon exchange model using an exchange degenerate combination of the Λ_α and Λ_γ trajectories. The 7.3 GeV/c cross section for reactions (2) through (4) is 0.26 ± 0.05 mb, 0.50 ± 0.05 mb, and 0.34 ± 0.08 mb, respectively. These $KN\pi$ final states are found to be dominated by N*(1236), K*(890), and K*(1420) resonance production. N*(1236) production is analyzed in terms of exchange degenerate ρ and A_2 trajectories, and the N*(1236) spin alignment is found to be in good agreement with the Stodolsky-Sakurai prediction. In connection with K*(890) resonance formation data, a two-parameter model is proposed to describe charged vector meson production in the reactions $\pi^\pm p \to \rho^\pm p$ and $K^\pm p \to K^{*\pm}(890)p$. It is argued that these processes are dominated by pion, ω, and f exchange, with negligible contributions from Pomeron and other natural parity exchanges. Trajectory and residue degeneracy are assumed for the ω and f exchanges, and SU(3) symmetry is imposed on the factorized residues. The K*(1420) production data are also discussed in the light of this model. The pion exchange contributions to K*(890) and K*(1420) production are successfully predicted on the basis of neutral K* production data. Cross sections of 22 ± 6 μb and 15 ± 5 μb are obtained for reactions (5) and (6), respectively. The $\bar{\Lambda}pp$ and ΛK^+K^+ final states are satisfactorily parameterized, using a conventional double-Regge model. These reactions have also been compared with the predictions of a spin-independent, generalized Veneziano model. The $\bar{\Lambda}pp$ data are in strong disagreement with the model. Using only two free (normalization) parameters, the Veneziano model provides a remarkably good description of the ΛK^+K^+ final state. (Diss. Abstr. Int., B)

14575 MOMENTUM-TRANSFER DEPENDENCE IN REACTIONS OF THE TYPE $A + p \to \Delta^{++} + A + \pi$. Ferbel, T.; Slattery, P.; Werner, B. (Univ. of Rochester, N. Y.). Phys. Rev. Lett.; 26: 344-6(8 Feb 1971).

The momentum-transfer distributions were examined in the reactions (1) $\pi^+ + p \to \Delta^{++}(1236) + \pi^+ + \pi^-$ at a π^+ beam momentum of 7 GeV/c, and (2) $K^+ + p \to \Delta^{++}(1236) + K^+ + \pi^-$ at an incident K^+ momentum of 12.7 GeV/c. In both instances the t dependence (proton to Δ) can be represented remarkably well by the simple form $(t + \mu^2)^{-2}$, where $\mu^2 \approx m_\pi^2$. (auth)

14576 SEARCH FOR ISOBAR STATE WITH T = $\frac{5}{2}$ IN THE REACTION $\pi^+ + p \to \pi^- + X^{3+}$. Birulev, V. K.; Vovenko, A. S.; Gus'kov, B. N.; (and others) (Joint Inst. for Nuclear Research, Dubna, USSR). Yadern. Fiz.; 12: 982-6(Nov 1970). (In Russian).

A search for the isobar state with T = $\frac{5}{2}$ is carried out measuring the spectrum of π^--mesons produced in the $\pi^+ + p \to \pi^- + X^{+++}$ reaction at the π^+-meson momentum of 3.88 GeV/c and at the angle of the π^--meson escape of 1.9° (lab. s.). In the obtained spectrum a maximum is observed that may be explained by a kinematic effect of associate production of Δ^{++} (1.24) and ρ^0-meson. Production of an isobar state with the isospin $\frac{5}{2}$ was not observed in the mass interval 1.2 to 2.2/GeV/c^2 within the experimental error limits. (auth)

14577 MEASUREMENT OF THE POLARIZATION PARAMETER IN BACKWARD π^+p ELASTIC SCATTERING AT 1.60, 1.80, 2.11 AND 2.31 GeV/c. Burleson, G. (Northwestern Univ., Evanston, Ill.); Hill, D.; Kato, S.; (and others). Phys. Rev. Lett.; 26: 338-40(8 Feb 1971).

Measurements of polarization in π^+p elastic scattering were made at 1.60, 1.80, 2.11, and 2.31 GeV/c. The data cover the entire angular range, with emphasis on the backward region. Comparisons were made with both u-channel and t-channel models, as well as with predictions of phase-shift analyses. While the agreement is generally poor in all cases, the best agreement is with some t-channel predictions. (auth)

14578 LONGITUDINAL PHASE-SPACE ANALYSIS OF 5 GeV/c π^+p REACTIONS. Rinaudo, G. (Univ., Turin. Istituto Nazionale di Fisica Nucleare, Turin); Werbrouck, A. E.; Bockmann, K.; (and others). Nucl. Phys.; B25: 351-73(1971).

The longitudinal phase-space analysis is applied to various three-body configurations produced in interactions of 5 GeV/c positive pions on protons. Distributions of the polar angle ω and of the average transverse momenta are presented. The dependence of cross sections upon incident momentum in different ω intervals is investigated for the final states $\pi^+\pi^0p$ and $\pi^+\pi^+n$. It is shown that in the ω-region where Pomeron exchange is expected these cross sections remain constant with energy and are dominated by the isospin $\frac{1}{2}$ amplitude. (auth)

14579 ELASTIC FORWARD AND BACKWARD SCATTERING OF π- AND K-MESONS AT 5.2 AND 7.0 GeV/c. Baker, W. F.; Berkelman, K.; Carson, P. J.; (and others) (CERN, Geneva). Nucl. Phys.; B25: 385-410(1971).

Results of measurements of the differential cross sections for the following elastic-scattering reactions: (i) π^+p at 5.2 and 7.0 GeV/c in the range $-1 < u < 0.02$ (GeV/c)^2, (ii) π^-p at 7.0 GeV/c in the range $-0.7 < u < 0.05$ (GeV/c)^2, (iii) K^+p at 5.2 and 7.0 GeV/c in the ranges $-1 < t < -0.01$ (GeV/c)^2 and $-1 < u < 0$ (GeV/c)^2, and K^-p at 7.0 GeV/c in the range $-1 < u < 0$ (GeV/c)^2. Backward peaks were observed in K^+p scattering with an energy dependence s^{-4}. No event was found in backward K^-p scattering. The angular distributions of forward K^+p elastic scattering show no structure. Backward π^+p elastic scattering shows the known dip at $u \approx -0.15$ (GeV/c)^2, which in this experiment was covered in one geometry. (auth)

14580 DECAY MODES OF THE ETA MESON. Kendall, Burton Nathaniel. Providence; Brown Univ. (1969). 116p. University Microfilms Order No. 70-8744.

Thesis.

A determination of the decay branching ratios of the eta meson into 2γ, $\pi^0\gamma\gamma$, $3\pi^0$, $\pi^+\pi^-\pi^0$, and $\pi^+\pi^-\gamma$ is reported. The etas were produced in the reaction $\pi^- + p \to \eta^0 + n$ with several incident pion momenta in the range 737.5 to 769.5 MeV/c. Counters and optical spark chambers were used to detect the reaction and decay particles. The measured branching ratios are: $2\gamma = 44.7 \pm 18.6\%$, $3\pi^0 = 31.7 \pm 12.5\%$, $\pi^+\pi^-\pi^0 = 18.6 \pm 11.9\%$, and $\pi^+\pi^-\gamma = 4.9 \pm 12.2\%$. The $\pi^0\gamma\gamma$ mode is consistent with zero. The systematic dependence of these values on the methods of analysis is discussed. (Diss. Abstr. Int., B)

14581 THE CHARGED PION LIFETIME MEASURED IN FLIGHT. Greenberg, Arthur Joel. Berkeley, Calif.; Univ. of California (1969). 161p. University Microfilms Order No. 70-13,058.

Thesis.

The lifetime of the charged pi meson was found by determining as a function of distance the number of surviving pions in a narrow beam. Measurements for both π^- and π^+ were made along a 36-ft decay path, equivalent ot 0.6 lifetime, using a movable pion detector. The monitor counters defining the beam were designed so that the measured attenuation with distance was due solely to pion decay and not to loss of scattered particles. The attenuation together with the pion velocity, derived from a precise time-of-flight measurement, determined the lifetime. The movable counter and the pion detector in the monitor system were differential Cerenkov counters with a liquid hydrogen radiator. The lifetime measured in this experiment with pions in flight, 26.02 ± 0.04 nsec, is in agreement with other equally precise experiments with positive pions at rest. Comparison of the lifetimes measured with pions in these two states of motion is relevant to the question of microcausality in field theory. (Diss. Abstr. Int., B)

14582 BACKWARD K^+P ELASTIC SCATTERING BETWEEN 1.0 AND 2.5 GeV/c. Tewksbury, Stuart K. Rochester, N. Y.; Univ. of Rochester (1969). 227p. University Microfilms Order No. 70-2916.

Thesis.

The backward elastic K^+p cross sections for $-1 \leq \cos\theta_{cm} \lesssim -.7$ with incident kaon laboratory momenta between 1.0 and 2.45 GeV/c, at intervals of ~0.1 GeV/c, were measured in the separated beam

XUM

of the Alternating Gradient Synchrotron at Brookhaven National Laboratory. Binned in $\cos\theta_{cm}$ intervals of 0.02, the distributions have a statistical uncertainty of 10%. A backward peak is seen at incident momenta above 1.8 GeV/c which becomes sharper at higher energies. At 2.33 GeV/c, $d\sigma/du \mathrel{\tilde{\propto}} e^{7u}$. The 180° cross section falls off with increasing s (center of mass energy squared) as $d\sigma/d\Omega \propto s^{-4}$, with no prominent structure other than three shoulders, at 1.2, 1.5, and 2.0 GeV/c. The distributions are interpreted in terms of Reggeized baryon exchange and indicate that exactly degenerate Λ_α and Λ_γ poles provide a better fit to the data than any single dominant pole. (Diss. Abstr. Int., B)

Particle Interactions and Properties (Theoretical)

Refer also to abstract 14925.

General

Refer also to abstract 14797.

14583 (AEC-tr-6882/1) 12th INTERNATIONAL CONFERENCE ON HIGH-ENERGY PHYSICS, DUBNA, 1964. VOLUME 1. Smorodinskii, Ya. A. (ed.). Translation of XII Mezhdunarodnaya Konferentsiya po Fizike Vysokikh Energii, Dubna, 1964. 1053p. (TT-68-50325/1; IPST-Cat-5130; CONF-550-(Vol.1)). Dep. NTIS.

The conference on high-energy physics covers theoretical and experimental interactions of pions and nucleons below and above 1 GeV, the method of complex angular momenta in field theory, resonances with strangeness zero, strange-particle resonances, and strange-particle physics. Other topics are theory of strong interaction symmetries, and experimental and theoretical studies of electromagnetic interactions. Abstracts of individual papers that have previously appeared in NSA may be found under CONF-550-(Vol. 1) in a cumulative report number index. (J.F.P.)

14584 (NP-18652) PHASE-SPACE INTEGRAL AND STATISTICAL QUANTITIES IN HIGH-ENERGY COLLISIONS. Research Report No. 14/1970. Suhonen, E. (Jyvaskyla Univ. (Finland). Dept. of Physics). Nov 1970. 11p. Dep. NTIS (U. S. Sales Only).

Quantities which are analogous to the numerical flux and energy-momentum tensor in relativistic statistical mechanics are derived from the generating function of the phase-space integral for n particles. The average energy in the rest frame of the particle system is calculated using the definition of the average value given in terms of phase-space. (auth) (Finland)

14585 EXISTENCE OF COMPLEX POLES AND OSCILLATORY AVERAGE MULTIPLICITY IN MULTIPERIPHERAL MODELS. Goldberger, Marvin L. (Princeton Univ., N. J.); Silverman, Dennis; Tan, Chung-i. Phys. Rev. Lett.; 26: 100-3(11 Jan 1971).

Using only the general factorization and nondegenerate threshold properties of multiperipheral models, the existence of damped oscillatory components is demonstrated for both the total cross section and the rate of growth of average multiplicity, with identical frequencies and relative amplitudes. For weak oscillation, however, they are shown to be 180° out of phase. Relevant experimental information on this fine structure is also discussed. (auth)

14586 DUAL MULTI-VENEZIANO SPINNING PARTICLE AMPLITUDES. Collop, D. J. (Cambridge Univ., Eng.). Nuovo Cim.; 1A: 217-37(21 Jan 1971).

Using a compact notation developed, multiparticle Veneziano amplitudes for spinning particles are obtained by factorization of the scalar-particle amplitudes. The general amplitude derived is shown to factorize in arbitrary tree diagrams provided that one introduces a different propagator. This propagator does not have matrix elements between spurious states but the factorization spectrum off mass shell is not clear. (auth)

14587 COMMENTS ON ISOSPIN-FACTORED CURRENT ALGEBRA AT INFINITE MOMENTUM. Garavaglia, T. (Colaiste Na Trionoide, Dublin). Phys. Rev., D; 3: 627-31(15 Jan 1971).

A solution of the isospin-factored current algebra at infinite momentum was given by Chang, Dashen, and O'Raifeartaigh, who assumed that one could project from the isospin-factored current algebra those solutions which contain a spacelike part which is definitely coupled to a timelike part by the current. This assumption was used to conclude that the operator M_3 vanishes. However, since the resulting solutions still contain a spacelike part which is coupled to the timelike part, it was suspected that this assumption may have excluded an important class of solutions. This, however, is shown not to be the case. (auth)

14588 BOHR QUANTIZATION OF RELATIVISTIC BOUND STATES OF TWO POINT PARTICLES. Degasperis, A. (Indiana Univ., Bloomington). Phys. Rev., D; 3: 273-80(15 Jan 1971).

The action-at-a-distance relativistic theory proposed by Van Dam and Wigner in its more general version discussed by Katz is considered. Exact bound-state solutions for systems of two particles are given. Bohr quantization of these solutions is also suggested. (auth)

14589 GENERAL PROPERTIES OF q-NUMBER SCHWINGER TERMS. Okubo, Susumu (Univ. of Rochester, N. Y.). Phys. Rev., D; 3: 409-19(15 Jan 1971).

A systematic study of properties of q-number Schwinger terms in the algebra of currents is carried out on the basis of Lorentz covariance. It is found that these terms can be expressed by means of a second-rank Lorentz tensor. As an application, the existence of a covariant time-ordered product of two currents is proven for a wide class of Schwinger terms. (auth)

14590 SOLUTION ON THE UNITARITY RELATION FOR SCATTERING AMPLITUDE OF PARTICLES WITH SPIN. Savrin, V. I.; Tyurin, N. E.; Khrustalev, O. A. (Inst. of High Energy Physics, Serpukhov, USSR). Yadern. Fiz.; 12: 1049-55 (Nov 1970). (In Russian).

On the basis of the unitarity relation the amplitude is calculated for the high-energy elastic scattering of a scalar particle on a spin-$\frac{1}{2}$ particle. A formula is given for the spinor particle polarization at scatterings to small and large angles. (auth)

14591 WEAKLY BOUND STATES OF THREE RESONANTLY INTERACTING PARTICLES. Efimov, V. N. (Ioffe Inst. of Physics and Tech., Leningrad). Yadern. Fiz.; 12: 1080-91(Nov 1970). (In Russian).

It is shown that if the pair forces provide a sufficiently strong resonance, the system of three identical particles has a family of bound states with low energies. The quantum numbers of all the states are identical; those are 0^+ for spinless bosons, and $\frac{1}{2}^+$, $T = \frac{1}{2}$, for nucleons. The range of the states is more than that of the pair forces. The best conditions for the family of levels exist in the system of three spinless neutral bosons; the conditions are less suitable in case of charged particles and of particles with spin and isospin. Possible existence of such levels in the three-α-particle system (the ^{12}C nucleus) and in the three-nucleon system (^3H) is discussed. (auth)

14592 KINEMATICAL SINGULARITIES OF THE THREE-BODY DECAY HELICITY AMPLITUDES. Jurkiewicz, J. Jagellonian Univ., Krakow). Acta Phys. Pol.; B1: 363-73(Oct-Dec 1970).

The kinematical behavior of the three-body decay helicity amplitudes at the boundary of the physical region and of the decay transversity amplitudes at the thresholds and pseudo-thresholds is discussed. The three-body decay amplitudes possess the threshold and pseudo-threshold singularities in s, t and u. (auth)

14593 DYNAMICAL CALCULATIONS IN CURRENT ALGEBRA. Rawls, John Marshall. Waltham, Mass.; Brandeis Univ. (1970). 111p. University Microfilms Order No. 70-24,653.

Thesis.

A number of problems are examined by use of the techniques of current algebra. The fact that neutral vector currents are the source of electromagnetism is used to prove that the scalar isovector spectrum is empty to zeroth order in α; in contrast, conservation of the axial vector current does not preclude the existence of massless (Goldstone) pseudoscalar excitations. The minimal electromagnetic coupling generalization of CVC is used to derive order α properties of the scalar isovector spectrum. The lowest order contributions to weak mass splittings of soft pseudoscalar mesons are calculated using the SU(3) × SU(3) algebra. The most divergent terms cancel in all cases considered; in the special case of the Cabbibo theory, the mass splittings vanish identically. Two generalizations of Sugawara models are discussed. In the first, new interactions are introduced by altering the current commutators but retaining the "free" form of $T_{\mu\nu}$, as exemplified by a simple effective $\pi^0 - 2\gamma$ interaction, which is compared with the standard triangle-diagram results. The second permits nonquadratic $T_{\mu\nu}$, which retain the "algebra" part of the current commutators; these models avoid the Dashen–Frishman parity degeneracy. Canonical techniques are employed in an analysis of commutators of currents and stress-energy tensor components in a variety of theories. It is concluded that, although terms of the required singularity structure are present, the

XUM

commutators involving the electromagnetic current in Pauli electrodynamics and the stress-energy tensor in a theory recently proposed by Callen, Coleman, and Jackiw both violate general principles of field theory. Hence, other (noncanonical) terms must also be present. (Diss. Abstr. Int., B)

14594 STUDY OF MANY-BODY CROSS SECTIONS AND LINK WITH TWO-BODY CROSS SECTIONS AND WITH THE REACTION MECHANISM. Hansen, J. D.; Kittel, W.; Morrison, D. R. O. (CERN, Geneva). Nucl. Phys.; B25: 605-20(1971).

Cross sections for many-body reactions were studied in an attempt to separate the effect of the reaction mechanism, i.e. the "physics," from phase-space effects. The cross section σ, is written as $\sigma = \sigma_A \times$ (phase-space term). The phase-space term is chosen such that at asymptotically high energies it tends to the value of one, and it has the form (phase-space volume)/P_L^{k-2}, where p_L is the incident laboratory momentum and k is the multiplicity of particles in the final state. The "physics" is then represented by σ_A which is found experimentally to have the form σ_A = (constant) $\times p_L^{-n_A}$ as in two-body reactions. Furthermore it is found that n_A is a constant independent of multiplicity, but depending on the reaction mechanism in a manner similar to that found for two-body reactions. (auth)

Electromagnetic

Refer also to abstracts 14800, 14802, and 14813.

14595 (ITF-70-63-P) SCATTERING OF HIGH-ENERGY γ QUANTA ON THE NUCLEONS AND NUCLEI. Akhiezer, A. I.; Rekalo, M. P. (Akademiya Nauk Ukrainskoi SSR, Kiev. Institut Teoreticheskoi Fiziki). 1970. 12p. (In Russian). Dep. NTIS (U. S. Sales Only).

The total cross sections of γ quanta interaction with the nucleons and nuclei are connected in the quark model with the total cross sections of π- and k-mesons interaction with the nucleons and nuclei. These relations agree well with existing experimental data about γp- and γd-interactions. The constant of the γp-interaction which is found by this method agrees with those values which are obtained in storage ring experiments or in the decays $V^0 \rightarrow e^+e^-$. However, the predicted A-dependence of total cross sections of γ-nuclei interaction contradicts experimental data which indicate breakdown of the vector dominance hypothesis. (auth)

14596 (JINR-E2-5424) RESONANT SCATTERING OF LIGHT BY LIGHT. Kunszt, Z.; Muradyan, R. M.; Ter-Atonyan, V. M. (Joint Inst. for Nuclear Research, Dubna (USSR). Lab. of Theoretical Physics). 1970. 8p. Dep. NTIS (U. S. Sales Only).

Resonant scattering of light by light due to exchange of C-even mesons, such as π^0 and η, is considered. The total cross section for $\gamma\gamma$-scattering at resonance point $s = m_\pi^2$ has the value $\sigma^\pi = (16\pi/m_\pi^2) \approx 1.1 \times 10^{-24}$ cm². Assuming 2% energy resolution, the cross section has the magnitude $10^{-30} \approx 10^{-31}$ cm². It is shown that the cross section for the reaction $\gamma\gamma \rightarrow \pi^+\pi^-$ near f(1260)-resonance has the value 10^{-29} cm². (auth)

14597 CONTRIBUTIONS OF INELASTIC CHANNELS TO THE PION'S EM FORM FACTOR AND PRODUCTION OF STRANGE PARTICLES IN PROTON-PROTON SCATTERING. Serio, Salvatore. Rochester, N. Y.; Univ. of Rochester (1970). 104p. University Microfilms Order No. 70-17,908.
Thesis.

It is shown that inelastic pion-pion scattering appreciably contributes to the electromagnetic form factor of the pion. The effect of inelasticity is computed by solving the dispersion relation for the pion form factor in the multichannel formalism with a suitable approximation for the left hand cut. The contributions of the $\pi\pi$-$K\bar{K}$ scattering are shown to be significant. Assuming equality of the couplings, a best fit analysis of the Orsay data gives $\Gamma_\rho = 95 \pm 10$ MeV. The reactions pp-YKN are studied under the hypothesis of a dominant contribution from the exchange of a pseudoscalar meson (π or K) between the initial protons. A simple multiplicative cut-off function is used to describe the various damping effects at large momentum transfer. It is found that the agreement with the experimental data is fairly good, within the limits of the model. (Diss. Abstr. Int., B)

14598 APPLICATION OF REGGE POLE THEORY TO LARGE-ANGLE POSITIVE PION PHOTOPRODUCTION. Solomonidou, Christina. Medford, Mass.; Tufts Univ. (1969). 126p. University Microfilms Order No. 70-17,394.
Thesis.

The nucleon and N* Regge poles and an even signature fixed pole at $J = -\frac{1}{2}$ are used to obtain a fit to the differential cross section of the photoproduction of positive pions off nucleons at large angles, at 4.3, 6.7, and 9.8 GeV. With the same parametrization agreement is also obtained with the magnitude but not the shape of the differential cross section for neutral pion photoproduction at large angles at 12 GeV. (Diss. Abstr. Int., B)

14599 PARTICLE MOTION IN THE ELECTROMAGNETIC FIELD. Souriau, Jean-Marie (CNRS, Orsay, France). Compt. Rend., Ser. A; 271: 1086-8(23 Nov 1970). (In French).

Two universal fields are associated with matter: X → T (T, symmetric momentum-energy tensor) and X → J (J, charge-current density vector). The two equations $\partial\mu J^\mu = 0$ and $\partial\mu T_\gamma^\mu + F\mu\gamma J^\mu = 0$, which express respectively the conservation of the electricity and the action of electromagnetic (F, electromagnetic field) and gravitational forces, are consistent with this principle. It is shown that the universality of this principle explains directly the dynamic and electromagnetic behavior of particles with spin. (France)

14600 BREMSSTRAHLUNG IN SCATTERING OF NEUTRINOS BY ELECTRONS TAKING INTO ACCOUNT RADIATIVE CORRECTIONS. Kerimov, B. K.; Tsvetkov, V. P. Vestn. Mosk. Univ., Ser. III. Fiz. Astron.; 11: 293-9(May-Jun 1970). (In Russian).

Angular and energy distribution of bremsstrahlung γ quanta in the scattering of neutrinos on electrons was calculated. Equations were obtained for radiative corrections of α order for the total effective cross section of neutrino-electron scattering considering the hard photon emission. (R.V.J.)

14601 COMMENTS ON SARACHIK AND SCHAPPERT'S EXACT RESULTS FOR SCATTERING OF LINEARLY POLARIZED RADIATION. Prakash, H.; Chandra, N.; Vachaspati (Univ. of Allahabad, India). Lett. Nuovo Cim.; 4: 1107-8(12 Dec 1970).

It is pointed out that the results of Sarachik and Schappert (Lett. Nuovo Cimento, 2: 7(1969)) for scattering of linearly polarized radiation by free electrons are not exact as claimed. (L.B.S.)

14602 INELASTIC PHOTOPRODUCTION ON NUCLEI AND THE DETERMINATION OF I_6/C. Rej, A. K. (Indian Statistical Inst., Calcutta). Lett. Nuovo Cim.; 4: 1119-22(12 Dec 1970).

It is pointed out that the quantity I_6/C can be studied experimentally from inelastic photoproduction of π^0 on ^{7}Li and ^{9}Be, leading to their respective second excited states, with linearly polarized photons parallel and perpendicular to the production plane. (L.B.S.)

14603 STRONG ABSORPTION CUT IN PHOTOPRODUCTION. Namyslowski, J. (Univ., Warsaw); Sawicki, M.; Staszel, M.; Wilk, G. Lett. Nuovo Cim.; 4: 1125-9(12 Dec 1970).

Two processes $\gamma p \rightarrow \pi^+ n$ and $\gamma p \rightarrow \pi^- \Delta^{2+}$ are investigated in the strong-cut Reggeized model. The main result of the best fit to the differential cross sections is that the ordinary coherent inelastic factor λ has to be quite large, not less than 2. (L.B.S.)

14604 EVIDENCE FOR AN ISOTENSOR ELECTROMAGNETIC CURRENT IN PION PHOTOPRODUCTION. Sanda, A. I.; Shaw, Graham (Columbia Univ., New York). Phys. Rev., D; 3: 243-9(1 Jan 1971).

An unambiguous and model-independent test for the presence of isotensor terms in pion photoproduction is suggested. It is also shown how the conventional theory of photoproduction can be generalized to include such a term, leaving the successful predictions for photoproduction on protons unchanged. Analysis of the available data on π^- photoproduction from neutrons yields evidence for striking effects due to such a term. Further experiments are discussed and, in particular, the importance of π^- radiative capture experiments, thus avoiding the use of a deuterium target, is stressed. (auth)

14605 s-CHANNEL HELICITY CONSERVATION WITH t-CHANNEL DYNAMICS. Thews, Robert L. (Univ. of Rochester, N. Y.). Phys. Rev., D; 3: 250-3(1 Jan 1971).

The compatibility of s-channel helicity conservation and t-channel exchanges in diffractive-type processes is examined. It is found that compatibility exists only in the infinite-energy limit. This requires specification of ratios of residue or vertex functions for t-channel helicity amplitudes. Assuming these conditions are satisfied, finite-energy corrections for ρ^0 polarized photoproduction are calculated and found to be consistent with data at 2.8 and 4.7 GeV. Predicted values of spin-density matrix elements for other diffractive processes are given for the usual t-channel analysis in unpolarized experiments. (auth)

14606 VECTOR-MESON EXCHANGE CONTRIBUTIONS TO THE $K_1 \rightarrow \gamma\gamma$ DECAY RATE. Uy, Zenaida Ebora Santos (State Univ. of New York, Stony Brook). Contract AT(30-1)-3668B. Phys. Rev., D; 3: 234-7(1 Jan 1971).

By assuming that (1) the decay $K_1 \rightarrow \gamma\gamma$ is saturated by the 2π intermediate state, (2) the $K\pi\pi$ vertex is of the first-order weak interaction, and (3) the $\pi\pi \rightarrow \gamma\gamma$ process goes by exchanges of ρ,

KUM

ω, and ϕ, the contributions to the decay rate of $K_1 \rightarrow \gamma\gamma$ from the three exchanges are calculated. It is found that the contributions do not alter in any significant way the result of the perturbation calculation using the Born term for the $\pi\pi \rightarrow 2\gamma$ reaction. (auth)

14607 FIELD-THEORETIC MODEL OF HIGH-ENERGY SCATTERING. III. INELASTIC ELECTRON–PROTON SCATTERING. Fried, H. M. (Brown Univ., Providence); Gaisser, T. K. Phys. Rev., D; 3: 224-9(1 Jan 1971).

A field-theoretic model of soft, neutral-meson production is used to bracket recent deep-inelastic electron–proton scattering data. (auth)

14608 FIXED POLE IN THE VIRTUAL COMPTON AMPLITUDE A_2. Rajaraman, R. (Delhi Univ.); Rajasekaran, G. Phys. Rev., D; 3: 266-8(1 Jan 1971).

The presence of a $J = 0$ fixed pole in the virtual Compton amplitude A_2 with a residue linear in the photon mass q^2 for all q^2 is suggested. The resultant sum rule is found to be consistent with the on-mass-shell ($q^2 = 0$) data, the scale-invariance requirement at $q^2 \rightarrow \infty$, and the electron scattering data for intermediate q^2. (auth)

14609 FORWARD PHOTOPRODUCTION OF A CHARGED PION AND N(1520). Clark, Robert Beck (Univ. of Texas, Austin). Phys. Rev., D; 3: 258-60(1 Jan 1971).

The analysis of the reaction $\gamma p \rightarrow \pi^+ N(1520)$ is considered and the influence of low-t theorems in the near forward direction is discussed. It is shown that present preliminary experimental results are not inconsistent with the dominance of the amplitudes whose forms near $t \approx \mu^2$ are determined by low-t theorems. Predictions are presented for $d\sigma/dt$ and the spin-density matrix $\rho_{\lambda\lambda'}$. (auth)

14610 POSSIBLE EXPLANATION FOR THE RAPID APPROACH TO "UNIVERSALITY" OF THE INELASTIC ELECTRON-SCATTERING STRUCTURE FUNCTIONS. Suri, Ashok (Stanford Univ., Calif. Univ. of California, Santa Cruz). Phys. Rev. Lett.; 26: 208-12(25 Jan 1971).

The single-variable analyticity of the inelastic electron-scattering structure functions in the complex x plane, with s kept fixed and real, to all orders of Feynman perturbation theory was determined. It is found that its Landau singularities, which move as a function of s, rapidly approach their asymptotic s-independent position once s is large. It is discussed how this observation offers a possible explanation for a rapid approach to "universality" of the inelastic electron-scattering structure functions and shows that $sW_2(s,q^2/s)$ should "scale" faster than $\nu W_2(s,x)$. (auth)

14611 WARD IDENTITIES FOR η DECAY IN PERTURBATION THEORY. Abers, Ernest S. (Univ. of California, Los Angeles); Dicus, Duane A.; Teplitz, Vigdor L. Contract AT(30-1)-2098. Phys. Rev., D; 3: 485-97(15 Jan 1971).

The process $\eta \rightarrow 3\pi$ is known to violate a simple prediction of partial conservation of axial-vector current. In many models, $\eta \rightarrow 3\pi$ proceeds through a fermion loop with electromagnetic corrections. The first radiative corrections to fermion loops give rise to divergent double-loop integrals with forms like $\int d^4r d^4k/[r^2 - m^2]^2[(r - k)^2 - m^2]^2$. As with single linearly divergent integrals, when a meaning is ascribed to them it may not always be possible to shift the origin of integration without changing the value of these integrals. Such integrals appear when one tries to check, in perturbation theory, Ward identities and low-energy theorems which follow from the formal manipulation of the equations of motions. They can cause anomalies similar to the one in the axial-vector-current two-photon vertex. Some applications to the $\eta\pi\sigma$ vertex, to the process $\eta \rightarrow 3\pi$, and to the corrections of order α^2 to $\pi^0 \rightarrow 2\gamma$ are studied. No anomalies which can be related to η decay are discovered. (auth)

14612 DEEP-INELASTIC e–p STRUCTURE FUNCTIONS IN A LADDER MODEL WITH SPIN-$^1/_2$ NUCLEONS. Blaha, Stephen (Rockefeller Univ., New York). Contract AT(30-1)-4204. Phys. Rev., D; 3: 510-23(15 Jan 1971).

The asymptotic behavior of the inelastic electron–proton structure functions W_1 and W_2 in the limit $|q^2| \rightarrow \infty$ with $\omega = 2q \cdot p/|q^2|$ fixed (q is the electron four-momentum transfer and p the target nucleon four-momentum) is found using a ladder model for the virtual Compton amplitude. Neutral vector mesons are exchanged between the (spin-$^1/_2$) proton legs. In addition, this model (with slight modifications) gives the asymptotic behavior for a ladder model in which pseudoscalar mesons are exchanged, and the asymptotic behavior for a truss-bridge-graph model in a mixed $\phi^3 - \phi^4$ field theory. In all of these models W_1 and νW_2 do not scale because of factors of $\ln |q^2|$ (with the exception of νW_2 in the truss-bridge model). In addition, it is found that the structure functions are essentially Bessel functions with the argument $\ln |q^2| \ln\omega$ in the $|q^2| \rightarrow \infty$ limit for fixed $\omega \gg 1$. (auth)

14613 BREMSSTRAHLUNG IN COULOMB FIELD: AN EXACT REGGE-MULTIPERIPHERAL PRODUCTION AMPLITUDE. Fronsdal, C.; Lundberg, L.-E. (International Centre for Theoretical Physics, Trieste, Italy). Phys. Rev., D; 3: 524-30(15 Jan 1971).

The exact matrix elements for Coulomb scattering, photoeffect, and bremsstrahlung in a Coulomb field are obtained by means of a very simple algebraic calculation. The method is closely related to current ideas on elementary particle physics, and Regge poles are particularly relevant in all three processes. Bremsstrahlung in a Coulomb field is a production amplitude that is given in its entirety by the contribution of a Reggeized multiperipheral diagram. Each internal line carries one value $\nu(\Xi)$ of the Reggeized principal quantum number n, or, equivalently, an infinite set of ordinary Regge poles with $\alpha(E) = \nu - 1, \nu - 2, \ldots$. This circumstance may be exploited to learn something about the Reggeon–Reggeon-particle vertex. (auth)

14614 SCALING, FIXED POLES, AND ELECTROPRODUCTION SUM RULES. Cornwall, John M.; Corrigan, Dennis; Norton, Richard E. (Univ. of California, Los Angeles). Phys. Rev., D; 3: 536-45(15 Jan 1971).

Bjorken's scale invariance is imposed on the general form of the Deser–Gilbert–Sudarshan (DGS) representation for forward current–hadron scattering amplitudes to deduce features of the scaling limit, the Regge limit, and the asymptotic limit for fixed total mass of the produced hadrons. Two sum rules are derived, whose validity essentially asserts that the residue of the $J = 0$ fixed pole in the virtual Compton amplitude is independent of the mass carried by the currents. One of these relations tests for the presence of operator Schwinger terms, and the other relates an integral over the total photoproduction cross section to an integral over a scale function observed in electroproduction. The significance of these ideas for the calculation of electromagnetic mass differences is also discussed. (auth)

14615 SPLITTING OF THE MAXWELL TENSOR. II. SOURCES. Teitelboim, Claudio (Princeton Univ., N. J.). Phys. Rev., D; 3: 297-8(15 Jan 1971).

The sources of the bound tensor $T_{I}^{\mu\nu}$ and the emitted tensor $T_{II}^{\mu\nu}$ introduced in the treatment of radiation reaction without advanced fields are investigated. It is found that both parts of the energy tensor have a δ-function-type source on the world line of the charged particle. The strength of the source is, in each case, the rate of change of the corresponding four-momentum. This is in sharp contrast with the situation in the advanced-field approach where the radiation field is source free and one has emission but not emitter. A very simple derivation of the Lorentz–Dirac equation based on the above results is presented. (auth)

14616 VACUUM-POLARIZATION CONTRIBUTIONS TO THE SIXTH-ORDER ANOMALOUS MAGNETIC MOMENT OF THE MUON AND ELECTRON. Brodsky, Stanley J. (Cornell Univ., Ithaca, N. Y. Stanford Linear Accelerator Center, Calif.); Kinoshita, Toichiro. Phys. Rev., D; 3: 356-62(15 Jan 1971).

The calculation of second-order vacuum-polarization contributions to the sixth-order electron and muon anomalous magnetic moments is reported. With these results the difference of muon and electron moments has now been completely calculated through sixth order in quantum electrodynamics. The only remaining sixth-order contributions to the electron moment which have not been completely calculated are those graphs without fermion loop insertions. (auth)

14617 ELECTROMAGNETIC CORRECTIONS TO NUCLEON TRANSITIONS OF THE VECTOR AND AXIAL-VECTOR CURRENTS. Pagels, Heinz (Rockefeller Univ., New York). Phys. Rev., D; 3: 610-14(15 Jan 1971).

The matrix elements of the divergences of the vector and axial-vector current between nucleon states are examined. These matrix elements are related to the nucleon mass difference and the corrections to the Goldberger–Treiman relation, respectively. For the nucleon mass difference it is indicated that for the sign of this quantity to be understood in terms of the electromagnetic interaction requires (i) comparable longitudinal and transverse virtual photon–nucleon cross sections, or (ii) $\sigma_t^p(q^2,\nu) - \sigma_t^n(q^2,\nu) < 0$ over a large region of the $(|q^2|,\nu)$ plane, where q^2 is the space-like virtual-photon mass and ν is the photon energy (this requirement is contraindicated by experimental data at $q^2 = 0$), or (iii) fixed J-plane poles at $J = 0$, $I - 1$ in the virtual Compton amplitude. The electromagnetic correction to the Goldberger–Treiman relation is also estimated, and it is shown to be very small. (auth)

14618 RELATIONSHIP OF FLUX QUANTIZATION TO CHARGE QUANTIZATION AND THE ELECTROMAGNETIC COUPLING CONSTANT. **Jehle, Herbert (George Washington Univ., Washington, D. C.). Phys. Rev., D; 3: 306-45(15 Jan 1971).**

The concept of a closed quantized flux loop (''elementary loop'') which avoids the implication of magnetic monopoles is investigated, leading to a theory of a charged lepton (muon or electron). In order to reconstruct a continuous magnetic dipole field of a source lepton, it is assumed that the flux loop adopts a statistical distribution of alternative forms characterized by a complex probability amplitude superposition, in a manner somewhat analogous to the superposition of path histories in Feynman's space–time approach to quantum mechanics. Flux quantization results from the equivalence of a line discontinuity of the phase factor of a ψ function of a field lepton (due to its phase multivaluedness by $\pm 2\pi$) to the presence of a line of quantized flux. On the same basis as quantized flux arises from such a singularity of that phase factor, so also an electric field arises when this singularity line is moving. In particular, the source's Coulomb field results from a spinning of the quantized flux loop (about the center of the source) with an angular velocity equal to the Zitterbewegung frequency $2mc^2/\hbar$, if the statistical distribution of flux loopforms properly represents the magnetic dipole field of a muon or of an electron. The reconstruction of the magnetic and electric fields of a charged lepton and the comparison of them with the quantized flux hc/e give a numerical estimate of the electromagnetic interaction constant $e^2/\hbar c$, i.e., an understanding of the relationship between e and $\hbar$. The energy mc^2 and angular momentum $\hbar/2$ may be interpreted as electromagnetic. The theory should work for both muon and electron and is expected to give some insight into the ratio of the masses of these two leptons. A representation of quarks in terms of linked quantized flux loops is suggested to describe a low-lying meson as a linkage of an elementary loop with an antiloop, and a low-lying baryon as three interlinked elementary loops. A model approach to problems of structure and conservation laws in particle physics is developed. A more abstract version of a quantized flux theory of particles should be preceded by such an heuristic model. (auth)

14619 CURRENT ALGEBRA AND PHOTOPRODUCTION OF π-MESONS ON HYPERONS. Tavluyev, G. V. Sb. Nauch. Rab. Aspir. Univ. Durzhby Narodov, Fak. Fiz.-Mat Estestv Nauk; No. 6, 213-17(1969). (In Russian).

Sum rules for the amplitudes of the photoproduction of π-mesons on hyperons are found within the framework of commutation relations of the quark model. The sum rules obtained are saturated by the low-level resonances in direct and intersecting channels. Values are selected for the coupling constants which give SU(3)-symmetry. The results are used to calculate the magnetic moments of hyperons. (JPRS)

14620 SIXTH-ORDER RADIATIVE CORRECTIONS TO $\alpha_\mu - \alpha_e$ Lautrup, B. E.; Peterman, A.; de Rafael, E. (CERN, Geneva). Nuovo Cim.; 1A: 238-42(21 Jan 1971).

The contribution to the anomalous magnetic moment of the muon from Feynman diagrams is given. (auth)

14621 INELASTIC ELECTRON SCATTERING AND THE MULTI-REGGE MODEL AND HADRONIC STATES OF EVEN CHARGE CONJUGATION FROM ELECTRON–POSITRON ANNIHILATION. **Creutz, Michael John. Stanford, Calif.; Stanford Univ. (1970). 97p. University Microfilms Order No. 70-22,160.**

Thesis.

The application of the multi-Regge model when a particle incident on a proton has a large negative four-momentum squared (p_1^2) is discussed. This kinematics occurs in inelastic electron scattering via single virtual photon exchange. I draw three main conclusions: Final states with only two hadrons will dominate the cross section in the limit of large center of mass energy squared (s) with the ratio s/p_1^2 constant. In the above limit, with s/p_1^2 much less than one, the final state will contain a baryon going backward with respect to the initial proton in the center-of-mass system. The vertex coupling a virtual photon to a hadron and a spacelike reggeon cannot fall rapidly with increasing photon momentum transfer if present data are to be described by the model. The production of hadronic states plus a photon in storage rings as a method of exploring even charge conjugation hadronic systems is discussed. The state of two charged pions and a photon is discussed in detail. It is found that storage ring production of this state will be a useful means with which to see the conjectured spin-zero epsilon resonance. (Diss. Abstr. Int., B)

14622 LOW ENERGY THEOREMS AND HIGH ENERGY PHOTOPRODUCTION. **Broadhurst, D. J.; Dombey, N.; Read, B. J. (Univ. of Sussex, Brighton, Eng.).** Phys. Lett.; 34B: 95-8(18 Jan 1971).

Following Damashek and Gilman, it is pointed out that low energy theorems can contribute at high energy. In forward pion photoproduction this contribution is dominant. (auth)

14623 POSSIBLE EFFECTS OF AN ELECTRIC DIPOLE MOMENT FOR A WEAK INTERMEDIATE BOSON. Tauber, Thomas Ernest. Bethlehem, Pa.; Lehigh Univ. (1970). 134p. University Microfilms Order No. 70-26,167.

Thesis.

Assuming that the observed CP-violation in the K_2^0-decays can be accounted for by an intrinsic electric dipole moment (EDM) of the (hypothetical) intermediate vector boson W, two consequences are examined. In spin-one electrodynamics, anomalous dipole moments cause the appearance of zero-order quadrupole moments. An EDM induces a magnetic quadrupole moment whose value is determined. The radiative multipole moment corrections are calculated to second order in e by using the ξ-limiting formalism. It is found that the magnetic dipole moment correction is independent of the value of the EDM and the result agrees with Lee, while being in disagreement with Bailin. By comparison, Bailin's value is verified for the electric quadrupole moment correction. The correction to the magnetic quadrupole moment is also determined. Since experimental accuracy in the measurement of the magnetic moments of the charged leptons could reach the level $(\alpha/\pi)^3$ in the not too distant future, all contributions of an order comparable to the sixth-order radiative corrections are of interest. An EDM of the W of about one magneton, as proposed by Salzman and Salzman, might be expected to cause such a contribution. However, it is found that there is no such correction to second-order in the semi-weak coupling constant, regardless of the magnitude of the W's EDM. Likewise, it is shown that possible intrinsic quadrupole moments of the W are not detectable through measurements of the dipole moments of the muon or the electron. (Diss. Abstr. Int., B)

14624 NONRELATIVISTIC TIME-DEPENDENT SCATTERING THEORY FOR LONG RANGE POTENTIALS. Mulherin, Denis Wren Mark. New York; Fordham Univ. (1969). 190p. University Microfilms Order No. 70-11,443.

Thesis.

The nonrelativistic scattering of two spinless particles in a time-dependent formalism is considered. In particular, a new time-dependent theory applicable to the Coulomb potential (λ/r) is developed. (TSS)

14625 COMMENT ON FIXED J-PLANE SINGULARITIES IN PHOTOPRODUCTION. **Bialas, A.; Golemo, A.; Gorczyca, B. (Jagellonian Univ., Krakow). Acta Phys. Pol.; B1: 383-6(Oct-Dec 1970).**

An experimental test of the hypothesis that fixed j-plane singularities dominate the high-energy photoproduction is discussed. (auth)

14626 PHOTOPRODUCTION OF SCALAR AND VECTOR MESONS IN THE REGION OF THE SECOND MAXIMUM IN ANGULAR DISTRIBUTION AND THE QUARK MODEL. **Gula, A. (Inst. of Nuclear Technique, Krakow). Acta Phys. Pol.; B1: 447-52 (Oct-Dec 1970).**

The assumption of antiquark–quark scattering dominance in the formation of the secondary maximum in angular distribution is applied to photoproduction processes. The SU(6) quark model is used to obtain simple relations between the differential cross sections for scalar and vector meson photoproduction in the momentum transfer region in which the secondary maximum appears. A qualitative explanation of the difference between the angular distributions of π^0 and η photoproduction on protons is presented. (auth)

14627 PHOTOPRODUCTION OF $K^+\Lambda$ AND $K^+\Sigma^0$ AND $g_{\Lambda KN}$, $g_{\Sigma KN}$ COUPLING CONSTANTS. Renard, F. M.; Renard, Y. (Univ., Montpellier, France). Nucl. Phys.; B25: 490-8(1971).

The reactions $\gamma p \to K^+\Lambda$ and $\gamma p \to K^+\Sigma^0$ are analyzed in the low and intermediate energy range with the help of a new isobaric coupling model which includes Born terms and s- and u-channel resonances only. The results are discussed in terms of the $g_{\Lambda KN}$ and $g_{\Sigma KN}$ coupling constants. The values $-12.7 \lessapprox g_{\Lambda KN} \lessapprox -8.5$ and $1.3 \lessapprox g_{\Sigma KN} \lessapprox 2.0$ are favored. (auth)

14628 LOCAL GAUGE-INVARIANT FORMULATION OF ELECTROMAGNETIC $\omega-\rho$ MIXING IN BROKEN SU(3) LAGRANGIAN THEORY. Burnel, A. (Univ., Liege). Nucl. Phys.; B25: 471-89(1971).

Electromagnetic interactions including first order $\omega-\rho$ mixing are introduced in broken SU(3) Lagrangian theory in such a way that the vector–meson mass term becomes invariant under the gauge transformations in the direction of the third component of isospin and of the hypercharge. The vector–meson dominance is contained in the diagonalization matrix. Assuming octet dominance and second-order $\rho-\omega$ mixing, three sum rules relating $g_{\omega\pi\pi}$, $g_{\phi\pi\pi}$, $g_{\rho_0 3\pi}$, $m_{\rho_+} - m_{\rho_0}$ and $m_{K_*+} - m_{K_{*0}}$ are obtained. Both current-mixing and mass-mixing are discussed. (auth)

14629 PHOTOPRODUCTION OF PSEUDOSCALAR MESONS ON PROTONS AND MIXING ANGLE OF ISOSINGLETS η_1 AND η_8. Kobylinskii, N. A. (Inst. of Theoretical Physics, Kiev). Yadern. Fiz.; 12: 1036-8(Nov 1970). (In Russian).

In order to determine the mixing angle for the isosinglets η_1 and η_8, the photoproduction of π^+, π^0, and η mesons on protons are considered in framework of the model which takes into account poles and cuts. (auth)

14630 SEMINAR DE FIZICA TEORETICA. 3. (Lectures in Theoretical Physics. III.). Novacu, V. Bucuresti; Editura Academiei Republicii Socialiste Romania (1970). 274p.

Eleven lectures on solid state and particle physics are included. The discussion of solid state theory covers the method of motion equation in many-body theory, the quantum theory of band ferromagnetism, theory of the excitonic insulator, high-field electrical conduction, the radial distribution function, the statistical theory of the evolution of macroscopic systems, and some applications of the pseudopotential method. The treatment of elementary particle theory includes the Veneziano amplitude, low-energy theorems for Compton scattering, radiative decays, and the Glauber model and the pion–deuteron scattering. (J.F.P.)

Weak

Refer also to abstract 14804.

14631 (ITF–70–64) DECAY $\mu \to e + \nu + \bar{\nu}$ AND LIMITATIONS ON THE NEUTRINO AND W BOSON MASSES AND ON THE VARIANTS OF THE WEAK INTERACTION. Rekalo, A. P. (Akademiya Nauk Ukrainskoi SSR, Kiev. Institut Teoreticheskoi Fiziki). 1970. 37p. Dep. NTIS (U.S. Sales Only). (In Russian).

An expression for the energy spectrum of the electrons, produced in the decay of polarized μ-meson, is obtained in a model of the weak interaction which transfers by charged vector boson (V- and A-interaction variants are arbitrary in the muon and electron vertex). Using experimental values of the spectrum parameters, the limitations are obtained on the masses of the muonic neutrino, intermediate boson and on the values of the deviation from V- A-variant of the weak interaction. Michel's parameter turned out very sensitive to m_ν: definite values of ρ limit m_ν from above better than in direct measurements of the neutrino mass. Parameter η is very sensitive to the values of the deviation from V–A theory: values of axial-vector constant greater or lesser than 20% in comparison with the constant of the vector interaction are excluded. Parameters ρ and η allow also reasonable limitations for mass of the W-boson. Analysis of the parameters of anistropic part δ and ξ confirms this conclusion. (auth)

14632 (KFKI–70–23–HEP) REMARKS ON "A NEW FIT OF THE PARAMETERS FOR CABIBBO'S THEORY." Frenkel, A.; Hasenfratz, P. (Magyar Tudomanyos Akademia Kozponti Fizikai Kutato Intezete, Budapest). [1970]. 7p. (CONF-700937-2). Dep. NTIS (U. S. Sales Only).

From Symposium on Hadron Spectroscopy, Balatonfured, Hungary.

Some of the theoretical uncertainties inherent in the theory of the weak interaction and their possible influence on the fitted value of the Cabibbo angle are discussed. Special attention is given to the problem of the q^2 dependence of the form factors. (auth)

14633 (NYO–2262–TA–233) ON THE CONSISTENCY OF HARD PION THEOREMS IN K_{l3} DECAYS. Olshansky, Robert; Kang, Kyungsik (Brown Univ., Providence, R. I. Dept. of Physics). [1970]. 18p. Dep. NTIS.

The K_{l3} scalar form factor is studied by the hard-pion method in the framework of a $(3,3^*) + (3^*,3)$ symmetry-breaking model using a modified pole dominance approximation. A set of consistency relations are found which provides a test of the reliability of the quadratic smoothness assumption as well as of the symmetry breaking model. In particular, it is found that the solution for the symmetry breaking-parameters which fit the data is inconsistent with the quadratic smoothness assumption. In addition, the status of other theoretical models is briefly reviewed. (auth)

14634 (NYO–4204–7) ASYMPTOTIC BEHAVIOR OF WEAK SPECTRAL FUNCTIONS AND HADRONIC DECAYS OF THE W BOSON. Li, Ling-Fong; Paschos, E. A. (Rockefeller Univ., New York). [1970]. Contract AT(30-1)-4204. 24p. Dep. NTIS.

Models of current algebra are employed to study the asymptotic properties of the spectral functions of weak currents. Asymptotically it is found that they all approach constant values closely related to each other. As an application, the results are used to estimate the hadronic decay of the intermediate vector boson. The branching ratio of the W-decay into hadrons to the decay into leptons is of order unity provided the electron-positron annihilation total cross section is point-like and predominantly isovector. Another contribution is a consequence of PCAC, which relates the decay rate of the W-boson into a soft pion plus any number of bosons to the decay into all bosons through a known constant independent of the W mass. (auth)

14635 (NYO–4204-9) REGGE MODEL FOR INELASTIC LEPTON–NUCLEON SCATTERING. Pagels, Heinz (Rockefeller Univ., New York). [1970]. Contract AT(30-1)-4204. 21p. Dep. NTIS.

Lepton nucleon scattering into hadrons is analyzed according to the simple Regge pole model. Assuming SU(3) for the factorized residues from a strong interaction analysis of tensor meson-baryon couplings $\sigma_T^{\gamma p}(\nu) - \sigma_T^{\gamma n}(\nu)/\sigma_T^{\gamma p}(\nu) - \sigma_T^{\gamma p}(\infty) = (0.26 \pm 0.05)$ is obtained to be compared with 0.31 obtained from the total photon nucleon photoproduction data. For the inelastic structure functions assuming all Regge poles couple in the deep inelastic region ${}^\gamma F_2^p(\rho) - {}^\gamma F_2^n(\rho) = +0.15\,\rho^{-1/2}$, $\rho = -\nu/q^2 > 4$ is found. In the analogous neutrino process from these assumptions ${}^\nu F_2^p(\rho) + {}^\nu F_2^n(\rho) \simeq 0.66 + (3.5 \pm 1.7)\rho^{-1/2}$, $\rho > 4$ is established. Analyzing the Adler and Gross–Llewellyn Smith sum rules the estimates ${}^{\bar\nu} F_2^p(\rho) - {}^\nu F_2^p(\rho) \simeq 1.5\,\rho^{-1/2}$, ${}^\nu F_3^p(\rho) + {}^\nu F_3^n(\rho) \simeq -8.9\,\rho^{1/2}$, $\rho > 4$ are obtained. Also it is concluded that if scaling behavior of the neutrino process occurs for $-q^2 > 1$ (GeV)^2 then these sum rules are saturated to 90% only for energies $\nu > 200$ GeV for $-q^2 > 1$ (GeV)^2. (auth)

14636 (NYO–4204-10) HADRONIC HELICITY CONSERVATION AND INELASTIC LEPTON–NUCLEON REACTIONS. Pais, A. (Rockefeller Univ., New York). [1970]. Contract AT-(30-1)-4204. 9p. Dep. NTIS.

It was suggested that hadronic s-channel helicity is conserved in the diffractive region. If applicable to inelastic lepton-nucleon processes, such conservation has many implications which are illustrated for π- and 2π-production. Polarization information is not needed for a first verification. (auth)

14637 (SU–1206–238) VAN HOVE MODEL AND NON-LEPTONIC HYPERON DECAYS. Goswami, D. N.; Schechter, J.; Ueda, Y. (Syracuse Univ., N. Y. Dept. of Physics). Nov 1970. 23p. (NYO–3399–238). Dep. NTIS.

An attempt is made to construct a pole model for nonleptonic decays where exchanged particles of all spins are included. Summation over the different spins is carried out by means of the Van Hove model, assuming that the Regge pole term is important. It is found that a number of trajectories do not contribute for a very simple, essentially kinematical reason. A discussion of some consequences of this approach is given. (auth)

14638 UPPER LIMIT FOR MAGNETIC-MONOPOLE PRODUCTION BY NEUTRINOS. Carrigan, R. A. Jr.; Nezrick, F. A. (National Accelerator Lab., Batavia, Ill.). Phys. Rev., D; 3: 56-9(1 Jan 1971).

Existing magnetic-monopole searches are re-evaluated in terms of monopole production by cosmic-ray neutrinos. The upper limit for the cross section for monopole production inside the best ocean-bed sample is $\sigma_D \leq 1.0 \times 10^{-38}\, E_T^2$ cm^2, where E_T is the threshold energy to produce a pair of monopoles expressed in BeV. An even lower limit of $\sigma_C \leq 3.0 \times 10^{-45}\, E_T^2$ cm^2 is established if the monopoles are collected on the sample from surrounding ocean water. (auth)

14639 NISHIJIMA'S MODEL WITH A FIFTH INTERACTION. Schorr, Amir (Tel-Aviv Univ., Israel); Ne'eman, Yuval. Phys. Rev., D; 3: 231-4(1 Jan 1971).

Nishijima's model for CP violation introduces a divergencelike term in the strong Hamiltonian and attributes the nonleptonic weak interaction to the second-order contribution due to that term (CP violation arises in third order). By using a unitary scalar density plus the fifth interaction for the original strong Hamiltonian, a current–current structure is induced in Nishijima's weak Hamiltonian somewhat similar to the conventional one. Moreover, it becomes equivalent to tadpole terms for $|\Delta S| = 1$. The $\Delta S = 0$ weak transitions are somewhat modified. The correct $|\Delta I| = 3/2$ admixture is obtained from a counter term which relegates the $|\Delta S| = 2$ contributions to fourth order (i.e., second-order weak interactions). $|\eta_{00}| \sim |\eta_\pm|$ to within 10% is found. (auth)

XUM

14640 CURRENT ALGEBRA, VECTOR DOMINANCE, AND THE DECAY $K_L^0 \rightarrow \pi^+\pi^-\pi^0\gamma$. Intemann, Gerald W. (State Univ. of New York, Binghamton). Phys. Rev., D; 3: 190-5(1 Jan 1971).

The decay rate and photon energy spectrum were calculated for the decay mode $K_L^0 \rightarrow \pi^+\pi^-\pi^0\gamma$. Neglecting small CP-violating effects, the E1 amplitude for $K_L^0 \rightarrow \pi^+\pi^-\pi^0\gamma$ is related to the amplitude for $K_L^0 \rightarrow \pi^0\gamma\gamma$ using current algebra and the hypothesis of a partially conserved axial-vector current. For the branching ratio $\Gamma(K_L^0 \rightarrow \pi^+\pi^-\pi^0\gamma)/\Gamma(K_L^0 \rightarrow \pi^0\gamma\gamma) = 0.16\%$ was found. Using the present experimental upper limit on $K_L^0 \rightarrow \pi^0\gamma\gamma$, $\Gamma(K_L^0 \rightarrow \pi^+\pi^-\pi^0\gamma)/\Gamma(K_L^0 \rightarrow \text{all}) < 3.7 \times 10^{-7}$ was estimated. The same branching ratio based on the ρ-dominance model was also determined and good agreement was found with the corresponding result of current algebra. (auth)

14641 INTERMEDIATE BOSON. I. THEORETICAL PRODUCTION CROSS SECTIONS IN HIGH-ENERGY NEUTRINO AND MUON EXPERIMENTS. Brown, R. W. (Brookhaven National Lab., Upton, N. Y.); Smith, J. Phys. Rev., D; 3: 207-23(1 Jan 1971).

The theoretical total cross sections are presented for W-boson production in the reactions $\nu + Z \rightarrow Z + W + \mu$ and $\mu + Z \rightarrow Z + W + \nu$ for a variety of Z. The emphasis is on the energies and corresponding W-boson masses pertinent to the National Accelerator Laboratory. The effects of the W's anomalous magnetic moment, the nucleon Fermi motion, the Pauli exclusion principle, inelastic channels (in particular, deep-inelastic ones), and the problem of incoherent versus coherent production are all discussed. A critique is given of some recent high-energy compilations. (auth)

14642 POSSIBLE TEST OF THE $\Delta S = DQ$ RULE IN $K_{\mu 3}^0$ DECAY IN A REGENERATION EXPERIMENT. Ebrahim, Abdul (Yale Univ., New Haven). Contract AT(30-1)-2726. Phys. Rev., D; 3: 109-13(1 Jan 1971).

The time dependence of the transverse component of muon polarization in $K_{\mu 3}^0$ decay is calculated under the assumption that the $\Delta S = \Delta Q$ rule is violated. The initial beam is taken to be an arbitrary superposition of K_L^0 and K_S^0 states. Four form factors, $f_\pm$ for the $\Delta S = \Delta Q$ amplitude and $g_\pm$ for the $\Delta S = -\Delta Q$ amplitude, enter into the description of the decay. It is shown that when $f_\pm$ and $g_\pm$ are not proportional, the transverse polarization is significantly different from zero for the first few lifetimes of K_S^0 even when there is no T violation in the decay. The possibility of experimentally observing this transverse polarization with muon decays from a regenerated K_L^0 beam is examined. It is found that the present experimental limits on $f_\pm$ and $g_\pm$ allow a transverse polarization as large as 15% at the exit face of the regenerator. This transverse polarization can, therefore, be used to test the $\Delta S = AQ$ rule in $K_{\mu 3}^0$ decay. (auth)

14643 WHY DO NEUTRINOS PRODUCE MORE W's THAN MUONS? Berends, F. A.; West, Geoffrey B. (Harvard Univ., Cambridge, Mass.). Contract AT(30-1)-2076. Phys. Rev., D; 3: 262-4(1 Jan 1971).

A simple model is used to expose the mechanism which makes W production by neutrinos at least an order of magnitude larger than the production by muons. This difference was noted by us in a full calculation of the muon-induced process. Using the model, it is noticed that the reaction $\mu^- + n \rightarrow p + W^- + \mu^-$ does not suffer from this damping effect. (auth)

14644 SUM RULES FOR $K_L - K_S$ DECAY. da Silveira, Adel (NEPEC, Rio de Janeiro). Phys. Rev., D; 3: 265(1 Jan 1971).

It is shown that the McVoy and McGlinn–Polis sum rules for $K_L - K_S$ decay are not equivalent. (auth)

14645 CHIRAL ALGEBRA, CHIRAL BREAKDOWN, AND ξ PARAMETER OF K_{l3} DECAY. Arnowitt, R. (Northeastern Univ., Boston); Friedman, M. H.; Nath, P.; Suitor, R. Phys. Rev. Lett.; 26: 104-7(11 Jan 1971).

Using hard-meson current algebra with single meson dominance of currents and the σ commutator, it is deduced that $0^\pm$ mesons must occur in nonets, and chiral symmetry is broken by only $(3,3^*) \oplus (3^*,3)$ terms (which then implies a small ξ parameter). Recent calculations which obtain a large negative ξ with only $(3,3^*)$ terms are seen to imply a violation of the current-algebra constraints. However, the large experimental ξ can be obtained by including additional nonpole $(1,8) \oplus (8,1)$ breaking terms. (auth)

14646 EXPERIMENTAL TEST OF RENORMALIZATION THEORY OF WEAK INTERACTIONS IN ep SCATTERING PROCESSES. Lobov, G. A.; Shabalin, E. P. (Inst. of Theoretical and Experimental Physics, Moscow). Yadern. Fiz.; 11: 1125-7(May 1970). (In Russian).

Renormalization theories predict the existence of a series of P-odd effects in ep-scattering. In particular they predict the occurrence of longitudinal ($P_\perp$) and transverse ($P_{||}$) polarizations in the scattering plane in the recoil proton after scattering of unpolarized electrons on unpolarized protons. In addition, the existence of a P-odd weak interaction leads to the appearance of asymmetry (K) in the distribution of recoil protons after scattering of electrons on the polarized proton target. The magnitude of this effect is estimated to be on the order of 1 to 10% which should be readily measurable experimentally. It is assumed that the most suitable experiment would be to determine the angular asymmetry of recoil protons after scattering of electrons on a polarized proton target. The asymmetry of recoil protons K is given as a function of scattering angle for a number of energy values. For convenience in selecting the optimum experimental conditions, the cross section for scattering of electrons on protons is also given as a function of scattering angle for energy values E = 6 and 15 (in nucleon mass units) in graphic form. An analytical expression for this relation is also presented. (TTT)

14647 HIGHER-ORDER TERMS IN THE CURRENT–CURRENT THEORY OF WEAK INTERACTIONS. Willey, R. S.; Tarter, J. M. (Univ. of Pittsburgh). Contract AT(30-1)-3829. Phys. Rev., D; 3: 559-66(15 Jan 1971).

An examination is made of the consequences of the hypothesis that, for some range of energies, the second-order terms in the perturbation expansion of the Fermi theory are small but nonnegligible corrections to the first-order terms, and responsible for reactions which violate first-order selection rules. Matrix elements are computed through second order in the weak coupling constant G and subtraction constants are introduced which are necessary to render the matrix elements finite to this order. From this point of view a number of weak-interaction problems are considered, including the experimental parameters of μ decay, the universality of the μ-decay coupling constant and the Fermi β-decay coupling constant, K_{l3} decays, and $\Delta S = \Delta Q$ and $\Delta S = 2$ semileptonic decays. (auth)

14648 V–A THEORY FOR NUCLEON RESONANCES. Clark, Robert Beck; Jaramillo, Ramios Rios; Yamada, Masao (Univ. of Texas, Austin). Phys. Rev., D; 3: 567-70(15 Jan 1971).

The conserved-axial-vector-current hypothesis and current commutation relations are used to predict that the weak-interaction coupling of nucleon resonances to nucleons is described by a V – A theory. (auth)

14649 K_{l3} DECAYS AND SU(3) BREAKING IN THE BANDT–PREPARATA APPROACH. Weinstein, Marvin (New York Univ., New York). Phys. Rev., D; 3: 481-4(15 Jan 1971).

A discussion of the decay $K^+ \rightarrow \pi^0 + l + \nu$ is presented, which makes clear that a recent calculation of the ξ parameter in K_3^0 decay depends upon the introduction of large SU(3) violation and not upon a modification of the hypothesis of partial conservation of the axial-vector current. In addition, a formula is derived giving a means of estimating $\xi(m_K^2)$ and its dependence upon SU(3) breaking. (auth)

14650 WEAK INTERACTION OF PHOTONS AND THE PHOTONEUTRINO PROCESS. Bandyopadhyay, P.; Chaudhuri, P. Ray (Indian Statistical Inst., Calcutta). Nuovo Cim.; 1A: 328-32 (21 Jan 1971).

Assuming that photons can interact weakly with neutrinos, the cross section for the photoneutrino process $e^- + \gamma \rightarrow e^- + \nu + \bar{\nu}$ was calculated. From this, the rate of stellar energy loss was derived and is compared with the result obtained on the basis of the current–current coupling theory. (auth)

14651 FULL EXPERIMENT IN WEAK SEMILEPTONIC HYPERON DECAYS. Dittrich, J.; Janouch, F. (Nuclear Research Inst., Rez, Czech.). Czech. J. Phys.; 21: 25-33(1971).

The possibilities of the realization of full experiment in weak semileptonic hyperon decays are investigated. Several proposals for the determination of constant form-factors are made. (auth)

14652 CALCULATION OF THE FORM FACTOR IN K_{e3} DECAY. Brene, N. (Univ. of Copenhagen). Nucl. Phys.; B25: 589-604(1971).

The form factor $f_+(0)$ is calculated from a set of assumptions of which the more important ones concern the saturation of the SU(3) × SU(3) charge algebra and the behavior of the $K\pi$ S-wave phase shift. It is assumed that it is dominated by a single resonance κ of finite width and coupled to both $K\pi$ and $K\eta$. Calculations are performed with resonance mass 900 MeV and 1100 MeV. In both cases, $f_+(0)$ is near 0.80 with a few percent uncertainty if the resonance width is around 150 MeV. If the width is around 450 MeV, $f_+(0)$ is between 0.90 and 1. (auth)

14653 DETERMINATION OF THE LEPTON-CHARGE VIOLATING COUPLING CONSTANTS IN MUON DECAY. Jarlskog,

XUM

Cecilia (Univ. of Lund, Sweden). Nucl. Phys.; B25: 543–50 (1971).

Muon decay, without requiring conservation of the lepton charge, is examined. The coupling constants occurring in the terms of the interaction Hamiltonian which can give rise to a pair of identical neutrinos (or antineutrinos) are referred to as the lepton-charge-violating coupling constants. Using the predicted V–A values for four decay parameters (which are close to the experimental values) it is shown that only four coupling constants, viz., g_V and g_A of the ordinary theory and $\tilde{g}_A$ and $\hat{g}_A$ of the lepton-charge violating interactions remain undetermined. Further, only the combination $|g_V|^2 + |g_A|^2 + 2|\tilde{g}_A|^2 + 2|\hat{g}_A|^2$ can be measured. The further assumption of the two-component theory for one of the decay neutrinos gives uniquely the V–A theory ($\tilde{g}_A = \hat{g}_A = 0$ and $g_V = -g_A$). Allowing for the experimental uncertainties, lepton-charge-violating scalar and pseudo-scalar interactions of about the same order of magnitude as the usual scalar and pseudoscalar interactions cannot be excluded. The significance of future measurements of η', one of the decay parameters for radiative muon decay, for finding upper limits to the scalar, pseudoscalar and tensor interactions is also discussed. (auth)

14654 ONCE-SUBTRACTED DISPERSION RELATIONS, CURRENT ALGEBRA, AND WEAK DECAYS OF HADRONS. Sebastian, Kunnat Joseph. College Park, Md.; Univ. of Maryland (1970). 186p. University Microfilms Order No. 70-23,315.

Thesis.

The application of current algebra, PCAC (partially conserved axial vector current) and dispersion relations, to the weak decays of hadrons is discussed, within the framework of the Cabibbo theory of weak interactions. Specifically, the work is to find the corrections to the soft pion predictions of current algebra in going from zero four momentum pion ($p_\pi = 0$) to zero mass pion ($p_\pi^2 = 0$) through the use of once subtracted dispersion relations. The dispersion relation is written in the appropriate variable keeping $P_\pi^2 = 0$. The subtraction point is chosen at the soft pion limit (i.e., $P_\pi^\mu = 0$) of the dispersion variable, so that the subtraction constant is given exactly by current algebra. The dispersion integrals are usually evaluated by saturating them with low mass single particle and resonance intermediate states. This program was applied specifically to three cases, K_{l3} decays, K_{l4} decays and nonleptonic decays of hyperons. It is found that the corrections to the soft pion results are important in each case. (TSS)

14655 DIVERGENCES OF THE AMPLITUDES OF WEAK NONLEPTONIC PROCESSES INVOLVING PHOTON EMISSION. Geshkenbein, B. V.; Ioffe, B. L. (Inst. of Theoretical and Experimental Physics, Moscow). Yadern. Fiz.; 12: 1011–24(Nov 1970). (In Russian).

Quadratically divergent terms in the amplitudes of nonleptonic processes involving one- and two-photon emission as well as in the amplitudes involving one virtual photon are studied in framework of a theory with the intermediate W boson. (auth)

Strong (General)

Refer also to abstract 14831.

14656 (SU–1206–237) EXCHANGE DEGENERACY AND OSCILLATING TOTAL CROSS SECTIONS. Amann, R. R. (Syracuse Univ., N. Y. Dept. of Physics). Nov 1970. 12p. (NYO–3399–237). Dep. NTIS.

The hypothesis that the Pomeron consists, in part, of a pair of complex conjugate Regge poles, as suggested by Chew and Snyder, is shown to allow exact exchange degenerate fits to the high energy total cross section data. A unique prediction of this hypothesis is that the ratio of real to imaginary parts for the amplitude for $\pi^- p \to \pi^- p$ scattering should not rise uniformly; but rather rise to plateau, remain approximately constant from 20 to 60 GeV, then resume its rise. (auth)

14657 (UCRL–20032) TWO REGGEON EXCHANGE CONTRIBUTIONS TO HADRON SCATTERING AMPLITUDES AT HIGH ENERGY. Quigg, Chris (California Univ., Berkeley. Lawrence Radiation Lab.). Oct 1970. Contract W-7405-eng-48. 186p. Dep. NTIS.

Thesis.

Regge cuts are discussed from a phenomenological point of view. Some attempts to derive amplitudes with Regge cuts are reviewed, including those of Amati, Stanghellini, and Fubini, and of Gribov. A phenomenological amplitude for the Regge cut from two Reggeon exchange is written down in a form that manifestly satisfies s-u crossing. The amplitude is formulated in terms of s-channel helicity partial-wave amplitudes, so the Reggeization of s-channel helicity amplitudes is discussed as a technical simplification. Implications of Regge cuts for various duality-breaking schemes (and vice versa) are summarized. Brief remarks are made on two Reggeon cuts and exotic exchange. These include model calculations of the $(P' + \rho) \otimes (P' + \rho)$ cut in $\pi\pi$ scattering, and of the single-meson-exchange "forbidden" reaction $K^- p \to K^+ \Xi^-$. (auth)

14658 SELECTION RULES IN DUAL-RESONANCE MODELS. Gliozzi, F. (Istituto Nazionale di Fisica Nucleare, Turin). Lett. Nuovo Cim.; 4: 1160–4(12 Dec 1970).

It is shown that in the coupling of scalar particles of lowest mass to resonances whose masses $\sqrt{s}$ satisfy the condition $\alpha(s) = n \geq n_0(k)$ a selection rule is operating that forbids the decay of a class of resonances θ_k into less than k + 1 scalar particles. A simple consequence of this selection rule is the appearance in the particle spectrum of a wide class of heavy stable particles, that is, particles that cannot spontaneously decay into particles of lower mass. Another class of selection rules which are expressible by means of sets of operators that annihilate the coherent state is mentioned. (L.B.S.)

14659 MOMENTUM SPECTRUM OF HADRONIC SECONDARIES IN THE MULTIPERIPHERAL MODEL. DeTar, Carleton E. (Univ. of California, Berkeley). Phys. Rev., D; 3: 128-44(1 Jan 1971).

Motivated by a simplified multiperipheral model, a general qualitative description of the momentum spectrum of secondaries, resulting from a collision of two hadrons at high energies is formulated. Arguing from two fundamental multiperipheral concepts, (a) that transverse momenta are limited and (b) that distant particles on the multiperipheral chain are uncorrelated, it is predicted that at sufficiently high incident energies, the momentum spectrum of particle X in the reaction $a + b \to X$ + anything, when presented in the variables $p_\perp$ and $y = \sinh^{-1}[p_{||}/(p_\perp^2 + m_X^2)^{1/2}]$, develops a central plateau in the y dependence, which elongates and flattens to a value that is normalized by the total cross section as the incident energy increases. Moreover, it is shown that the resultant particle density distribution is consistent with the hypothesis of limiting fragmentation. This description is contrasted with the predictions of the two-fireball model, the isobar-pionization model, and the statistical thermodynamical model. (auth)

14660 REGGE-POLE-CUT ANALYSIS OF TOTAL CROSS SECTIONS WITH SU(3) AND EXCHANGE DEGENERACY. Jackson, Jane C. (Arizona State Univ., Tempe). Phys. Rev., D; 3: 100-3(1 Jan 1971).

A phenomenological study of SU(3) and exchange degeneracy is made in a Regge-pole-cut model. The high-energy data of pion–nucleon, kaon–nucleon, nucleon–nucleon, and nucleon–antinucleon total cross sections, including the new Serpukhov data, are analyzed by means of least-squares fits with parameters corresponding to the P, P′, ρ, A_2, and ω Regge poles and subtractive vacuum cut. The data are fitted adequately with the assumptions of SU(3) and exchange degeneracy. For completeness, the data are analyzed with the assumptions of SU(3) alone, exchange degeneracy alone, and also without either of these assumptions. (auth)

14661 ANGULAR DISTRIBUTIONS FROM MULTIPARTICLE PRODUCTION MODELS. Lyon, Donald E. Jr. (Univ. of Michigan, Ann Arbor); Risk, Clifford; Tow, Don M. Phys. Rev., D; 3: 104-8(1 Jan 1971).

Using $\exp(-Ap_T^2)d^3p/E$ as the momentum distribution of secondaries produced in ultrahigh-energy collisions—a result predicted by the multiperipheral model, by Feynman's parton model, and by Cheng and Wu's consideration of hadrons as extended objects with many internal degrees of freedom—the characteristic features of the angular distribution are obtained. The dependence on incident energy, mass of secondaries, and the value of A is discussed. It is found that the c.m. angular distribution on the variables $\eta_{c.m.} = -\ln \tan\frac{1}{2}\theta_{c.m.}$ has a two-bump structure, whereas the lab angular distribution in $\eta = -\ln \tan\theta_l$ is flat. This difference leads to a discussion of the transformation between c.m. and lab angular distributions. It is found that the usual relativistic approximation of the exact transformation leads to incorrect results. Finally, it is pointed out that these momentum and angular distributions approach limiting distributions. (auth)

14662 NONLINEAR REGGE TRAJECTORIES. Grant, C. T.; Lomon, Earle L. (Massachusetts Inst. of Tech., Cambridge). Contract AT(30-1)-2098. Phys. Rev., D; 3: 260-1(1 Jan 1971).

Various assumptions for the mass dependence of Regge trajectories are compared with the data for the presumed trajectories. The possible observation of the asymptotic behavior of these trajectories with data which will be available in the near future is also discussed. (auth)

XUM

14663 NOTE ON EXTREME-ENERGY COLLISIONS. Hsu, J. P. (McGill Univ., Montreal). Phys. Rev., D; 3: 257-8(1 Jan 1971).

Within the framework of limiting fragmentation without pionization, the average multiplicity of hadron collisions is shown to be finite as the incident energy approaches infinity. (auth)

14664 N-POINT FUNCTIONS IN CHIRAL SU(3) x SU(3) CURRENT ALGEBRA. Arnowitt, R.; Friedman, M. H.; Nath, P.; Suitor, R. (Northeastern Univ., Boston). Phys. Rev., D; 3: 594-610(15 Jan 1971).

Hard-meson techniques are presented for calculating processes involving octets (nonets) of mesons under the assumptions of chiral SU(3) × SU(3) [U(3) × U(3)] current-algebra commutation relations, partial conservation of axial-vector currents, conservation and partial conservation of vector currents, and single-meson saturation of intermediate sums. Using these conditions and the usual smoothness hypothesis, the general procedure for constructing the arbitrary N-point function is given. If, in addition, one assumes that the "σ commutators" (i.e., the commutators of the time components of the currents with the scalar fields) are single-particle dominated, it is inconsistent to assume only octets of particles. A consistent formalism involving nonets of particles can be constructed, however. The spin-zero mesons must then belong to the $(3,3^*) + (3^*,3)$ representation. Hence the $(3,3^*) + (3^*,3)$ symmetry-breaking condition is deduced from the current-algebra conditions when combined with pole dominance. (auth)

14665 FACTORIZATION OF THE BALACHANDRAN DUAL-RESONANCE MODEL. Sinclair, D. K. (State Univ. of New York, Stony Brook). Contract AT(30-1)-3668B. Phys. Rev., D; 3: 384-94(15 Jan 1971).

The level structure of the Balachandran generalization of the N-point Veneziano model is considered. The model is shown to exhibit consistent factorization and level structure. Using the harmonic oscillator formalism, expressions are obtained for the vertices coupling one or two excited states to any number of ground-state particles. The form of the propagator is also obtained. Both vertices and propagators are seen to reduce to the Veneziano form when an appropriate limit is taken. Asymptotically, the degeneracy of the nth level is shown to behave like exp(const $n^{1/2}$) where the constant is given explicitly. The Gross model of N-point functions is seen to exhibit a similar asymptotic degeneracy, in contradiction to other results reported in the recent literature. (auth)

14666 DIVERGENCE OF THE TWO-LOOP PLANAR GRAPH IN THE DUAL-RESONANCE MODEL. Kaku, Michio; Scherk, Jooel (Univ. of California, Berkeley). Phys. Rev., D; 3: 430-9(15 Jan 1971).

The two-loop planar tadpole is constructed by inserting two projected planar tadpoles on a symmetric three-Reggeon vertex. The determinant, which is the generalization of the partition function appearing in the one-loop diagram, is studied as a function of the integration variables of the loops and propagators. It is found that although the determinant contains an infinite number of possibly exponentially divergent factors, only three of them actually diverge. The first two divergent factors are those associated with each tadpole. The additional divergence is associated with the closed path going around the two loops which does not cross itself. The calculation is also performed with the Koba–Nielsen variables of the original N-loop graph, and the same result is derived. (auth)

14667 VECTOR CURRENTS AND CURRENT ALGEBRA. III. DUAL-RESONANCE MODEL WITH UNIVERSALLY COUPLED VECTOR MESONS. Brower, Richard C. (Massachusetts Inst. of Tech., Cambridge); Weis, J. H. Phys. Rev., D; 3: 451-61(15 Jan 1971).

The model for conserved vector currents in the dual-resonance model is extended to include the infinite set of universally coupled vector mesons. One- and two-current amplitudes satisfying current algebra and factorizing on the M highest trajectories are constructed for a form factor falling like $(q^2)^{-M}$. Physically acceptable completely factorized amplitudes are not obtained in the limit $M \to \infty$, however. Complete factorization and unsubtracted dispersion relations in q^2 for single-current amplitudes are shown to indeed imply exponentially falling form factors. However, we then prove that no acceptable completely factorized two-current amplitudes can be constructed from a current coupling only to the universal vector mesons. (auth)

14668 DUALITY AND THE ADLER CONDITION. Cremmer, E. (Laboratoire de Physique Theorique et Hautes Energies, Orsay, France); Nuyts, J.; Sugawara, H. Phys. Rev., D; 3: 478-81(15 Jan 1971).

It is shown that the Adler condition is a natural consequence of duality. However, contrary to the usual expectations, it is not related to the existence of partially or totally conserved currents. (auth)

14669 SOME REMARKS ABOUT FIREBALLS. Miesowicz, M. (Inst. of Nuclear Physics, Krakow). Acta Phys. Pol.; A38: 495-9 (Nov 1970).

A definition of the fireball is proposed. It was shown that fireballs fulfilling this definition are produced in very wide energy range up to some tens TeV. Arguments were presented in favor of the fireball model as a model of pionization. (auth)

14670 QUARK-MODEL PREDICTIONS FOR THE MEASURABLE GENERALIZED STATISTICAL TENSORS. Kielanowski, P. (Univ., Warsaw). Acta Phys. Pol.; B1: 315-21(Oct-Dec 1970).

A set of linear relations for the measurable generalized statistical tensors completely equivalent to the quark model predictions for the transition amplitudes for the reaction $0^- + \frac{1}{2}^+ \to 1^- + \frac{3}{2}^+$ is given. The given relations can be tested directly by means of experimental data for joint decay distributions of the final particles. (auth)

14671 QUARK MODEL PREDICTIONS FOR THE TRANSVERSITY AMPLITUDES. Kupczynski, M. (Univ., Warsaw). Acta Phys. Pol.; B1: 301-13(Oct-Dec 1970).

A simple derivation of the quark model relations between the transversity amplitudes is given. The problem of the choice of the spin reference frame in which the additivity assumption holds is discussed. It is shown that all these quark model relations can be obtained from some simple geometrical postulates. (auth)

14672 LOW MOMENTS OF CURRENT ALGEBRA AT INFINITE MOMENTUM. Young, K. (California Inst. of Tech., Pasadena). Contract AT(11-1)-68. Phys. Lett.; 34B: 88-90 (18 Jan 1971).

It is shown that even the first few moments of the vector and axial vector charge density algebra at infinite momentum cannot be represented realistically in the space of the non-exotic states. (auth)

14673 LOCAL APPROXIMATION TO FIELD AND CURRENT COMMUTATORS. Dahmen, H. D.; Rothe, K. D.; Stech, B. (Univ., Heidelberg. Kernforschungszentrum, Karlsruhe, Ger.). Phys. Lett.; 34B: 83-7(18 Jan 1971).

Local approximations to commutators are constructed using a finite set of intermediate particle states. Thereby a solution of the saturation problem of current algebra is obtained. (auth)

14674 DUALITY AND THE BOOTSTRAP. Veneziano, G. (Inst. for Advanced Study, Princeton, N. J. Massachusetts Inst. of Tech., Cambridge). Contract AT(30-1)-2098. Phys. Lett.; 34B: 59-62(18 Jan 1971).

By extending the concept of duality nonlinear conditions in the coupling constant are obtained. In the dual model framework a sum rule for the coupling constant is obtained, which resembles the conditions derived in the multiperipheral bootstrap. (auth)

14675 NEW DUAL-RESONANCE AMPLITUDE. Rebbi, Claudio (Univ., Trieste, Italy). Nucl. Phys.; B25: 557-76(1971).

The existing n-point dual-resonance amplitude is modified so as to obtain a new amplitude, with a different spectrum of intermediate states. The generalization is achieved by replacing the vertices appearing in the old amplitude with operators transforming according to a different representation of the projective group. The resulting spectrum of excitations is given by the eigenvectors $L_0 + S_0$, where L_0 is one of the generators of the group of projective transformations already used in the construction of the former dual amplitude, and S_0 is an operator transforming as a $\frac{1}{2} \otimes \frac{1}{2}$ non-unitary representation of the same group. (auth)

14676 AN N/D CALCULATION USING THE DISCONTINUITY OF A SECOND ORDER FOUR-POINT INTERACTION AS INPUT. McColl, Daniel Clyde. Madison, Wis.; Univ. of Wisconsin (1969). 95p. University Microfilms Order No. 69-22,431.

Thesis.

An attempt is made to calculate the low-energy bound states occurring in the scattering of two massive particles. In particular, the discontinuity of a second-order Feynman graph was used as input for an N/D calculation with a cutoff. The Feynman graph is derived from a four-point interaction and is divergent even though its discontinuity is finite. Finally, the conditions for bound states are sought. First, a scalar ϕ^4 interaction is calculated and leads to a bound state whose position depends in the correct manner upon the coupling constant and the mass of the scattering particles. Next, the π^+ and ρ^+ are sought as bound states of a quark and an antiquark by using a relativistic interaction which correctly takes SU(3) and spin properties into account. The interaction Hamiltonian consists of two terms of the form $g\bar{\psi}o\psi\bar{\psi}o\psi$, where $o = \gamma_\mu$ for the first term, $o = i\gamma_\mu\gamma_5$ for the second term, and ψ is the field operator for a spin $\frac{1}{2}$ quark. This interaction is chosen to be invariant under the Fierz transformation in analogy with weak interactions. One may also note that this interaction is the interaction resulting from the product of two quark currents of the type introduced by Gell–Mann with the parity violating terms dropped. The bound state conditions show that π and ρ bound states do not exist for an SU(3) invariant interaction. A symmetry breaking term may be added which will cause the desired bound states to exist, but the coupling constant of this term must be greater than that of the original SU(3) invariant interaction Hamiltonian. The bound states π and ρ depend in the correct manner upon the coupling constants and masses of the quarks. (Diss. Abstr. Int., B.)

14677 THE COMPLEX ANGULAR MOMENTUM THEORY OF THE PRODUCTION OF THREE PARTICLES IN COLLISIONS OF TWO STRONGLY INTERACTING PARTICLES AT HIGH ENERGY. Luxton, Gary. Pasadena, Calif.; California Inst. of Tech. (1970). 115p. University Microfilms Order No. 70-12,490.

Thesis.

The problem of the continuation to complex values of the angular momentum of the partial wave amplitude is examined for the simplest production process, that of two particles → three particles. The presence of so-called "anomalous singularities" complicates the procedure followed relative to that used for quasi two-body scattering amplitudes. The anomalous singularities are shown to lead to exchange-degenerate amplitudes with possible poles in much the same way as "normal" singularities lead to the usual signatured amplitudes. The resulting exchange-degenerate trajectories would also be expected to occur in two-body amplitudes. The representation of the production amplitude in terms of the singularities of the partial wave amplitude is then developed and applied to the high energy region, with attention being paid to the emergence of "double Regge" terms. Certain new results are obtained for the behavior of the amplitude at zero momentum transfer, and some predictions of polarization and minima in momentum transfer distributions are made. A calculation of the polarization of the ρ^0 meson in the reaction $\pi^-p \rightarrow \pi^-\rho^0p$ at high energy with small momentum transfer to the proton is compared with data taken at 25 GeV by W. D. Walker and collaborators. The result is favorable, although limited by the statistics of the available data. (Diss. Abstr. Int., B)

14678 TOPICS IN THE DYNAMICS OF STRONG INTERACTIONS. Meggs, William Joel. Syracuse, N. Y.; Syracuse Univ. (1969). 112p. University Microfilms Order No. 70-12,795.

Thesis.

Calculational techniques in strong interaction physics are explored and applied to specific physical situations. It is found that overlapping resonances in three-particle final states can produce resonance-like structure for a certain spin configuration if a mass selection is made on the final state. Reported enhancements at 1080, 1169, and 1433 MeV in the missing mass plots of $\pi\pi\pi$, $K\pi\pi$, and $KK\pi$ final states, respectively may be understood by this mechanism. The Balachandran–Nuyts expansion of scattering amplitudes on the Mandelstam triangle is discussed for the case of equal masses. It is found that the eigenfunctions belong to a certain class of basis vectors of the (μ,μ) representations of the group SU(3). Possible applications of this method to the $\pi\pi$ bootstrap are indicated. The relation of Dolen–Horn–Schmid duality to the interference model of Barger and Olsson is discussed, and a class of resonances which is disjoint from the leading Regge effects from the cross channel is identified. Following an early suggestion by Gleeson, it is shown that these resonance towers have a Regge-like asymptotic behavior which does not have to be associated with cross channel effects. (Diss. Abstr. Int., B)

14679 THE INFINITE MOMENTUM LIMIT OF A SPINOR FIELD THEORY. Flory, David C. New York; Yeshiva Univ. (1969). 126p. University Microfilms Order No. 70-11,606.

Thesis.

A self-contained theory of Dirac fermions interacting with (pseudo)scalar bosons at infinite momentum was constructed. The theory is designed to give the correct relativistic dynamics when the space of intermediate states is restricted to those states which can be interpreted as the infinite momentum limit of sets of particles with finite momentum, that is, those states which correspond to the particle configurations observed in nature. The intermediate states which were eliminated are those containing particles moving away from the infinite momentum observer. The dynamical effect of these states is incorporated into a single counterterm in the interaction Hamiltonian. A complete set of generators of the Poincaré group in a basis appropriate to the infinite momentum limit is demonstrated. These generators satisfy the commutator algebra of the Poincaré group. In the context of old-fashioned perturbation theory the effect of the counterterm in the Hamiltonian is to produce a series of four-point vertices in the graphical representation of the perturbation expansion. A set of infinite momentum perturbation theory rules is given. In order to avoid the problems of renormalization a tree-graph approximation is made throughout. (Diss. Abstr. Int., B)

Strong (Baryon No. = 0)

14680 (INP–719) STATISTICAL MODEL AND CROSS SECTIONS FOR HIGH-ENERGY REACTIONS. Bartke, Jerzy (Institute of Nuclear Physics, Krakow (Poland)). 1970. 68p. Dep. NTIS (U. S. Sales Only).

Application of the statistical model to the calculation of cross sections for high-energy reactions is discussed. Comparison with the data includes branching ratios for various reaction channels within a given multiplicity and the energy dependence of partial cross sections. The obtained results indicate the usefulness of the statistical-model approach to the analysis of high-energy reaction cross sections. (auth)

14681 (INP–730) ON THE SPECTRUM OF RESONANCES IN THE GENERALIZED VENEZIANO MODEL. Bjorneboe, Jens (Institute of Nuclear Physics, Krakow (Poland)). Sep 1970. 35p. Dep. NTIS (U. S. Sales Only).

The spectrum of resonances with definite spin in the generalized Veneziano model is determined. Explicit formulae for the coupling of all normal-parity resonances to all channels are given. A set of selection rules for two-body reactions is found. (auth)

14682 (ITF-70-60-E) THE CONSEQUENCE OF ANALYTICITY OF THE $\pi\pi$-SCATTERING AMPLITUDE. Yatsun, V. A. (Akademiya Nauk Ukrainskoi SSR, Kiev. Institut Teoreticheskoi Fiziki). 1970. 16p. Dep. NTIS (U.S. Sales Only).

Some conditions on the partial π-π scattering amplitudes are deduced which follow from the analytical properties of the total amplitude in the plane of the transmitted impulse. These conditions have the form of the limit relations restricting the behavior of the partial amplitudes when the angular moment tends to infinity. (auth)

14683 (NYO–2262-TA-219) TWO LOOP APPROXIMATIONS TO PROPAGATORS IN THE σ MODEL. Wong, T. F. (Brookhaven National Lab., Upton, N. Y.); Guralnik, G. S. (Imperial Coll. of Science and Technology, London (England). Dept. of Physics. Brown Univ., Providence, R. I. Dept. of Physics). Dec 1970. 30p. Dep. NTIS.

A simple and systematic procedure is established for directly generating perturbation theory for the σ model order by order in the number of loops rather than in powers of the bare coupling constant. This self consistent Greens function method is demonstrated by deriving the already known tree and one loop approximations and then is applied to the much more complex problem of the two loop approximations to the propagators. The explicit form is displayed for these and it is demonstrated that in the limit of no symmetry breaking and zero pion bare mass the renormalized pion mass remains at zero as is required by the Goldstone theorem. These are the essential first steps toward calculating a unitary pion–pion scattering amplitude with this model to the two loop order. (auth)

14684 MASS SPECTRUM OF PARTICLES IN NONLINEAR QUARK THEORY. Bas'yuni, A. Kh.; Kurdgelaidze, D. F. Vestn. Mosk. Univ., Ser. III. Fiz. Astron.; 11: 256-61(May–Jun 1970). (In Russian).

Formulas for mass spectra of mesons and baryons in nonlinear quark theory of particles were obtained on the basis of relativistic and SU(3) invariant equations for mesons and baryons. Thus, within the limits of SU(3) and relativistic-invariant equations the results coincide with the results usually obtained only in nonrelativistic SU(6) invariant theory. (R.V.J.)

14685 ADLER CONDITION IN A DUAL RELATIVISTIC QUARK MODEL. Lebrun, J. P.; Venturi, G. (Cambridge Univ., Eng.). Lett. Nuovo Cim.; 4: 1133-5(12 Dec 1970).

The introduction of U_6-breaking mass splittings in a dual quark model characterized by a $U_6 \times U_6 \times O_3$ spectrum of states is discussed. It is then possible to treat the chiral $SU_3 \times SU_3$ limit for the nonet of pseudoscalar mesons and it is shown that, with a suitable off-shell extrapolation procedure, the usual soft-meson the-

XUM

orems are satisfied by meson–meson scattering amplitudes. (L.B.S.)

14686 RADIATIVE DECAYS OF MESONS IN A QUARK LOOP MODEL. Esteve, A.; Leon, J.; Tiemblo, A. (Instituto Rocasolano, Madrid. GIFT, Madrid). Lett. Nuovo Cim.; 1: 30-2(2 Jan 1971).

A quark loop model, breaking SU(3) through a larger mass for the strange quark, is used to calculate the radiative decays $\eta \rightarrow 2\gamma$ and vector meson decays producing γ and π^0. The widths, branching ratios, and coupling constant relations are found. (J.F.P.)

14687 POLE DOMINANCE CALCULATION OF πK SCATTERING LENGTHS. Lai, C. S.; Kiang, D. (Dalhousie Univ., Halifax, Nova Scotia). Can. J. Phys.; 47: 2715-8(1 Dec 1969).

The low-energy πK scattering is treated within the framework of the meson pole dominance with the inclusion of nonresonant S waves. The result obtained for the πK scattering lengths in the present method is somewhat different from that of current-algebra calculation. (auth) (Canada)

14688 VENEZIANO FORMULA FOR MESONS. Bassetto, A. (Univ., Padua. Istituto Nazionale di Fisica Nucleare, Padua). Fortschr. Phys.; 18: 185-235(1970).

A review is given of recent developments in strong interaction physics starting from the idea of duality. The finite-energy sum rules and the $\pi\pi \rightarrow \pi\omega$ process, derivation of the Veneziano formula from superconvergence relations, the Veneziano formula for the $\pi\pi \rightarrow \pi\omega$ scattering amplitude and for elastic $\pi\pi$ scattering, and quantization of the π and ρ trajectories from Adler self-consistency condition are discussed. Also the five-point amplitude in the scalar case and for the process $K\bar{K} \rightarrow 3\pi$, the six-point formula, factorization properties of the N-point scalar function, and the problem of ghosts are covered. (J.F.P.)

14689 SYMMETRY BREAKING AND SPIN-ZERO MASS SPECTRUM. Schechter, J.; Ueda, Y. (Syracuse Univ., N. Y.). Phys. Rev., D; 3: 168-76(1 Jan 1971).

The mass spectrum is discussed in a very general chiral SU(3) × SU(3) model of pseudoscalar and scalar mesons. The case of an exactly symmetric Lagrangian and spontaneous breakdown is covered, as well as the more realistic case when there is also some intrinsic symmetry breaking in the Lagrangian. The treatment is facilitated by the derivation of a mass formula which holds for all situations. In the realistic case the structure of the theory forces the mass of the ninth pseudoscalar meson to come out right and leaves us with the freedom to choose the masses of all scalar mesons (except the κ) as high as we like. The structure of the intrinsic symmetry breaking term is predicted. Some discussion of the baryons is included in this model and the corrections to the Cabibbo theory of semileptonic hyperon decay are estimated. (auth)

14690 ELECTROMAGNETIC PERTURBATION OF THE PSEUDOSCALAR-MASS SPECTRUM. Schechter, J.; Ueda, Y. (Syracuse Univ., N. Y.). Phys. Rev., D; 3: 176-82(1 Jan 1971).

Using the formalism developed in the preceding paper, electromagnetic perturbations are investigated in a rather general chiral SU(3) × SU(3) model of mesons. The meson and octet baryon mass shifts can be successfully correlated, and it is found that the electromagnetic breaking term in the Lagrangian may be of the same order of magnitude as the chiral-symmetry-breaking term. The speculation that all strong symmetry breaking may be of electromagnetic and weak origin is also investigated. (auth)

14691 STUDY OF THE $K\bar{K}\pi$ FINAL STATES FOR $N\bar{N}$ ANNIHILATION AT REST IN THE VENEZIANO LANGUAGE. Benfatto, C. (Univ., Rome); Cassandro, M.; Lusignoli, M.; Nicolo, F. Nuovo Cim.; 1A: 255-73(21 Jan 1971).

The $N\bar{N} \rightarrow K\bar{K}\pi$ processes are studied in terms of four-point Veneziano functions "à la Lovelace." A duality-breaking correction term is added to describe the φ bump. The theoretical mass spectra and angular distributions are in good qualitative agreement with the experimental data. The daughter resonances being a specific feature of any Veneziano model, their contributions to the various bumps were evaluated and found quite important. (auth)

14692 INTERFERENCE MODEL FOR RESONANCES SUGGESTED BY THE VENEZIANO AMPLITUDE. Kazes, E.; Wang, Kuo-hsiang (Pennsylvania State Univ., University Park). Nuovo Cim.; 1A: 345-56(21 Jan 1971).

Examination of the superposition of the Veneziano amplitude and satellite terms of sufficient generality to remove an arbitrary number of daughter resonances suggests a new model. The model has the same residue as the leading trajectory in the Veneziano amplitude for $\alpha(t) > -\frac{3}{2}$ it gives Regge behavior in almost every direction in the complex s-plane when applied to $\pi-\pi$ scattering, with two trajectories, it reproduces Weinberg's scattering lengths. (auth)

14693 USE OF FINITE-ENERGY SUM RULES FOR A NUMERICAL STUDY OF REGGE BEHAVIOR IN A UNITARIZED $\pi-\pi$ VENEZIANO MODEL. Griss, M. L. (Univ. of Illinois, Urbana). Phys. Rev., D; 3: 440-50(15 Jan 1971).

A simple single-channel K-matrix unitarization of the $\pi-\pi$ Veneziano model is performed. Inelastic effects corresponding to neglected channels are incorporated by giving the input, degenerate ρ and f^0 trajectories an imaginary part above the 4π inelastic threshold. Finite-energy sum rules are used to study the high-s behavior for $t < 0$, and corrected trajectories are extracted. The input degeneracy is broken, with the ρ being shifted up to an intercept of about 0.6 as against the input 0.483. The importance of nonleading terms in the Regge expansion, through interference effects at intermediate energies, is noted. The resulting deviation from crossing symmetry is examined. (auth)

14694 COMPARISON OF THE INTEGRAL CONSTRAINTS IMPOSED ON THE $\pi^0\pi^0$ s-WAVE BY CROSSING SYMMETRY AND POSITIVITY. Pennington, M. R. (London Univ.). Nucl. Phys.; B25: 621-33(1971).

The restrictiveness of the integral constraints imposed by positivity and crossing symmetry on the $\pi^0\pi^0$ s-wave obtained by Piguet–Wanders and Roskies are compared with those deduced by Balachandran–Blackmon and Pennington. The higher-order conditions are used to further constrain those lower-order restrictions found in the Piguet–Wanders–Roskies treatment alone. (auth)

14695 MESON–MESON SCATTERING IN THE VENEZIANO MODEL. Lasley, Eric Loren. Ithaca, N. Y.; Cornell Univ. (1970). 184p. University Microfilms Order No. 70-24,901.
Thesis.

Explicit, minimal Veneziano model amplitudes are constructed for the processes $\pi\pi \rightarrow \pi\pi$, $A_1\pi \rightarrow \pi\pi$, $A_1\pi \rightarrow A_1\pi$, $\omega\pi \rightarrow \pi\pi$, and $\omega\pi \rightarrow \omega\pi$. The reaction $\rho\pi \rightarrow \rho\pi$ is also discussed, but no explicit model is given. A set of invariant amplitudes is formed for each process by expansion of the type Σ (polynomials) × (beta functions). Contributing trajectories are identified from the known meson mass spectrum and quantum numbers. In every case, the leading trajectory poles have correct spin-parity as a consequence of enforcing the proper asymptotic behavior (corresponding to the dominant trajectory) on the invariant amplitudes. The asymptotic behavior of the various invariant amplitudes (in those cases where there is more than one) must be correlated in order to avoid parity doubling for the leading trajectory. Proper signature and factorization of the residues of the helicity amplitudes for the leading trajectory both imply further constraints on the invariant amplitudes. Minimal amplitudes are found, containing a small set of Veneziano terms, which satisfy the asymptotic behavior, signature, and factorization constraints, but do not overly restrict certain important low spin couplings. Multichannel factorization is satisfied for the two sets of coupled amplitudes $\pi\pi \rightarrow \pi\pi$, $A_1\pi \rightarrow \pi\pi$, $A_1\pi \rightarrow A_1\pi$ and $\pi\pi \rightarrow \pi\pi$, $\omega\pi \rightarrow \pi\pi$, $\omega\pi \rightarrow \omega\pi$. A method for obtaining models of the decays $A_1 \rightarrow 3\pi$ and $\omega \rightarrow 3\pi$ is also given. It is found that the Adler self-consistency condition is easily satisfied and does not restrict particle masses and trajectory parameters unless ad hoc assumptions about the number and type of Veneziano terms allowed in a given amplitude are invoked. The results are explicit, crossing-symmetric, Regge-behaved amplitudes parametrized in terms of certain important couplings. (Diss. Abstr. Int., B)

14696 CDD POLES IN PION–KAON DISPERSION RELATIONS. Hull, Patricia Groves. Atlanta; Georgia Inst. of Tech. (1970). 159p. University Microfilms Order No. 70-24,375.
Thesis.

The objective is to determine whether or not a CDD pole can be inserted into an existing single resonance solution for the pion–kaon scattering amplitude without destroying postulated properties of analyticity, unitarity or crossing symmetry. For the case of the pion–pion interaction, a program including inelastic scattering was run and solutions with a CDD pole appeared with the pole always occurring close to the original P-wave resonance position. The effect of the pole was to split the resonance into two parts, one on each side of the CDD pole. This split resonance solution implies that the theory allows for the existence of two particles with identical quantum numbers but slightly different masses. It is of considerable interest to verify the theoretical possibility for such a solution for interactions involving particles of unequal masses, particularly for pion–nucleon scattering, since it might help solve some of the difficulties that have been encountered in the mass formulas derived from SU(3) symmetry. The nucleon's spin angular momentum complicates the mathematics of the

XUM

analysis and since the kaon has the same I-spin as the nucleon, the pion–kaon interaction is analogous in all respects except spin angular momentum. It is for this reason that the pion–kaon interaction is chosen for consideration. (TSS)

14697 LAGRANGIAN APPROACH TO DUAL PION AMPLITUDES. Friedman, M. H.; Nath, P.; Srivastava, Y. N. (Northeastern Univ., Boston). Nucl. Phys.; B25: 374-84(1971).

A simple Lagrangian is constructed, which in the tree approximation produces a $\pi\pi$ scattering amplitude possessing (i) the correct iso-spin structure with no exotic resonances (ii) Regge asymptotic behavior $S^{\alpha_\rho(t)}$ and (iii) duality and satisfies (iv) the Adler condition. The last condition is satisfied without any restriction on the Regge-trajectory intercept. However, if $\alpha_\rho(m_\pi^2) = \frac{1}{2}$, the present model produces all the terms in the one of Lovelace–Veneziano plus a satellite term of $0(p^2/m_\rho^2)$ where p is the momentum of the off-shell pion. The ratio of I = 0 to I = 2 S-wave scattering lengths is $a_0^0/a_0^2 \approx -2$ and thus lies between the Schwinger value of $-\frac{3}{2}$ and the Weinberg value of $-\frac{7}{2}$. (auth)

14698 VENEZIANO MODEL FOR THE OFF-MASS-SHELL $A_1\pi \rightarrow \pi\pi$ PROCESS. Csikor, F. (Joint Inst. for Nuclear Research, Dubna, USSR). Yadern. Fiz.; 12: 1039-48(Nov 1970). (In Russian).

A Veneziano-type amplitude for the process $A_1\pi \rightarrow \pi\pi$ is obtained with the A_1-meson and a pion momenta off the mass shell. The model has the expected properties of the Veneziano-type amplitude off the mass shell, namely has only allowed poles in all the variables, satisfies the PCAC equation and is compatible with the current algebra. (auth)

14699 NONLINEAR FUNCTIONAL ANALYSIS AND NUMERICAL COMPUTATIONS OF THE STRONG-INTERACTION S-MATRIX; APPLICATIONS TO PION-PION DISPERSION RELATIONS. Chung, Kuk Pyo. Princeton, N. J.; Princeton Univ. (1970). 124p. University Microfilms Order No. 70-23,606.

Thesis.

The mathematical structure of the unitary, crossing-symmetric S-matrix is examined by means of nonlinear functional analysis. Constructive methods for actually finding the solutions without the N/D procedure are worked out and applied to solve the original and modified Chew–Mandelstam equations. Finally, a soluble model calculation for the pion–pion phase shifts for the S and P waves is performed on the basis of the twice-subtracted dispersion relations with a new form of crossing symmetry constraints. (Diss. Abstr. Int., B)

Strong (Baryon No. = 1)

Refer also to abstract 14648.

14700 (JINR–P1-5471) STATISTICAL ISOSPIN MODEL AND CROSS SECTIONS OF THE REACTIONS $\pi^-p \rightarrow N + (2, \ldots, 6)\pi$ WITHIN 1 TO 16 GeV ENERGY RANGE. Vinogradov, V. B.; Kutsidi, N. K.; Martinska, G.; Shandor, L. (Joint Inst. for Nuclear Research, Dubna (USSR). Lab. of Nuclear Problems). 1970. 17p. (In Russian). Dep. NTIS (U. S. Sales Only).

The ratios between the cross sections of different final charge states of $\pi^-p \rightarrow N + (2, \ldots, 6)\pi$ reactions were calculated on the basis of a statistical isospin model. The predictions of the model are compared with the experimental data for these reactions at different energies of incident π^--mesons. It is shown that the model predicts the ratios between different charge channels of $\pi^-p \rightarrow N + (2, \ldots, 6)\pi$ reactions in the energy range 1 to 16 GeV with an accuracy ≈ 10%. (auth)

14701 (KFKI--70-27-HEP) SPIN TEST FOR A FERMION ($J > \frac{1}{2}$) DECAYING INTO A SPIN-$\frac{1}{2}$ FERMION (Λ^0) PLUS A SPIN-1 PHOTON. Krasznovszky, S. (Magyar Tudomanyos Akademia Kozponti Fizikai Kutato Intezete, Budapest). [1970]. 7p. Dep. NTIS (U. S. Sales Only).

The decay of a fermion of arbitrary spin into an unstable spin-$\frac{1}{2}$ fermion (Λ^0) plus a photon is treated with density-matrix techniques and helicity formalism of Jacob and Wick. A complete determination of the multipole parameters of the parent fermion is possible only in terms of the particle—and polarization—angular distributions of the decay hyperon (Λ^0). (auth)

14702 (PAM–70-8) BREIT–WIGNER MODELS AND EFFECTIVE RANGE APPROXIMATIONS. Benayoun, M.; Leruste, Ph. (College de France, Paris. Laboratoire de Physique Atomique et Moleculaire). Oct 1970. 17p. (In French). Dep. NTIS (U. S. Sales Only).

Some of the methods used to analyze the experimental data are compared; namely the varying widths Breit–Wigner formula and the effective-range approximation of Ross and Shaw. In the D/D framework, the constraints arising from the use of these two models with the many-channel amplitude polology are indicated. Differences are pointed out. In this way, it is shown that it would be better to use a more flexible method for fitting the data which would contain these two models and which would also describe intermediate situations. The results obtained by the two methods for the η production by pions are compared. (France)

14703 (TID–25639) SU(3) × SU(3) CHIRAL LAGRANGIAN MODEL FOR $\bar{K}N$ INTERACTIONS. Hogan, Mary Elizabeth Mogge (Florida State Univ., Tallahassee). Jun 1970. 131p. Dep. NTIS.

Thesis.

A chiral Lagrangian model of meson-baryon scattering is used to develop a theory of $\bar{K}N$, $\pi\Sigma$, and $\pi\Lambda$ interactions. The meson and baryon fields are assumed to transform as nonlinear realizations of SU(3) × SU(3). In addition to pseudoscalar meson and $J^P = \frac{1}{2}^+$ baryon fields, vector meson, $J^P = \frac{1}{2}^-$ baryon, $J^P = \frac{3}{2}^+$ baryon and $J^P = \frac{3}{2}^-$ baryon fields are introduced in order to describe one particle exchange contributions. The chiral symmetry is broken by Lagrangians bilinear in either the baryon or pseudoscalar fields. An extensive formalism is developed in order to obtain physical predictions from the model. The partial wave amplitudes obtained from the chiral Lagrangian model are unitarized by a K-matrix formalism. Total cross sections are calculated for the processes $\bar{K}N \rightarrow \bar{K}N$, $\bar{K}N \rightarrow \pi\Sigma$, $\bar{K}N \rightarrow \pi\Lambda$, $\pi\Sigma \rightarrow \pi\Sigma$, $\pi\Lambda \rightarrow \pi\Sigma$, and $\pi\Lambda \rightarrow \pi\Lambda$. $\bar{K}N$, $\pi\Lambda$, and $\pi\Sigma$ scattering lengths are also calculated. Not all of the predictions agree with experiment. Methods of improving the model are suggested. (auth)

14704 REGGE-DIPOLE MODEL AND $\pi^-p \rightarrow \gamma n$ REACTION. Minami, S.; Ochiai, F.; Okabe, H. (Osaka City Univ.). Lett. Nuovo Cim.; 1: 33-6(2 Jan 1971).

The $\pi^- + p \rightarrow \eta + n$ reaction is described with the Regge dipole model of the A_2. This reaction is described in terms of the spin-nonflip and spin-flip amplitudes due to the A_2 dipole. The differential cross sections and the duality concept in this model are discussed. (J.F.P.)

14705 IMPLICATIONS OF THE PION GAUGE CONDITION FOR BARYONIC PARITY DOUBLETS. Uenal, B. C. (Univ. of Ankara, Turkey). Lett. Nuovo Cim.; 4: 1113-18(12 Dec 1970).

The $N^*(1470)$ $j = \frac{1}{2}^+$ and $N^*(1550)$ $j = \frac{1}{2}^-$ production from pion–nucleon ($\frac{1}{2}^+$) scattering $N(\kappa_1) + \pi(\kappa_2) \rightarrow N^*(\kappa_3) + \pi(\kappa_4)$ are considered and it is shown that the parity doublet trajectories decouple at the point $\kappa_2 = 0$ and $\kappa_4 = 0$. (L.B.S.)

14706 FIFTH INTERACTION AND BARYON MASSES. Nussinov, S. (Tel-Aviv Univ., Israel); Schorr, Amir; Ne'eman, Y. Phys. Rev., D; 3: 229-31(1 Jan 1971).

The fifth-interaction coupling is determined from large-angle high-energy nucleon–nucleon scattering, and the D/F value for baryon matrix elements of a current–current product is extracted from hyperon decays. Assuming symmetric-nonet conserved vector current, the baryon octet D/F value is predicted. The result fits observations to within 30%. The actual baryon masses fix $\sin\phi \approx \frac{1}{9} - \frac{1}{12}$ for the eighth-component admixture in the fifth-interaction current. (auth)

14707 BACKWARD πN SCATTERING: A REGGE-POLE-CUT MODEL WITHOUT PARITY DOUBLING. Durand III, Loyal; Lipinski, Hubert M. (Univ. of Wisconsin, Madison). Contract AT(11-1)-881. Phys. Rev., D; 3: 195-8(1 Jan 1971).

A very simple model in which the amplitude for backward πN scattering is described in terms of the exchange of the N_α and Δ_δ Regge trajectories and associated Regge cuts. The trajectory functions $\alpha(u)$ and the positions of the branch points $\alpha_c(u)$ are linear functions of u, but there are no odd-parity resonances associated with the resonances on the N_α and Δ_δ trajectories (no parity doubling). The model provides a good description of the data on backward $\pi^\pm p$ scattering, including the differential charge exchange cross section and the polarization observed in π^+p scattering. (auth)

14708 EXTENSION OF THE MASS OPERATOR IN THE SYMMETRIC QUARK MODEL FOR NEGATIVE-PARITY BARYON RESONANCES. Resnikoff, Marvin (State Univ. of New York, Buffalo). Phys. Rev., D; 3: 199-206(1 Jan 1971).

The two-body mass operators $M_{189}^{8_S L\cdot S}$, $M_{189}^{8_S L\cdot S}$, and three-body mass operators $M_{35}^{1 L\cdot S}$, $M_{35}^{1 L\cdot S}$, are considered in fitting the negative-parity baryon resonances in the SU(6) × O(3) multiplet (70, 1^-). The latter operators split the degeneracy of the Δ resonances in the decuplet. A least-squares fit to the latest experimental data is performed, and the results are in excellent agreement. It is suggested that a search be made for the two Ω^{-*}'s. (auth)

14709 DISPERSION SUM RULES FOR FIXED-u πN SCATTERING AMPLITUDES. Liu, Yu-chien; McGee, Ian J. (Univ. of Waterloo, Ont.). Phys. Rev., D; 3: 183-9(1 Jan 1971).

XUM

The fixed-u finite-energy sum rules for pion–nucleon scattering amplitudes are reviewed. The continuous-dispersion sum rules for these amplitudes are derived and tested. The real part of the amplitudes is restricted to appear on the right-hand cut ($N\pi \rightarrow N\pi$) only, because no information is available for the left-hand cut ($\pi\pi \rightarrow N\bar{N}$). The main result is an evaluation of the σ, f, and g coupling constants. (auth)

14710 FRAME DEPENDENCE OF VECTOR DOMINANCE IN THE VENEZIANO MODEL AND A NEW TEST OF ρ UNIVERSALITY. Contogouris, A. P. (McGill Univ., Montreal. CERN, Geneva); Gaskell, R.; Svec, M. Phys. Rev., D; 3: 145-50(1 Jan 1971).

Certain frame-dependent predictions of vector dominance are studied in terms of simple, parameter-free Veneziano models. It is shown that the transverse helicity-frame differential cross section for $\pi^-p \rightarrow \rho^0n$ has a sharp forward peak, in accord with recent experiments. Within our approach (which is more general than the Veneziano one) this peak is shown to provide a new test and verification of ρ universality. The ratio ρ_{1-1}/ρ_{11} of $\pi^-p \rightarrow \rho^0n$ density-matrix elements is also discussed. (auth)

14711 RELATIVISTIC HARMONIC OSCILLATORS AND THE STRUCTURE OF BARYONS. Cocho, G. (International Centre for Theoretical Physics, Trieste, Italy); Flores, J. Phys. Rev., D; 3: 157-65(1 Jan 1971).

A method, based on group theory, is proposed, by which a relativistic wave equation for a few-particle system can be related to a Schrödinger-like equation in such a way that solving the latter is equivalent to obtaining the solution to the first problem. The method is applied to studying the structure of the baryons considered as built from three quarks. The relativistic form factor of the proton is calculated and a simple two-quark effective interaction consistent with the form factor is obtained. Using this effective potential, an analysis of the baryon mass spectrum is then made. (auth)

14712 DECAY CORRELATIONS IN RESONANCE PRODUCTION USING QUARKS OF SPIN 3/2. Franklin, Jerrold (Technion-Israel Inst. of Tech., Haifa. Temple Univ., Philadelphia). Phys. Rev., D; 3: 166-8(1 Jan 1971).

The decay correlation predictions of Bialas and Zalewski for the process $P + B \rightarrow V + B^*$ are derived using spin-$\frac{3}{2}$ quarks, obeying normal Fermi statistics. An additional assumption is required of an approximate left-right symmetry in the transversity frame for quark–quark scattering. (auth)

14713 DOUBLE-REGGE ANALYSIS OF SINGLE-PION PRODUCTION IN π^-p INTERACTIONS AT 8 GeV/c. Shephard, W. D.; Dzierba, A. R.; Biswas, N. N.; (and others) (Univ. of Notre Dame, Ind.). Phys. Rev., D; 3: 113-27(1 Jan 1971).

A double-Regge model (DRM) was applied to $n\pi^+\pi^-$ and $p\pi^-\pi^0$ final states produced in π^-p interactions at 8 GeV/c incident beam momentum. Application of the model was limited to the energy region where all two-body final-state masses are large. Some difficulty exists in trying to understand the qualitative features of all the data in terms of the model. Parameters of the model were determined for those events which display features consistent with the DRM. These parameters are used to predict distributions in various kinematic variables. (auth)

14714 DOUBLE-PERIPHERAL-MODEL ANALYSIS OF THE REACTION $K^+p \rightarrow K^+\pi^-\Delta^{++}$ (1236) AT 9 GeV/c. Fu, Chumin (Univ. of California, Berkeley). Phys. Rev., D; 3: 92-100(1 Jan 1971).

Using a double-Regge-pole-exchange model, the low-$\Delta^{++}\pi^-$-mass enhancement in the reaction $K^+p \rightarrow K^+\pi^-\Delta^{++}_{1236}$ at 9 GeV/c is studied. It is found that P and π double exchange dominates the process. In general the model agrees with the data in the region where $M(K^+\pi^-) \geq 1.54$ GeV, $-t_{KK} < 0.5$ $(GeV/c)^2$, and $-t_{p\Delta} < 0.5$ $(GeV/c)^2$. The possibility of extending the model into the large-t region and problems involved in the extrapolation of the model to the $K\pi$ threshold are investigated. The importance of the contribution from the double-peripheral process in the low-$M(K^+\pi^-)$ region and its implications for the analysis of the $K\pi$ system are discussed. (auth)

14715 REGGE-POLE EIKONAL MODEL AND THE DOUBLE-CHARGE-EXCHANGE REACTIONS. Vossler, C. (Tokyo Univ. Univ. of Chicago). Nuovo Cim.; 1A: 357-67(21 Jan 1971).

The Regge-pole eikonal model is used to calculate the scattering amplitude for the double-charge-exchange process $n\pi^+ \rightarrow \Delta^{++}\pi^-$. To restrict the number of parameters needed to connect this reaction to other similar reactions, with a member of the $\frac{3}{2}$ decuplet in this final state, the quark model and exact SU_6 were used. It is indicated how these connections may be made, and predictions of cross sections for $n\pi^+ \rightarrow \Delta^{++}\pi^-$ are discussed. (auth)

14716 TOWARDS INCLUSION OF SPIN IN THE GENERALIZED VENEZIANO MODEL FOR $K^-p \rightarrow \pi^-\pi^+\Lambda$. Adjei, S. A.; Collins, P. A.; Hartley, B. J.; Moore, R. W.; Moriarty, K. J. M. (Imperial Coll. of Science and Tech., London). Phys. Rev., D; 3: 150-6(1 Jan 1971).

By combining the U(6,6) supermultiplet scheme with the Veneziano model, some of the arbitrariness of the Petersson–Törnqvist model is removed. The model is applied to $K^-p \rightarrow \pi^-\pi^+\Lambda$. (auth)

14717 PARTIAL WAVE ANALYSIS OF THE REACTION K $n \rightarrow \Sigma^-\pi^+\pi^-$ FROM 1.62 TO 1.74 GeV. Harrison, William Craig. Tallahassee; Florida State Univ. (1970). 84p. University Microfilms Order No. 70-20,068.

Thesis.

An explicit formalism was given for a relativistic partial wave analysis of the reaction $1 + 2 \rightarrow a + b + g$ with arbitrary spins incorporating an isobar or sequential decay model by the parametrization of the reduced matrix elements. This formalism was applied to a study of the reaction $K^-n \rightarrow \Sigma^-\pi^+\pi^-$ in the center-of-mass energy region from 1620 to 1740 MeV. The model is capable of reproducing all experimental distributions well and permits a straightforward interpretation of the reaction studied in this region, which is consistent with all available information on the $\bar{K}N$ system from two-body reactions. The analysis is consistent with the observation that the $\Sigma(1660)$ $J^P = \frac{3}{2}^-$ state formed from $\bar{K}N$ couples only weakly to $\Lambda(1405)\pi$ and supports the conclusion of Eberhard, et al., that there may exist two distinct $\Sigma(1660)$'s of $J^P = \frac{3}{2}^-$. (Diss. Abstr. Int., B)

14718 STUDY OF NEGATIVE-PARITY BARYON RESONANCES USING THE SYMMETRIC QUARK MODEL AND LOCAL TENSOR FIELDS AND GENERATORS OF THE LORENTZ GROUP. Divgi, Dattaprasad Ramdas. College Park, Md.; Univ. of Maryland (1970). 82p. University Microfilms Order No. 70-22,545.

Thesis.

The mass formula obtained by Greenberg and Resnikoff using the symmetric quark model, with one spin-orbit term added, is fitted using the masses of 13 negative-parity baryon resonances whose quantum numbers are known. The predicted masses are found to be within 12 MeV of the observed values in the root mean square sense. Predicted masses for other isospin multiplets in the same supermultiplet of SU(6) are given, along with the mixing amplitudes of the different SU(3) multiplets for all these resonances. These mixing angles are used to calculate partial decay widths for the resonances. It is found that the agreement with experimental values is satisfactory for D-wave decays but not for S-wave decays. Justification of the independent-particle formalism in terms of exact three-body states and the masses of resonances in the totally antisymmetric representation of SU(6) are discussed. The result of Orzalesi, Sucher and Woo that $\int d^3x\, f_{\mu\nu}(x)$ where $\partial^\mu f_{\mu\nu}(x) = 0$ is proportional to the energy-momentum operator P_ν under certain conditions is used. It is shown that, if $f_{\mu\nu} = f_{\nu\mu}$, the tensor $L_{\mu\nu} = \int d^3x(x_\mu f_{0\nu} - x_\nu f_{0\mu})$ is proportional to the tensor $M_{\mu\nu}$ which generates the Lorentz transformations. This relation is first proved for one-particle matrix elements and is then generalized to arbitrary states using field-theoretic arguments. It is used to obtain information about the one-particle matrix elements of $f_{\mu\nu}(0)$. (Diss. Abstr. Int., B)

14719 LIMITING DISTRIBUTION AND THE AVERAGE $\pi^\pm$ MULTIPLICITIES IN $\pi^- + p \rightarrow \pi^\pm$ + ANYTHING REACTIONS. Chen, Min-shih; Wang, Ling-lie; Wong, T. F. (Brookhaven National Lab., Upton, N. Y.). Phys. Rev. Lett.; 26: 280-3(1 Feb 1971).

The experimental data for the single-pion distribution in the reaction $\pi^- + p \rightarrow \pi^\pm$ + anything at incident energies between 2.5 and 6 GeV and at 25 GeV show evidence for a limiting distribution and scaling behavior. The slopes of the logarithmic increase of the average $\pi^\pm$ multiplicities calculated from the 25-GeV data are found to be comparable with those obtained from accelerator pp reactions and cosmic-ray experiments. Some comments are made on possible future experiments and on an apparent discrepancy between experiments at 10, 20, and 30 GeV and a limiting distribution. (auth)

14720 DETERMINATION OF THE $X^0(960)$ MESON SPIN–PARITY IN THE POLARIZATION EXPERIMENT. Klosinski, J.; Rembielinski, J.; Tybor, W. (Univ., Lodz, Poland). Acta Phys. Pol.; B1: 359-62(Oct-Dec 1970).

To establish the $X^0(960)$ meson spin-parity it is suggested to study the forward production of X^0 in the reaction $K^-p \rightarrow X^0\Lambda$ with the polarized proton. (auth)

14721 QUARK MODEL PREDICTIONS FOR PROCESSES $0^-\frac{1}{2}^+ \rightarrow J^P\frac{3}{2}^+$. Zalewski, K. (Inst. of Nuclear Research, Krakow). Acta Phys. Pol.; B1: 423-6(Oct-Dec 1970).

A simple method of deriving the quark model predictions for processes $0^{-}\frac{1}{2}^{+} \rightarrow J^{P}\frac{3}{2}^{+}$ is presented. The cases $J^P = 0^{\pm}$, $1^{\pm}$, and 2^{+} are discussed explicitly. The method is extended to cover the description of interfering resonances. As an example the $2^{+} - 0^{+}$ interference is described. (auth)

14722 FORWARD PEAK STRUCTURE IN QUASI TWO-BODY REACTIONS AND LONG RANGE PION EXCHANGE. Stevens, Paul Ronald. Los Angeles; Univ. of California (1969). 80p. University Microfilms Order No. 70-12,021.
Thesis.

The coherent droplet model with long range pion exchange to the following reactions: $\pi^{+}p \rightarrow \rho^{0}\Delta^{++}$, $\pi^{+}p \rightarrow f^{0}\Delta^{++}$, $\pi^{-}p \rightarrow \rho^{0}n$, $\pi^{+}p \rightarrow \rho^{+}p$, $K^{-}p \rightarrow K^{*-}(890)p$, $K^{-}p \rightarrow K^{*0}(890)n$, and $pp \rightarrow n\Delta^{++}$. The measured differential cross sections for $-t' < 0.02$ (GeV/c)^2 exhibit a variety of behaviors: spikes and dips and no structure. The model can account for these features. It provides fits to existing data for $-t' \leq 0.3$ (GeV/c)^2. For $\pi^{+}p \rightarrow \rho^{0}\Delta^{++}$, long range pion exchange accounts for the shape and magnitude of the spike and the droplet model accounts for the higher t′ data. In $\pi^{-}p \rightarrow \rho^{0}n$, the single helicity flip pion amplitudes dominate, accounting for the dip at $t' = 0$ and the peaking near $t' = -0.015$ (GeV/c)^2 in the 11.2 GeV/c data. The different behaviors near $t' = 0$ are due mainly to the kinematic structure of pion vertex functions. This kinematic structure is discussed. In some of the reactions detailed structures which need higher statistics data for confirmation are expected. At 8 GeV/c no structure is seen near $t' = 0$ in $\pi^{+}p \rightarrow f^{0}\Delta^{++}$. However, the physical region moves closer to the pion pole with increasing energy. The model predicts in $\pi^{+}p \rightarrow f^{0}\Delta^{++}$ at 16 GeV/c a spike similar in shape to that seen in $\pi^{+}p \rightarrow \rho^{0}\Delta^{++}$ at 8 GeV/c if there is no interference between long range pion exchange and the small impact parameter partial wave amplitudes. The detailed structure is sensitive to this interference. From the high statistics data for $\pi^{+}p \rightarrow \rho^{0}\Delta^{++}$ at 8 GeV/c, it is concluded that if one helicity amplitude dominates near $t' = 0$ the droplet amplitude is mainly imaginary. (Diss. Abstr. Int., B)

14723 LINEAR TRAJECTORY FITS OF PION NUCLEON SCATTERING AT HIGH ENERGIES. Gleiser, Reinaldo Jaime. Syracuse, N. Y.; Syracuse Univ. (1970). 122p. University Microfilms Order No. 70-24,080.
Thesis.

Pion–nucleon scattering at high energies is considered. A simple Regge pole model with linear trajectories is used. The trajectory parameters are fixed by the spins and masses of the particles lying on them. The necessity for bending the trajectories in order to reproduce the observed high energy dependence of the differential cross sections is avoided by not assuming that the continued partial wave amplitudes satisfy Mandelstam symmetry. The absence of this symmetry gives rise to extra terms in the asymptotic form of a given amplitude. These extra terms are unambiguously determined by the model, and do not require further parametrization or physical interpretation. At large momentum transfers these terms have an asymptotic behavior which dominates that of the pure Regge pole term. The effect on the scattering amplitudes is that a linear trajectory generates an asymptotic behaviour similar to that given by a "bent" trajectory. An explicit example is given showing that in relativistic scattering, Mandelstam symmetry is not a necessary consequence of the Froissart–Gribov representation. Fits for all the processes for which data are available were made. The fits are in reasonable agreement with experiment. In particular, in forward pion–nucleon charge-exchange scattering the model predicts a nonzero polarization with only rho exchange. The modification of the phase given by the extra terms results in the correct polarization in forward elastic scattering. In backward scattering there is good agreement except at small values of u, as expected because of the neglect of the problems associated with singularities at u equals zero. (Diss. Abstr. Int., B)

14724 EVIDENCE FOR VENEZIANO DIPS IN $K^{-}p$ SCATTERING. Odorico, R. (CERN, Geneva). Phys. Lett.; 34B: 65-8 (18 Jan 1971).

It is pointed out that $K^{-}p \rightarrow \overline{K}^{0}n$ and $K^{-}p$ elastic scattering exhibit structure at fixed u in the low-energy region ($\lesssim$2 GeV/c), where data of sufficient accuracy are available. No other known mechanism, besides the Veneziano model, seems to be able to account for this phenomenon. (auth)

14725 SPIN TEST FOR A FERMION ($J > \frac{1}{2}$) DECAYING INTO A SPIN-$\frac{1}{2}$ FERMION (Λ^{0}) PLUS A SPIN-1 PHOTON. Krasznovszky, S. (Central Research Inst. for Physics, Budapest). Nucl. Phys.; B25: 519-24(1971).

The decay of a fermion of arbitrary spin into an unstable spin-$\frac{1}{2}$ fermion (Λ^{0}) plus a photon is treated with density-matrix techniques and the helicity formalism of Jacob and Wick. A complete determination of the multipole parameters of the parent fermion is possible only in terms of the particle— and polarization—angular distributions of the decay hyperon (Λ^{0}). (auth)

14726 DUALITY AND THE COMPARISON OF RESONANCE AND REGGE MODELS FOR $\pi^{+}p$ BACKWARD SCATTERING. Tomlinson, P. G. (Indiana Univ., Bloomington); Sidwell, R. A.; Lichtenberg, D. B. (and others). Contract AT(11-1)-2009. Nucl. Phys.; B25: 443-59(1971).

The results of a resonance and a Regge model of $\pi^{+}p$ scattering are compared with cross section and polarization measurements at backward angles at incident momenta between 2.38 and 5.0 GeV/c. Both models agree qualitatively with the data. The $\pi^{+}p$ spin-flip and spin-non-flip amplitudes resulting from the two models are compared with each other. It is found that both the real and imaginary parts of these amplitudes are similar, a result which gives qualitative support to the concept of duality. (auth)

14727 PHASE-SHIFT ANALYSIS OF $\pi^{-}p \rightarrow K^{0}\Lambda$. Wagner, F.; Lovelace, C. (CERN, Geneva). Nucl. Phys.; B25: 411-27(1971).

A phase shift analysis of $\pi^{-}p \rightarrow K^{0}\Lambda$ was performed at twenty energies below 2 GeV/c. After extensive random searches, the single-energy solutions found were linked by a shortest path technique with smoothing. S_{11} and P_{11} resonances near 1700 MeV mass are definitely required, with an optional P_{13} or D_{13} resonance. The well-known D_{15} and F_{15} resonances decouple from $K\Lambda$. Details on the method are also given, which are important for appreciating recent $K^{+}p$ work. (auth)

14728 PARTIAL-WAVE ANALYSIS OF REACTION $\pi N \rightarrow \pi\pi N$ IN THE 339 TO 480 MeV ENERGY REGION. Kravtsov, A. V. (Ioffe Inst. of Physics and Tech., Leningrad). Yadern. Fiz.; 12: 1068-79(Nov 1970). (In Russian).

The results of the analysis of reaction $\pi N \rightarrow \pi\pi N$ are given. The analysis takes into account the s- and p-production of $\Delta(1236)$ and s-production of πN system with $T = J = \frac{1}{2}$, described in the scattering length approximation, from initial P_{11}, D_{13}, P_{31}, and D_{33} states of πN system. The obtained amplitudes of the process $\pi N \rightarrow \pi\Delta$ are compared with the predictions of $SU(6)_W$ and PCAC hypothesis. (auth)

Strong (Baryon No. ≥ 2)

Refer also to abstract 14918.

14729 (INR-P-1229) PROTON–PROTON AND PION–PROTON INELASTIC COLLISIONS AND THE PROTON AND PION FORM FACTORS. Sosnowski, R.; Wojcik, W. (Institute of Nuclear Research, Warsaw (Poland)). 1970. 13p. Dep. NTIS (U. S. Sales Only).

A model of proton–proton inelastic collisions at high energies is proposed. It assumes that the amplitude for a collision in which n secondary particles are produced is a product of n form factors identical with the charge form factor of the proton. The predictions of the model are compared with the experimental data. The main characteristics of the experimental distributions of secondary particles are well reproduced by the model. The experimental data on high energy pion–proton collisions are also compared with the prediction of the model. (auth)

14730 (JINR–P2-5444) COMMENT ON THE ELASTIC NN AND Nd SCATTERING. Dumbrais, O. V. (Joint Inst. for Nuclear Research, Dubna (USSR). Lab. of High Energy). 1970. 7p. (In Russian). Dep. NTIS (U. S. Sales Only).

The ratios are obtained connecting the product and difference of values $\alpha_{pn} \equiv [\mathrm{Re}\, f_{pn}(0)/\mathrm{Im}\, f_{pn}(0)]$, $\alpha_{pp} \equiv [\mathrm{Re}\, f_{pp}(0)/\mathrm{Im}\, f_{pp}(0)]$ with the differential and total cross sections of pn- and pp-scattering. It is shown, on this basis, how one can precisely estimate the term proportional to the product $\alpha_{pn}\alpha_{pp}$ in the Glauber correction in pd-scattering. (auth)

14731 (JINR–P2-5448) MODEL-INDEPENDENT DETERMINATION OF THE REAL PARTS OF THE INDEPENDENT OF SPIN pp-FORWARD SCATTERING AMPLITUDES. Dumbrais, O. V. (Joint Inst. for Nuclear Research, Dubna (USSR). Lab. of High Energy). 1970. 18p. (In Russian). Dep. NTIS (U. S. Sales Only).

A new method of analyzing the experimental data on proton-proton scattering is used to obtain an accurate determination of the real parts of the forward scattering amplitude in the momentum range $0.5 \leq k \leq 39$ GeV/c. The method exploits the known analyticity properties of the scattering amplitude and experimental data in a limited energy range. However, unlike conventional dispersion relation calculations, it requires no assumptions about the amplitudes in the unphysical and asymptotic regions and about π pole. Discrepancies between the experimental values of the real parts and earlier dispersion relation predictions in the momentum range 1.0 GeV/c $\leq k \leq$ 2.0 GeV/c are confirmed. (auth)

XUM

14732 (NP–18648) EFFECT OF NONLOCALITY OF NUCLEON–NUCLEON POTENTIAL ON THE TWO-BODY SUM RULES. Research Report No. 15/1970. Lilja, I. A.; Haemaelaeinen, R. M. K. (Jyvaskyla Univ. (Finland). Dept. of Physics). Dec 1970. 8p. Dep. NTIS (U. S. Sales Only).

It is found that the effect of nonlocality of the nucleon–nucleon interaction can be easily transformed into the coordinate operator in connection with the sum rule calculations. (J.F.P.)

14733 (NP–18660) ATLAS OF PARTICLE PRODUCTION SPECTRA. Grote, H.; Hagedorn, R. (European Organization for Nuclear Research, Geneva (Switzerland)); Ranft, J. (Leipzig Univ. (East Germany)). 1970. 116p. Dep. NTIS (U. S. Sales Only).

An atlas of momentum spectra of secondary particles produced in p + p below 800 GeV/c and proton reactions with nuclei below 70 GeV/c is presented. The calculations are based on the thermodynamic model. (J.F.P.)

14734 ANALYSIS OF MODERATE-ENERGY NUCLEON–NUCLEON DATA. Yoder, Neil Richard. University Park, Pa.; Pennsylvania State Univ. (1969). 95p. University Microfilms Order No. 70-19,492.

Thesis.

Several phenomenological aspects of the nucleon–nucleon interaction at moderate energies (0–350 MeV) are investigated. A faster minimization technique is developed for phase shift analysis and potential searches. This procedure uses a linear approximation to the data as a function of the search parameters when the vector to the minimum χ^2 is calculated. The application to the analysis of nucleon–nucleon scattering data of such statistical criteria as standard deviations, χ^2 test, F test, and Chauvenet's criterion is discussed. Phase shift analyses of pp and np scattering data are done using the methods described. Ordering of the phase shifts used as search parameters is studied. Charge splitting of the $^1S_0$ phase at 210 MeV is found to be indeterminate. The nucleon–nucleon potential is discussed, and the need for quadratic-angular-momentum dependence is demonstrated. Charge symmetry and charge independence in the zero-energy limit of scattering are studied. Charge symmetry of the nonelectromagnetic part of the potential is found to be valid within experimental limits, and a definite charge dependence is present. Several effects are found to be able to account for the charge dependence: charge splitting of the exchange-quantum masses and of the coupling constants. Quantitative estimates of the cause cannot be made because the predictions are sensitive to the various splittings and theoretical calculations are not available. Calculations of scattering length, pp bremsstrahlung, and the binding energy of nuclear matter are shown from qualitatively different but phase-equivalent potentials. Nuclear matter is very sensitive to the characteristics of the potential. Comparison of the fit to data of various nucleon–nucleon models is made. An energy-dependent representation of the phase shifts is used for comparison with models. It is shown that most models fall considerably outside the experimental errors. (Diss. Abstr. Int., B)

14735 MUON FLUX DEEP UNDERGROUND AND THE QUESTION OF STRONG W-INTERACTIONS. Kabir, P. K.; Kamal, A. N. (Rutherford High Energy Lab., Chilton, Eng.). Lett. Nuovo Cim.; 1: 1-8(2 Jan 1971).

It is shown that the hypothesis of strong W interactions with nuclei cannot be reconciled with the low muon flux found in deep mine experiments for boson mass less than or equal to 10 GeV. (J.F.P.)

14736 MULTIPLICITY IN VERY HIGH-ENERGY PARTICLE-NUCLEUS COLLISIONS. Fishbane, Paul M.; Trefil, J. S. (Univ. of Illinois, Urbana). Phys. Rev., D; 3: 238-42(1 Jan 1971).

The broad features of final multiplicity in high-energy inelastic particle-nucleus collisions are investigated. The A dependence of multiplicity is rather sensitive to the nature of the high-energy particle-nucleon reaction. In particular, consequences of the particle-nucleon reaction being of multiperipheral type are investigated. (auth)

14737 EIKONAL MODEL FOR LARGE-ANGLE np AND pp ELASTIC SCATTERING. Fried, H. M.; Raman, K. (Brown Univ., Providence). Phys. Rev., D; 3: 269-71(1 Jan 1971).

An eikonal model is described for large-angle np and pp elastic scattering at medium energies. Each amplitude is parametrized as a sum of one-boson exchanges modulated by the multiple virtual emission of soft neutral I = 0 and I = 1 vector mesons. Fits to the data are presented. (auth)

14738 MODELS FOR MESON–DEUTERON SCATTERING IN THE RESONANT REGION. Landau, Rubin H. (Univ. of Illinois, Urbana). Phys. Rev., D; 3: 81-92(1 Jan 1971).

A model is presented which extends the Glauber-theory description of meson scattering from deuterons to regions in which the meson–nucleon cross section varies rapidly or resonates. A Watson form of multiple-scattering theory is employed to derive a model which includes effects caused by the nucleons' Fermi momenta, nonforward intermediate scattering, and off-energy-shell scattering. It is concluded, after a numerical analysis, that the Glauber theory itself could generate the large oscillations in $\langle r^{-2}\rangle_d$ reported in the analysis of π^+d data around 1 GeV/c and could introduce small peaks into the deduced I = 0 channel of the K^+n cross section. Nevertheless, conclusions drawn by following the usual folding procedures are not altered significantly by this model, for the K^+d data of Cool et al. (auth)

14739 NUCLEON–NUCLEON S SCATTERING WITH THE HELP OF ONE-BOSON EXCHANGE POTENTIAL. Truebenbacher, E. (Univ., Mainz). Z. Naturforsch.; 25a: 1375-9 (Oct 1970). (In German).

An attempt is discussed to parametrize the low-energy nucleon–nucleon S-scattering data by a nonrelativistic potential corresponding to the exchange of quantum numbers J^P, with mass and coupling constants of a fictive "meson" as parameters. Whereas ^1S-scattering presents no difficulties, a final decision about the usefulness of the potentials was prevented by the instabilities of the numerical integrations in case of ^3S-scattering with respect to a unitarity test built into the computer program. As a byproduct, a multipole expansion of the one boson exchange potential is given in analogy to electrostatics. (auth)

14740 SPIN-DEPENDENT THREE-PARTICLE SCATTERING. Krauss, Jeffrey Allan. Cleveland; Case Western Reserve Univ. (1970). 72p. University Microfilms Order No. 70-25,881.

Thesis.

The effects of spin-dependent forces in nucleon–deuteron scattering are considered within the context of a three-body scattering formalism. Two-body S-wave and D-wave transition operators are included as input information; they are taken to be of a separable, Yamaguchi form for the sake of computational convenience. The particular formalism chosen, based upon the work of Sloan, avoids the numerical quadrature of an integral equation by forcing the deuteron to remain in its ground state during intermediate processes. The elastic scattering cross section and nucleon polarization are calculated at 14 and 23 MeV; the results for the polarization indicate that nucleon–deuteron scattering at these energies is suitably described with only modest two-body information. This constitutes the first successful calculation of the nucleon polarization at these energies. (Diss. Abstr. Int., B)

14741 ρ^0 PRODUCTION IN pn COLLISIONS AT 6.98 GeV/c. Yekutieli, G.; Yaffe, D.; Shapira, A.; (and others) (Weizmann Inst. of Science, Rehovot, Israel). Phys. Lett.; 34B: 101-4 (18 Jan 1971).

ρ^0 is produced in the final state pn $\pi^+\pi^-$ with a cross section of $\sigma = 100 \pm 30\ \mu b$. The ρ^0 is observed only when the neutron in pn $\pi^+\pi^-$ is emitted in the forward direction and the proton is emitted in the backward direction in the c.m.s. Single ρ^0 production in nucleon–nucleon collisions is discussed in terms of two I = 1 meson exchange diagrams, and is compared to ρ^0 production in pion–nucleon collisions. (auth)

14742 ASYMPTOTIC BEHAVIOR OF SINGLE PARTICLE DISTRIBUTIONS IN HADRON COLLISIONS. Abarbanel, H. D. I. (Princeton Univ., N. J.). Phys. Lett.; 34B: 69-71(18 Jan 1971).

The J-plane description of single particle distributions from hadronic reactions is discussed. It is shown how known Regge phenomenology allows one to exhibit the nature of the approach to the pionization of fragmentation limits. A precise specification emerges of the difference between the limiting distributions for $\pi^\pm$ production in pp collisions as a function of the longitudinal boost angle. (auth)

14743 CALCULATION OF nd SCATTERING LENGTHS WITH REALISTIC POTENTIALS. Belyaev, V. B.; Wrzecionko, J.; Zubarev, A. L. (Joint Inst. for Nuclear Research, Dubna, USSR). Yadern. Fiz.; 12: 923-6(Nov 1970). (In Russian).

The Faddeev equations for the neutron–deuteron scattering are solved with effective local potentials describing the $^3S_1$ and $^1S_0$ phase shifts for the NN scatterings in a wide energy range. The quartet and doublet scattering lengths are calculated; the dependence of the scattering lengths on the shape of the potential is studied. The obtained results are compared with the experiment. (auth)

14744 A MODEL NEUTRON DEUTERON SCATTERING CALCULATION ABOVE THE INELASTIC THRESHOLD. Webb, Jerry

Glen. College Station, Tex.; Texas A and M Univ. (1969). 61p. University Microfilms Order No. 70-11,589. Thesis.

The problem of three distinguishable spinless particles interacting by means of a short-range central potential is considered. The initial state is specified to be a free particle incident on a bound state of the other two with enough energy to create a three free particle final state. The aim is to calculate the elastic scattering amplitude in this energy region by means of the Kohn variational principle. For the asymptotic wave function, the simplest form available is used that still has some chance of leading to a correct result. The trial wave function chosen has a number of linear parameters and one nonlinear parameter. For the most complicated trial function used containing seventeen linear parameters and a range of values for the nonlinear parameter, it is found that it is not possible to produce a converged result, although evidence of convergence was present. (Diss. Abstr. Int., B)

14745 BINDING ENERGY OF A Λ PARTICLE IN NUCLEAR MATTER WITH NONCENTRAL ΛN FORCES. Dabrowski, J. (Univ., Warsaw); Hassan, M. Y. M. Acta Phys. Pol.; B1: 339-58(Oct-Dec 1970).

The binding energy of a Λ particle in nuclear matter $B_\Lambda(\infty)$, is calculated in the frame of the self-consistent Brueckner K matrix theory. In the K matrix equations pure kinetic energies in the intermediate states are used. The expression for $B_\Lambda(\infty)$, which includes the rearrangement energy, is derived in the case of a ΛN interaction which is spin dependent, has a tensor and spin-orbit part and contains a hard core. Calculations have been performed with the modified Herndon–Tang potentials and with a one-boson-exchange potential. The tensor suppression effect is estimated to be about 2 MeV, which includes important contributions of the ^3P ΛN interaction. The role of the self-consistency requirement in the tensor suppression effect is discussed. (auth)

14746 A FORM-FREE, SEMIPHENOMENOLOGICAL, ERROR-BOUNDED, POTENTIAL REPRESENTATION OF TWO-NUCLEON EXPERIMENTS. Stone III, Samuel Rollins. Berkeley, Calif.; Univ. of California (1969). 202p. University Microfilms Order No. 70-13,180. Thesis.

A study is made of how to obtain the most general potential which describes two-nucleon experiments. Motivation is to find the potential, not assuming a functional form, dictated entirely by experimental data. The study consists of two parts. The background, new developments, and conceptual components of a scheme which determines the potential from data are presented. The scheme is applied to proton–proton scattering and a potential is obtained in a numerical form which is designed for most rapid use by digital computer. The theory seeks a potential for use in the Schrödinger equation. It assumes only the usual invariance principles, the usual one-pion-exchange contribution (whose strength is not assumed), and moderate energies of interaction corresponding to laboratory beam energies less than 500 MeV. The potential so obtained has full generality as a spinor- and isospinor-operator. It is explicitly local, but nonlocality is accounted for through dependence on energy. It accounts for relativistic effects, mass splitting of pi mesons and of nucleons, lowest-ordered effects of magnetic moments and of extended nucleon size, and the proton–proton Coulomb force including the Uehling vacuum polarization correction. The scheme seeks a potential which is specifically designed for most rapid use by digital computer. Since wave functions, phase shifts, and scattering matrix elements depend on integrals of potential, a numerical quadrature is devised for maximum speed and accuracy. The quadrature, of Gaussian type, permits computation speed nearly two orders of magnitude faster than conventional integration of coupled, differential, Schrödinger equations. A precise numerical expression is given for vacuum polarization correction to proton–proton scattering. Finally the scheme produces not only the potential in numerical form but also error bounds. For each numerical value of potential the corresponding error bound is the statistically expected uncertainty. The scheme is applied to proton–proton scattering. Four separate solutions are obtained for the proton–proton, nuclear potential. The solutions differ in spinor-operator and energy forms. Each of the four numerical solutions is error-bounded. Each is well-fitted to experiment; chi-squared per datum is 1.89, 2.03, 5.22, and 5.63. The solutions approximate potentials predicted by one-boson-exchange, but the agreement is only qualitative. It is concluded that energy dependence is necessary for two-nucleon potentials. There seems little need for quadratic spin-orbit dependence. (Diss. Abstr. Int., B)

Particle Invariance Principles and Symmetries

General

Refer also to abstracts 14530, 14774, 14779, 14790, and 14798.

14747 (ITF-70-70) ON EQUATIONS OF MOTION INVARIANT WITH RESPECT TO THE GROUP P(1,n). [PART] II. Fushchich, V. I.; Sokur, L. P. (Akademiya Nauk Ukrainskoi SSR, Kiev. Institut Teoreticheskoi Fiziki). 1970. 26p. Dep. NTIS (U. S. Sales Only).

Equations are deduced which are generalization of the Dirac equation invariant with respect to the rotations and translations in (1 + N)-dimensional Minkowski space. The theoretical group analysis is carried out. The P-, and T- and C-properties of these equations are studied. (auth)

14748 (JINR-P2-5480) TEST OF SU3 - SYMMETRICAL STATISTICAL THEORY OF ELEMENTARY PARTICLE PRODUCTION. Beshtojev, H. M. (Joint Inst. for Nuclear Research, Dubna (USSR). Lab. of Theoretical Physics). 1970. 8p. (In Russian). Dep. NTIS (U. S. Sales Only).

The calculations performed previously were repeated and compared with new experimental data. The best agreement of calculations with experiment was obtained at $\lambda = 0.0407$. The calculation results are close to the experimental ones with the exception of data for channels with a small number of particles, where the statistical approach is not applied. (auth)

14749 SOME REMARKS ON THE THEORY OF INDUCED REALIZATIONS. Ndili, F. N. (Daresbury Nuclear Physics Lab., Eng.). Lett. Nuovo Cim.; 1: 13-16(2 Jan 1971).

Given the representations of a group H which is a subgroup of a given group G it is known that the Mackey theory of induced representations gives one a definite procedure for obtaining the linear representations of G from the linear representations of H. It is pointed out that recent developments in the theory of chiral symmetries in particle physics suggest an alternative procedure, which is to deduce from the linear representations of H, first the nonlinear representations of G, and then by a linearization technique to proceed to the linear representations of G. A discussion of the latter method is given. (J.F.P.)

14750 II LETNYAYA SHKOLA PO PROBLEMAM TEORII ELEMENTARNYKH CHASTITS, OTEPYA, AVGUST 1967. I CHAST'. PROBLEMY CP-SIMMETRII I SLABYE VZAIMODEISTVIYA. (Proceedings of the 1967 Summer School on Elementary Particle Physics, Held at Otepaa, Estonian SSR, August 1–13, 1967. Volume 1. Problems of CP Symmetry and weak Interactions). Ainsaar, A. (ed.). Tartu, USSR; Institut Fiziki i Astronomii, Akademiya Nauk Estonskoi SSR (1969). 167p.

Five articles are included on the problems of CP symmetry. The disturbance of the CP-invariance, phenomenological analysis of $K^\circ \to 2\pi$ decay and K° regeneration, unified electromagnetic-weak interactions of elementary particles, weak nucleon–nucleon interactions, and studies of the CP-invariance of nuclear and electromagnetic interactions are discussed. (R.V.J.)

14751 SPINOR SPACE AND MASS FORMULA FOR HADRONS. Tait, W.; Cornwell, J. F. (Univ. of St. Andrews, Fife, Scotland). Lett. Nuovo Cim.; 4: 1109-12(12 Dec 1970).

A representation of space-time as a bilinear product of spinors and a suggestion concerning the nature of space-time in the region occupied by an elementary particle are examined. The internal symmetry algebra U_3 has been defined by Smrz in terms of differential operators in the spinor variables and the GMO mass formula for hadrons was derived from the tensor properties of the mass operator of the external (de Sitter) space-time symmetry algebra. The relation of this approach to the way in which the problem was previously considered, i.e. by embedding the external and internal symmetry algebras in a larger higher-symmetry or noninvariance algebra, is considered. (L.B.S.)

14752 DIRAC REPRESENTATION OF THE RELATIVISTIC SYMMETRIES. Boehm, A.; Mainland, G. B. (Univ. of Texas, Austin). Fortschr. Phys.; 18: 285-304(1970).

The Dirac spinors are developed from a group theoretical point of view. The discussion is based on infinite-component wave equations and covers the definition of commutation relations, representation of the intrinsic part and of the whole relativistic symmetry, and the Dirac formalism. (J.F.P.)

14753 E(2) EXPANSION. Olshansky, Robert. Philadelphia; Univ. of Pennsylvania (1969). 108p. University Microfilms Order No. 70-16,193. Thesis.

A study is made of the crossed-channel E(2) expansion of the t = 0, unequal mass scattering amplitude. Assuming the scattering amplitude satisfies the Mandelstam representation and has a definite asymptotic behavior, the properties of the E(2) partial wave amplitude in the plane of the complex Casimir op-

XUM

erator are derived. Equations are found which relate the E(2) expansion to the 0(2,1) and Regge representations. From these it can be seen that the properties of the E(2) amplitude and the properties of the Froissart–Gribov partial wave amplitudes containing daughter trajectories are equivalent. (Diss. Abstr. Int., B)

14754 INTERNAL SYMMETRY BOOTSTRAPPED FROM THE VENEZIANO REPRESENTATION. Lee, Huan (Massachusetts Inst. of Tech., Cambridge). Contract AT(30-1)-2098. Phys. Rev., D; 3: 576-8(15 Jan 1971).

Starting with only charge conservation, SU(2) symmetry is obtained as a result of imposing unitarity constraints on a set of Veneziano amplitudes. (auth)

14755 SPINOR REPRESENTATIONS OF THE COMPLEX INHOMOGENEOUS LORENTZ GROUP. I. Burzynski, A. (Jagellonian Univ., Krakow). Acta Phys. Pol.; B1: 427-31(Oct-Dec 1970).

The spinor representations of the complex Poincaré group are investigated in the case when the complex mass of "the particle" is different from zero. The spinor representations of the complex Poincaré group are non-equivalent to the unitary representations, but they are equivalent to the unitary representations, when restricted to the real Poincaré group. (auth)

14756 SPINOR REPRESENTATIONS OF THE COMPLEX INHOMOGENEOUS LORENTZ GROUP. II. Burzynski, A. (Jagellonian Univ., Krakow). Acta Phys. Pol.; B1: 433-5(Oct-Dec 1970).

The spinor representation of the complex Poincaré group is constructed in the case when the complex mass of the "particle" is equal to zero. (auth)

14757 0(4) PROPERTIES OF SCATTERING AMPLITUDES FOR PARTICLES WITH SPIN. Abo-Shaeer, Muhsin A. R. Santa Barbara, Calif.; Univ. of California (1969). 142p. University Microfilms Order No. 70-24,224.

Thesis.

A set of vector functions analogous to the 3-dimensional vector spherical harmonics (VSH) is defined in 4 dimensions. The relation between 0(4) and 0(3) VSH is investigated. It is found, after Reggeization, that an 0(4) state with sense (nonsense) quantum numbers never couples to a nonsense (sense) 0(3) state. Two such states are always related through a sense–nonsense factor of $\sqrt{\alpha}$ near $\alpha = 0$. The 0(4) VSH are used to reduce the four-dimensional Bethe–Salpeter (BS) equation into a one-dimensional integral equation in the region of 0(4) symmetry. The angular parts of all possible tensor operators (symmetry-conserving and otherwise) are reduced. It is found after Reggeization that every one of these operators conserves the sense or nonsense of the 0(4) state it acts upon, i.e., a tensor operator connecting two 0(4) states differing in sense always produces a $\sqrt{\alpha}$ near $\alpha = 0$ when the angular part of its matrix element is reduced. Using this result and the relation between 0(4) and 0(3) vector spherical harmonics near $\alpha = 0$ the 0(3) content of an 0(4) pole is examined at and near K = 0 where nondegenerate perturbation theory is assumed to hold. It is thus found that only the nonsense part of the 0(3) content of the M = 1 residues at $\alpha = 0$ (where the M = 1 states are pure nonsense) survives for both vanishing and small total 4-momentum K. Finally a sum rule and a nondegenerate perturbation expression are given for the slopes of the trajectories at K = 0. A rough approximation applied to the expression of the slopes proves that the slope of the ground state is positive and makes the same result very plausible for the first few excited states. The invariants for the process $\pi N \rightarrow \rho N$ for both vanishing and nonvanishing momentum transfer are enumerated and put in 0(4) classes according to the quantum numbers of their leading poles. The leading s^{α} contributions to the various s-channel helicity amplitudes are calculated. After relating the Regge width to the coupling constants the differential cross section is calculated using the pion, the ω and the M = 1 exchange. No structure other than the already known peak resulting from the pion exchange is found. (Diss. Abstr. Int., B)

14758 DIMENSION OF SCALE SYMMETRY BREAKING. Ellis, J.; Weisz, P. H.; Zumino, B. (CERN, Geneva). Phys. Lett.; 34B: 91-4(18 Jan 1971).

Present theoretical understanding allows a c number δ term and any dimension for the chiral symmetry breaking term in the decomposition $\theta_{00} = \bar{\theta}_{00} + \epsilon(\delta + u)$. (auth)

14759 WIGNER FUNCTION FOR HYPERBOLIC ROTATIONS IN THE HOMOGENEOUS LORENTZ GROUP. Makarov, A. A.; Shepelev, G. I. Yadern. Fiz.; 12: 1092-5(Nov 1970). (In Russian).

The explicit form of the Wigner function for hyperbolic rotations in the Lorentz group and the addition theorem for the basis functions of the first-class irreducible representations of the Lorentz group are obtained. (auth)

14760 SU(n) ACTIONS ON DIFFERENTIABLE MANIFOLDS WITH VANISHING FIRST AND SECOND INTEGRAL PONTRYAGIN CLASSES. Grove, Edward Andrew. Providence; Brown Univ. (1969). 55p. University Microfilms Order No. 70-8728.

Thesis.

The following main results are derived: Theorem I. Suppose that SU(n) acts as a differentiable transformation group on a manifold M where $P_1(M;Z) = 0 = P_2(M;Z)$. Suppose that dim $M \leq n^2 - n - 2$, and that $n > 28$. Let G be the connected component of the identity of the principal isotropy subgroup of this action. Then G appears on a given list. Theorem II. Suppose that SU(n) acts as a differentiable transformation group on a manifold M, where $P_1(M;Z) = 0 = P_2(M;Z)$. Suppose that dim $M \leq n^2 - n - 2$, and that $n > 28$. Let $y \in U \subseteq M$ be a regular element, and let $x \in M$. Then after possibly conjugating G_x in G = SU(n), a list of possibilities is given. (TSS)

Applications (Electromagnetic and Weak)

Refer also to abstract 14649.

14761 SUPERWEAK INTERACTIONS AND TCP INVARIANCE. Kabir, P. K. (Rutherford High Energy Lab., Chilton, Eng.). Phys. Rev., D; 3: 256(1 Jan 1971).

The role of TCP invariance is examined in theories in which CP nonconservation arises solely through perturbation of the $K^0-\bar{K}^0$ effective Hamiltonian. While the assumption of TCP invariance requires that the observed CP nonconservation arise from an interaction obeying $|\Delta S| = 2$, the assumption that the super-weak interaction obeys $|\Delta S| = 2$ leads to the same predictions as TCP invariance, regardless of whether it possesses that symmetry. (auth)

14762 SEARCH FOR CP VIOLATION IN THE TIME DISTRIBUTION OF K(NEUTRAL) $\rightarrow \pi^+\pi^-\pi^0$. Meisner, Gerald W. (Univ. of Massachusetts, Amherst); Mann, W. Anthony; Hertzbach, Stanley S.; (and others). Phys. Rev., D; 3: 59-63(1 Jan 1971).

The time distribution of 50 unambiguous K(neutral) $\rightarrow \pi^+\pi^-\pi^0$ events was studied. Defining x + iy = amp $(K_S \rightarrow \pi^+\pi^-\pi^0)$/amp $(K_L \rightarrow \pi^+\pi^-\pi^0)$, $x = 2.75^{+0.66}_{-0.60}$, $y = 0.50^{+0.70}_{-0.55}$ were obtained by the maximum-likelihood technique; the results are roughly consistent with CP conservation. The kaons were produced by K^-p charge exchange at 400 MeV/c in the 30-in. BNL hydrogen bubble chamber. (auth)

14763 CHIRAL SYMMETRY BREAKING AND NONLINEAR REALIZATIONS. Barnes, K. J.; Dondi, P. H. (Queen Mary Coll., London). Nucl. Phys.; B25: 577-88(1971).

The application of PCAC to pions and kaons transforming non-linearly under SU(3) × SU(3) is shown to yield both octet symmetry breaking and the entire content of the Gell–Mann, Oakes and Renner scheme up to fourth order in an effective Lagrangian for pseudoscalar mesons. (auth)

14764 A THEORETICAL STUDY OF THE WEAK NONLEPTONIC DECAY MODES OF THE K MESON. Holstein, Barry Ralph. Pittsburgh; Carnegie-Mellon Univ. (1970). 220p. University Microfilms Order No. 70-12,428.

Thesis.

Techniques employing current algebra and partially conserved axial vector current are applied to nonleptonic decay processes. Both CP conserving and CP violating cases are considered. The Glashow model is employed throughout to describe the effects of CP violation. First the phenomenology of the effective kaon mass matrix is discussed and a theoretical estimate of the parameters of this matrix is given. The decay mode $K \rightarrow 2\pi$ is then discussed phenomenologically and a current algebra model is constructed to describe this process. It is shown that a $\Delta I = \frac{1}{2}$ rule is predicted in the CP conserving but not in the CP violating case, and reasons for this result are considered. Finally, the decay mode $K \rightarrow 3\pi$ is discussed phenomenologically and a current algebra model is constructed to describe also this process. Using two parameters determined from the experimental results for $K \rightarrow 2\pi$ decay, the predicted amplitudes and slopes in the various $K \rightarrow 3\pi$ decays are found to be in reasonable agreement with experiment for the CP conserving case. Predicted values for various CP violating parameters (e.g., the charge asymmetry in $K_L \rightarrow \pi^+\pi^-\pi^0$) are given in terms of one of the two Glashow phase angles. (Diss. Abstr. Int., B)

14765 ANALYTIC PROPERTIES OF INELASTIC HADRONIC FORM FACTORS AND BREAKING OF CP INVARIANCE IN ELECTROMAGNETIC INTERACTIONS. Bluvshtein, R. E.; Cheshkov,

A. A. (Moscow Aviation Inst.). Yadern. Fiz.; 12: 1025-35 (Nov 1970). (In Russian).

The inelastic hadronic form factor $\varphi(q^2, M, W)$ is assumed to be analytic in the final mass W. Existing models and the experimental data are not in contradiction with the hypothesis. The analyticity of $\varphi(q^2, M, W)$ in W is used with consideration of the model of electromagnetic CP violation (the BFL model). It is shown that in framework of the BFL model the ep inelastic scattering cross section has CP-odd terms in region of the N*(1470)-isobar production. (auth)

Applications (Strong)

Refer also to abstract 14583.

14766 A SIMPLE DUAL MODEL FOR MESON-BARYON SCATTERING IN SU_3. White, J. N. J. (Daresbury Nuclear Physics Lab., Eng.). Lett. Nuovo Cim.; 1: 20-2(2 Jan 1971).

Meson-baryon scattering in the SU(3) limit previously yielded two independent sets of exchange-degenerate baryon multiplets with opposite normality which through the duality hypothesis give no exotic resonances in any channel. It is assumed that the B amplitude is antisymmetric under s—u interchange, and simple expressions of the Veneziano type are found which summarize the given information. All baryons lie on a degenerate trajectory, and the amplitudes are regarded as first-approximation solutions. (J.F.P.)

14767 GENERALIZATIONS OF THE DIRAC REPRESENTATION. Boehm, A. (Univ. of Texas, Austin). Phys. Rev., D; 3: 367-76(15 Jan 1971).

Representation spaces of the relativistic symmetry are investigated, which are "infinite-dimensional" generalizations of the space of solutions of the Dirac equation. The representations are extended by the discrete operators C, P, and T. Application of these representations to the description of baryons and mesons is discussed. (auth)

14768 SYMMETRY BREAKING IN REPRESENTATIONS OF THE RELATIVISTIC SYMMETRY. Boehm, A. (Univ. of Texas, Austin). Phys. Rev., D; 3: 377-84(15 Jan 1971).

The symmetry breaking in representations of the relativistic symmetry which are generalizations of the Dirac representation is discussed. The symmetry-breaking relation is based on a generalization of the de Sitter model and leads to fine structure in the mass spectrum. (auth)

14769 POSSIBLE CONNECTION BETWEEN CHIRAL SYMMETRY BREAKING AND THE NONET OF TENSOR TRAJECTORIES. Gal-Ezer, E.; Gomberoff, L.; Nussinov, S. (Tel Aviv Univ., Israel). Phys. Rev., D; 3: 530-5(15 Jan 1971).

Pole dominance in the complex angular momentum plane is used in order to estimate deviations from a perturbative scheme based on the Gell-Mann—Oakes—Renner model of chiral symmetry breaking. It is seen that the deviation can be very large, leading to a mass pattern which corresponds to almost-conserved $SU(2) \times SU(2)$, even when the Hamiltonian originally deviates considerably from this limit. (auth)

14770 BROKEN CHIRAL AND CONFORMAL SYMMETRY AND THE KUO TRANSFORMATION. Rashid, A. M. Harun-Ar (International Centre for Theoretical Physics, Trieste, Italy. Univ. of Islamabad, Rawalpindi, Pakistan); Rashid, M. A. Phys. Rev., D; 3: 581-6(15 Jan 1971).

The breaking of conformal and chiral symmetry within the framework of effective Lagrangians is studied, and it is shown that the (8,8) type of symmetry breaking leads to unacceptable values of the pion—pion scattering lengths. A combination of $(3,\bar{3}) + (\bar{3},3)$ and (8,8) is then proposed, the particular form being uniquely fixed by the requirement of Kuo transformation. This is then shown to lead to improved scattering lengths for meson—meson scattering processes. (auth)

14771 STRAY BARYONIC RESONANCES AND SU(3). Meyer, J.; Plane, D. E. (CERN, Geneva). Nucl. Phys.; B25: 428-42 (1971).

An attempt is made to accommodate into SU(3), on the basis of their decay rates, those baryonic resonances which are presently without definitive multiplet assignments. It is shown that for a large fraction of them no SU(3) companions have yet been found. Certain regularities are however noted for most of the remaining resonances which are successfully accommodated in the scheme. (auth)

14772 ALGEBRAIC MODELS IN PARTICLE PHYSICS. Dickens, Elmer Douglas Jr. Morgantown, W. Va.; West Virginia Univ. (1970). 238p. University Microfilms Order No. 70-22,601.

Thesis.

The problem of the mass spectrum of mesons is considered from the point of view of algebraic models based on the Lie algebras of noncompact groups. After describing the group-theoretical approach to particle physics and difficulties encountered in applying it to the mass spectrum problem, especially the O'Raifeartaigh—Segal—Jost theorems, the class of algebraic models recently set forth is considered. These models employ the Lie algebras of certain, physically interesting Lie groups but go outside the Lie algebraic structure by allowing non-Lie algebraic "coupling" terms. The resulting associative algebraic models can be given a rigorous foundation as an algebra of continuous operators on a rigged Hilbert space and mass formulas can be derived. (TSS) (Diss. Abstr. Int., B)

Field Theories

General

Refer also to abstract 14718.

14773 HAMILTONIAN FORMALISM ON CHARACTERISTIC SURFACES. Eimers, Leroy Earl. Syracuse, N. Y.; Syracuse Univ. (1970). 150p. University Microfilms Order No. 70-24,075.

Thesis.

The problem of the construction of a Hamiltonian formalism suitable for propagation of a field off characteristic or null surfaces is considered. In the Hamiltonian theory of a massless scalar field, primary constraints arise. Certain integral combinations of these constraints generate the "news function" of the scalar field. Second-class combinations of constraints are eliminated by the construction of new variables differing from the original variables by the addition of constraints. Commutation relations are found for these variables. A Hamiltonian formalism for the electromagnetic field is developed on characteristic surfaces. Again new constraints, including those generating the "news function," are found, and are treated in a fashion similar to the scalar theory, leading to new commutation relations for the variables. A Hamiltonian for gravitation (general relativity) is constructed, first on null surfaces described only by the metric condition, $g^{00} = 0$, and then on null surfaces coordinatized in a manner analogous to Bondi's approach. In both cases constraints generating the "news" are found. The treatment of constraints is analogous to the electromagnetic and scalar theories and leads to new commutation relations for the variables. The meaning and possible application of these results is discussed. (Diss. Abstr. Int., B)

Quantum Field Theory

Refer also to abstracts 13829, 14514, 14583, 14759, and 14833.

14774 (KFKI-70-22-HEP) SUPERSELECTION RULES AND INTERNAL SYMMETRIES. Frenkel, A. (Magyar Tudomanyos Akademia Kozponti Fizikai Kutato Intezete, Budapest). [1970]. 9p. Dep. NTIS (U. S. Sales Only).

The discussion of superselection rules and internal symmetries covers superselection rules for angular momentum and fermion number, the relativization of superselection rules, and the relation of superselection rules and internal symmetries. (J.F.P.)

14775 FERMI'S GOLDEN RULE: AN EXERCISE IN QUANTUM FIELD THEORY. Stedman, G. E. (Queen Mary Coll., London). Amer. J. Phys.; 39: 205-14(Feb 1971).

The golden rule of time dependent perturbation theory is derived using the formalism of quantum field theory in statistical physics. The proof is more satisfying than that of some conventional presentations and is a simple illustration of the use of the quantum field theoretical formalism (e.g. Green's functions, linked cluster expansions, and Dyson's equation) in the context of solid state theory. (auth)

14776 QUANTIZATION OF LAGRANGIANS FOR CHARGES IN AN EXTERNAL FIELD. Hayes, C. F.; Craig, C. D. (Univ. of Hawaii, Honolulu). Aust. J. Phys.; 23: 951-2(Dec 1970).

A field theory correction for the coordinates and velocities of Lagrangians in classical mechanics, is outlined, giving Lagrangians to second order = $-mc^2 + \frac{1}{2}m(dR/dt)^2 + (m/8c^2)(dR/dt)^4 - (e^2/R) - (e^2/2c^2)(d^2R/dt^2)$. (Australia)

14777 FIELD EQUATIONS IN QUANTUM ELECTRODYNAMICS. Brandt, Richard A. (Univ. of Maryland, College Park). Fortschr. Phys.; 18: 249-83(1970).

A formulation of quantum electrodynamics is presented, based on finite local field equations. These Dirac and Maxwell equations

XUM

have the usual form except that the current operators $f(x)$ and $j^\mu(x)$ are explicitly expressed as local limits of sums of nonlocal field products and suitable subtraction terms. These limits are shown to exist and to yield finite operators in the sense that the iterative solutions to the field equations are equivalent to conventional renormalized perturbation theory. The various invariance properties of the theory, including Lorentz invariance, gauge invariance, charge conjugation invariance, and renormalization invariance, are discussed and related directly to the field equations and current definitions. Initially only the general forms of the currents, based on dimensional arguments, are given. The electric current, for example, contains the (suitably defined) term: $A^3(x)$:. The corresponding field equations are used to derive renormalized Dyson–Schwinger-type integral equations for the renormalized proper part functions Σ, $\Pi^{\mu\nu}$, Λ^μ, and $X^{\alpha\beta\gamma\delta}$ (the four-photon vertex function), etc. Application of the boundary conditions $\Sigma(\not{p} = m) = \Sigma'(\not{p} = m) = \Pi(0) = \Pi'(0) = \Pi''(0) = \Lambda(\not{p} = m, 0) = X(0,0,0,0) = 0$ completely specifies the current operators. Consistency is established by deriving the same equations from rigorous renormalization theory so that their iterative solutions are proved to reproduce the correct renormalized perturbation expansion. The electric current operator is exhibited in a manifestly gauge invariant form and in a form which is manifestly negative under charge conjugation. It is shown, in fact, that much of $j^\mu(x)$ can be determined directly from the requirements of gauge invariance and charge conjugation covariance, without recourse to the integral equations. It is suggested that equal time commutation relations can serve to similarly specify the rest of the current. (auth)

14778 FURTHER EVIDENCE AGAINST THE POSSIBILITY OF FASTER-THAN-LIGHT PARTICLES. Strnad, J. (Univ. of Ljubljana, Yugoslavia. Josef Stefan Inst., Ljubljana, Yugoslavia). Fortschr. Phys.; 18: 237-47(1970).

Arguments are added to the growing number of arguments against the possibility of faster-than-light particles. Causal loops with faster-than-light particles are discussed in the framework of nonquantum special relativity. Thought experiments with steady currents of faster-than-light particles show that the reinterpretation principle is incompatible with the causality principle. If both principles are used consequently paradoxial situations arise. These are visualized utilizing Brehme diagrams. The final conclusion is that particles cannot travel on a macroscopic scale faster than light if space and time are homogeneous and if the relativity and causality principles are valid. (auth)

14779 NONSTATIONARY YANG–MILLS FIELD ASSOCIATED WITH THE SO(3) GROUP. Kerbrat-Lunc, Helene. Compt. Rend., Ser. A; 271: 1093-6(23 Nov 1970). (In French).

A particular solution of the asymptotic at infinity field equation of Yang and Mills associated with the SO(3) group in Minkowski space-time is given. (France)

14780 EXTERNAL-LINE WAVE FUNCTIONS IN COULOMB-GAUGE ELECTRODYNAMICS AND EQUIVALENCE WITH THE LANDAU GAUGE. Smit, J. (Instituut voor Theoretische Fysica, Amsterdam). Lett. Nuovo Cim.; 1: 17-19(2 Jan 1971).

A form for the reduction formula for the spinor field in Coulomb or radiation gauge electrodynamics which differs from the one usually taken is proposed. The interaction picture method gives identical results, provided it is taken into account that the interaction is switched on and off adiabatically. With the correct form of the reduction formula equivalence with the Landau gauge can be demonstrated. This equivalence is explicitly checked to lowest nontrivial order. (J.F.P.)

14781 INVARIANCE OF THE VACUUM UNDER EXACT SCALE TRANSFORMATIONS. Wolsky, A. M. (New York Univ.). Lett. Nuovo Cim.; 1: 9-11(2 Jan 1971).

In studying the consequence of exact scale invariance it is shown that it is not true that the generator of scale transformations has the vacuum as an eigenstate. Errors are found in attempts to derive the consequences of exact scalar invariance for the N-point functions of quantum field theory. (J.F.P.)

14782 SYMMETRY CONDITIONS ON NONLINEAR SPINOR FIELD FUNCTIONALS. Stumpf, H.; Scheerer, K.; Maertl, H. G. (Univ., Tuebingen, Ger.). Z. Naturforsch.; 25a: 1556-61(Nov 1970).

The symmetry conditions of nonlinear spinor theory of elementary particles, i.e. the definitions of quantum numbers, are given for the nonlinear spinor field functionals. (auth)

14783 ZERO CHARGE AND SCALE INVARIANCE PROBLEMS IN THE SOLUBLE FIELD THEORY MODEL. Gribov, V. N.; Levin, E. M.; Migdal, A. A. (Ioffe Inst. of Physics and Tech., Leningrad). Zh. Eksp. Teor. Fiz.; 59: 2140-59(Dec 1970). (In Russian).

A number of static models are investigated and on the basis of their exact solutions a study is made of the possible behavior of the Green function and vertex parts in the region where perturbation theory is invalid. The analysis shows that the possible solutions suggested previously (weak coupling, strong coupling etc.) can in fact be realized. Moreover it can be explicitly studied how the solutions are matched with those of perturbation theory at high frequencies (energies). (auth)

14784 EFFECTIVE LAGRANGIANS, FIELD ALGEBRA, AND VECTOR-MESON DOMINANCE WITH UNSTABLE PARTICLES. Banyai, L. (International Centre for Theoretical Physics, Trieste, Italy). Phys. Rev., D; 3: 571-6(15 Jan 1971).

The finite-width mass distribution of the vector and axial-vector mesons is introduced in the phenomenological Lagrangian model. Tree-graph amplitudes becoming complex, unitarity constraints may be imposed. The $SU_2 \times SU_2$ algebra of fields and field-current identities is discussed. The well-known relation between the Schwinger term and the integral over the spectral density is identically obeyed in our tree-graph approach. A tentative unitary solution gives a rather broad A_1 resonance. A discussion of the $\pi\pi$ scattering amplitude and of the pion form factor in this approach is given. (auth)

14785 COMPOSITENESS, FEYNMAN DIAGRAMS, AND THE REGGEIZED ABSORPTION MODEL. Risk, Clifford (Univ. of California, Berkeley). Phys. Rev., D; 3: 546-59(15 Jan 1971).

The Reggeized absorption model is derived from field-theoretic diagrams. This model has been used to describe a large number of quasi-two-body reactions. It involves a Regge-cut correction to Regge-pole amplitude which is generated by the exchange of the Regge pole and a Pomeranchuk pole. The cut features the product of the Reggeon and Pomeranchon (without complex conjugation of either) and a large magnitude for the cut (coherent inelastic effects add to the original cut term). The fundamental physical assumption of our derivation is that physical particles are composite objects of constituent pieces of matter. In a scattering process, some of the constituent matter takes part in the scattering while the rest stands by as a spectator. These ideas lead to the double-scattering processes by a class of diagrams involving exchange of two Reggeons in the crossed channel and propagation of composite physical particles in the direct channel. When the direct-channel particles are Reggeized, an expression is obtained for the Regge box diagram. The analysis of diagrams begins with a discussion of the Amati–Fubini–Stanghellini diagram and similar diagrams to demonstrate how the absence of third double-spectral functions leads to the absence of a cut. For simple diagrams, it is found necessary to invoke properties of form factors to show absence of the cut, but that for sufficiently composite diagrams the absence of the cut rests solely on the absence of the third double-spectral functions. Next the Mandelstam diagram and similar diagrams are discussed to demonstrate how the presence of third double-spectral functions leads to cuts. For each diagram the expression for the amplitude is brought to the form of the absorption model. Finally, the general class of diagrams referred to above is studied. These diagrams feature compositeness in the direct channel (physical particles are composite), third double-spectral functions (physical particles have definite signature; no exchange degeneracy), and two-Reggeon exchange (double scattering and the Glauber spectator approximation). By assuming saturation of direct-channel amplitudes by physical states, an absorption formula (no complex conjugations) is obtained that includes the coherent inelastic factor λ (diffraction production of direct-channel resonances). (auth)

14786 METHOD OF EXTENDING THE BLANKENBECLER–SUGAR–LOGUNOV–TAVKHELIDZE APPROXIMATION TO THE BETHE–SALPETER EQUATION. Chen, T. C. (Brown Univ., Providence); Raman, K. Phys. Rev., D; 3: 505-9(15 Jan 1971). (NYO–2262TA–231).

A systematic method of obtaining accurate solutions to the Bethe–Salpeter (BS) equation is proposed, starting with the Blankenbecler–Sugar–Logunov–Tavkhelidze (BSLT) equation as the lowest-order approximation. For the equal-mass scattering problem, where the difference between the BS and the BSLT amplitudes is the most marked, the first-order correction gives good agreement with the BS amplitude. The method was also applied to the unequal-mass scattering problem, when the mass ratio is the pion–nucleon mass ratio. Here it is found that the BSLT amplitude itself is a good approximation to the BS amplitude. (auth)

14787 LORENTZ COVARIANCE AND THE CANONICAL QUANTIZATION OF NON-ABELIAN GAUGE THEORIES. Russo, Michael J. (Aerospace Research Labs., Wright-Patterson AFB, Ohio). Phys. Rev., D; 3: 400-8(15 Jan 1971).

One means of establishing the equivalence of the canonical and covariant quantization schemes for the massless, spin-1 non-Abelian guage field is to demonstrate that these formalisms yield identical S-matrix elements. It is explicitly demonstrated that to second order in the coupling constant the canonical formalism yields a Lorentz-covariant S-matrix element for the Compton scattering of a nucleon and a quantum of this gauge field. The need to modify the canonical formalism in order to obtain a consistent description of higher-order processes is then briefly discussed. (auth)

14788 QUANTIZED FIELDS AND PARTICLE CREATION IN EXPANDING UNIVERSES. II. Parker, Leonard (Univ. of Wisconsin, Milwaukee). Phys. Rev., D; 3: 346-56(15 Jan 1971).

The spin-$\frac{1}{2}$ field which satisfies the fully covariant generalization of the Dirac equation is considered. The metric, which is not quantized, is that of an expanding universe with Euclidean 3-space. The field is quantized in a manner consistent with the time development dictated by the equation of motion. Consideration of the special-relativistic limit then provides a new proof of the connection between spin and statistics. In general, there will be production of spin-$\frac{1}{2}$ particles as a result of the expansion of the universe. However, it is shown that in the limits of zero and infinite mass there is no spin-$\frac{1}{2}$ particle production. For arbitrary mass, an upper bound on the creation of particles of given momentum is obtained. The case of an instantaneous expansion is treated exactly (but not taking into account the reaction of the particle creation back on the gravitational field). For such an expansion, the created particle density, when integrated over all momenta, diverges as a result of the high-momentum behavior. The Friedmann expansion of a radiation-filled universe is also considered, emphasizing the effect of the initial stage of the expansion. The asymptotic form of the created particle density for large momenta is obtained, and thus it is shown that the particle density, integrated over all momenta, is finite, in contrast to the previous case. (auth)

14789 DILATON FIELD THEORY AND CONFORMALLY MINKOWSKIAN SPACE-TIME. Rosen, Gerald (Drexel Univ., Philadelphia). Phys. Rev., D; 3: 615-16(15 Jan 1971).

It is observed that conformal invariance of Lagrangians describing matter fields is a concomitant of general coordinate covariance, if space-time is a conformally Minkowskian Riemannian geometry on the level of hadron physics. The dilation field of Isham, Salam, and Strathdee is the mathematical object which fixes the local length-time scale in the prescribed system of coordinates. (auth)

14790 NOTE ON THE SCALE TRANSFORMATION. Takahashi, Yasushi (Univ. of Alberta, Edmonton). Phys. Rev., D; 3: 622-5(15 Jan 1971).

A simple dimensional relation on the canonical energy-momentum tensor is derived. This relation is used to express the deficiency of the scale invariance. It is shown that the scale transformation is not compatible with the Lorentz covariance in some cases which lie within the framework of the renormalizable field theory. (auth)

14791 COUPLING-CONSTANT ANALYTICITY IN THE CHARGED-SCALAR STATIC MODEL. James, P. B.; North, G. R. (Univ. of Missouri, St. Louis). Phys. Rev., D; 3: 587-93(15 Jan 1971).

The analytic properties of the two-point function for the charged-scalar static model in the bare coupling λ are investigated. The proper self-energy function appears to be an analytic function in the λ plane cut along the positive real λ axis, and the value of λ determined by mass renormalization lies well below the nearest branch point on the real λ line. The perturbation series will, therefore, converge at this point. The Padé approximants to the full propagator and to an important subsequence of graphs are studied. Although these approximants appear to converge in the cut λ plane, the convergence is not rapid. (auth)

14792 PROMOTION AND THRESHOLD SINGULARITIES IN MASSIVE QUANTUM ELECTRODYNAMICS. Aaron, R.; Pancheri-Srivastava, G.; Srivastava, Y. N. (Northeastern Univ., Boston). Phys. Rev., D; 3: 579-81(15 Jan 1971).

The threshold singularities are studied in the J plane for spinor and scalar massive quantum electrodynamics. It is found that they are responsible for the promotion phenomenon discussed recently by Cheng and Wu. (auth)

14793 POLARIZATION PHENOMENA IN VACUUM NONLINEAR ELECTRODYNAMICS. Brezin, E.; Itzykson, C. (CEN de Saclay, Gif-sur-Yvette, France). Phys. Rev., D; 3: 618-21 (15 Jan 1971).

The influence of the nonlinearities of vacuum quantum electrodynamics on the propagation of a low-frequency wave traversing an intense electromagnetic field is studied. Cotton-Mouton and Kerr effects on the polarization, as well as the associated birefringence, appear in analogy with the corresponding phenomena in material media. The magnitude of these effects is very small. It is not, however, excluded that they might provide a direct test of photon-photon scattering. (auth)

14794 WIGHTMAN FUNCTIONS IN A MODEL WITH MASS RENORMALIZATION. de Mottoni, P. (Centre de Physique Theorique, Paris); Tesei, A. Nuovo Cim.; 1A: 319-27(21 Jan 1971).

The volume and the ultraviolet cut-offs for a model with mass-changing interaction are investigated. A unitary operator plays the role of the usual dressing operator. Starting from the cut-off vacua, approximate Wightman functions are constructed, converging to the physical ones. (auth)

14795 CURRENT COMMUTATORS IN QUANTUM ELECTRODYNAMICS AND ELECTROMAGNETIC MASS DIFFERENCES OF THE PSEUDOSCALAR MESON AND BARYON OCTETS. Nagylaki, Thomas Andrew. Pasadena, Calif.; California Inst. of Tech. (1970). 96p. University Microfilms Order No. 70-12,492.
Thesis.

The operator structure of the singular terms in the equal-time commutator of space and time components of the electromagnetic current is investigated in perturbation theory by establishing a connection with Feynman diagrams. It is made very plausible that the singular term is a c number. Some remarks are made about the same problem in the electrodynamics of a spinless particle. An SU(3) symmetric multichannel calculation of the electromagnetic mass differences in the pseudoscalar meson and baryon octets is carried out with an attempt to include some of the physics of the crossed (pair annihilation) channel along the lines of the recent work by Ball and Zachariasen. The importance of the tensor meson Regge trajectories is emphasized. The agreement with experiment is poor for the isospin one mass differences, but excellent for those with isospin two.

14796 ON QUANTIZATION OF INTERACTING COVARIANT MASSLESS FIELDS WITH PRESCRIBED ASYMPTOTIC NULL DATA. Klarfeld, Joseph. New York; Yeshiva Univ. (1969). 100p. University Microfilms Order No. 70-11,607.
Thesis.

A covariant field theory is derived using the Lagrangian formalism for interacting massless fields with prescribed asymptotic null initial data at past null infinity, i.e., the incoming radiation fields. For noninteracting massless fields the incoming radiation fields and their commutation relations on a past null infinity hypersurface determined the field and the commutation relations at any finite points in space-time uniquely. Using the covariant perturbation expansion of the fields in powers of the coupling parameter and the retarded Green's function it was found that the interacting fields and their commutation relations are determined by the incoming radiation fields and their commutation relations at past null infinity. The commutation relations of the interacting fields are functionally dependent on the fields; they vanish for any two points in space with a space-like separation. It is believed that the dynamical theory of the massless fields, which is Lorentz covariant and causal, can be quantized. (Diss. Abstr. Int., B)

14797 FINITE FORMULATIONS OF FOUR-FERMION INTERACTIONS. Gomatam, Jagannathan. Syracuse, N. Y.; Syracuse Univ. (1969). 130p. University Microfilms Order No. 70-12,776.
Thesis.

Alternative formulations of a finite quantum field theory of interacting four-component spinor fields are studied, in particular the study of the interaction of four fermions. A theory of this nature based on the usual axioms of quantum field theory together with strong unitarity and strong Bogolyubov causality is developed. This theory describes renormalizable spinor interactions. The Federbush model, a theory of interacting spin $\frac{1}{2}$ particles in two dimensions, is discussed as an application. The four-fermion interaction in four-dimensional space-time, which is nonrenormalizable, is approached in two different ways. The "finite formulation I" employs higher order free-field equations and the "generalized step functions" or Π-functions in the framework of an indefinite metric Hilbert space, while retaining all the other assumptions mentioned earlier. This theory, though mathematically satisfactory, is so far, at least, not fully amenable to physical interpretation. The "finite formulation II" is a scattering operator theory, based on all the above-mentioned assumptions, except the notion of an interpolating field and uses a positive definite Hilbert space. This formulation is found to be mathematically and physically consistent for the example investigated. Whether this consistency will extend to all orders of perturbation expansion or to nonperturbative solutions is not known. (Diss. Abstr. Int., B)

14798 THE THEORY OF HIGHER SPIN FIELDS. Sipson, Roger Fredrick. Syracuse, N. Y.; Syracuse Univ. (1968). 123p. University Microfilms Order No. 70-12,816.
Thesis.

The theory of higher spin fields is analyzed starting from the representation theory of the Poincaré group rather than from the traditional starting point of a differential field equation. The complete theory of free fields is developed in parallel for spinors of the type (a,b) and (a,b) ⊕ (b,a). The generalization to other spinor types is indicated. Only the nonzero mass case is considered. A rather complete discussion of space and time reversal and charge conjugation is given, including many representations not usually considered. The plane waves for arbitrary spin and their completeness and orthogonality relations are given. With their aid the second quantized free fields are introduced by a Fock space approach. The generators of the Poincaré group for the quantized free fields are presented and the energy is shown to be positive definite. It is demonstrated that there exists a large class of differential equations which have the free fields as their only mass shell solutions but which also have extraneous solutions for other discrete masses. Based on these differential equations certain convolution operators are introduced. These have the important property of producing the δ-function when acting on a Lorentz invariant retarded commutator of two free fields. These convolution operators are used to generalize the operator derivative to arbitrary spin. The LSZ reduction formula can be generalized to arbitrary spin. Finally it is suggested that the concept of a current may be more closely associated with the retarded commutator of two free fields than with a differential field equation. (Diss. Abstr. Int., B)

14799 INFINITE-COMPONENT LOCAL FIELD THEORY WITH A RISING MASS SPECTRUM. Chodos, Alan Avrum. Ithaca, N. Y.; Cornell Univ. (1970). 62p. University Microfilms Order No. 70-24,029.
Thesis.

An infinite-component quantum field theory is studied for the purpose of describing the particles on a Regge trajectory and its daughters. Using the generators of the group 0(3,2), a class of first-order wave equations is obtained. The simplest of this class of equations is solved to yield a rising mass spectrum with a hydrogenlike accumulation point. Properties of the commutator, propagator, and electromagnetic form factor in this theory are discussed. It is shown that because only finite dimensional representations of the homogeneous Lorentz group appear in the theory, the commutator is a causal function. The form factor is shown to determine the weight functions that enter into the construction of the field. Finally, more general techniques for solving the class of wave equations are investigated, and the types of spectra given by these equations are classified according to the asymptotic behavior of a matrix which plays a role similar to that of the potential in nonrelativistic quantum mechanics. With an appropriate choice of this matrix, linearly rising trajectories are found to be possible. (Diss. Abstr. Int., B)

14800 SIMPLE RELATION BETWEEN THE BARE AND PHYSICAL MASS OF FERMIONS. Haberler, P. L. F. (Duke Univ., Durham, N. C.). Phys. Lett.; 34B: 75-8(18 Jan 1971).

Results obtained in various field-theoretic models of electrodynamics and pseudoscalar meson-nucleon theory with massless pions strongly suggest that the bare mass M_0 of the fermion involved is simply related to its physical mass M by $M_0 = Z_2M$. As a possible consequence of this relation it is suggested that the baryons as well as the electron and muon can be thought of as composite objects. (auth)

14801 MANIFESTLY GAUGE INVARIANT N-REGGEON VERTEX. Saito, S. (Univ. of Birmingham, Eng. Istituto Nazionale di Fisica Nucleare, Naples). Phys. Lett.; 34B: 72-4 (18 Jan 1971).

A simple expression for factorized N-reggion vertex is derived starting from the operator formalism. The gauge invariance is manifest and is equivalent to the invariance under the integral path deformation of the functional integral formalism. (auth)

14802 LEADING SINGULARITY IN COMPLEX ANGULAR MOMENTUM PLANE IN THE QUANTUM ELECTRODYNAMICS. Gribov, V. N.; Lipatov, L. N.; Grolov, G. V. (Ioffe Inst. of Physics and Tech., Leningrad). Yadern. Fiz.; 12: 994-1010 (Nov 1970). (In Russian).

High-energy asymptotics of the $\gamma\gamma$, $e\gamma$ and ee scatterings is found in the main logarithm approximation. In terms of the j-plane singularities the asymptotics corresponds to a standing branch point at $j > 1$. The reason for breaking the Froissart theorem in the present approach is discussed. (auth)

14803 TO THE QUESTION OF THE SOLVING BETHE-SALPETER'S SOLUTION IN LADDER APPROXIMATION IN FIELD THEORIES OF ARBITRARY DIVERGENCE. Gangnus, Yu. S. Vestn. Mosk. Univ., Ser. III. Fiz. Astron.; 11: 460-2 (Jul-Aug 1970). (In Russian).

Studies of Bethe–Salpeter type equations in unrenormalized theories of B. J. Schroer, J. Math. Phys. 5, 1361, 1966 and others have revealed the existence of nonphysical peculiarities of scattering amplitudes. An attempt is made to resolve this type of equation in a ladder approximation applied to the model theory with arbitrary power of divergence $n(n > 0)$ and in an approximation in which the peculiarities of the scattering amplitudes are not present. (R.V.J.)

14804 TRANSVERSALITY OF VECTOR AND AXIAL-VECTOR MESON FIELDS AND CHIRAL SYMMETRIES. Chkareuli, Dzh. L. (Inst. of Physics, Tbilisi, USSR). Yadern. Fiz.; 12: 1056-67 (Nov 1970). (In Russian).

The relation of the transversality condition for V and A meson fields to the chiral symmetries is established based on the Lagrangian approach. It is shown that in theories, where the V and A fields remain transversal while interacting, a chiral group arises, and, even more, the current algebra is valid. The form of the group is specialized. Contrary to the gauge theories, numbers of the vector and axial-vector fields may be different. Linear theory with massive baryons is discussed as well as the nonlinear theory (chiral dynamics). Masses of the baryons with opposite parities are to be equal. The case of the SU(2) ⊗ SU(2) symmetry is discussed in detail. A number of physical applications is considered; in particular, the axial part of the $\pi \rightarrow e\nu\gamma$ decay amplitude is calculated. (auth)

14805 GROUP GEOMETRY AND EFFECTIVE LAGRANGIANS GENERATED BY A MASSIVE GAUGE FIELD. Staunton, Lawrence Patrick. Los Angeles; Univ. of California (1969). 174p. University Microfilms Order No. 70-12,020.
Thesis.

The massive Yang–Mills gauge field is shown to be the Lagrangian equivalent of a composite massless field containing pseudoscalars as well as vector components which are minimally coupled to each other. In general, the total boson field consists of both vectors and pseudoscalars, but there exists a privileged gauge in which the pseudoscalars are transformed away. The vector field in this special gauge is formally identical to the right translation pseudoscalar current in the general gauge; therefore, the field algebra in the privileged gauge is identical to a current algebra in the general gauge. That is, vector fields go into pseudoscalar currents under a local gauge transformation. In this formalism the pseudoscalar field plays the role of a coordinate system on the group space while the vector field correlates the group space at distinct space-time points. The nonlinear Lagrangian may be expressed in terms of geometrical invariants defined on the group space and is manifestly invariant under general transformations of the pseudoscalar field. An SU(3) × SU(3) effective Lagrangian, generated by the massive gauge field discussed is formulated with the aid of the group geometrical method. The structure is manifestly invariant under nonlinear transformations and permits an exact and compact treatment of the nonlinear forms. In particular, the complete currents are presented. The SU(3) × SU(3) structure contains no free parameters that are not already necessary in an SU(2) × SU(2) model. These parameters are determined by a fitting of the linearized theory to the pion–nucleon system. Results for other members of the octets include a determination of the D/F ratio, the pseudoscalar–baryon coupling constants, which depend in a fundamental way on the masses of the vector meson multiplet, the kaon leptonic decay constant, and a simplified derivation of the Callen–Treiman formula. The results on the whole are in satisfactory agreement with experiment or with the current algebra, where these are different. (Diss. Abstr. Int., B)

14806 LOCALIZABLE AND NONLOCALIZABLE FIELD THEORIES. Kapuscik, E. (International Centre for Theoretical Physics, Trieste, Italy). Acta Phys. Pol.; B1: 293-300(Oct-Dec 1970).

XUM

The notion of localizability of field theory is discussed. New criteria for localizability are found and the relationship between Lagrangian and localizability is sketched. (auth)

Gravitation and General Relativity

Refer also to abstracts 13942, 13943, 13950, and 14508.

14807 (NP-18559) COMBINED BONDI AND FAST APPROXIMATION METHOD IN GENERAL RELATIVITY. II. THE GENERAL CASE. Preprint FAI-1 (1969). Unt, V. (Akademiya Nauk Estonskoi SSR, Tartu. Institut Fiziki i Astronomii). 1969. 32p. Dep. NTIS (U. S. Sales Only).

The gravitational field of a source with arbitrary time variations is considered, and a technique for integrating the Einstein equations is supplemented with the weak field fast approximation method. The main purpose is to describe the transport of mass and linear and angular momentum by gravitational waves in terms of the monotonic changes of the corresponding quantities characterizing the source. (J.F.P.)

14808 CONFORMAL FLATNESS OF THE SCHWARZSCHILD INTERIOR SOLUTION. Buchdahl, H. A. (Australian National Univ., Canberra). Amer. J. Phys.; 39: 158-62(Feb 1971).

It is shown that the only static distribution of fluid with nonnegative density and pressure which generates a conformally flat metric through Einstein's equations without cosmical term is that described by the Schwarzschild interior solution. The metric is exhibited in a form in which its conformal flatness is manifest. A transformation of coordinates which occurs in this work is used to obtain the optical point characteristic by a short-cut. (auth)

14809 PETROV'S CLASSIFICATION OF THE GRAVITATIONAL FIELDS AND TIME INVARIANTS. Polishchuk, R. F. Vestn. Mosk. Univ., Ser. III. Fiz. Astron.; 11: 350-2(May-Jun 1970). (In Russian).

A linear co-variant approximation for a gravitational field in a vacuum, in the vicinity of the universal point P, in a locally Galilean conic system of the semigeodezic region was examined. (R.V.J.)

14810 EXACT SOLUTION OF A STATIC CHARGED SPHERE IN GENERAL RELATIVITY. Wilson, S. J. (Univ. of Singapore). Can. J. Phys.; 47: 2401-4(Nov 1969).

An exact solution of the field equations of general relativity is obtained for a static, spherically symmetric distribution of charge and mass which can be matched with the Reissner–Nordström metric at the boundary. The self-energy contributions to the total gravitational mass are computed retaining only the first order terms in the gravitational constant. (auth) (Canada)

14811 COMMENT ON THE SPIN PRECESSION OF THE SCHIFF SATELLITE IN THE BRANS–DICKE THEORY. Morganstern, R. E. (Lunar Science Inst., Houston, Tex.). Phys. Rev., D; 3: 616-17(15 Jan 1971).

It is noted that the two versions of the Brans–Dicke (BD) theory yield different results for the de Sitter precession Ω_{DS} of an orbiting gyroscope, while the Lense–Thirring precession Ω_{LT} is unchanged, thus making the results unit dependent. This apparent inconsistency is resolved by showing that there exists a third term Ω_ϕ which arises from an anomalous scalar force term in the equations of motion. This latter term naturally combines with Ω_{DS} to make their sum independent of units, and agrees with previously published results. (auth)

14812 GRAVITATIONAL CONSTANT: EXPERIMENTAL BOUND ON ITS TIME VARIATION. Shapiro, Irwin I.; Smith, William B.; Ash, Michael B.; (and others) (Massachusetts Inst. of Tech., Cambridge. Massachusetts Inst. of Tech., Lexington). Phys. Rev. Lett.; 26: 27-30(4 Jan 1971).

Analysis of radar-echo time delays, primarily between Earth and Mercury, yields an upper limit on the fractional variation of the gravitational constant of 4 parts in 10^{10} per year. Continuation of these radar measurements for five more years—even at the present level of accuracy—would allow the uncertainty to be reduced reliably to 3 parts in 10^{11} per year, a limit close to the effect predicted by some theorists. (auth)

14813 MOTION AND STRUCTURE OF SINGULARITIES IN GENERAL RELATIVITY. Posadas, Roger. Pittsburgh; Univ. of Pittsburgh (1970). 128p. University Microfilms Order No. 70-20,354.

Thesis.

A new approach to equations of motion in general relativity is presented, in which matter is treated as singularities, of a particular kind, in the Weyl tensor and motion is described in terms of the behavior of the family of null cones emanating from a singular world line. This approach, which makes use of the spin coefficient formalism, provides an intrinsic description of the motion of a singularity in its own space-time and does not depend on a regular background space as in the usual approaches to motion. It is applied to the Robinson–Trautman solutions and their charged counterparts, the case of a general empty space, and the Einstein–Maxwell theory, and equations of motion for the singularity in each case are obtained. Two main results of this approach are the discovery of an internal structure for the singularity and the derivation of the Lorentz–Dirac equation of motion for a charged particle, with the Lorentz force appearing in terms of a unique background field and the Abraham radiation reaction force arising unexpectedly without the use of mass renormalization or ad hoc assumptions. (Diss. Abstr. Int., B)

14814 GENERAL-RELATIVISTIC FLUID SPHERES. III. A SIMULTANEOUS SOLVING OF TWO EQUATIONS. Kuchowicz, B. (Univ., Warsaw). Acta Phys. Pol.; B1: 437-46(Oct-Dec 1970).

Several new solutions of the gravitational field equations for space filled with matter are given. They are obtained under the following assumptions: (a) spherically symmetric distribution of a perfect fluid, (b) static gravitational field, (c) canonical Schwarzschild coordinates. These assumptions are the same as in the two preceding parts of the work; the procedure of deriving the solutions is modified to the extent that instead of dealing with one differential equation for one unknown function two such equations are dealt with. Only those solutions are presented which have such a simple form that a study of general features of relativistic stellar models may be easily performed with their help. Some of the solutions (being of an especially simple form) are examined in more detail; asymptotic equations of state of the ultrarelativistic matter in the central region of highest density are given. (auth)

14815 ASYMPTOTICALLY FLAT SPACES IN ASYMPTOTICALLY NULL-SPHERICAL COORDINATES. Persides, S. (Univ. of Chicago). Proc. Roy. Soc. (London), Ser. A; 320: 349-68(22 Dec 1970).

The behaviour of asymptotically flat gravitational fields in the framework of general relativity is studied by the use of tetrad formalism. For this, a system of coordinates u, r, θ and ϕ is used, such that at spatial infinity u = const. is a null hypersurface and r, θ and ϕ reduce to the usual spherical polar coordinates. A set of four vectors (a tetrad) is also chosen with the only restriction that they are everywhere null. The metric tensor and the four vectors are expanded in inverse powers of r; the rotation coefficients and the tetrad components of the Riemann tensor are then calculated in a similar expansion; and the first two terms in the expansion beyond their values for a flat space are retained. The field equations in these approximations are derived explicitly and their effect on the expansion of the tetrad components of the Riemann tensor is studied; and the total energy and linear momentum are examined. Three main results are derived: the form of the peeling theorem in the above-mentioned coordinates for an arbitrary null tetrad; the generalized expression for the news function of the field; a simple criterion for recognizing certain classes of nonradiating fields. (auth) (UK)

14816 TRANSFER OF ENERGY IN GENERAL RELATIVITY. Morgan, T. (Univ. of Nebraska, Lincoln); Bondi, H. Proc. Roy. Soc. (London), Ser. A; 320: 277-87(22 Dec 1970).

Time sequences of axially symmetric static configurations which can be continuously deformed into each other are studied. The restriction is found which characterizes those time sequences which are physically allowed. Only the regions of space surrounding a source are considered where, for quasi-static systems, the exact, static, empty space solutions of Weyl and Levi-Civita are good approximations at all times, and exact whenever the motion stops. The results are then valid for arbitrarily strong fields. The restriction was derived from the vanishing of a surface integral in much the same manner as the equations of motion are derived in post-Newtonian approximations. However, it holds in arbitrarily strong fields, whereas the usual post-Newtonian methods use in lowest order a trivial solution (flat space) and can only be used in weak fields. (UK)

Scattering Theory

Refer also to abstracts 14491, 14630, and 14754.

14817 (JINR-P4-5438) SCATTERING BY TWO CENTERS IN LONG-WAVE APPROXIMATION. Eganova, I. A.; Shirokov, M. I. (Joint Inst. for Nuclear Research, Dubna (USSR). Lab. of Theoretical Physics). 1970. 23p. (In Russian). Dep. NTIS (U. S. Sales Only).

Using the two-point functions, constructed previously, the scattering of a slow scalar particle by potentials of small radius separated by an arbitrary distance R is considered. It is shown that the multiple scattering approximation in the case, when the scattering phases are small, is valid even if the requirement kR ≫ 1 is not imposed (hk is the particle momentum). (auth)

14818 (N-70-40418) CONFIGURATION-SPACE THREE-BODY SCATTERING THEORY. Gerjuoy, E. (Pittsburgh Univ., Pa. Dept. of Physics). [1970]. Contract DA-31-124-ARO(D)-440. 10p. (NASA-CR-112667). NTIS.

Results are quoted for the physical three-body transition operator yielding the volume-independent three-body reaction coefficient. The three-body elastic scattering rate is computed when three initially free independently moving particles collide under the influence of short-range forces. (auth) (STAR)

14819 (N-70-40698) CONFIGURATION-SPACE THREE-BODY SCATTERING THEORY. Gerjuoy, E. (Pittsburgh Univ., Pa. Dept. of Physics). [1969]. Contract DA-31-124-ARO(D)-440. 115p. (NASA-CR-112362). NTIS.

The configuration space theory (nonrelativistic) three-body scattering is reviewed, with two main objectives: to derive from a very different approach, the general expressions for reaction rates customarily deduced via momentum space procedures; to determine the physical three-particle transition operator, to be distinguished from the conventional transition operator = V − VGV, where G is the Green's function. The matrix elements yield a reaction coefficient expressing the probability of true three-body reactions; contained in the matrix elements are terms representing, e.g., purely two-body scattering events. Although the possibility of inelastic processes is fully taken into account, for simplicity the detailed analysis is limited to those transition amplitudes representing elastic scattering under the influence of short range forces; however, the results are relevant to broader classes of reactions and forces. The analysis concentrates on the delta-functions occurring in transition amplitudes, as well as in expressions for a solution to Schroedinger's equation presumably satisfying the boundary conditions at real energy E for specified incident wave. It is found that these delta-functions (in a configuration space formulation) always are associated with (and in effect signal) previous illegitimate mathematical operations. (auth) (STAR)

14820 (RLO-1388-598) TROUBLES WITH STRICT CONFORMAL SYMMETRY. Boulware, David G.; Brown, Lowell S.; Peccei, R. D. (Washington Univ., Seattle. Dept. of Physics). 1970. Contract AT(45-1)-1388. 21p. Dep. NTIS.

Formal low-energy theorems for matrix elements involving the stress tensor can be used to derive the differential equations that express scale and conformal invariance. It is shown that these equations, when applied to a single particle matrix element of two fields, yield an integral representation that violates causality save for the trivial case where it reduces to the tree graphs of a free field. Although it is possible to construct conformally invariant, fully off-mass-shell amplitudes whose restriction to the mass shell yields a nontrivial result, these on-mass-shell amplitudes are not invariant under conformal transformations. This pathological behavior can be traced to an implicit assumption of analyticity when the stress tensor carries off small momenta that is, in general, false. (auth)

14821 DUAL, CROSSING-SYMMETRIC AMPLITUDE WITH MANDELSTAM ANALYTICITY. Cohen-Tannoudji, G.; Henyey, F.; Kane, G. L.; Zakrzewski, W. J. (Univ. of Michigan, Ann Arbor). Phys. Rev. Lett.; 26: 112-15(11 Jan 1971).

A class of scattering amplitudes is presented which are dual and crossing symmetric, have Regge asymptotic behavior and second-sheet poles for resonances in all channels, and satisfy a Mandelstam representation with correct double-spectral-function boundaries. The Regge trajectories and residues are essentially arbitrary. (auth)

14822 SYMMETRIES OF THE DUAL-RESONANCE AMPLITUDES. D'Adda, A. (Univ., Turin); Fubini, S. Lett. Nuovo Cim.; 4: 1174-8(12 Dec 1970).

The generalization of the permutation symmetry to n-point amplitudes in the dual-resonance model is considered. The symmetry structure for the generalized four-point amplitude containing one excited nonspurious level on the mass shell is examined. (L.B.S.)

14823 DIRECT- AND CROSS-DUALITY AMPLITUDES. Taha, M. O. (Miramare, Trieste, Italy). Phys. Rev., D; 3: 498-505(15 Jan 1971).

General considerations based on analyticity and asymptotic behavior lead to the construction of two crossing-symmetric model amplitudes for equal-mass spinless scattering, interpolating imposed asymptotic forms at low and high energy. One, the direct-duality amplitude, is a generalized Veneziano model. In the other, Regge-cut exchange is dual to the direct-channel resonances while Regge-pole exchange is dual to the direct-channel cut. (auth)

14824 PARTIAL BOOTSTRAP OF THE SCHIZOPHRENIC POMERANCHON. Chew, Geoffrey F.; Snider, Dale R. (Univ. of California, Berkeley). Phys. Rev., D; 3: 420-9(15 Jan 1971).

The Pomeranchuk (P) trajectory and residue near t = 0 are calculated through self-consistency requirements from properties of the P′. The calculation is based on a general multiperipheral model whose kernel is assumed to be nonsingular near J = 1, t = 0, apart from a small component associated with Pomeranchon exchange and containing the corresponding Amati–Fubini–Stanghellini (AFS) branch point. This small component of the kernel is treated by standard perturbation techniques. The self-consistent P trajectory turns out to have a slope smaller than normal and substantial positive curvature, whereas the logarithmic derivative of the residue is abnormally large. Although these effects result from proximity to the AFS branch point in the multiperipheral kernel, the corresponding branch point in the amplitude itself turns out to be relatively unimportant near t = 0. (auth)

14825 NONSINGULAR SCATTERING EQUATIONS. Osborn, T. A. (Stanford Univ., Calif. Oxford Univ.). Phys. Rev., D; 3: 395-9(15 Jan 1971).

Nonsingular integral equations are obtained for the two-body potential scattering problem. In momentum space the integral equations have square-integrable kernels and require only a finite range of integration. The integral equation is used to obtain bounds on the convergence of the Born series. (auth)

14826 LEVEL DEGENERACY OF THE GENERALIZED N-PARTICLE DUAL AMPLITUDE WITH SATELLITES. Rivers, R. J. (Univ. of Chicago). Phys. Rev., D; 3: 363-7(15 Jan 1971).

It is shown that the level degeneracy at $\alpha(s) = n$ for the general N-point function with satellites is $d_n \sim e^{n\gamma}$ as $n \rightarrow \infty$ where $\gamma = 1 - 1/(2k + 1)$, k = 1, 2, ... The form of the single loop constructed from such amplitudes is briefly discussed. (auth)

14827 BJORKEN LIMIT AND THE JIN–MARTIN LOWER BOUND. Bitar, Khalil M. (American Univ. of Beirut); Khuri, N. N. Contract AT(30-1)-4204. Phys. Rev., D; 3: 462-77(15 Jan 1971).

The restrictions that analyticity, unitarity (positivity), and current conservation place on the asymptotic behavior in q_0 at fixed q of the connected, covariant amplitude $\widetilde{M}^c_{\mu\nu}(q_0,q)$, where $\widetilde{M}^c_{\mu\nu}$ is the connected part of the forward amplitude for the scattering of a charged conserved current on a proton target, are investigated. The main tool is a theorem of Jin and Martin which was used to give lower bounds for forward amplitudes. The main result is to establish a rigorous lower bound on the contribution of the class-I intermediate states to $\widetilde{M}^c_{00}$. The bound gives $|M^I_{00} + p_0/mq_0| > C|q_0|^{-2}$, $C > 0$, for large complex q_0. This is larger by a factor $(q_0^{1+\epsilon})$ than the asymptotic behavior of $\widetilde{M}^c_{00}$ needed in order to have the Bjorken-limit definition of the space-space equal-time commutator agree with the naive quark commutator. This bound has the following consequences: (a) The existence of operator Schwinger terms is shown to be equivalent to the existence of a frame of reference for which the contribution of class-II intermediate states does not exactly cancel the $O(q_0^{-2})$ contribution of the class-I states. (b) The existence of the Bjorken-limit definition of the space-space commutator depends on yet another cancellation between the $O(q_0^{-3})$ contributions to $\widetilde{M}^c_{00}$ of the class-I and class-II states, and the cancellation also of all terms between $O(q_0^{-2})$ and $O(q_0^{-3})$. The sum rule whose validity is needed to guarantee this cancellation is known to diverge in perturbation theory. It is also shown to be divergent when the $P \rightarrow \infty$ limit is allowed. (c) The convergence of the Cottingham formula can only be guaranteed if in all frames of reference all the contributions between $O(q_0^{-2})$ and $O(q_0^{-4})$ of the class-I states are exactly canceled by the class-II contributions, and if in addition the remaining contribution at $O(q_0^{-4})$ of the class-I states is also exactly canceled out. The separation of the absorptive part of the amplitude into class-I and class-II contributions is carried out explicitly through a fully reduced Lehmann–Symanzik–Zimmermann formula. The class-I states are the usual s-channel states and the so-called Z-graph states. The class-II states are those that couple directly to the current, contribute only for timelike q, and are physically quite distinct from the class-I states. (auth)

14828 APPLICATIONS OF THE THEORY OF DIRICHLET SERIES TO THE SUPERPOSITION OF AN INFINITE NUMBER

OF REGGE POLES. Mandelbrojt, J. (CNRS, Marseille); Mandelbrojt, S. Nuovo Cim.; 1A: 274-84(21 Jan 1971).

A theorem is given, which proves, under certain general conditions, that the trajectories $\alpha_n(t)$ in the Chew–Frautschi diagram, are, asymptotically in n, parallel and spaced by one unit. (auth)

14829 DISCUSSION OF DUALITY AND ANALYTICITY. Boldrighini, C. (Univ., Rome); Sertorio, L. Nuovo Cim.; 1A: 293-318(21 Jan 1971).

It is first discussed how the Veneziano representation contains Regge poles. It does so in a very complicated way and even if the unitarization program were taken for granted extra problems would be expected. Second, the couplings of the elastic channel are studied as functions of the energy and of the angular momentum l. Appropriate average values of the angular momentum l seem to have a clear meaning and this is conserved also when the straight-line relationship among l and m^2 of the model is broken. Although the general coupling case is not studied it is thought that the dual model may have a more promising meaning if taken from this statistical point of view. (auth)

14830 ABOUT A SPACE-TIME OPERATOR IN COLLISION DESCRIPTIONS. Olkhovskii, V. S. (Kiev State Univ.); Recami, E. Lett. Nuovo Cim.; 4: 1165-73(12 Dec 1970).

A chronotopical coordinate operator was previously proposed for relativistic particles. An explicit analysis is made of the behavior of the operator with regard to relativistic spin-zero free particles. Anti-Hermitian operators, which may be added to the Hermitian operators, are taken into account. As a partial application to the nonrelativistic case, collision time durations are evaluated, and the results from the U-matrix and S-matrix formalisms are compared. (L.B.S.)

14831 EVALUATION OF THE ABSORPTION CORRECTIONS TO EXCHANGE MODELS. Bialas, A. (Jagellonian Univ., Krakow. Inst. of Nuclear Physics, Krakow); Zalewski, K. Acta Phys. Pol.; B1: 387-99(Oct-Dec 1970).

A method of evaluation of the absorption corrections by means of an expansion in a rapidly convergent power series is proposed. The resulting formulas are straightforward and easy for numerical calculations. (auth)

14832 A NEW APPROACH TO PARTIAL WAVE AMPLITUDES AND PHASE SHIFT ANALYSIS. Feldman, Frank Arthur. Boston; Boston Univ. (1970). 108p. University Microfilms Order No. 70-22,384.

Thesis.

A new method is developed for calculating partial-wave scattering amplitude and phase shifts for a particle interacting with an external time-independent potential of finite range. The most common intuitive formulation of quantum mechanics is examined. Its shortcomings when applied to scattering, in that bound states cannot be included in its formulation, are pointed out. Then the case of a potential of finite range is considered, and it is shown how a slight modification of the usual formalism allows the inclusion of bound states. A procedure is then developed for evaluating the partial wave phase shifts, which can be used to obtain the partial wave scattering amplitudes, or the partial wave S-matrix. The procedure leads to an approximation technique which is analytic in the complex k-plane at any order of approximation. Here $k^2 = (\hbar^2/2m)$ E, where E is the energy of the incoming particle. Next the singularities of the partial wave phase shifts in the complex k-plane are explored and interpreted. Then a spherically symmetric potential of range r = a, with an asymptotic expansion. $V(r) \underset{r \to a}{\approx} c(r - a)^\sigma$; $\sigma \geq 0$ is considered. A series of high energy results are derived which were previously obtained by Regge, who used the Jost function formalism. These results contain information about singularities of the partial wave S-matrix, which are inaccessible to the usual Lippmann–Schwinger formulation of scattering. Finally, use is made of the Bargmann inequality to show that for some potentials with n bound states it may be necessary to start the calculation with the solution of an n × n eigenvalue problem. Essentially it is demonstrated that the method of calculation converges rapidly enough to contain information about singularities of the scattering amplitude. Thus its rate of convergence is comparable to that of the Jost function approach and certainly faster than the convergence of the Born series when used in the Lippmann–Schwinger formalism. It is also noted that formulation allows for a weakening of the usual matching condition at the point where the potential vanishes. Although use is made of logarithmic derivative matching, it is found that continuity of the wave function and its derivative is not necessary. It is found natural, though not necessary, to drop this requirement and instead to normalize the interior wave function so that its integrated probability density is equal to the probability of scattering taking place (the total cross section). Thus the more natural result is that the probability of the particle interacting with the potential is the same as the total cross section. From the Schrödinger equation, one sees that the interior wave, penetrating the region of the potential, always interacts with the potential and thus scatters. (Diss. Abstr. Int., B)

14833 COMPLEX ANGULAR MOMENTUM ANALYSIS OF A FIELD-THEORETIC MODEL. Balakrishnan, V. Waltham, Mass.; Brandies Univ. (1970). 136p. University Microfilms Order No. 70-24,618.

Thesis.

The Regge pole structure of the Bethe–Salpeter amplitude for the scattering of scalar particles in the ladder approximation is studied. The leading Regge pole of the model is isolated by summing the ladder series in perturbation theory. Unequal-mass scattering in the s-channel is then considered. The first daughter pole is isolated by summing the series obtained from term-by-term analytic continuation in l (the complex angular momentum) of the original series. The relations between the positions and residua of the parent and daughter poles required by analyticity at s = 0 are verified to all orders in the coupling. The two other secondary poles near l = −2 in the case of weak coupling are also isolated after term-by-term continuation of the perturbation series. The special symmetry of the problem at s = 0 is exploited to isolate an infinite sequence of Regge poles of which the leading and daughter poles mentioned above are the first two members. The other secondary trajectories near l = −2 are again isolated (at s = 0), and weak-coupling expressions are given for the five Regge poles near l = −3. The origin of the daughter sequences corresponding to all the above poles is brought out from the representation for the partial-wave amplitude at s = 0. Finally, the threshold properties of the trajectories are considered. The "threshold accumulation" of Regge poles near l = −½ is demonstrated using the homogeneous partial-wave Bethe–Salpeter equation. Also discussed are the origin of the higher thresholds in the trajectory function and the question of "accumulations" of Regge poles in the l-plane at these thresholds in s. (Diss. Abstr. Int., B)

14834 STABILITY OF THE COMPLEX ANGULAR-MOMENTUM CONTINUATION. Miller, K. (Univ. of California, Berkeley); Viano, G. A. Nucl. Phys.; B25: 460-70(1971).

Stability estimates for the complex angular-momentum continuation are proved with the addition of a prescribed exponential bound or a prescribed uniform bound. Some numerical examples are given in order to show that the stability is quantitatively still extremely poor. (auth)

Particle Accelerators

Refer also to abstracts 13298, 13318, 14544, and 14925.

14835 (BNL-15423) 1000-GeV STORAGE RINGS. Blewett, J. P. (Brookhaven National Lab., Upton, N. Y.). 11 Nov 1970. 9p. Dep. NTIS.

Problems of injection at 30 GeV into intersecting storage rings are considered. A procedure is presented for acceleration in the storage rings to 1000 GeV. Questions of energy loss by synchrotron radiation and of space-charge limits are given preliminary treatment. It is shown that it is possible with feasible components to provide colliding beams of several amperes at 1000 GeV having energy spread lower by a large factor than the energy spread expected in the beams in the CERN ISR. (auth)

14836 (BNL-15424) METHOD FOR DECREASING THE ENERGY SPREAD IN THE AGS BEAM. Blewett, J. P. (Brookhaven National Lab., Upton, N. Y.). 25 Nov 1970. 5p. Dep. NTIS.

It is shown that the same procedure as is used in "debunching" linac beams can be used in synchrotrons to decrease the energy spread in the beam by a factor of about five. (auth)

14837 (BNL-50230) ANNUAL REPORT, JULY 1, 1970. (Brookhaven National Lab., Upton, N. Y.). Oct 1970. 233p. Dep. NTIS.

BIOLOGY—research at BNL
BROOKHAVEN ALTERNATING GRADIENT SYNCHROTRON—development and operation
BROOKHAVEN BEAM RESEARCH REACTOR—development and operation
BROOKHAVEN MEDICAL REACTOR—development and operation
CHEMISTRY—research at BNL
COMPUTERS—research at BNL
ENGINEERING—research at BNL
HIGH-ENERGY PHYSICS—research at BNL

INSTRUMENTS— development at BNL
MATHEMATICS— research at BNL
MEDICINE— research at BNL
METALLURGY— research at BNL
NUCLEAR PHYSICS— research at BNL
RADIATION CHEMISTRY— research at BNL
SOLID STATE PHYSICS— research at BNL (W.H.K.)

14838 (CERN–70–21(Vol.2), pp 525–37) ON-LINE COMPUTER FACILITIES AT ARGONNE. Rust, D. R. (Argonne National Lab., Ill.).

From International conference on data handling systems in high-energy physics, Cavendish Laboratory, Cambridge, March 23–25, 1970.

The basic philosophy of on-line computing at the Argonne ZGS is outlined, and a brief description of the system is given. The performance of the on-line computer system for wire spark chamber experiments is discussed. Two EMR 6050 computers and one XDS Sigma 2 computer are used. (W.H.K.)

14839 (CERN–70–21(Vol.2), pp 561–80) THE DATA HANDLING SYSTEM FOR THE OMEGA AND THE SFM PROJECTS. Davies, H.; Nierhaus, R.; Villemoes, P.; Zanella, P. (European Organization for Nuclear Research, Geneva (Switzerland)).

From International conference on data handling systems in high-energy physics, Cavendish Laboratory, Cambridge, March 23–25, 1970.

Problems in the development of data handling systems for the Omega project at the CERN PS and the Split Field Magnet project at the CERN ISR are discussed. The data handling requirements include film measurement, equipment checking and fault finding, data acquisition, sample checking, display of results and events, and simulation of experiments. The design proposal for the data handling system, based on data characteristics and requirements, is presented. (W.H.K.)

14840 (EUR–4286(Pt.2)) TRITIATED TITANIUM TARGETS PRODUCING 14-MeV NEUTRONS. PART II. STUDY OF MECHANISMS OF THE BEHAVIOR AND NEUTRON OUTPUTS. Final Report. Guillaume, M.; Delfiore, G.; Weber, G.; Cuypers, M. (Liege Univ. (Belgium). Laboratoire d'Application des Radioelements). Nov 1970. 60p. (In French). Dep. NTIS (U. S. Sales Only). EUR FF 11,–.

A great number of systematic manufacturing tests of tritiated titanium targets has been performed in order to know the optimal procedure for their preparation and their use with maximum performances under deuteron irradiation. The main factors that determine most of the parameters of a tritiated target are the purity and the thermal conductivity of the titanium layer. (auth)

14841 (JINR–P13–5353) APPARATUS FOR INVESTIGATION OF α-ACTIVE NUCLEI: THE PRODUCTS OF THE REACTIONS WITH HEAVY IONS. Kolesov, I. V.; Lobanov, Yu. Y.; Plotko, V. M. (Joint Inst. for Nuclear Research, Dubna (USSR). Lab. of Nuclear Reactions). 1970. 22p. (In Russian). Dep. NTIS (U. S. Sales Only).

An apparatus is described for investigation of α-active short-lived products of nuclear reactions induced by heavy ions. Recoil nuclei after stopping in a gas are collected on the fibrous filters, passed through by a gas stream (the collection coefficient is 40 to 70%) and are transferred, periodically, to two pairs of Si–Au detectors. The collectors are operated by pneumatic drive. The minimal transfer time is 0.02 s. The apparatus has the possibility of recording two series α-decays (parent and daughter nuclei). (auth)

14842 (LA–4571) QUARTERLY STATUS REPORT ON THE MEDIUM-ENERGY PHYSICS PROGRAM FOR THE PERIOD ENDING OCTOBER 31, 1970. (Los Alamos Scientific Lab., N. Mex.). Dec 1970. Contract W-7405-eng-36. 54p. Dep. NTIS.

The status of accelerator structures, rf power systems, accelerator control and instrumentation, and the experimental area is outlined. Also, accelerator physics research, LAMPF scheduling and facility construction, and the LAMPF users group are discussed. (W.H.K.)

14843 (LAL–RT–44–70) COLLIDING BEAM SET UP TO BE BUILT IN THE END STATION OF THE ORSAY LINAC. Arzelier, G.; Augustin, J. E.; Belbeoch, R.; (and others) (Paris Univ., Orsay (France). Laboratoire de l'Accelerateur Lineaire). 10 Sep 1970. 10p. Dep. NTIS (U. S. Sales Only).

The essential features of the colliding beam set up to be built in the end station of the Orsay Linac are described. In view of the cost, the energy envisaged has been reduced to the order of 2 × 1.5 GeV with a luminosity of 10^{32} cm^{-2} s^{-1}. The principle of space charge compensation using 4 beams and with a compensation factor of 12 is retained. A radiofrequency of 22.5 MHz and 8 harmonics is used. The injection energy of the positrons is 1.2 GeV. The length of the largest section (6 meters) compared with the diameter of the shielded room (36 meters) determined the geometry of the ring: 2 periods, 3 bending magnets, 7 quadrupoles per half period, magnetic radius 3.8 meters. (France)

14844 (MPS/Int. CO–68–1) STATISTICS OF PS OPERATION, 1967. (European Organization for Nuclear Research, Geneva (Switzerland)). 12p. Dep. NTIS (U. S. Sales Only).

A weekly time calendar for operation of the CERN Synchrotron in 1967 is presented. Tables are included which indicate the time dedicated to nuclear experiments, setting-up and parts tests, technical development, and maintenance. Also, the distribution of machine time to nuclear experiments, weekly statistics of beam intensity and number of pulses, weekly percentage of faults, fault repartition by system, and total distribution of beam intensity per target are presented. (W.H.K.)

14845 (NP–18601) ANNUAL REPORT, APRIL 1969–MARCH 1970. (Tokyo Univ., Japan. Inst. for Nuclear Study). 140p. Dep. NTIS (U. S. Sales).

COSMIC RADIATION— research at INS
CYCLOTRONS— operation of INS 160-cm
  — development of INS variable-energy
HIGH-ENERGY PHYSICS— research at INS
NUCLEAR EMULSIONS— development for detecting ultra-high energy air showers
NUCLEAR PHYSICS— research at INS
SYNCHROTRONS— development of INS 1.3-GeV electron
  — research at INS 1.3-GeV electron
  — development of INS proton, status of (W.H.K.)

14846 (NP–18651) POSSIBILITY OF COOLING WITH SUPERFLUID HELIUM IN TUBULAR SYSTEMS, FOR EXAMPLE, SUPERCONDUCTING HELIX WAVEGUIDES. Passow, C. (Kernforschungszentrum, Karlsruhe (West Germany). Institut fuer Experimentelle Kernphysik). Dec 1969. 48p. (In German). Dep. NTIS (U. S. Sales Only).

The technical feasibility of using superfluid helium with its high heat conductivity for cooling systems at temperatures between 1°K and 2°K is investigated theoretically. It is shown mathematically that the two-fluid model, which describes well the conductivity in capillaries and slits of very small dimensions, should be applicable in calculations for large-scale cooling systems also. On this basis, calculations for two different cooling systems are performed. In the first system there is no mass transport of helium. Therefore, the heat transport is due to the circulations in the pipe of the two quantum states, the superfluid and the normal fluid. In the second system the helium is pumped with small pressure through the system. Through a superleak, pure superfluid helium is fed to the heat source. The cooling system treated can be used, for example, to cool superconducting accelerator structures, especially helical waveguides. Numerical calculations for this applications have been done. (auth)

14847 (NP–18654) FREQUENCY DEPENDENCE OF THE RESIDUAL RESISTANCE OF A GALVANICALLY BEGUN LEAD LAYER IN A SUPERCONDUCTING STATE, MEASURED IN A TEM FIELD CONFIGURATION. Szecsi, L. (Kernforschungszentrum, Karlsruhe (West Germany). Institut fuer Experimentelle Kernphysik). Jul 1970. 73p. (In German). Dep. NTIS (U. S. Sales Only).

The frequency dependence of the surface resistance of a superconducting lead layer in a coaxial resonator (TEM field configuration) has been investigated for the range from 0.36 to 5 GHz. The same lead layer has always been used for the various frequencies of each series of measurements. A superconducting coupling system has been developed since the losses there have to be negligible compared to those in the resonator. Moreover, the system shows the required broad band width and adjustability of the coupling factor. In agreement with the BCS theory an ω^{α}-dependence with $\alpha \approx 1.8$ has been found for the superconducting fraction of the surface resistance. It was quite interesting to observe the not yet really understood residual resistance obeying approximately the same law. It follows from the above mentioned dependence of the rf losses that lower operating frequencies are advantageous when superconducting lead resonators are used for particle accelerators or particle separators. (auth)

14848 (PPAD–677–D) ON REGULATION OF MAGNET POWER SUPPLIES OR, WHY USE TRANSISTORS? Riedel, J. (Princeton-Pennsylvania Accelerator, Princeton, N. J.). 25 Nov 1970. Contract AT(30-1)-2137. 6p. Dep. NTIS.

The use of a series transistor bank to improve the ability of a silicon controlled rectifier (SCR) power supply to regulate the

XUM

current in typical beam transport magnets is discussed. It is concluded that the use of transistor banks from SCR magnet power supplies cannot be justified based on cost, maintenance, and reliability. (W.H.K.)

14849 (SJC-A-70-6) PROTOTYPE OF DRIFT TUBE QUADRUPOLE MAGNETS. Baba, H.; Kobayashi, M.; Nishikawa, T.; Tanaka, J.; Yamashita, S. (Tokyo Univ. (Japan). Inst. for Nuclear Study). Aug 1970. 40p. Dep. NTIS (U. S. Sales Only).

A prototype of the quadrupole magnet for the drift tubes at the injection end of the Tokyo 40-GeV proton linac has been fabricated. The design and construction and the pulsed current generator are described together with the measured magnetic properties including saturation, fringing field, harmonic contents and their axial distributions. (auth) (Japan)

14850 (SLAC–121) PHYSICS OF ELECTRON STORAGE RINGS: AN INTRODUCTION. Sands, Matthew (Stanford Linear Accelerator Center, Calif.). Nov 1970. Contract AT(04-3)-515. 172p. Dep. NTIS.

The basic principles of storage rings are discussed, and the theory of the basic single particle processes which determine the ultimate limits on the performance of storage rings are studied in detail. Betatron oscillations, energy oscillations, radiation damping, radiation excitation, and the luminosity of a high energy storage ring are discussed. (W.H.K.)

14851 (SLAC–128) TWO-MILE ACCELERATOR PROJECT. Quarterly Status Report, July 1–September 30, 1970. (Stanford Linear Accelerator Center, Calif.). Dec 1970. Contracts AT-(04-3)-400; AT(04-3)-515. 90p. Dep. NTIS.

A status report on the Stanford Linear Accelerator Project covering the period July 1, 1970 to September 30, 1970 is presented. Topics included are accelerator and research area operations, accelerator and research area equipment development, and physics research equipment development. (auth)

14852 (SLAC-Trans–126) AUTOMATING A 2-GeV ELECTRON LINAC. Grishaev, I. A.; Kobezskii, V. M.; Kolosov, V. I.; Krasnikov, V. D.; Mel'nichenko, V. V.; Myakota-Moskalev, V. I. (Akademiya Nauk Ukrainskoi SSR, Kharkov. Fiziko-Tekhnicheskii Institut). Translated by I. M. R. Jones for Stanford Linear Accelerator Center, Calif., from report KHFTI–70-16. 12p. Dep. NTIS.

Certain aspects of using an electronic digital computer for over-all automation of a 2-GeV electron linac are discussed. Data are given on existing and required beam stabilities. The basic automatic-control circuits and automation stages are analyzed. (auth)

14853 (UCRL–19919) MODIFICATION OF THE BERKELEY HILAC. Main, Robert M. (California Univ., Berkeley. Lawrence Radiation Lab.). Sep 1970. Contract W-7405-eng-48. 24p. (CONF-700929–4). Dep. NTIS.

From Proton Linear Accelerator Conference, Batavia, Ill.

A program is presently in progress for the modification of the Hilac to make possible the acceleration of ions of all masses to a maximum energy of 8.5 MeV/n. Present scheduling calls for the shut down of the existing Hilac in January 1971 and first beams from the modified system in August 1971. The improved accelerator will consist of a pressurized 2.5 MV Cockcroft–Walton injecting ions of minimum charge-to-mass ratio $\epsilon = 0.045$, at 0.112 MeV/n into an Alvarez linac. The linac will be separated at 1.2 MeV/n where particles will be stripped to a minimum $\epsilon = 0.16$. The second linac section will be partitioned into individual cavities of approximately equal velocity increments. Adjustment of rf phase and gradient in these cavities will provide variable energy from 2.6 to 8.5 MeV/n. All cavities will operate at 70.2 MHz and magnetic quadrupole focusing will be used throughout. (auth)

14854 (UCRL-Trans–1420) ON A TRANSIENT EFFECT OF THE ACCELERATING FIELD ON THE ELECTRON BUNCH CONTAINING IONS. Bonch-Osmolovskii, A. G. (Joint Inst. for Nuclear Research, Dubna (USSR)). Translated by G. Brodell (Univ. of California, Lawrence Radiation Lab., Berkeley), from report JINR–P9–5142. 14p. Dep. NTIS.

An abstract of this paper, prepared from the original language, appeared as NSA 24: 47530.

14855 (UCRL-Trans–1421) ON THE DYNAMICS OF CHARGED BUNCH COLLISIONS IN CONNECTION WITH THE IMPACT MECHANISM OF ACCELERATION. Bonch-Osmolovskii, A. G. (Joint Inst. for Nuclear Research, Dubna (USSR)). Translated by G. Brodell (Univ. of California, Lawrence Radiation Lab., Livermore), from report JINR–P9–5179. 17p. Dep. NTIS.

A detailed analysis of the impact mechanism of acceleration of a bunch of charged particles by the coherent method is presented. The dynamics of the collision of charged bunches and the chief characteristics of impact acceleration are studied. The kinematics of elastic collision of two bunches (electron ring and ion bunch), and the joint acceleration of ions and electrons by impact acceleration are discussed. (W.H.K.)

14856 (UCRL-Trans–1425) ELECTRON-BEAM SHAPING IN A LINEAR INDUCTION ACCELERATOR. Matora, I. M.; Merkulov, L. A.; Shelontsev, I. I. (Joint Inst. for Nuclear Research, Dubna (USSR)). Translated for Univ. of California, Lawrence Radiation Lab., Berkeley, from report JINR–P9-5268. 14p. Dep. NTIS.

Results of a study of beam losses in linear induction accelerators are briefly discussed. The study was undertaken for the development of the 30-MeV, 250-A LIU-30 electron linear induction accelerator, with a pulse recurrent frequency of 50 Hz and a mean beam power of 200 kW. (W.H.K.)

14857 MAGNETIC COIL COOLED BY A LIQUID FOR A PARTICLE ACCELERATOR. Andersson, Aarne; Klein, Hans; Tjerstrom, O. (to Allmanna Svenska Elektriska Aktiebolaget). French Patent 1,571,948. 12 May 1969. Priority date 12 Jul 1967, Sweden. (In French).

A description of a magnetic coil cooled by a liquid for a particle accelerator is presented. A schematic diagram of this coil and its cooling device is shown. (J.F.P.)

14858 GENERATION OF HIGH-INTENSITY BEAMS OF NANOSECOND PULSE DURATION BY ELECTRON LINACS. Irie, Koichi; Uetomi, Isamu (Mitsubishi Electric Corp., Amagasaki, Japan). Jap. J. Appl. Phys.; 9: 1391-8(Nov 1970).

Acceleration of electron beams with a very short pulse duration and high peak intensity is achieved in electron linacs. As pulse generators for very short pulse duration, a coaxial line-type pulser, a hard-tube pulser and a pulse sharpener are newly developed which can produce pulses of about 5 nanoseconds in pulse duration and about a few thousand volts in amplitude in 50-ohm load. In the Tohoku linac, a peak intensity of 1.3 amperes is obtained with a pulse duration of 7 nanoseconds and an energy of 75 MeV, while in the Mitsubishi linac, 2.0 amperes, 10 nanoseconds and 6.4 MeV, respectively, were achieved. These results agree with Leiss theory. As a parameter of transient beam loading, the ratios of the energy contained in a pulsed beam to the stored energy in the accelerating structure and of the peak beam power to the peak input RF power are presented. (auth)

14859 DEVELOPMENT OF A POLARIZED ION SOURCE. Smith III, Winfield Scott. Tucson, Ariz.; Univ. of Arizona (1970). 102p. University Microfilms Order No. 70-19,963.

Thesis.

A source of polarized protons and deuterons has been built for use on The University of Arizona's six-million-volt Van de Graaff accelerator. This source, operating on atomic beam principles, utilizes: an rf discharge for hydrogen (deuterium) dissociation, a permanent multipole magnet for atomic state selection, an adiabatic fast passage transition unit, and a high field solenoidal ionizer. A new two-frequency adiabatic fast passage transition unit has been developed for use on deuterium. The two-frequency technique has the advantage of using the same tapered-pole magnet and rf loop as used for the usual single frequency transitions in hydrogen. In addition, a new type of high field solenoidal ionizer is described, which utilizes an electron gun to inject electrons into the ionization region, resulting in a considerable power saving. (Diss. Abstr. Int., B)

14860 SUPERCONDUCTING QUADRUPOLE DOUBLET FOR THE LOS ALAMOS MESON PHYSICS FACILITY. Rogers, J. D.; Hassenzahl, W. V.; Laquer, H. L.; Novak, J. K.; Stokes, R. W. (Los Alamos Scientific Lab., N. Mex.). J. Appl. Phys.; 42: 73-9 (Jan 1971).

From Applied Superconductivity Conference, Boulder, Colo. See CONF-700618.

A superconducting quadrupole doublet for beam focusing was operated with a 30-kG field at the center of the 30-cm-long straight section of the magnets and a 3-kG/cm field gradient. The magnets used twisted multifilament Nb–Ti superconductor imbedded in a Cu matrix of 0.050-in. diameter and operate at currents up to 500 A. Each magnet is equipped with a persistent mode superconducting switch. The room-temperature beam aperture of the magnet–Dewar system is 15 cm. The focal length of the magnet pair is about 1 m for 500-MeV pions. The magnets are mounted in a Dewar with thermally compensated supports to minimize motion upon cooling and a soft iron shield reduces external fields to less than 60 G. (auth)

14861 NON-DESTRUCTIVE CONTROL OF CONCRETE STRUCTURES BY MEANS OF BETATRONS. Vorob'ev, V. A. Beton Zhelezobeton; 15: No. 9, 37-9(1969). (In Russian).

The design and performance of stationary, portable and transferable betatrons with a maximum energy of bremsstrahlung not exceeding 30 to 50 MeV are discussed. Basic parameters of the Tomsk Inst. betatron are included and the sensitivity of radiation defectoscopy using betatrons is estimated. (R.V.J.)

XUM

PHYSICS (NUCLEAR)

Neutron Interactions with Matter

Refer also to abstracts 13965, 14404, 14406, 14414, 14436, 14467, 14471, 14488, 14840, 15345–15350, 15396–15398, 15402, and 15405.

14862 (AERE-R-5770) COHERENT NEUTRON SCATTERING LENGTH OF ^{17}O. Valentine, T. M. (Atomic Energy Research Establishment, Harwell (England)). Apr 1968. 5p. Dep. NTIS (U. S. Sales Only).

The coherent neutron scattering length of ^{17}O was determined by the least-squares analysis of neutron diffraction data collected from a single crystal of UO_2 enriched in ^{17}O. The scattering length of ^{17}O is 5.78(15) fermis, which is virtually the same as the scattering length of the ^{16}O isotope. (auth) (UK)

14863 (CEA-N-1358) ANISN SYSTEM. DESCRIPTION AND USE OF THE DISCRETE ORDINATE PROGRAM ANISN AND OF THE AUXILIARY PROGRAMMES. Report No. 1. Devillers, Christian (Commissariat a l'Energie Atomique, Fontenay-aux-Roses (France). Centre d'Etudes Nucleaires). Oct 1970. 124p. (In French). Dep. NTIS (U. S. Sales Only).

Most of the data required for using the ANISN program (discrete ordinates) and the auxiliary programs, in the case of problems relating to one-dimensional transport of neutrons and gamma rays, are given. Detailed explanations concerning the preparation of the data and the cross-section library pre-processing are given and are illustrated by examples. The principle of the numerical method used by ANISN is presented in an appendix. (auth) (France)

14864 (CEA-N-1388) PROGRAM POKER. DESCRIPTION AND UTILIZATION. Lanore, Jeanne-Marie (Commissariat a l'Energie Atomique, Fontenay-aux-Roses (France). Centre d'Etudes Nucleaires). Dec 1970. 24p. (In French). Dep. NTIS (U. S. Sales Only).

The Monte-Carlo Code Poker allows the calculation of the propagation of polyenergetic neutrons in a plane or spherical geometry. It is particularly adapted to the problem of deep penetrations. The theoretical principles of the biasing method, the description of the code, and some advice on its use are given. (auth) (France)

14865 (COO-2049-2) ONE DIMENSIONAL S_n CALCULATIONS OF NEUTRON SPECTRA REFLECTED FROM THICK SLABS OF CONCRETE AND IRON, COMPARISON WITH MEASUREMENTS. Meyer, Walter; Timmons, Darrol H.; Shen, Peter K. (Kansas State Univ., Manhattan. Dept. of Nuclear Engineering). [1969]. 33p. (CONF-700608-23). Dep. NTIS.

From American Nuclear Society Meeting, Los Angeles, Calif.

For cases of near-normal incidence, the spectrum of neutrons reflected from (or transmitted through) semi-infinite slabs may be calculated by one-dimensional discrete ordinate, S_n, transport codes. Such reflected-spectrum calculations were completed for the materials, concrete (for slabs 9 inches and 24 inches thick) and cold roll steel (iron) (for slabs 6 and 24 inches thick) using the ANISN code. ANISN calculations for concrete were completed using the DLC-9 fine group cross section set compiled from the F.A.R. Schmidt cross section library. Calculations for iron were completed using the DLC-2, DLC-9, and the unpublished D.C. Irving evaluated Cerbonne cross section data. The incident neutron spectrum used in the S_n calculations was the spectrum measured for the fast beamport of the KSU TRIGA reactor. All ANISN calculations were made for qradrature order 16 (Gaussian-16 and Modified Lobatto-16) but P0, P4, P6, and P8 orders of anisotropy were considered. Reflected spectra for concrete and iron have previously been reported. These measurements, made with an NE-213 spectrometer, were completed for a 26 inch × 26 inch × 9 inch thick concrete slab of known composition and for a 26 inch × 26 inch × 6 inch thick cold roll (low carbon) steel slab. Neutrons obtained from the fast beamport of the KSU TRIGA and collimated through a 12 foot-long $1\frac{1}{4} \times 1\frac{1}{4}$ inch square duct were used as the incident source. A compilation of the ANISN calculated reflected spectra and the corresponding measured spectra for both the 6 inch thick steel (iron) and 24-inch thick (the measurements were made with a 9 inch thick slab) concrete slab are reported for reflected angles including θ = 106°, 120°, 127°, 146°, and 161°. The steel results exhibit good correspondence between the calculated and measured data at shallow angles of reflection, however, as θ increases, the calculated results become increasingly lower than the measurements. This disparity may be due only to truncation of the scattering cross section coefficients input to ANISN and the inherent oscillations at near back scatter. In comparing the iron data calculated with DLC-2, DLC-9 or the Irving fine group cross section sets, no significantly different results are noted, nor did changes in the order of anisotropy from 8 to 6 produce significantly different trends in the calculated results. Reducing the order of anisotropy to 4 or zero did produce significantly different trends. The measured results for concrete are also compared with 05R Monte Carlo calculated results. (auth)

14866 (LA-4567) TWOTRAN SPHERE: A FORTRAN PROGRAM TO SOLVE THE MULTIGROUP TRANSPORT EQUATION IN TWO-DIMENSIONAL SPHERICAL GEOMETRY. Lathrop, K. D.; Brinkley, F. W. (Los Alamos Scientific Lab., N. Mex.). Sep 1970. Contract W-7405-eng-36. 23p. Dep. NTIS.

Finite-difference techniques peculiar to the solution of the Boltzmann transport equation in two-dimensional spherical geometry are given. Programing information and input instructions are given for a FORTRAN program to solve the transport equation in this geometry. (auth)

14867 TWO-GROUP NEUTRON TRANSPORT THEORY FOR PLANE AND SPHERICAL GEOMETRY. Thielheim, K. O.; Bloecker, W. (Univ., Kiel). Z. Naturforsch.; 25a: 1370-4 (Oct 1970).

Two-group neutron transport theory is applied to critical problems in plane and spherical geometry. The neutron flux and the density transform for plane and spherical geometry respectively are expanded into singular eigenfunctions of the transport equation. With aid of the theory of singular integral equations the problem is reduced to one Fredholm integral equation for the expansion coefficients. The critical equations are presented as additional conditions. (auth)

14868 FORWARD MAGNETIC SCATTERING AMPLITUDE OF IRON FOR THERMAL NEUTRONS. Schneider, C. S.; Shull, C. G. (Massachusetts Inst. of Tech., Cambridge). Phys. Rev., B; 3: 830-6(1 Feb 1971).

The forward magnetic scattering amplitude of iron for thermal neutrons was determined on an absolute scale in two different experiments: the refractive bending of a polarized neutron beam by a small-angle prism (apex angle 32°) and the refractive bending of an unpolarized neutron beam by a large-angle biprism (apex angle 150°) of polycrystalline iron magnetized to saturation. This magnetic scattering amplitude, determined at 301°K, was established as being $0.589(6) \times 10^{-12}$ cm/atom and is in excellent agreement with the value of $0.587(<1) \times 10^{-12}$ cm/atom that is calculated from magnetization measurements. The measurement confirms the discrepancy between this value and that extrapolated by a 3d-electron form factor from earlier Bragg reflection measurements, namely 0.645×10^{-12} cm/atom, and this supports the presence of an anomalous magnetic form factor in iron at scattering angles smaller than permitted in Bragg reflection. Simultaneous measurement of the nuclear scattering amplitude yielded $0.954(6) \times 10^{-12}$ cm/atom in good agreement with previous powder measurements. The small refractive bending angles over a range of 20 sec of arc were measured by placing the prisms between the crystals of a double perfect-crystal spectrometer with torsion goniometer control. (auth)

14869 SEPARATION OF COHERENT AND INCOHERENT CROSS SECTIONS IN INELASTIC NEUTRON SCATTERING USING POLARIZED NUCLEAR TARGETS. Jauho, P.; Pirila, P. (Technical Univ., Helsinki). Phys. Status Solidi; 42: 757-66 (1 Dec 1970).

The coherent and incoherent neutron scattering cross sections have different dependences on the polarization of neutrons and target. This fact can be used to separate the coherent and incoherent part of the inelastic cross section and to enhance the otherwise very weak coherent scattering in the cases of ^{1}H and ^{51}V. Some details of this method are studied and the results are applied to the case of ZrH_2. It seems evident that the dispersion curves of phonons in ZrH_2 can be measured by this method. (auth)

14870 SLOWING DOWN OF NEUTRONS IN GRAPHITE. Sackett, John Irvin. Tucson, Ariz.; Univ. of Arizona (1970). 168p. University Microfilms Order No. 70-22,230.

Thesis.

A sinusoidally modulated source of fast neutrons has been used to determine the slowing-down time parameters of neutrons in graphite. In the traditional pulsed-neutron experiment, it is difficult to discriminate between responses due to several neutron energy groups. With wave modulation, the amplitude of the re-

XUM

sponse of neutrons with long slowing-down times decreases rapidly with increasing frequency. It is thereby possible to discriminate against neutrons slowing to low-energy groups by increasing the frequency of modulation. Measurement of the variance of the slowing-down time distribution using the pulsed experiment is difficult because of the effect of the pulse width on the width of the resulting distribution. This requires the use of short pulses requiring specialized equipment and resulting in a low duty factor for the experiment. With wave modulation, the variance of the slowing-down time distribution may be measured directly using small neutron generators common to university research. In this experiment, BF_3 detectors were respectively covered with cadmium, cadmium and indium, and cadmium and gold foils which acted as neutron filters, allowing only neutrons of characteristic energy groups to be transmitted to the detectors. By determining the response of the detectors to modulation of the source over a frequency range from 80 to 100,000 Hz, the slowing-down time parameters of neutrons to five energy groups were obtained. These measurements were performed in a 120 centimeter by 120 centimeter by 126 centimeter block of reactor grade graphite at spatial locations ranging from twenty to fifty centimeters from the centrally located source. Spatial dependence was observed in the mean slowing-down time and the standard deviation of each of the slowing-down time distributions. A 2.0-MeV Van de Graaff positive ion accelerator with a beam modulated by an electrostatic lens was used to produce the neutron source via the ^{7}Li(d,n)^{8}Be reaction in this experiment performed at the University of Arizona Department of Nuclear Engineering. A Monte Carlo program was written for the CDC 6400 and used at the University of Arizona Computing Center to numerically solve for the neutron slowing-down time distribution as a function of energy and position in graphite. The results supported those obtained from the experiment. (Diss. Abstr. Int., B)

14871 SEMI-ANALYTIC MONTE CARLO METHOD: EXTENSIONS IN LINEAR TRANSPORT THEORY. Jones, Dixon Douglas. Davis, Calif.; Univ. of California (1969). 105p. University Microfilms Order No. 70-21,894.

Thesis.

When particles interact with media which have macroscopically uniform compositions, their successive momentum states may be described without knowledge of the actual locations of their collisions. In Monte Carlo simulations, it is therefore possible to sample from momentum space, independent of coordinate space. The subsequent probability distributions for the spatial variable can be determined analytically, once the momentum part of a particle's history has been selected. This procedure is called semi-analytic Monte Carlo. Previously, this method has been studied for slab geometries and for a point source in infinite and semi-infinite media. In this work, the semi-analytic Monte Carlo method is extended to time dependent transport and transport in inhomogeneous media. The general method is described, with a point source in an infinite medium as an example. The probability density for (N + 1)st scatterings at any point in the medium is presented. A procedure is outlined for limiting the semi-analytic method to any desired order of scattering, and then continuing with analog Monte Carlo. The extension to time dependent transport employs a special four-dimensional space-time vector. A point source in space and time in an infinite homogeneous medium is studied. The probability density for the (N + 1)st collision, at any point in space and time, is derived by integrating over previous flight lengths. The extension to non-homogeneous media includes a discussion of general inhomogeneity, but attention is restricted primarily to one-dimensional density variations in media with constant relative compositions. The case of a plane source in an infinite slab is developed by utilizing a transformation of variables. Success in determining probabilities is limited in point source configurations. As examples, linear and exponential density variations illustrate transport in inhomogeneous media. (Diss. Abstr. Int., B)

14872 A ^{244}Cm–Be ISOTOPIC NEUTRON SOURCE. Stewart, D. C.; Horwitz, E. P.; Youngquist, C. H.; Wahlgren, M. A. (Argonne National Lab., Ill.). Nucl. Appl. Technol.; 9: 875-8(Dec 1970).

An (α,n) neutron source containing 0.63 grams of highly purified ^{244}Cm as the oxide and a 100 : 1 atom ratio of Be to Cm has been prepared. It emits 1.25 (±0.06) × 10^8 neutrons per second, corresponding to 66 neutrons per 10^6 alpha particles. (auth)

14873 TIME-DEPENDENT TRANSPORT SOLUTION IN PLANE GEOMETRY. Syros, C. (Univ. of Patras, Greece). Atomkernenergie; 16: 273-80(1970).

A solution of the time-, space-, and angle-dependent transport equation for neutrons is given. The method is based on the partition of the evolving system into subsystems obeying simpler equations. Infinite plane geometry is considered and integral transforms are applied. By obtaining the distribution function for each subsystem corresponding probabilities can easily be calculated. It has been possible to sum up explicitly the partial distributions and obtain the complete solution of the equation. (auth)

14874 NEUTRON THERMALIZATION MEASUREMENTS IN GRAPHITE BY THE REACTION RATES METHOD, USING A Ge(Li) GAMMA-RAY DETECTOR. Polley, M. V.; Walker, J. (Univ. of Birmingham, Eng.). J. Nucl. Energy; 24: 279-87(Oct 1970).

The thermalization of a burst of fast neutrons after injection into a graphite stack of dimensions 101 × 101 × 81 cm^3 was studied by the reaction rates method. The Cd/Hg reaction ratio was measured in the centre and near one face of the stack over the period 90–1290 μs after neutron injection. Characteristic prompt gamma rays from both indicator materials were detected simultaneously using a small Ge(Li) detector placed within the stack. The results compare favorably with previous theoretical determinations of the time-dependent Cd/Hg ratio and with ratios calculated from time-dependent differential neutron spectra. (auth) (UK)

14875 QUASI-CLASSICAL APPROXIMATION FOR SLOW NEUTRON SCATTERING. Nishigori, Takeo (Osaka Univ.). Progr. Theor. Phys. (Kyoto); 43: 1423-44(Jun 1970).

With the aid of a new method of the short-collision-time expansion, a quasi-classical formula for the differential scattering cross section of a slow neutron is derived along the line of reasoning of the well-defined quasi-classical prescription proposed in a previous paper. The formula satisfies the condition of detailed balance and a sum rule, and has the correct limit of weak binding of the target system. The scattering from a system of molecules is treated in the present formalism and a systematic method for the correction to the Krieger–Nelkin approximation is obtained. The effectiveness of this correction method is demonstrated in a numerical calculation for HCl gas. (auth)

14876 IMPORTANCE OF AND NEEDS FOR NEUTRON NUCLEAR DATA IN ASTROPHYSICS. Clayton, D. D. (Rice Univ., Houston, Tex.). pp 35-47 of Nuclear Data for Reactors. Vol. I. Vienna; International Atomic Energy Agency (1970).

From 2nd International Conference on Nuclear Data for Reactors, Helsinki, Finland. See STI/PUB-259(Vol.1); CONF-700605–(Vol.1).

Neutron nuclear data are of unique importance to astrophysics because many of the naturally occurring nuclei owe their origin to neutron reactions and because, unlike many charged-particle reactions, neutron cross-sections can be measured even at very low neutron energy. An enumeration of important neutron cross-sections within the context of the present state of the theory of nucleosynthesis is provided. It is also shown that certain dynamic details of exploding stars may be discovered by measurements of neutron cross-sections. 28 references. (auth)

14877 CROSS-SECTIONS AND TECHNIQUES FOR HIGH-PRECISION NEUTRON NUCLEAR DATA MEASUREMENTS. Deruytter, A. J. (EURATOM, Geel, Belg.). pp 127-49 of Nuclear Data for Reactors. Vol. I. Vienna; International Atomic Energy Agency (1970).

From 2nd International Conference on Nuclear Data for Reactors, Helsinki, Finland. See STI/PUB-259(Vol.1); CONF-700605–(Vol.1).

The accuracy requirements for cross-sections of structural and fuel materials needed for the design of nuclear reactors (and for precision neutron dosimetry) have stimulated the investigation and selection of standard cross-sections and the improvement of the precision in neutron flux measuring techniques. The present status in these fields is reviewed. Considerable attention is given to standard cross-sections, i.e. cross-sections that are used to obtain other cross-sections by comparison and especially to the so-called "primary" standards as, e.g. the cross-sections of the ^{10}B(n,α)^{7}Li-, H(n,n)H-reactions. Further, improvements in the knowledge of other "working standard" cross-sections such as ^{6}Li(n,α) and ^{3}He(n,p) are discussed. Some special attention is given to the normalization of ^{235}U(n,f) and ^{239}Pu(n,f)-reactions in the resonance region, as these cross-sections are both important reactor requests and, at the same time, may play the role of secondary standards. Also the situation of the absolute neutron-flux determination is briefly reviewed. Finally, stringent requirements for improvements are set forth for the preparation and handling of samples for precise measurements with respect to chemical definition, isotopical analysis and enrichment, and absolute counting (half-lives of α-active fissile isotopes). (92 references) (auth)

14878 PROGRESS IN INTERNATIONAL NUCLEAR DATA COMPILATION AND EXCHANGE. A REPORT OF THE FOUR NEUTRON DATA CENTERS. Pearlstein, S. (Brookhaven National Lab., Upton, N. Y.). pp 621-41 of Nuclear Data for Reactors. Vol. II. Vienna; International Atomic Energy Agency (1970).
From 2nd International Conference on Nuclear Data for Reactors, Helsinki, Finland. See STI/PUB-259(Vol.2); CONF-700605-(Vol.2).

There are four neutron data centers in the world, each responsible for collecting data from a particular geographic area. (A data collection is determined by where the measurements are performed, not where they are published.) The National Neutron Cross Section Center (NNCSC), supported by the United States Atomic Energy Commission and located at the Brookhaven National Laboratory, collects data measured in the USA and Canada. The Neutron Data Compilation Center (NDCC), operated by the European Nuclear Energy Agency and located at the Saclay Laboratory near Paris, France, collects data measured in Austria, Belgium, Denmark, France, Germany, Italy, Japan, The Netherlands, Norway, Spain, Sweden, Switzerland, and the United Kingdom. The Centr Po Jadernym Dannym (CJD), or Nuclear Data Center in translation, is the new name for the center located at Obninsk, USSR, and is responsible for collecting data from the Soviet Union. The Nuclear Data Section (NDS) of the International Atomic Energy Agency, Vienna, Austria, collects data from the remaining countries and acts as liaison between the CJD and other centers. The formal agreements for the exchange of experimental and evaluated data between Centers are reviewed. Individual reports covering the activities of each Center are also presented. (auth)

14879 APPLICATION OF INTERACTIVE COMPUTER GRAPHICS TO NUCLEAR DATA EVALUATION PROBLEMS. Alter, H.; Dunford, C. L. (Atomics International, Canoga Park, Calif.). Contract AT(04-3)-701. pp 643-65 of Nuclear Data for Reactors. Vol. II. Vienna; International Atomic Energy Agency (1970).
From 2nd International Conference on Nuclear Data for Reactors, Helsinki, Finland. See STI/PUB-259(Vol.2); CONF-700605-(Vol.2).

A comprehensive semi-automated data evaluation system is being developed at Atomics International, in order to overcome many of the deficiencies associated with the application of available nuclear data evaluation methods to the more detailed, systematic and accurate data evaluations currently required. Interactive computational techniques enable the computer to form displays on a screen, and to sense, interpret, and relate the displayed information in real time. These techniques not only permit the rapid display of data sets selected at random, but also allow the evaluator to perform a large number of sequential operations in a short time span. The evaluator can take full advantage of his experience in interpreting results at each operational step. Thus, a logical path may be followed through to conclusion, without intervening lengthy delays. A prototype interactive data evaluation system, SCORE, is being used in support of the ENDF/B national neutron cross-section evaluation effort. SCORE provides a unique data storage, manipulation, and retrieval system for experimental data stored on SCISRS I data tapes. Other operational modules include: (1) an interactive method for fitting multilevel resonance parameters, using either Breit-Wigner or Reich-Moore theory, (2) a method for fitting analytical cubic spline curves to experimental data, and (3) a method of intercomparing, by visually displayed overlays, ENDF/B evaluated data with SCISRS I experimental data tapes. The SCORE system is currently being further expanded in several ways. These include: (1) incorporating the Adler-Adler resonance region description and methods for obtaining model parameters from measured data, (2) developing methods to permit operation from remote graphic terminals, and (3) developing methods to produce hard-copy images of the cathode-ray tube displays. Future development includes the interfacing of SCORE with the SCISRS II experimental data files, and the incorporation of a module to perform both optical-model and compound-nucleus calculations to aid in nuclear cross-section data evaluation above the resonance region. (10 references) (auth)

Nuclear Properties and Reactions, A≤ 5

Refer also to abstracts 14573, 14591, 14746, 14891, and 14927.

14880 (COO-1764-105) STUDY OF N + α SYSTEM WITH THE RESONATING-GROUP METHOD. Reichstein, I.; Tang, Y. C. (Minnesota Univ., Minneapolis. School of Physics). [nd]. 41p. Dep. NTIS.

The n + α and p + α systems are considered with the resonating-group method in the one-channel approximation. The nucleon-nucleon potential used has both a central part and a spin-orbit component. From the results it is found that very good agreement with experiment can be obtained in the energy region below the reaction thresholds. In fact, even above the reaction thresholds where the one-channel approximation is expected to be less valid, the results are quite satisfactory. An effective potential between the clusters is also constructed. From this potential it is determined that the requirement of antisymmetry for the total wave function is very important. In particular, it creates an odd-even feature, wherein the effective central and the effective one-body spin-orbit potentials in the odd-l states are appreciably different from those in the even-l states. (auth)

14881 DIRECT NUMERICAL SOLUTION OF THE SCHROEDINGER EQUATION FOR H^3. Hill, Benny Joe. College Station, Tex.; Texas A and M Univ. (1969). 122p. University Microfilms Order No. 70-11,546.
Thesis.

The importance of the three-nucleon problem to understanding the nucleon-nucleon interaction is discussed. The general formulation of the three-nucleon problem is discussed. A reduction of the problem to a coupled set of two-dimensional equations with hard-core potentials is given. Calculations in the two-dimensional formulation are given showing difficulties with the two-dimensional approach. Alternatives are given for a direct solution of the Schrödinger equation with hard-core potentials including a discussion of the problem in three dimensions. (Diss. Abstr. Int., B)

14882 ELASTIC SCATTERING OF 100 MeV PROTONS FROM ^{3}He AND ^{4}He. Goldstein, N. P.; Held, A.; Stairs, D. G. (McGill Univ., Montreal). Can. J. Phys.; 48: 2629-39(1 Nov 1970).

Elastic scattering of 100 MeV protons by ^{3}He and ^{4}He was measured over a wide range of angles. Analysis of the small-angle results was carried out using a superposition of nucleon-nucleon amplitudes computed with both modern and old phase shifts. No significant differences were found in the accuracy of the predictions resulting from the two sets, but in both cases the ^{3}He results were better than those of ^{4}He. The peaking evident in the backward p-^{4}He scattering but not seen in heavy nuclei was interpreted in terms of an exchange interaction using an optical model analysis. (auth) (Canada)

14883 SECOND-ORDER CORRECTION OF THE PERTURBATION THEORY OF THE VARIATION OF BINDING ENERGY OF ^{3}H AND ^{4}He. Filippov, G. F.; Maksimenko, V. N. (Inst. of Theoretical Physics, Kiev). Ukr. Fiz. Zh.; 15: 1277-83(Aug 1970). (In Russian).

A general expression is found for the second-order correction of the perturbation theory to binding energy of the system of four nucleons determined by the variational method. This expression is used for calculations in the case of concrete variants of the pair potential found in the two-body problem. (auth)

14884 GROUND AND EXCITED STATES OF ^{4}He NUCLEUS. Gogsadze, G. Sh.; Kopaleishvili, T. I. (Tbilissi State Univ., USSR). Yadern. Fiz.; 12: 485-6(Sep 1970). (In Russian).

Higher configurations in calculation of energies of the ground (0^+, T = 0) and of the first excited (0^+, T = 0) states of the ^{4}He nucleus, its mean-square radius and integral cross section of the γ-quanta photoabsorption by this nucleus are taken into account within the translation-invariant shell model. It is shown that the account of several configurations leads to considerable improvement of results obtained in lower approximation. (auth)

14885 GAMMA-RAY YIELDS FROM THE REACTION D(p,γ)^{3}He AT LOW ENERGIES. Bailey, G. M.; Griffiths, G. M.; Olivo, M. A.; Helmer, R. L. (Univ. of British Columbia, Vancouver). Can. J. Phys.; 48: 3059-61(15 Dec 1970).

Total cross sections and measurements of the small isotropic component of the γ-ray yield from the reaction D(p,γ)^{3}He were determined in the energy range from 57 to 1100 keV using gas and deuterated polyethylene targets. The results are compared with some theoretical predictions. (auth) (Canada)

14886 INVESTIGATION OF REACTION ^{4}He(γ,p)^{3}H AT MAXIMAL γ-QUANTA ENERGY 120 MeV. Arkatov, Yu. M.; Vatset, P. I.; Voloshchuk, V. I.; Kirichenko, V. V.; Prokhorets, I. M.; Khodyachikh, A. F. (Physical-Technical Inst., Kharkov). Yadern. Fiz.; 12: 227-33(Aug 1970). (In Russian).

The reaction ^{4}He(γ,p)^{3}H was investigated by means of the diffusion chamber exposed to the photon beam from a 300-MeV electron linear accelerator. More than 10 thousand events were analyzed. Dependence of the reaction total cross section on the γ-quanta energy and the proton angular distributions in 14 energy regions were obtained. From analysis of the angular distributions the following quantities are obtained: asymmetry coefficient, total cross section of electrical quadrupole absorption of photons, and phase of interference between E1 and E2 absorptions as function of the γ-quanta energy. Four peaks beyond the triple standard error at energies 25, 26.5, 28.7, and 31 MeV are observed in the total cross section, plotted with 0.2-MeV energy step. (auth)

14887 DETERMINATION OF THE NEUTRON–NEUTRON SCATTERING LENGTH FROM A KINEMATICALLY COMPLETE EXPERIMENT ON THE REACTION $^2H(n,2n)H$. Zeitnitz, B.; Maschuw, R.; Suhr, P. (Univ., Hamburg). Nucl. Phys.; A149: 449-62(1970).

The coincident neutron spectra from the reaction $^2H(n,2n)H$ at $E_n = 18.5$ MeV ($\theta_1 = 24.2°$, $\theta_2 = 31.2°$) were measured with a double time-of-flight spectrometer. The data were analyzed in the Watson–Migdal approximation, using a Monte Carlo technique. The results give $a_{nn} = -16.4^{+2.6}_{-2.8}$ fm for the $^1S_0$ neutron–neutron scattering length. (auth)

14888 POLARIZATION AND SPIN-CORRELATION PARAMETERS IN PROTON-^{3}He ELASTIC SCATTERING AT 19.4 MeV. Baker, S. D.; Cahill, T. A.; Catillon, P.; Durand, J.; Garreta, D. (CEN de Saclay, Gif-sur-Yvette, France). Nucl. Phys.; A160: 428-36(1971).

Using a polarized proton beam and a polarized ^{3}He target, measurements of proton polarization, ^{3}He polarization, and the spin correlation parameters A_{yy} and A_{xx} in p-^{3}He elastic scattering at 19.4 MeV were obtained in a range of laboratory scattering angles from 38° to 115°. A phase-shift analysis, which is consistent with analyses at lower energies, is presented. (auth)

Nuclear Properties and Reactions, $6 \leq A \leq 19$

Refer also to abstracts 14527, 14528, 14573, 14591, 14602, 14845, 14916, 14920, 14982, 14983, 15103, 15163, and 15184.

14889 (CEA-CONF–1650) MEASUREMENTS OF THE DEPOLARIZATION PARAMETER D FOR ELASTIC PROTON SCATTERING. Beurtey, R.; Catillon, P.; Schnabel, P. (Commissariat a l'Energie Atomique, Saclay (France). Centre d'Etudes Nucleaires). 1970. 2p. (CONF-700811–4). Dep. NTIS (U. S. Sales Only).

From 3rd International Symposium on Polarization Phenomena in Nuclear Reactions, Madison, Wis.

An investigation was made of the conditions for which the depolarization parameter (D) is significantly different from unity, even when the spin-flip contribution is small. Measurements were made at scattering angles corresponding to the minima of the elastic-scattering cross-section, σ_{sf}/σ_{nsf} being relatively large. (σ_{sf} = cross section with spin-flip, σ_{nsf} = cross section without spin flip.) The beam of polarized protons was scattered by a target with a nonzero spin. D was measured for $^{27}Al(I = 5/2)$, $^{10}B(I = 3)$ and $^9Be(I = 3/2)$; the results are 0.964 ± 0.021, 0.926 ± 0.011 and 0.940 ± 0.016, respectively. Another measurement on ^{28}Si (I = 0) at 18.0 MeV gave a value of D = 1.027 ± 0.025, consistent with the theoretical value of unity. (France)

14890 (CEA-CONF–1651) MEASUREMENT AND MICROSCOPIC CALCULATIONS OF THE CROSS SECTIONS AND ASYMMETRIES FOR THE (p,p′) REACTION EXCITING THE 2.31-MeV (0^+, T = 1) STATE OF ^{14}N. Escudie, J-L.; Tarrats, A.; Raynal, J. (Commissariat a l'Energie Atomique, Saclay (France). Centre d'Etudes Nucleaires). 1970. 2p. (CONF-700811–6). Dep. NTIS (U. S. Sales Only).

From 3rd International Symposium on Polarization Phenomena in Nuclear Reactions, Madison, Wis.

Experimental evidence was obtained of nonresonant contributions to the $^{14}N(p,p')$ reaction at 24 MeV. Good fits could not be simultaneously obtained for both asymmetries and cross sections. A tensor force was found to be necessary to fit the cross section data. Experimental knowledge about the asymmetries removed important ambiguities in the nature of the force used and indicated the necessity of a spin–orbit term. The introduction of a nonscalar interaction necessitated the revision of the mixing generally chosen for the scalar potential. (France)

14891 (ORO–1316-97) INTERFERENCE AND RESCATTERING EFFECTS IN REACTIONS WITH THREE PARTICLES IN THE FINAL STATE. Valkovic, V.; Joseph C.; Niiler, A.; Phillips, G. C. Translated for Rice Univ., Houston, Tex., from Izv. Akad. Nauk SSSR, Ser. Fiz.; 32: 1976-89 1968). 13p. (CONF-680122–1). Dep. NTIS.

From 18th Annual Conference on Nuclear Structure and Spectroscopy, Riga, USSR.

The rescattering effect in reactions with three particles in the final state is discussed. The kinematic conditions for the observation of the contribution from the rescattering effect are given. Some experimental results are shown for the reactions $d + d \rightarrow n + p + d$ at 11 MeV and $^3He + {}^9Be \rightarrow 3\alpha$ at $E_{^3He} = 6.0$ MeV. Detailed experimental results of the $d + {}^7Li \rightarrow n + \alpha + \alpha$ reaction at deuteron bombarding energies $E_d = 3.0$, 3.2, and 5.9 MeV are presented. The experimental conditions were chosen in such a way that the neutron–alpha-particle rescattering after the decay of the $^8Be^*$ (16.63- and 16.9-MeV states) and the $^5He^*$ (16.70-MeV state) could be observed. An upper limit of ≤1% was established for the ratio of the neutron–alpha-particle rescattering contribution through an intermediate $^8Be^*$ or $^5He^*$ state to the sequential-decay contribution through that state. This rescattering effect is so small that it cannot be confused with any "new" resonance levels. (R.W.R.)

14892 (RLO–1388-600) FURTHER CALCULATIONS OF PROTON INELASTIC POLARIZATIONS AND ASYMMETRIES USING A SPIN-DEPENDENT INTERACTION OF THE FULL THOMAS FORM. Blair, J. S.; Sherif, H. (Alberta Univ., Edmonton. Nuclear Research Centre). Sep 1970. 9p. (CONF-700811–5). Dep. NTIS.

From 3rd International Symposium on Polarization Phenomena in Nuclear Reactions, Madison, Wis.

DWBA calculations in which the spin-dependent part of a collective interaction has the full Thomas form are extended to include new data. Calculated polarizations out to 45° are displayed for inelastic scattering of 155-MeV protons exciting the 2.62-MeV level of ^{208}Pb. These data suggest that the ratio of spin–orbit to real central deformation lengths should be slightly less than 1.0; however, scattering from ^{28}Si and ^{40}Ca indicates a ratio greater than 1.0. It is shown that, if the interaction Hamiltonian can be described in terms of collective coordinates only and if the inelastic amplitudes are computed in DWBA with only one multipolarity of angular-momentum transfer being predominant, then the inelastic relative cross sections, asymmetries, and polarizations from a nucleus with $J \neq 0$ are the same as those calculated for a hypothetical zero-spin nucleus with some optical and kinematic parameters. Calculated polarizations are given for inelastic scattering of 155-MeV protons from ^{11}B; and asymmetries, for scattering of 30.3-MeV protons from the same nucleus. (R.W.R.)

14893 ABSORPTION OF π MESONS AND α-CLUSTER STRUCTURE OF LIGHT NUCLEI. Kopaleishvili, T. I.; Machabeli, I. Z. (Tbilisi State Univ., USSR). Yadern. Fiz.; 12: 525-30(Sep 1970). (In Russian).

The reaction (π^-, 2nd) on ^{16}O, ^{14}N, and ^{12}C is studied assuming that the reaction proceeds with absorption of the π mesons by an (n,p) pair in an α cluster. The problem of what information on the cluster structure of the nucleus may by obtained and which features of the reactions are more suitable for the analysis is studied. It is shown that the angular correlation of the deuteron momentum and the total momentum of two neutrons depends essentially on "isolation" of the cluster. The spectrum of the deuterons depends less on this, and the spectrum of the residual nuclei is not sensitive to the "isolation." (auth)

14894 DOUBLE SCATTERING OF ^{3}He PARTICLES BY CARBON AND ALUMINUM. Burcham, W. E. (Univ. of Birmingham, Eng.); England, J. B. A.; Harris, R. G.; Evans, J. E. Acta Phys. Pol.; A38: 521-36(Nov 1970).

Experiments on the double scattering of ^{3}He particles of energy near 30 MeV by carbon and aluminium targets are described. Observed polarizations are less than 0.1 in the center of mass angular range 28–35° in the most reliable experiments. Implications for the spin-orbit potential in ^{3}He-nucleus scattering are discussed. (auth)

14895 INTEGRAL CROSS SECTIONS OF THE REACTION $^{11}B(n,\alpha)^8Li(\beta)^8Be^*(2\alpha)$. Scobel, W.; Bormann, M. (Univ., Hamburg). Z. Naturforsch.; 25a: 1406-10(Oct 1970). (In German).

The excitation function of the reaction $^{11}B(n,\alpha)^8Li(\beta)^8Be^*(2\alpha)$ was measured for neutrons with energies between 15.5 and 19 MeV. The reaction was identified by the α-decay of the $^8Be^*$ occurring with the lifetime of the residual nucleus ^{8}Li. The detector for the α-particles was a gridded ionization chamber. (auth)

14896 ANGULAR DISTRIBUTIONS OF DE-EXCITATION γ-RAYS IN ^{15}N AND ^{15}O PRODUCED FROM PARTICLE DECAYS

XUM

OF THE ^{16}O GIANT RESONANCE. Horowitz, Y. S.; McConnell, D. B.; Ssengabi, J.; Keller, N. (Univ. of Toronto). Nucl. Phys.; A151: 161-81(1970).

Angular distribution measurements were carried out on γ rays from ^{15}N and ^{15}O following the photodisintegration of ^{16}O. A bremsstrahlung spectrum with 27 MeV endpoint was used, and measurements were taken at three angles, 90, 120, and 150°. Values of the anisotropy coefficients a_2/a_0 were obtained for transitions through the states at 6.323, 5.299, and 5.270 MeV of ^{15}N, and the 6.180 MeV state of ^{15}O. The results for transitions to the 6.323 MeV state of ^{15}N and the 6.180 MeV state of ^{15}O produced revised values of the branching ratios to these states, and brought them into agreement with the estimates of Buck and Hill. (auth)

14897 PION CAPTURE ON ^{12}C WITH EMISSION NEUTRON PAIRS. Cheshire, David Lynn. Charlottesville, Va.; Univ. of Virginia (1969). 67p. University Microfilms Order No. 70-8094.

Thesis.

The energy spectra of neutron pairs from the $^{12}C(\pi^-,2n)^{10}B$ reaction have been measured. The ^{10}B excitation energy spectrum yields approximate energies for the residual two-hole states. Single neutron energy spectra for fixed excitation energies are used to test the theoretical treatment of the final state interaction. The data disagree with the theory for pion capture from 2P atomic states but agree well for capture from 1S atomic states. (Diss. Abstr. Int., B)

14898 FAST-NEUTRON INTERACTIONS WITH 1p, 2s, 1d NUCLEI. Roturier, Jacques (Faculte des Sciences, Bordeaux). Ann. Phys. (Paris); 4: 289-326(May-Jun 1969). (In French).

Thesis.

At the beginning of this study it was planned to evaluate the direct interaction mechanism and the mechanism of the compound nucleus at the time of the interaction of fast neutrons with light nuclei. The major effort has been directed toward reactions leading to the emission of neutral particles: neutrons and photons. Elastic scattering, inelastic scattering, and neutron radiative capture were studied particularly. A method based on the use of a rapid nuclear electronic technique was used. A time-of-flight spectrometer was developed in which the time resolution appears to have attained the theoretical limit. The elastic scattering of neutrons by beryllium, aluminum and silicon, potassium and calcium was analyzed by comparing the experimental results with the predictions from a nonlocal optical model proposed by Perey and Buck. Very good agreement was obtained in the case of the following reactions: $^{27}Al(n,n)^{27}Al$ and $^{28}Si(n,n)^{28}Si$. On the other hand, in the case of the $^{9}Be(n,n)^{9}Be$ reaction it was necessary, in order to improve the agreement between the experimental results, to interpose the contribution of an isotropic term, the origin of which is related either to the disintegration of the compound nucleus or to the formation of a "doorway" state. The agreement is not very satisfactory for the reactions $^{39}K(n,n)^{39}K$ and $^{40}Ca(n,n)^{40}Ca$. The studies of elastic scattering made by other investigators with different incident particles were confirmed. For these nuclei it appears that the optical model cannot be used unless account is taken of their structure. The introduction of deformations into the calculation analogous to that proposed by Taro Tamura would perhaps improve the agreement. In the case of inelastic scattering, two types of experiments were carried out. Neutron angular distributions were measured for the reactions $^{9}Be(n,n')^{9}Be$ ($Q = -2.43$ MeV) and $^{12}C(n,n')^{12}C$ ($Q = -4.43$ MeV), and they were compared with the theories of direct interaction based either on the DWBA method or on the method called "coupled channel approximation" proposed by Taro Tamura. Satisfactory agreement was obtained. Photons were also detected from deexcitation of levels obtained from inelastic scattering. It was shown that in more than one line spectrum there was observed a quasicontinuous gamma spectrum, the origin of which is probably dependent on the formation of a compound nucleus. The variation of the effective formation cross section of the compound nucleus was evaluated by comparison between the effective cross sections $\sigma_{n,n'}$ and $\sigma_{n,n'\gamma}$ for ^{24}Mg, ^{28}Si, or even by measuring the surface of the quasicontinuous gamma spectrum. This effective cross section varies in the 1d−2s levels; zero at the beginning of the 1d $^5/_2$ level, it passes through a maximum for $A \sim 28$ and decreases near the end of the 1d $^3/_2$ level. Such a variation reproduces fairly well the effects of levels observed by A. Chatterjee in the reactions (n,p) and (n,α). Finally, radiative capture was studied since the interest in it was increased by the intervention of a mechanism of semidirect capture. The gamma spectra resulting from radiative capture and having an energy in the approximate range 15 to 25 MeV were measured. The quantity $\int_{15\,MeV}^{25\,MeV}(d\sigma/dE_\gamma)dE$ was evaluated and compared with the effective cross section $\sigma_{n,n'}$ measured for others with an activation method. It was shown that for ^{9}Be and ^{12}C the effective radiative cross section is very small and of the order of magnitude that could be estimated by direct capture. For ^{23}Na, ^{28}Si, and ^{39}K the quantity $\int_{15\,MeV}^{25\,MeV}(d\sigma/dE_\gamma)$ is less than $\sigma_{n\gamma}$ measured by activation, whereas for ^{55}Mn these two quantities are practically equal. In addition, the effective radiation capture cross section with compound nucleus formation which produces very few high-energy photons becomes less and less probable, and it is a mechanism of semidirect capture that comes into play. (tr-auth)

14899 HELIUM-3 INELASTIC SCATTERING FROM SEVERAL LIGHT NUCLEI. Barengoltz, Jack Bennet. Urbana, Ill.; Univ. of Illinois (1970). 168p. University Microfilms Order No. 70-20,919.

Thesis.

^{9}Be, ^{10}B, ^{11}B, ^{12}C, ^{24}Mg, ^{25}Mg, ^{26}Mg, and ^{27}Al targets were employed to scatter a 20.5 MeV ^{3}He beam from the University of Illinois cyclotron. ^{3}He energy spectra were obtained through the use of solid state detectors in a $\Delta E-E$ telescope. Data were taken at laboratory angles of 15° to 115°, in 5° intervals, and also in 2.5° intervals in some cases. Angular distributions were derived for prominent levels corresponding to excitation energies up to 3.03 MeV for ^{9}Be, 6.03 MeV for ^{10}B, 8.57 MeV for ^{11}B, 9.64 MeV for ^{12}C, 8.44 MeV for ^{24}Mg, 3.41 MeV for ^{25}Mg, 7.32 MeV for ^{26}Mg, and 4.81 MeV for ^{27}Al. A DWBA analysis with the computer code JULIE was accomplished, and the collective model deformation parameters have been extracted. The experimental results are discussed in terms of the collective model of nuclear excitation. (Diss. Abstr. Int., B)

14900 STUDY OF CORE EXCITED STATES IN ^{17}O. Hirata, Michihiro (Tokyo Inst. of Tech.). Progr. Theor. Phys. (Kyoto); 43: 1526-38(Jun 1970).

The low-lying negative-parity states in ^{17}O are studied within the 1-hole−2-particle and 3-hole−4-particle configurations, the total angular momenta being restricted to $^1/_2$, $^3/_2$, and $^5/_2$. It is shown from energy spectra, the spectroscopic factor due to the reaction $^{18}O(p,d)^{17}O$, and the β transitions that the negative-parity states below 6 MeV are described mainly with 1-hole−2-particle configurations and that the states due to 3-hole−4-particle configurations may appear near 7 MeV. (auth)

14901 REACTION $^{12}C(d,\alpha)^{10}B$: REACTION MECHANISM AND CLUSTER STRUCTURE. Yang, Tien-fang. Ann Arbor, Mich.; Univ. of Michigan (1969). 132p. University Microfilms Order No. 70-14,689.

Thesis.

Angular distributions were measured from 15 to 165° for transitions to five low-lying $T = 0$ states in ^{10}B at $E_d = 21.2$, 25.0, and 28.9 MeV. Excitation functions were measured at 15 and 165° for all transitions from about 21 to 29 MeV. The angular distributions show diffraction-like patterns, and some exhibit pronounced backward peaks. The excitation functions show a smooth variation with energy, and the overall features of the angular distributions are preserved. Therefore the reaction mechanism was assumed to be predominantly direct. A DWBA analysis was carried out in which the total transition amplitude was taken as a coherent sum of a direct and an exchange amplitude. It was found that the "heavy-particle-stripping" part of the exchange process and its interference with the direct pick-up process is very important in reproducing the experimental angular distributions. Spectroscopic amplitudes were extracted from the DWBA analysis and compared with cluster model predictions calculated from a shell model basis. (Diss. Abstr. Int. B)

14902 STUDY OF THE (p,pα) AND (α,2α) REACTIONS IN ^{6}Li AND ^{7}Li AT 60 MeV. Jain, Mahavir. College Park, Md.; Univ. of Maryland (1969). 134p. University Microfilms Order No. 70-15, 374.

Thesis.

An investigation of the important reaction mechanisms, especially the contribution of the quasi-free cluster knockout-mechanism, at medium energies was undertaken. For this purpose both the (p,pα) and (α,2α) reactions on ^{6}Li and ^{7}Li were studied at about 60 MeV. The energy and angular correlations were obtained by measuring the energies of the two outgoing particles in coincidence. At the angles studied for various reactions, it is found that the quasi-free scattering reaction mechanism is more important than the sequential or two-step processes. The contribution due to the quasi-instantaneous break up, which is proportional to phase space, is estimated to be less than 5%. The analysis of the knock-out reactions was performed within the framework of the impulse approximation. The theoretical momentum distributions were derived from the cluster model wave function for ^{6}Li. For ^{7}Li an analytical expression for $l = 1$ was used. The impulse approximation for the cluster knock-out reaction seems to be fairly good for the (p,pα) reactions. For the (α,2α) reactions the effects of the off-energy-shell matrix element and multiple scattering are found to be significant. This makes the interpretation of the results obtained using this picture rather dubious for $(\alpha,2\alpha)$ reactions (especially ${}^{7}Li(\alpha,2\alpha){}^{3}H$ reactions). (Diss. Abstr. Int., B)

14903 REACTION ${}^{9}Be({}^{3}He,\alpha\alpha){}^{4}He$. Ehlers, David Henry. Pullman, Wash.; Washington State Univ. (1970). 67p. University Microfilms Order No. 70-16,803.

Thesis.

Coincidence spectra of α particles from the reaction ${}^{9}Be({}^{3}He,\alpha\alpha){}^{4}He$ were measured for several angular configurations at a bombarding energy of 1.55 MeV. The spectra suggest that the final state is formed primarily by sequential processes involving intermediate states of ${}^{8}Be$. Excitation functions at 140° laboratory angle were measured for the reactions ${}^{9}Be({}^{3}He,\alpha_0){}^{8}Be$(g.s.) and ${}^{9}Be({}^{3}He,\alpha_1){}^{8}Be$(2.9) between 1.0 and 1.9 MeV and showed no resonant behavior. Angular correlations of reactions proceeding through the unresolved 16.63- and 16.94-MeV states of ${}^{8}Be$ and through the first excited state of ${}^{8}Be$ were measured. The measured angular correlations were found to be inconsistent with theoretical predictions based on resonance formation of a compound-nuclear state, and with predictions based on an initial direct reaction. An initial reaction mechanism which includes both direct and compound nucleus modes is suggested by the data. An approximate treatment of the Coulomb interaction between the final-state particles indicates that the effect on the correlation due to this interaction is more pronounced than it is usually assumed to be. (Diss. Abstr. Int., B)

14904 STUDY OF REACTIONS ${}^{11}B({}^{3}He,p){}^{13}C$ AND ${}^{20}Ne({}^{3}He,p){}^{22}Na$ AT ≤ 3 MeV. Meynadier, C.; Allard, J. F.; Amiel, M.; (and others) (Institut d'Etudes Nucleaires, Algiers). Nucl. Phys.; A161: 305-20(1971). (In French).

Using a gas target with differential pumping, absolute differential cross sections were measured for 10 proton groups from the ${}^{20}Ne({}^{3}He,p){}^{22}Na$ reaction at 2.8 and 3 MeV and for 13 proton groups from the ${}^{11}B({}^{3}He,p){}^{13}C$ reaction at 3 MeV. Angular distributions of most groups were analyzed successfully by Hauser–Feshbach theory. The angular distribution of the ${}^{20}Ne({}^{3}He,p){}^{22}Na(E_{ex} = 3.944$ MeV) reaction was analyzed by double stripping DWBA, which gives 1^+ for this level. (auth)

14905 LIFETIMES AND GAMMA TRANSITIONS IN ${}^{19}O$. **Broude, C.; Karfunkel, U.; Wolfson, Y. (Weizmann Inst. of Science, Rehovot, Israel). Nucl. Phys.; A161: 241-51(1971).**

Gamma transitions were observed in ${}^{19}O$ and energies and branching ratios determined, following the ${}^{2}H({}^{18}O,p\gamma){}^{19}O$, and ${}^{3}H({}^{17}O,p\gamma){}^{19}O$ reactions. The lifetime of the 1470 keV second excited state in ${}^{19}O$ was measured from the Doppler line shape of its decay radiation to be 1.80 ± 0.29 ps, that of the 2774 keV state to be 70 ± 26 fs; a lower limit of 1.0 ps was set on the lifetimes of the 2367, 3066, and 3150 keV states. The lifetime of the ${}^{19}O$ 1470 keV level is in good agreement with the shell model, while that for the ${}^{19}O$ 2774 keV level is not consistent with ${}^{9}\!/_{2}{}^{+}$ usually assigned to it. (auth)

14906 DEUTERON STRIPPING AT 1.69 GeV/c. I. PROTON DISTRIBUTIONS. **Jafar, J. D.; Van Der Raay, H. B.; Ryan, D. G.; Stiegelmair, J. A.; Tandon, R. K. (Univ. of Birmingham, Eng.). Nucl. Phys.; A161: 105-22(1971).**

The angular distributions of stripped protons from the interaction of 1.69 GeV/c deuterons with various complex nuclei were measured. These angular distributions can be well fitted by compounding the incident nucleon momentum with its internal momentum in the deuteron. The observed momentum distribution may be similarly explained. However the absolute values of the cross sections are not in agreement with those predicted by the available theories. (auth)

14907 p–n CORRELATIONS IN THE ${}^{13}C(p,pn){}^{12}C$ REACTION. Otte, Victor Arthur. Houston, Tex.; Rice Univ. (1970). 122p. University Microfilms Order No. 70-23,562.

Thesis.

The three-body reaction ${}^{13}C(p,pn){}^{12}C$ was studied experimentally in a kinematically complete experiment. The p-n coincidence events were measured using associated time-of-flight techniques and a pulse shape discrimination system. Only in the region of 12.5-MeV bombarding energy is there an indication of sequential decay via singlet deuteron formation. Higher energies were not attainable with the available equipment and at lower energies sequential decays through levels in ${}^{13}C^*$ and ${}^{13}N^*$ were relatively strong and obstructed possible observation of the singlet deuteron. An upper limit, order of magnitude value is assigned to the (p,d^*) cross section. (Diss. Abstr. Int., B)

14908 π-CARBON ELASTIC SCATTERING NEAR THE 33 RESONANCE. Sternheim, Morton M. (Univ. of Massachusetts, Amherst); Auerbach, Elliott H. Phys. Rev. Lett.; 25: 1500-3 (23 Nov 1970).

Elastic π^--C scattering is calculated with the Kisslinger optical model from 120 to 280 MeV. With parameters obtained from π^--N phase shifts, general qualitative agreement is obtained with the recent Binon et al. data. Modifying the parameters further improves the fit. (auth)

14909 LOW-ENERGY NEUTRON SCATTERING CROSS-SECTION OF ${}^{6}Li$. Asami, A. (Japan Atomic Energy Research Inst., Tokai); Moxon, M. C. pp 153-60 of Nuclear Data for Reactors. Vol. I. Vienna; International Atomic Energy Agency (1970).

From 2nd International Conference on Nuclear Data for Reactors, Helsinki, Finland. See STI/PUB–259(Vol.1); CONF-700605–(Vol.1).

The neutron scattering cross-section of ${}^{6}Li$ was measured in the energy region between 1 keV and 110 keV with a scattering detector on a 50-m flight path of the Harwell Electron Linac neutron time-of-flight spectrometer. The detector consisted of eight ${}^{6}Li$-glass scintillators, and the measurements were made at four angles to the incident beam: 39°, 65°, 120° and 144°. The ${}^{6}Li$ sample had a thickness of 5.88×10^{-2} atoms/b (93.7% ${}^{6}Li$, 5.2% ${}^{7}Li$, and 1.1% others). The sample was canned with a thin aluminium plate of thickness of 1.47×10^{-3} atoms/b, which was sealed with Araldite. The measurements were made relative to a carbon sample with a thickness of 2.06×10^{-2} atoms/b. The data were analysed mainly with the IBM 7044 at JAERI. In the analysis corrections for the effects of the following were made: (1) self-absorption in the sample before and after primary scattering (assuming neutrons are lost by any further interaction after primary scattering, and this may be called the first-order multiple scattering; (2) multiple scattering (only for the twice-scattered neutrons in the sample, e.g. the second-order multiple scattering); (3) the sample impurities; (4) the sample can; (5) difference in attenuation caused by an aluminium neutron-beam tube between the neutrons scattered by the ${}^{6}Li$ and the carbon samples (above 40 keV); and (6) the energy dependence of the detector efficiency. Thus the differential scattering cross-section was obtained, which showed no significant angular dependence in the low-energy region below 10 keV. The angular distributions of the scattered neutrons were analysed in terms of the scattering lengths a_+ and a_- for the channel spin $3/2$ and $1/2$, respectively, and the resonance parameters of the 250-keV level in ${}^{6}Li(n,\alpha)$ cross-section from the 1/v law was obtained. (9 references) (auth)

14910 MEASUREMENT OF THE RATIO OF THE ${}^{6}Li(n,\alpha)$ AND ${}^{10}B(n,\alpha)$ CROSS-SECTIONS FROM 10 eV TO 80 keV AND RECOMMENDED VALUES OF THE CROSS-SECTIONS UP TO 200 keV. Sowerby, M. G.; Patrick, B. H.; Uttley, C. A.; Diment, K. M. (Atomic Energy Research Establishment, Harwell, Eng.). pp 161-73 of Nuclear Data for Reactors. Vol. I. Vienna; International Atomic Energy Agency (1970).

From 2nd International Conference on Nuclear Data for Reactors, Helsinki, Finland. See STI/PUB–259(Vol. 1); CONF-700605-(Vol. 1).

Measurements of the neutron spectrum produced by the Harwell 45 MeV Linear Accelerator were made, using time-of-flight techniques, with detectors based upon the ${}^{6}Li(n,\alpha)$ and ${}^{10}B(n,\alpha)$ reactions. A 2-inch-diameter ${}^{10}BF_3$ counter, a "boron-plug" detector with 0.003547 ${}^{10}B$ atoms/barn and a $1/8$-inch-thick ${}^{6}Li$ glass scintillator were used in the experiments, and their relative efficiencies as a function of neutron energy were calculated by Monte-Carlo methods. Since these detectors were "thin" $(n\sigma < 0.3)$ the multiple-scattering corrections were small and almost energy-independent, and hence the experimental data were used to obtain the ratio of the ${}^{6}Li(n,\alpha)$ to ${}^{10}B(n,\alpha)$ cross-sections in the energy range 10 eV to 80 keV. The ratio was normalized at 10 eV to a value of 0.245. The absorption cross-section of ${}^{6}Li$ was obtained from total and scattering cross-section data. By combining these values with the data from the ratio measurement, the ${}^{10}B(n,\alpha)$ cross-section was deduced with estimated errors ranging from 2-3%. The results are compared with other measurements, and there is very good agreement over the entire energy range. The data are all consistent with the ${}^{10}B(n,\alpha)$ cross-section falling below the $1/\sqrt{E}$ level, reaching a minimum at ~25 keV, where the deviation is about 4%. Above this energy the cross-section relative to the $1/\sqrt{E}$ level, rises and passes through a resonance at ~170 keV. The complete set of data was fitted by an analytic expression which includes the first three terms of the Shapiro expansion describing the low-energy dependence of such cross-sections together with an s-wave resonance at 170 keV. A least-squares fitting procedure was used with five free parameters, two of which are the energy and total width of the resonance. An expression for the ${}^{10}B(n,\alpha)$ cross-section up to 200 keV is given. The expression has an estimated accuracy ranging from ~1.5% at low energies to ~3% at the high-energy end. (29 references) (auth)

XUM

14911 MEASUREMENTS OF NEUTRON ELASTIC SCATTERING FROM CARBON IN THE ENERGY REGION OF 0.50 TO 2.00 MeV. Ahmed, N.; Coppola, M.; Knitter, H.-H. (EURATOM, Geel, Belg.). pp 177-89 of Nuclear Data for Reactors. Vol. I. Vienna; International Atomic Energy Agency (1970).

From 2nd International Conference on Nuclear Data for Reactors, Helsinki, Finland. See STI/PUB–259(Vol.1); CONF-700605–(Vol.1).

Thirty-one differential cross-section angular distributions for the elastic scattering of neutrons from carbon were measured at primary neutron energies between 0.50 and 2.00 MeV, using fast neutron time-of-flight techniques. The fully corrected points of each angular distribution were fitted with a five-term Legendre-polynomial expansion. The obtained B_L-coefficients were then fitted with suited functions of the energy in order to obtain a smooth dependence of the differential neutron-scattering cross-sections on the primary neutron energy using a limited number of parameters. A phase-shift analysis based on the present experimental B_L-coefficients was performed. The obtained phase shifts are compared with the ones predicted by a coupled-channel calculation of ^{12}C-neutron scattering and with phase shifts resulting from neutron-polarization measurements. (23 references) (auth)

14912 ANALYSIS OF THE TOTAL CROSS-SECTION OF CARBON FROM 70 eV TO 1.5 MeV. Uttley, C. A.; Diment, K. M. (Atomic Energy Research Establishment, Harwell, Eng.). pp 191-6 of Nuclear Data for Reactors. Vol. I. Vienna; International Atomic Energy Agency (1970).

From 2nd International Conference on Nuclear Data for Reactors, Helsinki, Finland. See STI/PUB–259(Vol.1); CONF-700605–(Vol.1).

The total cross-section of reactor grade graphite was measured from 0.07 keV to several MeV using the 120 m and 300 m flight paths on the Harwell 45 MeV Electron Linac. The data up to 1500 keV are well fitted with the following polynomial in energy (E in MeV): (1) $\sigma_{nT} = 4.744 - 3.707E + 2.389E^2 - 1.11E^3 + 0.242E^4$. The effective range expansion can be applied to the carbon cross-section by expressing $\sigma_{nT}(E)$ in terms of k cot δ_0, where $k(= k_0\sqrt{E})$ is the (c.m.) wave number and δ_0 is the s-wave phase shift. From effective range theory: (2) $k \cot \delta_0 = -1/a + r_0k^2/2 - P_0r_0^3k^4$; where a is the scattering length, r_0 is the effective range of the nuclear potential and P_0 is a potential shape factor. Application of Eq.(2) enables the s-wave scattering cross-section to be expressed as a polynomial in energy and by equating the coefficients of E^0 and E^1 with those in Equation (1) the scattering length and the effective range are found to be 6.14 fm and 3.06 fm, respectively. The coefficient of E^2 is determined by the value and sign of the shape factor P in addition to a and r_0 and furthermore p-wave scattering contributes a term α E^2. Assuming p-wave scattering to be negligible a value of $P = -0.071$ is obtained which is rather larger than the value (−0.033) expected for a sharply cut-off square well. If, however, $P = 0$ and p-wave scattering is interpreted as hard sphere scattering with radius R viz. $12\pi k^{-2} \sin^2 \delta_1$ with $\delta_2 = -k^3R^3/3$ a value of $R = 3.76$ fm is obtained corresponding to a p-wave cross-section of 0.2 barns at 1 MeV. Since P can be slightly positive for a well with a tail it is concluded that a significant p-wave interaction is present in the cross-section. A least-squares fit to the total cross-section was obtained after subtracting the above p-wave contribution, in terms of an s-wave potential scattering and the parameters of the $\frac{1}{2}^+$ state at −1.86 MeV (c.m.) in ^{13}C which yields a radius of 4.84 fm and a reduced neutron width of 0.51 MeV (c.m.). (auth)

14913 CROSS-SECTION OF THE $^6Li(n,\alpha)T$ REACTION IN THE 100 TO 500 keV ENERGY RANGE. Fort, E. (Centre d'Etudes Nucleaires, Cadarache, France). pp 253-62 of Nuclear Data for Reactors. Vol. I. Vienna; International Atomic Energy Agency (1970). (In French).

From 2nd International Conference on Nuclear Data for Reactors, Helsinki, Finland. See STI/PUB–259(Vol. 1); CONF-700605–(Vol. 1).

The cross-section for the $^6Li(n,\alpha)T$ reaction was determined from the efficiency of a ^6Li glass scintillator measured by a coincidence-version associated particle method, for which a description is given. The number of ^6Li atoms contained in the scintillator was determined by two methods of nuclear analysis: (a) By comparison with a glass whose ^6Li-content was calculated on the basis of a measurement of total absorption of thermal neutrons made in the ZOE reactor by the phase oscillation method; (b) a transmission method. In both cases it was assumed that the cross-section for the reaction at 2200 m/s was known. The multiple diffusion of the neutrons in the special case of the experiment was determined by a Monte-Carlo calculation. (12 references) (auth)

14914 STUDY OF STATES IN ^{16}O BY THE REACTIONS $^{17}O(\tau,\alpha)^{16}O$ AND $^{15}N(\tau,d)^{16}O$. Bohne, W.; Homeyer, H.; Lettau, H.; (and others) (Hahn–Meitner-Institut fuer Kernforschung, Berlin). Nucl. Phys.; A160: 257-73 (1971).

Spectroscopic factors were determined for 15 states in ^{16}O in the reaction $^{17}O(\tau,\alpha)$, and redetermined for 4 states in the reaction $^{15}N(\tau,d)$. From the DWBA fits to the measured angular distributions information on the transferred total spin could be deduced. The results are compared with predictions from the recent shell-model calculations of Zuker, Buck and McGrory and of older work of Gillet and Vinh–Mau. Good agreement is found in most cases. (auth)

14915 THE 14.2 AND 14.5 MeV LEVELS OF ^{15}O FORMED VIA ^3He BOMBARDMENT OF ^{12}C. Jackson, R. F.; Weller, H. R. (Univ. of Florida, Gainesville). Nucl. Phys.; A160: 247-56 (1971).

The alpha-particle core-excited threshold state (APCETS) model indicates that the 14.2 and 14.5-MeV levels in ^{15}O are formed by coupling an $L = 1$ alpha particle to the $\frac{1}{2}^-$ first excited state of ^{11}C. Detailed measurements of the cross section as a function of energy and angle for the $^{12}C(^3He, {}^3He)^{12}C$ and the $^{12}C(^3He, \alpha_0)^{11}C$ reactions were obtained for incident ^3He energies of 2.3 to 3.3 MeV. The elastic data were analyzed by means of an optical model plus resonance (OMPR) formulation. A Legendre polynomial analysis was performed on the α_0 data. The results indicate a $\frac{1}{2}^+$ assignment for the level at 14.2 MeV and a $(\frac{3}{2}^+, \frac{5}{2}^+)$ assignment for the 14.5-MeV level. These assignments are in accord with the APCETS model. (auth)

14916 THE $^{48}Ca(d,p)^{49}Ca$ REACTION ACROSS THE COULOMB BARRIER. Roy, G.; Bogaards, J. J. W. (Univ. of Alberta, Edmonton). Nucl. Phys.; A160: 289-304(1971).

Measurements were made on the $^{48}Ca(d, d)^{48}Ca$, $^{48}Ca(d, p_0)^{49}Ca$, and $^{48}Ca(d, p_1)^{49}Ca$ reactions between the energies of 2.5 MeV and 5.5 MeV in order to study the consistency of spectroscopic factors in stripping reactions above and below the Coulomb barrier. Some measurements were also performed with a polarized deuteron beam in order to better fix the optical-model parameters and test the j-dependence of the $^{48}Ca(d, p)^{49}Ca$ reaction. Very good fits to the data and consistent spectroscopic factors over the energy range were obtained provided energy-averaged deuteron optical-model parameters were used. Also, the j-dependence of the $^{48}Ca(d, p)^{49}Ca$ reaction was demonstrated for the ground and first excited states of ^{49}Ca. (auth)

14917 PROPERTIES OF THE LOW-LYING POSITIVE-PARITY STATES IN ^9Be AND ^{13}C. Gruebaum, L.; Tomaselli, M. (Technische Hochschule, Darmstadt, Ger.). Nucl. Phys.; A160: 437-44(1971).

Excitation energies and electromagnetic form factors of the low-lying positive-parity states were calculated in ^9Be and ^{13}C on the basis of a particle-core coupling model. The results are compared with recent electron scattering experiments and photon data. The first excited levels in the two nuclei show a large contribution from the spin term of the electromagnetic interaction at low-momentum transfer $q^2 < 0.6$ fm^{-2}. (auth)

14918 ELASTIC SCATTERING OF HIGH-ENERGY HADRONS FROM DEFORMED ^{12}C NUCLEUS. Lesniak, H.; Lesniak, L. (Inst. of Nuclear Physics, Krakow). Nucl. Phys.; B25: 525-34 (1971).

Elastic scattering of high-energy protons from deformed carbon nuclei is calculated using the multiple collision theory and deformed harmonic-oscillator wave functions. Calculated differential cross sections are compared with the experimental data. Good agreement is found for the oblate deformation. (auth)

Nuclear Properties and Reactions, $20 \leq A \leq 89$

Refer also to abstracts 14845, 14889, 14894, 14898, 14899, 14904, 14906, 14979, 14982, 14983, 15002, 15103, 15136, 15148, 15151, 15176, 15178, and 15196.

14919 (AWRE-O–78/70) $(n,n'\gamma)$ REACTIONS IN ^{51}V AND ^{89}Y. Porter, D.; Coles, R. E.; Gilboy, W. B. (Atomic Weapons Research Establishment, Aldermaston (England)). Oct 1970. 39p. Dep. NTIS (U. S. Sales Only). UK 5s. 6d.

A study of $(n,n'\gamma)$ reactions with ^{51}V and ^{89}Y for incident neutrons in the energy range 0.3 to 4 MeV is described. A 20-cc Ge(Li) spectrometer was used to detect de-excitation γ rays following inelastic scattering from samples in ring geometry. In all, 33 transitions in ^{51}V and 15 in ^{89}Y were observed; and production cross sections for these γ rays, at a mean angle of 100°, were derived as functions of incident neutron energy. Improved decay schemes, branching ratios, and level energies are presented and, where knowledge of these and appropriate γ-ray angular distributions permits, comparisons with the predictions of Hauser–Feshbach theory modified for level width fluctuations are made. Spin assignments of recent work are confirmed, and possible assignments for the other levels observed are discussed. (auth)

14920 (BNL-tr-380) A CONTRIBUTION TO THE STUDY OF THE INTERACTION OF FAST NEUTRONS WITH 1p, 2s, AND 1d NUCLEI. Roturier, Jacques. Translated for Brookhaven National Lab., Upton, N. Y., from Ann. Phys. (Paris); 4: 289-326(1969). 65p. Dep. NTIS.

Elastic scattering of neutrons by beryllium, aluminum, silicon, potassium, and calcium is analyzed; and the experimental results are compared with predictions based on the nonlocal optical model proposed by Perey and Buck. Very good agreement is obtained for the $^{27}Al(n,n)^{27}Al$ and $^{28}Si(n,n)^{28}Si$ reactions. In the case of the $^{9}Be(n,n)^{9}Be$ reaction, however, it is necessary to improve the agreement with the experimental results by invoking the contribution of an isotropic term whose origin involves either disintegration of the compound nucleus or formation of a "doorway" state. For the $^{39}K(n,n)^{39}K$ and $^{40}Ca(n,n)^{40}Ca$ reactions, although the agreement is not particularly satisfactory, the elastic-scattering studies carried out by other authors with various incident particles are confirmed. It appears that the optical model cannot be applied to these nuclei without taking their structure into account. Neutron angular distributions for the $^{9}Be(n,n')^{9}Be$ (Q = –2.43 MeV) and $^{12}C(n,n')^{12}C$ (Q = –4.43 MeV) reactions were measured and compared with the direct-interaction theories based either on the DWBA method or the so-called "coupled-channels approximation." Satisfactory agreement resulted. De-excitation gamma rays from the levels reached in inelastic scattering were also detected. In addition to a line spectrum there appears a quasi-continuous γ spectrum that apparently originates from formation of the compound nucleus. The variation of the effective cross section for compound-nucleus formation was determined by comparison between the effective cross sections $\sigma_{n,n'}$ and $\sigma_{n,n'\gamma}$ for ^{24}Mg, ^{28}Si or by measuring the area of this quasi-continuous γ spectrum. This effective cross section varies in the 1d–2s shells; it is zero at the beginning of the 1d 5/2 shell, passes through a maximum for A ~ 28, and decreases toward the end of the 1d 3/2 shell. This variation reproduces the shell effects observed in the (n,p) and (n,α) reactions quite well. γ spectra emitted on radiative capture with energies in the approximate range from 15 to 25 MeV were measured. The quantity $\int_{15\,MeV}^{25\,MeV}(d\sigma/dE_\gamma)dE_\gamma$ was determined and compared with the effective cross section $\sigma_{n,n'}$ measured by other authors by the activation method. The effective cross section for radiative capture is very small for ^{9}Be and ^{12}C, and of the order of magnitude of the cross section determined by direct capture. For ^{23}Na, ^{28}Si, and ^{39}K the quantity $\int_{15\,MeV}^{25\,MeV}(d\sigma/dE_\gamma)dE_\gamma$ is smaller than the $\sigma_{n\gamma}$ measured by activation, while the two are practically equal for ^{55}Mn. This means that with increasing A the effective cross section for radiative capture with formation of the compound nucleus, which produces very few high-energy photons, becomes less and less probable, and that we are dealing with a semidirect-capture mechanism. (R.W.R.)

14921 (CEA-CONF-1653) j-MIXING DETERMINATION IN (p,d) REACTIONS BY ASYMMETRY MEASUREMENTS. Gosset, J.; Kamitsubo, H.; Mayer, B. (Commissariat a l'Energie Atomique, Saclay (France). Centre d'Etudes Nucleaires). 1970. 2p. (CONF-700811-11). Dep. NTIS (U. S. Sales Only).

From 3rd International Symposium on Polarization Phenomena in Nuclear Reactions, Madison, Wis.

The $^{119}Sn(p,d)^{118}Sn$ reaction was studied at 24.5 MeV. The target spin and the spin in the final state being $1/2^+$ and 2^+, respectively, the l transferred equals 2. Two values are possible for j : j = 3/2 and j = 5/2. The spectroscopic factors $S_{3/2}$ and $S_{5/2}$ were calculated from the equations of the cross section σ and of the asymmetry A, the cross sections $\sigma_{3/2}$ and $\sigma_{5/2}$ and the asymmetries $A_{3/2}$ and $A_{5/2}$ being known. These were determined by using the experimental results from the reaction $^{118}Sn(p,d)^{117}Sn^*$ in which l = 2, j = 3/2 and j = 5/2. The shape of the cross-section angular distributions gave $\sigma_{3/2} \simeq \sigma_{5/2}$. The mean ratio $S_{3/2}/S_{5/2}$ was thus found to be 1.05 ± 0.18, the contributions of the two orbits $d_{3/2}$ and $d_{5/2}$ being nearly equal. The reaction $^{57}Fe(p,d)^{56}Fe^*$ was studied at 17.3 MeV. The target spin and the spin in the final state being $1/2^-$ and 2^+ respectively, the allowed values of l are 1 and 3 and the allowed values of j are 3/2 and 5/2. The spectroscopic factors were calculated with a least-squares χ^2 method and the mixing was determined using only cross section measurements. The reaction $^{61}Ni(p,d)^{60}Ni^*$ was also studied at 16.6 MeV. The target spin is 3/2 and both final spins are 2^+ so that the orbits involved are $p_{3/2}$, $p_{1/2}$, $f_{5/2}$, $f_{7/2}$. The fits between the cross sections and asymmetries and the determined spectroscopic factors are given. (France)

14922 (CEA-CONF-1655) STUDY OF (p,d) REACTIONS ON ^{48}Ca AND ^{49}Ti WITH POLARIZED PROTONS. Escudie, J. L.; Gosset, J.; Kamitsubo, H.; Mayer, B. (Commissariat a l'Energie Atomique, Saclay (France). Centre d'Etudes Nucleaires). 1970. 2p. (CONF-700811-8). Dep. NTIS (U. S. Sales Only).

From 3rd International Symposium on Polarization Phenomena in Nuclear Reactions, Madison, Wis.

The $^{48}Ca(p,d)^{47}Ca$ and $^{49}Ti(p,d)^{48}Ti$ reactions were induced with polarized proton beams at 22.9 MeV and 20.9 MeV, respectively. Cross sections and asymmetries were measured for transitions leading to the ground states of ^{47}Ca and ^{48}Ti and also to the first excited state of ^{48}Ti. The spin and parity of ^{47}Ca were deduced. A spin $7/2^-$ was assigned to ^{47}Ca by comparing the asymmetries for the two reactions $^{49}Ti(p,d)^{48}Ti$ and $^{48}Ca(p,d)^{47}Ca$. In the case of the $^{48}Ca(p,d)^{47}Ca$ reaction the stripping peak is at about 30°, the asymmetry is positive, and the total angular momentum transferred is j = 7/2. DWBA predictions are given for j = 5/2 and j = 7/2. The shape of the cross-section angular distribution is well reproduced, but the DWBA results do not give the correct ratio for the cross section at backward and forward angles. The optical-potential parameters were calculated to fit both cross section and polarization in the proton channel and cross section in the deuteron channel. The cross sections calculated in the DWBA are strongly j-dependent and the experimental results agree better with the j = $5/2^-$ curve than with the j = $7/2^-$ one. However, a good fit can be obtained with j = $7/2^-$ with different optical-potential parameters. Experimental results for the $^{49}Ti(p,d)^{48}Ti$ reaction leading to the first excited state of ^{48}Ti are presented. This latter transition involves a mixing of transferred j. (France)

14923 (CEA-CONF-1656) INELASTIC SCATTERING OF POLARIZED PROTONS BY ^{40}Ca AT 24.5 MeV. Escudie, J. L.; Gosset, J.; Kamitsubo, H.; Mayer, B. (Commissariat a l'Energie Atomique, Saclay (France). Centre d'Etudes Nucleaires). 1970. 2p. (CONF-700811-9). Dep. NTIS (U. S. Sales Only).

From 3rd International Symposium on Polarization Phenomena in Nuclear Reactions, Madison, Wis.

The asymmetry of the inelastic scattering of polarized protons by ^{40}Ca was measured. A beam energy of 24.5 MeV was used to reduce contribution from nondirect reactions. The experimental results and the DWBA macroscopic predictions are given. The calculated asymmetry is fairly sensitive to the optical-potential parameters, which were determined from the simultaneous fitting of both elastic scattering cross section and polarization measurements. Calculation with the full Thomas term gave satisfactory results for the first 3^- state. However, the same calculation gave an inferior fit for the 5^- state and failed completely for the second 3^- state. The microscopic calculation at 20.3 MeV using the wave functions of Gillet and Sanderson showed reasonable agreement for the asymmetry in the 5^- state at 4.48 MeV but not in the 3^- state at 3.73 MeV. These facts suggest that the 3^- state at 3.73 MeV is quasi-collective, contrary to the 5^- state at 4.48 MeV. (France)

14924 (COO-535-625) COMMENTS ON "SHAPES OF ANGULAR DISTRIBUTIONS OF (^3He,t) AND (p,n) TRANSITIONS TO 0^+ ANTI-ANALOG STATES". Rost, E. (Colorado Univ., Boulder. Dept. of Physics and Astrophysics). [1970]. Contract AT(11-1)-535. 9p. Dep. NTIS.

This comment on a recent Physical Review Letter points out that the assumptions used by Noble are not valid for the reaction considered; hence, the anomaly in the angular distributions remains to be explained. (auth)

14925 (MIT-2098-643) PHYSICS PROGRESS REPORT, DECEMBER 31, 1969. (Massachusetts Inst. of Tech., Cambridge. Lab. for Nuclear Science). Contract AT(30-1)-2098. 309p. Dep. NTIS.

Physics research and developments during the calendar year of 1969 at MIT are summarized. Activities are outlined for the cosmic ray group, accelerator physics collaboration, linear accelerator group, high energy accelerator physics group, ONR generator group, radioactivity group, charged particle reaction group, and the theoretical group. Personnel and publications are listed. (W.H.K.)

14926 ROTATION OF THE $\gamma\gamma$ ANGULAR CORRELATION OF THE CASCADES (570–797) keV, (570–797–605) keV AND (797–605) keV OF ^{134}Ba IN AN EXTERNAL MAGNETIC FIELD. Beer, H. (Technische Univ., Berlin). Z. Naturforsch.; 25a: 1513-24(Oct 1970). (In German).

The overall $\gamma\gamma$ angular correlation of the cascades (570–797) keV, (570–797–605) keV and (797–605) keV in ^{134}Ba was per-

XUM

turbed by an external magnetic field of 41.4 kG perpendicular to the directions of observation of the quanta. The rotation of the angular correlation was found to be $\omega\tau = 0.05 \pm 0.03$. This result could be due to the 2^+ 605 keV or the 4^+ 1400 keV energy level or to both levels with measurable portion. The aspects of these alternatives are discussed. (auth)

14927 ISOTOPE SHIFTS BETWEEN EVEN ISOTOPES $^{64\ 66\ 68\ 70}$Zn IN THE VISIBLE Zn II LINES. Les, Z.; Szewczyk, R. (Jagellonian Univ., Krakow). Acta Phys. Pol.; A38: 681-9(Nov 1970).

The isotope shifts between all four even stable isotopes of zinc, i.e. 64, 66, 68 and 70, were measured in three visible Zn II lines. λ 5894.35 Å, λ 6214.59 Å and λ 7478.79 Å corresponding to $3d^{10}4p\ ^2P^0_{1/2,3/2}-3d^9\ 4s^2\ ^2D_{3/2,5/2}$ transitions. Enriched isotopes were used. The light source was a Schüler lamp cooled with liquid nitrogen. A discussion is presented on the relative isotope shifts calculated on the basis of obtained data. The influence of the volume effect on the magnitude of the isotope shift in the Zn II spectrum is considered. (auth)

14928 40-MeV PROTON INELASTIC SCATTERING ON ^{50}Ti, ^{51}V, AND ^{52}Cr AND ITS MICROSCOPIC DESCRIPTION. Preedom, B. M.; Gruhn, C. R.; Kuo, T. Y. T.; Maggiore, C. J. (Michigan State Univ., East Lansing). Phys. Rev., C; 2: 166-86(Jul 1970).

Proton inelastic scattering for ^{50}Ti, ^{51}V, and ^{52}Cr was measured at 40 MeV. Angular distributions were obtained from 10 to 80° for states up to 8 MeV of excitation in ^{50}Ti and ^{52}Cr, and to 4.5 MeV in ^{51}V. The cross sections for exciting the low-lying states that have relatively simple wave functions were analyzed in terms of microscopic model, using realistic nucleon–nucleon forces. Core polarization is shown to be important, and it is seen that a strength obtained from the bound-state matrix elements of Kuo and Brown is adequate to describe the observed scattering. A macroscopic collective-model analysis of the data is also presented. (auth)

14929 NUCLEAR SPINS, NUCLEAR MOMENTS, AND HYPERFINE STRUCTURE OF ^{69}Ge AND ^{75}Ge, AND $^3P_2$ HYPERFINE STRUCTURE OF ^{71}Ge. Oluwole, Abiodun F.; Schmelling, Stephen G.; Shugart, Howard A. (Univ. of California, Berkeley). Contract W-7405-eng-48. Phys. Rev., C; 2: 228-37(Jul 1970).

The atomic-beam magnetic resonance method was used to measure the nuclear spin I and the hyperfine structure constants a and b in the $^3P_1$ atomic state of 38-h ^{69}Ge and 82-min ^{75}Ge, and in the $^3P_2$ atomic state of ^{75}Ge and 11-day ^{71}Ge. From these measurements, the nuclear moments μ_I and Q are deduced. The results are: for ^{69}Ge, $I = 5/2$, $a(^3P_1) = \mp 23.40(3)$ MHz, $b(^3P_1) = \pm 8.28(8)$ MHz, μ_I(uncorr) = $\pm 0.733(7)\mu_N$, and Q(uncorr) = $\pm 0.028(6)$ b; for ^{71}Ge, $a(^3P_2) = +360.53(4)$ MHz; and for ^{75}Ge, $I = 1/2$, $a(^3P_1) = -81.06(8)$ MHz, $a(^3P_2) = +335.94(9)$ MHz, and μ_I(uncorr) = $+0.508(5)\mu_N$. (auth)

14930 STUDY OF THE ODD STRONTIUM ISOTOPES WITH STRIPPING AND PICKUP REACTIONS. Bercaw, R. W. (Lewis Research Center, Cleveland); Warner, R. E. Phys. Rev., C; 2: 297-309(Jul 1970).

The (d,t) and (d,p) reactions induced by 20.65-MeV deuterons were used to study the levels of ^{87}Sr and ^{85}Sr up to an excitation of 3 MeV. The mass defect of ^{85}Sr was determined by the (d,t) reaction, and its level structure below 3 MeV was investigated. The cross sections were analyzed with the distorted-wave Born approximation (DWBA) to determine the l values of the neutron transfers and the spectroscopic factors. Tentative spin assignments were made on the basis of sum rules and the j dependence of the cross sections. (auth)

14931 EXCITED STATES IN ^{75}As. Paradellis, Th.; Hontzeas, S. (Univ. of Saskatchewan, Regina). Can. J. Phys.; 48:2254-64(1 Oct 1970).

The gamma-ray spectrum of ^{75}Se was studied with a variety of Ge(Li) detectors. The energies and intensities of 15 lines were accurately measured. Of these a 24.4 and 468.6 keV transition were substantiated for the first time in the gamma-ray spectrum. Ge(Li)–Ge(Li) coincidence measurements established the newly observed 24.4 keV transition. These experiments also substantiated the 80.8 keV transition (observed for the first time) deduced from electron conversion spectra. The accurate intensity values obtained in this work were combined with proper literature data and conversion coefficients for various transitions were determined. These data and recent half-life measurements of some excited states by other workers permitted us to calculate the transition rates in ^{75}As. The data obtained indicate that the 198.6, 279.5, and 400.5 keV levels in ^{75}As exhibit strong collective character, in contrast to the 264.6 keV level, which shows little influence of collective effects. (auth) (Canada)

14932 THERMAL-NEUTRON-CAPTURE GAMMA RAYS OF CADMIUM AND CHLORINE. Peak, Donald Wayne. Chapel Hill, N. C.; Univ. of North Carolina (1970). 84p. University Microfilms Order No. 70-21,220.

Thesis.

The thermal neutron capture gamma-ray spectra of cadmium and chlorine were investigated with a lithium-drifted germanium detector. The observed gamma-ray energies and intensities are in agreement with previous work by other investigators. The neutron separation energies of ^{114}Cd and ^{36}Cl were determined as 9040.6 ± 1.1 keV and 8582.6 ± 2 keV, respectively. Evaluation of the reduced strength of gamma rays from the capturing state of ^{114}Cd reveals the 5942, 5826, 5433, 5327 and 5155 keV gamma-rays to be E1 transitions. The ^{36}Cl gamma-ray spectrum shows the 6114 keV peak to be two unresolved gamma rays. The reduced strength of the 6114 keV gamma ray shows it to be an E1 transition. (Diss. Abstr. Int., B)

14933 SOME DOPPLER-SHIFT LIFETIMES IN ^{30}P. Lachaine, A.; Hird, B. (Univ. of Ottawa). Can. J. Phys.; 48: 2336-9(1 Oct 1970).

The Doppler-shift attenuation method was used to determine some lifetimes in ^{30}P which are populated by the decay of resonances in the ^{29}Si(p,γ)^{30}P reaction at 1505, 1643, and 1686 keV, and the 1773–5 keV doublet. There is evidence that either the 1775 keV component of the doublet has a measurable lifetime of 10 ± 5 fs or that all the observed radiation from this doublet contains γ rays from both components. (auth) (Canada)

14934 M1 TRANSITIONS AMONG THE $f_{7/2}d_{3/2}^{-1}$ STATES OF ^{40}K. Becker, J. A. (Lockheed Palo Alto Research Lab., Palo Alto, Calif.); Warburton, E. K. Phys. Rev. Lett.; 26: 143-5(18 Jan 1971).

The three experimentally known M1 transition rates among the $f_{7/2}d_{3/2}^{-1}$ 2^-, 3^-, 4^-, and 5^- quartet of ^{40}K are calculated to first order using the one-particle, one-hole wave functions of Perez. The calculations are in qualitative agreement with experiment and illustrate that the effective moment method is not valid when used with a zeroth-order (i.e., the pure $f_{7/2}d_{3/2}^{-1}$ configuration) calculation. This is expected since the effective moments correct for second-order effects and cannot simulate the first-order correction due to the presence of $f_{7/2}d_{5/2}^{-1}$ and $f_{5/2}d_{3/2}^{-1}$ impurities. (auth)

14935 THERMAL NEUTRON CAPTURE CROSS-SECTION MEASUREMENTS FOR ^{23}Na, ^{27}Al, ^{37}Cl, AND ^{51}V. Ryves, T. B.; Perkins, D. R. (National Physical Lab., Teddington, Eng.). J. Nucl. Energy; 24: 419-50(Nov 1970).

The 2200 m/s neutron capture cross sections of ^{23}Na, ^{37}Al, ^{37}Cl and ^{51}V were remeasured by the activation method in the NPL standard thermal neutron flux assembly. These cross sections refer to the total production of daughter isotopes in their ground states, both by direct formation and through isomeric transitions. The present results are more accurate than a previous set of measurements, and are for ^{23}Na, 526.9 ± 4.5 mb, for ^{27}Al, 230.5 ± 4.5 mb, for ^{37}Cl, 433 ± 6 mb and for ^{51}V, 4.88 ± 0.04 b, all relative to the ^{197}Au cross section of 98.8 ± 0.3 b. The half-lives of ^{28}Al and ^{52}V were also measured as 2.247 ± 0.018 min and 3.766 ± 0.008 min respectively. The quoted errors are the arithmetic sums of the estimated systematic errors and of the random errors expressed at a 99 percent confidence level. (auth) (UK)

14936 9480 AND 9495 keV LEVELS IN ^{28}Si. Forsblom, I.; Viitasalo, M. (Helsinki Univ.). Soc. Sci. Fenn., Comment. Phys.-Math.; 38: 131-4(1970).

The ^{27}Al(p,γ)^{28}Si reaction was investigated at proton energies of 742 and 1381 keV. Two different levels with excitation energies of 9480 ± 2 and 9495 ± 2 keV were found near 9.5 MeV. Furthermore, the Q-value of the reaction was determined as 11584.4 ± 0.9 keV. (auth) (Finland)

14937 NUCLEAR POLARIZATION ENERGY CORRECTION FOR MUONIC SPECTRA IN THE LEAD REGION. Skardhamar, H. F. (Univ. of Copenhagen). Nucl. Phys.; A151: 154-60(1970).

The nuclear polarization energy correction in muonic lead was calculated, employing a method in which the energy difference of the muonic states relative to the nuclear excitation energy was considered. To describe the nuclear states of excitation that are expected to contribute most significantly, the hydrodynamical model was used and the following modes of excitation, isovector and compression modes of multipolarity 0, 1, 2 and shape oscillations of multipolarity 2 and 3, were treated. (auth)

14938 STUDY OF THE REACTION ^{40}Ca(d,p)^{41}Ca USING THE WBP MODEL. Pearson, C. A.; Zissermann, D. (Univ. of Alabama, Birmingham). Nucl. Phys.; A154: 23-35(1970).

Predictions of the weakly bound projectile model were compared with measured differential cross sections, polarization and vector analyzing power for the reactions $^{40}Ca(d,p)^{41}Ca$ leading to the g.s., 1.95, 2.47, and 3.95 MeV states in ^{41}Ca at deuteron energies between 5 and 21 MeV. Optical potentials for the calculations are obtained by fitting nucleon–nucleus scattering from ^{40}Ca between 8 and 40 MeV. Uncertainties in these optical potentials are small and the corresponding (d,p) predictions are well defined. There is qualitative agreement with all the measurements and the spectroscopic factors extracted are independent of the deuteron energy. (auth)

14939 SPIN AND PARITY OF ^{41}Ca LEVELS FROM NEUTRON SCATTERING MEASUREMENTS. Kirouac, G. J.; Nebe, J. (Kernforschungszentrum, Karlsruhe, Ger.). Nucl. Phys.; A154: 36-48(1970).

The differential neutron scattering cross section for ^{40}Ca was measured at three angles with high-energy resolution from 0.55 to 2.0 MeV. The l- and J-values for about 70 levels of the compound nucleus ^{41}Ca were assigned from a study of the resonance shapes as a function of scattering angle. (auth)

14940 EXPERIMENTAL STUDY OF LOW-LYING LEVELS AND DECAY STRUCTURE IN THE NUCLEUS ^{62}Cu. Davidson, W. F.; Najam, M. R.; Dallimore, P. J.; Hellstroem, J.; Powell, D. L. (Australian National Univ., Canberra). Nucl. Phys.; A154: 539-50(1970).

The reaction $^{62}Ni(p,n\gamma)^{62}Cu$ was used to investigate the low-lying levels of ^{62}Cu and their γ decay. Gamma angular distributions were carried out using incident proton energies close to threshold for the states under investigation and comparison of these results were made with the predictions of the compound nucleus statistical model. In addition to levels seen in the β^+/EC decay of ^{62}Zn, namely the ground state (1^+), 40.84 keV (2^+), 243.43 keV (2^+), 287.86 keV (2^+), 548.25 keV (1^+), and 637.20 (1^+), other levels were found at 389.9, 426.1, 644.9, 675.1, 698.3, 727.5, 756.3, and 915.5 keV. The 426.1, 675.1, and 727.5 keV states are assigned to be 3^+, 3^+, and $2^{(+)}$ respectively, and possible spin values for the remaining levels are advanced. Gamma branching ratios were obtained, and a decay scheme for ^{62}Cu comprising 30 transitions is presented. (auth)

14941 INVESTIGATION OF THE ^{45}Sc LEVEL SCHEME BY MEANS OF INELASTIC PROTON SCATTERING. Broman, Lars (Chalmers Univ. of Tech., Goteborg); Al-Jadir, M. N. I.; Larsson, Curt; Ott, Aadu. Ark. Fys.; 40: 223-30(1970).

The $^{45}Sc(p,p')$ reaction at 8 MeV was studied with a magnetic spectrograph. Thirty-three proton groups feeding levels in ^{45}Sc between 1.65 and 4.13 MeV excitation energy were found. Gamma spectra were measured at a number of incident energies up to 4 MeV with a Ge(Li) detector; information was obtained concerning de-excitation modes for most levels up to 2.3 MeV. (auth) (Sweden)

14942 SPINS OF THE 0.46 AND 0.67 MeV LEVELS OF ^{34}Cl. Thirion, J. M.; Chouraqui, G.; Muller, Th.; Port, M. (Univ., Strasbourg). J. Phys. (Paris); 31: 743-8(Aug-Sep 1970). (In French).

The $^{32}S(^3He, p\gamma)^{34}Cl$ reaction was studied using a $^3He^{++}$ beam at 9, 9.5, and 10 MeV. The pγ coincidences were measured between protons detected at 0° and gamma rays, according to the Method II of Litherland and Ferguson. The interpretation of the angular correlations between the proton groups leading to the second and third excited states and the corresponding gamma rays leads to the unique value of unity for J for the 0.46 and 0.67 MeV levels of ^{34}Cl. These results are in good agreement with theoretical predictions of shell-model calculations with modified two-particle interaction. (France)

14943 OBSERVATION OF ANALOGUE STATES WITH T = 2 IN THE REACTIONS $^{26}Mg(^3He,n)^{28}Si$, $^{46}Ti(^3He,n)^{48}Cr$, AND $^{58}Ni(^3He,n)^{60}Zn$. Brill, O. D.; Vongai, A. D.; Romanov, V. S.; Faiziev, A. R. (Inst. of Atomic Energy, Moscow). Yadern. Fiz.; 12: 253-9(Aug 1970). (In Russian).

In ^{28}Si, ^{48}Cr, and ^{60}Zn, produced from the (^3He,n) reactions, an intensive excitation is observed of low-lying states with T = 2 and energies 15.29 ± 0.07, 8.77 ± 0.05, and 7.39 ± 0.125 MeV, respectively. (auth)

14944 REACTION ($^3He,\alpha$) ON NUCLEI WITH 1d–2s SHELL. Artemov, K. P.; Goldberg, V. Z.; Islamov, B. I.; Rudakov, V. P. (Inst. of Atomic Energy, Moscow). Yadern. Fiz.; 12: 239-52 (Aug 1970). (In Russian).

Differential cross sections of the ($^3He,\alpha$) reactions on $^{20,22}Ne$, ^{27}Al, and ^{28}Si were measured at ^3He energy of about 35 MeV. The experimental results are compared with calculations of the distorted wave method. Spectroscopic factors for a number of levels of the final nuclei are obtained. Dependence of the calculated differential cross sections and the spectroscopic factors on the parameters of the optical potential was studied. The measured cross sections are also compared with those calculated by means of the distorted wave method with account of the nuclear deformation. The spectroscopic properties of a number of levels in the final nuclei were determined. (auth)

14945 ANGULAR DEPENDENCES OF MANY-CHARGE PARTICLES PRODUCED BY 660-MeV PROTONS ON ^{27}Al NUCLEI. Milovanov, V. P.; Pokravskii, V. N.; Cherenkov, P. A.; Yutlandov, I. A. (Lebedev Inst. of Physics, Moscow). Yadern. Fiz.; 12: 234-8(Aug 1970). (In Russian).

Angular distributions of many-charge particles ^{11}C, ^{13}N, and ^{18}F resulting from reactions on ^{27}Al produced by 660-MeV protons were measured. Experimental results are compared with corresponding dependences which are due to the phase space of the reaction. (auth)

14946 REACTIONS $^{32}S(\gamma,p\gamma')$ AND $^{32}S(\gamma,n\gamma')$. Ishkhanov, B. S.; Kapitonov, I. M.; Lazutin, E. V.; (and others) (Inst. of Nuclear Physics, Moscow). Yadern. Fiz.; 12: 224-6(Aug 1970). (In Russian).

γ-quanta spectra from reactions $^{32}S(\gamma,p\gamma')$ and $^{32}S(\gamma,n\gamma')$ are obtained on the 35 MeV betatron of the Nuclear Physics Research Institute of the Moscow University using a 20 cm^3 Ge(Li) detector. The peaks are observed at the γ quanta energy 1.26 and 2.23 MeV. Absolute values of integral cross sections in these peaks are 40 and 90 MeV · mbn, respectively. (auth)

14947 UNIQUENESS OF THE REAL OPTICAL POTENTIAL. Watson, Brant Dennee. Tallahassee; Florida State Univ. (1970). 125p. University Microfilms Order No. 70-16,353.

Thesis.

Following a suggestion by Robson, α-particles were elastically scattered from ^{70}Ge, ^{90}Zr, ^{107}Ag, and ^{140}Ce at incident energies from ~0.6 to 1.2 times the classical Coulomb barrier height for each in an effort to resolve the problem of discrete real well depth ambiguities found in optical model analyses reported previously. The real and imaginary nuclear potential well radii and the Coulomb radius (assuming a uniformly charged sphere) for each nucleus were taken to be $R = R_c = r_o (A_{ALPHA}^{1/3} + A_{TARGET}^{1/3})$ where $r_o = 1.22$ fermi. A diffuseness of 0.57 fermi was used throughout. Consistently good fits were obtained to angular distributions and excitation functions for each nucleus. For three of the nuclei only one pair of real (U) and volume imaginary (W) potentials was found. However, the real well depth for ^{90}Zr showed a slight energy dependence. The potentials obtained were (in MeV): U = 23.5, W = 11.0 for ^{70}Ge; U ~ 22, W = 10.25 for ^{90}Zr; U = 25.5, W = 14.5 for ^{107}Ag, and U = 18.0, W = 6.0 for ^{140}Ce. Extensive grid searches on U and W were carried out for a representative highest-energy angular distribution for each nucleus. Contours of constant χ^2 were plotted and clearly indicate the absence of other solutions for the real well depth U. Since ambiguities were expected to occur at these higher energies, further calculations were performed in which the effect of absorption (W) was more generally explored. The usefulness of Robson's method was found to be limited to cases where the absorption required by the data is either small with respect to U or is ineffective. If the absorptive strength required by the data is a large fraction of U, then a preference for a particular pair of real and imaginary potentials may be indicated by the data, assuming the Woods-Saxon geometrical parameters to be fixed throughout. (Diss. Abstr. Int., B)

14948 SPINS AND PARITIES OF 1514- AND 1726-keV RESONANCES IN THE $^{27}Al(p,\gamma)^{28}Si$ REACTION. Snow, Peter Ballard. Provo, Utah; Brigham Young Univ. (1970). 132p. University Microfilms Order No. 70-15,694.

Thesis.

Spins and parities of resonance levels at 13047 and 13252 keV in ^{28}Si were studied. These were created at a proton energy of 1514 keV and 1726 keV respectively. Theoretical angular distributions for the first and second gamma rays from resonance were compared with the experimental angular distributions. A value of 2^- is assigned to the 1514 keV resonance, and 5^- is assigned to the 1726 keV resonance. (Diss. Abstr. Int., B)

14949 SPECTROSCOPY IN THE TITANIUM ISOTOPES VIA (p,d) AND (p,t) REACTIONS. Plauger, Phillip James. East Lansing, Mich.; Michigan State Univ. (1969). 86p. University Microfilms Order No. 70-15,111.

Thesis.

Deuteron angular distributions from $^{48}Ti(p,d)^{47}Ti$ were measured at incident proton energies of 24.80, 29.82, 35.15, 39.97 and 45.05 MeV to detect the presence of any energy dependence in various methods of extracting spectroscopic factors. Using optical param-

XUM

eters obtained from the literature, distorted wave Born approximation calculations were performed with the Oak Ridge code JULIE for the principal $L_n = 1$, 2 and 3 transitions observed. In all cases, significantly better agreement with the data was obtained in the zero-range approximation by using a lower integration cutoff at the nuclear surface. The variation of spectroscopic factors with cutoff radius also exhibited a plateau at the nuclear surface: however energy dependence of extracted spectroscopic factors was still present. The best agreement was obtained by applying finite range and non-locality corrections to the form factors used by JULIE. No integration cutoffs were required and energy dependence was removed. Partial angular distributions from ^{46}Ti(p,d)^{45}Ti at 34.78 MeV and ^{50}Ti(p,d)^{49}Ti at 45.05 MeV were also measured. Using the prescription obtained from the energy dependence study, spectroscopic factors were obtained for transitions to ^{45,47,49}Ti. The reactions ^{46,48,50}Ti(p,t)^{44,46,48}Ti were performed from 25 to 45 MeV in an attempt to excite $T = T_z + 2$ analog states. Only the $T = 2$ state at 9.31 MeV excitation in ^{44}Ti was observed. The ground state Q-value for ^{46}Ti(p,t)^{44}Ti was found to be −14.246(0.011) MeV. (Diss. Abstr. Int., B)

14950 STUDY OF THE ENERGY LEVELS OF ^{18}Ne, ^{23}Mg, ^{26}Si, ^{30}S, ^{34}Ar, AND ^{38}Ca BY THE (p,t) REACTION. Paddock, Robert Alton. East Lansing, Mich.; Michigan State Univ. (1969). 171p. University Microfilms Order No. 70-15,099.

Thesis.

A study of the (p,t) reaction on the even-even N = Z nuclei in the 2s1d shell was carried out. This reaction was used to study the energy levels of ^{18}Ne, ^{22}Mg, ^{26}Si, ^{30}S, ^{34}Ar and ^{38}Ca. Until recently little has been reported about these nuclei. Except for a few scattered reports of (p,t) experiments, only the (^{3}He,n) and (^{3}He,nγ) reactions have been used to study these nuclei. The excited states that were observed are reported along with the spin and parity assignments when possible. The two nucleon transfer distorted wave theory of N. K. Glendenning was studied with respect to these (p,t) reactions. It was found that the shapes of the predicted angular distributions are primarily dependent on the orbital angular momentum transfer and the optical model parameters. This fact was used to make the spin-parity assignments. It was also found that the magnitudes of the predicted cross-sections are strongly dependent on not only the optical model parameters, but also the bound state parameters of the transferred neutrons and the configuration mixing in the initial and final nuclear wave functions. It is concluded that the (p,t) reaction is useful to study the energy levels of nuclei two nucleons away from stability. It is also concluded that the two nucleon transfer distorted wave theory is useful to predict the general shapes of angular distributions but that the magnitudes are too dependent on parameters which are not well known to be predicted successfully. (Diss. Abstr. Int., B)

14951 TOTAL YIELD MEASUREMENTS FOR THE ^{24}Mg(α,γ)^{28}Si AND ^{27}Al(p,γ)^{28}Si REACTIONS. Lyons, Peter Bruce. Pasadena, Calif.; California Inst. of Tech. (1969). 169p. University Microfilms Order No. 70-561.

Thesis.

The ^{27}Al(p,γ)^{28}Si and ^{24}Mg(α,γ)^{28}Si reactions were investigated to provide the data needed for calculation of the ^{28}Si photodisintegration rate in astrophysical situations, particularly in the silicon-burning stage of stellar nucleosynthesis. A large solid angle NaI gamma ray spectrometer was employed which provided high detection efficiencies. The ^{27}Al(p,γ)^{28}Si reaction was investigated over the proton energy range 0.3 – 2.6 MeV; total gamma ray strengths were determined for 85 resonances. From 1.4 – 2.6 MeV, the gamma-ray yield curve was measured and an upper limit for the nonresonant cross section was determined. Where possible, total resonance widths were deduced from the data. The gamma-ray detection efficiencies and target purity were investigated experimentally. Comparison was made with resonance strengths, measured by other methods, in the reactions ^{30}Si(p,γ)^{31}P and ^{26}Mg(p,γ)^{27}Al. The reaction ^{24}Mg(α,γ)^{28}Si was investigated for alpha particle energies up to 2.8 MeV; total gamma ray strengths were determined for 16 resonances, including a previously unreported resonance at 1.358 ± 0.007 MeV. Stellar interaction and photodisintegration rates were calculated from the measured resonance strengths, and semiempirical fits to these rates were determined for use in astrophysical calculations. (Diss. Abstr. Int., B)

14952 ALPHA–γ ANGULAR CORRELATION STUDY OF ^{57}Ni USING THE REACTION ^{58}Ni(^{3}He,αγ)^{57}Ni. Gould, Christopher Robert. Philadelphia; Univ. of Pennsylvania (1969). 113p. University Microfilms Order No. 70-16,153.

Thesis.

The levels of ^{57}Ni populated in the reaction ^{58}Ni(^{3}He,α)^{57}Ni were studied using the method of particle γ-ray angular correlations. A 500 μgm/cm^2 nickel foil enriched to 99.9% ^{58}Ni was bombarded with a 15 MeV ^{3}He^{++} beam. The α particles were detected at zero degrees with respect to the incident beam by a position sensitive detector located at the focal point of a magnetic spectrometer. Four 7.6 cm × 10.2 cm NaI(Tl) crystals were simultaneously used to detect coincident γ-rays at angles between 90 and 160°. Using l-values known from previous work, the following spin-parity assignments are made for the levels indicated: 0.78 MeV $5/2^-$, 1.11 MeV $1/2^-$($3/2^-$), 2.59 MeV $7/2^-$, 3.24 MeV $7/2^-$, 3.71 MeV ($\geq 3/2$), 3.85 MeV ($3/2$, $5/2$), 4.23 MeV ($3/2$, $5/2$, $7/2$), 4.56 MeV ($\geq 7/2$), 5.22 MeV $7/2^-$, 5.56 MeV $3/2^+$, 6.00 MeV $3/2^+$. Branching ratios for the decays of these levels are presented, along with mixing ratios for the stronger transitions. (Diss. Abstr. Int., B)

14953 LIGHT RIGID ROTOR NUCLEI. Lindgren, Richard Arthur. New Haven; Yale Univ. (1969). 346p. University Microfilms Order No. 70-16,297.

Thesis.

In an attempt to empirically determine the degree to which the concepts of the simple rigid model approach to light collective nuclei is valid, a study of four similar, strongly deformed, prolate nuclei in the odd count $\zeta = 11$ nuclear multiplet was undertaken. Two members of this multiplet, ^{21}Na and ^{23}Na, were studied utilizing the ^{24}Mg(p,αγ)^{21}Na, ^{26}Mg(p,αγ)^{23}Na, ^{24}Mg(t,αγ)^{23}Na, and ^{23}Na(α,α′γ)^{23}Na reactions in the standard Method II angular correlation geometry of Litherland and Ferguson. New angular momentum quantum numbers and electromagnetic de-excitation properties were determined for levels and transitions in these nuclei. These data together with works of others were systematically examined by comparing model predictions based on the rotor, Coriolis, and shell models with experiment for the ^{21}Ne, ^{21}Na, ^{23}Na, and ^{23}Mg odd count $\zeta = 11$ nuclei. From these comparisons it was determined that the rotor and Coriolis model predictions of excitation spectra, electric quadrupole and magnetic dipole reduced transition probabilities in the $K^\pi = 3/2^+$ ground state rotational band in the $\zeta = 11$ nuclei are in better agreement with experiment than the shell model results. Further, the Coriolis results including other single particle configurations reproduce the magnetic dipole transitions matrix elements better than the pure rotor model calculation. Both models, rotor and Coriolis, are equally as effective in reproducing the electric quadrupole transitions as would be expected in a well deformed nuclear system. Despite the remarkably accurate predictions of the electromagnetic transition properties by the simple rotor model in this multiplet, validating the use of the model, there still remains an unexplained oscillatory perturbative deviation of the excitation energies from the $J(J + 1)$ rule in the mirror pair ^{23}Na and ^{23}Mg. Although only partially confirmed, a Coriolis based explanation appears appropriate to correct this anomaly as is seen by the improvement of the Coriolis model over the rotor model in reproducing the excitation spectra of the ground state rotational band. The large, almost limiting, rigid body values of the moment of inertia (>90%) and the strong prolate nuclear deformations ($\beta \sim +0.5$), completely supporting the premises on which the rigid rotor model is based, characterize the odd count $\zeta = 11$ group of collective nuclei without exception as perhaps the most rigid rotors in nature. (Diss. Abstr. Int., B)

14954 LIFETIMES OF THE 4.623 AND 4.688 MeV LEVELS IN ^{34}S. Sona, P.; Schrieder, G.; Kutschera, W. (Max-Planck-Institut fuer Kernphysik, Heidelberg. Univ., Heidelberg). Nucl. Phys.; A161: 283-8(1971).

The lifetimes of the 4.623 and the 4.688 MeV levels in ^{34}S were measured with the Doppler-shift attenuation method. A complete lineshape analysis was performed on the basis of a description of the stopping process of the recoiling nuclei, which is an extension of the Blaugrund method. The following lifetimes were found: τ (4.623 MeV) = 145 ± 50 fs, τ (4.688 MeV) = 110 ± 20 fs. (auth)

14955 LEVEL STRUCTURES OF ^{85} ^{87}Sr FROM (d,p) REACTIONS. Morton, J. M. (Nucl Physics Lab., Oxford); Davies, W. G.; McLatchie, W.; Darcey, W.; Kitching, J. E. Nucl. Phys.; A161: 228-40(1971).

The reactions ^{84}Sr(d,p)^{85}Sr and ^{86}Sr(d,p)^{87}Sr were studied at a bombarding energy of 12 MeV. Thirty-four levels below 4.5 MeV of excitation were identified in ^{87}Sr and fifty-four levels below 3.5 MeV were identified in ^{85}Sr. Transferred orbital angular momenta and spectroscopic information were deduced from a DWBA analysis of the proton differential cross sections. It was found that the lowest-lying excited states arise from $1g_{9/2}$, $2p_{1/2}$ and $2p_{3/2}$ configurations. The $1f_{5/2}$ shell appears to be completely filled in these low-mass strontium isotopes. (auth)

14956 CRANKED HARTREE–FOCK SOLUTIONS FOR COLLECTIVE EXCITATIONS. Stamp, A. P. (Nuclear Physics Lab., Oxford). Nucl. Phys.; A161: 81-92(1971).

The self-consistent solution for the nuclear Hamiltonian $H = H_0 - \omega J_x$ is determined for ^{20}Ne. The resulting energy spectrum and moment of inertia are compared with the predications of the simple cranking model and with experimental values. It is found that corrections to the self-consistent potential due to the rotation are important. The moment of inertia is shown to increase with ω, resulting in the lowering of the high-spin rotational states. However the frequency of the rotational motion for $I > 6$ approaches the intrinsic nucleon frequency and consequently the model breaks down. (auth)

14957 DECAY OF ^{56}Co AND ^{66}Ga: ENERGY AND INTENSITY STANDARDIZATION. Phelps, M. E.; Sarantites, D. G.; Winn, W. G. (Washington Univ., St. Louis). Nucl. Phys.; A149: 647-72(1970).

The energy and intensity of the γ transitions from the decay of 77.3 d ^{56}Co and of 9.3 h ^{66}Ga were carefully measured using a high-resolution Ge(Li) detector in conjunction with a split annular NaI(Tl) detector operated as a Compton suppression spectrometer or as a pair-three-crystal coincidence spectrometer. The following new γ transitions were observed in the decay of ^{56}Co and were assigned to the well-known level scheme of ^{56}Fe: 263.48 ± 0.11, 486.6 ± 0.4, 1160.06 ± 0.13, and 1640.3 ± 0.2 keV. More accurate values for the energy and intensity of the weaker transitions in the ^{56}Co decay are offered. Twenty-one new γ transitions were identified with the decay of ^{66}Ga. From singles anti-Compton and γ-γ coincidence measurements it was established that levels at 1039.24, 1872.70, 2372.24, 2780.2, 2938.4, 3105.07, 3229.05, 3332.2, 3381.32, 3433.08, 3688.90, 3791.29, 4046.5, 4086.19, 4295.52, 4461.5, and 4806.4 keV are populated in the decay of ^{66}Ga. A possible level at 3807.5 keV is also discussed. More accurate values for the energy and intensity of the γ rays from ^{66}Ga are offered for convenient high-energy and intensity standardization of Ge(Li) spectrometers. From the log ft values determined and from γ intensity information J^{π} values to many levels in ^{66}Zn are deduced. (auth)

14958 MUONIC INTERACTIONS IN ^{66}Zn AND ^{68}Zn. Jenkins, D. A.; Powers, R. J. (Virginia Polytechnic Inst., Blacksburg, Va.). Phys. Rev., C; 2: 458-61(Aug 1970).

The $J^P = 0^+$ nuclear excitation of ^{68}Zn in muonic atoms was searched for, as suggested by Henley and Wilets. ^{68}Zn was chosen because the energy of the 0^+ excitation is close to the energy difference of the 2s−1s muonic levels, thus allowing a dynamic interaction between a muon in a 2s state and the nucleus in the ground state. The 2s−1s level difference is 20 keV less than the nuclear excitation energy and, as a result, the dynamic interaction is too small to observe. The ^{66}Zn−^{68}Zn isotope shift was measured to be $\delta R/\delta R_{std} = 0.47 \pm 0.11$. (auth)

14959 INTERMEDIATE STRUCTURE IN THE PHOTON INTERACTION CROSS SECTIONS OF Sn AND Zr. Axel, P.; Min, K. K.; Sutton, D. C. (Univ. of Illinois, Urbana). Phys. Rev., C; 2: 689-711(Aug 1970).

Photon scattering cross sections were measured with 70-keV resolution from 6 to 9 MeV in Sn, and from 8.5 to 12.5 MeV in Zr. A new method of analysis is used to infer relatively reliable total photon interaction cross sections. Both the elastic scattering and the total interaction cross sections vary more rapidly with energy than had been anticipated; the best identified localization of transition strength is between 11.4 and 11.8 MeV in Zr. The average total interaction cross sections are qualitatively similar to, but about 50% larger than, an extrapolation of the electric dipole giant resonance. The cross sections are large enough to imply that electric dipole interaction dominates at most energies. The relative probability of photon scattering and photoproton emission is very sensitive to correlations between proton widths and ground-state γ widths. There is no evidence for width correlations associated with the additional strength concentrated near 11.5 MeV in ^{90}Zr. (auth)

14960 INELASTIC NEUTRON SCATTERING-(n,n′γ)-BY FLUORINE, IRON, COBALT, NICKEL, AND TANTALUM NUCLEI. Broder, D. L.; Gamaly, A. F.; Lashuk, A. I.; Sadokhin, I. P. (Inst. of Physics and Power Engineering, Obninsk, USSR). pp 295-300 of Nuclear Data for Reactors. Vol. II. Vienna; International Atomic Energy Agency (1970). (In Russian).

From 2nd International Conference on Nuclear Data for Reactors, Helsinki, Finland. See STI/PUB−259(Vol. 2); CONF-700605−(Vol. 2).

Using a Ge(Li) semiconductor spectrometer, the cross-sections were measured for the formation of gamma rays in inelastic neutron scattering by various nuclei: fluorine-for gamma lines with energies 110 and 200 keV in the neutron energy range 0.14-3.14 MeV; iron-for gamma lines with energies 847, 1030, 1240, 1250, 1410, 1810, 2100, 2112, 2280, 2350, 2430, 2545, 2610, 2775 and 3210 keV in the neutron energy range 0.90-6.0 MeV; cobalt-for gamma lines with energies 1095, 1190, 1280 and 1400 keV in the neutron energy range 1.14-2.68 MeV; nickel-for gamma lines with energies 1000, 1170, 1332, 1450, 1795, 2150 and 2210 keV in the neutron energy range 1.20-6.0 MeV; tantalum-for gamma lines with energies 137, 153, 302 and 482 keV in the neutron energy range 0.17-2.86 MeV. On the basis of the experimental data and of the energy level schemes of these nuclei conclusions are drawn regarding the excitation of individual levels and the total cross-section for inelastic neutron scattering. (auth)

14961 NEUTRON SCATTERING CROSS-SECTIONS OF IRON. Tomita, Y.; Tsukada, K.; Maruyama, M.; Tanaka, S. (Japan Atomic Energy Research Inst., Tokai). pp 301-4 of Nuclear Data for Reactors. Vol. II. Vienna; International Atomic Energy Agency (1970).

From 2nd International Conference on Nuclear Data for Reactors, Helsinki, Finland. See STI/PUB–259(Vol.2); CONF-700605–(Vol.2).

The differential cross-sections of elastic and inelastic scatterings by iron were measured at incident neutron energies from 1.43 to 2.15 MeV in steps of 40 keV with an energy resolution of 50 keV. Scattered neutrons and gamma rays produced in the inelastic process were observed at the same time with a Mobley bunching system of the JAERI 5.5-MV Van de Graaff accelerator and a time-of-flight spectrometer. The neutron scattering cross-sections were measured relative to the p-n cross sections, and the neutron-energy standard was the 2.08-MeV resonance of carbon. The cross-sections of gamma-ray production were measured with the same liquid-scintillation detector as the neutron detector, and normalized to the neutron scattering cross-sections. Both neutron and gamma-ray cross-sections were corrected for multiple scattering and attenuation of neutrons in the scattering sample, and source-to-sample angular spread. The angular distributions of the neutron and gamma-ray cross-sections thus obtained were fitted with Legendre expansions. Intermediate structures appear in the excitation functions of some of the expansion coefficients of the cross-sections. Energies of humps in the excitation functions are about 1.6 and 2.05 MeV. (9 references) (auth)

14962 WIDTH-FLUCTUATION AND RESONANCE-INTERFERENCE EFFECTS IN NEUTRON SCATTERING CROSS-SECTIONS OF ALUMINIUM, COPPER, AND ZINC. Tsukada, K.; Tomita, Y.; Tanaka, S.; Maruyama, M. (Japan Atomic Energy Research Inst., Tokai). pp 305-16 of Nuclear Data for Reactors. Vol. II. Vienna; International Atomic Energy Agency (1970).

From 2nd International Conference on Nuclear Data for Reactors, Helsinki, Finland. See STI/PUB–259(Vol.2); CONF-700605–(Vol.2).

Neutron scattering cross-sections of aluminium, copper and zinc were analysed in the energy region of 1 to 8 MeV by means of optical and statistical models, the width-fluctuation effect and the resonance-interference effect being taken into account. Data of the cross-sections used in the analysis include those at 4.81, 5.96, 7.03 and 8.03 MeV for aluminium, at 1.71 and 2.24 MeV for copper and at 1.71, 2.24, 4.48, 5.92, 6.97 and 7.99 MeV for zinc. Best-fit sets of optical-model parameters were sought for the angular distributions of elastic scattering, the inelastic scattering cross-sections and the total cross-sections at each energy. By using a computer code STAX2, calculations on the basis of Hauser−Feshbach's formulation and Moldauer's formulation were performed. In the latter formulation, the calculations were carried out with the maximum and zero values of Moldauer's parameter Q. Difference in fitting among the three calculations appears in backward angles in a limited energy region. Systematic energy variations of the optical-model parameters are seen more or less in the region below 4 MeV for all cases. In the region above 4 MeV, where the Moldauer effect is ineffective, the energy variations are not so pronounced. Judging from these two, the calculation with the maximum value of Q is considered to be best among the three calculations to reproduce the measured data, though fluctuations in the cross-sections and simple forms of the angular distributions in the lower energy region make the choice ambiguous. (12 references) (auth)

14963 FAST-NEUTRON SCATTERING FROM Al, Si, S, AND Zn. Tanaka, S.; Tsukada, K.; Maruyama, M.; Tomita, Y. (Japan Atomic Energy Research Inst., Tokai). pp 317-23 of Nuclear Data for Reactors. Vol. II. Vienna; International Atomic Energy Agency (1970).

From 2nd International Conference on Nuclear Data for Reactors, Helsinki, Finland. See STI/PUB–259(Vol.2); CONF-700605–(Vol.2).

Differential cross-sections for elastic and inelastic neutron scattering were measured for natural samples of Al, Si, S and Zn at incident energies from 4.5 to 8 MeV in about 1-MeV steps. Scattered neutrons were observed at angles from 30° to 150° in

10° steps with a Mobley bunching system of the JAERI 5.5-MV Van de Graaff accelerator and a time-of-flight spectrometer. The absolute differential cross-section scale was fixed with reference to the n-p scattering cross-section. The data were corrected for flux attenuation, multiple scattering in the samples and source-to-sample angular spread of neutron energy using a Monte-Carlo computer code. The differential cross-sections were analysed using the optical model for the elastic scattering, the statistical theory for the compound processes, and the coupled-channels and DWBA theories for the direct inelastic scattering. The optical-potential parameters were obtained by fitting the sum of the shape-elastic and compound-elastic scattering cross-sections to the measured elastic data. The inelastic data for low-lying levels are compared with the combined predictions by the Hauser–Feshbach and coupled-channels (or DWBA) calculations. The comparison shows good agreement for ^{27}Al and ^{32}S. For the first states in even isotopes of Zn, the direct processes are predominant in the energy region higher than 5.9 MeV. (17 references) (auth)

14964 NEUTRON ELASTIC-SCATTERING CROSS-SECTIONS OF VANADIUM, CHROMIUM, IRON, AND NICKEL. Holmqvist, B.; Wiedling, T. (Aktiebolaget Atomenergi, Studsvik, Swed.). pp 327-39 of Nuclear Data for Reactors. Vol. II. Vienna; International Atomic Energy Agency (1970).

From 2nd International Conference on Nuclear Data for Reactors, Helsinki, Finland. See STI/PUB–259(Vol.2); CONF-700605–(Vol.2).

A description, a compilation, and a discussion of elastic-scattering data obtained from measurements made in the energy range 1.8-8.1 MeV are presented. Between 1.8 and 3.0 MeV these measurements were performed at intervals of about 0.25 MeV while between 3.0 and 8.1 MeV, the corresponding intervals were generally 0.5 MeV. Time-of-flight techniques were employed. The differential scattering cross-sections are standardized with respect to well-established n-p scattering cross-sections. The experimental differential and total elastic cross-section data are compared with results deduced from optical-model calculations involving a spherical optical potential. The experimental elastic-scattering data and the calculated differential cross-sections are presented diagramatically. The optical-model parameters, total elastic cross-sections and total cross-sections are tabulated. (13 references) (auth)

14965 FAST-NEUTRON ELASTIC SCATTERING AT 8 MeV. Holmqvist, B.; Wiedling, T. (Aktiebolaget Atomenergi, Studsvik, Swed.). pp 341-8 of Nuclear Data for Reactors. Vol. II. Vienna; International Atomic Energy Agency (1970).

From 2nd International Conference on Nuclear Data for Reactors, Helsinki, Finland. See STI/PUB–259(Vol.2); CONF-700605–(Vol.2).

Fast-neutron elastic-scattering angular distributions were measured for 22 natural elements, ranging from Al to Bi, at 8 MeV neutron energy. Using time-of-flight techniques, differential scattering cross-sections were measured in the angular interval 20° to 160° in steps of 10° except in the forward angular region, where 5° steps were used. The angular distributions were corrected for neutron attenuation in the sample, for neutron multiple scattering and for geometrical effects. The experimental angular distributions are compared with distributions calculated using an optical potential with spherical symmetry. The potential parameters, i.e. the real and imaginary potential depths, the radii and the real diffuseness parameter were calculated with an automatic parameter search routine. The remaining parameters, namely the imaginary diffuseness parameter and the spin-orbit potential depth were held constant throughout the calculations. The results of these investigations demonstrate that the experimental cross-sections can be described satisfactorily in terms of the optical model. The geometrical parameters of the potential obtained by a best-fit procedure show no marked variations with mass number. The real potential depth slowly decreases with mass number and neutron excess. This shows the existence of a potential term depending upon isobaric spin. Its strength is 50 ± 10 MeV. The imaginary potential depth also decreases with mass number for values of the latter larger than about 55. Below this mass number the imaginary potential depth exhibits pronounced fluctuations. (8 references) (auth)

14966 FAST-NEUTRON INELASTIC SCATTERING IN THE ENERGY RANGE 2 TO 4.5 MeV. Almen, E.; Etemad, M. A.; Holmqvist, B.; Wiedling, T. (Aktiebolaget Atomenergi, Studsvik, Swed.). pp 349-55 of Nuclear Data for Reactors. Vol. II. Vienna; International Atomic Energy Agency (1970).

From 2nd International Conference on Nuclear Data for Reactors, Helsinki, Finland. See STI/PUB–259(Vol.2); CONF-700605–(Vol.2).

The inelastic scattering cross-sections were measured for 20 elements but the investigation of only six of them, i.e. Al, V, Mn, Fe, Nb, and Bi was completed. The measurements were made in the energy region 2 to 4.50 MeV in steps of roughly 0.25 MeV. Time-of-flight techniques were used. The inelastic cross-sections were determined relative to those established for the n-p reaction. The experimental cross-sections were corrected for the effects of the neutron-source anisotropy, attenuation of the neutron flux in the scatterer as well as for finite geometrical effects, using Monte-Carlo techniques. The experimental excitation functions are compared with those calculated with the Hauser–Feshbach formalism. The effects of level-width fluctuation were also taken into account. Optical-model parameters previously found in a systematic fast-neutron elastic-scattering investigation on the elements studied were used to obtain transmission coefficients for application in the Hauser–Feshbach calculations. (20 references) (auth)

14967 INELASTIC SCATTERING OF FAST NEUTRONS BY CHROMIUM, NICKEL, YTTRIUM, ZIRCONIUM, AND TUNGSTEN NUCLEI. Salnikov, O. A.; Lovchikova, G. N.; Kotelnikova, G. V.; Fetisov, N. I.; Trufanov, A. M. (Inst. of Physics and Power Engineering, Obninsk, USSR). pp 359-75 of Nuclear Data for Reactors. Vol. II. Vienna; International Atomic Energy Agency (1970). (In Russian).

From 2nd International Conference on Nuclear Data for Reactors, Helsinki, Finland. See STI/PUB–259(Vol.2); CONF-700605–(Vol.2).

The energy spectra of neutrons undergoing inelastic scattering by chromium, nickel, yttrium, zirconium, and tungsten nuclei were measured for five scattering angles: 30°, 60°, 90°, 120° and 150°. The measurements were made with a KG-300 cascade generator using the time-of-flight method. The initial energy of the neutrons was 14.4 MeV and the resolution 3 nsec/m at the half-height of the gamma peak. Knowing the energy spectra it was possible to determine the differential cross-section of the inelastically scattered neutrons for different spectrum energy intervals and to calculate the averaged temperature T_{eff} on the basis of the two neutron spectra from the reactions (n,n′) and (n,2n) and the temperature T of the residual nucleus after evaporation of the first neutron–i.e. the temperature characterizing inelastic scattering in a multi-level nucleon system. On the basis of the known angular distribution of the inelastically scattered neutrons the relationship between the contributions of direct processes, characterized by small incident neutron energy losses, and of processes involving a compound nucleus were determined. (11 references) (auth)

14968 FISSION-SPECTRUM-AVERAGED NEUTRON CROSS-SECTIONS FOR SOME THRESHOLD DETECTORS. Najzer, M.; Rant, J.; Solinc, H. (Inst. Jozef Stefan, Ljubljana, Yugoslavia). pp 571-5 of Nuclear Data for Reactors. Vol. II. Vienna; International Atomic Energy Agency (1970).

From 2nd International Conference on Nuclear Data for Reactors, Helsinki, Finland. See STI/PUB–259(Vol.2); CONF-700605–(Vol.2).

Neutron-activation cross-sections averaged over the ^{235}U fission spectrum for ^{115}In(n,n′)^{115}In, ^{64}Zn(n,p)^{64}Cu, ^{27}Al(n,p)^{27}Mg, ^{56}Fe(n,p)^{56}Mn, ^{24}Mg(n,p)^{24}Na and ^{19}F(n,2n)^{18}F reactions were measured relative to the ^{27}Al(n,α)^{24}Na reaction for which the averaged cross-section of 0.61 mb was assumed. The values obtained are 156 ± 5, 25.2 ± 1.3, 2.9 ± 0.3, 0.85 ± 0.05, 1.31 ± 0.05 and 0.053 ± 0.0005 mb, respectively. A standard fission-neutron source made of a 20% enriched uranium disk placed in the thermalizing column neutron beam was used for the irradiations. The converter was suspended in the exposure room in the reconstructed shielding facility of the TRIGA Mark II reactor. The large distance between the neutron source and the room walls makes fission-spectrum distortions due to scattered neutrons negligible. The induced gamma or positron-annihilation radiation was measured by a calibrated 3-in. diameter ×3-in. thick NaI(Tl) scintillation spectrometer. To obtain the activities, the spectra were unfolded by a technique similar to Health's technique. The measured cross-section values are compared with the results obtained by other authors as well as with values calculated by the available cross-section data and the fission spectrum given by $\Phi E = 0.513 \exp(-1.013\ E) \sinh(1.93\ E)^{1/2}$. (9 references) (auth)

14969 MULTILEVEL RESONANCE ANALYSIS OF THE TOTAL NEUTRON CROSS-SECTION OF ^{23}Na AND Ca BELOW 1 MeV. Nebe, J.; Kirouac, G. J. (Kernforschungszentrum, Karlsruhe, Ger.). pp 745-56 of Nuclear Data for Reactors. Vol. II. Vienna; International Atomic Energy Agency (1970).

From 2nd International Conference on Nuclear Data for Reactors, Helsinki, Finland. See STI/PUB–259(Vol.2); CONF-700605–(Vol.2).

The total neutron cross-sections of ^{23}Na and Ca were analysed below 1 MeV in order to provide neutron resonance parameters. The analysis uses the standard multilevel R-matrix formulas for a single open channel. A chi-squared fitting procedure is used for shape analysis. Resonance widths and energies were assigned for ^{23}Na up to 900 keV. The values of l and J were determined up to 439 keV; above this energy the inelastic channel opens and the assigned J values are only lower limits. In the case of Ca, the parameters of resonances between 0.5 and 1.2 MeV were determined. In many cases, new differential data for Ca were used to verify the l-value obtained by fitting the resonance. The channel radii and s and p-wave strength function of these nuclei are also discussed. (26 references) (auth)

14970 FAST-NEUTRON CAPTURE CROSS-SECTIONS OF Cr, Fe, Ni, AND Mo. Nishimura, K.; Asami, T.; Igarasi, S.; Hatchya, M.; Nakamura, H. (Japan Atomic Energy Research Inst., Tokai). pp 805-14 of Nuclear Data for Reactors. Vol. II. Vienna; International Atomic Energy Agency (1970).

From 2nd International Conference on Nuclear Data for Reactors, Helsinki, Finland. See STI/PUB-259(Vol.2); CONF-700605-(Vol.2).

In the keV-energy region, neutron radiative capture cross-sections for such reactor materials as Cr, Fe, Ni and Mo have been measured by a number of authors. A variety of standard cross-sections used in different groups of measurements makes a systematic comparison among their results difficult. The measurements of the Au(n,γ) cross-section curve by Poenitz et al. were adopted as a common standard cross-section. By multiplying the normalization factors to each (n,γ) cross-section in different groups of measurements, the renormalized (n,γ) cross-sections for Cr, Fe, Ni and Mo were obtained. By the use of the results of the systematic study of level density parameter a and strength function $1/\xi^{\circ}$, statistical model calculations were performed up to the region of about a few MeV. Calculations were made by the use of a computer code RACY. Collective and direct model calculations were performed in the region above a few MeV. The results of calculations from 10 keV to 20 MeV were adjusted to the renormalized (n,γ) cross-sections for Cr, Fe, Ni and Mo, and were compared with the curves of ENDF/B, KFK 750 and UK data. (47 references) (auth)

14971 CAPTURE CROSS-SECTIONS OF STRUCTURAL MATERIALS. Moxon, M. C. (Atomic Energy Research Establishment, Harwell, Eng.). pp 815-24 of Nuclear Data for Reactors. Vol. II. Vienna; International Atomic Energy Agency (1970).

From 2nd International Conference on Nuclear Data for Reactors, Helsinki, Finland. See STI/PUB-259(Vol.2); CONF-700605-(Vol.2).

The improvements in the cross-section data for fissile and fertile materials contrast strongly with the large discrepancies between different measurements of the absorption cross-sections of some of the elements used for fuel cladding and in the structure of nuclear reactors. The available data on the neutron absorption in these materials is examined, especially capture measurements which have shown the presence of many narrow capturing resonances in most of these elements. These results also indicate that in some cases the capture cross-section in the region of the large s-wave resonances could be an order of magnitude higher than the older results from the slowing-down spectrometer. Comment is about the corrections used to obtain the cross-sections from the γ-ray yield data, which in some cases can be very large. (25 references) (auth)

14972 ANALYSIS OF $2^- \rightarrow 2^+$ POSITON TRANSITIONS IN ^{84}Rb AND ^{74}As. De Beer, A.; Wooij, H. M. W.; Stuivenberg, J. H.; Blok, J. (Vrije Univ., Amsterdam). Nucl. Phys.; A160: 351-62 (1971).

Using new experimental data about spectrum shapes and $\beta\gamma$ angular correlations together with the intensity ratios of electron capture to positon decay, first-order forbidden transitions in ^{84}Rb and ^{74}As were reanalysed. The formalism used for the analysis is discussed with special emphasis on the formulas for the K/β^+ ratio. Three minima in the χ^2 surface with quite different sets of matrix elements were found for ^{84}Rb. The values of the parameters vary strongly with small variations in the experimental data, the K/β^+ ratio being no exception in this respect. In the case of ^{74}As a calculation based on the pairing model existed providing the non-relativistic matrix elements. The experiments could be fitted if the relativistic matrix elements were used as free parameters. If, however, the ratio between relativistic and non-relativistic matrix elements was limited to a reasonable region based on predictions of Fujita and Ahrens and Feenberg no fit to the experimental data could be obtained. (auth)

14973 PROPERTIES OF ^{55}Mn, ^{56}Mn, AND ^{57}Fe IN THE UNIFIED ROTATIONAL MODEL. Comfort, J. R. (Argonne National Lab., Ill.); Wasielewski, P.; Malik, F. B.; Scholz, W. Nucl. Phys.; A160: 385-408(1971).

A deformed single-particle model which includes the Coriolis coupling term is used to calculate the properties of ^{55}Mn and ^{57}Fe. The available experimental data are reviewed and compared with the calculated results. Good agreement is obtained for the energy levels, electromagnetic properties and stripping spectroscopic factors. An extension of the model to doubly odd nuclei, with inclusion of an n-p residual interaction, also produced good agreement with experimental quantities for ^{56}Mn. Consideration of these results in comparison with shell-model calculations leads to arguments that these nuclei may be statically deformed. (auth)

14974 ENERGY LEVELS OF ^{56}Mn. van Assche, P. H. M. (Technical Univ., Munich); Baader, H. A.; Koch, H. R.; (and others). Nucl. Phys.; A160: 367-84(1971).

The low-energy spectrum of the ^{55}Mn(n, γ)^{56}Mn reaction was studied with a γ-diffraction spectrometer. These data allowed the construction of a level scheme for ^{56}Mn with two previously unobserved doublets. High-energy γ-transitions to the low-energy states were measured for different neutron resonances at the BNL fast neutron chopper. For most states a unique spin and parity could be proposed. A shell-model calculation of the structure of the low-lying states of ^{56}Mn was carried out with the Oak Ridge-Rochester computer program; there are plausible theoretical analogues for 11 of the 12 experimentally observed states. Calculated spectroscopic factors and M1 transition probabilities are in qualitative agreement with the experiment. (auth)

14975 MEASUREMENT OF g-FACTORS FOR THE CASE OF UNSEPARABLE ENERGIES OF THE $\gamma\gamma$ CASCADE. Reuse, B. (Justus Liebig-Univ., Giessen, Ger.). Nucl. Phys.; A160: 363-6(1971). (In German)

The possibility of measuring the g-factors of nuclear levels with half-lives ($T_{½} \approx 1$ns) for a given $\gamma\gamma$ cascade, with energies which cannot be separated, is investigated. From the example of the 184-keV level of ^{67}Zn it is shown that a combination of a differential with an integral measurement of perturbed angular correlations allows one to determine the magnitude and the sign of such g-factors. (auth)

14976 SHAPES OF THE NON-UNIQUE AND UNIQUE FIRST-FORBIDDEN β-SPECTRA OF ^{84}Rb, ^{74}As AND ^{124}I. Booij, H. M. W.; Van Hoek, E. A.; van der Molen, H.; Slot, W. F.; Blok, J. (Vrije Univ., Amsterdam). Nucl. Phys.; A160: 337-50(1971).

The shapes of $2^- \rightarrow 2^+$ and $2^- \rightarrow 0^+$ positon and negaton spectra of ^{84}Rb, ^{74}As and ^{124}I were measured using a double focusing β-spectrometer. The spectrum shapes of the $2^- \rightarrow 2^+$ transitions were obtained by subtracting the unique spectra from the total spectra. The possible distortions of the spectra due to, for instance, scattering effects, influence of the iron of the spectrometer were investigated. As a final test the allowed spectra of ^{24}Na and ^{32}P were measured; the results for ^{32}P are presented. The non-unique spectra were analysed using the maximum β-energy W_0 and the coefficients k and a′ in the empirical shape factor $C(W) = k(1 + a'W)$ as adjustable parameters. For most unique transitions small deviations from the theoretical shape factor were found which were of the same order of magnitude as those reported for a number of other negaton transitions. (auth)

14977 PHOTOSPALLATION OF MEDIUM-HEAVY ELEMENTS WITH BREMSSTRAHLUNG OF MAXIMUM ENERGIES BETWEEN 0.8 AND 2.1 GeV. Kumbartzki, G. J.; Kim, Ung; Kwan, Ch. K. (Univ., Bonn). Nucl. Phys.; A160: 237-46(1971).

Yields of spallation products after irradiation of the elements ^{27}Al, ^{51}V, ^{55}Mn, ^{56}Fe, ^{59}Co and ^{75}As with bremsstrahlung of maximum energies between 0.8 and 2.1 GeV were measured by the activation method. For constant Z the yield as a function of the number of ejected particles is similar to that found for proton induced spallation. It is possible to reproduce the spallation data with an analytical formula, the parameters of which were determined for various energies and mass numbers. (auth)

14978 EMISSION OF ^{8}Li FRAGMENTS FROM K^- INTERACTIONS. Dhawan, M. M.; Gaur, R. K. (Univ. of Kurukshetra, India). Nucl. Phys.; B25: 535-42(1971).

About 190 hammer tracks from 1.5 and 3.5 GeV/c K^- interactions with emulsion nuclei were collected. After a careful analysis of possible losses the total emission frequency was evaluated. The production rate rises with the incident energy and so does the F/B ratio. The experimental studies suggest that production of short range hyperfragments needs some theoretical explanation other than evaporation theory. (auth)

Nuclear Properties and Reactions, A ≥ 90

Refer also to abstracts 13625, 13626, 13982, 14845, 14892, 14906, 14921, 14925, 14932, 14947, 14960, 14965, 14976, 14978, 15077, 15138, 15140, 15148, 15178, 15190, 15191, 15193, 15198, and 15399.

14979 (AAEC/E–198(Suppl.1)) RESONANCE PARAMETERS FOR MEASURED keV NEUTRON CAPTURE CROSS SECTIONS. Musgrove, A. R. de L. (Australian Atomic Energy Commission Research Establishment, Lucas Heights). Aug 1970. 60p. Dep. NTIS (U. S. Sales Only).

All available neutron capture cross sections in the keV region (~5 to 100 keV) have been fitted with resonance parameters using a nonlinear least squares fitting routine. Graphs of s-, p- and d-wave neutron strength functions are given. An appendix gives calculated best fits compared with experiment. (auth) (Australia)

14980 (CEA-CONF–1654) STUDY OF (p,d) REACTIONS ON ^{90}Zr AND ^{92}Mo WITH POLARIZED PROTONS. Escudie, J. L.; Gosset, J.; Kamitsubo, H.; Mayer, B. (Commissariat a l'Energie Atomique, Saclay (France). Centre d'Etudes Nucleaires). 1970. 2p. (CONF-700811–7). Dep. NTIS (U. S. Sales Only).

From 3rd International Symposium on Polarization Phenomena in Nuclear Reactions, Madison, Wis.

A study of (p,d) reactions with ^{90}Zr at 22.9 MeV and ^{92}Mo at 24.5 MeV is reported. The angular distributions of the cross sections and asymmetries for the first three levels of ^{89}Zr are similar to those of the corresponding levels in ^{91}Mo. The spin and parity assigned to the first three levels of ^{91}Mo are $\frac{9}{2}^+$ (ground state), $\frac{1}{2}^-$ and $\frac{3}{2}^-$. The strong j-dependence of the asymmetries for the two excited levels of ^{89}Zr and ^{91}Mo is shown. The DWBA satisfactorily explained the measured cross sections and asymmetries. The optical potentials used are listed. The proton potential fits the cross section and polarization for the elastic scattering of protons. The deuteron potential fits the cross section for the elastic scattering of deuterons at 12 MeV. Finite-range and nonlocality corrections are included but they do not significantly modify the asymmetry. (France)

14981 (IN–1448) GAMMA RAYS EMITTED BY THE FISSIONABLE NUCLIDES AND ASSOCIATED ISOTOPES. Cline, J. E. (Idaho Nuclear Corp., Idaho Falls). Dec 1970. Contract AT(10-1)-1230. 47p. Dep. NTIS.

Data on gamma-ray energies and intensities emitted by the nuclides present in nuclear fuel material are presented. These energies and intensities were measured using a high-resolution Ge(Li) spectrometer. Gamma-ray pulse-height spectra are given. (auth)

14982 (NCSAC–31) REPORTS TO THE AEC NUCLEAR CROSS SECTIONS ADVISORY COMMITTEE MEETING AT ARGONNE NATIONAL LABORATORY, CHICAGO, ILLINOIS, MAY 20–22, 1970. Chrien, R. E. (comp.) (Nuclear Cross Sections Advisory Committee (AEC)). 295p. (EANDC(US)–143-U; INDC(US)–22-U; CONF-700537). Dep. CFSTI.

ANTIMONY-121—neutron capture by, γ spectra for resonance, (E)
CARBON—neutron total cross section at 0.5 to 15 MeV, (E)
CERIUM-134—neutron capture by, γ spectra for resonance, (E)
CHROMIUM-50—neutron capture at 0.1 to 20 keV, cross section for, (E)
CHROMIUM-52—neutron total cross section up to 200 keV, (E)
CHROMIUM-53—photoneutron cross section for, (E)
CHROMIUM-54—neutron capture at 0.1 to 20 keV, cross section for, (E)
DYSPROSIUM-163—neutron capture up to 360 eV, γ spectra and resonance spin assignments for, (E)
GOLD-197—neutron capture up to 1 MeV, cross section for, (E)
INDIUM-115—neutron capture by, cross section calculations for, (T)
LUTETIUM-175—neutron capture by, resonance spin assignments for epithermal, (E)
—neutron capture by, cross section calculations for, (T)
NICKEL-60—neutron capture at 0.1 to 20 keV, cross section for, (E)
NITROGEN—neutron total cross section at 0.5 to 25 MeV, (E)
OXYGEN—neutron reactions (n,xγ) at 14.8 MeV, γ spectra from, (E)
OXYGEN-16—photon reactions (γ,n) at 30 MeV, neutron polarization from, (E)
—photodisintegration at 30 MeV, γ spectra from, (E)
PLUTONIUM-238—neutron fission at 15 to 500 eV, cross section for, (E)
PLUTONIUM-239—neutron capture by, γ spectra from, (E)
PLUTONIUM-240—neutron capture at 4 to 60 keV, average cross section for, (E)
PLUTONIUM-242—neutron total cross section up to 1 eV, (E)
SILVER-109—neutron capture by, γ spectra from, (E)
SILVER-110—energy-level scheme from silver-109 neutron capture, (E)
THULIUM-169—neutron capture by, cross section calculations for, (T)
TITANIUM-50—proton elastic scattering near 2.5 MeV with isobaric analog excitation, proton spectra from, (E)
URANIUM-233—neutron fission at 500 to 1500 keV, ratio to uranium-235 fission cross section, (E)
URANIUM-235—neutron fission at 500 to 1500 keV, ratio to uranium-233 fission cross section, (E)
—neutron fission at 1400 and 1500 keV, ratio to uranium-238 fission cross section, (E)
—neutron capture by, γ spectra from, (E)
URANIUM-238—neutron fission at 1400 and 1500 keV, ratio to uranium-235 fission cross section, (E)
—neutron capture by, cross section calculations for, (T)
VANADIUM-51—neutron capture at 0.1 to 20 keV, cross section for, (E) (J.W.R.)

14983 (NP–18492) SEARCH FOR CLASSES IN MAGNETIC QUADRUPOLE GAMMA TRANSITIONS. Letessier, Jocelyne (Paris Univ. (France). Faculte des Sciences). 14 May 1970. 112p. (In French). Dep. NTIS (U. S. Sales Only).

Thesis.

A limited number of transitions is known with certainty; an attempt was made to increase this number in order to find out whether distinct classes of M2 transitions existed and to relate these classes to certain nuclear properties. Automatic angular-correlation measuring equipment was developed, and two methods were used to measure mean lives ranging from some dozens of picoseconds to a few microseconds. One method involved using a time-amplitude converter; and the other, variable electronic delay-time techniques. In order to realize what were the limitations to the measurements of the weak proportions of E2 or M2 in the transitions M1 + E2 or E1 + M2, the 329 keV ^{40}Ce transition was studied in detail. It was shown that an accuracy of better than 50 percent could be achieved for mixings of a few parts per thousand when perturbations due to hyperfine coupling were eliminated. Most of the endeavors to detect M2 transitions were unsuccessful; however, fortuitously certain transitions led to the establishment of about twenty nuclear level schemes. Eighty-three M2 transitions which could be analyzed were found, and the periodicity of the forbidden transitions was already apparent. The periodicities were explained by the weak dependence of the M2 transition probabilities on the particular nuclear characteristics introduced: the deformation of the nucleus, the use of a Woods–Saxon deformed potential instead of that of a harmonic oscillator, and the force parameters used. Except for transitions between a two quasi-particle state and the ground state of an even–even nucleus, this probability is equally independent of the pair correlations in the region of the Fermi surface. The independent particle in spherical- or deformed-potential models yielded results for almost-magic or strictly rotational nuclei. The model of quasi-particles with convenient residual interactions led to an estimation of the M2 transition probabilities for nuclei of almost-closed shells. The shell model led to predictions on the regions of M2 isomerism, but it was difficult to construct collective M2 states except in the case of deformed nuclei. A high value of the forbiddenness factor may be explained by the coupling of a particle with vibrations of the core, in the region of ^{208}Pb and the semi-magic shells of N = 41 and Z = 41 and 43. Other explanations are possible, such as large deformations and instabilities in form. (74 references) (France)

14984 (NP–18536) PROPERTIES OF THE DEFORMED NUCLIDES PRODUCED IN THE DECAY OF ^{166}Ho, ^{166m}Ho, ^{166}Tm, ^{166}Yb, ^{180}Os, ^{180}Re, ^{181}Os, AND ^{181m}Os, AND BY CAPTURE OF THERMAL NEUTRONS IN ^{181}Ta. Goudsmit, Peter Frank Arnold (Amsterdam Univ. (Netherlands)). [1969]. 151p. Dep. NTIS (U. S. Sales Only).

Thesis.

Information about the properties of deformed nuclei is presented. After an introduction to the appropriate theoretical concepts, measurements on the decay of ^{166}Ho, ^{166m}Ho, and ^{166}Tm leading to ^{166}Er are discussed. Conversion coefficients and transition multipolarities are obtained, and special attention is directed to the properties of the gamma-vibrational and ground-state bands and to identifying states above 1 MeV with the calculated two-quasi-particle and collective excitations and with the members of their rotational bands. In the decay of ^{166}Yb, only an upper limit on the intensity could be estimated for any possible transitions other than the 82.3-keV one. The properties of states in ^{180}Re and ^{180}W excited in the decay of ^{180}Os and ^{180}Re were studied; they were consistent with theoretical predictions. Energy levels in ^{181}Re, from the beta decay of ^{181}Os, were examined. The spacing between certain odd-parity levels can be explained only if the rotation-particle coupling is taken into account. Finally, internal conversion in ^{182}Ta (following thermal neutron capture by ^{181}Ta) was measured with a semiconductor detector situated outside the region of high gamma flux. The conversion electrons were guided to the detector by a strong magnetic field (provided by a superconducting solenoid). This method results in a great reduction in the time required to make the measurements. (R.W.R.)

14985 (NP–18615) MULTIPOLE CHARACTER OF SOME GAMMA TRANSITIONS IN ^{152}Sm. Helppi, H.; Hattula, J. (Jyvaskyla Univ. (Finland). Dept. of Physics). Sep 1970. 15p. Dep. NTIS (U. S. Sales Only).

Multipole character of some transitions connecting the quadrupole and octupole vibrational bands to the ground-state rotational band in ^{152}Sm has been determined by measuring directional correlations using a Ge(Li)–NaI(Tl) spectrometer. A total of 14 correlations have been measured. From these measurements it can be concluded that the $2_\beta^+-2^+$, 689-keV, $2_\gamma^+-2^+$, 964-keV, and $3_\gamma^+-2^+$, 1112-keV transitions are essentially pure E2, and 3^--2^+, 1457-keV, 3^--4^+, 1213-keV, and 2^--2^+, 1408-keV transitions contain less than 2% M2. (auth) (Finland)

14986 (ORNL–tr–2408) ANISN SYSTEM, REPORT NO. 2. LGR/B PROGRAM: FOR UPDATING THE ANISN LIBRARY TAPES WITH PLOTTING OF CROSS SECTION CURVES. Brandicourt, Gilles; de Scheemaecker, Jacques (Commissariat a l'Energie Atomique, Fontenay-aux-Roses (France). Centre d'Etudes Nucleaires). Translated for Oak Ridge National Lab., Tenn., from report CEA-N–1335. 47p. Dep. NTIS.

The program LGR/B is an updating of the LGR program, which served to constitute and modify a library tape used by the program ANISN. LGR/B makes it possible to plot the total and absorption cross sections of the same element and to compare the cross sections of two different elements on the same graph. The program is listed in FORTRAN IV, and several examples of its use are given. Typical running time is of the order of one minute on an IBM 360/91, and the program uses 350K of core. (R.W.R.)

14987 (STI/PUB–259(Vol.1)) NUCLEAR DATA FOR REACTORS. VOL. I. Proceedings Series. Proceedings of the Second International Conference Held in Helsinki, 15–19 June 1970. (International Atomic Energy Agency, Vienna (Austria)). Oct 1970. 754p. (In several languages). (CONF-700605–(Vol.1)). IAEA $21.00.

Included are 55 papers on the results of basic neutron-physics investigations, especially basic data used in nuclear reactor design. A separate abstract was prepared for each of 48 papers. Seven papers were previously abstracted for NSA, and may be located under CONF–700605 in the Report Number Index. (H.D.R.)

For abstracts of individual papers see: 13215, 13216, 14357, 14876, 14877, 14909–14913, 15067–15101, 15206, 15345, and 15402.

14988 (STI/PUB–259(Vol.2)) NUCLEAR DATA FOR REACTORS. VOL. II. Proceedings Series. Proceedings of the Second International Conference Held in Helsinki, 15–19 June 1970. (International Atomic Energy Agency, Vienna (Austria)). Nov 1970. 972p. (In several languages). (CONF-700605–(Vol.2)). IAEA $24.00.

Included are 62 papers on the results of basic neutron-physics investigations, especially basic data used in nuclear reactor design. A separate abstract was prepared for each of 60 papers. Two papers were previously abstracted for NSA, and may be located under CONF–700605 in the Report Number Index. (H.D.R.)

For abstracts of individual papers see: 14878, 14879, 14960–14971, 15102–15135, 15207–15209, 15346–15350, and 15396–15399.

14989 (UCRL–50656(Suppl.)) FISSION GAS RELEASE CURVES: GROWTH AND DECAY FROM FISSION OF ^{239}Pu BY FISSION SPECTRUM NEUTRONS (SUPPLEMENT). Barg, D. C. (California Univ., Livermore. Lawrence Radiation Lab.). 9 Oct 1970. 150p. Dep. NTIS.

This supplement extends the scope of the original report to include times of release of radioactive gases as follows: 2, 4, 12, and 24 hr following fissioning. Tables and curves are presented for fission gas isotopes from ^{85}Kr through ^{88}Kr and from ^{133}Xe through ^{138}Xe, including growth and decay of the daughter products. (auth)

14990 THE ENERGY SPECTRUM OF PHOTONEUTRONS PRODUCED BY 140-MeV ELECTRONS INCIDENT ON TANTALUM. Burgart, C. E.; Straker, E. A.; Love, T. A.; Freestone, R. M. Jr. (Oak Ridge National Lab., Tenn.). Nucl. Sci. Eng.; 42: 421-3 (Dec 1970).

A tantalum target 8.3 radiation lengths in thickness was bombarded by 140-MeV electrons, and the neutron energy spectrum due to an electron–photon cascade was measured in the 0.7- to 20-MeV energy range. NE-213 liquid scintillator was utilized in a time-of-flight measurement. The spectrum, observed at the 165° flight station, is reported on an absolute basis. The results agree well with electron–photon cascade calculations. (R.W.R.)

14991 IN-BEAM GAMMA SPECTROSCOPY OF ^{161}Ho. Alonso, J.; Bakhru, H.; Bernthal, F. M.; (and others) (Yale Univ., New Haven). Contract AT(30-1)-3909. Nucl. Phys.; A160: 193-203 (1971).

Boron ion in-beam γ-spectroscopy studies are reported, leading to assignment of eight excited members of the ^{161}Ho ground rotational band. Energy spacings of ^{161}Ho and ^{165}Ho bands are analyzed in terms of perturbation expansions of the Coriolis interaction. Energies and intensities are compared with Stockholm work involving α-particle bombardments. (auth)

14992 LIFETIMES OF EXCITED STATES IN ^{101}Rh. Vaelivaara, K. G.; Marelius, A.; Kozyczkowski, J.; Sieniawski, J. (Uppsala Univ.). Phys. Scr.; 1: 89-90(1970).

Half-lives of the 181.8-keV level (1.91 ± 0.06 ns) and the 477.9-keV level (68 ± 16 ps) of ^{101}Rh were measured by the delayed-coincidence technique. Upper limits for the half-lives of two levels in ^{101}Ru are reported. (auth) (Sweden)

14993 STRENGTH-FUNCTION PHENOMENA IN ELECTRON-CAPTURE BETA DECAY. Duke, C. L. (Univ. of Aarhus, Denmark); Hansen, P. G.; Nielsen, O. B.; Rudstam, G. Nucl. Phys.; A151: 609-33(1970).

Approximate beta strength functions were derived from measurements of the electron-capture beta feed to the high-lying excited states in about 40 neutron-deficient nuclei. These nuclei ranged from isotopes of iridium ($Z = 77$) to those of radon ($Z = 86$). The beta feed was determined from the gamma spectra by a total absorption spectrometry technique involving two 15 cm diam. × 10 cm height NaI(Tl) crystals. Two sum spectra, one with and one without a coincidence demand, were recorded simultaneously for each isotope. An average multiplicity of three to four high-energy γ rays per cascade was deduced from the ratio of these two spectra. In general, the strength functions vary smoothly with energy as well as with the neutron number N and the proton number Z. Strong peaks appear in the energy region 1.5 to 3.5 MeV. Relatively little strength is found below an excitation energy in the daughter nucleus corresponding approximately to the energy required for forming a (pn) pair. This overall behavior can be understood by assuming that the main part of the strength is associated with transitions that excite protons that are initially in paired orbits. An average value $\bar{S}_\beta$ of the beta strength function for a given isotope may be calculated if the Q-value and the gross electron-capture half-life are known. $\bar{S}_\beta$ varies strongly but systematically with N and Z; from the light Pt isotopes with $N \approx 100$ to isotopes just below the 126-neutron closed shell, it decreases by a factor of about 300. Fine structure in this dependence may be evidence for subshell effects in deformed nuclei. The results are discussed in terms of the shell model. (auth)

14994 INVESTIGATION OF THE (n,α) REACTION ON Sm AND Nd ISOTOPES IN THE NEUTRON ENERGY REGION BELOW 1 keV. Kvitek, J.; Popov, Yu. P. (Joint Inst. for Nuclear Research, Dubna, USSR). Nucl. Phys.; A154: 177-90 (1970).

Alpha widths for sixteen resonances in the ^{149}Sm(n,α) reaction were measured on the IBR Pulsed Reactor of the Joint Institute for Nuclear Research. The results are discussed together with the improved data on α-widths for the ^{143}Nd, ^{145}Nd, and ^{147}Sm resonances in the neutron energy region 0.04 to 900 eV. From the dependence of α-widths on resonance spins, spin assignment of the ^{143}Nd resonances is made. The experimental values of the average α-widths for the given isotopes are compared with those calculated from the statistical nuclear model. The effect of neutron pairing correlations on the probability of α decay of excited states is discussed. Alpha-width fluctuations relative to the average value are considered. (auth)

14995 DECAY OF ^{205}At. Hopke, P. K.; Naumann, R. A.; Spejewski, E. H. (Frick Chemical Lab., Princeton, N. J. Princeton Univ., N. J.). Nucl. Phys.; A149: 63-4(1970).

The decay of ^{205}At to ^{205}Po was investigated and found to proceed entirely to a $^{9}/_{2}^{-}$ level at 718.8 ± 0.7 keV, with an estimated log ft of 6.1. (auth)

14996 TEST OF THE INDEPENDENCE HYPOTHESIS IN THE DECAY OF THE ^{210}Po COMPOUND NUCLEUS. Wong, P.; Daly, P. J.; Porile, N. T. (Purdue Univ., Lafayette, Ind.). Nucl. Phys.; A151: 549-60(1970).

The angular distributions, cross sections, and recoil ranges of ^{207}Po from the ^{206}Pb(^{4}He, 3n) and ^{207}Pb(^{3}He, 3n) reactions were measured over the energy intervals 32 to 44 and 21 to 33 MeV, respectively. The compound nuclear nature of these reactions was established by comparison of the average ranges with values expected for this mechanism. The angular distributions were used to derive values of the average total kinetic energy of the neutrons and photons emitted in these reactions. The partition of the excitation energy between these two decay modes was found to be equal for the two reactions to within at most 1.5 MeV. The expected difference in energy partition arising from angular momentum differences is approximately 0.5 MeV. (auth)

14997 INTERMEDIATE STRUCTURE EFFECTS IN THE FISSION OF SOME ACTINIDE NUCLEI. Sood, D. K.; Sarma, N. (Bhabha Atomic Research Centre, Bombay). Nucl. Phys.; A151: 532-48(1970).

High resolution cross-section measurements on neutron-induced fission of ^{233}U, ^{235}U, ^{239}Pu, ^{240}Pu, ^{241}Pu, and ^{242}Am were studied to investigate the intermediate structure effects arising from the double-humped nuclear deformation curve. An improved correlation analysis was used to determine the spacing, $\bar{D}_{II}$ of the class II levels built on the second minimum. The depth E_{II} of the second minimum was then derived by using a semi-empirical level spacing formula, and was re-evaluated for several other nuclei by using the $\bar{D}_{II}$ values obtained from the subthreshold fission cross sections on ^{234}U, ^{237}Np, ^{242}Pu, and ^{241}Am. Values of E_{II} resulting from fission isomer threshold measurements are also included to examine the variation of E_{II} as a function of Z and N in the actinide region. The results are compared with recent theoretical predictions. (auth)

14998 HIGH-RESOLUTION GAMMA SPECTROSCOPY IN THE DECAY OF ^{231}Pa. de Pinho, A. G.; da Silveira, E. F.; da Costa, N. L. (Pontificia Univ. Catolica, Rio de Janeiro). Phys. Rev., C; 2: 572-86(Aug 1970).

The decay of ^{231}Pa was reinvestigated by means of Ge(Li) singles and coincidence techniques. The spectrometer showed a resolution (full width at half maximum) of 850 eV for the 300-keV γ rays. 78 γ rays were attributed to the decay of ^{231}Pa. A level scheme for ^{227}Ac was proposed and interpreted in terms of rotation bands. Alternating terms in the K = $^{3}/_{2}$ bands were discussed in connection with Coriolis coupling to K = $^{1}/_{2}$ bands. (auth)

14999 SYMMETRY OF NEUTRON-INDUCED ^{235}U FISSION AT INDIVIDUAL RESONANCES. III. Cowan, G. A.; Bayhurst, B. P.; Prestwood, R. J.; Gilmore, J. S.; Knobeloch, G. W. (Los Alamos Scientific Lab., N. Mex.). Phys. Rev., C; 2: 615-20 (Aug 1970).

The symmetry of neutron-induced fission in ^{235}U was measured at a large number of epithermal levels with a time-of-flight energy-resolved beam from an underground nuclear explosion. The energy resolution was improved over previous similar "wheel" experiments. The symmetry of fission, as measured radiochemically by the ratio of ^{115}Cd to ^{99}Mo, shows a bimodel distribution. If the results are averaged separately for the two apparent groups, the first group (I) has an average ^{115}Cd/^{99}Mo ratio, which is 0.593 times the thermal value; the second-group (II) average is 1.11 times the thermal value. The average fission width in I is one-half the average fission width in II. The numbers of levels assigned to I and II are 24 and 14, respectively. The energies of levels assigned to I are 19.30, 21.07, 22.94, 23.63, 26.44, 27.81, 30.91, 32.10, 33.55, 34.85, 40.51, 41.91, 43.41, 44.04, 45.79, 46.93, 48.06, 48.82, 51.37, 56.58, 57.83, 58.15, 60.25, and 61.10 eV; assignments to II are at 24.23, 25.65, 28.35, 34.39, 35.21, 35.75, 36.64, 38.42, 39.44, 44.75, 49.51, 52.27, 53.56, and 58.68 eV. From analogy with conclusions based on a similar set of observations in the fission of ^{239}Pu and on arguments derived from fission–channel theory, it is hypothesized that J = 4 in I and 3 in II. (auth)

15000 TWO-QUASIPARTICLE STATES IN ^{168}Er. Michaelis, W.; Ottmar, H.; Weller, F. (Kernforschungszentrum, Karlsruhe, Ger.). Nucl. Phys.; A150: 161-86(1970).

The level structure of ^{168}Er and the de-excitation mechanism in this nucleus were studied by radiative capture of thermal neutrons in samples of natural erbium, which give a cross-section contribution of 89.8 ± 2.3% for ^{167}Er. Interference from the 9.1 ∓ 2.1% capture contribution of ^{166}Er was well known from a separate study with enriched ^{166}Er samples. High-resolution measurements of the γ spectrum were performed using the Karlsruhe Ge(Li) anti-Compton spectrometer below 2 MeV and a Ge(Li) double-escape spectrometer above 5.16 MeV. The high accuracy of the data allows the construction of a considerably extended transition diagram up to 2 MeV excitation energy. New levels were assigned to specific configurations and their superimposed rotational bands. Conclusive evidence is given that the previously known states at 1094 and 1542 keV are the two-quasiparticle neutron levels $[633\uparrow + 521\downarrow]_{nn}$ and $[633\uparrow - 521\downarrow]_{nn}$, respectively. Some aspects of the corresponding log ft values are discussed in detail. Rotational bands at 1354, 1569, and 1542 keV have to be identified with the $K^{\pi} = 1^{-}$, 2^{-} and 3^{-} octupole vibrational bands. The properties of the $K^{\pi} = 1^{-}$ state are presumably close to those of the neutron level $[512\uparrow - 633\uparrow]_{nn}$. The 3^{-} rotational member of the $K^{\pi} = 0^{-}$ octupole band probably occurs at 1914 keV. The simple model of pairing plus state-independent octupole force provides a surprisingly good microscopic description of the octupole excitation energies. The first $K^{\pi} = 0^{+}$ band was well established to occur at 1217 keV. Within the model of pairing plus quadrupole and spin-quadrupole force one obtains the interaction constants $\kappa_q = 5.3$ and $\kappa_t = 8.8$ (in units of $A^{-1/3}\hbar\omega_0$). The neutron level $[521\downarrow + 642\uparrow]_{nn}$ was tentatively assigned to a rotational band at 1893 keV. The properties of some other more or less collective states are discussed. No positive evidence was found for the occurrence of two-quasiparticle proton levels below 1820-keV excitation energy. The neutron separation energy was determined to be 7771.24 ± 0.48 keV. (auth)

15001 IDENTIFICATION OF A NEW ^{110}Rh ISOTOPE. Ward, T. E.; Takahashi, K.; Pile, P. H.; Kuroda, P. K. (Univ. of Arkansas, Fayetteville). Nucl. Phys.; A154: 665-72(1970).

Irradiation of enriched ^{110}Pd was found to produce a radioactive nucleide that was assigned to ^{110}Rh. The following radiation characteristics were observed to belong to the decay of the ^{110}Rh activity: half-life 34 ± 4 sec; β end-point energy 5.50 ± 0.30 MeV; γ energies 282 ± 2, 374 ± 1, 399 ± 1, 440 ± 1, 547 ± 1, 584 ± 1, 653 ± 1, 688 ± 1, 814 ± 2, 838 ± 1, and 905 ± 1 keV and relative intensities 3.9 ± 0.5, 100.0, 15.5 ± 1.5, 27.6 ± 2.5, 39.3 ± 3.6, 11.9 ± 1.5, 11.9 ± 1.6, 29.1 ± 3.2, ≈2.0, 18.0 ± 2.5, and 20.3 ± 2.8, respectively. (auth)

15002 RADIATIVE WIDTHS, SPINS, AND PARITIES OF NUCLEAR LEVELS IN THE 6 TO 9-MeV REGION EXCITED BY NEUTRON CAPTURE γ RAYS. Moreh, R.; Shlomo, S.; Wolf, A. (Nuclear Research Centre, Negev, Israel). Phys. Rev., C; 2: 1144-1144-56(Sep 1970).

Monochromatic photons obtained from thermal-neutron capture in iron were used for exciting nuclear levels in the energy region between 6 and 9 MeV. Angular distribution measurements on the elastically scattered radiation were carried out for determination of the spins of the resonance levels. Total and ground-state radiation widths of ten resonance levels in various isotopes were measured using self-absorption, temperature variation, and absolute scattering cross-section measurements. The parity of six resonance levels was measured using a Compton polarimeter, and strong M1 transitions were found in ^{141}Pr and ^{208}Pb; the character of four transitions was found to be E1. The observed total radiation widths Γ_γ of these bound levels were found to have the same magnitude as those of unbound levels obtained in neutron resonances, which indicate that Γ_γ is continuous across the (γ,n) threshold. (auth)

15003 ABSOLUTE DETERMINATION OF SPINS OF NEUTRON RESONANCES AND THE HYPERFINE COUPLING CONSTANT IN ^{167}Er. Brunhart, G.; Sailor, V. L. (Brookhaven National Lab., Upton, N. Y.). Phys. Rev., C; 2: 1137-43(Sep 1970).

The spins of the four lowest neutron resonances in ^{167}Er were determined by measuring the transmission of polarized neutrons through a sample of polarized erbium nuclei. The determination of the spins depends solely on the transmission effect and is independent of any assumption about the sign of the nuclear magnetic moment or the direction of the effective field at the target nuclei. The spins were found to be J = I + $^{1}/_{2}$ = 4 for the 0.460-eV resonance and J = I − $^{1}/_{2}$ = 3 for the resonances at 0.584, 6.10, and 9.6 eV. The nuclear polarization of the sample, obtained as function of the sample temperature at a fixed energy, was fitted to a theoretical curve, using the magnetic and electric hyperfine splitting constants as fitting parameters. The values found for the magnetic and electric hfs constants are, respectively, A/k = −0.085 ± 0.0005°K and P/k = −0.005 ± 0.001°K. Taking the nuclear magnetic moment of ^{167}Er to be $-0.56\mu_N$, the corresponding effective magnetic field at the nucleus is 7.26 × 10^{6} Oe. (auth)

15004 EXACT CALCULATION OF THE PENETRABILITY THROUGH TWO-PEAKED FISSION BARRIERS. Cramer, J. D.;

Nix, J. R. (Los Alamos Scientific Lab., N. Mex.). Phys. Rev., C; 2: 1048-57(Sep 1970).

The penetrability was computed exactly for a fission barrier V(ϵ) defined in terms of two parabolic peaks connected smoothly with a third parabola forming the intermediate well. The potential is specified by the peak energies E_1 and E_3 and the minimum energy E_2 of the connecting curve, along with the constants $\hbar\omega_1$, $\hbar\omega_3$, and $\hbar\omega_2$ related to the curvatures of the three parabolas. For an incident wave of unit amplitude, the amplitude of the transmitted wave is determined by requiring that the wave functions (expressed exactly in terms of parabolic-cylinder functions) and their first derivatives match at the points where the parabolas are connected. The penetrability is then obtained from the amplitude of the transmitted wave. The transmission is essentially an increasing exponential function exhibiting narrow resonances at the positions of quasibound states in the intermediate well. The widths of these resonances are extremely small (~10 eV) for the levels near the bottom of the well but increase dramatically as the energy increases. This trend continues in some cases above the top of the barrier, producing broad peaks in the penetrability function. The exact penetrabilities are accurately reproduced by the WKB approximation for energies well below the barrier tops, but for energies near the barrier tops the WKB approximation is found to overestimate the penetrability for the cases studied. (auth)

15005 STUDY OF THE DECAY ^{109}In → ^{109}Cd. Rivier, J.; Moret, R. (Institut des Sciences Nucleaires, Grenoble, France). Nucl. Phys.; A149: 337-49(1970). (In French).

The decay scheme of ^{109}In has been set up through a study of the γ-spectrum and by coincidence techniques. Several new transitions have been discovered with Ge(Li) detectors. Including these results into a summary of the observed low-lying levels of Cd odd-A isotopes and taking into account the Kisslinger and Sorensen calculations, an interpretation for these levels is suggested. (auth)

15006 STRONG L = 0 AND 2 TRANSITIONS IN (p,t) REACTIONS ON EVEN-MASS Ce ISOTOPES. Yagi, K.; Aoki, Y.; Sato, K. (Osaka Univ.). Nucl. Phys.; A149: 45-8(1970).

The pairing vibrational states near N = 82 were investigated by means of (p,t) reactions on the even-mass Ce isotopes of A = 140 and 142. Strong L = 0 and 2 transitions to the expected vibrational states were observed. (auth)

15007 DECAY OF 12.3 h ^{130g}I, 9.2 min ^{130m}I, AND 6.5 d ^{132}Cs. Quaim, Syed M. (Univ., Mainz). Nucl. Phys.; A154: 145-59(1970).

The decay of 12.3-hr ^{130g}I and 9.2-min ^{130m}I was investigated by $\beta\gamma$ and $\gamma\gamma$ coincidence studies using a plastic scintillator and large size Ge(Li) detectors. In the decay of ^{130g}I, three β groups and 18 γ transitions were observed. A decay scheme allowing placement of 13 of the emitted γ rays was constructed and the following excited levels of ^{130}Xe deduced: 536.0 (2^+), 1122.0 (2^+), 1204.5 (4^+), 1632.8 (4^+), 1808.0 (4^+), 1944.0 (5^+), 2170.5, and 2362.0 (6^+) keV. The 9.2-min ^{130m}I decays 84% by a highly converted isomeric transition to ^{130g}I and 16% by independent β-branching to levels of ^{130}Xe. Two β groups and four γ rays were observed. A partial decay scheme of this isomer is suggested. The 536.0 (2^+) and 1122.0 (2^+) levels of ^{130}Xe are populated directly by the two β groups from ^{130m}I. Extensive $\gamma\gamma$ coincidence measurements on 6.5 d ^{132}Cs were also carried out. A decay scheme is suggested that permits incorporation of all of the observed 12 γ transitions. In the electron capture and positon decay of this isotope ^{132}Xe is formed, the excited levels of which were adduced to be at 667.5 (2^+), 1297.5 (2^+), 1440.0 (4^+), 1803.0 (2, 3), and 1985.5 (2) keV. The first three excited states in ^{132}Ba at 464.5 (2^+), 1031.5 (2^+) and 1129.0 (4^+) keV are populated in the negaton decay of ^{132}Cs. (auth)

15008 STUDY OF THE STATES OF ^{116}In EXCITED THROUGH RADIATIVE RESONANCE NEUTRON CAPTURE IN ^{115}In. Wahrer, R. E.; King, J. D.; Kukoc, A. H.; Pan, P. J.; Taylor, H. W. (Univ. of Toronto). Nucl. Phys.; A154: 467-81(1970).

The γ radiation emitted following neutron capture by two low-energy resonances in ^{115}In was observed with a 33-cm^3 Ge(Li) spectrometer. A value of 6776 ± 4 keV for the neutron separation energy of ^{116}In was inferred from the data. Twenty-eight levels in ^{116}In were identified with primary transitions and a number of low-energy transitions. The energies of the 54-min and 2.2-sec isomeric states were inferred from the γ cascades to these states. The energies are 125 ± 4 and 292 ± 4 keV, respectively. Restrictions on the spin-parity assignments for some low-lying states are discussed. (auth)

15009 EXPERIMENTS ON PARITY NONCONSERVATION IN NUCLEAR FORCES. I. GAMMA TRANSITIONS IN ^{181}Ta AND ^{175}Lu. Vanderleeden, J. C.; Boehm, F. (California Inst. of Tech., Pasadena). Phys. Rev., C; 2: 748-60(Aug 1970).

The circular polarization of γ rays from unpolarized sources of ^{181}Hf and ^{175}Yb at 100 to 1000 Ci strength was measured, using a Compton polarimeter in a forward-scattering geometry. The technique consisted of integrating the total detector current and digitizing the charge. Several aspects of this method are discussed, such as the role of the switching pattern in optimizing the signal-to-noise ratio. All possible causes of false asymmetries were investigated. Control experiments were carried out with ^{103}Ru sources. The contribution to the observed circular polarization due to bremsstrahlung was calculated, as well as determined experimentally. Results for the circular polarization are $P_\gamma = (-3.9 \pm 1.2) \times 10^{-6}$ for the 482-keV transition in ^{181}Ta, and $P_\gamma = (6.3 \pm 1.0) \times 10^{-5}$ for the 396-keV transition in ^{175}Lu. These findings confirm the existence of a parity-nonconserving term in the nuclear Hamiltonian. (auth)

15010 FISSION OF ^{210}Po. Gadioli, E.; Iori, I.; Molho, N.; Zetta, L. (Univ., Milan. INFN, Milan). Nucl. Phys.; A151: 16-32(1970).

The excitation functions of the reactions ^{206}Pb(α,f) and ^{209}Bi(p,f) and the anisotropy parameters characterizing, at various excitation energies, the angular distributions of fragments emitted in both reactions are analyzed. In the analysis of the excitation functions the angular momentum of the fissioning nucleus is explicitly taken into account. In the calculation of the competing neutron decay width the influence of shell effects on the level density of ^{209}Pc was considered. The effective fission threshold of ^{210}Po (fission threshold plus pairing at the saddle point) is ≈21.95 MeV, corresponding to a fissility parameter $x \approx 0.72$, a value about 2% higher than the one recently proposed by Myers and Swiatecki. The ratio I_{rig}/I_{eff} at the saddle point seems to be about 15% higher than the one predicted by the liquid-drop-model calculations of Cohen and Swiatecki. (auth)

15011 ALPHA DECAY OF THE ^{221}Th AND ^{222}Th DECAY CHAINS. Torgerson, David F. (Texas A and M Univ., College Station); Macfarlane, Ronald D. Nucl. Phys.; A149: 641-6(1970).

The new isotopes ^{221}Th and ^{222}Th were produced in bombardments of ^{208}Pb targets with ^{16}O ions. From a study of the α decay chains of these nuclei, activities due to ^{217}Ra, ^{218}Ra, and ^{214}Rn were also observed. Accurate atomic masses were determined from the measurement of α-decay Q-values. (auth)

15012 DECAY OF ^{159}Dy: L-SUBSHELL X-RAY FLUORESCENCE AND COSTER–KRONIG YIELDS AT Z = 65; BRANCHING RATIO, AND K-CONVERSION OF THE 58 keV TRANSITION IN ^{159}Tb. McGeorge, J. C.; Freund, H. U.; Fink, R. W. (Georgia Inst. of Tech., Atlanta). Nucl. Phys.; A154: 526-38(1970).

Ultrahigh resolution Ge(Li) and Si(Li) detectors were used to study L-subshell x-ray fluorescence and Coster–Kronig yields in Tb from the EC decay of carrier-free ^{159}Dy. From singles and L x-ray spectra in coincidence with K_{α_1} and K_{α_2} x rays, the following L-subshell quantities were obtained: $\omega_3 = 0.188 \pm 0.016$, $\omega_2 \pm 0.160 \pm 0.018$, $f_{23} = 0.090 \pm 0.014$, $\nu_1 = 0.29 \pm 0.08$, $\nu_2 = 0.177 \pm 0.019$, $s_2 = 0.204 \pm 0.024$, $s_3 = 0.170 \pm 0.024$, and $\omega_{KL} = 0.184 \pm 0.016$. Corrections for nuclear cascading were made experimentally using an L x ray spectrum gated by K_β x rays. Angular correlation effects were taken into account. Taking a theoretical value of $s_1 = 0.270$, the present experiment allows estimates to be made of the following L_1 subshell quantities: $\omega_1 = 0.18 \pm 0.04$, $f_{12} = 0.41 \pm 0.36$ and $f_{13} = 0.43 \pm 0.28$. K x-ray spectra in coincidence with K x rays and with the 58.0-keV γ ray were taken to determine the EC branching to the 58.0-keV level (26.8 ± 1.4%) and the K-conversion coefficient of the 58.0-keV transition, $\alpha_K = 9.3 \pm 0.5$, which agrees with the theoretical value for an M1 + 1.4% E2 transition. (auth)

15013 OPTICAL-MODEL ANALYSIS OF ELASTIC SCATTERING AND POLARIZATION OF 49.5-MeV PROTONS ON ^{148}Sm. Woollam, P. B.; Griffiths, R. J.; Grace, Joan F.; Lewis, V. E. (King's Coll., London). Nucl. Phys.; A154: 513-25(1970).

The measurement and optical-model analysis of polarized and unpolarized proton elastic scattering data from ^{148}Sm at 49.5 MeV are presented as a preliminary to coupled channels calculations for all the even Sm isotopes. The differential cross-section and polarization measurements extend over an angular range of 10 to 118° c.m. Analysis was made in terms of the simple optical model and also the recent reformulation of Greenlees, Pyle, and Tang using nuclear-matter density distributions and a realistic two-body force. (auth)

15014 BETA BRANCH IN THE DECAY OF ^{141m}Nd AND STRUCTURE OF ^{141}Nd. Abulaffio, C.; Felsteiner, J.; Kalish, R.; Rosner, B.; Vourvopoulos, G. (Technion-Israel Inst. of Tech., Haifa). Nucl. Phys.; A151: 187-92(1970).

The allowed β-branch in the decay of ^{141m}Nd was observed and found to be strongly hindered. Comparison between log ft values for ^{141}Nd and ^{141m}Nd yields information on the proton part of the

XUM

^{141}Nd wave functions, which are in agreement with results deduced from direct reaction studies. (auth)

15015 FLUORESCENCE AND COSTER–KRONIG YIELDS OF L SUBSHELLS IN Hg FROM THE DECAY OF ^{198}Au AND ^{204}Tl. Palms, J. M. (Emory Univ., Atlanta); Wood, R. E.; Rao, P. Venugopala; Kostroun, V. O. Phys. Rev., C; 2: 592–4(Aug 1970).

Coincidences between L x rays and Kα x rays, emitted during the filling of K and L vacancies in Hg in the decay of ^{198}Au and ^{204}Tl, were measured with high-resolution Si(Li) and Ge(Li) x-ray spectrometers in a fast-coincidence arrangement. The following L-subshell fluorescence and Coster–Kronig yields are measured: $\omega_2 = 0.316 \pm 0.010$, $\omega_3 = 0.300 \pm 0.010$, and $f_{23} = 0.190 \pm 0.010$. (auth)

15016 DETERMINATION OF g FACTORS OF THE SECOND EXCITED STATES $^{11}/_{2}^{-}$ OF ^{147}Eu AND ^{149}Eu BY DIFFERENTIAL ANGULAR CORRELATION METHOD IN EXTERNAL MAGNETIC FIELD. Klimentovskaya, M. V.; Lebedev, N. A.; Sorokin, A. A. (Moscow State Univ.). Yadern. Fiz.; 12: 460-5(Sep 1970). (In Russian).

Using the differential angular correlation method in external magnetic field, g factors of the second isomeric states $^{11}/_{2}^{-}$ are measured in ^{147}Eu nuclei ($E = 625$ keV, $T_{1/2} = (0.765 \pm 0.015) \cdot 10^{-6}$ sec) and in ^{149}Eu nuclei ($E = 497$ keV, $T_{1/2} = (2.43 \pm 0.04) \cdot 10^{-6}$ sec). The values $g(^{147}Eu) = +(1.09 \pm 0.06)$ and $g(^{149}Eu) = +(1.10 \pm 0.03)$ are obtained taking into account the paramagnetic correction to the field $\beta(300°K) = 0.52$ acting on the nuclei. (auth)

15017 ON EFFECT OF α-RADIOACTIVE BACKGROUND AT INVESTIGATION OF THE α DECAY OF THE 104 ELEMENT. Akap'ev, G. N.; Druin, V. A.; Rud, V. I.; Sung-Tsing-Yang, G. Ya. (Joint Inst. for Nuclear Research, Dubna, USSR). Yadern. Fiz.; 12: 466-70(Sep 1970). (In Russian).

Experimental data on α decay of isotopes of the 104 element, obtained by Ghiorso et al. at Berkeley, are analyzed. It is shown that a number of isotopes of transuranium element were misidentified due to the presence of an α-radiactive background. The erroneous determination of half-life of some new isotopes is surmised. (auth)

15018 PROBABILITY OF FISSION WITH EMISSION OF LONG-RANGE PARTICLES. Bogdanov, V. G.; Solov'eva, Z. I. Yadern. Fiz.; 12: 471-3(Sep 1970). (In Russian).

The probability is calculated of the ^{238}U fission with emission of long-range particles by neutrons with energies 2.5 MeV (1/505), 7.6 MeV (1/505), and 14 MeV (1/475) and of ^{232}Th fission by neutrons with energy 14 MeV (1/470). Experimental data on probabilities of the fission by neutrons with energies 2.5 MeV (1/(835 ± 100)) and 7.6 MeV (1/(875 ± 100)) are presented. Disagreement between the calculated quantities with present values as well as with other experimental values is an evidence against validity of the calculation method of Doan et al. [Nucl. Phys., A96: 588(1967)]. (auth)

15019 FISSION OF ^{232}U BY NEUTRONS WITH ENERGY FROM 0.1 UP TO 1.5 MeV. Vorotnikov, P. E.; Dubrovina, S. M.; Otroshchenko, G. A.; (and others) (Inst. of Atomic Energy, Moscow). Yadern. Fiz.; 12: 474-6(Sep 1970). (In Russian).

Measured cross sections and fragment angular distributions for fission of ^{232}U by neutrons with energies from 0.1 up to 1.5 MeV are presented. The fission cross section is essentially constant in the neutron energy region 0.3–1.5 MeV and is found to be 2.2 ± 0.3 barn. It amounts to ~2.6 barn at $E_n \sim 0.1$ MeV. The fragment angular distributions have a small asymmetry that varies from 0.95 up to 1.2. (auth)

15020 MOESSBAUER EFFECT IN TUNGSTEN FOLLOWING COULOMB EXCITATION. Mekshes, M. W.; Hershkowitz, N. (Univ. of Iowa, Iowa City). Phys. Rev., C; 2: 289–96(Jul 1970).

Simultaneous Mössbauer-effect spectra of the first excited states of ^{182}W, ^{184}W, and ^{186}W were observed following Coulomb excitation by 6.0-MeV α particles. Tungsten nuclei were in tungsten metal targets at liquid-nitrogen temperature. An absorption spectrum of the first excited state of ^{183}W was also observed. Taking the half-life of the first excited state of ^{182}W to be 1.377 ± 0.014 nsec, the half-lives of the first excited states of ^{184}W, ^{186}W, and ^{183}W were determined to be 1.28 ± 0.13, 1.38 ± 0.12, and 0.174 ± 0.006 nsec, respectively. Data were consistent with electric quadrupole interactions in the targets. The Debye temperature of tungsten metal at liquid-nitrogen temperature was determined to be 329 ± 8°K. (auth)

15021 MEASUREMENT OF THE PROMPT NEUTRONS EMITTED IN THE FISSION OF ^{209}Bi AND ^{238}U INDUCED BY 155-MeV PROTONS. Cheifetz, E. (Weizmann Inst. of Science, Rehovot, Israel); Fraenkel, Z.; Galin, J.; Lefort, M.; Peter, J.; Tarrago, X. Phys. Rev., C; 2: 256–88(Jul 1970).

The energy distribution of the neutrons emitted in the fission of ^{209}Bi and ^{238}U induced by 155-MeV protons was measured at 0 and 90° with respect to the fission fragment direction. The neutron velocity was measured by the time-of-flight method in coincidence with the measurement of the kinetic energy of the two fission fragments. The number of postfission neutrons as a function of the fragment mass and the energy distribution of the postfission neutrons were determined without reference to any theoretical model. The number of prefission neutrons was determined on the assumption of isotropic emission from the excited nucleus. With this assumption it was found that 5.8 ± 1.0 prefission neutrons are emitted from U and 6.9 ± 1.0 from Bi. The number of postfission neutrons is 5.1 ± 0.5 for U and 4.2 ± 0.5 for Bi. The experimental results are compared with the results of calculations based on the usual model of a prompt intranuclear cascade followed by neutron evaporation–fission competition with several assumptions for Γ_f/Γ_n (ratio of fission width to neutron emission width). A consistent set of parameters which would give good agreement between the calculated results, the experimental results, radiochemical results for spallation residues, and total fission cross-section measurements could not be found. The experimental results indicate that Γ_f/Γ_n decreases at high excitation energies. It was found that the number of postfission neutrons increases rapidly with increasing fragment mass for both Bi and U. When the results for U are compared with low-energy fission data for this element, it is found that almost all the additional excitation energy available in high-energy fission is concentrated in the heavy fragment. (auth)

15022 SPECTROSCOPIC STUDY OF ^{105}Rh BY DIRECT (^{3}He,d) AND (p,α) REACTIONS. Dittmer, D. L.; Daehnick, W. W. (Univ. of Pittsburgh). Phys. Rev., C; 2: 239–49(Jul 1970).

The level structure of ^{105}Rh, below 2 MeV in excitation, was studied by ^{104}Ru(^{3}He,d)^{105}Rh at $E_{^3He} = 18$ MeV, and by ^{108}Pd(p,α)^{105}Rh at $E_p = 15$ MeV. An Enge split-pole spectrograph was used for high-resolution analysis of the reaction products. Particle detection for deuterons was achieved with nuclear emulsions, while position-sensitive "triode" counters were used for the α particles. Targets were kept thin enough to permit total experimental resolutions of 12–13 keV. Comparison of 17 measured (^{3}He,d) angular distributions with nonlocal, finite-range distorted-wave Born-approximation (DWBA) calculations indicated a predominance of $l = 2$ transfers, and yielded J^π limits for the more strongly excited states. Differential ^{108}Pd(p,α)^{105}Rh cross sections were obtained over the angular range of from 8 to 100° and complement the (^{3}He,d) measurements, frequently exciting levels not seen in proton stripping. DWBA triton-cluster transfer calculations reproduce the empirically observed $l = 1$ j dependence. A weaker, but detectable, j dependence is predicted for $l = 3$. The observed ^{105}Rh energy-level scheme is compared with weak-coupling-model expectations and the results of earlier β-decay studies. (auth)

15023 IDENTIFICATION AND STUDY OF RADIOACTIVE PROPERTIES OF Bi ISOTOPES USING ELECTROMAGNETIC MASS-SEPARATOR ON HEAVY ION BEAM. Tarantin, N. I.; Kabachenko, A. P.; Dem'yanov, A. V. (Joint Inst. for Nuclear Research, Dubna, USSR). Yadern. Fiz.; 12: 455-9(Sep 1970). (In Russian).

Results are presented of experiments performed with use of an electromagnetic mass-separator and a beam of heavy ions, on identification and measurement of the α-particle energies and the decay half-lifes of the Bi isotopes with the mass numbers A = 192 to 197, produced from the reactions ^{181}Ta + ^{20}Ne → $^{201-x}$Be + xn, with x = 4 to 9. (auth)

15024 NEW MODEL FOR THE MECHANISM OF FISSION OF HEAVY NUCLEI. Facchini, U.; Saetta-Menichella, E. (CISE Labs., Milan. Univ., Milan). Acta Phys. Pol.; A38: 537-61 (Nov 1970).

A new model of the scission mechanism for fission processes induced by slow and fast neutrons on ^{235}U is presented. In this model scission is considered a sudden process; the number of final states in which the fragments can be excited and a suitable scission barrier between the two fragments are taken into account. The experimental data are analyzed and the characteristics of the barrier are discussed. (auth)

15025 STUDY OF SEVERAL NEUTRON-DEFICIENT HAFNIUM NUCLIDES. Chu, Y. Y.; Reednick, J. (Brookhaven National Lab., Upton, N. Y.). Phys. Rev., C; 2: 310-14(Jul 1970).

The half-life of ^{169}Hf was found to be 3.26 ± 0.05 min. Several γ rays of ^{169}Hf were determined, and a partial decay scheme of ^{169}Hf proposed. The previously reported 1.5 h ^{169}Hf was found to be in error. The half-lives of ^{168}Hf, ^{170}Hf, and ^{171}Hf were redetermined to be 25.95 ± 0.20 min, 15.92 ± 0.15 h, and 12.09 ± 0.35 h, respectively. Several new γ rays of ^{168}Hf were observed. γ spectra of ^{170}Hf and ^{171}Hf were redetermined, and comparisons were made with previous investigations. (auth)

15026 NUCLEAR MAGNETIC MOMENT, HYPERFINE STRUCTURE, AND HYPERFINE-STRUCTURE ANOMALY OF ^{196}Au. Schmelling, Stephen G.; Ehlers, Vernon J.; Shugart, Howard A. (Univ. of California, Berkeley). Phys. Rev., C; 2: 225-8(Jul 1970).

The hfs separation and nuclear magnetic moment of 6.2-day ^{196}Au were measured. The results are: $\Delta\nu(^{196}\mathrm{Au}) = 21{,}347.2522(15)$ MHz and $\mu_I(^{196}\mathrm{Au};\ \mathrm{uncorr}) = +0.5823(14)\mu_N$. These values give the hfs anomaly with respect to ^{197}Au, $^{196}\Delta^{197} = -8.02(24)\%$. These measurements reconfirm the existence of large hfs anomalies in the gold isotopes. They also show that the ground-state nuclear structure of ^{196}Au is similar to that of ^{198}Au. (auth)

15027 K X-RAY YIELDS IN 0 TO 1 μs FROM ^{236}U FRAGMENTS. Kataria, S. K.; Kapoor, S. S.; Murthy, S. R. S.; Rama Rao, P. N. (Bhabha Atomic Research Centre, Bombay). Nucl. Phys.; A154: 458-66(1970).

The yields of K x rays emitted in the time range 0 – 1 μs by fragments of specified nuclear charges were determined in the thermal fission of ^{235}U with a high-resolution (0.9 keV FWHM at 26.25 keV) Si(Li) spectrometer. The fission fragments were detected in nearly 2π geometry by a silicon semiconductor detector placed at a distance of 0.5 mm from the source foil to ensure that the x rays were emitted close to the source foil after the fragments have come to rest. The spectra of K x rays in coincidence with fission were analyzed by a least-square fitting code to determine the total number of K x rays emitted per fission from fragments of different atomic numbers. Using the known fragment charge yield, the above results were transformed to obtain the K x-ray yield per fragment as a function of fragment charge. The present results are compared with those in the time interval 0 to 1 ns to obtain information on the x-ray half-lives for fragment nuclei of different atomic numbers. (auth)

15028 SEARCH FOR AFTER-EFFECTS OF THE ^{111}In EC DECAY ON THE ^{111}Cd $\gamma\gamma$ CORRELATION. Falk, F.; Linnfors, A.; Thun, J. E. (Uppsala Univ.). Nucl. Phys.; A152: 305-16(1970).

Three indium compounds: (i) In_2O_3, (ii) In_2S_3, and (iii) $In(C_9H_7NO)_3$ (indium hydroxyquinolate) were examined for evidence of after-effects on the 173 to 247 keV $\gamma\gamma$ correlation of the ^{111}In EC decay. The main experimental method was the application of a 23 kG decoupling magnetic field. The source temperature was also changed. No after-effects were found, although the correlation in case (iii) seems to be attenuated below the hard-core value. In the introduction after-effects and their detection are discussed at some length. (auth)

15029 RELATIVE K X-RAY TRANSITION PROBABILITIES AT Z = 96 FROM ^{249}Cf DECAY. Hansen, J. S.; Freund, H. U.; Fink, R. W. (Georgia Inst. of Tech., Atlanta). Nucl. Phys.; A153: 465-8(1970).

The relative intensities of the following K x-ray transitions were measured accurately at Z = 96 following ^{249}Cf alpha decay: $K_{\alpha 2}/K_{\alpha 1} = 0.626 \pm 0.006$, $K'_{\beta 1}/K_{\alpha 1} = 0.397 \pm 0.010$, $K'_{\beta 2}/K_{\alpha 1} = 0.133 \pm 0.005$, and $K_\beta/K_\alpha = 0.327 \pm 0.010$. A high-resolution Ge(Li) x-ray detector was used. The results were compared with theoretical calculations, and the systematic plot of the variation with Z of the K_β/K_α x-ray intensity ratio presented earlier was extended to Z = 96, where the experimental value is some 10% larger than the extrapolated theoretical prediction. (auth)

15030 DECAY OF ^{172}Lu AND THE ROTATIONAL BANDS OF ^{172}Yb. Sen, Dilip; Zganjar, E. F. (Louisiana State Univ., Baton Rouge). Nucl. Phys.; A148: 634-56(1970).

The γ spectra accompanying the electron capture decay of ^{172}Lu to levels in ^{172}Yb were studied using Ge(Li) detectors. The γ intensities reported were used in conjunction with the available conversion electron intensity data to compute internal conversion coefficients. Of the 128 transitions observed, 97 were placed in a decay scheme consisting of 28 levels. Multipolarity possibilities were determined for 86 transitions. Log ft values, reduced transition probability ratios, and inertial parameters were computed and used to identify rotational bands at 1172 keV (K = 3), 1466 keV (K = 2), 1609 keV (K = 2), 1662 keV (K = 3), 2073 keV (K = 4), and 2174 keV (K = 3). These bands and the ground state band contain 23 of the proposed levels. The five remaining levels at 1640, 1706, 2181, 2213, and 2343 keV were classified only according to spin-parity possibilities. The reduced B(E2) transition probability ratios and the band mixing parameters for transitions between levels of the K = 2 bands and the ground state rotational band were computed and compared to theoretical predictions. (auth)

15031 SHORT-LIVED FISSION ISOMERS FROM NEUTRON STUDIES. Elwyn, A. J. (Atomic Energy Research Establishment, Harwell, Eng. Argonne National Lab., Ill.); Ferguson, A. T. G. Nucl. Phys.; A148: 337-50(1970).

Spontaneously fissioning activities with half-lives of 4 to 67 ns were observed in neutron-induced reactions on isotopes of U and on ^{239}Pu. These activities were assigned to isomeric states in ^{234}U, ^{235}U, ^{236}U, and ^{240}Pu. In the case of ^{240}Pu, the data are consistent with the existence of two short-lived isomers. The cross sections for isomer production at $E_n \approx 2.2$ MeV were obtained, but only very approximate values of the isomer ratios were determined. These tentative values appear to be somewhat larger than isomer ratios found in charged-particle-induced fission. The present data along with the known spontaneous-fission properties of the ground state are consistent with the model of a one-dimensional double-humped fission barrier in which the excitation energy of the isomeric state relative to the ground state is ≤ 2.4 to 3.3 MeV (dependent on the final nucleus). (auth)

15032 LEVEL SCHEME OF ^{139}La STUDIED BY PHOTOEXCITATION WITH THERMAL NEUTRON CAPTURE GAMMA RAYS. Szichman, H. (Soreq Nuclear Research Centre, Yavne, Israel); Schlesinger, Y.; Ben-David, G.; Pavel, D. Nucl. Phys.; A148: 369-79(1970).

Nuclear resonant scattering of photons from several (n,γ) reactions was used to study bound nuclear levels in the 6 to 9 MeV region in ^{139}La. The results obtained in the de-excitation of six resonant levels at energies 6115, 6418, 6760, 7637, 8527, and 8582 keV are presented. From the angular distribution of the elastically scattered photons, a spin of $^9/_2$ was deduced for the 6115 and 6418 keV levels. On the basis of the angular distribution of the inelastically scattered photons the following spin assignments were made for four of the low-lying levels: 1219($^9/_2$), 1421($^7/_2$ or $^{11}/_2$), 1687($^7/_2$), and 1770($^9/_2$). Hitherto unknown levels were found at 1894 and 2159 keV. Total radiation widths were measured and found to be 79 ± 17 MeV for the 6115 keV resonant level, 45 ± 9 MeV for the 6418 keV level, and >60 MeV for the 6760 keV level. (auth)

15033 NEW EVIDENCE FOR VIBRATIONS IN EVEN Hg ISOTOPES. Covello, A.; Sartoris, G. (Univ., Naples. Istituto Nazionale di Fisica Nucleare, Naples). Nucl. Phys.; A149: 41-4 (1970).

The nuclear properties of the low-lying states of ^{204}Hg are calculated in a model of two proton holes coupled to a quadrupole vibrator. The calculated E2 excitation probability and the magnetic moment of the first 2^+ state are in good agreement with the experimental values recently reported by Kalish et al. (auth)

15034 NUCLEAR g FACTORS OF EXCITED 2+ LEVELS IN ^{194}Pt. Kenyon, D. B.; Keszthelyi, L.; Cameron, J. A. (McMaster Univ., Hamilton, Ont.). Can. J. Phys.; 48: 2730-4(15 Nov 1970).

The g factors of the 329 and 622 keV levels of ^{194}Pt were measured using perturbed angular correlations of gamma rays in the decay of ^{194}Ir detected with Ge(Li) and scintillation counters. The rotation angles for the two levels are 329 keV, $2+: \omega\tau = 0.087 \pm 0.004$ rad; and 622 keV, $2+': \omega\tau = 0.091 \pm 0.015$ rad. This is in agreement with earlier measurements using scintillation counters. Using recent values for the mean lifetimes of the levels, the g factors are $g(2+) = 0.28 \pm 0.03$ and $g(2+') = 0.22 \pm 0.04$. (auth) (Canada)

15035 COULOMB EXCITATION OF ^{107} ^{109}Ag. Robinson, R. L.; McGowan, F. K.; Stelson, P. H.; Milner, W. T. (Oak Ridge National Lab., Tenn.). Nucl. Phys.; A150: 225-46(1970).

Coulomb excitation effected with 10-MeV alpha particles and with 45.5-MeV oxygen ions was used to determine the properties of the low-lying $^3/_2{}^-$ and $^5/_2{}^-$ states in ^{107,109}Ag. The gamma energies and branching ratios, and the B(E2), B(M1) and $T_{1/2}$ values were extracted from the gamma yields, angular distributions, triple angular correlations, and Doppler shift measurements. The results were compared to the predictions of the single-particle core weak coupling model. The $^3/_2{}^-$ 786.5-keV and $^5/_2{}^-$ 949.7-keV levels in ^{107}Ag and the analogous states in ^{109}Ag at 702.0 and 862.5 keV are consistent with the interpretation that they are due to coupling of the odd $p_{1/2}$ proton to the second 2^+ core state. Another state of spin $^3/_2$ was observed at 1464.7 keV in ^{107}Ag and at 1324.2 keV in ^{109}Ag. Still other states were populated via multiple Coulomb excitation, as effected with oxygen ions, at 973.5 and 1146.8 keV in ^{107}Ag and at 912.3 and 1090.6 keV in ^{109}Ag. (auth)

15036 HIGH-SPIN ROTATIONAL AND THREE-QUASIPARTICLE EXCITATIONS IN ^{177}Ta. Skanberg, B.; Hjorth, S. A.; Ryde, H. (Research Inst. for Physics, Stockholm. Univ. of Stockholm). Nucl. Phys.; A154: 641-52(1970).

The γ spectrum from the ^{175}Lu(α,2n)^{177}Ta reaction was investigated at four angles relative to the incident beam and a search made for isomeric transitions. The rotational bands, which are built on the Nilsson states $\frac{7}{2}^+$[404], $\frac{5}{2}^+$[402], $\frac{9}{2}^-$[514], and $\frac{1}{2}^-$[541], were observed and their moment of inertia parameters discussed. A three-quasiparticle isomer with spin and parity tentatively suggested as $\frac{21}{2}^-$ is identified at an excitation energy of 1355.0 keV. (auth)

15037 AVERAGE NUMBER OF NEUTRONS EMITTED IN THE SPONTANEOUS FISSION OF SOME EVEN–EVEN HEAVY NUCLIDES. **Orth, C. J.** (Los Alamos Scientific Lab., N. Mex.). Nucl. Sci. Eng.; 43: 54-7(Jan 1971).

The values of the average number of prompt neutrons ($\bar{\nu}$) emitted in the spontaneous fission of some recently available even-even heavy nuclides have been determined by separately counting neutrons and spontaneous fissions and comparing these counts with similar counts from ^{252}Cf standards. The results are as follows: ^{244}Pu($\bar{\nu}$ = 2.30 ± 0.19), ^{248}Cm($\bar{\nu}$ = 3.11 ± 0.09), ^{250}Cm($\bar{\nu}$ = 3.31 ± 0.08), ^{250}Cf($\bar{\nu}$ = 3.53 ± 0.09), ^{254}Cf($\bar{\nu}$ = 3.93 ± 0.05), all on the basis of $\bar{\nu}$ = 3.77 for ^{252}Cf. A comparison of these results with existing $\bar{\nu}$ data for other heavy nuclides indicates that $\bar{\nu}$ is both Z and A dependent in a manner similar to that calculated by Bondarenko et al. (auth)

15038 INDEPENDENT YIELDS OF ^{124g}Sb, ^{126g}Sb, AND ^{160}Tb IN THE THERMAL NEUTRON INDUCED FISSION OF ^{235}U. Fahland, J.; Lange, G.; Herrmann, G. (Univ., Mainz). J. Inorg. Nucl. Chem.; 32: 3149-57(Oct 1970). (In German).

The following independent yields were measured: 60.4 d ^{124g}Sb 3.98(±0.30) × 10^{-6}%; 12.4 d ^{126g}Sb 8.8(±1.5) × 10^{-4}%, and 72.1 d ^{160}Tb 3(±2) × 10^{-6}%. The yields of the antimony isotopes indicate a slight enrichment of protons in heavy fragments formed in nearly symmetric fission, possibly due to a tendency of these fragments to preserve 50 protons. The yield of ^{160}Tb indicates an enrichment of neutrons in heavy fragments formed in extremely asymmetric fission. (auth) (UK)

15039 STUDY OF LEVELS IN ^{177}Lu FED IN THE β-DECAY OF 1.9 h ^{177}Yb. Brown, R. A. (Univ. of Manitoba, Winnipeg); Roulston, K. I.; Ewan, G. T.; Andersson, G. I. Nucl. Phys.; A154: 626-40(1970).

The γ spectrum of ^{177}Lu following the β decay of 1.9-h ^{177}Yb was studied with Ge(Li) detectors. Investigation of the singles spectrum with a high-resolution 44 cm^3 coaxial Ge(Li) detector revealed twenty-two transitions belonging to the β decay of ^{177}Yb. Seven of these, with energies 458.1 ± 0.5, 760.4 ± 0.3, 779.3 ± 0.3, 961.5 ± 0.5, 967.4 ± 0.5, 1214.8 ± 0.3, and 1336.4 ± 0.5 keV, respectively, are reported for the first time. Gamma-gamma coincidence experiments were performed with two large volume coaxial Ge(Li) detectors, using event by event data recording by an on-line computer, to position the γ rays in a level scheme. The present data, along with precision low-energy measurements, established levels in ^{177}Lu at 121.620 ± 0.003, 150.392 ± 0.003, 268.79 ± 0.01, 289.00 ± 0.01, 451.49 ± 0.01, 1049.5 ± 0.2, 1149.7 ± 0.2, 1230.65 ± 0.15, 1241.4 ± 0.2, and 1336.4 ± 0.3 keV. There is weak evidence for a level at 458.1 ± 0.5 keV. (auth)

15040 LOWER LIMIT ON THE HALF-LIFE OF THE 113.8-keV LEVEL OF ^{175}Lu BY THE MOESSBAUER EFFECT. Hardy, K. A.; Atzmony, U.; Walker, J. C. (Johns Hopkins Univ., Baltimore). Nucl. Phys.; A154: 497-8(1970).

The Mössbauer effect was observed in the 113.8 keV transition in ^{175}Lu following Coulomb excitation with 3 MeV protons. A lower limit on the half-life was determined as 96 ± 9 ps and the Debye temperature of Lu_2O_3 was found to be 174 ± 10°K. (auth)

15041 REORIENTATION MEASUREMENTS IN ^{116}Sn AND ^{124}Sn. Kleinfeld, A. M.; Covello-Moro, Renata; Ogata, H.; (and others) Rutgers-the State Univ., New Brunswick, N. J.). Nucl. Phys.; A154: 499-512(1970).

The first 2^+ states of ^{116}Sn and ^{124}Sn were studied by observing the γ decay to the ground states, following Coulomb excitation with backscattered ^{4}He, ^{16}O, and ^{32}S ions. The static electric quadrupole moment Q_{2^+} of the 2^+ states and the reduced electric transition probability B(E2, $0^+ \rightarrow 2^+$) were obtained by interpreting the results in terms of the reorientation effect. The values of Q_{2^+} found are +0.09 ± 0.13 b for ^{116}Sn and −0.24 ± 0.15 b for ^{124}Sn. The measured B(E2, $0^+ \rightarrow 2^+$) values are 0.22 ± 0.01 $e^2 \cdot b^2$ for ^{116}Sn and 0.19 ± 0.01 $e^2 \cdot b^2$ for ^{124}Sn. (auth)

15042 ^{135m}Ce AND ^{137m}Nd: ISOMERIC STATES IN N = 77 ISOTONES. Droste, Ch.; Neubert, W.; Lewitowicz, J.; Chojnacki, S.; Morek, T.; Wilhelmi, Z.; Alexander, K. F. (Joint Inst. for Nuclear Research, Dubna, USSR). Nucl. Phys.; A152: 579-87(1970).

Using the reaction ^{128}Te(^{12}C, 5n)^{135}Ce, the 20 s isomeric state was produced and studied with the Ge(Li) detector and the magnetic spectrometer on the beam line. A level scheme was constructed for ^{135m}Ce. In the reactions ^{119,122}Sn(^{20,22}Ne,xn) and ^{126}Te(^{16}O,xn), leading to ^{137}Nd, a new isomeric state with $T_{½}$ = 1.6 ± 0.15 s was found. In the decay of this state the following transitions were observed 108, 177, 232.8 (E3, isomeric transition), and 285 keV. The isomeric state was identified by analysis of excitation functions and determination of the energy difference between the K- and L-lines in the conversion electron spectrum. The systematics of isomeric states in the N = 77 isotones is discussed. (auth)

15043 ON LOW ENERGY LEVELS IN ^{185}W. **Malmskog, Sven G. (Aktiebolaget Atomenergi, Studsvik, Sweden); Hoejeberg, Mats; Berg, Valter.** Ark. Fys.; 40: 247-55(1970).

Gamma spectra in the decay of ^{185}Ta and ^{185m}W were studied with Ge(Li) detectors. The ^{185m}W isomeric transition of 131.6 keV was found to be of E3 multipolarity. A level scheme of ^{185}W is proposed with the following energy levels (energies in keV, spin, parity and K quantum numbers in brackets): 0 ($\frac{3}{2}^-$ $\frac{3}{2}$), 23.5 ($\frac{1}{2}^-$ $\frac{1}{2}$), 65.9 ($\frac{5}{2}^-$ $\frac{3}{2}$), 93.5 ($\frac{3}{2}^-$ $\frac{1}{2}$) (uncertain), 173.9 ($\frac{7}{2}^-$ $\frac{3}{2}$), 188.1 ($\frac{5}{2}^-$ $\frac{1}{2}$), 197.5 ($\frac{11}{2}^+$ $\frac{11}{2}$), 243.5 ($\frac{7}{2}^-$ $\frac{7}{2}$), and 390.8 ($\frac{9}{2}^-$ $\frac{7}{2}$). (auth) (Sweden)

15044 THERMAL-NEUTRON FISSION CROSS SECTION OF ^{227}Th. **Von Gunten, H. R. (Univ. of Bern); Flynn, K. F.; Schmid, A.** J. Inorg. Nucl. Chem.; 32: 3441-8(Nov 1970).

The thermal-neutron fission cross section of ^{227}Th was measured using both back to back fission counters and radiochemical techniques. A value of 200 ± 20 barns was obtained from eight independent measurements. (auth) (UK)

15045 MASS SYMMETRY IN THE SPONTANEOUS FISSION OF ^{257}Fm. **Balagna, J. P.; Ford, G. P.; Hoffman, D. C.; Knight, J. D. (Los Alamos Scientific Lab., N. Mex.).** Phys. Rev. Lett.; 26: 145-8(18 Jan 1971).

The kinetic energy distribution of coincident fragments from spontaneous fission of ^{257}Fm was measured with silicon detectors. The data reveal two significant features: (1) The mass-yield distribution is markedly more symmetric than for slightly lighter nuclei (e.g., ^{252}Cf, ^{254}Cf); (2) the average total kinetic energy increases monotonically with the approach to symmetric fission. (auth)

15046 SPONTANEOUSLY FISSIONING ISOMERS IN U, Pu, Am, AND Cm ISOTOPES. Plikanov, S. M.; Sletten, G. (Univ. of Copenhagen). Nucl. Phys.; A151: 656-72(1970).

Spontaneously fissioning isomers with microsecond half-lives were observed in ^{237}Pu, ^{239}Pu, ^{241}Pu, and ^{243}Am using a pulsed beam technique. Isomers having nanosecond half-lives were observed in ^{237}Am, ^{241}Cm, and ^{243}Cm using a DC beam and a fission-in-flight detection method. The isomers were studied through p- and d-induced reactions on thin targets of U, Np, Pu, and Am at energies varying from 9 to 14.2 MeV. The assignments are based on measured excitation functions and the important reactions were found to be (p, 2n), (d, 2n), (d, p), and (d, pn). The reaction ^{238}Pu + p shows threshold behavior typical for a (p,2n) reaction in the interval from 12 to 13 MeV. The difference E_{II} in the thresholds for the ground state and the isomeric state is 3.0 ± 0.3 MeV. A 300 ns isomer earlier assigned to ^{239}Np was reassigned to ^{238}U. A half-life systematics for fission isomers based on isomers reported in the literature and on isomers measured in the present work is presented. Odd-even effects on the spontaneous fission half-lives and the existence of excited states in the second potential well are discussed. (auth)

15047 HIGH SPIN ROTATIONAL LEVELS IN ^{177}Ta. Barneoud, D.; Foin, C.; Baudry, A.; Gizon, A.; Valentin, J. (Institut des Sciences Nucleaires, Grenoble, France). Nucl. Phys.; A154: 653-64(1970).

Gamma rays following the (α, 2n) reaction leading to the nucleus ^{177}Ta were studied by means of γγ coincidences. Unambiguous assignments were made for the bands built on the Nilsson states $\frac{7}{2}^+$[404], $\frac{9}{2}^-$[514], $\frac{5}{2}^+$[402], and $\frac{1}{2}^-$[541]. (auth)

15048 NUCLEAR DEFORMATION AND OPTICAL ISOTOPE SHIFTS IN THE REGION N = 88 TO 90. Saksena, G. D.; Ahmad, S. A. (Bhabha Atomic Research Centre, Trombay, India). Physica; 47: 92-8(29 Apr 1970).

Evidence concerning nuclear deformation from optical isotope shifts and reduced transition probabilities B(E2, 0 → 2) in the even–even nuclei of Nd, Sm, and Gd in the region of neutron number N = 88 to 90 are compared. Estimates of the nuclear deformation parameter β and optical isotope shift for ^{154}Dy are made from the rotational-energy values recently reported in the literature for this nucleus. The estimated value of β = 0.164 ± 0.02 shows that in dysprosium also the transition from single-particle model to collective model takes place when the 45th pair of neutrons enters. (auth)

15049 RECOIL STUDIES OF MEDIUM-ENERGY NUCLEAR REACTIONS INDUCED BY ^{3}He AND ^{4}He IONS. Montgomery, Daniel Michael. Lafayette, Ind.; Purdue Univ. (1969). 254p. University Microfilms Order No. 70-8928.
Thesis.

Excitation functions and average range measurements are reported for the (^{3}He, αn), (^{3}He, α), (^{4}He, 3n), and (^{3}He, 2n) reactions of ^{116}Cd. Isomer ratios for reactions leading to ^{115m,g}Cd are also reported. The energies of the ^{3}He and ^{4}He ions varied between 13 and 33, and 18 and 45 MeV, respectively. The results of the average range measurements are compared with ranges predicted by Lindhard, Scharff, and Schiott on the assumption of compound nucleus formation. Good agreement is obtained for the (^{4}He, 3n) and (^{3}He, 2n) reactions at all energies; this indicates that the mechanism is predominantly compound nucleus formation. The average ranges for the products of the (^{4}He, αn) and (^{3}He, α) reactions are much lower than expected at energies greater than about 25 MeV. These results are interpreted as involving low momentum transfer due to a direct interaction mechanism. These conclusions are also corroborated by the isomer ratios. In order to determine the energy range of compound nucleus formation, recoil techniques were used to measure excitation functions, isomer ratios, and average ranges for ^{137m,g}Ce produced by the ^{136}Ba(^{4}He,3n) and ^{137}Ba(^{3}He,3n) reactions. The energy range was from 14 to 33 MeV for the ^{3}He ions and from 27 to 44 MeV for the ^{4}He ions. The isomer ratio measurements were found to agree with predictions of the spin-dependent statistical theory of nuclear reactions for reasonable choices of parameters. The excitation functions and average range results were consistent with compound nuclear processes over the energy range studied. Angular distribution measurements of ^{137m}Ce and ^{137g}Ce from the reactions ^{136}Ba(^{4}He,3n) and ^{137}Ba(^{3}He,3n) were made over the energy range from 33.3 to 43.6 MeV and from 20.3 to 32.5 MeV, respectively. The results are analyzed to give the average total kinetic energy of the neutrons and average total kinetic energy of photons emitted in the reactions. Results indicate that the differences in average photon energies between ^{137m}Ce and ^{137g}Ce can be related to the rotational energy of the compound nucleus. The comparisons of the angular distributions of ^{137m}Ce from the (^{3}He, 3n) and (^{4}He, 3n) reactions indicate the independence hypothesis is valid for these reactions. The same results were found from the angular distributions of ^{137g}Ce. (auth) (Diss. Abstr. Int., B)

15050 ANOMALIES IN THE CROSS SECTIONS OF (d,n) REACTIONS LEADING TO ISOBARIC ANALOG STATES. Zaidi, S. A. A. (Univ. of Texas, Austin); Hollas, C. L.; Horton, J. L.; (and others). Phys. Rev. Lett.; 25: 1503-7(23 Nov 1970).

The (d,n) reactions on the nuclei ^{92}Mo, ^{94}Mo, ^{96}Mo, and ^{96}Zr leading to the isobaric analog states in the residual nuclei were studied. The observed (d,n)-reaction cross sections show strong deviations from the distorted-wave Born-approximation calculations based upon the known neutron spectroscopic factors of the corresponding parent analog states. (auth)

15051 NEUTRON-INDUCED FISSION OF ^{240}Pu NEAR THRESHOLD. Androsenko, Kh. D.; Smirenkin, G. N. Yadern. Fiz.; 12: 260-7(Aug 1970). (In Russian).

Fragment angular distributions from fission of ^{240}Pu and ^{239}Pu by neutrons with energies from 0.1 up to 1.5 MeV were measured. The angular distributions have square dependence on cos θ. An analysis of the cross section and angular anisotropy of the neutron-induced fission of ^{240}Pu near threshold was performed. The experimental results were interpreted in the framework of the two-humped fission barrier. (auth)

15052 RADIOACTIVE PROPERTIES OF ISOTOPES OF THE 103 ELEMENT. Druin, V. A. (Joint Inst. for Nuclear Research, Dubna, USSR). Yadern. Fiz.; 12: 268-71(Aug 1970). (In Russian).

Experimental results on α-decay of isotopes of the 103 element are analyzed. It is shown that the experiments, carried out in Dubna, on identification of three isotopes with the mass numbers 255, 256, and 257 of the 103 element give evidence that the first work on ^{257}103 by Ghiorso et al., [Phys. Rev. Lett., 6: 473 (1961)], performed at Berkeley, is not correct. (auth)

15053 ONE-NUCLEON STATES AND ENERGY SURFACES OF ^{238}U IN FISSION PROCESS. Adeev, G. D.; Gamalya, I. A.; Cherdantsev, P. A. (Tomsk Polytechnic Inst., USSR). Yadern. Fiz.; 12: 272-83(Aug 1970). (In Russian).

One-nucleon level spectra are calculated for a potential with equipotential surfaces as intersecting rotation ellipsoids of various volumes. Spin-orbit and I^{2} interactions are taken into account in diagonal approximation. The spectra are used to describe the shell correction to the droplet energy of ^{238}U. Energy surfaces of ^{238}U in a space of three shape parameters are calculated. The contour diagrams and the shape of the minimal barrier indicate the most probable values of the fission asymmetry, 0.85, and the ellipsoidal parameter for fragments, 0.55. (auth)

15054 DEPENDENCE OF INTERNAL CONVERSION COEFFICIENTS ON HIGH ENERGIES OF γ TRANSITIONS. Trusov, V. F. (Latvian State Univ., Riga). Yadern. Fiz.; 12: 284-6(Aug 1970). (In Russian).

The coefficients for internal conversion on K and L shells of Hg are presented; the maximum energies for γ transitions are the following: on K shell—16 MeV, on L_{I} subshell—12 MeV, on L_{II} and L_{III} subshells—6 MeV. Results are obtained on the basis of numerical integration of the Dirac equation with account of screening and finite dimensions. Ratios for conversion coefficients K/L_{I} for different Z and multipolarities are also given and compared with the ratios for electron densities on the boundary of the nucleus. (auth)

15055 LIFETIMES OF LEVELS OF ^{125}Te NUCLEUS. Berlovich, E. E.; Lukashevich, V. V.; Popov, A. V.; Romanov, V. M. (Ioffe Inst. of Physics and Tech., Leningrad). Yadern. Fiz.; 12: 217-23(Aug 1970). (In Russian).

By means of the differential time-amplitude convertor the lifetimes are measured of the ^{125}Te levels at 35.5, 321, and 463 keV with the results $(1.486 \pm 0.009) \cdot 10^{-9}$, $(7.6 \pm 0.2) \cdot 10^{-10}$, and $(19 \pm 3) \cdot 10^{-12}$ sec., respectively. Analyzing properties of the excited states, the presence of a weak negative deformation of the ^{125}Te nucleus is supposed. (auth)

15056 LIFETIME AND DECAY OF THE 23.8 keV STATE OF ^{119}Sn. Benczer-Koller, N. (Rutgers—The State Univ., New Brunswick, N. J.); Fink, T. Nucl. Phys.; A161: 123-8(1971).

The half-life of the 23.8 keV state in ^{119}Sn was measured by the delayed-coincidence technique. The observed value $\tau_{1/2} = 17.75 \pm 0.12$ ns corresponds to a natural line width for the state of $\Gamma = 0.325 \pm 0.002$ mm/sec. The internal conversion spectrum was measured; the ratios of internal conversion lines for both the 23.8 and 65.3 keV transitions agree with theoretical predictions and previous experiments. (auth)

15057 (^{3}He, α) REACTION ON Yb ISOTOPES WITH POSSIBLE OBSERVATIONS OF INDIRECT EXCITATIONS. Burke, D. G. (McMaster Univ., Hamilton, Can.); Alford, W. P.; O'Neil, R. A. Nucl. Phys.; A161: 129-54(1971).

Angular distributions of (^{3}He, α) reactions were measured with 28 MeV ^{3}He on targets of ^{172}Yb, ^{174}Yb and ^{176}Yb. The alpha spectra were analyzed with a magnetic spectrograph and levels up to excitation energies of 2 MeV were studied with a resolution (FWHM) of 25 keV. Distorted wave Born approximation (DWBA) calculations were carried out using optical-model parameters which had been found suitable in the lead region. The angular distributions obtained from these calculations were consistent with those measured for strongly populated states and the DWBA results were used to extract relative spectroscopic factors for a number of levels. The transitions with $l \approx 6$ yielded the largest cross sections so a comparison of the present results with earlier (d, t) data resulted in the identification of a number of new high spin states. Tentative assignments of the $\frac{5}{2}^{-}$ [523] and $\frac{5}{2}^{+}$ [642] Nilsson orbitals were made in each of the three final nuclei, although in most cases there is evidence for strong Coriolis mixing of the $j = \frac{13}{2}$ states. There may also be fragmentation of the single-particle states, as predicted by Soloviev and his coworkers. In each of the final nuclei studied, a state was observed at the expected position of the $j = \frac{11}{2}$ member of the $\frac{7}{2}^{+}$ [633] band. The data indicate that this state is not populated by a direct $l = 8$ neutron transfer. Further deviations from the simple direct reaction process are found in a comparison of (d, t) and (^{3}He, α) cross sections for the $\frac{5}{2}$ and $\frac{7}{2}$ members of the $\frac{5}{2}^{-}$ [512] band in ^{173}Yb. (auth)

15058 LEVEL STRUCTURE OF ^{181}W FROM THE DECAY OF ^{181}Re. Daly, P. J.; Ahlgren, Karin; Hofstetter, K. J.; Hochel, R. (Purdue Univ., Lafayette, Ind.). Nucl. Phys.; A161: 177-90 (1971).

The decay of ^{181}Re was investigated using Ge(Li) detectors in singles and coincidence γ-ray measurements. Conversion coefficients and multipolarities for all strong transitions were inferred using published conversion electron data. A ^{181}W level scheme was constructed which accommodates about 99% of the decay intensity and which differs in many respects from earlier proposals. An interpretation of the ^{181}W level structure in terms of the Nilsson model is presented, which is consistent with the results of recent independent neutron-transfer reaction studies as well as the decay data. (auth)

15059 LOW SPIN, NEGATIVE PARITY STATES IN THE N = 103 ISOTONES OF ^{171}Er, ^{173}Yb, AND ^{175}Hf IDENTIFIED BY THERMAL NEUTRON CAPTURE REACTIONS. Alenius, G.; Arnell, S. E.; Schale, C.; Wallander, E. (Chalmers Univ. of Tech., Goteborg). Nucl. Phys.; A161: 209-27(1971).

XUM

Energies and intensities of the γ-rays following thermal neutron capture in enriched samples of ^{170}Er, ^{172}Yb and ^{174}Hf were measured using internal reactor targets and a three-crystal Ge(Li) pair and anti-Compton spectrometer. The reaction Q-values, excitation energies and intensity values were deduced. Decay schemes of ^{171}Er, ^{173}Yb and ^{175}Hf are presented together with the spins and Nilsson assignments of the low-lying rotational bands populated from the capture states. (auth)

15060 DECAYS OF ^{159m}Ho AND ^{161m}Ho. Geiger, J. S.; Graham, R. L.; Johns, M. W. (Atomic Energy of Canada Ltd., Chalk River, Ont.). Nucl. Phys.; A161: 263-72(1971).

The half-life of the 205.9 keV state in ^{159}Ho is found to be 8.30 ± 0.08 sec. Studies of γ-ray singles spectra, conversion electron spectra and γe^- coincidences show that the 206 keV transition is paralleled by a 40 keV M3−166 keV E1 cascade of ≈5% intensity. The three levels are identified with Nilsson orbitals $\frac{1}{2}^+[411]$, $\frac{7}{2}^+[404]$ and $\frac{7}{2}^-[523]$ and their spacing indicates a quadrupole deformation of $\epsilon \approx 0.25$. The half-life of the 211.2 keV state in ^{161}Ho was measured with improved accuracy and is found to be 6.73 ± 0.10 sec. (auth)

15061 EVIDENCE FOR STATES OF PROLATE AND OBLATE DEFORMATION AND FOR SHAPE ISOMERISM IN ^{127}Cs. Conlon, T. W. (Atomic Energy Research Establishment, Harwell, Eng.). Nucl. Phys.; A161: 289-304(1971).

An isomeric state with a half-life of 55 μs was produced in ^{127}Cs. The spin-parities of all four excited states associated with the isomeric decay have been determined. Their values are indicative of the sequence of states predicted for the odd-proton cesium (Z = 55) isotopes at negative (oblate) values of the deformation. The nature of the deformation in the ground state however is shown to be probably prolate. Transitions observed between the probably prolate ground state and oblate excited states are discussed. (auth)

15062 DECAY SCHEMES OF ^{131}Ba AND ^{192}Ir NUCLEI. Lee, Sabrina V. J. Lin. Ann Arbor, Mich.; Univ. of Michigan (1969). 168p. University Microfilms Order No. 70-14,578.

Thesis.

In the study of the electron capture decay of ^{131}Ba to levels in ^{131}Cs, energy and relative intensity measurements were performed on 36 gamma-rays with a 4 cc Ge(Li) detector. New transitions at 797 keV and 954 keV were observed. Precision energy determinations were made for the four strongest transitions using a 2-meter curved-crystal spectrometer. Gamma-gamma coincidence studies were performed utilizing a 17 cc and a 40 cc coaxial Ge(Li) detector, a 4 cc planar Ge(Li) detector and NaI crystals. All observed gamma-rays were placed into the decay scheme, including the new transitions. The 1047 keV peak was concluded to be a doublet. A new decay scheme was proposed, which is consistent with the presently established decay scheme, with the addition of a new level at 1170 keV. The previously uncertain transitions at 323 keV, 461 keV and 969 keV were confirmed to belong to the decay. In the study of the beta decay and electron capture decay of ^{192}Ir to levels in ^{192}Pt and ^{192}Os respectively, 21 gamma transitions were observed, including new transitions at 110 keV, 177 keV and 280 keV. Energy and relative intensity measurements were made using a 17 cc and a 40 cc coaxial Ge(Li) detector. Precision curved-crystal gamma-ray energy determinations were made for 19 gamma transitions. In addition, a search was performed using curved-crystal spectrometer for all gamma-rays reported in Nuclear Data Sheets (1963) and by other authors, and for possible missing transitions between existing levels. Upper intensity limits are given. The singles and coincidence results confirm the presently established decay scheme. Furthermore, a level at 905 keV in ^{192}Os was confirmed by gamma-gamma coincidence results. While there is no experimental evidence for the existence of a 1055 keV and 1360 keV level in ^{192}Pt, there is some evidence for a level at 1090 keV. Half-life measurements were performed on all gamma-rays except the fore-mentioned possible new transitions. Transition multipolarities and spins and parities of excited states were deduced for ^{131}Cs, ^{192}Pt and ^{192}Os nuclei. The experimental results are compared with theoretical assignments of levels of these nuclei obtained from a consideration of various nuclear models. (Diss. Abstr. Int., B)

15063 EFFECT OF NUCLEAR DEFORMABILITY ON REACTION CROSS SECTIONS. Riesenfeldt, Peter W.; Thomas, T. Darrah (Princeton Univ., N. J. Princeton–Pennsylvania Accelerator, Princeton, N. J.). Phys. Rev., C; 2: 711-20 (Aug 1970).

The effect of nuclear deformability on the cross section was calculated for interaction of heavy ions with uranium. Static calculations indicated that these effects should be large; dynamic calculations with liquid-drop parameters indicate that they should be smaller, but measurable with currently available heavy ions (argon incident on uranium). Dynamic calculations with parameters derived from spectroscopic measurements indicate that the effects should be quite small, in agreement with experiment. Classical and quantum-mechanical calculations were carried out and the two methods gave the same results. The quantum-mechanical calculations also give the probability of Coulomb excitation to the vibrational states of the target nucleus. The value of several approximations used to estimate total reaction cross sections is discussed. (auth)

15064 EXPERIMENTAL DETERMINATION OF THE NORMALIZATION FOR (α, t) REACTIONS AND COMPARISON WITH THE THEORETICAL NORMALIZATION FACTOR. Hering, W. R.; Becker, H.; Wiedner, C. A.; Thompson, W. J. (Max-Planck-Institut fuer Kernphysik, Heidelberg). Nucl. Phys.; A151: 33-55 (1970).

The reaction ^{205}Tl(α, t) ^{206}Pb(g.s.) was measured between 20 and 25 MeV α energy, i.e. below and near the Coulomb barrier. It was possible to calculate the absolute experimental cross sections using a DWBA code with finite-range corrections provided that the (t + p) relative motion in the projectile is described by a Hulthén potential with $\beta/\alpha = 1.55 \pm 0.14$. This leads to an experimental normalization of $D_0^{exp}(\alpha, t) = -(272 \pm 14)$ MeV · fm$^{3/2}$, where the errors are due to uncertainties in the proton bound state potential parameters. A calculation of the theoretical normalization using only known properties of the α particle leads to $\beta/\alpha = 1.57 \pm 0.02$ and $D_0^{th}(\alpha, t) = -(269 \pm 2)$ MeV · fm$^{3/2}$. Using this value a proton bound state potential was deduced for the lead region of Woods-Saxon type with $r_0 = 1.27$ fm and a = 0.71 fm. A possible extension of the general results of this analysis to all transfer reactions from projectiles with $A \leqq 4$ is discussed. (auth)

15065 TEST OF THE INDEPENDENCE HYPOTHESIS BY ANGULAR DISTRIBUTION MEASUREMENTS. Montgomery, D. M.; Porile, N. T. (Purdue Univ., Lafayette, Ind.). Phys. Rev., C; 2: 595-607(Aug 1970).

Angular distributions, average projected ranges, and cross sections for the production of ^{137m}Ce and ^{137g}Ce from the ^{136}Ba(^{4}He, 3n) and ^{137}Ba(^{3}He, 3n) reactions were measured over the energy intervals 27 to 44 and 14 to 33 MeV, respectively. The average ranges were found to be consistent with a compound-nuclear process over the entire energy interval for both reactions. The isomer ratios are in good agreement with a calculation based on the spin-dependent statistical theory. Comparison was made with previous cross-section and isomer-ratio measurements, and various discrepancies are discussed. The angular distributions were analyzed to give the average total kinetic energy of the neutrons and photons emitted in the reactions. Comparison of these quantities at the same excitation energy and angular momentum of the compound nuclei shows that they are equal within the limits of error and thereby confirms the independence hypothesis. The observed differences in the average photon energies for reactions leading to ^{137m}Ce and ^{137g}Ce are quantitatively related to the difference in the average angular momentum of compound nuclei leading to each isomer. (auth)

15066 NEW TANTALUM ISOTOPES ^{170}Ta AND ^{171}Ta. Rezanka, I.; Ladenbauer-Bellis, I.-M.; Bernthal, F. M.; Rasmussen, J. O. (Yale Univ., New Haven). Contract AT(30-1)-3909. Phys. Rev. Lett.; 25: 1499-1500(23 Nov 1970).

The tantalum isotopes ^{170}Ta and ^{171}Ta were produced via the following reactions: ^{165}Ho(^{12}C, 6n)^{171}Ta, ^{159}Tb(^{16}O, 4n)^{171}Ta, ^{165}Ho(^{12}C, 7n)^{170}Ta, and ^{159}Tb(^{16}O, 5n)^{170}Ta. The half-life of ^{171}Ta was determined to be 25 ± 2 min and of ^{170}Ta, 7 ± 2 min. About 60 γ rays were assigned to the ^{171}Ta decay, while in ^{170}Ta decay, only the excitations of the first- and second-excited states of ^{170}Hf were observed. (auth)

15067 PRECISE 2200 m/s FISSION CROSS-SECTIONS OF ^{239}Pu AND ^{235}U. Deruytter, A. J.; Becker, W. (EURATOM, Geel, Belg.). pp 117-25 of Nuclear Data for Reactors. Vol. I. Vienna; International Atomic Energy Agency (1970).

From 2nd International Conference on Nuclear Data for Reactors, Helsinki, Finland. See STI/PUB-259(Vol.1); CONF-700605-(Vol.1).

A new precise measurement of the 2200 m/s fission cross-section of ^{239}Pu was performed with a slow chopper at the Belgian BR2-reactor (energy range from 0.005 to 0.1 eV). Simultaneous recordings of pulse-height and time-of-flight spectra of successively compared ^{239}Pu layers and standard natural boron layers were made. The detection of the ^{10}B(n,α)^{7}Li and ^{239}Pu(n,f) reaction fragments is made with excellent pulse-height resolution in low geometry with a surface barrier detector. The separation between the pile-up tail produced by the α-particles of ^{239}Pu and the fission-fragment pulse-height distribution was very good. The relative ^{10}B contents of several standard boron foils were checked by their neutron-induced reaction rates. The absolute ^{10}B contents were determined from direct weighing in vacuum combined with careful chemical and isotopic analysis of witness foils. The fission foils were checked by α- and fission counting. Their absolute weights were obtained from absolute low-geometry α-counting. A final value for the 2200 m/s fission cross-section of ^{235}U was also obtained, making use of a carefully redetermined value of the ^{234}U α-half-life. A comparison of the obtained 2200 m/s values with the up-dated IAEA review for these quantities is included. The fission cross-section of both isotopes was carefully studied down to 2 meV neutron energy and up to 0.1 eV and serves for the calculation of g-factors. (8 references) (auth)

15068 ABSOLUTE MEASUREMENT OF THE FISSION CROSS-SECTION FOR ^{235}U AND ^{239}Pu BETWEEN 0.025 AND 1 MeV. Szabo, I.; Marquette, J. P.; Fort, E.; Leroy, J. L. (Centre d'Etudes Nucleaires, Cadarache, France). pp 229–42 of Nuclear Data for Reactors. Vol. I. Vienna; International Atomic Energy Agency (1970). (In French).

From 2nd International Conference on Nuclear Data for Reactors, Helsinki, Finland. See STI/PUB–259(Vol.1); CONF-700605–(Vol.1).

The measurement was made using monokinetic neutrons from the Van-de-Graaff accelerator at Cadarache. The neutron flux was measured with standard counters. A special electronic assembly made it possible to reduce the fluctuations of the response time of the fission chamber to less than 7 ns, by detecting the current of electron migration due to ionization. In this way, use was made of the time-of-flight method to detect the fissions due to neutron background. The total error of the measurement points is ±3%. (27 references) (auth)

15069 CROSS-SECTIONS OF THE HEAVY NUCLEI IN THE RESONANCE REGION. James, G. D. (Atomic Energy Research Establishment, Harwell, Eng.). pp 267–86 of Nuclear Data for Reactors. Vol. I. Vienna; International Atomic Energy Agency (1970).

From 2nd International Conference on Nuclear Data for Reactors, Helsinki, Finland. See STI/PUB–259(Vol.1); CONF-700605–(Vol.1).

The available cross-section data of heavy nuclei of importance in reactor design are reviewed with particular emphasis on the fission-cross-section results. Data which indicate intermediate structure in the cross-sections of the heavy elements are presented and discussed. (54 references) (auth)

15070 MEASUREMENTS OF ALPHA AND OF FISSION CROSS-SECTION RATIOS FOR ^{233}U, ^{235}U, AND ^{239}Pu AT THERMAL ENERGIES. Lounsbury, M.; Durham, R. W.; Hanna, G. C. (Atomic Energy of Canada Ltd., Chalk River, Ont.). pp 287–94 of Nuclear Data for Reactors. Vol. I. Vienna; International Atomic Energy Agency (1970).

From 2nd International Conference on Nuclear Data for Reactors, Helsinki, Finland. See STI/PUB–259(Vol.1); CONF-700605–(Vol.1).

Measurements of alpha for ^{233}U, ^{235}U and ^{239}Pu, and of fission cross-section ratios for these nuclides, were made in the NRU reactor at Chalk River in a special temperature-controlled thermal-flux irradiation facility. Extensive thermalization calculations were carried out and the uncertainty in the neutron spectrum is believed to be equivalent to a temperature uncertainty of only ±4°C. The experiment consisted of irradiating mixtures of uranium and plutonium isotopes to approximately 0.7 neutrons per kilobarn, and measuring the changes in isotopic composition. With a ^{233}U$-$^{238}U mixture the change in the (233/238) ratio gives the 233 destroyed and that in (234/238) the 234 produced, from which α(233) can be calculated. Similarly a ^{239}Pu$-$^{242}Pu mixture gives α(239). When they are mixed, so that they receive the same irradiation, a comparison of the fractions of ^{233}U and ^{239}Pu destroyed gives the ratio of the absorption cross-sections. Both ^{233}U$-$Pu and ^{235}U$-$Pu mixtures are irradiated. By combining the α and σ_a data fission cross-section ratios are obtained that do not depend on the assay (e.g. by alpha particle counting) of thin deposits. The 2200 m/s α values obtained for ^{233}U, ^{235}U and ^{239}Pu were 0.0899 ± 0.0004, 0.1702 ± 0.0007, and 0.3597 ± 0.0021, respectively. The fission cross-section ratios were (239/233) = 1.4046 ± 0.0079, (239/235) = 1.2926 ± 0.0081 and (233/235) = 0.9203 ± 0.0057. Values of $g\sigma_\gamma = 95.6 \pm 2.1$ b for ^{234}U and $\sigma_\gamma = 289.5 \pm 1.4$ b for ^{240}Pu were also obtained. The errors include the uncertainties in the neutron spectrum and in other cross-sections (e.g. of ^{241}Pu and ^{242}Pu), as well as the experimental errors, but not the uncertainties in the g-factors. (15 references) (auth)

15071 MEASUREMENTS OF ^{233}U CROSS-SECTIONS FOR THERMAL NEUTRONS. Vidal, R.; Robin, M.; Carneiro Da Silva, C. (Centre d'Etudes Nucleaires, Fontenay-aux-Roses, France). pp 295–304 of Nuclear Data for Reactors. Vol. I. Vienna; International Atomic Energy Agency (1970). (In French).

From 2nd International Conference on Nuclear Data for Reactors, Helsinki, Finland. See STI/PUB–259(Vol.1); CONF-700605–(Vol.1).

The fission cross-section and the η of ^{233}U are determined for 2200 m/s by taking ^{235}U as a standard and using integral measurements made in a thermal neutron spectrum as a basis. This was done by using two complementary methods: (a) Measurement of fission cross-sections with fission chambers. The ratio of the fission cross-sections of ^{233}U and ^{235}U is determined by irradiating fission chambers containing ^{238}U in combination with either ^{233}U or ^{235}U in a Maxwellian spectrum. The originality of the method lies in the calibration of the chambers, which is carried out in a fast-neutron spectrum and takes advantage of the fissions produced in the ^{238}U. In this way, merely by knowing the isotopic contents of the foils, one can make a very accurate relative calibration. The results are $(\sigma_{f3}/\sigma_{f5})_{2200 m/s} = 0.914 \pm 0.005$.
(b) Measurement of η by the oscillation method. The ratio (η_3/η_5) is determined by measuring the variations in reactivity produced in a natural uranium-heavy water lattice by the oscillation of ^{238}U-samples containing between 0.1 and 0.7% of ^{233}U or ^{235}U. By weighting the differential cross-sections of ^{233}U and ^{235}U over the neutron spectrum in which the measurements were made, the ratio of the η from the ratios of the effective $\hat{\eta}$ were derived. The results are $(\eta_{233}/\eta_{235})_{2200 m/s} = 1.081 \pm 0.005$. From all these results the following cross-sections of ^{233}U are derived, considering the values of the ratio ν_3/ν_5, of σ_{f5} and η_5 given: $\sigma_{f3} = 530 \pm 4$ barns; $\eta_3 = 2.240 \pm 0.012$; $\sigma_{a3} = 589 \pm 7$ barns. (13 references) (auth)

15072 VALUE α FOR ^{239}Pu. Sukhoruchkin, S. I. (Moscow Inst. of Theoretical Experimental Physics). pp 307-13 of Nuclear Data for Reactors. Vol. I. Vienna; International Atomic Energy Agency (1970). (In Russian).

From 2nd International Conference on Nuclear Data for Reactors, Helsinki, Finland. See STI/PUB−259(Vol. 1); CONF-700605-(Vol. 1).

A short review of the results of the IAEA experts meeting on the α(^{239}Pu) problem held at Studsvik in Sweden on 12 June, 1970, is given. The findings and recommendations of the meeting are discussed, in particular the conclusion that the present accuracy in α can be assessed as ±10% up to 10 keV-neutron energy. (10 references) (auth)

15073 RATIO OF THE CAPTURE AND FISSION CROSS-SECTIONS OF ^{239}Pu IN THE ENERGY RANGE 100 eV TO 30 keV. Schomberg, M. G.; Sowerby, M. G.; Boyce, D. A.; Murray, K. J.; Sutton, D. L. (Atomic Energy Research Establishment, Harwell, Eng.). pp 315–30 of Nuclear Data for Reactors. Vol. I. Vienna; International Atomic Energy Agency (1970).

From 2nd International Conference on Nuclear Data for Reactors, Helsinki, Finland. See STI/PUB–259(Vol.1); CONF-700605–(Vol.1).

The ratio of the capture to fission cross-sections (alpha) of ^{239}Pu in the energy range 100 eV to 30 keV was measured using the Harwell 45-MeV Linear Accelerator time-of-flight spectrometer. The method used was previously described together with provisional results. The final results are presented and compared with the other available data. Most experiments to measure alpha in this energy range are normalized to the values of alpha at the peaks of the low-energy resonances. It was recognized at the meeting of specialists organized by the International Working Group on Fast Reactors in July 1969 that some of the discrepancies between the various experiments were due to differences in the values used for normalization. It was, therefore, recommended that a best set of normalization values should be obtained and that, for comparison purposes, all experiments should be normalized to these. An evaluation to produce a best set was performed, and the results are discussed. (23 references) (auth)

15074 MEASUREMENT OF ALPHA VALUES FOR ^{235}U AND ^{239}Pu. Belyaev, F. N.; Ignat'ev, K. G.; Sukhoruchkin, S. I.; (and others). (Moscow Inst. of Theoretical Physics). pp 339–44 of Nuclear Data for Reactors. Vol. I. Vienna; International Atomic Energy Agency (1970). (In Russian).

From 2nd International Conference on Nuclear Data for Reactors, Helsinki, Finland. See STI/PUB–259(Vol.1); CONF-700605–(Vol.1).

Because of inconsistences in alpha values for ^{239}Pu in the neutron energy range of several keV, measurements of this parameter for ^{235}U and ^{239}Pu were performed by means of the neutron spectrometer of the ITEF cyclotron. Fission and capture effects from metal foil were measured independently by two methods using different kinds of detectors, located on 14.6-meter path-flight. Alpha values for ^{235}U and ^{239}Pu were obtained in the energy range of neutrons from thermal to 10 keV. (auth)

XUM

15075 MEASUREMENTS OF THE RADIATIVE-CAPTURE-TO-FISSION CROSS SECTIONS (α) FOR ^{235}U AND ^{239}Pu IN THE NEUTRON ENERGY RANGE BELOW 30 keV. Kurov, M. A. (Joint Inst. for Nuclear Research, Dubna, USSR); Ryabov, Yu. V.; Sik, So Don; (and others). pp 345-55 of Nuclear Data for Reactors. Vol. I. Vienna; International Atomic Energy Agency (1970). (In Russian).

From 2nd International Conference on Nuclear Data for Reactors, Helsinki, Finland. See STI/PUB-259(Vol. 1); CONF-700605-(Vol. 1).

The results of measurements of the radiative-capture-to-fission cross sections $\alpha(E)$ for ^{239}Pu and ^{235}U in the neutron energy range below 30 keV are presented. The measurements were carried out with two different methods which are described in detail. (15 references) (auth)

15076 METHOD OF DIRECT MEASUREMENT OF THE CAPTURE-TO-FISSION CROSS-SECTION. Muradyan, H. V.; Mostovaya, T. A.; Mostovoi, V. I.; Shchepkin, Yu. G. (Inst. of Atomic Energy, Moscow). pp 357-72 of Nuclear Data for Reactors. Vol. I. Vienna; International Atomic Energy Agency (1970). (In Russian).

From 2nd International Conference on Nuclear Data for Reactors, Helsinki, Finland. See STI/PUB-259(Vol.1); CONF-700605-(Vol.1).

A method of direct measurement of the capture-to-fission (α) cross-section is described. The fission events are recorded by an ionization chamber. A layer of the substance to be studied is located along the neutron beam and, at the same line, serves as a sample for the capture measurements. Neutron capture is recorded by NaI(Tl) crystals. The α-values for ^{235}U obtained by the method are given in a neutron energy region of 0.3-5000 eV. (13 references) (auth)

15077 OBSERVATION OF AN ISOMERIC LEVEL IN ^{239}U BY MEANS OF THE ^{238}U(n,γ)^{239}U REACTION. Thomas, B. W.; Murray, J.; Rae, E. R. (Atomic Energy Research Establishment, Harwell, Eng.). pp 373-6 of Nuclear Data for Reactors. Vol. I. Vienna; International Atomic Energy Agency (1970).

From 2nd International Conference on Nuclear Data for Reactors, Helsinki, Finland. See STI/PUB-259(Vol. 1); CONF-700605-(Vol. 1).

Low-energy-capture gamma-ray spectra (<1 MeV) were measured for several resonances in ^{238}U up to a neutron energy of 350 eV. The data were obtained using a 25-cm^3 Ge(Li) detector at the Harwell 45 MeV Electron Linac. Capture events were recorded as functions of gamma-ray energy and neutron time-of-flight, and by suitable analysis of the data time-of-flight spectra were obtained for individual gamma-rays. The strongest low-energy gamma-ray, at 134 keV, depopulates a level in ^{239}U at the same energy by an E2-transition to the ground state. The time-of-flight spectrum for this transition indicates that the 134-keV level is isomeric with a half-life of approximately 1 microsecond. This is evident from the long tails on the low-energy side of each resonance, which are not present for other regions of the gamma-ray spectrum. The possibility of using low-energy gamma-rays as a measure of the total capture cross-section is investigated by comparing the time-of-flight spectrum for the 134-keV transition with that for a Moxon–Rae detector under the same experimental conditions. (auth)

15078 HIGH-ENERGY γ-RAYS FOLLOWING NEUTRON CAPTURE IN ^{239}Pu AND ^{235}U. Chrien, R. E. (Brookhaven National Lab., Upton, N. Y.); Wasson, O. A.; Dritsa, S.; Bokharee, S.; Garg, J. B. pp 377-86 of Nuclear Data for Reactors. Vol. I. Vienna; International Atomic Energy Agency (1970).

From 2nd International Conference on Nuclear Data for Reactors, Helsinki, Finland. See STI/PUB-259(Vol. 1); CONF-700605-(Vol. 1).

Primary high-energy γ-rays, representing direct transitions to low-lying states of the residual nucleus, in resonant neutron capture, were observed using the BNL fast-chopper time-of-flight facility. In ^{235}U such transitions are too weak to be easily observed; however, strong capture γ-rays are observed in ^{239}Pu resonances. Two of these transitions populate known states in ^{240}Pu at 597.4 keV (1^-) and at 42.8 keV (2^+), giving a neutron binding energy of 6533.7 ± 1.5 keV. Other γ-rays are seen which correspond to the population of levels heretofore unobserved in ^{240}Pu. These levels probably have spin 0^-, 1^-, or 2^- and are located at 858.1, 936.4, 958.5, 1241.4, and 1438.3 keV. There is weaker evidence for several additional levels. The observation of the M-1 transition permits the assignment of the spins of two resonances in ^{239}Pu. The 0.3-eV resonance and the 41.7 eV resonance are both assigned spin 1. These are in agreement with recent spin assignments derived from neutron-multiplicity measurements and scattering measurements; the former is in disagreement, however, with multilevel cross-section fitting. A comparison is made between the delayed fission γ-ray spectra of ^{235}U and ^{239}Pu, which appear as backgrounds in the time-of-flight studies. (13 references) (auth)

15079 TOTAL NEUTRON CROSS-SECTION OF ^{233}U FROM 0.7 eV TO 320 eV. Kolar, W.; Carraro, G.; Nastri, G. (EURATOM, Geel, Belg.). pp 387-402 of Nuclear Data for Reactors. Vol. I. Vienna; International Atomic Energy Agency (1970).

From 2nd International Conference on Nuclear Data for Reactors, Helsinki, Finland. See STI/PUB-259(Vol.1); CONF-700605-(Vol.1).

The total neutron cross-section of ^{233}U was measured in the energy range of 0.7-320 eV. The experiments were carried out at the 60-MeV electron linear accelerator of the CBNM. Two metal samples of ^{233}U with a thickness of 1.78 gr/cm^2 were available. The nominal resolution of the different measurements varied between about 50 ns/m at 0.7 eV and about 1 ns/m at 320 eV. Up to 93 eV, the results were analysed using the multilevel fit program CODILLI. In addition, from 2.5 eV to 53 eV a single-level analysis was performed. From the single-level resonance parameters up to 30 eV a mean level spacing $\langle D \rangle = 0.61 = 0.07$ eV was obtained. Assuming that all resonances in that energy range are due to s-wave neutrons the strength function is $S_0 = (2.25 \pm 0.55) \times 10^{-4}$. (14 references) (auth)

15080 NEUTRON WIDTHS OF ^{238}U FROM 60 eV TO 5.7 keV. Carraro, G.; Kolar, W. (EURATOM, Geel, Belg.). pp 403-12 of Nuclear Data for Reactors. Vol. I. Vienna; International Atomic Energy Agency (1970).

From 2nd International Conference on Nuclear Data for Reactors, Helsinki, Finland. See STI/PUB-259(Vol.1); CONF-700605-(Vol.1).

The neutron total cross-section of ^{238}U was measured from about 60 eV to about 14 keV and the resonance parameters were evaluated up to 5.7 keV. The experiments were carried out at the 60 MeV linear accelerator of the CBNM. The thickness of the ^{238}U sample (99.6% of ^{238}U) was 91 barn/at. The nominal resolution of the different measurements varied between 3.2 ns/m at 60 eV and 0.5 ns/m at about 5.7 keV. About 260 resonances were observed and the resonance parameters E_0 and Γ_n^0 were determined. The statistical properties for the resonances observed between 60-2000 eV are determined. A mean level spacing $\langle D \rangle = 17.8 \pm 0.9$ eV and a mean reduced neutron width $\langle \Gamma_n^0 \rangle = (1.95 \pm 0.27) \times 10^{-3}$ eV were calculated assuming that all resonances in that energy range are s-wave resonances. The s-wave strength function is determined to $S_0 = (1.09 \pm 0.15) \times 10^{-4}$. (10 references) (auth)

15081 RESONANCE PARAMETERS FROM NEUTRON RADIATIVE CAPTURE IN ^{238}U. Rohr, G.; Weigmann, H.; Winter, J. (EURATOM, Geel, Belg.). pp 413-16 of Nuclear Data for Reactors. Vol. I. Vienna; International Atomic Energy Agency (1970).

From 2nd International Conference on Nuclear Data for Reactors, Helsinki, Finland. See STI/PUB-259(Vol.1); CONF-700605-(Vol.1).

Neutron radiative capture in ^{238}U was studied in the neutron energy range from 50 eV to 1 keV. Combined area analysis of these data together with data from total cross-section measurements performed at the CBNM yields the resonance parameters of 28 resonances. A mean value of $\bar{\Gamma}_\gamma = (24.64 \pm 0.85)$ MeV was obtained. The results are compared with earlier measurements. No evidence for a non-statistical variation of the radiative widths with neutron energy was found. (8 references) (auth)

15082 FISSION-CROSS-SECTION MEASUREMENT OF ^{233}U. Cao, M. G.; Migneco, E.; Theobald, J. P.; Merla, M. (EURATOM, Geel, Belg.). pp 419-35 of Nuclear Data for Reactors. Vol. I. Vienna; International Atomic Energy Agency (1970).

From 2nd International Conference on Nuclear Data for Reactors, Helsinki, Finland. See STI/PUB-259(Vol.1); CONF-700605-(Vol.1).

The neutron-induced fission cross-section of ^{233}U was measured in the energy range between 0.018 eV and 2 keV. Up to 80 eV, a spark-chamber fission-fragment detector was used, the properties of which are described. From 10 eV up to 2 keV the data were taken with a fission neutron scintillator detector. A multilevel fit was performed for resonances below 65 eV. Resonance integrals are compared with results of other laboratories. (15 references) (auth)

15083 NEUTRON-INDUCED FISSION CROSS-SECTION OF ^{241}Pu. Migneco, E.; Theobald, J. P.; Wartena, J. A. (EURATOM, Geel, Belg.). pp 437-46 of Nuclear Data for Reactors. Vol. I. Vienna; International Atomic Energy Agency (1970).

From 2nd International Conference on Nuclear Data for Reactors, Helsinki, Finland. See STI/PUB-259(Vol.1); CONF-700605-(Vol.1).

A time-of-flight experiment was performed to measure the neutron-induced fission cross-section for neutrons of energies in the range 2-2000 eV. The CBNM linear accelerator with a mercury-cooled uranium target served as pulsed neutron source. The nominal resolution of the time-of-flight spectrometer was 20 ns/m between 2 and 46.5 eV and 2ns/m at higher energies. The fission events were detected by a liquid scintillation neutron detector. The reduced data are presented together with a set of resonance integrals, which are compared with results from other laboratories. (10 references) (auth)

15084 SCATTERING CROSS-SECTION OF ^{235}U BELOW 100 eV. DETERMINATION OF Γ_n AND J OF RESONANCES. Poortmans, F. (SCK-CEN, Mol, Belg.); Ceulemans, H.; Migneco, E.; Theobald, J. P. pp 449-60 of Nuclear Data for Reactors. Vol. I. Vienna; International Atomic Energy Agency (1970).

From 2nd International Conference on Nuclear Data for Reactors, Helsinki, Finland. See STI/PUB-259(Vol. 1); CONF-700605-(Vol. 1).

The detector array was composed of nine 10-atmosphere ^{3}He proportional counters with low jitter time. The measurements were performed below 100 eV at a 30 meter flight path of the liner electron accelerator of CBNM, Euratom, Geel. The main advantages of the detectors are their good discrimination properties against gamma rays and fission neutrons. The very low background allowed the measurements to be made with thin samples (7.81×10^{20} and 2.58×10^{20} nuclei/cm^2) so that the corrections for self-screening and absorption were small. The total error on the scattering cross-section data is of the order of 5%. In the whole energy range, the scattering cross-section is consistent with a potential scattering of 11.7 barn. The total cross-section was measured with the same samples and the same time-of-flight resolution. Taking the published values of resonance parameters $g\Gamma_n$ and Γ, the total cross-section and the scattering cross-sections corresponding to the two possible spin states were calculated, taking into account resolution and Doppler broadening. In general, the agreement with the experimental data is very good and the spin of 14 resonances below 60 eV was determined. For some resonances, the accuracy of the resonance parameters Γ_n and Γ was improved by the simultaneous fit of the scattering and total cross-section. The experimental results obtained and the correlation between their spin values and previously obtained data from different fission experiments (fission width, mass and kinetic energy of fission fragments, ternary-fission anisotropy of fission fragments from aligned nuclei and average number of neutrons per fission) are discussed. (10 references) (auth)

15085 SCATTERING CROSS-SECTION OF ^{235}U BETWEEN 0.025 eV AND 1 eV. Ceulemans, H.; Poortmans, F. (SCK-CEN, Mol, Belg.). pp 461-5 of Nuclear Data for Reactors. Vol. I. Vienna; International Atomic Energy Agency (1970).

From 2nd International Conference on Nuclear Data for Reactors, Helsinki, Finland. See STI/PUB-259(Vol.1); CONF-700605-(Vol.1).

In view of the importance of the ^{235}U scattering cross-section for cross checks between, for example, total and fission cross-sections, this quantity was measured at the BR2 reactor of SCK/CEN, Mol, in the energy region of 0.025 eV to 1 eV. The results of the experiments are presented together with a short description of the method and a discussion of the overall accuracy of the experiments. (auth)

15086 MEASUREMENT AND ANALYSIS OF ^{235}U AND ^{241}Pu FISSION CROSS-SECTIONS. Blons, J.; Debril, G.; Fermandjian, J.; Michaudon, A. (Centre d'Etudes Nucleaires, Saclay, France). pp 469-80 of Nuclear Data for Reactors. Vol. I. Vienna; International Atomic Energy Agency (1970). (In French).

From 2nd International Conference on Nuclear Data for Reactors, Helsinki, Finland. See STI/PUB-259(Vol.1); CONF-700605-(Vol.1).

The fission cross-sections of ^{235}U between 17 eV and 30 keV and of ^{241}Pu between 1 eV and 3 keV were measured by a time-of-flight method making use of a gas scintillator operated at a temperature of 77°K. The Saclay 45-MeV linear accelerator was used as pulsed neutron source. The experimental conditions are presented and the average fission cross-section is compared with those of other laboratories. Moreover, the fission cross-section of ^{241}Pu was analysed from 1 to 6 eV and from 14 to 63 eV by means of a least-squares program based on a single-level formalism, and from 6 to 14 eV by a least-squares program based on a multi-level formalism. Finally, the preliminary results of a higher-resolution measurement (2 ns/m) of ^{241}Pu are also presented. (15 references) (auth)

15087 SIMULTANEOUS ANALYSIS OF TOTAL AND FISSION CROSS-SECTIONS OF ^{239}Pu FROM 5.7 TO 160 eV USING A MULTI-LEVEL FORMALISM. Derrien, H.; Blons, J.; Michaudon, A. (Centre d'Etudes Nucleaires, Saclay, France). pp 481-93 of Nuclear Data for Reactors. Vol. I. Vienna; International Atomic Energy Agency (1970). (In French).

From 2nd International Conference on Nuclear Data for Reactors, Helsinki, Finland. See STI/PUB-259(Vol.1); CONF-700605-(Vol.1).

Total and fission cross-sections were measured at Saclay using the 45-MeV linear accelerator as a pulsed source of neutrons. The two measurements were carried out with a nominal resolution of 0.5 and 1 ns/m, respectively, the samples being held at the temperature of liquid nitrogen. In most cases analysis of the shape of the resonances by the Breit–Wigner single-level formula gave a satisfactory value for the parameters. However, this formula cannot always reproduce a cross-section shape in agreement with the measurements. More particularly, certain differences between the theoretical and experimental curves can be definitely reduced by adding resonances, the existence of which has not been definitely established. To reproduce as faithfully as possible the cross-section shape and thus define accurately certain parameters, the analysis was carried out using a multi-level formalism allowing for interference between resonances of the same spin; the formalism used is that of Reich and Moore. The program makes use of a least squares method of adjustment applied simultaneously to the total and fission cross-sections. Analytical results are presented, covering in particular: a comparison of the theoretical curves with the experimental results; a statistical study of the parameters and a comparison with an equivalent study made on the results of a single-level analysis; a determination of the spin of certain levels by systematic study of the shape of the interferences; the number of exit channels of the 0^+ and 1^+ states of the compound nucleus. (14 references) (auth)

15088 DETERMINATION OF THE SPIN OF SLOW-NEUTRON INDUCED RESONANCES IN ^{239}Pu. Trochon, J.; Derrien, H.; Lucas, B.; Michaudon, A. (Centre d'Etudes Nucleaires, Saclay, France). pp 495-511 of Nuclear Data for Reactors. Vol. I. Vienna; International Atomic Energy Agency (1970). (In French).

From 2nd International Conference on Nuclear Data for Reactors, Helsinki, Finland. See STI/PUB-259(Vol.1); CONF-700605-(Vol.1).

A high-resolution measurement of slow-neutron elastic scattering from ^{239}Pu was carried out by the time-of-flight method, using the Saclay 45-MeV linear accelerator as pulsed neutron source. An analysis of the experimental data, in conjunction with that of the total cross-section of Saclay, allowed the spin of 112 resonances in the energy range of 0-660 eV to be determined. With the help of certain assumptions, these results allow a classification of all resonances analysed into two groups corresponding to the two spins $J = 0^+$ and $J = 1^+$. A study of the mean widths $\langle\Gamma_f\rangle_{0^+}$ and $\langle\Gamma_f\rangle_{1^+}$ in energy intervals of 110 eV confirms the existence of an intermediate structure in the fission cross-section due to channel 1^+. This intermediate structure is responsible for the large fluctuations of α in the energy range of 0-660 eV. (23 references) (auth)

15089 HIGH-RESOLUTION MEASUREMENT AND ANALYSIS OF THE ^{239}Pu FISSION CROSS-SECTION. Blons, J.; Derrien, H.; Michaudon, A. (Centre d'Etudes Nucleaires, Saclay, France). pp 513-24 of Nuclear Data for Reactors. Vol. I. Vienna; International Atomic Energy Agency (1970). (In French).

From 2nd International Conference on Nuclear Data for Reactors, Helsinki, Finland. See STI/PUB-259(Vol.1); CONF-700605-(Vol.1).

The fission cross-section of ^{239}Pu was measured up to an energy of 30 keV with a gas scintillator containing 960 mg of ^{239}Pu and operated at a temperature of 77°K. The measurement was made with a resolution of 1 ns/m using the Saclay 45-MeV linear accelerator as pulsed neutron source. The resonances were analysed up to 660 eV by the shape method, by using a least-squares program based on a single-level formalism. A detailed study of the fission-width distribution for different energy intervals of 110 eV shows the existence of an intermediate structure in the fission cross-section due to the exit channel 1^+. This phenomenon is confirmed by measuring the spin of the resonances up to 660 eV. Finally, the fission cross-section averaged over different energy intervals is compared with those obtained in other laboratories. 18 references. (auth)

15090 FISSION AND CAPTURE CROSS-SECTIONS OF CURIUM. Moore, M. S. (Los Alamos Scientific Lab., N. Mex.); Brown, W. K.; Ennis, M. E.; (and others). pp 527-41 of Nuclear Data for Reactors. Vol. I. Vienna; International Atomic Energy Agency (1970).

XUM

From 2nd International Conference on Nuclear Data for Reactors, Helsinki, Finland. See STI/PUB–259(Vol.1); CONF-700605–(Vol.1).

In a recent experiment utilizing a nuclear explosion as the neutron source, both fission and capture cross-sections were measured for ^{244}Cm and ^{246}Cm, and fission cross-sections were measured for the other Cm isotopes in the production chain: ^{245}Cm, ^{247}Cm, and ^{248}Cm, from 20 eV to several MeV. Fission cross-sections were also determined for a number of other heavy isotopes, including ^{252}Cf. This technique appears to be reasonably well suited for such studies, since only limited quantities (20 to 100 μg) of separated target isotopes are required, and the sample activity (up to 10^8 fissions/s) is no problem. Analysis of the data in the resolved resonance region above 20 eV yields all the partial cross-sections for the isotopes ^{244}Cm, ^{246}Cm, and ^{247}Cm, under the assumption that the capture width for the odd-A target is constant and given by nuclear systematics. These measurements are also of interest because they offer experimental evidence concerning nuclear-structure-model predictions by Strutinsky and Nilsson on sub-barrier fission. The even curium and californium isotopes measured all show fission thresholds and appreciable sub-barrier resonance fission. However, the characteristic enhancement of sub-barrier resonance fission attributed to eigenstates in the second shape minimum does not seem to be present for the even Cm and Cf targets studied. (14 references) (auth)

15091 SIMULTANEOUS MEASUREMENT OF THE FISSION, CAPTURE, SCATTERING, AND TOTAL CROSS-SECTIONS OF ^{239}Pu. Farrell, J. A.; Auchampaugh, G. F.; Moore, M. S.; Seeger, P. A. (Los Alamos Scientific Lab., N. Mex.). pp 543-50 of Nuclear Data for Reactors. Vol. I. Vienna; International Atomic Energy Agency (1970).

From 2nd International Conference on Nuclear Data for Reactors, Helsinki, Finland. See STI/PUB–259(Vol.1); CONF-700605–(Vol.1).

The fission, capture, scattering, and total cross-sections of ^{239}Pu were measured from 14 eV to 1 MeV using an underground nuclear explosion as a pulsed neutron source. The flight path was 245 meters and the resolution was approximately 15 ns/meter in the resonance region. The cross-sections were measured simultaneously so that the source function is the same for each cross-section. All measurements were made with solid-state detectors. The current induced in the detectors by the detected particles was amplified with logarithmic amplifiers, displayed on oscilloscopes and photographed with moving film cameras. The capture and scattering cross-sections were measured from a ^{239}Pu sample which was 8.8×10^{-4} atoms/barn thick. The neutron flux was measured on each side of the sample by ^{6}LiF foils and solid-state detectors to determine the transmission through the sample and therefore the total cross-section and the self-absorption correction to the capture and scattering signals. The capture cross-section was measured with solid-state detectors equipped with Moxon–Rae converters. The fission gamma-ray sensitivity was determined from the broad 0^+ resonances which have very little capture. The ratio of capture to fission, alpha, was computed. The result from 1 to 30 keV is in good agreement with the measurements of other laboratories. The scattered-neutron detector was a stack of 10 thin solid-state detectors surrounded by 21 atmospheres of ^{3}He. The fission-neutron and gamma-ray background was measured by a similar detector filled with CH_4. The pressure of CH_4 was adjusted to match the responses of the two detectors to fission neutrons. The two signals were subtracted electronically in order to reduce recording errors. An additional transmission measurement was made on a thicker (6.1×10^{-3} atoms/barn) sample to provide a more accurate total cross-section in the valleys between resonances. 10 references. (auth)

15092 DETERMINATION OF RESONANCE PARAMETERS OF ^{240}Pu USING A CRYSTAL SPECTROMETER. Ramakrishna, D. V. S.; Navalkar, M. P. (Bhabha Atomic Research Centre, Bombay). pp 553-7 of Nuclear Data for Reactors. Vol. I. Vienna; International Atomic Energy Agency (1970).

From 2nd International Conference on Nuclear Data for Reactors, Helsinki, Finland. See STI/PUB–259(Vol.1); CONF-700605–(Vol.1).

Measurements of resonance parameters of ^{240}Pu were undertaken by using a high-resolution crystal spectrometer. Three different samples of plutonium in the form of Pu-Al alloy foils were used to study the important 1-eV resonance energy level of ^{240}Pu. The experimental data were analyzed by the method of area analysis and also by shape analysis incorporating Doppler broadening and the resolution function of the crystal spectrometer. The parameters $E_0 = 1.059$ eV, $\sigma_0 = 173{,}000$ barn, $\Gamma_n = 2.18$ MeV and $\Gamma = 31.0$ MeV show a best fit to the experimental transmission curve. The results are compared with the other data published. (auth)

15093 TEMPERATURE DEPENDENCE OF THE TOTAL CROSS-SECTION STRUCTURE OF ^{238}U IN THE UNRESOLVED RESONANCE REGION. Van'kov; A. A. (Inst. of Physics and Power Engineering, Obninsk, USSR); Grigor'ev, Yu. V.; Nikolaev, M. N.; (and others). pp 559-69 of Nuclear Data for Reactors. Vol. I. Vienna; International Atomic Energy Agency (1970). (In Russian).

From 2nd International Conference on Nuclear Data for Reactors, Helsinki, Finland. See STI/PUB–259(Vol.1); CONF-700605–(Vol.1).

The transmission of neutrons was measured in the range 1–100 keV through uranium-238 samples varying in thickness between 1 and 128 mM at −196°C, 20°C and 770°C using the time-of-flight neutron spectrometer at the Joint Institute for Nuclear Research, Dubna. The IBR pulsed fast reactor was used as neutron source. By using programs for calculating transmission and parameter optimization to process the experimental data, a set of average resonance parameters for uranium-238 describing the structure of the cross-section and its temperature dependence was obtained. (auth)

15094 EVALUATION IN THE RESONANCE RANGE OF NUCLEI WITH A MASS NUMBER ABOVE 220. Ribon, P. (Centre d'Etudes Nucleaires, Saclay, France). pp 571-99 of Nuclear Data for Reactors. Vol. I. Vienna; International Atomic Energy Agency (1970). (In French).

From 2nd International Conference on Nuclear Data for Reactors, Helsinki, Finland. See STI/PUB–259(Vol.1); CONF-700605–(Vol.1).

The problems posed by the evaluation of neutron data for fissile or fertile nuclei in the range of resolved or unresolved resonances are discussed. It appears to take several years until the data of an experiment are used by the reactor physicists. If one wants to have recent data at one's disposal, one cannot have recourse to evaluated-data libraries. Moreover, the existing parameter sets are only fragmentary. A new evaluation is, therefore, necessary for nearly all of these nuclei, but it cannot be based upon different parameter sets; these are indeed contradictory, and the evaluator will have to go back to the original data. For the set of σ_f of ^{235}U, it is shown that a careful comparison of the data shows up unsuspected local defects. Some examples illustrate the deviation between analyses carried out by different methods and between the results on the established divergences. The parameters or cross-sections are far from being known with the precision one would desire. This fact gives rise to anomalies in the interpretation of data necessary for understanding and simulation in the range of unresolved resonances. But the introduction of concepts connected with sub-threshold fission noticeably furthers this understanding. Therefore a comparison of the methods of analysis must be made in more and more accurate measurements (evaluation and correction of systematic errors). (auth)

15095 NEUTRON-SPECTROSCOPY STUDY OF NUCLEI WITH A < 220 IN THE RESONANCE ENERGY REGION. Muradyan, G. V.; Shchepkin, Yu. G.; Adamchuk, Yu. V. (Inst. of Atomic Energy, Moscow). pp 603-18 of Nuclear Data for Reactors. Vol. I. Vienna; International Atomic Energy Agency (1970). (In Russian).

From 2nd International Conference on Nuclear Data for Reactors, Helsinki, Finland. See STI/PUB–259(Vol.1); CONF-700605–(Vol.1).

The possibilities of neutron-spectroscopy experiments from the point of view of obtaining nuclear constants in the resonance energy range required for reactor calculations are discussed. It is shown that a further increase of accuracy of the constants is connected with the development of pulsed neutron sources. An analysis of the existing methods for selection of one system of levels is presented. Several reasons for the discrepancy between the experimental data and the theoretical prediction are considered. 65 references. (auth)

15096 NEUTRON CROSS-SECTIONS OF ISOTOPES USED AS ABSORBERS IN ATOMIC REACTORS. Vertebnyi, V. P. (Inst. of Physics, Kiev); Vlasov, M. F.; Gnidak, N. L.; (and others). pp 651-66 of Nuclear Data for Reactors. Vol. I. Vienna; International Atomic Energy Agency (1970). (In Russian).

From 2nd International Conference on Nuclear Data for Reactors, Helsinki, Finland. See STI/PUB–259(Vol.1); CONF-700605–(Vol.1).

The principal results of measurements of the energy dependence of the total neutron cross-sections, the neutron scattering cross-sections, and the radiative capture cross-sections of a large number of nonfissionable isotopes are presented. For the measurements, the VVR-M (water-moderated, water-cooled) reactor of the Physics Institute of the Ukrainian SSR Academy of Sciences and the time-of-flight method in the energy range 0.007 to 10 eV was used. Methods for increasing substantially the accuracy of total and partial cross-section measurements (reduction of multiple scattering, determination of the influence of impurities, irradiation of samples in the reactor core, etc.) are reviewed. Particular attention is paid to strong absorbers. In view of the fact that europium and dysprosium are used in reactor control, a careful analysis is made of all the neutron constants of these isotopes with a view of ascertaining the reasons for discrepancies between the results of different authors. Questions connected with the systematics of neutron cross-sections are discussed and experimental results are compared with theory. 18 references. (auth)

15097 ALPHA WIDTHS OF NEUTRON RESONANCES. Popov, Yu. P. (Joint Inst. for Nuclear Research, Dubna, USSR); Pshitula, M.; Rumi, R. F.; (and others). pp 669-78 of Nuclear Data for Reactors. Vol. I. Vienna; International Atomic Energy Agency (1970). (In Russian).

From 2nd International Conference on Nuclear Data for Reactors, Helsinki, Finland. See STI/PUB-259(Vol.1); CONF-700605-(Vol.1).

Radiation damages of the crystal lattice of construction materials due to the α-particle escaping after capture of a slow neutron are considerably more serious than in the case of γ-ray emission. Fortunately, in the region of heavy nuclei $\sigma(n,\alpha)/\sigma(n,\gamma) \leq 10^{-6}$. For light nuclei, however, the cross-sections become closer to each other, for which reason allowance for a possible contribution of the (n,α)-reaction to radiation damages will, in a number of cases, undoubtedly be of vital importance in choosing the construction materials for nuclear reactors. On the basis of the statistical and optical models of the atomic nucleus the problem of the mean values of α-widths of neutron resonances for various nuclei and the problem of α-width fluctuations are discussed. The results of calculations are compared with the experimental data. The possible reasons of the discrepancy between the calculated mean α-widths and the results of the measurements are discussed. A method of determining the spin of the nuclear resonance state from the values of total and partial α-widths measured in the (n,α)-reaction is proposed. The results of this spin identification are presented for a number of atomic nuclei. 12 references. (auth)

15098 MEASUREMENTS OF NEUTRON-RESONANCE TOTAL CROSS-SECTIONS FOR FISSION PRODUCT ISOTOPES. Jung, H. H.; Priesmayer, H. G.; Sulitze, H. (Kiel Univ.). pp 679-83 of Nuclear Data for Reactors. Vol. I. Vienna; International Atomic Energy Agency (1970).

From 2nd International Conference on Nuclear Data for Reactors, Helsinki, Finland. See STI/PUB-259(Vol.1); CONF-700605-(Vol.1).

The following measurements were made by means of the fast-chopper time-of-flight spectrometer at the FRG 1 to 5 MW research reactor. The spectrometer resolution was between 160 ns/m and 30 ns/m, depending on the rotor speed. (A) Total neutron cross-sections of ^{133}Cs, ^{135}Cs and ^{137}Cs: In the energy range from 1.7 to 1100 eV measurements were made on stable ^{133}Cs and a mixture of fission product ^{133}Cs, ^{135}Cs and ^{137}Cs. The isotopic abundance 133 : 135 : 137 was 0.488 : 0.171 : 0.341. Two resonances were found in $^{135/137}$Cs. Resonance parameters were determined. (B) Total neutron cross-sections of ^{100}Ru, ^{101}Ru and ^{104}Ru: In the energy range from 1 eV to 1.5 keV the total neutron cross-sections of the stable separated isotopes ^{100}Ru, ^{101}Ru, ^{102}Ru and ^{104}Ru were measured. These measurements are needed for fast-reactor burnup calculations since the yield for these isotopes of approximately 5% is relatively high. Several new resonances were found and known resonances could be assigned isotopically. Measurements with different sample thicknesses were made using natural ruthenium in order to determine resonance parameters. (C) Total neutron cross-sections of gross fission products: Samples of uranium enriched to 90% in ^{235}U were burned up to 40% in the FRG 2 to 15 MW research reactor. A first time-of-flight spectrum, taken after 70 days of cooling, is presented. The covered energy range is from 1 to 30 eV. (auth)

15099 EVALUATION OF FISSION PRODUCT YIELDS. Walker, W. H. (Atomic Energy of Canada Ltd., Chalk River, Ont.). pp 685-702 of Nuclear Data for Reactors. Vol. I. Vienna; International Atomic Energy Agency (1970).

From 2nd International Conference on Nuclear Data for Reactors, Helsinki, Finland. See STI/PUB-259(Vol.1); CONF-700605-(Vol.1).

The evaluation of yields from the thermal-neutron fission of ^{235}U are described, and these results, with yields from preliminary evaluations of ^{233}U and ^{239}Pu data, are used in the fission-product program, FISSPROD, to calculate fission-product absorption for comparison with reactivity measurements using irradiated fuel. Earlier evaluations of fission-product yields have taken weighted averages using both spectrometric and radiometric data. In the present evaluation the relative mass-spectrometric yields from different experimenters are normalized to the isotopes of an element near the maxima of the light and heavy mass peaks and compared. Very divergent relative yield values are rejected and the isotopic yields of a particular element are renormalized when the original normalization is suspect. This establishes the shape of the light and heavy mass peaks accurately. Final normalization requires an estimate of yields not included in mass-spectrometric data. The uncertainty in ^{235}U fission-product absorption calculations due to uncertainties in yields only is estimated to be about 1.4%. The major contributor is ^{135}Xe. 33 references. (auth)

15100 REDETERMINATION OF THE THERMAL-NEUTRON ABSORPTION CROSS-SECTIONS OF GROSS FISSION PRODUCTS OF ^{233}U, ^{235}U, AND ^{239}Pu. Okazaki, A. (Atomic Energy of Canada Ltd., Chalk River, Ont.); Sokolowski, E. K. pp 703-19 of Nuclear Data for Reactors. Vol. I. Vienna; International Atomic Energy Agency (1970).

From 2nd International Conference on Nuclear Data for Reactors, Helsinki, Finland. See STI/PUB-259(Vol.1); CONF-700605-(Vol.1).

The thermal cross-sections of the long-lived gross fission products from ^{233}U, ^{235}U and ^{239}Pu fission were determined by pile oscillator measurements on highly irradiated samples. The samples, consisting initially of a single fissile nuclide in a matrix of high-purity aluminum, had been irradiated to a depletion of 70 to 90%, which gave a fission product contribution to the total absorption cross-section of about 10%. Measurements with these samples had previously been performed at AECL, but were repeated under more favorable experimental conditions. The fission product cross-sections were determined with an accuracy of 5%. A comparison with a recent version of the calculational model FISSPROD shows that the calculated cross-sections are consistently about 7% higher than the measured ones. 14 references. (auth)

15101 NEUTRON CROSS-SECTION EVALUATION IN THE THERMAL AND RESONANCE ENERGY RANGE FOR NUCLIDES OF MASS LESS THAN 220. Story, J. S. (Atomic Energy Establishment, Winfrith, Eng.). pp 721-40 of Nuclear Data for Reactors. Vol. I. Vienna; International Atomic Energy Agency (1970).

From 2nd International Conference on Nuclear Data for Reactors, Helsinki, Finland. See STI/PUB-259(Vol.1); CONF-700605-(Vol.1).

Problems of the past and prospects for the near future in evaluation work for the thermal and resonance region in the mass range A less than 220 are discussed. In doing so, thermal-neutron scattering, moderator fast-neutron scattering and neutron age, and resonance cross-sections of other materials are treated. (auth)

15102 RECENT EXPERIMENTAL DATA FOR HEAVY NUCLEI. Poenitz, W. P. (Argonne National Lab., Ill.). pp 3-30 of Nuclear Data for Reactors. Vol. II. Vienna; International Atomic Energy Agency (1970).

From 2nd International Conference on Nuclear Data for Reactors, Helsinki, Finland. See STI/PUB-259(Vol.2); CONF-700605-(Vol.2).

The present knowledge of experimental nuclear data of fertile and fissile nuclei above the resonance energy region is critically reviewed. Recent request lists for nuclear data have been more and more demanding of the accuracy of such data as the capture cross section of ^{238}U and the fission cross sections of ^{235}U and ^{239}Pu. This situation reflects the importance of such cross sections in fast reactor calculations and design. Because of the large amounts of data involved, the review is mainly restricted to those heavy nuclei and their properties which have the strongest influence on the neutronics of fast reactors. 96 references. (auth)

15103 MEASUREMENT OF TOTAL NEUTRON CROSS-SECTIONS OF CARBON, NICKEL, ^{235}U, ^{238}U, AND ^{239}Pu BETWEEN 0.1 MeV AND 6 MeV. Cabe, J.; Cance, M.; Adam, A.; Beaufour, M.; Labat, M. (Centre d'Etudes, Bruyeres-le-Chatel, France). pp 31-7 of Nuclear Data for Reactors. Vol. II. Vienna; International Atomic Energy Agency (1970). (In French).

From 2nd International Conference on Nuclear Data for Reactors, Helsinki, Finland. See STI/PUB-259(Vol.2); CONF-700605-(Vol.2).

The total neutron cross-sections of carbon, natural nickel, uranium-235, uranium-238 and plutonium-239 was measured between 100 keV and 6 MeV with energy spreads of ±2 keV to ±40 keV depending on the element and the energy range. The error in the absolute values was less than 3%. The neutrons were obtained by the $T(p,n)^3He$ reaction, using protons (accelerated either by a

2-MeV Van de Graaff or by a 12-MeV pulsed-source tandem accelerator) to bombard a target of tritium adsorbed on a thin layer of titanium. The neutrons were detected by a 1 × 1.5 in. stilbene crystal used in combination with a 56 DVP 03 photomultiplier. The cross-section was derived, after appropriate correction, from the measurement of the transmission coefficient of the sample under study. 24 references. (auth)

15104 NEW TOTAL NEUTRON CROSS-SECTION MEASUREMENT OF URANIUM BETWEEN 0.5 TO 4.35 MeV. Kopsch, D.; Cierjacks, S.; Kirouac, G. J. (Kernforschungszentrum, Karlsruhe, Ger.). pp 39-47 of Nuclear Data for Reactors. Vol. II. Vienna; International Atomic Energy Agency (1970).

From 2nd International Conference on Nuclear Data for Reactors, Helsinki, Finland. See STI/PUB–259(Vol.2); CONF-700605–(Vol.2).

The total neutron cross-section of natural uranium was measured with the neutron time-of-flight facility at the Karlsruhe Isochronous Cyclotron (KIC). The measurement covers the energy range between 0.5 and 4.35 MeV with a resolution of 0.03 ns/m; this corresponds to an energy resolution between 290 eV at 0.5 MeV and 7.4 keV at 4.35 MeV. In the energy region 1.1 to 4.35 MeV the statistical error was between 1 and 0.5%, below 1.1 MeV the error increases up to 2.7% at 0.5 MeV. An extensive comparison with new available data is given. The existence of fluctuations in the cross-section in the lower energy range is investigated. 10 references. (auth)

15105 RADIATIVE CAPTURE OF NEUTRONS BY ^{238}U NUCLEI. Stavisskii, Yu. Ya. (Inst. of Physics and Power Engineering, Obninsk, USSR); Tolstikov, V. A.; Chelnokov, V. B.; Bergman, A. A.; Samsonov, A. E. pp 51-6 of Nuclear Data for Reactors. Vol. II. Vienna; International Atomic Energy Agency (1970). (In Russian).

From 2nd International Conference on Nuclear Data for Reactors, Helsinki, Finland. See STI/PUB–259(Vol.2); CONF-700605–(Vol.2).

The results of measurements of the energy dependence of average cross-sections for the radiative capture of neutrons by uranium-238 nuclei in the energy range 5 eV to 30 keV are presented. The measurements were made at the Lebedev Physics Institute of the USSR Academy of Sciences with a neutron spectrometer using the phenomenon of slowing-down in lead. The radiative capture of the neutrons was recorded by measuring the prompt capture gamma rays with a proportional gas-discharge counter in which the efficiency of gamma ray recording was linearly dependent on the gamma ray energy. Cylindrical samples of uranium-238 (U_3O_8) of different effective thicknesses ($\bar{n}_1 = 7.10 \times 10^{21}$ nuclei/cm^2, $\bar{n}_2 = 3.93 \times 10^{21}$ nuclei/cm^2 and $\bar{n}_3 = 1.29 \times 10^{21}$ nuclei/cm^2) were used. Normalization was carried out using the first resonance in the cross-section for radiative capture by uranium-238 ($E_0 = 6.67 + 0.02$ eV) and the cross-section for radiative capture by gold-197. The results are compared with those obtained by other authors. 21 references. (auth)

15106 RADIATIVE CAPTURE OF NEUTRONS BY ^{238}U IN THE ENERGY RANGE 24 TO 145 keV. Panitkin, Yu. G.; Tolstikov, V. A.; Stavisskii, Yu. Ya. (Inst. of Physics and Power Engineering, Obninsk, USSR). pp 57-61 of Nuclear Data for Reactors. Vol. II. Vienna; International Atomic Energy Agency (1970). (In Russian).

From 2nd International Conference on Nuclear Data for Reactors, Helsinki, Finland. See STI/PUB–259(Vol.2); CONF-700605–(Vol.2).

Measurements were made of the cross-section for the radiative capture by uranium-238 of neutrons in the energy range 24 to 145 keV, using a Van de Graaff generator and neutrons produced in the reaction ^{7}Li(p,n)^{7}Be. The target thickness was about 20 keV for protons of threshold energy. The induced activity was determined by measuring the gamma rays occurring in uranium-239 decay. The gamma radiation was detected by a Ge(Li) semiconductor detector. The neutron flux was monitored during the irradiation of uranium-238 samples. In the course of subsequent processing of the results a correction was introduced for fluctuations of the neutron flux during irradiation. The background of neutrons scattered in the target and in surrounding structural materials was also measured. (auth)

15107 MEASUREMENT OF THE FISSION CROSS-SECTION OF ^{241}Pu RELATIVE TO ^{235}U. Kaeppeler, F.; Pfletschinger, E. (Kernforschungszentrum, Karlsruhe, Ger.). pp 77-85 of Nuclear Data for Reactors. Vol. II. Vienna; International Atomic Energy Agency (1970).

From 2nd International Conference on Nuclear Data for Reactors, Helsinki, Finland. See STI/PUB–259(Vol.2); CONF-700605–(Vol.2).

The fission cross-section ratio ^{241}Pu : ^{235}U was measured as a function of neutron energy between 5 keV and 1 MeV by means of a pulsed 3-MeV Van de Graaff accelerator. The neutron energy was determined by time-of-flight technique. Fission events were detected in two identical argon-filled gas scintillation chambers in 4π-geometry. The accuracy of the cross-section ratios is estimated to be between 2.5 and 4%. 20 references. (auth)

15108 FISSION NEUTRON SPECTRUM FROM 0.01 TO 1.0 MeV. Jeki, L. (Hungarian Academy of Sciences, Budapest); Kluge, Gy.; Kozma, Gy.; (and others). pp 87-92 of Nuclear Data for Reactors. Vol. II. Vienna; International Atomic Energy Agency (1970).

From 2nd International Conference on Nuclear Data for Reactors, Helsinki, Finland. See STI/PUB–259(Vol.2); CONF-700605–(Vol.2).

Measurements of fission neutron spectra from 0.01 to 1 MeV for spontaneous fission of ^{252}Cf and thermal-neutron-induced fission of ^{235}U by time-of-flight technique are reported. A ^{6}Li-loaded glass scintillator and a gas scintillation detector (80% Ar + 20% Ni) were used for the detection of fission neutrons and fragments, respectively. The results are discussed in terms of the evaporation model. (auth)

15109 NEUTRON ENERGY SPECTRA FROM NEUTRON-INDUCED FISSION OF ^{238}U AT 1.35 AND 2.02 MeV. Almen, E.; Holmqvist, B.; Wiedling, T. (Aktiebolaget Atomenergi, Studsvik, Swed.). pp 93-101 of Nuclear Data for Reactors. Vol. II. Vienna; International Atomic Energy Agency (1970).

From 2nd International Conference on Nuclear Data for Reactors, Helsinki, Finland. See STI/PUB–259(Vol.2); CONF-700605–(Vol.2).

Results from a study of the energy spectrum of the neutrons emitted in the neutron-induced fission of natural uranium are presented. The measurements were performed at incident neutron energies of 1.35 and 2.02 MeV using time-of-flight techniques. The time-of-flight spectra were analyzed only above the position of the neutron elastic-scattering peaks. Corrections for neutron attenuation in the uranium sample were calculated using a Monte Carlo program. The corrected fission neutron spectra were fitted to Maxwellian temperature distributions. A temperature of 1.29 ± 0.03 MeV was obtained at 1.35 MeV incident neutron energy compared with 1.29 ± 0.02 MeV at 2.02 MeV. These values are consistent with previous results of ^{238}U. There are, thus, no indications that the ^{238}U fission spectra do not follow the generally observed temperature trend. 27 references. (auth)

15110 INELASTIC SCATTERING OF FAST NEUTRONS FROM ^{238}U. Barnard, E.; De Villiers, J. A. M.; Reitmann, D. (Atomic Energy Board, Transvaal, S. Afr.). pp 103-7 of Nuclear Data for Reactors. Vol. II. Vienna; International Atomic Energy Agency (1970).

From 2nd International Conference on Nuclear Data for Reactors, Helsinki, Finland. See STI/PUB–259(Vol.2); CONF-700605–(Vol.2).

The cross-sections for inelastic scattering of fast neutrons from ^{238}U were measured in the energy region below about 1.2 MeV. Neutrons with an energy spread of less than 10 keV were obtained from a pulsed 3-MeV Van de Graaff accelerator and the ^{7}Li(p,n)^{7}Be reaction. Time-of-flight techniques were employed and care was taken to ensure sufficient resolution of the neutron groups corresponding to the excitation of different energy levels in ^{238}U. Results were obtained for the levels at approximately 45, 150, 680 and 730 keV. All cross-sections were determined relative to the known cross-section for elastic scattering from carbon. Corrections were applied for flux attenuation and multiple scattering. The excitation curve for the first excited state in ^{238}U, measured in steps of 10 keV (or less) in incident energy, rises fairly smoothly with energy and only slight indications of structure were observed. The absolute values of the 90° differential inelastic-scattering cross-section for all the energy levels agree fairly well with the detailed results published by the Harwell group in 1966. (auth)

15111 MEASUREMENTS OF (n,2n) AND (n,3n) REACTION CROSS-SECTIONS OF FISSIONABLE MATERIALS USING A LARGE LIQUID SCINTILLATOR. Frehaut, J.; Gauriau, J.; Mosinski, G.; Soleilhac, M. (Centre d'Etudes, Bruyeres-le-Chatel, France). pp 109-17 of Nuclear Data for Reactors. Vol. II. Vienna; International Atomic Energy Agency (1970). (In French).

From 2nd International Conference on Nuclear Data for Reactors, Helsinki, Finland. See STI/PUB–259(Vol.2); CONF-700605–(Vol.2).

Working with the technique involving the use of a large liquid scintillator, a method for measuring (n,2n) and (n,3n) cross-sections relative to fission cross-section in fissionable materials was developed. The method consists in using the preferential time distribution of the instants at which the emitted neutrons are detected. By comparing the probability of detecting two (or three) neutrons with the previously measured probability of the emission of two (or three) fission neutrons, the relative cross-sections are derived. The first results obtained, particularly those for ^{238}U, are presented. (auth)

15112 STATUS OF IMPORTANT HEAVY-ELEMENT NUCLEAR DATA ABOVE THE RESONANCE REGION. Davey, W. G. (Argonne National Lab., Idaho Falls, Idaho). pp 119-37 of Nuclear Data for Reactors. Vol. II. Vienna; International Atomic Energy Agency (1970).

From 2nd International Conference on Nuclear Data for Reactors, Helsinki, Finland. See STI/PUB–259(Vol.2); CONF-700605–(Vol.2).

The status of $\bar{\nu}$-values, capture, and fission cross-sections for the most important heavy elements, ^{235}U, ^{238}U, ^{239}Pu, ^{240}Pu, and ^{241}Pu is evaluated to determine both the accuracy to which the data are known and to what degree the needs of reactor physicists are satisfied. Ratios of other fission cross-sections to that of ^{235}U are reasonably well known but the absolute value of the reference ^{235}U cross-section is very unsatisfactorily defined above 100 keV. The capture cross-section of ^{238}U is uncertain to about 15% below 100 keV if both ^{10}B(n,α) and ^{235}U(n,f) cross-sections are used as references. The ratio relative to ^{235}U(n,f) alone shows better consistency but even if this standard is correct the absolute capture cross-section suffers due to the stated uncertainties in ^{235}U(n,f) data. The ratio of capture-to-fission (α) in ^{235}U and ^{239}Pu is satisfactorily known, but the α-values for ^{240}Pu and ^{241}Pu remain unmeasured. Best values of $\bar{\nu}$ for the heavy isotopes at thermal energies are related to $\bar{\nu}$ for ^{252}Cf, but are not strongly affected by its precise value and tend to be incompatible with the ^{252}Cf data. The best values for $\bar{\nu}$ for ^{252}Cf have tended to lie in two groups differing by approximately 2% and a recent precise measurement gives additional support for the lower data which further emphasizes the incompatibility with the heavy element $\bar{\nu}$-data. Even if thermal-neutron $\bar{\nu}$-values are satisfactory, the variation of $\bar{\nu}$ with neutron energy may be of comparable importance for fast-reactor physicists. The evidence for nonlinear dependence of $\bar{\nu}$ for ^{235}U with neutron energy below 1 MeV is fairly clear, but better definition of the energy dependence for ^{235}U is needed. It is important to determine if similar behavior occurs in the $\bar{\nu}$-values for the other isotopes, particularly ^{239}Pu, but present experimental data are not sufficiently detailed to show if this occurs. 60 references. (auth)

15113 VALUE $\bar{\nu}$ OF ^{235}U AND ^{239}Pu IN A FAST-REACTOR SPECTRUM. Conde, H.; Widen, L. (Research Inst. of National Defense, Stockholm). pp 139-43 of Nuclear Data for Reactors. Vol. II. Vienna; International Atomic Energy Agency (1970).

From 2nd International Conference on Nuclear Data for Reactors, Helsinki, Finland. See STI/PUB–259(Vol.2); CONF-700605–(Vol.2).

The average number of prompt neutrons per ^{235}U and ^{239}Pu fission are measured at the fast zero-power reactor (FRO) at Studsvik, Sweden. Special attention is paid to the fission resonance region where earlier measurements with good energy resolution have given different $\bar{\nu}$-values for different groups of resonances. As fission neutron detector a large liquid scintillator is used. The reactor neutron energy spectrum is measured in separate time-of-flight and proton-recoil detector experiments. The experimental technique is described, and preliminary $\bar{\nu}$-values averaged over the fast reactor spectrum from 0 to 70 keV are given. 8 references. (auth)

15114 MEAN NUMBER OF PROMPT NEUTRONS AND RELATIVE CROSS-SECTIONS FOR THE FISSION OF ^{235}U AND ^{239}Pu BETWEEN 0.3 AND 1.4 MeV. Soleilhac, M.; Frehaut, J.; Gauriau, J.; Mosinski, G. (Centre d'Etudes, Bruyeres-le-Chatel, France). pp 145-56 of Nuclear Data for Reactors. Vol. II. Vienna; International Atomic Energy Agency (1970). (In French).

From 2nd International Conference on Nuclear Data for Reactors, Helsinki, Finland. See STI/PUB–259(Vol.2); CONF-700605–(Vol.2).

Using a spectrum of neutrons produced by the ^{7}Li(p,n)^{7}Be reaction on a thick lithium target, simultaneous measurements of $\bar{\nu}$ and of relative fission cross-sections on ^{235}U and ^{239}Pu were made. The energy of the incident neutrons was determined by the time-of-flight method, using a beam of pulsed protons at a frequency of 2.5 Mc/s. The energy resolution obtained varied from 10 keV to 50 keV between 0.3 and 1 MeV. The data were recorded on magnetic tape. The measurements of $\bar{\nu}$ are a follow-up of the results between 1.3 and 15 MeV which were published earlier. The findings are in agreement with most of the earlier measurements and confirm the nonlinear variation of $\bar{\nu}$ between 0.3 and 1 MeV. 20 references. (auth)

15115 AVERAGE NUMBER OF PROMPT NEUTRONS IN FAST-NEUTRON-INDUCED FISSION OF ^{235}U, ^{239}Pu, AND ^{240}Pu. Savin, M. V.; Khokhlov, Yu. A.; Zamyatnin, Yu. S.; Paramonova, I. N. (Inst. of Atomic Energy, Moscow). pp 157-65 of Nuclear Data for Reactors. Vol. II. Vienna; International Atomic Energy Agency (1970). (In Russian).

From 2nd International Conference on Nuclear Data for Reactors, Helsinki, Finland. See STI/PUB–259(Vol.2); CONF-700605–(Vol.2).

Measurements of $\bar{\nu}$ were made during fission of ^{235}U, ^{239}Pu and ^{240}Pu by fast neutrons with energies of 0.6 to 5 MeV. The measurements were carried out in a linear electron accelerator. The fission neutron detector was a liquid scintillator with a capacity of 400 liters. The fission neutron counting efficiency was approximately 70%. Virgin neutrons were selected by the time-of-flight method with a resolution of 1 nsec/m. The instant of fission was recorded from prompt fission gamma-ray pulses. The information was recorded by a two-dimensional AI-4096 amplitude analyzer (16 × 256). The measurements were based on comparison with the $\bar{\nu}$ value for spontaneous fission of ^{252}Cf ($\bar{\nu} = 3.772$). The measured values are accurate to within 1 to 3% for ^{235}U and ^{239}Pu and 3 to 5% for ^{240}Pu. The energy dependence of $\bar{\nu}$ for ^{235}U reveals a number of the irregularities noted previously. The average ($d\bar{\nu}/dE_n$) value for ^{239}Pu as measured is 0.15 MeV^{-1}. 17 references. (auth)

15116 AVERAGE NUMBER OF PROMPT NEUTRONS IN THE FISSION OF ^{235}U AND ^{239}Pu BY NEUTRONS. Nesterov, V. G.; Nurpeisov, B.; Prokhorova, L. I.; Smirenkin, G. N.; Turchin, Yu. M. (Inst. of Physics and Power Engineering, Obninsk, USSR). pp 167-75 of Nuclear Data for Reactors. Vol. II. Vienna; International Atomic Energy Agency (1970). (In Russian).

From 2nd International Conference on Nuclear Data for Reactors, Helsinki, Finland. See STI/PUB–259(Vol.2); CONF-700605–(Vol.2).

Results are given for measurements of the fission cross-section and the average number of prompt neutrons in the fission of ^{235}U and ^{239}Pu induced by neutrons. The fission cross-section was measured by a relative method used in conjunction with track methods in the 10 keV to 1 MeV neutron energy range. The fission cross-section of ^{235}U was taken as a reference. Between 0.3 and 5 MeV the average number of secondary neutrons was measured by means of ^{3}He counters in a paraffin block and between 0.08 and 0.7 MeV with a threshold detector (multilayer thorium chamber). 27 references. (auth)

15117 ANALYSIS OF THE NEUTRON ENERGY DEPENDENCE OF $\bar{\nu}$, ON THE BASIS OF THE ENERGY BALANCE IN NUCLEAR FISSION. Vorobeva, V. G. (Inst. of Physics and Power Engineering, Obninsk, USSR); Dyachenko, P. P.; Kolosov, N. P.; (and others). pp 177-81 of Nuclear Data for Reactors. Vol. II. Vienna; International Atomic Energy Agency (1970). (In Russian).

From 2nd International Conference on Nuclear Data for Reactors, Helsinki, Finland. See STI/PUB–259(Vol.2); CONF-700605–(Vol.2).

On the basis of experimental data relating to fission fragment yields and kinetic energies, the energy balance in thorium-232, uranium-235, uranium-238 and plutonium-239 fission by neutrons with energies in the 0 to 6 MeV range is discussed. Their findings, together with earlier results of direct measurements of $\bar{\nu}$, are used to plot a curve showing the dependence of $\bar{\nu}$ on neutron energy. 13 references. (auth)

15118 MEASUREMENT OF THE ENERGY SPECTRA AND THE AVERAGE NUMBER $\bar{\nu}$ OF PROMPT NEUTRONS PRODUCED IN THE FISSION OF ACTINIDE ELEMENTS. Zamyatnin, Yu. S.; Kroshkin, N. I.; Melnikov, A. K.; Nefedov, V. N. (Scientific-Research Inst. of Atomic Reactor, Melekess, USSR). pp 183-93 of Nuclear Data for Reactors. Vol. II. Vienna; International Atomic Energy Agency (1970). (In Russian).

From 2nd International Conference on Nuclear Data for Reactors, Helsinki, Finland. See STI/PUB–259(Vol.2); CONF-700605–(Vol.2).

Using the time-of-flight method, the spectra of prompt neutrons produced in the spontaneous fission of ^{244}Cm and ^{252}Cf and in the induced fission of ^{229}Th, ^{235}U, ^{238}Pu, ^{242m}Am, ^{245}Cm, and ^{249}Cf by thermal neutrons was measured. The pulse produced by the fission fragments in a gas-filled scintillation chamber was used as the starting signal. The neutrons were recorded by plastic detectors and by scintillation glass containing ^{6}Li. Using the expression $N(E) \sim \sqrt{E}e^{-E/T}$ to approximate the spectra, values of the parameter T for ^{244}Cm, ^{252}Cf, ^{229}Th, ^{238}Pu, ^{242m}Am, ^{245}Cm, and ^{249}Cf were, respectively: 1.38 ± 0.03; 1.48 ± 0.03; 1.24 ± 0.04;

XUM

1.35 ± 0.04; 1.42 ± 0.03; 1.50 ± 0.05; 1.55 ± 0.04 MeV. The values obtained for the average number $\bar{\nu}$ of neutrons for the above nuclei are, respectively: 2.77 ± 0.08; 3.77 ± 0.08; 2.05 ± 0.10; 2.92 ± 0.12; 3.28 ± 0.10; 3.83 ± 0.16 and 4.60 ± 0.21. The measurements were performed relative to ^{235}U, it being assumed that T = 1.29 MeV and $\bar{\nu}$ = 2.426 for this nuclide. The low-energy neutrons produced in the spontaneous fission of ^{252}Cf were measured by means of scintillation glass containing ^{6}Li. The spectrum was measured down to 5 keV. In the energy region below 100 keV it was noted that the neutron spectrum exceeds the expected distribution N(E) ~ $E^{1/2}$. Spectrum peaks were found at 80 to 90 keV, 0.5 MeV and 0.7 to 0.8 MeV. 31 references. (auth)

15119 NUMBER OF NEUTRONS PER FISSION, $\bar{\nu}$, FROM THERMAL TO 15 MeV. Colvin, D. W. (Atomic Energy Research Establishment, Harwell, Eng.). pp 195-213 of Nuclear Data for Reactors. Vol. II. Vienna; International Atomic Energy Agency (1970).

From 2nd International Conference on Nuclear Data for Reactors, Helsinki, Finland. See STI/PUB-259(Vol.2); CONF-700605-(Vol.2).

The principal papers submitted to the Conference on the parameter $\bar{\nu}$, the number of neutrons per fission, from thermal to 15 MeV and the findings of the IAEA Consultants Meeting on this subject, held at Studsvik in Sweden, are reviewed. The information is considered under the headings of thermal and absolute values, $\bar{\nu}$ as a function of energy, recent evaluation work on $\bar{\nu}$ as a function of energy, and some suggestions, or recommendations, of the Meeting for future work. 49 references. (auth)

15120 RADIATIVE NEUTRON CAPTURE CROSS-SECTIONS FOR NUCLEI WITH A < 220 ABOVE THE RESONANCE REGION. Abramov, A. I. (Inst. of Physics and Power Engineering, Obninsk, USSR). pp 245-63 of Nuclear Data for Reactors. Vol. II. Vienna; International Atomic Energy Agency (1970). (In Russian).

From 2nd International Conference on Nuclear Data for Reactors, Helsinki, Finland. See STI/PUB-259(Vol.2); CONF-700605-(Vol.2).

A review of the state of knowledge of radiative neutron capture cross-sections for nuclei with A < 220 in the nonresonance energy region (mainly above 1 keV) is given. The possibilities of various experimental methods and the results of the most recent measurements are considered. 86 references. (auth)

15121 MEASUREMENTS OF CROSS-SECTIONS FOR THE RADIATIVE CAPTURE OF 1-keV TO 1-MeV NEUTRONS BY Mo, Rh, Gd, Ta, W, Re, Au, AND ^{238}U. Fricke, M. P.; Lopez, W. M.; Friesenhahn, S. J.; Carlson, A. D.; Costello, D. G. (Gulf General Atomic Inc., San Diego, Calif.). pp 265-80 of Nuclear Data for Reactors. Vol. II. Vienna; International Atomic Energy Agency (1970).

From 2nd International Conference on Nuclear Data for Reactors, Helsinki, Finland. See STI/PUB-259(Vol.2); CONF-700605-(Vol.2).

Neutron average capture cross-sections were measured for eight elements in the energy range 1 keV to 1 MeV with a neutron time-of-flight spectrometer consisting of an electron-linear-accelerator pulsed-neutron source, a 230-meter evacuated neutron flight path, and a large liquid scintillator to detect the capture γ-rays. The intensity and energy dependence of the incident neutron flux were monitored during the capture measurements with ^{3}He-gas proportional counters calibrated against other counters containing boron trifluoride and methane. The measured energy variation of the neutron flux is, thus, based upon the cross-section for the $^{10}B(n,\alpha_0 + \alpha_1)^7Li$ reaction at neutron energies below 80 keV, and upon the n + p scattering cross-section at energies above 80 keV. The measurements extend to very low energies (~2 eV), and absolute capture cross-sections were obtained by normalization to the observed capture areas of resolved resonances. In most instances, a "saturated" resonance was available, which provides a normalization that does not depend strongly upon resonance parameters. These measurements yield a set of radiative capture cross-sections which span an exceptionally large neutron-energy interval with a relative accuracy of about 10% over the full range. 28 references. (auth)

15122 CALCULATIONS OF CROSS-SECTIONS FOR THE RADIATIVE CAPTURE OF FAST NEUTRONS. Fricke, M. P.; Lopez, W. M.; Friesenhahn, S. J.; Carlson, A. D.; Costello, D. G. (Gulf General Atomic Inc., San Diego, Calif.). pp 281-92 of Nuclear Data for Reactors. Vol. II. Vienna; International Atomic Energy Agency (1970).

From 2nd International Conference on Nuclear Data for Reactors, Helsinki, Finland. See STI/PUB-259(Vol.2); CONF-700605-(Vol.2).

Previously presented data together with some results of activation measurements, were analyzed in terms of the statistical model. It was not possible to reproduce most of the observed excitation functions using the customary energy dependence of the γ-ray penetrabilities. This result is independent of (1) different optical-model parameters used to describe the neutron channels and the effects of a nonspherical potential; (2) different level-density formulas and a wide variation in their parameters; (3) extreme assumptions of neutron width-fluctuation correlations; (4) extreme limits of the effect of the (n,γn') process; and (5) of any plausible spin or parity dependence of the total radiation width. If the usual form is retained for the γ-ray penetrabilities, $T_\gamma \sim 2\pi\langle\Gamma_\gamma\rangle/D$, then the most likely source of difficulty appears to lie with the conventional excitation-energy dependence of the average partial radiation widths that sum to $\langle\Gamma_\gamma\rangle$. 16 references. (auth)

15123 EVALUATION OF NUCLEAR DATA ABOVE THE RESONANCE ENERGY REGION: A < 220. Benzi, V. (CNEN, Bologna). pp 379-88 of Nuclear Data for Reactors. Vol. II. Vienna; International Atomic Energy Agency (1970).

From 2nd International Conference on Nuclear Data for Reactors, Helsinki, Finland. See STI/PUB-259(Vol.2); CONF-700605-(Vol.2).

The problem of nuclear data above the resonance energy region (A < 220) is discussed; total and elastic cross-sections, inelastic scattering, radiative capture and charged-particle and multiple-neutron emission are treated. The opinion is expressed that in the near future the evaluators' effort should be directed towards the determination of reliable parameter sets on the basis of systematic analyses of large amounts of data. 20 references. (auth)

15124 MEASUREMENT OF ACTIVATION RESONANCE INTEGRALS AT INFINITE DILUTION WITH A LITHIUM-DRIFTED GERMANIUM GAMMA-RAY SPECTROMETER AND COMPARISON WITH CALCULATED VALUES. Ricabarra, G. H.; Turjanski, R.; Ricabarra, M. D. (Comision Nacional de Energia Atomica, Buenos Aires). pp 589-601 of Nuclear Data for Reactors. Vol. II. Vienna; International Atomic Energy Agency (1970). (In Spanish).

From 2nd International Conference on Nuclear Data for Reactors, Helsinki, Finland. See STI/PUB-259(Vol.2); CONF-700605-(Vol.2).

The flux in the RA-1 reactor where the irradiations were made was sufficiently large (2×10^{12} n/cm^2 s) to permit the use of samples with negligible self-shielding correction. The reactor spectrum at the irradiation site was calculated by means of multigroup diffusion theory and a correction factor allowing for the slight deviation from the 1/E spectrum was applied to the resonance integral. In consequence the systematic errors which have been common in the majority of previous resonance integral determinations, such as insufficient discrimination of spurious activities, self-shielding of epithermal neutrons and uncertain or incomplete description of the thermal spectrum at the irradiation site were carefully avoided in the present method. This technique was used to obtain an accurate determination of the ratio of the activation resonance integral to the thermal cross-section either by measurement of the cadmium ratio or by comparing the ratios in a reactor spectrum and in a quasi-thermal spectrum in respect of 28 isotopes (of mass number less than 220). Where serious doubts exist on the accuracy of the published values for thermal activation cross-sections, an absolute determination of the activation resonance integral was performed. Up-to-date neutron resonance parameters were also used to calculate the resonance integrals for 23 isotopes. From the final results presented a better agreement is observed with the calculated values than in previous experimental determinations. Serious deviations from previous determinations are discussed in the light of present data on neutron resonance parameters. 39 references. (auth)

15125 CROSS-SECTIONS FOR RADIATIVE NEUTRON CAPTURE BY ^{238}U NUCLEI. Abagyan, L. P.; Abramov, A. I.; Nikolaev, M. N.; Stavisskii, Yu. Ya.; Tolstikov, V. A. (Inst. of Physics and Power Engineering, Obninsk, USSR). pp 667-85 of Nuclear Data for Reactors. Vol. II. Vienna; International Atomic Energy Agency (1970). (In Russian).

From 2nd International Conference on Nuclear Data for Reactors, Helsinki, Finland. See STI/PUB-259(Vol.2); CONF-700605-(Vol.2).

With a view to establishing reasonable energy resolution and measurement accuracy requirements in respect of cross-sections for the radiative capture of neutrons by uranium-238 nuclei, an analysis was made of the requests contained in RENDA and elsewhere for these cross-sections in the energy range 1 eV to 15 MeV. The published results of experimental work are considered and their reliability and possible reasons for discrepancies analyzed, particular attention being paid to the choice of reference cross-sections and to the calculation of the self-shielding effect. It is noted that the spread of $\sigma_\gamma(^{238}U)$ values remaining after all renormalizations far exceeds the uncertainty required by the users. Methods of calculating cross-sections for capture in uranium-238 are discussed. On the basis of selected experiments and calculations an evaluation is made of cross-sections for neutron capture by uranium-238 nuclei, the results being presented in the form of a smooth curve $\sigma_\gamma = \sigma_\gamma(E)$, recommended for use in various calculations. This curve is compared with similar curves obtained by other authors. Methods of obtaining group cross-sections and values of group cross-sections for neutron capture in uranium-238 are described. These are compared with the cross-sections from the 26-group system of constants which used to be employed. 63 references. (auth)

15126 EVALUATION OF ^{238}U NEUTRON CROSS-SECTIONS FOR THE ENDF/B FILE. Pitterle, T. A. (Westinghouse Electric Corp., Madison, Pa.). pp 687-701 of Nuclear Data for Reactors. Vol. II. Vienna; International Atomic Energy Agency (1970).

From 2nd International Conference on Nuclear Data for Reactors, Helsinki, Finland. See STI/PUB-259(Vol.2); CONF-700605-(Vol.2).

Neutron cross-section data for ^{238}U between 0.00001 eV and 15 MeV, available through August 1969, were evaluated in order to revise the ^{238}U file in the United States ENDF/B data library. Neutron data reevaluated are σ_t, σ_γ, σ_f, $\sigma_{nn'}$, σ_{ne}, σ_n, $\sigma_{n,2n}$, $\sigma_{n,3n}$ and $\bar{\nu}$. Emphasis is placed on the capture, fission and inelastic cross-section evaluations and existing experimental discrepancies. Resolved resonance parameters were reevaluated to include more p-wave resonances and recent radiation width measurements which lead to an average radiation width of 0.0235 eV for this evaluation. Measurements reported since the previous evaluation resulted in the following qualitative changes to the data relative to the previous ENDF/B ^{238}U evaluation: the capture cross-section is lower by 5 to 15% between 1 and 100 keV, the fission cross-section is consistently lower by 4 to 8%, the inelastic scattering cross-section, particularly for excited levels above 0.15 MeV, is lower by 5 to 15% between 1.3 and 2 MeV, and the total cross-section differs by up to ±10% above 100 keV. Uncertainties of at least 10% still exist in the capture cross-section below 150 keV. While the ^{238}U/^{235}U fission ratio is reasonably well known, uncertainties in the absolute ^{238}U fission cross-sections are relatively large owing to discrepancies in the ^{235}U fission cross-section above 2 MeV. 67 references. (auth)

15127 SIMULTANEOUS EVALUATION OF THE FISSION CROSS-SECTIONS OF ^{235}U, ^{239}Pu, AND ^{238}U AND THE CAPTURE CROSS-SECTION OF ^{238}U IN THE ENERGY RANGE 100 eV TO 20 MeV. Sowerby, M. G.; Patrick, B. H. (Atomic Energy Research Establishment, Harwell, Eng.). pp 703-16 of Nuclear Data for Reactors. Vol. II. Vienna; International Atomic Energy Agency (1970).

From 2nd International Conference on Nuclear Data for Reactors, Helsinki, Finland. See STI/PUB-259(Vol.2); CONF-700605-(Vol.2).

A simultaneous evaluation of the fission cross-sections of ^{235}U, ^{239}Pu and ^{238}U and the capture cross-section of ^{238}U and their ratios was performed. The experiments providing the data were critically examined so that doubtful experiments can be detected and their results eliminated or have their errors decreased. For this purpose an abstract of each experiment was prepared and examples of these are given. Account was taken in the evaluation of the structure observed in the keV fission cross-sections. To make the evaluation objective the cross-sections are found by a least-squares minimization procedure which has the advantage of allowing new data to be rapidly incorporated. 49 references. (auth)

15128 EVALUATION OF NEUTRON NUCLEAR DATA FOR SEVERAL ACTINIDES IN THE ENERGY RANGE FROM THERMAL TO 10 MeV. Hinkelmann, B. (Kernforschungszentrum, Karlsruhe, Ger.). pp 721-34 of Nuclear Data for Reactors. Vol. II. Vienna; International Atomic Energy Agency (1970).

From 2nd International Conference on Nuclear Data for Reactors, Helsinki, Finland. See STI/PUB-259(Vol.2); CONF-700605-(Vol.2).

The results of a first evaluation of experimental data on ^{231}Pa$_{91}$, ^{232}U$_{92}$, ^{234}U$_{92}$, ^{236}U$_{92}$, ^{237}U$_{92}$, ^{237}Np$_{93}$, ^{238}Np$_{93}$, ^{236}Pu$_{94}$, ^{238}Pu$_{94}$, ^{241}Am$_{95}$, and ^{242}Cm$_{96}$ are presented. Radiative capture cross-sections, fission cross-sections, (n,2n) cross-sections and $\bar{\nu}$, the mean number of secondary neutrons per fission, were evaluated and transformed into 5-group cross-sections. 44 references. (auth)

15129 CALCULATION OF ^{240}Pu NEUTRON CROSS-SECTIONS IN THE keV-RANGE. Caner, M.; Yiftah, S. (Israel Atomic Energy Commission, Yavne). pp 735-43 of Nuclear Data for Reactors. Vol. II. Vienna; International Atomic Energy Agency (1970).

From 2nd International Conference on Nuclear Data for Reactors, Helsinki, Finland. See STI/PUB-259(Vol.2); CONF-700605-(Vol.2).

A cross-section calculation for ^{240}Pu in the keV-range is presented. There are no experimental data in this region except for the fission cross-section. In addition to the experimental data evaluation, calculations are made by means of the optical model and the Hauser-Feshbach model; optical parameters are obtained from a fit to the ^{238}U cross-sections. The recommended curves are compared with the values in the ENDF/B library. 27 references. (auth)

15130 MULTILEVEL ANALYSIS OF THE ^{233}U AND ^{235}U CAPTURE AND FISSION CROSS-SECTIONS AND STATISTICAL PROPERTIES OF THE KAPUR-PEIERLS-TYPE RESONANCE PARAMETERS FOR THE S-WAVE CROSS-SECTIONS OF THE FISSILE ISOTOPES. de Saussure, G. (Oak Ridge National Lab., Tenn.); Perez, R. B.; Derrien, H. pp 757-75 of Nuclear Data for Reactors. Vol. II. Vienna; International Atomic Energy Agency (1970).

From 2nd International Conference on Nuclear Data for Reactors, Helsinki, Finland. See STI/PUB-259(Vol.2); CONF-700605-(Vol.2).

At the 1966 IAEA Conference on Nuclear Data for Reactors, simultaneous measurements of the capture and fission cross sections of ^{233}U and ^{235}U were presented. A multilevel analysis of a part of these data is described. The low-energy capture and fission cross sections were "least square-fitted" simultaneously using the multilevel formalism developed by Adler and Adler. In order to compare the Kapur-Peierls parameters obtained with the Adler formalism to the R-matrix parameters obtained by others, for the same cross sections, a method was developed to convert a set of R-matrix parameters into an equivalent set of Kapur-Peierls parameters. This same method was also used to numerically investigate the distribution of the Kapur-Peierls parameters by selecting R-matrix parameters from the appropriate distributions and converting those into equivalent Kapur-Peierls parameters. 42 references. (auth)

15131 CORRELATED ANALYSIS OF FISSILE-ELEMENT CROSS-SECTIONS AND INTERPRETATION IN TERMS OF R-MATRIX PARAMETERS. Adler, F. T.; Adler, D. B. (Univ. of Illinois, Urbana). Contract AEC(11-1)-2022. pp 777-88 of Nuclear Data for Reactors. Vol. II. Vienna; International Atomic Energy Agency (1970).

From 2nd International Conference on Nuclear Data for Reactors, Helsinki, Finland. See STI/PUB-259(Vol.2); CONF-700605-(Vol.2).

Fission, capture, and total cross-sections of ^{235}U in the energy region below 50 eV were analyzed by least-squares procedures with a multilevel expansion of the Kapur-Peierls type. The simultaneous analysis of three data sets allows constraints to be imposed which reflect the unitarity of the formalism, thus achieving compatibility among the resonance parameters and limiting uncertainties arising from possible quasi-resonances or hidden small levels. In a manner analogous to those earlier applied to the analysis of η in ^{239}Pu, the energy dependence of α can readily be interpreted. The multilevel parameters derived from data analysis cannot be used for statistical studies, however, as the pertinent distribution laws are as yet unknown. This fact makes it desirable to complement the analysis by deriving compatible R-matrix parameters, for which the distribution laws are well known. For this purpose, three independent approaches were investigated: (1) direct data fitting in terms of the complex amplitudes of the theory; (2) a perturbation method; and (3) an analysis of the mathematical structure of the transformations governing the relation of R-matrix and multilevel expansions. Numerical results for R-matrix parameters obtained in these ways and of the uncertainties involved are illustrated by examples based on the numerical analysis of theoretically prescribed cross-sections and by results obtained from the analysis of representative low-energy fissile-element cross-sections in the region below 50 eV. 21 references. (auth)

15132 METHOD OF SHAPE ANALYSIS OF CROSS-SECTIONS OF FISSILE NUCLEI. Krebs, J.; Le Coq, G.; L'Heriteau, J. P.; Ribon, P. (Centre d'Etudes Nucleaires, Saclay, France). pp 789-97 of Nuclear Data for Reactors. Vol. II. Vienna; International Atomic Energy Agency (1970). (In French).

From 2nd International Conference on Nuclear Data for Reactors, Helsinki, Finland. See STI/PUB-259(Vol.2); CONF-700605-(Vol.2).

The characteristics of a program permitting, by a least-squares method, the resonance parameters of fissile nuclei to be determined are presented. It performs the shape analysis of several experiments simultaneously. The inferences between the levels are treated as corrections and not taken into account in the least squares. A visualization unit allows simultaneous representation of theoretical curves and experimental points which permits the evolution of the calculation to be followed and, if necessary, the data with variable parameters to be modified. An example is given for some resonances of ^{235}U. (auth)

15133 ANALYSIS OF HIGH-ENERGY NEUTRON CROSS-SECTIONS FOR FISSILE AND FERTILE ISOTOPES. Prince, A. (Brookhaven National Lab., Upton, N. Y.). pp 825-62 of Nuclear Data for Reactors. Vol. II. Vienna; International Atomic Energy Agency (1970).

From 2nd International Conference on Nuclear Data for Reactors, Helsinki, Finland. See STI/PUB-259(Vol.2); CONF-700605-(Vol.2).

Based on the results of differential and integral data testing and the appearance of new significant experimental data, a program was established to revise the Evaluated Nuclear Data File (ENDF/B) on the major fissile and fertile isotopes. The various theoretical methods employed in calculating the total (σ_T), elastic (σ_{el}), inelastic ($\sigma_{nn'}$), radiative capture ($\sigma_{n\gamma}$), and fission (σ_{nf}) neutron cross-sections in the energy range of 10 keV to 15 MeV for ^{238}U, ^{239}Pu, ^{240}Pu, and ^{241}Pu are outlined. To describe the experimental data adequately, a deformed optical model potential was used in which the first three levels were coupled, i.e., ^{239}Pu($\frac{1}{2}^+$, $\frac{3}{2}^+$, $\frac{5}{2}^+$), ^{241}Pu($\frac{5}{2}^+$, $\frac{7}{2}^+$, $\frac{9}{2}^+$), and ^{240}Pu, ^{238}U(0^+, 2^+, 4^+). An equivalent local potential with the appropriate deformation was chosen so as to satisfy four important experimental constraints, i.e., the total scattering cross-section σ_T, the potential scattering cross-section σ_{pot}, and the s- and p-wave strength functions. The compound nuclear reactions were determined by employing a combined spherical potential and modified statistical model to describe the compound elastic, compound inelastic, radiative capture, and fission cross-sections. The application of the aforementioned phenomenological models, using a single set of parameters for each isotope, produced very good agreement with the experimental data at both low and high energies. The methods were extended into areas where no experimental data exist to provide a consistent set of nuclear data. 60 references. (auth)

15134 STUDY OF THE ^{239}Pu ANGULAR DISTRIBUTIONS IN THE ENERGY RANGE 0.2 TO 5.5 MeV. Benzi, V. (CNEN, Bologna); Zuffi, L.; Coppola, M.; Knitter, H.-H. pp 863-8 of Nuclear Data for Reactors. Vol. II. Vienna; International Atomic Energy Agency (1970).

From 2nd International Conference on Nuclear Data for Reactors, Helsinki, Finland. See STI/PUB-259(Vol.2); CONF-700605-(Vol.2).

The ^{239}Pu nucleus presents a structure in the low-lying nuclear levels which indicates a deformation of the collective type. The effects of such a deformation on the neutron-scattering angular distributions were studied by means of a non-spherical optical potential using the coupled-channel method, and the results of these calculations are compared with recently measured experimental values. 9 references. (auth)

15135 ANALYSIS OF NEUTRON INELASTIC SCATTERING BY ^{238}U. Igarasi, S.; Nakamura, H.; Murata, T.; Nishimura, K. (Japan Atomic Energy Research Inst., Tokai). pp 869-79 of Nuclear Data for Reactors. Vol. II. Vienna; International Atomic Energy Agency (1970).

From 2nd International Conference on Nuclear Data for Reactors, Helsinki, Finland. See STI/PUB-259(Vol.2); CONF-700605-(Vol.2).

Total and partial inelastic scattering cross-sections of ^{238}U are investigated in the range of neutron energy from 50 keV to 15 MeV, consistency being taken into account among total, elastic, inelastic and reaction cross-sections. In the present status there are few data to obtain a reliable data set from the experimental inelastic scattering cross-section. The optical model and Hauser-Feshbach's formula are mainly used in the energy range from 50 keV to 1.5 MeV and the evaporation model is used above 1.5 MeV. Values and trends of optical-potential parameters and level density parameters are sought by fitting the calculated values of the inelastic scattering cross-sections and the emitted neutron spectra to the experimental data. In order to obtain a curve of the inelastic scattering cross-section, detailed information is needed for spin, parity and energy of excited states from 1 MeV to 1.5 MeV. After surveying experimental and theoretical information, and comparing results of calculations with experimental data for excitation functions, values of these level parameters are tentatively determined. Calculations are performed by using a computer code ELIESE in the lower energy region. Effects of competitive processes, such as (n,γ), (n,f), etc., are taken into account in the calculations. Above the 1.5-MeV region, inelastic scattering cross-sections are obtained by using Hauser-Feshbach's model which includes contribution from the continuous state of the target nucleus, and by using cross-sections for compound formation and experimental data for (n,f), (n,2n), (n,3n) and (n,γ) cross-sections. 25 references. (auth)

15136 STUDY OF RADIATIONS OF ^{91}Y, ^{90}Y, AND ^{87}Y. Akhmed, M. R.; Baskova, K. A.; Vasil'ev, S. S.; (and others). Vestn. Mosk. Univ., Ser. III. Fiz. Astron.; 11: 386-90(Jul-Aug 1970). (In Russian).

Decay schemes for ^{91}Y, ^{90}Y, and ^{87}Y were verified using a β spectrometer with a fine lens and scintillation β and γ spectrometers. For measuring β−γ coincidences the scintillation β spectrometer was connected in coincidence with the scintillation γ spectrometer. Data obtained revealed a new γ transition of 1480 keV for ^{91}Y, and β−γ-coincidence studies confirmed the existence of the 1480-keV transition in the ^{91}Y decay scheme. The existence of the β transition for the isomeric state of ^{87}Y was also confirmed. (R.V.J.)

15137 DIRECTIONAL CORRELATIONS OF GAMMA RAYS IN ^{125}Sb FOLLOWING THE DECAY OF 9.6 d ^{125g}Sn. Macias, E. S.; Walters, W. B. (Massachusetts Inst. of Tech., Cambridge). Nucl. Phys.; A160: 274-88(1971).

A decay scheme for 9.6 d ^{125g}Sn was constructed that includes 20 previously unobserved γ-rays and two new levels. The angular correlation functions were determined for nine cascades and were utilized in conjunction with other data to establish spins and parities for nine levels. The level scheme is discussed in the context of the particle-core coupling model and the superconductor model. (auth)

15138 STUDY OF HIGH ANGULAR MOMENTUM STATES IN ^{155}Gd AND ^{157}Gd BY MEANS OF THE (^{3}He,α) REACTION. Loevhoeiden, G.; Waddington, J. C.; Ellegaard, C.; Tjoem, P. O. (Univ. of Copenhagen). Nucl. Phys.; A160: 305-20(1971).

Levels in ^{155}Gd and ^{157}Gd were studied by means of the (^{3}He,α) reaction with 20.3-MeV ^{3}He particles. The l-values were determined by comparing the measured (^{3}He,α) cross sections with that obtained in previous (d,t) experiment to the same nuclei, and by the ratio of the (^{3}He,α) cross section measured at 60° and 90°. Only one strong $\frac{13}{2}^+$ state was observed in each nucleus. This is readily explained by the strong Coriolis coupling between the N = 6 Nilsson orbitals. The previously unknown $\frac{11}{2}$ $\frac{9}{2}^-[514]$ state is assigned in both nuclei. (auth)

15139 LEVEL STRUCTURE OF ^{141}Pr STUDIED BY PHOTONUCLEAR EXCITATION. Pavel, D. (Soreq Nuclear Research Centre, Yavne, Israel. Bar-Ilan Univ., Ramat Gan, Israel); Ben-David, G.; Schlesinger, Y.; Szichman, H. Nucl. Phys.; A160: 409-16(1971).

Using the nuclear resonant scattering of photons from several (n,γ) reactions, bound nuclear levels in ^{141}Pr were studied. Five resonant levels, at energies 6111, 6115, 7188, 7256 and 8883 keV, were excited, and the results obtained in their de-excitation are presented. On the basis of the angular distribution of the scattered γ-rays the following spin assignments were made for three of the excited levels in ^{141}Pr: 1457.9 ($\frac{5}{2}$), 6115 ($\frac{7}{2}$) and 7188 ($\frac{5}{2}$). The total radiation width of the 6115-keV resonant level was measured and found to be 52 ± 10 MeV. (auth)

Nuclear Theory

Refer also to abstracts 14409, 14477, 14736, 14745, 14947, and 15024.

15140 (CU-1019-79) PRECOMPOUND DECAY FROM A TIME-DEPENDENT POINT OF VIEW. Harp, G. D. (Brookhaven National Lab., Upton, N. Y.); Miller, J. M. (Columbia Univ., New York. Dept. of Chemistry). Dec 1970. 29p. Dep. NTIS.

A model is proposed for following the progress of nucleon-induced nuclear reactions as a function of time. It predicts that the majority of protons and high-energy neutrons emitted from heavy targets in these reactions appear before internal statistical equilibrium has been established. For the 18-MeV (p,xn) reaction with ^{181}Ta, however, the model predicts fewer high-energy neutrons than are observed experimentally. Further, there is a difference in shape between the predicted and observed spectrum. The same differences arise when a comparison is made between the experimental spectrum and that predicted by Griffin's model for precompound decay. It is suggested that these differences arise because both models fail to consider surface reactions explicitly. It is suggested that this model might best be used in conjunction with Monte-Carlo cascade calculations of high-energy nuclear reactions to follow the complete equilibration of the nonequilibrated excited nuclei left after these cascades are

XUM

terminated. An example of using the model for this purpose is given. (auth)

15141 (DEMO–70/10) HERETRA: A COMPUTER PROGRAM FOR FISSION PRODUCTS CALCULATIONS. Antoniades, J.; Mavroyannakis, E. (Democritus Nuclear Research Center, Athens (Greece)). Mar 1970. 9p. Dep. NTIS (U. S. Sales Only).

A computer program is given which can be used for the calculation of the concentration of fission products. (auth)

15142 (DEMO–70/20) NEW DERIVATION OF AN APPROXIMATE EXPRESSION IN CLOSED FORM FOR THE BINDING ENERGY OF AN IMPURITY PARTICLE IN NUCLEAR MATTER. Grypeos, M. E. (Democritus Nuclear Research Center, Athens (Greece)). Sep 1970. 6p. Dep. NTIS (U. S. Sales Only).

A new derivation is given of an approximate expression in closed form for the binding energy of an impurity particle in nuclear matter. The advantage of this new derivation, in which no use is made of any cluster expansion, is that it is simpler than the original one. (auth)

15143 (LYCEN–7050) PROJECTION METHODS AND THEIR APPLICATIONS TO HARTREE–FOCK WAVE FUNCTIONS. Hage-Hassan, Mehdi (Lyon Univ. (France). Institut de Physique Nucleaire). Jun 1970. 81p. (In French). Dep. NTIS (U. S. Sales Only).

Thesis.

An attempt was made to use infinitesimal rotational projection operators in a calculation on the rotational band of deformed nuclei. A method of constructing these operators was developed; they were then associated with the destruction operators, which act as projectors in the case of axial symmetry. The use of these operators in rotational-band spectra led to complicated calculations. A new method was subsequently introduced, which led to a simpler calculation. The method of Lowdin, the theorem of Thouless, and the moments of inertia calculated by Yoccoz and by Villard were recovered. A formula for calculating the elements of the rotational matrix on the basis of an axially symmetric harmonic oscillator was established. A program was written for calculating the energy and the Hartree–Fock wave function; and another program for calculating the rotational-band spectrum using this method. The two programs may be used with a Series 1130, 8K IBM computer. (auth) (France)

15144 (NP–18618) LIMITS OF VALIDITY OF SIEGERT'S THEOREM IN THE NUCLEAR PHOTO-ABSORPTION. Haemaelaeinen, R. M. K.; Lilja, I. A. (Jyvaskyla Univ. (Finland). Dept. of Physics). Sep 1970. 6p. Dep. NTIS (U. S. Sales Only).

Siegert's theorem, which states that the current-density matrix element $\langle a|\vec{J}\cdot\vec{\epsilon}|b\rangle$ ($\vec{\epsilon}$ is a unit vector) in the electric multipole transition probability can be replaced by the charge-density matrix element $ick\langle a|\rho|b\rangle$ where k is the wave number of the radiation, is examined. It is concluded that the calculations of the absorption cross sections according to Siegert's theorem can contain errors which vary from the order of 10% at 50 MeV up to about 60% at 200 MeV. (Finland)

15145 (NYO–1082-25) FINE STRUCTURE IN HIGHLY EXCITED ANALOG STATES. Goulard, B. (Laval Univ. (Quebec)); Fallieros, S. (Brown Univ., Providence, R. I.). [1969]. 6p. Dep. NTIS.

The nature of the fine structure surrounding analog states at relatively high excitations is discussed and contrasted to the corresponding structure at lower energies. (auth)

15146 (NYO–1082-29) RESONANT ELASTIC SCATTERING OF PROTONS FROM ANALOGUE AND COMPOUND STATES. Fallieros, S. (Brown Univ., Providence, R. I. Dept. of Physics); Brown, G. E. (Nordisk Institut for Teoretisk Atomfysik, Copenhagen (Denmark). State Univ. of New York, Stony Brook. Inst. for Theoretical Physics). [1969]. Contract AT(30-1)-4032. 28p. Dep. NTIS.

A general derivation of the amplitude for elastic scattering in the presence of one analog state and many compound (T-lower) states is given. The form of the amplitude is derived in a rather general scattering formalism by using unitarity and invariance under time reversal. The assumptions necessary to make the transmission coefficient $P_A(\epsilon)$ vanish at some energy are stated. An additional assumption is necessary if it is to vanish at the unperturbed energy ϵ_A of the analog. (auth)

15147 (NYO–2171-333) GROUND STATE CORRELATIONS AS VARIATIONAL PARAMETERS IN THE NUCLEAR MANY-BODY PROBLEM. Dreizler, R. M.; Klein, Abraham; Krejs, F. R. (Pennsylvania Univ., Philadelphia. Dept. of Physics); Dreiss, Gerard J. (Northeastern Univ., Boston, Mass. Dept. of Physics). 14 Dec 1970. 40p. Dep. NTIS.

It is shown that amplitudes which normally occur in the Random Phase Approximation (RPA) can be considered as variational parameters in an approximate theory of the ground state, allowing arbitrary two-particle–two-hole excitations of a Hartree–Fock substrate. These amplitudes obey equations which differ in detail from the RPA, though the two sets are shown to coincide in the weak coupling limit. All the desirable mathematical and physical properties of the RPA have their counterpart in the new theory, but in addition correlations are guaranteed to be given correctly near the weak coupling limit. The method is applied to an exactly soluble model and some comparison with other approximation methods is made. (auth)

15148 (ORNL-tr–2399) SYSTEMATIZATION OF THE INELASTIC INTERACTIONS OF HIGH-ENERGY PIONS AND NUCLEONS WITH ATOMIC NUCLEI. Barashenkov, V. S.; Gudima, K. K.; Il'inov, A. S.; Toneev, V. D. (Joint Inst. for Nuclear Research, Dubna (USSR)). Translated for Oak Ridge National Lab., Tenn., from report JINR–P2-5118. 46p. Dep. NTIS.

A systematic study of the characteristics of inelastic nucleon and π-meson reactions with nuclei is presented in the energy range in which calculations with the usual cascade model are valid. The emphasis is on the region with projectile energy greater than 0.4 GeV where the processes of π-meson production are important. Comparison with previous results reveals that many secondary particle characteristics are quite dependent upon the details of the cascade model and, in particular, on the diffuseness of the nuclear boundary. (R.W.R.)

15149 COULOMB MIXING OF ISOSPIN STATES. Mekjian, A. Z. (Univ., Heidelberg. Rutgers–The State Univ., New Brunswick, N. J.). Nucl. Phys.; A146: 288-320(1970).

The Coulomb mixing of an analog state into states of different isospin and also into states of the same isospin is calculated. The dynamic distortion and isospin impurity of the analog state wave function is discussed. The sum of the squares of the matrix elements between the analog and states of the same and different isospin is given for various statistical model distributions of the nuclear matter density. These include a constant density model, a Thomas–Fermi model and a quadratic surface peaked model. The sum is also calculated using harmonic oscillator wave functions. The mixing of the analog to the configuration states is compared with the total transition strength of the analog into states of normal isospin. The transition strength to the configuration states is found to be only one percent or so of the sum rule. The energy of the configuration states is then compared with the c.m. energy of the normal isospin states which mix with the analog. The contribution of the configuration states to the spreading width of an analog is calculated. A statistical model calculation of the spreading, which takes into account the total transition strength of the analog, is also given. The conspiracies which enter into the statistical model description are discussed. (auth)

15150 CORRECTION OF THE FINITE VOLUME OF SCATTERER EFFECT ON THE MEASUREMENT OF DIFFERENTIAL ELASTIC AND INELASTIC NEUTRON CROSS SECTIONS. PART II. CORRECTION OF MULTIPLE-SCATTERING PROCESSES. Hermsdorf, D.; Hoehn, J.; Seeliger, D. (Technische Univ., Dresden). Kernenergie; 13: 283-7(Sep 1970). (In German).

15151 SEPARATION OF NUCLEAR-REACTION MECHANISMS. Corleo, G.; Pappalardo, G.; Rubbino, A. (Univ., Catania, Italy. Istituto Nazionale di Fisica Nucleare, Catania, Italy). Nuovo Cim.; 70A: 323-8(1 Dec 1970).

A few experimental data on nuclear reactions having ^{29}Si as intermediate system are analyzed in order to test the validity of some approximations usually made in comparing nuclear cross sections with theoretical predictions. The ratios $y_D = \sigma^{DI}/(\sigma^{DI} + \sigma^{fl})$ are deduced either through the analysis of averaged cross sections or through the analysis of statistical fluctuations. The results of the two methods are compared. (auth)

15152 TARGET SPIN DEPENDENCE OF THE OPTICAL POTENTIAL. Drigo, L.; Pisent, G. (Univ., Padua. Istituto Nazionale di Fisica Nucleare, Padua). Nuovo Cim.; 70A: 592-602(21 Dec 1970).

The problem of possible spin-dependent interactions in the optical-model description of a scattering process between nucleons and nuclei of spin $I \neq 0$ is considered, starting from the analysis of the usual $l \cdot s$ potential in the channel-spin representation. Then the effects of other potentials involving the target spin I are studied. The scattering equations are written down, and exactly solved under simplifying assumptions on the radial dependence of the phenomenological potentials. In the latter case some useful correlations among the scattering phase shifts are derived. (auth)

15153 PHENOMENOLOGICAL ANALYSIS OF QUASIROTATIONAL SPECTRA AND POSSIBLE EVIDENCE FOR HIGHER-PHONON STATES. Das, T. K. (Univ. of Pennsylvania, Philadelphia); Dreizler, R. M.; Klein, A. Phys. Rev., C; 2: 632-8 (Aug 1970).

A semiempirical description was developed for the ground-state band of even quasirotational nuclei, based on the picture of anharmonic vibrations, which agrees surprisingly well with experiment. Comparison with previous empirical and semiempirical formulas is presented. (auth)

15154 ISOSPIN DEPENDENCE OF THE PROTON OPTICAL POTENTIAL. Hodgson, P. E. (Oxford Univ.). Nucl. Phys.; A150: 1-10(1970).

Optical-model analyses of proton elastic scattering are analyzed to give an expression for the potential in terms of the nuclear symmetry parameter. It is shown that the usual method of obtaining the isospin dependence of the optical potential is invalid except in special circumstances and under very restrictive assumptions. (auth)

15155 NEW INTEGRAL EQUATIONS IN THE THEORY OF FOUR-PARTICLE SCATTERING. Avishai, Y. (Weizmann Inst. of Science, Rehovot, Israel). Nucl. Phys.; A150: 379-92(1970).

The four-particle problem is studied through the resolvent operator G of its Hamiltonian. The quantity G is decomposed into a product of five factors. Four of them may be found from the solutions of three-particle problems or the solutions of four-particle problems with less than six pair potentials. The fifth factor is shown to be a unique solution of an integral equation with a connected kernel. Along the same line a formal solution is presented for the components of the four-particle T-operator. The resulting system of integral equations is free of two-body potentials and contains only scattering operators. Finally an equation for the bound-state wave function is given, and its equivalence with the Schrödinger equation is explicitly demonstrated. (auth)

15156 QUASI-FREE SCATTERING PROCESSES AND THE HOLE STRUCTURE OF ATOMIC NUCLEI. Gross, D. H. E.; Lipperheide, R. (Hahn-Meitner-Institut fuer Kernphysik, Berlin). Nucl. Phys.; A150: 449-60(1970).

An expression for the cross section of quasi-free (p,2p) and (e,e′p) processes is given in the impulse approximation which takes account of arbitrary excitations of the residual nucleus. A formalism for the calculation of the hole structure of nuclei in the discrete and continuum parts of the excitation spectrum is developed. (auth)

15157 SEMI-MICROSCOPIC THEORY OF TWO-PHONON QUADRUPOLE–OCTUPOLE VIBRATIONS IN SPHERICAL NUCLEI. Raduta, A. (Inst. for Atomic Physics, Bucharest); Sandulescu, A.; Lipas, P. O. Nucl. Phys.; A149: 11-32(1970).

A microscopic description is given for the quintet of states (1^-, 2^-, 3^-, 4^-, 5^-) obtained by combining one quadrupole phonon and one octupole phonon. To the conventional shell-model Hamiltonian with pairing, quadrupole and octupole forces is added a quadrupole-octupole interaction term $H_{2,3}$ of the form $[Q_2Q_3Q_3]_0$. The multipole-moment operators Q_L are those defined through the ordinary pairing-multipole theory. The quadrupole-octupole coupling emerging directly from that theory is here neglected, as the quadrupole and octupole operators are assumed to commute. The spectral decomposition method of Do Dang and Klein is used to treat $H_{2,3}$ as a perturbation on the RPA. Expressions are derived for the splitting of the quintet and for the relevant B(E3) values. Also the effects of H_{23} on the lower phonon states are calculated. The theory is applied to ^{114}Sn and compared with experiment and phenomenology. (auth)

15158 NON-NORMAL PARITY STATES IN A = 15, 14, AND 13 NUCLEI. Hsieh, S. T. (National Tsing Hua Univ., Hsinchu, Taiwan); Horie, H. Nucl. Phys.; A151: 243-56(1970).

Shell-model calculations for the non-normal parity states of A = 15, 14 and 13 nuclei are carried out within the framework of the $1p^{n-1}$ (2s,1d) and $1s^3 1p^{n+1}$ configurations where $n = A - 4$. The matrix elements of the two-body interactions between the 1p nucleons are fixed to be those determined by Cohen and Kurath from a least-squares fit. In addition, the two-body interactions between inequivalent nucleons are assumed to arise from a central force. The results for energy levels, transition probabilities and spectroscopic factors are in good agreement with experiment. (auth)

15159 ISOSPIN MIXING IN NUCLEI. Mohan, Radhe. Durham, N. C.; Duke Univ. (1969). 124p. University Microfilms Order No. 70-20,279.

Thesis.

Isospin impurities in the ground states of even-even nuclei are calculated using a particle-hole basis in the shell model formalism. The calculated impurities are shown to decrease sharply with the inclusion of residual nuclear interactions. The results are compared to the results of the two-fluid (neutrons, protons) hydrodynamical model. It is shown that the two fluid model is not adequate for calculation of either isospin impurities or proton density distributions. A three-fluid model (protons, "married" neutrons and "bachelor" neutrons) is shown to give better results in both cases. Isospin mixing in analog states is also studied and it is shown that it can affect the spectroscopic factors deduced from the analog state experiments significantly. (Diss. Abstr. Int., B)

15160 PHENOMENOLOGICAL NUCLEAR THREE-BODY FORCES. Pask, C. (Univ. of New South Wales, Kensington, Australia). Aust. J. Phys.; 23: 465-74(Aug 1970).

The mathematical problem of constructing suitable expressions for nuclear three-body potentials is investigated. (auth) (Australia)

15161 MULTILEVEL FORMALISM FOR NEUTRON ELASTIC SCATTERING CROSS SECTIONS. Clayton, E. (Australian Atomic Energy Commission Research Establishment, Sutherland). Aust. J. Phys.; 23: 823-31(Dec 1970).

An extension of the Feshbach, Porter, and Weisskopf formalism was developed for neutron elastic scattering. The emphasis in this paper is on resonance–resonance interference and explicit use of the background R matrix. The results of this formulation are compared with experimental data in the resonance region for the nuclides ^{238}U, ^{197}Au, and ^{23}Na. (auth) (Australia)

15162 TOTAL HALF-LIFE PREDICTIONS FOR NEUTRON DEFICIENT ACTINIDE ISOTOPES. Keller, K. A.; Muenzel, H. (Kernforschungszentrum, Karlsruhe, Ger.). Nucl. Phys.; A148: 615-24(1970).

Equations for calculation of partial half-lives of electron capture and α decay in the actinide region are given. By introduction of a mean excitation energy of the daughter nuclei, an improved accuracy was obtained in comparison to Viola and Seaborg. With these relations and the partial half-lives of spontaneous fission, total half-lives for neutron deficient isotopes from actinium to element Z = 108 are calculated. The standard deviation of the mean for the total half-lives lies between a factor of 1.3 and 1.8, dependent on whether the nucleus is even or odd. (auth)

15163 REDUCED ISOSCALAR AND ISOVECTOR E2 MATRIX ELEMENTS IN THE A = 26, T = 1 TRIAD. Schulz, N.; Shapiro, M. H. (Univ. of Rochester, N. Y.). Nucl. Phys.; A148: 632-3 (1970).

Reduced isospin scalar and vector matrix elements can be extracted from comparison of electromagnetic transitions between analogous states in isospin triplets. Calculations for the transitions between the first 2^+, T = 1 and 0^+, T = 1 levels in the A = 26 triad indicate that only the isoscalar component shows collective enhancement. (auth)

15164 ISOSPIN MIXING OF HARTREE–FOCK SOLUTIONS. Brink, D. M. (Clarendon Lab., Oxford); Svenne, J. P. Nucl. Phys.; A154: 449-57(1970).

For nuclei with N > Z isobaric spin invariance is broken in the Hartree–Fock approximation even in the absence of charge dependent forces. A small modification of the usual Hartree–Fock procedure restores this symmetry. The modified procedure (constrained Hartree–Fock) is used to investigate isospin impurities due to the Coulomb interaction. (auth)

15165 ELECTRIC QUADRUPOLE TRANSITIONS IN ODD-MASS SPHERICAL NUCLEI. Reehal, Balbir S.; Sorensen, Raymond A. (Carnegie-Mellon Univ., Pittsburgh). Phys. Rev., C; 2: 819-27(Sep 1970).

Experimental B(E2) values are tabulated for transitions in odd-mass spherical nuclei and compared with predictions of the pairing-plus-quadrupole model including up to two phonons. Of the well over 100 cases, agreement within a factor of 2 was obtained for ≈⅔, indicating the general validity of the theory and suggesting its use as a guide to yet unmeasured cases. (auth)

15166 VIRTUAL NUCLEAR EXCITATION CORRECTIONS TO ELASTIC ELECTRON SCATTERING AT LOW ENERGIES. Rawitscher, G. H. (Univ. of Connecticut, Storrs). Phys. Lett.; 33B: 445-8(7 Dec 1970).

It is suggested that the energy region where virtual nuclear excitation corrections to the elastic electron scattering cross sections should be looked for experimentally is where the first diffraction minimum occurs at large angles. For Ca, Nd, and Pb this energy interval is in the vicinity of 120, 60, and 50 MeV, respectively. For the nucleus of Ca the correction to the cross section should be in the range of 5 to 15%. (auth)

15167 LOCAL SELF-CONSISTENT FIELD IN NUCLEI WITH A LARGE NUMBER OF NUCLEONS. Simenog, I. V.; Filippov, G. F. (Inst. of Theoretical Physics, Kiev). Ukr. Fiz. Zh.; 15: 1305-9(Aug 1970). (In Russian).

The local self-consistent field equations for nuclei with a large number of nucleons are deduced. (auth)

15168 CENTRIFUGAL TERMS IN RESIDUAL INTERACTION OF PARTICLES IN NUCLEUS. Isakov, V. I.; Guman, V. N.; Kharitonov, Yu. I.; Sliv, L. A. (Ioffe Inst. of Physics and Tech., Leningrad). Yadern. Fiz.; 12: 504-14(Sep 1970). (In Russian).

Various terms of the residual interaction are considered which are quadratic in relative angular momentum $L_{12} = (r_1 - r_2)\ (p_1 - p_2)/2$ of a pair of particles, i.e. $V(r)L_{12}$, $V(r)L_{12}^2\sigma_1\sigma_2$ and $V(r)(L_{12}^2S)^2$. Two-particle configuration splitting is studied under the action of these forces as a function from the radius of the action of the total momentum of the pair and the Nordheim number N. The contribution of these forces to the energy of the spin-orbital splitting of the intermediate field level is estimated. (auth)

15169 STUDY OF LOW-LYING LEVELS OF ANOMALOUS PARITY OF p-SHELL NUCLEI IN THE UNITARY SCHEME APPROXIMATION. Petrauskas, A. K.; Sabalyauskas, L. Yu. (Inst. of Physics and Mathematics, Vilnyus, USSR). Yadern. Fiz.; 12: 492-503(Sep 1970). (In Russian).

The levels of anomalous parity of nuclei in the unitary scheme approximation are interpreted. Assuming these levels to be described by the most symmetrical Young scheme and quantum numbers SU(3) of the Casimir operator, relative distances between low-lying levels of anomalous parity of p-shell nuclei with the number of nucleons n = 4m, n = 4m + 1 are calculated. Results of the calculations are compared with the experiment. (auth)

15170 ZERO-POINT OSCILLATIONS AND THE SHAPE OF NUCLEI IN TRANSITION REGIONS. Berlovitch, E. E. (Ioffe Inst. of Physics and Tech., Leningrad). Acta Phys. Pol.; A38: 645-9(Nov 1970).

The measured curves of the relationship between potential energy of even-even nuclei in transition regions as the neutron number varies show the existence of a distinct correlation with the change in mode of quasi-rotational bands and their conversion to rotational bands in strongly deformed nuclei. The existence of zero-point oscillations at an amplitude comparable to or larger than the deformation parameter and the asymmetry of potential energy curves result in a difference between the "center of oscillations" and the deformation conforming to the minimum curve. The position of this "center of oscillations" determines the true value of the nuclear deformation parameter. (auth)

15171 UNITARITY OF THE COLLISION MATRIX AND INTERDEPENDENCE OF RESONANCE PARAMETERS. Rosenfeld, L. (NORDITA, Copenhagen); Acta Phys. Pol.; A38: 603-19 (Nov 1970).

The cross sections for the reactions between the various channels of a compound nuclear system within a given energy interval are determined by contributions from a finite number of intrinsic resonant states of the system, superposed upon a smooth background. The unitarity and symmetry of the collision matrix impose a set of conditions on the parameters characterizing the resonant states and the background. These conditions are written explicitly in general form for the simple case of an energy interval far from the thresholds of all the open channels. (auth)

15172 BACKSCATTERING OF ALPHA PARTICLES. Budzanowski, A. (Jagellonian Univ., Krakow. Inst. of Nuclear Physica, Krakow); Grotowski, K.; Strzalkowski, A.; Hodgson, P. E. Acta Phys. Pol.; A38: 631-43(Nov 1970).

Angular distributions in the elastic scattering of alpha particles on atomic nuclei exhibit a complicated behavior. Some possible explanations are discussed. (auth)

15173 EMISSION OF ALPHA PARTICLES IN REACTIONS INDUCED BY MEDIUM-ENERGY NUCLEONS. Kulisic, P.; Cindro, N. (Inst. Rudjer Boskovic, Zagreb). Acta Phys. Pol.; A38: 621-30(Nov 1970).

The mechanism of the emission of alpha particles resulting from the bombardment of nuclei with medium energy nucleons was considered in view of some recent results on (n,α) and (p,α) reactions. It was found that in the region of heavy nuclei (A > 100) strong evidence exists for the preponderance of knockout processes involving the transfer of an alpha particle and the simultaneous capture of a nucleon in a single particle state. The situation is less clear in the medium mass region (20 < A < 100). In particular, for nuclei in the neighborhood of the $f_{7/2}$ shell, (p,α) reactions show features similar to one nucleon transfer reactions. This implies a pickup type process, where a single proton and a pair of neutrons are captured by the incident proton to form an alpha particle. No definite conclusions are possible at the moment for very light nuclei (A < 20). Arguments suggesting the knockout process can, however, be found. (auth)

15174 BOOTSTRAP THEORY OF VIBRATIONS. I. PERTURBATIVE SOLUTIONS AND QUASI-RANDOM-PHASE APPROXIMATION IN HEAVY SPHERICAL NUCLEI. Goswami, Amit (Univ. of Oregon, Eugene); Nalcioglu, Orhan; Sherwood, Arnold I. Nucl. Phys.; A153: 433-44(1970).

A self-consistent (bootstrap) theory of vibrations is developed for heavy spherical nuclei. The extended quasiparticle-phonon coupling (EQPC) theory is modified by introducing self-consistent potentials representing large matrix elements of the quadrupole operators between the even-core (ground and phonon) states. The bootstrap is completed by supplementing the EQPC equations with a new equation for the determination of the energy of the collective core states. These bootstrap equations are solved by using first order perturbation theory which leads to RPA. By employing second-order perturbation theory for the energy of the odd-mass states, the restoration of odd–even mass difference by backward coupling is shown. The "pushing-up effect" is also explicitly demonstrated. (auth)

15175 RADIATIVE CORRECTIONS TO BACK SCATTERING. Borie, Edith (National Bureau of Standards, Washington, D. C.). Phys. Rev., C; 2: 770-1(Aug 1970).

It is shown that the anomalous magnetic moment of the electron contributes to the radiative correction to scattering by a charge, even at high energies, when the scattering angle is 180°. This effect increases the radiative correction slightly as compared with the usual Schwinger correction. (auth)

15176 BOOTSTRAP THEORY OF VIBRATIONS. II. EXTENDED PARTICLE-PHONON COUPLING AND RPA IN CLOSED SHELL NUCLEAR REGIONS. Goswami, Amit (Univ. of Oregon, Eugene); Nalcioglu, Orhan; Sherwood, Arnold I. Nucl. Phys.; A153: 445-59(1970).

The bootstrap theory of vibrations was developed for closed-shell nuclei where the particle and phonon modes of these nuclei are generated simultaneously and self-consistently. It is shown that in first order the phonon solutions of this theory correspond to the random-phase approximation (RPA). The properties of the particle modes were also studied in this order. Particle (hole) states are pushed up in energy, which can account for the discrepancy between the shell-model particle-hole energies and the experimental ones. The non-normal parity states (particle-phonon coupled mode) were also studied and it was found that some of these can be expected to lie close in energy to the normal parity (particle mode) states, as it is experimentally found. The possibility of a different approach where the calculation of even- and odd-mass nuclei is carried out separately, the extended-particle-coupling theory (EPPC without bootstrap) was also pointed out. A numerical example using the perturbation theoretical solution of EPPC theory is given for ^{39,40,41}Ca. (auth)

15177 PROBABILITIES OF QUADRUPOLE TRANSITIONS AND THE MEAN VALUES OF QUADRUPOLE MOMENTS IN PHENOMENOLOGICAL NUCLEAR THEORY. Budnik, A. P.; Rabotnov, N. S.; Seregin, A. A. (Inst. of Physics and Power Engineering, Moscow). Yadern. Fiz.; 12: 477-84(Sep 1970). (In Russian).

Relative values of reduced probabilities of electric quadrupole transitions between 2^+ states and from 2^+ states into 0^+ states as well as the mean values of electric quadrupole moments of 2^+ states are calculated in the framework of the phenomenological collective nuclear model with the potential depending on both internal collective variables β and γ. The results obtained are compared with the experimental data for nuclei with intermediate deformations in which $\epsilon_2(2) = E_2(2^+)/E_1(2^+) \lesssim 8$. (auth)

15178 STRUCTURE OF PAIR STATES. Fomenko, V. N. (Leningrad State Univ.). Yadern. Fiz.; 12: 487-91(Sep 1970). (In Russian).

The quasiparticle structure of the ground state in even–even nuclei is investigated and compared with the random-phase method. The consideration is applied to cases of the Ni isotopes and ^{208}Pb. (auth)

15179 ANALOGUE RESONANCE IN REGION OF OVERLAPPING LEVELS OF THE COMPOUND NUCLEUS. Zaretskii, D. F.; Urin, M. G. (Moscow Inst. of Engineering Physics). Yadern. Fiz.; 12: 515-24(Sep 1970). (In Russian).

A description is presented of resonance (p,p′) and (p,n) reactions with excitation of analog states in the region of overlapping levels of the compound nucleus. Mechanisms of "internal" and "external" mixing of the analog and compound nuclear states are considered. Expressions for the cross sections of the resonance reactions are obtained with methods of the quantum damping theory. Microscopic interpretation of parameters in the expression is given. (auth)

15180 COUPLING CONSTANTS AND ELECTROMAGNETIC RADIATIVE CORRECTIONS IN BETA-DECAY AND THE MASS OF THE INTERMEDIATE VECTOR BOSON. Blin-Stoyle, R. J. (Univ. of Sussex, Brighton, Eng.); Freeman, J. M. Nucl. Phys.; A150: 369-78(1970).

Effective beta-decay coupling constants G'_V and G'_A are defined, which include renormalizing effects due to the electromagnetic interaction. Analysis of recent beta-decay data then gives $G'_V = 1.4150 \pm 0.0011 \times 10^{-49}$ erg · cm^3 and $|G'_A/G'_V| = 1.226 \pm 0.011$. It was concluded that only those theories of electromagnetic radiative corrections that take account of a very heavy intermediate vector boson are able to reconcile the values of G'_V, G_μ and the Cabibbo angle determined from polar vector strangeness changing semi-leptonic decays. (auth)

15181 COUPLED CHANNEL CALCULATIONS WITH COMPLEX EIGENVALUES. Lejeune, A.; Nagarajan, M. A. (Univ., Liege). Nucl. Phys.; A154: 602-12(1970).

The Kapur–Peierls dispersion theory was applied to the calculation of the S-matrix for a system of coupled square wells. The energy dependence of the complex eigenvalue was investigated. The validity of a single-level approximation to the S-matrix in the framework of Kapur–Peierls theory is studied. The correspondence between the complex eigenstates and the exact scattering wave function at resonance is discussed. The complex eigenvalues at resonance are compared with the poles of the S-matrix as the strength of the coupling interaction is varied. (auth)

15182 SYSTEMATIC ANALYSIS OF ISOMERIC RATIOS FOR (n,2n) REACTIONS AT 14 MeV. Guidetti, M.; Oldano, C. (Politecnico, Turin). Nucl. Phys.; A152: 387-94(1970).

Isomeric cross-section ratios for (n,2n) reactions at 14 MeV, in the medium mass range, were systematically analyzed in terms of various statistical models namely the shifted Fermi gas (SFGM), the independent pairing (IPM), and the superconductor (SM) models. The Huizenga and Vandenbosch method were adopted Comparison was made with available experimental values. (auth)

15183 HIGH-ENERGY SCATTERING OF HADRONS ON ^{6}Li. A POSSIBLE TEST FOR THE NEW CLUSTER MODEL. Cheon, Il-T.; Samaranayake, V. K. (International Centre for Theoretical Physics, Trieste, Italy). Nucl. Phys.; A154: 93-6 (1970).

Theoretical predictions are given for elastic scattering of high-energy pions on ^{6}Li. A possibility was shown for testing the new cluster model of ^{6}Li by high-energy scattering of hadrons. (auth)

15184 POSITIVE PION REACTIONS WITH ^{12}C. Jones, W. B.; Eisenberg, J. M. (Univ. of Virginia, Charlottesville). Nucl. Phys.; A154: 49-64(1970).

Positive pion scattering and absorption by spherical nuclei are considered. The optical-model treatment of the former process includes a nonlinear dependence on the density of scattering centers originally suggested by Kroll. Explicit results are given for the ^{12}C nucleus and compared with those obtained with the Kisslinger model. Pion optical-model wave functions, both with and without the Kroll modification, are used in a distorted wave calculation of differential cross sections for proton emission following pion absorption, and the results are compared with each other and with experiment for the case of ^{12}C. (auth)

15185 PROPERTIES OF 1s SHELL NUCLEI WITH MOMENTUM DEPENDENT INTERACTIONS. Bruels, Mark C.; Tripathi, Ram K.; Goldhammer, Paul (Univ. of Kansas, Lawrence). Nucl. Phys.; A153: 586-92(1970).

The Bolsterli–Feenberg perturbation procedure was applied to the momentum-dependent potentials of Nestor et al. Binding energies, rms radii, and percentage D-states were calculated for ^{2}H, ^{3}H, and ^{4}He, in addition to the Coulomb energies of ^{3}He and ^{4}He. A modified version of the separation method for solving the Bethe–Goldstone equation was also employed. This separation method was found to badly overestimate the binding energy, due to the explicit momentum dependence of the potentials. Second-order perturbation theory proves to yield results that are both quite accurate mathematically and in good agreement with experiment. (auth)

15186 SHELL MODEL WITH REALISTIC FORCES: SPECTRA AND THE EFFECTS OF CORRELATIONS IN A = 6 NUCLEI. Lawson, R. D. (Argonne National Lab., Ill.). Nucl. Phys.; A148: 401-27(1970).

Correlated wave functions that describe the motion of two nucleons outside an inert core were found by solving the coupled integro-differential equations describing the shell-model problem. The eigenvalues that emerge from the solution of this problem give the two-particle interaction energies relative to the closed shell, and the eigenfunctions contain all possible two-particle correlations that arise from exciting valence nucleons to states outside the Fermi sea. The theory was applied to ^{6}Li, and reasonable agreement with experiment was found when the Hamada–Johnston potential was used for the residual two-body force. The quantities compared with experiment are level scheme, E2 transition rates, M1 transition rates, and in ^{6}Be, the Coulomb energy of the two valence nucleons. It is argued that better agreement with experiment would emerge if the tensor component of the Hamada–Johnston potential were weakened. The variation of the effective-interaction matrix elements with both the single-particle level scheme and the oscillator constant $\hbar\omega$ is examined. This approach is shown to be equivalent to a reformulation of the Bloch–Horowitz theory in which not only the "model-space" states but also all other states allowed by the exclusion principle are treated on an equal footing. (auth)

15187 PARTICLE SPECTRUM IN NUCLEAR MATTER CALCULATIONS. Kao, Hsiao-wen. Pittsburgh; Carnegie-Mellon Univ. (1969). 115p. University Microfilms Order No. 70-12,430. Thesis.

The effect of energy spectrum on the nuclear matter binding energy was investigated. An accurate solution of the Bethe–Goldstone equation was obtained, from which one evaluated the reference spectrum reaction matrix G_r. One then solved the exact equation relating the exact reaction matrix G to the G_r by matrix inversion. The Pauli operator was treated exactly. The off-energy shell effect was also treated exactly by achieving a self-consistent energy spectrum for the two intermediate states. The particle energy was defined to cancel the bubble insertion, and the hole energy was evaluated from on-energy-shell matrix elements. Self-consistency of both the energy spectrum and the reaction matrix was obtained by iteration. The convergence was found to be fast and well-behaved. The binding energy per particle for the nuclear matter system was found to be 13.4, 16.0, 18.5 respectively at $k_F = 1.35, 1.4, 1.45$ fm^{-1}. The result shows a gain of 4 MeV per particle for the binding energy at $k_F = 1.4$ fm^{-1}. It is predictable that three-body contribution calculated from this exact G is going to be more positive, therefore, taking away some of the gain in binding. It is also believed that the three-body contribution is not going to offset all the gain in binding but hopefully significant enough to make nuclear matter saturate at the correct density. (Diss. Abstr. Int., B)

15188 TWO-NUCLEON POTENTIALS AND NUCLEAR SATURATION. Haftel, Michael Ivan. Pittsburgh; Univ. of Pittsburgh (1969). 233p. University Microfilms Order No. 70-11,815. Thesis.

A study of the properties of nuclear matter for potentials of varying smoothness and degree of nonlocality is presented. Numerical methods to handle the two-body and nuclear matter problems for general non-local potentials are developed. These numerical methods are used to calculate the binding energies and saturation densities for a number of phenomenological potentials. The binding energies and saturation densities are related to the wound integral $\varkappa$ and to contributions to $\varkappa$ arising from the central and tensor interactions. The principal result is that nuclear saturation near the empirical energy and density depends mainly on a strong tensor force in the $^3S_1 + {}^3D_1$ eigenchannel. A wound integral $\varkappa_{02}$, which is a measure of the strength of this tensor force, of between 0.05 and 0.07 is necessary for a potential to reproduce the empirical properties of nuclear matter. Potentials with very weak tensor forces are found to drastically overbind nuclear matter. The force with the weakest tensor force in this study overbinds nuclear matter, giving about −30 MeV per particle compared with the empirical value of −16 MeV per particle. The strength of the short-range repulsion is found to play only a secondary role in nuclear saturation. The strong tensor force necessary for nuclear saturation renders questionable the Hartree–Fock approach of calculating the properties of nuclei. (Diss. Abstr. Int., B)

XUM

15189 UNIFIED TREATMENT OF ROTATION, SURFACE VIBRATION, AND PAIRING VIBRATION OF ATOMIC NUCLEI. Ikeda, Akitsu (Osaka Univ.). Progr. Theor. Phys. (Kyoto); 43: 1539-59(Jun 1970).

The generator-coordinate method is formulated so as to be suitable for description of the nuclei in the transition region. To take into account the pairing correlation, the BCS wave function constructed with various single-particle states in a deformed potential well is used as an intrinsic wave function, from which eigenstates of angular momentum are projected out. Using the quadrupole deformation parameters, β and γ, and the gap parameters, Δ_n and Δ_p, as generator coordinates, the trial wave function is generated by superposing the projected wave functions with various values of the generator coordinates. Such a choice of the generator coordinates enables us to treat the rotation, the surface vibration, and the pairing vibration in a unified way. The generator function, which serves as a weight function, is obtained by solving an integral equation derived through the variational principle. It is shown that our projected wave functions have the same symmetry properties as those of wave functions given by the Bohr model. (auth)

15190 EFFECT OF INTERACTION OF NEUTRON WITH NUCLEUS IN COULOMB SPLITTING OF DEUTERON. Zhmailo, V. A. Yadern. Fiz.; 12: 293-301(Aug 1970). (In Russian).

Formulas are obtained for cross sections of various reactions accompanying deuteron splitting in the nuclear field and determined by the neutron interaction with the target nucleus. In the framework of the distorted wave approach, applied to the Coulomb splitting, quantitative estimates are obtained for the cross sections of splitting with production of the composite nucleus (A + n) and with potential scattering of the neutron on the nucleus A. The cross section of the ^{233}U(d,pf) reaction is calculated. The obtained cross sections are compared with the experiment. (auth)

15191 COUPLED-CHANNEL BORN-APPROXIMATION CALCULATION OF TWO-NUCLEON TRANSFER REACTIONS IN DEFORMED NUCLEI. Tamura, T. (Univ. of Texas, Austin); Bes, D. R.; Broglia, R. A.; Landowne, S. Contract AT(11-1)-1764. Phys. Rev. Lett.; 25: 1507-11(23 Nov 1970).

Two-neutron transfer reactions in strongly deformed nuclei are discussed in the framework of the coupled-channel Born approximation. In particular, the reaction ^{176}Yb(p,t)^{174}Yb is analyzed. (auth)

15192 STRIPPING REACTIONS WITH TWO TRANSFERRED NUCLEONS AND POLARIZABILITY OF t,^{3}He. Kadmenskii, S. G.; Kalechits, V. E.; Khlebostroev, V. G. (Voronezh State Univ., USSR). Yadern. Fiz.; 12: 302-7(Aug 1970). (In Russian).

Taking into account the distortion of the triton (^{3}He) internal wave function by the nuclear optical potential, a possible explanation of anomalous reactions of the type (t,p) and (^{3}He,n) on a number of nuclei of p-shell is studied when in the angular distribution for the case of momentum transfer L = 2 there is an anomalous peak at 0°. It is shown that the polarizability of the triton (^{3}He) is not large enough to explain these anomalies. Other possible approaches are considered to explain the anomalies and it is shown that no existing mechanisms of the reaction can explain them. The anomalies in reactions (t,p) and (^{3}He,n) can be understood only by account of the wave distortion not only of internal motion but also of the motion of center of mass of t, ^{3}He. (auth)

15193 MICROSCOPIC AND MACROSCOPIC ASPECTS OF NUCLEAR STRUCTURE WITH APPLICATIONS TO SUPERHEAVY NUCLEI. Tsang, Chin-fu. Berkeley, Calif.; Univ. of California (1969). 216p. University Microfilms Order No. 70-13,185. Thesis.

The relation between a microscopic approach and a macroscopic approach to the study of the nuclear binding energy as a function of neutron number, proton number and nuclear deformations is analyzed. A general discussion of the potential energy of a system which can be divided into a bulk region and a thin skin layer is given. This energy can be written down in the usual liquid drop type of expression, i.e., in terms of the volume, the surface area and other macroscopic properties of the system. The discussion is illustrated by a study of noninteracting particles in an orthorhombic potential well with zero potential inside and infinite potential outside. The total energy is calculated both exactly (a microscopic approach) and also from a liquid drop type of expression (a macroscopic approach). It turns out that the latter approach reproduces the smooth average of the exact results very well. The saddle point shapes of a charged conducting drop on a pure liquid drop model are studied. The properties of a conducting drop are compared with those of a drop whose charges are distributed uniformly throughout its volume. The latter is the usual model employed in the study of nuclear fission. Some of the more important symmetric saddle point shapes are also determined. A method due to Strutinski to synthesize a microscopic approach (the Nilsson model) and a macroscopic approach (the liquid drop model) is generalized. The results are applied to realistic nuclei. The possible occurrence of shape isomers comes as a natural consequence of the present calculation. Their trends as a function of neutron and proton members are discussed and the results are tabulated. The stabilities of the predicted superheavy nuclei with proton number around 114 and neutron number around 184 and 196 determined. Some of these nuclei appear to have extremely long life times. The possible experimental production of these superheavy nuclei is also discussed. (Diss. Abstr. Int., B)

15194 MOMENTUM DISTRIBUTION OF SHORT-LIVED NUCLEAR HOLE STATES. Herscovitz, Victoria E. (Univ. Federal do Rio Grande do Sul, Porto Alegre, Brazil). Nucl. Phys.; A161: 321-9(1971).

The influence of the lifetime of internal hole states, resulting from nuclear quasi-free scattering, on the corresponding momentum distributions is studied. The Schrödinger equation for bound states in complex potentials is solved by an iteration procedure. The momentum distribution of 1s hole states in 1p and 2s-1d shell nuclei is determined for some complex interactions, and leads to strongly model-dependent results. For imaginary potentials proportional to the density distributions of the shells less bound than the hole, the influence on the momentum distributions is very small, but sizable modifications result for potentials acting predominantly at the center or at the surface. (auth)

15195 CONVERGENCE OF RADIAL MATRIX ELEMENTS IN ELECTRON SCATTERING. Glossmann, N.; Toepffer, C. (Univ., Frankfurt am Main). Nucl. Phys.; A161: 330-6(1971).

New expressions for the radial matrix elements of electromagnetic electron-nucleus interaction are derived, which are more suitable for numerical purposes than the usual ones. (auth)

15196 PROJECTION OF ANGULAR MOMENTUM AND THE GENERATOR COORDINATE METHOD FOR LIGHT NUCLEI. Mihailovic, M. V. (Univ. of Maryland, College Park); Kujawski, E.; Lesjak, J. Nucl. Phys.; A161: 252-62(1971).

A method for studying collective states in light nuclei not describable in terms of a single intrinsic Slater determinant is presented. It is based on the generator coordinate method and makes use of "generating functions" obtained by projecting angular momentum from intrinsic deformed states. A useful procedure for projecting angular momentum from a generator coordinate wave function is presented. As an illustration the above method is applied to ^{20}Ne. (auth)

15197 M1 TRANSITION PROBABILITIES OF SINGLE-PARTICLE STATES IN THE LEAD REGION. Klemt, V.; Speth, J. (Technische Hochschule, Munich. Theoretisches Telinstitut, Munich). Nucl. Phys.; A161: 273-82(1971).

In the framework of the theory of finite Fermi systems the l-allowed and l-forbidden M1 transition probabilities in the lead region are calculated. With a projection formalism the transition density matrix of single-particle states of odd-mass nuclei from the response function of the doubly even nucleus is derived in a rigorous way. (auth)

15198 DYNAMIC COLLECTIVE MODEL OF PHOTOFISSION. Updegraff, W. E.; Onley, D. S. (Ohio Univ., Athens). Nucl. Phys.; A161: 191-205(1971).

A fissioning nucleus is described by a collective model with degrees of freedom which permit the nucleus to undergo internal oscillation, surface distension and rotation. Photoabsorption takes place primarily through the excitation of intrinsic charge density oscillations (as in the Steinwedel-Jensen model), but the nucleus is then unstable to fission, in that adiabatic distension of the surface may so drain the energy from the interior oscillation that the fission barrier effectively disappears. The same set of hydrodynamic assumptions are consistently applied to the system whether in a divided or coalesced state, and consequently the separation vector in the final state is continuously related to the collective variables of the parent nucleus. Calculation of the matrix element for photofission is then straightforward. Numerical calculations are confined to symmetric binary fission of ^{238}U. (auth)

15199 ONE-BOSON EXCHANGE POTENTIAL AND NUCLEAR MATTER PROPERTIES. Erkelenz, K.; Holinde, K.; Bleuler, K. (Univ., Bonn). Nucl. Phys.; A161: 155-76(1971).

The binding energy and saturation density of nuclear matter were calculated for a momentum dependent OBEP by the reference spectrum method of Bethe et al. The binding energy is calculated to first order in the Brueckner–Goldstone reaction matrix using self-consistent hole state energies in the effective mass approximation and zero intermediate-state potential energies. The second (Pauli term) and higher-order correction terms of the reference spectrum method were included; the latter in the geometric series approximation of Dahll et al. The potential energy contribution from first, second and third order are roughly in the ratio 80 : 20 : 2. A binding energy of −11.2 MeV per particle was found at a density corresponding to the Fermi momentum $k_F = 1.55\ fm^{-1}$. (auth)

15200 INVESTIGATION OF GROUND STATE CORRELATIONS IN AN EXTENDED LIPKIN–MESHKOV–GLICK MODEL. **Schalow, G.; Yamamura, M. (Hahn-Meitner-Institut fuer Kernforschung, Berlin. Sektor Kernphysik, Berlin). Nucl. Phys.; A161: 93-104(1971).**

The strength of ground state correlations calculated from the RPA and quasiboson approximation is known to differ by a factor of two from that calculated by various other methods. This contradiction is investigated in detail in an extended Lipkin–Meshkov–Glick model. It is proved that the RPA + quasiboson approximation formula gives the correct ground state correlations if only collective states are included, as suggested by Rowe. The notion of a collective state is defined quantitatively. (auth)

15201 REDUCED WIDTHS FROM ISOBARIC ANALOG RESONANCES. **Clarkson, R. G.; von Brentano, P.; Harney, H. L. (Max-Planck-Institut fuer Kernphysik, Heidelberg). Nucl. Phys.; A161: 49-72(1971).**

The parameter dependences of the shell-model expressions for the widths of analog resonances are examined. The expressions are reformulated so as to reduce the parameter dependences, and to make the remaining dependences as transparent as possible. A reduced width is defined which depends only very weakly on the parameters and which may hence be determined with high accuracy. This is demonstrated by numerical examples. A comparison is made of spectroscopy with analog resonances and sub-Coulomb stripping. (auth)

15202 HARTREE–BOGOLIUBOV CALCULATIONS WITH SPHERICAL RESTRICTION. **Schuetee, D. (Univ., Bonn). Nucl. Phys.; A161: 73-80(1971).**

The structure of the Hartree–Bogoliubov theory with spherical restrictions (SHB theory) is investigated. The SHB equations exhibit a strong instability if solutions are determined by iterations but this can be overcome by using the splitting of the SHB transformations according to Bloch and Messiah. Results of SHB calculations are presented for such nuclei where comparisons to deformed HB solutions are possible. It is shown that for light nuclei (18 < A < 40) the SHB solutions are energetically rather high (coexistence of spherical and deformed structures), whereas for ^{16}O and the Ca isotopes the SHB solutions have about the same binding compared to the deformed ones, indicating that these nuclei can be treated equivalently as spherical or (weakly) deformed structures. (auth)

15203 EQUIVALENCE OF THE CENTRIFUGAL STRETCHING MODEL AND THE VARIABLE MOMENT OF INERTIA MODEL FOR THE GROUND STATE BANDS OF DOUBLY EVEN NUCLEI. **Wold, Einar (Oslo Katedralskole). Nucl. Phys.; A154: 141-4 (1970).**

The centrifugal stretching model of Sood and the variable moment of inertia model of Mariscotti et al. for the ground state bands of doubly even nuclei are equivalent if the restoring force in the model of Sood is modified appropriately. (auth)

15204 ELECTRON-EXCITATION–GAMMA-DECAY REACTIONS IN HEAVY NUCLEI. **Griffy, T. A.; Whitehill, Don (Univ. of Texas, Austin). Phys. Rev., C; 2: 441-50(Aug 1970).**

The feasibility of using the reactions

$$\begin{array}{l} e + N(\epsilon_i, J_i) \rightarrow e' + N(\epsilon_f, J_f) \\ \qquad\qquad\qquad\qquad\qquad\quad \searrow N(\epsilon_{ff}, J_{ff}) + \gamma \end{array}$$

to investigate low-lying states of heavy nuclei is discussed. By detecting the decay photon, the problem of poor energy resolution for high-energy electrons can be circumvented. The formalism for the e'-γ coincidence cross section is given. The Coulomb distortion of the electron wave functions, which is important for heavy nuclei, is taken into account. Results for the e'-γ coincidence cross section and the γ-detection cross section for several nuclei are given. The e-γ coincidence cross section appears to be feasible when superconducting accelerators became operational. The γ-detection cross section offers a method for investigating low-lying states with present-day accelerators. (auth)

15205 ON THE MICROSCOPIC DESCRIPTION OF NUCLEAR VIBRATIONS WHEN PHONONS OCCUR AT RELATIVELY LOW ENERGY. II. OCTUPOLE STATES OF THE EVEN DEFORMED NUCLEI WITH A greater than or equal to 222. **Neergaerd, K. (Univ. of Copenhagen); Vogel, P. Nucl. Phys.; A149: 217-24(1970).**

Properties of the octupole vibrational states were calculated. It is possible to give a common description of all octupole states in the considered region including the very low-lying $K^\pi = 0^-$ states in the isotopes of Ra and Th. The Coriolis coupling between the states of the octupole quadruplet is taken into account in the calculations. The resulting theoretical spectra are compared with the experimental data. (auth)

15206 PROGRESS IN UNDERSTANDING NEUTRON INTERACTIONS WITH NUCLEI. **Lynn, J. E. (Atomic Energy Research Establishment, Harwell, Eng.). pp 93-113 of Nuclear Data for Reactors. Vol. I. Vienna; International Atomic Energy Agency (1970).**

From 2nd International Conference on Nuclear Data for Reactors, Helsinki, Finland. See STI/PUB-259(Vol.1); CONF-700605-(Vol.1).

The general development of neutron reactions is reviewed, with emphasis on the growing awareness of the importance of special, relatively simple, states of the nuclear motion in influencing the underlying microscopic structure of neutron cross-sections. The main illustrative case chosen is that of the coupling of single-particle motion and collective rotation of a heavy deformed nucleus. The description of this case is given in R-matrix theory, and it is shown how the coupling can give rise to correlation between elastic and inelastic scattering widths in the fine-structure resonances, thus influencing the average inelastic-scattering cross-section, provided that spreading of the special, coupled states into the fine structure is not too large. It is also shown how direct inelastic scattering cross-sections appear in the theory. The measured capture and inelastic scattering cross-sections of ^{238}U are discussed from the theoretical point of view, and it is pointed out how the capture data require a model of the radiative-capture process that favors high-energy transitions. This again may be evidence of the role of special modes that are not too strongly damped into the fine-structure levels. The recent developments in fission that strikingly demonstrate the role played by the special states corresponding to excitation of a highly-elongated quasi-stable shape of the nucleus are examined. 36 references. (auth)

15207 COMPOUND-NUCLEUS CALCULATIONS OF LOW-ENERGY NEUTRON REACTION CROSS-SECTIONS USING LEVEL DENSITIES FROM EXACT COUNTING OF SHELL-MODEL STATES. **Eriksson, J. R. (Aktiebolaget Atomenergi, Studsvik, Swed.). pp 881-4 of Nuclear Data for Reactors. Vol. II. Vienna; International Atomic Energy Agency (1970).**

From 2nd International Conference on Nuclear Data for Reactors, Helsinki, Finland. See STI/PUB-259(Vol.2); CONF-700605-(Vol.2).

The prediction of the energy-dependent (n,p) and (n,α) cross-sections from the compound-nucleus model is usually based on the assumption that the level density of the residual nucleus is of the Fermi-gas form $\rho_{FG}(E,I)$, where E is the nuclear excitation energy, and I is the spin. With this assumption, the integral mean of the (n,p) (or (n,α)) production cross-section $\langle\sigma_{n,p}\rangle_\Phi$ over a thermal-reactor neutron-flux distribution Φ (E) shows that the most important part of the level density is the residual excitation below 5 MeV. The level density ρ (E,I) is calculated at low excitation energies E by the method of exactly counting the spherical-model states. The single-particle shell-model levels are subject to a modified BCS calculation after which the quasi-particle states obtained are used as input in a level-counting program giving the level density ρ (E,I). The resulting ρ (E,I) shows pronounced effects arising from the specific neutron and proton single-particle-level schemes up to energies above 10 MeV. Despite this low-energy picture and the overall scatter of the values of ρ (E,I) an adequate $\rho_{FG}(E,I)$ can always be obtained at higher energies. It turns out that, except for a few cases, the Fermi-gas ground state lies above the ground state of the model nucleus indicating that $\rho_{FG}(E,I)$ tends to underestimate the low-energy level density. 8 references. (auth)

15208 DENSITY OF EXCITED STATES OF ATOMIC NUCLEI. **Ignatyuk, A. V.; Stavinskii, V. S.; Shubin, Yu. N. (Inst. of Physics and Power Engineering, Obninsk, USSR). pp 885-907 of Nuclear Data for Reactors. Vol. II. Vienna; International Atomic Energy Agency (1970). (In Russian).**

From 2nd International Conference on Nuclear Data for Reactors, Helsinki, Finland. See STI/PUB-259(Vol.2); CONF-700605-(Vol.2).

The results of calculations of the level density of atomic nuclei are discussed, in which systematic account is taken of the individual properties of nuclei associated with their shell structure. The calculations are based on the superfluid-nucleus model, which is being used with success in analyzing the properties of low-lying excited states of nuclei. The calculations do not involve the use of additional parameters and provide a means based on a single approach for correlating the properties of highly excited nuclei and those of nuclei in the ground and weakly excited states. The calculations performed show that the discrete structure of the single-particle spectrum leads to substantial changes in the energy dependence of level density as compared with the Fermi-gas model, provides a natural explanation for the anomalies observed in the spectra of inelastically scattered neutrons, and yields a qualitative description of the main characteristics of the nuclear fusion process, phase-transition range and so on. The spin dependence of nuclear level density and the dependence of the equilibrium deformation of nuclei on excitation energy are also considered. The internal consistency of the model and the fact that it explains the different average characteristics of excited nuclei justify the hope that the proposed method will provide a reliable basis for calculating and evaluating nuclear data. 27 references. (auth)

15209 AVERAGE RADIATION WIDTHS FOR EXCITATION ENERGIES OF THE ORDER OF NEUTRON BINDING ENERGY. **Zakharova, S. M.; Stavinskii, V. S.; Shubin, Yu. N.** (Inst. of Physics and Power Engineering, Obninsk, USSR). pp 909-16 of Nuclear Data for Reactors. Vol. II. Vienna; International Atomic Energy Agency (1970). (In Russian).

From 2nd International Conference on Nuclear Data for Reactors, Helsinki, Finland. See STI/PUB-259(Vol.2); CONF-700605-(Vol.2).

The behavior of the average radiation width is studied as a function of the number of nucleons in a nucleus. Nuclear level density is calculated in terms of the Fermi-gas model, allowance for residual interactions being made on a phenomenological basis. It is shown that the ratio of the average radiation width obtained from the experimental data on neutron resonances in the low-energy range to the average radiation width calculated with the Weisskopf model depends on the shell structure and correlates with the behavior of the width of a dipole giant resonance. Analytical treatment of the data yielded a semi-empirical expression for the average radiation width which can be used for calculating this quantity, in the case of a nuclear excitation energy of the order of neutron binding energy, to within ±40% in the range of A = 60 to A = 200. (auth)

15210 SUGGESTION FOR SOLVING THREE-BODY PROBLEMS. **Sasakawa, Tatuya** (CEN de Saclay, Gif-sur-Yvette, France). Nucl. Phys.; A160: 321-36(1971).

The possibility of solving three-body problems is discussed on the basis of symmetric kernels, especially for positive energies. For positive energies, it is concluded that it is preferable to solve the fully connected equation for the three-body wave function rather than the fully connected equation for the three-body t-matrix. This is because in the two-body t- or K-matrix, the Born term is of the same order of magnitude as the rest, and because the eigenfunction expansion of the Born term is slowly converging. It is shown that for positive energies the use of the symmetric kernel of Meetz and Weinberg is not practical. Another symmetric kernel, which yields very good convergence in any positive energy region, is proposed. For negative energies, one may solve either the fully connected t-matrix equation or the fully connected equation for the wave function. The method for separating the elastic channel is written. The validity of pole approximations is discussed. (auth)

REACTOR TECHNOLOGY

Commercial Power Reactors

15211 EVALUATION OF ISOCHECK AND INVENT FUEL INVENTORY CALCULATIONAL MODELS. Kern, R. C.; Bonaca, M. V. (Combustion Engineering, Inc., Windsor, Conn.). Nucl. Appl. Technol.; 9: 796-806(Dec 1970).

Two models which are designed to perform fuel inventory calculations without the use of detailed and expensive computer programs have been developed. The accuracies of these models have been evaluated by comparing results obtained with them to measurements of discharged fuel from the Yankee Rowe Reactor. In general, the models predict the ^{235}U depletion to within ±2% of the measured values and the total Pu production to within ±5% for fuel batches consisting of about 70 fuel assemblies. Uncertainties in the computational results have been ascertained to be about ±2% for the total ^{235}U content and ±3% for the total Pu production. 17 references. (auth)

15212 FUEL AND FUEL CYCLE FOR OSKARSHAMN. Almgren, B. Nucl. Eng. Int.; 15: 992-5(Dec 1970).

The fuel cycles for Units I & II are discussed and compared. Details are given of U procurement and conversion of UF$_6$; toll enrichment; fuel assembly design; fuel fabrication; core layout and reactivity control; fuel performance; monitoring of power distribution; and refuelling methods. (UK)

15213 TRANSVERSAL VIBRATIONS OF RODS EXCITED BY PARALLEL FLOW. Novak, J. (National Research Inst. for Machine Design, Bechovice, Czech.). Jad. Energ.; 17: 2-9 (1971). (In Czech).

Main test results of transversal vibration investigation of two smooth rods in parallel air or water flow are presented. One end of each rod (of circular cross section) was fixed and the other one was supported. Strain and deflection of the vibrating rod were examined as a function of the Reynolds number Re and turbulence intensity I. The investigation of rod vibration in the A-1 reactor is described. The results show that the rods vibrate with natural frequencies. Resulting vibration consists of several modes; the amplitudes and vibration directions depend on time. The modes associated with the lowest frequencies prevail. Resulting vibrations have a random character depending on the Reynolds number, turbulence intensity and rod length. It is concluded that the turbulence is the main cause of excitation of vibration. (auth)

Operation and Economics

15214 (DLCS-5000370) SHIPPINGPORT ATOMIC POWER STATION. Quarterly Operating Report, Third Quarter 1970. (Duquesne Light Co., Shippingport, Pa. Power Stations Dept.). Contract AT(11-1)-292. 20p. Dep. NTIS.

Operations and maintenance requirements during July to September 1970 are described. Coolant chemistry measurements are listed. (D.C.C.)

15215 (DOCKET-1151-39) ELK RIVER REACTOR. Status Report. (Rural Cooperative Power Association, Elk River, Minn.). 2 Feb 1971. 9p. Dep. NTIS.

Maintenance and surveillance activities for the deactivated reactor are reported for August 1970 to February 1971. (D.C.C.)

15216 (DOCKET-1155-89) LA CROSSE BOILING WATER REACTOR. Unplanned Reactor Scram. (Dairyland Power Cooperative, La Crosse, Wis.). 15 Jan 1971. 3p. (DPC-70-20). Dep. NTIS.

15217 (DOCKET-1155-92) LA CROSSE BOILING WATER REACTOR. Failure of Control Rod No. 13 to Scram Hydraulically at Normal Scram Speed. (Dairyland Power Cooperative, La Crosse, Wis.). 15 Jan 1971. 7p. (DPC-70-21). Dep. NTIS.

15218 (DOCKET-1155-93) LA CROSSE BOILING WATER REACTOR. Unplanned Reactor Scram. (Dairyland Power Cooperative, La Crosse, Wis.). 15 Jan 1971. 1p. (DPC-70-22). Dep. NTIS.

15219 (DOCKET-1155-94) LA CROSSE BOILING WATER REACTOR. Emergency Diesel Generator Failure to Start on First Crank During Monthly Test. (Dairyland Power Cooperative, La Crosse, Wis.). 15 Jan 1971. 1p. (DPC-70-23). Dep. NTIS.

15220 (DOCKET-1155-95) LA CROSSE BOILING WATER REACTOR. Failure of Control Rod No. 11 to Withdraw on Plant Startup. (Dairyland Power Cooperative, La Crosse, Wis.). 15 Jan 1971. 1p. (DPC-70-24). Dep. NTIS.

15221 (DOCKET-1155-96) LA CROSSE BOILING WATER REACTOR. Unplanned Reactor Scram. (Dairyland Power Cooperative, La Crosse, Wis.). 15 Jan 1971. 1p. (DPC-70-25). Dep. NTIS.

15222 (DOCKET-1155-97) LA CROSSE BOILING WATER REACTOR. Unplanned Reactor Scram. (Dairyland Power Cooperative, La Crosse, Wis.). 15 Jan 1971. 2p. (DPC-70-26). Dep. NTIS.

15223 (DOCKET-1155-98) LA CROSSE BOILING WATER REACTOR. Unplanned Reactor Scram. (Dairyland Power Cooperative, La Crosse, Wis.). 15 Jan 1971. 2p. (DPC-70-27). Dep. NTIS.

15224 (DOCKET-50003-62) INDIAN POINT STATION, UNIT NO. 1. Failure of a Reactor Outlet Stop Valve on No. 13 Loop to Function Properly. (Consolidated Edison Co. of New York, Inc., New York). 20 Jan 1971. 2p. Dep. NTIS.

15225 (DOCKET-50003-63) INDIAN POINT STATION, UNIT NO. 1. Foreign Material in Buffer Seal Housing of Control Rods. (Consolidated Edison Co. of New York, Inc., New York). 22 Jan 1971. 2p. Dep. NTIS.

15226 (DOCKET-50029-142) YANKEE NUCLEAR POWER STATION. Operation Report No. 120, December 1970. (Yankee Atomic Electric Co., Westboro, Mass.). 22 Jan 1971. 8p. Dep. NTIS.

15227 (DOCKET-50206-103) SAN ONOFRE NUCLEAR GENERATING STATION, UNIT 1. Semiannual Operating Report No. 7, July 1-December 31, 1970. (Southern California Edison Co., Los Angeles. San Diego Gas and Electric Co., Calif.). 15 Jan 1971. 10p. Dep. NTIS.

15228 (DOCKET-50206-105) SAN ONOFRE NUCLEAR GENERATING STATION, UNIT 1. Operation Report, January 1971. (Southern California Edison Co., Los Angeles). Feb 1971. Contract AT(30-1)-3270. 5p. (NYO-3270-46). Dep. NTIS.

15229 (DOCKET-50213-94) CONNECTICUT YANKEE ATOMIC POWER PLANT. Operation Report No. 70-12, December 1970. (Connecticut Yankee Atomic Power Co., Haddam). 22 Jan 1971. Contract AT(30-1)-3250. 15p. (NYO-3250-55). Dep. NTIS.

15230 (DOCKET-50237-132) DRESDEN NUCLEAR POWER STATION, UNIT 2. Report of Valve Failures. (Commonwealth Edison Co., Chicago, Ill.). 15 Jan 1971. 2p. Dep. NTIS.

Malfunctions of the isolation condenser outboard steam isolation valve, the torus spray valve, and the containment cooling heat exchanger bypass valve are reported. Corrective maintenance is described. (D.C.C.)

15231 (DOCKET-50237-140) DRESDEN NUCLEAR POWER STATION, UNIT 2. Abnormal Occurrence Report: Failure of Main Steam Isolation Valve 2D to Close. (Commonwealth Edison Co., Chicago, Ill.). 29 Jan 1971. 2p. Dep. NTIS.

15232 (DOCKET-50237-141) DRESDEN NUCLEAR POWER STATION, UNIT 2. High Pressure Coolant Injection Pump Flow Less Than That Specified. (Commonwealth Edison Co., Chicago, Ill.). 29 Jan 1971. 2p. Dep. NTIS.

15233 (DOCKET-50237-142) DRESDEN NUCLEAR POWER STATION, UNIT 2. Testing Program. (Commonwealth Edison Co., Chicago, Ill.). 2 Feb 1971. 2p. Dep. NTIS.

15234 (DOCKET-50245-53) MILLSTONE NUCLEAR POWER STATION, UNIT 1. Abnormal Occrrence No. A0-71-1: Failure of Core Spray Injection Valve to Close. (Millstone Point Co., Hartford, Conn.). 2 Feb 1971. 3p. Dep. NTIS.

15235 (DOCKET-50245-54) MILLSTONE NUCLEAR POWER STATION, UNIT 1. Abnormal Occurrence No. A0-71-2. (Millstone Point Co., Hartford, Conn.). 4 Feb 1971. 1p. Dep. NTIS.

Failure of the "B" system core spray injection valve to operate is described. The failure was due to galled threads on the valve stem. Replacement of the valve stem and yolk bushing on both the "A" and "B" core spray injection valves is described. (D.C.C.)

XUM

15236 (DOCKET-50263-51) MONTICELLO NUCLEAR GENERATING PLANT, UNIT 1. Unsafe Failure of Protection System Sensor. (Northern States Power Co., Minneapolis, Minn.). 12 Jan 1971. 1p. Dep. NTIS.

15237 (DOCKET-50266-39) POINT BEACH NUCLEAR PLANT, UNIT 1. Reactor Coolant Pump Fire. (Wisconsin Electric Power Co., Milwaukee). 22 Jan 1971. 3p. Dep. NTIS.

15238 (DOCKET-50266-40) POINT BEACH NUCLEAR PLANT, UNIT 1. Abnormal Occurrence Report: Failure of Containment Sump Suction Valves to Open. (Wisconsin Electric Power Co., Milwaukee). 22 Jan 1971. 3p. Dep. NTIS.

15239 (EUR-4580) GARIGLIANO NUCLEAR POWER PLANT. Annual Report, 1969. (Ente Nazionale per l'Energia Elettrica, Rome (Italy)). Dec 1970. 80p. (In Italian). Dep. NTIS (U. S. Sales Only). EUR Lit. 1,560.

Operations and maintenance requirements during March 1969 to February 1970 are described. Coolant chemistry measurements are presented. (D.C.C.)

15240 ELECTRICAL GENERATION WITH NUCLEAR ENERGY. Bainbridge, G. R. Australas. Eng.; 62: 16-21(Nov 1970).

Development of power generating reactors is briefly reviewed with reference to their introduction into Australia. A comparison of fuel data is given between Magnox, AGR and Mk III gas-cooled reactors, SGHWR, BWR and CANDU reactors and sodium cooled fast reactors. Reactor output, thermal efficiency, fuel rating and coolant properties for British gas-cooled reactors are tabulated. The features of a 500 MW(e) SGHWR power station are outlined. (Australia)

Safety and Siting

Refer also to abstract 13147.

15241 (DOCKET-1155-90) LA CROSSE BOILING WATER REACTOR. Provisional Operating Authorization No. DPRA-6; Technical Specifications Change No. 2. (Division of Reactor Licensing (AEC), Washington, D. C.). 19 Jan 1971. 4p. Dep. NTIS.

Authorization for use of an automatic gain control system for reactor instrumentation is presented. (D.C.C.)

15242 (DOCKET-1155-91) LA CROSSE BOILING WATER REACTOR. Reactor Low Flow Scram Bypass Key Switches. (Dairyland Power Cooperative, La Crosse, Wis.). 28 Jan 1971. 2p. Dep. NTIS.

15243 (DOCKET-50003-61) INDIAN POINT STATION, UNIT NO. 1. Completion of Thermal Sleeve Repairs. (Consolidated Edison Co. of New York, Inc., New York). 20 Jan 1971. 2p. Dep. NTIS.

15244 (DOCKET-50003-64) INDIAN POINT STATION, UNIT NO. 1. Facility Design Changes. (Consolidated Edison Co. of New York, Inc., New York). 26 Jan 1971. 4p. Dep. NTIS.

15245 (DOCKET-50010-76) DRESDEN NUCLEAR POWER STATION, UNIT 1. License No. DPR-2; Proposed Change No. 21 to Appendix A. (Commonwealth Edison Co., Chicago, Ill.). 18 Jan 1971. 4p. Dep. NTIS.

Revised release limits for airborne radioactive effluents are presented. Personnel requirements for normal reactor operation are listed. (D.C.C.)

15246 (DOCKET-50010-77) DRESDEN NUCLEAR POWER STATION, UNIT 1. License No. DPR-2; Proposed Change No. 22 to Appendix A. (Commonwealth Edison Co., Chicago, Ill.). 18 Jan 1971. 33p. Dep. NTIS.

Core configuration and fuel element performance characteristics for Cycle 8 operation are presented. (D.C.C.)

15247 (DOCKET-50016-89) ENRICO FERMI ATOMIC POWER PLANT, UNIT 1. Revised License Application, Part B. Vol. 1. Technical Information and Hazards Summary Report. (Power Reactor Development Co., Detroit, Mich.). 14 Jul 1961. 205p. Dep. NTIS.

Information on Fermi Fast Breeder Reactor is presented under the following topics: general description of plant; reactor vessel and associated structures; core and blanket design and performance; reactor physics; and control and neutron source components. (D.C.C.)

15248 (DOCKET-50016-90) ENRICO FERMI ATOMIC POWER PLANT, UNIT 1. Revised License Application, Part B. Vol. 7. Technical Information and Hazards Summary Report. (Power Reactor Development Co., Detroit, Mich.). [14 Jul 1961]. 128p. Dep. NTIS.

Information concerning hazards analysis for Fermi Fast Breeder Reactor is presented under the following topics: prevention of gross meltdown; credible accidents; hypothetical accidents; containment; and hazards external to reactor building. (D.C.C.)

15249 (DOCKET-50016-91) ENRICO FERMI ATOMIC POWER PLANT, UNIT 1. Revised License Application, Part B. Vol. 8. Proposed Technical Specifications. (Power Reactor Development Co., Detroit, Mich.). [14 Jul 1961]. 93p. Dep. NTIS.

15250 (DOCKET-50016-92) ENRICO FERMI ATOMIC POWER PLANT, UNIT 1. Sodium Service Piping, Additional Information. (Power Reactor Development Co., Detroit, Mich.). 18 Jan 1971. 16p. Dep. NTIS.

15251 (DOCKET-50016-93) ENRICO FERMI ATOMIC POWER PLANT, UNIT 1. Revised License Application, Part A. General Information and Request for License. (Power Reactor Development Co., Detroit, Mich.). Jul 1961. 37p. Dep. NTIS.

15252 (DOCKET-50016-94) ENRICO FERMI ATOMIC POWER PLANT, UNIT 1. Revised License Application, Part B. Vol. 2. Technical Information and Hazards Summary Report. (Power Reactor Development Co., Detroit, Mich.). 14 Jul 1961. 182p. Dep. NTIS.

Information on Fermi Fast Breeder Reactor is presented under the following topics: sodium coolant system; sodium and inert gas handling equipment; turbine and electrical system; and control and safety systems. (D.C.C.)

15253 (DOCKET-50016-95) ENRICO FERMI ATOMIC POWER PLANT, UNIT 1. Revised License Application, Part B. Vol. 3. Technical Information and Hazards Summary Report. (Power Reactor Development Co., Detroit, Mich.). 14 Jul 1961. 146p. Dep. NTIS.

Information on Fermi Fast Breeder Reactor is presented under the following topics: reactor building; shielding; fuel handling facilities; radioactive waste disposal systems; and auxiliary buildings and services. (D.C.C.)

15254 (DOCKET-50016-96) ENRICO FERMI ATOMIC POWER PLANT, UNIT 1. Revised License Application, Part B. Vol. 4. Technical Information and Hazards Summary Report. (Power Reactor Development Co., Detroit, Mich.). 14 Jul 1961. 109p. Dep. NTIS.

Information on Fermi Fast Breeder Reactor is presented under the following topics: startup and shutdown; sequence and control of loading and unloading; routine testing programs; programs to evaluate in-plant radiation effects; maintenance of radioactive equipment; radiological health and safety; and plant organization and training program (D.C.C.)

15255 (DOCKET-50016-97) ENRICO FERMI ATOMIC POWER PLANT, UNIT 1. Revised License Application, Part B. Vol. 5. Technical Information and Hazards Summary Report. (Power Reactor Development Co., Detroit, Mich.). 14 Jul 1961. 191p. Dep. NTIS.

Information on Fermi Fast Breeder Reactor is presented under the following topics: the critical experiment; fuel verification; reactor and system simulation; safety rod drop tests; APDA Component Test Facility; steam generator pilot unit tests; sodium reaction tests; coolant boiling and fuel meltdown tests; and containment vessel pressure and leak rate tests. (D.C.C.)

15256 (DOCKET-50016-98) ENRICO FERMI ATOMIC POWER PLANT, UNIT 1. Revised License Application, Part B. Vol. 6. Technical Information and Hazards Summary Report. (Power Reactor Development Co., Detroit, Mich.). 14 Jul 1961. 109p. Dep. NTIS.

Information on Fermi Fast Breeder Reactor is presented under the following topics: pre-operational test program; reactor startup and operational testing; verification of kinetic parameters and kinetic behavior; and site and environment. (D.C.C.)

15257 (DOCKET-50029-90) YANKEE NUCLEAR POWER STATION. Operating Plan in Event of Labor Strike. (Yankee Atomic Electric Co., Boston, Mass.). June 25, 1968. 3p. Dep. CFSTI.

15258 (DOCKET-50155-60) BIG ROCK POINT NUCLEAR PLANT. License No. DPR-6; Proposed Technical Specifications

UM

Change No. 25. (Consumers Power Co., Jackson, Mich.). 18 Jan 1971. 9p. Dep. NTIS.

Revised technical specifications concerning the use of auxiliary neutron sources are described. (D.C.C.)

15259 (DOCKET-50155-61) BIG ROCK POINT NUCLEAR PLANT. License No. DPR-6; Proposed Technical Specifications Change No. 26. (Consumers Power Co., Jackson, Mich.). 28 Jan 1971. 5p. Dep. NTIS.

Technical specifications concerning the use of Type 2A control elements are presented. (D.C.C.)

15260 (DOCKET-50155-62) BIG ROCK POINT NUCLEAR PLANT. License No. DPR-6; Proposed Technical Specifications Change No. 25, Additional Information. (Consumers Power Co., Jackson, Mich.). 1 Feb 1971. 2p. Dep. NTIS.

Additional information concerning the minimum initial neutron source strength required for reactor startup is presented. (D.C.C.)

15261 (DOCKET-50155-63) BIG ROCK POINT NUCLEAR PLANT. License No. DPR-6; Proposed Technical Specifications Change No. 27. (Consumers Power Co., Jackson, Mich.). 2 Feb 1971. 56p. Dep. NTIS.

Technical specifications concerning the modified emergency core cooling system and protection systems are presented. (D.C.C.)

15262 (DOCKET-50155-65) BIG ROCK POINT NUCLEAR PLANT. License No. DPR-6; Technical Specifications Change No. 21. (Division of Reactor Licensing (AEC), Washington, D. C.). 9 Feb 1971. 11p. Dep. NTIS.

Revised technical specifications concerning operations with Reload-F and Type J-1 fuel assemblies are presented. Design parameters of the fuel assemblies are listed. (D.C.C.)

15263 (DOCKET-50206-104) SAN ONOFRE NUCLEAR GENERATING STATION, UNIT 1. Cycle 2 Xenon Transient Analysis. (Southern California Edison Co., Los Angeles). 27 Jan 1971. 2p. Dep. NTIS.

15264 (DOCKET-50206-106) SAN ONOFRE NUCLEAR GENERATING STATION, UNIT 1. License No. DPR-13; Technical Specification Proposed Change No. 4, Request for Additional Information. (Division of Reactor Licensing (AEC), Washington, D. C.). 9 Feb 1971. 2p. Dep. NTIS.

Requests for additional information concerning control rod effectiveness during core lifetime are presented. (D.C.C.)

15265 (DOCKET-50213-95) CONNECTICUT YANKEE ATOMIC POWER PLANT. Examination and Evaluation of Capsule A for Pressure-Vessel Surveillance Program. Final Report. (Battelle Memorial Inst., Columbus, Ohio). 30 Oct 1970. 163p. Dep. NTIS.

For Connecticut Yankee Atomic Power Co., Hartford.

15266 (DOCKET-50213-96) CONNECTICUT YANKEE ATOMIC POWER PLANT. Preliminary Safety Analysis Report, Suppl. 2. (Connecticut Yankee Atomic Power Co., Hartford). 21 Jan 1971. 13p. Dep. NTIS.

Additional information concerning the site seismograph station, the spent fuel pool, land use, and liquid radioactive waste is presented. (D.C.C.)

15267 (DOCKET-50213-97) CONNECTICUT YANKEE ATOMIC POWER PLANT. License No. DPR-14. Technical Specifications Proposed Change No. 18. (Connecticut Yankee Atomic Power Co., Hartford). 3 Feb 1971. 11p. Dep. NTIS.

Design parameters and loading configuration for Core 3 are presented. (D.C.C.)

15268 (DOCKET-50219-120) OYSTER CREEK NUCLEAR POWER PLANT, UNIT NO. 1. Preliminary Safety Analysis Report, Amendment 65, Suppl. 1. (Jersey Central Power and Light Co., Morristown, N. J.). 26 Jan 1971. 5p. Dep. NTIS.

Revised information concerning the reactor protection system is presented. (D.C.C.)

15269 (DOCKET-50219-121) OYSTER CREEK NUCLEAR POWER PLANT, UNIT NO. 1. Summary Technical Report: Primary Containment Leakage Rate Test. (Jersey Central Power and Light Co., Morristown, N. J.). Jan 1971. 30p. Dep. NTIS.

15270 (DOCKET-50220-57) NINE MILE POINT NUCLEAR STATION. Petition Requesting Amendment of License, Amendment 5. Technical Supplement to Petition to Increase Power Level, Fifth Addendum. (Niagara Mohawk Power Corp., Syracuse, N. Y.). 26 Jan 1971. 15p. Dep. NTIS.

Requested additional information concerning performance capabilities of the emergency core cooling system is presented. (D.C.C.)

15271 (DOCKET-50231-68) SOUTHWEST EXPERIMENTAL FAST OXIDE REACTOR. License No. DR-15; Technical Specifications Proposed Change No. 3, Addendum No. 2. (General Electric Co., Sunnyvale, Calif. Breeder Reactor Development Operation). 27 Jan 1971. 23p. Dep. NTIS.

Technical specifications concerning modified safety limit settings for operations with guinea pig fuel rods are presented. (D.C.C.)

15272 (DOCKET-50231-69) SOUTHWEST EXPERIMENTAL FAST OXIDE REACTOR. Sodium Logging of Fuel Rods, Additional Information. (General Electric Co., Sunnyvale, Calif. Breeder Reactor Development Operation). 1 Feb 1971. 10p. Dep. NTIS.

15273 (DOCKET-50237-130) DRESDEN NUCLEAR POWER STATION, UNIT 2. Facility License DPR-19; Proposed Change No. 7 to Appendix A. (Commonwealth Edison Co., Chicago, Ill.). 18 Jan 1971. 16p. Dep. NTIS.

Revised safety limits for operation and surveillance requirements for radioactive effluents are presented. Operation personnel requirements are listed. (D.C.C.)

15274 (DOCKET-50237-131) DRESDEN NUCLEAR POWER STATION, UNIT 2. Facility License DPR-19; Proposed Change No. 8 to Appendix A. (Commonwealth Edison Co., Chicago, Ill.). 19 Jan 1971. 17p. Dep. NTIS.

Revised safety limits for fuel element cladding are presented. Trip level settings for protection instrumentation are listed. (D.C.C.)

15275 (DOCKET-50237-133) DRESDEN NUCLEAR POWER STATION, UNIT 2. Provisional Operating License No. DPR-19; Technical Specifications Change No. 8. (Division of Reactor Licensing (AEC), Washington, D. C.). 21 Jan 1971. 16p. Dep. NTIS.

Revised technical specifications concerning core thermal safety limits are presented. The revised specifications extend the core thermal safety limit to 120% of design recirculation flow and change the slope of the APRM flow biased scram and rod block curves. (D.C.C.)

15276 (DOCKET-50237-134) DRESDEN NUCLEAR POWER STATION, UNIT 2. Refueling. Proposed Modification No. 71-1 to Final Safety Analysis Report, Suppl. 1. (Commonwealth Edison Co., Chicago, Ill.). 25 Jan 1971. 12p. Dep. NTIS.

Requested additional information concerning the use of $Gd_2O_3-UO_2$ fuel rods is presented. A comparison of safety limits and operating characteristics for UO_2 fuel rods and $Gd_2O_3-UO_2$ fuel rods is included. (D.C.C.)

15277 (DOCKET-50237-135) DRESDEN NUCLEAR POWER STATION, UNITS 2 AND 3. Modifications on Control Rod Drives. (Commonwealth Edison Co., Chicago, Ill.). 18 Jan 1971. 5p. (DOCKET-50249-54). Dep. NTIS.

15278 (DOCKET-50237-136) DRESDEN NUCLEAR POWER STATION, UNIT 2. Proposed Change No. 5 to Appendix A of DPR-19, Suppl. 1. (Commonwealth Edison Co., Chicago, Ill.). 25 Jan 1971. 9p. Dep. NTIS.

Additional information concerning instrumentation for detecting a break in the main steam line and for signaling the main steam isolation valves is presented. The trip level settings for the instrumentation are discussed. (D.C.C.)

15279 (DOCKET-50237-137) DRESDEN NUCLEAR POWER STATION, UNIT 2. Proposed Modification No. 71-1 to Final Safety Analysis Report, Additional Information. (Commonwealth Edison Co., Chicago, Ill.). 28 Jan 1971. 2p. Dep. NTIS.

Additional information concerning coolant loss accident conditions while operating with $GD_2O_3-UO_2$ fuel elements is presented. (D.C.C.)

15280 (DOCKET-50237-138) DRESDEN NUCLEAR POWER STATION, UNIT 2. Provisional Operating License No. DPR-19; Technical Specifications Change No. 7. (Division of Reactor Licensing (AEC), Washington, D. C.). 1 Feb 1971. 15p. Dep. NTIS.

Revised release limits and monitoring requirements for radioactive effluents are presented. Personnel requirements for normal operation are listed. (D.C.C.)

15281 (DOCKET-50237-139) DRESDEN NUCLEAR POWER STATION, UNITS 2 AND 3. Secondary Containment Leak Rate

Test Summary. (Commonwealth Edison Co., Chicago, Ill.). 25 Jan 1971. 20p. (DOCKET-50249-55). Dep. NTIS.

15282 (DOCKET-50244-55) ROBERT EMMETT GINNA NUCLEAR POWER PLANT, UNIT NO. 1. Provisional Operating License No. DPR-18: Request for Technical Specification Change No. 4. (Rochester Gas and Electric Corp., N. Y.). 22 Jan 1971. 6p. Dep. NTIS.

Revised technical specifications for maximum allowable leak rates from the containment structure are presented. Leak rate testing schedule is included. (D.C.C.)

15283 (DOCKET-50244-56) ROBERT EMMETT GINNA NUCLEAR POWER PLANT, UNIT NO. 1. Provisional Operating License No. DPR-18: Request for Revision of Technical Specifications Change No. 5. (Rochester Gas and Electric Corp., N. Y.). 22 Jan 1971. 2p. Dep. NTIS.

Revised technical specifications concerning sampling schedules for the environmental monitoring program are presented. (D.C.C.)

15284 (DOCKET-50244-57) ROBERT EMMETT GINNA NUCLEAR POWER PLANT, UNIT NO. 1. Provisional Operating License No. DPR-18: Request for Revision of Technical Specifications Change No. 6. (Rochester Gas and Electric Corp., N. Y.). 22 Jan 1971. 2p. Dep. NTIS.

Revised technical specifications concerning testing requirements for reactor coolant samples are presented. (D.C.C.)

15285 (DOCKET-50244-58) ROBERT EMMETT GINNA NUCLEAR POWER PLANT, UNIT NO. 1. Provisional Operating License No. DPR-18: Request for Revision of Technical Specifications Change No. 7. (Rochester Gas and Electric Corp., N. Y.). 22 Jan 1971. 2p. Dep. NTIS.

Revised technical specifications concerning surveillance requirements for station batteries are described. (D.C.C.)

15286 (DOCKET-50244-59) ROBERT EMMETT GINNA NUCLEAR POWER PLANT, UNIT NO. 1. Petition Requesting Amendment of License and Extension of Expiration Date of Provisional Operating License (Includes Technical Supplement Accompanying Application to Increase Power). (Rochester Gas and Electric Corp., N. Y.). 8 Feb 1971. 395p. Dep. NTIS.

Design parameters and technical specifications for 1520 MW(t) operation are presented. Summaries of startup testing experience and operations during December 1969 to December 1970 are presented. (D.C.C.)

15287 (DOCKET-50245-52) MILLSTONE NUCLEAR POWER STATION, UNIT 1. Possibility of Inadvertent Opening of Core Spray System Valves. (Millstone Point Co., Wethersfield, Conn.). 23 Jan 1971. 1p. Dep. NTIS.

15288 (DOCKET-50249-56) DRESDEN NUCLEAR POWER STATION, UNIT 3. Facility Operating License No. DPR-25; Proposed Change No. 1 to Appendix A. (Commonwealth Edison Co., Chicago, Ill.). 10 Feb 1971. 5p. Dep. NTIS.

Revised release limits on gaseous radioactive effluents from the reactor are presented. (D.C.C.)

15289 (DOCKET-50250-38) TURKEY POINT PLANT, UNIT 3. Containment Dome Concrete Placement Program. (Florida Power and Light Co.). 25 Jan 1971. 47p. Dep. NTIS.

15290 (DOCKET-50254-26) QUAD-CITIES STATION, UNITS 1 AND 2. Notice of Availability of Environmental Report. (Division of Reactor Licensing (AEC), Washington, D. C.). 19 Jan 1971. 22p. (DOCKET-50265-22). Dep. NTIS.

15291 (DOCKET-50254-27) QUAD-CITIES STATION, UNITS 1 AND 2. Preliminary Safety Analysis Report, Amendment 16 (Includes Revisions to Final Safety Analysis Report). (Commonwealth Edison Co., Chicago, Ill. Iowa-Illinois Gas and Electric Co., Davenport, Iowa). 8 Feb 1971. 176p. (DOCKET-50265-23). Dep. NTIS.

Revised design parameters of the Quad Cities Power Reactor Units 1 and 2 are presented. Included also are additional data on the reactor requested by the Division of Reactor Licensing. (D.C.C.)

15292 (DOCKET-50261-50) H. B. ROBINSON UNIT NO. 2. Safety Injection System Performance at 2300 MWt and Reanalysis of Affected Fault Conditions. (Carolina Power and Light Co., Raleigh, N. C.). 25 Jan 1971. 18p. Dep. NTIS.

15293 (DOCKET-50263-52) MONTICELLO NUCLEAR GENERATING PLANT, UNIT 1. Provisional Operating License No. DPR-22, Amendment 1. (Division of Reactor Licensing (AEC), Washington, D. C.). 19 Jan 1971. 6p. Dep. NTIS.

15294 (DOCKET-50263-53) MONTICELLO NUCLEAR GENERATING PLANT, UNIT 1. Integrated Primary Containment Leak Rate Test, July 1970. (Northern States Power Co., Minneapolis, Minn.). 23 Dec 1970. 170p. Dep. NTIS.

15295 (DOCKET-50263-54) MONTICELLO NUCLEAR GENERATING PLANT, UNIT 1. Secondary Containment Leak Rate Test, August 1970. (Northern States Power Co., Minneapolis, Minn.). 5 Feb 1971. 5p. Dep. NTIS.

15296 (DOCKET-50266-38) POINT BEACH NUCLEAR PLANT, UNIT 1. Facility Operating License DPR-24, Amendment 1. (Division of Reactor Licensing (AEC), Washington, D. C.). 14 Jan 1971. 5p. Dep. NTIS.

Revised possession limits for radioactive by-product materials are presented. (D.C.C.)

15297 (DOCKET-50266-41) POINT BEACH NUCLEAR PLANT, UNIT 1. Environmental Monitoring Program Preoperational Report. (Eberline Instrument Co., Santa Fe, N. Mex.). 4 Feb 1971. 61p. Dep. NTIS.

For Wisconsin Electric Power Co., Milwaukee and Wisconsin Michigan Power Co., Appleton, Wis.

15298 (DOCKET-50271-36) VERMONT YANKEE NUCLEAR POWER STATION. Preliminary Safety Analysis Report, Amendment 18. (Vermont Yankee Nuclear Power Corp., Rutland). 22 Jan 1971. 97p. Dep. NTIS.

Personnel qualifications and responsibilities are listed. (D.C.C.)

15299 (DOCKET-50282-26) PRAIRIE ISLAND NUCLEAR GENERATING PLANT, UNITS 1 AND 2. Preliminary Safety Analysis Report, Amendment 7 (Includes Application for Operating License). (Northern States Power Co., Minneapolis, Minn.). 28 Jan 1971. 42p. (DOCKET-50306-26). Dep. NTIS.

Financial data on the owners of the Prairie Island Power Reactor Units 1 and 2 are presented in support of the application for operating license. The 1969 Annual Report for the Northern States Power Company is included. (D.C.C.)

15300 (DOCKET-50282-27) PRAIRIE ISLAND NUCLEAR GENERATING PLANT, UNITS 1 AND 2. Preliminary Safety Analysis Report, Amendment 7 (Includes Final Safety Analysis Report, Vol. 1). (Northern States Power Co., Minneapolis, Minn.). 28 Jan 1971. 555p. (DOCKET-50306-27). Dep. NTIS.

Information on Prairie Island Power Reactor Units 1 and 2 is presented under the following broad topics: site and environment; reactor; and reactor coolant system. (D.C.C.)

15301 (DOCKET-50282-28) PRAIRIE ISLAND NUCLEAR GENERATING PLANT, UNITS 1 AND 2. Preliminary Safety Analysis Report, Amendment 7 (Includes Final Safety Analysis Report, Vol. 2). (Northern States Power Co., Minneapolis, Minn.). 28 Jan 1971. 360p. (DOCKET-50306-28). Dep. NTIS.

Information on Prairie Island Power Reactor Units 1 and 2 is presented under the following main headings: containment; engineered safety features; and instrumentation and control. (D.C.C.)

15302 (DOCKET-50282-29) PRAIRIE ISLAND NUCLEAR GENERATING PLANT, UNITS 1 AND 2. Preliminary Safety Analysis Report, Amendment 7 (Includes Final Safety Analysis Report, Vol. 3). (Northern States Power Co., Minneapolis, Minn.). 28 Jan 1971. 359p. (DOCKET-50306-29). Dep. NTIS.

Information on Prairie Island Power Reactor Units 1 and 2 is presented under the following broad topics: auxiliary systems; steam and power conversion system; waste disposal and radiation protection; electrical systems; and conduct of operations. (D.C.C.)

15303 (DOCKET-50282-30) PRAIRIE ISLAND NUCLEAR GENERATING PLANT, UNITS 1 AND 2. Preliminary Safety Analysis Report, Amendment 7 (Includes Final Safety Analysis Report, Vol. 4). (Northern States Power Co., Minneapolis, Minn.). 28 Jan 1971. 324p. (DOCKET-50306-30). Dep. NTIS.

Information on Prairie Island Power Reactor Units 1 and 2 is presented under the following broad topics: initial tests and operations; and safety analysis. (D.C.C.)

15304 (DOCKET-50282-31) PRAIRIE ISLAND NUCLEAR GENERATING PLANT, UNITS 1 AND 2. Preliminary Safety Analysis Report, Amendment 7 (Includes Final Safety Analysis Report, Vol. 5). (Northern States Power Co., Minneapolis, Minn.). 28 Jan 1971. 384p. (DOCKET-50306-31). Dep. NTIS.

Information concerning the Prairie Island Power Reactor Units 1 and 2 is presented under the following topics: geology, hydrology, and seismology of the reactor site; design criteria for structures and systems; quality assurance program; and radiation sources. (D.C.C.)

15305 (DOCKET-50289-32) THREE MILE ISLAND NUCLEAR STATION, UNIT 1. Preliminary Safety Analysis Report, Amendment 17 (Includes Final Safety Analysis Report Modifications, Appendixes 6A and 12A). (Metropolitan Edison Co., Reading, Pa. Jersey Central Power and Light Co., Morristown, N. J. Pennsylvania Electric Co., Johnstown). 25 Jan 1971. 316p. Dep. NTIS.

Revised design parameters of the Three Mile Island Power Reactor Unit 1 are presented. Revised and additional information concerning the containment structures and systems, the reactor building fan cooler assembly, and the radiation emergency plan is included. (D.C.C.)

15306 (DOCKET-50293-34) PILGRIM NUCLEAR POWER STATION. Preliminary Safety Analysis Report, Amendment 18 (Includes Additions and Revisions to Final Safety Analysis Report). (Boston Edison Co., Mass.). 14 Jan 1971. 403p. Dep. NTIS.

Revised and additional information is presented under the following topics: containment system; instrumentation; control systems; plant layout; piping systems; protection systems; and emergency core cooling system. (D.C.C.)

15307 (DOCKET-50293-35) PILGRIM NUCLEAR POWER STATION. Preliminary Safety Analysis Report, Amendment 19 (Includes Additions and Revisions to Final Safety Analysis Report). (Boston Edison Co., Mass.). 1 Feb 1971. 67p. Dep. NTIS.

Revised design parameters of the Pilgrim Power Reactor are presented. Included also are additional data on the reactor requested by the Division of Reactor Licensing. (D.C.C.)

15308 (DOCKET-50302-16) CRYSTAL RIVER NUCLEAR GENERATING PLANT, UNIT 3. Environmental Report. (Florida Power Corp., St. Petersburg). Feb 1971. 37p. Dep. NTIS.

Information concerning chemical, radioactive, and thermal discharges from the reactor is presented. The effects of reactor operations on the environment are analyzed. (D.C.C.)

15309 (DOCKET-50305-12) KEWAUNEE NUCLEAR POWER PLANT. Environmental Report, Operating License Stage. (Wisconsin Public Service Corp., Green Bay). Jan 1971. 68p. Dep. NTIS.

Information concerning chemical, radioactive, and thermal discharges from the reactor is presented. The effects of reactor operations on the environment are analyzed. (D.C.C.)

15310 (DOCKET-50305-13) KEWAUNEE NUCLEAR POWER PLANT. Preliminary Safety Analysis Report, Amendment 7 (Includes Final Safety Analysis Report, Vol. 1). (Wisconsin Public Service Corp., Green Bay). 27 Jan 1971. 379p. Dep. NTIS.

Information on Kewaunee Power Reactor is presented under the following broad topics: site; reactor; and reactor coolant system. (D.C.C.)

15311 (DOCKET-50305-14) KEWAUNEE NUCLEAR POWER PLANT. Preliminary Safety Analysis Report, Amendment 7 (Includes Final Safety Analysis Report, Vol. 2). (Wisconsin Public Service Corp., Green Bay). 27 Jan 1971. 300p. Dep. NTIS.

Information on Kewaunee Power Reactor is presented under the following broad topics: containment systems; engineered safeguards; instrumentation and control; and electrical systems. (D.C.C.)

15312 (DOCKET-50305-15) KEWAUNEE NUCLEAR POWER PLANT. Preliminary Safety Analysis Report, Amendment 7 (Includes Final Safety Analysis Report, Vol. 3). (Wisconsin Public Service Corp., Green Bay). 27 Jan 1971. 272p. Dep. NTIS.

Information on Kewaunee Power Reactor is presented under the following main topics: auxiliary and emergency systems; steam and power conversion systems; waste disposal and radiation protection system; conduct of operations; and initial tests and operations. (D.C.C.)

15313 (DOCKET-50305-16) KEWAUNEE NUCLEAR POWER PLANT. Preliminary Safety Analysis Report, Amendment 7 (Includes Final Safety Analysis Report, Vol. 4). (Wisconsin Public Service Corp., Green Bay). 27 Jan 1971. 256p. Dep. NTIS.

Safety analysis of the Kewaunee Power Reactor is presented. Stand-by safety features and loss of coolant accident conditions are analyzed. (D.C.C.)

15314 (DOCKET-50305-17) KEWAUNEE NUCLEAR POWER PLANT. Preliminary Safety Analysis Report, Amendment 7 (Includes Final Safety Analysis Report, Vol. 5). (Wisconsin Public Service Corp., Green Bay). 27 Jan 1971. 386p. Dep. NTIS.

Information on Kewaunee Power Reactor is presented under the following headings: site geology; design codes for structures and components; quality assurance program; radioactive source base; and foundations for buildings and structures. (D.C.C.)

15315 (DOCKET-50315-26) DONALD C. COOK NUCLEAR PLANT, UNITS 1 AND 2. Preliminary Safety Analysis Report, Amendment 12 (Includes Application for Operating Licenses). (Indiana and Michigan Electric Co., Fort Wayne, Ind.). 1 Feb 1971. 16p. (DOCKET-50316-26). Dep. NTIS.

Application for operating license is presented. Financial data on the Indiana and Michigan Electric Company are included. (D.C.C.)

15316 (DOCKET-50315-27) DONALD C. COOK NUCLEAR PLANT, UNITS 1 AND 2. Environmental Report. (Indiana and Michigan Electric Co., Fort Wayne, Ind.). 1 Feb 1971. 132p. (DOCKET-50316-27). Dep. NTIS.

Information concerning chemical, radioactive, and thermal discharges from the reactor is presented. The effects of reactor operations on the environment are analyzed. (D.C.C.)

15317 (DOCKET-50315-28) DONALD C. COOK NUCLEAR PLANT, UNITS 1 AND 2. Preliminary Safety Analysis Report, Amendment 12 (Includes Final Safety Analysis Report, Vol. 1). (Indiana and Michigan Electric Co., Fort Wayne, Ind.). 1 Feb 1971. 400p. (DOCKET-50316-28). Dep. NTIS.

Information on Donald C. Cook Power Reactor Units 1 and 2 is presented under the following main headings: introduction and summary; site and environment; and reactor. (D.C.C.)

15318 (DOCKET-50315-29) DONALD C. COOK NUCLEAR PLANT, UNITS 1 AND 2. Preliminary Safety Analysis Report, Amendment 12 (Includes Final Safety Analysis Report, Vol. 2). (Indiana and Michigan Electric Co., Fort Wayne, Ind.). 1 Feb 1971. 335p. (DOCKET-50316-29). Dep. NTIS.

Information on Donald C. Cook Power Reactor Units 1 and 2 is presented under the following broad topics: reactor coolant system; containment; and engineered safety features. (D.C.C.)

15319 (DOCKET-50315-30) DONALD C. COOK NUCLEAR PLANT, UNITS 1 AND 2. Preliminary Safety Analysis Report, Amendment 12 (Includes Final Safety Analysis Report, Vol. 3). (Indiana and Michigan Electric Co., Fort Wayne, Ind.). 1 Feb 1971. 300p. (DOCKET-50316-30). Dep. NTIS.

Information on Donald C. Cook Power Reactor Units 1 and 2 is presented under the following broad topics: instrumentation and control; electrical systems; and auxiliary systems. (D.C.C.)

15320 (DOCKET-50315-31) DONALD C. COOK NUCLEAR PLANT, UNITS 1 AND 2. Preliminary Safety Analysis Report, Amendment 12 (Includes Final Safety Analysis Report, Vol. 4). (Indiana and Michigan Electric Co., Fort Wayne, Ind.). 1 Feb 1971. 178p. (DOCKET-50316-31). Dep. NTIS.

Information on Donald C. Cook Power Reactor Units 1 and 2 is presented under the following broad topics: steam and power conversion; waste disposal and radiation protection; conduct of operations; and initial tests and operations. (D.C.C.)

15321 (DOCKET-50315-32) DONALD C. COOK NUCLEAR PLANT, UNITS 1 AND 2. Preliminary Safety Analysis Report, Amendment 12 (Includes Final Safety Analysis Report, Vol. 5). (Indiana and Michigan Electric Co., Fort Wayne, Ind.). 1 Feb 1971. 493p. (DOCKET-50316-32). Dep. NTIS.

Information on Donald C. Cools Power Reactor Units 1 and 2 is presented under the following headings: safety analysis; design criteria for structures and equipment; auxiliary and waste disposal systems; and pressure vessel operation limits. (D.C.C.)

15322 (DOCKET-50315-33) DONALD C. COOK NUCLEAR PLANT, UNITS 1 AND 2. Preliminary Safety Analysis Report, Amendment 12 (Includes Final Safety Analysis Report, Vol. 6). (Indiana and Michigan Electric Co., Fort Wayne, Ind.). 1 Feb 1971. 356p. (DOCKET-50316-33). Dep. NTIS.

Information on Donald C. Cook Power Reactor Units 1 and 2 is presented under the following headings: geological data for site; dynamic analysis of containment structure for seismic loading; and general design criteria. (D.C.C.)

15323 (DOCKET-50341-25) ENRICO FERMI ATOMIC POWER PLANT, UNIT 2. Preliminary Safety Analysis Report, Amendment 15. (Detroit Edison Co., Mich.). 1 Feb 1971. 63p. Dep. NTIS.

Additional data on the reactor requested by the Division of Reactor Licensing are presented. Information on radwaste and radioactive effluents, environmental monitoring equipment, and auxiliary power supply systems is included. (D.C.C.)

15324 (DOCKET-50341-26) ENRICO FERMI ATOMIC POWER PLANT, UNIT 2. Preliminary Safety Analysis Report, Amendment 16. (Detroit Edison Co., Mich.). 3 Feb 1971. 37p. Dep. NTIS.

Additional data on the reactor requested by the Division of Reactor Licensing are presented. Information is presented on protection from turbine and coolant pump missiles, geological data for emergency cooling water reservoir, and tornado protection for spent fuel storage pool. (D.C.C.)

15325 (DOCKET-50344-19) TROJAN NUCLEAR PLANT. Construction Permit No. CPPR-79. (Division of Reactor Licensing (AEC), Washington, D. C.). 8 Feb 1971. 4p. Dep. NTIS.

15326 (DOCKET-50354-10) NEWBOLD ISLAND NUCLEAR GENERATING STATION, UNITS 1 AND 2. Preliminary Safety Analysis Report, Amendment 4. (Public Service Electric and Gas Co., Newark, N. J.). 28 Jan 1971. 307p. (DOCKET-50355-10). Dep. NTIS.

Revised design parameters of the Newbold Island Power Reactor Units 1 and 2 are presented. Included also are additional data on the reactor requested by the Division of Reactor Licensing. (D.C.C.)

15327 (DOCKET-50358-11) WM. H. ZIMMER NUCLEAR POWER STATION, UNIT 1. Environmental Report. (Cincinnati Gas and Electric Co., Ohio. Columbus and Southern Ohio Electric Co., Columbus, Ohio. Dayton Power and Light Co., Ohio). 15 Jan 1971. 542p. Dep. NTIS.

Information concerning chemical, radioactive, and thermal discharges from the reactor is presented. The effects of reactor operations on the environment are analyzed. (D.C.C.)

15328 (DOCKET-50358-12) WM. H. ZIMMER NUCLEAR POWER STATION, UNIT 1. Preliminary Safety Analysis Report, Amendment 5. (Cincinnati Gas and Electric Co., Ohio. Columbus and Southern Ohio Electric Co., Columbus, Ohio. Dayton Power and Light Co., Ohio). 12 Feb 1971. 307p. Dep. NTIS.

Revised and additional information concerning the single unit stackless design concept is presented. (D.C.C.)

15329 (DOCKET-50361-14) SAN ONOFRE NUCLEAR GENERATING STATION, UNITS 2 AND 3. Preliminary Safety Analysis Report, Amendment 6. (Southern California Edison Co., Los Angeles. San Diego Gas and Electric Co., Calif.). 29 Jan 1971. 185p. (DOCKET-50362-13). Dep. NTIS.

Requested seismological data for the reactor site and surrounding area are presented. Additional information is presented on core support structures and auxiliary and emergency systems. (D.C.C.)

15330 (DOCKET-50363-11) FORKED RIVER NUCLEAR GENERATING STATION, UNIT 1. Preliminary Safety Analysis Report, Amendment 5. (Jersey Central Power and Light Co., Morristown, N. J.). 29 Jan 1971. 60p. Dep. NTIS.

Revised design parameters of the Forked River Power Reactor Unit 1 are presented. Included also are additional data on the reactor requested by the Division of Reactor Licensing. (D.C.C.)

15331 (DOCKET-50367-9) BAILLY GENERATING STATION, NUCLEAR I. Preliminary Safety Analysis Report, Amendment 2. (Northern Indiana Public Service Co., Hammond). 25 Jan 1971. 621p. Dep. NTIS.

Revised design parameters of the Bailly Power Reactor Unit 1 are presented. Additional information related to the use of cooling towers is included. (D.C.C.)

15332 (DOCKET-50368-7) ARKANSAS NUCLEAR ONE, UNIT 2. Preliminary Safety Analysis Report, Suppl. 2. (Arkansas Power and Light Co., Little Rock). 3 Feb 1971. 69p. Dep. NTIS.

Revised meteorological data for the reactor site are presented. (D.C.C.)

15333 (DOCKET-50376-8) AGUIRRE NUCLEAR PLANT, UNIT NO. 1. Notice of Receipt of Application for Construction Permit and Facility License. (Division of Reactor Licensing (AEC), Washington, D. C.). 21 Jan 1971. 3p. Dep. NTIS.

15334 (DOCKET-50382-6) WATERFORD STEAM ELECTRIC STATION, UNITS 3 AND 4. Applicant's Environmental Report, Construction Permit Stage. (Louisiana Power and Light Co., New Orleans). 15 Jan 1971. 96p. (DOCKET-50383-6). Dep. NTIS.

Information concerning chemical, radioactive, and thermal discharges from the reactor is presented. The effects of reactor operations on the environment are analyzed. (D.C.C.)

15335 (NF-67-8) GUIDE FOR ENVIRONMENTAL SURVEILLANCE AROUND NUCLEAR FACILITIES. (National Center for Radiological Health, Rockville, Md.). Dec 1967. 21p.

The recommendations presented are for the purpose of providing guidance to health agencies in establishing environmental surveillance programs in the vicinity of nuclear power plants. The technology involved in the release of radioactivity from these plants and the dispersion through the environment are being investigated by the National Center for Radiological Health. The purpose of these studies is to optimize the requirements for environmental surveillance. Until these studies have been completed and the results evaluated the recommendations presented are considered adequate from a public health standpoint. 12 references. (auth)

15336 (NP-18636) JERVIS BAY NUCLEAR POWER STATION PROJECT INVESTIGATIONS AT SITE J.S1-SCOTTISH ROCKS. MacGregor, J. P.; Lamb, A. N.; McKinnon, C. K. (Electricity Commission of New South Wales (Australia). Civil Investigations Branch). Jun 1970. 159p. Dep. NTIS (U. S. Sales Only).

Results are presented of foundation and hydrographic investigations carried out in 1969 within an area designated Site J.S1 close to Scottish Rocks on the southern side of Jervis Bay to determine the suitability of this area for siting a 500 MW nuclear power station. Work on this site was curtailed when an alternative Site J.S2 was chosen at Murray's Beach. Sufficient drilling and geophysical work was completed at the Scottish Rocks site to permit the preparation of a contour plan of rock surface levels and selection of the most favorable area for siting the station, having regard for foundation conditions. Sufficient hydrographic work was carried out to show that a satisfactory cooling water system could be developed economically. A schematic station layout, based on results obtained, is depicted. (auth) (Australia)

15337 (STI/PUB-272) GUIDELINES FOR THE LAYOUT AND CONTENTS OF SAFETY REPORTS FOR STATIONARY NUCLEAR POWER PLANTS. Safety Series No. 34. Report Based on a Panel Held in Vienna, 30 June-4 July 1969. (International Atomic Energy Agency, Vienna (Austria)). Oct 1970. 56p. (CONF-690649). IAEA $2.00.

Guidelines for the organization and contents of the safety reports which support the request for authorization to construct and operate a nuclear power plant incorporating one or more reactors are presented. Safety Reports represent the principal communication between the applicant and the Regulatory Body, as outlined in the IAEA Code of Practice for the Safe Operation of Nuclear Power Plants. These Safety Reports will be a valuable document for the applicant. They should contain, therefore, precise information on the plant and its operating conditions. The writing of Safety Reports should be considered an opportunity to enhance the safety of the plant and its operating conditions. Their main purpose is to provide information to permit the assessment of the nuclear safety implications which may arise from the establishment of the plant at the chosen site with due consideration to the health and safety of the general public and the operating personnel. Safety Reports should include information such as design bases, site and plant characteristics, limits and conditions, conduct of operation and safety analyses, in such a way that the Regulatory Body may be able to evaluate the safety of the plant. (auth)

Power Reactor Development

Refer also to abstract 15406.

15338 (AAEC/LIB/Bib-258) JAPANESE A.T.R. REACTOR. ADVANCED THERMAL REACTOR. A Bibliography. Newland, E. A. (comp.) (Australian Atomic Energy Commission Research Establishment, Lucas Heights). Nov 1970. 3p. Dep. NTIS (U. S. Sales Only).

Sixteen references are listed, covering the period April 1966 to February 1970. The references are listed chronologically by year, and alphabetically by author within each year. References are also made to an abstract for each article. (Australia)

15339 (ANL-7765) REACTOR DEVELOPMENT PROGRAM PROGRESS REPORT, DECEMBER 1970. (Argonne National Lab., Ill.). 19 Jan 1971. Contract W-31-109-eng-38. 98p. Dep. NTIS.

Highlights of project activities for December 1970 are summarized. LMFBR physics development and component development are reviewed. Operations and analysis of ZPR-3, ZPR-6, ZPR-9, and ZPPR are described. The EBR-2 research and development projects and operations are summarized. Reactor fuels and materials development, engineering development, fuel cycle chemistry, and LMFBR safety studies are reported. (D.C.C.)

15340 (NEIC-RR-41) FAST BREEDING REACTORS. Bibliography, 1966-1969. Kowalski, A. (comp.) (Nuclear Energy Information Center, Warsaw (Poland)). 1970. 285p. Dep. NTIS (U. S. Sales Only).

The bibliography on Fast Breeding Reactors is the continuation of the compilation under the title Fast Reactors, published by the International Atomic Energy Agency in the Bibliographical Series No. 22 in 1966. This bibliography includes 2976 references registered in the Nuclear Science Abstracts vol. 20-23 in the period from 1966 to 1969. The Subject Index, Reactors Index, Author's Institution Index, Report Index and Patent Index are given. (auth)

15341 (SZS-20/70) HEAT GENERATION BY ABSORPTION OF IONIZING RADIATION IN NUCLEAR POWER PLANTS. Albrecht, L.; Schimmel, W. (Staatliche Zentrale fuer Strahlenschutz, Berlin (East Germany)). Sep 1970. 20p. (In German). Dep. NTIS (U. S. Sales Only).

The heat generation by absorption of ionizing radiation is particularly high where high energy flux densities occur. In reactors this is the case in and near the core. The individual contributions made to the heat generation by fission products, beta and gamma radiation as well as neutrons are discussed. The calculation methods are briefly outlined. (auth)

15342 ORGEL PROJECT 1959-1969. Leny, J. C. (European Atomic Energy Community, Ispra, Italy). Energ. Nucl. (Paris); 12: 406-12(Sep-Oct 1970). (In French).

The Commission of the European Communities decided in June 1969 not to build a large ORGEL prototype and to terminate the ORGEL project. The origin of ORGEL is briefly described and the principal developments discussed. The cost and a survey of the progress made within the frame of both the Community and its international context are recalled. (auth) (France)

Kinetics and Dynamics

Refer also to abstracts 14987, 14988, 15102, and 15396.

15343 (WHAN-IR-48) COMPARISON OF THE CODES RSYN AND 3DB. McCormick, N. J.; Hardie, R. W. (WADCO Corp., Richland, Wash.). Dec 1970. Contract AT(45-1)-2170. 28p. Dep. NTIS.

The Codes RSYN and 3DB have both been recently developed for the computation of fluxes and associated "bulk parameters" (such as k_{eff}) of fast reactors using three-dimensional diffusion theory. The R(eactor) SYN(thesis) code is based upon a spatial differencing of the matrix equations arising from a synthesis in one dimension of time-independent results calculated from a two-dimensional diffusion theory code. On the other hand, static calculations using the 3 D(imensional) B(urnup) code are based upon standard source iteration techniques, which are initiated with an initial fission source distribution and which utilize group rebalancing and successive line over-relaxation to accelerate convergence. The features and present operational status of RSYN are described. The utility of the codes for a series of (model) problems is discussed. 9 references. (auth)

15344 ENERGETICAL ANALYSIS OF A BHWR NUCLEAR POWER PLANT. Ninic, Neven; Studovic, Milovan (Boris Kidric Inst. of Nuclear Science, Belgrade). Nukl. Energ.; 4: No. 6, 1-7(1967). (In Serbo-Croatian).

A thermodynamic analysis of all processes taking place in a 500 MW(e) nuclear power plant has been made by following the energy flow in all components of the plant. The analysis includes the quantitative determination of the magnitudes of the availability losses (or energy losses) and their source during the whole process from supply of the nuclear fuel to output of the electrical work from the power plant. The magnitudes and the sources of the losses in the plant determine "the degree of validity" (the ratio of the produced work to the maximum possible amount of the work) both for the individual parts of the plant and for the plant as a whole. The degree of validity gives a quantitative figure how much the corresponding part of the plant reduces the theoretically possible power of the plant because of the conceptual or construction imperfection. (11 references) (auth)

15345 IMPLICATIONS OF NUCLEAR DATA UNCERTAINTIES TO REACTOR DESIGN. Greebler, P.; Hutchins, B. A.; Cowan, C. L. (General Electric Co., Sunnyvale, Calif.). pp 17-33 of Nuclear Data for Reactors. Vol. I. Vienna; International Atomic Energy Agency (1970).

From 2nd International Conference on Nuclear Data for Reactors, Helsinki, Finland. See STI/PUB-259(Vol.1); CONF-700605-(Vol.1).

Uncertainties in nuclear data require significant allowances to be made in the design and the operating conditions of reactor cores and of shielded-reactor-plant and fuel-processing systems. These allowances result in direct cost increases due to overdesign of components and equipment and reduced core and fuel operating performance. Compromising the allowances for data uncertainties has indirect cost implications due to increased risks of failure to meet plant and fuel performance objectives, with warrantees involved in some cases, and to satisfy licensed safety requirements. Fast breeders are the most sensitive power reactors to the uncertainties in nuclear data over the neutron energy range of interest for fission reactors, and the implications of the data uncertainties to design and operation of fast breeder reactors and fuel-processing systems are examined. The current status of uncertainty in predicted physics parameters due to data uncertainties is reviewed and compared with the situation in 1966 and that projected for within the next two years due to anticipated data improvements. Implications of the uncertainties in the predicted physics parameters to design and operation are discussed for both a near-term prototype or demonstration breeder plant (~300 MW(e)) and a longer-term large (~1000 MW(e)) plant. Significant improvements in the nuclear data have been made, the most important of these to fast power reactors being the ^{239}Pu alpha below 15 keV. The most important remaining specific data uncertainties are illustrated by their individual contributions to the computational uncertainty of selected physics parameters, and recommended priorities and accuracy requirements for improved data are presented. 55 references. (auth)

15346 RELATIONSHIP OF MICROSCOPIC AND INTEGRAL DATA. Campbell, C. G.; Rowlands, J. L. (Atomic Energy Establishment, Winfrith, Eng.). pp 391-425 of Nuclear Data for Reactors. Vol. II. Vienna; International Atomic Energy Agency (1970).

From 2nd International Conference on Nuclear Data for Reactors, Helsinki, Finland. See STI/PUB-259(Vol.2); CONF-700605-(Vol.2).

The ways in which UK reactor physicists have acquired group-averaged macroscopic cross-sections for use in reactor design calculations are reviewed and the role of integral experiments in this work is identified. The adequacy of these data for reactor design calculations is reviewed with particular reference to fast reactors, and the proposed use of both integral and evaluated differential data in meeting current needs is discussed. The program of work required to meet the needs of fast reactors bearing in mind the time scale for acquiring adequate information on cross-sections is reviewed. 12 references. (auth)

15347 COMPLEMENTARY ROLES OF INTEGRAL EXPERIMENTS AND DIFFERENTIAL MEASUREMENTS FOR A FAST-NEUTRON REACTOR PROJECT: THE CASE OF PLUTONIUM ISOTOPES. Barre, J. Y.; Bouchard, J. (Centre d'Etudes Nucleaires, Cadarache, France). pp 465-85 of Nuclear Data for Reactors. Vol. II. Vienna; International Atomic Energy Agency (1970). (In French).

From 2nd International Conference on Nuclear Data for Reactors, Helsinki, Finland. See STI/PUB-259(Vol.2); CONF-700605-(Vol.2).

Reactor physicists have two experimental sources at their disposal: differential measurements of the microscopic constants and results of integral experiments. A general analysis of the complementary role of these two types of measurement for the case of fast reactors is presented. The examples refer, above all, to plutonium isotopes. The essential conclusion is that the precision demanded by a project for the fundamental parameters (k_{eff}, breeding ratio) can be achieved by integral experiments and that, to obtain this result, it is not necessary to have very-high-precision differential measurements. 18 references. (auth)

15348 INTEGRAL MEASUREMENTS OF α FOR ^{239}Pu AND ^{235}U. Bouchard, J.; Barre, J. Y.; Darrouzet, M.; (and others). (Centre d'Etudes Nucleaires, Fontenay-aux-Roses, France). pp 487-511 of Nuclear Data for Reactors. Vol. II. Vienna; International Atomic Energy Agency (1970). (In French).

From 2nd International Conference on Nuclear Data for Reactors, Helsinki, Finland. See STI/PUB-259(Vol.2); CONF-700605-(Vol.2).

Two series of integral experiments on the α of ^{239}Pu were carried out in the medium-energy range. (a) Reactivity and reaction-rate measurements. These measurements were carried out in the coupled thermal-fast ERMINE assembly. An original method based on the use of a local chamber with a ^{238}U foil was developed to separate the capture and fission terms. This method, which is less sensitive to imprecision of $\bar{\nu}$ and to importance ratios than the boron calibration method used previously, can be used to obtain α for the true dilution of the sample without need for extrapolation to infinite dilution. (b) Irradiation. Two irradiation experiments were carried out, one in OSIRIS, a 70-MW, swimming-pool reactor, in a boron carbide capsule enriched such that the spectrum at the center resulted in a high capture rate in the energy range between 1 and 20 keV, and the other one in RAPSODIE, a fast reactor prototype, whose neutron spectrum corresponds to higher energies. Various samples of ^{235}U, ^{239}Pu and ^{238}U were irradiated during the two runs, the integrated fluxes for the one having been about 5×10^{21} n/cm² and about 1.5×10^{22} n/cm² for the other. The classical determinations of the capture rates by measuring the variation of the isotopic contents were supplemented by spectral-index measurements which allowed one to do without knowledge of the yields in determining the fission rates. In the case of the OSIRIS capsules, for which several difficulties in the calculation of the spectrum could be expected, the experimental checks were performed in an identical capsule placed at the center of the ISIS reactor, a faithful low-power model of OSIRIS. The results of this set of experiments are compared with the calculations made by the multigroup cross-section set of CADARACHE. For ^{239}Pu the experimental values of α are seen to be, in general, slightly lower than the calculated ones. 15 references. (auth)

15349 IMPLICATIONS OF FUNDAMENTAL INTEGRAL MEASUREMENTS ON HIGH-ENERGY NUCLEAR DATA FOR REACTOR PHYSICS. Fabry, A.; De Coster, M.; Minsart, G.; Schepers, J. C.; Vandeplas, P. (SCK-CEN, Mol, Belg.). pp 535-69 of Nuclear Data for Reactors. Vol. II. Vienna; International Atomic Energy Agency (1970).

From 2nd International Conference on Nuclear Data for Reactors, Helsinki, Finland. See STI/PUB-259(Vol.2); CONF-700605-(Vol.2).

Among the recent specific results obtained in the course of the SCK-CEN program of clean integral experiments, much attention is paid to new measurements of absolute average fission-spectrum cross-sections. An original procedure is described, which allows minimization and control of the sources of systematic errors. It is shown that this is probably the most precise and powerful method ever employed for this type of experiment, especially when reactions without threshold are investigated. A recommended set of data is tentatively presented and discussed for some high-energy nuclear reactions and for the ^{235}U-thermal-fission-neutron spectrum. This set is based on the requirement to fit simultaneously, whenever possible, within their respective confidence intervals, the most accurate differential measurements as well as the integral experiments performed in Belgian and other laboratories. The energy range extends from about 100 keV up to 10 MeV and the reactions include fission in ^{235}U, ^{238}U, ^{239}Pu, ^{232}Th, capture in a few important nuclides, inelastic scattering and charged-particle production in materials commonly used for reactor dosimetry. The long-standing reactor-theoretic underestimation of the ^{238}U-fission rates relative to ^{235}U- is also discussed. 131 references. (auth)

15350 INTEGRAL MEASUREMENT OF FISSION-PRODUCT REACTIVITY WORTHS IN SOME FAST REACTOR SPECTRA. Andersson, T. L. (Aktiebolaget Atomenergi, Studsvik, Swed.). pp 603-16 of Nuclear Data for Reactors. Vol. II. Vienna; International Atomic Energy Agency (1970).

From 2nd International Conference on Nuclear Data for Reactors, Helsinki, Finland. See STI/PUB-259(Vol.2); CONF-700605-(Vol.2).

The reactivity worth per atom for a number of fission-product isotopes relative to that of ^{235}U was measured in three various fast-reactor spectra. The following isotopes were studied: ^{95}Mo, ^{97}Mo, ^{99}Tc, ^{101}Ru, ^{102}Ru, ^{104}Ru, ^{103}Rh, ^{133}Cs, ^{147}Pm and ^{149}Sm. A fission product mock-up sample was also included in the measurements. The reactivity worths were measured by the pile-oscillator technique. The fundamental mode amplitude of the perturbation signal was obtained through Fourier analysis. The experimental results are compared with calculated values obtained from perturbation calculations using published cross-sections for the sample materials. From a comparison between the measured and the calculated reactivity worths it is concluded that only the ^{95}Mo, ^{104}Ru, and ^{149}Sm worths are well predicted in all three systems. For the other samples, the calculated values are generally too high. 19 references. (auth)

15351 CORE-OPTIMIZATION OF SODIUM COOLED FAST BREEDER REACTORS WITH METHODS OF NONLINEAR PROGRAMMING. Heusener, G. (Kernforschungszentrum, Karlsruhe, Ger.). Nucl. Eng. Design; 14: 3-11(Oct 1970).

Methods of solution of nonlinear optimization problems are described. In order to use one of these methods to optimize a fast breeder reactor, approximations in calculating the reactor for reasons of computer time are necessary. One of these approaches, which is used to estimate the results of the nuclear calculations, is discussed in more detail. Results of the optimization of a core of a 1000 MW(e) sodium cooled fast breeder reactor with oxide fuel are given. Two objective functions are considered and the different design characteristics are discussed. 14 references. (auth)

15352 EFFECT OF COLLAPSING CROSS-SECTION DATA ON FAST BREEDER PHYSICS PARAMETERS. Alcouffe, Raymond E.; Hirons, Thomas J.; O'Dell, R. Douglas (Los Alamos Scientific Lab., N. Mex.). Nucl. Sci. Eng.; 43: 173-85(Feb 1971).

A technique is demonstrated which is an alternative to the necessity of using many groups in order to perform an accurate fuel-cycle analysis on a fast breeder. This is accomplished by the consistent use of a space-dependent spectrum computed at the beginning-of-life of the system. The information thus generated is useful throughout the life of the system and allows an accurate and efficient analysis with very few energy groups. This technique is developed concisely for a finite differenced system of equations by the method of weighted residuals. (auth)

Control Systems

15353 (WAPD-TM-968) SPACE-TIME METHODS FOR MOVABLE FUEL PROBLEMS (LWBR DEVELOPMENT PROGRAM). Yasinsky, J. B.; Foulke, L. R. (Bettis Atomic Power Lab., Pittsburgh, Pa.). Dec 1970. Contract AT(11-1)-Gen-14. 21p. (CONF-700304-5). Dep. NTIS.

From Symposium on Dynamics of Nuclear Systems, Tucson, Ariz.

The need for a three-dimensional space-time computational capability for the design and analysis of a movable fuel controlled power reactor is examined, and the reasons leading to the selection of the space-time synthesis model over other existing space-time models is discussed. The mechanics for treating movable fuel and delayed neutron precursors within this model is outlined, and improvements that have been made in the associated spatial differencing model that result in improved accuracy are discussed. 9 references. (auth)

15354 (WHAN-IR-42) REACTOR ENGINEERING DEVELOPMENT PROGRESS REPORT, JUNE, JULY, AND AUGUST 1970: REACTOR ENVIRONMENT EFFECTS ON SIGNAL CABLES. Stringer, J. L. (WADCO Corp., Richland, Wash.). Dec 1970. Contract AT(45-1)-2170. 33p. Dep. NTIS.

Measurements of the radiation-induced noise in the Washington State University pulsed TRIGA Reactor ($\approx 2 \times 10^{16}$ nv and 10^{11} R hr^{-1} at the peak) showed the noise to be proportional to the induced insulator conductivity, but not to the induced direct current. The independence of the noise magnitude of cable dimensions noted in the ^{60}Co experiments (3.85×10^{7} R hr^{-1}) can be extended to include a combined neutron and gamma flux. The absence of the induced direct-current proportionality supports a model based on the amplitude and time distributions of the instantaneous positive and negative currents. Until this model is given a theoretical basis, the factor 2ϵ used to relate the noise magnitude to the sum of the induced direct-current components should be regarded as approximate. The ac and dc shunt resistance values for Cable 5E were measured with dc bias voltages of 10, 300 and 600 V dc applied over a temperature range of 1100 to 1500°F. Insulator polarization caused variations in the dc resistance of almost a factor of ten at 1100°F, reducing to about a factor of four at 1500°F. The general slope of the data suggests an interaction of the dc and ac resistance values above 1500°F. 5 references. (auth)

Cooling Systems

15355 (SAN-781-100) DEVELOPMENT AND VERIFICATION OF A DESIGN GUIDE FOR LMFBR SODIUM PIPING. (Braun (C. F.) and Co., Alhambra, Calif.). 23 Jul 1969. Contract AT-(04-3)-781. 75p. Dep. NTIS.

The overall objectives of the LMFBR Piping Design Guide are described. Steps considered necessary for the development and verification of the design guide are discussed. The detailed work plan is presented, together with the tentative schedule and organization chart. A review procedure, established by USAEC and LMEC, is described, and the manner in which identified research and development requirements will be handled is included. 3 references. (auth)

15356 (SAN-781-220) REVIEW OF FABRICATION AND INSTALLATION REQUIREMENTS FOR LMFBR PIPING. (Braun (C. F.) and Co., Alhambra, Calif.). 6 Jun 1969. Contract AT-(04-3)-781. 43p. Dep. NTIS.

Basic requirements for the fabrication and installation of LMFBR piping systems are described. Topics discussed include: welding; postweld heat treatment; examination; leak testing; repairs; marking; cleaning; packaging; handling and storage; certification; and dimensional and geometrical requirements. 48 references. (D.C.C.)

15357 (SAN–781-228) PIPING MATERIALS FOR LMFBR PLANTS. Technical Report 228 (Revision 1). (United Nuclear Corp., Elmsford, N. Y. Research and Engineering Center. Braun (C. F.) and Co., Alhambra, Calif.). 22 May 1970. Contract AT(04-3)-781. 244p. Dep. NTIS.

The effects of LMFBR environmental conditions on Type 304 and Type 316 stainless steels and Cr–Mo alloy are analyzed. The piping materials are studied for corrosion and erosion and changes in mechanical properties. 190 references. (D.C.C.)

15358 (SAN–781-234) STUDY OF MODEL TEST METHODS AS RELATED TO LMFBR PIPING SYSTEMS. (TRW Systems Group, Redondo Beach, Calif. Braun (C. F.) and Co., Alhambra, Calif.). 6 May 1970. Contract AT(04-3)-781. 97p. Dep. NTIS.

Model testing methods for LMFBR piping systems are described. Nine methods discussed include: photoelasticity; moire grid methods; X-ray diffraction; strain gages; brittle coatings; acoustoelasticity; extensometers; holographic interferometry; and scale models. 44 references. (D.C.C.)

15359 (SAN–781-243) REVEW OF IN-SERVICE SURVEILLANCE METHODS APPLICABLE TO LIQUID SODIUM PIPING. (Braun (C. F.) and Co., Alhambra, Calif.). 7 Jan 1970. Contract AT(04-3)-781. 56p. Dep. NTIS.

In-service surveillance requirements for LMFBR piping systems are described. Information on various types of surveillance methods is compared. Topics discussed include: sodium leak detection; pipe movement; alignment and vibration; material inspection; strain measurement and crack detection; and logging of records. Advantages and disadvantages of the various surveillance methods are outlined. 46 references. (auth)

15360 (SAN–781-500) PHILOSOPHY AND CRITERIA OF THE DESIGN GUIDE FOR LMFBR SODIUM PIPING. (Braun (C. F.) and Co., Alhambra, Calif.). 2 Oct 1970. Contract AT(04-3)-781. 44p. Dep. NTIS.

The philosophy and criteria adopted for the first issue of the Design Guide for LMFBR Sodium Piping are described. Topics discussed include: LMFBR piping design; stress categories; primary stresses; secondary stresses; thermal stress ratchet; peak stresses and fatigue; and inelastic analysis. 23 references. (D.C.C.)

15361 (SAN–781-518) SUMMARY OF RESEARCH AND DEVELOPMENT RECOMMENDATIONS FOR LMFBR PIPING. (Braun (C. F.) and Co., Alhambra, Calif.). 1 May 1970. Contract AT(04-3)-781. 42p. Dep. NTIS.

All those research and development programs which are considered prerequisite to the establishment of design procedures which provide adequate assurance of the safe design and operation of LMFBR piping are summarized. It has been recognized, however, that the proposed programs do not all deserve the same urgent priority, since conservative assumptions can in some cases be substituted for the needed information until the latter is available. Accordingly an attempt has been made to categorize the recommended R & D programs as to their relative priorities. These categories are as follows: first priority short-term investigations; first priority long-term investigations; second priority investigations; and investigations of peripheral interest. Each program is described in its appropriate category, with a brief background discussion and a proposed course of action. 33 references. (auth)

15362 (UNC–5231) STUDY OF DYNAMIC ANALYSIS METHODS AS RELATED TO LMFBR PIPING SYSTEMS. (United Nuclear Corp., Elmsford, N. Y. Research and Engineering Center. Braun (C. F.) and Co., Alhambra, Calif.). 14 May 1969. Contract AT(04-3)-781. 131p. (SAN–781-237; CFB–4122-237). Dep. NTIS.

The existing methods for computation of the deflection responses of LMFBR sodium piping systems under the influence of transient and steady-state time-dependent forcing functions such as arising from earthquakes, hydraulic shocks (sodium hammer), flow-induced vibration, and mechanical vibration of connected equipment are reviewed. The basis for selecting and developing dynamic analysis procedures for incorporation into the LMFBR Piping Design Guide is presented. 77 references. (auth)

15363 VELOCITY AND TEMPERATURE DISTRIBUTION IN TURBULENT FLOW IN SODIUM COOLED FUEL ELEMENTS WITH ECCENTRIC GEOMETRY. Hofmann, F. (Kernforschungszentrum, Karlsruhe, Ger.). Nucl. Eng. Design; 14: 43-50(Oct 1970).

A theoretical analysis of the velocity and temperature distribution in symmetrical and asymmetrical triangular rod clusters is presented. The analysis is applied to sodium as coolant with fully developed turbulent flow. Coolant mixing is taken into account by correlations for the diffusivities of momentum and energy. The thermal heat flux at the surface of the fuel pin is assumed to be uniform in circumferential direction and an arbitrary function in axial direction. The analysis is restricted to clusters of bare rods without spacers. The results show that already small deviations of the fuel rod in a tightly packed rod bundle cause considerable velocity and temperature differences of the coolant around the rod also in sodium cooled fuel elements. 8 references. (auth)

15364 NUCLEAR REACTOR PRESSURE VESSEL. **Shaw, James William Westgarth; Chapman, Dennis Arthur (to United Kingdom Atomic Energy Authority). British Patent 1,216,983. 23 Dec 1970. Filed 21 Jun 1967.**

Reference is made to concrete pressure vessels having heat exchangers in bores in the concrete. Conventionally the heat exchangers are formed by inserting banks of secondary coolant tubes into the bores, arranged to be swept by the primary coolant. These banks are carried by flanged domes bolted on the flanged collars anchored into the concrete. The flanges are located outside the pressure vessel, and introduce complex stress patterns, making them a possible source of weakness. In the system described anchorage is provided by a collar fixed in the concrete and extending within the bore. The collar has a ring of internal splines and a disk is provided that can be passed through these splines. Chocks bridging at least some of the splines, are provided to prevent removal of the disk. These chocks are normally in the form of a segmented ring. The disk itself may carry the bank of secondary coolant tubes and provide the only means of bore closure; on the other hand, the disk may be used merely to back a closure carrying the tubes. This closure may be a plain dome welded to the collar so as to seal off its end in such a way that the collar merges into the dome with gradual changes of curvature and thickness. (UK)

Fuels

15365 (NEDC–12111) PLUTONIUM UTILIZATION IN BOILING WATER REACTORS. PHASE II 1969 ANNUAL REPORT. O'Neill, G. L. (comp.) (General Electric Co., San Jose, Calif. Reactor Fuels and Reprocessing Dept.). Jul 1970. 56p. For Edison Electric Inst., New York.

Progress is reported on the joint EEI/GE program for utilization of plutonium in boiling water reactors. Design, fabrication, licensing, and Big Rock Point reactor irradiation experience to date is reported for 32 PuO_2-UO_2 fuel rods and three all PuO_2-UO_2 fuel rod bundles. The program includes planning for irradiation of four advance design bundles in a large boiling water reactor. 13 references. (auth)

15366 (WAPD-TM–986) IN-PILE DIMENSIONAL CHANGES OF ThO_2-UO_2 FUEL RODS WITH NON-FREE-STANDING CLADDING (LWBR DEVELOPMENT PROGRAM). Giovengo, J. F. (Bettis Atomic Power Lab., Pittsburgh, Pa.). Nov 1970. Contract AT(11-1)-Gen-14. 32p. Dep. NTIS.

Test data obtained from irradiation of bulk oxide Zircaloy clad fuel rods has been evaluated to determine the effect of several geometrical and environmental test variables on the observed post-irradiation dimensional changes. The major variables include clad-heat treatment, fast flux (nv), pellet end configuration, fuel center temperature, clad diameter-to-thickness ratio, accelerated power cycling and pressure cycles. Data indicates clad heat treatment, fast flux environment, pellet end configuration and fuel center temperature have a large effect on rod elongation believed to be caused by an "axial ratchetting" mechanism. The other test variables considered show much less of an effect, if any, on the observed dimensional changes resulting from "axial ratchetting" of the non-free-standing Zircaloy-4 cladding. 3 references. (auth)

15367 (WHAN-SA–51) PLUTONIUM FUELS FOR LMFBR: AN EXTRAPOLATION. Leggett, Robert D. (WADCO Corp., Richland, Wash.). 6 Oct 1970. Contract AT(45-1)-2170. 52p. (CONF-701001–15). Dep. NTIS.

From 4th International Conference on Plutonium and other Actinides, Santa Fe, N. Mex.

A brief summary of the "state of the knowledge" with regard to mixed oxide (UO_2-PuO_2) fuel clad with stainless steel for use in liquid-metal-cooled, fast breeder reactors (LMFBR's) is provided and areas of large uncertainty that must be resolved in meeting the needs of the reactor designer are pointed out. Three areas of general interest to fuel design are discussed: (1) Thermal performance; (2) Steady-state performance; and (3) Transient or off-normal performance. These three topics are considered separately with emphasis on typical values encountered in the design of fuel for FTR. (78 references) (auth)

XUM

15368 ^{233}U-BEARING SALT PREPARATION FOR THE MOLTEN SALT REACTOR EXPERIMENT. Chandler, J. M.; Bolt, S. E. (Oak Ridge National Lab., Tenn.). Nucl. Appl. Technol.; 9: 807-13(Dec 1970).

The Molten Salt Reactor Experiment was refueled with an enriching salt concentrate, ^{7}LiF-^{233}UF$_4$ (73-27 mole %). Sixty-three kilograms of this was prepared in a shielded cell in the Thorium-Uranium Recycle Facility at Oak Ridge National Laboratory. The preparation process involved reducing ^{233}UO$_3$ to UO$_2$ by treatment with hydrogen, converting the ^{233}UO$_2$ to ^{233}UF$_4$ by hydrofluorination, and fusing the ^{233}UF$_4$ with ^{7}LiF. Its preparation in a shielded cell was required because of the high ^{232}U content (222 ppM) of the ^{233}U. The product salt, containing 39 kg of uranium (91.4% ^{233}U), was low in oxide content (50 ppM) and the concentration of the corrosion products, chromium, iron, and nickel, was minimal at less than (0.05%) total. (auth)

15369 IMPROVEMENTS RELATING TO NUCLEAR REACTOR FUEL ELEMENTS. Linning, David Lees (to United Kingdom Atomic Energy Authority). British Patent 1,216,468. 23 Dec 1970. Filed 16 Dec 1966.

The fuel element described is intended primarily for fast reactors. Ceramic fuel is used with a high enrichment region surrounding a depleted or low enrichment region separated by sheathing. The high enrichment region has up to 40% voidage, including distributed voidage and that provided by an annular gap at the sheathing. Voidage associated with the low enrichment region may include a central hole. Two features giving economic advantages are realized. The radial temperature distribution is improved, permitting more fuel per unit length of pin, and this should result in a reduction of fabrication costs. The second resulting feature is a reduction in the creep strength of the cooler outer region of the fuel as a consequence of the intensification of fission rate in that region; thin high temperature cladding may be employed of sufficient strength to contain the swelling fuel without failure. Suitable fuel material may comprise Pu oxide or carbide, or ^{233}U oxide or carbide, for the high enrichment region, and U or Th oxide or carbide for the low enrichment region. Fabrication procedures are outlined. (UK)

15370 FLOW INDUCED ROD VIBRATIONS OF FAST REACTOR SUBASSEMBLIES. Kadlec, J.; Appelt, K. D. (Kernforschungszentrum, Karlsruhe, Ger.). Nucl. Eng. Design; 14: 136-50(Oct 1970).

The parallel flow induced vibration of fuel pins of the subassemblies of the Na 1 fast reactor study has been investigated. The procedure used includes calculation and experimental verification of natural frequencies and of normal modes, experimental investigation of resonance curves, experimental determination of the spectral density function of the reference strain of the vibrating pin, and calculation of the spectral density functions of the bending strain and of the displacement for all locations on the pin where peaks in the spectral density functions are expected. Typical results of experiments and of calculations as well as conclusions derived from this investigation are presented. 11 references. (auth)

15371 THERMAL, RADIATION, AND MECHANICAL ANALYSIS OF CYLINDRICAL OXIDE FUEL ELEMENTS OF FAST REACTOR IN UNSTEADY STATE. Cheng, Chi-kang. Ames, Iowa; Iowa State Univ. (1970). 175p. University Microfilms Order No. 70-25,775.

Thesis.

A computer program with code name ISUNE 1 was written for the analysis and has been proved useful and versatile. For a given irradiation time at constant linear power operation, the radius of the central void and the extents of the columnar-grain, the equiaxed-grain, and the unaffected-grain regions of a typical oxide cylindrical fuel rod are determined. The temperature distributions in the fuel element are obtained. A model postulated to analyze and calculate the irradiation swelling and fission-gas release for oxide fuels of fast reactor is developed. The effects of thermal-cycling growth and irradiation growth may be combined with the results of irradiation swelling. The thermal, radiation and stress analysis for the fuel elements is based on the thermal and radiation dilatation and an elastoplastic approach for the Prandtl–Reuss material. An iteration method of successive approximations is used to compute the stresses and strains developed in the fuel elements. The temperature at the fuel surface, the pressures in the central void and fuel-clad gap, and the gap thickness are determined through iteration processes. The size of fission gas bubbles, which can be affected by the hydrostatic stress surrounding them, are also determined by the iteration method in connection with the stress-strain calculations. (Diss. Abstr. Int., B)

Auxiliary and Emergency Systems

15372 (AE-408) METHOD FOR CALCULATING THE WASHOUT OF ELEMENTAL IODINE BY WATER SPRAYS. Bachofner, E.; Hesboel, R. (Aktiebolaget Atomenergi, Studsvik (Sweden)). Dec 1970. 23p. Dep. NTIS (U. S. Sales Only).

A model for calculating I$_2$ washout by spraying with pure as well as alkaline water is presented. With pure water the washout efficiency is largely dependent on the I$_2$ concentration in the gas phase. High initial I$_2$ concentrations decrease exponentially with a halftime expressed by $T_{½} = 0.693\ W/KF\ \alpha$, where W, K, F and α respectively mean gas volume, phase equilibrium constant, spray water flow and the saturation degree of I$_2$ in the drops. The decrease in concentration for low initial values is also exponential but with a halftime expressed by $T_{½} = 0.693\ W/B \cdot F$, where B is a water drop parameter. In an intermediate concentration range a third expression for the washout of I$_2$ is evaluated taking into account the degree of hydrolysis of I$_2$ in the water drops. (auth) (Sweden)

15373 (AERE-R-6475) PROPOSED METHOD FOR USING STANDARD BURST CARTRIDGE PRECIPITATOR EQUIPMENT FOR FUEL ACTIVITY RELEASE MONITORING ON A MK. III HIGH TEMPERATURE GAS COOLED REACTOR. Leake, J. W. (Atomic Energy Research Establishment, Harwell (England)). Dec 1970. 29p. Dep. NTIS (U. S. Sales Only). UK 4s. 6d.

A new method of using standard wire precipitation systems is proposed which will enable them to be used for fuel activity release monitoring (FARM) on the Mk. III high temperature gas cooled reactor. The method involves the division of the normal counting period into two parts (not necessarily equal) and the difference count is taken. It is shown that this permits the detection of releases of relatively small quantities of the short-lived Kr and Xe fission products in the presence of large activities of the long-lived Kr and Xe nuclides. The increased selectivity between short and long-lived activity should enable any significant additional release of activity from the fuel to be monitored. This method, with development, has limited potential for use on Mk. I and II gas cooled reactors. (auth) (UK)

15374 (BAW-10024) EFFECTIVENESS OF SODIUM THIOSULFATE SPRAYS FOR IODINE REMOVAL. (Nonproprietary Version of BAW-10022). (Babcock and Wilcox Co., Lynchburg, Va. Nuclear Power Generation Dept.). Jan 1971. 194p.

The design data and calculational methods used in evaluating the effectiveness of the iodine removal spray system as an engineered safety feature are examined. The data are generally applicable to all reactor plants using a spray system for iodine removal. The quantity and forms of the fission products airborne in the reactor building and the significance of these fission products individually and collectively are discussed. The significant experimental data available on the spray removal of the various forms of iodine are reviewed. The calculational models used by the various experimenters to correlate their results are presented. The calculational methods used by B&W to evaluate the iodine removal effectiveness of sodium thiosulfate sprays are described. Reasons for selecting the correlations used in the calculations are explained, the predicted effectiveness is compared with the experimental results obtained at various facilities, and the removal effectiveness expected in a typical plant is shown. 94 references. (auth)

Operation and Economics

15375 (CONF-691114-6) PLUTONIUM AS AN ALTERNATE FUEL IN LARGE WATER COOLED REACTORS. Sofer, G. A.; Tomonto, J. R.; Tulenko, J. S. (United Nuclear Corp., Elmsford, N. Y. Research and Engineering Center). [1969]. 8p. Dep. NTIS. ASME, New York, N. Y. $1.50.

From 90th Annual Meeting on American Society of Mechanical Engineers, Los Angeles, Calif.

Plutonium recycle in a thermal reactor promises to provide a safe and economic solution to the problem of accumulation of Pu discharged from thermal reactors. "Self-generation" Pu recycle designs appear to emerge as the preferable recycle scheme for the near-term future, with the implication that every reactor operator must concern himself with Pu recycle in his own reactor. (auth)

15376 LONG-TERM CHANGES IN THE FUEL ISOTOPE COMPOSITION IN A FAST POWER REACTOR STARTED UP WITH ^{235}U. Podpora, Jan (Inst. of Nuclear Research, Swirk, Poland). Nukleonika; 15: 489-97(1970). (In Polish).

Equations are formulated and solved describing the changes in the fuel isotope composition in the fast reactor started up with enriched U. Account was taken of various ways of fuel management between the core, blanket and environment. The knowledge of the isotopic composition will permit to investigate the gradual transformation of the reactor started up with enriched U to a Pu reactor, and to determine the time-dependence of certain reactor parameters such as unit charge, breeding gain as well as the exchange of the fuel streams between the reactor and the environment. (auth)

15377 LONG-TERM CHANGES IN THE PARAMETERS DESCRIBING THE FUEL BALANCE OF THE FAST POWER REACTOR STARTED UP WITH ^{235}U. **Podpora, Jan (Inst. of Nuclear Research, Swierk, Poland). Nukleonika; 15: 553-62 (1970). (In Polish).**

Diagrams of the isotopic compositions, considering the various ways of fuel management, are presented. They illustrate the gradual transformation of the reactor started up with ^{235}U into a plutonium reactor. Time-dependence curves of parameters describing the fuel balance of the reactor are also given. Basing on these data, the enriched-uranium fuelled fast reactor is characterized from the viewpoint of its fuel balance. (auth)

15378 BLANKET FUEL MANAGEMENT OPTIMIZATION OF A LIQUID METAL FAST BREEDER REACTOR IN A DYNAMIC ENVIRONMENT. Elais, David. College Park, Md.; Univ. of Maryland (1970). 216p. University Microfilms Order No. 70-23,294. Thesis.

Techniques developed for efficiently analyzing the detailed fuel management of liquid metal fast breeder reactors radial blankets in a dynamic environment are described. The results of applying those techniques to arrive at optimum fuel management decisions under a variety of realistic economic conditions are presented. An optimization procedure was developed, called a constrained ridge technique, which resulted in a capability to efficiently analyze fuel management decisions in any reactor model and subsequently arrive at the optimum policy decision to minimize fuel cycle costs. This technique has the capability of analyzing and optimizing a nuclear-economic model in a non-Euclidean hyperspace of continuous and discontinuous variables. It was programmed for a two dimensional space. A realistic nuclear-economic reactor model was also developed for calculating nuclide concentrations and fuel cycle costs as a function of time. It basically consists of a set of non-linear differential equations coupled with a fuel management policy. This model permits detailed and complete analysis of both radial out-in subassembly movement and radial blanket graphite content on total fuel cycle costs. Those fuel management related decisions are subjected to realistic engineering constraints on specific power, material concentrations and fissile material burnups. The nuclear-economic model and constrained ridge optimization technique were coupled to form a computational system called 2DBCOST. This system was then applied to an advanced, unspoiled 1000 MW(e) liquid metal fast breeder reactor and resulted in significant demonstrated fuel cycle cost savings in a dynamic economic environment. The effects of increasing or decreasing fabrication, reprocessing, shipping, interest, fuel handling and material costs in addition to inventory lead times and post irradiation lag times on optimum policy decisions can be studied. (Diss. Abstr. Int., B)

Safety and Siting

Refer also to abstract 13184.

15379 (EURFNR-785) SOLUBILITY OF INERT GASES IN THE REACTOR COOLANT SODIUM AND RELATED SAFETY PROBLEMS. Thormeier, K. (Kernforschungszentrum, Karlsruhe (West Germany). Institut fuer Reaktorentwicklung). Translation of report KFK-1166. 117p. Dep. NTIS.

Work Performed under United States-Euratom Fast Reactor Exchange Program.

A theoretical as well as experimental determination of the solubility of inert gases in liquid Na is presented. The investigation covers a wide range of temperatures and pressures. A theoretical relation for Henry's coefficient can be derived from statistical thermodynamics. This is used for calculation of the solubilities of inert gases in Na on the basis of the model concept that a dissolved gas atom requires a hole of its size in the liquid and that the gas atom, once it is placed in that hole, interacts with the ambient liquid and is made to vibrate. For experimental verification of these results a novel method has been developed for measurement of the solubility of gases in liquids which is suitable especially for determining the solubility of inert gases in liquid metals. The test facility set up allows the reliable measurement of gas concentrations in the range between 1.10^{-10} and 3.10^{-5} mole gas/mole liquid. The measured results, which are well reproducible, are in good agreement with the values derived theoretically. On the basis of the solubility data thus obtained the significance to safety of the cover gas bubbles (argon and helium, respectively) produced in the Na as a result of temperature changes and the capacity for the fission gases krypton and xenon in Na are regarded for the primary circuit of the fast sodium cooled breeder reactor SNR. 127 references. (auth)

15380 A BOOTSTRAP CONCEPT OF A SAFETY TEST FACILITY. **Kelber, Charles N. (Argonne National Lab., Ill.). Nucl. Appl. Technol.; 9: 780-5(Dec 1970).**

A concept of a facility for carrying out a series of in-pile tests of varying sizes for ensuring LMFBR safety is needed. The chief problems to be overcome are those arising from nuclear feedback from the test zone and the need to contain the test in a loop. The suggested solution involves using a zoned core coupled to the test region by a nickel reflector. This suggestion is based on the observation that as the test size is changed, the reactivity changes are easily accommodated by control rod movement if the loop wall thickness does not change much. To increase the test size safety without increasing test loop wall thickness requires the successful extrapolation of knowledge of energy yield and absorption gained on earlier, smaller tests. Such a procedure is termed a bootstrap procedure. 10 references. (auth)

15381 COOLING DISTURBANCES IN THE CORE OF SODIUM-COOLED FAST REACTORS AS CAUSES OF FAST FAILURE PROPAGATION. **Gast, K.; Smidt, D. (Kernforschungszentrum, Karlsruhe, Ger.). Nucl. Eng. Design; 14: 12-22(Oct 1970).**

As hypothetical cause of Bethe–Tait type excursions in sodium-cooled fast reactors local cooling failures are considered. Several mechanisms of failure propagation are discussed. The most important one is the thermal interaction between molten fuel and liquid sodium. The initial conditions starting from local failures or subassembly blockage are defined. A criterion for dryout in narrow channels is developed. The importance of sodium boiling superheat is rediscussed in this context. Finally the functional requirements for core instrumentation are given. It is concluded that the probability of failure propagation leading to Bethe-Tait excursions is sufficiently low. 11 references. (auth)

15382 INVESTIGATION ON DYNAMIC BOILING IN SODIUM COOLED FAST REACTORS. **Peppler, W.; Schlechtendahl, E. G.; Schultheiss, G. F. (Kernforschungszentrum, Karlsruhe, Ger.). Nucl. Eng. Design; 14: 23-42(Oct 1970).**

Experimental and theoretical investigations of the thermodynamics and hydrodynamics of cooling perturbations in fuel elements of sodium cooled fast reactors are described. Particular attention is given to bubble nucleation and to growth and shrinkage of the sodium vapor bubble volume. The theoretical model on which the digital computer code BLOW 2 is based, is described briefly. Boiling experiments which were carried out in a test loop under typical loss of coolant flow situations of a sodium cooled reactor are analysed with respect to the vapor bubble dynamics, the pressure pulses during the boiling process and the temperatures of the test section wall. The influence of artificial surface cavities and sodium impurities upon superheat is investigated in a separate experiment. 40 references. (auth)

Power Conversion Systems

15383 METHOD OF OPERATING A THERMAL POWER PLANT, MORE PARTICULARLY A NUCLEAR POWER PLANT. **Maillet, Ennemond (to Commissariat a l'Energie Atomique). British Patent 1,217,179. 31 Dec 1970. Priority date 28 Apr 1967, France.**

POWER CYCLES—evaluation of optimum, for direct cycle gas turbine gas cooled reactor

REACTORS, GAS-COOLED—power cycle for direct cycle gas turbine, analysis of optimum (D.L.C.)

Research and Test Reactors

Refer also to abstracts 13318, 14837, 15339, and 15367.

15384 (ANL-7578) APPARATUS FOR HIGH-SPEED PHOTOGRAPHIC EXPERIMENTS WITH IRRADIATED FAST-REACTOR FUEL SPECIMENS. **Robinson, L. E.; August, C. (Argonne National Lab., Ill.). Aug 1970. Contract W-31-109-eng-38. 16p. Dep. NTIS.**

The standard, transparent TREAT fuel-meltdown facility was redesigned for experimental use with irradiated fast-reactor fuel specimens. The stainless steel slot liner was formed of a

XUM

single sheet, with integral ribs rolled in, for greater rigidity and ease of fabrication. The redesigned test capsule has a fuel-holding frame automatically locked in position during remote loading. A Zircaloy auxiliary lining was added to ease decontamination and increase the reusability of the facility. A removable auxiliary flange was used to centralize inert gas and electrical connections and to clamp the refractory lining to the slot liner. An in-line, remotely operated assembly apparatus was designed to permit remote handling, spot welding, and fuel loading. 4 references. (auth)

15385 (DOCKET-50184-25) NATIONAL BUREAU OF STANDARDS REACTOR. Request Permission to Release Ten Additional Curies Per Year to the Sanitary Sewer. (National Bureau of Standards, Washington, D. C.). 20 Jan 1971. 1p. Dep. NTIS.

15386 (DOCKET-50231-67) SOUTHWEST EXPERIMENTAL FAST OXIDE REACTOR. Steady State Operation up to 20 MWt Approved. (Division of Reactor Licensing (AEC), Washington, D. C.). 1 Feb 1971. 1p. Dep. NTIS.

15387 (EURFNR-858) EVALUATION OF FAST CRITICAL EXPERIMENTS USING RECENT METHODS AND DATA. Kiefhaber, E.; Schmidt, J. J. (Kernforschungszentrum, Karlsruhe (West Germany). Institut fuer Neutronenphysik und Reaktortechnik). Sep 1970. 233p. (KFK-969; EANDC(E)-118(U)). Dep. NTIS (U. S. Sales Only).

Work Performed under United States-Euratom Fast Reactor Exchange Program.

The influence of changes in nuclear data on the calculated values for the criticality and other important parameters of critical assemblies is analyzed. The analysis is done for a variety of assemblies which differ in geometry, material composition, and energy distribution of the normal and adjoint flux. The primary objective is: to detect deficiencies in nuclear data and calculational methods; to get first preliminary improvements; and to get indications in which respect and in which way further long-range improvements should be carried on. The long-range aim of this kind of investigations is to provide or establish satisfactory nuclear data and calculational methods which can reliably be applied to the calculation of fast critical assemblies and of large fast power reactors. 91 references. (auth)

15388 (GULF-RT-10421) FAST REACTOR SPECTRUM MEASUREMENTS. Quarterly Progress Report for the Period Ending October 31, 1970. Young, J. C.; Borgonovi, G. M.; Crosbie, K. L. (Gulf Radiation Technology, San Diego, Calif.). 18 Nov 1970. Contract AT(04-3)-167. 36p. Dep. NTIS.

Time-of-flight measurements were made in STSF-7. These included spectrum measurements in the core, at the core-reflector interface, and in the reflector. Auxiliary measurements were also made of the dieaway of the system, and activation foils were used to determine the $^{235}U/^{238}U$ fission ratio. Calculations of the kinetics of the system using the computer code CAGE-2 were performed and compared to the measured data. The ^{3}He neutron spectrometer was placed in the STSF-7 core to measure the static spectrum as a check of this detector system. The design of STSF-8 was finalized and internal approvals were obtained to convert STSF-7 to STSF-8. The response function measurements for the proton recoil detectors were completed and the analysis of these data is well under way. Calculations were performed to compute the analytical response function for these detectors. The spectra measured in STSF-7 were partially analyzed and are reported. 16 references. (auth)

15389 (JAERI-1177-B(Pt.2)) JAERI's CONCEPTUAL DESIGN OF THE JAPAN EXPERIMENTAL FAST REACTOR. (Japan Atomic Energy Research Inst., Tokyo). Dec 1970. 273p. Dep. NTIS (U. S. Sales Only).

The primary objective of the present conceptual design (the second conceptual design of JFER) is to prepare for the construction of Japan Fast Experimental Reactor (JFER) which will enable various fast reactor engineering experiments such as fast flux irradiation work on fuels. The following subjects of the design are described: the general philosophy and specific aspects of the present design; the nuclear characteristics including burn-up behavior of the reactor core; the thermal hydraulic characteristics of the core; the mechanical design of the reactor vessel, the shielding plugs, the internal structure of the vessel, and the core structure including fuel assembly; the fuel handling system design; the design of the primary and secondary cooling loop systems which disperse the heat removed from the core into the air; the design of the fuel-monitoring facility which takes the fuel out of the reactor core periodically after a certain burn-up for various kinds of inspections; the design of shielding which shields neutrons and gamma-rays from the reactor, and gamma-rays from the primary sodium loop; the design of the instrumentation and control systems for the reactor operation, and some results of kinetic analysis of the reactor plant; and the description of the reactor containment building, the waste disposal facilities and other reactor service facilities for the reactor plant. Safety evaluation of the JFER such as the analyses of transient behavior, maximum credible accident and hypothetical accident is also described. 11 references. (auth)

15390 (JAERI-Memo-4141) CHARACTERISTIC MEASUREMENTS OF JRR-2. Sakurai, H. (Japan Atomic Energy Research Inst., Tokyo). Jul 1970. 307p. (In Japanese). Dep. NTIS (U. S. Sales Only).

JRR-2 is a thermal reactor using the plate-type fuel elements of 90% enriched uranium with heavy water both as moderator and coolant. The maximum thermal output of the reactor is 10 MW. The operating cycle of three weeks includes 300 hour operation, refueling, and exchange of irradiated samples. To improve the operation mode it has become necessary to increase the reactivity in JRR-2 by adding more fissile material. Therefore, the content of U-235 in the fuel was increased by 10%. Characteristics of the new core were measured during the period from December 1969 to February 1970. Main items of the measurements were as follows: critical mass measurements, control rods calibration, neutron and gamma flux measurements, measurements of various reactivity worths, power calibration and xenon buildup measurements. (auth)

15391 (JAERI-Memo-4180) NUCLEAR CALCULATION METHOD OF THE JMTR CORE. Oyamada, Rokuro; Tanaka, Toshiyuki; Iida, Hiromasa (Japan Atomic Energy Research Inst., Tokyo). Oct 1970. 112p. (In Japanese). Dep. NTIS (U. S. Sales Only).

The calculation method of the JMTR core is briefly described for the analysis of characteristics (excess reactivity, power distribution, CRD condition) and neutron flux distribution. In choosing the calculation method much attention has been given on how to evaluate geometrical and material heterogeneity of irradiation materials. Presently the THERMOS, the UGMG42 and the CDCPDQ codes are selected for the usual calculation of thermal group constants, fast group constants and two dimensional diffusion respectively. The calculation results by these codes are reliable in comparison with those of the JMTRC reactor physics experiment and the JMTR operation data. To evaluate the fine structure of neutron flux in unit cells a calculation method is to be developed, using the PANDORA, the METHUSELAH II, and the LEOPARD. (auth)

15392 (ORNL-TM-3286) HIGH FLUX ISOTOPE REACTOR QUARTERLY REPORT, JULY-SEPTEMBER OF 1970. McCord, R. V.; Corbett, B. L. (Oak Ridge National Lab., Tenn.). 19 Jan 1971. 26p. Dep. NTIS.

Operations and maintenance requirements for the reactor during July to September 1970 are described. System surveillance tests and design changes are discussed. Experimental work in the reactor is reviewed. (D.C.C.)

15393 (RCN-119) NEUTRON METROLOGY IN THE H.F.R. FLUX DENSITY INFORMATION FOR THE 45 MW CORE CONFIGURATION. Zijp, Willem L.; van der Werve, Hugo (Reactor Centrum Nederland, Petten). Sep 1970. 43p. Dep. NTIS (U. S. Sales Only).

A compilation of thermal and fast flux density values is presented for the 45 MW core configuration with 6 inner experiment positions. Data are given for the fuel region, the experiment positions occupied by S-assemblies, the poolside facility and the irradiation facilities for smaller capsules. No data are available for the beam tube arrangements. The values presented should be considered as estimates for nominal values, as the actual flux density values are dependent upon the fuel charge and its distribution over the core, the irradiation experiments installed and the position of the control members. Some results of multigroup neutron spectrum calculations performed with the TEDDI-M code are also presented. Furthermore data on the damage-to-activation ratio for graphite and steel irradiations in experiment positions are given. (auth)

15394 BASIC STATIC PARAMETERS FOR WWR-SM LATTICES WITH WATER CHANNELS. ESTIMATION OF HETEROGENEITY EFFECT ON NEUTRON AGE. Jozefowicz, Edward T. (Inst. of Nuclear Research, Swierk, Poland). Nukleonika; 15: 399-410(1970).

Investigations of the basic static characteristics of WWR-SM lattices (36% enriched multitube fuel, water moderated) with increased water-to-fuel ratio are described. Thermal microdistribution in the elementary cell, f, δ^{25}, ρ^{28}, ICR and B^2 components are measured, and some results are compared with the calculated values. The water content is increased by adding a regular lattice of water channels. A simple method of calculating the effect of heterogeneity of fission neutron sources on the neutron age as well as the interpretation of the results in the frames of the infinite multiplication factor and the two-group critical equation are presented. 17 references. (auth)

15395 TEMPERATURE MEASUREMENTS OF THE CLADDING OF WWR-SM TYPE FUEL ELEMENTS IN THE EWA-10 REACTOR CORE. Aleksandrowicz, Jerzy; Czerniewski, Michal; Labno, Leszek (Inst. of Nuclear Research, Swierk, Poland). Nukleonika; 15: 383-98(1970).

As part of the EWA-10 reactor start-up measurements program after its reconstruction connected with power increase, temperature measurements of the cladding of new type fuel elements were carried out. The main purpose of these measurements was to collect the necessary data for the elaboration of a hazard report and to estimate the core cooling conditions for the nominal value of the reactor power. The WWR-SM type fuel element was equipped with 8 thermocouples installed in the fuel cladding, and 2 thermocouples for measuring the inlet and outlet water temperatures. This instrumented fuel element was inserted during the experiment in hot places of the reactor core. Measurements for steady and transient states were performed at forced and natural convection flow. The dependence between the maximum power level and the values of flow rate and cooling water temperature were determined for the permissible temperature of fuel cladding assumed. (auth)

15396 THEORETICAL AND EXPERIMENTAL ANALYSIS OF FAST ZERO-POWER ASSEMBLIES. WITH SPECIAL CONSIDERATION OF NUCLEAR-DATA CHECK. Bohme, R. (Kernforschungszentrum, Karlsruhe, Ger.); Fischer, E. A.; Hinkelmann, B.; (and others). pp 427-57 of Nuclear Data for Reactors. Vol. II. Vienna; International Atomic Energy Agency (1970).

From 2nd International Conference on Nuclear Data for Reactors, Helsinki, Finland. See STI/PUB–259(Vol.2); CONF-700605–(Vol.2).

The correlation between microscopic data and integral quantities of interest for reactor physicists, from a general point of view, mainly in connection with experiments in fast zero-power assemblies, is discussed. The activities in the field of nuclear data and fast-reactor analysis performed in the Karlsruhe nuclear research centre are reviewed. The following points are discussed in detail: (1) The procedure followed by the nuclear-data evaluator to select best data from the given experimental microscopic cross-sections (a comparison of some specific cross-sections in various evaluated data files is given). (2) The procedure in calculating multi-group constants from these best data. (3) The influence of data uncertainties on integral nuclear parameters as criticality, reactivity coefficients, reaction-rate traverses and reaction-rate ratios. (4) The procedure and accuracy of the experimental assessment in spectrum measurements, reaction rate measurements, fine-structure measurements and in the determination of reactivity coefficients. (5) The evaluation of critical experiments with respect to checking the microscopic nuclear data and the possibility of improving these data by integral experiments. 62 references. (auth)

15397 CALCULATIONS OF JEZEBEL AND GODIVA WITH RECENT ENDF/B MICROSCOPIC DATA. Best, G. H.; Battat, M. E.; Labauve, R. J.; Seamon, R. E. (Los Alamos Scientific Lab., N. Mex.). pp 517-29 of Nuclear Data for Reactors. Vol. II. Vienna; International Atomic Energy Agency (1970).

From 2nd International Conference on Nuclear Data for Reactors, Helsinki, Finland. See STI/PUB–259(Vol.2); CONF-700605–(Vol.2).

Testing of the original ENDF/B data indicated deficiencies in the microscopic data for some materials. As a result, a reevaluation of the data for selected materials, including fissile and fertile nuclides, was performed by the ENDF/B working group. The experimental fast critical assemblies JEZEBEL and GODIVA were used as the calculational models for the initial testing of the reevaluated data files. To minimize uncertainties in the model specifications, the geometry and material specifications for these assemblies were based on a recent reevaluation by Hansen and Paxton, which resulted in modest changes in the critical masses of homogeneous spheres of the appropriate alloys. Multigroup constants were generated from the microscopic data using the MC^2 data processing code. The criticality calculations assumed spherical geometry and used isotropic transport theory. The effects of higher-order anisotropic scattering and quadrature order were taken into account in arriving at the final comparison. Central reactivity worths were computed using a perturbation-theory calculation. Certain physics parameters are calculated better with the reevaluated data, but the general lack of agreement between measured and calculated parameters indicates that deficiencies remain in the cross-section data. 23 references. (auth)

15398 INFLUENCE OF THE UNCERTAINTIES OF σ^f_{25} IN THE MONTE-CARLO CALCULATIONS OF SMALL CRITICAL ASSEMBLIES. Benzi, V.; Cupini, E.; De Matteis, A. (CNEN, Bologna). pp 531-4 of Nuclear Data for Reactors. Vol. II. Vienna; International Atomic Energy Agency (1970).

From 2nd International Conference on Nuclear Data for Reactors, Helsinki, Finland. See STI/PUB–259(Vol.2); CONF-700605–(Vol.2).

Recent measurements of the fission cross-section of ^{235}U in the energy range ~100 keV – 1 MeV give values ~15% lower than the results previously obtained. A Monte-Carlo analysis of some fully enriched small fast critical assemblies shows that such a reduction gives critical mass values which are in strong disagreement with the experimental ones. The possible influence of variations in the elastic and inelastic cross-sections is also discussed. (auth)

15399 INTEGRAL DATA FOR ^{235}U IN INTERMEDIATE NEUTRON SPECTRUM. Veselova, G. M.; Zakharova, S. M.; Kuznetsov, V. A.; (and others). (Inst. of Physics and Power Engineering, Obninsk, USSR). pp 577-87 of Nuclear Data for Reactors. Vol. II. Vienna; International Atomic Energy Agency (1970). (In Russian).

From 2nd International Conference on Nuclear Data for Reactors, Helsinki, Finland. See STI/PUB–259(Vol.2); CONF-700605–(Vol.2).

The results of measuring, on a PF-4 unit, the spectrum-average values of $\bar{\nu}_{eff}$ in intermediate uranium-beryllium physical assemblies with $\rho_{Be}/\rho_{^{235}U} = 84$ are presented. The work was performed as part of the program for improving the constants needed for building fast reactors. $\bar{\nu}_{eff}$ was measured by two methods. One of these made use of relationships which link the total statistical weight of the core and reflector components with the quantity K_∞. The expression used had the form: $S = 2(1/K_{eff} - 1/K^+)$, where S is the total statistical weight of the core and reflector components, K_{eff} is the effective multiplication factor, and $K^+ \simeq K_\infty$. This method was used for measurements in the PF-4 (F-8) assembly. In this assembly the core was surrounded with a steel reflector. In the PF-4(F-9) assembly, where the core was surrounded with a two-layer beryllium and steel reflector, work was performed by a method in which the values of neutron flux attenuation were measured by means of uranium and boron chambers in boron-10 and uranium-235 filters, respectively. The experimental values of $\bar{\nu}_{eff}/\nu_T = (\overline{\sigma_f \sigma_B})/(\overline{\sigma_a \sigma_B})$ were measured at the center and at the boundary of the core with the beryllium lateral reflector. The method used and the results of a multigroup calculation of these quantities employing three systems of constants are described. The results of the calculation are compared with the experimental data. 25 references. (auth)

Rocket and Space Reactors

15400 APPLICATIONS OF HEAT PIPES TO NUCLEAR REACTOR ENGINEERING. Parker, Monte Bryce. Ames, Iowa; Iowa State Univ. (1970). 86p. University Microfilms Order No. 70-25,816.

Thesis.

A feasibility study was made of the use of heat pipes as reactivity control devices for a nuclear reactor. The heat pipes contain uranium tetrafloride as the heat pipe working fluid. The evaporator section is within the reactor and the condenser section is outside the reactor. The reactor model used is based on a reactor used in rockets such as Nerva. Equations are derived relating the neutron flux and coolant temperature to the mass of fuel in the heat pipe evaporator section. The reactivity of the mass changes of the fuel is determined using a perturbation analysis. Other feedback effects are then added to the system and the time dependent behavior of the neutron density is determined for step and ramp reactivity inputs. (Diss. Abstr. Int. B)

15401 ANALYTICAL AND EXPERIMENTAL STUDIES RELATING TO THE SIMULATED STARTUP OF IN-CORE THERMIONIC REACTOR SYSTEMS. Guppy, James Garfield. Tucson, Ariz.; Univ. of Arizona (1970). 204p. University Microfilms Order No. 70-22,316.

Thesis.

An analytical representation of a nuclear reactor containing in-core thermionic devices suitable for transient studies is formulated. The resulting model is applicable to situations involving substantial changes in system operating conditions,

XUM

as would be experienced during start-up transients. Neutron kinetics and heat transfer are represented by "nodal" descriptions. Contributions from all system regions of importance are retained to produce realistic transient response. The resulting set of equations is coupled to a digital computer integration routine to solve for the dynamic response. The thermionic converter physics is described by a complex iterative numerical scheme based on a diffusion approximation to the plasma processes. Other thermionic processes included are surface and Schottky effects, plus an accounting of the electrostatic sheaths present. The analysis is extended to include general application to thermionic diodes undergoing transients. The digital description of the reactor model is tested against a comparable analog computer simulation and shown to yield better accuracy. The complex thermionic analysis is compared to a simpler converter physics description and found to be far superior in predicting the electrical characteristics of the converter for large changes in operating conditions. The thermionic analysis is also compared with transient experimental diode data over wide ranges of converter operations and shown to produce excellent agreement. Application of the model to system start-up is described for two postulated start-up approaches encompassing either constant diode voltage or constant emitter temperature. (Diss. Abstr. Int., B)

Reactor Theory

15402 GENERAL STATUS OF NUCLEAR DATA REQUIREMENTS. Schmidt, J. J. (International Atomic Energy Agency, Vienna). pp 3-15 of Nuclear Data for Reactors. Vol. I. Vienna; International Atomic Energy Agency (1970).

From 2nd International Conference on Nuclear Data for Reactors, Helsinki, Finland. See STI/PUB–259(Vol.1); CONF-700605–(Vol.1).

After a brief historical survey of developments in the last few years in reactor physics and technology, nuclear data requirements, and measurement techniques, the present status of nuclear data requirements is presented. Subjects discussed include e.g., the confidence level of important nuclear data, interpretation of fission resonances, ^{239}Pu resonances and α-values, the $\bar{\nu}$(^{252}Cf) standard, the energy dependence of $\bar{\nu}$, ^{235}U fast-neutron fission, ^{238}U fast-neutron capture, energy spectra of prompt fission neutrons. Also discussed are problems of compilation of experimental data and their detailed experimental characteristics, a task undertaken by the four neutron data centers at Brookhaven, Obninsk, Saclay and Vienna. 96 references. (auth)

15403 ERROR ESTIMATE IN REACTOR THEORY. Ronen, Yigal. Ithaca, N. Y.; Cornell Univ. (1970). 126p. University Microfilms Order No. 70-24,912.

Thesis.

A new analytic method for error estimate is presented and applied to reactor theory. The method is based on the functional analysis technique and gives upper bounds to the errors. There are two main advantages to the new method. First, error estimate can be obtained in cases for which no other known methods have succeeded. Second, when an estimate is obtained by this method it is a reliable one. This error estimate method finds a bound to the errors in the eigenvalues of homogeneous equations, and in the relative R.M.S. solutions of the inhomogeneous equations. The bound has the form of the norms of the operators of the exact and approximate equations. A generalization of the Schur test enables to find a low estimate to these operators' norms. By applying this test to integral transport operators, it is proven that these operators are always bounded in some L_2 Hilbert space. When the error estimate method is applied to the inhomogeneous integral transport equations, the results are bounds to the relative R.M.S. of the fluxes. Such errors are caused by neglecting linear (or any higher) anisotropic scattering, neglecting the scattering kernel of an absorber, changing the total cross section, and changing the scattering kernel. In the last case the error estimate due to a change in temperature is compared with the real error and found to be very close. The application of the method is further extended to homogeneous equations such as the integral transport equations and even to unbounded equations like diffusion equations. For these cases the errors in the reactivity and the time decay constants are studied. Some of the causes of these errors are the neglect of the scattering kernel of an absorber, space perturbation, neglect of delayed neutrons, xenon poisoning and fuel depletion. The effect of the error between B_N and B_{N+1} approximations is also studied. This method is successfully generalized for cases in which the solution of the approximate equation is included in the estimate. Thus a comparison between this method and perturbation theory is drawn. (Diss. Abstr. Int., B)

Kinetics

Refer also to abstracts 15343, 15352, and 15391.

15404 (EUR–4536) GEOMETRY ROUTINES FOR USE IN THE TIMOC CODE. Jaarsma, R. J.; Kschwendt, H. (European Atomic Energy Community, Ispra (Italy). Joing Nuclear Research Center). Dec 1970. 72p. Dep. NTIS (U. S. Sales Only). EUR FF 11,-.

For application in the Monte Carlo Code TIMOC a number of subroutines describing different geometrical configurations have been developed. Their description is presented. The first three subroutines were made a long time ago for special purposes and describe such simple geometries as cylinders, slabs and spheres, as well as more complicated configurations like concentric rings, ring sectors, lattices of cylinders or spheres. A complete description of the problems which can be handled, the way of linking to the main programme and the preparation of the input data are given. The adaptation of the subroutine GEOM of the O5R code, a more general geometry subroutine, to the TIMOC code is described. (auth)

15405 (LFEN-NI.–45-a) WESTCOTT FORMALISM. Jorge, H. Machado (Junta de Energia Nuclear, Sacavem (Portugal). Laboratorio de Fisica e Engenharia Nucleares). 1969. 49p. (In Portuguese). Dep. NTIS (U. S. Sales Only).

Neutron capture by a material in a well-moderated nuclear reactor is divided into a thermal portion and a 1/E portion. Westcott developed a prescription for the rate that requires a ratio and a gradual cut-off function Δ of the fluxes in the two parts, and the deviation from 1/v capture in the material that arises from resonance capture. This review of the prescription gives the formulas for the calculation of the several functions that are needed, presenting the Δ_4 function in the form of both table and graph. The range of validity of the formalism is indicated. 16 references. (TTT)

15406 (NP–18646) PARAMETER ADJUSTMENT BY THE GRADIENT METHOD ON THE HYBRID ANALOG COMPUTER. Katz, F. (Kernforschungszentrum, Karlsruhe (West Germany). Institut fuer Reaktorentwicklung). Sep 1970. 45p. (In German). Dep. NTIS (U. S. Sales Only).

The development of modern analog computers facilitates new iterative computing techniques, which enable the use of an analog computer to deal with many problems which so far could not be solved or only with great difficulty. To this class of problems belongs also the treatment of optimization problems. The applicability of the gradient method as an optimization strategy for use with analog computers is shown. In addition, the method is applied to a particular problem which arises in fast reactor core structure design, and the usefulness of the method is investigated in detail. (17 references) (auth)

15407 ENERGY MODELS FOR COMPUTING FAST-REACTOR PARAMETERS. Lorenzini, Paul Gilbert. Corvallis, Oreg.; Oregon State Univ. (1970). 171p. University Microfilms Order No. 70-22,769.

Thesis.

Because of the complicated form of the diffusion equation approximations are necessary to treat the energy dependence for practical problems. The standard model is the few group approximation. A second approximate form, the overlapping group or modal method, is examined and more fully developed to provide an alternative to this approach. The formalism developed is direct and straightforward. A computer code is presented to generate input that will enable the user to run a modal problem on any standard diffusion theory code that allows upscattering. Two fast reactor designs are studied. The results of one and two dimensional calculations using both energy models are presented. A comparison of the accuracy and the computer time requirements of each method is made. Numerical problems associated with the modal method are thoroughly studied. Results indicate that the two models are comparable. Improvements in the modal method are suggested and indications are that with further development, it may offer an attractive alternative to the few group approach. (Diss. Abstr. Int., B)

15408 HYBRID COMPUTER INVESTIGATION OF SPATIAL EFFECTS IN PROMPT CRITICAL REACTOR EXCURSIONS. Christenson, John Martin. Madison, Wis.; Univ. of Wisconsin (1970). 224p. University Microfilms Order No. 70-19,135.

Thesis.

Hybrid computer techniques were utilized to study spatial effects in a one-dimensional, one-group reactor undergoing a prompt critical excursion as the result of a step insertion of reactivity. Uniform, half-core, and quarter-core insertions

UM

were considered and the spatial effects are reported on as a function of two dimensionless variables: $B^2(e/c)$, a measure of excursions being induced by equal material changes, and $\Delta k(e/CL)$, a measure of excursions being induced by equal dynamic reactivity insertions. The relationship between the two variables is elucidated and the type of point kinetics formulation that gives a "best" description of the excursion is determined. A general conclusion is that for spatially uniform energy feedback a point kinetics formulation based on a $t = 0+$ buckling eigenvalue problem gives a relatively good estimate of the total energy release, even though it does not furnish a very good prediction of the final energy distribution. Several computer techniques were developed, including a method for using multiplexed digital-to-analog-convertors for the rapid establishment of integrator initial conditions, and a general purpose system for obtaining a self-calibrated, dynamic oscilloscope display of the outputs of arbitrary sequences of analog elements. (Diss. Abstr. Int., B)

Experimental Applications

Refer also to abstract 14877.

15409 MEASUREMENT OF THERMAL-NEUTRON SPECTRA IN HETEROGENEOUS LATTICES BY FOIL ACTIVATION. Dixon, Gregg Woodford. Stanford, Calif.; Stanford Univ. (1970). 153p. University Microfilms Order No. 70-22,162.
Thesis.

Thermal neutron spectra were measured with good spatial resolution within a unit cell of several H_2O-moderated natural uranium lattices and in one graphite-moderated lattice. Both activation ratios (or spectral indices) and differential spectra unfolded from these ratios were compared with integral transport theory calculations of the THERMOS computer code. The H_2O-moderated lattices had water-to-uranium volume ratios of 1 : 1, 2 : 1, and 3 : 1, with fuel-rod diameters of one inch. The graphite-moderated lattice had a square pitch of 5.75 inches. Dysprosium-164, europium-151, lutetium-176, and indium-115 were used as detectors. Dilute foils of 0.175 in. diameter were prepared containing the natural elements of these detectors, and packets of four foils each were irradiated in both the measured spectra and in a graphite thermal column reference spectrum. The activation ratio is defined as the ratio of the activity of a particular foil in the measured spectrum to the same foil's activity in the reference spectrum—normalized by the same ratio for dysprosium. This ratio depends only on the difference between the reference and the lattice spectra, not on flux intensities or counter efficiencies. The unfolded spectra were obtained from these ratios using a modified polynomial expansion scheme with a variable weighting function. The agreement between the results and the calculations is satisfactory; however, the agreement in the water regions is generally much better than in the fuel regions of the H_2O-moderated lattices. In the fuel regions, the measured spectra are consistently softer than the THERMOS-calculated spectra. The assumptions of a spatially constant "1/E" flux above ~0.7 eV, and the division of the space and energy variables into finite groups in the THERMOS calculations may contribute to these discrepancies. In the graphite lattice the experimental spectra are significantly harder than the THERMOS spectra calculated with a free gas kernel for graphite. Calculations with another code using a crystalline kernel show better agreement. (Diss. Abstr. Int., B)

Reactor Components, Fuels, and Accessories

Refer also to abstracts 12954, 13142, 13143, 13150, 13153, 13155, 13183, 13645, 13662, 13736–13738, 13745, 13780, 13782, 14970, 14971, and 15339.

15410 (ZJE–92) ROD MODELS OF FUEL ELEMENTS OF NUCLEAR REACTORS. Horcicka, J.; Krett, V.; Majer, J.; Sokol, J.; Stepanek, K.; Vlcek, J. (SKODA Concern, Pilsen (Czechoslovakia). Nuclear Power Plants Div.). 1970. 14p. Dep. NTIS (U. S. Sales Only).

A description of the individual types of fuel element models developed, as well as their manufacture and the manufacturing equipment used, is presented. Also described is the method of measuring thermal conductivity of fuel elements in isolation, and the thermocouples developed and now manufactured in the Nuclear Power Plants Division. (auth)

15411 DETERMINATION OF CERAMIC FUEL THERMAL CONDUCTIVITY AND GAP CONDUCTANCE BY THE BALANCED OSCILLATOR METHOD. **Daenner, Wolfgang (Kernforschungszentrum, Karlsruhe, Ger.). Nucl. Eng. Design; 14: 51-9(Oct 1970).**

The balanced oscillator method is described for in-pile application for measuring the thermal conductivity of ceramic fuels and the gap conductance. It is based upon a comparison of the experimentally and analytically determined transfer function between sinusoidal oscillations in coolant flow and specimen power at constant coolant temperatures. The analytical solution of the transfer function is deduced from the transient differential equation for heat conduction, taking into consideration radial variation of heat source, heat capacity of the cladding and time-dependence of the heat transfer coefficient. The results of out-of-pile experiments using carbon specimens prove the feasibility of the method and the completeness of the assumptions set up for the analytical solution. Suggestions for in-pile utilization of the method are also given. 27 references. (auth)

15412 GLASS-FIBRE-REINFORCED EPOXY LINER FOR SPENT-NUCLEAR-FUEL BAY. Williamson, A. S. (Ontario Hydro, Toronto). Ont. Hydro Res. Quart.; 22: No. 4, 1-5(1970).

Nuclear power stations require special facilities for storing spent fuel; these normally are large bays filled with demineralized water. An epoxy glass-fibre-reinforced coating system for the concrete bays has been developed, and following three years of laboratory tests the epoxy system has been installed in the spent-fuel bay at the Pickering nuclear generating station. (auth) (Canada)

15413 IMPROVEMENTS RELATING TO CONTROL SYSTEMS FOR NUCLEAR REACTORS. Dean, John Raymond (to A Reyrolle and Co. Ltd.). British Patent 1,216,993. 23 Dec 1970. Filed 15 Dec 1966.

In the system described the control rods are suspended individually or in groups by means of chains passed around a driving sprocket coupled to an actuating motor. The motor may be de-energised or declutched from the sprocket to allow descent of the rods under gravity. The braking means comprises a centrifugal governor mechanism, arranged to apply zero braking torque during the initial stage of downward acceleration of the rods until the sprocket rotation speed reaches a given value, and thereafter to apply a controlled braking torque. Various arrangements of governor mechanism and braking means are described. (UK)

15414 GRABHEADS FOR USE IN NUCLEAR REACTORS. Deacon, David; Evans, Timothy Lloyd; Peberdy, John Malcolm (to English Electric Co., Ltd.). British Patent 1,215,802. 16 Dec 1970. Filed 30 Dec 1966.

Improved solenoid-operated grabheads are described for reactor fuelling machines. (UK)

15415 NUCLEAR REACTOR FUEL ELEMENT STRINGERS. Butterfield, Colin Edgar (to United Kingdom Atomic Energy Authority). British Patent 1,215,750. 16 Dec 1970. Filed 19 Dec 1968.

Reference is made to stringers consisting of fuel element clusters tied together endwise by a central tie member. The improved tie member described comprises a wire rope the central core strand of which is tubular and provides access to the centre region of the member from one end of the stringer; such access may be required for a flux scanning wire or similar instrumentation. (UK)

15416 IMPROVEMENTS RELATING TO WINDING MECHANISMS FOR RAISING AND LOWERING SUSPENDED CONTROL RODS OF NUCLEAR REACTORS. Dean, John Raymond (to A, Reyrolle and Co., Ltd.). British Patent 1,216,994. 23 Dec 1970. Filed 11 Apr 1967.

The winding mechanism described comprises a driving sprocket or pulley around which the chain or cable attached to the control rod is passed, together with driving means to wind the control rod up and down. The excess length of chain or cable is wound around the pulley block system for storage as the control rod is wound up; this comprises a fixed pulley block having one or several pulley sheaves, and a movable pulley block with a corresponding number of pulley sheaves. The excess length of chain or cable leading from the driving sprocket or pulley is passed successively around the pulley sheaves of alternate blocks and is secured at its end to one of them. The moveable pulley block may be suspended below the fixed block by the suspension chain or cable to act as a tensioning weight. The driving sprocket or pulley is preferably mounted vertically above the fixed pulley block and the moveable block suspended vertically below the fixed block. Where the suspension means is a chain, a toothed driving sprocket is used, and the pulley sheaves, which need not be toothed sprockets, should be arranged one above another in line in each block, so that they

XUM

are generally coplanar. The diameters of the pulley sheaves in each block are graded so that the falls of chain will not cross or foul one another, but will remain substantially parallel. Such an arrangement enables a heavy duty chain to be used, which is only flexible in one plane. One pulley sheave may be resiliently mounted so as to be able to move transversely to its axis against spring means, to constitute a shock absorber for cushioning the control rod descent. (UK)

GENERAL

15417 (AEC-tr-7199) SPECTROSCOPY OF CHLOROPHYLL AND RELATED COMPOUNDS. Gurinovich, G. P.; Sevchenko, A. N.; Solov'ev, K. N. Translation of Spektroskopiya Khlorofilla i Rodstvennykh Soedinenii, Izdatel'stvo Nauka i Tekhnika, Minsk, 1968. 506p. Dep. NTIS.

15418 (ANL-Trans-871) ON THE PROBLEM OF THE ATOMIZATION OF A LIQUID BY A HIGH-VELOCITY GAS STREAM. Kunina, E. M.; Kheifets, M. I. Translated for Argonne National Lab., Ill.), from Inzh.-Fiz. Zh.; 19: 116-19(1970). 5p. Dep. NTIS.

15419 (BNL-15420) LIFT/DRAG RATIOS FOR MAGNETIC SUSPENSIONS. Powell, James R.; Danby, Gordon T. (Brookhaven National Lab., Upton, N. Y.). Dec 1970. 58p. Dep. NTIS.

15420 (BNL-tr-390) INVESTIGATION OF THE HEISENBERG MODEL OF THE IMPURE FERROMAGNETS. [PART] II. Provetski, E. (Joint Inst. for Nuclear Research, Dubna (USSR). Lab. of Theoretical Physics). Translated by S. J. Amoretty (Brookhaven National Lab., Upton, N. Y.), from Russian report. 15p. Dep. NTIS.

15421 (COO-1008-14) SULFONATE LEAVING GROUPS, STRUCTURE AND REACTIVITY: 2,2,2-TRIFLUOROETHANESULFONATE. Crossland, R. K.; Wells, W. E.; Shiner, V. J. Jr. (Indiana Univ., Bloomington. Dept. of Chemistry). [1970]. Contract AT(11-1)-1008. 11p. Dep. NTIS.

15422 (COO-1018-1219) SEQUENCE DETERMINATION FROM FRAGMENT DATA. Schwebel, John C. (Illinois Univ., Urbana. Dept. of Computer Science). 16 Nov 1970. Contract AT(11-1)-1018. 39p. Dep. NTIS.

15423 (COO-1198-775) TEMPERATURE CHANGES IN THIN FILMS DURING GROWTH BY PHYSICAL VAPOR DEPOSITION. Thornburg, David Devoe (Illinois Univ., Urbana. Dept. of Metallurgy and Mining Engineering). 1971. Contract AT(11-1)-1198. 211p. Dep. NTIS.

Thesis.

15424 (COO-1222-42) EFFECTS OF STRUCTURE OF PEPTIDE STATIONARY PHASES ON GAS-CHROMATOGRAPHIC SEPARATIONS OF AMINO-ACID ENANTIOMERS. Corbin, J. A.; Rhoad, J. E.; Rogers, L. B. (Purdue Univ., Lafayette, Ind. Dept. of Chemistry). [1970]. 20p. Dep. NTIS.

15425 (COO-1449-11) NATURE AND IMPORTANCE OF SELENIUM METABOLITES IN THE ANIMAL. Technical Progress Report, January 1, 1970–December 31, 1970. Halverson, A. W.; Palmer, I. S.; Whitehead, E. I. (South Dakota Agricultural Experiment Station, Brookings). Contract AT(11-1)-1449. 8p. Dep. NTIS.

15426 (COO-1473-4) GLACIOLOGICAL INVESTIGATIONS ON THE CASEMENT GLACIER, SOUTHEAST ALASKA. Final Report, May 1, 1965–October 31, 1969. Peterson, Donald N. (Ohio State Univ. Research Foundation, Columbus). Jul 1970. Contract AT(11-1)-1473. 172p. Dep. NTIS.

15427 (COO-1591-13) IMPURITY EFFECTS ON THE CREEP OF POLYCRYSTALLINE MAGNESIUM AND ALUMINUM OXIDES AT ELEVATED TEMPERATURES. Technical Progress Report, December 19, 1969–December 18, 1970. Gordon, Ronald S. (Utah Univ., Salt Lake City. Div. of Materials Science and Engineering). Contract AT(11-1)-1591. 85p. (UTEC-MSE-70-211). Dep. NTIS.

15428 (COO-1778-6) A STUDY OF GRAIN BOUNDARY SEGREGATION USING THE AUGER ELECTRON EMISSION TECHNIQUE. Annual Technical Progress Report, III. Stein, D. F.; Joshi, A.; Ramasubramanian, P. V. (Minnesota Univ., Minneapolis. School of Mineral and Metallurgical Engineering). 21 Dec 1970. Contract AT(11-1)-1778. 7p. Dep. NTIS.

15429 (COO-2026-4) KINETICS OF METHYLENE AND HYDROXYL RADICAL REACTIONS. Technical Progress Report. Carr, Robert W. Jr. (Minnesota Univ., Minneapolis. Dept. of Chemical Engineering). [1970]. Contract AT(11-1)-2026. 12p. Dep. NTIS.

15430 (COO-2118-2) ARITHMETIC UNIT OF ILLIAC III: SIMULATION AND LOGICAL DESIGN. PART II. Report No. 418. Koo, Ping L.; Atkins, Daniel E.; Goyal, Lakshmi N. (Illinois Univ., Urbana. Dept. of Computer Science). 28 Oct 1968; 10 Nov 1970. Contract AT(11-1)-2118. 165p. Dep. NTIS.

Revised and edited by Lakshmi N. Goyal. This report replaces Report No. 290.

15431 (CU-3954-3) PARTICLE-IN-CELL METHOD FOR MODEL KINETIC EQUATIONS. Mason, R. J. (Bell Telephone Labs., Inc., Whippany, N. J.); Chu, C. K. (Columbia Univ., New York). 1970. Contract AT(30-1)-3954. 9p. (CONF-700712-1). Dep. NTIS.

From 7th International Symposium on Rarefied Gas Dynamics, Pisa, Italy.

15432 (CU-3957-9) EFFECT OF CHEMICAL MODIFICATION OF DNA ON ITS MACROMOLECULAR STRUCTURE. Progress Report, May 1, 1970–January 15, 1971. Krasna, Alvin I. (Columbia Univ., New York. Dept. of Biochemistry). 9p. Dep. NTIS.

15433 (GJO-918-4) ELIPGRID: A FORTRAN IV PROGRAM FOR CALCULATING THE PROBABILITY OF SUCCESS IN LOCATING ELLIPTICAL TARGETS WITH SQUARE, RECTANGULAR, AND HEXAGONAL GRIDS. Final Report, Part 1b. Singer, Donald A. (Grand Junction Office (AEC), Colo.). [1970]. Contract AT(05-1)-918. 30p. Dep. NTIS.

15434 (JAB-99-35) SECOND PROGRESS REPORT ON RACKING TESTS OF WALL PANELS. (Blume (John A.) and Associates Research Div., San Francisco, Calif.). Jul 1968. Contract AT(26-1)-99. 148p. Dep. NTIS.

15435 (LA-4573) SOME ELEMENTARY ATTEMPTS AT NUMERICAL MODELING OF PROBLEMS CONCERNING RATES OF EVOLUTIONARY PROCESSES. Schrandt, R.; Ulam, S. (Los Alamos Scientific Lab., N. Mex.). Dec 1970. Contract W-7405-eng-36. 9p. Dep. NTIS.

15436 (NYO-2798-49) THYMINE PHOTOTRIMER. Wang, Shih Yi (Johns Hopkins Univ., Baltimore, Md. Dept. of Biochemistry). [1970]. 18p. Dep. NTIS.

15437 (NYO-3087-19) DISLOCATIONS IN CRYSTALS. Geiss, Roy H. (Virginia Univ., Charlottesville. Dept. of Materials Science). [nd]. 2p. (CONF-680905-5). Dep. NTIS.

From 26th Annual Meeting of the Electron Microscopy Society of America, New Orleans, La.

15438 (NYO-3360-55) CALCIUM KINETICS IN COWS. Annual Progress Report No. 7. Ramberg, C. F. Jr. (Pennsylvania Univ., Kennett Square. School of Veterinary Medicine). 22 Dec 1970. Contract AT(30-1)-3360. 9p. Dep. NTIS.

15439 (NYO-3827-18) CHARACTERISTICS OF THE NUCLEAR RNA POLYMERASE FROM RAT ANTERIOR PITUITARY TISSUE. Augustine, E. C.; Hymer, W. C. (Pennsylvania State Univ., University Park. Dept. of Biology). 30 Aug 1970. Contract AT(30-1)-3827. 32p. Dep. NTIS.

15440 (ORNL-TM-2484) FORTRAN PROGRAM FOR COMPUTING TWO-DIMENSIONAL MAGNETIC FIELDS. Stevens, S. S. (Oak Ridge National Lab., Tenn.). Jan 1971. 9p. Dep. NTIS.

15441 (ORNL-TM-3237) A SELECTION PROCEDURE BASED UPON WALD'S DOUBLE DICHOTOMY TEST. Hoel, David G. (Oak Ridge National Lab., Tenn.). Feb 1971. Contract W-7405-eng-26. 11p. Dep. NTIS.

15442 (ORNL-TM-3280) BIOLOGICAL MACROMOLECULAR SEPARATIONS TECHNOLOGY PROJECT. Progress Report, October 1, 1970–December 31, 1970. Kelmers, A. D. (comp.) (Oak Ridge National Lab., Tenn.). Feb 1971. Contract W-7405-eng-26. 24p. Dep. NTIS.

15443 (ORNL-tr-2426) XERODERMAL IDIOCY. De Sanctis, Carlo; Cacchione, Aldo. Translated by R. Gregg Mansfield (Oak Ridge National Lab., Tenn.), from Riv. Sper. Freniat. Med. Leg. Alienazioni Ment.; 56: 269-92(1932). 23p. Dep. NTIS.

15444 (ORNL-tr-2431) RESISTANCE TO SMALL SPHERES BY FRICTIONAL MEDIA. Sexl, Theodor. Translated by R. Gregg Mansfield (Oak Ridge National Lab., Tenn.), from Acta Phys. Austr.; 26: 59-62(1967). 4p. Dep. NTIS.

XUM

15445 (ORO–2036–21) IMPURITY DIFFUSION IN ALUMINUM AND ITS DILUTE ALLOYS. Alexander, W. B.; Slifkin, L. M. (North Carolina Univ., Chapel Hill). [1970]. Contract AT(40-1)-2036. 7p. (CONF-700639–1). Dep. NTIS.

From International Conference on Atomic Transport in Solids and Liquids, Marstrand, Sweden.

15446 (ORO–2410–18) NITRATE AND AMMONIUM UPTAKE AND ASSIMILATION, AND THEIR INFLUENCE ON STRONTIUM UPTAKE AND TRANSLOCATION BY HIGHER PLANTS. Annual Progress Report, May 1, 1970–April 30, 1971. Jackson, William A. (North Carolina State Univ., Raleigh). Jan 1971. Contract AT(40-1)-2410. 54p. Dep. NTIS.

15447 (ORO–2410–19) NITRATE AND AMMONIUM UPTAKE AND ASSIMILATION, AND THEIR INFLUENCE ON STRONTIUM UPTAKE AND TRANSLOCATION BY HIGHER PLANTS. Three-Year Summary Report, May 1, 1968–April 30, 1971. Jackson, William A. (North Carolina State Univ., Raleigh. Dept. of Soil Science). Contract AT(40-1)-2410. 16p. Dep. NTIS.

15448 (RLO–2017-3) TECHNETIUM AS A CATALYST IN ORGANIC REACTIONS. Final Report. Blackham, Angus U.; Palmer, James L. (Brigham Young Univ., Provo, Utah. Dept. of Chemistry). 30 Sep 1970. Contract AT(45-1)-2017. 83p. Dep. NTIS.

15449 (RLO–2214-1) NATURAL CONVECTIVE HEAT TRANSFER BETWEEN CONCENTRIC SPHERES. Annual Progress Report. Scanlan, J. A.; Bishop, E. H. (Montana State Univ., Bozeman). Jan 1971. Contract AT(45-1)-2214. 15p. Dep. NTIS.

15450 (RLO–2214-2) NATURAL CONVECTION HEAT TRANSFER BETWEEN CONCENTRIC SPHERES. Scanlan, J. A.; Bishop, E. H.; Powe, R. E. (Montana State Univ., Bozeman). [nd]. Contract AT(45-1)-2214. 33p. Dep. NTIS.

15451 (SAN–310-P-4-10) PATHWAYS OF TRACE ELEMENTS IN ARCTIC LAKE ECOSYSTEMS. Progress Report, April 15, 1970–April 14, 1971. Barsdate, Robert J. (Alaska Univ., College. Inst. of Marine Science). Jan 1971. Contract AT(04-3)-310. 151p. (R–71-2). Dep. NTIS.

15452 (SAN–781-2012(Pt.1)) ISOCHRONOUS STRESS–STRAIN CURVES FOR 2 $^1/_4$ Cr–1 Mo, TYPE 304-304H, AND TYPE 316-316H STEELS. PART I. (United Nuclear Corp., Elmsford, N. Y. Research and Engineering Center. Braun (C. F.) and Co., Alhambra, Calif.). 16 Oct 1970. Contract AT(04-3)-781. 37p. Dep. NTIS.

15453 (SC-DR-70-911) FUNCTIONAL TEST OF A ROCKET ENGINE MODULE (REM). Morgan, John H.; Bennett, Lawrence C. (Sandia Labs., Albuquerque, N. Mex.). Oct 1970. 20p. Dep. NTIS.

15454 (SC-RR–70-762) RAMAN SCATTERING IN LIQUID LASING MATERIAL CONTAINING $POCl_3$. Fitch, M. J. (Sandia Labs., Albuquerque, N. Mex.). Dec 1970. 14p. Dep. NTIS.

15455 (SC-T–71-3004) INTERNAL OXIDATION OF NICKEL ALLOYS CONTAINING SMALL AMOUNTS OF CHROMIUM. Goto, Shoji; Koda, Sigeyasu; Nomaki, Koji. Translated for Sandia Labs., Albuquerque, N. Mex., from J. Jap. Inst. Metals; 31: 600-6(1967). 25p. Dep. NTIS.

15456 (SC-T–71-3005) SYMMETRY AND MICROWAVE SPECTRA OF POLYATOMIC PARAMAGNETIC CENTERS. Kneubuehl, Fritz K. Translated for Sandia Labs., Albuquerque, N. Mex., from Phys. Kondens. Mater.; 1: 410-47(1963). 50p. Dep. NTIS.

15457 (SCL-T–71-209) ON THE PRODUCTION OF HIGH TEMPERATURES AND PRESSURES (7 kbar, 1600°C). Yasunami, M.; Fukuda, T.; Takahashi, O. Translated by K. Nakamura from 11th Symposium on High Pressure, Chemical Soc. of Japan, 24–26 October 1969, Sendai, Japan. 11p. (CONF-691048–2). Dep. NTIS.

15458 (SCL-T–71-210) HIGH-PRESSURE MEASUREMENT USING SEMICONDUCTOR STRAIN GAGES. Yasunami, K.; Moritoki, M. Translated by K. Nakamura from 11th Symposium on High Pressure, Chemical Soc. of Japan, 24–26 October 1969, Sendai, Japan. 11p. (CONF-691048–3). Dep. NTIS.

15459 (SCL-T–71-212) VAPOR-LIQUID EQUILIBRIA AT HIGH PRESSURE. Yorizane, M.; Yoshimura, S.; Masuoka, H. Translated by K. Nakamura from 11th Symposium on High Pressure, Chemical Soc. of Japan, 24–26 October 1969, Sendai, Japan. 6p. (CONF-691048–4). Dep. NTIS.

15460 (STI/DOC–11(Vol.8)(No.2)) LIST OF BIBLIOGRAPHIES ON NUCLEAR ENERGY. (International Atomic Energy Agency, Vienna (Austria)). 1970. 32p.

15461 (TID–25641) SOME ASPECTS OF THE BEHAVIOR OF COMPLEX COMPOUNDS. Final Report. Jones, Mark M. (Vanderbilt Univ., Nashville, Tenn.). 1 Jul 1970. Contract AT(40-1)-2676. 19p. Dep. NTIS.

15462 (UCRL–20202) DEVELOPMENT AND ORGANIZATION OF PHOTOSYNTHETIC PIGMENT SYSTEMS. Schultz, Alfred Joseph Jr. (California Univ., Berkeley. Lawrence Radiation Lab.). Nov 1970. Contract W-7405-eng-48. 142p. Dep. NTIS.

Thesis.

15463 (UCRL–20376) NUCLEAR RELAXATION IN NICKEL ALLOYS. Chornik, Boris (California Univ., Berkeley. Lawrence Radiation Lab.). Dec 1970. Contract W-7405-eng-48. 90p. Dep. NTIS.

Thesis.

15464 (UCRL–50937) RISK OF CARCINOGENESIS FROM LONG-TERM LOW-DOSE EXPOSURE TO POLLUTION EMITTED BY FOSSIL-FUELED POWER PLANTS. Watson, Donald E. (California Univ., Livermore. Lawrence Radiation Lab.). 1 Oct 1970. 14p. Dep. NTIS.

15465 (UCRL–50948) DETERMINATION OF BORON IN BORATES, BORON HYDRIDES, ORGANO-BORON COMPOUNDS, ELEMENTAL BORON AND REFRACTORY BORIDES. Rigdon, L. P.; Waggoner, M. C. (California Univ., Livermore. Lawrence Radiation Lab.). 8 Oct 1970. 10p. Dep. NTIS.

15466 (UCRL–50950) SHOCK–PULSE ATTENUATION AND HUGONIOT STUDIES OF THREE EXPLOSIVES AND THREE MOCK EXPLOSIVES. Wasley, Richard J.; Valentine, Robert H. (California Univ., Livermore. Lawrence Radiation Lab.). 12 Oct 1970. 20p. Dep. NTIS.

15467 (UCRL–72663) OPTIMUM DESIGN OF TWO-DIMENSIONAL NONRECURSIVE DIGITAL FILTERS. Ekstrom, M. P.; Algazi, V. R. (California Univ., Livermore. Lawrence Radiation Lab.). 19 Nov 1970. 8p. (CONF-701117–1). Dep. NTIS.

From 4th Asilomar Conference on Circuits and Systems, Pacific Grove, Calif.

15468 (UCSD–10-P-20-54) ECOLOGY OF THE PLANKTON OFF LA JOLLA, CALIFORNIA, IN THE PERIOD APRIL–SEPTEMBER 1967. Strickland, J. D. H. (ed.) (Scripps Institution of Oceanography, La Jolla, Calif.). 1970. 103p. Dep. NTIS.

15469 (Y–1748) REMOTE DATA STATION INTERFACE TO THE PRODUCTION CONTROL COMPUTER. Bowers, G. L.; Carver, D. W.; Davenport, C. M.; Falcon, J. P.; Stephens, A. E. (Union Carbide Corp., Oak Ridge, Tenn. Y-12 Plant). 20 Jan 1971. Contract W-7405-eng-26. 35p. Dep. NTIS.

XUM

CORPORATE AUTHOR INDEX

In the Corporate Author Index, technical report literature is indexed by the organization or institution responsible for issuing the report. Entries are given for all report literature and for published literature for which a corporate author approach is especially desirable, e.g., symposium and conference proceedings.

Each entry under a corporate author gives the publication title and the *NSA* volume and abstract numbers. Report numbers, where applicable, are given in parentheses at the end of the entry.

A

AEROJET-GENERAL CORP., SACRAMENTO, CALIF. MATERIALS RESEARCH LAB.
  Phase diagram for W--B--C, 25:13763 (AD-713154)
  Phase diagrams of Ti--Nb--C, Ti--Ta--C, and Ti--Mo--C, 25:13762 (AD-713153)
AEROSPACE CORP., EL SEGUNDO, CALIF.
  Prog. rpt. on 3.3-mm and soft x-ray bursts, 3/68--12/69, 25:13860 (AD-711784)
  Solar electron access to closed field lines, 25:14101 (AD-712045)
  Surface and bulk waves on axially magnetized plasma columns, 25:14360 (AD-711649)
AIR FORCE CAMBRIDGE RESEARCH LABS., L. G. HANSCOM FIELD, MASS.
  Stellar standards at 10 microns, 25:13788 (AD-711364)
AKADEMIYA NAUK ESTONSKOI SSR, TARTU. INSTITUT FIZIKI I ASTRONOMII.
  Combined Bondi and fast approximation method in general relativity. II, 25:14807 (NP-18559)
AKADEMIYA NAUK UKRAINSKOI SSR, KHARKOV. FIZIKO-TEKHNICHESKII INSTITUT.
  Automating a 2-GeV electron linac, 25:14852 (SLAC-Trans-126)
AKADEMIYA NAUK UKRAINSKOI SSR, KIEV. INSTITUT TEORETICHESKOI FIZIKI.
  Consequence of analiticity of the π π-scattering amplitude, 25:14682 (ITF-70-60-E)
  Decay μ + e + ν + anti ν and limitations on neutrino and w boson masses and on variants of weak interaction, 25:14631 (ITF-70-64)
  Equations of motion invariant with respect to group P(1,n). II, 25:14747 (ITF-70-70)
  Scattering of high-energy γ quanta on the nucleons and nuclei, 25:14595 (ITF-70-63-P)
AKTIEBOLAGET ATOMENERGI, STUDSVIK (SWEDEN).
  Method for calculating the washout of elemental iodine by water sprays, 25:15372 (AE-408)
ALASKA UNIV., COLLEGE. INST. OF MARINE SCIENCE.
  Prog. rpt. on pathways of trace elements in Arctic Lake ecosystems, annual, 4/15/70--4/14/71, 25:15451 (SAN-310-P-4-10)
ALBERTA UNIV., EDMONTON. NUCLEAR RESEARCH CENTRE.
  Further calculations of proton inelastic polarizations and asymmetries using a spin-dependent interaction of the full Thomas form, 25:14892 (RLO-1388-600)
AMSTERDAM UNIV. (NETHERLANDS).
  Properties of deformed nuclides produced in decay of ^{166}Ho, /sup 166m/Ho, ^{166}Tm, ^{166}Yb, ^{180}Os, ^{180}Re, ^{181}Os, and /sup 181m/Os, and by capture of thermal neutrons in ^{181}Ta, 25:14984 (NP-18536)
AMSTERDAM UNIV. (NETHERLANDS). ZEEMAN-LABORATORIUM.
  HPD--CDC 3200 system at Amsterdam, 25:13275 (CERN-70-21(Vol.2), pp 709-20)
ANSALDO S.p.A., GENOA (ITALY).
  Nuclear fuel with burnable poison. II, 25:13736 (EUR-4551)
ARGONNE NATIONAL LAB., ILL.
  Apparatus for high-speed photographic experiments with irradiated fast-reactor fuel specimens, 25:15384 (ANL-7578)
  Automatic scanning and measurement of bubble chamber film on Polly II, 25:13254 (CERN-70-21(Vol.1), pp 325-55)
  Chemical Engineering Division fuel cycle technology quarterly report, July--September 1970, 25:13077 (ANL-7755)
  Glossary of on-line measuring devices, 25:13294 (CERN-70-21(Vol.2), pp 963-77)
  Inversion of de Haas--van Alphen data. I, 25:14433 (ANL-7659)
  Multiple scattering of gamma radiation, 25:14393 (ANL-7689)
  On-line computer facilities at Argonne, 25:14838 (CERN-70-21(Vol.2), pp 525-37)
  Prog. rpt. on sodium technology, 7--9/70, 25:13651 (ANL/ST-4)
  Reactor development program progress report, December 1970, 25:15339 (ANL-7765)
ARKANSAS POWER AND LIGHT CO., LITTLE ROCK.
  Arkansas Nuclear One, Unit 2. Preliminary safety analysis report, Suppl. 2, 25:15332 (DOCKET-50368-7)
ARMY ELECTRONICS COMMAND, FORT MONMOUTH, N. J.
  High-order perturbation theory for a one-electron ion immersed in a plasma, 25:14283 (AD-710950)
ARMY ENGINEER NUCLEAR CRATERING GROUP, LIVERMORE, CALIF.
  Concept of row crater enhancement, 25:13135 (AD-713574)
  Seepage characteristics of explosively produced craters in soil and rock, 25:13102 (NCG-TR-27)
ARMY ENGINEER WATERWAYS EXPERIMENT STATION, VICKSBURG, MISS.
  Cratering in Greenland icecap snow, 25:13133 (AD-711861)
  Far-field characteristics of ground shock induced by explosions, 25:13129 (AD-713521)
  Neutron streaming through two-legged concrete ducts with baffles, 25:14391 (AD-710963)
  Seepage characteristics of explosively produced craters in soil and rock, 25:13102 (NCG-TR-27)
ATOMIC ENERGY COMMISSION, BAGHDAD (IRAQ). NUCLEAR RESEARCH INST.
  Effect of γ irradiation on phosphorous metabolism and nucleic acid synthesis in wheat seedlings, 25:13597 (NP-18606)
ATOMIC ENERGY OF CANADA LTD., CHALK RIVER (ONTARIO).
  Review of heavy water production processes, 25:13076 (AECL-2503)
ATOMIC ENERGY RESEARCH ESTABLISHMENT, HARWELL (ENGLAND).
  Coherent neutron scattering length of ^{17}O, 25:14862 (AERE-R-5770)
  Evacuable glove-box for handling of liquid sodium, and apparatus for analysis of carbon in sodium and other metals, 25:13185 (AERE-R-6338)
  Experimental study of spouting beds of spheres, 25:13139 (AERE-R-4852)
  Method for using standard burst cartridge precipitator equipment for fuel activity release monitoring on a Mk. III high temperature gas cooled reactor, 25:15373 (AERE-R-6475)
ATOMIC INDUSTRIAL FORUM, INC., NEW YORK.
  Legal framework for industrial Plowshare applications, 25:13137 (NP-18659)
ATOMIC WEAPONS RESEARCH ESTABLISHMENT, ALDERMASTON (ENGLAND).
  Reactions (n,n'γ) in ^{51}V and ^{89}Y, 25:14919 (AWRE-O-78/70)
ATOMICS INTERNATIONAL, CANOGA PARK, CALIF.
  Testing of a cascaded thermoelectric module, 25:14082 (N-70-39764)
AUSTRALIAN ATOMIC ENERGY COMMISSION RESEARCH ESTABLISHMENT, LUCAS HEIGHTS.
  Japanese A.T.R. Reactor, 25:15338 (AAEC/LIB/Bib-258)
  Physics of the dynamic growth of mushroom clouds, associated with nuclear explosions, 25:13131 (AAEC/LIB/Bib-255)
  Radiation-induced polymerization. I, 25:13029 (AAEC/LIB/Bib-259)
  Radiation-induced polymerization. II, 25:13030 (AAEC/LIB/Bib-260)
  Radiation-induced polymerization. III, 25:13031 (AAEC/LIB/Bib-261)
  Resonance parameters for measured keV neutron capture cross sections, 25:14979 (AAEC/E-198(Suppl.1))

B

BABCOCK AND WILCOX CO., LYNCHBURG, VA. NUCLEAR POWER GENERATION DEPT.
  Effectiveness of sodium thiosulfate sprays for iodine removal, 25:15374 (BAW-10024)

BALLISTIC RESEARCH LABS., ABERDEEN PROVING GROUND, MD.
- Effects of high-energy electron irradiation on single crystals of ammonium and sodium bifluoride, 25:14411 (AD-712321)
- Experimental comparison of fallout field simulation techniques, 25:13117 (AD-711532)

BATTELLE MEMORIAL INST., COLUMBUS, OHIO.
- Connecticut Yankee Atomic Power Plant. Examination and evaluation of Capsule A for pressure-vessel surveillance program. Final report, 25:15265 (DOCKET-50213-95)

BATTELLE-NORTHWEST, RICHLAND, WASH. PACIFIC NORTHWEST LAB.
- Analysis of hydrological factors influencing operation of 100-N emergency waste disposal Crib, 25:13186 (BNWL-1503)
- Criticality safety analysis: Model 60 shipping package for FFTF driver fuel, 25:13187 (BNWL-1512)
- Neutron radiography with ^{252}Cf, 25:13161 (BNWL-SA-3169)
- Survey of alpha waste generation and disposal as solids in the U. S. nuclear fuel industry, 25:13188 (BNWL-B-34)
- Water and sorbed-gas content of hypostoichiometric mixed oxide fuel pellets, 25:12925 (WHAN-SA-77)

BELL TELEPHONE LABS., INC., WHIPPANY, N. J.
- Particle-in-cell method for model kinetic equations, 25:15431 (CU-3954-3)

BETTIS ATOMIC POWER LAB., PITTSBURGH, PA.
- Fracture mechanics evaluation of stress intensity factors for various crack geometries and loading conditions, 25:13181 (WAPD-TM-976)
- In-pile dimensional changes of ThO_2--UO_2 fuel rods with non-free-standing cladding (LWBR Development Program), 25:15366 (WAPD-TM-986)
- Space--time methods for movable fuel problems (LWBR Development Program), 25:15353 (WAPD-TM-968)

BIRMINGHAM UNIV. (ENGLAND). DEPT. OF PHYSICS.
- Birmingham track analysis system, 25:13292 (CERN-70-21(Vol.2), pp 949-52)
- Vast: a video assisted scan table, 25:13238 (CERN-70-21(Vol.1), pp 47-58)

BLUME (JOHN A.) AND ASSOCIATES RESEARCH DIV., SAN FRANCISCO, CALIF.
- Prog. rpt. on racking tests of wall panels, 7/68, 25:15434 (JAB-99-35)

BONN UNIV. (WEST GERMANY). PHYSIKALISCHES INSTITUT.
- Experiences with coupled computers to control an HPD, 25:13276 (CERN-70-21(Vol.2), pp 721-7)

BOSTON EDISON CO., MASS.
- Pilgrim Nuclear Power Station. Preliminary safety analysis report, Amendment 18 (includes additions and revisions to final safety analysis report), 25:15306 (DOCKET-50293-34)
- Pilgrim Nuclear Power Station. Preliminary safety analysis report, Amendment 19 (includes additions and revisions to final safety analysis report), 25:15307 (DOCKET-50293-35)

BRAUN (C.F.) AND CO., ALHAMBRA, CALIF.
- Development and verification of design guide for LMFBR sodium piping, 25:15355 (SAN-781-100)
- Isochronous stress--strain curves for 2 $^1/_4$ Cr--1 Mo, type 304-304H, and type 316-316H steels. Part I, 25:15452 (SAN-781-2012(Pt.1))
- Philosophy and criteria of the design guide for LMFBR sodium piping, 25:15360 (SAN-781-500)
- Piping materials for LMFBR plants. Technical report 228 (Revision 1), 25:15357 (SAN-781-228)
- Review of fabrication and installation requirements for LMFBR piping, 25:15356 (SAN-781-220)
- Review of in-service surveillance methods applicable to liquid sodium piping, 25:15359 (SAN-781-243)
- Study of dynamic analysis methods as related to LMFBR piping systems, 25:15362 (UNC-5231)
- Study of model test methods as related to LMFBR piping systems, 25:15358 (SAN-781-234)
- Summary of research and development recommendations for LMFBR piping, 25:15361 (SAN-781-518)

BRIGHAM YOUNG UNIV., PROVO, UTAH. DEPT. OF CHEMISTRY.
- Technetium as a catalyst in organic reactions, 25:15448 (RLO-2017-3)

BROOKHAVEN NATIONAL LAB., UPTON, N. Y.
- 1000-GeV storage rings, 25:14835 (BNL-15423)
- Lift/drag ratios for magnetic suspensions, 25:15419 (BNL-15420)
- Method for decreasing energy spread in AGS beam, 25:14836 (BNL-15424)
- Operational experience with the Brookhaven On-Line Data Facility, 25:13289 (CERN-70-21(Vol.2), pp 921-30)
- Precompound decay from a time-dependent point of view, 25:15140 (CU-1019-79)
- Prog. rpt., annual, 7/70, 25:14837 (BNL-50230)
- Two loop approximations to propagators in the sigma model, 25:14683 (NYO-2262-TA-219)

BROWN UNIV., PROVIDENCE, R. I.
- Fine structure in highly excited analog states, 25:15145 (NYO-1082-25)

BROWN UNIV., PROVIDENCE, R. I. DEPT. OF PHYSICS.
- Consistency of hard pion theorems in K/sub 13/ decays, 25:14633 (NYO-2262-TA-233)
- Resonant elastic scattering of protons from analogue and compound states, 25:15146 (NYO-1082-29)
- Two loop approximations to propagators in the sigma model, 25:14683 (NYO-2262-TA-219)

BUREAU OF RADIOLOGICAL HEALTH, WINCHESTER, MASS. NORTHEASTERN RADIOLOGICAL HEALTH LAB.
- Liquid waste effluents from a nuclear fuel reprocessing plant, 25:12950 (BRH/NERHL-70-2)

C

CALIFORNIA UNIV., BERKELEY. COLL. OF ENGINEERING.
- Diagnostic studies in an induction-heated supersonic argon plasma, 25:14243 (AD-711127)

CALIFORNIA UNIV., BERKELEY. DIV. OF AERONAUTICAL SCIENCES.
- Cylindrical Langmuir-probe response in transition regime, 25:14242 (AD-711095)

CALIFORNIA UNIV., BERKELEY. LAWRENCE RADIATION LAB.
- Defects and phase transformations in cobalt ferrites, 25:13783 (UCRL-20369)
- Development and organization of photosynthetic pigment systems, 25:15462 (UCRL-20202)
- Energy spectra of backscattered electrons and positrons by Monte Carlo calculations, 25:13959 (UCRL-19719)
- Modification of Berkeley Hilac, 25:14853 (UCRL-19919)
- Nuclear relaxation in nickel alloys, 25:15463 (UCRL-20376)
- Performance of the DAPR system, 25:13280 (CERN-70-21(Vol.2), pp 761-804)
- Two Reggeon exchange contributions to hadron scattering amplitudes at high energy, 25:14657 (UCRL-20032)

CALIFORNIA UNIV., LIVERMORE. LAWRENCE RADIATION LAB.
- Determination of boron in borates, boron hydrides, organo-boron compounds, elemental boron and refractory borides, 25:15465 (UCRL-50948)
- Dispersion hardening of a Mo--1 at. percent Hf alloy by internal hardening, 25:13661 (UCRL-72627)
- Evaluation of trapping and tailing effects in Ge(Li) detectors, 25:13213 (UCRL-71508)
- Fate of Schooner fallout radionuclides ingested by the dairy cow, 25:13396 (UCRL-72511)
- Fission gas release curves: growth and decay from fission of ^{239}Pu by fission spectrum neutrons, 25:14989 (UCRL-50656(Suppl.))
- K-division experimental work. Part I. Geophysics research for underground explosion technology, 25:13104 (UCRL-50855)
- Optimum design of two-dimensional nonrecursive digital filters, 25:15467 (UCRL-72663)
- Plowshare and the environment, 25:13430 (UCRL-72830)
- Risk of carcinogenesis from long-term low-dose exposure to pollution emitted by fossil-fueled power plants, 25:15464 (UCRL-50937)
- Shock--pulse attenuation and hugoniot studies of three explosives and three mock explosives, 25:15466 (UCRL-50950)
- Weapons Effects Display System (WEDS MOD II): maintenance manual. I, 25:13322 (UCRL-50892(Vol.4)(Pt.1))
- Weapons effects display system (WEDS MOD II): maintenance manual. II, 25:13323 (UCRL-50892(Vol.4)(Pt.2))

CALIFORNIA UNIV., LOS ANGELES.
- UCLA SMP system, 25:13249 (CERN-70-21(Vol.1), pp 243-60)

CALIFORNIA UNIV., SANTA BARBARA.
- Optical spectroscopic investigation of helium and nitrogen plasmas, 25:14277 (AD-712024)

CAMBRIDGE UNIV. (ENGLAND). CAVENDISH LAB.
- Performance of Sweepnik I, 25:13252 (CERN-70-21(Vol.1), pp 293-308)
- Sweepnik II, an improved track measuring machine, 25:13251 (CERN-70-21(Vol.1), pp 285-92)

CAROLINA POWER AND LIGHT CO., RALEIGH, N.C.
- H. B. Robinson Unit No. 2. Safety injection system performance at 2300 MWt and reanalysis of affected fault conditions, 25:15292 (DOCKET-50261-50)

CENTRAL ELECTRICITY GENERATING BOARD, BERKELEY (ENGLAND). BERKELEY NUCLEAR LABS.
- Characterisation of the surface roughness of graphite, 25:13765 (RD/B/N-1770)

CENTRE NATIONAL DE LA RECHERCHE SCIENTIFIQUE, GRENOBLE (FRANCE).
- Magnetic properties and structures of CrB compounds Tb--$Ge_{0.2}Si_{0.8}$, HoSi, ErSi, and TmSi, 25:14434 (CEA-CONF-1701)

CENTRE NATIONAL DE LA RECHERCHE SCIENTIFIQUE, PARIS (FRANCE).
- Conference on structure and properties of the surfaces of solids, Paris, 7/69, 25:13734

CHALMERS TEKNISKA HOGSKOLA, GOTEBORG (SWEDEN).
- Damage in gold bombarded with medium mass ions, 25:14413 (NP-18645)

CHICAGO UNIV., ILL. ENRICO FERMI INST.
- Wire spark chamber design and performance using FET, capacitor readout, 25:13264 (CERN-70-21(Vol.2), pp 539-48)

CINCINNATI GAS AND ELECTRIC CO., OHIO.
- Wm. H. Zimmer Nuclear Power Station, Unit 1. Environmental report, 25:15327 (DOCKET-50358-11)
- Wm. H. Zimmer Nuclear Power Station, Unit 1. Preliminary safety analysis report, Amendment 5, 25:15328 (DOCKET-50358-12)

COLLEGE DE FRANCE, PARIS.
- Use of a simple geometry program for filtering HPD data,

25:13273 (CERN-70-21(Vol.2), pp 679-85)

COLLEGE DE FRANCE, PARIS. LABORATOIRE DE PHYSIQUE ATOMIQUE ET MOLECULAIRE.

Breit--Wigner models and effective range approximations, 25:14702 (PAM-70-8)

COLLEGE DE FRANCE, PARIS. LABORATOIRE DE PHYSIQUE NUCLEAIRE.

Automatic gain control in signal processing for bubble chamber pictures, 25:13257 (CERN-70-21(Vol.1), pp 383-97)

Use of Coccinelle to scan and measure big bubble chamber pictures, 25:13256 (CERN-70-21(Vol.1), pp 371-81)

COLORADO STATE UNIV., FORT COLLINS. DEPT. OF ATMOSPHERIC SCIENCE.

Atmospheric transport processes. II, 25:13121 (TID-25314)

COLORADO UNIV., BOULDER.

Prog. rpt. on models for magnetofluid dynamics, of the Sun, final, 6/15/67--6/15/70, 25:13858 (AD-710629)

COLORADO UNIV., BOULDER. DEPT. OF PHYSICS AND ASTROPHYSICS.

Comments on shapes of angular distributions of (^{3}He,t) and (p,n) transitions to 0^+ anti-analog states, 25:14924 (COO-535-625)

COLUMBIA UNIV., NEW YORK.

Particle-in-cell method for model kinetic equations, 25:15431 (CU-3954-3)

Progress in automatic scanning at Columbia, 25:13253 (CERN-70-21(Vol.1), pp 311-21)

COLUMBIA UNIV., NEW YORK. DEPT. OF BIOCHEMISTRY.

Prog. rpt. on effect of chemical modification of DNA on its macromolecular structure, 5/70--1/71, 25:15432 (CU-3957-9)

COLUMBIA UNIV., NEW YORK. PLASMA LAB.

Magnetic structure of oblique and normal ionizing shock waves, 25:14284 (AD-711086)

COLUMBUS AND SOUTHERN OHIO ELECTRIC CO., COLUMBUS, OHIO.

Wm. H. Zimmer Nuclear Power Station, Unit 1. Environmental report, 25:15327 (DOCKET-50358-11)

Wm. H. Zimmer Nuclear Power Station, Unit 1. Preliminary safety analysis report, Amendment 5, 25:15328 (DOCKET-50358-12)

COMITATO NAZIONALE PER L'ENERGIA NUCLEARE, ROME (ITALY).

Dosimetric use of beryllium oxide as a thermoluminescent material, 25:13304 (RT/PROT-(70)23)

COMMISSARIAT A L'ENERGIE ATOMIQUE, FONTENAY-AUX-ROSES (FRANCE). CENTRE D'ETUDES NUCLEAIRES.

Aerosols produced by evaporation of uranium wire, 25:13650 (AI-Trans-289)

ANISN system. Description and use of discrete ordinate program ANISN and of auxiliary programs, 25:14863 (CEA-N-1358)

Automation of a series of radioactive measurements on biological specimens, 25:13229 (CEA-CONF-1647)

LGR/B program: for updating the ANISN library tapes with plotting of cross section curves, 25:14986 (ORNL-tr-2408)

Measurement of the neutron albedo of ordinary concrete, 25:14394 (CEA-N-1382)

Program Poker. Description and utilization, 25:14864 (CEA-N-1388)

Study of a marine site with a view to radioactive effluent discharge, 25:13189 (CEA-CONF-1712)

COMMISSARIAT A L'ENERGIE ATOMIQUE, GRENOBLE (FRANCE). CENTRE D'ETUDES NUCLEAIRES.

Determination of internal and superficial oxygen content of molybdenum obtained using 54 MeV α particles and low energy deuterons, 25:12957 (LYCEN-7076)

Influence of radiation and amount of palmitate-1-^{14}C on distribution of this fatty acid in different lipid classes of Ehrlich ascites, 25:13362 (CEA-R-4039)

Magnetic properties and structures of CrB compounds Tb--$Ge_{0.2}Si_{0.8}$, HoSi, ErSi, and TmSi, 25:14434 (CEA-CONF-1701)

COMMISSARIAT A L'ENERGIE ATOMIQUE, SACLAY (FRANCE). CENTRE D'ETUDES NUCLEAIRES.

Ariane II: automatic device for the analysis of spark chamber photographs, 25:13285 (CERN-70-21(Vol.2), pp 859-78)

Inelastic scattering of polarized protons by ^{40}Ca at 24.5 MeV, 25:14923 (CEA-CONF-1656)

j-mixing determination in (p,d) reactions by asymmetry measurements, 25:14921 (CEA-CONF-1653)

Measurement and microscopic calculations of the cross sections and asymmetries for the (p,p') reaction exciting the 2.31-MeV (0^+,T = 1) state of ^{14}N, 25:14890 (CEA-CONF-1651)

Measurements of the depolarization parameter D for elastic proton scattering, 25:14889 (CEA-CONF-1650)

Preliminary tests with pictures from Mirabelle, 25:13291 (CERN-70-21(Vol.2), pp 941-8)

Simplified method of obtaining information from bubble chamber photographs, 25:13233 (CEA-N-1397)

Study of (p,d) reactions on ^{48}Ca and ^{49}Ti with polarized protons, 25:14922 (CEA-CONF-1655)

Study of (p,d) reactions on ^{90}Zr and ^{92}Mo with polarized protons, 25:14980 (CEA-CONF-1654)

COMMONWEALTH EDISON CO., CHICAGO, ILL.

Dresden Nuclear Power Station, Unit 1. License No. DPR-2; Proposed Change No. 21 to Appendix A, 25:15245 (DOCKET-50010-76)

Dresden Nuclear Power Station, Unit 1. License No. DPR-2; Proposed Change No. 22 to Appendix A, 25:15246 (DOCKET-50010-77)

Dresden Nuclear Power Station, Unit 2. Abnormal occurrence report: failure of Main Steam Isolation Valve 2D to close, 25:15231 (DOCKET-50237-140)

Dresden Nuclear Power Station, Unit 2. Facility License DPR-19; Proposed Change No. 7 to Appendix A, 25:15273 (DOCKET-50237-130)

Dresden Nuclear Power Station, Unit 2. Facility License DPR-19; Proposed Change No. 8 to Appendix A, 25:15274 (DOCKET-50237-131)

Dresden Nuclear Power Station, Unit 2. High Pressure Coolant Injection pump flow less than that specified, 25:15232 (DOCKET-50237-141)

Dresden Nuclear Power Station, Unit 2. Proposed Change No. 5 to Appendix A of DPR-19, Suppl. 1, 25:15278 (DOCKET-50237-136)

Dresden Nuclear Power Station, Unit 2. Proposed Modification No. 71-1 to final safety analysis report, additional information, 25:15279 (DOCKET-50237-137)

Dresden Nuclear Power Station, Unit 2. Refueling. Proposed modification No. 71-1 to final safety analysis report, Suppl. 1, 25:15276 (DOCKET-50237-134)

Dresden Nuclear Power Station, Unit 2. Report of valve failures, 25:15230 (DOCKET-50237-132)

Dresden Nuclear Power Station, Unit 2. Testing program, 25:15233 (DOCKET-50237-142)

Dresden Nuclear Power Station, Unit 3. Facility Operating License No. DPR-25; Proposed Change No. 1 to Appendix A, 25:15288 (DOCKET-50249-56)

Dresden Nuclear Power Station, Units 2 and 3. Modifications on control rod drives, 25:15277 (DOCKET-50237-135)

Dresden Nuclear Power Station, Units 2 and 3. Secondary containment leak rate test summary, 25:15281 (DOCKET-50237-139)

Quad-Cities Station, Units 1 and 2. Preliminary safety analysis report, Amendment 16 (includes revisions to final safety analysis report), 25:15291 (DOCKET-50254-27)

COMMONWEALTH SCIENTIFIC AND INDUSTRIAL RESEARCH ORGANIZATION, ADELAIDE (AUSTRALIA). DIV. OF SOILS.

Tritium content measurements on a variety of water samples, 25:13103 (NP-18639)

Tritium content measurements on a variety of water samples. Technical Memorandum 31/1969, 25:13120 (NP-18638)

CONNECTICUT YANKEE ATOMIC POWER CO., HADDAM.

Connecticut Yankee Atomic Power Plant. Operation report No. 70-12, December 1970, 25:15229 (DOCKET-50213-94)

CONNECTICUT YANKEE ATOMIC POWER CO., HARTFORD.

Connecticut Yankee Atomic Power Plant. Examination and evaluation of Capsule A for pressure-vessel surveillance program. Final report, 25:15265 (DOCKET-50213-95)

Connecticut Yankee Atomic Power Plant. License No. DPR-14. Technical specifications Proposed Change No. 18, 25:15267 (DOCKET-50213-97)

Connecticut Yankee Atomic Power Plant. Preliminary safety analysis report, Suppl. 2, 25:15266 (DOCKET-50213-96)

CONSOLIDATED EDISON CO. OF NEW YORK, INC., NEW YORK.

Indian Point Station, Unit No. 1. Completion of thermal sleeve repairs, 25:15243 (DOCKET-50003-61)

Indian Point Station, Unit No. 1. Facility design changes, 25:15244 (DOCKET-50003-64)

Indian Point Station, Unit No. 1. Failure of a reactor outlet stop valve on No. 13 loop to function properly, 25:15224 (DOCKET-50003-62)

Indian Point Station, Unit No. 1. Foreign material in buffer seal housing of control rods, 25:15225 (DOCKET-50003-63)

CONSUMERS POWER CO., JACKSON, MICH.

Big Rock Point Nuclear Plant. License No. DPR-6; proposed technical specifications Change No. 25, 25:15258 (DOCKET-50155-60)

Big Rock Point Nuclear Plant. License No. DPR-6; proposed technical specifications Change No. 27, 25:15261 (DOCKET-50155-63)

Big Rock Point Nuclear Plant. License No. DPR-6; proposed technical specifications Change No. 26, 25:15259 (DOCKET-50155-61)

Big Rock Point Nuclear Plant. License No. DPR-6; proposed technical specifications Change No. 25, additional information, 25:15260 (DOCKET-50155-62)

CONTINENTAL CAN CO., INC., CHICAGO, ILL. METAL DIV. RESEARCH AND DEVELOPMENT.

Prog. rpt. on growth characteristics of Clostridium botulinum, annual, 1/69--1/70, 25:13617 (COO-1183-32)

CORNELL UNIV., ITHACA, N.Y. LAB. OF PLASMA STUDIES.

Injection of relativistic electrons into Astron-like device, 25:14351 (AD-711822)

D

DAIRYLAND POWER COOPERATIVE, LA CROSSE, WIS.

La Crosse Boiling Water Reactor. Emergency diesel generator failure to start on first crank during monthly test, 25:15219 (DOCKET-1155-94)

La Crosse Boiling Water Reactor. Failure of control rod

- No. 13 to scram hydraulically at normal scram speed, 25:15217 (DOCKET-1155-92)
- La Crosse Boiling Water Reactor. Failure of control rod No. 11 to withdraw on plant startup, 25:15220 (DOCKET-1155-95)
- La Crosse Boiling Water Reactor. Reactor low flow scram bypass key switches, 25:15242 (DOCKET-1155-91)
- La Crosse Boiling Water Reactor. Unplanned reactor scram, 25:15216 (DOCKET-1155-89)
- La Crosse Boiling Water Reactor. Unplanned reactor scram, 25:15221 (DOCKET-1155-96)
- La Crosse Boiling Water Reactor. Unplanned reactor scram, 25:15222 (DOCKET-1155-97)
- La Crosse Boiling Water Reactor. Unplanned reactor scram, 25:15223 (DOCKET-1155-98)
- La Crosse Boiling Water Reactor. Unplanned reactor scram, 25:15218 (DOCKET-1155-93)

DANISH ATOMIC ENERGY COMMISSION, RISOE. RESEARCH ESTABLISHMENT.
- Prog. rpt. on electronics, semiannual, 10/69--3/70, 25:13321 (RISO-M-1270)

DARESBURY NUCLEAR PHYSICS LAB. (ENGLAND).
- On-line measuring system using visual displays for operator guidance, 25:13237 (CERN-70-21(Vol.1), pp 39-46)

DAYTON POWER AND LIGHT CO., OHIO.
- Wm. H. Zimmer Nuclear Power Station, Unit 1. Environmental report, 25:15327 (DOCKET-50358-11)
- Wm. H. Zimmer Nuclear Power Station, Unit 1. Preliminary safety analysis report, Amendment 5, 25:15328 (DOCKET-50358-12)

DEMOCRITUS NUCLEAR RESEARCH CENTER, ATHENS (GREECE).
- HERETRA: computer program for fission products calculations, 25:15141 (DEMO-70/10)
- New derivation of an approximate expression in closed form for the binding energy of an impurity particle in nuclear matter, 25:15142 (DEMO-70/20)

DETROIT EDISON CO., MICH.
- Enrico Fermi Atomic Power Plant, Unit 2. Preliminary safety analysis report, Amendment 15, 25:15323 (DOCKET-50341-25)
- Enrico Fermi Atomic Power Plant, Unit 2. Preliminary safety analysis report, Amendment 16, 25:15324 (DOCKET-50341-26)

DEUTSCHE AKADEMIE DER WISSENSCHAFTEN ZU BERLIN (EAST GERMANY). INSTITUT FUER HOCHENERGIEPHYSIK.
- Data processing for bubble chambers from the point of view of a small laboratory, 25:13272 (CERN-70-21(Vol.2), pp 665-73)

DEUTSCHES ELEKTRONEN-SYNCHROTRON, HAMBURG (WEST GERMANY).
- Experiences with coupled computers to control an HPD, 25:13276 (CERN-70-21(Vol.2), pp 721-7)
- Use of IBM data management to control bubble chamber data flow, 25:13277 (CERN-70-21(Vol.2), pp 729-34)

DIVISION OF MATERIALS AND LICENSING (AEC), WASHINGTON, D. C.
- West Valley Reprocessing Plant. Environmental sample data, 25:13080 (DOCKET-50201-62)
- West Valley Reprocessing Plant. License No. CSF-1. Technical specifications Change No. 13, 25:13078 (DOCKET-50201-60)

DIVISION OF REACTOR LICENSING (AEC), WASHINGTON, D. C.
- Aguirre Nuclear Plant, Unit No. 1. Notice of receipt of application for construction permit and facility license, 25:15333 (DOCKET-50376-8)
- Big Rock Point Nuclear Plant. License No. DPR-6; technical specifications Change No. 21, 25:15262 (DOCKET-50155-65)
- Dresden Nuclear Power Station, Unit 2. Provisional Operating License No. DPR-19; technical specifications Change No. 8, 25:15275 (DOCKET-50237-133)
- Dresden Nuclear Power Station, Unit 2. Provisional Operating License No. DPR-19; technical specifications Change No. 7, 25:15280 (DOCKET-50237-138)
- La Crosse Boiling Water Reactor. Provisional Operating Authorization No. DPRA-6; technical specifications Change No. 2, 25:15241 (DOCKET-1155-90)
- Monticello Nuclear Generating Plant, Unit 1. Provisional Operating License No. DPR-22, Amendment 1, 25:15293 (DOCKET-50263-52)
- Point Beach Nuclear Plant, Unit 1. Facility Operating License DPR-24, Amendment 1, 25:15296 (DOCKET-50266-38)
- Quad-Cities Station, Units 1 and 2. Notice of availability of environmental report, 25:15290 (DOCKET-50254-26)
- San Onofre Nuclear Generating Station, Unit 1. License No. DPR-13; technical specification proposed Change No. 4, request for additional information, 25:15264 (DOCKET-50206-106)
- Southwest Experimental Fast Oxide Reactor. Steady state operation up to 20 MWt approved, 25:15386 (DOCKET-50231-67)
- Trojan Nuclear Plant. Construction Permit No. CPPR-79, 25:15325 (DOCKET-50344-19)

DU PONT DE NEMOURS (E.I.) AND CO., AIKEN, S. C. SAVANNAH RIVER LAB.
- Self-radiation damage in ^{244}Cm oxide and aluminate, 25:13779 (DP-MS-70-44)

DUQUESNE LIGHT CO., SHIPPINGPORT, PA. POWER STATIONS DEPT.
- Shippingport Atomic Power Station operating report, 9/70, 25:15214 (DLCS-5000370)

E

EBERLINE INSTRUMENT CORP., SANTA FE, N. MEX.
- Point Beach Nuclear Plant, Unit 1. Environmental monitoring program pre-operational report, 25:15297 (DOCKET-50266-41)

EDISON ELECTRIC INST., NEW YORK.
- Prog. rpt. on Pu utilization in boiling water reactors, Phase II, annual, 1969, 25:15365 (NEDC-12111)

EIDGENOESSISCHES INSTITUT FUER REAKTORFORSCHUNG, WUERENLINGEN (SWITZERLAND).
- Corrosion of zirconium alloys in superheated steam: results of the prolonged experiments, 25:13629 (EIR-184)

ELECTRICITY COMMISSION OF NEW SOUTH WALES (AUSTRALIA). CIVIL INVESTIGATIONS BRANCH.
- Jervis Bay Nuclear Power Station project investigations at site J.S1-Scottish Rocks, 25:15336 (NP-18636)

ENTE NAZIONALE PER L'ENERGIA ELETTRICA, ROME (ITALY).
- Prog. rpt. on Garigliano Nuclear Power Plant, annual, 1969, 25:15239 (EUR-4580)

ENVIRONMENTAL SCIENCE SERVICES ADMINISTRATION, LAS VEGAS, NEV. AIR RESOURCES LAB.
- Weather for industrial nuclear explosions, 25:13136 (ARLV-351-15)

EUROPEAN ATOMIC ENERGY COMMUNITY.
- Comparison of radioactive contamination of total diet of adolescents in community. II, 25:13392 (EUR-3945(Pt.2))
- Geometry routines for use in the TIMOC code, 25:15404 (EUR-4536)
- Heat transfer coefficient as function of steam quality for high-pressure once through flow boiling, with determination of transition points between regions of particular heat transfer, 25:13149 (EUR-4561)
- Prog. rpt. on Garigliano Nuclear Power Plant, annual, 1969, 25:15239 (EUR-4580)

EUROPEAN ATOMIC ENERGY COMMUNITY, ISPRA (ITALY). JOINT NUCLEAR RESEARCH CENTER.
- Corrosion in high-temperature lithium heat pipes with niobium--zirconium and tantalum as wall material, 25:13630 (EUR-4298)
- Geometry routines for use in the TIMOC code, 25:15404 (EUR-4536)
- Heat transfer coefficient as function of steam quality for high-pressure once through flow boiling, with determination of transition points between regions of particular heat transfer, 25:13149 (EUR-4561)

EUROPEAN COMMUNITIES, LUXEMBOURG. COMMISSION.
- Comparison of radioactive contamination of total diet of adolescents in community. II, 25:13392 (EUR-3945(Pt.2))
- Thermal conductivity of uranium dioxide, 25:13749 (EUR-4568)

EUROPEAN COMPANY FOR THE CHEMICAL PROCESSING OF IRRADIATED FUELS, MOL (BELGIUM).
- Investigation of reprocessing input measurement using tracer technique, 25:13081 (NP-18577)

EUROPEAN ORGANIZATION FOR NUCLEAR RESEARCH, GENEVA (SWITZERLAND).
- Adam+Eva, scanning and measuring machine for film from the large bubble chambers, 25:13270 (CERN-70-21(Vol.2), pp 633-49)
- Atlas of particle production spectra, 25:14733 (NP-18660)
- Bubble chamber film measurement on HPDs at CERN, 25:13281 (CERN-70-21(Vol.2), pp 813-24)
- Calibration, precision, and filtering questions for the CERN Spiral Reader, 25:13235 (CERN-70-21(Vol.1), pp 5-18)
- Conference on data handling systems in high-energy physics, Cavendish Lab., Cambridge, 3/70, 25:13234 (CERN-70-21(Vol.1))
- Conference on data handling systems in high-energy physics, Cavendish Lab., Cambridge, 3/70, 25:13263 (CERN-70-21(Vol.2))
- Data handling system for the Omega and the SFM projects, 25:14839 (CERN-70-21(Vol.2), pp 561-80)
- Description and performance of the CERN Spiral Reader, 25:13236 (CERN-70-21(Vol.1), pp 19-36)
- Evaluation of reverse developed film measured on HPD 2, 25:13286 (CERN-70-21(Vol.2), pp 879-905)
- Focus remote access system, 25:13265 (CERN-70-21(Vol.2), pp 551-9)
- Geometrical reconstruction for the new bubble chambers, 25:13260 (CERN-70-21(Vol.1), pp 467-96)
- Lucy, a CRT film measuring device, 25:13259 (CERN-70-21(Vol.1), pp 427-65)
- Pattern recognition methods for Omega and SFM spark chamber experiments, 25:13283 (CERN-70-21(Vol.2), pp 831-50)
- Scanning and measuring of heavy liquid film on-line, 25:13271 (CERN-70-21(Vol.2), pp 651-64)
- Statistics of PS operation, 1967, 25:14844 (MPS/Int. CO-68-1)
- Status of the HPD minimum guidance programs at CERN, 25:13278 (CERN-70-21(Vol.2), pp 737-52)

F

FIAT, TURIN (ITALY). SEZIONE ENERGIA NUCLEARE.
  Nuclear fuel with burnable poison. II, 25:13736 (EUR-4551)
FLORIDA POWER AND LIGHT CO.
  Turkey Point Plant, Unit 3. Containment dome concrete placement program, 25:15289 (DOCKET-50250-38)
FLORIDA POWER CORP., ST. PETERSBURG.
  Crystal River Nuclear Generating Plant, Unit 3. Environmental report, 25:15308 (DOCKET-50302-16)
FLORIDA STATE UNIV., TALLAHASSEE.
  SU(3) x SU(3) chiral Lagrangian model for anti KN interactions, 25:14703 (TID-25639)
FLORIDA STATE UNIV., TALLAHASSEE. HIGH ENERGY PHYSICS LAB.
  Partial wave analysis of reaction $K^-n \to \Sigma^-\pi^+\pi^-$ from 1.62 to 1.74 GeV, 25:14557 (FSU-HEP-70-3-1)
FLORIDA UNIV., GAINESVILLE. DEPT. OF PHYSICS AND ASTRONOMY.
  Atomic physics and the polar cap, 25:14102 (N-70-19848)
FLORIDA UNIV., GAINESVILLE. ENGINEERING AND INDUSTRIAL EXPERIMENT STATION.
  Quantitative determination of the structure: property relationships in nuclear fuel element materials. Quarterly progress report, September 15--December 15, 1970, 25:13766 (SRO-552-6)

G

GENERAL ELECTRIC CO., CINCINNATI, OHIO. NUCLEAR SYSTEMS PROGRAMS.
  Design of nuclear Brayton turboalternator--compressor, 25:13168 (N-70-41276)
GENERAL ELECTRIC CO., PHILADELPHIA, PA. SPACE DIV.
  Prog. rpt. on large scale nonequilibrium MHD generator, annual, 8/69--7/70, 25:14081 (AD-711351)
GENERAL ELECTRIC CO., PLEASANTON, CALIF. NUCLEONICS LAB.
  Prog. rpt. on fission gas re-solution rates, 7--9/70, 25:13780 (GEAP-12147)
GENERAL ELECTRIC CO., SAN JOSE, CALIF. ATOMIC POWER EQUIPMENT DEPT.
  Two-phase flow and heat transfer in multirod geometries. Nineteenth Quarterly Progress Report, April 1--June 30, 1970, 25:13150 (GEAP-10253)
GENERAL ELECTRIC CO., SAN JOSE, CALIF. REACTOR FUELS AND REPROCESSING DEPT.
  Prog. rpt. on Pu utilization in boiling water reactors, Phase II, annual, 1969, 25:15365 (NEDC-12111)
GENERAL ELECTRIC CO., SCHENECTADY, N. Y.
  Operation of thermionic converter with tungsten emitter and niobium collector, 25:14083 (N-70-39884)
GENERAL ELECTRIC CO., SUNNYVALE, CALIF. BREEDER REACTOR DEVELOPMENT OPERATION.
  Southwest Experimental Fast Oxide Reactor. License No. DR-15; technical specifications Proposed Change No. 3, Addendum No. 2, 25:15271 (DOCKET-50231-68)
  Southwest Experimental Fast Oxide Reactor. Sodium logging of fuel rods, additional information, 25:15272 (DOCKET-50231-69)
GEOLOGICAL SURVEY, DENVER, COLO.
  Hydraulic testing of hole UAe-7h, Amchitka Island, Alaska, 25:13105 (USGS-474-84)
  Radiochemical analyses of water from selected streams, wells, springs, and precipitation collected prior to reentry drilling, Project Rulison, 25:12951 (USGS-474-83)
GESELLSCHAFT FUER KERNFORSCHUNG m.b.H., KARLSRUHE (WEST GERMANY).
  Plutonium-documentation, Vol. 4, No. 11, 1970, 25:13626
  Plutonium-documentation, Vol. 4, No. 9, 1970, 25:13625
GLASGOW UNIV. (SCOTLAND). DEPT. OF NATURAL PHILOSOPHY.
  Progress on Polly at Glasgow, 25:13255 (CERN-70-21(Vol.1), pp 357-70)
GOSUDARSTVENNYI KOMITET PO ISPOL'ZOVANIYU ATOMNOI ENERGII SSSR, MOSCOW.
  Cesium-137 from global fallout in foodstuffs and human organism, 25:13340 (NP-18382)
GOSUDARSTVENNYI KOMITET PO ISPOL'ZOVANIYU ATOMNOI ENERGII SSSR, SERPUKHOV. INSTITUT FIZIKI VYSOKIKH ENERGII.
  Observation of anti ^{3}He, 25:14540 (IFVE-SEF-70-16)
GRAND JUNCTION OFFICE (AEC), COLO.
  ELIPGRID: FORTRAN IV program for calculating probability of success in locating elliptical targets with square, rectangular, and hexagonal grids, 25:15433 (GJO-918-4)
  Preliminary reconnaissance for uranium in New Mexico, 1950--1958, 25:13125 (RME-160)
GULF GENERAL ATOMIC, INC., SAN DIEGO, CALIF.
  Instantaneous and time-dependent collapse of externally pressurized circular tubes with initial out-of-roundness, 25:13652 (GAMD-8219(Rev.))
  Thermodynamic data for carbonaceous systems, 25:13750 (GAMD-9335)
GULF RADIATION TECHNOLOGY, SAN DIEGO, CALIF.
  Prog. rpt. on fast reactor spectrum measurements, 10/70, 25:15388 (GULF-RT-10421)

H

HAMBURG UNIV. (WEST GERMANY). II. INSTITUT FUER EXPERIMENTALPHYSIK.
  Experiences with coupled computers to control an HPD, 25:13276 (CERN-70-21(Vol.2), pp 721-7)
HAWAII UNIV., HONOLULU.
  2400-MeV 5π mass enhancement in 6-prong π^-p events at 12 GeV/c, 25:14562 (TID-25640)
HEIDELBERG UNIV. (WEST GERMANY). INSTITUT FUER HOCHENERGIEPHYSIK.
  ARNULF: PDP-10 program for rapid acquisition of complete film information by a PEPR-device, 25:13242 (CERN-70-21(Vol.1), pp 113-24)
  BERTA: a FORTRAN program for automatic recognition and reconstruction of bubble chamber events. II, 25:13244 (CERN-70-21(Vol.1), pp 141-75)
  BERTA: a FORTRAN program for automatic recognition and reconstruction of bubble chamber events. I, 25:13243 (CERN-70-21(Vol.1), pp 125-39)
  CARL: a FORTRAN program for PEPR calibration using Chebyshev polynomials, 25:13245 (CERN-70-21(Vol.1), pp 177-86)
  ELKE: a grid guidance program for the rapid measurement of bubble chamber film, 25:13247 (CERN-70-21(Vol.1), pp 199-211)
  Heidelberg automatic event recognition, 25:13241 (CERN-70-21(Vol.1), pp 105-11)
  Present status of the Heidelberg-PEPR-Hardware and production system, 25:13246 (CERN-70-21(Vol.1), pp 187-96)

I

IBM SCIENTIFIC CENTER, HEIDELBERG (WEST GERMANY).
  BERTA: a FORTRAN program for automatic recognition and reconstruction of bubble chamber events. I, 25:13243 (CERN-70-21(Vol.1), pp 125-39)
  BERTA: a FORTRAN program for automatic recognition and reconstruction of bubble chamber events. II, 25:13244 (CERN-70-21(Vol.1), pp 141-75)
  Heidelberg automatic event recognition, 25:13241 (CERN-70-21(Vol.1), pp 105-11)
IDAHO NUCLEAR CORP., IDAHO FALLS.
  Gamma rays emitted by the fissionable nuclides and associated isotopes, 25:14981 (IN-1448)
ILLINOIS UNIV., URBANA. DEPT. OF COMPUTER SCIENCE.
  Arithmetic unit of ILLIAC III: simulation and logical design. II, 25:15430 (COO-2118-2)
  Sequence determination from fragment data, 25:15422 (COO-1018-1219)
ILLINOIS UNIV., URBANA. DEPT. OF METALLURGY AND MINING ENGINEERING.
  Temperature changes in thin films during growth by physical vapor deposition, 25:15423 (COO-1198-775)
IMPERIAL COLL. OF SCIENCE AND TECHNOLOGY, LONDON (ENGLAND). DEPT. OF PHYSICS.
  Operator intervention in the Imperial College HPD system, 25:13290 (CERN-70-21(Vol.2), pp 931-40)
  Two loop approximations to propagators in the sigma model, 25:14683 (NYO-2262-TA-219)
INDIANA AND MICHIGAN ELECTRIC CO., FORT WAYNE, IND.
  Donald C. Cook Nuclear Plant, Units 1 and 2. Environmental report, 25:15316 (DOCKET-50315-27)
  Donald C. Cook Nuclear Plant, Units 1 and 2. Preliminary safety analysis report, Amendment 12 (includes final safety analysis report, Vol. 1), 25:15317 (DOCKET-50315-28)
  Donald C. Cook Nuclear Plant, Units 1 and 2. Preliminary safety analysis report, Amendment 12 (includes application for operating licenses), 25:15315 (DOCKET-50315-26)
  Donald C. Cook Nuclear Plant, Units 1 and 2. Preliminary safety analysis report, Amendment 12 (includes final safety analysis report, Vol. 3), 25:15319 (DOCKET-50315-30)
  Donald C. Cook Nuclear Plant, Units 1 and 2. Preliminary safety analysis report, Amendment 12 (includes final safety analysis report, Vol. 5), 25:15321 (DOCKET-50315-32)
  Donald C. Cook Nuclear Plant, Units 1 and 2. Preliminary safety analysis report, Amendment 12 (includes final safety analysis report, Vol. 4), 25:15320 (DOCKET-50315-31)
  Donald C. Cook Nuclear Plant, Units 1 and 2. Preliminary safety analysis report, Amendment 12 (includes final safety analysis report, Vol. 2), 25:15318 (DOCKET-50315-29)
  Donald C. Cook Nuclear Plant, Units 1 and 2. Preliminary safety analysis report, Amendment 12 (includes final safety analysis report, Vol. 6), 25:15322 (DOCKET-50315-33)
INDIANA UNIV., BLOOMINGTON. DEPT. OF CHEMISTRY.
  Sulfonate leaving groups, structure and reactivity: 2,2,2-trifluoroethanesulfonate, 25:15421 (COO-1008-14)
INSTITUT FUER PLASMAPHYSIK, G.M.B.H. GARCHING (WEST GERMANY).
  Composition and electrical conductivity of combustion plasmas, 25:14285 (BMBW-FBK-70-29)

INSTITUT JOZEF STEFAN, LJUBLJANA (YUGOSLAVIA).
  Thermal treatment of Cr--SiO cermet thin films, 25:14435 (IJS-587)
INSTITUTE OF NUCLEAR PHYSICS, KRAKOW (POLAND).
  Comparison of K/π ratio in multiple production at energies 60 GeV and approximately 1000 GeV, 25:14509 (INP-718)
  Decay distributions in reaction $\pi^+p \to K^+Y^{*+}(1385)$ and polarization of Λ hyperon from $Y^{*+}(1385)$ decay at 8 GeV/c primary momentum, 25:14559 (INP-731)
  Pion production mechanism in high multiplicity π^+p interactions at 8 GeV/c, 25:14558 (INP-708)
  Spectrum of resonances in generalized Veneziano model, 25:14681 (INP-730)
  Statistical model and cross sections for high-energy reactions, 25:14680 (INP-719)
INSTITUTE OF NUCLEAR RESEARCH, WARSAW (POLAND).
  LCAC--SCF calculations of electron energies for transition states: bromine + aromatic molecule, 25:13064 (INR-1211)
  Proton--proton and pion--proton inelastic collisions and the proton and pion form factors, 25:14729 (INR-P-1229)
INTERNATIONAL ATOMIC ENERGY AGENCY, VIENNA (AUSTRIA).
  Conference on guidelines for the layout and contents of safety reports for stationary nuclear power plants, Vienna, 6--7/69, 25:15337 (STI/PUB-272)
  Conference on nuclear data for reactors, Helsinki, 6/70, 25:14987 (STI/PUB-259(Vol.1))
  Conference on nuclear data for reactors, Helsinki, 6/70, 25:14988 (STI/PUB-259(Vol.2))
  List of bibliographies on nuclear energy, 25:15460 (STI/DOC-11(Vol.8)(No.2))
IOWA-ILLINOIS GAS AND ELECTRIC CO., DAVENPORT, IOWA.
  Quad-Cities Station, Units 1 and 2. Preliminary safety analysis report, Amendment 16 (includes revisions to final safety analysis report), 25:15291 (DOCKET-50254-27)
ISTITUTO NAZIONALE DI FISICA NUCLEARE, BOLOGNA (ITALY).
  HDP--IBM 360/44 system at CNAF for bubble chamber data analysis. I, 25:13267 (CERN-70-21(Vol.2), pp 607-15)
  HPD--IBM 360/44 system at CNAF for bubble chamber data analysis. II, 25:13268 (CERN-70-21(Vol.2), pp 617-24)
  HPD--IBM 360/44 system at CNAF for bubble chamber data analysis. III, 25:13269 (CERN-70-21(Vol.2), pp 625-30)
ISTITUTO NAZIONALE DI FISICA NUCLEARE, TURIN (ITALY).
  IBM 1130 computer on-line system at Torino, 25:13288 (CERN-70-21(Vol.2), pp 911-20)

J

JAPAN ATOMIC ENERGY RESEARCH INST., TOKAI. TOKAI RESEARCH ESTABLISHMENT.
  Conference on inelastic neutron scattering, Tokai, 1969, 25:14436 (JAERI-1197)
JAPAN ATOMIC ENERGY RESEARCH INST., TOKYO.
  Bibliography on wastes of plutonium, 25:13190 (JAERI-Memo-4153)
  Characteristic measurements of JRR-2, 25:15390 (JAERI-Memo-4141)
  Environmental monitoring at JAERI, Tokai, 1969, 25:13119 (JAERI-Memo-4175)
  JAERI's conceptual design of Japan experimental fast reactor, 25:15389 (JAERI-1177-B(Pt.2))
  Joule heating in JFT-2, 25:14233 (JAERI-Memo-4186)
  Nondestructive testing of aircraft structures by radioisotopes, 25:13180 (JAERI-Memo-4163)
  Nuclear calculation method of the JMTR core, 25:15391 (JAERI-Memo-4180)
JERSEY CENTRAL POWER AND LIGHT CO., MORRISTOWN, N. J.
  Forked River Nuclear Generating Station, Unit 1. Preliminary safety analysis report, Amendment 5, 25:15330 (DOCKET-50363-11)
  Oyster Creek Nuclear Power Plant, Unit No. 1. Preliminary safety analysis report, Amendment 65, Suppl. 1, 25:15268 (DOCKET-50219-120)
  Oyster Creek Nuclear Power Plant, Unit No. 1. Summary technical report: primary containment leakage rate test, 25:15269 (DOCKET-50219-121)
  Three Mile Island Nuclear Station, Unit 1. Preliminary safety analysis report, Amendment 17 (includes final safety analysis report modifications, Appendixes 6A and 12A), 25:15305 (DOCKET-50289-32)
JET PROPULSION LAB., PASADENA, CALIF.
  Dopants for radiation-resistant silicon, 25:14412 (N-70-39456)
JOHNS HOPKINS UNIV., BALTIMORE, MD. DEPT. OF BIOCHEMISTRY.
  Thymine phototrimer, 25:15436 (NYO-2798-49)
JOINT INST. FOR NUCLEAR RESEARCH, DUBNA (USSR).
  Development of track chamber picture processing systems at JINR, 25:13279 (CERN-70-21(Vol.2), pp 753-60)
  Dynamics of charged bunch collisions in connection with impact mechanism of acceleration, 25:14855 (UCRL-Trans-1421)
  Electron-beam shaping in a linear induction accelerator, 25:14856 (UCRL-Trans-1425)
  Proportional chamber for compensation of counter geometry in the time-of-flight measurements, 25:13296 (JINR-P13-5472)
  Systematization of the inelastic interactions of high-energy pions and nucleons with atomic nuclei, 25:15148 (ORNL-tr-2399)
  Transient effect of accelerating field on electron bunch containing ions, 25:14854 (UCRL-Trans-1420)
JOINT INST. FOR NUCLEAR RESEARCH, DUBNA (USSR). LAB. OF HIGH ENERGY.
  Effective mass spectra of the $\gamma\gamma$, $\pi^0\gamma$, $\pi^0\gamma\gamma$, $\pi^0\pi^0$, π^0eta^0, $\pi^0\pi^0\gamma$, $\pi^0\pi^0\pi^0$ systems in mass value region M $(\gamma.......\gamma)$ less than or equal to 1.3 GeV, 25:14560 (JINR-E1-5349)
  Elastic NN and Nd scattering, 25:14730 (JINR-P2-5444)
  Experimental ionization chamber filled with liquid and solid argon, 25:13295 (JINR-P13-5404)
  Measurement of total cross sections of π^---p interaction, 25:14561 (JINR-P1-5460)
  Model-independent determination of the real parts of the independent of spin pp-forward scattering amplitudes, 25:14731 (JINR-P2-5448)
  Spectrometer channel of experimental ionization chambers with the argon and xenon condensates, 25:13211 (JINR-P13-5402)
  System of proportional wire chambers on-line with a computer, 25:13297 (JINR-P13-5473)
JOINT INST. FOR NUCLEAR RESEARCH, DUBNA (USSR). LAB. OF NEUTRON PHYSICS.
  Threshold detectors used for the neutron spectrum measurement, 25:13210 (JINR-P3-5421)
JOINT INST. FOR NUCLEAR RESEARCH, DUBNA (USSR). LAB. OF NUCLEAR PROBLEMS.
  Optimization of ion source and ion optical parameters of isotope separator, 25:13162 (JINR-P13-5369)
  Search for new type of radioactivity in aluminum and tungsten targets irradiated by 70-GeV protons, 25:14541 (JINR-P1-5399)
  Statistical isospin model and cross sections of reactions $\pi^-p \to N + (2,...,6)\pi$ within 1 to 16 GeV energy range, 25:14700 (JINR-P1-5471)
JOINT INST. FOR NUCLEAR RESEARCH, DUBNA (USSR). LAB. OF NUCLEAR REACTIONS.
  Apparatus for investigation of α-active nuclei: the products of reactions with heavy ions, 25:14841 (JINR-P13-5353)
JOINT INST. FOR NUCLEAR RESEARCH, DUBNA (USSR). LAB. OF THEORETICAL PHYSICS.
  Investigation of the Heisenberg Model of impure ferromagnets, 25:15420 (BNL-tr-390)
  Resonant scattering of light by light, 25:14596 (JINR-E2-5424)
  Scattering by two centers in long-wave approximation, 25:14817 (JINR-P4-5438)
  Test of SU(3) symmetrical statistical theory of elementary particle production, 25:14748 (JINR-P2-5480)
JUNTA DE ENERGIA NUCLEAR, SACAVEM (PORTUGAL). LABORATORIO DE FISICA E ENGENHARIA NUCLEARES.
  Westcott formalism, 25:15405 (LFEN-NI.-45-a)
JYVASKYLA UNIV. (FINLAND). DEPT. OF PHYSICS.
  Design, construction, and characteristics of some Ge(Li) detectors and spectrometers, 25:13212 (NP-18653)
  Effect of nonlocality of nucleon--nucleon potential on the two-body sum rules, 25:14732 (NP-18648)
  Limits of validity of Siegert's theorem in the nuclear photo-absorption, 25:15144 (NP-18618)
  Multipole character of some gamma transitions in ^{152}Sm, 25:14985 (NP-18615)
  Phase-space integral and statistical quantities in high-energy collisions, 25:14584 (NP-18652)

K

KANSAS STATE UNIV., MANHATTAN. DEPT. OF NUCLEAR ENGINEERING.
  Dimensional S/sub n/ calculations of neutron spectra reflected from thick slabs of concrete and iron, comparison with measurements, 25:14865 (COO-2049-2)
KERNFORSCHUNGSANLAGE, JUELICH (WEST GERMANY).
  Different models for calculation of nuclide transport in clad spherical fuel particles for high-temperature reactors, 25:13782 (JUL-685-PA)
KERNFORSCHUNGSANLAGE, JUELICH (WEST GERMANY). INSTITUT FUER FESTKOERPER- UND NEUTRONENPHYSIK.
  Lattice parameter measurements on aluminum after electron irradiation at low temperatures, 25:13723 (JUL-664-FN)
  Measurement of stored energy in electron-irradiated platinum below 40°K, 25:13722 (JUL-658-FN)
KERNFORSCHUNGSANLAGE, JUELICH (WEST GERMANY). INSTITUT FUER REAKTORENTWICKLUNG.
  Investigations of the diffusion of ^{6}Li from irradiated BeO, 25:13781 (JUL-677-RG)
KERNFORSCHUNGSZENTRUM, KARLSRUHE (WEST GERMANY). INSTITUT FUER EXPERIMENTELLE KERNPHYSIK.
  Frequency dependence of the residual resistance of a galvanically begun lead layer in a superconducting state, measured in a TEM field configuration, 25:14847 (NP-18654)
  Measurements on pulsed superconducting magnets, 25:14211 (KFK-1217)
  Possibility of cooling with superfluid helium in tubular systems, for example, superconducting helix waveguides,

25:14846 (NP-18651)

KERNFORSCHUNGSZENTRUM, KARLSRUHE (WEST GERMANY). INSTITUT FUER MATERIAL UND FESTKOERPERFORSCHUNG.
- Behavior of fission product Mo, Tc, Ru, Rh, and Pd in a carbide fuel element and structure of the system Mo--Ru--C, 25:13764 (KFK-1260)
- Precipitation of vanadium of UO_2 spheres from the gas phase, 25:13737 (KFK-1292)

KERNFORSCHUNGSZENTRUM, KARLSRUHE (WEST GERMANY). INSTITUT FUER NEUTRONENPHYSIK UND REAKTORTECHNIK.
- Evaluation of fast critical experiments using recent methods and data, 25:15387 (EURFNR-858)

KERNFORSCHUNGSZENTRUM, KARLSRUHE (WEST GERMANY). INSTITUT FUER REAKTORENTWICKLUNG.
- Parameter adjustment by the gradient method on the hybrid analog computer, 25:15406 (NP-18646)
- Solubility of inert gases in the reactor coolant sodium and related safety problems, 25:15379 (EURFNR-785)

KERNFORSCHUNGSZENTRUM, KARLSRUHE (WEST GERMANY). LABOR FUER ELEKTRONIK UND MESSTECHNIK.
- Fundamental principles on dimensioning of a counter--timer system, 25:13317 (NP-18655)

KUNGLIGA TEKNISKA HOGSKOLAN, STOCKHOLM (SWEDEN).
- Experimental evidence of element and isotope separation in a rotating plasma, 25:14278 (NP-18643)
- Texture and anisotropy of zirconium related to plastic deformation, 25:13655 (NP-18625)

L

LABORATOIRE CENTRAL DES INDUSTRIES ELECTRIQUES, FONTENAY-AUX-ROSES (FRANCE).
- Influence of various factors in determining the variation in the electrical characteristics of capacitors exposed to gamma radiation or electrons, 25:13327 (LCIE-364)

LAVAL UNIV. (QUEBEC).
- Fine structure in highly excited analog states, 25:15145 (NYO-1082-25)

LEIPZIG UNIV. (EAST GERMANY).
- Atlas of particle production spectra, 25:14733 (NP-18660)

LIEGE UNIV. (BELGIUM). LABORATOIRE D'APPLICATION DES RADIOELEMENTS.
- Tritiated titanium targets producing 14-MeV neutrons. II, 25:14840 (EUR-4286(Pt.2))

LOS ALAMOS SCIENTIFIC LAB., N. MEX.
- Adiabatic calorimetric enthalpy measurements for α, β, and γ uranium and heats of the transformations $\alpha \to \beta$ and $\beta \to \gamma$, 25:13653 (LA-4521)
- Production of Candida utilis with 93 at. percent ^{13}C acetic acid as the sole carbon source, 25:13331 (LA-4551)
- Prog. rpt. on Medium-Energy Physics Program, 10/31/70, 25:14842 (LA-4571)
- Some elementary attempts at numerical modeling of problems concerning rates of evolutionary processes, 25:15435 (LA-4573)
- TWOTRAN SPHERE: FORTRAN program to solve multigroup transport equation in two-dimensional spherical geometry, 25:14866 (LA-4567)

LOUISIANA POWER AND LIGHT CO., NEW ORLEANS.
- Waterford Steam Electric Station, Units 3 and 4. Applicant's environmental report, construction permit stage, 25:15334 (DOCKET-50382-6)

LYON UNIV. (FRANCE). INSTITUT DE PHYSIQUE NUCLEAIRE.
- Determination of internal and superficial oxygen content of molybendum obtained using 54 MeV α particles and low energy deuterons, 25:12957 (LYCEN-7076)
- Projection methods and their applications to Hartree--Fock wave functions, 25:15143 (LYCEN-7050)

M

MAGYAR TUDOMANYOS AKADEMIA KOZPONTI FIZIKAI KUTATO INTEZETE, BUDAPEST.
- Remarks on ''a new fit of the parameters for Cabibbo's theory'', 25:14632 (KFKI-70-23-HEP)
- Spin test for a fermion ($J > 1/2$) decaying into a spin-1/2 fermion, 25:14701 (KFKI-70-27-HEP)
- Superselection rules and internal symmetries, 25:14774 (KFKI-70-22-HEP)

MARYLAND UNIV., COLLEGE PARK. ENGINEERING MATERIALS GROUP.
- Total material variables influencing a ductile--brittle transition temperature for molybdenum, 25:13649 (AD-713191)

MASSACHUSETTS INST. OF TECH., CAMBRIDGE. DEPT. OF METALLURGY AND MATERIALS SCIENCE.
- Tunneling into superconducting rhenium single crystals, 25:14147 (AD-711826)

MASSACHUSETTS INST. OF TECH., CAMBRIDGE. ENGINEERING PROJECTS LAB.
- Refrigerant forced-convection condensation inside horizontal tubes, 25:13151 (NP-18642)

MASSACHUSETTS INST. OF TECH., CAMBRIDGE. LAB. FOR NUCLEAR SCIENCE.
- Prog. rpt. on physics, annual, 1969, 25:14925 (MIT-2098-643)
- Status of MIT's PEPR's, 25:13248 (CERN-70-21(Vol.1), pp 233-42)

MAX-PLANCK-INSTITUT FUER PHYSIK UND ASTROPHYSIK, MUNICH (WEST GERMANY).
- Brush system for automatic processing of bubble chamber pictures, 25:13274 (CERN-70-21(Vol.2), pp 689-707)
- Digitized microscope for evaluation of photo emulsions in high-energy physics, 25:13284 (CERN-70-21(Vol.2), pp 851-7)
- Present data analysis system of the bubble chamber group at the MPI Munich, 25:13287 (CERN-70-21(Vol.2), pp 907-9)

METROPOLITAN EDISON CO., READING, PA.
- Three Mile Island Nuclear Station, Unit 1. Preliminary safety analysis report, Amendment 17 (includes final safety analysis report modifications, Appendixes 6A and 12A), 25:15305 (DOCKET-50289-32)

MICHIGAN STATE UNIV., EAST LANSING.
- Coupling between pressure and temperature waves in liquid helium, 25:14129 (COO-1574-19)
- Dependence of He II film transfer rate on pressure head, film height, and substrate, 25:14128 (COO-1574-17)

MILLSTONE POINT CO., HARTFORD, CONN.
- Millstone Nuclear Power Station, Unit 1. Abnormal occurrence No. AO-71-1: failure of core spray injection valve to close, 25:15234 (DOCKET-50245-53)
- Millstone Nuclear Power Station, Unit 1. Abnormal occurrence No. AO-71-2, 25:15235 (DOCKET-50245-54)

MILLSTONE POINT CO., WETHERSFIELD, CONN.
- Millstone Nuclear Power Station, Unit 1. Possibility of inadvertent opening of core spray system valves, 25:15287 (DOCKET-50245-52)

MINNESOTA MINING AND MFG. CO., ST. PAUL. ELECTRICAL PRODUCTS GROUP.
- Prog. rpt. on thermoelectric converter development, final, 12/70, 25:13166 (MMM-4187-1)

MINNESOTA UNIV., MINNEAPOLIS. DEPT. OF CHEMICAL ENGINEERING.
- Prog. rpt. on kinetics of methylene and hydroxyl radical reactions, annual, 1970, 25:15429 (COO-2026-4)

MINNESOTA UNIV., MINNEAPOLIS. SCHOOL OF MINERAL AND METALLURGICAL ENGINEERING.
- Prog. rpt. on study of grain boundary segregation, 12/2/70, 25:15428 (COO-1778-6)

MINNESOTA UNIV., MINNEAPOLIS. SCHOOL OF PHYSICS.
- Study of N + α system with resonating-group method, 25:14880 (COO-1764-105)

MONTANA STATE UNIV., BOZEMAN.
- Natural convection heat transfer between concentric spheres, 25:15450 (RLO-2214-2)
- Prog. rpt. on natural convective heat transfer between concentric spheres, annual, 1/71, 25:15449 (RLO-2214-1)

MONTANA STATE UNIV., BOZEMAN. ENGINEERING RESEARCH LABS.
- Response of earth dams to seismic disturbances. II, 25:13130 (UCRL-13329(Pt.2))

MOUND LAB., MIAMISBURG, OHIO.
- Metallographic analysis of SNAP--15C heat source capsule, 25:13164 (MLM-1670)
- Metallographic analysis of SNAP-19B (IRHS) capsule, 25:13163 (MLM-1652)
- Prog. rpt. on stable gaseous isotope separation and purification, 4--6/70, 25:13165 (MLM-1753)
- Solubility of tritium in annealed and cold-worked copper, 25:13654 (MLM-1734)

N

NAGOYA UNIV. (JAPAN). INST. OF PLASMA PHYSICS.
- Diffusion of multipole magnetic fields through a conductive wall of a plasma container, 25:14352 (IPPJ-T-3)

NATIONAL ACCELERATOR LAB., BATAVIA, ILL.
- Safety report: 15-food bubble chamber, 25:13298 (NAL-48-2624)

NATIONAL AERONAUTICS AND SPACE ADMINISTRATION, CLEVELAND, OHIO. LEWIS RESEARCH CENTER.
- Thermal analysis of heat source for use with isotope Brayton space power system, 25:13167 (N-70-41092)

NATIONAL AERONAUTICS AND SPACE ADMINISTRATION, HUNTSVILLE, ALA. GEORGE C. MARSHALL SPACE FLIGHT CENTER.
- Heat transfer in convective envelope of Sun, 25:13862 (N-70-38381)
- Solar flow parameters, 25:13861 (N-70-37452)
- Solar x-ray astronomy summary and bibliography, 25:13863 (N-70-39828)
- Survey of classical Cepheid variable stars, 25:13789 (N-70-38166)

NATIONAL BUREAU OF STANDARDS, WASHINGTON, D. C.
- National Bureau of Standards Reactor. Request permission to release ten additional curies per year to the sanitary sewer, 25:15385 (DOCKET-50184-25)
- Review and updating of information on transmission and reflection of electrons by aluminum shields, 25:14396 (N-70-37470)

NATIONAL CENTER FOR RADIOLOGICAL HEALTH, ROCKVILLE, MD.
- Guide for environmental surveillance around nuclear facilities, 25:15335 (NF-67-8)

NAVAL POSTGRADUATE SCHOOL, MONTEREY, CALIF.
- Construction of a theta pinch for the generation of shock waves in a nitrogen plasma, 25:14350 (AD-711003)

Energy loss of high-energy electrons in Sn, Pb, and Gd, 25:14392 (AD-711005)

Laser-light scattering as a plasma diagnostic technique, 25:14241 (AD-710718)

NEBRASKA UNIV., LINCOLN. BEHLEN LAB. OF PHYSICS.

Unified track theory, 25:13209 (COO-1671-28)

NIAGARA MOHAWK POWER CORP., SYRACUSE, N. Y.

Nine Mile Point Nuclear Station. Petition requesting amendment of license, Amendment 5. Technical supplement to petition to increase power level, Fifth Addendum, 25:15270 (DOCKET-50220-57)

NORDISK INSTITUT FOR TEORETISK ATOMFYSIK, COPENHAGEN (DENMARK).

Resonant elastic scattering of protons from analogue and compound states, 25:15146 (NYO-1082-29)

NORTH AMERICAN CARBON, INC., COLUMBUS, OHIO. RESEARCH AND DEVELOPMENT DEPT.

Filter system design, installation and testing for radioactive contaminant removal, 25:13192 (NACAR-10012)

NORTH CAROLINA STATE UNIV., RALEIGH.

Prog. rpt. on nitrate and ammonium uptake and assimilation, annual, 5/70--4/71, 25:15446 (ORO-2410-18)

NORTH CAROLINA STATE UNIV., RALEIGH. DEPT. OF SOIL SCIENCE.

Prog. rpt. on nitrate and ammonium uptake and assimilation, summary, 5/68--4/71, 25:15447 (ORO-2410-19)

NORTH CAROLINA UNIV., CHAPEL HILL.

Impurity diffusion in aluminum and its dilute alloys, 25:15445 (ORO-2036-21)

NORTHEASTERN UNIV., BOSTON, MASS. DEPT. OF PHYSICS.

Ground state correlations as variational parameters in the nuclear many-body problem, 25:15147 (NYO-2171-333)

NORTHERN INDIANA PUBLIC SERVICE CO., HAMMOND.

Bailly Generating Station, Nuclear I. Preliminary safety analysis report, Amendment 2, 25:15331 (DOCKET-50367-9)

NORTHERN STATES POWER CO., MINNEAPOLIS, MINN.

Monticello Nuclear Generating Plant, Unit 1. Integrated primary containment leak rate test, Jul 1970, 25:15294 (DOCKET-50263-53)

Monticello Nuclear Generating Plant, Unit 1. Secondary containment leak rate test, August 1970, 25:15295 (DOCKET-50263-54)

Monticello Nuclear Generating Plant, Unit 1. Unsafe failure of protection system sensor, 25:15236 (DOCKET-50263-51)

Prairie Island Nuclear Generating Plant, Units 1 and 2. Preliminary safety analysis report, Amendment 7 (includes application for operating license), 25:15299 (DOCKET-50282-26)

Prairie Island Nuclear Generating Plant, Units 1 and 2. Preliminary safety analysis report, Amendment 7 (includes final safety analysis report, Vol. 1), 25:15300 (DOCKET-50282-27)

Prairie Island Nuclear Generating Plant, Units 1 and 2. Preliminary safety analysis report, Amendment 7 (includes final safety analysis report, Vol. 3), 25:15302 (DOCKET-50282-29)

Prairie Island Nuclear Generating Plant, Units 1 and 2. Preliminary safety analysis report, Amendment 7 (includes final safety analysis report, Vol. 2), 25:15301 (DOCKET-50282-28)

Prairie Island Nuclear Generating Plant, Units 1 and 2. Preliminary safety analysis report, Amendment 7 (includes final safety analysis report, Vol. 4), 25:15303 (DOCKET-50282-30)

Prairie Island Nuclear Generating Plant, Units 1 and 2. Preliminary safety analysis report, Amendment 7 (includes final safety analysis report, Vol. 5), 25:15304 (DOCKET-50282-31)

NORTHROP CORPORATE LABS., HAWTHORNE, CALIF.

Dopants for radiation-resistant silicon, 25:14412 (N-70-39456)

NUCLEAR CROSS SECTIONS ADVISORY COMMITTEE (AEC).

Reports to AEC Nuclear Cross Sections Advisory Committee meeting at Argonne National Lab., Chicago, Ill., 5/70, 25:14982 (NCSAC-31)

NUCLEAR ENERGY INFORMATION CENTER, WARSAW (POLAND).

Bibliography on fast breeding reactors, 1966--69, 25:15340 (NEIC-RR-41)

NUCLEAR FUEL SERVICES, INC., WEST VALLEY, N.Y.

West Valley Reprocessing Plant. Quarterly report, October 1--December 31, 1970, 25:13079 (DOCKET-50201-61)

NUCLEAR MATERIALS AND EQUIPMENT CORP., APOLLO, PA. ENERGY CONVERSION DIV.

Prog. rpt. on Radioisotope Powered Cardiac Pacemaker Program, final, 1/31/69--1/31/70, 25:13169 (NUMEC-3731-24)

O

OAK RIDGE NATIONAL LAB., TENN.

Analytical mass spectrometry at Oak Ridge National Laboratory, 25:13319 (ORNL-4643)

Discussions, 25:13659 (ORNL-4590, pp 233-48)

Effects of nuclear EMP on AM radio broadcast stations in the emergency broadcast system, 25:13328 (ORNL-TM-2830)

Fabrication procedures and acceptance data for ASTM A-533 welds and a 10-in. thick ASTM A-543 plate of the Heavy Section Steel Technology Program, Documentary Report 3, 25:13638 (ORNL-4313-3)

FORTRAN program for computing two-dimensional magnetic fields, 25:15440 (ORNL-TM-2484)

Heavy-Section Steel Technology Program. Semiannual progress report for period ending February 28, 1970, 25:13656 (ORNL-4590)

Instrumentation and Controls Division annual progress report for period ending September 1, 1970, 25:13318 (ORNL-4620)

Investigation of unirradiated materials, 25:13657 (ORNL-4590, pp 20-99)

Investigations of irradiated materials, 25:13724 (ORNL-4590, pp 100-34)

Personnel involved in development of nuclear standards in United States, 25:13469 (ORNL-NSIC-75(Rev.1))

Pressure vessel investigations, 25:13658 (ORNL-4590, pp 135-232)

Prog. rpt. on biological macromolecular separations technology project, 10--12/70, 25:15442 (ORNL-TM-3280)

Prog. rpt. on High Flux Isotope Reactor, 7--9/70, 25:15392 (ORNL-TM-3286)

Program administration and procurement, 25:13639 (ORNL-4590, pp 1-19)

Selection procedure based upon Wald's double dichotomy test, 25:15441 (ORNL-TM-3237)

Tensile and impact properties of thick-section plate and weldments, 25:13660 (ORNL-TM-3211)

OHIO AGRICULTURAL RESEARCH AND DEVELOPMENT CENTER, WOOSTER.

Detailed characterization of soil and vegetation on selected sites. Technical progress report, March 1, 1970--November 26, 1970, 25:13118 (COO-414-17)

OHIO STATE UNIV. RESEARCH FOUNDATION, COLUMBUS.

Glaciological investigations on the Casement Glacier, southeast Alaska, final, 1/65--10/69, 25:15426 (COO-1473-4)

OWENS VALLEY RADIO OBSERVATORY, PASADENA, CALIF.

Galactic hydrogen absorption at 21 cm wavelength in direction of Virgo A, 25:13831 (AD-711300)

Neutral hydrogen absorption in galaxy M82, 25:13911 (AD-711299)

Polarization of 3C10 and 3C58 at 1420 and 2880 MHz, 25:13833 (AD-711611)

OXFORD UNIV. (ENGLAND). DEPT. OF NUCLEAR PHYSICS.

PEPR for BEBC, 25:13240 (CERN-70-21(Vol.1), pp 89-104)

OXFORD UNIV. (ENGLAND). NUCLEAR PHYSICS LAB.

Oxford PEPR system, 25:13239 (CERN-70-21(Vol.1), pp 61-88)

P

PARIS UNIV. (FRANCE). FACULTE DES SCIENCES.

Search for classes in magnetic quadrupole gamma transitions, 25:14983 (NP-18492)

PARIS UNIV., ORSAY (FRANCE). INSTITUT DE PHYSIQUE NUCLEAIRE.

Pangloss, a CRT device for bubble chamber pictures, 25:13258 (CERN-70-21(Vol.1), pp 401-25)

Use of a simple geometry program for filtering HPD data, 25:13273 (CERN-70-21(Vol.2), pp 679-85)

PARIS UNIV., ORSAY (FRANCE). LABORATOIRE DE L'ACCELERATEUR LINEAIRE.

Amplitude discriminator on a large dynamic scale with precise time definition, 25:13320 (RI-70/13)

Colliding beam set up to be built in end station of Orsay linac, 25:14843 (LAL-RT-44-70)

PARIS UNIV., ORSAY (FRANCE). LABORATOIRE DE PHYSIQUE DES PLASMAS.

Study of an ionic instability in the plasma of a low pressure positive column subjected to a microwave resonating electric field, 25:14336 (NP-18662)

PENNSYLVANIA ELECTRIC CO., JOHNSTOWN.

Three Mile Island Nuclear Station, Unit 1. Preliminary safety analysis report, Amendment 17 (includes final safety analysis report modifications, Appendixes 6A and 12A), 25:15305 (DOCKET-50289-32)

PENNSYLVANIA STATE UNIV., UNIVERSITY PARK. DEPT. OF BIOLOGY.

Characteristics of nuclear RNA polymerase from rat anterior pituitary tissue, 25:15439 (NYO-3827-18)

PENNSYLVANIA UNIV., KENNETT SQUARE. SCHOOL OF VETERINARY MEDICINE.

Prog. rpt. on calcium kinetics in cows, annual, 12/22/70, 25:15438 (NYO-3360-55)

PENNSYLVANIA UNIV., PHILADELPHIA. DEPT. OF PHYSICS.

Ground state correlations as variational parameters in the nuclear many-body problem, 25:15147 (NYO-2171-333)

PITTSBURGH UNIV., PA. DEPT. OF PHYSICS.

Configuration-space three-body scattering theory, 25:14819 (N-70-40698)

Configuration-space three-body scattering theory, 25:14818 (N-70-40418)

POLYTECHNIC INST. OF BROOKLYN, N. Y. DEPT. OF AEROSPACE ENGINEERING AND APPLIED MECHANICS.

Difficulty and possibility of kinetic theory of quantum-mechanical systems. III and IV, 25:14490 (AD-711681)

PONTIFICIA UNIVERSIDADE CATOLICA DO RIO DE JANEIRO (BRAZIL). INSTITUTO DE FISICA.
- Prog. rpt. on study of natural radioactivity in Brazil, 11/70, 25:13393 (NYO-2577-12)

POWER REACTOR DEVELOPMENT CO., DETROIT, MICH.
- Enrico Fermi Atomic Power Plant, Unit 1. Revised license application, Part B. Vol. 1. Technical information and hazards summary report, 25:15247 (DOCKET-50016-89)
- Enrico Fermi Atomic Power Plant, Unit 1. Revised license application, Part A. General information and request for license, 25:15251 (DOCKET-50016-93)
- Enrico Fermi Atomic Power Plant, Unit 1. Revised license application, Part B. Vol. 2. Technical information and hazards summary report, 25:15252 (DOCKET-50016-94)
- Enrico Fermi Atomic Power Plant, Unit 1. Revised license application, Part B. Vol. 3. Technical information and hazards summary report, 25:15253 (DOCKET-50016-95)
- Enrico Fermi Atomic Power Plant, Unit 1. Revised license application, Part B. Vol. 7. Technical information and hazards summary report, 25:15248 (DOCKET-50016-90)
- Enrico Fermi Atomic Power Plant, Unit 1. Revised license application, Part B. Vol. 5. Technical information and hazards summary report, 25:15255 (DOCKET-50016-97)
- Enrico Fermi Atomic Power Plant, Unit 1. Revised license application, Part B. Vol. 6. Technical information and hazards summary report, 25:15256 (DOCKET-50016-98)
- Enrico Fermi Atomic Power Plant, Unit 1. Revised license application, Part B. Vol. 4. Technical information and hazards summary report, 25:15254 (DOCKET-50016-96)
- Enrico Fermi Atomic Power Plant, Unit 1. Revised license application, Part B. Vol. 8. Proposed technical specifications, 25:15249 (DOCKET-50016-91)
- Enrico Fermi Atomic Power Plant, Unit 1. Sodium service piping, additional information, 25:15250 (DOCKET-50016-92)

PRINCETON-PENNSYLVANIA ACCELERATOR, PRINCETON, N. J.
- Regulation of magnet power supplies, 25:14848 (PPAD-677-D)

PRINCETON UNIV., N.J. DEPT. OF PHYSICS.
- Princeton automatic track reader, 25:13250 (CERN-70-21(Vol.1), pp 273-83)

PUBLIC HEALTH SERVICE, LAS VEGAS, NEV. SOUTHWESTERN RADIOLOGICAL HEALTH LAB.
- Plant radioiodine relationships: a review, 25:13395 (SWRHL-90-r)

PUBLIC SERVICE ELECTRIC AND GAS CO., NEWARK, N.J.
- Newbold Island Nuclear Generating Station, Units 1 and 2. Preliminary safety analysis report, Amendment 4, 25:15326 (DOCKET-50354-10)

PURDUE UNIV., LAFAYETTE, IND. DEPT. OF CHEMISTRY.
- Effects of structure of peptide stationary phases on gas-chromatographic separations of amino-acid enantiomers, 25:15424 (COO-1222-42)

R

REACTOR CENTRUM NEDERLAND, PETTEN.
- Neutron metrology in H.F.R, 25:15393 (RCN-119)

ROCHESTER GAS AND ELECTRIC CORP., N. Y.
- Robert Emmett Ginna Nuclear Power Plant, Unit No. 1. Petition requesting amendment of license and extension of expiration date of provisional operating license (includes technical supplement accompanying application to increase power), 25:15286 (DOCKET-50244-59)
- Robert Emmett Ginna Nuclear Power Plant, Unit No. 1. Provisional Operating License No. DPR-18: request for revision of technical specifications Change No. 7, 25:15285 (DOCKET-50244-58)
- Robert Emmett Ginna Nuclear Power Plant, Unit No. 1. Provisional Operating License No. DPR-18: request for revision of technical specifications Change No. 5, 25:15283 (DOCKET-50244-56)
- Robert Emmett Ginna Nuclear Power Plant, Unit No. 1. Provisional Operating License No. DPR-18: request for revision of technical specifications Change No. 6, 25:15284 (DOCKET-50244-57)
- Robert Emmett Ginna Nuclear Power Plant, Unit No. 1. Provisional Operating License No. DPR-18: request for technical specification Change No. 4, 25:15282 (DOCKET-50244-55)

ROCKEFELLER UNIV., NEW YORK.
- Asymptotic behavior of weak spectral functions and hadronic decays of W boson, 25:14634 (NYO-4204-7)
- Hadronic helicity conservation and inelastic lepton--nucleon reactions, 25:14636 (NYO-4204-10)
- Regge model for inelastic lepton--nucleon scattering, 25:14635 (NYO-4204-9)

RURAL COOPERATIVE POWER ASSOCIATION, ELK RIVER, MINN.
- Elk River Reactor. Status report, 25:15215 (DOCKET-1151-39)

S

SAN DIEGO GAS AND ELECTRIC CO., CALIF.
- San Onofre Nuclear Generating Station, Unit 1. Semiannual operating report No. 7, July 1--December 31, 1970, 25:15227 (DOCKET-50206-103)
- San Onofre Nuclear Generating Station, Units 2 and 3. Preliminary safety analysis report, Amendment 6, 25:15329 (DOCKET-50361-14)

SANDERS NUCLEAR CORP., NASHUA, N.H.
- Development of SIREN capsule, Phase I, 25:13170 (SNC-2708-1)
- Prog. rpt. on development of SIREN capsule, phase IA, final, 9/69--1/70, 25:13171 (SNC-2708-2)

SANDIA LABS., ALBUQUERQUE, N. MEX.
- Functional test of a Rocket Engine Module, 25:15453 (SC-DR-70-911)
- Raman scattering in liquid lasing material containing $POCl_3$, 25:15454 (SC-RR-70-762)
- Study of the effect of the evaporative erosion on thermoelectric elements on the performance of thermoelectric generators, 25:14084 (SC-RR-70-804)

SANDVIK STEEL WORKS, SANDVIKEN (SWEDEN).
- Texture and anisotropy of zirconium related to plastic deformation, 25:13655 (NP-18625)

SCRIPPS INSTITUTION OF OCEANOGRAPHY, LA JOLLA, CALIF.
- Ecology of plankton off La Jolla, Calif., 4--9/67, 25:15468 (UCSD-10-P-20-54)

SKODA CONCERN, PILSEN (CZECHOSLOVAKIA). NUCLEAR POWER PLANTS DIV.
- Experimental investigation of film heat-transfer coefficient in the fuel element spacers area, 25:13153 (ZJE-66)
- Rod models of fuel elements of nuclear reactors, 25:15410 (ZJE-92)

SOCIEDAD PERUANA DE BIOLOGIA Y MEDICINA NUCLEAR, LIMA.
- Conference on first congress of Latin American Association of Societies of biology and nuclear medicine, Lima, Peru, 10/66, 25:13482 (CONF-661071)

SOUTH DAKOTA AGRICULTURAL EXPERIMENT STATION, BROOKINGS.
- Prog. rpt. on nature and importance of selenium metabolites in animal, 1--12/70, 25:15425 (COO-1445-11)

SOUTHERN CALIFORNIA EDISON CO., LOS ANGELES.
- San Onofre Nuclear Generating Station, Unit 1. Cycle 2 xenon transient analysis, 25:15263 (DOCKET-50206-104)
- San Onofre Nuclear Generating Station, Unit 1. Operation report, January 1971, 25:15228 (DOCKET-50206-105)
- San Onofre Nuclear Generating Station, Unit 1. Semiannual operating report No. 7, July 1--December 31, 1970, 25:15227 (DOCKET-50206-103)
- San Onofre Nuclear Generating Station, Units 2 and 3. Preliminary safety analysis report, Amendment 6, 25:15329 (DOCKET-50361-14)

STAATLICHE ZENTRALE FUER STRAHLENSCHUTZ, BERLIN (EAST GERMANY).
- Heat generation by absorption of ionizing radiation in nuclear power plants, 25:15341 (SZS-20/70)
- Illustration of specifications for transport of radioactive materials of high activity and fissionable materials, 25:13194 (SZS-19/70)
- Principles for control of nuclear material in GDR, 25:13193 (SZS-16/70)

STANFORD LINEAR ACCELERATOR CENTER, CALIF.
- Physics of electron storage rings, 25:14850 (SLAC-121)
- Prog. rpt. on two-mile accelerator project, 7--9/70, 25:14851 (SLAC-128)

STANFORD RESEARCH INST., MENLO PARK, CALIF.
- Evaluation of systems of fire development, 25:13134 (AD-713418)

STANFORD UNIV., CALIF. DEPT. OF MECHANICAL ENGINEERING.
- Prog. rpt. on radiation-induced nucleation of bubbles in superheated water, 12/70, 25:13152 (SU-326-P-13-5)

STANFORD UNIV., CALIF. INST. FOR PLASMA RESEARCH.
- Electron temperature and number density measurements in a nonequilibrium plasma boundary layer, 25:14244 (AD-711669)
- Model of pulsars, 25:13832 (AD-711397)
- Polarization measurements of solar Type-III radio bursts at 25.3 MHz, 25:13859 (AD-711398)
- Prog. rpt. on nonthermal phenomena of astrophysics, 5/66--6/70, 25:13936 (AD-711829)
- Theory of polarization transfer in inhomogeneous magnetized plasmas, 25:14286 (N-70-40979)

STATE UNIV. OF NEW YORK, STONY BROOK. INST. FOR THEORETICAL PHYSICS.
- Resonant elastic scattering of protons from analogue and compound states, 25:15146 (NYO-1082-29)

STOCKHOLM UNIV. (SWEDEN). INST. OF PHYSICS.
- System for on-line control of bubble chamber measurements, 25:13282 (CERN-70-21(Vol.2), pp 825-30)

SYDNEY UNIV. (AUSTRALIA). SCHOOL OF PHYSICS.
- Prog. rpt. on plasma physics, 7--12/70, 25:14231 (NP-18663)

SYRACUSE UNIV., N. Y. DEPT. OF PHYSICS.
- Exchange degeneracy and oscilliating total cross sections, 25:14656 (SU-1206-237)

  Van Hove model and non-leptonic hyperon decays, 25:14637 (SU-1206-238)

T

TECHNICAL UNIV. OF HELSINKI, OTANIEMI (FINLAND). DEPT. OF TECHNICAL PHYSICS.
  Determination of isotopic ratio ^{238}U/^{235}U by neutron activation, 25:12958 (TKK-F-A-136)
TECHNISCHE HOCHSCHULE, AACHEN (WEST GERMANY).
  Investigations of the diffusion of ^{6}Li from irradiated BeO, 25:13781 (JUL-677-RG)
TECHNISCHE HOCHSCHULE, HANOVER (WEST GERMANY). INSTITUT FUER TECHNISCHE CHEMIE.
  Influence of dimensions of gas fluidized beds on gas mixing, 25:13140 (BMBW-FBK-70-26)
TEXAS UNIV., AUSTIN. ELECTRONICS RESEARCH CENTER.
  Scattering amplitudes and spin polarizations of electrons scattered from H, He, C, Ne, Ar, Kr, Rb, Xe, Cs, Au, Hg, Pb, and Bi. I, 25:13995 (AD-711664)
TOKYO UNIV. (JAPAN). INST. FOR NUCLEAR STUDY.
  Prog. rpt., annual, 4/69--3/70, 25:14845 (NP-18601)
  Prototype of drift tube quadrupole magnets, 25:14849 (SJC-A-70-6)
TRW SYSTEMS GROUP, REDONDO BEACH, CALIF.
  Study of model test methods as related to LMFBR piping systems, 25:15358 (SAN-781-234)

U

UNION CARBIDE CORP., OAK RIDGE, TENN. COMPUTING TECHNOLOGY CENTER.
  Radiation Shielding Information Center program setup instructions manual, 25:14395 (CTC-INF-1017)
UNION CARBIDE CORP., OAK RIDGE, TENN. Y-12 PLANT.
  Remote data station interface to the production control computer, 25:15469 (Y-1748)
UNITED KINGDOM ATOMIC ENERGY AUTHORITY, SPRINGFIELDS (ENGLAND). REACTOR GROUP.
  Matrix precipitation of NbC in 20/25/Nb stainless steel, 25:13640 (TRG-Report-2040)
UNITED NUCLEAR CORP., ELMSFORD, N. Y. RESEARCH AND ENGINEERING CENTER.
  Isochronous stress--strain curves for 2 $^{1}/_{4}$ Cr--1 Mo, type 304-304H, and type 316-316H steels. Part I, 25:15452 (SAN-781-2012(Pt.1))
  Piping materials for LMFBR plants. Technical report 228 (Revision 1), 25:15357 (SAN-781-228)
  Plutonium as an alternate fuel in large water cooled reactors, 25:15375 (CONF-691114-6)
  Study of dynamic analysis methods as related to LMFBR piping systems, 25:15362 (UNC-5231)
UNITED STATES-EURATOM FAST REACTOR EXCHANGE PROGRAM.
  Evaluation of fast critical experiments using recent methods and data, 25:15387 (EURFNR-858)
  Solubility of inert gases in the reactor coolant sodium and related safety problems, 25:15379 (EURFNR-785)
UPPSALA UNIV. (SWEDEN). INST. OF PHYSICS.
  Approximation and accuracy in the design of a double-focusing flat spectrometer, 25:13324 (UUIP-715)
  Helium-3-cryostat for specific heat measurements, 25:14212 (UUIP-677)
URS RESEARCH CO., SAN MATEO, CALIF.
  Assessment of nuclear weapon requirements for assured destruction, 25:13132 (AD-711021)
UTAH UNIV., SALT LAKE CITY. DIV. OF MATERIALS SCIENCE AND ENGINEERING.
  Prog. rpt. on impurity effects on creep of polycrystalline magnesium and aluminum oxides at elevated temperatures, 12/19/69--12/18/70, 25:15427 (COO-1591-13)

V

VANDERBILT UNIV., NASHVILLE, TENN.
  Prog. rpt. on some aspects of the behavior of complex compounds, final, 7/1/70, 25:15461 (TID-25641)
VERMONT YANKEE NUCLEAR POWER CORP., RUTLAND.
  Vermont Yankee Nuclear Power Station. Preliminary safety analysis report, Amendment 18, 25:15298 (DOCKET-50271-36)
VIRGINIA UNIV., CHARLOTTESVILLE. DEPT. OF MATERIALS SCIENCE.
  Dislocations in crystals, 25:15437 (NYO-3087-19)

W

WADCO CORP., RICHLAND, WASH.
  Application of aqueous technology to LMFBR separations processes. Program plan for Task T-2: fuel dissolution characteristics, 25:13083 (WHAN-FR-33)
  Comparison of the codes RSYN and 3DB, 25:15343 (WHAN-IR-48)
  Determination of rare earths in plutonium--uranium mixed oxides, 25:12922 (WHAN-SA-44)
  Mock-up of remotely operated high-purity inert-atmosphere sodium analysis facility, 25:13195 (WHAN-SA-91)
  Plutonium fuels for LMFBR: an extrapolation, 25:15367 (WHAN-SA-51)
  Polarization effects in oxide insulators, 25:14437 (WHAN-SA-75)
  Prog. rpt. on reactor engineering, 6--8/70, 25:15354 (WHAN-IR-42)
  Use of amine extraction and emission spectrography in the analysis of plutonium, 25:12923 (WHAN-SA-47)
  Water and gas determinations in mixed oxides, 25:12924 (WHAN-SA-62)
  Water and sorbed-gas content of hypostoichiometric mixed oxide fuel pellets, 25:12925 (WHAN-SA-77)
WASHINGTON UNIV., SEATTLE. DEPT. OF NUCLEAR ENGINEERING.
  Prog. rpt. on dynamics of solvent extraction systems, III, annual, 10/69--9/70, 25:13082 (RLO-2225-T-11-1)
WASHINGTON UNIV., SEATTLE. DEPT. OF PHYSICS.
  Troubles with strict conformal symmetry, 25:14820 (RLO-1388-598)
WASHINGTON UNIV., SEATTLE. LAB. OF RADIATION ECOLOGY.
  Prog. rpt. on natural alpha-emitting radioisotopes in marine organisms, annual, 1969--1970, 25:13394 (RLO-2059-1)
WEIZMANN INST. OF SCIENCE, REHOVOTH (ISRAEL). DEPT. OF NUCLEAR PHYSICS.
  Weizmann Institute Spiral Reader system, 25:13293 (CERN-70-21(Vol.2), pp 953-62)
WESTFIELD COLL., LONDON (ENGLAND).
  Cost-effectiveness of different spark chamber read-out and digitising systems, 25:13266 (CERN-70-21(Vol.2), pp 581-606)
WESTINGHOUSE ELECTRIC CORP., PITTSBURGH, PA. NUCLEAR ENERGY SYSTEMS DIV.
  Prog. rpt. on plant instrumentation, 6/30/70, 25:13220 (WCAP-7562-1)
WESTINGHOUSE RESEARCH LABS., PITTSBURGH, PA.
  Prog. rpt. on basic plasma processes, final, 7/69--9/70, 25:14264 (AD-711828)
WISCONSIN ELECTRIC POWER CO., MILWAUKEE.
  Point Beach Nuclear Plant, Unit 1. Abnormal occurrence report: failure of containment sump suction valves to open, 25:15238 (DOCKET-50266-40)
  Point Beach Nuclear Plant, Unit 1. Environmental monitoring program pre-operational report, 25:15297 (DOCKET-50266-41)
  Point Beach Nuclear Plant, Unit 1. Reactor coolant pump fire, 25:15237 (DOCKET-50266-39)
WISCONSIN MICHIGAN POWER CO., APPLETON, WIS.
  Point Beach Nuclear Plant, Unit 1. Environmental monitoring program pre-operational report, 25:15297 (DOCKET-50266-41)
WISCONSIN PUBLIC SERVICE CORP., GREEN BAY.
  Kewaunee Nuclear Power Plant. Environmental report, operating license stage, 25:15309 (DOCKET-50305-12)
  Kewaunee Nuclear Power Plant. Preliminary safety analysis report, Amendment 7 (includes final safety analysis report, Vol. 1), 25:15310 (DOCKET-50305-13)
  Kewaunee Nuclear Power Plant. Preliminary safety analysis report, Amendment 7 (includes final safety analysis report, Vol. 2), 25:15311 (DOCKET-50305-14)
  Kewaunee Nuclear Power Plant. Preliminary safety analysis report, Amendment 7 (includes final safety analysis report, Vol. 3), 25:15312 (DOCKET-50305-15)
  Kewaunee Nuclear Power Plant. Preliminary safety analysis report, Amendment 7 (includes final safety analysis report, Vol. 5), 25:15314 (DOCKET-50305-17)
  Kewaunee Nuclear Power Plant. Preliminary safety analysis report, Amendment 7 (includes final safety analysis report, Vol. 4), 25:15313 (DOCKET-50305-16)
WISCONSIN UNIV., MADISON. DEPT. OF PHYSICS.
  Global method of fiducial recognition with fish-eye lenses, 25:13261 (CERN-70-21(Vol.1), pp 497-503)
  Status of SATR, 25:13262 (CERN-70-21(Vol.1), pp 505)

Y

YANKEE ATOMIC ELECTRIC CO., BOSTON, MASS.
  Yankee Nuclear Power Station: operating plan in event of labor strike, 25:15257 (DOCKET-50029-90)
YANKEE ATOMIC ELECTRIC CO., WESTBORO, MASS.
  Yankee Nuclear Power Station. Operation report No. 120, December 1970, 25:15226 (DOCKET-50029-142)

PERSONAL AUTHOR INDEX

Authors' names are indexed in the form appearing in the abstracted publication. Each entry under an author's name gives the publication title and the *NSA* volume and abstract numbers. Report numbers, where applicable, are given in parentheses at the end of the entry.

Because of problems involved in the mechanical preparation of this index, all accent marks are omitted. The following changes in spelling have been introduced to reduce some of the confusion which might result from omitting the accents:

Germanic	ä appears as	ae
Germanic	ö	oe
Germanic	ü	ue
Scandinavian	ϕ	oe

A

A. A., Temperature dependence of the total cross-section structure, 25:15093
AALTO, H., Determination of isotopic ratio ^{238}U/^{235}U by neutron activation, 25:12958 (TKK-F-A-136)
AARON, R., Promotion and threshold singularities in massive quantum electrodynamics, 25:14792
AARONSON, Stuart A., Inactivation of murine sarcoma and leukemia viruses by ultra-violet irradiation, 25:13609
AARSETH, S. J., Perturbation treatment of close binaries in N-body problem, 25:13802
ABAGYAN, L. P., Cross-sections for radiative neutron capture by ^{238}U nuclei, 25:15125
ABARBANEL, H. D. I., Asymptotic behavior of single particle distributions in hadron collisions, 25:14742
ABATE-DAGA, G., Nuclear fuel with burnable poison. II, 25:13736 (EUR-4551)
ABBADESSA, S., Action of ionizing radiations on CNS, 25:13561
ABBATI, A., Total body scanning for studies on regional distribution, 25:13503
ABDEL-AZIZ, A., Nuclear transformations of ^{35}S generated in neutron-irradiated alkali metal chlorides and oxychlorides, 25:13065
ABDEL-RASSOUL, A. A., Nuclear transformations of ^{35}S generated in neutron-irradiated alkali metal chlorides and oxychlorides, 25:13065
ABERS, Ernest S., Ward identities for eta decay in perturbation theory, 25:14611
ABO-SHAEER, Muhsin A. R., O(4) properties of scattering amplitudes for particle with spin, 25:14757
ABRAMOV, A. A., Kinetics of Sb(III and V) extraction, 25:12999
ABRAMOV, A. I., Cross-sections for radiative neutron capture by ^{238}U nuclei, 25:15125
  Radiative neutron capture cross-sections for nuclei with A < 220 above the resonance region, 25:15120
ABRAMS, Richard Henry Jr., Periodic pulling of the drift instability in a thermal plasma, 25:14337
ABULAFFIO, C., Decay of /sup 141m/Nd, 25:15014
ACCARY, A., Effects of neutron irradiation on U$_2$Ti, 25:13726
ADAM, A., Neutron cross-sections of ^{235}U, ^{238}U, and ^{239}Pu between 0.1 and 6 MeV, 25:15103
ADAMCHUK, Yu. V., Neutron-spectroscopy study of nuclei with A < 220 in resonance energy region, 25:15095
ADAMS, Donald R., Transfer of ^{85}Kr from air to grass, 25:13124
ADAMS, F., Applied γ ray spectrometry, 25:13231
ADAMS, W. H., Production of Candida utilis with 93 at. percent ^{13}C acetic acid as the sole carbon source, 25:13331 (LA-4551)
ADEEV, G. D., One-nucleon states and energy surfaces of ^{238}U in fission process, 25:15053
ADERHOLZ, M., Geometrical reconstruction for the new bubble chambers, 25:13260 (CERN-70-21(Vol.1), pp 467-96)
ADJEI, S. A., Toward inclusion of spin in generalized Veneziano model for $K^-p \to \pi^-\pi^+\Lambda$, 25:14716
ADLER, D. B., Correlated analysis of fissile-element cross-sections and interpretation in terms of R-matrix parameters, 25:15131
ADLER, F. T., Correlated analysis of fissile-element cross-sections and interpretation in terms of R-matrix parameters, 25:15131
ADLOFF, J. P., Aquoluminescence: release of energy stored in γ-irradiated crystals, 25:13026
AGOSTINELLI, Cataldo, Propagation of a plane wave in a plasma subjected to a magnetic field, 25:14379
AHLERS, Guenter, Heat capacity near the superfluid transition in ^{4}He, 25:14141
AHLGREN, Karin, Level structure of ^{181}W from the decay of ^{181}Re, 25:15058
AHMAD, S. A., Nuclear deformation and optical isotope shifts in the region N = 88 to 90, 25:15048
AHMED, N., Neutron elastic scattering from carbon in the energy region of 0.50 to 2.00 MeV, 25:14911
AHRENS, L. H., Composition of stony meteorites. IX, 25:13787
AINSAAR, A., Problems of CP symmetry and weak interactions, 25:14750
AINSLEY, R., Evacuable glove-box for handling of liquid sodium, and apparatus for analysis of carbon in sodium and other metals, 25:13185 (AERE-R-6338)
AISSA, M., Anisotropic spatial distribution of ions scattered by a single crystal, 25:13970
AKAP'EV, G. N., Effect of α-radioactive background at investigation of the α decay of the 104 element, 25:15017
AKHABABYAN, N., Effect of small magnetic storms on diurnal variations of neutron component, 25:14074
AKHIEZER, A. I., Fluctuations in a magnetohydrodynamic shock wave, 25:14287
  Scattering of high-energy γ quanta on the nucleons and nuclei, 25:14595 (ITF-70-63-P)
AKHMED, M. R., Study of radiations of ^{91}Y, ^{90}Y, and ^{87}Y, 25:15136
AKHTAR, M., Placentography: comparative investigations in nuclear medicine, 25:13517
AKITT, J. W., Quadrupole relaxation of ^{11}B and ^{10}B nuclei, 25:14479
ALBANO, Jorge Raul, Inverse Compton effect in electrons of Van Allen radiation belt, 25:14108
ALBERT, R. D., Auroral-particle precipitation and trapping caused by electrostatic double layers in the ionosphere, 25:14103
ALBRECHT, L., Heat generation by absorption of ionizing radiation in nuclear power plants, 25:15341 (SZS-20/70)
  Illustration of specifications for transport of radioactive materials of high activity and fissionable materials, 25:13194 (SZS-19/70)
ALCOUFFE, Raymond E., Effect of collapsing cross-section data on fast breeder physics parameters, 25:15352
ALCOX, Ray W., Results of 33,911 x-ray protection surveys of facilities with medical or dental diagnostic x-ray equipment, fiscal years 1961--1968, 25:13464
ALECU, Marian, Fuel element cladding, 25:13745
ALEFELD, G., Diffusion coefficients of H and D in V, Nb, and Ta by Gorsky-effect measurements, 25:14440
ALEKSANDROWICZ, Jerzy, Temperature measurements of cladding of WWR-SM type fuel elements in EWA-10 reactor core, 25:15395
ALENIUS, G., Low spin, negative parity states in the N = 103 isotones of ^{171}Er, ^{173}Yb, and ^{175}Hf, 25:15059
ALEXANDER, G., γn partial cross sections up to 12 GeV, 25:14519
ALEXANDER, K. F., Cerium-135m and /sup 137m/Nd: isomeric states in N = 77 isotones, 25:15042
ALEXANDER, W. B., Impurity diffusion in aluminum and its dilute alloys, 25:15445 (CRO-2036-21)
ALFEROV, M. V., Irradiation hazards produced by nonequilibrium emanations, 25:13435
ALFORD, W. P., Reaction (^{3}He,α) on Yb isotopes, 25:15057
ALGAZI, V. R., Optimum design of two-dimensional nonrecursive digital filters, 25:15467 (UCRL-72663)
ALIKHANOV, S. G., Plasma expansion in vacuum and the flow of a collisionless plasma stream around a plate, 25:14265
ALIMARIN, I. P., Methods for the analysis of natural materials containing ruthenium and osmium, 25:12939
AL-JADIR, M. N. I., Scandium-45 level scheme, 25:14941
ALLARD, J. F., Study of reactions ^{11}B(^{3}He,p)^{13}C and

^{20}Ne(^{3}He,p)^{22}Na at less than or equal to 3 MeV, 25:14904
ALLEN, J. E., Theory of a double sheath between two plasmas, 25:14320
ALLEN, Kenneth R., Scattering cross sections for multispecies quantum fluids, 25:13965
ALLEN, M. A., Magnetization and susceptibility measurements of polycrystalline niobium, 25:14195
ALLEN, Philip Brown, Mass enhancement and superconducting transition temperature calculations for metals and semiconductors, 25:14152
ALLEN, Philip W., Weather for industrial nuclear explosions, 25:13136 (ARLV-351-15)
ALLEN, Ralph Orville Jr., Multi-element neutron activation analysis: development and application to trace element study of Bruderheim chondrite, 25:12969
ALLES-BORELLI, V., Limits on the electromagnetic production of heavy leptons, 25:14517
  Validity of leptonic selection rules for $(\mu e \gamma)$ vertex at high four-momentum transfers, 25:14515
ALLEY, P. W., Measurement of the Σ^{+} magnetic moment, 25:14513
ALLIS, William P., Discharge maintained by a direct current and high frequency waves, 25:14266
ALLISON, A. C., Solution of coupled differential equations arising from Schroedinger equation, 25:14497
ALLISCN, W. W. M., Automatic scanning and measurement of bubble chamber film on Polly II, 25:13254 (CERN-70-21(Vol.1), pp 325-55)
ALLOIN, D., Physical parameters of emissive gas in nucleus of NGC 3031, 25:13918
ALLPRESS, J. G., Disordered crystallographic shear in WC/sub 3-x/ crystals, 25:13773
  Structural studies by electron microscopy: polymorphism of $ZrO_2.12Nb_2O_5$, 25:13774
ALMEN, E., Fast-neutron inelastic scattering in energy range 2 to 4.5 MeV, 25:14966
  Neutron energy spectra from neutron-induced fission of ^{238}U at 1.35 and 2.02 MeV, 25:15109
ALMGREN, B., Fuel and fuel cycle for Oskarshamn, 25:15212
ALONSO, J., In-beam gamma spectroscopy of ^{161}Ho, 25:14991
AL'PERT, Y. L., Double scattering of plasma streams in bi-thermal ionosphere, 25:14112
ALSTON-GARNJOST, Margaret, Test of $\Delta S = \Delta Q$ rule in leptonic decays of neutral K mesons, 25:14533
ALTABER, J., Adam+Eva, scanning and measuring machine for film from the large bubble chambers, 25:13270 (CERN-70-21(Vol.2), pp 633-49)
  Status of the HPD minimum guidance programs at CERN, 25:13278 (CERN-70-21(Vol.2), pp 737-52)
ALTER, H., Application of interactive computer graphics to nuclear data evaluation problems, 25:14879
ALTH, G., Irradiation of large surfaces with high-energy beams, 25:13538
  Irradiation planning for megavolt therapy of lymph nodes, 25:13535
  New radiotherapeutic aspects in the treatment of tumors in long bones, 25:13537
ALTMAN, G., Gamma-ray-induced spore germination of Dictyostelium discoideum, 25:13605
ALTSCHULER, Martin D., Coronal magnetic fields before and after solar proton events, 25:13893
ALVAREZ, F., Progress in automatic scanning at Columbia, 25:13253 (CERN-70-21(Vol.1), pp 311-21)
ALVENSLEBEN, H., Determination of photoproduction phase of rho^{0} mesons, 25:14527
  Observation of coherent interference pattern between rho,omega decays, 25:14528
  Photoproduction of pion pairs with high invariant mass, 25:14526
ALWORTH, C. W., Nuclear radiation detection using a superconducting resonant cavity, 25:14228
ALY, H. F., Nuclear transformations of ^{35}S generated in neutron-irradiated alkali metal chlorides and oxychlorides, 25:13065
AMANN, R. R., Exchange degeneracy and oscilliating total cross sections, 25:14656 (SU-1206-237)
AMATO, I., Nuclear fuel with burnable poison. II, 25:13736 (EUR-4551)
AMATO, Ignazio, Effect of gas trapped within pores during sintering and density regression of ceramic bodies, 25:13744
AMBERGER, E., B--C system in the kinetic formation region, 25:13767
  Carbon-induced lattices of B. I, 25:13739
  Formation of lattices of pure boron, 25:13740
AMELINCKX, S., Regular network of anti-phase boundaries in the x-phase of the system Fe--Cr--Mo--Ti, 25:13711
  Unusual dissociation of dislocations in Ni_3Ta, 25:13699
AMIEL, M., Study of reactions ^{11}B(^{3}He,p)^{13}C and ^{20}Ne(^{3}He,p)^{22}Na at less than or equal to 3 MeV, 25:14904
AMIN, M., Effects of deuteration on the specific heat of ADP crystals, 25:12998
AMPULSKI, G. W., Photon rest mass, 25:14510
ANAND, K. C., Is the 8°K background radiation universal, 25:13945
ANCELLIN, J., Study of a marine site with a view to radioactive effluent discharge, 25:13189 (CEA-CONF-1712)
ANDERS, H., Lucy, a CRT film measuring device, 25:13259 (CERN-70-21(Vol.1), pp 427-65)
ANDERSEN, B. V., Interference of medically administered ^{57}Co with transuranic element in vivo lung measurements, 25:13458
ANDERSEN, J. U., Channeling of positrcns, 25:14418
ANDERSON, Donald R., Implantable radiation assembly for circulating systems, 25:13529
ANDERSON, H. L., Cross sections for p + p + d + rho^{+} from 4.0 to 12.3 GeV/c and a search for the delta^{+}, 25:14542
ANDERSON, N. G., Radiation-enhanced onccgenesis by SV40, 25:13553
ANDERSON, R. W., Development cf SIREN capsule, Phase I, 25:13170 (SNC-2708-1)
ANDERSON, Robert W., Prog. rpt. on development cf SIREN capsule, phase IA, final, 9/69--1/70, 25:13171 (SNC-2708-2)
ANDERSSON, Aarne, Magnetic coil cooled by a liquid for a particle accelerator, 25:14857
ANDERSSON, G. I., Levels in ^{177}Lu, 25:15039
ANDERSSON, T. L., Integral measurement of fissicn-product reactivity worths in some fast reactor spectra, 25:15350
ANDRADE, P. da R., Angular correlation in nuclei with integral spin, 25:14477
ANDREEV, A. G., Concentration of uranium by living and dead peat-forming plants, 25:13116
ANDREEV, N. E., Excitation of Langmuir oscillations in plasma by field of transverse wave, 25:14370
  Theory of parametric resonance of plasma in a strong hf electric field, 25:14376
ANDREEVA, I. V., Mapping of uvr gene of S. typhimurium, 25:13408
ANDRESEN, E. G., Frequency of spurious alarms in radiation monitoring by the analog and by the digital methods, 25:13225
ANDREWS, J. G., Sheath growth in a low pressure plasma, 25:14299
  Theory of a double sheath between two plasmas, 25:14320
ANDROSENKO, Kh. D., Neutron-induced fission of ^{240}Pu near threshold, 25:15051
ANGELBERGER, P., Szilard--Chalmers effect for production of ^{203}Hg in high specific activity, 25:13060
ANISIMOV, S. I., Self-similar thermal wave in a two-temperature plasma heated by a laser pulse, 25:14237
ANTHONY, Anne-Marie, Influence of thermionic emission on measurements of electrical properties of refractory materials at high temperatures, 25:14455
ANTIPOV, Yu. M., Observation of anti ^{3}He, 25:14540 (IFVE-SEF-70-16)
ANTOINE, Pierre, Pangloss, a CRT device fcr bubble chamber pictures, 25:13258 (CERN-70-21(Vol.1), pp 401-25)
ANTONIADES, J., HERETRA: computer prcgram fcr fission products calculations, 25:15141 (DEMO-70/10)
ANTONINI, Gerard, Formation of a boundary layer dissipating magnetic energy near a neutral plane, 25:14099
AOKI, Y., Reactions (p,t) on even Ce isctopes, 25:15006
APIDIANAKIS, J., Liquid waste effluents from a nuclear fuel reprocessing plant, 25:12950 (BRH/NERHL-70-2)
APPARAO, Krishna M. V., Gamma radiation from x-ray source Sco X-1, 25:13856
  Is the 8°K background radiation universal, 25:13945
APPELT, K. D., Flow induced rod vibrations of fast reactor subassemblies, 25:15370
APTEKAR, R. L., Study of gamma radiation with Kosmos-135, 25:13951
ARAMS, F. R., Superconducting microstrip high-Q microwave resonators, 25:14230
ARBORELIUS, M. Jr., Simplified mobile equipment for ^{133}Xe-radiospirometry, 25:13514
ARKATOV, Yu. M., Investigation of reaction ^{4}He(γ,p)^{3}H at maximal γ-quanta energy 120 MeV, 25:14886
ARKHIPOV, R. G., Kinetic phenomena in propagaticn of second sound in He II, 25:14131
ARMANTROUT, G. A., Evaluation of trapping and tailing effects in Ge(Li) detectors, 25:13213 (UCRL-71508)
ARMSTRONG, James C., Electromagnetic instability in counterstreaming plasmas, 25:14342
ARMSTRONG, R. W., Total material variables influencing a ductile--brittle transition temperature for molybdenum, 25:13649 (AD-713191)
ARNELL, S. E., Low spin, negative parity states in the N = 103 isotones of ^{171}Er, ^{173}Yb, and ^{175}Hf, 25:15059
ARNOWITT, R., Chiral algebra, chiral breakdcwn, and xi parameter of K/sub 13/ decay, 25:14645
  N-point functions in chiral SU(3) x SU(3) current algebra, 25:14664
ARSENAULT, R. J., Preparation and some mechanical properties of high-purity vanadium, 25:13643
ARTEMOV, K. P., Reaction (^{3}He,α) on nuclei with 1d--2s shell, 25:14944
ARZELIER, G., Colliding beam set up to be built in end station of Crsay linac, 25:14843 (LAL-RT-44-70)
ASAMI, A., Low-energy neutron scattering crcss-section of ^{6}Li, 25:14909
ASAMI, T., Fast-neutron capture cross-sections cf Cr, Fe, Ni, and Mo, 25:14970
ASH, Michael B., Gravitational constant: experimental bound on its time variation, 25:14812
ASHOUR-ABDALLA, M., Nonlinear particle trajectories in a whistler-mode wave packet, 25:14122
ASHTON, F., Search for magnetic monopoles in cosmic rays,

25:14078

ASKAR, A., Time-dependent perturbation calculations based on the hydrodynamic analogy to quantum mechanics, 25:14054

ASKAR'YAN, G. A., Diamagnetic moment of a strong shock wave from a high-temperature light explosion in gases, 25:14282

ATKINS, Daniel E., Arithmetic unit of ILLIAC III: simulation and logical design. II, 25:15430 (COO-2118-2)

ATKINS, H., Technetium-labeled red blood cells, 25:13332

ATZMONY, U., Half-life of the 113.8-keV level of ^{178}Lu, 25:15040

AUBERT, A. E., Explanation of plasma densities high above critical density, 25:14333

AUCHAMPAUGH, G. F., Fission, capture, scattering, and total cross-sections of ^{239}Pu, 25:15091

AUDA, H., Effect of γ irradiation on phosphorous metabolism and nucleic acid synthesis in wheat seedlings, 25:13597 (NP-18606)

AUERBACH, Elliott H., Pi--carbon elastic scattering near the 33 resonance, 25:14908

AUGUST, C., Apparatus for high-speed photographic experiments with irradiated fast-reactor fuel specimens, 25:15384 (ANL-7578)

AUGUSTIN, J. E., Colliding beam set up to be built in end station of Orsay linac, 25:14843 (LAL-RT-44-70)

AUGUSTINE, E. C., Characteristics of nuclear RNA polymerase from rat anterior pituitary tissue, 25:15439 (NYO-3827-18)

AUGUSTYNIAK, W. M., Channeling of positrons, 25:14418

AULIN, I., Detectors in studies of regional lung function by ^{133}Xe radiospirometry, 25:13520

AURBACH, R. L., Inversion of de Haas--van Alphen data. I, 25:14433 (ANL-7659)

AVARGUES, M., Study of a marine site with a view to radioactive effluent discharge, 25:13189 (CEA-CONF-1712)

AVDON'KIN, V. V., Mass-spectrometric method for determining microimpurities in inert gases, 25:12941

AVELLONE, S., Action of ionizing radiations on CNS, 25:13561

AVISHAI, Y., Theory of four-particle scattering, 25:15155

AVOTIN, S. S., Twins of tetrahedral form in beryllium, 25:13718

AVRAIN, Ch., Kinetic study of oxidation of trivalent U sulfuric acid solutions, 25:12977

AVTONOMOV, V. A., Effects of γ rays on cotton at various light conditions, 25:13602

AXEL, P., Photon interaction cross sections of Sn and Zr, 25:14959

AYERS, Jack Duane, Transformations in Ag--Zn, Ag--Cd, and Cu--Zn alloys, 25:13720

B

BAADER, H. A., Energy levels of ^{56}Mn, 25:14974

BABA, H., Prototype of drift tube quadrupole magnets, 25:14849 (SJC-A-70-6)

BABB, Albert L., Prog. rpt. on dynamics of solvent extraction systems, III, annual, 10/69--9/70, 25:13082 (RLO-2225-T-11-1)

BABECKI, J., Comparison of K/π ratio in multiple production at energies 60 GeV and approximately 1000 GeV, 25:14509 (INP-718)

BABESHKIN, A. M., Nuclear gamma-resonance study of products of β-decay of /sup 121m/Sn, 25:13074

BABKINA, E. M., DNA synthesis and migration of cells in hair follicles in lambs, 25:13337

BABU, Ram, Ion--ion hybrid resonance, 25:14390

BACCHIN, Paolo, Diagnostic application of metabolic studies with isotopes, 25:13506

BACHOFNER, E., Method for calculating the washout of elemental iodine by water sprays, 25:15372 (AE-408)

BACON, M. E., Calculation of impact-broadening operator for Stark broadening of H/sub α/, 25:13978

BAD'IN, V. I., Irradiation hazards produced by nonequilibrium emanations, 25:13435

BAE, Soonhoon, Refrigerant forced-convection condensation inside horizontal tubes, 25:13151 (NP-18642)

BAGGIO-SAITOVITCH, E., Mechanism of formation of anomalous charge states of iron after ^{57}Co electron capture in Co complexes, 25:13075

BAIBULATOV, F. Kh., Educational aid for high-frequency plasma diagnostics, 25:14248

BAILEY, G. M., Gamma-ray yields from D(p,γ) ^{3}He, 25:14885

BAILLIE, David L., Gene conversion in higher organisms: half-tetrad analysis of recombination within the rosy cistron of Drosophila melanogaster, 25:13426

BAINBRIDGE, G. R., Electrical generation with nuclear energy, 25:15240

BAIRD, D. C., Current-induced intermediate state in Type-I superconductors, 25:14165

BAKER, John Michael, Leed intensities from cleaved surfaces of zinc and beryllium, 25:14472

BAKER, R. D., Performance of Sweepnik I, 25:13252 (CERN-70-21(Vol.1), pp 293-308)

BAKER, S. D., Polarization and spin-correlation parameters in proton-^{3}He elastic scattering at 19.4 MeV, 25:14888

BAKER, W. F., Elastic forward and backward scattering of π- and K-mesons at 5.2 and 7.0 GeV/c, 25:14579

BAKHRU, H., In-beam gamma spectroscopy of ^{161}Ho, 25:14991

BAKKER, A. M., Measurement of the lifetimes of the Σ^{+-}-hyperons, 25:14546

BALAGNA, J. P., Mass symmetry in the spontaneous fission of ^{257}Fm, 25:15045

BALAKIN, V. E., Experiment on 2 γ-quantum annihilation on VEEP-2, 25:14520

BALAKRISHNAN, V., Complex angular momentum analysis of a field-theoretic model, 25:14833

BALLANCE, Wilbur C., Hydraulic testing of hole UAe-7h, Amchitka Island, Alaska, 25:13105 (USGS-474-84)

BALLANTYNE, Graeme H., Gene conversion in higher organisms: half-tetrad analysis of recombination within the rosy cistron of Drosophila melanogaster, 25:13426

BALLARD, Harold N., Corrections to observed beta-ray atmospheric densitometer values as caused by cosmic rays, 25:13314

BALLINGER, Edwin R., Implantable radiation assembly for circulating systems, 25:13529

BALTAY, C., Progress in automatic scanning at Columbia, 25:13253 (CERN-70-21(Vol.1), pp 311-21)

BANCIU, A.-C., Spectrophotometric investigations of system $Th(NO_3)_4$--violuric acid, 25:13014

BANDO, Shoji, Determination of Sc, Cr, Fe, Co, Zn, and Sb in deposits and airborne particulate by neutron activation analysis, 25:12975

BANDYOPADHYAY, P., Weak interaction of photons and the photoneutrino process, 25:14650

BANFI, A., Clinical experiences in antineoplastic treatment with telecobalt therapy, 25:13546

BANKS, D. C., Seepage characteristics of explosively produced craters in soil and rock, 25:13102 (NCG-TR-27)

BANNISTER, M. J., Crystal structure and anisotropic thermal expansion of β-uranyl dihydroxide, $UO_2(OH)_2$, 25:13010

BANYAI, L., Effective Lagrangians, field algebra, and vector-meson dominance with unstable particles, 25:14784

BARABOSHKIN, A. N., Anodic dissolution of Mo in chloride--molybdate melts, 25:13631

BARAN, Z., Effects of neutron irradiation on U_2Ti, 25:13726

BARASHENKOV, V. S., Systematization of the inelastic interactions of high-energy pions and nucleons with atomic nuclei, 25:15148 (ORNL-tr-2399)

BARBER, D. J., Extralunar dust in Apollo cores, 25:13958

BARENGOLTZ, Jack Bennet, Helium-3 inelastic scattering from several light nuclei, 25:14899

BARFUSS, D. W., Melatonin synthesis in rat pineal glands inhibited by x-irradiation, 25:13559

BARG, D. C., Fission gas release curves: growth and decay from fission of ^{239}Pu by fission spectrum neutrons, 25:14989 (UCRL-50656(Suppl.))

BARKAT, Zalman, Clustering of nucleons in low-density neutron-star matter, 25:13819

BARKER, S. L., Retention of /sup 113m/In--^{59}Fe-ferric hydroxide in the mouse, 25:13486

BARLAT, A., Magnetic properties and structures of CrB compounds Tb--$Ge_{0.2}Si_{0.8}$, HoSi, ErSi, and TmSi, 25:14434 (CEA-CONF-1701)

BARNARD, E., Inelastic scattering of fast neutrons from ^{238}U, 25:15110

BARNEOUD, D., High spin rotational levels in ^{177}Ta, 25:15047

BARNES, Christopher Warren, Computer simulation of a spherically symmetric plasma, 25:14289

BARNES, K. J., Chiral symmetry breaking and nonlinear realizations, 25:14763

BAR-NIR, I., γn partial cross sections up to 12 GeV, 25:14519

BAROUCH, E., Influence of an interplanetary disturbance on solar flare proton propagation, 25:13869

BARRE, J. Y., Complementary roles of integral experiments and differential measurements for fast-neutron reactor project, 25:15347
  Integral measurements of α for ^{239}Pu and ^{235}U, 25:15348

BARRETT, Alan H., Studies of galactic interstellar formaldehyde, 25:13845

BARRETT, R. B., Ion-exchange selectivity of the synthetic zeolite Linde A in anhydrous and mixed media, 25:13091

BARSDATE, Robert J., Prog. rpt. on pathways of trace elements in Arctic Lake ecosystems, annual, 4/15/70--4/14/71, 25:15451 (SAN-310-P-4-10)

BARTKE, Jerzy, Statistical model and cross sections for high-energy reactions, 25:14680 (INP-719)

BAR'YAKHTAR, V. G., Associated-wave scattering of light and slow neutrons in semiconductor antiferromagnets, 25:14488

BASKOVA, K. A., Study of radiations of ^{91}Y, ^{90}Y, and ^{87}Y, 25:15136

BASS, F. G., Associated-wave scattering of light and slow neutrons in semiconductor antiferromagnets, 25:14488

BASS, R. F., Dopants for radiation-resistant silicon, 25:14412 (N-70-39456)

BASSETTO, A., Veneziano formula for mesons, 25:14688

BAS'YUNI, A. Kh., Mass spectrum of particles in nonlinear quark theory, 25:14684

BATALEVA, S. K., Phase diagram for Zr--Co system, 25:13712

BATES, D. R., Large angle scattering in slow H^+--H(1s) collisions, 25:14029
  Mutual neutralization at thermal energies, 25:14032

BATTAT, M. E., Calculations of Jezebel and Godiva with recent ENDF/B microscopic data, 25:15397
BAUDOIN, J.-C., Removable head for pneumatic device, 25:13203
BAUDRY, A., High spin rotational levels in ^{177}Ta, 25:15047
BAUMANN, Elizabeth W., Thermodynamic parameters of Th fluoride complexes from measurements with fluoride-selective electrode at 5, 25, and 45°C, 25:13022
BAURMANN, Karl-Wilhelm, Different models for calculation of nuclide transport in clad spherical fuel particles for high-temperature reactors, 25:13782 (JUL-685-PA)
BAUTISTA, Renato G., Extraction of Y in the system $Y(NO_3)_3$--HNO_3--H_2O--di(2-ethylhexyl) phosphoric acid, 25:13097
BAWA, S. R., Activities of prostates and seminal vesicles after x-irradiation of rat testes, 25:13366
BAYHURST, B. P., Neutron-induced ^{235}U fission at individual resonances. III, 25:14999
BAYINDIR, S., Angiographic diagnosis of hydatid disease of the liver, 25:13494
BAZIN, J., Effects of neutron irradiation on U_2Ti, 25:13726
BEALE, H. A., Preparation and some mechanical properties of high-purity vanadium, 25:13643
BEALL, W. T. Jr., High-current ac losses in large superconducting niobium tubes, 25:14225
BEAL-MONOD, M. T., Fluctuations of the order parameter in small superconducting samples, 25:14167
BEARZATTO, C., Ultrasonic attenuation of transverse waves in dirty superconductors, 25:14160
BEASLEY, Thomas M., Prog. rpt. on natural alpha-emitting radioisotopes in marine organisms, annual, 1969--1970, 25:13394 (RLO-2099-1)
BEAUDOIN, L., Detection of bone metastases by an isotopic method, 25:13513
BEAUFOUR, M., Neutron cross-sections of ^{235}U, ^{238}U, and ^{239}Pu between 0.1 and 6 MeV, 25:15103
BEAUFRERE, J., Test facility for sodium-heated steam generators, 25:13143
BECK, F., Automatic scanning and measurement of bubble chamber film on Polly II, 25:13254 (CERN-70-21(Vol.1), pp 325-55)
  Glossary of on-line measuring devices, 25:13294 (CERN-70-21(Vol.2), pp 963-77)
BECK, Robert N., Use of lithium-drifted germanium detectors for clinical radionuclide scanning, 25:13487
BECKER, H., Normalization for (α,t) reactions, 25:15064
BECKER, J. A., Ml transitions among the f/sub 7/2/d/sub $3/2/^{-1}$ states of ^{40}K, 25:14934
BECKER, R., Energy dependence of electron collision frequency on electrical conductivity of weakly ionized plasmas, 25:14308
BECKER, U., Determination of photoproduction phase of rho^0 mesons, 25:14527
  Observation of coherent interference pattern between rho,omega decays, 25:14528
BECKER, U. J., Photoproduction of pion pairs with high invariant mass, 25:14526
BECKER, W., Precise 2200 m/s fission cross-sections of ^{239}Pu and ^{235}U, 25:15067
BEDERSON, Benjamin, Line shifts and elastic scattering by slow electrons, 25:14057
BEER, H., Rotation of the γγ angular correlation of cascades of ^{134}Ba, 25:14926
BEGHI, Giorgio, Unidirectional solidification of eutectic alloys, 25:13692
BEGRAMBEKOV, L. B., Angular distribution of secondary electrons emitted by Nb due to bombardment with ions, 25:13969
BEHREND, H.-J., Photoproduction of ω mesons from hydrogen and deuterium, 25:14512
BEIGMAN, I. L., Electron excitation of transitions between excited states in Ba^+ and Sr^+ ions, 25:14000
BEKERUS, Milos, Late sequelae after exposure to ^{90}Sr skin irradiators observed eight and more years later, 25:13582
BELAN, V. G., Plasma expansion in vacuum and the flow of a collisionless plasma stream around a plate, 25:14265
BELBEOCH, R., Colliding beam set up to be built in end station of Orsay linac, 25:14843 (LAL-RT-44-70)
BELL, R. L., Grain boundary sliding during creep, 25:13675
BELOUSOVA, I. A., X-ray determination of the expansion coefficients of lanthanum and yttrium borides, 25:13760
BELOUSOVA, N. A., X-ray determination of the expansion coefficients of lanthanum and yttrium borides, 25:13760
BEL'TYUKOVA, S. V., Extraction of alkaline earth metals with thenoyltrifluoracetone and rhodamine S, 25:13098
BELYAEV, F. N., Measurement of alpha values for ^{235}U and ^{239}Pu, 25:15074
BELYAEV, V. B., Calculation of nd scattering lengths with realistic potentials, 25:14743
BENAYOUN, M., Breit--Wigner models and effective range approximations, 25:14702 (PAM-70-8)
BENBROOK, J. R., Measurement of the Σ^+ magnetic moment, 25:14513
BENCZER-KOLLER, N., Lifetime and decay of 23.8 keV state of ^{119}Sn, 25:15056
BEN-DAVID, G., Level scheme of ^{139}La, 25:15032
  Level structure of ^{141}Pr studied by photonuclear excitation, 25:15139
BENDORF, K., Experimental investigations of self-welding of structural materials under sodium, 25:13668
BENEDIKTOVA, G. P., Molybdenum treatment for increasing stability of steel No. Kh18N9T in liquid Li, 25:13634
BENETTA, R., Progress on Polly at Glasgow, 25:13255 (CERN-70-21(Vol.1), pp 357-70)
BENFATTO, C., K anti Kπ final states for N anti N annihilation at rest in the Veneziano language, 25:14691
BENGTSON, B., Plasma delay and plasma time jitter in subnanosecond timing with a surface barrier detector, 25:13228
BENHAMOU, Andre, Analysis of radioactive solutions, 25:12932
BENNETT, Lawrence C., Functional test of a Rocket Engine Module, 25:15453 (SC-DR-70-911)
BENSON, P. A., Particle size distribution in clouds from nuclear airbursts, 25:13138
BENZI, V., Evaluation of nuclear data above resonance energy region: A < 220, 25:15123
  Influence of uncertainties of $sigma_{28}$/sup f/ in Monte-Carlo calculations of small critical assemblies, 25:15398
  Plutonium-239 angular distributions in energy range 0.2 to 5.5 MeV, 25:15134
BERARDO, P. A., Analysis of negative-pion photoproduction near the P_{33} resonance: test of the ΔI less than or equal to 1 rule and time-reversal invariance, 25:14566
  Measurement of inverse pion photoproduction near the $P_{33}{}^0$(1236) resonance, 25:14567
BERCAW, R. W., Study of the odd strontium isotopes with stripping and pickup reactions, 25:14930
BERDOV, B. A., Investigation of vitamin B_{12}--^{60}Co radiometric method of whole body after resection of stomach, 25:13334
BERENDS, F. A., Why do neutrinos produce more W's than muons, 25:14643
BERG, Valter, Energy levels in ^{186}W, 25:15043
BERGAMASCO, Laura, Experimental results on stopping muons at 60 and 300 m.w.e, 25:14535
BERGE, J. P., Oxford PEPR system, 25:13239 (CERN-70-21(Vol.1), pp 61-88)
BERGER, Helmut, Electroretinogram of a frog exposed to ultraviolet light of about 366 nm, 25:13573
BERGER, R., Use of ^{238}Pu radiation sources in cardiac pacemakers, 25:13178
BERGERET, Henri, Local reinforcement of magnetic field near asperities of superconducting surface, 25:14205
BERGERET, Marcel, Coupling, 25:13199
  Remote manipulation tool, 25:13200
BERGERON, J., Photo-ionization of intergalactic matter, 25:13939
BERGGREN, R. G., Tensile and impact properties of thick-section plate and weldments, 25:13660 (ORNL-TM-3211)
BERGMAN, A. A., Radiative capture of neutrons by ^{238}U nuclei, 25:15105
BERGMANN, W., High resolution optical spark chamber, 25:13302
BERKELMAN, K., Elastic forward and backward scattering of π− and K-mesons at 5.2 and 7.0 GeV/c, 25:14579
BERLOVICH, E. E., Life times of levels of ^{128}Te nucleus, 25:15055
BERLOVITCH, E. E., Zero-point oscillations and the shape of nuclei in transition regions, 25:15170
BERNARD, A., Neutron yield of a focus discharge in various experiments, 25:14355
BERNARDINI, M., Limits on the electromagnetic production of heavy leptons, 25:14517
  Validity of leptonic selection rules for (μeγ) vertex at high four-momentum transfers, 25:14515
BERNSTEIN, G. J., Chemical Engineering Division fuel cycle technology quarterly report, July--September 1970, 25:13077 (ANL-7755)
BERNTHAL, F. M., In-beam gamma spectroscopy of ^{161}Ho, 25:14991
  New Ta isotopes ^{170}Ta and ^{171}Ta, 25:15066
BERONIUS, P., Reaction between methyl iodide and alkaline iodide, 25:12996
BERRY, H. G., Vacancy cascade spectroscopy: a convenient method of studying highly ionized atoms and molecules, 25:14038
BERRY, H. W., Elastic scattering of beryllium doubly charged ions in helium, 25:14027
BERRY, P. F., Portable nuclear gage for measuring cement content of plastic concrete, 25:13315
BERTIN, C. L., Comparison of superconducting and semiconducting bolometers, 25:14227
BERTRAM, William K., Observation of coherent interference pattern between rho,omega decays, 25:14528
  Photoproduction of pion pairs with high invariant mass, 25:14526
BES, D. R., Coupled-channel Born-approximation calculation of two-nucleon transfer reactions in deformed nuclei, 25:15191
BESEV, C., Approximation and accuracy in the design of a double-focusing flat spectrometer, 25:13324 (UUIP-715)
BESHTOJEV, H. M., Test of SU(3) symmetrical statistical theory of elementary particle production, 25:14748 (JINR-P2-5480)
BEST, G. H., Calculations of Jezebel and Godiva with recent ENDF/B microscopic data, 25:15397
BETTELS, J., Geometrical reconstruction for the new bubble

chambers, 25:13260 (CERN-70-21(Vol.1), pp 467-96)
BETTERTON, J. O. Jr., Eutectoid region of the Zr--Ga system, 25:13709
BETTINI, A., Annihilation anti pn → $\pi^+\pi^-\pi^-$ between 1.0 and 1.6 GeV/c, 25:14548
BETZ, G., Determination of the distribution of fission products in fuel particle coatings by the sputtering technique, 25:13758
BETZNER, J., Indirect parasternal lymphoscintigraphy in mammary carcinomas, 25:13515
BEURTEY, R., Measurements of the depolarization parameter D for elastic proton scattering, 25:14889 (CEA-CONF-1650)
BEVC, Vladislav, Surface and bulk waves on axially magnetized plasma columns, 25:14360 (AD-711649)
BEZDEK, Hugo Frank, Lattice dynamics of zirconium using thermal neutron scattering, 25:14467
BEZUS, V. A., Flows of 100- to 1500-MeV electrons at various heights in atmosphere, 25:14068
BHAGAT, S. M., He II--He I transition in the presence of a heat current, 25:14136
BHAGAVAT, G. K., Dc noise in plasma due to electron--ion collisions, 25:14303
BHAT, P. K., Guiding center of a charged particle in superposed heliotron and biconical cusp fields, 25:14330
BHATT, S. J., Fracture mechanics evaluation of stress intensity factors for various crack geometries and loading conditions, 25:13181 (WAPD-TM-976)
BHATTACHARJEE, S. B., Influence of chloramphenicol on irradiated bacteria, 25:13613
BIALAS, A., Evaluation of the absorption corrections to exchange models, 25:14831
  Fixed J-plane singularities in photoproduction, 25:14625
BIBLER, Ned E., Radiolysis of carbon tetrachloride. Radical yields and the formation of tetrachloroethylene as an initial product, 25:13045
BILAL, B. A., Separation of ^{131}Cs from irradiated Ba salts with help of counter current electrolysis, 25:13062
BILLARD, F., Some comments on the production and measurement of spheres of polystyrene latex, 25:13144
BILLETTE, J. J., Concerning a thought experiment violating Heisenberg's uncertainty principle, 25:14502
BILLING, H., Brush system for automatic processing of bubble chamber pictures, 25:13274 (CERN-70-21(Vol.2), pp 689-707)
BILLON, J. P., Correction coefficients for elementary quantitative analysis by spark mass spectrometry. Application to U and Pu dies, 25:12927
BIRKIGT, W., Conception of integrity of type A and B packaging for shipment of radioactive materials, 25:13201
  Illustration of specifications for transport of radioactive materials of high activity and fissionable materials, 25:13194 (SZS-19/70)
BIRKS, J. B., Triplet--triplet interactions in organic scintillators, 25:13220
BIRO, Tomas, Measurement of the radioactivity of natural waters, 25:13106
BIRULEV, V. K., Search for isobar state with $T = {}^5/_2$ in the reaction $\pi^+ + p \to \pi^- + X^{3+}$, 25:14576
BISHOP, E. H., Natural convection heat transfer between concentric spheres, 25:15450 (RLO-2214-2)
  Prog. rpt. on natural convective heat transfer between concentric spheres, annual, 1/71, 25:15449 (RLO-2214-1)
BISWAS, N. N., Double-Regge analysis of single-pion production in π^-p interactions at 8 GeV/c, 25:14713
BITAR, Khalil M., Bjorken limit and Jin--Martin lower bound, 25:14827
BITO, Janos, Plasma diagnostics with laser beams, 25:14255
BJORNEBOE, Jens, Spectrum of resonances in generalized Veneziano model, 25:14681 (INP-730)
BLACK, Paul H., Analysis of SV40-induced transformation of hamster kidney tissue in vitro. VII, 25:13615
BLACKBURN, M. J., Effect of microstructure on the strength, toughness, and stress-corrosion cracking susceptibility of a metastable beta titanium alloy (Ti--11.5Mo--6Zr--4.5Sn), 25:13672
BLACKHAM, Angus U., Technetium as a catalyst in organic reactions, 25:15448 (RLO-2017-3)
BLAHA, Stephen, Deep-inelastic e--p structure functions in ladder model with spin $^1/_2$ nucleons, 25:14612
BLAIR, J. S., Further calculations of proton inelastic polarizations and asymmetries using a spin-dependent interaction of the full Thomas form, 25:14892 (RLO-1388-600)
BLAIR, W. M. R., Bubble chamber film measurement on HPDs at CERN, 25:13281 (CERN-70-21(Vol.2), pp 813-24)
BLANCO, R. E., The feasibility of incorporating radioactive wastes in asphalt or polyethylene, 25:13197
BLANK, W. A., Irradiation injury to the bowel and rectum, 25:13589
BLAUGHER, R. D., Characteristics of NbN Dayem bridges, 25:14201
BLEULER, K., One-boson exchange potential and nuclear matter properties, 25:15199
BLEWETT, J. P., 1000-GeV storage rings, 25:14835 (BNL-15423)
  Method for decreasing energy spread in AGS beam, 25:14836 (BNL-15424)
BLIN-STOYLE, R. J., Mass of the intermediate vector boson, 25:15180
BLOBEL, V., Experiences with coupled computers to control an HPD, 25:13276 (CERN-70-21(Vol.2), pp 721-7)
BLOCH, J., Effects of neutron irradiation on U_2Ti, 25:13726
BLOCK, Melvin A., Functional autonomy in multinodular goiter, 25:13493
BLOECKER, W., Two-group neutron transport theory for plane and spherical geometry, 25:14867
BLOK, J., Analysis of $2^- \to 2^+$ positon transitions in ^{84}Rb and ^{74}As, 25:14972
  Shapes of the non-unique and unique first-forbidden β-spectra of ^{84}Rb, ^{74}As and ^{126}I, 25:14976
BLOMQVIST, G., System for on-line control of bubble chamber measurements, 25:13282 (CERN-70-21(Vol.2), pp 825-30)
BLONS, J., High-resolution measurement and analysis of ^{239}Pu fission cross-section, 25:15089
  Measurement and analysis of ^{235}U and ^{241}Pu fission cross-sections, 25:15086
  Total and fission cross-sections of ^{239}Pu from 5.7 to 160 eV, 25:15087
BLOOM, Bruce S., Combined therapy for cancer of the laryngopharynx, 25:13545
BLOOM, Eda T., Quantitative detection of cytotoxic antibodies against tumor-specific antigens of murine sarcomas induced by 3-methylcholanthrene, 25:13389
BLOW, S., Nuclear cross section requirements for fusion reactors, 25:14357
BLUDOVA, L. N., Mass-spectrometric method for determining microimpurities in inert gases, 25:12941
BLUM, A. S., Xenon-133 pulmonary-function analyzer, 25:13223
BLUVSHTEIN, R. E., Analytic properties of inelastic hadronic form factors and breaking of CP invariance in electromagnetic interactions, 25:14765
BOBROVSKII, G. A., Dependence of transport coefficients on plasma parameters in Tokamak, 25:14239
BOCKMANN, K., Longitudinal phase-space analysis of 5 GeV/c π^+p reactions, 25:14578
BOCKRATH, R. C., Specificity of uv mutagenesis in E. coli, 25:13406
BOECK, R. K., Calibration, precision, and filtering questions for the CERN Spiral Reader, 25:13235 (CERN-70-21(Vol.1), pp 5-18)
BOEHM, A., Dirac representation of the relativistic symmetries, 25:14752
  Generalizations of Dirac representation, 25:14767
  Symmetry breaking in representations of the relativistic symmetry, 25:14768
BOEHM, F., Parity nonconservation in nuclear forces. I, 25:15009
BOGAARD, Ronald Henry, Thermal resistivity of cadmium, magnesium, and alloys at low temperatures, 25:14473
BOGAARDS, J. J. W., ^{48}Ca(d,p)^{49}Ca reaction across the Coulomb barrier, 25:14916
BOGDANOV, D. D., Anomalies in the Z dependence of mean charges of heavy ions in helium and air, 25:14007
BOGDANOV, V. G., Probability of fission with emission of long-range particles, 25:15018
BOGUSLAVSKII, Yu. Ya., Acoustic flow in a superfluid liquid, 25:14130
BOHME, R., Theoretical and experimental analysis of fast zero-power assemblies, 25:15396
BOHNE, W., Study of states in ^{16}O, 25:14914
BOISSIER, Michele, Determination of internal and superficial oxygen content of molybendum obtained using 54 MeV α particles and low energy deuterons, 25:12957 (LYCEN-7076)
BOJSEN, J., Construction of instrument for more accurate, repeated blood volume determinations using HSA-^{131}I, 25:13218
BOKELUNG, H., Investigation of reprocessing input measurement using tracer technique, 25:13081 (NP-18577)
BOKHAREE, S., High-energy γ-rays following neutron capture in ^{239}Pu and ^{235}U, 25:15078
BOKRA, Yobou, Analytical study of dibromopyrogallolsulfonephthalein (DBPSP), 25:12926
BOLDRIGHINI, C., Discussion of duality and analyticity, 25:14829
BOLDUC, P. E., Interaction of electromagnetic wave with hot plasma half-space, 25:14361
BOLDUC, Paul Eugene, Interaction of plane electromagnetic wave with hot plasma half-space and plasma slab, 25:14386
BOLIVAR, Juan C., Value of scintiscans in the diagnosis of splenic abscess, 25:13512
BOLLINI, D., Limits on the electromagnetic production of heavy leptons, 25:14517
  Validity of leptonic selection rules for (μeγ) vertex at high four-momentum transfers, 25:14515
BOLT, S. E., ^{233}U-bearing salt preparation for the Molten Salt Reactor Experiment, 25:15368
BONACA, M. V., Evaluation of isocheck and invent fuel inventory calculational models, 25:15211
BONCH-OSMOLOVSKII, A. G., Dynamics of charged bunch collisions in connection with impact mechanism of acceleration, 25:14855 (UCRL-Trans-1421)
  Transient effect of accelerating field on electron bunch containing ions, 25:14854 (UCRL-Trans-1420)
BONDARENKO, B. V., Adsorption of Ba on a (110) face of Mo

single crystal, 25:13701
  Structure and work function of films of gadolinium on molybdenum, 25:13700
  Structure and work function of La films on a (110) Mo single crystal surface, 25:13702
BONDI, H., Transfer of energy in general relativity, 25:14816
BONET, Claude, Production of continuous high-power plasma flow, 25:14273
BONNEVIER, B., Experimental evidence of element and isotope separation in a rotating plasma, 25:14278 (NP-18643)
BOOIJ, H. M. W., Shapes of the non-unique and unique first-forbidden β-spectra of ^{84}Rb, ^{74}As and ^{124}I, 25:14976
BOOKBINDER, James H., Superfluidity in ^{3}He: inhibition by polarization, 25:14135
BOOLCHAND, Punit, Electric quadrupole interactions in single crystals of Te metal, Hf metal and $CaWO_4$, 25:14480
BOPP, C., Princeton automatic track reader, 25:13250 (CERN-70-21(Vol.1), pp 273-83)
BOPP, G. R., Effects of variable properties on MHD flow in finite ducts, 25:14090
BORGONOVI, G. M., Prog. rpt. on fast reactor spectrum measurements, 10/70, 25:15388 (GULF-RT-10421)
BORIE, Edith, Radiative corrections to back scattering, 25:15175
BORISOV, V. L., Inelastic scattering of slow electrons in germanium and silicon, 25:13967
BORISCVSKII, V. V., Release of stored energy in annealing of radiational defects in NaCl, 25:14424
BORMANN, M., Integral cross sections of reaction $^{11}B(n,\alpha)^{8}Li(\beta)^{8}Be^{*}(2\alpha)$, 25:14895
BORN, H.-J., Determination of impurities in boron carbide by neutron activation analysis, 25:12972
BORREL, Louis, Coupling, 25:13199
  Remote manipulation tool, 25:13200
BORTIN, Mortimer M., Skin allograft survival in mice after radioprotection with sodium S-(2-aminotheyl) phosphorothioate and supralethal total body x-irradiation, 25:13479
BOS, William G., Positron annihilation rates in lanthanum hydrides, 25:13988
BOSQUED, Jean-Michel, Low-energy proton flux parallel to field lines in auroral ionosphere, 25:14125
BOUCHARD, J., Complementary roles of integral experiments and differential measurements for fast-neutron reactor project, 25:15347
  Integral measurements of α for ^{239}Pu and ^{235}U, 25:15348
BOUCHER, R., Use of ^{238}Pu radiation sources in cardiac pacemakers, 25:13178
BOUCHEZ, Jacques, Simplified method of obtaining information from bubble chamber photographs, 25:13233 (CEA-N-1397)
BOUDKER, Guersch, By way of antiplasma towards antimatter, 25:14544
BOULWARE, David G., Troubles with strict conformal symmetry, 25:14820 (RLO-1388-598)
BOURASSEAU, D., Argon plasma generator with electron density within the range 5 x 10^{14} to 5 x 10^{17} cm^{-3}, 25:14335
BOURGEOIS, F., Pattern recognition methods for Omega and SFM spark chamber experiments, 25:13283 (CERN-70-21(Vol.2), pp 831-50)
BOVARD, P., Radiocontamination of soils and crops, 25:13402
  Study of a marine site with a view to radioactive effluent discharge, 25:13189 (CEA-CONF-1712)
BOWERS, G. L., Remote data station interface to the production control computer, 25:15469 (Y-1748)
BOWYER, A., Study of 200 patients with Pruitus ani, 25:13588
BOYCE, D. A., Ratio of capture and fission cross-sections of ^{239}Pu in energy range 100 eV to 30 keV, 25:15073
BOYD, R. E., Radiopharmaceuticals in nuclear medicine, 25:13519
BOZOKI, G., Proton momentum spectrum in πN inelastic interactions at 17.2 GeV/c, 25:14564
BRADLEY, Muriel V., Cytological effects of juice or puree from irradiated strawberries, 25:13621
BRADT, H., 1- to 10-keV x-ray sky near the galactic center, 25:13857
BRAFMAN, H., Weizmann Institute Spiral Reader system, 25:13293 (CERN-70-21(Vol.2), pp 953-62)
BRANDICOURT, Gilles, LGR/B program: for updating the ANISN library tapes with plotting of cross section curves, 25:14986 (CRNL-tr-2408)
BRANDCN, G., Description and performance of the CERN Spiral Reader, 25:13236 (CERN-70-21(Vol.1), pp 19-36)
BRANDT, John C., Gum nebula: fossil Stroemgren sphere of the Vela X supernova, 25:13851
BRANDT, Richard A., Field equations in quantum electrodynamics, 25:14777
BRAUN, J. D., Solubility of tritium in annealed and cold-worked copper, 25:13654 (MLM-1734)
BRAY, R. J., High-resolution photography of solar chromosphere. VIII, 25:13876
BRECHNA, H., Magnetization and susceptibility measurements of polycrystalline niobium, 25:14195
BREDOV, M. M., Study of gamma radiation with Kosmos-135, 25:13951
BREITLING, Gerhard, Additional radiation burden to the patient caused by shielding during deep x-ray therapy, 25:13460
BREITMAN, Z. M., Controlling the volumetric weight of light concretes in enclosing members by scattered gamma radiation, 25:13308
BRENE, N., Form factor in K/sub e3/ decay, 25:14652
BRETTEL, H., Digitized microscope for evaluation of photo emulsions in high-energy physics, 25:13284 (CERN-70-21(Vol.2), pp 851-7)
BREZIN, E., Polarization phenomena in vacuum nonlinear electrodynamics, 25:14793
BRILL, O. D., Observation of analogue states with T = 2 in the reactions $^{26}Mg(^{3}He,n)^{28}Si$, $^{46}Ti(^{3}He,n)^{48}Cr$, and $^{58}Ni(^{3}He,n)^{60}Zn$, 25:14943
BRINK, D. M., Isospin mixing of Hartree--Fock solutions, 25:15164
BRINKLEY, F. W., TWOTRAN SPHERE: FORTRAN program to solve multigroup transport equation in two-dimensional spherical geometry, 25:14866 (LA-4567)
BRISBOIS, Jacques, Measurement of the neutron albedo of ordinary concrete, 25:14394 (CEA-N-1382)
BRISSET, C., Desensitivity of a microwave cavity to measurements of hot-electron density, 25:14262
BROADHURST, D. J., Low energy theorems and high energy photoproduction, 25:14622
BROCKWELL, P. J., Multiple scattering of gamma radiation, 25:14393 (ANL-7689)
BRODER, D. L., Inelastic neutron scattering-$(n,n'\gamma)$-by F, Fe, Co, Ni, and Ta nuclei, 25:14960
BRODSKY, M. B., Possibility of magnetic ordering in delta-Pu, 25:14481
BRODSKY, Stanley J., Vacuum-polarization contributions to the sixth-order anomalous magnetic moment of the muon and electron, 25:14616
BROGLIA, R. A., Coupled-channel Born-approximation calculation of two-nucleon transfer reactions in deformed nuclei, 25:15191
BROKATE, K., BERTA: a FORTRAN program for automatic recognition and reconstruction of bubble chamber events. II, 25:13244 (CERN-70-21(Vol.1), pp 141-75)
  BERTA: a FORTRAN program for automatic recognition and reconstruction of bubble chamber events. I, 25:13243 (CERN-70-21(Vol.1), pp 125-39)
  Heidelberg automatic event recognition, 25:13241 (CERN-70-21(Vol.1), pp 105-11)
BROMAN, Lars, Scandium-45 level scheme, 25:14941
BROOKS, C. B., PEPR for BEBC, 25:13240 (CERN-70-21(Vol.1), pp 89-104)
BROOKS, R. D., Design of nuclear Brayton turboalternator--compressor, 25:13168 (N-70-41276)
BROSSIER, P., Experimental observation of drift instabilities in a collisionless plasma, 25:14345
BROUDE, C., Lifetimes and gamma transitions in ^{16}O, 25:14905
BROWER, Richard C., Vector currents and current algebra. III, 25:14667
BROWN, A. F., Solid-solution strengthening at 77°K in Cd single crystals containing Zn, 25:13670
BROWN, C. L., Criticality safety analysis: Model 60 shipping package for FFTF driver fuel, 25:13187 (BNWL-1512)
BROWN, D., Protactinium(V) fluorides, 25:12978
  Quinquevalent Pa and quadrivalent actinide tropolonates, 25:13009
BROWN, Donald P., Method for detecting one of heavy water and ordinary water in the presence of the other of heavy water and ordinary water, 25:12931
BROWN, G. E., Resonant elastic scattering of protons from analogue and compound states, 25:15146 (NYO-1082-25)
BROWN, Lowell S., Troubles with strict conformal symmetry, 25:14820 (RLO-1388-598)
BROWN, R. A., Levels in ^{177}Lu, 25:15039
BROWN, R. E., Laboratory and environmental mineral analysis using a ^{252}Cf neutron source, 25:12962
BROWN, R. W., Intermediate boson. I, 25:14641
BROWN, Robert L., Ultraviolet absorption-line spectra produced by H I regions, 25:13841
BROWN, Robert T., Electron temperature and number density measurements in a nonequilibrium plasma boundary layer, 25:14244 (AD-711669)
BROWN, Robert Thomas, Electron temperature and density nonequilibrium plasma boundary layer, 25:14258
BROWN, W. K., Fission and capture cross-sections of curium, 25:15090
BROWNING, G. K. S., Progress on Polly at Glasgow, 25:13255 (CERN-70-21(Vol.1), pp 357-70)
BRUELS, Mark C., Properties of 1s shell nuclei, 25:15185
BRUNHART, G., Spins of neutron resonances in ^{167}Er, 25:15003
BRUNING, H. A. C. M., Process for removal of gases held in interstitial sites from titanium, zirconium, hafnium, or thorium, 25:13641 (UCRL-Trans-10503)
BRUNO, G. A., Retention of /sup 113m/In--^{59}Fe-ferric hydroxide in the mouse, 25:13486
BRUYANT, F., Geometrical reconstruction for the new bubble chambers, 25:13260 (CERN-70-21(Vol.1), pp 467-96)
BUBNOV, L. Ya., Spectra of energy lost by slow electrons in aromatic hydrocarbons, 25:13968
BUCHDAHL, H. A., Conformal flatness of Schwarzschild interior solution, 25:14808
BUCHHOLZ, J. R., Production of Candida utilis with 93 at. percent ^{13}C acetic acid as the sole carbon source,

XUM

25:13331 (LA-4551)
BUCHLER, Jean-Robert, Clustering of nucleons in low-density neutron-star matter, 25:13819
BUDDE, R., Description and performance of the CERN Spiral Reader, 25:13236 (CERN-70-21(Vol.1), pp 19-36)
BUDKER, G. I., Experiment on 2 γ-quantum annihilation on VEEP-2, 25:14520
BUD'KO, N. I., Double scattering of plasma streams in bi-thermal ionosphere, 25:14112
BUDNIK, A. P., Probabilities of quadrupole transitions and the mean values of quadrupole moments in phenomenological nuclear theory, 25:15177
BUDZANOWSKI, A., Backscattering of alpha particles, 25:15172
BUDZIK, Dennis Michael, Construction of a theta pinch for the generation of shock waves in a nitrogen plasma, 25:14350 (AD-711003)
BUELL, U., Bloodpool scintigraphy with shortlived radionuclides, 25:13516
BULOS, F., Photoproduction of high-mass di-pion pairs at 15 GeV, 25:14511
BUNKIN, F. V., Electron heating in interaction between ultra-short intense laser pulses and matter, 25:14279
BURBACH, J., Cyclic deformation behavior of some engineering materials, 25:13683
BURCHAM, W. E., Double scattering of ^{3}He particles by C and Al, 25:14894
BURCHILL, C. E., Concerning kinetics of isopropyl alcohol radicals by electron spin resonance-flow techniques, 25:13032
BURCHULADZE, A. A., Search for magnetic monopoles in cosmic rays, 25:14078
BURD, D., Progress in automatic scanning at Columbia, 25:13253 (CERN-70-21(Vol.1), pp 311-21)
BURDANINA, N. A., Dielectric properties of a γ-irradiated KDP crystal, 25:14432
BURGART, C. E., The energy spectrum of photoneutrons produced by 140-MeV electrons incident on tantalum, 25:14990
BURGART, Calvin E., General method of importance sampling the angle of scattering in Monte Carlo calculations, 25:14404
BURKARD, O. M., Coupling between solar wind and ionosphere, 25:14110
BURKE, D. G., Reaction (^{3}He,α) on Yb isotopes, 25:15057
BURKEL, Richard H., Specific heat of superconducting transition metals containing nonmagnetic impurities at low temperatures, 25:14179
BURKHARDT, W., Principles for control of nuclear material in GDR, 25:13193 (SZS-16/70)
BURLESON, G., Polarization parameter in backward π^+p elastic scattering at 1.60, 1.80, 2.11, and 2.31 GeV/c, 25:14577
BURMEISTER, H., Scanning and measuring of heavy liquid film on-line, 25:13271 (CERN-70-21(Vol.2), pp 651-64)
BURNASHEVA, V. V., Phase diagram for Zr--Co system, 25:13712
BURNEL, A., Local gauge-invariant formulation of electromagnetic ω--rho mixing in broken SU(3) Lagrangian theory, 25:14628
BURNETT, B., 1- to 10-keV x-ray sky near the galactic center, 25:13857
BURNETTE, K. T., Observation of single fluxon drift through a superconductor, 25:14199
BURNS, John H., Refinement of the crystal structure of $AmCl_3$, 25:13011
BURNS, Raymond K., Thermal analysis of heat source for use with isotope Brayton space power system, 25:13167 (N-70-41092)
BURROWS, R. D., anti pd topological cross sections in momentum range 50 to 920 MeV/c, 25:14555
BURT, P. B., Perturbation theory for toroidal plasma, 25:14327
BURTON, W. B., Galactic structure derived from neutral H observations, 25:13930
BURZYNSKI, A., Spinor representations of complex inhomogeneous Lorentz group. I, 25:14755
  Spinor representations of complex inhomogeneous Lorentz group. II, 25:14756
BUSEV, A. I., Extraction--photometric determination of Fe, 25:12934
BUSSE, C. A., Corrosion in high-temperature lithium heat pipes with niobium--zirconium and tantalum as wall material, 25:13630 (EUR-4298)
BUSZA, W., Photoproduction of high-mass di-pion pairs at 15 GeV, 25:14511
BUTLER, Mary Ann, Genetic analysis of the histidine operon in Escherichia coli K12, 25:13422
BUTT, B. A., Reduction of sexual aggressiveness of male codling moths treated with tepa or gamma irradiation, 25:13557
BUTTEMER, D. R., Instantaneous and time-dependent collapse of externally pressurized circular tubes with initial out-of-roundness, 25:13652 (GAMD-8219(Rev.))
BUTTERFIELD, Colin Edgar, Fuel element stringers, 25:15415
BYRIKHIN, V. I., Metabolism of ^{14}C-dimecarbine in irradiated animals, 25:13576
BYRNE, W. F., Comparison of ^{46}Sc and ^{144}Ce as nonabsorbed reference materials in studies with cattle, 25:13352
BYRON, F. W. Jr., Theory of the quenching of metastable hydrogen atoms by helium, 25:14026

C

CABANNES, F., Argon plasma generator with electron density within the range 5 x 10^{14} to 5 x 10^{17} cm^{-3}, 25:14225
CABE, J., Neutron cross-sections of ^{235}U, ^{238}U, and ^{239}Pu between 0.1 and 6 MeV, 25:15103
CACAK, Robert Kent, Ionization cross sections, 25:13996
CACCHIONE, Aldo, Xerodermal idiocy, 25:15443 (ORNL-tr-2426)
CADIET, Francoise, Simplified method of obtaining information from bubble chamber photographs, 25:13233 (CEA-N-1397)
CAHILL, T. A., Polarization and spin-correlation parameters in proton-^{3}He elastic scattering at 19.4 MeV, 25:14888
CAHN, J. H., Distances and distribution of planetary nebulae, 25:13827
CALDAS, L. R., Effects of reductone on irradiated E. coli, 25:13610
CALDERINI, P., Effects of continuous exposure to radioactive phosphorus in ionic form, 25:13351
CAMERON, A. E., Analytical mass spectrometry at Oak Ridge National Laboratory, 25:13319 (ORNL-4643)
  Mass spectrometric investigation of surface ionization. VI. Desorption of Th$^+$, Np$^+$, and Pu$^+$ from W surfaces, 25:13686
CAMERON, J. A., Nuclear g factors of 2+ levels in ^{194}Pt, 25:15034
CAMPBELL, C. G., Relationship of microscopic and integral data, 25:15346
CAMPBELL, P. A., Plaque-forming cells of two different origins in single hemolytic foci, 25:13387
CAMPILLO, C., Concerning a thought experiment violating Heisenberg's uncertainty principle, 25:14502
CANCE, M., Neutron cross-sections of ^{235}U, ^{238}U, and ^{239}Pu between 0.1 and 6 MeV, 25:15103
CANER, M., Calculation of ^{240}Pu neutron cross-sections in keV-range, 25:15129
CANFIELD, R. C., Formation of solar rare-earth lines inside and outside the H and K, 25:13810
CANFIELD, Richard C., Deviations from LTE in weak complex spectra, 25:13816
CANGIANO, Sergio, Multiple scattering calculations of gamma photon transport, 25:14399
CANONICO, D. A., Measurement of residual stresses, 25:13697
  Tensile and impact properties of thick-section plate and weldments, 25:13660 (ORNL-TM-3211)
CANTU, A. M., Connection between N--S and E--W solar asymmetries, 25:13883
CANUTO, V., Theory of radiation mechanisms of pulsars. I, 25:13842
CAO, M. G., Fission-cross-section measurement of ^{233}U, 25:15082
CAPET, Henri, Transport flask for nuclear fuel elements, 25:13205
CARALP-AMILHAT, Francoise, Changes in the surface of uranium and its hydrides during successive hydrogenations and dehydrogenations at various temperatures, 25:13635
CARATHANASSIS, C., Digitized microscope for evaluation of photo emulsions in high-energy physics, 25:13284 (CERN-70-21(Vol.2), pp 851-7)
CARLSON, A. D., Calculations of cross-sections for the radiative capture of fast neutrons, 25:15122
  Measurements of cross-sections for radiative capture of 1-keV to 1-MeV neutrons by Mo, Rh, Gd, Ta, W, Re, Au, and ^{238}U, 25:15121
CARLSON, M. C. J., Water and sorbed-gas content of hypostoichiometric mixed oxide fuel pellets, 25:12925 (WHAN-SA-77)
CARLSON, P. J., Elastic forward and backward scattering of π^- and K-mesons at 5.2 and 7.0 GeV/c, 25:14579
CARLSON, Richard C., K-division experimental work. Part I. Geophysics research for underground explosion technology, 25:13104 (UCRL-50855)
CARNEIRO DA SILVA, C., Measurements of ^{233}U cross-sections for thermal neutrons, 25:15071
CARNEVALI, G., Clinical experiences in antineoplastic treatment with telecobalt therapy, 25:13546
CARO, D. E., anti pd topological cross sections in momentum range 50 to 920 MeV/c, 25:14555
CARR, H. A., Early visualization of /sup 99m/Tc-pertechnetate in metastatic thyroid cancer in a patient with Graves' disease, 25:13488
CARR, Matthew L., Inhibition of hepatic microsomal mixed function oxidases by D_2O, 25:13372
CARR, Robert W. Jr., Prog. rpt. on kinetics of methylene and hydroxyl radical reactions, annual, 1970, 25:15429 (COO-2026-4)
CARR, Thomas D., Jupiter's magnetospheric rotation period, 25:13957
CARRARO, G., Neutron widths of ^{238}U from 60 eV to 5.7 keV, 25:15080
  Total neutron cross-section of ^{233}U from 0.7 to 320 eV, 25:15079
CARRIGAN, R. A. Jr., Upper limit for magnetic-monopole production by neutrinos, 25:14638
CARROLL, P. J., Effect of specimen thickness on the

superconducting critical temperature of indium, 25:14173
CARTER, B., Axisymmetric black hole has only two degrees of freedom, 25:13828
CARTER, J. R. Jr., Effect of electron irradiation on lithium-doped silicon, 25:14423
CARVER, D. W., Remote data station interface to the production control computer, 25:15469 (Y-1748)
CARY, Arthur Simmons, The direct production of electron pairs in nuclear emulsion by 13.75 GeV electrons, 25:14525
CASBOLT, P. N., X rays from color television receivers in Britain, 25:13452
CASON, J. L., Neutron radiography with ^{252}Cf, 25:13161 (BNWL-SA-3169)
CASSANDRO, M., K anti Kπ final states for N anti N annihilation at rest in the Veneziano language, 25:14691
CASTAGNOLI, Carlo, Experimental results on stopping muons at 60 and 300 m.w.e, 25:14535
CASTELVETRI, A., HPD--IBM 360/44 system at CNAF for bubble chamber data analysis. II, 25:13268 (CERN-70-21(Vol.2), pp 617-24)
  HPD--IBM 360/44 system at CNAF for bubble chamber data analysis. III, 25:13269 (CERN-70-21(Vol.2), pp 625-30)
CASTMAN, B., Approximation and accuracy in the design of a double-focusing flat spectrometer, 25:13324 (UUIP-715)
CASTRILLON, J., Aromatic nitriles: a new family of scintillation solutes, 25:13214
CASWELL, J. L., Extended radio source in direction of pulsar CP 1919, 25:13834
  Unusual OH emission from a Mira variable, 25:13818
CATER, Margot S., Genetic analysis of the histidine operon in Escherichia coli K12, 25:13422
CATILLON, P., Measurements of the depolarization parameter D for elastic proton scattering, 25:14889 (CEA-CONF-1650)
  Polarization and spin-correlation parameters in proton-^{3}He elastic scattering at 19.4 MeV, 25:14888
CAVALLO, Giacomo, Consideration of observed isotropic γ-ray background, 25:14062
CEARLOCK, D. B., Analysis of hydrological factors influencing operation of 100-N emergency waste disposal Crib, 25:13186 (BNWL-1503)
CECCHET, G., HDP--IBM 360/44 system at CNAF for bubble chamber data analysis. I, 25:13267 (CERN-70-21(Vol.2), pp 607-15)
CECH, Jan, Pangloss, a CRT device for bubble chamber pictures, 25:13258 (CERN-70-21(Vol.1), pp 401-25)
CELINSKI, Zdzislaw, Electrical effects in electrode boundary layer in Faraday-type MHD generator, 25:14087
CEPOLINA, A. G., Measurement of residual stresses, 25:13697
CEULEMANS, H., Scattering cross-section of ^{235}U below 100 eV, 25:15084
  Scattering cross-section of ^{235}U between 0.025 and 1 eV, 25:15085
CHADHA, Sudha R., Effect of radiophosphorus on the development of gonads in mice, 25:13569
CHAKRAVORTY, D., Electrical conductivity in cubic Y_2O_3--ZrO_2 solid solutions, 25:14476
CHAMBERS, Carey A., Thermal desorption of atmospheric gases from plutonium dioxide. I, 25:13024
CHANDLER, Gerald David, $\pi^+\pi^0\pi^-$ production in K^-p interactions at 5.5 GeV/c, 25:14572
CHANDLER, J. M., ^{233}U-bearing salt preparation for the Molten Salt Reactor Experiment, 25:15368
CHANDRA, N., Density operator for unpolarized radiation, 25:14504
  Scattering of linearly polarized radiation, 25:14601
CHANDRASEKHAR, B. S., Properties of lead--indium alloys. II. Specific heat, 25:14180
CHANEL, G., Adam+Eva, scanning and measuring machine for film from the large bubble chambers, 25:13270 (CERN-70-21(Vol.2), pp 633-49)
CHANEY, K. F., Solubility of tritium in annealed and cold-worked copper, 25:13654 (MLM-1734)
CHANG, Chung-yueh, Demonstration of a circulating factor regulating blood platelet production using ^{35}S-sulfate in rats and mice, 25:13355
CHANUDET, L., Test facility for sodium-heated steam generators, 25:13143
CHAPELLE, J., Argon plasma generator with electron density within the range 5 x 10^{14} to 5 x 10^{17} cm^{-3}, 25:14335
CHAPMAN, Dennis Arthur, Nuclear reactor pressure vessel, 25:15364
CHAPMAN, J. W., Quasi-two-body production in π^+p interactions at 1.95 GeV/c, 25:14563
CHARLESTON, Donald B., Use of lithium-drifted germanium detectors for clinical radionuclide scanning, 25:13487
CHARLTON, B. G., Experimental study of spouting beds of spheres, 25:13139 (AERE-R-4852)
CHARLTON, G., Automatic scanning and measurement of bubble chamber film on Polly II, 25:13254 (CERN-70-21(Vol.1), pp 325-55)
CHATURVEDI, G. C., Ultraviolet absorption spectra of acetone and acetone-d_6, 25:13006
CHAUDHURI, P. Ray, Weak interaction of photons and the photoneutrino process, 25:14650
CHAUVIN, M., Test facility for sodium-heated steam generators, 25:13143
CHEBOTAEV, P. Z., Plasma expansion in vacuum and the flow of a collisionless plasma stream around a plate, 25:14265
CHEBOTAEV, V. P., Breakdown of 2^1P and 2^3P levels of He in a glow discharge, 25:13977
CHEIFETZ, E., Measurement of the prompt neutrons emitted in the fission of ^{209}Bi and ^{238}U induced by 155-MeV protons, 25:15021
CHEKHOVSKOI, V. Ya., Enthalpy and specific heat of the 80 percent W--20 percent Mo alloy at high temperatures, 25:13665
  Thermophysical properties of solids at high temperatures, 25:13667
CHELNOKOV, V. B., Radiative capture of neutrons by ^{238}U nuclei, 25:15105
CHEN, C. L., Prog. rpt. on basic plasma processes, final, 7/69--9/70, 25:14264 (AD-711828)
CHEN, Joseph C. Y., Faddeev equations for atomic problems. IV, 25:14010
CHEN, Juei-Teng, Electron-tunneling investigating of superconducting amorphous state of bismuth, 25:14210
CHEN, M., Determination of photoproduction phase of rho^0 mesons, 25:14527
CHEN, Min-shih, Limiting distribution and average π^{+-} multiplicities in $\pi^- + p \to$, 25:14719
CHEN, T. C., Method of extending Blankenbecler--Sugar--Logunov--Tavkhelidze approximation to Bethe--Salpeter equation, 25:14786
CHENG, Chi-kang, Thermal, radiation, and mechanical analysis of cylindrical oxide fuel elements of fast reactor in unsteady state, 25:15371
CHENG, K. L., Precipitation of tellurium with Bismuthiol II, 25:12943
CHEON, Il-T., Scattering of hadrons on ^{6}Li, 25:15183
CHERDANTSEV, P. A., One-nucleon states and energy surfaces of ^{238}U in fission process, 25:15053
CHERENKOV, P. A., Angular dependences of many-charge particles produced by 660-MeV protons on ^{27}Al nuclei, 25:14945
CHERNYKH, A. V., Dielectric permeability tensor of smoothly inhomogeneous electron plasma, 25:14291
CHESHIRE, David Lynn, Pion capture on ^{12}C, 25:14897
CHESHKOV, A. A., Analytic properties of inelastic hadronic form factors and breaking of CP invariance in electromagnetic interactions, 25:14765
CHESTER, C. V., Civil defense implications of a pressurized water reactor in a thermonuclear target area, 25:13184
CHESTER, R. O., Civil defense implications of a pressurized water reactor in a thermonuclear target area, 25:13184
CHEUNG, M. K., Specificity of uv mutagenesis in E. coli, 25:13406
CHEW, Geoffrey F., Partial bootstrap of schizophrenic Pomeranchon, 25:14824
CHEYLAN, J., Measurement of local enthalpy in an HF plasma, 25:14263
CHIBISOV, G. V., Galactic parameters as a consequence of cosmological turbulence, 25:13932
CHILDRESS, C. E., Fabrication procedures and acceptance data for ASTM A-533 welds and a 10-in. thick ASTM A-543 plate of the Heavy Section Steel Technology Program, Documentary Report 3, 25:13638 (ORNL-4313-3)
CHIN, Chao-wen, Low-mass white dwarfs and cooling sequences in Hyades cluster, 25:13799
CHIN, Y. C., Polarization measurements of solar Type-III radio bursts at 25.3 MHz, 25:13859 (AD-711398)
  Theory of polarization transfer in inhomogeneous magnetized plasmas, 25:14286 (N-70-40979)
CHIOCCHIO, O., Measurement of fast reactor type neutron spectra, 25:13226
CHIRKIN, Yu. M., Search for new type of radioactivity in aluminum and tungsten targets irradiated by 70-GeV protons, 25:14541 (JINR-P1-5399)
CHIU, H. Y., Theory of radiation mechanisms of pulsars. I, 25:13842
CHKAREULI, Dzh. L., Transversality of vector and axial-vector meson fields and chiral symmetries, 25:14804
CHODOS, Alan Avrum, Infinite-component local field theory with a rising mass spectrum, 25:14799
CHOJNACKI, S., Cerium-135m and /sup 137m/Nd: isomeric states in N = 77 isotones, 25:15042
CHONE, B., Iridium-192 contact irradiation with clinical sequelae (radiation accident), 25:13466
CHONG, Taisu, Vibronic transitions in radicals in irradiated naphthalene single crystals, 25:13047
CHORNIK, Boris, Nuclear relaxation in nickel alloys, 25:15463 (UCRL-20376)
CHOURAQUI, G., Spins of levels of ^{34}Cl, 25:14942
CHOVNICK, Arthur, Gene conversion in higher organisms: half-tetrad analysis of recombination within the rosy cistron of Drosophila melanogaster, 25:13426
CHOW, W. S., Specific heat of superconducting transition metals containing nonmagnetic impurities at low temperatures, 25:14179
CHRIEN, R. E., High-energy γ-rays following neutron capture in ^{239}Pu and ^{235}U, 25:15078
  Reports to AEC Nuclear Cross Sections Advisory Committee meeting at Argonne National Lab., Chicago, Ill., 5/70, 25:14982 (NCSAC-31)
CHRISTENSEN, R. N., Prog. rpt. on radiation-induced nucleation of bubbles in superheated water, 12/70, 25:13152 (SU-326-P-13-5)

CHRISTENSON, C. W., Production of Candida utilis with 93 at. percent ^{13}C acetic acid as the sole carbon source, 25:13331 (LA-4551)
CHRISTENSON, John Martin, Hybrid computer investigation of spatial effects in prompt critical reactor excursions, 25:15408
CHRISTIE, W. H., Analytical mass spectrometry at Oak Ridge National Laboratory, 25:13319 (ORNL-4643)
CHU, C. K., Particle-in-cell method for model kinetic equations, 25:15431 (CU-3954-3)
CHU, Y. Y., Study of several neutron-deficient hafnium nuclides, 25:15025
CHUBB, W., Mechanisms of swelling and gas release in uranium dioxide, 25:13785
CHUGUNOV, V. V., Attenuation of beta-particle fluxes in absorbers when measuring activities with 2π-geometry, 25:14403
CHUNG, Kuk Pyo, Nonlinear functional analysis and numerical computations of the strong-interaction S-matrix; applications to pion-pion dispersion relations, 25:14699
CHUVILO, I. V., Effective mass spectra of the $\gamma\gamma$, $\pi^0\gamma$, $\pi^0\gamma\gamma$, $\pi^0\pi^0$, π^0eta^0, $\pi^0\pi^0\gamma$, $\pi^0\pi^0\pi^0$ systems in mass value region M (γ.......γ) less than or equal to 1.3 GeV, 25:14560 (JINR-E1-5349)
CIERJACKS, S., New total neutron cross-section measurement of U between 0.5 to 4.35 MeV, 25:15104
CINDRO, N., Emission of alpha particles in reactions induced by medium-energy nucleons, 25:15173
CIRILLO, R., Effects of continuous exposure to radioactive phosphorus in ionic form, 25:13351
CIRKOVIC, Dimitrije, Protection by phytohemagglutinin of human blood lymphocytes irradiated in vitro, 25:13472
CIZEK, J., Stability conditions for solutions of Hartree--Fock equations for atomic and molecular systems. V, 25:14053
CLAASSEN, Hans C., Radiochemical analyses of water from selected streams, wells, springs, and precipitation collected prior to reentry drilling, Project Rulison, 25:12951 (USGS-474-83)
CLARK, Harold E., An empirical formula which predicts the critical parameters of a planar array of uranium-solution-filled cylinders, 25:13198
CLARK, Kenn E., Acceleration patterns in quasi-steady MPD arcs, 25:14281
CLARK, M. A., Observation of early-type stars from OGO-VI, 25:13813
CLARK, Robert Beck, Forward photoproduction of charged pion and N(1520), 25:14609
  V--A theory for nucleon resonances, 25:14648
CLARKSON, R. G., Reduced widths from isobaric analog resonances, 25:15201
CLAYTON, D. D., Importance of and needs for neutron nuclear data in astrophysics, 25:14876
CLAYTON, E., Multilevel formalism for neutron elastic scattering cross sections, 25:15161
CLIFFORD, Peter, Increase in antibody titer against the EBV-associated membrane antigen complex in Burkitt's lymphoma and nasopharyngeal carcinoma after local irradiation, 25:13391
CLIFTON, David G., Adiabatic calorimetric enthalpy measurements for α, β, and γ uranium and heats of the transformations $\alpha \to \beta$ and $\beta \to \gamma$, 25:13653 (LA-4521)
CLINE, J. E., Gamma rays emitted by the fissionable nuclides and associated isotopes, 25:14981 (IN-1448)
COATES, M. S., Neutron detector with a flat energy response for use in time-of-flight experiments, 25:13215
COBB, J. K., Magnetization and susceptibility measurements of polycrystalline niobium, 25:14195
COCHO, G., Relativistic harmonic oscillators and the structure of baryons, 25:14711
COFFEY, D. L., Comparison of NbTi and Nb_3Sn material tests, 25:14219
COGGIN, J. H., Radiation-enhanced oncogenesis by SV40, 25:13553
COGHEN, T., Pion production mechanism in high multiplicity π^+p interactions at 8 GeV/c, 25:14558 (INP-708)
COHEN, J. J., Plowshare: new challenge for health physicist, 25:13429
COHEN-TANNOUDJI, G., Dual, crossing-symmetric amplitude with Mandelstam analyticity, 25:14821
COHN, A., Effect of radiation escape on atomic state densities and electron distribution function, 25:14316
COLAIACE, Joyce D., Radiation dose fractionation, mitotic index, and multiple fixation studies on chromosome aberrations in Vicia faba, 25:13413
COLANGELO, S., Measurements of radioactivity in the sewage in Milan, 25:13454
COLES, R. E., Reactions (n,n'γ) in ^{51}V and ^{89}Y, 25:14919 (AWRE-O-78/70)
COLLINS, P. A., Toward inclusion of spin in generalized Veneziano model for $K^-p \to \pi^-\pi^+\Lambda$, 25:14716
COLLOP, D. J., Dual multi-Veneziano spinning particle amplitudes, 25:14586
COLTON, Eugene, Evidence for a narrow N*(1470), 25:14552
COLVIN, D. W., Number of neutrons per fission, anti ν, from thermal to 15 MeV, 25:15119
COLVIN, R. S., Galactic hydrogen absorption at 21 cm wavelength in direction of Virgo A, 25:13831 (AD-711300)
COMELLA, J. M., Pulsar NP 0532: disappearance of precursor pulse at 606 MHz, 25:13848
COMFORT, J. R., Properties of ^{55}Mn, ^{54}Mn, and ^{57}Fe in the unified rotational model, 25:14973
CONDE, H., Value anti ν of ^{235}U and ^{239}Pu in fast-reactor spectrum, 25:15113
CONLON, T. W., States of prolate and oblate deformation and for shape isomerism in ^{127}Cs, 25:15061
CONNOLLY, T. J., Prog. rpt. on radiation-induced nucleation of bubbles in superheated water, 12/70, 25:13152 (SU-326-P-13-5)
CONTOGOURIS, A. P., Frame dependence of vector dominance in Veneziano model and new test of rho universality, 25:14710
CONWAY, A. P., Progress on Polly at Glasgow, 25:13255 (CERN-70-21(Vol.1), pp 357-70)
CONWAY, John A., Cratering in Greenland icecap snow, 25:13133 (AD-711861)
COOK, V., Measurement of the Σ^+ magnetic moment, 25:14513
COOKE, W. T., Calcium-47 studies in adult coeliac disease and other gastrointestinal conditions with particular reference to osteomalacia, 25:13359
COOLEY, C. R., Survey of alpha waste generation and disposal as solids in the U. S. nuclear fuel industry, 25:13188 (BNWL-B-34)
COOPER, A. S., Instabilities of high-temperature superconductors, 25:14174
COOPER, Barbara, Demonstration of a circulating factor regulating blood platelet production using ^{35}S-sulfate in rats and mice, 25:13355
COOPER, George W., Demonstration of a circulating factor regulating blood platelet production using ^{35}S-sulfate in rats and mice, 25:13355
COOPER, J. A., Laboratory and environmental mineral analysis using a ^{252}Cf neutron source, 25:12962
COOPER, J. H., Weapons Effects Display System (WEDS MOD II): maintenance manual. I, 25:13322 (UCRL-50892(Vol.4)(Pt.1))
COPPOLA, M., Neutron elastic scattering from carbon in the energy region of 0.50 to 2.00 MeV, 25:14911
  Plutonium-239 angular distributions in energy range 0.2 to 5.5 MeV, 25:15134
CORBETT, B. L., Prog. rpt. on High Flux Isotope Reactor, 7--9/70, 25:15392 (ORNL-TM-3286)
CORBIN, J. A., Effects of structure of peptide stationary phases on gas-chromatographic separations of amino-acid enantiomers, 25:15424 (COO-1222-42)
CORDERO, P., Algebraic solution of a short-range potential problem, 25:14491
CORENZWIT, E., Instabilities of high-temperature superconductors, 25:14174
CORIOU, Henri, Selective growth of pits on a stainless steel in a chlorinated oxidizing medium, 25:13637
CORKE, Henry Edwin, Superfluid critical velocities in wide channels, 25:14146
CORLEO, G., Separation of nuclear-reaction mechanisms, 25:15151
CORNWALL, John M., Scaling, fixed poles, and electroproduction sum rules, 25:14614
CORNWELL, J. F., Spinor space and mass formula for hadrons, 25:14751
CORRIGAN, Dennis, Scaling, fixed poles, and electroproduction sum rules, 25:14614
CORTELLESSA, G. C., Measurements of radioactivity in the sewage in Milan, 25:13454
CORWIN, Stephen H., Experiences with ^{32}P in advanced carcinoma of the prostate, 25:13591
COSTA, Laurent, Measurement of the neutron albedo of ordinary concrete, 25:14394 (CEA-N-1382)
COSTELLO, D. G., Calculations of cross-sections for the radiative capture of fast neutrons, 25:15122
  Measurements of cross-sections for radiative capture of 1-keV to 1-MeV neutrons by Mo, Rh, Gd, Ta, W, Re, Au, and ^{238}U, 25:15121
COTTIER, H., Specificity of tritiated thymidine as a precursor of DNA under conditions of prolonged administration, 25:13358
COTTON, K. C., Radioactive tracers test nuclear steam turbines easier, better, 25:13148
COUDEVILLE, A., Neutron yield of a focus discharge in various experiments, 25:14355
COUGHLIN, Robert W., Enhancing the permeation characteristics of polyethylene by membrane irradiation in the fully swollen state, 25:13041
COUSSOT, G., Positron annihilation in a zirconium single crystal, 25:14441
COVELLO, A., Vibrations in even Hg isotopes, 25:15033
COVELLO-MORO, Renata, Reorientation measurements in ^{116}Sn and ^{124}Sn, 25:15041
COWAN, C. L., Implications of nuclear data uncertainties to reactor design, 25:15345
COWAN, G. A., Neutron-induced ^{235}U fission at individual resonances. III, 25:14999
COX, Donald Martin, Production of metastable 2s atoms by electron impact upon deuterium, 25:14045
CRAIG, C. D., Quantization of Lagrangians for charges in external field, 25:14776
CRAIG, G. B., Etching dislocations in zirconium, 25:13714
CRAMER, J. D., Exact calculation of the penetrability through two-peaked fission barriers, 25:15004
CRAWFORD, David L., Gum nebula: fossil Stroemgren sphere of the Vela X supernova, 25:13851
CRAWFORD, Frank S. Jr., Test of $\Delta S = \Delta Q$ rule in leptonic

decays of neutral K mesons, 25:14533
CREMMER, E., Duality and Adler condition, 25:14668
CRESTI, M., Annihilation anti pn $\to \pi^+\pi^-\pi^-$ between 1.0 and 1.6 GeV/c, 25:14548
CREUTZ, Michael John, Inelastic electron scattering and multi-Regge model and hadronic states of even charge conjugation from electron--positron annihilation, 25:14621
CROCKER, V. S., Nuclear cross section requirements for fusion reactors, 25:14357
CRONE, M., Radiation stimulated incorporation of ^{3}H-thymidine into diplotene oocytes of guinea-pig, 25:13367
CRONKITE, E. P., Specificity of tritiated thymidine as a precursor of DNA under conditions of prolonged administration, 25:13358
CROOM, D. L., 71-GHz solar radio bursts July 1967 to Dec. 1969, 25:13890
  Solar microwave bursts as indicators of the intensity of solar proton emissions, 25:13867
CROSBIE, K. L., Prog. rpt. on fast reactor spectrum measurements, 10/70, 25:15388 (GULF-RT-10421)
CROSSLAND, R. K., Sulfonate leaving groups, structure and reactivity: 2,2,2-trifluoroethanesulfonate, 25:15421 (COO-1008-14)
CROWE, Kenneth M., Slow muon depolarization in a single crystal of gypsum, 25:13989
CSIKOR, F., Veneziano model for the off-mass-shell $A_1\pi \to \pi\pi$ process, 25:14698
CULBERT, Harvey V., Properties of lead--indium alloys. II. Specific heat, 25:14180
CULHANE, J. L., Cooling of flare-produced plasmas in the solar corona, 25:13889
CULLEN, G. W., Compounds and alloys for superconducting applications, 25:14203
CUMMINGS, F. W., Beyond Hartree-liquid model of superfluid bosons, 25:14142
CUNDY, D. C., Scanning and measuring of heavy liquid film on-line, 25:13271 (CERN-70-21(Vol.2), pp 651-64)
CUPINI, E., Influence of uncertainties of sigma$_{28}$/sup f/ in Monte-Carlo calculations of small critical assemblies, 25:15398
CUPP, J. D., High-frequency limit of the Josephson effect, 25:14200
CURRIE, J., Princeton automatic track reader, 25:13250 (CERN-70-21(Vol.1), pp 273-83)
CURTIS, O. L. Jr., Dopants for radiation-resistant silicon, 25:14412 (N-70-39456)
CUYPERS, M., Tritiated titanium targets producing 14-MeV neutrons. II, 25:14840 (EUR-4286(Pt.2))
CZAPSKI, G., Contribution of H atoms to G/sub H2/ in the radiation chemistry of aqueous solutions, 25:13044
CZEMBIREK, H., Preparation of ^{85}Sr and /sup 87m/Sr for bone scintigraphy, 25:13061
CZERNIEWSKI, Michal, Temperature measurements of cladding of WWR-SM type fuel elements in EWA-10 reactor core, 25:15395
CZUBEK, Jan Andrzej, Investigation of the scattered gamma spectra in nuclear geophysics applications, 25:13113
CZYZEWSKI, O., Pion production mechanism in high multiplicity π^+p interactions at 8 GeV/c, 25:14558 (INP-708)

D

DABROWSKI, J., Binding energy of a Λ particle in nuclear matter with noncentral ΛN forces, 25:14745
DABROWSKI, L., Evaluation of Moessbauer spectra for ^{57}Fe, 25:14485
DACHS, J., Photometry of bright stars in Small Magellanic Cloud, 25:13921
DA COSTA, N. L., Decay of ^{231}Pa, 25:14998
D'ADDA, A., Symmetries of the dual-resonance amplitudes, 25:14822
DAEHNICK, W. W., Spectroscopic study of ^{105}Rh by direct (^{3}He,d) and (p,α) reactions, 25:15022
DAENNER, Wolfgang, Determination of ceramic fuel thermal conductivity and gap conductance by the balanced oscillator method, 25:15411
DAGAN, S., γn partial cross sections up to 12 GeV, 25:14519
DAHMEN, H. D., Local approximation to field and current commutators, 25:14673
DALLIMORE, P. J., Low-lying levels and decay structure in ^{62}Cu, 25:14940
DALY, P. J., Decay of ^{210}Po, 25:14996
  Level structure of ^{181}W from the decay of ^{181}Re, 25:15058
DAMERI, M., HDP--IBM 360/44 system at CNAF for bubble chamber data analysis. I, 25:13267 (CERN-70-21(Vol.2), pp 607-15)
DAMS, R., Applied γ ray spectrometry, 25:13231
DANBY, Gordon T., Lift/drag ratios for magnetic suspensions, 25:15419 (BNL-15420)
DANIEL, H., Pion finite size and mesic atoms, 25:13994
DANKO, M. I., Effect of optical quantum generator radiation on electrical parameters of fresh tissue, 25:13565
DANON, J., Mechanism of formation of anomalous charge states of iron after ^{57}Co electron capture in Co complexes, 25:13075
DARBY, I. A., Phase equilibria in the high magnesia corner of the system MgO--ThO$_2$--B$_2$O$_3$ at 1200°C, 25:13770
DARCEY, W., Level structures of ^{85} ^{87}Sr from (d,p) reactions, 25:14955
DARROUZET, M., Integral measurements of α for ^{239}Pu and ^{235}U, 25:15348
DAS, B. K., Phase transformations in near equiatomic Ta--Ru alloys, 25:13708
DAS, K. C., Contributions of conduction electrons to electric field and nuclear quadrupole interaction in rare earth metals, 25:14451
DAS, T. K., Phenomenological analysis of quasirotational spectra, 25:15153
DA SILVEIRA, Adel, Sum rules for K/sub L/--K/sub S/ decay, 25:14644
DA SILVEIRA, E. F., Decay of ^{231}Pa, 25:14998
DATTA, B., Greater vulnerability of the infecting viral strand of replicative-form deoxyribonucleic acid of bacteriophage phiX174, 25:13382
DAUER, Maxwell, Natural environmental radioactivity in south Florida sands and soils, February--June 1968, 25:13107
DAUVERGNE, J. P., Measurement of local enthalpy in an HF plasma, 25:14263
DAVENPORT, C. M., Remote data station interface to the production control computer, 25:15469 (Y-1748)
DAVEY, W. G., Status of important heavy-element nuclear data above the resonance region, 25:15112
DAVID, D. J., Correlated pseudo-potential approach for molecules, 25:14055
DAVID, F., Polarographic studies of lanthanides and cis- and transuranium elements, 25:13020
DAVID, G., Study of graphite oxidation by low energy electron diffraction, 25:13735
DAVIDOVIC, D. M., Influence of short-range atomic forces on molecular term splitting in (A,A) system, 25:14018
DAVIDSON, W. F., Low-lying levels and decay structure in ^{62}Cu, 25:14940
DAVIES, D. J. M., Performance of Sweepnik I, 25:13252 (CERN-70-21(Vol.1), pp 293-308)
  Sweepnik II, an improved track measuring machine, 25:13251 (CERN-70-21(Vol.1), pp 285-92)
DAVIES, H., Data handling system for the Omega and the SFM projects, 25:14839 (CERN-70-21(Vol.2), pp 561-80)
DAVIES, R. D., Observations of radio recombination lines with Δn = 1 to 5, 25:13840
DAVIES, W. G., Level structures of ^{85} ^{87}Sr from (d,p) reactions, 25:14955
DAVIS, K. G., Stability of planar solid/liquid interface for alloys of In in Sn, 25:13646
DAVIS, Stanley N., Transport of water away from a buried heat source with special reference to hydrologic phenomena observed at Aardvark nuclear detonation, 25:13111
DAVIS, Steven K., Shock tube experiments on the pyrolysi of deuterium-substituted ethylenes, 25:12993
DAVIS, T. Neil, Small-scale auroral arc distortions, 25:14119
DAVIS, W. Jr., The feasibility of incorporating radioactive wastes in asphalt or polyethylene, 25:13197
DAWSON, John M., Numerical model for toroidal plasma containment with flow, 25:14236
DEACON, David, Grabheads for reactors, 25:15414
DEAN, John A., Mass spectrometric investigation of surface ionization. VI. Desorption of Th$^+$, Np$^+$, and Pu$^+$ from W surfaces, 25:13686
DEAN, John Raymond, Improvements to control systems, 25:15413
  Mechanisms for control rods of reactors, 25:15416
DE BEER, A., Analysis of $2^- \to 2^+$ positon transitions in ^{84}Rb and ^{74}As, 25:14972
DE BOER, R. J., HPD--CDC 3200 system at Amsterdam, 25:13275 (CERN-70-21(Vol.2), pp 709-20)
DEBRIL, G., Measurement and analysis of ^{235}U and ^{241}Pu fission cross-sections, 25:15086
DE COSTER, M., Implications of fundamental integral measurements on high-energy nuclear data for reactor physics, 25:15349
DEDO, A., Etching dislocations in zirconium, 25:13714
DEERING, R. A., Gamma-ray-induced spore germination of Dictyostelium discoideum, 25:13605
DEFOUW, Richard John, Thermal instability and the convective stability of stellar chromospheres, 25:13822
DEGASPERIS, A., Bohr quantization of relativistic bound states of two point particles, 25:14588
DEHOFF, R. T., Quantitative determination of the structure: property relationships in nuclear fuel element materials. Quarterly progress report, September 15--December 15, 1970, 25:13766 (SRO-552-6)
DEIS, D. W., Alternating-current loss measurements in thin-film type II superconductors, 25:14189
DE JONGHE, Lutgard C., Defects and phase transformations in cobalt ferrites, 25:13783 (UCRL-20369)
DEKANENKO, V. M., Nature of solid solutions in the niobium--oxygen system, 25:14457
DELACHOUX, Jean-Claude, Amplitude discriminator on a large dynamic scale with precise time definition, 25:13320 (RI-70/13)
DE LA VAISSIERE, Ch., Use of a simple geometry program for filtering HPD data, 25:13273 (CERN-70-21(Vol.2), pp 679-85)

DELAVIGNETTE, P., Unusual dissociation of dislocations in Ni_3Ta, 25:13699
DELFIORE, G., Tritiated titanium targets producing 14-MeV neutrons. II, 25:14840 (EUR-4286(Pt.2))
DELHAYE, J., Some comments on the production and measurement of spheres of polystyrene latex, 25:13144
DELPECH, Andre, Continuous U precipitation process, 25:13012
DELVIGNETTE, P., Regular network of anti-phase boundaries in the x-phase of the system Fe--Cr--Mo--Ti, 25:13711
DEMARQUE, Pierre, Simultaneous determination of He and metal abundances in old open clusters, 25:13798
DE MATTEIS, A., Influence of uncertainties of sigma$_{28}$/sup f/ in Monte-Carlo calculations of small critical assemblies, 25:15398
DEMIRKHANOV, R. A., Resonance phenomena in an alkali plasma located in a variable electric field, 25:14368
DE MOTTONI, P., Wightman functions in a model with mass renormalization, 25:14794
DEM'YANOV, A. V., Identification and study of radioactive properties of Bi isotopes using electromagnetic mass-separator on heavy ion beam, 25:15023
  Search for new type of radioactivity in aluminum and tungsten targets irradiated by 70-GeV protons, 25:14541 (JINR-P1-5399)
DENNIS, Wiley Sam, Optical and infrared emission spectra of electron-bombarded liquid helium, 25:13973
DEO, M. G., Interaction of x-radiation and malnutrition. A study of kinetics of cellular proliferation in the jejunum of protein-deficient rats, 25:13562
DEORANI, S. C., Volume viscosity and structure of D_2O using ultrasonics, 25:12990
DE PINHO, A. G., Decay of ^{231}Pa, 25:14998
DE RAFAEL, E., Photon--photon scattering contribution to the decay rate of orthopositronium, 25:13992
  Sixth-order radiative corrections to a/sub μ/--a/sub e/, 25:14620
DER MATEOSIAN, E., Energy dependence of auto-ionization in beta decay, 25:13982
DERNIER, P. D., X-ray diffraction studies of the metal insulator transitions in Ti_4O_7, V_4O_7, and VO_2, 25:14442
DERRIEN, H., Determination of spin of slow-neutron induced resonances in ^{239}Pu, 25:15088
  High-resolution measurement and analysis of ^{239}Pu fission cross-section, 25:15089
  Multilevel analysis of the ^{233}U and ^{235}U capture and fission cross-sections, 25:15130
  Total and fission cross-sections of ^{239}Pu from 5.7 to 160 eV, 25:15087
DERUYTTER, A. J., Cross-sections and techniques for high-precision neutron nuclear data measurements, 25:14877
  Precise 2200 m/s fission cross-sections of ^{239}Pu and ^{235}U, 25:15067
DE SANCTIS, Carlo, Xerodermal idiocy, 25:15443 (ORNL-tr-2426)
DE SAUSSURE, G., Multilevel analysis of the ^{233}U and ^{235}U capture and fission cross-sections, 25:15130
DESCHAMPS, N. H., Development of SIREN capsule, Phase I, 25:13170 (SNC-2708-1)
DESCHAMPS, P., Experimental observation of drift instabilities in a collisionless plasma, 25:14345
DE SCHEEMAECKER, Jacques, LGR/B program: for updating the ANISN library tapes with plotting of cross section curves, 25:14986 (ORNL-tr-2408)
DE SOUZA, C. M., Effects of reductone on irradiated E. coli, 25:13610
DESTRIAU, Michel, Changes in the surface of uranium and its hydrides during successive hydrogenations and dehydrogenations at various temperatures, 25:13635
DETAR, Carleton E., Momentum spectrum of hadronic secondaries in the multiperipheral model, 25:14659
DEUTSCHER, R. L., Eight-coordinate complexes of niobium, tantalum, and uranium tetrahalides, 25:12979
DEVILLERS, Christian, ANISN system. Description and use of discrete ordinate program ANISN and of auxiliary programs, 25:14863 (CEA-N-1358)
DE VILLIERS, J. A. M., Inelastic scattering of fast neutrons from ^{238}U, 25:15110
DEVLIN, T. J., Proton--proton differential cross sections from 600 to 1800 MeV/c, 25:14543
DE YOUNG, D. S., Diffusion of energetic particles from radio galaxies, 25:13922
DHAWAN, M. M., Emission of ^{8}Li fragments from K-interactions, 25:14978
DICKENS, Elmer Douglas Jr., Algebraic models in particle physics, 25:14772
DICKSON, J. I., Etching dislocations in zirconium, 25:13714
DICUS, Duane A., Ward identities for eta decay in perturbation theory, 25:14611
DIERCKX, R., Measurement of fast reactor type neutron spectra, 25:13226
DIETRICH, Carl P., Production of heparin related mucopolysaccharides by mammalian cells in culture, 25:13357
DI GREGORIO, I., Action of ionizing radiations on CNS, 25:13561
DIKHTER, I. Ya., Specific heat and the heat of fusion of W at high temperatures, 25:13664
DILLARD, Bobby L., Priority system for the inspection of x-ray facilities, 25:13459
DILLET, A., Ariane II: automatic device for the analysis of spark chamber photographs, 25:13285 (CERN-70-21(Vol.2), pp 859-78)
DILLINGER, P., Radio-release determination of pH using radioactive kryptonate, 25:12955
DIMENT, K. M., Ratio of the ^{6}Li(n,α) and ^{10}B(n,α) cross-sections from 10 eV to 80 keV, 25:14910
  Total cross-section of carbon from 70 eV to 1.5 MeV, 25:14912
DINARDO, A. J., Superconducting microstrip high-Q microwave resonators, 25:14230
DITTMER, D. L., Spectroscopic study of ^{108}Rh by direct (^{3}He,d) and (p,α) reactions, 25:15022
DITTRICH, J., Full experiment in weak semileptonic hyperon decays, 25:14651
DIVGI, Dattaprasad Ramdas, Study of negative-parity baryon resonances using symmetric quark model and local tensor fields and generators of Lorentz group, 25:14718
DIXIT, M., Cross sections for p + p → d + rho$^+$ from 4.0 to 12.3 GeV/c and a search for the delta$^+$, 25:14542
DIXON, Gregg Woodford, Measurement of thermal-neutron spectra in heterogeneous lattices by foil activation, 25:15409
DJORDJEVIC, B., Temperature dependence of thymidine uptake and stability of thymidine incorporated during unscheduled DNA synthesis in irradiated and unirradiated HeLa cells, 25:13554
DMITREVSKII, L. L., Isotope exchange reactions in different BF_3-complex systems, 25:12992
DOBROTT, D., Magnetic and drift surfaces using a new stellarator expansion, 25:14234
DOBROZEMSKY, R., Determination of the distribution of fission products in fuel particle coatings by the sputtering technique, 25:13758
DOBRZYNSKI, L., Calibration, precision, and filtering questions for the CERN Spiral Reader, 25:13235 (CERN-70-21(Vol.1), pp 5-18)
DOCKTER, Juergen, Effects of an extract of calves-blood on radioinduced mucosa lesions in the area of larynx and pharynx, 25:13475
DODD, P., Adam+Eva, scanning and measuring machine for film from the large bubble chambers, 25:13270 (CERN-70-21(Vol.2), pp 633-49)
DOHERTY, James Edward, Acoustic and magnetic measurements of titanium and zirconium alloys, 25:14465
DOI, Toshio, Applied magnetic field vs critical current density characteristics of superconducting Nb--60 Ti--5 Zr alloy sheets, 25:14209
  Effects of V, Mo, or Ta additions on superconducting properties of Nb--40 Zr--10 Ti alloy, 25:14208
DOKE, N., Effects of tobacco mosaic virus infection on photosynthetic CO_2 fixation and $^{14}CO_2$ incorporation into protein in tobacco leaves, 25:13360
DOLGOV-SAVELEV, G. G., Electron-excitation cross sections for x-ray series of Cl, Ar, and Xe, 25:14008
DOMBEY, N., Low energy theorems and high energy photoproduction, 25:14622
DOMBROSKI, Daniel L., Scintiscanning in the diagnosis of rupture of the spleen, 25:13511
DOMOGATSKII, G. V., Hot-universe model and the Dirac monopole, 25:13953
  Observing neutrinos from collapsing stars and neutrino oscillations, 25:13830
DONAT, Klaus, Neutron streaming through two-legged concrete ducts with baffles, 25:14391 (AD-710963)
DONDI, P. H., Chiral symmetry breaking and nonlinear realizations, 25:14763
DONNELLY, Russell J., Motion of ions at finite velocities in helium II, 25:14144
DONNER, E. D., Optical properties and electron characteristics of niobium--tin alloys, 25:14149
DONOVAN, B. V., Decay processes in a high density argon afterglow, 25:14257
DORE, Earl K., Interval brain scanning with sodium pertechnetate /sup 99m/Tc for tumor detectability, 25:13505
DORMAN, I. V., Reaction of cosmic rays on the solar wind, 25:14076
DORMAN, L. I., Cosmic-ray anisotropy in the periods following proton outbursts, 25:14075
  Cosmic-ray meteorological effects, 25:14066
  Cosmic-ray variations, 25:14069
  Forbush decreases: theory and experiment, 25:14073
  Production of electrons in lower ionosphere by solar cosmic rays, 25:14124
  Reaction of cosmic rays on the solar wind, 25:14076
DORN, Gordon L., Genetic and morphological properties of undifferentiated and invasive variants of Aspergillus nidulans, 25:13423
DOROFEEV, V. M., Influence of exogenic serotonin on the aggregation of blood platelets and some blood coagulation indices in experimental acute radiation sickness, 25:13549
DOUGLASS, D. H., New class of gravitational wave detectors, 25:14547
DOWNS, G. L., Solubility of tritium in annealed and cold-worked copper, 25:13654 (MLM-1734)
DOWNS, W. E., How neutrons take on process control, 25:13177
DRAKE, J. L., Far-field characteristics of ground shock induced by explosions, 25:13129 (AD-713521)

DRASKOVIC, R., Possibilities of the application of activation analysis in medicine, 25:12964

DREISS, Gerard J., Ground state correlations as variational parameters in the nuclear many-body problem, 25:15147 (NYO-2171-333)

DREIZLER, R. M., Ground state correlations as variational parameters in the nuclear many-body problem, 25:15147 (NYO-2171-333)

Phenomenological analysis of quasirotational spectra, 25:15153

DRIEU, F., Removable head for pneumatic device, 25:13203

DRIGO, L., Target spin dependence of the optical potential, 25:15152

DRITSA, S., High-energy γ-rays following neutron capture in ^{239}Pu and ^{235}U, 25:15078

DROGOVOZ, S. M., Influence of total x-ray irradiation on synthesis of bile acids in albino female rats (chromatographic investigation), 25:13370

DRONOV, A. P., Electron excitation of transitions between excited states in Ba$^+$ and Sr$^+$ ions, 25:14000

DROSTE, Ch., Cerium-135m and /sup 137m/Nd: isomeric states in N = 77 isotones, 25:15042

DROZHENNIKOV, V. A., Comparative study of DNAse activity under treatment of cells E. coli K12 (lambda) with various inducing agents, 25:13371

DRUIN, V. A., Effect of α-radioactive background at investigation of the α decay of the 104 element, 25:15017

Radioactive properties of isotopes of the 103 element, 25:15052

DRUMINSKI, M., B--C system in the kinetic formation region, 25:13767

DRUZHININ, V. P., Emissivity of W, Mo, and Re single crystals, 25:13666

DRUZHININA, I. P., Thermocouple for accurate high-temperature measurements in a vacuum and in the presence of reactor radiation, 25:13326

DRYANCVSKA, O. A., Influence of temperature after irradiation of pollen from Nicotiana tabacum on formation of seeds and plants, 25:13601

DUBININ, G. N., Molybdenum treatment for increasing stability of steel No. Kh18N9T in liquid Li, 25:13634

DUBINSKII, V. E., Angular distribution of sputtered material in ion bombardment, 25:13966

DUBROVINA, S. M., Fission of ^{232}U by neutrons with energy from 0.1 up to 1.5 MeV, 25:15019

DUFFY, M. T., Vapor deposition and characterization of metal oxide thin films for electronic applications, 25:13748

DUFLO-PLISSONNIER, M., Kinetic study of oxidation of trivalent U sulfuric acid solutions, 25:12977

DUKE, C. L., Electron-capture beta decay, 25:14993

DULK, G. A., Galactic center region observed at 80 MHz, 25:13914

DUM, Christian T., Nonlinear beam--plasma interactions and stochastic acceleration, 25:14296

DUMBRAIS, O. V., Elastic NN and Nd scattering, 25:14730 (JINR-P2-5444)

Model-independent determination of the real parts of the independent of spin pp-forward scattering amplitudes, 25:14731 (JINR-P2-5448)

DUMONT, S., Influence of the line absorption on polarization of the continuum spectrum, 25:13898

DUNFORD, C. L., Application of interactive computer graphics to nuclear data evaluation problems, 25:14879

DUNN, W. L., Minimizing errors in gamma-ray backscatter density gages: existing gages and new design concepts, 25:13316

DURAND, J., Polarization and spin-correlation parameters in proton-^{3}He elastic scattering at 19.4 MeV, 25:14888

DURAND III, Loyal, Backward πN scattering, 25:14707

DURHAM, R. W., Measurements of alpha and of fission cross-section ratios for ^{233}U, ^{235}U, and ^{239}Pu at thermal energies, 25:15070

DUTHLER, Carl James, Dependence of He II film transfer rate on pressure head, film height, and substrate, 25:14128 (COO-1574-17)

DUTTA, Chizuko Matsubara, Many-body theory for properties of interacting atoms, 25:14046

DWORSCHAK, Heinz, Radiolytic degradation of toluene--nitric acid system, 25:13093

DYACHENKO, A. H., Investigation of spleen and liver polysomes of non-immunized and immunized rats with acute radiation damage, 25:13376

DYACHENKO, P. P., Analysis of neutron energy dependence of anti ν, on basis of energy balance in nuclear fission, 25:15117

DYAKINA, V. P., Scattering of conductivity electrons by spin waves in terbium and dysprosium single crystals, 25:14448

DYKHNC, N. M., Mass-spectrometric method for determining microimpurities in inert gases, 25:12941

DZHAVRSHYAN, Dzh. M., Optical properties of leaves of plants obtained from irradiated seeds, 25:13600

DZIERBA, A. R., Double-Regge analysis of single-pion production in π^-p interactions at 8 GeV/c, 25:14713

DZYUBENKO, I. I., Cesium-137 from global fallout in foodstuffs and human organism, 25:13340 (NP-18382)

E

EACHUS, R. S., Unstable intermediates. LXXX, 25:13028

EASEY, J. F., Protactinium(V) fluorides, 25:12978

EASTON, D. S., Eutectoid region of the Zr--Ga system, 25:13709

EASTWOOD, D., Adam+Eva, scanning and measuring machine for film from the large bubble chambers, 25:13270 (CERN-70-21(Vol.2), pp 633-49)

Evaluation of reverse developed film measured on HPD 2, 25:13286 (CERN-70-21(Vol.2), pp 879-905)

EBELING, W., Equation of state and ionization equilibrium hydrogen plasmas, 25:14319

Quantum statistical second virial coefficient for real gases and plasmas, 25:14322

EBERHARDT, P., Correlation between rock type and irradiation history of Apollo 11 igneous rocks, 25:13954

EBISAWA, Shigeo, Contact angles of gold and silver on a clean tungsten substrate, 25:13691

EBRAHIM, Abdul, Test of ΔS = ΔQ rule in K/sub μ3/^{0} decay, 25:14642

EBRAHIM, S., Thermal conductivity and total emittance of W from 1800 to 2800°K, 25:13663

ECHO, John B., Transfer of ^{85}Kr from air to grass, 25:13124

ECKELMAN, W., Technetium-labeled red blood cells, 25:13332

ECKELMEYER, Kenneth H., Deformation in wrought Mg--9 wt percent Y, 25:13710

EDELHEIT, Lewis Selig, Effect of point defects in copper on the anomalous transmission of x rays, 25:14427

EDWARDS, A. K., Two autodetaching states of O$^-$, 25:14009

EDWARDS, Joseph Lee, Formation and destruction of excited hydrogen atoms at high impact velocities, 25:14043

EDWARDS, M., On-line measuring system using visual displays for operator guidance, 25:13237 (CERN-70-21(Vol.1), pp 39-46)

EFIMOV, V. N., Weakly bound states of three resonantly interacting particles, 25:14591

EGANOVA, I. A., Scattering by two centers in long-wave approximation, 25:14817 (JINR-P4-5438)

EGELAND, A., Low-latitude whistlers generated by same lightning discharge, 25:14114

EGGEN, O. J., Stellar-polution samples at the galactic poles. II, 25:13935

EHLERS, David Henry, Reaction ^{9}Be(^{3}He,αα)^{4}He, 25:14903

EHLERS, Vernon J., Electron mass shift in ^{133}Cs, 25:14514

Nuclear magnetic moment, hyperfine structure, and hyperfine-structure anomaly of ^{198}Au, 25:15026

EICHMANN, E., Calibration, precision, and filtering questions for the CERN Spiral Reader, 25:13235 (CERN-70-21(Vol.1), pp 5-18)

EIMERS, Leroy Earl, Hamiltonian formalism on characteristic surfaces, 25:14773

EINHORN, Nina, Increase in antibody titer against the EBV-associated membrane antigen complex in Burkitt's lymphoma and nasopharyngeal carcinoma after local irradiation, 25:13391

EIPPER, Hermann Hans, Radiation protection against neutrons in a betatron beam, 25:13450

EISENBERG, J. M., Positive pion reactions with ^{12}C, 25:15184

EISENBERG, Y., Reactions $\gamma n \to p\pi^+\pi^-\pi^-$, $p\pi^+\pi^-\pi^-\pi^0$ and $n\pi^+\pi^+\pi^-\pi^-$ at 4.3 GeV, 25:14521

Weizmann Institute Spiral Reader system, 25:13293 (CERN-70-21(Vol.2), pp 953-62)

EISENRIEGLER, E., Temperature-dependent properties of isotopic defects in a cubic lattice, 25:14489

EITEL, W., Spin polarization and differential cross sections in inelastic electron--atom collisions, 25:14039

EKMAN, B., Roentgenologic-photometric method for bone mineral determinations, 25:13509

EKSTROM, M. P., Optimum design of two-dimensional nonrecursive digital filters, 25:15467 (UCRL-72663)

ELAIS, David, Optimization of liquid metal fast breeder reactor, 25:15378

ELLEGAARD, C., High angular momentum states in ^{156}Gd and ^{157}Gd, 25:15138

ELLINGER, F. H., Effective size of americium dissolved in lanthanum, 25:13705

ELLIS, J., Dimension of scale symmetry breaking, 25:14758

ELLIS, LeGrande C., Melatonin synthesis in rat pineal glands inhibited by x-irradiation, 25:13559

ELWYN, A. J., Short-lived fission isomers from neutron studies, 25:15031

ENCRENAZ, P. J., Attenuation of radio waves by atmosphere at frequency 1415 MHz, 25:13838

ENGELMANN, Ch., Determination of B, C, and O in Si by activation analysis, 25:12971

ENGLAND, J. B. A., Double scattering of ^{3}He particles by C and Al, 25:14894

ENGVOLD, O., Solar lithium abundance, 25:13870

ENNIS, M. E., Fission and capture cross-sections of curium, 25:15090

ENSTROM, R. E., Compounds and alloys for superconducting applications, 25:14203

EPELBOIN, I., Surface state of beryllium and faradaic yield of its anodic dissolution, 25:13704

EPSHTEIN, V. A., Investigation of a high-pressure laser spark ignited by an extraneous plasma source, 25:14331

XUM

EPSTEIN, Ervin, X-ray therapy and thyroid tumors, 25:13587
EPSTEIN, Leonard I., Value of scintiscans in the diagnosis of splenic abscess, 25:13512
EQUER, B., Use of Coccinelle to scan and measure big bubble chamber pictures, 25:13256 (CERN-70-21(Vol.1), pp 371-81)
ERBE, R., BERTA: a FORTRAN program for automatic recognition and reconstruction of bubble chamber events. I, 25:13243 (CERN-70-21(Vol.1), pp 125-39)
  BERTA: a FORTRAN program for automatic recognition and reconstruction of bubble chamber events. II, 25:13244 (CERN-70-21(Vol.1), pp 141-75)
  Heidelberg automatic event recognition, 25:13241 (CERN-70-21(Vol.1), pp 105-11)
ERIKSSON, J. R., Compound-nucleus calculations of low-energy neutron reaction cross-sections using level densities from exact counting of shell-model states, 25:15207
ERIKSSON, T., Potentiometric titration of fluoride with La and Th in unbuffered media, 25:12929
ERKELENZ, K., One-boson exchange potential and nuclear matter properties, 25:15199
ERMAN, P., Vacancy cascade spectroscopy: a convenient method of studying highly ionized atoms and molecules, 25:14038
ERMOLAEVA, N. V., Separation on phosphate cellulose of the products of degradation of deoxyribonucleoprotein formed after irradiation and enzymatic actin in vitro, 25:13363
ESCARD, J., Study of graphite oxidation by low energy electron diffraction, 25:13735
ESCHER, John S., Magnetic flux flow and fluctuation effects in thin-film superconductors, 25:14176
ESCUDIE, J. L., Inelastic scattering of polarized protons by ^{40}Ca at 24.5 MeV, 25:14923 (CEA-CONF-1656)
  Study of (p,d) reactions on ^{48}Ca and ^{48}Ti with polarized protons, 25:14922 (CEA-CONF-1655)
  Study of (p,d) reactions on ^{90}Zr and ^{92}Mo with polarized protons, 25:14980 (CEA-CONF-1654)
ESCUDIE, J-L., Measurement and microscopic calculations of the cross sections and asymmetries for the (p,p') reaction exciting the 2.31-MeV (0$^+$,T = 1) state of ^{14}N, 25:14890 (CEA-CONF-1651)
ESKOLA, K., Chemical separation of rutherfordium, 25:13088
ESKREYS, A., Pion production mechanism in high multiplicity π^+p interactions at 8 GeV/c, 25:14558 (INP-708)
ESTEVE, A., Radiative decays of mesons in a quark loop model, 25:14686
ETEMAD, M. A., Fast-neutron inelastic scattering in energy range 2 to 4.5 MeV, 25:14966
ETOURNEAU, Jean, Electronic structure of some hexaborides of the CaB$_6$ type, 25:14463
EUBANKS, Alfred Guion, Luminescence of uranium glasses, 25:13017
EVANI, Syamalarao, Mechanism of initiation in the thermal polymerization of styrene, 25:12983
EVANS, H. J., Cross sections for p + p + d + rho$^+$ from 4.0 to 12.3 GeV/c and a search for the delta$^+$, 25:14542
EVANS, J. E., Double scattering of ^{3}He particles by C and Al, 25:14894
EVANS, J. H., Quenching of vacancy defects into molybdenum, 25:13689
EVANS, R. G., Temperature dependence of thymidine uptake and stability of thymidine incorporated during unscheduled DNA synthesis in irradiated and unirradiated HeLa cells, 25:13554
EVANS, Stephen Anderson, Scattering between 2^{3}S metastable and ground-state He atoms, 25:14037
EVANS, Timothy Lloyd, Grabheads for reactors, 25:15414
EVENSON, K. M., High-frequency limit of the Josephson effect, 25:14200
EWAN, G. T., Levels in ^{177}Lu, 25:15039
EYRING, H., Solution of the time-dependent Schroedinger equation by the Laplace transform method, 25:14496

F

FABIE, Adrienne, Simplified method of obtaining information from bubble chamber photographs, 25:13233 (CEA-N-1397)
FABRE, F., UV-sensitivity of wild-type and different UVS mutants of Schizosaccharomyces pombe, 25:13606
FABRY, A., Implications of fundamental integral measurements on high-energy nuclear data for reactor physics, 25:15349
FACCHINI, U., New model for the mechanism of fission of heavy nuclei, 25:15024
FAHLAND, J., Independent yields of /sup 124g/Sb, /sup 126g/Sb, and ^{160}Tb in neutron fission of ^{235}U, 25:15038
FAINBERG, Joseph, Type-III solar radio burst storms observed at low frequencies. II, 25:13892
FAINSHTEIN, A. L., Influence of weak deformation of Cu films on channeling of protons, 25:14421
FAIRAND, Barry Philip, Fast-neutron sputtering from polycrystalline and monocrystalline gold, 25:14414
FAIZIEV, A. R., Observation of analogue states with T = 2 in the reactions ^{26}Mg(^{3}He,n)^{28}Si, ^{46}Ti(^{3}He,n)^{48}Cr, and ^{58}Ni(^{3}He,n)^{60}Zn, 25:14943
FALCON, J. P., Remote data station interface to the production control computer, 25:15469 (Y-1748)
FALK, F., Indium-111 EC decay, 25:15028
FALK, M., Infrared spectrum of HDO in water and in NaCl solution, 25:12994
FALLIEROS, S., Fine structure in highly excited analog states, 25:15145 (NYO-1082-25)
  Resonant elastic scattering of protons from analogue and compound states, 25:15146 (NYO-1082-29)
FARGES, L., Automation of a series of radioactive measurements on biological specimens, 25:13229 (CEA-CONF-1647)
FARKAS, T., Conference on corrosion, Budapest, 10/68, 25:13636
FARNSWORTH, R. K., Tritium in streams in the United States, 1961--1968, 25:13108
FARRELL, D. E., Properties of lead--indium alloys. II. Specific heat, 25:14180
FARRELL, J. A., Fission, capture, scattering, and total cross-sections of ^{239}Pu, 25:15091
FASANELLA, Edwin Lane, ESR studies of irradiated single crystals of L-tyrosine-HCl and L-phenylalanine-HCl, 25:13052
FATOME, Marc, Weight changes in spleen as a function of irradiation dose in mice, 25:13478
FAUGERAS, Pierre, Recovery of fissile materials, 25:13090
FEDUNOV, A. G., Search for new type of radioactivity in aluminum and tungsten targets irradiated by 70-GeV protons, 25:14541 (JINR-P1-5399)
FEENEY, J. A., Effect of microstructure on the strength, toughness, and stress-corrosion cracking susceptibility of a metastable beta titanium alloy (Ti--11.5Mo--6Zr--4.5Sn), 25:13672
FEESE, Klaus, Measurement of stored energy in electron-irradiated platinum below 40°K, 25:13722 (JUL-658-FN)
FEHRENTZ, D., Iridium-192 contact irradiation with clinical sequelae (radiation accident), 25:13466
FEHRENTZ, Dieter, Investigations about energy dependence of dosimeters in a 42-MeV betatron, 25:13446
FELDMAN, Frank Arthur, A new approach to partial wave amplitudes and phase shift analysis, 25:14832
FELKNER, Ira C., Isolation and characterization of thymineless mutants from ultraviolet-sensitive Bacillus subtilis strains, 25:13614
FELSTEINER, J., Decay of /sup 141m/Nd, 25:15014
FENGER, J., Chemical consequencies of the nuclear reactions in soluble Prussian Blue, 25:13068
FENYVES, E., Proton momentum spectrum in πN inelastic interactions at 17.2 GeV/c, 25:14564
FERBEL, T., Momentum-transfer dependence in reactions, 25:14575
FERGUSON, A. T. G., Short-lived fission isomers from neutron studies, 25:15031
FERGUSON, Lloyd N. Jr., Indirect exchange coupling of magnetic moments in rare-earth metals, 25:14487
FERMANDJIAN, J., Measurement and analysis of ^{235}U and ^{241}Pu fission cross-sections, 25:15086
FERNHOLZ, H.-J., Experimental animal studies concerning scintigraphic detection of acute thrombosis, 25:13518
FERRAN, P., Status of the HPD minimum guidance programs at CERN, 25:13278 (CERN-70-21(Vol.2), pp 737-52)
FERRERO, B., Effects of continuous exposure to radioactive phosphorus in ionic form, 25:13351
FERSE, Armin, Preparation of perfluorinated carboxylic acids, 25:13035
FESS, Lawrence R., Results of 33,911 x-ray protection surveys of facilities with medical or dental diagnostic x-ray equipment, fiscal years 1961--1968, 25:13464
FETISOV, N. I., Inelastic scattering of fast neutrons by Cr, Ni, Y, Zr, and W nuclei, 25:14967
FIELDS, Stanley A., Solar x-ray astronomy summary and bibliography, 25:13863 (N-70-39828)
FIGGER, H., Precision measurement of hyperfine structure of ^{175}Lu, 25:13986
FILE, J., Operation of a levitated superconducting ring in a plasma physics experimental device, 25:14356
FILIPPOV, G. F., Local self-consistent field in nuclei with a large number of nucleons, 25:15167
  Perturbation theory of variation of binding energy of ^{3}H and ^{4}He, 25:14883
FINDLAY, T., Progress on Polly at Glasgow, 25:13255 (CERN-70-21(Vol.1), pp 357-70)
FINK, M., Triple scattering for low-energy electrons, 25:14020
FINK, Manfred, Scattering amplitudes and spin polarizations of electrons scattered from H, He, C, Ne, Ar, Kr, Rb, Xe, Cs, Au, Hg, Pb, and Bi. I, 25:13995 (AD-711664)
FINK, R. W., Californium-249 decay, 25:15029
  Decay of ^{159}Dy, 25:15012
FINK, T., Lifetime and decay of 23.8 keV state of ^{119}Sn, 25:15056
FISCHEL, D., Outer layers of model moving atmospheres, 25:13792
FISCHER, E. A., Theoretical and experimental analysis of fast zero-power assemblies, 25:15396
FISCHER, G., Concerning a thought experiment violating Heisenberg's uncertainty principle, 25:14502
FISHBANE, Paul M., Multiplicity in very high-energy particle-nucleus collisions, 25:14736
FISHBURNE, E. S., Energy transfer between N$_2$ and electronically excited inert gas atoms and ions, 25:14012
FISHER, Michael E., Decay of order in isotropic systems of restricted dimensionality. II, 25:14493

Decay of order in isotropic systems of restricted dimensionality. I, 25:14492

FISHER, Raymond Kurt, Resonance cones in pattern of radio-frequency probe in a warm anisotropic plasma, 25:14259

FISZMAN, M., Radioactivity in diet in high background areas of Brazil, 25:13439

FITCH, M. J., Raman scattering in liquid lasing material containing $POCl_3$, 25:15454 (SC-RR-70-762)

FITZGERALD, C. L., The feasibility of incorporating radioactive wastes in asphalt or polyethylene, 25:13197

FIZGEER, B. M., Excitation functions for first negative system N_2^+ on excitation of N by fast electrons, 25:13998

FLENGAS, S. N., Potential chloride electrolytes for recovering the metals Ti, Zr, and Hf by fused salt electrolysis, 25:13089

FLIN, Piotr, Classification of galaxies, 25:13929

FLORES, J., Relativistic harmonic oscillators and the structure of baryons, 25:14711

FLORY, David C., The infinite momentum limit of a spinor field theory, 25:14679

FLYNN, K. F., Fission cross section of ^{227}Th, 25:15044

FOEX, Marc, Production of continuous high-power plasma flow, 25:14273

FOGEL, Ya. M., Collisions between fast protons or H atoms and O_2 molecules, 25:13999

Excitation functions for first negative system N_2^+ on excitation of N by fast electrons, 25:13998

FOIN, C., High spin rotational levels in ^{177}Ta, 25:15047

FOMENKO, V. N., Structure of pair states, 25:15178

FONTAINE, G., Automatic gain control in signal processing for bubble chamber pictures, 25:13257 (CERN-70-21(Vol.1), pp 383-97)

Use of Coccinelle to scan and measure big bubble chamber pictures, 25:13256 (CERN-70-21(Vol.1), pp 371-81)

FONTANA, Mars G., Perspectives on corrosion of materials, 25:13632

FONTI, L., HPD--IBM 360/44 system at CNAF for bubble chamber data analysis. II, 25:13268 (CERN-70-21(Vol.2), pp 617-24)

FORD, D. I., Partition function for systems of independent particles, 25:14494

FORD, G. P., Mass symmetry in the spontaneous fission of ^{257}Fm, 25:15045

FORMAN, W., Magnetic field structure around the Crab pulsar, 25:13850

FORMISANO, V., Alpha-particle observations in solar wind, 25:13895

FORNUSEK, Arthur Henry, Radiotherapy of malignant bone tumors, 25:13521

Studies of most efficient energies for irradiation of bone processes, 25:13536

FORSBLOM, I., Levels in ^{28}Si, 25:14936

FORSS, M., Isodose measurement of the bladder dose in radium therapy, 25:13448

FORT, E., Cross-section of ^{6}Li(n,α)T reaction in 100 to 500 keV energy range, 25:14913

Fission cross-section for ^{235}U and ^{239}Pu between 0.025 and 1 MeV, 25:15068

Measurements of fast neutron fluxes in the range of 10 keV to 1 MeV, 25:13216

FORTNEY, L. R., Quasi-two-body production in π^+p interactions at 1.95 GeV/c, 25:14563

FOULKE, L. R., Space--time methods for movable fuel problems (LWBR Development Program), 25:15353 (WAPD-TM-968)

FOWLER, E. C., Quasi-two-body production in π^+p interactions at 1.95 GeV/c, 25:14563

FOWLER, Eric B., Production of Candida utilis with 93 at. percent ^{13}C acetic acid as the sole carbon source, 25:13331 (LA-4551)

FRADIN, F. Y., Possibility of magnetic ordering in delta-Pu, 25:14481

FRAENKEL, Z., Measurement of the prompt neutrons emitted in the fission of ^{209}Bi and ^{238}U induced by 155-MeV protons, 25:15021

FRAKTOVNIKOVA, A. F., Thermocouple for accurate high-temperature measurements in a vacuum and in the presence of reactor radiation, 25:13326

FRANCOIS, Y., Sn--/sup 113m/In tracers in scintigraphies, 25:13501

FRANKE, J., Punched tape output of Vakutronik measuring equipment, 25:13224

FRANKEN, P. A., Photon rest mass, 25:14510

FRANKEVICH, E. L., Spectra of energy lost by slow electrons in aromatic hydrocarbons, 25:13968

FRANK-KAMENETSKII, D. A., Low-frequency instability of an electron-cyclotron wave in a plasma, 25:14343

FRANKLIN, Jerrold, Decay correlations in resonance production using quarks of spin $^{3}/_{2}$, 25:14712

FRANTSMAN, Yu. L., Structure and evolution of stars with various chemical compositions, 25:13821

FRANZ, Klaus-Dieter, Comparison of high-energy radiation applied through plaster casts, 25:13539

Investigations about energy dependence of dosimeters in a 42-MeV betatron, 25:13446

FRASER, Robert B., Diagnostic studies in an induction-heated supersonic argon plasma, 25:14243 (AD-711127)

FREEMAN, F. F., Grazing incidence spectra of the Sun, 25:13875

FREEMAN, G. R., Influence of temperature on the γ radiolysis of isopropyl alcohol vapor. Effect of molecular structure on the nonchain and chain decompositions of alcohol vapors, 25:13046

FREEMAN, J. M., Mass of the intermediate vector boson, 25:15180

FREESTON, I. L., Ion current to a plane probe in a flowing plasma, 25:14249

Measurement of ion density in a plasma torch using a plane probe, 25:14250

Variation of the admittance of a plasma capacitor with the amplitude of the measuring potential, 25:14251

FREESTONE, R. M. Jr., The energy spectrum of photoneutrons produced by 140-MeV electrons incident on tantalum, 25:14990

FREHAUT, J., Mean number of prompt neutrons and relative cross-sections for fission of ^{235}U and ^{239}Pu between 0.3 and 1.4 MeV, 25:15114

Measurements of (n,2n) and (n,3n) reaction cross-sections of fissionable materials using a large liquid scintillator, 25:15111

FRENKEL, A., Remarks on ''a new fit of the parameters for Cabibbo's theory'', 25:14632 (KFKI-70-23-HEP)

Superselection rules and internal symmetries, 25:14774 (KFKI-70-22-HEP)

FREUND, H. U., Californium-249 decay, 25:15029

Decay of ^{159}Dy, 25:15012

FREUND, P., Present data analysis system of the bubble chamber group at the MPI Munich, 25:13287 (CERN-70-21(Vol.2), pp 907-9)

FREUND, Robert S., Electron-impact excitation functions for states of N_2, 25:14013

FREY, K. W., Bloodpool scintigraphy with shortlived radionuclides, 25:13516

FREYSCHMIDT, P., Definition of toxic thyroid adenomas, 25:13594

FRICKE, M. P., Calculations of cross-sections for the radiative capture of fast neutrons, 25:15122

Measurements of cross-sections for radiative capture of 1-keV to 1-MeV neutrons by Mo, Rh, Gd, Ta, W, Re, Au, and ^{238}U, 25:15121

FRIDRICH, R., Radioisotopes in the diagnosis of gastric disease, 25:13495

FRIED, H. M., Eikonal model for large-angle np and pp elastic scattering, 25:14737

Field-theoretic model of high-energy scattering. III, 25:14607

FRIEDJUNG, M., Region of formation of narrow emission lines of Nova Delphini, 25:13820

FRIEDMAN, M. H., Chiral algebra, chiral breakdown, and xi parameter of K/sub 13/ decay, 25:14645

Lagrangian approach to dual pion amplitudes, 25:14697

N-point functions in chiral SU(3) x SU(3) current algebra, 25:14664

FRIEDMAN, Moshe, Injection of relativistic electrons into Astron-like device, 25:14351 (AD-711822)

FRIEDMAN, William H., Combined therapy for cancer of the laryngopharynx, 25:13545

FRIEDT, J. M., Mechanism of formation of anomalous charge states of iron after ^{57}Co electron capture in Co complexes, 25:13075

FRIEMAN, E. A., Magnetic and drift surfaces using a new stellarator expansion, 25:14234

FRIESENHAHN, S. J., Calculations of cross-sections for the radiative capture of fast neutrons, 25:15122

Measurements of cross-sections for radiative capture of 1-keV to 1-MeV neutrons by Mo, Rh, Gd, Ta, W, Re, Au, and ^{238}U, 25:15121

FRISCH, O. R., Sweepnik II, an improved track measuring machine, 25:13251 (CERN-70-21(Vol.1), pp 285-92)

FRISCHBIER, H.-J., Radiation injuries following electron therapy for mammary carcinomas, 25:13584

Results and complications in megavolt therapy of cervix carcinomas, 25:13531

FRISCHBIER, Hans-Joachim, Telecobalt irradiation of aortic lymph nodes, 25:13534

FRITZ, Garold F., Coupling between pressure and temperature waves in liquid helium, 25:14129 (COO-1574-19)

FROBEN, F. W., Paramagnetic species produced by ultraviolet irradiation of lithium, potassium, sodium, magnesium, and cadmium in 3-methylpentane at 77°K, 25:13025

FROEHLICH, H., What future for superconductivity, 25:14157

FROELING, Monika, Pendulum radiation with transversal shift of axis during ^{60}Co-teletherapy. III, 25:13447

FROESCHLE, C., Numerical study of the stochasticity of dynamical systems with two degrees of freedom, 25:13917

FROHMUELLER, H., High voltage therapy in bladder carcinomas, 25:13525

FROLOVA, L. V., Simultaneous determination of uranium(IV) and uranium(VI) by moving boundary method, 25:12938

FROMENT, M., Surface state of beryllium and faradaic yield of its anodic dissolution, 25:13704

FRONSDAL, C., Bremsstrahlung in coulomb field, 25:14613

FROSSARD, Henri, Weight changes in spleen as a function of irradiation dose in mice, 25:13478

FRYZUK, P., Stability of planar solid/liquid interface for alloys of In in Sn, 25:13646

FU, Chumin, Double-peripheral-model analysis of $K^+p \to K^+\pi^-\Delta^{++}$ (1236) at 9 GeV/c, 25:14714

FUBINI, S., Symmetries of the dual-resonance amplitudes, 25:14822

XUM

FUCCI, A., Adam+Eve, scanning and measuring machine for film from the large bubble chambers, 25:13270 (CERN-70-21(Vol.2), pp 633-49)
FUENTES, Kh., Realizing of z focusing in cylindrical electrostatic analyzers, 25:13325
FUESSY, E., Investigation of spontaneous silver precipitation on powdery platinum in nitric solutions, 25:13086
FUJII, Shoichi, Optimum planning for radiation facilities, 25:13461
FUJIIE, Yoichi, Decrease in intensity of Hg lines near source in weakly ionized flow, 25:14100
FUJITA, Dennis Ken, Some magnetic, spectroscopic, and crystallographic properties of Bk, Cf, and Es, 25:13018
FUJITA, Yoshiaki, Charge distribution produced by 4- to 24-MeV electrons in elemental materials, 25:13964
FUKATKO, Tomas, Improvement of responsive layer depth and energy resolution by cooling surface-barrier silicon detectors, 25:13217
FUKUDA, T., Production of high temperatures and pressures, 25:15457 (SCL-T-71-209)
FULTON, Thomas, Order corrections to muonium hyperfine structure, 25:13990
FUNCH-ROSENBERG, H., Construction of instrument for more accurate, repeated blood volume determinations using HSA-^{131}I, 25:13218
FUNG, P. C. W., Polarization measurements of solar Type-III radio bursts at 25.3 MHz, 25:13859 (AD-711398)
  Theory of polarization transfer in inhomogeneous magnetized plasmas, 25:14286 (N-70-40979)
FURENLID, Ingemar, Photometric recognition of rapid rotators and supergiants among B stars, 25:13790
FURMANSKA, B., Comparison of K/π ratio in multiple production at energies 60 GeV and approximately 1000 GeV, 25:14509 (INP-718)
FUSCHILLO, N., Electrical and tensile properties of Cu--ThO_2, Au--ThO_2, Pt--ThO_2, Au--Al_2O_3, and Pt--Al_2O_3 alloys, 25:13755
FUSHCHICH, V. I., Equations of motion invariant with respect to group P(1,n). II, 25:14747 (ITF-70-70)

G

GABUNIYA, R. I., Investigation of vitamin B_{12}--^{60}Co radiometric method of whole body after resection of stomach, 25:13334
GADIOLI, E., Fission of ^{210}Po, 25:15010
GADO, P., Disordered crystallographic shear in WO/sub 3-x/ crystals, 25:13773
GAISSER, T. K., Field-theoretic model of high-energy scattering. III, 25:14607
GALEEV, A. A., Diffusion-electric phenomena in plasma confined in Tokamak, 25:14238
GAL-EZER, E., Possible connection between chiral symmetry breaking and the nonet of tensor trajectories, 25:14769
GALIMOV, E. M., Carbon isotopes and the origin of petroleum, 25:13005
GALIN, J., Measurement of the prompt neutrons emitted in the fission of ^{209}Bi and ^{238}U induced by 155-MeV protons, 25:15021
GALKINA, O. S., Thermal magnetic effect and thermal emf of Gd at 90 to 250°K, 25:14458
GAL'PER, A. M., Flows of 100- to 1500-MeV electrons at various heights in atmosphere, 25:14068
GAMALY, A. F., Inelastic neutron scattering-$(n,n'\gamma)$-by F, Fe, Co, Ni, and Ta nuclei, 25:14960
GAMALYA, I. A., One-nucleon states and energy surfaces of ^{238}U in fission process, 25:15053
GAMBA, D., IBM 1130 computer on-line system at Torino, 25:13288 (CERN-70-21(Vol.2), pp 911-20)
GANDINI, F., Brush system for automatic processing of bubble chamber pictures, 25:13274 (CERN-70-21(Vol.2), pp 689-707)
GANGNUS, Yu. S., Solving Bethe--Salpeter's solution in ladder approximation in field theories of arbitrary divergence, 25:14803
GANICHEV, G. I., Fast-neutron thermalization time in silicate ores of varying moisture content, 25:13109
GANIVET, Michel, Analysis of radioactive solutions, 25:12932
GARAVAGLIA, T., Comments on isospin-factored current algebra at infinite momentum, 25:14587
GARCIA, Charles J., Mauna Loa coronagraph observations around the March 7, 1970 eclipse, 25:13888
GARCIA-GONZALES, F., Regular network of anti-phase boundaries in the x-phase of the system Fe--Cr--Mo--Ti, 25:13711
GARG, J. B., High-energy γ-rays following neutron capture in ^{239}Pu and ^{235}U, 25:15078
GARLICK, George F., Method for detecting one of heavy water and ordinary water in the presence of the other of heavy water and ordinary water, 25:12931
GARLID, Kermit L., Prog. rpt. on dynamics of solvent extraction systems, III, annual, 10/69--9/70, 25:13082 (RLO-2225-T-11-1)
GARNIER, G., Indium-113m-gelatine preparation for placental scintigraphy, 25:13502
GARNJOBST, Laura, New crisp genes and crisp-modifiers in Neurospora crassa, 25:13424
GARREAU, M., Surface state of beryllium and faradaic yield of its anodic dissolution, 25:13704
GARRETA, D., Polarization and spin-correlation parameters in proton-^{3}He elastic scattering at 19.4 MeV, 25:14888
GARRISON, John C., Statistical mechanics of persistent currents in quantum fluids, 25:14143
GASKELL, R., Frame dependence of vector dominance in Veneziano model and new test of rho universality, 25:14710
GASPARINI, Giulio M., Radiolytic degradation of toluene--nitric acid system, 25:13093
GASPARYAN, A. P., Reaction $np \to pp\pi^-$ for the incident neutron momenta from 2 up to 10 GeV/c, 25:14551
GASPERIC, J., Thermal treatment of Cr--SiO cermet thin films, 25:14435 (IJS-587)
GAST, K., Cooling disturbances in the core of sodium-cooled fast reactors as causes of fast failure propagation, 25:15381
GAST, P. W., Rare earth abundances in soil and rocks from Ocean of Storms, 25:13955
GATES, Gary F., Interval brain scanning with sodium pertechnetate /sup 99m/Tc for tumor detectability, 25:13505
GAUR, R. K., Emission of ^{8}Li fragments from K^- interactions, 25:14978
GAURIAU, J., Mean number of prompt neutrons and relative cross-sections for fission of ^{235}U and ^{239}Pu between 0.3 and 1.4 MeV, 25:15114
  Measurements of (n,2n) and (n,3n) reaction cross-sections of fissionable materials using a large liquid scintillator, 25:15111
GAUSTER, W. F., Comparison of NbTi and Nb_3Sn material tests, 25:14219
GAVALER, J. R., Alternating-current loss measurements in thin-film type II superconductors, 25:14189
  Characteristics of NbN Dayem bridges, 25:14201
GAVALIER, J. R., Very high critical current and field characteristics of niobium nitride thin films, 25:14193
GAVINI, A., Phonon effects in the far-infrared reflectivity of superconducting lead, 25:14175
GEBALLE, R., Two autodetaching states of O^-, 25:14009
GEGUSCH, M., Principles for control of nuclear material in GDR, 25:13193 (SZS-16/70)
GEGUZIN, Ya. E., Influence of weak deformation of Cu films on channeling of protons, 25:14421
GEIGER, J. S., Decays of /sup 159m/Ho and /sup 161m/Ho, 25:15060
GEILIKMAN, B. T., Collective oscillations in electronic mechanism for superconductivity, 25:14186
GEISS, J., Correlation between rock type and irradiation history of Apollo 11 igneous rocks, 25:13954
GEISS, Roy H., Dislocations in crystals, 25:15437 (NYO-3087-19)
GEISSLER, K., Description and performance of the CERN Spiral Reader, 25:13236 (CERN-70-21(Vol.1), pp 19-36)
GELLER, R., Desensitivity of a microwave cavity to measurements of hot-electron density, 25:14262
GEMBARZHEVSKII, G. V., Continuous absorption of partially ionized xenon in the visible region of the spectrum, 25:14280
GEMESY, T., Effective mass spectra of the $\gamma\gamma$, $\pi^0\gamma$, $\pi^0\gamma\gamma$, $\pi^0\pi^0$, π^0eta^0, $\pi^0\pi^0\gamma$, $\pi^0\pi^0\pi^0$ systems in mass value region M $(\gamma \ldots\ldots \gamma)$ less than or equal to 1.3 GeV, 25:14560 (JINR-E1-5349)
GENERALOV, N. A., Continuous absorption of partially ionized xenon in the visible region of the spectrum, 25:14280
GENTLE, K. W., Experimental test of quasi-linear theory, 25:14323
GEORGE, K. D., Iodine-131 reconcentration factor, 25:13347
GEORGE, Thomas Frederick, Dynamics of ion--molecule reactions, 25:14041
GERARD, Abadie, Weight changes in spleen as a function of irradiation dose in mice, 25:13478
GERARD, M., Status of the HPD minimum guidance programs at CERN, 25:13278 (CERN-70-21(Vol.2), pp 737-52)
GERBER, G. B., Proteolysis of partially denatured albumin in isolated perfused intestine of normal and irradiated rats, 25:13349
GERJUOY, E., Configuration-space three-body scattering theory, 25:14819 (N-70-40698)
  Configuration-space three-body scattering theory, 25:14818 (N-70-40418)
GERSHMAN, B. N., Electrostatic field theory under ionospheric conditions, 25:14123
GERSHWIN, Lawrence Kenneth, Asymmetry parameters in $\Sigma^- \to ne$ anti ν and $\Sigma^+ \to p\gamma$, 25:14539
GERSTEN, Joel I., Theory of the quenching of metastable hydrogen atoms by helium, 25:14026
GERSTNER, Joseph, Knight shift in beryllium metal, 25:14484
GERVOIS, A., Semi-circle' law for Gaussian random matrices, 25:14503
GESHKENBEIN, B. V., Divergences of the amplitudes of weak nonleptonic processes involving photon emission, 25:14655
GHEORGHIEV, Gheorghe, Some intrinsic motions important in magnetohydrodynamics. I, 25:14093
  Some intrinsic motions important in magnetohydrodynamics. II, 25:14094

GHIORSO, A., Chemical separation of rutherfordium, 25:13088
GHISELLI, A., HPD--IBM 360/44 system at CNAF for bubble chamber data analysis. II, 25:13268 (CERN-70-21(Vol.2), pp 617-24)
GHOSH, A. K., Applicability of single Born scattering theory, 25:14363
GIBBS, W. J., Radiation hazards, 25:13436
GIESE, R., Photoproduction of high-mass di-pion pairs at 15 GeV, 25:14511
GIESSEN, B. C., Metastable phase $(Al_{0.5}Nb_{0.5})Ni_3$, 25:13706
GIFFEN, W. C., Elastic scattering of beryllium doubly charged ions in helium, 25:14027
GILBERT, R. S., Radioactive tracers test nuclear steam turbines easier, better, 25:13148
GILBOY, W. B., Reactions $(n,n'\gamma)$ in ^{51}V and ^{89}Y, 25:14919 (AWRE-O-78/70)
GILCK, H., Determination of the radioactivity of samples, double-labeled with tritium, or ^{14}C, 25:12953
GILDEN, Raymond V., Inactivation of murine sarcoma and leukemia viruses by ultra-violet irradiation, 25:13609
GILLY, L., Malignant thyroid adenomas following x radiation during childhood, 25:13585
GILMAN, Peter A., Prog. rpt. on models for magnetofluid dynamics, of the Sun, final, 6/15/67--6/15/70, 25:13858 (AD-710629)
GILMORE, J. S., Neutron-induced ^{235}U fission at individual resonances. III, 25:14999
GIMPL, M. L., Electrical and tensile properties of Cu--ThO_2, Au--ThO_2, Pt--ThO_2, Au--Al_2O_3, and Pt--Al_2O_3 alloys, 25:13755
GINSBERG, D. M., Magnetic flux flow and fluctuation effects in thin-film superconductors, 25:14176
GINTSBURG, M. A., Self-similar waves in cold plasma with a magnetic field, 25:14369
GINZBURG, V. L., Problem of high-temperature superconductivity. II, 25:14156
  Theory of origin of cosmic rays, 25:14079
GIORDENESKU, N., Measurement of total cross sections of π^---p interaction, 25:14561 (JINR-P1-5460)
GIORGADZE, N. P., Propagation of a charged particle through weak nonlinear plasma, 25:14313
GIOVANIELLI, Damon Vincent, Helicon measurements in metals, 25:14468
GIOVENGO, J. F., In-pile dimensional changes of ThO_2--UO_2 fuel rods with non-free-standing cladding (LWBR Development Program), 25:15366 (WAPD-TM-986)
GIZON, A., High spin rotational levels in ^{177}Ta, 25:15047
GLEISER, Reinaldo Jaime, Linear trajectory fits of pion nucleon scattering at high energies, 25:14723
GLENISTER, P., Dose-response curve for the yield of translocations in mouse spermatogonia after repeated small radiation doses, 25:13404
GLIOZZI, F., Selection rules in dual-resonance models, 25:14658
GLOSSMANN, N., Convergence of radial matrix elements in electron scattering, 25:15195
GNIDAK, N. L., Neutron cross-sections of isotopes used as absorbers in atomic reactors, 25:15096
GODBEE, H. W., The feasibility of incorporating radioactive wastes in asphalt or polyethylene, 25:13197
GODDEN, Gerald Dean, Interaction $K^-d \to K^-\pi^-\pi^+d$ at 7.3 GeV/c, 25:14569
GODOLI, G., Connection between N--S and E--W solar asymmetries, 25:13883
GOGSADZE, G. Sh., Ground and excited states of ^4He nucleus, 25:14884
GOLD, E., anti pd topological cross sections in momentum range 50 to 920 MeV/c, 25:14555
GOLD, R. E., Varestraint test for refractory metals, 25:13695
GOL'DBERG, V. Z., Reaction $(^3He,\alpha)$ on nuclei with 1d--2s shell, 25:14944
GOLDBERGER, Marvin L., Existence of complex poles and oscillatory average multiplicity in multiperipheral models, 25:14585
GOLDBLITH, S. A., Recovery of salmonellae from irradiated and unirradiated foods, 25:13620
GOLDENBERG, G. J., Effect of irradiation on lymph flow and filtration function of lymph nodes, 25:13481
GOLDHAMMER, Paul, Properties of 1s shell nuclei, 25:15185
GOLDMAN, Joseph L., Combined therapy for cancer of the laryngopharynx, 25:13545
GOLDSCHMIDT, Eugene P., Genetic analysis of the histidine operon in Escherichia coli K12, 25:13422
GOLDSTEIN, Melvyn L., Theory of inverse Compton scattering in cold plasma, 25:13941
GOLDSTEIN, N. P., Scattering of protons from ^3He and ^4He, 25:14882
GOLDSZTAUB, S., Study of graphite oxidation by low energy electron diffraction, 25:13735
GOLDWASSER, M., Ariane II: automatic device for the analysis of spark chamber photographs, 25:13285 (CERN-70-21(Vol.2), pp 859-78)
GOLEMO, A., Fixed J-plane singularities in photoproduction, 25:14625
GOLOVANOV, L. B., Experimental ionization chamber filled with liquid and solid argon, 25:13295 (JINR-P13-5404)
GOLOVASHKIN, A. I., Optical properties and electron characteristics of niobium--tin alloys, 25:14149
GOLOVCHANSKII, E. M., Release of stored energy in annealing of radiational defects in NaCl, 25:14424
GOLOVIN, Yu. I., Mass-spectrometric method for determining microimpurities in inert gases, 25:12941
GOMATAM, Jagannathan, Finite formulations of four-fermion interactions, 25:14797
GOMBEROFF, L., Possible connection between chiral symmetry breaking and the nonet of tensor trajectories, 25:14769
GOMBOSI, E., Proton momentum spectrum in πN inelastic interactions at 17.2 GeV/c, 25:14564
GOMES, R. Alcantara, Effects of reductone on irradiated E. coli, 25:13610
GOODKIND, John M., Applications of superconductivity, 25:14155
GOODMAN, Gerald Joseph, Four-pronged antiproton-deuterium interactions at 7.0 GeV/c, 25:14554
GOODMAN, R. A., Weapons effects display system (WEDS MOD II): maintenance manual. II, 25:13323 (UCRL-50892(Vol.4)(Pt.2))
GOODMAN, Seymour Evan, Hydrokinetic theory of liquid helium II, 25:14137
GOPINATH, D. V., Radiation transport in one-dimensional finite systems. I. Development in the anisotropic source--flux iteration technique, 25:14406
  Radiation transport in one-dimensional finite systems. II. Gamma-ray transport studies with ASFIT, 25:14407
GORCZYCA, B., Fixed J-plane singularities in photoproduction, 25:14625
GORDELIER, S. C., Characterisation of the surface roughness of graphite, 25:13765 (RD/B/N-1770)
GORDEYEVA, N. V., Isotopic non-isomorphism of Rb(H/sub 1-x/D/sub x/)$_3$(SeO$_3$)$_2$ crystals, 25:12989
GORDON, C. M., Determination of Sr in sea water by photon activation analysis, 25:12974
GORDON, R. L., Polarization effects in oxide insulators, 25:14437 (WHAN-SA-75)
GORDON, Ronald S., Prog. rpt. on impurity effects on creep of polycrystalline magnesium and aluminum oxides at elevated temperatures, 12/19/69--12/18/70, 25:15427 (COO-1591-13)
GORE, M. S., Chemical and physical changes in irradiated and frozen Bombay duck, 25:13618
  Radiation pasteurization of fresh and blanched tropical shrimps, 25:13619
GORIN, Yu. P., Observation of anti ^3He, 25:14540 (IFVE-SEF-70-16)
GORODETSKII, A. A., Biological effects of fast neutrons. I, 25:13568
GORSKI, B., Complex formation between Tc and chelate-forming ligands. II, 25:13008
GORTEN, Ralph J., Significance of the total-body hematocrit in measurements of blood compartments, 25:13338
GORVAT, F. Yu., Lithium-6 incorporation into tissues, organs, and transplantable tumors, 25:13350
GOSS, W. M., Extended radio source in direction of pulsar CP 1919, 25:13834
  Unusual OH emission from a Mira variable, 25:13818
GOSSET, J., Determination of B, C, and O in Si by activation analysis, 25:12971
  Inelastic scattering of polarized protons by ^{40}Ca at 24.5 MeV, 25:14923 (CEA-CONF-1656)
  j-mixing determination in (p,d) reactions by asymmetry measurements, 25:14921 (CEA-CONF-1653)
  Study of (p,d) reactions on ^{48}Ca and ^{48}Ti with polarized protons, 25:14922 (CEA-CONF-1655)
  Study of (p,d) reactions on ^{90}Zr and ^{92}Mo with polarized protons, 25:14980 (CEA-CONF-1654)
GOSWAMI, Amit, Bootstrap theory of vibrations. I, 25:15174
  Bootstrap theory of vibrations. II, 25:15176
GOSWAMI, D. N., Van Hove model and non-leptonic hyperon decays, 25:14637 (SU-1206-238)
GOTO, Shoji, Internal oxidation of nickel alloys containing small amounts of chromium, 25:15455 (SC-T-71-3004)
GOTTSCHALK, Alexander, Use of lithium-drifted germanium detectors for clinical radionuclide scanning, 25:13487
GOTTSCHALK, W., Productivity of some mutants of pea and their hybrids, 25:13418
GOUACHE, J. C., Description and performance of the CERN Spiral Reader, 25:13236 (CERN-70-21(Vol.1), pp 19-36)
GOUDSMIT, Peter Frank Arnold, Properties of deformed nuclides produced in decay of ^{166}Ho, /sup 166m/Ho, ^{166}Tm, ^{166}Yb, ^{180}Os, ^{180}Re, ^{181}Os, and /sup 181m/Os, and by capture of thermal neutrons in ^{181}Ta, 25:14584 (NP-18536)
GOULARD, B., Fine structure in highly excited analog states, 25:15145 (NYO-1082-25)
GOULD, Christopher Robert, Alpha--γ angular correlation study of ^{57}Ni, 25:14952
GOULD, R. J., Atomic processes in a low-density hydrogen--helium plasma, 25:14302
GOVORUN, N. N., Development of track chamber picture processing systems at JINR, 25:13279 (CERN-70-21(Vol.2), pp 753-60)
GOYAL, Lakshmi N., Arithmetic unit of ILLIAC III: simulation and logical design. II, 25:15430 (COO-2118-2)
GOZAK, V. P., Low-frequency instability of an electron-cyclotron wave in a plasma, 25:14343
GRABOVSKII, Ya. K., Effect of ionizing radiation on the contents of ortho-oxyphenol in poplar shoots, 25:13598
GRACE, Joan F., Elastic scattering and polarization of

XUM

49.5-MeV protons on ^{148}Sm, 25:15013

GRAEBSCH, W., Data processing for bubble chambers from the pcint of view of a small laboratory, 25:13272 (CERN-70-21(Vol.2), pp 665-73)

GRAEFE, K. H., High voltage therapy in bladder carcinomas, 25:13525

GRAEME-BARBER, C., Grain boundary sliding during creep, 25:13675

GRAF, H., Correlation between rock type and irradiation history of Apollo 11 igneous rocks, 25:13954

GRAF, K. A., Simple model for calculating scatter, 25:14364

GRAHAM, R. L., Decays of /sup 159m/Ho and /sup 161m/Ho, 25:15060

GRANOVSKII, E. B., Molybdenum treatment for increasing stability of steel No. Kh18N9T in liquid Li, 25:13634

GRANT, C. T., Nonlinear Regge trajectories, 25:14662

GRAPPIOLO, G., Nuclear fuel with burnable poison. II, 25:13736 (EUR-4551)

GRASS, F., Szilard--Chalmers effect for production of ^{203}Hg in high specific activity, 25:13060

GRAUL, J., Radiation damage of semiconductor surface barrier detectors, 25:13329

GRAVIER, R., Experimental observation of drift instabilities in a collisionless plasma, 25:14345

GRECZ, Nicholas, Radiation survival of bacterial spores, 25:13611

GREEBLER, P., Implications of nuclear data uncertainties to reactor design, 25:15345

GREEN, A. E. S., Atomic physics and the polar cap, 25:14102 (N-70-19848)

GREEN, Louis C., Ordinary stars, white dwarfs, and neutron stars, 25:13797

  Starquakes: have they been observed, 25:13846

GREEN, R. O., Radiation Shielding Information Center program setup instructions manual, 25:14395 (CTC-INF-1017)

GREEN, Richard, Positron annihilation rates in lanthanum hydrides, 25:13988

GREENBERG, Arthur Joel, The charged pion lifetime measured in flight, 25:14581

GREENE, Anne, Genetic analysis of the histidine operon in Escherichia coli K12, 25:13422

GREENE, M. W., Production of ^{52}Fe for medical use, 25:13063

GREENIAUS, L. G., Measurement of proton--proton bremsstrahlung cross sections at 42 MeV, 25:14556

GREENSPAN, H., Multiple scattering of gamma radiation, 25:14393 (ANL-7689)

GREENWALD, Raymond Albert, Upper hybrid resonance scattering by magnetoplasma columns, 25:14382

GREGORY, W. D., Effect of specimen thickness on the superconducting critical temperature of indium, 25:14173

GRELOT, P., Interaction of a laser-created plasma with a strong magnetic induction, 25:14334

GREVE, A., Emission and absorption lines of Fe VIII, Fe XV, O III, O VII of the Sun, 25:13886

GRIBOV, V. N., Leading singularity in complex angular momentum plane in the quantum electrodynamics, 25:14802

  Zerc charge and scale invariance problems in the soluble field theory model, 25:14783

GRIEDER, A., Specificity of tritiated thymidine as a precursor of DNA under conditions of prolonged administration, 25:13358

GRIFFITHS, G. M., Gamma-ray yields from D(p,γ) ^{3}He, 25:14885

GRIFFITHS, R. J., Elastic scattering and polarization of 49.5-MeV protons on ^{148}Sm, 25:15013

GRIFFY, T. A., Electron-excitation--gamma-decay reactions in heavy nuclei, 25:15204

GRIGGS, Henry Gaston, Studies on recovery of Colpoda from pctentially lethal x and ultraviolet radiation induced damage, 25:13342

GRIGGS, James H., Emission spectrometric determination of trace elements in biological fluids, 25:12946

GRIGORENKO, L. P., Effect of x rays on cytological changes of bone marrow cells as a function of the immunobiological state of the reticulo-endothelial system, 25:13567

GRIGOR'EV, Yu. V., Temperature dependence of the total cross-section structure, 25:15093

GRIGOROV, N. L., Flows of 100- to 1500-MeV electrons at various heights in atmosphere, 25:14068

GRIMM, H.-J., ELKE: a grid guidance program for the rapid measurement of bubble chamber film, 25:13247 (CERN-70-21(Vol.1), pp 199-211)

GRISANTI, Alvaro, Measurement of the radioactivity of natural waters, 25:13106

GRISHAEV, I. A., Automating a 2-GeV electron linac, 25:14852 (SLAC-Trans-126)

GRISS, M. L., Regge behavior in unitarized π-π Veneziano mcdel, 25:14693

GRISSCM, John Thomas, Electron impact excitation and ionization studies of the rare gases, 25:14002

GROLOV, G. V., Leading singularity in complex angular momentum plane in the quantum electrodynamics, 25:14802

GROSFELD, Jay L., Liver scans after primary treatment of tumors in children, 25:13578

GROSS, D. H. E., Quasi-free scattering processes, 25:15156

GROSS, Franz, Overheating protection device for thermionic elements heated by nuclear energy, 25:13173

GROSS, S. H., Latitudinal and longitudinal variation of a planetary atmosphere, 25:13956

GROTE, H., Atlas of particle production spectra, 25:14733 (NP-18660)

  Pattern recognition methods for Omega and SFM spark chamber experiments, 25:13283 (CERN-70-21(Vol.2), pp 831-50)

GROTH, T., Approximation and accuracy in the design of a double-focusing flat spectrometer, 25:13324 (UUIP-715)

GROTOWSKI, K., Backscattering of alpha particles, 25:15172

GROVE, Edward Andrew, SU(n) actions on differentiable manifolds with vanishing first and second integral Pontryagin classes, 25:14760

GROZDANOVIC, J., Oscillopolarographic determination of cysteic acid level in the fingernails followed chronic irradiation in humans, 25:13369

GRUEBAUM, L., Properties of the low-lying positive-parity states in ^{9}Be and ^{13}C, 25:14917

GRUETTER, A., Corrosion of zirconium alloys in superheated steam: results of the prolonged experiments, 25:13629 (EIR-184)

GRUEVA, T., Effect of small magnetic storms on diurnal variations of neutron component, 25:14074

GRUHN, C. R., 40-MeV proton inelastic scattering on ^{50}Ti, ^{51}V, and ^{52}Cr and its microscopic descripticn, 25:14928

GRUTERS, M., Princeton automatic track reader, 25:13250 (CERN-70-21(Vol.1), pp 273-83)

GRYPEOS, M. E., New derivation of an approximate expression in closed form for the binding energy of an impurity particle in nuclear matter, 25:15142 (DEMO-70/20)

GUARDIOLA, R., Broken channels in π^+-photoproduction on ^{3}He, 25:14518

GUBATOVA, D. Ya., Determinaticn of the radiation loading in roentgenodiagnostic investigation with the aid of thermoluminescent dosimetry, 25:13453

GUBERNIEV, M. A., Comparative study of DNAse activity under treatment of cells E. coli K12 (lambda) with various inducing agents, 25:13371

GUDIMA, K. K., Systematization of the inelastic interactions of high-energy pions and nucleons with atomic nuclei, 25:15148 (ORNL-tr-2399)

GUECKEL, W., Determination of impurities in boron carbide by neutron activation analysis, 25:12972

GUEGUENIAT, P., Behavior of Ru in seawater, 25:13013

GUELIN, M., Neutral hydrogen absorption in galaxy M82, 25:13911 (AD-711299)

  Neutral hydrogen absorption in IRR II galaxy M82, 25:13927

GUENTHER, K., Diagnostics of xenon plasmas with higher precision, 25:14261

GUIDETTI, M., Isomeric ratios for (n,2n) reacticns, 25:15182

GUIGNARD, Claude, Pangloss, a CRT device for bubble chamber pictures, 25:13258 (CERN-70-21(Vol.1), pp 401-25)

GUILLAUME, M., Tritiated titanium targets producing 14-MeV neutrons. II, 25:14840 (EUR-4286(Pt.2))

GUINET, Philippe, Nuclear fuel based on UC, 25:13746

  Nuclear fuel based on UC, 25:13747

GUIOLLOT, Michel, Pangloss, a CRT device for bubble chamber pictures, 25:13258 (CERN-70-21(Vol.1), pp 401-25)

GULA, A., Photoproduction of scalar and victor mesons, 25:14626

GULYI, M. F., Avidin effect on intensity of ^{14}C incorporation from $NaH^{14}CO_3$ and glycine-1-^{14}C into proteins and lipids of rat liver homogenates, 25:13344

GUMAN, V. N., Centrifugal terms in residual interaction of particles in nucleus, 25:15168

GUNN, Robert B., Uptake curve in tracer kinetics, 25:13336

GUNSBERG, Melvin J., Combined therapy for cancer of the laryngopharynx, 25:13545

GUPPY, James Garfield, Simulated startup of in-core thermionic reactor systems, 25:15401

GUPTA, G. S., Activities of prostates and seminal vesicles after x-irradiation of rat testes, 25:13366

GUPTA, R. P., Electric field shielding and antishielding factors at rare-earth and heavy ions, 25:13983

GURALNIK, G. S., Two loop approximations to propagators in the sigma model, 25:14683 (NYO-2262-TA-219)

GURINOVICH, G. P., Spectroscopy of chlorophyll and related compounds, 25:15417 (AEC-tr-7199)

GUSEV, V. A., Collisions between fast protons or H atoms and O_2 molecules, 25:13999

GUSHEHIN, G. I., Thermocouple for accurate high-temperature measurements in a vacuum and in the presence of reactor radiation, 25:13326

GUS'KOV, B. N., Search for iscbar state with $T = {}^5/_2$ in the reaction $\pi^+ + p \to \pi^- + X^{3+}$, 25:14576

GUSMANO, E. A., Retention of /sup 113m/In--^{59}Fe-ferric hydroxide in the mouse, 25:13486

GUTHART, H., Simple model for calculating scatter, 25:14364

GUTMANN, Micheline, Pangloss, a CRT device fcr bubble chamber pictures, 25:13258 (CERN-70-21(Vcl.1), pp 401-25)

GUTMANN, Viktor, Ionization (heterolysis) of covalent compounds as coordination-chemical phenomenon, 25:13023

GUYER, R. A., Superfluidity in quantum crystals, 25:14145

XUM

H

HAAG, J., Chromosomal dosimetry on swine lymphocytes, 25:13417
HABANEC, Josef, Improvement of responsive layer depth and energy resolution by cooling surface-barrier silicon detectors, 25:13217
HABER, B., Reactions $\gamma n \to p\pi^+\pi^-\pi^-$, $p\pi^+\pi^-\pi^-\pi^0$ and $n\pi^+\pi^+\pi^-\pi^-$ at 4.3 GeV, 25:14521
HABERLER, P. L. F., Relation between bare and physical mass of fermions, 25:14800
HADDOCK, R. P., Analysis of negative-pion photoproduction near the P_{33} resonance: test of the ΔI less than or equal to 1 rule and time-reversal invariance, 25:14566
  Measurement of inverse pion photoproduction near the $P_{33}{}^0$(1236) resonance, 25:14567
HADEN, C. R., Nuclear radiation detection using a superconducting resonant cavity, 25:14228
HAEBERLI, W., Stopping power of Havar for 2.5 to 7.0 MeV deuterons, 25:14401
HAEMAELAEINEN, R. M. K., Effect of nonlocality of nucleon--nucleon potential on the two-body sum rules, 25:14732 (NP-18648)
  Limits of validity of Siegert's theorem in the nuclear photo-absorption, 25:15144 (NP-18618)
HAFTEL, Michael Ivan, Two-nucleon potentials and nuclear saturation, 25:15188
HAGEDCRN, R., Atlas of particle production spectra, 25:14733 (NP-18660)
HAGE-HASSAN, Mehdi, Projection methods and their applications to Hartree--Fock wave functions, 25:15143 (LYCEN-7050)
HAGENMULLER, Paul, Electronic structure of some hexaborides of the CaB_6 type, 25:14463
HAGERTY, Patrick Edwin, Antiproton--neutron annihilation at rest into final states of 5 and 6 pions, 25:14553
HAGGERTY, Herman Frederick, Bubble chamber search for K/sub S/^{0} $\to \pi^+\pi^-\pi^0$, 25:14537
HAGHIRI, F., Detailed characterization of soil and vegetation on selected sites. Technical progress report, March 1, 1970--November 26, 1970, 25:13118 (COO-414-17)
HAGOPIAN, Sharon Lee Ford, Single-pion production in π^-p interactions at 2.3 GeV/c, 25:14570
HAHN, Hong-sup, Quantum transport cross sections for ionized gases, 25:14297
HAIDT, D., Measurement of K/sub μ3/$^+$ decay parameters, 25:14534
HALBRITTER, J., Surface residual resistance of high-Q-superconducting resonators, 25:14222
HALFORD, W. D., Cosmological theory based on Lyra's geometry, 25:13947
HALL, D., Performance of the DAPR system, 25:13280 (CERN-70-21(Vol.2), pp 761-804)
HALL, Robert C., Scintiscanning in the diagnosis of rupture of the spleen, 25:13511
HALLINAN, Thomas J., Small-scale auroral arc distortions, 25:14119
HALVERSON, A. W., Prog. rpt. on nature and importance of selenium metabolites in animal, 1--12/70, 25:15425 (COO-1449-11)
HAMADA, Takeo, Some properties of tungsten--rhenium alloys, 25:13682
HAMLET, I. L., University of Virginia superconducting wind-tunnel balance, 25:14216
HAMMERMAN, Ira Saul, $n + p \to d + \pi^0$: a test of charge independence from threshold through resonance peak, 25:14549
HAMMITT, F. G., Behavior of liquid sodium in a sinusoidal pressure field, 25:13154
HAMMOND, J. P., Bonding graphite to metals with transition pieces, 25:13648
HANAK, J. J., Compounds and alloys for superconducting applications, 25:14203
HANCHEY, Penelope, Pinocytosis and membrane dilation in uranyl-treated plant roots, 25:13353
HAND, Russell E. Jr., Requirement of cellular synthesis for Kilham rat virus replication, 25:13608
HANDLEY, Thomas H., Fluid supported capsule holder for homogeneously irradiating samples, 25:13208
HANNA, G. C., Measurements of alpha and of fission cross-section ratios for ^{233}U, ^{235}U, and ^{239}Pu at thermal energies, 25:15070
HANSEN, C. J., Pulsational stability of pure-helium stars of low mass, 25:13793
HANSEN, J. D., Many-body cross sections, 25:14594
HANSEN, J. S., Californium-249 decay, 25:15029
HANSEN, Jean-Pierre, Fluid--solid phase transition of hard-sphere Bose system, 25:14500
HANSEN, P. G., Electron-capture beta decay, 25:14993
HANSEN, Richard T., Mauna Loa coronagraph observations around the March 7, 1970 eclipse, 25:13888
HANSEN, Shirley F., Mauna Loa coronagraph observations around the March 7, 1970 eclipse, 25:13888
HARADA, Takeo, Extraction of Y in the system $Y(NO_3)_3$--HNO_3--H_2O--di(2-ethylhexyl) phosphoric acid, 25:13097
HARBST, Hans, Postoperative radiotherapy of mammary carcinoma without irradiation of the thorax wall, 25:13533
HARDIE, R. W., Comparison of the codes RSYN and 3DB, 25:15343 (WHAN-IR-48)
HARDIN, Charles M., Priority system for the inspection of x-ray facilities, 25:13459
HARDY, K. A., Half-life of the 113.8-keV level of ^{176}Lu, 25:15040
HARGREAVES, J. K., Conjugate and closely-spaced observations of auroral radio absorption. IV, 25:14118
HARNEY, H. L., Reduced widths from isobaric analog resonances, 25:15201
HAROLD, Richard J., Ultraviolet-sensitive mutants of Streptomyces coelicolor. I, 25:13414
  Ultraviolet-sensitive mutants of Streptomyces coelicolor. II, 25:13407
HARP, G. D., Precompound decay from a time-dependent point of view, 25:15140 (CU-1019-79)
HARPER, M. W., Some unexpected dosimetric problems in an apparatus for mammalian radiobiology, 25:13456
HARRIS, J., Chemical separation of rutherfordium, 25:13086
HARRIS, J. F., Cxford PEPR system, 25:13239 (CERN-70-21(Vol.1), pp 61-88)
HARRIS, O. D., Calcium-47 studies in adult coeliac disease and other gastrointestinal conditions with particular reference to osteomalacia, 25:13359
HARRIS, R. G., Double scattering of ^3He particles by C and Al, 25:14894
HARRISON, Raymond, Studies of influence of wavelength on biological effects, 25:13583
HARRISON, William Craig, Partial wave analysis of reaction $K^-n \to \Sigma^-\pi^+\pi^-$ from 1.62 to 1.74 GeV, 25:14557 (FSU-HEP-70-3-1)
  Partial wave analysis of reaction $K^-n \to \Sigma^-\pi^+\pi^-$ from 1.62 to 1.74 GeV, 25:14717
HARROD, Donald Lee, Deformation of indium, 25:13698
HARTING, D., HPD--CDC 3200 system at Amsterdam, 25:13275 (CERN-70-21(Vol.2), pp 709-20)
HARTLEY, B. J., Toward inclusion of spin in generalized Veneziano model for $K^-p \to \pi^-\pi^+\Lambda$, 25:14716
HARTWICK, F. D. A., Radial variation in ratio of blue to red supergiants in Galaxy, 25:13791
HARTWIG, William H., Material-properties analyzers using superconducting resonators, 25:14229
HARUN-AR-RASHID, A. M., Broken chiral and conformal symmetry and Kuo transformation, 25:14770
HARVIE, Sylvia J., Ion exchange properties of crystalline zirconium phosphate, 25:13084
HARWOOD, S. E., Radiation-enhanced oncogenesis by SV40, 25:13553
HASEGAWA, Akira, Chemical and hygienic studies on natural radioactive spa. III, 25:13470
HASEGAWA, Keisuke, Radiation protection against x-ray diffraction apparatus, 25:13457
HASENFRATZ, P., Remarks on ''a new fit of the parameters for Cabibbo's theory'', 25:14632 (KFKI-70-23-HEP)
HASHEMI-TAFRESHI, Jafar, Energy source for the solar corona, 25:13907
HASSAN, H. A., Collisionless sheath near an electrode in the presence of a magnetic field, 25:14300
HASSAN, M. Y. M., Binding energy of a Λ particle in nuclear matter with noncentral ΛN forces, 25:14745
HASSENZAHL, W. V., Superconducting quadrupole doublet for LAMPF, 25:14860
HASTE, Glenn Roy, Ion cyclotron instabilities in finite plasmas, 25:14348
HATCHYA, M., Fast-neutron capture cross-sections of Cr, Fe, Ni, and Mo, 25:14970
HATHAWAY, D. O., Reduction of sexual aggressiveness of male codling moths treated with tepa or gamma irradiation, 25:13557
HATTULA, J., Multipole character of some gamma transitions in ^{152}Sm, 25:14985 (NP-18615)
HAUBOLD, Ulrich, Sequential scintigrams of kidney with ^{131}I- o-iodo-hippuric acid and /sup 113m/In-EDTA, 25:13499
HAUG, H., Hydrodynamic equations for condensate and depletion of He II, 25:14139
HAUGE, Oe., CuH lines in sunspot spectrum and solar isotope ratio of Cu, 25:13900
HAUSER, L. G., Evaluate your cost of cooling steam turbines, 25:13147
HAUSER, W., Technetium-labeled red blood cells, 25:13332
HAWKE, John, Iodine halides as radical scavengers, 25:13067
HAYASHI, Y., Unusual dissociation of dislocations in Ni_3Ta, 25:13699
HAYES, C. F., Quantization of Lagrangians for charges in external field, 25:14776
HAYES, Edward F., Noniterative solutions of integral equations for scattering. V, 25:14017
HAZARD, C., Radio structure of remnant of Kepler's supernova, 25:13854
HAZELTINE, R. D., Resistive plasma rotation and shock formation in toroidal geometry, 25:14235
HEAD, A., Status of the HPD minimum guidance programs at CERN, 25:13278 (CERN-70-21(Vol.2), pp 737-52)
HEARST, Joseph R., K-division experimental work. Part I. Geophysics research for underground explosion technology, 25:13104 (UCRL-50855)
HEASLEY, James N. Jr., Simultaneous determination of He and metal abundances in old open clusters, 25:13798
HEDRICK, Clyde Lewis, Interaction of quasi-transverse and

quasi-longitudinal waves in an inhomogeneous Vlasov plasma, 25:14388
HEGARTY, John Christopher, Gravitational interaction of em radiation and matter as cause of cosmological red shift, 25:13948
HEGER, N., Angiographic diagnosis of hydatid disease of the liver, 25:13494
HEIDENREICH, Roger, Results of radiotherapy for bronchial carcinoma obtained at the Giessen Univ. Clinic from 1962 to 1967, 25:13522
HEILES, Carl, Pulsar NP 0532: disappearance of precursor pulse at 606 MHz, 25:13848
HEIN, P., Data processing for bubble chambers from the point of view of a small laboratory, 25:13272 (CERN-70-21(Vol.2), pp 665-73)
HEINIS, P., Radioisotopes in the diagnosis of gastric disease, 25:13495
HEINZE, H. G., Struma maligna: 3, 5, and 8-year results in 259 cases, 25:13524
HEITZ, Ch., Effects of ^{60}Co γ radiation on Xe trioxide in aqueous solutions, 25:13049
HEJTMANEK, M., Genetic basis of virulence in dermatophytes, 25:13427
HELD, A., Scattering of protons from ^{3}He and ^{4}He, 25:14882
HELLAND, J., Analysis of negative-pion photoproduction near the P_{33} resonance: test of the ΔI less than or equal to 1 rule and time-reversal invariance, 25:14566
HELLMAN, K. B., Enhancement of viral transformation by ultraviolet light, 25:13552
HELLSTROEM, J., Low-lying levels and decay structure in ^{62}Cu, 25:14940
HELLWIG, B., Experiences with coupled computers to control an HPD, 25:13276 (CERN-70-21(Vol.2), pp 721-7)
HELMER, R. L., Gamma-ray yields from D(p,γ) ^{3}He, 25:14885
HELMICK, Larry S., Base-catalyzed hydrogen--deuterium exchange of N-substituted pyridinium ions. Inductive effects and internal return, 25:13000
HELPPI, H., Multipole character of some gamma transitions in ^{152}Sm, 25:14985 (NP-18615)
HENDERSON, David Michael, Pulse stimulated emission and echoes at upper hybrid resonance, 25:14381
HENDERSON, Thomas R., Serum organic acids in sheep exposed to neutron--gamma irradiation, air blast, or both, 25:13384
HENRIKSEN, R. N., Pulsar number-period distributions and oblique rotator, 25:13836
HENYEY, F., Dual, crossing-symmetric amplitude with Mandelstam analyticity, 25:14821
HERING, W. R., Normalization for (α,t) reactions, 25:15064
HERISTCHI, Dj., Upper cutoff in the spectrum of solar particles, 25:13910
HERMSDORF, D., Correction of finite volume of scatterer effect on measurement of differential elastic and inelastic neutron cross sections. II, 25:15150
HEROLD, J. S., Beyond Hartree-liquid model of superfluid bosons, 25:14142
HERRERA, J. C., Relativistic motion in constant field and Schott energy, 25:14507
HERRMANN, G., Independent yields of /sup 124g/Sb, /sup 126g/Sb, and ^{160}Tb in neutron fission of ^{235}U, 25:15038
HERSCCVITZ, Victoria E., Momentum distribution of short-lived nuclear hole states, 25:15194
HERSHKOWITZ, N., Moessbauer effect in tungsten following Coulomb excitation, 25:15020
HERTZBACH, Stanley S., CP violation in K(neutral) + $\pi^{+}\pi^{-}\pi^{0}$, 25:14762
HERTZBERG, Richard W., Deformation in wrought Mg--9 wt percent Y, 25:13710
HERTZBERGER, L. O., HPD--CDC 3200 system at Amsterdam, 25:13275 (CERN-70-21(Vol.2), pp 709-20)
HERZOG, W. G., Radioactive tracers test nuclear steam turbines easier, better, 25:13148
HESBOEL, R., Method for calculating the washout of elemental iodine by water sprays, 25:15372 (AE-408)
HESSER, James E., High-frequency stellar oscillations. VI, 25:13808
HETTNER, G., Geometrical arrangement of radiogold preparations in tumor implants, 25:13526
HEUSENER, G., Core-optimization of sodium cooled fast breeder reactors with methods of nonlinear programming, 25:15351
HEWISH, A., Spectrum of plasma-density irregularities in the solar wind, 25:13866
HICKEY, F. R., Muon experiments, 25:14532
HIJIKATA, Masayuki, Influence of temperature in the contact area on the static welding characteristics of electrical contacts, 25:13644
HILBERT, R. F., Mechanisms of swelling and gas release in uranium dioxide, 25:13785
HILDEBRANDT, J., Silver analyzer for discontinuous determination of the silver concentration in emulsion samples, 25:13312
HILGARD, Henry R., Dissociation of splenomegaly from graft-versus-host disease by host x-irradiation, 25:13390
HILGEMAN, Theodore William, Infrared observations of H II regions, 25:13826
HILL, Benny Joe, Numerical solution of the Schroedinger equation for ^{3}H, 25:14881
HILL, D., Polarization parameter in backward π^{+}p elastic scattering at 1.60, 1.80, 2.11, and 2.31 GeV/c, 25:14577
HILL, H. H., Effective size of americium dissolved in lanthanum, 25:13705
HILL, S. M. B., Medical supervision of radiation workers, 25:13465
HILLAND, Carl Boyd, Pulsed high-density kilovolt plasma employing noncylindrical Z pinch, 25:14359
HILLIARD, R. K., Survey of alpha waste generation and disposal as solids in the U. S. nuclear fuel industry, 25:13188 (BNWL-B-34)
HILLMAN, M., Production of ^{52}Fe for medical use, 25:13063
HILSCHER, Werner, Growth inhibition through gamma radiation on transplanted sarcomas in mice, 25:13473
HILTON, D. A., Identification of impurities in neutron-irradiated graphites by γ spectrometry, 25:12954
HIMMEL, L., Dispersion hardening of a Mo--1 at. percent Hf alloy by internal hardening, 25:13661 (UCRL-72627)
HINCKELMANN, Otto, Low-energy scattering by long-range potentials, 25:14019
HINDS, James J., Material-properties analyzers using superconducting resonators, 25:14229
HINKELMANN, B., Evaluation of neutron nuclear data for several actinides in energy range from thermal to 10 MeV, 25:15128
Theoretical and experimental analysis of fast zero-power assemblies, 25:15396
HINKSON, Thomas Clifford, Recoil reactions of ^{18}F in perfluorocyclobutane and perfluorocyclobutene, 25:13066
HIRAI, T., Effects of tobacco mosaic virus infection on photosynthetic CO_2 fixation and $^{14}CO_2$ incorporation into protein in tobacco leaves, 25:13360
HIRASAWA, Toshiaki, Radio spectra of quasi-stellar objects, 25:13843
HIRATA, Michihiro, Core excited states in ^{17}O, 25:14900
HIRD, B., Doppler-shift lifetimes in ^{30}P, 25:14933
HIRONS, Thomas J., Effect of collapsing cross-section data on fast breeder physics parameters, 25:15352
HIRTH, W., Interpretation of radio spectra of extragalactic sources, 25:13835
HJELLMING, R. M., Detection of radio emission from Antares, 25:13804
HJORTH, S. A., High-spin rotational and three-quasiparticle excitations in ^{177}Ta, 25:15036
HOANG-BINH, D., Stark broadening and radio recombination lines in NGC 7027, 25:13814
HOCH, M., Thermal conductivity and total emittance of W from 1800 to 2800°K, 25:13663
HOCHEL, R., Level structure of ^{181}W from the decay of ^{181}Re, 25:15058
HODGES, D., Automatic scanning and measurement of bubble chamber film on Polly II, 25:13254 (CERN-70-21(Vol.1), pp 325-55)
HODGSON, P. E., Backscattering of alpha particles, 25:15172
Isospin dependence of the proton optical potential, 25:15154
HOEFER-JANKER, Hans, Effects of an extract of calves-blood on radioinduced mucosa lesions in the area of larynx and pharynx, 25:13475
HOEGBERG, G., Damage in gold bombarded with medium mass ions, 25:14413 (NP-18645)
HOEHN, J., Correction of finite volume of scatterer effect on measurement of differential elastic and inelastic neutron cross sections. II, 25:15150
HOEJEBERG, Mats, Energy levels in ^{185}W, 25:15043
HOEL, David G., Selection procedure based upon Wald's double dichotomy test, 25:15441 (ORNL-TM-3237)
HOEL, Lars, Helium-3-crysotat for specific heat measurements, 25:14212 (UUIP-677)
HOEPER, Phillips Stephen, Observation and analysis of elastic resonance scattering of electrons by rare gases, 25:14035
HOER, G., Bloodpool scintigraphy with shortlived radionuclides, 25:13516
HOFFER, Paul B., Use of lithium-drifted germanium detectors for clinical radionuclide scanning, 25:13487
HOFFMAN, D. C., Mass symmetry in the spontaneous fission of ^{257}Fm, 25:15045
HOFFMANN, H., Equations of state of fuel materials UC and PuC, 25:13753
HOFFMANN, Klaus, Radiotherapy of esophagal fistulas caused by lumphogranulomatosis, 25:13542
HOFMANN, F., Velocity and temperature distribution in turbulent flow in sodium cooled fuel elements with eccentric geometry, 25:15363
HOFSTETTER, K. J., Level structure of ^{181}W from the decay of ^{181}Re, 25:15058
HOGAN, Mary Elizabeth Mogge, SU(3) x SU(3) chiral Lagrangian model for anti KN interactions, 25:14703 (TID-25639)
HOJMAN, S., Algebraic solution of a short-range potential problem, 25:14491
HOLINDE, K., One-boson exchange potential and nuclear matter properties, 25:15199
HOLLAND, P. T., Radiolysis of liquid hydrocarbons containing deuterium sulfide, 25:13048
HOLLAND, W. D., Particle size distribution in clouds from nuclear airbursts, 25:13138
HOLLAS, C. L., Anomalies in cross sections of (d,n) reactions leading to isobaric analog states, 25:15050
HOLLECK, H., Behavior of fission product Mo, Tc, Ru, Rh,

and Pd in a carbide fuel element and structure of the system Mo--Ru--C, 25:13764 (KFK-1260)
HOLLEVILLE, Patrick, Weight changes in spleen as a function of irradiation dose in mice, 25:13478
HOLLINGER, H. B., Effect of radiation escape on atomic state densities and electron distribution function, 25:14316
HOLLOWAY, J. H., Radioactive tracers test nuclear steam turbines easier, better, 25:13148
HOLM, David G., Gene conversion in higher organisms: half-tetrad analysis of recombination within the rosy cistron of Drosophila melanogaster, 25:13426
HOLMGREN, S. O., System for on-line control of bubble chamber measurements, 25:13282 (CERN-70-21(Vol.2), pp 825-30)
HOLMQVIST, B., Fast-neutron elastic scattering at 8 MeV, 25:14965
Fast-neutron inelastic scattering in energy range 2 to 4.5 MeV, 25:14966
Neutron elastic-scattering cross-sections of V, Cr, Fe, and Ni, 25:14964
Neutron energy spectra from neutron-induced fission of ^{238}U at 1.35 and 2.02 MeV, 25:15109
HOLROYD, P. M., Evacuable glove-box for handling of liquid sodium, and apparatus for analysis of carbon in sodium and other metals, 25:13185 (AERE-R-6338)
HOLSTEIN, Barry Ralph, A theoretical study of the weak nonleptonic decay modes of the K meson, 25:14764
HOLTHUIZEN, D. J., HPD--CDC 3200 system at Amsterdam, 25:13275 (CERN-70-21(Vol.2), pp 709-20)
HOLTZMAN, Jordan L., Inhibition of hepatic microsomal mixed function oxidases by D_2O, 25:13372
HOLWEGER, H., Damping and solar abundance of Na from Na I Fraunhofer lines, 25:13899
HOLZER, Alfred, Plowshare and the environment, 25:13430 (UCRL-72830)
HOLZER, Peter, Problem of zero-bias anomalies in the tunneling spectroscopy of superconductors, 25:14206
HOMEYER, H., Study of states in ^{16}O, 25:14914
HONIG, J. M., Plasma resonance in TiO, VO, and NbO, 25:14462
HONJI, Masahiro, Energy dissipation of electrons in Al and Cu targets, 25:14400
HONTZEAS, S., Excited states in ^{75}As, 25:14931
HONZAWA, T., Ion heating caused by ion-acoustic waves in an ion-streaming plasma, 25:14240
HOOGLAND, W., Measurement of the lifetimes of the Σ^{+}--hyperons, 25:14546
HOOKE, William H., Ionospheric response to an isotropic spectrum of internal gravity waves, 25:14121
HOPKE, P. K., Decay of ^{208}At, 25:14995
HOPWOOD, David A., Ultraviolet-sensitive mutants of Streptomyces coelicolor. II, 25:13407
Ultraviolet-sensitive mutants of Streptomyces coelicolor. I, 25:13414
HORAN, Donald Martin, Coronal electron temperatures associated with solar flares, 25:13902
HORCICKA, J., Rod models of fuel elements of nuclear reactors, 25:15410 (ZJE-92)
HORIE, H., Parity states in A = 15, 14, and 13 nuclei, 25:15158
HORIUCHI, Kensuke, Three cistrons in bacteriophage $Q\beta$, 25:13386
HORN, P. M., Vortex motion in the presence of thermodynamic fluctuations, 25:14207
HOROWITZ, Y. S., De-excitation γ-rays in ^{15}N and ^{15}O, 25:14896
HORTON, J. L., Anomalies in cross sections of (d,n) reactions leading to isobaric analog states, 25:15050
HORWITZ, E. P., A ^{244}Cm--Be isotopic neutron source, 25:14872
HOSHI, Michio, Precipitation of some actinide element complex ions by using hexammine cobalt (III) cation. I, 25:12980
HOSHINO, Yoshio, Electrochemical studies of Y and Y--Zn alloys in fused LiCl--KCl eutectic, 25:13095
HOT, M., Use of ^{238}Pu radiation sources in cardiac pacemakers, 25:13178
HOUTGAST, J., Observational method for absolute intensities in the solar spectrum, 25:13874
HSIEH, S. T., Parity states in A = 15, 14, and 13 nuclei, 25:15158
HSU, Chia-jung, Heat transfer in laminar flow through concentric annuli, 25:13159
HSU, J. P., Extreme-energy collisions, 25:14663
HUANG, Robert Y. M., Permeation of gases through modified polymer films. II, 25:13039
HUANG, W. F., Positron annihilation rates in lanthanum hydrides, 25:13988
HUBBARD, N. J., Rare earth abundances in soil and rocks from Ocean of Storms, 25:13955
HUBE, D. P., Places of origin of stars in Galaxy, 25:13926
HUBER, J. F. K., Microradiometric detector for column liquid chromatography, 25:12952
HUBER, J. G., Superconducting--normal phase boundary of superconductors containing nearly nonmagnetic impurities, 25:14159
HUBERT, Jerzy, Radioisotope measurements of the flow parameters of the postflotation slurry, 25:13176
HUEBENER, R. P., Ettingshausen effect in the intermediate state of thin superconducting Pb films, 25:14181
HUENERMANN, B., Placentography: comparative investigations in nuclear medicine, 25:13517
HUET, J. L., Measurements of fast neutron fluxes in the range of 10 keV to 1 MeV, 25:13216
HUGHES, M. P., Galactic hydrogen absorption at 21 cm wavelength in direction of Virgo A, 25:13831 (AD-711300)
HUGHES, M. W., Tritium content measurements on a variety of water samples. Technical Memorandum 31/1969, 25:13120 (NP-18638)
Tritium content measurements on a variety of water samples, 25:13103 (NP-18639)
HUGHEY, L. R., Adsorption of water vapor on polycrystalline tungsten, 25:13669
HULL, A. P., Invited comments on a derivation of the 'factor of 700' for ^{131}I, 25:13438
HULL, Patricia Groves, Odd poles in pion--kaon dispersion relations, 25:14696
HULTGREN, Ake, Process for recovering plutonium and uranium from reactor fuel elements irradiated at various degrees, 25:13101
HULTH, P. O., System for on-line control of bubble chamber measurements, 25:13282 (CERN-70-21(Vol.2), pp 825-30)
HUMPHREYS, Roberta M., Streaming motions in Carina--Centaurus region, 25:13928
HUNGERBUEHLER, V., High resolution wire spark chamber, 25:13301
HUNT, C. E. L., Continuous cooling transformation behaviour of zirconium--niobium--oxygen alloys, 25:13679
HUNT, G. J., Neutron detector with a flat energy response for use in time-of-flight experiments, 25:13215
HURAULT, J. P., Fluctuations of the order parameter in small superconducting samples, 25:14167
HUSAK, Vaclav, Review of commercial static systems of cameras used in nuclear medicine, 25:13222
HUTCHEON, I., Extralunar dust in Apollo cores, 25:13958
HUTCHINS, B. A., Implications of nuclear data uncertainties to reactor design, 25:15345
HUTTERER, Ferenc, Diagnostic application of metabolic studies with isotopes, 25:13506
HYLAND, G. J., Semiconductor reversible metal phase transitions, 25:14470
HYMER, W. C., Characteristics of nuclear RNA polymerase from rat anterior pituitary tissue, 25:15439 (NYO-3827-18)
HYMMEN, Ursula, Comparison of high-energy radiation applied through plaster casts, 25:13539
Megavolt therapy of malignant neoplasms of the stomach, 25:13532

I

IAFRATE, Gerald J., High-order perturbation theory for a one-electron ion immersed in a plasma, 25:14283 (AD-710950)
IBRAGIMOV, Sh. Sh., Electron-microscopic examination of Ni irradiated with α particles, 25:13728
ICHIKAWA, Haruko, Base-change mutagenesis and prophage induction in strains of Escherichia coli with different DNA repair capacities, 25:13421
ICHIKAWA, Ryushi, Fallout ^{90}Sr in beer, 25:13434
IGARASI, S., Analysis of neutron inelastic scattering by ^{238}U, 25:15135
Fast-neutron capture cross-sections of Cr, Fe, Ni, and Mo, 25:14970
IGNAT, Margareta, Some intrinsic motions important in magnetohydrodynamics. I, 25:14093
Some intrinsic motions important in magnetohydrodynamics. II, 25:14094
IGNAT'EV, K. G., Measurement of alpha values for ^{235}U and ^{239}Pu, 25:15074
IGNATYUK, A. V., Density of excited states of atomic nuclei, 25:15208
IIDA, Hiromasa, Nuclear calculation method of the JMTR core, 25:15391 (JAERI-Memo-4180)
IKEBUCHI, Hideharu, Chemical and hygienic studies on natural radioactive spa. III, 25:13470
IKEDA, Akitsu, Rotation, surface vibration, and pairing vibration of nuclei, 25:15189
IKEDA, Seiichi, Effect of Zr addition on the oxidation resistance and mechanical properties of Fe--Al--Cr alloys, 25:13680
IL'IN, N. P., Physicochemical model for element separation during mantle differentiation, 25:13115
IL'INOV, A. S., Systematization of the inelastic interactions of high-energy pions and nucleons with atomic nuclei, 25:15148 (ORNL-tr-2399)
IMAHASHI, Tsuyoshi, Determination of Sc, Cr, Fe, Co, Zn, and Sb in deposits and airborne particulate by neutron activation analysis, 25:12975
INFELD, E., Two-stream instability for arbitrary stream temperatures and densities, 25:14340
INKIN, V. D., Development of track chamber picture processing systems at JINR, 25:13279 (CERN-70-21(Vol.2), pp 753-60)
INOKUCHI, Hiroo, Catalytic activity of aromatic nitrile and alkali metal ion radical salt. I, 25:13001
INOKUTI, Mitio, Total cross sections for inelastic scattering of charged particles by atoms and molecules. V, 25:14022
INOZEMTSEVA, O. I., Cosmic-ray anisotropy in the periods

XUM

following proton outbursts, 25:14075
INTEMANN, Gerald W., Current algebra, vector dominance, and decay K/sub L/^{0} $\to$ $\pi^+\pi^-\pi^0\gamma$, 25:14640
IOFA, B. Z., Kinetics of Sb(III and V) extraction, 25:12999
IOFFE, A. I., Acoustic flow in a superfluid liquid, 25:14130
IOFFE, B. L., Divergences of the amplitudes of weak nonleptonic processes involving photon emission, 25:14655
IORI, I., Fission of ^{210}Po, 25:15010
IPOHORSKI, M., Vacancy tetrahedra in copper due to electron irradiation in the high-voltage microscope, 25:13731
IRIE, Koichi, Generation of high-intensity beams of nanosecond pulse duration by electron linacs, 25:14858
ISAENKO, V. I., X radiation effects on animals, 25:13574
ISAKOV, V. I., Centrifugal terms in residual interaction of particles in nucleus, 25:15168
ISHIKAWA, M., Effects of ultraviolet light and x rays on aqueous solutions of poly-L-glutamic acid, 25:13054
ISHIKAWA, Yoshiko, Causality and Lorentz invariance in relativistic quantum mechanics, 25:14508
ISHKHANOV, B. S., Reactions ^{32}S(γ,pγ') and ^{32}S(γ,nγ'), 25:14946
ISLAMOV, B. I., Reaction (^{3}He,α) on nuclei with 1d--2s shell, 25:14944
ISMAIL, H., Sputtering yield and secondary emission for metallic targets bombarded with Hg$^+$ ions, 25:13971
ISOUM, M., Lack of photoreactivation in human cells grown in vitro, 25:13377
ISRAEL, Harvey I., Photon cross sections from 1 keV to 100 MeV for elements Z = 1 to Z = 100, 25:14409
ISSERSTEDT, J., Optical spiral tracers and galactic structure, 25:13920
ISTOMIN, I. N., Collisionless heat wave, 25:14317
ISTOMINA, A. G., Problem of relative biological efficacy of tritium oxide, 25:13551
ITAGAKI, Takehiko, Some properties of tungsten--rhenium alloys, 25:13682
ITIKAWA, Yukikazu, Nonresonant vibrational excitation of CO$_2$ by electron collision, 25:14028
ITO, Albert Shunji, Photoproduction of eta mesons in the forward direction, 25:14522
ITO, Goro, Effect of Zr addition on the oxidation resistance and mechanical properties of Fe--Al--Cr alloys, 25:13680
ITO, Rinsuke, Charge distribution produced by 4- to 24-MeV electrons in elemental materials, 25:13964
ITOH, Noriaki, Vibronic transitions in radicals in irradiated naphthalene single crystals, 25:13047
ITOH, Satoshi, Joule heating in JFT-2, 25:14233 (JAERI-Memo-4186)
ITZYKSON, C., Polarization phenomena in vacuum nonlinear electrodynamics, 25:14793
IVANCHENKO, Yu. M., Josephson coupling energy in the presence of thermal fluctuations, 25:14184
IVANOV, A. A., Collisionless heat wave, 25:14317
  Low-frequency instability of an electron-cyclotron wave in a plasma, 25:14343
IVANOV, N. R., Isotopic non-isomorphism of Rb(H/sub 1-x/D/sub x/)$_3$(SeO$_3$)$_2$ crystals, 25:12989
IVANOV, S. I., Excitation functions for first negative system N$_2^+$ on excitation of N by fast electrons, 25:13998
IVANOV, V. I., Measurement of total cross sections of π^---p interaction, 25:14561 (JINR-P1-5460)
IVANOV, V. N., Lithium-6 incorporation into tissues, organs, and transplantable tumors, 25:13350
IVANOVSKAYA, I. A., Effective mass spectra of the $\gamma\gamma$, $\pi^0\gamma$, $\pi^0\gamma\gamma$, $\pi^0\pi^0$, π^0eta^0, $\pi^0\pi^0\gamma$, $\pi^0\pi^0\pi^0$ systems in mass value region M (γ........γ) less than or equal to 1.3 GeV, 25:14560 (JINR-E1-5349)
IVANOVSKII, L. E., Niobium precipitation on liquid zinc cathode, 25:13642
IWO, Kazuhiro, Base-change mutagenesis and prophage induction in strains of Escherichia coli with different DNA repair capacities, 25:13421
IZMEST'EV, A. A., Propagation of electromagnetic waves in Riemann space, 25:14499
IZQUIERDO, Miguel, Corrections to observed beta-ray atmospheric densitometer values as caused by cosmic rays, 25:13314

J

JAARSMA, R. J., Geometry routines for use in the TIMOC code, 25:15404 (EUR-4536)
JABLONSKI, Z., Effective mass spectra of the $\gamma\gamma$, $\pi^0\gamma$, $\pi^0\gamma\gamma$, $\pi^0\pi^0$, π^0eta^0, $\pi^0\pi^0\gamma$, $\pi^0\pi^0\pi^0$ systems in mass value region M (γ........γ) less than or equal to 1.3 GeV, 25:14560 (JINR-E1-5349)
JACKSON, Jane C., Regge-pole-cut analysis of total cross sections with SU(3) and exchange degeneracy, 25:14660
JACKSON, R. F., 14.2 and 14.5 MeV levels of ^{18}O, 25:14915
JACKSON, William A., Prog. rpt. on nitrate and ammonium uptake and assimilation, summary, 5/68--4/71, 25:15447 (ORO-2410-19)
  Prog. rpt. on nitrate and ammonium uptake and assimilation, annual, 5/70--4/71, 25:15446 (ORO-2410-18)
JACOBS, D., Lucy, a CRT film measuring device, 25:13259 (CERN-70-21(Vol.1), pp 427-65)
  Realizing of z focusing in cylindrical electrostatic analyzers, 25:13325
JACQUINOT, J., Growth rates of electrostatic waves in medium with or without cold plasma, 25:14384
JACQUOT, B., Desensitivity of a microwave cavity to measurements of hot-electron density, 25:14262
JACQUOT, C., Desensitivity of a microwave cavity to measurements of hot-electron density, 25:14262
JAFAR, J. D., Deuteron stripping at 1.69 GeV/c. I, 25:14906
JAHN, Robert G., Acceleration patterns in quasi-steady MPD arcs, 25:14281
JAIN, Mahavir, Reactions (p,pα) and (α,2α) in ^{6}Li and ^{7}Li at 60 MeV, 25:14902
JAMES, G. D., Cross-sections of the heavy nuclei in the resonance region, 25:15069
JAMES, P. B., Coupling-constant analyticity in the charged-scalar static model, 25:14791
JAMESON, Wayne R., Results of 33,911 x-ray protection surveys of facilities with medical or dental diagnostic x-ray equipment, fiscal years 1961--1968, 25:13464
JAMPSIN, B., Use of ^{238}Pu radiation sources in cardiac pacemakers, 25:13178
JANCSO, G., Determination of precise isotopic vapor pressure differences from -20 to 110°C, 25:12995
JANEV, R. K., Influence of short-range atomic forces on molecular term splitting in (A,A) system, 25:14018
JANNEY, Clinton D., Uptake studies in canine abdominal organs following ^{75}Se-selenomethionine administration by a variety of intravascular injection techniques, 25:13343
JANOCKO, M. A., Characteristics of NbN Dayem bridges, 25:14201
  Very high critical current and field characteristics of niobium nitride thin films, 25:14193
JANOUCH, F., Full experiment in weak semileptonic hyperon decays, 25:14651
JARAMILLO, Ramios Rios, V--A theory for nucleon resonances, 25:14648
JARLSKOG, Cecilia, Lepton-charge violating coupling constants in muon decay, 25:14653
JAROSCH, J. F., Mock-up of remotely operated high-purity inert-atmosphere sodium analysis facility, 25:13195 (WHAN-SA-91)
JASNOW, David, Decay of order in isotropic systems of restricted dimensionality. I, 25:14492
  Decay of order in isotropic systems of restricted dimensionality. II, 25:14493
JAUHO, P., Separation of coherent and incoherent cross sections in inelastic neutron scattering using polarized nuclear targets, 25:14869
JAYARAMAN, S., Computer method for calculating multi-field and rotational dose distributions in ^{60}Co teletherapy, 25:13449
JECH, C., Channeling patterns based on penetration of low-energy ions, 25:14417
JECH, J. J., Interference of medically administered ^{57}Co with transuranic element in vivo lung measurements, 25:13458
JEHLE, Herbert, Relationship of flux quantization to charge quantization and the electromagnetic coupling constant, 25:14618
JEKI, L., Fission neutron spectrum from 0.01 to 1.0 MeV, 25:15108
JENKINS, D. A., Muonic interactions in ^{64}Zn and ^{66}Zn, 25:14958
JESENAK, V., Radio-release determination of pH using radioactive kryptonate, 25:12955
JESTER, William A., Pulsed-neutron activation analysis system for short-lived radioisotopes, 25:12960
JOFFRIN, J., Ultrasonic attenuation of transverse waves in dirty superconductors, 25:14160
JOHANNES, E., On-line silver analyzer for non-destructive determination of silver surface density on current film strip, 25:13311
JOHANNSEN, K., Two-dimensional conduction heat transfer in liquid--metal bonded fast reactor fuel element with pellet and canning eccentricity, 25:13155
JOHANSSON, G., Potentiometric titration of fluoride with La and Th in unbuffered media, 25:12929
JOHNS, M. W., Decays of /sup 159m/Ho and /sup 161m/Ho, 25:15060
JOHNSON, A. D., 2400-MeV 5π mass enhancement in 6-prong π^-p events at 12 GeV/c, 25:14562 (TID-25640)
JOHNSON, Charles E., Electron mass shift in ^{133}Cs, 25:14514
JOHNSON, H. D., Whole body ^{40}K loss as a predictor of heat tolerance in cattle, 25:13339
JOHNSON, John L., Numerical model for toroidal plasma containment with flow, 25:14236
JOHNSON, Raleigh F., Significance of the total-body hematocrit in measurements of blood compartments, 25:13338
JOHNSON, Richard S., Emission spectrometric determination of trace elements in biological fluids, 25:12946
JOHNSON, Wayne R., Explosive welding plugs into heat exchanger tubes, 25:13647
JOHNSTON, Gerald S., Hot hepatic hemangioma, 25:13510
JOHNSTON, T. W., Applicability of single Born scattering theory, 25:14363

JOHRI, K. N., Trace metal analysis by combined thin-layer chromatography incorporating fluorescent support and ring oven colorimetry, 25:12944
JOLLES, Benjamin, Studies of influence of wavelength on biological effects, 25:13583
JONES, B. B., Grazing incidence spectra of the Sun, 25:13875
JONES, B. F., Membership in open cluster NGC 7062, 25:13801
JONES, C. K., Alternating-current loss measurements in thin-film type II superconductors, 25:14189
Characteristics of NbN Dayem bridges, 25:14201
Very high critical current and field characteristics of niobium nitride thin films, 25:14193
JONES, Dixon Douglas, Semi-analytic Monte Carlo method: extensions in linear transport theory, 25:14871
JONES, Eric Manning, Pulsational characteristics of low-mass Cepheid model, 25:13823
JONES, J. G., Radiation Shielding Information Center program setup instructions manual, 25:14395 (CTC-INF-1017)
JONES, Mark M., Prog. rpt. on some aspects of the behavior of complex compounds, final, 7/1/70, 25:15461 (TID-25641)
JONES, R. A., Mass motion in the solar chromosphere, 25:13877
JONES, Robert K., Serum organic acids in sheep exposed to neutron--gamma irradiation, air blast, or both, 25:13384
JONES, W. B., Positive pion reactions with ^{12}C, 25:15184
JONKE, A. A., Chemical Engineering Division fuel cycle technology quarterly report, July--September 1970, 25:13077 (ANL-7755)
JONKIERE, Nicole, Influence of thermionic emission on measurements of electrical properties of refractory materials at high temperatures, 25:14455
JORGE, H. Machado, Westcott formalism, 25:15405 (LFEN-NI.-45-a)
JOSEPH, C., Interference and rescattering effects in reactions with three particles in the final state, 25:14891 (ORO-1316-97)
JOSHI, A., Prog. rpt. on study of grain boundary segregation, 12/2/70, 25:15428 (COO-1778-6)
JOSHIMA, Hisamasa, Whole-body activation autoradiography, 25:13590
JOST, Heidemarie, Sequential scintigrams of kidney with ^{131}I- o-iodo-hippuric acid and /sup 113m/In-EDTA, 25:13499
JOVANCVICH, J. V., Measurement of proton--proton bremsstrahlung cross sections at 42 MeV, 25:14556
JOZEFCWICZ, Edward T., Basic static parameters for WWR-SM lattices with water channels, 25:15394
JUDD, B. R., Noncompact group for radial eigenfunctions, 25:14056
JUENGST, K. P., Measurements on pulsed superconducting magnets, 25:14211 (KFK-1217)
JUN, C. K., Thermal conductivity and total emittance of W from 1800 to 2800°K, 25:13663
JUNG, H. H., Measurements of neutron-resonance total cross-sections for fission product isotopes, 25:15098
JURKIEWICZ, J., Kinematical singularities of the three-body decay helicity amplitudes, 25:14592

K

KAAE, J. L., Structure and mechanical properties of isotropic pyrolytic carbons deposited below 1600°C, 25:13757
KABACHENKO, A. P., Identification and study of radioactive properties of Bi isotopes using electromagnetic mass-separator on heavy ion beam, 25:15023
KABAKCHI, A. M., Effect of kind and energy of irradiation on radiolysis of polypropylene, 25:13055
KABIR, P. K., Muon flux deep underground and the question of strong W-interactions, 25:14735
Superweak interactions and TCP invariance, 25:14761
KABIR, Syed M. Humayun, Effects of gamma radiation on egg and larval stages of rice weevil, 25:13558
KACHKOVA, V. G., Hygienic assessment of chicken meat irradiated with pasteurizing doses of γ-rays, 25:13624
KADLEC, J., Flow induced rod vibrations of fast reactor subassemblies, 25:15370
KADMENSKII, S. G., Stripping reactions with two transferred nucleons and polarizability of t,^{3}He, 25:15192
KAELLSTROEM, Krister, Texture and anisotropy of zirconium related to plastic deformation, 25:13655 (NP-18625)
KAEPPELER, F., Measurement of fission cross-section of ^{241}Pu relative to ^{235}U, 25:15107
KAERCHER, K. H., Irradiation of large surfaces with high-energy beams, 25:13538
Irradiation planning for megavolt therapy of lymph nodes, 25:13535
New radiotherapeutic aspects in the treatment of tumors in long bones, 25:13537
KAISER, Edward William Jr., Dipole moment and hyperfine parameters of $H^{35}Cl$ and $D^{35}Cl$, 25:12988
KAKKAR, L. R., Separation of Re from Mo, V, W, and other elements by tribenzylamine--chloroform extraction, 25:12921
KAKU, Michio, Divergence of the two-loop planar graph in the dual-resonance model, 25:14666
KALADZE, T. D., Propagation of a charged particle through weak nonlinear plasma, 25:14313
KALASHNIKOV, N. P., Theory of backscattering of fast electrons from a condensed medium. I, 25:13961
KALECHITS, V. E., Stripping reactions with two transferred nucleons and polarizability of t,^{3}He, 25:15192
KALER, J. B., Distances and distribution of planetary nebulae, 25:13827
KALININ, Yu. G., Current-interchange instability in turbulent heating of a plasma by a current, 25:14344
KALISH, R., Decay of /sup 141m/Nd, 25:15014
KALMYKOV, A. N., Thermal conductivity of 29NK-type alloy at temperatures between 80 and 239°K, 25:13685
KALVIUS, G. M., Hyperfine magnetic fields in USb, 25:14483
KAMAL, A. A., Azimuthal symmetry in 17.2-GeV/c π^- jets, 25:14565
KAMAL, A. N., Muon flux deep underground and the question of strong W-interactions, 25:14735
KAMAL, T. H., Whole body ^{40}K loss as a predictor of heat tolerance in cattle, 25:13339
KAMETANI, Katsuaki, Chemical and hygienic studies on natural radioactive spa. III, 25:13470
KAMINER, S. N., Cosmic-ray meteorological effects, 25:14066
KAMITSUBO, H., Inelastic scattering of polarized protons by ^{40}Ca at 24.5 MeV, 25:14923 (CEA-CONF-1656)
j-mixing determination in (p,d) reactions by asymmetry measurements, 25:14921 (CEA-CONF-1653)
Study of (p,d) reactions on ^{48}Ca and ^{49}Ti with polarized protons, 25:14922 (CEA-CCNF-1655)
Study of (p,d) reactions on ^{90}Zr and ^{92}Mo with polarized protons, 25:14980 (CEA-CCNF-1654)
KAMPER, R. A., Noise thermometry with the Josephson effect, 25:14198
KAMYSHEVA, L. N., Dielectric properties of a γ-irradiated KDP crystal, 25:14432
KANAPILLY, G. M., New method for the generation of aerosols of insoluble particles, 25:13145
KANAREK, T., Effective mass spectra of the $\gamma\gamma$, $\pi^0\gamma$, $\pi^0\gamma\gamma$, $\pi^0\pi^0$, π^0eta^0, $\pi^0\pi^0\gamma$, $\pi^0\pi^0\pi^0$ systems in mass value region M (γ.......γ) less than or equal to 1.3 GeV, 25:14560 (JINR-E1-5349)
KANE, G. L., Dual, crossing-symmetric amplitude with Mandelstam analyticity, 25:14821
KANE, R. P., Nature of the daily variation of geomagnetic field, 25:14111
KANG, Kyungsik, Consistency of hard pion thecrems in K/sub 13/ decays, 25:14633 (NYC-2262-TA-233)
KANITZ, Peter J. F., Permeaticn of gases through modified polymer films. II, 25:13039
KANOFSKY, A., Proton--proton differential cross sections from 600 to 1800 MeV/c, 25:14543
KAO, Hsiao-wen, Particle spectrum in nuclear matter calculations, 25:15187
KAPITONOV, I. M., Reactions $^{32}S(\gamma,p\gamma')$ and $^{32}S(\gamma,n\gamma')$, 25:14946
KAPLAN, M. A., Investigation of vitamin B_{12}--^{58}Co radiometric method of whole body after resection of stomach, 25:13334
KAPOOR, S. S., K x-ray yields from ^{236}U fragments, 25:15027
KAPSHUKOV, I. I., Activation energy of first stage of annealing of irradiated $^{238}PuO_2$, 25:13784
KAPUSCIK, E., Localizable and nonlocalizable field theories, 25:14806
KARASAWA, Takashi, Charge exchange of carbon and nitrogen ions in nitrogen gas, 25:14001
KARFUNKEL, U., Lifetimes and gamma transiticns in ^{19}O, 25:14905
KARGUTH, K., Definition of toxic thyroid adencmas, 25:13594
KARL, Brigitte, Telecobalt irradiation cf acrtic lymph nodes, 25:13534
KARNAUKHOV, V. A., Anomalies in the Z dependence of mean charges of heavy ions in helium and air, 25:14007
KARNEEV, A. N., Thermal magnetic effect and thermal emf of Gd at 90 to 250°K, 25:14458
KARPMAN, M. G., Molybdenum treatment for increasing stability of steel No. Kh18N9T in liquid Li, 25:13634
KARRAKER, D. G., Recovery of reactor-produced ^{231}Pa, 25:13100
KARTHA, Mukund, Liver scans after primary treatment of tumors in children, 25:13578
KARZHAVIN, Yu. A., Development of track chamber picture processing systems at JINR, 25:13279 (CERN-70-21(Vol.2), pp 753-60)
KASENTER, Albert G., Uptake studies in canine abdominal organs following ^{75}Se-selenomethionine administration by a variety of intravascular injection techniques, 25:13343
KASHIMA, Masatoshi, Whole-body activation autoradiography, 25:13590
KASHIWABARA, H., Molecular motion of peroxy radicals of polytetrafluoroethylene, 25:13034
KASSAL, T. T., Energy transfer between N_2 and electronically excited inert gas atcms and ions, 25:14012
KATAL'NIKOV, S. G., Isotope exchange reactions in different BF_3-complex systems, 25:12992
KATARIA, S. K., K x-ray yields from ^{236}U fragments, 25:15027

KATAYAMA, Toshikazu, Magnetic properties of Y/sub 1-x/Sm/sub x/Co$_5$ compounds, 25:14461
KATO, Kiyoshi, Bibliography on wastes of plutonium, 25:13190 (JAERI-Memo-4153)
KATO, S., Polarization parameter in backward π^+p elastic scattering at 1.60, 1.80, 2.11, and 2.31 GeV/c, 25:14577
KATO, Takesi, Base-change mutagenesis and prophage induction in strains of Escherichia coli with different DNA repair capacities, 25:13421
  Genetic and molecular characteristics of x-ray-sensitive mutants of Escherichia coli defective in repair synthesis, 25:13428
KATO, Y., Existence conditions of hydromagnetic shocks in Vlasov plasma, 25:14326
KATZ, F., Parameter adjustment by the gradient method on the hybrid analog computer, 25:15406 (NP-18646)
KATZ, Robert, Unified track theory, 25:13209 (COO-1671-28)
KAUFHCLD, R., Brush system for automatic processing of bubble chamber pictures, 25:13274 (CERN-70-21(Vol.2), pp 689-707)
KAUFMAN, A. J., Caesium plasma diodes seeded with Hg or Cd and the Penning effect, 25:14085
KAUFMAN, Allan N., Darwin model as a tool for electromagnetic plasma simulation, 25:14293
  Resonant interactions between particles and normal modes in a cylindrical plasma, 25:14362
KAUFMANN, Frank P., Problem of zero-bias anomalies in the tunneling spectroscopy of superconductors, 25:14206
KAUFMANN, Horst, Experimental tests about time factor effects, 25:13474
KAW, Predhiman K., Ponderomotive force on laser-produced plasmas, 25:14332
KAWAGUCHI, Toranosuke, Effect of high-temperature heating on magnetic properties of (Ce--MM)--Cu--Co ternary alloys, 25:14464
KAWAI, Y., Ion heating caused by ion-acoustic waves in an ion-streaming plasma, 25:14240
KAWASAKI, Koji, Contact angles of gold and silver on a clean tungsten substrate, 25:13691
KAWASAKI, Sunao, Diffusion of multipole magnetic fields through a conductive wall of a plasma container, 25:14352 (IPPJ-T-3)
KAZAKOV, A. E., Electron heating in interaction between ultra-short intense laser pulses and matter, 25:14279
KAZEEV, Yu. I., Inelastic scattering of slow electrons in germanium and silicon, 25:13967
KAZES, E., Interference model for resonances suggested by the Veneziano amplitude, 25:14692
KEEFER, Douglas H., Natural environmental radioactivity in south Florida sands and soils, February--June 1968, 25:13107
KEIGHTLEY, W. O., Response of earth dams to seismic disturbances. II, 25:13130 (UCRL-13329(Pt.2))
KELBER, Charles N., A bootstrap concept of a safety test facility, 25:15380
KELBG, G., Equation of state and ionization equilibrium hydrogen plasmas, 25:14319
KELK, J. E., Ion current to a plane probe in a flowing plasma, 25:14249
  Measurement of ion density in a plasma torch using a plane probe, 25:14250
KELLER, D. L., Mechanisms of swelling and gas release in uranium dioxide, 25:13785
KELLER, H. L., Geometrical arrangement of radiogold preparations in tumor implants, 25:13526
KELLER, J., Angular dependence of critical magnetic fields in superconducting films, 25:14163
KELLER, K. A., Half-life for neutron deficient actinide isotopes, 25:15162
KELLER, N., De-excitation γ-rays in ^{15}N and ^{15}O, 25:14896
KELLETER, H., Isolated lymphogranulomas of the stomach, 25:13541
KELLOFF, Gary, Inactivation of murine sarcoma and leukemia viruses by ultra-violet irradiation, 25:13609
KELLY, M. D., Metallographic analysis of SNAP--15C heat source capsule, 25:13164 (MLM-1670)
  Metallographic analysis of SNAP-19B (IRHS) capsule, 25:13163 (MLM-1652)
KELMERS, A. D., Prog. rpt. on biological macromolecular separations technology project, 10--12/70, 25:15442 (CRNL-TM-3280)
KENDALL, Burton Nathaniel, Decay modes of the eta meson, 25:14580
KENDRUP, I., Simplified mobile equipment for ^{133}Xe-radiospirometry, 25:13514
KENYON, D. B., Nuclear g factors of 2+ levels in ^{194}Pt, 25:15034
KEPERT, D. L., Eight-coordinate complexes of niobium, tantalum, and uranium tetrahalides, 25:12979
KEPPEL, E., BERTA: a FORTRAN program for automatic recognition and reconstruction of bubble chamber events. I, 25:13243 (CERN-70-21(Vol.1), pp 125-39)
  BERTA: a FORTRAN program for automatic recognition and reconstruction of bubble chamber events. II, 25:13244 (CERN-70-21(Vol.1), pp 141-75)
  Heidelberg automatic event recognition, 25:13241 (CERN-70-21(Vol.1), pp 105-11)
KERBRAT-LUNC, Helene, Nonstationary Yang--Mills field associated with the SO(3) group, 25:14779
KERIMOV, B. K., Bremsstrahlung in scattering of neutrinos by electrons taking into account radiative corrections, 25:14600
KERN, R. C., Evaluation of iscchek and invent fuel inventory calculational models, 25:15211
KESSER, G. M., Prog. rpt. on sodium technology, 7--9/70, 25:13651 (ANL/ST-4)
KESSLER, J., Spin polarization and differential cross sections in inelastic electron--atom collisions, 25:14039
KESZTHELYI, L., Nuclear g factors of 2+ levels in ^{194}Pt, 25:15034
KETTERSON, J. B., Inversion of de Haas--van Alphen data. I, 25:14433 (ANL-7659)
KHADR, F. H., Variation and covariation of seed weight and its components in wheat following irradiation, 25:13419
KHAIKOVICH, I. M., Fast-neutron thermalization time in silicate ores of varying moisture content, 25:13109
KHAMIDOV, D. Kh., Results of histochemical studies of glycogen and liver cells ultrastructure of irradiated rats, 25:13378
KHARITONOV, N. P., Testing of organosilicate press-material in reactor, 25:13330
KHARITONOV, Yu. I., Centrifugal terms in residual interaction of particles in nucleus, 25:15168
KHARITONOVA, V. N., Fine structure of terms for a sequence of states of light atoms, 25:14051
KHAZINS, D. M., Search for new type of radioactivity in aluminum and tungsten targets irradiated by 70-GeV protons, 25:14541 (JINR-P1-5399)
KHEIFETS, M. I., Problem of atomization of liquid by high-velocity gas stream, 25:15418 (ANL-Trans-871)
KHLEBOSTROEV, V. G., Stripping reactions with two transferred nucleons and polarizability of t,^{3}He, 25:15192
KHNYCHEV, S. S., Influence of exogenic serotonin on the aggregation of blood platelets and some blood coagulation indices in experimental acute radiation sickness, 25:13549
KHODYACHIKH, A. F., Investigation of reaction ^{4}He(γ,p)^{3}H at maximal γ-quanta energy 120 MeV, 25:14886
KHOKHLOV, Yu. A., Average number of prompt neutrons in fast-neutron-induced fission of ^{235}U, ^{239}Pu, and ^{240}Pu, 25:15115
KHORASANOV, G. L., Resonance phenomena in an alkali plasma located in a variable electric field, 25:14368
KHOURY, A. T., Gamma-ray-induced spore germination of Dictyostelium discoideum, 25:13605
KHRUSTALEV, O. A., Solution on the unitarity relation for scattering amplitude of particles with spin, 25:14590
KHURI, N. N., Bjorken limit and Jin--Martin lower bound, 25:14827
KHVOSTOVA, V. P., Methods for the analysis of natural materials containing ruthenium and osmium, 25:12939
KIANG, D., Pole dominance calculation of πK scattering lengths, 25:14687
KIBARSKA, T., Combined action of ethyleneimine and x rays on Aspergillus oryzae, 25:13381
KICHIGIN, G. N., Plasma expansion in vacuum and the flow of a collisionless plasma stream around a plate, 25:14265
KIDO, Yasumasa, Chemical and hygienic studies on natural radioactive spa. III, 25:13470
KIEFHABER, E., Evaluation of fast critical experiments using recent methods and data, 25:15387 (EURFNR-858)
KIELANOWSKI, P., Quark-model predictions for the measurable generalized statistical tensors, 25:14670
KIKINDAI, Tivadar, Recovery of fissile materials, 25:12090
KIKUCHI, Akira, Linac dynamic booster project and its application to medicine and biology, 25:13548
KILGORE, R. S., University of Virginia superconducting wind-tunnel balance, 25:14216
KIM, John Jungyu, Second-order shifts in frequency and amplitude in E X B instability, 25:14338
KIM, Ung, Photospallation of medium-heavy elements with bremsstrahlung of maximum energies between 0.8 and 2.1 GeV, 25:14977
KIM, Yong-ki, Total cross sections for inelastic scattering of charged particles by atoms and molecules. V, 25:14022
KING, J., Search for magnetic monopoles in cosmic rays, 25:14078
KING, J. D., States of ^{114}In, 25:15008
KINNEY, Ragon D., Study of the effect of the evaporative erosion on thermoelectric elements on the performance of thermoelectric generators, 25:14084 (SC-RR-70-804)
KINOSHITA, Toichiro, Vacuum-polarization contributions to the sixth-order anomalous magnetic moment of the muon and electron, 25:14616
KIRCHHOFF, R. H., Cylindrical Langmuir-probe response in transition regime, 25:14242 (AD-711095)
KIREEV, G. I., Kinetics of Sb(III and V) extraction, 25:12999
KIRICHENKO, V. V., Investigation of reaction ^{4}He(γ,p)^{3}H at maximal γ-quanta energy 120 MeV, 25:14886
KIRII, A. Yu., Theory of parametric resonance of plasma in a strong hf electric field, 25:14376
KIROUAC, G. J., Multilevel resonance analysis of total neutron cross-section of ^{23}Na and Ca below 1 MeV, 25:14969
  New total neutron cross-section measurement of U between 0.5 to 4.35 MeV, 25:15104
  Spin and parity of ^{41}Ca levels, 25:14939

KIRPICHNIKOVA, L. F., Isotopic non-isomorphism of Rb(H/sub 1-x/D/sub x/)$_3$(SeO$_3$)$_2$ crystals, 25:12989
KIRSCH, Karl A., Significance of the total-body hematocrit in measurements of blood compartments, 25:13338
KIRST, H., Data processing for bubble chambers from the point of view of a small laboratory, 25:13272 (CERN-70-21(Vol.2), pp 665-73)
KIRYUSHKINA, A. A., Mapping of uvr gene of S. typhimurium, 25:13408
KISH, P. P., Complex formation and extraction of bromotellurate, 25:12935
KISIELEWSKA, D., Decay distributions in reaction $\pi^+p \to K^+Y^{*+}(1385)$ and polarization of Λ hyperon from $Y^{*+}(1385)$ decay at 8 GeV/c primary momentum, 25:14559 (INP-731)
KITADA, Masahiro, Applied magnetic field vs critical current density characteristics of superconducting Nb--60 Ti--5 Zr alloy sheets, 25:14209
  Effects of V, Mo, or Ta additions on superconducting properties of Nb--40 Zr--10 Ti alloy, 25:14208
KITAMURA, T., Energy spectrum of a nova-like x-ray source, 25:13849
KITCHING, J. E., Level structures of ^{85} ^{87}Sr from (d,p) reactions, 25:14955
KITTEL, W., Many-body cross sections, 25:14594
KLAMANN, H., Laser beams as fiducial lines in bubble chambers, 25:13303
KLARFELD, Joseph, On quantization of interacting covariant massless fields with prescribed asymptotic null data, 25:14796
KLEIN, A., Phenomenological analysis of quasirotational spectra, 25:15153
KLEIN, Abraham, Ground state correlations as variational parameters in the nuclear many-body problem, 25:15147 (NYO-2171-333)
KLEIN, F., ARNULF: PDP-10 program for rapid acquisition of complete film information by a PEPR-device, 25:13242 (CERN-70-21(Vol.1), pp 113-24)
  BERTA: a FORTRAN program for automatic recognition and reconstruction of bubble chamber events. II, 25:13244 (CERN-70-21(Vol.1), pp 141-75)
  BERTA: a FORTRAN program for automatic recognition and reconstruction of bubble chamber events. I, 25:13243 (CERN-70-21(Vol.1), pp 125-39)
  CARL: a FORTRAN program for PEPR calibration using Chebyshev polynomials, 25:13245 (CERN-70-21(Vol.1), pp 177-86)
  Heidelberg automatic event recognition, 25:13241 (CERN-70-21(Vol.1), pp 105-11)
  Present status of the Heidelberg-PEPR-Hardware and production system, 25:13246 (CERN-70-21(Vol.1), pp 187-96)
KLEIN, George, Increase in antibody titer against the EBV-associated membrane antigen complex in Burkitt's lymphoma and nasopharyngeal carcinoma after local irradiation, 25:13391
KLEIN, Hans, Magnetic coil cooled by a liquid for a particle accelerator, 25:14857
KLEIN, Oskar, Arguments concerning relativity and ccsmology, 25:13950
KLEINFELD, A. M., Reorientation measurements in ^{116}Sn and ^{124}Sn, 25:15041
KLEMT, V., M1 transition probabilities of single-particle states in the lead region, 25:15197
KLEVANS, E. H., Interaction of electromagnetic wave with hct plasma half-space, 25:14361
  Plasma stability in bounded systems, 25:14339
KLIMENTOVSKAYA, M. V., Determination of g factors of second excited states $^{11}/_2{}^-$ of ^{147}Eu and ^{149}Eu by differential angular correlation method in external magnetic field, 25:15016
KLIMKCVA, O. A., Radiation-accelerated diffusion of gold in silicon, 25:14420
KLINK, R., Placentography: comparative investigations in nuclear medicine, 25:13517
KLOSINSKI, J., Determination of the $X^0(960)$ meson spin--parity in the polarization experiment, 25:14720
KLUEBER, O., Limiting the radial expansion of arc current by an axial magnetic field. I, 25:14267
KLUGE, Gy., Fission neutron spectrum from 0.01 to 1.0 MeV, 25:15108
KLUYVER, J. C., Measurement of the lifetimes of the Σ^{+-}-hyperons, 25:14546
KNACKE, Roger Fritz, Studies of interstellar extinction at infrared wavelengths, 25:13934
KNAPP, B., Princeton automatic track reader, 25:13250 (CERN-70-21(Vol.1), pp 273-83)
KNEUBUEHL, Fritz K., Symmetry and microwave spectra of pclyatomic paramagnetic centers, 25:15456 (SC-T-71-3005)
KNIGHT, J. D., Mass symmetry in the spontaneous fission of ^{257}Fm, 25:15045
KNITTER, H.-H., Neutron elastic scattering from carbon in the energy region of 0.50 to 2.00 MeV, 25:14911
  Plutonium-239 angular distributions in energy range 0.2 tc 5.5 MeV, 25:15134
KNOBELOCH, G. W., Neutron-induced ^{235}U fission at individual resonances. III, 25:14999
KO, Roy, Determination of rare earths in plutonium--uranium mixed oxides, 25:12922 (WHAN-SA-44)
  Use of amine extraction and emission spectrcgraphy in the analysis of plutonium, 25:12923 (WHAN-SA-47)
KOBAYASHI, M., Prototype of drift tube quadrupole magnets, 25:14849 (SJC-A-70-6)
KOBEZSKII, V. M., Automating a 2-GeV electron linac, 25:14852 (SLAC-Trans-126)
KOBYLINSKII, N. A., Photoproduction of pseudoscalar mesons on protons, 25:14629
KOCH, C. C., Superconductivity in Mo--Re and Nb--Ir sigma phases, 25:14177
KOCH, H., Complex formation between Tc and chelate-forming ligands. II, 25:13008
KOCH, H. R., Energy levels of ^{56}Mn, 25:14974
KOCH, W., Some practical results of ferrous-sulfate (Fricke) dosimetry, 25:13305
KOCH, Wolfgang, Preparation of perfluorinated carboxylic acids, 25:13035
KOCMIERSKA-GRODZKA, D., Protec1ysis of partially denatured albumin in isolated perfused intestine of normal and irradiated rats, 25:13349
KOCSIS, E., Reaction between methyl iodide and alkaline iodide, 25:12996
KODA, Sigeyasu, Internal oxidation of nickel alloys containing small amounts of chromium, 25:15455 (SC-T-71-3004)
KODOSKY, G., Metastability of the 2s state of mucnic hydrogen, 25:13991
KOESTER, John Kent, Studies of thermionically emitting electrodes in contact with plasmas, 25:14088
KOGA, Toyoki, Difficulty and possibility of kinetic theory of quantum-mechanical systems. III and IV, 25:14490 (AD-711681)
KOGAN, A. V., Heat capacity of gadolinium--lutetium alloys at superlow temperatures, 25:14450
KOGAN, E., Reactions $\gamma n \to p\pi^+\pi^-\pi^-$, $p\pi^+\pi^-\pi^-\pi^0$ and $n\pi^+\pi^+\pi^-\pi^-$ at 4.3 GeV, 25:14521
KOGAN, I. A., Influence of insulin on the sympatho-adrenal system of persons working with radiation sources, 25:13586
KOGAN, V. I., Stark broadening of H lines in plasma, 25:14310
KOHL, Fred J., Mass-spectrometric determination of the dissociation energy of ScC$_2$ and ScC$_4$, 25:13761
KOHNO, Isao, Charge exchange of carbon and nitrcgen ions in nitrogen gas, 25:14001
KOKADO, Masayuki, Thick-target yields of characteristic x rays by p, d, ^{3}He$^+$, and ^{4}He$^+$ bombardments, 25:13962
KOKH, I., System for processing meson-telescope data, 25:14067
KOLAR, W., Neutron widths of ^{238}U from 60 eV to 5.7 keV, 25:15080
  Total neutron cross-section of ^{233}U from 0.7 to 320 eV, 25:15079
KOLASKA, H., Recent results of cemented carbide research and problems encountered, 25:13752
KOLESOV, B. M., Fast-neutron thermalization time in silicate ores of varying moisture content, 25:13105
KOLESOV, I. V., Apparatus for investigation of α-active nuclei: the products of reactions with heavy ions, 25:14841 (JINR-P13-5353)
KOLIBALOVA, Anna, Changes in DNP histones after irradiation, 25:13385
KOLLMAN, V. H., Production of Candida utilis with 93 at. percent ^{13}C acetic acid as the sole carbon source, 25:13331 (LA-4551)
KOLLMEDER, L., Digitized microscope for evaluation of photo emulsions in high-energy physics, 25:13284 (CERN-70-21(Vol.2), pp 851-7)
KOLOKOL'TSOV, N. A., Designing multicomponent isotope separation cascades, 25:13179
KOLOSOV, N. P., Analysis of neutron energy dependence of anti ν, on basis of energy balance in nuclear fission, 25:15117
KOLOSOV, V. I., Automating a 2-GeV electron linac, 25:14852 (SLAC-Trans-126)
KOMAKI, Senichiro, Effect of Tathion on excretion of ^{203}Hg--MHP in kidney, 25:13341
KOMAROV, V. S., Concentration of uraniur by living and dead peat-forming plants, 25:13116
KONDO, Sohei, Base-change mutagenesis and prophage induction in strains of Escherichia coli with different DNA repair capacities, 25:13421
  Genetic and molecular characteristics of x-ray-sensitive mutants of Escherichia coli defective in repair synthesis, 25:13428
KONDORSKII, E. I., Thermal magnetic effect and thermal emf of Gd at 90 to 250°K, 25:14458
KONOTOP, Yu. F., Peculiarities of uranium deformation for tension at constant velocity, 25:13688
KONSTANTINOV, B. P., Study of gamma radiation with Kosmos-135, 25:13951
KOO, Ping L., Arithmetic unit of ILLIAC III: simulation and logical design. II, 25:15430 (COO-2118-2)
KOPALEISHVILI, T. I., Absorption of π mesons and α-cluster structure of light nuclei, 25:14893
  Ground and excited states of ^{4}He nucleus, 25:14884
KOPECKY, Karl R., Mechanism of initiaticn in the thermal polymerization of styrene, 25:12983
KOPECKY, V., Influence of the transformation of waves on the threshold currents of the beam instability, 25:14371
KOPPE, V. T., Excitation functions for first negative system N$_2{}^+$ on excitation of N by fast electrons,

25:13998
KOPSCH, D., New total neutron cross-section measurement of U between 0.5 to 4.35 MeV, 25:15104
KOR, S. K., Volume viscosity and structure of D_2O using ultrasonics, 25:12990
KORBEL, Kazimierz, Radioisotope measurements of the flow parameters of the postflotation slurry, 25:13176
KORENKOV, I. P., Radiational safety in the use of radioisotopic methods in engineering industry, 25:13467
KORNELSEN, E. V., Entrapment of He ions at (100) and (110) W surfaces, 25:14419
KORNIENKO, L. A., Impact strength and fracture structure of beryllium, 25:13684
KOROLEV, A. A., Diffusion of cesium in mono- and polycrystalline molybdenum, 25:13676
KOSHAEVA, K. K., Threshold detectors used for the neutron spectrum measurement, 25:13210 (JINR-P3-5421)
KOSLOWSKI, Leo, Investigations about combination injuries, 25:13368
KOSTA, L., Adsorption of V on oxides and its application to analytical separations, 25:12959
KOSTRCUN, V. O., L subshells in Hg from the decay of ^{198}Au and ^{204}Tl, 25:15015
KOTELNIKOVA, G. V., Inelastic scattering of fast neutrons by Cr, Ni, Y, Zr, and W nuclei, 25:14967
KOTOV, V. A., Simultaneous measurements of polar magnetic fields at Crimea and Mount Wilson, 25:13873
KOURA, Katsuhisa, Mott--Smith solution of Fokker--Planck equation, 25:14295
KOURI, Donald J., Noniterative solutions of integral equations for scattering. V, 25:14017
KOVACH, J. Louis, Filter system design, installation and testing for radioactive contaminant removal, 25:13192 (NACAR-10012)
KOVAL, A. G., Excitation functions for first negative system N_2^+ on excitation of N by fast electrons, 25:13998
KOVBA, L. M., Phase diagram of the uranium--oxygen system, 25:13777
KOWALSKI, A., Bibliography on fast breeding reactors, 1966--69, 25:15340 (NEIC-RR-41)
KOZLOV, F. N., Niobium precipitation on liquid zinc cathode, 25:13642
KOZLOV, G. I., Continuous absorption of partially ionized xenon in the visible region of the spectrum, 25:14280
KOZMA, Gy., Fission neutron spectrum from 0.01 to 1.0 MeV, 25:15108
KOZORCVITSKII, L. L., Collisionless heat wave, 25:14317
KOZYCZKOWSKI, J., Lifetimes of excited states in ^{101}Rh, 25:14992
KRAEFT, W. D., Quantum statistical second virial coefficient for real gases and plasmas, 25:14322
KRAEGELOH, U., Intermediate state of type-II superconductors, 25:14164
KRAETZIG, E., Angular dependence of critical magnetic fields in superconducting films, 25:14163
KRAFFT, G., Measurements on pulsed superconducting magnets, 25:14211 (KFK-1217)
KRAITCR, S. N., Threshold detectors used for the neutron spectrum measurement, 25:13210 (JINR-P3-5421)
KRAMER, Paul J., Faddeev equations for atomic problems. IV, 25:14010
KRAPF, Rudolf, Overheating protection device for thermionic elements heated by nuclear energy, 25:13173
KRASNA, Alvin I., Prog. rpt. on effect of chemical modification of DNA on its macromolecular structure, 5/70--1/71, 25:15432 (CU-3957-9)
KRASNIKOV, V. D., Automating a 2-GeV electron linac, 25:14852 (SLAC-Trans-126)
KRASNCVSKY, S., Effective mass spectra of the $\gamma\gamma$, $\pi^0\gamma$, $\pi^0\gamma\gamma$, $\pi^0\pi^0$, π^0eta^0, $\pi^0\pi^0\gamma$, $\pi^0\pi^0\pi^0$ systems in mass value region M (γ.......γ) less than or equal to 1.3 GeV, 25:14560 (JINR-E1-5349)
KRASZNOVSZKY, S., Spin test for a fermion (J > 1/2) decaying into a spin-1/2 fermion, 25:14701 (KFKI-70-27-HEP)
  Spin test for fermion (J > $^1/_2$) decaying, 25:14725
KRAUSS, Jeffrey Allan, Spin-dependent three-particle scattering, 25:14740
KRAVTSOV, A. V., Partial-wave analysis of reaction $\pi N \to \pi\pi N$ in the 330 to 480 MeV energy region, 25:14728
KRAVTSOV, Yu. A., Dielectric permeability tensor of smoothly inhomogeneous electron plasma, 25:14291
KREBS, J., Method of shape analysis of cross-sections of fissile nuclei, 25:15132
KREINICK, David Louis, High energy photoproduction of neutral mesons, 25:14524
KREITSBERG, Z. N., Effect of ionizing radiation on the contents of ortho-oxyphenol in poplar shoots, 25:13598
KREJS, F. R., Ground state correlations as variational parameters in the nuclear many-body problem, 25:15147 (NYO-2171-333)
KREMENEVA, S. G., Complex formation and extraction of bromotellurate, 25:12935
KREMP, D., Quantum statistical second virial coefficient for real gases and plasmas, 25:14322
KRESLCV, V. S., Change in composition of rat blood as affected by ^{237}Np, 25:13346
KRETT, V., Rod models of fuel elements of nuclear reactors, 25:15410 (ZJE-92)
KRETZSCHMANN, G., Nitrogen-15 program of the Inst. of Stable Isotopes, 25:13172
KRIEG, Rolf, Influence of dimensional inaccuracies on the stress calculation of piping systems, 25:13182
KRISCH, Robert E., Comparison of lethal effects of ^{32}P and ^{33}P decay in E. coli and in bacteriophages, 25:13612
KRISCHER, W., Calibration, precision, and filtering questions for the CERN Spiral Reader, 25:13235 (CERN-70-21(Vol.1), pp 5-18)
  Lucy, a CRT film measuring device, 25:13259 (CERN-70-21(Vol.1), pp 427-65)
  Status of the HPD minimum guidance programs at CERN, 25:13278 (CERN-70-21(Vol.2), pp 737-52)
KRISHNAMURTHY, G. T., Ureteral kinking and hydronephrosis in a transplanted kidney mimicking the rejection phenomenon, 25:13490
KRISHNAMURTHY, M. V., ESR study of irradiated single crystal of p-toluidinium chloride, 25:13051
KRISHNAN, C. S., Electrical conductivity in cubic Y_2O_3--ZrO_2 solid solutions, 25:14476
KRISHNASWAMY, M. R., Multiple muon events observed underground, 25:14060
KRISTAPSON, Ya. Zh., Temperature dependence of radiation colloid production in KCl crystals, 25:14429
KRISYUK, E. M., Cesium-137 from global fallout in foodstuffs and human organism, 25:13340 (NP-18382)
KRITSKAYA, V. K., Anomalous behavior of carbon atoms at low temperatures in martensite irradiated by electrons, 25:13729
  Radiation aging of chromium, 25:13730
KRIVOKONEVA, G. K., Phase transformations of brannerite during heating, 25:13128
KRONAST, B., Electron-drift velocities from ion and electron features of light scattering in z-pinch plasma, 25:14256
KROPP, D., BERTA: a FORTRAN program for automatic recognition and reconstruction of bubble chamber events. I, 25:13243 (CERN-70-21(Vol.1), pp 125-39)
  BERTA: a FORTRAN program for automatic recognition and reconstruction of bubble chamber events. II, 25:13244 (CERN-70-21(Vol.1), pp 141-75)
  Heidelberg automatic event recognition, 25:13241 (CERN-70-21(Vol.1), pp 105-11)
KROSHKIN, N. I., Measurement of energy spectra and average number anti ν of prompt neutrons produced in fission of actinide elements, 25:15118
KROTIKOV, V. A., Testing of organosilicate press-material in reactor, 25:13330
KRUPITSKAYA, T. M., Production of electrons in lower ionosphere by solar cosmic rays, 25:14124
KRYMSKII, G. F., Cosmic-ray variations and the interplanetary medium, 25:14070
KRZUK, Jerzy, Radioisotope measurements of the flow parameters of the postflotation slurry, 25:13176
KSCHWENDT, H., Geometry routines for use in the TIMOC code, 25:15404 (EUR-4536)
KUCHOWICZ, B., General-relativistic fluid spheres. III, 25:14814
KUDRYAVTSEV, A. P., Heat transfer during developed boiling of alkali metals, 25:13157
KUDRYAVTSEV, E. M., Electron excitation of transitions between excited states in Ba^+ and Sr^+ ions, 25:14000
KUEMMEL, Reiner, Electronic structure of the intermediate state in Type-I superconductors, 25:14169
KUGUSHEV, A. I., Dielectric permeability tensor of smoothly inhomogeneous electron plasma, 25:14291
KUHRY, J. G., Chemical behavior of hot atoms of ^{14}C and ^{13}N in several solid inorganic compounds. I, 25:13070
  Chemical behavior of hot atoms of ^{14}C and ^{13}N in several solid inorganic compounds. II, 25:13072
KUJAWSKI, E., Projection of angular momentum and the generator coordinate method for light nuclei, 25:15196
KUKIEL, E., Fission of natural uranium in neoplastic and normal tissue, 25:13361
KUKOC, A. H., States of ^{114}In, 25:15008
KUKULA, F., Use of diethyl dithiocarbamates for activation analysis with substoichiometric silver separation, 25:12963
KULIKOV, A. V., Search for new type of radioactivity in aluminum and tungsten targets irradiated by 70-GeV protons, 25:14541 (JINR-P1-5399)
KULISIC, P., Emission of alpha particles in reactions induced by medium-energy nucleons, 25:15173
KULKARNI, A. G., Compressibility studies in mixed aqueous electrolytes, 25:13015
KULSRUD, Russell M., Rotational deceleration of magnetized stars, 25:13800
KUMAR, Cidambi Krishna, Isotopic abundance of Mg in Sun, 25:13904
KUMBARTZKI, G. J., Photospallation of medium-heavy elements with bremsstrahlung of maximum energies between 0.8 and 2.1 GeV, 25:14977
KUMMER, J., Energy dependence of electron collision frequency on electrical conductivity of weakly ionized plasmas, 25:14308
KUMTA, U. S., Chemical and physical changes in irradiated and frozen Bombay duck, 25:13618
  Radiation pasteurization of fresh and blanched tropical shrimps, 25:13619
KUNINA, E. M., Problem of atomization of liquid by high-velocity gas stream, 25:15418 (ANL-Trans-871)
KUNSZT, Z., Resonant scattering of light by light,

25:14596 (JINR-E2-5424)
KUNZLER, J. E., Unusual strain dependence of T/sub c/ and related effects for high-temperature superconductors, 25:14183
KUO, T. Y. T., 40-MeV proton inelastic scattering on ^{50}Ti, ^{51}V, and ^{52}Cr and its microscopic description, 25:14928
KUPCZYNSKI, M., Quark model predictions for the transversity amplitudes, 25:14671
KUPIC, Edward A., Uptake studies in canine abdominal organs following ^{75}Se-selenomethionine administration by a variety of intravascular injection techniques, 25:13343
KUPRINA, V. V., Phase diagram for Zr--Co system, 25:13712
KUPTSCV, A. V., Search for new type of radioactivity in aluminum and tungsten targets irradiated by 70-GeV protons, 25:14541 (JINR-P1-5399)
KURDGELAIDZE, D. F., Mass spectrum of particles in nonlinear quark theory, 25:14684
KURNAEV, V. A., Angular distribution of secondary electrons emitted by Nb due to bombardment with ions, 25:13969
KURODA, P. K., New ^{110}Rh isotope, 25:15001
KUROV, M. A., Measurements of radiative-capture-to-fission cross sections (α) for ^{235}U and ^{239}Pu, 25:15075
KUTSCHERA, W., Lifetimes of 4.623 and 4.688 MeV levels in ^{34}S, 25:14954
KUTSIDI, N. K., Statistical isospin model and cross sections of reactions $\pi^- p \to N + (2,\ldots,6)\pi$ within 1 to 16 GeV energy range, 25:14700 (JINR-P1-5471)
KUTTIG, Helmut, Comparison of high-energy radiation applied through plaster casts, 25:13539
  Pendulum radiation with transversal shift of axis during ^{60}Co-teletherapy. III, 25:13447
  Postoperative radiotherapy of mammary carcinoma without irradiation of the thorax wall, 25:13533
  Radiotherapy of malignant bone tumors, 25:13521
  Studies of most efficient energies for irradiation of bone processes, 25:13536
KUYATT, C. E., Inelastic electron scattering from N_2O between 5.0 and 20.0 eV energy loss, 25:14014
KUZMINA, M. G., Milne problem for polarized radiation scattered according to Rayleigh's law, 25:14408
KUZNETSOV, E. I., Dependence of transport coefficients on plasma parameters in Tokamak, 25:14239
KUZNETSOV, V. A., Integral data for ^{235}U in intermediate neutron spectrum, 25:15399
KUZNETSOVA, A. P., Radiation aging of chromium, 25:13730
KVITEK, J., (n,α) reaction on Sm and Nd isotopes, 25:14994
KWAN, Ch. K., Photospallation of medium-heavy elements with bremsstrahlung of maximum energies between 0.8 and 2.1 GeV, 25:14977

L

LABAT, M., Neutron cross-sections of ^{235}U, ^{238}U, and ^{239}Pu between 0.1 and 6 MeV, 25:15103
LABAUVE, R. J., Calculations of Jezebel and Godiva with recent ENDF/B microscopic data, 25:15397
LABNO, Leszek, Temperature measurements of cladding of WWR-SM type fuel elements in EWA-10 reactor core, 25:15395
LABZOVSKII, L. N., Lamb level shift of inner electrons in heavy atoms, 25:14048
LACHAINE, A., Doppler-shift lifetimes in ^{30}P, 25:14933
LACHETEAU, Herve, Protective shell for the transport of lead casks, 25:13196
LACHMANN, Ute, Postoperative radiotherapy of mammary carcinoma without irradiation of the thorax wall, 25:13533
LACINA, J., Application of similarity rules to controlled fusion, 25:14354
  Similarity rules in plasma physics, 25:14318
LADENBAUER-BELLIS, I.-M., New Ta isotopes ^{170}Ta and ^{171}Ta, 25:15066
LADOV, Edwin Neil, Oxygen isotope effect in radiolysis of crystalline KNO_3, 25:13043
LAFOREST, J., Magnetic properties and structures of CrB compounds Tb--$Ge_{0.2}Si_{0.8}$, HoSi, ErSi, and TmSi, 25:14434 (CEA-CONF-1701)
LA GRUTTA, G., Action of ionizing radiations on CNS, 25:13561
LAI, C. K., Ground-state energy of mixture of fermions and bosons, 25:14501
LAI, C. S., Pole dominance calculation of πK scattering lengths, 25:14687
LAMB, A. N., Jervis Bay Nuclear Power Station project investigations at site J.S1-Scottish Rocks, 25:15336 (NP-18636)
LAMBERT, P. G., On-line measuring system using visual displays for operator guidance, 25:13237 (CERN-70-21(Vol.1), pp 39-46)
LAMOS, Jean, Production of continuous high-power plasma flow, 25:14273
LAMPSCN, Miles Landrum, Space-charge-limited electron currents in sodium chloride, 25:14449
LANDAU, Rubin H., Models for meson--deuteron scattering in the resonant region, 25:14738
LANDOLT, R. R., Activation analysis of counterfeit and genuine Japanese postage stamps, 25:12973
LANDOWNE, S., Coupled-channel Born-approximation calculation of two-nucleon transfer reactions in deformed nuclei, 25:15191
LANE, E. A., Radiopharmaceuticals in nuclear medicine, 25:13519
LANG, A. H., Roles of the Geological Survey of Canada in former U programs, 25:13127
LANG, Kenneth R., Pulse broadening due to angular scattering in the interstellar medium, 25:13853
LANG, W., Method of thermal shock analysis, 25:13183
LANGDON, T. G., Creep mechanisms in stoichiometric uranium dioxide, 25:13759
LANGE, D., Infrared thermography with a color scanner used in nuclear medicine, 25:13498
LANGE, Dieter, Simultaneous double-isotope scintigraphy with an Anger camera, 25:13500
LANGE, G., Independent yields of /sup 124g/Sb, /sup 126g/Sb, and ^{160}Tb in neutron fission of ^{235}U, 25:15038
LANGELIER, R., Detection of bone metastases by an isotopic method, 25:13513
LANGHAM, J., Production of Candida utilis with 93 at. percent ^{13}C acetic acid as the sole carbon source, 25:13331 (LA-4551)
LANGHAMMER, H., Bloodpool scintigraphy with shortlived radionuclides, 25:13516
LANGHOFF, H., Coulomb fragmentation following decay of ^{131}I, 25:13073
LANORE, Jeanne-Marie, Program Poker. Description and utilization, 25:14864 (CEA-N-1388)
LANZI, Giuseppe, Analysis of EPR spectra of oxidizing catalysts, 25:14482
LAPIDES, Jack, Treatment of delayed intractable hemorrhagic cystitis following radiation or chemotherapy, 25:13592
LAPPENBUSH, William L., Radiation response of rough-skinned newt Taricha granulosa, 25:13477
LAQUER, H. L., Superconducting quadrupole doublet for LAMPF, 25:14860
LARBALESTIER, D. C., Magnetisation studies of some cryogenic alloys, 25:14172
LARSON, R. E., Determination of Sr in sea water by photon activation analysis, 25:12974
LARSSON, Alf, Process for recovering plutonium and uranium from reactor fuel elements irradiated at various degrees, 25:13101
LARSSON, Curt, Scandium-45 level scheme, 25:14941
LARSSON, Mats, Helium-3-crysotat for specific heat measurements, 25:14212 (UUIP-677)
LASHUK, A. I., Inelastic neutron scattering-(n,n'γ)-by F, Fe, Co, Ni, and Ta nuclei, 25:14960
LASKEN, R. A., He II--He I transition in the presence of a heat current, 25:14136
LASKER, Barry M., High-frequency stellar oscillations. VI, 25:13808
LASLEY, Eric Loren, Meson--meson scattering in the Veneziano model, 25:14695
LASSALLE, J-C., Pattern recognition methods for Omega and SFM spark chamber experiments, 25:13283 (CERN-70-21(Vol.2), pp 831-50)
LASTOVICKA, J., X-ray control of the ionospheric absorption of hf radio waves, 25:13897
LATHROP, K. D., TWOTRAN SPHERE: FORTRAN program to solve multigroup transport equation in two-dimensional spherical geometry, 25:14866 (LA-4567)
LAUER, R. S., Carminic acid as a reagent for the photometric determination of the rare earth elements, 25:12937
LAURENS, Georges, Simplified method of obtaining information from bubble chamber photographs, 25:13233 (CEA-N-1397)
LAUTERBORN, D., Stars with central He burning and occurrence of loops in H--R diagram, 25:13815
LAUTRUP, B. E., Sixth-order radiative corrections to α/sub μ/--α/sub e/, 25:14620
LAVRENTOVICH, Ya. I., Effect of kind and energy of irradiation on radiolysis of polypropylene, 25:13055
LAVRUKHINA, A. K., Time and space variations of cosmic rays in the solar system, 25:14071
LAWSON, A. C., Superconductivity of the fcc transition metals, and of their alloys, and fcc carbides, 25:14148
LAWSON, R. D., Spectra and the effects of correlations in A = 6 nuclei, 25:15186
LAZAREV, A. V., Effect of Doppler broadening on line shape of spontaneous radiation, 25:14050
LAZORENKO, G. E., Accumulation of ^{90}Sr and ^{144}Ce from sea water by alginic acid, 25:13403
LAZUTIN, E. V., Reactions $^{32}S(\gamma,p\gamma')$ and $^{32}S(\gamma,n\gamma')$, 25:14946
LEAKE, J. W., Method for using standard burst cartridge precipitator equipment for fuel activity release monitoring on a Mk. III high temperature gas cooled reactor, 25:15373 (AERE-R-6475)
LEBEDEV, N. A., Determination of g factors of second excited states $^{11}/_2{}^-$ of ^{147}Eu and ^{149}Eu by differential angular correlation method in external magnetic field, 25:15016
LEBEDEV, R. A., Nuclear gamma-resonance study of products of β-decay of /sup 121m/Sn, 25:13074
LEBEDEV, S. V., Specific heat and the heat of fusion of W at high temperatures, 25:13664
LEBEDEV, S. Ya., Angular distribution of sputtered material in ion bombardment, 25:13966
LEBOWITZ, E., Production of ^{52}Fe for medical use, 25:13063

XUM

LEBRUN, J. P., Adler condition in a dual relativistic quark model, 25:14685

LECOCQ, P., Test facility for sodium-heated steam generators, 25:13143

LE COQ, G., Method of shape analysis of cross-sections of fissile nuclei, 25:15132

LEE, C., Concerning a thought experiment violating Heisenberg's uncertainty principle, 25:14502

LEE, C. K., Photoproduction of ω mesons from hydrogen and deuterium, 25:14512

LEE, E. P., Resistive plasma rotation and shock formation in toroidal geometry, 25:14235

LEE, Hong, Evaluation of systems of fire development, 25:13134 (AD-713418)

LEE, Huan, Internal symmetry bootstrapped from Veneziano representation, 25:14754

LEE, Kai Fong, Electromagnetic instability in counterstreaming plasmas, 25:14342

LEE, Patrick A., Theory of Josephson radiation. I, 25:14168

LEE, Sabrina V. J. Lin, Decay schemes of ^{131}Ba and ^{192}Ir nuclei, 25:15062

LEER, E., Low-latitude whistlers generated by same lightning discharge, 25:14114

LEFORT, M., Measurement of the prompt neutrons emitted in the fission of ^{209}Bi and ^{238}U induced by 155-MeV protons, 25:15021

LEGGETT, Robert D., Plutonium fuels for LMFBR: an extrapolation, 25:15367 (WHAN-SA-51)

LE GOFF, P., Measurement of local enthalpy in an HF plasma, 25:14263

LEGUEY, A., Use of a simple geometry program for filtering HPD data, 25:13273 (CERN-70-21(Vol.2), pp 679-85)

LEHERISSEY, E. S., Electron-impact excitation of rare gas atoms in the distorted-wave approximation, 25:14015

LEIBACHER, J., New description of the solar five-minute oscillation, 25:13901

LEIGH, B., Induction by x-rays of isochromosomes in germ cells of Drosophila melanogaster males, 25:13409

LEITH, J. T., Intracerebral temperature changes after x irradiation in the rabbit, 25:13575

LEJEUNE, A., Coupled channel calculations with complex eigenvalues, 25:15181

LELEU, C., Argon plasma generator with electron density within the range 5 x 10^{14} to 5 x 10^{17} cm^{-3}, 25:14335

LELOUP, C., Growth rates of electrostatic waves in medium with or without cold plasma, 25:14384

LEMBARES, Nicholas, Use of lithium-drifted germanium detectors for clinical radionuclide scanning, 25:13487

LE MIGNANT, A., Sn--/sup 113m/In tracers in scintigraphies, 25:13501

LENCHEK, Allen M., Theory of inverse Compton scattering in cold plasma, 25:13941

LENCHENKO, V. M., Electrification of substances by gamma radiation, 25:14430

LENHART, K., Genetic basis of virulence in dermatophytes, 25:13427

LENTZSCH, B., Influence of dimensions of gas fluidized beds on gas mixing, 25:13140 (BMBW-FBK-70-26)

LENY, J. C., ORGEL project 1959-1969, 25:15342

LENZ, D., Temperature dependence of dislocation attenuation in γ-irradiated Pb, 25:14459

LEON, J., Radiative decays of mesons in a quark loop model, 25:14686

LEON, M., Metastability of the 2s state of muonic hydrogen, 25:13991

LEONARD, B. P., Magnetic structure of oblique and normal ionizing shock waves, 25:14284 (AD-711086)

LEONG, C. L., Spectrophotometric determination of molybdenum with gallein and cetyltrimethylammonium bromide, 25:12930

LEPRINCE, Philippe, Discharge maintained by a direct current and high frequency waves, 25:14266

LERCH, R. E., Application of aqueous technology to LMFBR separations processes. Program plan for Task T-2: fuel dissolution characteristics, 25:13083 (WHAN-FR-33)

LEROY, J. L., Fission cross-section for ^{235}U and ^{239}Pu between 0.025 and 1 MeV, 25:15068
  Measurements of fast neutron fluxes in the range of 10 keV to 1 MeV, 25:13216

LEROY, Jean-Louis, Monochromatic photography of coronal emissions, 25:13887

LERUSTE, Ph., Breit--Wigner models and effective range approximations, 25:14702 (PAM-70-8)

LES, Z., Isotope shifts between even isotopes ^{64} ^{66} ^{68} ^{70}Zn in visible Zn II lines, 25:14927

LESJAK, J., Projection of angular momentum and the generator coordinate method for light nuclei, 25:15196

LESNIAK, H., Elastic scattering of high-energy hadrons from deformed ^{12}C nucleus, 25:14918

LESNIAK, L., Elastic scattering of high-energy hadrons from deformed ^{12}C nucleus, 25:14918

LESSMANN, G. G., Varestraint test for refractory metals, 25:13695

LESTER, Donald H., Constant voltage controller and transition monitor for superconducting magnets, 25:14221

LETESSIER, Jocelyne, Search for classes in magnetic quadrupole gamma transitions, 25:14983 (NP-18492)

LETFUS, V., Variations in lower ionosphere associated with cosmic-ray and geomagnetic variations, 25:14127

LETHUILLIER, Philippe, Magnetic susceptibility of intermetallic compounds of Sn--Sm system, 25:14453

LETOV, V. N., Lithium-6 incorporation into tissues, organs, and transplantable tumors, 25:13350

LETTAU, H., Study of states in ^{16}O, 25:14914

LEUNG, Cho Yuk, Positron diffusion and annihilation in helium gas, 25:13987

LEUTZ, H., Laser beams as fiducial lines in bubble chambers, 25:13303

LEVCHENKO, I. S., Optical properties and electron characteristics of niobium--tin alloys, 25:14149

LEVELUT, A., Ultrasonic attenuation of transverse waves in dirty superconductors, 25:14160

LEVENES, Guy, Measurement of film thickness by electron backscattering, 25:13141

LEVESQUE, Dominique, Fluid--solid phase transition of hard-sphere Bose system, 25:14500

LEVIN, E. M., Zero charge and scale invariance problems in the soluble field theory model, 25:14783

LEVIN, G., Gamma-ray-induced spore germination of Dictyostelium discoideum, 25:13605

LEVINSTEIN, H. J., Unusual strain dependence of T/sub c/ and related effects for high-temperature superconductors, 25:14183

LEVITZ, N. M., Chemical Engineering Division fuel cycle technology quarterly report, July--September 1970, 25:13077 (ANL-7755)

LEVSTEK, M., Adsorption of V on oxides and its application to analytical separations, 25:12959

LEVY, C. K., Intracerebral temperature changes after x irradiation in the rabbit, 25:13575

LEWIS, David Kenneth, Kinetics of isotope exchange reactions $D_2 + CH_4 + HD + CH_3D$, $D_2 + H_2S + HD + HDS$ and $HD + HD + H_2 + D_2$, 25:12987

LEWIS, V. E., Elastic scattering and polarization of 49.5-MeV protons on ^{148}Sm, 25:15013

LEWITOWICZ, J., Cerium-135m and /sup 137m/Nd: isomeric states in N = 77 isotones, 25:15042

LEWTHWAITE, G. W., Acceleration of climb-controlled creep by neutron irradiation, 25:13725

L'HERITEAU, J. P., Method of shape analysis of cross-sections of fissile nuclei, 25:15132

LI, Ling-Fong, Asymptotic behavior of weak spectral functions and hadronic decays of W boson, 25:14634 (NYO-4204-7)

LIBBY, D. R., Spectroscopic study of ion--neutral coupling in plasma acceleration, 25:14306

LICCIARDELLO, J. J., Recovery of salmonellae from irradiated and unirradiated foods, 25:13620

LICHTEN, William, Quantum mechanics of a double perturbation, 25:13981

LICHTENBERG, D. B., Duality and comparison of resonance and Regge models for π^+p backward scattering, 25:14726

LICHTENSTEIN, Carl Arthur, Wide-angle Bremsstrahlung: angular dependence, 25:14529

LIEBERMAN, D. S., Phase transformations in near equiatomic Ta--Ru alloys, 25:13708

LILJA, B., Detectors in studies of regional lung function by ^{133}Xe radiospirometry, 25:13520
  Simplified mobile equipment for ^{133}Xe-radiospirometry, 25:13514

LILJA, I. A., Effect of nonlocality of nucleon--nucleon potential on the two-body sum rules, 25:14732 (NP-18648)
  Limits of validity of Siegert's theorem in the nuclear photo-absorption, 25:15144 (NP-18618)

LIMPERT, J. C., Prog. rpt. on plant instrumentation, 6/30/70, 25:13230 (WCAP-7562-1)

LIN, D. N., Current-interchange instability in turbulent heating of a plasma by a current, 25:14344

LIN, R. P., Emission and propagation of approximately 40-keV solar-flare electrons, 25:13894

LIN, S. H., Solution of the time-dependent Schroedinger equation by the Laplace transform method, 25:14496

LIN, Sing-hsiung, Dipole radiation in compressible plasma, 25:14275

LIN, Tz-Hong, Chemical interactions of accelerated carbon-14 ions and atoms with benzene, 25:13038

LINDELL, S.-E., Detectors in studies of regional lung function by ^{133}Xe radiospirometry, 25:13520

LINDENBAUM, S. J., Operational experience with the Brookhaven On-Line Data Facility, 25:13289 (CERN-70-21(Vol.2), pp 921-30)

LINDGREN, Richard Arthur, Light rigid rotor nuclei, 25:14953

LINDL, John D., Ponderomotive force on laser-produced plasmas, 25:14332

LINDNER, Helmut, Radiation burden to the patient during a gastrointestinal passage, 25:13580

LINDQVIST, Torsten, Helium-3-cryostat for specific heat measurements, 25:14212 (UUIP-677)

LINDSTROM, P. J., Auroral-particle precipitation and trapping caused by electrostatic double layers in the ionosphere, 25:14103

LINETSKII, A. R., Nonlinear theory of excitation of plasma wave by electron beam, 25:14311

LINFORD, R. M. F., Alternating field losses in superconducting strip conductors, 25:14187

LINNFORS, A., Indium-111 EC decay, 25:15028

LINNING, David Lees, Improvements to fuel elements, 25:15369

LIOZNER, Alexander L., Tumor-induced skin heterogenization. III. Immunologic and immunogenetic mechanisms, 25:13388
LIPAS, P. O., Quadrupole--octupole vibrations in spherical nuclei, 25:15157
LIPATCV, L. N., Leading singularity in complex angular momentum plane in the quantum electrodynamics, 25:14802
LIPINSKI, Hubert M., Backward πN scattering, 25:14707
LIPPERHEIDE, R., Quasi-free scattering processes, 25:15156
LIPSON, S. G., Induced superconductivity in germanium films, 25:14161
LISITSA, V. S., Stark broadening of H lines in plasma, 25:14310
LISITSYN, V. N., Breakdown of 2^1P and 2^3P levels of He in a glow discharge, 25:13977
LITTENBERG, Laurence Stephen, Test of $\Delta S = \Delta Q$ rule in neutral K-e3 decay, 25:14538
LITTLE, J. B., Factors influencing exogenous nucleoside utilization in DNA synthesis by irradiated human cells, 25:13380
LIU, C. H., Trapping of electromagnetic waves by nonlinear resonant interactions with ion sound waves, 25:14374
LIU, Yu-chien, Dispersion sum rules for fixed-u πN scattering amplitudes, 25:14709
LJUNGQUIST, K. G., Roentgenologic-photometric method for bone mineral determinations, 25:13509
LLOYD, Robert C., Complex formation in Neodymium nitrate--water--di-(2-ethylhexyl) phosphoric acid, 25:13092
LO, Hai Hu., Electron capture and loss in collisions of heavy ions with atomic oxygen below 2 MeV, 25:14042
LOBANCV, Yu. V., Apparatus for investigation of α-active nuclei: the products of reactions with heavy ions, 25:14841 (JINR-P13-5353)
LOBAO, N., Radioactivity in diet in high background areas of Brazil, 25:13439
LOBKOWICZ, F, Photoproduction of ω mesons from hydrogen and deuterium, 25:14512
LOBOV, G. A., Experimental test of renormalization theory of weak interactions in ep scattering processes, 25:14646
LOCHER, J., Radioisotopes in the diagnosis of gastric disease, 25:13495
LOEVHOEIDEN, G., High angular momentum states in ^{155}Gd and ^{157}Gd, 25:15138
LOHBECK, H. U., Radiation injuries following electron therapy for mammary carcinomas, 25:13584
  Results and complications in megavolt therapy of cervix carcinomas, 25:13531
LOKEN, J. G., Automatic scanning and measurement of bubble chamber film on Polly II, 25:13254 (CERN-70-21(Vol.1), pp 325-55)
  Oxford PEPR system, 25:13239 (CERN-70-21(Vol.1), pp 61-88)
LOMINADZE, D. G., Propagation of a charged particle through weak nonlinear plasma, 25:14313
LOMON, Earle L., Nonlinear Regge trajectories, 25:14662
LONG, G., Evacuable glove-box for handling of liquid sodium, and apparatus for analysis of carbon in sodium and other metals, 25:13185 (AERE-R-6338)
LONG, H. M., Design features of ac superconducting cables, 25:14226
LONGINOTTI, L. D., Instabilities of high-temperature superconductors, 25:14174
LOPATKINA, A. P., Concentration of uranium by living and dead peat-forming plants, 25:13116
LOPEZ, W. M., Calculations of cross-sections for the radiative capture of fast neutrons, 25:15122
  Measurements of cross-sections for radiative capture of 1-keV to 1-MeV neutrons by Mo, Rh, Gd, Ta, W, Re, Au, and ^{238}U, 25:15121
LORD, D. H., Conference on data handling systems in high-energy physics, Cavendish Lab., Cambridge, 3/70, 25:13234 (CERN-70-21(Vol.1))
  Conference on data handling systems in high-energy physics, Cavendish Lab., Cambridge, 3/70, 25:13263 (CERN-70-21(Vol.2))
LORENTS, D. C., Charge-transfer excitation produced in collisions of He^+ and N_2^+ with alkali atoms, 25:14011
LORENZINI, Paul Gilbert, Energy models for computing fast-reactor parameters, 25:15407
LOS, J., Total cross section measurements of K on rare gases, 25:14005
LOSER, Robert W., Thermal desorption of atmospheric gases from plutonium dioxide. I, 25:13024
LOTT, Michel, Measurement of the neutron albedo of ordinary concrete, 25:14394 (CEA-N-1382)
LOUNSBURY, M., Measurements of alpha and of fission cross-section ratios for ^{233}U, ^{235}U, and ^{239}Pu at thermal energies, 25:15070
LOUP, J.-P., Influence of thermionic emission on measurements of electrical properties of refractory materials at high temperatures, 25:14455
LOUTIT, J. F., Malignancy from radium, 25:13593
LOVCHIKOVA, G. N., Inelastic scattering of fast neutrons by Cr, Ni, Y, Zr, and W nuclei, 25:14967
LOVE, T. A., The energy spectrum of photoneutrons produced by 140-MeV electrons incident on tantalum, 25:14990
LOVELACE, C., Phase-shift analysis of $\pi^- p \to K^0 \Lambda$, 25:14727
LUBELL, M. S., Comparison of NbTi and Nb_3Sn material tests, 25:14219
LUCA, Constantin, Analytical study of dibromopyrogallolsulfonephthalein (DBPSP), 25:12926
LUCAS, A. A., Multiple plasmon effects in the energy-loss spectra of electrons in thin films, 25:14486
LUCAS, B., Determination of spin of slow-neutron induced resonances in ^{239}Pu, 25:15088
LUCASSON, A., Directional dependence of atomic displacements in cobalt crystals, 25:13733
LUECKE, K., Temperature dependence of dislocation attenuation in γ-irradiated Pb, 25:14459
LUGININ, V. A., Simultaneous determination of uranium(IV) and uranium(VI) by moving boundary method, 25:12938
LUGININA, T. N., Variability of Bac. mesentericus, 25:13416
LUKAC, P., Radio-release determination of pH using radioactive kryptonate, 25:12955
  Solid-solution strengthening at 77°K in Cd single crystals containing Zn, 25:13670
LUKASHEVICH, V. V., Life times of levels of ^{128}Te nucleus, 25:15055
LUKENS, J. E., Versatile superconducting femtovolt amplifier and multimeter, 25:14217
LUNDBERG, L.-E., Bremsstrahlung in coulomb field, 25:14613
LUSIGNAN, B. B., Polarization measurements of solar Type-III radio bursts at 25.3 MHz, 25:13859 (AD-711398)
LUSIGNOLI, M., K anti Kπ final states for N anti N annihilation at rest in the Veneziano language, 25:14691
LUST, L. F., Mock-up of remotely operated high-purity inert-atmosphere sodium analysis facility, 25:13195 (WHAN-SA-91)
LUVISETTO, M. L., HDP--IBM 360/44 system at CNAF for bubble chamber data analysis. I, 25:13267 (CERN-70-21(Vol.2), pp 607-15)
  HPD--IBM 360/44 system at CNAF for bubble chamber data analysis. II, 25:13268 (CERN-70-21(Vol.2), pp 617-24)
LUXTON, Gary, The complex angular momentum theory of the production of three particles in collisions of two strongly interacting particles at high energy, 25:14677
LYARSKII, P. P., Radiational safety in the use of radioisotopic methods in engineering industry, 25:13467
LYASHCHENKO, A. B., Nature of solid solutions in the niobium--oxygen system, 25:14457
LYDIN, L. V., Reduction of sexual aggressiveness of male codling moths treated with tepa or gamma irradiation, 25:13557
LYNN, J. E., Progress in understanding neutron interactions with nuclei, 25:15206
LYON, Donald E. Jr., Angular distributions from multiparticle production models, 25:14661
LYON, Mary F., Dose-response curve for the yield of translocations in mouse spermatogonia after repeated small radiation doses, 25:13404
LYONS, L. R., Magnetospheric reflection of whistlers, 25:14120
LYONS, Peter Bruce, Yield measurements for $^{24}Mg(\alpha,\gamma)^{28}Si$ and $^{27}Al(p,\gamma)^{28}Si$ reactions, 25:14951
LYSIKOV, B. V., Testing of organosilicate press-material in reactor, 25:13330
LYTLE, C. D., Enhancement of viral transformation by ultraviolet light, 25:13552

M

MA, Z. Ming, Evidence for a narrow N*(1470), 25:14552
MACFARLANE, Ronald D., Alpha decay of the ^{221}Th and ^{222}Th decay chains, 25:15011
MACGREGOR, J. P., Jervis Bay Nuclear Power Station project investigations at site J.S1-Scottish Rocks, 25:15236 (NP-18636)
MACHABELI, I. Z., Absorption of π mesons and α-cluster structure of light nuclei, 25:14893
MACHI, Sueo, Mechanical properties of radiation-induced graft copolymers of styrene to polyethylene, 25:13042
MACIAS, E. S., Directional correlations of gamma rays in ^{125}Sb, 25:15137
MACKERT, B., Treating radiation-induced brachial plexus paresis, 25:13480
MACVICAR, Margaret L. A., Tunneling into superconducting rhenium single crystals, 25:14147 (AD-711826)
MADDOCK, A. G., Chemical consequencies of the nuclear reactions in soluble Prussian Blue, 25:13068
MADELAINE, G., Some comments on the production and measurement of spheres of polystyrene latex, 25:13144
MAERTL, H. G., Symmetry conditions on nonlinear spinor field functionals, 25:14782
MAGGIORE, C. J., 40-MeV proton inelastic scattering on ^{50}Ti, ^{51}V, and ^{52}Cr and its microscopic description, 25:14928
MAGNO, P., Liquid waste effluents from a nuclear fuel reprocessing plant, 25:12950 (BRH/NERHL-70-2)
MAGUIRE, W., Princeton automatic track reader, 25:13250 (CERN-70-21(Vol.1), pp 273-83)
MAHANTI, S. D., Self-polarization contribution to magnetic ordering in systems with singlet ground state, 25:14460
MAHE-PAILLERET, Paulette, Chemical and structural investigation of AB_2O_6 compounds of Mo--V--O, U--V--O,

and U--Mo--O systems, 25:13776
MAIER II, W. B., Production of N_2^+ in collisions between N^+ and N_2, 25:14030
MAILLET, Ennemond, Operating a nuclear power plant, 25:15383
MAIN, Robert M., Modification of Berkeley Hilac, 25:14853 (UCRL-19919)
MAINLAND, G. B., Dirac representation of the relativistic symmetries, 25:14752
MAITA, J. P., Unusual strain dependence of T/sub c/ and related effects for high-temperature superconductors, 25:14183
MAJER, J., Rod models of fuel elements of nuclear reactors, 25:15410 (ZJE-92)
MAJEWSKI, C., Fission of natural uranium in neoplastic and normal tissue, 25:13361
MAJKA, R., High resolution optical spark chamber, 25:13302
MAKAROV, A. A., Wigner function for hyperbolic rotations in the homogeneous Lorentz group, 25:14759
MAKHMUDOW, Z. Z., Associated-wave scattering of light and slow neutrons in semiconductor antiferromagnets, 25:14488
MAKHOV, V. I., Adsorption of Ba on a (110) face of Mo single crystal, 25:13701
  Structure and work function of films of gadolinium on molybdenum, 25:13700
  Structure and work function of La films on a (110) Mo single crystal surface, 25:13702
MAKI, K., Fluctuations of the order parameter in small superconducting samples, 25:14167
MAKINO, Isao, Thick-target yields of characteristic x rays by p, d, $^{3}He^+$, and $^{4}He^+$ bombardments, 25:13962
MAKSIMENKO, V. N., Perturbation theory of variation of binding energy of ^{3}H and ^{4}He, 25:14883
MALAKPUR, I., Region of formation of narrow emission lines of Nova Delphini, 25:13820
MALAMENT, Maxwell, Experiences with ^{32}P in advanced carcinoma of the prostate, 25:13591
MALIK, F. B., Properties of ^{55}Mn, ^{56}Mn, and ^{57}Fe in the unified rotational model, 25:14973
MALKOVA, A. I., Studies of zeolite cation influence on γ radiolysis of adsorbed ammonia by the EPR method, 25:13057
MALLIARIS, A. C., Spectroscopic study of ion--neutral coupling in plasma acceleration, 25:14306
MALMENDIER, Joseph William, Structures and properties of La_2O_3--BaO--B_2O_3 glasses, 25:13019
MALMSKOG, Sven G., Energy levels in ^{186}W, 25:15043
MALONEY, Joseph C., Experimental comparison of fallout field simulation techniques, 25:13117 (AD-711532)
MALTBY, P., Solar lithium abundance, 25:13870
MAMIDZHANYAN, E. A., Search for magnetic monopoles in cosmic rays, 25:14078
MANALIS, Melvyn Samuel, Optical spectroscopic investigation of helium and nitrogen plasmas, 25:14277 (AD-712024)
MANDEL, P., Superoperator transformation theory in quantum mechanics, 25:14505
MANDELBROJT, J., Applications of the theory of Dirichlet series to the superposition of an infinite number of Regge poles, 25:14828
MANDELBROJT, S., Applications of the theory of Dirichlet series to the superposition of an infinite number of Regge poles, 25:14828
MANEGOLD, Karlheinz, Radiation protection against neutrons in a betatron beam, 25:13450
MANELIS, R. M., X-ray determination of the expansion coefficients of lanthanum and yttrium borides, 25:13760
MANGENO, J. J., Disposal of radioactive wastes from U. S. naval nuclear-powered ships and their support facilities, 1969, 25:13444
MANN, W. Anthony, CP violation in K(neutral) $\to \pi^+\pi^-\pi^0$, 25:14762
MAPLE, M. B., Superconducting--normal phase boundary of superconductors containing nearly nonmagnetic impurities, 25:14159
MARACCI, G., Measurement of fast reactor type neutron spectra, 25:13226
MARAN, Stephen P., Gum nebula: fossil Stroemgren sphere of the Vela X supernova, 25:13851
MARATHE, S. G., Gamma spectrometric estimation of radionuclides in reactor coolant water, 25:12956
MARCHANDISE, H., Thermal conductivity of uranium dioxide, 25:13749 (EUR-4568)
MARCHENKO, V. A., Compensation effect in a protophilic deuterium-exchange reaction associated with a change in solvation of the catalyst cation, 25:13007
MARELIUS, A., Lifetimes of excited states in ^{101}Rh, 25:14992
MAREZIO, M., X-ray diffraction studies of the metal insulator transitions in Ti_4O_7, V_4O_7, and VO_2, 25:14442
MARGRAVE, Thomas E. Jr., Limb-darkening tables for F0--K0 main-sequence stars, 25:13806
MARINSKY, J. A., Ion-exchange selectivity of the synthetic zeolite Linde A in anhydrous and mixed media, 25:13091
MARK, Kai-keung, Relationship between synthesis of DNA and synthesis of phage lysozyme in E. coli infected by bacteriophage T4, 25:13616
MARKLUND, Kari, Helium-3-crysotat for specific heat measurements, 25:14212 (UUIP-677)
MARKOV, P. A., Thermal magnetic effect and thermal emf of Gd at 90 to 250°K, 25:14458
MARKUS, A. M., Influence of weak deformation of Cu films on channeling of protons, 25:14421
MARLBOROUGH, J. M., Results for Pleione's shell episode, 1938--1954, 25:13794
MARLIN, H., Removable head for pneumatic device, 25:13203
MARLOWE, M. O., Prog. rpt. on fission gas re-solution rates, 7--9/70, 25:13780 (GEAP-12147)
MARPLES, J. A. C., Effect of alloying additions on lattice parameters of α-U, 25:14452
  Structures of UN, UP, US, and USe at cryogenic temperatures, 25:14454
MARQUETTE, J. P., Fission cross-section for ^{235}U and ^{239}Pu between 0.025 and 1 MeV, 25:15068
MARSAULT, Jacques, Improvements in and relating to a transport flask especially for radioactive material, 25:13204
MARTIN, F., Calibration, precision, and filtering questions for the CERN Spiral Reader, 25:13235 (CERN-70-21(Vol.1), pp 5-18)
MARTIN, G. D., Operation of a levitated superconducting ring in a plasma physics experimental device, 25:14356
MARTIN, Margrit, Problems concerning radiological examination of the paranasal sinuses, 25:13507
MARTIN, P. G., Infrared spectra of interstellar grains, 25:13933
MARTINSKA, G., Statistical isospin model and cross sections of reactions $\pi^- p \to N + (2,\ldots,6)\pi$ within 1 to 16 GeV energy range, 25:14700 (JINR-P1-5471)
MARTYNOV, V. A., Anodic dissolution of Mo in chloride--molybdate melts, 25:13631
MARUYAMA, M., Fast-neutron scattering from Al, Si, S, and Zn, 25:14963
  Neutron scattering cross-sections of iron, 25:14961
  Width-fluctuation and resonance-interference effects in neutron scattering cross-sections of Al, Cu, and Zn, 25:14962
MASCHUW, R., Neutron--neutron scattering length, 25:14887
MASEK, K., Low-current helium discharge at low pressures, 25:14301
MASETTI, M., HDP--IBM 360/44 system at CNAF for bubble chamber data analysis. I, 25:13267 (CERN-70-21(Vol.2), pp 607-15)
  HPD--IBM 360/44 system at CNAF for bubble chamber data analysis. III, 25:13269 (CERN-70-21(Vol.2), pp 625-30)
  HPD--IBM 360/44 system at CNAF for bubble chamber data analysis. II, 25:13268 (CERN-70-21(Vol.2), pp 617-24)
MASEVICH, A. G., Structure and evolution of stars with various chemical compositions, 25:13821
MASHININ, V. A., Theory of backscattering of fast electrons from a condensed medium. I, 25:13961
MASHKOVA, E. S., Anisotropic spatial distribution of ions scattered by a single crystal, 25:13970
MASKER, W. E., Vortex motion in the presence of thermodynamic fluctuations, 25:14207
MASKER, Warren E., Fluctuation effects in one- and two-dimensional superconductors, 25:14162
MASON, Benjamin J., Plant radioiodine relationships: a review, 25:13395 (SWRHL-90-r)
MASON, E. A., Quantum transport cross sections for ionized gases, 25:14297
MASON, G. W., Extraction of U(VI) and selected M(III) cations by bis n-octyl phosphoric acid in two different hydrocarbon diluents, 25:13096
MASON, P. V., Effect of tin additive on indium thin-film superconducting transmission lines, 25:14223
MASON, R. J., Particle-in-cell method for model kinetic equations, 25:15431 (CU-3954-3)
MASUOKA, H., Vapor-liquid equilibria at high pressure, 25:15459 (SCL-T-71-212)
MATNEY, Thomas S., Genetic analysis of the histidine operon in Escherichia coli K12, 25:13422
MATORA, I. M., Electron-beam shaping in a linear induction accelerator, 25:14856 (UCRL-Trans-1425)
MATSCHKE, Siegfried, Interrelationship between cell survival, radiation portals, and dose gradients, 25:13451
MATSIBORKO, N. G., Nonlinear theory of excitation of plasma wave by electron beam, 25:14311
MATSUBARA, Tadao, X-ray excited optical luminescence analysis of trace rare earths in high purity yttrium and gadolinium oxides, 25:12948
MATSUHASHI, Sachiko, Three cistrons in bacteriophage Qβ, 25:13386
MATSUI, Hiroshi, X-ray excited optical luminescence analysis of trace rare earths in high purity yttrium and gadolinium oxides, 25:12948
MATSUOKA, Osamu, Whole-body activation autoradiography, 25:13590
MATSUURA, Keiichi, Effect of Tathion on excretion of ^{203}Hg--MHP in kidney, 25:13341
MATTHEW, J. A. D., Isotope dependence of self-trapping energy of light interstitial in metal, 25:14439
MATTHIAS, B. T., Instabilities of high-temperature superconductors, 25:14174
MATTHIEUSSENT, Gilles, Discharge maintained by a direct current and high frequency waves, 25:14266
MATTILA, K., Interpretation of the surface brightness of dark nebulae, 25:13919

MATULIS, A. Yu., Theory of perturbations of the autoionization levels of two-electron atoms, 25:14049
MAULBETSCH, John S., Refrigerant forced-convection condensation inside horizontal tubes, 25:13151 (NP-18642)
MAURY, F., Directional dependence of atomic displacements in cobalt crystals, 25:13733
  Recovery of low-temperature electron-irradiated cobalt crystals, 25:13713
MAURY, Roland, Compressibility of the rare earth-transition metal intermetallic compounds, 25:13694
MAVINKURVE, S. S., Radiation pasteurization of fresh and blanched tropical shrimps, 25:13619
MAVROYANNAKIS, E., HERETRA: computer program for fission products calculations, 25:15141 (DEMO-70/10)
MAYER, B., Inelastic scattering of polarized protons by ^{40}Ca at 24.5 MeV, 25:14923 (CEA-CONF-1656)
  j-mixing determination in (p,d) reactions by asymmetry measurements, 25:14921 (CEA-CONF-1653)
  Study of (p,d) reactions on ^{48}Ca and ^{49}Ti with polarized protons, 25:14922 (CEA-CONF-1655)
  Study of (p,d) reactions on ^{90}Zr and ^{92}Mo with polarized protons, 25:14980 (CEA-CONF-1654)
MAYER, W., 1- to 10-keV x-ray sky near the galactic center, 25:13857
MAYR, L. M., Effects of reductone on irradiated E. coli, 25:13610
MAZAGCL, Lyliane, Determination of internal and superficial oxygen content of molybendum obtained using 54 MeV α particles and low energy deuterons, 25:12957 (LYCEN-7076)
MAZOR, L., Spectrophotometric determination of fluorine in organic compounds wit: thorium chloranilate after hydropyrolytic decomposition of lead fluoride, 25:12936
MAZZARI, C., Adam+Eva, scanning and measuring machine for film from the large bubble chambers, 25:13270 (CERN-70-21(Vol.2), pp 633-49)
MAZZUCATO, M., Annihilation anti pn → $\pi^+\pi^-\pi^-$ between 1.0 and 1.6 GeV/c, 25:14548
MCANDLESS, J. M., Deuterium exchange of C-methyl protons in lumazine derivatives, 25:12982
MCCLAY, J. F., Resonant modes of a cavity and properties of micropulsations, 25:14117
MCCOLL, Daniel Clyde, An n/d calculation using the discontinuity of a second order four-point interaction as input, 25:14676
MCCOLL, I., Study of 200 patients with Pruitus ani, 25:13588
MCCONNELL, D. B., De-excitation γ-rays in ^{15}N and ^{15}O, 25:14896
MCCONNELL, R. D., Concerning a thought experiment violating Heisenberg's uncertainty principle, 25:14502
MCCORD, R. V., Prog. rpt. on High Flux Isotope Reactor, 7--9/70, 25:15392 (ORNL-TM-3286)
MCCORMACK, K. R., Changes in lung scan pattern related to free fluid and cardiac position, 25:13484
MCCORMICK, J. W. P., Progress on Polly at Glasgow, 25:13255 (CERN-70-21(Vol.1), pp 357-70)
MCCORMICK, N. J., Comparison of the codes RSYN and 3DB, 25:15343 (WHAN-IR-48)
MCDONALD, D. G., High-frequency limit of the Josephson effect, 25:14200
MCDOUGALL, F. H., Minimizing errors in gamma-ray backscatter density gages: existing gages and new design concepts, 25:13316
MCDOWELL, Richard B., Results of 33,911 x-ray protection surveys of facilities with medical or dental diagnostic x-ray equipment, fiscal years 1961--1968, 25:13464
MCFARLANE, James C., Plant radioiodine relationships: a review, 25:13395 (SWRHL-90-r)
MCGEE, Ian J., Dispersion sum rules for fixed-u πN scattering amplitudes, 25:14709
MCGEORGE, J. C., Decay of ^{159}Dy, 25:15012
MCGOWAN, F. K., Coulomb excitation of ^{107} ^{109}Ag, 25:15´35
MCGUIRE, Eugene J., Atomic L-shell Coster--Kronig, Auger, and radiative rates and fluorescence yields for Na through Th, 25:13980
MCINTYRE, D. R., Fate of Schooner fallout radionuclides ingested by the dairy cow, 25:13396 (UCRL-72511)
MCINTYRE, L. C., Stopping power of Havar for 2.5 to 7.0 MeV deuterons, 25:14401
MCKEOWN, J., Measurement of proton--proton bremsstrahlung cross sections at 42 MeV, 25:14556
MCKINNON, C. K., Jervis Bay Nuclear Power Station project investigations at site J.S1-Scottish Rocks, 25:15336 (NP-18636)
MCKOWN, David Melvin, Gamma--γ coincidence counting and activation analysis of meteoritic materials, 25:12967
MCKOWN, H. S., Analytical mass spectrometry at Oak Ridge National Laboratory, 25:13319 (ORNL-4643)
MCLATCHIE, W., Level structures of ^{85} ^{87}Sr from (d,p) reactions, 25:14955
MCLAUCHLIN, I. R., Recovery creep of niobium-stabilised austenitic stainless steels, 25:13674
MCNULTY, P. J., Muon experiments, 25:14532
MCWHAN, D. B., X-ray diffraction studies of the metal insulator transitions in Ti_4O_7, V_4O_7, and VO_2, 25:14442
MEATH, William J., Long-range intermolecular forces using Gaussian basis functions, 25:13984
MECHTLY, E. A., Changes of lower ionosphere electron densities with solar zenith angle, 25:14104
MEDVEDEV, I. G., Possibility of phase transitions in an imperfect multiply ionized plasma, 25:14304
MEESE, D., Malignant thyroid adenomas following x radiation during childhood, 25:13585
MEGGS, William Joel, Topics in the dynamics of strong interactions, 25:14678
MEHRA, Harish C., Trace metal analysis by combined thin-layer chromatography incorporating fluorescent support and ring oven colorimetry, 25:12944
MEHROTRA, P. N., Electrical transport in rare-earth oxides, 25:14469
MEISNER, Gerald W., CP violation in K(neutral) → $\pi^+\pi^-\pi^0$, 25:14762
MEKJIAN, A. Z., Coulomb mixing of isospin states, 25:15149
MEKSHES, M. W., Moessbauer effect in tungsten following Coulomb excitation, 25:15020
MELLEMA, Dwight Joel, Two- and three-body final states in K^+p interactions at 7.3 GeV/c, 25:14574
MEL'NICHENKO, V. V., Automating a 2-GeV electron linac, 25:14852 (SLAC-Trans-126)
MEL'NICHUK, D. O., Avidin effect on intensity of ^{14}C incorporation from $NaH^{14}CO_3$ and glycine-1-^{14}C into proteins and lipids of rat liver homogenates, 25:13344
MELNIKOV, A. K., Measurement of energy spectra and average number anti ν of prompt neutrons produced in fission of actinide elements, 25:15118
MELROSE, D. B., Theory of type II and type III solar radio bursts. II, 25:13872
  Theory of type II and type III solar radio bursts. I, 25:13871
MENON, M. G. K., Multiple muon events observed underground, 25:14060
MENZEL, Erhard Roland, Spectroscopy of Np^{4+} in crystalline electric fields, 25:14466
MERCER, Robert L., Diffusional deposition from a fluid flowing radially between concentric, parallel, circular plates, 25:13123
MERCER, T. T., Diffusional deposition from a fluid flowing radially between concentric, parallel, circular plates, 25:13123
MERCURIO, Jean-Pierre, Electronic structure of some hexaborides of the CaB_6 type, 25:14463
MEREDITH, John L., Experimental comparison of fallout field simulation techniques, 25:13117 (AD-711532)
MERICLE, L. W., Nuclear DNA complement in young proembryos of barley, 25:13405
MERICLE, R. P., Nuclear DNA complement in young proembryos of barley, 25:13405
MERKER, Milton, Solar-cycle modulation of fast neutrons in the atmosphere, 25:14064
MERKULOV, L. A., Electron-beam shaping in a linear induction accelerator, 25:14856 (UCRL-Trans-1425)
MERLA, M., Fission-cross-section measurement of ^{233}U, 25:15082
MESCHERYAKOV, M. G., Development of track chamber picture processing systems at JINR, 25:13279 (CERN-70-21(Vol.2), pp 753-60)
MESERVEY, R., Properties of very thin aluminum films, 25:14192
MESSERLI, R., Status of the HPD minimum guidance programs at CERN, 25:13278 (CERN-70-21(Vol.2), pp 737-52)
MESSERSCHMIDT, Otfried, Investigations about combination injuries, 25:13368
MESSIAEN, A. M., Explanation of plasma densities high above critical density, 25:14333
MESSIHA, S. A. S., Temperature field in magnetohydrodynamic oscillatory flow, 25:14095
METZGER, P. H., Observation of early-type stars from OGO-VI, 25:13813
MEUBUS, P., Temperature distributions in a helium plasma, 25:14254
  Velocity distributions in a gaseous plasma. II, 25:14253
  Velocity distributions in a gaseous plasma. I, 25:14252
MEULEMANS, M., Regular network of anti-phase boundaries in the x-phase of the system Fe--Cr--Mo--Ti, 25:13711
MEYER, J., Stray baryonic resonances and SU(3), 25:14771
MEYER, J. P., Chemical forms of ^{35}S resulting from neutron irradiation of LiCl in solution in methanol, 25:13071
MEYER, James W., Covariant classical motion of electron in a laser beam, 25:14506
MEYER, John W., Cratering in Greenland icecap snow, 25:13133 (AD-711861)
MEYER, Walter, Dimensional S/sub n/ calculations of neutron spectra reflected from thick slabs of concrete and iron, comparison with measurements, 25:14865 (COO-2049-2)
MEYERHOFF, R. W., High-current ac losses in large superconducting niobium tubes, 25:14225
MEYNADIER, C., Study of reactions ^{11}B(^{3}He,p)^{13}C and ^{20}Ne(^{3}He,p)^{22}Na at less than or equal to 3 MeV, 25:14904
MICHAELIS, W., Two-quasiparticle states in ^{168}Er, 25:15000
MICHAU, J. C., Ariane II: automatic device for the analysis of spark chamber photographs, 25:13285 (CERN-70-21(Vol.2), pp 859-78)
MICHAUDON, A., Determination of spin of slow-neutron induced resonances in ^{239}Pu, 25:15088
  High-resolution measurement and analysis of ^{239}Pu fission

XUM

cross-section, 25:15089
  Measurement and analysis of ^{235}U and ^{241}Pu fission cross-sections, 25:15086
  Total and fission cross-sections of ^{239}Pu from 5.7 to 160 eV, 25:15087
MICHELS, Charles J., Voltage--current characteristics of megawatt MPD-arc thruster, 25:14271
MICHOULIER, Jean, ESR of Er^{3+} ions in thoria crystal, 25:14478
MIELCZAREK, S. R., Inelastic electron scattering from N_2O between 5.0 and 20.0 eV energy loss, 25:14014
MIESOWICZ, M., Remarks about fireballs, 25:14669
MIGDAL, A. A., Zero charge and scale invariance problems in the soluble field theory model, 25:14783
MIGDISOV, A. A., Evolution of the chemical composition of the rocks in the shields and sediment cover of the Russian and North American platforms, 25:13114
MIGNECO, E., Fission-cross-section measurement of ^{233}U, 25:15082
  Neutron-induced fission cross-section of ^{241}Pu, 25:15083
  Scattering cross-section of ^{235}U below 100 eV, 25:15084
MIHAILOVIC, M. V., Projection of angular momentum and the generator coordinate method for light nuclei, 25:15196
MIHAJLOVIC, A., Activation energy of isothermal martensitic β--α' transformation, 25:13703
MIHALCV, J. D., Geomagnetic tail structure near the null sheet, 25:14113
MIKAMI, Yasuharu, Electron microscopy study of the precipitation processes in Cu--2 wt. percent Be alloy, 25:13715
MILANI, F., Clinical experiences in antineoplastic treatment with telecobalt therapy, 25:13546
MILES, M. E., Disposal of radioactive wastes from U. S. naval nuclear-powered ships and their support facilities, 1969, 25:13444
MILIOTIS, Demitrios M., Bulk-plasmon dispersion spectrum of Be using an x-ray scattering technique, 25:14443
MILKEY, Robert William, Heating of the chromospheric network by hydromagnetic waves, 25:13908
MILLER, A. J., Method for mapping the spatial distribution of stopping π^- mesons in tissue, 25:13547
MILLER, Carl F., Assessment of nuclear weapon requirements for assured destruction, 25:13132 (AD-711021)
MILLER, J. K., Comparison of ^{46}Sc and ^{144}Ce as nonabsorbed reference materials in studies with cattle, 25:13352
MILLER, J. M., Precompound decay from a time-dependent point of view, 25:15140 (CU-1019-79)
MILLER, J. Martin, Functional autonomy in multinodular goiter, 25:13493
MILLER, K., Stability of the complex angular-momentum continuation, 25:14834
MILLER, Kenneth J., Variational principle for scattering with bounds on the phase shift, 25:14024
MILLER, Morton W., Radiation dose fractionation, mitotic index, and multiple fixation studies on chromosome aberrations in Vicia faba, 25:13413
MILLER, N. C., Testing of a cascaded thermoelectric module, 25:14082 (N-70-39764)
MILLIAT, J. P., Test facility for sodium-heated steam generators, 25:13143
MILLIONSHCHIKOV, M. D., Turbulent heat exchange and mass transfer, 25:13160
MILLS, R. G., Operation of a levitated superconducting ring in a plasma physics experimental device, 25:14356
MILNER, W. T., Coulomb excitation of ^{107} ^{109}Ag, 25:15035
MILOVANOV, V. P., Angular dependences of many-charge particles produced by 660-MeV protons on ^{27}Al nuclei, 25:14945
MILSTEIN, Frederick, Indirect exchange coupling of magnetic moments in rare-earth metals, 25:14487
MIN, K. K., Photon interaction cross sections of Sn and Zr, 25:14959
MINAMI, Kentaro, Radiation protection against x-ray diffraction apparatus, 25:13457
MINAMI, S., Regge-dipole model and $\pi^-p + \gamma n$ reaction, 25:14704
MINENKO, V. P., Designing multicomponent isotope separation cascades, 25:13179
MINSART, G., Implications of fundamental integral measurements on high-energy nuclear data for reactor physics, 25:15349
MIOERNER, G., Detectors in studies of regional lung function by ^{133}Xe radiospirometry, 25:13520
MIRAKHMEDOV, A. K., Results of histochemical studies of glycogen and liver cells ultrastructure of irradiated rats, 25:13378
MIRJAN, J., Effect of γ irradiation on phosphorous metabolism and nucleic acid synthesis in wheat seedlings, 25:13597 (NP-18606)
MIROSHNICHENKO, Yu. T., Peculiarities of uranium deformation for tension at constant velocity, 25:13688
MIRSKI, U., Contribution of H atoms to G/sub H2/ in the radiation chemistry of aqueous solutions, 25:13044
MIRZA, Ishaq Muhammad, Excitation of N_2^+ first negative and Meinel bands by electron impact, 25:13997
MISCHKE, R. E., Proton--proton differential cross sections from 600 to 1800 MeV/c, 25:14543
MISHIN, E. V., Stabilization of universal instability, 25:14341
MISRI, Hassan, Comparison of high-energy radiation applied through plaster casts, 25:13539
  Postoperative radiotherapy of mammary carcinoma without irradiation of the thorax wall, 25:13533
MISURI, G., HDP--IBM 360/44 system at CNAF for bubble chamber data analysis. I, 25:13267 (CERN-70-21(Vol.2), pp 607-15)
  HPD--IBM 360/44 system at CNAF for bubble chamber data analysis. II, 25:13268 (CERN-70-21(Vol.2), pp 617-24)
MITANI, Hiroyasu, Electron microscopy study of the precipitation processes in Cu--2 wt. percent Be alloy, 25:13715
MITCHELL, Archer Sylvester Jr., Interaction of the solar wind with optically thin atmospheres, 25:13905
MITCHELL, J. B., Dispersion hardening of a Mc--1 at. percent Hf alloy by internal hardening, 25:13661 (UCRL-72627)
MITCHELL, T. E., Interstitial solution hardening in tantalum single crystals, 25:13690
MITO, Norio, Radiation protection against x-ray diffraction apparatus, 25:13457
MIURA, Akiko, Mutation and recombination of bacteriophage lambda: effect of ultraviolet radiation, 25:13412
MIURA, Y., Weld cracking and mechanical properties of 17 percent chromium steel weldment, 25:13696
MIYAZAWA, Yoshitoshi, Charge exchange of carbon and nitrogen ions in nitrogen gas, 25:14001
MIZUHARA, Takeshi, Magnetic properties of Y/sub 1-x/Sm/sub x/Co_5 compounds, 25:14461
MIZUHO, M., Fast neutron spectrometer, 25:13232
MKHEIDZE, Demuri M., Tumor-induced skin heterogenization. III. Immunologic and immunogenetic mechanisms, 25:13388
MKRTCHYAN, G. G., Search for new type of radioactivity in aluminum and tungsten targets irradiated by 70-GeV protons, 25:14541 (JINR-P1-5399)
MOE, Kjeldseth C., Solar lithium abundance, 25:13870
MOENKEMEYER, D., Experiences with coupled computers to control an HPD, 25:13276 (CERN-70-21(Vol.2), pp 721-7)
MOERSDORF, D., Infrared thermography with a color scanner used in nuclear medicine, 25:13498
MOGNASCHI, Ezio Roberto, Analysis of EPR spectra of oxidizing catalysts, 25:14482
MOHAN, Radhe, Isospin mixing in nuclei, 25:15159
MOISEITSEV, P. I., Radiational safety in the use of radioisotopic methods in engineering industry, 25:13467
MOLCHANOV, V. A., Anisotropic spatial distribution of ions scattered by a single crystal, 25:13970
MOLHO, N., Fission of ^{210}Po, 25:15010
MONNIER, Anne, Selective growth of pits on a stainless steel in a chlorinated oxidizing medium, 25:13637
MONTALBANO, M. E., Action of ionizing radiations on CNS, 25:13561
MONTES DE OCA, H., Production of heparin related mucopolysaccharides by mammalian cells in culture, 25:13357
MONTGOMERY, D. M., Test of the independence hypothesis by angular distribution measurements, 25:15065
MONTGOMERY, Daniel Michael, Recoil studies of medium-energy nuclear reactions induced by ^{3}He and ^{4}He ions, 25:15049
MOOK II, Delo Emerson, Study of Sco X-1, 25:13852
MOORE, Donald A., Metallographic preparation of uranium--silicon alloys, 25:13742
MOORE, J., Some unexpected dosimetric problems in an apparatus for mammalian radiobiology, 25:13456
MOORE, M. S., Fission and capture cross-sections of curium, 25:15090
  Fission, capture, scattering, and total cross-sections of ^{239}Pu, 25:15091
MOORE, R. W., Toward inclusion of spin in generalized Veneziano model for $K^-p + \pi^-\pi^+\Lambda$, 25:14716
MORCELLET, J. L., Sn--/sup 113m/In tracers in scintigraphies, 25:13501
MOREAU, Claude, Fuel element manufacturing process, 25:13741
MOREH, R., Nuclear levels excited by neutron capture γ rays, 25:15002
MOREK, T., Cerium-135m and /sup 137m/Nd: isomeric states in N = 77 isotones, 25:15042
MOREL, Colette, Aerosols produced by evaporation of uranium wire, 25:13650 (AI-Trans-289)
MORENO, G., Alpha-particle observations in solar wind, 25:13895
MORET, R., Study of the decay ^{109}In + ^{109}Cd, 25:15005
MORGAN, John H., Functional test of a Rocket Engine Module, 25:15453 (SC-DR-70-911)
MORGAN, Ora Billy Jr., Study of intense low-energy ion beams for fusion research, 25:14353
MORGAN, T., Transfer of energy in general relativity, 25:14816
MORGANSTERN, R. E., Spin precession of Schiff satellite in Brans--Dicke theory, 25:14811
MORIARTY, K. J. M., Toward inclusion of spin in generalized Veneziano model for $K^-p + \pi^-\pi^+\Lambda$, 25:14716
MORIMOTO, Ichiro, Influence of temperature in the contact area on the static welding characteristics of electrical contacts, 25:13644
MORIOKA, Shigeki, Finite-Larmor-radius hydromagnetic flow past an obstacle, 25:14329
MORITA, Kozo, Results of conformation radiotherapy in cervix carcinomas, 25:13530

MORITCKI, M., High-pressure measurement using semiconductor strain gages, 25:15458 (SCL-T-71-210)
MORIUCHI, S., Molecular motion of peroxy radicals of polytetrafluoroethylene, 25:13034
MORONEY, J. R., Radiation hazards, 25:13436
MOROZ, N. S., Measurement of total cross sections of π^---p interaction, 25:14561 (JINR-P1-5460)
MOROZ, V. I., Development of track chamber picture processing systems at JINR, 25:13279 (CERN-70-21(Vol.2), pp 753-60)
MORRIS, Charles Wayne, Anisotropy of diffuse solar radiation, 25:13903
MORRIS, D., Polarization of 150-MHz radiation from four pulsars, 25:13855
MORRIS, F. S., Radioactive tracers test nuclear steam turbines easier, better, 25:13148
MORRIS, J., Radiopharmaceuticals in nuclear medicine, 25:13519
MORRIS, J. B., Experimental study of spouting beds of spheres, 25:13139 (AERE-R-4852)
MORRISON, D. R. O., Many-body cross sections, 25:14594
MORRISON, Harry L., Statistical mechanics of persistent currents in quantum fluids, 25:14143
MORTON, J. M., Level structures of ^{85} ^{87}Sr from (d,p) reactions, 25:14955
MOSBRCOKER, Michael Lee, Energy loss of high-energy electrons in Sn, Pb, and Gd, 25:14392 (AD-711005)
MOSINSKI, G., Mean number of prompt neutrons and relative cross-sections for fission of ^{235}U and ^{239}Pu between 0.3 and 1.4 MeV, 25:15114
  Measurements of (n,2n) and (n,3n) reaction cross-sections of fissionable materials using a large liquid scintillator, 25:15111
IOSKALEV, Yu. I., Problem of relative biological efficacy of tritium oxide, 25:13551
MOSLEY, W. C., Self-radiation damage in ^{244}Cm oxide and aluminate, 25:13779 (DP-MS-70-44)
MOSS, F. E., University of Virginia superconducting wind-tunnel balance, 25:14216
MOSTOVAYA, T. A., Method of direct measurement of the capture-to-fission cross-section, 25:15076
MOSTOVOI, V. I., Method of direct measurement of the capture-to-fission cross-section, 25:15076
MOTULEVICH, G. P., Optical properties and electron characteristics of niobium--tin alloys, 25:14149
MOWAT, J. Richard, Electron mass shift in ^{133}Cs, 25:14514
MOXON, M. C., Capture cross-sections of structural materials, 25:14971
  Low-energy neutron scattering cross-section of ^{6}Li, 25:14909
MOXZYNSKI, M., Plasma delay and plasma time jitter in subnanosecond timing with a surface barrier detector, 25:13228
MUDD, R. D., Analysis of hydrological factors influencing operation of 100-N emergency waste disposal Crib, 25:13186 (BNWL-1503)
MUECK, H. J., Experiences with coupled computers to control an HPD, 25:13276 (CERN-70-21(Vol.2), pp 721-7)
MUEHLEISEN, Hermann, Effects of tanderil on radiosensitivity, 25:13476
MUELLER, F. M., Inversion of de Haas--van Alphen data. I, 25:14433 (ANL-7659)
MUELLER, G., Experimental animal studies concerning scintigraphic detection of acute thrombosis, 25:13518
MUELLER, Th., Construction of instrument for more accurate, repeated blood volume determinations using HSA-^{131}I, 25:13218
MUENZEL, H., Half-life for neutron deficient actinide isotopes, 25:15162
MUKHERJEE, B. K., Current-induced intermediate state in Type-I superconductors, 25:14165
MUKHERJEE, P., Influence of chloramphenicol on irradiated bacteria, 25:13613
MUKHERJEE, S. C., Electron capture by positrons from molecular hydrogen, 25:14006
MUL'CHENKO, B. F., Investigation of a high-pressure laser spark ignited by an extraneous plasma source, 25:14331
MULHERIN, Denis Wren Mark, Nonrelativistic time-dependent scattering theory for long range potentials, 25:14624
MULLER, Th., Spins of levels of ^{34}Cl, 25:14942
MULLIE, J., Ariane II: automatic device for the analysis of spark chamber photographs, 25:13285 (CERN-70-21(Vol.2), pp 859-78)
MUNECHIKA, Hirotsugu, Radiosensitivity and DNA metabolism inhibition, 25:13604
MUNTZ, James H., General alloy analysis with a gas sheathed tubular electrode arc, 25:12945
MURAD, E., Production of N_2^+ in collisions between N^+ and N_2, 25:14030
MURADYAN, G. V., Neutron-spectroscopy study of nuclei with A < 220 in resonance energy region, 25:15095
MURADYAN, H. V., Method of direct measurement of the capture-to-fission cross-section, 25:15076
MURADYAN, R. M., Resonant scattering of light by light, 25:14596 (JINR-E2-5424)
MURATA, Kenji, Energy dissipation of electrons in Al and Cu targets, 25:14400
MURATA, T., Analysis of neutron inelastic scattering by ^{238}U, 25:15135
MURPHY, Paul Henry, Thermally generated electrical currents in gamma-irradiated lucite, 25:13786
MURRAY, J., Isomeric level in ^{239}U, 25:15077
MURRAY, K. J., Ratio of capture and fission cross-sections of ^{239}Pu in energy range 100 eV to 30 keV, 25:15073
MURTHY, D. S. R., Incoherent scattering of gamma rays by K-shell electrons of Pt, 25:14410
MURTHY, S. Narasimha, Guiding center of a charged particle in superposed heliotron and biconical cusp fields, 25:14330
  Stability of cylindrical plasma in presence of monotonic field. II, 25:14346
MURTHY, S. R. S., K x-ray yields from ^{238}U fragments, 25:15027
MURTY, D. R. K., Retention of /sup 113m/In--^{59}Fe-ferric hydroxide in the mouse, 25:13486
MURTY, M. Sriramachandra, Effective atomic numbers for coherent scattering process of gamma rays in alloys, 25:14405
MUSCHLER, W., Simultaneous determination of electron concentration and electron collision frequency in a locally slowly varying magnetoplasma, 25:14315
MUSGRAVE, B., Automatic scanning and measurement of bubble chamber film on Polly II, 25:13254 (CERN-70-21(Vol.1), pp 325-55)
MUSGROVE, A. R. de L., Resonance parameters for measured keV neutron capture cross sections, 25:14979 (AAEC/E-198(Suppl.1))
MUSHKACHEVA, G. S., Change in composition of rat blood as affected by ^{237}Np, 25:13346
MUUSS, H., Laser beams as fiducial lines in bubble chambers, 25:13303
MYAKOTA-MOSKALEV, V. I., Automating a 2-GeV electron linac, 25:14852 (SLAC-Trans-126)

N

NAGAI, Hitoshi, Spectrophotometric determination of tantalum with methylene blue, 25:12947
NAGARAJAN, M. A., Coupled channel calculations with complex eigenvalues, 25:15181
NAGATA, Saburo, Structure of film prepared by low-energy sputtering of molybdenum, 25:14456
NAGEL, H.-H., Experiences with coupled computers to control an HPD, 25:13276 (CERN-70-21(Vol.2), pp 721-7)
NAGYLAKI, Thomas Andrew, Current commutators in quantum electrodynamics and electromagnetic mass differences of the pseudoscalar meson and baryon octets, 25:14795
NAIR, P. Madhusudanan, Asparagine synthetase from γ-irradiated potatoes, 25:13365
NAJAM, M. R., Low-lying levels and decay structure in ^{62}Cu, 25:14940
NAJZER, M., Fission-spectrum-averaged neutron cross-sections for some threshold detectors, 25:14968
NAKAGAWA, M., Energy spectrum of a nova-like x-ray source, 25:13849
NAKAMURA, H., Analysis of neutron inelastic scattering by ^{238}U, 25:15135
  Fast-neutron capture cross-sections of Cr, Fe, Ni, and Mo, 25:14970
NAKAMURA, M., Molecular motion of peroxy radicals of polytetrafluoroethylene, 25:13034
NAKAYAMA, Tadayuki, Structure of oxide films formed on niobium in high-temperature water and water vapor, 25:13771
NALCIOGLU, Orhan, Bootstrap theory of vibrations. I, 25:15174
  Bootstrap theory of vibrations. II, 25:15176
NAMYSLOWSKI, J., Strong absorption cut in photoproduction, 25:14603
NANCOLLAS, George H., Ion exchange properties of crystalline zirconium phosphate, 25:13084
NANDEDKAR, D. P., Dc noise in plasma due to electron--ion collisions, 25:14303
NAPPEY, P., Description and performance of the CERN Spiral Reader, 25:13236 (CERN-70-21(Vol.1), pp 19-36)
NARAIN, Jai Prakash, MHD of drop, in a cone, and sinks in uniform magnetic fields, 25:14096
NARASIMHACHARYULU, E., Incoherent scattering of gamma rays by K-shell electrons of Pt, 25:14410
NARASIMHAM, V. S., Multiple muon events observed underground, 25:14060
NARASIMHAN, S. L., Metastable constitution and superconducting transition behavior of Zr--Ta alloys, 25:13716
NARKHOV, A. V., Anomalous behavior of carbon atoms at low temperatures in martensite irradiated by electrons, 25:13729
NASLAIN, Roger, Electronic structure of some hexaborides of the CaB_6 type, 25:14463
NASTRI, G., Total neutron cross-section of ^{233}U from 0.7 to 320 eV, 25:15079
NATALE, E., Action of ionizing radiations on CNS, 25:13561
NATALI, S., Measurement of K/sub μ3/$^+$ decay parameters, 25:14534
NATH, P., Chiral algebra, chiral breakdown, and xi parameter of K/sub 13/ decay, 25:14645
  Lagrangian approach to dual pion amplitudes, 25:14697
  N-point functions in chiral SU(3) x SU(3) current algebra, 25:14664
NATHANS, M. W., Particle size distribution in clouds from nuclear airbursts, 25:13138
NATHRATH, Norbert, Displacement of wall-stabilized electric

arcs by curvature, 25:14269
NAUGHTON, William F., Pulsed-neutron activation analysis system for short-lived radioisotopes, 25:12960
NAUMANN, R. A., Decay of ^{209}At, 25:14995
NAVALKAR, M. P., Resonance parameters of ^{240}Pu, 25:15092
NAVINSEK, B., Thermal treatment of Cr--SiO cermet thin films, 25:14435 (IJS-587)
NAYAR, G. G., X-ray induced chlorophyll mutation in Sesamum orientale L, 25:13415
NAZARENKO, V. A., Extraction--photometric determination of Mo, 25:12933
NAZARYAN, A. Kh., Dielectric permittivity of plasma in a strong magnetic field, 25:14312
NDILI, F. N., Some remarks on the theory of induced realizations, 25:14749
NEBE, J., Multilevel resonance analysis of total neutron cross-section of ^{23}Na and Ca below 1 MeV, 25:14969
  Spin and parity of ^{41}Ca levels, 25:14939
NE'EMAN, Y., Fifth interaction and baryon masses, 25:14706
NE'EMAN, Yuval, Nishijima's model with fifth interaction, 25:14639
NEERGARD, K., Microscopic description of nuclear vibrations when phonons occur at relatively low energy. II, 25:15205
NEFEDOV, V. N., Measurement of energy spectra and average number anti ν of prompt neutrons produced in fission of actinide elements, 25:15118
NEFKENS, B. M. K., Measurement of inverse pion photoproduction near the P_{33}^0(1236) resonance, 25:14567
NEGANCV, B. S., Simple ^{3}He--^{4}He dilution refrigerator, 25:14214
NEGANCVA, N. L., Results of histochemical studies of glycogen and liver cells ultrastructure of irradiated rats, 25:13378
NEKRASOV, A. K., Radiative instability of a nonequilibrium plasma in magnetic traps, 25:14288
NELSON, D. B., Effects of nuclear EMP on AM radio broadcast stations in the emergency broadcast system, 25:13328 (CRNL-TM-2830)
NEMENCV, L. L., Search for new type of radioactivity in aluminum and tungsten targets irradiated by 70-GeV protons, 25:14541 (JINR-P1-5399)
NEMIRO, E. A., Determination of the radiation loading in roentgenodiagnostic investigation with the aid of thermoluminescent dosimetry, 25:13453
NESMEYANOV, An. N., Kinetics of Sb(III and V) extraction, 25:12999
  Nuclear gamma-resonance study of products of β-decay of /sup 121m/Sn, 25:13074
NESTEROV, V. G., Average number of prompt neutrons in fission of ^{235}U and ^{239}Pu by neutrons, 25:15116
NESTOROV, G., Variations in lower ionosphere associated with cosmic-ray and geomagnetic variations, 25:14127
NETHERY, C. M., Outer layers of model moving atmospheres, 25:13792
NEUBERT, W., Cerium-135m and /sup 137m/Nd: isomeric states in N = 77 isotones, 25:15042
NEUMANN, M., Wire spark chamber design and performance using FET, capacitor readout, 25:13264 (CERN-70-21(Vol.2), pp 539-48)
NEVSTRUEVA, M. A., Cesium-137 from global fallout in foodstuffs and human organism, 25:13340 (NP-18382)
NEWHOUSE, V. L., Noise analysis for amplifiers with superconducting input, 25:14224
  Observation of single fluxon drift through a superconductor, 25:14199
NEWKIRK, L. R., Transition temperatures and lattice parameters of metastable Te--Au solutions, 25:14178
NEWLAND, E. A., Japanese A.T.R. Reactor, 25:15338 (AAEC/LIB/Bib-258)
  Physics of the dynamic growth of mushroom clouds, associated with nuclear explosions, 25:13131 (AAEC/LIB/Bib-255)
  Radiation-induced polymerization. II, 25:13030 (AAEC/LIB/Bib-260)
  Radiation-induced polymerization. I, 25:13029 (AAEC/LIB/Bib-259)
  Radiation-induced polymerization. III, 25:13031 (AAEC/LIB/Bib-261)
NEWTON, G. J., New method for the generation of aerosols of insoluble particles, 25:13145
NEWTON, Roger G., Atoms in superstrong magnetic fields, 25:13829
NEZRICK, F. A., Upper limit for magnetic-monopole production by neutrinos, 25:14638
NGUYEN VAN NHUNG, Magnetic properties and structures of CrB compounds Tb--Ge$_{0.2}$Si$_{0.8}$, HoSi, ErSi, and TmSi, 25:14434 (CEA-CONF-1701)
NICKERSON, J. T. R., Recovery of salmonellae from irradiated and unirradiated foods, 25:13620
NICKLCW, R. M., Spin-wave dispersion relation in dysprosium metal, 25:14444
NICOL, K., Energy dependence of electron collision frequency on electrical conductivity of weakly ionized plasmas, 25:14308
NICOLC, F., K anti Kπ final states for N anti N annihilation at rest in the Veneziano language, 25:14691
NIEDERMEIER, William, Emission spectrometric determination of trace elements in biological fluids, 25:12946
NIELSEN, O. B., Electron-capture beta decay, 25:14993
NIELSEN, P., Experimental test of quasi-linear theory, 25:14323
NIEMINEN, U., Isodose measurement of the bladder dose in radium therapy, 25:13448
NIERHAUS, R., Data handling system for the Omega and the SFM projects, 25:14839 (CERN-70-21(Vol.2), pp 561-80)
NIESSEN, P., Continuous cooling transformation behaviour of zirconium--niobium--oxygen alloys, 25:13679
NIGMANOV, T. S., System of proportional wire chambers on-line with a computer, 25:13297 (JINR-P13-5473)
NIILER, A., Interference and rescattering effects in reactions with three particles in the final state, 25:14891 (CRO-1316-97)
NIKISHOV, A. I., Quantum processes in a constant electric field, 25:14498
NIKITIN, A. V., Reaction $np \to pp\pi^-$ for the incident neutron momenta from 2 up to 10 GeV/c, 25:14551
NIKITIN, E. E., Gyroscopic interpretation of two-state hypergeometric models of non adiabatic coupling, 25:14033
NIKOLAEV, B. I., Designing multicomponent isotope separation cascades, 25:13179
NIKOLAEV, M. N., Cross-sections for radiative neutron capture by ^{238}U nuclei, 25:15125
  Temperature dependence of the total cross-section structure, 25:15093
NIKULIN, E. I., Heat capacity of gadolinium--lutetium alloys at superlow temperatures, 25:14450
NINIC, Neven, Exergetical analysis of a BHWR nuclear power plant, 25:15344
NISHI, Tatsuo, Radiation protection against x-ray diffraction apparatus, 25:13457
NISHIGORI, Takeo, Quasi-classical approximation for slow neutron scattering, 25:14875
NISHIKAWA, Masahiro, Decrease in intensity of Hg lines near source in weakly ionized flow, 25:14100
NISHIKAWA, T., Prototype of drift tube quadrupole magnets, 25:14849 (SJC-A-70-6)
NISHIMURA, K., Analysis of neutron inelastic scattering by ^{238}U, 25:15135
  Fast-neutron capture cross-sections of Cr, Fe, Ni, and Mo, 25:14970
NISHIO, Y., Weld cracking and mechanical properties of 17 percent chromium steel weldment, 25:13696
NIX, J. R., Exact calculation of the penetrability through two-peaked fission barriers, 25:15004
NIYAZOVA, O. R., Radiation-accelerated diffusion of gold in silicon, 25:14420
NIZZA, P., Chromosomal dosimetry on swine lymphocytes, 25:13417
NOBEL, L., Heat transfer coefficient as function of steam quality for high-pressure once through flow boiling, with determination of transition points between regions of particular heat transfer, 25:13149 (EUR-4561)
NODA, Yutaka, Whole-body activation autoradiography, 25:13590
NOETHEL, H., Radiosensitive and radioresistant populations of Drosophila melanogaster. I, 25:13555
NOMAKI, Koji, Internal oxidation of nickel alloys containing small amounts of chromium, 25:15455 (SC-T-71-3004)
NORDEN, H., Damage in gold bombarded with medium mass ions, 25:14413 (NP-18645)
NORMAN, G. E., Possibility of phase transitions in an imperfect multiply ionized plasma, 25:14304
NORRIS, D. I. R., Dislocation loop growth in an electron irradiated thin foil, 25:13732
NORTH, G. R., Coupling-constant analyticity in the charged-scalar static model, 25:14791
NORTON, Richard E., Scaling, fixed poles, and electroproduction sum rules, 25:14614
NOTARO, J., Design features of ac superconducting cables, 25:14226
NOTKIN, G. E., Breakdown of 2^1P and 2^3P levels of He in a glow discharge, 25:13977
NOVACU, V., Lectures in theoretical physics. III, 25:14630
NOVAK, J., Transversal vibrations of rods exited by parallel flow, 25:15213
NOVAK, J. K., Superconducting quadrupole doublet for LAMPF, 25:14860
NOVIKOV, V. I., Irradiation hazards produced by nonequilibrium emanations, 25:13435
NOVIKOV, Yu. V., Hygienic investigation of the effect produced by small concentrations of uranium on the human body, 25:13595
NUCCIOTTI, Alessandro, Analysis of EPR spectra of oxidizing catalysts, 25:14482
NUNAMAKER, T. A., Wire spark chamber design and performance using FET, capacitor readout, 25:13264 (CERN-70-21(Vol.2), pp 539-48)
NURMIA, M., Chemical separation of rutherfordium, 25:13088
NURPEISOV, B., Average number of prompt neutrons in fission of ^{235}U and ^{239}Pu by neutrons, 25:15116
NUSSINOV, S., Fifth interaction and baryon masses, 25:14706
  Possible connection between chiral symmetry breaking and the nonet of tensor trajectories, 25:14769
NUYTS, J., Duality and Adler condition, 25:14668
NYSTROM, R. E., Behavior of liquid sodium in a sinusoidal pressure field, 25:13154

O

OBERTH, Ronald C., Acceleration patterns in quasi-steady MFD arcs, 25:14281
O'BRIEN, Brian J., Source of auroral energetic particles, 25:14116
OCHIAI, F., Regge-dipole model and $\pi^- p \to \gamma n$ reaction, 25:14704
OCHIAI, Shin I., Tunneling into superconducting rhenium single crystals, 25:14147 (AD-711826)
ODARTCHENKO, N., Specificity of tritiated thymidine as a precursor of DNA under conditions of prolonged administration, 25:13358
O'DELL, R. Douglas, Effect of collapsing cross-section data on fast breeder physics parameters, 25:15352
O'DONNELL, H. A., Progress on Polly at Glasgow, 25:13255 (CERN-70-21(Vol.1), pp 357-70)
O'DONNELL, Robert Michael, Multipion production in π^-rho interactions at 2.3 GeV/c, 25:14571
ODORICO, R., Evidence for Veneziano dips in $K^- p$ scattering, 25:14724
OESTERREICHER, H., Structural and magnetic characteristics of the pseudobinary system $PrMn_2$--$ErMn_2$, 25:13707
OGATA, H., Reorientation measurements in ^{116}Sn and ^{124}Sn, 25:15041
OGER, R., Removable head for pneumatic device, 25:13203
OHASHI, Shigeo, Effect of Zr addition on the oxidation resistance and mechanical properties of Fe--Al--Cr alloys, 25:13680
OHMAE, T., Weld cracking and mechanical properties of 17 percent chromium steel weldment, 25:13696
OKA, Janet A., Cytological effects of juice or puree from irradiated strawberries, 25:13621
OKABE, H., Regge-dipole model and $\pi^- p \to \gamma n$ reaction, 25:14704
OKABE, Shigeru, Charge distribution produced by 4- to 24-MeV electrons in elemental materials, 25:13964
OKAZAKI, A., Thermal-neutron absorption cross-sections of gross fission products of ^{233}U, ^{235}U, and ^{239}Pu, 25:15100
O'KEIFF, Gustav Mason, Acoustic oscillations in partially ionized argon columns, 25:14380
OKHRIMENKO, L. S., Effective mass spectra of the $\gamma\gamma$, $\pi^0\gamma$, $\pi^0\gamma\gamma$, $\pi^0\pi^0$, π^0eta^0, $\pi^0\pi^0\gamma$, $\pi^0\pi^0\pi^0$ systems in mass value region M (γ.......γ) less than or equal to 1.3 GeV, 25:14560 (JINR-E1-5349)
OKSYUK, A. A., Collisions between fast protons or H atoms and O_2 molecules, 25:13999
OKUBO, Susumu, General properties of q-number Schwinger terms, 25:14589
OLDANO, C., Isomeric ratios for (n,2n) reactions, 25:15182
OLIVER, William Parker, Measurement of the branching ratio K/sub L/^{0} $\to$ $2\pi^0$/K/sub L/^{0} $\to$ $3\pi^0$, 25:14530
OLIVO, M. A., Gamma-ray yields from D(p,γ) ^{3}He, 25:14885
OLKHOVSKII, V. S., Space--time operator in collision descriptions, 25:14830
OLSHANSKY, Robert, Consistency of hard pion theorems in K/sub l3/ decays, 25:14633 (NYO-2262-TA-233)
  E(2) expansion, 25:14753
OLSON, Lynn Mary, Near-steady oblique shock waves in a collisionless plasma, 25:14324
OLUWOLE, Abiodun F., Nuclear spins, nuclear moments, and hyperfine structure of ^{69}Ge and ^{75}Ge, and $^3P_2$ hyperfine structure of ^{71}Ge, 25:14929
O'MARA, Robert E., Scintiscanning in the diagnosis of rupture of the spleen, 25:13511
ONDERDELINDEN, D., Argon L-shell and Ne K-shell x-ray emission in heavy ion--atom collisions, 25:14004
O'NEIL, R. A., Reaction (^{3}He,α) on Yb isotopes, 25:15057
O'NEILL, G. L., Prog. rpt. on Pu utilization in boiling water reactors, Phase II, annual, 1969, 25:15365 (NEDC-12111)
O'NEILL, R., Progress on Polly at Glasgow, 25:13255 (CERN-70-21(Vol.1), pp 357-70)
ONISHCHENKO, I. N., Nonlinear theory of excitation of plasma wave by electron beam, 25:14311
ONISHI, Hiroshi, Spectrophotometric determination of tantalum with methylene blue, 25:12947
ONLEY, D. S., Dynamic collective model of photofission, 25:15198
OORT, J. H., Galaxies and the universe, 25:13913
O'RIORDAN, M. C., X rays from color television receivers in Britain, 25:13452
ORTH, C. J., Average number of neutrons emitted in the spontaneous fission of some even--even heavy nuclides, 25:15037
ORTH, Charles Douglas, Search for fractionally charged particles in cosmic rays, 25:14065
ORTOLANI, E. A., Action of ionizing radiations on CNS, 25:13561
OSAKA, Toshiaki, Structure of oxide films formed on niobium in high-temperature water and water vapor, 25:13771
OSBORN, T. A., Nonsingular scattering equations, 25:14825
OSHIUMI, Yoshihiko, Effect of Tathion on excretion of ^{203}Hg--MHP in kidney, 25:13341
OSIPOV, N. K., Nature of auroral magneto--ionospheric perturbations, 25:14106
OSMON, P. E., Cost-effectiveness of different spark chamber read-out and digitising systems, 25:13266 (CERN-70-21(Vol.2), pp 581-606)
OSTERMANN, G., Recent results of cemented carbide research and problems encountered, 25:13752
OSTRIKER, Jeremiah P., Nature of pulsars, 25:13844
OTROSHCHENKO, G. A., Fission of ^{232}U by neutrons with energy from 0.1 up to 1.5 MeV, 25:15019
OTSUKA, Kazuhiro, Electron microscopy study of the precipitation processes in Cu--2 wt. percent Be alloy, 25:13715
OTT, Aadu, Scandium-45 level scheme, 25:14941
OTT, Edward, Coupling theory of nonresonantly unstable waves, 25:14366
OTT, R. J., Precise measurement of K^+ lifetime, 25:14531
OTTE, Victor Arthur, p--n correlations in the ^{13}C(p,pn)^{12}C reaction, 25:14907
OTTMAR, H., Two-quasiparticle states in ^{168}Er, 25:15000
OUANNES, Claude, Pangloss, a CRT device for bubble chamber pictures, 25:13258 (CERN-70-21(Vol.1), pp 401-25)
OVCHINNIKOV, A. K., Fast-neutron thermalization time in silicate ores of varying moisture content, 25:13109
OWCZARCZYK, A., Electrical conductivity of 2-pentene irradiated at 77°K during warming, 25:13027
OWEN, Charles Scott, Dc currents and ac inductive coupling in Josephson junctions, 25:14204
OWEN, David A., Order corrections to muonium hyperfine structure, 25:13990
OYAMADA, Rokuro, Nuclear calculation method of the JMTR core, 25:15391 (JAERI-Memo-4180)
OZAKI, S., Operational experience with the Brookhaven On-Line Data Facility, 25:13289 (CERN-70-21(Vol.2), pp 921-30)
OZERNOI, L. M., Galactic parameters as a consequence of cosmological turbulence, 25:13932

P

PABST, H. W., Bloodpool scintigraphy with shortlived radionuclides, 25:13516
  Struma maligna: 3, 5, and 8-year results in 259 cases, 25:13524
PACHOLCZYK, A. G., Light variations of Seyfert galaxy NGC 4151. III, 25:13924
PADAWER, Gerald M., Proton microprobe analysis of the surface of stranded wire in the lunar module, 25:12961
PADDOCK, Robert Alton, Energy levels of ^{18}Ne, ^{22}Mg, ^{26}Si, ^{30}S, ^{34}Ar, and ^{38}Ca by (p,t) reaction, 25:14950
PAESCHKE, Karl-Dietrich, Problems concerning chemotherapy of cervical carcinomas based on experiences at gynecological clinic, Univ. of Goettingen, 25:13527
PAGE, Edward A., Electromagnetic interaction of superconductors near T/sub c/, 25:14154
PAGELS, Heinz, Electromagnetic corrections to nucleon transitions of the vector and axial-vector currents, 25:14617
  Regge model for inelastic lepton--nucleon scattering, 25:14635 (NYO-4204-9)
PAI, S. A., Gamma spectrometric estimation of radionuclides in reactor coolant water, 25:12956
PAIS, A., Hadronic helicity conservation and inelastic lepton--nucleon reactions, 25:14636 (NYO-4204-10)
PAKHTUSOVA, E. V., Experiment on 2 γ-quantum annihilation on VEEP-2, 25:14520
PAL, S. R., Latitude-wide enhancement of 6300-A emission in nightglow, 25:14109
PALAGYI, S., Separation of radioiodide, radioiodate, and radioperiodate by thin-layer chromatography, 25:13099
PALANDRI, E. M., Focus remote access system, 25:13265 (CERN-70-21(Vol.2), pp 551-9)
PALCZEWSKI, A., LCAO--SCF calculations of electron energies for transition states: bromine + aromatic molecule, 25:13064 (INR-1211)
PALDUS, J., Stability conditions for solutions of Hartree--Fock equations for atomic and molecular systems. V, 25:14053
PAL'GUEV, S. F., High-temperature radiographic studies of oxides. II, 25:13769
PALMER, I. S., Prog. rpt. on nature and importance of selenium metabolites in animal, 1--12/70, 25:15425 (COO-1449-11)
PALMER, James L., Technetium as a catalyst in organic reactions, 25:15448 (RLO-2017-3)
PALMIOTTO, F., Alpha-particle observations in solar wind, 25:13895
PALMS, J. M., L subshells in Hg from the decay of ^{198}Au and ^{204}Tl, 25:15015
PAN, P. J., States of ^{116}In, 25:15008
PANCHENKO, V. E., Electron-excitation cross sections for x-ray series of Cl, Ar, and Xe, 25:14008
PANCHERI-SRIVASTAVA, G., Promotion and threshold singularities in massive quantum electrodynamics, 25:14792
PANFILOV, A. S., Effect of pressure on Cr susceptibility of V--Cr and Cr--Mn alloys, 25:14447
PANITKIN, Yu. G., Radiative capture of neutrons by ^{238}U in energy range 24 to 145 keV, 25:15106
PAPAY, K. M., Spectrophotometric determination of fluorine in organic compounds with thorium chloranilate after hydropyrolytic decomposition of lead fluoride, 25:12936
PAPIROV, I. I., Impact strength and fracture structure of beryllium, 25:13684

XUM

  Twins of tetrahedral form in beryllium, 25:13718
PAPPALARDO, G., Separation of nuclear-reaction mechanisms, 25:15151
PARADELLIS, Th., Excited states in ^{75}As, 25:14931
PARAMONOVA, I. N., Average number of prompt neutrons in fast-neutron-induced fission of ^{235}U, ^{239}Pu, and ^{240}Pu, 25:15115
PARENT, J. R., Temperature distributions in a helium plasma, 25:14254
  Velocity distributions in a gaseous plasma. II, 25:14253
  Velocity distributions in a gaseous plasma. I, 25:14252
PARISEAU, G., Concerning a thought experiment violating Heisenberg's uncertainty principle, 25:14502
PARK, John T., Excitation of Schumann--Runge dissociation continuum in O_2 by 20 to 110-keV protons, 25:14023
PARKER, H. M., University of Virginia superconducting wind-tunnel balance, 25:14216
PARKER, H. S., Effect of oxide additions on the polymorphism of tantalum pentoxide. IV. The system Ta_2O_5--Ta_2WO_8, 25:13775
PARKER, Leonard, Quantized fields and particle creation in expanding universes. II, 25:14788
PARKER, Monte Bryce, Applications of heat pipes to nuclear reactor engineering, 25:15400
PARKER, W. H., Analog computer simulation of weakly connected superconducting rings, 25:14190
PARKS, R. D., Vortex motion in the presence of thermodynamic fluctuations, 25:14207
PARTHASARADHI, K., Effective atomic numbers for coherent scattering process of gamma rays in alloys, 25:14405
  Effective atomic numbers of alloys for pair-production process, 25:14402
PARTLOW, W. F., Changes in lung scan pattern related to free fluid and cardiac position, 25:13484
PASCHOS, E. A., Asymptotic behavior of weak spectral functions and hadronic decays of W boson, 25:14634 (NYO-4204-7)
PASCUAL, P., Photon--photon scattering contribution to the decay rate of orthopositronium, 25:13992
PASECHNIK, L. A., Economic effectiveness of using radioactive isotopes in industry, 25:13174
PASHEV, I., Combined action of ethyleneimine and x rays on Aspergillus oryzae, 25:13381
PASK, C., Phenomenological nuclear three-body forces, 25:15160
PASSENEAU, Jacques, Pangloss, a CRT device for bubble chamber pictures, 25:13258 (CERN-70-21(Vol.1), pp 401-25)
PASSOW, C., Possibility of cooling with superfluid helium in tubular systems, for example, superconducting helix waveguides, 25:14846 (NP-18651)
PATAKI, L., Reaction between methyl iodide and alkaline iodide, 25:12996
PATLAK, Clifford S., Uptake curve in tracer kinetics, 25:13336
PATRICK, B. H., Evaluation of fission cross-sections of ^{235}U, ^{239}Pu, and ^{238}U and the capture cross-section of ^{238}U, 25:15127
  Ratio of the ^{6}Li(n,α) and ^{10}B(n,α) cross-sections from 10 eV to 80 keV, 25:14910
PATRIKEEV, Yu. B., Heat capacity of gadolinium--lutetium alloys at superlow temperatures, 25:14450
PATRUSHEV, B. I., Low-frequency instability of an electron-cyclotron wave in a plasma, 25:14343
PATTERSON, A., Alternating-current loss measurements in thin-film type II superconductors, 25:14189
  Very high critical current and field characteristics of niobium nitride thin films, 25:14193
PAUL, D. A. L., Positron annihilation in methane gas, 25:13993
PAVEL, D., Level scheme of ^{139}La, 25:15032
  Level structure of ^{141}Pr studied by photonuclear excitation, 25:15139
PAVLINOV, L. V., Diffusion of cesium in mono- and polycrystalline molybdenum, 25:13676
PAVLOV, S. S., Intercrystalline corrosion of N70M28-type alloys, 25:13633
PEAK, Donald Wayne, Thermal-neutron-capture gamma rays of cadmium and chlorine, 25:14932
PEARLSTEIN, S., Progress in international nuclear data compilation and exchange, 25:14878
PEARSON, C. A., Reaction ^{40}Ca(d,p)^{41}Ca, 25:14938
PEASE, Alfred Anthony, Laser-light scattering as a plasma diagnostic technique, 25:14241 (AD-710718)
PEBERDY, John Malcolm, Grabheads for reactors, 25:15414
PECCEI, R. D., Troubles with strict conformal symmetry, 25:14820 (RLO-1388-598)
PECKER, J.-C., Influence of the line absorption on polarization of the continuum spectrum, 25:13898
PEE, A., Integrated program library for material property data, 25:13627
PELED, E., Contribution of H atoms to G/sub H2/ in the radiation chemistry of aqueous solutions, 25:13044
PELETSKII, V. E., Emissivity of W, Mo, and Re single crystals, 25:13666
PELLAT, R., Experimental observation of drift instabilities in a collisionless plasma, 25:14345
PENNA-FRANCA, E., Radioactivity in diet in high background areas of Brazil, 25:13439
PENNER, Thomas Lorne, Ions and excitations in organic radiation chemistry, 25:13037
PENNEY, B. K., Operator intervention in the Imperial College HPD system, 25:13290 (CERN-70-21(Vol.2), pp 931-40)
PENNINCQ, A., Removable head for pneumatic device, 25:13203
PENNINGTON, M. R., Comparison of integral constraints imposed on $\pi^0\pi^0$ s-wave by crossing symmetry and positivity, 25:14694
PENSELIN, S., Precision measurement of hyperfine structure of ^{175}Lu, 25:13986
PENZIAS, A. A., Attenuation of radio waves by atmosphere at frequency 1415 MHz, 25:13838
PEPPARD, D. F., Extraction of U(VI) and selected M(III) cations by bis n-octyl phosphoric acid in two different hydrocarbon diluents, 25:13096
PEPPLER, W., Investigation on dynamic boiling in sodium cooled fast reactors, 25:15382
PERCHERON, Annick, Magnetic susceptibility of intermetallic compounds of Sn--Sm system, 25:14453
PEREZ, A. G., Temperature dependence of thymidine uptake and stability of thymidine incorporated during unscheduled DNA synthesis in irradiated and unirradiated HeLa cells, 25:13554
PEREZ, R. B., Multilevel analysis of the ^{233}U and ^{235}U capture and fission cross-sections, 25:15130
PEREZ DE TEJADA, Hector Antonio, Magnetogasdynamic boundary layer, 25:14092
PEREZ-MENDEZ, V., Method for mapping the spatial distribution of stopping π^- mesons in tissue, 25:12547
PERKINS, Arthur Jeffery, Metastable phase transformations in bcc transition metal alloys, 25:13717
PERKINS, D. R., Neutron capture cross-section for ^{23}Na, ^{27}Al, ^{37}Cl, and ^{51}V, 25:14935
PERKINS, R. W., Laboratory and environmental mineral analysis using a ^{252}Cf neutron source, 25:12962
PERLES, Rene, Weight changes in spleen as a function of irradiation dose in mice, 25:13478
PEROVA, A. A., Cesium-137 from global fallout in foodstuffs and human organism, 25:13340 (NP-18382)
PERSIDES, S., Asymptotically flat spaces in asymptotically null-spherical coordinates, 25:14815
PERT, G. J., Collision free ionizing shock, 25:14298
PESCHEL, D. J., Weapons Effects Display System (WEDS MOD II): maintenance manual. I, 25:13322 (UCRL-50892(Vol.4)(Pt.1))
  Weapons effects display system (WEDS MOD II): maintenance manual. II, 25:13323 (UCRL-50892(Vol.4)(Pt.2))
PESHEKHONOV, V. D., Proportional chamber for compensation of counter geometry in the time-of-flight measurements, 25:13296 (JINR-P13-5472)
  System of proportional wire chambers on-line with a computer, 25:13297 (JINR-P13-5473)
PETER, J., Measurement of the prompt neutrons emitted in the fission of ^{209}Bi and ^{238}U induced by 155-MeV protons, 25:15021
PETERMAN, A., Sixth-order radiative corrections to α/sub μ/—α/sub e/, 25:14620
PETERS, Geraldine J., Observation of periodic shell activity by HR 2142, 25:13805
PETERS, M. W., 2400-MeV 5π mass enhancement in 6-prong π^-p events at 12 GeV/c, 25:14562 (TID-25640)
PETERSEN, D. A., Radiopharmaceuticals in nuclear medicine, 25:13519
PETERSON, Arsine Victoria, Spectroscopic investigation of four O-type subdwarfs, 25:13825
PETERSON, Donald N., Glaciological investigations on the Casement Glacier, southeast Alaska, final, 1/65--10/69, 25:15426 (CCO-1473-4)
PETERSON, E. W., Cylindrical Langmuir-probe response in transition regime, 25:14242 (AD-711095)
PETERSON, J. R., Charge-transfer excitation produced in collisions of He^+ and N_2^+ with alkali atoms, 25:14011
  Refinement of the crystal structure of $AmCl_3$, 25:13011
PETMEZAS, G., On-line measuring system using visual displays for operator guidance, 25:13237 (CERN-70-21(Vol.1), pp 39-46)
PETRAUSKAS, A. K., Study of low-lying levels of anomalous parity of p-shell nuclei in the unitary scheme approximation, 25:15169
PETRIKINA, R. Ya., Sintering of metals, carbides, and oxides by hot-pressing, 25:13743
PETROSYAN, R. A., Effect of x rays on cytological changes of bone marrow cells as a function of the immunobiological state of the reticulo-endothelial system, 25:13567
PETROV, G. D., Characteristic curve of the collective scattering of electromagnetic radiation in a plasma, 25:14375
PETROV, L. A., Anomalies in the Z dependence of mean charges of heavy ions in helium and air, 25:14007
PFLETSCHINGER, E., Measurement of fission cross-section of ^{241}Pu relative to ^{235}U, 25:15107
PHELPS, A. V., Prog. rpt. on basic plasma processes, final, 7/69--9/70, 25:14264 (AD-711828)
PHELPS, M. E., Decay of ^{56}Co and ^{66}Ga, 25:14957
PHILIP, Helen M., Calcium-47 studies in adult coeliac disease and other gastrointestinal conditions with particular reference to osteomalacia, 25:13359
PHILLIPS, G. C., Interference and rescattering effects in

reactions with three particles in the final state, 25:14891 (ORO-1316-97)
PHILLIPS, H. B., Automatic scanning and measurement of bubble chamber film on Polly II, 25:13254 (CERN-70-21(Vol.1), pp 325-55)
PHILLIPS, K. J. H., Cooling of flare-produced plasmas in the solar corona, 25:13889
PHILLIPS, Rita J. S., Dose-response curve for the yield of translocations in mouse spermatogonia after repeated small radiation doses, 25:13404
PIATTI, Giovanni, Unidirectional solidification of eutectic alloys, 25:13692
PICCHI, Pio, Experimental results on stopping muons at 60 and 300 m.w.e, 25:14535
PICCOTTI, F., Effects of continuous exposure to radioactive phosphorus in ionic form, 25:13351
PICHARD, B., Ariane II: automatic device for the analysis of spark chamber photographs, 25:13285 (CERN-70-21(Vol.2), pp 859-78)
PICHON, G., Calibration, precision, and filtering questions for the CERN Spiral Reader, 25:13235 (CERN-70-21(Vol.1), pp 5-18)
PICHUZHKIN, V. I., Effect of temperature on the composition of products in radiative induced oxidation of isooctane, 25:13040
PICKARDT, C. Renate, Thyroid gland growth and thyroid hyperfunction in anterior-pituitary insufficiency, 25:13579
PIEKOSZEWSKI, J., Evaluation of Moessbauer spectra for ^{57}Fe, 25:14485
PIELA, L., On the usefulness of approximate exchange integrals in calculations of the long-range forces, 25:13985
PIERCE, R. D., Chemical Engineering Division fuel cycle technology quarterly report, July--September 1970, 25:13077 (ANL-7755)
PIETRZYK, Z. A., Electron-drift velocities from ion and electron features of light scattering in z-pinch plasma, 25:14256
PIKEL'NER, L. B., Threshold detectors used for the neutron spectrum measurement, 25:13210 (JINR-P3-5421)
PILATI, D. A., Prog. rpt. on radiation-induced nucleation of bubbles in superheated water, 12/70, 25:13152 (SU-326-P-13-5)
PILE, P. H., New ^{110}Rh isotope, 25:15001
PILIPENKO, D. V., Collisions between fast protons or H atoms and O_2 molecules, 25:13999
PILLAY, K. K. Sivasankara, Activation analysis of airborne selenium as a possible indicator of atmospheric sulfur pollutants, 25:12965
PINARD-LEGRY, Gerard, Selective growth of pits on a stainless steel in a chlorinated oxidizing medium, 25:13637
PINK, E., Total material variables influencing a ductile--brittle transition temperature for molybdenum, 25:13649 (AD-713191)
PINT, P., Potential chloride electrolytes for recovering the metals Ti, Zr, and Hf by fused salt electrolysis, 25:13089
PINTER, G., Effective mass spectra of the $\gamma\gamma$, $\pi^0\gamma$, $\pi^0\gamma\gamma$, $\pi^0\pi^0$, π^0eta^0, $\pi^0\pi^0\gamma$, $\pi^0\pi^0\pi^0$ systems in mass value region M (γ.......γ) less than or equal to 1.3 GeV, 25:14560 (JINR-E1-5349)
PIOTROWSKI, A., Optimization of ion source and ion optical parameters of isotope separator, 25:13162 (JINR-P13-5369)
PIPES, Paul Bruce Jr., Experiments with ^{3}He--^{4}He dilution refrigeration, 25:14213
PIRILA, P., Separation of coherent and incoherent cross sections in inelastic neutron scattering using polarized nuclear targets, 25:14869
PIRRAGLIA, J., Latitudinal and longitudinal variation of a planetary atmosphere, 25:13956
PISAREV, Yu. N., Oxygen and hydrogen isotope exchange in alcohols, 25:12991
PISENT, G., Target spin dependence of the optical potential, 25:15152
PITTERLE, T. A., Evaluation of ^{238}U neutron cross-sections, 25:15126
PIVOVAROV, V. G., Nature of auroral magneto--ionospheric perturbations, 25:14106
PLAMBECK, James A., Electrochemical studies of Y and Y--Zn alloys in fused LiCl--KCl eutectic, 25:13095
PLANE, D. E., Stray baryonic resonances and SU(3), 25:14771
PLANEL, H., Development of Paramecium aurelia: influence of natural radiation, 25:13556
PLANICL, T., Indium-113m-gelatine preparation for placental scintigraphy, 25:13502
PLANTE, Georges, Selective growth of pits on a stainless steel in a chlorinated oxidizing medium, 25:13637
PLAUGER, Phillip James, Spectroscopy in Ti isotopes via (p,d) and (p,t) reactions, 25:14949
PLEKHANOV, A. F., Niobium precipitation on liquid zinc cathode, 25:13642
PLINER, Gerald A., Analysis of ^{131}I data in bovine thyroids, October 1964 through February 1969, 25:13397
PLOOG, K., B--C system in the kinetic formation region, 25:13767
  Carbon-induced lattices of B. I, 25:13739
  Formation of lattices of pure boron, 25:13740
PLOTKO, V. M., Apparatus for investigation of α-active nuclei: the products of reactions with heavy ions, 25:14841 (JINR-P13-5353)
PLUCINSKI, C. E., Water and gas determinations in mixed oxides, 25:12924 (WHAN-SA-62)
PODDAR, R. K., Greater vulnerability of the infecting viral strand of replicative-form deoxyribonucleic acid of bacteriophage phiX174, 25:13382
PODKULSKI, S. P., Operation of thermionic converter with tungsten emitter and niobium collector, 25:14083 (N-70-39884)
PODPORA, Jan, Long-term changes in fuel isotope composition in a fast power reactor started up with ^{235}U, 25:15376
  Long-term changes in parameters describing fuel balance of fast power reactor started up with ^{235}U, 25:15377
POENITZ, W. P., Recent experimental data for heavy nuclei, 25:15102
POINTU, Anne-Marie, Study of an ionic instability in the plasma of a low pressure positive column subjected to a microwave resonating electric field, 25:14336 (NP-18662)
POIZAT, J.-C., Dissociation of fast H_2^+ beam colliding with thin C targets, 25:13972
POKROVSKII, V. N., Angular dependences of many-charge particles produced by 660-MeV protons on ^{27}Al nuclei, 25:14945
  Mapping of uvr gene of S. typhimurium, 25:13408
POLETTO, G., Connection between N--S and E--W solar asymmetries, 25:13883
POLIKANOV, S. M., Spontaneously fissioning isomers in U, Pu, Am, and Cm, 25:15046
POLIKARPOV, G. G., Accumulation of ^{90}Sr and ^{144}Ce from sea water by alginic acid, 25:13403
POLISHCHUK, R. F., Petrov's classification of gravitational fields and time invariants, 25:14809
POLITIEK, J., Total cross section measurements of K on rare gases, 25:14005
POLITIS, C., Studies of the system uranium mononitride--molybdenum and uranium mononitride--tungsten at high temperatures, 25:13772
POLLARD, J. H., Epitaxial growth of Th on a W(100) substrate, 25:13719
POLLEY, M. V., Neutron thermalization in graphite, 25:14874
POLONIS, D. H., Metastable constitution and superconducting transition behavior of Zr--Ta alloys, 25:13716
POLOVIN, R. V., Fluctuations in a magnetohydrodynamic shock wave, 25:14287
POLUEKTOV, N. S., Carminic acid as a reagent for the photometric determination of the rare earth elements, 25:12937
  Extraction of alkaline earth metals with thenoyltrifluoracetone and rhodamine S, 25:13098
POLVERELLI, Michel, Influence of radiation and amount of palmitate-1-^{14}C on distribution of this fatty acid in different lipid classes of Ehrlich ascites, 25:13362 (CEA-R-4039)
PONSSEN, H., Description and performance of the CERN Spiral Reader, 25:13236 (CERN-70-21(Vol.1), pp 19-36)
PONTECORVO, B. M., Lepton charge and neutrino astrophysics, 25:13909
PONTEKORVO, B. M., Search for new type of radioactivity in aluminum and tungsten targets irradiated by 70-GeV protons, 25:14541 (JINR-P1-5399)
POORTMANS, F., Scattering cross-section of ^{235}U below 100 eV, 25:15084
  Scattering cross-section of ^{235}U between 0.025 and 1 eV, 25:15085
POPEA, Florica, Spectrophotometric investigations of system Th$(NO_3)_4$--violuric acid, 25:13014
POPIL'SKII, R. Ya., Phase relations and the electrical conductivity in the system ZrO_2--Sc_2O_3, 25:13778
POPOV, A. V., Life times of levels of ^{125}Te nucleus, 25:15055
POPOV, E. A., Nuclear gamma-resonance study of products of β-decay of /sup 121m/Sn, 25:13074
POPOV, Yu. P., (n,α) reaction on Sm and Nd isotopes, 25:14994
  Alpha widths of neutron resonances, 25:15097
POPOVA, E. A., Isotope effect in Raman spectra of a DKDP crystal, 25:12997
POPOVA, L. N., Phase relations and the electrical conductivity in the system ZrO_2--Sc_2O_3, 25:13778
POPPER, E., Microanalysis of cobalt by electrophoretic focussing with radioactive tracer, 25:12949
PORILE, N. T., Decay of ^{210}Po, 25:14996
  Test of the independence hypothesis by angular distribution measurements, 25:15065
PORT, M., Spins of levels of ^{34}Cl, 25:14942
PORTER, D., Reactions (n,n'γ) in ^{51}V and ^{89}Y, 25:14919 (AWRE-O-78/70)
PORTER, E. H., Rectangular moulds, 25:13455
PORTER, G. D., Plasma stability in bounded systems, 25:14339
PORTER, L. E., Stopping power of Havar for 2.5 to 7.0 MeV deuterons, 25:14401
PORTER, Newell S., Method for detecting one of heavy water and ordinary water in the presence of the other of heavy water and ordinary water, 25:12931
POSADAS, Roger, Motion and structure of singularities in general relativity, 25:14813
POSE, R., Development of track chamber picture processing

XUM

systems at JINR, 25:13279 (CERN-70-21(Vol.2), pp 753-60)
POSER, H., Infrared thermography with a color scanner used in nuclear medicine, 25:13498
POSSIN, George Edward, Superconductivity in nearly one-dimensional wires, 25:14151
POTTER, G. D., Fate of Schooner fallout radionuclides ingested by the dairy cow, 25:13396 (UCRL-72511)
POULARIKAS, A. D., Space-charge waves of bounded plasmas, 25:14372
POVER, W. F. R., Calcium-47 studies in adult coeliac disease and other gastrointestinal conditions with particular reference to osteomalacia, 25:13359
POWE, R. E., Natural convection heat transfer between concentric spheres, 25:15450 (RLO-2214-2)
POWELL, B. W., Bubble chamber film measurement on HPDs at CERN, 25:13281 (CERN-70-21(Vol.2), pp 813-24)
  Conference on data handling systems in high-energy physics, Cavendish Lab., Cambridge, 3/70, 25:13234 (CERN-70-21(Vol.1))
  Conference on data handling systems in high-energy physics, Cavendish Lab., Cambridge, 3/70, 25:13263 (CERN-70-21(Vol.2))
POWELL, D. L., Low-lying levels and decay structure in ^{62}Cu, 25:14940
POWELL, G. W., Solubility of tritium in annealed and cold-worked copper, 25:13654 (MLM-1734)
POWELL, James R., Lift/drag ratios for magnetic suspensions, 25:15419 (BNL-15420)
POWERS, R. J., Muonic interactions in ^{64}Zn and ^{66}Zn, 25:14958
PRAKASH, H., Density operator for unpolarized radiation, 25:14504
  Scattering of linearly polarized radiation, 25:14601
PREEDGM, B. M., 40-MeV proton inelastic scattering on ^{50}Ti, ^{51}V, and ^{52}Cr and its microscopic description, 25:14928
PRESMAN, A. S., Electromagnetic fields and life, 25:13570
PRESTWOOD, R. J., Neutron-induced ^{235}U fission at individual resonances. III, 25:14999
PRIBBLE, Mary Jo., New coordination compounds of uranium(V), 25:13016
PRICE, P. B., Extralunar dust in Apollo cores, 25:13958
PRICE, R., Production of Candida utilis with 93 at. percent ^{13}C acetic acid as the sole carbon source, 25:13331 (LA-4551)
PRICE, Stephan D., Stellar standards at 10 microns, 25:13788 (AD-711364)
PRIESMAYER, H. G., Measurements of neutron-resonance total cross-sections for fission product isotopes, 25:15098
PRILUTSKII, O. F., Cosmic rays in an expanding universe, 25:14080
PRINCE, A., Analysis of high-energy neutron cross-sections for fissile and fertile isotopes, 25:15133
PRINZIE, Michel, Pangloss, a CRT device for bubble chamber pictures, 25:13258 (CERN-70-21(Vol.1), pp 401-25)
PRITCHARD, J. A. V., Some unexpected dosimetric problems in an apparatus for mammalian radiobiology, 25:13456
PRITCHARD, T. W., Precise measurement of K^+ lifetime, 25:14531
PROKERT, K., Dosimetry of ionizing radiation through solid-dye systems, 25:13306
PROKHORETS, I. M., Investigation of reaction ^{4}He$(\gamma,p)^3$H at maximal γ-quanta energy 120 MeV, 25:14886
PROKHOROVA, L. I., Average number of prompt neutrons in fission of ^{235}U and ^{239}Pu by neutrons, 25:15116
PROKOF'EV, O. N., Cesium-137 from global fallout in foodstuffs and human organism, 25:13340 (NP-18382)
PROKOPCHIK, V. I., Neutron activation analysis in continuous determination of fluorite in a pulp flow, 25:12976
PRONINA, A. P., Paraprocess susceptibility of Gd and Ni_3Mn near Curie temperature, 25:14446
PROVETSKI, E., Investigation of the Heisenberg Model of impure ferromagnets, 25:15420 (BNL-tr-390)
PRUZANSKY, Jacob, Radiation treatment of mine waste waters, 25:13036
PSHEZHETSKII, S. Ya., Studies of zeolite cation influence on γ radiolysis of adsorbed ammonia by the EPR method, 25:13057
PSHITULA, M., Alpha widths of neutron resonances, 25:15097
PUGACHEVICH, V. P., System of proportional wire chambers on-line with a computer, 25:13297 (JINR-P13-5473)
PULCINELLI, Mario, Statistical considerations regarding medical judgments of unsuitability for work involving risks of radioactive exposure, 25:13468
PUPEZIN, J., Determination of precise isotopic vapor pressure differences from -20 to 110°C, 25:12995
PUSHKINA, N. N., Hygienic investigation of the effect produced by small concentrations of uranium on the human body, 25:13595
PUSTOVALOV, V. V., Anomalous absorption of electromagnetic waves by a plasma, 25:14373

Q

QUAIM, Syed M., Decay of /sup 130g/I, /sup 130m/I, and ^{132}Cs, 25:15007
QUEMADA, Daniel, Formation of a boundary layer dissipating magnetic energy near a neutral plane, 25:14099
QUERCI, F., Carbon star UU Aur, 25:13803
QUERCI, M., Carbon star UU Aur, 25:13803
QUIGG, Chris, Two Reggeon exchange contributions to hadron scattering amplitudes at high energy, 25:14657 (UCRL-20032)

R

RAABE, O. G., New method for the generation of aerosols of insoluble particles, 25:13145
RABEAU, M., Interaction of a laser-created plasma with a strong magnetic induction, 25:14334
RABINOWITZ, Mario, Analysis of critical power loss in a superconductor, 25:14194
RABOTNOV, N. S., Probabilities of quadrupole transitions and the mean values of quadrupole moments in phenomenological nuclear theory, 25:15177
RADERMACHER, Ernst, Radiotherapy of malignant bone tumors, 25:13521
RADHAKRISHNAN, V., Noise analysis for amplifiers with superconducting input, 25:14224
RAD'KOV, A. I., Thermal conductivity of 29NK-type alloy at temperatures between 80 and 239°K, 25:13685
RADOMANOV, V. B., Measurement of total cross sections of π^---p interaction, 25:14561 (JINR-P1-5460)
RADUTA, A., Quadrupole--octupole vibrations in spherical nuclei, 25:15157
RAE, E. R., Isomeric level in ^{239}U, 25:15077
  Neutron detector with a flat energy response for use in time-of-flight experiments, 25:13215
RAE, H. K., Review of heavy water production processes, 25:13076 (AECL-2503)
RAEDER, J., Composition and electrical conductivity of combustion plasmas, 25:14285 (BMBW-FBK-70-29)
RAETHJEN, H., Rocket instrument for measuring energy spectrum and directional distribution of medium energy protons in the auroral zone, 25:13227
RAGUIDEAU, J., Influence of an interplanetary disturbance on solar flare proton propagation, 25:13869
RAIKO, V. I., Optimization of ion source and ion optical parameters of isotope separator, 25:13162 (JINR-P13-5369)
RAINEY, W. T. Jr., Analytical mass spectrometry at Oak Ridge National Laboratory, 25:13319 (ORNL-4643)
RAISBECK, G. M., Decay of ^{7}Be in cosmic rays, 25:14059
RAIZER, Yu. P., Investigation of a high-pressure laser spark ignited by an extraneous plasma source, 25:14331
RAJARAMAN, R., Fixed pole in virtual Compton amplitude A_2, 25:14608
RAJASEKARAN, G., Fixed pole in virtual Compton amplitude A_2, 25:14608
RAJU, M. R., Method for mapping the spatial distribution of stopping π^- mesons in tissue, 25:13547
RAMAKRISHNA, D. V. S., Resonance parameters of ^{240}Pu, 25:15092
RAMALINGASWAMI, V., Interaction of x-radiation and malnutrition. A study of kinetics of cellular proliferation in the jejunum of protein-deficient rats, 25:13562
RAMAN, K., Eikonal model for large-angle np and pp elastic scattering, 25:14737
  Method of extending Blankenbecler--Sugar--Logunov--Tavkhelidze approximation to Bethe--Salpeter equation, 25:14786
RAMANAUSKAS, Algimantas, The ratio of negative to postive pions in forward pion photoproduction, 25:14523
RAMA RAO, J., Effective atomic numbers for coherent scattering process of gamma rays in alloys, 25:14405
RAMA RAO, P. N., K x-ray yields from ^{235}U fragments, 25:15027
RAMASUBRAMANIAN, P. V., Prog. rpt. on study of grain boundary segregation, 12/2/70, 25:15428 (COO-1778-6)
RAMBERG, C. F. Jr., Prog. rpt. on calcium kinetics in cows, annual, 12/22/70, 25:15438 (NYO-3360-55)
RAMBO, John T., K-division experimental work. Part I. Geophysics research for underground explosion technology, 25:13104 (UCRL-50855)
RAMDAS, S., Electrical transport in rare-earth oxides, 25:14469
RAMDOHR, B., Definition of toxic thyroid adenomas, 25:13594
RAMULU, K. Sree, Mutagenicity of radiations and chemical mutagens in sorghum, 25:13420
RANCITELLI, L. A., Laboratory and environmental mineral analysis using a ^{252}Cf neutron source, 25:12962
RANDHAWA, H. S., Ultraviolet absorption spectra of acetone and acetone-d_6, 25:13006
RANFT, J., Atlas of particle production spectra, 25:14733 (NP-18660)
RANKIN, J. M., Pulsar NP 0532: disappearance of precursor pulse at 606 MHz, 25:13848
RANT, J., Fission-spectrum-averaged neutron cross-sections for some threshold detectors, 25:14968
RAO, A. Lakshmana, Effective atomic numbers for coherent scattering process of gamma rays in alloys, 25:14405
RAO, B. K., Electric field shielding and antishielding factors at rare-earth and heavy ions, 25:13983
RAO, C. L., Gamma spectrometric estimation of radionuclides in reactor coolant water, 25:12956
RAO, C. N. R., Electrical transport in rare-earth oxides, 25:14469

Plasma resonance in TiO, VO, and NbO, 25:14462
Ultraviolet absorption spectra of acetone and acetone-d_6, 25:13006
RAO, G. V. Subba, Electrical transport in rare-earth oxides, 25:14469
RAO, P. Venugopala, L subshells in Hg from the decay of ^{198}Au and ^{204}Tl, 25:15015
RAO, Y. V., Azimuthal symmetry in 17.2-GeV/c π^- jets, 25:14565
RAPPAPORT, S., 1- to 10-keV x-ray sky near the galactic center, 25:13857
RASHID, M. A., Broken chiral and conformal symmetry and Kuo transformation, 25:14770
RASMUSSEN, J. O., New Ta isotopes ^{170}Ta and ^{171}Ta, 25:15066
RATKOCZY, Nandor, Unusual delay of metastases recurrence following radiotherapy of a mediastinal tumor, 25:13543
RAUBOLD, E., Experiences with coupled computers to control an HPD, 25:13276 (CERN-70-21(Vol.2), pp 721-7)
Use of IBM data management to control bubble chamber data flow, 25:13277 (CERN-70-21(Vol.2), pp 729-34)
RAVNIK, V., Adsorption of V on oxides and its application tc analytical separations, 25:12959
RAWITSCHER, G. H., Virtual nuclear excitation corrections to elastic electron scattering at low energies, 25:15166
RAWLS, John Marshall, Dynamical calculations in current algebra, 25:14593
RAY, D. K., Contributions of conduction electrons to electric field and nuclear quadrupole interaction in rare earth metals, 25:14451
RAY, R., Metastable phase $(Al_{0.5}Nb_{0.5})Ni_3$, 25:13706
RAYNAL, J., Measurement and microscopic calculations of the cross sections and asymmetries for the (p,p') reaction exciting the 2.31-MeV $(0^+, T = 1)$ state of ^{14}N, 25:14890 (CEA-CONF-1651)
RAZUMOVA, K. A., Dependence of transport coefficients on plasma parameters in Tokamak, 25:14239
READ, B. J., Low energy theorems and high energy photoproduction, 25:14622
REAVEY, T., Liquid waste effluents from a nuclear fuel reprocessing plant, 25:12950 (BRH/NERHL-70-2)
REBBI, Claudio, New dual-resonance amplitude, 25:14675
REBOUL, G., Automatic gain control in signal processing for bubble chamber pictures, 25:13257 (CERN-70-21(Vol.1), pp 383-97)
Use of Coccinelle to scan and measure big bubble chamber pictures, 25:13256 (CERN-70-21(Vol.1), pp 371-81)
RECAMI, E., Space--time operator in collision descriptions, 25:14830
REDDY, D. V. Krishna, Incoherent scattering of gamma rays by K-shell electrons of Pt, 25:14410
REDPATH, Bruce B., Concept of row crater enhancement, 25:13135 (AD-713574)
REED, D., Identification of impurities in neutron-irradiated graphites by γ spectrometry, 25:12954
REED, R. E., Spin-wave dispersion relation in dysprosium metal, 25:14444
REEDNICK, J., Study of several neutron-deficient hafnium nuclides, 25:15025
REEHAL, Balbir S., Electric quadrupole transitions in odd-mass spherical nuclei, 25:15165
REFSDAL, S., Stars with central He burning and occurrence of loops in H--R diagram, 25:13815
REGAD, G., Description and performance of the CERN Spiral Reader, 25:13236 (CERN-70-21(Vol.1), pp 19-36)
REICHSTEIN, I., Study of N + α system with resonating-group method, 25:14880 (COO-1764-105)
REINHARDT, M., Paradox in interaction of gravitational and electromagnetic fields, 25:13946
REINHARDT, Michael, Does a primeval magnetic field exist, 25:13944
REISS, G., ARNULF: PDP-10 program for rapid acquisition of complete film information by a PEPR-device, 25:13242 (CERN-70-21(Vol.1), pp 113-24)
BERTA: a FORTRAN program for automatic recognition and reconstruction of bubble chamber events. I, 25:13243 (CERN-70-21(Vol.1), pp 125-39)
BERTA: a FORTRAN program for automatic recognition and reconstruction of bubble chamber events. II, 25:13244 (CERN-70-21(Vol.1), pp 141-75)
Heidelberg automatic event recognition, 25:13241 (CERN-70-21(Vol.1), pp 105-11)
REITBERGER, T., Short-lived intermediates in methylcyclohexane radiolysis, 25:13050
REITER, Elmar R., Atmospheric transport processes. II, 25:13121 (TID-25314)
REITMANN, D., Inelastic scattering of fast neutrons from ^{238}U, 25:15110
REJ, A. K., Inelastic photoproduction on nuclei and the determination of I_0/C, 25:14602
REKALO, A. P., Decay μ + e + ν + anti ν and limitations on neutrino and w boson masses and on variants of weak interaction, 25:14631 (ITF-70-64)
REKALO, M. P., Scattering of high-energy γ quanta on the nucleons and nuclei, 25:14595 (ITF-70-63-P)
REMBIELINSKI, J., Determination of the $X^0(960)$ meson spin--parity in the polarization experiment, 25:14720
REME, Henri, Low-energy proton flux parallel to field lines in auroral ionosphere, 25:14125
REMEIKA, J. P., X-ray diffraction studies of the metal insulator transitions in Ti_4O_7, V_4O_7, and VO_2, 25:14442
REMILLIEUX, J., Dissociation of fast H_2^+ beam colliding with thin C targets, 25:13972
REMY-DEFRAIGNE, J., Proteolysis of partially denatured albumin in isolated perfused intestine of normal and irradiated rats, 25:13349
RENARD, F. M., Photoproduction of $K^+\Lambda$ and $K^+\Sigma^0$ and g/sub ΛKN, g/sub ΣKN/ coupling constants, 25:14627
RENARD, Y., Photoproduction of $K^+\Lambda$ and $K^+\Sigma^0$ and g/sub ΛKN, g/sub ΣKN/ coupling constants, 25:14627
RENAUD, C., Experimental observation of drift instabilities in a collisionless plasma, 25:14345
RENSE, W. A., Mass motion in the solar chromosphere, 25:13877
REPKO, Wayne W., Order corrections to muonium hyperfine structure, 25:13990
RESNIKOFF, Marvin, Extension of the mass operator in the symmetric quark model for negative-parity baryon resonances, 25:14708
REUSE, B., Measurement of g-factors for the case of unseparable energies of the $\gamma\gamma$ cascade, 25:14975
REUSS, Albrecht, Punch card control of telecobalt therapy, 25:13540
REUTER, B., Weizmann Institute Spiral Reader system, 25:13293 (CERN-70-21(Vol.2), pp 953-62)
REUTOV, V. F., Electron-microscopic examination of Ni irradiated with α particles, 25:13728
REVA, A. D., Cholinesterase activity of the spinal cord of animals after x-ray irradiation, 25:13333
REVA, O. D., Cholinesterase activity of spinal cord following radiation, 25:13375
REXFORD, H. E., Development of SIREN capsule, Phase I, 25:13170 (SNC-2708-1)
REXFORD, H. Eugene, Prog. rpt. on development of SIREN capsule, phase IA, final, 9/69--1/70, 25:13171 (SNC-2708-2)
REYNOLDS, John M., Solar x-ray astronomy summary and bibliography, 25:13863 (N-70-39828)
REZACOVA, V., Time-resolved measurements of electron energy distribution in unstable plasma. I, 25:14246
Time-resolved measurements of energy distribution in unstable plasma. II, 25:14247
REZANKA, I., New Ta isotopes ^{170}Ta and ^{171}Ta, 25:15066
RHINES, F. N., Quantitative determination of the structure: property relationships in nuclear fuel element materials. Quarterly progress report, September 15--December 15, 1970, 25:13766 (SRO-552-6)
RHOAD, J. E., Effects of structure of peptide stationary phases on gas-chromatographic separations of amino-acid enantiomers, 25:15424 (COO-1222-42)
RHOADES, Rodney A., Carbon-14-1-palmitate incorporation by rat lung: effect of nitrogen dioxide, 25:13356
RHODES, J. R., Portable radioisotope x-ray analyzers: techniques and applications, 25:13310
RHODES, R. G., Alternating field losses in superconducting strip conductors, 25:14187
RIBLET, G., Superconductivity and spin fluctuations in the Ir--Ni, Ir--Co, and Ir--Fe alloy systems, 25:14202
RIBON, P., Evaluation in the resonance range of nuclei with a mass number above 220, 25:15094
Method of shape analysis of cross-sections of fissile nuclei, 25:15132
RICABARRA, G. H., Measurement of activation resonance integrals at infinite dilution with a lithium-drifted germanium gamma-ray spectrometer and comparison with calculated values, 25:15124
RICABARRA, M. D., Measurement of activation resonance integrals at infinite dilution with a lithium-drifted germanium gamma-ray spectrometer and comparison with calculated values, 25:15124
RICCI, Enzo, Fluid supported capsule holder for homogeneously irradiating samples, 25:13208
RICCI, S. Basso, Clinical experiences in antineoplastic treatment with telecobalt therapy, 25:13546
RICCIONI, N., Diagnosis of malignant lesions of the liver by radiocolloid and ^{131}I fibrinogen, 25:13483
RICHARD, C., Applicability of single Born scattering theory, 25:14363
RICHARDS, P., Production of ^{52}Fe for medical use, 25:13063
Technetium-labeled red blood cells, 25:13332
RICHOILLEY, G., Development of Paramecium aurelia: influence of natural radiation, 25:13556
RICHTER, D., Conception of integrity of type A and B packaging for shipment of radioactive materials, 25:13201
Illustration of specifications for transport of radioactive materials of high activity and fissionable materials, 25:13194 (SZS-19/70)
RICHTER, J., Investigation of an improved iron arc, 25:14245
RICKARD, C. E. F., Quinquevalent Pa and quadrivalent actinide tropolonates, 25:13009
RIECK, G. D., Process for removal of gases held in interstitial sites from titanium, zirconium, hafnium, or thorium, 25:13641 (UCRL-Trans-10503)
RIEDEL, J., Regulation of magnet power supplies, 25:14848 (PPAD-677-D)
RIES, G., Measurements on pulsed superconducting magnets, 25:14211 (KFK-1217)
RIESENFELDT, Peter W., Effect of nuclear deformability on

reaction cross sections, 25:15063
RIGAUD, J. M., Determination of B, C, and O in Si by activation analysis, 25:12971
RIGDON, L. P., Determination of boron in borates, boron hydrides, organo-boron compounds, elemental boron and refractory borides, 25:15465 (UCRL-50948)
RIMM, Alfred A., Skin allograft survival in mice after radioprotection with sodium S-(2-aminotheyl) phosphorothioate and supralethal total body x-irradiation, 25:13479
RINAUDO, G., Longitudinal phase-space analysis of 5 GeV/c π^+p reactions, 25:14578
RINDI, A., Method for mapping the spatial distribution of stopping π^- mesons in tissue, 25:13547
RINGLEB, Dietrich, Results of radiotherapy for bronchial carcinoma obtained at the Giessen Univ. Clinic from 1962 to 1967, 25:13522
RIOLS, G., Ariane II: automatic device for the analysis of spark chamber photographs, 25:13285 (CERN-70-21(Vol.2), pp 859-78)
RIPA, A., Plants in national agriculture. V, 25:13599
RISK, Clifford, Angular distributions from multiparticle production models, 25:14661
  Compositeness, Feynman diagrams, and Reggeized absorption model, 25:14785
RISLEY, J. S., Two autodetaching states of O^-, 25:14009
RITCHIE, Burke, Nonadiabatic atom--atom collisions, 25:14021
RITZL, Friedrich, Growth inhibition through gamma radiation on transplanted sarcomas in mice, 25:13473
RIVERS, R. J., Level degeneracy of generalized N-particle dual amplitude with satellites, 25:14826
RIVIER, J., Study of the decay $^{109}In \to {}^{109}Cd$, 25:15005
ROBERSON, C., Experimental test of quasi-linear theory, 25:14323
ROBERT, Marie-Josee, Pangloss, a CRT device for bubble chamber pictures, 25:13258 (CERN-70-21(Vol.1), pp 401-25)
ROBERTS, J. T. A., Nature of activation volume-stress dependence in high temperature plasticity of UO_2, 25:13756
ROBERTS, Paul H., Motion of ions at finite velocities in helium II, 25:14144
ROBERTS, R. E., Nonstatistical behavior for H atom recombination, 25:14016
ROBERTSON, R. E., Heat capacity of activation for the hydrolysis of methanesulfonyl chloride and benzenesulfonyl chloride in light and heavy water, 25:12984
ROBIN, M., Measurements of ^{233}U cross-sections for thermal neutrons, 25:15071
ROBINSON, B. J., Unusual OH emission from a Mira variable, 25:13818
ROBINSON, C. J., Progress on Polly at Glasgow, 25:13255 (CERN-70-21(Vol.1), pp 357-70)
ROBINSON, Edgar Larry, Neutron-activation analysis using monoenergetic gamma-ray spectra, 25:12966
ROBINSON, L. E., Apparatus for high-speed photographic experiments with irradiated fast-reactor fuel specimens, 25:15384 (ANL-7578)
ROBINSON, Lawrence Baylor, Indirect exchange coupling of magnetic moments in rare-earth metals, 25:14487
ROBINSON, R. L., Coulomb excitation of $^{107}\ {}^{109}Ag$, 25:15035
ROBOZ, John, Diagnostic application of metabolic studies with isotopes, 25:13506
ROCKWOOD, Stephen Dell, Dilution refrigeration and measurement of quadrupole coupling constant in Re metal, 25:14474
RODIER, Jean, Antipollution and radioactive wastes, 25:13087
RODIONOV, K. P., Equation of state of solids, 25:13681
ROEHRIG, Heinz Dieter, Investigations of the diffusion of ^6Li from irradiated BeO, 25:13781 (JUL-677-RG)
ROESCH, D. L., Metallographic analysis of SNAP--15C heat source capsule, 25:13164 (MLM-1670)
ROESCH, Jean, Monochromatic photography of coronal emissions, 25:13887
ROESLER, F. L., Abundance of lithium in sunspots, 25:13865
ROGER, Robert Patrick, Amplitude effects for oscillating disk in liquid He II, 25:14134
ROGERS, J. D., Angular correlation in nuclei with integral spin, 25:14477
  Superconducting quadrupole doublet for LAMPF, 25:14860
ROGERS, L. B., Effects of structure of peptide stationary phases on gas-chromatographic separations of amino-acid enantiomers, 25:15424 (COO-1222-42)
ROGERSON, T. L., Half-minute counts for neutron probes, 25:13313
ROHR, G., Resonance parameters from neutron radiative capture in ^{238}U, 25:15081
ROHSENOW, Warren M., Refrigerant forced-convection condensation inside horizontal tubes, 25:13151 (NP-18642)
ROITENBURG, D. I., Continuous absorption of partially ionized xenon in the visible region of the spectrum, 25:14280
ROLLO, F. David, ^{125}I for measuring the radioiodine uptake of the thyroid, 25:13485
ROMAGNOLI, U., HDP--IBM 360/44 system at CNAF for bubble chamber data analysis. I, 25:13267 (CERN-70-21(Vol.2), pp 607-15)
  HPD--IBM 360/44 system at CNAF for bubble chamber data analysis. II, 25:13268 (CERN-70-21(Vol.2), pp 617-24)
ROMANOV, V. M., Life times of levels of ^{125}Te nucleus, 25:15055
ROMANOV, V. S., Observation of analogue states with T = 2 in the reactions $^{26}Mg(^3He,n)^{28}Si$, $^{46}Ti(^3He,n)^{48}Cr$, and $^{58}Ni(^3He,n)^{60}Zn$, 25:14943
ROMANOVA, L. V., Spectrographic determination of Se and Te in S, 25:12940
RONAT, E. E., Weizmann Institute Spiral Reader system, 25:13293 (CERN-70-21(Vol.2), pp 953-62)
RONEN, Yigal, Error estimate in reactor theory, 25:15403
RONOV, A. B., Evolution of the chemical composition of the rocks in the shields and sediment cover of the Russian and North American platforms, 25:13114
RONZHIN, A. I., Proportional chamber for compensation of counter geometry in the time-of-flight measurements, 25:13296 (JINR-P13-5472)
ROOSEN, Robert George, Gegenschein, 25:13906
ROSE, K., Comparison of superconducting and semiconducting bolometers, 25:14227
ROSE, Robert M., Tunneling into superconducting rhenium single crystals, 25:14147 (AD-711826)
ROSE, William K., Hydrogen-to-carbon ratios in accordance with CNO bi-cycle in carbon stars, 25:13795
ROSEN, Gerald, Dilaton field theory and conformally Minkowskian space--time, 25:14789
ROSENBERG, H., Evidence for mhd pulsations in the solar corona, 25:13868
ROSENBLUTH, M. N., Resistive plasma rotation and shock formation in toroidal geometry, 25:14235
ROSENFELD, L., Unitarity of the collision matrix and interdependence of resonance parameters, 25:15171
ROSNER, B., Decay of /sup 141m/Nd, 25:15014
ROSS, Sarah T., Cytological effects of juice or puree from irradiated strawberries, 25:13621
ROSSA, E., Calibration, precision, and filtering questions for the CERN Spiral Reader, 25:13235 (CERN-70-21(Vol.1), pp 5-18)
  Description and performance of the CERN Spiral Reader, 25:13236 (CERN-70-21(Vol.1), pp 19-36)
ROSSALL, B., Heat capacity of activation for the hydrolysis of methanesulfonyl chloride and benzenesulfonyl chloride in light and heavy water, 25:12984
ROSSI, A., Total body scanning for studies on regional distribution, 25:13503
ROST, E., Comments on shapes of angular distributions of $(^3He,t)$ and (p,n) transitions to 0^+ anti-analog states, 25:14924 (COO-535-625)
ROSTLER, Peter S., Darwin model as a tool for electromagnetic plasma simulation, 25:14293
ROTH, R. S., Effect of oxide additions on the polymorphism of tantalum pentoxide. IV. The system Ta_2O_5--Ta_2WO_8, 25:13775
  Structural studies by electron microscopy: polymorphism of $ZrO_2.12Nb_2O_5$, 25:13774
ROTHE, K. D., Local approximation to field and current commutators, 25:14673
ROTHER, Wolfgang, Method for determination of the viscosity of a plasma at atmospheric pressure, 25:14260
ROTHFELD, B., Unusual scan in cerebral infarction, 25:13489
ROTHSCHILD, Henry, Analysis of SV40-induced transformation of hamster kidney tissue in vitro. VII, 25:13615
ROTKOVSKA, D., Circadian variations in the effect of x-irradiation on the haematopoietic stem cells of mice, 25:13550
ROTURIER, Jacques, Fast-neutron interactions with 1p, 2s, 1d nuclei, 25:14898
  Interaction of fast neutrons with 1p, 2s, and 1d nuclei, 25:14920 (BNL-tr-380)
ROULSTON, K. I., Levels in ^{177}Lu, 25:15039
ROUX, G., Recovery of low-temperature electron-irradiated cobalt crystals, 25:13713
ROWCLIFFE, A. F., Matrix precipitation of NbC in 20/25/Nb stainless steel, 25:13640 (TRG-Report-2040)
ROWE, V. A., Ettingshausen effect in the intermediate state of thin superconducting Pb films, 25:14181
ROWLANDS, J. L., Relationship of microscopic and integral data, 25:15346
ROY, G., $^{48}Ca(d,p)^{49}Ca$ reaction across the Coulomb barrier, 25:14916
ROYSTON, R., Automatic scanning and measurement of bubble chamber film on Polly II, 25:13254 (CERN-70-21(Vol.1), pp 325-55)
ROZENTAL, I. L., Cosmic rays in an expanding universe, 25:14080
ROZGACHEV, K. I., Excitation functions of spectral lines of Kr II, 25:14040
ROZHKOV, V. V., Fluctuations in a magnetohydrodynamic shock wave, 25:14287
RUBBINO, A., Separation of nuclear-reaction mechanisms, 25:15151
RUBY, S. L., Hyperfine magnetic fields in USb, 25:14482
RUD, V. I., Effect of α-radioactive background at investigation of the α decay of the 104 element, 25:15017
RUDAKOV, L. I., Collective slowing down of an intense relativistic electron beam in a dense plasma target, 25:14292
  Current-interchange instability in turbulent heating of a

UM

plasma by a current, 25:14344
RUDAKOV, V. P., Reaction (^{3}He,α) on nuclei with 1d--2s shell, 25:14944
RUDSTAM, G., Electron-capture beta decay, 25:14993
RUDY, E., Phase diagram for W--B--C, 25:13763 (AD-713154)
  Phase diagrams of Ti--Nb--C, Ti--Ta--C, and Ti--Mo--C, 25:13762 (AD-713153)
RUDZIT, G. P., Extraction--photometric determination of Fe, 25:12934
RUEDIGER, A., Brush system for automatic processing of bubble chamber pictures, 25:13274 (CERN-70-21(Vol.2), pp 689-707)
RUEDIGER, O., Recent results of cemented carbide research and problems encountered, 25:13752
RUFFINI, Remo, Introducing the black hole, 25:13937
RUGE, I., Radiation damage of semiconductor surface barrier detectors, 25:13329
RUGGE, H. R., Variation in O VII x-ray line-emission from solar corona, 25:13885
RUMI, R. F., Alpha widths of neutron resonances, 25:15097
RUMMEL, Wulf, Punch card control of telecobalt therapy, 25:13540
RUSANCV, V. D., Collisionless heat wave, 25:14317
RUSH, C. M., Description of tidal effects in f_0F_2, 25:14105
RUSHBROOK, Peter Roys, Pulse radiolysis of N_2--NO and He--N_2, 25:13053
RUSSELL, B., Effect of radiation induced gas on the stress rupture properties of an aluminium--lithium alloy, 25:13678
RUSSELL, John L., Analysis of ^{131}I data in bovine thyroids, October 1964 through February 1969, 25:13397
RUSSO, Michael J., Lorentz covariance and canonical quantization of non-Abelian gauge theories, 25:14787
RUST, D. R., On-line computer facilities at Argonne, 25:14838 (CERN-70-21(Vol.2), pp 525-37)
RUZICKA, T., Low-current helium discharge at low pressures, 25:14301
RYABOV, Yu. V., Measurements of radiative-capture-to-fission cross sections (α) for ^{235}U and ^{239}Pu, 25:15075
RYABTSOV, V. D., Experimental ionization chamber filled with liquid and solid argon, 25:13295 (JINR-P13-5404)
  Spectrometer channel of experimental ionization chambers with the argon and xenon condensates, 25:13211 (JINR-P13-5402)
RYABUKHIN, Yu. S., Lithium-6 incorporation into tissues, organs, and transplantable tumors, 25:13350
RYAN, B. A., Proton--proton differential cross sections from 600 to 1800 MeV/c, 25:14543
RYAN, D. G., Deuteron stripping at 1.69 GeV/c. I, 25:14906
RYAN, John R., Combined therapy for cancer of the laryngopharynx, 25:13545
RYDE, H., High-spin rotational and three-quasiparticle excitations in ^{177}Ta, 25:15036
RYE, B. J., Physics of hot plasmas, 25:14305
RYE, Robert R., Mixed adsorption of ethylene and nitrogen on tungsten, 25:13687
RYUTOV, D. D., Asymptotic solution in the problem of anomalous plasma resistance, 25:14309
RYUTOV, V. D., Current-interchange instability in turbulent heating of a plasma by a current, 25:14344
RYVES, T. B., Neutron capture cross-section for ^{23}Na, ^{27}Al, ^{37}Cl, and ^{51}V, 25:14935

S

SABALYAUSKAS, L. Yu., Study of low-lying levels of anomalous parity of p-shell nuclei in the unitary scheme approximation, 25:15169
SACKETT, John Irvin, Slowing down of neutrons in graphite, 25:14870
SADOKHIN, I. P., Inelastic neutron scattering-(n,n'γ)-by F, Fe, Co, Ni, and Ta nuclei, 25:14960
SADOWSKI, G. S., Instrumentation and Controls Division annual progress report for period ending September 1, 1970, 25:13318 (ORNL-4620)
SADYKOV, S. S., Effects of γ rays on cotton at various light conditions, 25:13602
SAENDIG, R., Equation of state and ionization equilibrium hydrogen plasmas, 25:14319
SAETTA-MENICHELLA, E., New model for the mechanism of fission of heavy nuclei, 25:15024
SAFRATA, R. S., Simple ^{3}He--^{4}He dilution refrigerator, 25:14214
SAFRONOVA, U. I., Fine structure of terms for a sequence of states of light atoms, 25:14051
  Relativistic corrections to terms for a number of states of light atoms, 25:14052
  Theory of perturbations of the autoionization levels of two-electron atoms, 25:14049
SAGDEEV, R. Z., Asymptotic solution in the problem of anomalous plasma resistance, 25:14309
SAIKI, Masamichi, Safe control of environmental radioactivity around atomic energy plants, 25:13471
SAILOR, V. L., Spins of neutron resonances in ^{167}Er, 25:15003
SAITO, S., Manifestly gauge invariant N-Reggeon vertex, 25:14801
SAKANOUE, Masanobu, Nuclear track methods in solids and its development. I, 25:13219
SAKISAKA, Masakatsu, Thick-target yields of characteristic x rays by p, d, ^{3}He^{+}, and ^{4}He^{+} bombardments, 25:13962
SAKSENA, G. D., Nuclear deformation and optical isotope shifts in the region N = 88 to 90, 25:15048
SAKURAI, A., Far-field characteristics of ground shock induced by explosions, 25:13129 (AD-713521)
SAKURAI, H., Characteristic measurements of JRR-2, 25:15390 (JAERI-Memo-4141)
SALA, A., HDP--IBM 360/44 system at CNAF for bubble chamber data analysis. I, 25:13267 (CERN-70-21(Vol.2), pp 607-15)
SALNIKOV, O. A., Inelastic scattering of fast neutrons by Cr, Ni, Y, Zr, and W nuclei, 25:14967
SALOP, A., Charge-transfer excitation produced in collisions of He^{+} and N_2^{+} with alkali atoms, 25:14011
SALPETER, E. E., Photo-ionization of intergalactic matter, 25:13939
SALTZSTEIN, Edward C., Skin allograft survival in mice after radioprotection with sodium S-(2-aminotheyl) phosphorothioate and supralethal total body x-irradiation, 25:13479
SALZMAN, W. R., Time evolution of simple quantum-mechanical systems. II, 25:14495
SAMARANAYAKE, V. K., Scattering of hadrons on ^{6}Li, 25:15183
SAMBLES, A., Status of the HPD minimum guidance programs at CERN, 25:13278 (CERN-70-21(Vol.2), pp 737-52)
SAMSONOV, A. E., Radiative capture of neutrons by ^{238}U nuclei, 25:15105
SAMSONOV, A. V., Electrostatic field theory under ionospheric conditions, 25:14123
SAMSONOV, G. V., Sintering of metals, carbides, and oxides by hot-pressing, 25:13743
SAMUELS, Larry D., Liver scans after primary treatment of tumors in children, 25:13578
SANCHEZ-GOMEZ, J. L., Broken channels in π^{+}-photoproduction on ^{3}He, 25:14518
SANDA, A. I., Evidence for an isotensor electromagnetic current in pion photoproduction, 25:14604
SANDERS, H., Princeton automatic track reader, 25:13250 (CERN-70-21(Vol.1), pp 273-83)
SANDQUIST, David Lee, Energy loss of high-energy electrons in Sn, Pb, and Gd, 25:14392 (AD-711005)
SANDS, Matthew, Physics of electron storage rings, 25:14850 (SLAC-121)
SANDU, M. A., Carminic acid as a reagent for the photometric determination of the rare earth elements, 25:12937
SANDULESCU, A., Quadrupole--octupole vibrations in spherical nuclei, 25:15157
SANGAL, Satendra P., Composition and stability constants of cerium--chromotrope 2R chelate and the spectrophotometric determination of cerium, 25:12942
SANTAPPA, M., Photosensitization of vinyl polymerization by uranyl ions, 25:12981
SANTHANAM, K., Radiation transport in one-dimensional finite systems. I. Development in the anisotropic source--flux iteration technique, 25:14406
  Radiation transport in one-dimensional finite systems. II. Gamma-ray transport studies with ASFIT, 25:14407
SARAEVA, V. V., Effect of temperature on the composition of products in radiative induced oxidation of isooctane, 25:13040
SARANTITES, D. G., Decay of ^{56}Co and ^{66}Ga, 25:14957
SARFATT, J., Beyond Hartree-liquid model of superfluid bosons, 25:14142
SARGENT, F. P., Electron spin resonance studies of radiation damage. IV, 25:13033
SARIS, F. W., Argon L-shell and Ne K-shell x-ray emission in heavy ion--atom collisions, 25:14004
SARKOZI, Laszlo, Diagnostic application of metabolic studies with isotopes, 25:13506
SARMA, N., Fission of actinide nuclei, 25:14997
SARMA, Pranab K., Surface nucleation critical field H/sub c3/(T) of type II superconductors, 25:14171
SARTORIS, G., Vibrations in even Hg isotopes, 25:15033
SASAKAWA, Tatuya, Suggestion for solving three-body problems, 25:15210
SATO, K., Reactions (p,t) on even Ce isotopes, 25:15006
SATO, Matsuji, X-ray excited optical luminescence analysis of trace rare earths in high purity yttrium and gadolinium oxides, 25:12948
SATO, Mitsunori, Influence of temperature in the contact area on the static welding characteristics of electrical contacts, 25:13644
SATO, Noriyoshi, Low-frequency electrostatic waves in a weakly ionized plasma under a weak magnetic field, 25:14383
SAVATINOVA, I. T., Isotope effect in Raman spectra of a DKDP crystal, 25:12997
SAVCHENKO, M. M., Diamagnetic moment of a strong shock wave from a high-temperature light explosion in gases, 25:14282
SAVIN, M. V., Average number of prompt neutrons in fast-neutron-induced fission of ^{235}U, ^{239}Pu, and ^{240}Pu, 25:15115
SAVITSKII, I. V., Main results of investigations concerning radiation enzymology, 25:13379
SAVRIN, V. I., Solution on the unitarity relation for scattering amplitude of particles with spin, 25:14590

XUM

SAWICKI, M., Strong absorption cut in photoproduction, 25:14603
SAXENA, K. M. S., Screening numbers and scaled H-like wave functions for systems with large atomic numbers, 25:13976
SAYAPINA, R. Ya., Irradiation hazards produced by nonequilibrium emanations, 25:13435
SCANLAN, J. A., Natural convection heat transfer between concentric spheres, 25:15450 (RLO-2214-2)
  Prog. rpt. on natural convective heat transfer between concentric spheres, annual, 1/71, 25:15449 (RLO-2214-1)
SCARBROUGH, J. O., Superconductivity in Mo--Re and Nb--Ir sigma phases, 25:14177
SCARPA, G., Dosimetric use of beryllium oxide as a thermoluminescent material, 25:13304 (RT/PROT-(70)23)
SCHADEE, Aert, Upper limit of Swan band intensity in sunspot spectrum, 25:13881
SCHALE, C., Low spin, negative parity states in the N = 103 isotones of ^{171}Er, ^{173}Yb, and ^{175}Hf, 25:15059
SCHALCW, G., Ground state correlations in an extended Lipkin--Meshkov--Glick model, 25:15200
SCHATTEN, K. H., Mean solar field--interplanetary field correlation, 25:13896
SCHAUMANN, G., Diffusion coefficients of H and D in V, Nb, and Ta by Gorsky-effect measurements, 25:14440
SCHECHTER, J., Electromagnetic perturbation of the pseudoscalar-mass spectrum, 25:14690
  Symmetry breaking and spin-zero mass spectrum, 25:14689
  Van Hove model and non-leptonic hyperon decays, 25:14637 (SU-1206-238)
SCHEEF, Wolfgang, Effects of an extract of calves-blood on radioinduced mucosa lesions in the area of larynx and pharynx, 25:13475
SCHEERER, K., Symmetry conditions on nonlinear spinor field functionals, 25:14782
SCHEMMEL, R. R., Polarization effects in oxide insulators, 25:14437 (WHAN-SA-75)
SCHENCK, Alexander, Slow muon depolarization in a single crystal of gypsum, 25:13989
SCHENCK, Peter, Simultaneous double-isotope scintigraphy with an Anger camera, 25:13500
SCHENLEY, R. L., Role of pyridine nucleotides in the control of respiration in ultraviolet-irradiated Escherichia coli B/r cells, 25:13607
SCHEPERS, J. C., Implications of fundamental integral measurements on high-energy nuclear data for reactor physics, 25:15349
SCHERK, Jooel, Divergence of the two-loop planar graph in the dual-resonance model, 25:14666
SCHEUER, P. A. G., Small-scale irregularities in the interstellar gas, 25:13912
SCHIFF, Daniel, Fluid--solid phase transition of hard-sphere Bose system, 25:14500
SCHILLER, Karl, Behavior of uranium oxide particles in reducing flames, 25:13021
SCHILLING, R., Brush system for automatic processing of bubble chamber pictures, 25:13274 (CERN-70-21(Vol.2), pp 689-707)
SCHIMMEL, W., Heat generation by absorption of ionizing radiation in nuclear power plants, 25:15341 (SZS-20/70)
  Principles for control of nuclear material in GDR, 25:13193 (SZS-16/70)
SCHINDLER, R., Specificity of tritiated thymidine as a precursor of DNA under conditions of prolonged administration, 25:13358
SCHIPFER, J. J. M., Total cross section measurements of K on rare gases, 25:14005
SCHIRMANN, D., Interaction of a laser-created plasma with a strong magnetic induction, 25:14334
SCHLECHTENDAHL, E. G., DYSYS: digital computer program for simulation of general dynamic problems, 25:13158
  Investigation on dynamic boiling in sodium cooled fast reactors, 25:15382
SCHLEISIEK, Karl, Heat transfer and boiling during forced convection of sodium in an induction-heated tube, 25:13156
SCHLESINGER, Y., Level scheme of ^{139}La, 25:15032
  Level structure of ^{141}Pr studied by photonuclear excitation, 25:15139
SCHMELLING, Stephen G., Nuclear magnetic moment, hyperfine structure, and hyperfine-structure anomaly of ^{196}Au, 25:15026
  Nuclear spins, nuclear moments, and hyperfine structure of ^{69}Ge and ^{75}Ge, and $^{3}P_{2}$ hyperfine structure of ^{71}Ge, 25:14929
SCHMELZER, Ch., Laser beams as fiducial lines in bubble chambers, 25:13303
SCHMERLING, M. A., Phase transformations in near equiatomic Ta--Ru alloys, 25:13708
SCHMID, A., Fission cross section of ^{227}Th, 25:15044
SCHMIDT, G., New method for calculating the design strength of fuel cans for liquid metal cooled fast reactors, 25:13662
SCHMIDT, J. J., Evaluation of fast critical experiments using recent methods and data, 25:15387 (EURFNR-858)
  General status of nuclear data requirements, 25:15402
SCHMIDT, L., Facility for in-pile creep experiments on cladding tubes under thermal and stress cycling, 25:13142
SCHMIDT, R., ARNULF: PDP-10 program for rapid acquisition of complete film information by a PEPR-device, 25:13242 (CERN-70-21(Vol.1), pp 113-24)
  BERTA: a FORTRAN program for automatic recognition and reconstruction of bubble chamber events. II, 25:13244 (CERN-70-21(Vol.1), pp 141-75)
  BERTA: a FORTRAN program for automatic recognition and reconstruction of bubble chamber events. I, 25:13243 (CERN-70-21(Vol.1), pp 125-39)
  Heidelberg automatic event recognition, 25:13241 (CERN-70-21(Vol.1), pp 105-11)
SCHMIDT, W., Energy dependence of electron collision frequency on electrical conductivity of weakly ionized plasmas, 25:14308
SCHMIDT-HERMES, Heinz-Josef, Early results of telecobalt therapy of bronchial carcinomas, 25:13523
SCHMIEDEKAMP, C., Triple scattering for low-energy electrons, 25:14020
SCHNABEL, Klaus, Simultaneous double-isotope scintigraphy with an Anger camera, 25:13500
SCHNABEL, P., Measurements of the depolarization parameter D for elastic proton scattering, 25:14889 (CEA-CONF-1650)
SCHNEIDER, C. S., Forward magnetic scattering amplitude of iron for thermal neutrons, 25:14868
SCHNEIDER, G. J., Iridium-192 contact irradiation with clinical sequelae (radiation accident), 25:13466
SCHNEIDER, H., ARNULF: PDP-10 program for rapid acquisition of complete film information by a PEPR-device, 25:13242 (CERN-70-21(Vol.1), pp 113-24)
  BERTA: a FORTRAN program for automatic recognition and reconstruction of bubble chamber events. II, 25:13244 (CERN-70-21(Vol.1), pp 141-75)
  BERTA: a FORTRAN program for automatic recognition and reconstruction of bubble chamber events. I, 25:13243 (CERN-70-21(Vol.1), pp 125-39)
  Heidelberg automatic event recognition, 25:13241 (CERN-70-21(Vol.1), pp 105-11)
SCHNEIDER, Heidemarie, Pendulum radiation with transversal shift of axis during ^{60}Co-teletherapy. III, 25:13447
SCHNEIDER, Helga, Precipitation of vanadium of UO_2 spheres from the gas phase, 25:13737 (KFK-1292)
SCHNOPPER, H., 1- to 10-keV x-ray sky near the galactic center, 25:13857
SCHNOPPER, Herbert W., Hydrogen-to-carbon ratios in accordance with CNO bi-cycle in carbon stars, 25:13798
SCHNUPP, L., Brush system for automatic processing of bubble chamber pictures, 25:13274 (CERN-70-21(Vol.2), pp 689-707)
SCHOCKEN, Klaus, Heat transfer in convective envelope of Sun, 25:13862 (N-70-38381)
  Solar flow parameters, 25:13861 (N-70-37452)
SCHOENWALD, Dieter, Precipitation of vanadium of UO_2 spheres from the gas phase, 25:13737 (KFK-1292)
SCHOFER, N. L., Extraction of U(VI) and selected M(III) cations by bis n-octyl phosphoric acid in two different hydrocarbon diluents, 25:13096
SCHOLZ, W., Properties of ^{55}Mn, ^{56}Mn, and ^{57}Fe in the unified rotational model, 25:14973
SCHOMBERG, M. G., Ratio of capture and fission cross-sections of ^{239}Pu in energy range 100 eV to 30 keV, 25:15073
SCHOONOVER, D. R., Excitation of Schumann--Runge dissociation continuum in O_2 by 20 to 110-keV protons, 25:14023
SCHORR, Amir, Fifth interaction and baryon masses, 25:14706
  Nishijima's model with fifth interaction, 25:14639
SCHOWENGERDT, F. D., Excitation of Schumann--Runge dissociation continuum in O_2 by 20 to 110-keV protons, 25:14023
SCHRAMM, David N., Isotopic abundance of ^{26}Mg and limits on ^{26}Al in early solar system, 25:13864
SCHRANDT, R., Some elementary attempts at numerical modeling of problems concerning rates of evolutionary processes, 25:15435 (LA-4573)
SCHREIBER, D. S., Local magnetic fields in the vanadium--manganese alloy system, 25:14445
SCHRENK, G. L., Caesium plasma diodes seeded with Hg or Cd and the Penning effect, 25:14085
SCHRIEDER, G., Lifetimes of 4.623 and 4.688 MeV levels in ^{34}S, 25:14954
SCHUBARTH, A., Three-color photometry of field at border of Scutum Cloud, 25:13925
SCHUETEE, D., Hartree--Bogoliubov calculations with spherical restriction, 25:15202
SCHULHOF, M. P., Inelastic scattering of neutrons from antiferromagnets, 25:14471
SCHULMAN, LaDonne H., Structure and function of E. coli formylmethionyl tRNA. I, 25:13364
SCHULTE-BRINKMANN, Wolfgang, Radiation burden to the patient during a gastrointestinal passage, 25:13580
SCHULTE-FROHLINDE, Dietrich, Chemical effects of energetic radiation on frozen solutions and solid organic materials, 25:13056
SCHULTHEISS, G. F., Investigation on dynamic boiling in sodium cooled fast reactors, 25:15382
SCHULTZ, Alfred Joseph Jr., Development and organization of photosynthetic pigment systems, 25:15462 (UCRL-20202)
SCHULZ, N., Matrix elements in the A = 26, T = 1 triad, 25:15163
SCHULZ, Tilo, Longitudinal end effects of inductive three-

phase MHD converters, 25:14086
SCHUMANN, U., Integrated program library for material property data, 25:13627
SCHWARTZ, Marvin Jack, Instabilities in a hot electron plasma, 25:14349
SCHWARZ, U. J., Polarization of 150-MHz radiation from four pulsars, 25:13855
SCHWEBEL, John C., Sequence determination from fragment data, 25:15422 (COO-1018-1219)
SCHWENN, R., Measurement of the radial distribution of electric current density and temperature in hydrogen arcs with axial magnetic fields, 25:14268
SCIARAFFA, P. L., Automobile exhaust analysis for lead using a nuclear technique, 25:13309
SCOBEL, W., Integral cross sections of reaction $^{11}B(n,\alpha)^{8}Li(\beta)^{8}Be^{*}(2\alpha)$, 25:14895
SCOTT, F. A., Mock-up of remotely operated high-purity inert-atmosphere sodium analysis facility, 25:13195 (WHAN-SA-91)
SCRIBA, P. C., Thyroid gland growth and thyroid hyperfunction in anterior-pituitary insufficiency, 25:13579
SCULLY, Marlan O., Theory of Josephson radiation. I, 25:14168
SEABORG, Glenn T., The synthetic actinides: from discovery to manufacture, 25:13059
SEALS, R. K. Jr., Collisionless sheath near an electrode in the presence of a magnetic field, 25:14300
SEAMON, R. E., Calculations of Jezebel and Godiva with recent ENDF/B microscopic data, 25:15397
SEAR, R., Radio-iodine therapy to out-patients, 25:13596
SEBASTIAN, Kunnat Joseph, Once-substracted dispersion relations, current algebra, and weak decays of hadrons, 25:14654
SEBEK, J., Simple ^{3}He--^{4}He dilution refrigerator, 25:14214
SEEGER, P. A., Fission, capture, scattering, and total cross-sections of ^{239}Pu, 25:15091
SEELIGER, D., Correction of finite volume of scatterer effect on measurement of differential elastic and inelastic neutron cross sections. II, 25:15150
SEGALL, R. L., Dependence of radiation damage on deviation from Bragg angle, 25:13721
SEHGAL, Narender Kumar, Strange particle production in anti Pd annihilations in flight, 25:14550
SEIDEL, Karl-Heinz, Electroretinogram of a frog exposed to ultraviolet light of about 366 nm, 25:13573
SEIELSTAD, G. A., Polarization of 3C10 and 3C58 at 1420 and 2880 MHz, 25:13833 (AD-711611)
  Polarization properties of 3C 10 and 3C 58 at 1420 and 2880 MHz, 25:13839
SEIFERT, J., Indirect parasternal lymphoscintigraphy in mammary carcinomas, 25:13515
SEITE, G., Preliminary tests with pictures from Mirabelle, 25:13291 (CERN-70-21(Vol.2), pp 941-8)
SEKELY, M. E., Princeton automatic track reader, 25:13250 (CERN-70-21(Vol.1), pp 273-83)
SEKIGUCHI, Mutsuo, T4 endonuclease involved in repair of DNA, 25:13411
SEKULA, S. T., Low-frequency electromagnetic losses at 4.2°K of neutron-irradiated Nb, 25:14188
SELLE, J. E., Metallographic analysis of SNAP--15C heat source capsule, 25:13164 (MLM-1670)
  Metallographic analysis of SNAP-19B (IRHS) capsule, 25:13163 (MLM-1652)
SELLIER, J. C., Preliminary tests with pictures from Mirabelle, 25:13291 (CERN-70-21(Vol.2), pp 941-8)
SELONKE, F., Experiences with coupled computers to control an HPD, 25:13276 (CERN-70-21(Vol.2), pp 721-7)
SEN, Dilip, Decay of ^{172}Lu, 25:15030
SEN, S. K., Electric field shielding and antishielding factors at rare-earth and heavy ions, 25:13983
SEPTIER, Albert, Local reinforcement of magnetic field near asperities of superconducting surface, 25:14205
SEREGIN, A. A., Probabilities of quadrupole transitions and the mean values of quadrupole moments in phenomenological nuclear theory, 25:15177
SERGEEV, A. N., Concentration of uranium by living and dead peat-forming plants, 25:13116
SERGEEVA, V. N., Effect of ionizing radiation on the contents of ortho-oxyphenol in poplar shoots, 25:13598
SERIO, Salvatore, Contributions of inelastic channels to pion's and production of strange particles in proton--proton scattering, 25:14597
SERPI, A., Thermoluminescence of NaCl doped by stoichiometric excess, 25:14425
SERPI MACCIOTTA, P., Thermoluminescence of NaCl doped by stoichiometric excess, 25:14425
SEVCHENKO, A. N., Spectroscopy of chlorophyll and related compounds, 25:15417 (AEC-tr-7199)
SEXL, Theodor, Resistance to small spheres by frictional media, 25:15444 (ORNL-tr-2431)
SEXTON, M. C., Decay processes in a high density argon afterglow, 25:14257
SEYDEWITZ, Vera, Investigations about combination injuries, 25:13368
SEYERLEIN, J., Present data analysis system of the bubble chamber group at the MPI Munich, 25:13287 (CERN-70-21(Vol.2), pp 907-9)
SHABALIN, E. P., Experimental test of renormalization theory of weak interactions in ep scattering processes, 25:14646
SHADLEY, John Russell, Nucleation of cavitation by alpha-particle irradiation of liquid helium, 25:14133
SHADURSKII, K. S., Metabolism of ^{14}C-disecarbine in irradiated animals, 25:13576
SHAFER, J. Howard, Optical heterodyne measurement of xenon isotope shifts, 25:13004
SHAFER, Yu. G., Studies of cosmic plasma with Yakutsk complex, 25:14072
SHAH, Vasant L., Composition and stability constants of cerium--chromotrope 2R chelate and the spectrophotometric determination of cerium, 25:12942
SHAL'GIN, V. A., Oxygen and hydrogen isotope exchange in alcohols, 25:12991
SHAMRAI, E. F., Effect of sublethal and lethal doses of irradiation on extracellular and intracellular distribution of water in some tissues of rats, 25:13348
  Effect of sublethal and lethal radiation doses on extracellular and intracellular distribution of Na and K in brain, liver, kidneys, and muscular tissue of rats, 25:13566
SHANDOR, L., Statistical isospin model and cross sections of reactions $\pi^{-}p \to N + (2,\ldots,6)\pi$ within 1 to 16 GeV energy range, 25:14700 (JINR-P1-5471)
SHANER, John Wesley, Cyclotron echoes in Cs vapor, 25:14387
SHAPIRA, A., rho^{0} production in pn collisions at 6.98 GeV/c, 25:14741
  Weizmann Institute Spiral Reader system, 25:13293 (CERN-70-21(Vol.2), pp 953-62)
SHAPIRO, E. L., Cesium-137 from global fallout in foodstuffs and human organism, 25:13340 (NP-18382)
SHAPIRO, Irwin I., Gravitational constant: experimental bound on its time variation, 25:14812
SHAPIRO, H. H., Matrix elements in the A = 26, T = 1 triad, 25:15163
SHAPIRO, V. D., Nonlinear theory of excitation of plasma wave by electron beam, 25:14311
SHARAH, Abul, Electrode ablation in a spark discharge and in an electromagnetic shock tube, 25:14232
SHARMA, Urmil, Interaction of x-radiation and malnutrition. A study of kinetics of cellular proliferation in the jejunum of protein-deficient rats, 25:13562
SHAROV, B. V., Radiation aging of chromium, 25:13730
SHARPE, Thomas J., Standby milk surveillance network, 25:13443
SHATENSHTEIN, A. I., Compensation effect in a protophilic deuterium-exchange reaction associated with a change in solvation of the catalyst cation, 25:13007
SHAW, Graham, Evidence for an isotensor electromagnetic current in pion photoproduction, 25:14604
SHAW, James William Westgarth, Nuclear reactor pressure vessel, 25:15364
SHAYLOR, H. R., Vast: a video assisted scan table, 25:13238 (CERN-70-21(Vol.1), pp 47-58)
SHCHEPKIN, Yu. G., Method of direct measurement of the capture-to-fission cross-section, 25:15076
  Neutron-spectroscopy study of nuclei with A < 220 in resonance energy region, 25:15095
SHEFOV, N. N., Middle-latitude aurorae at the current solar maximum, 25:14115
SHEINDLIN, A. E., Thermophysical properties of solids at high temperatures, 25:13667
SHELBY, Robert Nelson, Direct muon production by neutral cosmic rays near sea level, 25:14063
SHELIKHINA, E. I., Extraction--photometric determination of Mo, 25:12933
SHELONTSEV, I. I., Electron-beam shaping in a linear induction accelerator, 25:14856 (UCRL-Trans-1425)
SHELTON, W. N., Electron-impact excitation of rare gas atoms in the distorted-wave approximation, 25:14015
  Total cross section for single-electron transfer in collisions of He^{+} with He, 25:14025
SHEN, Peter K., Dimensional S/sub n/ calculations of neutron spectra reflected from thick slabs of concrete and iron, comparison with measurements, 25:14865 (COO-2049-2)
SHENOY, G. K., Hyperfine magnetic fields in USb, 25:14483
SHEPARD, P. F., Proton--proton differential cross sections from 600 to 1800 MeV/c, 25:14543
SHEPELEV, G. I., Wigner function for hyperbolic rotations in the homogeneous Lorentz group, 25:14759
SHEPHARD, W. D., Double-Regge analysis of single-pion production in $\pi^{-}p$ interactions at 8 GeV/c, 25:14713
SHERIF, H., Further calculations of proton inelastic polarizations and asymmetries using a spin-dependent interaction of the full Thomas form, 25:14892 (RLO-1388-600)
SHERMAN, W. C., Seepage characteristics of explosively produced craters in soil and rock, 25:13102 (NCG-TR-27)
SHERWOOD, Arnold I., Bootstrap theory of vibrations. I, 25:15174
  Bootstrap theory of vibrations. II, 25:15176
SHEVCHENKO, V. I., Nonlinear theory of excitation of plasma wave by electron beam, 25:14311
SHIAU, Jeng-nan, Small-amplitude nonlinear theory of positive column spiral instability, 25:14347
SHIBATA, Tsugio, Magnetic properties of Y/sub 1-x/Sm/sub x/Co$_{5}$ compounds, 25:14461
SHIGAEV, V. N., Development of track chamber picture processing systems at JINR, 25:13279 (CERN-70-

XUM

21(Vol.2), pp 753-60)

SHIH, Pei-chong, MHD Rayleigh problem with unsteady wall motion, 25:14089

SHILLINGER, Yu. I., Hygienic assessment of chicken meat irradiated with pasteurizing doses of γ-rays, 25:13624

SHIMA, Kunihiro, Thick-target yields of characteristic x rays by p, d, $^3He^+$, and $^4He^+$ bombardments, 25:13962

SHIMABUKURO, F. I., Observation of 3.3-mm bursts and their correlation with soft x-ray bursts, 25:13891

SHIMABUKURO, Fred I., Prog. rpt. on 3.3-mm and soft x-ray bursts, 3/68--12/69, 25:13860 (AD-711784)

SHIMADA, S., Molecular motion of peroxy radicals of polytetrafluoroethylene, 25:13034

SHIMIZU, Ken'ichi, Electron microscopy study of the precipitation processes in Cu--2 wt. percent Be alloy, 25:13715

SHIMIZU, Ryuichi, Energy dissipation of electrons in Al and Cu targets, 25:14400

SHINER, V. J. Jr., Sulfonate leaving groups, structure and reactivity: 2,2,2-trifluoroethanesulfonate, 25:15421 (COO-1008-14)

SHIPL'RAIN, E. E., Thermophysical properties of solids at high temperatures, 25:13667

SHIRASHI, Yoshiyuki, Fallout ^{90}Sr in beer, 25:13434

SHIROKOV, M. I., Scattering by two centers in long-wave approximation, 25:14817 (JINR-P4-5438)

SHIVANANDAN, Kandiah, Cosmic-background measurements in the far infrared, 25:13949

SHIVPURI, R. K., Muon experiments, 25:14532

SHKAROFSKY, I. P., Applicability of single Born scattering theory, 25:14363

SHKUNDENKOV, V. N., Development of track chamber picture processing systems at JINR, 25:13279 (CERN-70-21(Vol.2), pp 753-60)

SHLENSKAYA, V. I., Methods for the analysis of natural materials containing ruthenium and osmium, 25:12939

SHLOMO, S., Nuclear levels excited by neutron capture γ rays, 25:15002

SHOAIB, K. A., Dependence of radiation damage on deviation from Bragg angle, 25:13721

SHOHET, J. L., Desensitivity of a microwave cavity to measurements of hot-electron density, 25:14262

SHOJI, Fumiya, Structure of film prepared by low-energy sputtering of molybdenum, 25:14456

SHOLIN, G. V., Stark broadening of H lines in plasma, 25:14310

SHOMODI, A., System for processing meson-telescope data, 25:14067

SHUBIN, Yu. N., Average radiation widths for excitation energies of the order of neutron binding energy, 25:15209

Density of excited states of atomic nuclei, 25:15208

SHUGART, Howard A., Electron mass shift in ^{133}Cs, 25:14514

Nuclear magnetic moment, hyperfine structure, and hyperfine-structure anomaly of ^{196}Au, 25:15026

Nuclear spins, nuclear moments, and hyperfine structure of ^{69}Ge and ^{75}Ge, and $^3P_2$ hyperfine structure of ^{71}Ge, 25:14929

SHUKLA, J. V., Electronic absorption spectra (π--π^*) of p-dibromobenzenes-D_4 and -H_4, 25:13003

SHULL, C. G., Forward magnetic scattering amplitude of iron for thermal neutrons, 25:14868

SHUNAILOV, A. F., Anodic dissolution of Mo in chloride--molybdate melts, 25:13631

SHUSTOVA, M. B., Extraction--photometric determination of Mo, 25:12933

SHUVALOV, L. A., Isotopic non-isomorphism of Rb(H/sub 1-x/D/sub x/)$_3$(SeO$_3$)$_2$ crystals, 25:12989

SHVARZ, K. K., Temperature dependence of radiation colloid production in KCl crystals, 25:14429

SHVYDKO, N. S., Cesium-137 from global fallout in foodstuffs and human organism, 25:13340 (NP-18382)

SIBGATULLIN, N., Development of inhomogeneities in axially symmetric models of the Universe, 25:13938

SICHA, M., Time-resolved measurements of electron energy distribution in unstable plasma. I, 25:14246

Time-resolved measurements of energy distribution in unstable plasma. II, 25:14247

SIDORIK, E. P., Effect of optical quantum generator radiation on electrical parameters of fresh tissue, 25:13565

SIDOROVA, I. K., Resonance phenomena in an alkali plasma located in a variable electric field, 25:14368

SIDWELL, R. A., Duality and comparison of resonance and Regge models for π^+p backward scattering, 25:14726

SIEGEL, Richard D., Enhancing the permeation characteristics of polyethylene by membrane irradiation in the fully swollen state, 25:13041

SIEKHAUS, Wigbert Josef, Range of Cs ions injected at 20 keV into Al, 25:13960

SIEKIERSKA, K. E., Chemical consequencies of the nuclear reactions in soluble Prussian Blue, 25:13068

SIENIAWSKI, J., Lifetimes of excited states in ^{101}Rh, 25:14992

SIGMON, Thomas William, Measurements of proton radiation damage and carrier diffusivities in Si, 25:14431

SIK, So Don, Measurements of radiative-capture-to-fission cross sections (α) for ^{235}U and ^{239}Pu, 25:15075

SILAEV, E. A., Experimental ionization chamber filled with liquid and solid argon, 25:13295 (JINR-P13-5404)

Spectrometer channel of experimental ionization chambers with the argon and xenon condensates, 25:13211 (JINR-P13-5402)

SILIN, V. P., Anomalous absorption of electromagnetic waves by a plasma, 25:14373

Theory of parametric resonance of plasma in a strong hf electric field, 25:14376

SILK, Joseph, Lyman-α production by suprathermal protons, 25:14061

Ultraviolet absorption-line spectra produced by H I regions, 25:13841

SILVA, R., Chemical separation of rutherfordium, 25:13088

SILVERMAN, Dennis, Existence of complex poles and oscillatory average multiplicity in multiperipheral models, 25:14585

SILVERMAN, Joseph, Mechanical properties of radiation-induced graft copolymers of styrene to polyethylene, 25:13042

SIMENOG, I. V., Local self-consistent field in nuclei with a large number of nucleons, 25:15167

SIMEONE, Marius, Coupling, 25:13199

Remote manipulation tool, 25:13200

SIMMONDS, M. B., Analog computer simulation of weakly connected superconducting rings, 25:14190

SIMMONS, J., Birmingham track analysis system, 25:13292 (CERN-70-21(Vol.2), pp 949-52)

SIMON, F., Effects of ^{60}Co γ radiation on Xe trioxide in aqueous solutions, 25:13049

SINANOGLU, Oktay, Oxygen auroral lines: new theory and experiment on forbidden transition probabilities, 25:14107

SINCLAIR, D. K., Factorization of Balachandran dual-resonance model, 25:14665

SINGER, Donald A., ELIPGRID: FORTRAN IV program for calculating probability of success in locating elliptical targets with square, rectangular, and hexagonal grids, 25:15433 (GJO-918-4)

SINGH, T. R., Long-range intermolecular forces using Gaussian basis functions, 25:13984

SINHA, B. K., Effect of irradiation on lymph flow and filtration function of lymph nodes, 25:13481

SINI, G. P., HPD--IBM 360/44 system at CNAF for bubble chamber data analysis. II, 25:13268 (CERN-70-21(Vol.2), pp 617-24)

SIPSON, Roger Fredrick, The theory of higher spin fields, 25:14798

SIVASUBRAMANIAN, A., Nonlinear instability of modulated waves in a magnetoplasma, 25:14367

SKAKUN, N. P., Influence of total x-ray irradiation on synthesis of bile acids in albino female rats (chromatographic investigation), 25:13370

SKANBERG, B., High-spin rotational and three-quasiparticle excitations in ^{177}Ta, 25:15036

SKARDHAMAR, H. F., Nuclear polarization energy correction for muonic spectra, 25:14937

SKAVRONSKAYA, A. G., Mapping of uvr gene of S. typhimurium, 25:13408

SKINNER, Gordon B., Shock tube experiments on the pyrolysis of deuterium-substituted ethylenes, 25:12993

SKIRDA, N. V., Relativistic increase of ionization and ionization effects in nuclear photoemulsions. III, 25:13299

SKORUPSKI, A., Two-stream instability for arbitrary stream temperatures and densities, 25:14340

SKORYUPIN, V. A., Current-interchange instability in turbulent heating of a plasma by a current, 25:14344

SKRIPKA,Yu. G., Anisotropic spatial distribution of ions scattered by a single crystal, 25:13970

SKROTSKII, G. V., Propagation of electromagnetic waves in Riemann space, 25:14499

SKRZYPCZAK, E., Search for resonant states p--/sub Λ/^4He and α--/sub Λ/^4He, 25:14573

SLATER, W. E., UCLA SMP system, 25:13249 (CERN-70-21(Vol.1), pp 243-60)

SLATTERY, P., Momentum-transfer dependence in reactions, 25:14575

SLAUGHTER, G. M., Bonding graphite to metals with transition pieces, 25:13648

SLETTEN, G., Spontaneously fissioning isomers in U, Pu, Am, and Cm, 25:15046

SLETTEN, H. I., Scanning and measuring of heavy liquid film on-line, 25:13271 (CERN-70-21(Vol.2), pp 651-64)

SLEVIN, James A., Elastic and inelastic differential scattering of low-energy electrons by potassium, 25:14034

SLIFKIN, L. M., Impurity diffusion in aluminum and its dilute alloys, 25:15445 (ORO-2036-21)

SLIV, L. A., Centrifugal terms in residual interaction of particles in nucleus, 25:15168

SLOT, W. F., Shapes of the non-unique and unique first-forbidden β-spectra of ^{86}Rb, ^{76}As and ^{126}I, 25:14976

SLOWINSKI, B., Effective mass spectra of the $\gamma\gamma$, $\pi^0\gamma$, $\pi^0\gamma\gamma$, $\pi^0\pi^0$, π^0eta^0, $\pi^0\pi^0\gamma$, $\pi^0\pi^0\pi^0$ systems in mass value region M (γ.......γ) less than or equal to 1.3 GeV, 25:14560 (JINR-E1-5349)

SMALL, Maurice, Experiences with ^{32}P in advanced carcinoma of the prostate, 25:13591

SMEETS, J., Comparison of radioactive contamination of total diet of adolescents in community. II, 25:13392 (EUR-3945(Pt.2))

SMIALEK, R. L., Interstitial solution hardening in tantalum single crystals, 25:13690

SMIDT, D., Cooling disturbances in the core of sodium-cooled fast reactors as causes of fast failure propagation, 25:15381

SMIRENKIN, G. N., Average number of prompt neutrons in fission of ^{235}U and ^{239}Pu by neutrons, 25:15116

  Neutron-induced fission of ^{240}Pu near threshold, 25:15051

SMIRNCV, B. M., Classical theory of resonant charge exchange, 25:14031

SMIRNCV, G. I., Search for new type of radioactivity in aluminum and tungsten targets irradiated by 70-GeV protons, 25:14541 (JINR-P1-5399)

SMIT, J., External-line wave functions in Coulomb-gauge electrodynamics and equivalence with the Landau gauge, 25:14780

SMITH, D. H., Analytical mass spectrometry at Oak Ridge National Laboratory, 25:13319 (ORNL-4643)

SMITH, David H., Mass spectrometric investigation of surface ionization. VI. Desorption of Th$^+$, Np$^+$, and Pu$^+$ from W surfaces, 25:13686

  Mass-spectrometric investigation of surface ionization. VII, 25:13979

SMITH, Francis J., Quantum transport cross sections for ionized gases, 25:14297

SMITH, I. L., On-line measuring system using visual displays for operator guidance, 25:13237 (CERN-70-21(Vol.1), pp 39-46)

SMITH, I. O., Effect of radiation induced gas on the stress rupture properties of an aluminium--lithium alloy, 25:13678

SMITH, J., Intermediate boson. I, 25:14641

SMITH, J. G., Superconducting microstrip high-Q microwave resonators, 25:14230

SMITH, Jack, Corrections to observed beta-ray atmospheric densitometer values as caused by cosmic rays, 25:13314

SMITH, L. G., Changes of lower ionosphere electron densities with solar zenith angle, 25:14104

SMITH, N. I., Search for magnetic monopoles in cosmic rays, 25:14078

SMITH, P. M., Positron annihilation in methane gas, 25:13993

SMITH, Richard Cecil, Experimental study of decay spectrum of K/sub L/^{0} $\to \pi^+\pi^-\pi^0$, 25:14536

SMITH, Roy H., Dose reduction factors of a lead-lined girdle, 25:13462

SMITH, T. D., Retention of /sup 113m/In--^{59}Fe-ferric hydroxide in the mouse, 25:13486

SMITH, William B., Gravitational constant: experimental bound on its time variation, 25:14812

SMITH, William Malcolm, Study of $K^- + p \to \Sigma^0 + \pi^0$ near 1670 MeV, 25:14568

SMITH III, Winfield Scott, Development of a polarized ion source, 25:14859

SMORODINSKII, Ya. A., Conference on high-energy physics, Dubna, 1964, 25:14583 (AEC-tr-6882/1)

SMUTZ, Morton, Extraction of Y in the system $Y(NO_3)_3$--HNO_3--H_2O--di(2-ethylhexyl) phosphoric acid, 25:13097

SNIDER, Dale R., Partial bootstrap of schizophrenic Pomeranchon, 25:14824

SNISAR, I. A., Cholinesterase activity of spinal cord following radiation, 25:13375

  Cholinesterase activity of the spinal cord of animals after x-ray irradiation, 25:13333

SNOEK, C., HPD--CDC 3200 system at Amsterdam, 25:13275 (CERN-70-21(Vol.2), pp 709-20)

SNOW, Peter Ballard, Spins and parities of 1514- and 1726-keV resonances in ^{27}Al(p,γ)^{28}Si reaction, 25:14948

SOBELS, F. H., Induction by x-rays of isochromosomes in germ cells of Drosophila melanogaster males, 25:13409

SOFER, G. A., Plutonium as an alternate fuel in large water cooled reactors, 25:15375 (CONF-691114-6)

SOHMA, J., Molecular motion of peroxy radicals of polytetrafluoroethylene, 25:13034

SOKOL, J., Rod models of fuel elements of nuclear reactors, 25:15410 (ZJE-92)

SOKOLCVA, V. I., Effect of sublethal and lethal doses of irradiation on extracellular and intracellular distribution of water in some tissues of rats, 25:13348

  Effect of sublethal and lethal radiation doses on extracellular and intracellular distribution of Na and K in brain, liver, kidneys, and muscular tissue of rats, 25:13566

SOKOLCWSKI, E. K., Thermal-neutron absorption cross-sections of gross fission products of ^{233}U, ^{235}U, and ^{239}Pu, 25:15100

SOKUR, L. P., Equations of motion invariant with respect to group P(1,n). II, 25:14747 (ITF-70-70)

SOLEILHAC, M., Mean number of prompt neutrons and relative cross-sections for fission of ^{235}U and ^{239}Pu between 0.3 and 1.4 MeV, 25:15114

  Measurements of (n,2n) and (n,3n) reaction cross-sections of fissionable materials using a large liquid scintillator, 25:15111

SOLINC, H., Fission-spectrum-averaged neutron cross-sections for some threshold detectors, 25:14968

SOLMITZ, Frank T., Test of $\Delta S = \Delta Q$ rule in leptonic decays of neutral K mesons, 25:14533

SOLOMCNIDOU, Christina, Application of Regge pole theory to large-angle π^+ photoproduction, 25:14598

SOLOV'EV, K. N., Spectroscopy of chlorophyll and related compounds, 25:15417 (AEC-tr-7199)

SOLOV'EVA, Z. I., Probability of fission with emission of long-range particles, 25:15018

SONA, P., Lifetimes of 4.623 and 4.688 MeV levels in ^{34}S, 25:14954

SONDEL, James A., Activation analysis of airborne selenium as a possible indicator of atmospheric sulfur pollutants, 25:12965

SONIN, E. B., Fluctuations, long-range order, and superfluidity, 25:14140

SOOD, D. K., Fission of actinide nuclei, 25:14997

SORANTIN, H., Preparation of ^{85}Sr and /sup 87m/Sr for bone scintigraphy, 25:13061

SORENSEN, Raymond A., Electric quadrupole transitions in odd-mass spherical nuclei, 25:15165

SOROKIN, A. A., Determination of g factors of second excited states $^{11}/_{2}^{-}$ of ^{147}Eu and ^{149}Eu by differential angular correlation method in external magnetic field, 25:15016

SOROKIN, D. N., Heat transfer during developed boiling of alkali metals, 25:13157

SOROKIN, Yu. A., Studies of zeolite cation influence on γ radiolysis of adsorbed ammonia by the EPR method, 25:13057

SOSNOWSKI, R., Proton--proton and pion--proton inelastic collisions and the proton and pion form factors, 25:14729 (INR-P-1229)

SOTNIKOV, V. M., Angular distribution of secondary electrons emitted by Nb due to bombardment with ions, 25:13969

SOUL, P. B., F-center saturation phenomena in KCl during low-energy electron irradiation, 25:14415

SOURIAU, Jean-Marie, Particle motion in the electromagnetic field, 25:14599

SOWERBY, M. G., Evaluation of fission cross-sections of ^{235}U, ^{239}Pu, and ^{238}U and the capture cross-section of ^{238}U, 25:15127

  Ratio of capture and fission cross-sections of ^{239}Pu in energy range 100 eV to 30 keV, 25:15073

  Ratio of the ^{6}Li(n,α) and ^{10}B(n,α) cross-sections from 10 eV to 80 keV, 25:14910

SPAHR, Kurt, Helium-3-crysotat for specific heat measurements, 25:14212 (UUIP-677)

SPALEK, Vaclav, Improvement of responsive layer depth and energy resolution by cooling surface-barrier silicon detectors, 25:13217

SPALINGER, D., Triple scattering for low-energy electrons, 25:14020

SPANGENBERG, W., Pulsational stability of pure-helium stars of low mass, 25:13793

SPARKS, W. M., Outer layers of model moving atmospheres, 25:13792

SPEJEWSKI, E. H., Decay of ^{205}At, 25:14995

SPENCER, Leo W. Jr., Preliminary survey of x-ray producing devices in Kansas schools, 1968, 25:13463

SPERINDE, J., Method for mapping the spatial distribution of stopping π^- mesons in tissue, 25:13547

SPETH, J., M1 transition probabilities of single-particle states in the lead region, 25:15197

SPIRIDONOV, F. M., Phase relations and the electrical conductivity in the system ZrO_2--Sc_2O_3, 25:13778

SPOSITO, Garrison, High-energy neutron scattering and Mihara--Puff theory of structure factor for liquid ^{4}He, 25:14138

SPRAGUE, James Alan, Properties of defect clusters in neutron-irradiated silicon, 25:14428

SPREVAK, D., Large angle scattering in slow H$^+$--H(1s) collisions, 25:14029

SPRING, M. S., Vacancy tetrahedra in copper due to electron irradiation in the high-voltage microscope, 25:13731

SPRUCH, Larry, Low-energy scattering by long-range potentials, 25:14019

SRIVASTAVA, Pratap N., Effect of radiophosphorus on the development of gonads in mice, 25:13569

SRIVASTAVA, Y. N., Lagrangian approach to dual pion amplitudes, 25:14697

  Promotion and threshold singularities in massive quantum electrodynamics, 25:14792

SROUR, J. R., Dopants for radiation-resistant silicon, 25:14412 (N-70-39456)

SSENGABI, J., De-excitation γ-rays in ^{15}N and ^{16}O, 25:14896

STAAB, E. V., Early visualization of /sup 99m/Tc-pertechnetate in metastatic thyroid cancer in a patient with Graves' disease, 25:13488

STACHOWICZ, W., Electrical conductivity of 2-pentene irradiated at 77^{0}K during warming, 25:13027

STAEHLER, Fritz, Metabolism of isolated perfused rat liver following irradiation in vitro. III, 25:13373

STAERK, H., Determination of impurities in boron carbide by neutron activation analysis, 25:12972

STAIRS, D. G., Scattering of protons from ^{3}He and ^{4}He, 25:14882

STAKEBAKE, Jerry L., Thermal desorption of atmospheric gases from plutonium dioxide. I, 25:13024

STALDER, G. A., Radioisotopes in the diagnosis of gastric disease, 25:13495

STAMP, A. P., Cranked Hartree--Fock solutions for collective excitations, 25:14956

STAREN'KII, A. G., Effect of kind and energy of irradiation on radiolysis of polypropylene, 25:13055

STASZEL, M., Strong absorption cut in photoproduction, 25:14603

STATNIKOV, Yu. G., Acoustic flow in a superfluid liquid, 25:14130
STAUNTON, Lawrence Patrick, Group geometry and effective Lagrangians generated by massive gage field, 25:14805
STAVINSKII, V. S., Average radiation widths for excitation energies of the order of neutron binding energy, 25:15209
  Density of excited states of atomic nuclei, 25:15208
  Measurement of total cross sections of π^---p interaction, 25:14561 (JINR-P1-5460)
STAVISSKII, Yu. Ya., Cross-sections for radiative neutron capture by ^{238}U nuclei, 25:15125
  Radiative capture of neutrons by ^{238}U nuclei, 25:15105
  Radiative capture of neutrons by ^{238}U in energy range 24 to 145 keV, 25:15106
STEARNS, Carl A., Mass-spectrometric determination of the dissociation energy of ScC$_2$ and ScC$_4$, 25:13761
STECH, B., Local approximation to field and current commutators, 25:14673
STECHER, Theodore P., Gum nebula: fossil Stroemgren sphere of the Vela X supernova, 25:13851
STECKENMESSER, R., Angiographic diagnosis of hydatid disease of the liver, 25:13494
STECKER, F. W., Are protars spinars, 25:13952
STEDMAN, G. E., Fermi's golden rule, 25:14775
STEIGMAN, Gary, Lyman-α production by suprathermal protons, 25:14061
STEIN, D. F., Prog. rpt. on study of grain boundary segregation, 12/2/70, 25:15428 (COO-1778-6)
STEIN, J., Measurement of K/sub μ3/$^+$ decay parameters, 25:14534
STEIN, John D., Ion-induced electron emission from metallic oxides, 25:13963
STEIN, John L., Standby milk surveillance network, 25:13443
STEIN, R. F., New description of the solar five-minute oscillation, 25:13901
STEIN, U., Roentgenologic-photometric method for bone mineral determinations, 25:13509
STEINBERG, Meyer, Radiation treatment of mine waste waters, 25:13036
STEINDLER, M. J., Chemical Engineering Division fuel cycle technology quarterly report, July--September 1970, 25:13077 (ANL-7755)
STEINOLFSON, Richard Steingrimur, Plasma acceleration and shock formation by electromagnetic force fields, 25:14274
STEKLY, Z. J. J., State of the art of superconducting magnets, 25:14220
STELSON, P. H., Coulomb excitation of ^{107} ^{109}Ag, 25:15035
STENFLO, J. O., Simultaneous measurements of polar magnetic fields at Crimea and Mount Wilson, 25:13873
STENFLO, Lennart, Kinetic theory of weakly ionized plasmas in electric field, 25:14328
STENGER, V. J., 2400-MeV 5π mass enhancement in 6-prong π^-p events at 12 GeV/c, 25:14562 (TID-25640)
STEPANEK, K., Rod models of fuel elements of nuclear reactors, 25:15410 (ZJE-92)
STEPANOV, A. V., Radiation intensity from the front of collisionless shock waves, 25:14314
STEPANOV, V. K., Diamagnetic moment of a strong shock wave from a high-temperature light explosion in gases, 25:14282
STEPANYAN, E. D., Effect of x rays on cytological changes of bone marrow cells as a function of the immunobiological state of the reticulo-endothelial system, 25:13567
STEPHENS, A. E., Remote data station interface to the production control computer, 25:15469 (Y-1748)
STEPIEN, Kazimierz, Quantitative classification of stars by Stroemgren photometry, 25:13809
STERNHEIM, Morton M., Pi--carbon elastic scattering near the 33 resonance, 25:14908
STEVENS, D. J., Radiation hazards, 25:13436
STEVENS, P. N., General method of importance sampling the angle of scattering in Monte Carlo calculations, 25:14404
STEVENS, Paul Ronald, Forward peak structure in quasi two-body reactions and long range pion exchange, 25:14722
STEVENS, S. S., FORTRAN program for computing two-dimensional magnetic fields, 25:15440 (ORNL-TM-2484)
STEWART, D. C., A ^{244}Cm--Be isotopic neutron source, 25:14872
STEWART, G. L., Tritium in streams in the United States, 1961--1968, 25:13108
STEWART, Ross, Deuterium exchange of C-methyl protons in lumazine derivatives, 25:12982
STIEGELMAIR, J. A., Deuteron stripping at 1.69 GeV/c. I, 25:14906
STILLEY, Jerry Lee, Free--free absorption coefficient of H-, 25:13974
STOCK, J., Line-intensity variations in spectrum of SX Phoenicis, 25:13812
  Radial velocity observations of SX Phoenicis, 25:13811
STOCKHAUSEN, Wolfgang, Growth inhibition through gamma radiation on transplanted sarcomas in mice, 25:13473
STOKES, R. W., Superconducting quadrupole doublet for LAMPF, 25:14860
STOLZ, W., Dosimetry of ionizing radiation through solid-dye systems, 25:13306
STONE, J. A., Radiolysis of liquid hydrocarbons containing deuterium sulfide, 25:13048
STONE, R. G., Type-III solar radio burst storms observed at low frequencies. II, 25:13892
STONE III, Samuel Rollins, A form-free, semiphenomenological, error-bounded, potential representation of two-nucleon experiments, 25:14746
STORHOK, V. W., Mechanisms of swelling and gas release in uranium dioxide, 25:13785
STORM, Derek Walton, Measurements of proton--proton bremsstrahlung at 20 MeV, 25:14545
STORM, Ellery, Photon cross sections from 1 keV to 100 MeV for elements Z = 1 to Z = 100, 25:14409
STORY, J. S., Neutron cross-section evaluation in the thermal and resonance energy range for nuclides of mass less than 220, 25:15101
STOTHERS, Richard, Low-mass white dwarfs and cooling sequences in Hyades cluster, 25:13799
STOYANOVA, M. N., Vertical structure of plages, 25:13882
STOYCHEFF, P. A., Total cross section for single-electron transfer in collisions of He$^+$ with He, 25:14025
STRAKER, E. A., The energy spectrum of photoneutrons produced by 140-MeV electrons incident on tantalum, 25:14990
STRATTON, L. P., Evacuable glove-box for handling of liquid sodium, and apparatus for analysis of carbon in sodium and other metals, 25:13185 (AERE-R-6338)
STRAUSS, Herbert D., Experiences with ^{32}P in advanced carcinoma of the prostate, 25:13591
STRAYER, Donald M., Motion of ions at finite velocities in helium II, 25:14144
STREET, G. S. B., Performance of Sweepnik I, 25:13252 (CERN-70-21(Vol.1), pp 293-308)
  Sweepnik II, an improved track measuring machine, 25:13251 (CERN-70-21(Vol.1), pp 285-92)
STREKALOVSKII, V. N., High-temperature radiographic studies of oxides. II, 25:13769
STRELIN, G. S., Dynamic of restoration of the bone marrow in its local irradiation in mice and rats, 25:13562
STRICKLAND, D. J., Atomic physics and the polar cap, 25:14102 (N-70-19848)
STRICKLAND, J. D. H., Ecology of plankton off La Jolla, Calif., 4--9/67, 25:15468 (UCSD-10-P-20-54)
STRINGER, J. L., Prog. rpt. on reactor engineering, 6--8/70, 25:15354 (WHAN-IR-42)
STRNAD, J., Further evidence against the possibility of faster-than-light particles, 25:14778
STROEBELE, H., CARL: a FORTRAN program for PEPR calibration using Chebyshev polynomials, 25:13245 (CERN-70-21(Vol.1), pp 177-86)
  Present status of the Heidelberg-PEPR-Hardware and production system, 25:13246 (CERN-70-21(Vol.1), pp 187-96)
STROHNER, G., Assay of B isotopes at the band heads of the BO molecule, 25:12928
STRONG, J. A., Cost-effectiveness of different spark chamber read-out and digitising systems, 25:13266 (CERN-70-21(Vol.2), pp 581-606)
STRUGALSKI, Z. S., Shower counters of gamma quanta and electrons, 25:13300
STRUGAL'SKII, Z. S., Effective mass spectra of the $\gamma\gamma$, $\pi^0\gamma$, $\pi^0\gamma\gamma$, $\pi^0\pi^0$, π^0eta^0, $\pi^0\pi^0\gamma$, $\pi^0\pi^0\pi^0$ systems in mass value region M (γ.......γ) less than or equal to 1.3 GeV, 25:14560 (JINR-E1-5349)
STRUKOV, B. A., Effects of deuteration on the specific heat of ADP crystals, 25:12998
STRZALKOWSKI, A., Backscattering of alpha particles, 25:15172
STUDOVIC, Milovan, Exergetical analysis of a BHWR nuclear power plant, 25:15344
STUERZINGER, P., Adam+Eva, scanning and measuring machine for film from the large bubble chambers, 25:13270 (CERN-70-21(Vol.2), pp 633-49)
STUIVENBERG, J. H., Analysis of 2$^-$ → 2$^+$ positon transitions in ^{84}Rb and ^{74}As, 25:14972
STUMPF, H., Symmetry conditions on nonlinear spinor field functionals, 25:14782
STUPEL, M. M., Induced superconductivity in germanium films, 25:14161
STURROCK, P. A., Model of pulsars, 25:13832 (AD-711397)
  Prog. rpt. on nonthermal phenomena of astrophysics, 5/66--6/70, 25:13936 (AD-711829)
SUARES, Kh. B., Realizing of z focusing in cylindrical electrostatic analyzers, 25:13325
SUBBOTIN, V. I., Heat transfer during developed boiling of alkali metals, 25:13157
SUDAKOV, L. V., Activation energy of first stage of annealing of irradiated ^{238}PuO$_2$, 25:13784
SUDAN, R. N., Nonlinear beam--plasma interactions and stochastic acceleration, 25:14296
SUGAI, Hideo, Low-frequency electrostatic waves in a weakly ionized plasma under a weak magnetic field, 25:14383
SUGAMORI, S. E., Heat capacity of activation for the hydrolysis of methanesulfonyl chloride and benzenesulfonyl chloride in light and heavy water, 25:12984
SUGAWARA, H., Duality and Adler condition, 25:14668
SUGITA, Toshio, Contact angles of gold and silver on a clean tungsten substrate, 25:13691
SUGIYAMA, Haruo, Monte Carlo calculation of electron slowing-down spectra at high energies, 25:14397
  Monte Carlo study of high energy electron spectra in water and Al, 25:14398

SUHONEN, E., Phase-space integral and statistical quantities in high-energy collisions, 25:14584 (NP-18652)
SUHR, P., Neutron--neutron scattering length, 25:14887
SUITA, Tokuo, Decrease in intensity of Hg lines near source in weakly ionized flow, 25:14100
SUITOR, R., Chiral algebra, chiral breakdown, and xi parameter of K/sub 13/ decay, 25:14645
  N-point functions in chiral SU(3) x SU(3) current algebra, 25:14664
SUKHORUCHKIN, S. I., Measurement of alpha values for ^{235}U and ^{239}Pu, 25:15074
  Value α for ^{239}Pu, 25:15072
SULABERIDZE, G. A., Designing multicomponent isotope separation cascades, 25:13179
SULITZE, H., Measurements of neutron-resonance total cross-sections for fission product isotopes, 25:15098
SUNDE, R. A., Automatic scanning and measurement of bubble chamber film on Polly II, 25:13254 (CERN-70-21(Vol.1), pp 325-55)
SUNG-TSING-YANG, G. Ya., Effect of α-radioactive background at investigation of the α decay of the 104 element, 25:15017
SUNJIC, M., Multiple plasmon effects in the energy-loss spectra of electrons in thin films, 25:14486
SUOMINEN, Pekka, Design, construction, and characteristics of some Ge(Li) detectors and spectrometers, 25:13212 (NP-18653)
SUPERATA, M. A., Effect of specimen thickness on the superconducting critical temperature of indium, 25:14173
SURAL, D. P., Electron capture by positrons from molecular hydrogen, 25:14006
SURI, Ashok, Possible explanation for the rapid approach to ''universality'' of the inelastic electron-scattering structure functions, 25:14610
SUTHERLAND, W. H., Some unexpected dosimetric problems in an apparatus for mammalian radiobiology, 25:13456
SUTTON, D. C., Photon interaction cross sections of Sn and Zr, 25:14959
SUTTON, D. L., Ratio of capture and fission cross-sections of ^{239}Pu in energy range 100 eV to 30 keV, 25:15073
SUTTON, J., Radio structure of remnant of Kepler's supernova, 25:13854
SUWALSKI, J., Evaluation of Moessbauer spectra for ^{57}Fe, 25:14485
SUZUKI, Masao, Fission track dating and U contents of obsidian. I, 25:13112
SVEC, K., Simple ^{3}He--^{4}He dilution refrigerator, 25:14214
SVEC, M., Frame dependence of vector dominance in Veneziano model and new test of rho universality, 25:14710
SVECHKAREV, I. V., Effect of pressure on Cr susceptibility of V--Cr and Cr--Mn alloys, 25:14447
SVEDIN, U., System for on-line control of bubble chamber measurements, 25:13282 (CERN-70-21(Vol.2), pp 825-30)
SVENNE, J. P., Isospin mixing of Hartree--Fock solutions, 25:15164
SVET-MOLDAVSKII, George J., Tumor-induced skin heterogenization. III. Immunologic and immunogenetic mechanisms, 25:13388
SVIRSKII, M. S., Uncertainty of pseudomultiplicity in the theory of superconductivity, 25:14185
SVISTUNOVA, T. V., Intercrystalline corrosion of N70M28-type alloys, 25:13633
SWANSCN, M. L., Stage I recovery of deformed metals. II, 25:14438
SWEET, Ronald C., Shock tube experiments on the pyrolysis of deuterium-substituted ethylenes, 25:12993
SWENSCN, P. A., Role of pyridine nucleotides in the control of respiration in ultraviolet-irradiated Escherichia coli B/r cells, 25:13607
SYMONS, M. C. R., Unstable intermediates. LXXX, 25:13028
SYROS, C., Time-dependent transport solution in plane geometry, 25:14873
SYROVATSKII, S. I., Theory of origin of cosmic rays, 25:14079
SZABO, A., Microanalysis of cobalt by electrophoretic focussing with radioactive tracer, 25:12949
SZABO, I., Fission cross-section for ^{235}U and ^{239}Pu between 0.025 and 1 MeV, 25:15068
  Measurements of fast neutron fluxes in the range of 10 keV to 1 MeV, 25:13216
SZANTAY, I., Phosphorated ^{32}P erythrocytic metabolism in GAS, 25:13335
SZECSI, L., Frequency dependence of the residual resistance of a galvanically begun lead layer in a superconducting state, measured in a TEM field configuration, 25:14847 (NP-18654)
  Measurement of dependence on frequency of residual resistance of superconducting layers of lead, 25:14170
SZENTGYOERGYI, P., Microanalysis of cobalt by electrophoretic focussing with radioactive tracer, 25:12949
SZEWCZYK, R., Isotope shifts between even isotopes ^{64} ^{66} ^{68} ^{70}Zn in visible Zn II lines, 25:14927
SZICHMAN, H., Level scheme of ^{139}La, 25:15032
  Level structure of ^{141}Pr studied by photonuclear excitation, 25:15139
SZIRMAI, E., Phosphorated ^{32}P erythrocytic metabolism in GAS, 25:13335
SZOCS, F., Decay of free radicals in irradiated PMMA at high pressures studied by ESR, 25:13058

T

TABARA, Hiroto, Radio spectra of quasi-stellar objects, 25:13843
TABASSO, M. Cristina, Experimental results on stopping muons at 60 and 300 m.w.e, 25:14535
TABATA, Tatsuo, Charge distribution produced by 4- to 24-MeV electrons in elemental materials, 25:13964
TAGGART, R., Metastable constitution and superconducting transition behavior of Zr--Ta alloys, 25:13716
TAHA, M. O., Direct- and cross-duality amplitudes, 25:14823
TAIT, G. Robert, Melatonin synthesis in rat pineal glands inhibited by x-irradiation, 25:13559
TAIT, W., Spinor space and mass formula for hadrons, 25:14751
TAJIRI, M., Existence conditions of hydromagnetic shocks in Vlasov plasma, 25:14326
TAKACS, J., Spectrophotometric determination of fluorine in organic compounds with thorium chloranilate after hydropyrolytic decomposition of lead fluoride, 25:12936
TAKAGISHI, K., Energy spectrum of a nova-like x-ray source, 25:13849
TAKAHASHI, K., New ^{110}Rh isotope, 25:15001
TAKAHASHI, Kanji, Environmental contamination associated with the development of nuclear power, 25:13437
TAKAHASHI, O., Production of high temperatures and pressures, 25:15457 (SCL-T-71-209)
TAKAHASHI, Shinji, Results of conformation radiotherapy in cervix carcinomas, 25:13530
TAKAHASHI, Yasushi, Note on the scale transformation, 25:14790
TAKATA, Shinzo, Effect of high-temperature heating on magnetic properties of (Ce--MM)--Cu--Co ternary alloys, 25:14464
TAKEDA, Tatsuoki, Joule heating in JFT-2, 25:14233 (JAERI-Memo-4186)
TALAKIN, O. G., Mass-spectrometric method for determining microimpurities in inert gases, 25:12941
TALBOT, L., Cylindrical Langmuir-probe response in transition regime, 25:14242 (AD-711095)
TALBOT, M., Development of SIREN capsule, Phase I, 25:13170 (SNC-2708-1)
TAMBOVTSEVA, A. M., Hygienic investigation of the effect produced by small concentrations of uranium on the human body, 25:13595
TAMMANN, G. A., Stephan's quintet or quartet, 25:13916
TAMURA, T., Coupled-channel Born-approximation calculation of two-nucleon transfer reactions in deformed nuclei, 25:15191
TAN, Chung-i., Existence of complex poles and oscillatory average multiplicity in multiperipheral models, 25:14585
TANAKA, Akira, Chemical and hygienic studies on natural radioactive spa. III, 25:13470
TANAKA, J., Prototype of drift tube quadrupole magnets, 25:14849 (SJC-A-70-6)
TANAKA, Koichi, Finite-Larmor-radius hydromagnetic flow past an obstacle, 25:14329
TANAKA, Nobuyuki, Recoil proton polarization from π^0 photoproduction on H, 25:14516
TANAKA, S., Fast-neutron scattering from Al, Si, S, and Zn, 25:14963
  Neutron scattering cross-sections of iron, 25:14961
  Width-fluctuation and resonance-interference effects in neutron scattering cross-sections of Al, Cu, and Zn, 25:14962
TANAKA, Toshiyuki, Nuclear calculation method of the JMTR core, 25:15391 (JAERI-Memo-4180)
TANDBERG-HANSSEN, Einer, Magnetic fields in quiescent prominences, 25:13884
TANDON, R. K., Deuteron stripping at 1.69 GeV/c. I, 25:14906
TANENBAUM, W., High resolution wire spark chamber, 25:13301
TANG, I-ming, Thermal conductivity in pure two-band superconductors in high magnetic fields, 25:14166
TANG, Ting-wei, Nonlinear instability of modulated waves in a magnetoplasma, 25:14367
TANG, Y. C., Study of N + α system with resonating-group method, 25:14880 (COO-1764-105)
TANIUTI, T., Existence conditions of hydromagnetic shocks in Vlasov plasma, 25:14326
TANNER, James Thomas, Determination of antimony in natural materials by neutron activation, 25:12968
TAPIA, S., Line-intensity variations in spectrum of SX Phoenicis, 25:13812
  Radial velocity observations of SX Phoenicis, 25:13811
TAPLIN, George V., Interval brain scanning with sodium pertechnetate /sup 99m/Tc for tumor detectability, 25:13505
TARANTIN, N. I., Identification and study of radioactive properties of Bi isotopes using electromagnetic mass-separator on heavy ion beam, 25:15023
TARASOV, V. D., Enthalpy and specific heat of the 80 percent W--20 percent Mo alloy at high temperatures, 25:13665
TARRAGO, X., Measurement of the prompt neutrons emitted in

XUM

the fission of ^{209}Bi and ^{238}U induced by 155-MeV protons, 25:15021
TARRATS, A., Measurement and microscopic calculations of the cross sections and asymmetries for the (p,p') reaction exciting the 2.31-MeV (0^+,T = 1) state of ^{14}N, 25:14890 (CEA-CONF-1651)
TARTER, J. M., Higher-order terms in the current--current theory of weak interactions, 25:14647
TATUM, E. L., New crisp genes and crisp-modifiers in Neurospora crassa, 25:13424
TAUBER, Thomas Ernest, Possible effects of an electric dipole moment for a weak intermediate boson, 25:14623
TAVLUYEV, G. V., Current algebra and photoproduction of π-mesons on hyperons, 25:14619
TAVROVSKAYA, T. V., Dynamic of restoration of the bone marrow in its local irradiation in mice and rats, 25:13563
TAYLOR, Benjamin Joseph, Scanner abundance study of late G and K dwarfs, 25:13824
TAYLOR, George Ormsbee, Scattering of He^+ ions by noble gases at high energies, 25:14044
TAYLOR, H. W., States of ^{114}In, 25:15008
TAYLOR, J. C., Crystal structure and anisotropic thermal expansion of β-uranyl dihydroxide, $UO_2(OH)_2$, 25:13010
Physics of hot plasmas, 25:14305
TAYLOR, J. W., Determination of precise isotopic vapor pressure differences from -20 to 110°C, 25:12995
TAYLOR, Robert John, Steepening of ion--acoustic waves and formation of collisionless electrostatic shocks, 25:14389
TEDROW, P. M., Properties of very thin aluminum films, 25:14192
TEITELBOIM, Claudio, Splitting of Maxwell tensor. II, 25:14615
TEL'KCVSKII, V. G., Angular distribution of secondary electrons emitted by Nb due to bombardment with ions, 25:13969
TELLES, N. C., Enhancement of viral transformation by ultraviolet light, 25:13552
TEMPLE, T. E., Early visualization of /sup 99m/Tc-pertechnetate in metastatic thyroid cancer in a patient with Graves' disease, 25:13488
TENNANT, Raymond W., Requirement of cellular synthesis for Kilham rat virus replication, 25:13608
TEOULE, Robert, Influence of radiation and amount of palmitate-1-^{14}C on distribution of this fatty acid in different lipid classes of Ehrlich ascites, 25:13362 (CEA-R-4039)
TEPLITZ, Vigdor L., Ward identities for eta decay in perturbation theory, 25:14611
TERA, F., Isotopic abundance of ^{26}Mg and limits on ^{26}Al in early solar system, 25:13864
TER-ATONYAN, V. M., Resonant scattering of light by light, 25:14596 (JINR-E2-5424)
TERRANI, S., Measurements of radioactivity in the sewage in Milan, 25:13454
TESEI, A., Wightman functions in a model with mass renormalization, 25:14794
TESTARDI, L. R., Unusual strain dependence of T/sub c/ and related effects for high-temperature superconductors, 25:14182
Unusual strain dependence of T/sub c/ and related effects fcr high-temperature superconductors, 25:14183
TEWKSBURY, Stuart K., Backward K^+p elastic scattering between 1.0 and 2.5 GeV/c, 25:14582
THAKUR, R. K., Atomic processes in a low-density hydrogen--helium plasma, 25:14302
THAKUR, S. N., Electronic absorption spectra (π--π^*) of p-dibromobenzenes-D_4 and -H_4, 25:13003
THEOBALD, J. P., Fission-cross-section measurement of ^{233}U, 25:15082
Neutron-induced fission cross-section of ^{241}Pu, 25:15083
Scattering cross-section of ^{235}U below 100 eV, 25:15084
THEWS, R., Particle size distribution in clouds from nuclear airbursts, 25:13138
THEWS, Robert L., s-channel helicity conservation with t-channel dynamics, 25:14605
THIBAULT, M., Detection of bone metastases by an isotopic method, 25:13513
THIEL, Manfred A. F., Does a primeval magnetic field exist, 25:13944
THIELHEIM, K. O., Two-group neutron transport theory for plane and spherical geometry, 25:14867
THIRION, J. M., Spins of levels of ^{34}Cl, 25:14942
THOMAS, B. W., Isomeric level in ^{239}U, 25:15077
THOMAS, Charles C. Jr., Activation analysis of airborne selenium as a possible indicator of atmospheric sulfur pollutants, 25:12965
THOMAS, T. Darrah, Effect of nuclear deformability on reaction cross sections, 25:15063
THOMAS, Thomas Jr., Carbon-14-1-palmitate incorporation by rat lung: effect of nitrogen dioxide, 25:13356
THOMPSON, A. R., Galactic hydrogen absorption at 21 cm wavelength in direction of Virgo A, 25:13831 (AD-711300)
THOMPSON, M. A., Global method of fiducial recognition with fish-eye lenses, 25:13261 (CERN-70-21(Vol.1), pp 497-503)
Status of SATR, 25:13262 (CERN-70-21(Vol.1), pp 505)
THOMPSON, Rodger I., Hydrogen-to-carbon ratios in accordance with CNO bi-cycle in carbon stars, 25:13795
THOMPSON, W. J., Normalization for (α,t) reactions, 25:15064
THOMSON, W. J., Effects of variable properties on MHD flow in finite ducts, 25:14090
THORMEIER, K., Solubility of inert gases in the reactor coolant sodium and related safety problems, 25:15379 (EURFNR-785)
THORNBURG, David Devoe, Temperature changes in thin films during growth by physical vapor deposition, 25:15423 (COO-1198-775)
THORNE, Kip S., Theoretical frameworks for testing relativistic gravity. I, 25:13942
THORNE, R. M., Magnetospheric reflection of whistlers, 25:14120
THUEMMLER, F., Studies of the system uranium mononitride--molybdenum and uranium mononitride--tungsten at high temperatures, 25:13772
THUN, J. E., Indium-111 EC decay, 25:15028
THURNAY, K., Equations of state of fuel materials UC and PuC, 25:13753
TICHY, M., Time-resolved measurements of energy distribution in unstable plasma. II, 25:14247
TIEMBLO, A., Radiative decays of mesons in a quark loop model, 25:14686
TIKHINSKII, G. F., Twins of tetrahedral form in beryllium, 25:13718
TILLEY, D. R., Superconducting proximity effect in layered systems with a magnetic field applied perpendicular to the interfaces, 25:14158
TILLMANN, Klaus-Dieter, Energy spectra of backscattered electrons and positrons by Monte Carlo calculations, 25:13959 (UCRL-19719)
TIMMONS, Darrol H., Dimensional S/sub n/ calculations of neutron spectra reflected from thick slabs of concrete and iron, comparison with measurements, 25:14865 (COO-2049-2)
TIMOFEEV, A. V., Radiative instability of a nonequilibrium plasma in magnetic traps, 25:14288
TIMOFEEVA, T. V., Fast-neutron thermalization time in silicate ores of varying moisture content, 25:13109
TIMUSHEV, G. F., Realizing of z focusing in cylindrical electrostatic analyzers, 25:13325
TIMUSK, T., Phonon effects in the far-infrared reflectivity of superconducting lead, 25:14175
TISCHER, Robert L., Behavior of uranium oxide particles in reducing flames, 25:13021
TITTERTON, E. W., Radiation hazards, 25:13436
TIXADOR, R., Development of Paramecium aurelia: influence of natural radiation, 25:13556
TJERSTROM, O., Magnetic coil cooled by a liquid for a particle accelerator, 25:14857
TJOEM, P. O., High angular momentum states in ^{155}Gd and ^{157}Gd, 25:15138
TKACHEV, A. V., Neutron-activation autoradiography of the thyroid gland in experimental radiation sickness, 25:13497
TODOROV, I. M., Investigation of spleen and liver polysomes of non-immunized and immunized rats with acute radiation damage, 25:13376
TOELGYESSY, J., Radio-release determination of pH using radioactive kryptonate, 25:12955
TOEPFFER, C., Convergence of radial matrix elements in electron scattering, 25:15195
TOLSTIKOV, V. A., Cross-sections for radiative neutron capture by ^{238}U nuclei, 25:15125
Radiative capture of neutrons by ^{238}U in energy range 24 to 145 keV, 25:15106
Radiative capture of neutrons by ^{238}U nuclei, 25:15105
TOMASELLI, M., Properties of the low-lying positive-parity states in ^{9}Be and ^{13}C, 25:14917
TOMITA, Y., Fast-neutron scattering from Al, Si, S, and Zn, 25:14963
Neutron scattering cross-sections of iron, 25:14961
Width-fluctuation and resonance-interference effects in neutron scattering cross-sections of Al, Cu, and Zn, 25:14962
TOMIZAWA, Jun-ichi, Mutation and recombination of bacteriophage lambda: effect of ultraviolet radiation, 25:13412
TOMLINSON, P. G., Duality and comparison of resonance and Regge models for π^+p backward scattering, 25:14726
TOMONTO, J. R., Plutonium as an alternate fuel in large water cooled reactors, 25:15375 (CONF-691114-6)
TONEEV, V. D., Systematization of the inelastic interactions of high-energy pions and nucleons with atomic nuclei, 25:15148 (ORNL-tr-2399)
TONON, G., Interaction of a laser-created plasma with a strong magnetic induction, 25:14334
TON THAT, B., Use of a simple geometry program for filtering HPD data, 25:13273 (CERN-70-21(Vol.2), pp 679-85)
TONUMA, Tadao, Charge exchange of carbon and nitrogen ions in nitrogen gas, 25:14001
TOPP, G. C., Soil water content from gamma ray attenuation, 25:13110
TORGERSON, David F., Alpha decay of the ^{221}Th and ^{222}Th decay chains, 25:15011
TORI, Paolo, Measurement of the radioactivity of natural waters, 25:13106
TOTH, G., Investigation of spontaneous silver precipitation on powdery platinum in nitric solutions, 25:13086
TOUSSET, Jean, Determination of internal and superficial

XUM

oxygen content of molybdenum obtained using 54 MeV α particles and low energy deuterons, 25:12957 (LYCEN-7076)
TOW, Don M., Angular distributions from multiparticle production models, 25:14661
TOWHEED, Syed Manzoor, Effects of gamma radiation on egg and larval stages of rice weevil, 25:13558
TOWNSEND, Eric, Improvements to master-slave manipulators, 25:13206
TRADOWSKY, K., Fundamental principles on dimensioning of a counter--timer system, 25:13317 (NP-18655)
TRAUB, W., Abundance of lithium in sunspots, 25:13865
TREBICHAVSKY, I., Effect of ionizing radiation on the frequency and ultrastructure of mast cells in mouse spleen, 25:13577
TREDER, H.-J., Elementary observations on gravitational collapse, 25:13940
TREFIL, J. S., Multiplicity in very high-energy particle-nucleus collisions, 25:14736
TREINDL, L., Heat capacity of activation for the hydrolysis of methanesulfonyl chloride and benzenesulfonyl chloride in light and heavy water, 25:12984
TREMBLEY, J., Description and performance of the CERN Spiral Reader, 25:13236 (CERN-70-21(Vol.1), pp 19-36)
TRET'YAK, S. A., Designing multicomponent isotope separation cascades, 25:13179
TRET'YAKOVA, S. M., Thermal conductivity of 29NK-type alloy at temperatures between 80 and 239°K, 25:13685
TRIFIRO, Ferruccio, Analysis of EPR spectra of oxidizing catalysts, 25:14482
TRIMBLE, Virginia, Mass of Crab Nebula, 25:13807
TRIPATHI, Ram K., Properties of 1s shell nuclei, 25:15185
TRISKA, P., X-ray control of the ionospheric absorption of hf radio waves, 25:13897
TROCHON, J., Determination of spin of slow-neutron induced resonances in ^{239}Pu, 25:15088
TROFIMOV, F. A., Metabolism of ^{14}C-dimecarbine in irradiated animals, 25:13576
TROSKO, J. E., Lack of photoreactivation in human cells grown in vitro, 25:13377
TROTTET, G., Upper cutoff in the spectrum of solar particles, 25:13910
TROUP, G. J., Nuclear magnetic resonance studies of irradiated beryllium oxide. II, 25:13754
TROYAN, Yu. A., Reaction $np \to pp\pi^-$ for the incident neutron momenta from 2 up to 10 GeV/c, 25:14551
TRUEBENBACHER, E., Nucleon--nucleon S scattering with help of one-boson exchange potential, 25:14739
TRUFANOV, A. M., Inelastic scattering of fast neutrons by Cr, Ni, Y, Zr, and W nuclei, 25:14967
TRULSEN, Jan Karsten, Test-particle radiation in magnetoplasma, 25:14325
TRUSOV, V. F., Dependence of internal conversion coefficients on high energies of γ transitions, 25:15054
TRUTTSE, Y. L., Middle-latitude aurorae at the current solar maximum, 25:14115
TSAI, Shih-tung, Thermal conductivity and low-frequency waves in collisional plasmas, 25:14385
TSANG, Chin-fu., Microscopic and macroscopic aspects of nuclear structure with applications to superheavy nuclei, 25:15193
TSENG, Raymond Chi-jen, Flat-plate boundary-layer studies in a partially ionized gas, 25:14276
TSERKOVNITSKAYA, I. A., Simultaneous determination of uranium(IV) and uranium(VI) by moving boundary method, 25:12938
TSINTSADZE, N. L., Possibility of parametric resonance in an electron plasma, 25:14377
TSISEK, Z., Proportional chamber for compensation of counter geometry in the time-of-flight measurements, 25:13296 (JINR-P13-5472)
TSUDA, Motoyuki, Catalytic activity of aromatic nitrile and alkali metal ion radical salt. I, 25:13001
  Catalytic activity of aromatic nitrile and alkali metal ion radical salt. II, 25:13002
TSUEI, C. C., Transition temperatures and lattice parameters of metastable Te--Au solutions, 25:14178
TSUKADA, K., Fast-neutron scattering from Al, Si, S, and Zn, 25:14963
  Neutron scattering cross-sections of iron, 25:14961
  Width-fluctuation and resonance-interference effects in neutron scattering cross-sections of Al, Cu, and Zn, 25:14962
TSURIKA, I. A., Extraction--photometric determination of Fe, 25:12934
TSVETKOV, V. P., Bremsstrahlung in scattering of neutrinos by electrons taking into account radiative corrections, 25:14600
TSVINEV, A. P., Experimental ionization chamber filled with liquid and solid argon, 25:13295 (JINR-P13-5404)
TSYTOVICH, V. N., Cosmic rays and plasma turbulence, 25:14077
  Small-scale irregularities in the interstellar gas, 25:13912
TUCK, Grover, An empirical formula which predicts the critical parameters of a planar array of uranium-solution-filled cylinders, 25:13198
TUCKER, Wallace H., Secular behavior of x-ray and radio emission from supernova remnants, 25:13847
TULENKO, J. S., Plutonium as an alternate fuel in large water cooled reactors, 25:15375 (CONF-691114-6)
TUPIKOV, V. I., Studies of zeolite cation influence on γ radiolysis of adsorbed ammonia by the EPR method, 25:13057
TURALA, M., Proportional chamber for compensation of counter geometry in the time-of-flight measurements, 25:13296 (JINR-P13-5472)
  System of proportional wire chambers on-line with a computer, 25:13297 (JINR-P13-5473)
TURBA, E., Total body scanning for studies on regional distribution, 25:13503
TURCANU, C. N., Reactions of recoiling ^{35}S and ^{32}P atoms, 25:13069
TURCHI, Peter J., Acceleration patterns in quasi-steady MPD arcs, 25:14281
TURCHIN, Yu. M., Average number of prompt neutrons in fission of ^{235}U and ^{239}Pu by neutrons, 25:15116
TURJANSKI, R., Measurement of activation resonance integrals at infinite dilution with a lithium-drifted germanium gamma-ray spectrometer and comparison with calculated values, 25:15124
TYBOR, W., Determination of the X^0(960) meson spin--parity in the polarization experiment, 25:14720
TYLER, V. E., Activation analysis of counterfeit and genuine Japanese postage stamps, 25:12973
TYMIENIECKA, T., Search for resonant states p--/sub Λ/^{8}He and α--/sub Λ/^{8}He, 25:14573
TYRROFF, H., Optimization of ion source and ion optical parameters of isotope separator, 25:13162 (JINR-P13-5369)
TYSON, J. A., New class of gravitational wave detectors, 25:14547
TYURIN, N. E., Solution on the unitarity relation for scattering amplitude of particles with spin, 25:14590

U

UEDA, Y., Electromagnetic perturbation of the pseudoscalar-mass spectrum, 25:14690
  Symmetry breaking and spin-zero mass spectrum, 25:14689
  Van Hove model and non-leptonic hyperon decays, 25:14637 (SU-1206-238)
UENAL, B. C., Implications of the pion gauge condition for baryonic parity doublets, 25:14705
UENO, Kaoru, Precipitation of some actinide element complex ions by using hexammine cobalt (III) cation. I, 25:12980
UETOMI, Isamu, Generation of high-intensity beams of nanosecond pulse duration by electron linacs, 25:14858
UGGERHOEJ, E., Channeling of positrons, 25:14418
ULAM, S., Some elementary attempts at numerical modeling of problems concerning rates of evolutionary processes, 25:15435 (LA-4573)
ULBERT, K., Oscillopolarographic determination of cysteic acid level in the fingernails followed chronic irradiation in humans, 25:13369
ULMANN, R., Rocket instrument for measuring energy spectrum and directional distribution of medium energy protons in the auroral zone, 25:13227
ULMANN, R. M., Commercialization of irradiated food, 25:13622
ULRICH, Marie-Helene J., Spectrographic observations of twenty-eight Markarian galaxies, 25:13923
UMEK, H., Preparation of ^{85}Sr and /sup 87m/Sr for bone scintigraphy, 25:13061
UNNERUS, C. E., Isodose measurement of the bladder dose in radium therapy, 25:13448
UNT, V., Combined Bondi and fast approximation method in general relativity. II, 25:14807 (NP-18559)
UPADHYA, K. N., Electronic absorption spectra (π--π^*) of p-dibromobenzenes-D_4 and -H_4, 25:13003
UPADHYAY, J., Radiation survival of bacterial spores, 25:13611
UPDEGRAFF, W. E., Dynamic collective model of photofission, 25:15198
URAMOTO, Johshin, Dependence of plasma density distribution on local decay time, 25:14294
URBAN, Eugene W., Flux flow and a new critical-current formula, 25:14197
URBAN, K., Voids in nickel after electron irradiation, 25:14416
URIN, M. G., Analogue resonance in region of overlapping levels of the compound nucleus, 25:15179
USPENSKII, V. A., Lithium-6 incorporation into tissues, organs, and transplantable tumors, 25:13350
UTTLEY, C. A., Ratio of the ^{6}Li(n,α) and ^{10}B(n,α) cross-sections from 10 eV to 80 keV, 25:14910
  Total cross-section of carbon from 70 eV to 1.5 MeV, 25:14912
UY, Zenaida Ebora Santos, Vector-meson exchange contributions to $K_L \to \gamma\gamma$ decay rate, 25:14606

V

VACEK, A., Circadian variations in the effect of x-irradiation on the haematopoietic stem cells of mice, 25:13550
VACHASPATI, Scattering of linearly polarized radiation, 25:14601
VAELIVAARA, K. G., Lifetimes of excited states in ^{101}Rh,

XUM

25:14992
VAGHIN, A. I., Adam+Eva, scanning and measuring machine for film from the large bubble chambers, 25:13270 (CERN-70-21(Vol.2), pp 633-49)
VAGNER, I., System for processing meson-telescope data, 25:14067
VAINSHTEIN, L. A., Electron excitation of transitions between excited states in Ba^+ and Sr^+ ions, 25:14000
VAJDA, P., Directional dependence of atomic displacements in cobalt crystals, 25:13733
  Recovery of low-temperature electron-irradiated cobalt crystals, 25:13713
VALASH, D., System for processing meson-telescope data, 25:14067
VALDEZ, Jesusa, Coronal magnetic fields before and after solar proton events, 25:13893
VALENTIN, J., High spin rotational levels in ^{177}Ta, 25:15047
VALENTINE, Robert H., Shock--pulse attenuation and hugoniot studies of three explosives and three mock explosives, 25:15466 (UCRL-50950)
VALENTINE, T. M., Coherent neutron scattering length of ^{17}O, 25:14862 (AERE-R-5770)
VALENTINI, H.-B., Amplification and damping of ionization waves in MHD channels, 25:14097
  Amplification and damping of magneto-acoustic waves in MHD channels, 25:14098
VALKOVIC, V., Interference and rescattering effects in reactions with three particles in the final state, 25:14891 (ORO-1316-97)
VALUEV, A. A., Possibility of phase transitions in an imperfect multiply ionized plasma, 25:14304
VAMPOLA, Alfred L., Solar electron access to closed field lines, 25:14101 (AD-712045)
VAN ALTENA, W. F., Membership in open cluster NGC 7062, 25:13801
VAN ASSCHE, P. H. M., Energy levels of ^{56}Mn, 25:14974
VAN DAM, P. H. A., HPD--CDC 3200 system at Amsterdam, 25:13275 (CERN-70-21(Vol.2), pp 709-20)
VAN DE GRAAF, M. Skorko, Search for resonant states p--/sub Λ/^{5}He and α--/sub Λ/^{5}He, 25:14573
VAN DE KIEFT, Lawrence J., Effects of high-energy electron irradiation on single crystals of ammonium and sodium bifluoride, 25:14411 (AD-712321)
VAN DEN BERGH, Sidney, Optical observations of galaxy associated with 3C 386, 25:13915
VANDENPLAS, P. E., Explanation of plasma densities high above critical density, 25:14333
VANDEPLAS, P., Implications of fundamental integral measurements on high-energy nuclear data for reactor physics, 25:15349
VANDERLEEDEN, J. C., Parity nonconservation in nuclear forces. I, 25:15009
VAN DER LINDE, H. J., Influence of temperature on the γ radiolysis of isopropyl alcohol vapor. Effect of molecular structure on the nonchain and chain decompositions of alcohol vapors, 25:13046
VAN DER MOLEN, H., Shapes of the non-unique and unique first-forbidden β-spectra of ^{84}Rb, ^{76}As and ^{126}I, 25:14976
VAN DER RAAY, H. B., Deuteron stripping at 1.69 GeV/c. I, 25:14906
VAN DER STRICHT, E., Comparison of radioactive contamination of total diet of adolescents in community. II, 25:13392 (EUR-3945(Pt.2))
VAN DER WERF-MESSING, B., Treatment of testicular tumors in Rotterdam, 25:13544
VAN DER WERVE, Hugo, Neutron metrology in H.F.R, 25:15393 (RCN-119)
VAN DER WIEL, M. J., Small-angle scattering of 10-keV electrons in He, Ne, and Ar, 25:14003
VAN DESSEL, E. L. J., Line profiles and flash intensities in photosphere--chromosphere transition region, 25:13878
VAN HOEK, E. A., Shapes of the non-unique and unique first-forbidden β-spectra of ^{84}Rb, ^{76}As and ^{126}I, 25:14976
VAN HOOK, W. A., Determination of precise isotopic vapor pressure differences from -20 to 110°C, 25:12995
VANICSEK, L., Proton momentum spectrum in πN inelastic interactions at 17.2 GeV/c, 25:14564
VAN'KOV, Temperature dependence of the total cross-section structure, 25:15093
VAN LEEUWEN, W. M., HPD--CDC 3200 system at Amsterdam, 25:13275 (CERN-70-21(Vol.2), pp 709-20)
VANN, D. C., Plaque-forming cells of two different origins in single hemolytic foci, 25:13387
VAN SOMEREN, L., Work function measurements on macroscopic tungsten specimens, 25:13693
VAN TUYL, H. H., Survey of alpha waste generation and disposal as solids in the U. S. nuclear fuel industry, 25:13188 (BNWL-B-34)
VAN URK-SCHOEN, A. M., Microradiometric detector for column liquid chromatography, 25:12952
VAN'YAN, L. L., Nature of auroral magneto--ionospheric perturbations, 25:14106
VAREY, R. H., Sheath growth in a low pressure plasma, 25:14299
VARGA, A., System for processing meson-telescope data, 25:14067
VARGA, S., Radio-release determination of pH using radioactive kryptonate, 25:12955
VARMA, C. M., Self-polarization contribution to magnetic ordering in systems with singlet ground state, 25:14460
VASILCHENKO, V. M., Investigation of spleen and liver polysomes of non-immunized and immunized rats with acute radiation damage, 25:13376
VASILENKO, L. S., Breakdown of 2^1P and 2^3P levels of He in a glow discharge, 25:13977
VASIL'EV, S. S., Study of radiations of ^{91}Y, ^{90}Y, and ^{87}Y, 25:15136
VASIL'EVA, E. S., Investigation of spleen and liver polysomes of non-immunized and immunized rats with acute radiation damage, 25:13376
VAS'KOV, V. V., Double scattering of plasma streams in bi-thermal ionosphere, 25:14112
VATSET, P. I., Investigation of reaction ^{4}He(γ,p)^{3}H at maximal γ-quanta energy 120 MeV, 25:14886
VATTUONE, G. M., Fate of Schooner fallout radionuclides ingested by the dairy cow, 25:13396 (UCRL-72511)
VAUGOYEAU, Henri, Nuclear fuel based on UC, 25:13746
  Nuclear fuel based on UC, 25:13747
VAVILOVA, V. V., Nature of solid solutions in the niobium--oxygen system, 25:14457
VEDRENNE, G., Development of Paramecium aurelia: influence of natural radiation, 25:13556
VEKSHTEIN, G. E., Asymptotic solution in the problem of anomalous plasma resistance, 25:14309
VELAZQUEZ, C., Aromatic nitriles: a new family of scintillation solutes, 25:13214
VELICHKO, I. A., Isotope effect in Raman spectra of a DKDP crystal, 25:12997
VELINOV, P., Effect of solar corpuscular streams on production of electrons in lower ionosphere, 25:14126
  Variations in lower ionosphere associated with cosmic-ray and geomagnetic variations, 25:14127
VENEZIANO, G., Duality and the bootstrap, 25:14674
VENKATARAMAN, Balu, ESR study of irradiated single crystal of p-toluidinium chloride, 25:13051
VENKATARAMAN, Krishnamurthi, Anelastic piezoresistance due to stress-induced ordering of defects, 25:13677
VENKATARAO, K., Photosensitization of vinyl polymerization by uranyl ions, 25:12981
VENOSA, Francesco, Food preservation with ionizing radiation, 25:13623
VENTURI, D., HDP--IBM 360/44 system at CNAF for bubble chamber data analysis. I, 25:13267 (CERN-70-21(Vol.2), pp 607-15)
  HPD--IBM 360/44 system at CNAF for bubble chamber data analysis. II, 25:13268 (CERN-70-21(Vol.2), pp 617-24)
VENTURI, G., Adler condition in a dual relativistic quark model, 25:14685
VENUS, W., Scanning and measuring of heavy liquid film on-line, 25:13271 (CERN-70-21(Vol.2), pp 651-64)
VERHEEST, Frank, Collisional drift waves in two-ion-species plasmas, 25:14365
VERKERK, C., Adam+Eva, scanning and measuring machine for film from the large bubble chambers, 25:13270 (CERN-70-21(Vol.2), pp 633-49)
VERMA, Kusum, Interaction of x-radiation and malnutrition. A study of kinetics of cellular proliferation in the jejunum of protein-deficient rats, 25:13562
VERMEER, Abraham, Excitation of ion oscillations by beam--plasma interaction, 25:14378
VERNHES, Claude, Antipollution and radioactive wastes, 25:13087
VERSCHUUR, G. L., Galactic hydrogen absorption at 21 cm wavelength in direction of Virgo A, 25:13831 (AD-711300)
VERTEBNYI, V. P., Neutron cross-sections of isotopes used as absorbers in atomic reactors, 25:15096
VESECKY, J. F., Cooling of flare-produced plasmas in the solar corona, 25:13889
VESELOVA, G. M., Integral data for ^{235}U in intermediate neutron spectrum, 25:15399
VESELY, D., Nucleation of cracks by a spark discharge in molybdenum single crystals, 25:13671
VESSELY, V., Time-resolved measurements of electron energy distribution in unstable plasma. I, 25:14246
VIANO, G. A., Stability of the complex angular-momentum continuation, 25:14834
VIDAL, R., Measurements of ^{233}U cross-sections for thermal neutrons, 25:15071
VIEHBOECK, F. P., Determination of the distribution of fission products in fuel particle coatings by the sputtering technique, 25:13758
VIITASALO, M., Levels in ^{28}Si, 25:14936
VIKLICKY, V., Effect of ionizing radiation on the frequency and ultrastructure of mast cells in mouse spleen, 25:13577
VILA, Samuel C., Deuterium burning as origin of outbursts of star HL Taurus 76, 25:13796
VILLEMOES, P., Data handling system for the Omega and the SFM projects, 25:14839 (CERN-70-21(Vol.2), pp 561-80)
VINOGRADOV, A. P., Carbon isotopes and the origin of petroleum, 25:13005
  Physicochemical model for element separation during mantle differentiation, 25:13115
VINOGRADOV, V. B., Statistical isospin model and cross sections of reactions $\pi^-p \to N + (2,\ldots,6)\pi$ within 1 to 16 GeV energy range, 25:14700 (JINR-P1-5471)
VISHNEVSKII, N. K., Observation of anti ^{3}He, 25:14540

(IFVE-SEF-70-16)
VISVANATHAN, N., Magnetic field structure around the Crab pulsar, 25:13850
VISWESWAR RAO, V., Effective atomic numbers of alloys for pair-production process, 25:14402
VLADIMIRSKAYA, T. M., Thermocouple for accurate high-temperature measurements in a vacuum and in the presence of reactor radiation, 25:13326
VLASOV, M. F., Neutron cross-sections of isotopes used as absorbers in atomic reactors, 25:15096
VLCEK, J., Experimental investigation of film heat-transfer coefficient in the fuel element spacers area, 25:13153 (ZJE-66)
  Rod models of fuel elements of nuclear reactors, 25:15410 (ZJE-92)
VODOLAZSKAYA, N. A., Separation on phosphate cellulose of the products of degradation of deoxyribonucleoprotein formed after irradiation and enzymatic actin in vitro, 25:13363
VOEGELI, Paul T. Sr., Radiochemical analyses of water from selected streams, wells, springs, and precipitation collected prior to reentry drilling, Project Rulison, 25:12951 (USGS-474-83)
VOELKL, J., Diffusion coefficients of H and D in V, Nb, and Ta by Gorsky-effect measurements, 25:14440
VOERTLER, Hans-Hellmut, Effects of tanderil on radiosensitivity, 25:13476
VOGEL, H. H. Jr., Tumors of rat adrenal gland induced by fission neutron irradiation, 25:13564
VOGEL, Karl-Heinz, Additional radiation burden to the patient caused by shielding during deep x-ray therapy, 25:13460
VOGEL, P., Microscopic description of nuclear vibrations when phonons occur at relatively low energy. II, 25:15205
VOGEL, R. C., Chemical Engineering Division fuel cycle technology quarterly report, July--September 1970, 25:13077 (ANL-7755)
VOGT, James Robert, Nondestructive determination of silicon and oxygen in meteorites by fast neutron-activation analysis, 25:12970
VOILLEQUE, Paul G., Transfer of ^{85}Kr from air to grass, 25:13124
VOLKENSHTEIN, N. V., Scattering of conductivity electrons by spin waves in terbium and dysprosium single crystals, 25:14448
VOLKOV, A. M., Propagation of electromagnetic waves in Riemann space, 25:14499
VOLKOV, Yu. N., Effect of optical quantum generator radiation on electrical parameters of fresh tissue, 25:13565
VOLKOVITSKAYA, V. V., Radiational safety in the use of radioisotopic methods in engineering industry, 25:13467
VOLOSHCHUK, A. I., Peculiarities of uranium deformation for tension at constant velocity, 25:13688
VOLOSHCHUK, A. M., Isotope exchange reactions in different BF_3-complex systems, 25:12992
VOLOSHCHUK, V. I., Investigation of reaction $^4He(\gamma,p)^3H$ at maximal γ-quanta energy 120 MeV, 25:14886
VOLPE, Joseph A., Hot hepatic hemangioma, 25:13510
VON ALBERT, H.-H., Treating radiation-induced brachial plexus paresis, 25:13480
VON BRENTANO, P., Reduced widths from isobaric analog resonances, 25:15201
VONGAI, A. D., Observation of analogue states with T = 2 in the reactions $^{26}Mg(^3He,n)^{28}Si$, $^{46}Ti(^3He,n)^{48}Cr$, and $^{58}Ni(^3He,n)^{60}Zn$, 25:14943
VON GUNTEN, H. R., Fission cross section of ^{227}Th, 25:15044
VON MEERWALL, E., Local magnetic fields in the vanadium--manganese alloy system, 25:14445
VONSOVSKII, S. V., Uncertainty of pseudomultiplicity in the theory of superconductivity, 25:14185
VOROB'EV, V. A., Non-destructive control of concrete structures by means of betatrons, 25:14861
VOROBEVA, V. G., Analysis of neutron energy dependence of anti ν, on basis of energy balance in nuclear fission, 25:15117
VOROTNIKOV, P. E., Fission of ^{232}U by neutrons with energy from 0.1 up to 1.5 MeV, 25:15019
VOSSLER, C., Regge-pole eikonal model and the double-charge-exchange reactions, 25:14715
VOURVOPOULOS, G., Decay of /sup 141m/Nd, 25:15014
VOVENKO, A. S., Search for isobar state with $T = {}^5/_2$ in the reaction $\pi^+ + p \to \pi^- + X^{3+}$, 25:14576
VSEVOLODOV, E. B., DNA synthesis and migration of cells in hair follicles in lambs, 25:13337
VU, Quat Thuong, Space-charge-limited current in fast-neutron-irradiated silicon, 25:14426

W

WACLAWSKI, B. J., Adsorption of water vapor on polycrystalline tungsten, 25:13669
WADDINGTON, J. C., High angular momentum states in ^{155}Gd and ^{157}Gd, 25:15138
WADE, C. M., Detection of radio emission from Antares, 25:13804
WADHWA, Y. D., Magnetohydrodynamic generalized couette flow (with uniform suction; time-dependent pressure gradient; and arbitrary initial velocity), 25:14091
WAGGONER, M. C., Determination of boron in borates, boron hydrides, organo-boron compounds, elemental boron and refractory borides, 25:15465 (UCRL-50948)
WAGNER, F., Phase-shift analysis of $\pi^-p \to K^0\Lambda$, 25:14727
WAGNER, Hans, Lattice parameter measurements on aluminum after electron irradiation at low temperatures, 25:13723 (JUL-664-FN)
WAGNER, R. L., Nitrogen diffusion and solubility in tungsten, 25:13673
WAHLGREN, M. A., A ^{244}Cm--Be isotopic neutron source, 25:14872
WAHNSIEDLER, W. E., Plasma resonance in TiO, VO, and NbO, 25:14462
WAHRER, R. E., States of ^{116}In, 25:15008
WAKABAYASHI, N., Spin-wave dispersion relation in dysprosium metal, 25:14444
WAKEFIELD, K. E., Operation of a levitated superconducting ring in a plasma physics experimental device, 25:14356
WALKER, A. B. C. Jr., Variation in O VII x-ray line-emission from solar corona, 25:13885
WALKER, Durham E. Y., Metallographic preparation of uranium--silicon alloys, 25:13742
WALKER, J., Neutron thermalization in graphite, 25:14874
WALKER, J. C., Half-life of the 113.8-keV level of ^{176}Lu, 25:15040
WALKER, W. H., Evaluation of fission product yields, 25:15099
WALLANDER, E., Low spin, negative parity states in the N = 103 isotones of ^{171}Er, ^{173}Yb, and ^{175}Hf, 25:15059
WALLERSTEIN, George, Optical spectrum of OH and infrared emitter VX Sagittarii, 25:13817
WALTER, J. A., Nuclear magnetic resonance studies of irradiated beryllium oxide. II, 25:13754
WALTERS, W. B., Directional correlations of gamma rays in ^{125}Sb, 25:15137
WANG, C. C., Vapor deposition and characterization of metal oxide thin films for electronic applications, 25:13748
WANG, Franklin F. Y., Calculation of the elastic moduli of binary composites, 25:13751
WANG, Jui-chang, Precipitation of tellurium with Bismuthiol II, 25:12943
WANG, Kuo-hsiang, Interference model for resonances suggested by the Veneziano amplitude, 25:14692
WANG, Ling-lie, Limiting distribution and average π^{+-} multiplicities in $\pi^- + p \to$, 25:14719
WANG, Shih Yi, Thymine phototrimer, 25:15436 (NYO-2798-49)
WARBURTON, E. K., Ml transitions among the f/sub 7/2/d/sub 3/2/$^{-1}$ states of ^{40}K, 25:14934
WARBURTON, R. J., Versatile superconducting femtovolt amplifier and multimeter, 25:14217
WARD, R., Superconducting proximity effect in layered systems with a magnetic field applied perpendicular to the interfaces, 25:14158
WARD, T. E., New ^{110}Rh isotope, 25:15001
WARING, J. L., Effect of oxide additions on the polymorphism of tantalum pentoxide. IV. The system Ta_2O_5--Ta_2WO_8, 25:13775
WARLIMONT, Hans, Principles of electron microscopy at high voltages and a comparison 100 to 200 kV, 25:13628
WARNER, R. E., Study of the odd strontium isotopes with stripping and pickup reactions, 25:14930
WARTENA, J. A., Neutron-induced fission cross-section of ^{241}Pu, 25:15083
WASIELA, Andre, ESR of Er^{3+} ions in thoria crystal, 25:14478
WASIELEWSKI, P., Properties of ^{55}Mn, ^{56}Mn, and ^{57}Fe in the unified rotational model, 25:14973
WASIM, Syed Mohammad, Thermal conductivity and thermal effects in superconducting niobium, 25:14153
WASLEY, Richard J., Shock--pulse attenuation and hugoniot studies of three explosives and three mock explosives, 25:15466 (UCRL-50950)
WASSERBURG, G. J., Isotopic abundance of ^{26}Mg and limits on ^{26}Al in early solar system, 25:13864
WASSON, O. A., High-energy γ-rays following neutron capture in ^{239}Pu and ^{235}U, 25:15078
WATSON, Brent Dennee, Uniqueness of the real optical potential, 25:14947
WATSON, C. J. H., Nuclear cross section requirements for fusion reactors, 25:14357
WATSON, Donald E., Risk of carcinogenesis from long-term low-dose exposure to pollution emitted by fossil-fueled power plants, 25:15464 (UCRL-50937)
WATSON, J. H. P., High-field superconductivity of alloys in porous glass, 25:14191
WATSON, Mary Beatrice Nelson, Theoretical study of ^{3}PI/sub g/ and ^{1}PI/sub g/ states of He_2, 25:13975
WATTEAU, J. P., Neutron yield of a focus discharge in various experiments, 25:14355
WATTS, T. L., Status of MIT's PEPR's, 25:13248 (CERN-70-21(Vol.1), pp 233-42)
WEBB, Jerry Glen, A model neutron deuteron scattering calculation above the inelastic threshold, 25:14744
WEBB, W. W., Mechanisms determining the critical current in hard superconductors, 25:14196
  Versatile superconducting femtovolt amplifier and multimeter, 25:14217
WEBBER, Bryan R., Test of $\Delta S = \Delta Q$ rule in leptonic decays of neutral K mesons, 25:14533
WEBER, G., Tritiated titanium targets producing 14-MeV

XUM

neutrons. II, 25:14840 (EUR-4286(Pt.2))
WEBER, P., Experimental investigation of film heat-transfer coefficient in the fuel element spacers area, 25:13153 (2JE-66)
WEBSTER, D. S., Chemical Engineering Division fuel cycle technology quarterly report, July--September 1970, 25:13077 (ANL-7755)
WEDEMEYER, H., Studies of the system uranium mononitride--molybdenum and uranium mononitride--tungsten at high temperatures, 25:13772
WEIGERT, A., Stars with central He burning and occurrence of loops in H--R diagram, 25:13815
WEIGMANN, H., Resonance parameters from neutron radiative capture in ^{238}U, 25:15081
WEILER, K. W., Polarization of 3C10 and 3C58 at 1420 and 2880 MHz, 25:13833 (AD-711611)
  Polarization properties of 3C 10 and 3C 58 at 1420 and 2880 MHz, 25:13839
WEINER, J. H., Time-dependent perturbation calculations based on the hydrodynamic analogy to quantum mechanics, 25:14054
WEINSTEIN, Marvin, K/sub 13/ decays and SU(3) breaking in Brandt--Preparata approach, 25:14649
WEIS, J. H., Vector currents and current algebra. III, 25:14667
WEISBECKER, Leo W., Evaluation of systems of fire development, 25:13134 (AD-713418)
WEISHAAR, Julius, Punch card control of telecobalt therapy, 25:13540
WEISS, Edward R., Ureteral kinking and hydronephrosis in a transplanted kidney mimicking the rejection phenomenon, 25:13490
WEISS, K., Hydrodynamic equations for condensate and depletion of He II, 25:14139
WEISS, M. J., Inelastic electron scattering from N_2O between 5.0 and 20.0 eV energy loss, 25:14014
WEISZ, P. H., Dimension of scale symmetry breaking, 25:14758
WELIACHEW, L., Neutral hydrogen absorption in galaxy M82, 25:13911 (AD-711299)
  Neutral hydrogen absorption in IRR II galaxy M82, 25:13927
WELLER, F., Two-quasiparticle states in ^{168}Er, 25:15000
WELLER, H. R., 14.2 and 14.5 MeV levels of ^{16}O, 25:14915
WELLS, J. S., High-frequency limit of the Josephson effect, 25:14200
WELLS, W. E., Sulfonate leaving groups, structure and reactivity: 2,2,2-trifluoroethanesulfonate, 25:15421 (COO-1008-14)
WENDENBURG, H.-H., Isolated lymphogranulomas of the stomach, 25:13541
WENNINGER, H., Laser beams as fiducial lines in bubble chambers, 25:13303
WENTZEL, Donat G., Acceleration and heating of interstellar gas by cosmic rays, 25:14058
WENZEL, M., Radiation effects on ^{75}Se incorporation in tumors following administration of $Na_2{}^{75}SeO_3$, 25:13354
WERBRCUCK, A., IBM 1130 computer on-line system at Torino, 25:13288 (CERN-70-21(Vol.2), pp 911-20)
WERBRCUCK, A. E., Longitudinal phase-space analysis of 5 GeV/c π^+p reactions, 25:14578
WERNER, B., Momentum-transfer dependence in reactions, 25:14575
WERNICK, J. H., Unusual strain dependence of T/sub c/ and related effects for high-temperature superconductors, 25:14183
WEST, Geoffrey B., Why do neutrinos produce more W's than muons, 25:14643
WESTERLUND, B. E., Structure of wing of Small Magellanic Cloud, 25:13931
WESTLAKE, D. G., Habit plane of vanadium hydride in vanadium, 25:13768
WHEELER, Harry, Pinocytosis and membrane dilation in uranyl-treated plant roots, 25:13353
WHEELER, John A., Introducing the black hole, 25:13937
WHITACRE, John, Corrections to observed beta-ray atmospheric densitometer values as caused by cosmic rays, 25:13314
WHITAKER, A., Phase equilibria in the high magnesia corner of the system MgO--ThO_2--B_2O_3 at 1200°C, 25:13770
WHITE, H. S., Performance of the DAPR system, 25:13280 (CERN-70-21(Vol.2), pp 761-804)
WHITE, J. N. J., Simple dual model for meson--baryon scattering in SU_3, 25:14766
WHITEHEAD, E. I., Prog. rpt. on nature and importance of selenium metabolites in animal, 1--12/70, 25:15425 (COO-1449-11)
WHITEHILL, Don, Electron-excitation--gamma-decay reactions in heavy nuclei, 25:15204
WHITEHOUSE, H. T., Prog. rpt. on radiation-induced nucleation of bubbles in superheated water, 12/70, 25:13152 (SU-326-P-13-5)
WHITNEY, E. D., Quantitative determination of the structure: property relationships in nuclear fuel element materials. Quarterly progress report, September 15--December 15, 1970, 25:13766 (SRO-552-6)
WHITNEY, James C., Finite-difference methods for the Fokker--Planck equation, 25:14307
WIDEN, L., Value anti ν of ^{235}U and ^{239}Pu in fast-reactor spectrum, 25:15113
WIEDLING, T., Fast-neutron elastic scattering at 8 MeV, 25:14965
  Fast-neutron inelastic scattering in energy range 2 to 4.5 MeV, 25:14966
  Neutron elastic-scattering cross-sections of V, Cr, Fe, and Ni, 25:14964
  Neutron energy spectra from neutron-induced fission of ^{238}U at 1.35 and 2.02 MeV, 25:15109
WIEDNER, C. A., Normalization for (α,t) reactions, 25:15064
WIELAND, Cuno, Comparison of high-energy radiation applied through plaster casts, 25:13539
  Megavolt therapy of malignant neoplasms of the stomach, 25:13532
WILCOX, Lowell Enrick, Experimental study of a traveling-wave magnetic-field plasma accelerator, 25:14358
WILDENBERG, Judith, Relation of mitotic recombination to DNA replication in yeast pedigrees, 25:13425
WILHELMI, Z., Cerium-135m and /sup 137m/Nd: isomeric states in N = 77 isotones, 25:15042
WILK, G., Strong absorption cut in photoproduction, 25:14603
WILKINSON, M. K., Spin-wave dispersion relation in dysprosium metal, 25:14444
WILL, Clifford M., Theoretical frameworks for testing relativistic gravity. I, 25:13942
  Theoretical frameworks for testing relativistic gravity. II, 25:13943
WILL, H., Facility for in-pile creep experiments on cladding tubes under thermal and stress cycling, 25:13142
WILLARD, J. E., Paramagnetic species produced by ultraviolet irradiation of lithium, potassium, sodium, magnesium, and cadmium in 3-methylpentane at 77°K, 25:13025
WILLDER, S. S., PEPR for BEBC, 25:13240 (CERN-70-21(Vol.1), pp 89-104)
WILLETT, K., Energy producers, 25:13126
WILLEY, Melvin G., Fluid supported capsule holder for homogeneously irradiating samples, 25:13208
WILLEY, R. S., Higher-order terms in the current--current theory of weak interactions, 25:14647
WILLHOIT, Donald G., Dose reduction factors of a lead-lined girdle, 25:13462
WILLIAMS, D., Status of the HPD minimum guidance programs at CERN, 25:13278 (CERN-70-21(Vol.2), pp 737-52)
WILLIAMS, G. H., Experimental study of spouting beds of spheres, 25:13139 (AERE-R-4852)
WILLIAMS, K. R., Recovery creep of niobium-stabilised austenitic stainless steels, 25:13674
WILLIAMSON, A. S., Glass-fibre-reinforced epoxy liner for spent-nuclear-fuel bay, 25:15412
WILLIS, David L., Radiation response of rough-skinned newt Taricha granulosa, 25:13477
WILLIS, W. J., High resolution optical spark chamber, 25:13302
  High resolution wire spark chamber, 25:13301
WILLNER, Birge, Early results of telecobalt therapy of bronchial carcinomas, 25:13523
WILSON, M. M., Radiation damage in copper bombarded with copper ions, 25:14422
WILSON, R. W., Attenuation of radio waves by atmosphere at frequency 1415 MHz, 25:13838
WILSON, Robert M., Solar x-ray astronomy summary and bibliography, 25:13863 (N-70-39828)
  Survey of classical Cepheid variable stars, 25:13789 (N-70-38166)
WILSON, S. J., Exact solution of a static charged sphere in general relativity, 25:14810
WILSON, T. L., Kinematic distance estimates for fourteen galactic supernova remnants using molecular absorption lines, 25:13837
WILSON, V. C., Operation of thermionic converter with tungsten emitter and niobium collector, 25:14083 (N-70-39884)
WINCHELL, P., Thermodynamic data for carbonaceous systems, 25:13750 (GAMD-9335)
WINDMILLER, L. R., Inversion of de Haas--van Alphen data. I, 25:14433 (ANL-7659)
WINEGARDNER, W. K., Survey of alpha waste generation and disposal as solids in the U. S. nuclear fuel industry, 25:13188 (BNWL-B-34)
WINER, Bette Marcia, Critical heat flux in liquid He II close to the lambda transition, 25:14132
WINKLER, C., Placentography: comparative investigations in nuclear medicine, 25:13517
WINKLER, K., Punched tape output of Vakutronik measuring equipment, 25:13224
WINN, W. G., Decay of ^{56}Co and ^{66}Ga, 25:14957
WINSOR, Niels K., Numerical model for toroidal plasma containment with flow, 25:14236
WINSTON, Martin A., Ureteral kinking and hydronephrosis in a transplanted kidney mimicking the rejection phenomenon, 25:13490
WINTER, J., Resonance parameters from neutron radiative capture in ^{238}U, 25:15081
WINTER, J. G., High-resolution photography of solar chromosphere. VIII, 25:13876
WINTERS, I. J., High resolution wire spark chamber, 25:13301
WINTON, J., Matrix precipitation of NbC in 20/25/Nb stainless steel, 25:13640 (TRG-Report-2040)
WISKOTT, D., Adam+Eva, scanning and measuring machine for

film from the large bubble chambers, 25:13270 (CERN-70-21(Vol.2), pp 633-49)
WITT, Inge, Growth inhibition through gamma radiation on transplanted sarcomas in mice, 25:13473
WIXON, N. J., Muon experiments, 25:14532
WOEHL, H., Continuum windows in spectra of umbrae (4000 to 8000 A), 25:13879
  Rotational temperatures of umbrae, 25:13880
WOELLGENS, P., Radiation effects on ^{75}Se incorporation in tumors following administration of Na$_2$^{75}SeO$_3$, 25:13354
WOJCIK, W., Proton--proton and pion--proton inelastic collisions and the proton and pion form factors, 25:14729 (INR-P-1229)
WOLBER, G., Precision measurement of hyperfine structure of ^{175}Lu, 25:13986
WOLD, Einar, Ground state bands of doubly even nuclei, 25:15203
WOLF, A., Nuclear levels excited by neutron capture γ rays, 25:15002
WOLF, L., Two-dimensional conduction heat transfer in liquid--metal bonded fast reactor fuel element with pellet and canning eccentricity, 25:13155
WOLF, Randolph John, Coaxial plasma accelerator and production of shock waves by dense Plasma Focus, 25:14270
WOLFENDEN, A., Damage in aluminum by 200 kV electrons, 25:13727
WOLFER, Wilhelm G., Annihilation and other interactions of positrons in a plasma, 25:14290
WOLFF, H., Concentration dependence of vapor pressure isotope effect of methylamine and N-deuteriomethylamine in hexane, 25:12985
WOLFF, Sheldon, Tertiary structure of chromosomes, 25:13410
WOLFGANG, Richard, Iodine halides as radical scavengers, 25:13067
WOLFSON, Y., Lifetimes and gamma transitions in ^{19}O. 25:14905
WOLSKY, A. M., Invariance of the vacuum under exact scale transformations, 25:14781
WOLTER, Helmut, Radiochemical processes in 6-ring compounds, 25:13374
WOLTJER, Lodewyk, Mass of Crab Nebula, 25:13807
WONG, Jack, Statistical mechanics of persistent currents in quantum fluids, 25:14143
WONG, P., Decay of ^{210}Po, 25:14996
WONG, T. F., Limiting distribution and average π^{+-} multiplicities in $\pi^- + p \to$, 25:14719
  Two loop approximations to propagators in the sigma model, 25:14683 (NYO-2262-TA-219)
WONG, Wing-hing, Dynamics of some exchange reactions, 25:12986
WOOD, R. E., L subshells in Hg from the decay of ^{198}Au and ^{204}Tl, 25:15015
WOODGATE, G. K., Elementary atomic structure, 25:14047
WOODS, M. J., Calibration figures for type 1383A ionization chamber, 25:13221
WOODWARD III, Benjamin Weston, Ionization of cesium atoms in collisions with atomic oxygen, 25:14036
WOOIJ, H. M. W., Analysis of $2^- \to 2^+$ positon transitions in ^{84}Rb and ^{74}As, 25:14972
WOOLLAM, P. B., Elastic scattering and polarization of 49.5-MeV protons on ^{148}Sm, 25:15013
WOTKE, H., Determination of the distribution of fission products in fuel particle coatings by the sputtering technique, 25:13758
WRIGHT, K., Princeton automatic track reader, 25:13250 (CERN-70-21(Vol.1), pp 273-83)
WRZECIONKO, J., Calculation of nd scattering lengths with realistic potentials, 25:14743
WSZOLEK, B., Fission of natural uranium in neoplastic and normal tissue, 25:13361
WU, Jung-tsung, Effect of ovarian steroids and x-ray irradiation on preimplantation blastocysts of the rat, 25:13560
WULFF, P., Investigation of an improved iron arc, 25:14245
WUNDERER, Bernd, Current density and field in quasi-neutral electron-beam plasma, 25:14321
WYERMAN, T. A., Tritium in streams in the United States, 1961--1968, 25:13108
WYSS, H. R., Infrared spectrum of HDO in water and in NaCl solution, 25:12994

Y

YAARI, R., Weizmann Institute Spiral Reader system, 25:13293 (CERN-70-21(Vol.2), pp 953-62)
YAFFE, D., rho^0 production in pn collisions at 6.98 GeV/c, 25:14741
YAGI, K., Reactions (p,t) on even Ce isotopes, 25:15006
YAKOVLEV, G. N., Activation energy of first stage of annealing of irradiated ^{238}PuO$_2$, 25:13784
YAKUSHIN, F. S., Compensation effect in a protophilic deuterium-exchange reaction associated with a change in solvation of the catalyst cation, 25:13007
YAMADA, Masao, V--A theory for nucleon resonances, 25:14648
YAMADA, Norikazu, Radiation protection against x-ray diffraction apparatus, 25:13457
YAMAMOTO, Hiroshi, Effect of high-temperature heating on magnetic properties of (Ce--MM)--Cu--Co ternary alloys, 25:14464
YAMAMOTO, Takehisa, Thick-target yields of characteristic x rays by p, d, ^{3}He$^+$, and ^{4}He$^+$ bombardments, 25:13962
YAMAMURA, M., Ground state correlations in an extended Lipkin--Meshkov--Glick model, 25:15200
YAMANAKA, T., Fast neutron spectrometer, 25:13232
YAMASHITA, S., Prototype of drift tube quadrupole magnets, 25:14849 (SJC-A-70-6)
YANG, C. N., Ground-state energy of mixture of fermions and bosons, 25:14501
YANG, Tien-fang, ^{12}C(d,α)^{10}B reaction: reaction mechanism and cluster structure, 25:14901
YANKULOV, Merko, Gamma radiosensitivity and mutability of barley, 25:13603
YAROSHEVSKII, A. A., Physicochemical model for element separation during mantle differentiation, 25:13115
YAROSLAVTSEVA, A. T., Excitation functions of spectral lines of Kr II, 25:14040
YASINSKY, J. B., Space--time methods for movable fuel problems (LWBR Development Program), 25:15353 (WAPD-TM-968)
YASUDA, Seiichi, T4 endonuclease involved in repair of DNA, 25:13411
YASUNAMI, K., High-pressure measurement using semiconductor strain gages, 25:15458 (SCL-T-71-210)
YASUNAMI, M., Production of high temperatures and pressures, 25:15457 (SCL-T-71-209)
YATES, Albert C., Scattering amplitudes and spin polarizations of electrons scattered from H, He, C, Ne, Ar, Kr, Rb, Xe, Cs, Au, Hg, Pb, and Bi. I, 25:13995 (AD-711664)
YATIRAJAM, V., Separation of Re from Mo, V, W, and other elements by tribenzylamine--chloroform extraction, 25:12921
YATSUN, V. A., Consequence of analiticity of the $\pi\pi$-scattering amplitude, 25:14682 (ITF-70-60-E)
YEE, A., 2400-MeV 5π mass enhancement in 6-prong π^-p events at 12 GeV/c, 25:14562 (TID-25640)
YEH, K. C., Trapping of electromagnetic waves by nonlinear resonant interactions with ion sound waves, 25:14374
YEKUTIELI, G., rho^0 production in pn collisions at 6.98 GeV/c, 25:14741
  Weizmann Institute Spiral Reader system, 25:13293 (CERN-70-21(Vol.2), pp 953-62)
YIFTAH, S., Calculation of ^{240}Pu neutron cross-sections in keV-range, 25:15129
YIOU, F., Decay of ^{7}Be in cosmic rays, 25:14059
YODA, Renpei, Some properties of tungsten--rhenium alloys, 25:13682
YODER, Neil Richard, Analysis of moderate-energy nucleon--nucleon data, 25:14734
YORIZANE, M., Vapor-liquid equilibria at high pressure, 25:15459 (SCL-T-71-212)
YOSHIDA, Y., Weld cracking and mechanical properties of 17 percent chromium steel weldment, 25:13696
YOSHIKAWA, S., Force-free configuration of a high-intensity electron beam, 25:14272
YOSHIMURA, S., Vapor--liquid equilibria at high pressure, 25:15459 (SCL-T-71-212)
YOUNG, J. C., Prog. rpt. on fast reactor spectrum measurements, 10/70, 25:15388 (GULF-RT-10421)
YOUNG, K., Low moments of current algebra at infinite momentum, 25:14672
YOUNGQUIST, C. H., A ^{244}Cm--Be isotopic neutron source, 25:14872
YURCHUK, E. F., Characteristic curve of the collective scattering of electromagnetic radiation in a plasma, 25:14375
YUTLANDOW, I. A., Angular dependences of many-charge particles produced by 660-MeV protons on ^{27}Al nuclei, 25:14945

Z

ZACHAROV, B., On-line measuring system using visual displays for operator guidance, 25:13237 (CERN-70-21(Vol.1), pp 39-46)
ZADUBAN, M., Separation of radioiodide, radioiodate, and radioperiodate by thin-layer chromatography, 25:13099
ZAGAMI, M. T., Action of ionizing radiations on CNS, 25:13561
ZAIDI, S. A. A., Anomalies in cross sections of (d,n) reactions leading to isobaric analog states, 25:15050
ZAININGER, K. H., Vapor deposition and characterization of metal oxide thin films for electronic applications, 25:13748
ZAKHAROVA, S. M., Average radiation widths for excitation energies of the order of neutron binding energy, 25:15209
  Integral data for ^{235}U in intermediate neutron spectrum, 25:15399
ZAKHARYAN, E. G., Effect of x rays on cytological changes of bone marrow cells as a function of the immunobiological state of the reticulo-endothelial system, 25:13567
ZAKOWICZ, W., Two-stream instability for arbitrary stream temperatures and densities, 25:14340
ZAKRZEWSKI, W. J., Dual, crossing-symmetric amplitude with Mandelstam analyticity, 25:14821
ZALDIVAR, R., Tumors of rat adrenal gland induced by

fission neutron irradiation, 25:13564
ZALEWSKI, K., Evaluation of the absorption corrections to exchange models, 25:14831
  Quark model predictions for processes $0^{-1}/_{2}^{+}$ + J/sup P/$^{3}/_{2}^{+}$, 25:14721
ZAMYATNIN, Yu. S., Average number of prompt neutrons in fast-neutron-induced fission of ^{235}U, ^{239}Pu, and ^{240}Pu, 25:15115
  Measurement of energy spectra and average number anti ν of prompt neutrons produced in fission of actinide elements, 25:15118
ZANELLA, P., Data handling system for the Omega and the SFM projects, 25:14839 (CERN-70-21(Vol.2), pp 561-80)
ZANEVSKII, Yu. V., Proportional chamber for compensation of counter geometry in the time-of-flight measurements, 25:13296 (JINR-P13-5472)
  System of proportional wire chambers on-line with a computer, 25:13297 (JINR-P13-5473)
ZANOTTI, U., HDP--IBM 360/44 system at CNAF for bubble chamber data analysis. I, 25:13267 (CERN-70-21(Vol.2), pp 607-15)
  HPD--IBM 360/44 system at CNAF for bubble chamber data analysis. II, 25:13268 (CERN-70-21(Vol.2), pp 617-24)
ZAPATA, R. N., University of Virginia superconducting wind-tunnel balance, 25:14216
ZARETSKII, D. F., Analogue resonance in region of overlapping levels of the compound nucleus, 25:15179
ZATSEPIN, G. T., Observing neutrinos from collapsing stars and neutrino oscillations, 25:13830
ZAUDERER, B., Prog. rpt. on large scale nonequilibrium MHD generator, annual, 8/69--7/70, 25:14081 (AD-711351)
ZAVADCVSKAYA, E. K., Release of stored energy in annealing of radiational defects in NaCl, 25:14424
ZECCHINA, L., Ettingshausen effect in rare-earth metals, 25:14475
ZEITNITZ, B., Neutron--neutron scattering length, 25:14887
ZELENSKII, V. F., Peculiarities of uranium deformation for tension at constant velocity, 25:13688
ZEL'VENSKII, Ya. D., Oxygen and hydrogen isotope exchange in alcohols, 25:12991
ZETTA, L., Fission of ^{210}Po, 25:15010
ZGANJAR, E. F., Decay of ^{172}Lu, 25:15030
ZHELEZNYKH, I. M., Hot-universe model and the Dirac monopole, 25:13953
ZHMAILO, V. A., Effect of interaction of neutron with nucleus in Coulomb splitting of deuteron, 25:15190
ZHUKOV, O. K., Dielectric properties of a γ-irradiated KDP crystal, 25:14432
ZHUKOVA, I. A., Enthalpy and specific heat of the 80 percent W--20 percent Mo alloy at high temperatures, 25:13665
ZHURAVLEV, N. N., X-ray determination of the expansion coefficients of lanthanum and yttrium borides, 25:13760
ZHURAVLEV, V. F., Problem of relative biological efficacy of tritium oxide, 25:13551
ZHURBIN, G. I., Determination of ^{14}C in tissues protein by low-effective counters, 25:13345
ZIEGER, K., Elementary integration of nonlinear transport equations in isotope separation. I, 25:13085
ZIEGLER, C. A., Automobile exhaust analysis for lead using a nuclear technique, 25:13309
ZIJP, Willem L., Neutron metrology in H.F.R, 25:15393 (RCN-119)
ZIL'BERMAN, L. A., Josephson coupling energy in the presence of thermal fluctuations, 25:14184
ZIMMERMAN, J. E., Noise thermometry with the Josephson effect, 25:14198
  Recent developments in superconducting devices, 25:14218
ZISSERMANN, D., Reaction ^{40}Ca(d,p)^{41}Ca, 25:14938
ZOLTEWICZ, John A., Base-catalyzed hydrogen--deuterium exchange of N-substituted pyridinium ions. Inductive effects and internal return, 25:13000
ZOOK, Elvin G., Value of scintiscans in the diagnosis of splenic abscess, 25:13512
ZOTOV, T. D., Paraprocess susceptibility of Gd and Ni$_3$Mn near Curie temperature, 25:14446
ZUBANKOV, V. N., High-temperature radiographic studies of oxides. II, 25:13769
ZUBAREV, A. L., Calculation of nd scattering lengths with realistic potentials, 25:14743
ZUBAREV, V. N., Measurement of total cross sections of π^---p interaction, 25:14561 (JINR-P1-5460)
ZUFFI, L., Plutonium-239 angular distributions in energy range 0.2 to 5.5 MeV, 25:15134
ZUMINO, B., Dimension of scale symmetry breaking, 25:14758
ZUM WINKEL, Karl, Sequential scintigrams of kidney with ^{131}I- o-iodo-hippuric acid and /sup 113m/In-EDTA, 25:13499
ZUNTER, Franjo, Postoperative radiotherapy of mammary carcinoma without irradiation of the thorax wall, 25:13533

SUBJECT INDEX

Cross references are included in cumulative subject indexes and in *Subject Headings Used by the USAEC Division of Technical Information* (USAEC report TID-5001).

The reader is also referred to *Guide to Abstracting and Indexing for Nuclear Science Abstracts* (USAEC report TID-4576).

Most headings in the subject index are specific materials, things, and processes. The headings are followed by modifiers that describe the properties of, or processes applied to, the headings.

All index entries cite *NSA* volume and abstract numbers; volume number precedes the colon and the abstract number follows it. The designation (R) following the abstract number indicates a progress report; (P) indicates a patent; and (T) indicates a translation. Abstracts for reports other than progress reports carry no letter designation. Report numbers, where applicable, are included in parentheses after the abstract number of the citation. Published literature (journal article or book) can be identified by the absence of a report number.

Ideas presented in the original literature, rather than key words, have been indexed. The indexers have selected what seemed the most probable and logical place to look for typical information. Since it is not always possible to anticipate where a user would look for information, the cumulative indexes include numerous cross references. Consideration of synonymous or closely related terms will prove valuable.

Information is indexed for the greatest use to the greatest number of users. This requires that a topic be indexed to headings that most specifically describe it and not ordinarily to the headings that describe its ultimate use or to the general class headings that include the specific headings. For example, information on boiler design for the Fermi Fast Breeder Reactor would be indexed under the headings BOILERS and FERMI FAST BREEDER REACTOR but not necessarily under the headings REACTORS, FAST or REACTORS, BREEDER.

General or broad headings are reserved for general summaries, reviews, comprehensive reports, and similar literature.

Subject Heading Styles

Generally, the direct form of subject entry is used rather than inverted headings; e.g., AMINO ACIDS rather than ACIDS, AMINO; HELIUM ISOTOPES He-4 rather than HELIUM—ISOTOPES He-4 or HELIUM—He-4 ISOTOPES. Note, however, that in some cases parenthetic modifying terms or inverted headings such as NEUTRONS, FAST, are used where the alphabetical arrangement of a direct entry would cause information to be scattered. In addition, organic compounds are usually entered in the index in the inverted form to facilitate grouping like or related compounds with the parent compounds; e.g., BENZENE, BROMO- rather than BROMOBENZENE. In general, the nomenclature used is that of the subject indexes to *Chemical Abstracts*.

Alphabetization

Subject headings are alphabetized word by word. Parenthetic qualifiers, numbers, and Greek letters within subject headings are disregarded in alphabetizing unless there are two or more headings that are otherwise identical, in which case the qualifier, numerical progression, or spelled names for the Greek letters determine the order.

Examples:

M-Capture
  see ELECTRON CAPTURE
MAGNESIUM
MAGNESIUM ALLOYS AND SYSTEMS
MANGANESE FLUORIDES
MANGANESE FLUORIDES MnF_2
MESONS
MESONS (π)
MESONS (ρ)
1-PENTANOL
2-PENTANOL

Modifying Phrases

The modifiers appearing under a subject heading are written specifically to show the relation between the item being indexed and the heading. The modifier therefore contains a maximum of useful information. Although the modifier begins with the word judged to be of greatest use to the greatest number of users, there is still need for the searcher to consider all modifiers under the heading(s) of interest.

Modifiers usually form meaningful phrases when combined with the subject heading. Some are intended to be read following the subject heading, e.g., the entry HYDROGEN—sorption by charcoal should be read "hydrogen sorption by charcoal." As a result of placing the important word first, however, many modifiers must be rearranged for smooth reading, e.g., FORMALDEHYDE—yields in radiolysis of ethyl ether, effects of deuterium on, should be read "effects of deuterium on formaldehyde yields in radiolysis of ethyl ether" and URANIUM—crystal structure of, effect of cooling rate on allotropic transformations in, should be read "effect of cooling rate on allotropic transformations in crystal structure of uranium."

Special characters are added to modifiers in the fields of physics and reactor technology; if the modifier does not establish the experimental or theoretical character of a reference, a symbol (E), (T), or (E/T) is placed immediately after the modifying phrase and before the abstract number.

XUM

Physical States and Configurations of Materials

The specific physical state, if other than normal, or the geometric configuration of the material is included in the modifying phrase; e.g., information on liquid metals is indexed under the specific metal with "liquid" in the modifier and carbon crucibles is indexed under CARBON with "crucibles" appropriately placed in the modifier. The information on carbon crucibles is also indexed under CRUCIBLES.

Nomenclature of Inorganic Compounds

Inorganic compounds are indexed to subject headings in the direct form. Cations are listed in the order of increasing valence for polycationic salts of varying valence and in alphabetic order for polycationic salts in which all cations have the same valence; e.g., SODIUM ALUMINUM SILICATES and POTASSIUM SODIUM SULFATES. If more than one anionic species is presented in a compound, the anions are arranged alphabetically, e.g., BERYLLIUM FLUORIDE HYDROXIDES.

Nomenclature of Organic Compounds

Organic compounds are indexed by subject headings based on the indexes to *Chemical Abstracts* except in the area of enzymes, in which specific enzymes, named according to the 1964 recommendations of the International Union of Biochemistry, are used. In many cases nonproprietary names for drugs are used as subject headings, and cross references are made from the systematic chemical names. Subject headings for hormones appear in the inverted style at HORMONES.

Nomenclature of Life Sciences

Subject headings for plants are names of phyla with one exception: members of the Phylum Tracheophyta are indexed under class or subclass names. Scientific names (genus and species) are used as the initial, or file, word in the modifying phrase. Scientific names are omitted only when the name is not available in the literature or cannot be found in available references.

Subject headings for animals are the names of phyla with the following exceptions: (1) members of Phylum Arthropoda and Phylum Chordata are indexed under appropriate class name, and (2) common names are used for members of Class Mammalia.

Subject headings are entered for various classes of commodities, and specific products are identified in the file-word position of the modifier. In the following examples, approved subject headings are capitalized and typical modifier file words are listed in lower case.

Example 1	Example 2
CEREALS	MEATS
bread	beef
flour	fish
oats	mutton
rice	pork
rye	poultry
wheat	seafood

Diseases, pathological conditions, and in vitro studies of atypical cells and tissues are indexed under subject headings for the organism affected, under the appropriate anatomical structure of physiological phenomenon affected, and under the appropriate disease heading. Subject headings for diseases (defined as any deviation from the norm) are DISEASES; DISEASES, INFECTIOUS; DISEASES, NEOPLASTIC; DISEASES, PHYSIOLOGICAL; DISEASES, PLANT; and DISEASES, TRAUMATIC.

Diseases of mixed etiology are treated in the following manner: neoplastic diseases that are also classified as infectious or physiological are indexed under DISEASES, NEOPLASTIC; diseases in which a microorganism is the etiologic agent are classified under DISEASES, INFECTIOUS; physiological anomalies that are neither neoplastic nor infectious are indexed under DISEASES, PHYSIOLOGICAL; the acute radiation syndrome, nonspecific radiation injuries, trauma, and wounds or incisions inflicted mechanically are indexed under DISEASES, TRAUMATIC.

Specific diseases or pathological conditions are named in the file-word position of the modifier, in the author's terminology, and are set off from the remainder of the modifier by commas. Neoplasms are designated as benign or malignant in the file-word position when more specific information is not available.

Multicomponent Alloys and Other Systems

Multicomponent alloys and systems, except well-known trade names, are indexed under a subject heading for each component in the form "element systems" for nonmetals or "element alloys and systems" for metals. The modifier begins with element symbols for each component arranged alphabetically. In addition, if significance is placed on the base metal of the alloy, this is indicated by adding "-base" to the element symbol.

Example: A 1.5C, 12Cr, 0.25V, 0.8Mo, bal Fe alloy is indexed as

```
CARBON SYSTEMS
  C--Cr--Fe-base--Mo--V, ...
CHROMIUM ALLOYS AND SYSTEMS
  C--Cr--Fe-base--Mo--V,...
IRON ALLOYS AND SYSTEMS
  C--Cr--Fe-base--Mo--V, ...
MOLYBDENUM ALLOYS AND SYSTEMS
  C--Cr--Fe-base--Mo--V, ...
VANADIUM ALLOYS AND SYSTEMS
  C--Cr--Fe-base--Mo--V, ...
```

Well-known alloys, such as ZIRCALOY-2, are indexed under the trade name; cross references from each component of the alloy to the trade name appear in cumulative indexes.

Multicomponent systems in which nonmetallic elements are present in large percentage and which are commonly referred to as systems or mixtures are indexed in a manner similar to alloys.

Example: A tungsten–silicon preparation is indexed as

```
TUNGSTEN ALLOYS AND SYSTEMS
  Si--W, ...
SILICON SYSTEMS
  Si--W, ...
```

Multicompound systems and mixtures of inorganic compounds are indexed under the subject heading for each component compound; the modifiers begin with an alphabetical listing of compound formulas.

Example: A lead titanate–lead zirconate mixture is indexed as

LEAD TITANATES
$PbTiO_3$--$PbZrO_3$
LEAD ZIRCONATES
$PbTiO_3$--$PbZrO_3$

A mixed system of compounds and elements is indexed by a combined form of the preceding conventions; e.g., a dispersion of copper and alumina would be indexed as

ALUMINUM OXIDES
  Al_2O_3--Cu, ...
COPPER ALLOYS AND SYSTEMS
  Al_2O_3--Cu, ...

Mixtures of organic compounds are indexed under subject headings for each component of the mixture; the modifiers begin with an alphabetical listing of compound names.

Example:

ACETIC ACID
  acetic acid--BF_3, ...
BORON FLUORIDES
  acetic acid--BF_3, ...

Example:

BENZENE, CHLORO-
  bromophenol--chlorobenzene, ...
PHENOL, BROMO-
  bromophenol--chlorobenzene, ...

If modifiers for alloys and systems are included with other modifiers under the same subject heading, they are filed last.

Example:

CARBON SYSTEMS
  deposition on nuclear fuel particles
  molecular structure of
  neutron total cross section for
  sorptive properties for xenon
  Young's modulus for
  Al--C--Cr, superconductivity in
  B--C, phase studies for
  C--U--Zr, fabrication and physical properties of

Nomenclature of High Energy Physics

Information on particle-particle events is indexed under subject headings for the specific particles involved. The modifier file word *interactions* is followed by the specific interaction written in symbolic form. Particle nomenclature and symbols follow that of Rosenfeld, et al. *Data on Particles and Resonant States,* UCRL-8030 (latest revision). For consistency the incident particle is always written first. The mass (in MeV) of a resonance state is included in parentheses after the symbol to avoid ambiguity. Hyperfragments are indicated in modifiers as in the following examples: Λ-He^5, Σ-H^3, $\Lambda\Lambda$-Be^{10}. The superscript on the right indicates the total number of baryons in the composite system.

Examples:

MESONS (π^-)
  interactions $\pi^- + p \rightarrow \Lambda + K^+ + \pi^-$ at 6 GeV/c in hydrogen bubble chamber, ΛK(1700) enhancement in, (E)
BARYONS, RESONANCE (N*)
  production of $\Delta^{++}(1236)$ and $\Delta^0(1236)$ from $K^- + p \rightarrow K^- + p + \pi^+ + \pi^-$ interactions at 2.63 and 2.70 GeV/c, (E)
HYPERFRAGMENTS
  binding energy of $\Lambda\Lambda$-He^6, three-body α--Λ--Λ model for

Subject headings are also provided for specific models and theories.

Examples:

ELEMENTARY PARTICLE MODELS (TRIPLET)
  hadron total cross sections in quark, numerical analysis of
CURRENT ALGEBRA
  PCAC hypothesis for A_1 and rho dominance in $\pi \rightarrow e + \nu + \gamma$ decay
REGGE POLE THEORY
  predictions for polarization in $K^- + p \rightarrow$ anti $K^0 + n$, $\pi^- + p \rightarrow \pi^0 + n$, and $\pi^- + p \rightarrow$ eta + n interactions at high energies
SYMMETRY GROUPS
  SU(2) × SU(4) intermediate-coupling model for nucleon and hyperon isobars

Nomenclature of Reactor Technology

Subject headings for reactors are of three types:

(1) Specific reactors, e.g., ARGONNE RESEARCH REACTOR, SAXTON POWER REACTOR

(2) Reactors having a common physics or engineering characteristic, e.g., REACTORS, FAST; REACTORS, ORGANIC-COOLED; REACTORS, PRESSURIZED-WATER

(3) Reactors having a common purpose, e.g., REACTORS, POWER; REACTORS, RESEARCH

Information on specific reactors, type (1), is indexed under the one specific subject heading. Information on classes or types of reactors, types (2) (characteristics) and (3) (purpose), is indexed under all applicable headings. For example, information on a heavy-water-moderated organic-cooled power reactor is indexed under REACTORS, HEAVY WATER-MODERATED; REACTORS, ORGANIC-COOLED; and REACTORS, POWER.

Subject headings exist for selected reactor components, e.g., REACTOR FUEL ELEMENTS. When applicable, headings for components are indexed even though they may have been included in a modifier under a type (1) or (2) heading. The materials in reactor components are indexed when the information is peculiar to the material.

Modifier file words under reactor headings are of two primary types: one type expresses reactor characteristics, e.g., reactivity; the other, components, e.g., control rod. If no subject heading appears for a reactor component, the heading REACTORS is used, and the component is used as the modifier file word.

A

ACCELERATORS
- cavity resonators for, frequency dependence of surface resistance of superconducting lead, 25:14847 (NP-18654)
- development and research at MIT, 1969, 25:14925(R) (MIT-2098-643)
- magnet for, design of liquid-cooled, 25:14857(P)
- research on crossed-beam, in Soviet Union, 25:14544
- waveguides for, superfluid helium cooling system for superconducting for helical, (T), 25:14846 (NP-18651)

ACETALDEHYDE
- yields from γ radiolysis of 2-propanol vapor at 124 to 400°C, 25:13046

ACETAMIDE, N,N-DIMETHYL-
- complexes with thorium halides or uranium halides in nitromethane, electric conductivity of, relation of composition and ionization capacity to, 25:13023

ACETIC ACID, (1,2-CYCLOHEXYLENEDINITRILO)TETRA-
- complexes with technetium, composition and stability of, 25:13008

ACETIC ACID, (ETHYLENEDINITRILO)TETRA-
- complexes with technetium, composition and stability of, 25:13008
- effectiveness of indium-113m-labeled, for kidney scintigraphy in man in comparison to iodine-131-labeled hippuran, 25:13499

ACETIC ACID, NITRILOTRI-
- complexes with technetium, composition and stability of, 25:13008

ACETONE
- yields from γ radiolysis of 2-propanol vapor at 124 to 400°C, 25:13046

ACETYLENE
- determination of trace amounts of, in argon, helium, hydrogen, krypton, and neon following freezing-out at liquid nitrogen temperature, mass spectrometric, 25:12941

ACETYLSEROTONIN METHYLTRANSFERASE
- radiation effects on activity of, in pineal glands in rats, x, 25:13559

ACID PHOSPHATES
- radioinduced decrease of content of, in dorso-lateral prostates of rats, x, 25:13366

ACRIDINE
- radiation effects on toxicity of, to biological materials, 25:13374

ACRIFLAVINE
- use for induction of SV40 virus from transformed hamster cell clones, 25:13615

ACRYLAMIDE
- polymerization following fluorescence quenching of uranyl ions, kinetics of, 25:12981

ACTIHAEMYL
- protective effects on brachial plexus in man following therapy for mammary carcinomas, 25:13480

ACTINIDES
- alpha and electron capture decay of, equations for calculations of half-lives of, 25:15162
- half-lives of neutron-deficient, calculation of, 25:15162
- production and uses of synthetic, review on, 25:13059

ACTINIUM
- reduction of trivalent, in perchlorate medium, polarographic studies on, 25:13020

ACTINIUM ISOTOPES Ac-227
- energy levels from alpha decay of protactinium-231, 25:14998

ACTIVATION ANALYSIS
- gamma spectra in neutron, computer programs for qualitative and quantitative analysis of, 25:12966
- uses in medicine, review on possibilities for, 25:12964
- uses of neutron, in process control industry, 25:13177

ADENOSINE, 2'-DEOXY-
- effects on growth of yeast cells, effects of cytidine monophosphates on, 25:13604

ADENOSINE 5'-TRIPHOSPHATE
- nicotinamide, effects on metabolism of NAD and NADP in irradiated organs of rabbits and rats, 25:13379

ADRENAL GLANDS
- radiation effects on human effects of insulin on, 25:13586
- radioinduced cortical carcinomas in rat, mixed whole-body fission neutron and γ, 25:13564

AERODYNAMICS
- lift--drag ratios for magnetic suspension systems, 25:15419 (BNL-15420)

AEROSOL GENERATORS
- performance for production of insoluble metal oxide aerosols, 25:13145
- performance for production of spherical polystyrene latex aerosols, 25:13144

AEROSOLS
- particle deposition from, flowing radially inward between concentric parallel circular plates, calculation of diffusional, 25:13123

AET
- radioprotective effects of, alone and in combination with other protectants on mice, use of spleen weight-radiation dose relation for testing, 25:13478

AGRICULTURE
- book: Plants in National Agriculture, 25:13599
- electromagnetic field effects in, 25:13572

AGUIRRE POWER REACTOR, UNIT 1
- construction of, notice of receipt of permit application for, 25:15333 (DOCKET-50376-8)
- operation of, notice of receipt of license application for, 25:15333 (DOCKET-50376-8)

AIR
- analysis for selenium by neutron activation as indicator of sulfur contamination, 25:12965
- analysis of deposits from, for antimony, chromium, cobalt, iron, scandium, and zinc by neutron activation and γ spectrometry, 25:12975
- analysis of particulates in, for antimony, chromium, cobalt, iron, scandium, and zinc by neutron activation and γ spectrometry, 25:12975
- heat transfer to, from fuel element bundles, effects of spacer arrangement on, 25:13153 (ZJE-66)
- ion reactions with, dependence of mean charges of ions from, on atomic number, (E), 25:14007
- krypton-85 deposition from, to grass in comparison to iodine-131, measurement of rate of, 25:13124

AIR SAMPLERS
- performance for lead determination in atmosphere by x-ray fluorescence analysis, 25:13309
- performance of impactor-type, for radon-contaminated atmosphere, (T), 25:13123

AIRCRAFT
- structure components for, gamma radiographic method for inspection of, 25:13180 (JAERI-Memo-4163)

AIRGLOW
- atomic energy level transition probabilities in night, forbidden nitrogen and oxygen, (E/T), 25:14107
- spectral enhancement of oxygen 6300-A emission in latitude-wide nightglow, (E), 25:14109

ALANINE, PHENYL-
- hydrochloride, radiation effects on single crystals of, ESR studies on free radicals produced from γ, 25:13052

ALANINE, 3-SULFO-
- radiation effects on content in fingernails of uranium miners, 25:13369

ALARM SYSTEMS
- spurious alarms in analog and digital, frequency of, 25:13225

ALASKA
- drill hole UAe-7h in Amchitka Island, hydraulic testing of, 25:13105 (USGS-474-84)
- glaciological studies of Casement Glacier, 25:15426 (COO-1473-4)

ALGAE
- contamination of marine, by sea-disposed liquid radioactive wastes, (E), 25:13189 (CEA-CONF-1712)

ALGINIC ACID
- radioisotope uptake by, in brown algae from sea water, 25:13403

ALKALI METAL HYDROXIDES
- analysis for molybdenum as complex trihydroxyfluoronate, extraction--photometric method for, 25:12933

ALKALI METALS
- distribution in atmosphere, use in tracer studies of global transport processes, (E), 25:13121 (TID-25314)
- heat transfer coefficients for boiling, equations for calculation of, 25:13157
- spectra of, relation of electron elastic scattering to Fermi theory of pressure shifts in, 25:14057

ALLOYS
- corrosion of, past and future perspectives on, 25:13632
- deformation behavior of, cyclic, 25:13683
- welding behavior of, effects of temperature in contact area on static, 25:13644

ALPHA PARTICLES
- detection in solar wind, (E), 25:13895
- dose to man following ingestion of spring water at Masutomi spa area in Japan, 25:13470
- effects on bubble nucleation in aqueous uranyl nitrate, 25:13152(R) (SU-326-P-13-5)
- effects on bubble nucleation in superheated water, 25:13152(R) (SU-326-P-13-5)
- effects on defects in nickel at 42 to 44 MeV, electron microscopy study of, 25:13728
- effects on human intestine following therapy of uterine carcinomas, treatment of complications from radium, 25:13589
- effects on polypropene, effects of energy on, 25:13055
- monitoring in airborne particulates in USA during 1969, plutonium-238 and plutonium-239, 25:13441
- monitoring in liquid effluent at Bettis Laboratory during 1969, 25:13431
- monitoring in surface waters of Kansas during 1969, 25:13432
- reactions (α,2α) with lithium-6 and -7 near 60 MeV, analysis for reaction mechanism in, (E), 25:14902
- reactions (α,2n) with lutetium-175 at 28 MeV, gamma spectra from, (E), 25:15036
- reactions (α,2n) with lutetium-175 at 28 MeV, gamma spectra from, (E), 25:15047
- reactions (α,3n) and (α,αn) with cadmium-116 at 18 to 45 MeV, excitation functions and average range measurements from, (E), 25:15049

  reactions (α,3n) with barium-136 at 27 to 44 MeV, excitation functions and average ranges from, (E), 25:15049
  reactions (α,3n) with barium-136 at 33 to 44 MeV, angular distributions and average total kinetic energies of neutrons and photons from, (E), 25:15049
  reactions (α,f) with lead-206, 25:15010
  reactions (α,γ) with magnesium-24 up to 2.8 MeV, γ-ray yield from, (E), 25:14951
  reactions (α,t) with thallium-205 at 20 to 25 MeV, cross sections and normalization for, (E), 25:15064
  scattering by cerium-140, germanium-70, silver-107, and zirconium-90, optical-model analysis of elastic, (E/T), 25:14947
  scattering by nuclei, analysis of backward elastic, (T), 25:15172
  scattering by silver-107 and silver-109 at 10 MeV, Coulomb excitation by inelastic, (E), 25:15035
ALPHA SOURCES
  design of implantable assembly containing, for irradiating body fluids, 25:13529(P)
  determination in precipitation, springs, streams, and wells in Project Rulison area, method for radiochemical, 25:12951 (USGS-474-83)
  monitoring at West Valley Processing Plant, Oct.--Dec. 1970, 25:13079 (DOCKET-50201-61)
  monitoring in environmental samples from West Valley Processing Plant, 1969, 25:13080 (DOCKET-50201-62)
ALPHA SPECTROMETERS
  design for analysis of alpha-emitting radioisotopes in marine organisms, 25:13394(R) (RLO-2099-1)
  development of surface-barrier silicon, for nuclear reaction product measurements, 25:14841 (JINR-P13-5353)
ALUMINUM
  abundance in chondrites, (E), 25:13787
  analysis for vanadium by neutron activation or spectrophotometry, separation methods for, 25:12959
  cesium-ion range at 20 keV in, effects of crystallinity and integrated flux on, (E/T), 25:13960
  complexes with bromopyrogallol red, formation constants and spectra of, 25:12926
  content and depth in crustal basalts and granites in USSR, 25:13115
  determination in copper-, magnesium-, nickel-, or titanium-base alloys using gas-sheathed tubular electrode arc, spectroscopic, 25:12945
  determination of trace amounts of, in blood serum by emission spectroscopy, 25:12946
  determination of trace amounts of, in boron carbide by neutron activation, 25:12972
  determination using bromopyrogallol red, spectrophotometric, 25:12926
  diffusion in, impurity, 25:15445 (ORO-2036-21)
  displacement damage in electron-irradiated, electron microscopy method for detection of, 25:13721
  effects of weld filler addition of, on mechanical properties of heat affected zone in ferritic stainless steel, 25:13696
  effects on backscattering during γ dosimetry to HeLa cells, 25:13456
  effects on gravimetric determination of tellurium, 25:12943
  electric conductivity of, at room temperature, (E), 25:14192
  electron backscattering at 1.0 MeV by thick targets of, Monte Carlo calculation of angular distributions and energy spectra from, 25:13959 (UCRL-19719)
  electron charge-deposition distribution at 4 to 24 MeV in, 25:13964
  electron reactions at 30 keV with, Monte Carlo calculation of energy losses and depth distribution of x-ray production in, 25:14400
  electron reflection and transmission by shields of, review data on, 25:14396 (N-70-37470)
  electron slowdown at 10 to 15 MeV in, Monte Carlo calculation of, 25:14397
  electron slowdown at 10 to 28 MeV, Monte Carlo study of spectra of, 25:14398
  gamma transport in, calculations using anisotropic source--flux iteration technique, 25:14407
  impedance in thin films of superconducting, rf, (E), 25:14151
  magnetic vortex pinning and motion in superconducting thin films of, 25:14176
  positron backscattering at 1.0 MeV by thick targets of, Monte Carlo calculation of angular distributions and energy spectra from, 25:13959 (UCRL-19719)
  proton reactions at 70 GeV, cross sections for antihelium-3 production, mass, and charge in, (E), 25:14540 (IFVE-SEF-70-16)
  proton reactions at 70 GeV, upper limits for cross sections for production of new-type radioactivity from, (E), 25:14541 (JINR-P1-5399)
  proton reactions below 70 GeV/c, atlas of particle-production-momentum spectra for, (T), 25:14733 (NP-18660)
  radiation effects on lattice parameters of, at low temperature, 3 MeV electron, 25:13723 (JUL-664-FN)
  radiation effects on microstructure of high-purity, 200 keV electron, 25:13727
  superconducting properties of thin films of, (E), 25:14192
  superconducting thermodynamic fluctuation effects in two-dimensional films of, (E/T), 25:14162
  superconducting vortex motion in presence of thermodynamic fluctuations in granular films of, (E), 25:14207
ALUMINUM ALLOYS AND SYSTEMS
  analysis for constituents using gas-sheathed tubular electrode arc, spectroscopic, 25:12945
  Al--Ca, mechanical properties of composite, 25:13692
  Al--Ce, mechanical properties of, 25:13692
  Al--Cr--Fe, mechanical properties of, effects of zirconium on, 25:13680
  Al--Cr--Fe, oxidation resistance to carbon dioxide at 600 to 900°C, effects of zirconium on, 25:13680
  Al--Cu, creep stress in, effects of velocity on, 25:13683
  Al--Nb--Ni, phase studies of, 25:13706
  Al--Pu-base, aluminum-27 NMR in delta-, 25:14481
  Al--Sb, mechanical properties of composite, 25:13692
  Al--Y, mechanical properties of composite, 25:13692
  Al-base--Li, stress rupture of dilute, at 175 to 300°C, effects of radioinduced gas bubbles on, 25:13678
ALUMINUM IONS
  reactions with oxygen atoms at 30 keV to 2 MeV, cross sections for electron capture and loss in, (E), 25:14042
ALUMINUM ISOTOPES Al-26
  abundance in early solar system, (E), 25:13864
  energy levels from aluminum-27 (He-3,α) reactions, spectroscopic factors for, (E), 25:14944
ALUMINUM ISOTOPES Al-27
  bremsstrahlung reactions at 0.8 to 2.1 GeV, spallation products from, (E), 25:14977
  deuteron reactions (d,p) at 650 MeV, proton angular distributions from, (E), 25:14906
  energy levels from helium-3 inelastic scattering, (E), 25:14899
  helium-3 double elastic scattering at 30 MeV, polarization in, (E), 25:14894
  helium-3 inelastic scattering at 20.5 MeV, energy spectra and angular distributions in, (E), 25:14899
  helium-3 reactions (He-3,α) at 35 MeV, differential cross sections for, (E), 25:14944
  neutron capture at 0.025 eV, cross section for, (E), 25:14935
  neutron elastic and inelastic scattering at 4.5 to 8 MeV, cross sections for, (E/T), 25:14963
  neutron elastic scattering at 14 MeV, optical-model analysis of differential cross sections for, (T), 25:14920(T) (BNL-tr-380)
  neutron elastic scattering at 8 MeV, cross sections for, (E/T), 25:14965
  neutron inelastic scattering at 2 to 4.5 MeV, cross sections for, (E/T), 25:14966
  neutron reactions (n,xγ) at 14 MeV, cross sections and gamma spectra from, (E/T), 25:14920(T) (BNL-tr-380)
  neutron scattering at 1 to 8 MeV, width fluctuation and resonance interference effects in cross sections for, (E/T), 25:14962
  nuclear magnetic resonance in stabilized delta-plutonium at 4 and 77°K, 25:14481
  proton elastic scattering at 18.0 MeV and 43°, depolarization parameter from polarized, (E), 25:14889 (CEA-CONF-1650)
  proton reactions (p,γ) at 0.3 to 2.6 MeV, γ-ray yield from, (E), 25:14951
  proton reactions (p,γ) at 742 and 1381 keV, Q-value for, (E), 25:14936
  proton reactions (p,γ) near 1.5 and 1.7 MeV, angular distributions for, (E), 25:14948
  proton reactions at 660 MeV, angular distributions of carbon-11, fluorine-18, and nitrogen-13 from, (E), 25:14945
ALUMINUM ISOTOPES Al-28
  half-life, (E), 25:14935
ALUMINUM OXIDES
  content in rocks of shields and sediment cover of Brazil, Canada, and USSR, relations with geological time, 25:13114
  creep at high temperatures in polycrystalline, effects of impurities on, 25:15427(R) (COO-1591-13)
  elastic properties of composites of pores in, 25:13751
  electric properties of commercial-grade, polarization effects in, 25:14437 (WHAN-SA-75)
  ion reactions at 10 to 40 keV with, secondary electron yields from, (E), 25:13963
  properties at high temperatures, review of physical, thermal, and thermodynamic, 25:13667
  sorptive properties for vanadium, 25:12959
  Al_2O_3--Au-base, properties of dispersion-strengthened, electric and tensile, 25:13755
  Al_2O_3--glass, elastic properties of composites of, 25:13751
  Al_2O_3--Pt-base, properties of dispersion-strengthened, electric and tensile, 25:13755
AMERICIUM
  deuteron reactions with thin targets of, at 9 to 14.2 MeV, (E), 25:15046
  precipitation in ammonium carbonate solutions using hexaamminecobalt chloride, evaluation of method for,

XUM

25:12980
  production and uses of, review on, 25:13059
  proton reactions with thin targets of, at 9 to 14.2 MeV, (E), 25:15046
  reduction of trivalent, in perchlorate medium, polarographic studies on, 25:13020
  separation from aqueous chloride solutions by solvent extraction using dioctyl phosphate in benzene or heptane, effects of variables on, 25:13096
  x-ray energies of, K, (E), 25:14981 (IN-1448)
AMERICIUM ALLOYS AND SYSTEMS
  Am--La-base, americium effective ionic size in, 25:13705
AMERICIUM CHLORIDES
  crystal structure of AmCl$_3$, 25:13011
AMERICIUM ISOTOPES Am-237
  half-lives of isomers of, (E), 25:15046
AMERICIUM ISOTOPES Am-241
  alpha decay of, gamma spectra and half-life for, (E), 25:14981 (IN-1448)
  determination in liquid waste effluents from nuclear fuel reprocessing plant by α spectrometry, 25:12950 (BRH/NERHL-70-2)
  neutron reactions at thermal energies to 10 MeV, evaluation of data on, (T), 25:15128
AMERICIUM ISOTOPES Am-242
  neutron fission of, energy spectra and mean prompt neutron production in thermal, (E), 25:15118
  neutron fission of, intermediate structure effects in, (E), 25:14997
AMERICIUM ISOTOPES Am-243
  fission of isomers of, spontaneous, (E), 25:15046
AMERICIUM OXIDES
  production of, design of equipment for, 25:13146
AMINO ACIDS
  separation of, effects of structure of peptide stationary phases on gas chromatographic, 25:15424 (COO-1222-42)
AMINOACYL TRANSFERASES
  recognition in Escherichia coli, effects of uv-irradiated pyrimidine residues on, 25:13364
AMMONIA
  effects on yields from γ radiolysis of carbon tetrachloride at 25°C, 25:13045
  radiolysis of, adsorbed on synthetic zeolites, EPR spectral studies on effects of alkali metals and hydrogen on γ, 25:13057
AMMONIUM ACID FLUORIDES
  radiation effects on single crystals of, ESR and optical absorption study of 1-MeV electron, 25:14411 (AD-712321)
AMMONIUM ACID PHOSPHATES
  thermal capacity of, effects of deuterium on, 25:12998
AMMONIUM CHLORIDES
  BaCl$_2$--NH$_4$Cl, electrolytic properties of aqueous solutions of, adiabatic compression and ultrasonic attenuation studies of, 25:13015
  MgCl$_2$--NH$_4$Cl, electrolytic properties of aqueous solutions of, adiabatic compression and ultrasonic attenuation studies of, 25:13015
AMMONIUM COMPOUNDS, SUBSTITUTED
  hexadecyltrimethylammonium bromide uses for spectrophotometric determination of molybdenum, 25:12930
  tetraethylammonium neptunium(IV) chloride, absorption spectra of single crystals of, 25:14466
AMMONIUM NITRATES
  KNO$_3$--NH$_4$NO$_3$, electrolytic properties of aqueous solutions of, adiabatic compression and ultrasonic attenuation studies of, 25:13015
  Mg(NO$_3$)$_2$--NH$_4$NO$_3$, electrolytic properties of aqueous solutions of, adiabatic compression and ultrasonic attenuation studies of, 25:13015
  NH$_4$NO$_3$--Pb(NO$_3$)$_2$, electrolytic properties of aqueous solutions of, adiabatic compression and ultrasonic attenuation studies of, 25:13015
  NH$_4$NO$_3$--UO$_2$(NO$_3$)$_2$, electrolytic properties of aqueous solutions of, adiabatic compression and ultrasonic attenuation studies of, 25:13015
AMMONIUM SULFATES
  MgSO$_4$--(NH$_4$)$_2$SO$_4$, electrolytic properties of aqueous solutions of, adiabatic compression and ultrasonic attenuation studies of, 25:13015
AMPHIBIA
  Rana sp., radiation effects on electroretinogram of, effects of fluorascein on uv, 25:13573
  Taricha granulosa, radiation effects on, protective effects of dimethyl sulfoxide against mixed cobalt-60 γ and x, 25:13477
AMPLIFIERS
  design of superconducting femtovolt, using quantum interference magnetometer, 25:14217
  noise analysis of, with superconducting inputs, 25:14224
  use of superconducting femtovolt, as multimeter, 25:14217
α-AMYLASE
  radiation effects on activity of, in Aspergillus oryzae, combined effects of ethylenimine and x, 25:13381
ANGIOSPERMIDAE
  Avena sativa, radioisotope uptake by, effects of ashed plants containing strontium-90 and yttrium-90 and soil pH on strontium-90 and yttrium-90, 25:13118(R) (COO-414-17)
  Avena sp., pinocytosis in root tip cells of, following uptake of uranyl ions, 25:13353
  Gossypium sp., radiation effects on time of ripening and yield of, effects of day length, dose, and seed exposure on γ, 25:13602
  grass, krypton-85 deposition from air to, in comparison to iodine-131, measurement of rate of, 25:13124
  grasses, effects on strontium-90 removal from soil, 25:13118(R) (COO-414-17)
  Hordeum distichum, radiation effects on DNA content of proembryo stages of, ionizing, 25:13405
  Hordeum sp., radiation effects on fertility, height, and survival of, effects of dose and dose rate on γ, 25:13603
  Nicotiana tabacum, fixation of carbon-14-labeled carbon dioxide in leaves of, effects of TMV infection on, 25:13360
  Nicotiana tabacum, radiation effects on seeds and plants of, following exposure of pollen, effects of temperature shock on γ, 25:13601
  Phaseolus sp., radiation effects on leaf mass and pigment content of, effects of seed exposure on x, 25:13600
  Pisum sativum, radioinduced mutations in, for increased productivity, economic value of x, 25:13418
  Populus trychocarpa, radiation effects on content of o-oxyphenols in shoots of, fast neutron and γ, 25:13598
  radiation effects on crop yield of, following plant or seed exposure, γ, 25:13599
  Sesamum orientale, radioinduced mutations in, for chlorophyll, fertility, and growth, x, 25:13415
  Sorghum sp., mutations induced in, for chlorophyll by chemical mutagens, 25:13420
  Sorghum sp., radioinduced mutations in, for chlorophyll production, γ and x, 25:13420
  Triticum sp., mutations induced by EMS in seeds of, for weight variations, 25:13419
  Triticum sp., radiation effects on metabolism of phosphates in seedlings of, γ, 25:13597 (NP-18606)
  Triticum sp., radioinduced mutations in seeds of, for weight variations, γ, 25:13419
  Vicia faba, chromosomes aberrations induced in, by γ-irradiated strawberry juice or puree, 25:13621
  Vicia faba, radioinduced chromosome aberrations in, effects of dose fractionation on x, 25:13413
ANTENNAS
  performance of cylindrical, in isotropic compressible plasma, (T), 25:14275
  radiation effects on Emergency Broadcast System, nuclear electromagnetic pulse, 25:13328 (ORNL-TM-2830)
ANTHRACENE
  electron energy loss spectra at 115 eV in single crystals of, 25:13968
9,10-ANTHRACENEDICARBONITRILE
  efficiency for liquid scintillation counting of tritium in toluene solution, 25:13214
ANTIBODIES
  radiation effects on titer of, against EBV-associated membrane antigen complex following therapy of Burkitt's lymphoma and nasopharyngeal carcinoma, γ, 25:13391
ANTIGENS
  effects of bacterial, on x-radiosensitivity of bone marrow and reticulo-endothelial system in rats, 25:13567
ANTIMONY
  determination in airborne and deposited particulates by neutron activation and γ spectrometry, 25:12975
  determination in natural materials by neutron activation and radiochemical separation, 25:12968
  energy-level excitation by neutron capture gamma rays, (E), 25:15002
  isomeric shifts for, produced by β decay of tin-121m in solid inorganic tin compounds, 25:13074
  neutron elastic scattering at 8 MeV, cross sections for, (E/T), 25:14965
  reactions with aqueous hydrochloric acid solutions, kinetics of extraction and isotopic exchange in, 25:12999
ANTIMONY ALLOYS AND SYSTEMS
  Al--Sb, mechanical properties of composite, 25:13692
  Bi--Pb--Sb, superconducting properties of, in porous glass, 25:14191
  Bi--Sb--Te, thermoelectric properties of BiSbTe, measurements for use in SNAP-23A, 25:13166(R) (MMM-4187-1)
  Sb--U, hyperfine magnetic fields in antiferromagnetic USb, Moessbauer effect study of, 25:14483
ANTIMONY ISOTOPES Sb-121
  Moessbauer spectrum in uranium antimonide, 25:14483
  neutron capture by, γ spectra for resonance, (E), 25:14982 (NCSAC-31)
ANTIMONY ISOTOPES Sb-124
  yields in thermal fission of uranium-235, independent, (E), 25:15038
ANTIMONY ISOTOPES Sb-125
  determination in liquid waste effluents from nuclear fuel reprocessing plant by γ spectrometry, 25:12950 (BRH/NERHL-70-2)
  energy levels from tin-125 decay, spin and parity of, (E/T), 25:15137
ANTIMONY ISOTOPES Sb-126
  yields in thermal fission of uranium-235, independent, (E), 25:15038

ARGININE
  dependence in uv-irradiated mutants of Escherichia coli, 25:13406
ARGON
  analysis for trace amounts of carbon dioxide following freezing-out at liquid nitrogen temperature, mass spectrometric, 25:12941
  analysis for trace amounts of hydrogen following condensation, mass spectrometric, 25:12941
  argon isotope concentration in, by thermal diffusion, 25:13165(R) (MLM-1753)
  argon-ion reactions at 50 to 300 keV with, absolute doubly differential ionization cross sections for, (E), 25:13996
  argon-ion reactions with, cross sections for L-shell x-ray emission in, (E), 25:14004
  determination in sodium, development of methods for, 25:13651(R) (ANL/ST-4)
  determination of trace amounts of, in xenon following condensation, mass spectrometric, 25:12941
  electron elastic scattering at 25 to 800 eV by, tables of amplitudes and spin polarizations for, (T), 25:13995 (AD-711664)
  electron elastic scattering by, resonances in, (E), 25:14035
  electron reactions at 10 keV with, determination of oscillator strengths from coincidence measurements of electrons and ions from, 25:14003
  electron reactions at 3 to 16 keV with, cross sections for excitation of K x rays in, (E), 25:14008
  electron reactions up to 150 eV with, excitation, ionization, and formation of negative-ion resonances in, (E), 25:14002
  helium-ion reactions at 120 to 830 keV with, differential cross sections for production of helium atoms, He^{+}, and He^{2+} in, (E), 25:14044
  neon-ion reactions with, cross sections for L-shell x-ray emission in, (E), 25:14004
  oxygen-ion (O^{-}) reactions in keV range with, formation of autodetaching states of Ar^{-} in, (E), 25:14009
  plasma jets of, electron density and temperature in boundary layer of seeded, 25:14244 (AD-711669)
  plasma jets of, generator for producing, 25:14335
  plasma jets of, Langmuir probe diagnostics of induction-heated supersonic, 25:14243 (AD-711127)
  plasma jets of, sheath dynamics near electrode in magnetic field, (T), 25:14300
  plasma of, Born theory for electromagnetic wave scattering on critical electron density fluctuations in, 25:14363
  plasma of, diagnostics using cylindrical Langmuir probes, (E), 25:14242 (AD-711095)
  plasma of, electron density and temperature in alkali-seeded, in nonequilibrium boundary layer, 25:14258
  plasma of, laser beam interaction threshold for spark maintenance, (E), 25:14331
  plasma of, microwave and spectroscopic measurements of afterglow, 25:14257
  plasma of, properties in wall-stabilized toroidal electric arcs, 25:14269
  plasma of, standing acoustic-wave propagation in column, (T), 25:14380
  proton reactions with, cross sections for L-shell x-ray emission in, (E), 25:14004
  solubility in liquid sodium, 25:15379(T) (EURFNR-785)
  thermal transpiration at 77 and 97°K, model for, 25:13165(R) (MLM-1753)
ARGON IONS
  effects on gold at 4 to 50 keV, defects induced in, 25:14413 (NP-18645)
  reactions with argon at 50 to 300 keV, absolute doubly differential ionization cross sections for, (E), 25:13996
  reactions with argon, cross sections for L-shell x-ray emission in, (E), 25:14004
  reactions with deuterium and hydrogen at 1 to 10 eV, cross sections for, (T), 25:14041
  reactions with gold and gold--copper single crystals at 70 keV, angular distributions of sputtering, 25:13966
  reactions with niobium single crystals at 25 keV, angular distribution of secondary electrons emitted in, 25:13969
  reactions with oxygen atoms at 30 keV to 2 MeV, cross sections for electron capture and loss in, (E), 25:14042
  scattering by copper single crystal at 30 keV, anisotropy in, 25:13970
ARGON ISOTOPES Ar-34
  energy levels from (p,t) reactions, spin-parity assignments for, (E), 25:14950
ARGON ISOTOPES Ar-36
  concentration in argon by thermal diffusion, 25:13165(R) (MLM-1753)
  proton reactions (p,t) with, angular distributions for, (E), 25:14950
ARGON ISOTOPES Ar-38
  concentration in argon by thermal diffusion, 25:13165(R) (MLM-1753)
ARGON ISOTOPES Ar-40
  concentration in argon by thermal diffusion, 25:13165(R) (MLM-1753)
  helium-3 reactions (He-3,t) with, form factors and distorted waves from DWBA analysis of, (T), 25:14924 (COO-535-625)
ARGON SYSTEMS
  Ar--H, mass separation effects in rotating plasma of, 25:14278 (NP-18643)
ARGONNE SYNCHROTRON (ZGS)
  experimental facilities for, on-line computer for, 25:14838 (CERN-70-21(Vol.2), pp 525-37)
ARKANSAS NUCLEAR ONE POWER REACTOR, UNIT 2
  site for, meteorological data for, 25:15332 (DOCKET-50368-7)
ARSENIC
  determination in neutron-irradiated graphite by γ spectrometry, 25:12954
  determination of trace amounts of, in boron carbide by neutron activation, 25:12972
  effects on gravimetric determination of tellurium, 25:12943
ARSENIC ISOTOPES As-74
  beta decay of, $2^{-} + 2^{+}$ positron transitions in, (E/T), 25:14972
  beta spectra from, shapes of nonunique and unique first-forbidden, 25:14976
  content of feces, milk, and urine of dairy cattle following ingestion of Schooner fallout, 25:13396 (UCRL-72511)
  distribution in fetal and maternal tissues of dairy cattle following ingestion of Schooner fallout, 25:13396 (UCRL-72511)
ARSENIC ISOTOPES As-75
  bremsstrahlung reactions at 0.8 to 2.1 GeV, spallation products from, (E), 25:14977
  energy levels and transitions from selenium-75 decay, internal conversion coefficients and transition rates for, (E), 25:14931
  energy-level excitation by neutron capture gamma rays, (E), 25:15002
  neutron elastic scattering at 8 MeV, cross sections for, (E/T), 25:14965
ARSINE, [o-(DIMETHYLAMINO)PHENYL]DIMETHYL-
  complexes with niobium tetrahalides, preparation and spectra of, 25:12979
ARSINE, 4-METHYL-o-PHENYLENEBIS[DIMETHYL-
  complexes with niobium tetrahalides, preparation and spectra of, 25:12979
ARSINE, o-PHENYLENEBIS[DIETHYL-
  complexes with niobium and tantalum tetrahalides, preparation and spectra of, 25:12979
ARSINE, o-PHENYLENEBIS[DIMETHYL-
  complexes with niobium, tantalum, and uranium tetrahalides, preparation and spectra of, 25:12979
ARSINE, o-PHENYLENEBIS[DIPHENYL-
  complexes with niobium tetrahalides, preparation and spectra of, 25:12979
ASPARAGINE SYNTHETASE
  radiation effects on activity of, in potatoes, effects of dose on γ, 25:13365
ASPHALT
  radioactive waste incorporation in, feasibility studies of, 25:13197
ASTATINE ISOTOPES
  electron-capture decay of neutron-deficient, (E/T), 25:14993
ASTATINE ISOTOPES At-205
  electron-capture decay of, energy levels of polonium-205 from, (E), 25:14995
ASTRON DEVICE
  electron-beam injection into, rotating relativistic cloud, 25:14351 (AD-711822)
ASTROPHYSICS
  neutron reaction analysis in, role of nuclear data in, 25:14876
ATMOSPHERE
  analysis for lead, filter collection and x-ray fluorescence method for, 25:13309
  anisotropy of diffuse solar radiation, (E), 25:13903
  density measurements of, beta radiometric gage for, 25:13314
  radiation monitoring of Los Alamos and Paducah environs, during 1969, β, 25:13431
  radiation monitoring of, in Canada, South America, and US during May, 1970, gross beta, 25:13122
  radiation monitoring of, in Guarapari region of Brazil, 25:13393(R) (NYO-2577-12)
  radiation monitoring of, in North, Central, and South America during July 1970, gross β, 25:13399
  radio-wave attenuation in, at 1415 MHz, (E), 25:13838
  radioactivity monitoring in surface, of Canada and USA during April, 1970, gross β, 25:13441
  radioactivity monitoring in surface, of North and South America during 1964 to 1970, monthly profiles of gross β, 25:13441
  sampling of radon-contaminated, performance of impactor-type sampler for, (T), 25:13123
  sulfur content in, neutron activation determination of selenium as indicator of, 25:12965
  transport processes in, chemical tracer studies of, 25:13121 (TID-25314)
ATMOSPHERIC PRECIPITATION
  radiation monitoring of Los Alamos and Paducah environs, during 1969, β, 25:13431

  - radiation monitoring of, in North, Central, and South America during July 1970, gross β, 25:13399
  - radioactivity monitoring in, of Canada and USA during April, 1970, gross β, 25:13441
- ATOMIC ABSORPTION SPECTROMETRY
  - equipment for analysis of radioactive solutions by, 25:12932(P)
- ATOMIC ENERGY
  - bibliographies on, 25:15460 (STI/DOC-11(Vol.8)(No.2))
- ATOMIC ENERGY, LEGAL ASPECTS
  - legislation for domestic and foreign uses of Plowshare technology, review of proposed, 25:13137 (NP-18659)
  - regulations for disposal of radioisotope-containing wastes, review of Italian, 25:13207
  - regulations for safe transport of highly radioactive and fissile materials, description of East German, 25:13194 (SZS-19/70)
- ATOMIC STRUCTURE
  - book: Elementary Atomic Structure, 25:14047
  - Hartree-Fock equations for, nonanalytic behavior of broken-symmetry solutions for, at branching point, 25:14053
- ATOMS
  - charged-particle inelastic scattering by, asymptotic expression for total cross sections for, 25:14022
  - electron correlation in, semiempirical pseudopotential procedure for calculation of, 25:14055
  - electron elastic scattering at very low energies by, relation of Fermi theory of line shifts to, 25:14057
  - electron reactions at 2 to 10 keV with, spectra from vacancy cascades produced in, (E), 25:14038
  - electron scattering at low energies by, phase shift to first order in long-range potential for, (T), 25:14019
  - energy levels of light, relativistic corrections to terms for, (T), 25:14052
  - energy levels of light, use of Breit operator in calculation of fine structure of terms for, 25:14051
  - energy levels of two-electron, perturbation theory of autoionizing, 25:14049
  - energy levels of Z = 1 to 100, tables of, 25:14409
  - energy-level transitions in Z = 11 through 90, calculated rates for L-shell Auger, Coster--Kronig, and radiative, 25:13980
  - interactions at large internuclear distances, calculation using approximate exchange integrals, 25:13985
  - ion reactions with excited, classical calculation of cross sections for resonant charge exchange in, 25:14031
  - ionization energies of, in superstrong magnetic fields, (T), 25:13829
  - Lamb shift of inner electrons in heavy, (T), 25:14048
  - neutron differential scattering cross sections using quasi-classical approximation for, slow, (T), 25:14875
  - perturbation of bound states, formulation of time-dependent, based on hydrodynamic analogy to quantum mechanics, 25:14054
  - photon reactions at 1 keV to 100 MeV with Z = 1 to 100, tables of cross sections for coherent and incoherent scattering, pair production, and photoelectric ejection in, 25:14409
  - properties of interacting, Brueckner--Goldstone many-body perturbation procedure for calculation of, 25:14046
  - radial properties of, use of noncompact group O(2,1) in eigenfunctions for, 25:14056
  - radiation emission from, effect of Doppler broadening on line shape of spontaneous, (T), 25:14050
  - reactions of hot, dynamics of exchange, 25:12986
  - scattering by molecules, homogeneous integral solution method of calculation of T-matrix for rotationally inelastic, 25:14017
  - spectra of Z = 1 to 100, tables of line energies and relative intensities for K and L x-ray, 25:14409
  - spectra of, deviations from LTE in weak complex, (T), 25:13816
  - wave functions for Z = 87 to 103, screening numbers for calculation of scaled hydrogen-like, 25:13976
- AURORAE
  - arc of, quasi-periodic small-scale distortions in, (E), 25:14119
  - atomic energy level transition probabilities in, forbidden nitrogen and oxygen, (E/T), 25:14107
  - charged particle acceleration in, relation of electrostatic and geomagnetic fields for production of, (E/T), 25:14116
  - emission following Mar. 23, 1969 geomagnetic disturbances, behavior of 6300- and 6394-A and OH, (E), 25:14115
  - proton flux measurement parallel to geomagnetic field lines in, 25:14125
  - radio-wave absorption in, conjugate and closely spaced observations of, (E), 25:14118
- AURORAL ZONE
  - disturbances in, nature of magneto-ionospheric, (T), 25:14106
  - electron precipitation into, (E), 25:14103
- AUSTRALIA
  - iodine-131 content of human thyroid in, following nuclear weapons testing during 1966 to 1968, 25:13436
  - strontium-90 content of stratosphere in, following nuclear weapons testing during 1966 to 1968, 25:13436
- AUTORADIOGRAPHY
  - development of neutron activation technique for whole-body, 25:13590
  - methods for diagnosis of thyroid disorders caused by radiation sickness, neutron, 25:13497
  - methods for studying DNA synthesis during growth of hair cells, 25:13337
- AVIDIN
  - effects on carbon-14 incorporation in lipids and proteins of rat liver homogenates, 25:13344

B

- B-66 (NIOBIUM ALLOY)
  - cracking sensitivity of, Varestraint testing of hot, 25:13695
- BACTERIOPHAGES
  - lambda, radioinduced mutations in, for clear forming mutants, effects of bacterial and phage genes on uv, 25:13412
  - phiX174, radiation damage to DNA of, inhibitory effects on reproduction of phosphorus-32 β, uv, and x, 25:13382
  - Qβ, effects on uv radiation effects on uracil incorporation in Escherichia coli, 25:13386
  - Qβ, isolation of amber mutants of, 25:13386
  - radiation effects on survival of, comparison of phosphorus-32 and phosphorus-33, 25:13612
  - T4, radiation effects on, effects of, on synthesis of DNA and phage lysozyme in Escherichia coli, uv, 25:13616
- BAILLY POWER REACTOR, UNIT 1
  - cooling towers for, safety analysis of, 25:15331 (DOCKET-50367-9)
  - design parameters of, revised and additional data on, 25:15331 (DOCKET-50367-9)
  - operations aspects of, revised and additional data on, 25:15331 (DOCKET-50367-9)
- BALANCES
  - design of electromagnetic, using superconducting coils for wind tunnel, 25:14216
- BARIUM
  - abundance in chondrites, achondrites, and Apollo 11 fines, (E), 25:13787
  - content and depth in crustal basalts and granites in USSR, 25:13115
  - determination of trace amounts of, in blood serum by emission spectroscopy, 25:12946
  - structure of films work function of adsorbed films of, on molybdenum (110) surface, 25:13701
- BARIUM CARBONATES
  - carbon-13 concentration in, system flowsheet for, 25:13165(R) (MLM-1753)
- BARIUM CHLORIDES
  - BaCl$_2$--NH$_4$Cl, electrolytic properties of aqueous solutions of, adiabatic compression and ultrasonic attenuation studies of, 25:13015
- BARIUM IONS
  - electron reactions with, effective cross sections for transitions between excited states in, (E), 25:14000
  - reactions with metallic oxides at 10 to 40 keV, secondary electron yields from, (E), 25:13963
  - reactions with oxygen atoms at 30 keV to 2 MeV, cross sections for electron capture and loss in, (E), 25:14042
- BARIUM ISOTOPES Ba-131
  - electron-capture decay of, γ singles and coincidence spectra from, (E), 25:15062
- BARIUM ISOTOPES Ba-132
  - energy levels from decay of cesium-132, (E), 25:15007
- BARIUM ISOTOPES Ba-134
  - energy-level transitions in, rotation of γ-γ angular correlations in magnetic field, 25:14926
- BARIUM ISOTOPES Ba-136
  - alpha reactions (α,3n) at 27 to 44 MeV, excitation functions and average ranges from, (E), 25:15049
  - alpha reactions (α,3n) at 33 to 44 MeV, angular distributions and average total kinetic energies of neutrons and photons from, (E), 25:15049
  - helium-4 reactions (He-4,3n) at 27 to 44 MeV, angular distributions, ranges, and cross sections for, (E), 25:15065
- BARIUM ISOTOPES Ba-137
  - helium-3 reactions (He-3,3n) at 14 to 33 MeV, angular distributions, ranges, and cross sections for, (E), 25:15065
  - helium-3 reactions (He-3,3n) at 14 to 33 MeV, excitation functions and average ranges from, (E), 25:15049
  - helium-3 reactions (He-3,3n) at 20 to 33 MeV, angular distributions and average total kinetic energies of neutrons and photons from, (E), 25:15049
- BARIUM ISOTOPES Ba-140
  - content of feces, milk, and urine of dairy cattle following ingestion of Schooner fallout, 25:13396 (UCRL-72511)
  - distribution in fetal and maternal tissues of dairy cattle following ingestion of Schooner fallout, 25:13396 (UCRL-72511)
- BARIUM OXIDES
  - BaO--B$_2$O$_3$, structure of glasses of, 25:13019
  - BaO--B$_2$O$_3$--La$_2$O$_3$, structure and properties of glasses of, 25:13019

BARYONS
  interactions with baryons, quark model relations between transversity amplitudes for, 25:14671
  interactions with mesons at high energies, review of statistical model for cross sections of single baryon and multimeson production in, (T), 25:14680 (INP-719)
  interactions with mesons in SU(3) symmetry, dual model for, (T), 25:14766
  interactions with mesons, use of spin-$^3/_2$ quarks for decay correlations in resonance production from, (T), 25:14712
  interactions with pseudoscalar mesons, quark model predictions for, 25:14721
  interactions with pseudoscalar mesons, quark model relations between transversity amplitudes for, 25:14671
  mass differences of octet, SU(3) symmetric multichannel calculation of electromagnetic, (T), 25:14795
  mass spectra and structure of, relativistic harmonic oscillators for, 25:14711
  mass spectra of, fifth interaction for, 25:14706
  mass spectra of, relativistic and SU(3)-invariant equations for nonlinear quark theory for, (T), 25:14684
  production in baryon interactions with mesons at high energies, review of statistical model for cross sections for, (T), 25:14680 (INP-719)
  production in N + N interactions at high energies, review of statistical model for cross sections for, (T), 25:14680 (INP-719)
  symmetry for, generalizations of Dirac representation of relativistic, 25:14767
BARYONS, RESONANCE
  classification in SU(3) multiplets, 25:14771
  coupling of normal-parity, to all channels in generalized Veneziano model, (T), 25:14681 (INP-730)
  decay of, selection rules for, 25:14658
  decay widths of negative-parity, symmetric quark model for partial, (T), 25:14718
  duality relation with interference model for, (T), 25:14678
  interactions of, generalized Veneziano model for selection rules for two-body, (T), 25:14681 (INP-730)
  mass of negative-parity, symmetric quark model for, (T), 25:14718
  mass operator in symmetric quark model, negative-parity, 25:14708
  mass spectra of, generalized Veneziano model for, (T), 25:14681 (INP-730)
  production in $\pi^- + p \to K^0 + \Lambda$ interactions at 0.90 to 1.95 GeV/c, phase shift analysis of, 25:14727
BARYONS, RESONANCE (N*)
  decay of, V--A theory for weak, 25:14648
  production and decay of, V--A theory for weak, 25:14648
  production in $\gamma + N \to \omega + N^*$ interactions at 9.1 GeV in deuterium and hydrogen targets, counter study of, (E), 25:14512
  production in $\pi^+ + p \to \Delta^{++}$ + rho^0(ω^0) interactions at 1.95 GeV/c, cross sections and density-matrix elements for, (E), 25:14563
  production of anti $\Delta^{--}\pi^+$(1470), anti $\Delta^{--}\pi^+$(1750), and pnπ^+(2250) enhancements in anti p + d → π^- + anti p + π^+ + p + n interactions at 7.0 GeV/c, (E), 25:14554
  production of dπ and drho enhancements in p + p → d + rho$^+$ (π^+) interactions at 4.0 to 12.3 GeV/c, spectrometer study of, (E), 25:14542
  production of Δ(1236) and Δ(1920) in anti p + d → π^- + anti p + 2p interactions at 7.0 GeV/c, (E), 25:14554
  production of Δ(1236) in anti p + d → anti p + 2p + π^0 interactions at 7.0 GeV/c, (E), 25:14554
  production of Δ(1236) in $K^+ + p$ interactions at 7.3 GeV/c in hydrogen bubble chamber, (E), 25:14574
  production of Δ(1236) in $\pi^- + p \to 2\pi + N$ at 2.3 GeV/c in hydrogen bubble chamber, (E), 25:14570
  production of Δ(1236), N(1470), and N(1688) in $n + p \to 2p + \pi^-$ interactions at 2 to 10 GeV/c, cross sections for, (E), 25:14551
  production of Δ^0 and anti Δ^{--} in anti p + d → $2\pi^-$ + 2p + anti n interactions at 7.0 GeV/c, (E), 25:14554
  production of Δ^-(1236) in $\pi^- + p \to 2\pi^- + 2\pi^+ + n$ interactions at 2.3 GeV/c in hydrogen bubble chamber, (E), 25:14571
  production of Δ^{++}, Δ^+, and Δ^0 in $K^- + p \to K^- + p + \pi^+ + \pi^- + \pi^0$ interactions at 5.5 GeV/c in hydrogen bubble chamber, (E), 25:14572
  production of Δ^{++}(1236) and d*(2170) enhancement in anti p + d → π^- + anti p + π^+ + d interactions at 7.0 GeV/c, (E), 25:14554
  production of Δ^{++}(1236) in $\pi^- + p \to 2\pi^- + p + \pi^+$ and $\pi^- + p \to 2\pi^- + p + \pi^+ + \pi^0$ interactions at 2.3 GeV/c in hydrogen bubble chamber, (E), 25:14571
  production of Δ^{++}(1236) in $\pi^+ + p$ and $K^+ + p$ interactions, momentum-transfer distributions in, (E), 25:14575
  production of Δ^{++}(1236) in π^- reactions with nuclei at 12 GeV/c in heavy-liquid bubble chamber, (E), 25:14562 (TID-25640)
  production of N(1520) in $\gamma + p \to \pi^+$ + N(1520) interactions, low-t theorems for forward, (T), 25:14609
  production of narrow N(1470) in p + p interactions at 6.6 GeV/c in bubble chamber, 25:14552
  search for $T = {}^3/_2$, in π^- spectrum in $\pi^+ + p \to \pi^- + X^{+++}$ interactions at 3.88 GeV/c, (E), 25:14576
  spin alignment of Δ(1236) in $K^+ + p$ interactions at 7.3 GeV/c in hydrogen bubble chamber, (E), 25:14574
BARYONS, RESONANCE (Y*)
  coupling of Σ(1660) to Λ(1405)π in partial wave analysis of $K^- + n \to \Sigma^- + \pi^+ + \pi^-$ interactions at 1.62 to 1.74 GeV, (T), 25:14717
  decay $\Lambda^0\gamma(1350) \to \Lambda^0 + \gamma$, density-matrix techniques and helicity formalism for spin test of Λγ(1350) from, (T), 25:14701 (KFKI-70-27-HEP)
  decay $\Sigma^+(1385) \to \pi^+ + \Lambda$ in bubble chamber, Λ polarization in, (E), 25:14559 (INP-731)
  existence of two distinct Σ(1660) in partial wave analysis of $K^- + n \to \Sigma^- + \pi^+ + \pi^-$ interactions at 1.62 to 1.74 GeV, (T), 25:14717
  production in $K^- + n \to \Sigma^-(\Sigma^+) + \pi^+(\pi^-) + \pi^-$ interactions at 670 to 835 MeV/c in deuterium bubble chamber, differential and total cross sections and partial-wave analysis for, (E/T), 25:14557 (FSU-HEP-70-3-1)
  production of Σ^+(1385) in $\pi^+ + p \to K^+ + \Lambda + \pi^+$ interactions at 8 GeV/c in bubble chamber, (E), 25:14559 (INP-731)
  search for Λ(1670) in $K^- + p \to \Sigma^0 + \pi^0$ interactions, (E), 25:14568
  spin of $\Lambda^0\gamma$(1350), density-matrix techniques and helicity formalism for $\Lambda^0\gamma(1350) \to \Lambda^0 + \gamma$ decay for test of, (T), 25:14701 (KFKI-70-27-HEP)
  spin test for $\Lambda^0\gamma$(1350) from multipole parameters, 25:14725
BASALT
  element concentration and depth in crustal, in USSR, 25:13115
  rare-earth abundances in Apollo 12, (E), 25:13955
BEAM SEPARATORS
  cavity resonators for, frequency dependence of surface resistance of superconducting lead, 25:14847 (NP-18654)
BEHAVIOR
  radiation effects on mating, of male codling moths, γ, 25:13557
BENZENE
  carbon-14 reactions with, at -196°C and 5 eV to 15 keV, mechanisms of, 25:13038
BENZENE, BROMO-
  reactions with recoil bromine-82, calculation of electron energies of transition states from, 25:13064 (INR-1211)
BENZENE, p-DIBROMO-
  spectra of, effects of deuterium on, 25:13003
BENZENE, NITRO-
  reactions with recoil bromine-82, calculation of electron energies of transition states from, 25:13064 (INR-1211)
BERKELIUM
  magnetic susceptibility of metallic and trivalent, 25:13018
  production and uses of, review on, 25:13059
BERKELIUM CHLORIDES
  spectra of hydrochloric acid solutions of, 25:13018
BERKELIUM ISOTOPES Bk-249
  compounds, preparation of microgram quantities of, 25:13018
BERYLLIUM
  deformation of single crystals of high-purity, formation of tetrahedral twins in plastic, 25:13718
  electron backscattering at 0.5 to 2.0 MeV by thick targets of, Monte Carlo calculation of angular distributions and energy spectra from, 25:13959 (UCRL-19719)
  electron charge-deposition distribution at 4 to 15 MeV in, (E/T), 25:13964
  electron diffraction intensities from cleaved surfaces of, low-energy, (LEED), 25:14472
  fracture structure of, 25:13684
  nuclear magnetic resonance Knight shift, nonlocal pseudopotential calculations, 25:14484
  photon reactions at 16 GeV, cross sections for high-mass di-pion pair and upper limits for cross sections for vector meson production in, 25:14511
  photon reactions at 4.1 to 6.1 GeV, phase of rho^0 production amplitude in, (E/T), 25:14527
  photon reactions at 5.1 GeV, coherent interference between rho → $e^+ + e^-$ and $\omega \to e^+ + e^-$ decays from production in, (E), 25:14528
  plasmon dispersion spectrum of, x-ray scattering study of bulk, 25:14443
  positron backscattering at 0.5 to 2.0 MeV by thick targets of, Monte Carlo calculation of angular distributions and energy spectra from, 25:13959 (UCRL-19719)
  proton reactions below 70 GeV/c, atlas of particle-production-momentum spectra for, (T), 25:14733 (NP-18660)
  solubility of, faradic yield of anodic, 25:13704
  superconducting transition temperature and mass enhancement, (T), 25:14152
  surface structure of, effects of anodic dissolution on, 25:13704
  tensile properties at 20 to 900°C, 25:13684

BERYLLIUM ALLOYS AND SYSTEMS
  Be--Cu-base, precipitation processes in, electron microscopy study of effects of aging on, 25:13715
BERYLLIUM CARBIDES
  Be_2C--UC, preparation of fuels of, containing intermetallic UBe_{13}, 25:13746(P)
  Be_2C--UC, production of fuels of, containing uranium dicarbide inclusions, 25:13747(P)
BERYLLIUM IONS
  scattering by helium at 100 to 800 eV of Be^{2+}, energy-loss spectra and interaction energy for, (E), 25:14027
BERYLLIUM ISOTOPES Be-6
  energy levels of, shell model with realistic forces for, 25:15186
BERYLLIUM ISOTOPES Be-7
  decay of, in cosmic rays, (T), 25:14059
  electron capture by, in cosmic rays, (T), 25:14059
BERYLLIUM ISOTOPES Be-9
  energy levels from helium-3 inelastic scattering, (E), 25:14899
  energy levels of, parity of low-lying, (T), 25:14917
  helium-3 inelastic scattering at 20.5 MeV, energy spectra and angular distributions in, (E), 25:14899
  helium-3 reactions (He-3,2α) at 1.55 MeV, analysis for reaction mechanism in, (E/T), 25:14903
  helium-3 reactions (He-3,2α) at 6.0 MeV, spectra from, (E/T), 25:14891(T) (ORO-1316-97)
  neutron capture at 14 MeV, cross sections for fast, (E/T), 25:14920(T) (BNL-tr-380)
  neutron elastic scattering at 14 MeV, optical-model analysis of differential cross sections for, (E/T), 25:14920(T) (BNL-tr-380)
  neutron inelastic scattering at 14 MeV, coupled-channels analysis of differential cross sections for, (E/T), 25:14920(T) (BNL-tr-380)
  photon reactions with, differential cross sections for π^0 production in polarized, 25:14602
  proton elastic scattering at 21.4 MeV and 58°, depolarization parameter from polarized, (E), 25:14889 (CEA-CONF-1650)
BERYLLIUM OXIDES
  defects in irradiated, NMR study of, 25:13754
  diffusion of lithium-6 from irradiated, mechanisms of, 25:13781 (JUL-677-RG)
  ion reactions at 10 to 40 keV with, secondary electron yields from, (E), 25:13963
  properties for thermoluminescence dosimetry, 25:13304 (RT/PROT-(70)23)
  BeO--U-base, deformation of, mechanisms for, 25:13688
BETA DECAY
  coupling constants of, effects of mass of intermediate vector boson on, 25:15180
  ionization following, energy dependence of auto-, 25:13982
BETA PARTICLES
  attenuation corrections for absorbers in 2π beta activity measurements, 25:14403
  dose to man from use of strontium-85 in scintigraphy of bone metastases, 25:13513
  dose to personnel following accidental exposure to iridium-192 vehicle, 25:13466
  effects on human pituitary gland function following implantation of yttrium-90, relation of, to thyroid function, 25:13579
  effects on human skin eight to ten years after therapy, strontium-90, 25:13582
  monitoring in air and precipitation of Los Alamos environs during 1969, 25:13431
  monitoring in air and water of Paducah environs during 1969, 25:13431
  monitoring in airborne particles and surface atmosphere of Central and South America during April, 1970, gross, 25:13441
  monitoring in atmosphere and atmospheric precipitation in Canada, South America, and US during May, 1970, 25:13122
  monitoring in atmosphere and precipitation in North, Central, and South America during July 1970, 25:13399
  monitoring in domestic water supplies in California during 1968, determination of gross, 25:13440
  monitoring in liquid effluent at Bettis Laboratory during 1969, 25:13431
  monitoring in precipitation and surface atmosphere in Canada and USA during April 1970, 25:13441
  monitoring in surface waters of Kansas during 1969, 25:13432
BETA SOURCES
  activity measurements of, absorber attenuation corrections for 2π, 25:14403
  design of implantable assembly containing, for irradiating body fluids, 25:13529(P)
  determination in precipitation, springs, streams, and wells in Project Rulison area, method for radiochemical, 25:12951 (USGS-474-83)
  monitoring at West Valley Processing Plant, Oct.--Dec. 1970, 25:13079 (DOCKET-50201-61)
  monitoring in environmental samples from West Valley Processing Plant, 1969, 25:13080 (DOCKET-50201-62)
BETA SPECTROMETERS
  development of lithium-drifted germanium, with superconducting solenoid for conversion electron spectroscopy, 25:14984 (NP-18536)
  magnetic field calculations for design of iron-free double-focusing, 25:13324 (UUIP-715)
BETATRONS
  design and performance for testing concretes, 25:14861
BEVERAGES
  beer, radioisotope content of Japanese, in relation to atmospheric deposition rates in Tokyo area during 1959 to 1969, comparison of fallout cesium-137 and strontium-90, 25:13434
BIBLIOGRAPHIES
  on fast breeder reactors covering 1966 to 1969, 25:15340 (NEIC-RR-41)
  on Japanese Advanced Thermal Reactor during April 1966 to February 1970, 25:15338 (AAEC/LIB/Bib-258)
  on physics of nuclear explosion cloud growth, 25:13121 (AAEC/LIB/Bib-255)
  on plutonium and transplutonium elements, Nov. 1970, 25:13626
  on plutonium and transplutonium elements, Sept. 1970, 25:13625
  on processing and disposal of plutonium-containing radioactive wastes, 25:13190 (JAERI-Memo-4153)
  on radioinduced curing of coatings, 25:13031 (AAEC/LIB/Bib-261)
  on radioinduced polymerization of concrete--plastics, 25:13030 (AAEC/LIB/Bib-260)
  on radioinduced polymerization of plastic--wood composites, 25:13029 (AAEC/LIB/Bib-259)
  on solar x-ray astronomy, 25:13863 (N-70-39828)
BIG ROCK POINT POWER REACTOR
  control elements for, revised technical specifications for Type 2A, 25:15259 (DOCKET-50155-61)
  emergency core cooling system for, technical specifications for modified, 25:15261 (DOCKET-50155-63)
  fuel element assemblies for, technical specifications for Reload-F and Type J-1, 25:15262 (DOCKET-50155-65)
  neutron sources for, minimum initial strength for startup, 25:15260 (DOCKET-50155-62)
  neutron sources for, revised technical specifications for auxiliary, 25:15258 (DOCKET-50155-60)
  protection systems for, technical specifications for modified, 25:15261 (DOCKET-50155-63)
BINDING ENERGY
  description of nuclear, synthesis of microscopic and macroscopic methods for, (T), 25:15193
BIOLOGICAL MATERIALS
  analysis for carbon-14 and tritium by liquid scintillation counting, 25:12953
  analysis of, development of data acquisition systems for radiometric, 25:13229 (CEA-CONF-1647)
  particle track formation in, theory of, 25:13209 (COO-1671-28)
BIOLOGICAL SYSTEMS
  radiation effects on, electromagnetic, 25:13572
BIOLOGY
  research at BNL, July 1969--June 1970, 25:14837(R) (BNL-50230)
4,4'-BIPHENYLDICARBONITRILE
  efficiency for liquid scintillation counting of tritium in toluene solution, 25:13214
BISMUTH
  determination using thin-layer chromatography and ring-oven colorimetry, 25:12944
  effects on gravimetric determination of tellurium, 25:12943
  electron elastic scattering at 25 to 800 eV by, tables of amplitudes and spin polarizations for, (T), 25:13955 (AD-711664)
  superconducting amorphous state of, electron tunneling in, 25:14210
BISMUTH ALLOYS AND SYSTEMS
  Bi--Pb--Sb, superconducting properties of, in porous glass, 25:14191
  Bi--Pr, magnetic ordering of intermetallic PrBi, self-polarization contribution to, (T), 25:14460
  Bi--Sb--Te, thermoelectric properties of BiSbTe, measurements for use in SNAP-23A, 25:13166(R) (MMM-4187-1)
BISMUTH ISOTOPES
  electron-capture decay of neutron-deficient, (E/T), 25:14993
BISMUTH ISOTOPES Bi-192
  alpha decay of, α energies and half-life for, (E), 25:15023
BISMUTH ISOTOPES Bi-193
  alpha decay of, α energies and half-life for, (E), 25:15023
BISMUTH ISOTOPES Bi-194
  alpha decay of, α energies and half-life for, (E), 25:15023
BISMUTH ISOTOPES Bi-195
  alpha decay of, α energies and half-life for, (E), 25:15023
BISMUTH ISOTOPES Bi-197
  alpha decay of, α energies and half-life for, (E), 25:15023
BISMUTH ISOTOPES Bi-209
  neutron elastic scattering at 8 MeV, cross sections for, (E/T), 25:14965
  neutron inelastic scattering at 2 to 4.5 MeV, cross

sections for, (E/T), 25:14966
proton fission at 155 MeV, prompt neutron spectra and yields from, (E), 25:15021
proton fission of, anisotropy and excitation functions for, 25:15010
BLACK HOLES
degrees of freedom of axisymmetric, two, (T), 25:13828
detection of, (T), 25:13937
formation of, (T), 25:13937
gravitational radiation emission from, (T), 25:13937
physics of, (T), 25:13937
BLADDER
radiation dose to human, during radium therapy, comparison of methods for determining, 25:13448
BLASTOCYSTS
radiation effects on preimplantation, of rats, whole-body x, 25:13560
ultrastructure of preimplantation, effects of estradiol on, 25:13560
BLOOD
composition changes in rat, following intravenous injections of neptunium-237, 25:13346
radiation effects on chemical composition of, in dogs, effects of preliminary exposure on uv and x, 25:13574
radiation effects on coagulation of, in rats, effects of serotonin on cobalt-60, 25:13549
radiation effects on histamine content in rat, effects of skin wounds on whole-body, 25:13368
radioisotope content of, of cattle following intravenous and oral administration, cerium-144 and scandium-46, 25:13352
volume determinations in human organs using iodine-131-labeled human serum albumen, detector system for, 25:13218
volume in human heart and placenta, comparison of metastable indium-131m and technetium-99 for scanning of, 25:13516
BLOOD PLASMA
calcium-47 retention in, of man, 25:13359
volume in patients in relation to erythrocyte mass, use of chromium-51 and iodine-125 in double tracer dilution method for measuring, 25:13338
BLOOD PLATELETS
production in mice and rats, sulfur-35 incorporation for determining effects of thrombopoietin on, 25:13355
radiation effects on formation of, in rats, effects of serotonin on cobalt-60, 25:13549
BLOOD SERUM
analysis for trace amounts of metals by emission spectroscopy, 25:12946
lithium-6 uptake by, of rats following intravenous injection, 25:13350
radiation effects on lactate and propionate content of, in sheep, effects of fasting and shock waves on γ and neutron, 25:13384
BODY FLUIDS
irradiation of, design of implantable assembly containing α or β sources for, 25:13529(P)
radiation effects on content and distribution of, in brain, kidneys, liver, and skeletal muscles of rats, effects of lethal and sublethal dose on x, 25:13348
BOHUNICE POWER REACTOR, UNIT 1
fuel elements for, effects of parallel flow turbulence on transverse vibrations of, 25:15213
BOILERS
heat transfer coefficients for once-through high pressure, effects of steam quality on, 25:13149 (EUR-4561)
leaks in sodium-heated, development of detection methods for, 25:13651(R) (ANL/ST-4)
testing of sodium-heated, description of facility for, 25:13143
BOILING
effects on forced convection heat transfer to sodium in heated tubes, 25:13156
BOLOMETERS
performance of semiconducting and superconducting, comparison of, 25:14227
BONE MARROW
radiation effects on chromosomes and mitosis rate in cells of, in rats, protective effects of bacterial antigens, epinephrine, and pilocarpine against x, 25:13567
radiation effects on, in mice and rats, effects of species on local x, 25:13563
radiation injuries to human, following phosphorus-32 therapy of prostate carcinoma, 25:13591
radioinduced leukemia and malignant myelosclerosis in, of man, radium, 25:13593
transplants of cells of, effects on hematopoiesis in x-irradiated mice, 25:13550
BONES
mineral content of human radius and ulna, use of radiography in combination with photometric scanning to determine, 25:13509
radioinduced osteosarcomas in, of personnel, radium, 25:13593
radiotherapy of tumors in long, effectiveness of 43.5 MeV x radiation for, evaluation of, 25:13537
scanning of human, use of strontium-85 for, review of, 25:13513
strontium-90 content of human, in United States during 1969, 25:13431
BORON
determination in borates, hydrides, organic compounds, or refractories, procedures for, 25:15465 (UCRL-50948)
determination in silicon by γ photon activation, 25:12971
neutron reactions (n,xγ) at 14 MeV with natural, cross sections for, (E/T), 25:14920(T) (BNL-tr-380)
preparation of pure lattices of, by pyrolysis of boron bromide--hydrogen mixture on tungsten wires at 900 to 1300°C, 25:13740
BORON BROMIDES
BBr_3--H, pyrolysis of carbon-containing, to prepare boron carbides at 900 to 1300°C, 25:13739
BBr_3--H, pyrolysis to prepare pure boron lattices on tungsten wires at 900 to 1300°C, 25:13740
BORON CARBIDES
analysis for impurities by neutron activation, 25:12972
preparation by pyrolysis of carbon-containing mixture of boron bromide--hydrogen at 900 to 1300°C, 25:13739
BORON FLUORIDES
complex with ethyl ether, analysis for boron-10/boron-11, emission spectroscopic method for, 25:12928
BORON ISOTOPES B-9
helium-3 inelastic scattering at 20.5 MeV, energy spectra and angular distributions in, (E), 25:14899
BORON ISOTOPES B-10
determination of abundance of, relative to boron-11 in boron trifluoride complex with ethyl ether, emission spectroscopic method for, 25:12928
energy levels from carbon-12 (π^-,2n) reactions, two-hole, (E), 25:14897
energy levels from helium-3 inelastic scattering, (E), 25:14899
exchange with boron-11 in boron trifluoride--substituted phenetole systems, 25:12992
helium-3 inelastic scattering at 20.5 MeV, energy spectra and angular distributions in, (E), 25:14899
neutron reactions (n,α) at 0.01 to 80 keV, cross sections for, (E)T), 25:14910
proton elastic scattering at 19.8 MeV and 60°, depolarization parameter from polarized, (E), 25:14889 (CEA-CONF-1650)
quadrupole relaxation speed relative to boron-11, 25:14479
scattering by holmium-165 at 50 MeV, γ spectra from inelastic, (E), 25:14991
BORON ISOTOPES B-11
determination of abundance of, relative to boron-10 in boron trifluoride complex with ethyl ether, emission spectroscopic method for, 25:12928
energy levels from helium-3 inelastic scattering, (E), 25:14899
exchange with boron-10 in boron trifluoride--substituted phenetole systems, 25:12992
helium-3 reactions (He-3,p) at 3 MeV, angular distributions for, (E), 25:14904
neutron reactions (n,α) at 15.5 to 19 MeV, cross section for, (E), 25:14895
proton inelastic scattering at 155 MeV, DWBA analysis of polarization angular distributions from, (T), 25:14892 (RLO-1388-600)
proton inelastic scattering at 30.3 MeV, DWBA analysis of asymmetry angular distributions from, (T), 25:14892 (RLO-1388-600)
quadrupole relaxation speed relative to boron-10, 25:14479
reactions (B-11,4nγ) with samarium-154 at 52 MeV, γ spectra from, (E), 25:14991
BORON NITRIDES
properties for use as electric insulation in SNAP-23A conversion system, 25:13166(R) (MMM-4187-1)
BORON OXIDES
B_2O_3--La_2O_3, lanthanum coordination structure in glasses of, 25:13019
B_2O_3--MgO-base--ThO_2, phase equilibria in magnesium oxide corner of, at 1200°C, 25:13770
B_2O_3--Na_2O--SiO_2--UO_2, luminescence of glasses of, 25:13017
BaO--B_2O_3, structure of glasses of, 25:13019
BaO--B_2O_3--La_2O_3, structure and properties of glasses of, 25:13019
BORON SYSTEMS
B--C--W, phase studies of, 25:13763 (AD-713154)
B--C-base, phase studies at 900 to 1200°C, 25:13767
BOSONS
bound states of three resonantly interacting spinless neutral, in carbon-12 and tritium, (T), 25:14591
ground-state energy of mixture of fermions and, in one-dimension with repulsive delta-function interaction, (T), 25:14501
interactions of spinless, nonrelativistic time-dependent theory for Coulomb potential in two-body, (T), 25:14624
interactions with Dirac fermions, infinite momentum limit of spinor field theory for, (T), 25:14679
model of superfluid, extension of Hartree-liquid, (T), 25:14142
order decay in Bose superfluids, effects of symmetry-breaking field on, (T), 25:14492
phase transition of hard-sphere Bose system, fluid--

XUM

  solid, (T), 25:14500
BOSONS, INTERMEDIATE-VECTOR
  decay of, asymptotic behavior of weak spectral functions for branching ratio for hadronic, (T), 25:14634 (NYO-4204-7)
  decay of, PCAC hypothesis for branching ratio for soft pion and bosons production in, (T), 25:14634 (NYO-4204-7)
  effects of mass of, on coupling constants in beta decay, 25:15180
  electric dipole moment of, effects of, (T), 25:14623
  interactions with hadrons, μ flux deep underground as evidence against hypothesis for strong, (T), 25:14735
  mass of, weak interaction model for electron energy spectrum in $\mu + e + \nu +$ anti ν decay for limitation on, (T), 25:14631 (ITF-70-64)
  production in neutrino reactions with nuclei at high energies, total cross sections for, 25:14641
  reactions with nuclei, μ flux in deep mines as evidence against hypothesis for strong interactions in, (T), 25:14735
  theory for divergences in amplitudes of nonleptonic weak interactions with one- and two-photon emission and virtual photon, 25:14655
BRAIN
  radiation effects on potassium and sodium content of, in rats, lethal and sublethal, 25:13566
  radiation effects on water content and distribution in, of rats, effects of lethal and sublethal dose on x, 25:13348
  scanning for differential diagnosis of benign and malignant neoplasms, use of metastable technetium-99 for, 25:13505
  scanning of human, for diagnosis of massive cerebral infarction, use of metastable technetium-99-labeled pertechnetate for, 25:13489
BRANNERITES
  phase transformations of, during heating at 600 to 1200°C, 25:13128
BRAZIL
  radiation monitoring of Guarapari region of, 25:13393(R) (NYO-2577-12)
  radioactivity in diet in high background areas in, 25:13439
BREMSSTRAHLUNG
  production in Coulomb field, exact Regge-multiperipheral amplitude for, 25:14613
  production in $\nu + e + \nu + e + \gamma$ interactions, γ energy and angular distribution and radiative corrections for total effective cross sections for, (T), 25:14600
  production in $p + p + p + p + \gamma$ at 20 MeV, cross sections and γ angular distributions and energy spectra for, (E), 25:14545
  production in $p + p + p + p + \gamma$ interactions at 42 MeV/c, wire-chamber spectrometer study of differential cross sections for, (E), 25:14556
  production in $p + p + p + p + \gamma$ interactions, N + N interactions below 350 MeV for, (T), 25:14734
  production of wide-angle, in electron reactions with nuclei at high energies, angular dependence of cross sections for, (E), 25:14529
  reactions (γ,n) with oxygen-16 at 30 MeV, neutron polarization from, (E), 25:14982 (NCSAC-31)
  reactions (γ,n) with tantalum up to 140 MeV, energy spectra from, (E), 25:14990
  reactions $(\gamma,n\gamma')$ and $(\gamma,p\gamma')$ with oxygen-16 at 27 MeV, angular distribution of γ rays from, (E), 25:14896
  reactions $(\gamma,n\gamma)$ and $(\gamma,p\gamma)$ with sulfur-32, γ spectra from, (E), 25:14946
  reactions (γ,p) with helium-4 at 120 MeV, angular distributions for, (E), 25:14886
  reactions with medium-heavy elements at 0.8 to 2.1 GeV, spallation products from, (E), 25:14977
  reactions with oxygen-16 at 19.5 to 26.5 MeV, γ spectra from photodisintegration, (E), 25:14982 (NCSAC-31)
BROMINE
  effects on yields from γ radiolysis of carbon tetrachloride at 25°C, 25:13045
BROMINE ISOTOPES Br-82
  reactions of recoil, with aromatic molecules, calculation of electron energies of transition states from, 25:13064 (INR-1211)
  use in tracer method for measuring density and flow velocity of postflotation slurry, 25:13176
BROMOPYROGALLOL RED
  complexes with aluminum and uranium, formation constants and spectra of, 25:12926
BROOKHAVEN ALTERNATING-GRADIENT SYNCHROTRON (AGS)
  beam energy spread in, method for decreasing, 25:14836 (BNL-15424)
  development and operation, July 1969--June 1970, 25:14837(R) (BNL-50230)
  storage rings for, proposal for 1000-GeV, 25:14835 (BNL-15423)
BROOKHAVEN BEAM RESEARCH REACTOR
  development and operation July 1969--June 1970, 25:14837(R) (BNL-50230)
BROOKHAVEN MEDICAL REACTOR
  development and operation July 1969--June 1970, 25:14837(R) (BNL-50230)
BUBBLES
  effects of radioinduced inert gas, on stress rupture of dilute aluminum--lithium alloy at 175 to 300°C, 25:13678
  radioinduced nucleation in superheated water, design of equipment for measuring alpha particle, 25:13152(R) (SU-326-P-13-5)
  radioinduced nucleation in superheated water, fission fragment, 25:13152(R) (SU-326-P-13-5)
BUILDING MATERIALS
  damage thresholds for concrete block, planter, plywood, and sheetrock, 25:15434(R) (JAB-99-35)
2,3-BUTANEDIOL, 2,3-DIMETHYL-
  yields from γ radiolysis of 2-propanol vapor at 124 to 400°C, 25:13046
BUTYRIC ACID, 4-AMINO-
  radiation effects on content of, in central nervous system of rabbits, ionizing, 25:13561

C

CABLES
  design features of ac superconducting, 25:14226
  electric insulation for instrumentation, effects of fast reactor environment on metal oxide, (E), 25:15354 (WHAN-IR-42)
CADMIUM
  determination of trace amounts of, in blood serum by emission spectroscopy, 25:12946
  determination using thin-layer chromatography and ring-oven colorimetry, 25:12944
  deuteron reactions (d,p) at 650 MeV, proton angular distributions from, (E), 25:14906
  effects on oxidation of trivalent uranium in sulfuric acid, 25:12977
  effects on performance of cesium plasma diodes, 25:14085
  neutron capture by, gamma spectra from thermal, (E), 25:14932
  neutron elastic scattering at 8 MeV, cross sections for, (E/T), 25:14965
  radiation effects on 3-methylpentane containing, at 77°K, comparative ESR studies on paramagnetic species produced from γ or uv, 25:13025
  superconducting transition temperature and mass enhancement, (T), 25:14152
  thermal conductivity at low temperatures, 25:14473
CADMIUM ALLOYS AND SYSTEMS
  Ag--Cd, phase transformations in, β--α massive, 25:12720
  Cd--In, superconducting flux trapping in region of martensitic transformation, 25:14172
  Cd-base--Zn, deformation of single crystals at 77°K, critical resolved shear stress and activation volume in, 25:13670
  Cd-base--Zn, thermal conductivity at low temperatures, 25:14473
CADMIUM ISOTOPES Cd-109
  energy levels from indium-109 decay, spin and parity of, (E), 25:15005
CADMIUM ISOTOPES Cd-111
  gamma spectra of, after-effects of indium-111 electron capture decay on, 25:15028
CADMIUM ISOTOPES Cd-112
  energy-level excitation by neutron capture gamma rays, (E), 25:15002
  neutron cross sections at 0.007 to 10 eV, energy dependence of, (E/T), 25:15096
CADMIUM ISOTOPES Cd-114
  neutron separation energy, (E), 25:14932
CADMIUM ISOTOPES Cd-115
  production from cadmium-116 (He-3,α) reactions at 13 to 33 MeV and (He-4,αn) reactions at 18 to 45 MeV, isomer ratios, (E), 25:15049
CADMIUM ISOTOPES Cd-116
  alpha reactions $(\alpha,\alpha n)$ and $(\alpha,3n)$ at 18 to 45 MeV, excitation functions and average range measurements from, (E), 25:15049
  helium-3 reactions (He-3,α) and (He-3,2n) at 13 to 33 MeV, excitation functions and average range measurements from, (E), 25:15049
CADMIUM PERCHLORATES
  radiation effects on frozen alcohol and aqueous acid solutions containing silver salts and, ESR studies on diatomic cations produced from γ, 25:13028
CAFFEINE
  effects on dark repair systems of x-irradiated colpoda, 25:13342
  effects on uv-radiosensitivity in Schizosaccharomyces pombe, 25:13606
  use for induction of SV40 virus from transformed hamster cell clones, 25:13615
CALCIUM
  abundance in chondrites, (E), 25:13787
  abundance in late G and K dwarfs, (E), 25:13824
  content and depth in crustal basalts and granites in USSR, 25:13115
  content of diet of human adolescents in EURATOM countries during 1965 to 1967, 25:13392 (EUR-3945(Pt.2))
  content of institutional diets of adults and children in USA during October to December 1969 as compared to annual average content for 1969, 25:13442
  electron elastic scattering by, effects of virtual nuclear excitation on cross section of, (T), 25:15166

  ion exchange behavior on zirconium phosphate crystals, 25:13084
  metabolism in cows, kinetics of, 25:15438(R) (NYO-3360-55)
  neutron elastic scattering at 8 MeV, cross sections for, (E/T), 25:14965
  neutron reactions (n,xγ) at 14 MeV with natural, cross sections for, (E/T), 25:14920(T) (BNL-tr-380)
  neutron total cross sections and resonance parameters at ·0.28 to 1.2 MeV, (T), 25:14969
  rehctions with oxygen dissolved in lithium, gettering, 25:13630 (EUR-4298)
  separation by solvent extraction using Rhodamine S and TTA, 25:13098
CALCIUM ALLOYS AND SYSTEMS
  Al--Ca, mechanical properties of composite, 25:13692
CALCIUM BORIDES
  electronic structure of CaB$_6$-type, 25:14463
CALCIUM CHLORIDES
  CaCl$_2$--CaMoO$_4$, solvent properties for molybdenum, kinetics of anodic, 25:13631
CALCIUM ISOTOPES Ca-38
  energy levels from (p,t) reactions, spin-parity assignments for, (E), 25:14950
CALCIUM ISOTOPES Ca-39
  energy level vibrations in, extended-particle-phonon-coupling theory of, 25:15176
CALCIUM ISOTOPES Ca-40
  deuteron reactions (d,p) at 5 to 21 MeV, weakly bound projectile model for, (E/T), 25:14938
  energy level vibrations in, extended-particle-phonon-coupling theory of, 25:15176
  neutron elastic scattering at 14 MeV, optical-model analysis of differential cross sections for, (T), 25:14920(T) (BNL-tr-380)
  neutron scattering at 0.55 to 2.0 MeV, differential cross sections for, (E), 25:14939
  proton inelastic scattering at 24.5 MeV, DWBA analysis of angular distributions and asymmetries from polarized, (E/T), 25:14923 (CEA-CONF-1656)
  proton reactions (p,t) with, angular distributions for, (E), 25:14950
CALCIUM ISOTOPES Ca-41
  energy level vibrations in, extended-particle-phonon-coupling theory of, 25:15176
  energy levels of, neutron scattering studies on spin and parity of, (E), 25:14939
CALCIUM ISOTOPES Ca-47
  nuclear spin and parity from calcium-48 (p,d) reactions, (E/T), 25:14922 (CEA-CONF-1655)
  retention in blood plasma of man, 25:13359
CALCIUM ISOTOPES Ca-48
  deuteron elastic scattering at 2.5 to 5.5 MeV, angular distributions from, (E), 25:14916
  deuteron reactions (d,p) at 2.5 to 5.5 MeV, angular distributions from, (E), 25:14916
  proton reactions (p,d) at 22.9 MeV, asymmetries from polarized, (E/T), 25:14922 (CEA-CONF-1655)
CALCIUM ISOTOPES Ca-49
  energy levels from deuteron reactions with calcium-48, (E), 25:14916
CALCIUM MOLYBDATES
  CaCl$_2$--CaMoO$_4$, solvent properties for molybdenum, kinetics of anodic, 25:13631
CALCIUM OXIDES
  content in rocks of shields and sediment cover of Brazil, Canada, and USSR, relations with geological time, 25:13114
CALCIUM TUNGSTATES
  electric quadrupole interactions in, Moessbauer effect study of, 25:14480
CALIFORNIA
  radiation monitoring of environs of Lawrence Radiation Laboratory at Berkeley, during 1969, 25:13398
  radioactivity monitoring in domestic water supplies in, during 1968, gross β, 25:13440
CALIFORNIUM
  magnetic susceptibility of trivalent, 25:13018
  production and uses of, review on, 25:13059
  reduction of trivalent, in perchlorate medium, polarographic studies on, 25:13020
CALIFORNIUM BROMIDES
  preparation and structure of crystalline, 25:13018
CALIFORNIUM CHLORIDES
  preparation of CfCl$_2$ by reduction of CfCl$_3$ by hydrogen, 25:13018
CALIFORNIUM FLUORIDES
  preparation and structure of crystalline, 25:13018
CALIFORNIUM ISOTOPES Cf-249
  alpha decay of, relative intensities of K x-ray transitions at $Z = 96$ following, 25:15029
  compounds, preparation of microgram quantities of, 25:13018
  neutron fission of, energy spectra and mean prompt neutron production in thermal, (E), 25:15118
CALIFORNIUM ISOTOPES Cf-250
  fission of, average number of prompt neutrons from spontaneous, (E), 25:15037
CALIFORNIUM ISOTOPES Cf-252
  fission of, energy spectra and mean prompt neutron production in spontaneous, (E), 25:15118
  fission of, neutron spectra from 0.01 to 1 MeV for spontaneous, (E), 25:15108
  neutron fission at 20 to 300 eV, cross sections for, (E), 25:15090
  performance as neutron source for radiography, 25:13161 (BNWL-SA-3169)
CALIFORNIUM ISOTOPES Cf-254
  fission of, average number of prompt neutrons from spontaneous, (E), 25:15037
CALIFORNIUM OXYBROMIDES
  preparation and structure of crystalline, 25:13018
CALIFORNIUM OXYCHLORIDES
  preparation and structure of crystalline, 25:13018
CALIFORNIUM OXYIODIDES
  preparation and structure of crystalline, 25:13018
CALORIMETERS
  design and operation of adiabatic, for measurement of heat effects on condensed-phase samples at 500 to 1000°C, 25:13653 (LA-4521)
  use for local enthalpy measurements in hf plasma, 25:14263
CANADA
  heavy water production at Glace Bay plant in, modification cost and time requirements for, 25:13175
  radiation monitoring of atmosphere of, during May, 1970, gross beta, 25:13122
  radioactivity monitoring in precipitaton and surface atmosphere in, during April, 1970, gross β, 25:13441
  radioisotope content of milk in, during 1969 and 1970, cesium-137, iodine-131, and strontium-90, 25:13433
  radioisotope content of milk in, during April 1970 as compared to average for previous 12-month period, cesium-137, iodine-131, and strontium-90, 25:13442
  uranium depoits in, role of Geological Survey of Canada in prospecting and development of, 25:13127
CARBIDES
  fabrication and properties of cemented, research on, 25:13752
  grain structure of cemented, qualitative and quantitative methods for determination of, 25:13752
  preparation of cemented, inspection and testing methods for starting materials for, 25:13752
  thermodynamic properties of, data compilation on high-temperature, 25:13750 (GAMD-9335)
CARBON
  abundance in four carbon stars, (E), 25:13795
  abundance in four O-Type subdwarf stars, (E), 25:13825
  abundance of molecular, in four carbon stars, (E), 25:13795
  determination in silicon by γ photon activation, 25:12971
  determination in sodium, calibration and design of meters for, 25:13651(R) (ANL/ST-4)
  deuteron reactions (d,p) at 650 MeV, proton angular distributions from, (E), 25:14906
  effects on backscattering during γ dosimetry, 25:13456
  electron elastic scattering at 25 to 800 eV by, tables of amplitudes and spin polarizations for, (T), 25:13995 (AD-711664)
  fission product distribution in fuel particle coating of pyrolytic, sputtering method for determination of, 25:13758
  fission product distribution in fuel particle coating of layered silicon carbide and pyrolytic, sputtering method for determination of, 25:13758
  hydrogen-ion (H_2^+) reactions at 2 MeV with films of, dissociation as function of film thickness in, (E), 25:13972
  mechanical properties of isotropic pyrolytic, deposited below 1600°C, relations of deposition conditions and structure with, 25:13757
  mercury-ion reactions at 5 to 30 keV, sputtering yield and secondary emission in, 25:13971
  meson (π^-) elastic scattering at 120 to 280 MeV, optical-model analysis of, (T), 25:14908
  neutron elastic scattering at 0.5 to 2 MeV, differential cross section angular distributions for, (E/T), 25:14911
  neutron reactions (n,xγ) at 14 MeV with natural, cross sections and gamma spectra from, (E/T), 25:14920(T) (BNL-tr-380)
  neutron total cross section at 0.07 to 1500 keV, (E/T), 25:14912
  neutron total cross section at 0.1 to 6 MeV, (E), 25:15103
  neutron total cross section at 0.5 to 15 MeV, (E), 25:14982 (NCSAC-31)
  photon reactions at high energies, spectrometer study of enhancement in high-invariant-mass π^---π^+ pair production in, (E), 25:14526
CARBON DIOXIDES
  content in rocks of shields and sediment cover of Brazil, Canada, and USSR, relations with geological time, 25:13114
  determination of trace amounts of, in argon, helium, hydrogen, krypton, and neon following freezing-out at liquid nitrogen temperature, mass spectrometric, 25:12941
  distribution in atmosphere, use in tracer studies of global transport processes, (E), 25:13121 (TID-25314)
  electron reactions with, nonresonant vibrational excitation in, (T), 25:14028

XUM

  fixation of carbon-14-labeled, in protein of tobacco leaves, effects of TMV infection on, 25:13360
  reactions with aluminum--chromium--iron alloys at 660 to 900°C, effects of zirconium on resistance to oxidation, 25:13680
CARBON IONS
  reactions with nitrogen gas at 39, 50, and 78 MeV, cross sections for electron capture and loss in, (E), 25:14001
CARBON ISOTOPES C-12
  abundance in UU Aur, (E), 25:13803
  concentration by Freon-11 distillation, 25:13165(R) (MLM-1753)
  deuteron reactions (d,α) at 21 to 29 MeV, analysis of reaction mechanism in, (E/T), 25:14901
  distribution in petroleum, correlation of theoretical method of formation and thermodynamics of, 25:13005
  effects on formation of petroleum, effects of temperature on thermodynamics of, 25:13005
  energy levels from helium-3 inelastic scattering, (E), 25:14899
  energy levels of, weakly bound states of three resonantly interacting particles in, (T), 25:14591
  helium-3 double elastic scattering at 30 MeV, polarization in, (E), 25:14894
  helium-3 elastic scattering at 2.3 to 3.3 MeV, angular distributions from, (E), 25:14915
  helium-3 inelastic scattering at 20.5 MeV, energy spectra and angular distributions in, (E), 25:14899
  helium-3 reactions (He-3,α) at 2.3 to 3.3 MeV, angular distributions from, (E/T), 25:14915
  meson (π^-) reactions (π^-,2nd) with, analysis using cluster model, (T), 25:14893
  meson (π^+) reactions with, optical-model calculations of, 25:15184
  meson reactions (π^-,2n) with, neutron energy spectra from, (E), 25:14897
  neutron capture at 14 MeV, cross sections for fast, (E/T), 25:14920(T) (BNL-tr-380)
  neutron inelastic scattering at 14 MeV, DWBA analysis of differential cross sections for, (E/T), 25:14920(T) (BNL-tr-380)
  proton elastic scattering at 1 GeV by deformed, differential cross sections for, 25:14918
  reactions (C-12,5n) with tellurium-128 at 78 MeV, energy levels of cerium-135 from, (E), 25:15042
CARBON ISOTOPES C-13
  abundance in UU Aur, (E), 25:13803
  concentration by carbon dioxide--carbamate exchange, 25:13165(R) (MLM-1753)
  concentration by Freon-11 distillation, 25:13165(R) (MLM-1753)
  concentration in barium carbonate, system flowsheet for, 25:13165(R) (MLM-1753)
  concentration in carbon monoxide using distillation columns, 25:13165(R) (MLM-1753)
  concentration in methane by carbon monoxide-to-methane conversion, 25:13165(R) (MLM-1753)
  concentration in methane by thermal diffusion, 25:13165(R) (MLM-1753)
  distribution in petroleum, correlation of theoretical method of formation and thermodynamics of, 25:13005
  effects on formation of petroleum, effects of temperature on thermodynamics of, 25:13005
  energy levels from boron-11 (He-3,p) reactions, spin-parity assignments for, (E), 25:14904
  energy levels of, parity of low-lying, (T), 25:14917
  incorporation in yeasts, 25:13331 (LA-4551)
  proton reactions (p,pn) with, p-n correlations in, (E), 25:14907
CARBON ISOTOPES C-14
  determination in tissue proteins, development of method for, 25:13345
  determination with tritium in double-labeled samples by liquid scintillation counting, 25:12953
  fixation of carbon dioxide-incorporated, into protein of tobacco leaves, effects of TMV infection on, 25:13360
  incorporation in glycerol and pyruvate for measuring incorporation into blood glucose in rats with cirrhosis, 25:13506
  incorporation in lipids and proteins of rat liver homogenates, effects of avidin on, 25:13344
  metabolism of palmitate-incorporated, in lungs of rats, effects of breathing nitrogen dioxide on, 25:13356
  reactions of recoil atoms and ions of, with benzene at -196°C and 5 eV to 15 keV, mechanisms of, 25:13038
  reactions of recoil, in neutron-irradiated nitrides, 25:13070
  reactions of recoil, in neutron-irradiated sodium and potassium cyanides, 25:13072
CARBON MONOXIDES
  abundance in four carbon stars, (E), 25:13795
  carbon-13 concentration in, distillation method for, 25:13165(R) (MLM-1753)
  distribution in atmosphere, use in tracer studies of global transport processes, (E), 25:13121 (TID-25314)
  thermal transpiration at 77 and 97°K, model for, 25:13165(R) (MLM-1753)
CARBON SYSTEMS
  thermodynamic properties of, data compilation on high-temperature, 25:13750 (GAMD-9335)
  B--C--W, phase studies of, 25:13763 (AD-713154)
  B--C-base, phase studies at 900 to 1200°C, 25:13767
  C--Mo--Ru, phase studies of, 25:13764 (KFK-1260)
  C--Mo--Ti, phase studies of, 25:13762 (AD-713153)
  C--Nb--Ti, phase studies of, 25:13762 (AD-713153)
  C--Ta--Ti, phase studies of, 25:13762 (AD-713153)
  C--ZrC, elastic properties of composites of, 25:13751
CARBON TETRACHLORIDE
  radiolysis at 25°C, effects of scavengers on yields from γ, 25:13045
CARDIAC PACEMAKERS
  design and performance of implantable plutonium-238-fueled, 25:13169(R) (NUMEC-3731-24)
  heat source for, design and safety testing of plutonium-238, 25:13178
  radiological safety of implantable plutonium-238-fueled, (E), 25:13169(R) (NUMEC-3731-24)
  testing of implantable plutonium-238-fueled, methods and results for drop, shock, and vibration, 25:13169(R) (NUMEC-3731-24)
CARMINIC ACID
  complexes with rare earths, spectrophotometric studies on, 25:12937
CASCADE SHOWERS
  particle azimuthal symmetry in 17.2-GeV/c π^--interaction-produced, (E/T), 25:14565
  production from π^- interactions at 17.2 GeV/c, azimuthal symmetry of particles in, 25:14565
  production of 60-GeV, from π reactions with nuclei in emulsions, K/π ratio of secondaries in, (E), 25:14509 (INP-718)
  propagation in matter, characteristics of electron--photon, 25:13300
CATALYSTS
  electron paramagnetic resonance spectra of reduced metal oxides, 25:14482
CATS
  radiation effects on cholinesterase activity in spinal cord of, partial and whole-body x, 25:13375
  radiation effects on cholinesterase activity in spinal cord, whole-body x, 25:13333
CATTLE
  iodine-131 content of thyroid gland in beef, use of, for monitoring fallout, 25:13397
  potassium-40 content of, accuracy of, as heat tolerance predictor, 25:13339
  radioisotope distribution in fetuses, milk, and tissues of dairy, following ingestion of Schooner Event fallout, 25:13396 (UCRL-72511)
  radioisotope metabolism in, following intravenous and oral administration, comparison of cerium-144 and scandium-46, 25:13352
CAVITY RESONATORS
  fabrication and testing of superconducting microstrip high-Q microwave, 25:14230
  surface residual resistance of high-Q superconducting, 25:14222
  surface resistance of superconducting lead, frequency dependence of residual, 25:14847 (NP-18654)
  use of superconducting, for material-properties analyzers, 25:14229
  use of superconducting, for nuclear radiation detection, 25:14228
CELLS
  migration in hair follicles of lambs, autoradiography of, using tritium-labeled thymidine, 25:13337
  mucopolysaccharide isolation from embryonic, of mice and rats, heparin-related, sulfur-35-labeled, 25:13357
  radiation effects on embryonic, of hamsters and mice, effects of, on SV40 tumorigenicity, x, 25:13553
  radiation effects on immune reactions following injection of lymphoid, into mice, effects of dose and splenomegaly on x, 25:13390
  radiation effects on survival of tumor, effects of dose distribution adjustment errors on fractionated, 25:13451
  radiation effects on ultrastructure of liver, in rats, histochemical studies on cobalt-60, 25:13378
  radiation effects on, electromagnetic, 25:13571
  radiation effects on, of hematopoietic stem in mice in relation to light and darkness, effects of transplantation of bone marrow cells on, 25:13550
  role of mast, in spleen regeneration in whole-body γ-irradiated mice, 25:13577
  uranyl binding in root tip, of oat plants, 25:13353
CELLS, CULTURED
  radiation effects on exogenous nucleoside utilization in DNA synthesis by human, x, 25:13380
  radiation effects on Kilham rat virus infectivity in rat embryo, effects of dose and 5-flurouracil on uv and x, 25:13608
  radiation effects on transformation of SV_{40}-infected, from mice, uv, 25:13552
  radiation effects on tumor, effects of, on immune reactions of mice to tumor cell grafts, γ, 25:13389
  radioinduced inhibition of DNA synthesis in human, photoreactivation of uv, 25:13377
  radioinduced SV40 virus induction from hamster kidney, uv and x, 25:13615
  SV40 virus induction from hamster kidney, using chemicals, 25:13615

CELLS, HeLa
  mucopolysaccharide isolation from, heparin-related, sulfur-35-labeled, 25:13357
  radiation dosimetry using, problems with apparatus during γ, 25:13456
  radiation effects on unscheduled DNA synthesis in, tritium tracer study of effects of temperature on uv, 25:13554
CELLS, KB
  radioinduced injuries to, in continuous culture, following exposure to phosphorus-32 ions, β, 25:13351
CELLS, L
  mucopolysaccharide isolation from, heparin-related, sulfur-35-labeled, 25:13357
CEMENTS
  determination in concrete, radiometric gage for, 25:13315
CENTRAL AMERICA
  radioactivity monitoring in surface atmosphere of, during April, 1970, gross β, 25:13441
  radioisotope content of milk in, during 1969 and 1970, cesium-137, iodine-131, and strontium-90, 25:13433
  radioisotope content of milk in, during April 1970 as compared to average for previous 12-month period, cesium-137, iodine-131, and strontium-90, 25:13442
CEREALS
  radiation processing of, effects of, on insects and microorganisms, review of, 25:13623
CERIUM
  complexes with carminic acid, spectrophotometric studies on, 25:12937
  complexes with disodium 4,5-dihydroxy-3-phenylazo-2,7-naphthalene disulfonate, composition, stability, and colorimetric properties of, 25:12942
  determination in plutonium oxide--uranium oxide fuels by solvent extraction and emission spectrography, 25:12922 (WHAN-SA-44)
  determination of trace amounts of, in plutonium and plutonium dioxide--uranium dioxide by solvent extraction and emission spectrography, 25:12923 (WHAN-SA-47)
  determination of trivalent, using Chromotrope 2R, spectrophotometric, 25:12942
  reactions with oxygen atoms, cross sections for ionization in, (E), 25:14036
  separation from aqueous chloride solutions by solvent extraction using dioctyl phosphate in benzene or heptane, effects of variables on, 25:13096
CERIUM ALLOYS AND SYSTEMS
  Al--Ce, mechanical properties of, 25:13692
CERIUM ISOTOPES Ce-134
  neutron capture by, γ spectra for resonance, (E), 25:14982 (NCSAC-31)
CERIUM ISOTOPES Ce-135
  energy levels from tellurium-128 (C-12,5n) reactions at 78 MeV, (E), 25:15042
CERIUM ISOTOPES Ce-137
  production from barium-136 (α,3n) reactions at 27 to 44 MeV and barium-137 (He-3,3n) reactions at 14 to 33 MeV, isomer ratios for, (E), 25:15049
CERIUM ISOTOPES Ce-138
  energy levels from cerium-140 (p,t) reactions, spin and parity of, (E), 25:15006
CERIUM ISOTOPES Ce-140
  alpha elastic scattering by, optical-model analysis of, (E/T), 25:14947
  energy levels from cerium-142 (p,t) reactions, spin and parity of, (E), 25:15006
  energy-level transitions in, angular correlations from, (E/T), 25:14983 (NP-18492)
  proton reactions (p,t) at 52.1 MeV, triton spectra and angular distributions from, (E), 25:15006
CERIUM ISOTOPES Ce-142
  proton reactions (p,t) at 52.1 MeV, triton spectra and angular distributions from, (E), 25:15006
CERIUM ISOTOPES Ce-144
  accumulation from sea water by alginic acid of brown algae, 25:13403
  determination in liquid waste effluents from nuclear fuel reprocessing plant by γ spectrometry, 25:12950 (BRH/NERHL-70-2)
  metabolism in calves and cattle following intravenous and oral administration, comparison of, to scandium-46 as nonabsorbed reference material, 25:13352
CERN SYNCHROTRON
  experimental facility for, development of data handling system for Omega project, 25:14839 (CERN-70-21(Vol.2), pp 561-80)
  operation of, statistics for 1967, 25:14844 (MPS/Int. CC-68-1)
CESIUM
  determination of trace amounts of, in blood serum by emission spectroscopy, 25:12946
  diffusion of low-solubility, in monocrystalline and polycrystalline molybdenum, mechanism of, 25:13676
  effects on γ radiolysis of ammonia adsorbed on synthetic zeolites, EPR spectral studies on, 25:13057
  electron elastic scattering at 25 to 800 eV by, tables of amplitudes and spin polarizations for, (T), 25:13995 (AD-711664)
  plasma of, cyclotron echoes in weakly ionized, (E/T), 25:14387
  plasma of, resonance phenomena in variable electric fields, 25:14368
  plasma of, resonant radiations from, (E/T), 25:14264(R) (AD-711828)
  separation from sodium in anhydrous and aqueous solutions of ethanol, methanol, and 1,2-propanediol by ion exchange using Zeolite Linde A, 25:13091
CESIUM IONS
  range in aluminum at 20 keV, effects of crystallinity and integrated flux on, (E/T), 25:13960
  reactions with metallic oxides at 10 to 40 keV, secondary electron yields from, (E), 25:13963
CESIUM ISOTOPES
  uses in fallout field simulation methods, 25:13117 (AD-711532)
CESIUM ISOTOPES Cs-122
  energy levels of, spin-parity assignments and transition multipolarities for, (E), 25:15061
  isomeric transition in, half-life and γ spectra for, (E), 25:15061
CESIUM ISOTOPES Cs-127
  energy levels of, spin-parity assignments and transition multipolarities for, (E), 25:15061
  isomeric transition in, half-life and γ spectra for, (E), 25:15061
CESIUM ISOTOPES Cs-131
  energy levels from barium-131 decay, spin-parity assignments for, (E), 25:15062
  production of carrier-free, by separation from barium-131 by countercurrent electrolysis, 25:13062
CESIUM ISOTOPES Cs-132
  electron-capture and positron decay of, energy levels of xenon-132 and barium-132 from, (E), 25:15007
CESIUM ISOTOPES Cs-133
  electron mass shift in intense electromagnetic field in, (E), 25:14514
  neutron total cross section and resonance parameters at 1.7 to 1100 eV, (E), 25:15098
  reactivity worths in fast reactor spectra, (E/T), 25:15350
CESIUM ISOTOPES Cs-134
  determination in liquid waste effluents from nuclear fuel reprocessing plant by γ spectrometry, 25:12950 (BRH/NERHL-70-2)
CESIUM ISOTOPES Cs-135
  neutron total cross section and resonance parameters at 1.7 to 1100 eV, (E), 25:15098
CESIUM ISOTOPES Cs-137
  accumulation by crops and soils in France from fallout and industrial wastes, 25:13402
  accumulation from sea water by alginic acid of brown algae, 25:13403
  accumulation in food, effects of uptake from soil on, 25:13340 (NP-18382)
  content of diet in USA during 1965 to 1970, 25:13401
  content of diet of human adolescents in EURATOM countries during 1965 to 1967, 25:13392 (EUR-3945(Pt.2))
  content of fish protein concentrates, 25:13394(R) (RLO-2099-1)
  content of institutional diets of adults and children in USA during October to December 1969 as compared to annual average content for 1969, 25:13442
  content of Japanese beer in relation to atmospheric deposition rates in Tokyo area during 1959 to 1969, comparison of fallout strontium-90 and, 25:13434
  content of milk in Canada, Central America, South America, and United States during 1969 and 1970, 25:13433
  content of milk in Western Hemisphere during April 1970 as compared to average for previous 12-month period, 25:13442
  content of milk sampled throughout Central, North, and South America during July 1970, 25:13401
  determination in liquid waste effluents from nuclear fuel reprocessing plant by γ spectrometry, 25:12950 (BRH/NERHL-70-2)
  neutron total cross section and resonance parameters at 1.7 to 1100 eV, (E), 25:15098
  uptake from soil by food chain, 25:13340 (NP-18382)
CESIUM NEPTUNIUM CHLORIDES
  spectra of single crystals of, absorption, 25:14466
CHARGED PARTICLES
  acceleration in auroral zone, mechanism for, (E/T), 25:14116
  distribution in Cytherean and Martian atmospheres and ionospheres, altitude- and angular coordinate-dependent, (E/T), 25:13956
  emission of relativistic, from radio galaxies, (T), 25:13922
  interactions with weakly nonlinear plasma, longitudinal fields from, (T), 25:14313
  motion in constant electric and magnetic fields, Schott energy effects in relativistic, (T), 25:14507
  motion in magnetoplasmas, radiations from test, (T), 25:14325
  motion in superposed Heliotron and biconical cusp fields, guiding center of, (T), 25:14330
  motion of, singularities in general relativity theory for Lorentz-Dirac equation of, (T), 25:14813
  reactions with helium, hydrogen, and lithium atoms and ions, ionization cross sections for, (T), 25:14022

scattering by atoms, ions, and molecules, asymptotic expression for total cross section for inelastic, 25:14022
scattering by Coulomb field, exact Regge-multiperipheral amplitude for bremsstrahlung production in, 25:14613
scattering by two-species quantum fluids, Born approximation to cross sections for, 25:13965
trajectories in whistler-mode wave packet, effect on loss-cone distortion, (T), 25:14122

CHEMICAL REACTIONS
dynamics of exchange, 25:12986

CHEMISTRY
research at BNL, July 1969--June 1970, 25:14837(R) (BNL-50230)

CHLORAMPHENICOL
effects on survival of uv and x-irradiated Escherichia coli, comparison of, 25:13613

CHLORINE
electron reactions at 3 to 16 keV with, cross sections for excitation of K x rays in, (E), 25:14008
neutron capture by, gamma spectra from thermal, (E), 25:14932
neutron reactions (n,xγ) at 14 MeV with natural, cross sections for, (E/T), 25:14920(T) (BNL-tr-380)

CHLORINE ISOTOPES Cl-34
energy levels at 0.46 and 0.67 MeV from sulfur-32 (He-3,p) reactions, spins of, (E), 25:14942

CHLORINE ISOTOPES Cl-36
neutron separation energy, (E), 25:14932

CHLORINE ISOTOPES Cl-37
neutron capture at 0.025 eV, cross section for, (E), 25:14935

CHLOROFORM
effects on yields from γ radiolysis of carbon tetrachloride at 25°C, 25:13045

CHLOROPHYLL
book: Spectroscopy of Chlorophyll and Related Compounds, 25:15417(T) (AEC-tr-7199)
content of x-radioinduced mutant, 25:13415
mutations induced in, of Sorghum by chemical mutagens, 25:13420
radiation effects on synthesis of ascaridine from, 25:13374
radioinduced mutations of, in Sorghum, γ and x, 25:13420

CHOLANTHRENE, 3-METHYL-
radiosensitivity of sarcomas induced with, in mice, β, 25:13473

CHOLIC ACID
radioinduced inhibition of synthesis of, in rat livers, 25:13370

CHOLINESTERASE
radiation effects on activity of, in blood and nervous system of rabbits, ionizing, 25:13561
radiation effects on activity of, in spinal cord of cats, partial and whole-body x, 25:13375
radiation effects on activity of, in spinal cord of cats, whole-body x, 25:13333

CHROMATOGRAPHY
detector for column liquid, microradiometric, 25:12952
methods for automated, high-resolution analyses, 25:13383

CHROMIUM
determination in airborne and deposited particulates by neutron activation and γ spectrometry, 25:12975
determination in aluminum-, cobalt-, iron-, or nickel-base alloys using gas-sheathed tubular electrode arc, spectroscopic, 25:12945
determination in neutron-irradiated graphite by γ spectrometry, 25:12954
determination of trace amounts of, in blood serum by emission spectroscopy, 25:12946
determination of trace amounts of, in boron carbide by neutron activation, 25:12972
effects on gravimetric determination of tellurium, 25:12943
energy-level excitation by neutron capture gamma rays, (E), 25:15002
neutron capture at 0.01 to 20 MeV, cross sections for, (T), 25:14970
neutron elastic scattering at 1.8 to 8.1 MeV, cross sections for, (E/T), 25:14964
neutron elastic scattering at 8 MeV, cross sections for, (E/T), 25:14965
neutron inelastic scattering at 14.5 MeV, cross sections for, (E), 25:14967
radioinduced aging in electrolytic, effects of deformation on fast neutron, 25:13730

CHROMIUM ALLOYS AND SYSTEMS
Al--Cr--Fe, mechanical properties of, effects of zirconium on, 25:13680
Al--Cr--Fe, oxidation resistance to carbon dioxide at 600 to 900°C, effects of zirconium on, 25:13680
Co-base--Cr--Fe--Mn, deuteron stopping power at 2.5 to 7.0 MeV for Havar foils, (E), 25:14401
Cr--Fe--Mo--Ti, microstructure of anti-phase boundaries in chi-phase of $Fe_{36}Cr_{12}Mo_5Ti_5$, 25:13711
Cr--Mn, pressure effects on magnetic susceptibility of, (E/T), 25:14447
Cr--Mo, corrosion by flowing liquid sodium, 25:15357 (SAN-781-228)
Cr--Ni-base, sealing leaks in tubes of, by explosive plug welding, 25:13647
Cr--Si--Zr-base, corrosion by steam at 350 to 450°C and 50 atm pressure, 25:13629 (EIR-184)
Cr--SiO, electric conductivity of thin films of, on alumina, fused quartz, and pyrex substrates, effects of thermal treatments on, 25:14435 (IJS-587)
Cr--V, pressure effects on magnetic susceptibility of, (E/T), 25:14447
Cr--Zr-base, corrosion by steam at 350 to 450°C and 50 atm pressure, 25:13629 (EIR-184)

CHROMIUM CARBIDES
properties for use in coating graphite for bonding to graphite or Hastelloy N using transition bonding layers, 25:13646

CHROMIUM ISOTOPES Cr-48
energy levels from titanium-46 (He-3,n) reactions, T = 2, (E), 25:14943

CHROMIUM ISOTOPES Cr-50
neutron capture at 0.1 to 20 keV, cross section for, (E), 25:14982 (NCSAC-31)

CHROMIUM ISOTOPES Cr-51
use with iodine-125 in double tracer dilution method for measuring blood plasma volume in relation to erythrocyte mass in patients, 25:13338

CHROMIUM ISOTOPES Cr-52
energy levels from proton inelastic scattering, (E), 25:14928
helium-3 reactions (He-3,3n) at 45.5 MeV, yields of iron-52 from, 25:13063
neutron total cross section up to 200 keV, (E), 25:14982 (NCSAC-31)
proton inelastic scattering at 40 MeV, microscopic description of, (E/T), 25:14928

CHROMIUM ISOTOPES Cr-53
photoneutron cross section for, (E), 25:14982 (NCSAC-31)

CHROMIUM ISOTOPES Cr-54
neutron capture at 0.1 to 20 keV, cross section for, (E), 25:14982 (NCSAC-31)

CHROMOSOMES
aberrations induced in Vicia faba, by γ-irradiated strawberry juice or puree, 25:13621
radioinduced aberrations in, of human lymphocytes, analysis of tertiary structure of x, 25:13410
radioinduced aberrations of, in Vicia faba, effects of dose fractionation on x, 25:13413
radioinduced dicentric and ring aberrations in swine lymphocytes, effects of dose on cobalt-60 γ, 25:13417
radioinduced isochromosome aberrations of, in Drosophila melanogaster, x, 25:13409
radioinduced translocation aberrations of, in spermatocytes of mice, effects of dose and dose rate on frequency of γ, 25:13404

CHROMOSPHERE
hydromagnetic-wave heating of network of, (T), 25:13508
mass motion in, (E), 25:13877
photography of, computer control for $^1/_8$-A tunable filter for high-resolution, (E), 25:13876
spectra of, high-resolution profile of O I 1304.9-A line in, (E), 25:13877
spicule formation in, (T), 25:13822
stability of stellar, convective, (T), 25:13822
transition region with photosphere, line profiles and flash intensities in, (T), 25:13878

CIRCADIAN CLOCK
radiation effects on, electromagnetic, 25:13572

CITRIC ACID
radioinduced decrease in content of, in seminal vesicles of rats, x, 25:13366

CLAYS
effects on vertical transfer of strontium-90 in soils, 25:13118(R) (COO-414-17)

COATINGS
book: Corrosion Week. 41st Manifestation of the European Federation of Corrosion, 7-12 October, 1968 in Budapest, 25:13636
radioinduced curing of, bibliography on, 25:13031 (AAEC/LIB/Bib-261)

COAXIAL CABLES
losses in large superconducting niobium tubes in, high-current ac, 25:14225

COBALT
complexes with 2,4-pentanedione, cobalt-57 electron-capture decay in, stabilization of anomalous charge states of iron after, 25:13075
determination by isotopic dilution and electrophoretic focusing, 25:12949
determination in airborne and deposited particulates by neutron activation and γ spectrometry, 25:12975
determination in iron- or nickel-base alloys using gas-sheathed tubular electrode arc, 25:12945
determination in meteoritic materials by neutron activation and γ--γ coincidence spectrometry, 25:12967
determination in neutron-irradiated graphite by γ spectrometry, 25:12954
determination of trace amounts of, in boron carbide by neutron activation, 25:12972
determination using thin-layer chromatography and ring-oven colorimetry, 25:12944
radiation effects on atomic displacements in monocrystalline, electron, 25:13733
recovery of electron-irradiated monocrystalline, effects of isochronal anneals on, 25:13713

COBALT ALLOYS AND SYSTEMS
analysis for constituents using gas-sheathed tubular electrode arc, spectroscopic, 25:12945
Co--Cu--misch metal, magnetic properties of, effects of heat treatments at 200 to 1220°C on, 25:14464
Co--Fe-base--Ni, thermal conductivity at 80 to 293°K, effects of cobalt content on, 25:13685
Co--Ir, superconductivity and spin fluctuations in, (E), 25:14202
Co--Sm--Y, lattice parameters and magnetic properties of Y/sub 1-x/Sm/sub x/Co_5, 25:14461
Co--Zr, phase diagram for, 25:13712
Co-base--Cr--Fe--Mn, deuteron stopping power at 2.5 to 7.0 MeV for Havar foils, (E), 25:14401
COBALT FERRATES
phase transformations in, electron microscopy study of, 25:13783 (UCRL-20369)
radioinduced defects in, dissociated ion, 25:13783 (UCRL-20369)
COBALT ISOTOPES
uses in fallout field simulation methods, 25:13117 (AD-711532)
COBALT ISOTOPES Co-56
electron-capture decay of, gamma spectra from, (E), 25:14957
COBALT ISOTOPES Co-57
effects on counter evaluations of transuranium element in lungs following internal deposition, 25:13458
electron-capture decay in cobalt complexes with 2,4-pentanedione, stabilization of anomalous charge states of iron after, 25:13075
electron-capture decay in doped Prussian Blue, reactions of iron-57 from, 25:13068
COBALT ISOTOPES Co-58
content of feces, milk, and urine of dairy cattle following ingestion of Schooner fallout, 25:13396 (UCRL-72511)
use as tracer for vitamin B-12 metabolism studies in man following stomach surgery, 25:13334
COBALT ISOTOPES Co-59
bremsstrahlung reactions at 0.8 to 2.1 GeV, spallation products from, (E), 25:14977
neutron elastic scattering at 8 MeV, cross sections for, (E/T), 25:14965
neutron inelastic scattering by, cross sections for fast, (E), 25:14960
COBALT ISOTOPES Co-60
content of fish protein concentrates, 25:13394(R) (RLO-2099-1)
determination in liquid waste effluents from nuclear fuel reprocessing plant by γ spectrometry, 25:12950 (BRH/NERHL-70-2)
effects on chromosomes of swine lymphocytes, effects of dose on aberrant, 25:13417
COLLISION PROCESSES
theory of, gyroscopic interpretation of two-state hypergeometric models of nonadiabatic coupling in, 25:14033
COMETS
solar-wind interactions with atmosphere of, (T), 25:13905
COMMUNICATION SYSTEMS
radiation effects on Emergency Broadcast System, nuclear electromagnetic pulse, 25:13328 (ORNL-TM-2830)
COMPLEXES
chemistry of coordination, Vanderbilt Univ. research on, 25:15461(R) (TID-25641)
COMPOSITE MATERIALS
properties of unidirectionally solidified, composed of eutectic alloys, 25:13692
COMPRESSORS
design for use in radioisotope-fueled Brayton cycle power system, 25:13168 (N-70-41276)
COMPTON EFFECT
electron emission in gamma irradiation, (T), 25:14430
theory of inverse, in cold collisionless plasma, (T), 25:13941
COMPUTER PROGRAMS
3DB, for fast reactor kinetics, 25:15343 (WHAN-IR-48)
ANISN, for solving Boltzmann equation in one dimension in plane, cylindrical, or spherical geometry, in FORTRAN IV, 25:14863 (CEA-N-1358)
ARNULF, for acquisition of bubble or spark chamber film information for PEPR system, 25:13242 (CERN-70-21(Vol.1), pp 113-24)
BERTA, for automatic recognition and reconstruction of bubble chamber events, 25:13244 (CERN-70-21(Vol.1), pp 141-75)
BERTA, for automatic recognition and reconstruction of bubble chamber events, 25:13243 (CERN-70-21(Vol.1), pp 125-39)
CARL, for calibration of PEPR system using Chebyshev polynomials, in FORTRAN, 25:13245 (CERN-70-21(Vol.1), pp 177-86)
CRECOL, for calculation of creep buckling characteristics of externally pressurized long thin tubes with initial ovalities, FORTRAN IV, 25:13652 (GAMD-8219(Rev.))
development for processing logging data on geophysical properties of earth materials, 25:13104 (UCRL-50855)
DYSYS, for simulation of general dynamic problems, 25:13158
ECFUEL, for calculation of fuel element heat transfer, 25:13155
ELIPGRID, for probability of locating elliptical targets with square, rectangular, or hexagonal grids, 25:15423 (GJO-918-4)
ELKE, for grid guidance for PEPR system for bubble chamber film analysis, 25:13247 (CERN-70-21(Vol.1), pp 199-211)
for inversion of de Haas--van Alphen data on closed Fermi surfaces with inversion symmetry, 25:14433 (ANL-7659)
HERETRA, for calculating concentrations of fission products, in FORTRAN, 25:15141 (DEMO-70/10)
LBCG, for geometrical reconstruction of particle tracks in large bubble chamber, in FORTRAN, 25:13260 (CERN-70-21(Vol.1), pp 467-96)
LGR/B, for updating ANISN library tapes with plotting of cross sections, in FORTRAN IV for IBM 360, 25:14986(T) (ORNL-tr-2408)
MAPLIB, for materials property library retrieval and storage, 25:13627
POKER, for calculating propagation of polyenergetic neutrons in plane or spherical geometry, 25:14864 (CEA-N-1388)
Radiation Shielding Information Center program setup instructions manual, 25:14395 (CTC-INF-1017)
RSYN, for fast reactor kinetics, 25:15343 (WHAN-IR-48)
SEISM, for predicting response of earth dams to seismic disturbances, FORTRAN, 25:13130 (UCRL-13329(Pt.2))
SEQ 1, for sequence determination from fragment data, 25:15422 (COO-1018-1219)
TIMOC, subroutines for various core geometries, FAD for IBM 7090, 25:15404 (EUR-4536)
TWOTRAN SPHERE, for solving Boltzmann transport equation in two-dimensional spherical geometry by finite-difference techniques, in FORTRAN, 25:14866 (LA-4567)
COMPUTERS
arithmetic unit of ILLIAC III, simulation and logic design for, 25:15430 (COO-2118-2)
development at Risoe, Oct. 1, 1969--March 31, 1970, 25:13321 (RISO-M-1270)
interface of production control, with remote data stations, 25:15469 (Y-1748)
research at BNL, July 1969--June 1970, 25:14837(R) (BNL-50230)
CONCRETES
analysis for cement, radiometric gage for, 25:13315
density measurements of, gamma radiometric gage for, 25:13308
gamma transport in, calculations using anisotropic source--flux iteration technique, 25:14407
neutron albedo of ordinary, (E), 25:14394 (CEA-N-1382)
neutron reflection by, one-dimensional S/sub n/ calculations of spectra of, (T), 25:14865 (COO-2049-2)
neutron streaming through two-legged ducts of, with baffles, (E), 25:14391 (AD-710963)
radioinduced polymerization of plastics in, bibliography on, 25:13030 (AAEC/LIB/Bib-260)
testing of, design and performance of betatrons for radiographic, 25:14861
CONNECTICUT YANKEE POWER REACTOR
core 3 for, design parameters and loading configuration for, 25:15267 (DOCKET-50213-97)
fuel storage pool for, additional information on spent, 25:15266 (DOCKET-50213-96)
operations history for December 1970, 25:15229 (DOCKET-50213-94)
pressure vessel steel for, radiation effects on, 25:15265 (DOCKET-50213-95)
radioactive waste from, modifications for handling liquid, 25:15266 (DOCKET-50213-96)
site for, additional information on land use and seismograph station for, 25:15266 (DOCKET-50213-96)
CONTROL SYSTEMS
design of heat-limiting, for radioisotope-fueled thermionic converters, 25:13173(P)
development at ORNL, Sept. 1969--Aug. 1970, 25:13318(R) (ORNL-4620)
COPPER
analysis of silver-coated wires of, on lunar module for fluorine by proton microprobe method, 25:12961
argon-ion scattering at 30 keV by single crystal of, effects of atomic-row packing density and separation on anisotropy of, 25:13970
content of human nails, determination by neutron activation analysis for diagnosis of cystic fibrosis, 25:13491
determination in aluminum-, cobalt-, iron-, or nickel-base alloys using gas-sheathed tubular electrode arc, spectroscopic, 25:12945
determination in neutron-irradiated graphite by γ spectrometry, 25:12954
determination of trace amounts of, in blood serum by emission spectroscopy, 25:12946
determination using thin-layer chromatography and ring-oven colorimetry, 25:12944
deuteron reactions (d,p) at 650 MeV, proton angular distributions from, (E), 25:14906
effects on backscattering during γ dosimetry to HeLa cells, 25:13456
effects on extraction--photometric determination of iron using tiron and diphenylguanidine, 25:12934
effects on gravimetric determination of tellurium,

  - 25:12943
  - electron backscattering at 1.0 MeV by thick targets of, Monte Carlo calculation of angular distributions and energy spectra from, 25:13959 (UCRL-19719)
  - electron charge-deposition distribution at 4 to 24 MeV in, 25:13964
  - electron reactions at 30 keV with, Monte Carlo calculation of energy losses and depth distribution of x-ray production in, 25:14400
  - electron slowdown at 10 to 15 MeV in, Monte Carlo calculation of, 25:14397
  - neutron elastic scattering at 8 MeV, cross sections for, (E/T), 25:14965
  - neutron scattering at 1 to 8 MeV, width fluctuation and resonance interference effects in cross sections for, (E/T), 25:14962
  - positron backscattering at 1.0 MeV by thick targets of, Monte Carlo calculation of angular distributions and energy spectra from, 25:13959 (UCRL-19719)
  - properties for brazing graphite to graphite or metals using transition bonding layers, 25:13648
  - proton channeling in single-crystal films of, effects of weak deformation on 170-keV, 25:14421
  - proton reactions below 70 GeV/c, atlas of particle-production-momentum spectra for, (T), 25:14733 (NP-18660)
  - radiation damage in, study of defects produced in copper-ion, 25:14422
  - radioinduced defects in single crystals of, anomalous x-ray transmission study of electron, 25:14427
  - radioinduced formation of vacancy tetrahedra in, high-voltage microscope electron, 25:13731
  - solvent properties of annealed and cold-worked, for tritium at 100 to 300°C, 25:13654 (MLM-1734)
- COPPER ALLOYS AND SYSTEMS
  - analysis for constituents using gas-sheathed tubular electrode arc, spectroscopic, 25:12945
  - Al--Cu, creep stress in, effects of velocity on, 25:13683
  - Au--Cu, sputtering by 70-keV argon ions of single crystals of, angular distributions of sputtered material in, 25:13966
  - Be--Cu-base, precipitation processes in, electron microscopy study of effects of aging on, 25:13715
  - Co--Cu--misch metal, magnetic properties of, effects of heat treatments at 200 to 1220°C on, 25:14464
  - Cu--Fe--Zr-base, corrosion by steam at 350 to 450°C and 50 atm pressure, 25:13629 (EIR-184)
  - Cu--Sn, photon reactions at 2.6 to 17.6 MeV with bell metal, effective atomic numbers for pair production in, (T), 25:14402
  - Cu--Zn, phase transformations in, β--α massive, 25:13720
  - Cu-base--ThO_2, properties of dispersion-strengthened, electric and tensile, 25:13755
- COPPER HYDRIDES
  - spectral lines due to, in sunspots, (E), 25:13900
- COPPER IONS
  - effects on copper at 30 and 90 keV, 25:14422
- COPPER ISOTOPES Cu-62
  - decay scheme for,(E), 25:14940
  - energy levels from nickel-62 (p,nγ) reactions, (E), 25:14940
- COPPER ISOTOPES Cu-63
  - abundance in Sun, (E), 25:13900
- COPPER ISOTOPES Cu-64
  - determination in reactor cooling water by γ spectroscopy, 25:12956
  - neutron reactions (n,p) with, fission-spectrum-averaged activation cross sections for, (E), 25:14968
- COPPER ISOTOPES Cu-65
  - abundance in Sun, (E), 25:13900
- CORROSION
  - book: Corrosion Week. 41st Manifestation of the European Federation of Corrosion, 7-12 October, 1968 in Budapest, 25:13636
- CORUNDUM
  - properties at high temperatures, review of physical, thermal, and thermodynamic, 25:13667
- COSMIC PARTICLES
  - acceleration of primary protons by spinars, (T), 25:13952
  - detection of multiple mesons (μ) at 1500 hg/cm^2, 25:14060
  - electron capture by beryllium-7, (T), 25:14059
  - electron capture in H I regions by protons, Lyman-α production in, (T), 25:14061
  - fluxes of 500- to 1500-MeV electrons in atmosphere, (E), 25:14068
  - magnetic monopole production by neutrinos in ocean bed, upper limit for cross sections for, 25:14638
  - monitoring of neutrons, meteorological effects in, (T), 25:14066
  - neutron intensity, effect of small magnetic storms on diurnal variation of, (E), 25:14074
  - scattering by interstellar gases, heating effects from, 25:14058
  - stopping of meson (μ) at 60 to 300 mwe, intensity and rate for, (E), 25:14535
- COSMIC RADIATION
  - Dirac monopoles in primary, (T), 25:13953
  - effects of primary, on 27-day variations of electron density at 50 to 80 km in ionosphere, (E/T), 25:14127
  - flux and temperature of background infrared, (E), 25:13949
  - intensity variations following proton flares, anisotropy of, (E), 25:14075
  - intensity variations of primary, meteorite data, (E/T), 25:14071
  - intensity variations of, methods for investigating, (T), 25:14069
  - interactions of primary, with astrophysical plasmas, (T), 25:14072
  - interactions with solar wind, (T), 25:14076
  - magnetic monopoles in primary, search for, (T), 25:14078
  - modulation of primary, by solar wind, (T), 25:14070
  - origin of isotropic gamma-ray background in, 25:14062
  - origin of primary, (T), 25:14079
  - origin of primary, (T), 25:14080
  - production of primary, by plasma turbulence, (T), 25:14077
  - propagation of primary, (T), 25:14080
  - quarks in primary, search for, (E), 25:14065
  - research at INS, April 1969--Mar. 1970, 25:14845(R) (NP-18601)
  - research at MIT, 1969, 25:14925(R) (MIT-2098-643)
  - spectra of primary electrons and ions, (T), 25:14077
- COSMIC RADIO SOURCES
  - Faraday rotation of, (E), 25:13944
  - galaxy associated with 3C 386, optical observations of, 25:13915
  - intensity of 3C 10 and 3C 58 at 2880 MHz, (T), 25:13839
  - polarization properties of 3C 10 and 3C 58 at 1420 and 2880 MHz, (E), 25:13833 (AD-711611)
  - polarization properties of 3C 10 and 3C 58, at 2880 Mhz, (E), 25:13839
  - search for small-diameter, in galactic center region, (E), 25:13914
  - spectra of extragalactic, interpretation of radio, (T), 25:13835
  - spectra of, detection of interstellar formaldehyde by absorption against, (E/T), 25:13845
  - spectral extinction of, as function of zenith angle, (E), 25:13838
  - spectral recombination lines at 6 cm in, (E), 25:13840
- COSMIC RAY TELESCOPES
  - data-processing system for, (E), 25:14067
  - operation of shower, for energy measurement of high-energy electrons and photons, 25:13300
- COSMIC SHOWERS
  - detection of ultra-high energy, development of nuclear emulsion chambers for, 25:14845(R) (NP-18601)
  - production of 1000-GeV, from proton reactions with nuclei in emulsions, K/π ratio of secondaries in, (E), 25:14509 (INP-718)
- COSMIC X-RAY SOURCES
  - GX 333 + 25, energy spectrum of, (E), 25:13849
  - properties of, near the galactic center, (E), 25:13857
  - Sco X-1, color--magnitude relation, distance, and interstellar reddening of, (E), 25:13852
  - Sco X-1, gamma emission from, due to Compton synchrotron process, (E/T), 25:13856
- COSMOLOGY
  - equivalence principle in, (T), 25:13950
  - galactic parameters as consequence of primeval turbulence, (T), 25:13932
  - Lyra's geometry in theory of, 25:13947
  - parameters of, cosmic-ray physics in, (T), 25:14080
- CRAB NEBULA
  - magnetic field in wisps, (E), 25:13850
  - mass of filamentary shell of, (T), 25:13807
  - properties of, (T), 25:13844
- CRACKS
  - geometry in solids, fracture mechanics evaluation of effects of stress on, 25:13181 (WAPD-TM-976)
- CRATERS
  - formation mechanisms and size of, produced by surface chemical explosions in Greenland icecap snow, 25:13133 (AD-711861)
  - formation of linear, with row-emplaced explosives, equations for predicting, 25:13135 (AD-713574)
  - slope stability of underground explosion-produced, effects of seepage characteristics of surrounding media on, 25:13102 (NCG-TR-27)
- CRITICAL ASSEMBLIES
  - neutron fission cross section of uranium-235 in fast, Monte Carlo analysis of, (E/T), 25:15398
  - operations summary for ZPR-3, ZPR-6, ZPR-9, and ZPPR during December 1970, 25:15339 (ANL-7765)
  - physics analysis of fast zero power, correlation of fast reactor microscopic and integral nuclear data by, (E/T), 25:15396
  - physics parameter measurements in Godiva and Jezebel, evaluation of ENDF/B data by, (E/T), 25:15397
  - physics parameters of fast, comparison of calculational methods for, (E/T), 25:15387 (EURFNR-858)
- CROPS
  - effects on strontium-90 removal from soil, 25:13118(R) (COO-414-17)
  - radioactive contamination of, in France from fallout and industrial wastes, cesium-137, iodine-131, and strontium-90, 25:13402
- CRUSTACEA
  - contamination by sea-disposed liquid radioactive waste,

(E), 25:13189 (CEA-CONF-1712)
CRYOSTATS
  description of use of helium-3, for specific heat measurements, 25:14212 (UUIP-677)
  development of superfluid helium, for superconducting helical waveguides, (T), 25:14846 (NP-18651)
CRYSTAL RIVER POWER REACTOR, UNIT 3
  effluents from, effects on environment of chemical, radioactive, and thermal, 25:15308 (DOCKET-50302-16)
CRYSTAL STRUCTURE
  model for three-dimensional, containing one-dimensional features, 25:13766(R) (SRO-552-6)
CRYSTALS
  dislocations in, fundamentals in collecting data on, 25:15437 (NYO-3087-19)
  ion channeling patterns of, autoradiographic method for determining, 25:14417
  isotopic defects in cubic lattice, temperature-dependent properties of, (T), 25:14489
CULTURE MEDIA
  effects on recovery of Salmonella from γ-irradiated food, 25:13620
  effects on uv-irradiated Escherichia coli, 25:13406
CURIUM
  ionization potential of, measurement by surface ionization comparison method, 25:13979
  production and uses of, review on, 25:13059
  reduction of trivalent, in perchlorate medium, polarographic studies on, 25:13020
  separation from aqueous chloride solutions by solvent extraction using dioctyl phosphate in benzene or heptane, effects of variables on, 25:13096
CURIUM ALUMINATES
  radiation effects on curium-244-incorporating, self-, 25:13779 (DP-MS-70-44)
CURIUM ISOTOPES
  neutron capture and fission cross sections for, (E), 25:15090
CURIUM ISOTOPES Cm-241
  half-lives of isomers of, (E), 25:15046
CURIUM ISOTOPES Cm-242
  determination in liquid waste effluents from nuclear fuel reprocessing plant by α spectrometry, 25:12950 (BRH/NERHL-70-2)
  neutron reactions at thermal energies to 10 MeV, evaluation of data on, (T), 25:15128
CURIUM ISOTOPES Cm-243
  half-lives of isomers of, (E), 25:15046
CURIUM ISOTOPES Cm-244
  determination in liquid waste effluents from nuclear fuel reprocessing plant by α spectrometry, 25:12950 (BRH/NERHL-70-2)
  fission of, energy spectra and mean prompt neutron production in spontaneous, (E), 25:15118
CURIUM ISOTOPES Cm-245
  neutron fission of, energy spectra and mean prompt neutron production in thermal, (E), 25:15118
CURIUM ISOTOPES Cm-248
  fission of, average number of prompt neutrons from spontaneous, (E), 25:15037
CURIUM ISOTOPES Cm-250
  fission of, average number of prompt neutrons from spontaneous, (E), 25:15037
CURIUM OXIDES
  production of, design of equipment for, 25:13146
  radiation effects on curium-244-incorporating, self-, 25:13779 (DP-MS-70-44)
  shipping of, design of shielded container for, 25:13202
CURRENT ALGEBRA
  Bjorken limit and Jin--Martin lower bound for forward amplitudes in, 25:14827
  calculations in, dynamical, 25:14593
  charge density at infinite momentum, low moments of vector and axial-vector, 25:14672
  chiral breakdown for nonet structure of 0⁻ and 0⁺ mesons in, 25:14645
  chiral breakdown for psi parameter for K → π + l + ν decay in, 25:14645
  commutation relations for sum rules for amplitudes of π production from photon-hyperon interactions in, quark model, 25:14619
  current and field commutators for saturation of, local approximation to, 25:14673
  hard-pion theorems in (3,3*) + (3,3*) symmetry-breaking model for scalar form factor for K → π + l + ν decay, 25:14633 (NYO-2262-TA-233)
  model with PCAC hypothesis for CP violation in phenomenological study of K → 2π(3π) decays, 25:14764
  PCAC hypothesis for branching ratio of W decay into soft pion and bosons in, 25:14634 (NYO-4204-7)
  Schwinger terms in, properties of q-number, 25:14589
  soft-pion predictions for weak decays of hadrons in, once-subtracted dispersion relations for corrections to, 25:14654
  solution of isospin-factored, at infinite momentum, 25:14587
  spectral functions for branching ratio of W hadronic decay in, asymptotic behavior of weak, 25:14634 (NYO-4204-7)
  SU(3) x SU(3) chiral Lagrangian model for total cross sections and scattering lengths for anti K + N, π + Σ, and π + Λ interactions, 25:14703 (TID-25639)
  SU(3) x SU(3), hard-meson method for N-point functions in chiral, 25:14664
  SU(3) x SU(3), weak mass splittings of soft pseudoscalar mesons in, 25:14593
  vector currents in dual-resonance model, 25:14667
CURRENT REGULATORS
  performance and use of transistor, for beam transport magnet power supplies, 25:14848 (PPAD-677-E)
CYANOGEN
  detection in UU Aur, (E), 25:13803
CYCLOBUTANE, OCTAFLUORO-
  reactions with recoil atoms of fluorine-18, effects of radical scavengers on, 25:13066
CYCLOBUTENE, HEXAFLUORO-
  reactions with recoil atoms of fluorine-18, effects of radical scavengers on, 25:13066
1,3-CYCLOHEXADIENE
  radiation effects on dimerization of, in benzene solutions, γ, 25:13037
CYCLOHEXANE
  radiolysis at 77 to 350°K, yields from γ, 25:13056
  radiolysis of liquid, containing deuterium sulfide, mechanism and yields from γ, 25:13048
CYCLOHEXANE, METHYL-
  radiolysis at 77°K, yields from γ, 25:13056
  radiolysis of, kinetics and transient spectra of short-lived intermediates produced by electron pulse, 25:13050
CYCLOPENTANE
  radiolysis of liquid, containing deuterium sulfide, mechanism and yields from γ, 25:13048
CYCLOTRONS
  development of INS variable-energy, 25:14845(R) (NP-18601)
  operation of INS 160-cm, April 1969--Mar. 1970, 25:14845(R) (NP-18601)
CYLINDERS
  critical diameter of uranyl fluoride- and uranyl nitrate-filled planar arrays of, empirical formula for prediction of, 25:13198
  gamma transport in, computer program for solving one-dimensional Boltzmann equation for, (T), 25:14863 (CEA-N-1358)
  neutron transport in, computer program for solving one-dimensional Boltzmann equation for, (T), 25:14863 (CEA-N-1358)
  thermal shock in hollow, comparison of experimental and predicted, 25:13183
CYTIDINE MONOPHOSPHATES
  synthesis in yeast cells, inhibition of, 25:13604

D

DAMS
  response of earth, to seismic disturbances, digital computer programs for predicting, 25:13130 (UCRL-13329(Pt.2))
DATA ACQUISITION SYSTEMS
  development at ORNL, Sept. 1969--Aug. 1970, 25:13318(R) (ORNL-4620)
  development for spectroscopic analysis of biological samples, 25:13229 (CEA-CONF-1647)
DATA DISPLAY SYSTEMS
  maintenance manual for Weapons Effects Display System for prompt effects from nuclear explosions, 25:13323 (UCRL-50892(Vol.4)(Pt.2))
  maintenance manual for Weapons Effects Display System for fallout from nuclear explosions, 25:13322 (UCRL-50892(Vol.4)(Pt.1))
DATA PROCESSING SYSTEMS
  description of Brookhaven On-Line Data Facility for high-energy physics experiments, 25:13289 (CERN-70-21(Vol.2), pp 921-30)
  description of FOCUS, for remote access, 25:13265 (CERN-70-21(Vol.2), pp 551-9)
  development at ORNL, Sept. 1969--Aug. 1970, 25:13318(R) (ORNL-4620)
DATA TABULATIONS
  energy levels for elements Z = 1 to 100, atomic, 25:14409
  evaluation of neutron use of interactive computer graphics in, 25:14879
  photon cross sections from 1 keV to 100 MeV for element Z = 1 to 100, 25:14409
  review of worldwide neutron data center activities, 25:14878
  x-ray energies and relative intensities for elements Z = 1 to 100, K and L, 25:14409
DENSIMETERS
  design and performance of gamma radiometric, for concretes, 25:13308
  design and performance of radiometric, for cement determination in concrete, 25:13315
  design of x-ray backscatter, for determining silver in photographic film, 25:13311
  design optimization of gamma backscatter, for soils, 25:13316
  development of beta radiometric, for density measurements of atmosphere, 25:13314

DEOXYRIBONUCLEASE
  effects on γ-radioinduced degradation of deoxyribonucleoproteins of rabbits, 25:13363
  radiation effects on activity of, in cells of Escherichia coli, comparison of γ, proton, and uv, 25:13371
DEUTERIUM
  argon--ion reactions at 1 to 10 eV with molecular, cross sections for, (T), 25:14041
  burning in HL Tau 76, central, (E/T), 25:13796
  deuteron reactions (d,dp) at 11 MeV, d--p coincidence spectra from, (E/T), 25:14891(T) (ORO-1316-97)
  diffusion in vanadium, niobium, and tantalum, Gorsky-effect measurements of, 25:14440
  effects on dipole moment and hyperfine parameters of chlorine-35-labeled hydrochloric acid, molecular-beam electric resonance spectral studies on, 25:12988
  effects on ethyl radical formations in solutions, 25:14837(R) (BNL-50230)
  effects on exchange reactions of chlorine with hydriodic acid, 25:12986
  effects on ferroelectric properties of rubidium selenites, $RbH_3(SeO_3)_2$, 25:12989
  effects on hydrolysis of methanesulfonyl and benzenesulfonyl chlorides, 25:12984
  effects on ir spectra of water, 25:12994
  effects on kinetics of argon--ion reactions with hydrogen at 1 to 10 eV, (T), 25:14041
  effects on Raman spectra of potassium dihydrogen phosphate crystals, 25:12997
  effects on spectra of p-dibromobenzene, 25:13003
  effects on thermal capacity of ammonium dihydrogen phosphate, 25:12998
  effects on thermal polymerization of styrene, 25:12983
  effects on uv spectra of acetone, 25:13006
  effects on vapor pressure of methylamine in hexane, effects of concentration on, 25:12985
  effects on vapor pressure of water, design of equipment for measuring, 25:12995
  effects on volume viscosity and structural relaxation of water, 25:12990
  effects on yields of molecular hydrogen from γ radiolysis of basic and neutral aqueous solutions of sodium azide, effects of scavengers on, 25:13044
  electron reactions at 10 to 500 eV with molecular, cross sections for production of 2s atoms in, (E), 25:14045
  exchange between ethanol, methanol, and propanol and water, at 200 to 300°C, activation energy for catalytic, 25:12991
  exchange between fluorene and 2-methyl-2-propanol in lithium tert-butoxide, effects of electron-donor additives on, 25:13007
  exchange between heavy water and N-substituted pyridinium ions, 25:13000
  exchange between methyl radicals in lumazine derivatives, 25:12982
  exchange with hydrogen in benzonitrile--alkali metal ion radical salt, effects of alkali metal on catalytic, 25:13002
  exchange with hydrogen in benzonitrile--cesium ion radical salt, mechanism of catalytic, 25:13001
  exchange with hydrogen in shock-tube pyrolysis of ethylenes, 25:12993
  neutron reactions (n,2n) at 18.5 MeV, neutron--neutron scattering length in, (E/T), 25:14887
  nuclear properties of, Bolsterli--Feenberg perturbation procedure for calculation of momentum-dependent, 25:15185
  oxygen-18 reactions (O-18,pγ) at 27 MeV, γ spectra from, (E), 25:14905
  plasma jets of, neutron and x-ray production in dense noncylindrical z pinch, (E), 25:14359
  proton reactions (p,γ) at 57 to 1100 keV, gamma yield and total cross section for, (E), 25:14885
  reactions with hydrogen sulfide at 1250 to 1590°K in shock tubes, kinetic studies on exchange, 25:12987
  reactions with methane at 1440 to 1755°K in single-pulse shock tubes, kinetic studies on exchange, 25:12987
  yields from γ radiolysis of liquid hydrocarbons containing deuterium sulfide, 25:13048
DEUTERIUM HYDRIDES
  exchange reactions in argon at 1120 to 1659°K in shock tubes, kinetic studies on, 25:12987
  yields from γ radiolysis of liquid hydrocarbons containing deuterium sulfide, 25:13048
DEUTERIUM SULFIDES
  effects on yields from γ radiolysis of liquid hydrocarbons, 25:13048
DEUTERIUM SYSTEMS
  D--H, mass separation effects in rotating plasma of, 25:14278 (NP-18643)
  D--H, reactions with recoil tritium, iodine bromide and iodine chloride as radical scavengers in, 25:13067
DEUTERON SOURCES
  development of polarized, for 6-MeV Van de Graaff accelerator, 25:14859
DEUTERONS
  interactions anti p + d → 2π^- + 2p + anti n at 7.0 GeV/c, Δ^0 and Δ^{--} production in, (E), 25:14554
  interactions anti p + d → anti p + 2p + π^0 at 7.0 GeV/c, Δ(1236) production in, (E), 25:14554
  interactions anti p + d → π^- + anti p + 2p at 7.0 GeV/c, Δ(1236) and Δ(1920) production in, (E), 25:14554
  interactions anti p + d → π^- + anti p + π^+ + d at 7.0 GeV/c, Δ^{--}(1236) and d*(2170) enhancement in, (E), 25:14554
  interactions anti p + d → π^- + anti p + π^+ + p + n at 7.0 GeV/c, anti $\Delta^{--}\pi^+$(1470), anti $\Delta^{--}\pi^+$(1750), and pnπ^+(2250) enhancements in, (E), 25:14554
  interactions anti p + d at 1.25 to 1.67 GeV/c, cross sections for Λ production in, (E), 25:14550
  interactions anti p + d, at 50 to 920 MeV/c in deuterium bubble chamber, total and topological cross sections for, (E), 25:14555
  interactions γ + d → p + p + π^+ + π^- + π^- at 1.1 to 3.5 GeV, total and resonance production cross sections for, (E), 25:14521
  interactions γ + d → $\pi^-(\pi^+)$ + 2p(2n) at 600 to 1700 MeV, π^-/π^+ cross section ratio, isoscalar and isovector amplitudes, and cross sections for γ + n → π^- + p interactions from forward, (E), 25:14523
  interactions K^- + d → K^- + π^- + π^+ + p at 7.3 GeV/c in deuterium bubble chamber, partial cross sections, high peripherality, and K*(890) production in, (E), 25:14569
  interactions K^- + d → p + $\Sigma^-(\Sigma^+)$ + $\pi^+(\pi^-)$ + π^- at 3 GeV/c in bubble chamber, cross sections for, (E), 25:14546
  interactions N + d → N + d, differential and total cross section relations for, (T), 25:14730 (JINR-P2-5444)
  interactions n + d above inelastic threshold, Kohn variational principle for calculating elastic amplitude of, (T), 25:14744
  interactions N + d at 14 and 23 MeV, elastic cross section and nucleon polarization in spin-dependent three-body, (T), 25:14740
  interactions n + d, realistic potentials for calculation of scattering lengths for, (T), 25:14743
  interactions p + d → p + d, Glauber correction in, (T), 25:14730 (JINR-P2-5444)
  interactions π + d, Glauber model for, (T), 25:14630
  interactions with mesons in resonant regions, Watson multiple-scattering theory for, 25:14738
  reactions (d,2α) with lithium-7 at 3.0 to 5.9 MeV, rescattering effects on α--α coincidence spectra from, (E/T), 25:14891(T) (ORO-1316-97)
  reactions (d,α) with carbon-12 at 21 to 29 MeV, analysis of reaction mechanism in, (E/T), 25:14901
  reactions (d,n) with molybdenum-92, -94, and -96 and zirconium-96 at 12 MeV with isobaric analog excitation, anomalies in cross sections for, (E), 25:15050
  reactions (d,p) and (d,t) with strontium-84, -86, and -88 at 20.7 MeV, DWBA analysis of, (E), 25:14930
  reactions (d,p) with aluminum-27, cadmium, carbon, copper, and lead at 650 MeV, proton angular distributions from, (E), 25:14906
  reactions (d,p) with calcium-40 at 5 to 21 MeV, weakly bound projectile model for, (E/T), 25:14938
  reactions (d,p) with calcium-48 at 2.5 to 5.5 MeV, angular distributions from, (E), 25:14916
  reactions (d,p) with strontium-84 and -86 at 12 MeV, angular distributions for, (E), 25:14955
  reactions (d,pf) with uranium-233, analysis of neutron-nucleus interaction in, (T), 25:15190
  reactions with americium, neptunium, plutonium, and uranium at 9 to 14.2 MeV, (E), 25:15046
  reactions with metallic thick targets at 90 to 360 keV, yields of characteristic x rays from, (E), 25:13962
  reactions with nuclei with Coulomb breakup, effect of neutron-nucleus interaction in, (T), 25:15190
  scattering by calcium-48 at 2.5 to 5.5 MeV, angular distributions from, (E), 25:14916
  stopping in Havar foils at 2.5 to 7.0 MeV, (E), 25:14401
DIAPHRAGMS
  radiation effects on selenium-75 incorporation in, in rats in vitro following incubation in sodium selenites, 25:13354
DIELECTRIC FILMS
  deposition and properties of thin metal-oxide, chemical vapor, 25:13748
DIET
  radioactive contamination of, of populations of high background areas in Brazil, 25:13439
  radioisotope content of human adolescent, sampled in EURATOM countries during 1965 to 1967, cesium-137, strontium-90, and radium-226, 25:13392 (EUR-3945(Pt.2))
  radioisotope content of institutional, of adults and children in USA during October to December 1969 as compared to annual average content for 1969, cesium-137 and strontium-90, 25:13442
  radioisotope content of, sampled throughout USA between 1965 and 1970, cesium-137, strontium-89, strontium-90, and radium-226, 25:13401
DISEASES
  conference on diagnosis and treatment of human intestinal, 25:13508
  pruritus ani, radiotherapy of human, damage to perianal skin following x, 25:13588
DISEASES, NEOPLASTIC
  adenocarcinomas, radiotherapy of human, effects on survival, effects on grid techniques on cobalt-60 γ, 25:13532
  adenomas, radiotherapy of human toxic thyroid, using iodine-131, effects on thyroid hormone synthesis,

25:13594
- adenomas, radiotherapy of lymph node, in children, effects of, on thyroid, x, 25:13585
- benign, radiodiagnosis of cystic and alveolar hydatid, of human liver, effectiveness of radiography and radioisotope scanning for, 25:13494
- benign, radiodiagnosis of human brain, using metastable technetium-99 scanning method, 25:13505
- benign, radiodiagnosis of human kidney, using metastable technetium-99 scanning method, 25:13504
- benign, radiodiagnosis of human stomach, use of scanning with phosphorus-32 or technetium-99 for, 25:13495
- Burkitt's lymphoma, radiotherapy of human, effects of, on titer of antibodies against EBV-associated membrane antigen complex, γ, 25:13391
- carcinomas, metastases, radiodiagnosis of human bone, use of scintillation counter and strontium-85 for, 25:13513
- carcinomas, radiodiagnosis of human metastatic papillary thyroid, use of metastable technetium-99-labeled pertechnetate with Anger camera for, 25:13488
- carcinomas, radioinduced cortical, in adrenal gland of buffalo rats, mixed whole-body γ and fission neutron, 25:13564
- carcinomas, radiotherapy in man, protective effects of tanderil against, 25:13476
- carcinomas, radiotherapy of bronchial, in man in combination with chemotherapy, effects on survival, megavoltage or orthovoltage, 25:13522
- carcinomas, radiotherapy of bronchial, in man, effects on survival, statistical evaluation of cobalt-60 γ, 25:13523
- carcinomas, radiotherapy of cervix, in man, effectiveness of conformation radiation in comparison to stationary techniques, 25:13530
- carcinomas, radiotherapy of human bladder, effects of, on survival, cobalt-60 γ, 25:13525
- carcinomas, radiotherapy of human bladder, treatment of cystitis following γ, 25:13592
- carcinomas, radiotherapy of human cervical and uterine, injuries to intestine following α and γ, 25:13589
- carcinomas, radiotherapy of human cervix, use of cobalt-60 γ for, development of computer methods for, 25:13540
- carcinomas, radiotherapy of mammary, in man, effects on brachial plexus, protective effects of actihemyl against, 25:13480
- carcinomas, radiotherapy of mammary, in man, effects on lungs, ribs, and skin, electron beam, 25:13584
- carcinomas, radiotherapy of nasopharyngeal, effects of, on titer of antibodies against EBV-associated membrane antigen complex, γ, 25:13391
- carcinomas, radiotherapy of peritoneal and pleural, dosimetry and methods for fast electrons, 25:13538
- carcinomas, radiotherapy of prostate, effects of, on bone marrow, 25:13591
- carcinomas, radiotherapy of thyroid, in man, effects of, on survival, 25:13524
- carcinomas, radiotherapy of thyroid, using iodine-131, 25:13596
- carcinomas, surgery of mammary, effectiveness of cobalt-60 γ radiotherapy following, 25:13533
- chondrosarcomas, radiotherapy in man, effectiveness of cobalt-60 γ for, 25:13521
- Ewing sarcomas, radiotherapy in man, effectiveness of cobalt-60 γ for, 25:13521
- fistulas, radiotherapy of esophageal, in patients with lymphogranulomatosis, effectiveness of cobalt-60 γ for, 25:13542
- hemangiomas, uptake of colloidal gold-198 by human liver, during scanning, 25:13510
- Hodgkin's disease, radiotherapy of, in man, in combination with stomach resection, evaluation of, 25:13541
- leukemia, radioinduced, in personnel, radium, 25:13593
- lymphogranulomas, radiotherapy in man, effects of dose and dose fractionation on, 25:13543
- lymphogranulomatosis, radiotherapy of human, effects on survival, effects on grid techniques on cobalt-60 γ, 25:13532
- malignant, radiodiagnosis of human brain, using metastable technetium-99 scanning method, 25:13505
- malignant, radiodiagnosis of human kidney, using metastable technetium-99 scanning method, 25:13504
- malignant, radiodiagnosis of human liver, methods using iodine-131-labeled fibrinogen for, 25:13483
- malignant, radiodiagnosis of human stomach, use of scanning with phosphorus-32 or technetium-99 for, 25:13495
- malignant, radioinduced, thyroid of children following therapy for lymph node adenomas, x, 25:13585
- malignant, radiotherapy in man, method for determining effects of cytostatic drugs on, 25:13527
- malignant, radiotherapy of advanced head and neck, in man, effects of sequential high or low dose methotrexate treatment on effectiveness of, 25:13528
- malignant, radiotherapy of bone, comparison studies on cesium-137 γ, cobalt-60 γ, and x, 25:13536
- malignant, radiotherapy of human children, effects of, on liver, γ, 25:13578
- malignant, radiotherapy of human laryngopharyngeal, combined use of dose fractionation followed by radical surgery for γ, 25:13545
- malignant, radiotherapy of oro-pharyngeal and thorax-abdominal, review of clinical experiences over ten-year period in telecobalt γ, 25:13546
- malignant, radiotherapy of skin, dosimetry and methods for fast electrons, 25:13538
- metastases, radiodiagnosis of human bone, use of scintillation counter and strontium-85 for, 25:13513
- metastases, radiotherapy of lung, dosimetry and methods for fast electrons, 25:13538
- metastases, radiotherapy of lymph node, methods for biaxial cobalt-60 γ, 25:13534
- myelosclerosis, radioinduced malignant, in personnel, radium, 25:13593
- osteosarcomas, radioinduced, in personnel, radium, 25:13593
- osteosarcomas, radiotherapy in man, effectiveness of cobalt-60 γ for, 25:13521
- radiodiagnosis of lung, using scintigraphy methods with Anger camera, evaluation of, in comparison with radioisotope ventilation tests, 25:13500
- reticulosarcomas, radiotherapy of human, effects on survival, effects on grid techniques on cobalt-60 γ, 25:13532
- sarcomas, γ-radiosensitivity of methyl cholanthrene-induced, in mice, 25:13473
- seminomas, radiotherapy of human testicular, using supervoltage radiation, 25:13544
- teratomas, radiotherapy of human testicular, using supervoltage radiation, 25:13544
- tumors, development of thyroid, in unexposed siblings of x-irradiated human children, 25:13587
- tumors, radiation effects on distribution of palmitates in phospholipids and triglycerides of Ehrlich ascites, effects of palmitate quantity on γ, 25:13362 (CEA-R-4039)
- tumors, radiation effects on selenium-75 incorporation in, of rats following administration of sodium selenites, 25:13354
- tumors, radiotherapy in man, comparison of interstitial gold-198 to radium for, 25:13526
- tumors, radiotherapy of, effects of dose distribution adjustment errors on effectiveness of, 25:13451

DISEASES, PHYSIOLOGICAL
- abscesses, radiodiagnosis of splenic, use of scanning for, 25:13512
- acne, radiotherapy in human children in relation to subsequent development of thyroid tumors, x, 25:13587
- calcium retention in patients with coeliac, effectiveness of calcium-47 for, 25:13359
- cirrhosis, radiodiagnosis of, advantages of using carbon-14 for measuring incorporation of precursors into glucose over determining concentration of metabolic end products, 25:13506
- cystic fibrosis, diagnosis of human, using copper content of nails determined by neutron activation analysis, 25:13491
- cystitis, treatment of γ-radioinduced, in man following therapy of bladder carcinoma, 25:13592
- infarctions, radiodiagnosis of massive cerebral, in human brain, use of metastable technetium-99-labeled pertechnetate for, 25:13489
- jaundice, radiodiagnosis of drug-induced, in man, use of angiography in combination with percutaneous transhepatic cholangiography for, 25:13492
- necrosis, radioinduced, in human ribs following therapy for mammary carcinomas, electron beam, 25:13584
- pyelonephritis, radiodiagnosis of human, use of iodine-131-labeled hippuran or indium-113m-labeled EDTA for, comparison studies on, 25:13499
- radiodiagnosis of, advantages of measuring incorporation of radioisotope-labeled precursors into glucose over determining concentration of metabolic end products, 25:13506
- radiotherapy for, dosimetry and methods for fast electrons, 25:13538
- ruptures, radiodiagnosis of splenic, use of metastable technetium-99-labeled sulfur colloid spleen scanning for, 25:13511
- thrombi, induced in animals, radiodiagnosis of, effectiveness of iodine-131-labeled fibrinogen for, 25:13518
- ulcers, radioinduced, in human skin following therapy for mammary carcinomas, electron beam, 25:13584
- xerodermal idiocy, case studies of, 25:15443(T) (ORNL-tr-2426)

DISEASES, TRAUMATIC
- radiation sickness, diagnosis in rats, neutron autoradiography method for, 25:13497
- skin wounds, effects on histamine content of blood, lungs, skin, and small intestine in rats in combination with radiation, 25:13368

DISPERSION RELATIONS
- interactions π + K, CDD pole effects on single resonance solution for, 25:14696
- interactions π + π, nonlinear functional analysis for numerical computations of S-matrix for, 25:14699
- sum rules for amplitudes of π + N interactions, fixed-u, 25:14709
- use of once-subtracted, for corrections to soft-pion predictions of current algebra for weak decays of

- hadrons, 25:14654

DOGS
- radiation effects on chemical composition of blood in, effects of preliminary exposure to uv on whole-body x, 25:13574
- selenium-75-labeled selenomethionine uptake by abdominal organs of, effects of injection method on, 25:13343

DONALD C. COOK POWER REACTOR, UNIT 1
- auxiliary systems for, final safety analysis of, 25:15319 (DOCKET-50315-30)
- auxiliary systems for, final safety analysis of, 25:15321 (DOCKET-50315-32)
- buildings and structures for, design specifications for, 25:15321 (DOCKET-50315-32)
- containment structure for, dynamic analysis of earthquake stresses on, 25:15322 (DOCKET-50315-33)
- containment systems for, final safety analysis of, 25:15318 (DOCKET-50315-29)
- control system for, final safety analysis of, 25:15319 (DOCKET-50315-30)
- cooling system for, final safety analysis of, 25:15318 (DOCKET-50315-29)
- design parameters for, requested information on, 25:15322 (DOCKET-50315-33)
- design parameters of, final safety analysis of, 25:15317 (DOCKET-50315-28)
- effluents from, effects on environment of chemical, radioactive, and thermal, 25:15316 (DOCKET-50315-27)
- electrical systems for, final safety analysis of, 25:15319 (DOCKET-50315-30)
- engineered safeguards for, final safety analysis of, 25:15318 (DOCKET-50315-29)
- instrumentation for, final safety analysis of, 25:15319 (DOCKET-50315-30)
- operation of, license application for, 25:15315 (DOCKET-50315-26)
- operations aspects of, final safety analysis of, 25:15320 (DOCKET-50315-31)
- owners of, financial statements of, 25:15315 (DOCKET-50315-26)
- pressure vessel for, operation limits for, 25:15321 (DOCKET-50315-32)
- radiation protection system for, final safety analysis of, 25:15320 (DOCKET-50315-31)
- radioactive waste disposal system for, final safety analysis of, 25:15321 (DOCKET-50315-32)
- radioactive waste disposal system for, final safety analysis of, 25:15320 (DOCKET-50315-31)
- safety analysis of, 25:15321 (DOCKET-50315-32)
- site for, final safety analysis of, 25:15317 (DOCKET-50315-28)
- site for, geology of, 25:15322 (DOCKET-50315-33)
- steam and power conversion systems for, final safety analysis of, 25:15320 (DOCKET-50315-31)
- testing programs for, final safety analysis of, 25:15320 (DOCKET-50315-31)

DONALD C. COOK POWER REACTOR, UNIT 2
- auxiliary systems for final safety analysis of, 25:15319 (DOCKET-50315-30)
- auxiliary systems for, final safety analysis of, 25:15321 (DOCKET-50315-32)
- buildings and structures for, design specifications for, 25:15321 (DOCKET-50315-32)
- containment systems for, final safety analysis of, 25:15318 (DOCKET-50315-29)
- control system for, final safety analysis of, 25:15319 (DOCKET-50315-30)
- cooling system for, final safety analysis of, 25:15318 (DOCKET-50315-29)
- design parameters of, final safety analysis of, 25:15317 (DOCKET-50315-28)
- electrical systems for, final safety analysis of, 25:15319 (DOCKET-50315-30)
- engineered safeguards for, final safety analysis of, 25:15318 (DOCKET-50315-29)
- instrumentation for, final safety analysis of, 25:15319 (DOCKET-50315-30)
- operation of, license application for, 25:15315 (DOCKET-50315-26)
- operations aspects of, final safety analysis of, 25:15320 (DOCKET-50315-31)
- owners of, financial statements of, 25:15315 (DOCKET-50315-26)
- pressure vessel for, operation limits for, 25:15321 (DOCKET-50315-32)
- radiation protection system for, final safety analysis of, 25:15320 (DOCKET-50315-31)
- radioactive waste disposal system for, final safety analysis of, 25:15320 (DOCKET-50315-31)
- radioactive waste disposal system for, final safety analysis of, 25:15321 (DOCKET-50315-32)
- safety analysis of, 25:15321 (DOCKET-50315-32)
- site for, final safety analysis of, 25:15317 (DOCKET-50315-28)
- steam and power conversion systems for, final safety analysis of, 25:15320 (DOCKET-50315-31)
- testing programs for, final safety analysis of, 25:15320 (DOCKET-50315-31)

DRESDEN POWER REACTOR, UNIT 1
- core for, physics measurements for Cycle 8, 25:15246 (DOCKET-50010-77)
- fuel elements for, performance characteristics for Cycle 8, 25:15246 (DOCKET-50010-77)
- personnel of, requirements for operation, 25:15245 (DOCKET-50010-76)
- radioactive effluents from, revised release limits for airborne, 25:15245 (DOCKET-50010-76)

DRESDEN POWER REACTOR, UNIT 2
- containment structure for, leak rate testing of secondary, 25:15281 (DOCKET-50237-139)
- control rod drives for, modifications of, 25:15277 (DOCKET-50237-135)
- core thermal safety limits for, revised technical specifications for, 25:15275 (DOCKET-50237-133)
- fuel element cladding for, revised safety limits for, 25:15274 (DOCKET-50237-131)
- fuel elements for, additional information for coolant loss accidents with gadolinium oxide (Gd_2O_3)--uranium oxide (UO_2), 25:15279 (DOCKET-50237-137)
- fuel elements for, operating characteristics and safety limits for gadolinium oxide (Gd_2O_3)--uranium oxide (UO_2), 25:15276 (DOCKET-50237-134)
- instrumentation for, trip level settings for main steam isolation valve system, 25:15278 (DOCKET-50237-136)
- operations incident of December 21, 1970, malfunction of isolation condenser outboard steam isolation valve, 25:15230 (DOCKET-50237-132)
- operations incident of December 9, 1970, malfunction of torus spray valve, 25:15230 (DOCKET-50237-132)
- operations incident of December 9, 1970, malfunction of containment cooling heat exchanger bypass valve, 25:15230 (DOCKET-50237-132)
- operations incident of January 19, 1971, high pressure coolant injection pump low flow rate, 25:15232 (DOCKET-50237-141)
- operations incident of January 22, 1971, malfunction of main steam isolation valve, 25:15231 (DOCKET-50237-140)
- personnel for, revised requirements for operation, 25:15280 (DOCKET-50237-138)
- personnel of, requirements for operation, 25:15273 (DOCKET-50237-130)
- protection instrumentation for, trip level settings for, 25:15274 (DOCKET-50237-131)
- radioactive effluents from, revised release limits and monitoring requirements for, 25:15280 (DOCKET-50237-138)
- radioactive effluents from, revised release limits and surveillance requirements for, 25:15273 (DOCKET-50237-130)
- testing program for, schedule for power, 25:15233 (DOCKET-50237-142)

DRESDEN POWER REACTOR, UNIT 3
- containment structure for, leak rate testing of secondary, 25:15281 (DOCKET-50237-139)
- control rod drives for, modifications of, 25:15277 (DOCKET-50237-135)
- radioactive effluents from, revised release limits for gaseous, 25:15288 (DOCKET-50249-56)

DRUGS
- effectiveness of cytostatic, for treatment of cancer in combination with x-ray therapy, methods for, 25:13527
- effects on survival of man following therapy for bronchial carcinomas in combination with megavoltage or orthovoltage radiation, 25:13522

DUSTS
- distribution in atmosphere, use in tracer studies of global transport processes, (E), 25:13121 (TID-25314)

DYSPROSIUM
- complexes with carminic acid, spectrophotometric studies on, 25:12937
- determination in plutonium oxide--uranium oxide fuels by solvent extraction and emission spectrography, 25:12922 (WHAN-SA-44)
- determination of trace amounts of, in plutonium and plutonium dioxide--uranium dioxide by solvent extraction and emission spectrography, 25:12923 (WHAN-SA-47)
- determination of trace amounts of, in yttrium oxide by x-ray-excited optical luminescence, 25:12948
- electric conductivity of single crystal, spin-wave scattering effects on, 25:14448
- electron band structure of, APW calculations for conduction electrons, 25:14451
- energy-level excitation by neutron capture gamma rays, (E), 25:15002
- Ettingshausen effect measurements on polycrystalline, 25:14475
- magnon dispersion relation for c-direction in ferromagnetic and helical magnetic phases, neutron spectral study of, 25:14444

DYSPROSIUM ISOTOPES
- nuclear deformation parameters and optical isotope shifts for, estimates of, (T), 25:15048

DYSPROSIUM ISOTOPES Dy-159
- electron-capture decay of, L-subshell x-ray fluorescence and Coster--Kronig yields in terbium-159 from, (E), 25:15012

DYSPROSIUM ISOTOPES Dy-161
- neutron cross sections at 0.007 to 10 eV, energy dependence of, (E/T), 25:15096

DYSPROSIUM ISOTOPES Dy-162
- neutron cross sections at 0.007 to 10 eV, energy

  dependence of, (E/T), 25:15096
DYSPROSIUM ISOTOPES Dy-163
  neutron capture up to 360 eV, γ spectra and resonance spin assignments for, (E), 25:14982 (NCSAC-31)
  neutron cross sections at 0.007 to 10 eV, energy dependence of, (E/T), 25:15096
DYSPROSIUM ISOTOPES Dy-164
  neutron cross sections at 0.007 to 10 eV, energy dependence of, (E/T), 25:15096

E

ECOSYSTEMS
  trace element pathways in Arctic Lake, 25:15451(R) (SAN-310-P-4-10)
EGGS
  radiation processing of, effects of culture medium on recovery of Salmonella following γ, 25:13620
  radiosensitivity of Sitophilus oryzae, cobalt-60 γ, 25:13558
EINSTEINIUM
  production and uses of, review on, 25:13059
EINSTEINIUM CHLORIDES
  preparation and structure of crystalline, 25:13018
  spectra of hydrochloric acid solutions of, 25:13018
EINSTEINIUM ISOTOPES Es-253
  compounds, preparation of microgram quantities of, 25:13018
EINSTEINIUM OXYCHLORIDES
  preparation and structure of crystalline, 25:13018
ELECTRIC ARCS
  construction of low-current, for measuremet of iron spectra, (E), 25:14245
  current expansion in axial magnetic fields, limitation of, 25:14267
  displacement of wall-stabilized, in toroidal geometries, 25:14269
  electric current density and temperature measurement in hydrogen, 25:14268
  plasma acceleration patterns in quasi-steady, argon, 25:14281
  properties of low-current, for measurement of iron spectra, (E), 25:14245
ELECTRIC CAPACITORS
  admittance in plasma, diagnostic use of, 25:14251
  radiation effects on, electron and gamma, 25:13327 (LCIE-364)
ELECTRIC CONDUCTIVITY
  measurement at high temperatures, correction for leakage currents due to thermionic emission, 25:14455
ELECTRIC DISCHARGE
  electrode ablation in, (E/T), 25:14232
  plasma in positive column, microwave-excited, (T), 25:14336 (NP-18662)
  plasma spiral instability in positive column, nonlinear theory of, 25:14347
ELECTRIC FIELDS
  electron motion in, differential probability quantum processes in, 25:14498
ELECTRIC GENERATORS
  design for use in radioisotope-fueled Brayton cycle power system, 25:13168 (N-70-41276)
ELECTRIC INSULATORS
  performance of metal oxide, effects of fast reactor environment on, (E), 25:15354 (WHAN-IR-42)
  polarization effects on oxide, 25:14437 (WHAN-SA-75)
  radioinduced electrification of, gamma, (T), 25:14430
  testing of organosilicate press-material VNPM-1, in reactor core, 25:13330
ELECTRIC PROBES
  ion current to plane, in flowing plasma, (T), 25:14249
  performance for ion density measurements in plasma torch, (E/T), 25:14250
  performance of cylindrical Langmuir, in transition regime, (E), 25:14242 (AD-711095)
  performance of Langmuir, for time-resolved electron energy distribution measurements, (E), 25:14246
ELECTRODES
  ablation in spark discharges and electromagnetic shock tubes, (E/T), 25:14232
  current--voltage properties of thermionic, in dense seeded plasmas, (E/T), 25:14088
ELECTRODYNAMICS
  Maxwell tensor in, sources of split, 25:14615
ELECTROMAGNETIC FIELDS
  book: Electromagnetic Fields and Life, 25:13570
  effects on cells and molecules, 25:13571
  effects on informational interconnections between organisms, 25:13572
  effects on nervous system of animals and man, 25:13571
  effects on reproduction and development of rats, 25:13571
  effects on vital activity of organisms, 25:13572
  electron motion in intense plane-wave, (T), 25:14506
  Hamiltonian formalism on characteristic surfaces for, 25:14773
  interactions with gravitational fields, (T), 25:13946
  particle motion in, spinning, (T), 25:14599
  physical characteristics of, 25:13581
  sources of, artificial and natural, 25:13581
ELECTROMAGNETIC SEPARATION
  ion sources for ISOLDE, design and optimization of, 25:13162 (JINR-P13-5369)
ELECTROMAGNETIC WAVES
  absorption in nonisothermal plasma, anomalous, (T), 25:14373
  interactions with half-space and slab plasma, oblique, (T), 25:14386
  interactions with inhomogeneous plasma column, upper hybrid resonance, (E/T), 25:14381
  interactions with ion--acoustic waves in isotropic plasma, trapping in resonant, (T), 25:14374
  interactions with matter in Universe, gravitational, (T), 25:13948
  interactions with plasma half-space, reflection and penetration of oblique incident, (T), 25:14361
  interactions with plasma, Darwin model for simulating, 25:14293
  propagation along cold collisionless axially magnetized plasma column, 25:14360 (AD-711649)
  propagation in Riemann space, 25:14499
  scattering by magnetoplasma columns, near upper hybrid resonance, (E/T), 25:14382
  scattering from turbulent plasma, model for calculating, 25:14364
  scattering in spin-wave resonances in semiconductor antiferromagnets, (T), 25:14488
  scattering on critical electron density fluctuations in plasma, use of born theory for, 25:14363
  scattering on plasma, characteristic curves for collective, (T), 25:14375
ELECTRON BEAMS
  equilibrium configuration of high-intensity, force-free, 25:14272
  interactions with dense plasma, collective slowing down of intense relativistic, (T), 25:14292
  interactions with plasma, current density calculation for, 25:14321
  interactions with plasma, instabilities from nonlinear, (T), 25:14296
  interactions with plasma, ion-wave excitation in, (E), 25:14378
  interactions with plasma, nonlinear theory for monochromatic wave excitation in, 25:14311
ELECTRON-DIFFRACTION ANALYSIS
  intensities of low-energy, from beryllium and zinc cleaved surfaces, 25:14472
ELECTRON MICROSCOPY
  methods at 100 to 200 kV, 25:13628
ELECTRON PAIRS
  production in electron reactions with nuclei at 13.75 GeV in emulsions, direct, (E), 25:14525
ELECTRON-RING ACCELERATORS
  ring dynamics in, transient effect of accelerating field on, 25:14854(T) (UCRL-Trans-1420)
  ring--bunch dynamics in, impact mechanism in, 25:14855(T) (UCRL-Trans-1421)
ELECTRONIC EQUIPMENT
  development at ORNL, Sept. 1969--Aug. 1970, 25:13318(R) (ORNL-4620)
ELECTRONIC FILTERS
  design of two-dimensional nonrecursive, algorithm for optimum, 25:15467 (UCRL-72663)
ELECTRONS
  acceleration in auroral zone, mechanism for, (E/T), 25:14116
  back scattering of radiative corrections to, (T), 25:15175
  charge-deposition distribution at 4 to 24 MeV in beryllium, aluminum, copper, silver, and gold, (E/T), 25:13964
  detection and measurement of secondary, method for, 25:13963
  effectiveness of fast, for therapy through plaster casts in comparison to cesium-137 γ, cobalt-60 γ, and x, 25:13539
  effects of 3-MeV, on anomalous x-ray transmission of copper, 25:14427
  effects of high-voltage microscope, on vacancy tetrahedra formation in copper, 25:13731
  effects of pulsed, on helium--nitric oxide and nitrogen--nitric oxide, yields from, 25:13053
  effects of pulsed, on methylcyclohexane, kinetics and transient spectra of short-lived intermediates produced by, 25:13050
  effects on ammonium and sodium acid fluoride single crystals at 1 MeV, 25:14411 (AD-712321)
  effects on atomic displacements in monocrystalline cobalt, 25:13733
  effects on crystal structure of martensitic carbon steel at 2 MeV, low-temperature, 25:13729
  effects on electric capacitors, 25:13327 (LCIE-364)
  effects on growth of large faulted dislocation loops in nickel, 25:13732
  effects on lattice parameters of aluminum at low temperatures and 3 MeV, 25:13723 (JUL-664-FN)
  effects on lithium-doped silicon at 1 MeV, 25:14423
  effects on lungs, ribs, and skin in man following therapy for mammary carcinomas, 25:13584
  effects on microstructure of high-purity aluminum at 200 keV, 25:13727
  effects on naphthalene monocrystals, vibronic structure

of radicals from, 25:13047
effects on nickel at 650 kV, oxidation effects on voi formation in, 25:14416
effects on poly(methyl methacrylate), ESR studies on decay of free radicals from, 25:13058
effects on potassium chloride crystals at 5 keV, saturation of F centers induced in, 25:14415
effects on specimens in microscopes at 100 to 200 kV, 25:13628
effects on stored energy in platinum at 3 MeV and less than 40^{0}K, 25:13722 (JUL-658-FN)
electric charge and flux quantization for, electromagnetic coupling constant from, 25:14618
emission by 400-eV electron-excited silicon and germanium, effects of temperature and free carrier density on secondary, 25:13967
emission by niobium single crystals bombarded by 25-keV argon ions, angular distribution of secondary, 25:13969
emission of 40-keV, in solar flares, (E), 25:13894
emission of secondary, from targets bombarded by mercury ions, 25:13971
energy loss spectra at 115 eV in anthracene, naphthacene, and pyrene, 25:13968
energy losses in gadolinium, lead, and tin at 52 to 92 MeV, (E), 25:14392 (AD-711005)
energy-loss spectra in thin films, multiple-plasmon effects in, (T), 25:14486
fluxes of 500- to 1500-MeV, at various levels in atmosphere, (E), 25:14068
interactions $e + e$ at high energies, leading singularity in complex angular momentum plane in quantum electrodynamics for asymptotics of, (T), 25:14802
interactions $e + N$, Regge pole model for hadron production from, (T), 25:14635 (NYO-4204-9)
interactions $e + N$, structure functions rapid approach to universality in inelastic, (T), 25:14610
interactions $e + p \to p + 2\pi$, hadronic s-channel helicity conservation in, (T), 25:14636 (NYO-4204-10)
interactions $e + p$ at high energies, field-theoretic model of soft, neutral-meson production for deep-inelastic, 25:14607
interactions $e + p$ near N(1470), analyticity of inelastic hadronic form factor and model of CP violation for, (T), 25:14765
interactions $e + p$, fixed pole in virtual Compton amplitude for, 25:14608
interactions $e + p$, ladder model for structure functions for deep-inelastic, 25:14612
interactions $e + p$, multi-Regge model for inelastic, (T), 25:14621
interactions $e + p$, test of weak interaction renormalization theories in, (T), 25:14646
interactions $e^+ + e^- \to 2\gamma$ at 1 GeV, validity limit of quantum electrodynamics, 25:14520
interactions $e^+ + e^- \to \mu + e$ at 0.8 to 1 GeV, test of validity of leptonic selection rules from colliding-beam, (E), 25:14515
interactions $e^+ + e^- \to \pi^+ + \pi^- + \gamma$ in storage rings, study of even-charge hadronic systems from, (T), 25:14621
interactions $e^+ + e^-$ at 0.8 to 1 GeV, production of heavy leptons in, (E), 25:14517
interactions $e^+ + e^-$, in storage rings, study of even-charge conjugation hadronic systems from production of hadronic states and photon in, (T), 25:14621
interactions $\gamma + e \to e + \nu +$ anti ν, stellar energy loss rate from cross sections for, (T), 25:14650
interactions $\gamma + e$ at high energies, leading singularity in complex angular momentum plane in quantum electrodynamics for asymptotics of, (T), 25:14802
interactions $\nu + e \to \nu + e + \gamma$, γ energy and angular distribution and radiative corrections for total effective cross sections for, (T), 25:14600
interactions with hadrons, scaling, fixed poles, and sum rules for, 25:14614
interactions with photons, kinetic theory of, 25:14490 (AD-711681)
interactions with plane-wave electromagnetic pulses, (T), 25:14506
magnetic moment of, vacuum polarization contributions to sixth-order anomalous, 25:14616
mass shift in cesium-133 in intense electromagnetic field, (E), 25:14514
motion in constant electric fields, differential probability of quantum processes in, 25:14498
motion in laser beams, covariant classical, (T), 25:14506
photon scattering by, in Van Allen belt, inverse Compton solar, (T), 25:14108
precipitation into auroral zone, (E), 25:14103
production in lower ionosphere by solar corpuscular streams, (T), 25:14126
production in lower ionosphere by solar particles, (E/T), 25:14124
production in $\mu \to e + \nu +$ anti ν decay, weak interaction model for energy spectrum for, (T), 25:14631 (ITF-70-64)
production of heavy, in electron reactions with nuclei at high energies, upper limits for coupling constant for, (E), 25:14529
propagation of 40-keV, in solar flares, (E), 25:13894
reactions (e,e'p) with nuclei, cross section expression for, (T), 25:15156
reactions with aluminum and copper at 30 keV, Monte Carlo calculation of energy losses and depth distribution of x-ray production in, 25:14400
reactions with argon, chlorine, and xenon at 3 to 16 keV, cross sections for excitation of K x rays in, (E), 25:14008
reactions with argon, helium, and neon at 10 keV, determination of oscillator strengths from coincidence measurements of electrons and ions from, 25:14003
reactions with argon, helium, and neon up to 150 eV, excitation, ionization, and formation of negative-ion resonances in, (E), 25:14002
reactions with atomic and molecular gas jets at 2 to 10 keV, spectra from vacancy cascades produced in, (E), 25:14038
reactions with barium and strontium ions, effective cross sections for transitions between excited states in, (E), 25:14000
reactions with carbon dioxide, nonresonant vibrational excitation in, (T), 25:14028
reactions with deuterium molecules at 10 to 500 eV, cross sections for production of 2s atoms in, (E), 25:14045
reactions with heavy nuclei, gamma spectra from, 25:15204
reactions with helium ions, experimental method for study of excitation to 2P state in, 25:14042
reactions with krypton and xenon up to 150 eV, ionization cross sections for, (E), 25:14002
reactions with krypton at 40 to 140 eV, excitation functions of spectral lines of Kr II in, (E), 25:14040
reactions with liquid helium at 160 keV, optical and infrared emission spectra from, (E), 25:13973
reactions with mercury atoms at 25 to 180 eV, differential cross sections and angular dependence of spin polarization in, (E), 25:14039
reactions with nitrogen molecules at 0.07 to 4.0 keV, cross sections for excitation of N_2^+ first negative and Meinel bands in, (E), 25:13997
reactions with nitrogen molecules at 0.5 to 20 keV, excitation functions for first negative bands of N_2^+ in, (E), 25:13998
reactions with nitrogen molecules at 16 eV, excitation functions for a ^{1}PI/sub g/ and D$^3\Sigma$/sub u/$^+$ states in, (E), 25:14013
reactions with nitrous oxide at 115 eV, energy-loss spectra and oscillator strengths for, (E), 25:14014
reactions with nuclei at 13.75 GeV in emulsions, direct production of electron pairs from, (E), 25:14525
reactions with nuclei at high energies, angular dependence of cross sections for wide-angle bremsstrahlung and upper limits for coupling constant for heavy electron production in, (E), 25:14529
reactions with potassium at 3.0 to 5.2 eV, differential cross sections for excitation of 4S--4P transition in, (E), 25:14034
reactions with rare gases, distorted-wave calculation of cross sections for excitation in, 25:14015
reflection and transmission by aluminum shields, review of data on, 25:14396 (N-70-37470)
scattering by atoms at 25 to 800 eV, tables of amplitudes and spin polarizations for elastic, (T), 25:13995 (AD-711664)
scattering by atoms at low energies, phase shift in first order in long-range potential for, (T), 25:14019
scattering by atoms at very low energies, relation of Fermi theory of line shifts to elastic, 25:14057
scattering by condensed media, nonrelativistic theory of back-, 25:13961
scattering by hydrogen atoms, variational calculation of bounds for phase shifts in, 25:14024
scattering by linearly polarized radiation, 25:14601
scattering by metallic thick targets at 0.5 to 2.0 MeV, Monte Carlo calculations of angular distributions and energy spectra from back-, 25:13959 (UCRL-19719)
scattering by nuclei, effects of virtual nuclear excitation on cross section of elastic, (T), 25:15166
scattering by nuclei, radial matrix elements for, (T), 25:15195
scattering by potassium at 1.0 to 5.2 eV, differential cross sections for elastic, (E), 25:14034
scattering by rare gases, resonances in elastic, (E), 25:14035
scattering by tungsten at 50 eV to 200 keV, depolarization due to spin flip in triple, (T), 25:14020
scattering gases at low energies, depolarization due to spin flip in triple, (T), 25:14020
slowing down in aluminum and water at 10 to 28 MeV, Monte Carlo study of spectra of, 25:14398
slowing down in aluminum, copper, and water at 10 to 15 MeV, Monte Carlo calculations of, 25:14397
trapping in ionospheric electrostatic double layers, (E), 25:14103
trapping of solar, in closed field lines of magnetosphere, (E/T), 25:14101 (AD-712045)
use for therapy of lung metastases, pleural and peritoneal carcinomas, and skin cancer, dosimetry and methods for fast, 25:13538

ELECTROPLATING
  book: Corrosion Week. 41st Manifestation of the European Federation of Corrosion, 7-12 October, 1968 in Budapest, 25:13636
ELECTROSTATIC ANALYZERS
  design of double-focusing, field considerations in, 25:13325
ELECTROSTATIC FIELDS
  relation to charged-particle acceleration in auroral zone, (E/T), 25:14116
  theory of, under ionospheric conditions, 25:14123
ELEMENT 104
  alpha decay of, effect of α radioactive background in studies of, 25:15017
  separation by cation exchange, chemistry of, 25:13088
ELEMENTARY PARTICLE MODELS
  coherent droplet, with long-range pion exchange for forward peak structure in quasi-two-body hadron interactions, 25:14722
  dual resonance, direct and crossing-symmetric amplitudes for equal-mass spinless scattering in, 25:14823
  dual resonance, Lagrangian approach to $\pi + \pi$ amplitudes in, 25:14697
  dual resonance, multiperipheral bootstrap conditions from coupling-constant sum rule in, 25:14674
  dual-resonance, Adler condition in, 25:14668
  dual-resonance, divergence of two-loop planar graph in, 25:14666
  dual-resonance, factorization and level structure of Balachandran, 25:14665
  dual-resonance, new amplitude in generalized, 25:14675
  dual-resonance, selection rules for resonance decay in, 25:14658
  dual-resonance, symmetry of n-point amplitude in, 25:14822
  dual-resonance, universally coupled vector mesons in, 25:14667
  exchange, convergent power series for absorption corrections to amplitudes in, 25:14831
  extended-particle, angular distribution of secondaries in, 25:14661
  fireball, definition of, 25:14669
  Glauber, for $\pi + d$ interactions, (T), 25:14630
  interference, for resonances in $\pi + \pi$ interactions, 25:14692
  interference, resonances in duality relation with, 25:14678
  multiparticle production, angular distributions from, 25:14661
  multiperipheral, angular distributions of secondaries in, 25:14661
  multiperipheral, complex Regge poles and oscillatory average multiplicity in particle interactions in, 25:14585
  multiperipheral, momentum spectra of hadron secondaries in, 25:14659
  Nishijima, with fifth interaction for nonleptonic weak Hamiltonian, 25:14639
  parton, angular distribution of secondaries in, 25:14661
  Regge dipole, for duality and differential cross sections for A_2 production in $\pi^- + p \to$ eta + n interactions, 25:14704
  Regge pole eikonal, for amplitude and differential cross sections for $\pi^+ + n \to \Delta^{++} + \pi^-$ interactions, 25:14715
  sigma, unitary amplitude of $\pi + \pi$ interactions in, two-loop approximations to propagators for, 25:14683 (NYO-2262-TA-219)
  statistical isospin, for final-charge-state cross section ratios for $\pi^- + p \to N + m\pi$ interactions at 1 to 16 GeV, (T), 25:14700 (JINR-P1-5471)
  statistical, for cross sections for meson and baryon production in N + N and meson-baryon interactions at high energies, 25:14680 (INP-719)
  statistical, for cross sections for meson production in anti N + N interactions at high energies, 25:14680 (INP-719)
  thermodynamic, for atlas of particle-production-momentum spectra from p + p interactions below 800 GeV/c and proton reactions with nuclei below 70 GeV/c, 25:14733 (NP-18660)
  Van Hove, nonleptonic hyperon decay in, 25:14637 (SU-1206-238)
  Veneziano amplitude, 25:14630
  Veneziano, amplitude of off-mass-shell $A_1 + \pi \to \pi + \pi$ interactions in, 25:14698
  Veneziano, coupling of normal-parity resonances to all channels in, 25:14681 (INP-730)
  Veneziano, duality and analyticity for Regge poles in representation of, 25:14829
  Veneziano, for amplitudes of meson interactions with mesons, 25:14695
  Veneziano, for mass and angular distributions in anti p + $n \to \pi^+ + 2\pi^-$ interactions at 1.0 to 1.6 GeV/c in deuterium bubble chamber, 25:14548
  Veneziano, four-point functions for mass spectra and angular distributions for anti N + N $\to$ K + anti K + π interactions at rest in, 25:14691
  Veneziano, frame dependence of vector dominance in, 25:14710
  Veneziano, interference model for resonances in $\pi + \pi$ interactions from amplitude in, 25:14692
  Veneziano, $K^- + p \to \pi^- + \pi^+ + \Lambda$ in generalized, 25:14716
  Veneziano, level degeneracy of generalized N-particle dual amplitude with satellites in generalized, 25:14826
  Veneziano, mass spectra of resonances in generalized, 25:14681 (INP-730)
  Veneziano, review of meson interactions with mesons in, 25:14688
  Veneziano, selection rules for two-body reactions in generalized, 25:14681 (INP-730)
  Veneziano, spinning particle amplitudes in dual multi-, 25:14586
  Veneziano, SU(2) symmetry from unitarity constraints on amplitudes in, 25:14754
ELEMENTARY PARTICLE MODELS (BOOTSTRAP)
  coupling constant sum rule from duality for, 25:14674
  interactions $\pi + \pi$ in, amplitude expansion on Mandelstam triangle for, 25:14678
ELEMENTARY PARTICLE MODELS (TRIPLET)
  Adler condition in dual relativistic quark, 25:14685
  baryon and meson mass spectra in nonlinear quark, relativistic and SU(3)-invariant equations for, 25:14684
  baryon resonance mass and partial decay widths in symmetric quark, negative-parity, 25:14718
  baryon--baryon and meson--baryon interactions in quark, relations between transversity amplitudes for, 25:14671
  commutation relations for sum rules for amplitudes of π production from photon-hyperon interactions in quark, 25:14619
  interactions γ + N in quark, total-cross-section relations for, 25:14595 (ITF-70-63-P)
  interactions γ + p at high energies in quark, constant of, 25:14595 (ITF-70-63-P)
  meson radiative decays in quark loop, coupling constant relations, branching ratios, and widths of, 25:14686
  photon reactions with nuclei in quark, total-cross-section relations for, 25:14595 (ITF-70-63-P)
  resonance decay correlations from meson--baryon interactions in quark, 25:14712
  statistical tensors for scattering amplitudes in quark, measurable, 25:14670
ELEMENTARY PARTICLES
  bound state of three resonantly interacting, in carbon-12 and tritium, (T), 25:14591
  decay helicity amplitudes of, kinematic singularities of, 25:14592
  decay of, phase space integral for quantities analogous to statistical parameters for, (T), 25:14584 (NP-18652)
  decay of, radiative, (T), 25:14630
  electromagnetic interactions of, angular distributions and differential cross sections for $\pi^- + p \to \gamma + n$ interactions at 1245 and 1337 MeV for validity of isospin rule for, (T), 25:14567
  interactions at high energies, conference on, (E/T), 25:14583(T) (AEC-tr-6882/1)
  interactions at high energies, phase space integral for quantities analogous to statistical parameters for, (T), 25:14584 (NP-18652)
  interactions at high energies, strict conformal symmetry for mass-shell amplitudes of, (T), 25:14820 (RLO-1388-598)
  interactions at rest, crossed-channel E(2) expansion of amplitude of, (T), 25:14753
  interactions of spinless, nonrelativistic time-dependent theory for Coulomb potential in two-body, (T), 25:14624
  interactions of spinning, dual multi-Veneziano amplitudes of, (T), 25:14586
  interactions of spinning, O(4) symmetry properties of amplitudes of, (T), 25:14757
  interactions of, effects of reaction mechanism and phase-space in cross sections for many-body, 25:14594
  interactions of, multiperipheral models for complex Regge poles and oscillatory average multiplicity in, (T), 25:14585
  interactions of, quark model predictions for measurable statistical tensors for amplitudes of, 25:14670
  interactions with scalar, at high energies and small and large angles, solution of unitarity relation for amplitude and spinor particle polarization in elastic, (T), 25:14590
  interactions with spin-$^1/_2$, at high energies and small and large angles, solution of unitarity relation for amplitude and spinor particle polarization in elastic, (T), 25:14590
  invariance principles for, conference on, 25:14750
  motion of, P, C, and T properties and invariance with respect to group P(1,n) for Dirac equations of, (T), 25:14747 (ITF-70-70)
  production in expanding universes, field quantization for, 25:14788
  production in interactions at high energies, phase space integral for quantities analogous to statistical parameters for multiple, (T), 25:14584 (NP-18652)
  production in particle interactions at high energies, multiperipheral models for complex Regge poles and oscillatory average multiplicity in, (T), 25:14585
  production of, angular distributions for multiple, 25:14661

  production of, test of SU(3) symmetrical statistical theory of, (T), 25:14748 (JINR-P2-5480)
  quantization of relativistic bound state of two point, Bohr, 25:14588
  reactions with nuclei at very high energies, multiplicity in, (T), 25:14736
  Regge trajectories of, mass dependence of, 25:14662
  scattering by Coulomb field, exact Regge-multiperipheral amplitude for bremsstrahlung production from, 25:14613
  search for quasi-stable, in new-type radioactivity from proton reactions with aluminum and tungsten at 70 GeV, (E), 25:14541 (JINR-P1-5399)
  strong interactions at high energies in multiperipheral model, momentum spectra of secondaries from, (T), 25:14659
  strong interactions at high energies, angular distributions of secondaries from multiparticle production in, (T), 25:14661
  strong interactions at high energies, complex angular momentum theory of three-particle production in two-body, (T), 25:14677
  strong interactions at high energies, Pomeron hypothesis for exchange degeneracy for oscillating total cross sections of, (T), 25:14656 (SU-1206-237)
  strong interactions at high energies, two-Reggeon exchange contributions to, (T), 25:14657 (UCRL-20032)
  strong interactions of equal-mass, amplitude expansion on Mandelstam triangle for, (T), 25:14678
  symmetry for, Dirac representation of relativistic, 25:14752
  symmetry for, induced realization theory for chiral, (T), 25:14749
  weak interactions of, higher-order terms in current--current theory of, 25:14647
  weak interactions of, Nishijima model with fifth interaction for nonleptonic, 25:14639
  weak interactions of, q^2 dependence of form factors for parameter fit for Cabibbo theory of, 25:14632 (KFKI-70-23-HEP)
  weak interactions with one- and two-photon emission and virtual photon, W-boson theory for divergences in amplitudes of nonleptonic, (T), 25:14655
ELEMENTARY PARTICLES (TRIPLET)
  interactions of quarks with antiquarks, N/D calculation using discontinuity of second-order four-point function interaction as input for π^+ and rho$^+$ bound states in, (T), 25:14676
  mass of, lower limits for, (E), 25:14065
  search for, in primary cosmic radiation, (E), 25:14065
ELEMENTS
  determination in minerals by neutron activation using californium-252 as neutron source, 25:12962
  determination of thirty-eight trace, in Bruderheim chondrite by neutron activation and radiochemical separation, 25:12969
  equations of state for 35 solid, calculation of baric coupling coefficients for, 25:13681
  photon reactions at 1 keV to 100 MeV with Z = 1 to 100, tables of cross sections for coherent and incoherent scattering, pair production, and photoelectric ejection in, 25:14409
ELK RIVER POWER REACTOR
  maintenance during August 1970 to February 1971, 25:15215 (DOCKET-1151-39)
  surveillance activities during August 1970 to February 1971, 25:15215 (DOCKET-1151-39)
EMBRYOS
  radiation effects on DNA content in pro-, stages of barley, ionizing, 25:13405
ENGINEERING
  research at BNL, July 1969--June 1970, 25:14837(R) (BNL-50230)
ENVIRONMENT
  contamination by gaseous wastes from conventionally-fueled and nuclearly-stimulated natural gas-fueled power plants, comparison of, 25:13430 (UCRL-72830)
  contamination by nuclear power plant effluents, recommendations for preventing, 25:13437
  radioactivity in nuclear power plants, control of, 25:13471
  radioactivity monitoring in, near AEC installations, 25:13445
  radioactivity monitoring in, of harbors containing support facilities for U. S. Naval nuclear-powered ships to determine adequacy of waste disposal limits and procedures during 1969, 25:13444
ENZYMES
  effects on DNA in uv-irradiated Escherichia coli, 25:13411
  effects on γ and x-radiosensitivity of human skin, 25:13583
EPOXY RESINS
  development of fiber glass reinforced, for lining spent fuel element storage tanks, 25:15412
  fabrication and use for testing simulated pressure vessels under complex stress, 25:13658 (ORNL-4590, pp 135-232)
EQUIPMENT AND PROCEDURES
  development of industrial process control, using neutrons, 25:13177
ERBIUM
  complexes with carminic acid, spectrophotometric studies on, 25:12937
  determination in plutonium oxide--uranium oxide fuels by solvent extraction and emission spectrography, 25:12922 (WHAN-SA-44)
  determination of trace amounts of, in plutonium and plutonium dioxide--uranium dioxide by solvent extraction and emission spectrography, 25:12923 (WHAN-SA-47)
  energy-level excitation by neutron capture gamma rays, (E), 25:15002
ERBIUM ALLOYS AND SYSTEMS
  Er--Mn--Pr, crystal structure of, 25:13707
  Er--Mn--Pr, magnetic properties of, 25:13707
ERBIUM IONS
  electron spin resonance in thoria single crystal, 25:14478
ERBIUM ISOTOPES Er-166
  energy levels from holmium-166 beta decay and thulium-166 beta and electron-capture decay, spin--parity assignments and mixing parameters for, (E/T), 25:14984 (NP-18536)
  energy-level transitions from holmium-166 beta decay and thulium-166 beta and electron-capture decay, multipolarities, log-ft values, and rates for E2, (E/T), 25:14984 (NP-18536)
ERBIUM ISOTOPES Er-167
  neutron capture by, energy levels of erbium-168 from thermal, (E), 25:15000
  neutron transmission by polarized, spins of resonances and hyperfine coupling constants for polarized, (E), 25:15003
ERBIUM ISOTOPES Er-168
  energy levels from thermal neutron capture by erbium-167, (E), 25:15000
ERBIUM ISOTOPES Er-170
  neutron capture by, γ spectra and Q-value for thermal, (E), 25:15059
ERBIUM ISOTOPES Er-171
  energy levels from erbium-170 thermal neutron capture, spin-parity assignments for, (E), 25:15059
ERBIUM SILICIDES
  magnetic properties and structure of ErSi, 25:14434 (CEA-CONF-1701)
ERYTHROCYTES
  mass in patients in relation to plasma volume, use of chromium-51 and iodine-125 in double tracer dilution method for measuring, 25:13338
  phosphorus-32 uptake by, of rats for determining correlation of phosphorated erythrocytic metabolism with second and third phase of general adaptation syndrome, 25:13335
  preparation of metastable technetium-99-labeled, for erythrocyte mass determinations, method for, 25:13332
ETHANE
  radiolysis of liquid, containing deuterium sulfide, mechanism and yields from γ, 25:13048
ETHANE, HEXACHLORO-
  yields from γ radiolysis of carbon tetrachloride, effects of scavengers on, 25:13045
ETHANE, HEXAPHENYL-
  radiation effects on radical formation in, 25:13374
ETHANESULFONIC ACID, 2,2,2-TRIFLUORO-
  preparation, reactivity, and structure of, for use in solvolysis studies on leaving groups, 25:15421 (COO-1008-14)
ETHANOL
  effects on separation of cesium from sodium by ion exchange using Zeolite Linde A, 25:13091
  radiolysis at 25°C, yields from γ, 25:13056
ETHYL ETHER
  complexes with boron trifluoride, analysis for boron-10/boron-11, emission spectroscopic method for, 25:12928
ETHYLENE
  effects on yields from γ radiolysis of carbon tetrachloride at 25°C, 25:13045
  sorption by polycrystalline tungsten surfaces, relations with nitrogen sorption, 25:13687
ETHYLENE POLYMERS
  radiation effects on gas permeation and separation properties of films of, γ, 25:13039
  radiation effects on permeation characteristics of fully swollen membrane of, γ, 25:13041
  radioactive waste incorporation in, feasibility studies of, 25:13197
  radioinduced graft polymerization of liquid styrene on films of, tensile properties of compounds produced by γ, 25:13042
  shielding effects of, against radiation dose from x-ray diffraction apparatus, 25:13457
ETHYLENE, TETRACHLORO-
  yields from γ radiolysis of carbon tetrachloride, effects of scavengers on, 25:13045
ETHYLENE, TETRAFLUORO-, POLYMERS
  radiation effects on wastes of, preparation of perfluorinated carboxylic acids by, 25:13035(P)
  radioinduced peroxy radicals in, ESR spectral studies on molecular motion of γ, 25:13034
ETHYLENIMINE
  effects on α-amylase activity in Aspergillus oryzae, combined effects of x radiation and, 25:13381

effects on Bacillus mesentericus in comparison with effects of fast neutrons and uv mutagenic, 25:13416
EUMYCOTA
  Aspergillus nidulans, radioinduced mutations in, for morphological changes, uv, 25:13423
  Aspergillus oryzae, radiation effects on α-amylase activity in, combined effects of ethylenimine and x, 25:13381
  Candida utilis, labeling with carbon-13, 25:13331 (LA-4551)
  Dictyostelium discoideum, radioinduced spore germination in, cobalt-60 γ, 25:13605
  Nannizzia incurvata, radioinduced mutations in, for reduced virulence, polyfactorial basis for uv, 25:13427
  Neurospora crassa, radioinduced mutations of, for morphological change, uv, 25:13424
  Saccharomyces cerevisiae, radioinduced mutations in, for prototrophs, relationship of DNA replication to x, 25:13425
  Saccharomyces sp., metabolism of DNA in, in relation of radiosensitivity, 25:13604
  Schizosaccharomyces pombe, radiosensitivity of, effects of caffeine and stage of growth on uv, 25:13606
EUROPIUM
  complexes with carminic acid, spectrophotometric studies on, 25:12937
  content and depth in crustal basalts and granites in USSR, 25:13115
  determination in neutron-irradiated graphite by γ spectrometry, 25:12954
  determination in plutonium oxide--uranium oxide fuels by solvent extraction and emission spectrography, 25:12922 (WHAN-SA-44)
  determination of trace amounts of, in gadolinium oxide and yttrium oxide by x-ray-excited optical luminescence, 25:12948
  determination of trace amounts of, in plutonium and plutonium dioxide--uranium dioxide by solvent extraction and emission spectrography, 25:12923 (WHAN-SA-47)
  reduction of trivalent, in perchlorate medium, polarographic studies on, 25:13020
  separation from aqueous chloride solutions by solvent extraction using dioctyl phosphate in benzene or heptane, effects of variables on, 25:13096
EUROPIUM ISOTOPES Eu-147
  energy level of, g-factor of second excited, (E), 25:15016
EUROPIUM ISOTOPES Eu-149
  energy level of, g-factor of second excited, (E), 25:15016
EUROPIUM ISOTOPES Eu-152
  beta and electron-capture decay of, gamma spectra and angular correlations in, (E), 25:14985 (NP-18615)
EVOLUTION
  rates of, numerical modeling of, 25:15435 (LA-4573)
EXPERIMENTAL BREEDER REACTOR-II
  operations summary for December 1970, 25:15339 (ANL-7765)
EXPLOSION CLOUDS
  bibliography on growth of nuclear, 25:13131 (AAEC/LIB/Bib-255)
  particle size distribution in nuclear, parameters for, 25:13138
EXPLOSIONS
  crater formation in Greenland icecap snow by chemical, dimensions and mechanisms of, 25:13133 (AD-711861)
  craters from underground, effects of seepage characteristics of surrounding media on slope stability of, 25:13102 (NCG-TR-27)
  effects of distant underground, on motion of earth dams, digital computer programs for predicting, 25:13130 (UCRL-13329(Pt.2))
  ground motion from distant underground chemical, equations for predicting, 25:13129 (AD-713521)
EXPLOSIVES
  crater formation by row-emplaced, equations for predicting linear, 25:13135 (AD-713574)
  response of solid, to sustained shock loading, 25:15466 (UCRL-50950)
EXPONENTIAL PILES
  neutron spectra in STSF-7, time-of-flight measurements of, 25:15388(R) (GULF-RT-10421)
EYES
  radiation effects on electroretinogram of, of frog, effects of fluorescein on uv, 25:13573

F

FALLOUT
  monitoring in USA, use of iodine-131 content of thyroid gland in beef cattle for, 25:13397
  monitoring of, maintenance manual for Weapons Effects Display System for, 25:13323 (UCRL-50892(Vol.4)(Pt.2))
  monitoring of, maintenance manual for Weapons Effects Display System for, 25:13322 (UCRL-50892(Vol.4)(Pt.1))
  simulation of field, using cesium, cobalt, or lanthanum isotopes, 25:13117 (AD-711532)
  tritium content of Australian, 1967 to 1969, 25:13120 (NP-18638)
  tritium content of Australian, 1969 to 1970, 25:13102 (NP-18639)
FAST FLUX TEST FACILITY
  cooling system for, design of remotely operated sodium analysis system for, 25:13195 (WHAN-SA-91)
  instrumentation for, development of, 25:13318(R) (ORNL-4620)
FAST TEST REACTOR
  fuel elements for, performance of stainless steel clad plutonium oxide (PuC_2)--uranium oxide (UO_2), (E/T), 25:15367 (WHAN-SA-51)
  fuel pins for, design of shipping container for, 25:13187 (BNWL-1512)
FECES
  radioisotope content of, of cattle following intravenous and oral administration, cerium-144 and scandium-46, 25:13352
FELDSPARS
  magnesium isotope abundances in lunar and terrestrial, (E), 25:13864
FERMI FAST BREEDER REACTOR
  boiler for, testing of, 25:15255 (DOCKET-50016-97)
  buildings and structures for, safety analysis of, 25:15253 (DOCKET-50016-95)
  components for, simulation testing of, 25:15255 (DOCKET-50016-97)
  containment structure for, leak rate testing of, 25:15255 (DOCKET-50016-97)
  control elements for, safety analysis of, 25:15247 (DOCKET-50016-89)
  control systems for, safety analysis of, 25:15252 (DOCKET-50016-94)
  coolant for, boiling and reaction testing of liquid sodium, 25:15255 (DOCKET-50016-97)
  cooling system for, safety analysis of, 25:15252 (DOCKET-50016-94)
  core for, safety analysis of, 25:15247 (DOCKET-50016-89)
  design parameters of, safety analysis of, 25:15247 (DOCKET-50016-89)
  electrical systems for, safety analysis of, 25:15252 (DOCKET-50016-94)
  fuel elements for, fabrication and testing of, 25:15255 (DOCKET-50016-97)
  fuel handling facilities for, safety analysis of, 25:15253 (DOCKET-50016-95)
  hazards analysis for, 25:15248 (DOCKET-50016-90)
  kinetics of, safety analysis of, 25:15256 (DOCKET-50016-98)
  operation of, license application for, 25:15251 (DOCKET-50016-93)
  operations aspects of, safety analysis of, 25:15254 (DOCKET-50016-96)
  personnel of, training program for, 25:15254 (DOCKET-50016-96)
  physics measurements for, safety analysis of, 25:15247 (DOCKET-50016-89)
  piping systems for, requested additional information on sodium service, 25:15250 (DOCKET-50016-92)
  pressure vessel for, safety analysis of, 25:15247 (DOCKET-50016-89)
  radioactive waste disposal system for, safety analysis of, 25:15253 (DOCKET-50016-95)
  shielding for, safety analysis of, 25:15253 (DOCKET-50016-95)
  site for, safety analysis of, 25:15256 (DOCKET-50016-98)
  steam and power conversion systems for, safety analysis of, 25:15252 (DOCKET-50016-94)
  technical specifications for, proposed, 25:15249 (DOCKET-50016-91)
  testing programs for, safety analysis of, 25:15256 (DOCKET-50016-98)
  testing programs for, safety analysis of, 25:15255 (DOCKET-50016-97)
  testing programs for, safety analysis of, 25:15254 (DOCKET-50016-96)
FERMI POWER REACTOR, UNIT 2
  auxiliary power supply for, preliminary safety analysis of, 25:15323 (DOCKET-50341-25)
  design parameters for, revised and additional data on, 25:15324 (DOCKET-50341-26)
  design parameters of, requested additional information on, 25:15323 (DOCKET-50341-25)
  fuel storage pool for, tornado protection for spent, 25:15324 (DOCKET-50341-26)
  operations aspects of, requested additional information on, 25:15323 (DOCKET-50341-25)
  pumps for, requested information on missile protection requirements for coolant, 25:15324 (DOCKET-50341-26)
  radioactive effluents from, preliminary safety analysis of, 25:15323 (DOCKET-50341-25)
  site for, geological data for emergency cooling water reservoir, 25:15324 (DOCKET-50341-26)
  site for, monitoring equipment for, 25:15323 (DOCKET-50341-25)
  turbine for, requested information on missile protection requirements for, 25:15324 (DOCKET-50341-26)
FERMIONS
  ground-state energy of mixture of, and bosons in one dimension with repulsive delta-function interaction, (T), 25:14501
  interactions of, finite formulation of four-body, (T),

  25:14797
  interactions with pseudoscalar bosons, infinite momentum limit of spinor field theory for, (T), 25:14679
  interactions with scalar particles at high energies and small and large angles, solution of unitarity relation for amplitude and spinor particle polarization in elastic, (T), 25:14590
  mass in field-theoretic models, relation between bare and physical, 25:14800
FERMIUM
  production and uses of, review on, 25:13059
FERMIUM ISOTOPES Fm-257
  fission of, fragment mass symmetry and kinetic energy distribution in spontaneous, (E), 25:15045
FERROMAGNETIC MATERIALS
  exchange coupling of magnetic moments in rare earths, modification of Ruderman--Kittel--Kasuya--Yoshida mechanism for pressure dependence, 25:14487
  model of impure, investigation of Heisenberg, 25:15420(T) (BNL-tr-390)
  neutron inelastic scattering by, conference on, Tokai, Japan, 12/69, (E/T), 25:14436 (JAERI-1197)
  ordering in small Heisenberg spin systems, effects of symmetry-breaking magnetic field on, (T), 25:14493
FETUSES
  radiation hazards to human, from placental localizaton using metastable indium-113, 25:13502
FIBRINOGEN
  effectiveness of iodine-131-labeled, for scanning of experimentally induced thrombi in animals, 25:13518
FIELD THEORY
  fields in, generators of Lorentz group for local tensor, 25:14718
  Hamiltonian formalism on characteristic surfaces in massless scalar, 25:14773
FILMS
  electron energy-loss spectra in thin, multiple-plasmon effects in, (T), 25:14486
  thickness of, electron backscatter method for measurement of, 25:13141
FILTERS
  cleaning of, used in removal of radioactive impurities, method for, 25:13094(P)
  design, installation, and testing of high-efficiency, for radioactive contaminant removal, 25:13192 (NACAR-10012)
FIRES
  propagation from nuclear explosions, evaluation of models for simulating, 25:13134 (AD-713418)
FISSION
  barrier to, exact calculation of penetrability through two-peaked, 25:15004
  theory of photoinduced, dynamic collective model for, 25:15198
  theory of, sudden model for, 25:15024
FISSION FRAGMENTS
  effects on bubble nucleation in superheated water, 25:13152(R) (SU-326-P-13-5)
  K x-ray emission at 0 to 1 μsec from uranium-235, 25:15027
  tracks in Japanese obsidian, rock age estimates from, (E), 25:13112
FISSION PRODUCTS
  content of, computer program for calculating, (T), 25:15141 (DEMO-70/10)
  distribution in fuel particle coatings of pyrolytic carbon and layered pyrolytic carbon and silicon carbide, sputtering method for determination of, 25:13758
  neutron absorption cross sections for gross, thermal, (E/T), 25:15100
  neutron absorption cross sections for gross, thermal, (T), 25:15099
  neutron total cross sections and resonance parameters for, (E), 25:15098
  production in neutron fission of plutonium-239, release curves for krypton and xenon, (T), 25:14989 (UCRL-50656(Suppl.))
  re-solution of gaseous, in uranium dioxide fuels, effects of neutron irradiation on, 25:13780(R) (GEAP-12147)
  reactivity worths in fast reactor spectra, (E/T), 25:15350
  separation of, development of electrochemical methods for, 25:13095
  yields from thermal neutron fission of uranium-235, (T), 25:15099
FISSIONABLE MATERIAL
  neutron cross sections for, least-squares method for shape analysis of, 25:15132
  neutron fission at thermal energies to 15 MeV, review of mean prompt neutron production from, 25:15119
  recovery from chemical decladding solutions, crystallization method for, 25:13090(P)
  shipping of, East German regulations for safe, 25:13194 (SZS-19/70)
FLORIDA
  radioisotope content of sands and soils of south, Feb. to June 1968 measurements of fission products and natural, 25:13107
FLUID FLOW
  effects on transversal vibrations of fuel rods, analysis of parallel flow turbulence, 25:15213
  equations for, particle-in-cell method for computer simulation of model, 25:15431 (CU-3954-3)
  heat and mass transfer in turbulent, theory for, 25:13160
  heat transfer in laminar, through concentric annuli, model for low Peclet number, 25:13159
  magnetic field from conducting, Joule dissipation at boundary layer of, 25:14099
  magnetohydrodynamic generalized Couette, with uniform suction, time-dependent pressure gradient, and arbitrary initial velocity, (T), 25:14091
  magnetohydrodynamic Rayleigh problem in, with unsteady wall motion, (T), 25:14089
  magnetohydrodynamic, effects of variable properties in finite ducts on, (T), 25:14090
  magnetohydrodynamic, in infinite cones, viscous incompressible, (T), 25:14096
  magnetohydrodynamic, intrinsic motions in, (T), 25:14093
  magnetohydrodynamic, motion due to line sink in uniform magnetic field in, (T), 25:14096
  magnetohydrodynamic, temperature field in boundary layer on porous wall in oscillatory, (T), 25:14095
  measurement of two-phase, in multirod fuel element bundles, 25:13150(R) (GEAP-10253)
  temperature distribution in turbulent liquid sodium, in triangular fuel rod clusters, (T), 25:15363
  velocity distribution of turbulent liquid sodium, in triangular fuel rod clusters, (T), 25:15363
FLUIDIZED BEDS
  design for vapor deposition of vanadium on uranium dioxide spheres, 25:13737 (KFK-1292)
  gas mixing in, effects of bed dimensions and gas velocity on, 25:13140 (BMBW-FBK-70-26)
  gas velocity for spouting, 25:13139 (AERE-R-4852)
  performance of shallow spouting, 25:13139 (AERE-R-4852)
FLUIDS
  charged-particle scattering by two-species quantum, Born approximation to cross sections for, 25:13965
  neutron scattering by two-species quantum, Born approximation to cross sections for, 25:13965
  photon scattering by two-species quantum, Born approximation to cross sections for, 25:13965
FLUORESCEIN
  effects on electroretinogram of frog following exposure of eyes to 366 nm uv, 25:13573
FLUORIDES
  determination by potentiometric titration using lanthanum or thorium, 25:12929
FLUORINE
  determination as contaminant on surface of silver-coated copper wiring on lunar module by proton microprobe method, 25:12961
  determination in organic compounds using thorium chloranilate, effects of iron on spectrophotometric, 25:12936
  determination in silicon by γ photon activation, 25:12971
  electron correlation in molecular, calculation using semiempirical pseudopotential procedure, 25:14055
FLUORINE ISOTOPES F-18
  reactions of recoil atoms of, in liquid octafluorocyclobutene and hexafluorocyclobutene, effects of radical scavengers on, 25:13066
FLUORINE ISOTOPES F-19
  determination by pulsed neutron activation and scintillation counting, 25:12960
  neutron inelastic scattering by, cross sections for fast, (E), 25:14960
  neutron reactions (n,2n) with, fission-spectrum-averaged activation cross sections for, (E), 25:14968
  neutron reactions (n,xγ) at 14 MeV, cross sections for, (E/T), 25:14920(T) (BNL-tr-380)
FLUORINE SYSTEMS
  F--Th, thermodynamic properties of cations formed in ammonium nitrate solutions of, at 5, 25, and 45°C, 25:13022
FLUORITES
  determination in pulp flow by fast neutron activation and γ spectrometry, 25:12976
FOOD
  cesium-137 accumulation in, effects of uptake from soil on, 25:13340 (NP-18382)
  effects of intake of, on iodine-131 uptake by perfused intestine and liver of irradiated rats, 25:13349
  radiation processing of packaged, for commercial sales, 25:13622
FORBUSH DECREASES
  effects on magnetic-field structure, (T), 25:14070
  model for, leaky-piston, (T), 25:14073
FORENSIC SCIENCE
  postage stamp analysis by neutron activation in, 25:12973
FORKED RIVER POWER REACTOR, UNIT 1
  design parameters of, revised and additional data on, 25:15330 (DOCKET-50363-11)
  operations aspects of, revised and additional data on, 25:15330 (DOCKET-50363-11)
FORMALDEHYDE
  detection of interstellar, by microwave absorption, (E/T), 25:13845
  spectral absorption lines due to, in supernova remnants,

UM

(E), 25:13837

FRANCE
  radioisotope accumulation by crops and soils in, from fallout and industrial wastes, cesium-137, iodine-131, and strontium-90, 25:13402

FREE RADICALS
  decay of radiolytic, in poly(methyl methacrylate), ESR studies on, 25:13058
  radioinduced in aqueous solutions of hydrogen peroxide and 2-propanol, effects of trivalent titanium on kinetics of reactions of γ, 25:13032
  radioinduced in glassy tetrahydro-2-methylfuran, ESR spectral studies on effects of photobleaching on trapped, 25:13033
  radioinduced in poly(tetrafluoroethylene), ESR spectral studies on molecular motion of peroxy, 25:13034
  radioinduced production in p-toluidine hydrochloride monocrystals, ESR spectral studies on γ, 25:13051

FRUCTOSE
  radioinduced decrease of content of, in dorso-lateral prostates of rats, x, 25:13366

FRUITS
  radiation processing of, effects of, on insects and microorganisms, review of, 25:13623
  strawberries, radiation processing of juice or puree of, effects of, on chromosomes of Vicia faba, aberrant, 25:13621

FS-85 (NIOBIUM ALLOY)
  cracking sensitivity of, Varestraint testing of hot, 25:13695

FUEL CAPSULES
  contamination of SNAP-15C, analysis of, 25:13164 (MLM-1670)
  corrosion of SNAP-19B, by seawater, 25:13163 (MLM-1652)
  design, development, and testing of SIREN radioisotope, 25:13170 (SNC-2708-1)
  testing of radioisotope SIREN, phase 1A final impact, 25:13171(R) (SNC-2708-2)
  testing of SNAP-23A, at 1450 to 1850°F, method for fire, 25:13166(R) (MMM-4187-1)

FURAN, TETRAHYDRO-2-METHYL-
  radioinduced trapped radicals in glassy, ESR spectral studies on effects of photobleaching on γ, 25:13033

FURNACES
  level indicator for blast, design of gamma radiometric, 25:13307

G

GADOLINIUM
  complexes with carminic acid, spectrophotometric studies on, 25:12937
  determination in plutonium oxide--uranium oxide fuels by solvent extraction and emission spectrography, 25:12922 (WHAN-SA-44)
  determination of trace amounts of, in plutonium and plutonium dioxide--uranium dioxide by solvent extraction and emission spectrography, 25:12923 (WHAN-SA-47)
  electron energy losses at 52 to 92 MeV in, (E), 25:14392 (AD-711005)
  Ettinghausen effect measurements on polycrystals and monocrystals of, 25:14475
  magnetic susceptibility near Curie point of single crystal of, temperature dependence of initial paraprocess, 25:14446
  neutron capture at 0.001 to 1 MeV, cross sections for, (E), 25:15121
  reduction of trivalent, in perchlorate medium, polarographic studies on, 25:13020
  structure of films work function of films of, on molybdenum (110) surface, 25:13700
  thermoelectromotive force at 90 to 250°K, effects of longitudinal magnetic field on, (E/T), 25:14458

GADOLINIUM ALLOYS AND SYSTEMS
  Gd--Lu, thermal capacity at 0.06 to 0.16°K, effective magnetic field at lutetium nuclei from, 25:14450

GADOLINIUM ISOTOPES
  nuclear deformation parameters and optical isotope shifts for, estimates of, (T), 25:15048

GADOLINIUM ISOTOPES Gd-155
  energy levels from (He-3,α) reactions, spins, parities, and angular momentum of, (E), 25:15138

GADOLINIUM ISOTOPES Gd-156
  helium-3 reactions (He-3,α) at 20.3 MeV, angular distributions from, (E), 25:15138

GADOLINIUM ISOTOPES Gd-157
  energy levels from (He-3,α) reactions, spins, parities, and angular momentum of, (E), 25:15138

GADOLINIUM ISOTOPES Gd-158
  helium-3 reactions (He-3,α) at 20.3 MeV, angular distributions from, (E), 25:15138

GADOLINIUM OXIDES
  analysis for trace amounts of rare earths by x-ray-excited optical luminescence, 25:12948
  coating of particulate, with molybdenum for use as burnable poison in fuels, 25:13736 (EUR-4551)

GALAXIES
  classification of, review on, 25:13929
  distribution in space, (T), 25:13913
  existence of NGC 7320 in Stephan's quintet, (E), 25:13916
  hydrogen in M82, radio-wave absorption by neutral, (E), 25:13927
  optical observations of, associated with 3C 386, (E), 25:13915
  parameters of, as consequence of primeval cosmological turbulence, (T), 25:13932
  radio-wave absorption in neutral hydrogen in M82, (E), 25:13911 (AD-711299)
  rotation of, (T), 25:13913
  spectrographic observations of 28 Markarian, (E), 25:13923
  stars in SMC, photometry of bright, (E), 25:13921
  stochasticity of dynamical systems with two degrees of freedom, (T), 25:13917
  structure of wing of the SMC, (E), 25:13931

GALLEIN
  uses for spectrophotometric determination of molybdenum, 25:12930

GALLIUM
  content and depth in crustal basalts and granites in USSR, 25:13115

GALLIUM ALLOYS AND SYSTEMS
  Ga--V, superconducting transition temperature of, strain dependence and related effects of, (E), 25:14183
  Ga--Zr-base, phase diagram of eutectoid region of, 25:13709

GALLIUM ISOTOPES Ga-66
  electron-capture decay of, gamma spectra from, (E), 25:14957

GALLIUM ISOTOPES Ga-67
  gamma angular correlations from, (E/T), 25:14975

GAMMA CAMERAS
  development of, review on, 25:13222

GAMMA RADIATION
  detection in tissues following administration of mesons (π) using plastic scintillators, 25:13547
  dose distribution and rate from cobalt-60 and radium slugs in rectangular molds, calculation of, 25:13455
  dose distribution of cobalt-60, in pendulum translation method for therapy, 25:13447
  dose to HeLa cells, effects of atomic number of material used in apparatus on, 25:13456
  dose to man following ingestion of spring water at Masutomi spa area in Japan, 25:13470
  dose to man in Australia and New Guinea following nuclear weapons testing during 1966 to 1968, fallout, 25:13436
  dose to personnel following accidental exposure to iridium-192 vehicle, 25:13466
  dosimetry in human urinary bladder during therapy, comparison of γ meter or isodose curve plotting methods for, 25:13448
  dosimetry in man during therapy, computer method for calculating cobalt-60, 25:13449
  effectiveness for postoperative irradiation of lymph system following surgical removal of mammary carcinomas, dosimetry for cobalt-60, 25:13533
  effectiveness for therapy of bone cancer in comparison to x, phantom studies on cesium-137 and cobalt-60, 25:13536
  effectiveness for therapy of bone tumors in man, evaluation of cobalt-60, 25:13521
  effectiveness for therapy of esophagus fistulas in patients with lymphogranulomatosis, cobalt-60, 25:13542
  effectiveness for therapy of stomach cancer, in relation to survival, effects of grid techniques on cobalt-60, 25:13532
  effectiveness for therapy through plaster casts in man in comparison to fast electrons and x, cesium-137 or cobalt-60, 25:13539
  effectiveness of biaxial pendulum, for therapy of lymph node metastases, effects of dose on cobalt-60, 25:13534
  effects on 1,3-cyclohexadiene in benzene, 25:13037
  effects on 2-pentene at 77 to 125°K, electric conductivity studies on transient species produced by, 25:13027
  effects on 2-propanol vapor at 124 to 400°C, yields from, 25:13046
  effects on 3-methylpentane containing cadmium, lithium, magnesium, potassium, or sodium at 77°K, ESR studies on paramagnetic species produced from, 25:13025
  effects on activity of asparagine synthetase in potatoes, effects of dose on, 25:13365
  effects on activity of hydrolases and content of DNA and protein in lambda strain of Escherichia coli K 12, 25:13371
  effects on ammonia adsorbed on synthetic zeolites, EPR spectral studies on effects of alkali metals and hydrogen on, 25:13057
  effects on antibody activity in spleen cells of mice, analysis of origin of plaque forming cells in, 25:13387
  effects on aqueous solutions of hydrogen peroxide and 2-propanol, effects of trivalent titanium on kinetics of free radical chain reactions in, 25:13032
  effects on basic and neutral aqueous solutions of sodium azide, effects of yields of hydrogen atoms on production of hydrogen molecules from, 25:13044
  effects on blood cells, weight of spleen, and weight of

thymus in rats in comparison to tritium oxide, RBE for cesium-137, 25:13551
effects on blood coagulation in rats, effects of serotonin on cobalt-60, 25:13549
effects on carbon tetrachloride at 25°C, effects of scavengers on yields from, 25:13045
effects on cell structure and glycogen in rat livers, cobalt-60, 25:13378
effects on chicken meat, effects of, on rats following ingestion, 25:13624
effects on chlorophyll production by Sorghum, mutagenic, 25:13420
effects on chromosomes of spermatocytes of mice, aberrant, 25:13404
effects on Clostridium botulinum spores, effects of dose, pH, and temperature on lethal cobalt-60, 25:13611
effects on content of lactate and propionate in blood serum of sheep, 25:13384
effects on content of o-oxyphenol in poplar shoots, 5000 R, 25:13598
effects on crystals of alkali metal salts, luminescence from aqueous release of stored energy produced by, 25:13026
effects on deoxyribonucleoproteins of rabbits, in vitro effects of nuclease on degrading, 25:13363
effects on development of eggs and larvae of Sitophilus oryzae, comparison of cobalt-60, 25:13558
effects on dielectric properties of potassium dihydrogen phosphate crystals, 25:14432
effects on drip loss in fish, effects of pre-dip treatment in sodium tripolyphosphate on, 25:13618
effects on electric capacitors, 25:13327 (LCIE-364)
effects on electric properties of lithium- and aluminum-doped silicon, (E), 25:14412 (N-70-39456)
effects on fertility height, and survival of two species of barley, effects of dose and dose rate on, 25:13603
effects on food, effects of culture medium on recovery of Salmonella following, 25:13620
effects on frozen alcohol and aqueous acid solutions of cadmium perchlorates and silver perchlorates, ESR studies on diatomic cations produced from, 25:13028
effects on frozen solutions and solid organic compounds, 25:13056
effects on gas permeation and separation properties of polyethylene films, 25:13039
effects on germination of Dictyostelium discoideum spores, cobalt-60, 25:13605
effects on glassy tetrahydro-2-methylfuran, ESR spectral studies on effects of photobleaching on trapped radicals produced by, 25:13033
effects on graft polymerization of liquid styrene on polyethylene films, tensile properties of compounds produced by, 25:13042
effects on human intestine following therapy of uterine carcinoma, treatment of cobalt and radium, 25:13589
effects on human pituitary gland function following implantation of yttrium-90, relation of, to thyroid function, 25:13579
effects on incidence of carcinomas in rat adrenal glands, mixed whole-body fission neutron and, 25:13564
effects on incorporation and distribution of palmitates in phospholipids and triglycerides of Ehrlich ascites tumors, effects of palmitate quantity on, 25:13362 (CEA-R-4039)
effects on induction of peroxy radicals in poly(tetrafluoroethylene), ESR spectral studies on, 25:13034
effects on isomerization of 1,2-diphenylpropene in cyclohexane, 25:13037
effects on liquid hydrocarbons containing deuterium sulfide, mechanism and yields from, 25:13048
effects on liver of children following therapeutic use of, effects of dactinomycin on, 25:13578
effects on mating behavior of male codling moths, 25:13557
effects on metabolism of carbon-14-labeled dimecarbine by rabbits, 25:13576
effects on metabolism of phosphates in wheat seedlings, effects of dose on, 25:13597 (NP-18606)
effects on methylcholanthrene-induced sarcomas in mice, in relation to fertility, cesium-137, 25:13473
effects on mice, role of mast cells in spleen regeneration following whole-body cobalt-60, 25:13577
effects on p-toluidine hydrochloride monocrystals, ESR spectral studies on free radicals produced by, 25:13051
effects on permeation characteristics of swollen polyethylene membranes, 25:13041
effects on pollen of tobacco plants, effects of temperature shock on damaging, 25:13601
effects on polypropene, effects of energy on, 25:13055
effects on rejection of transplants of virus-heterogenized skin in mice, 25:13388
effects on seeds of wheat, mutagenic, 25:13419
effects on single crystals of L-phenylalanine hydrochloride and L-tyrosine hydrochloride, ESR studies on free radicals produced by, 25:13052
effects on skin, RBE for, 25:13583
effects on storage life of shrimp, effects of blanching on, 25:13619
effects on strawberry juice or puree, effects of, on chromosomes of Vicia faba, aberrant, 25:13621
effects on substances, electrification, (T), 25:14430
effects on survival of man following therapy for bladder carcinomas, cobalt-60, 25:13525
effects on survival of man following therapy for bronchial carcinomas, statistical evaluation of cobalt-60, 25:13523
effects on Taricha granulosa, protective effects of dimethyl sulfoxide against mixed x and cobalt-60, 25:13477
effects on thermally generated electric currents in Lucite, 25:13786
effects on thyroid gland of rats, pathological, 25:13497
effects on time of ripening and yield of cotton, effects of day length, dose, and seed exposure on, 25:13602
effects on toluene in nitric acid, 25:13093
effects on tumor cells, effects of, on immune reactions of mice to tumor cell grafts, 25:13389
effects on xenon trioxide, yields of oxygen and xenon from, 25:13049
effects on yield of agricultural plants, effects of plant or seed exposure on, 25:13599
emission from antimatter in meteor streams, (E/T), 25:13951
emission from Sco X-1 due to Compton synchrotron process, (E/T), 25:13856
flux of isotropic component of cosmic, 25:14062
flux of, from protons reacting with microwave background, (T), 25:13945
monitoring in liquid effluent at Bettis Laboratory during 1969, 25:13431
monitoring in Paducah environs during 1969, 25:13431
origin of isotropic component of cosmic, 25:14062
reactions (γ,n) with chromium-53, cross section for, (E), 25:14982 (NCSAC-31)
reactions with alloys at 2.6 to 17.6 MeV, effective atomic numbers for pair production in, (T), 25:14402
scattering by alloys at 662, 1120, and 1330 keV, effective atomic number for coherent, (T), 25:14405
scattering by lanthanum-139, energy level studies by, 25:15032
scattering by platinum K-shell electrons at 662 keV, differential cross sections for incoherent, (E), 25:14410
scattering cross sections, Klein--Nishina multiple, (T), 25:14393 (ANL-7689)
scattering in rocks, use in radiometric well logging methods, 25:13113
transport in finite heterogeneous systems, calculations using anisotropic source--flux iteration technique, 25:14407
transport in heterogeneous media, multiple-scattering calculations of, 25:14399
transport in one-dimensional finite systems, anisotropic source--flux iteration technique for calculation of, 25:14406
transport in spheres, cylinders, and planes, computer program for solving one-dimensional Boltzmann equation for, (T), 25:14863 (CEA-N-1358)
use for therapy of bladder carcinoma, development of cystitis following, treatment of, 25:13592
use for therapy of Burkitt's lymphoma and nasopharyngeal carcinoma, effects of, on titer of antibodies against EBV-associated membrane antigen complex, 25:13391
use for therapy of cervix carcinomas, development of computer methods for cobalt-60, 25:13540
use for therapy of human cervix carcinomas in combination with radium or surgery, evaluation of cobalt-60, 25:13531
use for therapy of neoplasms of human laryngopharynx, dose fractionation method for, 25:13545
use for therapy of oro-pharyngeal and thorax-abdominal neoplasms, review of clinical experiences over ten-year period in telecobalt, 25:13546
GAMMA SOURCES
monitoring in environmental samples from West Valley Processing Plant, 1969, 25:13080 (DOCKET-50201-62)
GAMMA SPECTROMETERS
book: Applied Gamma Ray Spectroscopy, 25:13231
design and performance of lithium-drifted germanium, 25:13212 (NP-18653)
design of fast coincidence, 25:12967
development of lithium-drifted germanium, for scanning analysis of plutonium-bearing fuel rods and process waste, 25:13230(R) (WCAP-7562-1)
development of sodium iodide, for scanning analysis of plutonium-bearing fuel rods and process waste, 25:13230(R) (WCAP-7562-1)
GAMMA SPECTROSCOPY
book: Applied Gamma Ray Spectroscopy, 25:13231
GARIGLIANO POWER REACTOR
coolant chemistry during March 1969 to February 1970, 25:15239(R) (EUR-4580)
maintenance during March 1969 to February 1970, 25:15239(R) (EUR-4580)
operations during March 1969 to February 1970, 25:15239(R) (EUR-4580)
GAS ANALYZERS
design for pulmonary function studies using xenon-133 tracer, 25:13223
GAS FLOW
magnetohydrodynamic, boundary-layer problem in plasma,

(T), 25:14092
magnetohydrodynamic, magneto-acoustic wave damping and regenerative amplification in, 25:14098
magnetohydrodynamic, regenerative amplification and damping of magnetoacoustic waves in, (T), 25:14097
GASEOUS DIFFUSION PLANTS
cascades for, design of multicomponent, 25:13179
GASES
content of sorbed, in hypostoichiometric plutonium dioxide--uranium dioxide fuel pellets, effects of density and storage on, 25:12925 (WHAN-SA-77)
determination in mixed oxide fuels using residual gas analyzer, 25:12924 (WHAN-SA-62)
determination of sorbed, in hypostoichiometric plutonium dioxide--uranium dioxide fuel pellets, 25:12925 (WHAN-SA-77)
effects of trapped non-diffusible, on sintering density of uranium dioxide, 25:13744
electron triple scattering at low energies by, depolarization due to spin flip in, (T), 25:14020
equilibria at pressures to 600 atm, liquid-vapor, 25:15459(T) (SCL-T-71-212)
kinetic theory of, quantum statistical second virial coefficient for, 25:14322
leakage from Types A and B radioactive material shipping containers, method for calculating, 25:13201
mixing in fluidized beds, effects of bed dimensions and gas velocity on, 25:13140 (BMBW-FBK-70-26)
GENERATORS
evaluation as source of electromagnetic fields, 25:13581
GENES
effects of bacterial and phage, on uv-irradiated phage lambda, 25:13412
mapping in uv-irradiated Salmonella typhimurium, 25:13408
mapping in uv-radioinduced mutants of Streptomyces coelicolor, 25:13407
mapping of crisp, in Neurospora crassa, 25:13424
mapping of mutant, in uv and x-radiosensitive mutants of Escherichia coli defective in repair synthesis, 25:13428
radiation effects on conversion and recombination in, of Drosophila melanogaster, analysis of half-tetrad in x, 25:13426
GENETIC RECOMBINATION
radiation effects on, in Drosophila melanogaster, analysis of half-tetrad in x, 25:13426
GEOMAGNETIC FIELDS
hydromagnetic-wave propagation in, resonant mode theory for micropulsations, (T), 25:14117
pulsations in, resonant mode theory for micro-, (T), 25:14117
relation to charged particle acceleration in auroral zone, (E/T), 25:14116
variations of, effects on electron density at 50 to 80 km, (E/T), 25:14127
variations of, relation to ambient field weakening on night side, diurnal, (T), 25:14111
GERMANIUM
electron emission by 400-eV electron-excited doped, effects of temperature and free carrier density on, 25:13967
superconductivity in films of, sandwiched between metals, induced, (E), 25:14161
GERMANIUM ALLOYS AND SYSTEMS
Ge--Tb--Si, magnetic properties and structure of $TbGe_{0.2}Si_{0.8}$, 25:14434 (CEA-CONF-1701)
Ge--V, superconducting transition temperature of, strain dependence and related effects of, (E), 25:14183
Ge--V, superconducting transition temperature of, strain dependence and related effects of, (E/T), 25:14182
GERMANIUM ISOTOPES Ge-69
nuclear spin and magnetic and quadrupole moments of, determination from hyperfine structure, (E), 25:14929
GERMANIUM ISOTOPES Ge-70
alpha elastic scattering by, optical-model analysis of, (E/T), 25:14947
GERMANIUM ISOTOPES Ge-71
hyperfine structure of, 25:14929
GERMANIUM ISOTOPES Ge-74
energy-level excitation by neutron capture gamma rays, (E), 25:15002
GERMANIUM ISOTOPES Ge-75
nuclear spin and magnetic moment of, determination from hyperfine structure, (E), 25:14929
GERMANIUM TELLURIDES
superconducting transition temperature of, (T), 25:14152
GLASS
analysis of natural, for antimony by neutron activation and radiochemical separation, 25:12968
elastic properties of composites of pores in, 25:13751
luminescence of uranium-containing, 25:13017
Al_2O_3--glass, elastic properties of composites of, 25:13751
glass--W, elastic properties of composites of, 25:13751
GLOVE BOXES
design for handling liquid sodium and radioactive materials, 25:13185 (AERE-R-6338)
GLUCOSE
metabolism in rats with cirrhosis, use of carbon-14 for measuring incorporation of precursors into, 25:13506
GLUTAMATE DECARBOXYLASE
radiation effects on activity of, in central nervous system of rabbits, ionizing, 25:13561
GLUTAMIC ACID
polymers, photolysis of aqueous solutions of, uv, 25:13054
polymers, radiolysis of aqueous solutions of, x, 25:13054
GLUTATHIONE
effects on excretion of mercury-203-labeled merphyrin from kidney of mice in combination with 2,3-dimercapto-1-propanol, 25:13341
radioprotective effects of, in combination with other protectants on mice, use of spleen weight-radiation dose relation for testing, 25:13478
GLYCERIDES
radiation effects on incorporation of palmitates into, in ascites tumors, effects of palmitate quantity on γ, 25:13362 (CEA-R-4039)
GLYCOGEN
radiation effects on, in rat livers, cobalt-60, 25:13378
GLYCOLIC ACID
radioinduced inhibition of synthesis of, in rat livers, 25:13370
GOLD
contact angle for clean tungsten surface, sessile drop method for measurement of, 25:13691
determination in postage stamps by neutron activation, 25:12973
electron charge-deposition distribution at 4 to 24 MeV in, 25:13964
electron elastic scattering at 25 to 800 eV by, tables of amplitudes and spin polarizations for, (T), 25:13995 (AD-711664)
positron channeling in single-crystal films of, (E/T), 25:14418
radioinduced defects in foils of, 4-50 keV argon-, krypton-, and xenon-ion, 25:14413 (NP-18645)
sputtering by 70-keV argon ions of single crystals of, angular distributions of sputtered material in, 25:13966
sputtering by fast neutrons of polycrystalline and monocrystalline, atomic, (E), 25:14414
GOLD ALLOYS AND SYSTEMS
Al_2O_3--Au-base, properties of dispersion-strengthened, electric and tensile, 25:13755
Au--Cu, sputtering by 70-keV argon ions of single crystals of, angular distributions of sputtered material in, 25:13966
Au--Fe--Te, superconducting transition temperature and lattice parameters of liquid-quenched simple-cubic, 25:14178
Au--Mn--Te, superconducting transition temperature and lattice parameters of liquid-quenched simple-cubic, 25:14178
Au-base--ThO_2, properties of dispersion-strengthened, electric and tensile, 25:13755
GOLD IONS
crystal-field shielding and antishielding factors for Au^+ at electronic and nuclear sites, (T), 25:13983
GOLD ISOTOPES
electron-capture decay of neutron-deficient, (E/T), 25:14993
GOLD ISOTOPES Au-196
content of feces, milk, and urine of dairy cattle following ingestion of Schooner fallout, 25:13396 (UCRL-72511)
nuclear magnetic moment of, determination from hyperfine structure, (E), 25:15026
GOLD ISOTOPES Au-197
energy-level excitation by neutron capture gamma rays, (E), 25:15002
neutron capture at 0.001 to 1 MeV, cross sections for, (E), 25:15121
neutron capture up to 1 MeV, cross section for, (E), 25:14982 (NCSAC-31)
neutron elastic scattering at 8 MeV, cross sections for, (E/T), 25:14965
neutron elastic scattering by, calculation using multilevel formalism, (T), 25:15161
GOLD ISOTOPES Au-198
beta decay of, L-subshell fluorescence and Coster--Kronig yields in mercury from, (E), 25:15015
effectiveness for interstitial tumor therapy, effects of seed distance and dose distributions on, 25:13526
effectiveness of colloidal, for scanning of parasternal lymph nodes in patients with mammary carcinomas, 25:13515
uptake of colloidal, by hemangioma during human liver scanning, 25:13510
GONADS
radiation dose to human, during radiological examinations of intestine and stomach, 25:13580
radiation dose to, in personnel following accidental exposure to iridium-192 vehicle, β and γ, 25:13466
radiation shielding of, of female personnel, development of lead impregnated vinyl foundation garment for x, 25:13462
GRAIN STRUCTURE
boundary segregation analysis using Auger electron emission techniques, 25:15428(R) (COO-1778-6)

GRANITES
  element concentration and depth in crustal, in USSR, 25:13115
GRAPHITE
  analysis of neutron-irradiated, for impurities by γ spectrometry, 25:12954
  bonding to chromium carbide-coated graphite by copper brazing, 25:13646
  bonding to Hastelloy N using copper brazed nickel-base--tungsten alloy transition layers, 25:13648
  corrosion of SNAP-19B fuel capsule components of, by seawater, 25:13163 (MLM-1652)
  deposition on metallic fuel cladding, method for, 25:13745(P)
  neutron slowing down in, fast, (E), 25:14870
  neutron thermalization in, by the reaction rate method, (E), 25:14874
  neutron total cross section at 0.07 to 1500 keV, (E/T), 25:14912
  oxidation of, LEED study of, 25:13735
  performance of high-strength yarns of, in impact testing of SIREN fuel capsules, 25:13171(R) (SNC-2708-2)
  properties at high temperatures, review of physical, thermal, and thermodynamic, 25:13667
  surface roughness of, optical microscopy method for measurement of, 25:13765 (RD/B/N-1770)
GRAVITATION
  constant of, radar echo delay analysis for determination of bound on time variation of, (E), 25:14812
  experimental testing general relativistic, (T), 25:13942
  field equations for fluid spheres in general relativity theory, 25:14814
  mass of sphere in, self-energy contributions to total, 25:14810
  parametrized post-Newtonian hydrodynamics and Nordtvedt effect, (T), 25:13943
GRAVITATIONAL COLLAPSE
  equilibrium theory of, (T), 25:13940
  neutrino emission during, detection of, (T), 25:13830
  physics of, (T), 25:13940
GRAVITATIONAL FIELDS
  classification of, Petrov, 25:14809
  energy transfer in, time sequences of axially symmetric static configurations for, 25:14816
  Hamiltonian formalism on null surfaces for, 25:14773
  interactions with electromagnetic fields, (T), 25:13946
  sources of, combined Bondi and fast-approximation method for Einstein equations for transport of mass and linear and angular momentum from, 25:14807 (NP-18559)
  theory for asymptotically flat, asymptotically null-spherical coordinates in general relativity, 25:14815
GRAVITATIONAL RADIATION
  detection of, performance of class-1 and -2 detectors for, 25:14547
  emission from black holes, (T), 25:13937
  emission from pulsars, (T), 25:13846
GRAVITY WAVES
  propagation in ionosphere, response to isotropic spectrum of internal, (E/T), 25:14121
GROUND
  motion from distant underground chemical and nuclear explosions, equations for predicting, 25:13129 (AD-713521)
GROUND WATERS
  flow conditions near Hanford area Emergency Waste Disposal Crib, effects on safe waste disposal operations, (T), 25:13186 (BNWL-1503)
  flow into well at Nevada Test Site, effects of Aardvark Event on, (T), 25:13111
  tritium content of Australian, 1967 to 1969, 25:13120 (NP-18638)
  tritium content of Australian, 1969 to 1970, 25:13103 (NP-18639)
GROUP THEORY
  conformal symmetry for mass-shell amplitudes, strict, 25:14820 (RLO-1388-598)
  Lorentz group generators for local tensor fields, 25:14718
  Lorentz group in, addition theorem for basis functions of first-class irreducible representations of, 25:14759
  Lorentz group in, Wigner function for hyperbolic rotations in homogeneous, 25:14759
  symmetry conditions on nonlinear spinor field functionals, 25:14782
GUANIDINE, NITROSO-
  effects on Streptomyces coelicolor, mutagenic, 25:13414
GUANOSINE, 2'-DEOXY-
  effects on growth of yeast cells, effects of cytidine monophosphates on, 25:13604
GUINEA PIGS
  radiation effects on tritium incorporation into DNA of oocytes of, x, 25:13367
GYPSUMS
  meson (μ^+) depolarization in single crystals of, (E), 25:13989

H

H.B. ROBINSON POWER REACTOR, UNIT 2
  safety injection system for, design modifications for 2300 MW(t) operation, 25:15292 (DOCKET-50261-50)
HI REGIONS
  cosmic-ray heating and ionization of, (T), 25:14061
  dust content of, in Small Magellanic Cloud, (E), 25:13921
  heating of, x-ray, (T), 25:13841
  spectra of, ultraviolet absorption-line, (T), 25:13841
HII REGIONS
  helium abundance in M42, (E), 25:13826
  infrared observations of M42, (E), 25:13826
HADRONS
  interactions at extreme energies, hypothesis of limiting fragmentation for multiplicity of, 25:14663
  interactions at high energies in multiperipheral model, momentum spectra of secondaries from, (T), 25:14659
  interactions of, angular distributions and differential cross sections for $\pi^- + p + \gamma + n$ interactions at 1245 and 1337 MeV for time reversal invariance test in electromagnetic, (T), 25:14567
  interactions of, asymptotic behavior of single-particle distributions in, 25:14742
  interactions with electrons and photons, scaling, fixed poles, and sum rules for, 25:14614
  interactions with equal-mass hadrons, amplitude expansion of Mandelstam triangle for, (T), 25:14678
  interactions with hadrons at high energies, complex angular momentum theory of three-particle production in two-body, (T), 25:14677
  interactions with hadrons at high energies, Pomeron hypothesis for exchange degeneracy for oscillating total cross sections of, (T), 25:14656 (SU-1206-237)
  interactions with hadrons at high energies, two-Reggeon exchange contributions to, (T), 25:14657 (UCRL-20032)
  interactions with intermediate-vector boson, μ flux deep underground as evidence against hypothesis for strong, (T), 25:14735
  mass formula in space--time symmetry algebra, 25:14751
  production in anti $p + n$ and anti $p + p$ interactions at 1.25 to 1.67 GeV/c in deuterium bubble chamber, cross sections for, (E), 25:14550
  production with photon in $e^+ + e^-$ interactions in storage rings, study of even-charge conjugation hadronic systems from, (T), 25:14621
  scattering by lithium-6, testing of cluster model by, 25:15183
HAFNIUM
  abundance in chondrites, achondrites, and Apollo 11 fines, (E), 25:13787
  Debye temperature of, anisotropic, 25:14480
  electric quadrupole interactions in, Moessbauer effect study of, 25:14480
  neutron elastic scattering at 8 MeV, cross sections for, (E/T), 25:14965
  properties at high temperatures, review of physical, thermal, and thermodynamic, 25:13667
  separation from chlorides by fused salt electrolysis, 25:13089
  separation of nitrogen and oxygen from interstitial sites in, method for, 25:13641(T) (UCRL-Trans-10503)
HAFNIUM ALLOYS AND SYSTEMS
  Hf--Mo-base, microstructure of, effects of internal nitriding on, 25:13661 (UCRL-72627)
  Hf--Mo-base, tensile properties at 1100 to 1500°C, effects of internal nitriding on, 25:13661 (UCRL-72627)
  Hf--Re--Ta-base--W, cracking sensitivity of, Varestraint testing of hot, 25:13695
HAFNIUM CARBIDES
  Debye temperature of, 25:14480
HAFNIUM ISOTOPES Hf-168
  beta and electron-capture decay of, γ spectra and half-life for, (E), 25:15025
HAFNIUM ISOTOPES Hf-169
  beta and electron-capture decay of, γ spectra and half-life for, (E), 25:15025
HAFNIUM ISOTOPES Hf-170
  beta and electron-capture decay of, γ spectra and half-life for, (E), 25:15025
HAFNIUM ISOTOPES Hf-171
  electron-capture decay of, γ spectra and half-life for, (E), 25:15025
HAFNIUM ISOTOPES Hf-174
  neutron capture by, γ spectra and Q-value for thermal, (E), 25:15059
HAFNIUM ISOTOPES Hf-175
  energy levels from hafnium-174 thermal neutron capture, spin-parity assignments for, (E), 25:15059
HAFNIUM ISOTOPES Hf-178
  Moessbauer effect in hafnium single crystals at 4°K, electric quadrupole interactions from, 25:14480
HAFNIUM ISOTOPES Hf-181
  beta decay of, circular polarization of γ rays from, (E), 25:15009
HAIR
  growth in lambs, autoradiography of DNA synthesis and cell migration in follicles during, 25:13337
HALOGENS
  distribution in atmosphere, use in tracer studies of global transport processes, (E), 25:13121 (TID-25314)
HAMSTERS
  radiation effects on SV40 tumorigenicity in embryonic

cells of, x, 25:13553
HASTELLOY C
welds in contaminated SNAP-15C fuel capsule liner of, metallographic analysis of integrity of, 25:13164 (MLM-1670)
HASTELLOY N
bonding to graphite using copper brazed nickel-base--tungsten alloy transition layers, 25:13648
stresses in welds of, method for measuring residual, 25:13697
HASTELLOY X
collapse of externally pressurized long thin tubes of, with initial ovalities, computer program for calculation of, 25:13652 (GAMD-8219(Rev.))
HAYNES STELLITE NO. 6
welding in sodium at 500 to 700°C, tendency for self-, 25:13668
HAYNES 25 ALLOY
corrosion of SNAP-19B fuel capsule components of, by seawater, 25:13163 (MLM-1652)
HEAD
radiation effects on, of rabbits, intracerebral temperature changes following x, 25:13575
HEART
displacement of enlarged, equipment for lung scanning to demonstrate, 25:13484
scanning of blood pools in human, effectiveness of metastable indium-113 in comparison to metastable technetium-99 for, 25:13516
HEAT EXCHANGERS
tubes in, explosive plug sealing of leaking, 25:13647
HEAT EXCHANGERS (LIQUID-LIQUID)
design for use in helium isotope separation, 25:13165(R) (MLM-1753)
HEAT PIPES
corrosion testing at high temperatures, 25:13630 (EUR-4298)
use of evaporator, for reactivity control in rocket reactors, 25:15400
HEAT SOURCES
thermal analysis of aerodynamically-shaped radioisotope, designed for Brayton power cycles, 25:13167 (N-70-41092)
HEAT TRANSFER
analysis for turbulent fluid flow using mass transfer and laminar sublayer concepts, theory for, 25:13160
calculation for laminar flow through concentric annuli at low Peclet numbers, 25:13159
HEAT TRANSFER SYSTEMS
design for testing critical heat flux in multirod fuel element bundles, 25:13150(R) (GEAP-10253)
HELIUM
abundance in four O-Type subdwarf stars, (E), 25:13825
abundance in late G and K dwarfs, (E), 25:13824
abundance in M42, (E), 25:13826
abundance in old open clusters, (E), 25:13798
analysis for trace amounts of carbon dioxide following freezing-out at liquid nitrogen temperature, mass spectrometric, 25:12941
analysis for trace amounts of hydrogen following sorption on activated charcoal, mass spectrometric, 25:12941
beryllium-ion (Be^{2+}) scattering at 100 to 800 eV by, energy-loss spectra and interaction energy for, (E), 25:14027
book: Elementary Atomic Structure, 25:14047
burning in stars, central, (T), 25:13815
charged-particle reactions with, ionization cross sections for, (T), 25:14022
electric discharges in, breakdown of 2^1P and 2^3P levels in, (E), 25:13977
electron correlation in, calculation using semiempirical pseudopotential procedure, 25:14055
electron elastic scattering at 25 to 800 eV by, tables of amplitudes and spin polarizations for, (T), 25:13995 (AD-711664)
electron reactions at 10 keV with, determination of oscillator strengths from coincidence measurements of electrons and ions from, 25:14003
electron reactions at 160 keV with liquid, optical and infrared emission spectra from, (E), 25:13973
electron reactions up to 150 eV with, excitation, ionization, and formation of negative-ion resonances in, (E), 25:14002
energy levels of diatomic, quantum mechanical calculations on ^{3}PI/sub g/ and ^{1}PI/sub g/ states, 25:13975
energy levels of, energies and widths of autoionizing, (T), 25:14049
helium-ion reactions at 120 to 830 keV with, differential cross sections for production of helium atoms, He^+, and He^{2+} in, (E), 25:14044
helium-ion reactions at 2 to 22 keV with, total cross section for single-electron transfer in, (E), 25:14025
helium-ion reactions with metastable atoms of, elastic and inelastic cross sections for, (T), 25:14037
intermolecular force constants for, 25:13165(R) (MLM-1753)
ion reactions with, dependence of mean charges of ions from, on atomic number, (E), 25:14007
oxygen-ion (O^-) reactions in keV range with, formation of autodetaching states of O^- in, (E), 25:14009
plasma jets of, gas flow model for velocity distributions in, 25:14252
plasma jets of, gas flow model for velocity distributions in, 25:14253
plasma jets of, temperature distributions in, 25:14254
plasma of, energy balance in low-pressure discharges, (T), 25:14301
plasma of, optical spectra of, (E), 25:14277 (AD-712024)
polarizability of atomic, many-body calculation of frequency-dependent, 25:14046
positron annihilation and diffusion in, coincidence study of, 25:13987
proton reactions at 75 to 400 keV with, cross sections for formation and destruction of excited hydrogen atoms by charge exchange in, (E), 25:14043
reactions between ground-state and 2^3S metastable atoms of, at 10 to 200 eV, elastic and inelastic cross sections for, (T), 25:14037
reactions with hydrogen metastable atoms below 250 eV, quenching cross sections for, (T), 25:14026
solubility in liquid sodium, 25:15379(T) (EURFNR-785)
HELIUM IONS
charged-particle reactions with, ionization cross sections for, (T), 25:14022
electron reactions with, experimental method for study of excitation to 2P state in, 25:14042
reactions with helium at 2 to 22 keV, total cross section for single-electron transfer in, (E), 25:14025
reactions with helium metastable atoms, elastic and inelastic cross sections for, (T), 25:14037
reactions with metallic thick targets at 90 to 360 keV, yields of characteristic x rays from, (E), 25:13962
reactions with potassium and rubidium at 50 to 1600 eV, crossed-beam study of electron capture into excited states in, 25:14011
reactions with rare gases at 120 to 830 keV, diferential cross sections for production of helium atoms, He^+, and He^{2+} in, (E), 25:14044
reactions with tungsten (100) and (110) surfaces at 5 to 2000 eV, effects of lattice disorder and surface contamination on entrapment in, (E), 25:14419
HELIUM ISOTOPES He-3
concentration by distillation at low temperature, equipment and methods for, 25:13165(R) (MLM-1753)
interactions $\gamma + {}^3He + \pi^+ + 2n + p$, impulse approximation for π^+ angular distributions and total cross sections in, (T), 25:14518
interactions $\gamma + {}^3He + \pi^+ + n + d$, impulse approximation for π^+ angular distributions, total cross sections, and final-state interaction effects in, (T), 25:14518
mass and electric charge of antihelium-3 in proton reactions with aluminum at 70 GeV, (E), 25:14540 (IFVE-SEF-70-16)
nuclear magnetic susceptibility of pure solid, 25:14213
nuclear properties of, Bolsterli--Feenberg perturbation procedure for calculation of momentum-dependent, 25:15185
production of antihelium-3 in proton reactions with aluminum at 70 GeV, cross sections for, (E), 25:14540 (IFVE-SEF-70-16)
proton elastic scattering at 100 MeV, angular distributions for, (E), 25:14882
proton elastic scattering at 19.4 MeV, polarization and spin-correlation parameters for, (E/T), 25:14888
reactions (He-3,2α) with beryllium-9 at 1.55 MeV, analysis for reaction mechanism in, (E/T), 25:14903
reactions (He-3,2α) with beryllium-9 at 6.0 MeV, spectra from, (E/T), 25:14891(T) (ORO-1316-97)
reactions (He-3,3n) with barium-137 at 14 to 33 MeV, excitation functions and average ranges from, (E), 25:15049
reactions (He-3,3n) with barium-137 at 14 to 33 MeV, angular distributions, ranges, and cross sections for, (E), 25:15065
reactions (He-3,3n) with barium-137 at 20 to 33 MeV, angular distributions and average total kinetic energies of neutrons and photons from, (E), 25:15049
reactions (He-3,3n) with chromium-52 at 45.5 MeV, yields of iron-52 from, 25:13063
reactions (He-3,3n) with lead-207 at 21 to 33 MeV, angular distributions, cross sections, and recoil ranges for, (E), 25:14996
reactions (He-3,α) and (He-3,2n) with cadmium-116 at 13 to 33 MeV, excitation functions and average range measurements from, (E), 25:15049
reactions (He-3,α) with aluminum-27, neon-20, neon-22, and silicon-28 at 35 MeV, differential cross sections for, (E), 25:14944
reactions (He-3,α) with carbon-12 at 2.3 to 3.3 MeV, angular distributions from, (E/T), 25:14915
reactions (He-3,α) with gadolinium-156 and gadolinium-158 at 20.3 MeV, angular distributions from, (E), 25:15138
reactions (He-3,α) with nickel-58 at 15 MeV, α--γ angular correlations from, (E), 25:14952
reactions (He-3,α) with oxygen-17 at 11 MeV, angular distributions from, (E/T), 25:14914
reactions (He-3,α) with ytterbium-172, -174, and -176 at 28 MeV, angular distributions for, (E), 25:15057
reactions (He-3,d) with nitrogen-15 at 11 MeV, angular distributions from, (E), 25:14914
reactions (He-3,d) with ruthenium-104 at 18 MeV, angular distributions for, (E), 25:15022

  reactions (He-3,n) with magnesium-26, nickel-58, and titanium-46, neutron spectra from, (E), 25:14943
  reactions (He-3,n) with p-shell nuclei, analysis for distortion and polarization effects in, (T), 25:15192
  reactions (He-3,p) with boron-11 and neon-20 at 3 MeV, angular distributions for, (E), 25:14904
  reactions (He-3,p) with sulfur-32 at 9 to 10 MeV, p-γ angular correlations from, (E), 25:14942
  reactions (He-3,t) with argon-40, form factors and distorted waves from DWBA analysis of, (T), 25:14924 (COO-535-625)
  reactions of ions of, with metallic thick targets at 90 to 360 keV, yields of characteristic x rays from, (E), 25:13962
  scattering by aluminum-27 and carbon-12 at 30 MeV, polarization in double elastic, (E), 25:14894
  scattering by carbon-12 at 2.3 to 3.3 MeV, angular distributions from, (E), 25:14915
  scattering by several light nuclei, energy spectra and angular distributions for, (E), 25:14899
  superfluidity in, inhibition by polarization of, (T), 25:14135
HELIUM ISOTOPES He-4
  alpha-particle irradiation of superfluid, nucleation of cavitation by, 25:14133
  binding energy of, second-order correction of perturbation theory to, (T), 25:14883
  concentration by distillation at low temperature, equipment and methods for, 25:13165(R) (MLM-1753)
  coupling between pressure and temperature waves in superfluid, (E/T), 25:14129 (COO-1574-19)
  critical heat flux in superfluid, near lambda transition, (E/T), 25:14132
  disk oscillations in superfluid, amplitude effects for, (E), 25:14134
  energy levels of, calculation using translation-invariant shell model with higher configurations, (T), 25:14884
  hydrodynamic equations for condensate and depletion of superfluid, (T), 25:14139
  ion motion at finite velocities in superfluid, 25:14144
  kinetic theory of liquid II, hydro-, 25:14137
  neutron elastic scattering by, resonating-group calculations of phase shifts and effective potentials for fast, (T), 25:14880 (COO-1764-105)
  nuclear properties of, Bolsterli--Feenberg perturbation procedure for calculation of momentum-dependent, 25:15185
  photon reactions (γ,p) at 120 MeV, angular distributions for, (E), 25:14886
  proton elastic scattering at 100 MeV, angular distributions for, (E), 25:14882
  proton elastic scattering at 8 to 38 MeV, resonating-group calculations of phase shifts, differential cross sections, polarizations, and spin-rotation parameters for, (T), 25:14880 (COO-1764-105)
  reactions (He*4,3n) with lead-206 at 32 to 44 MeV, angular distributions, cross sections, and recoil ranges for, (E), 25:14996
  reactions (He-4,3n) with barium-136 at 27 to 44 MeV, angular distributions, ranges, and cross sections for, (E), 25:15065
  reactions of ions of, with metallic thick targets at 90 to 360 keV, yields of characteristic x rays from, (E), 25:13962
  scattering by tin-116 and tin-124, reorientation measurements following Coulomb excitation by inelastic, (E), 25:15041
  structure factor for liquid, Mihara--Puff theory of, 25:14138
  superfluid critical velocities of, in wide channels using phase coupling, (E/T), 25:14146
  superfluid film transfer rate in, dependence on pressure head, film height, and substrate of, (E), 25:14128 (COO-1574-17)
  superfluid transition in presence of heat current, (E), 25:14136
  thermal capacity near superfluid transition in, at saturated vapor pressure, 25:14141
  wave propagation in normal and superfluid, kinetic phenomena in second sound, (T), 25:14131
HELIUM SYSTEMS
  H--He, atomic processes in low-density plasma of, 25:14302
  H--He, thermal diffusion factors for, at 10 to 400°K, 25:13165(R) (MLM-1753)
  He--N, radiolysis of, yields from electron pulse, 25:13053
HEMATOPOIETINS
  effects on platelet production in mice and rats, demonstration of, using sulfur-35, 25:13355
HEPARIN
  effects on histone content of deoxyribonucleoproteins in liver, spleen, and thymus of x-irradiated rats, 25:13385
HEXANE
  radiolysis of liquid, containing deuterium sulfide, mechanism and yields from γ, 25:13048
HIGH-ENERGY PHYSICS
  book: Lectures in Theoretical Physics, (in Romanian), 25:14630
  research at BNL, July 1969--June 1970, 25:14837(R) (BNL-50230)
  research at INS, April 1969--Mar. 1970, 25:14845(R) (NP-18601)
  research at MIT, 1969, 25:14925(R) (MIT-2098-643)
HIPPURIC ACID, o-IODO-
  effectiveness of iodine-131-labeled, for kidney scintigraphy in man in comparison to indium-113m-labeled EDTA, 25:13499
HISTAMINE
  radiation effects on content of, in blood, lungs, skin, and small intestine in rats, effects of skin wounds on whole-body, 25:13368
HISTONES
  radiation effects on content of, in deoxyribonucleoproteins of liver, spleen, and thymus in rats, effects of heparin on x, 25:13385
HOLMIUM
  complexes with carminic acid, spectrophotometric studies on, 25:12937
  determination in plutonium oxide--uranium oxide fuels by solvent extraction and emission spectrography, 25:12922 (WHAN-SA-44)
  determination of trace amounts of, in plutonium and plutonium dioxide--uranium dioxide by solvent extraction and emission spectrography, 25:12923 (WHAN-SA-47)
HOLMIUM ISOTOPES Ho-159
  isomeric transition in, half-life and γ conversion electron spectra for, (E), 25:15060
HOLMIUM ISOTOPES Ho-161
  energy levels from samarium-154 (B-11,4nγ) reactions, spin-parity assignments for, (E), 25:14991
  isomeric transition in, half-life and γ conversion electron spectra for, (E), 25:15060
HOLMIUM ISOTOPES Ho-165
  boron-10 inelastic scattering at 50 MeV, γ spectra from, (E), 25:14991
  energy levels from boron-10 inelastic scattering, (E), 25:14991
HOLMIUM ISOTOPES Ho-166
  beta decay of, gamma spectra from, (E/T), 25:14984 (NP-18536)
HOLMIUM SILICIDES
  magnetic properties and structure of HoSi, 25:14434 (CEA-CONF-1701)
HORMONES, ADRENAL
  epinephrine, effects on x-radiosensitivity of bone marrow and reticulo-endothelial system in rats, 25:13567
  methylprednisolone, effects on repair processes in irradiated mice, mechanisms of, 25:13474
HORMONES, PANCREATIC
  insulin, effects on sympatho-adrenal system of irradiated man, 25:13586
HORMONES, PITUITARY
  follicle-stimulating hormone, effects on β-radiosensitivity of ovaries and testes in mice, 25:13569
HORMONES, SEX
  estradiol, effects on β-radiosensitivity of ovaries and testes in mice, 25:13569
  estradiol, effects on preimplantation blastocysts of rats, 25:13560
HORMONES, THYROID
  effects on survival of man following therapy for thyroid carcinomas, 25:13524
  radiation effects on synthesis of, in patients with toxic thyroid adenomas following therapy, iodine-131 β and γ, 25:13594
HOSPITALS
  radioactive waste disposal in sewage by, in Milan, Italy, 25:13454
HOT CELLS
  component assembly in, for dry processing of fuels, remote coupling device for, 25:13199(P)
  material transfer in, design of removable head for pneumatic device for, 25:13203(P)
  radioactive material handling in, design of equipment for remote, 25:13200(P)
HYDRIODIC ACID
  effects on yields from γ radiolysis of carbon tetrachloride at 25°C, 25:13045
HYDROCHLORIC ACID
  corrosive effects of boiling, on intercrystalline corrosion of molybdenum--nickel alloys, relations of temperature, titanium, tungsten, and zirconium with, 25:13633
  dipole moment and hyperfine parameters of chlorine-35-labeled, molecular-beam electric resonance spectral studies on effects of deuterium on, 25:12988
  neutron reactions at 20 and 90° with gaseous, differential cross sections from quasi-classical approximation for slow, (T), 25:14875
  reactions with antimony in aqueous solutions, kinetics of extraction and isotopic exchange in, 25:12999
HYDROCYANIC ACID
  detection in UU Aur, (E), 25:13803
HYDROFLUORIC ACID
  effects on solvent properties of trioctylamine for plutonium, 25:12923 (WHAN-SA-47)
  thermodynamic properties in solutions of ammonium nitrate at 5, 25, and 45°C, 25:13022

HYDROGEN
  abundance in four carbon stars, (E), 25:13795
  analysis for trace amounts of carbon dioxide following freezing-out at liquid nitrogen temperature, mass spectrometric, 25:12941
  argon--ion reactions at 1 to 10 eV with molecular, cross sections for, (T), 25:14041
  book: Elementary Atomic Structure, 25:14047
  charged-particle reactions with atomic, ionization cross sections for, (T), 25:14022
  content of sorbed, in hypostoichiometric plutonium dioxide--uranium dioxide fuel pellets, effects of density and storage on, 25:12925 (WHAN-SA-77)
  determination in sodium, calibration and design of meters for, 25:13651(R) (ANL/ST-4)
  determination of trace amounts of, in argon and krypton following condensation, mass spectrometric, 25:12941
  determination of trace amounts of, in helium and neon folowing sorption on activated charcoal, mass spectrometric, 25:12941
  determination of trace amounts of, in xenon following condensation, mass spectrometric, 25:12941
  diffusion in vanadium, niobium, and tantalum, Gorsky-effect measurements of, 25:14440
  distribution of neutral, in Milky Way, (T), 25:13930
  effects on determination of water in mixed oxide fuels, 25:12924 (WHAN-SA-62)
  effects on γ radiolysis of ammonia adsorbed on synthetic zeolites, EPR spectral studies on, 25:13057
  electron correlation in molecular, calculation using semiempirical pseudopotential procedure, 25:14055
  electron elastic scattering at 25 to 800 eV by, tables of amplitudes and spin polarizations for, (T), 25:13995 (AD-711664)
  electron scattering by atomic, variational calculation of bounds for phase shifts in, 25:14024
  energy levels of molecular, double-perturbation theory applied to Zeeman effect on metastable, 25:13981
  energy levels of μ-mesic atoms of, metastability of 2s state, 25:13991
  exchange with deuterium in benzonitrile--alkali metal ion radical salt, effects of alkali metal on catalytic, 25:13002
  exchange with deuterium in benzonitrile--cesium ion radical salt, mechanism of catalytic, 25:13001
  hyperfine interactions in rare gas atmospheres, calculation of fractional frequency shifts for, 25:14046
  intermolecular force constants for, 25:13165(R) (MLM-1753)
  intermolecular forces in ground-state, calculation of long-range, using Gaussian basis functions, 25:13984
  oxygen-ion (O^-) reactions in keV range with molecular, formation of autodetaching states of H^- in, (E), 25:14009
  plasma of, amplitude modulation and nonadiabaticity of Stark broadening in, (T), 25:14310
  plasma of, current density and temperature in arc, 25:14268
  plasma of, drft instabilities in collisionless, (E), 25:14345
  plasma of, effect of radiation escape on atomic state density and electron distribution function, (T), 25:14316
  plasma of, state equilibrium and ionization rates of, (T), 25:14319
  polarizability of atomic, many-body calculation of frequency-dependent, 25:14046
  polarizability of ground-state atom of, calculation using hydrodynamic analogy of quantum mechanics, 25:14054
  positron reactions at 50 to 544 eV with molecular, Born approximation calculation of cross sections for positronium formation by electron capture in, 25:14006
  positron reactions at low energies with atomic, convergence of separable-expansion method for solution of Faddeev equations for, 25:14010
  production by surface reactions of tungsten with water vapor, kinetics of, 25:13669
  proton scattering at low energies by atomic, large-angle, (T), 25:14029
  radio-wave absorption by neutral, in M82, (E), 25:13927
  radio-wave absorption in neutral, in direction of Virgo A, (E), 25:13831 (AD-711300)
  radio-wave absorption in neutral, in M82, (E), 25:13911 (AD-711299)
  reaction energies between atoms in ground and first excited state of molecular, calculation using approximate exchange integrals, 25:13985
  reactions between atoms of, at 1 to 56.25 eV, two-state impact-parameter calculation of cross section for 1s--2s excitation in, 25:14021
  reactions between atoms of, nonstatistical effect in resonance-theory calculation of recombination rates for three-body, 25:14016
  reactions with californium trichloride, preparation of californium dichloride by, 25:13018
  reactions with helium below 250 eV of metastable atoms of, quenching cross sections for, (E), 25:14026
  reactions with oxygen molecules at 3 to 50 keV of atomic, cross sections for O^- production in, (E), 25:13999
  reactions with uranium, surface changes during, 25:12635
  spectra of, classical-path calculation of Stark broadening of H/sub α/ line in, 25:13978
  yields from γ radiolysis of 2-propanol vapor at 124 to 400°C, 25:13046
  yields from γ radiolysis of basic and neutral aqueous solutions of sodium azide, effects of atomic hydrogen on molecular, 25:13044
  yields from γ radiolysis of liquid hydrocarbons containing deuterium sulfide, 25:13048
HYDROGEN ION CONCENTRATION
  determination by reaction with krypton-85-labeled thallium kryptonate, radiometric, 25:12955
HYDROGEN IONS (H^-)
  charged-particle reactions with, ionization cross sections for, (T), 25:14022
  photon absorption coefficients for, S--P and P--D contributions to free--free, (T), 25:13974
HYDROGEN IONS (H_2^+)
  intermolecular forces in ground-state, calculation of long-range, using Gaussian basis functions, 25:13984
  reactions with carbon films at 2 MeV, dissociation as function of film thickness in, (E), 25:13972
HYDROGEN PEROXIDES
  radioinduced reactions with aqueous 2-propanol, effects of trivalent titanium on kinetics of free radical chain reactions in γ, 25:13032
HYDROGEN SULFIDES
  reactions with deuterium at 1250 to 1590°K in shock tubes, kinetic studies on, 25:12987
HYDROGEN SYSTEMS
  Ar--H, mass separation effects in rotating plasma of, 25:14278 (NP-18643)
  BBr_3--H, pyrolysis of carbon-containing, to prepare boron carbides at 900 to 1300°C, 25:13739
  BBr_3--H, pyrolysis to prepare pure boron lattices on tungsten wires at 900 to 1300°C, 25:13740
  D--H, mass separation effects in rotating plasma of, 25:14278 (NP-18643)
  D--H, reactions with recoil tritium, iodine bromide and iodine chloride as radical scavengers in, 25:13067
  H--He, atomic processes in low-density plasma of, 25:14302
  H--He, thermal diffusion factors for, at 10 to 400°K, 25:13165(R) (MLM-1753)
  H--Na--O, phase studies of, 25:13651(R) (ANL/ST-4)
HYDROLASES
  radiation effects on activity of, in cells of Escherichia coli K 12, comparison of γ, proton, and uv, 25:13371
HYDROMAGNETIC WAVES
  effects on coupling of interstellar gas and cosmic rays, (T), 25:14058
  emission from magnetized stars, (T), 25:13800
  heating of chromospheric network by, (T), 25:13908
  propagation in magnetosphere, resonant mode theory for micropulsations, (T), 25:14117
HYDROXYL (HO)
  radio emission from, in R Hor, (E), 25:13818
  spectral absorption lines due to, in supernova remnants, (E), 25:13837
  spectral emission during Mar. 24, 1969 magnetic storm, behavior of, (E), 25:14115
HYPERFRAGMENTS
  decay $\Lambda\text{-}Be^9 \to \Lambda\text{-}He^5 + \alpha$ from meson (K^-) reactions with emulsion nuclei at rest, (E), 25:14573
  decay $\Lambda\text{-}Li^6 \to \Lambda\text{-}He^5 + p$ from meson (K^-) reactions with emulsion nuclei at rest, (E), 25:14573
  hyperon (Λ) binding energy in, Brueckner matrix theory for, 25:14745
HYPERICIN
  radiation effects on reactions of, in relation to human metabolism and radiotherapy, 25:13374
HYPERONS
  decay in broken SU(3) x SU(3) corrections to Cabibbo theory of semileptonic, 25:14689
  decay of, corrections to soft-pion productions of current algebra from once-subtracted dispersion relations for nonleptonic, (T), 25:14654
  decay of, full experiment and constant form factors for semileptonic, (T), 25:14651
  decay of, Van Hove model for nonleptonic, (T), 25:14637 (SU-1206-238)
  interactions with photons, quark model commutation relations for sum rules for amplitudes of π production from, (T), 25:14619
  magnetic moments of, sum rules for, (T), 25:14619
  production in $p + p \to Y + K + N$ interactions, π and K exchange contributions to, (T), 25:14597
HYPERONS (Λ)
  binding energy in nuclear matter with noncentral ΛN forces, Brueckner matrix theory for, 25:14745
  interactions $\pi + \Lambda \to \pi + \Lambda(\Sigma)$, SU(3) x SU(3) chiral Lagrangian model for total cross sections and scattering lengths for, (T), 25:14703 (TID-25639)
  polarization in $\Sigma^*(1385) \to \pi^+ + \Lambda$ decay in bubble chamber, (E), 25:14559 (INP-731)
  production in anti p + d interactions at 1.25 to 1.67 GeV/c, cross sections for, (E), 25:14550
HYPERONS (Σ)
  interactions $\pi + \Sigma \to \pi + \Sigma$, SU(3) x SU(3) chiral Lagrangian model for total cross sections and scattering lengths for, (T), 25:14703 (TID-25639)

XUM

HYPERONS (Σ^-)
  decay $\Sigma^- \to n + e +$ anti ν in hydrogen bubble chamber, asymmetry parameter and axial-vector-to-vector weak coupling constant ratio for, (E), 25:14539
  decay $\Sigma^- \to n + e(\mu) +$ anti ν in hydrogen bubble chamber, axial-vector-to-vector weak coupling constant ratio for, (E), 25:14539
  decay $\Sigma^- \to \pi^- + n$ in bubble chamber, lifetime determination from, (E), 25:14546
  lifetime determination from $\Sigma^- \to \pi^- + n$ decay in bubble chamber, (E), 25:14546
  production in $K^- + d \to p + \Sigma^- + \pi^+ + \pi^-$ interactions at 3 GeV/c in bubble chamber, cross sections for, (E), 25:14546
HYPERONS (Σ^+)
  decay $\Sigma^+ \to p + \gamma$ in hydrogen bubble chamber, asymmetry parameter and branching ratio for, (E), 25:14539
  decay $\Sigma^+ \to \pi^+ + n$ in bubble chamber, lifetime determination from, (E), 25:14546
  lifetime determination from $\Sigma^+ \to \pi^+ + n$ decay in bubble chamber, (E), 25:14546
  magnetic moment of, (E), 25:14513
  production in $K^- + d \to p + \Sigma^+ + \pi^- + \pi^-$ interactions at 3 GeV/c in bubble chamber, cross sections for, (E), 25:14546

I

IGNEOUS ROCKS
  composition of shields and sediment cover of Brazil, Canada, and USSR, relations with geological time, 25:13114
IMMUNE REACTIONS
  inhibition of tumor cell, in mice by tumor-specific antibody response to grafts, 25:13389
  radiation effects on graft-versus-host, in mice following injection of lymphoid cells, effects of dose and splenomegaly on x, 25:13390
  radiation effects on, in spleen cells of mice, analysis of origin of plaque forming cells following γ, 25:13387
  radiation effects on, of mice, effects of, on rejection of transplants of virus-heterogenized skin, γ, 25:13388
IMMUNIZATION
  effects on protein synthesis in liver and spleen cells in irradiated rats, 25:13376
IN-PILE LOOPS
  instrumentation for, development at ORNL of, 25:13318(R) (CRNL-4620)
INCONEL
  welding in sodium at 500 to 700°C, tendency for self-, 25:13668
INDIAN POINT POWER REACTOR, UNIT 1
  cooling system for, repair of thermal sleeves in, 25:15243 (DOCKET-50003-61)
  design modifications during April to September 1970, 25:15244 (DOCKET-50003-64)
  operations incident of January 11, 1971, foreign material in buffer seal housing of control rods, 25:15225 (DOCKET-50003-63)
  operations incident of January 4, 1971, malfunction of outlet stop valve, 25:15224 (DOCKET-50003-62)
INDIUM
  deformation of monocrystalline, at 4.28 to 406.6°K, 25:13698
  electrical transmission properties of superconducting, effect of tin additive on, 25:14223
  helicon-wave resonances in polycrystalline, (E), 25:14468
  magnetic vortex pinning and motion in superconducting thin films of, 25:14176
  neutron elastic scattering at 8 MeV, cross sections for, (E/T), 25:14965
  superconducting critical temperature of thin single-crystal and polycrystal plates of, effects of thickness and mean free path on, 25:14173
INDIUM ALLOYS AND SYSTEMS
  Cd--In, superconducting flux trapping in region of martensitic transformation, 25:14172
  Hg--In, ultrasonic attenuation of transverse waves in dirty superconducting, (E), 25:14160
  In--Pb, superconducting flux trapping in region of martensitic transformation, 25:14172
  In--Pb, thermal capacity and superconducting properties at low temperatures, 25:14180
  In--Sn, crystal growth in, stability of planar advancing solid/liquid interface in, 25:13646
  In--Tl, superconducting flux trapping in region of martensitic transformation, 25:14172
INDIUM ISOTOPES In-109
  decay scheme, (E), 25:15005
INDIUM ISOTOPES In-111
  electron-capture decay of, after-effects on cadmium $\gamma\gamma$ correlation from, 25:15028
INDIUM ISOTOPES In-113
  effectiveness of EDTA-incorporated metastable, for kidney scintigraphy in man in comparison to iodine-131-labeled o-iodo hippuric acid, 25:13499
  effectiveness of metastable, for blood pool scanning in human heart and placenta in comparison to metastable technetium-99, metastable, 25:13516
  effectiveness of metastable, for placental localization, 25:13502
  effectiveness of serum proteins-incorporated metastable, for scanning of human placenta in comparison to metastable technetium-99-labeled erythrocytes, 25:13517
  mixtures of metastable, with tin-113, evaluation for scanning liver, lungs, and spleen, 25:13501
INDIUM ISOTOPES In-115
  neutron capture by, cross-section calculations for, (T), 25:14982 (NCSAC-31)
  neutron capture by, gamma spectra from resonance, (E), 25:15008
  neutron inelastic scattering by, fission-spectrum-averaged activation cross sections for, (E), 25:14568
INDIUM ISOTOPES In-116
  energy levels from resonance neutron capture by indium-115, 25:15008
INDOLE-3-CARBOXYLIC ACID, 1,2-DIMETHYL-5-HYDROXY-, ETHYL ESTER
  radiation effects on metabolism of carbon-14-labeled, by rabbits, γ, 25:13576
INDUSTRIAL MANAGEMENT
  book: Economic Effectiveness of using Radioactive Isotopes in Industry (In Russian), 25:13174
INFORMATION RETRIEVAL SYSTEMS
  design of integrated, for materials property data, 25:13627
  Radiation Shielding Information Center program setup instructions manual, 25:14395 (CTC-INF-1017)
INFRARED RADIATION
  effectiveness of thermography in combination with x-radiography for diagnosis and nuclear medicine research, 25:13498
  emission from interstellar grains, (E/T), 25:13933
  flux and temperature of cosmic background, (E), 25:13949
  interstellar extinction of, (E), 25:13934
INSECTA
  Drosophila melanogaster, radioinduced gene conversions and recombinations in, analysis of half-tetrad in x, 25:13426
  Drosophila melanogaster, radioinduced isochromosome aberrations in, x, 25:13409
  Drosophila melanogaster, radiosensitivity of oocytes of, x, 25:13555
  Laspeyresia pomonella, radiation effects on mating behavior of male, γ, 25:13557
  radiation effects on, during processing of fruits, grains, and meats, review of, 25:13623
  Sitophilus oxyzae, radiosensitivity of eggs and larvae of, comparison of cobalt-60 γ, 25:13558
INSTRUMENTS
  development at BNL, July 1969--June 1970, 25:14837(R) (BNL-50230)
  development at CRNL, Sept. 1969--Aug. 1970, 25:13318(R) (ORNL-4620)
  development at Risoe, Oct. 1, 1969--March 31, 1970, 25:13321 (RISO-M-1270)
INTERNAL CONVERSION
  spectra measurements in high gamma fluxes with silicon detectors and superconducting solenoid, (E), 25:14584 (NP-18536)
INTERSTELLAR MATERIAL
  heating of gases by cosmic particles, (T), 25:14058
  infrared absorption in, (E), 25:13934
  infrared spectra of grains in, (E/T), 25:13933
INTESTINES
  diseases of human, conference on diagnosis and treatment of, 25:13508
  radiation effects on histamine content of, in rats, combined effects of skin wounds on whole-body, 25:13368
  radiation effects on iodine-131 uptake by perfused, of rats, effects of food intake on, 25:13349
  radiation effects on jejunal crypt cells of, in rats, x, 25:13562
  radiography of human, effects of, on gonads and skin, 25:13580
  radioinduced injuries of human, following therapy for uterine and cervical carcinoma, α and γ, 25:13589
INVARIANCE PRINCIPLES
  C, P, and T invariance for higher-spin fields, 25:14798
  C, P, and T invariance in Dirac equations for particle motion, 25:14747 (ITF-70-70)
  CP invariance for elementary particles, conference on, 25:14750
  CP violation in $e + p$ interactions near N(1470), model of, (T), 25:14765
  CP violation in $K \to 2\pi(3\pi)$ decays, current algebra model wth PCAC hypothesis for phenomenological study of, (T), 25:14764
  CP violation in $K^0 \to 2\pi^0$ decay, branching ratio for, (E), 25:14530
  CP violation in $K_2^0 \to \pi^+ + \pi^- + \pi^+$ decay, spark chamber search for, (E), 25:14536
  CP violation in time distribution of $K^0 \to \pi^+ + \pi^- + \pi^0$ decay, (E), 25:14762
  CPT invariance and superweak interaction for $K^0 \to 2\pi$ decay, 25:14761
  scale invariance in quantum field theory, incompatibility

    with Lorentz covariance, 25:14790
  time reversal invariance in hadron elctromagnetic interactions, angular distributions and differential cross sections for $\pi^- + p \to \gamma + n$ interactions at 1245 and 1337 MeV for test of, (E), 25:14567
  time reversal invariance test in angular distributions and differential cross sections for $\pi^- + p \to \gamma + n$ interactions at 1245 to 1363, 25:14566
INVERTEBRATES
  radioisotope content of marine, in Pacific Ocean, 25:13394(R) (RLO-2099-1)
IODATES
  separation of iodine-131-labeled, from iodides and periodates by thin-layer chromatography, 25:13099
IODIDES
  separation of iodine-131-labeled, from iodates and periodates by thin-layer chromatography, 25:13099
IODINE
  chemical state of, in irradiated oxide fuel elements, 25:13077(R) (ANL-7755)
  compounds, fragmentation by β^- decay of iodine-131 in, velocity spectra of Coulomb, 25:13073
  effects on reactions of recoil fluorine-18 in octafluorocyclobutane and hexafluorocyclobutene, scavenging, 25:13066
  effects on yields from γ radiolysis of carbon tetrachloride at 25°C, 25:13045
  removal from reactor containment systems, effectiveness of water sprays for, (T), 25:15372 (AE-408)
  removal from reactor containment systems, effectiveness of sodium thiosulfate sprays for, (E/T), 25:15374 (BAW-10024)
  sorption by zinc during pyrochemical head-end reprocessing of irradiated fuel elements, 25:13077(R) (ANL-7755)
IODINE BROMIDES
  properties as radical scavengers in reactions of recoil tritium with deuterium, hydrogen, or methane, 25:13067
IODINE CHLORIDES
  effects on yields from γ radiolysis of carbon tetrachloride at 25°C, 25:13045
  properties as radical scavengers in reactions of recoil tritium with deuterium, hydrogen, or methane, 25:13067
  yields from γ radiolysis of carbon tetrachloride, effects of scavengers on, 25:13045
IODINE ISOTOPES
  content of fallout, in plant tissues, role of species differences and standard methods of data expression in prediction of, 25:13395 (SWRHL-90-r)
  deposition of radioactive, on plant leaves from fallout, factors affecting foliar sorption following, 25:13395 (SWRHL-90-r)
  half-life of radioactive, on plant tissues following deposition from fallout, factors affecting, 25:13395 (SWRHL-90-r)
  uptake of radioactive, by human thyroid gland, use of iodine-125 for measuring, 25:13485
IODINE ISOTOPES I-124
  beta spectra from, shapes of nonunique and unique first-forbidden, 25:14976
IODINE ISOTOPES I-125
  uptake by thyroid in combination with iodine-131 as test for functional autonomy following therapy in patients with multinodular goiter, 25:13493
  use for measuring iodine radioisotope uptake by human thyroid gland, 25:13485
  use with chromium-51 in double tracer dilution method for measuring blood plasma volume in relation to erythrocyte mass in patients, 25:13338
IODINE ISOTOPES I-129
  monitoring at West Valley Processing Plant, Oct.--Dec, 1970, 25:13079 (DOCKET-50201-61)
IODINE ISOTOPES I-130
  beta and isomeric conversion decay of 9.2-min, energy levels of xenon-130 from, (E), 25:15007
  beta decay of 12.3-hr isomer, energy levels of xenon-130 from, (E), 25:15007
IODINE ISOTOPES I-131
  accumulation by crops and soils in France from fallout and industrial wastes, 25:13402
  beta decay of, velocity spectra of Coulomb fragmentation of diatomic iodine compounds by, 25:13073
  content in milk in Nuclear Fuel Services farm, West Valley, New York, 25:13079 (DOCKET-50201-61)
  content of feces, milk, and urine of dairy cattle following ingestion of Schooner fallout, 25:13396 (UCRL-72511)
  content of human thyroid from contaminated milk in Australia and New Guinea following nuclear weapons testing during 1966 to 1968, fallout, 25:13436
  content of milk in Canada, Central America, South America, and United States during 1969 and 1970, 25:13433
  content of milk in Western Hemisphere during April 1970 as compared to average for previous 12-month period, 25:13442
  content of milk sampled throughout Central, North, and South America during July 1970, 25:13401
  content of thyroid gland in children, reconcentration factor for, 25:13347
  deposition from air to grass in comparison to krypton-85, measurement of rate of, 25:13124
  distribution in fetal and maternal tissues of dairy cattle following ingestion of Schooner fallout, 25:13396 (UCRL-72511)
  effectiveness of fibrinogen-incorporated, for scanning of experimentally induced thrombi in animals, 25:13518
  effects on survival of man following therapy for thyroid carcinomas, 25:13524
  effects on thyroid hormone synthesis in patients with toxic thyroid adenomas following therapy, 25:13594
  exchange between iodomethane and potassium iodide in ethanol at 35°C, reaction order for components in, 25:12996
  excretion in human urine following use for therapy of thyroid carcinoma, 25:13596
  monitoring at West Valley Processing Plant, Oct.--Dec, 1970, 25:13079 (DOCKET-50201-61)
  radiation effects on uptake of albumin-incorporated, by perfused intestine of rats, effects of food intake on, 25:13349
  release in reactor effluents, application and basis of factor of 700 for, 25:13438
  removal from liquid radioactive wastes, effects of hydrological conditions on efficiency of Hanford Emergency Waste Disposal Crib for, (T), 25:13186 (BNWL-1503)
  separation of iodate, iodide, and periodate forms of, by thin-layer chromatography, 25:13099
  uptake by thyroid in combination with iodine-125 as test for functional autonomy following therapy in patients with multinodular goiter, 25:13493
  use for diagnosis of lesions in liver of man, methods for, 25:13483
  use for scanning liver of children following radiotherapy of neoplasms, 25:13578
  use of iodohippuric acid-incorporated, for scintigraphy of kidneys in man in comparison to indium-113m-labeled EDTA, 25:13499
  use with metastable technetium-99 and scintillation camera for diagnosis of ureteral obstruction following human kidney transplant, 25:13490
ION-ACOUSTIC WAVES
  absorption in nonisothermal plasma, anomalous, (T), 25:14373
  interaction with electromagnetic wave in isotropic plasma, trapping in resonant, 25:14374
  propagation in plasma, formation of collisionless electrostatic shock waves, in, (E/T), 25:14389
ION BEAMS
  design of proton, for plasma experiments, (E), 25:14253
ION SOURCES
  design and optimization of magnetron-type, for ISOLDE isotope separator, 25:13162 (JINR-P13-5369)
IONOSPHERE
  D region, effects of solar x rays on radio absorption at high frequencies in, (E), 25:13897
  distortions in quasi-periodic small-scale auroral arc, (E), 25:14119
  electric fields in auroral, proton flux-associated, (T), 25:14106
  electron density changes with solar-zenith angle in lower, (E), 25:14104
  electron density variations at 50 to 80 km in, cosmic-ray and geomagnetic effects on, (E/T), 25:14127
  electron production in lower, by solar corpuscular streams, (T), 25:14126
  electron production in lower, by solar particles, (E/T), 25:14124
  electron trapping in electrostatic double layers of, (E), 25:14103
  electrostatic fields in, theory for, 25:14123
  F2 layer, critical frequency of, tidal spectra effects during solar maximum and minimum in, (E), 25:14105
  F2 layer, relation of electron density with solar-wind velocity, Dec. 16 to May 10, 1966, daytime, (E), 25:14110
  interactions with bodies in, structure of far wake from double, (E/T), 25:14112
  polar-cap phenomena in, particle-stimulated processes in, (E/T), 25:14102 (N-70-19848)
  proton flux in auroral, parallel to geomagnetic field lines, (E), 25:14125
  radio-wave absorption in auroral, time variations of, (E), 25:14118
  wave propagation in, response to isotropic spectrum of internal gravity, (E/T), 25:14121
IONS
  charged-particle inelastic scattering by, asymptotic expression for total cross sections for, 25:14022
  electron correlation in two-electron, calculation using semiempirical pseudopotential procedure, 25:14055
  energy levels of two-electron, perturbation theory of autoionizing, 25:14049
  photon reactions with negative, long-range correction to matrix elements for dissociation in, 25:14019
  properties of highly ionized, technique of vacancy-cascade spectroscopy for study of, 25:14038
  reactions between negative and positive, at thermal energies, mutual neutralization in, (E/T), 25:14032
  reactions of heavy, with uranium, effects of nuclear deformability on cross sections for, (T), 25:15063
  reactions with air and helium of Z = 36 to 74, dependence

  of mean charges of ions from, on atomic number, (E), 25:14007
  reactions with excited atoms, classical calculation of cross sections for resonant charge exchange in, 25:14031
  reactions with molecules, kinetic model for, 25:14041
  spectra of, deviations from LTE in weak complex, (T), 25:13816
  wave functions for Z = 87 to 103, screening numbers for calculation of scaled hydrogen-like, 25:13976
IRIDIUM
  determination in meteoritic materials by neutron activation and γ--γ coincidence spectrometry, 25:12967
IRIDIUM ALLOYS AND SYSTEMS
  Co--Ir, superconductivity and spin fluctuations in, (E), 25:14202
  Fe--Ir, superconductivity and spin fluctuations in, (E), 25:14202
  Ir--Nb, superconducting transition temperature and low-temperature thermal capacity of sigma-phase, (E/T), 25:14177
  Ir--Ni, superconductivity and spin fluctuations in, (E), 25:14202
IRIDIUM ISOTOPES
  electron-capture decay of neutron-deficient, (E/T), 25:14993
IRIDIUM ISOTOPES Ir-192
  beta and electron-capture decay of, γ singles and coincidence spectra from, (E), 25:15062
  preparation and properties of gamma sources of, for radiography of aircraft parts, 25:13180 (JAERI-Memo-4163)
IRON
  abundance in late G and K dwarfs, (E), 25:13824
  abundance in solar wind, (E), 25:13958
  determination in airborne and deposited particulates by neutron activation and γ spectrometry, 25:12975
  determination in aluminum-, cobalt-, copper-, nickel-, or titanium-base alloys using gas-sheathed tubular electrode arc, spectroscopic, 25:12945
  determination of trace amounts of, in blood serum by emission spectroscopy, 25:12946
  determination of trace amounts of, in boron carbide by neutron activation, 25:12972
  determination using tiron and diphenylguanidine, extraction--photometric method for, 25:12934
  effects on fluorine determination in organic componds by spectrophotometry using thorium chloranilate, 25:12936
  effects on gravimetric determination of tellurium, 25:12943
  effects on oxidation of trivalent uranium in sulfuric acid, 25:12977
  electron backscattering at 1.0 MeV by thick targets of, Monte Carlo calculation of angular distributions and energy spectra from, 25:13959 (UCRL-19719)
  gamma transport in two-region systems with lead and water, calculations using iterative method, 25:14407
  gamma transport in, calculations using anisotropic source--flux iteration technique, 25:14407
  neutron capture at 0.01 to 20 MeV, cross sections for, (T), 25:14970
  neutron capture by, excitation of energy levels in 6- to 9-MeV region by gamma rays from thermal, (E), 25:15002
  neutron elastic and inelastic scattering at 1.43 to 2.15 MeV, cross sections for, (E), 25:14961
  neutron elastic scattering at 1.8 to 8.1 MeV, cross sections for, (E/T), 25:14964
  neutron elastic scattering at 8 MeV, cross sections for, (E/T), 25:14965
  neutron inelastic scattering at 2 to 4.5 MeV, cross sections for, (E/T), 25:14966
  neutron inelastic scattering by, cross sections for fast, (E), 25:14960
  neutron reflection by, one-dimensional S/sub n/ calculations of spectra of, (T), 25:14865 (COO-2049-2)
  neutron scattering by, forward amplitude for magnetic thermal, (E), 25:14868
  piezoresistance from stress-induced ordering of defects in alpha-, anelastic, (E/T), 25:13677
  positron backscattering at 1.0 MeV by thick targets of, Monte Carlo calculation of angular distributions and energy spectra from, 25:13959 (UCRL-19719)
  radiation effects on removal of divalent, from acidic mine waste waters, 25:13036(P)
  spectra of neutral, in low-current electric arcs, (E), 25:14245
  yields of multiply charged states of, from cobalt-57 electron-capture decay in cobalt complexes with 2,4-pentanedione, 25:13075
IRON ALLOYS AND SYSTEMS
  analysis for constituents using gas-sheathed tubular electrode arc, spectroscopic, 25:12945
  Al--Cr--Fe, mechanical properties of, effects of zirconium on, 25:13680
  Al--Cr--Fe, oxidation resistance to carbon dioxide at 600 to 900°C, effects of zirconium on, 25:13680
  Au--Fe--Te, superconducting transition temperature and lattice parameters of liquid-quenched simple-cubic, 25:14178
  Co--Fe-base--Ni, thermal conductivity at 80 to 293°K, effects of cobalt content on, 25:13685
  Co-base--Cr--Fe--Mn, deuteron stopping power at 2.5 to 7.0 MeV for Havar foils, (E), 25:14401
  Cr--Fe--Mo--Ti, microstructure of anti-phase boundaries in chi-phase of $Fe_{36}Cr_{12}Mo_5Ti_5$, 25:13711
  Cu--Fe--Zr-base, corrosion by steam at 350 to 450°C and 50 atm pressure, 25:13629 (EIR-184)
  Fe--Ir, superconductivity and spin fluctuations in, (E), 25:14202
IRON HYDROXIDES
  toxicity to mice in relation to use of metastable indium-113--iron-59-labeled ferric hydroxide particles for lung scanning, 25:13486
IRON IONS
  reactions with oxygen atoms at 30 keV to 2 MeV, cross sections for electron capture and loss in, (E), 25:14042
  spectra of Fe VIII and Fe XV in Sun, (E/T), 25:13886
IRON ISOTOPES Fe-52
  production for medical use by (He-3,3n) reactions with chromium-52 at 45.5 MeV, 25:13063
IRON ISOTOPES Fe-55
  content of fish protein concentrates, 25:13394(R) (RLO-2059-1)
IRON ISOTOPES Fe-56
  bremsstrahlung reactions at 0.8 to 2.1 GeV, spallation products from, (E), 25:14977
  energy levels from cobalt-56 electron capture decay, (E), 25:14957
  energy levels from iron-57 (p,d) reactions, spectroscopic factors for, (E/T), 25:14921 (CEA-CONF-1653)
  neutron reactions (n,p) with, fission-spectrum-averaged activation cross sections for, (E), 25:14968
IRON ISOTOPES Fe-57
  Moessbauer spectrum of, ambiguity problem in hyperfine parameters of, (T), 25:14485
  nuclear properties of, unified rotational model for, (T), 25:14973
  proton reactions (p,d) at 17.3 MeV, DWBA analysis of differential cross sections and asymmetries from, (E/T), 25:14921 (CEA-CONF-1653)
  reactions of recoil, from cobalt-57 electron-capture decay in doped Prussian Blue, 25:13068
IRON ISOTOPES Fe-59
  reactions of recoil, in neutron-irradiated potassium ferrocyanide or Prussian Blue, 25:13068
  retention in lungs of mice in relation to use of metastable indium-113--iron-59-labeled ferric hydroxide particles for lung scanning, 25:13486
IRON OXIDES
  content in rocks of shields and sediment cover of Brazil, Canada, and USSR, relations with geological time, 25:13114
IRON SULFATES $FeSO_4$
  properties and uses of dosimeters of, review on, 25:13305
  use in γ dosimetry, 25:13456
IRRADIATION FACILITIES
  sample holder for, design of fluid-supported spherical, 25:13208(P)
ISOTOPE EFFECTS
  measurement of precise vapor pressure, from -20 to 110°C, design of equipment for, 25:12995
ISOTOPE SEPARATION METHODS
  transport equations for, elementary integration of nonlinear, 25:13085
ISOTOPES
  diffusion in coated irradiated fuel spheres, models for calculation of, 25:13782 (JUL-685-PA)
ITALY
  radiation hazards to personnel at military nuclear establishment in Pisa, statistical analysis of medical judgments regarding, 25:13468
  radioactivity of natural waters and water supplies in, (E), 25:13106
  regulations for disposal of radioisotope-containing wastes in, review of, 25:13207

J

JAPAN
  radiation monitoring of environment of JAERI, Tokai, during 1969, 25:13119 (JAERI-Memo-4175)
  radioisotope content of beer in, in relation to atmospheric deposition rates in Tokyo area during 1959 to 1969, comparison of fallout cesium-137 and strontium-90, 25:13434
JAPANESE ADVANCED THERMAL REACTOR
  bibliography on, April 1966 to February 1970, 25:15338 (AAEC/LIB/Bib-258)
JAPANESE EXPERIMENTAL FAST REACTOR
  containment structures for, conceptual design parameters of, 25:15389 (JAERI-1177-B(Pt.2))
  control system for, conceptual design parameters of, 25:15389 (JAERI-1177-B(Pt.2))
  cooling system for, conceptual design parameters of, 25:15389 (JAERI-1177-B(Pt.2))
  design parameters of, conceptual, 25:15389 (JAERI-1177-B(Pt.2))
  instrumentation for, conceptual design parameters of, 25:15389 (JAERI-1177-B(Pt.2))
  radioactive waste disposal system for, conceptual design

- parameters of, 25:15389 (JAERI-1177-B(Pt.2))
- shielding for, conceptual design parameters of, 25:15389 (JAERI-1177-B(Pt.2))

JAPANESE MATERIALS TESTING REACTOR
- physics calculations for, comparison of computer programs for, 25:15391 (JAERI-Memo-4180)

JERVIS BAY POWER REACTOR
- siting of, foundation and hydrographic suitability of Scottish Rocks area for, 25:15336 (NP-18636)

JUPITER (PLANET)
- magnetosphere of, rotation period of, (E), 25:13957

K

KANSAS
- radiation monitoring of surface waters of, during 1969, α and β, 25:13432
- safety survey of x-ray equipment used in schools in, 25:13463

KEWAUNEE POWER REACTOR
- buildings and structures for, preliminary safety analysis of foundations for, 25:15314 (DOCKET-50305-17)
- buildings for, design codes for, 25:15314 (DOCKET-50305-17)
- components of, design codes for, 25:15314 (DOCKET-50305-17)
- containment systems for, final safety analysis of, 25:15311 (DOCKET-50305-14)
- control system for, final safety analysis of, 25:15311 (DOCKET-50305-14)
- coolant loss accident conditions in, final safety analysis of, 25:15313 (DOCKET-50305-16)
- cooling system for, final safety analysis of, 25:15310 (DOCKET-50305-13)
- design parameters of, final safety analysis of, 25:15310 (DOCKET-50305-13)
- effluents from, effects on environment of chemical, radioactive, and thermal, 25:15309 (DOCKET-50305-12)
- electrical systems for, final safety analysis of, 25:15311 (DOCKET-50305-14)
- emergency and auxiliary systems for, final safety analysis of, 25:15312 (DOCKET-50305-15)
- emergency systems for, final safety analysis of, 25:15313 (DOCKET-50305-16)
- engineered safeguards for, final safety analysis of, 25:15311 (DOCKET-50305-14)
- instrumentation for, final safety analysis of, 25:15311 (DOCKET-50305-14)
- operation aspects of, final safety analysis of, 25:15312 (DOCKET-50305-15)
- quality assurance program for, 25:15314 (DOCKET-50305-17)
- radiation protection system for, final safety analysis of, 25:15312 (DOCKET-50305-15)
- radioactive source base for, preliminary safety analysis of, 25:15314 (DOCKET-50305-17)
- radioactive waste disposal system for, final safety analysis of, 25:15312 (DOCKET-50305-15)
- safety analysis of, 25:15313 (DOCKET-50305-16)
- site for, final safety analysis of, 25:15310 (DOCKET-50305-13)
- site for, geology of, 25:15314 (DOCKET-50305-17)
- steam and power conversion systems for, final safety analysis of, 25:15312 (DOCKET-50305-15)
- testing programs for, final safety analysis of, 25:15312 (DOCKET-50305-15)

KIDNEYS
- indium-131--tin-113 distribution in rat, 25:13501
- lithium-6 uptake by, of rats following intraperitoneal and intravenous injections, 25:13350
- radiation effects on water content and distribution in, of rats, effects of lethal and sublethal dose on x, 25:13348
- scanning for differential diagnosis of benign and malignant neoplasms, use of metastable technetium-99 for, 25:13504
- scanning of human, effectiveness of iodine-131-labeled hippuran for, in comparison to indium-113m-labeled EDTA, 25:13499
- selenium-75-labeled selenomethionine uptake by dog, effects of route of administration on, 25:13343

KRYPTON
- analysis for trace amounts of carbon dioxide following freezing-out at liquid nitrogen temperature, mass spectrometric, 25:12941
- analysis for trace amounts of hydrogen following condensation, mass spectrometric, 25:12941
- chemical state of, in irradiated oxide fuel elements, 25:13077(R) (ANL-7755)
- electron elastic scattering at 25 to 800 eV by, tables of amplitudes and spin polarizations for, (T), 25:13995 (AD-711664)
- electron reactions at 40 to 140 eV with, excitation functions of spectral lines of Kr II in, (E), 25:14040
- electron reactions up to 150 eV with, ionization cross sections for, (E), 25:14002
- krypton isotope concentration in, by thermal diffusion, 25:13165(R) (MLM-1753)

KRYPTON IONS
- effects on gold at 4 to 42 keV, defects induced in, 25:14413 (NP-18645)
- reactions with oxygen atoms at 30 keV to 2 MeV, cross sections for electron capture and loss in, (E), 25:14042

KRYPTON ISOTOPES Kr-78
- abundance in Apollo 11 igneous rocks, (E), 25:13954

KRYPTON ISOTOPES Kr-83
- abundance in Apollo 11 igneous rocks, (E), 25:13954

KRYPTON ISOTOPES Kr-85
- deposition from air to grass in comparison to iodine-131, measurement of rate of, 25:13124
- ion channeling patterns in silicon, 25:14417
- monitoring at West Valley Processing Plant, Oct.--Dec, 1970, 25:13079 (DOCKET-50201-61)
- production in neutron fission of plutonium-239, release curves for, (T), 25:14989 (UCRL-50656(Suppl.))

KRYPTON ISOTOPES Kr-86
- concentration in krypton by thermal diffusion, 25:13165(R) (MLM-1753)
- production in neutron fission of plutonium-239, release curves for, (T), 25:14989 (UCRL-50656(Suppl.))

KRYPTON ISOTOPES Kr-87
- production in neutron fission of plutonium-239, release curves for, (T), 25:14989 (UCRL-50656(Suppl.))

KRYPTON ISOTOPES Kr-88
- production in neutron fission of plutonium-239, release curves for, (T), 25:14989 (UCRL-50656(Suppl.))

L

LA CROSSE BOILING-WATER REACTOR
- instrumentation for, authorization for automatic gain control system for, 25:15241 (DOCKET-1155-90)
- operations incident of December 18, 1970, failure of electric control rod drive system during startup, 25:15220 (DOCKET-1155-95)
- operations incident of December 20, 1970, unplanned scram from failure of power range instrument channel self-testing circuit, 25:15223 (DOCKET-1155-98)
- operations incident of December 21, 1970, unplanned scram from failure of water level safety channel, 25:15222 (DOCKET-1155-97)
- operations incident of December 9, 1970, unplanned scram from operator error in switching instrumentation channel range, 25:15221 (DOCKET-1155-96)
- operations incident of November 1, 1970, unplanned scram from operator error in switching power instrumentation range, 25:15218 (DOCKET-1155-93)
- operations incident of November 4, 1970, failure of emergency diesel generator to start on first crank, 25:15219 (DOCKET-1155-94)
- operations incident of October 28, 1970, failure of control rod drive hydraulic scram, 25:15217 (DOCKET-1155-92)
- operations incident of October 28, 1970, unplanned scram from on-power scram circuit test procedures, 25:15216 (DOCKET-1155-89)
- shutdown system for, modification of low flow bypass key switches for on-power testing of emergency, 25:15242 (DOCKET-1155-91)

LACTATE DEHYDROGENASE
- radiation effects on activity of, in central nervous system of rabbits, ionizing, 25:13561
- radiation effects on activity of, in human serum in combination with cytostatic drugs, x, 25:13527

LACTATES
- radiation effects on content of, in sheep serum, effects of air blast injury, and fasting on γ and neutron, 25:13384

LANTHANUM
- complexes with carminic acid, spectrophotometric studies on, 25:12937
- determination in neutron-irradiated graphite by γ spectrometry, 25:12954
- determination in plutonium oxide--uranium oxide fuels by solvent extraction and emission spectrography, 25:12922 (WHAN-SA-44)
- determination of trace amounts of, in plutonium and plutonium dioxide--uranium dioxide by solvent extraction and emission spectrography, 25:12923 (WHAN-SA-47)
- structure of films work function of films of, on molybdenum (110) surface, 25:13702
- uses in potentiometric titration for determination of fluoride ions, 25:12929

LANTHANUM ALLOYS AND SYSTEMS
- Am--La-base, americium effective ionic size in, 25:13705

LANTHANUM BORIDES
- electronic structure of CaB_6-type, 25:14463
- thermal expansion of LaB_4, LaB_6, and LaB_{12}, (E), 25:13760

LANTHANUM HYDRIDES
- positron annihilation rates in, effects of stoichiometry on, 25:13988

LANTHANUM ISOTOPES
- uses in fallout field simulation methods, 25:13117 (AD-711532)

LANTHANUM ISOTOPES La-139
- energy levels of, photon resonant scattering studies on, 25:15032

XUM

- energy-level excitation by neutron capture gamma rays, (E), 25:15002

LANTHANUM ISOTOPES La-140
- content of feces, milk, and urine of dairy cattle following ingestion of Schooner fallout, 25:13396 (UCRL-72511)

LANTHANUM OXIDES
- properties of aerosols of, measurement of chemical and physical, 25:13145
- B_2O_3--La_2O_3, lanthanum coordination structure in glasses of, 25:13019
- BaO--B_2O_3--La_2O_3, structure and properties of glasses of, 25:13019

LARVAE
- radiosensitivity of Sitophilus oryzae, cobalt-60 γ, 25:13558

LASER RADIATION
- interactions with argon plasma, spark maintenance in, (E), 25:14331
- interactions with plasma, effects of strong magnetic induction on, (E), 25:14334
- interactions with plasma, electron heating and bremsstrahlung radiations from, 25:14279
- interactions with plasma, ponderomotive force in, (T), 25:14332
- interactions with plasma, self-similar thermal wave in two-temperature, (T), 25:14237
- scattering on plasma, diagnostic use of, 25:14255
- scattering on plasma, diagnostic use of, 25:14241 (AD-710718)
- scattering on z-pinch plasma, electron drift velocity from, 25:14256

LASERS
- electron motion in, covariant classical, (T), 25:14506

LAWRENCIUM ISOTOPES
- alpha decay of, properties of, (E), 25:15052

LEACHING
- effects on strontium-90 removal from soils, 25:13118(R) (COO-414-17)

LEAD
- content of marine organisms in Pacific Ocean, 25:13394(R) (RLO-2099-1)
- determination in atmosphere, filter collection and x-ray fluorescence method for, 25:13309
- determination in copper-base alloys using gas-sheathed tubular electrode arc, spectroscopic, 25:12945
- determination of trace amounts of, in blood serum by emission spectroscopy, 25:12946
- determination using thin-layer chromatography and ring-oven colorimetry, 25:12944
- deuteron reactions (d,p) at 650 MeV, proton angular distributions from, (E), 25:14906
- effects on backscattering during γ dosimetry, 25:13456
- effects on gravimetric determination of tellurium, 25:12943
- electron elastic scattering at 25 to 800 eV by, tables of amplitudes and spin polarizations for, (T), 25:13995 (AD-711664)
- electron elastic scattering by, effects of virtual nuclear excitation on cross section of, (T), 25:15166
- electron energy losses at 52 to 92 MeV in, (E), 25:14392 (AD-711005)
- Ettingshausen effect in intermediate state of thin films of superconducting, thickness dependence of, 25:14181
- gamma transport in two-region systems with iron and water, calculations using iterative method, 25:14407
- gamma transport in, calculations using anisotropic source--flux iteration technique, 25:14407
- incorporation in vinyl panels, for fabrication of protective clothing for personnel against x radiation, 25:13462
- neutron elastic scattering at 8 MeV, cross sections for, (E/T), 25:14965
- nuclear polarization energy correction in muonic, (T), 25:14937
- properties for use in shielded containers, 25:13204(P)
- proton reactions below 70 GeV/c, atlas of particle-production-momentum spectra for, (T), 25:14733 (NP-18660)
- reflectivity of superconducting films of, phonon structure in far-infrared, 25:14175
- superconducting critical field in thin and thick films of, ultrasonic attenuation study of angular dependence of, (E/T), 25:14163
- superconducting layers of, frequency dependence of residual resistance of, (E), 25:14170
- ultrasonic attenuation of γ-irradiated monocrystalline, at 77 to 300°K, 25:14459

LEAD ALLOYS AND SYSTEMS
- Bi--Pb--Sb, superconducting properties of, in porous glass, 25:14191
- In--Pb, superconducting flux trapping in region of martensitic transformation, 25:14172
- In--Pb, thermal capacity and superconducting properties at low temperatures, 25:14180
- Mg-base--Pb, thermal conductivity at low temperatures, 25:14473
- Pb--Sn, photon scattering at 662, 1120, and 1330 keV by, effective atomic numbers for coherent, 25:14405
- Pb--Tl, superconducting intermediate state in, Meissner--Shubnikov domain patterns in, 25:14164

LEAD ISOTOPES Pb-203
- content of feces, milk, and urine of dairy cattle following ingestion of Schooner fallout, 25:13396 (UCRL-72511)

LEAD ISOTOPES Pb-206
- alpha fission of, anisotropy and excitation functions for, 25:15010
- energy levels of, quasiparticle structure of, (T), 25:15178
- helium-4 reactions (He-4,3n) at 32 to 44 MeV, angular distributions, cross sections, and recoil ranges for, (E), 25:14996

LEAD ISOTOPES Pb-207
- helium-3 reactions (He-3,3n) at 21 to 33 MeV, angular distributions, cross sections, and recoil ranges for, (E), 25:14996

LEAD ISOTOPES Pb-208
- energy-level excitation by neutron capture gamma rays, (E), 25:15002
- oxygen-16 reactions with, production of thorium-221 and thorium-222 by, 25:15011
- proton inelastic scattering at 155 MeV, DWBA analysis of polarization angular distributions from, (T), 25:14892 (RLO-1388-600)

LEAD ISOTOPES Pb-210
- content of fish protein concentrates, 25:13394(R) (RLO-2099-1)
- content of marine organisms in Pacific Ocean, 25:13394(R) (RLO-2099-1)

LEAD NITRATES
- KNO_3--$Pb(NO_3)_2$, electrolytic properties of aqueous solutions of, adiabatic compression and ultrasonic attenuation studies of, 25:13015
- NH_4NO_3--$Pb(NO_3)_2$, electrolytic properties of aqueous solutions of, adiabatic compression and ultrasonic attenuation studies of, 25:13015

LEAD OXIDES
- analysis for silver by neutron activation and radiochemical separation using diethyl dithiocarbamate, 25:12963
- deposition and properties of thin films of, chemical vapor, 25:13748

LEAD TELLURIDES
- thermoelectric properties of, measurements for use in SNAP-23A, 25:13166(R) (MPM-4187-1)

LEAD TIN TELLURIDES
- thermoelectric properties of, measurements for use in SNAP-23A, 25:13166(R) (MPM-4187-1)

LEAVES
- iodine radioisotopes deposition on plant, factors affecting foliar sorption following fallout, 25:13295 (SWRHL-90-r)

LECITHINS
- carbon-14-labeled palmitate incorporation into, of rat lungs, effects of breathing nitrogen dioxide on, 25:13356

LEPTONS
- charge conservation of, (T), 25:13909
- production of heavy, in $e^+ + e^-$ interactions at 0.8 to 1 GeV, (E), 25:14517

LEUCINE
- radiation effects on incorporation of tritium-labeled, in cytoplasm of perfused rat liver, x, 25:13373

LEUKOCYTES
- radiation effects on, in rats, RBE for cesium-137 and tritium oxide, 25:13551

LEVEL INDICATORS
- design of gamma radiometric, for blast furnaces, 25:13307

LIGHT
- deflection by solar gravitational field, (T), 25:13946
- effects on time of ripening and yield of γ-irradiated cotton, 25:13602
- scattering in spin-wave resonances in semiconductor antiferromagnets, (T), 25:14488

LIGHTNING
- discharges of, generation of low-latitude subprotonospheric and ion-cyclotron whistlers from same, (E), 25:14114

LINEAR ACCELERATORS
- beam losses in high-current induction electron, 25:14856(T) (UCRL-Trans-1425)
- control system for 2-GeV electron, automatic computer, 25:14852(T) (SLAC-Trans-126)
- control systems and instruments for ORELA, development of, 25:13318(R) (ORNL-4620)
- design modification of Berkeley Hilac for acceleration of ions of all masses, 25:14853 (UCRL-19919)
- development of 30-MeV, 250-A electron induction, 25:14856(T) (UCRL-Trans-1425)
- installation of pulsed reactor with, advantages to biology and medicine of, 25:13548
- pulse generators for electron, for high-intensity nanosecond beam pulsing, 25:14858
- storage ring at Orsay, proposal for colliding beam, 25:14843 (LAL-RT-44-70)

LIPIDS
- carbon-14 incorporation in, of rat liver homogenates, effects of avidin on, 25:13344

LIQUID FLOW
- magnetohydrodynamic, of viscous incompressible drops under axisymmetric current distribution, (T), 25:14096

LIQUID METAL FAST BREEDER REACTOR
  development of Argonne National Laboratory, December 1970, 25:15339 (ANL-7765)
  fuel elements for, performance of stainless steel clad plutonium oxide (PuO_2)--uranium oxide (UO_2), (E/T), 25:15367 (WHAN-SA-51)
  fuels for, effects of fabrication variables and irradiation history on dissolution in nitric acid, 25:13083 (WHAN-FR-33)
  piping systems for, comparison of dynamic analysis methods for, 25:15362 (UNC-5231)
  piping systems for, comparison of methods for in-service inspection of, 25:15359 (SAN-781-243)
  piping systems for, comparison of model testing methods for, 25:15358 (SAN-781-234)
  piping systems for, corrosive effects of liquid sodium on, 25:15357 (SAN-781-228)
  piping systems for, development and verification of design guide for, 25:15355 (SAN-781-100)
  piping systems for, fabrication and installation requirements for, 25:15356 (SAN-781-220)
  piping systems for, philosophy and criteria of design guide for, 25:15360 (SAN-781-500)
  piping systems for, review of research and development programs for, 25:15361 (SAN-781-518)
  safety of, bootstrap concept of facility for in-pile tests of, 25:15380
LIQUIDS
  atomization by gas streams at high velocities, 25:15418(T) (ANL-Trans-871)
LITHIUM
  abundance in Sun, (E), 25:13870
  content and depth in crustal basalts and granites in USSR, 25:13115
  corrosive effects of liquid, on stainless steel, relations of powdered molybdenum on resistance to, 25:13634
  corrosive effects on niobium-base--zirconium alloys, relations with dissolved oxygen content, 25:13630 (EUR-4298)
  corrosive effects on tantalum, relations with dissolved oxygen conent, 25:13630 (EUR-4298)
  effects on γ radiolysis of ammonia adsorbed on synthetic zeolites, EPR spectral studies on, 25:13057
  electron backscattering at 1.0 MeV by thick targets of, Monte Carlo calculation of angular distributions and energy spectra from, 25:13959 (UCRL-19719)
  ion exchange behavior on zirconium phosphate crystals, 25:13084
  positron backscattering at 1.0 MeV by thick targets of, Monte Carlo calculation of angular distributions and energy spectra from, 25:13959 (UCRL-19719)
  radiation effects on 3-methylpentane containing, at 77°K, comparative ESR studies on paramagnetic species produced from γ or uv, 25:13025
  radiation effects on silicon doped with, Hall-effect study of electron, 25:14423
  separation from fuel dissolver solution, 25:13081 (NP-18577)
LITHIUM ALLOYS AND SYSTEMS
  Al-base--Li, stress rupture of dilute, at 175 to 300°C, effects of radioinduced gas bubbles on, 25:13678
LITHIUM CHLORIDES
  radiation effects on methanol solutions of, chemical states of sulfur-35 from, 25:13071
LITHIUM FLUORIDES
  use in γ dosimetry, 25:13456
  LiF--UF_4, preparation of lithium-7 and uranium-233 enriched, 25:15368
LITHIUM HYDRIDES
  positron annihilation rates in, 25:13988
LITHIUM IONS
  charged-particle reactions with, ionization cross sections for, (T), 25:14022
  reactions with metallic oxides at 10 to 40 keV, secondary electron yields from, (E), 25:13963
LITHIUM ISOTOPES Li-6
  abundance in Sun, (E), 25:13870
  abundance in sunspots, (E), 25:13865
  alpha reactions (α,2α) near 60 MeV, analysis for reaction mechanism in, (E), 25:14902
  diffusion from irradiated beryllium oxide, mechanisms of, 25:13781 (JUL-677-RG)
  distribution in tissues and organs of rats following intraperitoneal and intravenous injections, 25:13350
  energy levels of, shell model with realistic forces for, 25:15186
  hadron scattering by, testing cluster model by, 25:15183
  meson (π) elastic scattering by, 25:15183
  neutron reactions (n,α) at 0.01 to 80 keV, cross sections for, (E)T), 25:14910
  neutron reactions (n,α) at 100 to 500 keV, cross section for, (E), 25:14913
  neutron scattering at 1 to 110 keV, cross sections for, (E), 25:14909
  proton reactions (p,pα) near 60 MeV, analysis for reaction mechanism in, (E), 25:14902
LITHIUM ISOTOPES Li-7
  abundance in Sun, (E), 25:13870
  abundance in sunspots, (E), 25:13865
  alpha reactions (α,2α) near 60 MeV, analysis for reaction mechanism in, (E), 25:14902
  deuteron reactions (d,2α) at 3.0 to 5.9 MeV, rescattering effects on α--α coincidence spectra from, (E/T), 25:14891(T) (CRO-1316-97)
  photon reactions with, differential cross sections for π^0 production in polarized, 25:14602
  proton reactions (p,pα) near 60 MeV, analysis for reaction mechanism in, (E), 25:14902
LITHIUM ISOTOPES Li-8
  production in meson (K^-) reactions with heavy emulsion nuclei at 1.5 and 3.5 GeV/c, 25:14978
LITHIUM NITRATES
  KNO_3--$LiNO_3$, electrolytic properties of aqueous solutions of, adiabatic compression and ultrasonic attenuation studies of, 25:13015
LIVER
  carbon-14 incorporation in lipids and proteins of homogenates of, of rats, effects of avidin on, 25:13344
  indium-113--tin-113 distribution in rat, 25:13501
  lithium-6 uptake by, of rats following intraperitoneal and intravenous injections, 25:13350
  radiation effects on histone content of deoxyribonucleoproteins in, of rats, effects of heparin on x, 25:13385
  radiation effects on iodine-131 uptake by perfused, of rats, effects of food intake on, 25:13349
  radiation effects on leucine incorporation and protein synthesis in perfused, of rats, x, 25:13373
  radiation effects on protein synthesis in cells of, in rats, alone and in combination with immunization, 25:13376
  radiation effects on regeneration of, in children following therapy of renal fossa, γ, 25:13578
  radiation effects on selenium-75 incorporation in, in rats in vitro following incubation in sodium selenites, 25:13354
  radiation effects on ultrastructure of cells in, of rats, histochemical studies on cobalt-60, 25:13378
  radiation effects on water content and distribution in, of rats, effects of lethal and sublethal dose on x, 25:13348
  radiodiagnosis of hydatid disease of, in man, combined use of biochemical and immunological tests, radiography, and radioisotope scanning for, 25:13454
  radioinduced damage to, of children following therapy of neoplasms, effects of dactinomycin on γ, 25:13578
  radioinduced inhibition of synthesis of bile acids in, of rats, inhibitory, 25:13370
  scanning of human, following radiotherapy of neoplasms using iodine-131 and metastable technetium-99, 25:13578
  scanning of human, for diagnosis of hemangiomas, uptake of colloidal gold-198 by tumor tissues during, 25:13510
  scanning of human, for diagnosis of malignancies, method for iodine-131, 25:13483
  selenium-75-labeled selenomethionine uptake by dog, effects of route of administration on, 25:13343
LOOPS
  description of sodium, for steam generator testing, 25:13143
LOS ALAMOS AREA (N. MEX.)
  radiation monitoring during 1969, 25:13431
LOS ALAMOS MESON PHYSICS FACILITY
  beam focusing magnets for, superconducting quadrupole doublet, 25:14860
  development of, Aug.--Oct., 1970, 25:14842(R) (LA-4571)
LUNAR MATERIALS
  ages of low- and high-potassium-containing Apollo 11, exposure, (E), 25:13954
  element abundance in Apollo 11 fines, refractory-, (E), 25:13787
  irradiation history of dust particles in Apollo 11 and 12 cores, (E), 25:13958
  magnesium isotope abundances in feldspars, (E), 25:13864
  rare-earth abundances in Apollo 12 basalts, (E), 25:13955
LUNGS
  function studies of, gas analyzer system using xenon-133 tracer for, 25:13223
  indium-113--tin-113 distribution in rat, 25:13501
  iron-59 retention in, of mice in relation to use of metastable indium-113--iron-59-labeled ferric hydroxide particles for lung scanning, 25:13486
  radiation dose to human, x, 25:13453
  radiation effects on histamine content in rat, effects of skin wounds on whole-body, 25:13368
  radioinduced fibrosis in human, following therapy for mammary carcinomas, 25:13584
  scanning of human, development of mobile detectors for xenon-133, 25:13514
  scanning of human, use of inferior probe on dual-headed rectilinear scanner for demonstrating displacement by enlarged heart and free fluids by, 25:13484
  scanning of human, use of xenon-133 with dorsal and ventral detectors for, 25:13520
  scintigraphy of, methods for, 25:13500
  transuranium element content of, effects of medically administered cobalt-57 on measurement of, 25:13458
LUTETIUM
  complexes with carminic acid, spectrophotometric studies

XUM

on, 25:12937
  determination in plutonium oxide--uranium oxide fuels by solvent extraction and emission spectrography, 25:12922 (WHAN-SA-44)
  determination in presence of ytterbium and yttrium using carminic acid, photometric, 25:12937
  determination of trace amounts of, in plutonium and plutonium dioxide--uranium dioxide by solvent extraction and emission spectrography, 25:12923 (WHAN-SA-47)
LUTETIUM ALLOYS AND SYSTEMS
  Gd--Lu, thermal capacity at 0.06 to 0.16°K, effective magnetic field at lutetium nuclei from, 25:14450
LUTETIUM ISOTOPES Lu-169
  energy-level transitions from hafnium-169 decay, multipolarities for, (E), 25:15025
LUTETIUM ISOTOPES Lu-172
  electron-capture decay of, gamma spectra from, (E), 25:15030
LUTETIUM ISOTOPES Lu-175
  alpha reactions (α,2n) at 28 MeV, gamma spectra from, 25:15036
  alpha reactions (α,2n) at 28 MeV, gamma spectra from, (E), 25:15047
  energy-level transitions from beta decay of ytterbium-175, circular polarization of γ rays from, 25:15009
  hyperfine structure of, atomic-beam magnetic-resonance measurement of, 25:13986
  neutron capture by, cross-section calculations for, (T), 25:14982 (NCSAC-31)
  neutron capture by, resonance spin assignments for epithermal, (E), 25:14982 (NCSAC-31)
  proton inelastic scattering at 3 MeV, Moessbauer effect following Coulomb excitation by, (E), 25:15040
LUTETIUM ISOTOPES Lu-177
  energy levels from beta decay of ytterbium-177, (E), 25:15039
LUTETIUM OXIDES
  Lu_2O_3--Yb_2O_3--Y_2O_3, analysis for lutetium and ytterbium using carminic acid, photometric, 25:12937
LYMPH NODES
  radiation effects on lymph flow and filtration function of, in rats, x, 25:13481
  radiotherapy of diseases of human, development of method for ultrahard x, 25:13535
  scanning of parasternal, in patients with mammary carcinomas, effectiveness of colloidal gold-198 for, 25:13515
LYMPH SYSTEM
  radiation effects on human, during therapy following surgical removal of mammary carcinomas, 25:13533
LYMPHOCYTES
  radiation effects on cultured human, protective effects of phytohemagglutinin against effects of dose on, 25:13472
  radiation effects on, in rats, RBE for cesium-137 and tritium oxide, 25:13551
  radioinduced chromosome aberrations in human, analysis of tertiary structure of x, 25:13410
  radioinduced chromosome aberrations in, of swine, effects of dose on cobalt-60 γ, 25:13417
LYSOZYME
  synthesis in Escherichia coli infected with uv-irradiated T4 phage, 25:13616

M

MAGNESIUM
  abundance in late G and K dwarfs, (E), 25:13824
  abundance in Sun, (E/T), 25:13899
  coating of fuel cladding of, method for graphite, 25:13745(P)
  content and depth in crustal basalts and granites in USSR, 25:13115
  determination in aluminum-base alloys using gas-sheathed tubular electrode arc, spectroscopic, 25:12945
  determination using Rhodamine S and TTA, extraction--photometric method for, 25:13098
  neutron reactions (n,xγ) at 14 MeV with natural, cross sections for, (E/T), 25:14920(T) (BNL-tr-380)
  radiation effects on 3-methylpentane containing, at 77°K, comparative ESR studies on paramagnetic species produced from γ or uv, 25:13025
  separation by solvent extraction using Rhodamine S and TTA, 25:13098
  thermal conductivity at low temperatures, 25:14473
MAGNESIUM ALLOYS AND SYSTEMS
  analysis for constituents using gas-sheathed tubular electrode arc, spectroscopic, 25:12945
  Mg--Zn, thermal conductivity at low temperatures, 25:14473
  Mg-base--Pb, thermal conductivity at low temperatures, 25:14473
  Mg-base--Y, deformation of wrought, 25:13710
MAGNESIUM CHLORIDES
  $MgCl_2$--NH_4Cl, electrolytic properties of aqueous solutions of, adiabatic compression and ultrasonic attenuation studies of, 25:13015
MAGNESIUM ISOTOPES Mg-22
  energy levels from (p,t) reactions, spin-parity assignments for, (E), 25:14950
MAGNESIUM ISOTOPES Mg-23
  energy levels of, rigid-rotor and Coriolis model predictions for, (T), 25:14953
MAGNESIUM ISOTOPES Mg-24
  abundance in early solar system, (E), 25:13864
  abundance in Sun, (E), 25:13904
  alpha reactions (α,γ) up to 2.8 MeV, γ-ray yield from, (E), 25:14951
  energy levels from helium-3 inelastic scattering, (E), 25:14899
  helium-3 inelastic scattering at 20.5 MeV, energy spectra and angular distributions in, (E), 25:14899
  neutron reactions (n,p) with, fission-spectrum-averaged activation cross sections for, (E), 25:14968
  proton reactions (p,t) with, angular distributions for, (E), 25:14950
MAGNESIUM ISOTOPES Mg-25
  abundance in Sun, (E), 25:13904
  energy levels from helium-3 inelastic scattering, (E), 25:14899
  helium-3 inelastic scattering at 20.5 MeV, energy spectra and angular distributions in, (E), 25:14899
MAGNESIUM ISOTOPES Mg-26
  abundance in early solar system, (E), 25:13864
  abundance in Sun, (E), 25:13904
  energy levels from helium-3 inelastic scattering, (E), 25:14899
  helium-3 inelastic scattering at 20.5 MeV, energy spectra and angular distributions in, (E), 25:14899
  helium-3 reactions (He-3,n) with, neutron spectra from, (E), 25:14943
MAGNESIUM NITRATES
  $Mg(NO_3)_2$--NH_4NO_3, electrolytic properties of aqueous solutions of, adiabatic compression and ultrasonic attenuation studies of, 25:13015
MAGNESIUM OXIDES
  content in rocks of shields and sediment cover of Brazil, Canada, and USSR, relations with geological time, 25:13114
  creep at high temperatures in polycrystalline, effects of impurities on, 25:15427(R) (COO-1591-13)
  elastic properties of composites of pores in, 25:13751
  properties at high temperatures, review of physical, thermal, and thermodynamic, 25:13667
  B_2O_3--MgO-base--ThO_2, phase equilibria in magnesium oxide corner of, at 1200°C, 25:13770
  MgO--ThO_2, phase equilibria at 1500°C, 25:13770
MAGNESIUM SULFATES
  $MgSO_4$--$(NH_4)_2SO_4$, electrolytic properties of aqueous solutions of, adiabatic compression and ultrasonic attenuation studies of, 25:13015
MAGNET COILS
  description of levitated superconducting, for Princeton Spherator, 25:14356
  design of prototype superconducting suspension, for Univ. of Virginia wind-tunnel balance, 25:14216
  fabrication and testing of superconducting, 25:14219
MAGNETIC FIELDS
  atom ionization energies in superstrong, (T), 25:13829
  components of two-dimensional, FORTRAN computer program for computing, 25:15440 (ORNL-TM-2484)
  effects of interplanetary, on coupling between solar wind and F2 layer, (E), 25:14110
  existence of intergalactic, Faraday rotation measurements of radio sources to confirm, 25:13944
  intensity of longitudinal, in quiescent prominences, (E), 25:13884
  maps of coronal, following proton flares, (E), 25:13893
  relation of mean solar and interplanetary, (T), 25:13856
  structure of interplanetary, (T), 25:14070
  structure of interplanetary, from cosmic-ray variations, (T), 25:14069
MAGNETIC MATERIALS
  excitation in, conference on collective, Tokai, Japan, 12/69, (E/T), 25:14436 (JAERI-1197)
  neutron inelastic scattering by, conference on, Tokai, Japan, 12/69, (E/T), 25:14436 (JAERI-1197)
MAGNETIC MIRROR MACHINES
  magnetic field diffusion through conductive walls of BSG, multipole, (T), 25:14352 (IPPJ-T-3)
  plasma instabilities in DCX devices, ion cyclotron, (T), 25:14348
  plasma instabilities in, hot electron, (E/T), 25:14349
MAGNETIC MONOPOLES
  production by cosmic neutrinos in ocean bed, upper limit for cross section for, 25:14638
  properties of Dirac, limitations on, (T), 25:13953
  search for relativistic, in primary cosmic radiation, (T), 25:14078
MAGNETIC STORMS
  effects of Mar. 24, 1969 on 6300- and 6394-A and OH midlatitude auroral emissions, (E), 25:14115
  effects of small, on diurnal variation of cosmic-ray neutron component, (E), 25:14074
MAGNETOHYDRODYNAMIC GENERATORS
  development of large-scale nonequilibrium, with rare gases, 25:14081(R) (AD-711351)
  electrical effects in electrode boundary layer in Faraday-type, (T), 25:14087
  end effects of inductive three-phase, with open magnetic

  circuit, longitudinal, (E/T), 25:14086
  gas flow in channel of, regenerative amplification and damping of magnetoacoustic waves in, (T), 25:14097
  gas flow in channel of, regenerative amplification and damping of magneto-acoustic waves in, 25:14098
MAGNETOHYDRODYNAMICS
  motions in, studies of free-force helicoidal and quasi-rigid, (T), 25:14094
  theory for cones and drops, 25:14096
MAGNETOMETERS
  use of superconducting quantum interference, as amplifier and multimeter, 25:14217
MAGNETOSPHERE
  electron trapping in closed field lines in, solar, (E/T), 25:14101 (AD-712045)
  hydromagnetic-wave propagation in, resonant mode theory for micropulsations, (T), 25:14117
  pulsations in, resonant mode theory for micro-, (T), 25:14117
  whistler propagation in, nonducted, (E/T), 25:14120
MAGNETOTAIL
  structure near null sheet, (E), 25:14113
MAGNETS
  design of quadrupole, for beam injection in Tokyo 40-GeV proton, 25:14849 (SJC-A-70-6)
  design of superconducting quadrupole doublet, for beam focusing at LAMPF, 25:14860
  design of superconducting, state of art of, 25:14220
  loss measurements on pulsed superconducting, 25:14211 (KFK-1217)
  performance of superconducting, state of art of, 25:14220
  power supplies for beam transport, use of transistors in, 25:14848 (PPAD-677-D)
  transition monitor for superconducting, 25:14221
  voltage controller for superconducting, constant, 25:14221
MAGNOX ALLOYS
  grain boundary sliding in polycrystalline AL80, at 200°C, effects of creep on, 25:13675
MAN
  calcium-47 retention in blood plasma of, 25:13359
  copper content of nails of, determination by neutron activation analysis for diagnosis of cystic fibrosis, 25:13491
  iodine-131 content of thyroid gland in children of, reconcentration factor for, 25:13347
  iodine-131 content of thyroid of, in Australia during 1966 to 1968, fallout, 25:13436
  iodine-131 excretion in urine of, following therapy of thyroid carcinoma, 25:13596
  metabolic indices of, effects of small quantities of uranium in drinking water on, 25:13595
  radiation dose to bladder in, comparison of methods for determining, 25:13448
  radiation dose to, following ingestion of spring water from Masutomi spa area in Japan, α and γ, 25:13470
  radiation dosimetry in lungs, mediastinum, and stomach of, x, 25:13453
  radiation dosimetry in, during therapy computer method for calculating cobalt-60 γ, 25:13449
  radiation dosimetry of, methods for residents of high natural background Guarapari region in Brazil, 25:13393(R) (NYO-2577-12)
  radiation effects on brachial plexus in, following therapy for mammary carcinomas, protective effects of actihemyl against paralyzing, 25:13480
  radiation effects on lungs, ribs, and skin of, following electron beam therapy, 25:13584
  radiation effects on mucosa in, following therapy, protective effects of solcoseryl against, 25:13475
  radiation effects on skin in, eight to ten years after therapy, strontium-90 β, 25:13582
  radiation effects on skin of, following therapy for carcinomas, protective effects of tanderil against, 25:13476
  radiation effects on sympatho-adrenal system of, effects of insulin on, 25:13586
  radiation effects on thyroid hormone synthesis in patients with toxic thyroid adenomes following therapy, iodine-131 β and γ, 25:13594
  radiation hazards to, from dental and medical x-ray facilities, priority system for state inspection to determine, 25:13459
  radiation hazards to, from lead shielding during therapy, 25:13460
  radiation injuries of perianal skin of, following therapy of pruritus ani, 25:13588
  radiography of paranasal sinuses in, methods for, for optimal results, 25:13507
  radioinduced carcinomas in thyroid of, following therapy for lymph node adenomas, carcinogenic, x, 25:13585
  radioinduced changes in thyroid gland function following yttrium-50 pituitary ablation, β and γ, 25:13579
  radioinduced fission of naturally occurring uranium-235 in neoplastic and normal tissues in kidney of, interstitial neutron, 25:13361
  radioinduced injuries to bowel and rectum of, following therapy for uterine carcinoma, α and γ, 25:13589
  radioinduced neoplasms in bones and bone marrow of, radium, 25:13593
  radioisotope scanning in, advantages of whole-body, 25:13503
  radiotherapy of advanced head and neck neoplasms in, effects of sequential high or low dose methotrexate treatment on effectiveness of, 25:13528
  radiotherapy of bladder carcinomas in, effects on survival, cobalt-60 γ, 25:13525
  radiotherapy of bone tumors in, effectiveness of cobalt-60 γ for, 25:13521
  radiotherapy of bronchial carcinomas in, effects on survival, statistical evaluation of cobalt-60, 25:13523
  radiotherapy of bronchial carcinomas in, in combination with chemotherapy, effects on survival, megavoltage or orthovoltage, 25:13522
  radiotherapy of Burkitt's lymphoma and nasopharyngeal carcinoma of, effects of, on titer of antibodies against EBV-associated membrane antigen complex, γ, 25:13391
  radiotherapy of cancer in, effectiveness of x radiation in combination with cytostatic drugs for, 25:13527
  radiotherapy of cervix carcinomas in female, development of computer methods for use of cobalt-60 γ for, 25:13540
  radiotherapy of cervix carcinomas in female, statistical evaluation of cobalt-60 γ, radium, and x, 25:13531
  radiotherapy of cervix carcinomas in, effectiveness of conformation radiation for, in comparison to stationary techniques, 25:13530
  radiotherapy of diseases of lymph nodes in, development of method for ultrahard x, 25:13535
  radiotherapy of Hodgkin's disease in, effectiveness of, in combination with stomach resection, 25:13541
  radiotherapy of lymph node metastases in, methods for biaxial pendulum cobalt-60 γ, 25:13534
  radiotherapy of lymphogranulomas in, relation of relapse time to effects of dose and dose fractionation during, 25:13543
  radiotherapy of lymphogranulomatosis fistulas in esophagus of, effectiveness of cobalt-60 γ for, 25:13542
  radiotherapy of mammary carcinomas in female, in combination with surgery, effects on lymph system, effects of dose on cobalt-60 γ, 25:13533
  radiotherapy of neoplasms of laryngopharynx in, combined use of dose fractionation followed by radical surgery for, 25:13545
  radiotherapy of oro-pharyngeal and thorax-abdominal neoplasms in, review of clinical experiences over ten-year period in telecobalt γ, 25:13546
  radiotherapy of stomach neoplasms in, effects on survival, effects on grid technique on cobalt-60 γ, 25:13532
  radiotherapy of testicular tumors of, effectiveness of supervoltage radiation for, 25:13544
  radiotherapy of thyroid carcinomas in, effects of, on survival, 25:13524
  radiotherapy of tumors in, comparison of interstitial gold-198 to radium for, 25:13526
  radium toxicity to, 25:13593
  scintigraphy in, use of indium-113 mixtures with tin-113 for, 25:13501
  shielding of gonads of female, development of lead impregnated vinyl foundation garment for, against x, 25:13462
  vitamin B-12 metabolism in, following stomach surgery, cobalt-58 tracer techniques for, 25:13334
MANGANESE
  determination in aluminum-, cobalt-, iron-, magnesium-, nickel-, or titanium-base alloys using gas-sheathed tubular electrode arc, spectroscopic, 25:12945
  determination in neutron-irradiated graphite by γ spectrometry, 25:12954
  determination in postage stamps by neutron activation, 25:12973
  determination of trace amounts of, in blood serum by emission spectroscopy, 25:12946
  determination of trace amounts of, in boron carbide by neutron activation, 25:12972
MANGANESE ALLOYS AND SYSTEMS
  Au--Mn--Te, superconducting transition temperature and lattice parameters of liquid-quenched simple-cubic, 25:14178
  Co-base--Cr--Fe--Mn, deuteron stopping power at 2.5 to 7.0 MeV for Havar foils, (E), 25:14401
  Cr--Mn, pressure effects on magnetic susceptibility of, (E/T), 25:14447
  Er--Mn--Pr, crystal structure of, 25:13707
  Er--Mn--Pr, magnetic properties of, 25:13707
  Mn--Ni, magnetic susceptibility near Curie point of Ni_3Mn single crystal, temperature dependence of initial paraprocess, 25:14446
  Mn--V, magnetic properties of, NMR and susceptibility study of band model of, (E/T), 25:14445
MANGANESE FLUORIDES
  spin fluctuations in antiferromagnetic MnF_2, neutron inelastic scattering study of dynamic, 25:14471
MANGANESE ISOTOPES Mn-54
  content of feces, milk, and urine of dairy cattle following ingestion of Schooner fallout, 25:13396 (UCRL-72511)
  content of fish protein concentrates, 25:13394(R) (RLO-

XUM

2099-1)
  determination in liquid waste effluents from nuclear fuel reprocessing plant by γ spectrometry, 25:12950 (BRH/NERHL-70-2)

MANGANESE ISOTOPES Mn-55
  bremsstrahlung reactions at 0.8 to 2.1 GeV, spallation products from, (E), 25:14977
  neutron capture by, gamma spectra from thermal and resonance, (E), 25:14974
  neutron elastic scattering at 8 MeV, cross sections for, (E/T), 25:14965
  neutron inelastic scattering at 2 to 4.5 MeV, cross sections for, (E/T), 25:14966
  nuclear magnetic resonance in vanadium--manganese alloys, 25:14445
  nuclear properties of, unified rotational model for, (T), 25:14973

MANGANESE ISOTOPES Mn-56
  determination in reactor cooling water by γ spectroscopy, 25:12956
  energy levels from neutron capture, spin and parity for, (E), 25:14974
  nuclear properties of, unified rotational model for, (T), 25:14973

MANGANESE OXIDES
  content in rocks of shields and sediment cover of Brazil, Canada, and USSR, relations with geological time, 25:13114

MANY BODY PROBLEM
  ground-state correlations as variational parameters in nuclear, (T), 25:15147 (NYO-2171-333)
  solutions for three-body, with positive energies, 25:15210

MARS (PLANET)
  atmosphere of, altitude, latitude, and longitude variations of neutral and ionized particles in, (E/T), 25:13956
  ionosphere of, altitude, latitude, and longitude variations of neutral and ionized particles in, (E/T), 25:13956

MARY KATHLEEN AREA (AUSTRALIA)
  economic history and uranium ore evaluation in, 25:13126

MASS SPECTROMETERS
  design for analysis of heavy metals for isotopes, 25:13319 (CRNL-4643)
  design for analysis of organic compounds, 25:13319 (CRNL-4643)
  design of, having multiple ion trajectories, 25:13963

MATERIALS TESTING
  equipment and method for Varestraint, for hot cracking of refractory alloys, 25:13695
  property data for, integrated computer program library of, 25:13627

MATERIALS TESTING ACCELERATORS
  design and performance of betatron, for testing concretes, 25:14861

MATERIALS TESTING, DESTRUCTIVE
  method for impact, of SIREN radioisotope fuel capsules, 25:13171(R) (SNC-2708-2)

MATHEMATICAL PHYSICS
  electromagnetic wave propagation in Riemann space, 25:14499

MATHEMATICS
  research at BNL, July 1969--June 1970, 25:14837(R) (BNL-50230)

MATRICES (MATHEMATICS)
  Gaussian random, proof of semi-circle law for, 25:14503

MATTER
  interaction with electromagnetic radiation in Universe, gravitational, (T), 25:13948
  nucleon clustering in low-density neutron-star, (T), 25:13819
  photoionization of intergalactic, by quasar uv radiation, (T), 25:13939

MATTER, ANTI-
  gamma emission from, in meteor streams, (E/T), 25:13951
  research in Soviet Union, 25:14544

MEATS
  fish, radiation processing of Bombay duck, effects of, on drip loss, effects of pre-dip treatment in sodium tripolyphosphate on γ, 25:13618
  poultry, radiation processing of chicken, effects of culture medium on recovery of Salmonella following γ, 25:13620
  poultry, radiation processing of, effects of, on rats following ingestion, 25:13624
  radiation processing of, effects of, on insects and microorganisms, review of, 25:13623
  seafood, radiation processing of inoculated packaged fresh cod, effects of, on organoleptic properties and type E toxin content, 25:13617(R) (COO-1183-32)
  seafood, radiation processing of shrimp, effects of, on storage life, effects of blanching on γ, 25:13619

MEDICAL SUPPLIES
  radiation doses and build-up effect in plaster casts, in relation to radiotherapy, comparison of electrons, γ, and x, 25:13539

MEDICINE
  activation analysis in, review on possibilities for use of, 25:12964
  conference on uses of radioisotopes in nuclear, 25:13482 (CONF-661071)
  research at BNL, July 1969--June 1970, 25:14837(R) (BNL-50230)
  review of radiopharmaceuticals in nuclear, in relation to cost, production, safety, techniques, and transport, 25:13519

MELATONIN
  radiation effects on synthesis of, in pineal glands in rats, x, 25:13559

MERCURY
  effects on gravimetric determination of tellurium, 25:12943
  effects on performance of cesium plasma diodes, 25:14085
  electron elastic scattering at 25 to 800 eV by, tables of amplitudes and spin polarizations for, (T), 25:13995 (AD-711664)
  electron reactions at 25 to 180 eV with, differential cross sections and angular dependences of spin polarization in, (E), 25:14039
  energy-level excitation by neutron capture gamma rays, (E), 25:15002
  fluorescence and Coster--Kronig yields of L subshells in, from decay of gold-198 and thallium-204, (E), 25:15015
  internal conversion coefficients for K- and L-shells of, dependence on γ transition energies, 25:15054
  spectra in discharge afterglows, line intensity in, 25:14100

MERCURY ALLOYS AND SYSTEMS
  Hg--In, ultrasonic attenuation of transverse waves in dirty superconducting, (E), 25:14160

MERCURY IONS
  reactions with polycrystalline metal targets at 5 to 30 keV, sputtering yield and secondary emission in, 25:13971

MERCURY ISOTOPES Hg-197
  production in high specific activity by Szilard--Chalmers reaction, 25:13060

MERCURY ISOTOPES Hg-203
  production in high specific activity by Szilard--Chalmers reaction, 25:13060
  radiation dose to kidneys of mice from Merphyrin-incorporated, effects of glutathione and 2,3-dimercapto-1-propanol on, 25:13341

MERCURY ISOTOPES Hg-204
  energy levels of, calculation using model of two proton holes coupled to a quadrupole vibrator, (T), 25:15033

MERPHYRIN
  effects of mercury-203-labeled, on kidneys of mice, effects of glutathione and 2,3-dimercapto-1-propanol on, 25:13341
  effects of mercury-203-labeled, on kidneys of mice, effects of glutathione on, 25:13341

MESIC ATOMS
  energy levels of hydrogen μ−, metastability of 2s state, 25:13991
  energy levels of π−, effects of meson (π) finite size on, (T), 25:13994

MESONS
  decays of vector, quark loop model for coupling constant relations and branching ratios for radiative, (T), 25:14686
  detection and measurement, data-processing system for cosmic-ray telescopes in, (E), 25:14067
  fields of, transversality condition for relation to SU(2) x SU(2) chiral symmetries fr vector and axial-vector, (T), 25:14804
  interactions with baryons at high energies, review of statistical model for cross sections for single baryon and multimeson production in, (T), 25:14680 (INP-719)
  interactions with baryons in SU(3) symmetry, dual model for, (T), 25:14766
  interactions with baryons, quark model predictions for pseudoscalar, 25:14721
  interactions with baryons, quark model relations between transversity amplitudes for pseudoscalar, 25:14671
  interactions with baryons, use of spin-$^{3}/_{2}$ quarks for decay correlations in resonance production from, (T), 25:14712
  interactions with deuterons in resonant regions, Watson multiple-scattering theory for, 25:14738
  interactions with mesons in dual relativistic quark model, Adler condition for, 25:14685
  interactions with mesons, overlapping resonance mechanism for production of 3π(1080), Kππ(1169), and KKπ(1433) enhancements in, (T), 25:14678
  interactions with mesons, review of Veneziano formula for, (T), 25:14688
  mass differences of octet of pseudoscalar, SU(3) symmetric multichannel calculation of electromagnetic, (T), 25:14795
  mass spectra in chiral SU(3) x SU(3) model, effect of electromagnetic perturbations on, 25:14690
  mass spectra of pseudoscalar and scalar, in broken SU(3) x SU(3) chiral symmetry, 25:14689
  mass spectra of, algebraic model based on SO(3,2) and SL(3,C) groups for, (T), 25:14772
  mass spectra of, relativistic and SU(3)-invariant equations for nonlinear quark theory for, (T), 25:14684
  mass splittings of soft pseudoscalar, SU(3) x SU(3) algebra for weak, (T), 25:14593
  production in anti N + N interactions at high energies,

review of statistical model for cross sections for, (T), 25:14680 (INP-719)
production in baryon interactions with mesons at high energies, review of statistical model for cross sections for, (T), 25:14680 (INP-719)
production in $\gamma + p$ interactions in SU(6)-quark model, relations between differential cross sections for scalar and vector, 25:14626
production in $N + N$ interactions at high energies, review of statistical model for cross sections for, (T), 25:14680 (INP-719)
production of vector, in photon reactions with beryllium at 16 GeV, upper limits for cross sections of, (E), 25:14511
Regge trajectories of tensor, relation between chiral symmetry breaking and, 25:14769
symmetry breaking in nonlinear realizations of SU(3) x SU(3) for pseudoscalar, 25:14763
symmetry for, generalizations of Dirac representation of relativistic, 25:14767
theory for 0^+ and 0^-, chiral algebra and breakdown for nonet, (T), 25:14645

MESONS (eta)
decay eta $\to 2\gamma$, counter and spark chamber study of branching ratio for, (E), 25:14580
decay eta $\to 2\gamma$, quark loop model for branching ratio and width of, (T), 25:14686
decay eta $\to 3\pi$ in perturbation theory, Ward identities for, 25:14611
decay eta $\to 3\pi^0$, counter and spark chamber study of branching ratio for, (E), 25:14580
decay eta $\to \pi$ + sigma, sigma $\to 2\pi$ in perturbation theory, Ward identities for, 25:14611
decay eta $\to \pi^0 + 2\gamma$, counter and spark chamber study of branching ratio for, (E), 25:14580
decay eta $\to \pi^+ + \pi^- + \gamma$, counter and spark chamber study of branching ratio for, (E), 25:14580
decay eta $\to \pi^+ + \pi^- + \pi^0$, counter and spark chamber study of branching ratio for, (E), 25:14580
decay of eta^0 in xenon bubble chamber, π^0 and γ production in, (E), 25:14560 (JINR-E1-5349)
exchange in $\gamma + \gamma$ interactions, effects on total cross sections from, (T), 25:14596 (JINR-E2-5424)
production in $\gamma + p \to$ eta $+ p$ interactions, model with poles and cuts for mixing angles of eta$_1$ and eta$_8$ isosinglets in, (T), 25:14629
production in $\pi + N \to$ eta $+ N$ interactions, Breit--Wigner models and effective-range approximations for, (T), 25:14702 (PAM-70-8)
production of eta^0 in $\gamma + p \to$ eta $+ p$ interactions at 5.0 to 10 GeV, cross sections for, (E), 25:14524
production of eta^0 in $\gamma + p \to$ eta$^0 + p$ and $\gamma + p \to \pi^0 +$ eta$^0 + p$ interactions at 1.465 to 1.815 GeV, cross sections for, (E), 25:14522
production of eta^0 in $\pi^+ + n$ interactions at 2.34 GeV/c in xenon bubble chamber, (E), 25:14560 (JINR-E1-5349)

MESONS (f)
decay of f^0 in xenon bubble chamber, π^0 and γ production in, (E), 25:14560 (JINR-E1-5349)
production of f^0 in $\pi^+ + n$ interactions at 2.34 GeV/c in xenon bubble chamber, (E), 25:14560 (JINR-E1-5349)

MESONS (K)
decay $K \to 2\pi + l + \nu$, corrections to soft-pion predictions of current algebra from once-subtracted dispersion relations for, (T), 25:14654
decay $K \to 2\pi(3\pi)$, current algebra model with PCAC hypothesis for CP violation in phenomenological study of, (T), 25:14764
decay $K \to \pi + e + \nu$, form factor in, 25:14652
decay $K \to \pi + l + \nu$, chiral algebra and breakdown for psi parameter of, (T), 25:14645
decay $K \to \pi + l + \nu$, consistency of hard-pion theorems in $(3,3^*) + (3^*,3)$ symmetry-breaking model for scalar form factor for, (T), 25:14633 (NYO-2262-TA-233)
decay $K \to \pi + l + \nu$, corrections to soft-pion predictions of current algebra from once-subtracted dispersion relations for, (T), 25:14654
decay $K \to \pi + l + \nu$, current--current theory for, 25:14647
decay $K \to \pi^+ + \pi^- + e +$ anti ν, soft-pion values of form factors for rate for, (T), 25:14654
exchange contributions to $p + p \to Y + K + N$ interactions, (T), 25:14597
interactions anti $K + N \to$ anti $K + N$, SU(3) x SU(3) chiral Lagrangian model for total cross sections and scattering lengths for, (T), 25:14703 (TID-25639)
interactions anti $K + N \to \pi + \Sigma(\Lambda)$, SU(3) x SU(3) chiral Lagrangian model for total cross sections and scattering lengths for, (T), 25:14703 (TID-25639)
interactions $K + N$, SU(3) and exchange degeneracy in Regge-pole-cut analysis of total cross sections for, (E/T), 25:14660
interactions $\pi + K$ at low energies, pole dominance calculation of scattering lengths for, (T), 25:14687
interactions $\pi + K$, CDD pole effects on single resonance solution in dispersion relations for, (T), 25:14696
mass of, phenomenology of effective matrix for, (T), 25:14764
production in 60- and 1000-GeV jets in emulsions, K/π ratio for secondary, (E), 25:14509 (INP-718)
production in $p + p \to Y + K + N$ interactions, π and K exchange contributions to, (T), 25:14597

MESONS (K^-)
interactions $K^- + d \to K^- + \pi^- + \pi^+ + p$ at 7.3 GeV/c in deuterium bubble chamber, partial cross sections, high peripherality, and $K^*(890)$ production in, (E), 25:14569
interactions $K^- + d \to p + \Sigma^-(\Sigma^+) + \pi^+(\pi^-) + \pi^-$ at 3 GeV/c in bubble chamber, cross sections for, (E), 25:14546
interactions $K^- + n \to \Sigma^- + \pi^+ + \pi^-$ at 1.62 to 1.74 GeV, $\Sigma(1660)$ weak coupling to $\Lambda(1405)\pi$ and existance of two distinct $\Sigma(1660)$ in partial wave analysis of, (T), 25:14717
interactions $K^- + n \to \Sigma^-(\Sigma^+) + \pi^+(\pi^-) + \pi^-$ at 670 to 835 MeV/c in deuterium bubble chamber, differential and total cross sections and partial-wave analysis for resonance production in, (E/T), 25:14557 (FSU-HEP-70-3-1)
interactions $K^- + p \to$ anti $K^0 + n$ at 0.45 to 1.8 GeV/c, Veneziano dips in angular distributions of, 25:14724
interactions $K^- + p \to$ anti $K^0 + n$, $K^0 \to \pi + l + \nu$, test of $\Delta S = \Delta Q$ rule from time distribution in, (E), 25:14533
interactions $K^- + p \to K^{*0}(890) + n$, coherent droplet model with long-range pion exchange for forward peak structure in, (T), 25:14722
interactions $K^- + p \to K^{*-}(890) + p$, coherent droplet model with long-range pion exchange for forward peak structure in, (T), 25:14722
interactions $K^- + p \to K^{*-}(890) + p$, two-parameter model for, (T), 25:14574
interactions $K^- + p \to K^- + p + \pi^+ + \pi^- + \pi^0$ at 5.5 GeV/c in hydrogen bubble chamber, total cross sections, resonance production, and quasi-two, -three, and -four body states in, (E), 25:14572
interactions $K^- + p \to K^- + p$ below 1.4 GeV/c, Veneziano dips in angular distributions of, 25:14724
interactions $K^- + p \to K^+ + \Xi^-$ interactions at high energies, two-Reggeon exchange contributions to, (T), 25:14657 (UCRL-20032)
interactions $K^- + p \to \pi^- + \pi^+ + \Lambda$ in generalized Veneziano model, 25:14716
interactions $K^- + p \to \Sigma^0 + \pi^0$, search for $\Lambda(1670)$ in, (E), 25:14568
interactions $K^- + p \to X^0 + \Lambda$ determination of spin and parity of $X^0(960)$ from, 25:14720
reactions with emulsion nuclei at rest, production and decay of Λ-Li^8 and Λ-Be^9 in, (E), 25:14573
reactions with heavy emulsion nuclei at 1.5 and 3.5 GeV/c, emission of lithium-8 fragments in, (E), 25:14978

MESONS (K^0)
decay $K^0 \to 2\pi$, CP violation from branching ratio for, (E), 25:14530
decay $K^0 \to 2\pi$, superweak interaction and TCP invariance for, 25:14761
decay $K^0 \to \pi + e + \nu$, test of $\Delta S = \Delta Q$ rule in spark chamber study of, (E), 25:14538
decay $K^0 \to \pi + l + \nu$, $\Delta S = \Delta Q$ rule from time distribution of, (E), 25:14533
decay $K^0 \to \pi^- + \mu^+ + \nu$, test of $\Delta S = \Delta Q$ rule from μ^+ transverse polarization in, 25:14642
decay $K^0 \to \pi^+ + \pi^- + \pi^0$, search for CP violation in time distribution of, (E), 25:14762
decay $K_1{}^0 \to \gamma + \gamma$, vector-meson exchange contributions to, (T), 25:14606
decay $K_1{}^0 \to \pi^+ + \pi^- + \pi^0$ in heavy-liquid bubble chamber, search for, (E), 25:14537
decay $K_2{}^0 \to 2\pi^0(3\pi^0)$, branching ratio for, (E), 25:14530
decay $K_2{}^0 \to \pi^+ + \pi^- + \pi^0 + \gamma$, rate, branching ratio, and γ spectra from current algebra and vector dominance for, 25:14640
decay $K_2{}^0 \to \pi^+ + \pi^- + \pi^0$, spark chamber study of $\Delta I = {}^1/_2$ rule and CP violation in asymmetry in, (E), 25:14536
decay $K_2{}^0$ and $K_1{}^0$, sum rules for, 25:14644

MESONS (K^+)
decay $K^+ \to \pi^0 + l + \nu$, SU(3) breaking for, 25:14649
decay $K^+ \to \pi^0 + \mu^+ + \nu$, Dalitz plot density and μ^+ polarization in, (E), 25:14534
interactions $K^+ + p \to$ anti $\Lambda + p + p$ at 7.3 GeV/c in hydrogen bubble chamber, (E), 25:14574
interactions $K^+ + p \to \Delta^{++}(1236) + K^+ + \pi^-$ at 12.7 GeV/c, momentum-transfer distributions in, (E), 25:14575
interactions $K^+ + p \to K^{*+}(890) + p$, two-parameter model for, (T), 25:14574
interactions $K^+ + p \to K^+ + p$ at 1.0 to 2.45 GeV/c, cross sections for backward, (E), 25:14582
interactions $K^+ + p \to K^+ + p$ at 7.3 GeV/c in hydrogen bubble chamber, cross sections for, (E), 25:14574
interactions $K^+ + p \to K^+ + \pi^- + \Delta^{++}(1236)$ at 9 GeV/c, double-peripheral model analysis of, (E/T), 25:14714
interactions $K^+ + p \to K^+ + \pi^+ + n$ at 7.3 GeV/c in hydrogen bubble chamber, cross sections and $\Delta(1236)$, $K^*(890)$, and $K^*(1420)$ production in, (E), 25:14574
interactions $K^+ + p \to \Lambda + K^+ + K^+$ at 7.3 GeV/c in hydrogen bubble chamber, (E), 25:14574
interactions $K^+ + p \to p + K^+(K^0) + \pi^0(\pi^+)$ at 7.3 GeV/c in hydrogen bubble chamber, cross sections and $\Delta(1236)$, $K^*(890)$, and $K^*(1420)$ production in, (E), 25:14574
interactions $K^+ + p$ at 5.2 and 7.0 GeV/c, differential cross sections for forward and backward elastic, (E), 25:14579
lifetime of, precise measurement of, (E), 25:14531

MESONS (μ)

- decay $\mu \to e + \nu + \text{anti } \nu$, weak interaction model for electron energy spectrum and limitations on masses of ν and W from, (T), 25:14631 (ITF-70-64)
- decay of, current--current theory for, 25:14647
- decay of, determination of lepton-charge-violating coupling constants in, 25:14653
- detection of multiple, at 1500 hg/cm², 25:14060
- electric charge and flux quantization for, electromagnetic coupling constant from, 25:14618
- fluxes deep underground as evidence against hypothesis for W strong interactions, 25:14735
- magnetic moment of, Feynman diagram sixth-order radiative corrections to anomalous, (T), 25:14620
- magnetic moment of, vacuum polarization contributions to sixth-order anomalous, 25:14616
- production by neutral cosmic particles at sea level, direct, (E), 25:14063
- reactions with zinc-66 and zinc-68, energy levels from, (E), 25:14958
- stopping of cosmic, at 60 to 300 mwe, intensity and rate for, (E), 25:14535

MESONS (μ^-)

- interactions in nuclear emulsions at 15.8 GeV/c, effect of discrepancy in primary beam momentum in, (E), 25:14532
- interactions $\mu^- + n \to p + W^- + \mu^-$, model for W^+ production in, 25:14643
- interactions $\mu^- + p \to p + W^- + \nu$, model for W^+ production in, 25:14643

MESONS (μ^+)

- depolarization in gypsum single crystals, (E), 25:13989
- interactions in nuclear emulsions at 10.1 GeV/c, effect of discrepancy in primary beam momentum on, (E), 25:14532

MESONS (ω)

- decay of ω^0 in xenon bubble chamber, π^0 and γ production in, (E), 25:14560 (JINR-E1-5349)
- decay $\omega \to 3\pi$, Veneziano model for, (T), 25:14695
- decay $\omega \to e^+ + e^-$ from production in photon reactions with beryllium at 5.1 GeV, 25:14528
- decay $\omega \to \pi^0 + \gamma$, quark loop model for coupling constant ratios and branching ratios for, (T), 25:14686
- interactions $\omega + \pi \to \omega(\pi) + \pi$, Veneziano model for amplitudes of, (T), 25:14695
- mixing of ω--rho in broken SU(3) Lagrangian theory, local gauge invariant formulation of electromagnetic, 25:14628
- production in $\gamma + N \to \omega + N(N^*)$ interactions at 9.1 GeV in deuterium and hydrogen targets, counter study of cross sections for, (E), 25:14512
- production in photon reactions with beryllium at 5.1 GeV, γωN coupling constants from, 25:14528
- production in $\pi^+ + p \to \Delta^{++} + \omega^0$ interactions at 1.95 GeV/c, cross sections and density-matrix elements for, (E), 25:14563
- production of ω^0 in $\text{anti } p + n \to 3\pi^- + 2\pi^+ + \pi^0$ interactions at rest in deuterium bubble chamber, (E), 25:14553
- production of ω^0 in $K^- + p \to K^- + p + \pi^+ + \pi^- + \pi^0$ interactions at 5.5 GeV/c in hydrogen bubble chamber, (E), 25:14572
- production of ω^0 in $\pi^+ + n$ interactions at 2.34 GeV/c in xenon bubble chamber, (E), 25:14560 (JINR-E1-5349)

MESONS (phi)

- production of phi^0 in $\gamma + p \to \text{phi}^0 + p$ interactions at 5.0 to 17.8 GeV, differential cross sections for, (E), 25:14524

MESONS (π)

- decay $\pi \to e + \nu + \gamma$, transversality condition for relation to SU(2) x SU(2) chiral symmetries for vector and axial-vector meson fields for calculation of axial part of amplitude of, (T), 25:14804
- electromagnetic radius of, effects on energy levels of π-mesic atoms, (T), 25:13994
- exchange contributions to $p + p \to Y + K + N$ interactions, (T), 25:14597
- exchange in quasi-two-body hadron interactions, coherent droplet model with, (T), 25:14722
- form factor of, contributions of $\pi + \pi$ inelastic channels to electromagnetic, (T), 25:14597
- interactions $A_1 + \pi \to A_1(\pi) + \pi$, Veneziano model for amplitudes of, (T), 25:14695
- interactions $A_1 + \pi \to \pi + \pi$, Veneziano amplitude for off-mass-shell, (T), 25:14698
- interactions $\omega + \pi \to \omega(\pi) + \pi$, Veneziano model for amplitudes of, (T), 25:14695
- interactions $\pi + d$, Glauber model for, (T), 25:14630
- interactions $\pi + K$ at low energies, pole dominance calculation of scattering lengths for, (T), 25:14687
- interactions $\pi + K$, CDD pole effects on single resonance solution in dispersion relations for, (T), 25:14696
- interactions $\pi + \Lambda \to \pi + \Lambda(\Sigma)$, SU(3) x SU(3) chiral Lagrangian model for total cross sections and scattering lengths for, (T), 25:14703 (TID-25639)
- interactions $\pi + N \to \text{eta} + N$, Breit--Wigner models and effective-range approximations for, (T), 25:14702 (FAM-70-8)
- interactions $\pi + N \to \pi + \Delta(\pi + N)$ at 339 to 480 MeV, partial-wave analysis of, (T), 25:14728
- interactions $\pi + N \to \pi + N^*$, pion gauge condition for baryon parity doublet in, 25:14705
- interactions $\pi + N \to \text{rho} + N$, O(4) classification of invariants and differential cross sections for, (T), 25:14757
- interactions $\pi + N$ at high energies, linear Regge trajectory fits of, (T), 25:14723
- interactions $\pi + N$, dispersion sum rules for fixed-u amplitudes of, 25:14709
- interactions $\pi + N$, Regge-pole-cut model without parity doubling for backward, 25:14707
- interactions $\pi + N$, solution to Bethe--Salpeter equation for, 25:14786
- interactions $\pi + N$, SU(3) and exchange degeneracy in Regge-pole-cut analysis of total cross sections for, (E/T), 25:14660
- interactions $\pi + \pi \to \pi + \pi$, Veneziano model for amplitudes of, (T), 25:14695
- interactions $\pi + \pi$ at high energies, two-Reggeon exchange contributions to, (T), 25:14657 (UCRL-20032)
- interactions $\pi + \pi$ in Veneziano model, finite-energy sum rules for Regge behavior of unitarized, 25:14693
- interactions $\pi + \pi$, amplitude expansion on Mandelstam triangle for bootstrap of, (T), 25:14678
- interactions $\pi + \pi$, analyticity in amplitudes of, (T), 25:14682 (ITF-70-60-E)
- interactions $\pi + \pi$, Lagrangian in tree approximation for dual amplitudes of, 25:14697
- interactions $\pi + \pi$, nonlinear functional analysis and numerical computations of S-matrix for dispersion relations for, (T), 25:14699
- interactions $\pi + \pi$, π electromagnetic form factor contributions from inelastic, (T), 25:14597
- interactions $\pi + \pi$, scattering lengths from broken chiral and conformal symmetry, 25:14770
- interactions $\pi + \pi$, two-loop approximations to propagators in sigma model for unitary amplitude of, (T), 25:14683 (NYO-2262-TA-219)
- interactions $\pi + \pi$, Veneziano amplitude for interference model for resonances in, (T), 25:14692
- interactions $\pi + \Sigma \to \pi + \Sigma$, SU(3) x SU(3) chiral Lagrangian model for total cross sections and scattering lengths for, (T), 25:14703 (TID-25639)
- interactions $\text{rho} + \pi \to \text{rho} + \pi$, (T), 25:14695
- production from photon interactions with hyperons, quark model commutation relations for sum rules for amplitudes of, (T), 25:14619
- production in 60- and 1000-GeV jets in emulsions, K/π ratio for secondary, (E), 25:14509 (INP-718)
- production in $\gamma + N \to \pi + \Delta$ interactions at high energies, contribution of low-energy theorem to, 25:14622
- production in $\gamma + N \to \pi + N$ interactions, isotensor electromagnetic current in, (T), 25:14604
- production in $\pi^+ + p$ interactions at 8 GeV/c in hydrogen bubble chamber, mechanism for, (E), 25:14558 (INP-708)
- production of high-mass di-pion pairs in photon reactions with beryllium at 16 GeV, cross sections for, (E), 25:14511
- reactions with nuclei at 60 GeV in emulsions, K/π ratio of secondaries in shower production from, (E), 25:14509 (INP-718)
- scattering by lithium-6, elastic, 25:15183
- spatial distribution of stopping, in tissues, method for, 25:13547

MESONS (π^-)

- beam profile of, computer-based wire proportional detector system for monitoring, 25:13297 (JINR-P13-5473)
- detection and spectroscopy of, liquid argon ionization chamber for, 25:13211 (JINR-P13-5402)
- interactions at 17.2 GeV/c, azimuthal symmetry of particles in showers produced from, (E/T), 25:14565
- interactions $\pi^- + n$ at 17.2 GeV/c in emulsions, proton momentum spectrum from, (E), 25:14564
- interactions $\pi^- + p \to 2\pi + N$ at 2.3 GeV/c in hydrogen bubble chamber, rho^-, rho^0, and Δ(1236) production in, (E), 25:14570
- interactions $\pi^- + p \to 2\pi^- + 2\pi^+ + n$ at 2.3 GeV/c in hydrogen bubble chamber, cross sections and $\Delta^-(1236)$ production in, (E), 25:14571
- interactions $\pi^- + p \to 2\pi^- + p + \pi^+ + \pi^0$ at 2.3 GeV/c in hydrogen bubble chamber, cross sections and $\omega^0(785)$, $N^{*++}(1236)$, and B(1220) production in, (E), 25:14571
- interactions $\pi^- + p \to 2\pi^- + p + \pi^+$ at 2.3 GeV/c in hydrogen bubble chamber, cross sections $\Delta^{++}(1236)$ and $\text{rho}^0(765)$ production and $\pi^- + \pi^-$ interaction cross sections for, (E), 25:14571
- interactions $\pi^- + p \to \text{eta} + n$, Regge dipole model of A_2 for differential cross sections and duality in, (T), 25:14704
- interactions $\pi^- + p \to \gamma + n$ at 1245 and 1337 MeV, spark chamber and neutron counter study of angular distributions and differential cross sections for, (T), 25:14567
- interactions $\pi^- + p \to \gamma + n$ at 1245 to 1363 MeV, test of ΔI less than or equal to 1 rule and time reversal invariance in angular distributions and differential cross sections for, (E), 25:14566
- interactions $\pi^- + p \to K^0 + \Lambda$ at 0.90 to 1.95 GeV/c, phase shift analysis of, 25:14727
- interactions $\pi^- + p \to N + m\pi$ at 1 to 16 GeV, statistical isospin model for final-charge-state cross section

ratios for, (T), 25:14700 (JINR-P1-5471)

- interactions $\pi^- + p \to n + \pi^+ + \pi^-$ at 8 GeV/c, double-Regge-model analysis of, (T), 25:14713
- interactions $\pi^- + p \to p + \pi^- + \pi^0$ at GeV/c, double-Regge-model analysis of, (T), 25:14713
- interactions $\pi^- + p \to \pi^- + p$ at high energies, Pomeron hypothesis for form of real-to-imaginary parts for amplitude of, (T), 25:14656 (SU-1206-237)
- interactions $\pi^- + p \to$ rho^0 + n in Veneziano model, test of rho universality from frame dependence of vector dominance in, 25:14710
- interactions $\pi^- + p \to$ rho^0 + n, coherent droplet model with long-range pion exchange for forward peak structure in, (T), 25:14722
- interactions $\pi^- + p \to$ rho^0 + n, fixed j-plane singularities in photoproduction from, (T), 25:14625
- interactions $\pi^- + p \to$ rho$^-$ + p, fixed j-plane singularities in photoproduction from, (T), 25:14625
- interactions $\pi^- + p \to$ rho$^-$ + p, two-parameter model for, (T), 25:14574
- interactions $\pi^- + p$ at 17.2 GeV/c in emulsions, proton momentum spectrum from, (E), 25:14564
- interactions $\pi^- + p$ at 2.5 to 25 GeV, limiting distribution, scaling behavior, and average multiplicities for π^- and π^+ production in, (T), 25:14719
- interactions $\pi^- + p$ at 4.0 to 6.0 GeV, Cherenkov hodoscope study of total cross sections of, (E), 25:14561 (JINR-P1-5460)
- interactions $\pi^- + p$ at 7.0 GeV/c, differential cross sections for backward elastic, (E), 25:14579
- interactions $\pi^- + \pi^-$ in $\pi^- + p \to 2\pi^- + p + \pi^+$ interactions at 2.3 GeV/c in hydrogen bubble chamber, cross sections for, (E), 25:14571
- lifetime of, Cherenkov counter in-flight study of, (E), 25:14581
- production in $e^+ + e^- \to \pi^+ + \pi^- + \gamma$ interactions in storage rings, study of even-charge hadronic systems from, (T), 25:14621
- production in $\gamma + d \to \pi^-(\pi^+) + 2p(2n)$ interactions at 600 to 1700 MeV, π^-/π^+ cross section ratio for, (E), 25:14523
- production in $\gamma + n \to \pi^- + p$ interactions, angular distributions and differential cross sections of $\pi^- + p \to \gamma + n$ interactions at 1245 and 1337 MeV for test of predictions for, (E), 25:14567
- production in $\gamma + p \to \pi^- + p$ interactions, π^-/π^+ cross section ratio in $\gamma + d \to \pi^-(\pi^+) + 2p(2n)$ interactions at 600 to 1700 MeV for cross sections for, (E), 25:14523
- production in $\pi^- + p$ interactions at 2.5 to 25 GeV, limiting distribution, scaling behavior, and average multiplicities for, (T), 25:14719
- production of π^---π^+ pairs in photon reactions with carbon at high energies, spectrometer study of, (E), 25:14526
- reactions (π^-,2n) with carbon-12, neutron energy spectra from, (E), 25:14897
- reactions (π^-,2nd) with carbon-12, nitrogen-14, and oxygen-16, analysis using cluster model, (T), 25:14893
- reactions with nuclei at 12 GeV/c in heavy-liquid bubble chamber, production of Δ^{++}(1236), rho^0(765), and rho rho π(2420) enhancement in, (E), 25:14562 (TID-25640)
- reactions with nuclei at high energies, review of, (T), 25:15148(T) (ORNL-tr-2399)
- scattering by carbon at 120 to 280 MeV, optical-model analysis of elastic, (T), 25:14908

MESONS (π^0)

- exchange in $\gamma + \gamma$ interactions, effects on total cross sections from, (T), 25:14596 (JINR-E2-5424)
- interactions $\pi^0 + \pi^0$, comparison of integral constraints from crossing symmetry and positivity on s-wave, 25:14694
- production in $\gamma + N \to \pi^0 + N$ interactions at 12 GeV at large angles, Regge pole theory for differential cross sections for, (T), 25:14598
- production in $\gamma + p \to$ eta^0 + $\pi^0 + p$ interactions at 1.465 to 1.815 GeV, cross sections for, (E), 25:14522
- production in $\gamma + p \to \pi^0 + p$ interactions at 1200 to 1800 MeV, spark chamber of recoil proton polarization from, (E), 25:14516
- production in $\gamma + p \to \pi^0 + p$ interactions at 5.0 to 17.8 GeV, differential cross sections for, (E), 25:14524
- production in $\gamma + p \to \pi^0 + p$ interactions, model with poles and cuts for mixing angles of eta$_1$ and eta$_8$ isosinglets in, (T), 25:14629
- production in polarized photon reactions with lithium-7 and beryllium-9, differential cross sections for, 25:14602
- production in $\pi^+ + n$ interactions at 2.34 GeV/c in xenon bubble chamber, (E), 25:14560 (JINR-E1-5349)

MESONS (π^+)

- decay of, radiative corrections to Goldberger--Freiman formula for, 25:14617
- interactions $\pi^+ + n \to \Delta^{++} + \pi^-$, Regge pole eikonal model for amplitude and differential cross sections for, (T), 25:14715
- interactions $\pi^+ + n$ at 2.34 GeV/c in xenon bubble chamber, neutral boson, π^+ and γ production in, (E), 25:14560 (JINR-E1-5349)
- interactions $\pi^+ + p \to \Delta^{++}$ + rho^0(ω^0) at 1.95 GeV/c, total and differential cross sections for, (E), 25:14563
- interactions $\pi^+ + p \to \Delta^{++}(1236) + \pi^+ + \pi^-$ at 7 GeV/c, momentum-transfer distributions in, (E), 25:14575
- interactions $\pi^+ + p \to K^+ + \Lambda + \pi^+$ at 8 GeV/c in bubble chamber, $\Sigma^+(1385)$ decay distributions and Λ polarization in, (E), 25:14559 (INP-731)
- interactions $\pi^+ + p \to n + 5\pi^+ + 3\pi^-$ at 8 GeV/c in hydrogen bubble chamber, π production mechanism for, (E), 25:14558 (INP-708)
- interactions $\pi^+ + p \to p + 4\pi^+ + 3\pi^- + \pi^0$ at 8 GeV/c in hydrogen bubble chamber, π production mechanism for, (E), 25:14558 (INP-708)
- interactions $\pi^+ + p \to p + 4\pi^+ + 3\pi^-$ at 8 GeV/c in hydrogen bubble chamber, π production mechanism for, (E), 25:14558 (INP-708)
- interactions $\pi^+ + p \to \pi^+ + \pi^0 + p$ at 5 GeV/c, longitudinal phase-space analysis of, (E/T), 25:14578
- interactions $\pi^+ + p \to \pi^+ + \pi^+ + n$ at 5 GeV/c, longitudinal phase-space analysis of, (E/T), 25:14578
- interactions $\pi^+ + p \to \pi^- + X^{+++}$ at 3.88 GeV/c, search for $T = {}^5/_2$ isobar from π^- spectrum in, (E), 25:14576
- interactions $\pi^+ + p \to$ rho^0 + Δ^{++}, fixed j-plane singularities in photoproduction from, 25:14625
- interactions $\pi^+ + p \to$ rho^0(f^0) + Δ^{++}, coherent droplet model with long-range pion exchange for forward peak structure in, (T), 25:14722
- interactions $\pi^+ + p \to$ rho$^+$ + p, coherent droplet model with long-range pion exchange for forward peak structure in, (T), 25:14722
- interactions $\pi^+ + p \to$ rho$^+$ + p, two-parameter model for, (T), 25:14574
- interactions $\pi^+ + p$ at 1.6 to 2.31 GeV/c, polarization parameter in backward elastic, (E), 25:14577
- interactions $\pi^+ + p$ at 2.38 to 5.0 GeV/c, test of duality from resonance and Regge models for, 25:14726
- interactions $\pi^+ + p$ at 5 GeV/c, longitudinal phase-space analysis of, 25:14578
- interactions $\pi^+ + p$ at 5.2 and 7.0 GeV/c, differential cross sections for backward elastic, (E), 25:14579
- interactions $\pi^+ + p$ at high energies, form factors in model for amplitude of inelastic, (T), 25:14729 (INR-P-1229)
- lifetime of, Cherenkov counter in-flight study of, (E), 25:14581
- production f bound-state, in quark interactions with antiquarks, N/D calculation using discontinuity of second-order four-point function interaction as input for, (T), 25:14676
- production in $e + p \to p + 2\pi$ interactions, hadronic s-channel helicity conservation in, (T), 25:14636 (NYO-4204-10)
- production in $e^+ + e^- \to \pi^+ + \pi^- + \gamma$ interactions in storage rings, study of even-charge hadronic systems from, (T), 25:14621
- production in $\gamma + {}^3\text{He} \to \pi^+ + n + d(n + p)$ interactions, impulse approximation for angular distributions for, (T), 25:14518
- production in $\gamma + p \to \pi^+ + n$ interactions at 4.3 to 9.8 GeV at large angles, Regge pole theory for differential cross sections for, (T), 25:14598
- production in $\gamma + p \to \pi^+ + n$ interactions, model with poles and cuts for mixing angles of eta$_1$ and eta$_8$ isosinglets in, (T), 25:14629
- production in $\gamma + p \to \pi^+ + N(1520)$ interactions, low-t theorems for forward, (T), 25:14609
- production in $\nu + p \to p + \pi^+ + \mu^-$ interactions, hadronic s-channel helicity conservation in, (T), 25:14636 (NYO-4204-10)
- production in $p + p \to d + \pi^+$ interactions at 4.0 to 12.3 GeV/c, spectrometer study of differential cross sections for, (E), 25:14542
- production in $\pi^- + p$ interactions at 2.5 to 25 GeV, limiting distribution, scaling behavior, and average multiplicities for, (T), 25:14719
- production of π^---π^+ pairs in photon reactions with carbon at high energies, spectrometer study of, (E), 25:14526
- reactions with carbon-12, optical-model calculations of, 25:15184
- reactions with spherical nuclei, optical model for, 25:15184

MESONS (rho)

- decay rho $\to e^+ + e^-$ from production in photon reactions with beryllium at 5.1 GeV, 25:14528
- decay rho^0 $\to 2\pi^+ + 2\pi^-$ in hydrogen bubble chamber, branching ratio for, (E), 25:14571
- decay rho^0 $\to 2\pi^- + \pi^+ + \pi^0$ in hydrogen bubble chamber, branching ratio for, (E), 25:14571
- interactions rho + $\pi \to$ rho + π, (T), 25:14695
- mixing of ω--rho in broken SU(3) Lagrangian theory, local gauge invariant formulation of electromagnetic, 25:14628
- polarization of rho$^-$ and rho^0 in $\pi^- + p \to 2\pi + N$ interactions at 2.3 GeV/c in hydrogen bubble chamber, (E), 25:14570
- production in $K^- + p \to K^- + p + \pi^+ + \pi^- + \pi^0$ interactions at 5.5 GeV/c in hydrogen bubble chamber, (E), 25:14572
- production in $p + n \to p + n + \pi^+ + \pi^-$ interactions, I = 1 meson exchange diagram for, 25:14741
- production in photon reactions with beryllium at 4.1 to 6.1 GeV, phase of amplitude for, (E/T), 25:14527
- production in photon reactions with beryllium at 5.1 GeV,

XUM

  - γrhoN coupling constants from, 25:14528
  - production in $\pi + p$ interactions, fixed j-plane singularities in photoproduction from, 25:14625
  - production in $\pi^+ + p \to \Delta^{++}$ + rho interactions at 1.95 GeV/c, cross sections and density-matrix elements for, (E), 25:14563
  - production of bound-state rho$^+$ in quark interactions with antiquarks, N/D calculation using discontinuity of second-order four-point function interaction as input for, (T), 25:14676
  - production of rho^0 in anti $p + n \to 3\pi^- + 2\pi^+$ interactions at rest in deuterium bubble chamber, (E), 25:14553
  - production of rho^0 in $\gamma + p \to$ rho^0 + p interactions at 5.0 to 17.8 GeV, differential cross sections for, (E), 25:14524
  - production of rho$^-$ and rho^0 in four-prong final states from $\pi^- + p$ interactions at 2.3 GeV/c in hydrogen bubble chamber, (E), 25:14571
  - production of rho$^-$ and rho^0 in $\pi^- + p \to 2\pi + N$ interactions at 2.3 GeV/c in hydrogen bubble chamber, angular distribution for, (E), 25:14570
  - production of rho$^+$ in $p + p \to d$ + rho$^+$ interactions at 4.0 to 12.3 GeV/c, spectrometer study of differential cross sections for, (T), 25:14542
  - production of rho$^+$ in $\pi^+ + p \to$ rho$^+$ + p interactions, two-parameter model for, (T), 25:14574
  - production of rho$^-$ in $\pi^- + p \to$ rho$^-$ + p interactions, two-parameter model for, (T), 25:14574
  - universality test from frame dependence of vector dominance in Veneziano model, 25:14710

- MESONS (X^0)
  - parity and spin of X^0(960) from production in $K^- + p \to X^0 + \Lambda$ interactions, 25:14720

- MESONS, RESONANCE
  - coupling of normal-parity, to all channels in generalized Veneziano model, (T), 25:14681 (INP-730)
  - decay $A_1 \to 3\pi$, Veneziano model for, (T), 25:14695
  - decay B(1220) $\to \omega^0 + \pi^-$ in hydrogen bubble chamber, (E), 25:14571
  - decay of rho rho π(2420) enhancement, branching ratio for, (E), 25:14562 (TID-25640)
  - decay of, selection rules for, 25:14658
  - duality relation with interference model for, (T), 25:14678
  - interactions $A_1 + \pi \to A_1(\pi) + \pi$, Veneziano model for amplitudes of, (T), 25:14695
  - interactions $A_1 + \pi \to \pi + \pi$, Veneziano amplitude for off-mass-shell, (T), 25:14698
  - interactions of, generalized Veneziano model for selection rules for two-body, (T), 25:14681 (INP-730)
  - mass spectra of, generalized Veneziano model for, (T), 25:14681 (INP-730)
  - mixing of eta$_1$ and eta$_8$ isosinglets in $\gamma + p \to \pi^0(\pi^+)$ + p(n) and $\gamma + p \to$ eta + p interactions, model with poles and cuts for, (T), 25:14629
  - production of 3π(1080), $K\pi\pi$(1169), and $KK\pi$(1433) enhancements in strong interactions, overlapping resonance mechanism for, (T), 25:14678
  - production of A_2 in $\pi^- + p \to$ eta + n interactions, Regge dipole model for differential cross sections and duality in, (T), 25:14704
  - production of B(1240) in $\gamma + p$ interactions at 5.0 to 17.8 GeV, (E), 25:14524
  - production of delta$^+$ in $p + p \to d$ + rho$^+$ (π^+) interactions at 4.0 to 12.3 GeV/c, spectrometer study of upper limits for, (E), 25:14542
  - production of enhancement in $\pi^- + \pi^+$ pair production in photon reactions with carbon at high energies, spectrometer study of, (E), 25:14526
  - production of f(1260) in photon reactions with beryllium at 16 GeV, upper limits for, (E), 25:14511
  - production of K^*(890) and K^*(1420) in $K^+ + p$ interactions at 7.3 GeV/c in hydrogen bubble chamber, (E), 25:14574
  - production of K^*(890) in $K^- + d \to K^- + \pi^- + \pi^+ + p$ interactions at 7.3 GeV/c in deuterium bubble chamber, (E), 25:14569
  - production of K^{*0} and K^{*-} in $K^- + p \to K^- + p + \pi^+ + \pi^- + \pi^0$ interactions at 5.5 GeV/c in hydrogen bubble chamber, (E), 25:14572
  - production of K^{*+}(890) in $K^+ + p \to K^{*+}$(890) + p interactions, two-parameter model for, (T), 25:14574
  - production of K^{*-}(890) in $K^- + p \to K^{*-}$(890) + p interactions, two-parameter model for, (T), 25:14574
  - production of ω^0(785) and B(1220) in $\pi^- + p \to 2\pi^- + p + \pi^+ + \pi^0$ interactions at 2.3 GeV/c hydrogen bubble chamber, (E), 25:14571
  - production of rho rho π(2420) enhancement in π^- reactions with nuclei at 12 GeV/c in heavy-liquid bubble chamber, (E), 25:14562 (TID-25640)
  - production of rho^0(765) in π^- reactions with nuclei at 12 GeV/c in heavy-liquid bubble chamber, (E), 25:14562 (TID-25640)
  - production of single, in $\pi + K$ interactions, CDD pole effects in solution for, (T), 25:14696
  - width of rho rho π(2420) enhancement in π^- reactions with nuclei at 12 GeV/c in heavy-liquid bubble chamber, (E), 25:14562 (TID-25640)

- METALLIC FILMS
  - deposition of thin, temperature changes during, 25:15423 (COO-1198-775)

- METALLURGY
  - research at BNL, July 1969--June 1970, 25:14837(R) (BNL-50230)

- METALS
  - abundance in late G and K dwarfs, (E), 25:13824
  - abundance in old open clusters, (E), 25:13798
  - corrosion of, past and future perspectives on, 25:13632
  - defects in deformed, stage I recovery of, 25:14438
  - deformation behavior of, cyclic, 25:13683
  - diffusion of light interstitial in, isotope effects in self-trapping energy in, (T), 25:14439
  - ion reactions at 90 to 360 keV with thick targets of, yields of characteristic x rays from, (E), 25:13962
  - welding behavior of, effects of temperature in contact area on static, 25:13644

- METAMORPHIC ROCKS
  - composition of shields and sediment cover of Brazil, Canada, and USSR, relations with geological time, 25:13114

- METEORITES
  - analysis for antimony by neutron activation and radiochemical separation, 25:12968
  - analysis for cobalt, iridium, nickel, scandium, and sodium by neutron activation and γ--γ coincidence spectrometry, 25:12967
  - analysis for oxygen and silicon by nondestructive fast neutron activation, 25:12970
  - analysis of major and minor phases of Bruderheim, for thirty-eight trace elements by neutron activation and radiochemical separation, 25:12969
  - element abundance in chondrites and achondrites, refractory-, (E), 25:13787
  - magnesium isotope abundances in, (E), 25:13864
  - use in determining time and space variations of cosmic rays in solar system, (E/T), 25:14071
  - use in study of cosmic-ray variations, (T), 25:14069

- METEORS
  - gamma emission from antimatter in streams of, (E/T), 25:13951

- METHACRYLIC ACID, METHYL ESTER, POLYMERS
  - effects on backscattering during γ dosimetry to HeLa cells, 25:13456
  - radiation effects on electric properties of Lucite, thermally generated currents following irradiation by gamma- and x-, 25:13786
  - radiolysis of, decay of free radicals from electron, 25:13058

- METHANE
  - carbon-13 concentration in, thermal diffusion method for, 25:13165(R) (MLM-1753)
  - distribution in atmosphere, use in tracer studies of global transport processes, (E), 25:13121 (TID-25314)
  - positron annihilation in, (E), 25:13993
  - reactions with deuterium at 1440 to 1775°K in single-pulse shock tubes, kinetic studies on exchange, 25:12987
  - reactions with recoil tritium, iodine bromide and iodine chloride as radical scavengers in, 25:13067
  - reactions with uranium to produce uranium carbide, 25:13738(P)
  - separation from nitrogen using γ-irradiated polyethylene films at 15 to 50°C, effects of dose on, 25:13039
  - yields from γ radiolysis of 2-propanol vapor at 124 to 400°C, 25:13046

- METHANE, CHLORO-
  - effects on yields from γ radiolysis of carbon tetrachloride at 25°C, 25:13045

- METHANE, CHLORODIFLUORO-
  - heat transfer in horizontal tubes, kinetics of forced-convection condensation, 25:13151 (NP-18642)

- METHANE, DICHLORO-
  - effects on yields from γ radiolysis of carbon tetrachloride at 25°C, 25:13045

- METHANE, DICHLORODIFLUORO-
  - heat transfer in horizontal tubes, kinetics of forced-convection condensation, 25:13151 (NP-18642)

- METHANE, IODO-
  - iodine-131 exchange between ethanol solutions of potassium iodide and, at 35°C, reaction order of components in, 25:12996

- METHANE, TRICHLOROFLUORO-
  - carbon-12 concentration in, by distillation, 25:13165(R) (MLM-1753)
  - carbon-13 concentration in, by distillation, 25:13165(R) (MLM-1753)

- METHANESULFONIC ACID, ETHYL ESTER
  - effects on chlorophyll production by Sorghum, mutagenic, 25:13420

- METHANESULFONIC ACID, METHYL ESTER
  - effects on chlorophyll production by Sorghum, mutagenic, 25:13420
  - effects on Escherichia coli, effects of DNA repair capacity on mutagenic, 25:13421
  - effects on seeds of wheat, mutagenic, 25:13419

- METHANOL
  - effects on separation of cesium from sodium by ion exchange using Zeolite Linde A, 25:13091

- METHOTREXATE
  - effects on radiotherapy of advanced head and neck neoplasms in man, sequential high or low dose, 25:13528

- METHYL SULFOXIDE
  - complexes with thorium halides or uranium halides in

  nitromethane, electric conductivity of, relation of composition and ionization capacity to, 25:13023
  radioprotective effects of, on Taricha granulosa, mixed cobalt-60 γ and x, 25:13477
METHYLENE
  detection in UU Aur, (E), 25:13803
  reactions with hydroxyl radicals, kinetics of, 25:15429(R) (COO-2026-4)
MEXICO
  radioactivity monitoring in airborne particulates in, during December, 1969, gross β, 25:13441
  radioisotope content of milk in, during April 1970 as compared to average for previous 12-month period, cesium-137, iodine-131, and strontium-90, 25:13442
MICE
  immune reactions to tumor cell grafts, effects of injection of γ-irradiated tumor cells on, 25:13389
  iron-59 retention in lungs of, in relation to use of metastable indium-113--iron-59-labeled ferric hydroxide particles for lung scanning, 25:13486
  radiation effects on antibody activity in spleen cells of, analysis of origin of plaque forming cells following γ, 25:13387
  radiation effects on bone marrow in, in comparison to rats, local x, 25:13563
  radiation effects on embryonic cells of, effects of, on SV40 tumorigenicity, x, 25:13553
  radiation effects on fertility in, following therapy of methyl cholanthrene-induced sarcomas, cesium-137 γ, 25:13473
  radiation effects on immune reactions of, effects of, on rejection of transplants of virus-heterogenized skin, γ, 25:13388
  radiation effects on immune reactions of, following injection of lymphoid cells, effects of dose and splenomegaly on x, 25:13390
  radiation effects on ovaries and testes of, following intrámuscular injection of phosphorus-32, effects of estradiol and FSH on β, 25:13569
  radiation effects on survival and skin transplants in, protective effects of sodium s-(2-aminoethyl) phosphorothioate against x, 25:13479
  radiation effects on tissues of, for whole-body neutron activation autoradiography, 25:13590
  radiation effects on tritium incorporation into DNA of oocytes of, x, 25:13367
  radiation effects on, protective effects of methylprednisolone against effects of dose fractionation on, 25:13474
  radiation effects on, role of mast cells in spleen regeneration following whole-body γ, 25:13577
  radioinduced chromosome aberrations in spermatocytes of, effects of dose and dose rate on frequency of translocations, γ, 25:13404
  sulfur-35 incorporation into blood platelets of, for determining effects of thrombopoietin on production of, 25:13355
  tritium-labeled thymidine incorporation into DNA of tissues of, effects of mitotic rate on specificity of, 25:13358
MICROORGANISMS
  radiation effects on, during processing of fruits, grains, and meats, review of, 25:13623
MICROSOMES
  activity of mixed oxidases from liver, in vitro, effects of deuterium oxide on, 25:13372
MICROWAVES
  implications of cosmic background, in relativistic cosmology, (T), 25:13950
  interactions of cosmic background, with high-energy protons, (T), 25:13945
  scattering by plasma, electron density measurement from, (E), 25:14262
MILK
  iodine-131 content of, in Australia and New Guinea during 1966 to 1968, fallout, 25:13436
  iodine-131 content, Nuclear Fuel Services farm, West Valley, New York, 25:13079 (DOCKET-50201-61)
  radioactivity monitoring in, during 1965 to 1968, operation of Standby Milk Surveillance Network of SWRHL in relation to, 25:13443
  radioisotope content of, in Canada, Central and South America, and United States during 1969 and 1970, cesium-137, iodine-131, and strontium-90, 25:13433
  radioisotope content of, in Western Hemisphere during April 1970 as compared to average for previous 12-month period, cesium-137, iodine-131, and strontium-90, 25:13442
  radioisotope content of, sampled in Central, North, and South America during July 1970, cesium-137, iodine-131, and strontium-90, 25:13401
MILKY WAY
  cosmic x-ray source distribution in central region of, (E), 25:13857
  illumination of Coalsack and Libra cloud by diffuse light of, (E), 25:13919
  interstellar extinction at infrared wavelengths, (E), 25:13934
  magnetic-field strength in, (E), 25:13855
  models of, based on density-wave theory, (T), 25:13930
  nebulae distribution in, planetary, (E), 25:13827
  radio observations of center region at 80 MHz, (E), 25:13914
  radio-wave absorption in neutral hydrogen in direction of Virgo A, (E), 25:13831 (AD-711300)
  star distances from center of, radial variation of red and blue supergiant, (E/T), 25:13791
  star field at border of Scutum Cloud, three-color photometry of, (E), 25:13925
  star formation in, positions of, (T), 25:13926
  star population from photometry near South Galactic Pole, M-, (E), 25:13935
  stellar motions in Carina--Centaurus region, streaming, (E), 25:13928
  structure derived from neutral hydrogen observations, (T), 25:13930
  structure of, up to 5 kpc from Sun, (E/T), 25:13920
MILLSTONE POINT POWER REACTOR, UNIT 1
  emergency core cooling system for, electrical interlock system for activating valves of, 25:15287 (DOCKET-50245-52)
  operations incident of January 19, 1971, failure of core spray injection valve to close, 25:15234 (DOCKET-50245-53)
  operations incident of January 25, 1971, failure of B system core spray injection valve, 25:15235 (DOCKET-50245-54)
MINERALS
  analysis by neutron activation using californium-252 as neutron source, 25:12962
  content of human radius and ulna, use of radiography in combination with photometric scanning to determine, 25:13509
MISCH METAL
  Co--Cu--misch metal, magnetic properties of, effects of heat treatments at 200 to 1220°C on, 25:14464
MITOMYCINS
  use for induction of SV40 virus from transformed hamster cell clones, 25:13615
MITOSIS
  radioinduced inhibition of, in crypt cells, effects of protein levels on x, 25:13562
  radioinduced inhibition of, in yeasts, carbon-13, 25:13331 (LA-4551)
MIXER-SETTLERS
  design for production of curium oxide and americium oxide, engineering drawings for, 25:13146
MOISTURE GAGES
  accuracy of, using one-half-minute count intervals, 25:13313
  performance of gamma ionization chamber-type, 25:13110
MOLDS
  radiation dose distribution and rate from cobalt-60 and radium slugs in rectangular, calculation of, 25:13455
MOLECULAR BEAMS
  design of nozzle--skimmer-type, 25:13165(R) (MLM-1753)
MOLECULAR STRUCTURE
  Hartree-Fock equations for, nonanalytic behavior of broken-symmetry solutions for, at branching point, 25:14053
MOLECULES
  atom scattering by, homogeneous integral solution method of calculation of T-matrix for rotationally inelastic, 25:14017
  charged-particle inelastic scattering by, asymptotic expression for total cross sections for, 25:14022
  electron correlation in, semiempirical pseudopotential procedure for calculation of, 25:14055
  electron reactions at 2 to 10 keV with, spectra from vacancy cascades produced in, (E), 25:14038
  ion reactions with, kinetic model for, 25:14041
  neutron differential scattering cross sections using quasi-classical approximation for, slow, (T), 25:14875
  radiation effects on, electromagnetic, 25:13571
  separation of biological macro-, 25:15442(R) (ORNL-TM-3280)
MOLLUSCA
  contamination by sea-disposed liquid radioactive waste, (E), 25:13189 (CEA-CONF-1712)
MOLTEN SALT REACTOR EXPERIMENT
  fuels for, preparation of lithium-7 enriched lithium fluoride--uranium-233-enriched uranium fluoride (UF_4), 25:15368
MOLYBDENUM
  analysis for internal oxygen by α activation and α spectroscopy, 25:12957 (LYCEN-7076)
  analysis for superficial oxygen by deuteron activation and α spectroscopy, 25:12957 (LYCEN-7076)
  barium films adsorbed on (110) surface of single crystals of, structure and work function of, 25:13701
  corrosion of SNAP-19B fuel capsule components of, by seawater, 25:13163 (MLM-1652)
  crack nucleation in single crystals of, by spark discharge, mechanism of, 25:13671
  defects in zone-refined, effects of high-speed quenching on vacancy, 25:13689
  deposition on gadolinium oxide particles, method for, 25:13736 (EUR-4551)
  determination in caustic alkalies and titanium as complex trihydroxyfluoronate, extraction--photometric method for, 25:12933
  determination in cobalt-, iron-, or nickel-base alloys using gas-sheathed tubular electrode arc,

spectroscopic, 25:12945
determination in neutron-irradiated graphite by γ spectrometry, 25:12954
determination of microgram amounts of, using galiein and cetyltrimethylammonium bromide, spectrophotometric, 25:12930
determination of trace amounts of, in blood serum by emission spectroscopy, 25:12946
diffusion of low-solubility cesium in monocrystalline and polycrystalline, mechanism of, 25:13676
effects on corrosion resistance of stainless steel to liquid lithium, 25:13634
effects on superconducting properties of niobium--titanium--zirconium alloy, 25:14208
emissivity of monocrystalline, at 1200 to 2600°K, total hemispherical, 25:13666
energy-level excitation by neutron capture gamma rays, (E), 25:15002
gadolinium films on (110) surface of single crystals of, structure and work function of, 25:13700
lanthanum films on (110) surface of single crystals of, structure and work function for, 25:13702
mercury-ion reactions at 5 to 30 keV, sputtering yield and secondary emission in, 25:13971
neutron capture at 0.001 to 1 MeV, cross sections for, (E), 25:15121
neutron capture at 0.01 to 20 MeV, cross sections for, (T), 25:14970
neutron elastic scattering at 8 MeV, cross sections for, (E/T), 25:14965
phase transition temperature of, effects of grain boundary strength and grain size on ductile--brittle, 25:13649 (AD-713191)
properties at high temperatures, review of physical, thermal, and thermodynamic, 25:13667
reactions of fission-product, with uranium carbide fuels, 25:13764 (KFK-1260)
separation from iron by solvent extraction, method for, 25:12934
separation from rhenium by solvent extraction using tertiary amines, 25:12921
solubility in calcium chloride--calcium molybdate melts, kinetics of anodic, 25:13631
structure of sputtered films of, effects of sputtering conditions on, 25:14456

MOLYBDENUM ALLOYS AND SYSTEMS
properties at high temperatures, review of physical, thermal, and thermodynamic, 25:13667
C--Mo--Ru, phase studies of, 25:13764 (KFK-1260)
C--Mo--Ti, phase studies of, 25:13762 (AD-713153)
Cr--Fe--Mo--Ti, microstructure of anti-phase boundaries in chi-phase of $Fe_{36}Cr_{12}Mo_5Ti_5$, 25:13711
Cr--Mo, corrosion of, by flowing sodium, 25:15357 (SAN-781-228)
Hf--Mo-base, microstructure of, effects of internal nitriding on, 25:13661 (UCRL-72627)
Hf--Mo-base, tensile properties at 1100 to 1500°C, effects of internal nitriding on, 25:13661 (UCRL-72627)
Mo--Ni, corrosion by boiling hydrochloric acid solution, effects of temperature, titanium, tungsten, and zirconium on intercrystalline, 25:13633
Mo--O--U, crystal structure of UMo_2O_8, 25:13776
Mo--O--V, crystal structure of $MoV_2O_{7.8}$ and MoV_2O_8, 25:13776
Mo--Re, superconducting transition temperature and low-temperature, thermal capacity of sigma-phase, (E/T), 25:14177
Mo--Sn--Ti-base--Zr, mechanical properties of metastable β, effects of microstructure on, 25:13672
Mo--U-base, phase transformation in dilute, kinetics of isothermal β--α' martensitic, 25:13703
Mo--UN, phase studies of eutectic of, at 2100 to 2700°C, 25:13772
Mo--W-base, enthalpy and thermal capacity of, at 1400 to 3000°K, 25:13665

MOLYBDENUM COUPLES
Mo--PT/Mo--Pt, performance of thermocouples of, for in-core high temperature measurements, 25:13326

MOLYBDENUM ISOTOPES Mo-91
energy levels from molybdenum-92 (p,d) reactions, spin--parity assignments for, (E/T), 25:14980 (CEA-CONF-1654)
nuclear spin and parity assignments for, (E/T), 25:14980 (CEA-CONF-1654)

MOLYBDENUM ISOTOPES Mo-92
deuteron reactions (d,n) at 12 MeV with isobaric analog excitation, anomalies in cross section for, (E), 25:15050
proton reactions (p,d) at 24.5 MeV, DWBA analysis of differential cross sections and asymmetries from, (E/T), 25:14980 (CEA-CONF-1654)

MOLYBDENUM ISOTOPES Mo-94
deuteron reactions (d,n) at 12 MeV with isobaric analog excitation, anomalies in cross section for, (E), 25:15050

MOLYBDENUM ISOTOPES Mo-95
reactivity worths in fast reactor spectra, (E/T), 25:15350

MOLYBDENUM ISOTOPES Mo-96
deuteron reactions (d,n) at 12 MeV with isobaric analog excitation, anomalies in cross section for, (E), 25:15050

MOLYBDENUM ISOTOPES Mo-97
reactivity worths in fast reactor spectra, (E/T), 25:15350

MOLYBDENUM OXIDES
spectra of reduced MoO_3, EPR, 25:14482

MONTE CARLO METHOD
use in transport problems, importance sampling angle of scattering in, 25:14404
use of semi-analytic, in linear transport theory, 25:14871

MONTICELLO POWER REACTOR, UNIT 1
containment structure for, integrated leak rate test of primary, 25:15294 (DOCKET-50263-53)
containment structure for, leak rate test of secondary, 25:15295 (DOCKET-50263-54)
operation of, provisional license for, 25:15293 (DOCKET-50263-52)
operations incident of December 23, 1970, failure of low water level scram switch, 25:15236 (DOCKET-50263-51)

MOON
solar-wind interactions with atmosphere of, (T), 25:13905

MUCOSA
radiation effects on human, following therapy, protective effects of solcoseryl against, 25:13475

MUONIUM
hyperfine structure of, corrections to, (T), 25:13990

MUSCLES
radiation effects on water content and distribution in, of skeleton of rat, effects of lethal and sublethal dose on x, 25:13348

MUTATIONS
induced by chemical mutagens for chlorophyll in Sorghum, 25:13420
induced by EMS for base-pair reversion and prophage induction in Escherichia coli, effects of DNA repair capacity on, 25:13421
induced in seeds of wheat by EMS for weight variations, 25:13419
induced in Streptomyces coelicolor by nitroguanidine, 25:13414
isolation of amber, of Qβ bacteriophages, 25:13386
isolation of thymine-deficient, from uv-radiosensitive strains of Bacillus subtilis, methods for, 25:13614
radioinduced and ethylenimine-induced, in Bacillus mesentericus, fast neutrons and uv, 25:13416
radioinduced, in Aspergillus nidulans for morphological changes, uv, 25:13423
radioinduced, in crisp strains of Neurospora crassa, for morphological change, uv, 25:13424
radioinduced, in Escherichia coli, for arginine dependence, effects of culture medium on uv, 25:13406
radioinduced, in Escherichia coli, for base-pair reversion and prophage induction, effects of DNA repair capacity on uv and x, 25:13421
radioinduced, in Escherichia coli, for histidine operon, uv and x, 25:13422
radioinduced, in Nannizzia incurvata for reduced virulence, polyfactorial basis for uv, 25:13427
radioinduced, in peas, for increased productivity, economic value of x, 25:13418
radioinduced, in phage lambda for clear forming mutants, effects of bacterial and phage genes on uv, 25:13412
radioinduced, in seeds of wheat for weight variations, γ, 25:13419
radioinduced, in Sesamum orientale affecting chlorophyll, fertility, and growth, x, 25:13415
radioinduced, in Sorghum for chlorophyll, γ and x, 25:13420
radioinduced, in Streptomyces coelicolor, genetic mapping of uv, 25:13407
radioinduced, in Streptomyces coelicolor, uv, 25:13414
radioinduced, in yeast for prototrophs, relationship of DNA replication to x, 25:13425

N

NAILS
cysteic acid content in uranium miner, chromatographic and oscillopolarographic studies on, 25:13369

NAPHTHACENE
electron energy loss spectra at 115 eV in polycrystalline, 25:13968

NAPHTHALENE
radiolysis of monocrystals of, vibronic structure of radicals from electron, 25:13047

2,7-NAPHTHALENEDISULFONIC ACID, 4,5-DIHYDROXY-3-(PHENYLAZO)-
complexes with cerium, composition, stability, and colorimetric properties of, 25:12942

NATURAL BACKGROUND RADIATION
effects on growth of Paramecium aurelia, shielding effects of underground laboratory on, 25:13556
monitoring in Guarapari region of Brazil, 25:13393(R) (NYO-2577-12)

NATURAL GAS
environmental contamination from, produced by nuclear stimulation, (T), 25:13430 (UCRL-72830)

NATURAL WATERS
  radiation dose to man following ingestion of, from Masutomi spa area in Japan, α and γ, 25:13470
  radioactivity of Italian, (E), 25:13106
NAVAL VESSELS
  radioactive waste disposal from U. S. nuclear-powered, and support facilities during 1969, environmental monitoring to determine adequacy of limits and procedures for, 25:13444
NBS RESEARCH REACTOR
  radioactive effluents from, request for increased release limits for, 25:15385 (DOCKET-50184-25)
NEBULAE
  model for Gum Nebula, (E), 25:13851
  surface brightness of Coalsack and Libra cloud, (E), 25:13919
NEODYMIUM
  complexes with carminic acid, spectrophotometric studies on, 25:12937
  determination in plutonium oxide--uranium oxide fuels by solvent extraction and emission spectrography, 25:12922 (WHAN-SA-44)
  determination of trace amounts of, in plutonium and plutonium dioxide--uranium dioxide by solvent extraction and emission spectrography, 25:12923 (WHAN-SA-47)
  electron elastic scattering by, effects of virtual nuclear excitation on cross section of, (T), 25:15166
  energy-level excitation by neutron capture gamma rays, (E), 25:15002
NEODYMIUM ISOTOPES
  nuclear deformation parameters and optical isotope shifts for, estimates of, (T), 25:15048
NEODYMIUM ISOTOPES Nd-137
  energy levels from tellurium-126 (O-18,xn), tin-119 (Ne-20,xn), tin-119 (Ne-22,xn), tin-122 (Ne-22,xn), and tin-122 (Ne-20,xn) reactions, 25:15042
NEODYMIUM ISOTOPES Nd-141
  beta decay of metastable, (E), 25:15014
  wavefunctions of, proton part of, (E), 25:15014
NEODYMIUM ISOTOPES Nd-143
  neutron reactions (n,α) at 0.04 to 900 eV, resonance, 25:14994
  neutron reactions (n,α) with, alpha widths of resonance, (E/T), 25:15097
NEODYMIUM ISOTOPES Nd-145
  neutron reactions (n,α) at 0.04 to 900 eV, resonance, 25:14994
NEODYMIUM NITRATES
  bis(2-ethylhexyl) phosphate--H_2O--$Nd(NO_3)_3$, complex formation in, 25:13092
NEON
  abundance in nucleus of NGC 3031, (E), 25:13918
  analysis for trace amounts of carbon dioxide following freezing-out at liquid nitrogen temperature, mass spectrometric, 25:12941
  analysis for trace amounts of hydrogen following sorption on activated charcoal, mass spectrometric, 25:12941
  electron elastic scattering at 25 to 800 eV by, tables of amplitudes and spin polarizations for, (T), 25:13995 (AD-711664)
  electron reactions at 10 keV with, determination of oscillator strengths from coincidence measurements of electrons and ions from, 25:14003
  electron reactions up to 150 eV with, excitation, ionization, and formation of negative-ion resonances in, (E), 25:14002
  helium-ion reactions at 120 to 830 keV with, differential cross sections for production of helium atoms, He^{+}, and He^{2+} in, (E), 25:14044
  neon-ion reactions at 50 to 300 keV with, absolute doubly differential ionization cross sections for, (E), 25:13996
  neon-ion reactions with, cross sections for K-shell x-ray emission in, (E), 25:14004
  polarizability of atomic, many-body calculation of frequency-dependent, 25:14046
NEON IONS
  reactions with argon and neon, cross sections for argon L-shell and neon K-shell x-ray emission in, (E), 25:14004
  reactions with neon at 50 to 300 keV, absolute doubly differential ionization cross sections for, (E), 25:13996
NEON ISOTOPES Ne-18
  energy levels from (p,t) reactions, spin-parity assignments for, (E), 25:14950
NEON ISOTOPES Ne-19
  energy levels from neon-20 (He-3,α) reactions, spectroscopic factors for, (E), 25:14944
NEON ISOTOPES Ne-20
  concentration in neon by thermal diffusion, 25:13165(R) (MLM-1753)
  energy levels of, calculation using angular momentum projection and generator coordinate method, (T), 25:15196
  energy levels of, cranked Hartree--Fock solution for collective, (T), 25:14956
  helium-3 reactions (He-3,α) at 35 MeV, differential cross sections for, (E), 25:14944
  helium-3 reactions (He-3,p) at 3 MeV, angular distributions for, (E), 25:14904
  proton reactions (p,t) with, angular distributions for, (E), 25:14950
  reactions (Ne-20,xn) with tin-119 and tin-122 at 60 to 160 MeV, energy levels of neodymium-137 from, (E), 25:15042
NEON ISOTOPES Ne-21
  concentration in neon by thermal diffusion, 25:13165(R) (MLM-1753)
  energy levels from neon-22 (He-3,α) reactions, spectroscopic factors for, (E), 25:14944
  energy levels of, rigid-rotor and Coriolis model predictions for, (T), 25:14953
NEON ISOTOPES Ne-22
  concentration in neon by thermal diffusion, 25:13165(R) (MLM-1753)
  helium-3 reactions (He-3,α) at 35 MeV, differential cross sections for, (E), 25:14944
  reactions (Ne-22,xn) with tin-119 and tin-122 at 60 to 160 MeV, energy levels of neodymium-137 from, (E), 25:15042
NEON SYSTEMS
  Ne--Xe, diffusion coefficients for, at 169 to 922°K, 25:13165(R) (MLM-1753)
NEPTUNIUM
  desorption from tungsten surfaces, modulated beam method for, 25:13686
  deuteron reactions with thin targets of, at 9 to 14.2 MeV, (E), 25:15046
  effects on lattice parameters of alpha-uranium at 43°K, 25:14452
  precipitation in ammonium carbonate solutions using hexaamminecobalt chloride, evaluation of method for, 25:12980
  production and uses of, review on, 25:13059
  proton reactions with thin targets of, at 9 to 14.2 MeV, (E), 25:15046
  x-ray energies of, K, (E), 25:14981 (IN-1448)
NEPTUNIUM IONS
  spectra in cubic and octahedral crystals of tetravalent, absorption, 25:14466
NEPTUNIUM ISOTOPES Np-237
  alpha decay of, gamma spectra and half-life for, (E), 25:14981 (IN-1448)
  neutron reactions at thermal energies to 10 MeV, evaluation of data on, (T), 25:15128
  toxicity to rats in relation to blood composition, 25:13346
NEPTUNIUM ISOTOPES Np-238
  neutron reactions at thermal energies to 10 MeV, evaluation of data on, (T), 25:15128
NEPTUNIUM ISOTOPES Np-239
  determination in reactor cooling water by γ spectroscopy, 25:12956
NERVOUS SYSTEM
  radiation effects on biochemical and bioelectric activities of, of rabbits, ionizing, 25:13561
  radiation effects on brachial plexus of human, following therapy for mammary carcinomas, protective effects of actihemyl against paralyzing, 25:13480
  radiation effects on, of rabbits, electromagnetic, 25:13571
NEUTRINOS
  astrophysical studies with, lepton charge conservation in, (T), 25:13909
  detection of, emitted during stellar gravitational collapse, (T), 25:13830
  interactions ν + N, Regge pole model for hadron production from, 25:14635 (NYO-4204-9)
  interactions $\nu + p + p + \pi^{+} + \mu^{-}$, hadronic s-channel helicity conservation in, (T), 25:14636 (NYO-4204-10)
  magnetic monopole production in ocean bed by cosmic, upper limit for cross sections for, 25:14638
  production in γ + e + e + ν + anti ν interactions, stellar energy loss rate from cross sections for, (T), 25:14650
  reactions with nuclei at high energies, total cross sections for W-boson production in, (T), 25:14641
NEUTRINOS (ANTI ν)
  interactions anti ν + N, Regge pole model for hadron production in, (T), 25:14635 (NYO-4204-9)
  production in γ + e + e + ν + anti ν interactions, stellar energy loss rate from cross sections for, (T), 25:14650
NEUTRINOS (ν/sub e/)
  interactions ν + e + ν + e + γ, γ energy and angular distribution and radiative corrections for total effective cross sections for, (T), 25:14600
NEUTRINOS (ν/sub μ/)
  interactions $\nu + p + \mu^{-} + p + W^{+}$, model for W^{+} production in, 25:14643
  mass of, weak interaction model for electron energy spectrum in μ + e + ν + anti ν decay for limitation on, (T), 25:14631 (ITF-70-64)
NEUTRON CROSS SECTIONS
  accuracy requirements for standards to be used in reactor design, 25:14877
  calculation of group-averaged macroscopic, for use in reactor design, 25:15346
  correction for multiple scattering processes in measurement of differential elastic and inelastic, (T), 25:15150

  data tabulations for heavy nuclei in resonance region, review of, (E), 25:15069
  evaluation for use in astrophysics, need for accurate, 25:14876
  evaluation of, use of interactive computer graphics in, 25:14879
  multilevel formalism for elastic scattering, (T), 25:15161
  plotting absorption and total, updating of LGR computer program for use with ANISN library tapes, (T), 25:14986(T) (ORNL-tr-2408)
  shape analysis for fissionable nuclei, least-squares method for, 25:15132
  statistical model analysis of radiative capture, (T), 25:15122
  tabulation of, review of data center activities in, 25:14878
NEUTRON SOURCES
  fabrication of curium-244--beryllium, 25:14872
  neutron flux of curium-244--beryllium, 25:14872
  targets for T(d,n), properties of tritiated titanium, 25:14840 (EUR-4286(Pt.2))
NEUTRON SPECTROMETERS
  development of gas-recoil proportional, with fast coincidence electronic collimation, 25:13232
  performance of helium-3 proportional, in fast subcritical assemblies, (E), 25:15388(R) (GULF-RT-10421)
NEUTRON STARS
  atom ionization energies in magnetic fields of, (T), 25:13829
  nucleon clustering in low-density matter of, (T), 25:13819
  properties of, (T), 25:13844
  properties of, (T), 25:13797
NEUTRONS
  capture by antimony-121 and cesium-134, γ spectra from resonance, 25:14982 (NCSAC-31)
  capture by chromium-50, chromium-54, nickel-60, and vanadium-51 at 0.1 to 200 keV, cross sections for, (E), 25:14982 (NCSAC-31)
  capture by curium, cross sections for, (E), 25:15090
  capture by dysprosium-163 up to 360 eV, γ spectra and resonance spin assignments for, (E), 25:14982 (NCSAC-31)
  capture by gold-197 up to 1 MeV, cross section for, (E), 25:14982 (NCSAC-31)
  capture by indium-115, gamma spectra from resonance, (E), 25:15008
  capture by indium-115, lutetium-175, thulium-169, and uranium-238, cross-section calculations for, (E), 25:14982 (NCSAC-31)
  capture by nuclei with $A < 220$, review of cross sections for non-resonance, 25:15120
  capture by plutonium-239 and uranium-235, γ spectra from, (E), 25:14982 (NCSAC-31)
  capture by reactor structural materials, evaluation of cross sections for, 25:14971
  capture by silver-109, γ spectra from, (E), 25:14982 (NCSAC-31)
  capture by uranium-233 and uranium-235, multilevel analysis of cross sections for, 25:15130
  capture by uranium-238 at 0.0001 to 20 MeV, evaluation of cross sections for, (E/T), 25:15127
  capture by uranium-238 at 0.005 to 30 keV, energy dependence of cross sections for, (E), 25:15105
  capture by uranium-238 at 1 eV to 15 MeV, cross sections for, (E/T), 25:15125
  capture by uranium-238 at 24 to 145 keV, cross sections for, (E), 25:15106
  capture by uranium-238, low-energy γ spectra from, (E), 25:15077
  capture in reactors, Westcott formalism for, (T), 25:15405 (LFEN-NI.-45-a)
  capture-to-fission ratio for plutonium-239, accuracy of values for, 25:15072
  detection at 100 to 700 keV with flat energy response, vaseline--boron-10 sphere with scintillation detector system for, 25:13215
  effects of photospheric, on heating of corona, (T), 25:13907
  effects on acceleration of climb-controlled creep in materials, (T), 25:13725
  effects on alkali metal chlorides and oxychlorides, chemical states of recoil sulfur-35 from, 25:13065
  effects on content of lactate and propionate in blood serum of sheep, 25:13384
  effects on fission of naturally occurring uranium-235 in neoplastic and normal tissues of human kidney, interstitial, 25:13361
  effects on iron-58-labeled potassium ferrocyanide and Prussian Blue, 25:13068
  effects on methanol solutions of lithium chloride, chemical states of sulfur-35 from, 25:13071
  effects on nitrides, reactions of recoil carbon-14 and nitrogen-13 from, 25:13070
  effects on potassium chloride crystals, colloid production in, 25:14429
  effects on sodium and potassium cyanides, reactions of recoil carbon-14 and nitrogen-13 from, 25:13072
  effects on structure of ordered hexagonal uranium--titanium phase, 25:13726
  effects on tissues of mice and rats for whole-body activation autoradiography, 25:13590
  emission from dense plasma focus discharge, parameters of, (E), 25:14355
  flux in fast reactors, comparison of three dimensional diffusion theory computer programs for, 25:15343 (WHAN-IR-48)
  flux measurements in reactors, techniques for high-precision, 25:14877
  intensity of cosmic, effects of small magnetic storms on diurnal variation of, (E), 25:14074
  interactions anti p + n $\to 3\pi^- + 2\pi^+ + \pi^0$ at rest in deuterium bubble chamber, production of ω^0 and branching ratio for, (E), 25:14553
  interactions anti p + n $\to 3\pi^- + 2\pi^+$ at rest in deuterium bubble chamber, production of rho^0 and branching ratio for, (E), 25:14553
  interactions anti p + n $\to$ K + anti K + π at rest, four-point Veneziano functions for mass spectra and angular distributions for, (T), 25:14691
  interactions anti p + n $\to \pi^+ + 2\pi^-$ at 1.0 to 1.6 GeV/c in deuterium bubble chamber, cross sections and Veneziano model for mass and angular distributions in, (E/T), 25:14548
  interactions anti p + n at 1.25 to 1.67 GeV/c in deuterium bubble chamber, cross sections for hadron production in, (E), 25:14550
  interactions $\gamma + n \to n + \pi^+ + \pi^- + \pi^-$ at 4.3 GeV, total and resonance production cross sections for, (E), 25:14521
  interactions $\gamma + n \to p + \pi^+ + \pi^- + \pi^- + \pi^0$ at 4.3 GeV, total and resonance production cross sections for, (E), 25:14521
  interactions $\gamma + n \to p + \pi^+ + \pi^- + \pi^-$ at 4.3 GeV, total and resonance production cross sections for, (E), 25:14521
  interactions $\gamma + n \to \pi^- + p$, angular distributions and differential cross sections of $\pi^- + p \to \gamma + n$ interactions at 1245 and 1337 MeV for test of predictions for, (E), 25:14567
  interactions $\gamma + n \to \pi^- + p$, π^-/π^+ cross section ratio in $\gamma + d \to \pi^-(\pi^+) + 2p(2n)$ interactions at 600 to 1700 MeV for cross sections of, (E), 25:14523
  interactions γ + n at 0.7 to 12 GeV in deuterium bubble chamber, isovector--isoscalar interference from partial cross sections for, (E), 25:14519
  interactions $K^- + n \to \Sigma^- + \pi^+ + \pi^-$ at 1.62 to 1.74 GeV, $\Sigma(1660)$ weak coupling to $\Lambda(1405)\pi$ and existance of two distinct $\Sigma(1660)$ in partial wave analysis of, (T), 25:14717
  interactions $K^- + n \to \Sigma^-(\Sigma^+) + \pi^+(\pi^-) + \pi^-$ at 670 to 835 MeV/c in deuterium bubble chamber, differential and total cross sections and partial-wave analysis for resonance production in, (E/T), 25:14557 (FSU-HEP-70-3-1)
  interactions $\mu^- + n \to p + W^- + \mu^-$, model for W^+ production in, 25:14643
  interactions n + d above inelastic threshold, Kohn variational principle for calculating elastic amplitude of, (T), 25:14744
  interactions n + d, realistic potentials for calculation of scattering lengths for, (T), 25:14743
  interactions $n + p \to 2p + \pi^-$ at 2 to 10 GeV/c, peripheral nature, zero-isospin exchange, total cross sections, and production cross sections for $\Delta(1236)$, N(1470), and N(1688) production in, (E), 25:14551
  interactions $n + p \to d + \pi^0$ from threshold through first resonance peak, spark chamber study of charge independence from differential and total cross sections for, (E), 25:14549
  interactions n + p below 350 MeV, phase shift analysis of, (T), 25:14734
  interactions n + p, eikonal model for large-angle elastic, 25:14737
  interactions $p + n \to p + n + \pi^+ + \pi^-$, $I = 1$ meson exchange diagram for rho^0 production in, 25:14741
  interactions π^- + n at 17.2 GeV/c in emulsions, proton momentum spectrum from, (E), 25:14564
  interactions π^+ + n at 2.34 GeV/c in xenon bubble chamber, neutral boson, π^+ and γ production in, (E), 25:14560 (JINR-E1-5349)
  mass difference (n - p) and transition matrix elements for, electromagnetic, 25:14617
  mesons (μ) production by cosmic, at sea level, (E), 25:14063
  monitoring of cosmic, meteorological effects in, (T), 25:14066
  reactions (n,2n) and (n,3n) with fissionable materials, cross sections for, (E), 25:15111
  reactions (n,2n) with deuterium at 18.5 MeV, neutron--neutron scattering length in, 25:14887
  reactions (n,2n) with fluorine-19, fission-spectrum-averaged cross sections for, (E), 25:14968
  reactions (n,2n) with uranium-238, cross sections for, (E), 25:15111
  reactions (n,α) with neodymium-143, samarium-147, and samarium-149, alpha widths of resonance, (E/T), 25:15097
  reactions (n,f) with actinide nuclei, intermediate structure effects in, (E), 25:14997
  reactions (n,f) with californium-252 at 20 to 300 keV, cross sections for, (E), 25:15090

reactions (n,f) with curium, cross sections for, (E), 25:15090
reactions (n,f) with fissionable materials from thermal energies to 15 MeV, review of mean prompt neutron production from, 25:15119
reactions (n,f) with plutonium-238 at 15 to 500 eV, cross section for, (E), 25:14982 (NCSAC-31)
reactions (n,f) with plutonium-239 and uranium-235 at 0 to 70 keV, mean prompt neutron production from, (E), 25:15113
reactions (n,f) with plutonium-239 and uranium-235 at 0.01 to 1 MeV, mean number of prompt neutrons and cross section for, (E), 25:15116
reactions (n,f) with plutonium-239 at 0.010 to 30 keV, cross sections and resonance parameters for, (E/T), 25:15089
reactions (n,f) with plutonium-239, thorium-232, uranium-235, and uranium-238 at 0 to 6 MeV, energy dependence of mean prompt neutron production from, (E), 25:15117
reactions (n,f) with plutonium-239, uranium-235, and uranium-238 at 0.0001 to 20 MeV, evaluation of cross sections for, (E/T), 25:15127
reactions (n,f) with plutonium-241 and uranium-235 at 0.005 to 1 MeV, ratio of cross sections for, (E), 25:15107
reactions (n,f) with plutonium-241 at 0.001 to 3 keV, cross sections for, (E/T), 25:15086
reactions (n,f) with uranium-233 and uranium-235, multilevel analysis of cross sections for, 25:15130
reactions (n,f) with uranium-235 at 0.017 to 30 keV, cross sections for, (E/T), 25:15086
reactions (n,f) with uranium-235, description using sudden model, (T), 25:15024
reactions (n,p) and (n,a) with nuclei, compound-nucleus calculations of cross sections for low-energy, 25:15207
reactions (n,p) with copper-64, iron-56, magnesium-24, and zinc-64, fission-spectrum-averaged activation cross sections for, (E), 25:14968
reactions (r,f) with plutonium-239, gas release curves from, (T), 25:14989 (UCRL-50656(Suppl.))
reactions with actinides at thermal energies to 10 MeV, evaluation of data on, (T), 25:15128
reactions with chromium-52 up to 200 keV, total cross section for, (E), 25:14982 (NCSAC-31)
reactions with fission product isotopes, total cross sections and resonance parameters for, (E), 25:15098
reactions with fissionable materials above resonance energies, review of data on, 25:15112
reactions with nuclei at A > 220, evaluation of data on resonance, 25:15094
reactions with nuclei at A < 220, evaluation of thermal and resonance cross sections for, 25:15101
reactions with nuclei at A < 220, neutron-spectroscopy analysis of resonance, 25:15095
reactions with nuclei with A < 220, activation resonance integrals for, (E/T), 25:15124
reactions with nuclei with A < 220, evaluation of data above resonance region, 25:15123
reactions with nuclei, energy dependence of average radiation widths for, (T), 25:15209
reactions with nuclei, energy dependence of energy level density from, (T), 25:15208
reactions with nuclei, role of special motion states in, 25:15206
reactions with plutonium-239 and uranium isotopes, yields of spontaneously fissioning isomers from, (E), 25:15031
reactions with plutonium-239 at 0.014 to 1000 keV, fission, capture, scattering, and total cross sections for, (E), 25:15091
reactions with plutonium-239 at 5.7 to 160 eV, simultaneous analysis of total and fission cross sections for, (E/T), 25:15087
reactions with plutonium-240 at 1 eV, resonance parameters for, (E), 25:15092
reactions with plutonium-242 up to 1 eV, total cross section for, (E), 25:14982 (NCSAC-31)
reactions with reactor control materials at 0.007 to 10 eV, energy dependence of cross sections for, (E/T), 25:15096
reactions with reactor materials, conference on basic data for, 25:14987 (STI/PUB-259(Vol.1))
reactions with reactor materials, conference on basic data for, 25:14988 (STI/PUB-259(Vol.2))
reactions with threshold detectors, fission-spectrum-averaged activation cross sections for, (E), 25:14968
reactions with uranium-233 and uranium-235, statistical distribution of Kapur-Peierls-type resonance parameters for, 25:15130
reactions with uranium-235, derivation of R-matrix parameters for cross sections for, 25:15131
reactions with uranium-238 at 0.00001 eV to 15 MeV, evaluation of cross sections for, 25:15126
reactions with uranium-238 at 1 to 100 keV, temperature dependence of total cross section and resonance parameters for, (E/T), 25:15093
reflection by concrete and iron, one-dimensional S/sub n/ calculations of spectra of, (T), 25:14865 (COO-2049-2)
reflection by concrete, albedo for, (E), 25:14394 (CEA-N-1382)
scattering by calcium-40 at 0.55 to 2.0 MeV, differential cross sections for, (E), 25:14939
scattering by indium-115, fission-spectrum-averaged activation cross sections for inelastic, (E), 25:14968
scattering by magnetic systems and high polymers, conference on inelastic, Tokai, Japan, 12/69, 25:14436 (JAERI-1197)
scattering by nuclei, correction for multiple scattering processes in measurement of differential cross sections for elastic and inelastic, (T), 25:15150
scattering by nuclei, multilevel formalism for elastic, (T), 25:15161
scattering by plutonium-239 at 0 to 660 eV, spin of resonances induced by, (E/T), 25:15088
scattering by polarized nuclei of polarized, separation of coherent and incoherent components of inelastic, (T), 25:14869
scattering by two-species quantum fluids, Born approximation to cross sections for, 25:13965
scattering from antiferromagnetic manganese(II) fluoride and rubidium manganese fluoride, inelastic, 25:14471
scattering in spin-wave resonances in semiconductor antiferromagnets, (T), 25:14488
spectra in fast subcritical assemblies, time-of-flight measurements of, 25:15388(R) (GULF-RT-10421)
spectra measurements of, characteristics of threshold activation and fission foil detectors for, 25:13210 (JINR-P3-5421)
streaming through two-legged concrete ducts with baffles, (E), 25:14391 (AD-710963)
transmission of polarized, by polarized erbium-167, spins of resonances and hyperfine coupling constants for, (E), 25:15003
transport calculations, comparison of discrete-angular-grid Monte Carlo, with other methods and experiment, 25:14404
transport equation in plane geometry, solution of time-dependent, (T), 25:14873
transport in one-dimensional finite systems, anisotropic source--flux iteration technique for calculation of, 25:14406
transport in plane and spherical geometry, two-group analysis of critical problem for, (T), 25:14867
transport in spheres, cylinders, and planes, computer program for solving one-dimensional Boltzmann equation for, (T), 25:14863 (CEA-N-1358)
transport in two-dimensional spherical geometry, computer program for solving Boltzmann equation for, (T), 25:14866 (LA-4567)
transport of polyenergetic, in spheres and planes, computer program for calculating, (T), 25:14864 (CEA-N-1388)
transport theory for, semi-analytic Monte Carlo method in linear, 25:14871
use for diagnosis of thyroid disorders caused by radiation sickness in rats, 25:13497
uses in process control industry, review of, 25:13177

NEUTRONS, COLD
  scattering by oxygen-17, length for coherent, (E), 25:14862 (AERE-R-5770)

NEUTRONS, EPITHERMAL
  capture by lutetium-175, resonance spin assignments for, (E), 25:14982 (NCSAC-31)
  reactions (n,f) with uranium-235, symmetry of, (E), 25:14999
  scattering by uranium-235 at 0.025 to 1 eV, cross section for, (E), 25:15085
  scattering by uranium-235 at 7 to 60 eV, resonance parameters for, (E), 25:15084

NEUTRONS, FAST
  book: Biological Effects of Fast Neutrons, 25:13568
  capture by beryllium-9, carbon-12, potassium-39, silicon-28, and sodium-23, cross sections for, (E/T), 25:14920(T) (BNL-tr-380)
  capture by chromium, iron, molybdenum, and nickel at 0.01 to 20 MeV, cross sections for, (T), 25:14970
  capture by gadolinium, gold, molybdenum, rhodium, rhenium, tantalum, tungsten, and uranium-238 at 0.001 to 1 MeV, cross sections for, (E), 25:15121
  capture cross sections at 0.001 to 1 MeV, statistical model analysis of, (T), 25:15122
  capture to fission ratio in plutonium-239 and uranium-235, integral measurements of, (E/T), 25:15348
  dosimetry in facility for evaluating radiaton protection measures, 42 MeV betaton, 25:13450
  effects on aging in electrolytic chromium, relations with deformation, 25:13730
  effects on Bacillus mesentericus, comparison with ethylenimine and uv, mutagenic, 25:13416
  effects on content of o-oxyphenol in poplar shoots, 1000 R, 25:13598
  effects on low-frequency electromagnetic losses in niobium at 40°C, 25:14188
  effects on mechanical properties of heavy-section Type A533B steel, 25:13724 (ORNL-4590, pp 100-34)
  effects on silicon, properties of defect clusters induced in, 25:14428
  effects on space-charge-limited currents in silicon at 14 MeV, 25:14426
  effects on swelling of Zircaloy clad thorium oxide (ThO_2)--uranium oxide (UO_2) rod type fuel elements, 25:15366 (WAPD-TM-986)

XUM

effects on welds of Type A533B steel, 25:13724 (ORNL-4590, pp 100-34)
flux density in 45 MW core of water cooled and moderated tank type reactor, (E/T), 25:15393 (RCN-119)
flux distribution in water cooled and moderated tank type reactors, comparison of computer programs for calculating, 25:15391 (JAERI-Memo-4180)
flux measurements at 10 keV to 1 MeV, development of detectors for absolute, 25:13216
production in atmosphere, solar-cycle modulation of, (E/T), 25:14064
reactions (n,2n) with nuclei at 14 MeV, isomeric cross-section ratios for, 25:15182
reactions (n,α) with boron-11 at 15.5 to 19 MeV, cross section for, (E), 25:14895
reactions (n,α) with lithium-6 at 100 to 500 keV, cross section for, (E), 25:14913
reactions (n,f) with plutonium-239 and -240 at 0.1 to 1.5 MeV, angular distributions of fragments from, (E), 25:15051
reactions (n,f) with plutonium-239 and uranium-235 at 0.3 to 1.4 MeV, mean prompt neutron production and relative cross sections for, (E), 25:15114
reactions (n,f) with plutonium-239 and uranium-235 at 0.025 to 1 MeV, total cross section for, (E), 25:15068
reactions (n,f) with plutonium-240, uranium-239, and uranium-235 at 0.6 to 5 MeV, mean prompt neutron production from, (E), 25:15115
reactions (n,f) with thorium-232 at 14 MeV with long-range particle emission, calculation of probability for, (T), 25:15018
reactions (n,f) with uranium-232 at 0.1 to 1.5 MeV, cross section and fragment angular distributions for, (E), 25:15019
reactions (n,f) with uranium-233 and -235 at 500 to 1500 keV, cross-section ratio for, 25:14982 (NCSAC-31)
reactions (n,f) with uranium-235 and -238 at 1400 and 1500 keV, cross-section ratio for, (E), 25:14982 (NCSAC-31)
reactions (n,f) with uranium-235, cross sections for, (E/T), 25:15398
reactions (n,f) with uranium-238 at 1.35 and 2.02 MeV, neutron spectra from, (E), 25:15109
reactions (n,f) with uranium-238 at 2.5, 7.6, and 14 MeV with long-range particle emission, calculation of probability for, (T), 25:15018
reactions (n,xγ) with nuclei at 14 MeV, cross sections and gamma spectra from, (E/T), 25:14920(T) (BNL-tr-380)
reactions with calcium and sodium-23 at 0.28 to 1.2 MeV, total cross sections and resonance parameters for, (T), 25:14969
reactions with carbon at 0.07 to 1500 keV, total cross sections for, (E/T), 25:14912
reactions with carbon at 0.5 to 15 MeV, total cross section for, (E), 25:14982 (NCSAC-31)
reactions with carbon, nickel, uranium-235, uranium-238, and plutonium-239 at 0.1 to 6 MeV, total cross sections for, (E), 25:15103
reactions with fast reactor materials, integral measurements of cross sections for, (E/T), 25:15349
reactions with fertile and fissionable nuclei, review of data on, 25:15102
reactions with gold polycrystals and monocrystals, atomic sputtering, (E), 25:14414
reactions with light nuclei, analysis for reaction mechanisms in, (E), 25:14898
reactions with nitrogen at 0.5 to 25 MeV, total cross section for, (E), 25:14982 (NCSAC-31)
reactions with plutonium-239, plutonium-240, plutonium-241, and uranium-238 at 0.01 to 15 MeV, cross sections for, (T), 25:15133
reactions with plutonium-240 at 0.001 to 1 MeV, cross sections for, (T), 25:15129
reactions with uranium at 0.5 to 4.35 MeV, total cross sections for, (E), 25:15104
scattering by aluminum, bismuth, iron, manganese, niobium, and vanadium at 2 to 4.5 MeV, cross sections for inelastic, (E/T), 25:14966
scattering by aluminum, copper, and zinc at 1 to 8 MeV, width fluctuation and resonance interference effects in cross sections for, (E/T), 25:14962
scattering by aluminum, silicon, sulfur, and zinc at 4.5 to 8 MeV, cross sections for elastic and inelastic, (E/T), 25:14963
scattering by aluminum-27, beryllium-9, calcium-40, potassium-39, and silicon-28 at 14 MeV, optical-model analysis of differential cross sections for elastic, (E/T), 25:14920(T) (BNL-tr-380)
scattering by beryllium-9 and carbon-12 at 14 MeV, differential cross sections for inelastic, (E/T), 25:14920(T) (BNL-tr-380)
scattering by carbon at 0.5 to 2 MeV, differential cross section angular distributions for elastic, (E/T), 25:14911
scattering by chromium, iron, nickel, and vanadium at 1.8 to 8.1 MeV, cross sections for elastic, (E/T), 25:14964
scattering by chromium, nickel, tungsten, yttrium, and zirconium at 14.4 MeV, cross sections for inelastic, (E), 25:14967
scattering by cobalt, fluorine, iron, nickel, and tantalum, cross sections for inelastic, (E), 25:14960
scattering by helium-4, resonating-group calculations of phase shifts and effective potentials for elastic, (T), 25:14880 (COO-1764-105)
scattering by iron at 1.43 to 2.15 MeV, cross sections for elastic and inelastic, (E), 25:14961
scattering by light nuclei, analysis for reaction mechanisms in elastic and inelastic, (E), 25:14898
scattering by nuclei at 8 MeV, cross sections for elastic, (E/T), 25:14965
scattering by plutonium-239 at 0.2 to 5.5 MeV, angular distributions in, (E/T), 25:15134
scattering by uranium-238 at 0.05 to 15 MeV, cross sections for inelastic, (E), 25:15135
scattering by uranium-238 below 1.2 MeV, cross sections for inelastic, (E), 25:15110
scattering by vanadium-51 and yttrium-89 at 0.3 to 4 MeV, gamma spectra and excitation functions at 100° for inelastic, (E), 25:14919 (AWRE-O-78/70)
slowing down in graphite, (E), 25:14870
thermalization in graphite by the reaction rate method, (E), 25:14874
thermalization in silicate ore boreholes, effects of moisture on, 25:13109

NEUTRONS, FISSION
effects on incidence of carcinomas in rat adrenal glands, mixed whole-body γ and, 25:13564

NEUTRONS, FUSION
production in dense deuterium noncylindrical z pinch, (E), 25:14359

NEUTRONS, INTERMEDIATE
capture by A = 45 to 204 nuclei, cross sections and resonance parameters for, (T), 25:14979 (AAEC/E-198(Suppl.1))
capture by plutonium-240 at 4 to 60 keV, average cross section for, (E), 25:14982 (NCSAC-31)
capture by uranium-238 at 0.05 to 1 keV, resonance parameters from radiative, (E), 25:15081
capture-to-fission ratio for plutonium-239 and uranium-235 at 0.1 to 30 keV, radiative, (E), 25:15075
capture-to-fission ratio for uranium-235 at 0.3 to 5000 eV, method for direct measurement of, 25:15076
capture-to-fission ratio in plutonium-239 at 0.1 to 30 keV, (E), 25:15073
capture-to-fission ratios for plutonium-239 and uranium-235 at 0.1 to 10 keV, (E), 25:15074
dosimetry in facility for evaluating radiaton protection measures, 42 MeV betaton, 25:13450
neutron reactions (n,f) with uranium-235, mean prompt neutron production from, (E/T), 25:15399
reactions (n,α) with boron-10 and lithium-6 at 0.01 to 80 keV, cross section ratios for, (E/T), 25:14910
reactions (n,f) with plutonium-241 at 2 to 2000 eV, cross section for, (E), 25:15083
reactions (n,f) with uranium-233 at 0.018 to 2000 eV, cross section for, (E), 25:15082
reactions with uranium-233 at 0.7 to 320 eV, total cross section for, (E), 25:15079
reactions with uranium-238 at 0.6 to 14 keV, total cross section for, (E), 25:15080
scattering by lithium-6 at 1 to 110 keV, cross sections for, (E), 25:14909

NEUTRONS, PILE
effects on re-solution of gaseous fission products in uranium dioxide fuels, 25:13780(R) (GEAP-12147)
flux monitoring of, radiation damage to surface-barrier semiconductor detectors during, 25:13329
spectra measurements in fast reactors, data unfolding methods for activation detectors for, 25:13226

NEUTRONS, THERMAL
absorption by gross fission products of uranium-233, uranium-235, and plutonium-239, cross sections for, (E/T), 25:15100
absorption cross sections for gross fission products of uranium-235, (T), 25:15099
absorption in uranium-233, neutron yield from, (E), 25:15071
capture by chlorine and cadmium, gamma spectra from, (E), 25:14932
capture by erbium-167, energy levels of erbium-168 from, (E), 25:15000
capture by erbium-170, hafnium-174, and ytterbium-172, γ spectra and Q-values for, (E), 25:15059
capture by iron, excitation of energy levels in 6- to 9-MeV region by gamma rays from, (E), 25:15002
capture by plutonium-239 and uranium-235, high-energy γ spectra from, (E), 25:15078
capture by samarium-149 and tantalum-181, conversion-electron spectra from, (E/T), 25:14984 (NP-18536)
capture by sodium-23, aluminum-27, chlorine-37, and vanadium-51 at 0.025 eV, cross sections for, (E), 25:14935
cpature to fission ratios for plutonium-239, uranium-233, and uranium-235, (E), 25:15070
dosimetry in facility for evaluating radiaton protection measures, 42 MeV betaton, 25:13450
effects on human nails for determination of copper content by activation analysis, 25:13491
flux density in 45 MW core of water cooled and moderated tank type reactor, (E/T), 25:15393 (RCN-119)
flux distribution in water cooled and moderated tank type

XUM

reactors, comparison of computer programs for calculating, 25:15391 (JAERI-Memo-4180)
reactions (n,f) with americium-242, californium-249, curium-245, plutonium-238, thorium-229, and uranium-235, energy spectra and mean prompt neutron production from, (E), 25:15118
reactions (n,f) with plutonium-239 and uranium-235 at 0.005 to 0.1 eV, (E), 25:15067
reactions (n,f) with plutonium-239, uranium-233, and uranium-235, cross section ratios for, (E), 25:15070
reactions (n,f) with thorium-227, cross section for, (E), 25:15044
reactions (n,f) with uranium-233, cross section for, (E), 25:15071
reactions (n,f) with uranium-235, fission product yields from, (T), 25:15099
reactions (n,f) with uranium-235, independent yields of antimony-124g and -126g and terbium-160 in, (E), 25:15038
reactions (n,f) with uranium-235, K x-ray yields from fragments from, (E), 25:15027
reactions with atoms and molecules, differential cross sections from quasi-classical approximation for, (T), 25:14875
reactions with hydrogen chloride gas at 0.010 and 0.025 eV at 20 and 90°, differential cross sections from quasi-classical approximation for, (T), 25:14875
scattering by iron, amplitude of forward magnetic, (E), 25:14868
scattering by zirconium, coherent inelastic, 25:14467
spectra measurements in graphite moderated and water moderated natural uranium lattices, foil activation method for, (E/T), 25:15409
use for therapy, advantages of pulsed reactor with electron-Linac for, 25:13548

NEW MEXICO
uranium deposits in, preliminary reconnaissance data on, 25:13125 (RME-160)

NEWBOLD ISLAND POWER REACTOR, UNIT 1
design parameters of, revised and additional data on, 25:15326 (DOCKET-50354-10)
operations aspects of, revised and additional data on, 25:15326 (DOCKET-50354-10)

NEWBOLD ISLAND POWER REACTOR, UNIT 2
design parameters of, revised and additional data on, 25:15326 (DOCKET-50354-10)
operations aspects of, revised and additional data on, 25:15326 (DOCKET-50354-10)

NICKEL
determination in cobalt- or iron-base alloys using gas-sheathed tubular electrode arc, spectroscopic, 25:12945
determination in meteoritic materials by neutron activation and γ--γ coincidence spectrometry, 25:12967
determination of trace amounts of, in blood serum by emission spectroscopy, 25:12946
determination using thin-layer chromatography and ring-oven colorimetry, 25:12944
effects on gravimetric determination of tellurium, 25:12943
mechanical properties of sintered powders of, 25:13766(R) (SRO-552-6)
microstructure of sintered powders of, 25:13766(R) (SRO-552-6)
neutron capture at 0.01 to 20 MeV, cross sections for, (T), 25:14970
neutron elastic scattering at 1.8 to 8.1 MeV, cross sections for, (E/T), 25:14964
neutron elastic scattering at 8 MeV, cross sections for, (E/T), 25:14965
neutron inelastic scattering at 14.5 MeV, cross sections for, (E), 25:14967
neutron inelastic scattering by, cross sections for fast, (E), 25:14960
neutron total cross section at 0.1 to 6 MeV, (E), 25:15103
porosity of sintered powders of, 25:13766(R) (SRO-552-6)
radioinduced defects in, electron microscopy study of 42 to 44 MeV α particle, 25:13728
radioinduced large faulted dislocation loops in, electron, 25:13732
radioinduced voids in thin foils of, effects of oxidation on electron, 25:14416

NICKEL ALLOYS AND SYSTEMS
analysis for constituents using gas-sheathed tubular electrode arc, spectroscopic, 25:12945
nuclear spin-lattice relaxation in, nickel-63 and palladium-105, 25:15463 (UCRL-20376)
welding in sodium at 500 to 700°C, tendency for self-, 25:13668
Al--Nb--Ni, phase studies of, 25:13706
Co--Fe-base--Ni, thermal conductivity at 80 to 293°K, effects of cobalt content on, 25:13685
Cr--Ni, internal oxidation of dilute, 25:15455(T) (SC-T-71-3004)
Cr--Ni-base, sealing leaks in tubes of, by explosive plug welding, 25:13647
Ir--Ni, superconductivity and spin fluctuations in, (E), 25:14202
Mn--Ni, magnetic susceptibility near Curie point of Ni_3Mn single crystal, temperature dependence of initial paraprocess, 25:14446
Mo--Ni, corrosion by boiling hydrochloric acid solution, effects of temperature, titanium, tungsten, and zirconium on intercrystalline, 25:13633
Ni--Ta, dislocation dissociation in ordered Ni_3Ta, 25:13699

NICKEL ISOTOPES Ni-57
energy levels from nickel-58 (He-3,α) reactions, spin-parity assignments for, (E), 25:14952

NICKEL ISOTOPES Ni-58
energy levels of, quasiparticle structure of, (T), 25:15178
helium-3 reactions (He-3,α) at 15 MeV, α--γ angular correlations from, (E), 25:14952
helium-3 reactions (He-3,n) with, neutron spectra from, (E), 25:14943

NICKEL ISOTOPES Ni-60
energy levels from nickel-61 (p,d) reactions, spectroscopic factors for, (E/T), 25:14921 (CEA-CONF-1653)
energy levels of, quasiparticle structure of, (T), 25:15178
neutron capture at 0.1 to 20 keV, cross section for, (E), 25:14982 (NCSAC-31)

NICKEL ISOTOPES Ni-61
energy-level excitation by neutron capture gamma rays, (E), 25:15002
proton reactions (p,d) at 16.6 MeV, DWBA analysis of differential cross sections and asymmetries from, (E/T), 25:14921 (CEA-CONF-1653)

NICKEL ISOTOPES Ni-62
energy levels of, quasiparticle structure of, (T), 25:15178
proton reactions (p,nγ) at 4.7 to 5.9 MeV, gamma spectra from, (E), 25:14940

NICKEL ISOTOPES Ni-64
energy levels of, quasiparticle structure of, (T), 25:15178

NICKEL ISOTOPES Ni-66
energy levels of, quasiparticle structure of, (T), 25:15178

NICOTINAMIDE-ADENINE DINUCLEOTIDE
radiation effects on content of, in organs of rabbits and rats, effects of injection of ATP and nicotinamide on, 25:13379

NICOTINAMIDE-ADENINE DINUCLEOTIDE PHOSPHATE
radiation effects on content of, in organs of rabbits and rats, effects of injection of ATP and nicotinamide on, 25:13379

NINE MILE POINT POWER REACTOR
emergency core cooling system for, requested additional information on, 25:15270 (DOCKET-50220-57)

NIOBIUM
abundance in chondrites, achondrites, and Apollo 11 fines, (E), 25:13787
argon-ion reactions at 25 keV of single crystals of, angular distribution of secondary electrons emitted in, 25:13969
complexes with diarsine-like ligands, preparation and spectra of tetrahalide, 25:12979
current losses in thin-film superconducting, alternating, (E), 25:14189
determination in cobalt- or nickel-base alloys using gas-sheathed tubular electrode arc, spectroscopic, 25:12945
diffusion of hydrogen and deuterium in, Gorsky-effect measurements of, 25:14440
effects of weld filler addition of, on mechanical properties of heat affected zone in ferritic stainless steel, 25:13696
electromagnetic losses at 4.2°K of fast-neutron-irradiated, low-frequency, 25:14188
losses in superconducting strip conductors, alternating field, 25:14187
magnetization and susceptibility measurements of polycrystalline superconducting, with tantalum impurities, 25:14195
oxidation during heating in deionized water and water vapor, electron diffraction study of structure of films formed by, 25:13771
preparation from niobium chlorides or potassium niobium fluorides by electrolytic reduction and by reactions with zinc, 25:13642
properties at high temperatures, review of physical, thermal, and thermodynamic, 25:13667
separation of tantalum from, by solvent extraction using 4-methyl-2-pentanone in hydrochloric acid or hydrofluoric acid, 25:12947
superconducting critical field of rolled foils of, (E), 25:14158
superconducting Josephson effect in, high-frequency limit of, (E/T), 25:14200
thermal conductivity and effects in superconducting, (E/T), 25:14153

NIOBIUM ALLOYS AND SYSTEMS
properties at high temperatures, review of physical, thermal, and thermodynamic, 25:13667
Al--Nb--Ni, phase studies of, 25:13706
C--Nb--Ti, phase studies of, 25:13762 (AD-713153)
Ir--Nb, superconducting transition temperature and low-temperature thermal capacity of sigma-phase, (E/T), 25:14177

XUM

  Nb--O--Zr-base, transformation temperatures of, effects on concentration on continuous cooling, 25:13679
  Nb--Sn, deposition of intermetallic Nb_3Sn on substrate for use as superconductor, 25:14150(P)
  Nb--Sn, electron characteristics and optical characteristics of superconducting, (E), 25:14149
  Nb--Sn, materials testing for use in superconducting coils of intermetallic Nb_3Sn, (E), 25:14219
  Nb--Sn, vapor deposition process for superconducting intermetallic Nb_3Sn, 25:14203
  Nb--Ti, materials testing for use in superconducting coils, 25:14219
  Nb--Ti, performance in superconducting magnets with various configurations, 25:14211 (KFK-1217)
  Nb--Ti-base--Zr, critical current density of superconducting rolled sheets of, relations with aging temperature, magnetic field, and time, 25:14209
  Nb--Zr, magnetic-flux flow through wall of, 25:14197
  Nb--Zr-base, corrosion by steam at 350 to 450°C and 50 atm pressure, 25:13629 (EIR-184)
  Nb-base--O, bonding in solid solutions of, use of modulus of elasticity data to study interatomic, 25:14457
  Nb-base--Ti--Zr, superconducting properties of, effects of molybdenum, tantalum, and vanadium additions on, 25:14208
  Nb-base--Zr, corrosion by lithium at 1500°C, effects of oxygen on, 25:13630 (EUR-4298)
NIOBIUM CARBIDES
  precipitation of homogeneous dispersions of, in Type 20-25 stainless steel, method for, 25:13640 (TRG-Report-2040)
NIOBIUM CHLORIDES
  reduction to niobium in melts, electrolytic and zinc, 25:13642
NIOBIUM ISOTOPES Nb-93
  neutron elastic scattering at 8 MeV, cross sections for, (E/T), 25:14965
  neutron inelastic scattering at 2 to 4.5 MeV, cross sections for, (E/T), 25:14966
NIOBIUM ISOTOPES Nb-95
  determination in reactor cooling water by γ spectroscopy, 25:12956
NIOBIUM NITRIDES
  current losses in thin-film superconducting, alternating, (E), 25:14189
  superconducting critical current and field characteristics of thin films of, very high, (E), 25:14193
  superconducting Josephson junction properties of, Dayem-bridge type, 25:14201
NIOBIUM OXIDES
  crystal structure of films of, formed on niobium by heating in deionized water and water vapor, electron diffraction study of, 25:13771
  deposition and properties of thin films of, chemical vapor, 25:13748
  plasma resonance in, effects of stoichiometry on, 25:14462
  spectra of reduced Nb_2O_5, EPR, 25:14482
  Nb_2O_5--ZrO_2, crystal structure of polymorphs of $ZrO_2 \cdot 12Nb_2O_5$, 25:13774
NITRIC ACID
  separation of yttrium from aqueous solutions of, by solvent extraction using bis(2-ethylhexyl) phosphate, 25:13097
  bis(2-ethylhexyl) phosphate--HNO_3--H_2O--$Y(NO_3)_3$, equilibrium in, extraction, 25:13097
NITRIDES
  radiation effects on, reactions of recoil carbon-14 and nitrogen-13 from neutron, 25:13070
NITROGEN
  abundance in four O-Type subdwarf stars, (E), 25:13825
  abundance in late G and K dwarfs, (E), 25:13824
  abundance in nucleus of NGC 3031, (E), 25:13918
  carbon-ion reactions at 39, 50, and 78 MeV with molecular, cross sections for electron capture and loss in, (E), 25:14001
  determination in silicon by γ photon activation, 25:12971
  determination of trace amounts of, in xenon following condensation, mass spectrometric, 25:12941
  diffusion in tungsten at 1000 to 1800°C, 25:13673
  electron reactions at 0.07 to 4.0 keV with molecular, cross sections for excitation of N_2^+ first negative and Meinel bands in, (E), 25:13997
  electron reactions at 0.5 to 20 keV with molecular, excitation functions for first negative bands of N_2^+ in, (E), 25:13998
  electron reactions at 16 eV with molecular, excitation functions for a ^{1}PI/sub g/ and D$^3\Sigma$/sub u/$^+$ states in, (E), 25:14013
  energy level transition probabilities in aurorae, night airglow, nebulae, and solar corona, forbidden, (E/T), 25:14107
  neutron reactions (n,xγ) at 14 MeV with natural, cross sections for, (E/T), 25:14920(T) (BNL-tr-380)
  neutron total cross section at 0.5 to 25 MeV, (E), 25:14982 (NCSAC-31)
  nitrogen-ion (N^+) reactions at 1 to 67 eV with molecular, cross sections and mechanisms for production of N_2^+ in, (E), 25:14030
  nitrogen-ion reactions at 45 and 85 MeV with molecular, cross sections for electron capture and loss in, (E), 25:14001
  plasma of, optical spectra of, (E), 25:14277 (AD-712024)
  plasma of, viscosity measurement at atmospheric pressure, 25:14260
  proton reaction at 75 to 400 keV with molecular, cross sections for formation and destruction of excited hydrogen atoms by charge exchange in, (E), 25:14042
  rare-gas-excited-atom and -ion reactions with molecular, energy transfer processes in, (E), 25:14012
  separation from methane using γ-irradiated polyethylene films at 15 to 50°C, effects of dose on, 25:13039
  separation of interstitial, from hafnium, 25:13641(T) (UCRL-Trans-10503)
  separation of interstitial, from thorium, 25:13641(T) (UCRL-Trans-10503)
  separation of interstitial, from titanium, 25:13641(T) (UCRL-Trans-10503)
  separation of interstitial, from zirconium, 25:13641(T) (UCRL-Trans-10503)
  solubility in tungsten at 1000 to 1800°C, 25:13673
  sorption by polycrystalline tungsten surfaces, relations with ethylene sorption, 25:13687
  thermal transpiration at 77 and 97°K, model for, 25:13165(R) (MLM-1753)
NITROGEN IONS
  effects of dissociated, on defects in cobalt ferrites, 25:13783 (UCRL-20369)
  reactions with nitrogen gas at 45 and 85 MeV, cross sections for electron capture and loss in, (E), 25:14001
NITROGEN IONS (N^+)
  reactions with nitrogen molecules at 1 to 67 eV, cross sections and mechanisms for production of N_2^+ in, (E), 25:14030
  reactions with oxygen atoms at 30 keV to 2 MeV, cross sections for electron capture and loss in, (E), 25:14042
NITROGEN IONS (N_2^+)
  reactions with potassium at 50 to 1600 eV, crossed-beam study of electron capture into excited states in, 25:14011
NITROGEN ISOTOPES N-13
  reactions of recoil, in neutron-irradiated nitrides, 25:13070
  reactions of recoil, in neutron-irradiated sodium and potassium cyanides, 25:13072
NITROGEN ISOTOPES N-14
  abundance in UU Aur, (E), 25:13803
  meson (π^-) reactions (π^-,2nd) with, analysis using cluster model, (T), 25:14893
  proton elastic and inelastic scattering at 24 MeV, DWBA analysis of differential cross sections and asymmetries for, (E/T), 25:14890 (CEA-CONF-1651)
NITROGEN ISOTOPES N-15
  abundance in UU Aur, (E), 25:13803
  energy-level transitions in, following photodecomposition of oxygen-16, angular distributions of γ rays from, (E), 25:14896
  helium-3 reactions (He-3,d) at 11 MeV, angular distributions from, (E/T), 25:14914
  production and uses of, 25:13172
NITROGEN ISOTOPES N-17
  beta decay of, log-ft values for, (T), 25:14900
NITROGEN OXIDES
  distribution in atmosphere, use in tracer studies of global transport processes, (E), 25:13121 (TID-25314)
NITROGEN OXIDES NO
  thermal desorption of radiolytically produced, from atmospheric gases on plutonium dioxide, mass spectrometric studies on, 25:13024
  N--NO, radiolysis of, yields from electron pulse, 25:13053
NITROGEN OXIDES NO_2 OR N_2O_4
  effects on metabolism of carbon-14-labeled palmitate in lungs of rats, 25:13356
NITROGEN OXIDES N_2O
  effects on oxidation of trivalent uranium in sulfuric acid, 25:12977
  electron reactions at 115 eV with, energy-loss spectra and oscillator strengths for, (E), 25:14014
NITROGEN SYSTEMS
  He--N, radiolysis of, yields from electron pulse, 25:13053
  N--NO, radiolysis of, yields from electron pulse, 25:13053
NOVAE
  spectra of Delphini 1967, region of formation of narrow emission lines in, (E), 25:13820
NUCLEAR AUXILIARY POWER SYSTEMS
  startup of in-core thermionic reactors, transient response during, (E/T), 25:15401
NUCLEAR ELECTRIC MOMENTS
  calculations using phenomenological collective model, (T), 25:15177
NUCLEAR EMULSIONS
  development for detecting ultra-high energy air showers, 25:14845(R) (NP-18601)
  electron reactions with nuclei at 13.75 GeV in, direct production of electron pairs from, (E), 25:14525
  ionization effects in, 25:13299

ionization in, relativistic increase of, 25:13299
meson (π) reactions with nuclei at 60 GeV in, K/π ratio of secondaries in shower production from, (E), 25:14509 (INP-718)
mesons(K⁻) reactions with heavy nuclei at 1.5 to 3.5 GeV/c in, emission of lithium-8 fragments in, (E), 25:14978
particle track formation in, theory of, 25:13209 (COO-1671-28)
proton reactions with nuclei at 1000 GeV in, K/π ratio of secondaries in shower production from, (E), 25:14509 (INP-718)

NUCLEAR ENGINEERING
book: Economic Effectiveness of using Radioactive Isotopes in Industry (In Russian), 25:13174

NUCLEAR EXPLOSIONS
effects of maintenance manual for Weapons Effects Display System for mapping prompt, 25:13323 (UCRL-50892(Vol.4)(Pt.2))
fallout from, maintenance manual for Weapons Effects Display System for mapping, 25:13322 (UCRL-50892(Vol.4)(Pt.1))
peaceful uses of, benefits versus risks during, 25:13429

NUCLEAR EXPLOSIONS, ATMOSPHERIC
cloud growth from, bibliography on, 25:13131 (AAEC/LIB/Bib-255)
clouds from, particle size distribution in, 25:13136
effects on pressurized-water reactor, civil defense implications of, 25:13184
fire spread from, evaluation of models for simulating, 25:13134 (AD-713418)

NUCLEAR EXPLOSIONS, UNDERGROUND
crater formation by row-emplaced, equations for predicting linear, 25:13135 (AD-713574)
craters from, effects of seepage characteristics of surrounding media on slope stability of, 25:13102 (NCG-TR-27)
effects of Aardvark, on water level in well near explosion site, (T), 25:13111
ground motion from distant, equations for predicting, 25:13129 (AD-713521)
testing at Semipalatinsk test area, seismic indications of Soviet, 25:13445
uses in industry, significance of weather prediction capabilities in, 25:13136 (ARLV-351-15)

NUCLEAR MAGNETIC RESONANCE
perturbed angular correlations in even-A nuclei with integral spin and combined static and time-dependent quadrupole interactions, (T), 25:14477

NUCLEAR MATTER
binding energy of an impurity particle in, approximate expression for, (T), 25:15142 (DEMO-70/20)
binding energy of, calculation using momentum-dependent one-boson exchange potential, (T), 25:15199
binding energy of, effect of particle energy spectrum on, (T), 25:15187
binding energy of, N + N potentials below 350 MeV for, (T), 25:14734
hyperon (Λ) binding energy in, Brueckner matrix theory for, 25:14745
two-nucleon potentials and nuclear saturation in, 25:15188

NUCLEAR MODELS
collective, unified treatment of rotations, surface vibrations, and pairing vibrations, (T), 25:15189
Fermi-gas, time-dependent decay of compound nucleus before equilibrium in, (T), 25:15140 (CU-1019-79)
optical, isospin dependence of the proton optical potential in elastic scattering, (T), 25:15154
shell, momentum distribution of hole states in, (T), 25:15194
shell, wavefunctions for motion of two nucleons outside inert core in, 25:15186

NUCLEAR PHYSICS
research at BNL, July 1969--June 1970, 25:14837(R) (BNL-50230)
research at INS, April 1969--Mar. 1970, 25:14845(R) (NP-18601)
research at MIT, 1969, 25:14925(R) (MIT-2098-643)

NUCLEAR POWER
contamination of environment by, 25:13437

NUCLEAR POWER PLANTS
contamination of environment by, comparison of thermal power stations and, 25:13437
cooling water requirements for, effects on power generation economics and plant site selection, 25:13147
environmental radioactivity around, control of, 25:13471
radioactive effluents from, guide for surveillance requirements for, 25:15335 (NF-67-8)
safety reports for, IAEA guidelines for organization and contents of, 25:15337 (STI/PUB-272)
turbines for, sodium-24 injection tracer method for measuring enthalpy of steam in, 25:13148

NUCLEAR REACTIONS
alpha emission in medium-energy nucleon-induced, analysis of mechanism for, (T), 25:15173
cross section expression for (p,2p) and (e,e'p), (T), 25:15156
description of two-nucleon transfer, using coupled-channel Born approximation, (T), 25:15191
mechanisms in, comparison of calculations using analysis of averaged cross sections and statistical fluctuations, (T), 25:15151
resonance parameters for compound system in, effect of unitarity of collision matrix on, (T), 25:15171
resonances in, reduced widths from isobaric analog, (T), 25:15201
S-matrix for system of coupled square wells, Kapur--Peierls dispersion theory for calculation of, 25:15181

NUCLEAR STRUCTURE
calculation for even--even nuclei using quasiparticle method, (T), 25:15178
calculations for light nuclei using Hartree--Bogoliubov calculations with spherical restriction, (T), 25:15202
calculations for p-shell nuclei using unitary scheme, (T), 25:15169
description for light nuclei using generator coordinate method and angular momentum projection, (T), 25:15196
description for transition region using zero-point oscillations, (T), 25:15170
hole structure from quasi-free scattering processes, (T), 25:15156
rotational spectra of deformed nuclei, Hartree-Fock calculation of, (T), 25:15143 (LYCEN-7050)

NUCLEAR THEORY
Coulomb mixing of analog states into isospin states, 25:15149
ground-state correlations as variational parameters in the many-body problem in, 25:15147 (NYO-2171-333)
ground-state correlations in extended Lipkin--Meshkov--Glick model, 25:15200
Hartree--Fock solutions in, isospin mixing of, 25:15164
isospin dependence of the proton optical potential, 25:15154
residual interaction in, centrifugal terms of, 25:15168
self-consistent fields in heavy nuclei, local, 25:15167
Siegert's theorem, limits of validity of, 25:15144 (NP-18618)
single-particle M1 transition probabilities in lead region, 25:15197
two-nucleon potentials and nuclear saturation in, 25:15188

NUCLEAR WEAPONS
hazards of fallout from testing of, in French Polynesia during 1966 to 1968, 25:13436
requirements for assured destruction of US population, assessment of, 25:13132 (AD-711021)

NUCLEI
alpha elastic scattering by, analysis of backward, (T), 25:15172
deuteron reactions with, effect of neutron-nucleus interaction on Coulomb breakup, (T), 25:15190
electric quadrupole transitions in odd-mass spherical, 25:15165
electron excitation reactions with heavy, gamma spectra from, 25:15204
electron reactions at 13.75 GeV in emulsions, direct production of electron pairs from, (E), 25:14525
electron reactions at high energies, angular dependence of cross sections for wide-angle bremsstrahlung and upper limits for coupling constant for heavy electron production in, (E), 25:14529
electron scattering by, radial matrix elements for, (T), 25:15195
energy levels of A = 13, 14, and 15, nonnormal-parity, 25:15158
energy levels of doubly even, centrifugal stretching model and variable moment of inertia model for, 25:15203
energy levels of even deformed, with A greater than or equal to 222, properties of octupole, 25:15205
energy levels of heavy spherical, bootstrap theory of vibrational, (T), 25:15174
energy levels of quasirotational, spectral studies on higher-phonon, 25:15153
energy levels of spherical, semi-microscopic theory of two-phonon quadrupole--octupole vibrational, (T), 25:15157
energy levels of, collective model calculation of quadrupole transition probabilities of, (T), 25:15177
energy levels of, nature of fine structure surrounding high-excitation analog, (T), 25:15145 (NYO-1082-25)
energy-level transitions in A = 26, reduced isoscalar and isovector E2 matrix elements in, 25:15163
energy-level transitions in, search for distinct classes of M2, (E/T), 25:14983 (NP-18492)
fission barrier of, exact calculation of penetrability of two-peaked, 25:15004
gamma angular correlations in even-A, influence of combined static and time-dependent quadrupole interactions on, (T), 25:14477
helium-3 reactions (He-3,n) with p-shell, analysis for distortion and polarization effects in, (T), 25:15192
intermediate-vector boson reactions with, μ flux in deep mines as evidence against hypothesis for strong interactions in, (T), 25:14735
isospin mixing in even--even, (T), 25:15159
meson (π) reactions at 60 GeV in emulsions, K/π ratio of secondaries in shower production from, (E), 25:14509 (INP-718)
meson (π⁺) reactions at high energies, review of, (T), 25:15148(T) (ORNL-tr-2399)

XUM

meson (π^+) reactions with spherical, optical model for, 25:15184
mesons (π^-) reactions at 12 GeV/c in heavy-liquid bubble chamber, production of Δ^{++}(1236), rho^0(765), and rho rho π(2420) enhancement in, (E), 25:14562 (TID-25640)
neutrino reactions at high energies, total cross sections for W-boson production in, 25:14641
neutron capture by A < 220, review of cross sections for non-radiative, 25:15120
neutron capture by A = 45 to 204, cross sections and resonance parameters for intermediate, (T), 25:14979 (AAEC/E-198(Suppl.1))
neutron cross sections for A < 220, evaluation of thermal and resonance, 25:15101
neutron elastic and inelastic scattering by light, analysis for reaction mechanisms in fast, (E), 25:14898
neutron inelastic scattering by polarized, separation of coherent and incoherent components in polarized, (T), 25:14869
neutron reactions (n,2n) at 14 MeV, isomeric cross-section ratios for, 25:15182
neutron reactions (n,p) and (n,α) with, compound-nucleus calculations of cross sections for low-energy, 25:15207
neutron reactions with A < 220, activation resonance integrals for, (E/T), 25:15124
neutron reactions with A < 220, evaluation of data above resonance region, 25:15123
neutron reactions with light, analysis for reaction mechanisms in fast, (E), 25:14898
neutron reactions with, energy dependence of average radiation widths for, (T), 25:15209
neutron reactions with, energy dependence of energy level density from, (T), 25:15208
neutron reactions with, role of special motion states in, 25:15206
neutron resonance parameters for A > 220, evaluation of data on, 25:15094
neutron resonance parameters for A < 220, neutron-spectroscopy analysis of, 25:15095
nucleon scattering by, target spin dependence in optical-model description of, 25:15152
particle reactions at very high energies, multiplicity in, (T), 25:14736
photon reactions with nuclei at high energies, quark model for total cross section relations for, (T), 25:14595 (ITF-70-63-P)
potentials in, phenomenological three-body, (T), 25:15160
properties of 1s shell, Bolsterli--Feenberg perturbation procedure for calculation of momentum-dependent, 25:15185
proton elastic scattering by analog and compound energy levels of, amplitudes for resonant, (T), 25:15146 (NYO-1082-29)
proton inelastic scattering by, description of analog resonances near compound-nucleus overlapping levels in, (T), 25:15179
proton reactions (p,n) with, description of analog resonances near compound-nucleus overlapping levels in, (T), 25:15179
proton reactions at 1000 GeV in emulsions, K/π ratio of secondaries in shower production from, (E), 25:14509 (INP-718)
proton reactions at high energies, review of, (T), 25:15148(T) (ORNL-tr-2399)
triton reactions (t,p) with p-shell, analysis for distortion and polarization effects in, (T), 25:15192
vibrations in closed-shell, bootstrap theory of, 25:15176
vibrations in closed-shell, extended-particle-phonon-coupling theory of, 25:15176

NUCLEI, ANTI-
mass and electric charge of antihelium-3 in proton reactions with aluminum at 70 GeV, (E), 25:14540 (IFVE-SEF-70-16)
production of antihelium-3 in proton reactions with aluminum at 70 GeV, cross sections for, (E), 25:14540 (IFVE-SEF-70-16)

NUCLEIC ACID, DEOXYRIBO-
effects on mutagenesis in EMS-treated and uv and x-irradiated Escherichia coli, 25:13421
metabolism in yeast cells, relation of radiosensitivity to inhibition of, 25:13604
photolysis of, thymine phototrimer production in uv, 25:15436 (NYO-2798-49)
radiation damage to, of phage phiX174, inhibitory effects of, on phage reproduction, phosphorus-32 β, uv, and x, 25:13382
radiation effects on content of, in cells of Escherichia coli K 12, comparison of γ, proton, and uv, 25:13371
radiation effects on content of, in proembryo stages of barley, ionizing, 25:13405
radiation effects on exogenous nucleoside utilization in, by cultured human cells, x, 25:13380
radiation effects on incorporation of tritium-labeled thymidine into, of oocytes of guinea pigs, x, 25:13367
radiation effects on synthesis of, in Escherichia coli, combined effects of reductone on uv, 25:13610
radiation effects on unscheduled synthesis of, in HeLa cells, tritium tracer study of effects of temperature on uv, 25:13554
radioinduced decrease of content of, in dorso-lateral prostates of rats, x, 25:13366
radioinduced inhibition of synthesis of, in cultured HeLa and human amnion cells, photoreactivation of uv, 25:13377
radioinduced single strand breaks in, of Escherichia coli, effects of T4 endonuclease on uv, 25:13411
radioprotective effects of, in combination with other protectants on mice, use of spleen weight-radiation dose relation for testing, 25:13478
repair synthesis of, genetic analysis of uv and x-radiosensitive mutants of Escherichia coli defective in, 25:13428
role in x-radioinduced prototrophic yeast mutants, 25:13425
structure of, effects of chemical modifications on macromolecular, 25:15432(R) (CU-3957-9)
synthesis in Escherichia coli infected with uv-irradiated T4 phage, 25:13616
synthesis in hair follicles of lambs, localization of, using autoradiography and tritium-labeled thymidine, 25:13337
tritium-labeled thymidine incorporation into, of tissues of mice, effects of mitotic rate on specificity of, 25:13358

NUCLEIC ACID, RIBO-
radiation effects on formylmethionyl, in Escherichia coli, uv, 25:13364
radiation effects on synthesis of, in Escherichia coli, effects of reductone on uv, 25:13610
radioinduced decrease of content of, in dorso-lateral prostates of rats, x, 25:13366

NUCLEONS
clustering in low-density neutron-star matter, (T), 25:13819
interactions anti K + N → anti K + N, SU(3) x SU(3) chiral Lagrangian model for total cross sections and scattering lengths for, (T), 25:14703 (TID-25639)
interactions anti K + N → π + Σ(Λ), SU(3) x SU(3) chiral Lagrangian model for total cross sections and scattering lengths for, (T), 25:14703 (TID-25639)
interactions anti N + N at high energies, review of statistical model for cross sections for meson production in, (T), 25:14680 (INP-719)
interactions anti N + N, SU(3) and exchange degeneracy in Regge-pole-cut analysis of total cross sections for, (E/T), 25:14660
interactions anti ν + N, Regge pole model for hadron production in, (T), 25:14635 (NYO-4204-9)
interactions e + N, Regge pole model for hadron production from, (T), 25:14635 (NYO-4204-9)
interactions e + N, structure functions rapid approach to universality in inelastic, (T), 25:14610
interactions γ + N → ω + N(N*) at 9.1 GeV in deuterium and hydrogen targets, counter study of cross sections for, (E), 25:14512
interactions γ + N → π + Δ at high energies, contribution of low-energy theorem, 25:14622
interactions γ + N → π + N, isotensor electromagnetic current in, (T), 25:14604
interactions γ + N → π^0 + N at 12 GeV at large angles, Regge pole theory for differential cross sections of, (T), 25:14598
interactions γ + N at high energies, quark model for total cross section relations for, (T), 25:14595 (ITF-70-63-P)
interactions γ + N, Regge pole model for hadron production from, (T), 25:14635 (NYO-4204-9)
interactions K + N, SU(3) and exchange degeneracy in Regge-pole-cut analysis of total cross sections for, (E/T), 25:14660
interactions N + d → N + d, differential and total cross section relations for, (T), 25:14730 (JINR-P2-5444)
interactions N + d at 14 and 23 MeV, elastic cross section and nucleon polarization in spin-dependent three-body, (T), 25:14740
interactions N + N → N + N, differential and total cross section relations for, (T), 25:14730 (JINR-P2-5444)
interactions N + N at high energies, fifth-interaction coupling from large-angle, 25:14706
interactions N + N at high energies, review of statistical model for cross sections for baryon and meson production in, (T), 25:14680 (INP-719)
interactions N + N at low energies, multipole expansion of one-boson exchange potential for, (T), 25:14739
interactions N + N at low energies, one-boson-exchange potential for S-scattering parametrization for, (T), 25:14739
interactions N + N below 350 MeV, phenomenological aspects of, (T), 25:14734
interactions N + N below 350 MeV, scattering length and nuclear matter binding energy from, (T), 25:14734
interactions N + N, effect on two-body sum rules from nonlocality of potential for, (T), 25:14732 (NP-18648)
interactions N + N, SU(3) and exchange degeneracy in Regge-pole-cut analysis of total cross sections for, (E/T), 25:14660
interactions ν + N, Regge pole model for hadron production from, 25:14635 (NYO-4204-9)
interactions π + N → eta + N, Breit--Wigner models and

  effective-range approximations for, (T), 25:14702 (FAM-70-8)
  interactions $\pi + N \to \pi + \Delta(\pi + N)$ at 339 to 480 MeV, partial-wave analysis of, (T), 25:14728
  interactions $\pi + N \to \pi + N^*$, pion gauge condition for baryon parity doublet in, 25:14705
  interactions $\pi + N \to$ rho + N, O(4) classification of invariants and differential cross sections for, (T), 25:14757
  interactions $\pi + N$ at high energies, linear Regge trajectory fits of, (T), 25:14723
  interactions $\pi + N$, dispersion sum rules for fixed-u amplitudes of, 25:14709
  interactions $\pi + N$, Regge-pole-cut model without parity doubling for backward, 25:14707
  interactions $\pi + N$, solution to Bethe--Salpeter equation for, 25:14786
  interactions $\pi + N$, SU(3) and exchange degeneracy in Regge-pole-cut analysis of total cross sections for, (E/T), 25:14660
  polarization in N + d interactions at 14 and 23 MeV, (T), 25:14740
  production in $p + p \to Y + K + N$ interactions, π and K exchange contributions to, (T), 25:14597
  scattering by nuclei, target spin dependence in optical-model description of, 25:15152
NUCLEONS (anti N)
  interactions anti N + N at high energies, review of statistical model for cross sections for meson production in, (T), 25:14680 (INP-719)
  interactions anti N + N, SU(3) and exchange degeneracy in Regge-pole-cut analysis of total cross sections for, (E/T), 25:14660
NUCLEOPROTEINS, DEOXYRIBO-
  radiation effects on histone content of, in liver, spleen, and thymus of rats, effects of heparin on x, 25:13385
  radioinduced degradation of, in rabbits, in vitro effects of nuclease on, 25:13363
NUCLEOSIDES
  radiation effects on utilization of, in DNA synthesis by cultured human cells, effects of growth phase of culture, nucleoside concentration, and precursors on x, 25:13380
NUCLEOTIDES
  effects on respiration in uv-irradiated Escherichia coli, 25:13607

O

OBSIDIAN
  age of Japanese, fission track estimates of, 25:13112
  uranium content of Japanese, (E), 25:13112
OOCYTES
  radiosensitivity of Stage 7, of Drosophila melanogaster, x, 25:13555
  tritium uptake by, of x-irradiated guinea pigs, autoradiographic study of, 25:13367
ORGANIC ACIDS
  radiation effects on content of, in sheep serum, effects of air blast injury, and fasting on γ and neutron, 25:13384
ORGANIC COMPOUNDS, FLUORO-
  analysis for fluorine using thorium chloranilate, effects of iron on spectrophotometric, 25:12936
  radioinduced preparation of perfluorinated carboxylic acids from polytetrafluoroethylene wastes, 25:13035(P)
ORGANISMS
  orientation of, effects of earth's electric and magnetic fields on, 25:13572
  radiation effects on, electromagnetic, 25:13570
  radiation effects on, electromagnetic, 25:13571
ORGANS
  radiation dose to human, 25:13503
  radiation effects on content of NAD and NADP in, of rabbits and rats, effects of ATP and nicotinamide on, 25:13379
ORGEL REACTOR
  development programs for, review of, 25:15342
ORNL HIGH-FLUX ISOTOPE REACTOR
  instrumentation for, development of, 25:13318(R) (ORNL-4620)
  maintenance during July to September 1970, 25:15392(R) (ORNL-TM-3286)
  operations during July to September 1970, 25:15392(R) (ORNL-TM-3286)
OSKARSHAMN POWER REACTOR
  fuel cycle for, 25:15212
  fuel elements for, design and fabrication of, 25:15212
OSMIUM
  determination in natural materials, methods for, 25:12939
OSMIUM ISOTOPES Os-180
  electron-capture decay of, gamma spectra and log-ft values from, (E/T), 25:14984 (NP-18536)
OSMIUM ISOTOPES Os-181
  beta decay of, gamma and conversion-electron spectra from, (E/T), 25:14984 (NP-18536)
  energy levels of, half-life of isomeric, (E/T), 25:14984 (NP-18536)
OSMIUM ISOTOPES Os-192
  energy levels from iridium-192 decay, spin-parity assignments for, (E), 25:15062
OSTEICHTHYES
  contamination by sea-disposed liquid radioactive waste, (E), 25:13189 (CEA-CONF-1712)
OVARIES
  radiation effects on, of mice, effects of estradiol and FSH on phosphorus-32 β, 25:13569
OXAZOLE, 2,5-DIPHENYL-
  efficiency for liquid scintillation counting of tritium in toluene solution, 25:13214
OXIDES
  electric conductivity of metal, effects of fast reactor environment on, (E), 25:15354 (WHAN-IR-42)
OXIDOREDUCTASES
  activity of mixed liver microsome, in vitro, effects of deuterium oxide on, 25:13372
OXYGEN
  abundance in four O-Type subdwarf stars, (E), 25:13825
  abundance in nucleus of NGC 3031, (E), 25:13918
  determination in meteorites by nondestructive fast neutron activation, 25:12970
  determination in silicon by charged particle activation, 25:12971
  determination in sodium, calibration and design of meters for, 25:13651(R) (ANL/ST-4)
  determination of internal, in molybdenum by α activation and α spectroscopy, 25:12957 (LYCEN-7076)
  determination of superficial, in molybdenum by deuteron activation and α spectroscopy, 25:12957 (LYCEN-7076)
  determination of trace amounts of, in xenon following condensation, mass spectrometric, 25:12941
  distribution in atmosphere, use in tracer studies of global transport processes, (E), 25:13121 (TID-25314)
  effects of dissolved, on corrosion of niobium--zirconium alloys and tantalum by lithium, 25:13630 (EUR-4298)
  energy level transition probabilities in aurorae, night airglow, nebulae, and solar corona, forbidden, (E/T), 25:14107
  hydrogen-atom reactions at 3 to 50 keV with, molecular, cross sections for O^- production in, (E), 25:13999
  ion reactions at 30 keV to 2 MeV with atomic, cross sections for electron capture and loss in heavy-, (E), 25:14042
  neutron reactions $(n,x\gamma)$ at 14 MeV with natural, cross sections and gamma spectra from, (E/T), 25:14920(T) (BNL-tr-380)
  neutron reactions $(n,x\gamma)$ at 14.8 MeV, γ spectra from, (E), 25:14982 (NCSAC-31)
  oxygen-ion (O^-) reactions with atomic, effects of short-range atomic forces on resonant charge exchange in, (T), 25:14018
  proton reactions at 20 to 110 keV with molecular, energy-loss spectra and cross sections for inelastic processes in, (E), 25:14023
  proton reactions at 3 to 50 keV with molecular, cross sections for O^- production in, (E), 25:13999
  reactions with cesium atoms of atomic, cross sections for ionization in, (E), 25:14036
  reactions with graphite, LEED study of, 25:13735
  separation of interstitial, from hafnium, 25:13641(T) (UCRL-Trans-10503)
  separation of interstitial, from thorium, 25:13641(T) (UCRL-Trans-10503)
  separation of interstitial, from titanium, 25:13641(T) (UCRL-Trans-10503)
  separation of interstitial, from zirconium, 25:13641(T) (UCRL-Trans-10503)
  spectra enhancement of 6300-A nightglow emission of, latitude-wide in Apr. and May 1967, (E), 25:14109
  spectral emission of 6300- and 6394-A, behavior during Mar. 23-24 magnetic disturbance, (E), 25:14115
  yields from γ radiolysis of xenon trioxide, 25:13049
OXYGEN IONS
  effects of dissociated, on defects in cobalt ferrites, 25:13783 (UCRL-20369)
  spectra of O III and O VII in Sun, (E/T), 25:13886
  x-ray emission from O VII, in solar corona, (E), 25:13885
OXYGEN IONS (O^+)
  reactions with oxygen atoms at 30 keV to 2 MeV, cross sections for electron capture and loss in, (E), 25:14042
OXYGEN IONS (O^-)
  reactions with argon and hydrogen molecules in keV range, formation of autodetaching states of Ar^- and H^- in, (E), 25:14009
  reactions with helium in keV range, formation of autodetaching states of O^- in, (E), 25:14009
  reactions with oxygen atoms, effects of short-range atomic forces on resonant charge exchange in, (T), 25:14018
OXYGEN ISOTOPES O-15
  energy levels from helium-3 reactions with carbon-12, spins and parities from, (E), 25:14915
  energy-level transitions in, following photodecomposition of oxygen-16, angular distributions of γ rays from, (E), 25:14896
OXYGEN ISOTOPES O-16
  determination by pulsed neutron activation and scintillation counting, 25:12960

XUM

  energy levels and transitions from oxygen-17 (He-3,α) and nitrogen-15 (He-3,d) reactions, (E), 25:14914
  meson (π^-) reactions (π^-,2nd) with, analysis using cluster model, (T), 25:14893
  photodisintegration at 30 MeV, γ spectra from, (E), 25:14982 (NCSAC-31)
  photon reactions (γ,n) at 30 MeV, neutron polarization from, (E), 25:14982 (NCSAC-31)
  photon reactions (γ,nγ') and (γ,pγ') at 27 MeV, angular distribution of γ rays from, (E), 25:14896
  reactions with lead-208, production of thorium-221 and thorium-222 by, 25:15011
  scattering by silver-107 and silver-109 at 45.5 MeV, Coulomb excitation by inelastic, (E), 25:15035
  scattering by tin-116 and tin-124, reorientation measurements following Coulomb excitation by inelastic, (E), 25:15041
OXYGEN ISOTOPES O-17
  energy levels from 1h--2p and 3h--4p configurations for, (T), 25:14900
  energy-level transitions from nitrogen-17 beta decay, (T), 25:14900
  helium-3 reactions (He-3,α) at 11 MeV, angular distributions from, (E/T), 25:14914
  neutron coherent scattering length for, cold, (E), 25:14862 (AERE-R-5770)
  reactions (O-17,pγ) with tritium at 22 MeV, γ spectra from, (E), 25:14905
OXYGEN ISOTOPES O-18
  determination in oxyanions by Raman spectroscopy, 25:13043
  effects on radiolysis of crystalline potassium nitrates, 25:13043
  exchange between ethanol, methanol, and propanol and water, at 200 to 300°C, activation energy for catalytic, 25:12991
  production of, by radiolysis of labeled crystalline potassium nitrates, 25:13043
  reactions (O-18,pγ) with deuterium at 27 MeV, γ spectra from, (E), 25:14905
  reactions (O-18,xn) with tellurium-126, energy levels of neodymium-137 from, (E), 25:15042
OXYGEN ISOTOPES O-19
  energy levels from deuterium (O-18,pγ) and tritium (O-17,pγ) reactions, lifetimes and γ-branching ratios for, (E), 25:14905
OXYGEN SYSTEMS
  Nb--O--Zr-base, transformation temperatures of, effects on concentration on continuous cooling, 25:13679
  H--Na--C, phase studies of, 25:13651(R) (ANL/ST-4)
  Mo--O--U, crystal structure of UMo_2O_8, 25:13776
  Mo--O--V, crystal structure of $MoV_2O_{7.8}$ and MoV_2O_8, 25:13776
  Nb-base--O, bonding in solid solutions of, use of modulus of elasticity data to study interatomic, 25:14457
  O--U, phase diagram of, 25:13777
  O--U--V, crystal structure of UV_2O_8, 25:13776
OYSTER CREEK POWER REACTOR, UNIT 1
  containment structure for, leak rate test of primary, 25:15269 (DOCKET-50219-121)
  protection system for, additional information on, 25:15268 (DOCKET-50219-120)
OZHENNITE (ZIRCONIUM ALLOY)
  corrosion by steam at 350 to 450°C and 50 atm pressure, 25:13629 (EIR-184)
OZONE
  distribution in atmosphere, use in tracer studies of global transport processes, (E), 25:13121 (TID-25314)

P

PACKAGING
  design of thermally insulated, for lead-shielded shipping container, 25:13196(P)
PADUCAH AREA (Ky.)
  radiation monitoring of environs of, during 1969, 25:13431
PALLADIUM
  reactions of fission-product, with uranium carbide fuels, 25:13764 (KFK-1260)
PALLADIUM ISOTOPES Pd-108
  proton reactions (p,α) at 15 MeV, angular distributions for, (E), 25:15022
PALMITATES
  metabolism of carbon-14-labeled, in lungs of rats, effects of breathing nitrogen dioxide on, 25:13356
  radiation effects on distribution of, in phospholipids and triglycerides of Ehrlich ascites tumors, effects of palmitate quantity on γ, 25:13362 (CEA-R-4039)
PANCREAS
  selenium-75-labeled selenomethionine uptake by dog, effects of route of administration on, 25:13343
PARAMAGNETIC MATERIALS
  paramagnetic centers in, symmetry and microwave spectra of polyatomic, 25:15456(T) (SC-T-71-3005)
PARANASAL SINUSES
  radiography of human, methods for, for optimal results, x, 25:13507
PARTICLE TRACKS
  analysis of bubble and spark chamber, computer program for acquisition of film information for PEPR system for, 25:13242 (CERN-70-21(Vol.1), pp 113-24)
  analysis of bubble and spark chamber, computer program for calibration of PEPR system for, 25:13245 (CERN-70-21(Vol.1), pp 177-86)
  analysis of bubble and spark chamber, computer-based HPD for, 25:13276 (CERN-70-21(Vol.2), pp 721-7)
  analysis of bubble and spark chamber, conference on data handling systems for, 25:13234 (CERN-70-21(Vol.1))
  analysis of bubble and spark chamber, conference on data handling systems for, 25:13263 (CERN-70-21(Vol.2))
  analysis of bubble and spark chamber, description and performance of CERN spiral reader for, 25:13236 (CERN-70-21(Vol.1), pp 19-36)
  analysis of bubble and spark chamber, development of data processing systems at JINR for, 25:13279 (CERN-70-21(Vol.2), pp 753-60)
  analysis of bubble and spark chamber, digitized microscope for, 25:13284 (CERN-70-21(Vol.2), pp 851-7)
  analysis of bubble and spark chamber, geometry reconstruction program for HPD, 25:13273 (CERN-70-21(Vol.2), pp 679-85)
  analysis of bubble and spark chamber, glossary of on-line measuring devices for, 25:13294 (CERN-70-21(Vol.2), pp 963-77)
  analysis of bubble and spark chamber, HPD system at Birmingham for, 25:13292 (CERN-70-21(Vol.2), pp 949-52)
  analysis of bubble and spark chamber, HPD system at Columbia Univ. for, 25:13253 (CERN-70-21(Vol.1), pp 311-21)
  analysis of bubble and spark chamber, on-line film plane digitizer for, 25:13237 (CERN-70-21(Vol.1), pp 39-46)
  analysis of bubble and spark chamber, PEPR system at Heidelberg for, 25:13241 (CERN-70-21(Vol.1), pp 105-11)
  analysis of bubble and spark chamber, performance of Sweepnik I for, 25:13252 (CERN-70-21(Vol.1), pp 293-308)
  analysis of bubble and spark chamber, performance of reverse-developed film for, 25:13286 (CERN-70-21(Vol.2), pp 879-905)
  analysis of bubble and spark chamber, performance of Oxford PEPR system for, 25:13239 (CERN-70-21(Vol.1), pp 61-88)
  analysis of bubble and spark chamber, POLLY system at Glasgow Univ. for, 25:13255 (CERN-70-21(Vol.1), pp 357-70)
  analysis of bubble and spark chamber, Princeton Automatic Track Reader for, 25:13250 (CERN-70-21(Vol.1), pp 273-83)
  analysis of bubble and spark chamber, SATR system at Wisconsin Univ. for, 25:13262 (CERN-70-21(Vol.1), pp 505)
  analysis of bubble and spark chamber, SMP system at UCLA for, 25:13249 (CERN-70-21(Vol.1), pp 243-60)
  analysis of bubble and spark chamber, spiral reader system at Weizmann Institute for, 25:13293 (CERN-70-21(Vol.2), pp 953-62)
  analysis of bubble and spark chamber, status of PEPR system at Heidelberg for, 25:13246 (CERN-70-21(Vol.1), pp 187-96)
  analysis of bubble and spark chamber, status of PEPR system at MIT for, 25:13248 (CERN-70-21(Vol.1), pp 233-42)
  analysis of bubble and spark chamber, Sweepnik II for, 25:13251 (CERN-70-21(Vol.1), pp 285-92)
  analysis of bubble and spark chamber, videc assisted scan table for, 25:13238 (CERN-70-21(Vol.1), pp 47-58)
  analysis of bubble chamber, Amsterdam HPD--CDC 3200 system for, 25:13275 (CERN-70-21(Vol.2), pp 709-20)
  analysis of bubble chamber, automatic gain control in signal processing for, 25:13257 (CERN-70-21(Vol.1), pp 383-97)
  analysis of bubble chamber, BRUSH automatic processing system for, 25:13274 (CERN-70-21(Vol.2), pp 689-707)
  analysis of bubble chamber, calibration and performance of CERN spiral reader for, 25:13235 (CERN-70-21(Vol.1), pp 5-18)
  analysis of bubble chamber, Coccinelle CRT digitizer for, 25:13256 (CERN-70-21(Vol.1), pp 371-81)
  analysis of bubble chamber, computer program for automatic recognition and reconstruction of events for, 25:13243 (CERN-70-21(Vol.1), pp 125-39)
  analysis of bubble chamber, computer program for automatic recognition and reconstruction of events for, 25:13244 (CERN-70-21(Vol.1), pp 141-75)
  analysis of bubble chamber, computer-based measuring projector for, 25:13272 (CERN-70-21(Vol.2), pp 665-73)
  analysis of bubble chamber, computer-based system at Munich for, 25:13287 (CERN-70-21(Vol.2), pp 907-9)
  analysis of bubble chamber, global method of fiducial recognition with fish-eye lenses for, 25:13261 (CERN-70-21(Vol.1), pp 497-503)
  analysis of bubble chamber, grid guidance program for PEPR film scanner for, 25:13247 (CERN-70-21(Vol.1), pp 199-211)
  analysis of bubble chamber, HPD Minimum Guidance programs for, 25:13278 (CERN-70-21(Vol.2), pp 737-52)
  analysis of bubble chamber, HPD--IBM 360/44 system at Bologna for, 25:13267 (CERN-70-21(Vol.2), pp 607-15)
  analysis of bubble chamber, HPD--IBM 360/44 system at

  - Bologna for, 25:13269 (CERN-70-21(Vol.2), pp 625-30)
  - analysis of bubble chamber, HPD--IBM 360/44 system at Bologna for, 25:13268 (CERN-70-21(Vol.2), pp 617-24)
  - analysis of bubble chamber, IBM data management system for, 25:13277 (CERN-70-21(Vol.2), pp 729-34)
  - analysis of bubble chamber, LUCY CRT system for, 25:13259 (CERN-70-21(Vol.1), pp 427-65)
  - analysis of bubble chamber, method for, 25:13233 (CEA-N-1397)
  - analysis of bubble chamber, on-line computer system in Sweden for, 25:13282 (CERN-70-21(Vol.2), pp 825-30)
  - analysis of bubble chamber, on-line IBM 1130 computer system in Italy for, 25:13288 (CERN-70-21(Vol.2), pp 911-20)
  - analysis of bubble chamber, operator intervention in HPD system for, 25:13290 (CERN-70-21(Vol.2), pp 931-40)
  - analysis of bubble chamber, PANGLOSS CRT device for, 25:13258 (CERN-70-21(Vol.1), pp 401-25)
  - analysis of bubble chamber, performance of DAPR system for, 25:13280 (CERN-70-21(Vol.2), pp 761-804)
  - analysis of bubble chamber, POLLY II system for, 25:13254 (CERN-70-21(Vol.1), pp 325-55)
  - analysis of bubble chamber, status of HPD systems at CERN for, 25:13281 (CERN-70-21(Vol.2), pp 813-24)
  - analysis of European 3.7-meter bubble chamber, performance of PEPR system for BEBC film, 25:13240 (CERN-70-21(Vol.1), pp 89-104)
  - analysis of Gargamelle bubble chamber, computer-based scanning and measuring system for, 25:13271 (CERN-70-21(Vol.2), pp 651-64)
  - analysis of large bubble chamber, ADAM + EVA scanning and measuring machine for, 25:13270 (CERN-70-21(Vol.2), pp 633-49)
  - analysis of Mirabelle bubble chamber, automatic gain control for HPD system for, 25:13291 (CERN-70-21(Vol.2), pp 941-8)
  - analysis of Omega spark chamber, development of pattern recognition programs for, 25:13283 (CERN-70-21(Vol.2), pp 831-50)
  - analysis of spark chamber, ARIANE II automatic system for, 25:13285 (CERN-70-21(Vol.2), pp 859-78)
  - formation in matter, unified theory of, 25:13209 (COO-1671-28)
  - reconstruction of large bubble chamber, computer program for geometrical, 25:13260 (CERN-70-21(Vol.1), pp 467-96)
- PARTICLES
  - deposition from aerosols flowing radially inward between concentric parallel circular plates, calculation of diffusional, 25:13123
  - motion of spinning, in electromagnetic field, (T), 25:14599
  - size distribution in atmospheric nuclear explosion clouds, 25:13138
- PEAT
  - strontium retention by, effects of saturation with potassium compounds on, 25:13118(R) (COO-414-17)
  - uranium content of, effects of humidity on, 25:13116
- PENICILLIN
  - radiation effects on action of in central nervous system of rabbits, ionizing, 25:13561
- PENNSYLVANIA
  - radiation monitoring of environs of Shippingport Atomic Power Station during 1969, 25:13398
- PENTANE, 3-METHYL-
  - radiation effects on, containing cadmium, lithium, magnesium, potassium, or sodium at 77°K, comparative ESR studies on paramagnetic species produced from γ or uv, 25:13025
- PENTANE, 2,2,4-TRIMETHYL-
  - radioinduced oxidation of, effects of temperature on composition of products from, 25:13040
- 2,4-PENTANEDIONE
  - complexes with cobalt, cobalt-57 electron-capture decay in, stabilization of anomalous charge states of iron after, 25:13075
- 2-PENTENE
  - radiation effects at 77 to 125°K, electric conductivity studies on transient species produced by γ, 25:13027
- PENTYLENETETRAZOLE
  - radiation effects on action of in central nervous system of rabbits, ionizing, 25:13561
- PEOPLE'S DEMOCRATIC REPUBLIC OF GERMANY
  - control of radioactive materials in, recommended regulations for, 25:13193 (SZS-16/70)
  - regulations for safe transport of highly radioactive and fissile materials in, 25:13194 (SZS-19/70)
- PERIODATES
  - separation of iodine-131-labeled, from iodates and iodides by thin-layer chromatography, 25:13099
- PERSONNEL
  - directory of nuclear standards development committees in USA, 25:13469 (ORNL-NSIC-75(Rev.1))
  - radiation dose to, following accidental exposure to iridium-192 vehicle, 25:13466
  - radiation effects on cysteic acid content of fingernails of uranium mining, methods for determining, 25:13369
  - radiation hazards to, at military nuclear establishment in Pisa, Italy, statistical analysis of medical judgments regarding, 25:13468
  - radiation protection for industrial, handling radioisotopes, 25:13467
  - radiosensitivity of atomic energy, value of pre-employment medical examination for prediction of, 25:13465
- PERTECHNETATES
  - use of metastable technetium-99-labeled, with Anger camera for diagnosis of human metastatic papillary thyroid carcinomas, 25:13488
- PERTURBATION THEORY
  - Fermi rule of time-dependent, quantum field theory formalism for derivation of, 25:14775
  - theorem for quantum mechanical system subject to two perturbations, 25:13981
- PETROLEUM
  - carbon-12 and carbon-13 distribution in, correlation of theoretical method of formation and thermodynamics of, 25:13005
- PHAEOPHYTA
  - radioisotope content of alginic acid of, following accumulation from sea water, 25:13403
- PHANTOMS
  - radiation dose distribution in human, measurement of, for therapy of bone cancer, comparison of cesium-137 γ, cobalt-60 γ, and x, 25:13536
- PHARMACEUTICALS
  - use of radioisotope-labeled, in nuclear medicine, review of economics and techniques for, 25:13519
- PHENOXY, HYDROXY-
  - radiation effects on content of, in shoots of poplars, fast neutron and γ, 25:13598
- PHOSPHATES
  - radiation effects on metabolism of, in wheat seedlings, γ, 25:13597 (NP-18606)
- PHOSPHOLIPIDS
  - radiation effects on incorporation of palmitates into, in ascites tumors, effects of palmitate quantity on γ, 25:13362 (CEA-R-4039)
- PHOSPHORIC ACID, BIS(2-ETHYLHEXYL) ESTER
  - solvent properties for rare earths, 25:13092
  - solvent properties for yttrium in aqueous nitric acid solutions, 25:13097
  - bis(2-ethylhexyl) phosphate--H_2O--$Nd(NO_3)_3$, complex formation in, 25:13092
  - bis(2-ethylhexyl) phosphate--HNO_3--H_2O--$Y(NO_3)_3$, equilibrium in, extraction, 25:13097
- PHOSPHORIC TRIAMIDE, HEXAMETHYL-
  - complexes with thorium halides or uranium halides in nitromethane, electric conductivity of, relation of composition and ionization capacity to, 25:13023
- PHOSPHOROTHIOIC ACID, S-(2-AMINOETHYL) ESTER
  - sodium salt, radioprotective effects of, on survival of skin transplants in mice, effects of dose on x, 25:13479
- PHOSPHORUS CHLORIDES
  - reactions with phosphorus-32 or sulfur-35 recoil atoms, direct labeling by, 25:13069
- PHOSPHORUS ISOTOPES P-30
  - energy levels from silicon-29 (p,γ) reactions, lifetime measurements using Doppler shift attenuation method, (E), 25:14933
- PHOSPHORUS ISOTOPES P-31
  - determination by pulsed neutron activation and scintillation counting, 25:12960
  - neutron reactions (n,xγ) at 14 MeV, cross sections for, (E/T), 25:14920(T) (BNL-tr-380)
- PHOSPHORUS ISOTOPES P-32
  - beta spectra from, shapes of nonunique and unique first-forbidden, 25:14976
  - effects on bacteriophages and Escherichia coli, 25:13612
  - effects on bone marrow following use for therapy of prostate carcinoma, 25:13591
  - effects on continuous cultures of KB cells, 25:13351
  - effects on DNA of phage phiX174, inhibitory effects of, on phage reproduction, 25:13382
  - effects on ovaries and testes of mice following intramuscular injection, effects of estradiol and FSH on, 25:13569
  - reactions of recoil atoms of, with phosphorus chlorides, phosphoryl chlorides, and thiophosphoryl chlorides, direct labeling by, 25:13069
  - uptake of phosphate ion-incorporated, by erythrocytes of rats for determining correlation of phosphorated erythrocytic metabolism with second and third phase of general adaptation syndrome, 25:13335
  - use for scanning human stomach for differential diagnosis of benign and malignant neoplasms, 25:13495
- PHOSPHORUS ISOTOPES P-33
  - effects on bacteriophages and Escherichia coli, 25:13612
- PHOSPHORUS OXIDES
  - content in rocks of shields and sediment cover of Brazil, Canada, and USSR, relations with geological time, 25:13114
- PHOSPHORYL CHLORIDES
  - Raman scattering by, in liquid lasing material, 25:15454 (SC-RR-70-762)
  - reactions with phosphorus-32 or sulfur-35 recoil atoms, direct labeling by, 25:13069
- PHOTOELECTRIC EFFECT
  - electron emission in gamma irradiation, (T), 25:14430
- PHOTOGRAPHIC EMULSIONS
  - analysis for silver, system for x-ray transmission, 25:13312

particle track formation in, theory of, 25:13209 (COO-1671-28)

PHOTOGRAPHIC FILM
  analysis for silver, on-line x-ray backscattering gage for, 25:13311

PHOTOMETRY
  stellar classifications by Stroemgren, (T), 25:13809

PHOTONS
  interactions $\gamma + {}^3\mathrm{He} \to \pi^+ + 2n + p$, impulse approximation for π^+ angular distributions and total cross sections in, (T), 25:14518
  interactions $\gamma + {}^3\mathrm{He} \to \pi^+ + n + d$, impulse approximation for π^+ angular distributions, total cross sections, and final-state interaction effects in, (T), 25:14518
  interactions $\gamma + d \to p + p + \pi^+ + \pi^- + \pi^-$ at 1.1 to 3.5 GeV, total and resonance production cross sections for, (E), 25:14521
  interactions $\gamma + d \to \pi^-(\pi^+) + 2p(2n)$ at 600 to 1700 MeV, π^-/π^+ cross section ratio, isoscalar and isovector amplitudes, and cross sections for $\gamma + n \to \pi^- + p$ interactions from forward, (E), 25:14523
  interactions $\gamma + e \to e + \nu + \mathrm{anti}\ \nu$, stellar energy loss rate from cross sections for, (T), 25:14650
  interactions $\gamma + e \to \gamma + e$, low-energy theorems for Compton, 25:14630
  interactions $\gamma + e$ at high energies, leading singularity in complex angular momentum plane in quantum electrodynamics for asymptotics of, (T), 25:14802
  interactions $\gamma + \gamma \to \pi^+ + \pi^-$ near f(1260), cross sections for, (T), 25:14596 (JINR-E2-5424)
  interactions $\gamma + \gamma$ at high energies, leading singularity in complex angular momentum plane in quantum electrodynamics for asymptotics of, (T), 25:14802
  interactions $\gamma + \gamma$, π^0 and eta exchange in total cross sections for, (T), 25:14596 (JINR-E2-5424)
  interactions $\gamma + n \to n + \pi^+ + \pi^- + \pi^-$ at 4.3 GeV, total and resonance production cross sections for, (E), 25:14521
  interactions $\gamma + N \to \omega + N(N^*)$ at 9.1 GeV in deuterium and hydrogen targets, counter study of cross sections for, (E), 25:14512
  interactions $\gamma + n \to p + \pi^+ + \pi^- + \pi^- + \pi^0$ at 4.3 GeV, total and resonance production cross sections for, (E), 25:14521
  interactions $\gamma + n \to p + \pi^+ + \pi^- + \pi^-$ at 4.3 GeV, total and resonance production cross sections for, (E), 25:14521
  interactions $\gamma + N \to \pi + \Delta$ at high energies, contribution of low-energy theorem, 25:14622
  interactions $\gamma + N \to \pi + N$, isotensor electromagnetic current in, (T), 25:14604
  interactions $\gamma + N \to \pi^0 + N$ at 12 GeV at large angles, Regge pole theory for differential cross sections of, (T), 25:14598
  interactions $\gamma + n \to \pi^- + p$, angular distributions and differential cross sections of $\pi^- + p \to \gamma + n$ interactions at 1245 and 1337 MeV for test of predictions for, (E), 25:14567
  interactions $\gamma + n \to \pi^- + p$, π^-/π^+ cross section ratio in $\gamma + d \to \pi^-(\pi^+) + 2p(2n)$ interactions at 600 to 1700 MeV for cross sections of, (E), 25:14523
  interactions $\gamma + n$ at 0.7 to 12 GeV in deuterium bubble chamber, isovector--isoscalar interference from partial cross sections for, (E), 25:14519
  interactions $\gamma + N$ at high energies, quark model for total cross section relations for, (T), 25:14595 (ITF-70-63-P)
  interactions $\gamma + N$, Regge pole model for hadron production from, (T), 25:14635 (NYO-4204-9)
  interactions $\gamma + p \to \mathrm{eta}^0 + p$ at 1.465 to 1.815 GeV, cross sections for, (E), 25:14522
  interactions $\gamma + p \to \mathrm{eta}^0 + p$ at 5.0 to 10 GeV, cross sections for, (E), 25:14524
  interactions $\gamma + p \to K^+ + \Lambda$ at low and intermediate energies, isobar analysis of ΛKN coupling constants from, 25:14627
  interactions $\gamma + p \to K^+ + \Sigma^0$ at low and intermediate energies, isobar analysis of ΣKN coupling constants from, 25:14627
  interactions $\gamma + p \to \pi^0 + \mathrm{eta}^0 + p$ at 1.465 to 1.815 GeV, cross sections for, (E), 25:14522
  interactions $\gamma + p \to \pi^0 + p$ at 1200 to 1800 MeV, spark chamber study of recoil proton polarization from, (E), 25:14516
  interactions $\gamma + p \to \pi^0 + p$ at 5.0 to 17.8 GeV, differential cross sections for, (E), 25:14524
  interactions $\gamma + p \to \pi^0(\pi^+) + p(n)$, model with poles and cuts for mixing angles of eta$_1$ and eta$_8$ isosinglets in, (T), 25:14629
  interactions $\gamma + p \to \pi^- + \Delta^{++}$ in strong-cut Reggeized model, 25:14603
  interactions $\gamma + p \to \pi^+ + n$ at 4.3 to 9.8 GeV at large angles, Regge pole theory for differential cross sections of, (T), 25:14598
  interactions $\gamma + p \to \pi^+ + n$ in strong-cut Reggeized model, 25:14603
  interactions $\gamma + p \to \pi^+ + N(1520)$, low-t theorems for forward π^+ production in, (T), 25:14609
  interactions $\gamma + p \to \mathrm{rho}^0 + p$ at 2.8 and 4.7 GeV, S-channel helicity conservation in polarized, 25:14605
  interactions $\gamma + p \to \mathrm{rho}^0(\mathrm{phi}^0) + p$ interactions at 5.0 to 17.8 GeV, differential cross sections for, (E), 25:14524
  interactions $\gamma + p$ at 5.0 to 17.8 GeV, B(1240) production in, (E), 25:14524
  interactions $\gamma + p$ at high energies, quark model for constant of, (T), 25:14595 (ITF-70-63-P)
  interactions $\gamma + p$ in SU(6)-quark model, relations between differential cross sections for scalar and vector meson production in, 25:14626
  interactions $\gamma + p$, fixed pole in virtual Compton amplitude for, 25:14608
  interactions of, fixed j-plane singularities in production, 25:14625
  interactions of, threshold singularities for Compton, 25:14792
  interactions with electrons, kinetic theory of, 25:14490 (AD-711681)
  interactions with hadrons, scaling, fixed poles, and sum rules for, 25:14614
  interactions with hyperons, quark model commutation relations for sum rules for amplitudes of π production from, (T), 25:14619
  mass of, very low-frequency parallel-resonance circuits for determining upper limits for rest, (E), 25:14510
  production in $e^+ + e^- \to \pi^+ + \pi^- + \gamma$ interactions in storage rings, study of even-charge hadronic systems from, (T), 25:14621
  production in $\nu + e \to \nu + e + \gamma$ interactions, γ energy and angular distribution and radiative corrections for total effective cross sections for, (T), 25:14600
  production in $p + p \to p + p + \gamma$ at 20 MeV, cross sections and γ angular distributions and energy spectra for, (E), 25:14545
  production in $p + p \to p + p + \gamma$ interactions, $N + N$ interactions below 350 MeV for, (T), 25:14734
  production in $\pi^+ + n$ interactions at 2.34 GeV/c in xenon bubble chamber, (E), 25:14560 (JINR-E1-5349)
  production of wide-angle, in electron reactions with nuclei at high energies, angular dependence of cross sections for, (E), 25:14529
  reactions (γ,f) with uranium-238, analysis using dynamic collective model, (T), 25:15198
  reactions with beryllium at 16 GeV, cross sections for high mass di-pion pair and upper limits for cross sections for vector meson production in, (E), 25:14511
  reactions with beryllium at 4.1 to 6.1 GeV, phase of rho^0 production amplitude in, (E/T), 25:14527
  reactions with beryllium at 5.1 GeV, coherent interference between $\mathrm{rho} \to e^+ + e^-$ and $\omega \to e^+ + e^-$ decays from production in, (E), 25:14528
  reactions with carbon at high energies, spectrometer study of enhancement in high-invariant-mass π^---π^+ pair production in, (E), 25:14526
  reactions with elements $Z = 1$ to 100 at 1 keV to 100 MeV, tables of cross sections for coherent and incoherent scattering, pair production, and photoelectric ejection in, 25:14409
  reactions with lithium-7 and beryllium-9, differential cross sections for π^0 production in polarized, 25:14602
  reactions with negative ions, long-range correction to matrix elements for dissociation in, 25:14019
  reactions with nuclei at high energies, quark model for total cross section relations for, (T), 25:14595 (ITF-70-63-P)
  scattering by praseodymium-141, angular distributions from inelastic, (E), 25:15139
  scattering by tin at 6 to 9 MeV and zirconium at 8.5 to 12.5 MeV, (E), 25:14959

PHOTOSPHERE
  disturbances of, connection between N--S and E--W asymmetries in, (E/T), 25:13883
  faculae in, spectra of, (E), 25:13882
  magnetic fields in, following proton flares, (E), 25:13893
  oscillations in, model for, (T), 25:13901
  plage structure in, vertical, (E), 25:13882
  transition region with chromosphere, line profiles and flash intensities in, (T), 25:13878

PHOTOSYNTHESIS
  pigment development and organization in, 25:15462 (UCRL-20202)

PHYTOHEMAGGLUTININ
  effects on x-radiosensitivity of cultured human lymphocytes, 25:13472

PICROTOXIN
  radiation effects on action of in central nervous system of rabbits, ionizing, 25:13561

PILGRIM POWER REACTOR
  containment system for, final safety analysis of, 25:15306 (DOCKET-50293-34)
  control systems for, final safety analysis of, 25:15306 (DOCKET-50293-34)
  design parameters of, revised and additional data on, 25:15307 (DOCKET-50293-35)
  emergency core cooling system for, final safety analysis of, 25:15306 (DOCKET-50293-34)
  instrumentation for, final safety analysis of, 25:15306 (DOCKET-50293-34)
  operations aspects of, revised and additional data on, 25:15307 (DOCKET-50293-35)
  piping systems for, final safety analysis of, 25:15306

(DOCKET-50293-34)
  protection systems for, final safety analysis of, 25:15306 (DOCKET-50293-34)
PILOCARPINE
  epinephrine, effects on x-radiosensitivity of bone marrow and reticulo-endothelial system in rats, 25:13567
PINCH DEVICES
  design of theta-, for shock-wave studies in nitrogen, 25:14350 (AD-711003)
PINCH EFFECT
  electron drift velocities in z, laser scattering measurement of, 25:14256
PINEAL GLAND
  radiation effects on activity of hydroxyindole methyltransferase and synthesis of melatonin in, in rats, x, 25:13559
PIPES
  design guide for liquid metal cooled fast breeder reactor systems, development and verification of, 25:15355 (SAN-781-100)
  design guide for liquid metal cooled fast breeder reactor, philosophy and criteria of, 25:15360 (SAN-781-500)
  design of bubble chamber, for studies of alpha-induced void nucleation in superheated water, 25:13152(R) (SU-326-P-13-5)
  design specifications for liquid metal cooled fast breeder reactor, comparison of dynamic analysis methods for, 25:15362 (UNC-5231)
  design specifications for liquid metal cooled fast breeder reactor, review of research and development programs for, 25:15361 (SAN-781-518)
  fabrication of liquid metal cooled fast breeder reactor, requirements for, 25:15356 (SAN-781-220)
  inspection of liquid metal cooled fast breeder reactor, comparison of methods for in-service, 25:15359 (SAN-781-243)
  installation of liquid metal cooled fast breeder reactor, requirements for, 25:15356 (SAN-781-220)
  stresses in systems of, effects of dimensional inaccuracies on calculation of, 25:13182
  testing methods for liquid metal cooled fast breeder reactor, comparison of model, 25:15358 (SAN-781-234)
PITUITARY GLAND
  radioinduced ablation of, in man, effects of, on thyroid function, yttrium-90 implant β and γ, 25:13579
PLACENTA
  scanning for localization using metastable indium-113 stabilized on gelatine at pH 4, 25:13502
  scanning of blood pools in human, effectiveness of metastable indium-113 for, in comparison to metastable technetium-99 for, 25:13516
  scanning of human, comparison of methods using metastable indium-113 or technetium-99 in combination with digital computer and scintillation camera for, 25:13517
PLANETARY NEBULAE
  atomic energy level transition probabilities in, forbidden nitrogen and oxygen, (E/T), 25:14107
  distances of 600, (E), 25:13827
  distribution of, (E), 25:13827
  infrared observations of NGC 7027 and IC 418, (E), 25:13826
  spectra of NGC 7027, Stark broadening and radio recombination lines in, (E/T), 25:13814
PLANKTON
  ecology of, off La Jolla, Calif., April--Sept., 1967, 25:15468 (UCSD-10-P-20-54)
PLANTS
  iodine radioisotopes uptake and half-life in tissues of, role of species differences and standard methods of data expression in prediction of fallout, 25:13395 (SWRHL-90-r)
  radioactivity monitoring of, West Valley, New York, 1969, 25:13080 (DOCKET-50201-62)
  uranium content of marsh, effects of humidity on, 25:13116
PLANTS (INDUSTRIAL)
  description of fuel cladding fabrication, at Norwegian Institute for Atomic Energy, 25:13645
PLASMA
  acceleration and shock wave formation by electromagnetic force fields, 25:14274
  antenna immersion in isotropic compressible, radiation from dipole, (T), 25:14275
  boundary sheath growth in low-pressure, limits of, (T), 25:14299
  boundary sheath kinetics between two, theory of, 25:14320
  boundary value problem for two-stream instability in spherical geometry, 25:14339
  charged particle motion in superposed Heliotron and biconical cusp fields, guiding center of, (T), 25:14330
  charged-particle interactions with weakly nonlinear, longitudinal fields from, (T), 25:14313
  charged-particle motion in magnetized, radiations from test, (T), 25:14325
  collisions in, dc noise from electron--ion, (T), 25:14303
  collisions in, quantum transport cross sections for, 25:14297
  conductivity of combustion, electric, 25:14285 (BMBW-FBK-70-29)
  conductivity of weakly ionized, effect of electron collision frequency on electric, (T), 25:14308
  conductivity of, asymptotic solutions for anomalous, 25:14309
  confinement in toroidal systems, numerical model for low-pressure, 25:14236
  cooling of flare-produced, in solar corona, (T), 25:13889
  diagnostics of argon afterglow, microwave and spectroscopic, 25:14257
  diagnostics of nonequilibrium boundary layer, electron temperature and density, 25:14258
  diagnostics of rotating mixtures, mass separation effects in, 25:14278 (NP-18643)
  diagnostics of warm anisotropic, resonance cones in field pattern of short rf probe for, 25:14259
  diagnostics of xenon, methods for temperature, 25:14261
  diagnostics of z-pinch, electron drift velocities from laser scattering, 25:14256
  diagnostics of, admittance of plane grid capacitor for nonlinear effects analysis, 25:14251
  diagnostics of, ion current to plane probe in, (T), 25:14249
  diagnostics of, performance of cylindrical Langmuir probes for, (E), 25:14242 (AD-711095)
  diagnostics of, viscosity measurement at atmospheric pressure, 25:14260
  diagnostics using calorimetric, gas-sampling probe, enthalpy profiles from, 25:14263
  diagnostics using cylindrical microwave cavities, electron density, (E), 25:14262
  diagnostics using hf radio waves, (E), 25:14248
  diagnostics using Langmuir probes, electron energy distribution, (E), 25:14246
  diagnostics using laser scattering and interferometry measurements, 25:14255
  diagnostics using laser-beam scattering, research on, 25:14241 (AD-710718)
  diagnostics using time-resolved sampling technique, ionization-wave, 25:14247
  dielectric permittivity in strong magnetic fields, (T), 25:14312
  diffusion in $l = 3$ stellarators, calculation using stellarator expansion technique, 25:13793
  diffusion in magnetic fields, density distribution effects on local decay time, (T), 25:14294
  diffusion in Tokamak devices, electric field effects on, (T), 25:14238
  diffusion of toroidal-confined, rotation and shock formation from resistive, (T), 25:14235
  electric discharges in helium, energy balance in low-pressure, (T), 25:14301
  electric discharges in, maintenance by dc and hf waves, 25:14266
  electron beam interactions with dense, collective slowing down of intense relativistic, (T), 25:14292
  electron beam interactions with, current density calculation for, 25:14321
  electron beam interactions with, instabilities from nonlinear, (T), 25:14296
  electron beam interactions with, ion-wave excitation in, (E), 25:14378
  electron beam interactions with, nonlinear theory for monochromatic wave excitation in, 25:14311
  electron density and collision frequency in varying magnetic fields, (T), 25:14315
  equilibrium of imperfect multiply ionized, equation of state for, (T), 25:14304
  flow past flat plates, boundary-layer studies of, (E/T), 25:14276
  flow past thin wedge, effects of finite Larmor radius on steady, (T), 25:14329
  heat transfer in collisionless, along magnetic field lines, (T), 25:14317
  heating by currents, current-interchange instability during turbulent, (E/T), 25:14344
  heating by electron cyclotron waves, lf wave excitation in, (E), 25:14343
  heating by ion--acoustic waves in streaming, ion, (E), 25:14240
  heating by laser beams, self-similar thermal wave in two-temperature, (T), 25:14237
  heating in laser-beam-irradiated, electron, 25:14279
  heating in tokamak-like JFT-2, Joule, 25:14233 (JAERI-Memo-4186)
  heating in variable electric fields, resonance phenomena in, 25:14368
  interactions of astrophysical, (T), 25:14072
  interactions of laser-produced, with strong magnetic induction, (E), 25:14334
  ionization equilibrium of hydrogen, (T), 25:14319
  kinetic theory of axially symmetric toroidal, perturbation, 25:14327
  kinetic theory of fully ionized, Mott--Smith solution of Fokker--Planck equation, 25:14295
  kinetic theory of weakly ionized, in external constant electric fields, 25:14328
  kinetic theory of, experimental test of quasi-linear, 25:14323
  kinetic theory of, finite-difference methods for Fokker--

Planck equation, 25:14307

- kinetic theory of, quantum statistical second virial coefficient for, 25:14322
- kinetic theory of, similarity rules in, 25:14318
- kinetics of hot, lectures on, 25:14305
- kinetics of hydrogen, equation of state, 25:14319
- kinetics of, asymptotic solutions for anomalous resistance, 25:14309
- laser beam interactions with argon, threshold for spark maintenance in, (E), 25:14331
- laser beam interactions with, electron heating and bremsstrahlung radiations from, 25:14279
- photon scattering in cold, theory of inverse Compton, (T), 25:13941
- polarization transfer in inhomogeneous magnetized, (T), 25:14286 (N-70-40979)
- positron annihilation in, theory for, 25:14290
- production by rf helix, density characteristics in, (T), 25:14333
- production using lasers, ponderomotive force in, (T), 25:14332
- properties in wall-stabilized toroidal electric arcs, 25:14269
- properties of hydrogen arc, current density and temperature, 25:14268
- properties of inhomogeneous electron, dielectric permeability tensor for, 25:14291
- properties of low-density hydrogen--helium, atomic processes in, 25:14302
- radiations from cesium, resonant, (E/T), 25:14264(R) (AD-711828)
- radiations from collisionless shock tubes, wave scattering effects on, (T), 25:14314
- radiations from electron--ion collisions in, dc noise, (T), 25:14303
- radiations from hydrogen, effects on atomic state density and electron distribution function, (T), 25:14316
- radiations from laser-beam-irradiated, bremsstrahlung, 25:14279
- radiations from nonequilibrium, in magnetic traps, (T), 25:14288
- research at Sydney Univ, 25:14231(R) (NP-18663)
- research on, similarity rules for, 25:14354
- rotation of toroidal-confined, from resistive diffusion, (T), 25:14235
- shock formation in toroidal-confined, from resistive diffusion, (T), 25:14235
- shock wave propagation in cold collisionless, near-steady oblique, (T), 25:14324
- shock wave propagation in collisionless Vlasov, existence conditions for hydromagnetic, (T), 25:14326
- shock wave propagation in, effect of fluctuations on MHD, (T), 25:14287
- shock wave structure in low-density, collisionless, (T), 25:14298
- shock wave structure in, oblique and normal ionizing, (T), 25:14284 (AD-711086)
- shock waves from light sparks in, diamagnetic moment of, (E/T), 25:14282
- simulation of electromagnetic wave interactions with, Darwin model for, 25:14293
- simulation of spherically symmetric, computer, 25:14289
- spectra of helium and nitrogen, optical, (E), 25:14277 (AD-712024)
- spectra of mercury, line intensity in discharge afterglows, 25:14100
- spectra of one-electron ion in, higher-order perturbation theory for, 25:14283 (AD-710950)
- spectra of partially ionized xenon, absorption, (E), 25:14280
- spectral-line broadening in hydrogen, amplitude modulation and nonadiabaticity of Stark, (T), 25:14310
- stability during turbulent heating by currents, current-interchange, (E/T), 25:14344
- stability in crossed electric and magnetic fields, frequency and amplitude shifts in, (T), 25:14338
- stability in microwave-excited positive columns, ion, (T), 25:14336 (NP-18662)
- stability in Q devices, periodic pulling of drift, (E), 25:14337
- stability of bounded, theory for two-stream instability in spherical geometry, 25:14339
- stability of collisionless, drift, (E), 25:14345
- stability of counter-streaming, electromagnetic, (T), 25:14342
- stability of finite mirror-confined, ion cyclotron, (T), 25:14348
- stability of hot-electron mirror-confined, (E/T), 25:14349
- stability of incompressible cylindrical, in monotonic fields, (T), 25:14346
- stability of positive column, nonlinear theory of spiral, 25:14347
- stability of two-stream, two pole models for, 25:14340
- stabilization of universal instability modes in large-shear magnetic field, 25:14341
- theory of turbulent, in interstellar space, 25:13912
- transport in Tokamak TM-3, diffusion and thermal conductivity effects on, (E/T), 25:14239
- turbulence in astrophysical, relation to primary cosmic radiation, (T), 25:14077
- wave absorption in nonisothermal, anomalous, (T), 25:14373
- wave coupling theory for, nonresonantly unstable, (T), 25:14366
- wave echoes in cesium, cyclotron, (E/T), 25:14387
- wave excitation by transverse waves in, Langmuir, (T), 25:14370
- wave excitation during electron cyclotron heating, lf, (E), 25:14343
- wave excitation in beam--plasma system, ion-, (E), 25:14378
- wave excitation in strong hf electric fields, parametric resonance, (T), 25:14376
- wave growth in infinite homogeneous, electrostatic, (T), 25:14384
- wave instabilities in magnetized, nonlinear, (T), 25:14367
- wave interaction in isotropic, electromagnetic and ion--acoustic, trapping in resonant, (T), 25:14374
- wave interactions in inhomogeneous Vlasov, quasi-transverse and quasi-longitudinal, (T), 25:14388
- wave interactions with column, deformation of resonance curves in, 25:14266
- wave interactions with half-space, reflection and penetration of oblique p-polarized electromagnetic, (T), 25:14361
- wave interactions with inhomogeneous column of, upper hybrid resonance, (E/T), 25:14381
- wave interactions with slab and half-space, oblique electromagnetic, (T), 25:14386
- wave interactions with, Darwin model for simulating electromagnetic, 25:14293
- wave propagation along cold collisionless axially magnetized, electromagnetic, 25:14360 (AD-711649)
- wave propagation and formation of collisionless electrostatic shocks in, ion--acoustic, (E/T), 25:14389
- wave propagation in argon column, standing acoustic-, (E), 25:14380
- wave propagation in magnetic fields, self-similar, (T), 25:14369
- wave propagation in magneto-, plane, (T), 25:14379
- wave propagation in two-ion-species, dispersion and stability of collisional drift-, (T), 25:14365
- wave propagation in weakly ionized magneto-, lf electrostatic, (E), 25:14383
- wave propagation on bounded, phase properties of space-charge, (T), 25:14372
- wave resonance phenomena in thermal cesium, in electric fields, 25:14368
- wave resonances in electron, in strong hf electric fields, 25:14377
- wave resonances in, ion--ion hybrid, (T), 25:14390
- wave scattering by magnetized columns of, near upper hybrid resonance, (E/T), 25:14382
- wave scattering from turbulent, model for calculating, 25:14364
- wave scattering on critical electron density fluctuations in, use of Born theory for, 25:14363
- wave scattering on, characteristic curves for collective electromagnetic, (T), 25:14375
- wave transformation in inhomogeneous, effect on threshold currents of beam instability in, (T), 25:14371
- wave--particle interactions with cylindrical, resonant, (T), 25:14362
- waves in collision-dominated slab, lf, (T), 25:14385

PLASMA ACCELERATORS

- design and performance of traveling-wave magnetic field, 25:14358
- jet diagnostics in dense focus, neutron and x-ray production, (E), 25:14359
- jet patterns in quasi-steady arcs, argon, 25:14281
- neutron yield from focus discharge, parameters of, (E), 25:14355
- properties of argon, electron density in, 25:14335
- properties of MW arc thruster, current--voltage, 25:14271
- shock wave production and properties in coaxial dense focus, 25:14270

PLASMA JETS

- diagnostics in dense noncylindrical z pinch, neutron and x-ray production in, (E), 25:14359
- diagnostics of helium, spectra measurement of temperature distribution, 25:14254
- diagnostics of induction-heated supersonic argon, using double Langmuir probe, 25:14243 (AD-711127)
- diagnostics of seeded-argon, electron density and temperature in boundary layer, 25:14244 (AD-711669)
- diagnostics using plane probes, ion density, (E/T), 25:14250
- flow around plates, one-dimensional solutions for, (E/T), 25:14265
- ion--neutral particle coupling in accelerating, (T), 25:14306
- production of argon, generator for, 25:14335
- production of continuous, discharge device for, 25:14272
- sheath dynamics near electrode in magnetic field, (T), 25:14300
- stability in crossed electric and magnetic fields, frequency and amplitude shifts in, (T), 25:14338
- velocity distributions in helium, gas flow model for, 25:14253

velocity distributions in helium, gas flow model for, 25:14252

PLASTICS
- book: Corrosion Week. 41st Manifestation of the European Federation of Corrosion, 7-12 October, 1968 in Budapest, 25:13636
- radioinduced polymerization in concrete, bibliography on, 25:13030 (AAEC/LIB/Bib-260)
- radioinduced polymerization in wood, bibliography on, 25:13029 (AAEC/LIB/Bib-259)
- shielding effects of vinyl, against radiation dose from x-ray diffraction apparatus, 25:13457

PLATES
- gamma transport in, computer program for solving one-dimensional Boltzmann equation for, (T), 25:14863 (CEA-N-1358)
- neutron transport in, computer program for calculating polyenergetic, (T), 25:14864 (CEA-N-1388)
- neutron transport in, computer program for solving one-dimensional Boltzmann equation for, (T), 25:14863 (CEA-N-1358)
- neutron transport in, two-group analysis of critical problem for, (T), 25:14867

PLATINUM
- photon incoherent scattering at 662 keV by K-shell electrons of, differential cross sections for, (E), 25:14410
- radiation effects on stored energy in, at less than 40°K, 3 MeV electron, 25:13722 (JUL-658-FN)

PLATINUM ALLOYS AND SYSTEMS
- Al_2C_3--Pt-base, properties of dispersion-strengthened, electric and tensile, 25:13755
- Pt--Rh, photon reactions at 2.6 to 17.6 MeV with, effective atomic numbers for pair production in, (T), 25:14402
- Pt-base--ThC_2, properties of dispersion-strengthened, electric and tensile, 25:13755

PLATINUM COUPLES
- Mo--PT/Mo--Pt, performance of thermocouples of, for in-core high temperature measurements, 25:13326

PLATINUM ISOTOPES
- electron-capture decay of neutron-deficient, (E/T), 25:14993

PLATINUM ISOTOPES Pt-192
- energy levels from iridium-192 decay, spin-parity assignments for, (E), 25:15062

PLATINUM ISOTOPES Pt-194
- energy levels at 329 and 622 keV, rotation angles and g factors for, (E), 25:15034

PLOWSHARE PROJECT
- fallout uptake from Schooner Event, distribution of, in fetuses, tissues, and milk following ingestion by dairy cattle, 25:13396 (UCRL-72511)
- geophysical research program for, 25:13104 (UCRL-50855)
- legal aspects of domestic and foreign uses of, review of proposed legislation on, 25:13137 (NP-18659)
- radiation safety problems encountered in, 25:13429
- water analysis in precipitation, springs, streams, and wells in Project Rulison area, methods for radiochemical, 25:12951 (USGS-474-83)

PLUTONIUM
- analysis for rare earth, tantalum, titanium, tungsten, and zirconium impurities by solvent extraction and emission spectrography, 25:12923 (WHAN-SA-47)
- bibliography on, Nov. 1970, 25:13626
- bibliography on, Sept. 1970, 25:13625
- content in solid wastes produced by reactor fuel fabrication and reprocessing plants, predictions to year 1990 of, 25:13188 (BNWL-B-34)
- desorption from tungsten surfaces, modulated beam method for, 25:13686
- determination in fuel dissolver solutions by tracer method and isotope dilution mass spectroscopy, 25:13081 (NP-18577)
- determination in fuel rods and process waste, development of spectrometer systems for, 25:13230(R) (WCAP-7562-1)
- determination of, correction coefficients for mass-spectrometric, 25:12927
- deuteron reactions with thin targets of, at 9 to 14.2 MeV, (E), 25:15046
- effects on lattice parameters of alpha-uranium at 43°K, 25:14452
- magnetic transition in delta-, aluminum-27 NMR search for, 25:14481
- precipitation in ammonium carbonate solutions using hexaamminecobalt chloride, chemical and crystallographic properties of compounds produced by, 25:12980
- production and uses of, review on, 25:13059
- proton reactions with thin targets of, at 9 to 14.2 MeV, (E), 25:15046
- recycle in thermal water cooled reactor fuels, economics of, (T), 25:15375 (CONF-691114-6)
- separation from irradiated fuel elements by solvent extraction using tertiary or quaternary amines, 25:13101(P)
- separation from radioactive wastes, bibliography on, 25:13190 (JAERI-Memo-4153)
- x-ray energies of, K, (E), 25:14981 (IN-1448)

PLUTONIUM ALLOYS AND SYSTEMS
- Al--Pu-base, aluminum-27 NMR in delta-, 25:14481

PLUTONIUM CARBIDES
- equations of state at 0 to 16,000°K, caloric and thermal, 25:13753

PLUTONIUM ISOTOPES
- neutron cross sections for, review of resonance, (E), 25:15069
- neutron reactions above resonance energies, review of data on, 25:15112
- neutron reactions with, review of data on fast, 25:15102

PLUTONIUM ISOTOPES Pu-236
- neutron reactions at thermal energies to 10 MeV, evaluation of data on, (T), 25:15128

PLUTONIUM ISOTOPES Pu-237
- fission of isomers of, spontaneous, (E), 25:15046

PLUTONIUM ISOTOPES Pu-238
- alpha decay of, gamma spectra and half-life for, (E), 25:14981 (IN-1448)
- content of airborne particulates in USA during 1969, 25:13441
- crystal lattice parameter annealing in self-irradiated dioxide of, activation energy of first stage of, 25:13784
- determination in liquid waste effluents from nuclear fuel reprocessing plant by α spectrometry, 25:12950 (BRH/NERHL-70-2)
- neutron fission at 15 to 500 eV, cross section for, (E), 25:14982 (NCSAC-31)
- neutron fission of, energy spectra and mean prompt neutron production in thermal, (E), 25:15118
- neutron reactions at thermal energies to 10 MeV, evaluation of data on, (T), 25:15128
- use as heat source for cardiac pacemaker, evaluation of, 25:13178

PLUTONIUM ISOTOPES Pu-239
- alpha decay of, gamma spectra and half-life for, (E), 25:14981 (IN-1448)
- content of airborne particulates in USA during 1969, 25:13441
- determination in liquid waste effluents from nuclear fuel reprocessing plant by α spectrometry, 25:12950 (BRH/NERHL-70-2)
- fission of isomers of, spontaneous, (E), 25:15046
- neutron capture by, γ spectra from, (E), 25:14982 (NCSAC-31)
- neutron capture by, high-energy γ spectra from, (E), 25:15078
- neutron capture to fission ratio at thermal energies, (E), 25:15070
- neutron capture to fission ratio in, integral measurements of fast, (E/T), 25:15348
- neutron capture-to-fission ratio at 0.1 to 10 keV, (E), 25:15074
- neutron capture-to-fission ratio at 0.1 to 30 keV, radiative, (E), 25:15075
- neutron capture-to-fission ratio at 0.1 to 30 keV, (E), 25:15073
- neutron capture-to-fission ratio for, accuracy of values for, 25:15072
- neutron cross sections at 0.01 to 15 MeV, (T), 25:15133
- neutron cross sections at 0.014 to 1000 keV, (E), 25:15091
- neutron elastic scattering at 0 to 660 eV, spin of resonances induced by, (E/T), 25:15088
- neutron fission at 0 to 6 MeV, energy dependence of mean prompt neutron production from, (E), 25:15117
- neutron fission at 0 to 660 eV, resonance parameters for, (E/T), 25:15089
- neutron fission at 0 to 70 keV, mean prompt neutron production from, (E), 25:15113
- neutron fission at 0.0001 to 20 MeV, evaluation of cross sections for, (E/T), 25:15127
- neutron fission at 0.005 to 0.1 eV, cross sections for, (E), 25:15067
- neutron fission at 0.01 to 1 MeV, mean number of prompt neutrons and cross section for, (E), 25:15116
- neutron fission at 0.010 to 30 keV, cross sections for, (E), 25:15089
- neutron fission at 0.025 to 1 MeV, total cross section for, (E), 25:15068
- neutron fission at 0.1 to 1.5 MeV, angular distribution of fragments from, (E), 25:15051
- neutron fission at 0.3 to 1.4 MeV, mean prompt neutron production and relative cross sections for, (E), 25:15114
- neutron fission at thermal energies, cross sections for, (E), 25:15070
- neutron fission of intermediate structure effects in, (E), 25:14997
- neutron fission of, gas release curves from, (T), 25:14989 (UCRL-50656(Suppl.))
- neutron reactions with, yields of spontaneously fissioning isomers from, (E), 25:15031
- neutron scattering at 0.2 to 5.5 MeV, angular distributions in, (E/T), 25:15134
- neutron total and fission cross sections at 5.7 to 160 eV, simultaneous analysis of, (E/T), 25:15087
- neutron total cross section at 0.1 to 6 MeV, (E), 25:15103
- nuclear magnetic resonance in stabilized delta-plutonium, search for, 25:14481

XUM

PLUTONIUM ISOTOPES Pu-240
- alpha decay of, gamma spectra and half-life for, (E), 25:14981 (IN-1448)
- fission of isomers of, spontaneous, (E), 25:15031
- neutron capture at 4 to 60 keV, average cross section for, (E), 25:14982 (NCSAC-31)
- neutron cross sections at 0.001 to 1 MeV, (T), 25:15129
- neutron cross sections at 0.01 to 15 MeV, (T), 25:15133
- neutron fission at 0.1 to 1.5 MeV, angular distribution of fragments from, (E), 25:15051
- neutron fission at 0.6 to 5 MeV, mean prompt neutron production from, (E), 25:15115
- neutron fission of intermediate structure effects in, (E), 25:14997
- neutron resonance parameters at 1 eV, (E), 25:15092

PLUTONIUM ISOTOPES Pu-241
- alpha and beta decay of, gamma spectra and half-life for, (E), 25:14981 (IN-1448)
- determination in liquid waste effluents from nuclear fuel reprocessing plant by scintillation counting, 25:12950 (BRH/NERHL-70-2)
- fission of isomers of, spontaneous, (E), 25:15046
- neutron cross sections at 0.01 to 15 MeV, (T), 25:15133
- neutron fission at 0.001 to 3 keV, cross sections for, (E/T), 25:15086
- neutron fission at 0.005 to 1 MeV, ratio of uranium-235 fission cross section to cross section for, (E), 25:15107
- neutron fission at 2 to 2000 eV, cross section for, (E), 25:15083
- neutron fission of intermediate structure effects in, (E), 25:14997

PLUTONIUM ISOTOPES Pu-242
- neutron total cross section up to 1 eV, (E), 25:14982 (NCSAC-31)

PLUTONIUM ISOTOPES Pu-244
- fission of, average number of prompt neutrons from spontaneous, (E), 25:15037

PLUTONIUM NITRATES
- analysis of solutions of, by atomic absorption spectrometry, equipment for, 25:12932(P)
- denitration of, fluidized bed process for, 25:13077(R) (ANL-7755)

PLUTONIUM OXIDES PuO$_2$
- crystal lattice parameter annealing in self-irradiated, activation energy of first stage of, 25:13784
- properties of plutonium-238 enriched, for use in SIREN fuel capsules, 25:13170 (SNC-2708-1)
- thermal desorption of radiolytically produced nitric oxide from, mass spectrometric studies on, 25:13024
- PuO$_2$--UO$_2$, analysis for rare earth impurities by solvent extraction and emission spectrography, 25:12923 (WHAN-SA-47)
- PuO$_2$--UO$_2$, analysis of fuels of, for rare earths by solvent extraction and emission spectrography, 25:12922 (WHAN-SA-44)
- PuO$_2$--UO$_2$, analysis of hypostoichiometric fuel pellets of, for sorbed gases and water, 25:12925 (WHAN-SA-77)
- PuO$_2$--UO$_2$, performance of stainless steel clad fast reactor fuels of, review of, 25:15367 (WHAN-SA-51)

PNEUMATIC SYSTEMS
- design for transferring materials in hot cells, 25:13203(P)

POINT BEACH POWER REACTOR, UNIT 1
- operations incident of January 12, 1971, failure of containment sump suction valves to open, 25:15238 (DOCKET-50266-40)
- operations incident of July 7, 1970, coolant pump fire, 25:15237 (DOCKET-50266-39)
- radioactive by-product materials for, revised possession limits for, 25:15296 (DOCKET-50266-38)
- site for, pre-operational environmental monitoring program for, 25:15297 (DOCKET-50266-41)

POLONIUM ISOTOPES Po-205
- energy levels from electron-capture decay of astatine-205, 25:14995

POLONIUM ISOTOPES Po-210
- angular distributions from lead-206 (He-4,3n) and lead-207 (He-3,3n) reactions, (E), 25:14996
- content of fish protein concentrates, 25:13394(R) (RLO-2099-1)
- content of marine organisms in Pacific Ocean, 25:13394(R) (RLO-2099-1)
- decay of, (E), 25:14996
- fission of, threshold and saddle point for, 25:15010

POLYMERS
- neutron inelastic scattering by, conference on, Tokai, Japan, 12/69, (E/T), 25:14436 (JAERI-1197)
- radioinduced curing of coatings of, bibliography on, 25:13031 (AAEC/LIB/Bib-261)

POLYSACCHARIDES
- isolation of heparin-related, sulfur-35-labeled, from embryonic cells of mice and rats, HeLa cells, and L cells, 25:13357

POPULATIONS
- destruction of US, by nuclear weapons, assessment of requirements for total, 25:13132 (AD-711021)
- radiation dose to human, of Britain from color television receivers, mutagenic x, 25:13452
- radiation protection of, in vicinity of nuclear installations, safety measures for, 25:13471
- radioactivity in diet of, in high background areas in Brazil, 25:13439

POSITRON CAMERAS
- development of, review on, 25:13222

POSITRONIUM
- decay rate of ortho-, photon--photon scattering contribution to 3-photon, (T), 25:13992

POSITRONS
- annihilation in helium gas, coincidence study of, 25:13987
- annihilation in methane gas, (E), 25:13993
- annihilation in plasma, theory for, 25:14290
- annihilation in zirconium single crystal, angular distribution of two-photon, 25:14441
- annihilation rates in lanthanum and lithium hydrides, 25:13988
- channeling in gold single-crystal films, (E/T), 25:14418
- diffusion in helium gas, coincidence study of, 25:13587
- interactions $e^+ + e^- \to 2\gamma$ at 1 GeV, validity limit of quantum electrodynamics, 25:14520
- interactions $e^+ + e^- \to \mu + e$ at 0.8 to 1 GeV, test of validity of leptonic selection rules from colliding-beam, (E), 25:14515
- interactions $e^+ + e^- \to \pi^+ + \pi^- + \gamma$ in storage rings, study of even-charge hadronic systems from, (T), 25:14621
- interactions $e^+ + e^-$ at 0.8 to 1 GeV, production of heavy leptons in, (E), 25:14517
- interactions $e^+ + e^-$, in storage rings, study of even-charge conjugation hadronic systems from production of hadronic states and photon in, (T), 25:14621
- reactions with hydrogen atoms at low energies, convergence of separable-expansion method for solution of Faddeev equations for, 25:14010
- reactions with hydrogen molecules at 50 to 544 eV, Born approximation calculation of cross sections for positronium formation by electron capture in, 25:14006
- scattering by metallic thick targets at 0.5 to 2.0 MeV, Monte Carlo calculations of angular distributions and energy spectra from back-, 25:13959 (UCRL-19719)

POTASSIUM
- content and depth in crustal basalts and granites in USSR, 25:13115
- content of diet of human adolescents in EURATOM countries during 1965 to 1967, 25:13392 (EUR-3945(Pt.2))
- content of institutional diets of adults and children in USA during October to December 1969 as compared to annual average content for 1969, 25:13442
- effects on γ radiolysis of ammonia adsorbed on synthetic zeolites, EPR spectral studies on, 25:13057
- electron elastic scattering at 1.0 to 5.2 eV by, differential cross sections for, (E), 25:14034
- electron reactions at 3.0 to 5.2 eV with, differential cross sections for excitation of 4S--4P transition in, (E), 25:14034
- helium-ion reactions at 50 to 1600 eV with, crossed-beam study of electron capture into excited states in, 25:14011
- ion exchange behavior on zirconium phosphate crystals, 25:13084
- neutron reactions $(n,x\gamma)$ at 14 MeV with natural, cross sections for, (E/T), 25:14920(T) (BNL-tr-380)
- nitrogen-ion (N_2^+) reactions at 50 to 1600 eV with, crossed-beam study of electron capture into excited states in, 25:14011
- prospecting for, development of instruments for, 25:13321 (RISO-M-1270)
- radiation effects on 3-methylpentane containing, at 77°K, comparative ESR studies on paramagnetic species produced from γ or uv, 25:13025
- radiation effects on content of, in brain and muscle tissues of rats, lethal and sublethal, 25:13566
- scattering by rare gases at 300 to 15000 m/sec, total cross sections for elastic, (E/T), 25:14005

POTASSIUM ACID PHOSPHATES
- radiation effects on dielectric properties of crystals of, gamma, 25:14432
- spectra of single crystals of, effects of deuterium on polarized Raman, 25:12997

POTASSIUM CHLORATES
- radiation effects on, chemical states of recoil sulfur-35 from neutron, 25:13065

POTASSIUM CHLORIDES
- colloid induced by impurity silver and thallium in crystals of, 25:14429
- radiation effects on, chemical states of recoil sulfur-35 from neutron, 25:13065
- radioinduced colloids in crystals of, reactor, 25:14426
- radioinduced F centers in crystals of, saturation of electron-, 25:14415
- KCl--NaCl, electrolytic properties of aqueous solutions of, adiabatic compression and ultrasonic attenuation studies of, 25:13015

POTASSIUM CYANIDES
- radiation effects on, reactions of recoil carbon-14 and nitrogen-13 from neutron, 25:13072

POTASSIUM FERROCYANIDES
- radiation effects on iron-58-labeled, reactions of recoil iron-59 from neutron, 25:13068

POTASSIUM IODIDES
- iodine-131 exchange between ethanol solutions of iodomethane and, at 35°C, reaction order of components

  in, 25:12996
POTASSIUM IONS
  reactions with oxygen atoms at 30 keV to 2 MeV, cross sections for electron capture and loss in, (E), 25:14042
POTASSIUM ISOTOPES K-39
  neutron capture at 14 MeV, cross sections for fast, (E/T), 25:14920(T) (BNL-tr-380)
  neutron elastic scattering at 14 MeV, optical-model analysis of differential cross sections for, (E/T), 25:14920(T) (BNL-tr-380)
POTASSIUM ISOTOPES K-40
  content in sands and soils of south Florida, 1968 measurements of natural, 25:13107
  content of cows, accuracy of, as heat tolerance predictor, 25:13339
  content of fish protein concentrates, 25:13394(R) (RLO-2099-1)
  energy-level transitions among f/sub 7/2/d/sub $3/2^{-1}$ states of, M1, (E), 25:14934
POTASSIUM NIOBIUM FLUORIDES
  reduction to niobium in melts, electrolytic and zinc, 25:13642
POTASSIUM NITRATES
  radiolysis of crystalline, effects of oxygen-18 on, 25:13043
  KNO_3--$LiNO_3$, electrolytic properties of aqueous solutions of, adiabatic compression and ultrasonic attenuation studies of, 25:13015
  KNO_3--NH_4NO_3, electrolytic properties of aqueous solutions of, adiabatic compression and ultrasonic attenuation studies of, 25:13015
  KNO_3--$Pb(NO_3)_2$, electrolytic properties of aqueous solutions of, adiabatic compression and ultrasonic attenuation studies of, 25:13015
POTASSIUM OXIDES
  content in rocks of shields and sediment cover of Brazil, Canada, and USSR, relations with geological time, 25:13114
POTASSIUM PERCHLORATES
  radiation effects on, chemical states of recoil sulfur-35 from neutron, 25:13065
POWER CYCLES
  design of radioisotope-fueled Brayton, incorporating compressor and turboalternator, 25:13168 (N-70-41276)
  evaluation of optimum, for direct cycle gas turbine gas cooled reactor, 25:15383(P)
  heat source for Brayton, thermal analysis of aerodynamically-shaped radioisotope, 25:13167 (N-70-41092)
POWER PLANTS
  effluents from natural gas-fueled, effects of nuclear stimulation of fuel gas on environmental contamination by, 25:13430 (UCRL-72830)
POWER SUPPLIES
  control circuit for, of superconducting magnets, 25:14221
PRAIRIE ISLAND POWER REACTOR, UNIT 1
  auxiliary systems for, final safety analysis of, 25:15302 (DOCKET-50282-29)
  buildings and structures for, design requirements of, 25:15304 (DOCKET-50282-31)
  components for, design requirements of, 25:15304 (DOCKET-50282-31)
  containment structures for, final safety analysis of, 25:15301 (DOCKET-50282-28)
  control system for, final safety analysis of, 25:15301 (DOCKET-50282-28)
  cooling system for, final safety analysis of, 25:15300 (DOCKET-50282-27)
  electrical systems for, preliminary safety analysis of, 25:15302 (DOCKET-50282-29)
  engineered safeguards for, final safety analysis of, 25:15301 (DOCKET-50282-28)
  instrumentation for, final safety analysis of, 25:15301 (DOCKET-50282-28)
  operation of, license application for, 25:15299 (DOCKET-50282-26)
  operations aspects of, final safety analysis of, 25:15302 (DOCKET-50282-29)
  operations of, safety analysis of initial, 25:15303 (DOCKET-50282-30)
  owners of, financial statements of, 25:15299 (DOCKET-50282-26)
  physics measurements for, final safety analysis of, 25:15300 (DOCKET-50282-27)
  quality assurance program for, 25:15304 (DOCKET-50282-31)
  quality assurance program for, 25:15304 (DOCKET-50282-31)
  radiation protection system for, final safety analysis of, 25:15302 (DOCKET-50282-29)
  radioactive waste disposal system for, final safety analysis of, 25:15302 (DOCKET-50282-29)
  safety analysis of, 25:15303 (DOCKET-50282-30)
  site for, final safety analysis of, 25:15300 (DOCKET-50282-27)
  site for, preliminary safety analysis of, 25:15304 (DOCKET-50282-31)
  steam and power conversion systems for, final safety analysis of, 25:15302 (DOCKET-50282-29)
PRAIRIE ISLAND POWER REACTOR, UNIT 2
  auxiliary systems for, final safety analysis of, 25:15302 (DOCKET-50282-29)
  buildings and structures for, design requirements of, 25:15304 (DOCKET-50282-31)
  components for, design requirements of, 25:15304 (DOCKET-50282-31)
  containment structures for, final safety analysis of, 25:15301 (DOCKET-50282-28)
  control system for, final safety analysis of, 25:15301 (DOCKET-50282-28)
  cooling system for, final safety analysis of, 25:15300 (DOCKET-50282-27)
  electrical systems for, preliminary safety analysis of, 25:15302 (DOCKET-50282-29)
  engineered safeguards for, final safety analysis of, 25:15301 (DOCKET-50282-28)
  instrumentation for, final safety analysis of, 25:15301 (DOCKET-50282-28)
  operation of, license application for, 25:15299 (DOCKET-50282-26)
  operations aspects of, final safety analysis of, 25:15302 (DOCKET-50282-29)
  operations of, safety analysis of initial, 25:15303 (DOCKET-50282-30)
  owners of, financial statements of, 25:15299 (DOCKET-50282-26)
  physics measurements for, final safety analysis of, 25:15300 (DOCKET-50282-27)
  quality assurance program for, 25:15304 (DOCKET-50282-31)
  quality assurance program for, 25:15304 (DOCKET-50282-31)
  radiation protection system for, final safety analysis of, 25:15302 (DOCKET-50282-29)
  radioactive waste disposal system for, final safety analysis of, 25:15302 (DOCKET-50282-29)
  safety analysis of, 25:15303 (DOCKET-50282-30)
  site for, final safety analysis of, 25:15300 (DOCKET-50282-27)
  site for, preliminary safety analysis of, 25:15304 (DOCKET-50282-31)
  steam and power conversion systems for, final safety analysis of, 25:15302 (DOCKET-50282-29)
PRASEODYMIUM
  complexes with carminic acid, spectrophotometric studies on, 25:12937
  determination in plutonium oxide--uranium oxide fuels by solvent extraction and emission spectrography, 25:12922 (WHAN-SA-44)
  determination of trace amounts of, in gadolinium oxide by x-ray-excited optical luminescence, 25:12948
  determination of trace amounts of, in plutonium and plutonium dioxide--uranium dioxide by solvent extraction and emission spectrography, 25:12923 (WHAN-SA-47)
PRASEODYMIUM ALLOYS AND SYSTEMS
  Bi--Pr, magnetic ordering of intermetallic PrBi, self-polarization contribution to, (T), 25:14460
  Er--Mn--Pr, crystal structure of, 25:13707
  Er--Mn--Pr, magnetic properties of, 25:13707
PRASEODYMIUM IONS
  crystal-field shielding and antishielding factors for Pr^{3+} at electronic and nuclear sites, (T), 25:13983
PRASEODYMIUM ISOTOPES Pr-141
  energy-level excitation by neutron capture gamma rays, (E), 25:15002
  energy-level structure of photo-excited, spin and parity for, (E), 25:15139
PRESSURE
  measurement of high, using semiconductor strain gages, 25:15458(T) (SCL-T-71-210)
PRESSURE VESSELS
  design of gas cooled reactor prestressed concrete, with provision for heat exchanger, 25:15364(P)
  materials for, development and testing of, 25:13724 (ORNL-4590, pp 100-34)
  testing of heavy-section epoxy models of, under complex stress, 25:13658 (ORNL-4590, pp 135-232)
PROCAINE
  radiation effects on action of in central nervous system of rabbits, ionizing, 25:13561
PROCESS EQUIPMENT
  development at ORNL, Sept. 1969--Aug. 1970, 25:13318(R) (ORNL-4620)
  development at Risoe, Oct. 1, 1969--March 31, 1970, 25:13321 (RISO-M-1270)
PROMETHIUM
  separation from aqueous chloride solutions by solvent extraction using dioctyl phosphate in benzene or heptane, effects of variables on, 25:13096
PROMETHIUM ISOTOPES Pm-147
  determination in liquid waste effluents from nuclear fuel reprocessing plant by scintillation counting, 25:12950 (BRH/NERHL-70-2)
  reactivity worths in fast reactor spectra, (E/T), 25:15350
1,2-PROPANEDIOL
  effects on separation of cesium from sodium by ion exchange using Zeolite Linde A, 25:13091
2-PROPANOL
  radioinduced reactions with aqueous hydrogen peroxide,

- effects of trivalent titanium on kinetics of free radical chain reactions in γ, 25:13032
- radiolysis at 77°K, yields from γ, 25:13056
- radiolysis of vapors of, at 124 to 400°C, yields from γ, 25:13046

1-PROPANOL, 2,3-DIMERCAPTO-
- effects on radiation dose from mercury-203-labeled merphyrin to kidneys of mice, effects of glutathione on, 25:13341

PROPENE
- yields from γ radiolysis of 2-propanol vapor at 124 to 400°C, 25:13046

PROPENE, 2-METHYL-
- effects on reactions of recoil fluorine-18 in octafluorocyclobutane and hexafluorocyclobutene, scavenging, 25:13066

PROPENE POLYMERS
- radiolysis of, effects of energy on α and γ, 25:13055

PROPIONATES
- radiation effects on content of, in sheep serum, effects of air blast injury, and fasting on γ and neutron, 25:13384

PROSPECTING
- equipment for, development of, 25:13321 (RISO-M-1270)

PROSTATE GLAND
- radiation effects on secretory activity of, in rats, x, 25:13366

PROTACTINIUM
- complexes with tropolone, chemical properties and preparation of, 25:13009
- x-ray energies of, K, (E), 25:14981 (IN-1448)

PROTACTINIUM FLUORIDES
- preparation of hydrates of, 25:12978

PROTACTINIUM ISOTOPES Pa-231
- alpha decay of, gamma spectra from, (E), 25:14998
- neutron reactions at thermal energies to 10 MeV, evaluation of data on, (T), 25:15128
- separation from irradiated fuels, 25:13100

PROTACTINIUM ISOTOPES Pa-233
- beta decay of, gamma spectra and half-life for, (E), 25:14981 (IN-1448)

PROTACTINIUM OXYFLUORIDES
- preparation and properties of, 25:12978

PROTECTIVE CLOTHING
- development of lead impregnated vinyl foundation garment for female personnel for protection of gonads against x, 25:13462

PROTEINS
- carbon-14 content of, in tissues, development of method for determining, 25:13345
- carbon-14 incorporation in, of rat liver homogenates, effects of avidin on, 25:13344
- content of human blood serum, effects of uranium content of drinking water on, 25:13595
- effects on x-irradiated jejunal crypt cells of rats, 25:13562
- radiation effects on content of, in cells of Escherichia coli K 12, comparison of γ, proton, and uv, 25:13371
- radiation effects on synthesis of, in Escherichia coli, combined effects of reductone on uv, 25:13610
- radiation effects on synthesis of, in perfused rat liver, x, 25:13373
- radioisotope content of fish, 25:13394(R) (RLO-2099-1)

PROTON BEAMS
- production for plasma experiments, (E), 25:14353

PROTON SOURCES
- development of polarized, for 6-MeV Van de Graaff accelerator, 25:14859

PROTONS
- acceleration in auroral zone, mechanism for, (E/T), 25:14116
- acceleration of primary cosmic, by spinars, (T), 25:13952
- channeling in copper single-crystal films at 170 keV, effects of weak deformation on, 25:14421
- detection and measurement in auroral zone at 0.15 to 8 MeV, rocket-borne silicon detector for, 25:13227
- effects on activity of hydrolases and content of DNA and protein in lambda strain of Escherichia coli K 12, 25:13371
- effects on silicon p^+-ν-n^+ diodes at 2.8 MeV, annealing of, 25:14431
- effects on sodium chloride crystals at 4.5 MeV, release of stored energy in annealing of defects induced in, 25:14424
- electron capture in H I regions by cosmic, Lyman-α production in, (T), 25:14061
- emission of solar, microwave bursts as indicators of intensity of, (E/T), 25:13867
- flux measurement parallel to geomagnetic field lines in auroral ionosphere, 25:14125
- form factor of, relativistic, 25:14711
- interactions anti $p + p \to K +$ anti $K + \pi$ at rest, four-point Veneziano functions for mass spectra and angular distributions for, (T), 25:14691
- interactions anti $p + p$ at 1.25 to 1.67 GeV/c in deuterium bubble chamber, cross sections for hadron production in, (E), 25:14550
- interactions $e + p \to p + 2\pi$, hadronic s-channel helicity conservation in, (T), 25:14636 (NYO-4204-10)
- interactions $e + p$ at high energies, field-theoretic model of soft, neutral-meson production for deep-inelastic, 25:14607
- interactions $e + p$ near N(1470), analyticity of inelastic hadronic form factor and model of CP violation for, (T), 25:14765
- interactions $e + p$, fixed pole in virtual Compton amplitude for, 25:14608
- interactions $e + p$, ladder model for structure functions for deep-inelastic, 25:14612
- interactions $e + p$, multi-Regge model for inelastic, (T), 25:14621
- interactions $e + p$, test of weak interaction renormalization theories in, (T), 25:14646
- interactions $\gamma + p \to \text{eta} + p$, model wth poles and cuts for mixing angles of eta_1 and eta_8 isosinglets in, (T), 25:14629
- interactions $\gamma + p \to \text{eta}^0 + p$ at 1.465 to 1.815 GeV, cross sections for, (E), 25:14522
- interactions $\gamma + p \to \text{eta}^0 + p$ at 5.0 to 10 GeV, cross sections for, (E), 25:14524
- interactions $\gamma + p \to K^+ + \Lambda$ at low and intermediate energies, isobar analysis of ΛKN coupling constants from, 25:14627
- interactions $\gamma + p \to K^+ + \Sigma^0$ at low and intermediate energies, isobar analysis of ΣKN coupling constants from, 25:14627
- interactions $\gamma + p \to \pi^0 + \text{eta}^0 + p$ at 1.465 to 1.815 GeV, cross sections for, (E), 25:14522
- interactions $\gamma + p \to \pi^0 + p$ at 1200 to 1800 MeV, spark chamber study of recoil proton polarization from, (E), 25:14516
- interactions $\gamma + p \to \pi^0 + p$ at 5.0 to 17.8 GeV, differential cross sections for, (E), 25:14524
- interactions $\gamma + p \to \pi^0(\pi^+) + p(n)$, model with poles and cuts for mixing angles of eta_1 and eta_8 isosinglets in, (T), 25:14629
- interactions $\gamma + p \to \pi^- + \Delta^{++}$ in strong-cut Reggeized model, 25:14603
- interactions $\gamma + p \to \pi^+ + n$ at 4.3 to 9.8 GeV at large angles, Regge pole theory for differential cross sections of, (T), 25:14598
- interactions $\gamma + p \to \pi^+ + n$ in strong-cut Reggeized model, 25:14603
- interactions $\gamma + p \to \pi^+ + N(1520)$, low-t theorems for forward π^+ production in, (T), 25:14609
- interactions $\gamma + p \to \text{rho}^0 + p$ at 2.8 and 4.7 GeV, S-channel helicity conservation in polarized, 25:14605
- interactions $\gamma + p$ at 5.0 to 17.8 GeV, B(1240) production in, (E), 25:14524
- interactions $\gamma + p$ at high energies, quark model for constant of, (T), 25:14595 (ITF-70-63-P)
- interactions $\gamma + p$ in SU(6)-quark model, relations between differential cross sections for scalar and vector meson production in, 25:14626
- interactions $\gamma + p$, fixed pole in virtual Compton amplitude for, 25:14608
- interactions $K^- + p \to$ anti $K^0 + n$ at 0.45 to 1.8 GeV/c, Veneziano dips in angular distributions of, 25:14724
- interactions $K^- + p \to$ anti $K^0 + n$, $K^0 \to \pi + l + \nu$, test of $\Delta S = \Delta Q$ rule from time distribution in, (E), 25:14533
- interactions $K^+ + p \to$ anti $\Lambda + p + p$ at 7.3 GeV/c in hydrogen bubble chamber, (E), 25:14574
- interactions $K^+ + p \to \Delta^{++}(1236) + K^+ + \pi^-$ at 12.7 GeV/c, momentum-transfer distributions in, (E), 25:14575
- interactions $K^- + p \to K^{*0}(890) + n$, coherent droplet model with long-range pion exchange for forward peak structure in, (T), 25:14722
- interactions $K^- + p \to K^{*-}(890) + p$, coherent droplet model with long-range pion exchange for forward peak structure in, (T), 25:14722
- interactions $K^+ + p \to K^{*+}(890) + p$, two-parameter model for, (T), 25:14574
- interactions $K^- + p \to K^{*-}(890) + p$, two-parameter model for, (T), 25:14574
- interactions $K^- + p \to K^- + p + \pi^+ + \pi^- + \pi^0$ at 5.5 GeV/c in hydrogen bubble chamber, total cross sections, resonance production, and quasi-two, -three, and -four body states in, (E), 25:14572
- interactions $K^+ + p \to K^+ + p$ at 1.0 to 2.45 GeV/c, cross sections for backward, (E), 25:14582
- interactions $K^+ + p \to K^+ + p$ at 7.3 GeV/c in hydrogen bubble chamber, cross sections for, (E), 25:14574
- interactions $K^- + p \to K^- + p$ below 1.4 GeV/c, Veneziano dips in angular distributions of, 25:14724
- interactions $K^+ + p \to K^+ + \pi^- + \Delta^{++}(1236)$ at 9 GeV/c, double-peripheral model analysis of, (E/T), 25:14714
- interactions $K^+ + p \to K^+ + \pi^+ + n$ at 7.3 GeV/c in hydrogen bubble chamber, cross sections and $\Delta(1236)$, $K^*(890)$, and $K^*(1420)$ production in, (E), 25:14574
- interactions $K^- + p \to K^+ + \Xi^-$ interactions at high energies, two-Reggeon exchange contributions to, (T), 25:14657 (UCRL-20032)
- interactions $K^+ + p \to \Lambda + K^+ + K^+$ at 7.3 GeV/c in hydrogen bubble chamber, (E), 25:14574
- interactions $K^+ + p \to p + K^+(K^0) + \pi^0(\pi^+)$ at 7.3 GeV/c in hydrogen bubble chamber, cross sections and $\Delta(1236)$, $K^*(890)$, and $K^*(1420)$ production in, (E), 25:14574
- interactions $K^- + p \to \pi^- + \pi^+ + \Lambda$ in generalized Veneziano model, 25:14716
- interactions $K^- + p \to \Sigma^0 + \pi^0$, search for $\Lambda(1670)$ in, (E), 25:14568

interactions $K^- + p \to X^0 + \Lambda$ determination of spin and parity of $X^0(960)$ from, 25:14720
interactions $K^+ + p$ at 5.2 and 7.0 GeV/c, differential cross sections for forward and backward elastic, (E), 25:14579
interactions $\mu^- + p \to p + W^- + \nu$, model for W^+ production in, 25:14643
interactions $n + p \to 2p + \pi^-$ at 2 to 10 GeV/c, peripheral nature, zero-isospin exchange, total cross sections, and production cross sections for $\Delta(1236)$, N(1470), and N(1688) production in, (E), 25:14551
interactions $n + p \to d + \pi^0$ from threshold through first resonance peak, spark chamber study of charge independence from differential and total cross sections for, (E), 25:14549
interactions n + p below 350 MeV, phase shift analysis of, (T), 25:14734
interactions n + p, eikonal model for large-angle elastic, 25:14737
interactions $\nu + p \to \mu^- + p + W^+$, model for W^+ production in, 25:14643
interactions $\nu + p \to p + \pi^+ + \mu^-$, hadronic s-channel helicity conservation in, (T), 25:14636 (NYO-4204-10)
interactions of primary cosmic, with microwave background, (T), 25:13945
interactions $p + d \to p + d$, Glauber correction in, (T), 25:14730 (JINR-P2-5444)
interactions $p + n \to p + n + \pi^+ + \pi^-$, I = 1 meson exchange diagram for rho^0 production in, 25:14741
interactions $p + p \to d + \text{rho}^+ (\pi^+)$ at 4.0 to 12.3 GeV/c, spectrometer study of differential cross sections, $d\pi$ and drho enhancements, and search for delta^+ in, (E), 25:14542
interactions $p + p \to n + \Delta^{++}$, coherent droplet model with long-range pion exchange for forward peak structure in, (T), 25:14722
interactions $p + p \to p + N(1470)$ at 6.6 GeV/c in bubble chamber, production of narrow N(1470) in, (E), 25:14552
interactions $p + p \to p + p + \gamma$ at 20 MeV, cross sections and γ angular distributions and energy spectra for, (E), 25:14545
interactions $p + p \to p + p + \gamma$ at 42 MeV, wire-chamber spectrometer study of differential cross sections for, (E), 25:14556
interactions $p + p \to p + p + \gamma$, N + N interactions below 350 MeV for, (T), 25:14734
interactions $p + p \to Y + K + N$, π and K exchange contributions to, (T), 25:14597
interactions p + p at 0.5 to 39 GeV/c, model-independent determination of real parts of spin independence of forward amplitudes of, (T), 25:14731 (JINR-P2-5448)
interactions p + p at 600 to 1800 MeV/c, differential cross sections for elastic, (E), 25:14543
interactions p + p at high energies, form factors in model for amplitude of inelastic, (T), 25:14729 (INR-P-1229)
interactions p + p below 350 MeV, phase shift analysis of, (T), 25:14734
interactions p + p below 500 MeV, form-free semiphenomenological error-bounded potential representation of, (T), 25:14746
interactions p + p below 800 GeV/c, atlas of particle-production momentum spectra for, (T), 25:14733 (NP-18660)
interactions p + p, eikonal model for large-angle elastic, 25:14737
interactions p + p, single-particle distributions for π^+ production in, 25:14742
interactions $\pi^- + p \to 2\pi + N$ at 2.3 GeV/c in hydrogen bubble chamber, rho^-, rho^0, and $\Delta(1236)$ production in, (E), 25:14570
interactions $\pi^- + p \to 2\pi^- + 2\pi^+ + n$ at 2.3 GeV/c in hydrogen bubble chamber, cross sections and $\Delta^-(1236)$ production in, (E), 25:14571
interactions $\pi^- + p \to 2\pi^- + p + \pi^+ + \pi^0$ at 2.3 GeV/c in hydrogen bubble chamber, cross sections and $\omega^0(785)$, $N^{*++}(1236)$, and B(1220) production in, (E), 25:14571
interactions $\pi^- + p \to 2\pi^- + p + \pi^+$ at 2.3 GeV/c in hydrogen bubble chamber, cross sections $\Delta^{++}(1236)$ and $\text{rho}^0(765)$ production and $\pi^- + \pi^-$ interaction cross sections for, (E), 25:14571
interactions $\pi^+ + p \to \Delta^{++} + \text{rho}^0(\omega^0)$ at 1.95 GeV/c, total and differential cross sections for, (E), 25:14563
interactions $\pi^+ + p \to \Delta^{++}(1236) + \pi^+ + \pi^-$ at 7 GeV/c, momentum-transfer distributions in, (E), 25:14575
interactions $\pi^- + p \to \text{eta} + n$, Regge dipole model of A_2 for differential cross sections and duality in, (T), 25:14704
interactions $\pi^- + p \to \gamma + n$ at 1245 and 1337 MeV, spark chamber and neutron counter study of angular distributions and differential cross sections for, (T), 25:14567
interactions $\pi^- + p \to \gamma + n$ at 1245 to 1363 MeV, test of ΔI less than or equal to 1 rule and time reversal invariance in angular distributions and differential cross sections for, (E), 25:14566
interactions $\pi^- + p \to K^0 + \Lambda$ at 0.90 to 1.95 GeV/c, phase shift analysis of, 25:14727
interactions $\pi^+ + p \to K^+ + \Lambda + \pi^+$ at 8 GeV/c in bubble chamber, $\Sigma^+(1385)$ decay distributions and Λ polarization in, (E), 25:14559 (INP-731)
interactions $\pi^+ + p \to n + 5\pi^+ + 3\pi^-$ at 8 GeV/c in hydrogen bubble chamber, π production mechanism for, (E), 25:14558 (INP-708)
interactions $\pi^- + p \to N + m\pi$ at 1 to 16 GeV, statistical isospin model for final-charge-state cross section ratios for, (T), 25:14700 (JINR-P1-5471)
interactions $\pi^- + p \to n + \pi^+ + \pi^-$ at 8 GeV/c, double-Regge-model analysis of, (T), 25:14713
interactions $\pi^+ + p \to p + 4\pi^+ + 3\pi^- + \pi^0$ at 8 GeV/c in hydrogen bubble chamber, π production mechanism for, (E), 25:14558 (INP-708)
interactions $\pi^+ + p \to p + 4\pi^+ + 3\pi^-$ at 8 GeV/c in hydrogen bubble chamber, π production mechanism for, (E), 25:14558 (INP-708)
interactions $\pi^- + p \to p + \pi^- + \pi^0$ at GeV/c, double-Regge-model analysis of, (T), 25:14713
interactions $\pi^- + p \to \pi^- + p$ at high energies, Pomeron hypothesis for form of real-to-imaginary parts for amplitude of, (T), 25:14656 (SU-1206-237)
interactions $\pi^+ + p \to \pi^+ + \pi^0 + p$ at 5 GeV/c, longitudinal phase-space analysis of, (E/T), 25:14578
interactions $\pi^+ + p \to \pi^+ + \pi^+ + n$ at 5 GeV/c, longitudinal phase-space analysis of, (E/T), 25:14578
interactions $\pi^+ + p \to \pi^- + X^{+++}$ at 3.88 GeV/c, search for $T = {}^5/_2$ isobar from π^- spectrum in, (E), 25:14576
interactions $\pi^- + p \to \text{rho}^0 + n$ in Veneziano model, test of rho universality from frame dependence of vector dominance in, 25:14710
interactions $\pi^- + p \to \text{rho}^0 + n$, coherent droplet model with long-range pion exchange for forward peak structure in, (T), 25:14722
interactions $\pi^- + p \to \text{rho}^0 + n$, fixed j-plane singularities in photoproduction from, (T), 25:14625
interactions $\pi^+ + p \to \text{rho}^0(f^0) + \Delta^{++}$, coherent droplet model with long-range pion exchange for forward peak structure in, (T), 25:14722
interactions $\pi^+ + p \to \text{rho}^+ + p$, coherent droplet model with long-range pion exchange for forward peak structure in, (T), 25:14722
interactions $\pi^- + p \to \text{rho}^- + p$, fixed j-plane singularities in photoproduction from, (T), 25:14625
interactions $\pi^+ + p \to \text{rho}^+ + p$, two-parameter model for, (T), 25:14574
interactions $\pi^- + p \to \text{rho}^- + p$, two-parameter model for, (T), 25:14574
interactions $\pi^+ + p$ at 1.6 to 2.31 GeV/c, polarization parameter in backward elastic, (E), 25:14577
interactions $\pi^- + p$ at 17.2 GeV/c in emulsions, proton momentum spectrum from, (E), 25:14564
interactions $\pi^+ + p$ at 2.38 to 5.0 GeV/c, test of duality from resonance and Regge models for, 25:14726
interactions $\pi^- + p$ at 2.5 to 25 GeV, limiting distribution, scaling behavior, and average multiplicities for π^- and π^+ production in, (T), 25:14719
interactions $\pi^- + p$ at 4.0 to 6.0 GeV, Cherenkov hodoscope study of total cross sections of, (E), 25:14561 (JINR-P1-5460)
interactions $\pi^+ + p$ at 5 GeV/c, longitudinal phase-space analysis of, 25:14578
interactions $\pi^+ + p$ at 5.2 and 7.0 GeV/c, differential cross sections for backward elastic, (E), 25:14579
interactions $\pi^- + p$ at 7.0 GeV/c, differential cross sections for backward elastic, (E), 25:14579
interactions $\pi^+ + p$ at high energies, form factors in model for amplitude of inelastic, (T), 25:14729 (INR-P-1229)
mass difference (n − p) and transition matrix elements for, electromagnetic, 25:14617
polarization of recoil, in $\gamma + p \to \pi^0 + p$ interactions at 1200 to 1800 MeV, spark chamber study of, (E), 25:14516
production in $p + p \to p + p + \gamma$ interactions at 42 MeV/c, wire-chamber spectrometer study of differential cross sections for, (E), 25:14556
production in $\pi^- + n$ and $\pi^- + p$ interactions at 17.2 GeV/c in emulsions, momentum spectrum from, (E), 25:14564
propagation of solar-flare, effect of interplanetary disturbance on, (T), 25:13869
reactions (p,2p) with nuclei, cross section expression for, (T), 25:15156
reactions (p,α) with palladium-108 at 15 MeV, angular distributions for, (E), 25:15022
reactions (p,d) and (p,t) with titanium-46, -48, and -50 at 25 to 45 MeV, angular distributions for, (E), 25:14949
reactions (p,d) with calcium-48 at 22.9 MeV, asymmetries from, (E/T), 25:14922 (CEA-CONF-1655)
reactions (p,d) with iron-57 at 17.3 MeV, DWBA analysis of differential cross sections and asymmetries from, (E/T), 25:14921 (CEA-CONF-1653)
reactions (p,d) with molybdenum-92 at 24.5 MeV, DWBA analysis of differential cross sections and asymmetries from, (E/T), 25:14980 (CEA-CONF-1654)
reactions (p,d) with nickel-61 at 16.6 MeV, DWBA analysis of differential cross sections and asymmetries from, (E/T), 25:14921 (CEA-CONF-1653)
reactions (p,d) with titanium-49 at 20.9 MeV, DWBA analysis of differential cross sections and asymmetries from, (E/T), 25:14922 (CEA-CONF-1655)

XUM

reactions (p,d) with zirconium-90 at 22.9 MeV, DWBA analysis of differential cross sections and asymmetries from, (E/T), 25:14980 (CEA-CONF-1654)
reactions (p,f) with bismuth-209, 25:15010
reactions (p,f) with bismuth-209 and uranium-238 at 155 MeV, prompt neutron spectra and yields from, (E), 25:15021
reactions (p,γ) with aluminum-27 at 0.3 to 2.6 MeV, γ-ray yield from, (E), 25:14951
reactions (p,γ) with aluminum-27 at 742 and 1381 keV, Q-value for, (E), 25:14936
reactions (p,γ) with aluminum-27 near 1.5 and 1.7 MeV, angular distributions for, (E), 25:14948
reactions (p,γ) with deuterium at 57 to 1100 keV, gamma yield and total cross section for, (E), 25:14885
reactions (p,γ) with silicon-29, resonance γ spectra from, (E), 25:14933
reactions (p,n) with nuclei, description of analog resonances near compound-nucleus overlapping levels in, (T), 25:15179
reactions $(p,n\gamma)$ with nickel-62 at 4.7 to 5.9 MeV, gamma spectra from, (E), 25:14940
reactions $(p,p\alpha)$ with lithium-6 and -7 near 60 MeV, analysis for reaction mechanism in, (E), 25:14902
reactions (p,pn) with carbon-13, p-n correlations in, (E), 25:14907
reactions (p,t) with argon-36, calcium-40, magnesium-24, neon-20, silicon-28, and sulfur-32, angular distributions for, (E), 25:14950
reactions (p,t) with cerium-140 and -142 at 52.1 MeV, triton spectra and angular distributions from, (E), 25:15006
reactions (p,t) with ytterbium-176, analysis using coupled-channel Born approximation, (T), 25:15191
reactions (p,xn) with tantalum-181 at 18 MeV, Fermi-gas-model calculations of high-energy-neutron cross sections from, (T), 25:15140 (CU-1019-79)
reactions (p,xn) with uranium-238 at 200 MeV, Fermi-gas-model calculations of neutron spectra and proton and neutron occupation numbers from, (T), 25:15140 (CU-1019-79)
reactions with aluminum and tungsten at 70 GeV, upper limits for cross sections for production of new-type radioactivity from, (E), 25:14541 (JINR-P1-5399)
reactions with aluminum at 70 GeV, cross sections for antihelium-3 production, mass, and charge in, (E), 25:14540 (IFVE-SEF-70-16)
reactions with aluminum-27 at 660 MeV, angular distributions of carbon-11, fluorine-18, and nitrogen-13 from, (E), 25:14945
reactions with americium, neptunium, plutonium, and uranium at 9 to 14.2 MeV, (E), 25:15046
reactions with argon, cross sections for L-shell x-ray emission in, (E), 25:14004
reactions with helium and nitrogen molecules at 75 to 400 keV, cross sections for formation and destruction of excited hydrogen atoms by charge exchange in, (E), 25:14043
reactions with metallic thick targets at 90 to 360 keV, yields of characteristic x rays from, (E), 25:13962
reactions with nuclei at 1000 GeV in emulsions, K/π ratio of secondaries in shower production from, (E), 25:14509 (INP-718)
reactions with nuclei at high energies, review of, (T), 25:15148(T) (ORNL-tr-2399)
reactions with nuclei below 70 GeV/c, atlas of particle-production-momentum spectra for, (T), 25:14733 (NP-18660)
reactions with oxygen molecules at 20 to 110 keV, energy-loss spectra and cross sections for inelastic processes in, (E), 25:14023
reactions with oxygen molecules at 3 to 50 keV, cross sections for O^- production in, (E), 25:13999
scattering by aluminum-27 at 18.0 MeV and 43° of polarized, depolarization parameter from elastic, (E), 25:14889 (CEA-CONF-1650)
scattering by analog and compound energy levels of nuclei, amplitudes for resonant elastic, (T), 25:15146 (NYO-1082-29)
scattering by beryllium-9 at 21.4 MeV and 58° of polarized, depolarization parameter from elastic, (E), 25:14889 (CEA-CONF-1650)
scattering by boron-10 at 19.8 MeV and 60° of polarized, depolarization parameter from elastic, (E), 25:14889 (CEA-CONF-1650)
scattering by boron-11 and lead-208 at 155 MeV, DWBA analysis of polarization angular distributions from inelastic, (T), 25:14892 (RLO-1388-600)
scattering by boron-11 at 30.3 MeV, DWBA analysis of asymmetry angular distributions from inelastic, (T), 25:14892 (RLO-1388-600)
scattering by calcium-40 at 24.5 MeV of polarized, DWBA analysis of angular distributions and asymmetries from inelastic, (E/T), 25:14923 (CEA-CONF-1656)
scattering by chromium-52, titanium-50, and vanadium-51 at 40 MeV, microscopic description of inelastic, (E), 25:14928
scattering by deformed carbon-12 at 1 GeV, differential cross sections for elastic, 25:14918
scattering by helium-3 and -4 at 100 MeV, angular distributions for elastic, (E), 25:14882
scattering by helium-4 at 8 to 38 MeV, resonating-group calculations of phase shifts, differential cross sections, polarizations, and spin-rotation parameters for elastic, (T), 25:14880 (COO-1764-105)
scattering by hydrogen atoms at low energies, large-angle, (T), 25:14029
scattering by lutetium-175 at 3 MeV, Moessbauer effect following Coulomb excitation by inelastic, (E), 25:15040
scattering by nitrogen-14 at 24 MeV, DWBA analysis of differential cross sections and asymmetries for elastic and inelastic, (E/T), 25:14890 (CEA-CONF-1651)
scattering by nuclei, description of analog resonances near compound-nucleus overlapping levels in inelastic, (T), 25:15179
scattering by nuclei, isospin dependence of the optical potential in elastic, (T), 25:15154
scattering by polarized helium-3 at 19.4 MeV, polarization and spin-correlation parameters of elastic, (E/T), 25:14888
scattering by samarium-148 at 49.5 MeV, optical-model analysis of elastic, (T), 25:15013
scattering by scandium-45 at 8 MeV, gamma spectra from inelastic, (E), 25:14941
scattering by silicon-28 at 18.0 MeV of polarized, depolarization parameter from elastic, (E), 25:14889 (CEA-CONF-1650)
scattering by titanium-50 near 2.5 MeV with isobaric analog excitation, proton spectra from elastic, (E), 25:14982 (NCSAC-31)
spectra of solar, upper cutoff in, (E/T), 25:13910

PROTONS (anti p)
interactions anti $p + d \to 2\pi^- + 2p +$ anti n at 7.0 GeV/c, Δ^0 and Δ^{--} production in, (E), 25:14554
interactions anti $p + d \to$ anti $p + 2p + \pi^0$ at 7.0 GeV/c, $\Delta(1236)$ production in, (E), 25:14554
interactions anti $p + d \to \pi^- +$ anti $p + 2p$ at 7.0 GeV/c, $\Delta(1236)$ and $\Delta(1920)$ production in, (E), 25:14554
interactions anti $p + d \to \pi^- +$ anti $p + \pi^+ + d$ at 7.0 GeV/c, $\Delta^{--}(1236)$ and $d^*(2170)$ enhancement in, (E), 25:14554
interactions anti $p + d \to \pi^- +$ anti $p + \pi^+ + p + n$ at 7.0 GeV/c, anti $\Delta^{--}\pi^+(1470)$, anti $\Delta^{--}\pi^+(1750)$, and $pn\pi^+(2250)$ enhancements in, (E), 25:14554
interactions anti $p + d$ at 1.25 to 1.67 GeV/c, cross sections for Λ production in, (E), 25:14550
interactions anti $p + d$, at 50 to 920 MeV/c in deuterium bubble chamber, total and topological cross sections for, (E), 25:14555
interactions anti $p + n \to 3\pi^- + 2\pi^+ + \pi^0$ at rest in deuterium bubble chamber, production of ω^0 and branching ratio for, (E), 25:14553
interactions anti $p + n \to 3\pi^- + 2\pi^+$ at rest in deuterium bubble chamber, production of rho^0 and branching ratio for, (E), 25:14553
interactions anti $p + n \to K +$ anti $K + \pi$ at rest, four-point Veneziano functions for mass spectra and angular distributions for, (T), 25:14691
interactions anti $p + n \to \pi^+ + 2\pi^-$ at 1.0 to 1.6 GeV/c in deuterium bubble chamber, cross sections and Veneziano model for mass and angular distributions in, (E/T), 25:14548
interactions anti $p + n$ at 1.25 to 1.67 GeV/c in deuterium bubble chamber, cross sections for hadron production in, (E), 25:14550
interactions anti $p + p \to K +$ anti $K + \pi$ at rest, four-point Veneziano functions for mass spectra and angular distributions for, (T), 25:14691
interactions anti $p + p$ at 1.25 to 1.67 GeV/c in deuterium bubble chamber, cross sections for hadron production in, (E), 25:14550
research in Soviet Union, 25:14544

PROTOZOA
Colpoda sp., radioinduced injuries to, effects of caffeine, temperature, and uv on dark repair systems following, 25:13342
Paramecium aurelia, radiation effects on growth of, shielding effects of underground laboratory on natural ionizing, 25:13556

PRUSSIAN BLUE
cobalt-57 electron capture decay in doped, reactions of iron-57 from, 25:13068
radiation effects on iron-58-labeled, reactions of recoil iron-59 from neutron, 25:13068

PUBLIC HEALTH
hazards from sewer disposal of radioactive wastes from hospitals in municipal sewers on, 25:13454

PULSARS
CP 0834, polarization at 150 MHz, (E), 25:13855
CP 0950, polarization at 150 MHz, (E), 25:13855
CP 1133, polarization at 150 MHz, (E), 25:13855
CP1919, detection of extended radio source in the direction of, (E), 25:13834
evolution of, spinars in, (T), 25:13952
gravitational radiation from, (T), 25:13846
model for, featuring rotating neutron stars, (T), 25:13832 (AD-711397)
models for, (T), 25:13846
motions in, crustal, (T), 25:13846
nature of, review on, (T), 25:13844
NP 0532, disappearance of precursor pulse at 606 MHz, (E), 25:13848

- NP 0532, magnetic-field structure around (E), 25:13850
- NP 0532, radiation emission from, (T), 25:13832 (AD-711397)
- number-period distribution of, prediction using oblique-rotator model, (T), 25:13836
- PSR 0628, polarization at 150 MHz, (E), 25:13855
- pulse broadening due to angular scattering in interstellar medium, (E/T), 25:13853
- radiation mechanisms for, (T), 25:13842
- radio brightness temperatures for, (T), 25:13842
- scintillations of, due to small-scale irregularities in interstellar space, (T), 25:13912

PULSE ANALYZERS
- development at ORNL, Sept. 1969--Aug. 1970, 25:13318(R) (ORNL-4620)

PULSE COLUMNS
- operation of sieve-plate, controlled cycling, 25:13082(R) (RLO-2225-T-11-1)

PULSE DISCRIMINATORS
- design and performance for large dynamic scale with precise time definition, 25:13320 (RI-70/13)

PULSE GENERATORS (ELECTRONICS)
- design for electron linac, for high-intensity nanosecond beam pulsing, 25:14858

3,5-PYRAZOLIDINEDIONE, 4-BUTYL-1-(p-HYDROXYPHENYL)-2-PHENYL-
- radioprotective effects of, on human skin following therapy for carcinomas, 25:13476

PYRENE
- electron energy loss spectra at 115 eV in polycrystalline, 25:13968

PYRIMIDINES
- radiation effects on residues of, effects of, on aminoacyl synthetase recognition in Escherichia coli, uv, 25:13364

Q

Q DEVICES
- plasma drift instability in, periodic pulling of, (E), 25:14337
- plasma wave structure in, thermal effects on if, (T), 25:14385

QUAD CITIES POWER REACTOR, UNIT 1
- design parameters of, revised and additional data on, 25:15291 (DOCKET-50254-27)
- effluents from, effects on environment of chemical, radioactive, and thermal, 25:15290 (DOCKET-50254-26)
- operations aspects of, revised and additional data on, 25:15291 (DOCKET-50254-27)

QUAD CITIES POWER REACTOR, UNIT 2
- design parameters of, revised and additional data on, 25:15291 (DOCKET-50254-27)
- effluents from, effects on environment of chemical, radioactive, and thermal, 25:15290 (DOCKET-50254-26)
- operations aspects of, revised and additional data on, 25:15291 (DOCKET-50254-27)

QUANTUM ELECTRODYNAMICS
- angular momentum plane in, asymptotics of $\gamma + \gamma$, $\gamma + e$, and $e + e$ interactions at high energies from leading singularity in complex, 25:14802
- current commutators in, operator structure of singular terms in equal-time, 25:14795
- formulation based on finite local field equations in, 25:14777
- singularities in spinor and scalar massive, promotion and threshold, 25:14792
- wave functions in Coulomb-gauge, equivalence with Landau gauge for external-line, 25:14780
- wave propagation in intense electromagnetic field in nonlinear, polarization phenomena in, 25:14793

QUANTUM FIELD THEORY
- Bethe-Salpeter equation in field theories of arbitrary divergence, ladder-approximation solution to, (T), 25:14803
- Bethe-Salpeter equation, method of extending Blankenbecler--Sugar--Logunov--Tavkhelidze approximation to, 25:14786
- complex angular momenta in, conference on, 25:14583(T) (AEC-tr-6882/1)
- coupling-constant analyticity in charged-scalar static model in, 25:14791
- dilaton field in conformally Minkowski space-time, 25:14789
- fermion bare and physical mass in, relation between, 25:14800
- Feynman diagrams in, Reggeized absorption model from, 25:14785
- field associated with SO(3) group in, nonstationary Yang--Mills, 25:14779
- field functionals in, symmetry conditions on nonlinear spinor, 25:14782
- field quantization and particle creation in expanding universes, spin-$^1/_2$, 25:14788
- fields in, higher-spin, 25:14798
- fields of mesons in, transversality condition for relation to SU(2) x SU(2) chiral symmetries for vector and axial-vector, 25:14804
- formalism for derivation of Fermi rule of time-dependent perturbation theory, 25:14775
- formalism for localizable and nonlocalizable, 25:14806
- formalism for massive Yang-Mills gauge field in, group geometry for effective Lagrangians in, 25:14805
- formulations of four-fermion interactions in, finite, 25:14797
- interactions of Dirac fermions with pseudoscalar bosons at infinite momentum in spinor, 25:14679
- Lagrangian formalism in broken SU(3), electromagnetic ω--rho mixing in local gauge-invariant, 25:14628
- Lagrangian model, field algebra and vector-meson dominance in, 25:14784
- Lagrangian quantization for charges in external field in, 25:14776
- Lagrangians generated by massive Yang-Mills gauge field in, group geometry for, 25:14805
- mass renormalization in model in, Wightman functions in, 25:14794
- microcausality in, Cherenkov counter in-flight study of meson (π^-) ad (π^+) lifetimes for, (E), 25:14581
- model in, complex angular momentum analysis of Regge pole structure of Bethe--Salpeter amplitude for scalar particle scattering in, 25:14833
- model of, zero charge and scale invariance in soluble, 25:14783
- model with mass renormalization in, Wightman functions for, 25:14794
- N-point functions in, vacuum invariance under exact scale transformations for, 25:14781
- quantization of interacting covariant massless fields in, with prescribed asymptotic null data, 25:14796
- quantization schemes for non-Abelian gauge field, equivalence of Lorentz covariant and canonical, 25:14787
- Regge trajectories for infinite-component local, with rising mass spectrum, 25:14799
- scale invariance in, incompatibility with Lorentz covariance, 25:14790
- scale transformations for N-point functions of, vacuum invariance under exact, 25:14781
- Wightman functions in model with mass renormalization in, 25:14794

QUANTUM MECHANICS
- causality and Lorentz invariance in relativistic, 25:14508
- differential probability of quantum processes for electrons moving in constant electric fields, 25:14498
- partition function for system of independent particles, 25:14494
- perturbation of bound states in, formulation based on hydrodynamic analogy, 25:14054
- Schroedinger equation for two-state system in, integration with respect to time of, 25:14495
- Schroedinger equation in, solution of coupled differential equations from, 25:14497
- Schroedinger equation solution by Laplace transform method, time-dependent, 25:14496
- Schroedinger equation with short-range central potential, SO(2,1) algebraic solution of, 25:14491
- superselection rules in, relation with internal symmetries for, 25:14774 (KFKI-70-22-HEP)
- theorem for double perturbations in, 25:13981
- transformation theory in, superoperator, 25:14505
- uncertainty principle in, thought experiment violation of, 25:14502

QUASARS
- evolution of, spinars in, (T), 25:13952
- radiation from, ionization of intergalactic matter by uv, (T), 25:13939
- spectra of, radio, (T), 25:13843
- synchrotron emission from, (T), 25:13936(R) (AD-711829)

R

RABBITS
- radiation effects on biochemical and bioelectrical activities of central nervous system of, ionizing, 25:13561
- radiation effects on content of NAD and NADP in organs of, effects of ATP and nicotinamide on, 25:13379
- radiation effects on head of, intracerebral temperature changes following x, 25:13575
- radiation effects on metabolism of dimecarbine by, γ, 25:13576
- radioinduced degradation of deoxyribonucleoproteins of, in vitro effects of nuclease on, 25:13363

RADIATION
- dose to human gonads and skin during radiological examinations of intestine and stomach, 25:13580
- dosimetry for tumor therapy, 25:13451
- effectiveness for therapy of Hodgkin's disease in man in combination with stomach resection, evaluation of, 25:13541
- effectiveness for therapy of lymphogranulomas in man, relation of recurrence latency to effects of dose and dose fractionation on, in relation to relapse time, 25:13543
- effectiveness of supervoltage, for therapy of human testicular tumors, 25:13544
- effects on biochemical and bioelectrical activities of central nervous system of rabbits, ionizing, 25:13561
- effects on brachial plexus in man following therapy for

XUM

  mammary carcinomas, protective effects of actihemyl against paralyzing, 25:13480
  effects on cell survival, effects of dose fractionation on, 25:13451
  effects on chemicals in relation to human metabolism and radiotherapy, 25:13374
  effects on DNA content in proembryo stages of barley, lethal, 25:13405
  effects on DNA synthesis in yeast cells, tracer study of, 25:13604
  effects on electric parameters of skin, histomorphological studies on, 25:13565
  effects on enzymes in organs of rabbits and rats, effects of injection of ATP and nicotinamide on, 25:13379
  effects on heating of reactor core components, (T), 25:15341 (SZS-20/70)
  effects on histamine content of blood, lungs, skin, and small intestine in rats, combined effects of skin wounds on whole-body, 25:13368
  effects on human intestine following therapy for uterine carcinoma, 25:13508
  effects on human skin following therapy for carcinomas, protective effects of tanderil against, 25:13476
  effects on mice, protective effects of dose fractionation and methylprednisolone against, 25:13474
  effects on mucosa in man following therapy, protective effects of solcoseryl against, 25:13475
  effects on oxidation of 2,2,4-trimethylpentane, effects of temperature on composition of products from, 25:13040
  effects on personnel, value of pre-employment medical examination for prediction of ionizing, 25:13465
  effects on potassium and sodium content of brain and muscular tissues of rats, lethal and sublethal, 25:13566
  effects on preparation of perfluorinated carboxylic acids from polytetrafluoroethylene wastes, 25:13035(P)
  effects on protein synthesis in liver and spleen cells of rats, alone and in combination with immunization, 25:13376
  effects on removal of ferrous iron compounds from acidic mine waste waters, 25:13036(P)
  effects on selenium-75 incorporation in diaphragms, livers, and tumors in rats following incubation in sodium selenites, 25:13354
  effects on shelf life of foods, review of, 25:13623
  effects on spleen weight in mice as function of close, use of function for testing protective effects of AET and combined AET, DNA, glutathione, and serotonin, 25:13478
  effects on survival of man following therapy for thyroid carcinomas, 25:13524
  effects on survival of man following therapy of bronchial carcinomas, combined effects of chemotherapy on megavoltage or orthovoltage, 25:13522
  effects on sympatho-adrenal system of personnel, effects of insulin on, 25:13586
  effects on synthesis of bile acids in rat livers, inhibitory, 25:13370
  effects on type E toxin production in inoculated, packaged, fresh cod fish, effects of incubation temperature, inoculum, and dose on ionizing, 25:13617(R) (COO-1183-32)
  effects on uptake of iodine-131 by perfused intestine and liver in rats, effects of food intake on, 25:13349
  hazards to personnel at military nuclear establishment in Pisa, Italy, statistical analysis of medical judgments regarding, 25:13468
  interactions of unpolarized, density operator for, 25:14504
  scattering according to Rayleigh's law, Milne problem for polarized, (T), 25:14408
  scattering by electrons, 25:14601
  use for therapy of advanced head and neck neoplasms in man, combined effects of sequential high or low dose methotrexate treatment on effectiveness of, 25:13528
  use of conformation, for therapy of uterine cervix cancer in comparison to stationary techniques, methods for, 25:13530
RADIATION CHEMISTRY
  research at BNL, July 1969--June 1970, 25:14837(R) (BNL-50230)
RADIATION DETECTORS
  book: Applied Gamma Ray Spectroscopy, 25:13231
  development at ORNL, Sept. 1969--Aug. 1970, 25:13318(R) (ORNL-4620)
  operation of shower, for energy measurement of high-energy electrons and photons, 25:13300
  performance of class-1 and -2 gravitational wave detectors, 25:14547
  performance of dorsal and ventral, during xenon-133 respirometry, 25:13520
  performance of mobile, for xenon-133 radiospirometry, 25:13514
RADIATION DETECTORS, ACTIVATION
  data unfolding methods for neutron spectra measurements in fast reactors, comparison of, 25:13226
  performance for neutron spectra measurements, 25:13210 (JINR-P3-5421)
  performance of manganese sulfate bath, for fast neutron flux measurements, 25:13216
RADIATION DETECTORS, BUBBLE CHAMBER
  cryogenic systems for NAL 15-foot hydrogen, safety analysis of, 25:13298 (NAL-48-2624)
  design modifications for studies of radioinduced bubble nucleation in superheated water, 25:13152(R) (SU-326-P-13-5)
  failure of NAL 15-foot hydrogen, safety analysis of rupture, 25:13298 (NAL-48-2624)
  fiducial system for large, using laser beams, 25:13303
  particle tracks in European 3.7-meter, performance of PEPR system for film analysis of, 25:13240 (CERN-70-21(Vol.1), pp 89-104)
  particle tracks in Gargamelle, computer-based scanning and measuring system for analysis of, 25:13271 (CERN-70-21(Vol.2), pp 651-64)
  particle tracks in large, ADAM + EVA scanning and measuring machine for analysis of, 25:13270 (CERN-70-21(Vol.2), pp 633-49)
  particle tracks in large, geometrical reconstruction program for, 25:13260 (CERN-70-21(Vol.1), pp 467-96)
  particle tracks in Mirabelle, automatic gain control for HPD system for analysis of, 25:13291 (CERN-70-21(Vol.2), pp 941-8)
  particle tracks in, Amsterdam HPD--CDC 3200 system of analysis of, 25:13275 (CERN-70-21(Vol.2), pp 709-20)
  particle tracks in, automatic gain control in signal processing for picture analysis of, 25:13257 (CERN-70-21(Vol.1), pp 383-97)
  particle tracks in, BRUSH system for automatic processing of, 25:13274 (CERN-70-21(Vol.2), pp 689-707)
  particle tracks in, calibration and performance of CERN spiral reader for analysis of, 25:13235 (CERN-70-21(Vol.1), pp 5-18)
  particle tracks in, Coccinelle CRT digitizer for analysis of, 25:13256 (CERN-70-21(Vol.1), pp 371-81)
  particle tracks in, computer program for acquisition of film information by PEPR system for analysis of, 25:13242 (CERN-70-21(Vol.1), pp 113-24)
  particle tracks in, computer program for automatic recognition and reconstruction of events for analysis of, 25:13243 (CERN-70-21(Vol.1), pp 125-39)
  particle tracks in, computer program for automatic recognition and reconstruction of events for analysis of, 25:13244 (CERN-70-21(Vol.1), pp 141-75)
  particle tracks in, computer program for calibration of PEPR system for analysis of, 25:13245 (CERN-70-21(Vol.1), pp 177-86)
  particle tracks in, computer-based HPD system for analysis of, 25:13276 (CERN-70-21(Vol.2), pp 721-7)
  particle tracks in, computer-based system at Munich for analysis of, 25:13287 (CERN-70-21(Vol.2), pp 907-9)
  particle tracks in, conference on data handling systems for analysis of, 25:13263 (CERN-70-21(Vol.2))
  particle tracks in, conference on data handling systems for analysis of, 25:13234 (CERN-70-21(Vol.1))
  particle tracks in, description and performance of CERN spiral reader for analysis of, 25:13236 (CERN-70-21(Vol.1), pp 19-36)
  particle tracks in, development of data processing systems at JINR for analysis of, 25:13279 (CERN-70-21(Vol.2), pp 753-60)
  particle tracks in, development of system in East Germany for analysis of, 25:13272 (CERN-70-21(Vol.2), pp 665-73)
  particle tracks in, digitized microscope for analysis of, 25:13284 (CERN-70-21(Vol.2), pp 851-7)
  particle tracks in, geometry reconstruction program for filtering HPD data for analysis of, 25:13273 (CERN-70-21(Vol.2), pp 679-85)
  particle tracks in, global method of fiducial recognition with fish-eye lenses for analysis of, 25:13261 (CERN-70-21(Vol.1), pp 497-503)
  particle tracks in, glossary of on-line measuring devices for analysis of, 25:13294 (CERN-70-21(Vol.2), pp 963-77)
  particle tracks in, grid guidance program for PEPR film scanner for analysis of, 25:13247 (CERN-70-21(Vol.1), pp 199-211)
  particle tracks in, HPD Minimum Guidance programs for analysis of, 25:13278 (CERN-70-21(Vol.2), pp 737-52)
  particle tracks in, HPD system at Birmingham for analysis of, 25:13292 (CERN-70-21(Vol.2), pp 949-52)
  particle tracks in, HPD system at Columbia Univ. for analysis of, 25:13253 (CERN-70-21(Vol.1), pp 311-21)
  particle tracks in, HPD--IBM 360/44 system at Bologna for analysis of, 25:13267 (CERN-70-21(Vol.2), pp 607-15)
  particle tracks in, HPD--IBM 360/44 system at Bologna for analysis of, 25:13268 (CERN-70-21(Vol.2), pp 617-24)
  particle tracks in, HPD--IBM 360/44 system at Bologna for analysis of, 25:13269 (CERN-70-21(Vol.2), pp 625-30)
  particle tracks in, IBM data management system for analysis of, 25:13277 (CERN-70-21(Vol.2), pp 729-34)
  particle tracks in, LUCY CRT system for analysis of, 25:13259 (CERN-70-21(Vol.1), pp 427-65)
  particle tracks in, method for analysis of, 25:13223 (CEA-N-1397)
  particle tracks in, on-line computer system in Sweden for analysis of, 25:13282 (CERN-70-21(Vol.2), pp 825-30)
  particle tracks in, on-line film plane digitizer for analysis of, 25:13237 (CERN-70-21(Vol.1), pp 39-46)
  particle tracks in, on-line IBM 1130 computer system in Italy for analysis of, 25:13288 (CERN-70-21(Vol.2), pp

911-20)
  particle tracks in, operator intervention in HPD system for analysis of, 25:13290 (CERN-70-21(Vol.2), pp 931-40)
  particle tracks in, PANGLOSS CRT device for analysis of, 25:13258 (CERN-70-21(Vol.1), pp 401-25)
  particle tracks in, PEPR system at Heidelberg for analysis of, 25:13241 (CERN-70-21(Vol.1), pp 105-11)
  particle tracks in, performance of DAPR system for analysis of, 25:13280 (CERN-70-21(Vol.2), pp 761-804)
  particle tracks in, performance of Oxford PEPR system for analysis of, 25:13239 (CERN-70-21(Vol.1), pp 61-88)
  particle tracks in, performance of reverse-developed film measured on HPD for analysis of, 25:13286 (CERN-70-21(Vol.2), pp 879-905)
  particle tracks in, performance of Sweepnik I for analysis of, 25:13252 (CERN-70-21(Vol.1), pp 293-308)
  particle tracks in, POLLY II system for automatic scanning and measurement of, 25:13254 (CERN-70-21(Vol.1), pp 325-55)
  particle tracks in, POLLY system at Glasgow Univ. for analysis of, 25:13255 (CERN-70-21(Vol.1), pp 357-70)
  particle tracks in, Princeton Automatic Track Reader for analysis of, 25:13250 (CERN-70-21(Vol.1), pp 273-83)
  particle tracks in, SATR system at Wisconsin Univ. for analysis of, 25:13262 (CERN-70-21(Vol.1), pp 505)
  particle tracks in, SMP system at UCLA for analysis of, 25:13249 (CERN-70-21(Vol.1), pp 243-60)
  particle tracks in, spiral reader system at Weizmann Institute for analysis of, 25:13293 (CERN-70-21(Vol.2), pp 953-62)
  particle tracks in, status of HPD systems at CERN for analysis of, 25:13281 (CERN-70-21(Vol.2), pp 813-24)
  particle tracks in, status of PEPR system at Heidelberg for analysis of, 25:13246 (CERN-70-21(Vol.1), pp 187-96)
  particle tracks in, status of PEPR system at MIT for analysis of, 25:13248 (CERN-70-21(Vol.1), pp 233-42)
  particle tracks in, Sweepnik II for analysis of, 25:13251 (CERN-70-21(Vol.1), pp 285-92)
  particle tracks in, video assisted scan table for analysis of, 25:13238 (CERN-70-21(Vol.1), pp 47-58)
  safety report on NAL 15-foot hydrogen, 25:13298 (NAL-48-2624)
  vacuum tank for NAL 15-foot hydrogen, stress analysis of, 25:13298 (NAL-48-2624)
RADIATION DETECTORS, CHERENKOV
  operation of shower, for energy measurement of high-energy electrons and photons, 25:13300
RADIATION DETECTORS, DIELECTRIC TRACK
  performance of glassy, for age estimation and uranium determination, 25:13219
  track formation and etching in, principles of, 25:13219
RADIATION DETECTORS, FISSION FOIL
  performance for neutron spectra measurements, 25:13210 (JINR-P3-5421)
RADIATION DETECTORS, IONIZATION CHAMBER
  calibration of type 1383A, for determination of radioisotopes in solution, 25:13221
  circuit for liquid argon, for meson (π^-) spectroscopy, 25:13211 (JINR-P13-5402)
  performance in soil water measurements, 25:13110
  performance of plane-parallel, filled with liquid and solid argon, 25:13295 (JINR-P13-5404)
  performance of proton recoil, in fast subcritical assemblies, (E/T), 25:15388(R) (GULF-RT-10421)
  sensitivity for measuring x rays from diffraction apparatus, 25:13457
RADIATION DETECTORS, PROPORTIONAL
  development for gas-recoil neutron spectroscopy, with fast coincidence electronic collimation, 25:13232
  development of wire, with on-line computer for meson (π^-) beam profile monitoring, 25:13297 (JINR-P13-5473)
  performance of proton-recoil, for fast neutron flux measurements, 25:13216
RADIATION DETECTORS, SCINTILLATION
  data recording system for liquid, 25:13224
  design for blood volume determinations in human organs using iodine-131-labeled human serum albumen, 25:13218
  development for flat-response neutron detection at 100 to 700 keV using vaseline--boron-10 sphere, 25:13215
  energy transfer in liquid organic, triplet-triplet, 25:13220
  geometry compensation for meson (π^-) time-of-flight spectroscopy using proportional detector, 25:13296 (JINR-P13-5472)
  neutrino detection in large underground, (T), 25:13830
  operation of shower, for energy measurement of high-energy electrons and photons, 25:13300
  performance of sodium iodide, for soil water measurements, 25:13110
  solutes for toluene-solvent liquid, aromatic nitrile, 25:13214
RADIATION DETECTORS, SEMICONDUCTOR
  design of, using superconducting resonant cavity, 25:14228
  radiation damage to surface-barrier, during in-core neutron flux monitoring, 25:13329
RADIATION DETECTORS, SEMICONDUCTOR (GERMANIUM)
  carrier trapping and tailing effects in lithium-drifted, 25:13213 (UCRL-71508)
  design and performance of lithium-drifted, 25:13212 (NP-18653)
  performance of lithium-drifted, for clinical radioisotope scanning, conditions and factors affecting, 25:13487
RADIATION DETECTORS, SEMICONDUCTOR (SILICON)
  design of rocket-borne, for measuring spectra and angular distribution of protons in auroral zone, 25:13227
  resolution and sensitivity enhancement of surface-barrier, by cooling, 25:13217
  time resolution of surface-barrier, plasma effects on, 25:13228
RADIATION DETECTORS, SPARK CHAMBER
  data acquisition and processing system for, on-line computer, 25:14838 (CERN-70-21(Vol.2), pp 525-37)
  data processing system for, FOCUS remote access system for, 25:13265 (CERN-70-21(Vol.2), pp 551-9)
  design and performance of high resolution magnetostrictive wire, 25:13301
  design and performance of high resolution optical, 25:13302
  design and performance using FET readout circuit, 25:13264 (CERN-70-21(Vol.2), pp 539-48)
  particle tracks in Omega, development of pattern recognition programs for analysis of, 25:13283 (CERN-70-21(Vol.2), pp 831-50)
  particle tracks in, ARIANE II automatic system for analysis of, 25:13285 (CERN-70-21(Vol.2), pp 859-78)
  particle tracks in, computer program for acquisition of film information by PEPR system for analysis of, 25:13242 (CERN-70-21(Vol.1), pp 113-24)
  particle tracks in, computer program for calibration of PEPR system for analysis of, 25:13245 (CERN-70-21(Vol.1), pp 177-86)
  particle tracks in, computer-based HPD system for analysis of, 25:13276 (CERN-70-21(Vol.2), pp 721-7)
  particle tracks in, conference on data handling systems for analysis of, 25:13234 (CERN-70-21(Vol.1))
  particle tracks in, conference on data handling systems for analysis of, 25:13263 (CERN-70-21(Vol.2))
  particle tracks in, description and performance of CERN spiral reader for analysis of, 25:13236 (CERN-70-21(Vol.1), pp 19-36)
  particle tracks in, development of data processing systems at JINR for analysis of, 25:13279 (CERN-70-21(Vol.2), pp 753-60)
  particle tracks in, digitized microscope for analysis of, 25:13284 (CERN-70-21(Vol.2), pp 851-7)
  particle tracks in, geometry reconstruction program for filtering HPD data for analysis of, 25:13273 (CERN-70-21(Vol.2), pp 679-85)
  particle tracks in, glossary of on-line measuring devices for analysis of, 25:13294 (CERN-70-21(Vol.2), pp 963-77)
  particle tracks in, HPD system at Birmingham for analysis of, 25:13292 (CERN-70-21(Vol.2), pp 949-52)
  particle tracks in, HPD system at Columbia Univ. for analysis of, 25:13253 (CERN-70-21(Vol.1), pp 311-21)
  particle tracks in, on-line film plane digitizer for analysis of, 25:13237 (CERN-70-21(Vol.1), pp 39-46)
  particle tracks in, PEPR system at Heidelberg for analysis of, 25:13241 (CERN-70-21(Vol.1), pp 105-11)
  particle tracks in, performance of Oxford PEPR system for analysis of, 25:13239 (CERN-70-21(Vol.1), pp 61-88)
  particle tracks in, performance of reverse-developed film measured on HPD for analysis of, 25:13286 (CERN-70-21(Vol.2), pp 879-905)
  particle tracks in, performance of Sweepnik I for analysis of, 25:13252 (CERN-70-21(Vol.1), pp 293-308)
  particle tracks in, POLLY system at Glasgow Univ. for analysis of, 25:13255 (CERN-70-21(Vol.1), pp 357-70)
  particle tracks in, Princeton Automatic Track Reader for analysis of, 25:13250 (CERN-70-21(Vol.1), pp 273-83)
  particle tracks in, SATR system at Wisconsin Univ. for analysis of, 25:13262 (CERN-70-21(Vol.1), pp 505)
  particle tracks in, SMP system at UCLA for analysis of, 25:13249 (CERN-70-21(Vol.1), pp 243-60)
  particle tracks in, spiral reader system at Weizmann Institute for analysis of, 25:13293 (CERN-70-21(Vol.2), pp 953-62)
  particle tracks in, status of PEPR system at Heidelberg for analysis of, 25:13246 (CERN-70-21(Vol.1), pp 187-96)
  particle tracks in, status of PEPR system at MIT for analysis of, 25:13248 (CERN-70-21(Vol.1), pp 233-42)
  particle tracks in, Sweepnik II for analysis of, 25:13251 (CERN-70-21(Vol.1), pp 285-92)
  particle tracks in, video assisted scan table for analysis of, 25:13238 (CERN-70-21(Vol.1), pp 47-58)
  readout systems for, cost-effectiveness study of, 25:13266 (CERN-70-21(Vol.2), pp 581-606)
RADIATION DOSE
  measurements in 42 MeV betatron, use of films, iron sulfate dosimeters, and lithium-fluoride thermoluminescence dosimeters for, 25:13446
RADIATION DOSIMETERS
  design for studies of electromagnetic field effects on biological and medical studies, 25:13581
  performance in 42 MeV betatron, effects of energy dependence on, 25:13446
RADIATION DOSIMETERS, CHEMICAL
  development of solid dye, using spectrophotometric readout, 25:13306

properties and uses of ferrous sulfate, review on, 25:13305
RADIATION DOSIMETERS, THERMOLUMINESCENT
  properties of beryllium oxide, 25:13304 (RT/PROT-(70)23)
RADIATION MONITORING
  methods for environmental, at JAERI, Tokai, Japan during 1969, 25:13119 (JAERI-Memo-4175)
  requirements for radioactive effluents from nuclear power plants, guide for, 25:15335 (NF-67-8)
RADIATION PROTECTION
  analysis for neutron uses in radiotherapy, 25:13450
  hazards from lead shielding, to patients during therapy, 25:13460
  methods for control of environmental radioactivity around nuclear power plants, 25:13471
  methods for industrial personnel handling radioisotopes, 25:13467
  methods for outpatients following iodine-131 therapy for thyroid carcinomas, 25:13596
  procedures for personnel and population at radioactive materials handling facilities, 25:13461
  programs for dental and medical x-ray facilities, priority system for state inspection in, 25:13459
  recommendations of Federal Radiation Council for environmental levels of cesium-137, iodine-131, strontium-89, and strontium-90, 25:13433
  standards in USA, directory of personnel involved in development of, 25:13469 (ORNL-NSIC-75(Rev.1))
RADIATION RATE METERS
  spurious alarms in analog and digital, frequency of, 25:13225
RADIATION STANDARDS AND UNITS
  factor of 700 for iodine-131 applied by AEC Division of Licensing and Regulation to annular release limits for halogens from power reactors, 25:13438
RADIATION TARGET CANS
  design for in-pile creep testing of fuel cladding under stress and thermal cycling, 25:13142
RADIATION TARGET CHAMBERS
  design for alpha spectroscopy of nuclear reaction products, 25:14841 (JINR-P13-5353)
RADIATION TARGETS
  properties of tritiated titanium, for 14-MeV neutron production, 25:14840 (EUR-4286(Pt.2))
RADIO GALAXIES
  evolution of, spinars in, (T), 25:13952
  particle emission from, relativistic, (T), 25:13922
  synchrotron emission from, (T), 25:13936(R) (AD-711829)
RADIO WAVES
  absorption of auroral, conjugate and closely spaced observations of, (E), 25:14118
  attenuation in atmosphere at 1415 MHz, (E), 25:13838
  emission from supernova remnants, secular behavior of, (T), 25:13847
  scattering on discharge plasma, diagnostic use of, (E), 25:14248
RADIOACTIVE CONTAMINATION
  removal from gases, design and testing of high-efficiency filters for, 25:13192 (NACAR-10012)
RADIOACTIVE MATERIALS
  control in East Germany, recommended regulations for, 25:13193 (SZS-16/70)
  handling facilities for, radiation protection measures for, 25:13461
  handling of, design of glove box for, 25:13185 (AERE-R-6338)
  handling of, design of remote handling equipment for, 25:13200(P)
  leakage from Types A and B radioactive material shipping containers, method for calculating, 25:13201
  shipping container for, design of protective packaging for, 25:13196(P)
  shipping of high-activity, East German regulations for safe, 25:13194 (SZS-19/70)
  shipping of, design of shielded container for, 25:13204(P)
  shipping of, method for calculating gas and radioactivity leakage from Types A and B containers for, 25:13201
RADIOACTIVE WASTE
  analysis for plutonium, development of spectrometer systems for gamma and neutron scanning, 25:13230(R) (WCAP-7562-1)
  analysis of liquid effluents from nuclear fuel reprocessing plant for radioisotopes, 25:12950 (BRH/NERHL-70-2)
  book: Antipollution and Radioactive Wastes, in French, 25:13087
  disposal from U. S. Naval nuclear-powered ships and support facilities during 1969, environmental monitoring to determine adequacy of limits and procedures for, 25:13444
  disposal of alpha-contaminated solid, from commercial reactor fuel fabrication and reprocessing plants, methods for, 25:13188 (BNWL-B-34)
  disposal of by hospitals, in sewage, public health aspects of, 25:13454
  disposal of liquid, from Hanford N Reactor incident, effects of hydrological factors on operation of Hanford area Emergency Waste Disposal crib for, (T), 25:13186 (BNWL-1503)
  disposal of liquid, into sea, contamination of marine species and seawater by, (E), 25:13189 (CEA-CONF-1712)
  disposal of radioisotope-containing, Italian regulations for, 25:13207
  filtration of, cleaning of filters used in, 25:13094(P)
  incorporation in asphalt and polyethylene, feasibility studies of, 25:13197
  plutonium content of solid, produced in reactor fuel fabrication and reprocessing plants, predictions to year 1990 of, 25:13188 (BNWL-B-34)
  plutonium separation from, bibliography on, 25:13190 (JAERI-Memo-4153)
  processing and disposal of low- and medium-level liquid and solid, methods for, 25:13191(T) (JPRS-51948)
  processing and disposal of plutonium-containing, bibliography on, 25:13190 (JAERI-Memo-4153)
  processing and disposal of, economics and methods of, 25:13087
  production of alpha-contaminated solid, by reactor fuel fabrication and reprocessing plants, predictions to year 1990 of, 25:13188 (BNWL-B-34)
RADIOACTIVITY
  monitoring at Lawrence Radiation Laboratory and Shippingport Atomic Power Station during 1969, 25:13398
  monitoring in environs of AEC installations, 25:13445
  monitoring in environs of harbors containing support facilities for U. S. Naval nuclear-powered ships to determine adequacy of waste disposal limits and procedures during 1969, 25:13444
  monitoring in milk during 1965 to 1968, operation of Standby Milk Surveillance Network of SWRHL in relation to, 25:13443
  monitoring in natural waters of Italy, 25:13106
  search for new-type, in proton reactions with aluminum and tungsten at 70 GeV, (E), 25:14541 (JINR-P1-5399)
RADIOAPPLICATORS
  design of implantable assembly containing, for irradiating body fluids, 25:13529(P)
RADIOBIOLOGY
  book: Biological Effects of Fast Neutrons, 25:13568
RADIOCHEMICAL PROCESSING PLANTS
  plutonium content of dissolver solutions fed into, tracer and mass spectrometric methods for determination of, 25:13081 (NP-18577)
  uranium content of dissolver solutions fed into, tracer and mass spectrometric methods for determination of, 25:13081 (NP-18577)
RADIOGRAPHY, BIOMEDICAL
  effectiveness for diagnosis of hydatid disease of human liver, 25:13494
  effectiveness for diagnosis of rare cases of Hodgkin's disease, x, 25:13541
  equipment safety survey in USA during 1961 to 1968, 25:13464
  images following myelographic, effects of diluted contrast media on improving quality of, 25:13496
  methods for diagnosis and nuclear medicine research, studies on infrared thermography and x, 25:13498
  methods for human paranasal sinuses for optimal results, x, 25:13507
  performance in combination with photometric scanning for determination of mineral content of human radius and ulna, 25:13509
  use of angiographic, in combination with percutaneous transhepatic cholangiography for diagnosis of drug-induced jaundice, 25:13492
RADIOGRAPHY, INDUSTRIAL
  method for inspecting aircraft structures using iridium-192 and thulium-170 gamma sources, 25:13180 (JAERI-Memo-4163)
  neutron sources for, performance of californium-252, 25:13161 (BNWL-SA-3169)
RADIOISOTOPE SCANNERS
  performance of dual-headed, with inferior probe for demonstration of pulmonary radioactivity displacement by enlarged heart and free fluids, 25:13484
RADIOISOTOPE SCANNING
  conference on uses of, in medicine, 25:13482 (CONF-661071)
  effectiveness for diagnosis of hydatid disease of human liver, 25:13494
  evaluation of whole-body, for determination of radioisotope distribution in man, 25:13503
  methods for clinical, using lithium-drifted germanium detectors, conditions and factors affecting, 25:13487
  methods for diagnosis of liver malignancies using iodine-131, 25:13483
  methods for inflated lung tissue using Anger camera in comparison with radioisotope ventilation tests, 25:13500
  use for diagnosis of human splenic abscesses, 25:13512
RADIOISOTOPES
  book: Economic Effectiveness of using Radioactive Isotopes in Industry (In Russian), 25:13174
  conference on uses in biology and nuclear medicine, 25:13482 (CONF-661071)
  content of alpha-emitting, in marine organisms, 25:13394(R) (RLC-2099-1)
  determination in sodium, development of methods for, 25:13651(R) (ANL/ST-4)
  determination using column liquid chromatography and counting, 25:12952

- distribution in man, scintigrams for, 25:13503
- environmental contamination by, MPC for, 25:13437
- handling by industrial personnel, protection methods for, 25:13467
- production by Linac dynamic booster in relation to application, 25:13548
- uptake curves for tracer studies, kinetics of, 25:13336
- use for diagnosis of liver diseases, advantages of measuring incorporation of precursors into glucose over determining concentration of metabolic end products, 25:13506
- use for medical diagnosis and therapy in relation to cost, production, safety, techniques, and transport, review of, 25:13519

RADIOMETRIC ANALYSIS
- book: Applied Gamma Ray Spectroscopy, 25:13231
- detectors for use with column liquid chromatography in, 25:12952

RADIOPAQUE AGENTS
- use of dilute, for improving quality of myelographic images, 25:13496

RADIOTHERAPY
- conference on uses of radioisotopes in nuclear, 25:13482 (CONF-661071)
- dose distribution in, evaluation of pendulum translation method for cobalt-60 γ, 25:13447

RADIUM
- effectiveness for interstitial therapy in comparison to gold-198, 25:13526
- effects on bones and bone marrow in personnel, neoplastic, 25:13593
- toxicity to personnel, 25:13593
- use for therapy of human cervix carcinomas in combination with γ and x radiations, statistical evaluation of, 25:13531

RADIUM ISOTOPES
- energy levels of, properties of octupole, 25:15205

RADIUM ISOTOPES Ra-217
- yields from alpha decay of thorium-221, 25:15011

RADIUM ISOTOPES Ra-218
- yields from alpha decay of thorium-222, 25:15011

RADIUM ISOTOPES Ra-226
- content in sands and soils of south Florida, 1968 measurements of natural, 25:13107
- content of diet in USA during 1965 to 1970, 25:13401
- content of diet of human adolescents in EURATOM countries during 1965 to 1967, 25:13392 (EUR-3945(Pt.2))
- content of institutional diet of adults and children in USA during 1969, annual average, 25:13442
- content of natural waters at Masutomi spa area in Japan in relation to daily ingestion limits, 25:13470

RADIUM ISOTOPES Ra-228
- content of food in Brazil, 25:13439
- decay products of, content of food in Brazil, 25:13439

RADON
- effects on cysteic acid content of fingernails of uranium miners, chromatographic and oscillopolarographic studies on, 25:13369

RADON ISOTOPES
- content in air of confined areas, maximum permissible, 25:13435
- electron-capture decay of neutron-deficient, (E/T), 25:14993
- radiation hazards of confined nonequilibrium, 25:13435

RADON ISOTOPES Rn-214
- yields from alpha decay of thorium-222, 25:15011

RADON ISOTOPES Rn-222
- content of natural waters at Masutomi spa area in Japan in relation to daily ingestion limits, 25:13470

RAINWATER
- tritium content of Australian, 1967 to 1969, 25:13120 (NP-18638)
- tritium content of Australian, 1969 to 1970, 25:13103 (NP-18639)

RARE EARTH ALLOYS AND SYSTEMS
- magnetic ordering of group V intermetallic compounds with, self-polarization contribution to, (T), 25:14460
- rare earths--transition metals, compressibility of intermetallic compounds of, strain gage measurements of, 25:13694

RARE EARTH OXIDES
- electron transport in sesquioxides and nonstoichiometric oxides of, 25:14469

RARE EARTHS
- abundance in chondrites, achondrites, and Apollo 11 fines, (E), 25:13787
- abundances in Apollo 12 basalts, (E), 25:13955
- ferromagnetism in, modification of Ruderman--Kittel--Kasuya--Yoshida exchange mechanism for pressure dependence of, 25:14487
- separation from aqueous solutions by solvent extraction using bis(2-ethylhexyl) phosphate, 25:13092
- spectral lines inside and outside H and K wings, formation of solar, (E/T), 25:13810

RARE GAS IONS
- reactions with nitrogen molecules of excited, energy transfer processes in, (E), 25:14012

RARE GASES
- electron elastic scattering by, resonances in, (E), 25:14035
- electron reactions with, distorted-wave calculation of cross sections for excitation in, 25:14015
- potassium-atom elastic scattering at 300 to 15000 m/sec by, cross sections for, (E/T), 25:14005
- reactions with nitrogen molecules of excited atoms of, energy transfer processes in, (E), 25:14012

RATS
- carbon-14 incorporation in lipids and proteins of homogenates of liver of, effects of avidin on, 25:13344
- carbon-14-labeled palmitate metabolism in lungs of, effects of breathing nitrogen dioxide on, 25:13356
- glucose metabolism in, with cirrhosis, use of carbon-14 for measuring incorporation of precursors, 25:13506
- lithium-6 distribution in organs and tissues of, following intraperitoneal and intravenous injections, 25:13350
- neptunium-237 toxicity in, following intravenous administration, 25:13346
- phosphorus-32 uptake by erythrocytes of, for determining correlation of phosphorated erythrocytic metabolism with second and third phase of general adaptation syndrome, 25:13335
- radiation effects on blood cells, weight of spleen, and weight of thymus in, comparison of RBE for cesium-137 and tritium oxide, 25:13551
- radiation effects on blood coagulation in, effects of serotonin on cobalt-60, 25:13549
- radiation effects on bone marrow and reticulo-endothelial system of, protective effects of bacterial antigens, epinephrine, and pilocarpine against x, 25:13567
- radiation effects on bone marrow in, in comparison to mice, effects of species on local x, 25:13563
- radiation effects on content of NAD and NADP in organs of, effects of ATP and nicotinamide on, 25:13379
- radiation effects on glycogen and ultrastructure of liver cells in, histochemical studies on cobalt-60, 25:13378
- radiation effects on histamine content of blood, lungs, skin, and small intestine in, combined effects of skin wounds on whole-body, 25:13368
- radiation effects on histone content of deoxyribonucleoproteins in liver, spleen, and thymus of, effects of heparin on, 25:13385
- radiation effects on iodine-131 uptake by perfused liver and intestine of rats, effects of food uptake on, 25:13349
- radiation effects on jejunal crypt cells of, effects of proteins on x, 25:13562
- radiation effects on leucine incorporation and protein synthesis by perfused liver of, x, 25:13373
- radiation effects on physiology of lymph system in, effects of dose on x, 25:13481
- radiation effects on potassium and sodium content of brain and muscular tissues in, lethal and sublethal, 25:13566
- radiation effects on preimplantation blastocysts of, 25:13560
- radiation effects on protein synthesis in liver and spleen cells of, alone and in combination with immunization, 25:13376
- radiation effects on reproduction of, electromagnetic, 25:13571
- radiation effects on secretion by accessory reproductive organs of, x, 25:13366
- radiation effects on synthesis of bile acids in livers of, inhibitory, 25:13370
- radiation effects on tissues of, for whole-body neutron activation autoradiography, 25:13590
- radiation effects on water content and distribution in organs of, effects of lethal and sublethal x, 25:13348
- radiation sickness in, neutron autoradiography for diagnosis of, 25:13497
- radioinduced cortical carcinomas in adrenal glands of buffalo, mixed whole-body fission neutron and γ, 25:13564
- sulfur-35 incorporation into blood platelets of, for determining effects of thrombopoietin on production of, 25:13355

REACTOR CONTAINMENT SYSTEMS
- spray systems for, effectiveness for iodine removal of sodium thiosulfate, (E/T), 25:15374 (BAW-10024)
- spray systems for, model for iodine washout by water, (T), 25:15372 (AE-408)

REACTOR CONTROL ELEMENTS
- drives for rod type, description of centrifugal governor for braking control during gravity accelerated operation of, 25:15413(P)
- drives for rod type, description of chain connected pulley block, 25:15416(P)

REACTOR CONTROL SYSTEMS
- development at ORNL, Sept. 1969--Aug. 1970, 25:13318(R) (ORNL-4620)
- development of movable fuel, for water cooled breeder reactors, (T), 25:15353 (WAPD-TM-968)
- performance of heat pipe evaporators for reactivity control in rocket, (T), 25:15400

REACTOR COOLANTS
- analysis of aqueous, for radioisotopes by γ spectroscopy, 25:12956

REACTOR EXPERIMENTAL FACILITIES
- design of photographic equipment for fuel meltdown observation, 25:15384 (ANL-7578)

- REACTOR FUEL ELEMENTS
  - analysis for plutonium, development of spectrometer systems for gamma and neutron scanning, 25:13230(R) (WCAP-7562-1)
  - burnup of boiling water reactor, cycle management procedures for optimum, 25:15212
  - cladding for, calculation of required strength of, 25:13662
  - cladding for, design of equipment and processes for Zircaloy, 25:13645
  - cladding for, design of in-pile stress and thermal cycling facility for testing, 25:13142
  - cladding for, DYSYS computer program for analysis of creep collapse of, 25:13158
  - cladding for, method for deposition of graphite coating on, 25:13745(P)
  - decladding of irradiated LMFBR, development of equipment and facilities for, 25:13077(R) (ANL-7755)
  - decladding of LMFBR, head-end process for, 25:13077(R) (ANL-7755)
  - design of boiling water reactor, 25:15212
  - enrichment regions of ceramic, description of central void low- and annular high-, 25:15369(P)
  - fabrication of carbon-matrix ceramic, method for, 25:13741(P)
  - fabrication of LMFBR, continuous conversion of plutonium nitrate--uranium nitrate to oxides for, 25:13077(R) (ANL-7755)
  - failure detection in gas cooled reactors, fission product activity release monitoring method for, 25:15373 (AERE-R-6475)
  - heat transfer from clad pellet-type, effects of bonding and configuration on, 25:13155
  - heat transfer from multirod bundles of, equipment and method for measuring, 25:13150(R) (GEAP-10253)
  - heat transfer to air from bundles of, effects of spacer arrangement on, 25:13153 (ZJE-66)
  - management in liquid metal fast breeder, optimization of radial blanket, 25:15378
  - meltdown experiments for, design of equipment for photographic observation of, 25:15384 (ANL-7578)
  - mockup of gas cooled finned, development of electrically heated, 25:15410 (ZJE-92)
  - performance of cylindrical oxide fast, thermal, radiation, and mechanical analysis of, (T), 25:15371
  - performance of plutonium oxide (PuO_2)--uranium oxide (UO_2), in boiling water reactors, (E), 25:15365(R) (NEDC-12111)
  - performance of stainless steel clad mixed oxide, review of, (E/T), 25:15367 (WHAN-SA-51)
  - radiation effects on swelling of Zircaloy-4 clad thorium oxide (ThO_2)--uranium oxide (UO_2) rod type, fast neutron, 25:15366 (WAPD-TM-986)
  - separation of plutonium and uranium from irradiated, by solvent extraction, method for, 25:13101(P)
  - shipping of, design of container for, 25:13187 (BNWL-1512)
  - shipping of, design of shielded container for, 25:13205(P)
  - storage tanks for spent, development of fiber glass reinforced epoxy liner for, 25:15412
  - stringers of cluster type, description of tubular wire rope connectors for, 25:15415(P)
  - vibrations in liquid sodium cooled pin type, analysis of coolant flow induced, (E/T), 25:15370
  - vibrations of rod type, effects of parallel flow turbulence on transverse, 25:15213
- REACTOR FUELS
  - analysis of mixed oxide, for gas and water, effects of density on, 25:12924 (WHAN-SA-62)
  - balance parameters in fast, long-term variations in, 25:15377
  - development of Argonne National Laboratory, December 1970, 25:15339 (ANL-7765)
  - dissolution of LMFBR, in nitric acid, effects of fabrication variables and irradiation history on, 25:13083 (WHAN-FR-33)
  - fabrication of, production reprocessing of, production and disposal of alpha-contaminated solid wastes from commercial, 25:13188 (BNWL-B-34)
  - isotopic composition of, long-term variations in, (T), 25:15376
  - radiation effects on isotope diffusion in coated-particle, models for calculation of, 25:13782 (JUL-685-PA)
  - reprocessing of, effects of radiolysis of toluene on zirconium extraction in, 25:13093
  - reprocessing of, tracer technique for determination of plutonium and uranium in dissolver solutions for, 25:13081 (NP-18577)
  - separation of protactinium-231 from, 25:13100
  - thermal conductivity of ceramic, balanced oscillator method for in-pile measurement of, (E/T), 25:15411
- REACTOR LOADING MACHINES
  - gratheads for, description of solenoid operated, 25:15414(P)
- REACTOR SAFETY
  - analyses of, IAEA guidelines for preparation of reports on, 25:15337 (STI/PUB-272)
  - development of Argonne National Laboratory, December 1970, 25:15339 (ANL-7765)
  - research at ORNL, Sept. 1969--1970, 25:13318(R) (ORNL-4620)
- REACTOR SAFETY EXPERIMENTS
  - design modifications of TREAT, for photographic observation of fuel meltdown experiments, 25:15384 (ANL-7578)
  - development for in-pile tests of LMFBR safety, bootstrap concept of, 25:15380
  - operations summary for TREAT, December 1970, 25:15339 (ANL-7765)
- REACTOR SIMULATORS
  - development at ORNL, Sept. 1969--Aug. 1970, 25:13318(R) (ORNL-4620)
  - use of hybrid analog computers, for optimum fast reactor core design, 25:15406 (NP-18646)
- REACTORS
  - design of, standard neutron cross sections and high-precision neutron flux measurements for, 25:14877
  - excursions in one-dimensional, hybrid computer analysis of spatial effects in prompt critical, 25:15408
  - instrumentation for, development at ORNL of, 25:13318(R) (ORNL-4620)
  - materials for, conference on basic neutron data for, 25:14987 (STI/PUB-259(Vol.1))
  - materials for, conference on basic neutron data for, 25:14988 (STI/PUB-259(Vol.2))
  - materials for, data compilation on thermal properties of carbonaceous, 25:13750 (GAMD-9335)
  - neutron capture in, Westcott formalism for, (T), 25:15405 (LFEN-NI.-45-a)
  - physics calculations for various core geometries, TIMOC computer program subroutines for, 25:15404 (EUR-4526)
  - physics of, analytic method for error estimate in, 25:15403
  - physics of, survey of nuclear data requirements for analysis of, 25:15402
  - structural materials for, evaluation of neutron capture cross sections for, 25:14971
- REACTORS, AGR-TYPE
  - economics of, comparison with other reactor types of, 25:15240
- REACTORS, BOILING
  - economics of, comparison with other reactor types of, 25:15240
  - fuel elements for, performance of plutonium recycle, (E), 25:15365(R) (NEDC-12111)
  - thermodynamics of 500 MW(e) heavy water, 25:15344
- REACTORS, BREEDER
  - bibliography on fast, 1966 to 1969, 25:15340 (NEIC-RR-41)
  - control of water cooled, three dimensional space-time analysis for movable fuel, (T), 25:15353 (WAPD-TM-968)
  - design of fast, effects of nuclear data uncertainties on, 25:15345
  - fuel cycle for fast, effect of collapsing cross section data on calculation of, (T), 25:15352
  - fuel elements for water moderated fast, radiation effects on swelling of Zircaloy-4 clad thorium oxide (ThO_2)--uranium oxide (UO_2) rod type, 25:15366 (WAPD-TM-986)
  - fuel management in 1000 MW(e), optimization of radial blanket, (T), 25:15378
- REACTORS, CANDU-TYPE
  - economics of, comparison with other reactor types of, 25:15240
- REACTORS, FAST
  - bibliography on breeder, 1966 to 1969, 25:15340 (NEIC-RR-41)
  - coolant boiling in, hydrodynamics and thermodynamics of liquid sodium, (E/T), 25:15382
  - coolant flow in triangular fuel rod clusters of, temperature and velocity distribution in turbulent liquid sodium, (T), 25:15363
  - coolant for liquid sodium cooled, solubility of inert gases in, (E/T), 25:15379(T) (EURFNR-785)
  - coolant loss accidents in liquid sodium cooled, analysis of Bethe-Tait type excursions from, 25:15381
  - cooling system for, DYSYS computer program for analysis of transient boiling in, 25:13158
  - core for, use of hybrid analog computers for optimum design parameters of, 25:15406 (NP-18646)
  - design of breeder, effects of nuclear data uncertainties on, 25:15345
  - design of, use of microscopic and integral nuclear data in, 25:15346
  - fission products in, reactivity worths of, (E/T), 25:15350
  - fuel cycle for breeder, effect of collapsing cross section data on calculation of, (T), 25:15352
  - fuel elements for water moderated breeder, radiation effects on swelling of Zircaloy-4 clad thorium oxide (ThO_2)--uranium oxide (UO_2) rod type, 25:15366 (WAPD-TM-986)
  - fuel elements for, description of central void low enrichment and annular high enrichment regions of ceramic, 25:15369(P)
  - fuel elements for, effects of cladding--pellet parameters on heat transfer from, 25:13155
  - fuel elements for, thermal, radiation, and mechanical analysis of cylindrical oxide, (T), 25:15371
  - fuel elements of liquid sodium cooled Na-1, coolant flow induced vibrations in pin type, (E/T), 25:15370
  - fuel management in 1000 MW(e), optimization of radial

  blanket, (T), 25:15378
  fuels for, integral measurements of α for, (E/T), 25:15348
  fuels for, long-term variations in balance parameters of, (T), 25:15377
  fuels for, long-term variations in isotopic composition of enriched uranium, (T), 25:15376
  instrumentation cables for, measurement of radiation induced noise in metal oxide insulation of, (E), 25:15354 (WHAN-IR-42)
  kinetics of, comparison of three dimensional diffusion theory computer programs for, 25:15343 (WHAN-IR-48)
  kinetics parameters of, few-group and modal method calculations of, 25:15407
  physics analysis of plutonium fueled, role of microscopic and integral nuclear data measurements in, 25:15347
  physics analysis of, integral measurements of high-energy nuclear data for, (E/T), 25:15349
  physics parameters of 1000 MW(e) liquid sodium cooled, nonlinear programming methods for optimum, (T), 25:15351
  physics parameters of, comparison of calculational methods for, (E/T), 25:15387 (EURFNR-858)
REACTCRS, GAS-COOLED
  fuel element failure detection for high temperature, fission product activity release monitoring method for, 25:15373 (AERE-R-6475)
  fuel elements for, development of electrically heated mockups of finned, 25:15410 (ZJE-92)
  power cycle for direct cycle gas turbine, analysis of optimum, 25:15383(P)
  pressure vessel for, description of heat exchanger containing concrete, 25:15364(P)
REACTCRS, GRAPHITE-MODERATED
  neutron spectra in natural uranium fueled lattices in, foil activation measurements of thermal, (E/T), 25:15409
REACTCRS, HEAVY WATER-MODERATED
  economics of, comparison with other reactor types of, 25:15240
  thermodynamics of 500 MW(e) boiling, 25:15344
REACTCRS, JAPAN
  uses in biology and medicine, advantages of Linac dynamic booster for, 25:13548
REACTCRS, LIQUID METAL-COOLED
  coolant boiling in fast, hydrodynamics and thermodynamics of liquid sodium, (E/T), 25:15382
  coolant flow in triangular fuel rod clusters of fast, temperature and velocity distribution in turbulent liquid sodium, (T), 25:15363
  coolant for fast, solubility of inert gases in liquid sodium, (E/T), 25:15379(T) (EURFNR-785)
  coolant loss accidents in fast, analysis of Bethe-Tait type excursions from, 25:15381
  economics of, comparison with other reactor types of, 25:15240
  fuel elements for, calculation of maximum pressure in, 25:13662
  fuel elements of fast, coolant flow induced vibrations in pin type, (E/T), 25:15370
  fuel management in 1000 MW(e), optimization of radial blanket, (T), 25:15378
  physics parameters of 1000 MW(e) fast, nonlinear programming methods for optimum, (T), 25:15351
REACTCRS, MAGNOX
  economics of, comparison with other reactor types of, 25:15240
REACTCRS, POWER
  core components for, radioinduced heating of, (T), 25:15341 (SZS-20/70)
  development in Australia of, economics of, 25:15240
  iodine-131 disposal from, basis of factor of 700 in hazard calculations for, 25:13438
  physics parameters of 1000 MW(e) liquid sodium cooled fast, nonlinear programming methods for optimum, (T), 25:15351
  thermodynamics of 500 MW(e) boiling heavy water, 25:15344
REACTCRS, PRESSURIZED-WATER
  hazards to population from nuclear weapons targeted, civil defense implications of, 25:13184
REACTCRS, RESEARCH
  fuel elements for WWR-SM, maximum cladding temperatures fcr, (E), 25:15395
  lattice parameters of WWR-SM, effects of increased water-tc-fuel ratio on, (E/T), 25:15394
  neutron age in WWR-SM, effects of source heterogeneity on, (T), 25:15394
  neutron flux density in 45 MW core of HFR (Netherlands), thermal and fast, (E/T), 25:15393 (RCN-119)
  neutron spectra in PF-4, value of anti ν/sub eff/ for uranium-235 in intermediate, (E/T), 25:15399
  physics measurements for 10 MW JRR-2, effects of 10 percent increase of uranium-235 on, 25:15390 (JAERI-Memo-4141)
REACTCRS, ROCKET
  reactivity control in, use of heat pipe evaporators for, (E), 25:15400
REACTCRS, THERMAL
  fuel recycle in water cooled, economics of plutonium, (T), 25:15375 (CONF-691114-6)
REACTORS, WATER-COOLED
  containment spray systems fcr, removal of iodine by sodium thiosulfate, (E/T), 25:15374 (BAW-10024)
  control of breeder, three dimensional space-time analysis for movable fuel, (T), 25:15353 (WAPD-TM-968)
  emergency core cooling systems for, effectiveness of water spray for removal of iodine in, (T), 25:15372 (AE-408)
  fuel elements for, performance of plutonium recycle, (E), 25:15365(R) (NEDC-12111)
  fuel recycle in, economics of plutonium, 25:15375 (CONF-691114-6)
REACTORS, WATER-MODERATED
  fuel elements for fast breeder, radiation effects on swelling of Zircaloy-4 clad thorium oxide (ThO_2)--uranium oxide (UO_2) rod type, 25:15366 (WAPD-TM-986)
  neutron spectra in natural uranium fueled lattices in, foil activation measurements of thermal, (E/T), 25:15409
RECOILS
  reactions in organic systems, mechanisms cf, 25:14837(R) (BNL-50230)
REDUCTONE
  effects on synthesis of DNA, RNA, and proteins in uv-irradiated Escherichia coli, 25:13610
REFRACTORY MATERIALS
  electric conductivity measurement at high temperatures, correction for leakage currents due to thermionic emission, 25:14455
  properties for use in SIREN radioisotope fuel capsules, 25:13170 (SNC-2708-1)
REFRIGERATION
  analysis of helium-3--helium-4 dilution, (E/T), 25:14213
  description of simple helium-3--helium-4 dilution, 25:14214
  design and performance of dilution, for temperatures less than 0.075°K, 25:14474
REGGE POLE THEORY
  absorption model from Feynman diagrams, 25:14785
  dual crossing symmetric amplitudes with Mandelstam analyticity in, 25:14821
  dual model for meson interactions with baryons in SU(3) symmetry in, 25:14766
  dual multi-Veneziano spinning particle amplitudes in, 25:14586
  duality and analyticity for poles in Venezianc representation in, 25:14829
  duality relation with interference model fcr resonances in, 25:14678
  model for differential cross sections and duality in A_2 production in $\pi^- + p \to$ eta + n interacticns in, dipole, 25:14704
  model for e + p inelastic interactions in, multi-Regge, 25:14621
  model for hadron production in l + N interactions in, 25:14635 (NYO-4204-9)
  multiperipheral amplitude fcr bremsstrahlung production in Coulomb field, 25:14613
  N-Reggeon vertex in, gauge-invariant, 25:14801
  pole eikonal model for amplitude and differential cross sections for $\pi^+ + n \to \Delta^{++} + \pi^-$ interacticns in, 25:14715
  pole structure of Bethe--Salpeter amplitude fcr scalar particle scattering, complex angular momentum analysis of, 25:14833
  pole-cut model with SU(3) and exchange degeneracy, 25:14660
  poles and oscillatory average multiplicity in particle interactions, multiperipheral models for complex, 25:14585
  poles in Veneziano representation in, duality and analyticity for, 25:14829
  poles in, Dirichlet series for superpositicn of infinite number of, 25:14828
  Pomeranchon in multiperipheral model, partial bootstrap of, 25:14824
  Pomeron hypothesis for exchange degeneracy for oscillating total cross sections for strong interactions in, (T), 25:14656 (SU-1206-237)
  Pomeron hypothesis for form of real-tc-imaginary parts for amplitude of $\pi^- + p \to \pi^- + p$ interacticns at high energies, 25:14656 (SU-1206-237)
  production of π^+ and π^0 in $\gamma + N$ interacticns at 4.3 to 12 GeV at large angles in, differential cross sections for, 25:14598
  Reggeon exchange contributicns to strong interactions at high energies, 25:14657 (UCRL-20032)
  trajectories for infinite-component lccal quantum field theory with rising mass spectrum in, 25:14799
  trajectories for $\pi + N$ interactions at high energies in, fits of, 25:14723
  trajectories in, mass dependence of, 25:14662
  Van Hove model for hyperon nonleptonic decay in, 25:14637 (SU-1206-238)
RELATIVE BIOLOGICAL EFFECTIVENESS
  comparison of cesium-137 γ and tritium oxide cn rats, 25:13551
  comparison of γ and x for effects on human skin, 25:13583
RELATIVITY THEORY
  Einstein equations in general, combined Bondi and fast-approximation method for, 25:14807 (NP-18559)

  Einstein equations in general, conformal flatness of Schwarzschild interior solution of, 25:14808
  experimental testing of general, (T), 25:13942
  gravitational energy transfer in general, time sequences of axially symmetric static configurations for, 25:14816
  gravitational field equations for fluid spheres in general, 25:14814
  gravitational fields in asymptotically null-spherical coordinates in general, tetrad formalism for asymptotically flat, 25:14815
  Hamiltonian formalism on null surfaces for, 25:14773
  Lorentz group in, addition theorem for basis functions of first-class irreducible representations of, 25:14759
  Lorentz group in, Wigner function for hyperbolic rotations in homogeneous, 25:14759
  motion in general, singularity structure from, 25:14813
  parametrized post-Newtonian hydrodynamics and Nordtvedt effect, (T), 25:13943
  satellite spin precession in Brans--Dicke theory, Shiff, 25:14811
  singularities in general, motion and structure of, 25:14813
  spheres in general, exact solution of static charged, 25:14810
  tachyons in special, causal loops for evidence against, 25:14778

REMOTE-CONTROL EQUIPMENT
  design for explosive plug welding of tubes, 25:13647
  design for monitoring chemical content and radioactivity in FFTF coolant sodium, 25:13195 (WHAN-SA-91)

REMOTE-HANDLING EQUIPMENT
  design for assembling components in hot cells, 25:13200(P)
  design for assembly of hot cell components for dry processing of reactor fuels, 25:13199(P)
  design for transporting multisample holder to irradiation position, 25:13208(P)
  design of improved master-slave-type, 25:13206(P)
  head for pneumatic, for transferring objects in hot cells, design of removable, 25:13203(P)

RESPIRATION
  radiation effects on cellular, effects of pyridine nucleotides on uv, 25:13607

RESPIRATORS
  design with gas analyzer for pulmonary function studies using xenon-133 tracer, 25:13223

RETICULO-ENDOTHELIAL SYSTEM
  radiation effects on phagocytic activity of cells of, in rats, protective effects of bacterial antigens, epinephrine, and pilocarpine against x, 25:13567

RHENIUM
  determination in neutron-irradiated graphite by γ spectrometry, 25:12954
  emissivity of monocrystalline and polycrystalline, at 1200 to 2800°K, total hemispherical, 25:13666
  neutron capture at 0.001 to 1 MeV, cross sections for, (E), 25:15121
  separation from other elements by solvent extraction using tertiary amines, 25:12921
  superconducting tunneling into single crystals of, 25:14147 (AD-711826)
  thermal capacity at low temperatures, quadrupole coupling in nuclear contribution to, 25:14474

RHENIUM ALLOY COUPLES
  Re--W/W, electromotive force of thermocouples of, effects of temperature on, 25:13682

RHENIUM ALLOYS AND SYSTEMS
  Hf--Re--Ta-base--W, cracking sensitivity of, Varestraint testing of hot, 25:13695
  Mo--Re, superconducting transition temperature and low-temperature, thermal capacity of sigma-phase, (E/T), 25:14177
  Re--W-base, mechanical properties of, 25:13682

RHENIUM ISOTOPES Re-180
  beta and electron-capture decay of, gamma spectra and branching ratios from, (E/T), 25:14984 (NP-18536)
  energy levels from osmium-180 electron-capture decay, spin--parity assignments and lifetimes for, (E/T), 25:14984 (NP-18536)
  energy-level transitions from osmium-180 electron-capture decay, multipolarities for, (E/T), 25:14984 (NP-18536)

RHENIUM ISOTOPES Re-181
  electron-capture decay of, γ singles and coincidence spectra from, (E), 25:15058
  energy levels from osmium-181 beta decay, spin--parity assignments for, (E/T), 25:14984 (NP-18536)
  energy-level transitions from osmium-181 beta decay, intensities, K- and L-conversion coefficients, and multipolarities for, (E/T), 25:14984 (NP-18536)

RHENIUM ISOTOPES Re-188
  content of feces, milk, and urine of dairy cattle following ingestion of Schooner fallout, 25:13396 (UCRL-72511)
  distribution in fetal and maternal tissues of dairy cattle following ingestion of Schooner fallout, 25:13396 (UCRL-72511)

RHODIUM
  reactions of fission-product, with uranium carbide fuels, 25:13764 (KFK-1260)

RHODIUM ALLOYS AND SYSTEMS
  Pt--Rh, photon reactions at 2.6 to 17.6 MeV with, effective atomic numbers for pair production in, (T), 25:14402

RHODIUM ISOTOPES Rh-101
  energy levels at 181.8 and 477.9 keV, half-lives of, (E), 25:14992

RHODIUM ISOTOPES Rh-103
  neutron capture at 0.001 to 1 MeV, cross sections for, (E), 25:15121
  reactivity worths in fast reactor spectra, (E/T), 25:15350

RHODIUM ISOTOPES Rh-105
  energy levels from palladium-108 (p,a) and ruthenium-104 (He-3,d) reactions, spin-parity assignments for, (E), 25:15022

RHODIUM ISOTOPES Rh-110
  beta decay of, half-life and gamma spectra for, 25:15001
  production and nuclear properties of, 25:15001

RHODOPSIN
  radiation effects on toxicity of, to biological materials, 25:13374

RIBONUCLEASE
  effects on γ-radioinduced degradation of deoxyribonucleoproteins of rabbits, 25:13363

RIVERS
  tritium content of US, (E), 25:13108
  tritium content of, in USA during 1970, 25:13400

RNA NUCLEOTIDYLTRANSFERASE
  characteristics of, from rat anterior pituitary tissue, 25:15439 (NYO-3827-18)

ROBERT E. GINNA POWER REACTOR, UNIT 1
  batteries for, revised surveillance requirements for station, 25:15285 (DOCKET-50244-58)
  containment structure for, revised leak rate limits and testing schedule for, 25:15282 (DOCKET-50244-55)
  coolant samples for, revised testing requirements for, 25:15284 (DOCKET-50244-57)
  design parameters for, revisions for 1520 MW(t) operation, 25:15286 (DOCKET-50244-59)
  operations history for 1969, 25:15286 (DOCKET-50244-59)
  site for, revised sampling schedules for environmental monitoring program for, 25:15283 (DOCKET-50244-56)
  startup testing of, review of, 25:15286 (DOCKET-50244-59)
  technical specifications for, revisions for 1520 MW(t) operation, 25:15286 (DOCKET-50244-59)

ROCKET MOTORS
  testing under controlled spin and torque profile environment, 25:15453 (SC-DR-70-911)

ROCKS
  gamma-scattering in, use in gamma and gamma--gamma well logging, 25:13113
  geophysical properties of, comparison of well logging methods for measuring, 25:13104 (UCRL-50855)
  permeability in and near explosion-produced craters, effects on crater slope stability, 25:13102 (NCG-TR-27)

RUBBER
  shielding effects of, against radiation dose from x-ray diffraction apparatus, 25:13457

RUBIDIUM
  content and depth in crustal basalts and granites in USSR, 25:13115
  electron elastic scattering at 25 to 800 eV by, tables of amplitudes and spin polarizations for, (T), 25:13555 (AD-711664)
  helium-ion reactions at 1 keV with, crossed-beam study of electron capture into excited states in, 25:14011

RUBIDIUM CHLORIDES
  radiation effects on, chemical states of recoil sulfur-35 from neutron, 25:13065

RUBIDIUM ISOTOPES Rb-84
  beta decay of $2^- \rightarrow 2^+$ positon transitions in, (E/T), 25:14972
  beta spectra from, shapes of nonunique and unique first-forbidden, 25:14976

RUBIDIUM MANGANESE FLUORIDES
  spin fluctuations in antiferromagnetic, neutron inelastic scattering study of dynamic, 25:14471

RUTHENIUM
  determination in natural materials, methods for, 25:12939
  reactions of fission-product, with uranium carbide fuels, 25:13764 (KFK-1260)

RUTHENIUM ALLOYS AND SYSTEMS
  C--Mo--Ru, phase studies of, 25:13764 (KFK-1260)
  Ru--Ta, phase transformations in near-equiatomic, effects of temperature on, 25:13708

RUTHENIUM ISOTOPES Ru-100
  neutron total cross section and resonance parameters at 1 to 1500 eV, (E), 25:15098

RUTHENIUM ISOTOPES Ru-101
  energy levels of, upper limits on half-lives for, (E), 25:14992
  neutron total cross section and resonance parameters at 1 to 1500 eV, (E), 25:15098
  reactivity worths in fast reactor spectra, (E/T), 25:15350

RUTHENIUM ISOTOPES Ru-102
  neutron total cross section and resonance parameters at 1 to 1500 eV, (E), 25:15098
  reactivity worths in fast reactor spectra, (E/T),

  25:15350
RUTHENIUM ISOTOPES Ru-103
  content of feces, milk, and urine of dairy cattle following ingestion of Schooner fallout, 25:13396 (UCRL-72511)
RUTHENIUM ISOTOPES Ru-104
  helium-3 reactions (He-3,d) at 18 MeV, angular distributions for, (E), 25:15022
  neutron total cross section and resonance parameters at 1 tc 1500 eV, (E), 25:15098
  reactivity worths in fast reactor spectra, (E/T), 25:15350
RUTHENIUM ISOTOPES Ru-106
  content in seawater, effects of sea-disposed liquid radioactive wastes on, (E), 25:13189 (CEA-CONF-1712)
  determination in liquid waste effluents from nuclear fuel reprocessing plant by γ spectrometry, 25:12950 (BRH/NERHL-70-2)
RUTHENIUM NITROSYLS
  physicochemical properties of, discharged into seawater by spent fuel processing plants, 25:13013

S

S-MATRIX
  functional analysis and numerical computations for $\pi + \pi$ dispersion relations, nonlinear, 25:14699
SAMARIUM
  complexes with carminic acid, spectrophotometric studies on, 25:12937
  determination in neutron-irradiated graphite by γ spectrometry, 25:12954
  determination in plutonium oxide--uranium oxide fuels by solvent extraction and emission spectrography, 25:12922 (WHAN-SA-44)
  determination of trace amounts of, in plutonium and plutonium dioxide--uranium dioxide by solvent extraction and emission spectrography, 25:12923 (WHAN-SA-47)
  energy-level excitation by neutron capture gamma rays, (E), 25:15002
SAMARIUM ALLOYS AND SYSTEMS
  Co--Sm--Y, lattice parameters and magnetic properties of Y/sub 1-x/Sm/sub x/Co_5, 25:14461
  Sm--Sn, magnetic susceptibility of $SmSn_3$, Sm_2Sn_3, and Sm_3Sn_3 at 2 to 900°K, 25:14453
SAMARIUM ISOTOPES
  nuclear deformation parameters and optical isotope shifts fcr, estimates of, (T), 25:15048
SAMARIUM ISOTOPES Sm-147
  neutron reactions (n,α) at 0.04 to 900 eV, resonance, 25:14994
  neutron reactions (n,α) with, alpha widths of resonance, (E/T), 25:15097
SAMARIUM ISOTOPES Sm-148
  proton elastic scattering at 49.5 MeV by, optical-model analysis of, (T), 25:15013
SAMARIUM ISOTOPES Sm-149
  neutron capture by, conversion-electron spectra from thermal, (E/T), 25:14984 (NP-18536)
  neutron reactions (n,α) at 0.04 to 900 eV, resonance, 25:14994
  neutron reactions (n,α) with, alpha widths of resonance, (E/T), 25:15097
  reactivity worths in fast reactor spectra, (E/T), 25:15350
SAMARIUM ISOTOPES Sm-152
  energy-level transitions from europium-152 beta and electron-capture decay, multipolarities and mixing ratios for, (E), 25:14985 (NP-18615)
SAMARIUM ISOTOPES Sm-154
  boron-11 reactions (B-11,4nγ) at 52 MeV, γ spectra from, (E), 25:14991
SAN ONOFRE POWER REACTOR, UNIT 1
  control rods for, requests for additional information on effectiveness of, 25:15264 (DOCKET-50206-106)
  operations history for January 1971, 25:15228 (DOCKET-50206-105)
  operations history for July 1 to December 31, 1970, 25:15227 (DOCKET-50206-103)
  xenon transient analysis for, Cycle 2, 25:15263 (DOCKET-50206-104)
SAN ONOFRE POWER REACTOR, UNIT 2
  auxiliary and emergency systems for, requested additional information on, 25:15329 (DOCKET-50361-14)
  core support structures for, requested additional information on, 25:15329 (DOCKET-50361-14)
  site for, seismological data for, 25:15329 (DOCKET-50361-14)
SAN ONOFRE POWER REACTOR, UNIT 3
  auxiliary and emergency systems for, requested additional information on, 25:15329 (DOCKET-50361-14)
  core support structures for, requested additional information on, 25:15329 (DOCKET-50361-14)
  site for, seismological data for, 25:15329 (DOCKET-50361-14)
SANDS
  fission product content of south Florida, measurements from Feb. to June 1968 of, 25:13107
  radioisotope content of south Florida, Feb. tc June 1968, measurement of natural potassium-40, radium-226, thorium-232, and uranium-238, 25:13107
SCALERS
  design specifications for scaler-timer system, 25:13217 (NP-18655)
SCANDIUM
  abundance in chondrites, achondrites, and Apollo 11 fines, (E), 25:13787
  determination in airborne and deposited particulates by neutron activation and γ spectrometry, 25:12975
  determination in meteoritic materials by neutron activation and γ--γ coincidence spectrometry, 25:12967
  determination in neutron-irradiated graphite by γ spectrometry, 25:12954
  determination of trace amounts of, in boron carbide by neutron activation, 25:12972
SCANDIUM CARBIDES
  dissociation energies of ScC_2 and ScC_4, 25:13761
SCANDIUM ISOTOPES Sc-45
  energy levels at 1.65 to 4.13 MeV from proton inelastic scattering, (E), 25:14941
  proton inelastic scattering at 8 MeV, gamma spectra from, (E), 25:14941
SCANDIUM ISOTOPES Sc-46
  metabolism in calves and cattle following intravenous and oral administration, comparison of, to cerium-144 as nonabsorbed reference material, 25:13352
SCANDIUM OXIDES
  Sc_2O_3--ZrO_2-base, electric conductivity of, effects of temperature on, 25:13778
  Sc_2O_3--ZrO_2-base, phase diagram of subsolidus region of, at 20 to 2000°C, 25:13778
SCATTERING
  amplitudes for equal-mass spinless, direct- and cross-duality, 25:14823
  amplitudes in dual-resonance model, derivation of new, 25:14675
  amplitudes in dual-resonance model, symmetry of n-point, 25:14822
  amplitudes in exchange models, convergent power series for absorption corrections to, 25:14831
  amplitudes of diffractive interactions, S-channel helicity conservation with t-channel dynamics for, 25:14605
  amplitudes of elastic, duality and analyticity for Regge poles in Veneziano representation fcr, 25:14829
  amplitudes of forward, Bjorken limit and Jin--Martin lower bound for, 25:14827
  amplitudes of potential, method for calculating partial-wave, 25:14832
  amplitudes of scalar-particle, complex angular momentum analysis of Regge pole structure of Bethe--Salpeter, 25:14833
  amplitudes of, stability of complex angular-momentum continuation of, 25:14834
  amplitudes of, strict conformal symmetry fcr mass-shell, 25:14820 (RLO-1388-598)
  amplitudes of, Veneziano, 25:14630
  amplitudes with Mandelstam analyticity, dual crossing-symmetric, 25:14821
  amplitudes with satellites, level degeneracy of generalized N-particle dual, 25:14826
  phase shift to first order in potential, (T), 25:14019
  phase shifts for, variational calculation of bounds for, 25:14024
  phase shifts of potential, method for calculating, 25:14832
  potential two-center, long-wave approximation for, 25:14817 (JINR-P4-5438)
  potential, method for calculating partial-wave amplitudes and phase shifts of, 25:14832
  potential, nonsingular integral equations for two-body, 25:14825
  Regge poles in, Dirichlet series for superposition of infinite number of, 25:14828
  space--time operator of, 25:14830
  theory of configuration-space three-body elastic, 25:14818 (N-70-40418)
  theory of configuration-space three-body, review of, 25:14819 (N-70-40698)
  theory of four-particle, integral equations in, (T), 25:15155
  wave function in vicinity of resonance energy for, Kapur--Peierls dispersion theory for studies on, 25:15181
SCb-291 (NIOBIUM ALLOY)
  cracking sensitivity of, Varestraint testing of hot, 25:13695
SCHIZOMYCOTA
  Bacillus mesentericus, mutations induced in, by ethylenimine, 25:13416
  Bacillus mesentericus, radioinduced mutations in, fast neutron and uv, 25:13416
  Bacillus subtilis, radiosensitive strains of, methods for isolation of thymine-deficient mutants from uv, 25:13614
  Clostridium botulinum Type C, marine isolates of, cultural outgrowth characteristics and nutritional requirements for, 25:13617(R) (COO-1183-32)
  Clostridium botulinum Type E, toxin production by, on irradiated packaged inoculated samples of fresh cod, 25:13617(R) (COO-1183-32)
  Clostridium botulinum, radiation effects on survival of

  spores of, effects of dose, pH, and temperature on cobalt-60 γ, 25:13611
  Escherichia coli K 12, radiation effects on hydrolase activity and content of DNA and proteins in, γ, protons, and uv, 25:13371
  Escherichia coli, radiation effects on incorporation of uracil into, effects of bacteriophage infection on, 25:13386
  Escherichia coli, radiation effects on respiration in, effects of pyridine nucleotides on uv, 25:13607
  Escherichia coli, radiation effects on sensitivity of, to subsequent treatment with chloramphenicol, comparison of uv and x, 25:13613
  Escherichia coli, radiation effects on survival of, comparison of phosphorus-32 and phosphorus-33, 25:13612
  Escherichia coli, radiation effects on synthesis of DNA, RNA, and proteins in, combined effects of reductone on uv, 25:13610
  Escherichia coli, radioinduced base-pair reversion and prophage induction mutations in, effects of DNA repair capacity on uv and x, 25:13421
  Escherichia coli, radioinduced mutations in, for arginine dependence, effects of culture medium on uv, 25:13406
  Escherichia coli, radioinduced mutations in, for histidine operon, uv and x, 25:13422
  Escherichia coli, radioinduced single strand breaks in DNA of, effects of T4 endonuclease on uv, 25:13411
  Escherichia coli, radiosensitive mutants of, defective in repair synthesis, genetic analysis of uv and x, 25:13428
  Escherichia coli, synthesis of DNA and phage lysozyme in, following infection with uv-irradiated T4 bacteriophage, 25:13616
  radiation effects on count of, in processed shrimp, γ, 25:13619
  Salmonella sp., recovery from γ-irradiated food, effects of culture medium on, 25:13620
  Salmonella typhimurium, radiation effects on host cell reactivation, genetic map for uv, 25:13408
  Streptomyces coelicolor, mutations induced in, by nitrosoguanidine, 25:13414
  Streptomyces coelicolor, radioinduced mutations in, genetic mapping of uv, 25:13407
  Streptomyces coelicolor, radioinduced mutations in, uv, 25:13414

SCINTILLATION CAMERAS
  development of, review on, 25:13222

SEALS AND GLANDS
  design of bubble chamber, for studies of alpha-induced void nucleation in superheated water, 25:13152(R) (SU-326-P-13-5)

SEAWATER
  analysis for strontium by photon activation, 25:12974
  corrosive effects on SNAP-19B fuel capsules, 25:13163 (MLM-1652)
  radioisotope accumulation from, by alginic acid of brown algae, 25:13403
  ruthenium-106 content of, effects of sea-disposed liquid radioactive wastes on, (E), 25:13189 (CEA-CONF-1712)
  tritium content of Australian, 1969 to 1970, 25:13103 (NP-18639)

SEDIMENTARY DEPOSITS
  analysis of deep-sea, for antimony by neutron activation and radiochemical separation, 25:12968

SEED
  mutations induced in wheat, by EMS for weight variations, 25:13419
  radiation effects on, of agricultural plants, latent γ, 25:13599
  radiation effects on, of beans, latent x, 25:13600
  radiation effects on, of tobacco following exposure of pollen, γ, 25:13601
  radioinduced mutations in, of wheat for weight variations, γ, 25:13419

SEISMIC WAVES
  effects on motion of earth dams, digital computer programs for predicting, 25:13130 (UCRL-13329(Pt.2))

SELENIUM
  determination in air by thermal neutron activation as indicator of sulfur contamination, 25:12965
  determination in sulfur, improvement in sensitivity of spectrographic, 25:12940
  effects on gravimetric determination of tellurium, 25:12943
  metabolism of, nature and importance of organic forms in, 25:15425(R) (COO-1449-11)

SELENIUM ISOTOPES Se-75
  electron capture decay of, γ coincidence spectra for, (E), 25:14931
  incorporation in diaphragms and livers in rats in vitro in comparison to incorporation in tumor cells following incubation in sodium selenites, 25:13354
  uptake of selenomethionine-incorporated, by abdominal organs in dogs, effects of route of administration on, 25:13343

SEMICONDUCTORS
  analysis of alloys of, for tellurium using Victoria Blue 4R, extraction--photometric method for, 25:12935
  neutron scattering in spin-wave resonances in antiferromagnetic, slow, (T), 25:14488
  wave scattering in spin-wave resonances in antiferromagnetic, electromagnetic, (T), 25:14488

SEMINAL VESICLES
  radiation effects on secretory activity of, in rats, x, 25:13366

SEROTONIN
  effects on blood coagulation in γ-irradiated rats, 25:13549
  radioprotective effects of, in combination with other protectants on mice, use of spleen weight-radiation dose relation for testing, 25:13478

SEWAGE
  radiation monitoring of, in Milan, Italy during 1968 and 1969, 25:13454

SEYFERT GALAXIES
  evolution of, spinars in, (T), 25:13952
  gas abundances in NGC 3031, neon, nitrogen, and oxygen, (E), 25:13918
  gas emission from nucleus of NGC 3031, (E), 25:13918
  luminosity of three Markarian, (E), 25:13923
  photographic B variations and infrared K data for NGC 4151, (E), 25:13924
  synchrotron emission from, (T), 25:13936(R) (AD-711829)

SHEEP
  hair follicle growth in, autoradiography of DNA synthesis and cell migration during, 25:13337
  radiation effects on lactate and propionate content of blood serum of, effects of shock waves and fasting on γ and neutron, 25:13384

SHELTERS
  protection factor for concrete, effects on requirements for nuclear weapons for total destruction of US population, 25:13132 (AD-711021)

SHIELDED CONTAINERS
  design for shipping curium oxide, 25:13202
  design for shipping FTR fuel pins, 25:13187 (BNWL-1512)
  design for shipping fuel elements, 25:13205(P)
  design for shipping radioactive materials, 25:13204(P)
  leakage from Types A and B radioactive materials shipping, method for calculating gas and radioactivity, 25:13201
  shipping of lead, design of protective packaging for, 25:13196(P)

SHIELDING
  gamma scattering cross sections, Klein--Nishina multiple, (T), 25:14393 (ANL-7689)
  Radiation Shielding Information Center program setup instructions manual, 25:14395 (CTC-INF-1017)

SHIPPING
  container for curium oxide, design of water-filled stainless steel, 25:13202

SHIPPINGPORT PRESSURIZED-WATER REACTOR
  coolant chemistry during July to September 1970, 25:15214(R) (DLCS-5000370)
  maintenance during July to September 1970, 25:15214(R) (DLCS-5000370)
  operations during July to September 1970, 25:15214(R) (DLCS-5000370)

SHOCK TUBES
  electrode ablation in electromagnetic, (E/T), 25:14222

SHOCK WAVES
  effects on content of lactate and propionate in serum of sheep, 25:13384
  production and properties in dense plasma focus, 25:14270
  production by ion--acoustic waves in plasma, (E/T), 25:14389
  production by light explosions in gases, diamagnetic moment of, (E/T), 25:14282
  production in plasma by electromagnetic force fields, 25:14274
  propagation along collisionless Vlasov plasma, existence conditions for hydromagnetic, (T), 25:14326
  propagation in cold collisionless plasma, near-steady oblique, (T), 25:14324
  propagation in magnetized plasma, effect of fluctuations on MHD, (T), 25:14287
  structure of collisionless ionizing, in low-density gas, (T), 25:14298
  structure of oblique and normal ionizing, magnetic, (T), 25:14284 (AD-711086)

SILICATE ROCKS
  neutron thermalization in borehole, effects of moisture on, 25:13109

SILICATES
  radiation history of grains of, in Apollo 11 and 12 cores, (E), 25:13958

SILICON
  abundance in Sun, (E/T), 25:13899
  analysis for boron, carbon, and oxygen by charged particle and γ photon activation, 25:12971
  carrier diffusivity and drift velocity measurements in p^{+}-ν-n^{+} diodes of, electron and hole, 25:14431
  content and depth in crustal basalts and granites in USSR, 25:13115
  determination in meteorites by nondestructive fast neutron activation, 25:12970
  determination of trace amounts of, in boron carbide by neutron activation, 25:12972
  electron emission by 400-eV electron-excited doped, effects of temperature and free carrier density on, 25:13967

  ion channeling patterns of [111], [110], and [100] surfaces of, krypton-85- and xenon-133-, 25:14417
  neutron elastic and inelastic scattering at 4.5 to 8 MeV, cross sections for, (E/T), 25:14963
  neutron reactions (n,xγ) at 14 MeV with natural, cross sections and gamma spectra from, (E/T), 25:14920(T) (BNL-tr-380)
  radiation damage in p^+-ν-n^+ diodes of, annealing of 2.8-MeV proton, 25:14431
  radiation effects on electric properties of lithium- and aluminum-doped, γ-, (E), 25:14412 (N-70-39456)
  radiation effects on gold diffusion in single crystals and surface-barrier diodes of, x, 25:14420
  radiation effects on lithium-doped, Hall-effect study of electron, 25:14423
  radiation effects on space-charge-limited currents in, 14-MeV neutron, 25:14426
  radioinduced defect clusters in doped Lopex, properties of fast-neutron, 25:14428
SILICON CARBIDES
  fission product distribution in fuel particle coating of layered pyrolytic carbon and, sputtering method for determination of, 25:13756
  properties at high temperatures, review of physical, thermal, and thermodynamic, 25:13667
SILICON ISOTOPES Si-26
  energy levels from (p,t) reactions, spin-parity assignments for, (E), 25:14950
SILICON ISOTOPES Si-27
  energy levels from silicon-28 (He-3,α) reactions, spectroscopic factors for, (E), 25:14944
SILICON ISOTOPES Si-28
  energy levels at 13.047 and 13.252 MeV from aluminum-27 (p,γ) reactions, spin-parity assignments for resonance, (E), 25:14948
  energy levels at 9480 and 9495 keV from aluminum-27 (p,γ) reactions, (E), 25:14936
  energy levels from magnesium-26 (He-3,n) reactions, T = 2, (E), 25:14943
  helium-3 reactions (He-3,α) at 35 MeV, differential cross sections for, (E), 25:14944
  neutron capture at 14 MeV, cross sections and gamma spectra from fast, (E/T), 25:14920(T) (BNL-tr-380)
  neutron elastic scattering at 14 MeV, diffraction- and optical-model analysis of differential cross sections for, (E/T), 25:14920(T) (BNL-tr-380)
  proton elastic scattering at 18.0 MeV, depolarization parameter from polarized, (E), 25:14889 (CEA-CONF-1650)
  proton reactions (p,t) with, angular distributions for, (E), 25:14950
SILICON ISOTOPES Si-29
  proton reactions (p,γ) with, resonance γ spectra from, (E), 25:14933
SILICON OXIDES
  content in rocks of shields and sediment cover of Brazil, Canada, and USSR, relations with geological time, 25:13114
  B_2O_3--Na_2O--SiO_2--UO_2, luminescence of glasses of, 25:13017
  Cr--SiO, electric conductivity of thin films of, on alumina, fused quartz, and pyrex substrates, effects of thermal treatments on, 25:14435 (IJS-587)
SILICON SYSTEMS
  Cr--Si--Zr-base, corrosion by steam at 350 to 450°C and 50 atm pressure, 25:13629 (EIR-184)
  Ge--Tb--Si, magnetic properties and structure of $TbGe_{0.2}Si_{0.8}$, 25:14434 (CEA-CONF-1701)
SILVER
  contact angle for clean tungsten surface, sessile drop method for measurement of, 25:13691
  determination in lead oxide and zinc sulfide by neutron activation and radiochemical separation using diethyl dithiocarbamate, 25:12963
  determination in photographic emulsion, x-ray transmission gage for, 25:13312
  determination in photographic film, on-line x-ray backscattering gage for, 25:13311
  effects on gravimetric determination of tellurium, 25:12943
  electron charge-deposition distribution at 4 to 24 MeV in, 25:13964
  energy-level excitation by neutron capture gamma rays, (E), 25:15002
  helicon-wave resonances in single-crystal, anisotropic electric resistivity tensor from, (E), 25:14468
SILVER ALLOYS AND SYSTEMS
  Ag--Cd, phase transformations in, β--α massive, 25:13720
  Ag--Zn, phase transformations in, β--α massive, 25:13720
SILVER ISOTOPES
  separation by spontaneous precipitation on platinum powder in nitric acid solutions, 25:13086
SILVER ISOTOPES Ag-107
  alpha elastic scattering by, optical-model analysis of, (E/T), 25:14947
  alpha inelastic scattering at 10 MeV, Coulomb excitation by, (E), 25:15035
  oxygen-16 inelastic scattering at 45.5 MeV, Coulomb excitation by, (E), 25:15035
SILVER ISOTOPES Ag-109
  alpha inelastic scattering at 10 MeV, Coulomb excitation by, (E), 25:15035
  neutron capture by, γ spectra from, (E), 25:14982 (NCSAC-31)
  oxygen-16 inelastic scattering at 45.5 MeV, Coulomb excitation by, (E), 25:15035
SILVER ISOTOPES Ag-110
  energy-level scheme from silver-109 neutron capture, (E), 25:14982 (NCSAC-31)
SILVER PERCHLORATES
  radiation effects on frozen alcohol and aqueous acid solutions containing cadmium salts and, ESR studies on diatomic cations produced from γ, 25:13028
SKIN
  lithium-6 uptake by, of rats following intravenous injection, 25:13350
  radiation dose to human, during radiological examinations of intestine and stomach, 25:13580
  radiation dose to, in personnel following accidental exposure to iridium-192 vehicle, β and γ, 25:13466
  radiation effects on electric parameters of, histomorphological studies on, 25:13565
  radiation effects on histamine content of, in rats, combined effects of skin wounds on whole-body, 25:13368
  radiation effects on human, comparison of REE of γ and x radiation for, 25:13583
  radiation effects on human, eight to ten years after therapy, strontium-90 β, 25:13582
  radiation effects on human, following therapy for carcinomas, protective effects of tanderil against, 25:13476
SLURRIES
  analysis of flotation, for fluorite by fast neutron activation and γ spectrometry, 25:12976
  density of postflotation, flow velocity of postflotation, bromine-82 tracer method for measuring, 25:13176
SNOW
  crater formation in Greenland icecap, mechanisms and size of chemical explosion-induced, 25:13133 (AD-711861)
SODIUM
  abundance in late G and K dwarfs, (E), 25:13824
  abundance in Sun from Fraunhofer lines, (E/T), 25:13899
  analysis for argon, development of methods for, 25:13651(R) (ANL/ST-4)
  analysis for carbon, calibration and design of meters for, 25:13651(R) (ANL/ST-4)
  analysis for hydrogen, calibration and design of meters for, 25:13651(R) (ANL/ST-4)
  analysis for oxygen, calibration and design of meters for, 25:13651(R) (ANL/ST-4)
  analysis for radioisotopes, development of methods for, 25:13651(R) (ANL/ST-4)
  analysis of FFTF coolant, design of remotely operated system for, 25:13195 (WHAN-SA-91)
  boiling of liquid, effects of cavitation and saturation temperature on initiation of nucleate, 25:13154
  boiling of liquid, hydrodynamics and thermodynamics of, 25:15382
  chemistry of heat transfer system, development of methods and standards for studies of, 25:13651(R) (ANL/ST-4)
  compatibility with stainless steel at high temperatures, effects of impurities on, 25:13651(R) (ANL/ST-4)
  content and depth in crustal basalts and granites in USSR, 25:13115
  corrosive effects on chromium--molybdenum alloy and stainless steels, 25:15357 (SAN-781-228)
  determination in meteoritic materials by neutron activation and γ--γ coincidence spectrometry, 25:12967
  determination in neutron-irradiated graphite by γ spectrometry, 25:12954
  determination in postage stamps by neutron activation, 25:12973
  determination of trace amounts of, in boron carbide by neutron activation, 25:12972
  distribution in atmosphere, use in tracer studies of global transport processes, (E), 25:13121 (TID-25314)
  effects on γ radiolysis of ammonia adsorbed on synthetic zeolites, EPR spectral studies on, 25:13057
  effects on self-welding in high temperature alloys and steel, 25:13668
  flow in triangular rod clusters of liquid, temperature and velocity distribution in, 25:15363
  handling of liquid, design of glove box for, 25:13185 (AERE-R-6338)
  heat transfer to liquid, effects of cavitation on, 25:13154
  heat transfer to, during forced convection in induction-heated tubes, 25:13156
  ion exchange behavior on zirconium phosphate crystals, 25:13084
  particle size distribution in aerosols of, at 400°C, 25:13651(R) (ANL/ST-4)
  properties for heating steam generators, description of facility for testing, 25:13143
  properties of nitrogen-bearing species of, 25:13651(R) (ANL/ST-4)
  radiation effects on 3-methylpentane containing, at 77°K, comparative ESR studies on paramagnetic species produced from γ or uv, 25:13025
  radiation effects on content of, in brain and muscle tissues of rats, lethal and sublethal, 25:13566

XUM

  separation from cesium in anhydrous and aqueous solutions of ethanol, methanol, and 1,2-propanediol by ion exchange using Zeolite Linde A, 25:13091
  solvent properties for inert gases of liquid, 25:15379(T) (EURFNR-785)
  solvent properties for xenon at 350 to 600°C, 25:13651(R) (ANL/ST-4)
SODIUM ACID FLUORIDES
  radiation effects on single crystals of, ESR and optical absorption study of 1-MeV electron, 25:14411 (AD-712321)
SODIUM ALLOYS AND SYSTEMS
  H--Na--O, phase studies of, 25:13651(R) (ANL/ST-4)
SODIUM AZIDES
  radiolysis of basic and neutral aqueous solutions of, effects of yields of hydrogen atoms on production of hydrogen molecules from γ, 25:13044
SODIUM CHLORIDES
  electric properties of crystals of, space-charge-limited electron currents in, 25:14449
  radiation effects on, chemical states of recoil sulfur-35 from neutron, 25:13065
  radioinduced defects in crystals of, release of stored energy in annealing of 4.5-MeV proton, 25:14424
  radioinduced thermoluminescence of crystals of, effects of sodium doping on x, 25:14425
  KCl--NaCl, electrolytic properties of aqueous solutions of, adiabatic compression and ultrasonic attenuation studies of, 25:13015
SODIUM CYANIDES
  radiation effects on, reactions of recoil carbon-14 and nitrogen-13 from neutron, 25:13072
SODIUM HYDROXIDES
  radiolysis at 77°K, yields from γ, 25:13056
SODIUM ISOTOPES Na-21
  energy levels of, angular momenta and transition properties of, (E), 25:14953
  energy levels of, rigid-rotor and Coriolis model predictions for, (T), 25:14953
SODIUM ISOTOPES Na-22
  energy levels from neon-20 (He-3,p) reactions, spin-parity assignments for, (E), 25:14904
SODIUM ISOTOPES Na-23
  determination by pulsed neutron activation and scintillation counting, 25:12960
  energy levels of, angular momenta and transition properties of, (E), 25:14953
  energy levels of, rigid-rotor and Coriolis model predictions for, (T), 25:14953
  neutron capture at 0.025 eV, cross section for, (E), 25:14935
  neutron capture at 14 MeV, cross sections for fast, (E/T), 25:14920(T) (BNL-tr-380)
  neutron elastic scattering by, calculation using multilevel formalism, (T), 25:15161
  neutron reactions $(n,x\gamma)$ at 14 MeV, cross sections for, (E/T), 25:14920(T) (BNL-tr-380)
  neutron total cross sections and resonance parameters at 0.28 to 1.2 MeV, (T), 25:14969
SODIUM ISOTOPES Na-24
  determination in reactor cooling water by γ spectroscopy, 25:12956
  use as tracer for measuring enthalpy of steam in nuclear power plant turbines, 25:13148
SODIUM OXIDES
  content in rocks of shields and sediment cover of Brazil, Canada, and USSR, relations with geological time, 25:13114
  B_2O_3--Na_2O--SiO_2--UO_2, luminescence of glasses of, 25:13017
SODIUM PHOSPHATES
  effects of pre-dip treatment using, on γ-irradiated fish, 25:13618
SODIUM THIOSULFATES
  sorptive properties for iodine in reactor containment atmospheres, (E/T), 25:15374 (BAW-10024)
SOILS
  density measurements of, design optimization of gamma backscatter gages for, 25:13316
  density of, gamma--gamma logging method for measurement of, 25:13104 (UCRL-50855)
  fission product content of south Florida, measurements from Feb. to June 1968 of, 25:13107
  geophysical properties of, comparison of well logging methods for measuring, 25:13104 (UCRL-50855)
  permeability in and near explosion-produced craters, effects on crater slope stability, 25:13102 (NCG-TR-27)
  radioactive contamination of, in France from fallout and industrial wastes, cesium-137, iodine-131, and strontium-90, 25:13402
  radioactivity monitoring at West Valley Processing Plant, 1969, 25:13080 (DOCKET-50201-62)
  radioisotope content of south Florida, Feb. to June 1968, measurement of natural potassium-40, radium-226, thorium-232, and uranium-238, 25:13107
  strontium-90 removal from, by leachate water, runoff water, and plant uptake, effects of crop management practices on, 25:13118(R) (COO-414-17)
  uranium content of marsh, effects of humidity on, 25:13116
  water content of, gamma ionization chamber measurements of, 25:13110
  water content of, neutron logging method for measurement of, 25:13104 (UCRL-50855)
SOLAR ACTIVE REGIONS
  electron emission structure of McMath 8905, (E), 25:13894
SOLAR CORONA
  atomic energy level transition probabilities in, forbidden nitrogen and oxygen, (E/T), 25:14107
  characteristics of, during eclipse of March 7, 1970, (E), 25:13888
  electron densities in, (E), 25:13885
  electron temperatures in, during solar flares, (E), 25:13902
  energy source for, (T), 25:13907
  heating by neutrons from photosphere, (T), 25:13907
  magnetic fields in, following proton flares, (E), 25:13893
  photography with interference filters, monochromatic, (T), 25:13887
  plasmas in, cooling of flare-produced, (T), 25:13889
  radio emission from, MHD pulsations of, (E/T), 25:13868
  x-ray line emission from, variation in O VII, (E), 25:13885
SOLAR DISTURBANCES
  asymmetries in, connection between N--S and E--W, (E/T), 25:13883
  effects on modulation of atmospheric neutron production, (E/T), 25:14064
SOLAR FLARES
  effects of proton-emitting, on diurnal variation of cosmic-rays, (E), 25:14075
  effects on coronal and photospheric magnetic fields, (E), 25:13893
  electron emission and propagation at 40 keV from, (E), 25:13894
  plasmas from, in corona, cooling of, (T), 25:13889
  proton propagation from, effect of interplanetary disturbance on, (T), 25:13869
  x-ray emission during, coronal electron temperatures associated with, (E), 25:13902
SOLAR PARTICLES
  interaction of streams of, in lower ionosphere, electron production by, (T), 25:14126
  interactions in lower ionosphere, electron production by, (E/T), 25:14124
  spectra of, upper cutoff in, (E/T), 25:13910
SOLAR PROMINENCES
  magnetic fields in quiescent, longitudinal, (E), 25:13884
SOLAR RADIATION
  anisotropy of diffuse, (E), 25:13903
  effects on biological activities, effects of electromagnetic fields on, 25:13572
  interactions in atmosphere, solar-cycle modulation of neutron production from, (E/T), 25:14064
SOLAR RADIO BURSTS
  average exciter speed for Type III, (E), 25:13892
  characteristics of 71 GHz, from July 1967 to Dec. 1969, (E), 25:13890
  effect of Mar. 23, 1969, on 6300- and 6394-A midlatitude auroral emission, (E), 25:14115
  energy of, as indicator of solar proton intensity, (E/T), 25:13867
  intensity fluctuations associated with Type IV, (E/T), 25:13868
  models for Type-II and -III, (T), 25:13872
  models for Type-II and -III, (T), 25:13871
  polarization characteristics at 25.3 MHz of Type-III, (E), 25:13859 (AD-711398)
  relation of 3.3-mm, to soft x-ray bursts, (E), 25:13860(R) (AD-711784)
  relation of 3.3-mm, to soft x-ray bursts, (E), 25:13891
SOLAR SPICULES
  formation of, mechanism for, (T), 25:13822
SOLAR SYSTEM
  cosmic-ray modulation by, primary, (E/T), 25:14071
  isotope abundances in early, magnesium-26 and aluminum-26, (E), 25:13864
SOLAR WIND
  alpha particles in, detection of, (E), 25:13895
  cosmic-ray interactions with primary, (T), 25:14076
  cosmic-ray modulation by, primary, (T), 25:14070
  flow parameters for, (T), 25:13861 (N-70-37452)
  interactions with lunar and cometary atmospheres, (T), 25:13905
  iron abundance in, (E), 25:13958
  plasma-density irregularities in, spectrum of, (T), 25:13866
  velocity of, relation with F2-layer electron density, daytime, (E), 25:14110
SOLAR X-RAY BURSTS
  relation of soft, to 3.3-mm bursts, (E), 25:13860(R) (AD-711784)
  relation of soft, to 3.3-mm radio bursts, (E), 25:13891
SOLCOSERYL
  effects on radioinduced lesions of mucosa following therapy, 25:13475
SOLDERS
  photon reactions at 2.6 to 17.6 MeV with, effective atomic numbers for pair production in, (T), 25:14402

SOLID STATE PHYSICS
  book: Lectures in Theoretical Physics, (in Romanian), 25:14630
  de Haas--van Alphen data inversion for closed Fermi surfaces with inversion symmetry, computer programs for, 25:14433 (ANL-7659)
  research at BNL, July 1969--June 1970, 25:14837(R) (BNL-50230)
SOLIDS
  conference on surface properties of, Paris, July 7 to 11, 1969, 25:13734
  crack geometries in, fracture mechanics evaluation of effects of stress on, 25:13181 (WAPD-TM-976)
  electron backscattering by, nonrelativistic theory of, 25:13961
  radiation effects on specimens of, in electron microscopes, 25:13628
  radioinduced acceleration of climb-controlled creep in, neutron, (T), 25:13725
  radioinduced energy storage in crystals of, luminescence from aqueous release of γ, 25:13026
SOLVENT EXTRACTION PROCESSES
  columns for, controlled cycling operation of pulsed, 25:13082(R) (RLO-2225-T-11-1)
  dynamics of, computer model for, 25:13082(R) (RLO-2225-T-11-1)
SOUND
  velocity in drill holes, well logging method using measurements of, 25:13104 (UCRL-50855)
SOUTH AMERICA
  radiation monitoring of atmosphere of, during May, 1970, gross beta, 25:13122
  radioactivity monitoring in surface atmosphere of, during April, 1970, gross β, 25:13441
  radioisotope content of milk in, during 1969 and 1970, cesium-137, iodine-131, and strontium-90, 25:13433
  radioisotope content of milk in, during April 1970 as compared to average for previous 12-month period, cesium-137, iodine-131, and strontium-90, 25:13442
SOUTHWEST EXPERIMENTAL FAST OXIDE REACTOR
  fuel elements for, transient operation with defective, 25:15272 (DOCKET-50231-69)
  operation of, authorization for 20 MW(t), 25:15386 (DOCKET-50231-67)
  safety limit settings for, effects of guinea pig fuel rods on, 25:15271 (DOCKET-50231-68)
SOVIET UNION
  nuclear explosions testing by, at Semipalatinsk test area, seismic indications of underground, 25:13445
SPACE
  magnetic field in intergalactic, (T), 25:13944
  plasma turbulence in interstellar, (T), 25:13912
  production of gegenschein in interplanetary, (E/T), 25:13906
  pulsar pulse broadening due to angular scattering in interstellar, (E/T), 25:13853
SPECIFIC HEAT
  measurement using conventional helium-3 cryostat, 25:14212 (UUIP-677)
SPECTROMETERS
  data acquisition systems for nuclear, for analysis of biological samples, 25:13229 (CEA-CONF-1647)
  design of grazing-incidence, for recording solar spectra, (E), 25:13875
  magnetic field calculations for design of iron-free double-focusing, 25:13324 (UUIP-715)
SPECTROSCOPY
  method for vacancy-cascade, 25:14038
SPERMATOCYTES
  radioinduced translocation chromosome aberrations in, of mice, effects of dose and dose rate on frequency of γ, 25:13404
SPHERES
  gamma transport in, computer program for solving one-dimensional Boltzmann equation for, (T), 25:14863 (CEA-N-1358)
  heat transfer between concentric, by natural convection, 25:15449(R) (RLO-2214-1)
  heat transfer between concentric, by natural convection, 25:15450 (RLO-2214-2)
  hydrodynamics of small, in frictional media, 25:15444(T) (CRNL-tr-2431)
  neutron transport in, computer program for calculating polyenergetic, (T), 25:14864 (CEA-N-1388)
  neutron transport in, computer program for solving Boltzmann equation for, (T), 25:14866 (LA-4567)
  neutron transport in, computer program for solving one-dimensional Boltzmann equation for, (T), 25:14863 (CEA-N-1358)
  neutron transport in, two-group analysis of critical problem for, (T), 25:14867
  radioinduced electrification of, gamma, (T), 25:14430
SPINAL CORD
  radiation effects on cholinesterase activity in, of cats, whole-body x, 25:13333
  radiation effects on cholinesterase activity in, of cats, partial and whole-body x, 25:13375
SPLEEN
  indium-113--tin-113 distribution in rat, 25:13501
  radiation effects on antibody activity in, cells of mice, analysis of origin of plaque forming cells following γ, 25:13387
  radiation effects on histone content of deoxyribonucleoproteins in, of rats, effects of heparin on x, 25:13385
  radiation effects on protein synthesis in cells of, in rats, alone and in combination with immunization, 25:13376
  radiation effects on weight of, in mice as function of dose, use of function for testing protective effects of AET and combined AET, DNA, glutathione, and serotonin, 25:13478
  radiation effects on weight of, in rats, comparison of RBE for cesium-137 and tritium oxide, 25:13551
  regeneration in whole-body γ-irradiated mice, role of mast cells in, 25:13577
  scanning of human, for diagnosis of rupture, use of metastable technetium-99-labeled sulfur colloid for, 25:13511
  scanning of human, for diagnosis of splenic abscesses, 25:13512
  selenium-75-labeled selenomethionine uptake by, in dogs, effects of route of administration on, 25:13343
SPORES
  radioinduced germination of Dictyostelium discoideum, cobalt-60 γ, 25:13605
STAINLESS STEEL
  collapse of externally pressurized long thin tubes of Type 316, with initial ovalities, computer program for calculation of, 25:13652 (GAMD-8219(Rev.))
  compatibility with sodium at high temperatures, effects of impurities on, 25:13651(R) (ANL/ST-4)
  corrosion by chlorinated oxidizing solution, effects of pitting on, 25:13637
  corrosion of Types 304 and 316, by flowing sodium, 25:15357 (SAN-781-228)
  corrosion of, past and future perspectives on, 25:13632
  corrosion resistance to liquid lithium, effects of powdered molybdenum on, 25:13634
  creep of niobium-stabilized austenitic, recovery theory for, 25:13674
  magnetic properties of austenitic, at 4.2 to 300°K, 25:14172
  mechanical properties of welds on ferritic, effects of aluminum, niobium, and titanium filler additions on, 25:13696
  niobium carbide precipitation in Type 20-25, method for, 25:13640 (TRG-Report-2040)
  removal of cladding of, on LMFBR fuel elements using zinc bath, 25:13077(R) (ANL-7755)
  stress-strain curves for types 304, 304H, 316, 316H and 2.25 percent chromium -1 percent molybdenum, 25:15452 (SAN-781-2012(Pt.1))
  welding in sodium at 500 to 700°C, tendency for self-, 25:13668
STANDARDS
  development of nuclear, in USA, directory of personnel involved in, 25:13469 (ORNL-NSIC-75(Rev.1))
STANFORD LINEAR ACCELERATOR
  development and operation, July 1 to Sept. 30, 1970, 25:14851(R) (SLAC-128)
STAR CLUSTERS
  cooling sequences in Hyades, (E/T), 25:13799
  helium abundances in old open, (E), 25:13798
  metal abundances in old open, (E), 25:13798
  star membership of NGC 7062, (E), 25:13801
STARS
  atmospheres of 4 O-Type subdwarf, model, (E), 25:13825
  atmospheres of, outer layers of model moving, (T), 25:13792
  characteristics of Cepheid variable, (E/T), 25:13789 (N-70-38166)
  chromospheres of, stability of, (T), 25:13822
  classification by Stroemgren photometry, quantitative, (T), 25:13809
  color--magnitude diagrams of, in open cluster NGC 7062, (E), 25:13801
  color-magnitude diagram for white-dwarf, in Hyades cluster, (E/T), 25:13799
  composition of, chemical, (T), 25:13821
  deceleration of magnetized, rotational, (T), 25:13800
  deuterium burning in HL Tau 76, (E/T), 25:13796
  distances of red and blue supergiant, from galactic center, (T), 25:13791
  energy loss of, cross sections of γ + e → e + anti ν + ν interactions for rate of, (T), 25:14650
  evolution of, (T), 25:13797
  evolution of, effects of chemical composition on, (T), 25:13821
  evolution of, occurrence of loops in H--R diagram, (T), 25:13815
  formation of late B-type, positions of, (T), 25:13926
  growth curves for UU Aur, (E), 25:13803
  helium abundances in, of old open clusters, (E), 25:13798
  helium burning in, central, (T), 25:13815
  hydrogen-to-carbon ratios in four carbon, in accordance with CNO bi-cycle, (E), 25:13795
  hydromagnetic-wave emission from magnetized, (T), 25:13800
  identification of blue, in wing of the Small Magellanic Cloud, (E), 25:13931
  infrared emission from, standard sources for, (E),

25:13788 (AD-711364)
  light curves for R548, (E), 25:13808
  limb-darkening tables for F0--K0 main-sequence, (E), 25:13806
  metal abundances in late G and K dwarf, (E), 25:13824
  metal abundances in, of old open clusters, (E), 25:13798
  model for Cepheid, pulsational characteristics of low-mass, (T), 25:13823
  model for VX Sgr, (E), 25:13817
  models for low-mass white-dwarf, evolutionary sequences for, (E/T), 25:13799
  motions of, in open cluster NGC 7062, proper, (E), 25:13801
  perturbation treatment of close-binary, in the N-body problem, (T), 25:13802
  photometric recognition of rapid rotators and supergiants among B, (E/T), 25:13790
  photometry of bright, in Small Magellanic Cloud, (E), 25:13921
  photometry of M, near South Galactic Pole, (E), 25:13935
  photometry of, at border of Scutum Cloud, (E), 25:13925
  properties of white-dwarf, 25:13797
  radio emission at 11.1 cm from Antares, detection of, (E), 25:13804
  radio emission from hydroxyl in Mira variable, (E), 25:13818
  shell activity in HR 2142, periodic, (E), 25:13805
  shell episode in Pleione, comparison of theoretical and observational results for, (E/T), 25:13794
  spectra of Cepheid variable, (E/T), 25:13789 (N-70-38166)
  spectra of SX Phoenicis, line intensity variations in, (E), 25:13812
  spectra of SX Phoenicis, radial velocity curve from, (E), 25:13811
  spectra of VX Sgr, (E), 25:13817
  spectra of, deviations from LTE in weak complex, (T), 25:13816
  spectra of, interstellar extinction in, (E), 25:13934
  stability of low-mass pure-helium, pulsational, (T), 25:14234
  ultraviolet emission from early-type, fluxes of, (E), 25:13813
STATISTICS
  selection procedure based on Wald's double dichotomy test, 25:15441 (ORNL-TM-3237)
STEAM
  corrosive effects on zirconium alloys at 350 to 450°C and 50 atm pressure, 25:13629 (EIR-184)
  enthalpy of wet, in nuclear power plant turbines, sodium-24 injection tracer method for measuring, 25:13148
  quality of steam generator, effects on heat transfer, 25:13149 (EUR-4561)
STEAM POWER PLANTS
  atmospheric contamination from fossil fueled, risk of carcinogenesis from long-term low-dose exposure to, 25:15464 (UCRL-50937)
  cooling water requirements for, effects on power generation economics and plant site selection, 25:13147
STEEL
  corrosion of, past and future perspectives on, 25:13632
  development of heavy-section, research program for, 25:13656(R) (ORNL-4590)
  fabrication of pressure vessels of heavy-section Type A533B, welding methods for, 25:13638 (ORNL-4313-3)
  mechanical properties of heavy-section pressure vessel, correlation of test data on, 25:13658 (ORNL-4590, pp 135-232)
  mechanical properties of heavy-section Type A533B, Charpy specimen testing for determination of, 25:13657 (ORNL-4590, pp 20-99)
  mechanical properties of Types A302B and A533B heavy-section, correlation of test data on, 25:13659 (ORNL-4590, pp 233-48)
  mechanical properties of welds on heavy-section Type A533B, 25:13639 (ORNL-4590, pp 1-19)
  mechanical properties of welds on heavy-section Type A533B, 25:13657 (ORNL-4590, pp 20-99)
  microstructure of rupture areas in Charpy specimens of Type A533B, 25:13657 (ORNL-4590, pp 20-99)
  properties of thick-section plates and weldments of Type A533B, impact and tensile, 25:13660 (ORNL-TM-3211)
  radiation effects on crystal structure of martensitic carbon, at low temperatures, 2 MeV electron, 25:13729
  radiation effects on mechanical properties of heavy-section Type A533B, fast neutron, 25:13724 (ORNL-4590, pp 100-34)
  radiation effects on welds on heavy-section Type A533B, fast neutron, 25:13724 (ORNL-4590, pp 100-34)
  welding in sodium at 500 to 700°C, tendency for self-, 25:13668
  welding of heavy-section Type A533B, methods for, 25:13639 (ORNL-4590, pp 1-19)
STELLARATORS
  plasma drift calculations for l = 3, using stellarator expansion technique, 25:13793
  superconducting ring for Spherator, operation of levitated, 25:14356
STILBENE, α-METHYL-
  radiation effects on isomerization of, in cyclohexane solutions, γ, 25:13037
STOMACH
  radiation dose to human, x, 25:13453
  radiography of human, effects of, on gonads and skin, 25:13580
STORAGE RINGS
  development of BNL 1000-GeV, 25:14835 (BNL-15423)
  development of colliding beam, at Orsay linac, 25:14843 (LAL-RT-44-70)
  experimental facility for CERN ISR, development of data handling system for Split Field Magnet project, 25:14839 (CERN-70-21(Vol.2), pp 561-80)
  research in Soviet Union, 25:14544
  theory of electron, 25:14850 (SLAC-121)
STRANGE PARTICLES
  properties of, conference on, (E), 25:14583(T) (AEC-tr-6882/1)
STRATOSPHERE
  strontium-90 content of, in Australia following nuclear weapons testing during 1966 to 1968, 25:13436
STRONTIUM
  abundance in chondrites, achondrites, and Apollo 11 fines, (E), 25:13787
  content and depth in crustal basalts and granites in USSR, 25:13115
  content of diet of human adolescents in EURATOM countries during 1965 to 1967, 25:13392 (EUR-3945(Pt.2))
  determination in seawater by photon activation, 25:12974
  determination of trace amounts of, in blood serum by emission spectroscopy, 25:12946
  ion exchange behavior on zirconium phosphate crystals, 25:13084
  separation by solvent extraction using Rhodamine S and TTA, 25:13098
  uptake by higher plants, effects of ammonium and nitrate uptake and assimilation on, 25:15447(R) (ORO-2410-19)
  uptake by higher plants, effects of ammonium and nitrate uptake and assimilation on, 25:15446(R) (ORO-2410-18)
STRONTIUM BORIDES
  electronic structure of CaB_6-type, 25:14463
STRONTIUM IONS
  electron reactions with, effective cross sections for transitions between excited states in, (E), 25:14000
  reactions with metallic oxides at 10 to 40 keV, secondary electron yields from, (E), 25:13963
STRONTIUM ISOTOPES Sr-83
  energy levels from strontium-84 (d,t) reactions, spin assignments for, (E), 25:14930
STRONTIUM ISOTOPES Sr-84
  deuteron reactions (d,p) and (d,t) at 20.7 MeV, DWBA analysis of, (E), 25:14930
  deuteron reactions (d,p) at 12 MeV, angular distributions for, (E), 25:14955
STRONTIUM ISOTOPES Sr-85
  effects on tissues of man following use for bone scanning, pathological β, 25:13513
  energy levels from (d,p) and (d,t) reactions, spin assignments for, (E), 25:14930
  energy levels from strontium-84 (d,p) reactions, spin-parity assignments and spectroscopic factors for, (E), 25:14955
  production for bone scintigraphy by activation of enriched or natural strontium, 25:13061
  use for scanning of human bones to detect metastases, review of, 25:13513
STRONTIUM ISOTOPES Sr-86
  deuteron reactions (d,p) and (d,t) at 20.7 MeV, DWBA analysis of, (E), 25:14930
  deuteron reactions (d,p) at 12 MeV, angular distributions for, (E), 25:14955
STRONTIUM ISOTOPES Sr-87
  energy levels from (d,p) and (d,t) reactions, spin assignments for, (E), 25:14930
  energy levels from strontium-86 (d,p) reactions, spin-parity assignments and spectroscopic factors for, (E), 25:14955
  production of metastable, for bone scintigraphy by activation of enriched or natural uranium, 25:13061
STRONTIUM ISOTOPES Sr-88
  deuteron reactions (d,p) and (d,t) at 20.7 MeV, DWBA analysis of, (E), 25:14930
STRONTIUM ISOTOPES Sr-89
  content of diet in USA during 1965 to 1970, 25:13401
  content of institutional diet of adults and children in USA during October to December 1969, 25:13442
  monitoring in stream silt at Bettis Laboratory during 1969, 25:13431
STRONTIUM ISOTOPES Sr-90
  accumulation by crops and soils in France from fallout and industrial wastes, 25:13402
  accumulation from sea water by alginic acid of brown algae, 25:13403
  content of diet in USA during 1965 to 1970, 25:13401
  content of diet of human adolescents in EURATOM countries during 1965 to 1967, 25:13392 (EUR-3945(Pt.2))
  content of fish protein concentrates, 25:13394(R) (RLO-2059-1)
  content of human bone in United States during 1969, 25:13431
  content of institutional diets of adults and children in USA during October to December 1969 as compared to

  annual average content for 1969, 25:13442
  content of Japanese beer in relation to atmospheric deposition rates in Tokyo area during 1959 to 1969, comparison of fallout cesium-137 and, 25:13434
  content of milk in Canada, Central America, South America, and United States during 1969 and 1970, 25:13433
  content of milk in Western Hemisphere during April 1970 as compared to average for previous 12-month period, 25:13442
  content of milk sampled throughout Central, North, and South America during July 1970, 25:13401
  content of stratosphere in Australia following nuclear weapons testing during 1966 to 1968, 25:13436
  determination in liquid waste effluents from nuclear fuel reprocessing plant by β counting, 25:12950 (BRH/NERHL-70-2)
  ionization following beta decay, energy dependence of auto-, (E), 25:13982
  monitoring at West Valley Processing Plant, Oct.--Dec. 1970, 25:13079 (DOCKET-50201-61)
  monitoring in environmental samples from West Valley Processing Plant, 1969, 25:13080 (DOCKET-50201-62)
  monitoring in stream silt at Bettis Laboratory during 1969, 25:13431
  removal from soil by leachate water, runoff water, and plant uptake, effects of crop management practices on, 25:13118(R) (COO-414-17)
  transfer in soils, effects of clay content on vertical, 25:13118(R) (COO-414-17)
  uptake by oats, effects of addition of ashed plants containing strontium-90 and yttrium-90 and soil pH on, 25:13118(R) (COO-414-17)
STRYCHNINE
  radiation effects on action of in central nervous system of rabbits, ionizing, 25:13561
STYRENE
  polymerization of, effects of deuterium on thermal, 25:12983
  radioinduced graft polymerization on polyethylene films, tensile properties of compounds produced by γ, 25:13042
STYRENE POLYMERS
  production of spherical aerosol particles of latex-type, effects of generation conditions on, (E), 25:13144
SULFUR
  analysis for selenium and tellurium, improvement in sensitivity of spectrographic, 25:12940
  content in atmosphere, neutron activation determination of selenium as indicator of, 25:12965
  content in rocks of shields and sediment cover of Brazil, Canada, and USSR, relations with geological time, 25:13114
  distribution in atmosphere, use in tracer studies of global transport processes, (E), 25:13121 (TID-25314)
  neutron elastic and inelastic scattering at 4.5 to 8 MeV, cross sections for, (E/T), 25:14963
  neutron elastic scattering at 8 MeV, cross sections for, (E/T), 25:14965
  neutron reactions (n,xγ) at 14 MeV with natural, cross sections for, (E/T), 25:14920(T) (BNL-tr-380)
SULFUR CHLORIDES
  reactions with sulfur-35 recoil atoms, direct labeling by, 25:13069
SULFUR ISOTOPES S-30
  energy levels from (p,t) reactions, spin-parity assignments for, (E), 25:14950
SULFUR ISOTOPES S-32
  helium-3 reactions (He-3,p) at 9 to 10 MeV, p-γ angular correlations from, (E), 25:14942
  photon reactions (γ,nγ) and (γ,pγ) with, γ spectra from, (E), 25:14946
  proton reactions (p,t) with, angular distributions for, (E), 25:14950
  scattering by tin-116 and tin-124, reorientation measurements following Coulomb excitation by inelastic, (E), 25:15041
SULFUR ISOTOPES S-34
  determination by pulsed neutron activation and scintillation counting, 25:12960
  energy levels at 4.623 and 4.688 MeV, lifetimes of, (E), 25:14954
SULFUR ISOTOPES S-35
  chemical states of recoil, in neutron-irradiated alkali metal chlorides and oxychlorides, 25:13065
  chemical states of recoil, in neutron-irradiated lithium chloride solutions, 25:13071
  incorporation into heparin-related mucopolysaccharides of mammalian cells, 25:13357
  labeling of blood platelets with, for determining effects of thrombopoietin on production of, 25:13355
  reactions of recoil atoms of, with phosphorus chlorides or oxychlorides, sulfur chlorides or oxychlorides, or thiophosphoryl chlorides, direct labeling by, 25:13069
SULFURIC ACID
  radiolysis at 77°K, yields from γ, 25:13056
SULFURYL CHLORIDE
  reactions with sulfur-35 recoil atoms, direct labeling by, 25:13069
SUN
  copper isotope abundances in, (E), 25:13900
  heat transfer in convective envelope of, (T), 25:13862 (N-70-38381)
  lithium abundance in, (E), 25:13870
  magnesium isotope abundances in, (E), 25:13904
  magnetic field of, relation to interplanetary field, (T), 25:13896
  magnetic fields of, comparison of Mt. Wilson and Crimean data on polar, (E), 25:13873
  magnetofluid dynamics of, model for, (T), 25:13858(R) (AD-710629)
  neutrino emission from, (T), 25:13909
  sodium abundance from Fraunhofer lines, (E/T), 25:13899
  spectra between 2962 and 4087 A, absolute intensities in, (E), 25:13874
  spectra of, effect of line absorption on polarization of continuum, (T), 25:13898
  spectra of, emission and absorption lines of Fe VIII, Fe XV, O III, and C VII in, (E/T), 25:13886
  spectra of, formation of rare-earth lines inside and outside H and K wings in, (E/T), 25:13810
  x-ray emission from, bibliography and review of, (T), 25:13863 (N-70-39828)
SUNSPOTS
  effects of maximum and minimum of, on F2 layer tidal spectra, (E), 25:14105
  lithium abundance in, (E), 25:13865
  spectra of lithium abundance in Sun from, (E), 25:13870
  spectra of umbrae of, continuum windows in, (E), 25:13879
  spectra of, copper hydride lines in, (E), 25:13900
  spectra of, upper limit of Swan band intensity in, (T), 25:13881
  temperatures of umbrae of, rotational, (E/T), 25:13880
SUPERCONDUCTIVITY
  conference on applied, Boulder, Colo., 6/70, 25:14215
  electronic mechanism of, collective oscillations in, (T), 25:14186
  theory of, review of, 25:14157
  theory of, uncertainty of pseudomultiplicity, 25:14185
SUPERCONDUCTORS
  critical current densities in hard, review of mechanisms determining, 25:14196
  critical field in films, angular dependence of, 25:14163
  critical field of Type-II, surface nucleation, (T), 25:14171
  critical power losses in, analysis of, (T), 25:14194
  critical-current formula for, flux flow and new, 25:14197
  current and inductive coupling in Josephson junctions, 25:14204
  current losses in thin-film, measurement technique for alternating, 25:14189
  electron tunneling in amorphous bismuth, 25:14210
  existence of high-temperature, review of mechanisms for possible, 25:14156
  fluxon drift in, single, 25:14199
  intermediate state in type-I, electron band structure of, 25:14169
  intermediate state in type-I, model of current-induced, 25:14165
  intermediate state in type-II, Meissner--Shubnikov domain patterns in, 25:14164
  Josephson effect in, high-frequency limit of, (E/T), 25:14200
  Josephson effect in, noise thermometry with, 25:14158
  Josephson junction in magnetic field, effects of thermal fluctuations on coupling energy of extended, (T), 25:14184
  Josephson junctions, characteristics of Dayem-bridge form of, 25:14201
  Josephson radiation from tunnel junction and microwave cavity, theory of, 25:14168
  losses in strip conductors, measurement technique for alternating field, 25:14187
  magnetic field near asperities of metallic surface, local reinforcement of hf, (T), 25:14205
  model for weakly connected rings of, analog computer simulation of, 25:14190
  order parameter fluctuations in zero-dimensional samples, mean field theory of, 25:14167
  phase boundary with normal state, containing nearly nonmagnetic impurities, 25:14159
  properties of one-dimensional wires, (E), 25:14151
  proximity effect in layered systems with perpendicular magnetic field, (T), 25:14158
  scattering matrix of, s-wave instabilities in, 25:14204
  statistical mechanics of persistent currents in quantum fluids, 25:14143
  thermal capacity of transition metals containing nonmagnetic impurities, (T), 25:14179
  thermal conductivity in pure two-band, Maki's theory of, 25:14166
  thermodynamic fluctuation effects in one- and two-dimensional, (E/T), 25:14162
  transition temperature of A-15-structure, strain dependence and related effects, (E/T), 25:14182
  transition temperature of A-15-structure, strain dependence and related effects, (E), 25:14183
  transition temperature of, correlation between conductivity electron concentration and, 25:14149
  transition temperatures and mass enhancements of, (T),

25:14152
transition temperatures, lattice instability of, with high, (E), 25:14174
tunneling spectroscopy of, zero-bias anomalies in, (T), 25:14206
use in devices, developments in, 25:14218
uses of, review of, 25:14155
wave attenuation in, hypersonic, (E/T), 25:14154

SUPERFLUIDITY
critical velocities in, in wide channels using phase ccupling, (E/T), 25:14146
fluctuations and long-range order in, (T), 25:14140
model of bosons in, extension of Hartree-liquid, (T), 25:14142
nucleation of cavitation by alpha-particle irradiation, 25:14133
occurrence in quantum crystals, (T), 25:14145
order decay in Bose system, effects of symmetry-breaking field on, (T), 25:14492
possibility of, in helium-3, (T), 25:14135
statistical mechanics of persistent currents in quantum fluids, 25:14143
wave propagation in, acoustic flow in first and second scund, (T), 25:14130

SUPERNOVA REMNANTS
Cas A, radio structure of, (E), 25:13854
detection of, associated with CP 1919, (E), 25:13834
distance estimates for fourteen, (E), 25:13837
polarization properties of 3C 10 and 3C 58 at 2880 MHz, (E), 25:13839
radio emission from, secular behavior of, (T), 25:13847
radio intensity of 3C 10 and 3C 58, at 2880 MHz, (E), 25:13839
Vela X, model for Gum Nebula associated with, (E), 25:13851
x-ray emission from, secular behavior of, (T), 25:13847

SUPERNOVAE
model for Gum Nebula, (E), 25:13851
neutrino emission during, detection of, (T), 25:13830

SURFACE WATERS
radiation monitoring of, in Kansas during 1969, α and β, 25:13432
radioactivity monitoring at West Valley Processing Plant, 1969, 25:13080 (DOCKET-50201-62)
tritium content of Australian, 1967 to 1969, 25:13120 (NP-18638)

SURFACES
book: Corrosion Week. 41st Manifestation of the European Federation of Corrosion, 7-12 October, 1968 in Budapest, 25:13636

SWINE
radioinduced chromosome aberrations in lymphocytes of, effects of dose on cobalt-60 γ, 25:13417

SYMMETRY GROUPS
$(3,3^*) + (3,3^*)$ symmetry-breaking model for scalar form factor for $K \to \pi + l + \nu$ decay, hard-pion theorems in, 25:14633 (NYO-2262-TA-233)
breaking in representations of Dirac relativistic symmetry, mass spectra from, 25:14768
breaking of chiral and conformal, for $\pi + \pi$ scattering lengths, 25:14770
breaking of chiral, relation between nonet of tensor trajectories and, 25:14769
breaking of chiral, scale dimension of, 25:14758
E(2), crossed-channel amplitude expansion of unequal-mass particle interactions at rest in, 25:14753
Lorentz, spinor representations of complex inhomogeneous, 25:14756
O(2,1) for radial eigenfunctions, 25:14056
O(4), amplitudes of particles with spin in, 25:14757
O(4), classification of invariants for $\pi + N \to$ rho + N interactions in, 25:14757
P(1,n), particle-motion Dirac equation invariance with respect to, 25:14747 (ITF-70-70)
Poincare, spinor representations of complex, 25:14756
Poincare, spinor representations of complex inhomogeneous, 25:14755
realizations of chiral, induced, 25:14749
representation of relativistic, Dirac, 25:14752
representations for baryons and mesons, generalization of Dirac, 25:14767
SL(3,C), meson mass spectra from algebraic model in, 25:14772
SO(2,1) algebra for short-range potential problem, 25:14491
SO(3), field associated with, nonstationary Yang--Mills, 25:14779
SO(3,2), meson mass spectra from algebraic model in, 25:14772
spinor representation of space--time algebra for hadron mass formula, 25:14751
SU(2) x SU(2) chiral, transversality condition for relation of vector and axial-vector meson fields to, 25:14804
SU(2), from unitarity constraints on Veneziano amplitudes, 25:14754
SU(3) x SU(3) breaking for pseudoscalar mesons, 25:14763
SU(3) x SU(3), meson mass spectra and hyperon semileptonic decay in, 25:14689
SU(3) x SU(3), meson mass spectra in chiral, electromagnetic perturbations on, 25:14690
SU(6) x O(3), mass operator for negative-parity baryon resonances in quark model in, 25:14708
SU(n), actions on differentiable manifolds with vanishing first and second integral Pontryagin classes, 25:14760
superselection rule relation with, 25:14774 (KFKI-70-22-HEP)

SYMMETRY GROUPS SU(3)
baryon and meson mass spectra in nonlinear quark theory in, 25:14684
baryon resonance classification in multiplets in, 25:14771
breaking for $K^+ \to \pi^0 + l + \nu$ decay, 25:14649
interactions of baryons with mesons in, dual model for, 25:14766
mass differences of octet baryons and mesons in multichannel calculation in, electromagnetic, 25:14795
statistical theory of elementary particle production in, test of, 25:14748 (JINR-P2-5480)

SYNCHROTRON RADIATION
emission from extragalactic radio scurces, (T), 25:13936(R) (AD-711829)
scattering in cold plasma, inverse Compton, (T), 25:13941

SYNCHROTRONS
beam injection in Tokyo 40-GeV proton, quadrupole magnet for transport system for, 25:14849 (SJC-A-70-6)
development of INS 1.3-GeV electron, April 1969--Mar. 1970, 25:14845(R) (NP-18601)
development of INS proton, status of, 25:14845(R) (NP-18601)
research at INS 1.3-GeV electron, April 1969--Mar. 1970, 25:14845(R) (NP-18601)

SYSTEMS FOR NUCLEAR AUXILIARY POWER (SNAP)
fuel capsule for, design, development, and testing of SIREN, 25:13170 (SNC-2708-1)

SYSTEMS FOR NUCLEAR AUXILIARY POWER (SNAP-15)
fuel capsules for, analysis of surface contamination of, 25:13164 (MLM-1670)

SYSTEMS FOR NUCLEAR AUXILIARY POWER (SNAP-19)
fuel capsules for, corrosion by seawater, 25:13163 (MLM-1652)

SYSTEMS FOR NUCLEAR AUXILIARY POWER (SNAP-23)
design, development, and testing of, final report on, 25:13166(R) (MMM-4187-1)

T

T-111 (TANTALUM ALLOY)
cracking sensitivity of, Varestraint testing of hot, 25:13695

T-222 (TANTALUM ALLOY)
cracking sensitivity of, Varestraint testing of hot, 25:13695

TACHYONS
existence of, causal loops in special relativity theory for evidence against, 25:14778

TANTALUM
abundance in chondrites, achondrites, and Apollo 11 fines, (E), 25:13787
complexes with diarsine-like ligands, preparation and spectra of tetrahalide, 25:12979
corrosion by lithium at 1500°C, effects of dissolved oxygen on, 25:13630 (EUR-4298)
corrosion of SNAP-19B fuel capsule components of, by seawater, 25:13163 (MLM-1652)
determination in cobalt- or nickel-base alloys using gas-sheathed tubular electrode arc, spectroscopic, 25:12945
determination in plutonium by solvent extraction and emission spectrography, 25:12923 (WHAN-SA-47)
determination using Methylene Blue, spectrophotometric, 25:12947
diffusion of hydrogen and deuterium in, Gorsky-effect measurements of, 25:14440
effects on superconducting properties of niobium--titanium--zirconium alloy, 25:14208
hardening of monocrystalline, at 4.2 to 550°K, interstitial solution, 25:13690
mercury-ion reactions at 5 to 30 keV, sputtering yield and secondary emission in, 25:13971
piezoresistance from stress-induced ordering of defects in, anelastic, (E/T), 25:13677
properties at high temperatures, review of physical, thermal, and thermodynamic, 25:13667
separation from niobium by solvent extraction using 4-methyl-2-pentanone in hydrochloric acid or hydrofluoric acid, 25:12947

TANTALUM ALLOYS AND SYSTEMS
properties at high temperatures, review of physical, thermal, and thermodynamic, 25:13667
C--Ta--Ti, phase studies of, 25:13762 (AD-713153)
Hf--Re--Ta-base--W, cracking sensitivity of, Varestraint testing of hot, 25:13695
Ni--Ta, dislocation dissociation in ordered Ni_3Ta, 25:13699
Ru--Ta, phase transformations in near-equiatomic, effects of temperature on, 25:13708
Ta--W, testing of fuel capsules of, for implantable plutonium-238-fueled cardiac pacemakers, metallographic and ultrasonic methods for, 25:13169(R) (NUMEC-3731-24)

Ta--Zr-base, phase studies of metastable structure of, 25:13716
Ta--Zr-base, superconducting transition temperature of, effects of concentration on, 25:13716
Ta-base--W, cracking sensitivity of, Varestraint testing of hot, 25:13695
Ta-base--W, welds in contaminated SNAP-15C fuel capsule liner of, metallographic analysis of integrity of, 25:13164 (MLM-1670)
Ta-base--Y, corrosion of dilute, by lithium at 1600°C, 25:13630 (EUR-4298)

TANTALUM ISOTOPES Ta-170
decay of, γ spectra and half-life for, (E), 25:15066

TANTALUM ISOTOPES Ta-171
decay of, γ spectra and half-life for, (E), 25:15066

TANTALUM ISOTOPES Ta-177
energy levels from lutetium-175 (α,2n) reactions, 25:15036
energy levels from lutetium-175 (α,2n) reactions, (E), 25:15047

TANTALUM ISOTOPES Ta-181
energy-level transitions from beta decay of hafnium-181, circular polarization of γ rays from, (E), 25:15009
neutron capture at 0.001 to 1 MeV, cross sections for, (E), 25:15121
neutron capture by, conversion-electron spectra from thermal, (E/T), 25:14984 (NP-18536)
neutron inelastic scattering by, cross sections for fast, (E), 25:14960
photon reactions (γ,n) up to 140 MeV, energy spectra from, (E), 25:14990
proton reactions (p,xn) at 18 MeV, Fermi-gas-model calculations of high-energy-neutron cross sections from, (T), 25:15140 (CU-1019-79)

TANTALUM ISOTOPES Ta-182
energy-level transitions from tantalum-181 thermal neutron capture, conversion coefficients and multipolarities from, (E/T), 25:14984 (NP-18536)

TANTALUM OXIDES
deposition and properties of thin films of, chemical vapor, 25:13748
spectra of reduced Ta_2O_5, EPR, 25:14482
Ta_2O_5--WO_3, phase diagram of Ta_2O_5--Ta_2WO_8 subsystem of, 25:13775

TAUROCHOLIC ACID
radioinduced inhibition of synthesis of, in rat livers, 25:13370

TECHNETIUM
catalytic properties in organic reactions, 25:15448 (RLO-2017-3)
complexes with CDTA, EDTA, or NTA, composition and stability of, 25:13008
reactions of fission-product, with uranium carbide fuels, 25:13764 (KFK-1260)

TECHNETIUM ISOTOPES Tc-99
effectiveness of erythrocyte-incorporated metastable, for scanning of human placenta in combination with digital computer and scintillation camera in comparison to metastable indium-113-labeled serum proteins, metastable, 25:13517
effectiveness of metastable, for blood pool scanning in human heart and placenta in comparison to indium-113, metastable, 25:13516
preparation of erythrocyte-incorporated metastable, for erythrocyte mass determinations, method for, 25:13332
reactivity worths in fast reactor spectra, (E/T), 25:15350
use of iron-ascorbic acid complex incorporated metastable, for scanning kidneys for differential diagnosis of benign and malignant neoplasms, 25:13504
use of metastable, for scanning human stomach for differential diagnosis of benign and malignant neoplasms, 25:13495
use of metastable, for scanning of liver of children following radiotherapy of neoplasms, 25:13578
use of metastable, with iodine-131 and scintillation camera for diagnosis of ureteral obstruction following human kidney transplant, 25:13490
use of pertechnetate-incorporated metastable, for scanning massive cerebral infarction in human brain, 25:13489
use of pertechnetate-incorporated metastable, with Anger camera for diagnosis of human metastatic papillary thyroid carcinomas, 25:13488
use of sodium pertechnetate-incorporated metastable, for scanning brain for differential diagnosis of benign and malignant neoplasms, 25:13505
use of sulfur colloid-incorporated metastable, for diagnosis of splenic rupture in man, 25:13511

TEKTITES
analysis for antimony by neutron activation and radiochemical separation, 25:12968

TELEVISION EQUIPMENT
evaluation as source of electromagnetic fields, 25:13581
radiation dose to human populations of Britain from color, mutagenic x, 25:13452

TELLURIUM
determination by precipitation using Bismuthiol II, 25:12943
determination in semiconductor alloys and tellurium salts using Victoria Blue 4R, extraction--photometric method for, 25:12935
determination in sulfur, improvement in sensitivity of spectrographic, 25:12940
electric quadrupole interactions in, Moessbauer effect study of, 25:14480
salts, analysis for tellurium using Victoria Blue 4R, extraction--photometric method for, 25:12935

TELLURIUM ISOTOPES Te-125
energy levels of, lifetime measurements for, (E), 25:15055

TELLURIUM ISOTOPES Te-126
oxygen-18 reactions (O-18,xn) with, energy levels of neodymium-137 from, (E), 25:15042

TELLURIUM ISOTOPES Te-128
carbon-12 reactions (C-12,5n) at 78 MeV, energy levels of cerium-135 from, (E), 25:15042

TELLURIUM ISOTOPES Te-132
content of feces, milk, and urine of dairy cattle following ingestion of Schooner fallout, 25:13396 (UCRL-72511)

TELLURIUM SYSTEMS
Au--Fe--Te, superconducting transition temperature and lattice parameters of liquid-quenched simple-cubic, 25:14178
Au--Mn--Te, superconducting transition temperature and lattice parameters of liquid-quenched simple-cubic, 25:14178
Bi--Sb--Te, thermoelectric properties of BiSbTe, measurements for use in SNAP-23A, 25:13166(R) (MMM-4187-1)

TEMPERATURE
production of 1600°C, at 7 kbar pressure, 25:15457(T) (SCL-T-71-209)

TERBIUM
complexes with carminic acid, spectrophotometric studies on, 25:12937
determination in plutonium oxide--uranium oxide fuels by solvent extraction and emission spectrography, 25:12922 (WHAN-SA-44)
determination of trace amounts of, in gadolinium oxide and yttrium oxide by x-ray-excited optical luminescence, 25:12948
determination of trace amounts of, in plutonium and plutonium dioxide--uranium dioxide by solvent extraction and emission spectrography, 25:12923 (WHAN-SA-47)
electric conductivity of single crystal, spin-wave scattering effects on, 25:14448
Ettingshausen effect measurements on polycrystalline, 25:14475

TERBIUM ALLOYS AND SYSTEMS
Ge--Tb--Si, magnetic properties and structure of $TbGe_{0.2}Si_{0.8}$, 25:14434 (CEA-CONF-1701)

TERBIUM ISOTOPES Tb-159
energy levels from dysprosium-159 electron-capture decay, L-subshell x-ray fluorescence and Coster--Kronig transitions of, (E), 25:15012

TERBIUM ISOTOPES Tb-160
yields in thermal fission of uranium-235, independent, (E), 25:15038

TERPHENYL
efficiency for liquid scintillation counting of tritium in toluene solution, 25:13214

TERPHENYL-4-CARBONITRILE
efficiency for liquid scintillation counting of tritium in toluene solution, 25:13214

TERPHENYL-4,4''-DICARBONITRILE
efficiency for liquid scintillation counting of tritium in toluene solution, 25:13214

TESTES
radiation effects on, of mice, effects of estradiol and FSH on phosphorus-32 β, 25:13569

TEXTILES
shielding effects of cotton, against radiation dose from x-ray diffraction apparatus, 25:13457

THALLIUM
magnetic vortex pinning and motion in superconducting thin films of, 25:14176

THALLIUM ALLOYS AND SYSTEMS
In--Tl, superconducting flux trapping in region of martensitic transformation, 25:14172
Pb--Tl, superconducting intermediate state in, Meissner--Shubnikov domain patterns in, 25:14164

THALLIUM ISOTOPES Tl-204
accumulation from sea water by alginic acid of brown algae, 25:13403
electron-capture decay of, L-subshell fluorescence and Coster--Kronig yields in mercury from, (E), 25:15015

THALLIUM ISOTOPES Tl-205
alpha reactions (α,t) at 20 to 25 MeV, cross sections and normalization for, (E), 25:15064
energy-level excitation by neutron capture gamma rays, (E), 25:15002

THERMAL CONDUCTIVITY
measurement of ceramic fuels, balanced oscillator method for in-pile, (E/T), 25:15411
measurement of gas cooled reactor fuel element, methods for, 25:15410 (ZJE-92)

THERMAL CYCLING APPARATUS
design of in-pile, for testing fuel cladding, 25:13142

THERMAL DIFFUSION
isotope separation by, effects of molecular inelastic

  collisions on, 25:13165(R) (MLM-1753)

THERMAL INSULATION
  development and testing for SNAP-23A conversion system, 25:13166(R) (MMM-4187-1)

THERMAL STRESSES
  calculation of transient, method for, 25:13183

THERMIONIC CONVERTERS
  heat limiting device for radioisotope-fueled, description of, 25:13173(P)
  performance of cesium, efffect of cadmium and mercury on, 25:14085
  performence of fluoride--vapor-deposited tungsten emitter, (E), 25:14083 (N-70-39884)

THERMCCOUPLES
  development at ORNL, Sept. 1969--Aug. 1970, 25:13318(R) (CRNL-4620)
  development of thermo-wire, for gas cooled reactor fuel element mockups, 25:15410 (ZJE-92)

THERMCELECTRIC CONVERTERS
  development of SNAP-23A experimental and prototype mockups, 25:13166(R) (MMM-4187-1)
  performance of, effects of evaporative erosion on thermoelectric elements on, (T), 25:14084 (SC-RR-70-804)
  testing of cascaded, life, 25:14082 (N-70-39764)

THERMCELECTRIC MATERIALS
  erosion of, effects on performance of thermoelectric ccnverters, (T), 25:14084 (SC-RR-70-804)

THERMCNUCLEAR EXPLOSIONS
  effects on tritium content in US river waters, 25:13108
  electromagnetic pulse from, effects on AM broadcast stations of, 25:13328 (ORNL-TM-2830)

THERMONUCLEAR REACTORS
  magnetic field diffusion through conductive walls of, multipole, (T), 25:14352 (IPPJ-T-3)
  nuclear cross section requirements for, 25:14357
  plasma confinement in toroidal, numerical model for low-pressure, 25:14236
  plasma equilibrium in toroidal, perturbation theory for, 25:14327
  plasma heating in tokamak-like JFT-2, Joule, 25:14233 (JAERI-Memo-4186)
  plasma rotation and shock formation in toroidal, from resistive diffusion, (T), 25:14235
  plasma simulation in injection-type, spherically symmetric, (T), 25:14289
  research on, similarity rules for, 25:14354

Δ^2-1,3,4-THIADIAZOLINE-5-THIONE, 2-MERCAPTO-4-PHENYL-
  use for quantitative determination of tellurium, 25:12943

THICKNESS GAGES
  description of electron backscatter, 25:13141

THIONYL CHLORIDE
  reactions with sulfur-35 recoil atoms, direct labeling by, 25:13069

THIOPHOSPHORYL CHLORIDE
  reactions with phosphorus-32 or sulfur-35 recoil atoms, direct labeling by, 25:13069

THORIUM
  abundance in chondrites, achondrites, and Apollo 11 fines, (E), 25:13787
  complexes with tropolone, chemical properties and preparation of, 25:13009
  content and depth in crustal basalts and granites in USSR, 25:13115
  content in rocks of shields and sediment cover of Brazil, Canada, and USSR, relations with geological time, 25:13114
  content of soil in Brazil, effects of, on food ccntamination, 25:13439
  descrption from tungsten surfaces, modulated beam method fcr, 25:13686
  determination of abundance of, relative to uranium in thorium dioxide--uranium dioxide by x-ray fluorescence spectrometry, 25:13077(R) (ANL-7755)
  determination using thin-layer chromatography and ring-oven colorimetry, 25:12944
  growth on tungsten (100) surface, Auger emission spectroscopy, LEED, and work function measurements of epitaxial, 25:13719
  precipitation in ammonium carbonate solutions using hexaamminecobalt chloride, chemical and crystallographic properties of compounds produced by, 25:12980
  prospecting for, development of instruments for, 25:13321 (RISO-M-1270)
  separation of nitrogen and oxygen from interstitial sites in, method for, 25:13641(T) (UCRL-Trans-10503)
  uses in potentiometric titration for determination of fluoride ions, 25:12929

THORIUM ALLOYS AND SYSTEMS
  F--Th, thermodynamic properties of cations formed in ammonium nitrate solutions of, at 5, 25, and 45°C, 25:13022

THORIUM BORIDES
  electronic structure of CaB_6-type, 25:14463

THORIUM FLUORIDES ThF_4
  thermodynamic poperties in solutions of ammonium nitrate at 5, 25, and 45°C, 25:13022

THORIUM HALIDES
  complexes with dimethylacetamide, methyl sulfoxide, or hexamethylphosphoric triamide in nitromethane, electric ccnductivity of, relation of composition and ionization capacity to, 25:13023

THORIUM ISOTOPES
  energy levels of, properties cf octupole, 25:15205
  neutron cross sections for, review of rescnance, (E), 25:15069

THORIUM ISOTOPES Th-221
  alpha decay of, 25:15011

THORIUM ISOTOPES Th-222
  alpha decay of, 25:15011

THORIUM ISOTOPES Th-227
  neutron fission of, cross section for thermal, (E), 25;15044

THORIUM ISOTOPES Th-228
  alpha decay of, gamma spectra and half-life fcr, (E), 25:14981 (IN-1448)

THORIUM ISOTOPES Th-229
  neutron fission of, energy spectra and mean prompt neutron production in thermal, (E), 25:15118

THORIUM ISOTOPES Th-232
  content in sands and soils of south Florida, 1968 measurements of natural, 25:13107
  neutron fission at 0 to 6 MeV, energy dependence of mean prompt neutron production from, (E), 25:15117
  neutron fission at 14 MeV with long-range particle emission, calculation of probability for, (T), 25:15018
  x-ray energies of, K, (E), 25:14981 (IN-1448)

THORIUM NITRATES
  complexes with violuric acid, composition and stability of, spectrophotometric studies on, 25:13014

THORIUM OXIDES ThC_2
  erbium-ion ESR in single crystal of, axially symmetric, 25:14478
  neptunium(IV) absorpticn spectra in single crystals of, 25:14466
  Au-base--ThO_2, properties of dispersicn-strengthened, electric and tensile, 25:13755
  B_2O_3--MgO-base--ThO_2, phase equilibria in magnesium oxide corner of, at 1200°C, 25:13770
  Cu-base--ThO_2, properties of dispersicn-strengthened, electric and tensile, 25:13755
  MgO--ThO_2, phase equilibria at 1500°C, 25:13770
  Pt-base--ThO_2, properties of dispersicn-strengthened, electric and tensile, 25:13755
  ThO_2--UO_2, analysis for thorium/uranium by x-ray fluorescence spectrometry, 25:13077(R) (ANL-7755)
  ThO_2--UO_2, radiation effects on swelling cf, fast neutron, 25:15366 (WAPD-TM-986)

THREE MILE ISLAND PCWER REACTCR, UNIT 1
  buildings for, design parameters of fan cccler assemblies for, 25:15305 (DOCKET-50289-32)
  containment structure and systems for, revised and additional data on, 25:15305 (DOCKET-50289-32)
  design parameters of, revised and additional data on, 25:15305 (DCCKET-50289-32)
  radiation emergency plan for, safety analysis of, 25:15305 (DCCKET-50289-32)

THULIUM
  complexes with carminic acid, spectrophotcmetric studies on, 25:12937
  determination in plutonium cxide--uranium oxide fuels by solvent extraction and emissicn spectrography, 25:12922 (WHAN-SA-44)
  determination of trace amounts of, in plutcnium and plutonium dioxide--uranium dicxide by sclvent extraction and emission spectrography, 25:12923 (WHAN-SA-47)
  separation from aqueous chlcride soluticns by solvent extraction using dioctyl phosphate in benzene or heptane, effects of variables on, 25:13096

THULIUM IONS
  crystal-field shielding and antishielding factors for Tm^{3+} at electronic and nuclear sites, (T), 25:13982

THULIUM ISOTOPES Tm-166
  beta and electron-capture decay of, gamma spectra from, (E/T), 25:14984 (NP-18536)

THULIUM ISOTOPES Tm-169
  neutron capture by, cross-section calculaticns for, (T), 25:14982 (NCSAC-31)

THULIUM ISOTOPES Tm-170
  preparation and properties of gamma scurces of, for radiography of aircraft parts, 25:13180 (JAERI-Memc-4163)

THULIUM SILICIDES
  magnetic properties and structure of TmSi, 25:14434 (CEA-CONF-1701)

THYMIDINE
  incorporation of tritum-labeled, into DNA cf tissues of mice, effects of mitotic rate on specificity of, 25:13358

THYMIDINE MONOPHOSPHATES
  effects on growth of yeast cells, 25:13604
  synthesis in yeast cells, inhibiticn cf, 25:13604

THYMINE
  isolation of mutants deficient for, from uv-radiosensitive strains of Bacillus subtilis, methods for, 25:13614

THYMUS GLAND
  radiation effects on histone content cf deoxyribonucleoproteins in, of rats, effects of heparin

XUM

  on x, 25:13385
  radiation effects on weight of, in rats, comparison of RBE for cesium-137 and tritium oxide, 25:13551
THYROID GLAND
  autoradiography of rat, for diagnosis of disorders caused by radiation sickness, method for neutron, 25:13497
  function of human, effects of radioinduced pituitary gland ablation on, 25:13579
  iodine radioisotope uptake by human, use of iodine-125 for measuring, 25:13485
  iodine-131 content of beef cattle, use of, for monitoring fallout, 25:13397
  iodine-131 content of, in children, reconcentration factor for, 25:13347
  radiodiagnosis of metastatic papillary carcinomas of human, use of metastable technetium-99-labeled pertechnetate for, 25:13488
  radioisotope uptake by, as test for functional autonomy following therapy in patients with multinodular goiter, iodine-125 and iodine-131, 25:13493
  radiotherapy of carcinomas of, using iodine-131, 25:13596
TIN
  compounds, tin-121m decay in solid inorganic, nuclear γ resonance studies on products from β, 25:13074
  determination in copper-base alloys using gas-sheathed tubular electrode arc, spectroscopic, 25:12945
  determination of trace amounts of, in blood serum by emission spectroscopy, 25:12946
  effects on backscattering during γ dosimetry to HeLa cells, 25:13456
  electron backscattering at 0.5 to 2.0 MeV by thick targets of, Monte Carlo calculation of angular distributions and energy spectra from, 25:13959 (UCRL-19719)
  electron energy losses at 52 to 92 MeV in, (E), 25:14392 (AD-711005)
  energy-level excitation by neutron capture gamma rays, (E), 25:15002
  fluxon drift through superconducting, observation of single, (E), 25:14199
  photon elastic scattering cross sections at 6 to 9 MeV, (E), 25:14959
  positron backscattering at 0.5 to 2.0 MeV by thick targets of, Monte Carlo calculation of angular distributions and energy spectra from, 25:13959 (UCRL-19719)
  superconducting critical current in one-dimensional thin films of, temperature dependence of, (E/T), 25:14162
  superconductivity in nearly one-dimensional wires, (E), 25:14151
  wave attenuation in, hypersonic, (E/T), 25:14154
TIN ALLOYS AND SYSTEMS
  Cu--Sn, photon reactions at 2.6 to 17.6 MeV with bell metal, effective atomic numbers for pair production in, (T), 25:14402
  In--Sn, crystal growth in, stability of planar advancing solid/liquid interface in, 25:13646
  Mo--Sn--Ti-base--Zr, mechanical properties of metastable β, effects of microstructure on, 25:13672
  Nb--Sn, deposition of intermetallic Nb_3Sn on substrate for use as superconductor, 25:14150(P)
  Nb--Sn, electron characteristics and optical characteristics of superconducting, (E), 25:14149
  Nb--Sn, materials testing for use in superconducting coils of intermetallic Nb_3Sn, (E), 25:14219
  Nb--Sn, vapor deposition process for superconducting intermetallic Nb_3Sn, 25:14203
  Pb--Sn, photon scattering at 662, 1120, and 1330 keV by, effective atomic numbers for coherent, 25:14405
  Sm--Sn, magnetic susceptibility of $SmSn_3$, Sm_2Sn_3, and Sm_5Sn_3 at 2 to 900°K, 25:14453
TIN ISOTOPES Sn-113
  mixtures with metastable indium-113, effectiveness for scanning, 25:13501
TIN ISOTOPES Sn-116
  helium-4 inelastic scattering by, energy-level reorientation following Coulomb excitation by, (E), 25:15041
  oxygen-16 inelastic scattering by, energy-level reorientation following Coulomb excitation by, (E), 25:15041
  sulfur-32 inelastic scattering by, energy-level reorientation following Coulomb excitation by, (E), 25:15041
TIN ISOTOPES Sn-118
  energy levels in, lifetimes for, (E/T), 25:14983 (NP-18492)
  energy-level transitions in, multipolarities of, (E/T), 25:14983 (NP-18492)
TIN ISOTOPES Sn-119
  energy level at 23.8 keV, lifetime measurement for, (E), 25:15056
  neon-20 reactions (Ne-20,xn) at 60 to 160 MeV, energy levels of neodymium-137 from, (E), 25:15042
  neon-22 reactions (Ne-22,xn) at 60 to 160 MeV, energy levels of neodymium-137 from, (E), 25:15042
TIN ISOTOPES Sn-121
  beta decay in solid inorganic tin compounds, nuclear γ resonance studies on products from, 25:13074
TIN ISOTOPES Sn-122
  neon-20 reactions (Ne-20,xn) at 60 to 160 MeV, energy levels of neodymium-137 from, (E), 25:15042
  neon-22 reactions (Ne-22,xn) at 60 to 160 MeV, energy levels of neodymium-137 from, (E), 25:15042
TIN ISOTOPES Sn-124
  helium-4 inelastic scattering by, energy-level reorientation following Coulomb excitation by, (E), 25:15041
  oxygen-16 inelastic scattering by, energy-level reorientation following Coulomb excitation by, (E), 25:15041
  sulfur-32 inelastic scattering by, energy-level reorientation following Coulomb excitation by, (E), 25:15041
TIN ISOTOPES Sn-125
  beta decay of, gamma spectra and angular correlations from, (E/T), 25:15137
TIN TELLURIDES
  superconducting transition temperature of, (T), 25:14152
TISSUES
  carbon-14 content of proteins in, development of method for determining, 25:13345
  electric properties of, values in different frequency ranges, 25:13581
  lithium-6 uptake by, of rats following intraperitoneal and intravenous injections, 25:13350
  meson (π) spatial distribution in, method for determination of, 25:13547
  radiation effects on potassium and sodium content of, in rats, lethal and sublethal, 25:13566
  radioinduced fission of naturally occurring uranium-235 in neoplastic and normal, of human kidney, interstitial neutron, 25:13361
  radioisotope content of, of cattle following intravenous and oral administration, cerium-144 and scandium-46, 25:13352
TITANIUM
  abundance in chondrites, achondrites, and Apollo 11 fines, (E), 25:13787
  analysis for molybdenum as complex trihydroxyfluoronate, extraction--photometric method for, 25:12933
  content and depth in crustal basalts and granites in USSR, 25:13115
  determination in aluminum-, cobalt-, iron-, or nickel-base alloys using gas-sheathed tubular electrode arc, spectroscopic, 25:12945
  determination in plutonium by solvent extraction and emission spectrography, 25:12923 (WHAN-SA-47)
  effects of trivalent, on kinetics of γ-radioinduced reactions of 2-propanol radicals with hydrogen peroxide, 25:13032
  effects of weld filler addition of, on mechanical properties of heat affected zone in ferritic stainless steel, 25:13696
  effects on intercrystalline corrosion of molybdenum--nickel alloys by boiling hydrochloric acid solution, relations with temperature, 25:13633
  mercury-ion reactions at 5 to 30 keV, sputtering yield and secondary emission in, 25:13971
  properties at high temperatures, review of physical, thermal, and thermodynamic, 25:13667
  separation from chlorides by fused salt electrolysis, 25:13089
  separation from iron by solvent extraction, method for, 25:12934
  separation of nitrogen and oxygen from interstitial sites in, method for, 25:13641(T) (UCRL-Trans-10503)
TITANIUM ALLOYS AND SYSTEMS
  analysis for constituents using gas-sheathed tubular electrode arc, spectroscopic, 25:12945
  phase transition and structure of, magnetic susceptibility and internal friction study of beta--omega, 25:14465
  C--Mo--Ti, phase studies of, 25:13762 (AD-713153)
  C--Nb--Ti, phase studies of, 25:13762 (AD-713153)
  C--Ta--Ti, phase studies of, 25:13762 (AD-713153)
  Cr--Fe--Mo--Ti, microstructure of anti-phase boundaries in chi-phase of $Fe_{36}Cr_{12}Mo_5Ti_5$, 25:13711
  Mo--Sn--Ti-base--Zr, mechanical properties of metastable β, effects of microstructure on, 25:13672
  Nb--Ti, materials testing for use in superconducting coils, 25:14219
  Nb--Ti, performance in superconducting magnets with various configurations, 25:14211 (KFK-1217)
  Nb--Ti-base--Zr, critical current density of superconducting rolled sheets of, relations with aging temperature, magnetic field, and time, 25:14209
  Nb-base--Ti--Zr, superconducting properties of, effects of molybdenum, tantalum, and vanadium additions on, 25:14208
  Ti--U, radiation effects on structure of ordered hexagonal U_2Ti, neutron, 25:13726
TITANIUM BORIDES
  properties at high temperatures, review of physical, thermal, and thermodynamic, 25:13667
TITANIUM ISOTOPES Ti-44
  energy level from titanium-46 (p,t) reactions, T = 2, (E), 25:14949
TITANIUM ISOTOPES Ti-45
  energy levels from titanium-46 (p,d) reactions, spectroscopic factors for, (E), 25:14949

- TITANIUM ISOTOPES Ti-46
  - helium-3 reactions (He-3,n) with, neutron spectra from, (E), 25:14943
  - proton reactions (p,d) at 35 MeV, angular distributions for, (E), 25:14949
  - proton reactions (p,t) at 25 to 45 MeV, angular distributions for, (E), 25:14949
- TITANIUM ISOTOPES Ti-47
  - energy levels from titanium-48 (p,d) reactions, spectroscopic factors for, (E), 25:14949
- TITANIUM ISOTOPES Ti-48
  - proton reactions (p,d) and (p,t) at 25 to 45 MeV, angular distributions for, 25:14949
- TITANIUM ISOTOPES Ti-49
  - energy levels from titanium-50 (p,d) reactions, spectroscopic factors for, (E), 25:14949
  - proton reactions (p,d) at 20.9 MeV, DWBA analysis of differential cross sections and asymmetries from polarized, (E/T), 25:14922 (CEA-CONF-1655)
- TITANIUM ISOTOPES Ti-50
  - energy levels from proton inelastic scattering, (E), 25:14928
  - proton elastic scattering near 2.5 MeV with isobaric analog excitation, proton spectra from, (E), 25:14982 (NCSAC-31)
  - proton inelastic scattering at 40 MeV, microscopic description of, (E/T), 25:14928
  - proton reactions (p,d) at 45 MeV, angular distributions for, (E), 25:14949
  - proton reactions (p,t) at 25 to 45 MeV, angular distributions for, (E), 25:14949
- TITANIUM OXIDES
  - content in rocks of shields and sediment cover of Brazil, Canada, and USSR, relations with geological time, 25:13114
  - crystal structure of Ti_4O_7, at 77 to 298°K, 25:14442
  - deposition and properties of thin films of, chemical vapor, 25:13748
  - ion reactions at 10 to 40 keV with, secondary electron yields from, (E), 25:13963
  - phase transitions in Ti_2O_3, review of thermally induced semiconductor--metal, 25:14470
  - phase transitions in Ti_4O_7, at 77 to 298°K, volume changes at metal--insulator, 25:14442
  - plasma resonance in, effects of stoichiometry on, 25:14462
- TOKAMAK DEVICES
  - plasma diffusion and thermal conductivity in TM-3, effects of transport coefficients on, (E/T), 25:14239
  - plasma diffusion in, electric field effects on, (T), 25:14238
- TOLUENE
  - radiolysis in nitric acid, effects on zirconium extraction of products from γ, 25:13093
  - reactions with recoil bromine-82, calculation of electron energies of transition states from, 25:13064 (INR-1211)
- p-TOLUIDINE
  - hydrochloride, radiolysis of monocrystals of, ESR spectral studies on free radicals produced by γ, 25:13051
- TRACER TECHNIQUES
  - development of bromine-82, for measuring density and flow velocity of postflotation slurry, 25:13176
  - development of sodium-24 injection, for measuring enthalpy of steam in nuclear power plant turbines, 25:13148
  - kinetics of biological, in relation to shape of uptake curves, 25:13336
  - use of chemical, for studying atmospheric transport processes, 25:13121 (TID-25314)
- TRANSACTINIDE ELEMENTS
  - stability of superheavy, calculations using generalized Strutinski method, (T), 25:15193
- TRANSITION METAL ALLOYS AND SYSTEMS
  - phase transformations in bcc, kinetics and morphology of, 25:13717
  - rare earths--transition metals, compressibility of intermetallic compounds of, strain gage measurements of, 25:13694
- TRANSITION METAL CARBIDES
  - sintering and hot pressing of powdered, factors controlling densification in, 25:13743
  - superconducting properties of fcc ternary, 25:14148
- TRANSITION METAL OXIDES
  - sintering and hot pressing of powdered, factors controlling densification in, 25:13743
- TRANSITION METALS
  - sintering and hot pressing of powdered, factors controlling densification in, 25:13743
  - thermal capacity of superconducting, containing nonmagnetic impurities, (T), 25:14179
- TRANSPLANTS
  - radiation effects on survival of skin, in mice, protective effects of sodium s-(2-aminoethyl) phosphorothioate against x, 25:13479
  - radioinduced delay of rejection of virus-heterogenized skin, in mice, γ, 25:13388
- TRANSPORT THEORY
  - equations for isotope separation, elementary integration of nonlinear, 25:13085
  - Milne problem for polarized-radiation scattering according to Rayleigh's law, 25:14408
  - Monte Carlo method in, importance sampling angle of scattering in, 25:14404
- TRANSURANIUM ELEMENTS
  - analysis of, design of mass spectrometer for, 25:12319 (ORNL-4643)
  - bibliography on, Nov. 1970, 25:13626
  - bibliography on, Sept. 1970, 25:13625
  - content of lungs, effects of medically administered cobalt-57 on measurement of, 25:13458
- TRIBENZYLAMINE
  - solvent properties for rhenium, 25:12921
- TRIBUTYLAMINE
  - solvent properties for rhenium, 25:12921
- TRIETHYLENEPHOSPHORAMIDE
  - effects on mating behavior of male codling moths, 25:13557
- TRIHEXYLAMINE
  - solvent properties for rhenium, 25:12921
- TRIISOOCTYLAMINE
  - solvent properties for rhenium, 25:12921
- TRIOCTYLAMINE
  - solvent properties for plutonium, effects of hydrofluoric acid on, 25:12923 (WHAN-SA-47)
  - solvent properties for rare earths, 25:12922 (WHAN-SA-44)
- TRITIUM
  - binding energy of, second-order correction of perturbation theory to, (T), 25:14883
  - chemical state of, in irradiated oxide fuel elements, 25:13077(R) (ANL-7755)
  - content in ground waters, rainwater and surface waters in Australia, 1967 to 1969, 25:13120 (NP-18638)
  - content in ground waters, rainwater, and seawater in Australia, 1969 to 1970, 25:13103 (NP-18639)
  - content in US river waters, (E), 25:13108
  - content of environment, nuclear power contribution to, 25:13437
  - content of river water in USA sampled during 1970, 25:13400
  - determination in liquid waste effluents from nuclear fuel reprocessing plant by scintillation counting, 25:12950 (BRH/NERHL-70-2)
  - determination in precipitation, springs, streams, and wells in Project Rulison area by scintillation counting, 25:12951 (USGS-474-83)
  - determination in toluene by liquid scintillation counting, efficiency of aromatic nitriles for, 25:13214
  - determination with carbon-14 in double-labeled samples by liquid scintillation counting, 25:12953
  - energy levels of, weakly bound states of three resonantly interacting particles in, (T), 25:14591
  - exchange bétween ethanol, methanol, and propanol and water, at 200 to 300°C, activation energy for catalytic, 25:12991
  - incorporation in thymidine for labeling DNA of tissues of mice, 25:13358
  - monitoring at West Valley Processing Plant, Oct.--Dec. 1970, 25:13079 (DOCKET-50201-61)
  - monitoring in environmental samples from West Valley Processing Plant, 1969, 25:13080 (DOCKET-50201-62)
  - nuclear properties of, Bolsterli--Feenberg perturbation procedure for calculation of momentum-dependent, 25:15185
  - oxygen-17 reactions (O-17,pγ) at 22 MeV, γ spectra from, (E), 25:14905
  - reactions of recoil, with deuterium, hydrogen, or methane, iodine bromide and iodine chloride as radical scavengers in, 25:13067
  - removal from liquid radioactive wastes, effects of hydrological conditions on efficiency of Hanford Emergency Waste Disposal Crib for, (T), 25:13186 (BNWL-1503)
  - Schroedinger equation for, direct numerical solution of, (T), 25:14881
  - solubility in annealed and cold-worked copper at 100 to 300°C, 25:13654 (MLM-1734)
  - targets for 14-MeV neutron production, properties of tritiated titanium, 25:14840 (EUR-4286(Pt.2))
  - uptake of thymidine-incorporated, by DNA of uv-irradiated HeLa cells, temperature dependence and stability during, 25:13554
  - uptake of thymidine-incorporated, by oocytes of x-irradiated guinea pigs, 25:13367
- TRITONS
  - reactions (t,p) with p-shell nuclei, analysis for distortion and polarization effects in, (T), 25:15192
- TROJAN POWER REACTOR, UNIT 1
  - construction of, permit for, 25:15325 (DOCKET-50344-19)
- TROPOLONE
  - complexes with protactinium or thorium, chemical properties and preparation of, 25:13009
- TUNGSTEN
  - Debye temperature of, 25:15020
  - desorption of neptunium, plutonium, and thorium from surfaces of, modulated beam method for, 25:13686
  - determination in cobalt- or iron-base alloys using gas-sheathed tubular electrode arc, spectroscopic, 25:12945
  - determination in neutron-irradiated graphite by γ

  - spectrometry, 25:12954
  - determination in plutonium by solvent extraction and emission spectrography, 25:12923 (WHAN-SA-47)
  - diffusion of nitrogen in, at 1000 to 1800°C, 25:13673
  - effects on backscattering during γ dosimetry to HeLa cells, 25:13456
  - effects on intercrystalline corrosion of molybdenum--nickel alloys by boiling hydrochloric acid solution, relations with temperature, 25:13633
  - electron triple scattering at 50 eV to 200 keV by, depolarization due to spin flip in, (T), 25:14020
  - emissivity of monocrystalline, at 1200 to 3200°K, total hemispherical, 25:13666
  - emittance of arc-cast and powdered, at 2500°K, total, 25:13663
  - gold contact angle for clean surface of, sessile drop method for measurement of, 25:13691
  - helium-ion reactions at 5 to 2000 eV with (100) and (110) surfaces of, effects of lattice disorder and surface contamination on entrapment in, (E), 25:14419
  - mechanical properties of doped, 25:13682
  - neutron capture at 0.001 to 1 MeV, cross sections for, (E), 25:15121
  - neutron inelastic scattering at 14.5 MeV, cross sections for, (E), 25:14967
  - properties at high temperatures, review of physical, thermal, and thermodynamic, 25:13667
  - proton reactions at 70 GeV, upper limits for cross sections for production of new-type radioactivity from, (E), 25:14541 (JINR-P1-5399)
  - separation from rhenium by solvent extraction using tertiary amines, 25:12921
  - silver contact angle for clean surface of, sessile drop method for measurement of, 25:13691
  - solvent properties for nitrogen at 1000 to 1800°C, 25:13673
  - sorptive properties of surfaces of polycrystalline, for ethylene and nitrogen, 25:13687
  - sorptive reactions of polycrystalline, with water vapor, hydrogen evolution kinetics in, 25:13669
  - thermal conductivity of arc-cast and powdered, at 1800 to 2800°K, 25:13663
  - thermal properties at 2600 to 3500°K, exploding wire method for measurement of, 25:13664
  - thorium growth on (100) surface of, Auger emission spectroscopy, LEED, and work function measurements of epitaxial, 25:13719
  - work functions for characterized macroscopic surfaces of, effects of surface preparation on, 25:13693

- TUNGSTEN ALLOY COUPLES
  - Re--W/W, electromotive force of thermocouples of, effects of temperature on, 25:13682
- TUNGSTEN ALLOYS AND SYSTEMS
  - properties at high temperatures, review of physical, thermal, and thermodynamic, 25:13667
  - B--C--W, phase studies of, 25:13763 (AD-713154)
  - glass--W, elastic properties of composites of, 25:13751
  - Hf--Re--Ta-base--W, cracking sensitivity of, Varestraint testing of hot, 25:13695
  - Mo--W-base, enthalpy and thermal capacity of, at 1400 to 3000°K, 25:13665
  - Re--W-base, mechanical properties of, 25:13682
  - Ta--W, testing of fuel capsules of, for implantable plutonium-238-fueled cardiac pacemakers, metallographic and ultrasonic methods for, 25:13169(R) (NUMEC-3731-24)
  - Ta-base--W, cracking sensitivity of, Varestraint testing of hot, 25:13695
  - Ta-base--W, welds in contaminated SNAP-15C fuel capsule liner of, metallographic analysis of integrity of, 25:13164 (MLM-1670)
  - UN--W, phase studies of eutectic of, at 2100 to 2700°C, 25:13772
- TUNGSTEN COUPLES
  - Re--W/W, electromotive force of thermocouples of, effects of temperature on, 25:13682
- TUNGSTEN IONS
  - crystal-field shielding and antishielding factors for W^+ at electronic and nuclear sites, (T), 25:13983
- TUNGSTEN ISOTOPES W-180
  - energy level at 1006.2 keV, lifetime of, (E/T), 25:14984 (NP-18536)
  - energy levels from rhenium-180 beta and electron-capture decay, spin--parity assignments for, (E/T), 25:14984 (NP-18536)
  - energy-level transitions from rhenium-180 beta and electron-capture decay, intensities, multipolarities, K-conversion coefficients, and angular correlations from, (E/T), 25:14984 (NP-18536)
- TUNGSTEN ISOTOPES W-181
  - content of feces, milk, and urine of dairy cattle following ingestion of Schooner fallout, 25:13396 (UCRL-72511)
  - distribution in fetal and maternal tissues of dairy cattle following ingestion of Schooner fallout, 25:13396 (UCRL-72511)
  - energy-level scheme from rhenium-181 decay, (E), 25:15058
- TUNGSTEN ISOTOPES W-182
  - Moessbauer effect in calcium tungstate, electric quadrupole interactions from, 25:14480
- TUNGSTEN ISOTOPES W-183
  - energy level of, Moessbauer measurement of lifetime for first-excited, (E), 25:15020
  - Moessbauer effect in calcium tungstate, electric quadrupole interactions from, 25:14480
- TUNGSTEN ISOTOPES W-184
  - energy level of, Moessbauer measurement of lifetime for first-excited, (E), 25:15020
- TUNGSTEN ISOTOPES W-185
  - distribution in fetal and maternal tissues of dairy cattle following ingestion of Schooner fallout, 25:13396 (UCRL-72511)
  - energy levels from tantalum-185 decay, spins and parities of, (E), 25:15043
- TUNGSTEN ISOTOPES W-186
  - energy level of, Moessbauer measurement of lifetime for first-excited, (E), 25:15020
- TUNGSTEN ISOTOPES W-187
  - content of feces, milk, and urine of dairy cattle following ingestion of Schooner fallout, 25:13396 (UCRL-72511)
- TUNGSTEN ISOTOPES W-188
  - content of feces, milk, and urine of dairy cattle following ingestion of Schooner fallout, 25:13396 (UCRL-72511)
  - distribution in fetal and maternal tissues of dairy cattle following ingestion of Schooner fallout, 25:13396 (UCRL-72511)
- TUNGSTEN OXIDES
  - crystal structure of WO/sub 3-x/, 25:13773
  - spectra of reduced WO_3, EPR, 25:14482
  - Ta_2O_5--WO_3, phase diagram of Ta_2O_5--Ta_2WO_8 subsystem of, 25:13775
- TURBINES
  - steam enthalpy in nuclear power plant, sodium-24 injection tracer method for measuring, 25:13148
- TURKEY POINT POWER REACTOR, UNIT 3
  - containment structure dome for, construction of prestressed and reinforced concrete, 25:15289 (DOCKET-50250-38)
- TYROSINE
  - hydrochloride, radiolysis of single crystals of, ESR studies on free radicals produced from γ, 25:13052
- TZM (MOLYBDENUM ALLOY)
  - welding in sodium at 500 to 700°C, tendency for self-, 25:13668

U

- ULTRASONIC TESTING
  - method for fuel capsules for implantable plutonium-238-fueled cardiac pacemaker, development of, 25:13169(R) (NUMEC-3731-24)
- ULTRASOUND
  - effects on initiation of cavitation in liquid sodium, 25:13154
- ULTRAVIOLET RADIATION
  - effects on 3-methylpentane containing cadmium, lithium, magnesium, potassium, or sodium at 77°K, ESR studies on paramagnetic species produced from, 25:13025
  - effects on activity of hydrolases and content of DNA and protein in lambda strain of Escherichia coli K 12, 25:13371
  - effects on aqueous solutions of poly-L-glutamic acid, 25:13054
  - effects on Aspergillus nidulans, mutagenic, 25:13423
  - effects on Bacillus mesentericus, comparison with ethylenimine and fast neutrons, mutagenic, 25:13416
  - effects on Colpoda, combined effects of x on, 25:13342
  - effects on crisp strains of Neurospora crassa, mutagenic, 25:13424
  - effects on DNA of Escherichia coli, effects of T4 endonuclease on degratory, 25:13411
  - effects on DNA of phage phiX174, inhibitory effects of, on phage reproduction, 25:13382
  - effects on DNA synthesis in cultured HeLa and human amnion cells, photoreactivation of inhibitory, 25:13377
  - effects on electroretinogram of frog, effects of fluorescein on 366 nm, 25:13573
  - effects on Escherichia coli formylmethionyl tRNA, 25:13364
  - effects on Escherichia coli, effects of culture medium on mutagenic, 25:13406
  - effects on Escherichia coli, effects of DNA repair capacity on mutagenic, 25:13421
  - effects on Escherichia coli, mutagenic, 25:13422
  - effects on host cell reactivation in Salmonella typhimurium, 25:13408
  - effects on incorporation of uracil into Escherichia coli, effects of bacteriophage Qβ infection on, 25:13386
  - effects on Kilham rat virus infectivity in rat embryo cells, effects of dose and 5-flurouracil on inhibiting, 25:13608
  - effects on mitosis of Colpoda, 25:13342
  - effects on phage lambda, effects of bacterial recB or recC and phage red or int genes on mutagenic, 25:13412
  - effects on pyrimidine residues, effects of, on aminoacyl synthetase recognition in Escherichia coli, 25:13364
  - effects on respiration in Escherichia coli, effects of pyridine nucleotides on inactivating, 25:13607

XUM

effects on sensitivity of Escherichia coli to subsequent treatment with chloramphenicol, 25:13613
effects on Streptomyces coelicolor, mutagenic, 25:13407
effects on Streptomyces coelicolor, mutagenic, 25:13414
effects on synthesis of DNA, RNA, and proteins in Escherichia coli, combined effects of reductone on, 25:13610
effects on T4 bacteriophage, effects of, on synthesis of DNA and phage lysozyme in Escherichia coli, 25:13616
effects on transformation of SV$_{40}$-infected cultured cells from mice, 25:13552
effects on transforming sarcoma virions and nontransforming leukemia virions of Murine sarcoma viruses, single-hit kinetics of inactivating, 25:13609
effects on unscheduled DNA synthesis in HeLa cells, effects of temperature on, tritium tracer study of, 25:13554
effects on virulence of Nannizzia incurvata, polyfactorial basis for mutagenic, 25:13427
effects on x-radiosensitivity of dogs, 25:13574
effects on yeast, effects of caffeine and stage of growth on lethal, 25:13606
spectra of solar extreme, (E), 25:13875
use for induction of SV40 virus from transformed hamster cell clones, 25:13615
UNITED KINGDOM
radiation dose to human populations of, from color television receivers, mutagenic x, 25:13452
UNITED STATES
radiation monitoring of atmosphere of, during May, 1970, gross beta, 25:13122
radioactivity monitoring in precipitaton and surface atmosphere in, during April, 1970, gross β, 25:13441
radioactivity monitoring in surface atmosphere of, during 1964 to 1970, gross β, and plutonium α, 25:13441
radioisotope content of institutional diet of adults and children in, during October to December 1969 as compared to annual average content for 1969, cesium-137 and strontium-90, 25:13442
radioisotope content of milk in, during 1969 and 1970, cesium-137, iodine-131, and strontium-90, 25:13433
radioisotope content of milk in, during April 1970 as compared to average for previous 12-month period, cesium-137, iodine-131, and strontium-90, 25:13442
tritium content in river waters of, (E), 25:13108
UNIVERSE
evolution of, 25:13950
expansion of, field quantization for particle creation in, 25:14788
model of, (T), 25:13950
model of, Dirac monopoles in hot, (T), 25:13953
models with a cosmological magnetic field, development of inhomogeneities in axially symmetric, (T), 25:13938
properties of, from study of galaxies, (T), 25:13913
URACIL
radiation effects on, in relation to biologic radiolesions or mutagenesis, 25:13374
URACIL, 5-FLUORO-
effects on virus infectivity in uv and x-irradiated rat embryo cells, 25:13608
URANIC ACID
crystal structure of, 25:13010
thermal expansion of monocrystals of, anisotropic, 25:13010
URANIUM
abundance in chondrites, achondrites, and Apollo 11 fines, (E), 25:13787
complexes with bromopyrogallol red, formation constants and spectra of, 25:12926
complexes with diarsine, preparation of tetrahalide, 25:12979
compounds of pentavalent, containing uranium--phosphorus, uranium--arsenic, uranium--nitrogen, and uranium--bismuth bonds, preparation of coordination, 25:13016
content and depth in crustal basalts and granites in USSR, 25:13115
content in Japanese obsidian, (E), 25:13112
content in marsh plants, soils, and water, effects of humidity on, 25:13116
content in rocks of shields and sediment cover of Brazil, Canada, and USSR, relations with geological time, 25:13114
content of diet of human adolescents in EURATOM countries during 1965 to 1967, 25:13392 (EUR-3945(Pt.2))
content of soil in Brazil, effects of, on food contamination, 25:13439
deformation of, mechanisms for, 25:13688
determination by dielectric track detectors, 25:13219
determination in fuel dissolver solutions by tracer method and isotope dilution mass spectroscopy, 25:13081 (NP-18577)
determination of abundance of, relative to thorium in thorium dioxide--uranium dioxide by x-ray fluorescence spectrometry, 25:13077(R) (ANL-7755)
determination of tetravalent and hexavalent, moving boundary method for simultaneous, 25:12938
determination of, correction coefficients for mass-spectrometric, 25:12927
determination using bromopyrogallol red, spectrophotometric, 25:12926
determination using thin-layer chromatography and ring-oven colorimetry, 25:12944
deuteron reactions with thin targets of, at 9 to 14.2 MeV, (E), 25:15046
effects on extraction--photometric determination of iron using tiron and diphenylguanidine, 25:12934
effects on metabolic indices in man when consumed in small quantities in drinking water, 25:13595
enthalpy of high-purity depleted α, β, and γ, adiabatic calorimeter for measurement of, 25:13653 (LA-4521)
evaporation of wires of, properties of aerosols produced by, 25:13650(T) (AI-Trans-289)
heavy ion reactions with, effects of nuclear deformability on cross sections for, (T), 25:15063
lattice parameters of alpha-, alloying effects of plutonium and neptunium on 43°K, 25:14452
monitoring in air and water of Paducah environs during 1969, 25:13431
neutron total cross section at 0.5 to 4.35 MeV, (E), 25:15104
oxidation of trivalent, in sulfuric acid solution, spectrophotometric study on, 25:12977
phase transformations in high-purity depleted, adiabatic calorimeter for measurement of heats of, 25:13653 (LA-4521)
precipitation as uranyl formate, design of equipment for continuous, 25:13012(P)
precipitation in ammonium carbonate solutions using hexaamminecobalt chloride, chemical and crystallographic properties of compounds produced by, 25:12980
prospecting for, development of instruments for, 25:13321 (RISO-M-1270)
proton reactions with thin targets of, at 9 to 14.2 MeV, (E), 25:15046
reactions with hydrogen, surface changes during, 25:13635
reactions with methane to produce uranium carbide, 25:13738(P)
separation from aqueous chloride solutions by solvent extraction using dioctyl phosphate in benzene or heptane, effects of variables on, 25:13096
separation from irradiated fuel elements by solvent extraction using organic phosphorus compounds, 25:13101(P)
x-ray energies of, K, (E), 25:14981 (IN-1448)
URANIUM ALLOYS AND SYSTEMS
coating of fuel cladding of, method for graphite, 25:13745(P)
BeO--U-base, deformation of, mechanisms for, 25:13688
Mo--O--U, crystal structure of UMo_2O_8, 25:13776
Mo--U-base, phase transformation in dilute, kinetics of isothermal β--α' martensitic, 25:13703
O--U, phase diagram of, 25:13777
O--U--V, crystal structure of UV_2O_8, 25:13776
Sb--U, hyperfine magnetic fields in antiferromagnetic USb, Moessbauer effect study of, 25:14483
Ti--U, radiation effects on structure of ordered hexagonal U_2Ti, neutron, 25:13726
URANIUM CARBIDES
equations of state at 0 to 16,000°K, caloric and thermal, 25:13753
production by carburizing metallic uranium, method for, 25:13738(P)
reactions with metallic fission products, 25:13764 (KFK-1260)
Be_2C--UC, preparation of fuels of, containing intermetallic UBe_{13}, 25:13746(P)
Be_2C--UC, production of fuels of, containing uranium dicarbide inclusions, 25:13747(P)
URANIUM CHLORIDES UCl_4
compounds with ligands containing arsenic, bismuth, nitrogen, or phosphorus, preparation and spectra of, 25:13016
URANIUM DEPOSITS
prospecting and development of Canadian, role of Geological Survey of Canada in, 25:13127
prospecting for New Mexico, preliminary reconnaissance data for, 25:13125 (RME-160)
URANIUM FLUORIDES UF_4
LiF--UF_4, preparation of lithium-7 and uranium-233 enriched, for MSRE, 25:15368
URANIUM HALIDES
complexes with dimethylacetamide, methyl sulfoxide, or hexamethylphosphoric triamide in nitromethane, electric conductivity of, relation of composition and ionization capacity to, 25:13023
URANIUM ISOTOPES
neutron cross sections for, review of resonance, (E), 25:15069
neutron reactions above resonance energies, review of data on, 25:15112
neutron reactions with, review of data on fast, 25:15102
URANIUM ISOTOPES U-232
alpha decay of, gamma spectra and half-life for, (E), 25:14981 (IN-1448)
determination in liquid waste effluents from nuclear fuel reprocessing plant by α spectrometry, 25:12950 (BRH/NERHL-70-2)
neutron fission at 0.1 to 1.5 MeV, cross section and fragment angular distributions for, (E), 25:15019
neutron reactions at thermal energies to 10 MeV, evaluation of data on, (T), 25:15128

URANIUM ISOTOPES U-233
- alpha decay of, gamma spectra and half-life for, (E), 25:14981 (IN-1448)
- deuteron reactions (d,pf) with, analysis of neutron-nucleus interaction in, (T), 25:15190
- neutron absorption at thermal energies, neutron yield from, (E), 25:15071
- neutron capture to fission ratio at thermal energies, (E), 25:15070
- neutron fission at 0.018 to 2000 eV, cross section for, (E), 25:15082
- neutron fission at 500 to 1500 keV, ratio to uranium-235 fission cross section, (E), 25:14982 (NCSAC-31)
- neutron fission at thermal energies, cross sections for, (E), 25:15070
- neutron fission of intermediate structure effects in, (E), 25:14997
- neutron fission of, multilevel analysis of cross sections for, 25:15130
- neutron reactions (n,f) at thermal energies, cross section for, (E), 25:15071
- neutron reactions with, yields of spontaneously fissioning isomers from, (E), 25:15031
- neutron resonance parameters for, statistical distributions of Kapur-Peierls, 25:15130
- neutron total cross section at 0.7 to 320 eV, (E), 25:15079

URANIUM ISOTOPES U-234
- alpha decay of, gamma spectra and half-life for, (E), 25:14981 (IN-1448)
- determination in liquid waste effluents from nuclear fuel reprocessing plant by α spectrometry, 25:12950 (BRH/NERHL-70-2)
- fission of isomers of, spontaneous, (E), 25:15031
- neutron reactions at thermal energies to 10 MeV, evaluation of data on, (T), 25:15128
- neutron reactions with, yields of spontaneously fissioning isomers from, (E), 25:15031

URANIUM ISOTOPES U-235
- alpha decay of, gamma spectra and half-life for, (E), 25:14981 (IN-1448)
- determination of abundance of, relative to uranium-238 by neutron activation and γ spectrometry, 25:12958 (TKK-F-A-136)
- fission of isomers of, spontaneous, (E), 25:15031
- neutron capture by, γ spectra from, (E), 25:14982 (NCSAC-31)
- neutron capture by, high-energy γ spectra from, (E), 25:15078
- neutron capture to fission ratio at thermal energies, (E), 25:15070
- neutron capture to fission ratio in, integral measurements of fast, (E/T), 25:15348
- neutron capture-to-fission ratio at 0.1 to 10 keV, (E), 25:15074
- neutron capture-to-fission ratio at 0.1 to 30 keV, radiative, (E), 25:15075
- neutron capture-to-fission ratio at 0.3 to 5000 eV, method for direct measurement of, 25:15076
- neutron cross sections for, multilevel analysis and derivation of R-matrix parameters for, 25:15131
- neutron fission at 0 to 6 MeV, energy dependence of mean prompt neutron production from, (E), 25:15117
- neutron fission at 0 to 70 keV, mean prompt neutron production from, (E), 25:15113
- neutron fission at 0.0001 to 20 MeV, evaluation of cross sections for, (E/T), 25:15127
- neutron fission at 0.005 to 0.1 eV, cross sections for, (E), 25:15067
- neutron fission at 0.01 to 1 MeV, mean number of prompt neutrons and cross section for, (E), 25:15116
- neutron fission at 0.017 to 30 keV, cross sections for, (E/T), 25:15086
- neutron fission at 0.025 to 1 MeV, total cross section for, (E), 25:15068
- neutron fission at 0.1 to 1 MeV, cross sections for, (E/T), 25:15398
- neutron fission at 0.3 to 1.4 MeV, mean prompt neutron production and relative cross sections for, (E), 25:15114
- neutron fission at 0.6 to 5 MeV, mean prompt neutron production from, (E), 25:15115
- neutron fission at 1400 and 1500 keV, ratio to uranium-238 fission cross section, (E), 25:14982 (NCSAC-31)
- neutron fission at 500 to 1500 keV, ratio to uranium-233 fission cross section, (E), 25:14982 (NCSAC-31)
- neutron fission at thermal energies, cross sections for, (E), 25:15070
- neutron fission in intermediate spectra, mean prompt neutron production from, (E/T), 25:15399
- neutron fission of intermediate structure effects in, (E), 25:14997
- neutron fission of, description using sudden model, (T), 25:15024
- neutron fission of, energy spectra and mean prompt neutron production in thermal, (E), 25:15118
- neutron fission of, fission product yields from thermal, (T), 25:15099
- neutron fission of, independent yields of antimony-124g and -126g and terbium-160 in thermal, (E), 25:15038
- neutron fission of, K x-ray yields from fragments from thermal, (E), 25:15027
- neutron fission of, multilevel analysis of cross sections for, 25:15130
- neutron fission of, symmetry of epithermal, (E), 25:14999
- neutron reactions with, yields of spontaneously fissioning isomers from, (E), 25:15031
- neutron resonance parameters for, statistical distributions of Kapur-Peierls, 25:15130
- neutron scattering at 0.025 to 1 eV, cross section for, (E), 25:15085
- neutron scattering at 7 to 60 eV, resonance parameters for, (E), 25:15084
- neutron total cross section at 0.1 to 6 MeV, (E), 25:15103
- radioinduced fission of naturally occurring, in neoplastic and normal tissues of human kidney, interstitial neutron, 25:13361

URANIUM ISOTOPES U-236
- fission of isomers of, spontaneous, (E), 25:15031

URANIUM ISOTOPES U-237
- beta decay of, gamma spectra and half-life for, (E), 25:14981 (IN-1448)
- neutron reactions at thermal energies to 10 MeV, evaluation of data on, (T), 25:15128

URANIUM ISOTOPES U-238
- content in sands and soils of south Florida, 1968 measurements of natural, 25:13107
- determination in liquid waste effluents from nuclear fuel reprocessing plant by α spectrometry, 25:12950 (BRH/NERHL-70-2)
- determination of abundance of, relative to uranium-235 by neutron activation and γ spectrometry, 25:12958 (TKK-F-A-136)
- energy levels of, calculation for one-nucleon, (T), 25:15053
- fission of, potential energy surface for, (T), 25:15053
- Moessbauer spectrum in uranium antimonide, 25:14483
- neutron capture at 0.0001 to 20 MeV, evaluation of cross sections for, (E/T), 25:15127
- neutron capture at 0.001 to 1 MeV, cross sections for, (E), 25:15121
- neutron capture at 0.005 to 30 keV, energy dependence of cross sections for, (E), 25:15105
- neutron capture at 0.05 to 1 keV, resonance parameters from radiative, (E), 25:15081
- neutron capture at 1 eV to 15 MeV, cross sections for, (E/T), 25:15125
- neutron capture at 24 to 145 keV, cross sections for, (E), 25:15106
- neutron capture by, cross-section calculations for, (T), 25:14982 (NCSAC-31)
- neutron capture by, low-energy γ spectra from, (E), 25:15077
- neutron cross sections at 0.00001 eV to 15 MeV, evaluation of, 25:15126
- neutron cross sections at 0.01 to 15 MeV, (T), 25:15123
- neutron elastic scattering by, calculation using multilevel formalism, (T), 25:15161
- neutron fission at 0 to 6 MeV, energy dependence of mean prompt neutron production from, (E), 25:15117
- neutron fission at 0.0001 to 20 MeV, evaluation of cross sections for, (E/T), 25:15127
- neutron fission at 1.35 and 2.02 MeV, neutron spectra from, (E), 25:15109
- neutron fission at 1400 and 1500 keV, ratio to uranium-235 fission cross section, (E), 25:14982 (NCSAC-31)
- neutron fission at 2.5, 7.6, and 14 MeV with long-range particle emission, calculation of probability for, (T), 25:15018
- neutron fission of, cross sections for (n,2n) reaction, (E), 25:15111
- neutron inelastic scattering at 0.05 to 15 MeV, cross sections for, (T), 25:15135
- neutron inelastic scattering below 1.2 MeV, cross sections for, (E), 25:15110
- neutron reactions with, yields of spontaneously fissioning isomers from, (E), 25:15031
- neutron total cross section and resonance parameters at 1 to 100 keV, temperature dependence of, (E/T), 25:15093
- neutron total cross section at 0.1 to 6 MeV, (E), 25:15103
- neutron total cross section at 0.6 to 14 keV, (E), 25:15080
- photofission of, analysis using dynamic collective model, (T), 25:15198
- proton fission at 155 MeV, prompt neutron spectra and yields from, (E), 25:15021
- proton reactions (p,xn) at 200 MeV, Fermi-gas-model calculations of neutron spectra and proton and neutron occupation numbers from, (T), 25:15140 (CU-1019-79)

URANIUM ISOTOPES U-239
- energy-level transitions from uranium-238(n,γ) reactions at low energies, low-energy γ spectra from, (E), 25:15077
- neutron fission at 0.6 to 5 MeV, mean prompt neutron production from, (E), 25:15115

URANIUM NITRIDES
- structure at 4 to 300°K, 25:14454
- Mo--UN, phase studies of eutectic of, at 2100 to 2700°C, 25:13772
- UN--W, phase studies of eutectic of, at 2100 to 2700°C,

- 25:13772

URANIUM ORES
- uranium oxide content of Mary Kathleen Mine, evaluation of, 25:13126

URANIUM OXIDES
- emissivity in nitrogen-diluted hydrogen--oxygen flames, 25:13021
- porosity of sintered powders of, 25:13766(R) (SRO-552-6)

URANIUM OXIDES UO_2
- activation volumes in sintered polycrystalline, at 1324 tc 1800°C, effects of stress on, 25:13756
- coating of spheres of, with vanadium by fluidized bed reduction of vanadium chloride vapors, 25:13737 (KFK-1292)
- creep in stoichiometric polycrystalline, at 1430 to 1666°C, mechanisms of, 25:13759
- mechanical properties of sintered powders of, 25:13766(R) (SRC-552-6)
- preparation of gadolinium oxide-poisoned fuels of, 25:13736 (EUR-4551)
- radiation effects on fission gas re-solution in fuels of, pile neutron, 25:13780(R) (GEAP-12147)
- radiation effects on gas release and swelling in rhenium--tungsten-clad, at 1325 to 1900°C, 25:13785
- sintering density of, effects of trapped non-diffusible gases on, 25:13744
- thermal conductivity at 300 to 900°K, 25:13766(R) (SRO-552-6)
- thermal conductivity of sintered and vibro-compacted fuels of, review of, 25:13749 (EUR-4568)
- B_2O_3--Na_2O--SiO_2--UO_2, luminescence of glasses of, 25:13017
- PuO_2--UO_2, analysis for rare earth impurities by solvent extraction and emission spectrography, 25:12923 (WHAN-SA-47)
- PuO_2--UO_2, analysis of fuels of, for rare earths by solvent extraction and emission spectrography, 25:12922 (WHAN-SA-44)
- PuO_2--UO_2, analysis of hypostoichiometric fuel pellets of, for sorbed gases and water, 25:12925 (WHAN-SA-77)
- PuO_2--UO_2, performance of stainless steel clad fast reactor fuels of, review of, 25:15367 (WHAN-SA-51)
- ThO_2--UO_2, analysis for thorium/uranium by x-ray fluorescence spectrometry, 25:13077(R) (ANL-7755)
- ThO_2--UO_2, radiation effects on swelling of, fast neutron, 25:15366 (WAPD-TM-986)

URANIUM OXIDES U_3O_8
- content of uranium ores from Mary Kathleen Mine, 25:13126

URANIUM PHOSPHIDES
- structure at 4 to 300°K, 25:14454

URANIUM RESERVES
- economic history and estimates of Mary Kathleen Mine, 25:13126

URANIUM SELENIDES
- structure at 4 to 300°K, 25:14454

URANIUM SILICIDES
- etching and polishing for metallography, methods for, 25:13742

URANIUM SULFIDES
- structure at 4 to 300°K, 25:14454

URANYL ACETATES
- uptake by pinocytosis in root tips of oat plants, 25:13353

URANYL FLUORIDES
- criticality of planar arrays of cylinders filled with uranium-235 enriched, empirical formula for prediction of, 25:13198

URANYL FORMATES
- precipitation of, design of equipment for continuous, 25:13012(P)

URANYL IONS
- binding in plant cells, use of electron-dense crystals formed in plant roots exposed to uranyl acetate for determining sites of, 25:13353
- flucrescence quenching of, effects of acrylamide on kinetics of, 25:12981
- toxicity to root tip cells in oat plants, 25:13353

URANYL NITRATES
- bubble nucleation in aqueous, effects of alpha particles on, 25:13152(R) (SU-326-P-13-5)
- criticality of planar arrays of cylinders filled with uranium-235 enriched, empirical formula for prediction of, 25:13198
- denitration of, fluidized bed process for, 25:13077(R) (ANL-7755)
- NH_4NO_3--$UO_2(NO_3)_2$, electrolytic properties of aqueous solutions of, adiabatic compression and ultrasonic attenuation studies of, 25:13015

UREA, 1-ETHYL-1-NITROSO-
- effects on chlorophyll production by Sorghum, mutagenic, 25:13420

UREA, HYDROXY-
- effects on growth of yeast cells, effects of cytidine monophosphates on, 25:13604

URETER
- radiodiagnosis of obstruction of, following human kidney transplant, use of iodine-131 and metastable technetium-99 with scintillation camera for, 25:13490

URIDINE, 5-BROMO-2'-DEOXY-
- effects on irradiated yeast cells, 25:13604
- use for induction of SV40 virus from transformed hamster cell clones, 25:13615

URIDINE, 5-FLUORO-
- effects on irradiated yeast cells, 25:13604

URIDINE MONOPHOSPHATES
- effects on growth of yeast cells, 25:13604

URINE
- iodine-131 excretion in human, following use for therapy of thyroid carcinoma, 25:13596
- radioisotope content of, of cattle following intravenous and oral administration, cerium-144 and scandium-46, 25:13352

V

VAN ALLEN RADIATION BELTS
- electrons in, inverse Compton effect in, (T), 25:14108

VAN DE GRAAFF ACCELERATORS
- control systems and instruments for ORNL, development of, 25:13318(R) (ORNL-4620)
- ion source for, development of polarized, 25:14859

VANADIUM
- deposition on uranium dioxide spheres by reduction of vanadium chloride vapors, 25:13737 (KFK-1292)
- determination in aluminum by neutron activation or spectrophotometry, separation methods for, 25:12959
- determination in cobalt-, iron-, or titanium-base alloys using gas-sheathed tubular electrode arc, spectroscopic, 25:12945
- determination of trace amounts of, in boron carbide by neutron activation, 25:12972
- diffusion of hydrogen and deuterium in, Gorsky-effect measurements of, 25:14440
- effects on superconducting properties of niobium--titanium--zirconium alloy, 25:14208
- mechanical properties of high-purity, 25:13643
- neutron elastic scattering at 1.8 to 8.1 MeV, cross sections for, (E/T), 25:14964
- neutron elastic scattering at 8 MeV, cross sections for, (E/T), 25:14965
- neutron inelastic scattering at 2 to 4.5 MeV, cross sections for, (E/T), 25:14966
- preparation of high-purity, electron beam melting method for, 25:13643
- separation from iron by solvent extraction, method for, 25:12934
- separation from rhenium by solvent extraction using tertiary amines, 25:12921
- sorption on aluminum and zirconium oxides, 25:12959

VANADIUM ALLOYS AND SYSTEMS
- Cr--V, pressure effects on magnetic susceptibility of, (E/T), 25:14447
- Ga--V, superconducting transition temperature of, strain dependence and related effects of, (E), 25:14183
- Ge--V, superconducting transition temperature of, strain dependence and related effects of, (E), 25:14183
- Ge--V, superconducting transition temperature of, strain dependence and related effects of, (E/T), 25:14182
- Mn--V, magnetic properties of, NMR and susceptibility study of band model of, (E/T), 25:14445
- Mo--O--V, crystal structure of $MoV_2O_{7.8}$ and MoV_2O_8, 25:13776
- O--U--V, crystal structure of UV_2O_8, 25:13776

VANADIUM CHLORIDES
- reduction by hydrogen for deposition of vanadium on uranium dioxide spheres, 25:13737 (KFK-1292)

VANADIUM HYDRIDES
- crystal structure of habit plane of, 25:13768

VANADIUM ISOTOPES V-51
- bremsstrahlung reactions at 0.8 to 2.1 GeV, spallation products from, (E), 25:14977
- energy levels from neutron inelastic scattering, spin--parity assignments for, (E), 25:14919 (AWRE-O-78/70)
- energy levels from proton inelastic scattering, (E), 25:14928
- energy-level transitions from neutron inelastic scattering, relative intensities of, (E), 25:14919 (AWRE-O-78/70)
- neutron capture at 0.025 eV, cross section for, (E), 25:14935
- neutron capture at 0.1 to 20 keV, cross section for, (E), 25:14982 (NCSAC-31)
- neutron inelastic scattering at 0.3 to 4 MeV, gamma spectra and excitation functions at 100° for, (E), 25:14919 (AWRE-O-78/70)
- nuclear magnetic resonance in vanadium--manganese alloys, 25:14445
- proton inelastic scattering at 40 MeV, microscopic description of, (E/T), 25:14928

VANADIUM ISOTOPES V-52
- half-life, (E), 25:14935

VANADIUM OXIDES
- crystal structure of V_4O_7, at 77 to 298°K, 25:14442
- phase transitions in VO_2 and V_2O_3, review of thermally induced semiconductor--metal, 25:14470
- phase transitions in VO_2 and V_4O_7, at 77 to 298°K, volume changes at metal--insulator, 25:14442
- plasma resonance in, effects of stoichiometry on, 25:14462

VANADIUM SILICIDES
- superconducting transition temperature of, strain

  - dependence and related effects of, (E/T), 25:14182
  - superconducting transition temperature of, strain dependence and related effects of, (E), 25:14183
- VAPOR PRESSURE
  - measurement of precise isotopic, from -20 to 110°C, design of equipment for, 25:12995
- VEGETABLES
  - mushroom, radiation processing of, for commercial sales, 25:13622
  - potatoes, radiation effects on activity of asparagine synthetase in, effects of dose on γ, 25:13365
  - potatoes, radiation processing of, for commercial sales, reduction of dose for, 25:13622
- VENUS (PLANET)
  - atmosphere of, altitude, latitude, and longitude variations of neutral and ionized particles in, (E/T), 25:13956
  - ionosphere of, altitude, latitude, and longitude variations of neutral and ionized particles in, (E/T), 25:13956
- VERMONT YANKEE POWER REACTOR
  - personnel for, qualifications and responsibilities of, 25:15298 (DOCKET-50271-36)
- VERTEBRATA
  - radioisotope content of marine, in Pacific Ocean, 25:13394(R) (RLO-2099-1)
- VESSELS
  - design of annular centrifugal contactor for use in LMFBR fuel reprocessing, 25:13077(R) (ANL-7755)
- VIOLURIC ACID
  - complexes with thorium nitrate, composition and stability of, spectrophotometric studies on, 25:13014
- VIRUSES
  - Kilham rat, radiation effects on infectivity of, in rat embryo cells, effects of 5-flurouracil on uv and x, 25:13608
  - Murine sarcoma, radioinduced inactivation of transforming sarcoma virions and nontransforming virions of, rates for uv, 25:13609
  - SV40, effects on transformation of uv-irradiated cultured cells from mice, 25:13552
  - SV40, induction from transformed hamster cell clones using chemicals, uv and x radiation, 25:13615
  - SV40, radiation effects on tumorigenicity of, for embryonic cells of hamsters and mice, 25:13553
  - TMV, effects on fixation of carbon-14-labeled carbon dioxide in protein of tobacco leaves, 25:13360
- VITAMIN B GROUP
  - B_1, radiation effects on action of, in central nervous system of rabbits, ionizing, 25:13561
  - folic acid, radiation effects on action of, in central nervous system of rabbits, ionizing, 25:13561
  - metabolism in man following stomach surgery, cobalt-58 tracer studies of, 25:13334
  - nicotinamide, effects on metabolism of NAD and NADP in irradiated organs of rabbits and rats, 25:13379
- VITAMINS
  - content of human body, effects of uranium content of drinking water on, 25:13595

W

- WATER
  - analysis and sampling of, Public Health Service programs for, 25:13432
  - analysis for gross α, gross β, and tritium in Project Rulison area, methods for radiochemical, 25:12951 (USGS-474-83)
  - bubble nucleation in superheated, effects of alpha particles on, 25:13152(R) (SU-326-P-13-5)
  - content in earth materials, neutron logging method for measurement of, 25:13104 (UCRL-50855)
  - content in hypostoichiometric plutonium dioxide--uranium dioxide fuel pellets, effects of density and storage on, 25:12925 (WHAN-SA-77)
  - content in rocks of shields and sediment cover of Brazil, Canada, and USSR, relations with geological time, 25:13114
  - content in soils, gamma scintillation chamber measurements of, 25:13110
  - determination in hypostoichiometric plutonium dioxide--uranium dioxide fuel pellets, 25:12925 (WHAN-SA-77)
  - determination in mixed oxide fuels using moisture analyzer, effects of hydrogen on, 25:12924 (WHAN-SA-62)
  - determination in presence of heavy water by microwave methods, 25:12931(P)
  - electron slowdown at 10 to 15 MeV in, Monte Carlo calculation of, 25:14397
  - electron slowdown at 10 to 28 MeV, Monte Carlo study of spectra of, 25:14398
  - gamma transport in two-region systems with iron and lead, calculations using iterative method, 25:14407
  - gamma transport in, calculations using anisotropic source--flux iteration technique, 25:14407
  - neutron thermalization by ore-contained, time characteristics of, 25:13109
  - radiation effects on removal of iron from acidic mine drainage, 25:13036(P)
  - radiation monitoring of Paducah environs during 1969, β, 25:13431
  - volume viscosity of, 25:12990
  - yields from γ radiolysis of 2-propanol vapor at 124 to 400°C, 25:13046
  - bis(2-ethylhexyl) phosphate--H_2O--$Nd(NO_3)_3$, complex formation in, 25:13092
  - bis(2-ethylhexyl) phosphate--HNO_3--H_2O--$Y(NO_3)_3$, equilibrium in, extraction, 25:13097
- WATER-d
  - spectra of, ir, 25:12994
- WATER-d_2
  - determination in presence of normal water by microwave methods, 25:12931(P)
  - effects on activity of mixed liver microsome oxidases, inhibitory, 25:13372
  - production in Canada, Glace Bay plant modification cost and time requirements for, 25:13175
  - production of, evaluation of processes for, 25:13076 (AECL-2503)
  - volume viscosity of, 25:12990
- WATER-t
  - effects on blood cells, weight of spleen, and weight of thymus in rats in comparison to cesium-137, RBE for, 25:13551
- WATER SUPPLIES
  - radioactivity monitoring in domestic, in California during 1968, gross β, 25:13440
  - radioactivity of Italian, (E), 25:13106
- WATER VAPOR
  - distribution in atmosphere, use in tracer studies of global transport processes, (E), 25:13121 (TID-25314)
  - sorption by polycrystalline tungsten, hydrogen evolution kinetics in, 25:13669
- WATERFORD POWER REACTOR, UNIT 3
  - effluents from, effects on environment of chemical, radioactive, and thermal, 25:15334 (DOCKET-50382-6)
- WATERFORD POWER REACTOR, UNIT 4
  - effluents from, effects on environment of chemical, radioactive, and thermal, 25:15334 (DOCKET-50382-6)
- WELL LOGGING
  - gamma--gamma method for measuring density of earth materials, 25:13104 (UCRL-50855)
  - method using acoustic wave velocity in drill holes, 25:13104 (UCRL-50855)
  - methods for gamma and gamma--gamma, use of gamma-scattering in rocks for, 25:13113
  - methods for measuring geophysical properties of earth materials at underground nuclear explosion sites, comparison of, (E), 25:13104 (UCRL-50855)
  - neutron method for measuring water content in earth materials, 25:13104 (UCRL-50855)
  - neutron thermalization in silicate ore borehole, effects of moisture on, 25:13109
- WEST VALLEY PROCESSING PLANT
  - effluent and environmental monitoring for, changes in technical specifications for, 25:13078 (DOCKET-50201-60)
  - radiation monitoring at, Oct.--Dec. 1970, 25:13079 (DOCKET-50201-61)
  - radiation monitoring in environs of, 1969, 25:13080 (DOCKET-50201-62)
- WHISTLERS
  - production of low-latitude subprotonospheric and ion-cyclotron, by same lightning discharge, (E), 25:14114
  - propagation in ambient magnetic field direction, nonlinear particle trajectories in, (T), 25:14122
  - propagation in magnetosphere, nonducted, (E/T), 25:14120
- WILLIAM H. ZIMMER POWER REACTOR, UNIT 1
  - design parameters of single unit stackless concept for, revised and additional data on, 25:15328 (DOCKET-50358-12)
  - effluents from, effects on environment of chemical, radioactive, and thermal, 25:15327 (DOCKET-50358-11)
  - operations aspects of single unit stackless concept for, revised and additional data on, 25:15328 (DOCKET-50358-12)
- WIRES
  - performance of indium thin-film superconducting transmission, effect of tin additive on, 25:14223
- WOOD
  - radioinduced polymerization of plastics in, bibliography on, 25:13029 (AAEC/LIB/Bib-259)

X

- X RADIATION
  - dose from diffraction apparatus, surveymeters for measuring scattered, 25:13457
  - dose to human populations of Britain from color television receivers, mutagenic, 25:13452
  - dosimetry in human lungs, mediastinum, and stomach, 25:13453
  - effectiveness for therapy of bone cancer in comparison to cesium-137 and cobalt-60 γ, phantom studies on, 25:13536
  - effectiveness for therapy of malignancies in man in combination with cytostatic drugs, 25:13527
  - effectiveness for therapy through plaster casts in man in comparison to cesium-137 γ, cobalt-60 γ, and fast electrons, 25:13539
  - effectiveness of 43.5 MeV, for therapy of tumors in long

bones, 25:13537
effects of solar, on high-frequency radio absorption in D region, (E), 25:13897
effects on activity of hydroxyindole methyltransferase and synthesis of melatonin in pineal glands in rats, 25:13559
effects on aqueous solutions of poly-L-glutamic acid, 25:13054
effects on α-amylase activity in Aspergillus oryzae, combined effects of ethylenimine on inhibitory, 25:13381
effects on bone marrow and reticulo-endothelial system in rats, protective effects of bacterial antigens, epinephrine, and pilocarpine against, 25:13567
effects on bone marrow in mice and rats, effects of species on local, 25:13563
effects on chemical composition of blood in dogs, effects of preliminary exposure to uv on, 25:13574
effects on chlorophyll production by Sorghum, mutagenic, 25:13420
effects on chlorophyll, fertility, and growth of Sesamum orientale, mutagenic, 25:13415
effects on cholinesterase activity in spinal cord of cats, whole-body, 25:13333
effects on cholinesterase activity in spinal cord of cats, partial and whole-body, 25:13375
effects on chromosomes of Drosophila melanogaster, aberrant, 25:13409
effects on chromosomes of human lymphocytes, aberrant, 25:13410
effects on chromosomes of Vicia faba, effects of dose fractionation on aberrant, 25:13413
effects on Colpoda, effects of caffeine, temperature, and uv on dark repair systems following, 25:13342
effects on DNA of phage phiX174, inhibitory effects of, on phage reproduction, 25:13382
effects on embryonic cells of hamsters and mice, effects of, on SV40 tumorigenicity, 25:13553
effects on Escherichia coli, effects of DNA repair capacity on mutagenic, 25:13421
effects on Escherichia coli, mutagenic, 25:13422
effects on exogenous nucleoside utilization in DNA synthesis by cultured human cells, effects of growth phase of culture, nucleoside concentration, and precursors on, 25:13380
effects on genes of Drosophila melanogaster, mutagenic, 25:13426
effects on gold diffusion in silicon, 25:14420
effects on head of rabbits, intracerebral temperature changes following, 25:13575
effects on heating of H I regions, (T), 25:13841
effects on hematopoietic stem cells in mice in relation to light and darkness, effects of transplantation of bone marrow cells on, 25:13550
effects on histone content of deoxyribonucleoprotein in liver, spleen, and thymus of rats, effects of heparin on, 25:13385
effects on human lymphocytes in vitro, protective effects of phytohemagglutinin against effects of dose on, 25:13472
effects on human skin, RBE for, 25:13583
effects on human thyroid following therapy for lymph node adenomas in children, carcinogenic, 25:13585
effects on incorporation of tritium-labeled thymidine into diplotene ooctyes, 25:13367
effects on jejunal crypt cells of rats, effects of protein contents on recovery from, 25:13562
effects on Kilham rat virus infectivity in rat embryo cells, effects of dose and 5-flurouracil on inhibiting, 25:13608
effects on leaf mass and pigment content of beans, effects of dose for seed exposure on, 25:13600
effects on leucine incorporation and protein synthesis in isolated perfused rat liver, 25:13373
effects on lymph flow and filtration function of lymph nodes in rats, effects of dose on, 25:13481
effects on oocytes of Drosophila melanogaster, lethal, 25:13555
effects on perianal skin following therapy of pruritus ani, x, 25:13588
effects on preimplantation blastocysts of rats, whole-body, 25:13560
effects on productivity of peas, mutagenic, 25:13418
effects on protrophy in yeast, relationship of DNA replication to mutagenic, 25:13425
effects on secretion by accessory reproductive organs in rats, 25:13366
effects on sensitivity of Escherichia coli to subsequent treatment with chloramphenicol, 25:13613
effects on sodium chloride crystals, effects of sodium doping on thermoluminescence, 25:14425
effects on splenomegaly in mice, effects of, on graft-versus-host reactions following injection with spleen or thymus cells, 25:13390
effects on survival and skin transplants in mice, protective effects of sodium s-(2-aminoethyl) phosphorothioate against 400 to 1100 R, 25:13479
effects on Taricha granulosa, protective effects of methyl sulfoxide against mixed cobalt-60 γ and, 25:13477
effects on thermally generated electric currents in Lucite, 25:13786
effects on water content and distribution in brain, kidneys, liver, and skeletal muscles of rats, lethal and sublethal, 25:13348
emission during solar flares, coronal electron temperatures associated with, (E), 25:13902
emission from hot coronal plasmas, (T), 25:13889
emission from O VII in solar corona, (E), 25:13885
emission from Sun, bibliography and review of, (T), 25:13863 (N-70-39828)
emission from supernova remnants, secular behavior of, (T), 25:13847
origin of cosmic background, in radiogalaxies, (T), 25:13922
production in dense deuterium noncylindrical z pinch, (E), 25:14359
protection of patients against, during deep therapy, 25:13460
scattering by two-species quantum fluids, Born approximation to cross sections for, 25:13965
shielding of gonads of female personnel against, development of lead impregnated vinyl foundation garment for, 25:13462
spectra of solar soft, (E), 25:13875
use for induction of SV40 virus from transformed hamster cell clones, 25:13615
use for theory of acne in human children in relation to subsequent development of thyroid tumors, 25:13587
use for therapy of human cervix carcinomas in combination with radium or surgery, evaluation of addition of 15 MV x or cobalt-60 γ for effectiveness of, 25:13531

X-RAY-ABSORPTION ANALYSIS
equipment for silver determination in photographic emulsion, 25:13312

X-RAY EQUIPMENT
dose from diffraction, protective effects of shielding materials against, 25:13457
inspection of dental and medical, priority system for state, 25:13459
safety survey of dental and medical diagnostic, in USA during 1961 to 1968, 25:13464
safety survey of, used in schools in Kansas, 25:13463

X-RAY FLUORESCENCE ANALYSIS
equipment for, review of portable radioisotope source, 25:13310

XENON
analysis for trace amounts of argon, hydrogen, nitrogen, and oxygen by condensation, mass spectrometric, 25:12941
chemical state of, in irradiated oxide fuel elements, 25:13077(R) (ANL-7755)
electron elastic scattering at 25 to 800 eV by, tables of amplitudes and spin polarizations for, (T), 25:13955 (AD-711664)
electron reactions at 3 to 16 keV with, cross sections for excitation of K x rays in, (E), 25:14008
electron reactions up to 150 eV with, ionization cross sections for, (E), 25:14002
plasma of, absorption spectra of partially ionized, (E), 25:14280
plasma of, diagnostic methods for temperature measurement in, 25:14261
solubility in sodium at 350 to 600°C, 25:13651(R) (ANL/ST-4)
xenon isotope concentration in, by thermal diffusion, 25:13165(R) (MLM-1753)
yields from γ radiolysis of xenon trioxide, 25:13049

XENON IONS
effects on gold at 12 to 30 keV, defects induced in, 25:14413 (NP-18645)
reactions with oxygen atoms at 30 keV to 2 MeV, cross sections for electron capture and loss in, (E), 25:14042

XENON ISOTOPES Xe-124
concentration in xenon by thermal diffusion, 25:13165(R) (MLM-1753)

XENON ISOTOPES Xe-126
abundance in Apollo 11 igneous rocks, (E), 25:13954

XENON ISOTOPES Xe-130
energy levels from decay of iodine-130 isomers, (E), 25:15007

XENON ISOTOPES Xe-131
abundance in Apollo 11 igneous rocks, (E), 25:13954
concentration in xenon by thermal diffusion, 25:13165(R) (MLM-1753)

XENON ISOTOPES Xe-132
effects on spectra of xenon, optical heterodyne measurement of, 25:13004
energy levels from decay of cesium-132, (E), 25:15007

XENON ISOTOPES Xe-133
ion channeling patterns in silicon, 25:14417
production in neutron fission of plutonium-239, release curves for, (T), 25:14989 (UCRL-50656(Suppl.))
use for scanning of human lung function, performance of dorsal and ventral detectors during, 25:13520
use for scanning of human lungs, development of mobile detectors for, 25:13514

XENON ISOTOPES Xe-134
effects on spectra of xenon, optical heterodyne measurement of, 25:13004
production in neutron fission of plutonium-239, release curves for, (T), 25:14989 (UCRL-50656(Suppl.))

- XENON ISOTOPES Xe-135
  - production in neutron fission of plutonium-239, release curves for, (T), 25:14989 (UCRL-50656(Suppl.))
- XENON ISOTOPES Xe-136
  - effects on spectra of xenon, optical heterodyne measurement of, 25:13004
  - production in neutron fission of plutonium-239, release curves for, (T), 25:14989 (UCRL-50656(Suppl.))
- XENON ISOTOPES Xe-137
  - production in neutron fission of plutonium-239, release curves for, (T), 25:14989 (UCRL-50656(Suppl.))
- XENON ISOTOPES Xe-138
  - production in neutron fission of plutonium-239, release curves for, (T), 25:14989 (UCRL-50656(Suppl.))
- XENON OXIDES
  - radiolysis of aqueous solutions of xenon trioxide, yields of oxygen and xenon from γ, 25:13049
- XENON SYSTEMS
  - Ne--Xe, diffusion coefficients for, at 169 to 922°K, 25:13165(R) (MLM-1753)

Y

- YANKEE POWER REACTOR
  - fuel inventory in, evaluation of ISOCHECK and INVENT codes for isotopic, (E/T), 25:15211
  - operation of, staffing procedures during labor strike, 25:15257 (DOCKET-50029-90)
  - operations history for December 1970, 25:15226 (DOCKET-50029-142)
- YTTERBIUM
  - complexes with carminic acid, spectrophotometric studies on, 25:12937
  - determination in plutonium oxide--uranium oxide fuels by solvent extraction and emission spectrography, 25:12922 (WHAN-SA-44)
  - determination in presence of lutetium and yttrium using carminic acid, photometric, 25:12937
  - determination of trace amounts of, in plutonium and plutonium dioxide--uranium dioxide by solvent extraction and emission spectrography, 25:12923 (WHAN-SA-47)
  - energy-level excitation by neutron capture gamma rays, (E), 25:15002
  - reduction of trivalent, in perchlorate medium, polarographic studies on, 25:13020
- YTTERBIUM BORIDES
  - electronic structure of CaB_6-type, 25:14463
- YTTERBIUM ISOTOPES Yb-171
  - energy levels from ytterbium-172 (He-3,α) reactions, spectroscopic factors and spin-parity assignments for, (E), 25:15057
- YTTERBIUM ISOTOPES Yb-172
  - energy levels from electron-capture decay of lutetium-172, (E), 25:15030
  - helium-3 reactions (He-3,α) at 28 MeV, angular distributions for, (E), 25:15057
  - neutron capture by, γ spectra and Q-value for thermal, (E), 25:15059
- YTTERBIUM ISOTOPES Yb-173
  - energy levels from ytterbium-172 thermal neutron capture, spin-parity assignments for, (E), 25:15059
  - energy levels from ytterbium-174 (He-3,α) reactions, spectroscopic factors and spin-parity assignments for, (E), 25:15057
- YTTERBIUM ISOTOPES Yb-174
  - helium-3 reactions (He-3,α) at 28 MeV, angular distributions for, (E), 25:15057
- YTTERBIUM ISOTOPES Yb-175
  - beta decay of, circular polarization of γ rays from, (E), 25:15009
  - energy levels from ytterbium-176 (He-3,α) reactions, spectroscopic factors and spin-parity assignments for, (E), 25:15057
- YTTERBIUM ISOTOPES Yb-176
  - helium-3 reactions (He-3,α) at 28 MeV, angular distributions for, (E), 25:15057
  - proton reactions (p,t) with, analysis using coupled-channel Born approximation, (T), 25:15191
- YTTERBIUM ISOTOPES Yb-177
  - beta decay of 1.9-hr, gamma spectra from, (E), 25:15039
- YTTERBIUM OXIDES
  - Lu_2C_3--Yb_2O_3--Y_2O_3, analysis for lutetium and ytterbium using carminic acid, photometric, 25:12937
- YTTRIUM
  - abundance in chondrites, achondrites, and Apollo 11 fines, (E), 25:13787
  - complexes with carminic acid, spectrophotometric studies on, 25:12937
  - electric potential of trivalent/neutral couple of, 25:13095
  - Ettingshausen effect measurements on polycrystalline, 25:14475
  - separation from aqueous chloride solutions by solvent extraction using dioctyl phosphate in benzene or heptane, effects of variables on, 25:13096
  - separation from aqueous nitric acid solutions by solvent extraction using bis(2-ethylhexyl) phosphate, 25:13097
- YTTRIUM ALLOYS AND SYSTEMS
  - Al--Y, mechanical properties of composite, 25:13692
  - Co--Sm--Y, lattice parameters and magnetic properties of Y/sub 1-x/Sm/sub x/Co_5, 25:14461
  - Mg-base--Y, deformation of wrought, 25:13710
  - Ta-base--Y, corrosion of dilute, by lithium at 1600°C, 25:13630 (EUR-4298)
  - Y--Zn, thermodynamic properties of intermetallic YZn_{12} in molten chlorides, 25:13095
- YTTRIUM BORIDES
  - thermal expansion of YB_2, YB_4, YB_6, and YB_{12}, (E), 25:13760
- YTTRIUM ISOTOPES Y-87
  - beta and electron-capture decay of, gamma spectra from, (E), 25:15136
  - beta and electron-capture decay of, Kurie plot of beta spectra from, (E), 25:15136
- YTTRIUM ISOTOPES Y-88
  - beta and electron-capture decay of, gamma spectra from, (E), 25:15136
  - content of feces, milk, and urine of dairy cattle following ingestion of Schooner fallout, 25:13396 (UCRL-72511)
- YTTRIUM ISOTOPES Y-89
  - energy levels from neutron inelastic scattering, spin--parity assignments for, (E), 25:14919 (AWRE-O-78/70)
  - energy-level transitions from neutron inelastic scattering, relative intensities of, (E), 25:14919 (AWRE-O-78/70)
  - neutron inelastic scattering at 0.3 to 4 MeV, gamma spectra and excitation functions at 100° for, (E), 25:14919 (AWRE-O-78/70)
  - neutron inelastic scattering at 14.5 MeV, cross sections for, (E), 25:14967
- YTTRIUM ISOTOPES Y-90
  - beta decay of, gamma spectra from, (E), 25:15136
  - uptake by oats, effects of addition of ashed plants containing strontium-90 and yttrium-90 and soil pH on, 25:13118(R) (COO-414-17)
- YTTRIUM ISOTOPES Y-91
  - beta decay of, gamma spectra, branching ratios, and log-ft values for, (E), 25:15136
- YTTRIUM ISOTOPES Y-92
  - ionization following beta decay, energy dependence of auto-, (E), 25:13982
- YTTRIUM NITRATES
  - bis(2-ethylhexyl) phosphate--HNO_3--H_2O--$Y(NO_3)_3$, equilibrium in, extraction, 25:13097
- YTTRIUM OXIDES
  - analysis for trace amounts of rare earths by x-ray-excited optical luminescence, 25:12948
  - elastic properties of composites of pores in, 25:13751
  - Lu_2O_3--Yb_2O_3--Y_2O_3, analysis for lutetium and ytterbium using carminic acid, photometric, 25:12937
  - Y_2O_3--ZrO_2, electric conductivity at 700 to 1250°C of solid solutions of, mechanism of, 25:14476
  - Y_2O_3--ZrO_2, phase studies of, 25:13769

Z

- ZINC
  - determination in airborne and deposited particulates by neutron activation and γ spectrometry, 25:12975
  - determination in aluminum-, copper-, or magnesium-base alloys using gas-sheathed tubular electrode arc, spectroscopic, 25:12945
  - determination of trace amounts of, in blood serum by emission spectroscopy, 25:12946
  - effects on oxidation of trivalent uranium in sulfuric acid, 25:12977
  - electron diffraction intensities from cleaved surfaces of, low-energy, (LEED), 25:14472
  - energy-level excitation by neutron capture gamma rays, (E), 25:15002
  - neutron elastic and inelastic scattering at 4.5 to 8 MeV, cross sections for, (E/T), 25:14963
  - neutron elastic scattering at 8 MeV, cross sections for, (E/T), 25:14965
  - neutron scattering at 1 to 8 MeV, width fluctuation and resonance interference effects in cross sections for, (E/T), 25:14962
  - reactions with niobium halides to produce niobium, 25:13642
  - reactions with potassium niobium chloride to produce niobium, 25:13642
  - sorptive properties for iodine released during pyrochemical head-end reprocessing of irradiated fuel elements, 25:13077(R) (ANL-7755)
  - superconducting transition temperature and mass enhancement, (T), 25:14152
- ZINC ALLOYS AND SYSTEMS
  - Ag--Zn, phase transformations in, β--α massive, 25:13720
  - Cd-base--Zn, deformation of single crystals at 77°K, critical resolved shear stress and activation volume in, 25:13670
  - Cd-base--Zn, thermal conductivity at low temperatures, 25:14473
  - Cu--Zn, phase transformations in, β--α massive, 25:13720
  - Mg--Zn, thermal conductivity at low temperatures, 25:14473
  - Y--Zn, thermodynamic properties of intermetallic YZn_{12} in molten chlorides, 25:13095

XUM

ZINC ISOTOPES
- isotope shift between A = 64, 66, 68 and 70, (E), 25:14927

ZINC ISOTOPES Zn-60
- energy levels from nickel-58 (He-3,n) reactions, T = 2, (E), 25:14943

ZINC ISOTOPES Zn-64
- neutron reactions (n,p) with, fission-spectrum-averaged activation cross sections for, (E), 25:14968

ZINC ISOTOPES Zn-65
- accumulation from sea water by alginic acid of brown algae, 25:13403

ZINC ISOTOPES Zn-66
- energy levels from gallium-66 electron capture decay, (E), 25:14957
- meson (μ) reactions with, energy levels from, (E), 25:14958

ZINC ISOTOPES Zn-67
- energy level at 184 keV, g-factor for, (E/T), 25:14975

ZINC ISOTOPES Zn-68
- meson (μ) reactions with, energy levels from, (E), 25:14958

ZINC SULFIDES
- analysis for silver by neutron activation and radiochemical separation using diethyl dithiocarbamate, 25:12963

ZIRCALOY
- anisotropy and texture of tubes of, effects of plastic deformation on, 25:13655 (NP-18625)
- production of fuel cladding tubes of, design of equipment and processes for, 25:13645

ZIRCALOY-2
- corrosion by steam at 350 to 450°C and 50 atm pressure, 25:13629 (EIR-184)

ZIRCALOY-4
- radiation effects on tubes of, fast neutron, 25:15366 (WAPD-TM-986)

ZIRCONIUM
- abundance in chondrites, achondrites, and Apollo 11 fines, (E), 25:13787
- anisotropy and texture of, effects of plastic deformation on, 25:13655 (NP-18625)
- coating of fuel cladding of, method for graphite, 25:13745(P)
- determination in nickel-base alloys using gas-sheathed tubular electrode arc, spectroscopic, 25:12945
- determination in plutonium by solvent extraction and emission spectrography, 25:12923 (WHAN-SA-47)
- dislocations in α-, etching method for revealing glide, 25:13714
- effects on intercrystalline corrosion of molybdenum--nickel alloys by boiling hydrochloric acid solution, relations with temperature, 25:13633
- effects on mechanical properties and oxidation resistance of aluminum--chromium--iron alloys, 25:13680
- elastic constants from phonon dispersion curves, 25:14467
- neutron inelastic scattering at 14.5 MeV, cross sections for, (E), 25:14967
- phonon dispersion curves from thermal neutron inelastic scattering, 25:14467
- photon elastic scattering cross sections at 8.5 to 12.5 MeV, (E), 25:14959
- positron annihilation in single crystal of, angular distribution of two-photon, 25:14441
- properties at high temperatures, review of physical, thermal, and thermodynamic, 25:13667
- separation from aqueous fuel reprocessing solutions by solvent extraction, effects of radiolysis of toluene on, 25:13093
- separation from chlorides by fused salt electrolysis, 25:13089
- separation of nitrogen and oxygen from interstitial sites in, method for, 25:13641(T) (UCRL-Trans-10503)

ZIRCONIUM ALLOYS AND SYSTEMS
- phase transition and structure of, magnetic susceptibility and internal friction study of beta--omega, 25:14465
- properties at high temperatures, review of physical, thermal, and thermodynamic, 25:13667
- Co--Zr, phase diagram for, 25:13712
- Cr--Si--Zr-base, corrosion by steam at 350 to 450°C and 50 atm pressure, 25:13629 (EIR-184)
- Cr--Zr-base, corrosion by steam at 350 to 450°C and 50 atm pressure, 25:13629 (EIR-184)
- Cu--Fe--Zr-base, corrosion by steam at 350 to 450°C and 50 atm pressure, 25:13629 (EIR-184)
- Ga--Zr-base, phase diagram of eutectoid region of, 25:13709
- Mo--Sn--Ti-base--Zr, mechanical properties of metastable β, effects of microstructure on, 25:13672
- Nb--O--Zr-base, transformation temperatures of, effects on concentration on continuous cooling, 25:13679
- Nb--Ti-base--Zr, critical current density of superconducting rolled sheets of, relations with aging temperature, magnetic field, and time, 25:14209
- Nb--Zr, magnetic-flux flow through wall of, 25:14197
- Nb--Zr-base, corrosion by steam at 350 to 450°C and 50 atm pressure, 25:13629 (EIR-184)
- Nb-base--Ti--Zr, superconducting properties of, effects of molybdenum, tantalum, and vanadium additions on, 25:14208
- Nb-base--Zr, corrosion by lithium at 1500°C, effects of oxygen on, 25:13630 (EUR-4298)
- Ta--Zr-base, phase studies of metastable structure of, 25:13716
- Ta--Zr-base, superconducting transition temperature of, effects of concentration on, 25:13716

ZIRCONIUM CARBIDES
- C--ZrC, elastic properties of composites of, 25:13751

ZIRCONIUM HYDRIDES
- neutron inelastic scattering by polarized ZrH_2 single crystals, coherent and incoherent cross sections of polarized, (T), 25:14869

ZIRCONIUM ISOTOPES Zr-89
- content of feces, milk, and urine of dairy cattle following ingestion of Schooner fallout, 25:13396 (UCRL-72511)

ZIRCONIUM ISOTOPES Zr-90
- alpha elastic scattering by, optical-model analysis of, (E/T), 25:14947
- proton reactions (p,d) at 22.9 MeV, DWBA analysis of differential cross sections and asymmetries from, (E/T), 25:14980 (CEA-CONF-1654)

ZIRCONIUM ISOTOPES Zr-91
- energy levels from yttrium-91 beta decay, (E), 25:15136
- energy-level transitions from yttrus-91 beta decay, (E), 25:15136

ZIRCONIUM ISOTOPES Zr-95
- determination in liquid waste effluents from nuclear fuel reprocessing plant by γ spectrometry, 25:12950 (BRH/NERHL-70-2)
- determination in reactor cooling water by γ spectroscopy, 25:12956

ZIRCONIUM ISOTOPES Zr-96
- deuteron reactions (d,n) at 12 MeV with isobaric analog excitation, anomalies in cross section for, (E), 25:15050

ZIRCONIUM OXIDES
- corrosion of SNAP-19B fuel capsule components of, by seawater, 25:13163 (MLM-1652)
- properties at high temperatures, review of physical, thermal, and thermodynamic, 25:13667
- properties of aerosols of, measurement of chemical and physical, 25:13145
- sorptive properties for vanadium, 25:12959
- Nb_2O_5--ZrO_2, crystal structure of polymorphs of $ZrO_2 \cdot 12Nb_2O_5$, 25:13774
- Sc_2O_3--ZrO_2-base, electric conductivity of, effects of temperature on, 25:13778
- Sc_2O_3--ZrO_2-base, phase diagram of subsolidus region of, at 20 to 2000°C, 25:13778
- Y_2O_3--ZrO_2, electric conductivity at 700 to 1250°C of solid solutions of, mechanism of, 25:14476
- Y_2O_3--ZrO_2, phase studies of, 25:13769

ZIRCONIUM PHOSPHATES
- properties as ion exchange material, 25:13084

ZODIACAL LIGHT
- mechanism for production of gegenschein, (E/T), 25:12906

REPORT NUMBER INDEX

Reports, conference papers and proceedings, numbered translations, and patents are included in this index. Each item is listed by report number; this is followed by the abstract number and a brief notation regarding public availability. The index entries show which reports are on file in the institutions listed on the back of the front cover (Dep.), which reports have been published in open-literature journals (journal citation), and which reports can be purchased (source and price). Whenever a report is identified by more than one number, the availability is given under the primary number, and a cross reference is given under the secondary report number.

The report number codes apply to USAEC reports unless designated otherwise. Non-USAEC reports are identified by parenthetical notes after the report codes; e.g., (non-AEC), (British), (Canadian), (French). The note (Misc.) identifies the codes used for both USAEC and non-USAEC reports. Patents are listed under the heading "PATENTS"; the country of origin is included in parentheses.

A comprehensive list of both USAEC and non-USAEC report codes is contained in the latest revision of TID-85, *Report Number Series Used by the Division of Technical Information in Cataloging Reports.* This information is also included in the Cumulative Report Number Index (issued annually).

Availability of USAEC Reports

All USAEC Reports abstracted in *Nuclear Science Abstracts* are available through one or more of the following sources:

(1) University and public libraries in the United States. A list of these organizations appears on the inside front cover of each issue of *NSA*.

(2) NCR Microcard Editions in Microcard and micronegative form. Orders and inquiries should be sent to: Order Processing Department, 365 South Oak Street, West Salem, Wisconsin 54669.

(3) National Technical Information Service, U. S. Department of Commerce, Springfield, Virginia 22151.

(4) Superintendent of Documents, U. S. Government Printing Office, Washington, D. C. 20402.

(5) National Cash Register Co., P. O. Box 3111, Oak Ridge, Tenn. 37830, in micronegative form. Purchase details available on request.

Availability of Non-USAEC Reports

U. S. Reports. Reports of U. S. Government agencies are available to the public from the National Technical Information Service (NTIS). If specific availability is not shown, inquiries may be directed to NTIS.

Non-U. S. Reports. Reports of atomic energy organizations of other countries are available from NTIS for U. S. sale only. Specific availability in the country of origin is shown, when known, at the report number entry. Otherwise, inquiries should be made to the organizations listed below:

AUSTRALIA

Australian Atomic Energy Commission Research Establishment. Available upon request from the Library, Australian Atomic Research Establishment, Private Mail Bag, Sutherland, New South Wales, Australia.

BELGIUM

Centre d'Étude de l'Energie Nucléaire. Available upon request to individuals and organizations from the Centre d'Etude de l'Energie Nucléaire (C.E.N.), Studiecentrum voor Kernenergie (S.C.K.), Technical Information Dept., MOL-DONK (Belgium).

CERN

CERN European Organization for Nuclear Research. Available without charge from CERN European Organization for Nuclear Research, Geneva 23, Switzerland. Copies are deposited in libraries throughout the world.

FRANCE

Commissariat à l'Energie Atomique. Inquiries for reports numbered 1-2199 should be addressed to Service Central de Documentation du C.E.A., Centre d'Etudes Nucléaires de Saclay, Boîte postale n° 2, 91. GIF-sur-YVETTE, FRANCE. Reports numbered 2200 and above are available from La Documentation Française, 31 quai Voltaire, 75, PARIS (7e), FRANCE.

Service Central de Protection contre les Rayonnements Ionisants. Copies are available from Ministère de la Santé Publique, Service Central de Protection contre les Rayonnements Ionisants, B.P. n° 78 Le Vesinet (France) Telex 25667.

GERMANY

Deutsches Elektronen-Synchrotron DESY. Copies are available from Deutsches Elektronen-Synchrotron DESY, Dokumentation, 2000 Hamburg 52, Notkestieg 1, Germany.

Gesellschaft für Kernforschung mbH (KFK). Copies are available from Gesellschaft für Kernforschung mbH, 75 Karlsruhe, Postfach 947, Germany. Copies are also deposited in many national nuclear centers in the world.

Kernforschungsanlage. Copies may be ordered from Zentralbibliothek der Kernforschungsanlage Jülich, Jülich, Bundesrepublik Deutschland.

Hahn-Meitner-Institute für Kernforschung. Available without charge from Hahn-Meitner-Institute für Kernforschung Ber-

XUM

lin, Bibliothek, Glienicker Strasse 100, 1 Berlin 39, Germany. Copies are deposited in many national nuclear centers in the world.

Johann-Wolfgang-Goethe Universität, Frankfurt Am Main, Institut für Kernphysik, (IKF). Copies are available from Gmelin Institut, 40–42 Varrentrappstrasse, Frankfurt (Main), West Germany.

ISRAEL

Israel Atomic Energy Commission. Available without charge from Israel Atomic Energy Commission, Soreq Nuclear Research Centre, Yavne, Israel.

ITALY

Centro Informazioni Studi Esperienze (CISE). For sale at CISE Press Office, Casella Postale 3986, Milano, Italy. Copies are deposited in the libraries of various nuclear centers in Italy and abroad.

Comitato Nazionale per l'Energia Nucleare. Copies are available from Comitato Nazionale per l'Energia Nucleare, Divisione Affari Internazionali e Studi Economici, Ufficio Pubblicazioni, Via Belisario, 15, Roma, Italy.

JAPAN

Japan Atomic Energy Research Institute (JAERI). Available from the Staff Supply Cooperative of Japan Atomic Energy Research Institute (JAERI), Tokai-mura, Naka-gun, Ibaraki-ken, Japan. Copies are deposited in depositories in Tokyo, Nagoya, and Osaka.

Nagoya University. Copies are available from Research Information Center, Institute of Plasma Physics, Nagoya University, Nagoya, Japan.

University of Tokyo. Available free of charge from Institute for Nuclear Study, University of Tokyo, Tanashi-Machi, Kitatama-gun, Tokyo, Japan.

NETHERLANDS

Reactor Centrum Nederland. For sale by Reactor Centrum Nederland, 112 Scheveningseweg, 's-Gravenhage, The Netherlands. Copies are deposited in university libraries in Holland and in many national nuclear centers in the world.

NEW ZEALAND

Institute of Nuclear Sciences. Copies are available from Librarian, N. Z. Institute of Nuclear Sciences, D.S.I.R., Private Bag, Lower Hutt, New Zealand. Copies are deposited in other countries.

PAKISTAN

Atomic Energy Center. Copies are available from Atomic Energy Center, P. O. Box 658, Lahore, (West Pakistan).

POLAND

Reports of the Polish nuclear institutes are published by the Nuclear Energy Information Center of the Government Commissioner for Use of Nuclear Energy. Copies are available free of charge from Nuclear Energy Information Center, Palace of Culture and Science, Warsaw, Poland.

SPAIN

Junta de Energia Nuclear. "JEN" reports are available without charge from Servicio de Documentation, Junta de Energia Nuclear, Ciudad Universitaria, Madrid (3), España.

SWITZERLAND

Eidgenössisches Institut für Reaktorforschung. "EIR" reports are available from Eidgenössisches Institut für Reaktorforschung, c/o Bibliothek, 5303 Würenlingen/Switzerland.

TURKEY

Turkish Atomic Energy Commission. Copies are available free of charge from T.A.E.C., Çekmece Nuclear Research Center, P. O. Box 1, Airport, Istanbul, Turkey.

Conferences

Published conference proceedings as well as individual unpublished papers from conferences are included in this index. A CONF number is assigned to the conference if published proceedings are received and also if only a single paper is received. The base number used is year-month-sequence. Thus, the number CONF-650101 indicates that the conference was held in 1965, in January, and that this was the first January 1965 conference so received. This number would be assigned to complete published proceedings. If individual papers are received, the base number is extended to include a paper number, e.g., CONF-650101-1. As additional papers are received, they will be assigned consecutive numbers in the series, CONF-650101-1, CONF-650101-2, etc. This numbering system ensures that all papers received from a conference will be associated with that conference in this index.

If published proceedings are received after the receipt of individual papers, the complete proceedings will be abstracted and the abstract number will appear in this index with the base CONF number.

Abbreviations Used in Availability Column

AECL	Reports of the Atomic Energy of Canada Limited are for sale by the Scientific Document Distribution Office, Atomic Energy of Canada Limited, Chalk River, Ontario, Canada.
CFSTI	See NTIS
DENM	Reports of the Atomic Energy Commission Research Establishment, Risö, are available on exchange from the Library, Danish Atomic Energy Commission, Risö, Roskilde, Denmark. Also for sale at the price shown from Jul. Gjellerup, Booksellers, 87 Sölvgade, Kobenhavn K., Denmark. Reports of Danatom are available on loan from Research Establishment, Risö, Roskilde, Denmark. Copies are available from Danatom, Aurehojvej 2, Hellerup, Denmark.
Dep.	AEC reports so designated are maintained in the organizations listed on the inside front cover of *NSA*. Prior to July 1, 1965, reports were deposited either in printed copy form or in microform. After that time, all reports have been in the form of micronegatives. Reports from other countries so designated are available in the United States at the organizations listed on the inside front cover of *NSA*.

DTIE	Available from the U. S. Atomic Energy Commission, Division of Technical Information Extension, P. O. Box 62, Oak Ridge, Tennessee 37830. (Conference papers are available on loan only.)
EM	Blueprints of AEC engineering drawings are available from NTIS, U. S. Department of Commerce, Springfield, Virginia 22151. Current prices of the CAPE-packages may be obtained from this address. TID-4100, available from the Division of Technical Information Extension, P. O. Box 62, Oak Ridge, Tennessee 37830, contains information on all the CAPE-packages for sale.
EUR	For sale by Centrale de vente des publications des Communautés européennes 37, rue Glesener-Luxembourg.
GPO	For sale by the Superintendent of Documents, Government Printing Office, Washington, D. C. 20402.
IAEA	Available from the International Atomic Energy Agency, Vienna, Austria, and from its sales agencies in various countries throughout the world. A list of these agencies is found in each STI/DOC and STI/PUB publication.
NORW	Reports from Forsvarets Forskningsinstitutt are available from Norwegian Defense Research Establishment, Library, P. O. Box 25, Kjeller, Norway. "KR" reports are available on an exchange basis from the Library, Institutt for Atomenergi, Box 40, Kjeller, Norway. Reports of the Norwegian Reactor School are available from the Library, Institutt for Atomenergi, P. O. Box 40, Kjeller, Norway.
NRC	For sale by the National Research Council of Canada, Ottawa, Ontario, Canada.
NTIS	For sale by the National Technical Information Service (NTIS), U. S. Department of Commerce, Springfield, Virginia 22151 at the following prices for eye legible copy: 1–300 pages $3.00 301–600 pages $6.00 601–900 pages $9.00 Documents over 900 pages have special prices which may be obtained from NTIS. Microfiche copy of each separately bound document can be purchased for $0.95. Reports issued by organizations outside the United States will be sold by NTIS *only to purchasers within the United States.* Purchasers outside the United States may acquire such reports from the sources described elsewhere in these columns.
OECD	Available from O. E. C. D., Publications 2, rue, André-Pascal, 75 Paris 16^{e}, France, and from its sales agencies in various countries throughout the world. A list of these agencies is found in each OECD publication.
SWED	"AE" reports are for sale from Aktiebolaget Atomenergi, Library Section, Box 43041, Stockholm 43, Sweden. Microcopy of these reports is available from the International Documentation Center, Tumba, Sweden. Reports of the VDDIT-series may be obtained from Aktiebolaget Atomenergi, Information Office, Scientific and Technical Information, Box 43041, Stockholm 43, Sweden. Other series are not generally available to the public. Organizations in the Atomic Energy field may obtain copies from Aktiebolaget Atomenergi.
UK	United Kingdom Atomic Energy Authority reports generally may be purchased from Her Majesty's Stationery Office, P. O. Box 569, London S.E.1. Copies of many UKAEA reports (particularly earlier ones) may be purchased in microcopy form from Micro Methods Ltd., East Ardsley, Wakefield, Yorkshire, England. Copies of UKAEA reports are deposited with the National Lending Library for Science and Technology and 10 public libraries in England; with the USAEC and (through USAEC) with NTIS; and in most national nuclear centers throughout the world. In the USA, UKAEA reports are available on a subscription basis, by subject category, from UNIPUB, Inc., P. O. Box 433, New York, N. Y. 10016, USA.
UN	Mail orders should be directed to the Sales Section, Room 1059, United Nations Headquarters, New York, New York 10017.
ZAED	Available from Zentralstelle für Atomkernenergie Dokumentation, 6000 Frankfurt/Main 90, P. O. Box 901069, Westendstr. 21, West Germany

XUM

Report No.	Abstract No.	Availability
AAEC/E-	(Australian)	
198(Suppl. 1)	25-14979	Dep. NTIS (U. S. Sales Only), 60p.
AAEC/LIB/Bib-	(Australian)	
255	25-13131	Dep. NTIS (U. S. Sales Only), 8p.
258	25-15338	Dep. NTIS (U. S. Sales Only), 3p.
259	25-13029	Dep. NTIS (U. S. Sales Only), 22p.
260	25-13030	Dep. NTIS (U. S. Sales Only), 6p.
261	25-13031	Dep. NTIS (U. S. Sales Only), 24p.
AD-	(Misc.)	
710629	25-13858	NTIS, 18p.
710718	25-14241	NTIS, 99p.
710950	25-14283	NTIS, 84p.
710963	25-14391	NTIS, 31p.
711003	25-14350	NTIS, 35p.
711005	25-14392	NTIS, 82p.
711021	25-13132	NTIS, 144p.
711086	25-14284	NTIS, 68p.
711095	25-14242	NTIS, 59p.
711127	25-14243	NTIS, 87p.
711299	25-13911	NTIS, 20p.
711300	25-13831	NTIS, 18p.
711351	25-14081	NTIS, 15p.
711364	25-13788	NTIS, 19p.
711397	25-13832	NTIS, 82p.
711398	25-13859	NTIS, 42p.
711532	25-13117	NTIS, 130p.
711611	25-13833	NTIS, 57p.
711649	25-14360	NTIS, 50p.
711664	25-13995	NTIS, 156p.
711669	25-14244	NTIS, 257p.
711681	25-14490	NTIS, 37p.
711784	25-13860	NTIS, 27p.
711822	25-14351	NTIS, 16p.
711826	25-14147	NTIS, 13p.
711828	25-14264	NTIS, 58p.
711829	25-13936	NTIS, 31p.
711861	25-13133	NTIS, 37p.
712024	25-14277	NTIS, 161p.
712045	25-14101	NTIS, 27p.
712321	25-14411	NTIS, 36p.
713153	25-13762	NTIS, 148p.
713154	25-13763	NTIS, 62p.
713191	25-13649	NTIS, 22p.
713418	25-13134	NTIS, 88p.
713521	25-13129	NTIS, 9p.
713574	25-13135	NTIS, 15p.
AE-	(Non-AEC)	
408	25-15372	Dep. NTIS (U. S. Sales Only), 23p.
AEC-tr-		
6882/1	25-14583	Dep. NTIS
7199	25-15417	Dep. NTIS
AECL-	(Canadian)	
2503	25-13076	Dep. NTIS (U. S. Sales Only). AECL $1.00, 21p.
3699	25-13033	Can. J. Chem.; 48: 3453-9(1 Nov 1970)
AERE-R-	(British)	
4852	25-13139	Dep. NTIS (U. S. Sales Only), 35p.
5770	25-14862	Dep. NTIS (U. S. Sales Only), 5p.
6338	25-13185	Dep. NTIS (U. S. Sales Only), 25p.
6475	25-15373	Dep. NTIS (U. S. Sales Only). UK 4s. 6d, 29p.
AFCRL-	(Non-AEC)	
70-260	25-13858	See AD-710629
70-0402	25-13788	See AD-711364
AFCRL-AFSIG-	(Non-AEC)	
221	25-13788	See AD-711364
AFML-TR-	(Non-AEC)	
69-117(Pt. 1)	25-13762	See AD-713153
69-117(Pt. 5)	25-13763	See AD-713154
AFOSR-	(Misc.)	
70-1652-TR	25-13995	See AD-711664
70-2284-TR	25-14284	See AD-711086
70-2371-TR	25-14244	See AD-711669
AI-Trans-	(Misc.)	
289	25-13650	Dep. NTIS
AL-		
70-56	25-14082	See N-70-39764
ANL-		
7578	25-15384	Dep. NTIS, 16p.
7659	25-14433	Dep. NTIS, 311p.
7689	25-14393	Dep. NTIS, 31p.
7755	25-13077	Dep. NTIS, 55p.
7765	25-15339	Dep. NTIS, 98p.
ANL/ST-		
4	25-13651	Dep. NTIS, 67p.
ANL-Trans-		
871	25-15418	Dep. NTIS
ARLV-		
351-15	25-13136	Dep. NTIS, 23p.
AS-	(Non-AEC)	
69-13	25-14242	See AD-711095
70-5	25-14243	See AD-711127
AWRE-O-	(British)	
78/70	25-14919	Dep. NTIS (U. S. Sales Only). UK 5s. 6d, 39p.
B-	(Misc.)	
1	25-13597	See NF-18606
BAW-	(Misc.)	
10024	25-15374	
BMBW-FBK-	(West German)	
70-26	25-13140	Dep. NTIS (U. S. Sales Only), 80p.
70-29	25-14285	Dep. NTIS (U. S. Sales Only), 52p.
BNL-		
15420	25-15419	Dep. NTIS, 58p.
15423	25-14835	Dep. NTIS, 9p.
15424	25-14836	Dep. NTIS, 5p.
50230	25-14837	Dep. NTIS, 233p.
BNL-tr-		
380	25-14920	Dep. NTIS
350	25-15420	Dep. NTIS
BNWL-		
1503	25-13186	Dep. NTIS, 34p.
1512	25-13187	Dep. NTIS, 16p.
BNWL-B-		
34	25-13188	Dep. NTIS, 43p.
BNWL-SA-		
3169	25-13161	Dep. NTIS, 10p.
3173	25-12962	Nucl. Appl. Technol.; 9: 861-74(Dec 1970)
3437	25-13195	See WHAN-SA-91
BRH/NERHL-	(Non-AEC)	
70-2	25-12950	NTIS, 59p.
BRL-	(Misc.)	
1485	25-13117	See AD-711532
1490	25-14411	See AD-712321
CAPE-		
2046	25-13202	EM
2047	25-13146	EM
CEA-CONF-	(French)	
1647	25-13229	Dep. NTIS (U. S. Sales Only), 22p.
1650	25-14889	Dep. NTIS (U. S. Sales Only), 2p.
1651	25-14890	Dep. NTIS (U. S. Sales Only), 2p.
1653	25-14921	Dep. NTIS (U. S. Sales Only), 2p.
1654	25-14980	Dep. NTIS (U. S. Sales Only), 2p.
1655	25-14922	Dep. NTIS (U. S. Sales Only), 2p.
1656	25-14923	Dep. NTIS (U. S. Sales Only), 2p.
1701	25-14434	Dep. NTIS (U. S. Sales Only), 13p.
1712	25-13189	Dep. NTIS (U. S. Sales Only), 18p.
CEA-N-	(French)	
1335	25-14986	For translation see ORNL-tr-2408
1358	25-14863	Dep. NTIS (U. S. Sales Only), 124p.
1382	25-14394	Dep. NTIS (U. S. Sales Only), 27p.
1388	25-14864	Dep. NTIS (U. S. Sales Only), 24p.
1397	25-13233	Dep. NTIS (U. S. Sales Only), 28p.
CEA-R-	(French)	
3473	25-13650	For translation see AI-Trans-289
4039	25-13362	Dep. NTIS (U. S. Sales Only), 22p.
CERN-	(European Organization for Nuclear Research)	
70-21(Vol. 1)	25-13234	
70-21(Vol. 2)	25-13263	
CFB-		
4122-237	25-15362	See UKC-5231
CONF-550-	(The International Conference on High-Energy Physics, Dubna, Aug. 5-15, 1964)	
(Vol.1)	25-14583	See AEC-tr-6882/1
CONF-651019-	(15th Canadian Chemical Engineering Conference, Quebec City, Canada, Oct. 25, 1965)	
1	25-13076	See AECL-2503

Report No.	Abstract No.	Availability
CONF-661071-	(1st Conference of the Latin American Association of the Biology and Nuclear Medicine Societies, Lima, Peru, Oct. 2-8, 1966)	
	25-13482	
CONF-680122-	(18th Annual Conference on Nuclear Structure and Spectroscopy, Riga, U.S.S.R., Jan. 25-Feb. 2, 1968)	
1	25-14891	See ORO-1316-97
CONF-680905-	(26th Annual Meeting of the Electron Microscopy Society of America, New Orleans, La., Sept. 16-19, 1968)	
5	25-15437	See NYO-3087-19
CONF-681084-	(41st Manifestation of the European Federation of Corrosion, Budapest, Hungary, Oct. 7-12, 1968)	
	25-13636	Budapest; Akademiai Kiado (1970). 1084p
CONF-690645-	(International Conference on Proctology, London, England, June 23-26, 1969)	
Suppl.	25-13508	Proc. Roy. Soc. Med.; 63: Suppl., 1-160(1970)
CONF-690649-	(Panel on Guidelines for The Layout and Contents of Safety Reports for Stationary Nuclear Power Plants, Vienna, Austria, June 30-July 4, 1969)	
	25-15337	See STI/PUB-272
CONF-690728-	(Conference on Structure and Properties of the Surfaces of Solids, Paris, France, July 7-11, 1969)	
	25-13734	Paris; Centre National de la Recherche Scientifique (1970). 232p
CONF-691048-	(11th Symposium on High Pressure, Sendai, Japan, Oct. 24--26, 1969)	
2	25-15457	See SCL-T-71-209
3	25-15458	See SCL-T-71-210
4	25-15459	See SCL-T-71-212
CONF-691114-	(90th Annual Meeting on American Society of Mechanical Engineers, Los Angeles, Calif., Nov. 16-20, 1969)	
6	25-15375	Dep. NTIS. ASME, New York, N. Y. $1.50
CONF-691219-	(3rd Conference on Inelastic Neutron Scattering, Tokai, Japan, Dec. 6-8, 1969)	
	25-14436	See JAERI-1197
CONF-700304-	(Symposium on Dynamics of Nuclear Systems, Tucson, Ariz., Mar. 23-25, 1970)	
5	25-15353	See WAPD-TM-968
CONF-700323-	(10th International Conference on Data Handling Systems in High Energy Physics, Cambridge, England, Mar. 23-25, 1970)	
(Vol.1)	25-13234	See CERN-70-21(Vol.1)
(Vol.2)	25-13263	See CERN-70-21(Vol.2)
CONF-700334-	(2nd Annual Symposium on Automated, High-Resolution Analyses in the Clinical Laboratory, Oak Ridge, Tenn., Mar. 12-13, 1970)	
	25-13383	Clin. Chem.; 16: 623-725(Aug 1970)
CONF-700503-	(3rd International Conference on Magnet Technology, Hamburg, Germany, May 19-22, 1970)	
8	25-14211	See KFK-1217
CONF-700505-	(2nd Congress of the International Radiation Protection Association, Brighton, England, May 3-8, 1970)	
15	25-13304	See RT/PROT-(70)23
CONF-700537-	(Meeting on the AEC Nuclear Cross Sections Advisory Committee, Chicago, Ill., May 20-22, 1970)	
	25-14982	See NCSAC-31
CONF-700605-	(2nd International Conference on Nuclear Data for Reactors, Helsinki, Finland, June 15-19, 1970)	
(Vol.1)	25-14987	See STI/PUB-259(Vol.1)
(Vol.2)	25-14988	See STI/PUB-259(Vol.2)
CONF-700608-	(American Nuclear Society Meeting, Los Angeles, Calif., June 29-July 2, 1970)	
23	25-14865	See COO-2049-2
CONF-700618-	(Applied Superconductivity Conference, Boulder, Colo., June 15-17, 1970)	
	25-14215	J. Appl. Phys.; 42: 1-189(Jan 1971)
CONF-700639-	(International Conference on Atomic Transport in Solids and Liquids, Marstrand, Sweden, June 16-20, 1970)	
1	25-15445	See CRO-2036-21
CONF-700705-	(7th International Conference on Corpuscular Photography and Visual Solid Detectors, Barcelona, Spain, July 7-11, 1970)	
1	25-13209	See CCO-1671-28
CONF-700712-	(7th International Symposium on Rarefied Gas Dynamics, Pisa, Italy, July, 1970)	
1	25-15431	See CU-3954-3
CONF-700806-	(15th International Conference on High Energy Physics, Kiev, U.S.S.R., Aug. 26-Sept. 4, 1970)	
55	25-14558	See INP-708
CONF-700811-	(3rd International Symposium on Polarization Phenomena in Nuclear Reactions, Madison, Wis., Aug. 31-Sept. 4, 1970)	
4	25-14889	See CEA-CONF-1650
5	25-14892	See RLO-1388-600
6	25-14890	See CEA-CONF-1651
7	25-14980	See CEA-CONF-1654
8	25-14922	See CEA-CONF-1655
9	25-14923	See CEA-CONF-1656
11	25-14921	See CEA-CONF-1653
CONF-700819-	(2nd International Conference on the Strength of Metals and Alloys, Pacific Grove, Calif., Aug. 30-Sept. 4, 1970)	
9	25-13661	See UCRL-72627
CONF-700929-	(Proton Linear Accelerator Conference, Batavia, Ill., Sept. 28-Oct. 2, 1970)	
4	25-14853	See UCRL-19919
CONF-700935-	(Symposium on the Technology of Pressure-Retaining Steel Components, Vail Village, Colo., Sept. 21-23, 1970)	
2	25-13660	See CRNL-TM-3211
CONF-700937-	(Symposium on Hadron Spectroscopy, Balatonfured, Hungary, Sept. 6-11, 1970)	
2	25-14632	See KFKI-70-23-HEP
CONF-700940-	(International Conference on Magnetism, Grenoble, France, Sept. 14-19, 1970)	
2	25-14434	See CEA-CONF-1701
CONF-701001-	(4th International Conference on Plutonium and Other Actinides, Santa Fe, N. Mex., Oct. 5-9, 1970)	
15	25-15367	See WHAN-SA-51
CONF-701017-	(14th Annual Conference on Analytical Chemistry in Nuclear Technology, Gatlinburg, Tenn., Oct. 13-15, 1970)	
2	25-12925	See WHAN-SA-77
3	25-12922	See WHAN-SA-44
4	25-12924	See WHAN-SA-62
CONF-701023-	(Symposium on The Use of Nuclear Techniques in The Measurement and Control of Environmental Pollution, Salzburg, Austria, Oct. 26-30, 1970)	
1	25-13229	See CEA-CONF-1647
CONF-701025-	(Conference on Chemistry and Spectroscopy, San Francisco, Calif., Oct. 6, 1970)	
2	25-12923	See WHAN-SA-47
CONF-701032-	(Conference on Thin Films, Cannes, France, Oct. 5-10, 1970)	
1	25-14435	See IJS-587
CONF-701102-	(Meeting of the American Nuclear Society, Washington, D.C., Nov. 15-19, 1970)	
5	25-13430	See UCRL-72830
6	25-13396	See UCRL-72511
9	25-14437	See WHAN-SA-75
14	25-13195	See WHAN-SA-91
CONF-701115-	(American Association of Contamination Control North Central Conference, Chicago, Ill., Nov. 15-17, 1970)	
1	25-13192	See NACAR-10012
CONF-701116-	(Basic Science and Nuclear Division Meeting of the American Ceramic Society, Gatlinburg, Tenn., Nov. 3-6, 1970)	
1	25-13779	See DF-MS-70-44
CONF-701117-	(4th Asilomar Conference on Circuits and Systems, Pacific Grove, Calif., Nov. 18-20, 1970)	
1	25-15467	See UCRL-72663

Report No.	Abstract No.	Availability
CONF-701203-	(Conference on Marine Pollution and its Effects on Living Resources and Fishing, Rome, Italy, Dec. 9-18, 1970)	
1	25-13189	See CEA-CONF-1712
COO-		
414-17	25-13118	Dep. NTIS, 45p.
535-625	25-14924	Dep. NTIS, 9p.
1008-14	25-15421	Dep. NTIS, 11p.
1018-1219	25-15422	Dep. NTIS, 39p.
1183-32	25-13617	Dep. CFSTI, 59p.
1198-775	25-15423	Dep. NTIS, 211p.
1222-42	25-15424	Dep. NTIS, 20p.
1400-29	25-13405	Mutat. Res.; 10: 515-18(Nov 1970)
1449-11	25-15425	Dep. NTIS, 8p.
1473-4	25-15426	Dep. NTIS, 172p.
1574-17	25-14128	Dep. NTIS, 81p.
1574-19	25-14129	Dep. NTIS, 90p.
1591-13	25-15427	Dep. NTIS, 85p.
1671-28	25-13209	Dep. NTIS, 29p.
1764-105	25-14880	Dep. NTIS, 41p.
1778-6	25-15428	Dep. NTIS, 7p.
2026-4	25-15429	Dep. NTIS, 12p.
2049-2	25-14865	Dep. NTIS, 33p.
2118-2	25-15430	Dep. NTIS, 165p.
CRL-	(Canadian)	
91	25-13076	See AECL-2503
CTC-INF-		
1017	25-14395	Dep. NTIS, 108p.
CU-	(Misc.)	
1019-79	25-15140	Dep. NTIS, 29p.
3954-3	25-15431	Dep. NTIS, 9p.
3957-9	25-15432	Dep. NTIS, 9p.
DEMO-	(Greek)	
70/10	25-15141	Dep. NTIS (U. S. Sales Only), 9p.
70/20	25-15142	Dep. NTIS (U. S. Sales Only), 6p.
DLCS-		
5000370	25-15214	Dep. NTIS, 20p.
DOCKET-1151-	(Elk River Reactor) (AEC)	
39	25-15215	Dep. NTIS, 9p.
DOCKET-1155-	(LaCrosse Boiling Water Reactor) (AEC)	
89	25-15216	Dep. NTIS, 3p.
90	25-15241	Dep. NTIS, 4p.
91	25-15242	Dep. NTIS, 2p.
92	25-15217	Dep. NTIS, 7p.
93	25-15218	Dep. NTIS, 1p.
94	25-15219	Dep. NTIS, 1p.
95	25-15220	Dep. NTIS, 1p.
96	25-15221	Dep. NTIS, 1p.
97	25-15222	Dep. NTIS, 2p.
98	25-15223	Dep. NTIS, 2p.
DOCKET-50003-	(Indian Point Station; See Also DOCKET-50247, DOCKET-50286) (Non-AEC)	
61	25-15243	Dep. NTIS, 2p.
62	25-15224	Dep. NTIS, 2p.
63	25-15225	Dep. NTIS, 2p.
64	25-15244	Dep. NTIS, 4p.
DOCKET-50010-	(Dresden Nuclear Power Station; See also DOCKET-50237 and DOCKET-50249) (Non-AEC)	
76	25-15245	Dep. NTIS, 4p.
77	25-15246	Dep. NTIS, 33p.
DOCKET-50016-	(Enrico Fermi Atomic Power Plant) (Non-AEC)	
89	25-15247	Dep. NTIS, 205p.
90	25-15248	Dep. NTIS, 128p.
91	25-15249	Dep. NTIS, 93p.
92	25-15250	Dep. NTIS, 16p.
93	25-15251	Dep. NTIS, 37p.
94	25-15252	Dep. NTIS, 182p.
95	25-15253	Dep. NTIS, 146p.
96	25-15254	Dep. NTIS, 109p.
97	25-15255	Dep. NTIS, 191p.
98	25-15256	Dep. NTIS, 109p.
DOCKET-50029-	(Yankee Atomic Electric Co.) (Non-AEC)	
90	25-15257	Dep. CFSTI, 3p.
142	25-15226	Dep. NTIS, 8p.
DOCKET-50155-	(Big Rock Point Reactor) (Misc.)	
60	25-15258	Dep. NTIS, 9p.
61	25-15259	Dep. NTIS, 5p.
62	25-15260	Dep. NTIS, 2p.
63	25-15261	Dep. NTIS, 56p.
65	25-15262	Dep. NTIS, 11p.
DOCKET-50184-	(National Bureau of Standards Reactor) (Non-AEC)	
25	25-15385	Dep. NTIS, 1p.
DOCKET-50201-	(West Valley Reprocessing Plant--Formerly Spent Fuel Processing Plant) (Misc.)	
60	25-13078	Dep. NTIS, 11p.
61	25-13079	Dep. NTIS, 8p.
62	25-13080	Dep. NTIS, 122p.
DOCKET-50206-	(San Onofre Nuclear Generating Station) (Misc.)	
103	25-15227	Dep. NTIS, 10p.
104	25-15263	Dep. NTIS, 2p.
105	25-15228	Dep. NTIS, 5p.
106	25-15264	Dep. NTIS, 2p.
DOCKET-50213-	(Connecticut Yankee Atomic Power Plant) (Misc.)	
94	25-15229	Dep. NTIS, 15p.
95	25-15265	Dep. NTIS, 163p.
96	25-15266	Dep. NTIS, 13p.
97	25-15267	Dep. NTIS, 11p.
DOCKET-50219-	(Oyster Creek Nuclear Power Plant) (Non-AEC)	
120	25-15268	Dep. NTIS, 5p.
121	25-15269	Dep. NTIS, 30p.
DOCKET-50220-	(Nine Mile Point Nuclear Station) (Non-AEC)	
57	25-15270	Dep. NTIS, 15p.
DOCKET-50231-	(Southwest Experimental Fast Oxide Reactor) (Non-AEC)	
67	25-15386	Dep. NTIS, 1p.
68	25-15271	Dep. NTIS, 23p.
69	25-15272	Dep. NTIS, 10p.
DOCKET-50237-	(Dresden Nuclear Power Station, See also DOCKET-50249) (Non-AEC)	
130	25-15273	Dep. NTIS, 16p.
131	25-15274	Dep. NTIS, 17p.
132	25-15230	Dep. NTIS, 2p.
133	25-15275	Dep. NTIS, 16p.
134	25-15276	Dep. NTIS, 12p.
135	25-15277	Dep. NTIS, 5p.
136	25-15278	Dep. NTIS, 9p.
137	25-15279	Dep. NTIS, 2p.
138	25-15280	Dep. NTIS, 15p.
139	25-15281	Dep. NTIS, 20p.
140	25-15231	Dep. NTIS, 2p.
141	25-15232	Dep. NTIS, 2p.
142	25-15233	Dep. NTIS, 2p.
DOCKET-50244-	(Robert Emmett Ginna Nuclear Power Plant, Formerly Brookwood Nuclear Station) (Non-AEC)	
55	25-15282	Dep. NTIS, 6p.
56	25-15283	Dep. NTIS, 2p.
57	25-15284	Dep. NTIS, 2p.
58	25-15285	Dep. NTIS, 2p.
59	25-15286	Dep. NTIS, 395p.
DOCKET-50245-	(Millstone Point Nuclear Power Station) (Non-AEC)	
52	25-15287	Dep. NTIS, 1p.
53	25-15234	Dep. NTIS, 3p.
54	25-15235	Dep. NTIS, 1p.
DOCKET-50249-	(Dresden Nuclear Power Station; See also DOCKET-50237) (Non-AEC)	
54	25-15277	See DOCKET-50237-135
55	25-15281	See DOCKET-50237-139
56	25-15288	Dep. NTIS, 5p.
DOCKET-50250-	(Turkey Point, See also DOCKET-50251) (Non-AEC)	
38	25-15289	Dep. NTIS, 47p.
DOCKET-50254-	(Quad-Cities Station; See also DOCKET-50265) (Non-AEC)	
26	25-15290	Dep. NTIS, 22p.
27	25-15291	Dep. NTIS, 176p.
DOCKET-50261-	(H. B. Robinson) (Non-AEC)	
50	25-15292	Dep. NTIS, 18p.
DOCKET-50263-	(Monticello Nuclear Generating Plant) (Non-AEC)	
51	25-15236	Dep. NTIS, 1p.
52	25-15293	Dep. NTIS, 6p.
53	25-15294	Dep. NTIS, 170p.
54	25-15295	Dep. NTIS, 5p.
DOCKET-50265-	(Quad-Cities Station; See also DOCKET-50254) (Non-AEC)	
22	25-15290	See DOCKET-50254-26
23	25-15291	See DOCKET-50254-27
DOCKET-50266-	(Point Beach Nuclear Plant) (Non-AEC)	
38	25-15296	Dep. NTIS, 5p.
39	25-15237	Dep. NTIS, 3p.
40	25-15238	Dep. NTIS, 3p.
41	25-15297	Dep. NTIS, 61p.
DOCKET-50271-	(Vermont Yankee Nuclear Power Station) (Non-AEC)	
36	25-15298	Dep. NTIS, 97p.

Report No.	Abstract No.	Availability
DOCKET-50282-	(Prairie Island Nuclear Generating Plant, See also DOCKET-50306) (Non-AEC)	
26	25-15299	Dep. NTIS, 42p.
27	25-15300	Dep. NTIS, 555p.
28	25-15301	Dep. NTIS, 360p.
29	25-15302	Dep. NTIS, 359p.
30	25-15303	Dep. NTIS, 324p.
31	25-15304	Dep. NTIS, 384p.
DOCKET-50289-	(Three Mile Island Nuclear Station) (Non-AEC)	
32	25-15305	Dep. NTIS, 316p.
DOCKET-50293-	(Pilgrim Nuclear Power Station) (Non-AEC)	
34	25-15306	Dep. NTIS, 403p.
35	25-15307	Dep. NTIS, 67p.
DOCKET-50302-	(Crystal River Nuclear Plant; see DOCKET-50303) (Non-AEC)	
16	25-15308	Dep. NTIS, 37p.
DOCKET-50305-	(Kewaunse Nuclear Power Plant) (Non-AEC)	
12	25-15309	Dep. NTIS, 68p.
13	25-15310	Dep. NTIS, 379p.
14	25-15311	Dep. NTIS, 300p.
15	25-15312	Dep. NTIS, 272p.
16	25-15313	Dep. NTIS, 256p.
17	25-15314	Dep. NTIS, 386p.
DOCKET-50306-	(Prairie Island Nuclear Generating Plant, See also DOCKET-50282) (Non-AEC)	
26	25-15299	See DOCKET-50282-26
27	25-15300	See DOCKET-50282-27
28	25-15301	See DOCKET-50282-28
29	25-15302	See DOCKET-50282-29
30	25-15303	See DOCKET-50282-30
31	25-15304	See DOCKET-50282-31
DOCKET-50315-	(Donald C. Cook Nuclear Power Plant, See also DOCKET-50316) (Non-AEC)	
26	25-15315	Dep. NTIS, 16p.
27	25-15316	Dep. NTIS, 132p.
28	25-15317	Dep. NTIS, 400p.
29	25-15318	Dep. NTIS, 335p.
30	25-15319	Dep. NTIS, 300p.
31	25-15320	Dep. NTIS, 178p.
32	25-15321	Dep. NTIS, 493p.
33	25-15322	Dep. NTIS, 356p.
DOCKET-50316-	(Donald C. Cook Nuclear Power Plant, See also DOCKET-50315) (Non-AEC)	
26	25-15315	See DOCKET-50315-26
27	25-15316	See DOCKET-50315-27
28	25-15317	See DOCKET-50315-28
29	25-15318	See DOCKET-50315-29
30	25-15319	See DOCKET-50315-30
31	25-15320	See DOCKET-50315-31
32	25-15321	See DOCKET-50315-32
33	25-15322	See DOCKET-50315-33
DOCKET-50341-	(Enrico Fermi Atomic Power Plant) (Non-AEC)	
25	25-15323	Dep. NTIS, 63p.
26	25-15324	Dep. NTIS, 37p.
DOCKET-50344-	(Trojan Nuclear Plant) (Non-AEC)	
19	25-15325	Dep. NTIS, 4p.
DOCKET-50354-	(Newbold Island Nuclear Generating Station) (See also DOCKET-50355) (Non-AEC)	
10	25-15326	Dep. NTIS, 307p.
DOCKET-50355-	(Newbold Island Nuclear Generating Station) (See also DOCKET-50354) (Non-AEC)	
10	25-15326	See DOCKET-50354-10
DOCKET-50358-	(Wm. H. Zimmer Nuclear Power Station, Units 1 and 2) (See also DOCKET-50359) (Non-AEC)	
11	25-15327	Dep. NTIS, 542p.
12	25-15328	Dep. NTIS, 307p.
DOCKET-50361-	(San Onofre Nuclear Generating Station) (Units 2 and 3) (See also Docket-50362) (Docket-50206) (Unit 1) (Non-AEC)	
14	25-15329	Dep. NTIS, 185p.
DOCKET-50362-	(San Onofre Nuclear Generating Station) (Units 2 and 3) (See also Docket-50361) (Docket-50206) (Unit 1) (Non-AEC)	
13	25-15329	See DOCKET-50361-14
DOCKET-50363-	(Forked River Nuclear Station) (Unit 1) (Non-AEC)	
11	25-15330	Dep. NTIS, 60p.
DOCKET-50367-	(Bailly Generating Station Nuclear 1), (Non-AEC)	
9	25-15331	Dep. NTIS, 621p.
DOCKET-50368-	(Arkansas Nuclear One) (Non-AEC) (Unit 2)	
7	25-15332	Dep. NTIS, 69p.

Report No.	Abstract No.	Availability
DOCKET-50376-	(Aguirre Nuclear Plant) (Non-AEC)	
8	25-15333	Dep. NTIS, 3p.
DOCKET-50382-	(Louisiana Power and Light Plant) (Non-AEC) (See also DOCKET-50383)	
6	25-15334	Dep. NTIS, 96p.
DOCKET-50383-	(Louisiana Power and Light Plant) (Non-AEC) (See also DOCKET-50382)	
6	25-15334	See DOCKET-50382-6
DP-MS-		
70-44	25-13779	Dep. NTIS, 21p.
DPC-		
70-20	25-15216	See DOCKET-1155-89
70-21	25-15217	See DOCKET-1155-92
70-22	25-15218	See DOCKET-1155-93
70-23	25-15219	See DOCKET-1155-94
70-24	25-15220	See DOCKET-1155-95
70-25	25-15221	See DOCKET-1155-96
70-26	25-15222	See DOCKET-1155-97
70-27	25-15223	See DOCKET-1155-98
EANDC(E)-	(European-American Nuclear Data Committee)	
118(U)	25-15387	See EURFNR-858
EANDC(US)-	(European-American Nuclear Data Committee)	
143-U	25-14982	See NCSAC-31
ECOM-	(Non-AEC)	
3305	25-14283	See AD-710950
EIR-	(Swiss)	
184	25-13629	Dep. NTIS (U. S. Sales Only), 62p.
ETR-	(Belgian)	
266	25-13081	See NP-18577
EUR-	(European Atomic Energy Community)	
3945(Pt.2)	25-13392	Dep. NTIS (U. S. Sales Only), 70p.
4286(Pt.2)	25-14840	Dep. NTIS (U. S. Sales Only). EUR FF 11,-, 60p.
4298	25-13630	Dep. NTIS (U. S. Sales Only), 32p.
4536	25-15404	Dep. NTIS (U. S. Sales Only). EUR FF 11,-, 72p.
4551	25-13736	Dep. NTIS (U. S. Sales Only). EUR FF 6.65, 40p.
4561	25-13149	Dep. NTIS (U. S. Sales Only). EUR FF 11,-, 70p.
4568	25-13749	Dep. NTIS (U. S. Sales Only). EUR FF 23,35µ 158p.
4580	25-15239	Dep. NTIS (U. S. Sales Only). EUR Lit. 1.560, 80p.
EURFNR-	(European Atomic Energy Community)	
785	25-15379	Dep. NTIS
858	25-15387	Dep. NTIS (U. S. Sales Only), 233p.
FSU-HEP-		
70-3-1	25-14557	
GAMD-	(Misc.)	
8219(Rev.)	25-13652	Dep. NTIS, 32p.
9335	25-13750	Dep. NTIS, 46p.
GEAP-	(Misc.)	
10253	25-13150	Dep. NTIS, 40p.
12147	25-13780	Dep. NTIS, 10p.
GESP-	(Non-AEC)	
493	25-13168	See N-70-41276
9006	25-14083	See N-70-39884
GJO-		
918-4	25-15433	Dep. NTIS, 30p.
GULF-RT-		
10421	25-15388	Dep. NTIS, 36p.
IFVE-SEF-	(Russian)	
70-16	25-14540	Dep. NTIS (U. S. Sales Only), 31p.
IJS-	(Yugoslavian)	
587	25-14435	Dep. NTIS (U. S. Sales Only), 8p.
IN-		
1448	25-14981	Dep. NTIS, 47p.
INDC(US)-		
22-U	25-14982	See NCSAC-31
INP-	(Polish)	
708	25-14558	Dep. NTIS (U. S. Sales Only), 22p.
718	25-14509	Dep. NTIS (U. S. Sales Only), 8p.
719	25-14680	Dep. NTIS (U. S. Sales Only), 68p.
730	25-14681	Dep. NTIS (U. S. Sales Only), 35p.
731	25-14559	Dep. NTIS (U. S. Sales Only), 9p.
INR-	(Non-AEC)	
1211	25-13064	Dep. NTIS (U. S. Sales Only), 11p.

Report No.	Abstract No.	Availability
INR-P-	(Polish)	
1229	25-14729	Dep. NTIS (U. S. Sales Only), 13p.
IPPJ-T-	(Japanese)	
3	25-14352	Dep. NTIS (U. S. Sales Only), 19p.
IPST-Cat.-	(Russian)	
5130	25-14583	See AEC-tr-6882/1
ITF-	(Russian)	
70-60-E	25-14682	Dep. NTIS (U. S. Sales Only), 16p.
70-63-P	25-14595	Dep. NTIS (U. S. Sales Only), 12p.
70-64	25-14631	Dep. NTIS (U. S. Sales Only), 37p.
70-70	25-14747	Dep. NTIS (U. S. Sales Only), 26p.
JAB-	(Non-AEC)	
99-35	25-15434	Dep. NTIS, 148p.
JAERI-	(Japanese)	
1177-B(Pt. 2)	25-15389	Dep. NTIS (U. S. Sales Only), 273p.
1197	25-14436	Dep. NTIS (U. S. Sales Only), 117p.
JAERI-Memo-	(Japanese)	
4141	25-15390	Dep. NTIS (U. S. Sales Only), 307p.
4153	25-13190	Dep. NTIS (U. S. Sales Only), 19p.
4163	25-13180	Dep. NTIS (U. S. Sales Only), 153p.
4175	25-13119	Dep. NTIS (U. S. Sales Only), 34p.
4180	25-15391	Dep. NTIS (U. S. Sales Only), 112p.
4186	25-14233	Dep. NTIS (U. S. Sales Only), 20p.
JINR-	(Russian)	
E1-5349	25-14560	Dep. NTIS (U. S. Sales Only), 45p.
E2-5424	25-14596	Dep. NTIS (U. S. Sales Only), 8p.
P1-5399	25-14541	Dep. NTIS (U. S. Sales Only), 11p.
P1-5460	25-14561	Dep. NTIS (U. S. Sales Only), 14p.
P1-5471	25-14700	Dep. NTIS (U. S. Sales Only), 17p.
P2-5118	25-15148	For translation see ORNL-tr-2399
P2-5444	25-14730	Dep. NTIS (U. S. Sales Only), 7p.
P2-5448	25-14731	Dep. NTIS (U. S. Sales Only), 18p.
P2-5480	25-14748	Dep. NTIS (U. S. Sales Only), 8p.
P3-5421	25-13210	Dep. NTIS (U. S. Sales Only), 25p.
P4-5438	25-14817	Dep. NTIS (U. S. Sales Only), 23p.
P9-5142	25-14854	For translation see UCRL-Trans-1420
P9-5179	25-14855	For translation see UCRL-Trans-1421
P9-5268	25-14856	For translation see UCRL-Trans-1425
P13-5353	25-14841	Dep. NTIS (U. S. Sales Only), 22p.
P13-5369	25-13162	Dep. NTIS (U. S. Sales Only), 16p.
P13-5402	25-13211	Dep. NTIS (U. S. Sales Only), 12p.
P13-5404	25-13295	Dep. NTIS (U. S. Sales Only), 12p.
P13-5472	25-13296	Dep. NTIS (U. S. Sales Only), 11p.
P13-5473	25-13297	Dep. NTIS (U. S. Sales Only), 11p.
JPRS-	(Non-AEC)	
51948	25-13191	NTIS
JUL-	(German)	
658-FN	25-13722	Dep. NTIS (U. S. Sales Only), 47p.
664-FN	25-13723	Dep. NTIS (U. S. Sales Only), 58p.
677-RG	25-13781	Dep. NTIS (U. S. Sales Only), 123p.
685-PA	25-13782	Dep. NTIS (U. S. Sales Only), 73p.
KFK-	(German)	
969	25-15387	See EURFNR-858
1166	25-15379	For translation see EURFNR-785
1217	25-14211	Dep. NTIS (U. S. Sales Only), 13p.
1260	25-13764	Dep. NTIS (U. S. Sales Only), 31p.
1292	25-13737	Dep. NTIS (U. S. Sales Only), 19p.
KFKI-	(Hungarian)	
70-22-HEP	25-14774	Dep. NTIS (U. S. Sales Only), 9p.
70-23-HEP	25-14632	Dep. NTIS (U. S. Sales Only), 7p.
70-27-HEP	25-14701	Dep. NTIS (U. S. Sales Only), 7p.
KHFTI-	(Russian)	
70-16	25-14852	For translation see SLAC-Trans-126
LA-		
4521	25-13653	Dep. NTIS, 13p.
4551	25-13331	Dep. NTIS, 9p.
4567	25-14866	Dep. NTIS, 23p.
4571	25-14842	Dep. NTIS, 54p.
4573	25-15435	Dep. NTIS, 9p.
LAL-RT-	(French)	
44-70	25-14843	Dep. NTIS (U. S. Sales Only), 10p.
LCIE-	(French)	
364	25-13327	Dep. NTIS (U. S. Sales Only), 34p.
LF-	(Misc.)	
24	25-14413	See NP-18645
LFEN-NI.-	(Portuguese)	
45-a	25-15405	Dep. NTIS (U. S. Sales Only), 49p.
LP-	(Misc.)	
118	25-14336	See NP-18662
LPS-	(Non-AEC)	
47	25-14351	See AD-711822

Report No.	Abstract No.	Availability
LYCEN-	(French)	
7050	25-15143	Dep. NTIS (U. S. Sales Only), 81p.
7076	25-12957	Dep. NTIS (U. S. Sales Only), 14p.
MIT-	(Misc.)	
2098-643	25-14925	Dep. NTIS, 309p.
MLM-		
1652	25-13163	Dep. NTIS, 28p.
1670	25-13164	Dep. NTIS, 23p.
1734	25-13654	Dep. NTIS, 6p.
1753	25-13165	Dep. NTIS, 51p.
MMM-		
4187-1	25-13166	Dep. NTIS, 360p.
MPS/Int. CO-	(European Organization for Nuclear Research)	
68-1	25-14844	Dep. NTIS (U. S. Sales Only), 12p.
MSFC-IN-SSL-T-	(Non-AEC)	
68-4	25-13861	See N-70-37452
68-16	25-13789	See N-70-38166
MSFC-R-SSL-INT-		
67-8	25-13862	See N-70-38381
N-	(Misc.)	
70-19848	25-14102	CFSTI, 87p.
70-37452	25-13861	NTIS, 30p.
70-37470	25-14396	NTIS, 53p.
70-38166	25-13789	NTIS, 89p.
70-38381	25-13862	NTIS, 18p.
70-39456	25-14412	NTIS, 59p.
70-39764	25-14082	NTIS, 14p.
70-39828	25-13863	NTIS, 143p.
70-39884	25-14083	NTIS, 78p.
70-40418	25-14818	NTIS, 10p.
70-40698	25-14819	NTIS, 115p.
70-40979	25-14286	NTIS, 21p.
70-41092	25-13167	NTIS, 38p.
70-41276	25-13168	NTIS, 543p.
NACAR-	(Non-AEC)	
10012	25-13192	
NAL-		
48-2624	25-13298	Dep. NTIS, 147p.
NASA-CR-	(Misc.)	
1661	25-14083	See N-70-39884
72700	25-14082	See N-70-39764
108236	25-14102	See N-70-19848
112362	25-14819	See N-70-40698
112667	25-14818	See N-70-40418
112838	25-14396	See N-70-37470
113550	25-14412	See N-70-39456
113823	25-14286	See N-70-40979
113925	25-13168	See N-70-41276
NASA-TM-X-	(Misc.)	
52891	25-13167	See N-70-41092
53916	25-13861	See N-70-37452
53920	25-13789	See N-70-38166
53928	25-13862	See N-70-38381
53991	25-13863	See N-70-39828
NCG-TR-	(Non-AEC)	
27	25-13102	Dep. NTIS, 75p.
NCL-	(Misc.)	
70-51-R	25-14412	See N-70-39456
NCSAC-	(Nuclear Cross Section Advisory Committee)	
31	25-14982	Dep. CFSTI, 295p.
NEDC-	(Non-AEC)	
12111	25-15365	
NEIC-RR-	(Polish)	
41	25-15340	Dep. NTIS (U. S. Sales Only), 285p.
NF-	(Non-AEC)	
67-8	25-15335	
NP-	(AEC File No. for Non-AEC Reports)	
18382	25-13340	Dep. CFSTI (U. S. Sales Only), 21p.
18492	25-14983	Dep. NTIS (U. S. Sales Only), 112p.
18536	25-14984	Dep. NTIS (U. S. Sales Only), 151p.
18559	25-14807	Dep. NTIS (U. S. Sales Only), 32p.
18577	25-13081	Dep. NTIS (U. S. Sales Only), 31p.
18601	25-14845	Dep. NTIS (U. S. Sales), 140p.
18606	25-13597	Dep. NTIS (U. S. Sales Only), 16p.
18615	25-14985	Dep. NTIS (U. S. Sales Only), 15p.
18618	25-15144	Dep. NTIS (U. S. Sales Only), 6p.
18625	25-13655	Dep. NTIS (U. S. Sales Only), 40p.
18636	25-15336	Dep. NTIS (U. S. Sales Only), 159p.
18638	25-13120	Dep. NTIS (U. S. Sales Only), 10p.

Report No.	Abstract No.	Availability
18639	25-13103	Dep. NTIS (U. S. Sales Only), 7p.
18642	25-13151	
18643	25-14278	Dep. NTIS (U. S. Sales Only), 28p.
18645	25-14413	Dep. NTIS, 12p.
18646	25-15406	Dep. NTIS (U. S. Sales Only), 45p.
18648	25-14732	Dep. NTIS (U. S. Sales Only), 8p.
18651	25-14846	Dep. NTIS (U. S. Sales Only), 48p.
18652	25-14584	Dep. NTIS (U. S. Sales Only), 11p.
18653	25-13212	Dep. NTIS (U. S. Sales Only), 115p.
18654	25-14847	Dep. NTIS (U. S. Sales Only), 73p.
18655	25-13317	Dep. NTIS (U. S. Sales Only), 10p.
18659	25-13137	Atomic Industrial Forum, Inc. $6.00
18660	25-14733	Dep. NTIS (U. S. Sales Only), 116p.
18662	25-14336	Dep. NTIS (U. S. Sales Only), 134p.
18663	25-14231	Dep. NTIS (U. S. Sales Only), 11p.
NUMEC-		
3731-24	25-13169	Dep. NTIS, 149p.
NYO-		
1082-25	25-15145	Dep. NTIS, 6p.
1082-29	25-15146	Dep. NTIS, 28p.
2171-333	25-15147	Dep. NTIS, 40p.
2262-TA-219	25-14683	Dep. NTIS, 30p.
2262-TA-231	25-14786	Phys. Rev., D; 3: 505-9(15 Jan 1971)
2262-TA-233	25-14633	Dep. NTIS, 18p.
2577-12	25-13393	Dep. NTIS, 30p.
2798-49	25-15436	Dep. NTIS, 18p.
3087-19	25-15437	Dep. NTIS, 2p.
3250-55	25-15229	See DOCKET-50213-94
3270-46	25-15228	See DOCKET-50206-105
3360-55	25-15438	Dep. NTIS, 9p.
3399-237	25-14656	See SU-1206-237
3399-238	25-14637	See SU-1206-238
3827-18	25-15439	Dep. NTIS, 32p.
4204-7	25-14634	Dep. NTIS, 24p.
4204-9	25-14635	Dep. NTIS, 21p.
4204-10	25-14636	Dep. NTIS, 9p.
ORNL-		
4313-3	25-13638	Dep. NTIS, 86p.
4590	25-13656	Dep. NTIS, 256p.
4620	25-13318	Dep. NTIS, 169p.
4643	25-13319	Dep. NTIS, 67p.
ORNL-NSIC-		
75(Rev.1)	25-13469	Dep. NTIS, 626p.
ORNL-TM-		
2484	25-15440	Dep. NTIS, 9p.
2830	25-13328	Dep. NTIS, 77p.
3211	25-13660	Dep. NTIS, 30p.
3237	25-15441	Dep. NTIS, 11p.
3280	25-15442	Dep. NTIS, 24p.
3286	25-15392	Dep. NTIS, 26p.
ORNL-tr-		
2399	25-15148	Dep. NTIS
2408	25-14986	Dep. NTIS
2426	25-15443	Dep. NTIS
2431	25-15444	Dep. NTIS
ORO-		
1316-97	25-14891	Dep. NTIS
2036-21	25-15445	Dep. NTIS, 7p.
2410-18	25-15446	Dep. NTIS, 54p.
2410-19	25-15447	Dep. NTIS, 16p.
PAM-	(French)	
70-8	25-14702	Dep. NTIS (U. S. Sales Only), 17p.
PATENTS	(British)	
1,214,498	25-13035	
1,215,397	25-13094	
1,215,750	25-15415	
1,215,802	25-15414	
1,216,425	25-13200	
1,216,426	25-13199	
1,216,468	25-15369	
1,216,633	25-13738	
1,216,983	25-15364	
1,216,993	25-15413	
1,216,994	25-15416	
1,217,179	25-15383	
1,219,876	25-13206	
1,220,027	25-13205	
1,220,041	25-13204	
PATENTS	(French)	
1,560,128	25-13101	
1,571,948	25-14857	
1,572,805	25-14150	
1,586,431	25-13090	
1,586,726	25-13196	
1,586,737	25-13745	
1,586,938	25-12932	
1,587,616	25-13203	
1,588,604	25-13746	
1,588,605	25-13747	
1,588,611	25-13741	
1,588,805	25-13012	
PATENTS	(German)	
1,188,301	25-13641	For translation see UCRL-Trans-10503
PATENTS	(U. S.)	
3,434,467	25-13529	
3,537,966	25-13036	
3,538,434	25-12931	
3,546,496	25-13173	
3,549,492	25-13208	
PIBAL-	(Non-AEC)	
70-35	25-14490	See AD-711681
PNE-R-		
42	25-12951	See USGS-474-83
PPAD-		
677-D	25-14848	Dep. NTIS, 6p.
PR-	(Non-AEC)	
20	25-14231	See NF-18663
R-	(Misc.)	
71-2	25-15451	See SAN-310-P-4-10
RCN-	(Dutch)	
119	25-15393	Dep. NTIS (U. S. Sales Only), 42p.
RD/B/N-	(British)	
1770	25-13765	Dep. NTIS (U. S. Sales Only), 35p.
RI-	(Misc.)	
70/13	25-13320	Dep. NTIS (U. S. Sales Only), 58p.
RISO-M-	(Danish)	
1270	25-13321	Dep. NTIS (U. S. Sales Only), 14p.
RLO-		
1388-598	25-14820	Dep. NTIS, 21p.
1388-600	25-14892	Dep. NTIS, 9p.
2017-3	25-15448	Dep. NTIS, 83p.
2059-1	25-13394	Dep. NTIS, 7p.
2214-1	25-15449	Dep. NTIS, 15p.
2214-2	25-15450	Dep. NTIS, 33p.
2225-T-11-1	25-13082	Dep. NTIS, 83p.
2225-T-13-3	25-13716	J. Nucl. Mater.; 38: 83-7(Jan 1971)
RME-		
160	25-13125	Dep. GPO $1.75
RT/PROT-	(Italian)	
(70)23	25-13304	Dep. NTIS (U. S. Sales Only), 32p.
SAMSO-TR-	(Non-AEC)	
70-309	25-14360	See AD-711649
70-331	25-13860	See AD-711784
70-352	25-14101	See AD-712045
SAN-		
310-P-4-10	25-15451	Dep. NTIS, 151p.
781-100	25-15355	Dep. NTIS, 75p.
781-220	25-15356	Dep. NTIS, 43p.
781-228	25-15357	Dep. NTIS, 244p.
781-234	25-15358	Dep. NTIS, 97p.
781-243	25-15359	Dep. NTIS, 56p.
781-500	25-15360	Dep. NTIS, 44p.
781-518	25-15361	Dep. NTIS, 42p.
781-2012 (Pt.1)	25-15452	Dep. NTIS, 37p.
SC-DR-		
70-911	25-15453	Dep. NTIS, 20p.
SC-RR-		
70-762	25-15454	Dep. NTIS, 14p.
70-804	25-14084	Dep. NTIS, 19p.
SC-T-		
71-3004	25-15455	Dep. NTIS
71-3005	25-15456	Dep. NTIS
SCL-T-		
71-209	25-15457	Dep. NTIS
71-210	25-15458	Dep. NTIS
71-212	25-15459	Dep. NTIS
SJC-A-	(Non-AEC)	
70-6	25-14849	Dep. NTIS (U. S. Sales Only), 40p.
SLAC-		
121	25-14850	Dep. NTIS, 172p.
128	25-14851	Dep. NTIS, 90p.
SLAC-Trans-		
126	25-14852	Dep. NTIS
SM-	(Misc.)	

Report No.	Abstract No.	Availability
142/46	25-13229	See CEA-CONF-1647
SNC-		
2708-1.	25-13170	Dep. NTIS, 372p.
2708-2	25-13171	Dep. NTIS, 54p.
SRO-	(Misc.)	
552-6	25-13766	Dep. NTIS, 22p.
STI/DCC-	(International Atomic Energy Agency)	
11(Vol.8)(No.2)	25-15460	
STI/PUB-	(International Atomic Energy Agency)	
259(Vol.1)	25-14987	IAEA $21.00
259(Vol.2)	25-14988	IAEA $24.00
272	25-15337	IAEA $2.00
SU-	(Misc.)	
326-P-13-5	25-13152	Dep. NTIS, 38p.
1206-237	25-14656	Dep. NTIS, 12p.
1206-238	25-14637	Dep. NTIS, 23p.
SU-IPR-		
338	25-13859	See AD-711398
350	25-14244	See AD-711669
365	25-13832	See AD-711397
378	25-14286	See N-70-40979
382	25-13936	See AD-711829
SWRHL-		
90-r	25-13395	Dep. CFSTI, 53p.
SZS-	(German)	
16/70	25-13193	Dep. NTIS (U. S. Sales Only), 24p.
19/70	25-13194	Dep. NTIS (U. S. Sales Only), 34p.
20/70	25-15341	Dep. NTIS (U. S. Sales Only), 20p.
TID-		
25314	25-13121	Dep. NTIS, 382p.
25639	25-14703	Dep. NTIS, 131p.
25640	25-14562	Dep. NTIS, 9p.
25641	25-15461	Dep. NTIS, 19p.
TKK-F-A-	(Finnish)	
136	25-12958	Dep. NTIS, 31p.
TR-	(Misc.)	
1	25-13649	See AD-713191
2	25-14147	See AD-711826
31	25-14277	See AD-712024
59(6230-30)-5	25-13860	See AD-711784
59(6260-20)-8	25-14101	See AD-712045
59(9220-2)-1	25-14360	See AD-711649
88	25-13995	See AD-711664
TRG-Report-	(British)	
2040	25-13640	Dep. NTIS (U. S. Sales Only). UK 3s. 0d, 12p.
TT-	(Misc.)	
68-50325/1	25-14583	See AEC-tr-6882/1
UCRL-		
13329(Pt.2)	25-13130	Dep. NTIS, 101p.
19719	25-13959	Dep. NTIS, 36p.
19919	25-14853	Dep. NTIS, 24p.
20032	25-14657	Dep. NTIS, 186p.
20202	25-15462	Dep. NTIS, 142p.
20369	25-13783	Dep. NTIS, 138p.
20376	25-15463	Dep. NTIS, 90p.
50656(Suppl.)	25-14989	Dep. NTIS, 150p.
50855	25-13104	Dep. NTIS, 172p.
50892(Vol.4)(Pt.1)	25-13322	Dep. NTIS, 79p.
50892(Vol.4)(Pt.2)	25-13323	Dep. NTIS, 185p.
50937	25-15464	Dep. NTIS, 14p.
50948	25-15465	Dep. NTIS, 10p.
50950	25-15466	Dep. NTIS, 20p.
71508	25-13213	Dep. NTIS, 11p.
72511	25-13396	Dep. NTIS, 18p.
72627	25-13661	Dep. NTIS, 7p.
72663	25-15467	Dep. NTIS, 8p.
72830	25-13430	Dep. NTIS, 23p.
UCRL-Trans-		
1420	25-14854	Dep. NTIS
1421	25-14855	Dep. NTIS
1425	25-14856	Dep. NTIS
10503	25-13641	Dep. NTIS
UCSD-		
10-P-20-54	25-15468	Dep. NTIS, 103p.
UNC-	(Misc.)	
5231	25-15362	Dep. NTIS, 131p.
URS-	(Non-AEC)	
757-6	25-13132	See AD-711021
USGS-		
474-83	25-12951	Dep. NTIS, 16p.
474-84	25-13105	Dep. NTIS, 35p.
UTEC-MSE-		
70-211	25-15427	See CCO-1591-13
UUIP-	(Swedish)	
677	25-14212	Dep. NTIS (U. S. Sales Only), 26p.
715	25-13324	Dep. NTIS (U. S. Sales Only), 20p.
WAPD-TM-	(Misc.)	
968	25-15353	Dep. NTIS, 21p.
976	25-13181	Dep. NTIS, 79p.
986	25-15366	Dep. NTIS, 32p.
WCAP-	(Misc.)	
7562-1	25-13230	Dep. NTIS, 58p.
WHAN-FR-		
33	25-13083	Dep. NTIS, 38p.
WHAN-IR-		
42	25-15354	Dep. NTIS, 33p.
48	25-15343	Dep. NTIS, 28p.
Y-		
1748	25-15469	Dep. NTIS, 35p.
ZJE-	(Czechslovakian)	
66	25-13153	Dep. NTIS (U. S. Sales Only), 24p.
92	25-15410	Dep. NTIS (U. S. Sales Only), 14p.

XUM

Appendix I

JOURNAL LIST

This list of journals supplements the listing which appeared as Appendix II in Volume 25, Number 1. The journals are arranged alphabetically by abbreviation. Additional supplements will be included in numbers 13 and 19 of this volume.

The title abbreviations are based on the National Clearinghouse for Periodical Title Word Abbreviations, *Word Abbreviation List* published by the Standards Committee Z-39 of the American National Standards Institute.

TID-4579 (5th Ed.) *Serial Titles Cited in Nuclear Science Abstracts* lists the titles and abbreviations of the journals regularly scanned for *NSA* as well as those from which an occasional item is taken. This publication is available from the National Technical Information Service (NTIS), U. S. Department of Commerce, Springfield, Virginia, 22151, for $6.00 for full size or reproduction copy and $0.95 for microfiche copy.

A

Acta Math. (Uppsala)
Acta Mathematica (Uppsala) (Sweden)

Acta Neurol. (Naples)
Acta Neurologica (Naples) (Italy)

Acta Pathol. Microbiol. Scand., Sect. A
Acta Pathologica et Microbiologica Scandinavica,
Section A. Pathology (Denmark)

Acta Pathol. Microbiol. Scand., Sect. A, Suppl.
Acta Pathologica et Microbiologica Scandinavica,
Section A. Pathology, Supplementum (Formerly Acta
Pathologica et Microbiologica Scandinavica, Supplementum)
(Denmark)

Acta Pathol. Microbiol. Scand., Sect. B
Acta Pathologica et Microbiologica Scandinavica,
Section B. Microbiology and Immunology (Denmark)

Acta Univ. Upsal., Abstr. Uppsala Diss. Med.
Acta Universitatis Upsaliensis, Abstracts of Uppsala
Dissertations in Medicine (Sweden)

Acta Vet. (Brno)
Acta Veterinaria (Brno) (Czechoslovakia)

Actinides Lanthanides Rev.
Actinides and Lanthanides Reviews (Netherlands)
Supersedes Actinides Reviews

Advan. Hum. Genet.
Advances in Human Genetics (U. S.)

Advan. Mater. Res.
Advances in Materials Research (U. S.)

Advan. Microbial Physiol.
Advances in Microbial Physiology (England)

Advan. Oto-Rhino-Laryngol.
Advances in Oto-Rhino-Laryngology (Switzerland)
Supersedes Bibliotheca Oto-Rhino-Laryngologica

Agents Actions
Agents and Actions (Switzerland)

Agrochimica
Agrochimica (Italy)

Amer. Fam. Physician - GP
American Family Physician - GP (U. S.)
Supersedes GP, Journal of the American Academy of
General Practice

Ann. Chim. Appl.
Annali di Chimica Applicata (Italy)
Superseded by Annali di Chimica (Rome)

Ann. Gastroenterol. Hepatol.
Annales de Gastroenterologie et d'Hepatologie (France)

Ann. Med. Interne
Annales de Medecine Interne (France)
Supersedes Bull. Mem. Soc. Med. Hop. Paris

Ann. Meteorol.
Annalen der Meteorologie (West Germany)

Annu. Bull., Int. Dairy Fed.
Annual Bulletin, International Dairy Federation (Belgium)

Arch. De Vecchi Anat. Patol. Med. Clin.
Archivio De Vecchi Anatomia Patological e la Medicina Clinic
(Italy)

Argonne Rev.
Argonne Reviews (U. S.)
Supersedes Argonne National Laboratory Reviews

At. Energy Law Rep.
Atomic Energy Law Reports (U. S.)

Atherosclerosis
Atherosclerosis (Netherlands)
Supersedes Journal of Atherosclerosis Research

Aust. Chem. Process. Eng.
Australian Chemical Processing and Engineering (Australia)

Australas. J. Pharm., Sci. Suppl.
Australasian Journal of Pharmacy, Science Supplement
(Australia)

B

Beitr. Pathol.
Beitraege zur Pathologie (West Germany)
Supersedes Beitraege zur Pathologischen Anatomie und zur
Allgemeinen Pathologie

Beitr. Radioastron.
Beitraege zur Radiostronomie (West Germany)

Bol. Estud. Med. Biol.
Boletin de Estudios Medicos y Biologicos (Mexico)

Brit. J. Occup. Saf.
British Journal of Occupational Safety (England)

Bull. Inst. Int. Froid
Bulletin de l'Institut International du Froid (France)

Bull., Int. Union Cancer
Bulletin, International Union Against Cancer (Switzerland)

Bygg
Bygg (Norway)

Byull. Gl. Bot. Sada
Byulleten Glavnogo Botanicheskogo Sada (U.S.S.R.)

C

Californium-252 Progr.
Californium-252 Progress (U. S.)

Carbohyd. Res.
Carbohydrate Research (Netherlands)

Cesk. Pediat.
Ceskoslovenska Pediatrie (Czechoslovakia)

Cesk. Zdrav.
Ceskoslovenske Zdravotnictvi (Czechoslovakia)

Chem. N. Z.
Chemistry in New Zealand (New Zealand)
Supersedes Journal of the New Zealand Institute of Chemistry

Chest (Chicago)
Chest (Chicago) (U. S.)
Supersedes Diseases of the Chest

Chirurgie
Chirurgie (France)
Supersedes Memoires de l'Academie de Chirurgie

Chutanzo
Chutanzo (Casting and Forging) (Japan)

Ciel Terre
Ciel et Terre (Belgium)

Civil Eng. Trans., Inst. Eng., Aust.
Civil Engineering Transactions, Institution of Engineers, The, Australia (Australia)

Constructeur
Constructeur, De (Absorbed Constructiematerialen) (Netherlands)

D

Denshi Tsushin Gakkai Ronbunski, C
Denshi Tsushin Gakkai Ronbunshi, C (Japan)

Develop. Appl. Spectrosc.
Developments in Applied Spectroscopy (U. S.)

Diastema
Diastema (South Africa)

E

Eclogae Geol. Helv.
Eclogae Geologicae Helvetiae (Switzerland)

ELDO/ESRO Sci. Tech. Rev.
ELDO/ESRO Scientific and Technical Review (France)

Electro
Electro (Norway)
Supersedes Elektroteknisk Tidsskrift

Electromedica
Electromedica (West Germany)

Elektronika
Elektronika (Formerly Przeglad Elektroniki) (Poland)

Energomashinostroenie
Energomashinostroenie (U.S.S.R.)

Eur. J. Clin. Invest.
European Journal of Clinical Investigation (West Germany)
Supersedes Archiv fuer Klinische Medizin

F

Farbe Lack
Farbe und Lack (West Germany)

Farm. Obz.
Farmaceuticky Obzor (Czechoslovakia)

Faserforsch. Textiltech.
Faserforschung und Textiltechnik (East Germany)

Fiziol. Biokhim. Kul't. Rast.
Fiziologiya i Biokhimiya Kul'turnykh Rastenii (Ukrainian S. S. R.)

Fiz.-Khim. Mekh. Mater.
Fiziko-Khimicheskaya Mekhanika Materialov (Ukrainian S.S.R.)
Issued in English translation as Soviet Materials Science

Fonderia Ital.
Fonderia Italiana (Italy)

Food Ind. J.
Food Industries Journal (India)

Forsk. Framsteg
Forskning och Framsteg (Sweden)

Frequenz
Frequenz (West Germany)

Fukushima Igaku Zasshi
Fukushima Igaku Zasshi (Fukushima Medical Journal) (Japan)

G

Gas- Wasserfach, Wasser - Abwasser
Gas- und Wasserfach, Wasser - Abwasser (West Germany)
Continues in part Gas- und Wasserfach, Das

Geol. Pruzkum
Geologicky Pruzkum (Czechoslovakia)

G. Psichiat. Neuropatol.
Giornale di Psichiatria e di Neuropatologia (Italy)

Gradbeni Vestn.
Gradbeni Vestnik (Yugoslavia)

Gynecol. Invest.
Gynecologic Investigation (Switzerland)
Supersedes Gynaecologia

H

Hoshasen Kagaku
Hoshasen Kagaku (Japan)

I

Iden
Iden (Heredity) (Japan)

Indian J. Math.
Indian Journal of Mathematics (Indian)

Indian J. Pure Appl. Math.
Indian Journal of Pure and Applied Mathematics (India)

Indian J. Sci. Ind.
Indian Journal of Science and Industry (India)

Industriekurier
Industriekurier (West Germany)

Infec. Immunity
Infection and Immunity (U. S.)

Int. J. Magn.
International Journal of Magnetism (England - U. S.)

Irrig. Power
Irrigation and Power (India)

Isotope Ind. Landwirt.
Isotope in Industrie und Landwirtschaft (Austria)

Izv. Akad. Nauk Arm. SSR, Geol. Geogr. Nauki
Izvestiya Akademii Nauk Armyanskoi SSR, Geologicheskie i Geograficheskie Nauki (Armenian S.S.R.)
Superseded by Izv. Akad. Nauk Arm. SSR, Nauki Zemle

Izv. Akad. Nauk Kirg. SSR
Izvestiya Akademii Nauk Kirgizskoi SSR (Kirgiz S.S.R.)

Izv. Akad. Nauk SSSR, Mekh. Tverd. Tela
Izvestiya Akademii Nauk SSSR, Mekhanika Tverdogo Tela (U.S.S.R.)

Izv. Akad. Nauk Turkm. SSR, Ser. Biol. Nauk
Izvestiya Akademiya Nauk Turkmenskoi SSR, Seriya Biologicheskikh Nauk (Turkmen S.S.R.)

J

J. Brit. Astron. Ass.
Journal of the British Astronomical Association (England)

J. Helminthol.
Journal of Helminthology (England)

J. Lumin.
Journal of Luminescence (Netherlands)

J. Med. Microbiol.
Journal of Medical Microbiology (Scotland)

J. Membrane Biol.
Journal of Membrane Biology (U. S.)

J. Norw. Med. Ass.
Journal of the Norwegian Medical Association (Norway)

J. Oil Colour Chem. Ass.
Journal of the Oil and Colour Chemists' Association (England)

XUM

J. Polym. Sci., Part D
Journal of Polymer Science, Part D. Macromolecular Reviews (U. S.)

J. Range Manage.
Journal of Range Management (U. S.)

J. Roy. Coll. Surg. Ireland
Journal of the Royal College of Surgeons in Ireland (Ireland)

J. Therm. Anal.
Journal of Thermal Analysis (England)

J. Univ. Poona
Journal of the University of Poona (India)

K

Kaijo Hoan Daigakko Kenkyu Hokoku, Dai-2-Bu
Kaijo Hoan Daigakko Kenkyu Hokoku, Dai-2-Bu (Journal of Maritime Safety Academy, Part 2) (Japan)

Kansai Ika Daigaku Zasshi
Kansai Ika Daigaku Zasshi (The Journal of the Kansai Medical School) (Japan)

Kazan. Med. Zh.
Kazanskii Meditsinskii Zhurnal (U.S.S.R.)

Kerntech. Atomprax.
Kerntechnik und Atompraxis (West Germany)
Supersedes Atompraxis and Kerntechnik from Jan. 1971

Khim. Drev.
Khimiya Drevesiny (Latvian S.S.R.)

Kratk. Soobshch. Fiz.
Kratkie Soobshcheniya po Fizike (U.S.S.R.)

Kyushu Ketsueki Kenkyu Dokokaishi
Kyushu Ketsueki Kenkyu Dokokaishi (Journal of Kyushu Hematological Society) (Japan)

L

Lantbrukshogsk. Ann.
Lantbrukshogskolans Annaler (Sweden)

M

Manuscr. Math.
Manuscripta Mathematica (West Germany)

Maroc Med.
Maroc Medical (Morocco)

Mar. Pollut. Bull.
Marine Pollution Bulletin (England)

Maschinemarkt
Maschinemarkt (West Germany)

Mecan. Mater. Elec.
Mecanique Materiaux Electricite (France)
Supersedes Mecanique Electricite

Methods Comput. Phys.
Methods in Computational Physics (U. S.)

Microvasc. Res.
Microvascular Research (U. S. - England)

Minerva Oftalmol.
Minerva Oftalmologica (Italy)

Munkavedelem
Munkavedelem (Hungary)

N

Nat. Saf. News
National Safety News (U. S.)

Natuurwetensch. Tijdschr. (Ghent)
Natuurwetenschappelijk Tijdschrift (Ghent) (Belgium)

Neuropharmacology
Neuropharmacology (England)
Supersedes International Journal of Neuropharmacology

Nucl. Technol.
Nuclear Technology (U. S.)
Supersedes Nuclear Applications and Technology

Nutr. Metab.
Nutrition and Metabolism (Switzerland)
Supersedes Nutritio et Dieta

O

Oceans
Oceans (U. S.)

Organometal. Chem. Rev., Sect. A
Organometallic Chemistry Reviews, Section A. Subject Reviews (Netherlands)
Supersedes in part Organometallic Chemistry Reviews

P

Period. Polytech., Mech. Eng.
Periodica Polytechnica, Mechanical Engineering (Hungary)
Supersedes Periodica Polytechnica, Engineering

Pharmacol. Res. Commun.
Pharmacological Research Communication (England)

Physiol. Chem. Phys.
Physiological Chemistry and Physics (U. S.)

Postepy Astronaut.
Postepy Astronautyki (Poland)

Powder Met. Int.
Powder Metallurgy International (West Germany)

Probl. Arktiki Antarktiki
Problemy Arktiki i Antarktiki (U.S.S.R.)

Probl. Kosm. Phys.
Probleme der Kosmichen Physik (West Germany)

Probl. Sov. Geol.
Problemy Sovetskoi Geologii (U.S.S.R.)

Proc. Indian Nat. Sci. Acad., Part A
Proceedings of the Indian National Science Academy, Part A. Physical Sciences (Formerly Proceedings of the National Institute of Sciences of India, Part A) (India)

Proc. Indian Nat. Sci. Acad., Part B
Proceedings of the Indian National Science Academy, Part B. Biological Sciences (Formerly Proceedings of the National Institute of Sciences of India, Part B) (India)

Proc., Inst. Teknol. Bandung
Proceedings, Institut Teknologi Bandung (Indonesia)

Proc. Roy. Soc. Med., Suppl.
Proceedings of the Royal Society of Medicine, Supplement (England)

Progr. Nucl. Acid Res. Mol. Biol.
Progress in Nucleic Acid Research and Molecular Biology (Formerly Progress in Nucleic Acid Research) (U. S.)

R

Reakts. Metody Issled. Org. Soedin.
Reaktsii i Metody Issledovaniya Organicheskikh Soedinenii (U.S.S.R.)

Recherche (Paris)
Recherche, La (Paris) (France)
Supersedes Atomes (Paris)

Rev. Agroquim. Tecnol. Aliment.
Revista de Agroquimica y Tecnologia de Alimentos (Spain)

Rev. Fr. Allergol.
Revue Francaise d'Allergologie (France)
Supersedes Revue Francaise d'Allergie

Rev. Med. (Tirgu-Mures)
Revista Medicala (Tirgu-Mures) (Romania)

Rev. Venez. Sanid. Asistencia Soc.
Revista Venezolana de Sanidad y Asistencia Social (Venezuela)

Riv. Sper. Freniat. Med. Leg. Alienazioni Ment.
Rivista Sperimentale di Freniatria e Medicina Legale delle Alienazioni Mentali (Italy)

S

Safety (London)
Safety (London) (England)

Schweiz. Bauztg.
Schweizerische Bauzeitung (Switzerland)

Search
  Search. Science, Technology and Society (Australia)
  Supersedes Australian Journal of Science

Seibutsu Kagaku
  Seibutsu Kagaku (Biological Science) (Japan)

Showa Igakkai Zasshi
  Showa Igakkai Zasshi (The Journal of the Showa Medical Association) (Japan)

Shoyakugaku Zasshi
  Shoyakugaku Zasshi (Journal of Pharmacognosy) (Japan)

Soobshch. Byurakan. Observ., Akad. Nauk Arm. SSR
  Soobshcheniya Byurakanskoi Observatorii, Akademiya Nauk Armyanskoi SSR (Armenian S.S.R.)

Spec. Publ., Geol. Soc. Aust.
  Special Publication, Geological Society of Australia (Australia)

Springer Tracts Mod. Phys.
  Springer Tracts in Modern Physics. Ergebnisse der Exakten Naturwissenschaften (West Germany)

Stahlbau
  Stahlbau (West Germany)

Strength Mater. (USSR) (Engl. Transl.)
  Strength of Materials (USSR) (English Translation of Problemy Prochnosti) (U. S.)

Stud. Cercet. Met.
  Studii si Cercetari de Metalurgie (Romania)

Sumitomo Search
  Sumitomo Search (Japan)

Symp. Zool. Soc. London
  Symposia of the Zoological Society of London and The Malacological Society of London (England)

Synthesis
  Synthesis (West Germany)

T

Tekniikka
  Tekniikka (Finland)
  Supersedes Teknillinen Aikakauslehti

Teplofiz. Teplotekh.
  Teplofizika i Teplotekhnika (Ukrainian S.S.R.)

Termoproch. Mater. Konstr. Elem.
  Termoprochnost Materialov i Konstruktivnykh Elementov (U.S.S.R.)

TNO Nieuws
  TNO Nieuws (Netherlands)

Tokyo Toritsu Eisei Kenkyusho Nempo
  Tokyo Toritsu Eisei Kenkyusho Nempo (Annual Report of Tokyo Metropolitan Labs. for Medical Science) (Japan)

Tool. Prod.
  Tooling and Production (U. S.)

Tr. Gidrometeorol. Nauch.-Issled. Tsent. SSSR
  Trudy Gidrometeorologicheskogo Nauchno-Issledovatel'skogo Tsentra SSSR (U.S.S.R.)

Tr. Inst. Fiz. Zemli, Akad. Nauk SSSR
  Trudy Instituta Fiziki Zemli, Akademiya Nauk SSSR (U.S.S.R.)

Tr. Mosk. Obshchest. Ispyt. Prir.
  Trudy Moskovskogo Obshchestva Ispytatelei Prirody (U.S.S.R.)

Tr. Tbilis. Gos. Univ.
  Trudy Tbilisskogo Gosudarstvennogo Universiteta (Georgian S.S.R.)

U

Urologe, Ausg. A
  Urologe, Der, Ausgabe A (West Germany)
  Supersedes in part Urologe, Der

V

Vestn. Khar'kov. Politekh. Inst.
  Vestnik Khar'kovskogo Politekhnicheskogo Instituta (Ukrainian S.S.R.)

Vigyan Pragati
  Vigyan Pragati (India)

Vod. Hospod., B
  Vodni Hospodarstvi, B (Czechoslovakia)

Vop. Magmat. Metamorfiz.
  Voprosy Magmatizma i Metamorfizma (U.S.S.R.)

W

Wasser, Luft Betr.
  Wasser, Luft und Betrieb (West Germany)

Weather (London)
  Weather (London) (England)

Werkstatt Betr.
  Werkstatt und Betrieb (West Germany)

Z

Zairyo Kagaku
  Zairyo Kagaku (Japan)

Z. Tierphysiol. Tierernaehr. Futtermittelk.
  Zeitschrift fuer Tierphysiologie Tierernaehrung und Futtermittelkunde (West Germany)

Z. Wasser- Abwasserforsch.
  Zeitschrift fuer Wasser- und Abwasserforschung (West Germany)

Z. Wirt. Fertigung
  Zeitschrift fuer Wirtschaftliche Fertigung (West Germany)

☆U. S. GOVERNMENT PRINTING OFFICE: 1971—436-213/21

XUM

UNITED STATES
ATOMIC ENERGY COMMISSION
P. O. BOX 62
OAK RIDGE, TENNESSEE 37830

OFFICIAL BUSINESS

POSTAGE AND FEES PAID
U. S. ATOMIC ENERGY COMMISSION

POSTAGE AND FEES PAID
U. S. GOVERNMENT PRINTING OFFICE

UNIVERSITY MICROFILMS
ATTN MRS. MARLENE HURST
MANAGER, PUBLISHER RELATIONS
ANN ARBOR MICHIGAN 48106

1

AEC Symposium Series

PRECIPITATION SCAVENGING (1970)

Coordinators: R. J. Engelmann and W. G. N. Slinn

This volume contains the proceedings of the 1970 Precipitation Scavenging Meeting, Battelle–Northwest, Richland, Washington, June 2–4, 1970. Thirty-eight papers assess the state-of-the-art and provide a wide perspective of research and projects, including experimental techniques, experimental data, microphysics in scavenging, and models for predicting scavenging. Available as CONF-700601 for $6.00 a copy from the National Technical Information Service, Springfield, Virginia 22151. (512 pages, 194 illus., 6 by 9 in., Library of Congress Catalog Card No. 70-609397)

CONTENTS

Scavenging in Perspective, *J. J. Fuquay*
Priorities in Scavenging Research, *R. J. Engelmann*
Radar Observations of Convective Storm Circulation and Its Relation to Precipitation Scavenging, *R. M. Lhermitte*
Scavenging of Tracer in Severe Storms, *A. N. Dingle*
Interactions of Cloud Condensation Nuclei and Ice Nuclei with Cloud and Precipitation Elements: A Review, *L. F. Radke, W. D. Scott, and C. E. Robertson*
Entry of Freezing Nuclei into Precipitation, *G. Vali*
In-Cloud Scavenging Analysis from Cosmogenic Radionuclide Measurements, *R. W. Perkins, C. W. Thomas, J. A. Young, and B. C. Scott*
Stable Elements of the Atmosphere as Tracers of Precipitation Scavenging, *L. A. Rancitelli, R. W. Perkins, T. M. Tanner, and C. W. Thomas*
Concentration Variation of Some Trace Metals in Precipitation from Great Plains Thunderstorms, *D. H. Steffe*
Scavenging by Snow and Ice Crystals, *S. K. Sood and M. R. Jackson*
Scavenging of Soluble Dye Particles by Rain, *M. T. Dana*
Collection Efficiencies of Raindrops for Submicron Particulates, *J. R. Adam and R. G. Semonin*
Collection Efficiency of Water Droplets in AgCl Aerosol, *M. Kerker, E. Matijević, V. Hampl, and D. Cooke*
Collection Efficiency in Washout by Rain, *T. G. Owe Berg*
Scavenging of Aerosol Particles by Sprays, *J. D. McCormack and R. K. Hilliard*
Continuous Charged Cloud-Particle Sampler, *C. P. R. Saunders, M. H. Smith, and J. Latham*
Pulsed-Laser Holography for Analysis of Particle Size and Distribution, *F. R. Reich and B. P. Hildebrand*
Thermal-Diffusion Chambers as Cloud-Nuclei Counters, *V. K. Saxena and J. L. Kassner, Jr.*
Automatic Sequential Rain Sampler for Scavenging Studies, *D. F. Gatz, R. F. Selman, R. K. Langs, and R. B. Holtzman*
Effect of Solubilities of Gases on Their Scavenging by Raindrops, *A. K. Postma*
Laboratory Investigations on Washout of Trace Gases, *S. Beilke*
Washout of Gaseous Iodine Species, *L. F. Coleman and A. K. Postma*
European Interest in Acidic Precipitation, *H. Reiquam*
Washout of SO_2 from the Plume of a Coal-Fired Power Plant, *J. M. Hales, J. M. Thorp, and M. A. Wolf*
Scavenging of SO_2 by Convective Storms, *P. W. Summers*
Mechanisms of Iodine Injection from the Sea Surface, *C. S. Martens and R. C. Harriss*
Model for Variations with Particle Size of Halogen-Ion Ratios in Marine Aerosols, *J. A. Robbins*
Theory of Diffusive and Impactive Scavenging, *G. M. Hidy*
Attachment of Trace Substances on Atmospheric Aerosols, *J. R. Brock*
Recent Calculations of Collision Efficiencies, *L. M. Hocking*
Processes Influencing Evolution of Droplet or Aerosol Spectrum, *R. L. Drake*
Particle-Free Space in Stefan Flow, *O. A. Vittori and V. Prodi*
Phoretic Processes in Scavenging, *W. G. N. Slinn and J. M. Hales*
Precipitation Scavenging in a Large-Cloud Diffusion Code, *K. R. Peterson and T. V. Crawford*
Scavenging of Aerosols by Rain: A Numerical Study, *R. N. Kortzeborn and F. F. Abraham*
Tropospheric Scavenging of ^{90}Sr and ^{3}H, *P. W. Krey and B. Krajewski*
Use of Natural Radioactivities To Estimate Large-Scale Precipitation Scavenging, *L. Machta, R. J. List, M. E. Smith, Jr., and H. Oeschger*
Scavenging Prediction Using Ratios of Concentrations in Air and Precipitation, *R. J. Engelmann*
Closing Remarks, *R. J. Engelmann*

XUM

XUM